Journal of Inorganic & Nuclear Chemistry

VOLUME 24 1962

EDITORS

JOSEPH J. KATZ Argonne · A. G. MADDOCK Cambridge · L. E. J. ROBERTS Harwell · E. J. W. VERWEY Eindhoven

EDITORIAL ADVISORY BOARD

U.K. and Commonwealth: J. S. ANDERSON, F.R.S., Teddington · C. C. ADDISON, Nottingham · C. B. AMPHLETT, Harwell · F. M. BREWER, Oxford · G. E. COATES, Durham · J. F. DUNCAN, Melbourne · H. J. EMELÉUS, F.R.S., Cambridge · F. FAIRBROTHER, Manchester · J. H. GREEN, Kensington, N.S.W. · H. M. N. H. IRVING, Leeds · L. E. ORGEL, Cambridge · A. R. POWELL, F.R.S., Wembley · P. L. ROBINSON, Newcastle-upon-Tyne · R. SPENCE, Harwell · H. G. THODE, F.R.S., Hamilton · L. YAFFE, Montreal

U.S.A.: L. F. AUDRIETH and JOHN C. BAILAR JR., Univ. of Illinois · F. BASOLO, Northwestern Univ. · E. O. BRIMM, Linde Air Products · HERBERT C. BROWN, Purdue · ANTON B. BURG, Univ. South Calif. · CHARLES D. CORYELL, M.I.T. · R. W. DODSON, Brookhaven · W. CONARD FERNELIUS, Koppers Company, Penn. · WARREN C. JOHNSON, Chicago · H. B. JONASSEN, Tulane Univ. · JACOB KLEINBERG, Univ. of Kansas · K. A. KRAUS, Oak Ridge · W. F. LIBBY, Los Angeles · W. M. MANNING, Argonne · THERALD MOELLER, Univ. of Illinois · EARL L. MUETTERTIES, Wilmington, Delaware · EUGENE G. ROCHOW, Harvard · GLENN T. SEABORG, Univ. of California · P. W. SELWOOD, Evanston · F. H. SPEDDING, Ames · R. W. STOUGHTON, Oak Ridge · J. R. VAN WAZER, Missouri · DON M. YOST, Pasadena, Calif. · W. H. ZACHARIASEN, Chicago · R. A. PENNEMAN and B. B. CUNNINGHAM, Univ. of California · H. TAUBE, Chicago

Austria: E. BRODA, Vienna · BERTHA KARLIK, Vienna · V. GUTMANN, Vienna
Denmark: J. BJERRUM, Copenhagen
France. J. BÉNARD, Paris · J. CHÉDIN, Paris · J. GUÉRON, Paris · M. MAGAT, Paris
Germany: W. HIEBER, Munich · G. JANDER, Berlin · A. MUENSTER, Frankfurt
Netherlands: A. E. VAN ARKEL, Leiden · A. H. W. ATEN JR., Amsterdam
J. H. DE BOER, Geleen · J. H. VAN SANTEN, Eindhoven
Israel: M. BOBTELSKY, Jerusalem · *Italy:* V. CAGLIOTI, Rome
Norway: H. HARALDSEN, Oslo · ODD HASSEL, Oslo
Persia: H. A. C. McKAY, Tehran
Sweden: G. HÄGG, Uppsala · L. G. SILLÉN, Stockholm
Switzerland: G. SCHWARZENBACH, Zurich

PERGAMON PRESS OXFORD · LONDON · NEW YORK · PARIS

NOTES FOR CONTRIBUTORS

I. General

1. Papers should, in general, be concerned with original work in the field of inorganic and nuclear chemistry. They should be submitted to the Editors, whose names and addresses follow (papers not in the English language to Dr. E. J. W. Verwey):—

Joseph J. Katz: *Argonne National Laboratory, 9700 South Cass Avenue, Argonne, Illinois, U.S.A.*
A. G. Maddock: *University Chemical Laboratory, Lensfield Road, Cambridge, England*
L. E. J. Roberts: *Atomic Energy Research Establishment, Harwell, Didcot, Berks, England*
E. J. W. Verwey: *Philips Research Laboratories, Eindhoven, The Netherlands*

2. Fifty free reprints of each paper are supplied. Additional copies can be supplied at a reasonable cost if ordered at the time when the first proofs are returned. A reprint order form will accompany proofs.

II. Script Requirements

1. Scripts should be submitted in duplicate. They must be typewritten, and double-spaced. Authors are requested to make clear any Greek characters which may be confused with ordinary letters or with other characters. Authors will receive proofs for correction when their contribution is first set, but there is rarely time for page proofs also to be sent for checking. This will be done, however, where the amount of alteration makes it advisable.

2. Illustrations should be placed at the end of the manuscript, and legends should be typed on a separate sheet. It is requested that photographs should be kept to the minimum necessary. Line drawings or good photo-prints may be provided. Line drawings must include all relevant details: if they are already well drawn it may be possible to reproduce them direct from the original. It is not possible to reproduce from "dye-line" prints, or from prints with weak lines. Illustrations for reproduction should normally be about twice the final size required. Any lettering on diagrams—other than Greek letters, symbols, etc.—should be stencilled and should be sufficiently large and bold to permit reproduction when the diagram has been reduced to a size suitable for inclusion in the journal.

3. References should be clearly indicated in the text by superior numbers. Full references should be given in numbered footnotes containing author's name, initials, title of paper (where desired), abbreviated title of journal, year, volume number, and page number.

4. The text of articles submitted must be concise and in a readily understandable style. The technical description of the methods used should only be given in detail when such methods are new. The essential contents of each paper should be briefly recapitulated in an abstract. French and German papers should be submitted with English abstracts. **Four copies of the English abstracts are required with all papers, including those in the English language.**

5. To conserve space, authors are requested to mark less important portions of the paper (such as description of methods, record of experimental results, etc.) for printing in smaller type.

Publishing Offices: Headington Hill Hall, Oxford (Oxford 64881)

Issued in parts. Subscription per annum, including postage: (*A*) £33 (*U.S.A.* $100); (*B*) *for subscribers who write direct to the publisher certifying that the subscription is for their personal use,* £5.5s. (*U.S.A.* $15). *Back numbers, price on application.*

Copyright © 1962 *Pergamon Press Ltd.*

PRINTED IN NORTHERN IRELAND AT THE UNIVERSITIES PRESS, BELFAST

LIST OF CONTENTS

Pages 1-112 (January, 1962)

J. M. **Ferguson**, D. L. **Love** and D. **Sam**: γ-Ray spectra of ^{123m}Te and ^{124}Te 1
K. E. **Siekierska** and A. **Sokolowska**: Reaction of neutron activated arsenic atoms in organic media—II. AsPh$_3$–benzene system 13
E. **Whipple** and A. **Wold**: Preparation of stoicheiometric chromites 23
A. E. **Ogard**, W. C. **Pritchard**, R. M. **Douglass** and J. A. **Leary**: The preparation of uranium monocarbide–plutonium monocarbide solid solutions, plutonium sesquicarbide and plutonium monocarbide 29
E. J. **Felten** and E. A. **Aitken**; The mechanism and kinetics of the formation of $UO_{2.00} \cdot 6YO_{1.5}$ 35
J. W. **Frazer**, B. E. **Holder** and E. F. **Worden**: The preparation and identification of N-fluoro-N′-trifluoromethyldiazine-N′-oxide 45
T. J. **Mao**, R. D. **Dresdner** and J. A. **Young**: The preparation of polyfluoroalkyl phosphonitrilates and N-(perfluoroacyl) phosphoramidic dichlorides 53
R. C. **Johnson**, F. **Basolo** and R. G. **Pearson**: Base hydrolysis of some chloroammineplatinum(IV) complexes 59
W. Z. **Heldt**: Reactions of co-ordinated ligands—III. Reactions of iron isonitrile complexes with nucleophiles 73
E. R. **Clark**: Complex formation between germanic acid and α-hydroxy acids—II. Mandelic acid 81
J. O. **Wear**, J. T. **Curtis**, Jr. and E. S. **Amis**: A study of transference and solvation phenomena—VI. Hydrochloric acid in water and water–ethanol solvents 93
S. C. **Chattoraj**, C. A. **Hollingsworth**, D. H. **McDaniel** and G. B. **Smith**: The lithium aluminium hydride–ethyl ether system at 25°C 101
R. L. **Martin** and J. B. **West**: Solubility of magnesium oxide in molten salts . . . 105

Pages 113–220 (February, 1962)

S. J. **Nassif**, S. **Abecasis** and A. **Mocoroa**: Yield ratios for the isomeric pair ^{121m}Te, ^{121}Te produced in *^{121}Sb(d,2n) ^{121}Te nuclear reaction* 113
E. **Hagebø**, A. **Kjelberg** and A. C. **Pappas**: Radiochemical studies of isotopes of antimony and tin in the mass region 127–130 117
C. W. **Owens** and F. S. **Rowland**: The chemical state of chlorine-36 in neutron-irradiated minerals 133
M. **Vlatković** and A. H. W. **Aten**, Jr: Thermal annealing of neutron-irradiated chlorine oxyanions 139
A. V. **Grosse**: The relationship between the surface tensions and energies of liquid metals and their critical temperatures 147
J. E. **Fergusson**, G. M. **Pratt**, G. A. **Rodley** and C. J. **Wilkins**: Selenium-sulphur solid solutions 157
A. D. **Craig** and A. G. **MacDiarmid**: Application of the Wurtz reaction to the synthesis of disilane and 1,2-dimethyldisilane 161
R. S. **Feinberg** and E. G. **Rochow**: Halogen rearrangement in organosilicon halides . . 165
G. B. **Deacon** and B. O. **West**: The reactions of metal complexes with alkyl halides—I. Reactions of halo(triphenylphosphine)mercury(II) and quaternary halomercurate(II)complexes 169
F. G. **Sherif** and A. M. **Awad**: Revaluation of the continuous variation method as applied to the uranyl azide complexes 179
J. E. **Powell**: The separation of lithium isotopes by ion exchange 183
J. **Shankar** and B. C. **de Souza**: Isotopic exchange in the cobaltous–cobaltic system in perchloric acid 187
C. **Grigorescu-Sabău**: Ion exchange equilibria in the presence of organic solvents—I. The influence of organic solvents on the distribution constant of praseodymium . . . 195
S. **Siekierski**: The influence of diluent on extraction of europium and thorium nitrates by tri-*n*-butylphosphate 205

Note:
K. S. Bhatki, K. P. Gopinathan and A. T. Rane: Preparation of high activity terbium^{161} from gadolinium 215
Notice 218
Errata 219

Pages 221–336 (March, 1962)

I. F. Croall and H. H. Willis: The fission products of ^{81}Se and ^{83}Se 221
K. Buijs: Infra-red study of some oxy-ions of sulphur attached to an ion-exchange resin 229
R. J. Morrow and A. Palm: Infra-red absorption of water of hydration in lanthanide trichlorides 239
L. I. Katzin: Infra-red spectra of nitrate salts in tributyl phosphate solution . . . 245
L. H. Brixner: Preparation and properties of the single crystalline AB_2-type selenides and tellurides of niobium, tantalum, molybdenum and tungsten 257
W. Z. Heldt: Reactions of co-ordinated ligands—IV. Synthesis of iron isonitrile complexes by the transalkylation reaction 265
L. Maier: Organo-phosphorous compounds—IV. The preparation of isomeric tetra-alkyldiphosphines and tetra-alkyldiphosphine monosulphides, a new class of phosphorous compounds 275
R. D. Whitaker and J. R. Ambrose: Iodine monochloride and iodine trichloride systems involving pyridine and quinoline 285
C. A. Crutchfield, Jr., W. M. McNabb and J. F. Hazel: Complexes of uranyl ion with some simple organic acids 291
R. D. Joyner, R. G. Linck, J. N. Esposito and M. E. Kenney: Dichloro- and siloxygermanium phthalocyanines 299
E. H. P. Cordfunke: On the uranates of ammonium—I. The ternary system NH_3–UO_3–H_2O 303
T. A. O'Donnell and D. F. Stewart: Chemical reactions of molybdenum hexafluoride . 309
T. Moeller and J. E. Huheey: Some reactions of diphosphorus tetraiodide . . . 315
D. F. Peppard, G. W. Mason, S. McCarty and F. D. Johnson: Extraction of Ca(II), Sr(II) and Ba(II) by acidic esters of phosphorus oxyacids 321
A. D. Kirshenbaum, J. A. Cahill and A. V. Grosse: The density of liquid silver from its melting point to its normal boiling point 2450°K 333

Pages 337–460 (April, 1962)

E. N. Sloth, D. L. Horrocks, E. J. Boyce and M. H. Studier: Tritium in the thermal neutron fission of uranium-235 337
M. S. Foster and A. F. Voigt: Photoproduction of beryllium-7 343
T. R. P. Gibb, Jr: A model for the rationalization of saline and metallic hydride formation 349
L. F. Dahl, G. L. Davis, D. L. Wampler and R. West: The molecular and crystal structure of thallium(I) methoxide 357
B. P. Block and G. Barth-Wehrenalp: Inorganic co-ordination polymers—I. General considerations 365
B. P. Block, R. A. Florentine, J. Simkin and G. Barth-Wehrenalp: Inorganic co-ordination polymers—II. Monoamminedichlorozinc (II) 371
E. Giesbrecht, W. G. R. de Camargo, G. Vicentini and M. Perrier: Dioxane addition compounds of some bivalent metal perchlorates 381
M. D. Taylor and C. P. Carter: Preparation of anhydrous lanthanide halides, especially iodides 387
R. E. Greene and G. S. Petit: High pressure fluorination of uranium oxides . . . 393
B. Jaselskis and J. G. Lanese: Nature of the anodic tellurate wave at the dropping mercury electrode 399
F. Baroncelli, G. Scibona and M. Zifferero: The extraction of nitric acid by long chain tertiary amines 405
C. E. Higgins and W. H. Baldwin: Interactions between tributyl phosphate, phosphoric acid and water 415
D. F. Peppard, E. P. Horwitz and G. W. Mason: Comparative liquid–liquid extraction behaviour of europium (II) and europium (III) 429
D. A. Collins, J. J. Hillary, J. S. Nairn and G. M. Phillips: The development and application of a process for the recovery of over 100g of protactinium-231 from a uranium refinery waste material 441

Pages 461–588 (November, 1962)

G. R. A. Johnson: The nitrous oxide radiation dosimeter 461
P. de Santis, E. Giglio and A. Ripamonti: The crystal structure of trimeric phosphonitrilic bromide 469
J. R. Ferraro: Infra-red spectra of several salts of acidic organophosphorus compounds . . 475
S. Califano: Infra-red spectra and vibration assignment of phosphonitrilic halides—I. Trimeric phosphonitrilic chloride 483
S. Califano and A. Ripamonti: Vibrational spectra of phosphonitrilic halides—II. The crystal spectra of $(NPCl_2)_3$ in polarized light 491
T. Moeller and L. C. Thompson: Observations on the rare earths—LXXV. The stabilities of diethylenetriaminepentaacetic acid chelates 499
W. R. May and M. M. Jones: The stability constants of several copper(II) complexes with aromatic carboxylic acids and their correlation with the Hammett relationship . . . 511
D. T. Peterson and J. Rexer: Ternary compounds between thorium monocarbide and thorium dihydride 519
D. A. Everest, R. A. Mercer, R. P. Miller and G. L. Milward: The chemical nature of sodium beryllate solutions 525
N. K. Shastri, J. O. Wear and E. S. Amis: Kinetics of the reduction of neptunium(V) with iodide ion 535
F. Baroncelli, G. Scibona and M. Zifferero: The extraction of Pu(IV) nitrate by long chain tertiary amines nitrates 541
F. Baroncelli, G. Scibona and M. Zifferero: The extraction of hexavalent uranium from nitric acid solutions by tri-*n*-dodecylamine nitrate 547
W. E. Keder: Extraction of tetra- and hexavalent actinides from hydrochloric acid by tri-*n*-octylamine in xylene 561
M. F. Barrett, D. Sweasey and N. E. Topp: The extraction of lanthanons with alkali metal amalgams—I. Samarium and ytterbium 571

Note:

W. W. Wendlandt and G. R. Horton: On the nature of the solvated 8-quinolinol and 2-methyl-8-quinolinol chelates of thorium(IV) 587

Pages 589–748 (November, 1962)

I. L. Preiss and P. M. Strudler: New neutron deficient barium isotopes 589
R. C. Poller: Infra-red spectra and structure of some phenyltin compounds . . . 593
J. T. Spence and E. R. Peterson: Infra-red spectra of metal complexes of riboflavin . . 601
N. Naqvi, E. L. Amma and Q. Fernando: Charge-transfer spectra of certain metal chelates of pyrazylmethyl ketones 609
Z. Libuś: Absorption spectra of uranium(VI) complexes in solutions 619
P. B. Hart and E. G. Steward: Compound formation in the system cadmium oxide–boric oxide 633
J. R. Witt and E. I. Onstott: Preparation of anhydrous lanthanon acetates by desolvation . 637
H. Selig and J. G. Malm: The vapour-pressure and transition points of TcF_6 641
W. F. Sullivan and J. R. Coleman: Effect of sulphur trioxide on the anatase–rutile transformation 645
G. P. Haight, Jr.: A spectrophotometric study of the dimerization of pentavalent molybdenum in hydrochloric acid 663
G. P. Haight, Jr.: Polarography of hexavalent molybdenum in hydrochloric acid . . . 673
Y. Murakami: Complexing behaviour of kojic acid with metal ions–II. Fe(III) chelates . 679
O. D. Bonner, H. Dolyniuk, C. F. Jordan and G. B. Hanson: The determination of ion association constants from cation exchange measurements–I. The cadmium chloride and cadmium bromide systems 689
J. Shankar and B. C. de Souza: Isotopic exchange in the cobaltous–cobaltic system in perchloric acid—II. Heats and entropies of exchange 693
T. Sato: The extraction of uranium(VI) from sulphuric acid solutions by di-(2-ethylhexyl)-phosphoric acid 699
C. F. Baes, Jr.: The extraction of metallic species by dialkylphosphoric acids . . . 707
M. T. Sardiña, R. F. Cellini and T. Batuecas Rodriguez: Extraction of uranium from solutions of complex uranylcarbonate by cetyl-dimethylbenzyl-ammonium chloride . . 721
G. W. Latimer, Jr. and N. H. Furman: Extractions from HCl—I. Adiponitrile as an extraction solvent 729
A. V. Grosse and A. D. Kirshenbaum: The temperature range of liquid lead and silver and an estimate of their critical constants 739

Pages 749–936 (December, 1962)

M. J. Cabell: Neutron capture cross-section data for ^{149}Sm 749
M. H. Studier, C. Postmus, Jr., J. Mech, R. R. Walters and E. N. Sloth: The use of ^{129}I as an isotopic tracer and its determination along with normal ^{127}I by neutron activation—the isolation of iodine from a variety of materials 755
R. G. Inskeep: Infra-red spectra of metal complex ions below 600 cm^{-1}—I. The spectra of the tris complexes of 1,10-phenanthroline and 2,2-bipyridine with the transition metals iron(II) through zinc(II) 763
M. Barrachina: Echange hétérogène d'ions isotopiques sur colonne. Application radiochimiques: separation du phosphore-32 et du soufre-35 sur colonne de sulfate de barium . 777
N. C. Stephenson: The crystal structure of di-iododi-(*o*-phenylenebisdimethylarsine) platinum (II) $Pt(C_6H_4[As(Ch_3)_2]_2)_2I_2$ 791
N. C. Stephenson: The structure of the di-iododi-(*o*-phenylenebisdimethylarsine)-palladium(II) molecule 797
N. C. Stephenson: The crystal structure of diammine bis(acetamidine)platinum(II) chloride monohydrate, $Pt(NH_3)_2$ $CH_3.C.(NH_2).NH]_2Cl_2H_2O$ 801
K. O. Watkins and M. M. Jones: Use of the method of continuous variations with mixed ligand complexes 809
R. P. Agarwal and R. C. Mehrotra: Study of catechol derivatives of thorium . . 821
W. E. Ohnesorge and A. Capotosto, Jr.: Fluorescence of metal chelate compounds of 8-quinolinol—III. The mono-(8-quinolinol)-aluminum species in absolute ethanol . . 829
E. J. Felten, E. F. Juenke and S. F. Bartram: The system Cr_2O_3–UO_2O_2 839
S. Z. Haider, M. H. Khundkar and K. De: Preparation and properties of chromyl borate . 847
R. C. Wilhoit, J. R. Burton, Fu-tien Kuo, Sui-rong Huang and A. Viquesnel: Properties of aluminium ethoxide 851
D. C. Bradley, R. N. Kapoor and B. C. Smith: Alkoxides of uranium(IV) 863
M. W. Nathans and W. W. Wendlandt: The thermal decomposition of the rare-earth sulphates. Thermogravimetric and differential thermal analysis studies up to 1400°C. . 869
D. F. Peppard, G. W. Mason and I. Hucher: Stability constants of certain lanthanide(III) and actinide(III) chloride and nitrate complexes 881
W. L. Marshall, J. S. Gill and R. Slusher: Aqueous systems at high temperature—VI. Investigations on the system NiO–SO_3–H_2O and its D_2O analogue from 10^{-4} to 3 m SO_3, 150–450°C 889
E. K. Dukes and G. A. Burney: Solubility of neptunium(IV) peroxide 899
J. O. Wear and E. S. Amis: A study of transference and solvation phenomena—VII. A determination of true transference numbers and relative solvation numbers in mixed solvents . 903
R. L. Angstadt and S. Y. Tyree: The nature of zirconyl chloride in strong hydrochloric acid: light scattering 913
D. K. Straub, H. H. Sisler and G. E. Ryschkewitsch: Metal-dinitrogen tetroxide reactions in acetonitrile and dimethylsulphoxide 919

Notes:

H. Shapiro and H. E. Podall: Reductive carbonylation synthesis of metal carbonyls—VI. A sodium-naphthalene complex route to Group VI-B metal carbonyls 925
E. R. Corey, M. V. Evans and L. F. Dahl: Preparation and structure of ruthenium tetracarbonyldiiodide 926
D. J. Apers, F. G. Dejehet, B. S. van Outryve d'Ydewalle and P. C. Capron: Chemical effects of nuclear recoil: metal phthalocyanines 927
D. E. Lavalle: Preparations of nitrides and phosphides of rare-earth metals . . . 930
Book Reviews: 935

Pages 937–1024 (December, 1962)

G. Pilcher and H. A. Skinner: Valence-states of boron, carbon, nitrogen and oxygen . 937
J. P. Oliver and L. G. Stevens: The preparation and characterization of tri-n-propyl-, tri-isopropyl- and trivinylgallium 953
R. C. Mehrotra and A. K. Rai: Studies in heavy metal soaps—II. Molecular weights of aluminium soaps 961
G. W. Mason, S. McCarty and D. F. Peppard: Synergistic effects in the extraction of selected metallic cations by mono (2-ethyl hexyl) phosphoric acid 967
D. F. Peppard, M. N. Namboodiri and G. W. Mason: Extraction of Th(IV) as a mixed complex nitrate of chloride, by 2-ethylhexyl hydrogen 2-ethylhexyl phosphonate . . 979
D. D. Gilbert and E. B. Sandell: Benzene extraction of stannic iodine 989

W. L. Marshall, E. V. Jones, G. M. Hebert and **F. J. Smith**: Aqueous systems at high temperature—VII. Liquid-liquid immiscibility and critical phenomena in the systems UO_3-SO_3-H_2O, UO_3-SO_3-D_2O and CuO-SO_3-D_2O, 270–430°C . . . 995
D. Nicholls: The ammonolysis of vanadium(III) bromide . . . 1001

Notes:

L. Lynds: Preparation of stoichiometric UO_2 by thermal decomposition of UO_2I_2 . . . 1007
J. G. Cuninghame, L. E. Glendenin and **A. L. Harkness**: Neutron capture cross-section of 36 hr ^{105}Rh . . . 1009
J. F. Tate and **M. M. Jones**: The Nernst law in concentrated sodium perchlorate solutions 1010
J. E. Huheey: Concerning acid-base theories . . . 1011
P. J. McGonical, J. A. Cahill and **A. D. Kirshenbaum**: The liquid range density, observed normal boiling point and estimated critical constants of indium . . . 1013
D. Shanefield: Solubilities of metal trichloracetates in polar and nonpolar liquids . 1014
L. J. Wittenberg and **R. H. Steinmeyer**: The solubility of plutonium(VI) carbonate in lithium acid carbonate . . . 1015
J. H. Balthis: Preparation of molybdenum(III) acetylacetonate . . . 1016
R. E. Vallee and **D. H. McDaniel**: The anhydrous hydrochloride salts of dichlorobis (ethylenediamine)cobalt (III) chloride . . . 1017
R. Prasad and **A. K. Dey**: Amphoterism of hydrous thorium oxide and the adsorption of fuchsine by the hydrous oxide . . . 1018

Letter to the Editor

T. Costea and **I. Dema**: The relationship between retention and chemical constitution . 1021
Errata . . . 1023

Pages 1025–1174 (December, 1962)

D. B. McWhan, B. B. Cunningham and **J. C. Wallmann**: Crystal structure, thermal expansion and melting point of americium metal . . . 1025
B. Kamenar and **D. Grdenić**: The crystal structure of potassium chloride trichlorostannite hydrate, KCl, $KSnCl_3$, H_2O . . . 1039
P. B. Hart and **S. E. F. Smallwood**: An examination of the infra-red spectra of borate anions . . . 1047
P. B. Hart and **C. S. Brown**: The synthesis of new calcium borate compounds by hydrothermal methods . . . 1057
G. W. Watt, E. P. Helvenston and **L. E. Sharif**: Ammines of iridium(O) . . . 1067
L. Maier: Organophosphorus compounds—V. A new synthesis of tertiary phosphines and arsines, phosphonic and thiophosphonic as well as phosphinic and thiophosphinic halides 1073
L. C. Thompson: Complexes of the rare earths—II. N,N'-ethylenediaminediacetic acid 1083
H. B. Gray, E. Billig, R. Hall and **L. C. King**: Metal complexes of pyrones and thiopyrones 1089
K. Suzuki and **K. Yamasaki**: The stability of some metal complexes incorporating oxygen or sulphur as donor atoms . . . 1093
R. J. Kern: Tetrahydrofuran complexes of transition metal chlorides . . . 1105
J. Selbin and **L. H. Holmes, Jr.**: Complexes of oxovanadium(IV) . . . 1111
R. F. Riley and **L. Ho**: Evidence for a pentacyanonitrosyl complex of molybdenum . 1121
G. R. Hennig: Catalytic oxidation of graphite . . . 1129
J. Krtil: Exchange properties of ammonium salts of 12-heteropolyacids—IV. Cs exchange on ammonium phosphotungstate and phosphomolybdate . . . 1139
H. Kakihana, T. Nomura and **Y. Mori**: The separation factor of lithium isotopes with ion exchangers . . . 1145
J. Selbin and **B. Shamburger**: Higher oxidation states of silver—II. Reaction of ozone with silver(I) complexes in non-aqueous solvents . . . 1153
J. D. Ray: Heat of isomerization of peroxynitrite to nitrate and kinetics of isomerization of peroxynitrous acid to nitric acid . . . 1159
P. A. Tierney, D. W. Lewis and **D. Berg**: Some physical properties of boron trichloride-phosphine . . . 1163

Notes:

G. Kakadadse and **H. J. Wilson**: Investigation of isopolyacids by a new conductometric technique . . . 1171
A. G. Massey: Pentacarbonlyacrylonitriletungsten . . . 1172

Pages 1175–1300 (December, 1962)

V. Maxia, W. H. Kelly and **D. J. Horen**: The neutron-deficient yttrium isotopes ^{83}Y, ^{82}Y and ^{84}Y . . . 1175
D. J. Silvester and **G. C. Jack**: Relative cross-sections for the ^{127}I(*d,p*) reaction . . 1181

M. V. Ramaniah and A. C. Wahl: Fission of ^{232}Th by 9·5 MeV deuterons. Yield-mass curve 1185
R. Benz: Thermodynamics of $PuCl_3$ from transpiration data 1191
V. Y. Labaton, E. V. Garner and E. Whitehead: Phase and equilibrium pressure studies of the zirconium-titanium-hydrogen system 1197
E. J. Frihauf and J. C. Bailar, Jr.: The heat stabilities of some polymeric metal complexes 1205
A. J. Strauss and L. B. Farrell: Hg–Se system 1211
T. Williams: Spectrophotometric studies of ion pair formation 1215
G. B. Deacon: The reactions of metal complexes with alkyl halides—III. The reactions of halo(triphenylphosphine)cadmium(II) complexes 1221
J. S. Oh and J. C. Bailar, Jr.: Some co-ordination polymers prepared from bis-(β-diketones) 1225
K. O. Watkins and M. M. Jones: A generalized formulation of the method of continuous variations for mixed ligand complexes 1235
F. Monacelli, F. Basolo and R. G. Pearson: Acid catalysis of the hydrolysis of acetatopentammine complexes of cobalt(III), rhodium(III) and iridium(III) 1241
M. Halpern, T. Kim and N. C. Li: The extraction of hydrochloric acid and some metal chlorides by tri-*n*-butoxyethyl phosphate 1251
H. Yoshida: Solvent extractions studies of thiocyanate complex of the lanthanides . . 1257
T. Sato: The extraction of uranium (VI) from sulphuric acid solutions by tri-*n*-dodecylamine 1267
H. T. Baker and C. F. Baes, Jr.: An infra-red and isopiestic investigation of the interaction between di(2-ethylhexyl)phosphoric acid and tri-*n*-octylphosphine oxide in octane . . 1277
A. D. Kirshenbaum, J. A. Cahill, P. J. McGonigal and A. V. Grosse: The density of liquid NaCl and KCl and an estimate of their critical constants together with those of the other alkali halides 1287

Notes:

G. A. Dupetit: Preparation of neptunium targets by electrodeposition 1297
R. R. Filler and L. Gorelic: Alkylammonium complexes of copper(II) 1297
Book Reviews 1299

Pages 1301–1484 (December, 1962)

B. J. Dropesky and C. J. Orth: A summary of the decay of some fission product tin and antimony isotopes 1301
E. T. Bramlitt and R. W. Fink: Isometric states of ^{92}Nb 1317
E. T. Bramlitt and R. W. Fink: Absolute activation cross sections for reactions of niobium with 14·5 MeV neutrons 1321
J. E. C. Macrae and P. F. D. Shaw: Neutron-induced reactions in iodobenzene . . . 1327
J. E. C. Macrae and P. F. D. Shaw: Effects of neutron capture upon benzene solutions of organic iodides 1337
G. Vicentini, J. V. Valarelli, M. Perrier and E. Giesbrecht: Dioxane addition compounds of hydrated yttrium, lanthanum and rare earth perchlorates 1351
W. C. Erdman and B. E. Douglas: The racemization of complex ions on activated carbon—I. The racemization of potassium D-ethylenediaminetetra-acetatocobaltate(III) 1355
W. C. Erdman, H. E. Swift and B. E. Douglas: The racemization of complex ions on activated carbon—II. The racemization of D-tris(ethylenediamine)cobalt(III) chloride and other complexes 1365
F. G. Sherrif, W. M. Oraby and H. Sadek: Spectrophotometric study of the chromium(III) azide reaction 1373
E. R. Clark: The basicity and dissociation constants of some complex molybdic acids . 1381
D. F. Peppard, G. W. Mason, I. Hucher and F. A. J. A. Brandao: Comparative extraction of U(VI) by neutral and mono-acidic phosphates and phosphonates 1387
R. Hering: Über Ionenaustauscherharze mit kompexbildenen Ankergruppen—IV. Die Bindungsverhältnisse der Seltenerd-Ionen am IDE-Austauscherharz 1399
B. Chu, D. C. Whitney and R. M. Diamond: On anion-exchange resin selectivities . 1405
A. S. Kertes and I. T. Platzner: Distribution of nitric acid between water and Amberlite LA-1 liquid anion exchanger 1417
T. V. Healy, D. F. Peppard and G. W. Mason: Synergism in the solvent extraction of di, tri and tetravalent metal ions—III. Antisynergism with thenoyl trifluoracetone . . . 1429
T. V. Healy and J. R. Ferraro: Synergism in the solvent extraction of di, tri tetravalent metal ions—IV. Absorption spectral studies of the synergistic complexes 1449
J. R. Ferraro and T. V. Healy: Synergism in the solvent extractions of di, tri- and tetravalent metal ions—V. Infra-red studies of the isolated complexes 1463

Notes:

M. M. Markowitz: The ammono-deliquescence of lithium metal 1475

J. D. R. Thomas: The solubilities of alkali metal iodides in ethanol 1477
L. D. Pettit and S. Bruckenstein: A cryoscopic study in ethylenediamine . . . 1478
Book Reviews 1481

Pages 1485–1690 (December, 1962)

J. B. Laidler and F. Brown: Mass distribution in the spontaneous fission of ^{240}Pu . . 1485
M. J. Cabell and L. J. Slee: The ratio of neutron capture to fission for uranium-235 . 1493
I. Mádi: Deposition of various radioactive elements on the surface of the platinum anode . 1501
S. R. Veljković and G. Harbottle: Low-temperature studies of recoil reactions . . 1517
M. A. Wahlgren and W. W. Meinke: Radiation from short-lived rare gas fission products 1527
N. Saito, T. Tominaga and H. Sano: Hot-atom chemistry of cobalt complexes—I. Hot-atom chemistry of nitroammine cobalt(III) complexes 1539
J. N. Maclean, F. J. C. Rossotti and H. S. Rossotti: The self-association of hydrogen fluoride vapour 1549
A. G. Galinos: Some mixed complex halogen acids with pseudohalogens . . . 1555
W. P. Thistlethwaite and W. T. Watson: The formation and composition of some metal 12-molybdophosphates 1559
M. Hillman, D. J. Mangold and J. H. Norman: Interaction of boranes. The diborane-pentaborane (9) reaction 1565
Chr. K. Jørgensen: Absorption spectra of transition group complexes of sulphur-containing ligands 1571
Chr. K. Jørgensen: Solvent effects on the absorption bands of iridium (IV) hexabromide and other *5d*-hexahalides 1587
E. J. Gonzales and H. B. Jonassen: Mixed complexes of copper(II) with *O*-azophenol and ethanolamine or ethylenediamine 1595
J. L. Bear, G. R. Choppin and J. V. Quagliano: Complexes of lanthanide elements with mercapto acetate ligands 1601
K. O. Watkins and M. M. Jones: An experimental test of a more generalized formulation of the method of continuous variations 1607
A. S. Ghosh Mazumdar, K. P. R. Pisharody and R. N. Singh: Kinetics of reaction between plutonium(II) and chlorine in chloride solutions 1617
C. Ferriera de Miranda and A. G. Maddock: The chemistry of protactinium—VI. The polarography of protactinium 1623
T. Moeller and T. M. Hseu: Observations on the rare earths—LXXVI. The stabilities of the *trans*-1,2-diaminocyclohexane-N,N′-tetraacetic acid chelates of the tri-positive ions . . 1635
C. E. Meloan and W. W. Brandt: The association of water molecules with the extracted benzohydroxamic acid chelates of uranium(VI) and iron(III) 1645
W. Smulek and S. Siekierski: The influence of diluent on the extraction of iron(III) from hydrochloric acid solution by tertiary amines 1651
A. I. Popov and J. C. Marshall: Potentiometric determination of basicity constants in anhydrous formic acid 1667
M. B. Brodsky and B. G. F. Carleson: Electrodeposition of plutonium and uranium from molten salt solutions of di-chlorides 1675

Notes:

M. L. Good and F. F. Holland: Anomolous solvent effects in the extraction of Co(II) from aqueous chloride solutions by long chain alkyl amines 1683
W. W. Wendlandt and J. K. Fisher: The kinetics and heats of olation of some hydroxoaquotetramminecobalt(III) complexes 1685
W. K. Schropp: Derivatives of nickelocene with thiols 1688
W. K. Schropp: Cyclopentadienyl iodo nickel phosphines 1690

AUTHOR INDEX

Abecasis, S. p. 113
Agarwal, R. P. p. 821
Aitken, E. A. p. 35
Ambrose, J. R. p. 285
Amis, E. S. pp. 93, 535, 903
Amma, E. L. p. 609
Angstadt, R. L. p. 913
Apers, D. J. p. 927
Aten, A. H. W. Jr. p. 139
Awad, A. M. p. 179

Baes, C. F. Jr. pp. 707, 1277
Bailar, J. C. Jr. pp. 1205, 1225
Baker, H. T. p. 1277
Baldwin, W. H. p. 415
Balthis, J. H. p. 1016
Baroncelli, F. pp. 405, 541, 547
Barrachina, M. p. 777
Barrett, M. F. p. 571
Barth-Wehrenalp, G. pp. 365, 371
Bartram, S. F. p. 839
Basolo, F. pp. 59, 1241
Batuecas Rodriguez, T. p. 721
Bear, J. L. p. 1601
Benz, R. p. 1191
Berg, D. p. 1163
Bhatki, K. S. p. 215
Billig, E. p. 1089
Block, B. P. pp. 365, 371
Bonner, O. D. p. 689
Boyce, E. J. p. 337
Bradley, D. C. p. 863
Bramlitt, E. T. pp. 1317, 1321
Brandao, F. A. J. A. p. 1387
Brandt, W. W. p. 1645
Brixner, L. H. p. 257
Brown, C. S. p. 1057
Brown, F. B. p. 1485
Bruckenstein, S. p. 1478
Buijs, K. p. 229
Burney, G. A. p. 899
Burton, J. R. p. 851

Cabell, M. J. pp. 749, 1493
Cahill, J. A. pp. 333, 1012, 1287
Califano, S. pp. 483, 491
Capotosto, A. Jr. p. 829
Capron, P. C. p. 927
Carleson, B. G. F. p. 1675
Carter, C. P. p. 387
Cellini, R. F. p. 721
Chattoraj, S. C. p. 101
Choppin, G. R. p. 1601
Chu, B. p. 1405
Clark, E. R. pp. 81, 1381
Coleman, J. R. p. 645
Collins, D. A. p. 441
Cordfunke, E. H. P. p. 303
Corey, E. R. p. 926
Costea, T. p. 1021
Craig, A. D. p. 161
Croall, J. F. p. 221
Crutchfield, C. A. Jr. p. 29
Cuninghame, J. G. p. 1009
Cunningham, B. B. p. 1025
Curtis, J. T. Jr. p. 93

Dahl, L. F. pp. 357, 926
Davies, G. L. p. 357
De, K, p. 847
Deacon, G. B. pp. 169, 1221
de Camargo, W. G. R. p. 381
Dejehet, F. G. p. 927
Dema, I. p. 1021
de Santis, P. p. 469
de Souza, B. C. pp. 187, 693
Dey, A. K. p. 1018
Diamond, R. M. p. 1405
Dolyniuk, H. p. 689
Douglas, B. E. pp. 1355, 1365
Douglass, R. M. p. 29
Dresdner, R. D. p. 53
Dropesky, B. J. p. 1301
Dukes, E. K. p. 899
Dupetit, G. A. p. 1297

Erdman, W. C. pp. 1355, 1365
Esposito, J. N. p. 299
Evans, M. V. p. 926
Everest, D. A. p. 525

Farrell, L. B. p. 1211
Feinberg, R. S. p. 165
Felten, E. J. pp. 35, 839
Ferguson, J. M. p. 1
Fergusson, J. E. p. 157
Fernando, Q. p. 609
Ferraro, J. R. pp. 475, 1449, 1463
Ferriera de Miranda, C. p. 1623
Filler, R. R. p. 1297
Fink, R. W. pp. 1317, 1321
Fischer, J. K. p. 1685
Florentine, R. A. p. 371
Foster, M. S. p. 343
Frazer, J. W. p. 45
Frihauf, E. J. p. 1205
Furman, N. H. p. 729
Fu-Tien Kuo p. 851

Galinos, A. G. p. 1555
Garner, E. V. p. 1197
Ghosh Mazumdar, A. S. p. 1617
Gibb, T. R. P. Jr. p. 349
Giesbrecht, E. p. 381, 1351
Giglio, A. p. 469
Gilbert, D. D. p. 989
Gill, J. S. p. 889
Glendenin, L. E. p. 1009
Gonzales, E. J. p. 1595
Good, M. L. p. 1683
Gopinathan, K. P. p. 215
Gorelic, L. p. 1299
Gray, H. B. p. 1089
Grdenić, D. p. 1039
Green, R. E. p. 393
Grigorescu-Sabău, C. p. 195
Grosse, A. V. pp. 147, 333, 739, 1287

Hagebø, E. p. 117
Haider, S. Z. p. 847
Haight, G. P. Jr. pp. 663, 673
Hall, R. p. 1089
Halpern, M. p. 1251
Hanson, G. B. p. 689
Harbottle, G. p. 1517
Harkness, A. L. p. 1009
Hart, P. B. pp. 633, 1047, 1057
Hazel, J. F. p. 291
Healy, T. V. pp. 1429, 1449, 1463
Hebert, G. M. p. 995
Heldt, W. Z. pp. 73, 275
Helvenston, E. P. p. 1067
Hennig, G. R. p. 1129
Hering, R. p. 1399
Higgins, C. E. p. 415
Hillary, J. J. p. 441
Hillman, M. p. 1565
Ho, L. p. 1121
Holder, B. E. p. 45
Holland, F. F. Jr. p. 1683
Hollingsworth, C. A. p. 101
Holmes, L. H. Jr. p. 1111
Horen, D. J. p. 1175
Horrocks, D. L. p. 337
Horton, G. R. p. 587
Horwitz, E. P. p. 429

Hseu, T. M. p. 1635
Hucher, I. pp. 881, 1387
Huheey, J. E. pp. 315, 1011

Inskeep, R. G. p. 763

Jack, G. C. p. 1181
Jaselskis, B. p. 399
Johnson, F. D. p. 321
Johnson, G. R. A. p. 461
Johnson, R. C. p. 59
Jonassen, H. B. p. 1595
Jones, E. V. p. 995
Jones, M. M. pp. 511, 809, 1010, 1235, 1607
Jordan, C. F. p. 689
Jørgenson, C. K. pp. 1571, 1587
Joyner, R. D. p. 299
Juenke, E. F. p. 839

Kakadadse, G. p. 1171
Kakihana, H. p. 1145
Kamenar, B. p. 1039
Kapoor, R. N. p. 863
Katzin, L. I. p. 245
Keder, W. E. p. 561
Kelly, W. H. p. 1175
Kenney, M. E. p. 299
Kern, R. J. p. 1105
Kertes, A. S. p. 1417
Khundkar, M. H. p. 847
Kim, T. p. 1251
King, L. C. p. 1089
Kirshenbaum, A. D. pp. 333, 739, 1012, 1287
Kjelberg, A. p. 117
Krtil, J. p. 1139

Labaton, V. Y. p. 1197
Laidler, J. B. p. 1485
Lanese, J. G. p. 399
Latimer, G. W. Jr. p. 729
Lavalle, D. E. p. 930
Leary, J. A. p. 29
Lewis, D. W. p. 1163
Li, N. C. p. 1251
Libuš, Z. p. 619
Linck, R. G. p. 299
Love, D. L. p. 1
Lynds, L. p. 1007

MacDiarmid, A. G. p. 161
Maclean, J. N. p. 1549
Macrae, J. E. C. pp. 1327, 1337
Maddock, A. G. p. 1623
Mádi, I. p. 1501
Maier, L. pp. 275, 1073
Malm, J. G. p. 641
Mangold, D. J. p. 1565
Mao, T. J. p. 53
Markowitz, M. M. p. 1475
Marshall, J. C. p. 1667
Marshall, W. L. pp. 889, 995
Martin, R. L. p. 105
Mason, G. W. pp. 321, 429, 881, 967, 979, 1387, 1429
Massey, A. G. p. 1172
Maxia, V. p. 1175
May, W. R. p. 511
McCarty, S. pp. 321, 967
McDaniel, D. H. pp. 101, 1017
McGonigal, P. J. pp. 1012, 1287
McNabb, W. M. p. 291
McWhan, D. B. p. 1025
Mech, J. p. 755
Mehrotra, R. C. pp. 821, 961
Meinke, W. W. p. 113
Meloan, C. E. p. 1645
Mercer, R. A. p. 525
Miller, R. P. p. 525
Milward, G. L. p. 525
Mocoroa, A. p. 113
Moeller, T. pp. 315, 419, 1635
Monacelli, F. p. 1241
Mori, Y. p. 1145
Morrow, R. J. p. 239
Murakami, Y. p. 679

Nairn, J. S. p. 441
Namboodiri, M. N. p. 979
Naqvi, N. p. 609
Nassif, S. J. p. 113
Nathans, M. W. p. 869
Nicholls, D. p. 1001
Nomura, T. p. 1145
Norman, J. H. p. 1565

O'Donnell, T. A. p. 309
Ogard, A. E. p. 29
Oh, J. S. p. 1225
Ohnesorge, W. C. p. 829
Oliver, J. P. p. 953
Onstott, E. I. p. 637
Oraby, W. M. p. 1373
Orth, C. J. p. 1301
Owens, C. W. p. 133

Palm, A. p. 239
Pappas, A. C. p. 117
Pearson, R. G. pp. 59, 1241
Peppard, D. F. pp. 321, 429, 881, 967, 979, 1387, 1429
Perrier, M. pp. 381, 1351
Peterson, D. T. p. 519
Peterson, E. R. p. 601
Petit, G. S. p. 393
Pettit, L. D. p. 1478
Phillips, G. M. p. 441
Pilcher, G. p. 937
Pisharody, K. P. R. p. 1617
Platzner, I. T. p. 1417
Podall, H. E. p. 925
Poller, R. C. p. 593
Popov, A. I. p. 1667
Postmus, C. Jr. p. 755
Powell, J. E. p. 183
Prasad, R. p. 1018
Pratt, G. M. p. 157
Preer, I. L. p. 589
Pritchard, W. C. p. 29

Quagliano, J. V. p. 1601

Rai, A. K. p. 961
Ramaniah, M. V. p. 1185
Rane, A. T. p. 215
Ray, J. D. p. 1159
Rexer, J. p. 519
Riley, R. F. p. 1121
Ripamonti, A. pp. 469, 491
Rochow, E. G. p. 165
Rodley, G. A. p. 157
Rossotti, F. J. C. p. 1549
Rossott, H. S. p. 1549
Rowland, F. S. p. 133
Ryschkewitsch, G. E. p. 919

Sadek, H. p. 1373
Saito, N. p. 1539
Sam, D. p. 1
Sandell, E. B. p. 989
Sano, H. p. 1539
Sardiña, M. T. p. 721
Sato, T. pp. 699, 1267
Schropp, W. K. pp. 1688, 1690
Scibona, G. pp. 405, 541, 547
Selbin, J. pp. 1111, 1153
Selig, H. p. 641
Shamburger, B. p. 1153
Shanefield, D. p. 1014
Shankar, J. pp. 187, 693
Shapiro, H. p. 925
Sharif, L. E. p. 1067
Shastri, N. K. p. 535
Shaw, P. F. D. pp. 1327, 1337
Sherif, F. G. pp. 179, 1373
Siekierska, K. E. p. 13
Siekierska, S. pp. 205, 1651
Silvester, D. J. p. 1181
Simkin, J. p. 371
Singh, R. N. p. 1617
Sisler, H. H. p. 919
Skinner, H. A. p. 937
Slee, L. J. p. 1493
Sloth, E. N. pp. 337, 755
Slusher, R. p. 889
Smallwood, S. E. F. p. 1047
Smith, B. C. 863
Smith, F. J. p. 995
Smith, G. B. p. 101
Smulek, W. p. 1651
Sokowska, A. p. 13
Spence, J. T. p. 601
Steinmeyer, R. H. p. 1015
Stephenson, N. C. pp. 791, 797, 801
Stevens, L. G. p. 953
Steward, E. G. p. 633
Stewart, D. F. p. 309
Straub, D. K. p. 919
Straus, A. J. p. 1211
Strudler, P. M. p. 589
Studier, M. H. pp. 337, 755
Sui-rong Huang p. 851

Sullivan, W. F. p. 645
Suzuki, K. p. 1093
Sweasey, D. p. 571
Swift, H. E. p. 1365

Tate, J. F. p. 1010
Taylor, M. D. p. 387
Thistlethwaite, W. P. p. 1559
Thomas, J. D. R. p. 1477
Thompson, L. C. p. 499, 1083
Tierney, P. A. p. 1163
Tominaga, T. p. 1539
Topp, N. E. p. 571
Tyree, S. Y. p. 913

Valarelli, J. V. p. 1351
Vallee, R. E. p. 1017
van Outryve d'Ydewalle, B. S. p. 927
Veljkovic, S. R. p. 1517
Vicentini G. p. 381, 1351
Viquesnel, A. p. 851
Vlatković, M. p. 139
Voigt, A. F. p. 343

Wahl, A. C. p. 1185
Wahlgreen, M. A. p. 1527
Wallman, J. C. p. 1025
Walters, R. R. p. 755
Wampler, D. L. p. 357
Watkins, K. O. pp. 809, 1235, 1607
Watson, W. T. p. 1559
Watt, G. W. p. 1067
Wear, J. O. pp. 99, 535, 903
Wendlandt, W. W. pp. 587, 869, 1685
West, B. O. p. 169
West, J. B. p. 105
West, R. p. 357
Whitaker, R. D. p. 285
Whitehead, E. p. 1197
Whitney, D. C. p. 1405
Whipple, E. p. 23
Wilhoit, R. C. p. 851
Wilkins, C. J. p. 157
Williams, T. p. 1215
Willis, H. H. p. 221
Wilson, H. J. p. 1171
Witt, J. R. p. 637
Wittenberg, L. J. p. 1015
Wold, A. p. 23
Worden, E. F. p. 45

Yamasaki, K. p. 1093
Yoshida, H. p. 1257
Young, J. A. p. 53

Zifferero, M. pp. 405, 541, 547

J. inorg. Nucl. Chem., 1962, Vol. 24, pp. 1 to 11. Pergamon Press Ltd. Printed in Northern Ireland

γ-RAY SPECTRA OF ^{133m}Te AND ^{134}Te

J. M. Ferguson, D. L. Love and D. Sam
U.S. Naval Radiological Defense Laboratory, San Francisco 24, California

(*Received* 28 *November* 1960; *in revised form* 2 *August* 1961)

Abstract—Tellurium radionuclides were separated from ^{235}U fission products and their γ-ray energies and abundances measured by scintillation techniques. ^{134}Te has four γ-rays ranging in energy from 79 to 262 keV. An equilibrium mixture of ^{133m}Te and ^{133}Te has eleven γ-rays ranging in energy from 309 to 973 keV. A partial decay scheme for ^{133m}Te is proposed. The half periods of ^{133m}Te and ^{134}Te were remeasured as 50 and 42 min, respectively.

Background

It has become obvious that there are serious gaps in the available data on the decay properties of many important fission products.(1) The data on many nuclides are so sparse that estimates of total γ-emissions are unreliable.(2) Hence a programme to determine the γ-ray spectra of some of these radionuclides has been undertaken.

The tellurium isotopes are major contributors to the gross fission-product activity at 1 hr after fission; yet most of their γ-ray spectra are unknown or poorly known.(3,4) These isotopes include ^{131}Te, ^{131m}Te, ^{132}Te, ^{133}Te, ^{133m}Te, and ^{134}Te. A chart of the properties of these and neighbouring nuclides is shown in Fig. 1. The decay properties of ^{132}Te and ^{131m}Te are fairly well known.(4,6) The γ-ray spectrum of ^{131}Te has been studied in a separate experiment.(7) An investigation of the γ-ray spectra of ^{133m}Te and ^{134}Te is the subject of this report.

Previous work

Most of the decay data for ^{133m}Te comes from the work of Pappas(8), and consists of the measurement of a 63 min half-period and rough measurements of the β-ray and γ-ray spectra using absorbers (see Table 1). He found that ^{133m}Te may decay either by β-emission to ^{133}I or by γ-emission to the ^{133}Te ground level. This ground level in turn undergoes β-decay with a half-period of 2 min.(8) Since the measurements by Pappas were done with an equilibrium source, the radiations he observed can be attributed either to $^{133m}\mathrm{Te} \xrightarrow{e,\gamma} {}^{133}\mathrm{Te} \xrightarrow{\beta,\gamma} {}^{133}\mathrm{I}$ or to $^{133m}\mathrm{Te} \xrightarrow{\beta,\gamma} {}^{133}\mathrm{I}$. The branching between these two modes was investigated by Alväger and Oelsner(9). They found that 13 per cent of the ^{133m}Te transitions go to the ^{133}Te ground level. The energy of the isomeric transition is 0·334 MeV. These results are included in Table 1 and in the decay scheme in Fig. 4.

---

(1) C. F. Miller, Report USNRDL-TR-247 (1958).
(2) P. D. LaRivere. Private communication.
(3) D. Strominger, J. M. Hollander and G. T. Seaborg, *Revs. Modern Phys.* **30**, 585 (1958).
(4) K. Way, *et al.*, *Nuclear Data Sheets.* National Academy of Sciences, National Research Council, Washington, D.C. (1959).
(5) *Chart of the Nuclides*, General Electric Co., Schenectady, New York (1956).
(6) A. Bedesen, K. P. Mitrofanos, A. A. Sorokin and V. S. Shpinel, *J. Exptl. Theoret. Phys* (*USSR*) **37**, 314 (1959).
(7) J. M. Ferguson and F. M. Tomnovec, Report USNRDL-TR-490 (1960).
(8) A. C. Pappas, *Phys. Rev.* **87**, 162 (1952); **81**, 299 A (1951).
(9) T. Alväger and C. Oelsner, *Arkiv Fysik* **12**, 319 (1957).

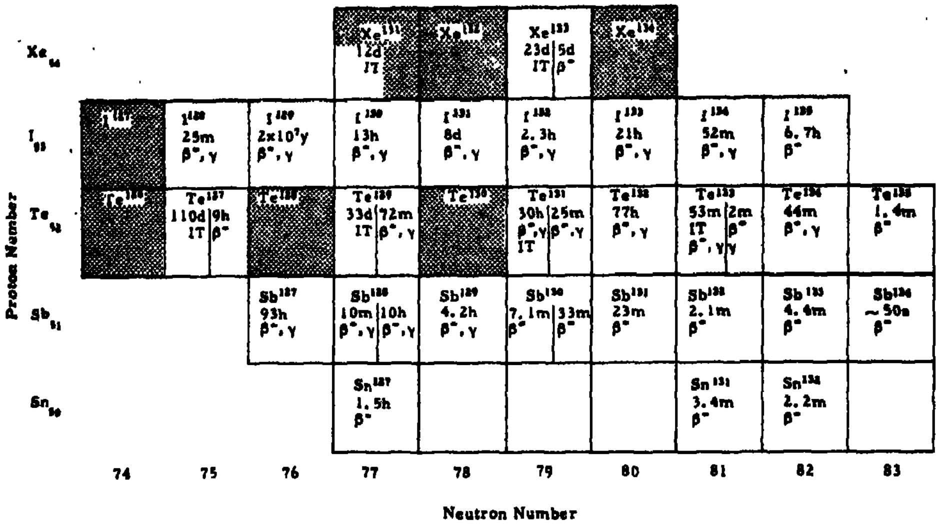

Fig. 1.—Decay properties of nuclides in the region of interest. The format of this figure is taken from the General Electric Chart of the Nuclides.[4]

Table 1.—Previous data on ^{133m}Te–^{133}Te

Type of irradiation	Energy	Abundance (%)	Reference
β_1	~1·3	~70	8
β_2	~2·4	~30	8
γ	0·334*	13	9
γ_1	~0·4	—	8
γ_2	~0·6	—	8
γ_3	~1·0	—	8

* This gamma is the transition from ^{133m}Te to ^{133}Te. The total transition intensity (gammas and conversion electrons) was found to be 13 per cent.

There are no previous measurements pertaining to the nature of the radiations from ^{134}Te. The half-period was found to be 44 min.(10–12)

EXPERIMENTAL

Description of experiment

The physics and chemistry equipment necessary for the experiment was taken to the General Electric reactor at Vallecitos, California. Three samples of ^{235}U (93·2 per cent enriched) were irradiated in the reactor. The tellurium fission products were chemically separated from the ^{235}U. These tellurium activities consisted of approximately equal amounts of ^{133m}Te and ^{134}Te. The γ-radiations from each of these samples were studied with a NaI(Tl) crystal. The pulse-height spectrum from the crystal was analysed and recorded with a 100-channel analyser. Each sample was counted in a series of 5 min runs starting about 20 min after the neutron irradiation and continuing for 3 hr.

The pulse-height spectra were analysed to give each sample's γ-ray spectrum as a function of time. From these data the energies and abundances of the ^{133m}Te and ^{134}Te γ-rays were computed.

(10) A. C. Pappas and C. D. Coryell, *Phys. Rev.* **81**, 329 A (1953).
(11) P. H. Abelson, *Phys. Rev.* **56**, 1 (1939).
(12) J. L. Mackin, *et al.*, "Early Time Decay of Fission Product Mixtures. III. Gamma Ionization Chamber Measurements Following Thermal Neutron Fission of ^{235}U," US NRDL-TR (in press).

Neutron irradiation and chemistry

The tellurium activities were produced by thermal neutron fission of 2 mg samples of ^{235}U. The flux at the sample position was about 10^{10} neutrons per cm^2 per sec, and each sample was irradiated for 300 sec. The method of irradiation is described by MACKIN *et al.*(12)

Since ^{133m}Te and ^{134}Te were to be studied, it was desirable to exclude the other tellurium fission products as much as possible. These other interfering tellurium activities are formed mainly by decay of their long-lived antimony parents. Therefore, the antimony was separated from the tellurium and other fission products as soon as possible after the irradiation. Iodine separations were made as the last part of the radio-chemical procedure in order to minimize the magnitude of the iodine peaks that grow into the tellurium samples.

Of the three samples irradiated, the first two were treated according to steps 1, 2 and 3 below. The third sample was treated as described in steps 1 and 4.

1. *Preparation of fission product mixture.* Uranium metal (93·2 per cent ^{235}U) was dissolved in hydrochloric acid and the acidity adjusted to 1 N. About 0·1 ml of this solution containing 2 mg of uranium was sealed in a polyethylene capsule. This capsule was placed in a nylon rabbet and irradiated in the reactor for 300 sec. After irradiation the fission products were removed from the capsule and washed into a centrifuge tube.

2. *Separation of tellurium.* A rapid separation of radiochemically pure tellurium was obtained from a modification of a procedure by NEWTON(13). Tellurium was separated from the fission products by precipitation of the metal with sulphur dioxide from a solution of 3 N hydrochloric acid and hydrazine hydrochloride. The tellurium metal was dissolved in warm 6 N nitric acid and the solution evaporated to dryness. These steps were repeated. Additional decontamination was achieved by an iron hydroxide scavenge. Tellurium metal was again precipitated. This tellurium separation required about 10 min.

3. *Separation of iodine from tellurium.* The iodine daughters of tellurium were separated by solvent extraction into carbon tetrachloride. Ten ml of the tellurium solution in 9 N hydrochloric acid and triiodide was extracted twice with 10 ml portions of carbon tetrachloride. The time required for the removal of iodine was less than 3 min.

4. *Separation of tellurium enriched in* ^{133m}Te. To identify the ^{133m}Te gamma peaks from those of ^{134}Te advantage was taken of the different half-periods of the parent isotopes, ^{133}Sb ($T_{\frac{1}{2}}$ = 4·1 min) and ^{134}Sb ($T_{\frac{1}{2}}$ = 0·8 min). A rapid separation of tellurium metal from irradiated ^{235}U fission products about 3 min old leaves enriched ^{133}Sb in the supernate since most of the ^{134}Sb had already decayed to ^{134}Te. The antimony separation from tellurium consisted of adding antimony and tellurium carriers to a 9 N hydrochloric acid solution of irradiated ^{235}U. This solution was saturated with hydrogen sulphide for 1 min and the tellurium sulphide was filtered through No. 4 Whatman filter paper. Two min were required for this separation. The ^{133}Sb in the supernate decayed to ^{133m}Te. This ^{133m}Te was separated from the other fission products by the procedure described in step 2 above.

Data taking

The γ-ray detector is a 4 in. high, 4 in. diameter NaI(Tl) crystal. The crystal is housed in a 6 in. lead shield. The source was mounted outside the crystal housing, and the γ-rays were collimated through a 1·5 in. diameter port to the top of the crystal. The crystal is coupled to a photomultiplier tube. The pulses from the photomultiplier are amplified and then recorded in a 100 channel pulse-height analyser.

The γ-ray measurements were begun within 5 min after the final iodine separation. Each sample was counted for 5 min, and the data in the analyser were then recorded on paper tape. The read-out of the data was completed in about 3 min, and another 5 min run was begun. This procedure was continued for 3 hr after the irradiation. More runs were made the next day to measure long-lived activities. Three different amplifier gains were used to cover different ranges of γ-ray energies. The ranges were 0–0·4 MeV, 0–1·5 MeV and 0–3 MeV. Every third run was made at the same gain setting.

---

(13) W. W. MEINKE, *Chemical Procedures Used in Bombardment Work at Berkeley*, U.S. Atomic Energy Commission Report AECD-2738 (1949); Newton, "Chemical Separations of Tellurium", procedure 52–4.

DATA ANALYSIS AND RESULTS

Analysis procedure

Only the data from the second sample were completely analysed. The following procedure was used for the first sample. After the first set of γ-spectra had been obtained, a second iodine–tellurium separation was made. Both the iodine and tellurium were analysed to obtain their spectra after a period of decay. However, it was found that the loss of activity and the time delay in the separations resulted in counting rates too low for proper data analyses. On the following runs, therefore, the ^{134}I was allowed to grow in as the counting continued. There was too little activity in the first sample.

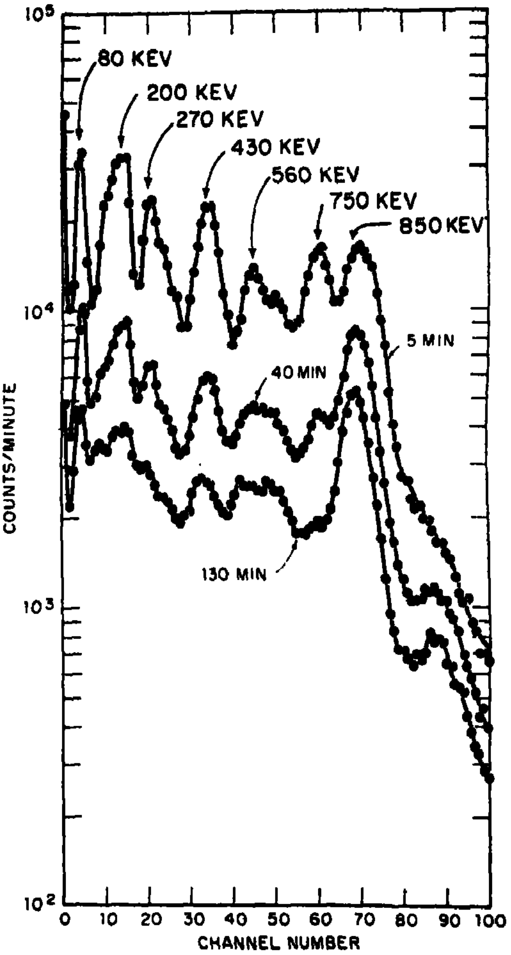

Fig. 2.—Three pulse-height spectra of the separated tellurium. The time between the final chemical separation and the taking of the spectra is indicated on the figure. The 5-min data have been multiplied by three so that the curves won't overlap. The prominent peak at 850 keV is due to 850 and 890 keV γ-rays from ^{134}I. The prominent γ-rays at 80 and 200 keV are assigned to ^{134}Te, and the others are assigned to ^{133m}Te–^{133}Te.

The third sample contained a strong ^{131}Te component, and was used only for comparisons with the second run. This third sample had a higher ratio of ^{133m}Te to

^{134}Te than the other samples, and so was used to check on the assignment of individual peaks to ^{133m}Te or ^{134}Te.

The raw data consist of pulse-height spectra taken at 8 min intervals. About thirty γ-rays from seven different nuclides are present in each spectrum. The pulse-height spectrum from typical runs are shown in Fig. 2 and 3.

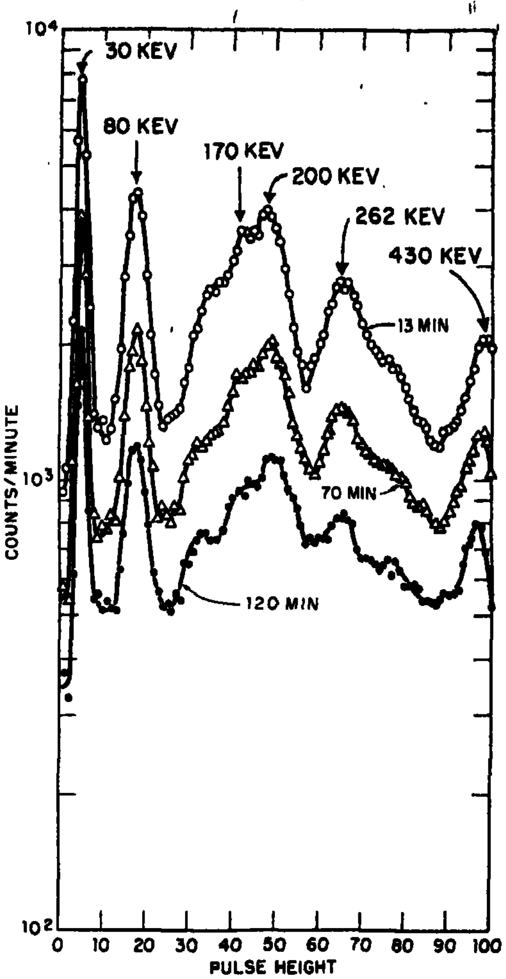

FIG. 3.—Three pulse-height spectra of the separated tellurium. The time between the final chemical separation and the taking of the spectra is indicated on the figure. These spectra were taken on an expanded gain to analyse the low-energy γ-ray spectrum.

The pulse-height distribution for single-energy γ-rays consists of a Gaussian-shaped peak and a continuous spectrum below the peak. A typical single-energy pulse-height spectrum of ^{137}Cs is shown in Fig. 4. The energy and intensity of the γ-ray determine the position and size of the peak. To analyse a given peak in a complex spectrum one must subtract out the contribution from neighbouring γ-rays. The method used was to analyse each γ-ray individually, starting with the highest energy γ-ray. After the first γ-ray abundance and energy had been determined, its contribution to the pulse-height spectrum was subtracted on the basis of the known spectrum for single-energy γ-rays. The same procedure was then applied to the next highest energy γ-ray, and so on. The data taken at later times were analysed first. The results were then used to subtract the long-lived activities from earlier runs.

The γ-intensities from ^{132}I, ^{133}I and ^{132}Te were obtained from data taken the day after the irradiation. These later spectra are relatively simple, and the γ-ray intensities were obtained by successive subtraction, as described above. These intensities are then used to subtract the three activities from all the earlier runs.

The remaining activities are ^{134}I, ^{131}Te, ^{133m}Te (the ^{133m}Te is actually an equilibrium mixture of ^{133}Te and ^{133m}Te, and ^{134}Te. Of these, ^{134}I is the most prominent at times greater than one hour after the chemical separation.

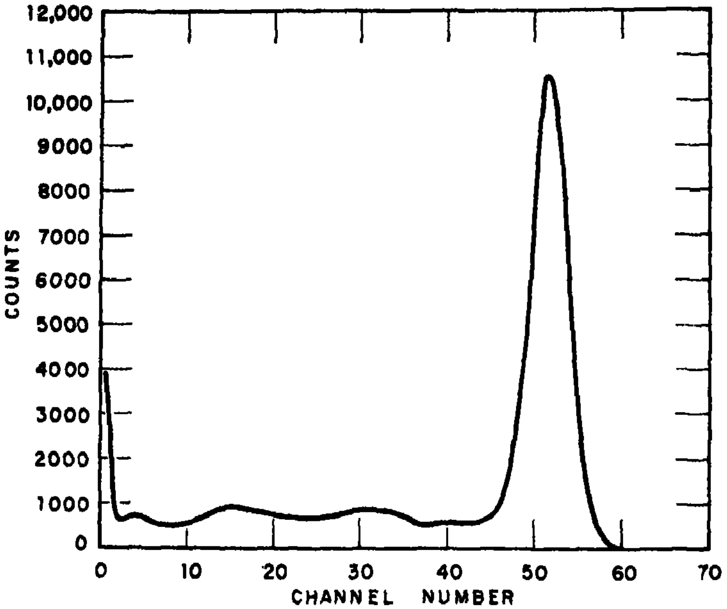

FIG. 4.—Pulse-height spectrum from the ^{137}Cs 0·662 MeV γ-ray. The rise in channel one is due to the barium *K* X-ray.

The γ-ray spectrum of ^{134}I is not well known. However, a list of γ-ray energies and intensities has been reported by O'KELLEY *et al.* and they are continuing work on this nuclide.(14) In our work we have not completely analysed the ^{134}I spectrum but have subtracted the ^{134}I on the basis of the prominent γ-rays and the raw pulse-height spectra obtained at later times.

The ^{134}I was subtracted out by the following procedure. The relative amount of ^{134}I present in each counting run can be determined by a knowledge of the half-periods involved and the times of the different runs. Thus the ^{134}I contribution could be subtracted from the earlier runs simply by multiplying one of the later runs by the approximate factor and subtracting it from the early run. With this method part of the tellurium contribution is also subtracted from the early run. However, in general, this is a small part of the total contribution, since the tellurium is decaying away while the iodine is growing in. This procedure was followed using different pairs of counting runs to make sure that the results were consistent.

(14) G. D. O'KELLEY, E. EICHLER and N. R. JOHNSON, Ann. Conf. 15/P/672, Chemistry Div. Ann. Progress Report for Period Ending June 20, 1959 (ORNL-1782)(1959); (private communication).

After the subtraction of ^{134}I only the γ-rays of ^{131}Te, ^{133m}Te and ^{134}Te remain. (See Fig. 5.) The ^{131}Te spectrum is known from another experiment,(7) and it was subtracted on the basis of the intensity of its strong γ-ray at 145 keV. This leaves ^{133m}Te and ^{134}Te. The full-energy peaks were initially assigned to ^{133m}Te or ^{134}Te by run number 3, and confirmed on the basis of half-periods. The reported half-periods are 63 min for ^{133m}Te and 44 min for ^{134}Te. Because of the similar half-periods, each γ-ray must be followed for at least one half-hour to be identified. The γ-ray intensity was measured for the first run, assigned to ^{133m}Te or ^{134}Te, and subtracted from the succeeding runs on the basis of the half-period. It was found that new half-periods had to be assigned to both ^{133m}Te and ^{134}Te to make the analysis consistent.

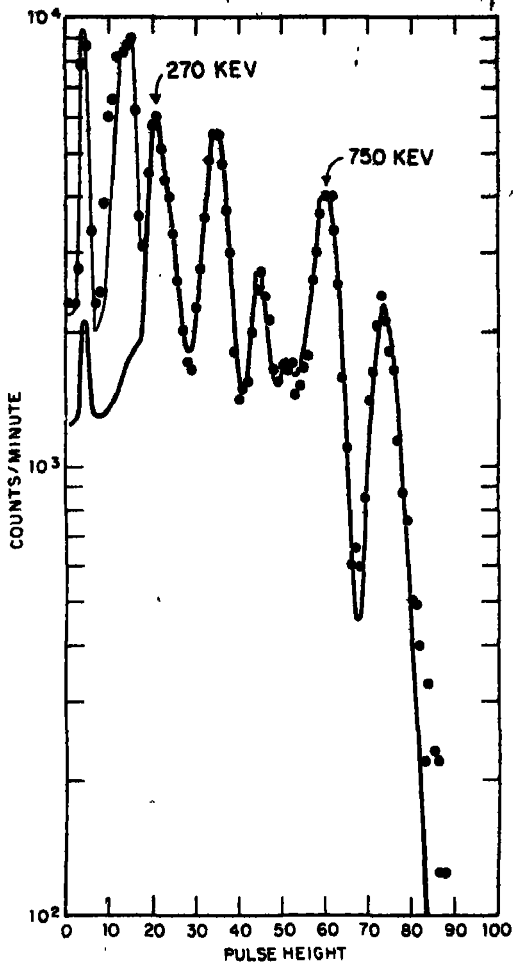

Fig. 5.—These points are the data from the top curve of Fig. 2 after subtraction of the ^{134}I. The light solid line is the ^{133m}Te spectrum calculated from the pulse-height spectra of mono-energetic γ-rays and the energies and intensities given in Table 2. The heavy solid line is a combined ^{133m}Te and ^{134}Te spectrum constructed from the data of Table 2. The 75 keV peak in the ^{133m}Te *spectrum is due to lead K X-rays fraom the collimator.* The discrepancy in channels 10 and 11 is due to the 145 keV γ-ray from ^{131}Te.

The analysis was quite sensitive to small changes in energy, intensity, or half-period assignments. γ-rays with abundances of only a few per cent showed up quite well in the analysis. However, in these cases it is more difficult to determine the half-period; thus we are not certain whether some of the weak γ-rays belong to ^{133m}Te or to ^{134}Te.

The above analysis gives the nuclide assignment and relative abundances of the γ-rays. To obtain the number of γ-rays per disintegration we compare the results with those for ^{133}I and ^{134}I. The abundance of the ^{133}I 0·53 MeV γ-ray is taken to be 0·94 γ-rays per disintegration;(15) the sum of the abundances of the 0·85 and 0·98 MeV γ-ray in ^{134}I is taken to be 1·6 gammas per disintegration.(14) Since the iodine comes from the decay of the tellurium, we can determine the amount of tellurium present from these numbers. This is the basis for the absolute gamma-ray intensities given below.

RESULTS

The energies and abundances of the γ-rays are given in Tables 2 and 3. The errors represent standard deviations. Two errors are listed for the abundances. The first of these represents the error relative to the abundances of the other γ-rays from the same nuclide. The second error represents the uncertainty in the number of γ-rays per disintegration. Since our samples were mixtures of ^{133m}Te and ^{134}Te, there is the danger that one of the γ-rays is assigned to the wrong isotope. However, we found that when the "wrong" assignment was made, either in the preliminary analysis or later as a check, there was a pronounced discrepancy in the analysis, corresponding to oversubtraction or undersubtraction of the peak from later runs.

Table 2.—^{133m}Te–^{133g}Te (equilibrium mixture)

Gamma energy (keV)	Abundance γ-rays per disintegration	Error for relative abundance	Error for absolute abundance
309 ± 8	0·207	±0·03	±0·05
343 ± 10	0·041	±0·007	±0·009
387 ± 10	0·057	±0·008	±0·012
432 ± 5	0·50	±0·05	±0·10
468 ± 10	0·22	±0·02	±0·04
557 ± 5	0·35	±0·04	±0·05
632 ± 10	0·18	±0·02	±0·03
698 ± 10	0·24	±0·03	±0·05
754 ± 5	0·85	±0·09	±0·16
910 ± 10	0·57	±0·06	±0·12
973 ± 10	0·10	±0·015	±0·02

Table 3.—^{134}Te

Gamma energy (keV)	Abundance γ-rays per disintegration	Error for relative abundance	Error for absolute abundance
30 (*K* X-ray)	0·35	±0·05	±0·07
79 ± 8	0·126	±0·015	±0·020
174 ± 10	0·16	±0·02	±0·04
204 ± 5	0·21	±0·02	±0·04
262 ± 5	0·19	±0·02	±0·04

It was necessary to use different half-periods in the data analysis to obtain consistent results. The new half-period for ^{134}Te is 42 min and for ^{133m}Te is 50 min.

---

(15) A. R. Brosi and P. M. Gross, Jr. Report ORNL-499 (1959).

DISCUSSION

^{133m}Te

Since no β-ray or coincidence measurements were made, we cannot establish a complete decay scheme. However, our data together with a knowledge of nuclear systematics in this region tell us what the principal features of the decay scheme are likely to be. Way, *et al.*, have given a tentative partial decay scheme based on previous data and nuclear level systematics.$^{(4)}$ We will first review this information and then apply it to our results.

^{133m}Te may decay either by beta emission to levels in ^{133}I or by an isomeric transition to the 2 min ground level of ^{133}Te. Alväger and Oelsner found that 13 ± 3 per cent of the decays go by the isomeric transition.$^{(9)}$ This transition is a member of the well-known "island of isomerism" of nuclides just below the shell closure at 82 neutrons. It is well-established that this group of isomers has a common basis. Each consists of an excited level with a character of $\frac{11}{2}-$ above a $\frac{3}{2}+$ ground level. The 50 min level is then expected to have a character of $\frac{11}{2}-$, and the isomeric transition should be of the magnetic 2^4-pole type. The energy of this transition was measured to be 0·3340 MeV by Alväger and Oelsner.

The only other data on the decay of ^{133m}Te are some absorber measurements by Pappas. He found β-rays with energies of about 1·3 and 2·4 MeV and abundances of about 70 and 30 per cent, respectively. The total energy available for β-decay of the ground level may be estimated by extrapolating the decay energies of other odd-A tellurium isotopes to $A = 133$; by this method Way, *et al.*, obtained a value of 3·0 MeV.$^{(4)}$ Using somewhat the same method, we obtained 3·1 MeV. Since ^{133m}Te is 0·33 MeV above ^{133}Te, this method gives 3·3 or 3·4 MeV for the total decay energy.

Now we consider the data from this report. Apparently the weak 0·343 MeV γ-rays in our spectrum is the 0·334 isomeric transition. The energy discrepancy is within the experimental error. Rose's theoretical internal conversion coefficient for this transition is 1·4.$^{(16)}$ Thus, for 13 ± 3 per cent decay by isomeric transition, we would expect $0{\cdot}054 \pm 0{\cdot}012$ γ-rays per disintegration. Our experimental value is $0{\cdot}041 \pm 0{\cdot}009$ γ-rays per disintegration, so we are in agreement with Alväger and Oelsner.

Since only 13 per cent of the decays go through the ^{133}Te ground level, all the intense γ-rays result from the direct beta decay of ^{133m}Te. There are three γ-rays with an intensity greater than 50 per cent. These γ-rays can be fitted into a consistent scheme only by putting them in cascade. They are arranged in order of increasing abundance in Fig. 6. This type of scheme agrees well with the other information we have. The intense β-ray energy observed by Pappas is about 1·3 MeV, yet we expect to have about 3·4 MeV available. Thus, we must account for about 2 MeV by γ-transitions. Since there are no intense γ-rays with energies greater than 1 MeV, cascade transitions can be expected to dominate.

Four of the eleven observed γ-rays have been placed in the decay scheme. The other γ-rays can be fitted into various possible level schemes by energy and abundance balancing. However, there is no sound basis for choosing one level scheme over another, so all but the three intense γ-rays were omitted.

---

(16) M. E. Rose, *Internal Conversion Coefficients.* Interscience, New York (1958).

^{134}Te

The only previous data for ^{134}Te are half-period determinations, ABELSON and PAPPAS give values of 43 and 44 min, respectively.(10,11)

WAY *et al.* estimate the total energy available for β-decay to be 1·4 MeV on the basis of beta-ray systematics.(4) A 1·4 MeV transition with a 44 min half-period would have a log *ft* of 5·4. Hence the half-period indicates an allowed transition to the ground level and/or one or more low-energy excited levels. However, we do not expect an allowed beta transition to the ground level for the following reason: The ^{134}I ground level decays by beta emission to ^{134}Xe. It is known that ^{134}I does not have an allowed transition to the O + ^{134}Xe ground level.(14) Since the transition from ^{134}I to this O+ level is forbidden, the transition from the O+ ground level of ^{134}Te to the ^{134}I ground level must also be forbidden. Hence it is expected that the ^{134}Te decay goes predominantly to excited levels in ^{134}I that have energies less than, say 0·5 MeV.

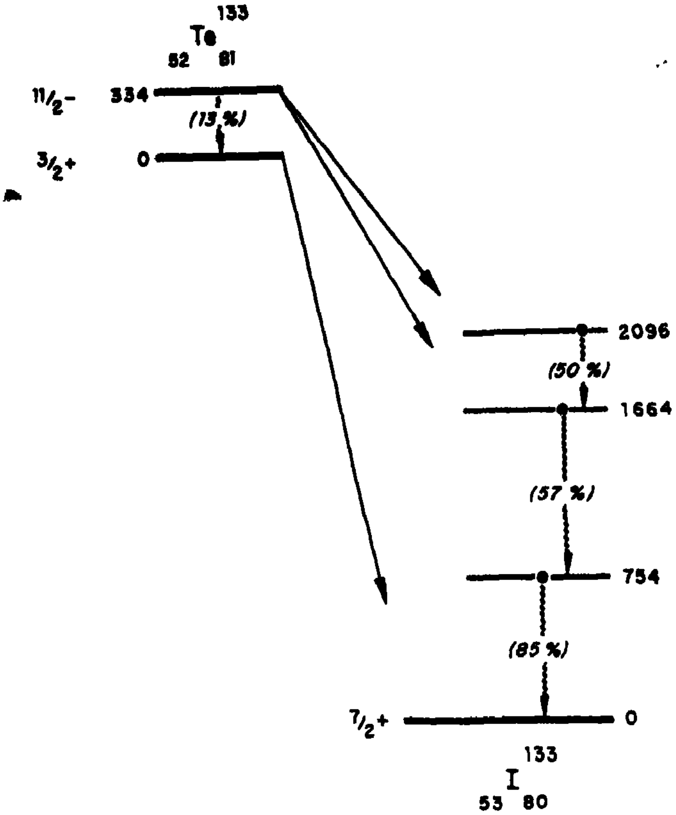

FIG. 6.—Proposed decay scheme of ^{133m}Te. The isomeric transition energy and intensity are taken from the work of ALVÄGER and OELSNER.(9) Seven γ-rays from our work are not shown.

These expectations agree with our data. All the γ-rays are below 300 keV. Their intensities suggest that they come from "parallel" or competing transitions rather than from cascade transitions.

The sum of the γ-ray and *K* X-ray intensities is 1·04. If we take the fluorescence field of iodine to be 0·86,(17) the sum of γ-ray and K-shell transitions is 1·09. The X-rays are assumed to come from internal conversion. If we further assume that the ratio of K-shell internal conversions to all the internal conversions is 0·9,(18) 1·14 is obtained for the sum of the intensities of all the γ-rays and internal conversions.

To see if the ratio of X-rays to γ-rays is reasonable, first assume all the γ-transitions are of the magnetic dipole or $M1$ type. Using Rose's theoretical internal conversion coefficients and a 0·86 fluorescence yield, 0·27 K X-rays per disintegration are expected from internal conversion. If the 79 keV transition is taken to be of the $E2$ type, 0·37 K X-rays per disintegration are expected. Hence the extimated intensities are of the same order as the measurements. The high intensity of the X-rays suggests that there may be other, highly converted transitions in the decay scheme. However, the energy and intensity of the X-rays are not well known since the spectrometer was not really designed for this energy region. Also, the X-ray intensity is uncertain because of contributions to X-ray peak from other activities in the sample.

No order of the γ-rays in the level scheme is proposed except to say that the abundances suggest they are parallel or competing transitions. If there are no cascade transitions, and the total energy available for beta decay is 1·4 MeV, there are four beta groups with energy endpoints of 1·3, 1·2, 1·2 and 1·15 MeV, with log ft values of 5·6, 6, 5·9 and 5·9, respectively.

Acknowledgements—The authors would like to express their gratitude to J MACKIN *et al.*, for the reactor irradiations, to A GREENDALE for his preliminary work on the chemical procedures; and to Mr. R A TAYLOR for his help with the electronic equipment

---

(17) A. H WAPSTRA, G J NIJGH, and R VAN LIESHOUT, *Nuclear Spectroscopy Tables*. Interscience, New York (1959)

J. Inorg. Nucl. Chem., 1962, Vol. 24, pp. 13 to 22. Pergamon Press Ltd. Printed in Northern Ireland

REACTION OF NEUTRON ACTIVATED ARSENIC ATOMS IN ORGANIC MEDIA—II

AsPh$_3$–BENZENE SYSTEM

K. E. Siekierska and A. Sokolowska
Department of Radiochemistry, Institute of Nuclear Research, Warsaw, Poland

(*Received* 2 *May* 1961; *in revised form* 20 *September* 1961)

Abstract—The quantitative distribution of the active products following the neutron irradiation of solutions of arsenic triphenyl and arsenic trichloride in benzene has been investigated. The scavenging action of dissolved oxygen has been explored and the results interpreted in terms of the different kinds of reaction in which the radioactive fragments can participate. Comparative measurements on the behaviour of a solution of diphenyl arsine oxide have also been made. A new method of paper chromatographic separation of the products has been used.

The chemical effects following thermal neutron capture can be considered, in the first approximation, as a combination of several processes accompanying the different stages of slowing down of the recoiling atoms. These processes are generally divided into: primary retention—due to the failure of bond rupture, high energy processes including radical, hot exchange and bimolecular reactions and thermal reactions controlled by diffusion.(1,2) The participation of these phenomena in determining the yields of individual organic and inorganic products has been extensively studied(3,4,5) as well as the problem of whether elastic(6) or inelastic collisions between the recoiling atoms and the surrounding molecules play a dominant role. The contribution from the primary retention to the total organic yields has also been investigated.(7) The experimental study of these problems can be carried out by investigating the influence of various factors on the distribution of activity amongst the products in a given system. The parameters generally studied influencing the qualitative and quantitative distribution of products are as follows: the influence of added substances, the effect of temperature, density, phase, structure, dilution and finally the post irradiation effects. Most of the papers concerning the mechanism of the processes in liquids are exclusively devoted to organic halide systems, but as has been pointed out previously(8) the study of systems containing polyvalent atoms may offer certain advantages in studying the relative roles of elastic and inelastic collisions. They present some new features in respect of the primary retention and the possibility of bond reformation. The primary retention in such systems depends on the survival of, not only one, but several bonds, and the reformation of the bonds is possible, either in one or more steps.

---

(1) J. E. Willard, *Ann. Rev. Nucl. Sci.* **3**, 193 (1953).
(2) S. Goldhaber and J. E. Willard, *J. Amer. Chem. Soc.* **74**, 318 (1952).
(3) G. Levy and J. E. Willard, *J. Phys. Chem.* **74**, 6161 (1953).
(4) M. Milman and P. F. D. Shaw, *J. Chem. Soc.* 1303–1317 (1957).
(5) J. Chien and J. E. Willard, *J. Amer. Chem. Soc.* **79**, 4872 (1957).
(6) W. F. Libby, *J. Amer. Chem. Soc.* **69**, 2523 (1947).
(7) R. S. H. Chiang and J. E. Willard, *J. Amer. Chem. Soc.* **74**, 6213 (1952).
(8) K. E. Siekierska, A. Halpern, and A. Siuda, Symposium Intern. Atomic Energy Agency Cent/30, Prague, October 1960.

For these reasons it was decided to examine the chemical effects following the (n, γ) reaction in phenylarsenic compounds.(9) In previous investigations, MADDOCK and SUTIN(10) had shown that the arsenic activity after the irradiation of crystalline $AsPh_3$ is distributed between tri-, di-, and mono-phenyl compounds and the inorganic form. *A priori* it seemed reasonable to assume that the comparison of the results for an irradiation of an $AsCl_3$–benzene system with those for a tri-phenylarsine-benzene system would allow some conclusions to be drawn about the mechanism of these processes. In the first system the formation of organic compounds would only be possible by radical reactions, while in the latter system the organic yield could arise from many processes. Thus it seemed that such a comparison would render it possible to determine the rôle of the various types of processes in the reformation of organic bonds. However, the results previously obtained were insufficient to draw unambiguous conclusions. It was found that the yield of the triphenyl derivative was higher in the case of triphenylarsine irradiated as crystals than in benzene solution. This, as well as the quite different distribution of activity obtained for $AsCl_3$ in benzene, needed further explanation. Also the influence of oxygen, which was present in all the irradiated solutions had not been studied. The purpose of the second part of the work, reported below, was to resolve these questions and if possible to determine the rôle and importance of the various processes mentioned above in the yield of individual organic products.

EXPERIMENTAL

Materials

Arsenic trichloride, triphenylarsine [TPA], diphenylarsine oxide [DPO], phenyloxide [PO], diphenylarsonic acid [DPA], phenylarsonic acid [PA] used as target substances and as carriers, were prepared and purified by the previously described methods.(9) All inorganic carriers and other reagents were analytical grade. Solvents were dried and redistilled before use. Technical oxygen used to saturate some samples was washed with an aqueous solution of $KMnO_4$ and with benzene, dried with $CaCl_2$ and silica gel and finally saturated with benzene. Whatman's No. 1 paper, used for chromatography, was previously washed with 0·5 per cent sodium *versene* solution, rinsed with distilled water and air dried. The sizes of paper strips and sheets used for chromatography were 2·5 × 30 cm and 30 × 30 cm respectively.

Irradiations

The samples placed in sealed quartz ampoules were irradiated in the thermal column of the Polish reactor "EWA" at 4×10^9 neutrons/cm^2 sec for 40 hr. The sealing of the ampoules containing the samples was carried out under the following conditions: (1) at atmospheric pressure, (2) after degassing the frozen samples *in vacuo* at 10^{-4} mm pressure. Liquid samples were frozen in liquid air before sealing.

Paper chromatograms were activated at 10^{13} n/cm^2 sec for 2 hr. The counting of the activity of liquid samples was carried out with a GM annular tube-type MG. The paper chromatograms were scanned with an end-window GM tube (thickness of window: 5 mg/cm^2). Between the strip and the counter there was a brass diaphragm (with a window 0·5 cm wide). During the measurements the strip was pulled under this diaphragm, so that the activity was determined for each 0·5 cm of the strip.

(9) K. E. SIEKIERSKA, A. SOKOLOWSKA and I. G. CAMPBELL, *J. Inorg. Nucl. Chem.* **12**, 18 (1959).
(10) A. G. MADDOCK and N. SUTIN, *Trans. Faraday Soc.* 51, 184 (1955).

Separation methods

A new method, based on extraction of the sample into aqueous KOH solution and paper chromatography of the separated phases has been used to separate the following products: TPA, DPO, PO, DPA, PA, AsO_3^{3-}, AsO_4^{3-}.

Extraction. Using radioactivation analysis the partition coefficients, for all the compounds cited above, in the system benzene—KOH aq. have been determined. The best separation has been obtained using extraction with 1% KOH solution. The partition coefficients presented in Table 1, show that in the case of both the oxides the separation error was only 0·5 per cent, which was within the counting error limits. Equilibrium between the phases was attained after 2 hr shaking. In order to avoid loss of activity caused by adsorbtion after emptying, the ampoules were filled twice with 1% KOH for 2 hr. These washings were subsequently used for extraction and after shaking the phases were centrifuged and separated. The following solutions were obtained: a benzene phase containing TPA and DPO, and two aqueous phases containing PO, DPA, PA and the inorganic forms.

TABLE 1.—PARTITION COEFFICIENTS OF VARIOUS PRODUCTS IN THE SYSTEM BENZENE/1 PER CENT KOH AQ.

Substance	$K_{Benz}KOH_{aq.}$
As inorg.	0
PA	0
DPA	0
PO	0·0058
DPO	178
$AsPH_3$	∞

Chromatography. In order to achieve a further separation of the products paper chromatography was employed. Using activation analysis the R_F values were determined for all substances, both singly and in mixtures. The detection and location of the active arsenic compounds on the strip was carried out by the procedure described above. The identification of the irradiation products, in the samples investigated, was done by comparison of their R_F values with those of the activated substances. In order to separate the components of the benzene phase ascending, one dimensional paper chromatography was supplemented by an additional procedure, since the R_F values of TPA and DPO are very similar in most solvents. Before use, the strips of paper were moistened at the starting position with 0·02 ml of 0·1% $HgCl_2$ in ethyl alcohol. TPA was precipitated by the $HgCl_2$ in alcoholic media, whereas DPO gave no precipitate. Thus, when the chromatograms were developed in absolute alcohol, the addition compound $AsPh_3{\cdot}HgCl_2$ remained at the starting point and the DPO migrated with the front.

In order to separate the substances contained in the aqueous phase ascending, two-dimensional paper chromatography was employed. The chromatogram was developed in butyl alcohol saturated with 5% NH_3 aq. and then in butyl alcohol saturated with 20% CH_3COOH aq. Before counting the sheets were cut into strips and then the activity was measured as above. The R_F values obtained for both dimensions are presented in Table 2.

RESULTS

The results were calculated, assuming the total activity on the strip or sheet was equal to the activity of the benzene or water phase respectively. The activity of individual products was calculated as a percentage of the total activity. The results of irradiations are presented as the distribution of activity between tri-, di-, and mono-organic derivatives and the inorganic form. The deviations observed are caused by the relatively large error of the separation and measurement procedure, which is greater than the statistical errors for counting. In the case of samples containing air the deviations were especially high, probably because of different amounts of oxygen in various samples, acting as scavenger. Standard deviations are several per cent, in some cases 30 per cent, depending on the individual product and the number of experiments. The tables present all values obtained and the average values for individual species.

Table 2.—R_F values for various substances in the solvents used

Substance	R_F in butanol saturated with 20% CH_3COOH aq.	R_F in butanol saturated with 5% NH_3 aq.
AsO_4^{---}	0·1	0
AsO_3^{---}	0·47	0·21
PA	0·78	0·02
DPA	0·9	0·35
PO	0·9	0·92

Scavenger effect

It has been pointed out by many authors[3,4] that the addition of certain substances, which are able to combine with free radicals diminishes the organic activity in two stages. The rapid fall in activity occurring at very low concentration of scavenger has been attributed to the suppression of thermal reactions, and the subsequent very slow decrease of activity with increasing scavenger concentrations to the influence on hot reactions. The contributions of hot and thermal reactions can be separately determined by extrapolation of the second, nearly linear, part of the curve representing the dependence of the organic yield on the scavenger concentration to zero concentration. The form of these curves permits an approximate evaluation of the contribution from diffusion controlled reactions being made from the drop in the yield, without establishing the dependence on the scavenger concentration.

In the experiments described air, oxygen and arsenic trichloride were used as scavengers in benzene solutions of TPA. The distribution of activity between the individual products in the absence (samples degassed), and in the presence of scavengers are presented in Tables 3, 4 and 5 respectively. As can be seen from a comparison of these results, the presence of scavenger diminishes the yield of tri- and diphenyl derivatives indicating that there is some contribution from thermal reactions to the formation of these forms. The decrease in activity in the case of the tri- derivative is about 14 per cent of the total arsenic activity, and in the case of di- form 16 per cent. The decrease in activity for individual forms does not depend, within the limits of the experimental errors, on the concentration of the target substance. Only in very highly concentrated solutions is this drop lower, which might be caused by an insufficient amount of oxygen in such solutions. On the other hand the presence of scavenger increases slightly the yield of the mono- derivative form.

DISTRIBUTION OF ACTIVITY AFTER IRRADIATION OF TPA IN BENZENE AT VARIOUS CONCENTRATIONS

TABLE 3.—DEGASSED

CONCENTRATIONS		I/S*	PER CENT OF ACTIVITY IN THE FORM OF:			
m/l	% mol		$AsPh_3$	$—AsPh_2$	$=AsPh$	As inorganic
1·0	9·19	3/9	19·7 ± 4·0	18·2 ± 1·4	17·9 ± 1·9	44·1 ± 5·0
0·4	3·43	2/6	18·0 ± 1·8	21·9 ± 1·9	20·2 ± 0·6	38·3 ± 1·9
0·1	0·88	7/21	16·0 ± 3·2	23·6 ± 1·9	16·6 ± 2·4	43·2 ± 3·7
0·01	0·088	3/9	12·4 ± 2·0	21·1 ± 1·9	16·2 ± 3·8	50·4 ± 4·0
0·005	0·044	2/6	20·5 ± 1·3	22·2 ± 2·2	10·5 —	49·6 ± 2·0

TABLE 4.—SATURATED WITH OXYGEN

CONCENTRATIONS		I/S*	PER CENT OF ACTIVITY IN THE FORM OF:			
m/l	% mol		$AsPh_3$	$—AsPh_2$	$=AsPh$	As inorganic
1·0	9·19	3/9	4·0 ± 1·1	12·3 ± 1·6	21·9 ± 2·4	62·6 ± 4·0
0·4	3·43	4/12	2·3 ± 1·2	9·4 ± 0·8	23·2 ± 1·1	64·9 ± 1·2
0·1	0·88	2/6	2·1 ± 0·2	6·8 ± 0·4	22·3 ± 0·4	68·8 ± 0·5
0·005	0·044	2/6	1·4 ± 0·1	5·4 ± 0·5	27·5 ± 3·0	65·7 ± 2·5

TABLE 5.—IN THE PRESENCE OF AIR

CONCENTRATIONS		I/S*	PER CENT OF ACTIVITY IN THE FORM OF:			
m/l	% mol		$AsPh_3$	$—AsPh_2$	$=AsPh$	As inorganic
2·0	15·08	3/9	10·1 ± 1·7	12·0 ± 2·7	24·3 ± 2·0	53·9 ± 2·4
1·0	2·19	4/12	11·3 ± 3·4	12·7 ± 1·1	19·1 ± 2·7	56·9 ± 4·5
0·4	3·43	7/21	2·6 ± 0·5	8·8 ± 2·6	19·6 ± 2·8	68·9 ± 4·0
0·2	1·74	2/6	4·0 ± 1·4	22·0 —	16·2 —	57·5 —
0·15	1·31	2/6	3·3 ± 0·4	—	—	—
0·1	0·83	10/30	2·4 ± 0·8	5·8 ± 0·8	24·5 ± 4·8	67·7 ± 3·8
0·05	0·44	3/9	2·3 ± 0·5	7·6 ± 0·8	17·7 ± 1·9	72·7 ± 2·2
0·005	0·044	2/6	2·5 ± 0·5	—	—	—

* I/S = Number of irradiations/Number of separations

The distribution of activity for TPA benzene solution containing $AsCl_3$ at various concentrations is presented in Table 6. These data indicate that $AsCl_3$ behaves like a scavenger, but only at concentrations about 0·001 M. The distribution of activity in this case is very similar to the distribution in the presence of oxygen. This result is in agreement with the data of ČIFKA(11) who had investigated the yields of di- and monophenyl derivatives in benzene solutions of $AsCl_3$, as a function of the arsenic trichloride concentration. The curve obtained by that author is quite similar to the curves of organic yield versus scavenger concentration.

---

(11) J. ČIFKA, Symposium I.A.E.A., CENT/5, Prague, October 1960.

Dilution effect

The conclusions about the fate of the recoil atom, which can be drawn from dilution experiments are two fold. The extent to which hot exchange contributes to the retention may be estimated by comparing the yield of parent substance in concentrated and in diluted solutions; also the yield of the parent compound in weak solutions (diluted with a diluent unable to reform the parent compound in reactions with the recoil atoms) and containing a scavenger should permit evaluation of the primary retention. However, by using a diluent that is able to reform the parent substance in reactions with the recoiling atoms in solutions containing scavenger only the sum of the contributions from primary retention and hot processes can be determined.

Table 6.—The distribution of activity after irradiation of degassed benzene solutions of TPA and $AsCl_3$ at various concentrations

Concentration of:		Per cent of activity in form of			
TPA M	$AsCl_3$ M	$AsPh_3$	$—AsPh_2$	$=AsPh$	As inorg.
0·1	—	16·02	23·57	16·63	43·77
0·099	0·001	17·63	26·32	13·73	42·33
0·05	0·05	1·62	7·02	18·44	72·92
—	0·1	0·86	5·05	16·01	78·07

The results of experiments on dilution of TPA with benzene (concentration range 1–0·005 M) presented in Tables 3, 4 and 5 indicate that in degassed solutions the yields of the organic forms are independent, within the limits of experimental error, of the concentration of TPA. It suggests, especially in the case of the tri- derivative form, that the contribution from hot exchange processes to the formation of active organic forms is not of great importance. In solutions containing oxygen as a scavenger (Table 4) the yields of tri- and di- derivative decrease slightly with dilution, while the yield of mono-derivative is slightly increased. In solutions saturated with air (Table 5) the changes in the yield of tri- and di- forms upon dilution are greater, and may be due to the smaller concentrations of oxygen in these solutions. Nevertheless, the distribution of activity is similar in weak solutions of TPA whether saturated with oxygen or air.

The irradiation of $AsCl_3$ *in benzene*

The organic retention in a solution of arsenic trichloride in benzene may be attributed only to highly energetic reactions, owing to (1) the scavenging action of $AsCl_3$, (2) no possibility of hot exchange reactions leading to organic combinations and (3) no primary organic retention. Assuming that simple chemical reactions between $AsCl_3$ and benzene do not occur and that the mechanism of the slowing-down processes of the recoiling atom is similar in both systems, it may be expected that the yield of each organic product in the case of arsenic trichloride irradiation should be nearly equal to the contribution from hot processes in the case of TPA in benzene.

The results presented in Table 6 show that the yields of tri-, di- and mono-phenyl-derivatives in irradiated solutions of $AsCl_3$ in benzene are about 1, 5 and 16 per cent respectively.

The irradiation of less substituted forms

It should be observed that in the complete absence of hot exchange, the distribution of activity should be independent of the kind of compound activated, that is, of the number of radicals attached to the activated atom. If, however, the hot exchange process and failure of bond rupture are not of negligible importance, the distribution of activity should be changed, and then the yield of the parent form would be higher in the case of each activated compound.

In order to obtain some data concerning these problems experiments with benzene solutions of DPO have been carried out. The results present in Table 7 indicate that: (1) the yield of the tri- derivative is slightly increased by dilution of the DPO and is lower than in the case of benzene solutions of TPA at similar concentrations, (2) the yield of the di- form decreases with dilution and in dilute solution attains the same value as in the TPA-benzene system, (3) the yield of the mono- form is slightly decreased by dilution and is nearly equal to the value obtained in TPA-benzene solutions.

TABLE 7.—THE DISTRIBUTION OF ACTIVITY AFTER IRRADIATION OF DEGASSED BENZENE SOLUTIONS OF DPO

Concentration	Per cent of activity in form of:			
M	$AsPh_3$	$\cdot$—$AsPh_2$	=AsPh	As inorg.
0·5	9·16	32·97	7·38	50·48
	9·14	28·78	10·05	52·02
0·01	10·52	23·06	15·71	50·70
	15·48	27·91	12·59	44·01
0·003	12·60	23·64	16·50	47·25
	10·89	24·23	14·41	50·45

Effect of γ-radiation

As was shown in the first part of this work,⁽⁹⁾ the organic retention in irradiated, degassed samples of crystalline TPA increases with increasing γ dose. In order to obtain some data on the effect of radiation on the liquid systems under investigation, benzene solutions of TPA, degassed and in the presence of oxygen, were irradiated with various γ doses. The results obtained are presented in Table 8. It can be seen from these data, that: (1) only for the lower γ doses does the presence of oxygen diminish the yields of the tri- and di-derivative, (2) in the higher γ-doses, the yields of these two forms increase from 16 to 21 per cent in the case of the tri- derivative and from 23 to 27 per cent in the case of the di- derivative. The yield of the mono- form decreases slightly with increasing γ-dose.

DISCUSSION

The results presented above can be explained by assuming the following reactions occur:

1. The processes due to primary retention:

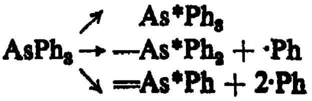

$$AsPh_3 \begin{array}{l} \nearrow \; As^*Ph_3 \qquad\qquad\qquad \text{(A)} \\ \rightarrow \text{—}As^*Ph_2 + \cdot Ph \qquad \text{(B)} \\ \searrow \; =As^*Ph + 2\cdot Ph \qquad \text{(C)} \end{array}$$

2. The processes due to radical recombination, which can occur in both the thermal and high energy region:

$$\mathrm{As}^* + \cdot\mathrm{Ph} \rightarrow {=}\mathrm{As}^*\mathrm{Ph} \tag{A}$$

$$\mathrm{As}^* + 2\cdot\mathrm{Ph} \rightarrow {-}\mathrm{As}^*\mathrm{Ph}_2 \tag{B}$$

$$\mathrm{As}^* + 3\cdot\mathrm{Ph} \rightarrow \mathrm{As}^*\mathrm{Ph}_3 \tag{C}$$

$$={}\mathrm{As}^*\mathrm{Ph} + \cdot\mathrm{Ph} \rightarrow {-}\mathrm{As}^*\mathrm{Ph}_2 \tag{D}$$

$$-\mathrm{As}^*\mathrm{Ph}_2 + \cdot\mathrm{Ph} \rightarrow \mathrm{As}^*\mathrm{Ph}_3 \tag{E}$$

3. Hot exchange reactions such as

$$\mathrm{As}^* + \mathrm{AsPh}_3 \rightarrow \mathrm{As} + \mathrm{As}^*\mathrm{Ph}_3$$

4. Reactions with oxygen or other scavengers:

$$\mathrm{As}^* + 4\mathrm{O} \rightarrow \mathrm{AsO}_4^{3-} \tag{A}$$

$$={}\mathrm{As}^*\mathrm{Ph} + 2\mathrm{O} + \mathrm{H}_2\mathrm{O} \rightarrow \mathrm{AsPhO(OH)}_2 \tag{B}$$

$$={}\mathrm{As}^*\mathrm{Ph} + \cdot\mathrm{Ph} + \mathrm{X} \rightarrow \mathrm{AsPh}_2\mathrm{X} \tag{C}$$

$$\cdot\mathrm{Ph} + \mathrm{O} \rightarrow \mathrm{PhO}^- \tag{D}$$

TABLE 8.—THE EFFECT OF γ-DOSE ON THE ACTIVITY DISTRIBUTION IN 0·1 M BENZENE SOLUTION OF TPA

Conditions of irradiation	Thermal neutron flux: n/cm² sec	Total γ and fast neutron dose: rads	Percentage of activity in form			
			AsPh_3	$-\mathrm{AsPh}_2$	$=\mathrm{AsPh}$	As inorg.
degassed (1)	$4{\cdot}0 \times 10^9$	$3{\cdot}4 \times 10^{5(2)}$	16·02	23·57	16·63	43·17
satur. with O_2 (1)	$4{\cdot}0 \times 10^9$	$3{\cdot}4 \times 10^{5(2)}$	2·09	6·78	22·26	68·77
degassed	$3{\cdot}0 \times 10^{11}$	$3{\cdot}8 \times 10^{6(3)}$	19·04	28·08	20·06	32·81
	$3{\cdot}0 \times 10^{11}$	$3{\cdot}8 \times 10^{6(3)}$	19·99	24·55	19·00	36·45
	$3{\cdot}0 \times 10^{11}$	$3{\cdot}8 \times 10^{6(3)}$	17·49	30·74	18·90	32·31
satur. with O_2			4·87	9·54	29·27	56·31
degassed	$1{\cdot}7 \times 10^{12}$	$4{\cdot}1 \times 10^7$	23·13	27·32	16·19	33·34
	$1{\cdot}7 \times 10^{12}$	$4{\cdot}1 \times 10^7$	21·30	25·05	16·31	37·34
	$1{\cdot}7 \times 10^{12}$	$4{\cdot}1 \times 10^7$	19·62	26·27	16·08	38·01
satur. with O_2	$1{\cdot}7 \times 10^{12}$	$4{\cdot}1 \times 10^{7(4)}$	23·54	29·08	18·25	29·11
	$1{\cdot}7 \times 10^{12}$	$4{\cdot}1 \times 10^{7(4)}$	27·50	26·07	19·33	27·26
	$1{\cdot}7 \times 10^{12}$	$4{\cdot}1 \times 10^{7(4)}$	23·13	28·05	15·42	33·39

(1) Average values from Tables 3 & 4
(2) Dose rate $5{\cdot}4 \times 10^3$ rads/h
(3) Dose rate $4{\cdot}7 \times 10^5$ rads/h
(4) Dose rate $1{\cdot}1 \times 10^6$ rads/h

The influence of oxygen (i) depresses the total organic yield due to reactions of the second type by decreasing the concentration of both free atomic arsenic via process 4A and phenyl radicals via reaction 4D; (ii) it depresses the yield of the tri- and di-derivative by the reaction 4B; this leads to an increase of the yield of mono- derivative. Since the increase of the $=\mathrm{As}^*\mathrm{Ph}$ yield is not equal to the sum of the decreases of the $-\mathrm{As}^*\mathrm{Ph}_2$ and $\mathrm{As}^*\mathrm{Ph}_3$ yields, processes of the 2nd and 4th type must exist simultaneously.

The experiments on dilution of TPA with benzene in the presence of oxygen show that at very low concentration the yield of $\mathrm{As}^*\mathrm{Ph}_3$ (1–2 per cent) is probably due to the reaction 1A. At higher concentrations, (1·0 M TPA), the yield of this product increases since (i) reactions of the 2nd type are not entirely scavenged (lower solubility of oxygen in the concentrated solutions), (ii) the hot exchange reaction (3) can occur. The yield of the di- derivative decreases with dilution, probably for these same reasons. The yield of mono- derivative does not decrease and is equal to 22 per cent. Under these conditions the mono- derivative can be formed as a result of processes 1C, 4B and 2A occurring in the high energy region. On the other hand, the results obtained for experiments on dilution in the absence of oxygen, when $=\text{As}^*\text{Ph}$ can be formed only as a result of processes 1C and 2A, indicate that the total contribution to the yield of $=\text{As}^*\text{Ph}$ from these two processes is equal to 16 per cent. This means that the difference between the yield of the mono- form, in the presence and in the absence of oxygen, is due to the reaction 4B and is equal to 6 per cent.

The yield of the mono- form in irradiated AsCl_3– benzene systems is equal to 16 per cent. As mentioned above, $=\text{As}^*\text{Ph}$ can be formed only as a result of reaction 2A in the higher energy region. This can be interpreted as evidence that the contribution from primary retention (1C) to the formation of this product is negligible.

In the irradiated DPO-benzene system, the tri- derivative can be formed by reactions of the 2nd type and the di- derivative by reactions 1B, 2B, 2D and 3. Now the yield of the latter is dependent on the concentration and the distribution of the products in this system and is different from the TPA-benzene system. Thus it is possible to say that there is some contribution from hot exchange reactions to the formation of the di- form and that the probability of this reaction increases as the number of organic bonds in the parent molecule decreases.

In degassed solution, an increase in γ-dose accentuates processes of the 2nd type, thereby increasing the yield of the di- and tri- derivative. The yield of the mono- derivative is practically independent of the γ-dose. These effects confirm the previous conclusions.

TABLE 9.—THE APPROXIMATE CONTRIBUTION FROM VARIOUS PROCESSES TO THE YIELD OF INDIVIDUAL PRODUCTS IN IRRADIATED TPA-BENZENE SYSTEM

(A) AS A PERCENTAGE OF TOTAL ARSENIC ACTIVITY
(B) AS A PERCENTAGE OF THE YIELD OF INDIVIDUAL PRODUCTS

Type of process	Per cent of activity in form of: AsPh_3		$—\text{AsPh}_2$		$=\text{AsPh}$	
	A	B	A	B	A	B
Bond rupture failure	1–2	10	2	10	0	0
Hot reactions	>1	>5	5	20	16	70
Thermal reactions	14	85	16	70	0	0
Processes caused by presence of scavenger	0	0	0	0	6	30

The contributions from the various processes to the yield of individual products have been evaluated as a percentage of the total arsenic activity (Table 9a) and as a percentage of the yield of individual products (Table 9b). The results obtained indicate that the mono- form is produced exclusively by hot radical processes, that the di- form has an intermediate character and that the tri- form is created mainly by radical processes in the thermal energy region. This can be explained on a model of consecutive reformation of organic bonds, which follows successive stages of the slowing down of the recoiling atom, as discussed previously.(8)

It is possible that this conclusion has a more general character [illegible] similar results for other organic liquid systems containing polyvalent [illegible]. For example, comparison of our results with those obtained for crystalline [illegible] by MADDOCK and SUTIN(19) reveals some similarities, especially with regard to the shape of the annealing curves.

Acknowledgements—The authors wish to express their gratitude to Dr. I. G. CAMPBELL for his encouragement and discussions throughout this work, and Dr. A. G. MADDOCK and Dr. S. SIEKIERSKI for helpful discussion. They would like also to thank Mr J. ROJEK for his technical assistance and the operation group of the Polish Reactor EWA for irradiations.

PREPARATION OF STOICHEIOMETRIC CHROMITES

E. Whipple and A. Wold
Lincoln Laboratory,* Massachusetts Institute of Technology
Lexington 73, Massachusetts

(*Received* 21 *June* 1961; *in revised form* 1 *August* 1961)

Abstract—The preparation of pure stoicheiometric chromites MCr_2O_4 ($M = Mg^{2+}, Zn^{2+}, Cu^{2+}, Mn^{2+}, Fe^{2+}, Co^{2+}, Ni^{2+}$) from suitable precursors is discussed. Atomic ratios Cr/M very close to the theoretical values were obtained. The chromites were examined by chemical analysis and several physical constants were measured.

THE chromites are a group of compounds which have the formula MCr_2O_4 and possess the spinel structure. The symbol M can indicate magnesium, copper, manganese, iron, cobalt, nickel and zinc. Unlike the ferrites, these compounds show magnetic properties which do not conform to the Néel model for ferrimagnetism. In particular, the chromites rather than giving saturation moments at 10,000 oersted, as most ferrites do, give high field susceptibilities as measured by JACOBS.[1] Furthermore, the observed net moments disagreed with the values calculated on the basis of an antiparallel alignment of *A* and *B*-site moments. They are extremely sensitive to homogeneity and chemical purity. It is believed that these differences in behaviour arise from stronger *B-B* interactions[2,3] in the chromites than in the ferrites. It is reasonable that definitive magnetic studies should be made of compounds of the highest available purity and homogeneity.

Previous methods employed for the synthesis of chromites consisted simply of preparing an intimate physical mixture of two appropriate oxides and heating this mixture to a sufficiently high temperature (1400–1700°C) to cause the two oxides to react and form the desired product. This method does not yield pure products easily because of the refractory nature of chromium (III) oxide and of many of the divalent-metal oxides involved. Tedious grinding procedures and firings must be done, and extraneous impurities are usually introduced as a result of the grinding. Ignition at elevated temperatures occasionally results in the preferential loss of some of the divalent oxides, e.g. ZnO, CuO.

The synthetic techniques, discussed in this paper, achieve excellent stoicheiometry, low trace impurity content, and homogeneity approaching the maximum theoretically possible. The principle advantage of the "precursor" method is that the two metals are mixed on an atomic scale so that greater reactivity and more homogeneous products result than by heating a mixture of ball-milled (or mortar-ground) oxides. The procedures involve the crystallization from solution of compounds containing chromium and another metal in the atomic ratio 2:1. Any other element which may be present is volatilized at elevated temperatures. Decomposition of these crystalline

---

* Operated with support from the U.S. Army, Navy, and Air Force.

[1] I. S. JACOBS, *J. Phys Chem. Solids* **15**, 54 (1960).

[2] T. R. MCGUIRE and S. W. GREENWALD, *The Substitution of Chromium in Ferrites, Solid State Physics in Electronics and Telecommunications*, Part 1, Vol. 3, p. 50. Academic Press, London (1960).

[3] D. G. WICKHAM and J. B. GOODENOUGH, *Phys. Rev.* **115**, 1156 (1959).

precursors yields a mixture of the oxides $M^{2+}O$ and Cr_2O_3 which are finely divided and intimately mixed. The ignition of these compounds, at a relatively low temperature ($<$ 1200°C), results in the formation of the crystalline chromite.

EXPERIMENTAL SECTION

Procedures

1. *Magnesium chromite.* The precursor $(NH_4)_2Mg(CrO_4)_2 \cdot 6H_2O$(4) (see Table 1) was prepared by dissolving 0·079 mole $Mg(NO_3)_2 \cdot 6H_2O$, 0·158 mole $(NH_4)_2CrO_4$, 0·325 g $(NH_4)_2SO_4$ and 5 g of $NH_4C_2H_3O_2$ (buffer) in 125 ml of water, using gentle heat. The salt was crystallized in the cold and a yield of 70 per cent was obtained. The product was ignited to the corresponding chromite at 1100–1200°C.

Magnesium chromite can also be prepared from $MgCr_2O_7 \cdot 5H_2O$.(5) The product was carefully dehydrated and first heated at 530°C in a hydrogen–nitrogen atmosphere (1 : 9), in order to reduce the chromium to the trivalent state. The product was then reheated in air at 1100°C to give the desired product.

2. *Manganese chromite.* The precursor used for the preparation of manganese chromite, $MnCr_2O_4$ was $MnCr_2O_7 \cdot 4C_5H_5N$. This compound was obtained, well crystallized and in good yield, according to the method by BRIGGS.(6) Upon gentle ignition over a flame, the salt decomposed vigorously to the mixed oxides and a little carbon. The oxides were fired to the chromite at 1100°C in air and quenched from 800°C or higher. A final firing at 1100°C in an atmosphere of hydrogen diluted with nitrogen (1 : 3) converted all the manganese to the divalent state.

3. *Cobalt chromite.* The chromite was best prepared from the precursor $CoCr_2O_7 \cdot 4C_5H_5N$,(6) which crystallized poorly and was found to be deficient in chromium. After determining the total chromium present in a sample of cobalt chromite prepared from the precursor, enough $(NH_4)_2Cr_2O_7$ was dissolved in approximately 10 ml of water and the solution was added to the remaining oxides. This resulted in a corrected chromium-cobalt ratio. The mixture was ignited, ground, fired at 1200° for 3 days and then quenched from 800°C.

4. *Nickel chromite.* $(NH_4)_2Ni(CrO_4)_2 \cdot 6H_2O$(7) was prepared by mixing separate solutions of ·084 moles $Ni(C_2H_3O_2)_2 \cdot 4H_2O$ dissolved in 135 ml of water, and 0·158 mole $(NH_4)_2CrO_4$ plus 0·32 g $(NH_4)_2SO_4$ dissolved in 70 ml of water. The solutions are mixed at 25–30°C. The product was crystallized at 0°C overnight, and the yield was 75 per cent of theoretical. The precursor was ignited over a flame and fired at 1100°C to yield the desired chromite $NiCr_2O_4$.

5. *Copper chromite.* The precursor $(NH_4)_2Cu(CrO_4)_2 \cdot 2NH_3$ was prepared according to the method of BRIGGS.(7) The crust which formed above the solution was discarded and the product was washed with dilute ammonia. The precursor was then heated carefully to form the mixed oxides and then fired at 800°C, and finally at 700°C for one day. The final firing temperature is important since a mixture of $CuCrO_2$ and Cr_2O_3 was observed to form if the product was heated to 1100°C.

6. *Zinc chromite.* The precursor $(NH_4)_2Zn(CrO_4)_2 \cdot 2NH_3$, prepared according to the procedure of BRIGGS(7) gave a chromite which contained excess chromium. In order to enrich the precursor with ZnO, 0·12 mole $ZnSO_4 \cdot 7H_2O$, 0·18 mole $(NH_4)_2CrO_4$ and 0·18 mole $(NH_4)_2SO_4$ were added to 250 ml of strong ammonia. The ammonium sulphate was used instead of ammonium nitrate to salt out the precursor. The solution was allowed to stand and evaporate. The product was then ignited at 1100°C and showed the presence of excess zinc oxide. The sample was then fired at 1400°C, which volatilized the excess zinc oxide and the stoicheiometric zinc chromite remained. Pure zinc chromite possesses a brown colour; whereas chromium-rich zinc chromite is grey-green.

7. *Ferrous chromite.* The precursor $NH_4Fe^{3+}(CrO_4)_2$(8) was readily prepared from 0·04 mole $(NH_4)_2Cr_2O_7$ and 0·08 mole $Fe(NO_3)_3 \cdot 9H_2O$ dissolved in 200 ml water, and 0·16 mole $(NH_4)_2CrO_4$ dissolved in 100 ml of water. The ammonium chromate was added slowly to the stirred hot solution containing ferric nitrate and ammonium dichromate. The first product was a brown sludge which changed to the dark red product. The conversion appeared to proceed only in the absence of excess ammonium chromate. When delayed, this change was achieved by the addition of 2 ml of conc.

---

(4) F. J. MALAGUTI and M. SARZEAU, *Ann. Chim. Phys.* (3) 9, 431 (1843).

(5) W. H. HARTFORD, *J. Amer. Chem. Soc.* 68, 2192 (1946).

(6) S. H. C. BRIGGS, *Anorg. Chem.* 56, 246 (1907).

(7) S. H. C. BRIGGS, *Trans. Chem. Soc.* 83, 391 (1903).

(8) R. WEINLAND and E. MERGENTHALER, *Dtsch. Ges.* 57, 777 (1924).

nitric acid and boiling the solution 3½ hours. The $(NH_4)Fe(CrO_4)_2$ was not washed in order to avoid any loss of chromium. The product, which was obtained in good yield, was ignited to the mixed oxide $Fe_2O_3{\cdot}2Cr_2O_3$. Chemical analysis of the fired chromite sometimes showed a slight excess of iron. In those cases, the mixed oxides were then corrected by the addition of an ammonium dichromate solution, and ignited to destroy the dichromate. The final product was ground and fired in a CO–CO_2 atmosphere (1:2) at 1150°C for 6 hr.

The effect of SO_4^{2-} *on the preparation of chromite precursors*

The crystalline compounds used as precursors in the synthesis of the chromites did not always have a metal ratio suitable for the formation of a stoicheiometric chromite. When the chromium was in excess, advantage could often be taken of the isomorphism of sulphate and chromate to correct the metal ratio. The sulphate could then be volatilized completely by careful ignition in air.

The precursor $(NH_4)_2Ni(CrO_4)_2{\cdot}6H_2O$ crystallizes with a slight excess of chromium. The addition of a small, measured quantity of $(NH_4)_2SO_4$ to the preparation replaces a little chromate with sulphate, thus correcting the ratio. This procedure is applicable to the magnesium precursor also.

For the double salt series $(NH_4)_2M(CrO_4)_2{\cdot}2NH_3$ a large amount of $(NH_4)_2SO_4$ must be used for a small reduction of chromium. In the synthesis of $ZnCr_2O_4$ by this type of precursor, the effect was used to prepare a precursor deficient in chromium.

Chemical and physical measurements

In order to identify the products, each of the chromites was chemically analysed. The chromites are very inert chemically as well as very refractory; they require prolonged hot fusion with molten sodium hydroxide in order to be thoroughly attacked. The total chromium was then done according to the procedure of LINGANE and DAVIS.(9) In order to analyse for M^{2+}, a separate sample of the chromite was dissolved by prolonged attack with sodium bromate(10) in a very dilute sulphuric acid solution.

The lattice constants were determined with a Philips Norelco diffractometer using Cr-K_α radiation. The magnetization values were determined in a field of 10,000 oersteds using the vibrating coil magnetometer.(11) The results of these measurements are given in Table 2.

RESULTS AND DISCUSSION

The results of the chemical analyses summarized in Table 1 indicate that the "precursor" methods described above were successful for the preparation of nickel, copper, zinc and iron chromites. Three of the seven systems studied, namely, cobalt, zinc and iron chromites were obtained by "doctoring" the precursors slightly. The somewhat high values for the Cr/M ratio obtained for manganese, and magnesium chromite were believed to be a consequence of the presence of excess chromium in the precursors. Careful X-ray examination of thoroughly fired samples, by step-counting techniques over the intense Cr_2O_3 peaks, indicated that no Cr_2O_3 was present in the final products. However, a large sample (60 g) of $MnCr_2O_4$ prepared for neutron diffraction studies showed the presence of a small amount of Cr_2O_3 (< 1 per cent).

The lattice constants listed in Table 2 are in good agreement with those reported in the literature. The cubic to tetragonal transformation point of iron chromite was found to be $-138°C \pm 3°C$. This is considerably lower than $-90°C$ reported by FRANCOMBE(12). The lower value would indicate some important differences in the chemistry of the two compounds.

The saturation magnetic moments (n_B) for nickel, manganese and iron chromites are in good agreement with those reported by Lotgering(13). The values given in Table 2 for magnesium, cobalt, copper and zinc chromites have not been previously reported. Lotgering has indicated that the chromite (oxygen) spinels have a *B-B* interaction which is of the same order of magnitude as the *AB* interaction. This usually results in lower saturation moments than are predicted by the Néel theory of ferrimagnetism. Preliminary neutron diffraction experiments(14) on $MnCr_2O_4$ showed a complex spin configuration which could not be explained by the Yafet-Kittel model. Unfortunately, the more recent theoretical study made by Kaplan, *et al.*(15) applies only to pure, normal, stoicheiometric spinels. Hence, it seemed desirable to have as "good" a sample as possible available for further neutron diffraction study. Such an investigation of our sample of $MnCr_2O_4$ is presently being undertaken by Corliss and Hastings.

---

(9) J. J. LINGANE and D. G. DAVIS. *Analyt. Chim. Acta* **15**, 201 (1956).

(10) R. LYDÉN, *Z. Anorg. Chem.* **223**, 28 (1935).

(11) K. DWIGHT, N. MENYUK and D. O. SMITH, *J. Appl. Phys.* **29**, 491 (1958).

(12) M. H. FRANCOMBE, *J. Phys. Chem. Solids* **3**, 37 (1957).

Table 1.—Preparation of the stoicheiometric chromites

Chromite	Precursor	Cr/M^{2+}	Yield of precursor (%)	Ref.
$MgCr_2O_4$	$(NH_4)_2Mg(CrO_4)_2\cdot 6H_2O$	2·010* ± 0·002	70	4
$NiCr_2O_4$	$(NH_4)_2Ni(CrO_4)_2\cdot 6H_2O$	1·999 ± 0·002	75	7
$MnCr_2O_4$	$MnCr_2O_7\cdot 4C_5H_5N$	2·015† ± 0·002	90	6
$CoCr_2O_4$	$CoCr_2O_7\cdot 4C_5H_5N$	2·012* ± 0·002	90	6
$CuCr_2O_4$	$(NH_4)_2Cu(CrO_4)_2\cdot 2NH_3$	2·000 ± 0·003	43	7
$ZnCr_2O_4$	$(NH_4)_2Zn(CrO_4)_2\cdot 2NH_3$	1·995 ± ·0006	77	7
$FeCr_2O_4$	$NH_4Fe(CrO_4)_2$	1·995 ± 0·003	80	8

* Based on total Cr only
† Based on total Mn only

Table 2.—Crystallographic and magnetic properties of the chromites

Compound	Lattice constants (25°C)		Transformations	$\mu\left(\begin{array}{c}\text{Bohr mag/mole}\\ \text{10,000 oe., 4·2°K}\end{array}\right)$
	Cubic(a_0) Å	Tetragonal*		
$MgCr_2O_4$	8·333 ± ·002			0·15
$NiCr_2O_4$		a = 8·248 ± 0·002 c = 8·454 ± 0·002	Tet. to cubic at 37°C ± 2°C	0·33
$MnCr_2O_4$	8·437 ± 0·002			1·20
$CoCr_2O_4$	8·332 ± 0·002			0·18
$CuCr_2O_4$		a = 8·532 ± 0·003 c = 7·788 ± 0·003		0·72
$ZnCr_2O_4$	8·327 ± 0·002			0·12
$FeCr_2O_4$	8·377 ± 0·002		Tet. to cubic at −138°C ± 3°C	0·84

* Based on pseudocubic cell

These compounds have not been examined for trace impurities and spectroscopic analyses were not performed. However, the precursors are prepared from very pure salts which contain very little trace impurities, and are themselves purified by crystallization. Where analyses of both metals were accurately determined, the total oxides did not deviate by more than 0·15 per cent from 100 per cent.

---

(13) F. K. Lotgering, *Phillips Res. Rpts.* **11**, 190 (1956).
(14) L. Corliss and J. Hastings. Private communication (1961).
(15) T. A. Kaplan, K. Dwight, D. Lyons and N. Menyuk, *J. Appl. Phys. Supp.* **32**, 13S (1961).

Acknowledgements—The authors would like to thank Dr. D. G. WICKHAM, who conceived the "precursor" technique for the synthesis of chromites. They wish to acknowledge the assistance of Dr. R. J. ARNOTT and N. MENYUK who made the crystallographic and magnetic measurements.

J. Inorg. Nucl. Chem., 1962, Vol. 24, pp. 29 to 34. Pergamon Press Ltd. Printed in Northern Ireland

THE PREPARATION OF URANIUM MONOCARBIDE–PLUTONIUM MONOCARBIDE SOLID SOLUTIONS, PLUTONIUM SESQUICARBIDE AND PLUTONIUM MONOCARBIDE

A. E. Ogard, W. C. Pritchard, R. M. Douglass and J. A. Leary*
Los Alamos Scientific Laboratory, University of California Los Alamos,
New Mexico

(*Received* 19 *June* 1961; *in revised form* 17 *August* 1961)

Abstract—Hypostoicheiometric† uranium monocarbide–plutonium monocarbide solid solutions with no impurities detectable by X-ray diffraction or metallographic examination have been prepared simply by sintering at 1450–1850°C mixtures of uranium dioxide, plutonium dioxide and graphite. Pellets with densities up to 12·85 g/cm^3 (94·5 per cent of theoretical density) were achieved by a second sintering of pressed pellets of the reaction product. By a similar procedure single-phase stoicheiometric plutonium sesquicarbide has been prepared with pellet densities up to 12·6 g/cm^3 (99 per cent of theoretical density). However, hypostoicheiometric plutonium monocarbide prepared in the same manner always contained plutonium sesquicarbide as the only impurity. Arc melting of the sintered uranium monocarbide–plutonium monocarbide solid solutions and plutonium sesquicarbide yielded comparably pure materials of near theoretical density. Arc melting of the sintered plutonium monocarbide eliminated the plutonium sesquicarbide impurity resulting in a single-phase hypostoicheiometric plutonium monocarbide.

Although the practical importance of plutonium–containing ceramics is based on their potential use as a nuclear fuel, the form of such a fuel is uncertain at this time. A variety of carbide fuels in different forms has been proposed, such as uranium monocarbide and plutonium monocarbide in solid solution as a ceramic fuel rod for power reactors, plutonium carbide fuel rods for specialized reactors, and either the solid solution or plutonium carbide in a dispersion fuel system.

A review of the literature shows that the preparation of uranium monocarbide has been studied quite extensively. Various methods which have been used are the reaction of graphite and uranium powders,(1) uranium dioxide and graphite,(1,2) uranium hydride and methane,(2) and direct arc melting of uranium metal and graphite.(3) Much less work has been reported on plutonium monocarbide and plutonium sesquicarbide, but similar preparative methods have been used, such as the reaction of graphite and plutonium powder,(4) plutonium dioxide and graphite,(4,5) and direct arc melting of plutonium metal and graphite.(5) However, it was not definitely shown with the plutonium carbides that single phase materials were achieved in these preparations.

---

* Work performed under the auspices of the U.S. Atomic Energy Commission

† Carbon deficient

(1) H. A. Wilhelm, P. Chiotti, A. I. Snow and A. H. Daane, *J. Chem. Soc.* S318 (1949).

(2) L. M. Litz, A. B. Garrett and F. C. Croxton, *J. Amer. Chem. Soc.* **70**, 1718 (1948).

(3) A. C. Secrest, Jr., E. L. Foster and R. F. Dickerson, Report BMI-1309 (1959).

(4) J. L. Drummond, B. J. McDonald, H. M. Ockenden and G. A. Welch, *J. Chem. Soc.* 4785 (1957).

(5) R. N. R. Mulford, F. H. Ellinger, G. S. Hendrix, and E. D. Albrecht, *Conférence International sur le Métallurgie du Plutonium*, Mémoire n° 32, Grenoble (1960).

Uranium monocarbide is reported by RUNDLE(6) as being face-centred-cubic (NaCl type) with a lattice dimension of 4·951 Å. Plutonium monocarbide is reported by ZACHARIASEN(7) and MULFORD(5) as also being face-centred-cubic (NaCl type) with lattice dimension in the range 4·92–4·97 Å. Because of the same crystal structure and similar lattice dimensions, uranium monocarbide and plutonium monocarbide could form a solid solution, possibly over the complete range of composition. However, nothing has appeared in the literature on the preparation of uranium monocarbide–plutonium monocarbide solid solutions. Plutonium sesquicarbide is body-centred-cubic with lattice dimension of 8·129 Å.(8)

In this work powder metallurgical techniques, together with arc melting procedures were used for the preparation of the carbides after preliminary work indicated that these methods were the most satisfactory.

EXPERIMENTAL

Generally the same powder metallurgical techniques were used in the preparation of sintered pellets of each of the carbides. The respective powdered dioxides were ball-milled with less than 325-mesh spectrographic grade graphite and pressed at 60 tons/in^2 into 0·4 in. high right cylinders using a 0·407 in. diameter tungsten carbide floating die. Plutonium dioxide was prepared by heating plutonium(IV) peroxide in air at 950°C to constant weight. Uranium dioxide was prepared by heating triuranium octaoxide to constant weight at 1200°C in a hydrogen atmosphere. The average particle sizes of the plutonium dioxide and uranium dioxide obtained from these preparations were 1 μ and 4·4 μ, respectively. The amounts of materials used (approximately 25 g) were computed on the basis of the following reactions:

$$xUO_2 + (1 - x)PuO_2 + (2 + y)C \rightarrow (U_xPu_{1-x})C_y + 2CO \qquad (0{\cdot}7 < x < 0{\cdot}9)$$
$$(0{\cdot}95 < y < 1)$$

$$2PuO_2 + 7C \rightarrow Pu_2C_3 + 4CO$$

$$PuO_2 + (2 + x)C \rightarrow PuC_x + 2CO \qquad (0{\cdot}71 \leqslant x < 1)$$

The pressed pellets were loaded into a degassed, 1 in. inside diameter graphite crucible with a 0·010 in. thick tantalum plate separating the pellets from the crucible, and sintered in a vacuum induction furnace. Reaction of the materials started at 1100–1200°C but the bulk of the reaction was carried out at 1250–1450°C. The materials were sintered at these temperatures until the pressure of the system under full pumping decreased and approached the starting pressure of 0·01–0·05 μ. In the uranium–plutonium carbide system the temperature was raised to 1850°C after the major portion of the reaction was over in order to complete the conversion to carbide.

The product obtained from the first sintering was usually a porous, hour glass shaped pellet which clearly exhibited voids and lateral laminations. These pellets were ground in a flowing helium atmosphere, passed through a 325-mesh screen, re-pressed in a vacuum pressing can and re-sintered for several hours at temperatures and pressures similar to the first sintering. The pellets obtained from this second sintering were dense, right cylinders with no visible laminations or voids. X-ray powder diffraction and metallographic examinations were obtained on these specimens to evaluate purity and homogeneity of the sintered products. In addition, the pellet densities were measured by displacement in bromobenzene. In some cases the second sintered materials were arc melted to determine the quality of product obtainable by this method.

RESULTS

Uranium monocarbide–plutonium monocarbide solid solutions

Single-phase hypostoicheiometric uranium monocarbide–plutonium monocarbide solid solutions in the range 35·9 atom per cent uranium–15·4 atom per cent plutonium

---

(6) R. E. RUNDLE, N. C. BAENZIGER, A. S. WILSON, R. A. MCDONALD, *J. Amer. Chem. Soc.*, 70, 99 (1948).

(7) W. H. ZACHARIASEN, *The Transuranium Elements*, (Edited by G. T. Seaborg, J. J. Katz and W. M. Manning) NNES, Div. IV, Vol. 14 B, Paper 20.2, McGraw-Hill, New York (1949).

(8) W. H. ZACHARIASEN, *Acta Cryst.* 5, 17 (1952).

($U_{0·7}Pu_{0·3}C_{0·95}$) to 46·1 atom per cent uranium–5·1 atom per cent plutonium ($U_{0·9}Pu_{0·1}C_{0·95}$) have been prepared by simply sintering a mixture of uranium dioxide, plutonium dioxide, and graphite at 1450–1850°C for 6 hr. This range of composition is of principal interest for breeder reactor fuels.

X-ray powder diffraction photographs of the first-sintered hypostoicheiometric materials showed no impurities except for one 41·0 atom per cent uranium–10·2 atom per cent plutonium monocarbide ($U_{0·8}Pu_{0·2}C_{0·95}$) preparation in which a few, very weak, extraneous lines appeared due to a trace of uranium dioxide or to the $CuK\beta_1$ lines of the monocarbide solid solution. No impurities of any kind were detected by X-ray diffraction or metallographic examination in the materials after a second sintering. Pellet densities up to 12·58 g/cm^3 (94·5 per cent of theoretical) have been achieved after a second sintering. Thus it has been shown that hypostoicheiometric uranium monocarbide–plutonium monocarbide solid solutions can easily be prepared from the dioxides and graphite in a single sintering. The re-pressing and re-sintering serves to densify the product and to control shrinkage of the specimen.

Arc melting of a $U_{0·8}Pu_{0·2}C_{0·95}$ pellet that had been sintered twice yielded a button that was homogeneous when examined metallographically. Only one phase was detected by X-ray diffraction, and metallographic examination showed it to contain less than 3 per cent impurities. The measured density of this material is 3 per cent higher than the theoretical density. Impurities which could possibly be present to give this high density are uranium, plutonium, tungsten or tungsten carbides. However none of these were detected in the X-ray diffraction pattern.

In contrast to these preparations, a stoicheiometric 45 atom per cent uranium–5 atom per cent plutonium preparation ($U_{0·9}Pu_{0·1}C$) contained approximately 15 per cent of sesquicarbide solid–solution impurity after each of two sinterings.

The crystal structure of the solid solutions was determined to be face-centred-cubic with lattice dimension of 4·955 to 4·963 Å and isomorphous with uranium monocarbide and plutonium monocarbide. Densities calculated from these lattice dimensions vary from 13·63 to 13·59 g/cm^3, respectively. Results of X-ray powder diffraction and metallographic analyses and density determinations are compiled in Table 1.

Plutonium sesquicarbide

In preparations using stoicheiometric amounts of starting materials, two sinterings were done at 1250–1450°C and a third sintering at 1650–1750°C to test the effect of multiple sinterings on the purity and density of the product. Between the first and second sinterings the material was re-ground and re-pressed. X-ray diffraction analyses showed the sintered material to be plutonium sesquicarbide with a trace of plutonium monocarbide as the only impurity present in the amounts: first sinter $\leqslant$ third sinter $<$ second sinter. Metallographic examination of the third sintered pellet showed the plutonium monocarbide impurity as a matrix and also as a thin outer surface of zetaplutonium monocarbide.(5) The difference in impurity level between the three sinterings is probably due to the ease of oxidation of powdered plutonium carbides during handling. During the grinding of the first-sintered material in the flowing helium atmosphere, some oxygen and water vapour were undoubtedly adsorbed. Upon re-sintering, the oxygen would have reacted with the carbide and decreased the amount of carbon in the product, thereby increasing the amount of plutonium monocarbide impurity. The third sintering at 1650–1750°C was above the incongruent melting point of the monocarbide,(5) and a plutonium-rich dissociation product was found to distill out of the material, thereby lowering the PuC impurity level. Sintered pellet densities up to 12·6 g/cm³ (99 per cent of theoretical) were achieved after the third sintering.

Single-phase plutonium sesquicarbide was prepared by a 6 hr sintering at 1250–1450°C of pressed compacts of plutonium dioxide and graphite. It was found that a slight excess of graphite was needed to react with any excess oxygen that might be present due to adsorption during handling of the various materials. Therefore the starting mixture contained 1 per cent excess graphite over that needed to form stoicheiometric plutonium sesquicarbide. No impurities were detected by X-ray diffraction or metallographic examination in this first sintered material using the excess graphite. The immersion density of this sintered product was 11·3 g/cm³ (89 per cent of theoretical).

TABLE 1.—ANALYSES OF URANIUM MONOCARBIDE–PLUTONIUM MONOCARBIDE PREPARATIONS

Preparation	Density g/cm³	a_0 (Å) MC	a_0 (Å) M_2C_3	Impurity* (%)
$U_{0.9}Pu_{0.1}C$				
1st sinter		4·963	8·094	15
2nd sinter		4·963	8·094	15
$U_{0.9}Pu_{0.1}C_{0.95}$				
1st sinter		4·957	N.D.†	<5
2nd sinter	12·85	4·960	N.D.	<3
$U_{0.8}Pu_{0.2}C_{0.95}$				
1st sinter		4·955	N.D.	<5
2nd sinter	12·7	4·956	N.D.	<5
Arc melted	14·0	4·955	N.D.	3
$U_{0.7}Pu_{0.3}C_{0.95}$				
1st sinter		4·961	N.D.	<5
Theoretical	13·6			

* Amounts of M_2C_3 impurity estimated by X-ray diffraction and metallographic examination.

† N.D. – not detected in powder pattern.

Arc melting of these sintered materials produced a shattered material with density of 12·7 g/cm³ (essentially 100 per cent theoretical) and less than 5 per cent impurity as determined by metallographic examination.

The lattice dimension of the body-centred-cubic plutonium sesquicarbide phase was found to vary from 8·122 to 8·139 Å, including all values for this phase whether present as the predominant constituent or as an impurity. Densities calculated from these lattice dimensions vary correspondingly from 12·57 to 12·67 g/cm³. Results of

X-ray powder diffraction, metallographic analyses and density determinations are compiled in Table 2.

Plutonium monocarbide

Single phase plutonium monocarbide has not been successfully achieved solely by sintering compacts of the dioxide and graphite. In a series of preparations of 41·5, 45·0, 47·0 and 50·0 atom per cent carbon, the products formed by a single sintering at 1450°C contained plutonium sesquicarbide as the only impurity found in the X-ray diffraction pattern. The estimated amount of this impurity varied from 20 to 50 per cent. Grinding, re-pressing and re-sintering of these preparations did not materially alter the amount of plutonium sesquicarbide. However, arc melting of the second-sintered 45·0 and 47·0 per cent carbon materials did yield virtually single phase materials. No plutonium sesquicarbide was detected in this material by X-ray diffraction and only a trace amount was detected by metallographic examination. Arc melting yielded buttons with densities up to 13·4 g/cm^3 (98·5 per cent of theoretical density) for the hypostoicheiometric plutonium monocarbide.

TABLE 2.—ANALYSES OF PLUTONIUM SESQUICARBIDE PREPARATIONS

Preparation	Density (g/cm^3)	a_0 (Å) PuC	a_0 (Å) Pu_2C_3	[illegible]
60·0 atom per cent carbon, Pu_2C_3				
1st sinter No. 1		T.Q.†	8·130	[illegible]
1st sinter No. 2		T.Q.	8·127	[illegible]
2nd sinter No. 2	11·3	4·967	8·130	[illegible]
3rd sinter No. 2	12·6	T.Q.	8·129	[illegible]
Arc melted 2nd sinter	12·7			<3
1st sinter No. 3 excess carbon used	11·3	N.D.†	8·122	<3
Theoretical	12·7			

* Amounts of PuC impurity estimated by X-ray powder diffraction and metallographic examination.

† T.Q. = *trace quantity, too small an amount of measure* a_0.

‡ N.D. = not detected in powder pattern.

The lattice dimension of the face-centred-cubic plutonium monocarbide phase was found to vary from 4·960 to 4·977 Å, including all values for this phase whether present as the predominant constituent or as an impurity in other carbide preparations.

CONCLUSIONS

1. Single-phase hypostoicheiometric uranium monocarbide–plutonium monocarbide solid solutions of the compositions $U_{0·9}Pu_{0·1}C_{0·95}$, $U_{0·8}Pu_{0·2}C_{0·95}$ and $U_{0·7}Pu_{0·3}C_{0·95}$ have been prepared by sintering the dioxides and graphite. It was determined that uranium dioxide, plutonium dioxide and graphite can be reacted to form a monocarbide solid solution without first making the monocarbides separately or the solid solution of the dioxides. Sintered pellet densities up to 12·85 g/cm^3 (94·5 per cent of theoretical) were achieved. Arc melting of the sintered product yielded a comparably pure single-phase macroscopically homogeneous button.

2. Single-phase plutonium sesquicarbide has been prepared in a single sintering

by powder metallurgical techniques from plutonium dioxide and graphite. A slight excess of graphite over that needed to form a stoicheiometric compound was used in the preparation to insure complete reaction of all oxygen present.

3. Completely single-phase hypostoicheiometric plutonium monocarbide has not been prepared solely by powder metallurgical techniques. The preparations always contained plutonium sesquicarbide but no other impurities were detected by X-ray diffraction. The resulting sintered material is, however, a good material to arc melt into single-phase plutonium monocarbide. Arc melted button densities of 13·4 g/cm^3 (98·5 per cent of theoretical) for single-phase plutonium monocarbide have been achieved.

4. Powdered plutonium carbides are easily oxidized and are pyrophoric in some cases, necessitating a highly inert system for the procedures in which the powders are handled such as grinding and compacting.

Acknowledgements—The authors wish to thank W. J. MARAMAN for frequent, helpful consultations on this project, Group CMB-1 for chemical and X-ray diffraction analyses, and Group CMF-5 for metallographic examinations.

J. Inorg. Nucl. Chem., 1962, Vol. 24, pp. 35 to 43. Pergamon Press Ltd. Printed in Northern Ireland

THE MECHANISM AND KINETICS OF THE FORMATION OF $UO_{2.90}\cdot 6YO_{1.5}$

E. J. Felten and E. A. Aitken
General Electric Nuclear Materials and Propulsion Operation
(formerly Aircraft Nuclear Propulsion Department)
Cincinnati 15, Ohio

(*Received* 14 *June* 1961; *in revised form* 4 *August* 1961)

Abstract—Above 1200°C four phases are present in the UO_2–Y_2O_3–O_2 system, namely; U_3O_8, a mixed oxide phase having the fluorite structure, a rhombohedral phase and Y_2O_3. The fluorite phase was found to exist between 30 and 72·5 mole per cent $YO_{1.5}$. Between 74·5 and 81·0 mole per cent $YO_{1.5}$ the fluorite phase and the rhombohedral phase co-exist. The ideal composition of the rhombohedral phase is $UO_{2.90}\cdot 6YO_{1.5}$ (85·7 mole per cent $YO_{1.5}$). The rhombohedral phase is found between 81·0 and 87·7 mole per cent $YO_{1.5}$, and co-exists with yttrium oxide between 87·7 and 95·6 mole per cent $YO_{1.5}$.

X-ray diffraction methods were used to determine the mechanism and kinetics of the reaction between UO_2 or U_3O_8 and Y_2O_3 to form the rhombohedral phase. Between 1000 and 1100°C a fluorite phase having an approximate composition $UO_{2.90}\cdot 2YO_{1.5}$ is formed as an intermediate in the reaction with only a slow conversion to the rhombohedral phase. At 1200°C and above the formation of the rhombohedral phase proceeds more rapidly, going to completion in 8 hr or less at 1400°C.

The X-ray diffraction data indicate good agreement with the Jander model for the formation of the rhombohedral phase. The reaction proceeds at least in part by diffusion of gaseous UO_3 to the surface of the Y_2O_3 particles. Further reaction involves bulk diffusion of uranium through the surface layer. An activation energy of 91 kcal/mole was obtained for the diffusion process.

Previous investigations into the UO_2–Y_2O_3–O_2 system above 1200°C have revealed the presence of three phases, namely; U_3O_8, a mixed oxide phase having the fluorite structure, and Y_2O_3.(1) In studies at 1200°C, Hund *et al.*(1) found the fluorite phase exists between 30 and 65 mole per cent of $YO_{1.5}$. In this range the lattice parameter of the face-centered cubic cell decreases regularly from 5·376 to 5·317 Å. These values were converted from the original results reported in kX units. The fluorite phase has a cation sub-lattice which is statistically fully occupied. At low yttrium oxide content, oxygen is statistically distributed in the octahedral vacancies. At about 55 mole per cent of $YO_{1.5}$ the cation and anion locations are both fully occupied. At still higher $YO_{1.5}$ concentrations vacancies occur in the oxygen sub-lattice. The authors(1) report the inability to attain complete conversion, presumably to the fluorite phase, on the side of the system which is rich in yttrium oxide.

In work performed at this laboratory the system was studied by reacting the mixed powders in air at approximately 1700–1800°C. In addition to the phases found by Hund *et al.*(1), a phase exhibiting rhombohedral symmetry was also found. Here the fluorite phase was found to exist between 30 and 72·5 mole per cent $YO_{1.5}$. The lattice parameters obtained from solid solutions in this region are in good agreement with those of HUND *et al.*(1) Between 74·5 and 81·0 mole per cent $YO_{1.5}$ the fluorite phase and the rhombohedral phase co-exist. The ideal composition of the rhombohedral phase is $UO_{2.90}\cdot 6YO_{1.5}$ (85·7 mole per cent $YO_{1.5}$). The rhombohedral phase is found between 81·0 and 87·7 mole per cent $YO_{1.5}$, and co-exists with yttrium oxide between 87·7 and 95·6 mole per cent $YO_{1.5}$. Thermal balance studies have been conducted on blended UO_2–$6YO_{1.5}$ powders.(2) No change in the stoicheiometry of the yttrium oxide was obtained in the temperature range of these experiments. Thermogravimetric analyses (TGA) indicated that $UO_{2.0}$ was oxidized to U_3O_8 prior to its reaction with Y_2O_3. This oxidation was found to proceed in two distinct stages: a rapid oxidation of $UO_{2.0}$ to $UO_{2.35}$ between 130 and 280°C; a constant weight plateau between 280 and 330°C and an extremely rapid oxidation to $UO_{2.65}$ between 330 and 348°C. Oxidation to $UO_{2.67}$ was completed by 450°C. Above 600°C, a slight loss of oxygen was observed, and by 1200°C the oxygen–uranium ratio was reduced to a value of about 2·60. Further heating above 1200°C resulted in an increase in weight with temperatures to 1460°C. This is in sharp contrast with undiluted $UO_{2.0}$ which undergoes weight loss above 1250°C (presumably due to volatilization of UO_3). The UO_{2+x}–$6YO_{1.5}$ composition attains an equilibrium weight of 1460°C corresponding to an oxygen-uranium ratio of 2·90. During 22 hr at 1460°C the sample weight remained constant (*i.e.* no volatilization of urania occurred). Upon cooling to room temperature a slight oxidation occurred increasing the oxygen–uranium ratio to 2·92.

---

* Present address: Pratt and Witney Aircraft, North Haven, Connecticut.

(1) F. Hund, V. Peetz and G. Kottenhahn, *Z. Anorg. Chem.* **278**, 184–191, 1955.

X-ray diffraction analysis indicated the product of the TGA runs to be the rhombohedral phase. Chemical analysis for U^{4+} and U^{6+} in a sample prepared by reaction in air at 1460°C gave an oxygen–uranium ratio of 2·90, in excellent agreement with the thermal balance results. The lattice parameters of the rhombohedral phase are $a_0 = 6{\cdot}530$ Å and $\alpha = 99°4'$ as determined from X-ray diffraction powder patterns.(3) The more convenient hexagonal lattice constants are $a_0 = 9{\cdot}93_5$ Å and $c_0 = 9{\cdot}36_0$ Å. These have been confirmed by the analysis of diffraction patterns obtained from single crystals. X-ray patterns for the rhombohedral phase, a representative fluorite phase ($UO_{2.90}\cdot 2YO_{1.5}$) and yttrium oxide are presented in Table 1.

The potential usefulness of the rhombohedral phase led to an investigation of its preparation. Analysis of the results gave a better understanding of the kinetics and mechanism of the formation of the phase.

EXPERIMENTAL

The materials used in this investigation consisted of Mallinckrodt UO_2 powder (purity: >99·99 per cent) and Y_2O_3 powder obtained from the Dow Chemical Co. (99·9 per cent pure). The powders were blended in the dry state by means of a Mix-R-Mill (Spex Industries, Inc., Scotch Plains, New Jersey). This is a specially designed device for blending and grinding of ceramic powders. After blending, the homogenous mixtures were fired in platinum cups for various periods of time in air at a number of temperatures. The products obtained were examined both visually and by X-ray diffraction.

RESULTS

The discussion of the results can be divided into two sections, depending on whether the experiments were conducted above or below 1200°C. Below this temperature important information is obtainable regarding the mechanism of the formation of $UO_{2.90}\cdot 6YO_{1.5}$, while above 1200°C the kinetics of the reaction were studied.

---

(2) E. F. JUENKE, To be published.

(3) S. F. BARTRAM and G. A. CHASE, Private communication (1961).

The results of the X-ray diffraction analysis of mixtures fired below 1200°C are found in Table 2. On experiments using equimolar mixtures of UO_2 or $UO_{2.67}$ and Y_2O_3 fired for 120 hr at 1100°C and 64 hr at 1310°C a single, face-centred cubic phase was obtained having a lattice parameter, $a_0 = 5·33$ Å. This suggests that the cubic phase formed in the UO_2–$3Y_2O_3$ reaction at 1000 and 1080°C has a composition close to that of $UO_{2·90}·2YO_{1·5}$.

TABLE 1.—X-RAY DIFFRACTION PATTERNS FOR $UO_{2·90}·2YO_{1·5}$; $UO_{2·90}·6YO_{1·5}$ AND Y_2O_3

$UO_{2·90}·2YO_{1·5}$ Face-centred cubic phase		$UO_{2·90}·6YO_{1·5}$ Rhombohedral phase		Y_2O_3 Body-centred cubic phase	
d(Å)	*hkl*	*d*(Å)	*hkl**	*d*(Å)	*hkl*
		6·35	011		
		4·97	110		
				4·34	211
		4·12	102		
		3·92	201		
		3·16	022		
		3·12	003		
3·08	111	3·08	121	3·06	222
		2·87	300		
2·665	200	2·673	212	2·652	400
		2·644	113		
				2·500	411
				2·372	420
		2·313	311		
				2·261	332
				2·165	422
		2·125	132		
		2·111	303		
		2·056	204	2·080	510
		1·943	223	1·936	521
		1·900	124		
1·884	220	1·877	410	1·874	440
1·607	311	1·609	413	1·599	622
		1·602	421		

* Indexed on basis of hexagonal cell.

Transpiration experiments conducted in an oxidizing atmosphere show U_3O_8 to have a high volatility at relatively low temperatures.[4] The vapour species in equilibrium with U_3O_8 is assumed to be UO_3. To determine the importance of the vapour phase in reactions between $UO_{2·67}$ and Y_2O_3 in air, Y_2O_3 pellets were fired in a platinum boat in close proximity, but not physically in contact with U_3O_8 powder. This experiment was conducted at 1310°C for 64 hr during which time the exposed portions of the Y_2O_3 pellet were completely covered by a blue-black skin. X-ray examination of the skin showed it to be face-centred cubic with a lattice parameter of 5·32 Å which corresponds approximately to the $UO_{2·90}·2YO_{1·5}$ composition.

The reaction between $UO_{2·67}$ and $3Y_2O_3$ is thus assumed to proceed as outlined in

---

[4] R. J. ACKERMANN, R. J. THORN, C. ALEXANDER and M. TETENBAUM, *J. Phys. Chem.* **64**, 350–55 (1960).

Fig. 1. As shown by the X-ray results the conversion of the mixtures to the rhombohedral phase is extremely slow at 1000°C but becomes more rapid at 1200° and above. Complete conversion was apparently obtained after 64 hr at 1310°C. Visual inspection of $UO_{2.67}$–$3Y_2O_3$ mixtures fired between 1000° and 1420°C very often gave a good indication as to how far the reaction had proceeded. Where more than one phase was present a salt and pepper effect was observed, the reacted powder becoming more homogeneous in appearance as the time at temperature was increased.

TABLE 2.—PHASE RELATIONS FOR UO_2–$3Y_2O_3$ AFTER REACTING IN AIR BETWEEN 1000° AND 1420°C

Exp. no.	Temp. (°C)	Time (hr)	Phases found
76	1000	100	Y_2O_3 + F.C. cubic phase ($a_0 = 5{\cdot}33_4$ Å) + trace rhombohedral phase
78	1000	480	Y_2O_3 + F.C. cubic phase ($a_0 = 5{\cdot}32_6$ Å) + trace rhombohedral phase
1	1080	16	Y_2O_3 + F.C. cubic phase ($a_0 = 5{\cdot}32_9$ Å) + trace rhombohedral phase
108	1100	65	Y_2O_3 + rhombohedral phase
121	1100	120	Y_2O_3 + rhombohedral phase
40	1190	6	Y_2O_3 + rhombohedral phase
44	1190	36	Y_2O_3 + rhombohedral phase
9	1310	64	Rhombohedral phase
31	1420	6	Rhombohedral phase + trace Y_2O_3

A comparison of the X-ray diffraction patterns for the rhombohedral phase and Y_2O_3 (see Table 1) show that both patterns have a common peak at about 3·08 Å (Peak *A*). The rhombohedral phase has a peak at 3·12 Å (Peak *B*) to which Y_2O_3 makes no contribution.

By measuring the ratio of the intensities of Peak *A* to Peak *B* one can determine the extent to which the reaction proceeded. Therefore, synthetic mixtures were prepared, composed of varying quantities of U_3O_8, Y_2O_3 and the rhombohedral phase. As seen in Fig. 2, this peak ratio varies from 10 at 30 per cent of completion to 3·4 at 100 per cent of completion. This empirical curve was used to determine the extent of reaction in fired $UO_{2.67}$–$3Y_2O_3$ mixtures. An example of the results obtained in this way is shown in Fig. 3 for two mixtures fired for 2 and 18 hr at 1190°C and which have gone to 35 and 72 per cent of completion, respectively. As seen in Fig. 4 the time dependency for the formation of $UO_{2.90}{\cdot}6YO_{1.5}$ is non-linear.

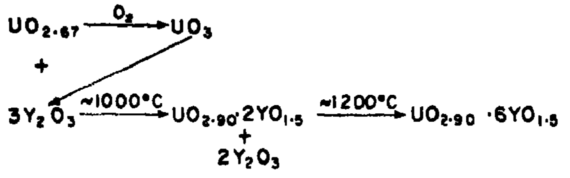

FIG. 1.

The data suggest that JANDER's model for the kinetics of solid-state reactions be tested.[5] A number of other workers have analysed their data in terms of this

---

[5] W. JANDER, *Z. Anorg. Chem.* 163, 1 (1927).

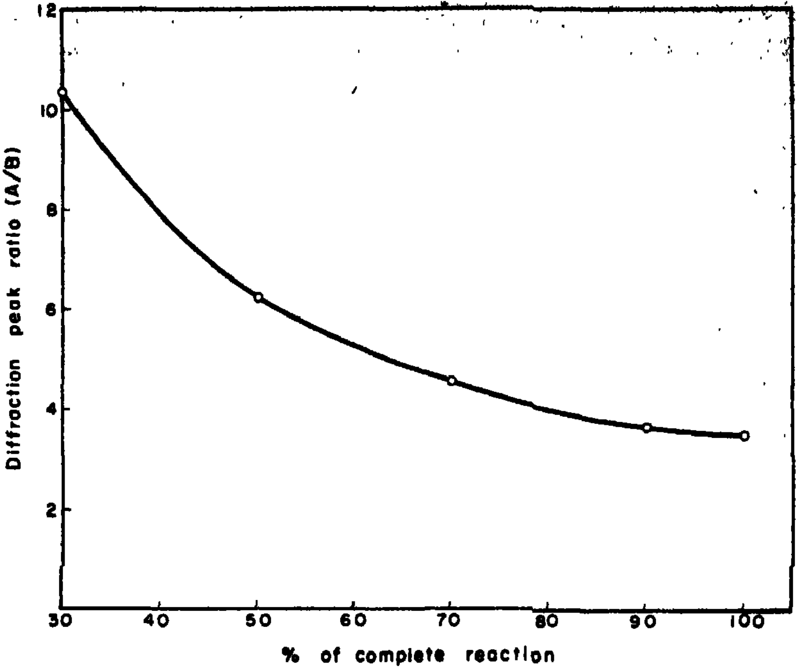
Diffraction peak ratio (A/B)
12
10
8
6
4
2
30
40
50
60
70
80
90
100
% of complete reaction

FIG. 2.

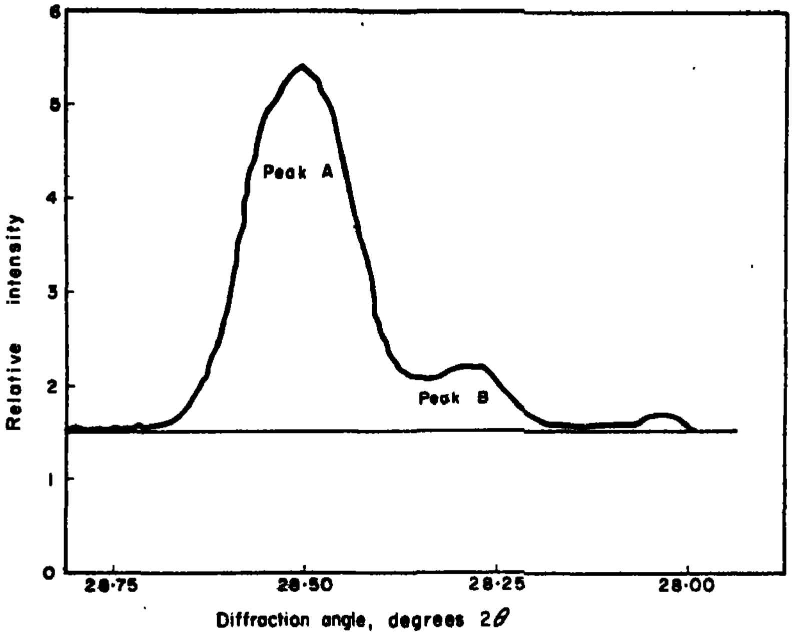
Relative intensity
6
5
4
3
2
1
0
Peak A
Peak B
28·75
28·50
28·25
28·00
Diffraction angle, degrees 2θ

FIG. 3(a).

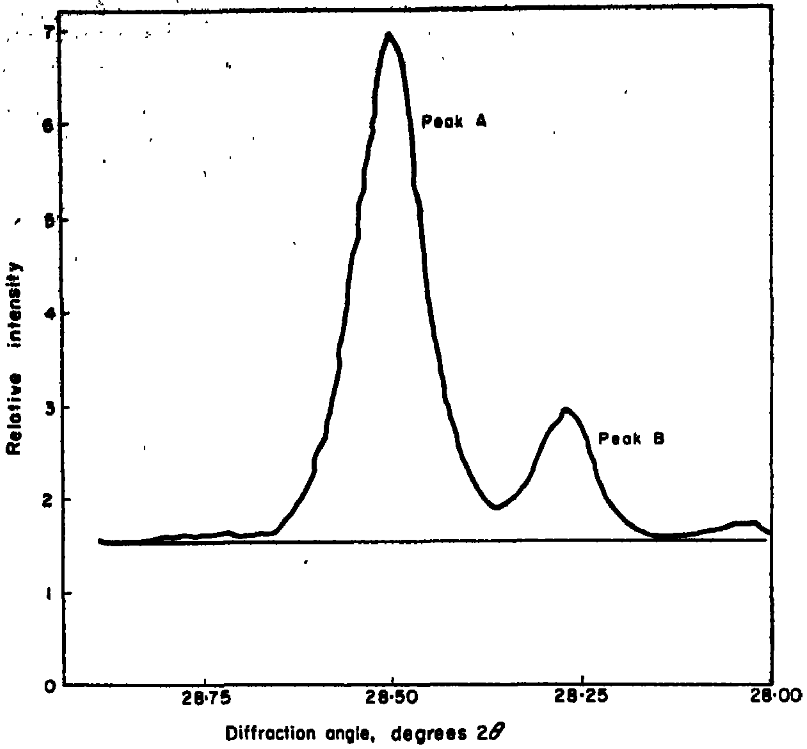
Peak A
Peak B
Relative intensity
0
1
2
3
4
5
6
7
28·75
28·50
28·25
28·00
Diffraction angle, degrees 2θ

FIG. 3(b).

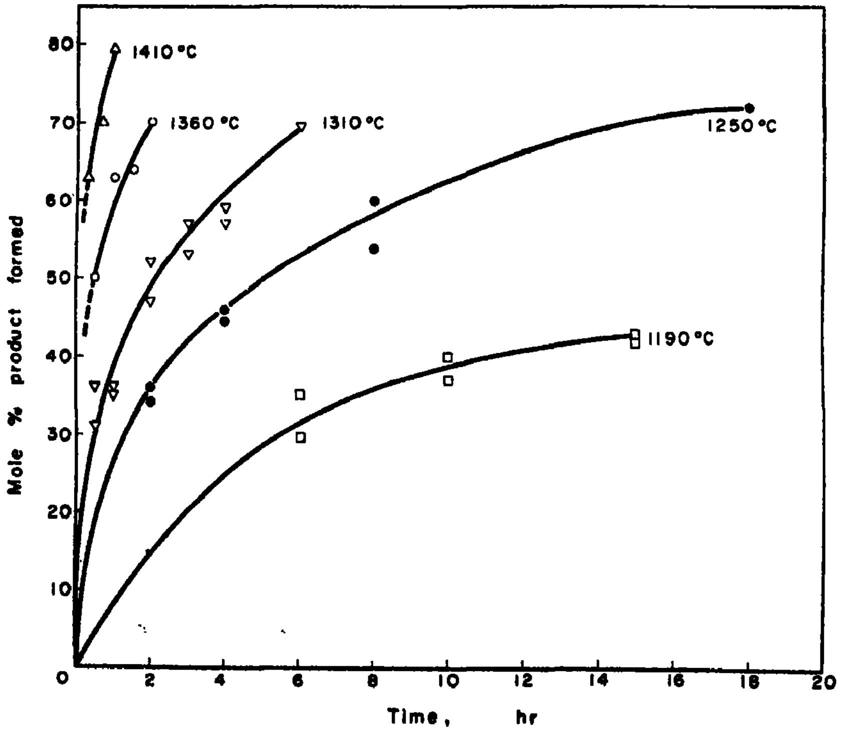
1410 °C
1360 °C
1310 °C
1250 °C
1190 °C
Mole % product formed
0
10
20
30
40
50
60
70
80
0
2
4
6
8
10
12
14
16
18
20
Time, hr

FIG. 4.

model.[6-9] JANDER considered a sphere of radius r which develops a reaction product of thickness y over its entire surface. One can relate x, the fraction of the sphere reacted, to r and y by the following relationship:

$$x = \frac{\text{volume of original sphere}-\text{volume unchanged after time } t}{\text{volume of original sphere}}$$

$$x = \frac{\dfrac{4\pi r^3}{3} - \dfrac{4\pi}{3}(r-y)^3}{\dfrac{4\pi r^3}{3}}$$

$$x = 1 - \frac{(r-y)^3}{r^3}$$

Solving for y

$$y = r(1 - \sqrt[3]{(1-x)}) \tag{1}$$

The rate of thickening of the reaction product was assumed to be inversely proportional to its thickness:

$$\frac{dy}{dt} = \frac{k}{y} \tag{2}$$

Integration of (2) gave:

$$y^2 = 2kt \tag{3}$$

Substituting for y^2 in (3):

$$(1 - \sqrt[3]{(1-x)})^2 = \frac{2k}{r^2}\, t = Kt \tag{4}$$

A plot of $(1 - \sqrt[3]{(1-x)})^2$ vs t should therefore be a straight line. For convenience the results have been plotted on logarithmic paper, and as seen in Fig. 5, a linear relationship having the expected slope of unity was obtained for the family of curves.

The expression relating the parameter $(1 - \sqrt[3]{(1-x)})^2$ to time is a true rate expression since it relates the fraction of the sphere converted to the rhombohedral phase per unit time. Therefore the values of K are related to the absolute temperature (T) by the standard Arrhenius equation:

$$K = A \exp\left(\frac{-\Delta E}{RT}\right) \tag{5}$$

An average value of K at each temperature was obtained from individual $(1 - \sqrt[3]{(1-x)})^2$ and t values. A plot of log K against $1/T$ (Fig. 6) gives an activation energy, ΔE, for the reaction of 91 kcal/mole.

In a practical sense the kinetics data allow one to predict the time required to convert $UO_{2.67}$–$3Y_2O_3$ mixtures to the rhombohedral phase if the particle size of the Y_2O_3 is known. For the material used in this investigation the time varies from 670 hr at 1190°C to 8 hr at 1420°C.

---

(6) G. ECONOMOS and T. R. CLEVENGER, JR., *J. Amer. Ceram. Soc.* **43**, 48 (1960).

(7) Y. IIDA, *J. Japan Soc. Powder Metall.* **6**, No. 2, 11 (1959).

(8) P. J. JORGENSEN, M. E. WADSWORTH and I. B. CUTLER, *J. Amer. Ceram. Soc.* **42**, 613 (1959).

(9) H. KEDESDY and A. DRUKALSKY, *J. Amer. Chem. Soc.* **76**, 5941 (1954).

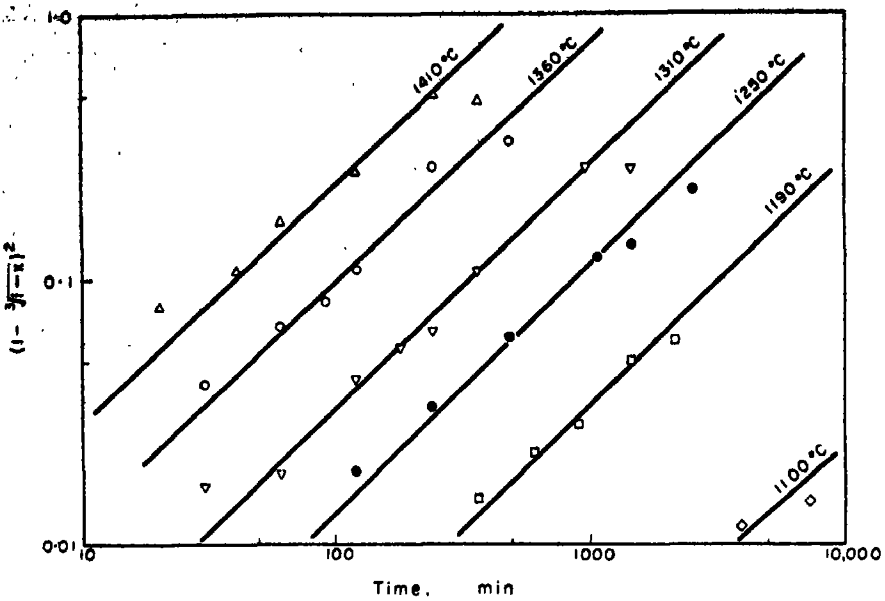
1·0
0·1
0·01
$(1-\sqrt[3]{1-x})^2$
10
100
1000
10,000
Time, min
1410 °C
1360 °C
1310 °C
1250 °C
1190 °C
1100 °C

Fig. 5.

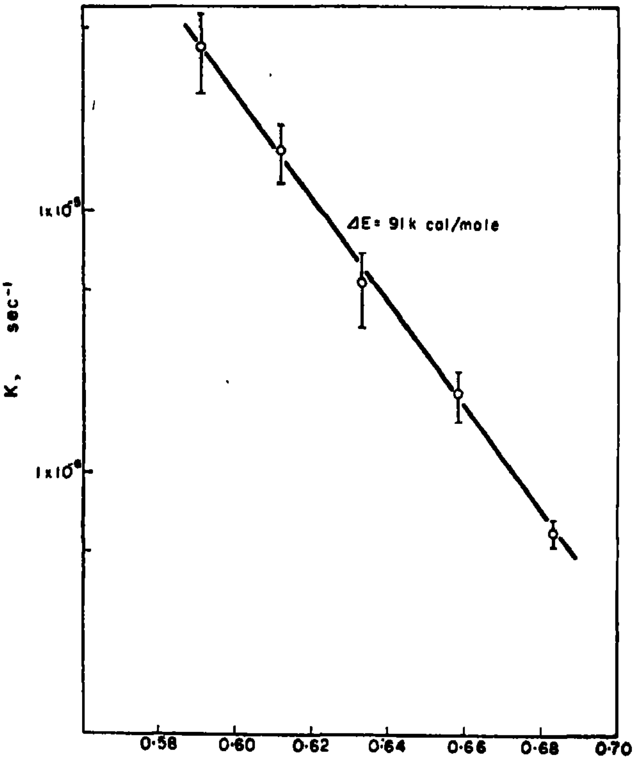
1×10^{-5}
1×10^{-6}
K, sec^{-1}
ΔE= 91 k cal/mole
0·58
0·60
0·62
0·64
0·66
0·68
0·70
$1/T \times 10^3$, °K

Fig. 6.

DISCUSSION AND CONCLUSION

In the results presented here the reaction between UO_2 or $UO_{2.67}$ and $3Y_2O_3$ proceeds by means of an intermediate face-centred cubic phase having the fluorite structure and an approximate composition of $UO_{2.90}{\cdot}2YO_{1.5}$. At 1000°C, even after 480 hr, this phase is present in major amounts and only a very small amount of the rhombohedral phase is found to be present. At 1100°C after 65 and 120 hr, the major phases are Y_2O_3 and a measurable amount of the rhombohedral phase. Thus, the reaction between the $UO_{2.67}$ and Y_2O_3 to form the rhombohedral phase is very sluggish at 1000°C, but proceeds more rapidly at 1100°C, and still more rapidly above 1200°C. The experiment in which the isolated Y_2O_3 and U_3O_8 were fired suggests that the initial reaction involves the oxidation of U_3O_8 to volatile UO_3, which reacts on the surface of the Y_2O_3 particles to form the $UO_{2.90}{\cdot}2YO_{1.5}$. As the temperature or time at temperature is increased additional uranium reacts with the surface layer by both vapour phase and bulk diffusion to form $UO_{2.90}{\cdot}6YO_{1.5}$ on the surface of the Y_2O_3 particles. As indicated by the agreement of the experimental data with the JANDER model,(5) the urania rich phase formed on the surface of Y_2O_3 particles acts as a diffusion barrier to the transport of uranium ions to the interior of the particles. An activation energy of 91 kcal/mole was obtained for the reaction process. It should be kept in mind that in order for the JANDER model to be rigorously obeyed uniformly sized particles must be used. This assumption cannot be made in the present case. However, the apparent agreement with the model allows one to predict, in a practical manner, the kinetics of the UO_{2+x}–$3Y_2O_3$ reaction. A more detailed description of the diffusion process must await the determination of the structure of the rhombohedral phase.

The results obtained here help to explain the observations of HUND *et al.*(1) regarding the sluggish reactivity of mixtures on the side of the system rich in yttrium oxide. As indicated in Table 2 and Fig. 5, only a portion of the mixture would have been converted to the rhombohedral phase at 1200°C. An increase of either the temperature or the time at temperature would have converted the oxide mixture to the rhombohedral phase.

Acknowledgements—The authors wish to extend their thanks to G. CHASE, S. BARTRAM and R. HAAG for their help during the course of this investigation.

J. Inorg. Nucl. Chem., 1962, Vol. 24, pp. 45 to 52. Pergamon Press Ltd. Printed in Northern Ireland

THE PREPARATION AND IDENTIFICATION OF N-FLUORO-N'-TRIFLUOROMETHYLDIAZINE-N'-OXIDE*

J. W. Frazer, B. E. Holder and E. F. Worden
Lawrence Radiation Laboratory, University of California, Livermore, California

(*Received* 14 *June* 1961; *in revised form* 17 *August* 1961)

Abstract—The compound N-fluoro-N'-trifluoromethyldiazine-N'-oxide (CF_3NONF) has been prepared from the reaction of CF_3I, NO, and N_2F_4 by ultra-violet and thermal activation. Its structure has been shown by NMR and ultra-violet absorption data to be $CF_3—\overset{\overset{O}{\uparrow}}{N}=NF$.

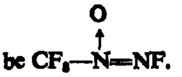
$CF_3—\overset{\overset{O}{\uparrow}}{N}=NF$

N-Fluoro-N'-trifluoromethyldiazine-N'-oxide (CF_3NONF) was first found as a by-product of reaction (1) when the starting compounds

$$CF_3I + N_2F_4 \rightarrow CF_3NF_2 + I + NF_2 \qquad (1)$$

were activated by ultra-violet light (≥ 2750 Å) in Pyrex. The necessary nitric oxide was supplied by reaction (2).

$$N_2F_4 + SiO_2 \rightarrow 2NO + SiF_4. \qquad (2)$$

Thermal activation of CF_3I and N_2F_4 in Pyrex can also be used for the synthesis of CF_3NONF.

EXPERIMENTAL

Apparatus and reagents. The syntheses by ultra-violet excitation were carried out in a 310 cm³ 4π Pyrex reactor which was thermostated at 26 ± 5°C or 46 ± 5°C by circulating water. A 200 W low-pressure mercury arc was used as an excitation source.

All thermally induced reactions were carried out in hermetically-sealed Pyrex bombs of ~75 cm³ capacity.

The starting materials were always at a total pressure of less than 1 atm and present in mole-ratios equivalent to the indicated stoicheiometry. Research grade chemicals were used in all reactions. The N_2F_4† had a purity of ≥99·5 per cent.⁽¹⁾

Analytical procedure. Identification of the reaction products was made by gas chromatography, mass spectrometry and infra-red data. Usually the initial separation and purification of the reaction products was made by gas chromatography and the quantity of the purified compounds determined by P-V-T measurements. Preliminary separations of the reaction products were made using a 20 ft column of di-n-decylphthalate on C-22 firebrick (15:100 ratio by weight) Final purification was accomplished by a 10 ft activated silica gel column (40–60 mesh). The columns were operated at ambient temperature and a helium flow rate of ~100 cm³/min.

The by-products from the synthesis often reacted with the chromatographic columns. Because of this problem and the difficulty of separating and determining all the products, only carbon containing compounds obtained in appreciable yields were quantitatively determined.

RESULTS

Synthesis data. Tables 1 and 2 list the ultra-violet and thermally activated reactions explored during the synthesis of CF_3NONF. Synthesis conditions are indicated with

---

* This work was performed under the auspices of the U.S. Atomic Energy Commission.

† N_2F_4 may be purchased from Peninsular Chemical Research Inc., P.O. Box 3597, Gainsville, Florida.

⁽¹⁾ J. W. Frazer, *J. Inorg. Nucl. Chem.* **11**, 166, (1959).

TABLE 1—REACTIONS ACTIVATED BY ULTRA-VIOLET EXCITATION (>2750 Å)

$$CF_3I + N_2F_4 \xrightarrow[26°C]{\text{ultra-violet 1 hr}} CF_3NF_2 + CF_3NO + CF_3NONF + I_2 \tag{3}$$

22·8%* NM† 6·5%

$$CF_3I + NO + N_2F_4 \xrightarrow[26°C]{\text{ultra-violet 1 hr}} CF_3NO + CF_3NONF + (CF_3NF_2) + I_2 \tag{4}$$

12% 17% NM

$$CF_3I + NO \xrightarrow[26°C]{\text{ultra-violet 1 hr}} CF_3NO + I_2 \tag{5}$$

29%

$$CF_3NO + N_2F_4 \xrightarrow[46°C]{\text{ultra-violet 1 hr}} CF_3NONF \tag{6}$$

14%

$$CF_3NF_2 + NO \xrightarrow[46°C]{\text{ultra-violet 2 hr}} \text{No reaction} \tag{7}$$

$$CF_3NF_2 + NO + N_2F_4 \xrightarrow[26°C]{\text{ultra-violet 1 hr}} \text{No reaction} \tag{8}$$

$$CF_3NO + N_2F_2 \xrightarrow[46°C]{\text{ultra-violet 2 hr}} \text{No reaction} \tag{9}$$

$$CF_3NONF \xrightarrow[26°C]{\text{ultra-violet 1 hr}} 36\% \text{ decomposition [including } 22\%\ CF_3NF_2 \text{ and } 35\%\ CF_3NO] \tag{10}$$

---

* Yield values as based on the available CF_3 groups.

† NM—not measured quantitatively.

TABLE 2—REACTIONS ACTIVATED BY HEATING IN PYREX AT 120°C FOR 1 HR

$$CF_3I + N_2F_4 \rightarrow CF_3NONF + CF_3NF_2 + I_2 \tag{11}$$

35% 11%

$$CF_3I + NO + N_2F_4 \rightarrow CF_3NONF + CF_3NF_2 + I_2 \tag{12}$$

45%* NM†

$$CF_3NO + N_2F_4 \rightarrow CF_3NONF + CF_3NF_2 \tag{13}$$

45% 20%

$$CF_3I + NO \rightarrow \text{No reaction} \tag{14}$$

$$CF_3NF_2 + NO \rightarrow \text{No reaction} \tag{15}$$

$$CF_3NONF \rightarrow \text{No decomposition in 24 hr} \tag{16}$$

---

* Yield values as based on the available CF_3-groups.

† NM—not measured quantitatively.

each reaction plus yield data based on the available (CF_3—). It should be noted that the synthesis of CF_3NONF can be accomplished by either ultra-violet excitation or thermal activation of CF_3I plus N_2F_4 in a Pyrex reaction vessel (reactions 3 and 11 in Tables 1 and 2). The addition of NO to the starting materials (CF_3I plus N_2F_4) enhances the CF_3NONF yield (reactions 4 and 12). If NO is not added as a starting material CF_3NONF cannot be synthesized until the NO is produced by reaction (2).

The CF_3NONF yield of the thermally activated reaction is considerably greater than that of the ultra-violet activated reaction. This is due at least in part to the difference in the stability of CF_3NONF with respect to ultra-violet excitation and to heat. When the CF_3NONF is very pure, there is no decomposition in Pyrex at 120°C in 24 hr (reaction 16), but the ultra-violet irradiation of the compound results in a 35 per cent decomposition in 1 hr (reaction 10).

From the synthesis of CF_3NONF the only other compounds of interest were CF_3NF_2 and CF_3NO. N,N-difluorotrifluoromethylamine (CF_3NF_2) was present regardless of whether the synthesis was carried out by ultra-violet excitation or thermal activation. However, CF_3NO was only present when the synthesis was carried out by ultra-violet excitation. The thermally induced reaction of CF_3I and NO did not yield CF_3NO (reaction 14).

When CF_3NF_2 plus NO are subjected to the same conditions used for the synthesis of CF_3NONF no reaction occurs (see reactions 7 and 15). It is therefore concluded that CF_3NF_2 is an end-product in the synthesis of CF_3NONF. These observations suggest that the groups in CF_3NONF are not arranged in the order of (CF_3)—(NF)—(NO).

When CF_3NO plus N_2F_4 are ultra-violet or thermally activated (reactions 6 and 13) CF_3NONF is synthesized. This suggests that the groups in CF_3NONF are arranged in the order (CF_3)—(NO)—(NF).

Since CF_3NO can only be an intermediate compound in the uv activated reactions, there must be at least two different mechanisms by which CF_3NONF can be synthesized. Two such possible mechanisms are suggested below:

$$CF_3I \xrightarrow{\text{ultra-violet}} CF_3 + I \tag{17}$$

$$CF_3 + NO \xrightarrow{\text{ultra-violet}} CF_3NO \tag{18}$$

$$N_2F_4 \leftrightarrows 2NF_2 \tag{19}$$

$$CF_3NO + NF_2 \xrightarrow{\text{ultra-violet or }\Delta} CF_3NONF + F \tag{20}$$

and

$$NO + NF_2 \overset{\text{ultra-violet or }\Delta}{\rightleftarrows} NONF_2 \tag{21}$$

$$CF_3I + NONF_2 \xrightarrow{\text{ultra-violet or }\Delta} CF_3NONF + F + I. \tag{22}$$

JOHNSON and COBURN[8] have reported the thermal free-radical decomposition of N_2F_4 at ambient temperature, making these overall mechanisms attractive.

Analytical and physical property data. From the mass spectrum data (Table 3) CF_3NONF was shown to contain (CF_3), (NO), and (NF) groups. The infrared spectrum (Fig. 1) showed absorption bands in the regions where these groups are normally active. A determination of the molecular weight by the method of limiting densities yielded a value of 132·1 versus 132·0 calculated for a compound CF_4N_2O-(CF_3NONF). This agrees with the molecular weight (132) obtained by mass spectrum data. The compound is therefore limited to just one of each of the groups (CF_3), (NO), and (NF).

---

[8] F. A. JOHNSON and C. B. COLBURN, "*The tetrafluorohydrazine-difluoro-amino radical equilibrium.*" Presented at the American Chemical Society Meeting, St. Louis, Missouri, March 21–30, 1961.

TABLE 3.—MASS SPECTRUM DATA FOR CF_3NONF

		Pattern (%)	
m/e	Ion assignment	$I_m = 247$ mA	$I_m = 426$ mA
12	C^+	2·89	
14	N^+	4·20	
16	O^+	4·56	
19	F^+	1·75	
28	N_2^+	7·28	
30	NO^+	36·87	
31	CF^+	10·13	
33	NF^+	3·89	
44	N_2O^+	10·92	8·60
45	CFN^+	1·04	1·39
47	N_2F^+	16·35	16·88
50	CF_2^+	9·74	12·10
63	$NONF^+$		0·12
64	CF_2N^+		0·82
66	CF_2O^+		0·59
69	CF_3^+	100·0	100·0*
		—	—
99	CF_3NO^+		0·94
132	CF_3NONF^+		1·83

* CF_3^+ sensitivity = 73·9 div/μ.

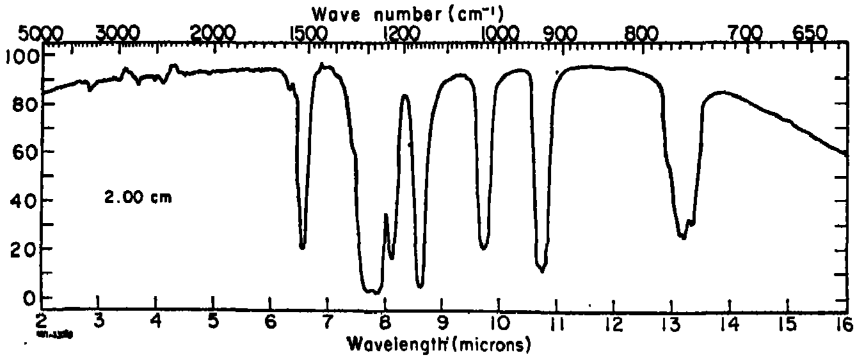

FIG. 1.—The infra-red spectrum of CF_3NONF.

This compound is a gas at room temperature and a clear liquid in the condensed phase. The vapour-pressure can be expressed by $\log_{10\,\text{cm}} P = 5{\cdot}0989 - \frac{415{\cdot}09}{T} - \frac{116667}{T^2}$ over the range 238–267°K. The boiling point is $-7{\cdot}5 \pm 0{\cdot}2$°C.

Some of the most reasonable structures of CF_3NONF are

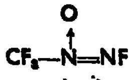

$CF_3\text{—}\overset{\overset{\displaystyle O}{\uparrow}}{N}\text{=}NF$

I

$CF_3\text{—}O\text{—}N\text{=}N\text{—}F$

II

$CF_3\text{—}N\text{=}N\text{—}O\text{—}F$

III

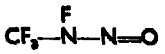

$CF_3\text{—}\overset{F}{N}\text{—}N\text{=}O$

IV

shown by I through IV. From the synthesis data structure I was preferred; this assignment was confirmed by nuclear magnetic resonance and ultra-violet absorption spectra data.

Nuclear magnetic resonance data. The ^{19}F spectrum of the two fluorine resonance peaks was observed at 40·0 Mc/s (Fig. 2). The chemical shift of the two peaks relative to the CF$_3$ in trifluoroacetic acid is given in parts per million. The peak at −118·7 p.p.m. is broad and shows no structure, while the signal at −7·0 p.p.m. shows six peaks and appears to be three sets of doublets. Double irradiation at a nitrogen frequency of 3,072,050 ± 25 cycles changed the −7·0 peak to a doublet. From this behaviour it is evident that the −7·0 p.p.m. peak is coupled to a nitrogen and also to another nucleus of spin ½. The only nuclear species present of spin ½ is fluorine, and it therefore must be a single fluorine at −118·7 p.p.m. coupled to the fluorines at −7·0 p.p.m. It is concluded that the peak at −7·0 p.p.m. arises from a —CF$_3$ group and from measurements on the original and decoupled spectra the spin coupling constants are:

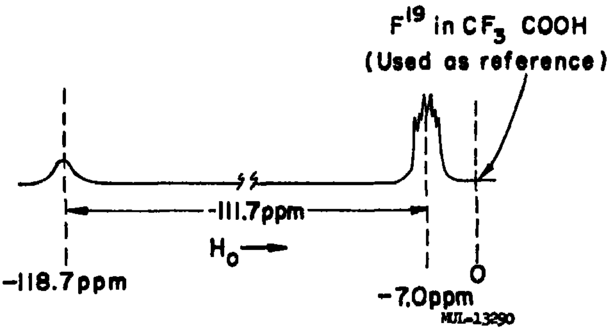

FIG. 2.—The nuclear magnetic resonance spectrum of CF$_3$NONF at 40·0 Mc/s.

$$J_{\mathrm{CF_3-F_{-118\cdot7}}} = 7{\cdot}1 \pm 0{\cdot}5\ \mathrm{cs}$$

$$J_{\mathrm{CF_3-N}} = 11{\cdot}9 \pm 0{\cdot}5\ \mathrm{cs}$$

The broadness of the single fluorine at −118·7 is reasonable if it is split into a quartet by the —CF$_3$ group and then further coupled to a nitrogen giving a broad unresolvable set of lines.

Additional double irradiation experiments were performed to show that the −118·7 p.p.m. peak is indeed coupled to a nitrogen and, furthermore, this is a different nitrogen than the one coupled to the —CF$_3$ group. One irradiation was already mentioned previously as detecting a N—CF$_3$ coupling which could be removed by saturating a particular nitrogen at 3,072,050 ± 25 cycles. For the purposes of identification this nitrogen has been labelled N(CF$_3$).

Another frequency was found in the nitrogen region which would sharpen the ^{19}F peak at −118·7 p.p.m. The nitrogen irradiation frequency was 3,071,930 ± 25 cycles. Since it was necessary to reduce the dc magnetic field 111·7 p.p.m. (118·7 − 7·0 p.p.m.) to go from the CF$_3$ peak to the single fluorine, the precession frequency of the N(—CF$_3$) would have also been reduced by $(111{\cdot}7 \times 10^{-6}) \times (3{\cdot}072 \times 10^{6}) = 342$ cycles, and its precession frequency during the time we were observing the single fluorine decoupling was then 3,072,050 − 342 cycles = 3,071,708 cycles. This precession frequency is 222 cycles different from the 3·071930 Mc/s frequency which did have a decoupling influence on the −118·7 peak. Therefore, the two types of fluorines are coupled to two different nitrogens. The magnitude of the coupling of the F(−118·7 p.p.m.) to its nitrogen, N(F), is not known accurately but is estimated to be of the order of 50 cycles from the fact that the F(−118·7 p.p.m.) peak begins to show structure if the sample is examined at room temperature. Most of the initial measurements were made near zero degrees centigrade.

Double irradiation of the nitrogens while holding the field constant were carried out to confirm the above conclusions. In this case the dc magnetic field was held constant while using just enough sweep field to span the peak under observation. The fluorine resonances were stimulated with a variable but stable 40 Mc/s oscillator and the output of the probe observed through the nuclear magnetic resonance receiver. With the field fixed, the 40·0 Mc/s oscillator frequency was adjusted to bring one of the fluorine resonances on to the oscilloscope. The nitrogen frequency was searched until a decoupling of the fluorine was observed. With the field still unchanged and the nitrogen saturating oscillator fixed at its decoupling value, the 40·0 Mc/s oscillator was changed to bring the other fluorine signal on to the oscilloscope to see if there was any decoupling of the second fluorine. The observed results are given in Table 4.

TABLE 4.—VALUES OF THE DOUBLE IRRADIATION EXPERIMENTS

Nitrogen frequency	Effect on CF_3 peak ^{19}F at 40·000100 Mc/s	Effect on single ^{19}F, ^{19}F at 40·004571 Mc/s
3·072025 Mc/s ± 25 cycles	Decoupled to a doublet	*No effect*
3·072225 Mc/s ± 25 cycles	*No effect*	Peak sharpened

The two approaches for measuring the chemical shift of the nitrogens relative to each other gave 222 (frequency constant) and 200 (field constant) cycles respectively. Because the strength of the saturating rf must be high in order to achieve the decoupling, the frequency position of maximum decoupling effect is sufficiently uncertain to make this deviation reasonable.

The observed spectra and decouplings are most consistent with structure I. Structure II is unlikely because it is felt that a N—CF_3 spin coupling of the observed magnitude would not be carried through a F—C—O—N bond system. The apparently large N—F coupling (about 50 cycles) is much larger than would be expected through a —N—O—F bond arrangement as in structure III. On the other hand the −118·7 chemical shift is in the region commonly measured for fluorines bonded to nitrogen. Structure IV would indicate that both types of fluorine should be spin coupled to the same nitrogen. The double irradiation experiments proved that the two types of fluorines were actually coupled to different nitrogens thus ruling out structure IV.

Ultra-violet absorption data. The absorption spectrum of CF_3NONF consists of a weak absorption band with a maximum at 2770 Å (ϵ_{max} = 7·3) and a shallow minimum at 2670 Å (ϵ_{min} = 6·9) followed by a strong ultraviolet absorption with a maximum at 2125 Å ($\epsilon_{max} \sim 4500$). The compound exhibits no absorption bands with $\epsilon > 0·05$ between 3500 Å and 12,000 Å.

The ultraviolet spectrum of CF_3NONF yields strong evidence for the identification of the compound with structure I.

Structure IV contains the group X — N = O where X has a nonbonded pair of electrons. Compounds containing this group have absorptions with considerable band

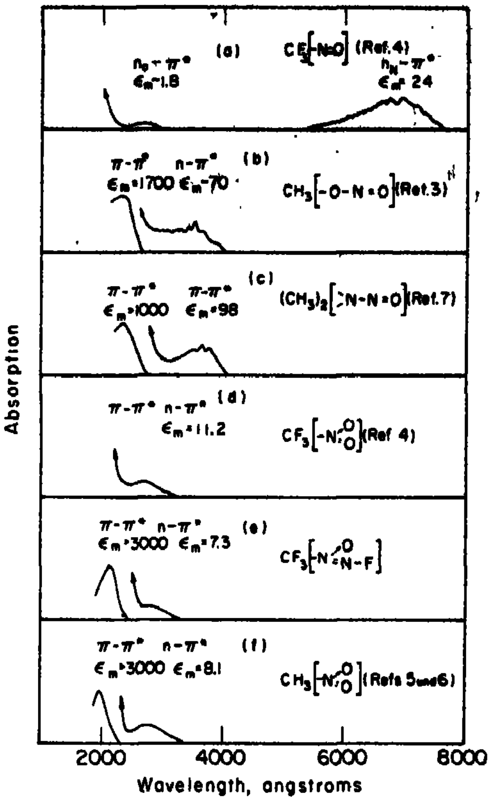

FIG. 3.—The absorption spectrum of CF_4N_2O and the absorptions of compounds containing various nitrogen–oxygen groups. The type of transition and absorption coefficient at maximum (ϵ_m) is given above each absorption band.

TABLE 5.—ABSORPTION CHARACTERISTICS OF CF_3NONF, CF_3NO_2, AND CH_3NO_2

Compound	Weak continuum					Strong continuum	
	λ_{max}	ϵ_{max}	λ_{min}	ϵ_{min}	$f \times 10^4$	λ_{max}	ϵ_{max}
CF_4N_2O (I)	2770	7·3	2670	6·9	2	2125	>3000
CF_3NO_2(4)	2775	11·2	2370	2·0	—	—	>3000
CH_3NO_2(5, 6)	2750	8·1	2450	3·9	2·5	1975	>3000

structure in the 3000–4000 Å region,(3) see Fig. 3 (b, c). Structure II is electronically similar to IV and to methyl nitrite and would be expected to have a similar absorption spectrum. Since the spectrum of CF_3NONF does not have an absorption with band structure in this region of the spectrum, structures II and IV seem unlikely.

The 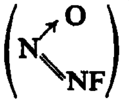 group of structure I is electronically similar to the nitro group

---

(3) C. H. PURKIS and H. W. THOMPSON, *Trans. Faraday Soc.* **32**, 674, 1466 (1936).
(4) J. MASON, *J. Chem. Soc.* 3904 (1957).
(5) N. S. BAYLISS and E. G. MCRAE, *J. Phys. Chem.* **58**, 1006 (1954).
(6) S. NAGAKURA, *Mole. Physics* **3**, 152 (1960).
(7) R. N. HASELDINE and B. J. H. MATTINSON, *J. Chem. Soc.* 4172 (1955).

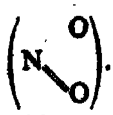

. Compounds containing the nitro group have a weak continuous absorption with a maximum at roughly 2750 Å followed by a strong continuum. This is the type of absorption exhibited by CF_4N_2O. The similarity in position and strength of the ultraviolet absorptions of CF_3NONF and those of the nitro compounds (see Fig. 3 (d, e, f) and Table 5) is strong evidence in favour of structure I as the structure of the compound CF_3NONF described.

Conclusions. We conclude that structure I is the structure of the compound CF_3NONF since it is the only structure of those considered which is consistent with all the data. It is thought the reactions described are quite general and will result in a series of new compounds containing the group —NONF.

Acknowledgements—The authors wish to acknowledge the able assistance of J. A. Happe and C. J. Dooley for their help in obtaining the nuclear magnetic resonance mass spectra data.

J. Inorg. Nucl. Chem., 1962, Vol. 24, pp. 53 to 58. Pergamon Press Ltd. Printed in Northern Ireland

THE PREPARATION OF POLYFLUOROALKYL PHOSPHONITRILATES AND N-(PERFLUOROACYL) PHOSPHORAMIDIC DICHLORIDES

T. J. Mao,* R. D. Dresdner and J. A. Young
Departments of Chemistry and Chemical Engineering
University of Florida, Gainesville, Florida

(*Received* 14 *June* 1961; *in revised form* 31 *August* 1961)

Abstract—The phosphonitrilic fluorides can be made to react readily with sodium polyfluoroalkyl alcoholates, $CHF_2(CF_2)_nCH_2ONa$, to give high yields of the corresponding phosphonitrilic esters, viscous, high boiling liquids, which are soluble in a variety of organic and fluorocarbon solvents, but insoluble in water.

The end product of reactions between fluorocarbon amides and PCl_5 are N-(perfluoroacyl)-phosphoramidic dichlorides, $R_fCONHPOCl_2$, where R_f is a perfluoroalkyl radical. The structure of this type of compound was confirmed by their reactions with fluoroalcohols and hydrazine.

Reactions of phosphonitrilic chloride trimer, $(NPCl_2)_3$, with fluorocarbon amides, an imide and the barium salt of trifluoroacetic acid were studied. Amides undergo the same chemistry as benzamide, the salt acts similarly to sodium benzoate, while perfluoroglutarimide was converted to the acid–amide adduct of pyridine when pyridine was used as a solvent.

The so-called fluoroalcohols are prepared by the free radical telomerization of tetrafluoroethylene with ethylene.(1) These trihydrofluoroalcohols are about 10^4 times as acidic as ethanol.(2) They exhibit both the properties of alcohols and weak acids. The alcohols and their sodium derivatives can be made to react with cyanuric chloride, $(CNCl)_3$, to form tri-(polyfluoroalkyl)cyanurates.(3) Ratz and Grundmann reported(4) that the alcoholates could be made to react with phosphonitrilic chlorides to form the corresponding phosphonitrilate esters, which are viscous liquids at room conditions. Dishon reported(5) a preparation for the dibutyl and dimethyl phosphonitrilic trimers. These trimers are hydrolytically and thermally unstable. On the contrary, the polyfluoroalkyl phosphonitrilates are quite stable. In the work reported here, a route to the polyfluoroalkyl phosphonitrilates was obtained by a reaction involving the sodium alcoholate and phosphonitrilic fluorides. These reactions proceeded quite readily to give product yields in excess of 70 per cent.

For many years numerous investigators have studied the reactions of amides with phosphorous chlorides, particularly PCl_5.(6–12) However, it was through the work of Kirsanov(9,10) that a reasonable reaction mechanism became available. The stability of the intermediate trichlorophosphazoacyl compounds and their hydrolysates, the phosphoramidic dichlorides, seemed to be dependent on the nature of the organic radical involved. Work with the fluorocarbon amides seems to confirm a relationship between stability and the character of the electronegative substituents.

---

* Present address, General Motors Research Laboratories, Warren, Michigan.

(1) R. M. Joyce, U.S. Pat. 2 599 628 (1951).

(2) A. L. Henne and R. L. Pelly, *J. Amer. Chem. Soc.* **74**, 1426 (1952).

(3) H. S. Holt and J. T. Maynard, U.S. Pat. 2 741 606 (1956).

(4) R. Ratz and C. J. Grundmann, U.S. Pat. 2 876 247 (1959).

(5) B. Dishon, *J. Amer. Chem. Soc.* **71**, 2251 (1949).

(6) O. Wallach, *Ann.* **184**, 1 (1877).

(7) W. Steinkopf, *Ber. Dtsch. Chem. Ges.* **41**, 3571 (1908).

(8) A. W. Titherly and E. J. Worrall, *J. Chem. Soc.* 1143 (1909).

(9) A. V. Kirsanov, *Acad. Sci. U.S.S.R. Div. Chem. Sci.*, **551** (1954).

(10) A. V. Kirsanov and R. G. Makirta, *Gen. Chem. (USSR)*, **26**, 1033 (1956).

(11) D. C. England, R. V. Lindsey and L. R. Melby, *J. Amer. Chem. Soc.*, **80**, 6443 (1958).

(12) J. Braun, *Ber. Dtsch. Chem. Ges.* **67 B**, 1762 (1934).

WALLACH(6) reported that benzamide was converted to benzonitrile with the liberation of HCl and $POCl_3$ in a reaction with PCl_5. He postulated $C_6H_5CCl_2NH_2$ as an intermediate in the reaction. STEINKOPF(1) investigated reactions between halogenated amides, $RCONH_2$, where R was $CHCl_2$, CCl_3 or CBr_3. He claimed products of the type $RCX{=}NPOX_2$ where X is halogen, assuming that the formation of such derivatives was due to the influence of halogens in the starting amides. TITHERLY and WORRALL(8) made a more critical study of the reaction with benzamide and explained the results via an intermediate, $C_6H_5CCl_2NH_2$, which reacted with the $POCl_3$ formed to produce $C_6H_5CCl_2NHPOCl_2$ and HCl, where upon another mole of HCl was eliminated with the formation of $C_6H_5CCl{=}NPOCl_2$, which hydrolysed readily to $C_6H_5CONHPOCl_2$ and another mole of HCl. More recently KIRSANOV(9,10) repeated the reaction with benzamide, taking every precaution to exclude water from his system. He did not isolate Wallach's intermediate, $C_6H_5CCl_2NH_2$, but did succeed in isolating and identifying a product $C_5H_6CON{=}PCl_3$, isomeric with $C_6H_5CCl{=}NPOCl_2$ proposed by TITHERLY and WORRALL. This compound was described as a remarkably reactive substance, which decomposed on heating to benzonitrile and $POCl_3$ which would account for Wallach's results. Also, this material hydrolysed so readily to N-phenyl phosphoramidic dichloride, that only by storing it over a mixture of phosphorous pentoxide and fused KOH could hydrolysis be prevented for any reasonable period. It was also noted that this sensitive material reacted with formic acid to form the phosphoramidic dichloride, HCl and CO.

By employing the so-called KIRSANOV method, ENGLAND and co-workers(11) prepared halogenated phosphoramidic dichlorides such as $CHCl_2CF_2CONHPOCl_2$. However, earlier attempts by BRAUN(12) to prepare simple unhalogenated hydrocarbon phosphoramidic dichlorides were unsuccessful. Accordingly, it would appear that successful attempts to prepare dichlorides require amides with negative substituents and conditions under which the intermediate trichloride is stable. It is not surprising therefore, that N-(perfluoroacyl) phosphoramidic dichlorides were prepared in good yields.

Materials and apparatus

C5 and C7 Fluoroalcohols, $CHF_2(CF_2)_nCH_2OH$ where *n* is 3 or 5, boil at 140·5° and 169·5° respectively. Samples of these two materials were supplied without charge by the E. I. duPont de Nemours Co., as technical grade samples which were purified by fractionation.

Perfluorocarboxylic acid amides R_fCONH_2 (R_f is CF_3 or C_3F_7) were prepared from the corresponding acids, which were first esterified. Treatment of the ester with ammonia produced the amide.

Phosphonitrilic chloride trimer, $(NPCl_2)_3$ was purchased from the Millmaster Chemical Corp., New York, as a mixture of trimer and tetramer. The trimer was obtained by a process of vacuum sublimation not unlike that described by Burg and CARON(13). It melted at 113°.

Phosphonitrilic fluorides, $(NPF_2)_{3,4}$, were prepared from P_3N_5 as described in a prior paper.(14)

Perfluoroglutarimide was prepared by the method of HENNE and ZIMMER(15). The original ethyl perfluoroglutarate was purchased from the Hooker Chemical Co., Niagara Falls, N.Y. Treatment with ammonia forms the diamide, which, when heated with sulphuric acid forms the imide.

(13) A. B. BURG and A. P. CARON, *J. Amer. Chem. Soc.* **81**, 836 (1959).

(14) T. J. MAO, R. D. DRESDNER and J. A. YOUNG, *J. Amer. Chem. Soc.* **81**, 1020 (1959).

(15) A. L. HENNE and W. F. ZIMMER, *J. Amer. Chem. Soc.* **73**, 1103 (1951).

Barium trifluoroacetate was prepared in almost quantitative yields by neutralizing trifluoroacetic acid in an aqueous solution of barium hydroxide.

Most of the reported reactions were performed in a 150 ml round bottom flask equipped with a water cooled condenser, magnetic stirrer and a delivery system. Cold-traps were attached to the condenser exit. The cold-traps were protected from atmospheric moisture with drying tubes filled with phosphoric anhydride. These were backed by a sulphuric acid bubbler.

Reactions

The preparation of polyfluoroalkyl phosphonitrilates. (A) *From fluoroalcohol C7 and* $(NPF_2)_3$. In this experiment 14 g (0·042 mole) C7 fluoroalcohol in 15 ml of N-43 (Minnesota Mining fluorocarbon tertiary butyl amine solvent b.p. ca. 170°) was caused to react with 1·0 g (0·042 mole) sodium at 130° for 4 hr. At this time, 1·7 g (0·007 mole) of $(NPF_2)_3$ in 10 ml of N-43 was added to the flask, and the reaction continued for 8 hr at 125°. The cool reaction mixture was filtered to remove NaF and vacuum stripped of solvent. The crude product amounting to 10 g was a clear, amber, viscous liquid. It distilled at 170–172° and 0·8 mm. Its infra-red spectrum was very similar to the starting alcohol but showed no OH assignment at 3·0 μ. It was soluble in acetone, ether, chloroform, benzene, toluene, freon-113 as well as N-43 but insoluble in water. The yield was 70 per cent. (Found: N, 2·08%; mol. wt. 2180. Calc. for $C_{42}H_{18}F_{72}P_3N_3O_6$; N, 1·98% (Kjeldahl); mol. wt. 2121 (Rast)).

(B) In a similar reaction 20 g (0·06 mole) C7 fluoroalcohol, 1·4 g (0·06 mole) sodium and 2·5 g (0·0075 mole) $(NPF_2)_4$ were involved, producing 16 g of crude product which distilled at 201–203° and 0·5 mm and demonstrated the same solubility character, and manifested a similar infra-red spectrum as the trimer ester. The yield was 73 per cent. (Found: N, 2·18%; mol. wt. 2760. calc. for $C_{56}H_{24}F_{96}P_4N_4O_8$: N 1·98% (Kjeldahl) mol. wt. 2828 (Rast)).

Preparation of fluorocarbon N-(acyl) phosphoramidic dichlorides. (A) *From* $C_3F_7CONH_2$ and PCl_5. Twenty-one and three tenths grammes of (0·10 mole) amide and 20·8 g (0·10 mole) chloride in 50 ml dry benzene were refluxed for 6 hr when the solids disappeared. The cool reaction mixture was filtered and stripped of benzene. Thirty grammes of white crystals melting at 85–90° were retained. These were purified by vacuum sublimation to a m.p. of 89–90°. Twenty-two grammes were recovered. The gas which condensed in the liquid air cooled tail trap amounted to 7 g of HCl, equivalent to 3 mole per mole of reagent. The above reaction was repeated in the presence of excess formic acid and the same products along with carbon monoxide were obtained. An infra-red spectrum of the solid product as a melt had prominent peaks at 5·70, 3·25 and 6·80 μ. The yield was 66 per cent. (Found: C, 14·20; F, 39·92; Cl, 20·85; P, 9·70; N, 4·09; H, 0·57%; mol. wt. 346. (f.p. depression in Freon 112) Calc. for $C_3F_7Cl_2PNHO_2$: C, 14·55; F, 40·30; Cl, 21·50; P, 9·40; N, 4·24; H, 0·30; mol. wt. 330).

(B) From CF_3CONH_2 and PCl_5. In a reaction similar to that described above, 11·3 g (0·1 mole) CF_3CONH_2 and 20·8 g (0·1 mole) PCl_5 were reacted to yield 17 g of purified crystals melting at 83–84·5°. The infra-red spectrum of the crystals had prominent peaks at 5·66, 3·25 and 6·77 μ. The yield was 74 per cent. (Found: N, 5·97; Cl, 30·40%; mol. wt. 248. Calc. for $C_2F_3Cl_2PNO_2H$; N, 6·08; Cl, 30·84%; mol. wt. 230.

Reaction of $C_3F_7CONH_2$ *with* $POCl_3$. Four grammes of (0·02 mole) amide and 3·1 g (0·02 mole) $POCl_3$ in 20 ml benzene were refluxed for 8 hr. Low boiling gases, condensed in the liquid air cooled tail trap, amounting to 2·0 g were determined to be a mixture of HCl and C_3F_7CN. Filtration of the reaction mixture and vacuum stripping of the solvent left 4 g solids, part of which was the starting amide.

Reaction of $C_3F_7CONHPOCl_2$ *with C5 fluoroalcohol.* Three and three tenths grammes of dichloride (0·01 mole) and 4·6 g (0·02 mole) C5 fluoroalcohol in 20 ml benzene were refluxed for 8 hr. The cooled reaction mixture was filtered and the solvent vacuum stripped. A white crystalline solid was observed on the walls of the vessel above a liquid phase. It was identified as $C_3F_7CONH_2$. The remaining liquid was a viscous yellow tinted material whose infra-red spectrum was very similar to the starting fluoro alcohol but that it showed no band in the 3·0 μ region. It contained phosphorous, and its properties were similar to the liquid formed when the alcohol was reacted with $POCl_3$. This product was believed to be the phosphoric acid ester, $(C_5H_3F_8O_2)_3P$ prepared by Benning.(18) An equivalent quantity of HCl was found in the liquid air cooled tail trap.

Reaction of $C_3F_7CONHPOCl_2$ *with hydrazine.* To a suspension of 1·9 g (0·06 mole) anhydrous hydrazine in 15 ml benzene cooled in an ice bath was added a solution of 6·6 g (0·02 mole) of dichloride in 20 ml benzene. The reaction was carried out at this temperature for 3 hr. The solid material that formed was filtered off and extracted with absolute ethanol. The ethanol was evaporated on a steam bath. The solid crystalline residue was purified by vacuum sublimation. It contained no

---

(18) A. F. Benning, U.S. Pat., 2 597 702 (1952).

[illegible] and melted at 73–74° in good agreement with a sample prepared from $C_3F_7COOCH_3$ and hydrazine(17). The infra-red spectra of the two samples of $C_3F_7CONHNH_2$ were identical.

Reaction of $(NPCl_2)_3$ *with perfluoroglutarimide in pyridine.* Two and six tenths grammes of (0·0075 mole) chloride in 25 ml pyridine was cooled with an ice-bath. To this was added dropwise 10 g (0·045 mole) imide in 25 ml benzene. The reaction was allowed to proceed for 10 hr at room temperature. The reaction mixture was filtered and the solvents were vacuum stripped. A solid product was washed with benzene and ether and recrystallized from acetone. It amounted to 9 g. An infra-red spectrum of the white crystals between salt plates had definite absorptions at 5·78 and 5·96 μ and at 6·71 and 3·2 μ. The solid had an equivalent weight of 317–320 and released pyridine in basic solution. (Found: N, 8·55; F, 35·71%; equiv. wt. 317–320 (titration). Calc. for $C_{10}F_6N_2O_3H_6$: N, 8·83; F, 35·95% mol. wt. 320);

Reaction of $(NPCl_2)_3$ *with* CF_3CONH_2. Eleven and three tenths grammes of (0·1 mole) amide was added to a suspension containing 5·8 g (0·017 mole) chloride in 25 ml N-43. The mixture was refluxed at 170° for 10 hr. The starting materials went into solution and an insoluble white precipitate appeared. The solvent was vacuum stripped. Five grammes of the amide were recovered by ether extraction. The residual solids amounted to 4·5 g and did not melt up to 360° but showed some decomposition starting at 300°. Further attempts to categorize the material were unsuccessful, although it did contain carbon and nitrogen and gave weak tests for phosphorus and fluorine. Gases condensed in the tail trap were HCl and CF_3CN.

Reaction of $(NPCl_2)_3$ *with barium trifluoroacetate.* Ninety grammes of (0·25 mole) barium salt and 20 g (0·057 mole) chloride were pulverized, mixed thoroughly and placed in a large (6·0 cm i.d. × 30 cm) test tube. Closure was made with a rubber stopper, which was connected to a trap cooled in a mixture of dry-ice and acetone. A phosphoric anhydride drying tube completed the system. The mixture was heated with a mantle for several weeks at 130–150°. White crystals, amounting to 7·5 g., deposited on the cool walls of the tube, and were removed from the system by vacuum sublimation. The m.p. of the crystals was the same as a sample of $(CF_3CO)_2NH$ made by reacting trifluoroacetonitrile with trifluoroacetic acid. The tail trap contained 3 g of a mixture of CF_3CN, CF_3COCl, and $(CF_3CO)_2O$. (Found: N, 6·3; C, 23·0; H, 0·48. Calc. for $C_4F_6NO_2H$: N, 6·7; C, 23·0; H, 0·62%).

DISCUSSION OF THE RESULTS

Both trimeric and tetrameric phosphonitrilic fluorides were shown to react with sodium salt of trihydrododecafluoro-1-heptanol in a fluoro-carbon solvent, yielding the corresponding tri- and tetra-(polyfluoroalkyl)phosphonitrilates. When this work was completed, RATZ and GRUNDMANN(4) reported in a patent that similar alcohols could be made to react with phosphonitrilic chlorides in an organic solvent to give the same types of compounds. The results reported here are significant in at least two respects. The fluoro compounds are much more stable than the hydrocarbon esters reported by DISHON(5). Hydrolytic stability can be attributed to lack of solubility in water and in part to the steric protection of the large polyfluoroalkyl groups in the molecules. Thermal stability is attributed partly to ring stabilization by the electronegative polyfluoroalkyl group and partly to the inherent stability of the polyfluoroalkyl group itself. Phosphonitrilic fluorides behave in a similar manner to the other halogen analogues in their reactions with these alcohols but the free energy involved in their reactions favor higher product yields.

In this work, it was observed that CF_3CONH_2 and $C_3F_7CONH_2$ underwent reactions with PCl_5 readily. The formation of the reaction intermediate, $R_fCON{=}PCl_3$, was strongly suggested. The gaseous products were consistently two equivalents of HCl, until recovery was attempted. The liberation of a third equivalent on addition to formic acid to the reaction mixture seemed to confirm the precursory existence of N-(perfluoroacyl)trichlorophosphine imide, $R_fCON{=}PCl_3$.

The characterization of the products was based on a combination of physical and chemical tests. Analyses were satisfactory. However, the possibility of isomeric

---

(17) L. PARCELL and H. C. BROWN, Private communication.

[illegible] such as $R_fC(OH)=NPOCl_2$ or $R_fCCl=NP(OH)Cl_2$ were [illegible] primary and secondary amides can in theory exist in either a keto or [illegible] infrared data all support the ketonic structure.(18) In the spectrum of [illegible] $POCl_2$, a strong absorption at 5·77 μ corresponds to a C=O assignment.[illegible] There were no bands below 3·0 μ where most OH absorptions appear.(18) Existence of an NH assignment was indicated by an absorption at 3·25 μ.(18) The other functional group, P=O, could not be uniquely ascertained because of the strong C–F bands in the 7–9 μ region. Additional supporting evidence for the ketonic structure was the facile reaction of $C_3F_7CONHPOCl_2$ with both a C_5 fluoroalcohol and hydrazine to form the amide and hydrazide in which the C_3F_7CONH grouping was retained.

$C_3F_7CONH_2$ was caused to react with $POCl_3$ to see if the phosphoramidic dichloride could be prepared by a simple substitution reaction. If the sought after product had formed, it should have been stable in benzene at reflux. As the products were C_3F_7CN and HCl, it is assumed that dehydration occurred by some process similar to that noted by BRAUN.(12)

Making use of the suggestion(12) that the initial attack by PCl_5 on amides is on the carbonyl oxygen, the fact that PCl_5 exists as the ions $(PCl_4)^+(PCl_6)^-$ and the evidence submitted by KIRSANOV that $RCON=PCl_3$ is a reaction product in the absence of moisture, a logical reaction mechanism for the reaction between fluorocarbon amides and PCl_5 can be summarized in the following steps:

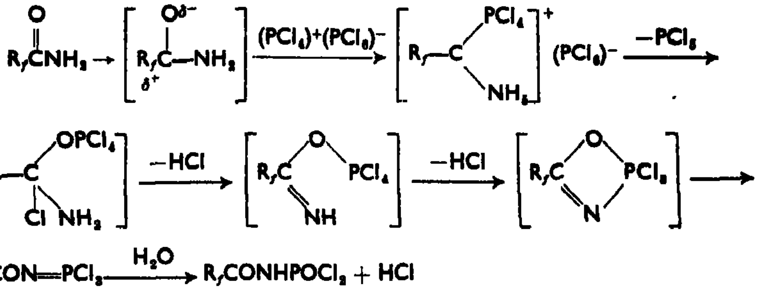

In the reaction between $(NPCl_2)_3$ and perfluoroglutarimide an excess of pyridine was used partly as a solvent, partly as a base. It would appear from the unexpected results of this reaction that an initial substitution occurred to form an intermediate of the type

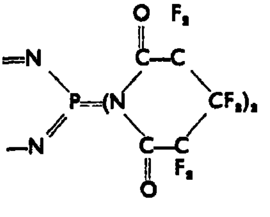

which hydrolysed in the presence of small amounts of water to form the acid–amide which complexed readily with pyridine. This reaction is of interest as there is no report in the literature of the free acid–amide having been prepared. The elemental

(18) L. J. BELLAMY, *The Infra-red Spectra of Complex Molecules* (2nd. Ed.), pp. 95, 203, and 205. J. Wiley, New York (1958).

(19) J. H. SIMONS (Editor), *Fluorine Chemistry*, Vol. 2, Chap. 7, p. 452 and p. 490. Academic Press, New York (1954).

analysis, equivalent weight data and infra-red spectral data indicating two different carbonyl absorptions offer supporting evidence that the compound formed is $H_2NCO(CF_2)_3COOH{\cdot}C_5H_5N$.

When $(NPCl_2)_3$ was reacted with trifluoroacetamide the only identifiable products were the corresponding nitrile and HCl. The solid products formed were not isolated or identified. As in the case with $POCl_3$ it is improbable that a simple dehydration occurred.

The reaction between $(NPCl_2)_3$ and barium trifluoroacetate gave results not unlike those observed by BEZMAN and REED[20] using sodium benzoate as the salt. They proposed a mechanism that substituted oxygen for nitrogen in the PN ring via a bond shift through ring closure with the eventual release of a nitrile. Attack of another equivalent of the salt on the residue accounted for the formation of an anhydride. Should the same process be repeated at the three quivalent ring sites, the final residue would be a metaphosphate salt. As the solid product in this case was a diacyl imide it can be assumed that small amounts of moisture converted some of the anhydride or acid chloride to trifluoroacetic acid which reacted readily with the trifluoroacetonitrile present in the reaction environment to form $(CF_3CO)_2NH$.

The accompanying table presents the C=O and N—H infrared absorptions in microns for a number of compounds. Spectra for a number of fluorocarbon amides can be found in Reference (20).

INFRA-RED SPECTRAL DATA FOR SOME COMPOUNDS

Compound	Carbonyl absorption (μ)	N—H absorptions (μ)
$CF_3CONHPOCl_2$	5·66	3·25 and 6·77
$C_3F_7CONHPOCl_2$	5·70	3·25 and 6·80
pyr. $HOOC(CF_2)_3CONH_2$	5·78 and 5·96	3·2 6·71 (broad)
$(CF_3CO)_2NH$	5·63	3·08 none

---

[20] I. I. BEZMAN and W. R. REED, 136th Meeting, *American Chemical Society*, Atlantic City, September, 1959.

J. Inorg. Nucl. Chem. 1962, Vol. 24, p. 59 to 71. Pergamon Press Ltd. Printed in Northern Ireland

BASE HYDROLYSIS OF SOME CHLOROAMMINE-PLATINUM(IV) COMPLEXES*

R. C. Johnson,† F. Basolo and R. G. Pearson

(*Received* 27 *June* 1961; *in revised form* 22 *August* 1961)

Abstract—The rates of base hydrolysis of $[Pt(NH_3)_5Cl]^{3+}$, *cis* and *trans*-$[Pt(NH_3)_4Cl_2]^{2+}$, *trans* $[Pt(NH_3)_3Cl_3]^+$, and *trans*-$[Pt(en)_2Cl_2]^{2+}$ were measured. The acid dissociation constants of these complexes were also measured. These data show that in the basic solutions used for the kinetic studies amido complexes (e.g. $[Pt(NH_3)_4NH_2Cl]^{2+}$) were the predominant species. Under such basic reaction conditions considerable reduction accompanied hydrolysis of those compounds which contained *trans* chloro groups. Probable mechanisms of base hydrolysis and of reduction are discussed.

The hydrolysis of inert co-ordination compounds has been the subject of considerable recent interest. Cobalt(III) complexes have been studied(1) extensively and some work has also been reported on Cr(III),(2) Rh(III),(3) Ir(III),(2) and Pt(II).(4) The studies on chloroamminecobalt(III) complexes indicated that under acidic conditions the rate of hydrolysis was essentially independent of the $[H^+]$; in basic solution a first order hydroxide ion dependence was found. The kinetics observed for base hydrolysis were explained in terms of an acid base pre-equilibrium followed by dissociation of the conjugate base of the complex (S_N1CB).(5)

$$[Co(NH_3)_5Cl]^{2+} + OH^- \rightleftharpoons [Co(NH_3)_4NH_2Cl]^+ + H_2O \tag{1}$$

$$[Co(NH_3)_4NH_2Cl]^+ \rightarrow [Co(NH_3)_4NH_2]^{2+} + Cl^- \tag{2}$$

$$[Co(NH_3)_4NH_2]^{2+} + H_2O \rightarrow [Co(NH_3)_5OH]^{2+} \tag{3}$$

An alternative suggestion was that the reaction proceeds by a displacement (S_N2) process.(6) The base hydrolysis reactions of chloroamminecobalt(III) complexes are very much faster than the reactions in acid. Data on chloroamminemetal(III) complexes of Cr(III)(2) and Rh(III)(3) show a much smaller effect of $[OH^-]$ on their rate of hydrolysis. In Pt(II) square planar complexes the acid and base hydrolysis rates are the same.(4)

---

* Presented in part before the Division of Inorganic Chemistry at the 139th Meeting of the American Chemical Society, St. Louis, Missouri, April, 1961.

† Taken in part from the Ph.D. thesis of R. C. Johnson, Northwestern University, June, 1961.

(1) F. Basolo and R. G. Pearson, *Mechanisms of Inorganic Reactions*, p. 128. J. Wiley, New York (1958).

(2) F. Basolo and R. G. Pearson, *Mechanisms of Inorganic Reactions*, p. 137. J. Wiley, New York (1958).

(3) A. B. Lamb, *J. Amer. Chem. Soc.* **61**, 699 (1939); S. A. Johnson. Private Communication (1961).

(4) D. Banerjea, F. Basolo, R. G. Pearson, *J. Amer. Chem. Soc.* **79**, 4055 (1957); A. A. Grinberg, *J. Inorg. Chem.* (*U.S.S.R.*) **4**, 683 (1959).

(5) F. Basolo and R. G. Pearson, *Mechanisms of Inorganic Reactions*, p. 124–132. J. Wiley, New York (1958); R. G. Pearson, H. H. Schmidtke and F. Basolo, *J. Amer. Chem. Soc.* **82**, 4434 (1960).

(6) D. D. Brown, C. K. Ingold and R. S. Nyholm, *J. Chem. Soc.* 2678 (1953).

This study reports the rate of hydrolysis of the following compounds:

$[Pt(NH_3)_5Cl]^{3+}$,
cis and *trans*-$[Pt(NH_3)_4Cl_2]^{2+}$,
trans-$[Pt(NH_3)_3Cl_3]^{+}$,
$[Pt(NH_3)_4ClOH]^{2+}$,
trans-$[Pt(en)_2Cl_2]^{2+}$
and $[Pt(en)_2ClOH]^{2+}$.

Hydrolysis under neutral and acid conditions at room temperature was observed to be negligible for the compounds studied. Therefore the kinetics were studied under basic conditions. It was observed that for some of the compounds the base hydrolysis was accompanied by reduction of Pt(IV) to Pt(II), and this behaviour was also investigated.

EXPERIMENTAL

Preparation of compounds. The preparation of $[Pt(NH_3)_6]Cl_4$, $[Pt(NH_3)_5Cl]Cl_3$, $[Pt(NH_3)_5Cl](NO_3)_3$, and *cis*-$[Pt(NH_3)_4Cl_2](NO_3)_2$ reported here are all modifications of preparations described in the literature.(7)

Hexammineplatinum (IV) chloride was prepared by the reaction of 18·0 g of $(NH_4)_2[PtCl_6]$ and 12·0 g of $(NH_4)_2CO_3$ with 50 ml of liquid ammonia in a glass lined rotating autoclave. The reaction took place at room temperature in 18 hr. Ammonia was allowed to evaporate leaving a white product (a mixture of $(NH_4)_2CO_3$, $[Pt(NH_3)_6](CO_3)_2$, $[Pt(NH_3)_5Cl]_2(CO_3)_3$, and conjugate bases of these complexes). The residue was extracted with dilute NH_4OH. The remaining residue was treated with 6 N HCl to form $[Pt(NH_3)_6]Cl_4$ and $[Pt(NH_3)_5Cl]Cl_3$. These can be separated by fractional crystallization; the $[Pt(NH_3)_6]Cl_4$ separated first as a monohydrate. The product was dried at 100° in a vacuum. Yield was 5·0 g (28 per cent of theory). (Found: Pt, 44·3; Cl, 32·2. Calc. for $[Pt(NH_3)_6]Cl_4$: Pt, 44·3; Cl, 32·3%.)

Chloropentammineplatinum(IV) chloride was obtained as the major product from the preceding preparation of $[Pt(NH_3)_6]Cl_4$. Yield was 8·6 g of dried material (50 per cent of theory). (Found: Pt, 45·8; Cl(ionic), 25·3. Calc. for $[Pt(NH_3)_5Cl]Cl_3$: Pt, 46·2; Cl(ionic), 25·2%.)

Chloropentammineplatinum(IV) nitrate was prepared by dissolving $[Pt(NH_3)_5Cl]Cl_3$ in a minimum amount of hot water, cooling, and precipitating with excess HNO_3.

Trans-dichlorotetrammineplatinum(IV) chloride was prepared by the reaction of chlorine with $Pt(NH_3)_4]Cl_2$ in dilute HCl.(7) (Found: Pt, 48·2. Calc. for $[Pt(NH_3)_4Cl_2]Cl_2$: Pt, 48·2%.)

Trans-dichlorotetrammineplatinum(IV) nitrate was prepared by mechanically stirring a mixture of 0·66 g of *trans*-$[Pt(NH_3)_4Cl_2]Cl_2$ and 0·56 g of $AgNO_3$ in 25 ml of water for 1 hr. Unreacted starting material and AgCl were removed on a filter. The filtrate was evaporated in vacuum until pale yellow crystals of product formed. After drying the crystals at 100°C, 0·50 g of product was obtained (66 per cent of theory). (Found: Pt, 42·9; Cl, 15·6. Calc. for $[Pt(NH_3)_4Cl_2](NO_3)_2$: Pt, 42·5; Cl, 15·5%.)

Trans-chlorohydroxotetrammineplatinum(IV) nitrate was prepared by bubbling Cl_2 through a solution of 1·0 g of $[Pt(NH_3)_4]Cl_2$ in 20 ml of 0·2 N NaOH. An orange precipitate resulted. Nitric acid was added to the solution and the product was collected. This material was dissolved in hot dilute HNO_3, cooled, and precipitated with excess HNO_3 and acetone. The product was recrystallized and dried. (Found: Cl, 9·80; Cl^-(ionic) 0·53. Calc. for $[Pt(NH_3)_4ClOH](NO_3)_2$:Cl, 8·06%.) The product contained some $[Pt(NH_3)_4Cl_2](NO_3)_2$, but the ultra-violet spectrum and the rate of hydrolysis of the mixture indicate that it did not contain $[Pt(NH_3)_4(OH)_2]^{2+}$.

Cis-dichlorotetrammineplatinum(IV) nitrate was prepared by the addition of 39 ml of 20% NH_4OH solution to 8·29 g of *trans*-$[Pt(NH_3)_4Cl_2]Cl$. The product immediately becomes orange. The solution was stirred from time to time for 3 hr and was then filtered to remove a yellow product. The filtrate was cooled to 0° and then acidified with HCl. A white product resulted and was collected. The product was purified by adding it to a little water and 0·5 M NaOH at 0°. A yellow orange product was formed and collected. This was acidified with 6 N HCl until the product turned white. The white solid was dissolved in dilute HNO_3 and precipitated upon addition of excess HNO_3. (Found: Pt, 43·6; Cl, 15·5. Calc. for $[Pt(NH_3)_4Cl_2](NO_3)_2$: Pt, 42·6; Cl, 15·5%.)

Chlorotriammineplatinum(II) chloride was prepared from *cis*-$[Pt(NH_3)_2Cl_2]$ and KCNO.(7) (Found: Pt, 61·8; Cl(ionic), 11·3. Calc. for $[Pt(NH_3)_3Cl]Cl$: Pt, 61·5; Cl(ionic), 11·2%.)

---

(7) *Gmelin's Handbuch der Anorganischen Chemie*, Vol. 68 D, pp. 41–68, 467–530, (1957).

Trans-trichlorotriammineplatinum(IV) chloride was prepared by chlorine oxidation of $[Pt(NH_3)_3Cl]Cl$ in dilute HCl solution.(7) (Found: Pt, 50·0; Cl(ionic), 9·15. Calc. for $[Pt(NH_3)_3Cl_3]Cl$: Pt, 50·2; Cl(ionic), 9·40%.)

Trans-trichlorotriammineplatinum(IV) nitrate was prepared by dissolving *trans*-$[Pt(NH_3)_3Cl_3]Cl$ in a minimum amount of water and adding excess HNO_3.

Trans-dichlorobis(ethylenediamine)platinum(IV) chloride was prepared by oxidation of $[Pt(en)_2]Cl_2$ with chlorine.(7)

Trans-dichlorobis(ethylenediamine)platinum(IV) nitrate was prepared by dissolving *trans*-$[Pt(en)_2Cl_2]Cl_2$ in a minimum amount of water and precipitating with HNO_3. (Found: Pt, 38·6; Cl, 13·7. Calc. for $[Pt(en)_2Cl_2](NO_3)_2$: Pt, 38·2; Cl, 13·9%.)

Chloroaquobis(ethylenediamine)platinum(IV) nitrate was prepared by heating 5·50 g (0·0108 mole) of *trans*-$[Pt(en)_2Cl_2](NO_3)_2$ with 1·835 g. (0·0108 mole) of $AgNO_3$ in 100 ml of water at 80°C for five days in the dark. The solution was filtered and evaporated to 10 ml in the dark and then filtered again. Addition of HNO_3 to the filtrate gave a white precipitate (3·5 g). This product was contaminated with $AgNO_3$. It was recrystallized from HNO_3 and washed carefully with alcohol. After drying at 100° in vacuum, 2·5 g of crystalline white product remained (42 per cent of theory). (Found: Pt, 36·8; Cl, 6·96. Calc. for $[Pt(en)_2ClH_2O](NO_3)_3$: Pt, 35·1; Cl, 6·40%.) This product was dissolved in water and neutralized with NH_4OH. A pale yellow product was obtained upon the addition of alcohol and ether. This material ($[Pt(en)_2ClOH](NO_3)_2$) was recrystallized from water by precipitation with alcohol. The material was dried at 100°C in vacuum. (Found: Pt, 39·3; Cl, 7·23. Calc. for $[Pt(en)_2ClOH](NO_3)_2$: Pt, 39·6; Cl, 7·22%.)

Bis(ethylenediamine)platinum(II) chloride and $[Pt(NH_3)_4]Cl_2$ were prepared as described in the literature.(7)

The Na_2HPO_4 was Mallinckrodt $Na_2HPO_4 \cdot 7H_2O$ analytical reagent. The phenol was Baker and Adamson USP fused crystals.

Rates of reaction. The kinetic data were collected by preparing the appropriate solutions in aluminium foil wrapped volumetric flasks and thermostating these (±0·1°C). The release of chloride was followed by titrating aliquots of these solutions by the Volhard method for chloride determination. Bis(ethylenediamine)platinum(II) and $[Pt(NH_3)_4]^{2+}$ were quantitatively detected by titration with a standard ceric solution in 1 M H_2SO_4 to which excess chloride had been added. Ionic chloride catalyses the oxidation of Pt(II) salts into the corresponding dichloro Pt(IV) complex. Ferroin was used as the indicator. The method does not work for $[Pt(tetrameen)_2]^{2+}$ or $[Pt(py)_4]^{2+}$,* since they are not oxidized rapidly under the titration conditions. The rate constants were determined from the slopes of plots of $\ln(Cl_\infty^- - Cl^-/Cl_\infty^-)$ vs. time where Cl^- is moles of chloride ion at time t and Cl_∞^- is moles of chloride at infinite time. Experimental Cl_∞^- values agreed with calculated values (±5 per cent); in a few cases the experimental Cl_∞^- values did not agree, but the deviations could be accounted for by release of chloride by other reactions (reduction or subsequent hydrolysis).

Determination of acid dissociation constants. The pK_a's of several complexes were measured by potentiometric titration using a Beckman Model G pH meter with an E-2 glass electrode which is designed to have a small Na^+ error in basic solution. As a reference determination phenol was titrated and the pK_a found at μ (ionic strength) $= 0{\cdot}11$ was 10·0 and at $\mu = 0{\cdot}005$ was 9·95. A literature value is 9·98.(8) The ionic strength reported is the ionic strength at which the acid is half titrated. The pK_a's reported are the pH values at which the acid is half neutralized.

In order to measure pK_a's much above ten by a titration technique, the concentration of the acid must be increased to the extent that the ionic strength of the solution becomes very large (especially when the acids are multiply charged). Since this then gives a rather meaningless pK_a, a conductivity method, similar to the technique of BALLINGER and LONG,(9) was used to measure the acid dissociation constants of some very weak acids. The method was slightly different since multiple positively charged acids were studied rather than neutral acids. The method works because in the reaction

$$RH^{n+} + OH^- \rightleftharpoons R^{(n-1)+} + H_2O \tag{4}$$

the acid species (RH^{n+}) decreases in charge and OH^- is consumed; both effects lead to a decrease in conductivity. The theoretical conductivity for a complex, e.g., $[Pt(NH_3)_4Cl_2](NO_3)_2$ in a solution of NaOH is

$$\kappa = 10^{-3}[[Na^+]\lambda_{Na+} + [NO_3^-]\lambda_{NO_3-} + (C - [A^-])\lambda_{HA} + ([Na^+] - [A^-])\lambda_{OH-} + [A^-]\lambda_{A-}]. \tag{5}$$

---

* Symbols used are en $= NH_2CH_2CH_2NH_2$, tetrameen $= NH_2C(CH_3)_2C(CH_3)_2NH_2$, and py = pyridine.

(8) W. J. BLAEDEL and V. W. MELOCHE, *Elementary Quantitative Analysis*, p. 786. Row Peterson, Evanston, Illinois (1957).

(9) P. BALLINGER and F. A. LONG, *J. Amer. Chem. Soc.* **81**, 1050–3, (1959).

HA represents the complex, A^- its conjugate base ($[Pt(NH_3)_3NH_2Cl_2]^+$), and C the original concentration of complex. The λ's are ionic conductivities for the species at the ionic strength of the solution. These were estimated from tables of conductivities of salts as a function of concentration.[10]

The conductivities of the acids were experimentally measured and the conductivities of the conjugate bases were estimated from conductivities of similar complexes. A list of λ's used is reported in Table 1. If a function

$$\kappa_s = 10^{-3}[[Na^+]\lambda_{Na^+} + [NO_3^-]\lambda_{NO_3^-} + C\lambda_{HA} + [Na^+]\lambda_{OH^-}] \tag{6}$$

TABLE 1.—VALUES OF SPECIFIC CONDUCTIVITIES USED IN CONDUCTOMETRIC pK_a DETERMINATIONS AT 25·0°C

Ionic Strength (μ)	0·005	0·010	0·016	0·020	0·050
λ_{Na^+}	47·7	46·9	46·2	45·7	44·1
$\lambda_{NO_3^-}$	68·5	68·5	64·0	64·0	62·5
λ_{OH^-}	192	191	185	182	—

Ion	λ	Ion	λ
trans-$[Pt(NH_3)_4Cl_2]^{2+}$	90	*trans*-$[Pt(en)_2Cl_2]^{2+}$	76
trans-$[Pt(NH_3)_3NH_2Cl_2]^+$	60	*trans*-$[Pt(en)(en{-}H)Cl_2]^+$	50
cis-$[Pt(NH_3)_3NH_2Cl_2]^+$	50	$[Pt(NH_3)_4NH_2Cl]^{2+}$	82
cis-$[Pt(NH_3)_2(NH_2)_2Cl_2]^0$	0	$[Pt(NH_3)_3(NH_2)_2Cl]^+$	55
$[PO_4]^{3-}$	105	$[PO_4]^{2-}$	90

is defined (this corresponds to the conductivity if the acid remains entirely in the acid form when treated with NaOH), then the concentration of the conjugate base of the acid

$$[A^-] = 10^{-3}\frac{(\kappa_s - \kappa_e)}{(\lambda_{OH^-} + \lambda_{HA} - \lambda_{A^-})} \tag{7}$$

in which κ_e is the experimental conductivity. From these data and the known C and the original $[OH^-]$ concentration, K_a's can be calculated. A summary of experimental data and calculations is presented in Table 2.

A Leeds and Northrup Jones Bridge, oscillator, and amplifier were used with an oscilloscope as the null detector. The cell constant of the cell used was 0·546. The conductivity of the carbonate free NaOH used in the study agreed with published values.

RESULTS

The reaction between OH^- and $[Pt(NH_3)_5Cl]^{3+}$ is the method of choice for the preparation of $[Pt(NH_3)_5OH]^{3+}$.

$$[Pt(NH_3)_5Cl]^{3+} + OH^- \rightarrow [Pt(NH_3)_5OH]^{3+} + Cl^- \tag{8}$$

For simplicity the hydrolysis reactions will be written as reactions of the complex with hydroxide ion. However it is known that the species present in basic solution were the conjugate bases of the complex, e.g., $[Pt(NH_3)_4NH_2Cl]^{2+}$ or $[Pt(NH_3)_3(NH_2)_2Cl]^+$.

$$[Pt(NH_3)_3(NH_2)_2Cl]^+ + OH^- \rightarrow [Pt(NH_3)_3(NH_2)_2OH]^+ + Cl^- \tag{9}$$

The hydrolysis of $[Pt(NH_3)_5Cl]^{3+}$ at these experimental conditions gave no evidence for the formation of any other products than $[Pt(NH_3)_5OH]^{3+}$. Table 3 gives the rate data that were collected. Both chloride and nitrate salts were studied and were found to give similar kinetic results. A plot of the rate constants obtained in the pOH range 3–6 is shown in Fig. 1. These data were collected at 80·0°C in buffers containing 0·10 M ammonium or n-butylammonium acetate and sufficient free amine to give the desired pH. In every case all of the coordinated chloride was replaced and linear

---

[10] B. E. CONWAY, *Electrochemical Data*, pp. 141–142. Elsevier, Amsterdam (1952).

TABLE 2.—SUMMARY OF CONDUCTIVITY DATA AND CALCULATIONS AT 25·0°C

C_0	$\kappa_s \times 10^3$ (Ω^{-1})	$\kappa_e \times 10^{-3}$ (Ω^{-1})	[Na$^+$]	pK_a
trans-[Pt(NH$_3$)$_4$Cl$_2$](NO$_3$)$_2$				
0·0100	2·48	3·32	0·00504	11·2
0·00500	1·70	2·25	0·00504	11·3
0·00250	1·39	1·74	0·00504	11·3
0·00125	1·28	1·46	0·00504	11·4
trans-[Pt(en)$_2$Cl$_2$](NO$_3$)$_2$				
0·0100	2·18	3·01	0·00421	10·8
0·00500	1·44	1·99	0·00421	11·1
0·00250	1·15	1·48	0·00421	11·1
[Pt(NH$_3$)$_5$Cl](NO$_3$)$_3$				
0·00600	2·32	2·39	0·00810	12·5
0·00500	2·21	2·30	0·00810	12·5
0·00400	2·13	2·22	0·00810	12·5
0·00300	2·04	2·13	0·00810	12·5
0·00200	1·98	2·02	0·00810	12·7
cis-[Pt(NH$_3$)$_4$Cl$_2$](NO$_3$)$_2$				
0·00500	1·73	1·87	0·00817	12·3
0·00400	1·76	1·88	0·00817	12·3
0·00300	1·79	1·90	0·00817	12·4
0·00200	1·84	1·91	0·00817	12·5
0·00100	1·87	1·93	0·00817	12·3
Na$_2$HPO$_4$				
0·00600	2·66	2·93	0·00817	12·1
0·00500	2·54	2·75	0·00817	12·1
0·00400	2·42	2·56	0·00817	12·3
0·00300	2·31	2·48	0·00817	12·5
0·00200	2·18	2·27	0·00817	12·3

TABLE 3.—PSUEDO FIRST-ORDER RATE CONSTANTS FOR THE REACTION

$$[Pt(NH_3)_5Cl]^{3+} + OH^- \xrightarrow{k} [Pt(NH_3)_5OH]^{3+} + Cl^-$$

[Pt(IV)]	[OH$^-$]	T (°C)	$k \times 10^5$ (sec^{-1})
0·00500	0·49	25·0	2·0
0·00500	0·10*	25·0	0·70
0·00500	0·10	25·0	0·85
0·00500	0·10	50	36·0
0·00500	0·050	50·0	32·0
0·00500	pH = 11·0	50·0	3·9
0·00500	pH = 11·0	80·0	94·0
0·0100	pH = 11·0	80·0	91·0
0·00500	pH = 10·4	80·0	27·0
0·0100	pH = 10·4	80·0	33·0

* [KNO$_3$] = 0·40 M.

[illegible] order kinetic plots were obtained. A slightly acidic (pH ~ 4) solution of $[Pt(NH_3)_5OH]Cl_3$ was heated at 80·0° for four days. The ionic chloride concentration remained constant during this period. Thus either the anation reaction must be very slow, or the equilibrium lies far toward the hydroxo complex under these conditions.

The reaction of *cis*-$[Pt(NH_3)_4Cl_2](NO_3)_2$ in NaOH solution to yield ionic chloride goes to completion at 25·0° and is fast enough to be conveniently studied. The kinetic

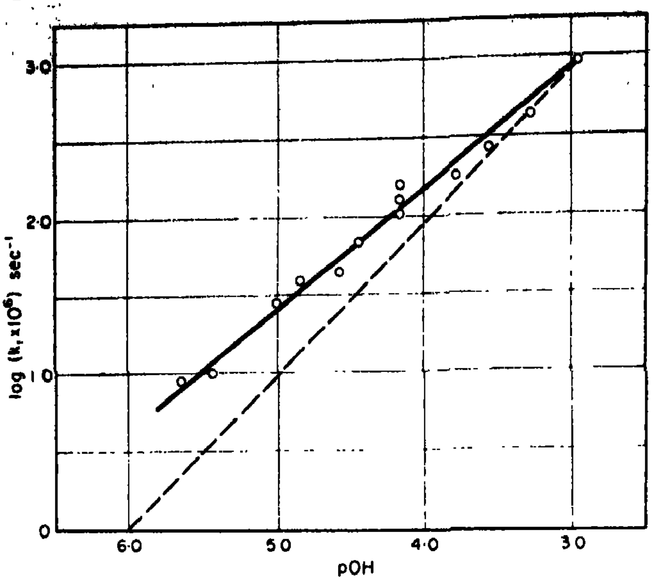

Fig. 1.—Rates of hydrolysis of $[Pt(NH_3)_5Cl]^{3+}$ in amine-acetate buffers at 80°C. The dashed line is drawn with a slope of unity.
The pH of the buffers was measured at 25·0°C. The ionization constants of primary amines and ammonia are essentially independent of temperature between 25–80°C. Therefore the pOH of the solutions is independent of temperature[13].

data collected indicated that the two chlorides are released at different rates. By means of Powell plots[11] it was possible to evaluate the rate constants for the consecutive reactions (equations 10 and 11).

$$cis\text{-}[Pt(NH_3)_4Cl_2]^{2+} + OH^- \xrightarrow{k_1} cis\text{-}[Pt(NH_3)_4ClOH]^{2+} + Cl^- \quad (10)$$

$$cis\text{-}[Pt(NH_3)_4ClOH]^{2+} + OH^- \xrightarrow{k_2} [Pt(NH_3)_4(OH)_2]^{2+} + Cl^- \quad (11)$$

Although the products of these reactions were not isolated, the chlorohydroxo product is probably the *cis* isomer since it hydrolyses much faster than the initial hydrolysis product of *trans*-$[Pt(NH_3)_4Cl_2]^{2+}$ which presumably is *trans*-$[Pt(NH_3)_4ClOH]^{2+}$. The rate data are presented in Table 4. No Pt(II) was detected as a result of the reactions of the *cis*-compounds; the rate of chloride release was not affected by the addition of $[Pt(NH_3)_4]Cl_2$.

The remaining compounds studied contained *trans* chloro groups. In all cases reduction as well as hydrolysis occurred in basic solution. The hydrolysis of *trans*-$[Pt(NH_3)_4Cl_2]^{2+}$ was found to be catalysed by $[Pt(NH_3)_4]^{2+}$. The rate of chloride

---

[11] A. A. Frost and R. G. Pearson, *Kinetics and Mechanism*, p. 169. J. Wiley, New York (1961).
[12] J. R. Hall and R. A. Plowman, *Aust. J. Chem.* **8**, 168–172 (1955); **9**, 14–24 (1956).
[13] I. M. Kolthoff and P. J. Elving, *Treatise on Analytical Chemistry*, Part I, Vol. 1, pp. 435–36. Interscience Encyclopedia, New York (1960), pp, 435–36.

[illegible] had a first-order dependence on the concentration of [illegible] independent of [OH^-] in NaOH solutions. The product of this [illegible] [$Pt(NH_3)_4ClOH]^{2+}$ (probably the trans isomer). A sample of *trans*-[illegible] was prepared; its hydrolysis was slow at 50·0°. ($k = 1 \times 10^{-[illegible]}$ sec^{-1}). In the [illegible] of added $[Pt(NH_3)_4]^{2+}$ the rate of release of chloride ion increased as a function of time, and 8–10 per cent of the original Pt(IV) was reduced to $[Pt(NH_3)_4]^{2+}$. (In the presence of added $[Pt(NH_3)_4]^{2+}$ reduction no longer was an important process). The formation of $[Pt(NH_3)_4]^{2+}$ explained the increase in the rate of chloride release as a function of time. The initial rate observed for the reactions to which no Pt(II) had been added are reported in Table 5. As indicated by these data the initial rate of the uncatalysed reaction was dependent on the concentration of *trans*-$[Pt(NH_3)_4Cl_2]^{2+}$. This may be a real dependence on Pt(IV); but the dependence may also be due to the presence of some catalyst in the *trans*-$[Pt(NH_3)_4Cl_2]^{2+}$. (Most Pt(IV) compounds contain small amounts of Pt(II)). Samples of *trans*-$[Pt(NH_3)_4Cl_2]^{2+}$ prepared at different times did not give the same rates of hydrolyses. That different samples reacted at different rates was not very surprising since the samples may contain small amounts of $[Pt(NH_3)_4]^{2+}$ which catalyses the hydrolysis reaction. However the second-order rate constants for the Pt(II) catalysed reaction were the same for all samples studied.

TABLE 4.—PSEUDO FIRST-ORDER RATE CONSTANTS FOR THE RELEASE OF CHLORIDE AT 25·0°C IN THE REACTIONS

$$cis\text{-}[Pt(NH_3)_4Cl_2]^{2+} + OH^- \xrightarrow{k_1} cis\text{-}[Pt(NH_3)_4ClOH]^{2+} + Cl^-$$

$$cis\text{-}[Pt(NH_3)_4ClOH]^{2+} + OH^- \xrightarrow{k_2} [Pt(NH_3)_4(OH)_2]^{2+} + Cl^-$$

[Pt(IV)]	[OH^-]	[KNO_3]	$k_1 \times 10^5$ (sec^{-1})	$k_2 \times 10^5$ (sec^{-1})
0·00500	0·49	—	13·7	1·8
0·00500	0·10	0·30	5·7	0·4
0·00500	0·10	—	6·0	0·6
0·00500	0·050	0·050	3·4	0·3

TABLE 5.—RATE CONSTANTS FOR THE HYDROLYSIS OF *trans*-$[Pt(NH_3)_4Cl_2]^{2+}$ IN BASIC SOLUTION AT 25·0°C

[Pt(IV)]	[Pt(II)]*	[OH^-]	$k_1 \times 10^5$ (sec^{-1})	$k_1' \times 10^2$ M^{-1} (sec^{-1})§
0·00500	—	0·40	1·3	—
0·00250	—	0·40	0·6	—
0·00250	0·00210	0·40	2·7	10
0·00500	0·00204	0·40	3·0	8
0·00500	0·00279	0·20†	3·4	8
0·00500	0·00210	0·10‡	3·1	9
0·00500	0·00109	0·40	2·3	9
0·00500	0·00052	0·40	1·8	10

* Pt(II) = $[Pt(NH_3)_4]^{2+}$.
† [KNO_3] = 0·20 M
‡ [KNO_3] = 0·30 M.
§ Values of k_1' were calculated by subtracting the uncatalysed rate constant from the catalysed rate constant and dividing by [Pt(II)].

The reaction of *trans*-$[Pt(NH_3)_3Cl_3]^+$ with dilute NaOH gave 6–8 per cent reduction to Pt(II) as well as hydrolysis. The hydrolysis of two chlorides was rapid whereas the third chloride was released only after weeks at 25·0°C (equations 12 and 13).

$$trans\text{-}[Pt(NH_3)_3Cl_3]^+ + OH^- \xrightarrow{k_1} [Pt(NH_3)_3Cl_2OH]^+ + Cl^- \tag{12}$$

$$[Pt(NH_3)_3Cl_2OH]^+ + OH^- \xrightarrow{k_2} [Pt(NH_3)_3Cl(OH)_2]^+ + Cl^- \tag{13}$$

By means of Powell plots rate constants were evaluated for the release of the first and second chlorides. The kinetic analysis was made assuming that hydrolysis was the only process releasing chloride. Since the reduction process was not extensive, the rate constants reported should be reasonably accurate (±10 per cent for k_1 and ±20 per cent for k_2). When relatively large quantities of Pt(II) ($[Pt(NH_3)_4]^{2+}$ or $[Pt(NH_3)_3Cl]^+$) were added to the reaction mixtures a relatively rapid initial release of chloride was observed. The extent of the rapid chloride release was dependent on the relative amounts of Pt(IV) and Pt(II) present. About one chloride ion was released rapidly for each molecule of Pt(II) added to the reaction mixture. When this initial chloride release was neglected, rate constants calculated for the subsequent reaction were very similar to the rate constants for the reaction mixtures to which no Pt(II) had been added. The rate data are reported in Table 6.

TABLE 6.—PSUEDO FIRST-ORDER RATE CONSTANTS FOR THE REACTIONS (T = 25·0°C.)

$$trans\text{-}[Pt(NH_3)_3Cl_3]^+ + OH^- \xrightarrow{k_1} [Pt(NH_3)_3Cl_2OH]^+ + Cl^-$$

$$[Pt(NH_3)_3Cl_2OH]^+ + OH^- \xrightarrow{k_2} [Pt(NH_3)_3Cl(OH)_2]^+ + Cl^-$$

[Pt(IV)]	$[OH^-]$	$[KNO_3]$	$k_1 \times 10^5$ (sec^{-1})	$k_2 \times 10^5$ (sec^{-1})
0·00500	0·49	—	6·4	—
0·00500	0·10	0·40	3·0	0·7
0·00500	0·10	—	4·3	0·5
0·00500	0·050	0·050	3·2	0·5
0·00254	0·265	—	6·1	—
0·00250*	0·265	—	6·2	—

* $[Pt(NH_3)_4]Cl_2$ = 0·00058 M.

The most prevalent reaction of *trans*-$[Pt(en)_2Cl_2]^{2+}$ in basic solution was its reduction to $[Pt(en)_2]^{2+}$. The kinetics of this reaction were studied by titration of the $[Pt(en)_2]^{2+}$ formed with a standard Ce(IV) solution. The rate of chloride release was also followed. Linear first-order plots were obtained for chloride release using the integrated form of the expression $d[Cl^-]/dt = k[Pt(en)_2Cl_2^{2+}]$. If the reduction and hydrolysis reactions were competing first-order reactions, then the k in the rate equation would be equal to the sum of the first-order rate constants for reduction and chloride release. Furthermore the ratio of chloride released to $[Pt(en)_2]^{2+}$ formed would be constant. Experimental ratios were not constant. Evidence to be discussed later showed that the reduction process was complicated and did not show first-order kinetics. The kinetic data are presented in Table 7. The rate constants for the reduction process were obtained from plots of ln $(Pt(IV)^\circ/Pt(IV)^\circ\text{-}Pt(II))$ vs. time, where $Pt(IV)^\circ$ is the initial concentration of *trans*-$[Pt(en)_2Cl_2]^{2+}$ and Pt(II) is the experimental concentration of $[Pt(en)_2]^{2+}$ at time t. This empirical equation gives a linear plot for one half-life. It was found that increasing the concentration of Pt(IV) increased the rates of both Cl^- release and reduction; the extent of reduction also increased. At Pt(IV) concentrations of 0·0100 M or higher, linear first-order kinetic plots for chloride release were not obtained. At higher Pt(IV) concentrations the reaction solutions darkened and degradation of the complex began to occur. The addition of $[Pt(en)_2]^{2+}$ to the reaction mixture slightly decreased the rate and extent of reduction. Both the rate of reduction and chloride release were slightly OH^- dependent. The extent of reduction increased with increasing hydroxide ion concentration. At the end of the reactions at least 95 per cent of the calculated coördinated chloride was found as ionic chloride.

TABLE 7.—PSUEDO FIRST-ORDER RATE CONSTANTS FOR THE REACTIONS (T = 25·0°.)

$$trans\text{-}[Pt(en)_2Cl_2]^{2+} \xrightarrow{k_{Cl^-}} Cl^- + [Pt(en)_2]^{2+} + [Pt(en)_2(OH)_2]^{2+}$$

$$trans\text{-}[Pt(en)_2Cl_2]^{2+} \xrightarrow{k_{Pt(II)}} [Pt(en)_2]^{2+}$$

[Pt(IV)]	[NaOH]	$k_{Cl^-} \times 10^5$ (sec^{-1})	$k_{Pt(II)} \times 10^5$ (sec^{-1})	%Pt as Pt(II) at t_∞
0·0200	0·40	(25)	fast	89
0·0100	0·40	(11)	(7·1)	70
0·00500	0·40	7·0	3·8	64
0·00250	0·40	5·5	(3)	47
0·00500	0·20	5·6*	2·9	58
0·00500	0·10	4·7‡	2·3	53
0·00500†	0·40	6·4	3·0	51

* $[KNO_3]$ = 0·20 M.
† $[Pt(en)_2]Cl_2$ = 0·00250 M.
‡ $[KNO_3]$ = 0·30 M.

It was found that $trans\text{-}[Pt(en)_2Cl_2]^{2+}$, $trans\text{-}[Pt(en)_2ClOH]^{2+}$, and $trans\text{-}[Pt(en)_2(OH)_2]^{2+}$ can be identified polarographically. The complex $[Pt(en)_2]Cl_2$ is reduced at a more negative potential than the former compounds,[12] and they can be determined in its presence. The half-wave potentials for the Pt(IV) complexes are respectively <0·08 V, −0·22 V, and −0·82 V vs. SCE. Polarographs taken on neutralized samples from hydrolysis kinetic runs indicated that the final hydrolysis product of $trans\text{-}[Pt(en)_2Cl_2]^{2+}$ was $trans\text{-}[Pt(en)_2(OH)_2]^{2+}$.

TABLE 8.—PSUEDO FIRST-ORDER RATE CONSTANTS FOR THE REACTION
$[Pt(en)_2ClOH]^{2+} + OH^- \rightarrow [Pt(en)_2(OH)_2]^{2+} + Cl^-$
(Pt(IV) = 0·00500 M, T = 25·0°C.)

[NaOH]	$[KNO_3]$	$k \times 10^5$ (sec^{-1})	%Pt as Pt(II) at t_∞
0·40	—	0·60	40
0·20	0·20	0·33	25
0·10	0·30	0·27	28

The hydrolysis of $[Pt(en)_2ClOH]^{2+}$ was also studied. The data are presented in Table 8. The data indicate that this compound was also reduced in basic solution. The rate of chloride release was OH^- dependent.

It was found that *trans*-$[Pt(en)_2(OH)_2]^{2+}$ was not reduced when dissolved in NaOH solution.

DISCUSSION

In order to understand the kinetics of reactions of these Pt(IV) complexes in basic solution, it is important to realize that they are weak polybasic acids.

$$[Pt(NH_3)_5Cl]^{3+} \overset{K_1}{\rightleftharpoons} [Pt(NH_3)_4NH_2Cl]^{2+} + H^+ \tag{14}$$

$$[Pt(NH_3)_4NH_2Cl]^{2+} \overset{K_2}{\rightleftharpoons} [Pt(NH_3)_3(NH_2)_2Cl]^{+} + H^+ \tag{15}$$

Table 8 lists values of pK_a's for some Pt(IV) ammine complexes. These were obtained by titration, conductivity studies, or from the literature. The simplest type of rate equation for hydrolysis which can be written for these compounds would be one of the following:

TABLE 9.—ACID DISSOCIATION CONSTANTS OF PLATINUM(IV) COMPLEXES AT 25·0°C

Complex	Ionic strength	$pK_a^{(1)}$	$pK_a^{(2)}$	Method
$[Pt(NH_3)_6]Cl_4$	0·020	7·20	10·5	Titration
	0·032	7·25	10·6	Titration
	0·40	7·80	11·1	Titration
	dilute	7·9	10·1	Reference[14]
$[Pt(NH_3)_5Cl]Cl_3$	0·020	8·40	>11·0	Titration
	0·020	—	12·5	Conductivity
	0·12	8·65	>12·4	Titration
	dilute	8·1	10·3	Reference[14]
trans-$[Pt(NH_3)_4Cl_2](NO_3)_2$	0·016	11·3	—	Conductivity
	0·017	>11·0	—	Titration
	0·16	11·3	—	Titration
	dilute	9·8	—	Reference[14]
cis-$[Pt(NH_3)_4Cl_2](NO_3)_2$	0·011	—	12·4	Conductivity
	0·016	9·70	>10·7	Titration
	—	9·40	10·3	Reference[15]
trans-$[Pt(NH_3)_3Cl_3]Cl$	0·0050	>11·1	—	Titration
trans-$[Pt(en)_2Cl_2]Cl_2$	0·010	>11·0	—	Titration
	0·016	11·0	—	Conductivity
	0·16	11·3	—	Titration
	dilute	10·4	—	Reference[15]
trans-$[Pt(en)_2ClH_2O](NO_3)_3$	0·022	3·70	>10·8	Titration

$$d[Cl^-]/dt = k_1[H_nA] + k_2[H_{n-1}A^-] + k_3[H_{n-2}A^=] + \ldots \tag{16}$$

$$d[Cl^-]/dt = k_1'[H_nA][OH^-] + k_2'[H_{n-1}A^-][OH^-] + k_3'[H_{n-2}A^=][OH^-] + \ldots \tag{17}$$

These general equations are written for a neutral acid (H_nA) but are applicable to any charge type. Equation (16) would apply to a complex in which the complex (acid) and its conjugate bases all react by a dissociative mechanism (S_N1) and therefore corresponds to the S_N1CB process. Equation (17) corresponds to a mechanism in which each species reacts by a displacement process (S_N2). The k's are rate constants for the hydrolysis of each species in solution. The observed rate therefore in either case will be the sum of rates of the hydrolyses of the free acid and of its conjugate bases; and the rate will depend on the concentrations of the respective species (i.e., on their pK_a's and the OH^- ion concentration) and on the relative values of the k's. The rates of these two processes as a function of H^+ for a dibasic acid are

---

[14] J. BJERRUM, G. SCHWARZENBACH and L. G. SILLÉN, *Stability Constants*, Part II *Inorganic Ligands*, pp. 14, 57. The Chemical Society Special Publication 7, London (1958).

[15] A. A. GRINBERG, L. V. VRUBLEVSKAYA, KH. I. GIL'DENGERSHEL' and A. I. STETSENKO, *Russian J. Inorg. Chem.* (translation) 462–66 (1959).

$$d[Cl^-]/dt = \frac{1}{[H^+]^2 + K_1[H^+] + K_1K_2}(k_1[H^+]^2 + k_2[H^+]K_1 + k_3K_1K_2) \qquad (18)$$

$$d[Cl^-]/dt = \frac{[OH^-]}{[H^+]^2 + K_1[H^+] + K_1K_2}(k_1'[H^+]^2 + k_2'[H^+]K_1 + k_3'K_1K_2) \qquad (19)$$

The experimental data presented in the previous sections show the hydroxide dependences for the hydrolyses of the different complexes. It was thought that this information might provide a clue to the mechanism of these reactions. By plotting equations (18) and (19) as a function of pH using appropriate values for the acid ionization constants (K's) and trying a variety of combinations of rate constants (k's), one should be able to match the experimentally determined hydroxide dependence with one of the equations. This would provide evidence that the reaction obeys either a first or second-order rate equation. Unfortunately for all the compounds studied (except *trans*-$[Pt(NH_3)_4Cl_2]^{2+}$) the observed hydroxide dependence was intermediate between zero and first order. This type of behaviour can be adequately explained by either mechanism and both rate equations (18 and 19). Therefore the observed hydroxide dependences can be explained in terms of the acid base equilibria, but assignment of mechanism cannot be made in terms of hydroxide dependence data.

The hydrolysis of $[Pt(NH_3)_5Cl]^{3+}$ and *cis*-$[Pt(NH_3)_4Cl_2]^{2+}$ did not involve any side reactions and the rates were only dependent on the concentrations of complex and hydroxide ion. It appears that these reactions proceed by a simple substitution type process, but the data are not adequate to provide a more detailed mechanistic interpretation. The Pt(II) independent hydrolysis of *trans*-$[Pt(NH_3)_3Cl_3]^+$ is similar to these reactions and probably proceeds by a simple substitution mechanism.

The *trans*-dichloro complexes react in a manner quite different from the other complexes. The fact that the hydrolysis of *trans*-$[Pt(NH_3)_4Cl_2]^{2+}$ has a first-order dependence on $[Pt(NH_3)_4]^{2+}$ and is independent of OH^- suggests that a bridge mechanism as outlined in equations (20), (21) and (22) is operative.

$$[Pt(NH_3)_4]^{2+} + H_2O \rightleftharpoons [Pt(NH_3)_4H_2O]^{2+} \qquad (20)$$

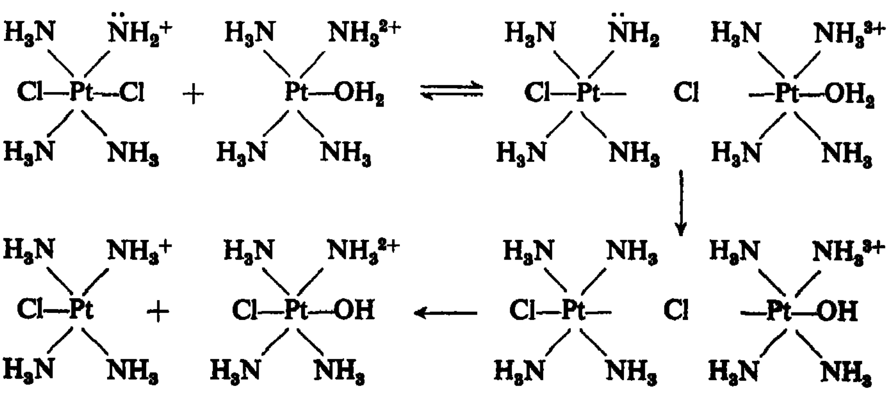

(21)

(22)

This mechanism is very similar to those used to explain chloride exchange(16) and certain substitution reactions(17) of this type of dichloro Pt(IV) complexes. The conjugate base $[Pt(NH_3)_3NH_2Cl_2]^+$ is almost certainly the reactive Pt(IV) species since at a pH over 13, the complex is at least 90 per cent in this form or in the form of more dissociated acids. The mechanism is consistent with the Pt(II) and OH^- dependence observed. It also explains why only one Cl^- is replaced, assuming that OH^- is not a good bridging group in Pt(IV)–Pt(II) systems. This assumption seems justified on the basis that platinum exchange between $[Pt(en)_2(OH)_2]^{2+}$ and $[Pt(1\text{—}pn)_2]^{2+}$, in which OH^- would have to serve as a bridging group, was not observed.(16)

The reactions of *trans*-$[Pt(en)_2Cl_2]^{2+}$ in basic solution led to extensive reduction. Hydrolysis was observed to be essentially Pt(II) independent. A small hydroxide dependence was observed for Cl^- release and reduction to $[Pt(en)_2]^{2+}$. It seems probable that hydrolysis is essentially OH^- independent and that the OH^- dependence observed for Cl^- release was due to the reduction process.

The kinetic data for this system are best explained by assuming that reduction and hydrolysis to $[Pt(en)_2(OH)_2]^{2+}$ are competing processes. If this assumption is correct, the increase in the rate of Cl^- release as [Pt(IV)] was increased was due to an increase in the rate of reduction, since the extent of reduction increased. The fact that an increase in OH^- concentration increases the extent of reduction supports the assumption that reduction and hydrolysis are competing reactions. It also indicates that the hydroxide dependence is primarily in the reduction process.

The mechanism for the reduction process was also of interest. Reduction occurred only in complexes which contained *trans* chlorides. This suggested that a mechanism involving a bridged intermediate was a plausible path. The fact that at infinite time in all the hydrolyses runs on *trans*-$[Pt(en)_2Cl_2]^{2+}$ all the calculated chloride was found as ionic chloride indicates that neither Cl_2, OCl^-, nor ClO_3^-, which are likely oxidation products in this reaction, are formed. Oxygen is not a likely direct product of the reaction since neither Pt(IV) complexes nor Cl_2 are observed to oxidize water to O_2 in basic solution. Equations (23) and (24) present a mechanism that is consistent with the data collected on *trans*-$[Pt(en)_2Cl_2]^{2+}$. This mechanism is analogous to the type of bridge mechanism proposed for chloride exchange and other substitution reactions of this type of Pt(IV) complexes.(16,17)

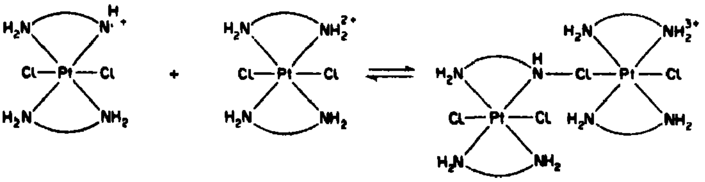

(23)

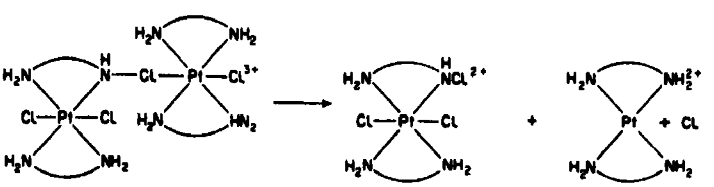

(24)

---

(16) F. BASOLO, M. L. MORRIS and R. G. PEARSON, *Disc. Faraday Soc.* **29**, 80, (1960).

(17) R. C. JOHNSON and F. BASOLO, *J. Inorg. Nucl. Chem.*, **13**, 36 (1960).

The fact that only *trans* dichloro-Pt(IV) compounds are reduced is consistent with observations that Cl^- exchange is rapid only for Pt(IV) compounds containing *trans* chlorides. This type of mechanism would also explain the Pt(IV) dependence observed for chloride release and reduction, since a second-order Pt(IV) dependence is expected if reaction (23) is rate determining. The chloroamine formed is a strong oxidizing agent and may either oxidize the organic group further or oxidize water to O_2. In this way most of the Cl^- would reappear in the solution. A small loss in ligand would not be detected by the analytical methods used. Oxidation of coordinated ammines by Cl_2 has recently been reported.(18)

SUMMARY

The chloroammineplatinum(IV) complexes studied were found to release chloride ion in basic solution by at least three different processes. In the basic reaction mixtures the predominant platinum containing species were conjugate bases, amido complexes; these ions were involved in the hydrolysis reactions and may have been the only reactive platinum species. One reaction process involves the simple replacement of coordinated chloride ion by hydroxide ion. This occurs with the complexes $[Pt(NH_3)_5Cl]^{3+}$, *cis*-$[Pt(NH_3)_4Cl_2]^{2+}$ and *trans*-$[Pt(NH_3)_3Cl_3]^+$. A second process is one catalysed by the presence of Pt(II), which was found for the complex *trans*-$[Pt(NH_3)_4Cl_2]^{2+}$. A third method of chloride ion release is that resulting from the reduction of six-coordinated platinum(IV) to four-coordinated platinum(II) complexes. This decrease in coordination number is accompanied by the loss of two chloro groups in *trans* positions. Such a path is responsible for approximately 10 per cent of the Cl^- released from *trans*-$[Pt(NH_3)_4Cl_2]^{2+}$ and *trans*-$[Pt(NH_3)_3Cl_3]^+$ and up to 90 per cent of the Cl^- released from *trans*-$[Pt(en)_2Cl_2]^{2+}$.

Note added in proof—While this paper was in the proof stage, an article presenting base hydrolysis data on a similar series of compounds was found. (A. A. GRINBERG and YU. N. KUKUSHKIN, *Dokl. Akad. Naur. SSSR*, **132**, 1071 (1960)). The experimental data reported were in general agreement with our work.

Acknowledgements—This research was supported in part by the U.S. Atomic Energy Commission under contract No. AT(11-1)-89-Proj. No. 2. R. C. J. wishes to thank the American Cyanamid Corporation and the National Science Foundation for fellowships. We are also grateful to Professor J. O. EDWARDS for helpful discussions and for the suggested mechanism of reduction of *trans*-dichloro systems.

---

(18) YU. N. KUKUSHKIN, *J. Inorg. Chem. U.S.S.R.* (translation), 1131 (1959).

J. Inorg. Nucl. Chem., 1962, Vol. 24, pp. 73 to 79. Pergamon Press Ltd. Printed in Northern Ireland

REACTIONS OF CO-ORDINATED LIGANDS—III

REACTIONS OF IRON ISONITRILE COMPLEXES WITH NUCLEOPHILES

W. Z. Heldt
E. I. du Pont de Nemours and Company, Incorporated
Explosives Department, Experimental Station Laboratory
Wilmington, Delaware

(*Received* 17 *August* 1961)

Abstract—Nucleophiles reacted with cyanopentabenzylisonitrileiron(II) bromide (X) in three different fashions: bases such as sodium hydroxide and sodium bicarbonate decomposed X to tarry polymers; potassium cyanide caused polymer formation and generated benzyl isonitrile from the complex; weak bases which form only moderately stable complexes with iron(II), e.g. methanol, ethyl mercaptan or ammonia, were benzylated.

In a previous communication we have described the synthesis of a new class of iron isonitrile complexes.(1) Relatively little work is reported on the reactions of organic ligands when co-ordinated to a metal ion; no such work was found in the literature on metal isonitrile complexes.(2) Yet considerable double bond formation has been observed between iron and the isonitrile ligand which could modify the reactivity of the organic ligand in the aliphatic, and even more so, in the aromatic series.(3) This paper describes the reactions of cyano pentabenzylisonitrileiron(II)bromide with various nucleophiles.(4)

EXPERIMENTAL

Reaction of potassium cyanide with cyanopentabenzylisonitrileiron(II) bromide (X) *in* 90 *per cent ethyl alcohol*

To a solution of 54 g (0·071 mole) of X in 90 per cent ethyl alcohol was added 30 g (0·45 mole) of potassium cyanide. The reaction mixture was refluxed and stirred for 72 hr. The excess solvent was then evaporated under 0·1 mm pressure and room temperature to yield as a residue a black tarry material. The distillate was Fraction *A*. Extraction of the residue with boiling chloroform (5 × 100 ml) and subsequently with boiling ethyl alcohol (3 × 100 ml) and evaporation of the extracts yielded 33·7 g of black material (*B*), which refused to crystallize, despite numerous attempts to purify it. The infra-red spectrum of *B* indicated the presence of several nitrile and/or isonitrile groups (in μ): 3·00 (*s*) 3·40 (*s*), 3·50 (*s*), 4·58 (*vs*), 4·68 (*vs*), 5·10 (*s*), 6·00 (*sh*), 6·30 (*s*), 6·18 (*s*), 6·88 (*s*), 7·22 (*m*), 7·42 (*s*), 9·03 (*s*), 14·40 (*s*). Attempts to hydrolyse this material by prolonged refluxing with 80 per cent sulphuric acid failed.

The ethanol, chloroform insoluble material, 27 g, Fraction C, gave a positive prussian blue test with ferric chloride. When 26·5 g of *C* was dissolved in 100 ml of 2 N hydrochloric acid and an excess of zinc chloride was added a white precipitate appeared which, after drying at 120°C/30 mm, consisted of 10 g of solid. Since about 70 per cent of this precipitate accounted for zinc ferrocyanide, the conversion to ferrocyanide anion must be about 40 per cent.(5)

Fraction *A* was distilled at 760 mm and then at reduced pressure through a spinning band column, yielding 6 g of N benzyl formamide, b.p. 88–90°C, 21 mm Hg, identified by comparison of its spectrum with that of an authentic sample. (Found: N, 10·98. Calc. for $C_6H_5CH_2NHCOH$: N, 10·36%).

---

(1) W. Z. Heldt, *J. Inorg. Nucl. Chem.* In press.

(2) L. Malatesta, *Isocyanide Complexes of Metals*, in "*Progress in Inorganic Chemistry*". (Edited by F. A. Cotton) p. 283. Interscience, New York (1959).

(3) (a) H. M. Powell and G. W. R. Bartindale, *J. Chem. Soc.*, 799 (1945).
(b) F. A. Cotton and F. Zingales. *J. Amer. Chem. Soc.*, **83**, 351 (1961).

(4) C. K. Ingold, *Structure and Mechanism of Organic Chemistry*, p. 197. Cornell University Press (1953).

(5) H. E. Williams, *Cyanogen Compounds* (2nd Ed.) p. 364, Edward Arnold, London (1948).

Exchange experiments with X and labelled potassium cyanide

Labelled $K^{14}CN$ was obtained from New England Nuclear Corporation. Twenty one and seven tenths milligrams (= 0·32 mmole) of $K^{14}CN$ were dissolved in 4 ml of H_2O; 1·9898 g (30·6 mmole) of inactive KCN dissolved in 4 ml of H_2O were added to the solution; the solution was stirred for several minutes and subsequently 125 ml of absolute ethanol was added, whereby $K^{14}CN$ (1·310 g) crystallized out. The $K^{14}CN$ was washed with absolute ethanol, dried and analysed by the scintillation method in methanol as described by HAYES(4). The sample contained 500 μc/g of ^{14}C. Analysis for ^{14}C in the reaction mixtures was performed according to the same method under the same conditions.

(a) To 383 mg of X (0·5 mmole) dissolved in 13 ml of 100 per cent methanol was added a solution of 33 g (0·5 mmole) of $K^{14}CN$ containing 16·5 μc in 7 ml of distilled water, and the homogenous solution was allowed to stir in a stoppered bottle for 60 hr at room temperature. The reaction mixture was then poured into 400 ml of water, the aqueous solution was extracted with chloroform, the chloroform extracts were dried with magnesium sulphate, filtered, and evaporated to dryness under reduced pressure at 28°C. The oily residue, 250 mg, was then dried at 25°C/1·1 mm overnight; analysis indicated 11·6 μc which represented an accounting for ^{14}C of 70·4 per cent in the sample isolated from the reaction mixture.

(b) Same as in (a) but the homogeneous solution was allowed to stir for 5 min instead of 60 hr before the reaction mixture was poured into water and processed. Total material isolated was 210 mg; in this case the product was crystallized after drying. Radioactive analysis gave 4·3 μc indicating an exchange of 26·1 per cent in the sample isolated from the reaction mixture.

(c) To a solution of 3·83 g (5 mmole) of X in 130 ml of methanol was added a solution of 337 mg (5·3 mmole, 20·0 μc) of $K^{14}CN$ in 70 ml of water and the homogeneous solution was stirred in a closed vessel for 60 hr at room temperature. The solution was then evaporated to dryness under reduced pressure. To the residual green oil was added 100 ml of 85 per cent sulphuric acid and the reaction mixture was heated on a steam bath for 4 hr. The reaction mixture was then cooled to room temperature and was poured onto about 400 g of ice whereby a yellow oil precipitated out. This yellow oil was dissolved in chloroform, the chloroform solution was dried with magnesium sulphate and product was crystallized from chloroform–methyl ethyl ketone. After one recrystallization from methyl ethyl ketone, 1·8 g of yellow crystals were obtained with a m.p. 156–158°C. This material did not give any melting point depression upon admixture with $(C_6H_5CH_2NC)_5FeCNHSO_4{\cdot}H_2O$(1) and their infra-red spectra were identical. Radioactive analysis indicated $8{\cdot}5 \times 10^{-4}$ μc/mg, or 7·6 per cent exchange of the cyanide group in the isonitrile complex.

Reaction of X *with* $K^{14}CN$ *in ethylene glycol dimethyl ether*

To a solution of 30·6 g (0·04 mole) of X in 250 ml of dry ethylene glycol dimethyl ether (distilled over Na) in a stainless steel vessel was added 8·463 g (0·13 mole) of potassium cyanide labelled with ^{14}C having a radioactivity of 65 μc. The reaction mixture was heated for 5 hr at 150°C under 700 atm nitrogen pressure. The reaction mixture was then cooled to room temperature and was filtered from the ethylene glycol dimethyl ether insoluble materials (*A*). The filtrates were poured onto 500 ml of ether in order to precipitate any unreacted isonitrile complexes which were ether insoluble. A light brown ether soluble mixture was obtained (Fraction I) and a dark brown ether insoluble material precipitated out which was dissolved in chloroform (*B*). Fraction *A* was then extracted with 2 × 75 ml of boiling chloroform and the chloroform extracts were combined with Fraction *B* which, after evaporation and drying at 25°C/1·0 mm, yielded 10·8 g of isonitrile complexes (Fraction II). The infra-red spectrum of Fraction II: (KBr) 2·92 (*vs*), 3·42 (*s*), 4·56 (*v*), 4·62 (*s*), 4·88 (*vs*), 6·14 (*s*), 6·68 (*s*), 6·88 (*s*), 7·42 (*s*), 8·92 (*m*), 13·60 (*s*), 14·36 (*s*), (μ). The chloroform insoluble fraction of *A*, Fraction III, was mainly an inorganic bluish-white material, 16·8 g. Fraction I was distilled first at 760 mm and subsequently under reduced pressure.

DISTILLATION

Fraction	mm Hg	Boiling point (°C)	Distilled (g)	n_D^{25}
I*a*	15	42–80	1·35	1·4640
I*b*	15	80–95 main 90–95	3·0	1·5167
I*c*	1·0	115–140 main 138–140	2·7	1·5419
I*d*			4·3	
Residue				

---

(4) F. N. HAYES *Int. J. Appl. Radiation and Isotopes*, **1**, 46 (1956).

The totals of Fractions I, II, and III were 38·95 g which accounted for 98 per cent of the materials used in the reaction. Fraction Ib consisted of about 80–90 per cent of benzyl isonitrile, identified by comparison with the spectra of a reference sample,(7) and an unknown alcohol (ethylene glycol?) Infra-red spectrum (liquid): 2·95 (*vs*), 3·29 (*s*), 3·42 (*s*), 3·49 (*s*), 4·63 (*vs*), 5·98 (*w*), 6·22 (*w*), 6·68 (*vs*), 6·88 (*vs*), 7·08 (*w*), 7·40 (*w*), 8·32 (*s*), 9·29 (*s*), 9·82 (*vs*), 10·55 (*w*), 11·08 (*w*), 12·28 (*broad*), 12·68 (*vs*), 14·40 (*vs*), (μ). Fraction *Ic* consisted of a mixture of benzyl isonitrile (about 20–30 per cent) and N-benzylformamide, identified by comparison of the reference spectra of these two compounds. Radioactive analysis gave the following results:

Fractions (g)	μc	% of total radioactivity
I*b* (3·0)	3·86	5·94
Ic (2·7)	1·28	1·97
II (10·8)	7·63	11·73
III (16·8)	16·15	24·85
Total	28·92	44·5

The balance of radioactivity must be present in the nonanalysed pot-residue I*d*, which contained products of polymerization of benzyl isonitrile.

Reaction of X *with methanol under carbon monoxide pressure*

A solution of 54 g (0·07 mole) of X in 200 ml of methanol was pressurized with carbon monoxide to 700–850 atm and the reaction mixture was heated at 175°C for 6 hr in a stainless steel autoclave. During this period a total of 350 atm of carbon monoxide was consumed by the reaction mixture. The reaction vessel was washed well with methyl alcohol and the reaction mixture was filtered from a solid compound *A* (10·05 g). This white material was insoluble in all organic solvents such as ether, chloroform, acetonitrile, methanol, dimethylformamide and dimethylsulphoxide, but dissolved in concentrated sulphuric acid and dilute, hot sodium hydroxide. A solution of *A* in concentrated sulphuric acid evolved a gas when heated on a steambath. The infra-red spectrum in KBr showed three peaks in the nitrile, isonitrile and carbon monoxide region: 2·98 (*vs*), 3·05 (*vs*), 4·50 (*s*), 4·75 (*vs*), 4·92 (*vs*), 6·02 (*w*), 6·20 (*s*), 6·70 (*s*), (μ). The material did not melt up to 320°C. (Found: C, 29·94; H, 3·29; N, 23·91; Fe, 31·00. Calc. for $H_5Fe_2(CN)_6(CO)_3$: C, 30·28; H, 1·41; N, 23·55; Fe, 31·29. Calc. for $H_{11}\,Fe_2(CN)_6(CO)_3$: C, 29·78; H, 3·05; N, 23·16; Fe, 30·77%). Specific magnetic susceptibility (as solid) $\chi = 34{\cdot}1 \times 10^{-6}$ c.g.s. at 25°C.

When 512 mg of *A* were added to 5·0 ml of 1·9786 N sodium hydroxide and the solution was stirred for 1·5 hr at room temperature, then filtered from the very slight precipitates, and back titrated with 0·113 N hydrochloric acid potentiometrically, 66·5 ml of hydrochloric acid were necessary to neutralize the excess of sodium hydroxide. That means that there were 1·5 active hydrogens in the above formula weight of *A*.

On the other hand, when 277 mg of *A* were added to 3·0 ml of 1·9786 N sodium hydroxide and the mixture was heated on a hot plate to boiling, cooled to room temperature, filtered, and back titrated potentiometrically with 0·113 N hydrochloric acid, 34·5 ml of hydrochloric acid were necessary to neutralize the excess of sodium hydroxide; here the solid consumed 2·037 meq. of base or it contained about 2·65 active hydrogens. The blue residue which precipitated after acidification was filtered, washed throughly with water and was dried at 0·1 mm/25°C for several hours. (Found: C, 21·69; H, 2·23; N, 16·86; Fe, 29·26. Calc. for $Fe_7C_{24}H_{32}N_{16}O_{24}$: C, 21·84; H, 2·44; N, 16·98; Fe, 29·62%) The infra-red spectrum in KBr of this material also differed considerably from A: 2·95 (*vs*), 4·70–4·90 (*vs*, broad), 6·20 (*w*), 9·30 (*w*), 9·75 (*w*), (μ).

The filtrate of *A* was distilled through a fractionating column first at 760 mm, then at reduced pressure yielding as the main fraction 25·1 g of a colourless liquid, b.p. 104–106°C/90 mm Hg, n_D^{27} = 1·4967. Infra-red spectrum: 3·00 (*w*), 3·50 (*vs*), 5·92 (*vs*), 6·25 (*w*), 6·70 (*s*), 6·89 (*vs*), 7·25 (*vs*), 7·32 (*s*), 8·40 (*s*), 9·10 (*vs*), 9·72 (*s*), 10·40 (*s*), 10·82 (*s*), 11·07 (*s*), 13·50 (*s*), 14·35 (*vs*), (μ). The infra-red spectrum of the distillate indicated the presence of a keto or acid group. The distillate did not saponify when boiled with base and did not give a 2,4-dinitrophenylhydrazone or a semicarbazone. Finally, the distillate was purified by reduction of all contaminants with lithium aluminium hydride. To a slurry of 4·0 g (0·1 mole) of lithium aluminium hydride in 100 ml of anhydrous ether and a three neck flask (stirrer, condenser, additional funnel) was added a solution of 7·5 g of the distillate in 50 ml of ether, at such a rate the ether just refluxed. The reaction mixture was then refluxed overnight. After this time the reaction mixture was cooled to room temperature and the excess lithium aluminium hydride was decomposed with water, and the hydroxides were dissolved by the addition of 50 ml of 20 per cent sulphuric acid. The ether layer was separated and the water layer was extracted three times with 100 ml of ether. The ether extracts were combined, dried with magnesium sulphate and distilled. Only one material was obtained in the vacuum distillation; 6·7 g, b.p. 101–103°C/80 mm, n_D^{27} = 1·4992. Infra-red spectrum of this material was nearly superimposable with that of methyl benzyl ether. The nuclear magnetic resonance spectrum of this material was identical with that of an authentic sample of benzyl methyl ether; it indicated only aromatic, methylene and methyl hydrogen in a ratio of 5:2:3.

---

(7) I. Ugi and R. Meyer *Ber. Dtsch. Chem. Ges.* **93**, 239 (1960).

Reaction of tetrabenzhydrylisonitrileiron(II) cyanide with anhydrous methanol

A solution of 11 g (0·0125 mole) of $((C_6H_5)_2CHNC)_4Fe(CN)_2$,(1) m.p. 242–244°C, in 70 ml of absolute methanol (Baker's analysed methanol was distilled from magnesium methoxide) was heated for 4 hr at 140°C under 780–800 atm nitrogen. The reaction mixture was then cooled to room temperature and was filtered from 2·9 g of methanol insoluble material. The methanol soluble filtrates were distilled under 16 mm pressure. Only one fraction was isolated; b.p. 148–150°C/16 mm, 4·4 g, 44 per cent conversion for $(C_6H_5)_2CHOCH_3$, n_D^{25} = 1·5650. There remained 1·8 g of pot residue which was not further identified. (Found: C, 84·27; H, 6·96. Calc. for $(C_6H_5)_2CHOCH_3$: C, 84·79; H, 7·12%). Infra-red: 3·30 (*s*), 3·40(*s*), 3·55 (*s*), 5·12(*w*), 5·30(*w*), 5·55(*w*), 6·22(*m*), 6·70(*vs*), 6·99(*vs*), 7·42 (*m*), 7·65 (*s*), 8·42 (*s*), 9·12 (*s*), 9·32 (*vs*), 9·72 (*vs*), 10·35 (*vs*), 10·85 (*w*), 10·95 (*w*), 11·55 (*w*), 12·05 (*w*), 13·25 (*vs*), 13·55 (*vs*), 14·35 (vs, broad), (μ).

Reported for $(C_6H_5)_2CHOCH_3$; b.p. 147–148/17 mm Hg.(8)

Reaction of potassium thiocyanate with X

To a solution of 15·2 g (0·02 mole) of X in 150 ml of dry (see above) ethylene glycol dimethyl ether was added 7·8 g (0·08 mole) of potassium thiocyanate (dried at 120°C/20 mm for 24 hr), and the reaction mixture was heated at 150°C for 5 hr under 700 atm nitrogen pressure. The reaction mixture was then filtered from 11·5 g of a black solid. The filtrates were distilled under 1·0 mm pressure. Only one fraction was collected, b.p. 75–155°C (main fraction, b.p. 152–155°C) 4·5 g (38 per cent conversion in reference to KSCN added). There remained 5·5 g of a black residue in the still. The infra-red spectrum of the distillate was: 3·00 (*w*), 3·30 (*w*), 3·42 (*w*), 4·62 (*w*), 4·85 (*w*), 5·95 (*w*), 6·22 (*w*), 6·68 (*s*), 6·88 (*s*), 7·25 (*s*), 7·52 (*w*), 8·20 (*s*), 9·36 (*w*), 9·75 (*w*), 14·40 (*s*), (μ).

A synthetic sample of benzyl thiocyanate was prepared from benzyl bromide and potassium thiocyanate according to the procedure of JOHNSON(9), b.p. 117–119·5/5 mm, m.p. 39–40°C (reported m.p. 41°C(10)). (Found: N, 9·58; S, 21·29. Calc. for $C_6H_5CH_2NCS$: N, 9·25; S, 21·21%). Benzyl thiocyanate showed a strong band ar 4·62 μ characteristic of the $-S-C{\equiv}N$ absorption. The band at 4·85 μ in the reaction mixture appeared therefore to belong to benzyl isothiocyanate.(11) Judging from the intensity of the two bands at 4·62 μ and 4·85 μ, the reaction mixture consisted of approximately 3:1 ratio of benzyl isothiocyanate and benzyl thiocyanate.(12)

RESULTS AND DISCUSSION

Nucleophiles may displace the cyanide group or the isonitrile group from $(C_6H_5CH_2NC)_5FeCNBr$(X), or may react with the isonitrile group, the methylene group, or, least probably, attack the aromatic nucleus in X.

When X was heated with sodium hydroxide or sodium bicarbonate in water or dimethylformamide as the solvent (see Table 1) only polymer formation took place. Interestingly, the polymer exhibited strong infrared bands at 4·58 μ and 4·70 μ, indicating the presence of isonitrile groups. The iron was so strongly complexed it could nor be dissolved out of this polymer with 80 per cent sulphuric acid.

When X was refluxed for 16 hr with a five molar excess of triphenylphosphine, triphenylarsine or pyridine in a chloroform solution, X was recovered in 90–100 per cent.

(8) E. BERGMANN and J. HERVEY, *Ber. Dtsch. Chem. Ges.* 62, 915 (1929).

(9) T. B. JOHNSON and R. B. DOUGLASS, *J. Amer. Chem. Soc.* 61, 2548 (1939).

(10) L. HENRY, *Ber. Dtsch. Chem. Ges.* 2, 636 (1869).

(11) (a) E. LIEBER, C. N. R. RAO and J. RAMACHANDRAN, *Spectrochim. Acta*, 13, 296 (1959).
(b) L. S. LUSKIN, G. E. GANTERT and W. E. CRAIG, *J. Amer. Chem. Soc.* 78, 4965 (1956).

(12) W. Z. HELDT, Unpublished results (1959).

Under similar conditions carbon monoxide is easily displaced from iron carbonyls.(18)

When X was boiled with six moles of potassium cyanide in 90 per cent ethyl alcohol, potassium ferrocyanide and *N*-benzylformamide, which is a hydrolysis product of benzyl isonitrile were identified in about 40 and 14 per cent conversions, respectively. In addition to these compounds a polymeric material formed which still contained iron and showed three strong bands in the triple bond stretching region at 4·58 μ, 4·68 μ and at 5·10 μ. Attempts to hydrolyse this polymer with 80 per cent sulphuric acid failed. Under the same reaction conditions, X underwent hydrolysis to benzyl amine with no difficulty.(1) When the KCN/X ratio was decreased from 10 to 3, the amount of benzyl isonitrile or N-benzylformamide isolated increased from 1 to 30 per cent (Table 1 and Experimental). Polymeric iron-containing products which showed two strong bands in the 4·50–4·85 region were formed when the KCN/X ratio exceeded 4; little polymer formation was observed when the KCN/X ratio remained below 3½. Potassium cyanide, therefore, when present in more than four molar excess, polymerizes the benzyl isonitrile and the concurrent iron isonitrile complexes.

FIG. 1.—Reaction of $K^{14}CN$ with $(C_6H_5CH_2NC)_5FeCNBr$.

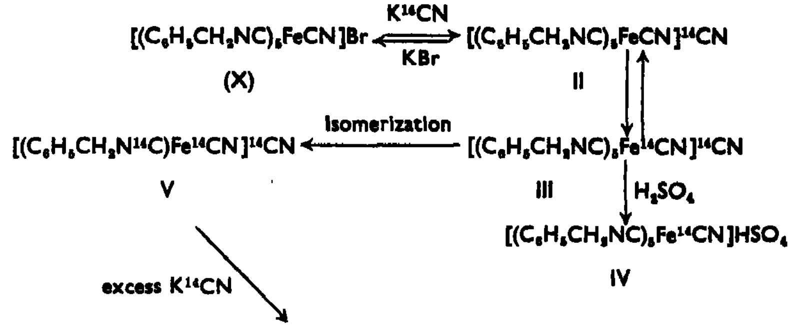

	$C_6H_5CH_2N^{14}C$	$C_6H_5CH_2NH^{14}COH$	Benzyl Isonitrile polymer	Iron Isonitrile complexes	Inorganic cyanides and complexes
conversion	12·8%	11·0%	18·3%	10·8 g	16·8 g
radioactivity (%)	6·0	2·0	55·5(?)	11·7	24·8

The relative ease of preparation of an iron–alkyl isonitrile complex and the formation of an alkyl isonitrile in the reaction of potassium cyanide with the complex indicates a novel route for the synthesis of alkyl isonitriles. It was therefore of interest to investigate the mode of isonitrile formation from X in some detail with $K^{14}CN$ (see Fig. 1). The metathetical exchange of the bromide in X against radio cyanide (II, III), one of the first intermediates in the formation of alkyl isonitriles from X, was not instantaneous; after 5 min at room temperature only 26 per cent of bromide was exchanged against labelled cyanide, and after 60 hr only 70·5 per cent. When the products of the metathesis of X, i.e., II, III (Fig. 1) was converted into the hydrosulphate(1) IV, it was found that 7·6 per cent of the cyanide bound to iron was exchanged against radio-cyanides. Products accounting in all three experiments was only 46–65 per cent.

---

(18) (a) W. HIEBER and R. BREU, *Ber. Dtsch. Chem. Ges.* **90**, 1259 (1957).
(b) W. HIEBER and N. KAHLEN, *Ber. Dtsch. Chem. Ges.* **91**, 2234 (1958).

TABLE 1.—REACTIONS OF $(C_6H_5CH_2NC)_5FeCNBr$ WITH NUCLEOPHILES

Experiment no.	$(C_6H_5CH_2NC)_5FeCNBr$		Reactant		Reaction conditions				Products and identification of products
	(g)	(mole)	(g)	(mole)	Solvent (ml)	Time (hr)	Temp. (°C)	Pressure (atm)	
1	15·0	(0·02)	NaOH	0·25	H_2O 100	6	150	800 CO	Tar
2	15·0	(0·02)	$NaHCO_3$	0·2	D.M.F. 100	4·6	150	800 CO	Tar
3	14·4	(0·02)	KCN 8·58	0·13	HCN 120	5	90	closed autoclave	Tar only
4	14·6	(0·02)	KCN 10·0	0·16	CH_3OH 50 H_2O 50	5	150	closed autoclave	2·6 g N-benzylformamide (0·009 mole)
5	22·8	(0·03)	KCN 19·3	0·3	$(CH_2OCH_3)_2$ 120	6	100		0·6 g N-benzylformamide
6	15·0	(0·02)	KCN 5·2	0·08	$(CH_2OCH_3)_2$ 100	1	200	700 N_2	3·8 g of a mixture of $C_6H_5CH_2NC$ (about 35%) and $C_6H_5CH_2NHCHO$
7	15·0	(0·02)	KCN 3·9	0·06	$(CH_2OCH_3)_2$ 150	3	150	700 N_2	2·1 g of a mixture of $C_6H_5CH_2NC$ and $C_6H_5CH_2NHCHO$
8	15·0	(0·02)	CH_3OH 100 ml		none	6	175	850 N_2	FI 8·6 g solid precipitate; filtrate distilled, yielded = 3·624 g (= 36%) of $C_6H_5CH_2OCH_3$
9	30·0	(0·04)	$(CH_3)_2CHOH$ 100 ml		none	6	175	840 N_2	FI 10·65 g solid; filtrate distilled yielded = 11·91 g (42%) $C_6H_5CH_2OCH(CH_3)_2$, identified by N.M.R., I.R. analysis
10	15·0	(0·02)	CH_3CO_2H 100 ml $(CH_3CO)_2O$ 4 ml		none	2	150	850 N_2	FI 6.60 g solid; filtrate distilled yielded = 2·24 g (= 14%) of $C_6H_5CH_2OCOCH_3$; identified by I.R., N.M.R. analysis
11	15·0	(0·02)	NH_3	3·0	none	5	130	350 N_2	6·1 g of tars and 6·5 g (61% conversion) of $C_6H_5CH_2NH_2$, b.p. 103–105°C./18 mm identified as p-toluene sulphone amide. m.p. 113·4–114·0°C.
12	22·5	(0·03)	$CH_3(CH_2)_2CH_2NH_2$	1·0	none	6	175	380 N_2	17·4 g of tars, 9·8 g of benzylamine and N-(n)butyl benzylamine; identified as 9·8 g of p-toluene sulphonimides; b.p. 113·4–114·0°C. and m.p. 157·5–159·4°C, respectively
13	15·0	(0·02)	CH_3CH_2SH	1·01	none	4	130	400 N_2	2·55 g tars and 6·2 g (= 44% conversion) of benzyl ethyl thioether, b.p. 80–82°C./10 mm Hg n_D^{20} = 1·5415; analysis found C = 65·66; H = 7·86; and 1·5 g of $C_6H_5CH_2NC$; Analysis Calc. for $C_6H_5CH_2SCH_2CH_3$: C = 64·36; H = 7·56
14	15·0	(0·02)	CH_3CONH_2	1·0	none	6	175	closed vessel	Tars

The polymerizations of the liberated benzyl isonitrile and of the concurrent isonitrile complexes were diminished when the solvent was ethylene glycol dimethyl ether rather than ethyl or methyl alcohol. When X was heated with 3·25 molar excess of $K^{14}CN$ in ethylene glycol dimethyl ether in an autoclave there were formed: benzyl isonitrile, N-benzylformamide, a polymer resulting from benzyl isonitrile, iron isonitrile complexes and unreacted labelled potassium cyanide insoluble in chloroform (Fig. 1). In a simple displacement of benzyl isonitrile by $K^{14}CN$ from X all the labelled atoms should appear in the isonitrile complex and none in the displaced benzyl isonitrile. Since the benzyl isonitrile and N-benzylformamide were both labelled, an internal isomerization of III–V must have preceded the formation of isonitrile from V. Furthermore, the radioactive label was present in all of the products isolated but in each to a different extent. For example, the benzyl isonitrile was more radioactive than the N-benzylformamide which must have been formed by addition of water to benzyl isonitrile. The results indicated, therefore, the internal isomerization and the generation of benzyl isonitrile, N-benzylformamide and the polymerization of benzyl isonitrile (?) are concurrent processes in this reaction.

When the nucleophile was a weak base, and a weak complexing agent with Fe(II), then benzylation of the nucleophile was observed (see Table 1).

$$\mathrm{(C_6H_5CH_2NC)_5FeCNBr + H\overset{\cdot\cdot}{\underset{\cdot\cdot}{X}}R \rightarrow C_6H_5CH_2XR}$$

$$\mathrm{HXR = HOCH_3,\ HOCH(CH_3)_2,\ HO_2CCH_3,\ HNH_2,\ HNH(CH_2)_2CH_3,\ HSCH_2CH_3}$$

When X was heated in methanol for 6 hr at 175°C under 700–850 atm of carbon monoxide pressure, methyl benzyl ether was isolated in 60 per cent conversion with the formation of a white methanol insoluble residue which gradually became blue:

$$\mathrm{(C_6H_5CH_2NC)_5FeCNBr + CH_3OH \xrightarrow{CO} C_6H_5CH_2OCH_3 + H_{(5-11)}Fe_2(CN)_6(CO)_2}$$

This new carboxyl cyanide complex (or complex mixture?) exhibited three strong bands in the triple bond region: 4·50 μ, 4·75 μ and 4·92 μ and was paramagnetic χ (specific) $= 34·1 \times 10^{-6}$ c.g.s. at 25°C. The complex was insoluble in the usual organic solvents (see Experimental) but dissolved in sodium hydroxide and concentrated sulphuric acid, in sulphuric acid, with the evolution of a gas. Back-titration of the alkaline solution of the complex with standard acid indicated the presence of 1·5 acidic hydrogens per mole.of complex. When heated with 2·0 N sodium hydroxide, the complex decomposed. Further work is therefore required to identify this composition definitely as a complex or as a complex mixture.

A similar displacement was observed for a tetracoordinated isonitrile complex, tetrabenzhydrylisocyanoiron(II) cyanide, which yielded benzhydryl methyl ether in 44 per cent conversion. Various highly coloured inorganic residues were obtained in these reactions which were not identified any further.

When X was reacted with potassium thiocyanate both benzyl thiocyanate and benzyl isothiocyanate were formed. Benzyl isothiocyanate was probably formed by thermal rearrangement of benzyl thiocyanate under the reaction conditions employed.[14]

Acknowledgement—The author wishes to thank Dr. G. R. Coraor for many helpful discussions and suggestions and Mr. R. S. Blake of the Central Research Department for the radioactive analysis.

---

[14] (a) H. Hennicke *Ann.* **344**, 24 (1906).
(b) P. A. S. Smith and D. W. Emerson *J. Amer. Chem. Soc.* **82**, 3076 (1960).
(c) C. N. R. Rao *Chem. and Industr.* p. 625 (1960).

J. Inorg. Nucl. Chem., 1962, Vol. 24, pp. 81 to 91. Pergamon Press Ltd. Printed in Northern Ireland

COMPLEX FORMATION BETWEEN GERMANIC ACID AND α-HYDROXY ACIDS—II

MANDELIC ACID*

E. R. Clark
Wolverhampton and Staffordshire College of Technology, Wolverhampton.
College of Advanced Technology, Gosta Green, Birmingham, 4

(*Received* 11 *July* 1961; *in revised form* 22 *August* 1961)

Abstract—The system germanic acid/mandelic acid has been investigated in aqueous solution between pH 2 and 7. Solubility, pH and conductivity studies have shown that germanic acid reacts with mandelic acid to form a 1:3 complex in solutions of acid pH value. Potentiometric titration of the complex acid indicated that it behaves as a dibasic acid. $pK_1 = 2{\cdot}53$ and $pK_2 = 3{\cdot}83$ in 0·1 M KCl using a ligand concentration of 0·02 M. Crystallization of a solid complex acid was found possible from solutions containing 0·1 M mandelic acid. The solid complex acid was found to contain 1 mole Ge to 2 moles mandelic acid together with 4 moles of water of crystallization.

It has long been known that many α-hydroxy acids form complex acids with many acids such as boric acid, arsenious acid, etc. A summary of the earlier work in this field has been given in Britton.(1) The lactic, glycollic, malic and citric acid complexes of niobium and tantalum have been described by Fairbrother and Taylor(2) whilst more recently the citric, tartaric, malic and mandelic complexes of molybdic acid and tungstic acid prepared by ion exchange have been investigated by Richardson.(3)

In comparison with other α-hydroxy acids, mandelic acid as a complexing agent has received much less attention although it has been noted that zirconium forms an insoluble mandelate(4,5,6) and so does hafnium.(7) The mandelate complex of indium has been described by Cozzi and Raspi.(8)

First mention of the mandelic acid complex of germanium was made by Vartapetian.(9) By using conductivity and pH measurements and a method of continuous variations, a complex acid containing 1 mole Ge/2 moles mandelic acid was identified in aqueous solution. Furthermore, a solid complex acid was described of the same molar ratio Ge/acid.

The present paper describes the Ge/mandelic acid system in more detail. The observations do not agree with those of Vartapetian.

EXPERIMENTAL

Materials

Spectrographically pure quartz-type GeO_2 was used for all experiments. The purity of the DL-mandelic acid as determined by titration was 100 per cent and that of the L-mandelic acid 99·2 per cent.

---

* Part of a Ph.D. thesis (London) 1960

(1) H. T. S. Britton, *Hydrogen Ions*, (4th Ed.) Vol. 2, p. 166–77. Chapman and Hall (1956).

(2) F. Fairbrother and J. Taylor, *J. Chem. Soc.* 4946–54 (1956).

(3) E. Richardson, *J. Inorg. Nucl. Chem.* **13**, 84–90 (1960).

(4) R. E. Oesper, *Analyt. Chem.* **21**, 1509 (1949).

(5) R. B. Hahn and E. S. Baginski, *Analyt. Chem. Acta.* **14**, 45–7 (1956).

(6) R. B. Hahn and L. Weber, *J. Amer. Chem. Soc.* **77**, 4777–9 (1955).

(7) R. B. Hahn and P. T. Joseph, *J. Amer. Chem. Soc.* **79**, 1298–9 (1957).

(8) D. Cozzi and G. Raspi, *Ricerca Sci.* **27**, 2392–8 (1927).

(9) O. Vartapetian, *C.R. Acad. Sci., Paris* **239**, 1139–41 (1954).

The mandelic acid and GeO_2 solutions were prepared using conductivity water which had been obtained by passing distilled water through a mixed bed deionisation column.

Methods

The methods used for the solubility, conductivity and pH studies were similar to those described in a previous paper.(10)

Solubility experiments. These were carried out by mixing 0·06 g samples of GeO_2 with 3 ml of an aqueous solution of DL-mandelic acid of various concentrations contained in 10 ml centrifuge tubes. The germanium which had passed into solution after one week was determined using the phenylfluorone method.(11)

Conductivity and pH *studies.* Mandelic acid, 0·04 M, was mixed in various molar proportions with an 0·04 M solution of GeO_2. The conductivities and pH values of these solutions were determined after 4 hr although experiments indicated that the solutions were stable up to at least three weeks.

A conductivity cell and standard Wheatstone bridge circuit as described by FINDLAY(12) was used, the balance point being detected by a cathode ray oscilloscope.(13) All measurements were made at 20 ± 0·1°C and are given in $\Omega^{-1}\,cm^{-1}$.

pH measurements on solutions of GeO_2 and mandelic acid were made on a Cambridge portable pH meter (range 0–14 pH) using a glass and calomel electrodes which were standardized with a British Drug Houses buffer of pH 4 or 6·5 at 21° or 25°C.

Potentiometric titration. Glass/silver–silver electrodes were used. These were standardized against a mixture of 0·01 N HCl and 0·09 N KCl (Veibels solution) which has a pH of 2·10 at 25°C.(14) The silver–silver chloride electrodes were prepared from a paste of pure silver oxide as described by NAIR.(15)

The cell used (Fig. 1), which was immersed in a thermostat kept at 25°C, has a capacity of about 70 ml and is provided with two inlets for nitrogen. The gas, which has previously been saturated with water and then passed through the presaturater (P) containing the same liquid as that being titrated, can, by opening or closing taps T_1 and T_2, either sweep over the surface of the liquid or be used to stir it. The glass electrode (G) and Ag/AgCl electrode (S) are mounted in two B14 sockets whilst a third B14 socket provides an inlet for the alkali solution and a fine capillary tube (C) provides an outlet for the nitrogen gas.

Fifty ml portions of mixtures of germanomandelic acid of ligand concentration 0·02 M and 0·1 M KCl contained in the cell were titrated with 0·315 N NaOH delivered from a semi-automatic grade A burette capable of reading to 0·02 ml. The pH was measured after each successive small addition of NaOH solution, the mixture being stirred by the nitrogen. It was found that equilibrium was attained within 1 min.

The titration was repeated on 50 ml samples of mixtures of 0·02 M mandelic acid and 0·1 M KCl.

Thermogravimetric analysis. Thermogravimetric analysis of the crystalline complex acid was made using a Stanton Thermobalance with a heating rate of 5° per min.

X-ray powder analysis. Powder photographs were made using cobalt K_α radiation (λ = 1·7889 Å) or copper K_α radiation (λ = 1·5405) and 11·46 cm diameter or 19·0 cm diameter cameras.

Chemical analysis of crystalline materials. The germanium content was determined by the phenylfluorone method(11) using a small sample weight or alternatively by ashing 100–200 mg of sample at 900°C.

The carbon and hydrogen analyses were determined by the usual combustion methods.

DISCUSSION AND RESULTS

(a) *Reactions in solution*

The solubility of quartz-type GeO_2 in solutions of mandelic acid is shown in Fig. 2. Over the sloping part of the curve excess solid GeO_2 is present whilst over the horizontal part there is an excess of soluble acid in the presence of germanium. Equilibrium occurs at a mole ratio Ge: mandelic acid of 1 : 3.

The results of conductivity and pH experiments on mixtures of 0·04 M DL-mandelic acid and 0·04 M GeO_2 (Figs. 3 and 4) by the method of continuous variations

---

(10) E. R. CLARK, *J. Inorg. Nucl. Chem.* (1961).

(11) H. J. CLULEY, *Analyst* **76**, 523–30 (1951).

(12) A. FINDLAY, *Practical Phys. Chem.* 161 (1945).

(13) R. N. HASZELDINE and A. A. WOOLF, *Chem. & Industr.* 544–5 (1950).

(14) R. G. BATES, *Electrometric* pH *determinations* p. 73–4. J. Wiley, New York (1954).

(15) V. S. K. NAIR, *Talanta.* **9**, 27 (1962).

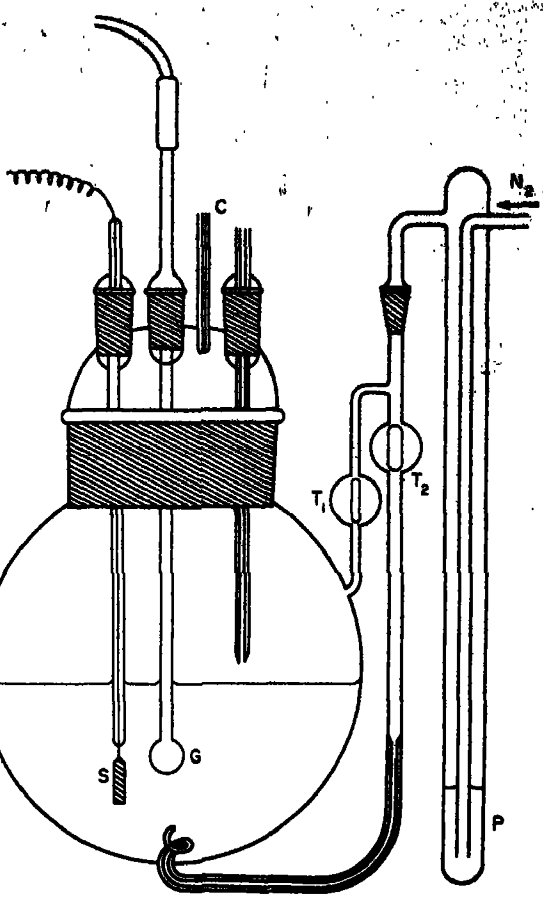

Fig. 1.—Cell used for potentiometric titration of the complex acid.

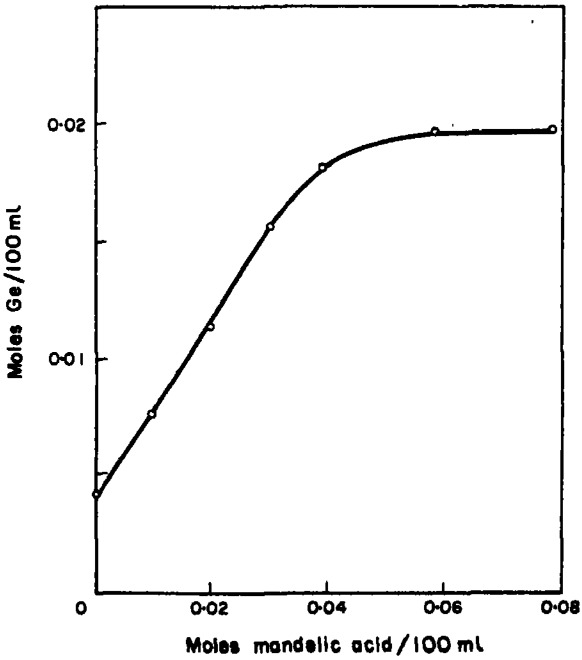

Fig. 2.—Solubility of quartz type germanium dioxide in solutions of mandelic acid of various concentrations at 20°C.

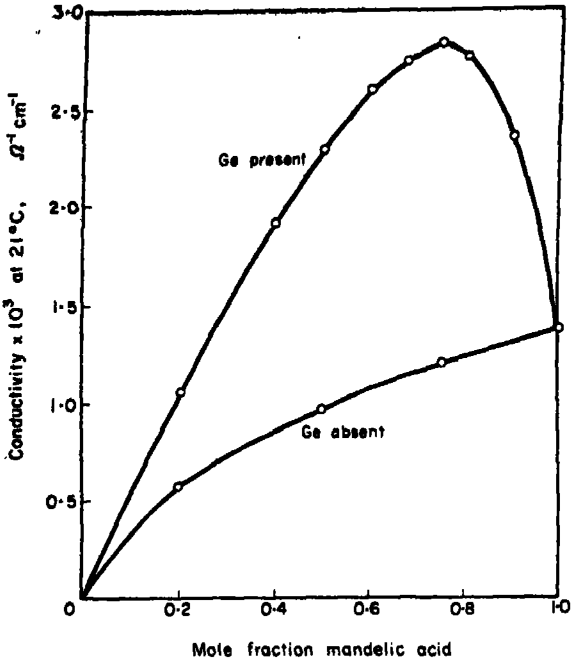

FIG. 3.—Conductivities of mixtures of 0·04 M GeO_2 and 0·04 M mandelic acid at 21°C.

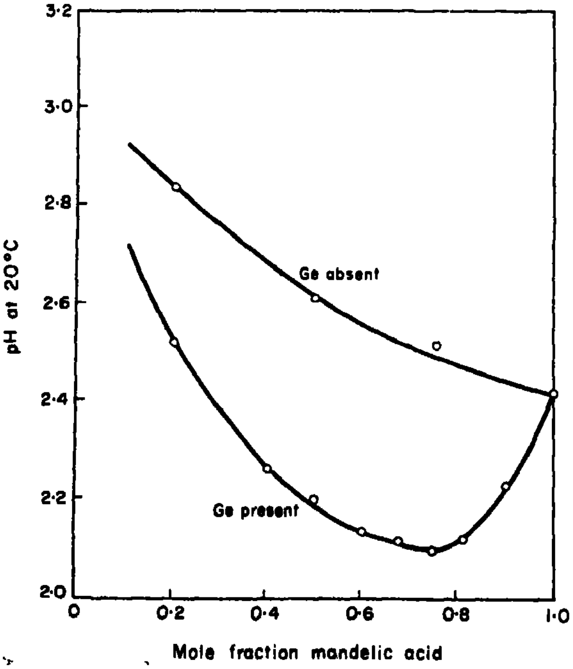

FIG. 4.—pH values of mixtures of 0·04 M GeO_2 and 0·04 M mandelic acid at 20°C.

show a well-defined maximum on the conductivity curve and a minimum on the pH curve at a molar fraction of mandelic acid of 0·75, indicating the existence of a 1:3 complex. These observations do not agree with those of VARTAPETIAN who showed by pH and conductivity measurements that a 1:2 complex existed. Similar results are obtained when germanic acid and L-mandelic acid are mixed. The 1:3 complex is also formed if the solutions of 0·04 M GeO_2 and 0·04 M DL-mandelic acid are heated on a water bath for four hours, and then cooled and made up to their original volume.

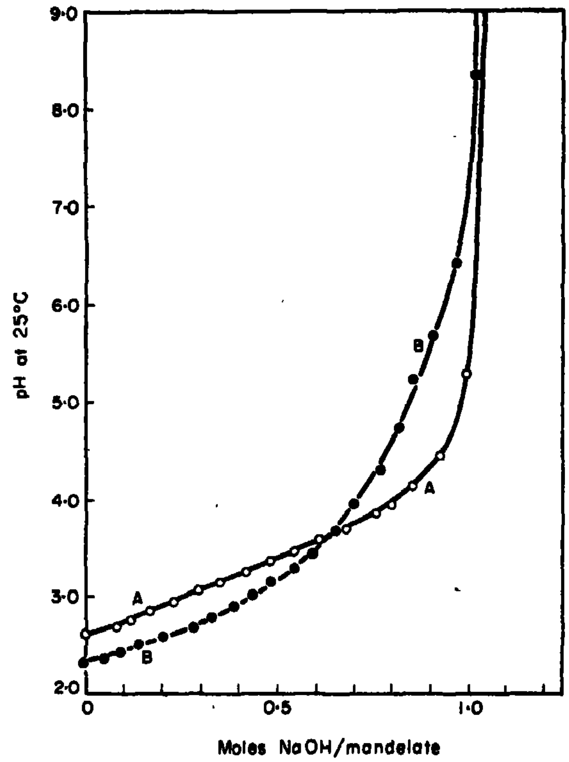

FIG. 5.—Potentiometric titration of 0·02 M mandelic acid in 0·1 M KCl (Curve *A–A*) and 0·02 M mandelic acid and 0·00666 M GeO_2 in 0·1 M KCl (Curve *B–B*) at 25°C.

The results of the potentiometric titration of the complex acid and mandelic acid are given in Fig. 5. Clearly, the primary dissociation constant K_1 of the complex acid is larger than that of the parent acid. It is significant that the two titration curves intersect at a mole ratio of NaOH/mandelate of 0·66/l., i.e. two thirds of the way towards complete neutralization. Analysis of the titration curve for the complex acid by using the procedure recommended by GAGE[16] indicates that the acid is behaving as a dibasic acid over the pH range 2·3–7·0. The dissociation constants for the complex acid can be calculated by rearranging the Henderson equation thus:

$$hx = Kc - Kx$$

where K = the classical dissociation constant

c = total concentration of acid

---

[16] J. C. GAGE, *Analyst* **82**, 219 (1957).

and
$$x = a + h - Kw/h$$

where a = concentration of added alkali

h = hydrogen ion concentration

Kw/h = hydroxyl ion concentration.

A plot of hx against x should be a straight line of slope K. Fig. 6 shows the results for mandelic acid alone when pK is found to be 3·30. Analysis of the results for the complex acid (Fig. 7) indicates that titration takes place in two stages, pK_1 and pK_2 being 2·53 and 3·83 respectively.

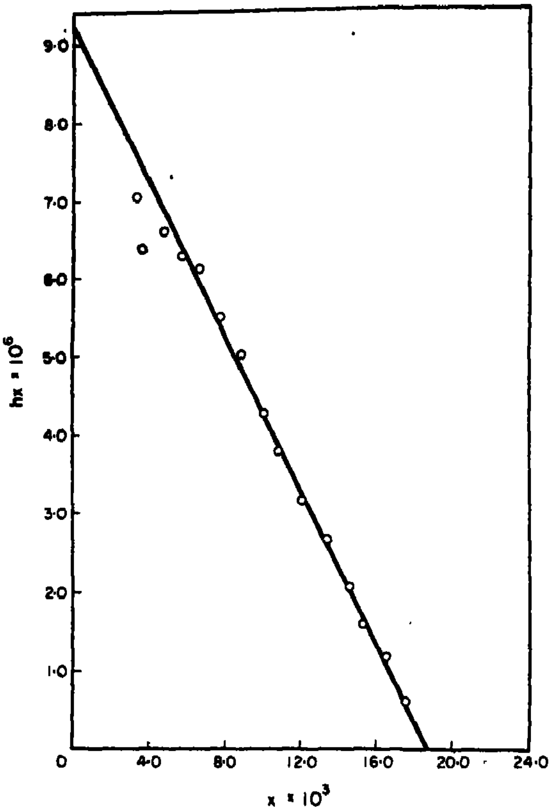

Fig. 6.—Plot of hx against x for mandelic acid.

A possible formula for the complex acid is therefore:—

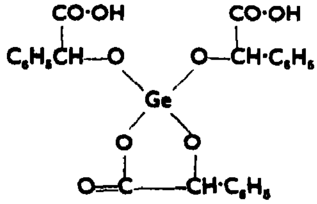

(b) *The crystalline complex of* GeO_2 *and mandelic acid*

The solubility experiments reported above have indicated that germanomandelic acid is very soluble in water. Crystallization of a solid complex can therefore only be produced from a concentrated solution of the acid. Two methods were used for the production of a crystalline complex of germanomandelic acid:

(1) slow evaporation of solutions of the complex acid on a water bath followed by cooling, and

(2) isothermal evaporation of solutions of the complex acid at room temperature in a desiccator using silica gel as absorbent.

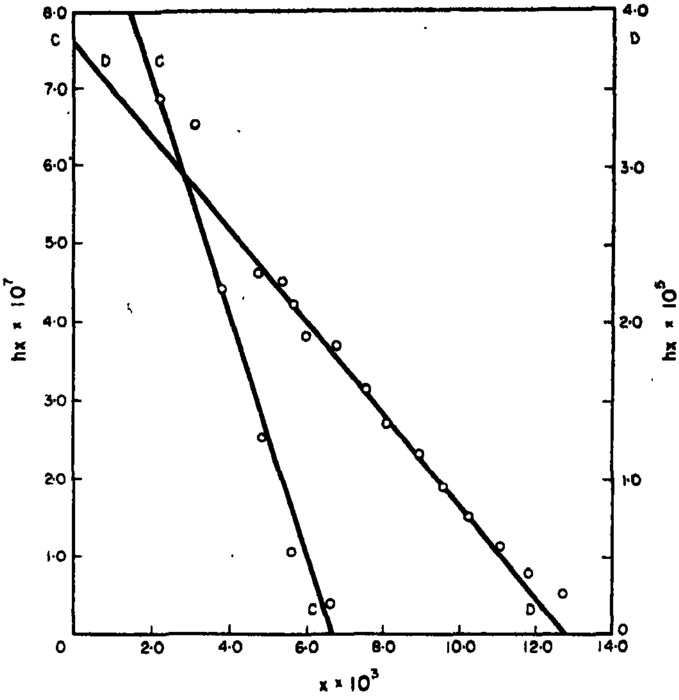

FIG. 7.—Plot of *hx* against *x* for germanomandelic acid. Line *D–D* first stage of titration $pK_1 = 2{\cdot}53$. Line *C–C* second stage of titration $pK_2 = 3{\cdot}83$.

In both methods a crystalline material was obtained when the mandelic acid concentration had reached ≏0·1 M. The white crystalline precipitate was filtered off, washed, recrystallized from water and dried at 60°C. The *d* spacings for this compound together with those of mandelic acid are given in Table 1. Chemical analysis of the substance gave C, 43·45 H, 4·65 Ge, 16·35%. Required for $C_{16}H_{20}O_{10}Ge$: C, 43·19 H, 4·53 Ge, 16·32%.

Thermogravimetric analysis of the material showed that a loss in weight occurred at two different temperatures. The results are shown in differential form in Fig. 8, i.e. a plot of weight loss (g)/per 100 g per °C against temperature. The loss in weight at 130–140°C and that around 200°C was subsequently shown to be due to a loss in water content, and not the evolution of carbon dioxide. At temperatures around 210–220°C the complex acid begins to decompose. Differential thermal analysis of the crystalline germanomandelic acid was carried out by Dr. WITTMAN of the Technische Hochschule, Vienna. The results (Fig. 9) show that there are two endothermic points corresponding to the evolution of water at the two different temperatures.

TABLE 1

d spacings for germanomandelic acid heated to			*d* spacings for mandelic acid
80°C	105°C	140°C	
s(*d*) 10·31	*s*(*d*) 10·19	*s*(*d*) 14·52	*m* 8·17
s(*d*) 8·02	*s*(*d*) 8·00	*f* 10·35	*m* 6·38
m 6·77	*m* 6·63	*m* 7·38	*s* 5·28
m 5·48	*m* 5·90	*s*(*d*) 5·89	*s* 4·84
s 5·15	*s* 5·17	*ms* 4·88	*m* 4·64
f 4·71	*f* 4·72	*ms* 4·59	*m* 4·43
m 4·37	*m* 4·37	*ms* 4·16	*m* 4·26
m 3·98	*m* 3·98	*ms* 3·76	*s* 4·08
m 3·70	*m* 3·72	*m* 3·45	*s* 4·02
m 3·47	*m* 3·45	*f* 3·13	*m* 3·89
m 3·12	*m* 3·10	*vf* 2·90	*f* 3·61
m 2·85	*m* 2·84	*vf* 2·75	*m* 3·50
m 2·76	*m* 2·62	*m* 2·57	*m* 3·39
m 2·61	*f* 2·25	*vf* 2·38	*s* 3·19
m 2·57		*m* 2·25	*f* 3·09
m 2·37		*vf* 2·16	*f* 3·00
f 2·25		*vf* 2·07	*m* 2·92
f 2·17		*vf* 1·97	*m* 2·70
m 2·05		*vf* 1·87	*vf* 2·61
			f 2·51
			m 2·41
			f 2·36
			m 2·31

Abbreviations used: *s*–strong, *ms*–medium to strong, *m*–medium, *f*–faint, *vf*–very faint, (*d*)–diffuse (broad line).

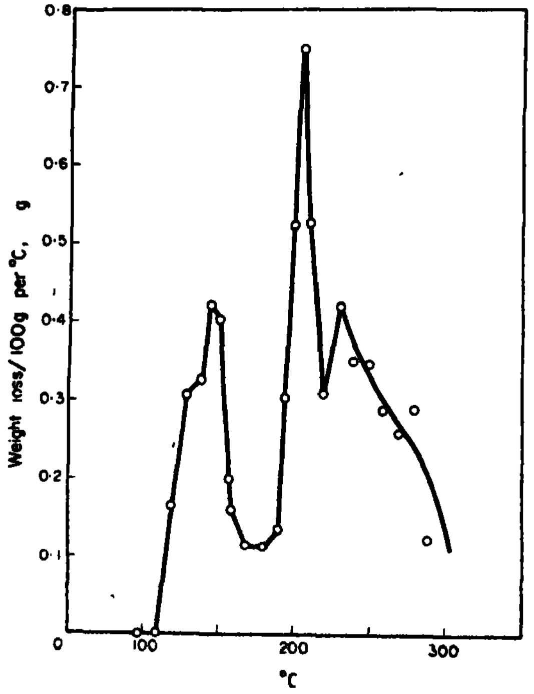

FIG. 8.—Thermogravimetric analysis of germanomandelic acid.

A sample of the crystalline germanomandelic acid was heated in nitrogen for half an hour at 140°C. Analysis of the material produced gave C, 47·00 H, 3·95 Ge, 17·75; required for $C_{16}H_{16}O_8Ge$: C, 46·56 H, 4·03 Ge, 17·50%. This compound differs from the first by $2H_2O$ and it therefore seems likely that this quantity of water per mol.

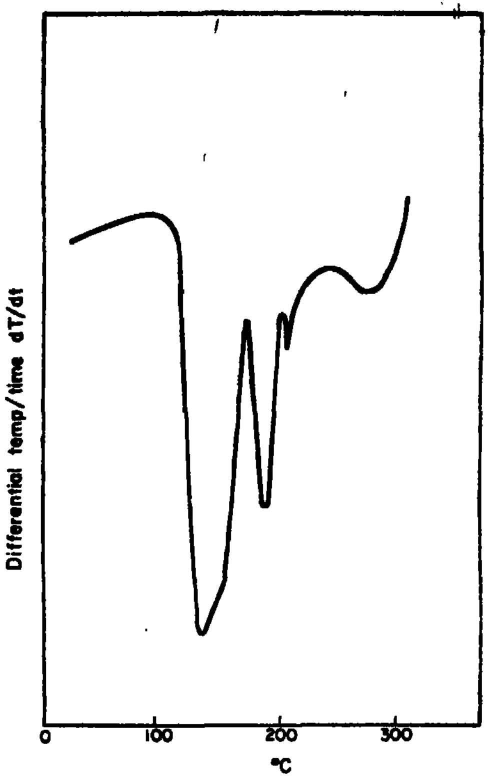

FIG. 9.—Differential thermal analysis of germanomandelic acid.

of Ge is released at the first endothermic point and a further two at the second endothermic point. The following two reactions therefore occur at 140°C and 200°C:

$$C_{16}H_{12}O_6Ge4H_2O \xrightarrow{140°\,C} C_{16}H_{12}O_6Ge2H_2O + 2H_2O$$

$$C_{16}H_{12}O_6Ge2H_2O \xrightarrow{200°\,C} C_{16}H_{12}O_6Ge + 2H_2O$$

Possible structural formulae for these acids are therefore:

(i) the first acid

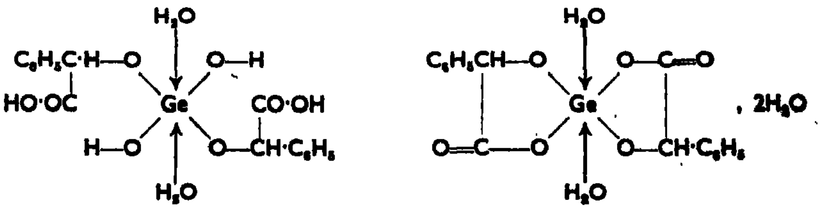

(ii) the acid produced by heating the first at 140°C

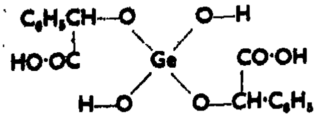

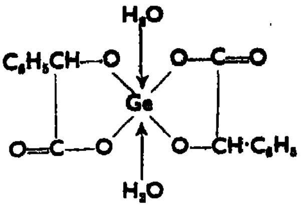

(iii) the compound produced at 200°C

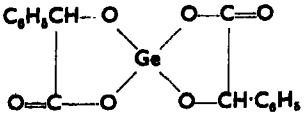

VARTAPETIAN[9] has also prepared a crystalline germanomandelic acid and gives a formula for it based solely on a germanium determination. No mention was made of any water of crystallization.

Since water is evolved at two different temperatures, it is probably that the two pairs of water molecules are linked in different ways, the first being only loosely bound, the second more firmly held. The indication is, therefore, that two molecules of water may be associated as water of crystallization or lattice water and two more may be co-ordinated to the central germanium atom or released by ring formation. The extent to which hydrogen bonding occurs cannot be deduced but it probably plays an important part in the structure of this acid.

It will be noted that although a 1:3 complex is identified in aqueous solution, it is a 1:2 complex acid which is isolated from solution. The following reaction occurs during crystallization:

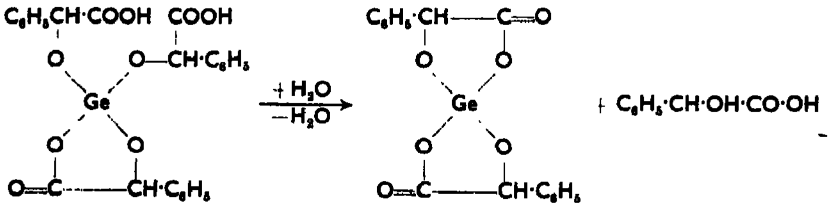

One molecule of mandelic acid is split off to give a more stable complex containing two five-membered rings.

Attempts to produce crystalline samples of other complex hydroxy acids of germanium have, with one exception, always given a crystalline complex acid containing the same number of moles Ge/acid as that found for the complex acid identified in solution. For example, the complex acids of germanium with both α-hydroxycaprylic acid and benzilic acid contain 1 mole Ge/2 moles acid both in solution and in the crystalline state.[17,18] More recently the complexes with α-hydroxy caproic acid $CH_3(CH_2)_3CH(OH)COOH$, α-hydroxy heptylic acid $CH_3(CH_2)_4CH(OH)COOH$, α-hydroxy decoic acid $CH_3(CH_2)_7CH(OH)COOH$ and α-hydroxy lauric acid

---

[17] E. R. CLARK, Thesis, London (1960).

[18] E. R CLARK, *Nature Lond.* 183, 536–7 (1959).

$CH_3(CH_2)_nCH(OH)COOH$ have been prepared.(19) In all cases the complex acid identified in solution was found to contain the same ratio of moles Ge/acid as that in the crystalline material, i.e. 1 mole Ge/2 moles acid.

Germanobromomandelic acid behaves in a similar way to germanomandelic acid. Both acids dissolve in excess of water to give a strongly acid solution. Presumably hydrolysis occurs with the formation of the 1:3 complex and the parent acid, e.g. for germanomandelic acid:

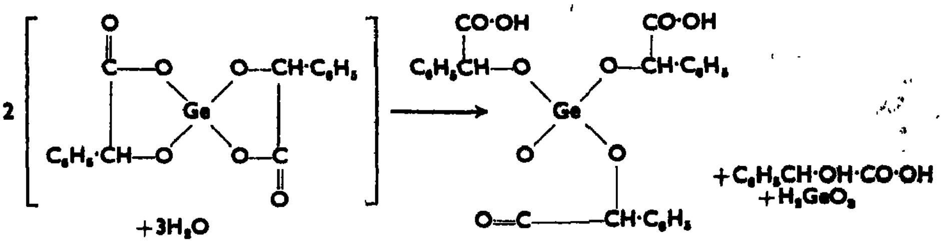

Germanomandelic acid and germanobromomandelic acid are probably hexa-co-ordinated complexes of germanium, the two molecules of water being co-ordinated to the germanium atom and the other two being held as lattice water. The infra-red spectra analysis of the mandelic acid complexes of germanium and some of the other complex acids are being carried out and will be reported later.

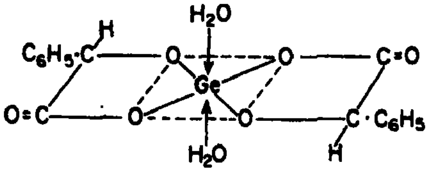

Acknowledgements—The author wishes to thank Mrs. S. Taylor for preparing the silver-silver chloride electrodes and the Veibels solution and Mr. S. Greenfield for carrying out the carbon and hydrogen analyses.

(19) J. W. Denman, Thesis, Birmingham College of Advanced Technology (1961).

J. Inorg. Nucl. Chem., 1962, Vol. 24, pp. 93 to 99. Pergamon Press Ltd. Printed in Northern Ireland

A STUDY OF TRANSFERENCE AND SOLVATION PHENOMENA—VI

HYDROCHLORIC ACID IN WATER AND WATER–ETHANOL SOLVENTS

J. O. Wear, J. T. Curtis, Jr. and E. S. Amis
Department of Chemistry, University of Arkansas, Fayetteville, Arkansas

(*Received* 14 *June* 1961; *in revised form* 16 *August* 1961)

Abstract—Transference and solvation phenomena for the ions of hydrochloric acid in water, 99·7 weight per cent ethanol, and water–ethanol solvents have been studied. The transference number of the cation as a function of acid concentration in water and in 99·7 weight per cent ethanol and as a function of solvent composition are presented graphically and discussed in relation to Grotthus and ordinary conduction of the hydrogen ion and in relation to relative solvation of hydrogen and chloride ions. The amount of solvent transferred from anode to cathode is also presented graphically and discussed in relation to the transference numbers of the ions.

Transport and solvation phenomena have been previously studied for the ions of silver perchlorate, uranyl chloride, and alkali chlorides in water, water–ethanol and ethanol.(1–5) In this contribution to the series of investigations the transport and solvation phenomena of the ions of hydrochloric acid in water, water–ethanol, and ethanol have been observed. some solvation of hydrochloric acid is often referred to and also since the study of solvation has not been done thoroughly over a wide range of concentration in water, it seemed that a study of transport and solvation phenomena would be worth while. Also the work normally referred to is that of Buchböck,(6) which was done in 1906. It was thought that a study of solvation with respect to concentration might give additional information on the solvation of the hydrogen ion.

A Hittorf transference measurement with the use of an inert reference substance was the method chosen for the determination of the transport and solvation data. This is the same method used in the previous studies.(1–5)

EXPERIMENTAL

The hydrochloric acid was prepared by bubbling hydrogen chloride gas through either water or ethanol. The hydrogen chloride gas was prepared in a generator from Fisher Certified Reagent sodium chloride and reagent sulfuric acid. The absolute ethanol used was 99·7 weight per cent ethanol. The inert reference substance, α-Methyl-D-glucoside, was prepared by Nutritional Biochemical Corporation. The silver wire and all other chemicals were of reagent quality.

The experimental procedure used was the same as used previously(3).

TREATMENT OF DATA

The symbols used in this paper are the same as were used in the lithium chloride study(3).

---

(1) W. V. Childs and E. S. Amis, *J. Inorg. Nucl. Chem.* **16**, 114 (1960).

(2) D. M. Mathews, J. O. Wear and E. S. Amis, *J. Inorg. Nucl. Chem.* **13**, 298 (1960).

(3) J. O. Wear, C. V. McNully and E. S. Amis, *J. Inorg. Nucl. Chem.* **18**, 48 (1961).

(4) J. O. Wear, C. V. McNully and E. S. Amis, *J. Inorg. Nucl. Chem.* **19**, 278 (1961).

(5) J. O. Wear, C. V. McNully and E. S. Amis, *J. Inorg. Nucl. Chem.* **20**, 100 (1961).

(6) G. Buchböck, *Z. Phys. Chem.* **55**, 563 (1960).

Using methods already described(1,2) the Hittorf transference number of the anion and cation, respectively and the grammes of solvent transferred per faraday of electricity were calculated using the following equations:

$$t_c = \left(\frac{p_s{}^m}{100 - p_s{}^m} - \frac{p_s{}^a}{100 - p_s{}^a}\right)\frac{W(100 - p_s{}^a)\,A_{Ag}}{100W_{Ag}M_s} \qquad (1)$$

$$t_a = 1 - t_c \qquad (2)$$

$$\Delta G^F_{sol} = \frac{\left[\alpha_a \dfrac{d_m}{d_a} - \alpha_m \dfrac{(1 - f_s{}^a)}{(1 - f_s{}^m)}\right] W}{F\alpha_m} \qquad (3)$$

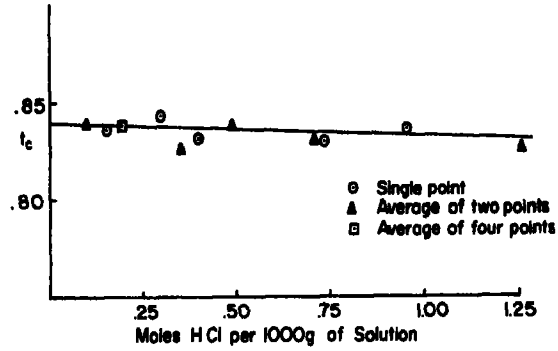

Fig. 1.—Cation transference number plotted against moles HCl per 1000 g of solution in aqueous solution at 25°C.

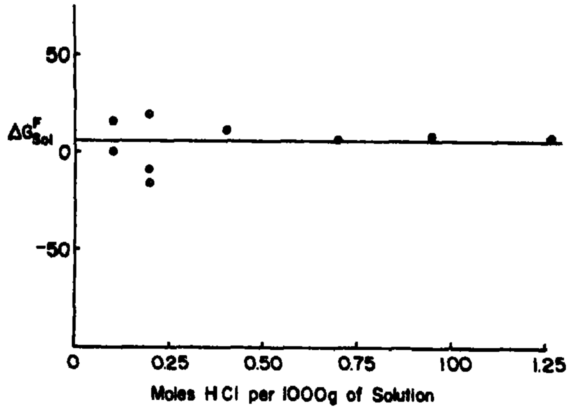

Fig. 2.—Grammes of water transported from anode to cathode per faraday of electricity plotted against moles HCl per 1000 g of solution in aqueous solution at 25°C.

In pure water, the moles of water transported per faraday could be calculated by dividing equation (3) by the molecular weight of water. In pure ethanol a similar calculation could be made. This could not be done in the case of mixed solvents since no molecular weight could be calculated for the solvent in the solvation sheath.

In Table 1 are the data for Figs. 1 and 2. Figs. 1 and 2, respectively, give the cation transference numbers and grammes of water transferred per faraday from the anode

TABLE 1.—HITTORF TRANSFERENCE NUMBERS AND GRAMMES OF SOLVENT TRANSPORTED FROM THE ANODE TO THE CATHODE FOR HCl SOLUTE IN WATER

Conc. HCl moles per 1000g of solution	0·1014	0·1014	0·1542	0·1983	0·1983	0·1988	0·1988
α_m	13·243	13·243	—	—	13·489	12·434	12·434
α_a	13·246	13·250	—	—	13·491	12·442	12·436
Ag_1	0·40203	0·42053	0·43093	0·40106	0·40522	0·42530	0·40557
Ag_2	0·40293	0·41947	0·43120	0·40006	0·40411	0·42557	0·40520
$F \times 10^3$	3·731	3·893	3·996	3·713	3·751	3·944	3·758
p_s^m	0·36960	0·36960	0·56214	0·72311	0·72311	0·72482	0·72482
p_s^a	0·31439	0·31337	0·50413	0·67024	0·66897	0.66758	0·66758
W	206·8915	211·7376	208·7526	209·3526	208·5993	210·1279	202·7667
t_c	0·835	0·842	0·836	0·824	0·831	0·842	0·853
t_a	0·165	0·158	0·164	0·176	0·169	0·158	0·147
d_m	1·00188	1·00188	—	—	1·00737	1·00685	1·00685
d_a	1·00157	1·00159	—	—	1·00730	1·00654	1·00658
$\Delta G_{H_2O}^F$	0·00	16·4	—	—	−16·5	19·7	—8·2
$\Delta N_{H_2O}^F$	0·00	0·91	—	—	−0·92	1·09	−0·45

Conc. HCl moles per 1000 g of solution	0·2975	0·3579	0·3579	0·4002	0·4981	0·4981
α_m	—	—	—	13·373	—	—
α_a	—	—	—	13·380	—	—
Ag_1	0·41228	0·30402	0·41330	0·43055	—	0·33384
Ag_2	0·41212	0·30373	0·41350	0·43109	0·31354	0·33507
$F \times 10^3$	3·821	2·817	3·832	3·993	2·906	3·100
P_s^m	1·08469	1·30487	1·30487	1·45914	1·81615	1·81615
P_a^s	1·02963	1·26491	1·24992	1·40040	1·77389	1·77316
W	210·9046	209·7328	210·4253	203·0965	210·8287	211·2487
t_c	0·843	0·827	0·824	0·831	0·856	0·819
t_a	0·157	0·173	0·176	0·169	0·144	0·181
d_m	—	—	—	1·01087	—	—
d_a	—	—	—	1·01057	—	—
$\Delta G_{H_2O}^F$	—	—	—	11·4	—	—
$\Delta N_{H_2O}^F$	—	—	—	0·63	—	—

Conc. HCl moles per 1000 g of solution	0·7067	0·7067	0·7355	0·9537	1·2617	1·2617
α_m	—	13·051	—	13·430	—	13·025
α_a	—	13·057	—	13·436	—	13·027
Ag_1	0·30059	0·32731	0·40148	0·41741	0·33270	0·33596
Ag_2	0·30085	0·32742	0·40165	0·41875	0·33219	0·33504
$F \times 10^3$	2·788	3·034	3·722	3·875	3·082	3·110
P_s^m	2·57666	2·57666	2·68174	3·47746	4·60009	4·60009
P_s^a	2·53470	2·53291	2·62986	3·42404	4·55914	4·55812
W	210·8741	211·0808	211·1581	213·4053	213·1040	215·8061
t_c	0·851	0·809	0·829	0·836	0·814	0·837
t_a	0·149	0·191	0·164	0·164	0·186	0·163
d_m	—	1·01625	—	1·02073	—	1·02597
d_a	—	1·01625	—	1·02048	—	1·02556
$\Delta G_{H_2O}^F$	—	5·3	—	7·5	—	5·3
$\Delta N_{H_2O}^F$	—	0·29	—	0·42	—	0·29

to the cathode plotted against concentration of hydrochloric acid in moles per 1000 g of solution. No significant dependence of the cation transference with HCl concentration is evident from data shown in Figs. 1 and 2. The lack of significant dependence of transference number on concentration agrees well with the existing literature.(7)

The data of Fig. 1 can be easily explained in view of the data of Fig. 2. The data of Fig. 2 shows no change in solvation with change in concentration, therefore, the ions keep the same relative size and mobility. The data of Fig. 2 at first does not appear to agree with the existing theory that solvation is higher at lower concentration,(8) but since most of the current is carried by hydrogen ions moving by Grotthus type conduction, a change in solvation might not be significant enough to show in the case of the predominance of this type of conduction. This is because very little solvent is actually moving since hydrogen ions transferred by Grotthus conduction convey no solvent.

TABLE 2.—HITTORF TRANSFERENCE NUMBERS AND GRAMMES OF SOLVENT TRANSPORTED FROM THE ANODE TO THE CATHODE FOR HCl SOLUTE

Weight per cent Ethanol	12·2	12·2	25·3	25·3	55·7	55·7	88·0	88·0
Conc. HCl moles per 1000 g of solution	0·1473	0·1473	0·1907	0·1907	0·1947	0·1947	0·2032	0·2032
α_m	12·453	—	12·921	12·921	6·534	0·534	4·802	4·802
α_a	12·469	—	12·924	12·923	6·541	6·541	4·815	4·816
Ag_1	0·40873	0·38800	0·31557	0·32947	0·32786	0·33980	0·31004	0·31001
Ag_2	0·41084	0·38852	0·31584	0·32650	0·32748	0·33859	0·31092	0·31141
$F \times 10^8$	3·799	3·599	2·926	3·040	3·037	3·144	2·878	2·880
P_s^m	0·53695	0·53695	0·69515	0·69515	0·70991	0·70991	0·74094	0·74094
P_s^a	0·47894	0·48277	0·64480	0·64173	0·66313	0·66135	0·69872	0·69719
W	202·0591	204·6821	198·6533	198·2695	186·4152	189·2168	170·0728	170·4381
t_c	0·851	0·850	0·944	0·962	0·793	0·807	0·690	0·715
t_a	0·149	0·150	0·056	0·038	0·207	0·193	0·310	0·285
d_m	1·01250	—	0·96020	0·96020	0·90688	0·90688	0·82603	0·82603
d_a	1·01277	—	0·95930	0·96003	0·90652	0·90661	0·82581	0·82590
ΔG^F_{sol}	25·6	—	47·3	−20·2	65·7	55·4	147·9	148·2

Another explanation of this independence of concentration might be that the hydrogen ion and chloride ion lose solvation at compensating rates with change in concentration. Therefore, the net relative size would be the same and hence the transference number as well as the net solvation change would remain the same.

In Table 2 are recorded the data plotted in Figs. 3 and 4. Figs. 3 and 4, respectively, give the cation transference number and the grammes of solvent transported from the anode to the cathode per faraday as a function of weight per cent ethanol at about 0·19 mole hydrochloric acid per 1000 g of solution.

In Fig. 3 the transference number of the cation at first increases to a maximum at about 25 weight per cent ethanol and then decreases regularly to 99·7 weight per cent ethanol. This increase can be explained as due to the increase in the viscosities of the water-ethanol solvent with increase in ethanol with the consequent influence on the transference number on the chloride ion while the Grotthus conduction of the hydrogen ion remains relatively unaffected. There is a maximum in the viscosity of water-ethanol mixtures between 40 and 50 weight per cent ethanol which would indicate the actual maximum in Fig. 3 should be in the same region. If Grotthus conduction is not affected very much out to 25 weight per cent ethanol, the chloride ion would be slowed down by this viscosity increase and make the mobility of the hydrogen ion relatively greater.

---

(7) (a) E. H. Riesenfeld and B. Reinhold, *Z. Phys. Chem.* **68**, 440 (1910).
(b) Z. Szabo, *Mag. chem. Föly.* **41**, 52.

(8) H. Ulich, *Z. Phys. Chem.* A **168**, 141 (1934).

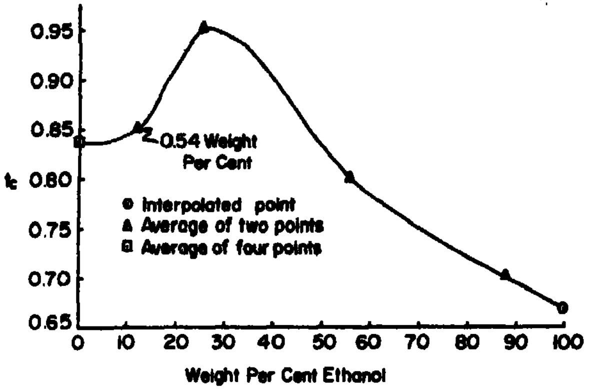

FIG. 3.—Cation transference number at 0·7 weight per cent HCl plotted against weight per cent ethanol in solvent at 25°C.

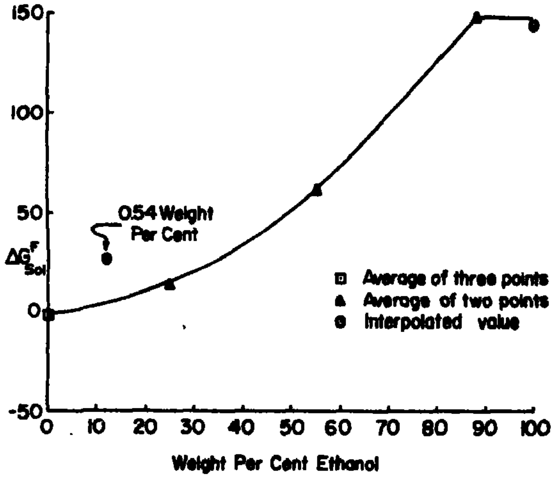

FIG. 4.—Calculated grams of solvent transferred from anode to cathode per faraday of electricity at 0·7 weight per cent HCl plotted against weight per cent ethanol in solution at 25°C.

Beyond 25 weight per cent ethanol, the decrease in Grotthus conduction and increase in solvation mass of the hydrogen ion (see Fig. 4) cause a decrease in the transference number of the hydrogen ion. Further decrease in the transference number of the hydrogen is brought about by a decrease in the viscosity of the mixture above 45 weight per cent ethanol. This decrease is continued on out to 99·7 weight per cent ethanol.

The data of Fig. 4 indicates an increase in the mass of solvent carried by the hydrogen ion up to 88 weight per cent ethanol. This is quite different from the sine-like curves previously obtained.(2–6) From water to 25 weight per cent ethanol the increase is rather small so that it can be explained as an exchange, in those hydrogen ions moving normally and not by Grotthus conduction, of water in the hydrogen ion solvation sheath for ethanol. Next a decrease would be expected due to a similar exchange on the chloride ion, but instead a more rapid increase was found. This as well as the continual increase up to 88 weight per cent ethanol is probably due mostly to a decrease in Grotthus type conduction. This would let more solvated hydrogen ions move through the solution and consequently convey more solvent from anode to cathode. Replacement of water by ethanol in the solvent sheath of the normally moving hydrogen ions could play some part.

TABLE 3.—HITTORF TRANSFERENCE NUMBERS AND GRAMMES OF SOLVENT TRANSPORTED FROM THE ANODE TO THE CATHODE FOR HCl SOLUTE IN 99·7 WEIGHT PER CENT ETHANOL

Conc. HCl moles per 1000 g of solution	0·1492	0·2919	0·2919	0·3206	0·4561	0·5033	0·6413
α_m	5·523	—	—	5·433	5·521	—	6·251
α_a	5·509	—	—	5·445	5·537	—	6·268
Ag_1	0·31280	0·32279	0·31516	0·40534	0·41249	0·39557	0·41034
Ag_2	0·31181	0·32514	0·31644	0·40534	0·41179	0·39492	0·41009
$F \times 10^3$	2·895	3·003	3·927	3·757	3·820	3·664	3·803
P_r^m	0·54384	1·06423	1·06423	1·16902	1·66294	1·83492	2·33818
P_s^a	0·50158	1·02048	1·02048	1·11458	1·60460	1·77899	2·27911
W	167·3488	164·6062	164·4874	166·6707	168·8217	166·6069	167·5381
t_c	0·674	0·665	0·681	0·670	0·719	0·710	0·730
t_a	0·326	0·335	0·329	0·330	0·281	0·290	0·270
d_m	0·79806	—	—	0·79952	0·80602	—	0·803502
d_a	0·79383	—	—	0·79835	0·80581	—	0·804267
ΔG_{EtOH}^F	144·1	—	—	138·9	112·0	—	63·4
ΔN_{EtOH}^F	3·1	—	—	3·0	2·4	—	1·4

The lack of any apparent change in solvation from 88 to 99·7 weight per cent ethanol is either because Grotthus conduction has completely disappeared and all water in the solvation sheaths have been replaced by ethanol (though the latter is unlikely) or the reference substance is being incorporated into the solvation sheath of the hydrogen ion. In the case of lithium chloride this last reason was assumed to be the case.(3)

The data for Figs. 5 and 6 are recorded in Table 3. Figs. 5 and 6, respectively, give the cation transference and grammes of ethanol transported from anode to cathode per faraday plotted against moles of hyrochloric acid per 1000 grammes of solution in 99·7 weight per cent ethanol. Together the data of Figs. 5 and 6 can be explained very well.

From 0·15 to 0·32 mole hyrochloric acid per 1000 grammes of solution there is no appreciable change in either transference number or solvation. This would be expected since a change in solvation would change the relative size of the solvated ions and therefore change the transference number. From 0·32 to 0·64 mole hydrochloric acid per 1000 g of solution a smooth increase in cation transference number is observed as well as a smooth decrease in grams of solvent transported from anode to cathode. This indicates a decrease in relative solvation of the hydrogen ion and therefore the hydrogen ion will be smaller relative to the chloride ion and therefore more mobile.

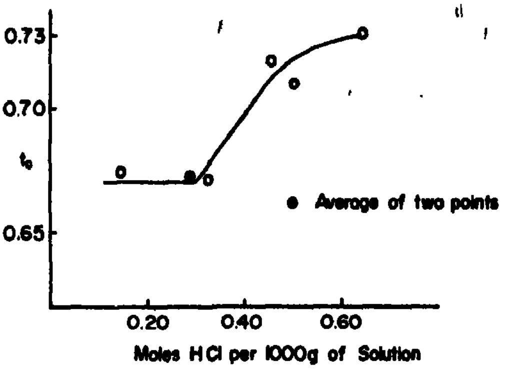

Fig. 5.—Cation transference number plotted against moles HCl per 1000 g of solution of 99·7 weight per cent ethanol solution at 25°C.

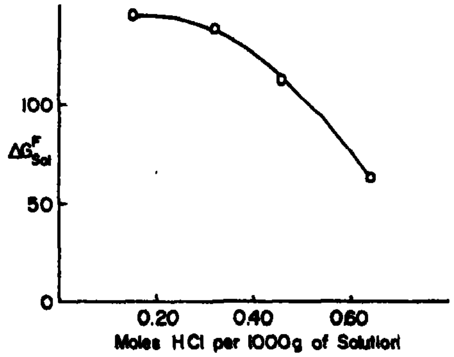

Fig. 6.—Grammes of ethanol transported from anode to cathode per faraday of electricity plotted against moles HCl per 1000 g of solution in 99·7 weight per cent ethanol solution at 25°C.

ACCURACY AND PRECISION

From comparing cation transference numbers at equal salt concentrations the average deviation is ±1·0 per cent which is well within the ±2·0 per cent accuracy of the method. Not enough values of grams of solvent transferred at equal salt concentrations exist to determine precision, but a value of ±25 per cent on accuracy is probably a good value.

Acknowledgements—The authors wish to thank the Atomic Energy Commission for Contract AT-(40-1)-2069 which supported this research financially. One of us (J. O. W.) wishes to thank the National Science Foundation for a Co-operative Fellowship.

J. Inorg. Nucl. Chem., 1962, Vol. 24, pp. 101 to 104. Pergamon Press Ltd. Printed in Northern Ireland

THE LITHIUM ALUMINIUM HYDRIDE–ETHYL ETHER SYSTEM AT 25°C*

S. C. Chattoraj, C. A. Hollingsworth, D. H. McDaniel and G. B. Smith
Department of Chemistry, University of Pittsburgh, Pittsburgh 13

(*Received* 19 *June* 1961; *in revised form* 4 *August* 1961)

Abstract—The vapour pressure–composition isotherm for the lithium aluminum hydride-ethyl ether system was determined at 25°C using vacuum line techniques. The vapour pressure of the solid–liquid region was determined as a function of the temperature, and these data give a value of 8170 cal/m for the heat of vaporization of ether from the two-phase system. The possibility of a liquid compound $LiAlH_4 \cdot n(C_2H_5)_2O$ is discussed. The solubility of lithium aluminum hydride in ethyl ether was found to be much greater than that reported in the literature.

INTRODUCTION

The usual solvents for lithium aluminium hydride are diethyl ether, tetra hydrofuran, pyridine, dioxane and dimethyl ether of ethylene glycol. The object of the present study was to measure the vapour-pressures of solutions of lithium aluminium hydride in diethyl ethyl to determine whether or not a complex, as a well defined species, is formed. Search of the literature revealed reports of the existence of etherates of closely analogous compounds, namely, those of $LiBH_4$,(1–3) $LiBH_4 \cdot 2(CH_3)_2O$, $LiBH_4 \cdot (CH_3)_2O$, $(LiBH_4)_2 \cdot (CH_3)_2O$, $LiBH_4 \cdot (C_2H_5)_2O$ and $(LiBH_4)_2 \cdot (C_2H_5)_2O$. Wiberg, *et al.*(4) reported the existence of mono and dietherates of lithium aluminium hydride: $LiAlH_4 \cdot 2(C_2H_5)_2O$ (in the temperature range −60°—25°C), $LiAlH_4 \cdot (C_2H_5)_2O$ (in the temperature range −15°C to a temperature somewhere below 40°C). However, it is not clear how Wiberg *et al.* established the molecular formula of these substances.

RESULTS AND DISCUSSION

Vapour-pressure–composition data at 24·95°C are given in Table 1. Composition is expressed in terms of the ratio of number of moles of ether in the solid or liquid phase to the number of moles of lithium aluminium hydride. These results check well with those of three other experiments at temperatures 25·00 ± 0·01°C, 24·95 ± 0·01°C and 24·71 ± 0·01°C. The vapour-pressure–composition isotherms are shown in Fig. 1.

The curve at 25°C may be interpreted as showing a saturation plateau of solid lithium aluminium hydride in contact with solution followed by the curve for the unsaturated solution. According to the results of four experiments, the plateau intersects the unsaturated solution curve at between 1·14 and 1·35 for the mole ratio. The solubility of lithium aluminium hydride calculated from this mole ratio is about

---

* This work was sponsored by the U.S. Army Research Office (Durham)

(1) H. I. Schlesinger, H. C. Brown, H. R. Hoekstra and L. R. Rapp, *J. Amer. Chem. Soc.* 75, 199 (1953).

(2) G. W. Schaeffer, T. L. Kolski and D. L. Ekstedt, *J. Amer. Chem. Soc.* 79, 5912 (1957).

(3) T. L. Kolski, H. B. Moore, L. E. Roth, K. J. Martin and G. W. Schaeffer, *J. Amer. Chem. Soc.* [illegible], 549 (1958).

(4) E. Wiberg, H. Noth and R. Uson, *Z. Naturforsch.* 11 b, 488 (1956).

41 g per 100 g of diethyl ether and is much greater than the value,(8) (25–30 g per 100 g of ether) reported in the literature.

Table 1.—Vapour-pressure isotherms for the lithium aluminium-diethyl ether system at 24·95 ± 0·01°C

Mole ratio*	Mole ratio†	Vapour-pressure (mm.)
3·19	3·25	495·7
1·89	1·92	372·6
1·65	1·68	299·3
1·49	1·51	239·7
1·38	1·40	199·9
1·12	1·14	139·9
0·89	0·90	140·0
0·55	0·56	140·0
0·20	0·20	139·9
0·003	0·003	29·7
0·00	0·00	0·0

* Calculated from weight of sample and total weight of ether removed from the sample flask.

† Calculated from aluminium analysis data.

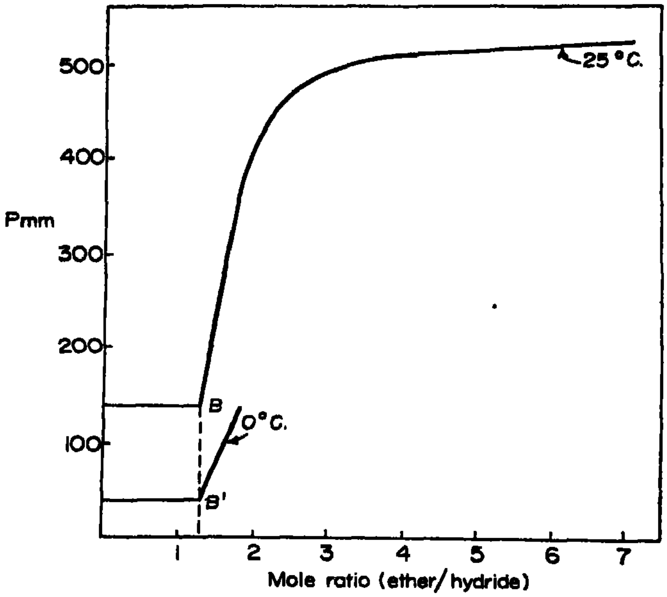

Fig. 1.—Vapour-pressure-composition isotherms for the lithium aluminium hydride–ethyl ether system.

An alternative interpretation of Fig. 1 is that the plateau represents lithium aluminium hydride and ether vapour in equilibrium with a liquid etherate of lithium aluminium hydride. The etherate would have to be completely miscible with ether to explain the curve.

Some difficulty has been experienced in trying to establish precisely the mole ratio of ether to lithium aluminium hydride at the point *B*. Whether the very small amount of precipitate or cloudiness present in the sample (and which could not be avoided as described in the experimental part) caused this variation is not known.

---

(8) N. G. Gaylord, *Reduction with Complex Metal Hydrides*, p. 11. Interscience, New York (1956).

If the value for the plateau point *B* were a small integer or the ratio of small whole numbers, this would support an interpretation of a simple stoichiometric complex. Our values for the mole ratio (1·35–1·14) at the point *B* are not greatly different from the result (a 1:1 complex) which WIBERG *et al.*⁽⁴⁾ reported.

At 0°C the pressure–composition isotherm in the vicinity of plateau point *B* shows a break at virtually the same value for the mole ratio as at 25°C. This offers some support for a complex, although it could be explained by a low value for the differential heat of solution of lithium aluminium hydride in the saturated solution.

TABLE 2.—PLATEAU VAPOUR PRESSURES AT VARIOUS TEMPERATURES

t(°C)	*P*(cm)	Direction of approach	*t*°C	*P*(cm)	Direction of approach
−23·6	0·952	Cooling	23·28	12·818	Cooling
−23·6	0·937	Warming	23·28	12·826	Warming
0·07	3·832	Cooling	29·88	17·297	Cooling
0·04	3·945	Warming	29·88	17·290	Warming
9·83	6·58	Cooling	42·74	29·83	Cooling
9·84	6·600	Warming	42·74	29·83	Warming

The vapour–pressure of the plateau was determined at several temperatures (Table 2). The plot of log *P* vs. $1/T$ is linear, and the slope gives $\Delta H_{\text{vap}} = 8{,}170$ cal/mole. Using 6,220 cal/mole for the heat of vapourization of pure ether, and assuming that the ether vapour is an ideal gas, one obtains the following approximate values for the thermodynamic quantities associated with the mixing of one mole of liquid ether with sufficient solid hydride to obtain the saturated solution (or liquid etherate): $\Delta H = -1{,}950$, $\Delta F \simeq -800$ and $\Delta S \simeq -3{\cdot}8$ e.u. This negative entropy change indicates a large amount of order in the solution. This is consistent with, but not proof of, the proposition that the liquid is a compound of well defined composition.

EXPERIMENTAL

Materials. Lithium aluminium hydride was obtained from Metal Hydrides, Inc. Mallinckrodt diethyl ether was dried over sodium wire.

Preparation of solution. Lithium aluminium hydride was pulverized in an atmosphere of dry nitrogen. A mixture of this lithium aluminium hydride and anhydrous diethyl ether was refluxed for 6–8 hr under dry nitrogen. The resulting solution was allowed to settle, filtered through a sintered glass filter stick under nitrogen pressure and then stored in a brown glass bottle fitted with a serum stopper and covered with wax. This served as the stock solution.

In spite of precautions taken to keep moisture and carbon dioxide from the solution, the formation of a very small amount of cloudiness (insoluble material) in the solution could not be avoided. One difficulty is the high viscosity of concentrated solutions of lithium aluminium hydride in diethyl ether. This causes filtering difficulties.

Introduction of the sample into the apparatus. A known volume, about 5 ml of the stock solution, was transferred in a dry-box by means of an hypodermic syringe into a serum capped, tared, small (110 ml) sample flask containing 10–15 ml of dry ether and a glass enclosed magnetic stirrer. The flask with the sample was weighed, the serum stopper was removed and the flask was quickly attached to the vacuum line apparatus, which had been previously flushed with dry nitrogen. The sample flask was then cooled in liquid nitrogen and the apparatus was degassed.

The general techniques are similar to these described in SANDERSON's monograph.⁽⁶⁾ The apparatus

---

⁽⁶⁾ R. T. SANDERSON, *Vacuum Manipulation of Volatile Compounds*, J. Wiley, New York (1948).

essentially consists of two volume-calibrated sections separated by a porous partition mercury valve. Each section was provided with a manometer.

Determination of isotherms. After the apparatus had been degassed the system was isolated from the rest of the line by closing the proper stock valves and raising the mercury level in the left manometer. The sample flask thermostated at temperatures close to 25°C and in one experiment close to 0°C. When equilibrium was attained the pressure reading on the manometer was measured by means of a cathetometer.

Ether was transferred, a little at a time, to a standard bulb by opening the porous partition mercury valve. When the pressure in the standard bulb was within 2/3 of the vapour-pressure of pure ether, the ether in the standard bulb was transferred to an upper bulb.

From the volume, pressure and temperature data the number of moles of ether removed from the reaction flask and the number of moles of ether present in the gas phase in the sample flask were calculated assuming ideal gas laws.

When all the ether had been removed the residue of lithium aluminium hydride was taken out and allowed to stand exposed to the atmosphere for a day, during which time it underwent slow hydrolysis. The residue was then dissolved in dilute hydrochloric acid and analysed for aluminium by the gravimetric oxide method(7) to determine the total amount of lithium aluminium hydride present in the sample. This analysis served as a check for the total amount of lithium aluminium hydride in the sample calculated from the weight of the sample and the total weight of ether removed from the reaction flask.

All the necessary data thus having been obtained the composition was computed in terms of mole ratio of ether present in liquid or solid phase to the total lithium aluminium hydride in the sample corresponding to each equilibrium vapour-pressure reading of the system in the reaction flask.

Plateau vapour-pressure at various temperatures. The plateau vapour-pressures were determined by approaching each temperature from above (cooling) and also from below (warming). The average of the two vapour-pressures was used for calculating ΔH_{vap}.

---

(7) A. Vogel, *Quantitative Inorganic Analysis*, p. 411. Longmans Green, New York (1951).

J. Inorg. Nucl. Chem., 1962, Vol. 24, pp. 105 to 111. Pergamon Press Ltd. Printed in Northern Ireland

SOLUBILITY OF MAGNESIUM OXIDE IN MOLTEN SALTS

R. L. Martin* and J. B. West†

(*Received* 2 *March* 1961; *in revised form* 24 *August* 1961)

Abstract—The solubility of magnesium oxide in a variety of molten salts was determined by a visual method. Only mixtures containing cryolite or sodium metaphosphate were found to dissolve greater than 0·2 per cent of magnesium oxide.

The direct electrolysis of magnesium oxide offers attractive commercial possibilities for the production of magnesium, due to the availability of the magnesium oxide as a cheap raw material and its relatively low decomposition potential (Table 1). However, a successful commercial process using MgO has not been developed, partially because a suitable solvent for MgO has not been found. A number of investigations of the solubility of magnesium oxide in various melts are reported in the literature. However, many of the published values are not in agreement. The purpose of this work was to determine approximately the solubility of magnesium oxide in a variety of molten salt solvents.

TABLE 1.—THEORETICAL DECOMPOSITION POTENTIALS OF MAGNESIUM OXIDE AND MAGNESIUM CHLORIDE

Reaction	Decomposition potential (V)	Reference
$MgCl_2(liq.) = Mg(liq.) + Cl_2$	2·50 @ 1000°K	(1)
$MgO = Mg + 1/2\,O_2$	2·45 @ 1000°K	(2)
$MgO + C = Mg(liq.) + CO$	1·52 @ 1000°K	(1)

APPARATUS AND METHOD

The Aluminum Laboratories Limited developed a method for determining the liquidus curves for the binary system cryolite–alumina⁽³⁾ which could be adapted to magnesium oxide–molten salt systems. The method consisted of directing a beam of light through a clear melt of known cryolite–alumina composition and, as the melt cooled, observing with a telescope the first appearance of crystals. This method, with modifications, was used for the magnesium oxide solubility determinations reported herein.

1. *Description of apparatus*

The molten solvent was contained in a 10 per cent rhodium–platinum crucible which fitted inside an electric crucible furnace. (See Fig. 1). Dimensions of the furnace chamber were 3 in. i.d. by 3½ in. deep. The furnace temperature was manually controlled to ±10°F by means of a rheostat. The crucible was supported in the furnace by a silica triangle formed by three ¼ in. o.d. by 2 in. silica rods. The platinum, 10 per cent rhodium–platinum thermocouple was in a ¼ in. protection tube, also of 10 per cent rhodium–platinum, because of its greater rigidity. A light beam from an arc lamp was directed into the molten solvent, and the melt was observed through a telescope with a magnification of 20 diameters.

---

* Research Department, Jersey Production Research Company, Tulsa, Oklahoma.

† School of Chemical Engineering, Oklahoma State University, Stillwater, Oklahoma.

⁽¹⁾ K. K. Kelley, U.S. Bureau of Mines Technical Paper 676 (1945).

⁽²⁾ G. Fuseya, and S. Kunazo, *J. Electrochem. Assoc.* (*Japan*) **2**, 76–81 (1934). Original not seen. Abstracted in *Chem. Abstr.* **28**, 3307 (1934).

⁽³⁾ N. W. F. Phillips, R. H. Singleton, and E. A. Hollingshead. *J. Electrochem. Soc.* **102**, 690–692 (1955).

The apparatus also included a variable speed stirring motor, a Model 141P 0–1000°C, Wheelco pyrometer with automatic cold junction compensator that was calibrated for use with the above thermocouple, and a steel reflector for directing the light beam from the arc lamp into the furnace.

2. *Method*

A 100 g sample of solvent was prepared and heated in the platinum crucible to a temperature at which a clear melt was obtained. Then the liquidus temperature of the solvent was determined by slowly cooling the melt at a rate of approximately 1°F per min while observing through the telescope the appearance of crystals. The temperature at which the first crystals began to form was recorded as the liquidus temperature of the solvent. Supersaturation was minimized by seeding the cooling melt with a few particles of magnesium oxide. The melt was stirred gently and continuously during the liquidus determination.

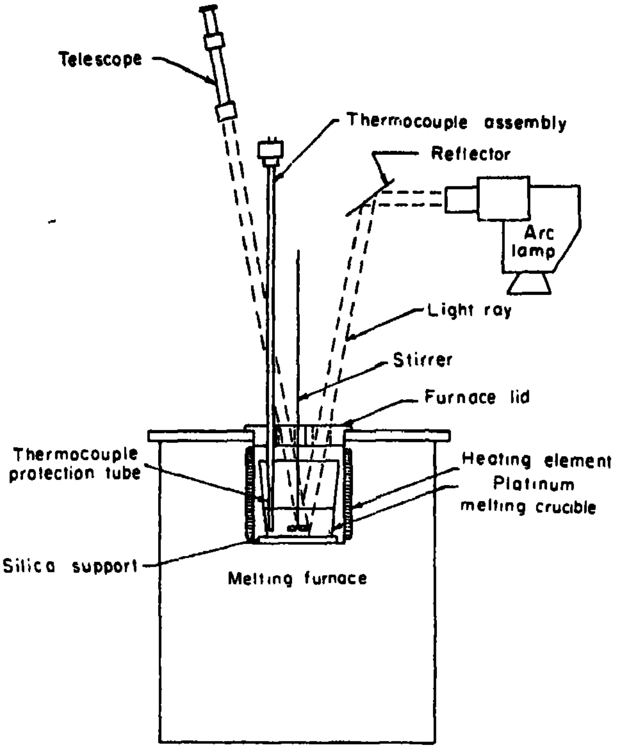

Fig. 1.—Solubility apparatus.

A small amount of magnesium oxide from a weighed portion was added to the solvent. The temperature of the melt was increased until the melt was again clear. Then the melt was slowly cooled and the liquidus temperature of the system was determined in the same manner as the liquidus temperature of the solvent was determined. Again supersaturation was minimized by seeding with a few particles of magnesium oxide. A negligible amount of magnesium oxide was added during seeding. The liquidus temperature and the magnesium oxide content of the system was recorded. Additional magnesium oxide was added and again the liquidus temperature determined. Thus by repeating this procedure for each magnesium oxide addition a temperature–magnesium oxide solubility relationship was obtained for the desired temperature range. This range included the approximate temperatures from the liquidus temperature of the solvent to the temperature at which fuming occurred. All liquidus temperatures were established by duplicate determinations.

The thermocouple was initially calibrated and regularly checked at the freezing point of reagent-grade sodium chloride which was taken to be 801°C. The thermocouple calibration was also checked at the melting point of potassium chloride (776°C) and lithium chloride (613°C.)

The accuracy of the solubility method and technique was checked by determining the solubility of aluminium oxide in cryolite. This system was chosen because the solubility of aluminium oxide in cryolite has been recently determined as 10 wt per cent at 963°C.[3] Using this method and technique, agreement with the published value was obtained. Reproducibility of the liquidus temperature was within ±5°C.

With the exception of the cryolite, the solvent constituents and magnesium oxide used in the solubility determinations were anhydrous reagent-grade chemicals. The cryolite was taken from selected natural lump and had the following analysis as determined by Aluminum Laboratories Limited.[4]

Loss of ignition at 700°C.	0·13%
Fe	0·006%
Si	0·007%
Ca	0·01%
Mg	Not detected
Pb	0·01%
K	0·030%
Li	0·007%
Freezing point	1009°C ± 1°C.

RESULTS

The results of this study are summarized in Tables 2 through 6. In these tables the solubility of magnesium oxide is often recorded as a maximum value. As an example, the solubility of magnesium oxide in the first listed solvent is recorded as "<0·05", that is, the solubility lies between 0 and 0·05 wt per cent. More accurate determinations were not necessary for the purposes of this study because these solubilities were negligible. Any solvent dissolving less than 0·5 per cent magnesium oxide probably would not make a suitable electrolytic cell bath.

It was found that magnesium oxide is appreciably soluble in molten mixtures of cryolite and sodium chloride. As a means of finding the optimum cryolite content, the solubilities of magnesium oxide in binary mixtures of cryolite and sodium chloride were determined as functions of composition and temperature. The solubilities are tabulated in Table 6.

TABLE 2.—SOLUBILITY OF MAGNESIUM OXIDE IN PURE HALIDES

Composition of solvent	Wt (%)	Liquidus temp. of MgO free solvent (°C)	MgO solubility wt (%)	Temp. at which MgO solubility was determined (°C)
KF	100·0	880	<0·04	890
LiCl	100·0	615	<0·05	688
NaCl	100·0	801	<0·05	900
KCl	100·0	774	<0·05	900
$MgCl_2$	100·0	Hydrolysed with moisture in the atmosphere and resulting MgO was not miscible		
$CaCl_2$	100·0	772	0·05	870
$SrCl_2$	100·0	870	<0·05	900
KBr	100·0	730	<0·05	890
NaBr	100·0	745	0·04	780

The workers of the United States Bureau of Mines have conducted extensive research into the solubilities of MgO in molten alkali and alkaline earth fluoride and chloride systems. The only systems in which appreciable solubilities were found were those of magnesium oxide in magnesium chloride containing boric oxide. Later work has indicated that these were not true solubilities but suspensions due to the dispersing action of the boric oxide.

---

(4) N. W. F. PHILLIPS, Arvida, Quebec, Canada. Private communication (1956).

TABLE 3.—SOLUBILITY OF MAGNESIUM OXIDE IN BINARY MIXTURES OF PURE HALIDES

Composition of solvent	Wt (%)	Liquidus temp. of MgO free solvent (°C)	MgO solubility wt (%)	Temp. at which MgO solubility was determined (°C)
KF	60·0	768	0·1–0·2	870
NaF	40·0			
KF	67·4	740	<0·1	870
NaF	32·6			
KF	74·1	740	0·1	870
NaF	25·9			
NaF	52·3	830	0·05	935
CaF_2	47·7			
NaF	69·6	960	<0·05	975
MgF_2	30·4			
LiCl	66·5	563	<0·05	718
NaCl	33·5			
KCl	56·0	372	<0·05	678
LiCl	44·0			
MgF_2	53·0	Solvent not completely miscible at 970°C		
LiF	47·0			
$CaCl_2$	79·7	603	0·10	853
LiCl	20·3			
$CaCl_2$	60·0	499	<0·10	850
LiCl	40·0			
$CaCl_2$	59·8	845	<0·05	870
KCl	40·2			

TABLE 4.—SOLUBILITY OF MAGNESIUM OXIDE IN TERNARY AND QUATERNARY MIXTURES OF PURE HALIDES

Composition of solvent	Wt (%)	Liquidus temp of MgO free solvent (°C)	MgO solubility wt (%)	Temp. at which MgO solubility was determined °C
BaF_2	50·0	750	0·05	940
NaF	32·0			
MgF_2	18·0			
BaF_2	60·0	Solvent not completely miscible at 970°C		
CaF_2	16·4			
MgF_2	16·0			
NaF	7·6			
$CaCl_2$	59·9	499	0·20	850
LiCl	39·9			
NH_4BF_4	0·2*			
$CaCl_2$	59·95	499	0·10	850
LiCl	39·95			
NH_4BF_4	0·10*			
NaCl	48·3	670	0·05	890
$CaCl_2$	48·3			
NH_4F	3·4†			
Cryolite	60·0	882	3·16	920
NaF	40·0		4·20	962

* Fuming was noted, probably due to the decomposition of NH_4BF_4

† Loss of some NH_4F as the mixture was melted

TABLE 5.—SOLUBILITY OF MAGNESIUM OXIDE IN BINARY AND TERNARY MIXTURES OF HALIDES WITH OTHER SUBSTANCES

Composition of solvent	Wt/%	Liquidus temp. of MgO free solvent (°C)	MgO solubility wt (%)	Temp. at which MgO solubility was determined (°C)
CaCl$_2$	99·0	772	0·18	870
B$_2$O$_3$	1·0			
CaCl$_2$	59·7	845	0·05	870
KCl	40·1			
B$_2$O$_3$	0·2			
CaCl$_2$	59·6	845	0·05	870
KCl	40·1		0·10	920
B$_2$O$_3$	0·2			
NH$_4$BF$_4$	0·1*			
MgF$_2$	70·2	655	2·0	708
NaPO$_3$	29·8		3·9	795
KF	99·9	880	0·04	890
KBF$_4$	0·1			

* Fuming was noted, probably here to the decomposition of NH$_4$BF$_4$

TABLE 6.—SOLUBILITY OF MAGNESIUM OXIDE IN MIXTURES OF CRYOLITE AND SODIUM CHLORIDE

Cryolite wt (%)	NaCl wt (%)	MgO added to mixture wt (%)	Liquidus temp. of mixture (°C)
80·0	20·0	0	920
		2·94	920
		3·40	910
		3·85	910
		4·30	925
		4·77	935
		5·20	960
70·0	30·0	0	880
		2·37	838
		2·94	830
		4·00	920
68·5	31·5	0	740
		0·52	790
		1·05	835
60·0	40·0	0	848
		2·56	820
		3·15	880
50·0	50·0	0	802
		0·94	795
		1·25	790
		1·95	810
		2·55	870

The high solubilities reported by BECK,(5) GRUBE,(6) and BAUXITBANYA(7) were not found in this study. BECK reported the solubility of magnesium oxide in a melt of 60 per cent potassium fluoride and 40 per cent sodium fluoride to be 11·4 per cent at 677°C. The Bureau of Mines researchers attempted to reproduce BECK'S work and found a solubility of only 0·5 per cent at 870°C. The solubility was found to be 0·1–0·2 per cent during this study.

BECK determined the solubility of magnesium oxide in the fluoride melt by use of blind cell liquidus determinations.(5) The blind cell liquidus determinations rely upon the precipitation of relatively large amounts of magnesium oxide at the liquidus temperature. The latent heat of this precipitation causes a point of inflexion on the time-cooling temperature curve which is taken as the liquidus temperature. In many systems the precipitation is slight at the liquidus temperature and heavy precipitation does not occur until the temperature has dropped considerably below the visually observed liquidus temperature. This could account for the unusually large value of 11·4 per cent at 677°C reported by BECK.

The solubility of 0·1–0·2 per cent magnesium oxide in the potassium fluoride–sodium fluoride-melt at 870°C is of the same order of magnitude as the value of 0·5 per cent at 870°C reported by the Bureau of Mines. The Bureau of Mines' value might have included some magnesium oxide in suspension which could account for the difference between the two values. Solubility values for magnesium oxide in other solvents investigated are in similar agreement with the Bureau of Mines' work.

GRUBE reported the solubility of magnesium oxide in a melt of 50 per cent barium fluoride, 32 per cent sodium fluoride, and 18 per cent magnesium fluoride to be 1 per cent at approximately 750°C. From this study, a solubility of less than 0·05 per cent is indicated. BAUXITBANYA reported the solubility of magnesium oxide in a melt of 48·3 per cent sodium chloride, 48·3 per cent calcium chloride and 3·4 per cent ammonium fluoride to be 10 per cent. A maximum solubility of 0·05 per cent at 890°C was found using the visual solubility method.

ILINSKII and ANTIPINE(8) reported the solubility of magnesium oxide exceeded 10 per cent in a eutectic of 53 per cent magnesium fluoride and 47 per cent lithium fluoride. The Bureau of Mines workers reported a solubility of only 0·4 per cent(8) when they attempted to reproduce this work. The magnesium fluoride–lithium fluoride eutectic was not completely miscible of 970°C, the maximum temperature obtainable with the furnace used in this work.

It was assumed in the solubility determinations that magnesium oxide precipitated at the liquidus temperature. In the event that some of the solvent constituents precipitated at the liquidus temperature, the reported magnesium oxide solubilities would be less than the actual values.

A possible source of error in the results would be compositional changes due to evaporation of the melt during the time period required to melt the solvent and to determine the magnesium oxide solubility. To minimize such error, the temperature of the system was held below the temperature at which fuming could be detected. Also, there could have been minor compositional changes in some of the melts due to reaction between constituents of the melt and the platinum crucible and/or the constituents of the atmosphere.

---

(5) E. BECK, *Metallurgie*, 5, 504 (1908).

(6) G. GRUBE, *Z. Elecktrochem, Agnew, Physik. Chem.* 33, 481–487 (1927). Abstracted in *Chem. Abstr.* 22, 732 (1928).

(7) M. BAUXITBANYA, Hungarian Patent 135 408 (1949). Translated by R. M. HELMANN, The John Crerar Library, Chicago (Aug. 30, 1956).

(8) Unpublished U.S. Bureau of Mines War Minerals Report (1943).

(9) K. K. KELLEY, K. P. MISHCHENKO and A. I. FENLINOV, *J. Applied Chem.* (*U.S.S.R.*), 19, 363–370 (1946). Abstracted in *Chem. Abstr.* 41, 1140d.

(10) Unpublished U.S. Bureau of Mines War Minerals Report (1943).

Of the solvents investigated only those containing cryolite or sodium metaphosphate ($NaPO_3$) dissolved appreciable quantities of magnesium oxide. The others show little or no promise as solvents. A 60 per cent cryolite–40 per cent sodium chloride melt dissolved 3·15 per cent magnesium oxide at 880°C. The 60 per cent cryolite–40 per cent sodium fluoride melt dissolved 4·2 per cent magnesium oxide at 962°C. A sodium metaphosphate–magnesium fluoride melt dissolved 4·8 per cent magnesium oxide at 880°F. The maximum solubility in any of the remaining solvents was found to be 0·2 per cent.

Acknowledgements—The authors would like to acknowledge the generous support of Mr. R. M. WHEELER of the Standard Magnesium Corporation whose encouragement and financial support made this work possible. The co-operation of the U.S. Bureau of Mines, in providing access to much unpublished data, is sincerely appreciated.

J. Inorg. Nucl. Chem., 1962, Vol. 24, pp. 113 to 116. Pergamon Press Ltd. Printed in Northern Ireland

YIELD RATIOS FOR THE ISOMERIC PAIR ^{121m}Te, ^{121}Te PRODUCED IN ^{121}Sb(d,2n)^{121}Te NUCLEAR REACTION

S. J. **Nassiff**, S. **Abecasis** and A. **Mocoroa**
Comisión Nacional de Energía Atómica, Buenos Aires
and
Dto. de Física de la Universidad Nacional de la Plata, La Plata

(*Received* 6 *July* 1961)

Abstract—The cross-section ratio for the isomeric pair ^{121m}Te, ^{121}Te produced in the ^{121}Sb(d,2n) ^{121}Te nuclear reaction has been determined experimentally for deuterons from 9 up to 28 MeV.

Nuclear reactions are usually considered as proceeding by intermediate formation of a compound nucleus at low energies, <30 Mev.

If energetically possible the nucleus emits one or more particles and generally the residual nucleus remains in an excited state from which it reaches the ground or isomeric state through a gamma cascade.

At low energies of the nuclear projectile the spins of the target nucleus and of the isomers are the most important factors for determining the population ratio of the isomeric states. The isomer whose spin is closest to the spin of the compound nucleus will be favoured. At higher energies, where the compound nucleus is produced with a wider spin range, this effect is not so remarkable.(2–6)

The statistic theory suggests that the above mentioned ratio should approach the statistical weights ratio of the isomeric states.(7,8)

In this work, the ratio of the yields of the isomeric pair Te^{121m}, ^{121}Te, formed in the ^{121}Sb(d,2n) ^{121}Te nuclear reaction is studied as a function of the energy of the bombarding particle.

EXPERIMENTAL

a. *Bombarding procedure*

Samples of antimony oxide were irradiated in the internal beam of the 180 cm synchrocyclotron of the C.N.E.A. (Buenos Aires) with deuterons from 9 up to 28 MeV energy.

The experiment was performed using the stacked foil technique. The Sb_2O_3 was slurried on silver foils of approximately 30 mg/cm^2 which were then folded over and stacked together. The deuteron energy on each sample of the stack was calculated from Rich and Madey range–energy curves.(9)

The exposure was performed at the orbit corresponding to 28·1 MeV. The maximum spread of the beam was estimated to be $\pm 1{\cdot}2$ MeV, for 28·1 MeV energy. The modification of the curvature across the target was not enough to change the thickness of the absorber traversed by the particles.

Owing to the flux variations throughout the different thickness of the target the excitation function of each single isomer was not determined.

(1) J. M. Blatt and V. F. Weisskopf, *Theoretical Physics*. J. Wiley, New York (1952).
(2) B. Linder and R. James, *Phys. Rev.* **114**, 322 (1959).
(3) R. M. Diamond, J. W. Meadows and R. A. Sharp, *Phys. Rev.* **102**, 190 (1956).
(4) J. R. Huizenga and R. Vanderbosch, *Phys. Rev.* **120**, 1305 (1960).
(5) A. C. Pappas and R. A. Sharp, *J. Inorg. Nucl. Chem.* **10**, 173 (1959).
(6) S. M. Bailey: A.E.C.U. U.S. Report UCRL 8710 (1959).
(7) E. Segrè and A. C. Helmholtz: *Revs. Mod. Phys.* **21**, 271 (1949).
(8) H. B. Levy. Ph. D. Thesis, Report UCRL 2305 (1953).
(9) M. Rich and R. Madey, Report UCRL 2301 (1954).

The stable isotopes for antimony are: ^{121}Sb (57·25 per cent) and ^{123}Sb (42·75 per cent). On account of the different cross-sections for the (d,4n) and (d,2n) reactions the ^{121}Te activity from ^{123}Sb(d,4n) ^{121}Te reaction is negligible in regard to the ^{121}Sb(d,2n) ^{121}Te reaction activity.

b. *Chemical separation*

The irradiated antimony tri-oxide was dissolved in 6N HCl and tellurium carrier was added. After the reduction with HBr, metallic tellurium was precipitated with hydrazinehydrochloride.

The precipitate was dissolved and reprecipitated several times always using antimony as hold-back-carrier.

c. *Counting procedure*

The decay scheme$^{(10)}$ of ^{121}Te is sketched in Fig. 1.

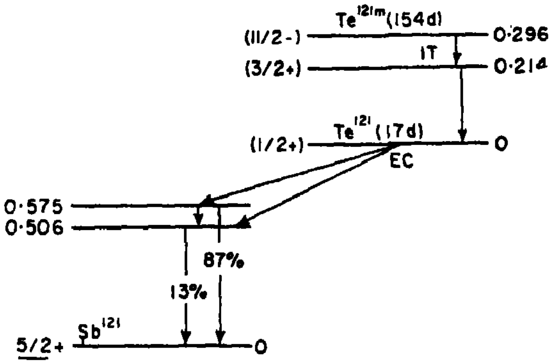

Fig. 1.—Disintegration scheme of $^{121m/121}$Te

By measurement of the 0·214 and 0·575 MeV γ-rays, the populations of the 154 and 17 days half-lives levels respectively can be determined.

The γ-spectra were obtained with a 2 in. × 2 in. NaI (Tl) scintillation counter coupled to a one channel pulse height analyser.

Fig. 2 shows as example the gamma spectrum of $^{121m/121}$Te corresponding to a 18·7 ± 0·3 MeV deuteron energy measured 72 days after irradiation. Peaks corresponding to 0·575, 0·506, 0·214 and 0·159 MeV energies are observable. The two first peaks correspond to radiation emitted in the ground level disintegration of the ^{121}Te; the 0·214 MeV ray to the de-excitation of the isomeric state and the 0·159 MeV ray is from ^{123}Te produced in the ^{123}Sb(d,2n)^{123}Te reaction.

The areas under the 0·214 and 0·575 MeV photopeaks were integrated graphically. Counting corrections and those corresponding to the disintegration scheme were made in order to calculate the relative intensities of the two levels under investigation.

RESULTS AND DISCUSSION

The values of the cross section ratios for the excited [(11/2) −] and ground ($\frac{1}{2}$+) levels with contribution of the intermediate level ($\frac{3}{2}$ +), for different deuteron energies, are given in Table 1.

The $\sigma(11/2)/(\sigma\frac{1}{2} + \sigma\frac{3}{2})$ (indicated as σ_m/σ_g) represent an average of data obtained at different times from the end of irradiation. The listed errors are the deviation of the single values from the average.

In Fig. 3 the σ_m/σ_g ratio is shown as a function of the deuteron energies. A slight increase in the population of the highest spin level is noticeable with growing deuteron energy. This is in agreement with earlier experimental work$^{(2-8)}$, i.e. at low deuteron energies the states of the residual nucleus closest to the spin of the target nucleus are the most favoured.

---

(10) D. Strominger, J. M. Hollander and G. T. Seaborg, *Revs. Mod. Phys.* **30**, 585 (1958).

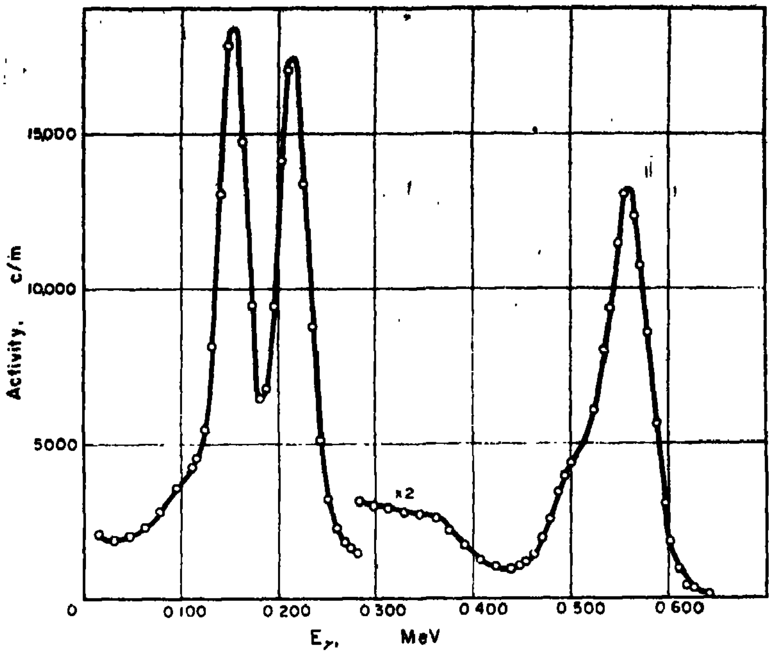

FIG. 2.—γ-spectrum of $^{121m/121}$Te corresponding to 18·7 MeV deuteron energy, measured 72 days after the end of irradiation.

TABLE 1.

Deuteron energy (MeV)	σ_m/σ_h
27·30 ± 0·1	0·793 ± 0·087
25·80 ± 0·2	0·747 ± 0·064
24·20 ± 0·2	0·653 ± 0·079
22·80 ± 0·2	0·720 ± 0·093
21·50 ± 0·1	0·720 ± 0·060
20·30 ± 0·1	0·623 ± 0·024
18·70 ± 0·3	0·653 ± 0·032
16·60 ± 0·2	0·603 ± 0·009
14·30 ± 0·3	0·560 ± 0·015
11·70 ± 0·3	0·470 ± 0·025
9·20 ± 0·2	0·560 ± 0·095

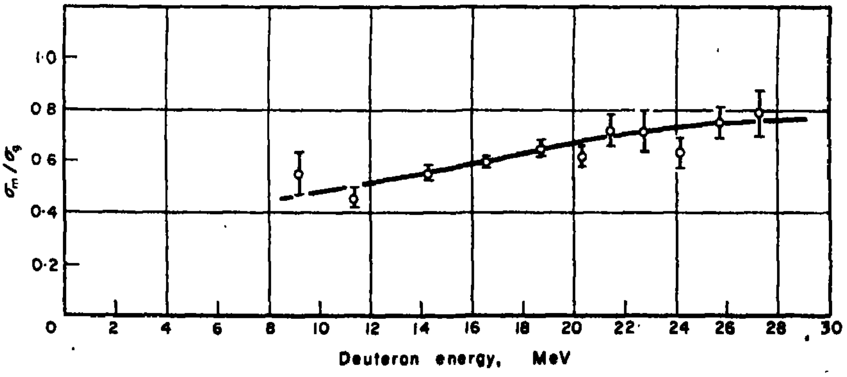

FIG. 3.—σ_m/σ_g ratio as a function of the deuteron energies.

It is not possible to conclude if this ratio tends to the limit $(2I_m + 1)/(2I_g + 1 + 2I_i + 1)^{(7,8)}$, were I_m, I_g and I_i are the spins of the metastable, ground and intermediate states respectively.

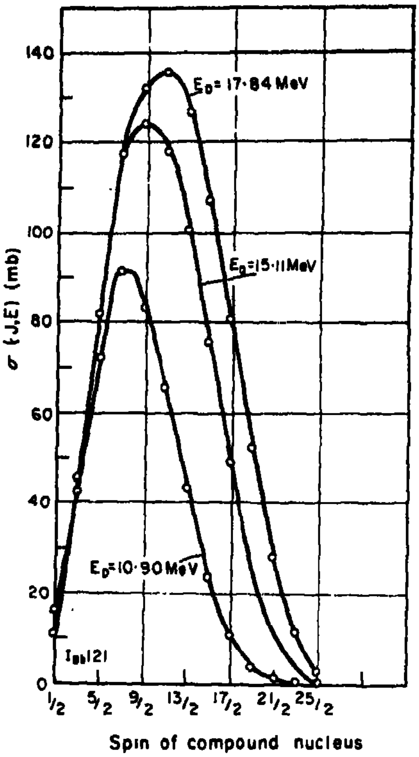

Fig. 4.—*Distribution of angular momentum in compound nuclei for deuteron energies* of 10·90, 15·11 and 17·80 MeV

Assuming that every particle penetrating into the potential barrier is captured, the angular momentum distribution of the compound nucleus was calculated from:

$$\sigma(J, E) = \pi\lambda^2 \sum_{S=|I-s|}^{I+s} \sum_{l=|J-S|}^{J+S} g(S)\frac{2J+1}{2S+1} \cdot T_l(E)$$

where $T_l(E)$ is the barrier transmission coefficient of a particle with orbital angular momentum l and energy E.

S is the spin entrance-channel.

J is the angular momentum of the compound nucleus.

I is the spin of the target nucleus.

s is the spin of the deuteron.

$g(S)$ is the statistical weight for S.

Fig. 4 shows such distribution for incident deuteron energies of 10·90 MeV, 15·11 MeV and 17·84 MeV (in the centre-of-mass system).

The trend observed from the curves in Fig. 4 agrees with the experimental results sketched in Fig. 3.

Acknowledgements—The authors are obliged to the Synchro-cyclotron group who kindly performed the irradiations for them.

J. Inorg. Nucl. Chem., 1962, Vol. 24, pp. 117 to 131. Pergamon Press Ltd. Printed in Northern Ireland

RADIOCHEMICAL STUDIES OF ISOTOPES OF ANTIMONY AND TIN IN THE MASS REGION 127–130

E. Hagebø*, A. Kjelberg† and A. C. Pappas‡
Department of Chemistry, University of Oslo, Blindern, Norway
and
The Gustaf Werner Institute for Nuclear Chemistry, Uppsala, Sweden

(*Received* 24 *July* 1961; *in revised form* 4 *September* 1961)

Abstract—Rapid radiochemical methods based on isopropyl ether–hydrochloric acid extraction for separation of antimony from enriched tellurium targets, and on ethyl ether–ammonium thiocyanate extraction for separation of tin from fission product mixture were developed. Antimony daughters were periodically milked from tin by stripping of the ether phase with ammonium thiocynate.

The nuclides reported are: 9·9 ± 0·5 min ^{128m}Sb, 9·9 ± 0·5 hr ^{128g}Sb, 7·1 ± 0·4 min ^{130m}Sb, 33 ± 2 min ^{130g}Sb, 4·6 ± 0·4 min and 2·2 ± 0·2 hr ^{127}Sn, 57 ± 4 min ^{128}Sn, and 8·8 ± 0·6 min and 1·0 ± 0·1 hr ^{129}Sn.

Assignment of isomeric states in ^{127}Sn and ^{129}Sn cannot be made with present evidence.

The principal groups of nuclear isomers appear just below the closed nucleon shells (50, 82, 126) where two levels of very different spin compete for the ground state. Thus the odd-neutron nuclei with less than 82 neutrons have low ground-state spins ($s\frac{1}{2}$ or $d\frac{3}{2}$) and due to the proximity of the $h(11/2)$ level, isomerism will be possible in the corresponding isotopes of tin and antimony as well as tellurium, iodine, xenon and cesium.

The isomerism in isotopes of tellurium and heavier elements is well established. For isotopes of tin and antimony in the mass region 126–130, however, contradictory observations have been reported, not only where isomerism is concerned but also with respect to half-lives, genetic relationships and mass assignments. Isotopes of antimony in the mass region 131 to 134 have independently been studied by Cook(1) and by Pappas.(2,3) Their results are in all aspects in full agreement. The isotopes of tin in the mass region 130 to 132 have only been studied by Pappas and Wiles.(4)

Due to the short half-lives of these isotopes of tin and antimony, further information seems to be limited by the availability of rapid chemical methods for their isolation. This particularly refers to those nuclides that can only be produced through fission and spallation reactions.

On the basis of experience gained through earlier work(2,4) and during the investigation of fission yields in this mass region,(3) it was found fruitful to continue studies of isotopes of tin and antimony with mass number 127–130. Some of the results of the present work, the observation of isomerism in antimony-128 and antimony-130, have earlier been reported as personal communications to collectors of nuclear data(5,6,7) and also briefly described in reference (8).

---

* Present address: The Gustaf Werner Institute for Nuclear Chemistry.

† Research Fellow, Royal Norwegian Council for Scientific and Industrial Research.

‡ Permanent address: Department of Chemistry, University of Oslo.

(1) G. B. Cook Report AERE C/R-729 (1951).

(2) A. C. Pappas *Phys. Rev.* **81**, 299 (1951).

(3) A. C. Pappas Report AECU-2806, MIT-LNS-63 (1953), (Inaugural Dissertation, University of Oslo).

(4) A. C. Pappas and D. R. Wiles *J. Inorg. Nucl. Chem.* **2**, 69 (1956).

Previous studies of isotopes of antimony with mass number 127–130

In 1951 BARNES and FREEDMAN(9) found 40 min and 9 hr antimony activities in a fission mixture but did not assign a mass number to the former. The 9 hr activity, however, was given mass number 126 from the observed change in the activity ratio 9 hr Sb ^{99}Mo when going from thermal to 14 MeV neutron-induced fission of uranium. In the decay of the 9 hr activity, however, FRAENZ *et al.*(10) were able to identify the γ-ray from the first excited level in tellurium-128. Thus the 9 hr activity should be ascribed to antimony-128.

Isotopes of antimony with half-life of about 10 min, also with contradictory mass assignments, have been reported by different authors. BARNES and FREEDMAN(9,11) proposed mass number 126 or 130 for a 10 min activity found in fission, and PAPPAS(3) reported a half-life of about 12 min for an activity decaying to stable tellurium. Of the two possible mass assignments 128 and 130, the latter was suggested on the basis of fission yield measurements. During studies of short-lived isotopes of tin PAPPAS and WILES(4) measured the half-life of antimony-130 in samples milked from fission-product tin and found it to be 9·2 min.

An activity with a half-life of about 10 min and mass number 130 was also reported by FRAENZ *et al.*(12) Subsequently a study of the γ-spectrum of the 10 min activity indicated, however, that the mass assignment should be changed to 128.(10) The latter assignment was supported by WINCHESTER(13) as a result of a study of long-lived tin isotopes in fission and on the basis of measured fission yield of its mother nuclide, the 57 min tin.

It appears that antimony activities with a half-life of about 10 min cannot all be ascribed to either antimony-128 or antimony-130. Thus the picture seems highly complex and has not been improved by BOSCH(14) who quite recently reported 330 min for the half-life of antimony-130.

This review has been concerned only with antimony isotopes of odd neutron number. These are the isotopes in which nuclear isomerism should occur, and this phenomenon might be responsible for the present confusion. In the mass region concerned, the isotopes of even neutron number, i.e. 93 hr ^{127}Sb, 4·6 hr ^{129}Sb and 22 min ^{131}Sb, are all well known and no discrepancy has been reported.

---

(5) D. STROMINGER, J. M. HOLLANDER and G. T. SEABORG *Table of Isotopes*, *Revs. Mod. Phys.* **30**, 585, (1958).

(6) W. H. SULLIVAN *Trilinear Chart of Nuclides*, USAEC, Washington 1957 and revisions.

(7) K. WAY, G. ANDERSSON, C. H. FULLER, N. B. GOVE, J. B. MARION, C. L. MCGINNIS and M. YAMADA *Nuclear Data Sheets*, NAS-NRC, Washington (1958) and later.

(8) A. C. PAPPAS *Beitr. Phys. Chem. d.* 20. *Jahrh.:* L. MEITNER, O. HAHN, M. VON LAUE z. 80. Geburtstag, p. 85, Fr. Vieweg, Braunschweig (1959).

(9) J. W. BARNES and A. J. FREEDMAN *Phys. Rev.* **84**, 365 (1951).

(10) I. FRAENZ, J. RODRIGUEZ and R. RADICELLA Z. *Naturforsch.* **11** a, 1037 (1956).

(11) J. W. BARNES Personal communication to C. D. CORYELL (1953) quoted in Reference (3).

(12) I. FRAENZ, J. RODRIGUEZ and H. CARMINATTI *Z. Naturforsch.* **10** a, 82 (1955).

(13) J. WINCHESTER Progress Report MIT-LNS, p. 14, Aug. (1955).

(14) H. BOSCH Semi-annual Report UCRL-8867 p. 40 (1958).

Previous studies on isotopes of tin with mass number 127–130

Tin activities with 50 min and 1·5 hr half-lives were first reported by Barnes and Freedman(9) who assigned to these activities the mass numbers 126 and 127 respectively by studying their antimony daughters. Fraenz *et al.*(12) found a tin activity with a half-life of 57 min and gave it mass number 130. Later(10) these authors ascribed this activity to tin-128. This was done by identification in the decay of its antimony daughter of the γ-ray from the first excited state in tellurium-128. This assignment was also corroborated by Winchester(13) through fission-yield measurements. Carminatti *et al.*(15) report a half-life of 2·05 hr for tin-127 instead of 1·5 hr when produced by fast-neutron irradiation of tellurium.

For 4·6 hr ^{129}Sb Pappas(3) found a low fission yield, which could be explained if its tin parent has a relatively long half-life (minutes). This explanation was supported by Barnes(11) who found indications that the half-life of tin-129 may be of the order of several minutes.

The isotopes of tin with mass number 130 and higher have only been studied by Pappas and Wiles(4). They reported 2·6 min for the half-life of tin-130.

As in the isotopes of antimony one should expect nuclear isomerism to be present in isotopes of odd number, but no isomerism has yet been reported beyond mass number 125.

With the exception of a few experiments carried out at the Institute for Nuclear Research in Amsterdam in 1955, the experiments reported in this paper were performed at the authors' institutions in different periods during the years 1955 to 1960.

ISOTOPES OF ANTIMONY

Experimental

A fission-product mixture(2,3,4,9,10,12,13) or irradiated natural tellurium(10) was used as the source for the nuclides of interest in the previous work, but these complicated systems should if possible be avoided. The present study was therefore concentrated on inducing (n, p) reactions in highly enriched tellurium-128 and tellurium-130, reactions which give antimony-128 and antimony-130, respectively.

The target were obtained from Oak Ridge National Laboratory. Their isotopic analyses are given in Table 1.

(n, p) reactions were induced in the targets by fast neutrons produced in the irradiation of beryllium with 21 MeV deuterons accelerated in the Amsterdam cyclotron. Interfering activities result from side reactions such as $(n, 2n)$, (n, pn) and (n, α) in the major constituents and moreover from these and (n, p) reactions in the isotopic impurities present in the targets.

Table 1 summarizes the reactions involved and shows which radioactive isotopes of tellurium, antimony and tin can be formed. A radiochemical separation of antimony from the irradiated targets was therefore required.

In the chemically separated and purified samples one should expect antimony-128 or 130 (depending on which target is used) to be responsible for the main activity. The low content of tellurium-126 in both targets would by the (n, p) reaction give antimony-126 in only very small amounts. The influence, however, of interfering activities arising from the presence of tellurium-128 in tellurium-130 and *vice versa* should be considered in the analysis of the decay curve of the isolated antimony.

Cross-sections for the reactions where charged particles are emitted are not known for the actual target nuclei, but one would on the basis of the types of nuclides involved expect (n, p) reactions to be favoured. Moreover, antimony-127 and antimony-129 formed by (n, pn) reactions have half-lives which are longer than those expected for the unknown isotopes of antimony.

Thus, isotopes of antimony formed by (n, pn) reactions in the major target isotope and in addition by the (n, p) reaction in the minor constituent would merely be present as background activities when short irradiation times are used. (Cf. Table 1.)

Chemical separation. The chemical isolation of antimony should be fast and give good decontamination, particularly from tin and tellurium. In addition a very good recovery of the costly target materials was required.

(15) H. Carminatti, I. Fraenz, R. Radicella and J. Rodrigues *Z. Naturforsch.* **11 a**, 419 (1956).

Previous radiochemical methods for antimony are based mostly on distillation, precipitation and stibine generation, requiring 1–3 hr.

Wilkinson and Grummitt$^{(16)}$, however, claim 80 per cent chemical yield for a 10–15 min stibine method, but the applicability of the method is rather strongly dependent on the experimental conditions.

Pappas$^{(8)}$ developed a still faster method which, however, often gives poor chemical yields. This method is based on previous work by Stanley and Glendenin$^{(17)}$ and uses the extraction of antimony(V) chloride by isopropyl ether (IPE). Further work along this line was found worthwhile, and from this study the following method was developed.

Table 1.—Nuclear reactions in tellurium targets

Target: Tellurium-128

	(n, p)	$(n, 2n)$	(n, pn)	(n, α)
Major component:				
95·6 ± 0·4% ^{128}Te	^{128}Sb	^{127m}Te 105 days ^{127g}Te 9·4 hr	^{127}Sb 93 hr	^{125}Sn 9·5 min ^{125}Sn 10 days
Minor components:*				
3·0 ± 0·2% ^{130}Te	^{130}Sb	^{129m}Te 33·3 days ^{129g}Te 72 min	^{129}Sb 4·6 hr	^{127}Sn ~ 2 hr
1·1 ± 0·2% ^{126}Te	^{126}Sb	^{125m}Te 58 days ^{125g}Te stable	^{125}Sb 2·0 years	^{123}Sn 40 min ^{123}Sn 136 days

Target: tellurium-130

	(n, p)	$(n, 2n)$	(n, pn)	(n, α)
Major component:				
95·6 ± 1·7% ^{130}Te	^{130}Sb	^{129m}Te 33·3 days ^{129g}Te 72 min	^{129}Sb 4·6 hr	^{127}Sn ~ 2 hr
Minor components:*				
3·8 ± 0·7% ^{128}Te	^{128}Sb	^{127m}Te 105 days ^{127g}Te 9·4 hr	^{127}Sb 93 hr	^{125}Sn 9·5 min ^{125}Sn 10 days
0·3 ± 0·2% ^{126}Te	^{126}Sb	^{125m}Te 58 days ^{125g}Te stable	^{125}Sb 2·0 years	^{123}Sn 40 min ^{123}Sn 136 days

* ^{120}Te, ^{122}Te, ^{123}Te, ^{124}Te and ^{125}Te all $< 0·1$ per cent

After 10–30 min irradiation the target is dissolved in hydrochloric acid and antimony(V) carrier added. Tin(II) in excess is used to precipitate tellurium from the cold solution. This was found superior to the use of sulphur dioxide or hydrazine. The precipitate is later easily purified for repeated use as target material.

As shown by Edwards and Voigt$^{(18)}$ antimony(V) can be extracted from 6–9 N hydrochloric acid into IPE. As the antimony carrier after precipitation of tellurium is in the +3 oxidation state, an oxidation to the +5 state must be performed. Tellurate, ceric, and permanganate ions and chlorine and bromine were tried as oxidizing agents. Bromine dissolved in benzene was found most suitable, especially as the IPE used in the extraction can be mixed with the benzene. Thus oxidation and extraction is performed in a single step. The bromine colour also facilitates a rapid checking of complete oxidation or reduction in the different steps of the procedure.

There are also other advantages of mixing the two organic solvents. IPE is quite soluble in 9 N hydrochloric acid, and the separation of the two phases after the extraction is relatively slow. Both effects are, however, counteracted by mixing the IPE with benzene. This also makes it possible to use a very small volume of IPE. Thus 1 ml IPE in 10 ml benzene is sufficient for the extraction of 2 mg antimony in the presence of 200–300 mg tin, the latter from the reduction step.

For reduction and back-extraction of antimony, a solution of tin(II) in 9 N hydrochloric acid was found superior to the hydrazine used previously. The tin also acts as a holdback carrier for possible tin activities. In the case of a final precipitation of antimony as metal, part of the tin will be co-precipitated, but as samples were mostly counted in the liquid form, this was of no particular concern.

(16) G. Wilkinson and W. E. Grummitt *Nucleonics* **9**, No. 3, 52 (1951).

(17) S. W. Stanley and L. E. Glendenin *Radiochemical Studies: The Fission Products* (Edited by C. D. Coryell and N. Sugarman) NNES, Div. IV, Vol. 9, Papers 134 and 271, McGraw-Hill, New York (1951).

(18) F. C. Edwards and A. F. Voigt *Analyt. Chem.* **21**, 1204 (1949).

The detailed procedure is given in the Appendix.

Tracer tests showed that the decontamination factors with respect to tellurium and tin obtained by this procedure are 5 × 10^4 and 10^4 respectively. The chemical yield is 60–70 per cent and less than 5 min is needed for the entire separation.

Liquid samples were counted in a 20th Century Electronics Ltd. type M6H liquid β-counter, and solid samples using a Philips end-window Geiger–Mueller tube.

Results and discussion

Half-lives. The gross decay curves of the antimony samples resulting from the fast neutron irradiation of the tellurium-128 target showed half-lives of about 10 min, 10 hr and a long-lived tail by a first analysis. The long-lived activity, present in low abundance, was presumably due to the 93 hr ^{127}Sb formed by the (n, pn) reaction in the target. In order to correct for this, a growth-decay curve for the 93 hr ^{127}Sb–9·4 hr ^{127g}Te pair was constructed on the basis of appropriate relative counting efficiencies, taking into account the branched decay of the 93 hr ^{127}Sb. The influence in this decay of the 105 days ^{127m}Te is insignificant during the first days and was therefore neglected. This constructed curve was fitted to the tail of the decay curve as shown in Fig. 1 and subtracted. A minor correction for the presence of tellurium-130 in the target was next made by subtracting 3·0 per cent of the gross decay curve of antimony separated from a sample of tellurium-130 of equal weight irradiated for the same length of time. The resulting curve was then easily analysed into a 10·7 ± 0·5 min and a 9·9 ± 0·5 hr activity (averages of three runs). The former half-life has also been determined in connection with the studies of tin isotopes reported in the latter part of this paper.

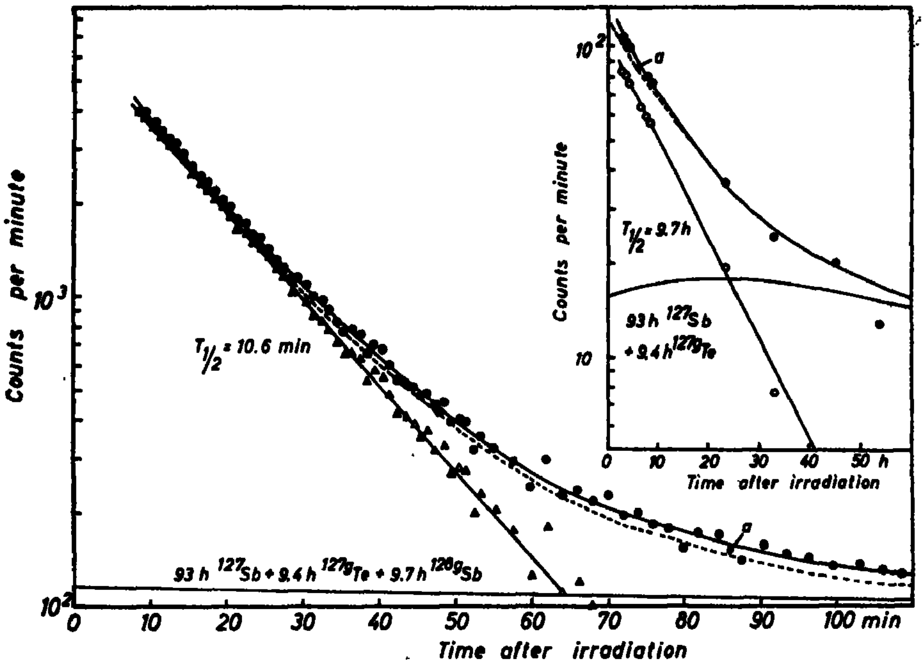

FIG. 1.—Typical decay curve for antimony separated from bombarded tellurium-128. Curves (a) are gross curves corrected for the 3·0 per cent tellurium impurity in the target.

A first analysis of the gross decay curve of antimony samples obtained from the fast neutron irradiation of the tellurium-130 target disclosed half-lives of 10–15 min, about 5 hr and in addition traces of a long-lived tail. The last two components were evidently due to the decay of the 4·6 hr ^{129}Sb formed by the (*n*, *pn*) reaction in tellurium-130. Corrections for the 129-chain and also for the activity formed by reactions in the 3·8 per cent tellurium-128 in the target were performed in a way similar to that described for the antimony-128 decay curve. The final analysis of the antimony decay curves gave two components of 7·1 ± 0·4 min and 33 ± 2 min.

The mass assignments of these four antimony activities follow in a straightforward manner from their production, i.e. ^{128}Te (*n*, *p*) ^{128}Sb and ^{130}Te (*n*, *p*) ^{130}Sb, and isomerism is obviously present both in antimony-128 and in antimony-130.

The half-lives found for the two states of antimony-128 are in full agreement with those independently observed by FRAENZ *et al.*(12) during the course of the present work, namely 10·3 min and 9·6 hr. These authors studied antimony from 30 MeV deuteron-induced fission in natural uranium and from (*d*, α) reactions on natural tellurium. Their mass assignment is based on investigations of the γ-spectra involved(10,19) and is supported by the results of the present work.

The 10·7 min and the 7·1 min isomers found in antimony-128 and 130 respectively show that the different mass assignments given to an activity of antimony with a half-life of about 10 min are justified and that the contradictions were caused by the similarity in the half-lives involved. The 40 min species observed by BARNES and FREEDMAN(9) in γ–γ coincidence measurements must have been the 33 min ^{130}Sb. Furthermore the 9·2 min,(4) the 12 min(3) and the 10 min(9) species observed in fission mixture are probably mixtures of the 7·1 min ^{130}Sb and the 33 min ^{130}Sb with a large proportion of the former.

No support is found in the present work for the 330 min half-life recently reported by BOSCH.(14)

Decay energies. The decay characteristics of the 10·7 min ^{128}Sb and the 9·9 hr ^{128}Sb have been studied by BARNES and FREEDMAN(9), FRAENZ *et al.*(12,19) and also by the present authors. The measurements give 2·7–2·9 MeV and 1·0–1·5 MeV for the β-energies of the short- and long-lived species respectively. Moreover, both species show γ-energies of 0·32 MeV and 0·75 MeV in about equal relative intensities and in addition higher energies with low intensities. The 0·75 MeV γ has also been measured by Coulomb excitation in ^{128}Te, thus confirming the mass assignment.

No direct study of the decay characteristics of the 7·1 min ^{130}Sb and the 33 min ^{130}Sb is available. Assuming, however, that the absorption of lower energy β's relative to high energy β's was larger in the liquid samples than in the solid samples studied in the present work, the following qualitative information is obtained: E^{β} (7·1 min) $\gg$ E^{β} (33 min) $\geqslant$ 1 MeV.

Assignment of isomeric states. The decay curves (Fig. 1) do not provide information to decide which half-lives correspond to the isomeric states of antimony-128 and antimony-130. The observations on the energies suggest strongly, however, that there is a significant β-branch from both isomers of mass numbers 128 and 130, and that the short-lived species in these pairs probably are the metastable states, while no information is available on eventual isomeric transitions. Therefore other approaches were tried.

---

(19) I. FRAENZ, J. RODRIGUES and R. RADICELLA *Proceedings of the Second International Conference on the Peaceful Uses of Atomic Energy, Geneva* 1958, Vol. 14, p. 187, United Nations, Geneva (1958).

Preliminary experiments confirmed the observations by Bonner(20) that isotopic exchange between the two oxidation states involved (+3 and +5) is very slow. Therefore a very good isomer separation could be visualized if the antimony (originally present in the +5 state) were to change its oxidation state (to +3) as the result of a converted γ-transition. This is known to occur in tellurium where a reduction from the +6 to the +4 state is the result of the internal conversion of the γ-ray.(21)

Attempts were therefore made to separate chemically the two oxidation states of antimony-128 from a solution of antimony in the +5 state. First, antimony(V) was extracted with isopropyl ether and antimony(III) back-extracted with 8 M hydrochloric acid at an appropriate time. Secondly, antimony(III) sulphide was precipitated in presence of hydrofluoric acid from a solution containing antimony(V). In this case about 10 per cent of antimony(V) followed the antimony(III) sulfide. This was proved to be purely a co-precipitation phenomenon, and may explain the discrepancies which appear in two papers by Fraenz *et al.*(10,12)

None of these approaches gave measureable activities in the antimony(III) fractions. This may indicate very low conversion of the γ-rays involved or no isomeric transition, provided the transition does result in a change of oxidation state as is the case for tellurium.

As experimental studies have not given any firm basis for isomeric state (level) assignments, an empirical approach was tried.

It is known that the ground states of both antimony-122 and -124 have longer half-lives than the metastable states.(7) The *Nuclear Data Sheets*(7) seem to prefer tentatively to assign the longer half-life in antimony-126 and in antimony-128 to the metastable state, while for antimony-130 the ground state is given the longer half-life. These assignments were considered in the context of the half-life systematics described below.

In the case of same spin and parity the logarithm of the half-lives of even or odd mass numbered isotopes for a given element seems often to be a linear function of mass number as shown by different authors.(22,23,24) Andersson(24) has worked out this method to give a simple systematics applicable to many series of alternate isotopes of the elements and indicated its usefulness in suggesting level assignments in certain cases of isomerism. Fig. 2(24) shows the neutron-rich isomers of antimony which are of even mass number. For a given mass number these are found on two different curves depending on their half-lives (long or short). In the case of antimony-124 the 60 day ^{124}Sb is well established as the ground state with level assignment 3–.(25) The relationships in Fig. 2 therefore suggest strongly that the spin and parity of the 6·2 day ^{126}Sb, the 9·9 hr ^{128}Sb, and the 33 min ^{130}Sb is 3–. Therefore these nuclides may represent the corresponding ground states. These results are in accordance with the energy considerations given above. Little support seems to be left for the level assignments tentatively given in *Nuclear Data Sheets*(7) for antimony-126 and -128.

(20) N. A. Bonner *J. Amer. Chem. Soc.* 71, 3909 (1949).

(21) R. R. Williams *Radiochemical Studies: The Fission Products* (Edited by C. D. Coryell and N. Sugarman) NNES, Div. IV, Vol. 9, Paper 20, McGraw-Hill, New York (1951).

(22) A. F. Stehney and G. J. Perlow *Proceedings of the Second International Conference on the Peaceful Uses of Atomic Energy, Geneva* 1958, Vol. 15, p. 348. United Nations, Geneva (1958).

(23) A. C. Pappas, G. Rudstam and Å. Svanheden To be published.

(24) G. Andersson *Nucl. Phys.* 24, 666 (1961).

(25) P. C. B. Fernando, G. K. Rochester and K. F. Smith *Phil. Mag.* 5, 1309 (1960).

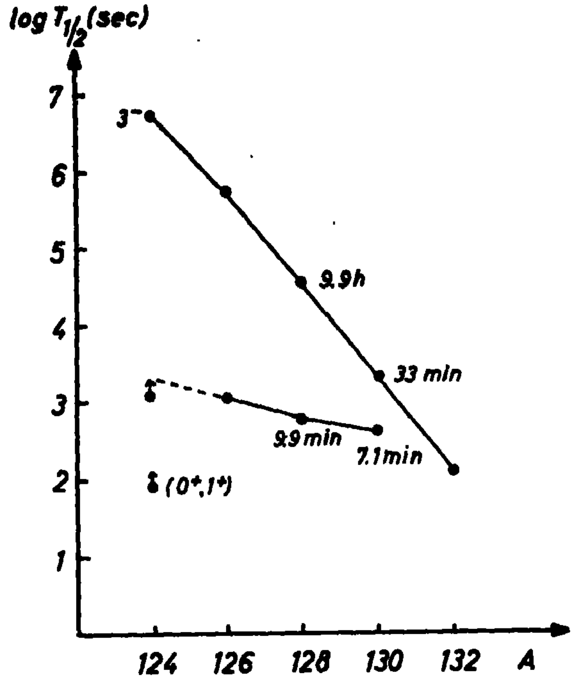

FIG. 2.—Log$T_{1/2}$ versus mass number for neutron-rich isomers of antimony of even mass number. Reproduced with slight alterations from reference (2).

ISOTOPES OF TIN

Experimental

The tin isotopes of interest are produced in fission or spallation reactions only and are preferably studied through their respective antimony daughters described in the previous part of this paper. The daughter milking technique offers a feasible approach to the study provided that the chemical procedure for isolation of tin from fission mixture gives complete separation from antimony in a single step. The radiochemical purity of tin with respect to activities other than antimony, however, is a minor requirement. This is because the half-lives involved allow time for further purification of the milked antimony.

Chemical separations. During studies of short-lived isotopes of tin, PAPPAS and WILES developed an extremely fast procedure for the isolation of fission-product tin in a pure state. This method, however, requires the uranium target to be in the +4 state; the chemical form of the target was pyridinium hexachloro uranate(IV).

In order to avoid these difficulties a new procedure was developed on the basis of a study of the ethyl ether thiocyanate system. According to BOCK[36] tin(IV) will be extracted completely (more than 99·9 per cent) by ethyl ether from 7 M ammonium thiocyanate solution 0·5 M in hydrochloric acid, while only 2·2 per cent of antimony(III) is extracted. Preliminary tracer tests also showed that only 0·9 per cent of antimony(V) is extracted under these conditions.

The most important step in the entire procedure is the milking of antimony from tin as it is required that no tin be carried over with the antimony. If this should happen, however, the half-lives obtained would be too short. Using the 118 day ^{113}Sn as tracer*, two series of milking experiments were performed under conditions exactly like those to be used during the actual milking experiment. Each series consisted of ten successive milkings. In one case the ether phase after the end of the final milking contained 98·0 per cent and in the second case 99·2 per cent of the original total tin activity. These results support the high extractability given by BOCK[36]. Thus the loss of tin in each milking can be neglected.

Tin was therefore isolated from a fission mixture using one extraction of tin(IV) thiocyanate into ethyl ether. In some cases, however, one sulphide precipitation preceded this extraction. From the ether solution, antimony was milked at regular intervals and further purified by extraction with isopropyl ether as already described for separation of antimony from tellurium. The details of the procedure are given in the Appendix.

---

* Ample consideration was given to the presence of its daughter, the 1·7 hr ^{113m}In.

[36] R. BOCK *Z. Anal. Chem.* **113**, 110 (1951).

Two series of experiments were performed, using thermal neutrons, 50 or 170 MeV protons to induce fission in the uranium targets.

A. Tin was isolated about 1 hr after the end of the irradiation and antimony milked at 1 hr intervals (growth periods) in order to look for long-lived tin parents. The antimony samples were purified immediately in order to include also the short-lived isomer of antimony-128 formed by decay of tin.

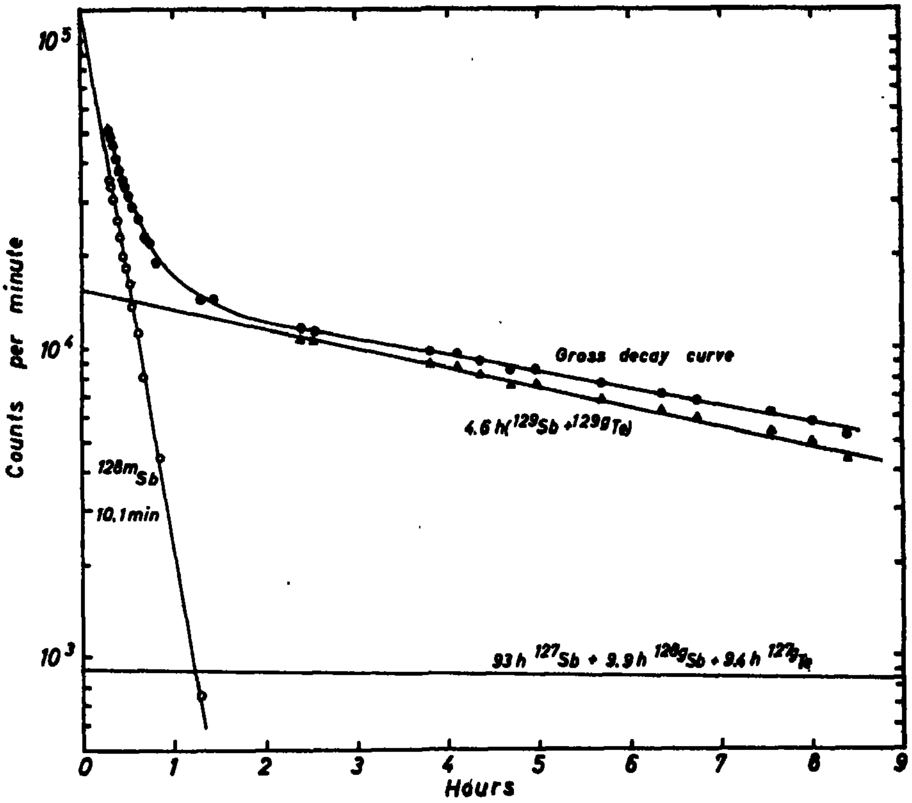

Fig. 3.—Typical decay curve for antimony milked from tin (Series A).

B. Tin was isolated a few minutes after the end of the irradiation and antimony milked from the tin at regular short (5 min) intervals (growth periods). As the tin isotopes of interest were tin-127 and tin-129, the milked antimony samples were purified and counted when the 22 min ^{131}Sb had decayed.

The relative chemical yields of antimony in the milked samples were determined either spectrophotometrically by the method of van Aman *et al.*(37) or gravimetrically as antimony(III) sulphide.

The antimony samples were counted in a standard counting arrangement using end-window proportional or Geiger–Mueller Tubes.

Results and discussion

Half-lives. A typical gross decay curve of the antimony samples milked in series A experiments is shown if Fig. 3. It is possible to identify the presence of three antimony components in the samples i.e. 93 hr ^{127}Sb, 10 min ^{128m}Sb and 4·6 hr ^{129}Sb.

The gross decay curves of the different antimony samples milked in series B

---

(37) R. E. van Aman, F. D. Hollibaugh and J. H. Kanzelmeyer *Analyt. Chem.* 31, 1783 (1959).

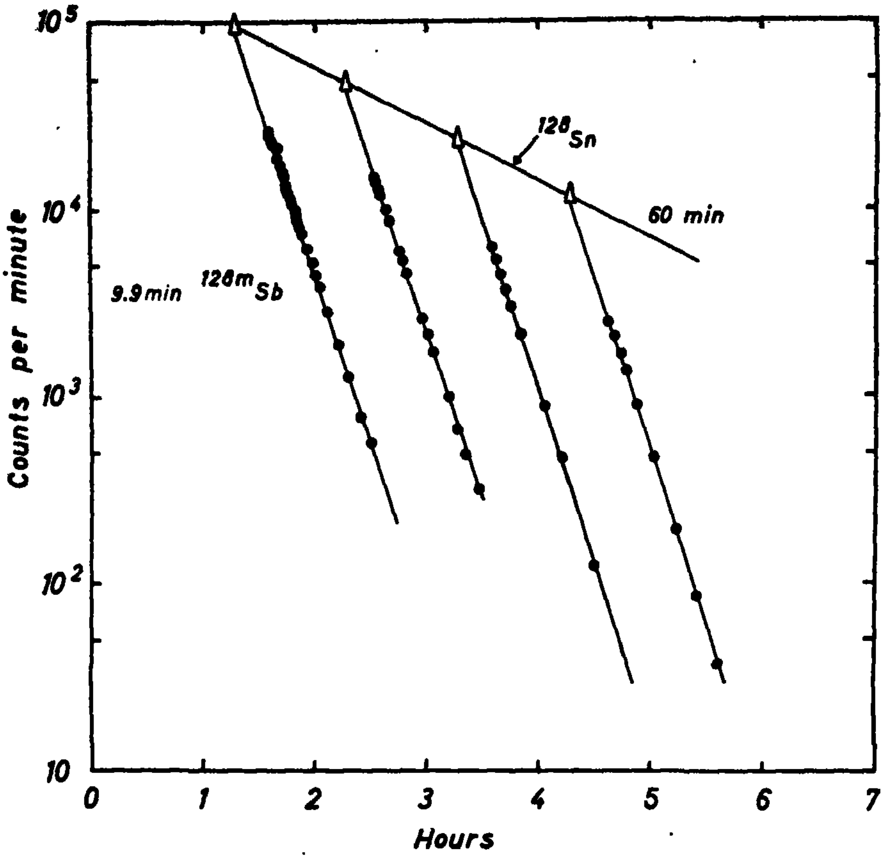

Fig. 4.—Typical decay curve for ^{128}Sn (Series A).

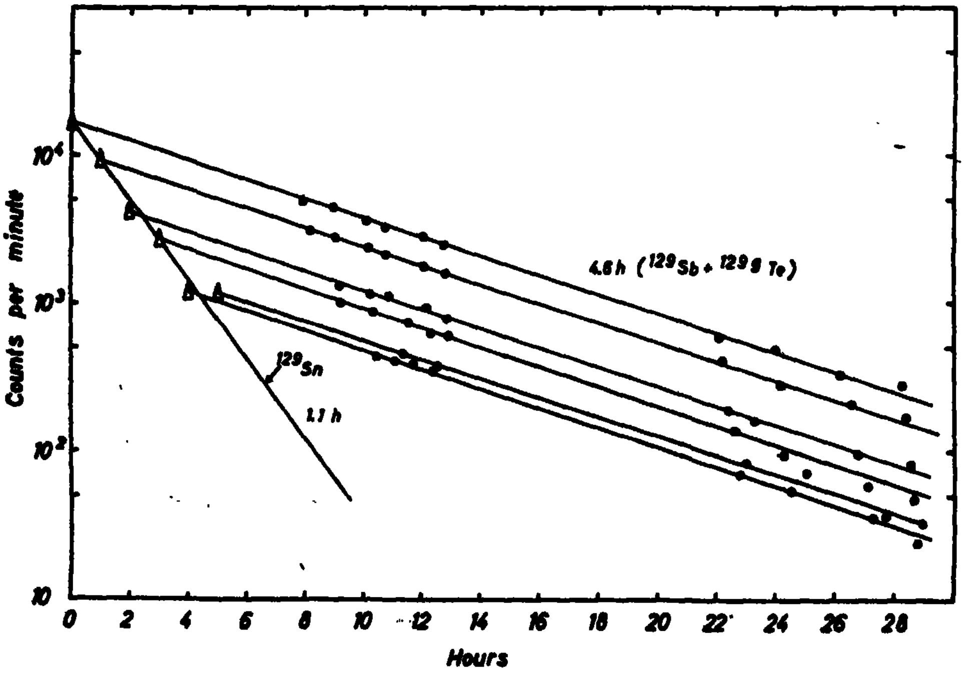

Fig. 5.—Typical decay curve for ^{129}Sn (Series A).

experiments were similar to those observed in series A experiments. Due to the long decay, however, of the antimony before counting, the 10 min ^{128m}Sb did not show up in series B samples. Otherwise the method of curve analysis used was the same as described above.

The zero time activities of the different antimony isotopes present in the milked samples were corrected only for the chemical loss of antimony occurring during the purification of the samples. This can be done because of the complete separation of antimony from tin without loss of either in the milking step.

The values so obtained are proportional to the disintegration rates of the respective tin parents at the beginning of the growth of antimony.(4)

In the present investigation all growth periods in each run were of equal length. Thus by plotting the corrected zero-time activities as a function of time for the start of each growth period, the half-life of the corresponding tin parent is obtained in a straightforward manner. Four to eight milkings were performed from each tin stock solution giving the same number of points on each tin decay curve.

The average values of the half-lives of ^{127}Sb and ^{129}Sb observed in the present work are 93 hr and 4·6 hr respectively, thus confirming previously published data.(3,28) *Concerning* ^{128m}*Sb, the average half-life measured in these milking experiments is* somewhat shorter, i.e. 9·8 min, than the value obtained from irradiation of enriched tellurium samples. The average of all our experiments is 9·9 ± 0·5 min as compared to 10·3 ± 0·3 min given by FRAENZ *et al.*(12) The limits of error were estimated on the basis of a non-rigorous evaluation of the reliability of the data. The limits of errors as calculated from a statistical treatment of the data are smaller than the limits listed. The same applies for the limit of errors given for antimony-128 and antimony-130 earlier in the paper.

Typical decay curves of the tin isotopes having antimony daughters with mass numbers 128 and 129 are shown in Figs. 4 and 5 (corrected for chemical yield of antimony). The half-lives found in the various experiments are given in Tables 2, 3 and 4.

Milking experiments have the great advantage of immediately disclosing parent–daughter relationships. Since the mass numbers of the antimony daughters are well known, mass assignments of the tin isotopes can be made unambigously, i.e. both the 4·6 min and 2·2 hr have mass number 127, the 57 min is ^{128}Sn, and both the 8·8 min and 1·0 hr have mass number 129.

The 57 ± 4 min half-life measured for ^{128}Sn is in full agreement with the previously reported value 57 ± 2 min.(12,13) It is interesting to note that in samples of antimony milked from tin the 9·9 min ^{128m}Sb was observed, but not the 9·9 hr ^{128g}Sb. This shows that ^{128}Sn mainly decays to the isomeric state of ^{128}Sb. Branching to the ground state of at most a few per cent is estimated on the basis of the milking experiments. FRAENZ *et al.*(10) found approximately 3 per cent.

These experiments prove the existence of isomerism both in ^{127}Sn and ^{129}Sn as should be expected from their nuclear constitution. Only one state has previously been reported in ^{127}Sn with a half-life of 1·5 hr(9) to 2·05 ± 0·05 hr.(15) The present value 2·2 ± 0·2 hr confirms the latter. Tin-129 has not been reported previously.

---

(28) N. R. SLEIGHT and W. H. SULLIVAN *Radiochemical Studies: The Fission Products* (Edited by C. D. CORYELL and N. SUGARMAN) NNES, Div. IV, Vol. 9, Paper 131. McGraw-Hill, New York (1951).

TABLE 2.—HALF-LIFE OF TIN-127

Series A		Series B	
Run*	Half-life (hr)	Run†	Half-life (min)
1	1·8	1	4·3
2	2·3	2	4·4
3	2·5	3	4·9
4	2·3		
5	2·3		
Average	2·2 ± 0·2 hr	Average	4·6 ± 0·4 min

* Runs 1–3 U(*n*,*f*). Run 4–5 U(170 MeV *p*, *f*).
† Runs 1–3 U(170 MeV *p*, *f*).

TABLE 3.—HALF-LIFE OF TIN-128

Series A	
Run*	Half-life (min)
1	57
2	58
3	60
4	54
5	54
Average	57 ± 4 min

* Runs 1–3 U(*n*,*f*). Run 4 U(50 MeV *p*, *f*). Run 5 U(170 MeV *p*, *f*).

TABLE 4.—HALF-LIFE OF TIN-129

Series A		Series B	
Run*	Half-life (hr)	Run†	Half-life (min)
1	1·0	1	8·5
2	1·1	2	8·3
3	0·8	3	9·3
4	0·9	4	9·0
6	1·0		
Average	1·0 ± 0·1	Average	8·8 ± 0·6

* Runs 1–3 U(*n*, *f*). Run 4 U(50 MeV *p*, *f*). Run 5 U(170 MeV *p*, *f*).
† Runs 1–4 U(170 MeV *p*, *f*).

Assignments of isomeric states. No data are yet available which allow conclusions to be drawn concerning metastable and ground-state assignments for the isomers found in ^{127}Sn and ^{129}Sn. The same difficulty applies to ^{121}Sn, ^{123}Sn and ^{125}Sn.

Some observations made during the course of the present study will, however, be reported here as they might throw some light on this problem.

1. In the experiments where the nuclides of interest were produced in fission of uranium induced by 170 MeV protons, the long-lived state in ^{127}Sn is much more abundant than the short-lived. The opposite is observed for the isomers of ^{129}Sn.

On the basis of previous studies of yields of isomers in fission induced by high energy protons(29,30), these observations might be taken to indicate that 2·2 hr ^{127}Sn and 8·8 min ^{129}Sn are either both ground states or both isomeric states.

2. The milking experiments disclose significant β-decay both in the 4·6 min ^{127}Sn and the 8·8 min ^{129}Sn. If in addition a comparison with previously known isomers of tin isotopes is made, one would expect that the isomers concerned for a given mass are nuclides very close in energy and that both states decay by β-emission only.

3. The disintegration rate at saturation of a fission product is proportional to its fission yield. Therefore, the experiments described in this paper allowed an evaluation of relative fission yields of ^{128}Sn and the long-lived isomers of ^{127}Sn and ^{129}Sn in fission of uranium induced by thermal neutrons. Appropriate corrections were made of the counting rates observed and the fission yields obtained in duplicate measurements, relative to that of the 57 min ^{128}Sn are 0·32 and 0·20 for the 2·2 hr ^{127}Sn and the 1·0 hr ^{129}Sn, respectively.

The yield-mass curve for fission of uranium induced by thermal neutrons and the charge-distribution curve valid for this process(31,32) can be used to obtain an estimate of the expected fission yield of both isomers together in ^{127}Sn and ^{129}Sn relative to the fission yield of ^{128}Sn. The values obtained are 0·4 and 2·1, respectively.

A comparison between measured and estimated values seems to suggest a low relative fission yield of the 4·6 min ^{127}Sn and a high relative fission yield of the 8·8 min ^{129}Sn. These results might be taken to support the conclusions already made concerning the occurrence of the nuclides involved among the products from fission of uranium induced by 170 MeV protons (paragraph 1 above), but no definite conclusion can be drawn.

TABLE 5.—Present knowledge of half-lives and genetic relationships for isotopes of tin and antimony in the mass region 127–130

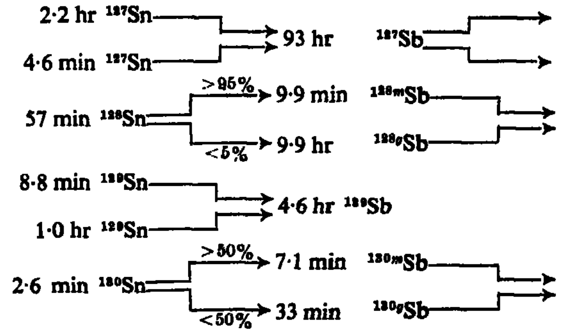

4. A plot similar to Fig. 2 does not give any decisive contribution to the present problem, and shows that this form of systematics is not always applicable.(34)

Work is now in progress in attempting to improve the measurements of the fission yields of ^{127}Sn, ^{128}Sn, ^{129}Sn and of their antimony daughters in addition to a study of isomer yield ratios.

---

(29) I. B. HÄLLER and G. ANDERSSON *J. Inorg. Nucl. Chem.* **20**, 12 (1961).

(30) E. HAGEBØ Unpublished data (1961).

(31) S. KATCOFF *Nucleonics* **18**, no. 11, 201 (1960).

(32) A. C. PAPPAS *Proceedings of the International Conference on the Peaceful Uses of Atomic Energy, Geneva* 1955, Vol. 7, p. 19. United Nations, New York (1956).

In the meantime Table 5 summarizes the present state of knowledge about the parts of the decay chains with mass numbers 127, 128, 129 and 130 which have been investigated in this paper. In this table no assignments are made concerning the isomers in ^{127}Sn and ^{129}Sn in accordance with the previous discussion. However, nuclides which are likely to be of similar character are placed in the same vertical order; that is, 2·2 hr ^{127}Sn and 8·8 min ^{129}Sn are either both ground states or both isomeric states and vice versa for the pair 4·6 min ^{127}Sn and 1·0 hr ^{129}Sn.

Acknowledgements—We are indebted to Professor A. H. W. ATEN JR. for his kindness and the excellent working facilities given us at the Institute for Nuclear Research in Amsterdam. The authors want to thank Director G. RANDERS and the staff at the Institute for Atomic Energy, Kjeller for irradiation facilities. Thanks are also due to Professor THE SVEDBERG and his staff at The Gustaf Werner Institute for Nuclear Chemistry, Uppsala for interest and helpful co-operation.

The work has been financially supported by the Royal Norwegian Council for Scientific and Industrial Research and the authors are glad to take this opportunity to express their sincere thanks to the Council for this support. One of us (E. H.) is also indebted to the Swedish Atomic Research Council for financial support.

APPENDIX: RADIOCHEMICAL PROCEDURES

Procedure 1. *Separation of antimony from irradiated enriched tellurium*

1. Dissolve the target (TeO_2) in 5 ml 9 N HCl to which is added 2 mg Sb(V) carrier. Add with vigorous stirring 2·5 ml $SnCl_2$ solution (100 mg Sn^{++} per ml) per 100 mg target. After about ½ min filter with suction through a Gooch, and wash twice with 2 ml 9 N HCl.

2. Transfer the filtrate to a separatory funnel containing 10 ml C_6H_6, 1·0 ml IPE and also 0·1 ml Br_2 per 100 mg target. Shake the funnel for about 10 sec. (Distinct brown colour of Br_2 should remain in the organic phase, showing complete oxidation). Discard the water phase and wash with 1 ml 9 N HCl.

3. Transfer the organic phase to a separatory funnel containing 5 ml 9 N HCl and 1·0 ml $SnCl_2$ solution and shake. (The organic phase should be colourlesss after the extraction, showing complete reduction).

4. Transfer the water phase to a separatory funnel containing 10 ml C_6H_6, 1·0 ml IPE and 0·05 ml Br_2 (or as little as possible) and shake for 10 sec. (Permanent brown colour.) Discard the water phase and wash with 1 ml 9 N HCl.

5. Transfer the organic phase to a separatory funnel containing 5 ml 9 N HCl and add dropwise a minimum amount of $SnCl_2$ solution (0·5–1·0 ml). Shake, and if necessary add $SnCl_2$ such that the organic phase just becomes colourless.

This solution can either be used for liquid β-counting, or for preparing solid samples. In the latter case:

6. Add 2–3 mg Sb(III) carrier, heat the solution and add approx. 15 ml boiling hot Cr^{2+} solution. Filter the solution and wash the precipitate carefully in boiling hot 9 N HCl, then with H_2O, alcohol and ether. (Some metallic Sn is also precipitated.)

Regeneration of tellurium target. The metallic tellurium precipitate in step 1 above is washed with hot water and dissolved in HNO_3, heated to dryness and precipitated by $N_2H_4 \cdot 2HCl$ from hot dilute HCl. The precipitate is dissolved in HNO_3 and transformed to TeO_2 by heating, and the target material is ready for use for further irradiation.

Procedure 2. *Separation of tin from fission-product mixture, and milking of antimony from tin*

I. Target: $UO_2(NO_3)_2 \cdot 6H_2O$

1. Dissolve the irradiated target in 10 ml 0·5 N HCl to which is added 5 mg each of Sn(IV), Sb(III) and As(III) carriers. Precipitate the sulphides by H_2S. Centrifuge and discard the solution. Wash the precipitate by stirring with 5 ml 0·5 N HCl and centrifuge once more.

2. Add 2 ml hot 6 N HCl, stir and filter by suction. Discard the As_2S_3 precipitate.

3. Dilute the solution to 25 ml by adding 7 M NH_4SCN solution, and transfer it to a separatory funnel containing 25 ml ethyl ether. Shake for one minute, discard the water phase and shake the organic phase twice for 10 sec with 10 ml 7 M NH_4SCN, 0·5 N in HCl and containing 5 mg Sb(III) carrier.

Zero time for growth of antimony from tin to be taken at the end of the last shaking period.

4. Series A: Wait 1 hr. Series B: Wait 5 min.

5. Add 10 ml 7 M NH_4SCN solution, 0·5 N in HCl and containing 5 mg Sb(III) carrier. Shake for 1 min. End of shaking is milking time.

6. Add about 1 ml concentrated HF to the water phase and precipitate Sb_2S_3 by H_2S. Centrifuge and discard the solution. Wash the precipitate with 0·5 N HCl.

7. Series A: Continue with step 8. Series B: Wait 5–6 hr, then continue with step 8.

8. Dissolve the precipitate in 10 ml 8 N HCl, boil rapidly to expel H_2S, cool and shake in a separatory funnel about 30 sec with 1:1 isopropylether:benzene to which is added 3–5 drops of bromine. Discard the water phase, and wash the organic phase with 8 N HCl.

9. Series A: Add 5 ml 8 N HCl containing about 50 mg $SnCl_2$. Series B: Add 5 ml 8 N HCl and about 4 drops of saturated $N_2H_4 \cdot 2HCl$ solution.

10. Shake vigorously until the Br_2 colour vanishes. Discard the organic phase.

11 Dilute the water phase to about 20 ml, add about 1 ml concentrated HF and precipitate Sb_2S_3 by H_2S.

12. Filter the precipitate onto a small filter paper, and wash with water, alcohol and ether.

13. Series A: Dry by suction, mount and count. Series B: Dry for 10 min at 110°C, weigh filter paper and precipitate, mount and count.

II. Target UO_3

1. Dissolve the irradiated target in 2 ml 6 N HCl containing 5 mg Sb(III) and 5 mg Sn(IV) carrier. Continue with step 3 in procedure 2 I above.

J. Inorg. Nucl. Chem. 1962. Vol. 24, pp. 133 to 137. Pergamon Press Ltd. Printed in Northern Ireland

THE CHEMICAL STATE OF CHLORINE-36 IN NEUTRON-IRRADIATED MINERALS†

C. W. OWENS and F. S. ROWLAND
Department of Chemistry, University of Kansas, Lawrence

(*Received* 24 *August* 1961)

Abstract—The oxidation state assumed upon solution by ^{36}Cl formed by thermal neutron irradiation of chlorine-containing minerals was determined. Except for about 0·2 and 0·9 per cent as ClO_3^- in carnallite and chlorapatite, respectively, all the ^{36}Cl radioactivity was found in the chloride state. The ^{36}Cl radioactivity in the chloride state in carnallite and chlorapatite was reduced by thermal annealing.

THE discovery that cosmic ray produced secondary neutrons form ^{36}Cl in barely detectable amounts in some terrestrial minerals[(1)] has prompted an investigation into the possibilities of natural Szilard-Chalmers enrichment of the specific activity of ^{36}Cl. An appreciable percentage of the ^{36}Cl activity in an oxidation state other than that normally found for chlorine in a mineral would permit the development of carrier-free separations of the enriched ^{36}Cl. However, as described below, the ^{36}Cl formed in irradiated chlorine-containing minerals by pile neutron irradiation is almost exclusively in the chloride form when the mineral is placed in solution. Since this is a common oxidation state for the stable chlorine isotopes in each mineral studied, very little isotopic enrichment can be obtained. Although about 0·2 per cent of the ^{36}Cl formed in irradiated carnallite, and about 0·9 per cent of that formed in chlorapatite, was found in the ClO_3^- fraction, the percentages are so small as to be useless for any enrichment purposes.

TABLE 1.—CHLORINE-CONTAINING MINERALS INVESTIGATED

Mineral	Chlorine*(%)	Origin	Composition
Carnallite	39	Spain	$KCl{\cdot}MgCl_2{\cdot}6H_2O$
Chlorapatite	0·5	Norway	$CaFCa_4(PO_4)_3$ with Cl for some F
Halite	54	Kansas	NaCl
Lazurite	0·05	Chile	$3NaAlSiO_4{\cdot}Na_2S$ with some ·NaCl and ·$CaSO_4$
Mimetite	0·02	Mexico	$9PbO{\cdot}3As_2O_5{\cdot}PbCl_2$
Nitratite	14	Chile	$NaNO_3$ (with Cl^- and ClO_4^-)
Scapolite	0·004	Massachusetts	$Na_4Al_3Si_9O_{24}Cl$ (with $Ca_4Al_6Si_6O_{25}$)
Scapolite	0·004	Quebec	same as above
Sodalite in Nepheline Syenite	1·0	New Hampshire	$3NaAlSiO_4{\cdot}NaCl$
Sylvite with Halite	38	Texas	KCl with NaCl

* By weight as determined by using ^{36}Cl activity for activation analysis measurement.

---

† This research has been supported in part by A.E.C. Contract No. AT(11-1)-407.

[(1)] R. DAVIS, JR. and O. A. SCHAEFFER, BNL 340 (T-59) (1955). See also O. A. SCHAEFFER, S. O. THOMPSON, and N. L. LARK, *J. Geophys. Research* **65**, 4013 (1960).

EXPERIMENTAL

Irradiation of minerals

Ten chlorine-containing minerals and C.P. sodium chloride were selected for the initial neutron irradiation. The halite sample was obtained from the Department of Geology of the University of Kansas, while the remainder of the minerals were obtained from Ward's Natural Science Establishment, Inc., Rochester, N.Y. The minerals are listed in Table 1, with their place of origin, usual chemical composition, and chlorine content. The chlorine content was determined from the data in Table 2 using the ^{38}Cl activity as a basis for activation analysis measurement.

Table 2.—^{38}Cl radioactivity in different oxidation states from ^{37}Cl (n, γ) in irradiated minerals

Sample						
			cpm/mg AgCl Precipitate†			
Compound or mineral	Aliquot size (mg)	Solvent	Cl^- fraction	ClO_3^- fraction	ClO_4^- fraction	mg NaCl carrier
(a) Irradiated for 10 days at 1·5 × 10^{13} neutrons cm^{-2} sec^{-1}.						
NaCl (C.P.)	7·49	H_2O	76·6 ± 1·4	0·02 ± 0·04	0·03 ± 0·05	122
Carnallite	20·3	H_2O	123 ± 2	0·33 ± 0·02	0·02 ± 0·01	126
Carnallite	84·4	H_2O	416 ± 7·5	1·32 ± 0·04	0·04 ± 0·06	118
Chlorapatite†	79·3	conc. HNO_3	6·46 ± 0·12	0·06 ± 0·01	0·04 ± 0·04	121
Halite	3·88	H_2O	24·7 ± 0·5	−0·01 ± 0·02	0·00 ± 0·02	182
Lazurite	242	dilute HCl	2·06 ± 0·04	−0·1 ± 0·2	0·01 ± 0·02	118*
Mimetite	680	conc. HNO_3	2·38 ± 0·04	−0·01 ± 0·01	0·00 ± 0·04	131
Nitratite†	28·4	H_2O	53·2 ± 1·0	0·01 ± 0·02	−0·01 ± 0·02	121
Scapolite (Mass.)	464	conc. HNO_3	0·33 ± 0·02	0·00 ± 0·01	−0·01 ± 0·04	122
Scapolite (Que.)	653	conc. HNO_3	0·50 ± 0·02	−0·02 ± 0·02	0·00 ± 0·05	116
Sodalite	105	dilute HCl	19·4 ± 0·4	0·03 ± 0·03	0·00 ± 0·02	118*
Sylvite	22·6	H_2O	148 ± 3	0·01 ± 0·02	0·02 ± 0·03	113
(b) Irradiated for 10 days at 0·5 × 10^{11} neutrons cm^{-2} sec^{-1}.						
$KClO_4$ (C.P.)	86·5	H_2O	1·90 ± 0·04	0·38 ± 0·03	0·06 ± 0·01	122
$NaClO_3$ (C.P.)	142	H_2O	4·38 ± 0·08	0·40 ± 0·01	0·00 ± 0·01	125
Carnallite	109	H_2O	3·11 ± 0·06	0·13 ± 0·01	0·00 ± 0·01	119
Lazurite	452	dilute HCl	0·20 ± 0·01	0·00 ± 0·01	0·00 ± 0·01	117*
Nitratite	186	H_2O	2·10 ± 0·04	0·00 ± 0·01	0·00 ± 0·01	117
Sodalite	379	dilute HCl	0·39 ± 0·01	0·00 ± 0·01	0·00 ± 0·01	117*
(c) Irradiated for 10 days at 1·5 × 10^{13} neutron cm^{-2} sec^{-1}. and annealed 14 days at 200 ± 5°C						
Carnallite†	6·91	H_2O	34·1 ± 1·0	0·00 ± 0·02	0·00 ± 0·02	125
Chlorapatite†	111	conc. HNO_3	2·50 ± 0·08	0·02 ± 0·01	0·00 ± 0·02	131

* NaCl equivalent, actually added as HCl.

† The assigned error is the statistical counting error, or ±1·8 per cent, whichever is greater. The efficiency in (b) is 34 per cent, in (a) and (c), 18 per cent, except for samples marked with † for which the efficiency was 14 per cent (Plexiglas backing).

Before irradiation, the minerals were crushed into medium fine powders and individually wrapped in aluminium foil. Several grammes of each were then irradiated in the Brookhaven reactor at a flux of $1{\cdot}5 \times 10^{13}$ neutrons cm^{-2} sec^{-1}. for a period of ten days. After irradiation, the samples were allowed to decay for several months, and then transferred to weighing bottles and stored in a desiccator. Those samples with a large chlorine content showed appreciable discoloration from radiation damage.

Additional samples of some of the minerals, as well as C.P. sodium chlorate and potassium perchlorate, were subsequently irradiated for ten days at a flux of approximately $0{\cdot}5 \times 10^{13}$ neutrons cm^{-2} sec^{-1}. in the Argonne CP-5 reactor. These minerals samples showed slight discoloration from irradiation, the sodium chlorate and potassium perchlorate developing a light amber colour.

Separation of oxidation states

A portion of each irradiated sample was dissolved in the mildest solvent thought to be capable of taking the chlorine containing compounds into solution, as shown in Table 2. The solution was then filtered and mixed with a carrier solution containing approximately 0·002 mole each of the sodium salts of Cl^-, ClO_3^- and ClO_4^-. No NaCl was added for the samples dissolved in dilute HCl. For samples dissolved in acid, the fitrate was neutralized with 6M NaOH prior to the addition of the carrier solution.

Silver chloride was precipitated from the sample plus carrier solution through the addition of an excess of 0·5 M $AgNO_3$ solution, after being made slightly acid with HNO_3. This silver chloride precipitate was filtered and set aside for purification. More NaCl was added to the filtrate, and this additional AgCl was filtered and discarded, insuring removal of the ^{36}Cl in the Cl^- state.

Sulphur dioxide was then bubbled through the filtrate for several minutes, reducing ClO_3^- to Cl^-, without chemically affecting ClO_4^-. Again, AgCl was precipitated through the addition of excess 0·5 M $AgNO_3$ solution, filtered, and set aside for purification.

The ClO_4^- fraction was isolated by two separate methods. Originally, the filtrate containing the ClO_4^- carrier was evaporated to a volume of 50 ml, filtered to remove residue, and then further evaporated to about 10 ml. A solution containing 1 gramme of KNO_3 in 3 ml water was then added to the evaporated solution, and cooled slowly to room temperature, and then to 0°C. The crystallized $KClO_4$ was filtered on glass fibre filter paper, dried at 100°C for 10 min, and, in a test tube over a burner, decomposed to KCl and oxygen. The residue was dissolved, filtered, acidified with nitric acid, and AgCl was precipitated with excess 0·5 M $AgNO_3$ solution.

Later, a second procedure was developed for the ClO_4^- fraction. After the filtrate from the chlorate separation was freed from silver ions by standing overnight in ammoniacal solution over magnesium turnings, the perchlorate was precipitated by the addition of tetraphenyl arsonium chloride. The tetraphenyl arsonium perchlorate was filtered, dried at 100°C and then reduced to Cl^- by a method similar to that suggested by CRUMP and JOHNSON(2). The dry precipitate was placed in a flame-ignition Parr bomb with an excess of sodium peroxide and the two solids were thoroughly mixed by shaking the closed bomb. The mixture was ignited by heating with a Fischer burner, the heating being stopped when a few ml of water in the recess of the head of the bomb began to boil. After cooling the residue was dissolved, filtered, and the filtrate acidified. Again, a precipitate of AgCl was obtained upon the addition of excess 0·5 M $AgNO_3$ solution.

Radiochemical purification

The silver chloride precipitates from the chloride and chlorate fractions were dissolved in 6 M aqueous ammonia and the diammine silver ions were then reduced to metallic silver through the addition of purified magnesium turnings. After standing overnight, the solution was filtered, added to an excess of concentrated sulphuric acid, and distilled. The distillate contained primarily the HCl-water azeotrope but could also have carried the HF-, HBr-, and HI-water azeotropes, if present. Silver chloride was then precipitated in acidic solution and dissolved in ammoniacal solution until constant radioactivity was obtained.

The silver chloride precipitate from the ClO_4^- fraction was dissolved in 6 M aqueous ammonia, and reprecipitated in acidic solution until constant radioactivity was obtained.

Radiochemical assay

Aliquots of purified ammoniacal sample solutions were acidified and collected on weighed glass fibre filter paper. The precipitates were washed with three separate 20 ml portions of absolute ethanol, dried for 10 min at 100°C, weighed, mounted on aluminium or Plexiglas disks, and covered with cellophane tape. The radioactivity of the samples irradiated at the higher flux was determined with an end-window Geiger counter. The measurements on the samples irradiated at the lower flux were carried out on a 2 in. diameter low-level Geiger counter with a background of 1·0 counts/min, produced by Sharp Laboratories, Inc., La Jolla, California. The Plexiglas backings gave a lower background count than the available aluminium disks.

---

(2) L. CRUMP and C. JOHNSON, *Analyt. Chem.* **27**, 1007-8 (1955).

Corrections of the experimentally determined count rates were made to the activity expected for a precipitate of thickness 11·0 mg/cm^2. The precipitate thicknesses varied from 1·17 to 28·9 mg/cm^2, for which the empirically determined thickness correction was never larger than 16 per cent. The correction factors are precise to 1·8 per cent. The standard area of the Cl^- and ClO_3^- precipitates was 2·27 cm^2, while that of the perchlorate precipitates was 3·30 cm.^{2} The efficiency of the regular end-window Geiger counter is approximately 18 per cent, while the low-level Geiger counter has an efficiency under our conditions of approximately 34 per cent. The diminution in observed count rates through aluminium absorbers was consistent in each case with the 0·7 MeV. β-ray of ^{36}Cl.

Annealing studies

Possible effects of thermal annealing on the relative radioactivity in the chloride, chlorate, and perchlorate fractions were investigated by holding the irradiated samples of carnallite and chlorapatite at 200 ± 5°C for a period of two weeks. The samples were then dissolved and assayed in the normal manner.

RESULTS AND DISCUSSION

The ^{36}Cl activity found in each of the three chlorine oxidation states is shown in Table 2. The oxidation state, of course, is that found after solution of the irradiated crystals and does not necessarily imply the oxidation state of the radioactivity prior to solution. The chloride fraction includes through rapid isotopic exchange all ^{36}Cl in the solution in an oxidation state lower than $+5$. The listed count rates are the averages of those considered constant for the given fraction.

No ^{36}Cl radioactivity is found in the oxidized states from any of the minerals except for approximately 0·2 and 0·9 per cent of the total radioactivity as ClO_3^-, in carnallite and chlorapatite, respectively. Although the percentage in the ClO_3^- fraction from carnallite is very small, it is reproducible and independent of irradiation time in the range studied, as shown in Table 3. No significant ClO_4^- radioactivity was found in any of the minerals.

Thermal annealing of the carnallite and chlorapatite samples reduced the already small percentages of ^{36}Cl found as ClO_3^-, as shown in Table 3. The radiation damage discolouration disappeared during the thermal annealing, and the samples resumed their original appearance.

Irradiated minerals are not very satisfactory matrices in which to study the actual "hot" atom reactions occurring for the ^{36}Cl atoms, but the observation of chloride as the predominant oxidation state is consistent with those made for other chlorine isotopes in various inorganic compounds. The radioactivity distribution obtained for $NaClO_3$ and $KClO_4$ is shown in Table 4, together with several distributions obtained

TABLE 3.—^{36}Cl AS ClO_3^- IN IRRADIATED CARNALLITE AND CHLORAPATITE

Mineral	Irradiation time	(mg) sample	(mg) $NaClO_3$ carrier	$Cl^{36}O_3^-$ (%)
Carnallite	10 days at 1·5 × 10^{12} n cm^{-2} sec^{-1}	20·3	218	0·23 ± 0·02
Carnallite	10 days at 1·5 × 10^{12} n cm^{-1} sec^{-1}	84·4	228	0·23 ± 0·02
Carnallite	10 days at 0·5 × 10^{11} n cm^{-1} sec^{-1}	109	209	0·24 ± 0·02
Carnallite	10 days at 1·5 × 10^{12} n cm^{-2} sec^{-1} Annealed 14 days at 200 ± 5°C	6·91	251	0·00 ± 0·03
Chlorapatite	10 days at 1·5 × 10^{12} n cm^{-2} sec^{-1}	79·3	217	0·9 ± 0·2
Chlorapatite	10 days at 1·5 × 10^{12} n cm^{-2} sec^{-1} Annealed 14 days at 200 ± 5°C	111	218	0·6 ± 0·3

previously by other experimenters. The $NaClO_3$ results are quite consistent with those obtained by SHARMAN and McCALLUM, whose sample had an even heavier neutron and γ-ray exposure than ours.

TABLE 4.—OXIDATION STATES OF CHLORINE ISOTOPES IN IRRADIATED COMPOUNDS

Compound	Isotope	Activity in oxidation state			Reference
		Cl^-	ClO_3^-	ClO_4^-	
KIO_3	$^{41}K\ (n, \alpha)\ ^{38}Cl$	"Practically All"	$<1\%$	—	(6)
$NaClO_3$	$^{35}Cl\ (n, \gamma)\ ^{36}Cl$	$86{\cdot}5 \pm 3{\cdot}0\%$	$12{\cdot}7 \pm 0{\cdot}3\%$	$0{\cdot}5 \pm 0{\cdot}05\%$	(3)
$NaClO_3$	$^{35}Cl\ (\gamma, n)\ ^{34}Cl$	~90%†	~10%†	0	(4)
Na_2SO_4	$^{34}S\ (p, n)\ ^{34}Cl$	13743 ± 115 cpm	22 ± 3* cpm	40 ± 3 cpm	(7)
$K_2S_2O_8$	$^{34}S\ (p, n)\ ^{34}Cl$	1047 ± 24 cpm	0 ± 2* cpm	9 ± 2 cpm	(7)
1·0 M $NaClO_3$	$^{37}Cl\ (n, \gamma)\ ^{38}Cl$	$100 \pm 2\%$	—	—	(8)
1·0 M $NaClO_4$	$^{37}Cl\ (n, \gamma)\ ^{38}Cl$	$100 \pm 10\%$	$0 \pm 10\%$	—	(8)
$NaClO_3$	$^{35}Cl\ (n, \gamma)\ ^{36}Cl$	$87{\cdot}6 \pm 0{\cdot}4\%$	$12{\cdot}4 \pm 0{\cdot}4\%$	$0{\cdot}0 \pm 0{\cdot}3\%$	This work.
$KClO_4$	$^{35}Cl\ (n, \gamma)\ ^{36}Cl$	$79{\cdot}9 \pm 1{\cdot}5\%$	$17{\cdot}9 \pm 1{\cdot}3\%$	$2{\cdot}2 \pm 0{\cdot}4\%$	This work.

* Reported as chlorine having oxidation state zero to +5.

† Experiments were conducted over a range of conditions; these values are representative.

(3) L. J. SHARMAN and K. J. McCALLUM, *J. Chem. Phys.* **23**, 597 (1955).

(4) K. J. McCALLUM and O. G. HOLMES, *Canad. J. Chem.* **29**, 691 (1951).

(6) O. D'AGOSTINO, *Gazz. Chim. Ital.* **65**, 1071 (1935).

(6) M. VLATKOVIC and A. H. W. ATEN, JR., *J. Inorg. Nucl. Chem.* **13**, 331-2 (1960).

(7) D. MEIER and C. GARNER, *J. Chem. Phys.* **17**, 1344 (1949).

(8) W. F. LIBBY, *J. Amer. Chem. Soc.* **62**, 1930 (1940).

J. Inorg. Nucl. Chem., 1962, Vol. 24, pp. 139 to 146. Pergamon Press Ltd. Printed in Northern Ireland

THERMAL ANNEALING OF NEUTRON-IRRADIATED CHLORINE OXYANIONS*

M. VLATKOVIĆ† and A. H. W. ATEN, JR.
Institute for Nuclear Physics Research, Amsterdam, Netherlands

(*Received* 17 *July* 1961)

Abstract—Thermal annealing of the products of the Szilard-Chalmers process in neutron irradiated alkali chlorates is similar to annealing in most salts containing oxyanions. In perchlorates and in sodium chlorite, on the other hand, an "inverse" type of annealing is observed, which means that the percentage of the activity in the chlorate + chlorite + hypochlorite fraction decreases on heating.

THERMAL annealing behaviour has been investigated in a number of neutron irradiated halogen oxyanions, like bromates,(1) iodates(2) and periodates(3) but no data have been published concerning the annealing of chlorates or perchlorates. We thought that it would be of interest to fill this gap and in the course of these experiments we observed some cases of "inverse" annealing. The general shape of the "inverse" annealing curve has been shown to be quite similar to that of a "normal" one.

EXPERIMENTAL

Materials

Potassium chlorate, sodium chlorate and potassium perchlorate were of "Merck" p.a. origin. The crystals were ground in a mortar. The powdered chlorates were oven dried at 140°C for 2 days and the potassium perchlorate was dried at 160°C for 3 days. Sodium perchlorate monohydrate $NaClO_4{\cdot}H_2O$ was supplied by B.D.H. The wet crystals were washed with dry ether and dried in a vacuum desiccator for 10 hr at room temperature. Anhydrous sodium perchlorate was prepared from the monohydrate form by thermal dehydration. The compound loses its crystal water at ca. 54°.(4) Our sample of anhydrous material was obtained by drying at 160° for 3 days. Cases of different thermal pre-treatment are mentioned later.

Sodium chlorite was prepared from the trihydrate $NaClO_2{\cdot}3H_2O$ by thermal dehydration at 140° for 1 day. The dried sodium chlorite contained ca. 2 per cent of the chloride calculated as sodium chloride.

Neutron bombardment

The irradiations were performed with neutrons moderated in paraffin, from the Amsterdam synchrocyclotron. For irradiation salts were sealed in soft glass tubes in the presence of the air. Some of the samples of $NaClO_4{\cdot}H_2O$ had cork stoppers.

Thermal annealing

For heating above 300°C we used a thermostatically controlled oven where the temperature was constant ±5°. For lower temperatures refluxing boiling liquids were used with a constant temperature of ±1°. The irradiated salts were heated in the closed glass tubes in which they had been irradiated except for annealing above 460° where the glass tubes had to be replaced by Pyrex glass after irradiation. Quick cooling of the heated samples was done by dipping the samples into liquid air.

---

* Work performed in partial fulfilment of the requirements for the degree of doctor of chemical sciences at the University of Zagreb of M. VLATKOVIĆ.

† Present address: Institute "Ruder Bosković", Zagreb, Yugoslavia.

(1) J. COBBLE and G. E. BOYD, *J. Amer. Chem. Soc.* **74**, 1282 (1952); R. HENRY, C. AUBERTIN and E. de la GUERONNIERE, *J. Phys. Rad.* **18**, 320 (1957); J. JACH and G. HARBOTTLE, *Trans. Faraday Soc.* **54**, 520 (1958); A. G. MADDOCK and H. MULLER, *Trans. Faraday Soc.* **56**, 509 (1960).

(2) R. E. CLEARY, W. H. HAMILL and R. R. WILLIAMS, *J. Amer. Chem. Soc.* **74**, 4675 (1952).

(3) A. H. W. ATEN, G. K. KOCH, G. A. WESSELINK and A. M. de ROOS, *J. Amer. Chem. Soc.* **79**, 63 (1957).

(4) GMELINS, *Handbuch der Anorganischen Chemie*, Verlag Chemie, Berlin (1927). Band 8 Auflage, Cl, 6, No. 341.

Analysis

One mmole of irradiated $NaClO_3$, $KClO_3$ and $NaClO_2$ respectively was dissolved in ca. 100 ml of water containing 1 mmole chloride carrier. The chloride was precipitated with nitric acid and silver nitrate (except in the case of $NaClO_2$ where nitric acid was not added) and after the addition of another portion of chloride carrier a second silver chloride precipitate was obtained. The chlorate ion and the chlorite ion were reduced in the filtrate by passing through sulphur dioxide, the excess of which was later boiled off, and the chlorine was precipitated as silver chloride.

Three to six hundred milligrams of $NaClO_4{\cdot}H_2O$, $NaClO_4$ or $KClO_4$ were dissolved in water containing 1 mmole of chloride and chlorate each as carriers. The precipitation of the chloride and the chlorate as silver chloride containing ^{36}Cl was performed as described above. The excess of silver ions in the filtrate containing the perchlorate was removed by adding chloride ions and subsequent filtration. This was followed by precipitation of the perchlorate ion as tetraphenylarsonium perchlorate[5] by means of tetraphenylarsonium hydrochloride.

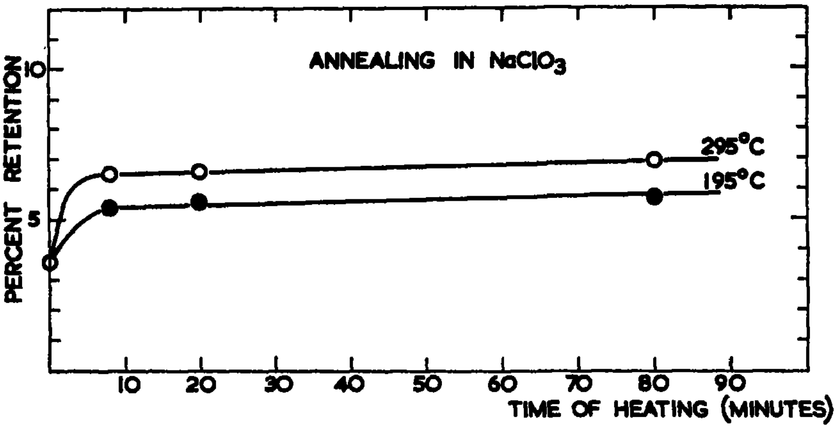

FIG. 1.—Annealing in $NaClO_3$. Per cent retention vs. time of heating (min.).

We should point out that our chemical separation was carried out under conditions in which the exchange of chlorine atoms between chloride, chlorite, chlorate and perchlorate was slow.[6] All precipitates were washed with acetone and ether, dried for a few minutes at 120° and weighed for the chemical yield. Then the corrections of the activity for the incomplete recovery of the precipitates could be applied.

Counting

The precipitates were covered with cellophane tape and counted in aluminium dishes with a β-GM counter. Decay curves were drawn for all samples and the relative activities were determined from them. Half-life curves of ^{36}Cl obtained with some silver chloride samples which had been precipitated in a neutral solution showed a tail attributed to ^{32}P formed by the reaction of fast neutrons with ^{35}Cl. Although this activity was not very important a correction was made for it.

RESULTS

Thermal annealing of $NaClO_3$ *and* $KClO_3$

The heating of the neutron irradiated chlorates before analysis resulted in a slight increase in the retention. Plots of the retention against the time of annealing are shown in Figs. 1 and 2. Initial retention was found to be identical for both chlorates. Obviously the retention increases in two stages, but we did not measure with any precision the slope for the first and fast part of the reaction.

---

[5] F. J. WELCHER, *Organic Analytical Reagents*, Vol. 4., p. 362. van Nostrand, New York (1953).

[6] H. TAUBE and H. DODGEN, *J. Amer. Chem. Soc.* 71, 3330 (1949); D. A. LEE, *J. Amer. Chem. Soc.* 76, 2590 (1954).

Sodium chlorate melts at ca. 250°C so that one of the annealing curves (Fig. 1) was obtained on the melt. On heating at 295° for 80 min it was found that the salt started decomposing, which was observed by a very slight opalescence, when ca. 300 mg of the heated salt was dissolved in water and nitric acid and silver nitrate were added. Potassium chlorate is more stable to heat; it did not melt during the annealing experiment, but slight decomposition was observed on heating the irradiated salt at 350° for 80 min.

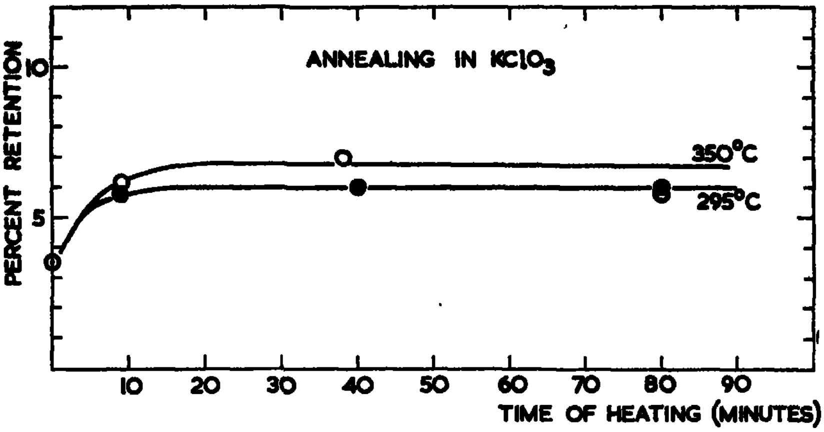

Fig. 2.—Annealing of $KClO_3$. Per cent retention vs. time of heating (min.).

Thermal annealing in $NaClO_4$ *and* $KClO_4$

No activity was found in the perchlorate fraction even after thermal annealing of the irradiated salts. The real retention was very uncertainly measured after the thermal annealing of potassium perchlorate at 490° for 80 min (ca. 2·5 per cent) and in the case of sodium perchlorate at 460° for 80 min (ca. 1·5 per cent). Most of the activity was found in the chloride fraction and the rest followed the chlorate fraction. When the percentage of activity which was found to follow chlorate is plotted against the time of annealing, we obtain curves like those in Figs. 3 and 4. In the case of sodium perchlorate heated at 295°, a small increase in the activity of the chlorate fraction was observed. When either irradiated perchlorate is heated to a higher temperature, the activity of the chlorate fraction decreases appreciably and part of the radioactivity passes into chloride. It is worth mentioning that alkali perchlorates are exceptionally stable to heat and the annealing experiments could be done without, or with very slight decomposition of the heated salts. The treatment before neutron irradiation for all samples used in these experiments was drying at 160° for 3 days. In two experiments the neutron irradiated potassium perchlorate was dissolved in the carrier solution, $NaHAsO_3$ was added and the solution was left for 20 min at room temperature. By adding acetic acid, nitric acid and silver nitrate, the silver chloride was precipitated. Further separation of the chlorate and the perchlorate was performed as was described before. By this method of analysis any existing active chlorite or hypochlorite would have been reduced and would have joined the Cl-fraction. The percentage of the active chlorate fraction did not change significantly; hence we may conclude that the "chlorate" radioactivity in general consists of ions having the actual composition ClO_3^-.

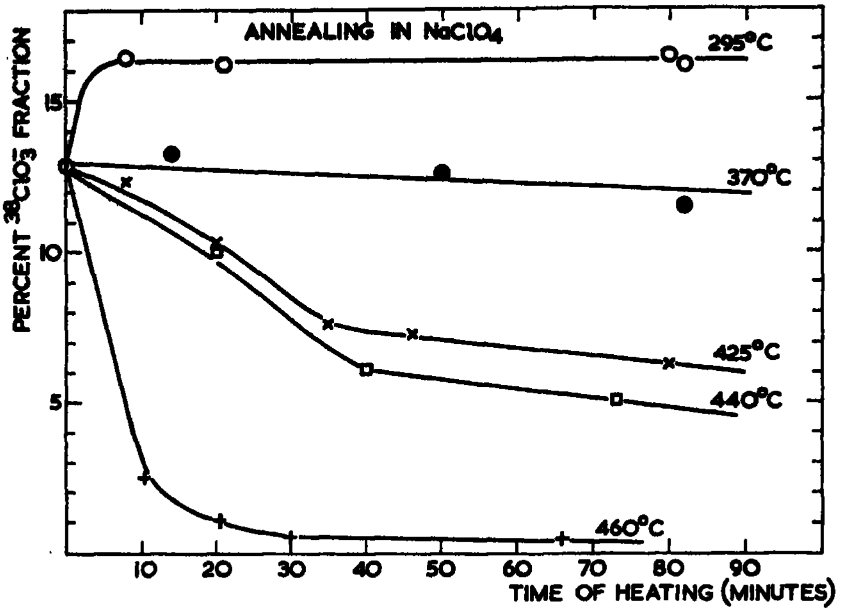

FIG. 3.—Annealing of NaClO$_4$. Per cent of ^{38}Cl in the chlorate fraction vs. time of heating (min).

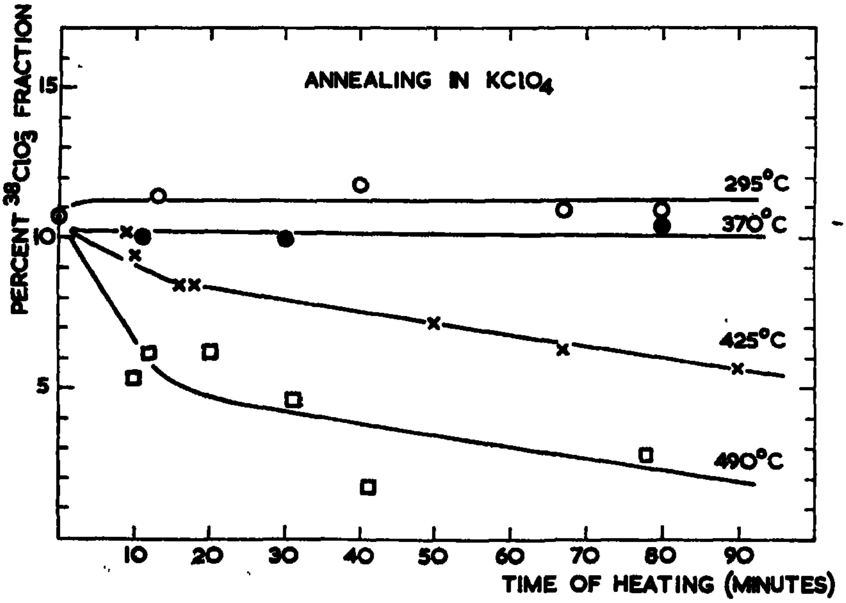

FIG. 4.—Annealing of KClO$_4$. Per cent of ^{38}Cl in the chlorate fraction vs. time of heating (min).

The influence of preirradiation treatment on the thermal annealing behaviour of $NaClO_4$

Sodium perchlorate monohydrate dehydrated at 160° for 3 days (pre-treatment a) was subsequently either dried in an oven at 370° for 12 hr (pre-treatment b) or dissolved in dry acetone; ether was added and the precipitated salt was filtered off, washed with dry ether and dried at room temperature in a vacuum dessicator for 4 hr (pre-treatment c). The salt prepared according to (c) contained about 2 per cent of moisture and acetone.

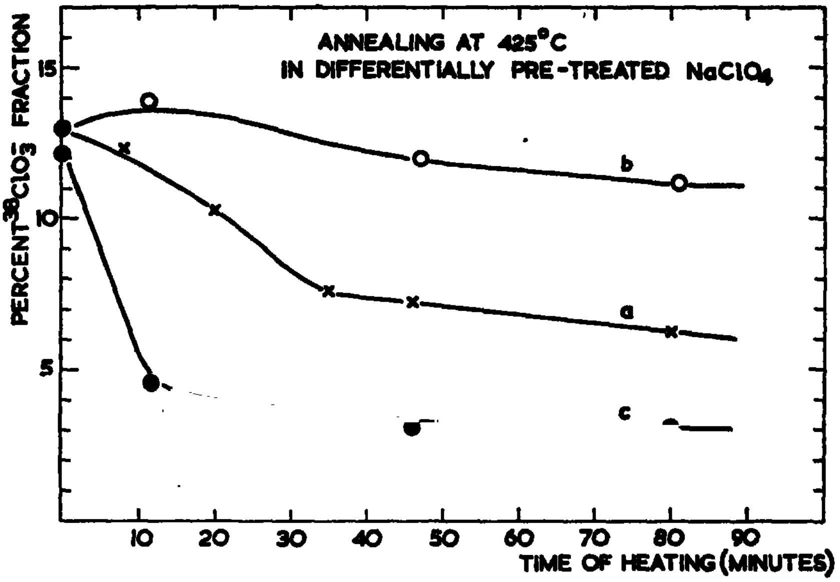

FIG. 5.—Annealing of $NaClO_4$ at 425°C. Per cent of ^{38}Cl in the chlorate fraction vs. time of heating (min). Pre-irradiation treatment of $NaClO_4$: dried 160°C, 72 hr (a) and subsequently either dried at 370°C, 12 hr (b) or recrystallized from organic solvents and dried at a vacuum (c).

Sodium perchlorate samples prepared by treatment (b) and (c) were irradiated with neutrons and annealing was carried out at 425°. The annealing curves obtained (b and c, Fig. 5) were compared with one (a) taken from Fig. 3 corresponding to the same temperature. Initial activity percentages in the chlorate fraction were almost the same in all samples, whatever the thermal pretreatment had been.

Thermal annealing of $NaClO_4{\cdot}H_2O$

The percentages of the activity found in the chlorate fraction in the various experiments with sodium perchlorate monohydrate are given in the third column of Table 1. The rest of the activity was found in the chloride fraction.

Thermal annealing of $NaClO_2$

If the analysis of the irradiated sodium chlorite is performed as described above, it is possible to distinguish only between the chloride fraction and the higher oxidation states of chlorine ($ClO^- + ClO_2^- + ClO_3^-$). The relation between the percentage of radioactivity in the higher oxidation states of chlorine and the time of annealing is presented in Fig. 6. Sodium chlorite is said to decompose at 180–200°(4) but considerable decomposition was caused by keeping the salt at 154° for a period of 50 min or longer.

TABLE 1.—ACTIVITY IN THE CHLORATE FRACTION IN NEUTRON-IRRADIATED $NaClO_4 \cdot H_2O$

Group of experiments	Description of experiments	Percentage of activity in the $ClO_3^- + ClO_2^- + ClO^-$ fraction
1	No annealing, room temperature	8·1
2	No annealing, $NaAsO_2$ was added to the solution of irradiated salt, Cl^- and ClO_3^- carriers, left 40 min. Percentage includes ClO_3^- only, without ClO^- and ClO_2^-.	7·1
3	Annealing in stream of nitrogen:	
a	at 100° for 80 min (partial dehydration occurred during annealing	8·0
b	at 154° for 40 and 83 min (partial dehydration occurred during annealing)	5·0; 3·7
c	at 292° for 40, 80 and 95 min (at the end of annealing the salt was completely dehydrated)	2·8; 2·2; 2·5
4	Annealing under vacuum:	
a	at 76° for 80 min (79 % of the crystal water was lost)	8·0
b	at 100° for 80 min (at the end of annealing the salt was completely dehydrated)	8·1
5	Annealing in small glass ampoules at 292°, for 80 min, dehydration prevented (during annealing salt melted)	6·4

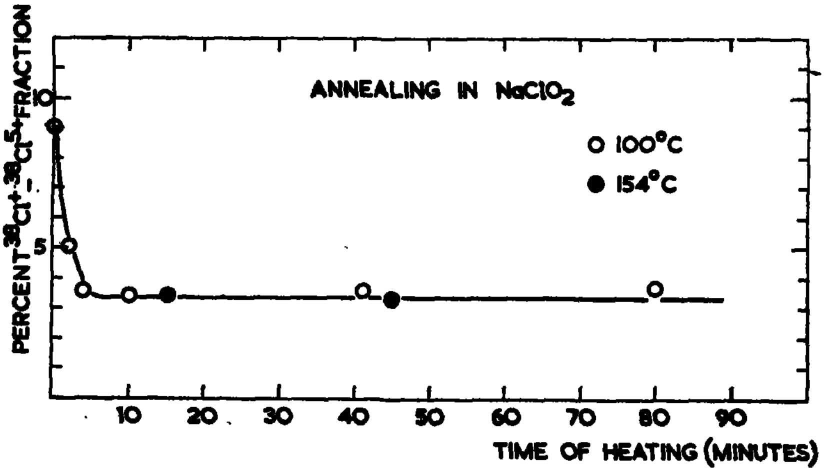

FIG. 6.—Annealing in $NaClO_2$. Per cent of ^{38}Cl in $ClO^- + ClO_2^- + ClO_3^-$ fraction vs. time of heating (min).

DISCUSSION

The low retention amounting to 3·5 per cent found in neutron irradiated sodium chlorate and potassium chlorate supports the earlier results(7) for the $^{37}Cl(n, \gamma)^{38}Cl$ reaction in sodium chlorate where 1·5 per cent of retention was reported. The same authors, however, obtained 9 per cent retention for betatron irradiation of sodium chlorate, $^{35}Cl(\gamma, n)^{34}Cl$. This significantly higher value may well have been caused by radiation annealing when chlorate was irradiated by a betatron as is supposed in the original paper.

In the post recoil thermal annealing experiments with chlorates we obtained a slight increase of the retention; the isothermal curves (Figs. 1 and 2) show that a plateau which amounts to about double the initial retention could be reached.

An interesting feature of the neutron irradiated perchlorate is the practical absence of any retention in the strictest sense of the word (in the ClO_4-fraction) even after the annealing. This shows once more that the chemical bonds are completely ruptured by the recoil. It is of interest that in the case of a perchlorate the parent compound could not be reformed from the radioactive nucleus. This might perhaps be attributed to the fact that the formation of ClO_4^- in the crystal lattice would require a high positive charge on the chlorine atom and that sufficiently highly charge radio-chlorine atoms are not produced by the recoil process or by the internal conversion of capture γ-rays. The fact that formation of radioactive ClO_4^- is practically absent in the case of slow neutron irradiation of alkali perchlorates provides an interesting parallel to the low yield of radioactive IO_4^- in the activation of potassium periodate.(8)

Another interesting phenomenon is the decrease of the chlorate activity in the thermal annealing curves obtained (Figs. 3 and 4). These curves show fairly good reproducibility when pre-irradiation thermal treatment of the samples is identical. It is of special interest that these "inverse" annealing curves, in which the percentage activity in the oxidized fraction decreases, have the same shape as "normal" annealing curves.(8) At first we observe a fast reaction, which involves only a part of the total activity available for the reaction, followed by a second much slower process with the same general trend. The decrease in the activity of the chlorate fraction may perhaps be explained by thermal decomposition of radioactive chlorate formed in the perchlorate lattice in which the ClO_3^- ion will be less stable than the ClO_4^- ions.

The thermal decomposition of chlorate in the pure condition takes place between 400° and 500°(4) according to $4KClO_3 \rightarrow KCl + 3KClO_4$ followed by $KClO_4 \rightarrow KCl + 4O$ and the low activity of ca. 2 per cent found in the perchlorate fraction might possibly be ascribed to such a decomposition, if, at least, the latter may be assumed to take place according to the normal mechanism.(9)

There is one special feature about the "inverse" annealing, which is illustrated in Fig. 5. Although preliminary heat-treatment of the sample to be irradiated hardly affects the initial retention, the influence of heat pre-treatment on the shape of the annealing curve is most pronounced. It is quite evident that some component of the crystal participates in the annealing, which component is very sensitive to preliminary heating. The suggestion comes to mind that faults in the crystal lattice play a part in the annealing process and that these lattice faults are "ironed out" during the preliminary heat treatment. At any rate the component in question cannot be a product of the irradiation during neutron activation.

---

(7) K. J. McCallum and O. G. Holmes, *Canad. J. Chem.* **29**, 691 (1951).

(8) G. Harbottle and N. Sutin, *Adv. Inorg. Chem. Radiochem.* **1**, 267 (1959).

(9) A. Vanden Bosch and A. H. W. Aten Jr., *J. Amer. Chem. Soc.* **75**, 3835 (1953).

A few explanatory remarks should be made in this connection. It might be suggested that the difference between the three curves in Fig. 5 might be caused by the retention of different quantities of moisture which would mean that the "inverse" annealing would be due entirely to the action of very rare H_2O molecules left in the crystals. However a moisture content of any importance could hardly be expected to occur in the salt dried at 160° for 72 hr, and thus the difference between the two upper curves would remain unexplained. Some authors have reported the influence of pre-irradiation degassing on the initial oxidation states of ^{32}P and of ^{35}S produced in neutron irradiated alkali chlorides,(10) which seems to be due to the influence on the retention of small quantities of various gases within the crystal lattice.(11) However, in those experiments the initial retention was found to be very different in samples which had undergone different pre-irradiation treatment.

In the case of sodium perchlorate monohydrate the percentage of the total activity found initially in the oxidized fraction (8 per cent) is appreciably lower than in the anhydrous compound (Table 1). This is similar to observations made on other salts, but a rule of general validity does not seem to exist (cf. the discussions given by HARBOTTLE and SUTIN(8) and by MADDOCK and MÜLLER(1)).

As the presence of arsenite did not significantly affect the activity in the chlorate fraction we may assume that this activity goes into solution in a chemical form which is essentially ClO_3^-.

Dehydration in itself does not much influence the activity of the chlorate fraction. This is in agreement with the behaviour in the case of dehydration or hydration of other irradiated salts.(11)

The thermal annealing behaviour of the monohydrate is roughly similar to that of the anhydrous material, but there is a difference in that in the former case a lower temperature is required for "inverse" annealing than in the latter case. It should, however, be kept in mind that in the $NaClO_3 \cdot H_2O$ the annealing takes place—at least in part—during the dehydration process. It seems that the removal of water from the lattice during the annealing contributes to the lowering of the activity in the chlorate fraction.

Sodium chlorite also shows "inverse" annealing (Fig. 5). It is tempting to look for an explanation in the posibility that most of the activity in the $ClO^- + ClO_2^- + ClO_3^-$ fraction is present as ClO^- ions and that these ions in the $NaClO_2$ lattice easily decompose on heating.

Acknowledgement—This investigation was performed as part of the program of the Foundation for Fundamental Research of Matter (F.O.M.) with the financial support of the Organization for Pure Research (Z.W.O.).

One of the authors (M. VLATKOVIĆ) wishes to give thanks to the International Atomic Energy Agency, Vienna, which made it possible to carry out the work described in this paper.

(10) W. S. KOSKI, *J. Amer. Chem. Soc.* 71, 4042 (1949); T. A. CARLSON and W. S. KOSKI, *J. Chem. Phys.* 23, 1596 (1955); R. H. HERBER, I.A.E.A. Prague Symposium, Oct. 1960.

(11) L. LINDNER. Thesis, Amsterdam (1959).

J. Inorg. Nucl. Chem., 1962, Vol. 24, pp. 147 to 156. Pergamon Press Ltd. Printed in Northern Ireland

THE RELATIONSHIP BETWEEN THE SURFACE TENSIONS AND ENERGIES OF LIQUID METALS AND THEIR CRITICAL TEMPERATURES*

A. V. GROSSE
Research Institute of Temple University, Philadelphia, Pennsylvania

(*Received* 16 *August* 1961)

Abstract—It is shown that a general relationship exists between the surface tension (σ) and surface energy (σ_A) of a liquid metal and its critical temperature (T_c) and atomic volume (V_A). The relationship (except for Hg, Cd and Zn) is:

$$\sigma_A{}^o = \sigma^o \cdot V_A{}^{o\,2/3} = 0{\cdot}64 \text{ (ergs/gramme atom}^{2/3}\text{)}.\ T_c \text{ (in °K)},$$

where the superscript o refers to the extrapolated value at 0°K.

THERE is at present no recognised simple and general relationship between the surface tension of a *liquid metal* and any of its other physical properties. The metals constitute about 80 per cent of all the elements, and the surface tensions of only a small number have been measured.

As inorganic chemists we are interested in a general relationship applicable to all metals which will permit us to estimate at least approximately the surface tension and surface energy of any metal at any specified temperature over its whole liquid range, i.e. from its melting point to its critical point. In contrast, many of physical-chemical studies, and justifiably so, had the aim of correlating the surface tension of one metal over a very narrow temperature range, but with great precision. In view of the many high temperature studies on liquid metals being carried out at the Institute, where the surface tension enters only as a correction factor, such a general relationship would be particularly valuable.

The surface tensions of liquid metals are substantially higher than those of normal liquids, e.g. a large number of homopolar organic and inorganic compounds, and the well known law of EÖTVOS(1), RAMSAY and SHIELDS(2) is usually considered *not to apply* to liquid metals and salts.(3) It will be shown in this paper that the *law of* EÖTVOS *does apply to liquid metals*, provided that certain adjustments are made.

The law of EÖTVOS for homopolar molecules, with surface tension, σ, and molar volume, V_M, states that

$$\sigma_M = \sigma \cdot \mathrm{V}_M{}^{2/3} = K_{E\ddot{o}}(T_c - T), \qquad (1)$$

where T_c is the critical temperature in °K., T the temperature at which σ_M, σ, and V_M are measured and $K_{E\ddot{o}}$, the EÖTVOS constant:

$$K_{E\ddot{o}} = 2{\cdot}12 \text{ erg per mole}^{2/3} \text{ per °K.}$$

---

* This work was supported in part by the National Science Foundation under Grant NSF-G 15540.

(1) EÖTVOS, *Wiedeman's Ann. Phys.* 27, 452 (1886).

(2) W. RAMSAY and J. SHIELDS, *Z. Phys. Chem.* 12, 443 (1893).

(3) See for example A. EUCKEN, *Principles of Physical Chemistry* (7th Ed.). p. 128. Akadem. Verlagsgesellschaft, Leipzig (1951).

If σ_M and σ and V_M, respectively, are extrapolated as an undercooled liquid to 0°K., the EÖTVOS relationship becomes:

$$\sigma_M{}^0 = \sigma^0 \cdot V_M{}^{0\frac{2}{3}} = K_{E\ddot{o}} \cdot T_c \tag{2}$$

It will be demonstrated here that for liquid metals

$$\sigma_A{}^0 = \sigma^0 \cdot V_A{}^{0\frac{2}{3}} = C \cdot T_c, \tag{3}$$

where $\sigma_A{}^0$, σ^0 and $V_A{}^0$ are the extrapolated surface energy, tension and volume per gramme atom at 0°K., respectively. In the case of metals the universal constant C is about 3 times smaller than $K_{E\ddot{o}}$ and $\simeq 0{\cdot}64$ *erg per g at.*$^{\frac{2}{3}}$ *per °K.* That the constant for metals should be different from the EÖTVOS constant is understandable since the nature of metallic bonding is quite different from the weak Van der Waals' forces in homopolar molecules. The reason that this relationship was not recognised earlier is probably due to two causes.

First, there was no clear understanding of the critical temperatures of metals. In a recent paper(4) it was shown that the critical temperature of metals can be reasonably estimated from a number of available experimental data. It was demonstrated that the law of Cailletet and Mathias or the law of rectilinear diameters applies to liquid mercury, the only metal whose critical temperature had been determined experimentally. In this respect mercury follows most other thermally stable liquids and it is assumed that other metals behave similarly.

One can readily calculate the ideal density of the saturated metal vapour in equilibrium with the liquid from its known vapour-pressure. As long as the vapour density is small compared to the liquid density, one is far away from the critical point, since at the critical temperature the density of the liquid metal and that of the saturated vapour are identical. By plotting liquid and ideal vapour density vs. temperature one can readily obtain an *upper limit* of the critical temperature.

In addition, the theory of corresponding states requires that the entropy of vaporization of two metals be equal at the same reduced temperature. The heat of vaporization, as well as the entropy are known for mercury over a substantial temperature range. Since both the energy and the entropy of vaporization equal 0 at the critical temperature, it is feasible to construct the entropy vs. temperature curve of mercury. Assuming that the other metals will have the same entropy values at the same reduced temperatures, it is possible to estimate the critical temperature of any metal, since vapour-pressure and heat of vaporization data of all elements are now available.(5) The critical temperatures obtained by the two methods are in reasonable agreement. Tables 1 and 2 give the critical temperatures ranging form 1733°K for mercury to about 23,000°K for tungsten. In contrast to homopolar molecules, the normal boiling points of which are about ⅔ of the critical temperatures, the metals have critical temperatures of 2·75–4 times higher than the normal boiling points (629·9°K and 5800°K for Hg and W, respectively).

Second, comparatively few reliable data are available on the surface tensions of metals.

---

(4) A. V. GROSSE, *J. Inorg. Nucl. Chem.* **22**, 23 (1961); see also A. V. GROSSE, Report on "The Liquid Range of Metals and Some of Their Physical Properties at High Temperatures," The Research Institute of Temple University, Philadelphia, Pa., Sept 5, 1960.

(5) D. R. STULL and G. C. SINKE, *The Thermodynamic Properties of the Elements*, Advances in Chemistry Series, Vol. 18. Amer. Chem. Soc., Washington, D.C. (1956).

We will consider here the simplest, and also practically the most important case, namely, the surface tension of a metal vs. its saturated vapour, which at low temperatures is identical to a vacuum. In a number of cases the atmosphere can be a noble gas, such as argon or helium, provided that the noble gas used is pure. Other requirements for reliable measurements, particularly at high temperatures are:

1. That the metal be not contaminated by the material of the container or other equipment during the experiment.

2. That due consideration be given to the presence of surface active impurities. It has been demonstrated that the presence of other metals or nonmetals, even in trace amounts, can influence not only the actual values of the surface tension, but change the nature of the whole surface tension vs. temperature curve.

In view of the above requirements, good experimental data are available primarily on low-melting metals such as tin, lead, bismuth, cadmium, zinc and mercury, the latter being the classical example. Recently, in view of its importance to nuclear reactor technology, the surface tension of liquid sodium has been accurately measured. The most reliable data on sodium, described by TAYLOR(6) are given below:

SURFACE TENSION OF SODIUM

T(°C)	σ(dynes/cm)
100	190·4
150	185·4
200	180·4
250	175·4
300	170·6
350	165·6
400	160·8
450	156·0

It was shown originally by van der Waals (1894) and developed recently by GUGGENHEIM(7) that for most organic liquids the EÖTVOS law can be made more exact by using the relationship:

$$\sigma = \sigma^0(1 - T/T_c)^n \text{ or in its logarithmic form} \qquad (4)$$

$$\log_{10} \sigma = \log_{10}\sigma^0 + n \log_{10}(1 - T/T_c), \qquad (5)$$

where the exponent $n = 11/9$ or 1·222.

The surface tensions of the metals referred to above are given in Fig. 1 in logarithmic form, and the exponent n or the slope is given alongside each line. The data on which the line is based are given in Table 2 and the experimental temperature ranges are also given in Table 1. One notices immediately, *in contrast* to organic compounds that the slope n is not constant, but varies from 1·28 in case of sodium down to 0·25 in case of cadmium. It is believed that it is too early to judge whether the same slope will prevail for a larger temperature ranges, because at present the experimental ranges covers only small percentages, i.e. about 5 per cent, of the total liquid temperature ranges.

Both the surface tension and the surface energy vanish at the critical temperature.

---

(6) J. W. TAYLOR, AERE Report M/TN24 (1954); see also Liquid Metals Handbook, Na–K-suppl., 1 July 1955, p. 28.

(7) E. A. GUGGENHEIM, *J. Chem. Phys.* 13, 259 (1945).

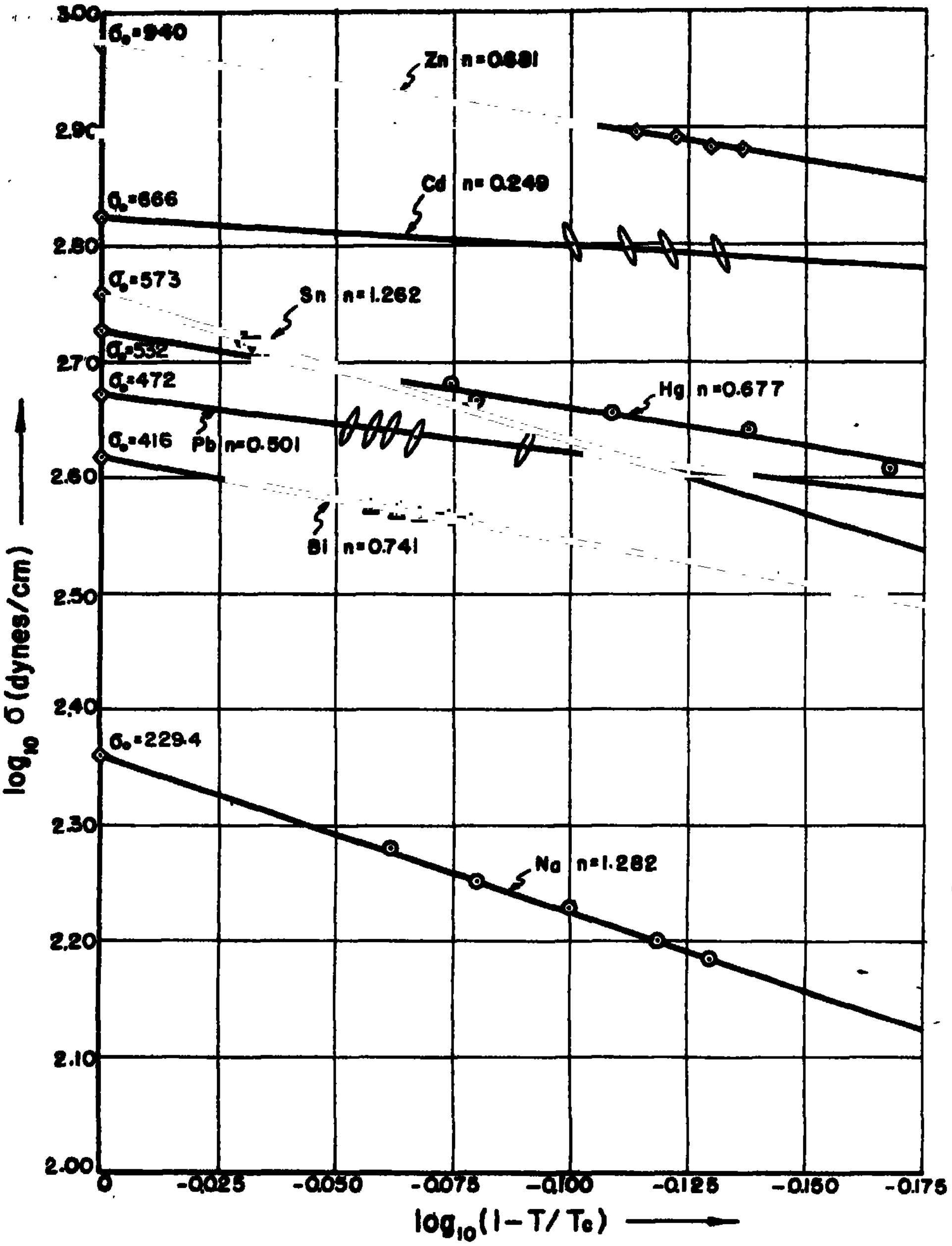

FIG. 1.—Surface tension of zinc, cadmuim, mercury, tin, lead, bismuth and sodium

This fact is taken advantage of in Fig. 2, where the actual data for the same low melting metals are plotted from the experimental range down to the critical temperature and *extrapolated* to 0°K, assuming that we have a straight line σ vs. T relationship. The data so obtained are compared in Table 1 with those obtained by logarithmic extrapolation to 0°K in Fig. 1. In all cases, with the exception of mercury, the agreement between the two methods of obtaining σ^0 is fairly good. Both the logarithmic and straight-line plot reproduce the presently available experimental data, with the exception of mercury, similarly well.

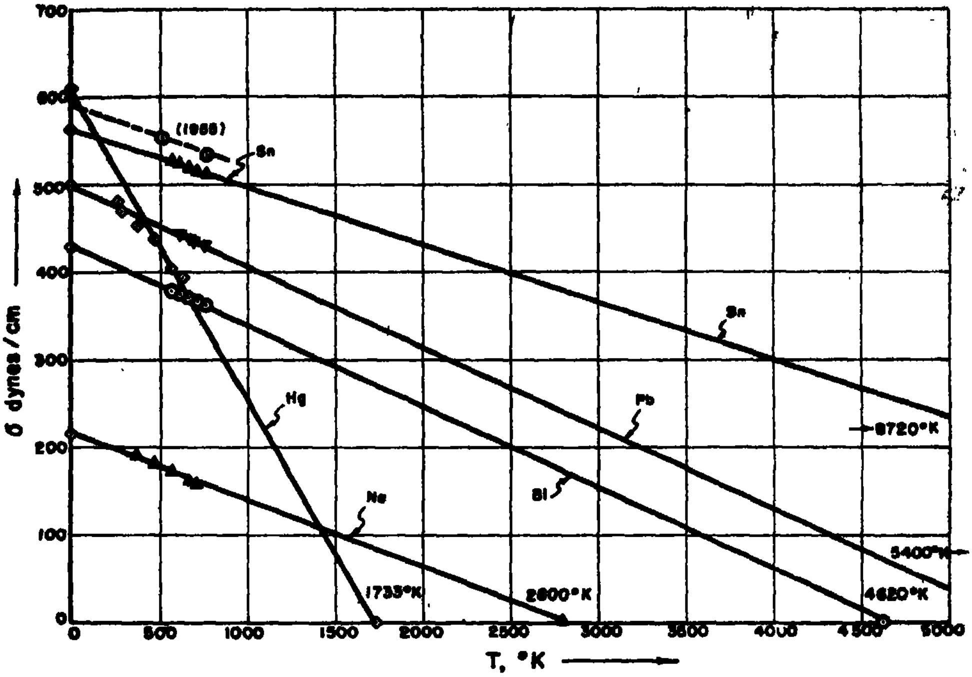

Fig. 2.—Surface temp vs. temp. of liquid metals

Table 1.—Comparison of σ^0(log) (see Fig. 1) and σ^0 (see Fig. 2)

Metal	Exp. range of σ, (°C)	% of Total liquid range	Tm.p. (°K)	T_c (°K)	Total liquid range (°K)	Log^{10} σ^0(log)	n = log slope	σ^0(log) (see Fig. 1) dyne/cm)	σ^0 (see Fig. 2) (dyne/cm)
Zn	510–640	4·8	692·7	3380	2690	2·9731	0·681	940	1030
Cd	350–500	6·3	594	2960	2370	2·8235	0·249	666	810
Sn	300–500	2·4	505	8720	8215	2·7582	1·262	573	578
Hg	0–354	23·6	234·29	1733	1500	2·7260	0·677	532	608
Pb	350–750	9·4	600·6	5400	4800	2·6722	0·501	470	498
Bi	300–500	4·9	544·5	4620	4075	2·6186	0·741	416	428
Na	100–450	14·4	370·97	2800	2430	2·3610	1·282	229·4	216

The straight line plot of σ vs. T, expressed algebraically, is of course:

$$\sigma = \sigma^0(1 - T/T_c) \tag{6}$$

and assumes for metals, in contrast to Fig. 1, an exponent $n = 1$.

It embraces however in principle the critical point and does permit one to obtain, at least in first approximation, the *surface tension at any temperature*. As mentioned previously, the logarithmic equation covers at present only a small percentage of the total liquid range of the metal (see Table 1). Furthermore, if extended over a larger temperature range it ceases to be a straight line relationship: ($\log_{10} \sigma$ at $T_c = -\infty$).

Regardless of what the final accurate temperature function of surface tension will be (we believe it is likely to be slightly convex or concave towards the T-axis) we chose for our present purposes the simple straight line relationship, shown in Fig. 2, to obtain σ^0 or the extrapolated surface tension at 0°K.

All the experimental values of σ^0 of twenty metals, as well as the atomic surfaces and the atomic surface energies of these metals are given in Table 2. The source of the experimental data on each metal is given in an appendix to Table 2.

In order to obtain $\sigma_A{}^0 = \sigma^0 \cdot V_A{}^{2/3}$ it would be best to use atomic volumes or areas of the respective metals extrapolated as undercooled liquids also to 0°K. Unfortunately accurate liquid density data are not yet available for a large number of metals. Thus, we will use, with a small error, atomic volumes of the solid metal at room temperature. (A later correction to the true $V_A{}^0$ values will probably improve the relationship). It is in this manner that the atomic areas, given in Table 2, have been calculated.

(It is to be noted that our $V_A{}^{2/3}$ is not the *true atomic area*, but only a number proportional to it. For a close-packed surface of close packed spheres the *true* atomic surface area, A, at the temperature T,

$$A_T = 1{\cdot}091\ V_A{}^{T2/3} \cdot N^{1/3}, \text{ in cm}^2/\text{g} \cdot \text{at.}$$

where N is Avogadro's number. The true surface free energy per gramme atom at any temperature T, would be

$$F\sigma = \sigma_T \cdot A_T \text{ and in the case of close packed spheres}$$

$$F\sigma = \frac{\sigma_T \cdot 1{\cdot}091\ V_A{}^{T2/3} N^{1/3}}{4{\cdot}181 \times 10^7}\ \frac{\text{g cal}}{\text{g atom}},$$

if σ_T is in dynes/cm and $V_A{}^T$ in cm³/g atom. For simplicity we will retain for the present our definition of σ_A).

The plot of the atomic surface energy vs. critical temperature is shown in Fig. 3. It will be noted that with the exception of mercury, cadmium and zinc, all the metals for which data are available fall essentially on a straight line, from the lowest experimental surface energy of mercury, at a critical temperature of 1733°K, to tungsten with the highest value, at a critical temperature of approximately 23000°K. The experimental surface tension of tungsten was determined in an elegant way by the drop-weight method by CALVERLEY⁽⁸⁾. The greatest deviation from the line is noted in the case of tin. Recent investigations by POKROVSKY and SAIDOV⁽⁹⁾ have shown that traces of surface active metal inpurities, like lead and bismuth, lower the surface tension appreciably; their highly purified tin showed higher values (shown as a dotted line (1955) in Fig. 2). In view of the many difficulties mentioned previously in making

(8) A. CALVERLEY, *Proc. Phys. Soc.* **70 B**, 1040–44 (1957).

(9) N. L. POKROVSKY and M. SAIDOV, *J. Phys. Chem., U.S.S.R.* **29**, 1601–1609 (1955).

TABLE 2.—EXPERIMENTAL SURFACE TENSIONS AND ATOMIC SURFACE ENERGIES OF LIQUID METALS

	Metal	T_c (°K)	Atomic volume at room temp., (cm^3/g atom)	Atomic surface, (cm^2/g atom$^{2/3}$)	σ^0, Surface tension (dynes/cm)	σ_A, atomic surface energy (ergs/g atom$^{2/3}$)
1	Hg	1733	13·9	5·78	608	(3510)
2	K	2440	45·3	12·60	100	1260
3	Na	2880	22·9	8·05	216	1735
4	Cd	2960	13·0	5·53	810	(4480)
5	Zn	3380	9·2	4·39	1030	(4530)
6	Bi	4620	21·3	7·66	428	3280
7	Te	4840	17·2	6·65	460	3060
8	Sb	5070	18·2	6·91	476	3300
9	Pb	5400	18·2	6·91	498	3440
10	In	6730	15·1	6·10	608	3650
11	Ag	7480	10·3	4·73	1100	5210
12	Ga	7620	11·8	5·18	770	3990
13	Ge	8400	13·6	6·45	770	4950
14	Al	8550	10·2	4·65	945	4400
15	Sn	8720	16·3	6·42	578	3710
16	Cu	8980	7·1	3·68	1260	4640
17	Au	9500	10·2	4·71	1325	6290
18	Fe	10350	7·053	3·678	2100	7730
19	Pt	14650	8·7	4·24	2160	9160
20	W	23200	9·8	4·59	2840	13050

APPENDIX TO TABLE 2

Source of Experimental Data

Na, K	*Liquid Metals Handbook*, *Na-Nak Supplement*, U.S.A.E.C.- Dept. of the Navy, Washington, D.C. (1955).
Zn, Cd, Pb, Sn, Bi	T. HOGNESS. *J. Amer. Chem. Soc.* 43, 624 (1921).
Hg, Au, Ag, Tl, Sb	*Liquid Metals Handbook*, (2nd Ed.)., U.S.A.E.C.- Dept. of the Navy, Washington, D.C. (1952).
Fe	F. A. HALDEN and W. D. KINGERY, *J. Phys. Chem.* 59, 557-9 (1955).
Al	A. PORTEVIN and P. BASTIEN, *C. R. Acad. Sci.*, Paris 202, 1072-4 (1936).
Ga	O. A. TIMOFEEVITCHEVA and P. P. PUGATCHEVITCH, *D.A.N. of the U.S.S.R.* 134, No. 4, 840-843 (1960).
Ge	T. P. KOLESNIKOVA, *Chem. Abstr.* 55, 9995 (1961). (*Izvest. V. U. Zavedenii, Chernaya Met.*, No 9, 14-17 (1960)).
In	O. A. TIMOFEEVITCHEVA and P. P. PUGATCHEVITCH, *D.A.N. of the U.S.S.R.* 124, No. 5, 1093-6 (1959).
W	A. CALVERLEY, *Proc. Phys. Soc.* 70B, 1040-4 (1957).
Pt	QUINCKE, *Ann. Phys.* 134, 356 (1868).
Cu	SAUERWALD and DRATH, *Z. Anorg. Chem.* 154, 79 (1926).

(Data for Mg vary from 560–990 dynes/cm at 700°C, see II Liq. Met. H. B., and have not been considered!).

accurate measurements particularly at the higher temperatures (see p. 149), the present agreement is satisfactory.

The data for mercury, cadmium and zinc fall on a parallel line. The reason for their exceptional positions may be that whereas on the surface of all other metals each atom is surrounded by six closest neighbours, a surface atom of mercury is surrounded by fewer, approximately four atoms(10); thus in such cases, in view of the greater insaturation of surface forces one would expect the surface tension to be higher. Most of the metals however crystallize in a cubic or hexagonal close packed lattice, and it is to be expected that at least near the melting point the geometric pattern of the solid is preserved in the liquid. A rigorous explanation for the behaviour of Hg, Cd and Zn *will have to wait* additional study.

---

(10) See J. A. CAMPBELL and J. H. HILDEBRAND, *J. Chem. Phys.* 11, 330 (1943).

In order to extend the experimental foundation of this relationship it would be particularly desirable to obtain experimental data on metals above gold, i.e. having critical temperatures above 10,000°K. Maximum surface tensions are expected for metals having high critical temperatures and low atomic volumes and thus atomic areas; data for liquid molybdenum, tantalum, columbium, rhenium and other noble metals (Os, Ir, etc.) would be particularly desirable. Low values are conversely expected for metals with a low critical temperature and high atomic volumes; therefore rubidium, cesium and francium are expected to fall on the lowest end of the line.

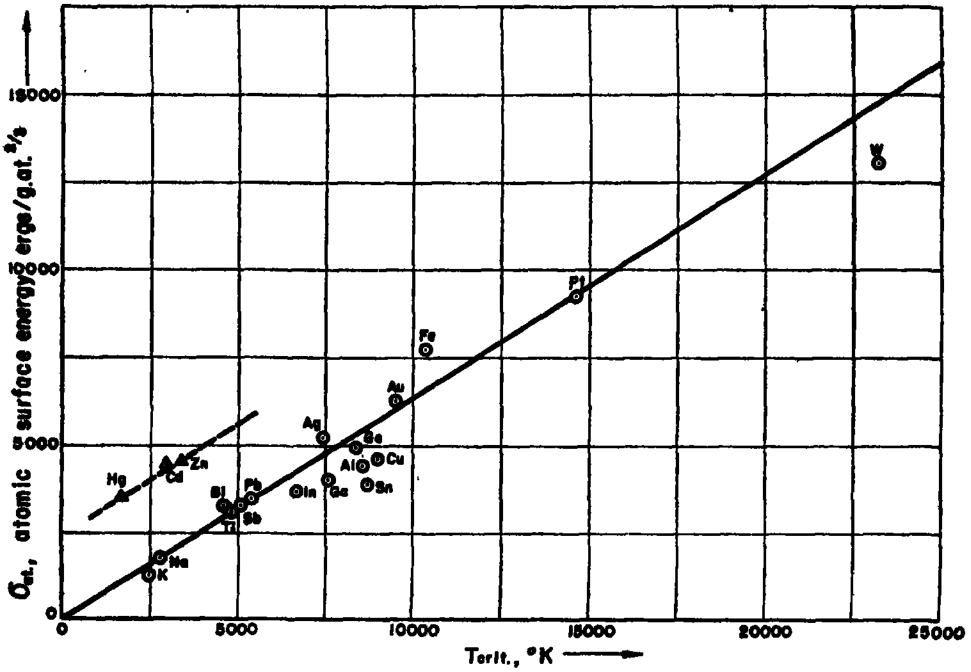

FIG. 3—Atomic surface energy, $\sigma_{\text{at.}}$ $(= \sigma^0 \cdot V^{2/3}_{\text{at.}}$ vs. $T_c)$.

The slope of the line for each metal or $d\sigma/dT = -\sigma^0/T_c$ and σ vs. T relationship can be expressed as:

$$\sigma = \sigma^0 + \frac{d\sigma}{dT} \cdot T \tag{7}$$

where the average temperature coefficients over the whole liquid range of each metal are given in Table 3. (They are compared with experimental values obtained over a narrow temperature range given in the last column of the Table.)

The general relationship between σ_A vs. T_c permits us to estimate the surface tension of any metal at any temperature. We will illustrate this point by a specific example—namely, *lanthanum* and *europium*.

In view of the close similarity of the rare earth metals one would expect superficially similar values of their surface tension.

TABLE 3.—THE AVERAGE TEMPERATURE COEFFICIENTS OF SURFACE TENSION OVER THE WHOLE LIQUID RANGE

$$d\sigma/dT = -\sigma^{\circ}/T_{0}$$

(σ° and T_0 taken from Table 2)

(arranged in ascending order and comparison with experimental values over limited temp. range)

Metal	$d\sigma/dT$, (dyne per cm per °K)	Exp. values dynes per cm per °K	Range (°C)
K	—0·041		
Na	—0·077	—0·098	100–450
Sn	—0·065	—0·049 (S.U. 1960)	250–500
		—0·080 (Hogness)	300–500
In	—0·086	—0·085	170–500
Ge	—0·092		
Pb	—0·092	—0·073	350–500
Bi	—0·093	—0·065	300–500
Sb	- 0·094		
Tl	—0·095		
Ga	—0·101	—0·047	30–505
Al	—0·111		
W	—0·123		
Au	—0·140		
Cu	—0·140		
Ag	—0·147		
Pt	—0·148		
Fe	—0·203		
Cd	—0·274	—0·067	350–500
Zn	—0·305	—0·185	510–640
Hg	- 0·352	—0·243	0·354

The pertinent data on the two elements, with an estimate of their critical temperatures, are given in Table 4.

From our relationship it follows that σ_{A}° for

La = 7500 ergs per cm per g. at$^{\frac{2}{3}}$.

and Eu = 3300 ergs per cm per g. at$^{\frac{2}{3}}$.

The respective surface tensions at 0°K., $\sigma^{0} = 940$ and 350 dynes/cm. At 1200°K the surface tensions will be, in line with Equation 7:

850 dynes/cm for La

270 dynes/cm for Eu;

thus La will have a value approximately three times greater than liquid europium.

Since both metals are now available in a high degree of purity the above values can be determined experimentally.

TABLE 4.

				Data from reference. 5				
Z	Density at 20°C.	V_A. (cms^3)	Crystal form	M.P. (°K)	N.B.P. (°K)	ΔS Vap.	T_{red}.	T_0(°K).
La 57	6·19	22·42	face centred cubic	1193	3640	26·25	0·312	11,700
Eu 63	5·244	29·00	body centred cubic	1100	1700	24·70	0·330	5,150

The original EÖTVOS law cannot be checked experimentally for metals *at the moment*, because so far the surface tensions of metals have been measured over a very narrow temperature range, i.e. 5–10 per cent of the total liquid range. In contrast, σ_M and σ of typical homopolar molecules like CO_2, CCl_4 and benzene have been measured over the *whole liquid range*, up to their critical point.

Note. A publication by TAYLOR⁽¹¹⁾ with an estimation of the unknown surface of 27 metals at their melting points, was brought to our attention. Taylor uses five physical correlations, of which the closest one to ours is a relationship between the surface energy and the heat of sublimation of the solid metal. Since the estimation of the surface tension of 27 metals, where experimental data are now lacking, is important but would require the presentation of a large number of additional experimental data, we intend to compare our estimates with those of Taylor in a separate publication.

(11) J. W. TAYLOR, *Metallurgia*, **50**, 161–165 (1954).

J. Inorg. Nucl. Chem. 1962, Vol. 24, pp. 157 to 160. Pergamon Press Ltd. Printed in Northern Ireland

SELENIUM-SULPHUR SOLID SOLUTIONS

J. E. Fergusson, G. M. Pratt, G. A. Rodley and C. J. Wilkins
Department of Chemistry, University of Canterbury, Christchurch, New Zealand

(*Received* 24 *May* 1961)

Abstract—Selenium and sulphur form a series of solid solution phases, mostly based on known structures of the elements. Some of these phases contain eight-membered cyclic molecules with selenium–sulphur bonds, but no stoichiometric compounds were isolated. The behaviour of the phases under thermal and solvent treatment has been determined.

The formation of solid solutions in regions of the selenium-sulphur system is well established.(1–5)

In carrying out an X-ray powder examination over the entire composition range we have sought also information on the thermal stability and the constitution of the phases. The results confirm the chief solid solution phases to be those described recently be de Haan and Visser.(6) Some of these phases contain eight-membered cyclic molecules with selenium-sulphur bonds, but isolation of stoichiometric compounds was found not possible. Even the product of composition SeS_2 from the reaction between selenious acid and hydrogen sulphide gives a powder photograph characteristic of the solid solution phase (II, Table 1) formed in the range within which this composition falls.

Table 1.

Phase	Structure type	Se contents of melts producing phase (%)	Se contents of phases crystallized from CS_2 (%)
I	α-Sulphur(a)	0–14	0–18
II	γ-Sulphur(b)	17–55	20–49
III	α-Selenium(a)	60	50–68
IV	Modified hex. selenium(c)	$66\frac{2}{3}$	53(d)
V	Unknown(e)	75–85	—(f)
VI	Hex. selenium(a)	93–100	—(f)

(a) Identified from powder photograph. (b) Identified from cell dimensions determined from single crystal photographs. (c) Indices of lines in powder photograph were established by comparison with the rather similar pattern from hexagonal selenium. For phase IV axial lengths are: $a = 4{\cdot}77 \pm 0{\cdot}05$ Å; $c = 5{\cdot}03 \pm 0{\cdot}08$ Å. (d) Residue after extraction. (e) Not based on any known sulphur or selenium structure. (f) Cannot be recrystallized from carbon disulphide.

Crystallization (under standardized conditions) of melts of increasing selenium content* produced the succession of solid solution phases listed in Table 1. The cell dimensions of all phases increased with increasing selenium content.

---

* All compositions are given as atomic percentages.

(1) B. Rathke, *Liebigs Ann.* **49**, 253 (1844).
(2) W. Muthmann, *Z. Krist.* **17**, 357 (1890).
(3) W. E. Ringer, *Z. Anorg. Chem.* **32**, 183 (1902).
(4) F. Halla and F. X. Bosch, *Z. Phys. Chem.* **10 B**, 149 (1930).
(5) F. Halla, E. Mehl and F. X. Bosch, *Z. Phys. Chem.* **12 B**, 377 (1931).
(6) Y. M. de Haan and M. P. Visser, *Physica* **26**, 127 (1960).

Phase IV, the chief constituent of solidified melts of composition 66⅔ per cent selenium is present to some extent in melts within the range 33–72 per cent selenium and remains after solvent extraction. Samples obtained in this way contained about 53 per cent selenium. Powder photographs from samples of composition near 70 per cent were variable. The few weak lines superimposed upon diffuse scattering characteristic of non-crystalline material were not identifiable with lines from phases IV, V or VI.

Ringer's melting point curve for the system,(3) though not revealing some of the peritectic breaks through difficulties of measurement, places the eutectic composition slightly greater than 40 per cent selenium. The composition ranges now found for the more important phases show that I and II lie on the sulphur-rich side of the eutectic and III, V and VI on the selenium-rich side.

Phases I, II and III dissolve readily in carbon disulphide and are subject to composition change and consequent interconversion upon recrystallization, the fractions of highest selenium content being the least soluble. Fractionation likewise occurs upon vacuum sublimation. Phases IV, V and VI differ in being much less soluble. They undergo partial decomposition to I, II and III upon solvent treatment (Table 2).

Table 2.—Transformation of phases

Initial phase†	Products from			
	Extraction by CS_2 at 46°	Extraction by CS_2 at 160°	Heating at 160°	Vacuum sublimation
I	I	I, (II), (III)	Unchanged	I
II	III, II, I	(III), II, (I)	Unchanged	II, I
III	III, II, (I)	(VI*), III, (II), (I)	VI, V	II
IV	IV*, III, II, (I)	(VI*), III, (II), (I)	VI, V	II
V	V*, III, (II), (I)	(V*), III, (II), (I)	VI	I
VI	VI*, III, (II), (I)	(VI*), III, (II), (I)	Unchanged	Unidentified

* Insoluble residue. Brackets indicate minor products only.

† The results are for phases I, II and III recrystallized from solution, but for IV, V and VI as solidified melts.

Constitution of the solid solutions

There is evidence that phases II and III contain cyclic molecules Se_nS_{8-n}, rather than a mixture of S_8 and Se_8 molecules. Evaporation of a carbon disulphide solution of α-sulphur and α-selenium in appropriate proportions yields phase I rather than α-sulphur only after heating overnight to 100–120°. Phases II and III are obtained after heating to 160°. The occurrence of a considerable change at this latter temperature may be significant since it is the temperature at which disruption of the sulphur-sulphur bond occurs freely. Also, whereas a sample of phase II (33 per cent Se) sublimes at 80° under vacuum without change, a mixture of sulphur and selenium in the same proportion gave phase I (of low selenium content). Phase I differs from II and III only in so far as it may contain a proportion of S_8 molecules, as shown by its crystallization from a solution of phase II to which α-sulphur has been added.

The interconversion of phases I, II and III upon recrystallization could arise either through concentration of molecules according to their composition type, or

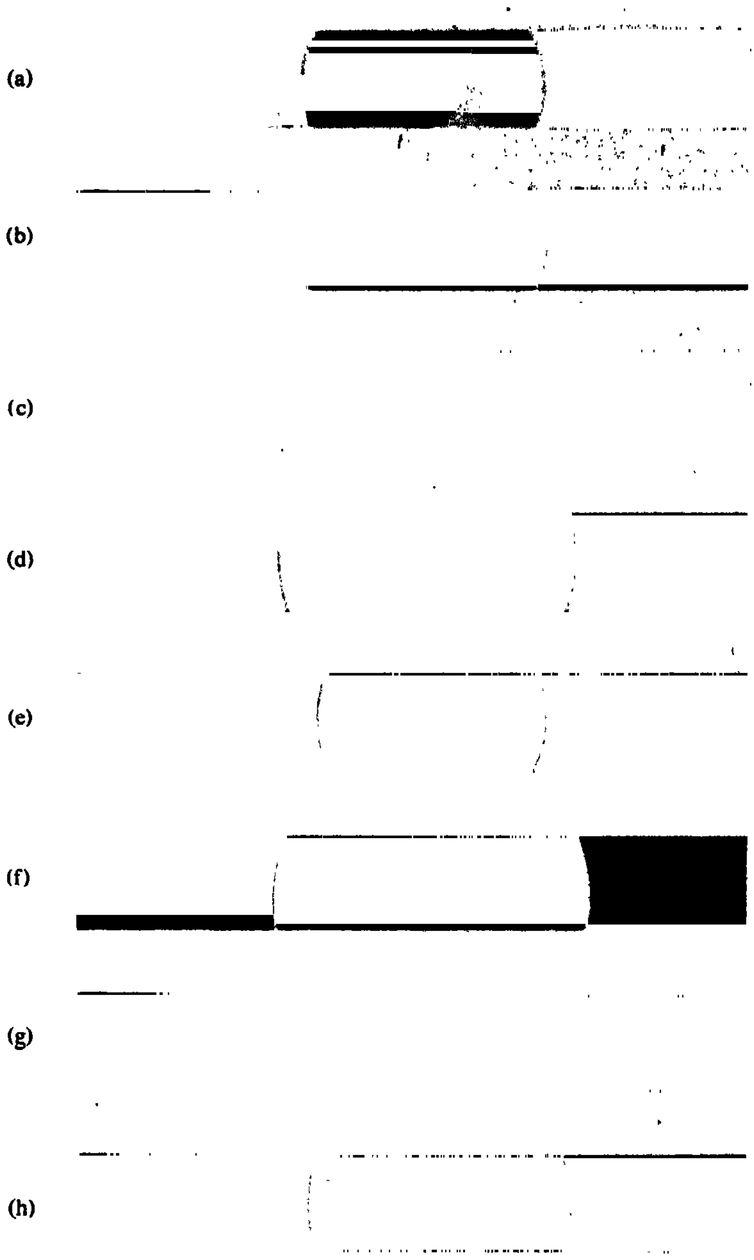

Fig. 2.—X-ray powder photographs (a–f) of phases I–VI, having respective compositions 7·5, 32·5, 68, 53, 80, and 95 atomic per cent selenium. (g) The product from very slow cooling of phase IV. The spotted and full lines show the existence of (at least) two constituents. (h) The sublimate from phase VI.

atomic rearrangement. The latter may be less important, because the of a process $8Se_nS_{8-n} \rightarrow nSe_8 + (8-n)S_8$ at low temperatures could lead to of sparingly soluble selenium; but this does not occur.

he absorption spectra (Fig. 1) of phases I, II and III, and of α-monoclinic in carbon disulphide are qualitatively similar, as are some features of the of phases I and II, and of α-sulphur in chloroform. (Phase III absorbs much strongly than phase II in the latter solvent and shows a subsidiary maximum at mμ with ε ≈ 1800). The absence of quantitative relationships amongst the sorption intensities once again excludes structural interpretation in terms of Se_8 and

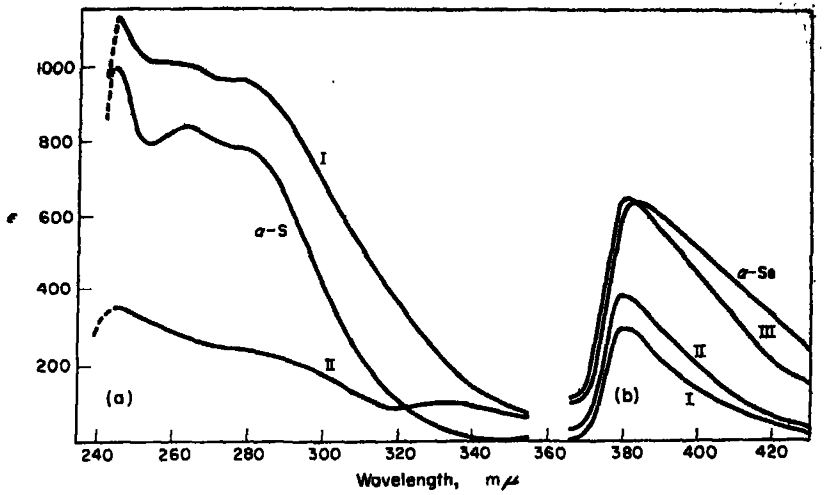

FIG. 1.—(a) Absorption spectra of phase I, phase II, and α-sulphur in chloroform. (b) Absorption spectra of phases I, II and III, and α-selenium in carbon disulphide. For (a) the concentration of sulphur in gram-atoms per litre was used in calculating extinction coefficients, and for (b) the concentration of selenium in gram-atoms per litre. Compositions of phases I, II and III were 14, 27·5 and 68 atomic per cent respectively.

S_8 molecules alone. The distinctive maximum, $\varepsilon = 100$ at 333 mμ in a region of otherwise low absorption on the curve for phase II can be attributed to Se—S bonds. The infra-red stretching frequency (471 cm^{-1}) of the sulphur–sulphur bond in α-sulphur becomes progressively weaker in phases I, II and III. Yet its presence (at 463 cm^{-1}) even in III, of composition 68 per cent Se, indicates random distribution rather than alternation of the atoms within the mixed molecules.

Phase V, of unknown structure but of low solubility like IV and VI, may be assumed polymeric. The slow decomposition of these phases by boiling carbon disulphide reflects the low bond strengths on the selenium-rich phases.

Thermal behaviour of the phases

There is no evidence that phases I, II, III, V and VI, within their normal composition limits, are not stable at room temperature. Phase IV differs in being metastable. A sample photographed after five months had partially decomposed to phase III.

At 160° phases III (68 per cent Se) and IV (53 per cent Se) are unstable, changing through intermediate formation of VI to V. A sample of phase V obtained by cooling a melt containing 80 per cent Se converts on the other hand to VI at this temperature. It reverts to V on cooling the melt from high temperature (360°), when crystallization occurs at about 140°. This behaviour is indicative of a peritectic transition where the high temperature phase (VI) does not revert quickly to the lower temperature phase (V). The peritectic temperature between these phases lies between 140° and 160°, and the miscibility gap extends from about 85 to 93 per cent. No evidence has been obtained on the peritectic temperature between phases III and V owing to difficulty in ensuring equilibrium.

Phase IV seems to result from crystallization of a residual component present in the melt in highest proportion at high temperatures. A sample which has been isolated as an extraction residue can, after heating to 360°, be partially recrystallized by rapid cooling (15 min). Normal cooling in the furnace produced phase V, and very slow cooling (5 days) gave two unidentified products (Fig. 2g).

EXPERIMENTAL

Preparation of samples. Mixtures of sulphur and selenium were heated overnight to 360° in sealed tubes which had been flushed with carbon dioxide. The samples were normally allowed to cool in the tube furnace (taking 90 min over the range 200–100°). Solvent extractions were made with carbon disulphide. Vacuum sublimations were made at 80° onto a water-cooled finger.

The sample from the reaction between hydrogen sulphide and selenious acid was obtained by Nordlander's procedure.(7) It contained 32·5 per cent selenium.

For selenium determination samples were dissolved by nitric acid and reduced with hydrazine hydrate.

X-ray powder photographs. These were taken with a Philips 114·83 mm camera using copper radiation. Photographs of the chief products are reproduced in Fig. 2.

d-Values of principal lines from less well-known products follow. Phase IV (53% Se): 4·15 (*m*), 3·19 (*s*), 3·01 (*w*), 2·16 (*m*), 2·09 (*w*), 1·59 (*w*). Phase V (80% Se): 4·71 (*w*), 4·11 (*s*), 3·41 (*s*), 3·03 (*m*), 2·94 (*m*), 2·77 (*s*), 2·39 (*m*). "70% Phase" (70% Se): 2·02 (*s*), 1·76 (*m*), 1·24 (*w*), 1·06 (*w*). Products from very slow cooling of phase IV: spotted lines (Fig. 2 g), 3·51 (*m*), 3·04 (*s*), 2·15 (*s*), 1·83 (*m*), 1·75 (*m*), 1·36 (*m*); full lines, 2·80 (*m*), 2·71 (*w*), 2·62 (*w*), 1·63 (*m*). Sublimate from phase VI (Fig. 2 h): 4·13 (*m*), 3·58 (*s*), 3·22 (*w*), 3·00 (*w*), 2·77 (*w*), 2·19 (*s*), 1·87 (*m*). Values calculated for the β-monoclinic selenium structure,(8) but not found in any products, are: 4·65, 4·03, 3·87, 3·79, 3·78, 3·67, 3·49, 3·42.

Spectra. For measuring absorption spectra chloroform was useful as solvent over the range 240–360 mμ. Carbon disulphide was used at longer wavelengths. Monoclinic selenium is insoluble in chloroform, and the selenium absorption at 370–420 mμ is not shown by solutions even of selenium-rich phases in this solvent.

Infra-red spectra were provided by Drs. N. S. Ham and A. L. G. Rees of the Division of Chemical Physics, C.S.I.R.O., Melbourne. The absorption bands recorded over the range 720–420 cm^{-1} on a Perkin–Elmer 12C spectrometer with potassium bromide optics were: α-sulphur, 471 cm^{-1} (*w*); phase I, 17% Se, 469 cm^{-1} (*w*); phase II, 35% Se, 467 cm^{-1} (*vw*); phase III, 68% Se, 463 cm^{-1} (*vvw*).

Acknowledgement—Assistance from the research fund of the University of New Zealand is acknowledged.

(7) B. W. Nordlander, *Indust. Engng. Chem.* **19**, 518 (1927).

(8) R. E. Marsh, L. Pauling and J. D. McCullough, *Acta Cryst.* **6**, 73 (1953).

J. Inorg. Nucl. Chem., 1962, Vol. 24, pp. 161 to 164. Pergamon Press Ltd. Printed in Northern Ireland

APPLICATION OF THE WURTZ REACTION TO THE SYNTHESIS OF DISILANE AND 1,2-DIMETHYLDISILANE*

A. D. CRAIG and A. G. MACDIARMID†
John Harrison Laboratory of Chemistry
University of Pennsylvania
Philadelphia

(*Received* 19 *July* 1961; *in revised form* 26 *August* 1961)

THE Wurtz reaction has been used frequently in organosilicon chemistry to prepare disilanes and higher silanes which contain no Si—H bonds.(1,2,3) It has been reported that when SiH_3Cl was shaken with a 0·74 per cent sodium amalgam, at room temperature, all the chlorine was abstracted but only a 1·7 per cent yield of Si_2H_6 was obtained. When a sodium–potassium alloy was used, little or no Si_2H_6 was obtained.(4)

Later it was found that SiH_3I would react with solid sodium(5) at room temperature *to yield* Si_2H_6. *It was suggested that the formation of a film of NaI on the surface of* the sodium prevented 62 per cent of the SiH_3I employed from undergoing reaction. This method does not show great promise for the synthesis of relatively large quantities of Si_2H_6 since very large surface areas of sodium would be required. The present study was undertaken to investigate the necessary conditions for obtaining good yields of disilanes containing Si—H bonds by means of the Wurtz reaction.

In this investigation attempts to obtain higher yields and greater quantities of Si_2H_6 than those previously reported by allowing SiH_3I to react with sodium or sodium–potassium alloy were unsucessful. However, very good yields and relatively large quantities of Si_2H_6 resulted when SiH_3I *vapour* was permitted to react with liquid sodium amalgam at room temperature. Good yields of the new compound dimethyldisilane, presumably the 1,2 isomer, $CH_3SiH_2SiH_2CH_3$, were obtained in an analogous reaction. It would appear that the experimental method developed may be conveniently employed for the synthesis of considerably larger quantities of volatile disilanes.

A reaction mechanism involving an intermediate silylmetallic compound rather than one based on the production of free silyl radicals such as

$$2SiH_3I + 2Na \rightarrow 2NaI + 2SiH_3\cdot \qquad (1)$$

$$2SiH_3\cdot \rightarrow Si_2H_6 \qquad (2)$$

is suggested for the following reasons: (a) during the course of the reaction the surface of the amalgam became coated with a thick slush which disappeared when nearly all of the SiH_3I had been consumed; (b) SiH_4 was slowly evolved when the nonvolatile reaction products were allowed to stand for several days; (c) treatment of the nonvolatile residues from two SiH_3I experiments with dilute hydrochloric acid produced a gas presumed to be a silicon hydride. These observations suggest that an intermediate species such as $(SiH_3)_2Hg$ or SiH_3HgI is probably involved in the course of the reaction. This appears to be reasonable since a silyl–metallic compound, $KSiH_3$, has recently been isolated as a stable species.(6) Although the proposed silyl–mercury compounds have not been isolated, it seems very likely that a reaction-scheme such as that described below is involved in the preparation of volatile disilanes by the method described in this paper.

---

* This work was supported in part by the U.S. Air Force, Contract No. AF 33-(616)-6516. Reproduction in whole or in part is permitted for any purpose of the United States Government. The results are based on portions of a thesis to be submitted by A. D. CRAIG to the Graduate School of the University of Pennsylvania in partial fulfillment of the requirements for the degree of Doctor of Philosophy.

† Alfred P. Sloan Research Fellow.

(1) H. GILMAN, R. K. INGHAM and A. G. SMITH, *J. Org. Chem.* **18**, 1743 (1953).

(2) H. GILMAN, D. J. PETERSEN, A. W. JARVIE and H. J. S. WINKLER, *J. Amer. Chem. Soc.* **82**, 2076 (1960).

(3) M. P. BROWN and G. W. A. FOWLES, *J. Chem. Soc.* 2811 (1958).

(4) A. STOCK and K. SOMIESKI, *Ber. Dtsch. Chem. Ges.* **54**, 524 (1921).

(5) H. J. EMELÉUS, A. G. MADDOCK and C. REID, *J. Chem. Soc.* 353 (1941).

The highest yields of the disilanes were obtained when the vapour, only, of the silyl iodide was permitted to react with liquid sodium amalgam. It is proposed that the presence of liquid SiH_3I on the amalgam surface facilitates the mechanical removal of the possible intermediate compounds SiH_3HgI and/or $(SiH_3)_2Hg$ as a suspension in the liquid SiH_3I. This then allows the surface of the amalgam to become more accessible to attack by SiH_3I according to equations (3) or (4) below, and hence more of the SiH_3 groups undergo reaction (6) with consequent increased yields of SiH_4 and decreased yields of Si_2H_6. When SiH_3I vapour only is present, reaction (5) is favoured.

$$SiH_3I + Na/Hg\ (excess) \rightarrow SiH_3HgI\ (fast) \quad (3)$$

$$2SiH_3I + Na/Hg\ (excess) \rightarrow (SiH_3)_2Hg + 2NaI\ (fast) \quad (4)$$

$$SiH_3I + (SiH_3)_2Hg \rightarrow Si_2H_6 + SiH_3HgI\ (slower) \quad (5)$$

$$(SiH_3)_2Hg \rightarrow SiH_4 + (SiH_2)_x + Hg\ (slow) \quad (6)$$

EXPERIMENTAL

All work was carried out in a Pyrex glass vacuum system. Stopcocks were lubricated with Apiezon N grease in preference to silicone grease in order to eliminate the possibility of foreign silicon compounds appearing through attack on the grease by the substances handled. All pressure readings were made with a glass Bourdon gauge in order to eliminate contamination and possible reaction of compounds with mercury. All temperatures below 0° were measured by an iron-constantan thermocouple, standardized by the National Bureau of Standards.

Silyl iodide was prepared from SiH_4 and HI. Its purity was checked by determining its vapour pressure at 0° (found, 123·6 mm; lit. value, 123·9 mm(5)). Liquid sodium amalgam was prepared by dissolving sodium metal in mercury, the sodium content being subsequently determined by analysis.

Methylsilyl iodide was prepared from CH_3SiH_3 and HI. Its purity was checked by determining its vapour-pressure at 0° (found, 42·9 mm; lit. value, 43·0 mm(7)).

(a) *Reaction of silyl iodide (liquid and vapour phase) with sodium amalgam.* In a typical experiment SiH_3I (11·65 mmoles) was condensed into a 250 ml round-bottom flask containing 50 g of sodium amalgam (0·65% Na w/w). Initially, 50 per cent of the SiH_3I was in the liquid phase, the remainder being in the vapour phase. The reaction was allowed to proceed for 1·5 hr at room temperature during which time the flask was constantly agitated. Some liquid SiH_3I was present on the surface of the amalgam during the first 0·5 hr. Separation and identification of all the volatile products showed that 75·8 per cent of the SiH_3I had undergone reaction to give SiH_4, 32·7,* and Si_2H_6, 39·5 per cent. No hydrogen was evolved. The above substances were identified by their molecular weight, vapour pressure, and/or infrared spectra. In another experiment, where 75 per cent of the SiH_3I was in the liquid phase, the yield of Si_2H_6 was only 12·8%.

(b) *Reaction of silyl iodide (vapour phase only) with sodium amalgam.* A side arm was attached to the neck of a 0·5 l. flask which was used as the reaction vessel. A manometer, adjacent to the flask in the vacuum system, served as a means of detecting pressure changes in the reaction vessel.

---

* All the percentages given are based on the quantity of silicon originally in the silyl iodide or methylsilyl iodide consumed, which appeared in the given product. In the case of hydrogen gas, the percentage is based on the quantity of hydrogen in the silyl iodide or Si—H hydrogen in the methylsilyl iodide consumed.

(6) M. A. Ring and D. M. Ritter, *J. Amer. Chem. Soc.* **83**, 802 (1961).

(7) H. J. Emeléus, M. Onyszchuck and W. Kuchen, *Z. Anorg. Chem.* **283**, 74 (1956).

Sodium amalgam, 225·0 g (0·752% Na w/w) was introduced into the reaction vessel under dry nitrogen gas. The vessel was then evacuated and SiH_3I (6·75 mmole; 1·0662 g) was condensed into the side arm. This amount of SiH_3I was completely vapourized at room temperature and produced a resulting pressure of 18·7 cm on the manometer after 15 min. The amalgam was stirred continuously by means of a glass covered magnetic stirring bar. A thick silvery film soon began to form on the amalgam and this film became slushy as the reaction proceeded. After 8·9 hr at room temperature (normal laboratory fluorescent lighting) the pressure in the reaction vessel had dropped to 10·4 cm and a large amount of black powder appeared on the surface quite suddenly (within 5 min) at the end of this period.

Separation of all the volatile products yielded SiH_4 (0·861 mmole; 13·1%; mol. wt. found, 32·3. calc., 32·1; confirmed by infra-red spectrum$^{(8)}$), Si_2H_6 (2·19 mmole; 66·8%, mol. wt. found, 62·5. calc., 62·2; confirmed by infra-red spectrum;$^{(9)}$ vapour pressure at −63·5°, found, 64·6 mm, lit. value, 65·4 mm$^{(10)}$), SiH_3I (0·20 mmole; 3·0% vapour pressure at −23·0° found, 33·1 mm., lit. value, 34·8 mm$^{(8)}$) and hydrogen (0·342 mmole, 3·4 per cent). The non-volatile products of this experiment were stirred intermittently for eight days *in vacuo* at room temperature without removal from the reaction vessel. The vessel was opened to the vacuum system and it was found that a small amount of hydrogen and SiH_4 (6·9 mg, 0·215 mmole; identified by infra-red spectrum$^{(8)}$) were present. Another experiment similar to that described above, was carried out employing 14·36 mmole (2·2700 g) of SiH_3I. The yield of Si_2H_6 was 55·4 per cent (3·79 mmole). Addition of dilute HCl to the non-volatile residue in the reaction vessel caused the evolution of a gas, presumably a silane, which was spontaneously inflammable in air.

(c) *Reaction of methylsilyl iodide with sodium amalgam.* The apparatus used was identical to that described in (b) above except that a 1 l. flask was employed. In a typical experiment, sodium amalgam, 289·6 g (0·752% Na w/w) was allowed to react with 3·13 mmole (0·5393 g) of CH_3SiH_2I at room temperature. This amount was completely vapourized in the flask and produced a pressure of 6·20 cm after 19 min. A silvery slush, similar to that noted in the above experiment, formed during the reaction and after 7·7 hr it suddenly (within 5 min) decomposed to a black powder which floated on the surface of the amalgam. The pressure at the conclusion of the experiment was 3·70 cm.

After separation of all the volatile products, it was found that 97·9 per cent of the CH_3SiH_2I had undergone reaction to form CH_3SiH_3 (0·782 mmole, 25·5%; mol. wt. found, 45·3. Calc., 46·1; confirmed by infra-red spectrum$^{(7)}$) and $CH_3SiH_2SiH_2CH_3$ (0·764 mmoles, 49·7% mol. wt. Found, 91·0, Calc. 90·28). No hydrogen or other noncondensable gas was formed. In order to remove the last traces of CH_3SiH_2I from the $CH_3SiH_2SiH_2CH_3$ it was necessary to add to the mixture 0·1 ml of $(n\text{-}C_3H_7)_3N$, which forms an only slightly volatile addition compound with the iodide. (Found* C, 26·75; H, 11·38. Calc. C, 26·61; H, 11·17%).

A sample of $CH_3SiH_2SiH_2CH_3$ of mol. wt., 91·0 exerted a vapour-pressure of 107·0 mm at 0° and melted below −144°. In contrast to compounds containing an Si_2H_5 group,$^{(11)}$ $Si_2H_4(CH_3)_2$ was not spontaneously inflammable in air. It was found that the material decomposed slowly at, and above 0°, and in this respect it is similar to $Si_2H_5CH_3$ which also decomposed under similar experimental conditions.$^{(12)}$

The non-volatile products of the reaction between CH_3SiH_2I and sodium amalgam were stirred intermittently for eight days *in vacuo* at room temperature without removal from the reaction vessel. A small amount of hydrogen and a trace of material, presumably CH_3SiH_3, was found on opening the vessel.

It was found by Stock,$^{(4)}$ and also in this laboratory, that 2–10 per cent of a sample of Si_2H_6 was decomposed by sodium amalgam during 24 hr at room temperature Under similar experimental conditions, $CH_3SiH_2SiH_2CH_3$ decomposed much more extensively.

In four experiments, two with SiH_3I and two with CH_3SiH_2I, the decrease in total pressure was recorded throughout each entire experiment at 15 min intervals as the iodide underwent reaction with the amalgam. The volume of the apparatus employed was essentially constant throughout each experiment and the temperature variation was ±0·5°. It was found that a plot of $\log (P - P_\infty)$ vs. time was linear in each case. It appears from these results that the rate-determining step of these reactions is first order with respect to SiH_3I or CH_3SiH_2I respectively.

---

* The analysis was carried out by the Schwarzkopf Microanalytical Laboratory, Woodside 77, New York. Samples were transported in liquid nitrogen.

(8) C. H. Tindal, J. W. Straley and H. H. Nielsen, *Phys. Rev.* **62**, 151 (1942).

(9) G. W. Bethke and M. K. Wilson, *J. Chem. Phys.* **26**, 1107 (1957).

(10) K. Stokland, *Kgl. Norske Videnskab. Selskabs Skrifter*, No. 3, 1, 47 (1950).

(11) L. G. L. Ward and A. G. MacDiarmid, *J. Amer. Chem. Soc.* **82**, 2151 (1960).

(12) S. Isenberg Ph.D. Dissertation, University of Chicago (1937).

Vapour pressure of 1,2-*dimethyldisilane*. Vapour pressures in the range −65·8°–0·0° are represented by the equation $\log P_{mm} = -(1288{\cdot}10/T) + 6{\cdot}74345$ and are given in Table 1. The extrapolated boiling point is 60·3°. The molar heat of vaporization is 5·89 kcal $mole^{-1}$ and Trouton's constant, 17·7 cal °C^{-1} $mole^{-1}$. The Trouton's constant is therefore somewhat similar to that reported for $Si_2H_5CH_3$ (14·0 cal °C^{-1} $mole^{-1}$).(12) The irreversibility of the vapour-pressure curve found upon decreasing the temperature indicated that slight decomposition had taken place.

TABLE 1.—VAPOUR-PRESSURE OF 1,2-DIMETHYLDISILANE*

Temp (°C)	Vapour pressure (mm)	
	Observed	Calculated
−46·2	11·8	11·7
−41·8	15·1	15·0
−38·8	17·7	17·7
−25·2	35·6	35·5
−18·4	48·7	48·7
−13·8	60·7	60·0
1·2	120·2	112·0
0·0	114·5†	106·8
− 196	0·3†	—
0·0	107·0‡	106·8

* Duration of the determination, approximately 8 hr.

† Pressure observed on decreasing the temperature.

‡ Vapour pressure of pure sample immediately after purification.

Thermal stability. A 40 mg sample of $CH_3SiH_2SiH_2CH_3$ was held at 0° for 4·7 hr, after which time the vapour-pressure had increased from 110·2 to 111·3 mm. Upon cooling the sample to −196°, 0·1 mm pressure of non-condensable gas was observed.

Infra-red spectrum. Infra-red measurements were made with a Perkin Elmer Infracord double beam recording spectrophotometer, employing a sodium chloride optical system. The measurements were made on the gaseous phase at 25° with the sample confined in a 10 cm cell with 0·5 cm potassium bromide windows cemented with glyptal resin. The absorption maxima are summarized in Table II below.

TABLE 2.—INFRA-RED SPECTRUM OF 1,2-DIMETHYLDISILANE (PRESSURE = 8·0 mm)

cm^{-1}	Strength	Assignment(13)
2980	Medium	C—H stretch
2950	Shoulder	C—H stretch
2150	Very strong	Si—H stretch
1420	Weak	CH_3 deformation
1253	Medium	CH_3 deformation
946	Shoulder	SiH_2 deformations
931	Strong	
919	Strong	
912	Shoulder	
878	Shoulder	CH_3 rock
861	Very strong	SiH_2 deformations
853	Very strong	
845	Very strong	
728	Shoulder	Si—C stretch and/or SiH_2 deformations
724	Strong	
720	Shoulder	
698	Medium	

---

(13) E. A. V. Ebsworth, M. Onyszchuk and N. Sheppard, *J. Chem. Soc.* 1453 (1958).

J. Inorg. Nucl. Chem., 1962, Vol. 24, pp. 165 to 168. Pergamon Press Ltd. Printed in Northern Ireland

HALOGEN REARRANGEMENT IN ORGANOSILICON HALIDES

R. S. Feinberg* and E. G. Rochow
Mallinckrodt Laboratory, Harvard University, Cambridge, Massachusetts

(*Received* 17 *January* 1961; *in revised form* 24 *August* 1961)

Abstract—To test (1) whether there is any halogen rearrangement in a pure organosilicon halide, and (2) whether such a compound undergoes solvolytic dissociation in ethers or nitrogeneous solvents, methylbromodichlorosilane ($CH_3SiBrCl_2$) was prepared and then was tested for rearrangement under a variety of conditions. At reflux temperature for 43 hr, in the absence of metals and metal chlorides, it generated no detectable methyltrichlorosilane, indicating that there was no exchange of halogen through self-ionization. The presence of traces of aluminum chloride or the halides of other metals caused rearrangement and consequent evolution of CH_3SiCl_3. In all-glass equipment, addition of *n*-butyl ether, 1,3 dioxane, N,N dimethylaniline, or N,N dimethylformamide brought about formation of trichlorosilane at reflux temperature; the rate of such rearrangement increased with the basicity of the solvent and with its dielectric constant.

Although silicon has an extensive ionic chemistry, almost its only ionic form is that of a large anion containing a major proportion of oxygen or fluorine. Positive (siliconium) ions seem to be a rare species,(1) frequently adduced to explain the reactions of some silicon compounds but elusive in the face of deliberate attempts to find them.(2,3) Undoubtedly they exist as structural components in the silicon and organosilicon acetylacetonates,(4,5) where they are stabilized by chelation, and they very probably exist as solvated cations in 100% H_2SO_4.(6) Conductometric studies in nitrogenous solvents at room temperature show that under such conditions the measurable concentration of siliconium ions is extremely low, so low as to be obscured by the effect of residual moisture in even the most carefully purified solvents.(7)

One sensitive test which might be applied to the existence or nonexistence of siliconium ions in pure silicon compounds, or in solutions of them, is halogen rearrangement or exchange. Such exchange is known to occur during the reactions of bromine-containing Grignard reagents with silicon tetrachloride in ether, resulting in a complex mixture of (organo) chlorobromosilanes,(8) and in the action of organomagnesium bromides on methyltrichlorogermane, but this can be ascribed to the action of magnesium bromide as a Lewis acid.(9,10) Free iodine is also known to exchange slowly with silicon tetraiodide at 130° in xylene solution.[11] Aluminium chloride, moreover, brings about a rapid redistribution of halogen atoms on silicon at elevated temperatures.[12]

---

* Harvard College, 1961.

(1) E. G. Rochow, *Introduction to the Chemistry of the Silicones*, p. 118. J. Wiley, New York (1951).

(2) H. Gilman and G. E. Dunn, *J. Amer. Chem. Soc.* 72, 2178 (1950).

(3) R. C. West, Thesis, Harvard (1954).

(4) R. C. West, *J. Amer. Chem. Soc.* 80, 3246 (1958).

(5) S. K. Dhar, V. Doron and S. Kirschner, *J. Amer. Chem. Soc.* 81, 6372 (1959).

(6) F. P. Price, *J. Amer. Chem. Soc.* 70, 781 (1948).

(7) A. B. Thomas and E. G. Rochow, *J. Amer. Chem. Soc.* 79, 1843 (1957).

(8) E. Krause and A. von Grosse, *Die Chemie der metallorganischen Verbindungen*, p. 259. Borntraeger, Berlin, (1937); Edwards Bros., Ann Arbor (1943).

(9) S. O. Lawesson, *Arkiv Kemi* 11, 317 (1957); *Chem. Abstr.* 52, 1135e (1958).

(10) V. A. Ponomarenko and G. Ya. Vzenkova, *Izvest. Akad. Nauk SSSR* Otdel. Khim. Nauk, 994 (1957). *Chem. Abstr.* 52, 4473 (1958).

What is desired here is to find out whether there is any perceptible halogen rearrangement in a pure halosilane at moderately elevated temperatures and in the absence of metallic salts.* Furthermore, it might be that co-ordinating solvents of appropriate dielectric constant could bring about solvolytic dissociation of the halosilane at ambient or moderately elevated temperatures, producing such rearrangement. In view of the experiments on conductivity[7] it seemed interesting to look into this point.

The compound chosen for investigation was methylbromodichlorosilane, $CH_3SiBrCl_2$, which was prepared by the bromination of methyldichlorosilane, CH_3SiHCl_2,† a product of the reaction of methyl chloride with silicon. The preparation turned out to be considerably more difficult than was anticipated, but 300 g eventually were made available for the study of halogen exchange.

EXPERIMENTAL

Preparation of $CH_3SiBrCl_2$

Addition of bromine to CH_3SiHCl_2 at its boiling point, 41°, resulted in preferential bromination of the methyl group and a complex mixture of products. When freshly-prepared[14] anhydrous iron(III) chloride was used as catalyst, reaction occurred only at high concentrations of bromine and could not be brought to completion. It was found necessary to use aluminium chloride as catalyst in order to achieve satisfactory bromination, despite the undesirability of its presence later and the difficulty of separating it from the product. Combination of three methods for removal, in sequence, was found necessary: inactivation of $AlCl_3$ by addition of NaCl, flash distillation at reduced pressure, and fractionation in a twenty-plate column. The following procedure describes the more successful runs:

Four grammes of aluminium chloride and 348·0 g (3·0 mole) of redistilled methyldichlorosilane were stirred together in a 500 ml three-neck flask, and 480·0 g (3·0 mole) of bromine were added at a rate sufficient to maintain reflux. Completion of the reaction was indicated by persistence of the bromine colour.‡ Twenty grams of dry powdered sodium chloride then were added, and the liquid distilled off immediately at room temperature. The distillate was shaken with mercury to remove the small amount of distilled bromine, distilled at room temperature again to separate it from the mercury bromide, and finally subjected to fractional distillation in a vacuum-jacketed column packed with glass helices. Fractions boiling at 86·5–88·0° were combined and re-fractionated, giving 166·1 g of $CH_3SiBrCl_2$, b.p. 86·5,° a yield of 28·6 per cent based on CH_3SiHCl_2 or 31·3 per cent based on Br_2.§

---

* It would be expected that rearrangement would occur as the temperature of thermal dissociation is approached, but since the bond energies of Si–Br and Si–Cl bonds are high, 74 and 91 kcal, respectively,[13] this should be a distinctly separate kind of reaction.

† The authors are grateful to Dr. W. F. Gilliam of the General Electric Company for a generous supply of this compound.

‡ In this example, decolourization of bromine stopped after addition of 454 g (2·84 mole) of Br_2. The difference represents loss of CH_3SiHCl_2 carried off by evolved HBr. In one run these vapours were condensed in a dry-ice trap and the CH_3SiHCl_2 was returned to the flask after evaporation of the HBr, but the yield was not improved appreciably by this procedure.

§ The high-boiling material consisted in part of CH_3SiBr_2Cl and CH_3SiBr_3, both of which evolved bromine on standing. These were formed by unavoidable halogen rearrangement during the refluxing with $AlCl_3$, the other product being CH_3SiCl_3 (which was recovered early in the distillation).

(11) Yu. P. Nozarenko and T. V. Vovk, *Ukrain. Khim. Zhur.* **21**, (1955); *Chem. Abstr.* **49**, 13003b (1955).

(12) F. C. Whitmore, L. H. Sommer and J. R. Gold, *J. Amer. Chem. Soc.* **69**, 1176 (1947); R. O. Sauer and E. M. Hadsell, *Ibid.* **70**, 3590 (1948).

(13) C. Eaborn, *Organosilicon Compounds*, p. 90, Butterworth, London; Academic Press, New York (1960).

(14) A. Pray, *Inorganic Syntheses*, Vol. V, p. 153. McGraw Hill, New York (1957).

The same compound was prepared by the KUMADA(15) by the redistribution of CH_3SiCl_3 and CH_3SiBr_3 with $AlCl_3$; b.p. 86·5°. (Found;(16) Halogen 77·60. Calc. for $CH_3SiBrCl_2$, Halogen 77·78%).

Refluxing of pure $CH_3SiBrCl_2$.

Early experiments showed that $CH_3SiBrCl_2$ purified as described above could be refluxed at atmospheric pressure in a vacuum-jacketed column (1·3 × 18·0 cm) packed with glass helicies for 22 hr without change of boiling point. In an effort to detect even minute quantities of CH_3SiCl_3 (b.p. 65·7°) which might accumulate at the column head, an adiabatic column 1·0 × 120 cm packed with glass helices and fitted with a partial-takeoff head was used. Thirty-five grammes of $CH_3SiBrCl_2$, purified as described, was stirred continuously in the stillpot and heated to reflux at atmospheric pressure for 43 hr. During this time the boiling point fell only from 86·5 to 85·0°. At this point 3·4 g of distillate were taken off, and the boiling point rose at once to 86·5°, where it stayed during the next hour. The 3·4 g of distillate had a halogen content of 78·71 per cent, calculated on the basis of 2Cl:1Br (theor. for $CH_3SiBrCl_2$ = 77·78 per cent.

The same halosilane, refluxed with toluene in a fractionating column packed with stainless steel helices, which had been used for many previous distillations of chlorosilanes and had a visible coating of metal chlorides, underwent marked rearrangement.* Thirty-two grammes of $CH_3SiBrCl_2$ (b.p. 86·3°, 77·45 per cent halogen) and 150 ml of pure, dried toluene were heated on an oil bath to which a vacuum-jacketed column (2·2 × 100 cm) was affixed. Using a total reflux-partial take-off head, the vapour temperature on total reflux became stable at 65°. Two milliliters of distillate were withdrawn, and the reflux temperature rose rapidly to 86° again. Within 30 min the temperature had dropped once more to 65°, and another increment of several drops was removed, whereupon the temperature again rose rapidly. This process was repeated until over 20 ml of distillate had been removed, with no change in the behaviour of the column.

Refluxing with basic solvents

(1) N,N *dimethylformamide*. To the 31·4 g of $CH_3SiBrCl_2$ left in the all-glass fractionation assembly after the refluxing experiment, 3 g of $HCON(CH_3)_2$ was added. A white addition compound formed, not all of which dissolved on heating. The first stable reflux temperature to be reached was 65·3°. Eight grammes of CH_3SiCl_3 were taken off over a period of 2 hr, b.p. 65·3–65·5°. (Found, Cl, 71·08. Calc. for CH_3SiCl_3, Cl, 71·17%). When 40 ml of bromocyclohexane was added to the stillpot as chaser and the distillation was resumed, solid addition compound condensed in the column and plugged it.

(2) N,N *dimethylaniline*. Nineteen grammes of $C_6H_5N(CH_3)_2$ was added to 21 g of pure $CH_3SiBrCl_2$ in the all-glass fractionation assembly. Distillation was begun and the following fractions were obtained:

Sample	Wt. (g)	Boiling range	Cl (%)
1	2·0	64–65°	69·69
2	2·8	64–65°	68·36
3	3·0	64–65°	
4	2·0	65·5°	69·66
5	0·9	65·5–66·0°	69·73

After fraction 5 was taken, the experiment had to be terminated because solid co-ordination compound collected in the column and a green gelatinous solid collected in the stillpot.

(3) 1,4 *dioxane*. Five grammes of $C_4H_8O_2$ (distilled from CaH_2) were added to 28 g of $CH_3SiBrCl_2$ in the same apparatus. There was no sign of reaction, but the reflux temperature dropped slowly to 65·8°. At very high reflux ratio, 3·8 g of low-boiling material were taken off at 65·8–66·0° over a period of 36 hr. (Found, Cl, 70·96. Calc. for CH_3SiCl_3; Cl, 71·17%).

A second fraction, b.p. 66·0°, 70·04% Cl, was taken off, and then the distillation was stopped. A sample taken from the stillpot was fractionally distilled in small-scale equipment, and 1 g of CH_3SiBr_3, b.p. 131°, was isolated. (Found, Br, 83·59. Calc. for CH_3SiBr_3; Br, 84·4%.)

* This experiment was conducted by Mr. A. L. LANE in this Laboratory.

(15) M. KUMADA, *J. Inst. Polytech. Osaka City Univ.*, Ser. C. **2**, 131–8 (1952); *Chem. Abstr.* **48**, 11303f (1954).

(16) E. G. ROCHOW, *An Introduction to the Chemistry of the Silicones*, (2nd ed.), p. 165. J. Wiley, New York (1951).

(4) *n-Butyl ether*. Using 38 g of $(n\text{-}C_4H_9)_2O$ (distilled from CaH_2) and 16·1 g of $CH_3SiBrCl_2$ in the same apparatus, the reflux temperature dropped slowly to 66·0° in 20 hr. At this temperature, 4·2 g of CH_3SiCl_3 were taken off. (Found, Cl, 68·97. Calc. for CH_3SiCl_3; Cl, 71·17%). In another experiment, a much larger amount of the ether (250 ml) was added to 16·1 g of $CH_3SiBrCl_2$ and refluxed. A stable vapour temperature of 67° was reached, but removal of only 1 g of CH_3SiCl_3 caused it to rise swiftly. After 1½ hr of further reflux, the temperature fell only 1°. The contents of the column were washed back into the stillpot with warm butyl ether, and the distillation continued. An equilibrium temperature of 66·7° again was reached at the head, but only 0·6 g of distillate (69·84% Cl) could be taken off at 66·7–68·0° before the temperature again rose.

CONCLUSIONS

The catalytic effect of aluminium chloride in bringing about halogen exchange through an ionic mechanism is too well known(12,14) to require comment here. The similar but weaker effect of transition-metal halides on the column packing is not surprising, in view of the known (but rather slow) exchange brought about by magnesium bromide.(8,10) Considering the undoubted presence of at least some transition-metal ions in glass, the possibility of forming surface layers of boron and aluminium halides on the surface of Pyrex, and the difficulty of separating the very last of the aluminium chloride from the methylbromodichlorosilane used in these experiments, the behaviour of this halosilane during the total-reflux experiment in all-glass equipment should be considered only as an approximation to the behaviour of the thoroughly pure substance. Extrapolation then would indicate that really pure $CH_3SiBrCl_2$ does not undergo halogen exchange and rearrangement at its boiling point, 86·5°.

In the four basic solvents used, methylbromodichlorosilane undergoes halogen exchange and subsequent rearrangement to methyltrichlorosilane and methyltribromosilane. One plausible mechanism for this action is that of solvolytic dissociation to an ionic species, and this view is supported by the observation that the rate of rearrangement increases with the dielectric constant of the solvent.* At the same time, a limitation on the process is imposed by the formation of solid coordination products by the more basic solvents, like N,N dimethylformamide and N,N dimethylaniline, so no quantitative relation to dielectric constant becomes feasible. An alternative explanation is one similar to that of Allen and Modena,(17) who found rapid exchange between ^{36}Cl and R_3SiCl in dioxane solutions of water or alcohols, and attributed it to release of chloride ion from a complex of the chlorosilane with the basic solvent. In the present instance, however, where no hydroxyl-containing liquid is present and no ions are demonstrable by conductivity, the Allen-Modena mechanism must be altered to a point where it differs little from one of solvolytic dissociation.

---

* The dielectric constants at room temperature are dioxane 2·21, n-Bu_2O 3·06, $C_6H_5N(CH_3)_2$ 4·48, and $HCON(CH_3)_2$ 36·7. The rates of CH_3SiCl_3 formation were: from dioxane, 0·038 g/g^{-1}/hr^{-1}; from n-butyl ether 0·055 g/g^{-1}/hr^{-1}; from dimethyl aniline, unknown; from dimethylformamide 0·128 g/g^{-1}/hr^{-1}.

(17) A. D. Allen and G. Modene *J. Chem. Soc.* 3671 (1957).

J. Inorg. Nucl. Chem., 1962, Vol. 24, pp. 169 to 178. Pergamon Press Ltd. Printed in Northern Ireland

THE REACTIONS OF METAL COMPLEXES WITH ALKYL HALIDES—I

REACTIONS OF HALO(TRIPHENYLPHOSPHINE)MERCURY(II) AND QUATERNARY HALOMERCURATE(II)COMPLEXES

G. B. DEACON and B. O. WEST
Department of Physical and Inorganic Chemistry
University of Adelaide

(*Received* 20 *July* 1961; *in revised form* 15 *September* 1961)

Abstract—The conversion of halo(triphenylphosphine)mercury(II) complexes to quaternary halomercurate(II) complexes by alkyl halides has been studied. Halogen exchange frequently occurs where the halogens of the reactants differ. Reaction between quaternary halomercurate(II) complexes, and alkyl halides containing a different halogen, has been shown to occur.

THE conversion of di-iodo*bis*(*p*-dimethylaminophenyldimethylphosphine)mercury(II) and di-iodo*bis*(phenyldimethylphosphine)mercury(II) to the corresponding *bis*(aryltrimethylphosphonium) tetraiodomercurate(II) complexes by methyl iodide in acetone has been reported.⁽¹⁾

$$(ArMe_2P)_2HgI_2 + 2MeI \rightarrow [ArMe_3P]_2HgI_4$$

We have studied the reactions with alkyl halides of the complexes $(Ph_3P)_2HgX_2$ and $(Ph_3P{\cdot}HgX_2)_2$* (where X is Cl, Br, I). The occurrence of halogen exchange in reactions where the halogens of the reactants differ has led to a study of the reactions of quaternary halomercurate(II) complexes with alkyl halides. For comparison the reactions of quaternary halides and mercuric bromide with alkyl halides have also been attempted.

EXPERIMENTAL

The iodo(triphenylphosphine)mercury(II) complexes were prepared by reaction between stoicheiometric amounts of the phosphine and mercuric iodide in benzene and were recrystallized from the same solvent.

1. Di-iodobis(triphenylphosphine)mercury(II). White microcrystalline powder, m.p. 246–247° (lit.⁽²⁾ ca. 250°) (Found: C, 44·0; H, 3·3; I, 26·4. Calc. for $C_{36}H_{30}P_2HgI_2$: C, 44·1; H, 3·1; I, 26·0%).

2. Di-μ-iododi-iodobis(triphenylphosphine)dimercury(II). White microcrystalline powder, m.p. 242° (Found: C, 30·0; H, 2·25; I, 35·3; Hg, 27·9. Calc. for $C_{36}H_{30}P_2Hg_2I_4$: C, 30·15; H, 2·1; I, 35·5; Hg, 28·0%).

Chloro and Bromo(triphenylphosphine)mercury(II) complexes

These were precipitated on mixing ethanol solutions of the stoicheiometric amounts of the mercuric halide and triphenylphosphine.

---

* The bromo and chloro complexes were assumed dimeric by EVANS *et al.*⁽²⁾ by analogy with the structure found for similar trialkylphosphine and trialkylarsine complexes. The iodo complex is not sufficiently soluble in suitable solvents for determination of the molecular weight,⁽³⁾ but is similarly written as the dimer.

⁽¹⁾ R. C. CASS, G. E. COATES and R. G. HAYTER, *J. Chem. Soc.* 4007 (1955).

⁽²⁾ R. C. EVANS, F. G. MANN, H. S. PEISER and D. PURDIE, *J. Chem. Soc.* 1209 (1940).

⁽³⁾ G. B. DEACON and B. O. WEST. Unpublished observations (1961); *J. Chem. Soc.* 5127 (1961).

⁽⁴⁾ G. V. WITTIG and D. WITTENBERG, *Liebigs Ann.* 606, 1 (1957).

1. Dibromobis(triphenylphosphine)mercury(*II*). White powder, m.p. 258–259° (Found: C, 48·2; H, 3·4; Hg, 22·7. Calc. for $C_{36}H_{30}P_2HgBr_2$: C, 48·8; H, 3·4; Hg, 22·7%).

2. Di-μ-bromodibromobis(triphenylphosphine)dimercury(II). White powder, m.p. 251–252° (lit.$^{(3)}$ 240–250°) (Found: C, 34·8; H, 2·8. Calc. for $C_{36}H_{30}P_2Hg_2Br_4$: C, 34·7; H, 2·4%).

3. Dichlorobis(triphenylphosphine)mercury(II). Recrystallized from acetone, white needles, m.p. ca. 270° (lit.$^{(3)}$ 273°) (Found: C, 53·8; H, 3·8. Calc. for $C_{36}H_{30}P_2HgCl_2$: C, 54·3; H, 3·8%).

4. Di-μ-chlorodichlorobis(triphenylphosphine)dimercury(II). White powder, m.p. ca. 300–310° (lit.$^{(3)}$ 306–309°) (Found: C, 40·7; H, 3·05. Calc. for $C_{36}H_{30}P_2Hg_2Cl_4$: C, 40·5; H, 2·8%).

Preparation of quaternary halomercurates

All preparations were effected by reaction between stoicheiometric amounts of appropriate reagents (the specific reagents used are given in parenthesis after the name of the compound) in acetone. The required complex was crystallized, generally after the addition of ethanol to lower the solubility, and recrystallized from acetone or acetone/ethanol.

1. Triphenylethylphosphonium tribromomercurate(II). ($Ph_3EtPBr—HgBr_2$). White microcrystalline powder, m.p. 136·5° (Found: C, 32·7; H, 2·8; Hg, 26·9. Calc. for $C_{20}H_{20}PHgBr_3$: C, 32·8; H, 2·7; Hg, 27·4%).

2. Triphenylmethylphosphonium dibromoiodomercurate(II). ($Ph_3MePI—HgBr_2$). Cream plates, m.p. 137·5° (Found: C, 29·8; H, 2·4. Calc. for $C_{19}H_{18}PHgBr_2I$: C, 29·8; H, 2·4%).

3. Triphenylmethylphosphonium bromodi-iodomercurate(II). ($Ph_3MePI—HgBr_2—HgI_2$). Pale yellow fine needles, m.p. 140° (Found: C, 27·9; H, 2·2. Calc. for $C_{19}H_{18}PHgBrI_2$: C, 28·1; H, 2·2%).

4. Triphenylethylphosphonium bromodi-iodomercurate(II). ($Ph_3EtPBr—HgI_2$). Pale yellow microcrystalline powder, m.p. 93–94° (Found: C, 29·0; H, 2·5. Calc. for $C_{20}H_{20}PHgBrI_2$: C, 29·1; H, 2·4%).

5. Triphenylmethylphosphonium tri-iodomercurate(II). ($[Ph_3MeP]_2[HgI_4]—HgI_2$). Yellow needles, m.p. 146–146·5° (Found: C, 26·2; H, 2·1; Hg, 22·9. Calc. for $C_{19}H_{18}PHgI_3$: C, 26·55; H, 2·1; Hg, 23·4%).

6. Triphenylethylphosphonium tri-iodomercurate(II). ($Ph_3EtPI—HgI_2$). Yellow needles, m.p. 127·5–128° (Found: C, 27·3; H, 2·3; Hg, 22·7; I, 43·7. Calc. for $C_{20}H_{20}PHgI_3$: C, 27·5; H, 2·3; Hg, 23·0; I, 43·7%).

7. Bis(triphenylmethylphosphonium) tetraiodomercurate(II). ($Ph_3MePI—HgI_2$). Pale yellow plates, m.p. 172–173° (Found: C, 37·1; H, 2·8. Calc. for $C_{38}H_{36}P_2HgI_4$: C, 36·1; H, 2·85%). Further recrystallization failed to improve the purity of the complex.

8. Bis(triphenylethylphosphonium) tetraiodomercurate(II). ($Ph_3EtPHgI_3—Ph_3EtPI$). Very small, pale yellow plates, m.p. 135–136° (Found: C, 36·9; H, 3·3. Calc. for $C_{40}H_{40}P_2HgI_4$: C, 37·2; H, 3·1%).

Triphenylethylphosphonium bromide was obtained by refluxing triphenylphosphine with excess ethyl bromide. In a typical preparation triphenylphosphine (1·19 g) was converted to triphenylethylphosphonium bromide (0·87 g, 52 per cent), recrystallized from ether/ethanol, m.p. 204–204·5° (lit.$^{(4)}$ 203·5°) (Found: C, 64·6; H, 5·5. Calc. for $C_{20}H_{20}PBr$: C, 64·7; H, 5·5%), after reacting with ethyl bromide for 10 hr.

Reactions of Halo(triphenylphosphine)mercury(II) complexes with alkyl halides

The reactions were carried out by refluxing the solid complex (0·2–1 g) with a large excess of redistilled reagent grade alkyl halide (10–30 ml). In some reactions an additional solvent was employed. If the reaction product was insoluble it was filtered off and recrystallized from acetone/ethanol (except in the case of attempted reactions with ethyl bromide). If the product was soluble the solution was evaporated to dryness under reduced pressure and the residue recrystallized from acetone/ethanol.

Methyl iodide

In all reactions the yield was >90 per cent.

1. $(Ph_3P)_2HgI_2$ was refluxed as a suspension in methyl iodide for 2 hr. The resulting pale yellow solid precipitated was bis(triphenylmethylphosphonium) tetraiodomercurate(II), m.p. and mixed m.p. 172–172·5° (Found: C, 36·6; H, 3·1%). The product was converted to the tri-iodomercurate, m.p. and mixed m.p. 146–146·5° (Found: C, 26·4; H, 2·2%) by reaction with mercuric iodide in acetone. The methyl iodide was evaporated and contained negligible solute.

2. $(Ph_3P·HgI_2)_2$ dissolved on refluxing to give a yellow solution. After 2 hr the solvent was evaporated and triphenylmethylphosphonium tri-iodomercurate(II) was obtained, m.p. and mixed m.p. 146–146·5° (Found: C, 26·8; H, 2·2%).

3. $(Ph_3P)_2HgBr_2$ was refluxed as a suspension for 1½ hr. The yellow precipitate was bis(triphenylmethylphosphonium) tetraiodomercurate(II), m.p. 172°, mixed m.p. 171·5–172° (Found: C, 37·0; H, 3·2%). Conversion to the tri-iodomercurate gave m.p. 145·5–146°, mixed m.p. 146° (Found: C, 26·3; H, 2·2%).

4. $(Ph_3P{\cdot}HgBr_2)_2$ dissolved on refluxing to give a yellow solution. After 1 hr the solvent was evaporated and triphenylmethylphosphonium tri-iodomercurate(II), was obtained, m.p. 146°, mixed m.p. 146–146·5° (Found: C, 26·7; H, 2·4%).

5. $(Ph_3P)_2HgCl_2$ was refluxed with methyl iodide and acetone. After 5 min the bulk of the complex had dissolved to give a pale yellow solution, then slow precipitation of pale yellow crystals commenced. After 1 hr the volatiles were evaporated and bis(triphenylmethylphosphonium) tetraiodomercurate(II) was obtained, m.p. and mixed m.p. 173–173·5° (acetone only) (Found: C, 36·9; H, 3·3%). Conversion to the tri-iodomercurate gave m.p. 146·5–147°, mixed m.p. 146·5° (Found: C, 26·45; H, 2·2%).

6. $(Ph_3P.HgCl_2)_2$ dissolved on refluxing to give a yellow solution. After 2 hr triphenylmethylphosphonium tri-iodomercurate(II) was obtained, m.p. 146–146·5°, mixed m.p. 146° (Found: C, 26·5; H, 2·4%).

Ethyl iodide

Except in 1., yields of crude product were >95 per cent.

1. $(Ph_3P)_2HgI_2$ (0·96 g 0·98 mmoles) was refluxed as a suspension in ethyl iodide (25 ml) for 8 hr. The pale yellow precipitate was bis(triphenylethylphosphonium) tetraiodomercurate(II) (1·03 g, 0·80 mmole, ca. 80%), m.p. 126–130° (by direct synthesis, 135–136°), unaltered by further recrystallization (Found: C, 37·9; H, 3·6%). Evaporation of the ethyl iodide yielded a small amount of pale yellow solid, not further investigated.

2. $(Ph_3P{\cdot}HgI_2)_2$ dissolved on refluxing to give a yellow solution. After 2·5 hr the ethyl iodide was evaporated and triphenylethylphosphonium tri-iodomercurate(II) was obtained, recrystallized three times from acetone/ethanol, m.p. 131–133° (by alternate synthesis 127·5–128°) (Found: C, 26·9; H, 2·2; HgI_2*, 52·7. Calc. for $C_{20}H_{20}PHgI_3$: HgI_2, 52·1%).

3. $(Ph_3P{\cdot}HgBr_2)_2$ dissolved on refluxing to give a yellow solution. The residue, after removal of the solvent, was impure triphenylethylphosphonium tri-iodomercurate(II), m.p. 124–124·5°. 0·402 g of impure product was decomposed by excess triphenylphosphine in ethanol to yield di-iodobis(triphenylphosphine)mercury(II) (0·436 g 0·446 mmole, 97 per cent based on $C_{20}H_{20}PHgI_3$), m.p. and mixed m.p. 248–249° (Found: C, 44·1; H, 3·2%) as a precipitate. The ethanol solution was evaporated to dryness, yielding triphenylethylphosphonium iodide (0·178 g, 0·426 mmole, 92%), recrystallized from acetone/ether, m.p. 166° (lit.[5] 164–165°), mixed m.p. 166° (Found: C, 57·7; H, 5·0. Calc. for $C_{20}H_{20}PI$: C, 57·6; H, 4·8%), which was separated from unreacted triphenylphosphine. Refluxing the impure triphenylethylphosphonium tri-iodomercurate(II) from the original reaction with more ethyl iodide gave a purer product, m.p. 126–127° (Found: C, 27·2; H, 2·3; I, 44·0%).

Reactions with ethyl bromide

The complexes $(Ph_3P)_2HgX_2$ and $(Ph_3P{\cdot}HgX_2)_2$ (where X is I, Br) were refluxed as suspensions in ethyl bromide. Certain reactions were also attempted in the presence of benzene or acetone to ensure partial solution of the complexes. In most of the experiments the bulk of the reactant was recovered unchanged from suspension by filtration, the results being given in Table 1 (nos. 1–7). The filtrate from 2, 3, 4, 6, was evaporated to dryness, the residue obtained being primarily unchanged reactant in each case. No more than a trace of product could be detected. In expt. 8 the volatiles were removed *in vacuo* and the residue extracted with 3 ml. cold acetone. The bulk of the material was insoluble, and was unchanged reactant. The soluble material was also primarily unchanged reactant.

$(Ph_3P)_2HgBr_2$ was also recovered substantially unchanged after refluxing with ethyl bromide in benzene for 2 hr, m.p. 260–261° (Found: C, 48·7; H, 3·5%).

Reactions with n-*butyl bromide*

1. $(Ph_3P)_2HgI_2$ (0·53 g) was refluxed with *n*-butyl bromide. After 2½ hr a pale brown–yellow melt formed. This solidified on cooling, and white crystals were deposited from solution. After a further 1½ hr heating, the product was a white

---

* By decomposition of the complex with excess triphenylphosphine giving a quantitative yield of $(Ph_3P)_2HgI_2$[5].

[5] A. Michaelis and H. V. Soden, *Liebigs Ann.* **229**, 295 (1885).

crystalline suspension, which was filtered off (0·53 g), m.p. 189–190°. On fractional recrystallization from acetone/ethanol, di-bromo*bis*(triphenylphosphine)mercury(II) m.p. 258–259° and *mixed* m.p. 258° (*after two recrystallizations from acetone*), (Found: C, 47·9; H, 3·5 %) crystallized first, followed by a much smaller amount of white microcrystalline solid, m.p. 117·5–118° (after two recrystallizations from acetone/ethanol) (Found: C, 36·5; H, 3·2 %), not identified. When $(Ph_3P)_2HgI_2$ (0·57 g) was refluxed with *n*-butyl bromide for 2 hr, the solid product (0·54 g) was iodine free and only gave one fraction on recrystallization, viz., impure $(Ph_3P)_2HgBr_2$, m.p. 253°.

TABLE 1.—ATTEMPTED REACTION OF COMPLEXES WITH ETHYL BROMIDE

Expt.	Complex	W_1(g)	Time (hr). [conditions]	W_2(g)	m.p.* (°C)	Product mixed m.p.	Found (%)	
							C	H
1	$(Ph_3P)_2HgI_2$	0·73	6 [a]	0·67	249–250	250	—	—
2	$(Ph_3P)_2HgI_2$	0·56	7 [b]	0·47	247–248	247–248	43·8	3·2
3	$(Ph_3P)_2HgI_2$	0·40	5 [c]	0·36	247–247·5	248–248·5	44·2	3·2
4	$(Ph_3P{\cdot}HgI_2)_2$	0·14	11 [a]	0·10	241–242	241–242	—	—
5	$(Ph_3P)_2HgBr_2$	0·44	14 [a]	0·38	258	257–257·5	—	—
6	$(Ph_3P)_2HgBr_2$	0·37	3·5 [c]	0·33	260–260·5	258·5–260	48·8	3·6
7	$(Ph_3P{\cdot}HgBr_2)_2$	0·64	13 [a]	0·62	252–253	252–253·5	—	—
8	$(Ph_3P{\cdot}HgI_2)_2$	0·47	6 [c]	0·41	240·5–241	240–240·5	30·4	2·2

W_1 initial weight complex.
W_2 weight complex recovered (see text).
a reflux with ethyl bromide.
b reflux with ethyl bromide in benzene.
c reflux with ethyl bromide in acetone.
* Nos. 4, 8 recrystallized from benzene. Others as isolated.

2. When $(Ph_3P)_2HgBr_2$ (0·59 g) was refluxed with *n*-butyl bromide for 7½ hr, a pale yellow–brown melt slowly formed. On cooling this became semi-solid, and was filtered off. After drying (80°) to remove solvent the product (0·71 g) did not completely solidify. Considerable difficulty was experienced in crystallizing the product. White crystals were eventually obtained from acetone/ethanol. The product again softened on oven drying to remove solvent, but solidified on cooling. It analysed as tris(triphenyl-*n*-butylphosphonium) heptabromodimercurate(II), m.p. 111–112° (Found: C, 41·2; H, 3·8; P, 4·8; Hg, 20·5; Br, 29·4. Calc. for $C_{66}H_{72}P_3Hg_2Br_7$: C, 41·3; H, 3·75; P, 4·85; Hg, 20·9; Br, 29·2 %). The weight of semi-solid product was in excess of that required for the formation of the heptabromodimercurate alone (0·64 g). Another compound must also be present, but has not been identified.

Attempted reaction with iodobenzene

$(PPh_3)_2HgI_2$ (0·69 g) was refluxed with iodobenzene for ca. 2 hr. The compound dissolved but no yellow iodomercurate colour developed in the solution. When the iodobenzene was removed by distillation, a pale glue was obtained which could not be crystallized.

Reactions of quaternary trihalomercurate(II) complexes with alkyl halides

For reactions in absence of an added solvent, a considerable excess of alkyl halide (10–20 ml: 0·1–0·6 g complex) was employed. Where acetone was added 0·1–0·4 g complex was initially dissolved in

10 ml of acetone and 5 ml (nos. 1, 2, 3, 5, 8) or 10 ml (no. 6) of the alkyl halide was added. Except where stated the yields were 90–100 per cent. All products were recrystallized from acetone/ethanol.

1. A solution of triphenylethylphosphonium tribromomercurate(II) in acetone and methyl iodide was refluxed. After heating for 15 min, the initially colourless solution had become bright yellow. Evaporation of the solvent gave a residue of triphenylethylphosphonium tri-iodomercurate(II), m.p. 127–127·5°, mixed m.p. 127·5–128° (Found: C, 28·0; H, 2·8%).

2. The same reaction occurred when a similar solution was kept at 25° for 1 hr. Triphenylethylphosphonium tri-iodomercurate(II) was obtained, m.p. 127·5–128°, mixed m.p. 128° (Found: C, 27·9; H, 2·6%).

3. Triphenylmethylphosphonium dibromo-iodomercurate(II) reacted with methyl iodide in acetone in 1 hr at 25° to give triphenylmethylphosphonium tri-iodomercurate(II), m.p. and mixed m.p. 146·5° (Found: C, 26·45; H, 2·3%).

4. Triphenylmethylphosphonium bromodi-iodomercurate(II) was converted to the tri-iodomercurate, m.p. 146°, mixed m.p. 146–146·5° (Found: C, 26·3; H, 2·2%) by refluxing with methyl iodide for 2½ hr.

5. Triphenylethylphosphonium bromodi-iodomercurate(II) reacted with methyl iodide in acetone in 1 hr at 25° to give triphenylethylphosphonium tri-iodomercurate(II), m.p. 127·5–128°, mixed m.p. 128° (Found: C, 27·5; H, 2·4%).

6. Triphenylmethylphosphonium tri-iodomercurate(II) (0·21 g) was refluxed with ethyl bromide in acetone for 2 hr and allowed to stand for 10 hr at room temperature. The volatiles were removed *in vacuo* and 0·20 g of a yellow solid, m.p. 143·5° was obtained. On crystallization from acetone/ethanol the first fraction had m.p. 143·5–144° (Found: C, 27·3; H, 2·5; I, 38·5; Br, 4·6%), the second had m.p. 143·5–144° (Found: C, 27·0; H, 2·7; I, 38·9; Br, 4·3%. Calc. for $Ph_3MePHgI_3$: C, 26·5; H, 2·1; I, 44·4%. Calc. for $Ph_3MePHgBrI_2$: C, 28·1; H, 2·2; I, 31·3; Br, 9·9%). The ultraviolet spectrum in methanol of the first fraction in the region 240–320 mμ shows features intermediate between the spectra of $[Ph_3PMe][HgBrI_2]$ and $[Ph_3PMe][HgI_3]$ (Fig. 1).

7. Triphenylmethylphosphonium tri-iodomercurate(II) was refluxed with excess *n*-butyl bromide for 4 hr. Partial solution of the complex occurred. On cooling pale yellow crystals of triphenylmethylphosphonium bromodi-iodomercurate(II) were obtained, m.p. 140°, mixed m.p. 139–140° (Found: C, 27·8; H, 2·2%).

8. A solution of triphenylethylphosphonium tri-iodomercurate(II) (0·14 g) in acetone and ethyl bromide was maintained at 25° for 1 hr. No colour change was observed. When the solvents were removed *in vacuo*, the complex was recovered unchanged, m.p. 127–127·5°, mixed m.p. 128–128·5° (Found: C, 27·6; H, 2·6%).

Reaction of mercuric bromide with methyl iodide

1. Mercuric bromide was refluxed with excess methyl iodide for 10 hr. A yellow residue was obtained after removal of the methyl iodide by distillation. Impure bromoiodomercury(II) was partly separated from unreacted mercuric bromide by ether extraction, recrystallized from the same solvent and obtained as a yellow microcrystalline powder still impure, m.p. 212–214° (lit.(6) 229°) (Found: Hg, 50·2; Br, 24·7; I, 24·8. Calc. for HgBrI: Hg, 49·2; Br, 19·6; I, 31·2%).

2. A solution of mercuric bromide (0·184 g) in acetone and methyl iodide (10 ml and 5 ml respectively) was maintained at 25° for 1 hr. When the solvents were removed *in vacuo* the residual solid (0·186 g) showed only a faint yellow colouration, hence very little halogen exchange occurred.

Reactions of quaternary halides with alkyl halides

In all reactions ca. 5 per cent of ethanol (v/v) was added to the system to increase the solubility of the quaternary halide. The yields were near quantitative (>90 per cent) and all products were recrystallized from ether/ethanol.

1. Triphenylethylphosphonium bromide was converted to the iodide, m.p. 166·5–167°, mixed m.p. 166–166·5° (Found: C, 57·0; H, 5·0%), by refluxing with ethyl iodide in acetone for 1 hr.

2. A solution of triphenylethylphosphonium bromide (0·14 g) in acetone (10 ml) and methyl iodide (5 ml) was maintained at 25° for 1 hr. Triphenylethylphosphonium iodide, m.p. 166·5°, mixed m.p. 166–166·5°, (Found: C, 57·3; H, 4·8%) was obtained.

3. A solution of triphenylethylphosphonium iodide (0·11 g) in acetone (10 ml) and ethyl bromide (5 ml) was maintained at 25° for 1 hr. Triphenylethylphosphonium bromide, m.p. and mixed m.p. 203–204° (Found: C, 64·7; H, 5·5%) was obtained.

---

(6) *Handbook of Chemistry and Physics* (39th Ed.), Chemical Rubber Publishing Co., Cleveland, Ohio (1957).

Ultra-violet spectra

Ultra-violet spectra were measured in 1 mm silica cells, using a Unicam SP500 spectrophotometer. Reagent grade methanol was refluxed over and distilled from sodium hydroxide.

Microanalyses

Microanalyses were determined by the C.S.I.R.O. Microanalytical Laboratories, Melbourne.

RESULTS AND DISCUSSION

The reactions studied and the results obtained are collected in Table 2. The complexes $(Ph_3P)_2HgI_2$ and $(Ph_3P{\cdot}HgI_2)_2$ react with methyl iodide or ethyl iodide to yield the corresponding triphenylalkylphosphonium iodomercurates.

$$(Ph_3P)_nHgI_2 + nRI \rightarrow [Ph_3RP]_nHgI_{n+2}$$

where n is 1 or 2, R is Et or Me.

The complexes $(Ph_3P)_2HgX_2$ and $(Ph_3P{\cdot}HgX_2)_2$ (where X is Cl or Br) are converted by methyl iodide to the corresponding triphenylmethylphosphonium iodomercurates. The reactions involve halogen exchange* as well as quaternization.

$$(Ph_3P)_nHgX_2 + (n + 2)MeI \rightarrow [Ph_3PMe]_nHgI_{n+2} + 2MeX$$

where n is 1 or 2.

None of the bromo or iodo(triphenylphosphine)mercury(II) complexes react with ethyl bromide under reflux. Addition of solvents to ensure partial solution of the complexes does not induce reaction, hence failure to react is not due to insolubility in ethyl bromide.

$(Ph_3P)_2HgI_2$ undergoes halogen exchange with n-butyl bromide to yield $(Ph_3P)_2HgBr_2$. The quaternization of the latter complex by n-butyl bromide requires a much longer time. The crude product from this reaction gave a compound with analytical composition corresponding to the complex $[n\text{-Bu—PPh}_3]_3Hg_2Br_7$ on recrystallization. The formation of this complex is surprising, as the reaction of the analogous complex $(Ph_3P)_2HgI_2$ with ethyl iodide yields a tetraiodomercurate. Lattice energies evidently favour crystallization of the heptabromodimercurate rather than the tetrabromomercurate. The weight of crude product obtained was in excess of that calculated for the formation of the heptabromodimercurate alone. Probably triphenyl-n-butylphosphonium bromide is also formed in the reaction.

Halo(triphenylphosphine)mercury(II) complexes react more readily with alkyl iodides than with alkyl bromides. This can be attributed to two factors. The bond energy of C—Br is greater than that of C—I,⁽⁷⁾ and iodomercurate complexes are more stable than bromomercurate complexes.⁽⁸,⁹⁾ Though the presence of Hg—Hal bonds has been shown to facilitate C—Hal bond rupture,⁽¹⁰⁾ the failure of $(Ph_3P)_2HgI_2$ to react with iodobenzene shows that the effect in this system is insufficient to cause quaternization to occur. Iodobenzene does not react with triphenylphosphine directly.⁽¹¹⁾

---

* Throughout this paper this term is used only to describe reactions in which the inter-changing halogens are different.

(7) T. L. COTTRELL, *The Strength of Chemical Bonds*. Butterworths, London (1958).
(8) L. G. SILLÉN, *Acta Chem. Scand.* 3, 539 (1949).
(9) I. LEDEN and J. CHATT, *J. Chem. Soc.* 2936 (1955).
(10) R. ANANTARAMAN, *Bull. Central Research Inst. Univ. Travancore*, Ser. A, 3, 159 (1954).
(11) G. M. KOSOLAPOFF, *Organophosphorus Compounds*, p. 78. Wiley, New York (1950).

For the quaternization step in the reactions there are two possible mechanisms.

(a) The complex dissociates to give a free triphenylphosphine molecule, which is quaternized by the alkyl halide. The halide ion, so formed, complexes to give the halomercurate. Dissociation of halo(triphenylphosphine)mercury(II) complexes in ethyl bromide must be negligible, as the formation of the Ph_3PEt^+ cation cannot be detected. Triphenylphosphine reacts significantly with ethyl bromide to form triphenylethylphosphonium bromide using comparable conditions.

(b) The reactions proceed via co-ordination of the alkyl halide with mercury followed by rearrangement of the intermediate, e.g., for $(Ph_3P)_2HgX_2$ (where X is a halogen),

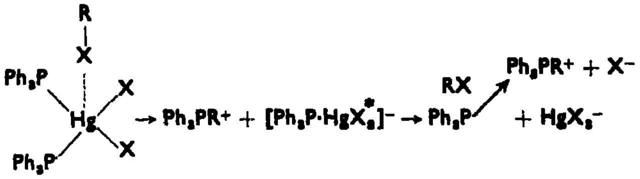

An analogous scheme can be written for $(Ph_3P\cdot HgX_2)_2$ complexes. At present there is not sufficient evidence to decide which mechanism applies. The use of kinetic measurements to decide the mechanism would be difficult due to the low solubility of the halo(triphenylphosphine)mercury(II) complexes.

Where halogen exchange occurs in addition to quaternization two reaction paths are possible depending on which step occurs first, e.g., for $(Ph_3P\cdot HgBr_2)_2$,

Path 1: $(Ph_3P\cdot HgBr_2)_2 \xrightarrow{MeI} (Ph_3P\cdot HgI_2)_2 \xrightarrow{MeI} [Ph_3PMe][HgI_3]$

Path 2: $(Ph_3P\cdot HgBr_2)_2 \xrightarrow{MeI} [Ph_3PMe][HgBr_2I] \xrightarrow[A]{MeI} [Ph_3PMe][HgI_3]$

The conversion of $(Ph_3P)_2HgI_2$ to a bromomercurate by *n*-butyl bromide must proceed by path 1, as the intermediate formation of $(Ph_3P)_2HgBr_2$ has been demonstrated. Intermediates have not been isolated in the reactions with alkyl iodides. The reaction A, and others similar have been shown to occur. They are summarized in Table 2, and may be represented by the equation

$$M\cdot[HgBr_nI_{3-n}] + nMeI \rightarrow M[HgI_3] + nMeBr$$

where $n = 3$, 2 or 1, and M is Ph_3MeP or Ph_3EtP.

The reverse reaction does not occur readily. Under conditions similar to those which permit complete exchange between triphenylethylphosphonium tribromomercurate(II) and methyl iodide, triphenylethylphosphonium tri-iodomercurate(II) fails to react with ethyl bromide. Boiling ethyl bromide only induces slight bromination of triphenylmethylphosphonium tri-iodomercurate(II). The more extreme conditions of the reaction using *n*-butyl bromide only introduce one bromine atom.

We consider that the mechanism of these trihalomercurate/alkyl halide exchange reactions is a dissociation and recombination process of the following type,

$$[HgX_3]^- \rightleftharpoons HgX_2 + X^- \qquad (1)$$

$$X^- + RY \rightarrow RX + Y^- \qquad (2)$$

$$Y^- + HgX_2 \rightleftharpoons [HgX_2Y]^- \rightleftharpoons HgXY + X^-, \text{ etc.} \qquad (3)$$

---

* Mixtures of $[PMe_4][HgI_3]$ and triphenylphosphine in methanol (ca. 5×10^{-4} M) have been examined spectroscopically, and show no evidence for the formation of the ion $[Ph_3P\cdot HgI_3]^-$, hence the dissociation should be complete.[8]

TABLE 2.—REACTIONS OF COMPLEXES AND RELATED COMPOUNDS WITH ALKYL HALIDES

Complex	Reagent (Conditions)	Product	Complex	Reagent (Conditions)	Product
$(Ph_3P)_2HgI_2$	MeI*	$[Ph_3PMe]_2HgI_4$	$(Ph_3P)_2HgI_2$	n-BuBr*	$(Ph_3P)_2HgBr_2$
$(Ph_3P{\cdot}HgI_2)_2$	MeI*	$[Ph_3PMe]HgI_3$	$(Ph_3P)_2HgBr_2$	n-BuBr*	$[Ph_3P{\cdot}n\text{-}Bu]_2Hg_2Br_6$
$(Ph_3P)_2HgBr_2$	MeI*	$[Ph_3PMe]_2HgI_4$	$[Ph_3PEt]HgBr_3$	MeI†**	$[Ph_3PEt]HgI_3$
$(Ph_3P{\cdot}HgBr_2)_2$	MeI*	$[Ph_3PMe]HgI_3$	$[Ph_3PMe]HgBr_2I$	MeI**	$[Ph_3PMe]HgI_3$
$(Ph_3P)_2HgCl_2$	MeI†	$[Ph_3PMe]_2HgI_4$	$[Ph_3PMe]HgBrI_2$	MeI*	$[Ph_3PMe]HgI_3$
$(Ph_3P{\cdot}HgCl_2)_2$	MeI*	$[Ph_3PMe]HgI_3$	$[Ph_3PEt]HgBrI_2$	MeI**	$[Ph_3PEt]HgI_3$
$(Ph_3P)_2HgI_2$	EtI*	$[Ph_3PEt]_2HgI_4$	$[Ph_3PMe]HgI_3$	EtBr†	Slight Br substitution
$(Ph_3P{\cdot}HgI_2)_2$	EtI*	$[Ph_3PEt]HgI_3$	$[Ph_3PMe]HgI_3$	n-BuBr*	$[Ph_3PMe]HgBrI_2$
$(Ph_3P{\cdot}HgBr_2)_2$	EtI*	$[Ph_3PEt]HgI_3$	$[Ph_3PEt]HgI_3$	EtBr**	No reaction
$(Ph_3P)_2HgI_2$	PhI*	No product identified	$HgBr_2$	MeI*	HgBrI (impure)
$(Ph_3P)_2HgI_2$	EtBr*†‡	No reaction	$HgBr_2$	MeI**	Slight reaction
$(Ph_3P{\cdot}HgI_2)_2$	EtBr*†	No reaction	$[Ph_3PEt]Br$	MeI**	$[Ph_3PEt]I$
$(Ph_3P)_2HgBr_2$	EtBr*†‡	No reaction	$[Ph_3PEt]Br$	EtI†	$[Ph_3PEt]I$
$(Ph_3P{\cdot}HgBr_2)_2$	EtBr*	No reaction	$[Ph_3PEt]I$	EtBr**	$[Ph_3PEt]Br$

* Reflux reagents at boiling point.

† Reflux reagents in acetone.

‡ Reflux reagents in benzene.

** Reagents at 25° in acetone.

where X ≠ Y and X, Y are Br or I. The dissociations represented by equations (1) and (3) are well known.(8,12) Reaction (2) has been shown to occur readily under the conditions of the present experiments (Table 2), and has been the subject of considerable kinetic investigation.(13) Tri-iodomercurate complexes do not react with alkyl bromides as extensively as the bromomercurates react with alkyl iodides, since the stability of iodomercurates is greater than that of the bromomercurates.(8,9) This factor favours equilibrium positions to the left hand side of equations (1) and (3) when X = I and Y = Br, and inhibits the further dissociation illustrated in equation (3), by which complete exchange could occur. In particular the species $[HgI_2Br]^-$ tends to dissociate into HgI_2 and Br^- rather than HgBrI and I^-. Conversely when X = Br and Y = I, the greater stability of iodomercurates over bromomercurates favours equilibrium positions to the right hand side of equations (1) and (3), and the reactions can proceed to completion, Exchange between mercuric halides and alkyl halides does not provide an alternative route for substitution, as the direct exchange between mercuric bromide and methyl iodide occurs very slowly. The

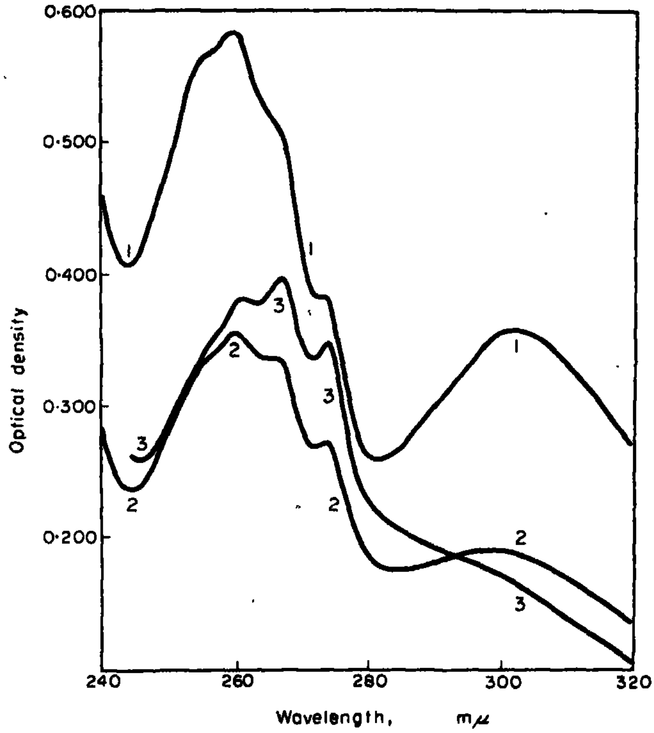

Fig. 1.—Absorption spectra in methanol.

1. $[Ph_3PMe]HgI_3$ 3·31 × 10^{-4} M
2. Reaction product of $[Ph_3PMe]HgI_3$ and EtBr ca. 2·6 × 10^{-4} M
3. $[Ph_3PMe]HgBrI_2$ 3·66 × 10^{-4} M

---

[12] Y. Marcus, *Acta Chem. Scand.* 11, 598, 610 (1957).

[13] e.g. J. B. Conant, W. R. Kirner, R. E. Hussey, *J. Chem. Soc.* 47, 476 488 (1925); P. B. D. de la Mare, L. Fowden, E.D. Hughes, C. K. Ingold, and J. D. H. Mackie, *J. Chem. Soc.* 3169, 3173, 3177, 3180, 3187, 3193, 3196 (1955).

quaternary cations used in the exchange reactions are unaffected by the alkyl halides, and are not considered to be involved in the reactions.

It is planned to extend these investigations to the reactions of analogous complexes of other transition metals. At present the reactions of the complexes $(Ph_3P)_2CdX_2$ (where X is Br or I) with alkyl halides are being studied.

Ultra-violet spectra. The ultra-violet spectra of triphenylmethylphosphonium bromodi-iodomercurate(II), triphenylmethylphosphonium tri-iodomercurate(II), and the partially brominated product from the reaction of the tri-iodomercurate with ethyl bromide, have been measured in methanol (Fig. 1). The spectrum of the bromodi-iodomercurate(II) compound shows no feature that can be conclusively allocated to the presence of the $[HgBrI_2]^-$ ion, thus the dissociation $[HgBrI_2]^- \rightleftharpoons HgI_2 + Br^-$ must be considerable. The peaks at 261–262 mμ, 267 mμ and 274 mμ are close to those given for the triphenylmethylphosphonium cation in ethanol.(14) The mercuric iodide band at 270–271 mμ (15) is masked by the sharp changes in cation absorption in this region. The spectrum of the tri-iodomercurate is similar to that of tetramethylphosphonium tri-iodomercurate in methanol,(15) both complexes showing a maximum at 302–304 mμ ($\varepsilon_{PMe_4HgI_3} = 1{\cdot}09 \times 10^4$, $\varepsilon_{Ph_3MePHgI_3} = 1{\cdot}08 \times 10^4$) due to the $[HgI_3]^-$ ion. The differences between the spectra are considered due to the absorption of the $[Ph_3PMe]^+$ ion. The spectrum of the product from the reaction of $[Ph_3PMe][HgI_3]$ with ethyl bromide is intermediate between those of the tri-iodo and bromodi-iodo derivatives. The $[HgI_3]^-$ band at ca. 300 mμ is still present, though weaker and slightly displaced, indicating that some substitution had occurred.

Acknowledgement—We are grateful to the Australian Atomic Energy Commission and to the Imperial Chemical Industries of Australia and New Zealand for awards to one of us (G. B. D.) and to Dr. A. A. DIAMANTIS for helpful discussions.

(14) F. G. MANN, J. T. MILLAN and B. B. SMITH, *J. Chem. Soc.* 1130 (1953).

(15) G. B. DEACON and B. O. WEST, *J. Chem. Soc.* 3929 (1961).

J. Inorg. Nucl. Chem. 1962, Vol. 24, pp. 179 to 182. Pergamon Press Ltd. Printed in Northern Ireland

REVALUATION OF THE CONTINUOUS VARIATION METHOD AS APPLIED TO THE URANYL AZIDE COMPLEXES

F. G. SHERIF and A. M. AWAD
Faculty of Science, Alexandria University, Alexandria,
Egypt, U.A.R.

(*Received 5 July* 1961; *in revised form 28 August* 1961)

Abstract—The method of continuous variation is discussed critically, particularly when applied to solutions containing more than one complex. The deformations in the curves obtained can be interpreted by following the contours of these curves at different wavelengths and concentrations. The presence of mono-, di- and tri-azido uranyl complex ions is revealed.

ONE of the general spectrophotometric methods by means of which complex formation in coloured solutions may be established, is the method of continuous variation of JOB$^{(1)}$. This method, as it is now applied, requires the plotting of Y values (the difference between the total absorbance measured for each mixture and the absorbance of ions corresponding to no reaction) vs. the mole fraction of the metallic ion. During our investigation of the uranyl azide$^{(2)}$ and other metallic azide complexes,$^{(3)}$ we found that there is no difference between plotting the values of Y and plotting directly the measured absorbances, when the general contours of the curves in both cases are compared. When VOSBURGH and COOPER$^{(4)}$ modified the method, they stated that if all wavelengths lead to the same result, then a single compound is formed and only one maximum (or minimum) in the curves will be obtained. When more than one compound is formed, the results obtained are dependent on the wavelength and for useful conclusions the wavelengths must be carefully selected. The stepwise formation of many complexes can be represented by

$$\mathrm{A} + n\mathrm{B} = \mathrm{AB}_n \tag{1}$$

$$\mathrm{AB}_n + q\mathrm{B} = \mathrm{AB}_{n+q} \tag{2}$$

in which A is a metallic ion and B is the ligand; n and q are the numbers of ligand molecules. In order to get a maximum corresponding to a higher complex, such as AB_{n+q}, the absorption contribution made by the lower complex AB_n was calculated using known stability constants and subtracted from the total assuming that Beer's law would be obeyed for the lower complex. However, we think that the last assumption would be unlikely in case of highly dissociated complex ions. This might be why the method of continuous variation did not always give full information about complex formation and could only be relied upon for cases such as the formation of relatively stable complex ions whose absorption bands were widely separated from each other and from that of the metallic ion, and that should conform to Beer's law. Unfavourable conditions would lead to deformed curves. However, in our case, by following the contours of the curves at a wide range of wavelength and at different total concentrations, these deformations can be interpreted to show the possible formation of complexes of different molecular ratios. They may appear as one or more maxima, a shoulder or a kink in the same curve. Each maximum, shoulder or kink should correspond to a certain coloured species, or to the interference of absorbance of one ion with the other. The relative intensities of these deformations may indicate the relative stabilities of the different ions at different concentrations of reagents, especially when measurements on a single solution are repeated after a certain time. A shoulder that appears at one concentration can grow up to a maximum by concentrating the solutions, while the already present maximum might fade away to a shoulder or disappear completely. These changes might also appear when the shapes of the curves at different wavelengths and for the same concentration are compared. The appearance of a shoulder can be interpreted as a slight formation of a particular species at a certain concentration or as a weak absorbance at a certain wavelength. Likewise, an accompanying sharp maximum would mean a stable complex or one with a strong absorbance at a particular wavelength. For any concentration, the change in position of one oı more irregularity in the curves would reflect the difference in stabilities of the different complexes.

---

(1) P. JOB, *C. R. Acad. Sci., Paris* **180**, 928 (1925).

(2) F. G. SHERIF and A. M. AWAD, *J. Inorg. Nucl. Chem.* **19**, 94 (1961).

(3) F. G. SHERIF and W. M. ORABY, *J. Inorg. Nucl. Chem.* **17**, 152 (1961); H. K. EL-SHAMY and F. G. SHERIF, *Egypt J. Chem.* **2**, 217 (1959).

(4) W. C. VOSBURGH and G. R. COOPER, *J. Amer. Chem. Soc.* **63**, 437 (1941).

In this investigation, JOB's continuous variation method was applied to the uranyl azide system at different concentrations. The formation of different complex ions containing different ratios of uranium to azide was suggested.

EXPERIMENTAL

The preparation and analysis of the different solutions used, together with the experimental procedures applied were given in a previous article (2). A Unicam Spectrophotometer S.P. 500, with glass cells 0·1 cm thick, was used.

RESULTS

The existence of a 1-uranyl:1-azide coloured species at a total concentration of 0·016 M was confirmed previously(2) by one sharp maximum at a mole fraction of 0·5 for UO_2^{2+}. In this investigation, the total concentration of uranyl and azide ions was kept constant at 0·08 M and the ionic strength at 0·224 by adding the required amounts of sodium perchlorate. Measurements were taken in the wavelength range of 370–470 mμ. Representative curves are given in Fig. 1. If the two maxima at the wavelength 380 mμ are extrapolated, a single maximum that lies at a mole fraction of 0·33 for UO_2^{2+} is formed and would indicate the formation of a 1-uranyl:2-azide complex. However, the maximum to the right of Fig. 1 falls at a ratio of 1:1·5 and can represent a mixture of 1:1 and 1:2 complexes. The other maximum, being at a ratio of 1:2·3, can be the result of a contribution of a slight formation of a 1:3 complex ion to the 1:2 form. Indications for higher complexes are clearer at shorter than at longer wavelengths as shown by the disappearance of the maximum at 440 μ.

For the total concentration of 0·16 M, Fig. 2, the curves at 280, 390 and 400 μ possess definite maxima substantiating the existence of the 1:3 complex $UO_2(N_3)_3^-$. Shoulders corresponding to a ratio of 1:1 are also observed. As we approach longer wavelengths the maxima are reduced gradually. For the total concentration of 0·32 M, Fig. 3, there is sufficient contribution from the 1:1 form to produce a definite asymmetry in the curves. As well as the sharp maximum at the 1:3 ratio at 400 μ,

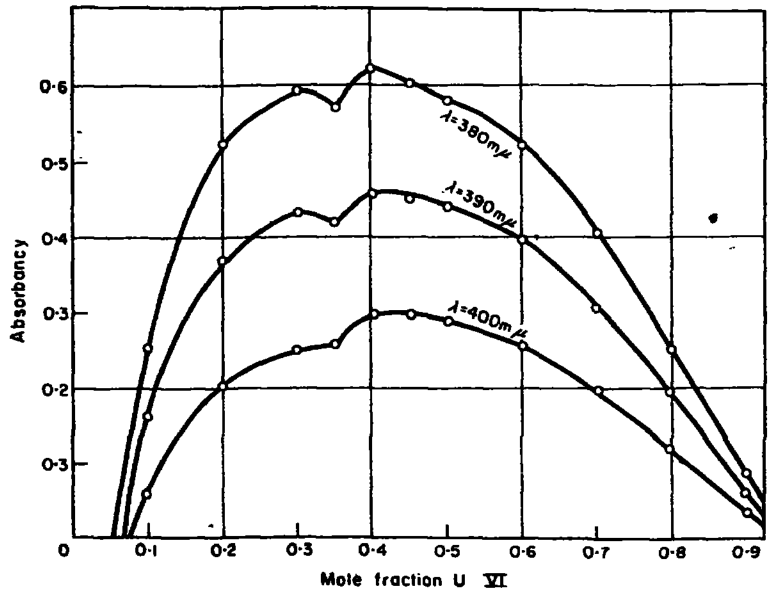

Fig. 1.—Continuous variation method; total concentration of uranyl and azide ions is 0·08 M. The ionic strength was kept constant at 0·224.

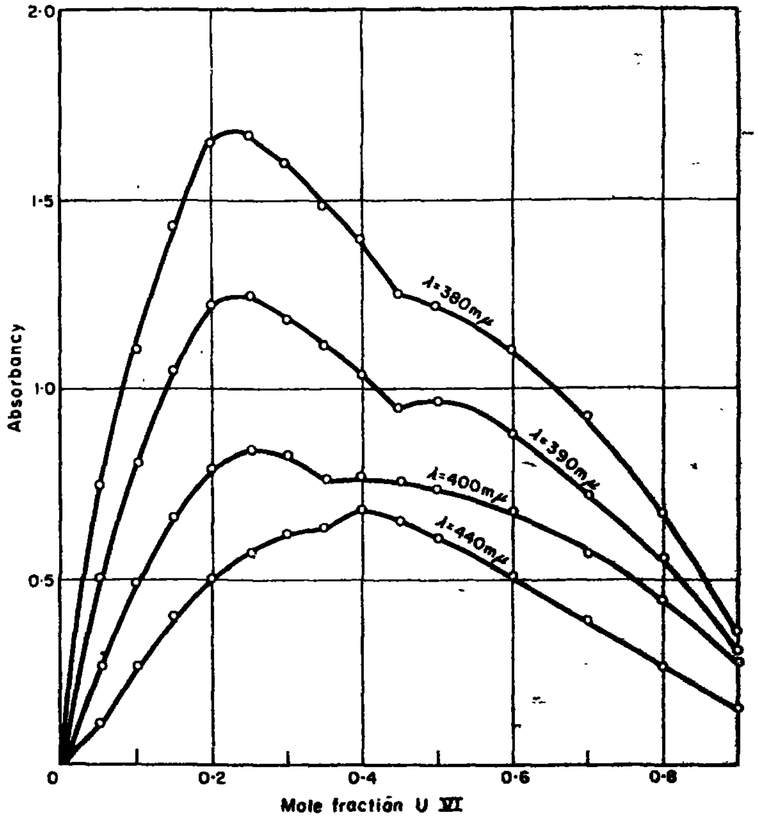

Fig. 2.—Continuous variation method; total concentration of uranyl and azide ions is 0·16 M. The ionic strength was kept constant at 0·448.

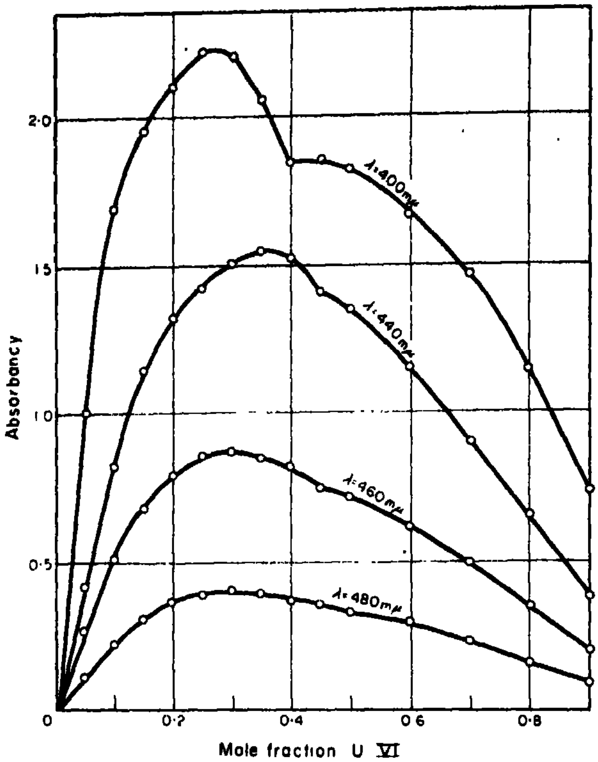

FIG. 3.—Continuous variation method; total concentration of uranyl and azide ions is 0·32 M. The ionic strength was kept constant at 0·896.

there is a well defined maximum at 440 mμ for a 1:2 complex. When the absorbancies of these solutions were measured after 24 hr, a shift in the position of these maxima towards lower azide ratio was observed while the shoulders representing the 1:1 form got clearer. This indicates the relative stability of the mono-azido uranyl complex ion, $UO_2N_3^-$.

These data are generally explained by proposing the possible reaction of the UO_2^{2+} and N_3^- ions in a consecutive order, forming three types of complexes in aqueous solutions, where the ratio of UO_2^{2+} to N_3^- varies from 1:1 to 1:3. The increase in concentration of both reagents leads to the formation and stabilization of higher complexes.

J. Inorg. Nucl. Chem., 1962, Vol. 24, pp. 183 to 186. Pergamon Press Ltd. Printed in Northern Ireland

THE SEPARATION OF LITHIUM ISOTOPES BY ION EXCHANGE*

J. E. Powell
Institute for Atomic Research and Department of Chemistry
Iowa State University, Ames, Iowa

(*Received* 2 *May* 1961; *in revised form* 31 *August* 1961)

Abstract—The single-stage separation factor for the separation of ^{6}Li and ^{7}Li by distribution between *a solution of lithium acetate and the lithium form of a sulphonated styrene–divinylbenzene copolymer* (Dowex 50 X24) has been measured by a method of frontal analysis. The value obtained was 1·0026 ± 0·0003. The comparative merits of elution and displacement chromatography as means of resolving lithium isotopes have been discussed.

Lee and Begun(1) recently summarized previous work related to the separation of ^{6}Li and ^{7}Li by ion exchange. They examined the effect of crosslinkage (DVB content) of sulphonated styrene–divinylbenzene copolymers upon the ^{6}Li–^{7}Li separation factor and concluded that separation was promoted by dehydration of the lithium ion when it was sorbed by the resin. Sorption of lithium ions on resins of low crosslinkage, which imbibe water freely, produced almost negligible separation effects. As crosslinkage of the resin increased and the water content decreased, a substantial increase in the ^{6}Li–^{7}Li separation factor was observed. It rose from 1·0006 for X2 resin to 1·0038 for X24 resin. Lee(2) also proposed that the hydrating tendency of co-sorbed ions directly affected the ^{6}Li–^{7}Li separation factor. Indeed, his data showed that α for the separation of lithium isotopes increased as the heat of hydration of the co-sorbed ion increased. With X16 resin α was observed to be 1·0023 with NH_4^+ as the co-sorbed ion and about 1·005 with Al^{3+} or Cr^{3+}.

DISCUSSION

Elution of a given ionic species down an ion-exchange bed charged with some counter ion by means of a salt solution of that counter ion is the simplest case of elution chromatography. Under such conditions a bell-shaped elution curve is generally obtained, and, as the elution distance increases, local non-equilibrium between the solution phase and the resin causes the band to spread and the concentration maximum to diminish. Diffusion processes and channeling also contribute to this effect. Because of the bell-shaped character of the elution curve the greatest enrichment is found where the sorbate concentration is lowest. Consequently, isotope enrichments by elution chromatography are notoriously inefficient from the viewpoint of chemical economy.

A distinct advantage of displacement chromatography over elution chromatography is the change of the elution curve from bell-shaped to nearly rectangular. Another is the increased utilization of column capacity. This type of elution is obtained when the front and rear displacement reactions both have favourable equilibrium constants.

---

* Work was performed in the Ames Laboratory of the U.S. Atomic Energy Commission.

(1) D. A. Lee and G. M. Begun, *J. Amer. Chem. Soc.* **81**, 2332 (1959).

(2) D. A. Lee, *J. Amer. Chem. Soc.* **83**, 1801 (1961).

$$n\bar{A}^{m+} + mB^{n+} \rightleftharpoons nA^{m+} + m\bar{B}^{n+}; \quad K_I > 1 \tag{I}$$

$$o\bar{B}^{n+} + nC^{o+} \rightleftharpoons oB^{n+} + n\bar{C}^{o+}; \quad K_{II} > 1 \tag{II}$$

The barred symbols refer to the resin phase and the unbarred symbols refer to the aqueous phase in these equilibria. That is to say, the order of affinity of the resin for a given ion increases from ion A^{m+} (the retaining ion) to ion B^{n+} (the sorbed ion species being eluted) and to ion C^{o+} (the driving ion of the eluant). The larger the respective equilibrium constants, the more rectangular becomes the elution curve. According to SPEDDING *et al.*[3]

$$\log (B/A)_f = (f - i) \log \alpha + \log (B/A)_i \tag{1}$$

The symbols f and i are arbitrary plate numbers where the concentration ratios $(B/A)_f$ and $(B/A)_i$ are observed, and α is the separation factor. For a million-fold change in the concentration ratio,

$$(f - i) = 6/\log_{10}\alpha \tag{2}$$

The major problem encountered in the elution of lithium by displacement chromatography is that of providing a suitable retaining ion for lithium. Sulphonated styrene–divinylbenzene copolymer has the least affinity for lithium; so, while lithium is displaced cleanly from a resin bed by any other cationic species, a means must be provided to promote redeposition of the lithium. Redeposition is readily brought about by use of hydrogen ion as the retaining ion if the eluant is a salt of a weak acid. Although the equilibrium constant for the reaction

$$Li^+ + \bar{H}^+ \rightleftharpoons \bar{Li}^+ + H^+ \tag{III}$$

is slightly less than unity, the formation of a weak acid assures a sufficiently large separation factor to provide a steep concentration gradient at the leading edge of the lithium band. In the presence of an anion of a weak acid:

$$\alpha = \frac{[\bar{Li}^+]\{[H^+] + [HA]\}}{[\bar{H}^+][Li^+]} = \frac{[\bar{Li}^+][H^+]\{1 + K_{HA}[A^-]\}}{[\bar{H}^+][Li^+]}; \tag{3}$$

If the anion is acetate, then,

$$\alpha = K_{i.ex.}\{1 + K_{HA}[A^-]\} \cong 10^4[A^-] \tag{4}$$

EXPERIMENTAL

An experiment was carried out at this laboratory in order to determine the separation factor for ^{6}Li and ^{7}Li distributing between 0·5-molar lithium acetate and saturated lithium state Dowex 50-X24, a sulphonated styrene–divinylbenzene coplymer. A bed of 100–200 mesh resin, 120 cm long and 2·54 cm in diameter and originally in the hydrogen cycle, was saturated with Li$^+$ from a 0·5 molar solution of lithium acetate. When the lithium-ion breakthrough occurred, the effluent was collected in fractions which were first analysed gravimetrically for lithium content (converted to anhydrous LiCl and weighed in fused silica ware) and then assayed mass-spectrometrically for ^{6}Li and ^{7}Li (after conversion to LiI by careful evaporation with HI). The flow-rate during saturation of the bed was maintained at about 90 ml per hour. A depletion of ^{6}Li in the effluent lithium acetate occurred in the first four samples (360 ml) collected after breakthrough and the ^{6}Li–^{7}Li ratio returned to normal 4 hr after the first lithium was detected at the bottom of the column. The value of ε was determined as follows:

---

[3] F. H. SPEDDING, J. E. POWELL and H. J. SVEC, *J. Amer. Chem. Soc.* **77**, 6125 (1955).

$$\varepsilon = \alpha - 1 = \sum_{i=1}^{m} \frac{V_i C_i (R_0 - R_i)}{Q R_0} = 0{\cdot}0026 \pm 0{\cdot}0003 \tag{5}$$

where α = the ^{6}Li–^{7}Li separation factor.
V_i = the volume of the ith fraction collected (in litres).
C_i = the molar concentration of lithium in the ith fraction.
R_i = the ratio of ^{6}Li to ^{7}Li in the ith fraction.
R_0 = the ratio of ^{6}Li to ^{7}Li in the original lithium acetate.
Q = the total capacity of the resin bed in equivalents.

CONCLUSIONS

In a situation where there is a scant supply of water, as in a highly crosslinked ion-exchange resin, three singly charged ions might be expected to be nearly as effective as a single triply charged ion at orienting solvent molecules. Hence there appears to be little advantage in using sorbed co-ions in the separation of lithium isotopes by displacement chromatography.

It is not difficult to devise a system whereby lithium can be co-eluted with a polyvalent cation under conditions where simultaneous band displacements occur. One such system involves elution of an equimolar mixture of lithium and erbium down a bed of H$^+$-state resin by means of an eluant solution which is 0·015 molar in both $(NH_4)_3$ Cit and NH_4OH(pH = 8·8–8·9). A ratio of three equivalents of erbium to one of lithium is maintained by the following reactions which occur at the band boundaries.

$$(NH_4)_3Cit + NH_4OH + \overline{Er}^{3+} + \overline{Li} \rightleftarrows Li^+ + ErCitOH^- + 4\overline{NH}_4{}^+ \tag{IV}$$

$$Li^+ + ErCitOH^- + \overline{4H}^+ \rightleftarrows \overline{Li}^+ + \overline{Er}^{3+} + H_3Cit + H_2O \tag{V}$$

In a situation like this where lithium occupies only one-fourth of the exchange sites, the value of ε would have to be four times as large as in the simple elution of lithium ion by displacement chromatography in order to just break even in terms of chemicals expended per mole of lithium resolved into its isotopic constituents. This is a consequence of the fact that the consumption of chemicals is directly proportional to the product of the number of band displacements required and the length of the sorbed band, while the minimum number of displacements required is inversely proportional to ε.(8) Comparing the isotopic separation factor for simple elution of lithium by displacement chromatography (1·0026) to the best factor obtained by Lee in the presence of triply charged ions (1·005), it is apparent that co-elution of lithium and multiply-charged ions is impractical.

Actually, the prospect of separating lithium isotopes by elution of lithium down a hydrogen-state resin bed by displacement chromatography with ammonium–acetate solution is rather promising. Making use of the equation,

$$\nu = (1 + \varepsilon N_0)/\varepsilon \sim = 1/\varepsilon \qquad (\text{when } \varepsilon \ll 1), \tag{6}$$

and the abundance of ^{6}Li in natural lithium sources, one concludes that the isolation of one mole of ^{6}Li (6 g) requires the expenditure of approximately 5000 mole (85 kg) of anhydrous ammonia and perhaps 10,000 equivalents or 5000 mole (500 kg) of sulphuric acid, the hundred per cent excess of acid required for regeneration being due to a somewhat unfavorable equilibrium constant for the displacement of ammonium ions by hydrogen ions.

It is of interest that the effluent solution during most of the elution process contains only acetic acid. This effluent solution can be restored to its original form simply by bubbling in gaseous ammonia until a pH corresponding to ammonium acetate is reached. The solution can then be reused as eluant. Consequently, very little ammonium acetate need be expended and the consumption of water depends primarily upon the concentration of the acid regenerant chosen.

Acknowledgements—The author is indebted to Dr. H. SVEC and Mr. A. ANDERSON of the mass-spectrometric group for the determination of ^{6}Li–^{7}Li ratios.

J. Inorg. Nucl. Chem., 1962, Vol. 24, pp. 187 to 193. Pergamon Press Ltd. Printed in Northern Ireland

ISOTOPIC EXCHANGE IN THE COBALTOUS–COBALTIC SYSTEM IN PERCHLORIC ACID

J. Shankar and B. C. de Souza
Chemistry Division, Atomic Energy Establishment, Trombay, Bombay

(*Received* 5 *June* 1961, *in revised form* 28 *August* 1961)

Abstract—Systematic investigations are reported on the isotopic exchange in the cobaltous–cobaltic system using cobalt-60. Ammonia and ethylenediamine were found to be satisfactory quenchers of this fast exchange, even though some zero-time exchange was observed. In the concentration range studied the reaction was found to be of the first order with respect to each reactant. At a high fixed ionic strength (3·1), variation of perchloric acid concentration from 0·25 F to 0·7 F showed an inverse first-order dependence. Possible mechanisms for the exchange are discussed.

Several studies[1,2,3] have been reported on the isotopic exchange between different oxidation states of metal ions in aqueous solutions. However, the information available on $Co(II)_{aq}$–$Co(III)_{aq}$ system is rather meagre and requires clarification. McCallum[4] reported some preliminary observations on this system, while Bonner and Hunt[5,6] studied the dependence of the exchange on certain parameters. The latter work suffers from a number of limitations, e. g.

(i) it does not show whether the exchange rate is independent of the quencher employed;

(ii) the exchange was found to follow an overall second-order rate equation, but Stranks and Wilkins[7] have pointed out that in such reactions it is advisable to determine the order with respect to each of the reactants;

(iii) the results of Bonner and Hunt on the inverse dependence of the exchange rate on hydrogen ion concentration can be explained either by the participation of hydrolysed species or by the variation in activity coefficients. Furthermore, their results on the effects of heavy water and ionic strength would bear closer investigation.

The experiments described here commenced long before the publication of the paper of Bonner and Hunt[6], and our results clear up many of the above points. Probable mechanisms are also suggested.

EXPERIMENTAL

The reagents used were of the purest grade available, and the tracer employed was ^{60}Co. Cobaltic perchlorate was prepared by electrolytic oxidation of the corresponding cobaltous salt in perchloric acid. The reactants were prepared afresh periodically to avoid hydrolysis and decomposition.

The method for quenching and chemical separation described by Bonner and Hunt[6] is rather lengthy, and a simplified rapid procedure developed by the authors for quenching and separation is described below.

The temperature of the reaction was maintained at 0·0 ± 0·2°C by using crushed ice in a Dewar

---

[1] C. B. Amplett, *Quart. Rev.* **8**, 219 (1954).
[2] R. R. Edwards, *Ann. Rev. Nucl. Sci.* **1**, 301 (1952).
[3] F. Basalo and R. G. Pearson, *Mechanism of Inorganic Reactions*, pp. 303-331 J. Wiley, New York (1958).
[4] K. J. McCallum, Brookhaven Nat. Lab. Chem. Conf. No. 2 BNL-C-8 (1948).
[5] N. A. Bonner and J. P. Hunt, *J. Amer. Chem. Soc.* **74**, 1866 (1952).
[6] N. A. Bonner and J. P. Hunt, *J. Amer. Chem. Soc.* **82**, 3826 (1960).
[7] D. R. Stranks, and R. G. Wilkins, *Chem. Rev.* **57**, 743 (1957).

flask. Predetermined volumes of the prepared cobaltic and cobaltous perchlorates were added to a known volume of perchloric acid sodium perchlorate solution. After allowing 15 min for the temperature to stabilize, ^{60}Co tracer (as Co(II)) was added to the mixture and the time of addition taken as the zero time. The final total volume was always 50 ml. Two ml aliquots of the reaction mixture were pipetted at suitable intervals and rapidly transferred into 20 ml of the quencher (0·1 F ethylenediamine dihydrochloride, containing sufficient alkali to make the final quenched mixture 0·15 F with respect to the alkali). In some experiments 0·4 F ammonia was used as an alternative quencher. The quenched reaction mixture was then acidified with hydrochloric acid to pH $\sim$ 3, to allow the separations to be done at leisure without oxidation or reduction taking place in the system during storage. No effect of storage on the exchange rate was found up to three days.

One ml of 6 F hydrochloric acid and 5 g of ammonium-thiocyanate were added to the quenched solution, which was then extracted thrice with 1:1 (v/v) amyl alcohol–ether. The two phases were separately collected in two volumetric flasks. The extraction efficiency was 98 ± 1 per cent.

The concentrations of the reactants in the original reaction mixture were determined spectrophotometrically using a Beckmann DU instrument. Cobaltous ion was determined by the thiocyanate method(8), and cobaltic ion by oxidation of ferrous ion and measurement at 2250 Å of the equivalent amount of ferric ions formed. The course of the exchange was followed by measuring the γ-activity of ^{60}Co, distributed in the two phases on a NaI(Tl) scintillation counting assembly.

RESULTS

The principle involved in quenching is the conversion of the rapidly-exchanging $Co(II)_{aq}$–$Co(III)_{aq}$ system into the very slowly–exchanging complex systems. With this end in view, only those reagents were tried which could be used homogeneously and which did not need specific pH conditions for rapid and efficient complexing. Among the complexing agents tried were acetylacetone, ethylenediamine tetra-acetic acid, ammonia and ethylenediamine, and only the last two were found to be satisfactory quenchers which fulfilled the above conditions.

The fraction of the activity exchanged was determined at different times with the results shown in Fig. 1. It will be seen that the plots of $\log (1 - F')$ against t are straight lines. The parallel lines A and B refer to the lower cobalt concentration using ammonia and ethylenediamine as quenchers respectively: at the higher cobalt concentration the points obtained with the two quenchers lie on one line C. The results indicate that the nature of the quencher and the concentration of the reactants influence the zero-time exchange. The half-time of exchange is not affected by the quencher, since the slopes of the plots for ammonia and ethylenediamine using the same cobalt concentration are identical, showing that these values of $t_{\frac{1}{2}}$ are correct ones.

Fig. 2 shows typical straight lines obtained when $\log R$ is plotted against $\log C$, R being the rate of exchange and C the concentration of Co(II) at constant Co(III) concentration and vice-versa. The slopes of the straight lines give directly the order of the reaction with respect to each of the reactants. The order was determined at various concentrations of reactants ($0{\cdot}3 \times 10^{-3}$ to $4{\cdot}0 \times 10^{-3}$ F), acidities (0·25 to 3·0 F $HClO_4$) and ionic strength (0·25 to 3·0 μ), and its value was found to be 1 with respect to each reactant within this range of conditions. As such the exchange is an overall second-order process.

Biedermann and **Sillan**(9) have shown that replacement of sodium ions by hydrogen ions up to 0·6 F at a total concentration of 3·0 F sodium perchlorate does not cause any variation in the activity coefficient of the acid. Advantage was taken of this observation to make definitive experiments on the acid dependence of the exchange at an ionic strength of 3·0. The results shown at A in Fig. 3 clearly indicate an inverse first-order dependence of the exchange rate on the hydrogen ion concentration. The

(8) J. B. Hoag, *Nuclear Reactor Experiments*, p. 429. Van Nostrand, Princeton, New Jersey (1958).
(9) G. Biedermann and L. G. Sillen, *Arkiv. For Kemi*, 5, 425 (1953).

straight line shows an appreciable intercept, indicating the simultaneous presence of an acid-independent path for the exchange. Also shown at B is a similar plot for a heavy water medium. The rates of exchange by both the acid-dependent and acid-independent paths appear to be lowered by a factor of ~2 in heavy water compared with those in light water.

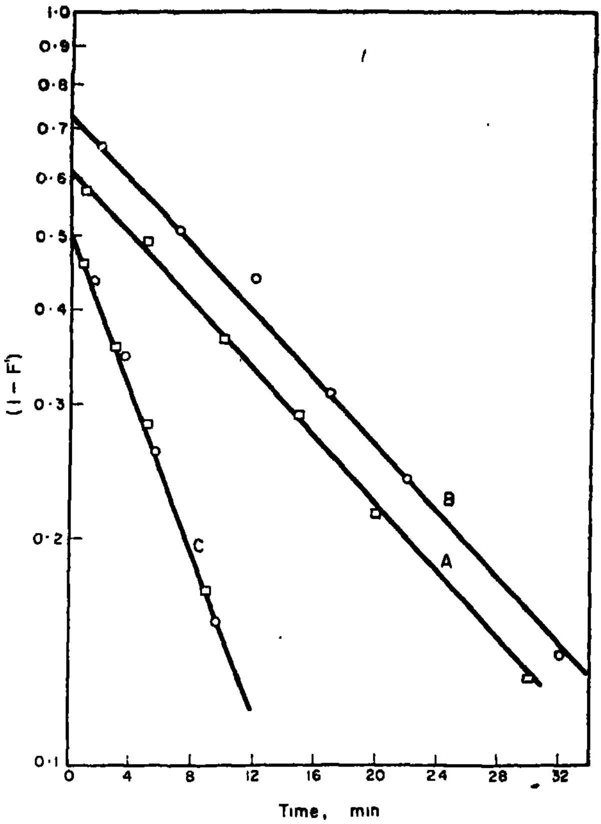

FIG. 1.—Effect of different quenchers on exchange rate.
A, B. Co(II) = $0{\cdot}7 \times 10^{-3}$ F, Co(III) = $0{\cdot}65 \times 10^{-3}$ F, $HClO_4$ = 1·0 F, $t_{\frac{1}{2}}$ = 12 min, μ = 1·0. Temperature = 0·0°C.
C. Co(II) = $2{\cdot}39 \times 10^{-3}$ F, Co(III) = $0{\cdot}45 \times 10^{-3}$ F, $HClO_4$ = 1·0 F $t_{\frac{1}{2}}$ = 5·7 min, μ = 1·0. Temperature = 0·0°C.

In order to determine the variation of the exchange rate with ionic strength, two sets of experiments were carried out using sodium and lithium perchlorates. The results for sodium perchlorate given in Table 1 indicate that there is an increase in the exchange rate with increasing ionic strength. Similar results were obtained with lithium perchlorate.

DISCUSSION

The data presented in the preceding section show that the reaction is of first order with respect to each reactant, with an inverse first-order dependence on hydrogen ion concentration together with a simultaneous acid-independent path. The reaction

TABLE 1.—EFFECT OF VARIATION OF IONIC STRENGTH ON EXCHANGE RATE
Concentration of total cobalt $1\cdot2 \times 10^{-3}$ F
Concentration of perchloric acid 0·28 F
Ionic strength adjusted using sodium perchlorate
Temperature 0·0 ± 0·2°C

Conc. of $NaClO_4$ (F)	Ionic strength (μ)	$0\cdot16\,\mu$	Velocity constant (k, $F^{-1}\,min^{-1}$)	log k	log $k - 0\cdot16\,\mu$
0·43	0·71	0·11	54	1·73	1·62
0·86	1·14	0·18	68	1·84	1·66
1·30	1·58	0·25	76	1·88	1·63
1·73	2·01	0·32	107	2·03	1·71
2·65	2·93	0·47	131	2·12	1·65
3·43	3·71	0·59	177	2·25	1·65
4·19	4·47	0·72	244	2·37	1·67

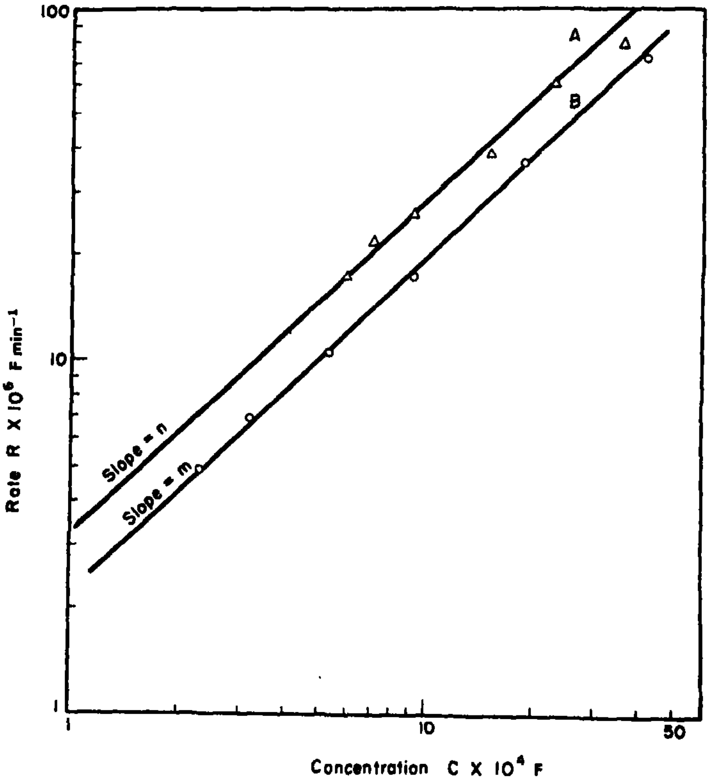

FIG. 2.—Determination of m and n in the equation
$R = k[Co(II)]^m[Co\,III]^n$
A. $Co(II) = 0\cdot68 \times 10^{-3}$ F, $HClO_4 = 1\cdot0$ F, $\mu = 1\cdot0$ Co(III) varied from $0\cdot6 \times 10^{-3}$ to $3\cdot6 \times 10^{-3}$ F, $n = 0\cdot93 \pm 0\cdot08$
Temperature = 0·0°C.
B. $Co(III) = 0\cdot53 \times 10^{-3}$ F, $HClO_4 = 1\cdot0$ F, $\mu = 1\cdot0$ Co(II) varied from $0\cdot23 \times 10^{-3}$ to $4\cdot17 \times 10^{-3}$ F, $m = 0\cdot96 \pm 0\cdot07$
Temperature = 0·0°C

can thus be expressed by an equation of the type:

$$R = (\text{Co(II)})(\text{Co(III)})\left[a + \frac{b}{(\text{H}^+)}\right] \tag{1}$$

where *a* and *b* are constants. An inverse acid dependence indicates the participation of hydrolysed species in the exchange. While the hydrolysis of Co^{2+} can be neglected under the working conditions, SUTCLIFFE and WEBER$^{(10)}$ have shown that Co^{3+} partially exists as CoOH^{2+}. Hence the exchange may occur through the following two paths:

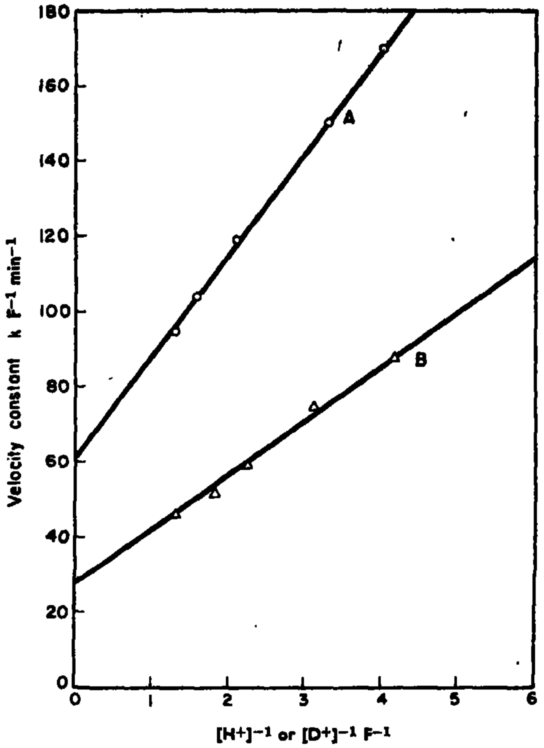

FIG. 3.—Effect of variation of acid concentration on exchange rate.

A. Solvent: light water Co = $0{\cdot}53 \times 10^{-3}$ F
HClO_4 varied from 0·25 to 0·78 F, $\mu = 3{\cdot}0$
$a = 61\ \text{F}^{-1}\ \text{min}^{-1}$, $b = 27\ \text{min}^{-1}$

B. Solvent: heavy water. Co = $1{\cdot}0 \times 10^{-3}$ F
HClO_4 varied from 0·24 to 0·76 F, $\mu = 3{\cdot}0$.
Temperature 0·0°C
$a = 28\ \text{F}^{-1}\ \text{min}^{-1}$, $b = 14\ \text{min}^{-1}$

$$\text{A}: \ {}^*\text{Co}^{2+} + \text{CoOH}^{2+} \rightleftharpoons \text{Co}^{2+} + {}^*\text{CoOH}^{2+} \qquad k_1$$

$$\text{B}: \ {}^*\text{Co}^{2+} + \text{Co}^{3+} \rightleftharpoons \text{Co}^{2+} + {}^*\text{Co}^{3+} \qquad k_2$$

It can be easily shown that if these are the most important paths under the working conditions the exchange rate is given by

$$R = (\text{Co(II)})(\text{Co(III)})\left[k_2 + \frac{k_1 K_h}{(\text{H}^+)}\right] \tag{2}$$

---

(10) L. H. SUTCLIFFE and J. R. WEBER, *Trans. Faraday Soc.* **52**, 1225 (1956).

where K_h($\sim$4 × 10^{-3} at 0°C), the first hydrolysis constant of Co^{3+}, is much less than (H^+). A comparison of equations (1) and (2) shows that $a = k_2$ and $b = k_1K_h$. SUTCLIFFE and WEBER(11) have postulated that Co(III) species also exist as the dimer $(Co—O—Co)^{4+}$. Equation (2) for the exchange rate is valid even if the dimerization constant is 100 times more than the hydrolysis constant.

In aqueous solutions, the cobaltic species $Co(H_2O)_6{}^{3+}$ and $Co(H_2O)_5OH^{2+}$ are spin paired while the cobaltous species $Co(H_2O)_6{}^{2+}$ is a spin-free complex. The observed rapid exchange in the case under consideration compared with systems involving most other cobaltic complexes suggests that these aquo-complexes are rather easily transformed into the spin-free state. FRIEDMAN *et al*(12)., on the basis of magnetic susceptibility data, have postulated a vibrational activation energy of 4 kcal for this rearrangement. Once the reactants and products are in similar electronic and geometrical arrangement, exchange can occur with ease through a bridge mechanism.

For the acid-dependent path, two possible mechanisms can be visualized for the exchange:

$$Co^{3+} + CoOH^{2+} \rightleftharpoons (Co—O—Co)^{5+} + H^+ \qquad (1)$$

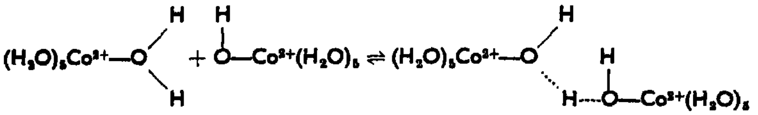
(2)

Mechanism (1) is a modified form of the equilibrium that has been postulated for the Co(III) dimer in perchloric acid solutions, while (2) is similar to the one proposed by HUDIS and DODSON(13) for the aqueous Fe(II)–Fe(III) exchange. There is no conclusive evidence for the existence of the dimer $(Co—O—Co)^{5+}$ and therefore mechanism (1) is a speculative one. The isotopic effect observed when heavy water is substituted for light water cannot serve as a distinguishing pointer between these two mechanisms as both of them are expected to show similar isotope effects. In the acid-independent exchange, a mechanism similar to (2) is ruled out on crystal field and enthalpy considerations.(14)

An alternative mechanism,(15) which may operate in systems like the present one, is based on the coupling of the hydration shells by hydrogen bonding, which makes it easier for direct electron transfer in certain systems. The hydrogen bonding may take place as shown below:

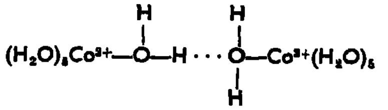

$$(H_2O)_5Co^{3+}—\overset{H}{\overset{|}{O}}—H\cdots\underset{\underset{H}{|}}{\overset{H}{\overset{|}{O}}}—Co^{2+}(H_2O)_5$$

In this mechanism the observed D_2O–H_2O isotopic effect may be due to the difference in the stretching of the O—H or O—D bonds.

In the present case, the overall picture suggests an H- or O- atom bridge mechanism for the acid-dependent path and a true electron transfer for the acid-independent path.

The effect of varying the ionic strength on the velocity constant was studied to determine the product of the charges of the interacting species. Since the ionic strengths involved were high, the extended Debye–Huckel equation

---

(11) L. H. SUTCLIFFE and J. R. WEBER, *J. Inorg. Nucl. Chem.* 12, 281 (1960).

(12) H. L. FRIEDMAN, J. P. HUNT, R. A. PLANE and H. TAUBE, *J. Amer. Chem. Soc.* 73, 4028 (1957).

(13) J. HUDIS, and R. W. DODSON, *J. Amer. Chem. Soc.* 78, 911 (1956).

(14) J. HALPERN, and L. E. ORGEL, *Disc. Farad. Soc.* No. 39, p.7 (1960).

(15) D. R. STRANKS, *Modern Co-ordination Chemistry*, p. 78. Interscience, New York (1960).

$$\log k = \log k_0 + \frac{2AZ_AZ_B\mu^{\frac{1}{2}}}{1 + B\mu^{\frac{1}{2}}} + C\mu$$

was employed. Using the values of C determined by NASANEN[16] for lithium and sodium perchlorate media, the results given in Table 1 show that $(\log k - C\mu)$ is nearly constant, i.e. the plot of $[\mu^{\frac{1}{2}}/(1 + B\mu^{\frac{1}{2}})]$ vs $(\log k - C\mu)$ is a straight line of zero slope. In other words (Z_AZ_B) is zero. This indicates that the charge on at least one of the reacting species, probably the cobaltic ones, tends to become zero in solutions of high perchlorate ion concentration as a result of appreciable perchlorate complexing.

Acknowledgement—The authors would like to thank Dr K. S. VENKATESWARLU for helpful discussions.

(16) R. NASANEN, *Acta. Chem. Scand.* 3, 959 (1949).

J. Inorg. Nucl. Chem., 1962, Vol. 24, pp. 195 to 203. Pergamon Press Ltd. Printed in Northern Ireland

ION EXCHANGE EQUILIBRIA IN THE PRESENCE OF ORGANIC SOLVENTS—I

THE INFLUENCE OF ORGANIC SOLVENTS ON THE DISTRIBUTION CONSTANT OF PRASEODYMIUM

C. Grigorescu-Sabău
Institute for Atomic Physics, Bucharest, Rumania

(*Received* 8 *August* 1961)

Abstract—A systematic study was made of the influence of the addition of organic solvents on the distribution coefficients of praseodymium between the resin KU_2 in H-, NH_4-, Na- and K-forms) and solutions containing HCl, organic solvent and H_2O.

It was observed that the organic solvents do not influence the character of the reaction between cations and resin but only modify the value of the ion-exchange constants.

Several papers describe studies of the distribution of alkali metal ions between different resins and solutions containing methyl alcohol, ethyl alcohol or acetone,(1–4) and Sakaki and Kakihana(5) have extended these studies to include alkaline earth metals. Panchenkov *et al.*(6) have made a systematic study of the influence of the above solvents on the uptake of alkali metals in the presence of different anions (SO_4^{2-}, Cl^-, I^-) on different resins (SBS, SDV-3, Espapit-1), and have also measured the change in K_d as the dielectric constant of the medium is changed. In 1961 Rusi and Ionescu(7) studied the influence of acetone on the uptake of the trivalent ions cerium (III) and praseodymium (III).

In all cases the distribution coefficient K_d varied linearly with the concentration of the organic solvent, increasing as the latter increased. This dependence was explained either on the basis of decreasing hydration of the ions or on the basis of the formation of oxonium complexes.

The present paper reports a systematic study of the influence of various organic solvents upon the distribution of praseodymium ions between resin and solution, with the aim of following the mechanism of ion exchange in the presence of various organic solvents and on resins in different forms.

EXPERIMENTAL

The procedure was the same as that described previously.(8,9) Solutions were shaken in contact with the resin for 6 hr at 20°C. The Russian resin KU_2 (sulphonated polystyrene), particle size approximately 0·43–0·25 mm, was used; ^{143}Pr ($t_{½}$ = 13·5 days) was added to a solution of $PrCl_3$ containing 0·000969 equiv. Pr, pH = 2·1

(1) G. Vigner, *Izbranie raboti, Moskva, Izd. A.N. SSSR.*, 1941, p. 109.
(2) T. R. Kressman and J. A. Kitchener, *J. Chem. Soc.* 1211 (1949).
(3) S. L. Bafna *J. Sci. Industr. Res.* **12**, 613 (1953).
(4) E. A. Materova, J. L. Vert and G. P. Grinberg, *Zh. Obshei Khim.* **24**, 953 (1954).
(5) T. Sakaki, H. Kakihana, *Kogaku, Bull. Chem. Soc. Japan* **28**, 217 (1955).
(6) G. M. Panchenkov, V. I. Gorshkov and M. V. Kuklanova, *Zh. fiz. Khim.* **32**, 361 and 616 (1958).
(7) A. Rusi, and S. Ionescu. *Studii Si Cercetări Fizică*, **4**, 735, (1961).
(8) S. Ionescu, O. Constantinescu, D. Topor and E. Gird, *Proceedings of the Second International Conference on the Peaceful uses of Atomic Energy, Geneva*, 1958 **28**, P/1424. United Nation (1958).
(9) I. Dema, M. Dumitru, E. Gird, E. Găinar, A. Rusi, S. Spiridon, C. Sabău, O. Constantinescu and S. Ionescu, *Studii Si Cercetări Fizică* **2**. 397 (1960).

Solvents used were: methyl alcohol (Analar), ethyl alcohol (Merck), isopropyl alcohol (Lodz), acetone (Merck), methyl ethyl ketone (Reanal), glycol (Gliwice).

The solutions used were ternary mixtures of water, hydrochloric acid and the organic solvent having the following composition: 0·5 and 1·0 M. HCl containing 0, 20, 40, 60 and 80 per cent of the organic solvent, and 1·5 and 2·0 M. HCl containing 0, 20, 40, 60 and 70 per cent organic solvent.

In order to study the influence of the form of the resin at the time of contact with the solution the former was used in hydrogen-, ammonium-, sodium-, and potassium-forms. The resin was converted into these forms by shaking with 5 N HCl and with saturated solutions of NH_4Cl, NaCl, KCl (Merck) respectively for 6 hr. Distilled and deionized water was used to wash the resin and to prepare solutions.

RESULTS

The distribution constant was calculated from the experimental data rising the standard formula:

$$K_d = \frac{A_i - A_f}{A_f} \cdot \frac{V}{m}$$

where A_i = initial specific activity of the solution, A_f = final specific activity, V = the volume of the solution (4 ml), m = mass of resin (0·02 g = 0·1 mequiv.).

Fig. 1 shows log K_d versus solvent concentration for the different solvents used,

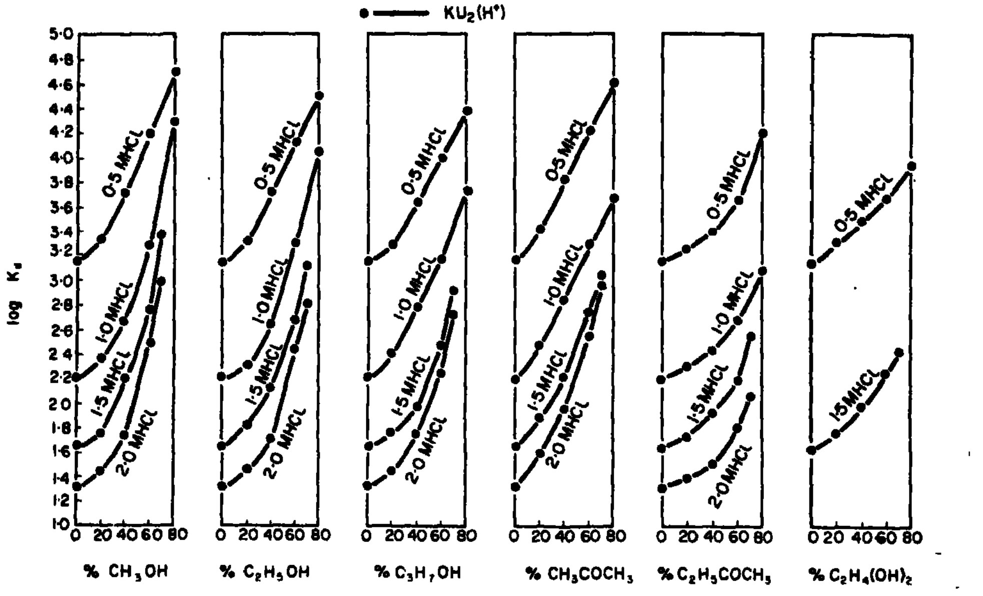

FIG. 1.—Variation of log K_d for RH versus the concentration of organic solvent, in the concentrations: 0·5, 1·0, 1·5, 2·0 M HCl and the solvents CH_3OH, C_2H_5OH, C_3H_7OH, CH_3COCH_3, $CH_3COC_2H_5$, $C_2H_4(OH)_2$.

on the hydrogen-form resin RH, showing that for concentrations greater than 40 per cent the distribution coefficient varies almost linearly (within the limits of experimental error) with solvent concentration, except for methylethyl ketone and for polyfunctional solvents (glycol). Furthermore, for the same percentage of solvent the difference between the values of the distribution coefficients become less as the acid concentration increases, while for the same acid concentration the greatest variation is for 1 M acid. For different solvents at the same acid concentration the values of K_d decrease slightly as the number of C atoms in the molecule increases

(CH_3OH—C_2H_5OH—C_3H_7OH; CH_3COCH_3—$CH_3COC_2H_5$). In the case of acetone however, the values are greater than for izopropyl-alcohol, although both solvents have the same number of C atoms, since the chemical functionality differs. Diols exert a smaller influence upon K_d than do monofunctional solvents. The net result is that the absorption of cations on the resin is greater when the number of C atoms is small.

Fig. 2 shows the variation of log K_d with the solvent concentration at two acid concentrations (0·5 M and 1·5 M) on the NH_4^+, Na^+ and K^+ forms of the resin. The RNH_4 resin shows the same regularities as does RH, with the one difference that the nature of the solvent has less influence on the K_d values. At higher acid concentrations the influence of the solvent is less, since the NH_4^+ ions displaced from the resin combine with the excess HCl to form NH_4Cl. In the case of RNa and RK we observe the smallest range of variation of K_d with concentration of the solvent, together with inversion of the influence of the acid on K_d: this influence is greater for 1·5 M HCl than for 0·5 M HCl.

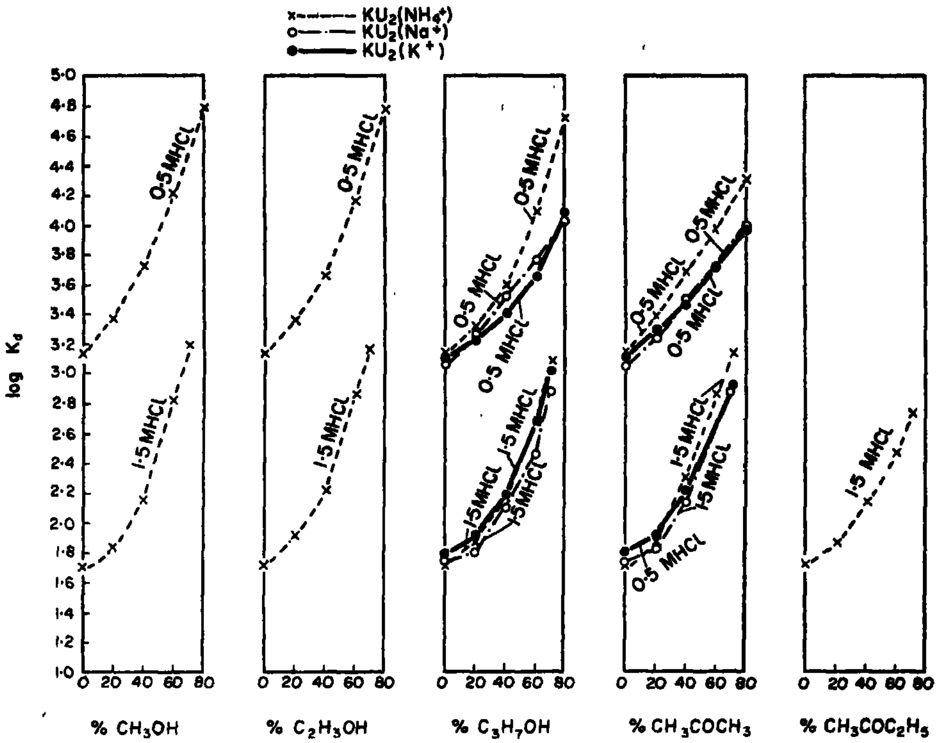

Fig. 2.—Log K_d versus solvent concentration for resins in NH_4-, Na- and K-forms in 0·5 and 1·5 M HCl for CH_3OH, C_2H_5OH, C_3H_7OH, CH_3COCH_3, $CH_3COC_2H_5$.

DISCUSSION

The experimental data show that the reaction between resin and Pr^{3+} ions in acid solution is strongly influenced by the presence of organic solvents. A number of conclusions can be drawn from the results.

Assuming(10) *that the law applies to the reaction*

$$3RH + Pr^{3+} \rightleftharpoons R_3Pr + 3H^+$$

we have

$$K_s = \frac{[R_3Pr]}{[Pr^{3+}]} \cdot \frac{[H^+]^3}{[RH]^3} \cdot \frac{[f_{Pr}]_r}{[f_{Pr}]_s} \cdot \frac{[f_H]_s^3}{[f_H]_r^3} \cong K_a \frac{[H^{3+}]}{[RH]^3} \tag{1}$$

where f represent the activity coefficients, r refers to resin and s to the solution. At the low concentrations studied the activity coefficient ratio can be considered approximately equal to unity.

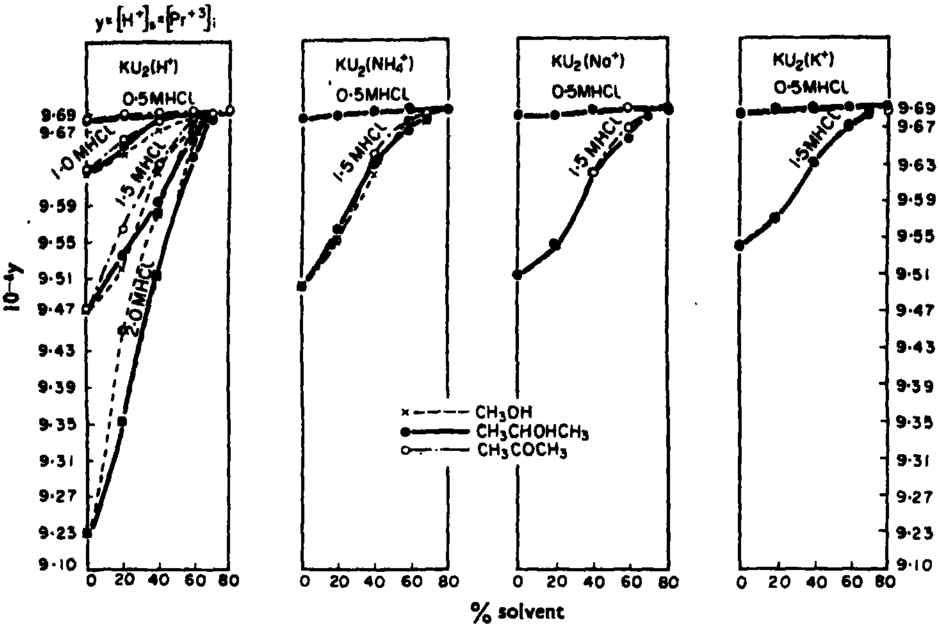

FIG. 3.—Amount of Pr^{3+} absorbed as a function of the percentage organic solvent in the solution

K_a was determined experimentally and the quantity of hydrogen ions released on exchange equals that of praseodymium absorbed by the resin. The quantity of resin remaining in the hydrogen form at equilibrium equals that initially taken minus the final hydrogen ion concentration in solution. All these quantities were expressed in mequiv/g.

The curves in Fig. 3 show the quantity of praseodymium absorbed from a medium of given acidity as a function of the proportion of organic solvent. These curves show clearly that the effect of the solvent is much greater at higher acidities as previously observed.(7) This suggests that it would be interesting to examine the quantity of praseodymium absorbed as a functioning of the acidity, and Fig. 4 shows the absorbed praseodymium (y) versus the acidity (x). A family of curves is obtained for pure acid and for 20, 40, 60 and 80 per cent organic solvent. Each of these curves fits an equation of the form

$$y = -ax^3 + b \tag{2}$$

---

(10) E. R. TOMPKINS and S. W. MAYER, *J. Amer. Chem. Soc.* **69**, 2866 (1947).

where y is the quantity of absorbed ions, b is the maximum quantity absorbed at zero acidity, x is the initial acid concentration, and a is a constant which is characteristic of the amount of organic solvent present in the solution. These curves show that the presence of the organic solvent does not change the character of the reaction which takes place, but only increases the uptake of absorbed ions.

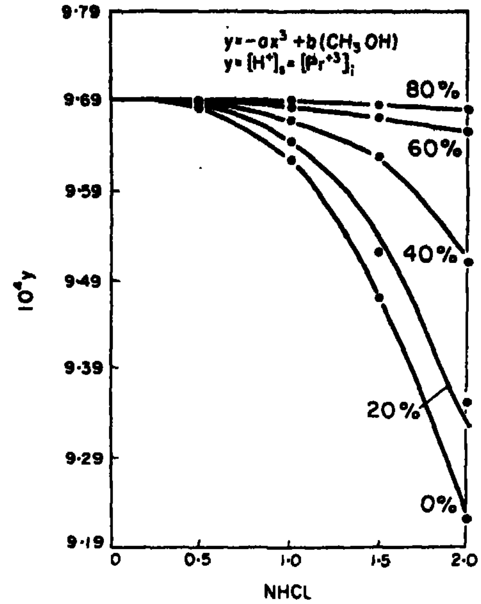

FIG. 4.—Amount of Pr^{3+} absorbed as a function of the initial acidity (Curves: $y = -ax^3 + b$)

If b represents the total amount of trivalent ions absorbed from the neutral ionic solution, then on introducing a quantity of acid x the amount of absorbed ions decreases by ax^3. We may speculate that in the case of doubly-charged cations the decrement will equal ax^2, and for singly-charged cations with ax. Experiments have been started to verify these suppositions.

In Fig. 5 the values of a corresponding to each curve in Fig. 4 are plotted versus the concentration of the organic solvent; they fall on a straight line, with a value a_{max} in the absence of organic solvent, decreasing to the value $a_0 = 0$, corresponding to the maximum concentration of the organic solvent for which absorption takes place in a neutral medium, i.e. the concentration at which the organic solvent has probably removed all the hydrogen ions initially present in the solution.

These observations suggest that it should be possible to calculate from the values of a the amount of organic solvent necessary to fix the quantity of ions which it is desired to retain on the resin in the case of elution or absorption of an element on a column when carrying out separations from other ions present in the solution.

An equation may be derived theoretically which has the same form as equation (2), which was deduced empirically form the experimental data, by substituting for the ionic concentrations in equation (1):

$$K_e = \frac{[P_3Pr]}{[Pr^{3+}]} \cdot \frac{[H^+]^3}{[RH]^3} = \frac{y}{b-y} \cdot \frac{x^3}{k^3} \tag{3}$$

where y, b and x have the same significance as in equation (2), K_e is the equilibrium constant, and k the quantity of resin taken (in mequiv/g). This equation may be converted to the form

$$y = \frac{K_e k^3 b}{x^3 + k^3 K_e} = \frac{a'b}{x^3 + a'} \tag{4}$$

which is also verified by the experimental data.

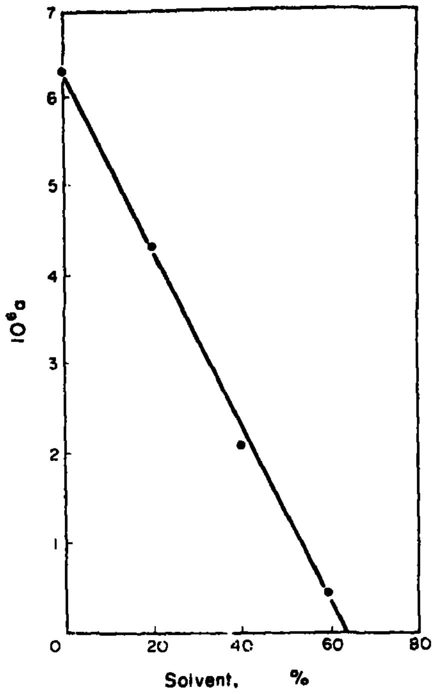

FIG. 5.—a versus solvent concentration.

TABLE 1.—VALUES OF a FOR DIFFERENT CONCENTRATIONS OF ORGANIC SOLVENT.

$a \times 10^6$	$b \times 10^4$	Solvent (%)
6·3	9·691	0
4·3	9·690	20
2·08	9·6908	40
0·45	9·6899	60
0·036	9·6899	80

The variation of K_e as a function of K_d is given by the relationship

$$\frac{K_e}{K_d} = \frac{[H^+]^3}{[RH]^3}$$

and in Fig. 6 log K_e is plotted versus log K_d, since their values vary widely with respect to the percentage of organic solvent.

We observe that

(1) for each initial acidity the values corresponding to the different proportions of organic solvent lie on a straight line which may be represented by the equation

$$\log K_e = \log K_d + 3 \log \frac{[\mathrm{H}^+]}{[\mathrm{RH}]} \tag{5}$$

(2) These straight lines are parallel, showing that the effect of the organic solvent is the same for each concentration of acid. However, the separation between the lines is not proportional to the concentration of the acid used, the curves being less widely spaced at the higher acid concentrations. If we substitute in equation (5) y for the acid concentration released on exchange we obtain

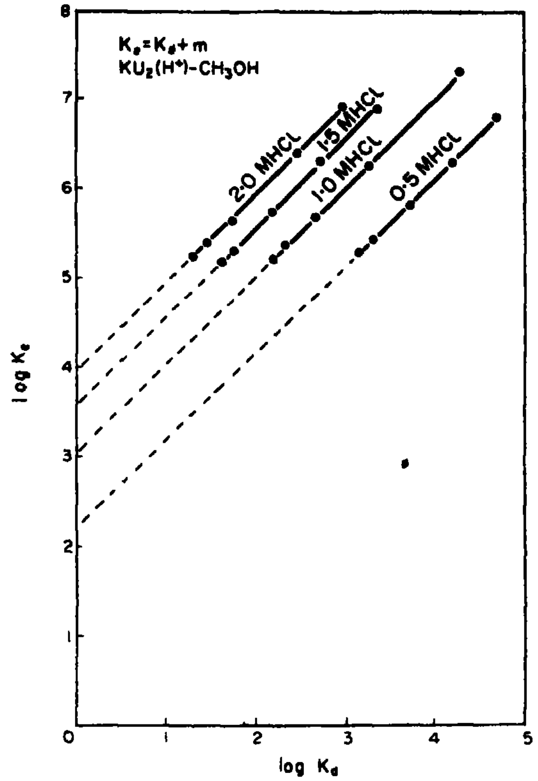

FIG. 6.—Log K_e vs log K_d for various organic solvent concentrations (Curves: $K_e = K_d + m$)

$$\log K_e = \log K_d + 3 \log \frac{x + y}{k - y} \tag{6}$$

where k is the initial concentration of resin in mequiv/g. Substituting for y from equation (2), we obtain

$$\log K_e = \log K_d + 3 \log \frac{x - ax^3 + b}{k + ax^3 - b} \tag{7}$$

Using this formula and the shape of the curves in Fig. 4, we may explain the closer spacing of the curves at higher acidities. The value of $-ax^3 + b$ is seen to increase

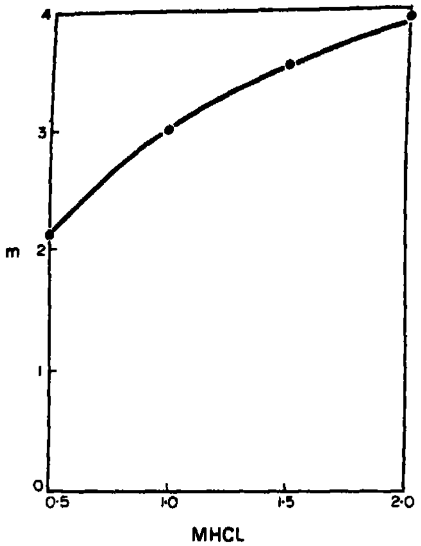

FIG. 7.—m vs HCl concentration.

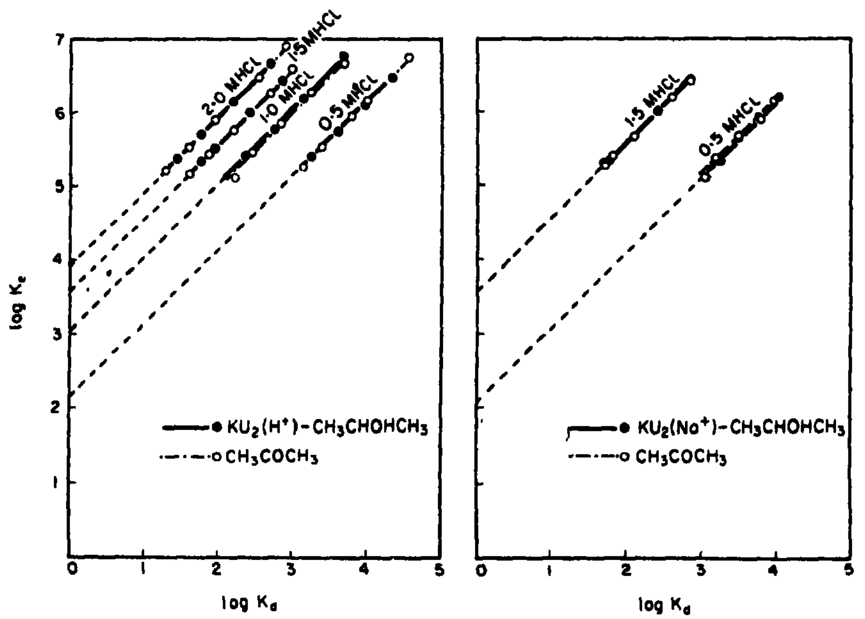

FIG. 8.—Log K_e as a function of log K_d for different forms of resin and for different organic solvents.

slightly at low acid concentrations and much more so at high acid concentrations (Fig. 4). Equation (7) can be written simply in the form

$$K_e = K_d + m \tag{8}$$

with m varying in the family of curves with the amount of acid (Fig. 7).

We observe that m tends to a limiting value (x/k) as x increases to the given by $ax^3 = b$. This is the maximum acidity at which the cations are no longer absorbed, and depends upon a.

(3) The conclusions previously expressed are valid for different organic solvents The linear plots of K_e vs K_d are superimposed although the values of K_e are different, being situated above or below those represented in Fig. 6. These values are represented in Fig. 8. The curves are independent of the form of the resin and of the nature of the solvent.

CONCLUSIONS

(i) The presence of organic solvents in acid media does not influence the manner in which praseodymium ions interact with the polystyrene sulphonic acid resin.

(ii) However, organic solvents modify the constant a in equation (2) from the value which it has in the pure acid to the value zero, by decreasing the concentration of hydrogen ions up to their complete elimination from the solution.

(iii) Absorption processes on polystyrene sulphonic acid resins which take place in the presence of organic oxygen-containing solvents in acid media are independent of the nature of the solvent.

J. Inorg. Nucl. Chem., 1962, Vol. 24, pp. 205 to 214. Pergamon Press Ltd. Printed in Northern Ireland

THE INFLUENCE OF DILUENT ON EXTRACTION OF EUROPIUM AND THORIUM NITRATES BY TRI-*n*-BUTYLPHOSPHATE

S. SIEKIERSKI
Department of Radiochemistry, Institute of Nuclear Research, Warsaw

(*Received* 8 *June* 1961)

Abstract—The partition coefficients of europium and thorium extracted from 4 M $NaNO_3$ into 5% (by volume) TBP in a number of diluents have been determined. Using the values of the partition coefficients and of the activity of TBP in the same diluents activity coefficients of the metal complexes in the organic phase have been calculated. It has been shown that both the activity coefficient of the complex in the organic phase and the activity of TBP are related to the solubility parameter of the diluent used. The influence of diluent on the partition coefficient is relatively small since both the activity of TBP and the activity coefficient of the complex change into the same direction with diluent.

THE influence of diluent on the extraction of nitrates by tri-*n*-butylphosphate (TBP) is of both practical and theoretical importance, and has been investigated by several authors$^{(1-7)}$. Most of these papers were dealing with the extraction of uranyl nitrate, but some of them dealt also with the extraction of Pu(IV), Zr, Ce(III), Np(IV) and Np(VI) from nitric acid solutions. In these studies various diluents including aliphatic and aromatic hydrocarbons, halogen substituted hydrocarbons and in a few cases esters and ethers have been used. The experiments have clearly shown that the extraction rate by TBP depends on the diluent used, being generally higher for aromatic and aliphatic hydrocarbons than for halogen substituted hydrocarbons. Especially low extraction has been observed in the case of chloroform used as diluent. Among the aliphatic hydrocarbons the extraction seems to decrease with increasing number of carbon atoms in the chain, and among benzene derivatives it seems to decrease with increasing number of methyl groups.$^{(3)}$ It should be stressed that the influence of the diluent depends to some extent on the method of expressing the TBP concentration in the organic phase.$^{(3)}$ Several attempts at introducing some correlation between the extraction and physicochemical properties of the diluent have been made. In their first paper SHEVTCHENKO *et al.*$^{(2)}$ connected the extractability by TBP with the dielectric constant of diluent, but in their second paper they pointed out as well the parallel between the extraction and the polarizability of the diluent. On the other hand PUSHLENKOV *et al.*$^{(6)}$ did not observe any correlation between the extraction by TBP and dielectric constant, dipole moment, or refractive index of the diluent. An important advance has been made by TAUBE$^{(4)}$ from this Department, who pointed out that the extraction depends on the electrostatic interaction between the complex

---

(1) Z. I. DIZDAR, J. K. RAJNVAIN and O. S. GAL, *Bull. Inst. Nucl. Sci. Boris Kidrich* **8**, 59 (1958).
(2) V. B. SHEVTCHENKO, A. S. SOLOVKIN, I. V. SHILIN, L. M. KIRILLOV, A. V. RADIONOV and V. V. BALANDINA, *Radiokhim.* **1**, 257 (1959).
(3) V. B. SHEVTCHENKO, A. S. SOLOVKIN, I. V. SHILIN, L. M. KIRILLOV, A. V. RADIONOV and V. V. BALANDINA, *Radiokhim.*, **2**, 281 (1960).
(4) M. TAUBE, *J. Inorg. Nucl. Chem.* **12**, 174 (1959).
(5) M. TAUBE, *J. Inorg. Nucl. Chem.* **15**, 171 (1960).
(6) M. F. PUSHLENKOV, E. V. KOMAROV and O. N. SHIVALOV, *Radiokhim.* **2**, 537 (1960).
(7) T. V. HEALY and G. M. WAIND, AERE/C/R 773.

and permanent or induced dipoles in the molecules of diluent and on the work which is needed to form a hole in the organic phase. In the case of slightly polar complexes with TBP the second factor is more important and the extraction into polar liquids is therefore lower than the extraction into non-polar ones.

Nevertheless it seems that the role of the diluent in the extraction by TBP has not yet been satisfactorily elucidated. This is probably because all the authors so far tried to explain the differences between various diluents, whereas the similarities in the extraction behaviour of diluents should be explained. The experimental data collected by various authors show that the partition coefficient of uranyl nitrate into diluted TBP changes by a factor of two to seven for such different solvents as heptane, benzene, ethyl bromide, dichlorethylene or carbon tetrachloride. The only exceptions are $CHCl_3$ and $CHBr_3$, for which the partition coefficients are considerably lower. The differences observed in partition coefficients are much lower than those to be expected from the activities of TBP in various diluents. It has been shown by ALCOCK *et al.*(8) that the activity of 5% (by volume) TBP in benzene is about ten times lower than its activity in heptane. Assuming the activity of TBP to be the only factor determining extraction, one should expect about a 100 times higher partition coefficient into heptane than into benzene because two molecules of TBP are attached to each $UO_2(NO_3)_2$ molecule. This conclusion however is in complete disagreement with the experimental results. This fact leads to the conclusion that there must exist another factor acting in the opposite direction, and it should be explained that these two factors nearly cancel each other, so that partition coefficient changes only a little with diluent. The extraction of many nitrates by TBP can be described by the following equation:(9)

$$\mathrm{Me}^{z+}_{\mathrm{aq}} + z\mathrm{NO}^-_{3\,\mathrm{aq}} + n\mathrm{TBP}_0 \rightarrow \mathrm{Me(NO_3)}_z \,.\, n\mathrm{TBP}_0$$

The equilibrium constant is then:

$$K = \frac{a_c}{a'_{\mathrm{Me}} \cdot a'^{z}_{\mathrm{NO}_3} \cdot a^n_{\mathrm{TBP}}} \tag{1}$$

and the partition coefficient:

$$k = K \,.\, \frac{y^{z+1}_{\pm}\, c'^{z}_{\mathrm{NO}_3} \cdot a^n_{\mathrm{TBP}}}{y_c} \tag{2}$$

or at constant composition of the aqueous phase:

$$k = A \,.\, \frac{a^n_{\mathrm{TBP}}}{y_c} \tag{3}$$

In the above equation a and c denote activities and concentrations in the organic phase, respectively, and when dashed-in the aqueous phase. y_c is the molar activity coefficient of the complex in the organic phase and $y_{\pm}$ is the mean molar stoichiometrical activity coefficient of the salt in the aqueous phase and A and K are constants, the former for an aqueous phase of fixed composition.

Equation (3) shows that the partition coefficient depends on a_{TBP} and y_c. These factors may both change with diluent. The activity of TBP in the ternary mixture: TBP–diluent–H_2O has been determined for several diluents(8) from the solubility in the equilibrium aqueous phase. By measuring the partition coefficient into the organic phase of the same composition, the value of y_e can be calculated from equation (3), and its dependence on diluent revealed. Since in this procedure the composition of the organic phase must be the same for both k and a_{TBP} determinations, extraction cannot be carried out from HNO_3 because it is well extracted into TBP and can change its activity. $NaNO_3$ which is not extracted by dilute TBP solutions can be used instead. For the same reason microamounts of extractable cations should be used. In this paper the activity of TBP in several additional diluents has been measured, and partition coefficients for Th^{4+} and Eu^{3+} from 4 M $NaNO_3$ into the same organic phases determined. Partition coefficient determinations have also been carried out for the TBP–diluent–H_2O systems studied by ALCOCK *et al.*(8) The other possibility was to determine the TBP activity in mixtures: TBP–diluent–H_2O–HNO_3, and to extract cations from HNO_3 solutions. But this procedure seemed to have certain disadvantages. The interaction between partially hydrated TBP and diluent appeared to be of more general interest than that between TBP, HNO_3 and diluent. Data concerning the activity of TBP in the system TBP–diluent–H_2O can be applied, under appropriate experimental conditions, to extraction from salts other than nitrates. The solubility of TBP in HNO_3 solutions is lower than in water and that would diminish the accuracy of TBP activity determinations for certain diluents.

---

(8) K. ALCOCK, S. S. GRIMLEY, T. V. HEALY, J. KENNEDY and H. A. C. MCKAY, *Trans. Faraday Soc.* 52, 39 (1956).

(9) E. HESFORD and H. A. C. MCKAY, *Trans. Faraday. Soc.* 54, 573 (1958).

EXPERIMENTAL

Materials. The TBP and solvents used were purified by standard methods. $NaNO_3$ and HNO_3 were Analar grade. ^{234}Th tracer was separated from uranium nitrate. $^{152,154}Eu$ tracer has been used. ^{32}P-labelled TBP was supplied by The Radiochemical Centre, Amersham.

TBP *solubility determinations*. One ml of the solution of ^{32}P- labelled TBP in a diluent has been shaken with 15 ml of water for several minutes. After a short period of standing, the phases were centrifugated and after separation, the activity of the aqueous phase was measured with a liquid counter. Then the organic phase was shaken with a fresh portion of water. This was repeated seven times, the first wash being done with 0·1% NaOH. The activities of the aqueous phases from the last 3–4 equilibrations did not generally differ by more than a few percent. The mean value has been calculated. The measurements were done at 18–22°C.

Partition coefficient determinations. Partition coefficients for Th and Eu were determined by measuring the activities of both phases with a liquid counter. An appropriate correction was introduced to compensate for density changes. The total concentration of metal in the extraction experiments was $3{\cdot}5 \times 10^{-4}$ M. At least three independent equilibrations were carried out for each composition of the organic phase. The standard deviation of the mean value was about 5 per cent.

RESULTS AND DISCUSSION

The activity of TBP

The activity of 5 per cent (by volume) or 0·183 molar TBP in a number of diluents, as determined from its solubility in water, is shown in Table 1. The activity of TBP in kerosene, hexane and cyclohexane was taken from the paper of ALCOCK *et al.*(8) Our data for benzene and toluene are in good agreement with those already published.(8) In calculating the activity of TBP from its solubility in water it has been assumed that the activity of undiluted TBP is equal to unity, and that the activity coefficient of TBP in water is always equal to unity, because of the very low concentration of TBP in water.

The following conclusions can be drawn from the data shown in Table 1:

The diluents used can be divided into three groups: (1) aliphatic hydrocarbons, (2) aromatic and substituted aliphatic, or substituted aromatic hydrocarbons, (3) $CHCl_3$ and $CHBr_3$. The highest activity of TBP is observed in aliphatic hydrocarbons; it decreases in this group with the length of the chain. The lowest activity is observed in $CHCl_3$ and $CHBr_3$ both of which can form hydrogen bonds with TBP molecules. The activity is intermediate in aromatic and substituted aromatic or substituted aliphatic hydrocarbons. The differences in the TBP activity among various members of this group seem to be small as compared to the differences in such physico-chemical properties as the dipole moment or the dielectric constant.

There is no simple relation between TBP activity and dipole moment, or polarizability of the molecule of diluent taken separately. But it can be stated that TBP activity is generally high in diluents with both small polarizability and dipole moment and low in diluents with high dipole moment, or high polarizability (excluding nitrobenzene).

TABLE 1.

Diluent	Activity a_{TBP}	Dipole moment μ_{dil}	Solubility parameter		$\frac{M_{H_2O}}{M_{TBP}}$
			δ_{dil}	δ_{TBP}	
Kerosene	0·35	0·0	7·8*	10·1	0·15
Heptane	0·21	0·0	7·45	9·8	0·19
Hexane	1·155	0·0	7·30	9·6	0·20
Cyclohexane	0·12	0·0	8·20	10·5	0·18
Nitrobenzene	0·036	3·99	10·0	11·7	1·0
Toluene	0·029	0·39	8·90	10·4	0·34
Carbon tetrachloride	0·0245	0·0	8·6	10·1	0·21
Ethyl iodide	0·0245	1·78	9·4	11·4	—
Benzene	0·0215	0·0	9·15	10·8	0·41
o-Dichlorobenzene	0·016	2·26	10·0	10·6	—
Chlorobenzene	0·0137	1·56	9·5	10·2	0·35
1,2-Dibromoethane	0·0133	1·12	10·4	11·7	—
Bromoform	0·0049	0·99	10·5	—	0·47
Chloroform	0·0012	1·15	9·3	—	0·49

* value for dodecane

There seems to exist a relation between the TBP activity and the Hildebrand solubility parameter of the diluent used (Fig. 1). Generally, the activity is higher in diluents with small solubility parameters. To examine this relation more closely the solubility parameter of TBP in mixtures has been calculated from the activity data. This calculation has been carried out on the basis of the following equation;(10)

$$\ln a_{TBP} = \ln \varphi_{TBP} + \varphi_{dil}\left(1 - \frac{V_{TBP}}{V_{dil}}\right) + V_{TBP}\varphi_{dil}^2(\delta_{TBP} - \delta_{dil})^2/RT \qquad (4)$$

where φ is the volume fraction, V—molar volume, δ—solubility parameter. It has been assumed that there is no volume change on mixing. The results obtained are shown in Table 1. It is not possible to calculate δ_{TBP} in the case of $CHCl_3$ and $CHBr_3$ because the second term in the right hand side of equation (4) is negative for these two diluents. The negative value of the partial molar energy of mixing means that forces acting between unlike molecules (TBP–diluent) are different in their character from those between like molecules. It has been shown experimentally by PUSHLENKOV(6) that hydrogen bond is formed between TBP and $CHCl_3$ molecules. The formation of this bond is responsible for the especially small activity of TBP in $CHCl_3$ or $CHBr_3$. The data in Table 1 show that the solubility parameter of TBP (δ_{TBP}) is not constant, as it should be, but changes with diluent. The mean value of δ_{TBP} is 10·6. The changes in solubility parameter with diluent are probably caused by the different content of water in the organic phase (different degree of hydration of TBP, see Table 1). The other cause might be the use of the first term in the right hand side of equation (4) as the partial molar entropy of mixing. Nevertheless equation (4) represents the trend which exists in the dependence of a_{TBP} on δ_{dil}. This follows from Fig. 2 where ln a_{TBP} has been plotted against

---

(10) I. H. HILDEBRAND and R. L. SCOTT, *The Solubility of Nonelectrolytes*. Reinhold, Amsterdam (1950).

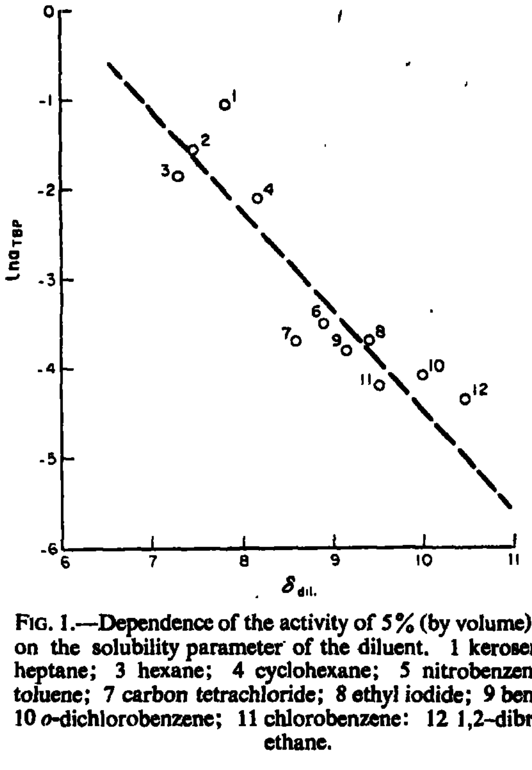

FIG. 1.—Dependence of the activity of 5% (by volume) TBP on the solubility parameter of the diluent. 1 kerosene; 2 heptane; 3 hexane; 4 cyclohexane; 5 nitrobenzene; 6 toluene; 7 carbon tetrachloride; 8 ethyl iodide; 9 benzene; 10 o-dichlorobenzene; 11 chlorobenzene: 12 1,2-dibromoethane.

$$Z = \ln \varphi_{TBP} + \varphi_{dil}\left(1 - \frac{V_{TBP}}{V_{dil}}\right) + V_{TBP}\varphi_{dil}^2 (\bar{\delta}_{TBP} - \delta_{dil})^2/RT$$

for various diluents. $\bar{\delta}_{TBP}$ is the mean value of the solubility parameter of TBP calculated from the data in Table 1. Fig. 2 shows that there is a general tendency for ln a_{TBP} to decrease with Z, as expected from equation (4).

It is interesting to note that the solubility parameter of unhydrated TBP as calculated from the boiling point is about 7·7, which is considerably lower than the value determined above. The discrepancy may be accounted for by the fact that the diluted TBP is partially hydrated when in equilibrium with water. The small value of the solubility parameter of pure TBP deserves some explanation because the TBP molecule has a rather high dipole moment $\mu = 3·1$. A possible explanation is that the P=O group in the TBP molecule is hidden in some sort of a cage formed by the hydrocarbon

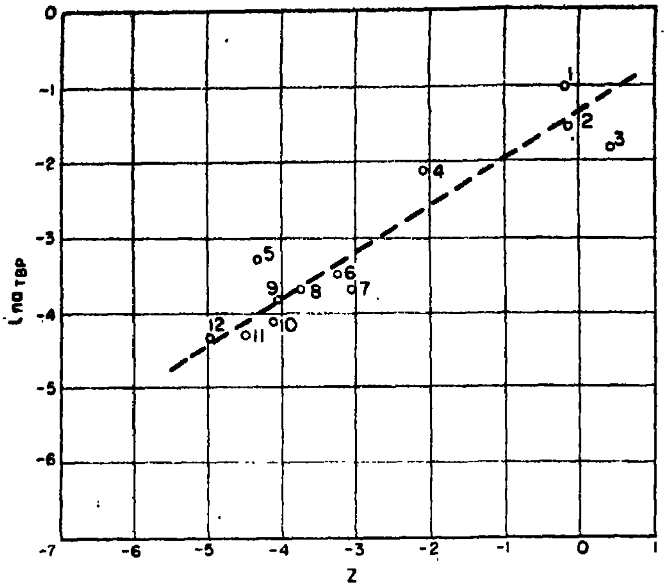

FIG. 2.—Dependence of ln a_{TBP} and Z.

chains. Such a structure for esters of phosphoric acids has been suggested by ARBUZOV and VINOGRADOVA.(11)

Partition coefficients of Eu, Th *and* HNO_3

Partition coefficients into 5% (by volume) TBP in various diluents and the composition of the aqueous phase before extraction are listed in Table 2. In the case of

TABLE 2.

	Partition coefficient				
	Eu aq. phase: 4 M $NaNO_3$+ 0·06 M HNO_3	Eu aq. phase: 6 M $NaNO_3$+ 0·06 M HNO_3	Th aq. phase: 4 M $NaNO_3$+ 0·37 M HNO_3	Th aq. phase: 4 M HNO_3	HNO_3 aq. phase: 4 M $NaNO_3$+ 0·37 HNO_3
Kerosene	0·020	—	0·46	0·080	0·13
Heptane	0·019	0·11	0·51	0·075	0·14
Hexane	0·019	—	0·52	0·070	0·15
Cyclohexane	0·020	—	0·55	0·075	0·155
Nitrobenzene	0·0095	—	0·28	0·075	0·14
Toluene	0·0038	—	0·19	0·035	0·14
Carbon tetrachloride	0·0020	0·0095	0·080	0·040	0·11
Ethyl iodide	0·0028	—	0·080	0·016	0·15
Benzene	0·0031	0·015	0·24	0·048	0·15
o-Dichlorobenzene	0·0039	0·024	0·12	—	—
Chlorobenzene	0·0032	0·0175	0·14	0·028	0·13
Bromoform	<0·001	0·004	<0·001	—	—
Chloroform	<0·001	—	<0·001	0·0026	0·013
Tributylphosphate	22·0	—	570	38·0	9·1

---

(11) B. A. ARBUZOV and V. S. VINOGRADOVA, *Izv. Akad. Nauk. U.S.S.R.* 459, (1947).

Th extraction the concentration of HNO_3 was 0·37 M, since at lower acidities the reproducibility of results was poor. The results obtained may be summarized as follows:

Extraction of europium from 4 M $NaNO_3$. As before the diluents used can roughly be divided into the same three classes. The highest partition coefficients were obtained for diluents of the first group, lower for diluents of the second group and much lower still for $CHCl_3$ and $CHBr_3$. In the case of the last two diluents only the upper limit of the partition coefficient could be given. Since the order observed is also the order of decreasing activity of the TBP it may be stated that the partition coefficient decreases with the activity of TBP. But the differences in k_{Eu} are much smaller than those expected from differences in the TBP activity. There is no influence of TBP activity inside each class since for aliphatic hydrocarbons the partition coefficient is practically constant, and it changes irregularly for diluents of the second group. It is worth noting that CCl_4 belongs to the second class of diluents. Only a few data were obtained for europium extraction from 6 M $NaNO_3$ but the picture seems to be generally the same.

Extraction of Th *from* 4 M $NaNO_3$ + 0·37 M HNO_3. The influence of diluent reveals a close similarity to that in the case of europium extraction, but the difference between partition coefficients for diluents of the first group and partition coefficients for diluents of the second group is smaller for thorium than for europium.

Extraction of Th *from* 4 M HNO_3. The influence of diluents of the first and second group is almost the same as in extraction from sodium nitrate, although partition coefficients are lower. It means that the change of the activity of $TBP{\cdot}HNO_3$ with diluent is nearly the same as the change of the activity for hydrated TBP. Quite different is the case of $CHCl_3$. For this diluent partition coefficient from nitric acid is considerably higher than from sodium nitrate.

Extraction of HNO_3 *from* 4 M $NaNO_3$. There is no difference between diluents of the first and second group. The partition coefficient into $CHCl_3$ as diluent is smaller but the difference is not great.

Activity coefficient of the complex in the organic phase. Activity coefficients of the complex in various diluents can be calculated from equation (3) provided k, a_{TBP}, and n are known, an appropriate standard state is chosen, and composition of the aqueous phase is constant for each equilibration. In the case of europium it has been assumed that $y_{Eu} = 1$ for undiluted TBP in equilibrium with 4 M $NaNO_3$ containing 0·06 M HNO_3 before extraction. Since the content of nitric acid in the equilibrium organic phase is very low (about 0·009 M in diluted TBP) the activity of TBP previously calculated (Table 1) was used. The results of HESFORD *et al.*[12] and of our own investigations have shown that n = 3 for europium. Under these assumptions the following expression for y_{Eu} can be obtained from equation (3):

$$y_{Eu} = a^3_{TBP,x} \cdot \frac{k_{100}}{k_x} \qquad (5)$$

where $a_{TBP,x}$ denotes the activity of 5% TBP in diluent x, k_{100} and k_x are partition coefficients into undiluted TBP and into TBP in diluent x respectively.

In the case of thorium extraction from 4 M $NaNO_3$ + 0·37 M HNO_3 the concentration of HNO_3 in diluted TBP was about 0·056 M and it was not possible to use the a_{TBP} values from Table 1. a_{TBP} has been calculated from the following expression: $a_{TBP} = c_f \cdot y_{TBP}$, where c_f is the concentration of free TBP and y_{TBP} is the molar activity coefficient of TBP in the absence of HNO_3. This expression can be used for a_{TBP} calculations provided y_{TBP} does not change much with c_{TBP} which is true for small TBP concentration. As the state for which $y_{Th} = 1$ the undiluted TBP in equilibrium with an aqueous phase containing 4 M $NaNO_3$ and 0·37 M HNO_3 before extraction has been used. Under these assumptions one obtains for the activity coefficient of thorium the following equation:

---

[12] E. HESFORD, E. E. JACKSON and H. A. C. MCKAY, *J. Inorg. Nucl. Chem.* **9**, 279 (1959).

$$y_{Th} = \frac{a^2_{TBP,x}}{a^2_{TBP,100}} \cdot \frac{k_{100}}{k_x} \tag{6}$$

where $a_{TBP,100}$ is the activity of undiluted TBP in equilibrium with the aqueous phase containing 4 M $NaNO_3$ and 0·37 M HNO_3. It has been assumed that the limiting value of n for thorium is two,[13] although our experiments even with dilute TBP showed that n is somewhat higher and is not a whole number. In the case of thorium extraction from 4 M HNO_3 the same procedure has been adopted for the calculation of y_{Th}. Since in the case of extraction from HNO_3 solution the concentration of HNO_3 in the equilibrium organic phase was very near to the total concentration of TBP, the values of y_{Th} are rather approximate. The difference in the absolute value of the activity coefficients of the complexes in the organic phase when extracted from $NaNO_3$ and from HNO_3 are chiefly caused by the different standard states chosen.

Activity coefficients of europium and thorium complexes in the various diluents are plotted in Fig. 3, as a function of y_{TBP}, where y_{TBP} is the molar activity coefficient of TBP. Activity coefficients in $CHBr_3$ and $CHCl_3$ were not calculated because only the upper limit of the partition coefficient into these diluents was known.

There is a general tendency for y_c to decrease with y_{TBP}. In the case of aliphatic hydrocarbons the dependence of y_c on y_{TBP} is approximately linear. In the case of aromatic and substituted hydrocarbons a similar straight line can be drawn, but the points are much more scattered. The two classes of diluents coincide with those observed in the case of TBP activity. At constant y_c value, the y_{TBP} value is smaller for diluents of the second class.

It has been shown that the influence of the diluent on the activity of TBP can be accounted for by assuming that the solubility parameter of TBP is about 10·6. The data in Fig. 3, show that there is a parallel between the influence of diluent on y_{TBP} and on y_c. For this reason one might try to explain the influence of diluent on y_c, assuming that the complex has a solubility parameter (δ_c) higher than about eleven. With this assumption y_c should decrease with increase of δ_{dil} for most diluents because the difference ($\delta_c - \delta_{dil}$) would decrease. The existence of such a general tendency is supported by data in Fig. 4. The similarity between TBP molecules and molecules of complex in their interaction with diluent may well be accounted for by the fact that co-ordinated TBP molecules constitute the bulk of the complex, and that the interaction of the complex with surrounding molecules is due chiefly to the presence of co-ordinated TBP molecules. This similarity shows also that the function of the P=O group in the interaction of free TBP molecules with diluent does not play an important role, because this group disappears in the case of co-ordinated TBP molecules.

[13] E. HESFORD, H. A. C. MCKAY and D. SCARGIL, *J. Inorg. Nucl. Chem.* **4**, 321 (1957).

The influence of diluent on the partition coefficient. Provided the extraction can be represented by equation (1) the partition coefficient is a function of the ratio a^n_{TBP}/y_c. Both factors change with diluent in the same direction since the interaction forces with diluent molecules are similar for both TBP and complex. The result is that k does not change very much with diluent. But since the compensation of the y_c and a_{TBP} factors is not complete some influence of diluent is observed. The magnitude of this influence depends on the structure and physicochemical properties of the complex, on the diluent used, and should be investigated for each specific case. There is for example no compensation at all in the case of $CHCl_3$ and $CHBr_3$ as diluents. These two diluents form hydrogen bonds with TBP molecules, but in their interaction with the molecules of the complex they probably behave as liquids with solubility parameter of 10·5 and 9·3 respectively.

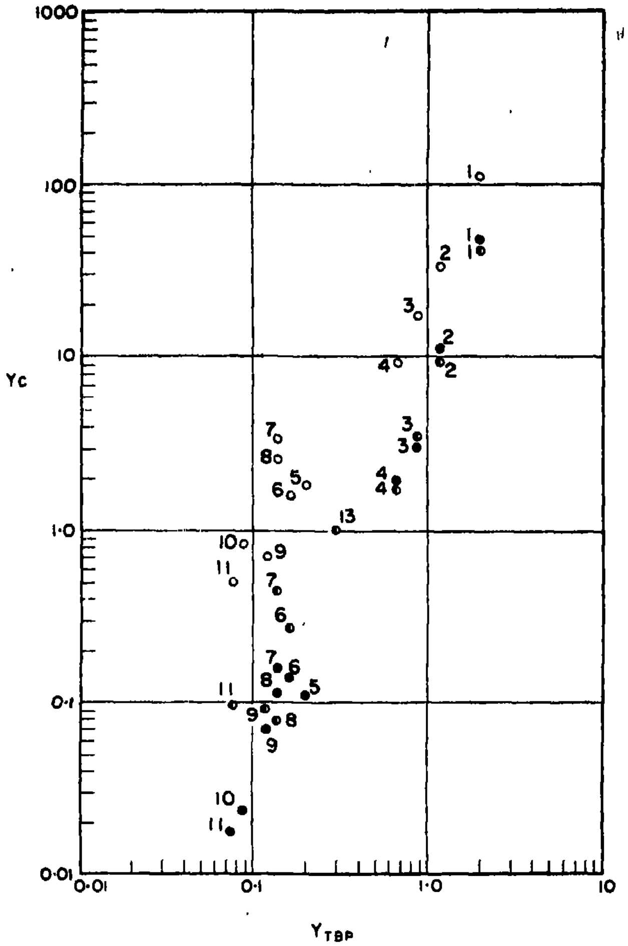

FIG. 3.—Relation between the activity coefficient of europium, or thorium complex and the the activity coefficient of 5% (by volume) TBP in various diluents. 13-denotes TBP.

●—data for europium extracted from 4 M $NaNO_3$ + 0·06 M HNO_3.
○—data for thorium extracted from 4 M $NaNO_3$ + 0·37 M HNO_3
◐—data for thorium extracted from 4 M HNO_3

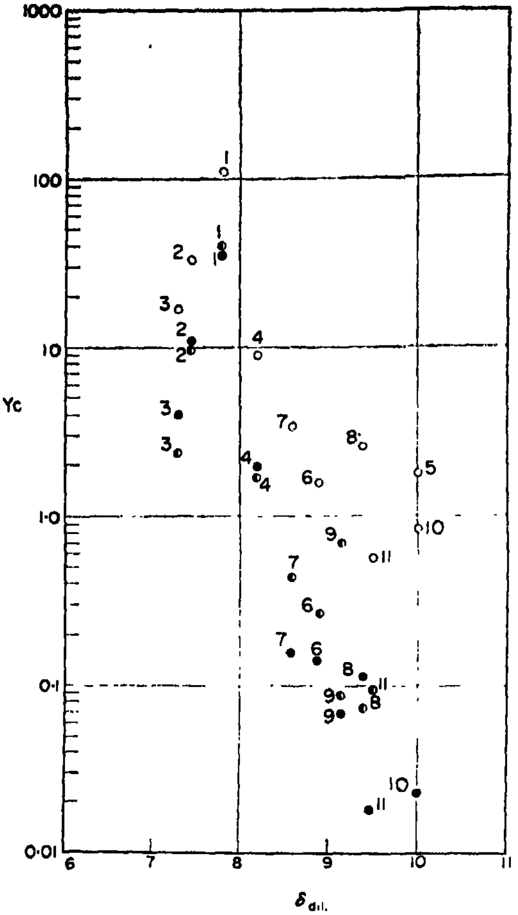

Fig. 4.—Dependence of the activity coefficient of europium or thorium complex in the organic phase on the solubility parameter of the diluent.

● —data for europium extracted from 4 M $NaNO_3$ + 0·06 M HNO_3.
○ —data for thorium extracted from 4 M $NaNO_3$ + 0·37 M HNO_3
◐ —data for thorium extracted from 4 M HNO_3

Generally, the influence of diluent on extraction should increase with differences between the molecules of extracting agent and of complex, with respect to the interaction with the molecules of diluent. Therefore as long as the interaction of both species with diluent is due to dispersion forces, or weak dipole-dipole interactions the resulting effect of diluent on extraction is relatively small. This mode of interaction for both complex and extracting agent may be expected for other extractants similar to TBP, which form uncharged and only slightly polar complexes with metal ions. A strong influence of diluent may be however expected in all cases where either the extractant or the extracted complex is strongly polar, or one of them interacts with the molecules of diluent by specific chemical forces such as hydrogen bonds.

Acknowledgements—Acknowledgement should be made to Dr. A. G. Maddock for valuable suggestions and helpful discussion and to Mrs. J. Szydłowska for her skilled technical assistance.

J. Inorg. Nucl. Chem., 1962, Vol. 24, pp. 215 to 217. Pergamon Press Ltd. Printed in Northern Ireland

NOTE

Preparation of high specific activity terbium^{161} from gadolinium*

(*Received* 29 *May* 1961; *in revised form* 18 *September* 1961)

Sources of high specific activity and purity are necessary for the study of resonance absorption of low energy γ-rays. The present paper describes an attempt to prepare a high specific activity source of Tb^{161} from Gd for studying the recoil-less emission and absorption of the 26 Kev gamma-ray of Dy^{161} (1).

The preparation of pure and high specific activity Tb^{161} has been reported by various workers. Sheline *et al.*(2) have prepared terbium^{161} by deuteron bombardment of enriched gadolinium and by using the chemical separation method developed by Thompson *et al.*(3) Smith *et al.*(4) have followed the methods of Nervick(5) and Choppin *et al.*(6) for separating terbium activity from other rare earths. Butement(7) has used the method of Ketelle and Boyd(8) for the purification of terbium and gadolinium isotopes in the study of β and γ-ray energies.

Recently, Maslova *et al.*(9) separated rare earth activities in fission products on a sulphonated polystyrene resin (KU-2) on a 100 cm column using 0·25 M lactic acid at pH 4·0 and showed that elution with 0·01 M pyrophosphoric acid at pH 5·2–8·0 was as effective as lactic acid for rare earths separation.

Most of the procedures(3,5,6) quoted above can handle only a few mg ($<$ 5 mg) of the rare earth and require high mesh resin at elevated temperatures. But since the flux of the reactor "Apsara" at Trombay, Bombay, is about hundred times lower than that available at DIDO, Harwell, about 100–150 mg of gadolinium had to be used. This paper describes the details of the experimental procedure developed in this laboratory to purify terbium^{161} in carrier-free form using a Dowex-50 resin at a room temperature.

EXPERIMENTAL

The lactic acid and ammonium hydroxide used were of B. D. H. AnalaR quality, and were not further purified.

Dowex-50 resin was used, sieved to between 80 and 120 mesh. It was twice cycled through the hydrogen and ammonium forms using pure dil HCl and ammonium chloride solution and then treated with a 5% solution of NH$_4$CNS to remove any impurities like iron and copper and finally cycled again through the hydrogen and ammonium forms. Before putting activity on the column in the ammonium form it was equilibrated with the lactate solution which was to be used for elution.

A pyrex glass tube of 16·4 mm internal diameter with a stop cock at the bottom and a ground glass joint for connecting the reservoir at the top was used. The resin (80–120 mesh) was filled in the tubing to 185 mm height. The volume of water occupying the space between the resin particles and the glass tubing was exactly 22 ml. For collecting equal volumes of the eluant, a syphon tube of about 2·5 ml capacity was introduced between the outlet of the column and the collecting tube.

To a lactic acid solution containing 0·4 per cent phenol (added to prevent any fungus formation) was added concentrated ammonium hydroxide to adjust to the required pH and the volume made up in the standard volumetric flask. The final concentration of the lactate solution was 0·5 molar. Several such solutions were prepared from pH 3·0 to pH 4·0.

---

* Presented at the 48th Session of the Indian Science Congress held at Roorkee in January 1961.

(1) S. Jha, R. K. Gupta, H. G. Devare, G. C. Pramila and R. S. Raghavan, Nuovo Cimento XIX, 682 (1961).

(2) P. G. Hansen, O. Nathan, O. B. Nielsen and R. K. Sheline, *Nucl. Phys.* **6**, 630 (1958).

(3) S. G. Thompson, B. G. Harvey, G. R. Choppin, and G. T. Seaborg, *J. Amer. Chem. Soc.* **76**, 6229 (1954).

(4) W. G. Smith, J. H. Hamilton, R. L. Robinson and L. M. Langor, *Phys. Rev.* **104**, 1020 (1956).

(5) W. E. Nervik, *J. Phys. Chem.* **59**, 690 (1955).

(6) G. R. Choppin, B. G. Harvey and S. G. Thompson, *J. Inorg. Nucl. Chem.* **2**, 66 (1956).

(7) F. D. S. Butement, *Phys. Rev.* **75**, 1276 (1949).

(8) H. B. Ketelle and G. E. Boyd, *J. Amer. Chem. Soc.*, **69**, 2800 (1947).

(9) G. B. Maslova, P. P. Nazrov and K. V. Chruntov, *Zh. Neorg. Khim*, **5**, 359 (1960).

100 mg of specpure Gd_2O_3 was irradiated in the "Apsara" Reactor at Trombay, Bombay, for one week with a neutron flux of approximately 10^{12} n cm^{-2} sec^{-1}. It was dissolved in a minimum amount of hot 5N HCl and evaporated to dryness. The residue was taken up in distilled H_2O. This solution, containing all Gd and Tb activities, was adsorbed on the resin column at a rate of about 0·3 ml/min, and the column then washed thoroughly with sufficient distilled water to remove unadsorbed ions. The lactate solution of the appropriate pH was put in the reservoir connected to the column and elution started at a definite time. The rate of elution was controlled by the stop cock. 5 ml portions of the eluant were collected in pyrex tubes and the time taken for collecting a certain number of tubes was noted occasionally.

The activity of each fraction of approximately 5 ml was measured by γ-counting, using a 1 in. thick and 1·5 in. diameter NaI(Tl) crystal with a Dumont 6292 photomultiplier. The γ-ray spectrum of representative fractions from each elution peak was also taken to identify the different activities.

Differential elution curves corresponding to different pH values of the lactate solution were plotted and representative curves are given in Figures 1, 2 and 3.

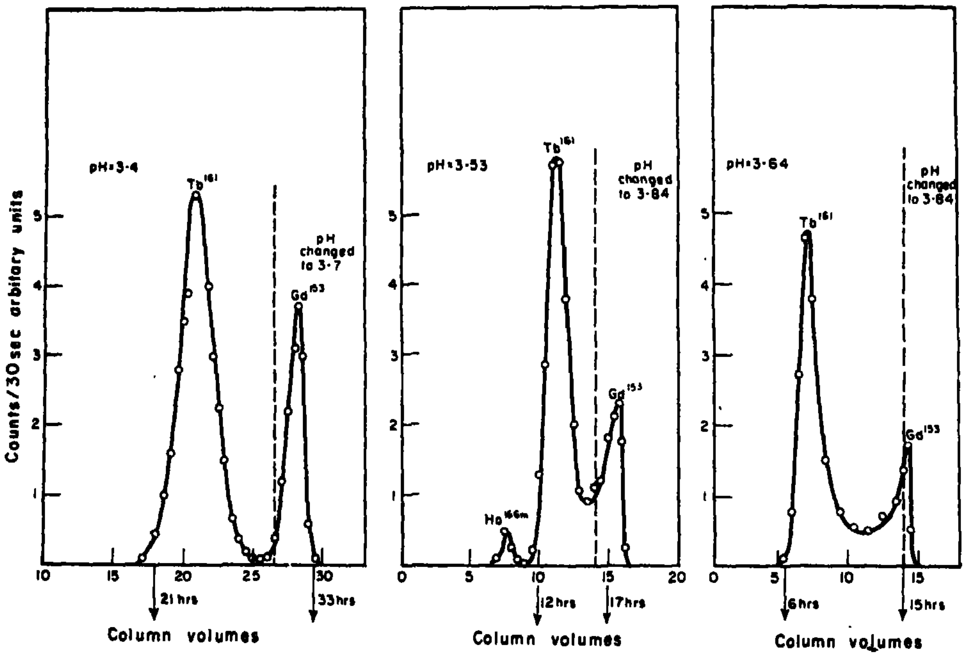

FIGS. 1–3.—Elution curves of Tb^{161} and Gd^{153} from Dowex-50 by 0·5 M lactate at various pH.

All the tubes containing pure terbium^{161} activity were combined in one beaker; the pH of this solution was adjusted between 1 and 2 by adding concentrated HCl and the activity again absorbed on a very small column 2 × 0·4 cm of Dowex-50 resin (about 120 mesh) in the H^+ form. This process adsorbed all the terbium activity. After washing the column thoroughly with double distilled water to remove the adhering lactate solution, the adsorbed activity was eluted with minimum amount of 5N HCl or dil HNO_3 and the solution evaporated to dryness. This was taken up in water and evaporated on the source holder.

In the actual experiment of studying the Mössbauer effect, the carrier-free Tb^{161} was mixed with 1 mg of dysprosium oxide, the mixture dissolved in nitric acid and converted into oxide. The transmission of the 26 KeV gamma-ray was measured$^{(1)}$ using Dy_2O_3 absorbers of thickness varying from 7·9 mg/cm^2 to 78·8 mg/cm^2.

DISCUSSION

It can be seen from Figs 1–3 that there is a critical pH of the semi-molar lactate solution which could separate terbium from even 100 mg of gadolinium in a shorter time at room temperature using

Dowex-50 resin (80–120 mesh). Though solutions having pH less than 3·53 could give well-separated elution curves, this pH(3·53) is the most suitable one, when the time factor becomes important because of the short half-life of the isotope.

In Fig. 3, though the peaks look to be well-separated, it was observed that from column volume 8 (i. e. in the descending portion of the Tb peak) some Gd started coming out with the Tb activity, as detected by the γ-ray spectrum, and hence the entire portion of five column volumes (5–10 c.v.) could not be mixed together for pure Tb^{161}.

After elution of all the active terbium from the column, the pH of the eluting solution was changed to a higher value, 3·7–3·84, in order to remove the bulk activity of Gd^{159} in a shorter time interval. To test the purity of the separated samples obtained by these experiments, gamma-ray spectra of fractions were taken using a 6292 Dumont photomultiplier and a NaI(Tl) crystal of 1·5 cm diameter. The data obtained agreed with that reported⁽¹³⁾.

A low intensity γ-ray of 70 KeV, reported earlier⁽¹⁰⁾ in the decay of Gd^{159}, has been confirmed to be belonging to Gd^{159} by this chemical separation and also by coincidence studies⁽¹¹⁾.

The procedure of using 0·5 M lactate solution at the proper pH for the separation of adjacent rare-earths at a room temperature (~30°C) on Dowex-50 resin was first developed⁽¹²⁾ for Pm^{148} produced by successive neutron capture on Nd^{146}.

Acknowledgements—The authors are indebted to Professor B. V. THOSAR and Dr. S. JHA for the interest they have taken in the work.

K. S. BHATKI*
K. P. GOPINATHAN*
A. T. RANE

Tata Institute of Fundamental Research
Bombay-5 India

* Seconded by Chemistry Division, Atomic Energy Establishment Trombay, Bombay.

(10) S. K. BHATTACHERJEE and S. RAMAN, *Nucl. Phys.* **1**, 486 (1956).

(11) K. P. GOPINATHAN, Presented at the Symposium on Nuclear and Radiaton Chemistry, Calcutta, India (December 1960).

(12) K. S. BHATKI, K. P. GOPINATHAN and A. T. RANE, Presented at the Symposium on Low Energy Nuclear Physics, Waltair, India (February 1960).

(13) H. LENTZ, *Z. Phys.* **159**, 462 (1960).

J. Inorg. Nucl. Chem., 1962, Vol. 24, p. 218. Pergamon Press Ltd. Printed in Northern Ireland

NOTICE

Waverley Gold Medal Essay Competition 1962

Research is again organizing the Waverley Gold Medal Essay Competition this year in order to encourage the clear presentation of new scientific work in a form which may be readily understood by scientists working in other fields and by the layman.

Leaflets setting out the aims of the Competition and conditions of entry can be obtained from the following address:—

Research, 88 Kingsway, London W.C.2.

J. Inorg. Nucl. Chem., 1962, Vol. 24, p. 219. Pergamon Press Ltd. Printed in Northern Ireland

ERRATA

L. P. O'Connor and J. L. Perkin, Cross-sections for the reactions ^{226}Ra $(n,2n)$ ^{225}Ra and ^{226}Ra$(n,3n)$ ^{224}Ra with 14·5 MeV neutrons, *J. Inorg. Nucl. Chem.* **13**, 5–12 (1960).

Page 8, lines 8 and 9; read 'Details are given in Section 2. 5. 2. The mean time . . .'
Page 11, line 5; for 'milligrams' read 'micrograms'.

R. L. Bedford, A. E. Martell and M. Calvin, Influence of fluorine substitution on the properties of metal chelate compounds—III, *J. Inorg. Nucl. Chem.* **14**, 169–178 (1960).

Page 173, caption to Fig. 3; for '10^{-4}' read '10^{-3}' and for '10^{-3}' read '10^{-2}'. In Fig. 3; for '10^{3}' read '10^{2}' and for '10^{4}' read '10^{3}'.
Page 174. $\varepsilon_{\max}$ column of Table 1 following 4200; for '36, 28, 25, —, ~9, ~7' read '360, 280, 250, —, ~50, ~30'. Following 7300; for '33, 33, 28, 18, ~7, ~6', read '330, 330, 280, 180, ~45, ~34'.

D. J. MacDonald and C. S. Garner, Kinetic of aquation of *trans*-dichlorobis-(ethylenediamine) chromium(III) cation, *J. Inorg. Nucl. Chem.* **18**, 219–225 (1961).

Page 223, footnote to Table 5; for '0·018' read '0·108'.
Page 225, line 4; for '$10^{-5(3)}$' read '$10^{-4(3)}$'.

N. D. Dudey and T. T. Sugihara, Half lives of ^{117}In and ^{117m}In, *J. Inorg. Nucl. Chem.* **20**, 157–159 (1961).

Page 158, line 11; for 'Sb^{117}' read '^{117}Sn'.

R. E. Panzer and J. F. Suttle, The compound $UCl_5 \cdot PCl_5$, *J. Inorg. Nucl. Chem.* **20**, 229–241 (1961).

Pages 235, 237; captions for Figures 5 and 6 should be interchanged.

T. C. Ichniowski and A. F. Clifford, A polarographic study of chromium(III) in ammonia solvents (Divers liquids), *J. Inorg. Nucl. Chem.* **22**, 133–139 (1961).

Pages 136, 137; Figures 1 and 2 should be interchanged.

J. Inorg. Nucl. Chem., 1962, Vol. 24, pp. 221 to 227. Pergamon Press Ltd. Printed in England

THE FISSION PRODUCTS ^{81}Se AND ^{83}Se

I. F. Croall and H. H. Willis
A.E.R.E. Harwell, Didcot, Berks.

(*Received 5 October* 1961)

Abstract—The cumulative yields of the isomers of ^{81}Se and ^{83}Se have been measured in the thermal neutron fission of ^{233}U and ^{235}U and in the 20 MeV proton fission of ^{235}U. It is shown that for both these isomer pairs the independent yield of the high spin isomer is greater than that of the low spin isomer in 20 MeV proton fission of ^{235}U.

^{81}Se and ^{83}Se both have two nuclear isomers. Those of ^{81}Se have half-lives of 57 min (^{81m}Se) and 18 min (^{81}Se): the 57 min isomer undergoes an isomeric transition to the 18 min lower level.⁽¹⁾ ^{83m}Se has a half-life of 69 sec, and no isomeric transition between this state and the 25 min ground state has been observed.⁽¹, ²⁾ The cumulative yields of the two isomers of ^{81}Se and of the 25 min isomer of ^{83}Se have previously been reported for the thermal neutron fission of ^{235}U.⁽³⁾ No measurements for the thermal neutron fission of ^{233}U or for 20 MeV proton fission of ^{235}U have been described.

The cumulative yield measurements described here form the first stage of a study of the independent yields of the isomers of ^{81}Se and ^{83}Se. Previous work⁽⁴, ⁵, ⁶⁾ has indicated different independent yields for the members of an isomer pair: in some cases the high spin isomer has the highest yield, in others the low spin isomer is favoured. From the results obtained here some preliminary information concerning the independent yields of the isomers has been derived.

EXPERIMENTAL

^{235}U *thermal neutron fission*

Two series of experiments were carried out; one was designed to give the fission yields of 69 sec ^{83m}Se and 25 min ^{83}Se and the other to give the cumulative fission yields of the isomers of ^{81}Se and of 25 min ^{83}Se. The first series also gave the yield of 32 min ^{84}Br.

The fission mass chains involved are given below.

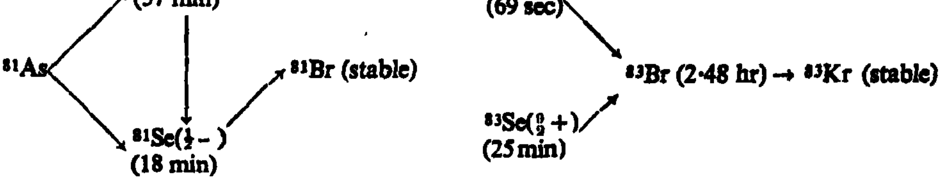

The spins and parities of the selenium isomers are taken from reference (2).

---

(1) D. Strominger, J. M. Hollander and G. T. Seaborg, *Rev. Mod. Phys.* 30, 585 (1958).
(2) K. Way, R. W. King, C. L. McGinnis and R. van Lieshout, U.S.A.E.C. Report, TID 5300 (1955).
(3) S. Katcoff, *Nucleonics*, 18 (11), 201 (1960).
(4) M. Talat-Erben, L. E. Glendenin and E. P. Steinberg. Private communication (1958).
(5) L. E. Glendenin. Private communication (1959).
(6) I. F. Croall and L. E. Glendenin. To be published.

1. *^{83}Se isomer cumulative yields.* These yields were measured indirectly in the following way. A sample of ^{235}U in solution as uranyl nitrate was irradiated in the pneumatic "rabbit" assembly in the graphite pile BEPO for times varying from 30 sec to 2 min. At a known time interval after the end of the irradiation an aliquot of the solution was taken and bromine was separated and purified radiochemically. The bromine samples were then counted using a 2π-gas flow proportional counter, the decay curve being followed until background was reached. From this decay curve the amount of ^{83}Br activity at the time of the bromine separation was obtained. The ^{84}Br (32 min) activity at the end of the irradiation was also obtained from the experiments in which there was only a short delay between the end of the irradiation and the bromine separation. These counting rates were corrected for self-absorption and back-scattering to those corresponding to a weight of 10 mg of silver bromide on the sample tray. These corrections were taken from those derived by Cuninghame *et al.*(7, 8) for identical counting arrangements. The radiochemical procedure for bromine was based on that given by Glendenin *et al.*(9) The final silver bromide precipitate was mounted on a filter paper disk, the area of the precipitate being defined as 2 cm^2 by a standard filter stick. For counting the filter paper was held in a standard aluminium tray.

Duplicate radiochemical analysis for ^{140}Ba were carried out in each experiment, using a procedure based on that of Glendenin(10) but mounting finally as barium sulphate. The barium activity at the end of the irradiation was calculated, corrections for self-absorption and back-scattering being made as in reference (7), to give the counting-rate corresponding to 10 mg of barium sulphate on the tray. A final correction was made to the ^{140}Ba counting-rate to make it comparable on an absolute basis with the ^{83}Br counting rate.(7)

The following expression was derived for the ratio of ^{83}Br to ^{140}Ba counting rates, the former at the time of bromine separation, the latter at the end of the irradiation.

$$\frac{A_{Br}}{A_{Ba}} = \frac{1}{Y_{Ba}(1-e^{-\lambda_{Ba}t})}\Bigg[e^{-\lambda_3 T}(1-e^{-\lambda_3 t})(Y_1+Y_2)+\frac{Y_1\lambda_3}{\lambda_3-\lambda_1}(1-e^{-\lambda_1 t})(e^{-\lambda_1 T}-e^{-\lambda_3 T})$$
$$+\frac{Y_2\lambda_3}{\lambda_3-\lambda_2}(1-e^{-\lambda_2 t})(e^{-\lambda_2 T}-e^{-\lambda_3 T})+\frac{Y_1\lambda_3}{\lambda_3-\lambda_1}e^{-\lambda_3 T}(e^{-\lambda_3 t}-e^{-\lambda_1 t})$$
$$+\frac{Y_2\lambda_3}{\lambda_3-\lambda_2}e^{-\lambda_3 T}(e^{-\lambda_3 t}-e^{-\lambda_2 t})\Bigg]$$

Where A_{Br} and A_{Ba} are the counting rates of ^{83}Br and ^{140}Ba as defined above.

Y_1 : cumulative fission yield of 69 sec ^{83m}Se.
Y_2 : cumulative fission yield of 25 min ^{83}Se.
Y_{Ba} : cumulative fission yield of ^{140}Ba, taken as 6·35 per cent.(3)
t : length of the irradiation.
T : time interval from the end of the irradiation to the bromine separation.
λ_1 : decay constant of 69 sec ^{83m}Se.
λ_2 : decay constant of 25 min ^{83}Se.
λ_3 : decay constant of 2·48 hr ^{83}Br.
λ_{Ba} : the decay constant of 12·8 day ^{140}Ba.

The contribution due to the independent yield of ^{83}Br was ignored, as it is less than 1 per cent of the total chain yield.

In the early stages of this work the half-life of ^{83}Br was observed to be considerably greater than the value of 2·3 hr(2) which is usually accepted. A careful redetermination of this half-life was therefore carried out using ^{83}Br prepared both by fission and by an (n, γ) reaction on enriched selenium (86 per cent ^{82}Se). The samples were counted on a number of

(7) J. G. Cuninghame, M. L. Sizeland and H. H. Willis, AERE/C/R 2054 (1957).

(8) J. G. Cuninghame. Private communication (1959).

(9) L. E. Glendenin, R. R. Edwards and H. Gest, NNES, Div. IV, Vol. 9, Paper 232. McGraw-Hill (1951).

(10) L. E. Glendenin, NNES, Div. IV, Vol. 9, Paper 288.

different types of counter, including end-window Geiger, 2π-gas flow and 4π-gas flow proportional counters. The observed decay curves were analysed by least squares methods, the final result being a value of 2·48 ±0·05 hr for the half-life. This value is confirmed in recent work by Bowles(11), and has been used throughout the studies reported here.

In the equation given above the only unknowns in a given experiment are Y_1 and Y_2, and hence a series of experiments in which t and T are varied gives a set of equations of the form $y = Y_1 + x\,Y_2$, where x and y are variables. A plot of this gives Y_1 and Y_2 directly as the intercept and slope respectively; Fig. 1 shows the present results plotted in this form.

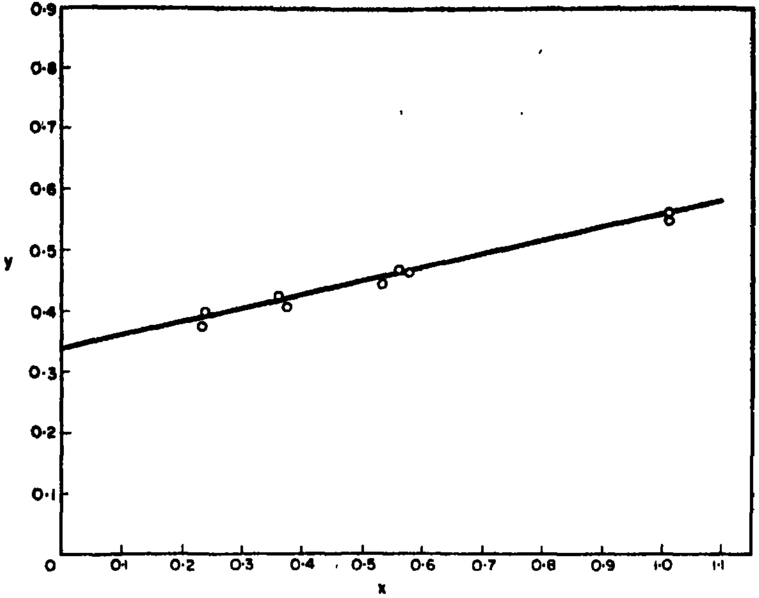

Fig. 1.

A straight line fitted to these results by the method of least square, gives

Y_1 = 0·34 per cent (cumulative yield of 69 sec ^{83m}Se)

Y_2 = 0·21 per cent (cumulative yield of 25 min ^{83}Se)

^{84}Br (32 min) was observed in a number of these experiments, and its cumulative fission yield relative to ^{140}Ba = 6·35 per cent was found to be 0·93 ±0·05 per cent.

2. ^{81}Se *isomer cumulative yields.* These yields were measured directly by separating selenium from the fission products. Samples in which the selenium separation was carried out immediately after the irradiation gave decay curves which could be analysed for 18 min ^{81}Se and 25 min ^{83}Se. Those in which some 2 hr of decay elapsed before separation gave decay curves from which the amounts of 57 min ^{81}Se and 25 min ^{83}Se could be obtained.

In some early experiments using irradiation times of the order of 0·25 min evidence was found of some hold-up in the mass 81 chain. Further work(12) led to a half-life of 30 ±4 sec for ^{81}As, in good agreement with the value later published by Morinaga *et al.*(13) of 31 ±2 sec. The mode of decay of ^{81}As was estimated to be ~ 97 per cent to 18 min ^{81}Se and ~ 3 per cent to 57 min ^{81m}Se.

The experimental procedure in this series was exactly the same as that above except that now selenium and barium were separated. Irradiation times varied between 30 sec and 2 min. The radiochemical separation scheme used for selenium was based on the precipitation of elementary selenium from hydrochloric acid solution by reduction with sulphur dioxide, tellurium and iron scavenging steps being incorporated. The sample used for chemical yield determination and counting was elementary selenium.

(11) B. J. Bowles. AERE, Harwell, private communication (1960).

(12) I. F. Croall and H. H. Willis. To be published.

(13) H. Morinaga, T. Kuroyanagi, H. Mitsui and K. Shoda, *J. Phys. Soc. Japan*, **15**, 213 (1960)

All samples were counted with a 2π-gas flow proportional counter, the decay curves being followed to the background level. From the samples in which the selenium was separated immediately after the end of the irradiation, the amount of 18 min ^{81}Se was obtained by subtraction of a composite 25 min ^{83}Se–2·48 hr ^{83}Br growth-decay curve from the observed curve. The amount of 25 min ^{83}Se was also determined. The decay curves of the samples separated some 2 hr after the end of the irradiation were more complex, due to the presence of the growth-decay curve of ^{81m}Se–^{81}Se. The procedure adopted was to subtract the contribution of ^{83}Se–^{83}Br as determined from the later stages of the decay curve, leaving the complex curve due to the ^{81m}Se–^{81}Se system. Previous calibration of the counter for ^{81m}Se–^{81}Se, where the counting efficiency for the ^{81m}Se conversion electrons (0·105 MeV) is much less than that for the β-particles of ^{81}Se, enabled the final resolution of the curve into its components to be made.

All counting rates were corrected for self-absorption and back-scattering to the values corresponding to 10 mg weight on the counting tray, and finally for the differences in absolute counting efficiency between the selenium isotopes and ^{140}Ba under these conditions. The ^{140}Ba counting-rates were also corrected for self-absorption and back-scattering to the value corresponding to 10 mg of barium sulphate on the tray.

RESULTS

All results for the thermal neutron fission of ^{235}U are given below with estimated overall errors: literature values(3) are also shown for comparison. The ^{83}Se yield is derived from both the series of experiments described above.

Table 1.—Thermal neutron fission of ^{235}U

Nuclide	Cumulative yield (%) This work	Reference (7)
^{81m}Se	0·0076 ± 0·0009	0·0084
^{81}Se	0·21 ± 0·02	0·14
^{83m}Se	0·34 ± 0·02	—
^{83}Se	0·218 ± 0·022	0·22
^{84}Br	0·93 ± 0·05	0·92

These results lead to a value of 0·56 per cent for the total chain yield of mass 83, as ^{83}Br has a negligible independent yield. This is somewhat higher than the value of 0·51 per cent quoted by Katcoff.(3)

The thermal neutron fission of ^{233}U

The cumulative fission yields of ^{81}Se, ^{81m}Se and ^{83}Se were measured in a series of experiments analogous to those reported above in Section (2) of the ^{235}U work, the yields being relative to ^{140}Ba = 6·52 per cent.(14) This is the total chain yield of mass 140 less 0·3 per cent for the independent yield of ^{140}La. This value was selected in preference to the value of 5·4 per cent(7) as it is more consistent with the yields at neighbouring mass numbers.

The cumulative fission yields of the three isomers are given below.

Table 2.

^{81m}Se	0·014 ± 0·002 %
^{81}Se	0·322 ± 0·040 %
^{83}Se	0·40 ± 0·03 %

---

(14) D. R. Bidinosti, D. E. Irish and R. H. Tomlinson, *Canad. J. Chem.* 39, 628 (1961).

20 *MeV proton fission of* ^{235}U

The cumulative yields of ^{81m}Se, ^{83}Se, ^{83}Br and ^{84}Br were measured for 20 MeV proton fission of ^{235}U. Twenty milligram samples of enriched (93 per cent ^{235}U) uranium metal wrapped in aluminium were irradiated in the internal cyclotron beam at a mean proton energy of 20 MeV for times between 5 and 10 min. Separate irradiations were carried out for the selenium and bromine determinations. The target was dissolved in a mixture of nitric and hydrochloric acids under a reflux condenser to prevent loss of bromine; both bromine or selenium and molybdenum carriers were present at this stage. The radiochemical procedures for bromine and selenium were those used in the earlier stages of this work. Molybdenum was separated using a procedure based on precipitation of molybdenum with α-benzoinoxime followed by ferric hydroxide scavenging steps and a final precipitation as the 8-hydroxyquinolinate.

The selenium decay curves showed only 57 min and 2·48 hr activities, owing to the length of time which elapsed between the end of the irradiation and the start of counting. The bromine decay curves were analysed for 2·48 hr ^{83}Br and 32 min ^{84}Br. All counting rates were corrected for self-absorption and back-scattering effects, and for the differences in absolute efficiencies between the selenium and bromine isotopes and ^{99}Mo.

Four separate determinations were made for both selenium and bromine. Table 3 shows the yields relative to ^{99}Mo = 1·00.

TABLE 3.

^{81m}Se	0·034 ± 0·006
^{83}Se	0·123 ± 0·020
^{83}Br	0·21 ± 0·02
^{84}Br	0·43 ± 0·04

DISCUSSION

In the thermal neutron fission of ^{235}U the value predicted for the fractional chain yield of ^{81}Se on the basis of the equal charge displacement rule(15, 16) is 0·01. Essentially all the observed ^{81}Se is therefore formed through the decay of its precursor ^{81}As, and the ratio of the cumulative yields of the isomers of ^{81}Se is simply determined by the branching ratio for this decay. Similarly the predicted fractional chain yield of ^{81}Se for ^{233}U thermal neutron fission is 0·02, and we would therefore expect the ratio of the cumulative yields of the two isomers of ^{81}Se to be the same as that observed for ^{235}U fission.

Taking a total chain yield for mass 81 in ^{233}U fission of 0·34 per cent, the two ratios are given below.

	^{233}U	^{235}U
$\dfrac{^{81}\text{Se}}{^{81m}\text{Se}}$	∼ 23	28

In view of the uncertainty in the total chain yield for the ^{233}U case the agreement is satisfactory.

For ^{83}Se the predicted fractional chain yields in the thermal neutron fission of ^{233}U and ^{235}U are 0·12 and 0·13 respectively. The observed ratios of the cumulative yields of ^{83}Se/^{83m}Se for the two species undergoing fission include a contribution from

---

(15) L. E. GLENDENIN, C. D. CORYELL and R. R. EDWARDS, reference 9, paper 52.

(16) A. C. WAHL, *J. Inorg. Nucl. Chem.* 6, 263 (1958).

the independent formation of the isomers. Taking the total chain yield of mass 83 in ^{233}U thermal neutron fission as 1·0 per cent (average of the values from (7) and (16)), these ratios are:

	^{233}U	^{235}U
$\dfrac{^{83}Se}{^{83m}Se}$	0·67	0·62

JONES *et al.*(17), in a study of the fission of ^{235}U with protons in the energy range 12–20 MeV, have given a mass yield curve for the 20 MeV proton fission of ^{235}U. The results reported here are consistent with their results, but lead to a somewhat broader mass-yield curve. The total chain yield of mass 81 was estimated from a mass-yield curve using both JONES' and the present results. The total number of neutrons emitted in the 20 MeV proton fission of ^{235}U is ~ 5,(18) and using the equal charge displacement rule it is estimated that > 95 per cent of the total chain yield is found in the cumulative yields of ^{81}Se and ^{83}Se. The fractional chain yields of ^{81}Se and ^{83}Se are estimated to be $\sim 0{\cdot}14$ and $\sim 0{\cdot}25$ respectively. The contributions by the selenium isotopes to the observed cumulative yields in 20 MeV proton fission are thus much larger than those in thermal neutron fission.

The observed cumulative yield ratios are:

$$\frac{^{81}Se}{^{81m}Se} \approx 0{\cdot}57 \qquad \frac{^{83}Se}{^{83m}Se} = 1{\cdot}41$$

For thermal neutron fission these ratios were ~ 25 and 0·65 respectively.

The change in these ratios in going from thermal neutron fission to 20 MeV fission is due to the increased independent formation of the selenium nuclides at higher energies. For the ratios to change in the observed directions it is necessary that for 20 MeV proton fission the isomer ^{81m}Se be formed in higher independent yield than ^{81}Se, and ^{83}Se in higher independent yield than ^{83m}Se. Both ^{83m}Se and ^{83}Se are the high-spin isomers of their respective pairs.(2)

VALLIS(19) has found the ratio $^{81}Se/^{81m}Se$ to be ~ 9 in the 14 MeV neutron fission of ^{235}U, a value which is intermediate between those reported above for thermal neutron and for 20 MeV proton fission of ^{235}U. A similar argument suggests that in this case also the high spin isomer is favoured in independent formation.

Very few other determinations of independent isomer ratios are available. TALAT-ERBEN *et al.*(4) found that in the thermal neutron fission of ^{233}U, ^{235}U and ^{239}Pu, and in the pile neutron fission of ^{232}Th the high spin isomer of ^{131}Te was formed in greater independent yield than the low spin isomer. In contrast to these results CROALL and GLENDENIN(6) found that the low spin isomer of ^{106}Rh was favoured in independent formation from the thermal neutron fission of ^{233}U and ^{239}Pu. It has also been observed that the low spin isomer of ^{111}Pd is favoured in the thermal neutron fission of ^{233}U and of ^{239}Pu.(14) For high energy (> 45 MeV) fission the only isomer pair studied is ^{115}Cd, and BAILEY concludes(20) that at these high energies the high spin isomer is favoured.

---

(17) W. H. JONES, A. TIMNICK, J. H. PAEHLER and T. H. HANDLEY, *Phys. Rev.* **99**, 184 (1955).

(18) B. J. BOWLES, F. BROWN and J. P. BUTLER, *Phys. Rev.* **107**, 751 (1957).

(19) D. G. VALLIS, AWRE, Aldermarston, Berkshire, England, private communication (1961).

(20) S. M. BAILEY. Report UCRL 8710 (1959).

Whilst the results are too few to enable firm conclusions to be drawn about the independent formation of nuclear isomers, it does appear that there is a difference between nuclides near the trough of the mass-yield curve, and those near the peaks; this certainly seems to be the case for the few measurements in low and medium energy fission. For nuclides near the trough (^{106}Rh and ^{111}Pd) the low spin isomer is favoured, while for nuclides formed in more asymmetric fission (^{131}Te, ^{83}Se and ^{81}Se), the high spin isomer is the favoured one. It is possible that this difference is associated with differences found in other properties of the fission products, for example, their kinetic energy.

Acknowledgements—The authors are indebted to Mr. G. N. Walton for discussions throughout this study, and to Mr. R. Pollard for experimental assistance in the early stages of the work.

J. Inorg. Nucl. Chem., 1962, Vol. 24, pp. 229 to 238. Pergamon Press Ltd. Printed in England

INFRA-RED STUDY OF SOME OXY-IONS OF SULPHUR ATTACHED TO AN ION-EXCHANGE RESIN

K. Buijs

Chemical Physics Group of the National Chemical and Physical Research Laboratories,
C.S.I.R., Pretoria, South Africa

(*Received* 9 *August* 1961; *in revised form* 26 *October* 1961)

Abstract—The infra-red spectra of sulphate, sulphite, thiosulphate, metabisulphite, dithionate and tetrathionate ions attached to the anion-exchanger, Amberlite IRA-400, have been studied. The spectra are different from those of the ions in the crystalline state as regards number and positions of absorption bands. Sulphate, thiosulphate and dithionate ions are readily exchanged for bromide ions, if a sample of Amberlite IRA-400 is pressed into KBr. Tetrathionate ions do not react in this way. If sulphite, thiosulphate and metabisulphite ions are attached to the anion-exchanger, Amberlite IRA-400, and the ion-exchanger is dried, these ions are easily oxidized by atmospheric oxygen to sulphate, tetrathionate and sulphate plus dithionate respectively. The infra-red spectra of potassium sulphate, metabisulphite, dithionate and tetrathionate are discussed briefly with special attention to the assignment of the overtones in the 2000–2500 cm^{-1} region.

Complex inorganic ions are generally studied either in the crystalline state or in solutions. An ion-exchanger provides a matrix for the complex ions, which is basically very different from the two other matrices. The ions are much more accessible, for instance, for various reagents, than in a rigid crystal lattice. The forces on the ions, exerted by the surrounding medium, are different in the three cases. Consequently, the infra-red spectra of the ions attached to an ion-exchanger differ from those in a crystal lattice or in solution. In this study the infra-red spectra of sulphate, thiosulphate, metabisulphite, dithionate and tetrathionate ions attached to the anion-exchanger, Amberlite IRA-400, as well as the spectra of K_2SO_4, $K_2S_2O_5$, $K_2S_2O_6$ and $K_2S_4O_6$, are discussed. It is shown that SO_3^{2-}, $S_2O_3^{2-}$ and $S_2O_5^{2-}$ are very easily oxidized by atmospheric oxygen if they are attached to Amberlite IRA-400.

EXPERIMENTAL

Samples of Amberlite IRA-400 with the appropriate anions attached to it, were prepared by treating the resin with solutions of salts of these anions. The saturated resin was then thoroughly washed with water, dried and ground using a liquid-grinding technique.⁽¹⁾ It was dried finally in vacuum over phosphorous pentoxide. Infra-red spectra of these samples were recorded using dispersions in vaseline or KBr. The dispersions in KBr were prepared by applying a pressure of 10,000 kg/cm^2 for 2 min. The potassium salts were studied only as vaseline mulls. The spectra were recorded with a Perkin Elmer 21 double-beam infra-red spectrometer, fitted with a NaCl prism.

RESULTS AND DISCUSSION

Potassium sulphate, metabisulphite, dithionate and tetrathionate

As the spectra of the potassium salts are of interest for the discussion of the spectra of the ions attached to Amberlite IRA-400, they are presented first with a discussion of new features. The infra-red spectra of K_2SO_4, $K_2S_2O_5$, $K_2S_2O_6$,

---

(1) A. Strasheim and K. Buijs, *Spectrochim. Acta*, **16**, 1010 (1960).

and $K_2S_4O_6$ in the regions 650–1350 and 2000–2500 cm^{-1}, are shown in Fig. 1. The very weak bands in the region 1350–2000 cm^{-1}, are not reported because of the uncertainties due to atmospheric water and vaseline bands.

The frequencies and assignments for K_2SO_4 are given in Table 1.

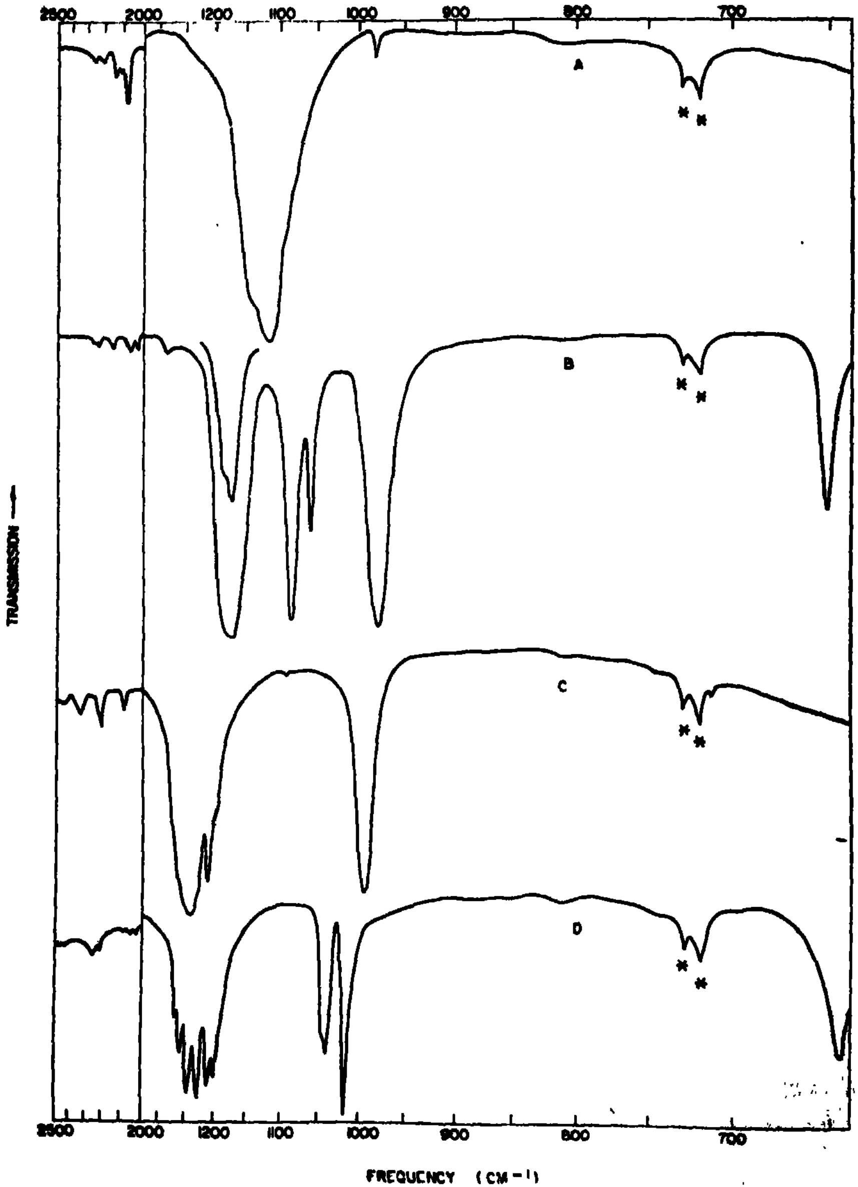

Fig. 1.—The infra-red spectra of K_2SO_4 (*A*), $K_2S_2O_5$ (*B*), $K_2S_2O_6$ (*C*) and $K_2S_4O_6$ (*D*).
* Bands due to vaseline.

TABLE 1.—FREQUENCIES AND ASSIGNMENTS FOR K_2SO_4

Frequency	Rel. intensity*	Assignment
983	*vw*	$\nu_1\,(A_1)$
1113	*vs*	$\nu_3\,(F_2)$
1142	*s sh*	
2083	*vw*	$\nu_1+\nu_3\,(F_2)$
2117		
2146		
2210	*vw*	$2\nu_3\,(A_1+E+F_2)$
2265		

* *s*: strong, *m*: medium, *w*: weak, *v*: very, *sh*: shoulder, *br*: broad.

K_2SO_4 has been studied previously by DUVAL and LECOMTE (2) in the region 6–15 μ and MILLER and WILKINS(3), who found only the ν_3 band at 1110 cm^{-1}. K_2SO_4 crystallizes in the space group V_h^{16}–*Pnma* with four molecules in the unit cell.(4) The site group (5) of SO_4^{2-} is C_s. All degenerate levels are thus split and all modes become infra-red active.

The frequencies and assignments for $K_2S_2O_5$ are listed in Table 2. The bands are numbered with Roman figures, as no assignments of species could be given.

TABLE 2.—THE FREQUENCIES AND ASSIGNMENTS FOR $K_2S_2O_5$

Frequency (cm^{-1})	Rel. intensity	Assignment
652	*s*	I
980	*vs*	II
1058	*s*	III
1084	*vs*	IV
1173	*vs*	V
1183	*s sh*	VI
1289	*vw*	2×I
2022	*vw*	II+III
2060	*vw*	II+IV
2149	*vw*	III+IV
2227	*vw*	III+V
2257	*vw*	IV+V

The spectrum of $K_2S_2O_5$ has been studied by SIMON *et al.*(6) and MILLER and WILKINS.(3) The latter authors found bands at 1105 cm^{-1} and 1250 cm^{-1} which are due to dithionate and sulphate impurities respectively, as will be discussed later in this paper. The crystal structure of $K_2S_2O_5$ has been determined by ZACHARIASEN(7) and confirmed and refined recently by LINDQVIST and MÖRTSELL.(8) They found that the space group is C_{2h}^2–$p2_1/^m$, with two molecules per unit cell. The site group is C_s, as is the ionic point group. The X-ray analysis shows unambiguously that a S-S bond is present in the metabisulphite ion. Simon *et al.* concluded from their Raman and infra-red studies that the ion contains a S-O-S bond and has symmetry C_{2v}. Their evidence is based mainly on the occurrence of four stretching vibrations and on the intensity ratios of the Raman lines. The intensity of Raman lines in the solid state, however, is a rather dangerous criterion. If the band at 1183 cm^{-1} is regarded as a fundamental, there are five fundamentals present in the S-O stretching region as is expected for a $S_2O_5^{2-}$ ion with C_s symmetry and containing a S-S bond.

---

(2) M. DUVAL and J. LECOMTE, *C.R. Acad. Sci., Paris*, **227**, 1153 (1948).

(3) F. A. MILLER and C. H. WILKINS, *Analyt. Chem.* **24**, 1253 (1952).

(4) L. ANDOLT BÖRNSTEIN, *Zahlenwerte und Funktionen*, Band IV. Springer Verlag, Berlin (1955).

(5) R. S. HALFORD, *J. Chem. Phys.* **14**, 8 (1946).

(6) A. SIMON, K. WALDMANN and E. STEGER, *Z. anorg. Chem.* **288**, 131 (1956).

(7) W. ZACHARIASEN, *Phys. Rev.* **40**, 923 (1932).

(8) I. LINDQVIST and M. MÖRTSELL, *Acta Cryst.* **10**, 406 (1957).

It is impossible from the infra-red spectrum, to distinguish between the three stretching modes of species A' and the two of species A''.

The frequencies and assignments for $K_2S_2O_6$ are given in Table 3. The assignments of the symmetry species are given for the symmetry of the free ion (D_{3d}).

Table 3.

Frequency (cm^{-1})	Rel. intensity	Assignment
712	*vw*	$\nu_2\ (A_{1g})$
994	*s sh*	$\nu_7\ (E_u)$
998	*s*	
1093	*vw*	
1200	*w sh*	$\nu_1\ (A_{1g})$
1212	*m*	$\nu_{10}\ (E_g)$
1230	*sh*	$\nu_5\ (A_{2u})$
1243	*vs*	
1268	*w sh*	Combin. band
2086	*vw*	$\nu_1+\nu_7\ (E_u)$
2208	*vw*	$\nu_7+\nu_{10}\ (A_{1u}+A_{2u}+E_u)$
2329	*vw*	$\nu_1+\nu_5\ (A_{2u})$
2450	*vw br*	$\nu_5+\nu_{10}\ (E_u)$, $2\nu_5\ (A_{1g})$ and $2\nu_{10}\ (A_{1g}+E_g)$

The frequency values differ slightly from those reported by Duval and Lecomte(9) who studied the region 6–15 μ. The space group of $K_2S_2O_6$ is D_3^2–$P321$, with three molecules per unit cell.(10) The dithionate ions in the unit cell are not all equivalent: one has site symmetry D_3, the other two C_3. The splitting of ν_5, ν_7 and ν_{10}, which is caused by this phenomenon, is discussed elsewhere.(11) The assignment of ν_2 is based on the occurrence of a polarized Raman line at 710 cm^{-1} for aqueous solutions.(9) It is further seen from Table 3 that the symmetry species of all overtones contain one of the species which are active under D_{3d} symmetry (A_{2u} and E_u).

The frequencies and assignments for $K_2S_4O_6$ are given in Table 4.

No reference to the infra-red spectrum of crystalline $K_2S_4O_6$ has been found in the literature. In $BaS_4O_6 \cdot 2H_2O$, the chain of sulphur atoms in the $S_4O_6^{2-}$ ion is non-planar,(12) so that the ion has symmetry C_1. The space group of $K_2S_4O_6$ is C_s^4–Cc. There are eight molecules per unit cell.(13) The space group C_s^4 contains

---

(9) C. Duval and J. Lecomte, *Bull. Soc. Chim. France*, **11**, 376 (1944).

(10) E. Stanley, *Acta Cryst.* **9**, 897 (1956).

(11) K. Buijs, *J. Chem. Phys.* **36**, 861 (1962).

(12) O. Foss, S. Furberg and H. Zachariasen, *Acta Chem. Scand.* **8**, 459 (1954).

(13) G. Tunell, H. E. Merwin and C. J. Ksanda, *Amer. J. Sci.* **35** A, 361 (1938).

TABLE 4.—FREQUENCIES AND ASSIGNMENTS FOR $K_2S_4O_6$

Frequency (cm^{-1})	Rel. intensity	Assignment
646	*m*	v_7
1016	*vs*	v_6
1040	*s*	v_5
1044	*sh*	Combination or overtone band
1198	*vs*	v_4
1209	*vs*	v_3
1225	*vs*	v_2
1245	*vs*	v_1
1259	*s*	Combination or overtone bands
1267	*m*	
2033	*vw*	$2v_6$
2053	*vw*	v_5+v_6
2086	*vw*	$2v_5$
2212	*vw*	v_4+v_6
2250	*vw*	v_3+v_5
2439	*vw*	v_1+v_4, v_2+v_3
2469	*vw*	v_1+v_2

only sites with C_1 symmetry, which is thus the same symmetry as the $S_4O_6^{2-}$ ion in $BaS_4O_6 \cdot 2H_2O$. As a consequence, all modes are infra-red active and belong to the species *A*. The assignment of the bands in the 1000–1300 cm^{-1} region is based on the following considerations.

Firstly, the strongest bands generally arise from the fundamentals. Secondly, the bands assigned to the fundamentals give the best agreement for the combinations and overtones in the 2000–2500 cm^{-1} region. Thirdly, it can be expected that the S-O stretching modes in $S_4O_6^{2-}$ have frequencies very similar to those in $S_2O_6^{2-}$. As only six fundamentals are S-O stretching modes, the bands at 1259 and 1267 cm^{-1} and the shoulder at 1044 cm^{-1} have to be assigned to combinations or overtones.

Ions attached to Amberlite IRA-400

In Fig. 2 are shown the spectra of SO_4^{2-}, $S_2O_6^{2-}$ and $S_4O_6^{2-}$ attached to Amberlite IRA-400. A number of bands in the mull spectra arises from the ion-exchange resin, the spectrum of which has been discussed elsewhere.(14) In the spectra of the KBr disks, these bands are compensated for by placing the appropriate amount of the bromide form of Amberlite IRA-400 in the reference beam of the spectrometer.

The mull spectrum of the sulphate ions attached to Amberlite IRA-400 shows only a strong broad band at 1093 cm^{-1} (Fig. 2A). No splitting is observed, the broadness of the band is due to the differences in the interaction forces to which the ion is subjected at different positions on the resin.(14)

---

(14) A. STRASHEIM and K. BUIJS, *Spectrochim. Acta*, **17**, 388 (1961).

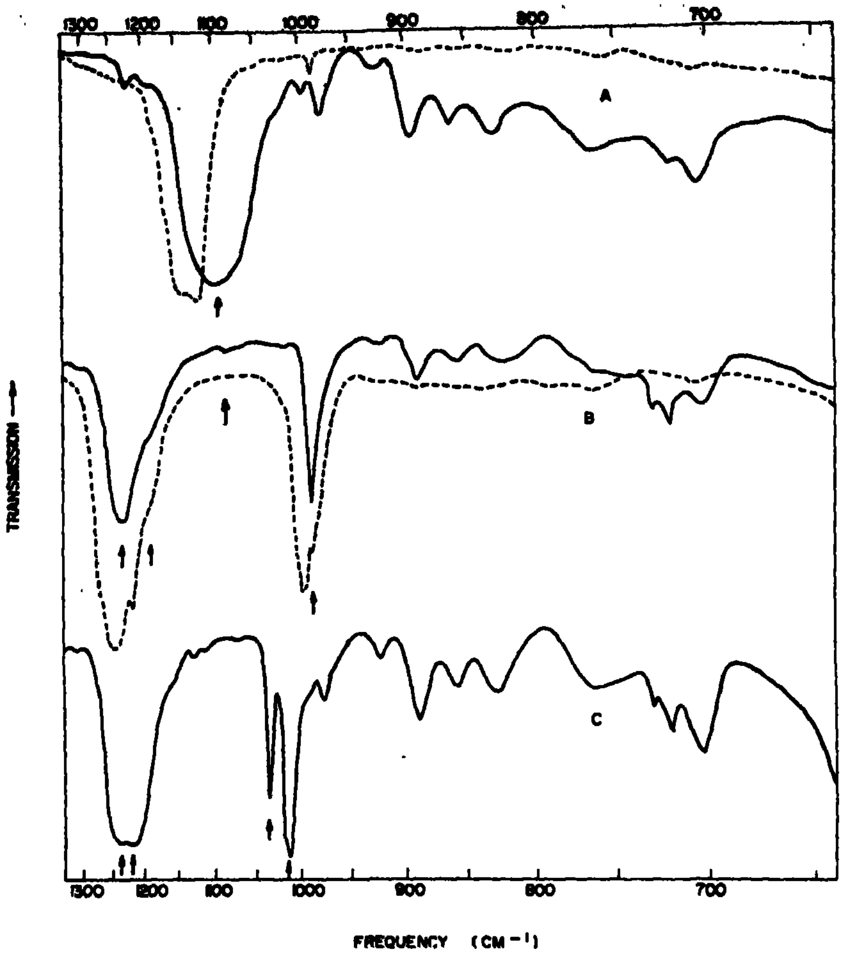

FIG. 2.—The infra-red spectra of SO_4^{2-} (*A*), $S_2O_6^{2-}$ (*B*) and $S_4O_6^{2-}$ (*C*) ions attached to Amberlite IRA-400.

Full lines: Vaseline mulls.
Broken lines: KBr disks.
Arrows indicate the relevant bands in the mull spectra.

The KBr spectrum is identical with the spectrum of K_2SO_4. Two different reactions can occur if an ion-exchanger is pressed together with KBr. In the first case the ions which were attached to the resin dissolve in the KBr, giving a solid solution, as do for instance NO_3^- ions.(15) In the second case, as is found here, an exchange takes place, leading to the formation of the potassium salt of the ions. From spatial considerations it is evident that SO_4^{2-} ions cannot form a solid solution in KBr.

The frequencies of the bands for $S_2O_6^{2-}$ and $S_4O_6^{2-}$ ions are given in Table 5.

---

(15) A. STRASHEIM and K. BUIJS, *J. Chem. Phys.* 34, 691 (1961).

TABLE 5.—THE FREQUENCIES OF ABSORPTION BANDS OF $S_2O_6^{2-}$ AND $S_4O_6^{2-}$ IONS ATTACHED TO AMBERLITE IRA-400 WITH THE FREQUENCIES OF $K_2S_2O_6$ AND $K_2S_4O_6$ LISTED FOR COMPARISON

$S_2O_6^{2-}$				
Mull		KBr		$K_2S_2O_6$
Frequency (cm^{-1})	Rel. intensity	Frequency (cm^{-1})	Rel. intensity	
986	*s*	985	*sh*	
		994	*sh*	994
		998	*s*	998
1087	*vw*			1093
1185	*sh*	1200	*sh*	1200
		1212	*m*	1212
1230	*vs*	1243	*vs br*	1230 1243

$S_4O_6^{2-}$			
Frequency (cm^{-1})			
Mull	KBr	Rel. intensity	$K_2S_4O_6$
1013	1014	*vs*	1016
1039	1041	*s*	1040; 1044
1220	1221	*vs*	1198; 1209
1233	1233	*vs*	1225; 1245

Some distortion of the ion is evident from the intensity (which is somewhat higher than in $K_2S_2O_6$) of the A_{1g} mode (1087 cm^{-1}) in the mull spectrum of $S_2O_6^{2-}$ attached to Amberlite IRA-400. The spectrum of the $S_2O_6^{2-}$ form of Amberlite IRA-400 pressed in KBr, clearly shows the presence of $K_2S_2O_6$. The broadness of the 1234 cm^{-1} band and the shoulder at 985 cm^{-1} are due to $S_2O_6^{2-}$ ions still attached to the resin.

The high frequency stretching modes are not resolved for $S_4O_6^{2-}$ attached to Amberlite IRA-400. The spectra of vaseline and KBr disks are identical. Thus in the series SO_4^{2-}, $S_2O_6^{2-}$, $S_4O_6^{2-}$ the ions tend to stick more to the ion-exchanger. In the same way tetrathionate ions in solution are able to poison anion-exchange resins. They can then only be removed after decomposition.

Oxidation of ions attached to Amberlite IRA-400

When an attempt was made to record the spectrum of sulphite ions attached to Amberlite IRA-400, it was found that the spectrum was identical with that of sulphate ions. An analysis of sulphite, using the method of WEST and GAEKE (16), indicated that immediately after drying, 0·2 micro equivalents of SO_3^{2-} were present per mg of sample—about 10 per cent of the capacity of the ion-exchanger. After 24 hr of exposure to the atmosphere, however, only 0·08 micro equivalents per mg were found. In a KBr pellet containing 2 mg of a fresh sample, no sulphite was found. From these observations it is concluded that SO_3^{2-} ions attached to Amberlite IRA-400 are very rapidly oxidized by atmospheric oxygen, if the resin has been dried.

(16) P. W. WEST and G. C. GAEKE, *Analyt. Chem.* **28**, 1816 (1956).

Similar reactions have been observed with thiosulphate and metabisulphite ions. The spectra of $S_2O_3^{2-}$ and $S_2O_5^{2-}$ attached to Amberlite IRA-400 are shown in Fig. 3. The occurrence of hydrates of $K_2S_2O_3$ hampers the observation of the infra-red spectrum of this compound. However, from measurements on partly hydrated samples and from data on other thiosulphates,(17) it is known that no strong thiosulphate bands occur in the region 1200–1300 cm^{-1}. The band occurring in this region for $S_2O_3^{2-}$ attached to Amberlite IRA-400 should accordingly be assigned to tetrathionate ions as is also in agreement with the positions of other bands. The frequencies found and compounds identified are listed in Table 6.

The intensity ratios of the strong bands clearly show the substitution of thiosulphate by tetrathionate on the resin. Thiosulphate ions are thus oxidized by atmospheric oxygen if they are attached to an ion-exchange resin in the same way as they are oxidized by iodine in aqueous solution. The spectra of the KBr disk and

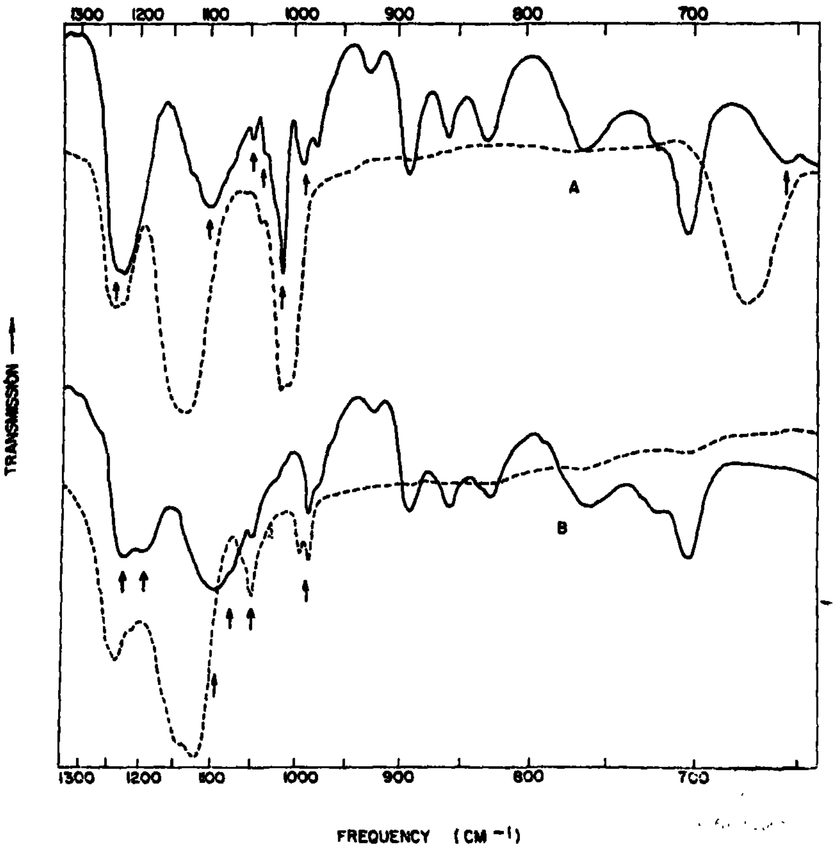

FIG. 3.—The infra-red spectra of Amberlite IRA-400 treated with $S_2O_3^{2-}$ (A) and $S_2O_5^{2-}$ (B) ions.
Full lines: Vaseline mulls.
Broken lines: KBr disks.
Arrows indicate the relevant bands in the mull spectra.

[illegible] Duval and J. Lecomte, *C.R. Acad. Sci., Paris*, 213, 998 (1941).

TABLE 6.—THE FREQUENCIES AND COMPOUNDS FOR AMBERLITE IRA-400 TREATED WITH THIOSULPHATE (FREQUENCIES FOUND FOR PURE COMPOUNDS INDICATED IN BRACKETS)

Frequency (cm^{-1})		
KBr	Mull	Compound
	654	$S_2O_3^{2-}$
671		$K_2S_2O_3$
	990	$S_2O_3^{2-}$
1006		$K_2S_2O_3$
	1013	$S_2O_3^{2-}+S_4O_6^{2-}$ (1013)
1015		$S_4O_6^{2-}$ (1014) $+K_2S_2O_3$
1039	1036	$S_4O_5^{2-}$ (1040)
	1047	?
	1099	$S_2O_3^{2-}$
1129		$K_2S_2O_3$
1234	1233	$S_4O_6^{2-}$ (1233)

the vaseline mull show successive stages of the oxidation process. The oxidation process evidently is much slower than is the case with sulphite ions. From the different positions of $S_2O_3^{2-}$ bands in the mull and in the KBr disk, it follows that thiosulphate is also exchanged readily with bromide on the resin.

The frequencies found and compounds identified in Amberlite IRA-400 treated with $S_2O_5^{2-}$ ions are listed in Table 7.

TABLE 7.—THE FREQUENCIES AND COMPOUNDS FOR AMBERLITE IRA-400 TREATED WITH $S_2O_5^{2-}$ IONS (FREQUENCIES FOUND FOR PURE COMPOUNDS INDICATED IN BRACKETS)

Frequency (cm^{-1})		Compound
KBr:	985	K_2SO_4 (983)
	996	$K_2S_2O_6$ (998)
	1048	?
	1118	K_2SO_4 (1113)
	1140	K_2SO_4 (1142)
	1213	$K_2S_2O_6$ (1212)
	1241	$K_2S_2O_6$ (1243)
Mull:	985	$S_2O_5^{2-}$ ($K_2S_2O_5$: 980) + $S_2O_6^{2-}$ (986)
	1046	?
	1073	$S_2O_5^{2-}$ ($K_2S_2O_5$: 1084)
	1093	SO_4^{2-} (1093)
	1189	$S_2O_5^{2-}$ ($K_2S_2O_5$: 1173 and 1183)
	1228	$S_2O_6^{2-}$ (1230)

The spectrum shown in Fig. 3(B) is fully compatible with the occurrence of $S_2O_6^{2-}$ and SO_4^{2-} on the ion-exchanger. According to BASSET and HENRY (18) crystals of potassium metabisulphite are slowly oxidized in a humid atmosphere with formation of K_2SO_4 and $K_2S_2O_6$. This slow process is thus accelerated considerably if ions are attached to Amberlite IRA-400. The rate of oxidation in this case is greater than that of thiosulphate ions, as no metabisulphite is found in the spectrum of the sample in a KBr disk.

---

(18) H. BASSET and A. J. HENRY, *J. Chem. Soc.* 914 (1935).

CONCLUSION

Infra-red studies of ions attached to an ion-exchanger offer the possibility of observing these ions in a very special medium. The special conditions prevailing in this medium are clearly shown by the very high sensitivity towards atmospheric oxygen displayed by sulphite, thiosulphate and metabisulphite ions attached to Amberlite IRA-400.

J. Inorg. Nucl. Chem. 1962, Vol. 24, pp. 239 to 244. Pergamon Press Ltd. Printed in England

INFRA-RED ABSORPTION OF WATER OF HYDRATION IN LANTHANIDE TRICHLORIDES*

R. J. Morrow and A. Palm
Lawrence Radiation Laboratory, University of California,
Livermore and Berkeley, California

(*Received* 12 *September* 1961; *in revised form* 12 *October* 1961)

Abstract—The absorption spectra of the hydrated lanthanide trichlorides were examined in the region between 4000–400 cm^{-1} by the KBr disk technique. The major bands are assigned to vibrations characteristic of the water molecules on the basis of the consistent pattern of the observed spectra, and isotopic frequency shifts upon deuteration.

While the majority of spectroscopic investigations of the rare earth salts reported in the literature treat electronic transitions, this survey deals with vibrational transitions. A recent study of hydrated praseodymium zinc nitrate and cerous nitrate(1) is similarly concerned with internal vibrations. The absorption bands observed here are only indirectly associated with the lanthanides, since they arise essentially from the water molecules which form a hydration shell about the central cation. During the past ten years absorptions characteristic of water of hydration have been investigated extensively, particularly the OH stretching and the HOH bending modes. Some of the recent work refers to these as well as to the vibrations occurring in the CsBr region.(2)

EXPERIMENTAL

Spectroscopic measurements

The spectra were obtained from samples dispersed in a KBr matrix by customary techniques. Several spectra of Nujol mulls were recorded also in order to establish effects of sample preparation. The Perkin-Elmer Models 21 and 221 double-beam instruments equipped with NaCl, KBr, and CsBr optics were employed. In some cases the error in the reported frequencies is greater than the instrumental error because of the unresolved broad envelopes of many of the bands.

Sample preparation

Lanthanide oxides (99·9 per cent purity) purchased from Lindsay Chemical were employed. The trichlorides were prepared by dissolving the respective oxides in an excess of concentrated HCl while being heated. Water was added and the excess acid was removed by slow evaporation. The final crystalline material was obtained after storing in an evacuated desiccator for several days. The cerous salt was prepared via the ammonium hexanitrato cerate according to the procedure outlined by Smith.(3)

The deuterated hydrates were prepared by sweeping dry HCl and argon past the lanthanide trichlorides while being heated in a furnace to 300°C in the course of an hour. This temperature was maintained for another hour before the sample was cooled slowly under a continuous stream of gas. Subsequently, a small quantity of D_2O was added to the crystalline material which was then transferred to a dry box and pressed into a KBr pellet.

---

* This work was performed under the auspices of the U.S. Atomic Energy Commission.

(1) H. G. Haefele, *Z. Physik*. **148**, 262 (1957).

(2) See for example, F. A. Miller, G. L. Carlson, F. F. Bentley and W. H. Jones, *Spectrochim. Acta*. **16**, 135 (1960).

(3) G. F. Smith, *Cerate Oxidimetry*. Smith Chemical Company, Columbus, Ohio (1942).

RESULTS

The prominent absorption maxima, summarized in Table 1, persist throughout the series of compounds studied. Because of the close resemblance between the individual spectra, only a representative set is reproduced in Figs. 1 and 2. The

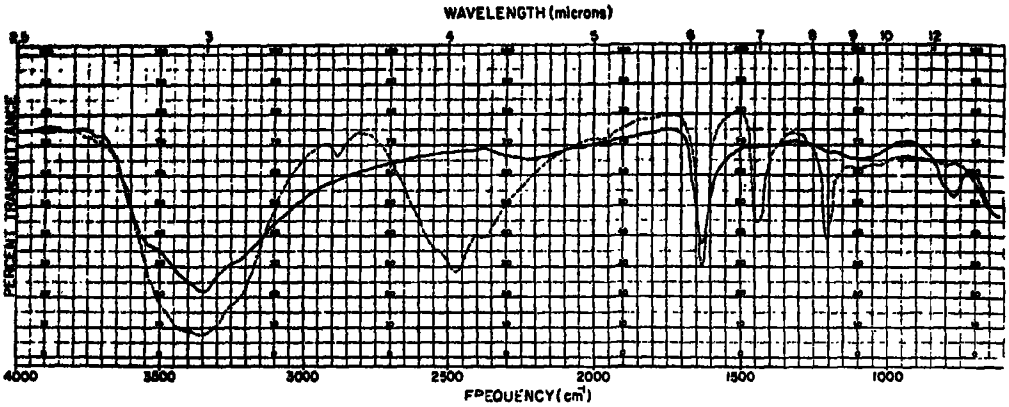

Fig. 1.—The infra-red absorption spectra of hydrated holmium trichloride: ordinary water; partially deuterated water.

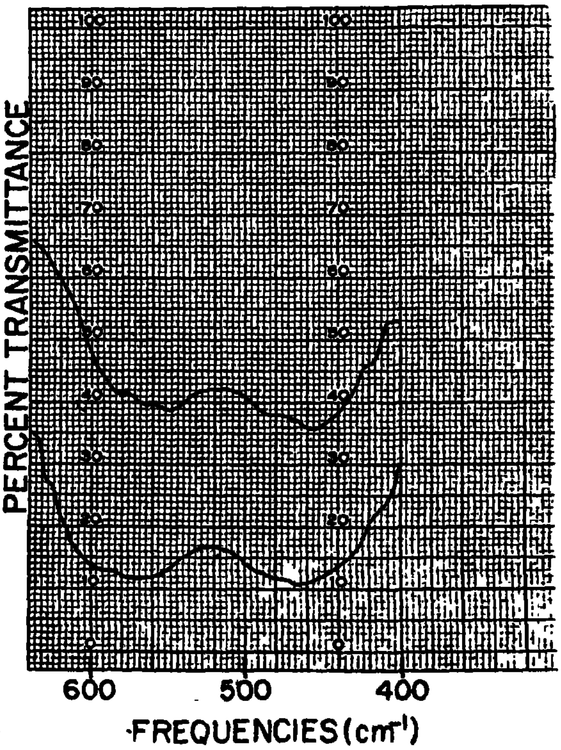

Fig. 2.—The infra-red absorption spectra of hydrated praseodymium trichloride; lower curve; ordinary water; upper curve: partially deuterated water.

bands occurring in the KBr region exhibit broader contours than those in the NaCl region with the exception of the 3340 cm^{-1} band which has an apparent half-width of about 280 cm^{-1}. The half-width of the low-frequency bands varies between 104 and 126 cm^{-1}. The poor spectral quality appears to be inherent in the nature of the material investigated rather than caused by sample preparation since both KBr disks and Nujol mulls yielded similar band envelopes and relative intensities. The frequencies appear but slightly altered, except for the absorption peak near 1090 cm^{-1} which is shifted to about 1150 cm^{-1} in the Nujol spectra of the majority of compounds investigated.

Although the gross features of the spectra recur within the series, dissimilarities as a result of the hygroscopic nature of these salts are observed. The lanthanide trichlorides form monoclinic hexahydrated crystals,(4) $[M(H_2O)_6]^{3+}$ Cl_3^-: however, the rare earth ion concentrations of our samples determined by complexometric titrations (EDTA)(5b) indicate a trihydrate of praseodymium, a nonahydrate of holmium, and hexahydrates of the remaining chlorides. In terms of cation concentration, deviations from stoichiometric ratios vary between —3·2 per cent for ytterbium and —0·43 per cent for dysprosium.

DISCUSSION

The common features of the spectra and the fact that absorptions arising from forbidden 4f electronic transitions are attenuated by many orders of magnitudes, evince that none of the prominent bands are of electronic origin.

The spectra are identified as shown in the last column of Table 1. The peak ascribed to the OH antisymmetric stretching mode occurs near 3340 cm^{-1} throughout the series, indicating moderately strong hydrogen bonding of 5–6 kcal per mole.(5a) On the basis of an empirical relation between the OH stretching frequency and known interatomic distances,(6) the hydrogenbonded O–Cl distance, O–H · · · Cl, is estimated to be about 3·07 Å. This value agrees reasonably well with the interatomic distances O–H · · · Cl of 3·14 to 3·24 Å derived from X-ray diffraction analyses of gadolinium trichloride hexahydrate.(7) The spectra of the neodymium, gadolinium, and terbium salts are particularly intense. There the OH stretching band exhibits distinct maxima at about 3500 and 3240 cm^{-1}. In accord with similar suggestions advanced recently,(8) the former can possibly be assigned to the symmetric stretching vibration and the latter to the first overtone of the bending mode. The structure of the OD stretching band observed in the spectra of the samarium and holmium salts is interpreted analogously. Then, the high and low frequency peaks would correspond to ν_1 and to $2\nu_2$, respectively.

The well-defined band near 1620 cm^{-1} is associated with the in-plane bending mode and that near 770 cm^{-1} with an OH libration about an axis perpendicular to the symmetry axis. Spectroscopic investigations of ice,(8) hydrated aluminium chloride,(9) and silicates and phosphates,(10) for instance, corroborate this assignment.

(4) A. Pabst, *Amer. J. Science*, **222**, 426 (1931).

(5) (a) R. M. Badger, *J. Chem. Phys.* **8**, 288 (1940); (b) J. S. Fritz, R. T. Oliver and D. J. Pietrzyk, *Analyt. Chem.* **30**, 1111 (1958).

(6) O. Glemser and E. Hartert, *Naturwissenschaften*, **42**, 534 (1955).

(7) M. Marezio, H. A. Plettinger and W. H. Zachariasen, *Acta Cryst. Camb.* **14**, 234 (1961).

(8) D. F. Hornig, H. F. White and F. P. Reding, *Spectrochim. Acta* **12**, 338 (1958).

(9) E. Hartert and O. Glemser, *Z. Elektrochem.* **60**, 746 (1956).

(10) Ya I. Ryskin and G. P. Stavitskaya, *Opt. and Spectrosc.* **8**, 320 (1960).

TABLE 1.—ABSORPTION BANDS OF HYDRATED LANTHANIDE TRICHLORIDES

Ce	Pr	Pr**	Nd	Nd**	Sm	Sm**	Eu	Assignments	
			$\left.\begin{array}{l}3484\\3348\\3218\end{array}\right\}$ *vs*					ν_1	$OH\sigma_s$
3343 *vs**	3323 *vs*, *bd*	3390 *vs*		3370 *vs*	3338 *vs*	3330 *vs*	3347 *vs*, *bd*	ν_3	$OH\sigma_a$
3230 *sh*								$2\nu_2$	
				2865 *w*					
		2500 *s*		2495 *m*		2455 *vs*, *bd*		ν_3	$OD\sigma_a$
						2372 *vs*		$2\nu_2$	
2205 *w*, *bd*	2180 *m*		2205 *m*		2205 *w*		2215 *m*	$\nu_2+\nu_L$	
						1960 *w*			
1613 *s*	1614 *vs*	1615 *s*	1621 *s*	1617 *m*	1622 *s*	1632 *m*	1624 *s*	ν_2	$HOH\delta$
		1418 *s*		1413 *w*				ν_2	$HOD\delta$
		1190 *w*		1195 *w*		1202 *vs*		ν_2	$DOD\delta$
1048 *w*, *bd*	1078 *m*	1090 *w*	1088 *m*		1098 *m*	1015 *w*	1089 *w*	$\nu_L+\nu_T$	
740 *vs*†	723 *m*	550 *m*	750 *vs*	568 *s*	760 *s*‡	578 *m*	761 *m*	ν_L	OH, OD L
680 *vs*†			687 *vs*		693 *s*‡		697 *m*	ν_L	OH L
578 *s*	564 *vs*		567 *s*		573 *m*		577 *s*		
462 *s*	465 *vs*	455 *m*	469 *s*	474 *s*	476 *s*	460 *m*	472 *vs*, *bd*		

* Estimated intensities: *vs* = very strong, *s* = strong, *m* = medium, *w* = weak, *bd* = broad, *sh* = shoulder.

† Observed in Nujol spectra only.

‡ Not observed in anhydrous salt.

** Partially deuterated salts.

TABLE 1 (*continued*).—ABSORPTION BANDS OF HYDRATED LANTHANIDE TRICHLORIDES

Gd	Dy	Tb	Ho	Ho**	Er	Tm	Yb	Assignments	
3517		3542			3484 *sh*			v_1	OHσ_s
3333 } *vs*	3333 *vs, bd*	3347 } *vs, bd*	3343 *s, bd*	3350 *vs*	3346 *vs, bd*	3346 *vs, bd*	3341 *vs, bd*	v_3	OHσ_a
3248		3238				3240 *sh*	3238 *sh*	$2v_2$	
				2875 *w*					
				2530				v_1	ODσ_s
				2468 } *s*				v_3	ODσ_a
				2375				$2v_2$	
2217 *w*	2220 *m*	2225 *m*	2225 *w, bd*		2215 *m, bd*	2230 *m, bd*	2223 *m*	v_2+v_L	
2040 *w*						2050 *w*	2030 *w*		
1625 *vs*	1625 *s*	1626 *s*	1628 *m*	1624 *s*	1627 *s*	1623 *s*	1623 *s*	v_2	HOHδ
				1438 *s*				v_2	HODδ
				1199 *s*				v_2	DODδ
1109 *w, bd*	1100 *m*	1086 *m*	1083 *w, bd*		1088 *m, bd*	1083 *m*	1083 *m, bd*	v_L+v_T	
			805 *w*		815 *m*				
767 *s*	772 *s*	770 *s*	770 *m*		760 *s*	780 *m, bd*	775 *s*$^{\Delta}$	v_L	OH, OD L
			714 *m*†						
700 *s*	693 *m*	700 *w*	698 *m*†				710 *s*$^{\Delta}$	v_L	OH L
583 *vs*	596 *s*	592 *vs*	605 *m*	602 *vs*	615 *vs*	607 *w*	607 *m*		
475 *s, bd*	479 *s, bd*	467 *s*	468 *s*	483 *vs*	477 *s*	478 *m, bd*	483 *s*		

** Partially deuterated salts.

† Observed in Nujol spectra only.

Δ Not observed in one of the samples.

The spectra of the deuterated salts demonstrate the expected isotopic frequency shifts (*R_D* ~ 1·32). A band near 690 cm^{-1} which appears in some of the spectra may likewise be identified as a librational mode.⁽⁸⁾

Undoubtedly, the low-frequency maxima are associated also with the water of hydration, but the deuteration studies did not clarify their identification. Presumably, displacements of the oxygen atoms of the octahedral complex [$M(OH_2)_6$] contribute largely to these absorptions.⁽¹¹⁾

The summation band near 2220 cm^{-1} is tentatively ascribed to a combination of the bending mode near 1620 cm^{-1} with a band near 600 cm^{-1}, observed throughout the series, rather than to the second overtone of a librational mode.⁽⁸⁾ The peak at about 1090 cm^{-1} is probably a combination of the libration band near 770 cm^{-1} with a calculated band at about 320 cm^{-1}, characteristic of the octahedral complex.⁽¹¹⁾

Acknowledgement—The authors are grateful to E. SMATHERS for her assistance in the preparation of the lanthanide trichlorides and F. B. STEPHENS for the analyses of these compounds.

(11) R. LAFONT, *Ann. Phys.* **4**, 905 (1959).

J. Inorg. Nucl. Chem., 1962, Vol. 24, pp. 245 to 256. Pergamon Press Ltd. Printed in England

INFRA-RED SPECTRA OF NITRATE SALTS IN TRIBUTYL PHOSPHATE SOLUTION*

L. I. Katzin†
Chemistry Division, A.E.R.E., Harwell, Berks.‡

(*Received* 24 *January* 1961)

Abstract—The infra-red spectra of some sixteen nitrates are observed in tributyl phosphate solvent. The splitting of the ν_3 band of the nitrate ion is followed in particular. The findings are shown to be consistent with the concept that in general in these solutions a co-ordinate bond is formed between the anion and the metallic cation. The exceptions are pointed out, and it is established that a splitting of about 100 cm^{-1} serves as a defensible division between essentially electrostatic splitting (lower) and splitting due to co-ordinate binding (higher). The correlation between the tributyl phosphate spectra and the vibrational spectra in the solid crystals is pointed out, and with it the apparent fact that even in the conventionally ionic crystals the interaction with the cation is sufficient to modify the vibrational pattern to that of the co-ordinately bound ligand.

Details of the nature and the characteristics of the interaction between cations and anions have always been vague. Part of the difficulty has been due to the barrier of the classical theoretical conception of the interaction as a purely electrostatic one, between point charges. Part of the difficulty has come because most studies have been conducted in water, with its special ionizing and solvating characteristics. Use of semipolar solvents of low dielectric constant (e.g., alcohols) has made it possible to demonstrate characteristic alterations of the absorption spectrum of nitrate ion(1) and of other anions, including the monatomic halides,(2, 3) due to interaction with cations.

The theoretical interpretations of the infra-red spectra of many polyatomic groupings have been worked out. In particular, the infra-red spectrum of nitrate ion in dilute aqueous solution has been related to the vibrations of the planar triangular configuration.(4) The infra-red spectra of substances like methyl nitrate, in which the nitrato group is tightly bonded to carbon, have also been observed and analysed.(5) There exists therefore a standard to which interpretations of infra-red spectra found for nitrates can be referred.

One or two surveys of infra-red spectra of solid nitrates for analytical and identification purposes have been made,(6) and a few solids have been looked at for alterations in the nitrate spectrum, some reports appearing since this work was completed.(7-11) In relatively few cases have the infra-red spectra of nitrate salts in nonaqueous solution been looked at.(12-14) The observations to be reported in this paper make systematic use of the relative ease of solution of nitrate salts in organic solvents, particularly the alkyl phosphates, exemplified in tri-n-butyl phosphate (TBP). Observations have been made on some sixteen nitrates of interest which are sufficiently soluble in this medium. Observations are also reported on the spectra of some of these nitrates in other media, for comparison. Some conclusions of theoretical interest will be pointed out, making supplemental use of the literature data on Raman spectra.

---

* Based on Report AERE-R 3031 (Aug., 1959).

† Permanent address: Argonne National Laboratory, 9700 South Cass Avenue, Argonne, Illinois.

‡ Exchange Research Scientist at A.E.R.E., 1958–59.

(1) L. I. Katzin, *J. Chem. Phys.* **18**, 789 (1950).

(2) L. I. Katzin, *J. Chem. Phys.* **20**, 1165 (1952).

(3) L. I. Katzin, *J. Chem. Phys.* **23**, 2055 (1955).

(4) G. Herzberg, *Infra-red and Raman Spectra.* Van Nostrand, New York (1945).

(5) J. C. D. Brand and T. M. Cawthon, *J. Amer. Chem. Soc.* **77**, 319 (1955).

(6) F. A. Miller and C. H. Wilkins, *Analyt. Chem.* **24**, 1253 (1952).

EXPERIMENTAL

After some preliminary trials with NaCl-plates, thin films of solution between plates of CaF_2 were used, permitting observation down to ca. 950 cm^{-1}.* The instrument used was the Hilger double-beam infra-red spectrophotometer, model H80D. A single plate of CaF_2 was used in the reference light beam. Wavelength calibration was against the spectrum of a polystyrene film.(15) After the frequencies of the essentially invariant carbon skeletal peaks of the organic medium were well established, these could be used for internal frequency standard for the nitrate peaks. Frequency accuracy is on the order of ±1–2 cm^{-1}. I am deeply indebted to Mr. A. M. DEANE for technical advice on the measurements.

RESULTS

The vibration frequencies agreed for the nitrate ion in dilute aqueous solution(4) are the symmetrical stretching, 1050 cm^{-1}, the out-of-plane vibration (deformation) of the nitrogen atom, 831 cm^{-1}, and the asymmetric stretch and planar rock, 1390 and 720 cm^{-1}. The last two, generally identified as υ_3 and υ_4, are doubly degenerate. The symmetrical stretch (υ_1) is the principal line of the Raman spectrum. In principle it is not to be seen in the infra-red spectrum, and in our system would be lost in the P–O–C absorptions of the phosphate. The strongest line of the infra-red spectrum is υ_3, which is relatively broad.

As can be seen in Table 1, where the new data for nitrates in solution are compiled, the υ_3 band is split into two in all cases, even for lithium nitrate. The nominal single peak has only been found as an artefact when rocksalt plates are used. If the corresponding chloride of the cation in solution is at all soluble, reaction with the rocksalt takes place which gives a strong $NaNO_3$ peak around 1360 cm^{-1}. Weak additional peaks are also usually shown at 835 and at 1790 cm^{-1}. The first is the sodium nitrate υ_2 and the latter a combination band (υ_1 and υ_4). A similar behaviour has been noted with hydrated nitrates in Nujol mulls,(8, 10) and may constitute a source of error in earlier work, as in the survey of MILLER and WILKINS.(6)

---

*BaF_2 (1·5mm) has good transmission through the NaCl region, but etches, as it is about 100 times as soluble as CaF_2, and many cations complex fluoride. A thin coating of CaF_2 on BaF_2 proves only partially satisfactory for work below 950 cm^{-1}.

(7) B. M. GATEHOUSE, S. E. LIVINGSTONE and R. N. NYHOLM, *J. Chem. Soc.* 4222 (1957).

(8) B. M. GATEHOUSE and A. E. COMYNS, *J. Chem. Soc.* 3965 (1958).

(9) C. C. ADDISON and B. M. GATEHOUSE, *Chem. and Industr.* 464 (1958).

(10) J. G. ALLPRESS and A. N. HAMBLY, *Austral. J. Chem.* 12, 569 (1959).

(11) F. VRATNY, *Appl. Spectrosc.* 13, 59 (1959).

(12) L. L. BURGER and R. H. MOORE, U.S.A.E.C. Report HW–18260 (1955).

(13) YA. I. RYSKIN, *Optiki i spektroskopiya*, 6, 113 (1959).

(14) J. R. FERRARO, *J. Inorg. Nucl. Chem.* 10, 319 (1959).

(15) E. K. PLYLER, L. R. BLAINE and M. NOWAK, *J. Research Natl. Bur. Standards*, 58, 195 (1957).

Allowing for the fact that in some instances exact frequency assignment of peaks is complicated by interference from solvent peaks, it is still clear that although there may be strong resemblances between the effects of chemically related cations, the alterations of the nitrate spectrum are on the whole individual, and do not just represent one, two or three spectra. The intensity ratios of the peaks are difficult to assign, because of the complications of the solvent interferences, and variable broadening. The impression is obtained, however, that the intensities are crudely equal for lithium nitrate, that for slightly greater splittings the lower-frequency band is more intense than is the higher, and that for the highest splittings, the two bands may be equal in intensity, and in some cases the higher-frequency band may be slightly stronger. The columns of Table 1 have been arranged to accentuate the observation that when the lower-frequency band is above 1300 cm^{-1} the higher-frequency band is generally below 1450 cm^{-1}, whereas with lower-band frequencies in the range 1270–1300 cm^{-1} the upper band ranges from 1460 to 1550 cm^{-1}. Occasionally, in addition to the high-frequency member of the split υ_3 band there are seen shoulders or other indications of another absorption frequency. Sometimes, in different preparations, the roles of main peak and shoulder seem to be reversed. These may be indications of a chemical equilibrium involving more than one environment for a nitrate group.

Some salts, principally those whose chlorides are rather insoluble in the phosphate, showed no differences in the nitrate spectra above 950 cm^{-1} between measurements on fluorite and on rocksalt plates. For these, peaks appearing below 950 cm^{-1} in the rocksalt plate observations are taken to be peaks belonging to the nitrate in solution. Where such appeared, they are listed in Table 1. The absence of such peaks for a given salt may mean that they were not seen, or that because of reaction on the rocksalt, no statement can be made as to their presence or absence. For uranyl nitrate and ferric nitrate, some measurements were made on BaF_2 partially protected by evaporated coatings of CaF_2. These plates had transmittance useful over the entire rocksalt region, but allowance had to be made for $Ba(NO_3)_2$ lines at 1350 and 1406 cm^{-1} (lines at lower frequencies were not seen).

Combination frequency peaks are sometimes seen above 1600 cm^{-1}. It is not certain whether the characteristic 1660 cm^{-1} peak of magnesium nitrate is a nitrate absorption or an unusual water peak.(16) Occasional small peaks at about 1714 cm^{-1} are open to the suspicion that they represent traces of acetone accidentally present. Thorium and uranyl nitrates show small peaks near 1028 cm^{-1} in the nonphosphate solvents, where this region is viewable, and ferric nitrate shows one at about 943 cm^{-1} in dibutyl carbitol. This last could be an HNO_3 peak, if hydrolysis is significant in this solvent. The strong P–O–C band of the phosphate in the 1000 cm^{-1} region does not allow a systematic check at these frequencies with the tributyl phosphate solutions.

DISCUSSION

In their analysis of the vibrational spectrum of methyl nitrate,(5) Brand and Cawthon reported nitrate frequencies 1672 (*vs*) (N–O asymmetrical stretch), 1287 (*s*) (symmetrical N–O stretch), 854, 759, 657 and 578 cm^{-1}. (Other nitrate esters show similar frequencies.(17)) If this is taken as the exemplar of a "truly" co-ordinately bound nitrate, it bears some resemblances to the sort of spectra reported above, but also shows some marked differences. The pair of N–O stretch peaks resemble some of those in Table 1. The symmetrical stretch has a frequency which is very like that of a number of the nitrates in Table 1, but in our data it is associated with quite a range of higher-frequency peaks attributable to the asymmetric stretch. Some of these are lower by about 200 cm^{-1} than methyl nitrate's 1672 cm^{-1}, and none is closer than about 120 cm^{-1}. Further, the nitrate salts show a persistence of frequencies related to the nitrate ion symmetrical stretch, with the infra-red 1028 cm^{-1} of the thorium and uranyl nitrates in methylisobutyl ketone and in dibutyl carbitol, and the considerable body of data from Raman spectral investigations (see below).

---

(16) L. I. Katzin. *J. Inorg. Nucl. Chem.* **20**. 300 (1961)

(17) J. F. Brown, Jr., *J. Amer. Chem. Soc.* **77**, 6341 (1955).

Table 1.—Observed nitrate infra-red spectra in solutions

System*	Vibrational frequencies								
$LiNO_3$—TBP		828			1329	1394			
$Mg(NO_3)_2$—TBP		829			1310	1400			1660 1709
$Ca(NO_3)_2$—TBP		825			1315	1442			
$Co(NO_3)_2$—TBP				(~ 1290?)†				1502	
$Ni(NO_3)_2$—TBP				(~ 1290?)†				1503	1705?
$Cu(NO_3)_2$—TBP				1285			1495	1543	
—Hexone				1290			1500		
—DBC				1290			1500		
$Zn(NO_3)_2$—TBP				1287			1497		1713
$Cd(NO_3)_2$—TBP				1293			1463		~ 1710
$Fe(NO_3)_3$—TBP				1273		??		1549	
—Hexone				1296				1555	
—DBC		815	943**	1293				1551	
$Cr(NO_3)_3$(v)—TBP				(1290?)		1450			1714
$Cr(NO_3)_3$(gr)TBP				1281				1508	
$La(NO_3)_3$—TBP	733	818		1293	1306		1482		1716
$Ce(NO_3)_3$—TBP	732	822		1290			1490	(1512)	1729 1757
$Ce(NO_3)_4$—TBP‡				1279				1514	1714
$Th(NO_3)_4$—TBP				1299	(1318)			1514 (1548)	1621, 1667 1715, 1773
—Hexone			1027	1287				1531	
—DBC			1029	1290				1528	
$UO_2(NO_3)_2$—TBP	740	812		1282				1524	1617 1720
—Hexone			1028	1278				1531	
—DBC	739	804	1026	1280				1531	

* Hydrated salts were used in preparing the solutions, and a second aqueous phase generally formed which was separated off, together with undissolved solid.

TBP = tributyl phosphate
Hexone = methyl isobutyl ketone
DBT = dibutyl "carbitol" (dibutyl ether of di-ethylene glycol).

† Concentration low, peak may be lost on P–O peak.

‡ Leached from $(NH_4)_2Ce(NO_3)_6$.

** May be HNO_3 frequency.

For many, if not all, of the nitrates concerned, there is chemical and ultraviolet absorption spectral evidence(1) that the anions are co-ordinately bound (as distinguished from being held purely electrostatically) to the cations. It seems necessary therefore to recognize that there are differences in the total effects of two or more examples in both of which good electron-sharing bonds are formed. This could correspond perhaps to what the theoreticist means when he calculates "percentage electrostatic character" of a bond, though the author hesitates to use this terminology because of the connotations of the term electrostatic. In a descriptive sense one might perhaps talk of the *elasticity* of a bond. In methyl nitrate, the carbon-oxygen bond is *inelastic*, relative to the O–N bond, in this sense, and the result is loss of the vibratory character of the nitrate group as such. Hydrolysis of organic nitrates gives no uniform trend—in some instances the nitrate takes the ester oxygen with it, in some instances it may not.(18) With the usual labile sort of inorganic nitrate, there is no question of scission of the nitrate group. In the metal nitrates, the bonding of the oxygen by the metal atom is more *elastic*, and the character of the nitrate group can manifest itself, though obviously distorted in detail. From this view it is not surprising that the *nitrato* symmetrical N–O stretching frequency (not to be confused with the nitrate symmetrical stretch at 1050 cm^{-1}) should for many salts approximate that of methyl nitrate, while the asymmetrical stretch, involving the relative movement of the nitrogen and the oxygen bound to an external atom, and therefore sensitive to the elasticity of that bond, should be highly variable and fall far short of the limit set in methyl nitrate. The Raman spectrum of nitric acid(19) shows a vibrational peak at 1680 cm^{-1}, resembling methyl nitrate, but also shows a peak at 1538 cm^{-1}, similar to many of the nitrates in our work, and a peak at 1301 cm^{-1}. The retention of something like the symmetrical stretch frequency of the nitrate in salts and its apparent loss by the organic nitrate then follow reasonably from the difference in "elasticity". It may be noted that in the nitric acid spectrum(19) the 1050 cm^{-1} vibration is replaced by one at 926 cm^{-1}. This is the reason for suspecting the 943 cm^{-1} absorption for ferric nitrate in dibutyl carbitol to be an indication of hydrolysis.

A conclusion of this argument is that one may expect considerable gradation in elasticity of the bond to the metal ion, and therefore a corresponding gradation in the effect on the nitrate ion. There is thus no *a priori* criterion for a decision on which splitting of the 1390 cm^{-1} nitrate ion vibration represents the largest one due purely to asymmetry of the external electrical field, and which represents the smallest splitting due to an elastic co-ordinate bond. One must therefore develop a criterion empirically.

The co-ordination number of lithium, in the lithium nitrate solutions in tributyl phosphate, is probably four. From observations of the water absorption peaks in the solutions,(16) and chemical evidence,(20) it is concluded that there are probably two molecules of water and two of tributyl phosphate in the co-ordination sphere, filling it. One may take it tentatively, therefore, that in this instance the nitrate is held electrostatically, and that the splitting found (65 cm^{-1}) is characteristic only of the effect of electrical asymmetry. Magnesium nitrate(16) also brings water into the solution, but the co-ordination number may be six, and one cannot say certainly whether or not the nitrate is in the co-ordination sphere. The splitting is somewhat larger, 90 cm^{-1}. For calcium nitrate the splitting is over 125 cm^{-1}, and chemical evidence(16, 20) suggests that nitrate is in the co-ordination sphere, as the species in solution is probably not hydrated. Nickelous nitrate also takes water into the tributyl phosphate,(16) but in this instance the peak splitting is near maximal. The nickel co-ordination number may more certainly be six than it is in the case of

(18) M. Anbar, I. Dostrovsky, D. Samuel and A. D. Yoffe, *J. Chem. Soc.* 3603 (1954).

(19) T. F. Young, L. F. Maranville and H. M. Smith, *The Structure of Electrolytic Solutions* (Edited by W. J. Hamer), p. 35. J. Wiley, New York (1959).

(20) T. V. Healy and P. E. Brown, AERE Report C/R 1970 (1956).

magnesium, but chemical evidence for a difference in nitrate co-ordination between them is lacking. They could therefore both be instances of co-ordinated nitrate. One may therefore tentatively say that splittings between 65 cm^{-1} (lithium nitrate) and 125 cm^{-1} (calcium nitrate) cannot yet be certainly assigned, but that below this region they almost certainly represent electrostatic or second-sphere effects, and that above this value we are undoubtedly dealing with the effects of co-ordinate bonding.

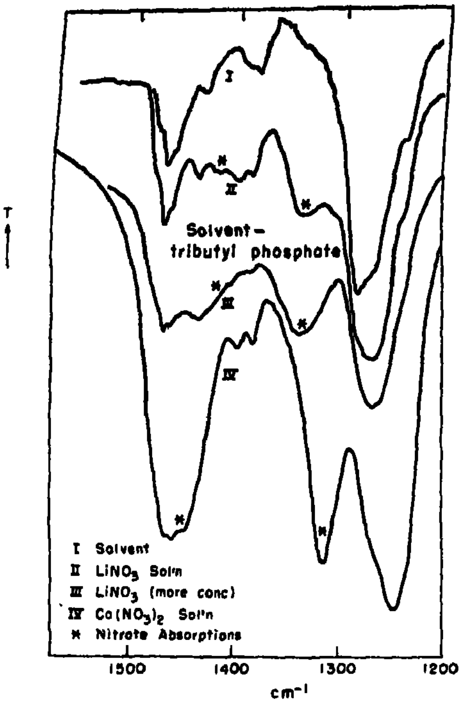

FIG. 1.—Transmission curves of $LiNO_3$ and $Ca(NO_3)_2$ solutions in tributyl phosphate, to illustrate small splittings of the band of the nitrate group.

MATHIEU and LOUNSBURY,[21] from Raman spectral studies on nitrates, have laid stress on the apparent splitting of the 720 cm^{-1} (υ_4) vibration. They believe that their analysis of splitting dependence on solution concentration gives evidence for transition to a single second form of nitrate. If one simply takes this "second form" to represent co-ordinated nitrate, as distinguished from ionic nitrate, the dilemma presented by the splitting of the υ_3 band is not resolved. In their results the splitting can be seen when the υ_3 band shows no splitting, or only a minimal splitting, and no simple correlation is evident. The appearance of a second component in the vicinity of the 1050 cm^{-1} υ_1 vibration, observed in the Raman work, also fails to be diagnostic, as it is seen in the infra-red absorption with uranyl nitrate and with thorium nitrate (hexone and dibutyl carbitol), but not with ferric nitrate or cupric nitrate. In the Raman studies, the second component is quite prominent with copper nitrate. From the infra-red spectra, all four nitrates would be judged rather similar.

---

[21] J. P. MATHIEU and M. LOUNSBURY, *Dis. Faraday Soc.* **9**, 196 (1950).

TABLE 2.—SUMMARY OF DATA AND LITERATURE ON NITRATE PEAKS

	Vibrational frequencies									
LiNO$_3$(TBP) Infra-red		828			1330		1395			
·3H$_2$O(21) Raman	717		1054		1332		1416			
·3H$_2$O(26) Raman			1061		1336		1417			
NH$_4$NO$_3$ (cryst)(6) Infra-red		830*w*			1340		1390			1630*w* 1740*w*
(cryst)(26) Raman			1050		1354					
Mg(NO$_3$)$_2$(TBP) Infra-red		829			1310		1400			1660 1709
(sat. aq.)(24) Raman			1052		1346		1427			
·2H$_2$O(26) Raman			1064		1352		1431			
·6H$_2$O(26) Raman			1063		1355		1428			
Ca(NO$_3$)$_2$ (TBP) Infra-red		825			1315		1442			
·4H$_2$O(21) Raman	721		1052		1354		1424			
·4H$_2$O(26) Raman			1052		1353		1422			
Ca(NO$_3$)$_2$(6) Infra-red		820*w*	1044*w*		1350		1430			1640
(sat. aq.)(24) Raman	717 742		1052		1346		1439			
(16N aq.)(21) Raman	716 746		1050		1358		1428			
Ba(NO$_3$)$_2$ Infra-red	731	823			1355		1425			
Co(NO$_3$)$_2$ (TBP) Infra-red				(~1290?)		(1385?)			1502	
·6H$_2$O(25) Infra-red		807*vw* 836*w*				1372				
Co(NO$_3$)$_2$(25) Infra-red	799 762 792					1366				
Ni(NO$_3$)$_2$ (TBP) Infra-red				(~1290?)		(1385?)			1504	1705?
·6H$_2$O(25) Infra-red		837	1048*w*			1383				
Cu(NO$_3$)$_2$ (anhyd)(25) Infra-red	770 781		1016	(1264) (1289)					1546 1565	
Cu(NO$_3$)$_2$ (TBP) Infra-red				1285				1495	1543	
(sat. aq.)(21) Raman	719 757	1024	1048		1315		1405	1480		
·9H$_2$O(21) Raman	720 755	1020	1047	1284	1325		1381	1440	1498	
·3H$_2$O(6) Infra-red		836				1378*vs*			1587	1790

---

(24) A. SILVEIRA and E. BAUER, *C.R. Acad. Sci., Paris*, 195, 416 (1932).

(25) B. M. GATEHOUSE. These On Air for University (1957).

(26) O. THEIMER, *Monatsh.* 81, 301 (1950).

TABLE 2 (*continued*).

$Cu(NO_3)_2$ *cont.*	Vibrational frequencies									
(Hexone) Infra-red				1290					1500	
(DBC)				1290±					1500±	
$Zn(NO_3)_2$ (TBP) Infra-red				1287				1497		1713
(conc. aq.)(21) Raman	719		1050		1340		1408			
$\cdot 6H_2O$(21) Raman	710–20		1053		1350		1370			
$\cdot 6H_2O$(25) Infra-red		835				1377				
(anhyd)(25) Infra-red	763	793 800	1040	1299					1546	
$\cdot 6H_2O$(26) Raman			1051		1333					
$Co(NO_3)_2$ (TBP) Infra-red				1293				1466		~ 1710
$\cdot 4H_2O$(25) Infra-red		834				1370		1463		
$\cdot 4H_2O$(26) Raman			1054		1357		1435			
(anhyd)(25) Infra-red	751*m*	802*w*	1028*w*		1348		1376			
(anhyd)(26) Raman			1073		1379		1403			
$Fe(NO_3)_3$ (TBP) Infra-red				1273			??		1549	
(hexone) Infra-red				1296					1555	
(DBC) Infra-red				1293					1551	
$\cdot 9H_2O$(6) Infra-red		835*w*				1361				1685
$Cr(NO_3)_3$ (violet)(TBP) Infra-red				(1290?)			1450			1785
$Cr(NO_3)_3$ (green)(TBP) Infra-red				1281					1508	1714
$La(NO_3)_3$ (TBP) Infra-red	733	818		1293	1306			1482		1716
$Ce(NO_3)_3$ (TBP) Infra-red	732	822		1290				1490	(1512)	1729
(aq. sat.)(21) Raman	714 741		1047(22)		1348			1468		1757
$\cdot 6H_2O$(13) Infra-red	735	826	1044		1330				1505	
$\cdot 6H_2O$(21) Raman	716 738		1044 1054		1353		1444			
(33% Me Et CO)(13) Infra-red	736	823	1034		1310			1488		
$Ce(NO_3)_4$ (TBP) Infra-red	740			1279					1514	1714
$K_2(Ce(NO_3)_6)$(7) Infra-red		804	1034	(1277) 1290	1387				1531	
$NH_4Ce(NO_3)_6$ sic(25) Infra-red	739	804	1032	1263						
$Th(NO_3)_4$ (TBP) Infra-red				1279 1299					1534 1560	
(Hexone) Infra-red				(1318)					1514	1621, 1667, 1715, 1773
(DBC)			1027	1287					(1548)	
(conc. aq.)(21) Raman	(716)		1029 1034	1290	(1370)				1531 1528	
$\cdot 4H_2O$(21) Raman	751 714 748		(1050) 1036					1487	1500 1543 1542	

TABLE 2 (*continued*).

	Vibrational frequencies								
$UO_2(NO_3)_2$ (TBP) Infra-red		823		1282				1524	1617 1720
(DBC) Infra-red			1026	1280				1531	
(Hex) Infra-red			1028	1278				1531	
(Hex)(12) Infra-red	746	807	1020	1268				1531	
(Ether)(12) Infra-red	747	811	1030	1274				1532	
$\cdot 2H_2O$(12) Infra-red	750*w*	803*w*	1030	1296	1389*w*			1520	
$\cdot 2H_2O$(8) Infra-red	706; (743)748	801	1026; 1044	1280	1311			1515 1547	
$\cdot 2H_2O$(10) Infra-red	752; 743, 707	803	1029	1268				1540	1605*w*
$\cdot 3H_2O$(8) Infra-red	720; 743(747)	800	1029; 1043	1284	1308			1517 1545	
$\cdot 3H_2O$(10) Infra-red	744; 751	800; 804	1032; 1045	1276; 1306				1506; 1540	
$\cdot 6H_2O$(8) Infra-red	748	803 835	1030			1366			
$\cdot 6H_2$(10) Infra-red	705	809; 788	1042; 1052	1297; 1333				1497; 1536	
$RbUO_2(NO_3)_3$(8) Infra-red	(711) 736	803	1023	1276				1536	
$NaNO_3$(22) Raman	713		1048		1340; 1354		1379 } infra- 1387 } red 1404		
$NaNO_3$(6) Infra-red		836				1358			1790
(conc. aq.)(21) Raman					1357		1410		
KNO_3 Infra-red		824				1380			1767
$AgNO_3$(6) Infra-red	733	835 803				1348			
$AgNO_3$(25) Infra-red	733	801			1362		1471		
$Sr(NO_3)_2$ (aq.)(21) Raman					1353		1423		
$\cdot 4H_2O$(26) Raman			1058		1363		1432		
I(anhyd.?)(6) nfra-red	737	815			1382		1441		1795
$Hg(NO_3)_2$; H_2O(23) Infra-red	700	806 837	1036		1375		1460		1789
$Pb(NO_3)_2$(26) Raman	731	800	1048						
$Al(NO_3)_3$ (aq.)(21) Raman	719		1050		1315		1410		
$\cdot 9H_2O$(31) Raman	730		1058		1321		1434		
			1046		1388				
$\cdot 9H_2O$(26) Raman			1056		1382		1420		

---

(22) L. COUTURE, *Ann. Phys.* 2 (12th), *5* (1947).

(23) R. B. BERNSTEIN, H. G. PARS and D. C. BLUMENTHAL, *J. Amer. Chem. Soc.* 79, 1579 (1957).

Some thought-provoking relations are to be seen if one compiles the available literature on inorganic nitrate vibration spectra, without limitation with respect to physical state, or to whether the spectrum has been obtained by Raman or by infra-red techniques (Table 2).

The only instances in which an unsplit ν_3 line is seen are the sodium and potassium nitrates, and the infra-red spectra of salts taken on rocksalt plates, for which there is a strong suspicion (see above) that one is seeing the spectrum of sodium nitrate. In fact, for most such systems, Raman spectra, generally taken in silica, show the split ν_3 band and fail to show the single band around 1370 cm^{-1} often found in the infra-red measurements. One may conclude that aside from perhaps sodium and potassium nitrates, the environment of the nitrate ion in crystals is sufficiently asymmetric to split the ν_3 vibration. The sodium and potassium nitrate crystals are known to be cubic,(27) but unfortunately the structures of most other nitrates are not known.

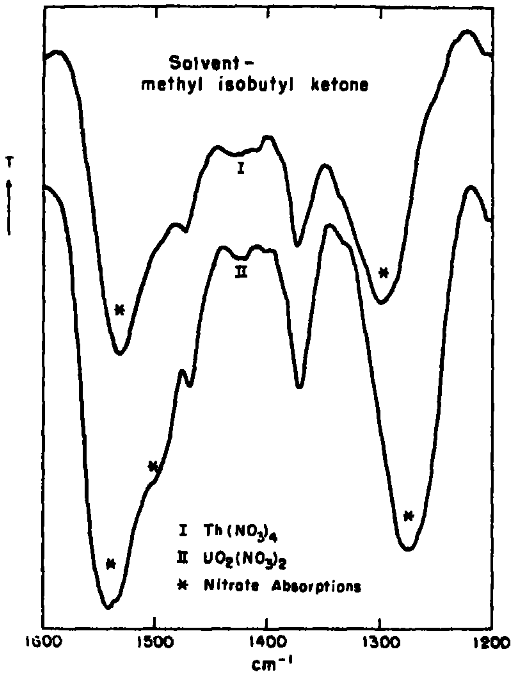

FIG. 2.—Transmission curves of $Th(NO_3)_4$ and $UO_2(NO_3)_2$ in methyl isobutyl ketone, to illustrate the large splittings of the band of the nitrate group. (Ketone spectra given to avoid the interference of the P = O vibrations in the 1200 cm^{-1} region in the tributyl phosphate solutions.)

For hydrated, crystalline lithium nitrate, the splitting and the peak wavelengths are much the same as for TBP solution. For magnesium nitrate, the splitting in the TBP solution is perhaps 10 cm^{-1} greater than that in the saturated aqueous solution, which in turn is slightly greater than that of the two hydrated solids, which are about equal. For saturated aqueous strontium nitrate the splitting is about 70 cm^{-1}, and for the solid phases it is about the same. With aluminum nitrate in saturated aqueous solution the splitting is slightly larger, 95 cm^{-1}, and (though the two sets of Raman data are not completely concordant) this is considerably reduced in the hydrated solid. The saturated aqueous calcium nitrate and the solid phases show a definite reduction from the TBP solution, down to less than 95 cm^{-1}. These relations are consistent with the limits suggested before—a dissymmetry splitting of 70 cm^{-1} or less for ions related only by electrostatic forces, and an uncertain region of 70–100 cm^{-1}. The calcium nitrate in TBP is thus clearly in the co-ordinate-bonding region, as demanded by the experimental data. The situation in the aqueous solution, with splitting above 90 cm^{-1}, and for aluminum nitrate solution, splitting 95 cm^{-1}, is undefined, though the difference between the latter solution and the crystalline solid is suggestive.

---

(27) R. W. G. WYCKOFF, *Phys. Rev.* **16**, 149 (1920); D. A. EDWARDS, *Z. Krist.* **80**, 154 (1931).

Further examples of this region in Table 2 are barium nitrate (splitting 70 cm^{-1}) and silver nitrate (slightly over 100 cm^{-1}). There is an expectation in the latter that as with the silver halides there may be some component of co-ordination in the crystal structure, so that the splitting may actually reflect this. Mercuric nitrate monohydrate, however, which might perhaps also be assumed to have some co-ordinate properties, has a splitting about that of magnesium nitrate. The hexahydrated zinc nitrate and the tetrahydrated cadmium nitrate show very low splittings, even less than that of lithium nitrate. These might represent, by our criteria, ionic nitrate in nearly symmetrical crystal lattice positions.

With these exceptions, however, the largest number of entries in Table 2 show characteristically much higher splittings of ν_3, in solid states and in concentrated aqueous solutions, as well as in TBP solution. Strikingly, in most instances the maximum splittings in the solid state are not significantly different from those for the TBP solution. Metals represented are transition elements with incomplete *d*-shells, rare earths, and members of the last row of the periodic table.

Anydrous cupric nitrate is known to be blue and volatile,(28) and presumably nitrate groups are multiply co-ordinated to the copper. In the solid state the spectrum is not significantly different from that of the solution of cupric nitrate in TBP, which in turn has a ν_3 splitting not significantly greater than for the hydrated solids, or the concentrated aqueous solution. Recent structural studies show the nitrates in crystalline anhydrous $Cu(NO_3)_2$ to be largely ionic, and only fractionally covalently held.(29)

The rare-earths are poor complex-formers among cations, and the nitrate ion is considered to be a poor complexing group in general. Yet in the solid state there is indication that hydrated cerous nitrate shows splittings approaching that of the solution of cerous nitrate in tributyl phosphate, and not much short of the splittings shown by the known complexes such as green chromic nitrate, or the solid hexanitratocerate salt. In fact, the ν_3 splittings for these known complexes cannot be differentiated from the solution or the solid phase splittings of salts for which one is reasonably certain that the solid phase does not in fact contain such defined complex groupings, and for which the solid shows every normal indication of behaving as a traditional ionic lattice material. Further, the solutions, which we know contain single molecules with anions co-ordinated to cation, show almost identical splitting spectra.

---

(28) C. C. Addison and B. J. Hathaway, *Proc. Chem. Soc.* 19 (1959).

(29) S. C. Wallmark, *Proc. Chem. Soc.* 311 (1959).

That some sort of interaction may exist between anion and cation in crystals, without involving direct consideration of bonding between them, is indicated by the usefulness of ligandfield theory, which has been applied widely to the description of compounds of cations with nonbonding *d*-electrons. Thus, the easily distinguishable appearance of the fully hydrated perchlorate, nitrate and chloride of Co(II) could probably be ascribed to crystal field symmetry effects, without considering detailed differences in orbital interaction of the ions. On the other hand, even in a matrix such as MgO, a detailed analysis⁽³⁰⁾ of the paramagnetic resonance and optical absorption spectra of Ni(II) shows that some of the *d*-electrons must spend almost one-fourth their time on the surrounding oxygen atoms, rather than entirely on the Ni, a symptom of bonding. Ligand-field theory in general gracefully avoids this complication by allowing it to be absorbed into parameters which are adjusted for fit to data. However, it has not to our knowledge been pointed out previously that inter-ionic interactions in normal crystals are sufficient to affect the vibrational spectrum of complex groups such as the nitrate ion not only to an extent greater than might be expected for purely electrostatic interaction, but to an extent almost identical with that for the co-ordinately bound group in free solution. In the case of $COCl_2 \cdot 6H_2O$, it has been shown⁽³¹⁾ that the structural unit is not the $CO(H_2O)_6{}^{2+}Cl_2$ which would be anticipated, but $(COCl_2(H_2O)_4) \cdot 2H_2O$. Detailed structures on nitrates might show correlations with the degree of cation influence on spectrum.

SUMMARY

It has been shown that when a wide variety of nitrate salts are dissolved in solvents such as tributyl phosphate, the nitrate ions are largely held co-ordinately by the cation, and the infra-red vibration spectrum of the nitrate shows characteristic changes. A survey of the literature on both infra-red and Raman spectra of nitrates shows that even in the crystalline state many nitrates show alterations of the vibrational spectrum hardly distinguishable from those shown by the TBP solutions. Implications for the ion interactions both in solution and in the crystalline state are discussed.

(30) W. Low, *Ann. N.Y. Acad. Sci.* 72, 69 (1958).

(31) E. V. STROGANOV, I. I. KOZHINA and S. N. ANDREEV, *Vestnik Leningrad Univ.* 13, No. 10, *Ser. Fiz. i Khim.*, No. 2, 109–16; *Chem. Abstr.* 52, 17880 f (1958).

J. Inorg. Nucl. Chem., 1962, Vol. 24, pp. 257 to 263. Pergamon Press Ltd. Printed in England

PREPARATION AND PROPERTIES OF THE SINGLE CRYSTALLINE AB_2-TYPE SELENIDES AND TELLURIDES OF NIOBIUM, TANTALUM, MOLYBDENUM AND TUNGSTEN*

L. H. BRIXNER
Pigments Department, E. I. du Pont de Nemours & Co., Inc., Wilmington, Delaware

(*Received* 7 *August* 1961; *in revised form* 25 *September* 1961)

Abstract—The AB_2-type selenides and tellurides of niobium, tantalum, molybdenum and tungsten have been prepared in single crystalline form by means of transport reactions. Lattice parameters were determined on the basis of single crystal patterns and are given for the eight compounds. Pertinent thermoelectric parameters, such as electrical resistivity, Seebeck coefficient and thermal conductivity were measured on compacted polycrystalline aggregates and are given together with the calculated "Figure of Merit".

THE recent resurgence of interest in the phenomenon of thermoelectricity has initiated a rather detailed study of practically all metal tellurides and selenides from lithium to uranium. It appeared that the group Va and VIa compounds, particularly those of niobium, tantalum, molybdenum and tungsten, had been somewhat neglected during these investigations. The reason for this may be the fact that the selenides and tellurides of these metals thermally dissociate rather than melt and therefore pose a problem with regard to the preparation of single crystalline material. It is probably for this same reason that the structural parameters of only four of the eight compounds have been reported in the literature. Only the X-ray work on WTe_2 was based on a single crystal, which was found by KNOP and HARALDSEN(1) in an otherwise polycrystalline reaction product. Crystallographic parameters have also been reported for WSe_2 by GLEMSER *et al.*(2): for $TaTe_2$ by UKRAINSKII *et al* (3): and for $MoTe_2$ by PUOTINEN and NEWNHAM(4). $MoSe_2$ has been described by WENDEHORST(5), $TaSe_2$ by ARIYA(6) and an undefined niobium selenide was mentioned by BOLTON (7). Electrical properties have only been investigated for the Ta/Te system by UKRAINSKII *et al.* It was therefore our intention to attempt the preparation of all eight compounds in single crystalline form and to determine their structural and electrical properties.

* Parts of this Paper have been presented at the XVIIIth International Congress of Pure and Applied Chemistry at Montreal, Canada.

(1) O. KNOP and H. HARALDSEN, *Canad. J. Chem.* 34, 1142–45 (1956).

(2) O. GLEMSER, H. SAUER and P. KÖNIG, *Z. Anorg. Chem.* 257, 241–46 (1948).

(3) YU. M. UKRAINSKII, L. M. KOVBA, YU. P. SIMANON and A. V. NOVOSELOVA, *Russian J. Inorg. Chem.* 4, 1305–6 (1959).

(4) D. PUOTINEN and R. E. NEWNHAM, *Acta Cryst.* 14, 691–2 (1961).

(5) E. WENDEHORST, *Z. Anorg. Chem.* 173, 268–72 (1928).

(6) S. M. ARIYA, A. I. ZASLAVSKII and I. I. MATVEEVA, *Zh. Obsch. Khim.* 26, 2373 (1956).

(7) W. VON BOLTON, *Z. Elektrochem.* 15, 145–49 (1907).

EXPERIMENTAL

1. *Preparation and analysis*

The standard experimental technique for the preparation of all polycrystalline compounds was to seal the constituent elements, weighed to the nearest milligram, into a quartz ampoule, 15 mm diameter, 20 cm long, under a vacuum of ~10^{-5} mm Hg. The compounds were of the best commercially available purity, usually 99·9%+ and were not given any special purification treatment prior to the reaction. Charges of about 20 g were fired at 600–700°C for 10–15 hr, after which time usually a black-looking, free-flowing reaction product was obtained that could be remixed easily inside the quartz tube by shaking. A second firing at 1000–1200°C for another 10–15 hr assured completeness of the reaction and a homogeneous polycrystalline product of grey metallic lustre was obtained.

For the preparation of single crystalline material a portion (about 5–10 g) of this primary reaction product was again charged into a quartz tube together with about 1–3 mg of iodine in the case of Nb, Ta and W, or bromine in the case of Mo. No transport of $MoTe_2$ was observed when iodine was used. Bromine, however, was successfully used for the transport of all compounds. The quartz tube was placed into a double wound 1 in. diameter furnace. With one end at 900°C, the other at 700°C, transport proceeded from the hot to the cold end according to the probable reaction:

$$NbTe_{2(s)}+5/2\ I_{2(g)} \rightleftharpoons NbI_{5(g)}+2\ Te_{(g)}$$

This is in concordance with the experience of SCHAFER⁽⁸⁾, who transported CrTe via $CrTe + I_2 \longrightarrow CrI_2 + 0{\cdot}5\ Te_2$ over a temperature drop from 1025 to 850°C. The only metal which apparently did not form a volatile iodide, under the reaction conditions was molybdenum, and the transport with bromine probably took place via $MoBr_3$ or $MoBr_4$.

Quantities up to 10 g could be transported during some 10–15 hr. The brightly shining crystals with edges up to 5 mm usually had the shape of flat hexagonal plates. In the case of WTe_2 both needles and plates were observed. The compositional character of the transported crystals was established both by X-ray and chemical analysis. Selenium can be determined by completely oxidizing the corresponding selenide and vaporizing selenium in form of SeO_2 at about 350–400°C. This effects a rather clean separation from the remaining metal oxides. Tellutium was determined by precipitation as such with SO_2 after the corresponding telluride had been brought into solution with a mixture of HNO_3/HCl and a few drops of HF. In most cases, however, only the metals were determined: niobium and tantalum with cupferron, molybdenum by precipitation with H_2S and subsequent conversion into MoO_3, and tungsten with cinchonine. Within the analytical error, the metal content of all transported compounds agreed with theory and we shall therefore only give one typical result: Found: Ta, 53·31; Se, 47·02%. Calc. for $TaSe_2$: Ta, 53·39; Se, 46·61%.

2. *Crystallographic characterization*

X-ray powder diffraction patterns were taken with a Philips 114·6 mm diameter camera at 25°C. The samples were sealed in 0·2 mm diameter Lindemann glass capillaries and were exposed to the $K\alpha$ radiation of copper ($\lambda = 1{\cdot}5418$ Å) for between 5–8 hr. For the single crystal patterns, Weissenberg, Sauter-Schiebold and precession camera techniques were used. Densities were determined by vacuum distilling CCl_4 onto the sample contained in a 5 ml pycnometer. Table 1 summarizes some of the crystallographic data. The parameters given can be considered accurate to ±0·005 Å.

The parameters for WTe_2 had been reported earlier in the literature by KNOP and HARALDSEN⁽¹⁾, those of WSe_2 by GLEMSER *et al* ⁽²⁾, those of $MoTe_2$ by PUOTINEN and NEWNHAM⁽⁴⁾ and we are in good agreement with those data; $TaTe_2$ was reported by UKRAINSKII⁽³⁾ as orthorhombic pseudohexagonal with

$$a_o = 6{\cdot}41_5\ \text{kX};\ b_o = 10{\cdot}9_0\ \text{kX};\ c_o = 6{\cdot}68\ \text{kX}.$$

It is apparent that $a_o \times \sqrt{3}$ and b_o correspond to our a_o and our c_o is three times the value of c_o given in reference ⁽³⁾.

---

(8) H. SCHAFER and T. P. DISMUKES, *Chemische Transportreaktionen*, p. 66 (1961). Velog der Chemie, Weinheim, Bergstrasse, West Germany. We thank Prof. Schafer for the opportunity of having read the manuscript in advance of publication.

TABLE 1—PARAMETERS, SPACE GROUPS, AND DENSITIES OF THE INVESTIGATED SINGLE CRYSTALLINE AB_2 (A=Nb, Ta, Mo, W; B=Se, Te) COMPOUNDS

Compond	a_o (Å)	b_o (Å)	c_o (Å)	p, X-ray (g·ml⁻¹)	p, Pycn. (g·ml⁻¹)	Molecule Per unit cell, Z	Unit cell Volume	Space group	Type
$NbTe_2$	10·904	—	19·888	7·62	7·6	27	2047·8	D_{3d}^5–$R\bar{3}m$	Related to $CdCl_2$
$TaTe_2$	10·904	—	20·075	9·46	9·4	27	2067·1	D_{3d}^5–$R\bar{3}m$	Related to $CdCl_2$
$MoTe_2$	3·517	—	13·949	7·80	7·7	2	149·4	D_{6h}^4–$P63/mmc$	MoS_2
WTe_2	14·028	3·495	6·270	9·49	9·4	4	307·4	D_{2h}^{13}–$Pmmn$*	Unknown
α–$NbSe_2$†	3·449	—	12·998	6·22	—	2	133·9	D_{6h}^4–$P6$	MoS_2
β–$NbSe_2$	3·439	—	25·188	6·46	6·3	4	258·0	D_{6h}^4–$P63/mmc$	Related to MoS_2
α–$TaSe_2$	3·431	—	12·737	8·66	8·6	2	129·8	D_{6h}^4–$P63/mmc$	MoS_2
β–$TaSe_2$†	3·428	—	19·100	8·6	—	3	194·4	D_{3d}^5–$R\bar{3}m$	$CdCl_2$
$MoSe_2$	3·288	—	12·900	6·98	6·9	2	120·8	D_{6h}^4–$P63/mmc$	MoS_2
WSe_2	3·280	—	12·950	9·40	9·0	2	120·7	D_{6h}^4–$P63/mmc$	MoS_2

* Since the exact structure of WTe_2 is not known, this space group only represents the most likely one consistent with the observed systematic absences.

† These modifications were found on the basis of powder patterns; whether we are dealing with metastable high temperature modifications (obtained by quenching) or whether these compounds crystallize in polymorphic modifications is not yet established.

TABLE 2.—CRYSTALLOGRAPHIC PARAMETERS OF THE AB (A=Nb, Ta; B=Se, Te) COMPOUNDS

Compound	a_0 (Å)	c_0 (Å)	Space group
NbSe	3·437	13·030	D_{6h}^4-$P6_3/mmc$
NbTe	10·904	20·119	D_{3d}^5-$R\bar{3}m$
TaSe	3·425	12·746	D_{6h}^4-$P6_3/mmc$
TaTe	10·904	20·102	D_{3d}^5-$R\bar{3}m$

In the case of niobium and tantalum we also prepared the monochalcogenides and on the basis of powder patterns the parameters summarized in Table 2 were obtained.

It appears that the parameters of these monochalcogenides are essentially identical with those of the corresponding diselenides and ditellurides, and we may deal with a case similar to the one EHRLICH[9] observed for the TiTe/TiTe$_2$ system, where he established a continuous transition from the nickel-arsenide structure of TiTe to the cadmium iodide structure of TiTe$_2$.

Contrary to the dichalcogenides, which exhibited metallic lustre, these mono-compounds were usually black and in some cases even pyrophoric. We therefore did not investigate these compositions to the same extent as the di-compounds and even the presented parameters should only be considered as preliminary results.

3. *Electrical properties and thermal conductivity*

Since our original objective was to evaluate the title compounds as possible thermoelectric materials, we determined the pertinent parameters, namely, electrical resistivity ρ (Ω cm), SEEBECK coefficient S (μV/°C) and thermal conductivity κ (W°C^{-1} cm^{-1}) in order to be able to compute a "Figure of Merit", given by $Z = S^2\rho^{-1}\kappa^{-1}$. The samples used for the electrical measurements were bars, ¼ in. × ¼ in. × 2 in., which were cold pressed at 80,000–100,000 lb in $^{-2}$ and subsequently sintered at 600–800°C for 10–15 hr. The green densities of the as-pressed bars were usually 85–88 per cent. of the theoretical value and increased only slightly upon sintering. In one case (NbTe$_2$) it was demonstrated that hot pressing at 1000°C under inert conditions can produce specimens of greater than 98 per cent density. The samples for thermal conductivity were ¾ in. diameter × 1 in. long cylinders, pressed and prepared in the same fashion as described for the bars.

The d.c. resistivities were measured by the two-point method, using a standard 0·01 Ω resistance, a 1½ V battery as power source, and determining the potential drop with a Leeds and Northrup Type K2 Potentiometer. The surface of the bar was checked for homogeneity with a four-point probe, which indicated that there was a 5–10 per cent scatter. The resistivity measurements should therefore be considered reliable only within these limitations. Resistivities were determined at room temperature and at liquid nitrogen temperature. The data are summarized in Table 3. These data, as well as the thermal conductivity data are characteristic only of the direction in which they have been measured. This statement is necessary because later studies on solid solutions of these compounds indicated that even in the powder compacts a very pronounced anisotropy of properties, both electrical and thermal, does exist.

The Seebeck coefficient was measured with a Type K2 Potentiometer in combination with a galvanometer. Thermal EMF was generated by butting the bars between two copper blocks, turned from the same piece of stock, one of which was heated by means of a heating tape, the other, water-cooled by a coil soldered onto the block. The temperature gradient was measured by means of two thermocouples located in holes drilled to the centre of the bar immediately behind the contact faces. The data which were obtained in reference to copper and were corrected to absolute values are given together with the resistivity values in Table 3. The numbers can be considered accurate to ±10 per cent, which was the maximum scatter experienced in running S as a function of temperature.

[9] P. EHRLICH, *Z. Anorg. Chem.* **260**, 1–18 (1949).

Thermal conductivity was measured at elevated temperatures by the technique described by KINGERY(10). The test cylinder was sandwiched between two standard alumina rods of the same dimensions, which were obtained from the Norton Company and had a reported thermal conductivity over the investigated temperature range of 0·02 W°C^{-1} cm^{-1}. As soon as the thermal current was established as equal through both standards, the thermal current through the sandwiched unknown, together with the temperature difference, gave the thermal conductivity. The room temperature values were obtained by extrapolation from the lowest point of the measurement, which usually was obtained at 50–80°C. Accuracy cannot be claimed better than ±20 per cent.

The ΔT across the sample was kept between 10–20°C. The data are summarized together with the electrical parameters in Table 3.

For $NbSe_2$ the Seebeck coefficient stayed constant over the measured temperature range (25–130°C for $T_{av.}$). $NbTe_2$ changed type from p to n at an average temperature of about 80°C and the Seebeck coefficient increased from this temperature on. We therefore measured all three properties (S, ρ, κ) for $NbTe_2$ as a function of temperature and the results are represented by Fig. 1.

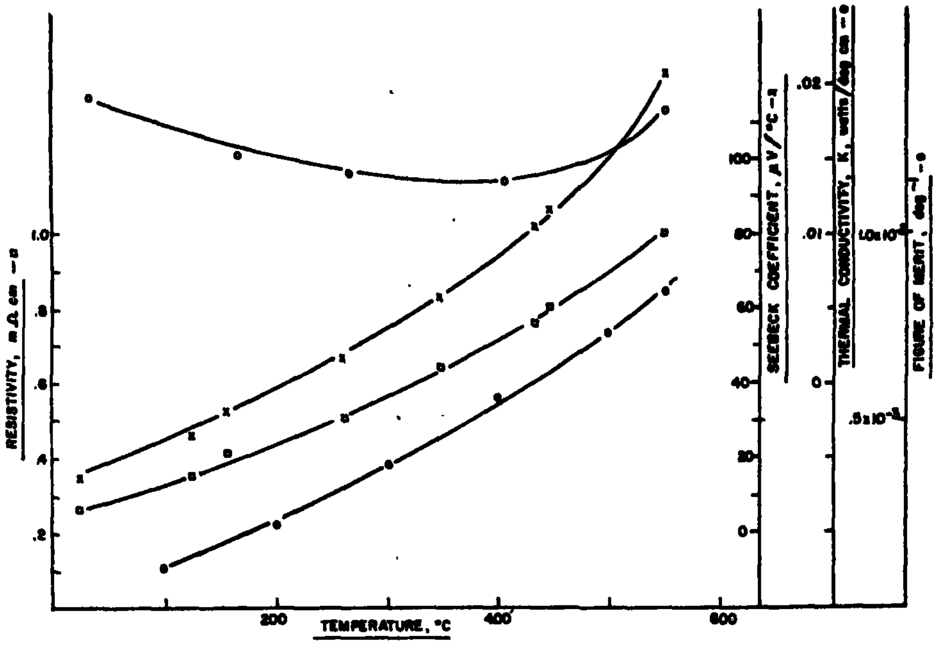

FIG. 1.—Thermoelectric properties of NbTe^2 as a function of temperature

The Seebeck coefficient for $MoTe_2$ and WSe_2 increased with rising temperature, whereas the Seebeck coefficient for $MoSe_2$ decreased over the same measured temperature range. WTe_2 repeatedly exhibited the behaviour represented by Fig. 2. A change of type from n to p occurred usually at a mean temperature of about 100°C.

(10) J. FRANCL and W. D. KINGERY, *J. Amer. Ceram. Soc.* 37, No. 2, 80–84 (1954).

TABLE 3.—ELECTRICAL PROPERTIES AND THERMAL CONDUCTIVITY OF THE INVESTIGATED AB_2 COMPOUNDS

Compound	Electrical resistivity, ρ in mΩ cm at 25°C	Electrical resistivity, ρ in mΩ cm at −196°C	Seebeck coefficient (μ V/°C)	Type	Thermal Conductivity (W°C^{-1} cm^{-1})	Figure of Merit, Z (°C^{-1}) at 25°C
$NbSe_2$	0·35	0·18	12	*n*	0·021	$1{\cdot}96 \times 10^{-5}$
$TaSe_2$	0·40	0·31	13	*n*	0·017	$2{\cdot}48 \times 10^{-5}$
$MoSe_2$	$3{\cdot}44{\cdot}10^3$	$4{\cdot}76{\cdot}10^5$	900	*n*	0·023	$1{\cdot}02 \times 10^{-5}$
WSe_2	$5{\cdot}00{\cdot}10^2$	$1{\cdot}50{\cdot}10^4$	990	*p*	0·017	$1{\cdot}15 \times 10^{-4}$
$NbTe_2$	0·26	0·077	15	*p*	0·019	$4{\cdot}55 \times 10^{-5}$
$TaTe_2$	0·36	0·12	14	*p*	0·014	$3{\cdot}89 \times 10^{-5}$
$MoTe_2$	$8{\cdot}5{\cdot}10^3$	$1{\cdot}34{\cdot}10^6$	780	*n*	0·020	$3{\cdot}66 \times 10^{-6}$
WTe_2	2·87	0·36	57	*n*	0·016	$7{\cdot}08 \times 10^{-4}$

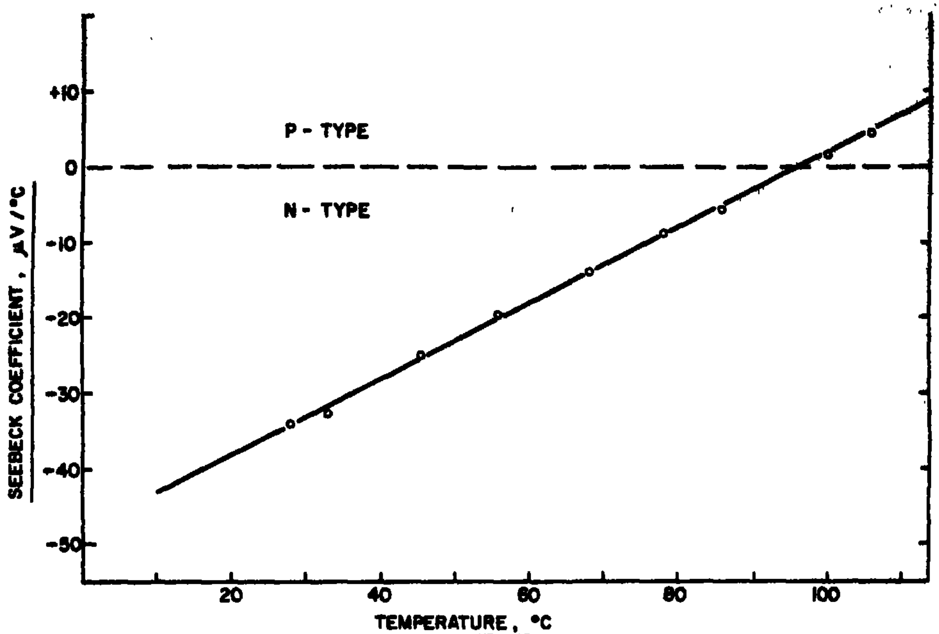

FIG. 2.—Seebeck coefficient, as a function of temperature for WTe$_2$

DISCUSSION

It is apparent from the data presented in Table 3 that electronically we are dealing with two classes of materials: the semiconductors MoSe$_2$, MoTe$_2$ and WSe$_2$ and the metal-like conductors NbSe$_2$, TaSe$_2$ NbTe$_2$ and TaTe$_2$, with WTe$_2$ taking a somewhat intermediate position. If one assumes all metals to be in the quadrivalent state, this can be explained on the grounds that the Va group elements would have a free electron contributing to the metal-like conductivity, whereas the paired electrons of the VIa Group elements are more difficult to promote into the conduction band. It is interesting to note the large difference in the properties of MoTe$_2$ and WTe$_2$ (see Table 3). In view of the fact that we are dealing with different structures, this is of course not necessarily surprising, even if the chemical formulas appear to be similar: cf. the pair grey tin-metallic tin which demonstrates the effect of structural differences on solid state properties in its most extreme form.

Since the discussed compounds are either isomorphic or very closely related structurally, it should be of particular interest to prepare solid solutions between the electronically different materials and thus possibly find compositions of improved electrical characteristics, particularly with respect to the Figure of Merit. This concept is presently being pursued, and the results on systems such as Mo$_x$Nb$_{1-x}$Te$_2$ or$_x$W$_x$ Ta$_{1-x}$Se$_2$ will be the subject of a future publication.

Acknowledgement—The author gratefully acknowledges the cooperation of Dr. G. TEUFER of the Engineering Research Laboratory, who determined all X-ray parameters.

J. Inorg. Nucl. Chem., 1962, Vol. 24, pp. 265 to 274. Pergamon Press Ltd. Printed in England.

REACTIONS OF CO-ORDINATED LIGANDS—IV

SYNTHESIS OF IRON ISONTRILE COMPLEXES BY THE TRANSALKYLATION REACTION

W. Z. Heldt
E. I. du Pont de Nemours & Company, Inc.
Explosives Department, Experimental Station Laboratory

(*Received* 11 *September* 1961)

Abstract—When tetrabenzylisocyano iron (II) cyanide or cyanopentabenzylisocyano iron (II) bromide is heated with an alkyl halide (R'X) and if the benzylhalide formed is continuously removed during the reaction, products of the general formulae $(R'NC)_x(C_6H_5CH_2NC)_y FeCNX$ $(x+y=5)$ (X = halogen); $(R'NC)_5FeBr_2$ and $(R'NC)_4Fe(CN)_2$ are formed.

Iron isonitrile complexes are prepared by:

(1) addition of isontriles to iron II salts such as Fe $(C10_4)_2$ (1)
(2) addition of isonitriles to iron carbonyls,(2) and
(3) alkylation of ferro-cyanides with alkylhalides(3), or alkyl sulphates(1a)

Few alkyl isonitriles were prepared having substituent groups in the alkyl chain probably because of the poor synthetic methods available for their preparation.(4) No iron (II) complexes of substituted alkyl isonitriles appear to have been prepared thus far.(1a) This paper reports a new, relatively simple method for the preparation of a wide variety of alkyl isonitrile complexes.

EXPERIMENTAL

Reaction of $(C_6H_5CH_2NC)_5FeCNBr$ (I) *with p-carbomethoxybenzyl bromide*

To 15·4 g (0·02 mole) of $(C_6H_5CH_2NC)_5FeCNBr$ (I) was added 23·0 g (0·1 mole) of *p*-carbomethoxybenzyl bromide. The reaction mixture was well mixed and was then dry distilled at 4 mm, the pot-temperature of the reaction vessel being held at 95–120°C. During a period of 70 min, 8·5 g (0·05 mole) of benzyl bromide distilled over, identified by its b.p. and infra-red spectrum. The residue from the distillation, a brown oil, 28·6 g, was dissolved in chloroform and was then chromatographed on 500 g of alumina suspended in chloroform. The column was washed with 7 × 50 ml of chloroform, 5 × 50 ml of 50 per cent chloroform acetone, 3 × 50 ml acetone, 3 × 50 ml 50 per cent acetone-methanol and finally with 6 × 50 ml of methanol. Three distinct compounds were eluted; Fraction I, 10·5 g with chloroform; Fraction II, 9·5 g, with acetone and acetone–methanol; and Fraction III, 3·7 g, with methanol.

Fractions II and III were combined and were fractionally crystallized from methyl ethyl ketone (250 ml). The less soluble fractions (A) 2·5 g, were recrystallized once more from chloroform–carbon tetrachloride and were dried at 100°C/1·0 mm, melting at 234–237·5°C. Found: C, 58·86; H, 4·68; N, 8·11; Fe, 5·74; Br, 8·01. Calc. for $(p\text{-}CH_3OCOC_6H_4CH_2NC)_5FeCNBr$: C, 59·03; H, 4·37; N, 8·10; Fe, 5·38; Br, 7·70%.

---

(1) (*a*) L. Malatesta, *Isocyanide Complexes of Metals*, Progress in Inorganic Chemistry. (Edited by F. A. Cotton) p. 283. Interscience, New York (1959).
(*b*) L. Malatesta and A. Sacco, *Ann. Chim.* 43, 622 (1953).

(2) W. Hieber and D. von Pigenot, *Ber. Dtsch. Chem. Ges.* 89, 193, 610, 616 (1956).

(3) (a) E. G. J. Hartley and H. M. Powell, *J. Chem. Soc.* 101 (1933).

(4) (a) I. Ugi and R. Meyr, *Angew. Chem.* 70, 702 (1958);
(b) H. R. Hertler and E. J. Corey, *J. Org. Chem.* 23, 1221 (1958).

The infra-red spectrum of this material was nearly identical with that of p-$(CH_3OCOC_6H_4CH_2NC)_5FeCNBr \cdot H_2O$,(5) m.p. 185–186·2°C, although the large discrepancies of the melting points of the monohydrate with the nonhydrated form are of interest. When samples of both compounds were mixed and dried at 100°C/1·0 mm for a prolonged time, the mixed melting point was 232–236°C, i.e., there was no melting point depression.

From the mother liquors of Fraction A there crystallized upon reduction of the volume of solvent a material, Fraction B, 1·5 g. After one recrystallization from methyl ethyl ketone this material melted at 141–142·5°C. Found: C, 61·09; 61·29; H, 4·61, 4·44; N, 8·93, 9·01; Fe, 6·00, 5·91; Br.9·81.

$$\text{Calc. for}\left[\begin{matrix}(p\text{-}CH_3OCOC_6H_4CH_2NC)_3\\(C_6H_5CH_2NC)_2\end{matrix}\right]FeCNBr:$$

C, 61·25; H, 4·48; N, 9·12; Fe, 6·06; Br, 8·67%.

Infra-red (KBr): 3·40 (*s*), 4·45 (*vs*), 4·72 (*vs*), 5·78 (*vs*), 6·18 (*s*), 6·32 (*w*), 6·68 (*w*), 6·88 (*s*), 6·98 (*vs*), 7·08 (*s*), 7·42 (*s*), 7·62 (*s*), 7·82 (*vs*), 8·46 (*s*), 9·03 (*vs*), 9·82 (*s*), 10·38 (*s*), 12·00 (*w*), 12·55 (*w*), 13·35 (*w*), 14·35 (*s*), μ.

Further reduction of the mother liquors of Fraction B yielded C, 2·0 g. After one recrystallization from methyl ethyl ketone this material melted at 123–126°C. Found: C,58·79; H, 4·80; N, 89·5; Fe, 5·89; Br, 9·01.

$$\text{Calc. for}\left[\begin{matrix}(C_6H_5CH_2NC)\\(p\text{-}CH_3OCOC_6H_4CH_2NC)_4\end{matrix}\right]FeCNBr \cdot H_2O:$$

C, 58·99; H, 4·55; N, 8·42; Fe, 5·60; Br, 8·01%.

Except for a strong OH band at 2·92μ, the infra-red spectrum of the latter materials was practically identical with Fraction I of the following experiment.

Reaction of tetrabenzylisocyano iron (II) cyanide (II) with p-carbomethoxybenzyl bromide

To 11·5 g (0·05 mole) of p-carbomethoxybenzyl bromide were added 5·6 g (0·01 mole) of II, m.p. 229–230°C. The reaction mixture was well mixed and was dry-distilled under a vacuum of 5·0 mm and an oil-bath temperature of 135–162°C. After 2·0 ml of benzyl bromide (b.p. 78–80°C/5·0 mm) had distilled over, the dry-distillation was discontinued. The distillation residue was dissolved in chloroform and was chromatographed on 450 g of alumina suspended in chloroform. The column was washed with 700 ml of 50 per cent acetone–chloroform, 150 ml of acetone and finally with 350 ml of 50 per cent acetone–methanol. Two fractions were eluted: Fraction I with acetone–chloroform, 2·14 g; and Fraction II with acetone–methanol, 4·9 g. Fraction I was recrystallized from methanol and methyl ethyl ketone. After several recrystallizations from these solvents the compound melted at 226–230°C (dried at 100°C/1·0 mm). Found: C, 60·85; H, 5·42; N, 8·59; Fe, 5·21; Br, 8·54.

$$\text{Calc. for}\left[\begin{matrix}p\text{-}CH_3OCOC_6H_4CH_2NC)_4\\C_6H_5CH_2NC\end{matrix}\right]FeCNBr:$$

C, 60·07; H, 4·43; N, 8·58; Fe, 5·70; Br, 8·16%.

Infra-red (KBr): 2·92 (*w*), 3·40 (*m*), 4·56 (*vs*), 4·70 (*s*), 5·79 (vs), 6·18 (*s*), 6·32 (*w*), 6·68 (*w*), 6·96 (*s*), 7·05 (*s*), 7·45 (*m*), 7·61 (*m*), 7·80 (*w*), 8·07 (*m*), 8·46 (*m*), 9·00 (*s*), 9·82 (*m*), 10·35 (*m*), 11·98 (*w*), 14·40 (*m*) μ.

Reaction of II with α-bromo-p-xylene

To 11·5 g (0·02 mole) of II, m.p. 229–230°C were added 20·5 g (0·11 mole) of α-bromo-p-xylene. The reactants were well mixed and were dry-distilled at 8 mm, maintaining the oil-bath temperature at 125°C. After 20 min, 8 ml of a material distilled over b.p. 85–87°/8 mm. The infra-red spectrum of the distillate indicated a mixture of benzyl bromide and α-bromo-p-xylene, the latter being by far the major constituent in the reaction mixture.

The residue was taken up in chloroform and was crystallized from chloroform–carbon tetrachloride. A white material crystallized out, m.p. 130–134°C. After several more recrystallizations from methyl ethyl ketone it had a m.p. 135–136·5°C. Found: C, 66·55; H, 5·80; N, 11·07; Fe, 6·68; Br, 9·94.

$$\text{Calc. for}\begin{bmatrix}(p\text{–}CH_3C_6H_4CH_2NC)_4\\ C_6H_5CH_2NC\end{bmatrix}FeCNBr:$$

C, 67·25; H, 5·39; N, 10·47; Fe, 6·96; Br, 9·95%.

Infra-red (KBr): 2·90 (*w*), 3·30 (*s*), 3·42 (*s*), 3·50 (*s*), 4·56 (*vs*), 4·71 (*s*), 6·10 (*s*), 6·25 (*w*), 6·45 (*s*), 7·08 (*s*), 7·25 (*w*), 7·42 (*s*), 7·60 (*w*), 8·05 (*w*), 8·35 (*w*), 8·45 (*w*), 8·95 (*w*), 9·62 (*w*), 9·81 (*w*), 10·40 (*w*), 11·93 (*w*), 12·45 (*s*), 12·62 (*s*), 13·33 (*s*) 13·79 (*m*), 14·40 (*m*) μ.

This material depressed the melting point of $(p\text{–}CH_3C_6H_4CH_2NC)_5FeCNBr\cdot H_2O$(5) upon admixture.

Partial transalkylation of I with α-bromo-p-xylene

To 22·8 g (0·03 mole) of I were added 22·5 g (0·12 mole) of α-bromo-p-xylene. The reactants were heated and stirred overnight on a steambath in a vessel closed by a calcium chloride tube and were dry-distilled at 6–9 mm pressure and an oil-bath temperature of 115–117°C. After 11 min, 3·5 ml of distillate, b.p. 82–84°C were collected. Infra-red spectrum of the distillate indicated a mixture of α-bromo-*p*-xylene and benzyl bromide. The residue was then crystallized from chloroform-carbon tetrachloride, yielding ca. 5 g of $(p\text{–}CH_3C_6H_4CH_2NC)_5FeCNBr\cdot H_2O$, identified by mixed melting point with a reference sample and by its infra-red spectrum.(5)

Reaction of I with α-bromo-o-xylene

To 15·2 g (0·02 mole) of I were added 22·0 g (0·12 mole) of α-bromo-*o*-xylene and the reaction mixture was dry distilled under 9 mm and an oil bath temperature of 120°C. After 43 min there distilled 13 ml of a material, b.p. 84–86°C. The distillate was identified by infra-red as a mixture of α-bromo-*o*-xylene, benzyl bromide (about 20–35 per cent) and a nonidentified isonitrile (about 5 per cent). The residue from the distillation was then crystallized from methyl ethyl ketone. After several crystallizations a material was obtained with a melting point of 235–237°C. This material did not depress, upon admixture, the melting point of the previously prepared $(o\text{-}CH_3C_6H_4CH_2NC)_4Fe(CN)_2$ and the infra-red spectra of these two materials were superimposable.

Reaction of p-nitrobenzyl bromide with I

To 22·8 g (0·03 mole) of I were added 25 g (0·12 mole) of *p*-nitrobenzyl bromide. The reactants were well mixed and were distilled under 6 mm Hg and an oil bath temperature of 115–141°C. A total of 3·5 ml of distillate was collected. The distillate consisted solely of benzyl bromide, i.e. the reaction proceeded to about 20 per cent completion. The brown residue in the distillation flask was then chromatographed in the usual fashion on alumina suspended in chloroform. The column was washed with 850 ml of chloroform, 5 × 250 ml 50 per cent acetone–chloroform, 4 × 250 ml of acetone, 7 × 250 ml of acetone–methanol and finally with 2 × 250 ml of methanol. Fraction I, 12·3 g was eluted with chloroform, and was identified as starting material (i.e., 50 per cent recovery), Fraction II, 13·7 g was eluted with 50 per cent chloroform-acetone and acetone; and Fraction III, 18·7 g, with 50 per cent acetone–methanol.

Infra-red spectrum of Fraction II ($CHCl_3$): 3·00 (*s*), 3·45 (*s*), 4·58 (*vs*), 4·72 (*w*), 6·25 (*w*), 6·58 (*s*), 6·72 (*m*), 6·92 (*m*), 6·98 (*m*), 7·45 (*s*), 8·10–8·35 (*m*), 14·45 (*s*) μ. The infra-red spectrum of this material indicates definitely an isonitrile complex. All attempts to crystallize this fraction remained unsuccessful.

Fraction III was crystallized from acetone yielding 8·7 g of a solid (Fraction A). After several recrystallizations from methanol–methyl ethyl ketone, the melting point of this solid was 139–143°C. Found: C, 57·87, 57·83; H, 4·48, 4·49; N, 13·44, 13·41; Fe, 6·60; Br, 9·44.

$$\text{Calc. for}\begin{bmatrix}(p\text{-}NO_2C_6H_4CH_2NC)_2\\ (C_6H_5CH_2NC)_3\end{bmatrix}FeCNBrH_2O:$$

C, 57·55; H, 4·12; N, 13·10; Fe, 6·53; Br, 9·35%.

Infra-red (KBr): 3·00 (*w*), 3·40 (*s*), 4·58 (*vs*), 4·72 (*w*), 6·25 (*m*), 6·58 (*s*), 7·00 (*m*), 7·10 (*m*), 7·45 (*s*), 8·20–8·30 broad (*s*), 14·45 (*s*) μ.

From the mother liquors of Fraction A there crystallized 5·0 g of a yellow material which was very soluble in methyl ethyl ketone. After several recrystallizations and drying, this material melted at 85–88°C. Found: C, 46·88, 46·92; H, 3·93, 3·69; N, 12·59, 12·32; Fe, 5·14; Br. 13·50.

$$\text{Calc. for}\left[\begin{matrix}(p\text{-NO}_2\text{C}_6\text{H}_4\text{CH}_2\text{NC})_4\\ \text{C}_6\text{H}_5\text{CH}_2\text{NC}\end{matrix}\right]\text{FeBr}_2\cdot 2\text{H}_2\text{O}$$

C, 47·18; H, 3·46; N, 12·38; Fe, 5·48; Br, 15·70%.

Infra red (KBr): 2·90 (*s*), 4·54 (*vs*), 4·72 (*w*), 6·22 (*s*), 6·58 (*vs*), 6·69 (*w*), 6·88 (*w*), 7·44 (*vs*), 9·02 (*w*), 9·85 (*w*), 11·65 (*w*), 12·55 (*w*), 13·65 (*s*), 14·40 (*s*) μ.

The appearance of a cyanide band at 4·72μ, which is found to be typical of a cyanide group, makes a structural assignment of this compound uncertain.

Reaction of I with β-naphthyl bromomethane

To 15·5 g (0·02 mole) of I were added 18·00 g (0·08 mole) of β-naphthyl bromomethane, m.p. 44–45°, which was prepared according to the procedure of SCHULZE[6]. The well-mixed reaction mixture was then dry-distilled at 115–130°C and 2·0 mm vacuum. A total of 9·9 ml, 13·1 g (0·076 mole) of benzyl bromide was collected, identified by its infra-red spectrum and boiling point. The distillation residue was dissolved in chloroform and was chromatographed as usual on 450 g of alumina. Two distinct compounds were eluted: Fraction I, 7·45 g with acetone; and Fraction II, 6·4 g, with 50 per cent acetone–methanol. Fraction I was recrystallized several times from methyl ethyl ketone, and melted after drying at 165–167°C. Found: C, 71·31; H, 4·85; N, 8·79; Fe, 5·92; Br, 7·98. Calc. for $(\beta\text{-C}_{10}\text{H}_7\text{CH}_2\text{NC})_5\text{FeCNBr}\cdot\text{H}_2\text{O}$: C, 72·12; H, 4·66; N, 8·26; Fe, 5·49; Br, 7·87.

$$\text{Calc. for}\left[\begin{matrix}(\beta\text{-C}_{10}\text{H}_7\text{CH}_2\text{NC})_4\\ \text{C}_6\text{H}_5\text{CH}_2\text{NC}\end{matrix}\right]\text{FeCNBr}\cdot\text{H}_2\text{O}:$$

C, 70·96; H, 4·60; N, 8·71; Fe, 5·79; Br, 8·28%.

Infra-red (KBr): 2·90 (*w*), 3·35 (*m*), 3·40 (*m*), 4·55 (*vs*), 4·72 (*s*), 6·20 (*w*), 6·30 (*m*), 6·62 (*s*), 6·60 (*s*), 6·89 (*s*), 6·99 (*s*), 7·28 (*s*), 7·50 (*s*), 7·85 (*s*), 8·95 (*w*), 9·85 (*w*), 10·42 (*w*), 10·55 (*w*), 11·25 (*w*), 11·70 (*s*), 12·25 (*vs*), 13·00 (*w*), 13·20 (*s*), 13·40 (*vs*), 14·45 (*s*) μ.

Fraction II was crystallized several times from methyl ethyl ketone and melted at 216–218°C after drying at 100°C/1·0 mm. Found: C, 69·58; H, 4·39; N, 9·76; Fe, 6·94.

$$\text{Calc. for}\left[\begin{matrix}\beta\text{-C}_{10}\text{H}_7\text{CH}_2\text{NC})_2\\ (\text{C}_6\text{H}_5\text{CH}_2\text{NC})_3\end{matrix}\right]\text{FeCNBr}:$$

C, 69·43; H, 4·64; N, 9·91; Fe, 65·9%.

The infra-red spectrum (KBr) of Fraction II was almost identical with that of Fraction I; here the 2·90μ band is very weak; the isonitrile band is split slightly into two bands: 4·52μ and 4·57μ.

Reaction of I with α-bromoacetophenone

To 15·5 g (0·02 mole) of I were added 16·4 g (0·082 mole) of α-bromoacetophenone, the reaction mixture was well mixed, fused and dry-distilled at 2·8 mm and an oil-bath temperature of 135–140°C. After heating for 90 min at this temperature, 2·5 ml of distillate (b.p. 42–60°C) were collected and the reaction was discontinued. The infra-red spectrum of the distillate indicated benzyl bromide as the major constituent and acetophenone, probably an impurity in the commercial α-bromoacetophenone. The residue of the distillation was dissolved in chloroform and was chromatographed on neutral alumina suspended in chloroform. The column was then washed with 6×50 ml of chloroform, 13×50 ml of 50 per cent chloroform–acetone, 3×50 ml of acetone, 12×50 ml of 50 per cent acetone–methanol and finally with 7×50 ml of methanol. Two fractions were eluted: with chloroform, Fraction I, 25·3 g and with 50 per cent chloroform–acetone, Fraction II, 7·6 g. Fraction I was crystallized from methyl ethyl ketone, m.p. 105–120°C. After several recrystallizations from methyl ethyl ketone and drying at 25°C/1 mm, the material melted at 219–220°C. Found: C, 57·05; 57·35, H, 3·96, 4·06; N, 7·72, 7·70; Fe, 5·88; halogen, 17·56. Calc. for $(C_6H_5COCH_2NC)_3FeBr_2$: C, 57·41; H, 3·75; N, 7·44; Fe, 5·93; Br, 16·98%.

Infra-red (KBr): 2·95 (*w*), 3·40 (*s*), 3·50 (*s*), 3·75 (*w*), 4·52 (*s*), 4·60 (*vs*), 5·99 (*s*), 6·15 (*w*), 6·25 (*s*), 6·68 (*vs*), 6·80 (*vs*), 6·89 (*m*), 7·45 (*s*), 7·80 (*s*), 8·35 (*m*), 8·85 (*s*), 8·92 (*vs*), 9·05 (*s*), 9·15 (*s*), 9·60 (*s*), 9·85 (*s*), 10·60 (*vs*), 10·80 (*s*), 13·20 (*vs*), 13·40 (*s*), 13·60 (*s*), 13·90 (*s*), 14·05 (*vs*), 14·35 (*vs*), 14·60 (*vs*) μ.

Reaction of I with hexadecyl iodide

To 11·5 g (0·015 mole) of I were added 42 g (0·12 mole) of hexadecyl iodide (Eastman Chem. Co.) and the reaction mixture was distilled at an oil-bath temperature of 120–156°C under 0·5 mm vacuum. After 98 min there distilled at 44–46°C, 3 ml of a yellowish liquid. The infra-red spectrum of the distillate indicated the presence of benzyl bromide and hexadecyl iodide.

Analysis of distillate: Br, 6·93; I, 47·18%.

The reaction residue was then boiled with chloroform, the solution was filtered hot, whereby a chloroform insoluble material, Fraction I, 0·69 g, m.p. 145–210°C was isolated. This material was recrystallized from methanol–chloroform; after drying at 25°C/1·0 mm it melted at 230–231·5°C. Upon admixture of this material with $(C_6H_5CH_2NC)_4Fe(CN)_2$ the melting point was not depressed and the two materials showed identical infra-red spectra.

The chloroform soluble material was cooled to room temperature and was chromatographed on 750 g of neutral alumina suspended in chloroform. The column was washed with 7×50 ml of chloroform, 6×50 ml 50 per cent chloroform–acetone, 10×50 ml of acetone, 13×50 ml 50 per cent acetone–methanol and 3×50 ml of methanol. Three fractions were eluted: Fraction I, 34 g a liquid, with chloroform and 50 per cent chloroform–acetone; Fraction II, 7·3 g a solid, m.p. 265–278, with acetone; and Fraction III, 6·6 g with 50 per cent methanol–acetone and methanol. Fraction I seemed to consist mainly of hexadecyl iodide and hexadecyl or benzyl isonitrile as evidenced by a strong band at 4·58μ. Fraction II was not processed any further.

Fraction III was dissolved in about 100 ml of hot methyl ethyl ketone and was filtered. The methyl ethyl ketone insoluble material, Fraction IIIA was a compound melting at 229–231·5°C, after drying in a vacuum oven. Found: C, 69·90, 69·77; H, 10·97, 10·93; N, 6·85, 6·65; Fe, 3·82; I, 8·34. Calc. for $[CH_3(CH_2)_{14}CH_2NC]_5FeCNI$: C, 70·46; H, 11·36; N, 5·73; Fe, 3·81; I, 8·66%.

Infra-red ($CHCl_3$): 3·47 (*vs*), 3·51 (*vs*), 4·55 (*vs*), 4·72 (*w*), 6·31 (*w*), 7·46 (*w*), 8·12–8·30 (*w*), 13·75 (*m*), 15·25 (*w*) μ.

From the filtrates of compound Fraction IIIA there crystallized a yellow material, Fraction IIIB; after several recrystallizations from methyl ethyl ketone, the material melted after drying at 90·5–93·0°C. Found: C, 68·94, 68·97; H, 11·26, 11·07; N, 6·10, 6·14; Fe, 4·37; I, 8·34.

$$\text{Calc. for} \begin{bmatrix} (CH_3(CH_2)_{14}CH_2NC)_4 \\ C_6H_5CH_2NC \end{bmatrix} FeCNI\text{:}$$

C, 69·44; H, 10·52; N, 6·31; Fe, 4·19; I, 9·53%.

Infra-red ($CHCl_3$): 3·40 (*vs*), 4·57 (*vs*), 4·70 (*s*), 6·25 (*w*), 6·70 (*vs*), 7·27 (*s*), 13·60 (*s*), 14·40 (*s*) μ. Fraction IIIB gave a melting point depression with Fraction IIIA upon admixture.

Reaction of I with 3-phenoxy-l-bromopropane

To 15·0 g (0·02 mole) of I were added 37·6 g (0·12 mole) of 3-phenoxy-l-bromopropane and the reaction mixture was heated on a steam bath overnight in a reaction vessel closed by a calcium chloride drying tube. Subsequently, the reaction mixture was dry-distilled at 6–9 mm the oil-bath temperature being kept at 134–160°C. After 40 min, 8 ml of liquid, b.p. 78–103°C (main fraction 78–79°C), distilled over. The infra-red spectrum of the distillate indicated a mixture of 3-phenoxy-l-bromopropane and benzyl bromide, the latter constituting about 90 per cent of the distillate. The pot-residue was dissolved in chloroform and was chromatographed on a column prepared from about 450 g of neutral alumina suspended in chloroform. The column was then washed with 4×50 ml of chloroform, 7×50 ml of 50 per cent chloroform–acetone, 4×50 ml of acetone, 8×50 ml of 50 per cent acetone–methanol and finally with 7×50 ml of methanol. Three different fractions were eluted: Fraction I, 11·8 g with chloroform; Fraction II, 8·5 g with 50 per cent chloroform–acetone; and Fraction III with 4·9 g with 50 per cent acetone–methanol. All attempts to crystallize Fraction I, Fraction II, and Fraction III failed. Fraction II, a yellow oil, was dried for 60 hr at 25°C/1·0 mm Hg and was then analysed. Found: C, 62·28; H, 6·10; N, 8·52; Fe, 6·19; Br, 8·00. Calc. for $(C_6H_5OCH_2CH_2CH_2NC)_5FeCNBr \cdot H_2O$: C, 62·13; H, 5·82; N, 8·53; Fe, 5·66; Br, 8·11%.

Infra-red ($CHCl_3$): 2·95 (*m*), 3·40 (*s*), 4·53 (*vs*), 4·73 (*s*), 6·28 (*s*), 6·72 (*s*), 6·84 (*s*), 6·98 (*s*), 7·25 (*m*), 7·50 (*m*), 7·80 (*m*), 8·10 (*vs*), 8·25 (*vs*), 8·56 (*s*), 9·25 (*s*), 9·56 (*s*), 10·38 (*m*), 10·79 (*m*), 11·38 (*m*), 14·40 (*s*) *μ*.

Reaction of I with 12-bromo-n-dodecanoic acid

To 15·0 g (0·02 mole) of I were added 33·5 g (0·12 mole) of 12-bromo-n-dodecanoic acid and the reaction mixture was dry-distilled at 1·0 mm and 140°C oil-bath temperature in the usual fashion. After 90 min, 8 ml of benzyl bromide (11·6 g or 68 per cent conversion based on exchange of all benzyl groups), b.p. 40–42°C, distilled over as the sole product (identified by the infra-red spectrum of the distillate). The residue of the reaction was then extracted with ether to remove the unreacted 12-bromo-n-dodecanoic acid. The ether insoluble material was dissolved in chloroform, was filtered several times through charcoal, and was crystallized from chloroform methyl ethyl ketone.

The material melted, after drying at 1·0 mm Hg at 61–63°C. Found: C, 55·16; 55·34, 55·61; H, 8·81, 8·95, 8·95; N, 5·65, 5·45; Fe, 3·68; Br, 13·73. Calc. for $(HCO_2(CH_2)_{10}CH_2NC)_5FeBr_2 \cdot 3H_2O$: C, 55·90; H, 8·20; N, 5·02; Fe, 3·99; Br, 11·45%.

Infra-red (KBr): 2·95 (*s*), 3·26 (*sh*), 3·41 (*vs*), 3·51 (*vs*), 4·50 (*vs*), 5·78 (*vs*), 6·81 (*s*), 6·94 (*w*), 7·16 (*w*), 7·41 (*w*), 7·62 (*w*), 7·96 (*w*), 8·10 (*w*), 8·30 (*w*), 8·59 (*s*), 9·06 (*w*), 9·55 (*w*), 11·26 (*w*), 12·35 (*w*), 13·50 (*w*), 13·88 (*w*) *μ*.

Simultaneous reaction of allyl bromide and p-carbomethoxybenzyl bromide with $K_4Fe(CN)_6$.

To 11·45 g (0·05 mole) of *p*-carbomethoxybenzyl bromide and 6·05 g (0·05 mole) of allyl bromide were added 15·0 g (0·015 mole) of dry $K_4Fe(CN)_6$ and the reaction mixture was heated on the steam bath with stirring in a vessel closed by a calcium chloride tube for two days. The reaction mixture was then extracted with petroleum ether to remove the unreacted bromides. The petroleum ether insoluble material was extracted with boiling chloroform and the chloroform extracts were evaporated to dryness. All attempts to crystallize this material failed. Finally it was pressed on a clay-plate and was crystallized yielding about 2·0 g of a material melting at 220–230°C. After several more recrystallizations from carbon tetrachloride–chloroform the material melted at 233–237°C. The material did not depress, upon mixture, the melting point of $(CH_3O_2CC_6H_4CH_2NC)_5FeCNBr \cdot H_2O$ and the infra-red spectra of these two materials were identical.

Reaction of $(C_6H_5CH_2NC)_6FeBr_2$ *with p-nitrobenzyl bromide*

To 6·75 g (7·2 mmole) of $(C_6H_5CH_2NC)_6FeBr_2$ were added 9·33 g (43 mmole) of *p*-nitrobenzyl bromide, the reaction mixture was well mixed and was distilled under reduced pressure at 1·0 mm in the usual fashion. The reaction was stopped after about 1·5 ml of a liquid distilled over; the liquid was identified as benzyl bromide, (1·5 ml = 2·15 g = 1·3 mmole of benzyl bromide or 18 per cent of total benzyl bromide). The residue was extracted with ether, which yielded, upon evaporation, 10·1 g of wet *p*-nitrobenzyl bromide. The ether insoluble material was then crystallized from acetone yielding 3·3 g of N-benzyl formamide and a non-identified oil. The N-benzyl formamide was identified by infra-red spectrum of an authentic sample.

RESULTS AND DISCUSSION

It was noticed earlier that the alkylations of tetrabenzylisonitrile iron (II) cyanide (II) to cyanopentabenzylisonitrile iron (II) bromide (I) and of cyanopentabenzylisonitrile iron (II) bromide to hexabenzylisontrile iron II bromide (III) with benzyl bromide are equilibrium reactions: (5,7)

$$(C_6H_5CH_2NC)_4Fe(CN)_2 \xrightleftharpoons{C_6H_5CH_2Br} (C_6H_5CH_2NC)_5FeCNBr \xrightleftharpoons{C_6H_5CH_2Br}$$

$$(C_6H_5CH_2NC)_6FeBr_2$$

When a foreign alkyl halide was introduced into the system, these alkylation reactions could be tailored into a synthesis of new isonitrile complexes by a "transalkylation reaction."

$$(RNC)_5FeCNBr + R'Br \rightleftharpoons \left[\begin{array}{ll} \text{a.} & \begin{matrix}(RNC)_4\\ R'NC\end{matrix}\ FeCNBr \\ \text{b.} & \begin{matrix}(RNC)\\ (R'NC)_2\end{matrix}\ FeCNBr \\ \text{c.} & \begin{matrix}(RNC)_2\\ (R'NC)_3\end{matrix}\ FeCNBr \\ \text{d.} & \begin{matrix}RNC\\ (R'NC)_4\end{matrix}\ FeCNBr \\ \text{e.} & (R'NC)_5\ FeCNBr \end{array}\right] + RBr \qquad (2)$$

The transalkylation of isonitrile complexes could be accomplished with an alkyl halide R'X, which is higher boiling then RBr, by a continuous distillation of RBr from the reaction mixture to yield b, c, d and e. The reaction is, in form, similar to the transalkylations and transesterifications found, for example, in carbon (8,9) and boron chemistry (10,11). Since the separation and crystallization of the reaction products were laborious each reaction is described in some detail in the Experimental Part and the reaction products isolated are summarized in Table 1. Considerable difficulty was encountered with the purification of these products.

A typical reaction profile is given in Fig. 1 for the transalkylation of I with *p*-nitrobenzyl bromide, and *β*-naphthyl bromomethane. The reactants were well mixed and were placed into a still equipped with a magnetic stirrer and two thermometers: one to measure the temperature in the distillation vessel and the other to measure the temperature of the distilling vapour. The still was connected to a graduated cylinder and was evacuated and placed into a constant temperature bath. The constant bath temperature was brought to about 120°C, at which temperature the reaction started. The temperature was maintained at about 120°C or was increased by about 15–30°C after the distillation of three moles of benzyl bromide. The progress of the reaction was followed by the rate of distillation of benzyl bromide.

(5) W. Z. Heldt, *J. Inorg. Nucl. Chem.* **22**, 305 (1961).

(6) K. E. Schulze, *Ber. Dtsch. Chem. Ges.* **17**, 1527 (1884).

(7) E. G. J. Hartley, *J. Chem. Soc.* **101**, 705 (1912).

(8) A. Schneider, *U.S. Pat.* 2742512, J. T. Kelly, F. T. Wadsworth and R. J. Lee, *U.S. Pat.* 2759027.

(9) J. H. Halsam, *U.S. Pat.* 2822348.

(10) H. C. Brown and B. C. Subba Rao, *J. Org. Chem.* **22**, 1137 (1957).

(11) P. D. George and J. R. Ladd, *J. Amer. Chem. Soc.* **77**, 1900 (1955).

In each of the cases investigated (see Table 1) the rate of distillation of benzyl bromide decreased after about three to four moles of benzyl bromide had distilled over. Hexadecyl bromide transalkylated about twice as fast as hexadecyl chloride. No comparison was made between the relative velocity of transalkylation of hexadecyl iodide and hexadecyl bromide. The initiation period of the "transalkylation" reaction was shorter the more polar R'X suggesting perhaps a medium effect.

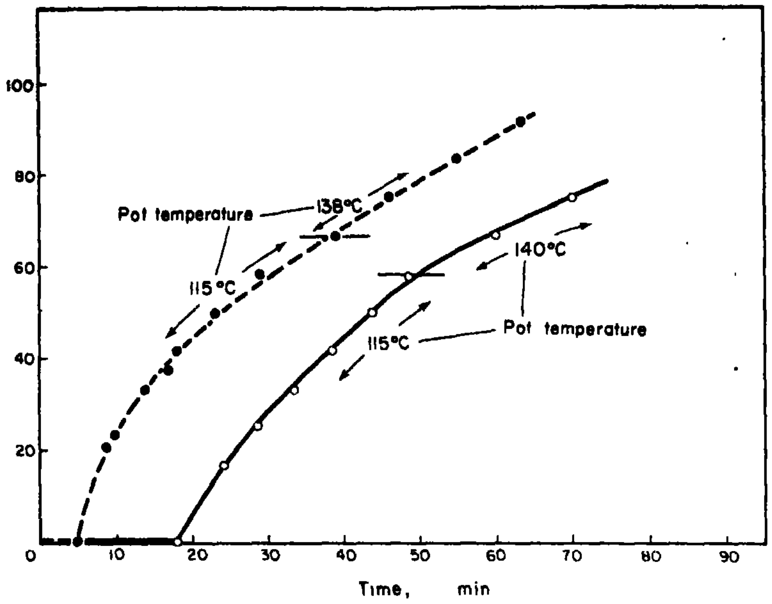

FIG. 1.—Rate of transalkylation of I with *p*-nitrobenzyl bromide (•) and with *β*-naphthyl bromoethane (∘) as measured by the rate of distillation of benzyl bromide.

TABLE 1.—TRANSALKYLATION REACTIONS, SUMMARY

Moles R'X/ moles I*	R'X	Products isolated
4	*p*-$NO_2C_6H_4CH_2Br$	$(R'NC)_2(RNC)_3FeCNBr$; $(R'NC)_4(RNC)FeBr_2\cdot 2H_2O$
5	*p*-$CH_3CO_2C_6H_4CH_2Br$	$(R'NC)_5FeCNBr$; $(R'NC)_4RNCFeCNBr\cdot H_2O$; $(R'NC)_3(R'NC)_3(RNC)_2FeCNBr$
4	$C_6H_5COCH_2Br$	$(R'NC)_5FeBr_2$
6	*o*-$CH_3C_6H_4CH_2Br$	$(R'NC)_4Fe(CN)_2$
4	*p*-$CH_3C_6H_4CH_2Br$	$(R'NC)_5FeCNBr\cdot H_2O$
4	*β*-naphthyl CH_2Br	$(R'NC)_5FeCNBr\cdot H_2O$; $(R'NC)_2(RNC)_3FeCNBr$
8	$CH_3(CH_2)_{14}CH_2I$	$(R'NC)_5FeCNI$; $(R'NC)_4RNCFeCNI$
6	$C_6H_5O(CH_2)_2CH_2Br$	$(R'NC)_5FeCNBr\cdot H_2O$
6	$HCO_2(CH_2)_{12}CH_2Br$	$(R'NC)_5FeBr_2\cdot 3H_2O$
Moles R'X/ moles II*		
5	*p*-$CH_3CO_2C_6H_4CH_2Br$	$(R'NC)_4RNCFeCNBr$
5·5	*p*-$CH_3C_6H_4CH_2Br$	$(R'NC)_4(RNC)FeCNBr$

* I = $(C_6H_5CH_2NC)_5FeCNBr$; II = $(C_6H_5CH_2NC)_4Fe(CN)_2$; R = benzyl

All compounds which could be isolated from the solid reaction mixtures are summarized in Table 1. The structures of the transalkylated products were determined by ultimate analysis, infra-red spectra and frequently by comparison with samples prepared by an independent route.⁽⁵⁾ Some of the samples contain water of crystallization which was absorbed from the solvent of crystallization. Iron isonitrile complexes of types II and III and probably also I are clathrate compounds⁽¹²⁾ and we have found that the water of crystallization is frequently difficult to remove. In addition to these compounds expected from equation (2), materials in which the cyano group was replaced by bromide with structures tentatively assigned as $[(p\text{-}O_2NC_2H_4CH_2NC)_4C_6H_5CH_2NC]FeBr_2{\cdot}H_2O$, $(C_6H_5COCH_2NC)_5FeBr_2$, and $(p\text{-}O_2NC_2H_4CH_2NC)_5FeBr_2{\cdot}3H_2O$ were isolated as major constituents. The mode of formation of these materials is thus far not clear. In the reaction of I with *o*-xylyl bromide and with n-hexadecyl iodide, an isonitrile was identified among the distillation products.

The scope of the transalkylation reaction is clearly broader than the alkylation of alkali ferrocyanides with alkyl halides. The alkyl group in R'X may be activated by a carbon–carbon double bond in the α-position or may be nonactivated: it may bear a substituent such as a carboxy group. X may be chloride, bromide, or iodide.

The mechanism of the transalkylation reaction is very complex because of the multitude of products involved and the possibility of internal rearrangement within the complex.⁽¹³⁾ The first step in the reaction may be the alkylation of I to III or elimination of benzyl bromide to form either II or IV. (See Fig. 2). The alkylation of I with benzyl bromide was slower than the total transalkylation reaction with either *p*-nitrobenzyl bromide or *p*-xylyl bromide. Furthermore, no transalkylated products were obtained in the reaction of III with *p*-nitrobenzyl bromide. Therefore, the alkylation of I to III cannot be a principal step in transalkylation. Only one tetrabenzylisonitrile iron II cyanide was synthesized, m.p. 229–230°C: on the basis of infra-red, nuclear magnetic spectra, ⁽¹⁴⁾ and its thermal stability, it is most probably

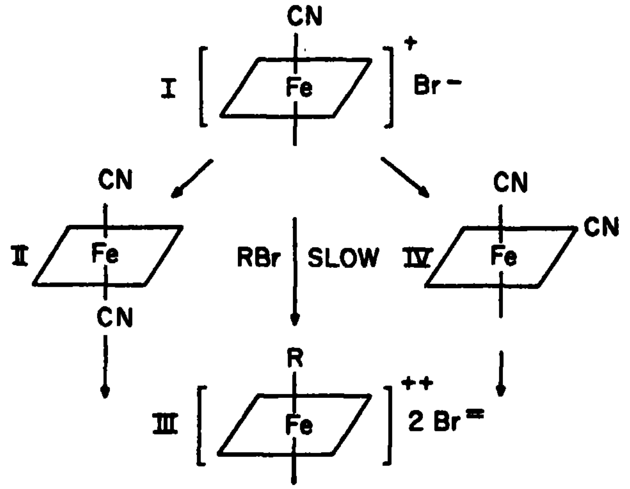

FIG. 2.—The stereochemistry of the transalkylation reaction.

⁽¹²⁾ H. M. POWELL and G. W. R. BARTINDALE, *J. Chem. Soc.* 799 (1945).

⁽¹³⁾ W. Z. HELDT, *J. Inorg. and Nucl. Chem.* In print.

⁽¹⁴⁾ W. Z. HELDT. Unpublished results, (1960).

the "trans-isomer". Transalkylation of II with *p*-carbomethoxybenzyl bromide and *p*-xylyl bromide was slower than the corresponding transalkylation of I, and different products were isolated from the two reactions. Furthermore, II was isolated in the transalkylation of hexadecyl iodide even when an excess of hexadecyl iodide was used. Hence the first step in the transalkylation of I is most probably the formation of IV. Transalkylation of I with less than stoichiometric amounts of *p*-xylyl bromide yielded the totally transalkylated product $(p\text{-}CH_3C_6H_5CH_2NC)_5FeCNBr\cdot\cdot H_2O$. The experiment suggests that the formation of IV may indeed be rate determining.

It was found previously⁽⁵⁾ that electron withdrawing groups in $p\text{-}XC_6H_4CH_2Br$ impede the alkylation of $K_4Fe(CN)_6$ to form $R_4Fe(CN)_2$, $R_5Fe(CN)Br$ and R_6FeBr_2 and electron-donating groups accelerate the alkylation of $K_4Fe(CN)_6$. Electron withdrawing groups, $-NO_2$, $-CO_2CH_3$, in $p\text{-}XC_6H_4CH_2Br$ do not impede the transalkylation reaction but perhaps even accelerate it as compared to an electron donating group, $X = CH_3$.

The qualitative results obtained thus far seem to indicate that either (a) the electronic effects involved in the elimination reaction (I→IV) are cancelled by the electronic requirements for the alkylation of IV or (b) the rate-determining step in the reaction is the concerted displacement of the benzyl group by the halide anion in the formation of IV: the para substituent in a–d (equation 2) should then have a relatively small influence on the rate of elimination.

Acknowledgement—The author wishes to thank Drs. J. A. C. ALLISON and G. R. CORAOR for many helpful discussions and suggestions.

J. Inorg. Nucl. Chem., 1962, Vol. 24, pp. 275 to 283. Pergamon Press Ltd. Printed in England

ORGANO-PHOSPHORUS COMPOUNDS—IV

THE PREPARATION OF ISOMERIC TETRA-ALKYLDIPHOSPHINES AND TETRA-ALKYLDIPHOSPHINE MONOSULPHIDES, A NEW CLASS OF PHOSPHORUS COMPOUNDS(1)

L. Maier*
Monsanto Chemical Company, Research Department Inorganic Chemicals Division,
St. Louis, Missouri; and Monsanto Research S.A. Zurich, Switzerland

(*Received* 1 *September* 1961; *in revised form* 26 *October* 1961)

Abstract—Organic substituted diphosphine disulphides are reduced by tributylphosphine, when heated in the ratio 1:2 to give excellent yields of tetra-alkyldiphosphines. In this reaction, tetra-alkyldiphosphine disulphides of the type RR'P(S)-(S)PRR' yield two isomeric diphosphines, the structure of which has been proved without question by nuclear magnetic resonance (n.m.r.) and chemical reactions. It is believed this to be the first time that such isomerism has been observed with triply connected phosphorus compounds.

If tetra-alkyldiphosphine disulphides are caused to react with tributylphosphine in the ratio 1:1 at elevated temperatures a new class of phosphorus compounds, the tetra-alkyldiphosphine monosulphides are produced. The structures and some of the chemical reactions of these compounds are discussed. A number of new n.m.r. chemical shifts are reported.

Although diphosphine, H_2P–PH_2, has been known for a long time, the first organic substituted diphosphine $(C_6H_5)_2P$–$P(C_6H_5)_2$ originally described in 1888(2) was thoroughly investigated only recently.(3) It was prepared by the following reaction:

$$(C_6H_5)_2PH + ClP(C_6H_5)_2 \rightarrow (C_6H_5)_2P\text{–}P(C_6H_5)_2 + HCl \qquad (1)$$

Later Issleib and Seidel(4) extended this method to the preparation of aliphatic diphosphines. Other methods for preparing tetra-alkyldiphosphines involve the reduction of tetra-alkyldiphosphine disulphides. As reducing agents, Zn-dust,(5)† Na,(6) Fe, Cu(7) and most conveniently tertiary phosphines(8a,c) have been used, especially n–tributylphosphine, which is available commercially.

---

* On leave of absence during 1960 from Monsanto Research S.A., Zürich.

† We observed that with Zn dust as a desulphurizing agent many by-products are formed, caused probably by a decomposition reaction(8a). This observation was confirmed by H. Nöth,(9). The boiling point of 54·5°C for P, P'–dimethyl-P, P'–diethylphosphine, reported in our preliminary communication,(8a) is erroneous. This is the boiling point of methylethylphosphine $CH_3(C_2H_5)PH$. The correct boiling point of $CH_3(C_2H_5)P$–$P(C_2H_5)CH_3$ is 188–190°C at normal pressure. We believe that the boiling point of $(n\text{–}C_3H_7)_2P$–$P(C_3H_7\text{–}n)_2$ given by Kuchen(5) as 108°C is also wrong. This is probably the boiling point of dipropylphosphine $(n\text{–}C_3H_7)_2PH$. The correct boiling point of $(n\text{–}C_3H_7)_2P$–$P(C_3H_7\text{–}n)_2$ is 144–145°C/16 mm Hg.(6)

(1) Part 3 of this series L. Maier, *Ber. Dtsch. Chem. Ges.* **94**, 3056 (1961).

(2) C. Dörken, *Ber. Dtsch. Chem. Ges.* **21**, 1509 (1888).

(3) W. Kuchen and H. Buchwald, *Ber. Dtsch. Chem. Ges.* **91**, 2871 (1958).

(4) K. Issleib and W. Seidel, *Ber Dtsch. Chem. Ges.* **92**, 2681 (1959).

(5) W. Kuchen and H. Buchwald, *Angew. Chem.* **71**, 162 (1959).

(6) K. Issleib and A. Tzschach, *Ber.* **93**, 1852 (1960).

(7) H. Niebergall, *Angew. Chem.* **72**, 210 (1960).

(8) (a) L. Maier, *Angew. Chem.* **71**, 575 (1959); (b) L. Maier, *Ber. Dtsch. Chem. Ges.* **94**, 3043, (1961); (c) G. W. Parshall, *J. Inorg. Nucl. Chem.* **14**, 291 (1960).

1. ***Stereoisomeric organic substituted diphosphine***

The reduction of asymmetric tetraalkyl- or dialkyl-diaryldiphosphine disulphides with tributylphosphine yields asymmetric diphosphines according to Equation (2);

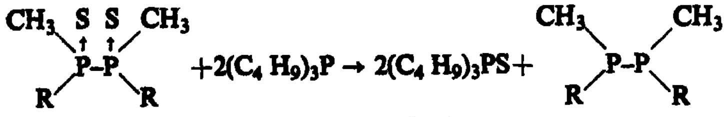

(2)

$R = C_2H_5, C_6H_5$

In investigating the ^{31}P nuclear magnetic resonance (n.m.r.) spectra of diphosphines which are believed to exhibit two different organic groups on each phosphorus, we found two distinct peaks of the same intensity. Fig. 1 gives the n.m.r. spectra of P,P′-dimethyl-P, P′-diphenyldiphosphine and P, P′-dimethyl-P, P′-diethyldiphosphine.

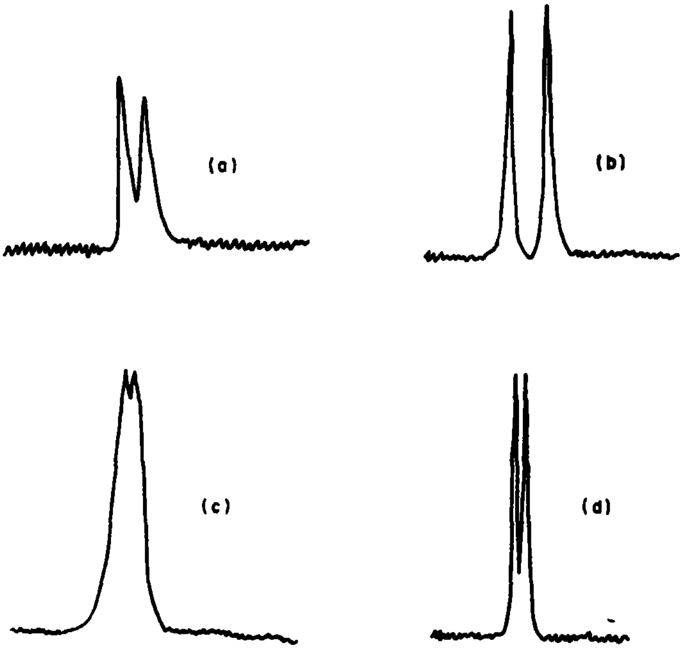

FIG. 1.—a. ^{31}P nuclear magnetic resonance spectrum of

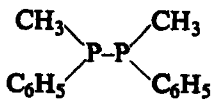

b. same spectrum decoupled

c. ^{31}P nuclear magnetic resonance spectrum of

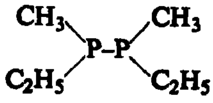

d. same spectrum decoupled

Although two peaks with the same area can be clearly seen (*a*, *c*) in the normal spectra their resolution is not as good as in the spectra *b* and *d* because of the spin–spin splitting of the hydrogens attached to the carbon atoms with the phosphorus. This makes the peaks somewhat broader and not as high as in *b* and *d*.

However, using the spin decoupler to superimpose a radiofrequency so as to decouple the spin–spin splitting of the hydrogens attached to the carbon atoms with the phosphorus, the two peaks become much sharper and higher and the resolution increases (spectra *b*, *d*). The separation of the two peaks changes with the groups attached to the phosphorus atoms. The two peaks in P, P′-dimethyl P, P′-diphenyldiphosphine are separated by 3·5 p.p.m. while in P, P′-dimethyl-P, P′-diethyldiphosphine the separation is 1·5 p.p.m. The existence of two peaks of the same area for these asymmetric diphosphines can be explained on the basis that:

(1) two isomeric forms are present in a 1:1 ratio

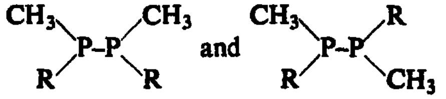

(I)

$R = C_2H_5$, C_6H_5 or

(2) rearrangement occurred to give a structure of the following type:

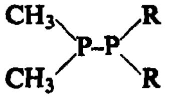

(II)

Four or more peaks would normally be expected for structure II, although two peaks would be possible for a certain combination of chemical shifts and the P–P coupling constant.

However, structure II could be ruled out since upon going to higher frequencies with the n.m.r. spectrometer (from 16·2 to 24·3 Mc/s) the separation of the two peaks remained the same in p.p.m. If the two peaks were caused by P–P spin splitting, as in structure II, the separation in p.p.m. of the two peaks would have changed. Further evidence for structure I was obtained by cleaving the asymmetric diphosphines with bromine; only one product, a mixed dialkyl- or alkylarylbromophosphine was produced.

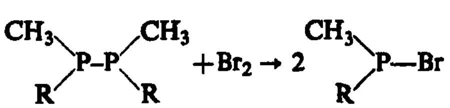

(3)

$R = C_2H_5$, C_6H_5

It is interesting to note that both the meso and the racemic tetra-alkyldiphosphine disulphides(8a,b) gave on reduction with tributylphosphine the asymmetric diphosphines in a 1:1 ratio. This means that either the reduction temperature is high enough to effect conversion, or a breakage of the P–P bond is involved to give first a dialkylphosphine radical ($CH_3RP\cdot$), which would then combine with another dialkylphosphine radical in a statistical manner to give a 1:1 mixture of the asymmetric diphosphines.

We believe this to be the first time that stereoisomers have been observed with triply connected phosphorus compounds. Separation of the two isomers could not be achieved by distillation.

2. *Tetra-alkyldiphosphine monosulphides*

When the tetra-alkyldiphosphine disulphides were made to react with tributylphosphine at 170°C at exactly a 1:1 ratio a new class of phosphorus compounds, the tetra-alkyldiphosphine monsulphides

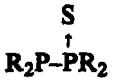

$$R_2P\text{-}\overset{S}{\overset{\uparrow}{P}}R_2$$

were obtained in nearly quantitative yield. Only a very small amount of the completely reduced diphosphine disulphide, the tetra-alkyldiphosphine and traces of unreduced diphosphine disulphide were present.

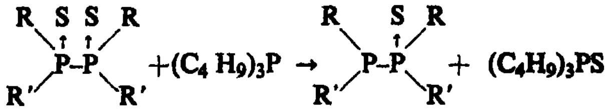

(4)

(III)

R = CH_3, C_2H_5
R′= CH_3, C_2H_5, C_6H_5

The structure of III was proved unequivocably by n.m.r. Since this is an AB type compound, the theory predicts(10) that the spectrum consists of a pair of doublets, the doublet splitting being equal to the spin-coupling constant. Indeed, a spectrum of this kind was obtained. Fig. 2 gives the n.m.r. spectrum of tetramethyldiphosphine monosulphide and dimethyl-diethyldiphosphine monosulphide. The undecoupled spectrum indicated two pairs of peaks, but especially spectrum *c* is not too well resolved because of spin–spin splitting of the hydrogens attached to the carbon atoms with the phosphorus. However, the decoupled spectrum shows clearly that we have two pairs of peaks, whereby the inner peaks (4, 5) being larger in area than the outer peaks (2, 7 b and 1, 7 d). It should be pointed out that the entire spectrum cannot be decoupled at one superimposed frequency. The negative part of the spectrum, attributable to the quadruply connected phosphorus compounds (peak 2–4a or 1–4b) decouples at a different frequency than the positive part of the spectrum assignable to triply connected phosphorus compounds. The spincoupling constant (*J*) (No. of cycles between 2 and 4, 1 and 4, or 5 and 7) was measured as 243 c/s. Knowing *J*, the relative intensities of the four observed peaks can be calculated according to the following equations:

$$C \cdot \sin\theta = \tfrac{1}{2} J \qquad (5)$$

and

$$C = [1/2(\gamma_o\delta)^2 + J^2]^{\frac{1}{2}} \qquad (6)$$

This equation solved according to Hamiltonian gives the energies for the transitions(10):

	Energy	*Relative intensity*
5 → 2	$\frac{1}{2}J+C$	$1-\sin\theta$
7 → 4	$-\frac{1}{2}J+C$	$1+\sin\theta$
4 → 2	$\frac{1}{2}J-C$	$1+\sin\theta$
7 → 5	$-\frac{1}{2}J-C$	$1-\sin\theta$

---

(9) H. NÖTH, *Z. Naturforsch.* 15 B, 327 (1960).

(10) J. A. POPLE, W. G. SCHNEIDER and H. J. BERNSTEIN, *High Resolution Nuclear Magnetic Resonance*, p. 119. McGraw Hill, New York (1959).

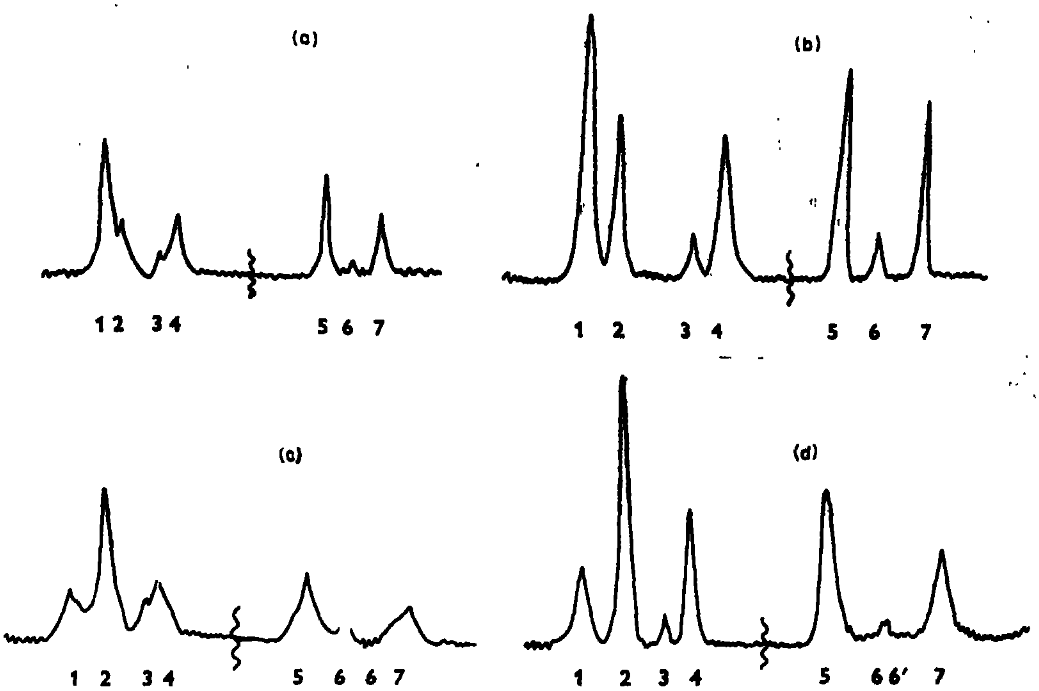

FIG. 2.—a. ^{31}P magnetic resonance spectrum of $(CH_3)_2P\text{-}\overset{\overset{S}{\uparrow}}{P}(CH_3)_2$ (peak 2, 4—5, 7) together with $(C_4H_9)_3PS$ (peak 1), unreduced $[(CH_3)_2PS]_2$ (peak 3) and completely reduced $[(CH_3)_2P]_2$ (peak 6)

b. same spectrum decoupled.

c. ^{31}P magnetic resonance spectrum of

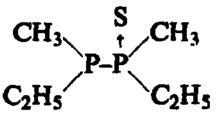

(peak 1, 4—5, 7) together with $(C_4H_9)_3PS$ (peak 2), unreduced $[CH_3(C_2H_5)PS]_2$ (peak 3) and completely reduced $[CH_3C_2H_5P]_2$ (peak 66′).

d. same spectrum decoupled.

Table 1 summarizes the theoretical relative intensities expected for $J = 243$ c/s and $C = 811{\cdot}5$ c/s (C was calculated from the correlation $2C—J = 1380$ c/s whereby $2C—J$ is the distance between the two inner peaks (4 and 5): this gives for sin θ a value of 0·15) with the intensities observed for tetramethyldiphosphine monosulphide and tetraethyldiphosphine monosulphide. The agreement between theory and experiment is excellent.

Provided that, during the preparation, an "umbrella-type" inversion of the molecule occurs at the triply connected phosphorus atom to give:

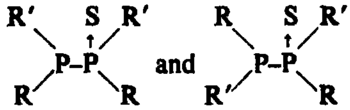

(IV)

tetra-alkyldiphosphine monosulphides with two different groups on the phosphorus atoms should theoretically give 8 peaks in the m.m.r. with the four inner peaks being larger in area than the four outer peaks. In reality only four peaks (the two

TABLE 1.—THE CALCULATED RELATIVE INTENSITIES FOR $J = 243$ c/s AND $C = 811{\cdot}5$ c/s ARE COMPARED WITH THE INTENSITIES OBSERVED FOR

$$(CH_3)_2P\text{–}\overset{\overset{\displaystyle S}{\uparrow}}{P}(CH_3)_2 \text{ AND } (C_2H_5)_2P\text{–}\overset{\overset{\displaystyle S}{\uparrow}}{P}(C_2H_5)_2$$

Peak	Calc. relative intensities	Observed for $(CH_3)_2P\text{–}\underset{\underset{\displaystyle S}{\downarrow}}{P}\text{–}(CH_3)_2$	$(C_2H_5)_2P\text{–}\underset{\underset{\displaystyle S}{\downarrow}}{P}(C_2H_5)_2$
2	0·85	0·85	0·81
4	1·15	1·17	1·14
5	1·15	1·18	1·13
7	0·85	0·85	0·85
Intensity ratio	1·353	1·37	1·33

inner ones being large) were observed. This might be due to the fact that molecular inversion did not occur (perhaps being prevented by the bulky sulphur atom) or the n.m.r. resolution was not high enough to resolve the eight peaks.

3. *Properties of the tetra-alkyldiphosphine monosulphides*

Tetramethyldiphosphine monosulphide could be distilled without decomposition under reduced pressure. However, because of the closeness of the boiling points no quantitative separation from tributylphosphine sulphide was achieved. The compound ignites in air. Oxidation with O_2 in acetone solution caused destruction of the molecule and no compound of the structure

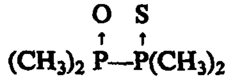

$$(CH_3)_2\overset{\overset{\displaystyle O}{\uparrow}}{P}\text{—}\overset{\overset{\displaystyle S}{\uparrow}}{P}(CH_3)_2$$

could be identified. However, a chemical proof of the structure was obtained by cleavage of the diphosphine monosulphides with bromine in benzene solution.

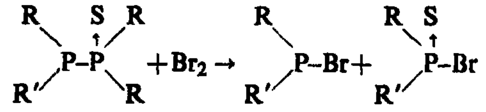

(7)

A 1:1 mixture of dialkylbromophosphine and dialkylthiophosphinic bromide was obtained.

EXPERIMENTAL

The tetra-alkyldiphosphine disulphides $[(CH_3)_2PS]_2$,(11) $[(C_2H_5)_2PS]_2$,(12) $[CH_3(C_2H_5)PS]_2$ and $[CH_3(C_6H_5)PS]_2$(8a,b) were prepared as described in the literature, and carefully purified by recrystallizing them several times.*

---

* The main impurities, which are dialkylthiophosphinic acids, $R_2P(S)SH$ and $R_2P(S)OH$, were first removed by treatment with alkaline solution.(12a) It was found in this work that they are reduced by $(C_4H_9)_3P$ to give a secondary phosphine (R_2PH).

(11) (a) M. I. KABACHNIK and E. S. SHEPELEVA, *Izvestia Akad. Nauk* 56 (1949); (b) H. REINHARDT, D. BIANCHI and D. MOLLE, *Ber. Dtsch. Chem. Ges.* 90, 1657 (1957).

(12) (a) P. J. CHRISTEN, L. M. VAN DER LINDE and F. N. HOOGE, *Rec. Trav. Chim.* 78, 161 (1959); (b) K. ISSLEIB and A. TZSCHACH, *Ber. Dtsch. Chem. Ges.* 92, 704 (1959).

1. *Preparation of*

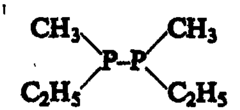

(V)

A mixture of 12 g of $[CH_3C_2H_5PS]_2$—the high and low melting form(8a, b) gave upon reduction the same 1:1 mixture of stereoisomeric diphosphines—and 23 g of tributylphosphine* was slowly heated in an atmosphere of nitrogen. The mixture became a homogenous liquid at 150°C. Continued heating yielded 8 g of liquid, spontaneously inflammable in air, which on redistillation gave 5·5 g (65·4 per cent.) of clear colourless (V) b.p. 188–190°C at 740 mm Hg. (Found: C, 48·32; H, 11·06. Calc. for $C_6H_{16}P_2$ (150·15): C, 47·99; H, 10·74%). N.m.r. indicated that the reduction of the diphosphine disulphides with tributylphosphine is quantitative. However, due to the high solubility of the tetra-alkyldiphosphines in tributylphosphine sulphide only a 60–70 per cent yield could be obtained by distillation. For n.m.r. investigation mixtures of the diphosphine disulphides and tributylphosphine in the ratio of 1:2·1 (5 per cent excess of $(C_4H_9)_3P$) were sealed under nitrogen in thick-walled Pyrex tubes of 15 mm diameter and heated for 1½–3 hours to 170°C. Heating of the tubes for 20 hr at 170°C did not decompose the tetra-alkyldiphosphines. The tubes were opened under nitrogen and the tetra-alkyldiphosphines were obtained by fractional distillation. Table 2 summarizes the results.

TABLE 2.—BOILING POINTS AND ^{31}P CHEMICAL SHIFTS OF TETRA-ALKYLDIPHOSPHINES

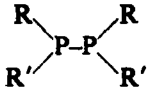

R	R′	b.p. (°C)	Yield (%)	^{31}P chemical shift in p.p.m. relative to 85% H_3PO_4
CH_3	CH_3	38–40/16 mm Hg*	62	+59·5
C_2H_5	C_2H_5	220–3/740 mm Hg†	68	+34·3
CH_3	C_2H_5	188–190/740 mm Hg	65·4	+44·7, +46·2
CH_3	C_6H_5	128–130/0·5 mm Hg‡	70	+38·2, +41·7

* Reported b.p. 140°C.(13)

† Reported b.p. 221–222°C.(4)

‡ m.p. 73–76°C; reported m.p. 75–77°C.(14)

2. *Cleavage of* $[CH_3(C_2H_5)P]_2$ (V) *with bromine*

A solution of 6·9 g of bromine in 20 ml of benzene was slowly added to 6·5 g of V dissolved in 20 ml of benzene. A strong exothermic reaction ensued (excess of bromine has to be avoided, otherwise $CH_3(C_2H_5)PBr_3$ is formed). Fractional distillation of the colourless solution yielded 8·7 g (= 65 per cent.) of $CH_3C_2H_5PBr$, a colourless liquid which fumes heavily in moist air, b.p. 129°C/740 mm Hg, n.m.r. chemical shift—98·5 p.p.m. (reported b.p. 128–129°C/720 mm, chemical shift—98·5 p.p.m.).(15) (Found: C, 23·25; H, 5·20. Calc. for C_3H_8BrP(154·99): C, 23·04; H, 5·47%). In the same way 4·3 g of $[CH_3(C_6H_5)P]_2$ dissolved in 15 ml of benzene with 2·2 g of bromine in 15 ml of benzene gave 4 g (= 61 per cent) of $CH_3C_6H_5PBr$, bp. 65°C/0·5 mm (reported b.p. 215°C/15 mm Hg(16), chemical shift—77 p.p.m.**

* The tributylphosphine used in these experiments was supplied by Westvaco, Mineral Products Division of F.M.C. Corporation.

** This agreed well with a sample synthesized by an independent method which will be reported in the near future.

(13) A. B. BURG, P. J. SLOTA and W. MAHLER, *Abstracts of Paper presented at 134th meeting of the American Chemical Society*, p. 78 P. September (1958).

(14) J. W. B. REESOR and G. F. WRIGHT, *J. Org. Chem.* **22**, 385 (1957).

(15) H. ULMER, L. C. D. GROENWEGHE, and L. MAIER *J. Inorg. Chem.* **20**, 82 (1961)

(16) G. M. KOSOLAPOFF, *Organophosphorus Compounds*, J. Wiley, New York (1950).

3. *Preparation of* $(CH_3)_2\overset{S}{\overset{\uparrow}{P}}-P(CH_3)_2$ (VI)

A mixture of 11·5 g of tributylphosphine and 10·5 g of tetramethyldiphosphine disulphide was sealed under nitrogen in a thick-walled Pyrex tube and heated for 20 hr to 170°C (n.m.r. analysis after 3 hr heating indicated that the reduction was not complete after this period). Then the tube was opened under nitrogen and the content fractionally distilled under reduced pressure. A fraction boiling at 65–70°C/0·5 mm contained mostly VI (90 per cent.) but also 10 per cent. of $(C_4H_9)_3PS$ as analyzed by n.m.r. The compound ignites in air and solidifies at room temperature. Other tetra-alkyldiphosphine monosulphides were synthesized similarly and analysed by n.m.r. The results are summarized in Table 3.

TABLE 3.—^{31}P CHEMICAL SHIFT OF TETRA-ALKYLDIPHONPHINE MONOSULPHIDES $RR'\overset{S}{\overset{\uparrow}{P}}-PRR'$

R	R′	^{31}P chemical shift in p.p.m. relative to 85% H_3PO_4*	
CH_3	CH_3	—43·9, —30·3	+54·7, +69·5
C_2H_5	C_2H_5	—62·8, —47·8	+29·5, +44·6
CH_3	C_2H_5	—53·9, —40·2	+40·9, +55·8
CH_3	C_6H_5	—43·7, —33·9	+37·5, +47·4

* The negative shift is due to the quadruply connected phosphorus atom and the positive shift to the triply connected phosphorus atom.

Through careful fractionation P, P′-dimethyl-P, P′-diethyldiphosphine-monosulphide $[CH_3(C_2H_5)P-\overset{S}{\overset{\uparrow}{P}}(C_2H_5)CH_3]$ was obtained in a pure state, b.p. 85–86°C/0·025 mm and analysed. (Found: C, 39·21; H, 8·79; S, 17·74. Calc. for $C_6H_{16}P_2S$(181·2): C, 39·76; H, 8·90; S, 18·11%).

4. *Oxidation of VI with oxygen*

Oxygen was bubbled through a solution of 1 g of VI dissolved in 5 ml of acetone. An extremely exothermic reaction occured. Acetone came to reflux. N.m.r. analysis of the crude product in acetone solution gave nine peaks all on the negative side. The two peaks on the positive side had disappeared. Since for a compound of the structure

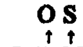

$$R_2\overset{O}{\overset{\uparrow}{P}}-\overset{S}{\overset{\uparrow}{P}}R_2$$

only four peaks on the negative side would be expected, the P–P bond was probably oxidized to give a P–O–P bond which hydrolysed partly with trace amounts of water to give phosphinic and monothiophosphinic acid. No isolation of the species was attempted.

5. *Cleavage of* $R_2\overset{S}{\overset{\uparrow}{P}}-PR_2$ *with bromine*

(a) *Cleavage of* $CH_3(C_2H_5)P-\overset{S}{\overset{\uparrow}{P}}(C_2H_5)CH_3$ (VII) *with bromine.* To a solution of 0·9 g of VII in 1 ml of benzene was added 0·7 g of bromine in 1 ml of benzene. An exothermic reaction occurred. N.m.r. analysis showed two peaks of the same area, one at —98·5 p.p.m. ($CH_3C_2H_5PBr$ see experiment 2 and Reference 15) and one at —85 p.p.m.($CH_3C_2H_5P(S)Br$.) The latter compound was also obtained when $[CH_3(C_2H_5)PS]_2$ was cleaved with bromine;[8a] the chemical shift was the same.

(b) *Cleavage of* $(C_2H_5)_2P\text{–}\overset{\overset{S}{\uparrow}}{P}(C_2H_5)_2$ (VIII) *with bromine.* To 0·72 g of VIII in 1 ml of C_6H_6 was added 0·63 g of bromine in 1 ml of benzene. Diethylbromopshophine, $(C_2H_5)_2PBr$, chemical shift —117 p.p.m. (and diethylthiophosphinic bromide (chemical shift—96 p.p.m.), this compound was also obtained when $[(C_2H_5)_2PS]_2$ was cleaved with bromine;(5) the chemical shift was the same) were produced in a 1:1 ratio.

Acknowledgement—I especially wish to thank Dr. J. R. VAN WAZER for helpful discussions and for correcting the English text. This research was supported in part by the United States Air Force under Contract AF 33(616)-6950 monitored by the Materials Laboratory, Wright Air Development Center, Wright Patterson Air Force Base, Ohio, U.S.A.

J. Inorg. Nucl. Chem., 1962, Vol. 24, pp. 285 to 289. Pergamon Press Ltd. Printed in England

IODINE MONOCHLORIDE AND IODINE TRICHLORIDE SYSTEMS INVOLVING PYRIDINE AND QUINOLINE

R. D. Whitaker and J. R. Ambrose*
Department of Chemistry, Washington and Lee University, Lexington, Virginia

(*Received* 1 *September* 1961; *in revised form* 5 *October* 1961)

Abstract—Spectrophotometric studies indicate that only addition compounds with 1:1 stoicheiometries are present in significant concentrations in carbon tetra-choride solutions of iodine monochloride or iodine trichloride with heterocyclic amines. However, thermal studies reveal that in the solid state, in addition to the expected 1:1 type compounds, the system iodine trichloride-pyridine forms $C_5H_5N{\cdot}2ICl_3$ (m.p. 140°) and $ICl_3{\cdot}2C_5H_5N$ (m.p. 69° incongruent) and the system iodine trichloride–quinoline forms $ICl_3{\cdot}2C_9H_7N$ (m.p. 81°). The system iodine monochloride–quinoline forms only the 1:1 type compound, and a reinvestigation of part of the system iodine monochloride-pyridine confirmed the absence of a compound with a mole ratio of 1:2 of iodine monochloride to pyridine.

In a previous publication⁽¹⁾ from this Laboratory, the preparation of molecular addition compounds of the type $D{\cdot}ICl$ and $D{\cdot}ICl_3$, where D is a molecule of one of several heterocyclic amines, was reported. These compounds were prepared by mixing carbon tetrachloride solutions of the iodine chlorides and amines at concentrations such that precipitation of the addition compounds occurred. It was of interest to investigate further some of these systems in order to study; (1) the possible presence in solution of addition compounds with stoichiometries other than 1:1, and (2) the formation of compounds in the absence of a solvent.

Carbon tetrachloride solutions of iodine monochloride with quinoline and of iodine trichloride with pyridine, quinoline, and 2,6–lutidine were studied spectrometrically using Job's method of continuous variation.⁽²⁾ Similar studies involving iodine monochloride with pyridine and 2,6–lutidine as well as other interhalogen-amine solutions have been reported.⁽³⁾ These studies indicated that addition compounds of 1:1 stoicheiometries only are present in significant concentration in solutions of these amines with iodine monochloride and iodine monobromide. One of the purposes of the present work was to determine whether or not iodine trichloride behaves in a manner analogous to the other interhalogen compounds in this respect. Phase diagrams were constructed for the binary systems of iodine monochloride and quinoline and of iodine trichloride with pyridine and quinoline. The phase diagram for iodine monochloride-pyridine has been reported.⁽⁴⁾ A reinvestigation of this system over part of the concentration range was undertaken.

---

*Taken in part from a thesis presented by J. R. Ambrose to Washington and Lee University in partial fulfilment of the requirements for the degree of Bachelor of Science in Chemistry.

(1) R. D. Whitaker, J. R. Ambrose and C. W. Hickam, *J. Inorg. Nucl. Chem.* **17**, 254 (1961).
(2) P. Job, *Ann. Chim.* [10] **9**, 113 (1928).
(3) A. I. Popov and R. H. Rygg, *J. Amer. Chem. Soc.* **79**, 4622 (1957).
(4) Ya. A. Fialkov and I. D. Muzyka, *J. Gen. Chem., Moscow*, **18**, 1205 (1948).

RESULTS

Continuous variation studies

These studies were carried out using carbon tetrachloride solutions of the iodine chlorides and amines in which the initial concentrations of components were varied over a ten-fold range, 10^{-4}–10^{-5} M. The absorbance was measured as a function of mole ratio of components at several wavelengths in the 290–330 mμ region. Maxima in the absorbances due to the complexes alone occurred at a mole ratio of 1:1 in every case.

Thermal studies

ICl_3*–pyridine system.* In addition to the expected 1:1 compound, the phase diagram (Fig. 1) shows that two other compounds are formed, $C_5H_5N{\cdot}2ICl_3$ which melts at 140°, and $ICl_3{\cdot}2C_5H_5N$ which melts incongruently at 69°. Eutectics occur at —47·2° with a composition of about 97 mole per cent pyridine, at 129° with a composition of 36 mole per cent pyridine, and at —24·6° with a composition of about 2 mole per cent pyridine. Some decomposition was noticed with compositions rich in iodine trichloride. The evolution of chlorine, accompanied by darkening of the usual yellow colour, was sometimes detected, and it was necessary to frequently prepare fresh mixtures in order to obtain consistent results. Even so, somewhat less than the usual accuracy must be ascribed to the values obtained with iodine trichloride-rich mixtures.

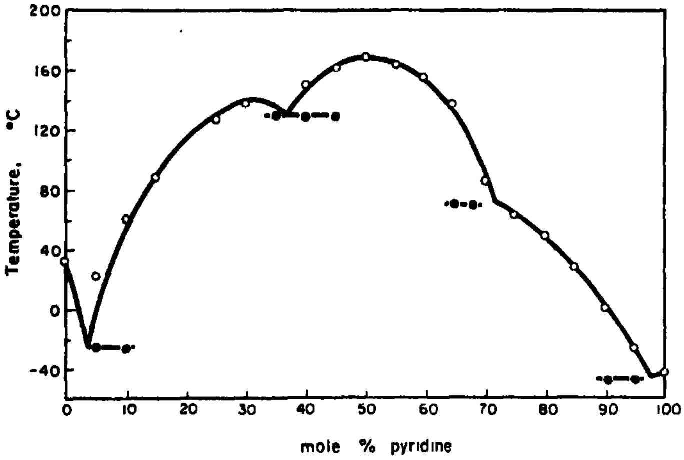

FIG. 1.—The system iodine trichloride–pyridine.

The melting point of the 1:1 compound was found to be 168·2°. This value is a bit lower than the melting point of 175–177°(1) as determined on a small sample of the 1:1 compound, prepared by precipitation from solution. However, the agreement is close enough to resolve the discrepancy between this latter value and the value given by ZAPPI and FERNANDEZ,(5) who reported a decomposition point of 196° for this compound. It is clear that the more nearly correct melting point for the pure 1:1 compound is 175–177°.

(5) E. V. ZAPPI and M. FERNANDEZ, *Ann. Ass. Quim. Argentina*, **27**, 102 (1939).

ICl_3–*quinoline system.* The phase diagram (Fig. 2) shows that a compound $ICl_3 \cdot 2C_9H_7N$ which melts at 81° is formed, as well as the expected 1:1 compound. Mixtures containing more than 60 mole per cent iodine trichloride reacted explosively when heated. However, the system possesses a eutectic at 82° with a composition of 43 mole per cent quinoline, so that it is likely that another, somewhat unstable compound exists. The other eutectics occur at —42·7° with a composition of 95 mole per cent quinoline and at 60° with a composition of 59·5 mole per cent quinoline. The melting point of the 1:1 compound was found to be 128·4°, which compares reasonably well with the previously reported value of 134–139°.⁽¹⁾

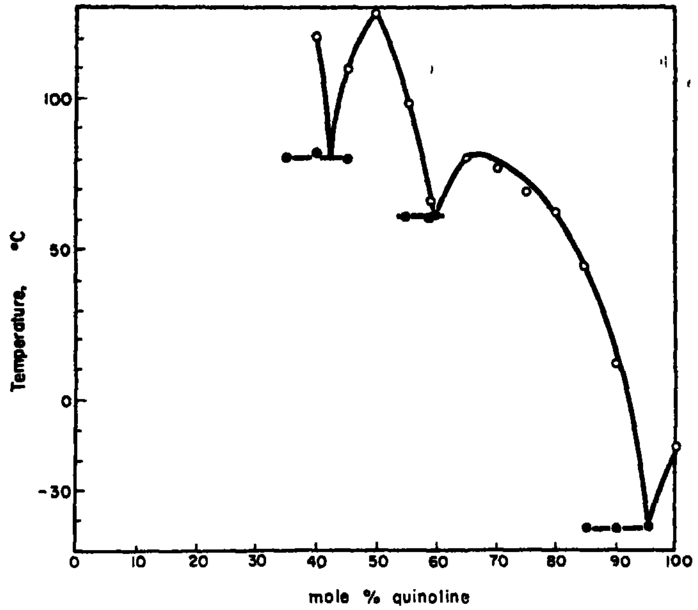

Fig. 2.—The system iodine trichloride–quinoline.

ICl–*quinoline system.* Only the 1:1 compound was found to exist. (Fig. 3.) Its apparent melting point of 132·2° is far below the previously reported value of 150–152°.⁽¹⁾ Although the freezing points of mixtures close to the 50 mole per cent composition were reproducible, it was observed that some decomposition did occur when these mixtures were liquified. The characteristic bright yellow colour of the solid mixtures changed to brown after liquification. However, this darkening became less pronounced as the compositions became richer in either component. The dashed line indicates the region where significant decomposition occurred. The remaining regions of the diagram possess the usual accuracy. Eutectics occur at precisely the same temperature of —31·8°, with compositions of 22 mole per cent and approximately 97 mole per cent quinoline.

ICl–*pyridine system.* Fialkov and Muzyka⁽⁴⁾ have published this phase diagram. Their work revealed two compounds—the 1:1 compound and a compound of the type $C_5H_5N \cdot 2ICl$ which melts at 35·1°. However, the freezing curve shows a rather abrupt change in slope in the region 70–80 mole per cent pyridine. Thinking that an incongruently melting compound consisting of a mole ratio of pyridine to iodine monochloride of 2:1 might have been overlooked, the present authors reinvestigated this system in the region 65–85 mole per cent pyridine. No meritectic halt was observed and no significant deviations from the previously reported results were obtained.

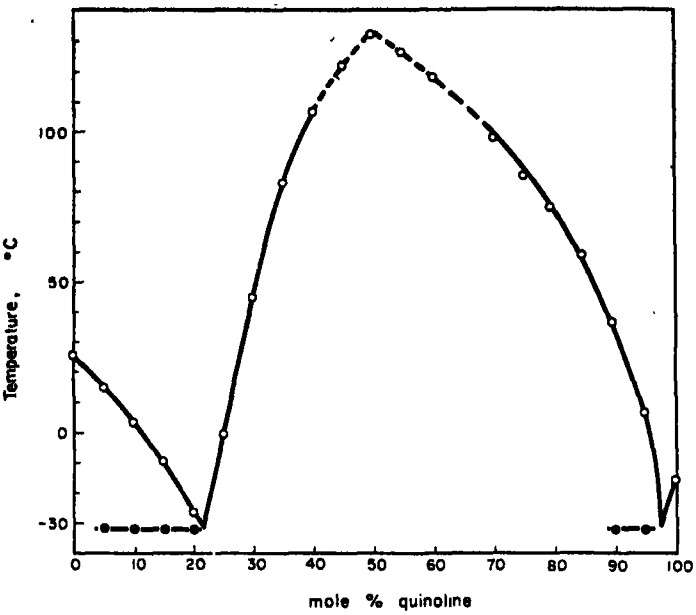

FIG. 3.—The system iodine monochloride–quinoline.

DISCUSSION

The continuous variation studies indicate that in non-polar solvents, the only important equilibrium in solutions of iodine monochloride or iodine trichloride–heterocyclic amine systems is;

$$D + A \rightleftharpoons DA$$

where D is the donor molecule and A is the acceptor molecule. The usual assumption made in connexion with work on relatively weak donor-acceptor systems has been that in non-polar solvents, the only complex in solution in significant concentration is the 1:1 species.* The situation is apparently the same for comparatively strong donor-acceptor systems. Although factors such as the relative donor-acceptor strengths of the molecules and the relative sizes of the molecules usually do not alter the stoicheiometries of the complexes which are formed in solution, the comparative degrees of dissociation of the complexes will, of course, depend strongly on these factors.(3)

In the absence of a solvent, however, the formation of compounds occurs in which stoicheiometries not solely of 1:1 are realized. The higher melting point of $C_5H_5N{\cdot}2ICl_3$ as compared with that of $C_5H_5N{\cdot}2ICl$ is similar to the case for the analogous 1:1 type compounds.(1) Iodine monochloride forms only the 1:1 compound with quinoline. If iodine trichloride forms a compound in which the mole ratio of iodine trichloride to quinoline is greater than one, such a compound is rather unstable, as evidenced by the explosive nature of some of the iodine trichloride-rich mixtures.

---

* It is not implied that there may not be several complexes with 1:1 stoicheiometries in equilibrium, each with different orientations of donor and acceptor molecules. For a discussion of such isomerism see, ORGEL and MULLIKEN.(6)

(6) L. E. ORGEL and R. S. MULLIKEN, *J. Amer. Chem. Soc.* **79**, 4839 (1957).

The most striking part of this comparison is to be found in the fact that with pyridine and quinoline, iodine trichloride forms compounds of the type $ICl_3 \cdot 2D$, whereas iodine monochloride does not. A superficial consideration of spatial factors would lead to the conclusion that the reverse situation should be favoured. Iodine monochloride should offer less steric hindrance than iodine trichloride to the addition of two large donor groups. With regard to steric effects, several points must be considered, however. It should be noted that it is indeed unlikely that the iodine atom has a co-ordination number of five in these compounds of iodine trichloride. The partial or complete ionization of chlorine could lead to one of two possible situations which we may represent;

$$D_2ICl_2^+ \cdots\cdots Cl^- \quad [I] \qquad D_2I^+ \cdots\cdots Cl_3^- \quad [II]$$

Either of the structures represented by [I] or [II] would lessen the "crowding" about the iodine atom, but we should expect [II] to be favoured somewhat from this standpoint. The configuration D_2I^+ is well known, a fact which again would seem to favour [II] as more nearly correct. However, because of these very reasons, it is difficult to understand why iodine monochloride does not form analogous compounds since the configurtiaon D_2I^+ would result in such cases. The absence of compounds of the type $D_2 \cdot ICl$ seems to suggest that the configuration D_2I^+ may not be correct for the iodine trichloride compounds. In the light of this consideration, the authors tend to favour [I] as more nearly correct, although definitive evidence which would allow a positive choice between the two possibilities is lacking.

One last point which should be considered is that the $ICl_3 \cdot 2C_5H_5N$ compound melts incongruently and the maximum of the freezing curve corresponding to the $ICl_3 \cdot 2C_9H_7N$ compound is fairly broad. Thus neither of these compounds is particularly stable at its melting point.

EXPERIMENTAL

Chemicals

The preparation and purification of iodine chlorides and the purification of the amines have been described.(1) Eastman Kodak Co. spectro-grade carbon tetra-chloride was used as the solvent in the spectrophotometric studies.

Spectrophotometric studies

A Beckman Model DB Spectrophotometer was used. The light path length of the glass-stoppered silica cells was 1 cm. The temperature of the cell compartment was held at 26·0 ± 0·1°.

Thermal studies

Phase diagrams for the binary systems were constructed by the cooling-curve method. Temperature–time plots were obtained by means of an iron–constantan thermocouple in conjunction with an E. H. Sargent Model SR Recorder. The apparatus was calibrated using as standards the melting points of benzene, naphthalene, and salicylic acid. Mixtures of known composition were prepared by direct weighing in a stoppered, glass tube fitted with glass stirrer and thermocouple well. The stirrer was operated manually. At lower temperatures, n-heptane, and at higher temperatures, dibutylphthalate, were used to insure thermal equilibrium in the thermocouple well. The cold junction temperature was maintained at 0°. All points were determined at least twice, and the reported temperatures are believed to be accurate to within ±2·5°.

Acknowledgment—We wish to express our appreciation to the Research Corporation for the financial support of this work.

J. Inorg. Nucl. Chem., 1962, Vol. 24, pp. 291 to 298. Pergamon Press Ltd. Printed in England

COMPLEXES OF URANYL ION WITH SOME SIMPLE ORGANIC ACIDS

C. A. Crutchfield, Jr.,(1) W. M. McNabb and J. F. Hazel
University of Pennsylvania, Philadelphia, Pennsylvania

(*Received* 8 *May* 1961; *in revised form* 9 *October* 1961)

Abstract—Stepwise formation constants were determined for complexes of uranyl ion with lactic, β-OH-propionic, α-OH-butyric, and β-OH-butyric acids. The constants were determined by pH titration, and some qualitative information was also obtained by polarography.

The investigation by Ahrland(2) of the uranyl-glycolic acid system indicated the formation of complexes having metal-ligand ratios of 1:1, 1:2 and 1:3. It was shown that the ligand was the glycolate anion and not the unionized molecule. Where the glycolic acid-glycolate ion ratio was 4 or greater, no perceptible hydrolysis was found. Li, *et al.*(3) studied this and other systems by ion exchange methods and drew similar conclusions. Both Ahrland and Li found evidence of only mononuclear complexes under the conditions used.

In a spectrophotometric study of the uranyl-lactate system, Feldman and co-workers(4) found only a 1:1 complex up to pH = 3·5 with no evidence of polymeric forms until the pH was increased. A subsequent study(5) of pH titration curves indicated the presence of polymeric forms up to the trimer. In this latter study, an equimolar (0·05 M) mixture of uranyl salt and lactic acid was used—these conditions, perhaps, being conducive to the formation of polymeric forms.

In the work described here, stepwise formation constants were determined for complexes of uranyl ion with a group of four closely related organic acids.

EXPERIMENTAL

Material. The uranyl perchlorate was purchased from the G. F. Smith Chemical Co. and some was also prepared from uranyl nitrate by the method of Salvadori.(6) The uranyl perchlorate solution was assayed by a lead reductor method,(7) and any acid impurity present was determined by a cation resin exchange method.(8) Carbonate-free sodium

(1) a. Abstract from a dissertation by C. A. Crutchfield, Jr., submitted in partial fulfillment for the degree of Ph.D. at the University of Pennsylvania, Phila., Penna., June (1960).
b. This work was aided, in part, by a scholarship to C. A. Crutchfield, Jr., from the Edgar Fahs Smith Scholarship Fund of the University of Pennsylvania.
c. Present address: Stanford Research Institute, Southern California Laboratories, South Pasadena, California.

(2) S. Ahrland, *Acta Chem. Scand.* 7, 485 (1953).

(3) N. C. Li, W. M. Westfall, A. Lindenbaum, J. M. White and J. Schubert, *J. Amer. Chem. Soc.* 79, 5864 (1957).

(4) I. Feldman and J. Havill, *J. Amer. Chem. Soc.* 76, 2114 (1954).

(5) I. Feldman, J. Havill and W. Neuman, *J. Amer. Chem. Soc.* 76, 4726 (1954).

(6) R. Salvadori, *Chem. Z.* 36, 513 (1912).

(7) W. D. Cook, J. F. Hazel and W. M. McNabb, *Analyt. Chem.* 22, 654 (1950).

(8) H. Day, J. Gill, E. Jones and W. Marshall, *Analyt. Chem.* 26, 611 (1954).

hydroxide was prepared from saturated sodium hydroxide and was stored in and dispensed from an all plastic container. The sodium hydroxide was standardized against primary standard potassium hydrogen phthalate. The organic acids were of C.P. grade and were standardized against sodium hydroxide. Carbonate free water was used in all titrations and polarograms. The Triton X-100, a gift from the Rohm and Haas Corp., Philadelphia, Pa., was used as a maximum suppressor in the polarographic work.

Apparatus and procedure. A Leeds and Northrup pH meter, catalogue number 7664, was used for the pH titration. The meter was standardized against a 0·05 M potassium hydrogen phthalate buffer (pH = 4·01 at 31°). All titrations and pH measurements were made in a thermostated sample cell which had a cover fitted with inlets for electrodes, etc. There was also an inlet for nitrogen, which was continually passed over the solution to exclude atmospheric carbon dioxide. Solutions were allowed to stand, with stirring, for about 15 min to insure that equilibrium had been attained.

Because of the possibility of photochemical reduction of the uranyl ion, solutions used in pH titrations and polarography were tested for the presence of uranous ion by titration with dichromate.(9) No reduction was detected.

The Leeds and Northrup Electrochemograph E was used for polarographic measurements. It was fitted with a thermostated sample cell, and the reference electrode had an e.m.f. of +0·223 V against a normal hydrogen electrode. A dropping mercury electrode was used.

RESULTS AND DISCUSSION

pH and activity corrections. Because of the difficulty of obtaining activity coefficients for all of the ions involved, the "concentration" constants were determined rather than the thermodynamic constants.(10) The molar concentrations of all terms in the Calvin and Wilson equation(11) could be easily determined from the stoicheiometry of the solution with the exception of the H^+ ion and the acid ionization constants of the ligands. Since the ready hydrolysis of the uranyl ion made it necessary to work with pH less than 3·5, it was considered unsafe to neglect activity coefficients for the H^+ ion. Therefore, it was assumed that pH meter readings expressed hydrogen ion activity: these values were converted to molar concentration by calculation of the activity coefficient from the Debye-Hückel equation. Constant terms used in this equation were obtained from Bates' *Electrometric pH Determination.*(12)

This method of converting pH meter values to H^+ ion concentrations is admittedly not exact, but it is at least a partial correction and serves to make the H^+ ion term in the Calvin and Wilson equation more consistent with the other terms. A more elaborate treatment of this would have been futile because of the uncertainty of the pH measurements themselves.

While the authors admit that modern instruments will furnish formal pH values to a precision of ±0·001 units, they feel that presentation of pH values of precision better than ±0·01 units would have been overly optimistic in view of the uncertainties in the complex systems examined in this work. Except for the most rigidly controlled studies on fairly simple systems, unknown liquid junction potentials alone will probably contribute an uncertainty of at least ±0·01 units.(13) Moreover, N.B.S. standard buffer solutions have a precision of only ±0·01 pH units.(12)

---

(9) G. Rao, V. Rao and M. Rao, *Analyt. Chim. Acta*, **15**, 97 (1956).

(10) H. Irving and H. Rossotti, *J. Chem. Soc.* 2904 (1954).

(11) M. Calvin and K. Wilson, *J. Amer. Chem. Soc.* **67**, 2003 (1945).

(12) R. Bates, *Electrometric pH Determination*, p. 89. J. Wiley, New York (1954).

(13) J. Lingane, *Electroanalytical Chemistry* (2nd Ed.), p. 74. Interscience, New York (1958).

In order to check this procedure, the thermodynamic ionization constants of the organic acids were determined. These values were used also to obtain the concentration ionization constants of the acids, which were needed for the Calvin and Wilson equation. The thermodynamic ionization constant for lactic acid was the only one available in the literature for 31°. The constant for monochloracetic acid was determined as an additional check.

Experimental values, averaged from six or more determinations, are compared with literature data in Table 1.

Table 1.—Thermodynamic ionization constants, 31°

Acid	Calculated p*K*a	Literature p*K*a⁽¹⁴⁾
Lactic	3·83 ±0·03 S.D.	3·864
Monochloracetic	2·81 ±0·06	2·875
β-OH-propionic	4·52 ±0·03	—
α-OH-butyric	3·81 ±0·03	—
β-OH-butyric	4·40 ±0·01	—

pH titrations. Known amounts of uranyl perchlorate, the organic acid, and sodium perchlorate were pipetted into the titration cell. Water was added to make an initial volume of 100 ml with ionic strength of about 0·10. This mixture was titrated with strong (about 1·0 N) sodium hydroxide and the pH was recorded after the system had reached equilibrium.

In order to detect polymerization and mixed (i.e., hydroxy) complexes, the pH titrations for each acid studied were obtained for various concentrations of both uranyl ion and the ligand.⁽¹⁵⁾ The total uranyl ion concentration ranged from 0·003 M to 0·009 M, or by a factor of two or better in each system. The data obtained for each acid agreed with the limits of accuracy of the measurements which indicated that polynuclear and mixed complexes could be neglected. The stability constants obtained from the titration data showed no apparent trending related to the various metal–ligand concentrations. To minimize the possibility of hydroxy-complex formation, no data were used in which the pH was greater than 3·5.

Ahrland's work⁽²⁾ with the uranyl–glycolate system indicated that no polymeric forms were present to any appreciable extent when the glycolic acid–glycolate ion ratio was greater than about four. Acid-ion ratios for the systems studied in this work were kept above five, except for two titrations of the α-OH-butyric acid system, which had minimum ratios of 3 and 2·5. These, however, showed no significant differences from the other titrations for this system with minimum ratios of five and six.

The exact behaviour of the uranyl ion on hydrolysis is still uncertain. However, assuming Sutton's⁽¹⁶⁾ value of $K = 1{\cdot}14 \times 10^{-6}$ for the reaction:

$$2\,UO_2^{2+} + 2\,H_2O = U_2O_5^{2+} + 2H^+ \qquad \text{(I)}$$

the per cent of uranyl ion hydrolysed, even if no complexation at all occurred, would be about 1·5 per cent under the most adverse conditions used in this work. It was

---

⁽¹⁴⁾ B. Conway, *Electrochemical Data*, p. 184. Elsevier, New York (1952).

⁽¹⁵⁾ R. Tobias, *J. Chem. Educ.* **35**, 592 (1958).

⁽¹⁶⁾ J. Sutton, *J. Chem. Soc., Suppl.* **2**, S-275 (1949).

considered that this small amount could safely be ignored: there was no evidence of polymeric or hydrolysed forms in significant amounts, and the principal complex species appear to be of the type $UO_2(A)_n^{2-n}$, where the ligand A is the anion of the organic acid.

The amount of ligand bound to the uranyl ion was calculated from pH titration data by the equation of Calvin and Wilson.(11) From this, values of Bjerrum's "formation function", $\bar{n}$, were calculated along with corresponding values of (A), the ligand ion concentration.(17) The stability constants were then determined from a smoothed plot of $\bar{n}/(A)$ vs. (A) by Fronaeus' graphical extrapolation method.(18)

A condensed set of data from a typical titration for each acid is presented in Table 2.

Table 2.—pH titration solutions and data

All titrations performed under nitrogen at 31° C Lactic acid—99·84 ml solution containing 0·00883 M $UO_2(ClO_4)_2$, 0·1325 M lactic acid, 0·01083 M $HClO_4$, 0·1000 M $NaClO_4$, titrated with 0·8250 M NaOH

NaOH (ml)	pH	$\bar{n}$	$(A)^- \times 10^3$	$\bar{n}/(A)^-$
0·302	1·83	0·954	1·48	647
0·517	1·87	0·962	1·61	597
0·713	1·91	0·964	1·76	548
1·119	1·99	1·022	2·09	488
1·554	2·07	1·144	2·48	462
1·994	2·18	1·213	3·14	386
2·913	2·40	1·487	4·98	298
3·877	2·61	1·858	7·61	244
4·541	2·75	2·101	9·96	211

β-OH-propionic acid—99·85 ml solution containing 0·00484 M $UO_2(ClO_4)_2$, 0·0557 M β-OH-propionic acid, 0·00539 M $HClO_4$, 0·1000 M $NaClO_4$, titrated with 1·234 M N OH

NaOH (ml)	pH	$\bar{n}$	$(A)^- \times 10^3$	$\bar{n}/(A)^-$
0·083	2·30	0·278	0·421	660
0·168	2·37	0·292	0·493	593
0·333	2·52	0·359	0·688	521
0·516	2·71	0·481	1·045	460
0·605	2·81	0·554	1·30	426
0·681	2·89	0·632	1·54	409
0·891	3·10	0·864	2·40	361
1·117	3·28	1·154	3·24	335

Because of the inaccuracy of the data at low $(A)^-$ values, a lower limit of integration was chosen in all cases. Also, the erratic behaviour of the higher functions, due to compounding of errors, prevented in most cases the direct determination of values of K_2 and K_3.

---

(17) J. Bjerrum, *Metal Ammine Formation in Aqueous Solution*. Haase, Copenhagen (1941).
(18) S. Fronaeus, *Acta Chem. Scand.* 4, 74 (1950).

α–OH–butyric acid—99·90 ml solution containing 0·00338 M $UO_2(ClO_4)_2$, 0·0557 M α–OH–butyric acid, 0·00539 M $HClO_4$, 0·1000 M $NaClO_4$, titrated with 0·4418 M NaOH

NaOH (ml)	pH	$\bar{n}$	$(A)^- \times 10^3$	$\bar{n}/(A)^-$
0·901	2·11	0·787	1·00	785
1·503	2·22	0·874	1·26	692
1·899	2·31	0·899	1·54	585
2·504	2·48	0·904	2·22	408
2·939	2·60	0·988	2·84	348
3·272	2·70	1·035	3·48	297
3·743	2·82	1·194	4·18	286
4·112	2·93	1·225	5·42	226
4·760	3·11	1·238	7·57	164
5·732	3·31	1·501	10·42	144

β–OH–butyric acid—99·85 ml solution containing 0·00528 M $UO_2(ClO_4)_2$, 0·0595 M β–OH–butyric acid, 0·00539 M HC lO_4, 0·1000 M $NaClO_4$, titrated with 1·234 M NaOH

0·000	2·22	0·281	0·494	568
0·151	2·33	0·296	0·633	468
0·400	2·56	0·354	1·059	334
0·576	2·75	0·434	1·61	327
0·703	2·88	0·525	2·13	247
0·851	3·03	0·628	2·93	214
0·968	3·12	0·748	3·52	213
1·156	3·28	0·861	4·93	175

For these reasons, and because of the rather abrupt rise of $\bar{n}/(A)^-$ values at very low $(A)^-$, the constants were also calculated by a "best fit" method. Approximate values for the constants were inserted into equation II, the equation for the $\bar{n}/(A)^-$ vs. $(A)^-$ curve.

$$\frac{\bar{n}}{(A)} = \frac{K_1+2K_1K_2(A)+3K_1K_2K_3(A)^2+\ldots}{1+K_1(A)+K_1K_2(A)^2+K_1K_2K_3(A)^3+\ldots} \qquad \text{(II)}$$

The approximate values were then adjusted until a curve was obtained which fit the experimentally determined points within ±5 per cent of the $\bar{n}/(A)$ values, corresponding to a pH error of ±0·02 units. Space limitations prevent the presentation of graphs of these data. Values for the stability constants obtained by this method and by graphical extrapolation are given in Table 3. The values obtained from the titration data listed in Table 2 are those listed first for each ligand in Table 3.

The accuracy of the log K values is limited by that of the pKa values (±0·03) and by pH measurements (±0·02). Thus the values for log K_1 are probably accurate to about ±0·1 log units. The values of log K_2 and log K_3 are dependent on the values for log K_1, and since errors compound rapidly by both methods of calculation, log

[illegible]

[illegible] $K_n = \frac{[UO_2(A)_n]}{[UO_2(A)_{n-1}][A]}$

Ionic strength 0·12–0·13, temperature [illegible]

Fronaeus			Curve fitting		
log K_1	log K_2	log K_3	log K_1	log K_2	log K_3
Lactic acid					
3·31	2·14	1·70	3·32	2·13	1·84
3·34	2·30	1·89	3·37	2·26	1·98
3·42	1·70	1·77	3·41	2·45	2·26
3·34	1·77	2·36	3·31	2·04	1·70
α–OH–butyric acid					
3·28	1·60	—	3·32	1·78	—
3·26	1·96	—	3·29	1·81	—
3·29	1·92	—	3·29	1·85	—
3·18	1·49	—	3·26	1·48	—
β–OH–propionic acid					
2·90	—	—	2·74	2·18	2·00
2·98	—	—	2·74	2·18	2·08
2·86	—	—	2·70	2·08	2·00
2·96	—	—	2·76	2·18	2·08
β–OH–butyric acid					
2·71	1·23	—	2·70	1·40	—
2·73	1·23	—	2·71	1·40	—
2·83	—	—	2·78	1·40	—
2·62	1·18	—	2·61	1·30	—

K_2 should be accurate only to ±0·3 units, and log K_3 to ±1 unit (that is, log K_3 values should be considered as indicating only the order of magnitude).

Average values for each system, calculated from the curve fitting method are presented in Table 4.

TABLE 4.—AVERAGED STABILITY CONSTANTS

	log K_1	log K_2	log K_3	pK_a
Lactic acid	3·36 ± 0·05	2·2 ± 0·3	2 ± 1	3·83 ± 0·03
α–OH–butyric acid	3·29	1·7	0 (< 1)	3·81
β–OH–propionic acid	2·74	2·2	2	4·52
β–OH–butyric acid	2·70	1·4	0 (< 1)	4·42

For both α- and β-hydroxy butyric acids, no third complex was detected. In both cases it was possible to construct a curve to fit the experimental data by assuming the presence of the species MA and MA_2 only. Also, the plot of the function from which K_2 was calculated was a straight line with a zero slope.(17) If any third complex, MA_3, is formed in these systems, log K_3 must be less than one, else it would have been detected.

[illegible] In addition, the plot of the [illegible] straight line with positive slope.

The values calculated for the lactic acid systems are compared [illegible] those found for the uranyl–glycolic acid system by AHRLAND[2] and LI[3].

TABLE 5.

Source	log K_1	log K_2	log K_3	log K_1/K_2	Ligand	Ionic strength	[illegible]
AHRLAND(2)	2·42	1·53	1·26	0·89	Glycolate	1	20°
LI *et al.*(3)	2·75	1·52	—	1·23	Glycolate	0·16—0·19	25°
This work	3·36	2·22	1·94	1·14	Lactate	0·12—0·13	31°

Polarography. The solutions used for polarography were similar to those used in the pH titrations except for the addition of 0·01 per cent of maximum suppressor and the use of a much smaller uranyl ion concentration (about 0·001 M). No quantitative information could be obtained by polarography due to the irreversibility of the U(V)–U(IV) reduction.

The polarographic results for the two α-hydroxy acids were quite similar (see Table 6). The U(VI)–U(V) waves were symmetrical and plots of $E_{d.e.}$ vs. log $[i/(i_d-i)]$ were good straight lines with slopes close to that expected for a one-electron reduction. This linearity indicated that no dimeric forms were present in detectable amounts.(19) Where the pH was above about 4·2 in these systems, a slight degree of irreversibility appeared for both acids. This was indicated by increasing deviation from the theoretical slope and the appearance of some curvature as the current approached the limiting value. This irreversibility of U(VI) reduction at high pH values has been reported by others, and has been ascribed to the formation of some hydrolysed form of the uranyl ion.(20,21) If hydrolysis is the true explanation of this irreversibility, then the least stable complex should show the greatest effect as it would be less effective in shielding the uranyl ion from attack by hydroxyl ion, etc.

The $E_{\frac{1}{2}}$ values became more negative as the acid anion concentration increased, indicating that the ligand was the ion of the acid and not the unionized molecule. When the $E_{\frac{1}{2}}$ values were plotted against log(A) values, a fairly straight line was formed with a slope close to the theoretical value for a one-electron reduction with the loss of one ligand. Data for solutions of different total organic acid concentration were coincident within experimental error.

The polarograms of the two β-hydroxy acids were less satisfactory. The plots of $E_{d.e.}$ versus log $[i/(i_d-i)]$ were linear at low pH, but they showed very definite irreversibility at about pH 3·5 and above. This was more pronounced for systems with low organic acid concentration. Where the slopes of these plots could be determined, they were close to the theoretical value for a one-electron reduction.

---

(19) G. BOOMAN and W. HOLBROOK, *Analyt. Chem.* 31, 10 (1959).

(20) E. BREDA, L. MEITES, T. REDDY and P. WEST, *Analyt. Chim. Acta*, 14, 390 (1956).

(21) P. SUBBARAMAN, N. JOSHI and J. GUPTA, *Analyt. Chim. Acta*, 20, 89 (1959).

This is in agreement with the pH titration results, especially since the β-OH-butyric acid polarograms showed more irreversibility than did those for β-OH-propionic acid.

TABLE 6.—POLAROGRAPHIC RESULTS, SLOPE IN (—) VOLTS

Acid	$E_{d.e.}$ vs. log $[i/(i_d-i)]$	$E_{\frac{1}{2}}$ vs. log (A)
Lactic	0·068–0·056	0·054
α–OH–butyric	0·068–0·055	0·056
β–OH–propionic	0·069–0·055	0·076
β–OH–butyric	0·083–0·068	0·111
Theoretical (31°)	0·0603*	0·0603† 0·1206‡

* $M^{+n}+\bar{e}=M^{+n-1}$

† $M(A)_n^{2-n}+\bar{e}=M(A)_{n-1}^{2-n}+A^-$

‡ $M(A)_n^{2-n}+\bar{e}=M(A)_{n-2}^{2-n+1}+2A^-$

Plots of $E_{\frac{1}{2}}$ versus log (A) indicated that the ligand was the anion of the organic acid. The slope of this data for the β-OH-propionic system was slightly greater than that expected for a one-electron reduction with loss of one ligand, and showed a very slight curvature in the direction of increasing slope as log (A) was increased by increasing the pH. The same data for β-OH-butyric acid showed definite curvature and the "average" slope was only slightly less than the expected value for a one-electron reduction with the loss of two ligands. This deviation from the expected $E_{\frac{1}{2}}$ vs. log(A) data is very probably caused by irreversibility, which would have the effect of increasing the apparent $E_{\frac{1}{2}}$ shift. This irreversibility is in turn caused by the lower stability of the complexes formed by the β-hydroxy acids.

CONCLUSIONS

In the case of the two α-hydroxy acids, the first ligand attaching may be a chelate. Evidence for this is the larger value of log K_1 for these two acids as compared with the log K_1 values for the two β-hydroxy acids, even though the latter are weaker acids.(22) This is probably due to the greater stability of the five-membered chelate rings which would be formed by the α-hydroxy acids as opposed to the six-membered rings which would be formed by the β-hydroxy acids.(23)

Rather definite evidence was found for the formation of a third complex, MA_3, for both α- and β-OH-propionic acids but not for either of the hydroxy-butyric acids. This difference is perhaps due to steric hindrance by the larger hydroxy-butyrate ions.(24) The examination of molecular models gave some indication of steric hindrance, but not enough for definite conclusions to be drawn. It should not be concluded that the third complex does not exist for these acids, but it is more probable that their stability constants are too small to be detected by the methods and conditions used.

(22) R. CANNAN and A. KILBRICK, *J. Amer. Chem. Soc.* **60**, 2314 (1938).

(23) G. SCHWARZENBACH, *Analyt. Chem.* **32**, 6 (1960).

(24) H. IRVING and H. ROSSOTTI, *J. Chem. Soc.* 2910 (1954).

J. Inorg. Nucl. Chem., 1962, Vol. 24, pp. 299 to 302. Pergamon Press Ltd. Printed in England.

DICHLORO- AND SILOXYGERMANIUM PHTHALOCYANINES*

R. D. JOYNER, R. G. LINCK, J. N. ESPOSITO and M. E. KENNEY
Department of Chemistry, Case Institute of Technology, Cleveland, Ohio

(*Received* 21 *August* 1961)

Abstract—Two syntheses of dichlorogermanium phthalocyanine are given, one of which is especially advantageous. In addition several siloxy germanium phthalocyanines are described. The properties of one member of this group suggest that it is polymeric.

RECENTLY it has been reported that dichlorogermanium phthalocyanine is produced when phthalonitrile and $GeCl_4$ are reacted together in refluxing quinoline.(1) Further work has uncovered two additional methods for the synthesis of dichlorogermanium phthalocyanine. One method depends on the reaction of *o*-cyanobenzamide with $GeCl_4$ in refluxing 1-chloronaphthalene and the other on the reaction occurring between phthalocyanine and $GeCl_4$ in refluxing quinoline. The second of these two methods appears to be especially advantageous in terms of yield, convenience and purity of product.

In the same paper which reported dichlorogermanium phthalocyanine, bis-(triphenylsiloxy)-germanium phthalocyanine also was reported. Related compounds containing siloxy groups of the type $-OSi(Ph)_2O-$ in place of the $OSi(Ph)_3$ groups have now been prepared. As expected these new compounds show properties markedly influenced by the specific nature of the siloxy groups.

EXPERIMENTAL

Dichlorogermanium phthalocyanine

o-Cyanobenzamide method. To 10 g (0·07 mole) of *o*-cyanobenzamide in 100 ml of 1-chloronaphthalene, 2·4 ml (0·021 mole) of germanium tetrachloride was added. This was heated slowly to 180° (1½ hr) and held at this temperature for 2 hr. The mixture was then slowly heated to reflux (1 hr) and held at this temperature for 2 hr. After cooling, the reaction mixture was filtered and the crystalline product obtained was washed with acetone, water and dimethylformamide and dried. The crystals were identified by their infra-red spectrum.(2) Yield 2·5 g (0·0038 mole).

Metal-free phthalocyanine method. A mixture of 2·6 g (0·0051 mole) of phthalocyanine, 0·60 ml (0·0052 mole) of $GeCl_4$ and 30 ml of technical quinoline was heated to reflux in 10 min. and held at this temperature for 110 min. The crystalline product was separated

---

* This work was partially supported by the Research Corporation and by the National Science Foundation. Further support was obtained from the United States Air Force through the Air Force Office of Scientific Research of the Air Research and Development Command, under Contract No. AF 49 (638)-773. Reproduction in whole or in part is permitted for any purpose of the United States Government.

(1) R. D. JOYNER and M. E. KENNEY, *J. Amer. Chem. Soc.* **82**, 5790 (1960). Phthalonitrile is incorrectly given as phthalocyanine in this synthesis.

(2) R. D. JOYNER, Ph.D. Thesis, University Microfilms 61-3317.

from the hot reaction mixture by filtration and washed with quinoline, benzene and acetone. An infra-red spectrum of it showed that the conversion of the phthalocyanine was essentially complete. Yield 2·7 g (0·0041 mole). The use of synthetic quinoline did not affect the product or change the yield materially, but the use of an increased ratio of $GeCl_4$ gave a product containing green impurities.

Siloxygermanium phthalocyanines

Bis-(diphenylhydroxysiloxy)-germanium phthalocyanine bisdioxanate. A mixture of 30 g (0·048 mole) of powdered dihydroxygermanium phthalocyanine, 30 g (0·14 mole) of diphenylsilanediol and 400 ml of benzene was refluxed for 3½ hr. The resultant mixture yielded when filtered a crystalline reaction product. A 3 g portion of this was dissolved in 30 ml of refluxing dioxane. The resultant solution after being filtered and cooled yielded 1·4 g of thin platelets which were greenish-blue by transmitted light and reddish by reflected light. These were filtered off and vacuum dried at 50°C. A portion of these was then crushed and further vacuum dried at room temperature, Found: C, 64·74; H, 4·98; N, 9·58. Calc: for $C_{56}H_{38}N_8GeSi_2O_4{\cdot}2C_4H_8O_2$: C, 64·49; H, 4·57; N, 9·40%.

Both 1 : 2 and 1 : 6 hydroxide-diol mole ratio mixtures yielded reaction products which were the same as those obtained with the 1 : 3 mole ratio mixture but a 1 : 1 mixture gave some unreacted hydroxide and no crystalline siloxide. The highest percentage yield was obtained with the 1 : 2 mixture.

Bis-(diphenylhydroxysiloxy)-germanium phthalocyanine. The unsolvated diphenylhydroxysiloxide was obtained from the product solvated with dioxane by vacuum drying it at 80° for 6 hr. Found: C, 66·01 and 66·04; H, 3·89 and 3·94; N, 11·50 Calc. for $C_{56}H_{38}N_8GeSi_2O_4$: C, 66·22; H, 3·77; N, 11·03%.

The infra-red spectrum of this compound (Table 1) matched with the spectra of the 1 : 6, 1 : 3 and 1 : 2 hydroxide-diol reaction products and showed that they were the unsolvated diphenylhydroxysiloxide. When the compound was treated with $LiAlH_4$ in butyl ether no hydrogen was evolved.

Samples of the diphenylhydroxysiloxide were also crystallized from dimethylformamide and pyridine but the crystals obtained in both cases broke upon washing with acetone. The product obtained from dimethylformamide showed a 10% weight loss on vacuum drying at room temperature. The solubility of the diphenylhydroxysiloxide in these two solvents when hot was approximately 1g/10 ml.

Bis-(diphenylbenzyloxysiloxy)-germanium phthalocyanine. A 0·5 g (0·0005 mole) sample of the diphenylhydroxysiloxide was placed in 25 ml (0·24 mole) of benzyl alcohol and the mixture heated to reflux. The resultant solution yielded on cooling 280 mg of the diphenylbenzyloxysiloxide, a blue-green compound by transmitted light. The infra-red spectrum of this compound (Table 1) showed several important differences when compared with the diphenylhydroxysiloxide. Found: C, 70·76; H, 4·50; N, 9·08. Calc: for $C_{70}H_{50}N_8GeSi_2O_4$: C, 70·30; H, 4·21; N, 9·37%.

Thermal decomposition of the diphenylhydroxysiloxide. A sample of the crude diphenylhydroxysiloxide was immersed in a heating bath at 385° while under vacuum. Gas was evolved and a blue-green product (by transmitted light) was obtained which was non-volatile and insoluble in dioxane. It gave an infra-red spectrum (Table 1) which was related to that of the diphenylhydroxysiloxide in the 700–1150 cm^{-1} region but which lacked an absorption band in the 3500 cm^{-1} region. These observations suggested that a polygermanosiloxane had been formed.

DISCUSSION

The basic conclusions concerning the nature of these germanophthalocyaninosiloxanes rest principally on the synthetic methods used to obtain them and on the results of their elemental analyses. However, a consideration of some of the other data available provides support for these conclusions and further amplifies them.

In the case of the diphenylhydroxysiloxide, its formulation as a silanol is substantiated by its solubility in solvents generally good for polar materials, by its solvation with dioxane and apparently also with dimethylformamide and pyridine, and by its facile reaction with benzyl alcohol. In addition, the fact that it shows infra-red absorptions in the 830–900 cm^{-1} region and at 3545 cm^{-1} is in accord with such a structure.(3)

The short wave length of the 3545 cm^{-1} OH band compared to the OH band in diphenylsilandiol (3238 cm^{-1} in a Nujol mull) may indicate a reduction in hydrogen bonding. If this is the case it is not surprising in view of the steric requirements of the molecule as a whole.

The infra-red spectrum of the diphenylhydroxysiloxide also shows prominent bands in the 700 to 1150 cm^{-1} region at 702, 734, 760, 905, 1091 and 1126 cm^{-1} (Table 1). An examination of the spectra of the germanium phthalocyanines previously reported (1) shows that bands in positions similar to all but the first of these are characteristic of germanium phthalocyanines. (Silicon,(4) aluminum (5) and other (6) phthalocyanines also have similar spectral absorptions.) The 702 cm^{-1} band in the diphenylhydroxysiloxide is undoubtedly due to the presence of phenyl rings.

TABLE 1—PROMINENT INFRA-RED BANDS*

$PcGe[OSi(OH)(Ph)_2]_2$ (KBr)	$PcGe[OSi(OCH_2Ph)(Ph_2]_2$ (Nujol)	$[PcGe(OSi(Ph)_2O)_2]_n$ (Nujol)
	Common Bands	
702	700	705
734	729	730
760	759	760
905	903	906
1091	1089	1093
1126	1125	1125
	Characteristic Bands	
783	717	1000
830	777	
866	838	
999	998	
1016	1018	
1038	1035	
	1069	

* Reproductions of these spectra are available in reference (2)

Although the spectra of analogous silicon and germanium phthalocyanines are usually very similar,(4) the sharp band common to them near 900 cm^{-1} can be used to

(3) L. J. BELLAMY, *The Infra-red Spectra of Complex Molecules* (2nd Ed.) p. 341. J. WILEY, New York (1958); A. L. SMITH, *Spectrochim. Acta.* 16, 102 (1960).

(4) R. D. JOYNER, J. CEKADA, Jr., R. G. LINCK and M. E. KENNEY, *J. Inorg. Nucl. Chem.* 15, 387 (1960).

(5) J. E. Owen and M. E. KENNEY, *Abstracts of* 138*th National Meeting of the American Chemical Society*, New York (1960).

(6) A. N. SIDOROV and I. P. KOTLYAR, *Opt. i Spektr.* 11, 175 (1961); *Optics and Spectroscopy* 11, 92 (1961).

distinguish between the two types. In the cases examined so far the germanium compounds absorb in the 900–906 cm^{-1} region and the analogous silicon compounds in a similar narrow region about 10 cm^{-1} higher.

The spectrum of the diphenylhydroxysiloxide solvated with dioxane is very similar to that of the unsolvated diphenylhydroxysiloxide except for the presence of a band at 1260 cm^{-1}, a band assignable to the ether oxygen of the dioxane.

The fact that the diphenylhydroxysiloxide forms in high yields shows that under the conditions chosen, the condensation reaction between the OH groups attached to Si and Ge atoms is easier than that between pairs of silanol groups and pairs of GeOH groups. While this result may be due partly to steric and solubility factors the mildness of the conditions required suggests that other factors are also important. Perhaps the GeOH groups are relatively basic compared to the SiOH groups and an acid-base reaction which splits out water therefore takes place easily.

With regard to structure it may be concluded that the siloxy groups attached to the germanium atoms must be *trans* to each other because the bulk of the groups precludes a *cis* arrangement unless the unlikely assumption is made that the Ge atoms are very far out of the plane of the phthalocyanine rings. This same *trans* arrangement can be assumed for the remaining germanium phthalocyanines because in all cases similar considerations argue for it.

The infra-red spectrum of the diphenylbenzyloxysiloxide shows bands which are characteristic of a metal phthalocyanine (729, 759, 1089, 1125 cm^{-1}), of a germanium phthalocyanine (903 cm^{-1}) and of phenyl rings (700 cm^{-1}), but shows no bands in the 3500 cm^{-1} OH region and only one prominent band in the 830–900 cm^{-1} SiOH region. All these observations are consistent with the structure assigned to the compound on the basis of synthetic and analytical data. The bands at 998, 1018 and 1035 cm^{-1} are positioned very similarly to analogous bands in the spectrum of the diphenylhydroxysiloxide (999, 1016 and 1038 cm^{-1}) and the triphenylsiloxide (997, 1012 and 1034 cm^{-1}) thus suggesting a common origin. It may be that these bands are associated with the GeOSi grouping since other similar groups show absorptions in this region.(7) The backbone of this compound is unusual in that it contains C, Si and Ge linked together with oxygen in order of increasing atomic number, i.e., COSiOGeOSiOC.

The postulated formation of a polygermanosiloxane by the thermal decomposition of the diphenylhydroxysiloxide is supported by several pieces of data. Among these are the nonvolatility of the product and its insolubility in dioxane. Similarly in accord with this hypothesis is the fact that its preparation is accompanied by the release of gas. The presence of bands in its infra-red spectrum at positions which are characteristic of phthalocyaninogermanium groups and of a band at 1000 cm^{-1} which can be assigned to siloxy groups (and perhaps to GeOSi groups as well) also point to a polygermanosiloxane. As expected on the basis of the structure postulated for the polymer, no bands are visible in the OH region around 3500 cm^{-1}. The backbone of the polymer, $(GeOSiOSiO)_n$, and the fact that the polymer can be considered to be formed from relatively long siloxy units bridging phthalocyaninogermanium units combine to make it unique.

---

(7) L. J. BELLAMY, *The Infra-red Spectra of Complex Molecules* (2nd Ed.) p. 340. J. Wiley, New York (1958).

J. Inorg. Nucl. Chem., 1962, Vol. 24, pp. 303 to 307. Pergamon Press Ltd. Printed in England

ON THE URANATES OF AMMONIUM—I

THE TERNARY SYSTEM NH_3–UO_3–H_2O

E. H. P. CORDFUNKE
Reactor Centre of the Netherlands (R.C.N.), Petten

(*Received* 18 *October* 1961)

Abstract—The ternary system NH_3–UO_3–H_2O has been studied in aqueous solutions. From chemical and X-ray analysis four compounds, having the bruto-formulae:

$UO_3 \cdot 2\,H_2O$ (I)
$3\,UO_3 \cdot NH_3 \cdot 5\,H_2O$ (II)
$2\,UO_3 \cdot NH_3 \cdot 3\,H_2O$ (III)
$3\,UO_3 \cdot 2\,NH_3 \cdot 4\,H_2O$ (IV)

were found to exist in this system at 40° C. The stability of these phases is discussed.

The reaction of a solution of uranylnitrate with ammonia has also been studied. The precipitates thus formed could be identified as I (pH = 3·5), II (pH = 4–7) and III (pH > 7). However, they cannot be isolated in a pure form, owing to the presence of nitrate, which cannot be removed completely by washing with water.

A MINIMUM of reliable information is available on the composition and properties of the uranates, precipitated from aqueous solutions.

Addition of ammonia to a solution of uranylnitrate yields a product that originally was believed to be ammoniumdiuranate: $(NH_4)_2U_2O_7$.* For instance TRIDOT(1) found some evidence for its formation.

On the contrary, recent investigations(2, 3, 4) have shown the complex nature of this precipitate. These studies give sufficient evidence that $(NH_4)_2U_2O_7$ cannot be obtained from aqueous solutions, even in the presence of a large excess of ammonia. Several compositions, including hydrated polyuranates,(4) are reported as a result of various methods of investigation.

However, little or no attention has been given to conditions of equilibrium and to the possibility of hydrolysis of the precipitates by washing with water. On this latter fact EWING c.s.(5) have drawn the attention. Consequently most analyses must have failed to give a correct view of the compositions. It was therefore considered worthwhile to make a systematic study of the uranates of ammonium, combined with extensive X-ray work.(6) In this paper the results of these investigations, especially on the ternary system NH_3–UO_3–H_2O (at 40° C), will be presented.

EXPERIMENTAL

Samples, containing UO_3, water and ammonia were equilibrated at 40° C.

As starting material the amorphous form of UO_3 was chosen, because of its high reactivity. This UO_3 can be prepared easily from $UO_4 \cdot 2H_2O$ by heating in air at 450–500° C.(7)

---

*In the technical literature generally indicated as ADU.

(1) G. TRIDOT, *Ann. Chim.* 358, 12e Série (5), (1950).

(2) A. M. DEANE, AERE/R–3411 (1960).

(3) F. J. ARMSON, H. E. DIBBEN and H. MASON, S.C.S.–R-30 (1959).

(4) K. J. NOTZ e.o. T.I.D., report 6228.

(5) R. A. EWING e.o. Report BMI–1115 (1956).

(6) To be published separately by P. C. DEBETS and B. O. LOOPSTRA in this journal.

(7) E. H. P. CORDFUNKE, *J. Inorg. Nucl. Chem.* 23, 285 (1961).

Pure UO_3 (99·9 per cent) was weighed into screw-cap bottles of 100 ml in fixed quantities of 2·86 g (0·01 mole). After placing measured volumes of water and ammonia of various concentrations into the bottles, they were closed and sealed with paraffine-wax. These bottles were continuously shaken in a thermostat at 40 ± 1° C for various periods of time (1–4 weeks).

After that, the solids were filtered off, washed with waterfree acetone until free of ammonium ions and dried in air and finally over concentrated H_2SO_4; it was checked that the products do not change composition by this treatment.

Most of the samples, thus obtained, were examined by X-ray diffraction, using a Philips diffractometer with a recorder. The different phases detected, are labelled as I, II and so on, merely as a matter of convenience.

The uranium content of the solids was determined by the weight change on ignition of the samples in air at 750–800° C, the compounds being converted to U_3O_8.

The ammonia content was analysed by means of a semi-micro technique, according to Conway.(8) By this method small amounts of ammonia can be determined accurately. The water content of the solids was obtained by difference.

The most relevant experimental data are presented in Table 1.

Table 1.—Experimental data of the ternary system NH_3–UO_3–H_2O (40° C)

Initial solution $\frac{NH_3}{UO_3}$ (molar ratio) (±1%)	Solid phase $\frac{NH_3}{UO_3}$ (molar ratio) (±1·5%)	Solid phase By X-ray
0·000	0·000	I
0·062	0·058	„
0·110	0·108	„
0·166	0·162	I (+II)
0·218	0·216	„
0·321	0·319	„
0·323	0·320	II (+I)
0·326	0·322	„
0·333	0·333	II
0·335	0·333	„
0·346	0·333	„
0·382	0·355	II (+III)
0·383	0·350	„
0·394	0·376	„
0·414	0·379	„
0·422	0·378	„
0·468	0·432	III (+II)
0·514	0·474	„
0·730	0·508	III
0·770	0·493	„
0·829	0·504	„
0·834	0·515	III (+IV ?)
0·834	0·512	„
1·511	0·539	III (+IV)
4·64	0·587	„
7·73	0·636	„
33·25	0·653	IV
80·0	0·660	„

---

(8) E. J. Conway, *Microdiffusion analysis and volumetric error*. London (1950).

DISCUSSION

The experimental results show that there are four solid phases in the area of the system NH_3–UO_3–H_2O studied, each of them having a different X-ray diffraction pattern⁽⁶⁾ (Table 1).

The compound I was identified by chemical and X-ray analysis⁽⁹⁾ as the well known hydrate $UO_3 \cdot 2H_2O$. This hydrate is rapidly formed by the action of water on amorphous UO_3.

The average composition of the pure uranates II, III and IV, is given in Table 2. It was shown experimentally that the compounds are stable when dried over concentrated H_2SO_4, the molar ratio HN_3/UO_3 being constant with time (Fig. 1 and 2).

TABLE 2.—THE COMPOSITION OF THE COMPOUNDS IN THE TERNARY SYSTEM NH_3–UO_3–H_2O (40° C)

Type	Composition		Bruto-formula
	wt% UO_3 (±0·5%)	wt% NH_3 (±1%)	
I	88·9	—	$UO_3 \cdot 2H_2O$
II	88·9	1·75	$3UO_3 \cdot NH_3 \cdot 5H_2O$
III	89·2	2·65	$2UO_3 \cdot NH_3 \cdot 3H_2O$
IV	88·8	3·38	$3UO_3 \cdot 2NH_3 \cdot 4H_2O$

The uranates II, III and IV are closely related to $UO_3 \cdot 2H_2O$: the number of moles NH_3 and H_2O per mole of UO_3 is 2 in all cases. This is in agreement with structural data, obtained from the X-ray analysis.⁽⁶⁾

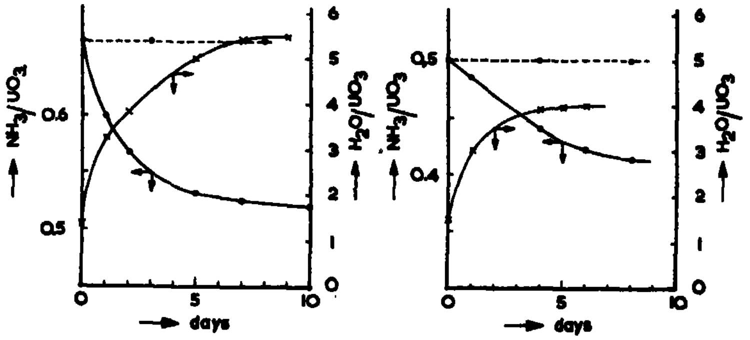

FIG. 1.—Compound IV. FIG. 2.—Compound III.
---NH_3/UO_3-ratio over conc. H_2SO_4.

The compounds III and IV are hygroscopic: upon prolonged standing in air, saturated with water vapour, they can attract considerable amounts of water. An illustration of this phenomenon is given for product IV in Fig. 1, from which can be seen that IV can take up approximately 4 moles of water per mole of UO_3 over the theoretical amount (H_2O/UO_3 = 1·33; Table 2). The behaviour of compound III is quite analogous (Fig. 2).

⁽⁹⁾ J. K. DAWSON e.o. *J. Chem. Soc.* 3531 (1956).

It is interesting to note that both III and IV are not only hygroscopic, but also unstable in contact with water vapour (e.g. moist air), since it was found that the molar ratio NH_3/UO_3 of these compounds gradually decreases with time. In Fig. 1 this is illustrated for the compound IV. Apparently the $NH_3 \cdot UO_3$-ratio approaches asymptotically a value, approximately corresponding with that of III. However, the NH_3/UO_3-ratio of a pure III also decreases in contact with moist air (Fig. 2). The phenomenon must be due to an exchange of part of the NH_3 in the lattice for water.

The excess of water, taken up by IV can easily be removed by pumping off. The substance so obtained is probably mainly III. Bringing this phase in contact with moist air results in a further decrease of the NH_3/UO_3-ratio. This can be repeated until finally the composition of II is reached.

The behaviour of compound II is quite different. Freshly prepared II may contain much water in excess. Upon standing in air, it begins to shrink gradually, water being expelled: the molar ratio NH_3/UO_3, however, remains constant. This was observed on several II-preparations of which an example is given in Table 3.

TABLE 3.—THE COMPOSITION OF COMPOUND II

Molar ratio	II freshly prepared	Same precipitate after 2½ month in air	Theor. composition (Table 2)
NH_3/UO_3	0·33	0·33	0·33
H_2O/UO_3	4·87	1·83	1·67

It must be concluded therefore that towards moist air, compound II is the only stable one of the three uranates found in the ternary system NH_3–UO_3H_2O.

The reaction between a solution of uranylnitrate and ammonia has been studied by several authors, as already mentioned. Owing to the contradictory results we have investigated this reaction, using the information obtained from the ternary system NH_3–UO_3–H_2O.

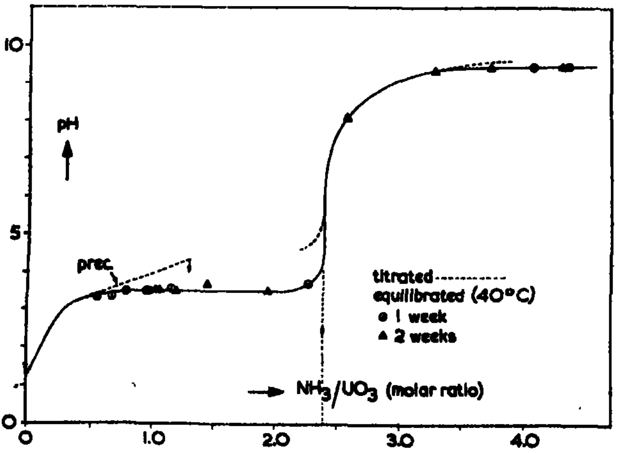

FIG. 3.—pH-curve, obtained on addition of ammonia to $UO_2(NO_3)_2$.

We have studied this precipitation at various concentrations of uranylnitrate and ammonia in the same way by allowing the products to attain the equilibrium in a thermostat at 40° C. Some results are given in Fig. 3, in which the pH of the saturated solution is plotted against the molar ratio NH_3/UO_3 of the initial solution.

In Fig. 3 the pronounced effect of the waiting time on pH during the precipitation ($pH < 5$) is illustrated. The pH after equilibration is obviously lower than can be obtained by direct titration (dotted line): this has not been generally recognized.(10) An explanation of this phenomenon can possibly be found in a slow transformation via complex uranyl ions (e.g. $U_2O_5^{2+}$, $U_3O_8^{2+}$ etc., according to Sutton(11)) into solid uranates of a different composition.*

The precipitation, starting at $pH = 3{\cdot}5$ is completed at $pH = 4$. For a complete precipitation ~ 2·3 moles of NH_4OH per mole of $UO_2(NO_3)_2$ are required (ammonia for neutralization of the small amounts of free acid not included); X-ray analysis revealed that this precipitate is of type II, whereas at $pH = 3{\cdot}5$ (incomplete precipitation) product I is precipitated. It is evident that the quantity of ammonia, required for complete precipitation of II, corresponding with a bruto-ratio $NH_3/UO_3 = 2{\cdot}3$, is in agreement with the composition found for product II in the ternary system. Above $pH = 7$ this precipitate is gradually converted into a mixture of the solids II and III, as revealed by X-ray analysis.

The analytical data of the precipitates appeared to be more difficult to interpret, owing to the fact that in all cases appreciable, but not reproducible amounts of NO_3^--ions are strongly retained. Most of these NO_3^--ions can be removed by washing the precipitates with water, but this results at the same time in a rapid conversion of III into II, as already noted. Notwithstanding thorough washing, it appeared to be impossible to remove nitrate completely.

We must conclude therefore that the results obtained from a study of the reaction of a solution of $UO_2(NO_3)_2$ with ammonia do not give a true picture of the uranates of ammonium. This must be the reason for the contradictory results, described in the literature.

Acknowledgement—The author wishes to thank Prof. J. P. W. Houtman for his stimulating interest in this work, and Dr. B. O. Loopstra for many valuable discussions.

The author is much indebted to Mr. P. Aling for his assistance in much of the experimental work.

*The nature of these slow transformations has been studied extensively by M. E. A. Hermans *et al.* (KEMA, Arnhem, Netherlands) as part of their work on the ADU-like precipitates, which provided the stimulus for the present investigation. The work of Mr. Hermans will be published as a thesis: Delft Technical University.

(10) J. Maly and V. Vesely, *J. Inorg. Nucl. Chem.* **7**, 119 (1958).

(11) J. Sutton, *J. Chem. Soc.* S 275 (1949).

J. Inorg. Nucl. Chem., 1962, Vol. 24, pp. 309 to 314. Pergamon Press Ltd. Printed in England

CHEMICAL REACTIONS OF MOLYBDENUM HEXAFLUORIDE

T. A. O'DONNELL and D. F. STEWART
Chemistry Department, University of Melbourne, Parkville, N.2, Melbourne

(*Received* 10 *August* 1961; *in revised form* 18 *October* 1961)

Abstract—Previous accounts of the chemical properties of molybdenum hexafluoride are restricted to comments on the ease of hydrolysis of the compound and to a few very simple observations on its reactions with a short series of unrelated substances. This paper describes a systematic study of the chemical reactions of the hexafluoride with the lower fluorides of some elements of Groups V and VI and with Group V trichlorides.

Some new techniques for studying the reactions of volatile fluorides and for fractionation of the products within the reaction system are described.

THE preparation of molybdenum hexafluoride was first reported by RUFF and EISNER,(1) who used platinum apparatus for the reaction. With the limited experimental procedures then available, they were not able to provide any worthwhile account of the chemical reactivity of the hexafluoride, apart from a comment on the ease of hydrolysis and some very simple observations on its apparent reaction with a few unrelated compounds. Some physical properties of the hexafluoride were studied by RUFF and ASCHER(2) and very recently CADY and HARGREAVES(3) have measured vapour pressures and related properties. Spectroscopic studies, such as those of GAUNT(4) have been carried out for structure determination. BRADY and co-workers(5) have provided thermodynamic data for this and other volatile fluorides.

Recent Russian work(6) provides the most detailed account of the hydrolysis of molybdenum hexafluoride and the formation of oxyfluorides. The ready hydrolysis of the volatile fluorides of the metallic elements accounts for the slow progress in the study of the reactions of these compounds because of the difficulty of handling them in glass apparatus. Etching reactions lead to complete hydrolysis of the compounds. Techniques employing glass vacuum systems based on packless all-metal valves, and in which the glass was carefully dried by evacuation and flaming, were developed specifically for the handling and characterization of molybdenum hexafluoride.(7)

Most of the published work on the higher fluorides of the metallic elements, such as that on the hexafluorides of osmium,(8) platinum(9) and the transuranic elements,(10) has been concerned primarily with identification and with physical properties.

---

(1) O. RUFF and F. EISNER, *Z. Anorg. Chem.* **52**, 256 (1907).

(2) O. RUFF and E. ASCHER, *Z. Anorg. Chem.* **196**, 413 (1931).

(3) G. H. CADY and G. B. HARGREAVES, *J. Chem. Soc.* 1563 (1961).

(4) J. GAUNT, *Trans. Faraday Soc.* **49**, 1122 (1953).

(5) a. A. P. BRADY, O. E. MYERS and J. K. CLAUSS, *J. Phys. Chem.* **64**, 588 (1960).
b. O. E. MYERS and A. P. BRADY, *J. Phys. Chem.* **64**, 591 (1960).

(6) N. S. NIKOLAEV and A. A. OPALOVSKII, *Russian J. Inorg. Chem.* (Eng. trans.), **5**, 532 (1959).

(7) T. A. O'DONNELL, *J. Chem. Soc.* 4681 (1956).

(8) B. WEINSTOCK and J. G. MALM, *J. Amer. Chem. Soc.* **80**, 4466 (1958).

(9) B. WEINSTOCK, H. H. CLAASSEN and J. G. MALM, *J. Amer. Chem. Soc.* **79**, 5832 (1957).

(10) B. WEINSTOCK and J. G. MALM, *J. Inorg. Nucl. Chem.* **11**, 104 (1959).

Fischer and Rudzitis[11] have shown that bismuth pentafluoride is a very vigorous fluorinating agent converting sulphur and iodine to fluorides rapidly at room temperature. However, there is little published work on the chemical reactions of the higher fluorides to form a basis for discussion of the reactions of molybdenum hexafluoride. This difficulty is illustrated by recent observations[12] that tungsten hexafluoride, which might be expected to be almost identical with the molybdenum compound, differs markedly in its chemical reactivity.

Early observations of the reactions of molybdenum hexafluoride with carbon disulphide and phosphorus pentachloride indicated vigorous reactivity, although it was subsequently shown that iodine dissolved readily without change in molybdenum hexafluoride and that sulphur was also unaffected. It was then decided to study the ability of molybdenum hexafluoride to oxidize the lower fluorides of some non-metals to higher fluorides and surprisingly small reactivity was observed. The present investigation was then completed by a study of the reactions between the hexafluoride and trichlorides of some Group V elements. In these cases reactions occurred which could be related to those of the corresponding trifluorides and to the known chemistry of the halides of the Group V elements concerned.

EXPERIMENTAL

Preparation of reagents

Molybdenum hexafluoride was prepared by direct fluorination of the metal in a copper reactor and collected in a glass trap containing sodium fluoride and cooled to −78° C. It was then purified by distillation in a glass system. Hydrolysis was prevented by using the rigorous precautions previously reported.(7) The sample was stored in a carefully dried glass-trap fitted with a metal valve.

Phosphorus trifluoride was prepared by a method which was essentially that of Chatt and Williams,[13] phosphorus trichloride being added to an excess of antimony trifluoride. The product was fractionated to remove phosphorus trichloride. Reaction of a stoicheiometric mixture of arsenious oxide and calcium fluoride with excess concentrated sulphuric acid produced arsenious trifluoride. Commercial laboratory reagent grade antimony trifluoride was sublimed at 180° C and 10^{-5} mm pressure. Bismuth trifluoride was prepared by condensing anhydrous hydrogen fluoride on to bismuth hydroxide in a polyethylene container, which was then sealed for 15 hr. Water and excess hydrogen fluoride were removed subsequently by evaporation.

Sulphur tetrafluoride was obtained commercially in a cylinder and purified by shaking with mercury and by fractionation. Direct fluorination of selenium at 0° C using a 1:1 mixture of fluorine and nitrogen[14] resulted in the formation of selenium tetrafluoride.

Phosphorus trichloride was a laboratory reagent grade chemical, purified by re-distillation. The reaction of arsenious oxide and hydrochloric acid was used to prepare arsenic trichloride, which was then distilled.

Antimony trichloride was prepared by direct chlorination of antimony, maintaining an excess of the metal, followed by sublimation.

Apparatus and experimental

The reactions of molybdenum hexafluoride were studied in a glass vacuum system fitted with Hoke valves (No. 432), which were incorporated in the system through copper–glass seals brazed directly to the valves or joined with unions. The glass was carefully dried by evacuation and flaming before the reagents were admitted.

---

[11] J. Fischer and E. Rudzitis, *J. Amer. Chem. Soc.* 81, 6375 (1959).

[12] C. Pallaghy. Unpublished observations.

[13] J. Chatt and A. A. Williams, *J. Chem. Soc.* 3061 (1951).

[14] E. E. Aynsley, R. D. Peacock and P. L. Robinson, *J. Chem. Soc.* 1231 (1952).

For each reaction, a special reaction system was designed to handle the particular reagents and the expected products. A typical system fitted with Hoke valves at V is shown in Fig. 1. A bulb of volume appropriate to the quantities of reagents used was connected to a conventional vacuum system at K and to it were attached various side-tubes, each connected through a capillary, so that these side-tubes could be removed subsequently by heating the capillary. If both reagents were volatile, the less volatile was first distilled from its source trap. For example, some molybdenum hexafluoride might be distilled from the trap D to the side-arm F and subsequently exposed to a volatile reactant such as phosphorus trifluoride, contained in a trap B of appropriate size and fitted with a break-seal C. In the case of a reaction involving an involatile compound, e.g. bismuth trifluoride, the main part of the system was evacuated and flamed and then filled with carefully dried air. The involatile reactant was introduced into G from a tube fitted at J through a ground joint. The system was then sealed at H, evacuated and flamed and some molybdenum hexafluoride distilled from D to G.

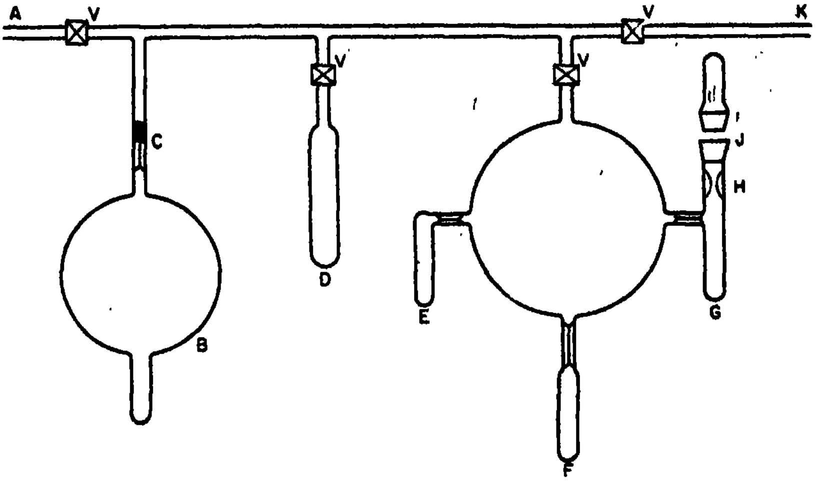

FIG. 1.—System for study of reactions of molybdenum hexafluoride.

When a particular reaction was complete, the main bulk of the involatile products of reaction would be in one side-tube, e.g. G. Partial fractionation of the products was then achieved by maintaining G at room temperature and cooling E or F to —183° C. Tube G, containing the involatile products of reaction, was then drawn off by sealing the capillary and its contents analysed. By use of suitable coolants, the products of intermediate volatility could be fractionated between the remaining tubes E and F and isolated in these tubes. The very volatile products remained in the bulb and could be removed at A for examination by infra-red spectroscopy or some other procedure.

Analytical methods

Involatile products of reactions were identified usually by chemical analysis. Fluoride was determined by the null-point potentiometric method.(15) Molybdenum was determined gravimetrically with 8-hydroxyquinoline and volumetrically by the method of RAO and SURYANARAYANA.(16) Hydrogen peroxide was used to ensure that molybdenum was present initially as Mo(VI), which was then reduced to Mo(V) with hydrazine sulphate and Mo(V) was titrated against ceric sulphate. Potentiometric titration against silver nitrate was used for chloride because molybdate interferes with Mohr and Volhard methods.

Volatile products were identified by infra-red and ultra-violet spectroscopy and by their physical properties, such as melting and boiling points.

---

(15) T. A. O'DONNELL and D. F. STEWART, *Analyt. Chem.* **33**, 337 (1961).

(16) G. G. RAO and M. SURYANARAYANA, *Z. Analyt. Chem.* **168**, 177 (1959).

REACTIONS OF MOLYBDENUM HEXAFLUORIDE

Phorphorus trifluoride

The trifluoride was added gradually to a known amount of molybdenum hexafluoride in a vacuum system fitted with Hoke valves. Controlled addition of phosphorus trifluoride was achieved by admitting it to a bulb of known volume, measuring the pressure and condensing this aliquot of the reactant in the side-arm containing the hexafluoride. The reaction was studied under conditions ranging from excess molybdenum hexafluoride to excess phosphorus trifluoride. The only products of reaction were molybdenum pentafluoride and phosphorus pentafluoride which was identified by its infra-red spectrum. With excess molybdenum hexafluoride, molybdenum pentafluoride was present in yellow solution in the hexafluoride, while with excess phosphorus trifluoride the yellow solid, molybdenum pentafluoride, was isolated and identified by chemical analysis and by its melting point, previously reported by PEACOCK.(17)

Arsenious trifluoride

There was no reduction of molybdenum hexafluoride even when the two fluorides were heated to 150°C in a sealed thick-walled glass tube. The two compounds remained as colourless, immiscible liquids.

Antimony trifluoride

The solid trifluoride and liquid hexafluoride did not react at temperatures up to 150°C.

Bismuth trifluoride

No reaction on heating to 80°C.

Sulphur tetrafluoride

There was no evidence of reaction at room temperature.

Selenium tetrafluoride

The two fluorides remained as immiscible colourless liquids on heating in a sealed tube to 150°C. At 200°C, there was extensive glass attack but no colouration indicative of formation of lower molybdenum fluorides.

Phosphorus trichloride

In this case, the reaction appeared to proceed in two steps, the nature of the second step depending on which of the two reactants was in excess. The first step was a metathetical reaction producing phosphorus trifluoride and a mixture of lower molybdenum chlorides and chlorine. Frequently, it appeared that the first molybdenum chloride produced was the black pentachloride, which in a few hours changed to the brown or red tetrachloride or trichloride.

When molybdenum hexafluoride was in excess, the second step in the reaction was reduction of the hexafluoride to molybdenum pentafluoride by the phosphorus trifluoride produced in the first step. Under these conditions, infra-red spectroscopy showed that the volatile products of reaction contained phosphorus pentafluoride, but no phosphorus trifluoride, and chlorine was identified by its ultra-violet spectrum.

---

(17) R. D. PEACOCK, *Proc. Chem. Soc.* 59 (1957).

However, when there was excess phosphorus trichloride, only phosphorus trifluoride was found in the volatile products. There was no formation of phosphorus pentafluoride and the chlorine reacted with excess trichloride to form phosphorus pentachloride. Analysis indicated that the involatile reaction products contained phosphorus pentachloride and molybdenum pentachloride. The colour of this residue also indicated the presence of the pentachloride rather than lower chlorides.

Arsenic trichloride

Analysis of the involatile products of reaction indicated the formation of molybdenum trichloride. The volatile products were arsenic trifluoride and chlorine. There was no evidence in the infra-red spectrum of the presence of arsenic pentafluoride.

Antimony trichloride

There was no formation of antimony pentafluoride. The reaction appeared to give lower molybdenum chlorides and chlorine, which then reacted with antimony (III) to produce mixed chlorofluorides of antimony(V). The formation of one such compound was indicated when a white sublimate was isolated with a melting point close to that of SbF_2Cl_3.

DISCUSSION OF REACTIONS

Oxidation of lower fluorides

Molybdenum hexafluoride was shown to be relatively inert as an oxidant. Of the lower fluorides studied, only phosphorus trifluoride was oxidized and there was no evidence of the formation in that reaction of a molybdenum fluoride lower than MoF_5. The reaction $2MoF_6+PF_3 \rightarrow 2MoF_5+PF_5$ provides a more satisfactory method for preparing molybdenum pentafluoride than that previously reported by PEACOCK.(17) The observation that the hexafluoride does not oxidize bismuth trifluoride is in general agreement with the reaction reported by FISCHER and RUDZITIS(11) in which bismuth pentafluoride readily oxidized UF_4 to UF_6.

Nature of molybdenum chlorides formed

The compound $MoCl_6$ is unstable and has never been isolated. In many of these reactions, there was evidence of the initial formation of $MoCl_5$ which usually dissociated within a few hours to lower chlorides, for which the chloride to molybdenum ratio varied for different reactions. The ratio, which appeared to depend on experimental conditions such as the volume of the reaction system and the relative proportions and nature of reagents, ranged from five in the reaction with excess phosphorus trichloride to about three in reactions in which molybdenum hexafluoride was in great excess.

Under the experimental conditions it might be expected that the pentachloride should be formed. However, the formation of lower chlorides can be explained in the light of the recent work of PEARSON and GARNER(18), who have shown that chlorine is released when $MoCl_5$ is dissolved in carbon tetrachloride at room temperature, to produce lower molybdenum chlorides of indefinite stoicheiometry. In the introduction to this present paper it was stated that $MoFCl_5$ is an excellent solvent for iodine,

(18) I. M. PEARSON and C. S. GARNER, *J. Phys. Chem.* **65**, 690 (1961).

resembling CCl_4 in this respect. Also WF_6 and CCl_4 have been shown to mix mutually without reaction.(12) It seems very reasonable then to suggest that MoF_6 acts as an inert solvent for the $MoCl_5$ formed initially and that the pentachloride then dissociates to lower chlorides.

Scheme of reactions with trichlorides

The general reaction with trichlorides was in the first instance a metathetical one:

$$4\,XCl_3+2\,MoF_6 \rightarrow 4\,XF_3+2\,MoCl_5+Cl_2.$$

Subsequent reaction depended on the nature and proportion of the reactants.

Only in the case of the PCl_3 reaction was the trifluoride, formed initially, oxidized to the pentafluoride and then only when MoF_6 was in excess. Also, in excess MoF_6, $MoCl_5$ dissociated to $MoCl_4$ or $MoCl_3$ and chlorine. These reaction steps can be represented as:

$$4\,PCl_3+2\,MoF_6 \rightarrow 4\,PF_3+2\,MoCl_5+Cl_2$$
$$2\,MoCl_5 \rightarrow 2\,MoCl_4\ (\textit{or}\ MoCl_3)+Cl_2$$
$$2\,MoF_6+PF_3 \rightarrow PF_5+2\,MoF_5.$$

The overall reaction could be written:

$$2\,PCl_3+5\,MoF_6 \rightarrow 4\,MoF_5+MoCl_4+2\,PF_5+Cl_2.$$

When PCl_3 was in excess a simpler reaction occurred. No PF_5 was formed and the chlorine formed initially reacted with excess PCl_3 to form PCl_5. In the absence of excess MoF_6, the $MoCl_5$ did not dissociate.

$$4\,PCl_3+2\,MoF_6 \rightarrow 4\,PF_3+2\,MoCl_5+Cl_2$$
$$PCl_3+Cl_2 \rightarrow PCl_5$$

Overall reaction: $5\,PCl_3+2\,MoF_6 \rightarrow 4\,PF_3+2\,MoCl_5+PCl_5$.

As expected from the earlier work on reactions between MoF_6 and the trifluorides, there was no oxidation of the trifluorides first formed in the reaction of MoF_6 with $AsCl_3$ and with $SbCl_3$. In the $AsCl_3$ reaction, chlorine did not react with excess $AsCl_3$, due to the instability of $AsCl_5$, and AsF_3 and Cl_2 were observed as separate volatile products. DESS *et al.*(19) state that reaction occurs between AsF_3 and Cl_2 only in the presence of small amounts of water. KOLDITZ(20) in earlier work, while not commenting on the possible role of water, suggested that $[AsCl_4]^+[AsF_6]^-$ is formed at 0°C in the presence of a large excess of chlorine. It seems reasonable that, at room temperature and reduced pressures and with water rigorously excluded, there should be no interaction between AsF_3 and Cl_2. The overall reaction in the presence of excess MoF_6 can be summarized as:

$$2\,AsCl_3+MoF_6 \rightarrow 2\,AsF_3+MoCl_4\ (\textit{or}\ MoCl_3)+Cl_2.$$

A reaction similar to the above could be written for $SbCl_3$ with the addition of a representative equation:

$$SbF_3+Cl_2 \rightarrow SbF_3Cl_2.$$

The identity of the mixed halides of Sb (V) will depend on the relative proportions of reagents. For example, SbF_3 and chlorine formed in the initial reaction could react with $SbCl_3$ to form SbF_2Cl_3, indicated experimentally as one of the products.

$$SbCl_3+2\,SbF_3+3\,Cl_2 \rightarrow 3\,SbF_2Cl_3.$$

---

(19) H. M. DESS, R. W. PARRY and G. L. VIDALE, *J. Amer. Chem. Soc.* **78**, 5730 (1956).

(20) L. KOLDITZ, *Z. Anorg. Chem.* **280**, 313 (1955).

J. Inorg. Nucl. Chem., 1962, Vol. 24, pp. 315 to 319. Pergamon Press Ltd. Printed in England

SOME REACTIONS OF DIPHOSPHORUS TETRAIODIDE

T. MOELLER and J. E. HUHEEY
Noyes Chemical Laboratory, University of Illinois, Urbana, Illinois

(*Received* 13 *July* 1961; *in revised form* 25 *October* 1961)

Abstract—The reactions of diphosphorus tetraiodide with phenol and certain aliphatic alcohols, Grignard reagents, and amines have been investigated. Although small quantities of the expected substituted diphosphorus compounds have been detected spectrophotometrically among the products from some of the reactions, the major products are monophosphorus compounds and amorphous, highly polymerized solids related to red phosphorus and the solid phosphorus hydrides. Reaction paths resulting in the cleavage of the P–P bond and ultimate polymer formation are considered.

ALTHOUGH diphosphines and diphosphorus tetraiodide are well-characterized compounds, information on other tricovalent diphosphorus compounds is scanty.⁽¹⁾ This may be due, at least in part, to the small number of synthetic routes available for their preparation. The only potentially generally applicable methods described involve the coupling of two phosphorus-containing moieties under the influence of sodium⁽²˒ ³⁾ or Grignard reagents.⁽⁴⁻⁸⁾ Thus a convenient synthesis involving only the substitution of other functional groups for those already present in an easily prepared diphosphorus compound might open routes to compounds difficult or impossible to synthesize by existing methods.

The diphosphorus tetrahalides would appear to be ideal for this purpose. However, only the chloride and the iodide have been described, and only the iodide is readily prepared. In this compound, the P–P bond has a length of 2·21 Å, and the configuration of iodine atoms is such that the lone electron pairs on the two phosphorus atoms are *trans* to each other.⁽⁹⁾ Attempts to prepare the chloride from the iodide⁽¹⁰⁾ and the fluoride from the chloride⁽¹¹⁾ have lead to rupture of the P–P bond. However, this bond appears to be retained in at least one of the hydrolysis products ($H_2P_2O_4$) of the tetraiodide.⁽¹²⁾ This suggests that esters of the type $(RO)_2P–P(OR)_2$, obtainable ordinarily by a Wurtz-type reaction,⁽¹³⁾ might result from analogous alcoholysis reactions or that organodiphosphines or the unknown amides, $(R_2N)_2P–P–(NR_2)_2$, might be similarly obtainable.

---

(1) J. R. VAN WAZER, *Phosphorus and Its Compounds.* Vol. 1. *Chemistry*, pp. 215–219, 234–235. Interscience, New York (1958).

(2) K. ISSLEIB and W. SEIDEL, *Ber. Dtsch. Chem. Ges.* **92**, 2681 (1959).

(3) W. KUCHEN and H. BUCHWALD, *Ber. Dtsch. Chem. Ges.* **92**, 227 (1959).

(4) P. J. CHRISTEN, L. M. VAN DER LINDE and F. N. HOOGE, *Rec. Trav. Chim.* **78**, 161 (1959).

(5) K. ISSLEIB and A. TZSCHACH, *Ber. Dtsch. Chem. Ges.* **92**, 704 (1959).

(6) M. I. KABACHNIK and J. S. SHEPELEVA, *Izv. Akad. Nauk. S.S.S.R., Otdl. Khim. Nauk*, 56 (1949).

(7) W. KUCHEN and H. BUCHWALD, *Angew. Chem.* **71**, 162 (1959).

(8) H. NIEBERGALL, *Angew. Chem.* **72**, 210 (1960).

(9) Y. C. LEUNG and J. WASER, *J. Phys. Chem.* **60**, 539 (1956).

(10) A. GAUTIER, *C.R. Acad. Sci., Paris*, **78**, 286 (1874).

(11) A. FINCH, *Canad. J. Chem.* **37**, 1793 (1959).

(12) M. BAUDLER, *Naturforsch.* **14 b**, 464 (1959).

(13) E. F. ENGELKE, U.S. Pat. 2403792 (1946).

Accordingly, diphosphorus tetraiodide has been caused to react with alcohols, phenol, various amines, and Grignard reagents. Unfortunately, none of these reactions follows a simple path, and each yields principally a tricovalent monophosphorus compound and highly polymeric solids which resemble the lower phosphorus hydrides(14, 15) in their physical and chemical properties. Although the chemical compositions of these polymers depend upon the reaction conditions, they all agree approximately with those of the polymeric hydrides with greater or lesser substitution by both iodine and the entering group for hydrogen. In a few experiments, small quantities of diphosphorus compounds could be detected by ultraviolet spectroscopy, but only the solvolysis of the tetraiodide with phenol yielded any of the desired product, specifically the diphosphate (II–II) ester,(16) $(C_6H_5O)_2P\text{–}P(OC_6H_5)_2$.

EXPERIMENTAL

Materials, apparatus and techniques. All chemicals were of reagent quality. Solvents were dried over sodium. Commercially available "anhydrous" alcohols were dried over magnesium and distilled prior to use.

All ultra-violet spectra were measured with a Cary Model 14 recording spectrophotometer, using solutions in n-hexane, n-heptane, methanol, ethanol, n-propanol or n-butanol. Infra-red spectra were obtained with a Perkin-Elmer Model 21 instrument using either Nujol mulls or solutions in chloroform, methylene chloride, or chloroform. X-ray diffraction data were obtained with a Standard X-Ray Co. unit, using copper $K\alpha$ radiation and a nickel filter.

Moisture-sensitive materials were handled in a Berkeley-type gloved box, the atmosphere of which had been dried with sodium carbonate, alumina, and phosphorus (V) oxide.

Synthesis of diphosphorus tetraiodide. The procedure employed was a modification of that described by GERMANN and TRAXLER.(17) A stock solution containing ca. 1 gramme atom of iodine per litre was prepared by adding 254 g of iodine to 2 l. of dry benzene, warming at 45–50° C, and stirring until dissolution was complete. A stock solution containing ca. 1 gramme-atom of phosphorus per litre was prepared by dissolving 60 g of white phosphorus (weighed under acetone and dried momentarily in air) in 2 l. of dry benzene. For a specific synthesis, two volumes of the iodine solution were added to one volume of the phosphorus solution. The initially dark-coloured solution turned slowly to a clear orange-red and deposited crystals of the product on standing. These crystals were removed, washed several times with n-heptane, and dried *in vacuo*. M. p. 125·0–125·5° C. Yield 68–75 per cent. Re-crystallization was effected from dry bromobenzene. Reactions were carried out either with the initial benzene solution or the solid.

Properties of diphosphorus tetraiodide. The compound proved to be slightly soluble without decomposition in rigorously dried benzene, liquid alkanes, chloroform, diethyl ether, tetrahydrofuran, acetonitrile, N, N–dimethylformamide, and liquid sulphur dioxide. Solubility in bromo- or chlorobenzene is greater, and these solvents can be used for recrystallization. Nitrobenzene is a moderately good solvent at low temperatures, but at higher temperatures, it oxidizes diphosphorus tetraiodide rapidly. Any moisture present in any of the systems effects immediate solvolytic decomposition of the solute. Acetone, methyl ethyl ketone, cyclohexanone, acetophenone, and dimethyl sulphoxide react rapidly to give uncharacterized dark solutions and precipitate apparently polymeric substances.

(14) E. WIBERG and G. MÜLLER-SCHIEDMAYER, *Ber. Dtsch. Chem. Ges.* **92**, 2372 (1959).

(15) (a) E. C. EVERS and E. H. STREET, *J. Amer. Chem. Soc.* **78**, 5726 (1956); (b) E. H. STREET, D. M. GARDNER and E. C. EVERS, *J. Amer. Chem. Soc.* **80**, 1819 (1958); (c) G. J. BEICHL and E. C. EVERS, *J. Amer. Chem. Soc.* **80**, 5344 (1958).

(16) For a comprehensive discussion of the nomenclature of these compounds, see J. E. HUHEEY, Doctoral Dissertation, University of Illinois (1961).

(17) F. E. E. GERMANN and R. N. TRAXLER, *J. Amer. Chem. Soc.* **49**, 307 (1927).

The ultra-violet absorption spectrum of diphosphorus tetraiodide in cyclohexane has a characteristic maximum (λ_{max}) at 228 mμ. Air oxidation to iodine (λ_{max} = 520 mμ) is so rapid that exact evaluation of the extinction co-efficient was not attempted.

Reaction of diphosphorus tetraiodide with phenol. A 96 g (0·17 mole) sample of diphosphorus tetraiodide was prepared as outlined in a one-litre round-bottomed flask equipped with a stirrer and a reflux condenser. To the flask was added 500 ml of hexane and 78 ml (83 g, or 0·89 mole) of phenol. The reaction mixture was heated at reflux temperature for 10 hr by means of an oil-bath. Copious quantities of hydrogen iodide were evolved. Refluxing was stopped when the evolution of hydrogen iodide had practically ceased. The resulting solution was decanted from the red solid that had separated.

The red solid was insoluble in benzene, diethyl ether, acetone, and methanol. It did not melt below 235° C, but upon being heated strongly in a tube, it yielded a reddish sublimate, an oil, and the odour of phenol. Upon treatment with bromine water, it gave tribromophenol. (Found: C, 10·10; H, 6·11; I, 25·3, 26·5%.) A second sample, prepared after only 4 hr of refluxing, behaved similarly but contained only 2·07%C and 0·76%H. Both samples, when examined by X-ray diffraction, gave the diffuse halos of amorphous substances plus a few weak lines for unreacted diphosphorus tetraiodide.

The supernatant solution from the reaction was added to a ca. 5·0 × 100 cm chromatographic column of acid-washed alumina, and the adsorbed material was eluted in 50 ml fractions with diethyl ether-n-heptane (50 per cent each). Each of the first six fractions yielded a single drop of oil upon evaporation. Each was then dissolved in heptane and examined spectrophotometrically. Absorption maxima (in mμ) noted were, respectively, 226; 229; 232; none; 265, 272, 278 and 265, 271, 277. The values for the last two samples are those of phenol, but the peaks at ca. 230 mμ for the first three samples indicate the presence of one or more species containing a P–P bond.(18) Most reasonably, they could be ascribed to the tetraphenyldiphosphate (II–II) ester. The infra-red spectra of these three fractions were different from those of phenol and triphenylphosphite, but no assignments of observed frequencies can yet be made.

Although the chromatographic fractions were too small for accurate analysis, fractions obtained by distilling the reaction product under reduced pressure were analysed.

Found for Fraction 1 : C, 67·01; H, 5·15%
for Fraction 2 : C, 68·00; H, 5·09%
for Fraction 3 : C, 66·82; H, 5·01%
Calcd. for $(C_6H_5O)_2P–P(OC_6H_5)_2$: C, 66·36; H, 4·64%
for $(C_6H_5O)_3P$: C, 69·67; H, 4·87%
for C_6H_5OH : C, 76·57; H, 6·43%

Reaction of the supposed tetraphenyl ester with hydrogen iodide. Two 5 ml samples of a solution of Fraction 1 in n-heptane (0·6 ml) were frozen in ampoules attached to a vacuum line. The system was evacuated. A 40 per cent aqueous solution of hydrogen iodide was dehydrated by being dropped slowly into a flask containing phosphorus (V) oxide and cooled to −78° C. This flask was attached to the vacuum system and the hydrogen iodide distilled into another flask containing fresh phosphorus (V) oxide. The dry hydrogen iodide was then distilled into one of the ampoules containing the heptane solution. The other sample was retained untreated as a control. Both samples were allowed to warm to room temperature and then to stand for 1 hr. A separate phase appeared in the treated sample. Each tube was then treated with 5 ml of n-heptane, and a 5 ml aliquot was withdrawn. Excess hydrogen iodide was removed from the aliquot from the treated sample with a current of dry nitrogen. Spectrophotometric examination showed the untreated sample to be unchanged but indicated a substantial decrease in the intensity of the P–P absorption peak and an overall increase in general absorbancy in the 210–270 mμ region for the treated sample. In addition, a red solid, resembling that noted in the original reaction, was found on the walls of the tube containing the hydrogen iodide-treated sample.

(18) A. B. Burg, L. R. Grant, J. E. Griffiths, K. K. Joshi, G. L. Juvinall and W. Mahler in R. I. Wagner, F. F. Casserio and L. D. Freeman, WADC Tech. Report 57–126, Pt. III, 82 (1959).

Reactions of diphosphorus tetraiodide with aliphatic alcohols. Addition of crystalline diphosphorus tetraiodide to aliphatic alcohols resulted in vigorous reactions with the formation of amorphous, polymeric, red solids. In an attempt to detect the presence of any diphosphorus solvolysis products, aliquots of a solution of 152·6 mg of the tetraiodide in 500 ml of cyclohexane were diluted with various dried aliphatic alcohols to a uniform concentration of $2{\cdot}14 \times 10^{-4}$ M and examined spectrophotometrically. The following λ_{max} values (in mμ) were obtained: methanol, 220; ethanol, 227; 1-propanol, 234; 2-propanol, 240; 1-butanol, 244; 2-methyl-2-propanol, 236. All extinction coefficients were ca. 1×10^4.

Reaction of diphosphorus tetraiodide with phenylmagnesium bromide. A solution of 0·082 mole of phenylmagnesium bromide in diethyl ether was prepared by the procedure of Fieser.(19) Benzene was added as the ether was removed by distillation until the distillate was essentially pure benzene. The solution was cooled to room temperature, and 500 ml of a 0·04 M solution of diphosphorus tetraiodide in benzene was added slowly with stirring. A yellow solid separated immediately. When all of the tetraiodide had been added, the mixture was forced through a fritted-glass filter on to a column of acid-washed alumina.

The remaining solid, after being washed with ether and dried, was found to be amorphous and insoluble in all common solvents. Its melting point was above 200° C, but upon being heated strongly, it yielded a condensate of white phosphorus. (Found: C, 19·41; H, 3·08; P, 19·41%.)

The chromatographic column was treated in order with benzene, diethyl ether, and acetone. The first fractions were shown to contain biphenyl by infra-red examination. Subsequent fractions were shown to contain phosphorus by the *o*-anisidine–molybdate test.(20) Most, if not all, of this phosphorus was identified as triphenylphosphine by treating the sample with a solution of sulphur in carbon disulphide, recovering and recrystallizing the reaction product, and determining a mixed melting point with triphenylphosphine sulphide from an independent synthesis.

Reaction of diphosphorus tetraiodide with n-*propylamine.* To a solution of 101 g (0·178 mole) of diphosphorus tetraiodide in 1400 ml of benzene contained in a two-litre, three-necked, round-bottomed flask equipped with a stirrer, a dropping funnel, and a reflux condenser, a solution of 100 g (1·7 mole) of n-propylamine in 200 ml of benzene was added slowly with stirring. The brownish white precipitate that formed was removed by filtration and dried. Treatment with ethanol gave an insoluble, amorphous, brown residue, melting above 200° C and yielding a sublimate of white phosphorus at higher temperatures, and a solution that deposited white crystals of n-propylammonium iodide upon evaporation. (Found: C, 19·28; H, 5·39; N, 7·49. Calc. for $n\text{-}C_3H_7NH_3I$: C, 19·18; H, 5·35; N, 7·54%).

Substitution of N-methylaniline for n-propylamine gave a similar reaction except that an orange, amorphous polymeric material resulted and the N-methylanilinium iodide remained in solution. In neither case could an identifiable phosphorus-containing product be isolated from solution.

DISCUSSION

These observations indicate clearly that although phenol, alcohols, Grignard reagents, and amines attack diphosphorus tetraiodide readily the major products are polymeric derivatives related to the solid phosphorus hydrides (and, therefore, red phorphorus) and monophosphorus compounds rather than the expected diphosphorus derivatives. Although the latter have been detected spectrophotometrically in small quantities, these reactions cannot be used for their syntheses.

This type of cleavage of the phosphorus–phosphorus bond has been reported for other systems. Thus, Emeléus and coworkers(21) reported complete cleavage when tetrakis (trifluoromethyl) diphosphine is hydrolyzed in alkaline solution.

(19) L. F. Fieser, *Experiments in Organic Chemistry* (3rd Ed.), p. 79. Heath, Boston (1955).

(20) C. M. Welch and P. W. West, *Analyt. Chem.* **29**, 874 (1957).

(21) F. W. Bennett, H. J. Emeléus and R. N. Hazeldine, *J. Chem. Soc.* 3896 (1954).

Similarly, t-butyl alcohol reacts quantitatively with this diphosphine to yield bis(trifluoromethyl)-phosphine and *O*–t-butyl-bis(trifluoromethyl) phosphate (–I),(22) and treatment of the same diphosphine with trimethylphosphine and hydrogen chloride yields bis(trifluoromethyl)phosphine.(18) Furthermore, biphosphine gives phosphine and solid polymeric hydrides when treated with liquid ammonia,(15b) and diphosphorus tetraiodide yields trimethylphosphine when treated with methyllithium.(22) These reactions and those involving alcohols, amines, and Grignard reagents are apparently all examples of attack by basic reagents which invariably cleave the P–P bond and may or may not result in polymerization of the fragments.

It is difficult to assume that phenol supplies a sufficient concentration of phenoxide ion to sustain an entirely comparable reaction. It is probably for this reason that diphosphorus species can be distinguished in the reaction products. Subsequent cleavage either by released or added hydrogen iodide may then occur.

Although the exact structures of the polymeric products are unknown, three structures seem most reasonable, namely a single chain of phosphorus atoms: a double chain, cross-linked at alternate phosphorus atoms: or a chain of P_4X_2 groups based upon a proposed structure for red phosphorus.(23) Irrespective of the true structure, greater or lesser substitution by iodide and other groups is probable, with the degree of iodide substitution decreasing with increasing time of reaction. The reaction paths for the formation of such polymeric products are not clear. With the Grignard reaction, coupling may occur by the same mechanism that is involved in the reaction of thiophosphoryl chloride with alkyl Grignard reagents to yield diphosphine disulfides.(4–8) Whether a parallel exists to the assumed mechanisms for the formation of the much more complicated solid hydrides(14) cannot be determined.

The facts that cleavage of diphosphines is apparently favoured by both acidic and basic conditions, that biphosphine itself is quite unstable with respect to this reaction, and that organic diphosphines are moderately to very stable may be accounted for by assuming that at some stage in the reaction of a diphosphorus compound the electron pair between the two phosphorus atoms is somewhat displaced toward one atom and that this is then followed by migration of a group to this more negative atom and heterolytic cleavage of the bond.

---

(22) A. B. Burg, G. Brendel, A. P. Caron, G. L. Juvinall, W. Mahler, K. Moedritzer and P. J. Slota, Jr., WADC Tech. Report 56–82, Pt. II (1957).

(23) L. Pauling and M. Simonetta, *J. Chem. Phys.* **20**, 29 (1952).

J. Inorg. Nucl. Chem., 1962, Vol. 24, pp. 321 to 332. Pergamon Press Ltd. Printed in England

EXTRACTION OF Ca(II), Sr(II) AND Ba(II) BY ACIDIC ESTERS OF PHOSPHORUS OXY ACIDS*

D. F. PEPPARD, G. W. MASON, S. MCCARTY and F. D. JOHNSON
Argonne National Laboratory, Argonne, Illinois

(*Received* 18 *August* 1961)

Abstract—The extraction of Ca(II), Sr(II) and Ba(II) from aqueous mineral acid, in the presence and absence of the corresponding sodium salt, into xylene solutions of $(GO)_2PO(OH)$, G = 2-ethyl hexyl and para (1,1,3,3 tetramethyl butyl) phenyl, and of $(GO)G'PO(OH)$, G = n-octyl and G′ = phenyl and chloro methyl, has been investigated radiometrically. The distribution ratio, *K*, has been found to be inversely second-power dependent upon the hydrogen ion concentration in the equilibrated aqueous phase.

The dependency of *K* upon the concentration of extractant in the equilibrated xylene phase was found to be 2·5-power for Ca and Sr and 3·0-power for Ba in systems involving bis [para (1,1,3,3 tetramethyl butyl) phenyl] phosphoric acid or n-octyl hydrogen chloromethyl phosphonate; 3·0-power for Ca, Sr and Ba in systems involving n-octyl hydrogen phenyl phosphonate; and 3·0-power for Ca (Sr and Ba not proved) in systems involving bis(2-ethyl hexyl) phosphoric acid.

The effect of structural differences in the extractants is discussed, and the extraction of alkaline earths (II) is compared with that of Pm(III) and Cm(III).

THE extraction of a metallic cation of charge $+b$ from an aqueous mineral acid phase into an opposing phase consisting of a weakly dissociated mono acidic chelating extractant (bi-dentate) dissolved in a liquid carrier diluent has been studied extensively. If the extractant remains essentially quantitatively in the organic phase and if complexing of the metallic cation by the extractant in the aqueous phase is negligible, then, in general, the distribution ratio, *K*, for the metallic cation varies directly with the concentration of extractant raised to the *b*th–power.(1) The extraction of the $+b$ charged cation is said to have a *b*th–power extractant dependency. The extraction may be generalized as:

$$M_A^{b+} + bHCh_O \rightleftharpoons MCh_{bO} + bH_A^+ \qquad (1)$$

where HCh is the unionized chelating extractant and the subscripts A and O refer, respectively, to mutually equilibrated aqueous and organic phases.

However, if the extractant is dimeric in the carrier diluent but may be found in the extracted species as monomers, dimers or both, the extractant dependency may be *b*th-power, 0·5*b*th-power or something intermediate, even though the co-ordination number, *C.N.*, of the extracted cation is 2*b*. If, in addition, the *C.N.* of the cation is different from 2*b*, the probability of an extractant-dependency other than *b*th-power is increased.

---

* Based on work performed under the auspices of the U.S. Atomic Energy Commission.

(1) E. B. SANDELL and P. F. CUMMINGS, *Analyt. Chem.* 21, 1356 (1949). N. H. FURMAN, W. B. MASON and J. S. PEKOLA, *Ibid* 21, 1325 (1949).

In systems employing a dimeric mono-acidic ester of ortho phosphoric acid as extractant, the extractant dependency for trivalent lanthanides⁽²⁾ and actinides⁽²⁾, M^{3+}, is reported as third-power. However, that for tetravalent thorium, Th^{4+}, is also third-power.⁽³⁾ This dependency of less than b is presumably to be explained in terms of geometrical difficulties in placing four mono-ionized dimers about the thorium atom.

Conversely, an expectant-dependency of greater than b might be expected for M^{2+} if the *C.N.* is 6. Consequently, a study of the extraction of the M(II) alkaline earths was undertaken.

The investigation presently described encompassed both mono-acidic esters, $(GO)_2PO(OH)$, of ortho phosphoric acid and mono-acidic esters, (GO)G'PO(OH), of two different G' organo phosphonic acids. These extractants in a liquid carrier diluent were used in opposition to an aqueous phase containing a mineral acid, with and without the corresponding sodium salts.

Nomenclature

The distribution ratio, *K*, of a specific nuclide is defined as the concentration of nuclide in the upper divided by the concentration of nuclide in the lower of two equilibrated sensibly-immiscible liquid phases, the concentration being considered proportional to the β-activity per ml of the given phase.

Symbolic formulae, consistent with those employed in previous papers of this series, are used. A mono-acidic ortho phosphate ester in which the two groups are alike is represented as $(GO)_2PO(OH)$, or HDGP, where the H represents the acidic hydrogen, G is the organic group and D signifies the prefix di. A mono-acidic organo phosphonate is represented as (GO)G'PO(OH) where the G' is an organic group attached to the P atom through a C–P bond. This C–P mode of attachment is indicated by the bracketed expression in HG [G'P].

The two mono-acidic esters of ortho phosphoric acid employed and their symbolic formulae are; bis 2-ethyl hexyl phosphoric acid, $[(C_2H_5)C_6H_{12}O]_2PO(OH)$, HDEHP, (di 2-ethyl hexyl), and bis [para (1,1,3,3, tetramethyl butyl) phenyl] phosphoric acid, $[(C_8H_{17})C_6H_4O]_2$ PO(OH), HDOΦP, (di octylphenyl). The two mono-acidic esters of organo phosphonic acids studied are, correspondingly: n-octyl hydrogen phenyl phosphonate, $(n\text{-}C_8H_{17}O)(C_6H_5)$ PO(OH) Hn–O [ΦP], and n-octyl hydrogen chloromethyl phosphonate, $(n\text{-}C_8H_{17}O)$ $(ClCH_2)$ PO(OH), Hn–O [ClMP].

Sources of materials

A mixture of the mono and di para (1,1,3,3 tetramethyl butyl) phenyl esters of ortho phosphoric acid was obtained from Victor Chemical Co. and the di ester, HDOΦP, isolated as described previously.⁽⁴⁾ The bis 2-ethyl hexyl phosphoric acid, obtained from Virginia Carolina Chemical Corp. and assaying greater than 98% HDEHP was subjected to further purification.⁽⁴⁾ The acidic phosphonates, Hn-O[ΦP] and Hn-O[ClMP], were prepared by the method for preparation and purification of HG[G'P] compounds described previously⁽⁵⁾, utilizing $ΦPOCl_2$ and $ClCH_2POCl_2$ obtained from Victor Chemical Co. and n-octyl alcohol.

⁽²⁾ (a) D. F. PEPPARD, G. W MASON, J. L. MAIER and W. J. DRISCOLL, *J. Inorg. Nucl. Chem.* **4**, 334 (1957).
(b) D. F. PEPPARD, G. W. MASON, W. J. DRISCOLL and R. J. SIRONEN, *J. Inorg. Nucl. Chem.* **7**, 276 (1958).

⁽³⁾ D. F. PEPPARD, G. W. MASON and S. MCCARTY, *J. Inorg. Nucl. Chem.* **13**, 138 (1960).

⁽⁴⁾ D. F. PEPPARD, J. R. FERRARO and G. W. MASON, *J. Inorg. Nucl. Chem.* **7**, 231 (1958).

⁽⁵⁾ D. F. PEPPARD, J. R. FERRARO and G. W. MASON, *J. Inorg. Nucl. Chem.* **12**, 60 (1959).

The β-active nuclides, 160 day ^{45}Ca, 28 year ^{90}Sr (and accompanying β-active 64 hr ^{90}Y) and 8 year ^{133}Ba were obtained from the Isotopes Division of the Oak Ridge National Laboratory.

Determination of distribution ratios

The distribution ratio, *K*, of a specific nuclide was determined radiometrically, the data being obtained both by "direct" and "reverse" extractions in order to confirm the attainment of equilibrium. That is, data were obtained both for the pregnant aqueous phase vs. barren organic phase and for the barren aqueous phase vs. pregnant organic phase conditions. The H$^+$ion concentrations reported are those for the equilibrated aqueous phases. Xylene was used as diluent throughout.

In general, 2-ml portions of the pertinent aqueous and organic phases, one of the phases containing 10^5–10^6 counts/min of the tracer nuclide per ml, were mutually agitated by manual shaking for a 2 min period in a 15 ml stoppered polypropylene centrifuge tube. Following centrifugations, a portion of each phase was transferred by means of a transfer pipette to separate polypropylene centrifuge tubes and each sample centrifuged again. Aliquots of each phase were then taken for assay.

Assays were ultimately performed by evaporating an aliquot on a platinum disk for β-counting.(2a) However, only organic phases and aqueous mineral acid phases were assayed directly. Salt-containing aqueous phases were assayed as specifically described.

In the acid-dependency studies, all made at $\mu = 1 \cdot 0$, the Ca content of the equilibrated aqueous salt-plus-acid phase was determined by extraction into an organic phase following addition of a buffer as follows. A 1·0 ml portion of the equilibrated aqueous phase was transferred to a small stoppered vial containing 1·0 ml of 0·1 F HDOΦP in xylene and 0·20 ml of 10 M ammonium acetate. Greater than 99 per cent of the Ca reported to the organic phase, even under the most adverse of the conditions, i.e. highest initial H$^+$ concentration of salt phase. An aliquot of the resulting pregnant HDOΦP phase was then evaporated on a platinum disk for β-counting. The resultant count per minute corresponded to a count per minute assay of an equal aliquot of the equilibrated salt phase.

Since, even under buffered conditions, the extraction of Sr and Ba into 0·1 F HDOΦP in xylene was found to be far below 99 per cent from aqueous salt phases initially containing more than 0·05 M H$^+$, the Sr and Ba contents of such aqueous salt phases were obtained by a difference method.

In general the *K* for Ba was determined as follows. The tracer Ba was extracted from an aqueous phase approximately 0·005 M in H$^+$ into a suitable volume of the organic phase to be investigated. This pregnant organic phase was then assayed for Ba by contacting an aliquot with an equal volume of 0·25 M HCl causing the tracer to report in greater than 99·9 per cent yield to the aqueous phase. An aliquot of this aqueous phase was then evaporated on a platinum disk for β-counting.

A 2·0 ml portion of the assayed pregnant organic phase was then equilibrated with a 2·0 ml portion of the aqueous salt-plus-acid phase to be investigated. Following separation of the equilibrated phases, the Ba content of the equilibrated organic phase was determined by extracting the tracer from a 1·0 ml portion of organic phase into a 1·0 ml portion of 0·25 M HCl and assaying the resultant HCl phase. The Ba content (per ml) of the equilibrated salt phase was then taken as the difference between the assays (per ml) of initial and final organic phases.

The Sr data were obtained in an identical manner except for a modification introduced for ^{90}Y removal. The 64 hr β-active ^{90}Y daughter of ^{90}Sr is far more extractable than ^{90}Sr under the conditions employed. Therefore, in the determination of *K* values less than unity, ^{90}Y–contamination leads to erroneous results, the measured *K* being too large and the relative error increasing with decreasing *K*. Consequently, the ^{90}Y is removed just prior to the *K*-determination experiment by contacting the aqueous 0·005 F H$^+$ solution containing ^{90}Sr with a 0·05 F solution of the extractant under study. Under these conditions well over 99·9 per cent of the ^{90}Y is extracted and well over 97 per cent of the ^{90}Sr remains in the aqueous phase. The resultant aqueous phase is then contacted with a solution of the extractant under study (in the proper F range) in order to prepare a pregnant organic phase containing ^{90}Sr but no ^{90}Y except for that quantity which has grown since the ^{90}Y removal step.

This pregnant organic phase is then utilized as described for Ba. It should be noted that this technique also eliminates interference from ^{90}Y which has grown after the ^{90}Y removal step; since, in the assay of a pregnant organic phase by re-extraction into an aqueous HCl phase, the ^{90}Y remains nearly quantitatively in the depleted organic phase.

RESULTS AND CONCLUSIONS

The K for Ca into 0·3F HDEHP from an aqueous 1M(HCl + NaCl) phase is seen to be inverse second-power dependent upon the equilibrium concentration of H^+ ion in the aqueous phase, Fig. 1. This inverse second-power acid dependency of the *K* for Ca is also displayed by the systems involving 0·10F HDOΦP in xylene and an opposing aqueous HX + NaX phase in which X = ClO_4^-, Cl^-, and NO_3^-, Fig. 2. It will be noted that the *K* is highest from perchlorate, lowest from nitrate and of intermediate value from chloride solutions. Whether these small differences are a reflexion of weak complexing of Ca or of a general μ-effect upon the activity of H^+ and/or Ca^{2+} is unknown.

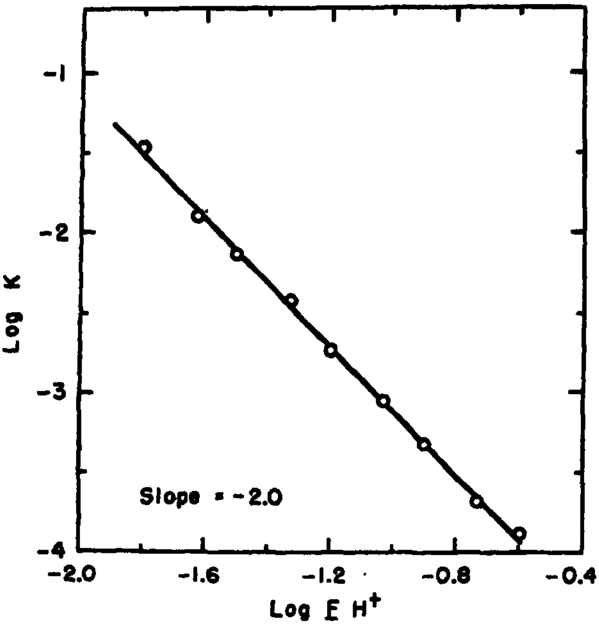

FIG. 1.—Hydrogen ion dependency of the extraction of Ca into 0·30 F HDEHP in xylene from HCl + NaCl. μ = 1·0.

Due to the mutual proximity of the three curves of Fig. 2 and to the fact that an inverse second-power acid dependency was manifested in all three systems, the remainder of the study was restricted to systems involving an aqueous chloride phase, since, for many nuclear and analytical applications, a chloride-containing phase is to be preferred to one containing nitrate or perchlorate. Extensive studies of Sr and Ba in HDEHP systems were not considered feasible due to the very low *K* values for these elements.

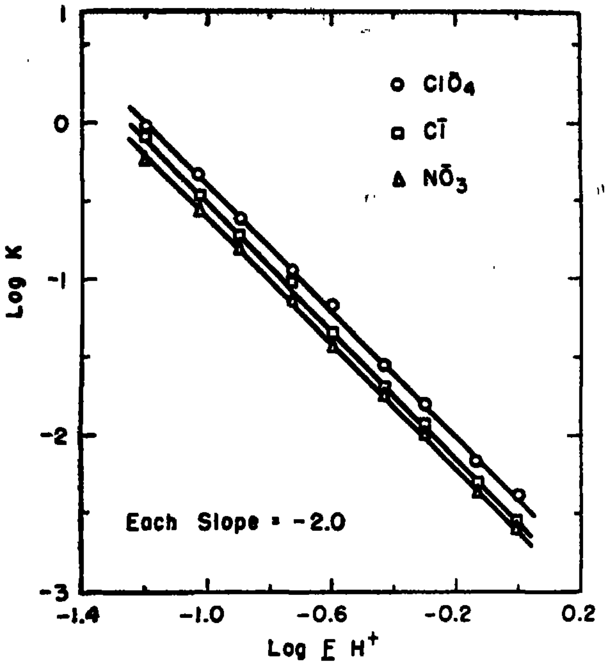

FIG. 2.—Hydrogen ion dependence of the extraction of Ca into 0·10 F HDOΦP in xylene from HX+NaX; X=ClO$_4$. μ = 1·0.

In Fig. 3, the *K* values for Ca, Sr and Ba in an HDOΦP vs. aqueous chloride system are compared. An inverse second-power H$^+$ ion dependency is followed closely. In this system, all three elements are relatively well extracted, consequently the extraction behaviour of Sr and Ba may be studied with precision.

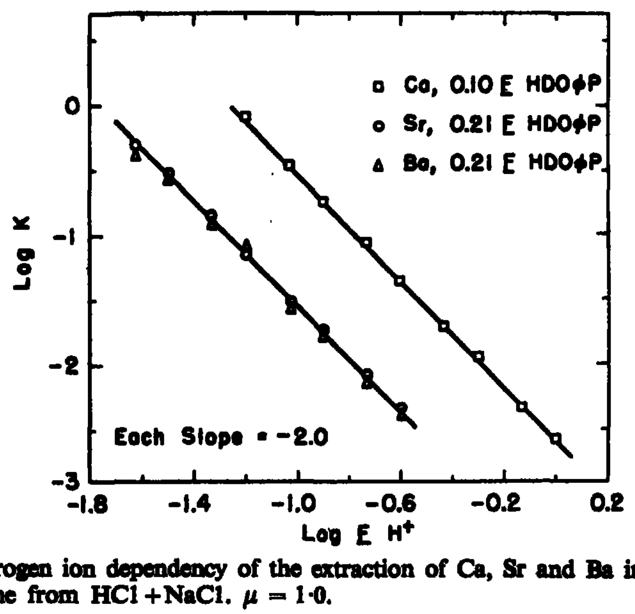

FIG. 3.—Hydrogen ion dependency of the extraction of Ca, Sr and Ba into HDOΦP in xylene from HCl+NaCl. μ = 1·0.

Similarly to the two mono-acidic phosphates, HDEHP and HDOΦP, the two mono-acidic phosphonates, Hn-O[ΦP] and Hn-O[ClMP], also extract these elements from a 1·0 μ chloride phase with an inverse second-power H^+ ion dependency, Figs. 4 and 5.

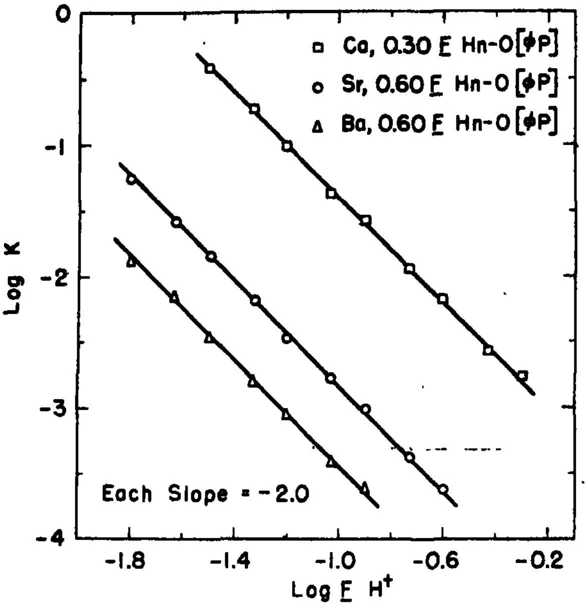

Fig. 4.—Hydrogen ion dependency of the extraction of Ca, Sr, and Ba into Hn-O [ΦP] in xylene from HCl + NaCl. $\mu = 1·0$.

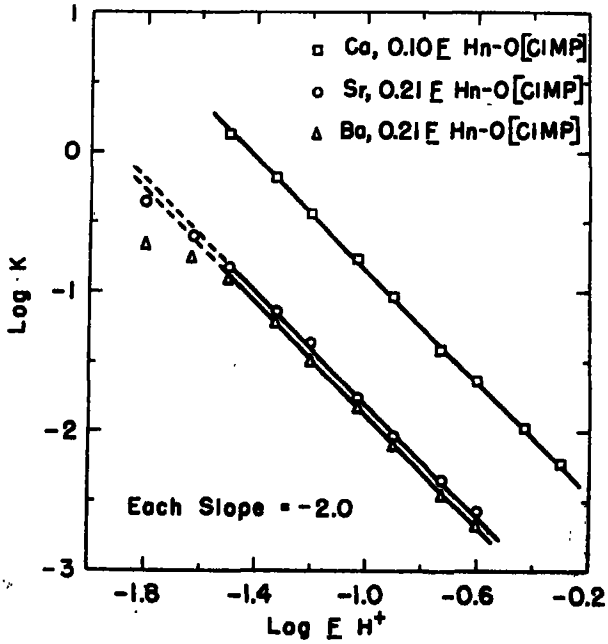

Fig. 5.—Hydrogen ion dependency of the extraction of Ca, Sr, and Ba into Hn-O [ClMP] in xylene from HCl + NaCl. $\mu = 1·0$.

From these data, considering the fact that the extractants are dimeric,(4-6) the extraction of Ca, Sr and Ba might now be generalized as:

$$\mathrm{M}_{\mathrm{A}}^{2+}+b(\mathrm{HY})_{2o} \rightleftharpoons \mathrm{M}(\mathrm{HY}_2)_2(\mathrm{HY})_{2b-4o}+2\mathrm{H}_{\mathrm{A}}^{+} \tag{2}$$

where $(\mathrm{HY})_2$ represents the dimeric extractant and the subscripts A and O refer respectively to mutually equilibrated aqueous and organic phases.

The coefficient *b*, the extractant dependency, of Expression 2 is found to be either 2·5 or 3·0, depending upon the elements and upon the extractant. In Figs. 6 and 8, pertaining to HDEHP and Hn–O[ΦP], the data indicate a third-power extractant dependency, $b = 3{\cdot}0$. In Figs. 7 and 9 pertaining to HDOΦP and Hn–O[CIMP], the extractant dependency is shown to be 2·5-power for Ca and Sr and 3·0-power for Ba.

The distribution ratio, *K*, corresponding to Expression (2), for a constant μ chloride system, may be expressed in the form: (2b)

$$K = \mathrm{K_S F_{Ex,o}^{b}}/[\mathrm{H}^+]_{\mathrm{A}}^{2} \tag{3}$$

where $\mathrm{F_{Ex}}$ represents the concentration in formality units of the extractant in the xylene phase and K_{S} is a composite constant characteristic of the system. Utilizing Expression (3), the values of *b* obtained from Figs. 6–9, and the *K* values read from the straight lines of Figs. 1–5 (and certain additional Sr data), K_{S} values were calculated

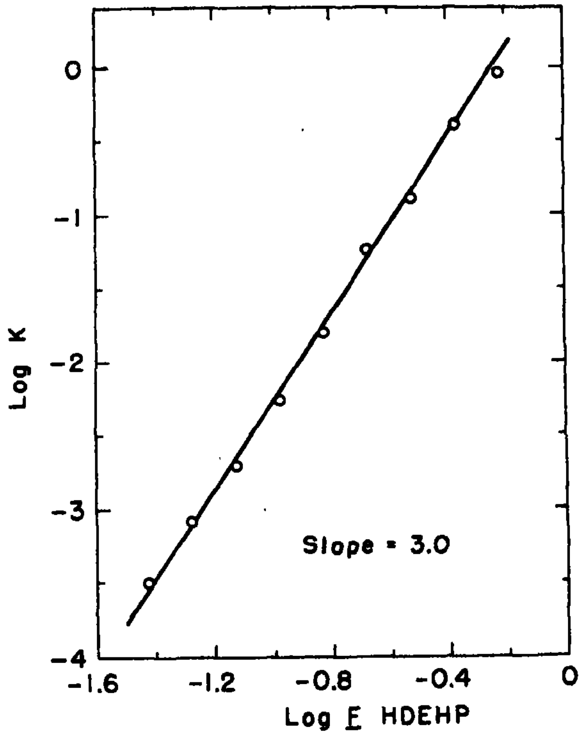

FIG. 6.—Extractant dependency of the extraction of Ca into HDEHP in xylene from 0·01 M HCl.

---

(6) D. DRYSSEN, *Acta. Chem. Scand.* 11, 1771 (1957); D. F. PEPPARD, J. R. FERRARO and G. W. MASON, *J. Inorg. Nucl. Chem.* 4, 371 (1957).

for the elements for 1·0 μ chloride systems, Fig. 10. (Numerically, K_S is the hypothetical value of K in a 1·0F extractant vs. 1·0M H^+ system. Actually, gross departures from the dependencies indicated by Expression (2) are noted under these conditions).

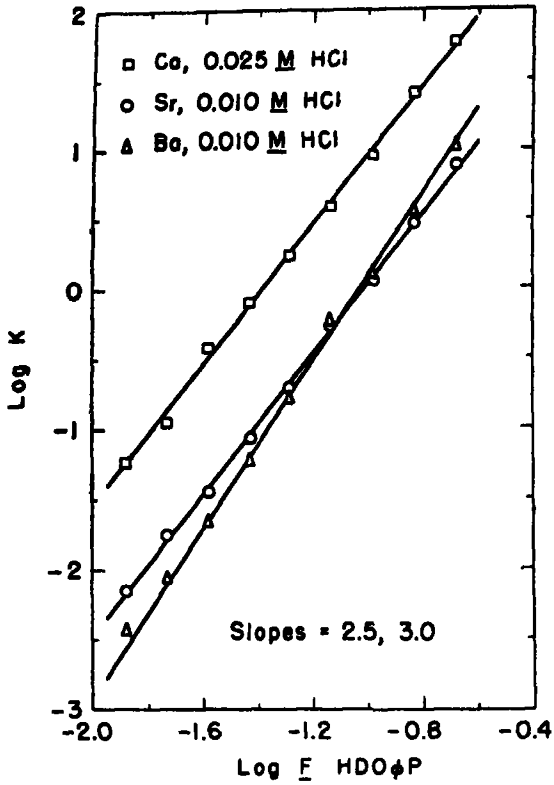

Fig. 7.—Extractant dependency of the extraction of Ca, Sr, and Ba into HDOΦP in xylene from dilute HCl.

In making comparisons in Fig. 10, it should be remembered that for a given extractant, the stoicheiometry of extraction is identical for Ca and Sr but not, in every case, for Ca, Sr and Ba. The approximate β-values, i.e., the ratio of their respective K values, for Ca with respect to Sr are, respectively: > 100, 55, 220, and 55 for a 1·0 μ chloride system versus xylene solutions of HDEHP, HDOΦP, Hn–O[ΦP] and Hn–O[ClMP].

It is apparent, from Fig. 10, that the mutual separation of Ca and Sr may be accomplished readily. These systems, however, show little promise for the mutual separation of Sr and Ba, although they may be used advantageously in isolating a composite fraction containing Sr and Ba or Ca, Sr and Ba as a group from less extractable elements.

DISCUSSION

Since no radioactive isotope of Mg was available during this study, the behaviour of Mg can be discussed in a qualitative fashion only. In gross extraction experiments (successive extractions and scrubs), involving the simultaneous presence of Ca, Mg and Sr, the Mg concentrated with the Sr in the aqueous phase when the effective distribution ratio, *E*, for Ca was set at approximately unity. ($E = RK$ where R is the volume ratio of organic phase to aqueous phase). In this way, the *K* for Mg was shown to be considerably lower than that for Ca in each of the systems studied. It may be noted that Kimura (7) reports that in the 50 per cent HDEHP (toluene) vs. 0·1M HCl system, the *K* for Ca is approximately eighty times that for Mg.

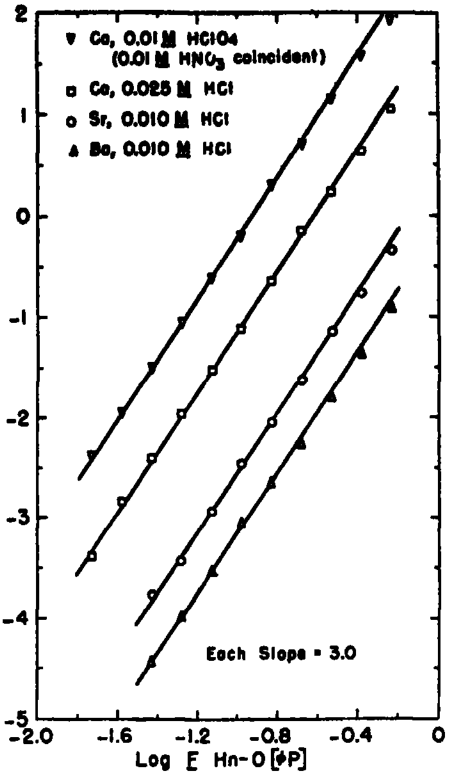

FIG. 8.—Extractant dependency of the extraction of Ca, Sr, and Ba into Hn-O[ΦP] in xylene from dilute HX; X = ClO_4^-, Cl^-, NO_3^-.

Kimura (8) further finds the extractant dependencies for the alkaline earths to be second-power in the HDEHP (toluene) vs. 0·05M HCl system. In the present study, the *K* for Ca was found to be third-power extractant dependent. The studies differ in the diluent employed and the range of concentrations of extractant.

Since the *K* for Ba is consistently third-power dependent upon the concentration of extractant in all of the cases presently reported, whereas the *K* values for Ca and Sr are 2·5 power extractant-dependent for two of the extractants, it seems logical to assume that the extractant dependency is partially dependent upon the ionic size of the cation. If the extractant dependency decreases with decreasing size of the cation, it is perhaps logical to surmise that Be and/or Mg is sufficiently small to display

(7) K. Kimura, *Bull. Chem. Soc. Japan* 33, 1038 (1960).

(8) K. Kimura, *Bull. Chem. Soc. Japan* 34, 63 (1961).

a second-power extractant dependency. In their comprehensive investigation of the extraction of Be from aqueous mineral acid phases into solutions of HDGP in toluene, HARDY, *et al* ⁽⁹⁾ found the *K* to be second-power dependent for systems in which G was n-butyl, n-octyl and 2-ethyl hexyl. It is apparent, from their data, that under comparable conditions, the *K* for Be should be considerably higher than that for Ca in HDEHP systems.

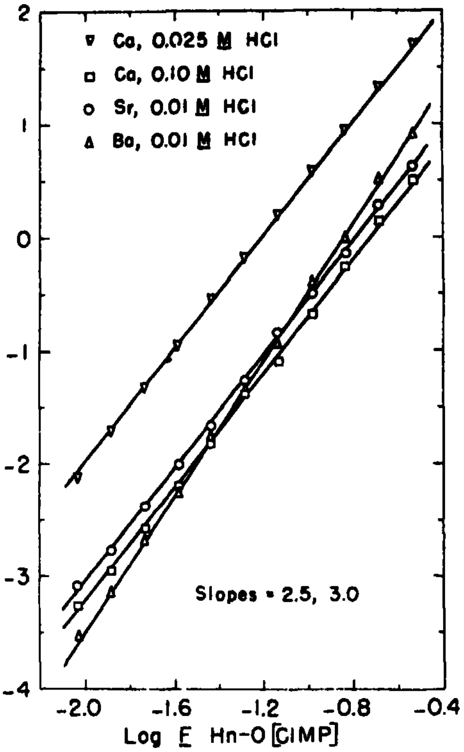

FIG. 9.—Extractant dependency of the extraction of Ca, Sr, and Ba into Hn-O[ClMP] in xylene from dilute HCl.

CATTRALL⁽¹⁰⁾, in his studies of the extraction of Be into solutions of HDEHP in kerosene, employed an aqueous sulphate phase. Since the effect of sulphate complexing of Be upon his data is not known, no direct comparisons are possible.

With respect to the extractant dependencies that are greater than two for Ca, Sr and Ba, it may be noted that DYRSSEN⁽¹¹⁾ has "shown that Sr^{2+} is extracted from an aqueous solution into an oxine–chloroform solution in the form of $SrA_2 \cdot 2HA$", (HA is the oxine molecule). He states, "Bearing in mind that the co-ordination number of Sr^{2+} is 6, it is not surprising that the two water molecules left after the complexing with two oxinate ligands, A, may be exchanged for two HA, thus giving an uncharged complex that is soluble in organic solvents".

---

(9) C. J. HARDY, B. F. GREENFIELD and D. SCARGILL, *J. Chem. Soc.* 174 (1961).

(10) R. W. CATTRALL, *Aust. J. Chem.* 14, 163 (1961).

(11) D. DYRSSEN, *Svensk. Kem Tidskr.* 67, 311 (1955).

It is, therefore, suggested that the extracted species are, respectively, $M(HY_2)_2(HY)$ and $M(HY_2)_2(HY)_2$ for the systems involving 2·5-power and 3·0-power extractant dependencies.

The effect of varying the nature of the phosphorus-based extractant is large, the K_s for Ca in the HDOΦP and HDEHP systems differing by a factor of nearly 4×10^3, Fig. 10. This difference is probably attributable to a combination of an acidity factor and a steric hindrance factor.

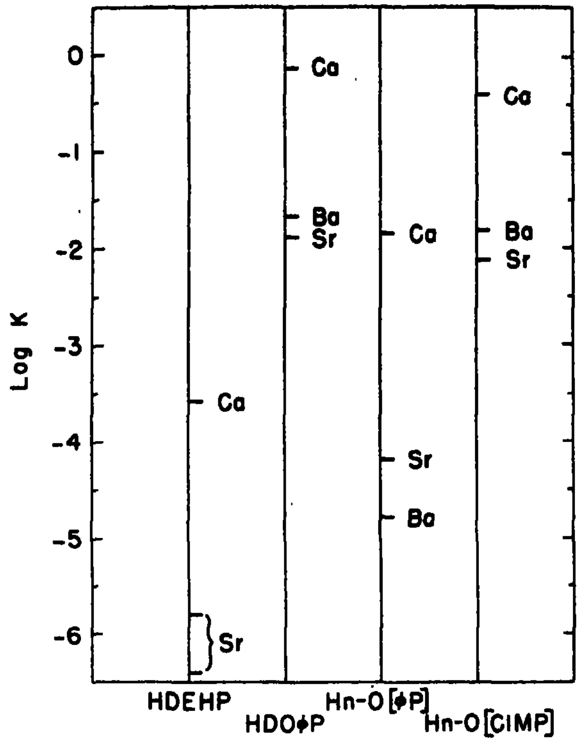

FIG. 10.—K_s values for extraction of Ca, Sr, and Ba from HCl + NaCl ($\mu = 1{\cdot}0$) into solutions of $(GO)_2PO(OH)$ and (GO) G′PO(OH) in xylene. (Based upon data in 0·05–0·25 M H^+ range).

Considering the relative electronegative character of the G groups, HDOΦP is expected to be much more acidic than HDEHP. Assuming, for simplification, the bonding of the ionized residue to M^{b+} to be of comparable strength for the two extractants the more highly acidic extractant should display the higher K_s. On the other hand, the steric hindrance due to branching of the octyl group might be expected to result in lowered strength of bonding to M^{b+}. (It seems logical that steric hindrance should affect the bonding to a relatively large M^{b+} much more drastically than that to a proton).

Of the two acidic phosphonates, Hn–O[ClMP] is expected to be more acidic than Hn–O[ΦP]. Whether there is an important difference in the steric factors is questionable.

PEPPARD, *et al* ⁽¹²⁾ reported K_s values for the extraction of Pm (III) and Cm (III) from an aqueous $HClO_4+NaClO_4$ ($\mu = 1{\cdot}0$) phase into toluene solutions of selected HDGP and HG [G'P] extractants. Since an aqueous perchlorate rather than chloride phase and toluene diluent rather than xylene were employed, direct comparisons are impossible. In addition, the HG [G'P] extractants employed in the previous study⁽¹²⁾ were the 2-ethyl hexyl, rather than the n-octyl, derivatives of phenyl and chloromethyl phosphonic acids. Nevertheless, an interesting relationship between the effects of structural changes in the extractant upon the K_s for M^{3+} and M^{2+} ions may be expressed, in approximate fashion, as:

$$(Ks_2/Ks_1)_{M3+} \cong (Ks_2/Ks_1)^{3/2}_{M2+} \tag{4}$$

where the subscripts 1 and 2 refer to two different extractants. For example, using HDOΦP as Extractant 1 and HDEHP as Extractant 2, and the La^{3+} and Ca^{2+} data, the left and right sides of Expression (4) are respectively 4×10^5 and 3×10^5.

The effect of steric hindrance upon the acidity of HDGP and HG [G'P] extractants and the effects of both steric hindrance and increasing acidity upon the K_s of a number of M^{b+} ions are now being investigated. It is anticipated that large changes in specificity may be realized through variation of the steric hindrance and acidity factors.

(12) D. F. PEPPARD, G. W. MASON and I. HUCHER. *J. Inorg. Nucl. Chem.* **18**, 245 (1961).

J. Inorg. Nucl. Chem., 1962, Vol. 24, pp. 333 to 336. Pergamon Press Ltd. Printed in England

THE DENSITY OF LIQUID SILVER FROM ITS MELTING POINT TO ITS NORMAL BOILING POINT 2450°K*

A. D. Kirshenbaum, J. A. Cahill and A. V. Grosse
The Research Institute, Temple University, Philadelphia 44, Pa.

(*Received* 1 *August* 1961; *in revised form* 9 *October* 1961)

Abstract—The density of liquid silver was determined, by the Archimedean principle, over the whole range from its melting point to its normal boiling point. It can be best expressed by the linear equation

$$D\ (\text{g/cm}^3) = 10{\cdot}465 - 9{\cdot}067 \times 10^{-4}\ T^\circ\text{K}$$

with a probable error of $\pm 0{\cdot}009$ g/cm³.

The density of liquid silver is 9·346 g/cm³ at its melting point (1234° K) and 8·244 g/cm³ at its normal boiling point (2450° K).

Recently, as part of our high temperature density studies of liquid oxides⁽¹⁾ fluoride⁽²˒ ³˒ ⁴˒ ⁵⁾ and metals,⁽⁵⁾ we have reported the density of liquid lead from its melting point to its normal boiling point.⁽⁶⁾ Since then, we have measured the density of liquid silver from its melting point (1234°K) to its normal boiling point (2450°K) with a precision of $\pm 0{\cdot}009$ g/cm³ or 0·1 per cent.

EXPERIMENTAL PROCEDURE

These measurements were made with the same graphite crucible, chimney and sinker used in the lead experiments.⁽⁶⁾ The liquid silver was heated in the graphite crucible. The sinker was immersed into the liquid silver and the silver refluxed at atmospheric pressure for ½–1 hr in order to remove all entrapped and dissolved gases. The temperature was then dropped below the boiling point of silver in approximately 50–100° K intervals and the density measurements made from the apparent loss in weight and the volume of the graphite sinker.

The volume of the sinker was 3·535 g/cm³ at 20° C as determined by the apparent loss in weight in mercury. The volume was corrected for thermal expansion at the operating temperature as described previously.⁽⁶⁾ The volume of the sinker depended upon its depth of immersion in the liquid silver. This was determined by electrical contact as described in the paper on lead.⁽⁶⁾

The apparent losses in weight were corrected for surface tension. The values used at the boiling point of silver (750 dyn/cm at 2450° K)⁽⁷⁾ were obtained by extrapolating the data reported by Krause and Sauerwald.⁽⁸⁾ A contact angle of 140° was assumed in these calculations since, as with lead and mercury, the silver did not wet the graphite. The correction at the boiling point was 0·319 g (= 1·0 per cent of total apparent weight loss).

---

* This research was sponsored by the National Science Foundation under Grant 15540.

(1) A. D. Kirshenbaum and J. A. Cahill, *J. Inorg. Nucl. Chem.* **14**, 283 (1960).

(2) A. D. Kirshenbaum, J. A. Cahill and C. S. Stokes, *J. Inorg. Nucl. Chem.* **15**, 297 (1960).

(3) A. D. Kirshenbaum and J. A. Cahill, Technical Note No. 9, Contract No. AF 18(600)-1475, the Research Institute of Temple University, April 30, 1959.

(4) A. D. Kirshenbaum and J. A. Cahill, *J. Inorg. Nucl. Chem.* **19**, 65 (1961).

(5) A. D. Kirshenbaum, Second Annual Report on High Temperature Inorganic Chemistry to the National Science Foundation, Research Grant NSF-G6278, the Research Institute of Temple University, Dec. 15, 1960.

(6) A. D. Kirshenbaum, J. A. Cahill and A. V. Grosse, *J. Inorg. Nucl. Chem.* **22**, 33 (1961).

(7) D. R. Stull and G. C. Sinke, *Thermodynamic Properties of the Elements, Advances in Chemistry Series*, Vol. 19. Amer. Chem. Soc. (1956).

(8) W. Krause and F. Sauerwald, *Z. Anorg. Chem.* **181**, 347, 353 (1929).

The lower temperatures (1250–1400° K) were measured by means of a chromel–alumel thermocouple calibrated by measuring the melting point of silver and had an accuracy of ±0·2° K. An optical pyrometer was used for the higher temperatures (1700–2450° K); black body conditions were attained by using a graphite well. The pyrometer was standardized by measuring the melting points of silver and platinum and the boiling points of lead and silver. The probable average temperature deviation from the fixed points was ±5° K.

The silver used in these experiments was obtained from Hagstoz and Sons, Phila., and had a purity of 99·95 per cent silver; the main impurity being copper (~ 0·04 per cent). Any oxide present in the silver was reduced to the metal and the oxygen removed as CO when the silver was refluxed in the graphite crucible and chimney. Graphite was used as construction material for silver because it had been shown by Ruff and Bergdahl(9) that the solubility of carbon in silver is negligible. At its boiling point, it is only 0·0022 wt. per cent and thus no correction for dissolved C was required.

RESULTS

Table 1.—Experimental density values of liquid silver

Temperature (° K)	Density (g/cm³)	Temperature (° K)	Density (g/cm³)
1285	9·261	2093	8·549
1311	9·233	2163	8·483
1332	9·216	2228	8·475
1339	9·207	2263	8·422
1352	9·192	2293	8·428
1362	9·206	2308	8·409
1384	9·164	2323	8·386
1396	9·169	2338	8·353
1408	9·156	2358	8·347
1409	9·151	2388	8·323
1717	8·891	2393	8·300
1730	8·861	2423	8·317
1812	8·820	2438	8·278
2013	8·671	2438	8·266

Table 2.—Density, specific volume, atomic volume and volume coefficient of expansion of liquid silver

Temperature °(K)	Density (g/cm³)	Specific volume (cm³/g)	Atomic volume (cm³/g-atom)	Volume coefficient of Expansion ×10⁶ (°K⁻¹)
1234 (m.p.)	9·346 ± 0·009	0·10700 ± 0·00011	11·543 ± 0·013	97·0 ± 0·09
1400	9·196	0·10874	11·731	98·6
1500	9·105	0·10983	11·848	99·6
1600	9·014	0·11094	11·968	100·6
1800	8·833	0·11321	12·213	102·6
2000	8·652	0·11558	12·470	104·8
2200	8·470	0·11806	12·736	107·0
2400	8·289	0·12064	13·015	109·4
2450 (n.b.p.)	8·244 ± 0·009	0·12130 ± 0·00013	13·086 ± 0·014	110·0 ± 0·1
2500	8·198	0·12198	13·159	110·6

The results obtained are tabulated in Table 1. Least square treatment of the data gave the following straight line density–temperature relationship:

$$D\,(\text{g/cm}^3) = 10{\cdot}465 - 9{\cdot}067 \times 10^{-4}\,T^\circ\,\text{K}$$

$$\text{or } D\,(\text{g/cm}^3) = 9{\cdot}346 - 9{\cdot}067 \times 10^{-4}\,(T - 1234^\circ\,\text{K})$$

with a probable error of ±0·009 g/cm³.

---

(9) O. Ruff and B. Bergdahl, *Z. Anorg. Chem.* **106**, 91 (1919).

TABLE 3.—LITERATURE DATA ON THE DENSITY OF LIQUID SILVER

Literature reference	Author	Year	Temperature range (°K)	Density at m.p. (g/cm³)	Density equation	Method used
10	SAUERWALD	1922	1298–1367	9·32	$D = 10{\cdot}77 - 11{\cdot}74 \times 10^{-4}$ T°K.	Archimedean principle
12	MATSUYAMA	1929	1233–1343	9·294	$D = 10{\cdot}439 - 9{\cdot}279 \times 10^{-4}$ T°K.	—
13	JOUNIAUX	1930	1365–1575	9·33	$D = 10{\cdot}50 - 9{\cdot}52 \times 10^{-4}$ T°K.	Archimedean principle
	This paper	1961	1285–2438	9·346	$D = 10{\cdot}465 - 9{\cdot}067 \times 10^{-4}$ T°K.	" "
10	Solid (SAUERWALD)			9·685		

Thus at the melting point of silver (1234°K), the density is 9·346 g/cm^3. Extrapolation of the solid density data reported by SAUERWALD(10) with the X-ray ($a = 4{\cdot}07787$ Å,(11) 4 atoms/cell) density data (10·5668 g/cm^3 at 25°C) gives a solid density at the melting point of 9·665 g/cm^3. Therefore the volumetric expansion on melting $(V_l - V_s/V_l)$ equals 3·30 per cent.

The atomic volumes were calculated for various temperatures from the smoothed density values obtained from the liquid silver density equation. These values are summarized in Table 2, together with the cubical coefficient of expansion values or β, calculated from the equation:

$$dD/dT = \beta \cdot D_t.$$

COMPARISON OF OUR RESULTS WITH LITERATURE DATA

A literature survey of the data on liquid silver showed that very few data have been published. A comparison of our results with the literature is made in Fig. 1 and Table 3. Only these investigators, SAUERWALD,(10) MATSUYAMA(12) and JOUNIAUX,(13) made more than one measurement over a temperature range of at least 50°. The density equations obtained by these investigators are presented in the table together with their values at the melting point. They are in good agreement with the value of 9·346 g/cm^3 found in this paper (see Table 3).

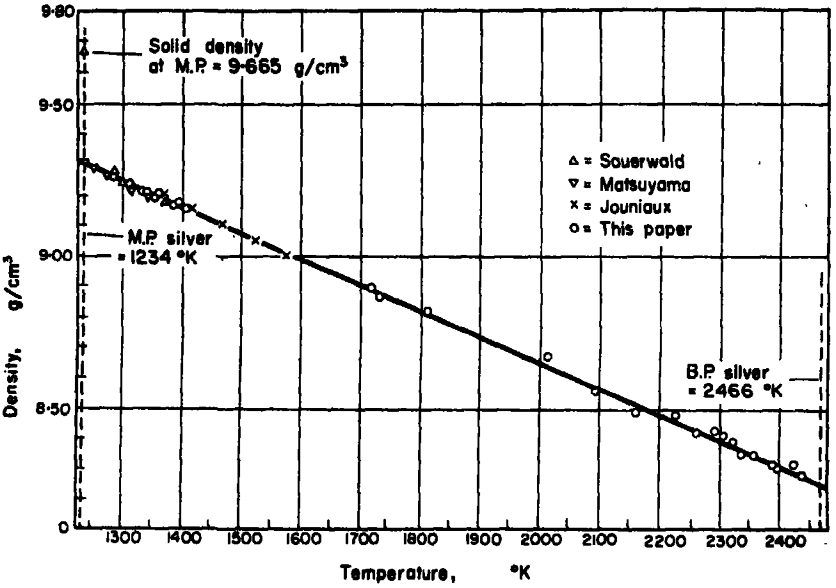

FIG. 1.—Density of liquid silver.

Their temperature coefficients are also in reasonable agreement with our data, if one considers that they were obtained only over a temperature range between 60–200° whereas ours were obtained over a 1200° range.

(10) F. SAUERWALD, *Z. Metallk.* 14, 457 (1922).

(11) F. FOOTE and E. R. JETTE, *Phys. Rev.* 38, 81 (1940).

(12) Y. MATSUYAMA, *Sci. Rep. Tôhoku. Univ.* 18, 737 (1929).

(13) A. JOUNIAUX, *Bul. Soc. Chim.* 47, 528 (1930).

J. Inorg. Nucl. Chem., 1962, Vol. 24, pp. 337 to 341. Pergamon Press Ltd. Printed in England

TRITIUM IN THE THERMAL NEUTRON FISSION OF URANIUM-235*

E. N. SLOTH, D. L. HORROCKS, E. J. BOYCE and M. H. STUDIER
Argonne National Laboratory, Argonne, Illinois

(*Received* 8 *September* 1961; *in revised form* 30 *October* 1961)

Abstract—The existence of tritium as a product of fission, first reported by ALBENESIUS,(1) has been verified. A ratio of $1{\cdot}25 \pm 0{\cdot}15 \times 10^4$ fissions per atom of tritium was found for the thermal neutron-induced fission of ^{235}U. Tritium was converted to water in a closed system and its activity measured by liquid scintillation techniques. The number of fissions was determined by assay of the 0·537 MeV γ-ray of ^{140}Ba.

THE existence of ternary fission has been well established.(2) In particular, the long range alpha particles arising from thermal neutron-induced fission(3–6) and spontaneous fission of californium-252(2, 7) have been studied by nuclear emulsion techniques, ionization measurements and magnetic analysis. The abundance of this type of tripartite fission is roughly one in 300 of the normal binary fission events.

Triple fission in which the third fragment is the triton was first reported by ALBENESIUS.(1) A frequency range of one tritium atom per $1\text{–}2 \times 10^4$ fissions was given. While our experiments were in progress ALBENESIUS and ONDREJCIN(8) reported a value of $1{\cdot}05 \pm 0{\cdot}09 \times 10^4$ for the ratio of fissions to tritium atoms. They isolated tritium and determined it by liquid scintillation techniques. They calculated the number of fissions from reactor data. We determined tritium in a similar manner and in addition isolated the fission product ^{140}Ba to determine the number of fissions.

EXPERIMENTAL PROCEDURE

Sample preparation and irradiation

The uranium was irradiated as U_3O_8 powder in 0·2, 0·5 and 1·0 gramme quantities. National Bureau of Standards (MSST) U_3O_8 and U_3O_8 prepared from commercial uranyl nitrate hexahydrate were used. The commercial uranium was purified by dissolution in nitric acid followed by an ether extraction and subsequent ignition to U_3O_8.

The uranium oxide was irradiated in platinum vials manufactured from 6 mm o.d. platinum tubing. One end of a 4 in. section of tubing was sealed off by heating in the flame of a torch and closed by means of a small hammer. After introduction of the sample the open end was closed in a like manner. Prior to irradiation the vials were subjected to a leak test by immersion in paraffin oil under vacuum.

* Based on work performed under the auspices of the U.S. Atomic Energy Commission.

(1) E. L. ALBENESIUS, *Phys. Rev. Letters*, **3**, 274 (1959).

(2) M. L. MUGA, H. R. BOWMAN and S. G. THOMPSON, *Phys. Rev.* **121**, 270 (1961). This paper contains a brief summary of earlier work on the subject.

(3) K. W. ALLEN and J. T. DEWAN, *Phys. Rev.* **80**, 181 (1950).

(4) E. W. TITTERTON, *Nature, Lond.* **168**, 590 (1951).

(5) D. L. HILL, *Phys. Rev.* **87**, 1049 (1952).

(6) C. B. FULMER and B. L. COHEN, *Phys. Rev.* **108**, 370 (1957).

(7) E. W. TITTERTON and T. A. BRINKLEY, *Nature, Lond.* **187**, 229 (1960).

(8) E. L. ALBENESIUS and R. S. ONDREJCIN, *Nucleonics* **18**, No. 9, 100 (1960).

Because of the lithium impurity in quartz, of the order of 5–10 p.p.m., quartz tubes were not suitable as irradiation containers. The thermal neutron cross-section of ^{6}Li (950 barns) is so large that the tritium produced by the reaction ^{6}Li (n, α)H^3 would mask the results for tritium produced by the fission process. The concentration of lithium in the NBS uranium oxide was measured by emission spectrographic analysis to be less than 5 parts per billion, giving rise to a tritium production of less than 5 per cent of that observed from fission.

The irradiations were carried out in Argonne's CP–5 reator at a flux of $2{\cdot}54 \times 10^{13}$ neutrons per square centimeter per second for periods of 1–2 days. The irradiated vials were cooled for about one month to allow short lived isotopes to decay.

Isolation and determination of tritium-apparatus

After rinsing a vial successively in nitric acid, water, drying with acetone and again leak testing as previously described, the vial was placed in the apparatus schematically diagrammed in Fig. 1. The traps are standard liquid air traps 25 × 200 mm with 24/40 taper joints and 10 mm o.d. connecting tubing. Traps 2 and 3 contained a plug of Pyrex glass wool at the bottom to minimize bumping during the vacuum distillation process. All traps contained plugs of Pyrex glass wool at the top to hold back possible entrained solids. Halogen holdback carriers in 2N nitric acid and 5N sodium hydroxide were added to trap 2 and trap 3 respectively. Preliminary experiments showed radioactive halogens were found to be troublesome contaminants in the isolated tritiated water.

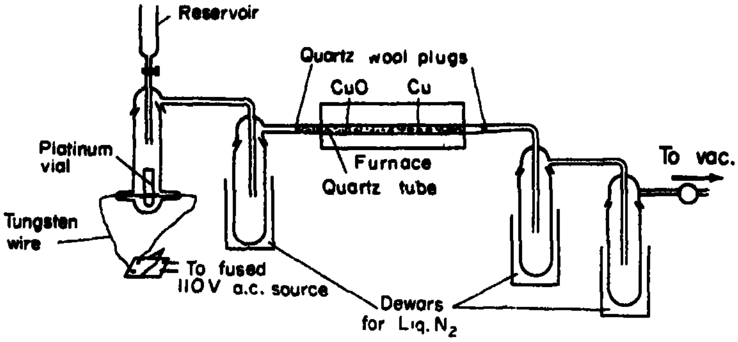

FIG. 1.—Apparatus for isolation of tritium.

The combustion tube, approximately 40 cm long and 15 mm o.d. with graded quartz to Pyrex seals, was filled with cupric oxide in wire form, and plugged with quartz wool. The cupric oxide was reduced to copper metal by heating in a stream of hydrogen gas. After complete reduction and cooling, a stream of oxygen was used with heating to convert one-half of the copper metal to cupric oxide to give a cleaner and more active oxide surface. The combustion tube was then placed in the furnace on the vacuum system as shown in Fig. 1. A heating tape was woven about the upper part of trap 2 and the connecting tubing leading to the combustion furnace to minimize condensation in this section of the apparatus.

The combustion tube serves two purposes. Any tritium present as tritium gas is converted to tritium oxide on passing through the heated cupric oxide. Radioactive halogens, if present as organic halides, are decomposed by the cupric oxide and removed by adsorption on the copper metal.

The platinum vial is placed between the 20 mil tungsten wires of trap 1. The tungsten wires were sealed in Hard Green Sealing Glass No. 3321 tubing and sealed directly to Pyrex. Leads were attached from the tungsten wires through a switch to a 110 V source protected with a 20 A fuse. Upon closure of the switch a short circuit resulted across the platinum vial and melted a small hole in it.

Procedure

With liquid nitrogen in place under traps 2, 3 and 4, the system was checked for leaks at a pressure of 1–2 μ of mercury. The furnace was set at 750–800° C. The system was brought to atmospheric pressure after isolating it from the vacuum pump. A small hole was melted in the platinum vial by means of the short-circuit device. The reagents were added to trap 1 under vacuum through the reservoir. First, 2 ml of concentrated nitric acid plus 2 ml of water were added. By repeated evacuation and bleeding air into the system, the acid solution was forced back and forth inside the platinum vial, dissolving all of the uranium oxide. The solution was then neutralized by the addition of 5 N sodium hydroxide. Neutralization was completed when further addition of base caused no further precipitation of the orange sodium diuranate. Mixing of the solution was accomplished by gentle heating with a torch.

The solution was then distilled under vacuum into trap 2. No bumping was observed if trap 1 was maintained at room temperature. Any residual moisture in trap 1 was driven into trap 2 by the application of heat. Trap 1 was then removed from the system by sealing off the connecting tube, and set aside for ^{140}Ba determination on the residue.

The liquid nitrogen was then removed from trap 2 and a beaker of hot water inserted in its place. The heating tape was set at 110° C and the tritiated water was distilled through the combustion tube into trap 3. After sealing off the combustion tube, vacuum distillation into trap 4 was accomplished.

The volume of tritiated water was measured in a graduated cylinder. An aliquot (2 ml) was removed and analysed for tritium activity as earlier described by two of us.⁽⁹⁾

Determination of the number of fissions—isolation of ^{140}Ba

The procedure for isolation of the ^{140}Ba fission product is that due to GLENDENIN.⁽¹⁰⁾ Analyses were made in triplicate and the time of the barium chloride precipitation was noted as the separation time. The barium chloride was dissolved and an aliquot removed for radioactive assay, the remaining solution was treated to bring about a barium carbonate precipitation from which a chemical yield was determined.

Activity of ^{140}Ba. The gamma activity of the barium sample was measured as soon as possible after separation time, using a 5 in. sodium iodide well-type scintillator coupled to a single channel analyser. Since the increase in the ^{140}La daughter activity is nearly linear with time for about the first 10 hr of growth, the observed γ activity can be corrected to zero ^{140}La by extra polation to the time of the barium separation.

Counts were taken at suitable intervals over a period of 4 hr. The extrapolation was carried out conveniently by employing an unweighted least squares computation using the IBM 610 Analogue Computer. The standard deviations for the ^{140}Ba activities at time of separation were less than 1·2 per cent.

The counting efficiency for the ^{140}Ba in the sodium iodide crystal spectrometer was determined by counting equal aliquots of a separated ^{140}Ba solution simultaneously in the sodium iodide crystal spectrometer and in the "Tri-Carb" liquid scintillation spectrometer. For the liquid scintillation spectrometer the barium chloride solution was made basic and the barium extracted into a 50 per cent solution of di(2-ethylhexyl) orthophosphoric acid in toluene. Aliquots of the dioctyl phosphate solution containing the barium were added to a toluene base scintillator and counted. All beta particles emanating from ^{140}Ba were counted by the liquid scintillation spectrometer with 100 per cent efficiency⁽⁹⁾ and compared to the γ-ray count in the 0·35–0·65 MeV range obtained from the sodium iodide crystal spectrometer. Any contribution from the growth of ^{140}La was negligible inasmuch as the standardization was accomplished within one-half hour of the barium separation. The counting efficiency for the ^{140}Ba was found to be 18·6 per cent of the total disintigration rate.

Number of fissions. Appropriate corrections for decay, chemical yield, volume of aliquots, and efficiency of detection were applied to the observed ^{140}Ba activity to obtain

---

⁽⁹⁾ D. L. HORROCKS and M. H. STUDIER, *Analyt. Chem.* 33, 615 (1961).

⁽¹⁰⁾ L. E. GLENDENIN, *Radiochemical Studies: The Fission Products* (Edited by C. D. CORYELL and N. SUGARMAN). NNES, Plutonium Project Record, Paper 236 McGraw-Hill, New York (1951).

the ^{140}Ba activity present upon termination of irradiation of the uranium oxide in the reactor. The number of fissions is then calculated from the equation:

$$\text{Number of fissions} = \frac{At}{Y(1-e^{-\lambda t})} \tag{1}$$

where A = activity of ^{140}Ba upon termination of irradiation in disintegration/min
t = time of irradiation in minutes
λ = decay constant of ^{140}Ba = $3{\cdot}76\times10^{-5}$ min^{-1}
$(1-e^{\lambda t})$ = growth and decay of ^{140}Ba during irradiation
Y = fission yield of ^{140}Ba from thermal neutron-induced fission of ^{235}U = 6·35 per cent[11]

RESULTS AND DISCUSSION

The results obtained for the fission to tritium ratio in the thermal neutron-induced fission of ^{235}U are shown in Table 1. The first five samples were heated to 900° C, prior to the isolation of tritiated water in an open flow system, on the assumption that any tritium gas would be converted to water through reaction with U_3O_8. The results suggest that tritium was not completely converted to water and that varying amounts of tritium were lost. In the last eight samples the tritium was isolated in the closed vacuum system, as previously described, in which any tritium gas present was converted to tritiated water on passing through the cupric oxide combustion tube.

TABLE 1.

Sample*	U_3O_8 (g)	Tritium atoms† (T × 10^{-11})	Ba activity‡ (disintegration/ min × 10^{-10})	No. fissions** (F × 10^{-15})	F/T × 10^{-4}
M–1	0·2006	3·63	2·025	8·937	2·46
M–2	0·5126	10·06	5·307	23·42	2·33
M–3	1·0227	37·34	10·78	47·57	1·27
K–1	0·4915	7·755	3·553	15·68	2·02
K–2	1·0775	2·093	11·13	49·12	23·47
M–4	0·1969	8·430	2·020	8·915	1·06
M–5	0·5972	20·32	5·950	26·26	1·29
M–6	1·0256	36·67	10·50	46·34	1·26
M–7	0·5314	5·929	2·752	11·82	1·99
M–8	1·0211	18·84	5·082	21·83	1·16
K–3	0·5616	10·73	2·910	12·50	1·16
K–4	0·4873	8·516	2·641	11·34	1·33
K–5	1·1114	16·87	5·936	25·50	1·51

* M and K represent commercial and NBS (MSST) U_3O_8 respectively.
† The standard deviation of the tritium activity was 1 per cent.
‡ Average of three determinations ±3 per cent.
** From Equation 1.

The numerical values of the fission to tritium ratio in the last eight samples were analysed by the statistical method of DEAN and DIXON.[12] Sample M–7 may be rejected with 90 per cent confidence and the resulting average value is $1{\cdot}25\pm0{\cdot}15\times10^4$

---

[11] KATCOFF and SEYMOUR, *Nucleonics* **18**, No. 11, 201 (1960).
[12] R. B. DEAN and W. J. DIXON, *Analyt. Chem.* **23**, 636 (1951).

with approximately 95 per cent confidence. This value is in good agreement with that of Albenesius and Ondrejcin;(8) $1{\cdot}05 \pm 0{\cdot}09 \times 10^4$ for the thermal neutron-induced fission of ^{235}U.

Recently Watson(13) and Wegner(14) have observed a fission to tritium ratio of approximately $0{\cdot}5 \times 10^4$ in the spontaneous fission of californium–252. The frequency of triton emission appears to be significantly greater than that associated with thermal neutron fission of ^{235}U. Titterton and Brinkley(6) suggest the same trend in the frequency of long-range alpha emission.

Acknowledgement—We wish to acknowledge J. Faris for the emission spectrographic analysis.

(13) J. C. Watson, *Phys. Rev.* **121**, 230 (1961).

(14) H. E. Wegner, *Bull. Amer. Phys. Soc.* **6**, 307 (1961).

J. Inorg. Nucl. Chem., 1962, Vol. 24, pp. 343 to 347. Pergamon Press Ltd. Printed in England

PHOTOPRODUCTION OF BERYLLIUM-7

M. S. Foster and A. F. Voigt
Institute for Atomic Research and Department of Chemistry*
Iowa State University, Ames, Iowa

(*Received* 4 *October* 1961)

Abstract—The nuclide ^{7}Be has been produced by photoactivation of ^{9}Be, B and ^{12}C using the bremsstrahlung beam of an electron synchrotron operated at 45 MeV. Integrated cross sections for the formation of ^{7}Be have been estimated by comparison with the ^{181}Ta (γ, n) ^{180m}Ta reaction. The reaction ^{12}C (γ, $2p3n$) ^{7}Be has also been observed in irradiations at 30, 35 and 40 MeV maximum energy. Its yield has been compared with that of the ^{12}C (γ, n) reaction at 45 MeV. The reaction ^{27}Al (γ, $2p3n$) ^{22}Na was observed at 45 MeV.

Experimental and theoretical investigations of the phenomena of photonuclear reactions have been the subject of a large number of studies since the first observed photodisintegrations of deuterium and beryllium.$^{(1)}$ The reactions which have been studied most thoroughly are the (γ, n) and (γ, p) reactions. Less completely examined are the "exotic" reactions in which two or more nucleons are emitted as the result of photoexcitation.

A singular neutron-deficient isotope in the region of $Z < 10$ is the beryllium isotope of mass seven. It is separated from the other known beryllium isotopes by the completely unstable ^{8}Be nucleus. Also, it has recently been observed as a spallation product in a number of high energy processes.$^{(2)}$ Beryllium-7 decays with a half-life of 53 days by K-capture with a 477 keV γ-ray accompanying 12 per cent of the decay processes.$^{(3)}$

The production of ^{7}Be by the ^{9}Be (γ, $2n$) reaction has been reported by Lokan,$^{(4)}$ who bombarded a block of beryllium metal in a bremsstrahlung beam of 30 MeV maximum energy for a total of 16 hr to obtain a counting rate of only 10 counts/min. By comparison with the ^{63}Cu (γ, n) reaction he estimated the integrated cross section to 30 MeV to be $1{\cdot}2\pm0{\cdot}2$ MeV-mbarns. To our knowledge no other photonuclear reactions producing ^{7}Be have been reported.

It was the purpose of this investigation to determine if ^{7}Be might be produced in a medium energy bremsstrahlung beam using as target materials the light elements, beryllium, boron, carbon, oxygen and aluminium. It was also desired to determine the yields of the reactions relative to other photonuclear reactions of known yields, and, if possible, to estimate the integrated cross sections.

EXPERIMENTAL

Target materials of metallic beryllium from the Beryllium Corporation, powdered boron from Fairmont Chemical Company, carbon spectrograph rods from National Carbon Company, "Fisher Certified Reagent" boric acid, "Baker's Analysed" cupric oxide, 2S grade aluminium rods, and fused silica rods were used in these irradiations.

---

*Contribution No. 978. Work was performed in part in the Ames Laboratory of the U.S. Atomic Energy Commission.

(1) J. Chadwick and M. Goldhaber, *Proc. Roy. Soc.* (*Lond.*), **151** A, 479 (1935).

(2) P. A. Benioff, *Phys. Rev.* **119**, 316 (1960).

(3) D. Strominger, J. M. Hollander and G. T. Seaborg, *Rev. Mod. Phys.* **30**, 585 (1958).

(4) K. H. Lokan, *Proc. Phys. Soc.* (*Lond.*), **70** A, 415 (1957).

They were irradiated in a probe extending into the donut of the Iowa State University synchrotron(5) which was operated at an electron energy of 45 ±2 MeV or less as determined by an energy control device. Bremsstrahlung were produced in a Pb radiator which was 2·8 mm thick. All irradiations were monitored by the use of tantalum foils of 0·0005 in. thickness which were wrapped around the sample. In the case of the powdered samples, the monitor foil was wrapped around the brass container used to hold the sample.

All samples in which ^{7}Be was anticipated were counted in a well-type NaI(Tl) scintillation counter to detect radiation with photon energy in excess of 40 KeV. γ-spectra were taken using an RCL 256 channel pulse-height analyser which was calibrated with standard activities of ^{7}Be, ^{22}Na, ^{137}Cs, ^{203}Hg, ^{54}Mn and ^{60}Co. The tantalum monitor foils were counted in a conventional GM counting arrangement. Two foils were counted also with the scintillation counter used for the ^{7}Be samples to obtain conversion factors for the two instruments.

RESULTS

The number of radioactive nuclei, α (E_0), formed during an irradiation at a particular bremsstrahlung of maximum energy E_0, is given by

$$\alpha(E_0) = \eta\int_0^{E_0} \sigma(E)\, N\,(E_0, E)\, dE \qquad (1)$$

in which η = the number of target nuclei, σ (E) = the cross-section as a function of photon energy E, and $N(E_0, E)$ = the number of photons per unit area with energy between E and $(E+dE)$.

Various workers have estimated the integrated cross sections for photonuclear processes by comparing the yields of two reactions, one of which has a cross-section which has been determined independently. One such comparison method has been used for cases in which the cross-sections are sharply peaked functions at energies well below the maximum in the bremsstrahlung spectrum, which is assumed to have a $1/E$ shape. With these assumptions the ratio of the yields can be expressed as;

$$\frac{\alpha_2}{\alpha_1} = \frac{\eta_2\, E_p\,(1)\int_0^{E_0} \sigma_2\, dE}{\eta_1\, E_p\,(2)\int_0^{E_0} \sigma_1\, dE} \qquad (2)$$

in which E_p represents the energy at the peak in the cross section curve.(6) If the integral is known for the monitor reaction, the integral for the unknown reaction can be estimated. In these calculations the reaction ^{181}Ta (γ, n)^{180m}Ta was used for the comparison with the work of Carver and co-workers(7, 8, 9) taken as standard.

Estimates of the cross sections for the ^{9}Be (γ, $2n$) and B (γ, pxn) reactions were obtained from the relative yields of product and monitor activity, Equation(2), and the data in Table 1 on peak energies and cross-sections.

---

(5) A. J. Bureau and C. L. Hammer, *Rev. Sci. Instrum.* **32**, 93 (1961).

(6) T. T. Sugihara and I. Halpern, *Phys. Rev.* **101**, 1768 (1956).

(7) J. H. Carver, R. D. Edge and K. H. Lokan, *Proc. Phys. Soc.* (*Lond.*), **70A**, 415 (1957).

(8) J. H. Carver and W. Turchinetz, *Proc. Phys. Soc.* (*Lond.*), **71A**, 613 (1958); **73**, 69 (1959).

(9) J. H. Carver. Private communication (1961).

For the production of ^{7}Be from ^{12}C the yield relative to the tantalum monitor reaction increased with energy up to 45 MeV. Hence, it was not considered legitimate to use Equation (2) for the estimation of the integrated cross-section. Instead the relative yields of ^{7}Be in the sample and ^{180m}Ta in the monitor were used with Equation (1), the **Penfold** and **Leiss** tables of bremsstrahlung spectra (10) and the data of **Carver** and **Turchinetz** on the cross-section of the Ta reaction(8, 9) to obtain values for the integrated cross section of the ^{12}C (γ, $2p3n$)^{7}Be reaction. The average yield ratios per target nucleus were calculated relative to the ^{181}Ta (γ, n) ^{180m}Ta and ^{12}C (γ, n) ^{11}C reactions. In order to determine the number of nuclei of sample and monitor in the beam it was assumed that equal areas of each were struck by the beam, and the number of nuclei of each type was calculated from the densities, molecular weights and isotopic abundances.

Table 1.—Comparison data for calculations

Reaction	E_p peak energy (MeV)	Integrated cross-section to 45 MeV (MeV-barns)	Reference
^{9}Be (γ, $2n$) ^{7}Be	24		4
B (γ, pxn) ^{7}Be	33		Est. from threshold
^{181}Ta (γ, n) ^{180m}Ta	14	$1{\cdot}6 \pm 0{\cdot}3$	9

The net counting rates for the tantalum monitoring foils were plotted to obtain the intercepts used for the determination of relative yields. These semi-log plots were very close to straight lines and gave an average half-life of 8·19 hr, comparing well with the accepted value of 8·15 hr.(3)

Beryllium results

Two beryllium rods were irradiated for periods of 4 hr in the bremsstrahlung beam at 45±2 MeV and subsequently counted in the well-type scintillation counter. The decay of the 477 keV peak was followed for 45 days and the data so obtained were analysed using a weighted least squares treatment. With the use of Equation (2) the average of two values for the integrated cross section to 45 MeV was found to be 3·2±1·0 Mev-mbarns.

Boron results

Duplicate samples of powdered boron were irradiated at 45 MeV for periods of 6 hr each and counted as previously described. The integrated cross section for the production of ^{7}Be from boron was estimated with the help of Equation(2) giving the results shown in Table 2. For this calculation it was assumed that ^{10}B was the isotope involved in the reaction.

In the γ-ray spectra of these samples, two peaks were visible at 130 and 830 keV which were considered to be due to impurities. From qualitative spectroscopic analysis of the boron and the observed γ-ray energies, it is considered likely that the peak at 130 keV was due to ^{57}Co and the one at 830 keV to ^{54}Mn. These peaks were resolved completely from the 477 keV peak of ^{7}Be and were neglected in the calculations.

(10) A. S. **Penfold** and J. E. **Leiss**, *Analysis of Photo Cross Sections*. Physics Research Laboratory University of Illinois, Champaign (1958).

TABLE 2.—RELATIVE YIELDS* AND INTEGRATED CROSS-SECTIONS FOR FORMATION OF ^{7}Be

Material	E_0	$T\frac{1}{2}$ (days)	Activity at end of irrad. (counts/min)	$\int_0^{E_0} \sigma(E)dE$ (MeV mbars)	Yield, rel. to Ta $\times 10^4$	Yield, rel. to C $\times 10^2$
Be	45	57	4530	$3{\cdot}2 \pm 1$	12 ± 2	8 ± 2
B	45	52	953	$1{\cdot}2 \pm 0{\cdot}4$	$3{\cdot}2 \pm 0{\cdot}6$	$2{\cdot}0 \pm 0{\cdot}6$
HBO_2	45	56	108	$1{\cdot}6 \pm 0{\cdot}5$	$4{\cdot}3 \pm 0{\cdot}5$	$2{\cdot}7 \pm 0{\cdot}7$
C	45	51	1987	$8{\cdot}1 \pm 2{\cdot}6$	18 ± 3	12 ± 4
C	40	53	1080	$5{\cdot}2 \pm 1{\cdot}6$	12 ± 2	
C	35	59	707	$2{\cdot}5 \pm 0{\cdot}8$	7 ± 1	
C	30	56	175	$0{\cdot}5 \pm 0{\cdot}2$	$1{\cdot}1 \pm 0{\cdot}3$	

* Average of two experiments except for C at 30 MeV which is the result of a single experiment.

Carbon results

Duplicate samples of carbon were irradiated at 45, 40 and 35 MeV maximum bremsstrahlung energy and a single sample at 30 MeV. The time of irradiation varied from 4 to 7 hr. Results of these experiments are summarized in Table 2. A second pair of samples was irradiated at 45 MeV for 30 min and counted immediately in order that the ^{11}C content might be determined and compared directly with the amount of ^{7}Be produced. The yield of ^{7}Be relative to the ^{12}C (γ, n) reaction was found to be $0{\cdot}10 \pm 0{\cdot}03$. Comparison with the tantalum monitor was also made in these irradiations, giving a $^7\mathrm{Be}/^{180m}\mathrm{Ta}$ ratio of $(16 \pm 3) \times 10^{-4}$. The γ-ray spectra of these samples were identical with that of the standard ^{7}Be used for calibration purposes. The average half life of ^{7}Be as determined in all irradiations, including both carbon series, was 53 ± 2 days.

Irradiation of oxygen and aluminium

In an attempt to see whether the energy available was sufficient to produce ^{7}Be as a spallation product from oxygen, samples of metaboric acid (HBO_2), cupric oxide and silica were irradiated at 45 MeV. The metaboric acid showed the presence of the 477 keV peak in an amount expected for its boron content. The cupric oxide and silica did not show any peak at this energy, indicating that the reaction ^{16}O $(\gamma, 4p5n)$ ^{7}Be was not observed.

Aluminium metal was also irradiated under similar conditions and observed with well scintillation counter. In this case there was a strong annihilation peak at 511 keV with a half-life of approximately two years. Since these properties are characteristic of ^{22}Na and no isotopes of aluminium or magnesium with these properties are known, it was concluded that the reaction ^{27}Al $(\gamma, 2p3n)$ ^{22}Na was observed. Its yield relative to the tantalum reaction at 45 Mev was estimated to be $(14 \pm 3) \times 10^{-4}$ and relative to the ^{12}C (γ, n) ^{11}C reaction $(9 \pm 3) \times 10^{-2}$. The peak at 511 keV did not show any distortion on the low energy side which could be attributed to the 477 keV γ-ray of ^{7}Be and it seems unlikely that any ^{7}Be was produced in the irradiation of aluminium.

DISCUSSION

It is noteworthy that the yield ratios for the production of ^{7}Be from carbon are higher than those for its production from ^{9}Be. The yield ratio for the production of ^{7}Be and ^{11}C from ^{12}C shows that the reaction which gives rise to ^{7}Be is about 10 per cent as probable as the (γ, n) reaction yielding ^{11}C. This seems surprisingly high.

A calculation of mass thresholds for various types of reactions using the masses listed by SULLIVAN(11) shows the following;

(a) For the reaction ^{9}Be $(\gamma, 2n)$ ^{7}Be, $-Q_m = 20{\cdot}6$ MeV.

(b) For the production of ^{7}Be from ^{10}B and ^{11}B the values of $-Q_m$ for all particle emission paths lie below 45 MeV, from 18·6 for the ^{10}B (γ, t) reaction to 38·6 for the ^{11}B $(\gamma, p3n)$ reaction. The present data do not provide sufficient information for any decision regarding the pathway, but it is probable that ^{10}B is the parent isotope.

(c) For the production of ^{7}Be from ^{12}C, the only paths which have mass thresholds below 45 MeV are the $(\gamma, \alpha n)$, $(\gamma, {}^5\text{He})$ and (γ, td) reactions with the thresholds at 26·3, 27·2 and 43·9 MeV respectively. Since ^{5}He is unstable with respect to ^{4}He and a neutron, its emission as a single entity seems unlikely. Over the range of energies investigated, the yield of ^{7}Be from carbon varied smoothly indicating that a single mechanism is involved for the reaction up to 45 MeV. This fact and the nearness of its threshold to 45 MeV would appear to eliminate the (γ, td) reaction from consideration. Thus the reaction by which ^{7}Be is produced from ^{12}C appears to be the excitation of the ^{12}C nucleus followed by the ejection of an α-particle and a neutron. If the reaction proceeds with the α-particle emission step first, a neutron emitting state of ^{8}Be would be involved. If the neutron is emitted first, an α-emitting state of ^{11}C would be involved. From the fact that the cross-section of the ^{12}C $(\gamma, 2p3n)$ reaction is considerably larger than that for ^{9}Be $(\gamma, 2n)$ reaction (8 compared to 3 MeV-mbarns) it would seem likely that the two reactions do not involve the same intermediates. Hence the pathway involving neutron emission first to an α-emitting state of ^{11}C would appear to be the most likely for the photoproduction of ^{7}Be from ^{12}C.

Acknowledgement—The authors wish to express their appreciation to Dr. A. J. BUREAU and others of the synchrotron crew for their aid in the irradiations.

(11) W. H. SULLIVAN, *Trilinear Chart of Nuclides*. U.S. Govt. Printing Office (1957).

J. Inorg. Nucl. Chem., 1962, Vol. 24, pp. 349 to 356. Pergamon Press Ltd. Printed in England

A MODEL FOR THE RATIONALIZATION OF SALINE AND METALLIC HYDRIDE FORMATION*

T. R. P. Gibb, Jr.
Department of Chemistry, Tufts University, Medford 55, Mass.

(*Received* 2 *September* 1959; *in revised form* 19 *September* 1961)

Abstract—The exothermic, reversible formation of solid hydrides from the elements is rationalized on the basis of a model in which the hydride consists of hydrogen anions and metal cations, the latter likewise engaging in metal–metal bonding in the metallic hydrides. The lattice energy is evaluated as the sum of the Madelung energy and this metal–metal interaction energy. Two empirical methods of estimating the latter are suggested, one involving crystal field stabilization. The total lattice energy so calculated is compared semi-quantitatively with the sum of the endothermic factors in a Born-Haber cycle. The energy balance is favourable with few exceptions for hydrides known to form directly, and unfavourable for hydrides which evidently do not form directly from the elements.

The action of hydrogen gas on some forty metals, including groups I–VI, the lanthanides and actinides, results in reversible exothermic formation of solids containing stoicheiometric or nearly-stoicheiometric proportions of hydrogen. The metals Be, Mo, W are exceptions in that they do not behave in this manner, and Pd is exceptional in that apparently it alone in the groups to the right of Group VI takes up hydrogen readily. A few solid hydrides are known which are not formed by direct synthesis from the metals and which decompose irreversibly, e.g. hydrides of Be, Al, Ni, Cu and possibly Ge (GeH_2), together with several reported hydrides which are stable only at very low temperatures.

It seems of interest to attempt a rationalization of these hydrides based on a model which, while not rigorous, does permit more or less quantitative estimations which would be extremely difficult on a more rigorous level. The model chosen is one in which the principal contribution to the lattice energy is coulombic, i.e. Madelung energy, and therefore easily calculable by the method of Born *et al.*(1) In the case of metallic hydrides where electron delocalization is evidently present, it is assumed for simplicity that there remains an attractive metal–metal interaction similar to that in the original metal, but involving a smaller number of electrons. This interaction is further weakened by the increased metal–metal distance necessary to accommodate H^- in the structure, as observed in the case of nearly all metallic hydrides. In cases where *d*-orbitals are involved, the stabilization due to splitting of the *d*-orbital in the crystal field of H^- may be estimated by the same procedure used for lower-valent oxides, etc.(2, 3)

---

* This research was supported by the United States Atomic Energy Commission. Part of the substance of this paper was reported at the XVIIth International Congress of Pure and Applied Chemistry at Munich in September, 1959, as Paper A–227.

(1) (a) M. Born and J. E. Mayer, *Z. Phys.* **75**, 1 (1932) *et seq.*
(b) cf. J. Sherman, *Chem. Rev.* **11**, 94 (1932).

(2) D. E. O'Reilly, *J. Chem. Educ.* **38**, 312 (1961).

(3) F. J. Morin, *Bell System Tech. J.* **37**, 1047 (1958).

This model provides at least a rationalization of the energy of the formation of stoicheiometric (MH, MH_2, MH_3) hydrides as shown below and in the accompanying figures. The rationalization is merely the comparison of the relative magnitude of the endothermic steps of a Born-Haber cycle with the lattice energy which must pay, energy-wise, for these steps. If the lattice energy calculated from the proposed model numerically exceeds the endothermic steps, the hydride is expected to form exothermically. An additional lattice-energy contribution must be included for non-stoicheiometric hydrides such as $VH_{1\cdot 63}$, $PdH_{0\cdot 6}$ or the several lanthanide H-rich phases, $MH_{>2}$ for example, where vacancy-vacancy⁽⁴⁾ or possibly H-vacancy interactions must be included. Stabilization due to the presence of vacancies results in the existence of several non-stoicheiometric hydrides, whose stoicheiometric H-content is not achieved at room temperature. Thus the limiting composition of the Pd–H_2 system is about $PdH_{0\cdot 6}$ at room temperature, but is $PdH_{0\cdot 9}$ at −78°C.⁽⁵⁾

Lattice energy and the Born-Haber cycle

Lattice energies are calculated from the Born-Lande or the Born-Mayer equations ⁽¹⁾, neglecting VAN DER WAALS (attractive), and zeropoint contributions. When Madelung constants are not known, the approximate KAPUSTINSKII equation is employed.⁽⁶⁾ The constant ρ in the Born-Mayer equation is evaluated by two methods, viz. from the equivalence $(1-1/n') = (1-\rho/d)$ where n' is the Born exponent (arithmetic mean from reference 1b), and d the M–H distance: and by working backwards from the known heats of formation and internuclear distances in the alkali metal hydrides. The value of $\rho = 0\cdot 46$ is used herein, which is considerably larger, as one would expect, than the value of 0·345 generally employed for ions of higher atomic number. Internuclear distances are taken from standard sources⁽⁷, ⁸⁾ or were determined experimentally by X-ray diffraction. Internuclear distances in unknown hypothetical hydrides are estimated.⁽⁹⁾ Note that accurate prediction of internuclear distance generalizes the calculation of lattice energies to the extent that observed and predicted distances are substantially identical.

Ionization potentials are obtained from the N.B.S. Tables supplemented by calculated values from references ⁽¹⁰, ¹¹, ¹²⁾. Heats of sublimation of metals are taken from STULL and SINKE's tables⁽¹³⁾ and from KITTEL.⁽¹⁴⁾ Heats of formation,

---

(4) G. G. LIBOWITZ, *J. Chem. Phys.* **27**, 514 (1957). (An amplified and corrected version of this reference was presented at the International Conference on Nonmetallic Crystals at Northwestern Univ. August 1961.)

(5) Data of PERMINOV, ORLOV and FRUMKIN, cf. P. L. LEVINE and K. E. WEALE, *Trans. Faraday Soc.* **56**, 357 (1960).

(6) A. F. KAPUSTINSKII, *Quart. Rev.* (*Lond.*) **10**, 283 (1956).

(7) W. B. PEARSON, *A Handbook of Lattice Spacings and Structures of Metals and Alloys.* Pergamon Press, New York (1958).

(8) R. E. ELSON, H. C. HORNIG, W. L. JOLLY, J. W. KURY, W. J. RAMSAY and A. ZALKIN, UCRL 4519 Rev. (1956).

(9) T. R. P. GIBB, Jr. and D. P. SCHUMACHER, *J. Phys. Chem.* **64**, 1407 (1960).

(10) L. L. QUILL (Editor), *Chemistry and Metallurgy of Miscellaneous Materials, Thermodynamics.* McGraw-Hill, New York (1950).

(11) W. FINKELNBURG *et al.*, *Naturwissenschaften*, **42**, 35 (1955); *Phys. Rev.* **77**, 303 (1950).

(12) M. A. ELYASHEVICH, *Spectra of Rare Earths.* Government Press, Moscow (1953).

(13) D. R. STULL and G. C. SINKE, *Thermodynamic Properties of Elements*, Amer. Chem. Soc. Washington, D.C. (1956).

(14) C. KITTEL, *Introduction to Solid State Physics*, p. 89. J. Wiley, New York (1957).

when necessary, are from reference (8) or calculated from equilibrium pressures by the VAN'T HOFF equation. The electron affinity of hydrogen is taken to be $-16{\cdot}5$ kcal/g-atom and the dissociation energy of hydrogen to be $+51{\cdot}5$ kcal/g-atom. Thus the energy required to convert a gramme-atom of metal and M/2 mols of molecular hydrogen to gaseous M^{n+} and nH^- ions is given by $L+I_n+35{\cdot}0\,n$ where L is the latent heat of sublimation of the metal, I_n is the ionization potential summed to the ion charge n. This energy requirement is plotted as x in the figures. When the gaseous ions condense to form the postulated ionic hydride, the exothermic energy is the lattice energy of that solid whose calculated value is plotted as open circles in the figures. If the hydride is truly saline and is formed exothermically, the open circle should be above the x, the difference in height being the heat of formation of the hydride. In view of the approximate nature of the calculated energies in most cases, the difference between these rather large numbers is not given numerical significance here. The relative positions of the x and o symbols in the figures serve to indicate trends in the heat of formation. The figures do not include crystalline trihydrides, which are reported for Group III (A and B), the lanthanides, and some actinides. For AlH_3, the ionic model predicts a heat of formation close to zero, the other members of Group IIIA have predicted endothermic heats of formation. ScH_3 and YH_3 are predicted by the model to be formed exothermically. In the lanthanide and actinide series, the necessary constants for a Born-Haber calculation are not available except for a few elements whose trihydrides are predicted to be formed exothermically, in agreement with observation.

Contribution of metal–metal interaction to the lattice energy

It is evident that in the metallic hydrides to the right of Group III the full bonding potentialities, i.e. the maximum valences of the metal, are not realized in an ionic model. The exothermic Madelung energy from the formation of an ionic lattice involving H^- and metal ions of maximum charge is not sufficient to overcome the higher ionization energies of the metal, so that TiH_3 and TiH_4, for example, are not formed. We suggest that in the metallic hydrides, e.g. TiH_2, the unused orbitals (here principally *d*-orbitals) of the metal are involved in covalent or metallic metal–metal bonding. The expanded metal lattice in the hydride is then held together by similar forces to those in the original metal, but diminished by the increased intermetallic distance and by the loss of some of the outer electrons to hydrogen. Naively, one may assume that the energy contributed by such bonding is proportional to the cohesive energy of the metal, the number of available electrons and inversely proportional to some function of the internuclear distance such as given by the Morse function or 6–12 relation. For the purpose of this correlation, and particularly since one is dealing with metal–metal distances only a few per cent larger than in the original metal, the latter function may be simplified to $1/d^x$ where d is internuclear distance and x is between 1 and 2. The higher exponent is more likely, inasmuch as the attenuation of metal–metal attractive energy is due both to increasing internuclear distance and the presence of intervening or partially-intervening H^- ions. The residual metal–metal cohesive energy U_{MM} in the hydride is then given as:

$$U_{MM} = L{d^x}_{MM}\,(z_M - n)/{d^x}_{MMH}z_M$$

where L is the cohesive energy of the metal, d_{MM} the intermetallic distance in the metal, d_{MMH} is the intermetallic distance in the hydride, z_M the number of electrons involved in bonding in the metal, and n is the H/M atomic ratio. It should be pointed out that this gross oversimplification is permissible only because the metal–metal interaction energy is usually small relative to the lattice energy, and because quantitative results are not needed for present purposes. The value of z_M has been taken as the Pauling metallic valence of the metal. Data for a more rigorous approximation are lacking for all but a few metals and the unsettled state of modern theories of alloys(15) indicates that it will be some time before really rigorous calculations of such an interaction energy will be feasible. No central-force model appears applicable to metals.

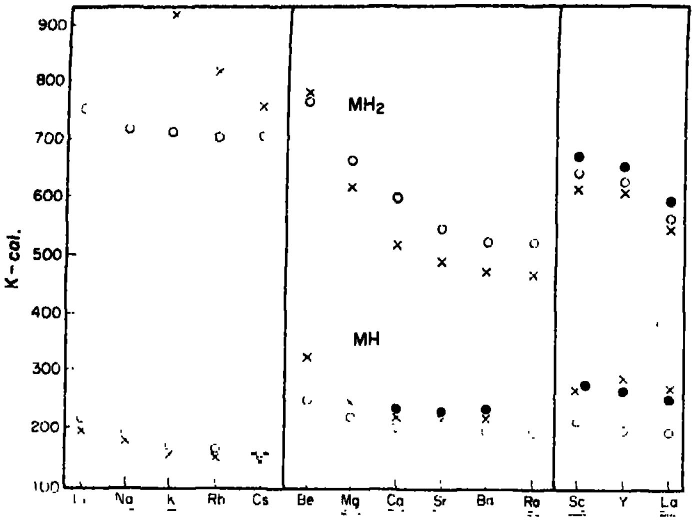

Fig. 1.

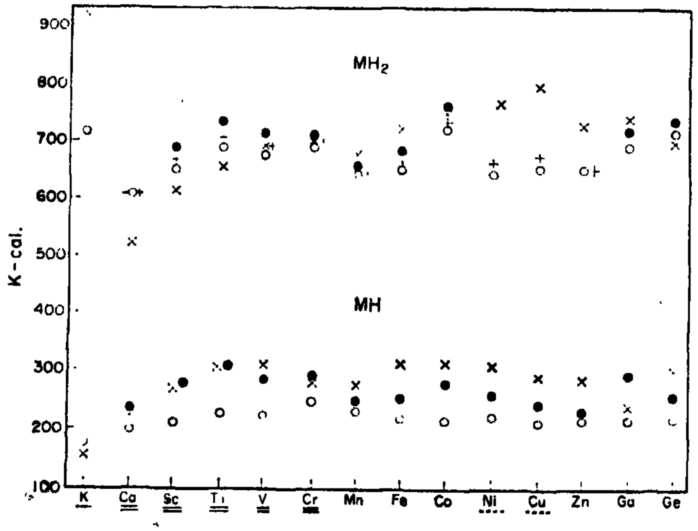

Fig. 2.

---

(15) R. A. Oriani, *J. Phys. Chem. Solids*, **2**, 327 (1957).

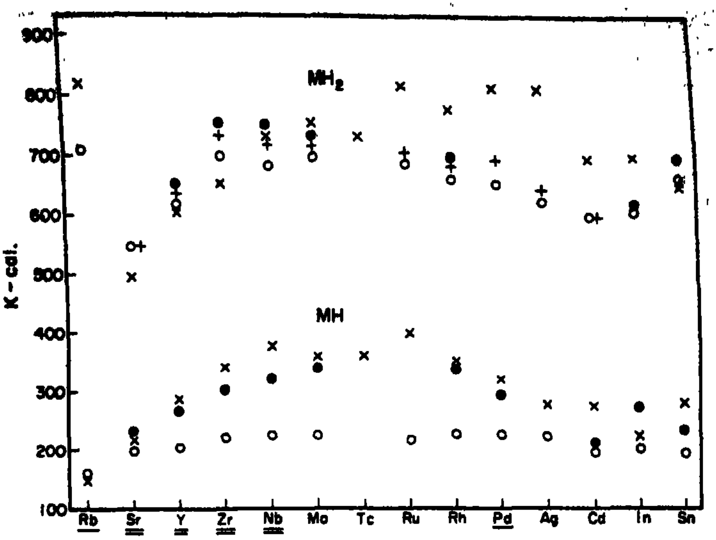

Fig. 3.

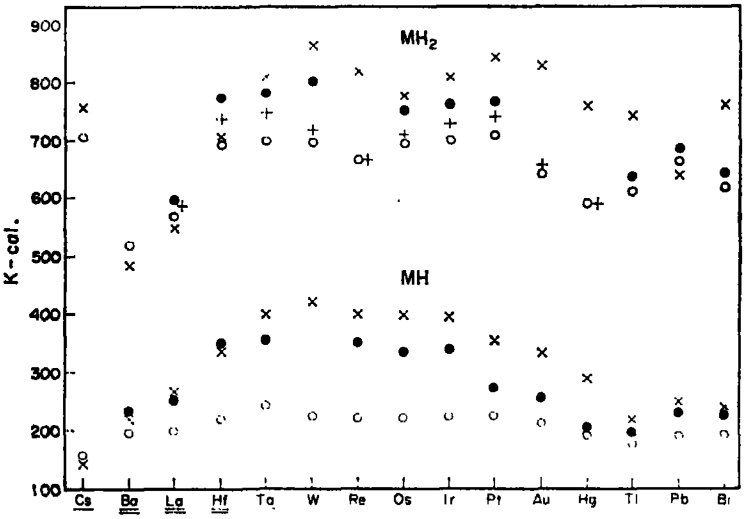

Fig. 4.

Figs. 1–4.—The figures show the Medelung energy of real and hypothetical mono- and di-hydrides as open circles, the sum of Madelung and empirically calculated metal–metal interaction energies as solid circles, the sum of Madelung and crystal field stabilization energies as plus signs. The opposing energies calculated as the sum of the endothermic steps of a Born–Haber cycle are shown as x. Elements forming monohydrides are underlined. Those forming dihydrides are double underlined. (The full stoicheiometry may not be achieved.)

Figs. 1–4 show as black circles the sum of the metal–metal interaction energy estimated by the above equation, and the Madelung energy. It is clear that this sum gives a much better rationalization of the existence of six known hydrides of Groups V and VI and of the heat of formation of several others, notably from

Groups III and IV. On the other hand, it indicates an exothermic formation of GeH_2, InH, SnH_2, GaH, and CoH_2, none of which is known to form exothermically. The estimation of internuclear distances in the first three of these compounds is particularly unreliable, which may account for large errors in the predicted lattice energy. It is also evident that the assumed metal–metal interaction energy makes no provision for directed bonding, which is certainly present in the original metals.

Crystal field stabilization energy

The foregoing suggestion that an attractive metal–metal interaction exists in partly ionic solids is also made in current discussions of crystal field theory.(2, 3, 16, 17, 18) In this theory, interpreted simply, the repulsion of anion neighbours (here H^-) in the lattice may "squeeze out" metal orbitals oriented towards *next*-nearest neighbour metal ions, so that these orbitals have lower energies. Metal–metal ("covalent") attractive interaction along these directions is energetically favoured provided the orbitals are appropriately oriented, and available for bonding. The crystal field stabilization energy (C.F.S.E.) for an octahedral environment, assuming a small field and maximum spin, is given as a parameter $-D_q$ multiplied by $4\,t-6\,e$ where in the octahedral case, t is the number of electrons in the t_{2g} orbitals and e is the number of electrons in the antibonding e-orbitals. For a tetrahedral environment the higher and lower energy orbitals are interchanged and the D_q reduced by a factor of about $\frac{4}{9}$, and for a cubic environment D_q is reduced by a factor of about $\frac{8}{9}$ (reference 17, p. 415). It is reasonable that the crystal field due to H^- is not as large as that due to F^- or O^{2-} so that the assumption of a weak field and consequent maximum spin is likely. (This, however, is being examined experimentally.) Estimation of D_q by an equation involving the effective radius of the d electrons is probably not warranted in the case of metallic hydrides, and no experimental (spectroscopic) values are available. One may, however, use the C.F.S.E. of the crystallographically similar fluorides and oxides to estimate a value for hydrides. The spectroscopic value of D_q for divalent oxides, fluorides and hydrates(19) of the left-hand portion of the period Sc–Cu is reasonably consistent, so that an average value of $3{\cdot}8+0{\cdot}3$ kcal mole for Sc, Ti, V, Cr and an average value of $2{\cdot}7\pm0{\cdot}1$ for Fe, Co and Ni may be used. The higher value is again applicable to Cu at the end of this period. More accurate treatment appears not to be justified at present, since the C.F.S.E. calculated thermodynamically is considerably higher than that observed spectroscopically, at least for several oxides(2) and fluorides.(17, 18) The assumption is made that the value of D_q for compounds of H^- is about $\frac{2}{3}$ that for F^- and $O^=$, in keeping with the lower electronegativity of H which is partly offset by the tenuousity of the electron distribution about H^-. It is also assumed, following Orgel (reference 18, p. 45) that the value of D_q increases about 30 per cent in the second period and an additional 30 per cent in the third period. The ease of spin-pairing also increases in descending to the lower periods and it is likely that in the field of H^-, pairing may occur in the higher atomic number inner transition metal hydrides, although in such cases the C.F.S.E. is more difficult to estimate and no estimations are made for the low-spin cases.

(16) cf. W. Moffitt and C. J. Ballhausen, *Ann. Rev. Phys. Chem.* **7**, 107 (1956).

(17) P. George and D. S. McClure, *Progress Inorg. Chem.* **1**, 381 (1959).

(18) L. E. Orgel, *Transition Metal Chemistry*. J. Wiley, New York (1960).

(19) D. Polder, *Physica* **9**, 709 (1942).

TABLE 1.—ESTIMATED C.F.S.E. VALUES (kcal per mole) FOR ACTUAL AND HYPOTHETICAL DIHYDRIDES

	D_q	Multiplier Octahed.	 Cubic	C.F.S.E. (rounded) Octahed.	 Cubic
ScH_2	2·5	4	6	10	13 *jt*
TiH_2	2·5	7	12	17	27
VH_2	2·5	12	7	30	16
CrH_2	2·5	6	4	15	9
MnH_2	—	0	0	0	0
FeH_2	1·8	4	6	7	10 *jt*
CoH_2	1·8	7	12	13	19
NiH_2	1·8	12	7	22	11
CuH_2	2·5	6	4	15 *jt*	9
ZnH_2	—	0	0	0	0

In Table 1 the crystal field stabilization energies estimated in accordance with current practices and the above assumptions are listed for the divalent metal hydrides, real and hypothetical, of the first period. Those configurations which are particularly likely to show Jahn-Teller distortions are indicated by the symbol *jt*. Since the majority of known dihydrides have the fluorite structure or an approximation thereof, it is reasonable to assume a cubic environment. For the hypothetical dihydrides from MnH_2 to ZnH_2, however, no *a priori* choice of structure has been made, but the maximum C.F.S.E. is taken.

The C.F.S.E. values from Table 1 added to the estimated lattice energy are plotted as small + signs in Fig. 2. Note that the C.F.S.E. trends are in the right direction to account for the formation of hydrides by elements to the left of Mn, although it would appear that the C.F.S.E. for VH_2 is too low and for hypothetical FeH_2 and CoH_2 slightly too high. Values of the C.F.S.E. for periods II and III have been calculated in the same way and the highest reasonable value added to the lattice energy to give the points represented as + signs in Figs. 3 and 4. It is evident that the C.F.S.E. improves the rationalization of the known hydrides of Groups III, IV and V (notably HfH_2), but is not of sufficient magnitude to alter the predictions based on lattice energy alone for other (hypothetical) dihydrides.

It is difficult to perform the same sort of estimations for the monohydrides, since no D_q values are available for halides of the univalent cations (Group II–VIII). Moreover, it is likely that the foregoing considerations are not applicable if the *s*-level is partly occupied. Presumably hybridization would occur and, naively, increased stability should be observed for d^3s, d^4s, d^8s and d^9s^1, the former due to hybridization and half-filling of the *d*-orbitals as in VH and Cr^+H^-, the latter due to near-filling of the *d*-orbitals in NiH and Cu^+H^-. These are just the monohydrides which require extra stabilization according to Fig. 2, since VH, CrH, NiH and CuH have been reported although the latter decomposes at room temperature and NiH is also unstable. In the second period similar stabilizations are needed to rationalize NbH and $PdH_{<1}$, but the gap between the lattice energies and *x*-factors (Fig. 3) is so large for MoH and AgH that these hydrides are not likely, nor indeed have they been found. The same considerations apply to WH and PtH, but the well known $TaH_{\sim 1}$ remains anomalous. It is tempting to extend the C.F.S.E. estimation employed for divalent ions to isoelectronic ions of smaller charge, and with an *increased* D_q, but there is no acceptable reason for doing this.

SUMMARY AND DISCUSSION

Two obvious points concerning the suggested model remain to be further clarified: evidence for the primarily hydridic (as opposed to protonic or covalent) character of hydrogen in metallic hydrides, and evidence that neglect of the screening of the ionic charges by conduction (or metallic) electrons is justified. The first of these points will be dealt with elsewhere (see also reference 4 and 20), but the second is justified, in part at least, by the lack of any major energy change (ΔH) accompanying the sudden appearance of metallic character in sulphides(21) or in oxides(22) as the non-metal content is decreased. The lattice energy of many such compounds is given fairly accurately by the Born method, whether the substance is a conductor or not. Furthermore, there is some question as to the actual number of conduction electrons, since one would expect many "metallic" oxides, sulphides and hydrides to conduct by a vacancy mechanism.

The assumption that the energetics of hydride formation are primarily due to Madelung energy supplemented by metal–metal bonding, provides a rationalization of the existence of most primary hydrides and interprets the hydrogenation-catalytic ability of Mo and the Group VIII elements whose hypothetical hydrides are predicted to have close to zero heat of formation. The uncertainties arising from the approximate nature of the Born–Haber and Madelung energy estimations are generally considerably less than the proposed additional contributions, and are small compared to the total cohesive energy. The oxidation number of the cation is uncertain for the Ga and Ge groups particularly, and the lattice energies are correspondingly less reliable for these groups. The predicted Madelung energies for unknown hydrides are obviously subject to large errors and serve mainly to indicate trends. Several hydrides predicted by this rationalization have subsequently been prepared ($VH_{\sim 2}$, NbH_2, GeH_2) and others whose prediction is indecisive have been reported (AlH_3, NiH).

It should be kept in mind that the choice of an ionic model is dictated by the difficulty of estimating cohesive energies by other means. The model is naive at the moment, but suggests the means for its improvement through more careful evaluation of lattice energies and refinement of the evaluation of metal–metal interaction energies. The crystal field stabilization energy has the particular merit that it includes directional character which is obviously necessary to the explanation of observed distortions of hydride crystal structures. Further, it provides maximum stabilization in just those periodic groups where hydride formation occurs. Evaluation of D_q by reflexion-spectroscopy and confirmation of the weak-field maximum-spin assumption by magnetic measurements should greatly aid in the quantitative application of the theory to the metallic hydrides.

---

(20) R. A. ORIANI, E. MCCLIMENT and J. F. YOUNGBLOOD, *J. Chem. Phys.* **27**, 330 (1957).

(21) cf. M. LAFFITTE and J. BENARD, *XVIth Congress International Union of Pure and Applied Chemistry*. Paris (1957); *The Physical Chemistry of Metallic Solutions and Intermetallic Compounds*, p. 418. Chem. Publishing, New York (1960).

(22) F. J. MORIN, *Phys. Rev.* **3**, 34 (1959).

J. Inorg. Nucl. Chem., 1962, Vol. 24, pp. 357 to 363. Pergamon Press Ltd. Printed in England

THE MOLECULAR AND CRYSTAL STRUCTURE OF THALLIUM (I) METHOXIDE*

L. F. DAHL, G. L. DAVIS, D. L. WAMPLER† and R. WEST
Department of Chemistry, University of Wisconsin, Madison 6, Wisconsin

(*Received* 31 *July* 1961; *in revised form* 5 *October* 1961)

Abstract—An X-ray single-crystal structural study of thallium (I) methoxide, $TlOCH_3$, has yielded the thallium arrangement along with a proposed over-all configuration of the molecule. Thallium (I) methoxide is orthorhombic with $a = 13{\cdot}80$ Å, $b = 6{\cdot}98$ Å, and $c = 13{\cdot}66$ Å. The probable space group is $Pca2_1$; the unit cell contains sixteen $TlOCH_3$ species. Two-dimensional Patterson and Fourier projections and least squares analyses gave the atomic positions of the heavy thallium atoms; the X-ray data were not sufficient to allow detection of the methoxide positions.

Crystalline thallium (I) methoxide consists of tetrameric molecules in which the thallium atoms are at the corners of a regular tetrahedron. In this structure the average Tl–Tl distance is 3·84 Å. A structure is proposed for $(TlOCH_3)_4$ in which thallium and methoxide groups each occupy the corners of two interpenetrating concentric tetrahedra of different size resulting in a distorted cube such that the Tl–O–Tl angle is > 90° and the O–Tl–O angle is < 90°.

THALLIUM(I) alkoxides were first prepared by LAMY nearly one hundred years ago.(1) Unlike the alkali metal alkoxides, which are ionic solids, most of the thallium compounds are liquids with low volatility. Freezing point depression measurements have shown that thallium(I) alkoxides exist as tetranuclear compounds in benzene solution.(2) Recent boiling point elevation experiments(3) confirm the tetrameric nature of thallium(I) alkoxides in solution and indicate that the degree of polymerization apparently is not affected by the size and shape of the alkyl substituent. In contrast, branching of the alkyl group sterically hinders association and lowers the degree of polymerization for many other covalent metal alkoxides.(3)

On the basis of their molecular weight determinations, SIDGWICK and SUTTON(2) proposed a cubic structure for the tetrameric thallium(I) alkoxide molecules. Although no direct support for the SIDGWICK–SUTTON structure has appeared, it has been frequently reprinted(3, 4) and widely accepted.

---

* Presented in part at the National Meeting of American Crystallographic Association at Washington D.C., January 1960.

† National Science Foundation Predoctoral Research Fellow.

(1) A. LAMY, *Ann. Chim. Phys.* 67, 365 (1863).

(2) N. V. SIDGWICK and L. E. SUTTON, *J. Chem. Soc.* 1461 (1930).

(3) D. C. BRADLEY, *Metal-Organic Compounds*, American Chemical Society Advances in Chemistry Series, 23, 10 (1959).

(4) See, for example, M. J. EMELEUS and J. S. ANDERSON, *Modern Aspects of Inorganic Chemistry* (2nd Ed.), p. 119. Van Nostrand, New York (1952); A. F. WELLS, *Structural Inorganic Chemistry* (2nd Ed.), p. 635. Clarendon, Oxford (1950); N. V. SIDGWICK, *Chemical Elements and Their Compounds*, p. 485. Clarendon, Oxford (1950); R. J. GILLESPIE and R. S. NYHOLM, *Quart. Rev.* 11, 367 (1957); W. HÜCKEL, *Structural Chemistry of Inorganic Compounds*, p. 149. Elsevier, New York (1950).

The present X-ray diffraction investigation was undertaken to obtain more definite evidence for the structure of thallium(I) alkoxides. Thallium(I) methoxide was chosen for study because it is a solid at room temperature.* This compound was obtained by the action of methanol on thallium(I) ethoxide which was prepared from thallium metal and ethanol in the presence of air.

EXPERIMENTAL PROCEDURE

(a) *Preparation and analysis*

Thallium(I) ethoxide. The method of preparation used was an improvement over that of Sidgwick and Sutton.(2) Thallium metal was beaten with a hammer into a thick foil and then cut into turnings with scissors. In a specially built apparatus (Fig. 1) 30·6 g (0·15 g atom) of freshly-cut thallium was suspended in a Gooch crucible over refluxing ethanol while a slow stream of dry, CO_2 free air was passed through. During 16 hr of refluxing most of the thallium reacted to form thallium(I) ethoxide, which dripped through the crucible into the reflux pot. The ethanol was cooled to room temperature, and the lower layer of thallium (I) ethoxide was separated as a heavy oil. The yield of crude ethoxide, containing some ethanol, was 18 g (50 per cent). For infra-red spectral work the ethanol was removed by pumping on the crude ethoxide.

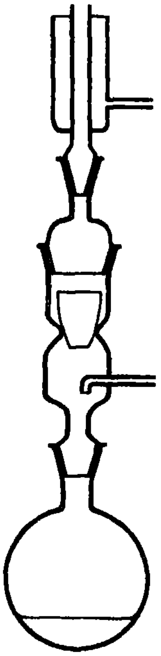

Fig. 1.—Apparatus for the preparation of thallium (I) ethoxide.

Thallium (I) methoxide. Crude thallium (I) ethoxide was added to approximately twice its weight of dry methanol. A white precipitate of thallium (I) methoxide formed immediately. After a few minutes the alcohol was decanted and the thallium (I) methoxide was twice recrystallized from dry benzene to give colourless prisms. The crystals could be kept for several months under benzene without serious decomposition, although they decompose very rapidly in air. They were dried *in vacuo* as needed. The substance was analysed gravimetrically by precipitation of thallium as thallium chromate. (Found: Tl, 86·4, 85·9 per cent. Calc.: for $TlOCH_3$: Tl, 86·8 per cent.)

---

* The tetrameric nature of thallium (I) methoxide in solution has been firmly established.(2) However, it should be noted that association in the solid state may differ from that in solution.(5, 6)

(5) M. E. Kenney and A. W. Laubengayer, *J. Amer. Chem. Soc.* **76**, 4839 (1954).

(6) G. S. Smith and J. L. Hoard, *J. Amer. Chem. Soc.* **81**, 3907 (1959).

(b) *Infra-red spectra of thallium (I) alkoxides*

Thallium (I) methoxide and ethoxide were both studied in the 625–4000 cm^{-1} region. The spectrum of thallium (I) methoxide as a mull in white petroleum oil was obtained; thallium (I) ethoxide was examined as a liquid film between sodium chloride plates. By far the strongest band in both spectra is the one at 1030 cm^{-1} which is probably due to the C–O stretching vibration.(7) Both compounds show the usual C–H stretching absorptions near 2950 and O–H bending modes at 1450 and 1380 cm^{-1}, although these bands are partly obscured by mull bands in the case of the methoxide. The methoxide has weak bands of unknown origin at 720 cm^{-1} and at about 620 cm^{-1}, while the ethoxide shows a prominent band at 870 cm^{-1}.

(c) *Isolation of single crystals and collection of X-ray data*

Crystals were quickly removed from benzene and immersed in vaseline without allowing the protective film of benzene to evaporate completely. They were then loaded into Lindemann glass capillaries which were subsequently sealed. The crystals were found to decompose in the X-ray beam after several exposures. Although Mo$K\alpha$ radiation was tried, suitable X-ray pictures were obtained only with Cu$K\alpha$ radiation. In addition most of the crystals were found to be twinned. As a result of these difficulties two-dimensional Weissenberg intensity data were obtained for the (*hol*) and (*okl*) zones from two crystals together with limited three-dimensional data from other crystals by application of the usual multiple film technique. The intensities were visually estimated with a calibrated standard set of intensities and corrected for Lorentz and polarization effects.

(d) *Structural determination*

Weissenberg and precession X-ray pictures taken with Cu$K\alpha$ radiation revealed the crystals to be orthorhombic with lattice constants $a = 13{\cdot}80$ Å, $b = 6{\cdot}98$ Å and $c = 13{\cdot}66$ Å. Sixteen $TlOCH_3$ species per unit cell give a calculated density of 4·75 g/cm^3. The indexed data showed the occurrence of the following systematic absences: $\{okl\}$ for l odd; $\{hol\}$ for h odd; and $\{ool\}$ for l odd. The indicated probable space group $Pca2_1$ (C_{2v}^{5}) was confirmed by the structure ultimately found. Since the space group $Pca2_1$ contains four general equivalent points (i.e. x, y, z; $\bar{x}, \bar{y}, \frac{1}{2}+z$; $\frac{1}{2}-x, y, \frac{1}{2}+z$; $\frac{1}{2}+x, \bar{y}, z$), the positions of four thallium atoms had to be determined.

The thallium atoms were located from Patterson and Fourier projections and were refined by the method of least squares on an IBM 650 computer.(8) The scattering factors used for Tl are those of JAMES–BRINDLEY(9) corrected for dispersion.(10)

The electron-density maps and corresponding unit cell projections are given in Figs. 2 and 3. The asymmetric part of the projected unit cell is outlined by dotted lines. The [010] electron-density map clearly shows the tetrameric arrangement of the thallium atoms. Although the thallium atoms overlap on the [100] electron-density map, the tetrameric molecules still can be discerned.

(7) L. J. BELLAMY, *The Infra-red Spectra of Complex Molecules* (2nd Ed.), Chap. 7. Methuen, London (1958).

(8) M. E. SENKO and D. H. TEMPLETON, *A Crystallographic Least Squares Programme for the IBM 650 Computer*, University of California Radiation Laboratory (1956).

(9) *Internationale Tabellen zur Bestimmung von Kristallstrukturen*, Rev. E. Band 2, p. 573. Gebruder Borntraeger, Berlin (1944).

(10) C. H. DAUBEN and D. H. TEMPLETON, *Acta Cryst.* **8**, 841 (1955).

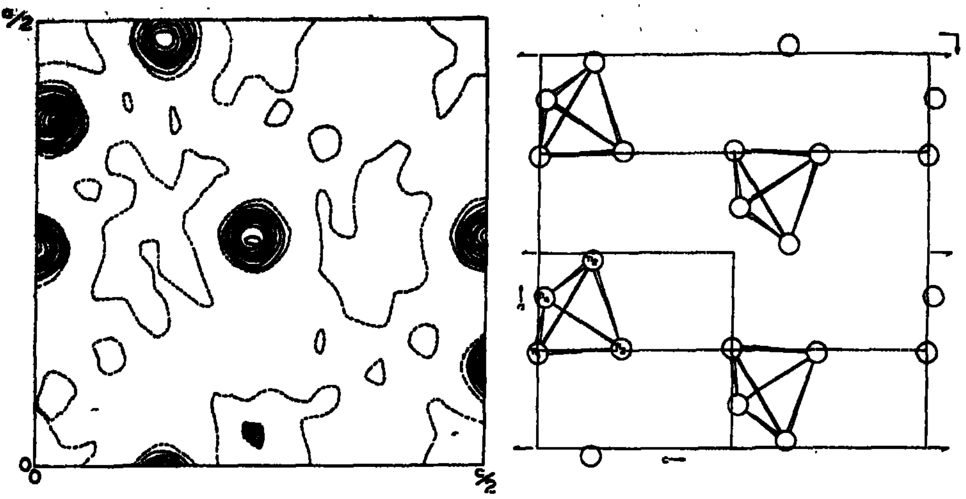

Fig. 2.—(a) [010] Fourier projection.
(b) [010] Projection of Tl atoms.

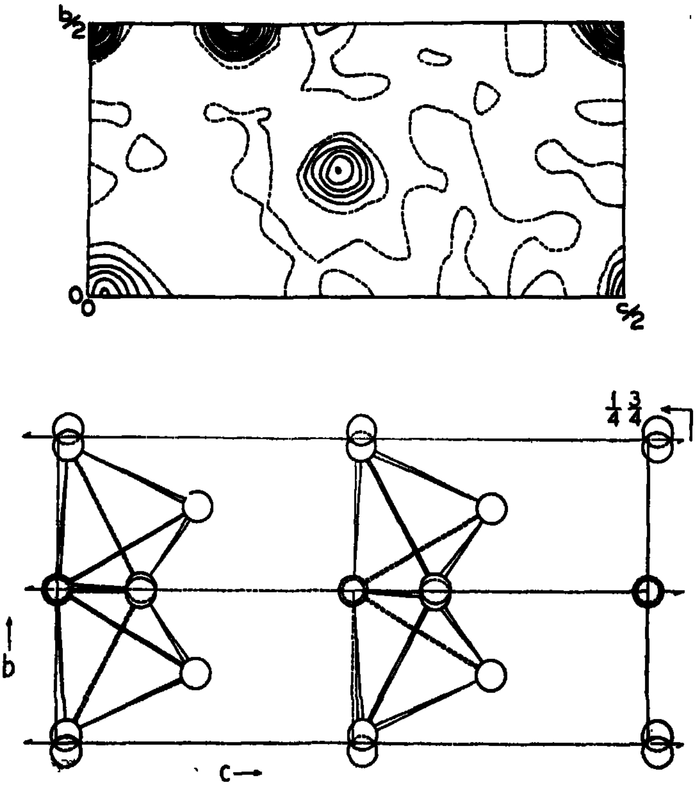

Fig. 3.—(a) [100] Fourier projection.
(b) [100] Projection of Tl atoms.

The final x and z positional parameters were obtained for the four asymmetric thallium atoms from least squares refinement of the (*hol*) data. The y parameters then were obtained from least squares analysis of the (*okl*) data; lack of resolution limited the usefulness of these latter data, but structure factor calculations for (*h*1*l*), (*h*2*l*), (2*kl*) reflexions based on the final parameters showed good qualitative agreement with the observed intensities and also eliminated possible ambiguities of structure imposed by consideration of only axial projections. For instance, since (*hol*) data for which $h = 2n+1$ are systematically absent, *in projection the origin can be shifted by* $a/4$. However, examination of general reflexions for which $h = 2n+1$ clearly showed the correct choice of x co-ordinates. The common z co-ordinates for both zones agree to within one standard deviation. The final discrepancy factor, $R_1 = (\sum||Fo| - |Fc||/\sum|Fo|) \times 100$, based only on observed reflexions is 13·7 per cent for the (*hol*) data and 15·9 per cent for the (*okl*) data.*

Since the crystals dissolved somewhat in the vaseline and possessed irregular shapes, no absorption corrections were applied to the intensity data; the effect was minimized as much as possible by the use of small crystals. The final parameters and their standard deviations⁽¹¹⁾ are listed in Table 1. The individual isotropic temperature factors given are the unweighted averages of the results of the two least squares refinements. Table 2 lists the intramolecular and intermolecular Tl–Tl distances and their probable errors.⁽¹²⁾

TABLE 1.—FINAL PARAMETERS, STANDARD DEVIATIONS, AND ATOM TEMPERATURE FACTORS

Atom	x	y	z	$\sigma(x)$	$\sigma(y)$	$\sigma(z)$	B(Å^2)
Tl_1	0·243	0·500	0·000	0·001	0·002	0·002	0·17
Tl_2	0·481	0·485	0·143	0·001	0·003	0·001	0·13
Tl_3	0·256	0·221	0·241	0·001	0·002	0·002	0·21
Tl_4	0·389	0·028	0·016	0·001	0·002	0·001	0·26

TABLE 2.—NEAREST INTERATOMIC Tl–Tl DISTANCES

Intramolecular	
Tl_1–Tl_2	3·81 ±0·02 Å
Tl_1–Tl_3	3·83 ±0·02
Tl_1–Tl_4	3·86 ±0·02
Tl_2–Tl_3	3·86 ±0·02
Tl_2–Tl_4	3·84 ±0·02
Tl_3–Tl_4	3·83 ±0·02
Intermolecular	
Tl_1–3 Tl	4·04, 4·11, 4·20 Å
Tl_2–3 Tl	4·11, 4·36, 4·52
Tl_3–3 Tl	4·04, 4·46, 4·52
Tl_4–3 Tl	4·20, 4·36, 4·46

---

* A record of the 106 (*hol*) structure factors (7 of which were unobserved) and 62 (*okl*) structure factors (4 of which were unobserved) and the calculated structure factors has been deposited as a Document with ADI Auxiliary Publications project, Photo-duplication Service, Library of Congress, Washington 25, D.C., USA.

(11) D. W. J. CRUICKSHANK, *Acta Cryst.* 2, 154 (1949).

(12) D. W. J. CRUICKSHANK and A. P. ROBERTSON, *Acta Cryst.* 6, 698 (1953).

DESCRIPTION OF THE STRUCTURE

Crystalline thallium methoxide consists of tetrameric molecules, $[Tl(OCH_3)]_4$, in in which within experimental error the thallium atoms are at the corners of a regular tetrahedron. The average intramolecular Tl–Tl distance is 3·84 Å. The X-ray intensity data obtained are not sufficiently sensitive to allow the determination of the methoxide positions in the presence of the heavy thallium atoms.

The configuration of the thallium atoms is consistent with the structure proposed by SIDGWICK and SUTTON.(2) In their structure the thallium and oxygen atoms occupy the eight corners of a cube formed by two *regular*, *equal-sized*, interpenetrating concentric tetrahedra of thallium and oxygen atoms. Each thallium atom is equally bonded to three oxygen atoms. Each oxygen is bonded to three thallium atoms and a methyl group. This four-co-ordinated oxygen with three 90° bond angles appears most unlikely. Furthermore, in basic beryllium acetate(13) ($Be_4O(OOCCH_3)_6$), the only four-co-ordinated oxygen compound whose structure has been unambiguously determined by X-ray diffraction, the oxygen atom is tetrahedrally co-ordinated.

We feel that the structure is better represented by a *distorted* cube in which the oxygen atoms occupy the corners of the smaller tetrahedron (Fig. 4). This distortion is achieved by pushing the oxygen atoms in along the threefold axes of the cube resulting in a Tl–O–Tl angle greater than 90° and an O–Tl–O angle less than 90°. Trimethylplatinum chloride, $[(CH_3)_3PtCl]_4$, has a similar structure.(14) The platinum and chlorine atoms occupy corners of two interpenetrating concentric tetrahedra of different size resulting in a Pt–Cl–Pt angle of 97½° and a Cl–Pt–Cl angle of 82½°.

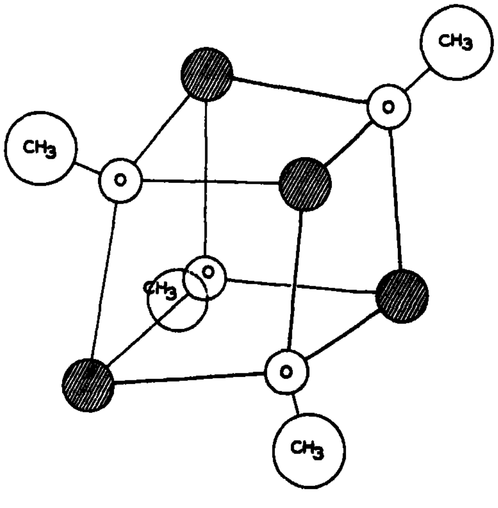

FIG. 4.—Proposed molecular structure for $[Tl(OCH_3)]_4$.

To ascertain the packing for thallium(I) methoxide a three-dimensional molecular model of the unit cell was constructed to scale from the refined thallium positions and estimated methoxide positions. The structure was found to be most reasonable from packing considerations, and yielded satisfactory van der Waals distances of approximately 4 Å for the methyl–methyl contacts.(15) Our proposed molecular model is in accord with the apparent lack of steric hindrance of the alkoxide groups to tetranuclear association.(3)

---

(13) A. TULINSKY and C. R. WORTHINGTON, *Acta Cryst.* **12**, 626 (1959).

(14) R. E. RUNDLE and J. H. STURDIVANT, *J. Amer. Chem. Soc.* **69**, 1561 (1947).

The structure for thallium(I) methoxide is unusual for thallium(I) since all other thallium(I) compounds known, including the halides, nitrate, and sulphate, have co-ordination number six or eight. In these latter cases the thallium(I) acts as a pseudo-alkali metal ion. The exact positions of the methoxide groups probably can best be determined by neutron diffraction studies.

Acknowledgement—The authors wish to thank Miss H. WHITTAKER for assistance with the preparation of the thallium (I) alkoxides used in this study and also are grateful to the Research Corporation for financial support obtained from a Frederick Gardner Cottrell grant.

(15) L. PAULING, *The Nature of the Chemical Bond*, Cornell University Press, Ithaca, New York (1960).

J. Inorg. Nucl. Chem., 1962, Vol. 24, pp. 365 to 369. Pergamon Press Ltd. Printed in England

INORGANIC CO-ORDINATION POLYMERS—I

GENERAL CONSIDERATIONS

B. P. Block and G. Barth-Wehrenalp
Research and Development Department, Pennsalt Chemicals Corporation, Wyndmoor, Pa.

(*Received* 14 *September* 1961; *in revised form* 30 *October* 1961)

Abstract—Synthetic approaches to co-ordination polymers are classified as condensation polymerizations, addition-type polymerizations involving co-ordinatively-unsaturated intermediates, and degradation polymerizations. The first two classes are further subdivided into homocondensations and heterocondensations and into elimination–additions, substitution–additions, oxidation–additions, redistribution–additions and rearrangement–additions, respectively. These various classes are discussed.

In our Laboratories we are investigating the synthesis of inorganic co-ordination polymers, where we define co-ordination polymers as substances with repeating units containing atoms in the backbone acting as acceptors in co-ordinate covalent bonds. This definition is more restrictive than that used by Sowerby and Audrieth,(1) "polymeric materials containing co-ordinated metal ions", for it excludes polymers which do not contain co-ordination centres in the backbone such as $[-CH_2CH(C_5H_4FeC_5H_5)-]_x$.(2) We do not include the latter type in our definition, for the co-ordinated portion is not an integral part of the polymer backbone, but rather an adjunct to a substance which is a polymer in its own right.

To systematize our synthetic approaches to co-ordination polymers we have formulated a classification scheme which we wish to present in this initial communication in order to provide the framework for succeeding papers in this series, in which we will report the results of our studies. Sowerby and Audrieth(1) and Berlin and Matveeva(3) have also presented such schemes for somewhat different situations. Their treatments were, however, less detailed because of the nature of their reviews.

Broadly speaking, organic polymerization reactions are classified as condensation or addition reactions. These two types of reactions involve the elimination of small molecules between units in the first case and the union of unsaturated molecules in the latter. In general, the central element of a co-ordination compound does not form double or triple bonds leading to the chemical behaviour classed as unsaturation in organic chemistry, so that addition polymerization in the foregoing sense is not expected for co-ordination compounds. There is another kind of unsaturation conceivable in co-ordination compounds, co-ordinative unsaturation, in which there are not sufficient ligands present to meet the co-ordination number requirements of the co-ordination centre. In the classification that follows the addition-type polymerizations can be pictured as involving the creation of co-ordinative unsaturation and its satisfaction by polymerization.

---

(1) D. B. Sowerby and L. F. Audrieth, *J. Chem. Educ.* 37, 134 (1960).

(2) F. S. Arimoto and A. C. Haven, Jr., *J. Amer. Chem. Soc.* 77, 6295 (1955).

(3) A. A. Berlin and N. G. Matveeva, *Russ. Chem. Revs.* 29, 119 (1960).

The term "condensation polymerization" will be used in the same sense that it is for organic polymerization, i.e., to designate those reactions in which small molecules are split out between molecules. We propose two classes of inorganic condensation polymerizations: "homocondensations" and "heterocondensations", referring to reactions in which the elimination takes place between like molecules and between different kinds of molecules, respectively. Examples of both these classes have been reported in the literature. JOYNER and KENNEY found⁽⁴⁾ that the compound $Ge(C_{32}H_{16}N_8)(OH)_2$, where $C_{32}H_{16}N_8$ is the phthalocyanine anion, loses water when heated, presumably forming $(-Ge(C_{32}H_{16}N_8)O-)_x$. This reaction, by definition, is a homocondensation. There do not seem to be any simple examples of heterocondensation polymerizations leading to co-ordination polymers known, although several reactions which probably should be so classified have been reported. For illustrative purposes a reaction which has been attempted in our Laboratories will be used. The desired reaction was to take place between $[Pt(NH_3)_2Cl_2(OH)_2]$ and $(C_6H_5)_2SiCl_2$ by splitting out HCl to yield $(-Pt(NH_3)_2Cl_2OSi(C_6H_6)_2O-)_x$. It will be noted that in this reaction the co-ordination sphere about the metallic element would not be disturbed.

The second broad class is that of "addition-type polymerizations." This term will be applied to reactions which can be pictured as involving co-ordinatively unsaturated intermediates in the formation of the backbone. Obviously all homocondensations as well as those heterocondensations in which the co-ordination sphere of the metal is disturbed must involve co-ordinatively unsaturated intermediates, but in deference to established usage these classes will be arbitrarily maintained for reactions obviously analogous to organic condensations. There are different addition-type polymerizations conceivable: accordingly, we have made the following subdivision based on different ways of achieving co-ordinative unsaturation; elimination–addition, substitution–addition, oxidation–addition, redistribution–addition and rearrangement–addition.

An *elimination–addition polymerization* is a reaction in which a polymer is formed from a fully co-ordinated monomer by the loss of neutral ligands. For example, ELVIDGE and LEVER have found⁽⁵⁾ that $(C_5H_5N)Mn(C_{32}H_{16}N_8)O$ another phthalocyanine-containing co-ordination compound, loses pyridine when heated at reduced pressure to give the polymer $(-Mn(C_{32}H_{16}N_8)O-)_x$. This reaction differs from a homocondensation in that the molecule eliminated from the monomer is not split out from between two units but originates from only one molecule, suggesting that a co-ordinatively unsaturated intermediate, presumably pentaco-ordinate $Mn(C_{32}H_{16}N_8)O$ in the example, is formed at least transitorily. We will arbitrarily base the distinction between elimination–addition and homocondensation on this difference, i.e., the small molecule is eliminated from a single unit in the former and from between two units in the latter. The difference between the two is schematically shown in Fig. 1.

The second addition-type polymerization, *substitution–addition*, designates reactions in which a catenating group which cannot act as a multidentate ligand replaces either a multidentate ligand or an appropriate combination of unidentate ligands. There are several polymerization reactions in the literature which appear

---

⁽⁴⁾ R. D. JOYNER and M. E. KENNEY, *J. Amer. Chem. Soc.* **82**, 5790 (1960).

⁽⁵⁾ J. A. ELVIDGE and A. B. P. LEVER, *Proc. Chem. Soc.* 195 (1959).

to fall into this classification, but, as with heterocondensation, no simple example has been reported. Another reaction that has been investigated in our Laboratories was designed to be of this type and can serve as an illustration of the basic concept. It is the reaction of diphenylphosphinic acid with beryllium acetylacetonate in one-to-one molar ratio in order to displace one acetylacetonate ion from each beryllium

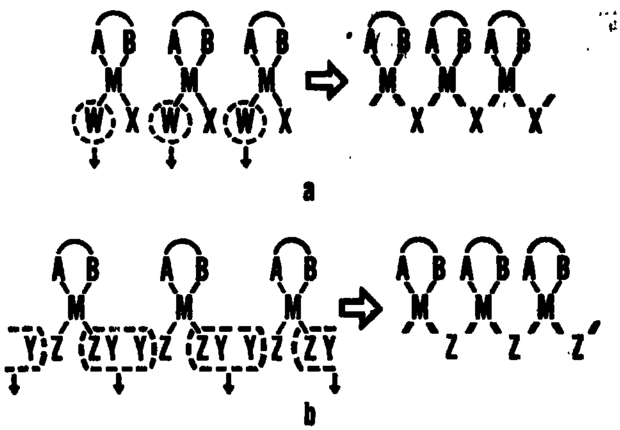

FIG. 1.—Polymerization by (a) elimination-addition and (b) homocondensation.

and produce $(-Be(C_5H_7O_2)OP(C_6H_5)_2O-)_x$, a composition which could correspond to a high molecular weight polymer. Here the replacement of the bidentate acetylacetonate ion with the diphenylphosphinate ion is expected to lead momentarily to a trico-ordinated intermediate which then polymerizes in order to give beryllium(II) its usual co-ordination number of four, it being assumed that the diphenylphosphinate ion will not act as a chelating agent with beryllium(II).

The example just cited is not a heterocondensation because all new bonds are not formed by elimination of molecules: instead, the process is unsymmetrical, forming both co-ordinate covalent and covalent bonds to beryllium. Although there are reactions which are definitely either substitution-additions (Fig. 2a) or heterocondensations (Fig. 2b), some reactions reported in the literature involving bis(chelates) can be classified as either, on the basis of the preceding criteria. Thus, the reaction of

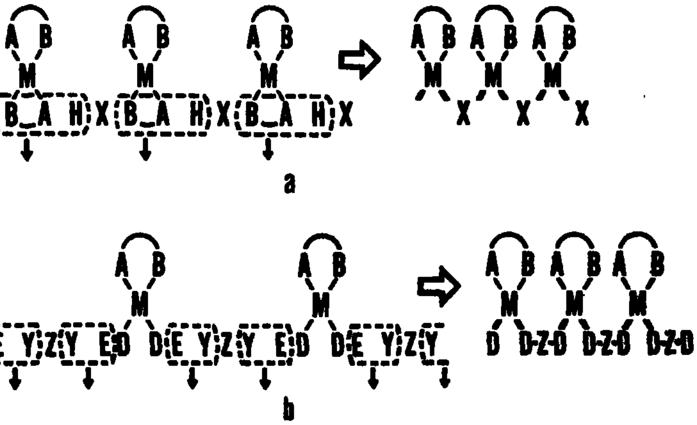

FIG. 2.—Polymerization by (a) substitution-addition and (b) heterocondensation.

beryllium acetylacetonate with terephthaloyldiacetone to yield the polymer ($>$ BeCH$_3$COCHCOC$_6$H$_4$COCHCOCH$_3$ $<$)$_x$⁽⁶⁾ could be classified either as a substitution–addition (replacement of two bidentate ligands by a bis(bidentate) catenating agent) or a heterocondensation (splitting out of acetylacetone). We prefer the first classification. Consequently, our criterion for distinguishing between substitution–addition and heterocondensation polymerization in such cases will be that in the former co-ordinate covalent bonds are formed in the polymer backbone.

Oxidation–addition polymerization (short for oxidation-number-change-addition) is a unique process in which the co-ordination number of an element is increased by a change in oxidation state in an environment such that there are not sufficient ligands present to satisfy the new co-ordination number without sharing of ligands and polymerization. No examples of this type have yet been reported, so a hypothetical system will be used as the example. The reaction of [Pt(NH$_3$)$_2$Cl$_2$] with sulphur to yield (—Pt(NH$_3$)$_2$(Cl)$_2$S—)$_x$ would involve the oxidation of four-co-ordinate platinum(II) to six-co-ordinate platinum(IV). For the latter to have a co-ordination number of six, platinum atoms must share sulphur or chlorine atoms. Although, in principle, an increase in co-ordination number could be achieved by reduction of the central atom, e.g., by conversion of four-co-ordinate chromium(VI) to six-co-ordinate chromium(III), we do not believe that at this time such reactions warrant separate classification as reduction–addition polymerizations.

The fourth of the addition-type processes, *redistribution–addition polymerization*, has not been reported either. The reaction of zinc(II) cyanide with zinc(II) acetylacetonate to form (—Zn(C$_5$H$_7$O$_2$)CN—)$_x$ would be an example of this class. Superficially, this process seems to be a low probability method since it is the reverse of disproportionation, which frequently appears to be spontaneous. It should be noted, however, that in many of the formation constant data⁽⁷⁾ there is sufficient difference between K_1 and K_2 to indicate that redistribution–addition polymerizations are possible.

The last addition-type class, which we term "rearrangement–addition polymerization", has recently been used to prepare beryllium(II) bis-β-diketone polymers.⁽⁸⁾ The basic principle of this method is the conversion of a cyclic compound to a linear polymer by opening the ring under such conditions that the radicals recombine into chains. In the work cited macrocyclic beryllium chelates with bis-β-diketones were converted to polymers by heating them above their melting points. Although this seems to be the only example of the use of such a reaction for the preparation of a co-ordination polymer it is, of course, also the kind of reaction involved in the formation of plastic sulphur and elastomeric phosphonitrilic halides.

Another classification which we wish to use is that of "degradation polymerization". This category embraces those reactions in which a co-ordinating agent converts a two- or three-dimensional polymeric structure into a less-cross-linked system. We have found no examples of this class in the literature, so we will again cite a reaction which we have investigated. In this case the plan was to displace one half the cyanide from zinc(II) cyanide, a three-dimensional co-ordination polymer,⁽⁹⁾ by acetylacetone

---

⁽⁶⁾ J. P. WILKINS and E. L. WITTBECKER, U.S. Pat. 2659711 (1953).

⁽⁷⁾ J. BJERRUM, G. SCHWARZENBACH and L. G. SILLÉN, Special Publication No. 6. The Chemical Society, London (1957).

⁽⁸⁾ R. W. KLUIBER and J. W. LEWIS, *J. Amer. Chem. Soc.* **82**, 5777 (1960).

⁽⁹⁾ G. S. ZHDANOV, *Dokl. Akad. Nauk SSSR*, **31**, 352 (1941).

to give polymeric (—$Zn(C_5H_7O_2)CN$—)$_x$. Although hydrogen cyanide was liberated, the reaction produced a mixture of $Zn(C_5H_7O_2)_2$ and $Zn(CN)_2$ rather than the desired polymer. Degradation polymerizations are not of the addition-type because, even though co-ordinative unsaturation may be involved in the reaction, it is not essential to the formation of the backbone, which already existed in the original polymer.

We have investigated and are investigating many reactions from this point of view and will report on them in succeeding papers in this series. Part II, which follows, is an investigation of the product formed either by an elimination–addition polymerization or by a redistribution–addition polymerization.

Acknowledgement—We are greatly indebted to Dr. L. W. BUTZ and our colleagues at Pennsalt for valuable discussion of the preceding concepts. Our thanks are due to the Office of Naval Research for partial support of our studies in the area of co-ordination polymers.

J. Inorg. Nucl. Chem., 1962, Vol. 24, pp. 371 to 380. Pergamon Press Ltd. Printed in England.

INORGANIC CO-ORDINATION POLYMERS—II

MONOAMMINEDICHLOROZINC(II)

B. P. BLOCK, R. A. FLORENTINE, J. SIMKIN and G. BARTH-WEHRENALP
Research and Development Department, Pennsalt Chemicals Corporation, Wyndmoor, Pa.

(*Received* 14 *September* 1961)

Abstract—Diamminedichlorozinc(II) was converted to monoamminedichlorozinc(II) by thermal loss of one mole of ammonia or by reaction with one mole of zinc chloride. The monoammine does not distill without decomposition as reported in the literature. Its physical appearance, melt viscosity as a function of temperature, and melt conductivity as a function of temperature suggest a polymeric structure. Molecular weight determinations and solution conductivity indicate that the structure is depolymerized in co-ordinating solvents. A branched chain structure is proposed.

IN Part I of this series(1) different ways of synthesizing co-ordination polymers were discussed. The present study is an investigation of the product which is formed either by the loss of one molecule of ammonia from $[Zn(NH_3)_2Cl_2]$, an elimination–addition reaction, or by the reaction of zinc(II) chloride with $[Zn(NH_3)_2Cl_2]$ in one-to-one mole ratio, a redistribution–addition reaction. The composition formed, $Zn(NH_3)Cl_2$, has been known for over a century.(2) KANE's original observation that $Zn(NH_3)Cl_2$ distills at red heat without decomposition has been reasserted(3) and is generally accepted.(4) Recent Russian work(5) reports that $Zn(NH_3)Cl_2$ partially sublimes at 400° C. No investigations directed toward elucidation of its structure have been reported although MÜLLER refers to "polymeric zinc monoammine chloride" in a German patent.(6)

EXPERIMENTAL

General

The moisture sensitivity of many of the compounds studied required their handling under anhydrous conditions. Reactions were run in closed systems, transfers were made either in a dry box or a dry bag,(7) and measurements were made in an apparatus protected from moisture. All changes in apparatus outside the dry-box or dry-bag were made while a positive nitrogen pressure was maintained in the system.

Synthesis of $ZnCl_2$ *and* $[Zn(NH_3)_2Cl_2]$

Initially commercial anhydrous $ZnCl_2$ was used as the starting material for the preparation of the $[Zn(NH_3)_2Cl_2]$, but even after dehydration with $SOCl_2$ satisfactorily low water contents could not be attained, so it was necessary to prepare the $ZnCl_2$ from metallic Zn.

---

(1) B. P. BLOCK and G. BARTH-WEHRENALP, *J. Inorg. Nucl. Chem.* **24**, 365 (1962).

(2) R. J. KANE, *Ann. Chim. Phys.* [2] **72**, 290 (1839).

(3) W. BLITZ and C. MESSERKNECHT, *Z. Anorg. Chem.* **129**, 161 (1923); M. T. SCHMIDT and L. F. AUDRIETH, *Trans. Illinois State Acad. Sci.* **28**, 133 (1935).

(4) J. N. FRIEND (Editor), *A Textbook of Inorganic Chemistry*, Vol. 10, p. 48. Griffin, London (1928).

(5) G. G. URAZOV, A. K. KIRAKOSYAN and R. S. MKHITARYAN, *Dokl. Akad. Nauk SSSR*, **114**, 564 (1957).

(6) W. MÜLLER, German Pat. 936332 (1955).

(7) L. R. OCONE and J. SIMKIN, *J. Chem. Educ.* (In Press).

The transformation from Zn through $ZnCl_2$ to ammoniated $ZnCl_2$ was made in a system protected from atmospheric moisture. First 30·0 g of Zn was placed in a 500 ml, three-necked, ball-joint flask, and then the system was dried by repeatedly evacuating and flushing it with nitrogen passed through P_2O_5. Next 125 ml of $(C_2H_5)_2O$ was distilled from sodium and condensed onto the Zn through a Dewar-type condenser, and then anhydrous P_2O_5-dried HCl was introduced. The delivery tube had an opening small enough so that the gas turbulence would provide adequate mixing. After all the Zn had disolved, $(C_2H_5)_2O$ was distilled off until the residue became viscous. The remaining $(C_2H_5)_2O$ was removed by heating at 170–180° C in vacuum until the residue was dry. (Samples of $ZnCl_2$ for moisture analysis (Karl-Fischer technique) were removed at this stage by using a sampling tube which could be connected to the reaction flask through a ball-joint, filled by inverting the flask, and then removed by sealing off the tube.) Sufficient ammonia was distilled from sodium through a trap to prevent sodium carry-over and condensed onto the $ZnCl_2$ at Dry-ice temperature so that a liquid phase was present. It was necessary to stir the mixture occasionally in order to ensure complete reaction. Excess NH_3 was then removed by allowing the flask to come to room temperature while nitrogen slowly passed through the system. In two to three hours the evolution of NH_3 was slow enough that the product could be transferred to a weighing dish and brought to constant weight over concentrated H_2SO_4 in a vacuum desiccator. The yield of $[Zn(NH_3)_2Cl_2]$ was essentially quantitative.

Synthesis of $Zn(NH_3)Cl_2$

(a) *Elimination–addition.* For this route to $Zn(NH_3)Cl_2$ 100 g of $[Zn(NH_3)_2Cl_2]$ was kept in a vacuum oven at 200° C until a 10·0 g loss in weight had occurred.

(b) *Redistribution–addition.* In an alternate procedure $Zn(NH_3)Cl_2$ was made by the fusion of 6·8 g of $ZnCl_2$ with 8·5 g of $[Zn(NH_3)_2Cl_2]$ in a sealed tube at 300° C for 16 hr.

It is particularly important to maintain anhydrous conditions during the synthesis of $Zn(NH_3)Cl_2$ and its manipulation because it is extremely sensitive to water. The product is an amber-coloured, transparent, glassy solid at room temperature. It does not have a sharp melting point but softens at approximately 80–90° C into a syrup which is rather viscous up to 100° C but then becomes quite mobile at higher temperatures.

	Analysis							
	Zn (%)		Cl (%)		NH_3 (%)		H_2O (%)	
	Found	Calc.	Found	Calc.	Found	Calc.	Found	Calc.
$ZnCl_2$	47·8	47·97	51·8	52·03	—	—	0·024	—
$[Zn(NH_3)_2Cl_2]$	37·9	38·38	41·1	41·62	20·1	20·00	0·04	—
$Zn(NH_3)Cl_2$	42·6	42·64	45·5	46·25	11·3	11·11	0·25	—

Thermal stability

(a) *Thermobalance.* In Fig. 1 is reproduced the weight–temperature plot obtained by heating $Zn(NH_3)Cl_2$ on a Chevanard Thermobalance modified to permit the use of a nitrogen atmosphere. The heating rate was 2·5° C/min; other details of operation are described elsewhere.(8) Another sample was heated at 5°/min to 475° C and then immediately removed from the thermobalance and put into a nitrogen-filled desiccator. Analysis of the residue: Zn, 47·6; Cl, 49·6; NH_3, 1·6 per cent. This residue, corresponding to 89 per cent of the original weight, still contained 100 per cent of the original amount of Zn. Samples were also heated at the standard rate in nitrogen to 165 and 200° C and then held at those temperatures for long periods of time. The weight loss in 60 hr at 165° C corresponded to the change in water content. The weight-time curve at 200° is reproduced in Fig. 2. Analysis of the residue after 85 hr at 200° C: Zn, 46·5; Cl, 48·9; NH_3, 5·8 per cent; after 170 hr at 200° C: Zn, 44·0; Cl, 47·6; NH_3, 5·1 per cent. The original amount of zinc was still present in the residues.

---

(8) J. R. Soulen and I. Mockrin, *Analyt. Chem.* 33, 1909 (1961).

(b) *Furnaces.* The monoammine was kept in an oven for 200 hr at 200 ± 5° C. There was a weight loss of approximately 0·3 per cent per hour for the first 30 hr, followed by a significant levelling off to approximately 0·03 per cent per hour. Analysis of residue: Zn, 52·1; Cl, 40·5; NH_3, 0·1 per cent. The residue still contained 100 per cent of the Zn originally present. At 400° C in a nitrogen atmosphere $Zn(NH_3)Cl_2$ lost 26·9 per cent of its weight in 5 hr. A moderate amount of a white sublimate was deposited on the walls of the reaction tube beyond the heating zone, and a substantial amount of liquid NH_3 condensed in a cold trap. The residue analysed Zn, 48·1; Cl, 48·5; and NH_3, 3·0 per cent or $Zn:Cl:NH_3$ = 1:1·86:0·24 and still contained 82·5 per cent of the original amount of Zn. In the sublimate the ratio of $Zn:Cl:NH_3$ was 1:2·06:0·725. A small amount of sublimate collected during a 300° C run was identified by its X-ray pattern as $[Zn(NH_3)_2Cl_2]$ and the sublimate obtained from a 600° C run gave a $Zn:Cl:NH_3$ ratio of 1:2·05:0·23. A sam[illegible] of $ZnCl_2$ treated in an identical manner at 400° C also deposited a white powder on t[illegible] reaction tube walls.

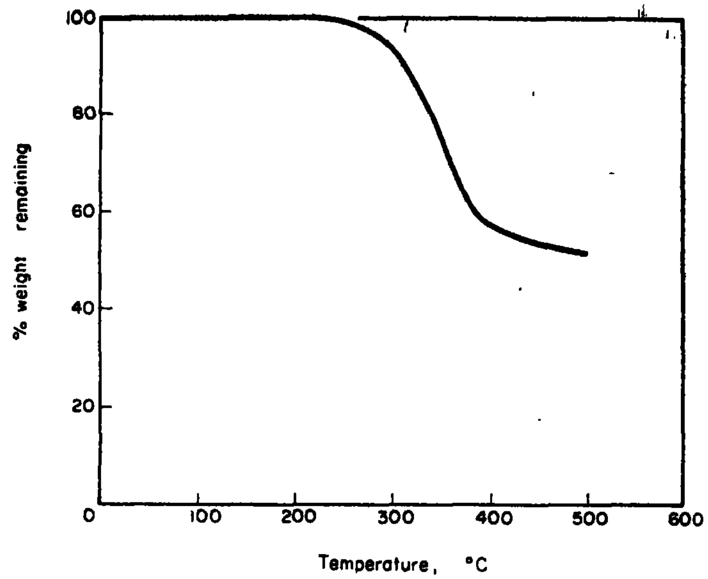

FIG. 1.—Thermogravimetric analysis of monoamminedichlorozinc(II).

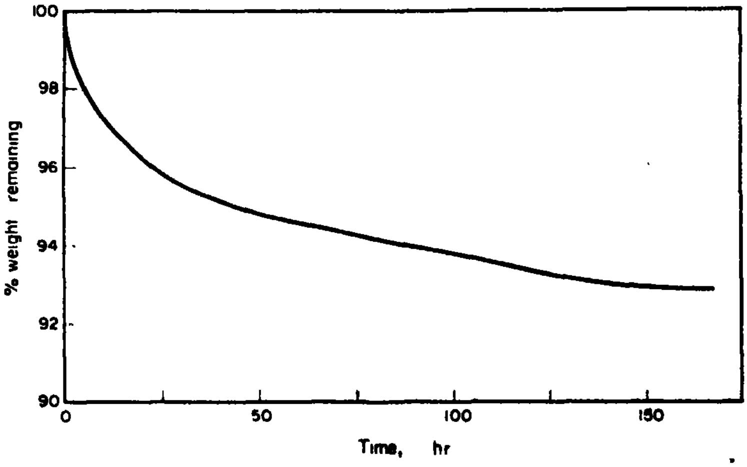

FIG. 2.—Weight loss of monoamminedichlorozinc(II) at 200° C.

Solubility and molecular weight

For some studies it was necessary to work with solutions of $Zn(NH_3)Cl_2$. A detailed investigation of solubilities was not carried out, but, in cases where sufficient $Zn(NH_3)Cl_2$ did not dissolve to give at least a 1 per cent solution, weighed samples of the saturated solutions were evaporated to dryness in order to permit estimation of solubility. It was possible to make a 7 per cent solution in acetamide at 85° C and 1 per cent solutions in N, N-dimethylformamide, dimethyl sulphoxide, pyridine, and n-butylamine at 30° C so the solubility of $Zn(NH_3)Cl_2$ is at least as great as indicated in these solvents. In all other solvents tried the solubility was less than 0·1 per cent. These included benzene, carbon tetrachloride, trichloroethylene, dioxane, and tetrahydrofuran. There was decomposition with water.

The only solvents that dissolve sufficient $Zn(NH_3)Cl_2$ to permit molecular weight determinations are good co-ordinating agents. The values found by colligative methods, 150 ± 5 in N, N-dimethylformamide (I), 150 ± 10 in acetamide (II), 155 ± 5 in n-butylamine (III), and 167 ± 5 in dimethyl sulphoxide (IV), all correspond to the value of 153·3 calculated for monomeric $Zn(NH_3)Cl_2$. The molecular weight determinations I and III were made by measurement of elevation of the boiling point with the equipment as described by Dimbat and Stross.(9) IV was made by conventional cryoscopic techniques, and II was made by the Rast procedure.(10)

Viscosity

Preliminary melt viscosity determinations were made in capillary viscometers of the Ostwald-Cannon-Fenske type(11) A. H. Thomas Type 500–A18). The U-tube viscometers were filled with $Zn(NH_3)Cl_2$ in a dry-box. The outlets were protected with drying tubes filled with an Anhydrone-Drierite mixture and were connected to a manifold that permitted tandem measurements without breaking a gas line leading to the nitrogen pressure source or the mercury manometer. The pressures applied ranged from −100 to 200 mm Hg. An oil-filled thermostat was maintained at ±0·05° C in the temperature range 100–165° C. The data are plotted in Figs. 3 and 4.

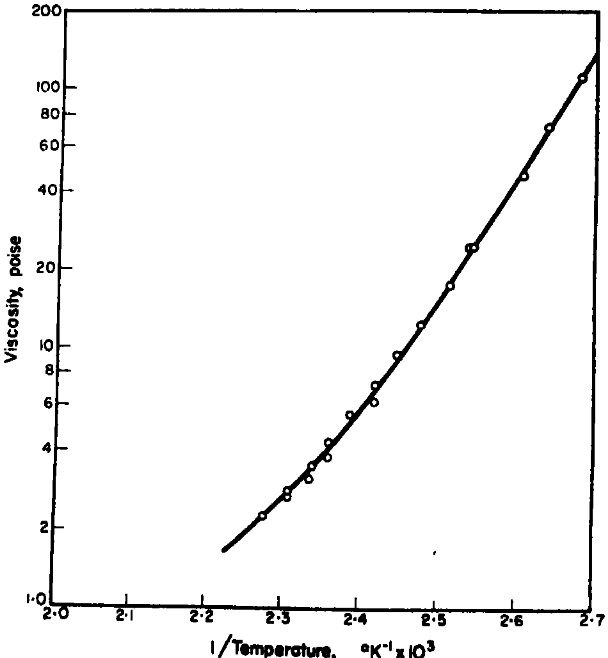

Fig. 3.—Viscosity of molten monoamminedichlorozinc(II) as a function of temperature.

(9) M. Dimbat and F. H. Stross, *Analyt. Chem.* **29**, 1517 (1957).

(10) K. Rast, *Ber. Dtsch. Chem. Ges.* **55** B, 1051 (1922).

(11) M. R. Cannon and M. R. Fenske, *Oil Gas J.* **33**, 52 (1935); **34**, 45 (1936). Also M. R. Cannon, *Industr. Engng. Chem., Analyt. Ed.* **16**, 708 (1944).

For the determination of molecular weights from the shear-dependence of viscosity,[12] a double cone viscometer was constructed and used to measure the viscosity of molten $Zn(NH_3)Cl_2$ at various rates of shear at temperatures from 110 to 150° C. The results are shown in Fig. 5. Procedural details were as described by BUECHE and HARDING.[12]

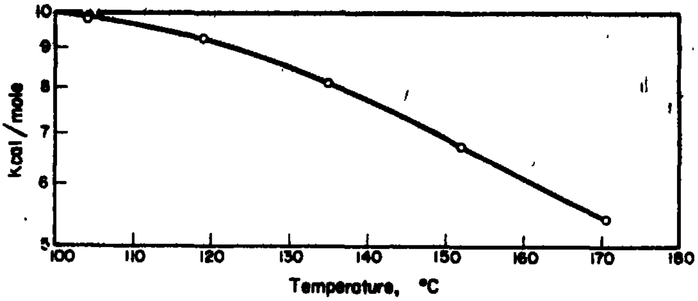

FIG. 4.—Activation energy of flow of monoamminedichlorozinc(II) as a function of temperature.

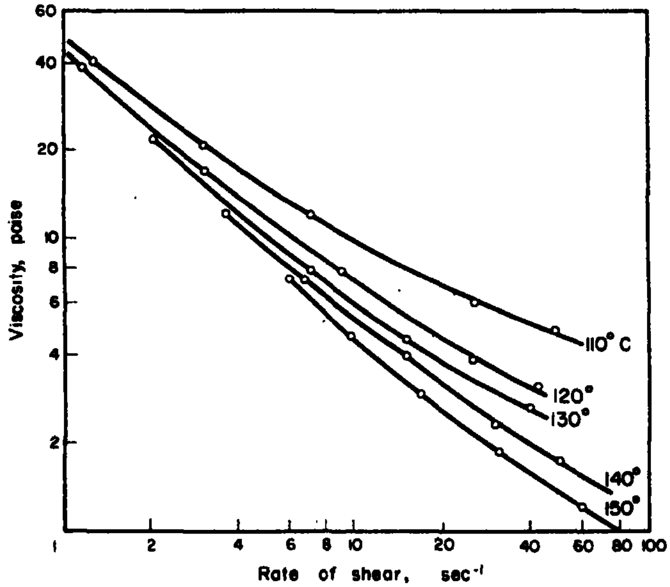

FIG. 5.—Viscosity-shear behaviour of molten monoamminedichlorozinc(II) at various temperatures.

Conductance

The conductance of molten samples was measured using a Sunderman pipette-form conductivity cell[13] with a cell constant of 13·0. Each molten sample was drawn by suction into the pipette, the ends of which were then protected by rubber caps. A thermocouple was inserted through one of the caps and positioned near the electrodes. The cell was wrapped on one side with aluminium foil and laid in a horizontal position under an infra-red lamp controlled through a Variac in order to hold the temperature (read on a recording potentiometer) constant during measurement. In operation the conductivity was measured as a function of decreasing and increasing temperature. The results are shown in Fig. 6.

Solution conductances were measured in the solvent N, N-dimethylformamide in a Type 4918 Leeds and Northrup conductivity cell with a cell constant of 0·196. The work was performed in a dry-box with leads through the vapour barrier outlet panel. The curves are reproduced in Fig. 7.

[12] F. BUECHE and S. W. HARDING, *J. Polymer Sci.* **32**, 177 (1958).

[13] F. W. SUNDERMAN, *Amer. J. Clin. Path.* **15**, 219 (1945); **19**, 659 (1949).

Miscellaneous

Infra-red spectra were run on films of samples held between sodium chloride plates using a Model 21 Perkin-Elmer Infra-red Spectrophotometer. X-ray diffraction patterns were made on powdered samples placed on a wedge and covered with thin tightly taped Mylar film. Powder samples in glass capillaries were also used. Fibre and film samples were sealed in Mylar and run as such. $(NH_4)_2ZnCl_4$ was identified in some samples, but otherwise the results suggested amorphous products. Fibres of $Zn(NH_3)Cl_2$ were extruded from a glass pipette held at 150° C.

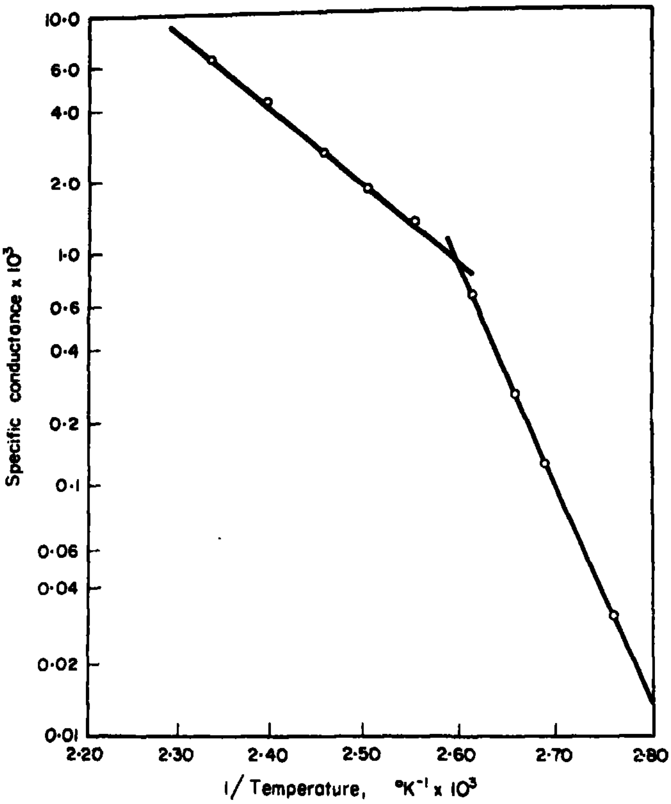

FIG. 6.—Conductance of molten monoamminedichlorozinc(II) as a function of temperature.

DISCUSSION

First, the thermal properties of the product will be considered and then its structure. The statement that $Zn(NH_3)Cl_2$ can be distilled without decomposition is not accurate. The present results clearly show that almost all the ammonia can be liberated without the loss of any zinc and that the distillate contains zinc compounds only at temperatures high enough for volatilization of $ZnCl_2$. At such temperatures the zinc-containing product is not uniquely $Zn(NH_3)Cl_2$ but may contain a varying number of ammonia molecules per zinc atom. It is thus most likely that in a first step $Zn(NH_3)Cl_2$ loses NH_3, then at sufficiently high temperatures $ZnCl_2$ also sublimes over, and that NH_3 and $ZnCl_2$ subsequently recombine in the receiver to form a number of products depending on conditions. In all probability KANE observed only $Zn(NH_3)Cl_2$ in the distillate because his system was at such a temperature that $Zn(NH_3)Cl_2$ was stable in his receiver.

The elucidation of the structure of $Zn(NH_3)Cl_2$ is more difficult. For the established compositions on either side of $Zn(NH_3)Cl_2$, $[Zn(NH_3)_2Cl_2]$ and $ZnCl_2$, X-ray structure investigations show that zinc has a co-ordination number of four; i.e., in the monomer $[Zn(NH_3)_2Cl_2]$$^{(14)}$ and in $ZnCl_2$,$^{(15)}$ a three-dimensional polymer. It is consequently likely that zinc also has a co-ordination number of four in $Zn(NH_3)Cl_2$. Possibilities for the structure are (i) a polymer with sufficient degree of polymerization so that end groups do not affect the analysis, (ii) a cyclic structure, (iii) a glass, or (iv) a mixture of $[Zn(NH_3)_2Cl_2]$ and $ZnCl_2$.

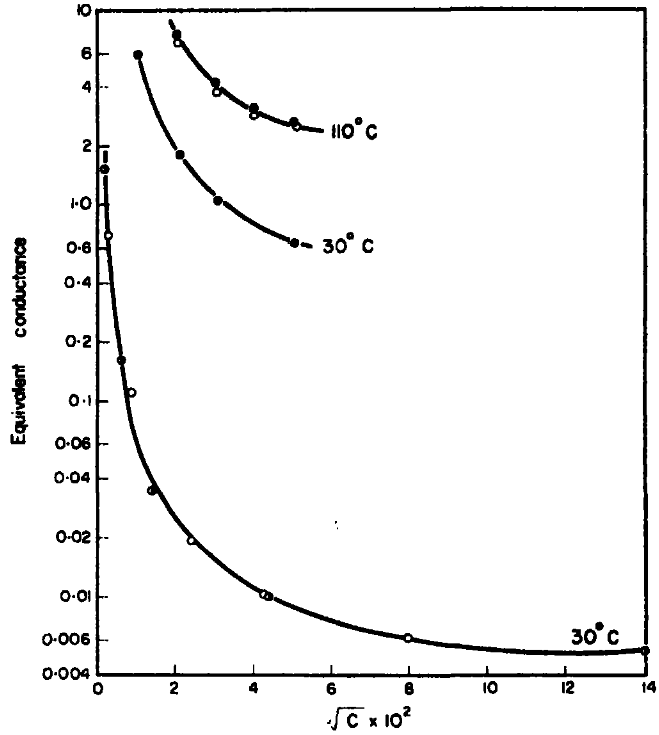

Fig. 7.—Equivalent conductances in N,N-dimethylforamide of monoamminedichlorozinc(II) (open circles), zinc chloride (filled circles) and a one-to-one mixture of diamminedichlorozinc(II) and zinc chloride (half-filled circles).

The physical properties of $Zn(NH_3)Cl_2$ correspond to those of an organic polymer with a rather low degree of polymerization. Thus, it softens over a range of temperatures and when just molten can be drawn into fine monofilaments which exhibit plasticity and flexibility after cooling. It can also be cast in films. It is interesting that initial stress-relaxation measurements by Tobolsky$^{(16)}$ indicate that $Zn(NH_3)Cl_2$ has a glass transition temperature of 6° C and a rubbery modulus at room temperature

(14) C. H. MacGillavry and J. M. Bijvoet, *Z. Krist.* **94**, 249 (1936).

(15) B. Brehler, *Fortschr. Mineral.* **38**, 198 (1960); H. R. Oswald and H. Jaggi, *Helv. Chim. Acta*, **43**, 72 (1960). It is to be noted that these single crystal structure studies disprove the generally accepted $CdCl_2$ structure for $ZnCl_2$ (A. F. Wells, *Structural Inorganic Chemistry* (2nd Ed.), p. 278, Oxford University Press, London (1950)) which had been questioned by J. D. MacKenzie and W. K. Murphy, *J. Chem. Phys.* **33**, 366 (1960).

(16) A. V. Tobolsky and co-workers. Private communication (1961).

but exhibits no rubbery plateau. Preliminary approximate calculations of molecular weight based on stress-relaxation times yield a value of thirty monomer units if it is assumed that the flow mechanism is not bond interchange. On the other hand molecular weight determinations in n-butylamine, N, N-dimethylformamide, acetamide, and dimethyl sulphoxide all give values corresponding to a monomer. These two apparently contradictory observations are not incompatible however, for the molecular weight determinations had to be carried out in solvents which are capable of co-ordinating with zinc. Thus the monomeric molecular weights could well be due to degradation of a polymeric structure by the solvent.

A similar effect is noted in the conductivity studies. In N, N-dimethylformamide at 110° C $Zn(NH_3)Cl_2$ and $ZnCl_2$ both have essentially the same equivalent conductance. The solution of a one-to-one mixture of $ZnCl_2$ and $[Zn(NH_3)_2Cl_2]$ also exhibits identical behaviour, so it may be concluded that all the solutions contain approximately the same species. Again this can most reasonably be attributed to complete degradation by the solvent of the structures present prior to dissolution. The melt conductance behaviour of $Zn(NH_3)Cl_2$, however, offers support for a polymeric structure, for there is a discontinuity in the temperature-conductivity curve. CROOK(17) has interpreted a similar curve for $ZnCl_2$ to mean that molten $ZnCl_2$ is appreciably polymerized, with the steep initial rise being due to the breaking up of a non-conducting or poorly conducting polymer into ions. The slower increase beyond the discontinuity is due to less dramatic changes with further temperature increase. A corresponding interpretation of the $Zn(NH_3)Cl_2$ data seems justified.

The viscosity–shear curve does not show non-Newtonian behaviour characteristic of a polymer in the molten state. Consequently, the Bueche–Harding technique cannot be used to determine the molecular weight of $Zn(NH_3)Cl_2$ and, in fact, suggests that the molecular weight is low because only at much lower shear rates would the curve have the proper shape for molecular weight determinations. The temperature dependence of viscosity, nevertheless, does show a dependence of the energy of activation of flow to be expected from a polymer, going from 10 kcal/mole at 105° C to 5·4 at 170° C. This supports a polymeric structure for $Zn(NH_3)Cl_2$ in that other polymers such as polyethylene and polyesters show comparable behaviour.

Taken together the properties investigated are best interpreted in terms of a polymer or a glass which is easily degraded, either by dissolution or by heat. A simple cyclic structure does not seem to explain the properties. The assumption that the product is a mixture does not account for some of the physical properties although such a picture could be true. The intuitively attractive concept that in $Zn(NH_3)Cl_2$ a polymeric structure should arise by sharing of chloride ions between zinc atoms to give the latter a co-ordination number of four is not definitely established by the data. Neither is it denied, however, and it seems the best explanation of the properties. The major question remaining is that relating to the possibility of considering $Zn(NH_3)Cl_2$ a glass. There are a number of definitions of the term "glass", some of which permit little distinction between a glass and a polymer. In the broadest sense a glass is a polymer, so a real distinction is difficult and probably rests on the nature of the bonding in the material in question. It is probable that $Zn(NH_3)Cl_2$ is a borderline material with substantial covalent character to its bonding, but less so than a typical organic polymer. In both $[Zn(NH_3)_2Cl_2]$ and $ZnCl_2$ the zinc-to-chlorine distance within the tetrahedral co-ordination sphere is 2·30 Å. This is less than the sum of the ionic radii of Zn^{2+} and Cl^-, 2·42 Å, corrected for tetrahedral co-ordination(18) and suggests at least partial covalent character in the bonds. Similar bond distance and bond type are probable in $Zn(NH_3)Cl_2$.

---

(17) E. H. CROOK. Thesis, University of Pennsylvania (1960).

(18) L. PAULING, *The Nature of the Chemical Bond* (3rd Ed.), pp. 514 and 598. Cornell University Press, Ithaca, New York (1960).

Such a polymeric structure can be regarded as the result of the replacement of one-fourth of the zinc–chlorine bonds in $ZnCl_2$ with zinc–ammonia bonds. This has the net effect of giving the average zinc atom an environment of one ammonia, one unshared chloride ion and two shared chloride ions if a co-ordination number of four is maintained for the zinc. Statistically it is not probable that only the simple linear chains 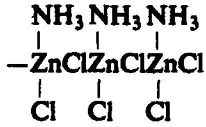 $-\underset{Cl}{\overset{NH_3}{Zn}}Cl\underset{Cl}{\overset{NH_3}{Zn}}Cl\underset{Cl}{\overset{NH_3}{Zn}}Cl-$ are present but that there is more or less branching to give a sort of cross-linking. Because of the stoicheiometry requirements there will be one additional terminal zinc atom for every branching zinc introduced, i.e., for every 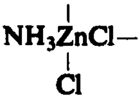 $NH_3\underset{Cl}{\overset{|}{Zn}}Cl-$ there must be one more 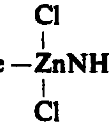 $-\underset{Cl}{\overset{Cl}{Zn}}NH_3$ unit. These, of course, do not have to be directly bonded to one another, there can be any number of $-Zn(NH_3)(Cl)Cl-$ units in between them. Below a portion of such a structure containing three branching points is shown. It will be noted that there are three terminal units to compensate for them.

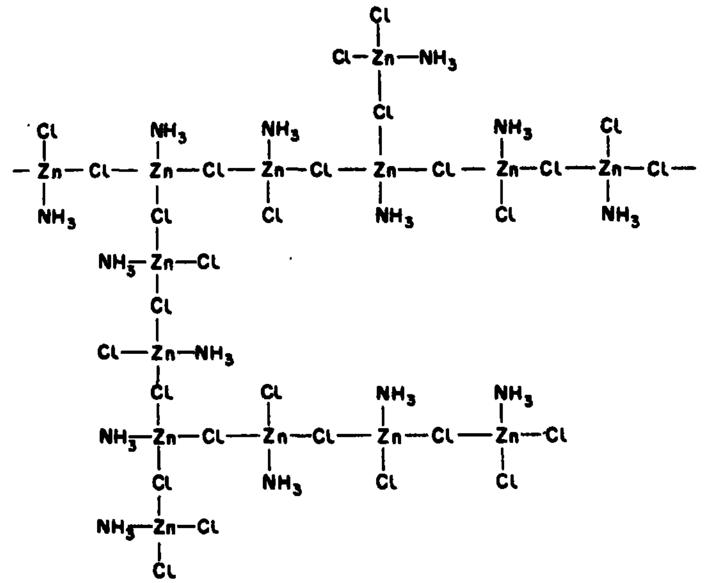

We have in progress a study of a series of ammines of zinc chloride containing up to 1·5 molecules of ammonia per zinc which we expect will help elucidate the structure of the monoammine.

Acknowledgement—We are indebted to the Office of Naval Research for partial support of this investigation under Contract Nonr 2687(00), Task No. 356–408 and to Dr. J. R. SOULEN and his co-workers for the thermogravimetric analysis, the Pennsalt Analytical Department for chemical analyses, molecular weight determinations and infra-red and X-ray spectra, and Messrs. P. T. FLINT, A. J. HAMILTON, G. C. MINCARELLI and J. W. SIMMONS for assistance with the experimental work.

J. Inorg. Nucl. Chem., 1962, Vol. 24, pp. 381 to 386. Pergamon Press Ltd. Printed in England

DIOXANE ADDITION COMPOUNDS OF SOME BIVALENT METAL PERCHLORATES

E. GIESBRECHT, W. G. R. DE CAMARGO, G. VICENTINI and M. PERRIER
Departamento de Química e Departamento de Mineralogia e Petrografia
da Faculdade de Filosofia, Ciências e Letras da Universidade de São
S. Paulo, Brazil

(*Received* 25 *September* 1961)

Abstract—The reactions between dioxane and the hydrated beryllium, magnesium, calcium, copper, zinc, strontium, cadmium, barium, mercury and lead perchlorates are described.

X-ray powder patterns and infra-red absorption spectra of the obtained compounds are also presented, together with data for Mn, Fe, Co and Ni, similar compounds already described elsewhere.

ADDITION compounds are formed when dioxane reacts with several hydrated perchlorates.(1,2,3) This paper discusses the reaction of dioxane with Be, Mg, Ca, Cu, Zn, Sr, Cd, Ba, Hg and Pb perchlorates.

It was observed that beryllium and calcium perchlorates by reacting with dioxane form compounds, which, upon analysis, approach the following compositions: $Be(ClO_4)_2{\cdot}4H_2O{\cdot}4C_4H_8O_2$ and $Ca(ClO_4)_2{\cdot}4H_2O{\cdot}6C_4H_8O_2$. However, they are very unstable as well as hygroscopic, and they lost dioxane when submitted to a vacuum in order to remove the excess solvent.

The copper compound corresponds to the formula... $Cu(ClO_4)_2{\cdot}4H_2O{\cdot}5C_4H_8O_2$. SMEETS(4) obtained a substance with the formula $Cu(ClO_4)_2{\cdot}6H_2O{\cdot}12C_4H_8O_2$, however this substance has not been observed in our experiments.

The remaining compounds which usually are more stable and less hygroscopic than Be and Ca compounds have the following composition;

$$M(ClO_4)_2{\cdot}6H_2O{\cdot}5C_4H_8O_2 \qquad (M = Mg, Zn, Cd)$$

$$M'(ClO_4)_2{\cdot}2C_4H_8O_2 \qquad (M' = Sr, Ba, Pb)$$

$$Hg(ClO_4)_2{\cdot}2H_2O{\cdot}4C_4H_8O_2$$

All compounds lose dioxane, when heated slowly and carefully, but explode violently at higher temperatures.

X-ray powder patterns. The X-ray powder procedure has been used, not only for characterization through *d*-spacings, but also for correlating the compounds. The results have pointed out the existence of isomorphism between some of these substances as well as with other substances previously reported,(2) whose X-ray diagrams were also determined in this study.

---

(1) G. VICENTINI, M. PERRIER, W. G. R. DE CAMARGO and J. M. V. COUTINHO, *Ber. Dtsch. Chem. Ges.* **94**, 1063 (1961).

(2) G. VICENTINI, M. PERRIER and E. GIESBRECHT, *Ber. Dtsch. Chem. Ges.* **94**, 1153 (1961).

(3) M. PERRIER, E. GIESBRECHT, W. G. R. DE CAMARGO and G. VICENTINI, *Ber. Dtsch. Chem. Ges.* **95**, 257 (1962).

(4) C. SMEETS, *Natuurwet. Tijdschr.* **19**, 12 (1937); *Chem. Abstr.* **31**, 1815 (1937).

The compounds with the general formula $M(ClO_4)_2 \cdot 6H_2O \cdot 5C_4H_8O_2$ (M = Mg, Mn, Fe, Co, Ni, Zn, Cd) gave diffraction patterns, all of which were so nearly identical as to suggest complete isomorphism among these substances. See the values of d(Å) and I in Table 2.

The strontium and lead compounds also showed nearly identical X-ray diagrams (see Table 3).

The X-ray data for the other compounds are presented in Tables 4, 5 and 6.

Infra-red spectra. The dioxane spectra were observed without essential modification in all compounds including those of manganese, iron (II), cobalt and nickel. The peaks at 875 and 1122 cm^{-1}(5) appeared in the infra-red spectra of all substances.

If the dioxane actually is co-ordinated, the binding must be relatively weak as evidence by the ease of its removal under heating (and under vacuum for the beryllium and calcium compounds) and by the occurrence of the —O—stretching frequency essentially unaltered in the infra-red spectrum of the solvated addition compounds.

EXPERIMENTAL

1. *Dioxane addition compound of hydrated beryllium perchlorate.*

Beryllium nitrate—$Be(NO_3)_2 \cdot 3H_2O$—and excess 70 per cent perchloric acid were carefully heated until fumes of perchloric acid were evolved. After cooling, the crystals were collected in a sintered glass funnel, well pressed and intimately ground with excess dioxane. The resulting crystals were filtered and recrystallized from hot dioxane.

2. *Dioxane addition compound of hydrated magnesium perchlorate*

Magnesium perchlorate—$Mg(ClO_4)_2 \cdot xH_2O$—was humidified with water and then intimately ground with excess dioxane. After filtration, the resulting crystals were recrystallized from hot dioxane.

3. *Dioxane addition compounds of calcium, strontium, cadmium, barium and lead perchlorates.*

All perchlorates were obtained from the appropriate carbonates and dilute perchloric acid. The solutions were evaporated to near dryness on a water bath. The residues were intimately ground with excess dioxane, and the resulting crystals washed with cold dioxane. Only the cadmium compound could be recrystallized from hot dioxane.

4. *Dioxane addition compounds of copper, zinc and mercury perchlorates.*

They were prepared by the same procedure described in (3), using the corresponding oxide as starting material. The mercury oxide reacted only with a great excess of perchloric acid. All compounds were recrystallized from hot dioxane.

In order to remove the excess of dioxane all substances were stored in a vacuum desiccator over calcium chloride, except for the beryllium and calcium compounds which slowly lost dioxane during this procedure.

Analytical data. The metals were determined by usual procedures. Water and perchlorate were determined by methods described in a previous paper.(1) The analytical results are tabulated in Table 1.

Solubilities. All substances described above are very soluble in water, methanol, ethanol, acetone and tetrahydrofuran. They are less soluble in ether and almost insoluble in benzene, chloroform, carbon tetrachloride and carbon disulphide. The calcium compound is insoluble in cold dioxane; the others, except for strontium, barium and lead compounds, are moderately soluble in hot dioxane and could be recrystallized from this solvent.

(5) S. C. BURKET and R. M. BADGER, *J. Amer. Chem. Soc.* **72**, 4397 (1950).

TABLE 1.—SUMMARY OF ANALYTICAL RESULTS

Compound	Aspect	Formula Weight	Analysis (%)					
			Metal		Perchlorate		Water	
			Theor.	Exp.	Theor.	Exp.	Theor.	Exp.
$Mg(ClO_4)_2{\cdot}6H_2O{\cdot}5C_4H_8O_2$	Colourless needles (from dioxane)	771·8	3·15	3·12	25·77	25·35	14·00	14·26
$Zn(ClO_4)_2{\cdot}6H_2O{\cdot}5C_4H_8O_2$	„ „ „ „	812·9	8·04	7·93	24·46	24·42	13·29	13·62
$Cd(ClO_4)_2{\cdot}6H_2O{\cdot}5C_4H_8O_2$	„ „ „ „	859·9	13·07	12·78	23·13	23·47	12·57	12·97
$Cu(ClO_4)_2{\cdot}4H_2O{\cdot}5C_4H_8O_2$	Blue needles (from dioxane)	775·0	8·19	8·26	25·66	25·73	9·29	9·15
$Sr(ClO_4)_2{\cdot}2C_4H_8O_2$	Colourless crystals	462·7	18·93	18·98	42·98	42·74	—	—
$Ba(ClO_4)_2{\cdot}2C_4H_8O_2$	„ „	512·5	26·80	26·94	38·81	38·73	—	—
$Pb(ClO_4)_2{\cdot}2C_4H_8O_2$	„ „	582·3	35·58	35·36	34·16	34·13	—	—
$Hg(ClO_4)_2{\cdot}2H_2O{\cdot}4C_4H_8O_2$	Colourless needles (from dioxane)	788·0	25·45	25·22	25·24	24·85	4·57	4·41

X-ray diffraction patterns. These patterns were obtained with a NORELCO unit, Buerger powder camera (114·6 mm), Cu *Kα*. The very deliquescent substances were enclosed, without grinding, in Lindemann glass capillary tubes (0·5 mm diameter). Due to the grain size of crystals, some lines on the films were very grainy. Therefore it was not feasible to assign numerical values to the relative intensities. The X-ray diffraction data are summarized in Tables 2-6. The errors for *d*-spacings values are approximately the following:

d (Å)	*Error* (Å)
18–9	0·35
9–3	0·10
3–1	0·01
1–0·5	0·002

The *d* values were not corrected for systematic or random errors (film shrinkage, absorption, eccentricity, etc.).

Infra-red spectra. These spectra were measured with a Perkin-Elmer Model 137 Double Beam Recording Spectrophotometer, using Nujol suspensions between rock salt plates.

TABLE 2.—X-RAY DIFFRACTION PATTERNS FOR THE COMPOUNDS OF TYPE: $M(ClO_4)_2 \cdot 6H_2O \cdot 5C_4H_8O_2$—(M = Mg, Mn, Fe, Co, Ni, Zn, Cd)

Mg	Mn	Fe	Co	Ni	Zn	Cd
—	—	9·30	—	—	9·40	9·52
—	9·06	—	8·86	8·90	—	8·78
—	—	—	—	—	7·75	—
—	7·30	—	—	7·26	—	7·16
—	—	6·48	6·52	6·72	—	—
—	—	—	—	—	6·10	—
—	5·80	—	5·78	5·74	—	5·84
5·01	—	5·22	—	5·22	4·92	—
4·72 *m*	4·78 *m*	—	4·72 *m*	4·68 *m*	4·74 *m*	4·76 *m*
—	4·62 *m*	4·66 *m*	—	—	—	4·64 *m*
4·44 *s*	4·48 *s*	4·50 *s*	4·50 *s*	4·46 *s*	4·55 *s*	4·50 *s*
—	4·40 *m*	—	4·28 *m*	4·28 *m*	—	4·40 *m*
4·09 *m*	4·24 *m*	4·22 *m*	—	4·16 *m*	4·25 *m*	4·16 *m*
3·91 *m*	4·06 *m*	4·06 *m*	4·02 *m*	4·02 *m*	4·13 *m*	4·08 *m*
—	—	—	3·88 *m*	3·88 *m*	—	—
—	3·68 *m*	3·64 *m*	3·70 *m*	3·70 *m*	3·69 *m*	3·66 *m*
—	3·50	—	3·50	3·48	—	—
—	—	3·26	3·32	—	—	3·36
—	2·98	—	—	2·96	—	—
2·81	2·82	—	—	2·82	—	—
2·74	2·75	2·74	2·72	2·70	—	—
—	—	—	2·64	2·62	2·66	—
—	—	—	2·54	—	—	—
—	—	—	2·48	—	2·45	—
—	—	—	2·40	2·38	—	—
—	—	—	2·08	—	2·22	—
—	—	—	2·04	—	—	—
—	—	—	1·94	—	—	—

s = Strong *m* = Medium; the others weak

TABLE 3.—X-RAY DIFFRACTION PATTERNS FOR THE COMPOUNDS $Sr(ClO_4)_2 \cdot 2C_4H_8O_2$ AND $Pb(ClO_4)_2 \cdot 2C_4H_8O_2$

Sr		Pb	
*I**	*d*(Å)	*I**	*d*(Å)
—	—	3	7·47
10	6·65	10	6·68
5	5·82	3	5·77
1	5·18	2	5·26
1	4·35	2	4·30
2	4·04	—	—
10	3·85	10	3·87
1	3·52	2	3·50
2	3·31	2	3·34
2	3·22	2	3·25
—	—	1	3·12
3	2·89	2	2·89
3	2·81	3	2·82
2	2·74	½	2·67
—	—	½	2·63
8	2·53	4	2·53
2	2·37	1	2·38
½	2·28	—	—
1	2·23	2	2·23
—	—	1	2·16
5	2·02	2	2·06
2	1·928	1	1·945
—	—	½	1·911
2	1·854	1	1·870
1	1·809	—	—
2	1·671	½	1·681
—	—	½	1·634
2	1·524	½	1·539
1	1·388		

* The values of *I* are relative for each film.

TABLE 4.—X-RAY DIFFRACTION PATTERN FOR THE COMPOUND $Cu(ClO_4)_2 \cdot 4H_2O \cdot 5C_4H_8O_2$

I	*d*(Å)
Weak	8·22
,,	6·40
,,	5·48
Strong	4·58
,,	4·32
,,	4·16
Weak	3·62
,,	3·30
,,	2·82
,,	2·70
,,	2·62

TABLE 5.—X-RAY DIFFRACTION PATTERN FOR THE COMPOUND $Ba(ClO_4)_2 \cdot 2C_4H_8O_2$

I	*d*(Å)
8	7·89
10	7·31
8	6·65
3	6·14
5	5·64
3	4·17
8	3·93
5	3·78
8	3·66
5	3·56
5	3·21
1	3·01
8	2·86
1	2·72
1	2·39
5	2·32
1	2·08
1	1·935
1	1·939
1	1·879
1	1·773
1	1·711
1	1·682
½	1·622
½	1·601
1	1·529
½	1·328
½	1·303

TABLE 6.—X-RAY DIFFRACTION PATTERN FOR THE COMPOUND $Hg(ClO_4) \cdot 2H_2O \cdot 4C_4H_8O_2$

I	*d*(Å)
10	9·86
8	8·96
3	8·07
3	7·22
3	6·77
3	4·93
3	4·30
8	4·01
3	3·34
3	2·69

Acknowledgements—The authors wish to acknowledge indebtedness to the Rockefeller Foundation and Conselho Nacional de Pesquisas (Rio de Janeiro) for financial support. They also wish to express their appreciation to Mr. J. V. Valarelli and Mr. L. C. Santos for their collaboration in the determination of x-ray powder patterns.

J. Inorg. Nucl. Chem. 1962, Vol. 24, pp. 387 to 391. Pergamon Press Ltd. Printed in England

PREPARATION OF ANHYDROUS LANTHANIDE HALIDES, ESPECIALLY IODIDES*

M. D. TAYLOR† and C. P. CARTER
Department of Chemistry, Howard University, Washington D.C.

(*Received* 29 *September* 1961; *in revised form* 2 *November* 1961)

Abstract—A general method is described which can be used to synthesize nearly all the lanthanide halides in high purity and good yield. It involves heating *in vacuo*, a molecularly dispersed mixture of hydrated lanthanide halide with the proper ammonium halide until the water and ammonium halide are expelled to leave pure, anhydrous lanthanide halide. All tri-halides except the iodides of samarium and europium are obtained. These are obtained as di-halides. Optimum condition for synthesis are discussed. The procedure is the only one which has been reported for preparing pure anhydrous iodides with relatively simple apparatus and technique.

MUCH interest exists in the preparation of anhydrous lanthanide halides. These compounds are used widely for the production of the lanthanide metals both by electrolytic and metallothermic methods. They are the starting materials from which many other anhydrous compounds, especially the divalent halides, are prepared. Anhydrous halides also are required for thermochemical and physicochemical studies of the lanthanide compounds, especially in non-aqueous solutions.

Though methods for preparing anhydrous lanthanide compounds have been the subject of many investigations, these compounds are still difficult to prepare. The hydrated salts are obtained readily by reaction between the oxides and hydrohalic acid solutions. Attempts to dehydrate them usually lead to their hydrolysis in accordance with the equation:

$$LnCl_3+H_2O \rightleftharpoons LnOCl\times 2HCl \qquad (1)$$

or decomposition in accordance with the equation:

$$LnI_3+\tfrac{1}{2}O_2 \rightleftharpoons LnOI+I_2 \qquad (2)$$

Hydrolysis of chlorides and some bromides can be prevented by performing the dehydration in an atmosphere of HCl or HBr, but the iodides can not be dehydrated this way. In such dehydration the hydrogen halide must be completely free of moisture and oxygen to prevent reactions (1) and (2) from occurring.

The methods which have been reported for preparing anhydrous lanthanide halides have been presented mainly as individual examples applicable to the preparation of a few special compounds. Except for the preparation of the chlorides, few methods of general applicability have been published. A review which attempts to summarize, classify and evaluate the various methods has been submitted for publication.⁽¹⁾

---

* Major support for this work was from Research Grant G7334 from the National Science Foundation.

† Robert A. Welch Visiting Scholar at Prairie View Agricultural and Mechanical College, Prairie View, Texas, 1960–61.

(1) M. D. TAYLOR, *Chem. Revs.* To be published.

Except for a few miscellaneous ones, the known methods for preparing anhydrous lanthanide halides generally involve either converting the oxide to the halide with a suitable halogenating reagent or dehydrating the wet halide.

Up to now no single general method has been reported which can be applied to the preparation of all anhydrous lanthanide halides; the iodides are especially difficult to prepare. We have succeeded in developing such a method. It consists in heating, *in vacuo*, a molecularly dispersed mixture of hydrated lanthanide halide with the appropriate ammonium halide to expel first the water, then the ammonium halide. The ammonium halide environment prevents hydrolysis of the lanthanon halide and a perfectly pure product is obtained. Variations of the procedure have been reported(2-8) but no systematic studies have been made either to ascertain if the procedure is suitable for preparing all the lanthanide halides or what the optimum conditions are for maximum yield and purity. Such conditions have been ascertained in this study.

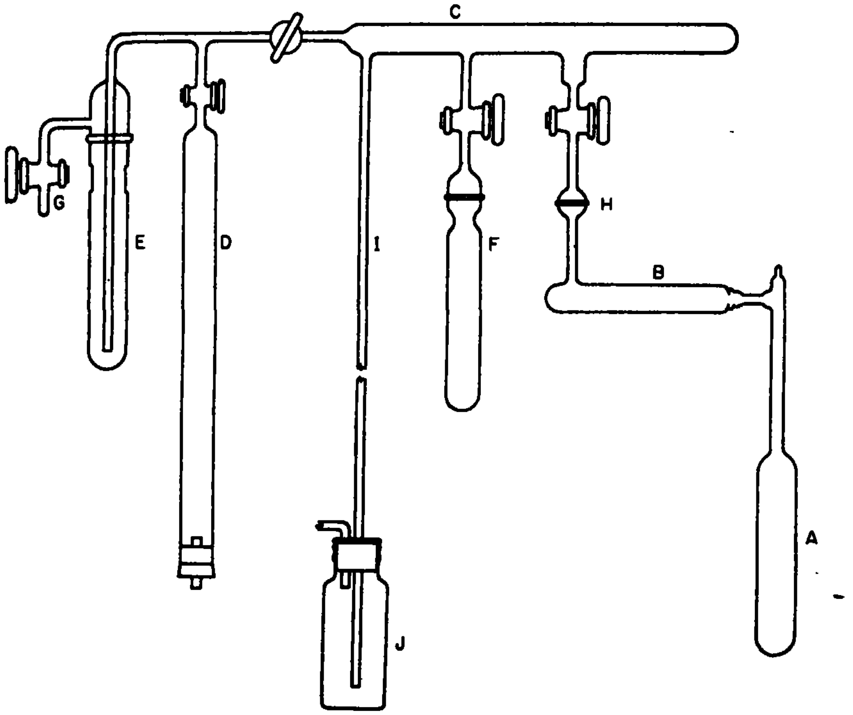

FIG. 1.

EXPERIMENTAL

Starting materials. The source of the lanthanide materials was lanthanide oxides, 98–100 per cent pure. They were obtained either from Research Chemicals, Inc., Burbank,

---

(2) DUBOIN, *Annales Scientific d'Ecole Normal Superieure*, Paris [3] **5**, 416 (1888).
(3) F. EPHRAIM and P. RAY, *Ber. Dtsch. Chem. Ges.* **62**, 1509, 1520, 1639 (1929).
(4) R. HERMANN, *J. Prakt. Chem.* **82**, 385 (1861).
(5) W. R. HODGKINSON, *J. Soc. Chem. Industr.* (London), **33**, 445 (1914).
(6) G. JANTSCH, H. JAWREK, N. SKALLA and H. GAWALOWSKY, *Z. Anorg. Chem.* **207**, 353 (1932).
(7) G. JANTSCH, N. SKALLA and H. JAWUREK, *Z. Anorg. Chem.* **201**, 207 (1931).
(8) M. C. MARIGNAC, *Ann. Chim. Phys.* [3] **38**, 148 (1853).

California, or Lindsay Chemical Division, West Chicago, Illinois. Ammonium halides and hydrochloric acid were reagent grade. Hydrobromic and hydroiodic acids were prepared by the reaction of tetrahydronaphthalene with bromine or iodine⁽⁹⁾ in accordance with equation:

$$C_{10}H_{12}+2_2 \rightleftharpoons C_{10}H_8+4HI \tag{3}$$

General procedure. The general procedure consisted in dissolving the oxide in dilute hydrohalic acid, adding about 6·0 mole of ammonium halide per mole of lanthanide metal, and adding next about 50 ml of relatively concentrated hydrohalic acid. The mixture was evaporated to dryness. Toward the end of the evaporation it must be stirred sufficiently vigorously to prevent its sticking to the walls of the beaker since it is nearly impossible to remove stuck material without breaking the beaker. The water and ammonium halide are removed in the special apparatus shown in Fig. 1. It consists of a Pyrex reaction vessel (A), with an attached sublimation tube (B), that is attached to a vacuum line manifold (C), with a ball and socket joint, (H). The vacuum line consisted of a manifold, a manometer (I), a drying tube (D), a trap (E), and an outlet to the pump (G). The operating details will be described below for a specific example.

Preparation of $YbCl_3$. Ytterbium oxide, 10·0 g was dissolved with heating in 35·0 ml of 6 N HCl. Next 15·0 g NH_4Cl was added. It failed to dissolve completely. Addition of 50·0 ml of conc. HCl caused more precipitation but most of the precipitate dissolved on heating. The mixture was evaporated to dryness and heated to 200° C on the hot plate. Then it was transferred to the reaction vessel (A), which was sealed. The trap (E) was cooled by a liquid nitrogen or dry-ice bath and the system was evacuated. The reaction vessel was surrounded by an electric furnace and heated to 200° C during 1·5 hr. All the water was driven off and NH_4Cl began to evolve. Now a cover was placed over the furnace. The temperature was raised to 430° over a period of 8 hr to sublime all the NH_4Cl away. The apparatus was permitted to cool, filled with pure dry N_2, and the reaction vessel was removed to the dry-box. The product weighed 13·2 g for a yield of 82 per cent. It was completely soluble in water. Some $YbCl_3$ was swept into the sublimation tube by the subliming NH_4Cl. It was isolated as the oxalate from which 1·8 g of Yb_2O_3 was recovered.

Eighteen lanthanide halides have been prepared. Quantitative data for these are recorded in Table 1. In addition, qualitative data have been obtained for the preparation of iodides of H_o, Dy, and Tb. The results obtained supports the conclusion that the ammonium halide method can be used to prepare all anhydrous lanthanide halides.

Analysis. Halide is precipitated with $AgNO_3$. Divalent lanthanide halides must be oxidized before this precipitation is made. The excess silver was precipitated with hydrohalic acid. The residual solution is evaporated to proper volume and the lanthanide ion is precipitated with oxalic acid. The oxalate is ignited and weighed as the lanthanide oxide.

DISCUSSION

An examination of Table 1 shows that the yields are generally greater than 60 per cent and may exceed 95 per cent. Most material is lost by passing over along with the subliming ammonium halide. The process appears to be more electrical than mechanical in nature. A space charge develops between the product and the sublimate during sublimation. When the product particles are finely divided, they jump vigorously and continuously as long as the ammonium halide sublimes. Indeed, a slight tap on the vessel will cause considerable quantity of the product to leap to the far end of the sublimation tube. Such jumping is negligible in samples where the particle size is large. One obtains nearly quantitative yield from such samples.

---

(9) J. Hauben, J. Baedler and W. Fischer, *Ber. Dtsch. Chem. Ges.* 69 B, 1772 (1936).

TABLE 1.—DATA ON ANYYDROUS LANTHANIDE HALIDES

Compd.	Wt. of oxide (g)	m Moles lanthanide metal	m Moles NH_4X	m Moles halides obtained	Yield (%)	Purity (%)	Colour	Water solution
$LaCl_3$	5·0	30·7	187	16·4	53·5	100·1	White	Clear
$CeCl_3$	5·0	29·1	225	26·0	90	99·2	White	Clear
$PrCl_3$	5·0	29·3	331	28·6	98·7	99·8	Light green	Clear
$NdCl_3$	5·0	29·7	187	28·4	96	99·8	Pink	Slightly cloudy
$SmCl_3$	10·1	58·0	187	51·4	88·5	99·6	White	Very slightly cloudy
$EuCl_3$	4·75	26·6	187	20·6	78	100	Pale yellow	Clear
$YbCl_3$	10·0	57·4	281	47·0	82	—	White	Clear
$LaBr_3$	2·0	12·2	59	6·4	54	99·4	White	Clear
$SmBr_3$	1·5	8·8	44	5·38	61·5	99·8	Light gray	Clear
$EuBr_3$	2·0	11·8	59	6·4	54	99·7	Light gray	Clear
$YbBr_3$	1·4	7·2	36	4·86	67·5	99·6	Light gray	Clear
LaI_3	5·0	30·7	207	25·6	83	—	Gray	Slightly cloudy
CeI_3	5·0	29·1	207	18·1	62·3	99·7	Bright yellow	Clear
NdI_3	5·0	29·7	308	25·2	85	100	Light green	Slightly cloudy
SmI_2	2·0	11·2	56	8·0	70	99·2	Yellow	Cloudy
EuI_2	1·5	8·4	42	4·83	59	99·7	Pale green	Cloudy
GdI_3	2·0	11·0	55	8·5	78	99·5	Light greenish-yellow	Clear
YbI_3	2·0	10·2	51	3·26	33	99·8	Greenish-yellow	Cloudy

Data in Table 1 show that instead of the tri-iodides, the di-iodides of Sm and Eu are obtained. Other experiments have shown that when the reaction temperature is too high, instead of pure $EuCl_3$, a mixture of $EuCl_2$ and $EuCl_3$ is obtained. Thus SmI_3 and EuI_3 can not be prepared by the ammonium halide method. It is doubtful if any method is known which yields pure samples of these compounds.

The method described above is the only one known to the author which produces nearly all the anhydrous lanthanide halides pure and in good yield by a relatively simple procedure.

J. Inorg. Nucl. Chem., 1962, Vol. 24, pp. 393 to 398. Pergamon Press Ltd. Printed in England

HIGH PRESSURE FLUORINATION OF URANIUM OXIDES*

R. E. GREENE and G. S. PETIT
Technical Division, Oak Ridge Gaseous Diffusion Plant,
Union Carbide Nuclear Company, Oak Ridge, Tennessee

(*Received* 28 *November* 1960; *in revised form* 9 *October* 1961)

Abstract—A new method for the fluorination of uranium oxides to uranium hexafluoride has been developed. It uses gaseous fluorine at a pressure of about 1000 lbin^{-2}. The pressure is obtained by vapourization of liquid fluorine which has been condensed onto the oxide and an activator, potassium chloride, in a metal reactor at liquid nitrogen temperature. When the closed reactor warms within a safety shield, the fluorine vaporizes and a fluorination takes place very rapidly, usually before the reactor reaches room temperature. The reactor is again cooled and oxygen and unconsumed fluorine are separated from the condensed uranium hexafluoride by pumping. Based upon uranium, a 95 per cent yield of uranium hexafluoride, pure enough for isotopic analysis with the gas-type mass spectrometer, is obtained. The reactor also serves as the sample tube after the fluorination, which is completed in 15 min or less. Although the method is primarily used for the conversion of laboratory samples for uranium isotopic analysis, other applications may be feasible.

ONE of the oldest and most widely used methods for preparing uranium hexafluoride from uranium oxides uses colbaltic fluoride.⁽¹⁾

$$U_3O_8+18CoF_3 \xrightarrow{375°C} 3UF_6+18CoF_2+4O_2 \qquad (1)$$

Another uses gaseous fluorine at a pressure of one atmosphere or less.⁽²⁾

$$U_3O_8+9F_2 \xrightarrow{370°C} 3UF_6+4O_2,\ \Delta H = -223{\cdot}3 \text{ kcal/mole} \qquad (2)$$

These methods require about 3 hr for the preparation of 2 g of uranium hexafluoride with an expenditure of a minimum of one man hour per sample. A third method⁽³⁾ uses liquid bromine trifluoride in a bomb reactor.

$$\tfrac{1}{3}\ U_3O_8+2BrF_3 \longrightarrow UF_6+Br_2+\tfrac{4}{3}O_2,\ \Delta H = -73{\cdot}3 \text{ kcal/mole} \qquad (3)$$

It has been used routinely to fluorinate a sample in 30 min, but a larger amount of oxide is required, since some uranium hexafluoride is lost with the bromine in the purification step. A transfer of the uranium hexafluoride to a mass spectrometer sample tube is also necessary to separate the uranium hexafluoride from halogen compounds which interfere with the isotopic analysis.

---

* This document is based on work performed at the Oak Ridge Gaseous Diffusion Plant operated by Union Carbide Corporation for the U.S. Atomic Energy Commission.

⁽¹⁾ A. E. CAMERON, "Determination of the Isotopic Composition of Uranium", TID-5213, Chapter 2, Office of Technical Services, Department of Commerce, Washington D.C. (1950).

⁽²⁾ J. J. KATZ and E. RABINOWITCH, *Chemistry of Uranium*, NNES, Div. VIII, Vol. 5, p. 399. McGraw-Hill, New York (1951).

⁽³⁾ R. E. GREENE and G. S. PETIT, *Fluorination of Uranium Oxides With Bromine Trifluoride for Mass Spectrometer Assaying*, Carbide and Carbon Chemicals Company, K-25 Plant, August 25, 1954 (K-1137).

Although the chemistry and heat of reaction of the new method are essentially the same as that of equation (2), the reaction rate is much greater because of the high fluorine pressure; therefore, much higher temperatures are developed at the site of the reaction.

The new method has a number of advantages over the older ones. It eliminates tedious glass blowing, furnace heating, and lengthy distillation techniques. It produces a very pure product in high yield and eliminates transfer of the sample, since the reactor also serves as the spectrometer sample tube. With it, a fluorination can be completed in less than 15 min. A large heavy wall nickel reactor has been used to fluorinate as much as 10 g of oxide in one batch and temperatures as high as 550°C have been observed.

EXPERIMENTAL

Apparatus

The reactor is made from a packless diaphragm Monel angle valve. A connector seat is silver soldered to the diaphragm side of the valve and a standard $\frac{3}{8}$ or $\frac{1}{8}$ in. copper male flare fitting to the other. A section of copper tubing, 0·049 in. wall thickness and 4 in. long is pinched closed, Heliarc welded or silver soldered pressure tight, and fastened to the valve with a flare nut (Fig. 1).

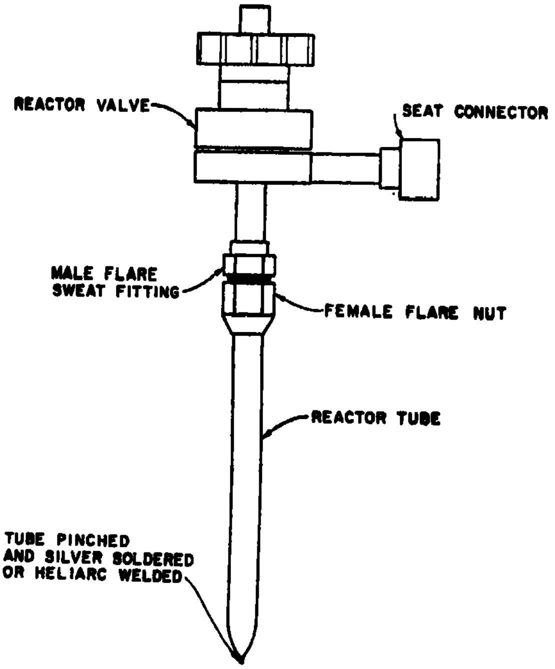

Fig. 1.—Reactor.

The vacuum manifold (Fig. 2) and the fluorination manifold (Fig. 3) are constructed primarily of nickel and Monel. The fluorination system, except the fluorine tank, is installed in a fume hood.

A thermocouple is clamped to the lower portion of the reactor tube and connected to a suitable pyrometer.

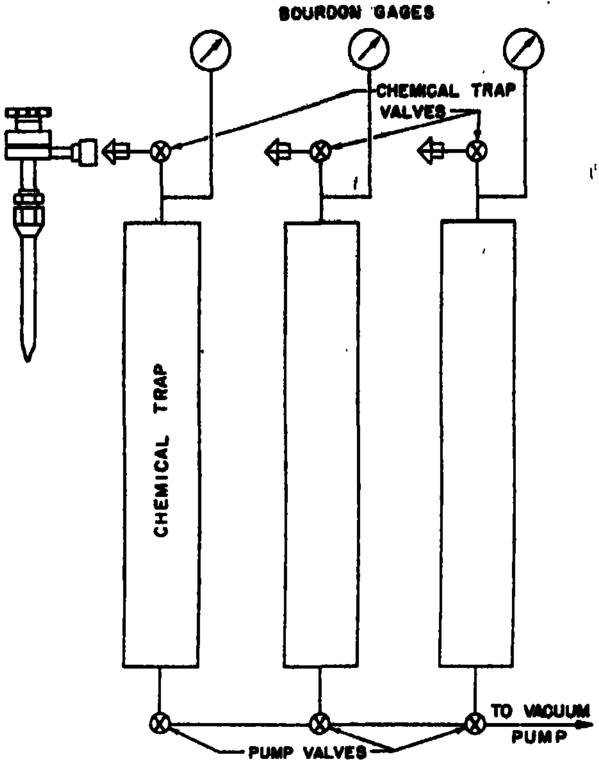

FIG. 2.—VACUUM MANIFOLD.

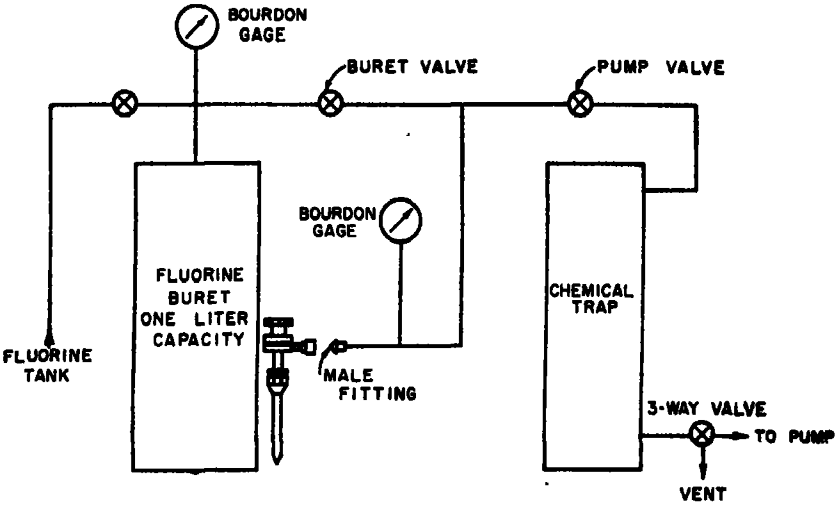

FIG. 3.—FLUORINE MANIFOLD.

An explosion shield encompasses the lower portion of the reactor during the reaction. It is made of 4 in. steel pipe so that a Dewar flask containing liquid nitrogen can be raised and lowered within it. The rear of the shield is perforated to relieve pressure in event of an explosion (Fig. 4).

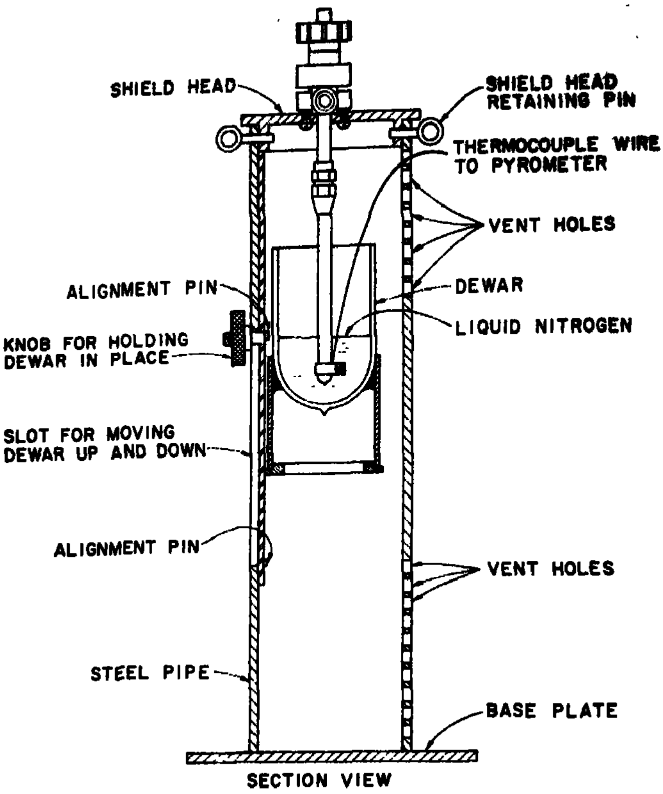
SHIELD HEAD
SHIELD HEAD RETAINING PIN
THERMOCOUPLE WIRE TO PYROMETER
VENT HOLES
ALIGNMENT PIN
DEWAR
LIQUID NITROGEN
KNOB FOR HOLDING DEWAR IN PLACE
SLOT FOR MOVING DEWAR UP AND DOWN
ALIGNMENT PIN
VENT HOLES
STEEL PIPE
BASE PLATE
SECTION VIEW

FIG. 4.—EXPLOSION SHIELD.

Procedure

A weighed quantity of uranium oxide, from 1 to 3 g, is mixed with about 1 mg of potassium chloride and transferred to the reactor (Fig. 1). The reactor is then assembled and evacuated without heating. The thermocouple is attached and the reactor placed in the safety shield. A quantity of fluorine which is at least three times the stoicheiometric amount required and sufficient to develop a fluorine pressure of at least 750 lbin^{-2} within the reactor, is measured into the burette. Some of this fluorine is admitted to the sample at room temperature to desensitize impurities that are highly reactive with fluorine. After 1 min, the Dewar within the shield is raised to immerse the lower portion of the reactor in liquid nitrogen, and the remainder of the fluorine is admitted. When the fluorine pressure drops to about 300 mm of mercury, the approximate vapour-pressure of fluorine at liquid nitrogen temperature, the valve of the reactor is closed. The line between the reactor and the burette is then evacuated, and the reactor is disconnected from the fluorine manifold. The Dewar containing the liquid nitrogen is lowered, permitting the liquid fluorine to boil and build up pressure. When the reaction takes place (usually before the reactor reaches room temperature), the reactor tube heats almost instantaneously to 200–400° C.

The reactor is cooled for about a minute in air, and then in liquid nitrogen to liquefy the fluorine and oxygen, which reduces the pressure. These gases are then removed using the vacuum manifold (Fig. 2). Reheating to about 100° C with the valve closed, followed by flash pumping at ice-brine temperature, purifies the uranium hexafluoride adequately for admission into gas-type mass spectrometers.

RESULTS

Several thousand oxide samples have been fluorinated by this method. The uranium hexafluoride is of high purity, and the yield is approximately 95 per cent.

Rush samples have been prepared for introduction into the mass spectrometer in less than 15 min. A 2 g sample of uranium oxide can be fluorinated with a total of 0·4 man hours of labour, including fabricating the reactor tube and cleaning the reactor valve.

DISCUSSION

Activators

The potassium chloride activator apparently serves only as an igniter or energy supplier rather than a catalyst since many materials initiate the reaction between uranium oxide and fluorine under high pressure. Iron oxides, potassium tartrate, and silicic acid in addition to the chlorides, bromides and iodides of potassium and sodium, have been observed to promote this reaction. Some impure samples of uranium oxides reacted with fluorine without the addition of an activator; however, purified oxide samples under the same conditions would not react with fluorine without the presence of some starter material.

All of the uranium oxides can be fluorinated using potassium chloride as the activator but potassium iodide is a much better activator for uranium tetrafluoride. With potassium iodide, yields of approximately 85 per cent have been achieved. With the proper activator the method may be useful for fluorinating a variety of other materials.

Fluorination of uranium metal

Fine turnings of metallic uranium react violently with fluorine under high pressure, usually bursting the reactor, whereas massive pieces do not fluorinate at room temperature with potassium chloride as an activator. Metal samples should be ignited to uranium oxide before fluorination.

Purity

Impurities in uranium hexafluoride prepared by the described method have been determined using recording gas-type mass spectrometers. Mass spectrum data show only trace amounts of chlorine, hydrofluoric acid, and chloryl fluoride (ClO_2F). The purity of the product is dependent upon that of the starting material, the fluorine, the amount and type of activator used, and the purification treatment after fluorination. The method has consistently produced samples that meet the stringent purity requirements for highly precise uranium isotopic measurements by mass spectrometry.

Explosions

Occasionally the reaction may burst the reactor tube. For this reason fluorinations are performed with the reactor tube in a shield of steel pipe. The cause of these infrequent explosions has not been determined, but they may result from an impurity that activates the entire charge of the reactor at once, producing a reaction more violent than the usual rapid burning. Some of the impurities that have been suspected are carbon, platinum, silver, chromium and boron. These impurities have been added in a concentration of approximately fifty parts per million to test samples of pure oxide, but these adulterated samples produced no explosions. Alteration of oxide surface area and slight traces of moisture appeared to make little difference in explosion susceptibility.

The tendency of impure oxides to cause explosions during fluorination can be reduced by treating them with hydrofluoric acid. This treatment consists of placing a few grammes of the oxide in a platinum dish, and covering with 48 per cent hydrofluoric acid, drying under an infra-red lamp, and igniting to the oxide in a steam atmosphere at 800°C. Uranium trioxide samples usually do not require the hydrofluoric acid treatment. The frequency of explosions has also been reduced by modifying the procedure in such a manner as to expose the sample first to gaseous fluorine at room temperature, which renders inactive those impurities which are highly reactive with fluorine.

Reactor tubes

Experience has shown that increasing the wall thickness of the copper reactor tubes from 0·032 to 0·049 in. reduced the frequency of tube ruptures to less than one in 500. The heavier walled tube withstands a pressure of nearly 9000 lbin^{-2} at room temperature, while the thinner ones rupture at approximately 5500 lbin^{-2}.

A new reactor tube is used for each sample, since a new tube costs no more than cleaning a used one.

Operating pressures

A special fluorination reactor was constructed with an attached pressure gauge for studying minimum initial reaction pressures with pure urano-uranic oxide. Reactions could not be produced below 750 lbin^{-2} of fluorine pressure at room temperature with potassium chloride as the activator: however, in routine operations where approximately 1000 lbin^{-2} fluorine pressure is used, the majority of the reactions start below room temperature. The reactions begin at a lower pressure with potassium iodide than with potassium chloride as the activator.

Prevention of isotopic and chemical contamination

In a laboratory where a range of isotopic concentrations of uranium is handled, care must be taken to prevent contamination of one sample by another. For this reason several vacuum systems are used to minimize accidental contamination. All reactor valves are coded and each valve is used for samples in a limited isotopic range. Each vacuum system is also restricted to a designated isotopic range.

The reactor, after being charged with fluorine and while still within the shield, is disconnected from the fluorine manifold before the reaction to avoid contamination of the manifold in event a leak of the reactor valve occurs. The use of a new reactor tube for each sample also greatly reduces the possibility of isotopic contamination.

Heat should not be used in the evacuation of the sample before fluorination. Heating the sample during evacuation causes a sudden rise in pressure, probably due to rapid vapourization of contained water, forcing some of the powdered sample into the evacuation lines and contaminating them. This phenomenon was observed with uranium trioxide in a glass system.

Contamination with organic materials must be prevented where fluorine is used. Organic solvents are never used in cleaning fluorination apparatus, as even small amounts of such material can cause serious explosions with fluorine.(4)

(4) R. H. LAFFERTY, J. C. BARTON and J. A. WESTBROOK, *Liquid Fluorine-CottonExplosion, Chemical and Engineering News*, Vol. 26, p. 3336. Amer. Chem. Soc. (1948).

J. Inorg. Nucl. Chem., 1962, Vol. 24, pp. 399 to 404. Pergamon Press Ltd. Printed in England

NATURE OF THE ANODIC TELLURATE WAVE AT THE DROPPING MERCURY ELECTRODE

B. Jaselskis and J. G. Lanese
Department of Chemistry, University of Michigan, Ann Arbor, Michigan

(*Received* 11 *September* 1961)

Abstract—Tellurate solutions at the dropping mercury electrode show an adsorption type anodic wave in the vicinity of zero volts vs. S.C.E. The presence of this anodic wave is attributed to depolarization of mercury electrode and the formation of an insoluble mercurous tellurate film given by the reaction $2\ Hg^{\circ} + H_6TeO_6 \rightarrow Hg_2H_4TeO_6 + 2H^+ + 2e$. Under similar conditions an anodic wave is not observed with tellurite, selenate, selenite and arsenate.

At the dropping mercury electrode tellurate shows a well defined cathodic wave. The nature of this wave and analytical applications have been described by Norton *et al.*⁽¹⁾ Closer examination of dilute tellurate solutions reveals the presence of an anodic wave in the vicinity of zero volts vs. S.C.E. in addition to the reported cathodic wave. In a limited concentration range this wave is proportional to the concentration. The nature of this anodic wave is of interest and is described in this paper.

EXPERIMENTAL

Apparatus. Polarograms were recorded by a Sargent Model XXI polarograph using a thermostated polarographic H cell with an external reference electrode. Both the saturated calomel and the saturated mercury–mercurous sulphate electrode were used. Oxygen was eliminated by passing a purified nitrogen through the solution.

Materials. Buffer solutions of a desired ionic strength were prepared from the reagent grade chemicals. The ionic strength was adjusted with potassium sulphate. Telluric acid was obtained from the Amend Drug and Chemical Co. and also was prepared from a pure metallic tellurium by the oxidation procedure described in the Brauer's *Handbuch der Praeparativen Anorganischen Chemie.*⁽²⁾ Mercurous tellurate (later referred as a black precipitate) was prepared by electrolysis of tellurate buffered solutions using mercury pool electrode at the potential set slightly more positive than the calomel electrode or by reacting metallic mercury with tellurate without an applied potential.

Polarograms of tellurate solutions. The anodic portion of polarogram was recorded by changing the potential of the dropping mercury electrode from negative towards positive potentials. In this manner smooth curves were obtained. Otherwise at high concentrations of tellurate the anodic curve shows some irregularities.

EXPERIMENTAL RESULTS

Anodic tellurate waves. In Britton and Robinson buffer solutions at pH 10 in the presence of chloride the tellurate ion shows a well defined anodic wave in the vicinity of zero volts vs. S.C.E. At lower pH's this wave is poorly defined and can be overlooked. Better results can be obtained when the mercury-mercurous sulphate reference electrode is used in the bicarbonate-carbonate buffer solutions containing potassium sulphate. A typical polarogram of a dilute tellurate solution is shown in

---

⁽¹⁾ E. Norton, R. W. Stoenner and A. I. Medalia, *J. Amer. Chem. Soc.* 75, 1821 (1953).

⁽²⁾ G. Brauer, *Handbuch der Praparativen Anorganischen Chemie*, pp. 348, 349. Ferdinand Enke, Stuttgart (1954).

Fig. 1. At higher concentrations of tellurate than 8×10^{-5} M the anodic wave forms a poorly defined prewave. Similar prewave for halide solutions has been observed by KOLTHOFF and OKINAKA(3) and has been attributed to the formation of a monomolecular layer of the mercurous halide.

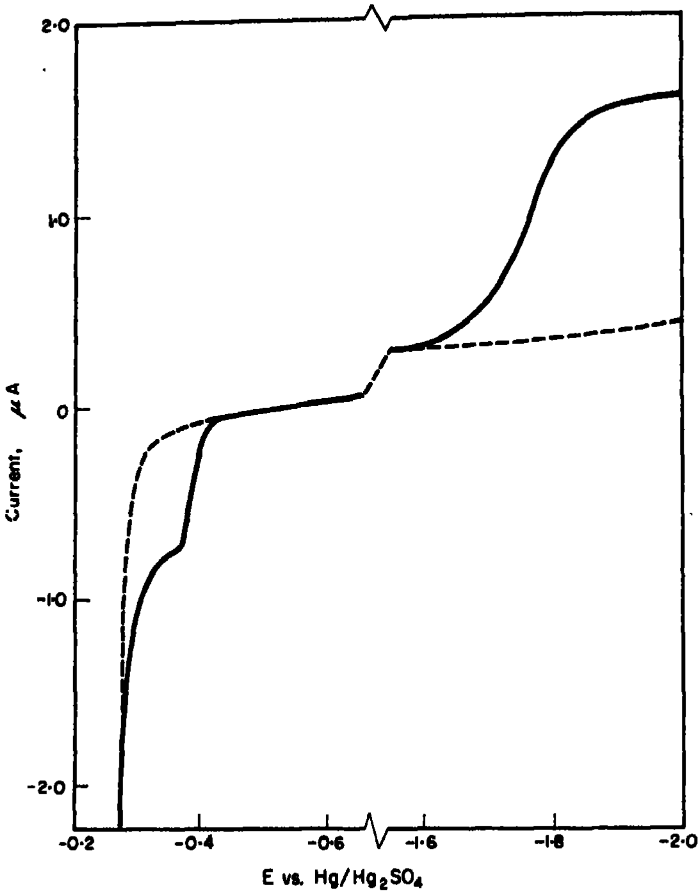

FIG. 1.—Polarogram of $5 + 10^{-5}$ M tellurate in bicarbonate-carbonate buffer.

The limiting current is directly proportional to the height of mercury column and it is inversely proportional to the temperature if the concentration of tellurate is above 8×10^{-5} M. At temperatures over 65°C the anodic wave disappears. Temperature effect on the anodic diffusion current changes somewhat with the concentration of tellurate. Changes become pronounced when the tellurate ion concentration is less than 8×10^{-5} M.

Electrocapillary characteristics. Electrocapillary characteristics of the tellurate solutions are considerably different from those of the supporting electrolyte alone as shown in Fig. 2. The electrocapillary curve for the tellurate solution shows a maximum at approximately the half-wave potential of the anodic wave and also a broad shoulder in the vicinity of the electrocapillary maximum of the supporting electrolyte. Similar electrocapillary behaviour has been reported by BENESCH and

---

(3) I. M. KOLTHOFF and Y. OKINAKA, *J. Amer. Chem. Soc.* **83**, 47 (1961).

Benesch[4] for the reduction of organic mercury compounds. The drop time of mercury decreases progressively by increasing the concentration of tellurate until a saturation concentration is reached, approximately 8×10^{-5} M. The addition of various maximum suppressors have no effect on the diffusion current. Some effect is observed with Triton X–100 and camphor. In the presence of 0·1 per cent of Triton X-100 electrocapillary curve for tellurate is somewhat depressed but the general shape remains the same as for the tellurate alone. The results indicate that mercurous tellurate and Triton X-100 are both absorbed simultaneously and that no replacement of the one film by the other takes place. In the presence of chelating agents such as ethylenediaminetetracetate the anodic wave disappears.

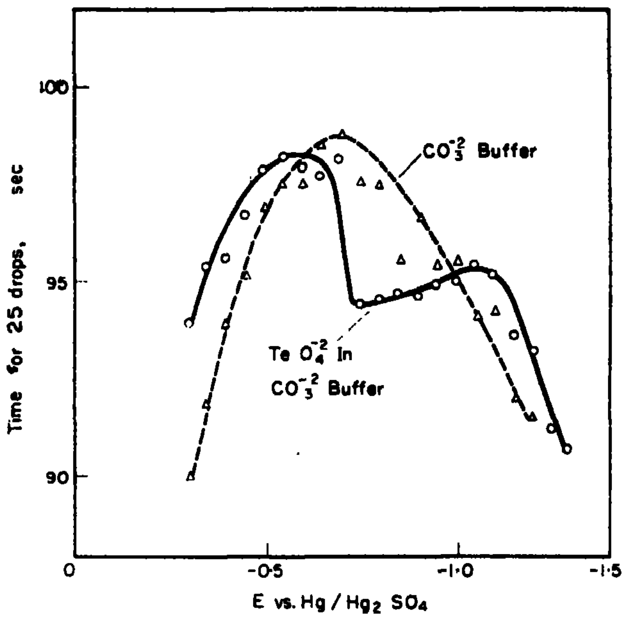

FIG. 2.—Electrocapillary curves: 0·1 M carbonate–bicarbonate and 0·1 M potassium sulphate buffer solution in the presence and in the absence of tellurate.

Dependence of the limiting current and half-wave potential on concentration, pH and ionic strength. The limiting current for the anodic wave increases with the concentration of tellurate until a saturation value is reached. Approximately the same values of saturation currents are obtained with the buffer solutions investigated. However, the dependence of a limiting current on concentration is somewhat affected by the composition of the buffer as shown in Fig. 3. In phosphate buffer solutions the reproducibility of the limiting current is poor. The half-wave potential for the anodic wave becomes more negative with the increasing pH. It changes in a linear manner with pH. The slope for the curve of the half-wave potential vs. pH is approximately 0·062. The half-wave potential also varies in a linear manner with the logarithm of the tellurate ion concentration. The slope for this curve is approximately 0·020. Variation of the half-wave potential with the pH and with the logarithm of

---

[4] R. E. Benesch and R. Benesch. *J. Phys. Chem.* **56**, 648 (1952).

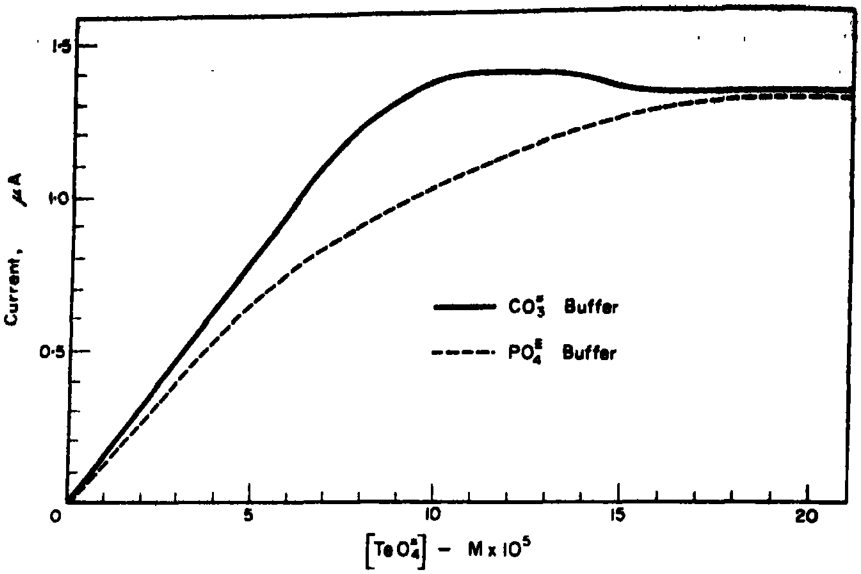

Fig. 3.—Height of the anodic wave as a function of tellurate ion concentration.

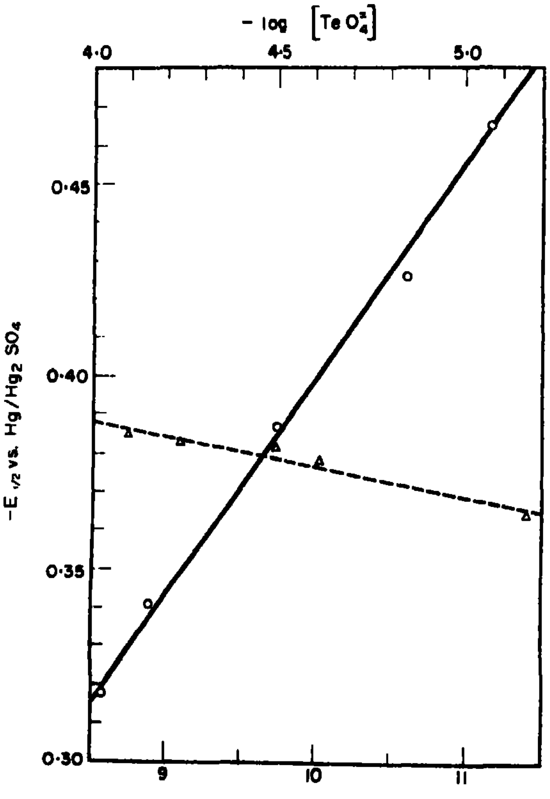

Fig. 4.—Half-wave potential of the anodic wave as a function of pH and the negative logarithm of the tellurate ion concentration. (Solid line—$E_{\frac{1}{2}}$ vs. pH and the dashed line—$E_{\frac{1}{2}}$ vs. $-\log(TeO_4^=)$).

the tellurate ion concentration is shown in Fig. 4. The limiting current and the half-wave potential dependence on the concentration of tellurate and pH is shown in Table 1.

TABLE 1.—POLAROGRAPHIC MEASUREMENTS ON TELLURATE SOLUTIONS

Concentration of tellurate (mM)	Anodic diffusion current i (μA)	Anodic half-wave potential* (v)	pH of the supporting electrolyte
0·0069	0·10	0·364	9·70†
0·0245	0·37	0·378	,,
0·0323	0·46	0·381	,,
0·0578	0·88	0·383	,,
0·0804	1·19	0·385	,,
0·050	0·71	0·318	8·58†
0·050	0·69	0·341	8·89†
0·050	0·71	0·387	9·74†
0·050	0·71	0·426	10·61†
0·050	0·73	0·465	11·16†

* Anodic potentials are measured against mercury–mercurous sulphate reference electrode.

† All buffer solutions contain potassium bicarbonate–carbonate and potassium sulphate.

Variation of the ionic strength by a factor of ten has no effect on the half-wave potential.

DISCUSSION

Diffusion current dependence on concentration, electrocapillary characteristics and visual observation of mercury droplets suggest that the anodic wave is due to the formation of an isoluble film and adsorption of tellurate ions. During polarographic scanning of tellurate solutions mercury droplets are covered with a black precipitate. LINGANE and NIEDRACH(5) report a similar precipitate for the reduction of the tellurite ion in the vicinity of the tellurite reduction wave. The nature of this precipitate has been attributed to the formation of the metallic tellurium. However, the black precipitate, which is formed by the reaction of tellurate with the metallic mercury without or with an electrical potential applied, is quite different from that reported by LINGANE and NIEDRACH.(5) This precipitate contains mercurous and tellurate ions. The composition of this precipitate corresponds to 65 per cent mercury and 18 per cent tellurium. The empirical formula of the black precipitate cannot be ascertained unambiguously since it appears to vary somewhat with the conditions of the preparation. These results compare favourably with the mercurous tellurate. ($Hg_2H_4TeO_6$; 64% Hg: 20·3% Te.)

Formation of anodic waves at the dropping mercury electrode by halide solutions have been described by KOLTHOFF and MILLER(6) and by RAVENDA.(7) Similar

(5) J. J. LINGANE and L. M. NIEDRACH, *J. Amer. Chem. Soc.* 71, 196 (1949).

(6) I. M. KOLTHOFF and C. S. MILLER, *J. Amer. Chem. Soc.* 63, 1405 (1941).

(7) J. RAVENDA, *Coll. Trav. Chim. Tchecosl.* 6, 453 (1934).

anodic waves have been reported for periodate by JENSOVSKY[8] and for organic mercury compounds by BENESCH and BENESCH.[4] In all cases the mercury electrode is depolarized by the formation of an insoluble mercurous salt. Thus, the nature of the anodic wave of tellurate solutions at the dropping mercury electrode is attributed to the depolarization of mercury and the formation of an insoluble film of mercurous tellurate by the reaction:

$$2Hg^{\circ}+H_6TeO_6 \rightarrow Hg_2H_4TeO_6+2H^{+}+2e.$$

Hence the half wave potential is related to the concentration of tellurate and pH by the equation:

$$E_{\frac{1}{2}} = \text{constant} - \frac{0{\cdot}0591}{2} \log \frac{\text{Te(VI)}}{2} - 0{\cdot}0591 \text{ pH}.$$

Thus the half wave potential should vary as the logarithm of the tellurate concentration and as the pH. Experimentally determined slopes for these variations are 0·020 and 0·062 respectively.

The reversibility of the anodic depolarization by tellurate has been evaluated from the slope in the plot of the logarithm of (i_d-i) vs. potential of the dropping mercury electrode:

$$E_{\text{d.m.e.}} = \text{constant} - \frac{0{\cdot}0591}{2} \log (i_d-i).$$

The slope for the anodic tellurate wave in the concentration ranges below 8×10^{-5} is approximately 60 mV. For more concentrated tellurate solutions than 8×10^{-5} M two slopes are obtained; 60 mV for the major portion of the wave and 125 mV for the prewave. These results clearly indicate that the tellurate anodic wave is irreversible, and the adsorption wave is still much more drawn out.

All these observations suggest that the anodic tellurate wave is a surface-film limited wave not, strictly speaking, an adsorption wave.

---

(8) L. JENSOVSKY, *Coll. Trav. Chim. Tchecosl.* **22**, 311 (1957).

J. Inorg. Nucl. Chem., 1962, Vol. 24, pp. 405 to 413. Pergamon Press Ltd. Printed in England

THE EXTRACTION OF NITRIC ACID BY LONG CHAIN TERTIARY AMINES

F. Baroncelli, G. Scibona and M. Zifferero
Gruppo Reprocessing del C.N.E.N. c/o Istituto di Chimica Farmaceutica
dell'Università di Roma

(*Received* 23 *August* 1961)

Abstract—Nitric acid is extracted into benzene solutions of long chain tertiary amines to an extent which is in excess of the quantity required for salt formation. This excess is due partly to the extractive properties of the benzene and partly to the properties of the amine nitrate solution.

For the portion of acid extracted by the amine salt a partition co-efficient is introduced which is a linear function of the amine concentration.

Simple equations are given to compute the amount of HNO_3 extracted into the organic phase in a wide range of acid concentration (0–16 M) and amine concentration (0·05–1 M). To obtain information on the nature of the nitric acid present in the organic phase, infra-red spectroscopy was used. The existence of ion pairs $[R_3NH^+NO_3^-]^0$ was shown. An increase of the amine nitrate concentration promotes the formation of higher orders of association.

The extraction of nitric acid from aqueous solutions, using long chain aliphatic amines dissolved in a hydrocarbon diluent, has received increasing attention from the time it was first reported by Smith and Page.(1) A number of papers have appeared(2–12) on nitric, hydrochloric, sulphuric acid extraction mainly in connexion with the use of amine-diluent systems in the recovery of uranium and thorium from ores and with the potential application of amines in the reprocessing of irradiated fuels. From a survey of this literature it is quite evident that the amine-diluent system is capable to extract the acid to a greater extent than that compatible with a salt formation reaction.

This investigation was undertaken with the aim to study the partition of nitric acid between an aqueous phase and a benzene solution of tri-n-dodecylamine (TLA) and to gather information on the physical state of nitric acid in the organic phase by means of infra-red spectroscopy.

(1) E. L. Smith and J. E. Page, *J. Soc. Chem. Industr.* **67**, 48 (1948).
(2) F. L. Moore, Report ORNL 1314 (1952).
(3) K. A. Allen, *J. Phys. Chem.* **60**, 239 (1956).
(4) K. A. Allen, *J. Phys. Chem.* **60**, 943 (1956).
(5) F. L. Moore, *Analyt. Chem.* **29**, 1660 (1957).
(6) K. A. Allen, *J. Phys. Chem.* **62**, 1119 (1958).
(7) U. Bertocci, Report AERE/R/2933 (1959).
(8) C. Boirie, *Bull. Soc. Chim., France*, 980 (1959).
(9) M. de Trentinian and A. Chesne, Compte rendu du colloque de extraction par solvent J.E.N. Madrid 29–30 oct. 1959—Pag. 319.
(10) G. Scibona, Report CNC-43 (1950).
(11) M. Zifferero and F. Baroncelli, Report CNC-41 (1960).
(12) D. J. Carswell and G. G. Lawrance, *J. Inorg. Nucl. Chem.* **11**, 69 (1959).

Our results indicate that nitric acid in a benzene solution of a tertiary long chain amine (°) is partly free as molecular nitric acid and partly bound to form ion pairs $[R_3NH^+NO_3^-]^\circ$.

(°) The investigation was extended also to other aliphatic amines: they all followed closely the TLA behaviour.

EXPERIMENTAL

Reagent source and purity

Trilaurylamine was supplied by Rhône & Poulenc in a special high purity batch. The amine purity was checked with a determination of the equivalent weight as resulting from a potentiometric non aqueous titration, the agreement with the calculated molecular weight being within 1 per cent.

The benzene and the other chemicals were reagent grade products.

Extraction procedure

Equal volumes of aqueous and organic phase were stirred at constant temperature (25 ±0·1° C). Phase equilibrium was reached in less than 1 min in all the cases. Phases were separated by centrifugation and suitable aliquots were taken for analysis. A similar procedure was adopted to determine the solubility of nitric acid in benzene.

Method of analysis

A normal volumetric procedure was followed to obtain the acid content of the aqueous phase.

A potentiometric titration with potassium isopropilate was chosen for the organic phase after a dilution with a mixture of ethylene glicol and isopropanol.

A two steps titration pattern was noticed due to the excess acid titration (first step) and to the amine nitrate titration (second step).

Water determination

H_2O was determined using the Karl Fischer method with a Townson & Mercer apparatus. The results are only indicative due to the interference of nitric acid.

Infra-red spectroscopy

All spectra were recorded by means of a Perkin-Elmer Model 221 double beam spectrophotometer, equipped with rock salt optic. Cells 0·055 and 0·062 mm thick were employed.

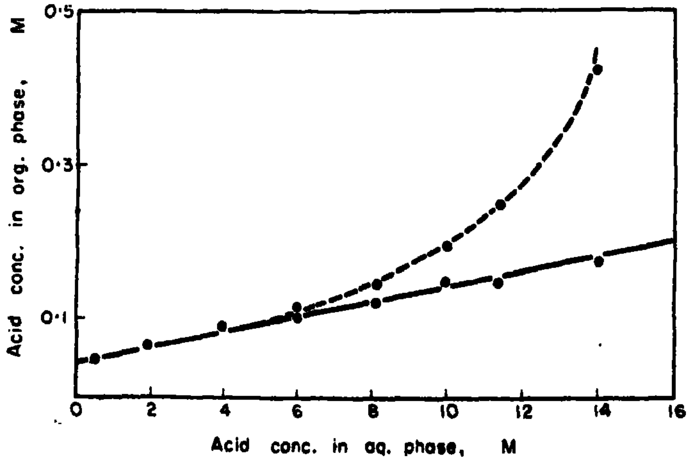

Fig. 1.—Equilibrium isotherm for the system: 0·05 M TLA in benzene—aqueous nitric acid.

RESULTS AND DISCUSSION

Nitric acid isotherms

The equilibrium isotherms for nitric acid–TLA at different amine concentration (Fig. 1–4) substantiate the hypothesis that the acid extraction is characterized by salt formation reaction, followed by the extraction of more acid from the organic phase, depending on the amine concentration. The isotherms in fact are straight lines whose intercepts with the vertical axis correspond to an organic nitric acid molarity equal to the amine molarity. This coincidence (within the limit of the experimental error) unambiguously attests the formation of the amine mononitrate.

A partition co-efficient α_a^o can be therefore introduced for the excess nitric acid extraction, which is a linear function of the amine molarity;

$$\alpha_a^o = z \cdot R_3N = \frac{HNO_{3\,org}}{HNO_{3\,aq}} \tag{1}$$

where $$HNO_{3\,org} = \alpha_a^o \cdot HNO_{3\,aq} = z \cdot R_3N \cdot HNO_{3\,aq} \tag{2}$$

indicates the concentration of nitric acid extracted in a reversible way (which can be washed back by water scrubs).

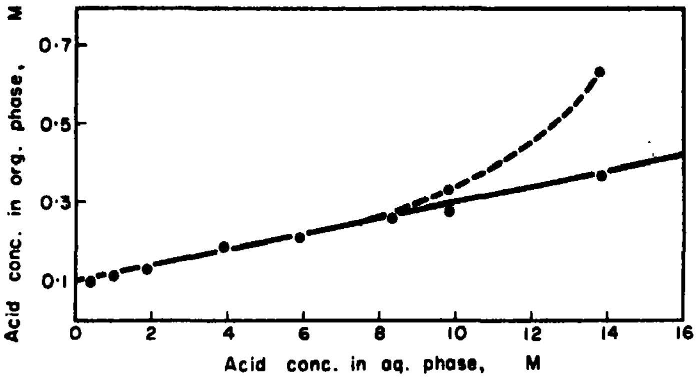

FIG. 2.—Equilibrium isotherm for the system: 0·1 M TLA in benzene—aqueous nitric acid.

The angular co-efficient α_a^o of equation (1) can be calculated from the slope of the isotherms. If one plots the angular coefficients α_a^o as a function of the amine concentration (Fig. 5), straight lines are obtained, passing through the origin, whose slope is the experimental parameter z.

If now a new, more general, partition coefficient D_a^o is introduced, relating the distribution of the nitric acid between water and a hydrocarbon solution of the free amine, it will be:

$$D_a^o = \frac{HNO_{3\,total\,org}}{HNO_{3\,aq}} \tag{3}$$

$HNO_{3\,total\,org}$ now indicating the concentration of the total extractable nitric acid.

Equation (3) can therefore be written:

$$D_a^o = \frac{R_3NHNO_3 + \alpha_a^o \cdot HNO_{3\,aq}}{HNO_{3\,aq}} \tag{4}$$

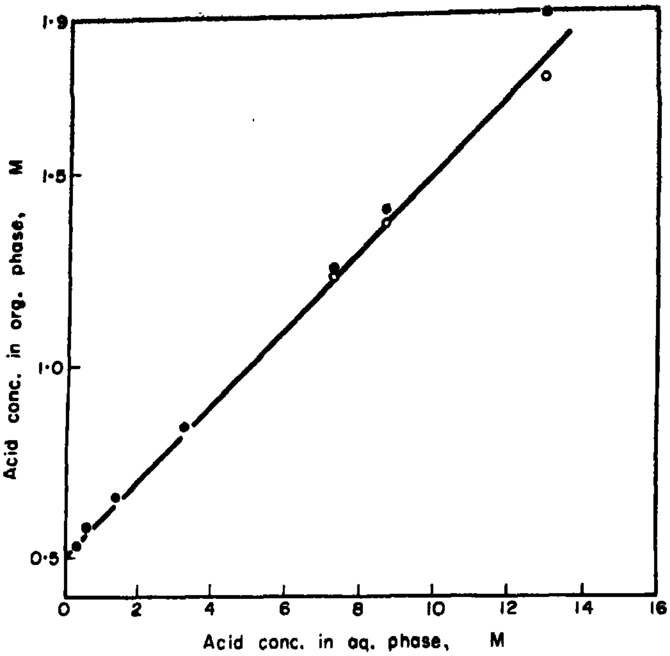

FIG. 3.—Equilibrium isotherm for the system: 0·5 M TLA in benzene—aqueous nitric acid.° are points corrected for HNO_3 extraction in pure benzene.

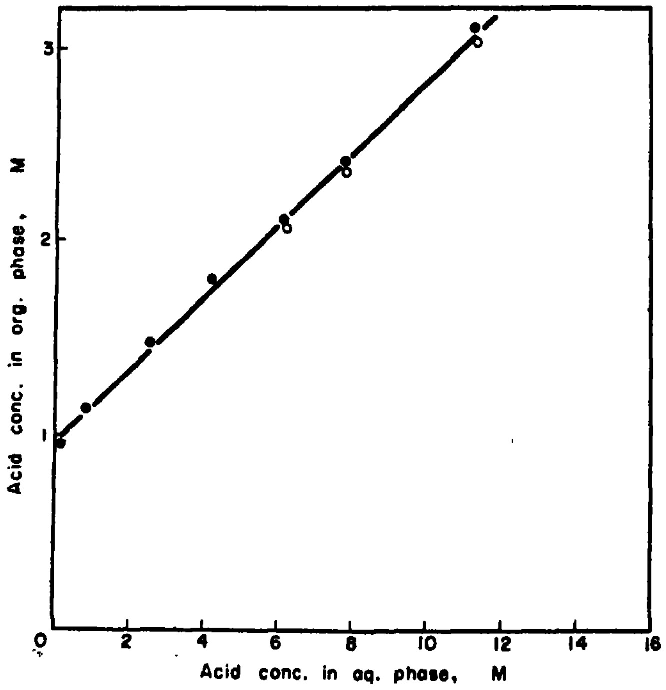

FIG. 4.—Equilibrium isotherm for the system: 1·0 M TLA in benzene—aqueous nitric acid. ° are points corrected for HNO_3 extraction in pure benzene.

In presence of sufficient nitric acid, is:

$$R_3NHNO_3 = R_3N, \text{ and}$$

$$D_a^o = R_3N \cdot \left(\frac{1}{HNO_{3\,aq}} + z \right) \tag{5}$$

Therefore this partition coefficient D_a^o is an hyperbolic function whose limits (HNO$_3$ concentration varying from O to ∞) are;

D_a^o approaches ∞ when $HNO_{3\,aq}$ approaches O
D_a^o approaches $z \cdot R_3N$ when HNO_3 approaches ∞.

z is an experimental parameter which can be calculated, as shown, from the equilibrium isotherms. These in fact are (equation 5) straight lines with intercept R_3N and slope $z \cdot R_3N$.

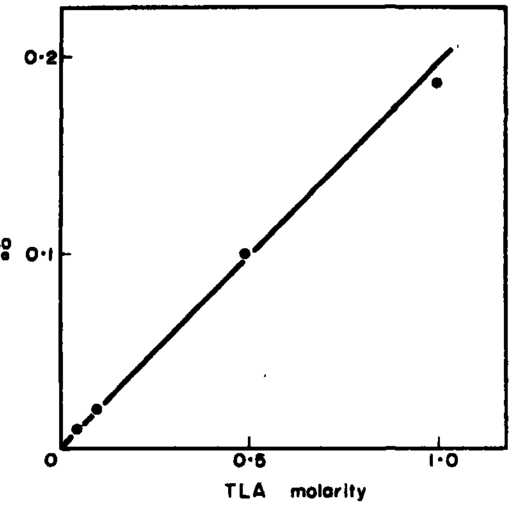

FIG. 5.—α_a^o versus amine concentration.

It is worth noticing that a few isotherms (Fig. 1 and 2) show a parabolic course. This deviation from linearity may be explained in terms of additional nitric acid extraction due to the benzene itself.

A short investigation on this matter (Fig. 6) has shown that the equilibrium isotherm of the benzene–HNO$_3$ system is described by the following equation:

$$HNO_{3\,aq} = a_0 + b \cdot HNO_{3\,\text{benzene}} + c(HNO_3)^2_{\text{benzene}} \tag{6}$$

with $a_0 = 6{\cdot}075$, $b = 75{\cdot}238$, $c = -165{\cdot}9$ obtained with the compensation method.

The extraction of nitric acid into benzene has been studied in the nitric acid concentration range 6–14M since the quantity of nitric acid ectracted at lower acidity is quite negligible. In Table 1 a summary of the equilibrium data is given.

If one takes into account this additional extraction due to the amine diluent, equation (5) must be suitably modified to include this new variable; equation (7) is so obtained:

$$D_a^o = \frac{R_3N(1 + zHNO_{3\,aq}) + F\,(HNO_{3\,aq})}{HNO_{3\,aq}} \tag{7}$$

$F(HNO_{3\,aq})$ taking care of the extraction of nitric acid into the benzene.

Once known, the contribution of the benzene to the extracted nitric acid can be substracted and in this case the course (dotted lines) of isotherms in Fig. 1 and 2 is brought back to linearity. As told before the effect of additional nitric acid caused by the extraction in benzene is noticeable only at high molar aqueous acidity for low amine molarities. This explains the linear course of most isotherms.

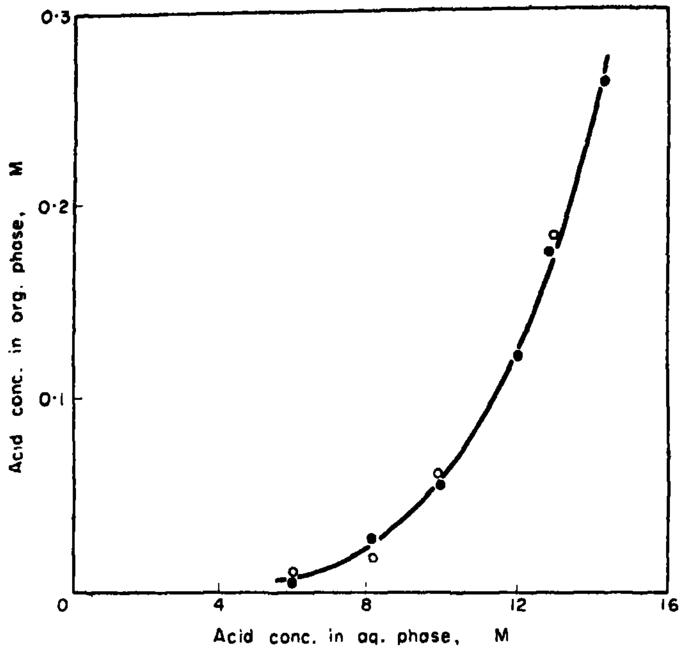

Fig. 6.—Extraction of HNO_3 in pure benzene as a function of HNO_3 concentration in the aqueous phase. Experimental ° calculated with equation (6).

Table 1.—Extraction of HNO_3 in benzene at increasing HNO_3 concentration in the aqueous phase

aq. HNO_3 at equil. (M)	org. HNO_3 at equil. (M)
6·10	$6{\cdot}7 \times 10^{-3}$
8·24	$2{\cdot}6 \times 10^{-2}$
10·03	$5{\cdot}1 \times 10^{-2}$
11·52	$1{\cdot}0 \times 10^{-1}$
13·02	$1{\cdot}8 \times 10^{-1}$
14·35	$2{\cdot}6 \times 10^{-1}$

In Fig. 7 the distribution coefficients D_a^0 are plotted against $HNO_{3\,aq}$ (the asymptotic lines for the nitric acid (0–14 M) are in agreement with the value $z{\cdot}R_3N$ within a 10 per cent error); dotted lines departing from solid lines showing the actual behaviour if the effect of nitric acid extraction in benzene is deducted.

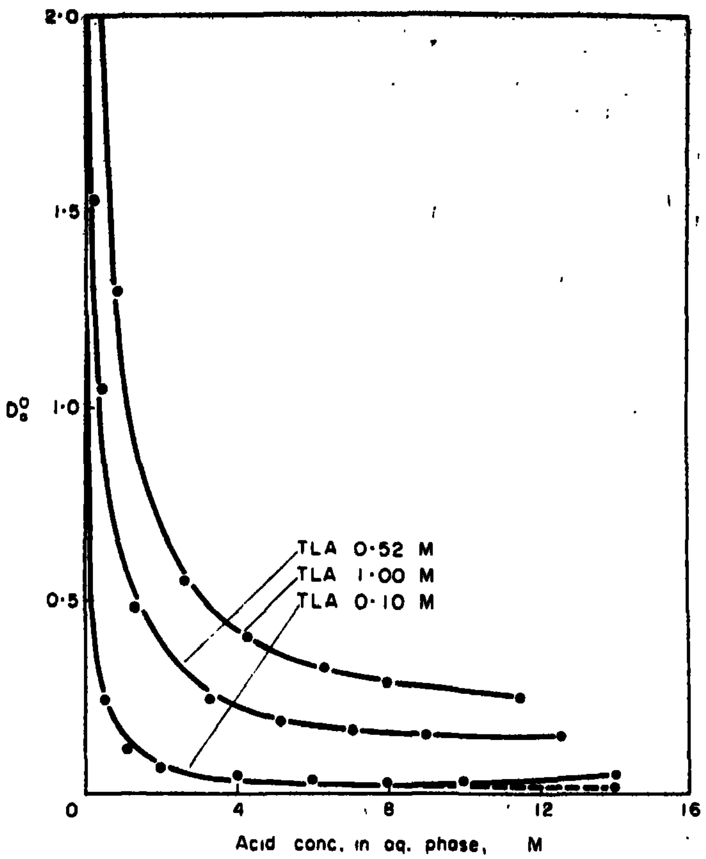

FIG. 7.—D_a^0 as a function of HNO_3 concentration in the aqueous phase for three different TLA concentrations.

The fact that nitric extracts appreciably in benzene was recently reported:[13] the authors explain the increase of the extraction at higher acidities of the aqueous phase as due to a concurrent decrease of the acid dissociation.

Infra-red spectra

The spectra were all recorded in benzene solution. Mixtures of TLA and HNO_3 with a ratio ρ (nitric acid conc./amine conc.) between 1 and 3 were used, a value of $\rho = 1$ corresponding to the stoicheiometry of the salt formation reaction.

The vibrations of HNO_3 are reported in Table 2. The spectra of benzene solutions at different concentration of TLA–HNO_3 with $\rho = 1$ show a band at 833 cm^{-1}. From a survey of the data reported in references,[14-17] this band can be ascribed to the nitrate ion. In fact, the nitrate ion has four fundamental modes of vibration, all of which may be observed in the infra-red in suitable cases, but only two are generally sufficiently sharp to be used for identification purposes. These are the vibration which occur near 1350 cm^{-1} and 830 cm^{-1}. In our case, we use only the 830 cm^{-1} because the benzene absorbency is strong in the 1350 cm^{-1} region. (On the other hand, it is not advisable to change the solvent, since the isotherms were studied in benzene solutions.)

---

[13] A. A. GRINBERG and G. S. LOZHKINA, *Zh. Neorg. Khim.* **5**, 738–44 (1960).

[14] O. RIEDLICH and L. E. NIELSEN, *J. Amer. Chem. Soc.* **65**, 654 (1943).

[15] D. A. MARCUS and J. M. FRESCO, *J. Chem. Phys.* **27**, 564 (1957).

[16] S. A. STERN and J. T. MULLHAUPT, *Chem. Rev.* **60**, April (1960).

[17] L. J. BELLAMY, *Infra-red spectra of complexes molecules.* J. Wiley, New York (1954).

TABLE 2.—VIBRATIONS AND FREQUENCIES OF NITRIC ACID (cm^{-1})*

No.	Symmetry and assignment			Infra-red liquid
1	A_1	NO_2	stretch	1300 *s*
2	A_1	N–O	stretch	922 *s*
3	A_1	NO_2	bend	690 *m*
4	B_2	NO_2	stretch	1670 *s*
5	B_2	N–OH	bend	—
6	B_1	out of plane	bend	769 *m*
7	A_1	O–H	stretch	3380 *m*
8	A_1	O–H	bend	1340
9	A_1	O–H	torsion	—

* For a description of these vibrations see references (14), (15), (16).
The 1350 cm^{-1} and the 830 cm^{-1} frequencies are assigned to the NO_3 ion.(14, 16)

The presence of the 833 cm^{-1} band and the absence of the symmetrical and asymmetrical NO_2 stretching modes,(17–19) and of the N–O stretch confirm the existence in solution of $[TLAH^+NO_3^-]^c$ ion pairs.

By increasing the concentration ($\rho = 1$) of TLA and HNO_3 from 0·05 to 0·5, besides the 833 cm^{-1} band, a new band appears at 825 cm^{-1}. This fact should be ascribed to an order of association higher than the simple ion pair. Such an assumption is in agreement with the behaviour of alkyl ammonium salts whose solutions, in low dielectric constant solvents, form ion pairs, triple ions, quadruple and greater orders of association.

By increasing the concentration of the nitric acid in the organic phase, the mass action law of association can suffer a reversal resulting in a decrease of the degree of association. This occurs in the case of TLA–HNO_3 mixtures with $\rho > 1$. In fact the infra red spectra of systems in which ρ is gradually increased from 1 to 3 (Table 2 gives a summary of the main frequencies) yield the following observations;

(i) the 825 cm^{-1} band vanishes:
(ii) the 940 cm^{-1}, 1300 cm^{-1}, 1650 cm^{-1} bands increase strongly in intensity:
(iii) the 833 cm^{-1} band increases very weakly.

The disappearance of the 825 cm^{-1} band is in agreement with the previous picture, depending on a decrease of the degree of association.

The presence of ν_1, ν_2, ν_4 stretching modes is characteristic of the case $\rho > 1$. They can be used to establish if the concentration of nitric acid in solution exceeds the amine molarity. These frequencies are due to molecules of nitric acid which may be free and in dimer form. The presence of water in solution suggests the possibility of a hemihydrate $(HNO_3)_2 \cdot H_2O$ (Table 3), and the shift of the ν_2 mode to 940 cm^{-1},

---

(18) E. Lieber, D. R. Levering and L. J. Patterson, *Analyt. Chem.* **23**, 1594 (1951).
(19) F. Pristera, *Analyt. Chem.* **25**, 844 (1953).

probably due to the hydrogen bonding formation, is in agreement with this hypothesis. The split of ν_2 in two strong bands as pointed out in reference⁽²⁰⁾ was not verified in our spectra. The very weak increase of the 833 cm^{-1} band suggests that only a little amount of this nitric acid is in the form of nitrate ions.

TABLE 3.—EXTRACTION OF H_2O IN BENZENE AT DIFFERENT HNO_3 MOLARITIES OF THE AQUEOUS PHASE

HNO_3 aqueous (M)	H_2O in benzene (M)	HNO_3 in benzene (M)
6·200	$1 \cdot 1 \times 10^{-2}$	$6 \cdot 7 \times 10^{-3}$
8·160	$1 \cdot 5 \times 10^{-2}$	$2 \cdot 6 \times 10^{-2}$
10·02	$2 \cdot 6 \times 10^{-2}$	$5 \cdot 2 \times 10^{-2}$
11·63	$4 \cdot 3 \times 10^{-2}$	$1 \cdot 1 \times 10^{-1}$
14·50	$12 \cdot 1 \times 10^{-2}$	$2 \cdot 6 \times 10^{-1}$

CONCLUSION

Nitric acid extracts into benzene solution of long chain tertiary aliphatic amines to an extent which is greatly in excess of the acid requested for the salt formation.

This excess acid is due partly to the extractive properties of the benzene itself and partly to the properties of the amine mononitrate solution.

For the portion of acid which is extracted by the amine salt a partition coefficient α has been introduced which is a linear function of the amine concentration. α is defined with the help of an experimental parameter z.

The infra-red spectra in benzene solutions indicate that when the HNO_3/TLA ratio is > 1, nitric acid is present both free under molecular form and bound to the amine to form ion pairs. At $HNO_3/TLA = 1$, an increase of the salt concentration promotes the formation of higher orders of association. From this fact we are induced to consider α only as a partition coefficient between the two phases, bearing in mind that its linear dependence on the amine concentration can be explained with the increase of the dielectric constant of the amine phase.

⁽²⁰⁾ C. J. HARDY, B. F. GREENFIELD and D. SCARGILL, *J. Chem. Soc.* 90 (1961).

J. Inorg. Nucl. Chem., 1962, Vol. 24, pp. 415 to 427. Pergamon Press Ltd. Printed in England

INTERACTIONS BETWEEN TRIBUTYL PHOSPHATE, PHOSPHORIC ACID AND WATER*

C. E. HIGGINS and W. H. BALDWIN
Chemistry Division, Oak Ridge National Laboratory, Tennessee

(*Received* 2 *October* 1961; *in revised form* 1 *November* 1961)

Abstract—The distribution co-efficient for phosphoric acid between tributyl phosphate (TBP) and water increased with the acid concentration in the inorganic phase and correlated with the water behaviour in the organic phase. Water accompanying the acid into the TBP was salted out after the ratio 3 $TBP{\cdot}H_3PO_4{\cdot}6\ H_2O$ was reached but levelled off at one water per TBP regardless of the phosphoric acid concentration over the range 1–4 moles H_3PO_4 per mole TBP. Evidence for a high degree of association in solutions of anhydrous H_3PO_4 and TBP was obtained from ebullioscopic molecular weight determinations in ether and the viscosity of undiluted solutions. The maximum viscosity occurred at the 3 H_3PO_4 to 1 TBP ratio and was about three times that of anhydrous, super-cooled H_3PO_4.

AN EARLIER investigation⁽¹⁾ into the interactions between TBP, monovalent electrolytes, and water has been extended now to include the polyvalent orthophosphoric acid. With the exception of sulphuric acid⁽²⁾ all of the many TBP–acid studies have been concerned with the monobasic acids, thus information gained from distribution tests with a tribasic acid should be of interest. The industrial potential of TBP for the purification of phosphoric acid has recently been shown by DOUMAS.⁽³⁾

The previously noted miscibility of anhydrous phosphoric acid and TBP⁽⁴⁾ made possible the investigation of interactions between these compounds in the absence of water. The method of continuous variation was employed for ebullioscopic molecular weight determinations and refractive index and viscosity measurements.

EXPERIMENTAL

Chemicals. Reagent grade orthophosphoric acid (86·1 per cent H_3PO_4) was used to prepare the stock aqueous solutions. Removal of water by vacuum pump treatment of the 86 per cent H_3PO_4 gave solutions in the 86 to 100 per cent range. Anhydrous phosphoric acid—^{32}P was prepared by mixing 5 mc H_3PO_4—^{32}P in weak HCl with 1·14 g of 86·1 per cent H_3PO_4 (0·010 mole) in a 50 ml Pyrex round-bottomed flask, freezing, then pumping off the volatile materials until the correct weight loss had been achieved, warming no higher than 50° C during the drying operation. Solutions containing tracer ^{32}P were then prepared over the concentration range 10^{-3} M to 15 M H_3PO_4, having specific activities of 0·25 to 12 mc per mole throughout the period of test.

The organic chemicals were of reagent grade or were distilled before use. TBP was purified as before.⁽¹⁾

---

* This paper is based upon work performed for the United States Atomic Energy Commission at the Oak Ridge National Laboratory operated by Union Carbide Corporation.

⁽¹⁾ W. H. BALDWIN, C. E. HIGGINS and B. A. SOLDANO, *J. Phys .Chem.* 63, 118 (1959).

⁽²⁾ E. HESFORD and H. A. C. MCKAY, *J. Inorg. Nucl. Chem.* 13, 156 (1960).

⁽³⁾ B. C. DOUMAS, *Purification of Phosphoric Acid by Solvent Extraction*, University Microfilms, Ann Arbor, Mich. (1961).

⁽⁴⁾ C. E. HIGGINS and W. H. BALDWIN, *J. Org. Chem.* 21, 1156 (1956).

Distribution and solubility determinations. The distribution of phosphoric acid between water and TBP was accomplished by equilibrating the aqueous stock solutions with equal volumes (5–20 ml) of pure TBP and with TBP in various concentrations in organic diluents. The equilibration time was 1 hr in a water-bath at 25 ±0·2° C. A sharp phase layering was obtained by centrifugation for 20–30 sec at 2,000 rev/min in an open centrifuge at a room temperature of 25° C without materially altering the solution equilibrium.(5) Any volume changes were noted, following which the phases were separated and stored in the bath.

The distribution co-efficient, E_a°, in all cases refers to the ratio, after equilibration, of the concentration (moles per litre) of phosphoric acid in the organic phase to that in the aqueous phase. M_o and M_a refer to molar concentrations of H_3PO_4 in the organic and aqueous phases, respectively, while m_o and m_a refer to molalities.

Approximate amounts of tributyl phosphate dissolved in the high concentration equilibrium phosphoric acid solutions were determined by extracting duplicate 50 ml samples several times with equal volumes of C.P. carbon tetrachloride, concentrating, and pumping to constant weight at room temperature in weighed 50 ml round-bottomed flasks. The solubility of TBP in dilute phosphoric acid solutions was previously determined with TBP-^{32}P after the manner used for the reported solubilities in monovalent electrolyte solutions.(6)

Dry TBP and anhydrous phosphoric acid mixed in mole ratios varying from 1:20 to 100:1 formed clear, homogeneous solutions.

Analysis of solutions. The phosphoric acid concentration in most solutions was determined by titration of aliquots (aqueous phases in water and organic phases in 50 per cent ethyl alcohol) with standard sodium hydroxide using a Fisher Titrimeter, others by solution counting the beta activity, correcting, when necessary, for the effect of solution density on counting rate after the manner of Dyrssen.(7) Some equilibrium aqueous solutions were analysed by interpolation of their densities on a density vs. stock phosphoric acid concentration curve. Values thus found agreed within ±1 per cent of the values found by titration.

Water content in the equilibrium organic solutions (no diluent) was determined by use of the Karl Fischer reagent.* The TBP content was then found by subtracting from the weight of a known volume of organic solution the weights of water and phosphoric acid.

Densities were determined at 25·0 ±0·2° C using calibrated weight pipettes of 0·500–4 ml capacities.

Solutions of TBP and anhydrous phosphoric acid in varying molar proportions were prepared for physical measurements. Refractive indices were obtained at 25·0° C with an Abbé refractometer. Molecular weights were determined in ether by the ebullioscopic method of Menzies and Wright.(8, 9) An estimation of the viscosities at 25° was obtained by comparing the time to deliver ~0·4 ml between two marks 20 cm apart on a straight upright tube of 1·6 mm i.d. with that of glycerine (170 sec) as a standard. The viscosities were calculated from the relationship: $\frac{\pi_1}{\pi_2} = \frac{d_1 t_1}{d_2 t_2}$, where d_1, d_2 and t_1, t_2 are densities and delivery times, respectively, and π_2 for glycerine (d_4^{25} 1·255) is 954 cpoise.(10)

RESULTS AND DISCUSSION

The distribution of phosphoric acid between pure TBP and water as a function of the equilibrium aqueous phase acid concentration is shown in Table 1. The semi-log plot, Fig. 1, shows E_a° falling into three separate sections depending upon

---

* We are indebted to W. R. Laing and co-workers of the Analytical Chemistry Division for the water analysis.

(5) C. E. Higgins and W. H. Baldwin, *Analyt. Chem.* 32, 236 (1960).

(6) C. E. Higgins, W. H. Baldwin and B. A. Soldano, *J. Phys. Chem.* 63, 113 (1959).

(7) D. Dyrssen, *Acta Chem. Scand.* 11, 1771 (1957).

(8) A. W. C. Menzies and S. L. Wright, Jr., *J. Amer. Chem. Soc.* 43, 2314 (1921).

(9) W. T. Smith, Jr. and R. L. Shriner, *The Examination of New Organic Compounds*, pp. 63–66. J. Wiley, New York (1956).

(10) H. Ley and U. Kirchner, *Z. Anorg. Chem.* 173, 395 (1928).

TABLE 1.—EXTRACTION OF PHOSPHORIC ACID AND WATER BY 100% TBP AT 25°C

Equilibrium aqueous phase			Equilibrium organic phase					
Density (g/ml)	H_3PO_4 concn. (M)	Mole fraction H_3PO_4	Density (g/ml)	H_3PO_4 concn. (M)	Mole fraction H_3PO_4	Mole fraction H_2O	Mole fraction TBP	E_a^0
0·9971	0·000	0·0000	0·9767	0·0000	0·0000	0·499	0·501	0·0000
1·018	0·406	0·0074	0·9780	0·0375	0·0055	0·492	0·502	0·0924
1·041	0·838	0·0155	0·9815	0·106	0·0150	0·502	0·483	0·126
1·062	1·26	0·0233	0·9864	0·198	0·0257	0·538	0·436	0·157
1·066	1·33	0·0250	0·9875	0·214	0·0255	0·582	0·393	0·161
1·127	2·56	0·0500	1·006	0·583	0·0654	0·574	0·361	0·228
1·193	3·91	0·0801	1·029	1·02	0·105	0·576	0·320	0·261
1·319	6·50	0·147	1·068	1·84	0·218	0·415	0·367	0·283
1·445	9·18	0·233	1·110	2·71	0·312	0·346	0·342	0·295
1·546	11·4	0·324	1·151	3·62	0·388	0·312	0·299	0·318
1·615	12·9	0·398	1·193	4·53	0·463	0·267	0·270	0·351
1·646	13·6	0·439	1·220	5·09	0·500	0·252	0·248	0·374
1·743	15·9	0·609	1·342	7·71	0·654*	0·175*	0·175*	0·485
1·752	16·2	0·643	1·360	8·10	0·670	0·165	0·165	0·500

* Graphical interpolation.

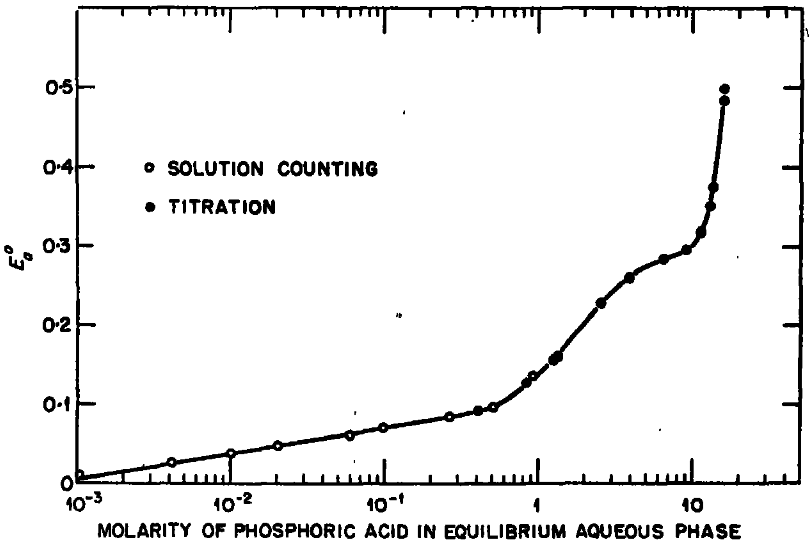

FIG. 1.—The relationship between distribution co-efficient and the equilibrium aqueous phase H_3PO_4 concentration.

the aqueous phase concentration. Each section also mirrors the water extraction behaviour (columns 7 and 8, Table 1 and Fig. 2). At first E_a^0 increased linearly from 0·01 to 0·1 over the range 10^{-3}–0·5 M_a, with the TBP–H_2O ratio remaining constant at one in the organic phase. In the second section E_a^0 increased more rapidly with co-extraction of water and H_3PO_4. The maximum water to TBP ratio of 2 in the organic phase occurred at 4 M_a. E_a^0 then began to level off as the addition of more phosphoric acid salted water out of the organic phase rapidly. In the last section E^o_a rose rapidly from 0·3 at ~ 10 M_a to 0·5 at 16 M_a. Through this range the TBP–H_2O ratio was that of the monohydrate regardless of the accompanying phosphoric acid concentration. When the phosphoric acid concentrations in each phase were converted to mole fractions, columns 3 and 6, Table 1, it was noted that generally the mole fraction of phosphoric acid in the organic phase was nearly the same as that in the corresponding aqueous phase.

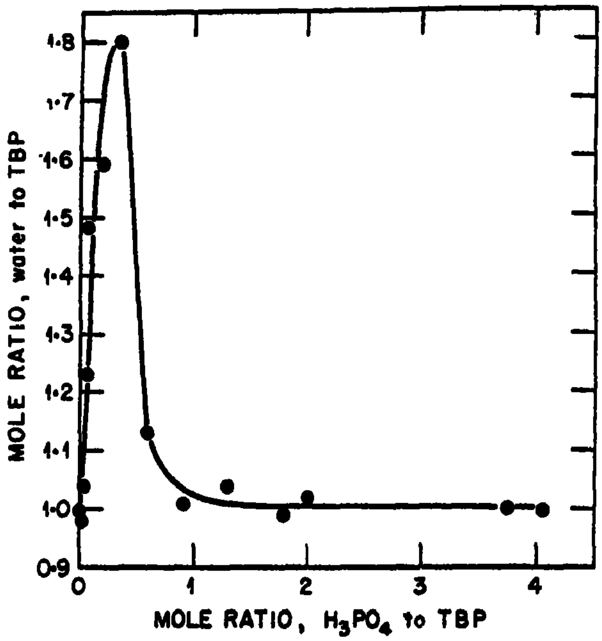

FIG. 2.—Water behaviour in the organic phase.

The amount of TBP going into the aqueous phase was not appreciable over the range 0–15 M_a H_3PO_4 (see Table 2). Phosphoric acid dissolved less TBP than water alone until the concentration exceeded 15 M_a H_3PO_4. Anhydrous H_3PO_4 dissolved TBP in all proportions at 25° C.

TABLE 2.—SOLUBILITY OF TBP IN PHOSPHORIC ACID SOLUTIONS AT 25° C

Equilibrium concentrations	
H_3PO_4 in queous (M)	TBP in aqueous (mg/l.)
0·00	414*
0·12	388*
0·29	370*
0·58	336*
1·14	290*
12·4	110†
14·8	390†
TBP miscible with anhydrous H_3PO_4	

* Determined using TBP–^{32}P.

† Determined by weight recovery.

The water behaviour in acid systems extracted by TBP is peculiar to the acid itself. Phosphoric acid carried water into the organic phase to the extent of about five molecules per molecule of acid (initial slope, Fig. 2). Water co-extracted with the halogen acids in ratios varying from 3:1 to 4:1 (1). From evidence obtained by an organic volume change technique,(11) TUCK and DIAMOND(12) have recently postulated the presence of a trihydrated hydronium ion in the TBP phase after contact with aqueous HBr, HCl, and $HClO_4$. Small differences were found, however, and from these and other results(1, 2) the amount of water initially co-extracted by each acid appears to decrease in the order $H_3PO_4 > HI > HBr > HCl > HClO_4 > H_2SO_4 > HNO_3$.

Nitric acid is a special case since it forces water from the TBP phase until the 1:1 ratio of TBP and HNO_3 is reached.(13, 1) As additional nitric acid goes into the organic phase the water content begins to increase.(13) The TBP appears to have approached its original monohydrated state when the organic phase is about 8 M HNO_3.

The organic phase acid concentration at which water is squeezed out by additional acid also varies with the acid. From the water–phosphoric acid curve (Fig. 2) the maximum appears to have occurred when the organic phase has the approximate composition 3 $TBP \cdot H_3PO_4 \cdot 6\,H_2O$. If the organic solutions resulting from the extraction of perchloric and sulphuric acids by HESFORD and MCKAY(2) have densities similar to those reported here for the organic solutions containing phosphoric acid and water then recalculating their data on a molal basis results in maxima at compositions of approximately 2 $TBP \cdot HClO_4 \cdot 4\,H_2O$ and $TBP \cdot 2\,H_2SO_4 \cdot 2\,H_2O$. The former does agree with the $HClO_4$ extraction data of SIEKIERSKI and GWOZDZ.(14) Maxima for the halides(1) occur at roughly $TBP \cdot 0{\cdot}7HX \cdot 3\,H_2O$. The aforementioned minimum in nitric acids' water curve, for which the densities of the equilibrium organic solutions are known up to about 5 M_a HNO_3,(15) occurs when the composition of the organic phase is close to $TBP \cdot HNO_3 \cdot \frac{1}{3}\,H_2O$. The exact ratio of HNO_3 to TBP at the minimum water content is actually 1·2.(13)

In previous work(1) most of the univalent electrolytes tested approached a 1:1 TBP–electrolyte composition in the organic phase, nitric acid alone exceeding this ratio. Here the polyvalent phosphoric acid to TBP ratio was ~ 1 at 9 M H_3PO_4 in the equilibrium aqueous phase, rose to 2:1 at 13·6 M_a, and continued to increase rapidly. This indicates polymerization in the organic phase at the higher acidities. Other evidence will be given in a later section. The maximum ratio obtained here was four, at an equilibrium aqueous phase H_3PO_4 concentration of 16 M. Polymerization increased and the distribution ratio rose rapidly since the limiting condition in the aqueous phase was being approached, that is, anhydrous phosphoric acid which was miscible with TBP.

The extraction of nitric acid by TBP up to as much as 2½ HNO_3 molecules per TBP has been previously noted by ALCOCK *et al.*(13) TUCK(15) has postulated addition of the extra nitric acid molecules to the P–O–C oxygen atoms. KORPAK and DEPTULA,(16) in presenting evidence for the formation of the complexes TBP·HNO_3, TBP·$2HNO_3$, TBP·$3HNO_3$, and possibly TBP·$4HNO_3$, have made the same suggestion. Such a bonding arrangement would appear to be consistent with the observed viscosities of the organic solutions. As shown by HESFORD and McKAY,(2) the viscosity increased very little, in fact beyond 1 M_0 HNO_3 decreasing until at 5 M_0 it was the same as the viscosity of monohydrated TBP itself.

---

(11) D. G. TUCK, *J. Chem. Soc.* 3202 (1957).

(12) D. G. TUCK and R. M. DIAMOND, *J. Phys. Chem.* 65, 193 (1961).

(13) K. ALCOCK, S. S. GRIMLEY, T. V. HEALY, J. KENNEDY and H. A. C. MCKAY, *Trans. Faraday Soc.* 52, 39 (1956).

(14) S. SIEKIERSKI and R. GWOZDZ, *Nukleonika* 5, 205 (1960).

(15) D. G. TUCK, *J. Chem. Soc.* 2783 (1958).

(16) W. KORPAK and C. DEPTULA, *Nucleonika* 5, 63 (1960).

The extraction of phosphoric acid by TBP is a somewhat different case in that the TBP is contacting an inorganic relative which also has a phosphoryl group. Its dative bonded P → O provides the opportunity for hydrogen bonding by an additional phosphoric acid molecule: at the higher acidities this results in several phosphoric acid molecules being associated with each TBP molecule. Furthermore, cross linkages must be present since the structure of liquid phosphoric acids is known to consist of a complicated hydrogen bridge system.(17) The water curve, Fig. 2, though, does lead one to suspect that by the time the 1:1 ratio of TBP to H_3PO_4 has been attained the phosphoric acid is connected to the P → O of the TBP by a hydronium ion.

The acid extraction data in Table 1 have been recalculated on a molal basis and plotted in Fig. 3. Two straight lines result, the one of steeper slope lying between 1 and 7 molal in the aqueous phase having the equation:

$$m_o = -0{\cdot}17+0{\cdot}295\,m_a$$

where m_0 and m_a are moles H_3PO_4 per kg of TBP in the organic phase and moles H_3PO_4 per kg H_2O in the aqueous phase, respectively. The other, above 7 m_a, is linear out to nearly 100 molal and bears the relationship:

$$m_o=0{\cdot}75+0{\cdot}157m_a$$

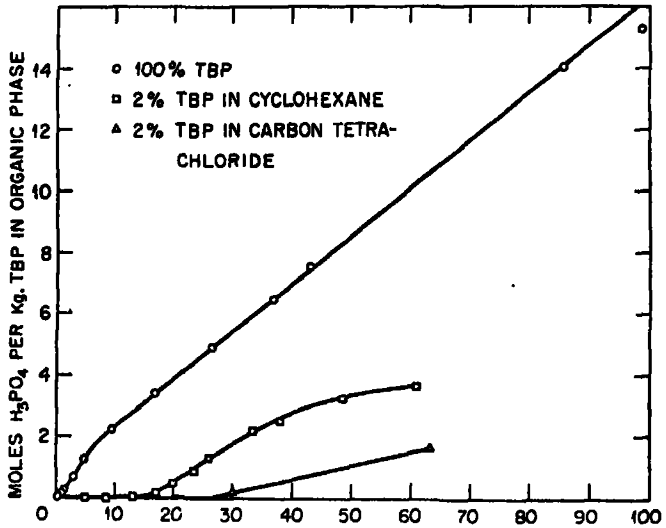

FIG. 3.—The distribution of H_3PO_4 between TBP and water.

The difference in slopes in Fig. 3 suggests that perhaps differences in extraction mechanism exist in the two regions covered. The intersection of the lines occurs at 1·8 molal H_3PO_4 in the organic phase, representing a mole ratio of H_2PO_4 to TBP of 0·5. From Fig. 2 it can be seen that this point is essentially the boundary between the region where the H_3PO_4 is highly hydrated and that in which only the one water molecule per TBP is tolerated. The steeper sloped line covers the region where the multihydrated H_3PO_4 is extracted. The lesser sloped line, which covers the bulk of the plot, applies to the region in which compound formation between TBP and the phosphoric acid is probable. In phosphoric acid, then, we have a specimen apparently exhibiting both the Class I and Class II properties previously mentioned,(1) i.e., behaviour strongly affected by hydration (up to 1·2 *m* in the organic phase), and specific TBP–acid complex formation (above 3·4 *m*), respectively. The stipulation in the latter case here is that a molecule of water is involved regardless of the number of phosphoric acid molecules in the polymer, presumably as a hydronium ion bridge between the TBP and the first phosphoric acid molecule in the chain.

---

(17) J. R. VAN WAZER, *Phosphorus and Its Compounds*; *Chemistry*, Vol. 1, p. 489. Interscience, New York (1958).

Additional evidence of two different extraction mechanisms was found by extracting at different temperatures solutions representative of each region in Fig. 3. When stock solutions of 2·92 M and 15 M H_3PO_4 were extracted with TBP at 2, 25 and 55° C the distribution co-efficient for the sample in the multi-hydrated H_3PO_4 region varied considerably, being 0·33, 0·23 and 0·14, respectively. In the region 2 case, on the other hand, the distribution co-efficient was totally unaffected, remaining at 0·37 over the temperature span tested. The bonds in the concentrated region are thus found to be stronger than those in the dilute range. Water analysis divulged the information that the region 2 sample likewise was unaltered from the 1:1 TBP–H_2O ratio at the temperatures of the test, but the water content of the region 1 sample was affected greatly by temperature. At 55° the ratio was one. At 2° the water to TBP ratio was 1·30, considerably less than the ratio obtained when an equivalent amount of H_3PO_4 was extracted at 25° C, and not greatly different than the 1·2 H_2O's/TBP found for TBP saturated with water at 0° C. The water curve at the low temperature is at least displaced, while at 55° it appears to have flattened.

The effect of a change in diluents on the extraction of H_3PO_4 by TBP was obtained using 12 M stock H_3PO_4 and 2 per cent (by volume) solutions of TBP in carbon tetrachloride, hexane, cyclohexane, dibutyl ether and methyl ethyl ketone. The equilibrium organic phase acid concentrations were 0·003 M, 0·034 M and 0·036 M when the equilibrations were made with TBP in carbon tetrachloride, hexane, and cyclohexane, respectively—while the diluents alone extracted no acid. TBP in dibutyl ether extracted the most and was 0·46 M, but dibutyl ether alone accounted for over half of this value, being 0·25 M in H_3PO_4 when no TBP was present. Methyl ethyl ketone was miscible with the 12 M H_3PO_4. The oxygen-containing solvents such as ethanol,(18) butanol, ethyl acetate and acetone,(19) oxygenated cycloparaffins(20) and ketones, esters and ethers(21) have all been used as solvents in the commercial production and purification of phosphoric acid. The distribution of phosphoric acid between water and ether has also been reported.(22, 23) A detailed survey of solvents and extraction processes for phosphoric acid has been published by Doumas.(24)

(18) P. J. Fox, *J. Industr. Engng. Chem.* **6**, 828 (1914).

(19) J. H. Gravell, U.S. Pat. 1499611 (1924). *Chem. Abstr.* **18**, 2790 (1924).

(20) C. A. Vana, U.S. Pat. 1968544 (1934). *Chem. Abstr.* **28**, 5937 (1934).

(21) C. H. Keller, U.S. Pat. 1981145 (1934). *Chem. Abstr.* **29**, 559 (1935).

(22) M. Bachelet, E. Cheylan and J. Le Bris, *J. Chim. Phys.* **44**, 302 (1947).

(23) B. Helferich and U. Baumann, *Ber. Dtsch. Chem. Ges.* **85**, 461 (1952).

(24) B. C. Doumas, *Purification of Phosphoric Acid by Solvent Extraction*, p.p. 56–64. University Microfilms Ann Arbor, Mich. (1961).

Pronounced differences were found in the abilities of pure and diluted TBP to extract H_3PO_4. With a 2 per cent solution of TBP in cyclohexane E°_{a} increased from 2×10^{-6} at 4 M_a to 5×10^{-3} at 15 M_a (Table 3). This is more than a two thousandfold increase whereas with pure TBP E°_{a} rose only from 0·26 to 0·37 over this same concentration range. In Fig. 3 is shown the extraction behaviour of TBP alone and diluted with cyclohexane and carbon tetrachloride. An aqueous phase molality of 16 is necessary before the 2 per cent TBP in cyclohexane begins to extract the H_3PO_4 appreciably, while 27 *m* is required for the same concentration of TBP in CCl_4. The difference in pure and diluted TBP's extracting ability must be a result of the concentration change, since in a diluent the TBP molecules are much fewer and farther apart, combined with a decrease in polarity in the organic phase. The poorer extraction obtained when TBP is dissolved in carbon tetrachloride instead of cyclohexane is probably attributable to the effect of the diluent in altering the polarity of the phosphoryl group.

TABLE 3.—EXTRACTION OF H_3PO_4—^{32}P BY 2% TBP IN CYCLOHEXANE, $t = 25°$ C

H_3PO_4 concentration (M)		
Aqueous phase	Organic phase	E°_{a}
4·02	8×10^{-6}	2×10^{-6}
6·00	$8{\cdot}4 \times 10^{-5}$	$1{\cdot}4 \times 10^{-5}$
7·62	$3{\cdot}60 \times 10^{-4}$	$4{\cdot}7 \times 10^{-5}$
8·02	$6{\cdot}53 \times 10^{-4}$	$8{\cdot}14 \times 10^{-5}$
9·20	$3{\cdot}59 \times 10^{-3}$	$3{\cdot}90 \times 10^{-4}$
10·0	$9{\cdot}57 \times 10^{-3}$	$9{\cdot}57 \times 10^{-4}$
11·3	$2{\cdot}64 \times 10^{-2}$	$2{\cdot}34 \times 10^{-3}$
12·5	$4{\cdot}34 \times 10^{-2}$	$3{\cdot}47 \times 10^{-3}$
13·1	$5{\cdot}05 \times 10^{-2}$	$3{\cdot}85 \times 10^{-3}$
14·9	$7{\cdot}28 \times 10^{-2}$	$4{\cdot}89 \times 10^{-3}$

From Fig. 3 it is evident that the H_3PO_4:TBP ratio did not exceed 1 in the dilute TBP solutions. With cyclohexane as diluent the H_3PO_4 concentration levelled off at 3·64 mole per kg TBP, very close to the 1:1 complex. The extraction of TBP from a 2 per cent solution in cyclohexane by phosphoric acid solutions was negligible over the range shown in Fig. 3, although anhydrous H_3PO_4 removed all the TBP from the diluents.

The usual method of determining the species extracted is to obtain the slope of a log–log plot of E°_{a} vs. TBP concentration, keeping the aqueous phase at a constant composition.(25) Normally the plot holds good up to 5 or 10 volume per cent TBP before deviations occur. However, from Fig. 4, in which values of E°_{a} resulting from the extraction of 13·1 M H_3PO_4—^{32}P stock solution by TBP in cyclohexane are plotted over the range 0·2–100 per cent TBP, it appears that the complex here extracted depends on the amount of TBP present. The slope over the range 0·2–0·4 per cent TBP is 3·4, from 0·8 to 4 per cent it is 1·6 to 1·4, and from 9 to 100 per cent it is 1·04. The organic phase was saturated with one H_3PO_4 molecule per TBP at 9·27% TBP, increasing somewhat above 1:1 at 20 and 100% TBP, the resultant aqueous phase concentrations being 13·0, 12·9 and 11·9 M, respectively. The other aqueous acidities remained at 13·1 M.

(25) T. V. HEALY and H. A. C. MCKAY, *Rec. Trav. Chim.* **75**, 730 (1956).

The solvation numbers for a multitude of metal–TBP complexes have been established(26) and good evidence of 1:1 species of HNO_3(25, 15), HCl, etc(2) has also been presented. The charge distribution on the cation is uniform in these instances, however, whereas phosphoric acid has three hydrogen atoms, all ionizable to different degrees.

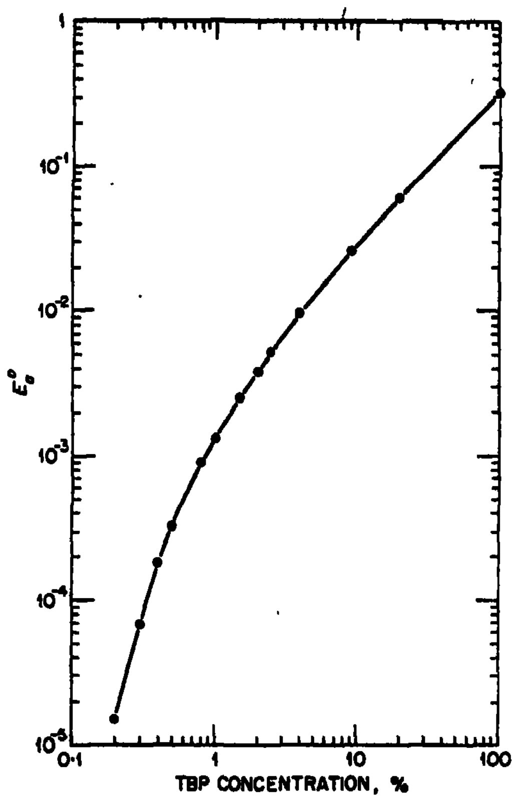

Fig. 4.—Variation in distribution co-efficient as a function of TBP concentration in cyclohexane. Initial aqueous phase H_3PO_4 concentration was 13·1 M.

The extraction of a higher concentration solution of H_3PO_4–^{32}P (15 M) as a function of TBP concentration in cyclohexane (Table 4) led to the formation of a third phase, between the aqueous and cyclohexane phases, when the TBP concentration was 4–35+ per cent. The TBP to H_3PO_4 ratio in the third phase over this range was 1:2, the same as in 100% TBP after contact with 15 M H_3PO_4. Upon raising the temperature the third phase disappeared at 40° C.

Molecular weight determinations were made on anhydrous phosphoric acid-TBP mixtures of varying mole proportions in the hopes that some clue as to a preferred species might be obtained. The mixtures weren't sufficiently stable in boiling cyclohexane or soluble enough when the H_3PO_4 to TBP ratio was greater than one; however, when mixtures of ratios 1·5–3 were extracted with cyclohexane at temperatures of 10–55° C the material recovered from the cyclohexane phase had the composition of roughly one H_3PO_4 molecule per TBP.

---

(26) See for example Reference 25; D. F. Peppard, J. P. Faris, P. R. Gray and G. W. Mason, *J. Phys. Chem.* 57, 294 (1953); D. Scargill, K. Alcock, J. M. Fletcher, E. Hesford and H. A. C. McKay, *J. Inorg. Nucl. Chem.* 4, 304 (1957); H. A. C. McKay and T. V. Healy, *Progress in Nuclear Energy, Series III, Process Chemistry*, (Edited by F. R. Bruce, J. M. Fletcher and H. H. Hyman), Vol. 2, pp. 551–552. Pergamon Press, New York, London, Paris, Los Angeles (1958).

TABLE 4.—EXTRACTION OF H_3PO_4—^{32}P FROM 15 M H_3PO_4—^{32}P AT VARIOUS TBP CONCENTRATIONS IN CYCLOHEXANE $t = 25°$ C

TBP concn. (vol. %)	Third phase volume (% of total)	Equilibrium H_3PO_4 concentrations (M) Organic phase	Third phase	Aqueous phase	E°_{a}
0	0	0	0	15·0	0
0·5	0	0·0068	0	14·9	0·00046
1·0	0	0·0285	0	14·9	0·00191
1·5	0	0·0514	0	14·9	0·00345
2·0	0	0·0780	0	14·9	0·00523
2·5	?	0·0864	?	14·9	0·00580
4·0	2·5*	0·0935	—	14·9	0·00628†
9·3	8·1*	0·118	3·32	14·8	0·00797†
20·0	21*	0·155	3·12	14·8	0·0105†
35·0	42*	0·260	2·69	14·5	0·0179†
50·0	0	2·84	0	14·4	0·197
100	0	5·12	0	13·7	0·374

* Third phase miscible with organic phase at 40° C.

† Moles H_3PO_4/l. in lighter org. phase ÷ moles H_3PO_4/l. in aq. phase.

Ether was then used as the solvent for the molecular weight determinations by boiling point elevation. TBP, used as standard, behaved ideally over the range tested (0·2–1·5 g solute per 30 ml ether) while increasing association manifested itself as the mole per cent of phosphoric acid increased. Molecular weights at the upper limit of 1·5 g of mixture per 30 ml ether increased from the 266 of the TBP to 330, 360, 420, 480, 510 and 570 for solutions of H_3PO_4 in TBP of 25, 33·3, 50, 66·7, 75 and 100 mole per cent H_3PO_4, respectively. Similar behaviour previously was noted by KOSOLAPOFF and POWELL(27) when determining molecular weights of organophosphonic acids cryoscopically in naphthalene. They found the molecular weight to exceed that of a hexamer and to still be rising at the higher concentrations. Dibasic organophosphoric acids polymerized in like manner in naphthalene.(28) Our ebullioscopically determined values, which varied directly with the concentration over the range studied, all fell within the molecular weight region of 265–300 when extrapolated to infinite dilution. It thus appeared that the phosphoric acid behaved as a trimer at infinite dilution in ether, and no specific complex between TBP and anhydrous phosphoric acid was detected by the ebullioscopic method of molecular weight determination.

(27) G. M. KOSOLAPOFF and J. S. POWELL, *J. Chem. Soc.* 3535 (1950).

(28) D. F. PEPPARD, J. R. FERRARO and G. W. MASON, *J. Inorg. Nucl. Chem.* 7, 231 (1958).

The refractivity of solutions comprised of two substances in varying mole proportions in a diluent(29) and of mixtures of the pure substances themselves(30) has been used to demonstrate hydrogen bonding and to indicate the resultant species. In Table 5 are listed the refractive indices of anhydrous mixtures of H_3PO_4 and TBP. The refractive index increased linearly from 1·4225 (pure TBP) to 1·4314 at 66·7% H_3PO_4, then curved rapidly up to the value of 1·4508 at 100% H_3PO_4. The maximum deviation between the observed refractive indices and those calculated from either the Gladstone and Dale(31) or Lorenz and Lorentz(31) refractivities occurred at 66·7 mole per cent H_3PO_4 (Table 5). The values obtained from the empirical Gladstone and Dale mixture rule are listed because they were closer to the observed refractivities. As noted by HOLMES,(32) the maximum deviation between observed and calculated refractive indices corresponded to the greatest change in volume on mixing, in this case as shown by the difference in calculated and observed densities (Table 5, column 4). Calculating the refractivity differences by other methods, however, caused the maximum deviation in (*n* obs.–*n* calc.) to occur at different mole fractions of H_3PO_4.

TABLE 5.—DENSITY AND REFRACTIVE INDEX OF ANHYDROUS H_3PO_4–TBP SOLUTIONS AT 25° C

Mole % H_3PO_4	Density (g/ml)			n_D^{25}		
	Observed	Calc.*	Diff.	Observed	Calc.†	Diff.
0	0·9722			1·4225		
25·0	1·031	1·026	0·005	1·4258	1·4263	−0·0005
33·3	1·057	1·050	0·007	1·4270	1·4277	−0·0007
50·0	1·126	1·116	0·010	1·4287	1·4307	−0·0020
66·7	1·233	1·220	0·013	1·4314	1·4347	−0·0033
75·0	1·306	1·299	0·007	1·4337	1·4350	−0·0013
80·0	1·367	1·361	0·006			
84·3	1·424			1·4371	1·4361	0·0010
90·0	1·540	1·539	0·001	1·4404	1·4406	−0·0002
91·4				1·4415		
95·2	1·680	1·681	−0·001	1·4448	1·4445	0·0003
100·0	1·868			1·4508		

* Calculated assuming no volume change.

† From the Gladstone and Dale mixture rule, (31).

The results of simple viscometric measurements on the anhydrous H_3PO_4–TBP mixtures have been plotted in Fig. 5. The viscosity increased slowly up to 33% H_3PO_4, then rapidly increased to the maximum of 630 cpoise at 75% H_3PO_4, almost thrice the viscosity of liquid 100% H_3PO_4 itself. The values obtained can be considered only approximate due to the type of apparatus employed and the use of a single standard in calculating viscosities of vastly different magnitude. Nonetheless, the results for TBP, dibutyl phosphoric acid, and H_3PO_4—3·7, 70 and 226 cpoise, respectively—are not unreasonably different than the reported results of 3·422,(33) 71 (at 20° C),(28) and 200 cpoise (by graphical interpolation).(34)

---

(29) F. M. ARSHID, C. H. GILES, E. C. MCLURE, A. OGILVIE and T. J. ROSE, *J. Chem. Soc.* 67 (1955).

(30) N. A. PUSCHIN and P. G. MATAVULJ, *Z. Phys. Chem.* A **158**, 290 (1932); N. A. PUSHIN, P. MATAVULJ, I. I. RIKOVSKI and M. NENADOVIC, *Bull. Soc. Chim. Belgrade*, **11**, No. 3/4, 72 (1940–46), *Chem. Abstr.* **42**, 2167 (1948); N. A. PUSHIN, P. MATAVULJ and I. I. RIKOVSKI, *Bull. Soc. Chim. Belgrade*, **13**, 45 (1948), *Chem. Abstr.* **46**, 4298 (1952).

(31) J. R. PARTINGTON, *An Advanced Treatise on Physical Chemistry*; *Physico-Chemical Optics*, Vol. 6, p. 72. Longmans, Green, London, New York, Toronto (1953).

(32) J. HOLMES, *J. Chem. Soc.* **103**, 2165 (1913); **107**, 1471 (1915).

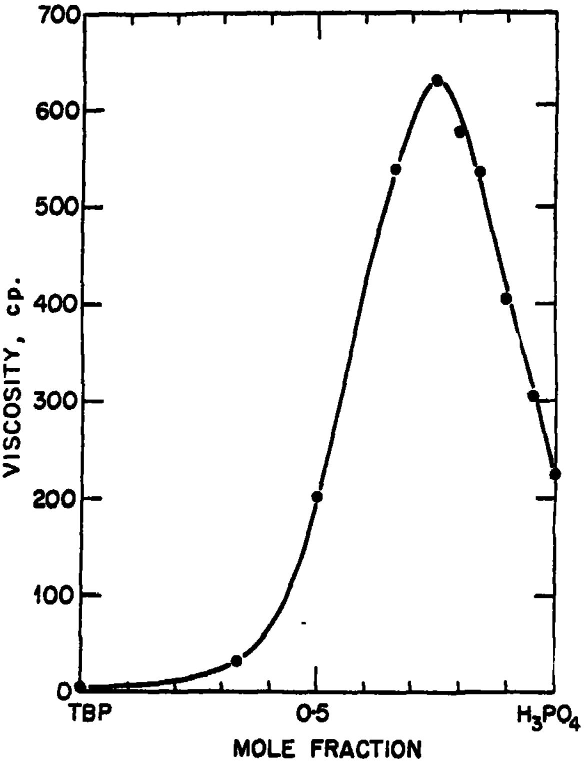

FIG. 5.—The viscosity of anhydrous TBP–H_3PO_4 solutions.

Monobutyl- and dibutyl phosphates, the partial esters of phosphoric acid, were tested and compared with the dry TBP–H_3PO_4 solutions of 66·7 and 33·3% H_3PO_4 respectively, said solutions having the same ratio of butoxy and hydroxy groups per phosphoryl group as do the corresponding partial esters. Monobutyl phosphate, $C_4H_9OP(O)(OH)_2$, has a density at 25° C of 1·226 g/ml and a refractive index of 1·4309 compared with 1·240 g/ml and n_D^{25} 1·4314 for the TBP–$2H_3PO_4$ solution. Dibutyl phosphate, $(C_4H_9O)_2P(O)OH$, at the same temperature has a density of 1·061 g/ml and n_D of 1·4268 compared with 1·057 g/ml and n_D^{25} of 1·4270 for the H_3PO_4·2TBP solution. The viscosity found for dibutyl phosphate, 70 cpoise, was about twice that of its corresponding mixture, but monobutyl phosphate's viscosity,

---

(33) D. P. EVANS and W. J. JONES, *J. Chem. Soc.* 985 (1932).

(34) J. R. VAN WAZER, *Phosphorus and its Compounds*; *Chemistry*, Vol. 1, p. 485. Interscience, New York (1958).

500 cpoise, was close to that of the TBP·$2H_3PO_4$ solution, 538 cpoise. Dibutyl phosphoric acid's viscosity can be attributed to the fact that it dimerizes,(7, 28, 35) thus exhibiting more structure than the 2TBP·H_3PO_4 solution. Monobutyl phosphoric acid, on the other hand, is a dibasic acid such as has been shown to readily polymerize.(27, 28) The TBP·$2H_3PO_4$ solution may be polymerized in such a fashion that its structure resembles that of monobutyl phosphoric acid.

Associated liquids have greater viscosities because of their hydrogen bonding.(36) The most association in the system reported here occurred at one TBP per three phosphoric acid molecules (Fig. 5). Although the ratio at which a maximum is found does not necessarily agree with the ratio of a known complex in the system investigated, as shown by ADDISON and SMITH,(37) the degree of deviation of the viscosity curve is nevertheless an indication of the amount of association. FERRARO and PEPPARD(38) have shown by the method of continuous variation, cryoscopically with benzene and by infra-red with cyclohexane, that TBP and mono-(2 ethylhexyl) phosphoric acid (H_2MEHP) form associated complexes having the ratio $(TBP)_2/(H_2MEHP)_6$ in benzene and $(TBP)_4/(H_2MEHP)_{12}$ in cyclohexane. While we cannot tell the number of units of each substance involved in the undiluted solutions of TBP and H_3PO_4, the basic ratio of one TBP to three acid units is likewise indicated by the viscosity curve. It may be of interest to note that in X-ray diffraction structure studies on anhydrous phosphoric acid four formula weights were found per unit cell of crystals.(39) The TBP·$3H_3PO_4$ ratio (four units total) giving the maximum viscosity may be a fortuitous circumstance. From the density and viscosity results it is evident, though, that the major interactions between TBP and anhydrous H_3PO_4 do occur at 67–75 mole per cent H_3PO_4.

(35) B. J. THAMER, *J. Phys. Chem.* **64**, 694 (1960).

(36) G. C. PIMENTEL and A. L. MCCLELLAN, *The Hydrogen Bond*, pp. 61–63. Freeman, San Francisco and London (1960).

(37) C. C. ADDISON and B. C. SMITH, *J. Chem. Soc.* 1783 (1960).

(38) J. R. FERRARO and D. F. PEPPARD, *J. Phys. Chem.* **65**, 539 (1961).

(39) J. R. VAN WAZER, *Phosphorus and Its Compounds; Chemistry*, Vol. 1, p. 486. Interscience, New York (1958).

J. Inorg. Nucl. Chem., 1962, Vol. 24, pp. 429 to 439. Pergamon Press Ltd. Printed in England

COMPARATIVE LIQUID–LIQUID EXTRACTION BEHAVIOUR OF EUROPIUM (II) AND EUROPIUM (III)*

D. F. Peppard, E. P. Horwitz and G. W. Mason
Argonne National Laboratory, Argonne, Illinois

(*Received* 21 *September* 1961)

Abstract—The liquid–liquid extraction behaviour of Eu(II) into solutions of acidic phosphoric and phosphonic esters has been investigated both on a macro-scale and tracer-scale. The distribution ratio of Eu(II) was investigated as a function of extractant concentration in the organic phase and HCl concentration in the aqueous phase using β-active 13, 16 year $^{152,\,154}$Eu.

Advantage was taken of the large separation factors Pm(III)/Eu(II), Sm(III)/Eu(II), and Gd(III)/Eu(II) in effecting the mutual separation of ^{147}Pm and $^{152,\,154}$Eu, the high purification of ^{147}Pm with respect to $^{152,\,154}$Eu, and the enrichment, concentration and recovery in high yield of europium from a rare earth oxide containing 0·1 per cent Eu.

It is generally assumed that separation techniques involving more than a single oxidation state are rapid and yield pure products. Of those lanthanides which may exist in the dipositive oxidation state, europium(II) is the most readily obtained. Thus, several procedures for separating europium from other lanthanides are based on oxidation–reduction cycles. For example, the following procedures have shown varying degrees of effectiveness:

(1) reduction of Eu(III) by a mercury cathode or by amalgamated zinc followed by precipitation of $EuSO_4$ or $EuCl_2 \cdot 2H_2O$, (2) direct reduction of Eu(III) to a metal amalgam by either sodium amalgam or electrolysis at a mercury cathode or lithium amalgam cathode, and (3) reduction of Eu(III) with zinc powder followed by precipitation of the lanthanides(III) as hydroxides with conc. NH_4OH.(1)

However, all of these procedures suffer from one or more difficulties due to:

(1) mechanical complications attendant upon multiplication of the separation effect, (2) carrying lanthanides(III) on Eu(II) solid or vice versa, and (3) incomplete reduction at low concentrations of Eu.

All but the last of these phenomena may, in principle, be eliminated by effecting the separation by liquid–liquid extraction.

---

* Based on work performed under the auspices of the U.S. Atomic Energy Commission.

(1) a. R. C. Vickery, *Chemistry of the Lanthanons*. Academic Press, New York (1953);
b. D. M. Yost, H. Russell and C. S. Garner, *The Rare Earth Elements and their Compounds*. J. Wiley, New York (1947);
c. P. C. Stevenson and W. E. Nervik, *The Radiochemistry of the Rare Earths, Scandium, Yttrium, and Actinium*. Nuclear Science Series NAS–NS3020, National Research Council, National Academy of Sciences (1961).

The use of acidic phosphoric and phosphonic esters in a carrier diluent as extractants for lanthanides(III)[(2-3)] and Ca(II), Sr(II), and Ba(II)[(4)] has been studied. It was found that the distribution ratio for a lanthanide(III) exceeds that for Ca(II), Sr(II), and Ba(II) by a factor of 10^4–10^7 depending upon which lanthanide(III) and alkaline earth ions are involved. Since Eu(II) behaves more like a heavy alkaline earth ion than a lanthanide(III) ion,[(1)] particularly with respect to complexing ability, one would expect a liquid–liquid extraction technique, using acid phosphoric and phosphonic esters, to be applicable to the separation of Eu(II) from lanthanides(III).

However, in order to achieve a high purification of a given lanthanide with respect to europium or in order to apply the separation technique to tracers, one must be able to reduce Eu(III) and maintain it as Eu(II) at concentrations as low as 10^{-10} M. Consequently, assuming that a system exists in which the organic solvent differentiates strongly in favour of lanthanides(III) as opposed to Eu(II), the over-all problem of separating Eu(II) from lanthanides(III) is reduced, in its essentials, to the two problems of reducing Eu(III) to Eu(II) in high yield and preventing Eu(II) from oxidizing to Eu(III).

Thus, an investigation of the stabilization of Eu(II) at tracer concentration and an investigation of the extraction characteristics of both Eu(III) and Eu(II) in several liquid–liquid extraction systems were undertaken.

EXPERIMENTAL

Nomenclature

Throughout this discussion, HDGP represents a general orthophosphoric acid diester, $(GO)_2PO(OH)$, and HG[G′P] represents a general phosphonic acid ester (GO)G′PO(OH), in which G and G′ are generalized organic groups, D signifies di and H represents an ionizable hydrogen. G′ is linked to the P by a C–P bond.

The specific extractants utilized in this investigation, with their symbolic representations are: di(2-ethyl hexyl) orthophosphoric acid, $[2\text{-}(C_2H_5)C_6H_{12}O]_2PO(OH)$, HDEHP; di-para-(1, 1, 3, 3-tetramethyl butyl) phenyl orthophosphoric acid, HDOϕP; 2-ethyl hexyl hydrogen phenyl phosphonate $[2\text{-}(C_2H_5)C_6H_{12}O](C_6H_5)PO(OH)$, HEH[$\phi$P]; and n-octyl hydrogen chloromethyl phosphonate, $(C_8H_{17}O)(ClCH_2)PO(OH)$, Hn-O[ClMP].

Since the HDGP and HG[G′P] esters are dimeric[(5-7)] and appear to function as mono-ionized dimers in the extractions studied, the ionization of the extractants may be generalized as $(HY)_2$ yielding $H^+ + HY_2^-$.

The distribution ratio, K, of a specific nuclide is defined as the concentration of nuclide in the upper divided by the concentration of nuclide in the lower of two mutually equilibrated sensibly-immiscible liquid phases, the upper phase in this study being the organic, as opposed to the aqueous, phase. The separation factor, β, is defined for two solutes A and B as K_A/K_B.

Source of materials

Each of the (GO)G′PO(OH) compounds was prepared by hydrolysis of $(GO)_2G'PO$. The neutral esters, bis (2-ethyl hexyl) phenyl phosphonate and bis (2-ethyl hexyl) chloromethyl phosphonate, were obtained from Victor Chemical Works. Each of the phosphoric esters studied was obtained in a mixture of the mono-ester and di-ester containing variable

---

(2) D. F. Peppard, G. W. Mason, J. L. Maier and W. J. Driscoll, *J. Inorg. Nucl. Chem.* **4**, 334 (1957).

(3) D. F. Peppard, G. W. Mason, I. Hucher, *J. Inorg. Nucl. Chem.* **18**, 245 (1961).

(4) D. F. Peppard, G. W. Mason, S. McCarty and F. D. Johnson, *J. Inorg. Nucl. Chem.* To be published.

(5) D. F. Peppard, J. R. Ferraro and G. W. Mason, *J. Inorg. Nucl. Chem.* **12**, 60 (1959).

(6) D. F. Peppard, J. R. Ferraro and G. W. Mason, *J. Inorg. Nucl. Chem.* **4**, 371 (1957).

(7) D. F. Peppard, J. R. Ferraro and G. W. Mason, *J. Inorg. Nucl. Chem.* **7**, 231 (1958).

quantities of pyro esters, neutral orthoesters, and free alcohol. Both of the phosphoric ester mixtures, the 2-ethyl hexyl and the p-octyl phenyl, i.e. para (1, 1, 3, 3-tetramethyl butyl) phenyl, were obtained from Victor Chemical Company.

The β active nuclides, 2·6 year ^{147}Pm, and (13, 16 year) ^{152,154}Eu were obtained from the Isotopes Division of the Oak Ridge National Laboratory. α-active ^{241}Am was obtained from A.N.L. stocks. The ^{147}Pm and ^{241}Am tracers were repurified by liquid–liquid extraction techniques.

Samples of Eu_2O_3 (98 per cent) and of a rare earth oxide containing essentially Sm and Gd, together with small amounts of other lanthanons, were obtained from Lindsay Rare Earth Chemical Division of American Potash and Chemical Corporation.

The HCl and NaCl were purified as described previously.(8) Baker Analysed Reagent chromium(III) chloride hexahydrate was used as a source of Cr(III). (The salt was green and thus presumably contained Cr largely in the form of $CrCl^+$ ion.) Mallinckrodt Analytical Reagent 30 mesh zinc was used to make the zinc amalgam. All other reagents employed were analytical reagent grade.

Liquid Carbonic Corporation high purity nitrogen (99·9 per cent N_2) was used as a source of nitrogen for all experiments.

Preparation and purification of extractants

The preparation and purification of n-octyl hydrogen chloromethyl phosphonate, Hn-O[ClMP], and 2-ethyl hexyl hydrogen phenyl phosphonate, HEH[ϕP], have been described previously.(4, 5) The purification of bis[para(1,1,3,3-tetramethyl butyl) phenyl] phosphoric acid, i.e. di(octyl phenyl) phosphoric acid, HDOϕP, and bis (2-ethyl hexyl) phosphoric acid, i.e. di octyl phosphoric, HDEHP, has also been described previously.(9)

Preparation of zinc amalgam

Amalgamation of zinc was accomplished by washing 30 mesh zinc for 1 min in sufficient 1 M hydrochloric acid to cover it, followed by adding the proper amount of $HgCl_2$ solution to give 0·5 per cent by weight of mercury and stirring for 3 min.(10) The resultant amalgam was washed successively with three portions of water and stored under 0·05M HCl. In no case was the amalgamated zinc stored for more than 8 hrs.

Determination of distribution ratios

Following separation of the mutually equilibrated liquid phases, the distribution ratio, *K*, was determined radiometrically by evaporating aliquots of each phase on 3 mil platinum disks 1⅜ in. in diameter, by means of induction-heating, for β- and α-counting. In instances in which ^{241}Am was used as an internal normalizing nuclide, the beta activity was counted through 10 mg of aluminium absorber. (A correction of 13 counts/min per 10^3 counts/min of ^{241}Am was still required.)

All equilibrations and centrifugations of phases, transfer of solutions and withdrawal of aliquots were performed in the presence of nitrogen. In the acid and solvent dependency determinations, the aliquot of aqueous phase was titrated with standard 0·0100 M NaOH, using bromthymol blue indicator, in order to obtain the acidity of the aqueous phase at equilibrium.

In each experiment involving an aqueous phase with salt content, a 0·5 ml portion of the separated aqueous phase was contacted with a 0·5 ml portion of 0·2 F Hn–O[ClMP] in toluene in the presence of air. The 0·2 F Hn-O[ClMP] extracts Eu(III) with a *K* in excess of 10^3 from each of the salt phases investigated. Consequently, the analysis of an aliquot of the 0·2 F Hn-O[ClMP] is equivalent to the analysis of an identical aliquot of the equilibrated aqueous phase.

---

(8) D. F. Peppard, G. W. Mason and S. McCarty, *J. Inorg. Nucl. Chem.* **13**, 138 (1960).

(9) D. F. Peppard, G. W. Mason, W. J. Driscoll and R. J. Sironen, *J. Inorg. Nucl. Chem.* **7**, 276 (1958).

(10) H. W. Stone and D. N. Hume, *Industr. Engng. Chem.* **11**, 598 (1939).

Separations

The separation of ^{152,154}Eu from ^{147}Pm and the separation of gross europium from gross rare earths were performed with the same apparatus and under essentially the same conditions as employed in the determination of the distribution ratios, except that three equilibration assemblies were used simultaneously.

In the separation of ^{152,154}Eu and ^{147}Pm, the β-activity was counted first without an absorber and then through 60 mg of aluminium absorber. The 60 mg aluminium absorber lowered the contribution of ^{147}Pm sufficiently to permit the detection of ^{152,154}Eu alone, after a small correction. Once the contribution of ^{152,154}Eu to the total activity was established, the activity due to ^{147}Pm was obtained by difference.

For the assay of gross rare earths, the metal content of the organic phase was returned to an aqueous phase by re-extraction into 5 M HCl. The re-extract and the pertinent aqueous phase were analysed by the spectroscopic copper-spark technique of FRIED *et al.*(11) In some instances, in order to increase the sensitivity of assay, a product was subjected to further extractions in order to concentrate the metal content. The per cent yield of Eu in the experiment involving gross rare earths was determined by performing a separate experiment under the same conditions using ^{152,154}Eu, together with gross rare earths, and using radiometric assay.

Apparatus and procedure

The apparatus used for measuring distribution ratios and performing separations is shown in Fig. 1. Tube *A* is a modified centrifuge tube and *G* is a modified syringe.

The general procedure used for measuring distribution ratios and performing separations was the following: Amalgamated zinc was placed in Tube *A*. The tube was then flushed with N_2 for 5 min by opening stopcocks *C* and *D*. (The N_2 was first passed through a gas washing bottle containing toluene or xylene and 0·05 M HCl in order to reduce evaporation of the aqueous and organic phases.) The aqueous solution was transferred to tube *A* by first attaching a pipette to the Tygon tube connexion *E*, opening stopcock *F*, and then flushing the pipette for one minute. The pipette was then inserted into the beaker or flask containing the aqueous solution so that the tip of the pipette was almost touching the bottom of the container. The flow of nitrogen through the pipette was regulated by stopcock *F*. After two minutes of bubbling N_2 through the solution, stopcock *F* was closed while holding the tip of the pipette in the solution. The solution was then drawn into the pipette by means of syringe *G*. With stopcock *C* opened and stopcock *D* closed, plug *B* was removed and the pipette introduced into tube *A*. After expelling the solution, the pipette was removed, plug *B* replaced and stopcock *C* closed.

The aqueous phase and Zn(Hg) were mixed for 2 min, by shaking manually, before the organic phase or feed was introduced in order to reduce Cr(III) to Cr(II) and in order to allow time for Cr(II) to scavenge traces of oxygen.

The organic solution, which served as the feed in separation experiments, was introduced into tube *A* by using the same procedure as described for the aqueous phase. After expelling the organic solution from the pipette, the pipette was removed, plug *B* replaced, stopcock *C* closed, and the N_2 tubing, which was connected to stopcock *C*, removed.

Equilibration of phases was achieved through manual shaking. Phase disengagement was facilitated by placing the apparatus in a clinical centrifuge and centrifuging at a low speed for 30 sec.

The N_2 tube was connected to stopcock *C* after centrifuging. The organic phase was withdrawn from Tube *A* by attaching a new pipette at connection *E* and flushing the pipette for 1 min with N_2. Then with stopcock *F* open, stopcock *C* was opened, and plug *B* removed. After the pipette was inserted into tube *A*, stopcock *F* was closed, and the organic phase drawn into the pipette. A similar procedure was used to remove the aqueous phase.

RESULTS AND DISCUSSION

The stabilization of Eu(II) and determination of its distribution ratio

The ease in maintaining europium in the di-positive oxidation state was found to increase with increasing concentration of Eu(II) in the system. Little difficulty was encountered in maintaining europium in the reduced state at concentrations of ten millimolar and higher. The removal of atmospheric and dissolved oxygen was sufficient to prevent Eu(II) from oxidizing in 0·05 M HCl for a period of 10–15 min and probably longer, a period sufficiently long for completion of a distribution ratio determination or separation. However, procedures for working with 10^{-2} M Eu(II) were found to be completely inadequate for working with 10^{-10} M Eu(II).

---

(11) M. FRIED, N. H. NACHTRIEB and F. S. TOMKINS, *J. Opt. Soc. Amer.* 37, 279 (1947).

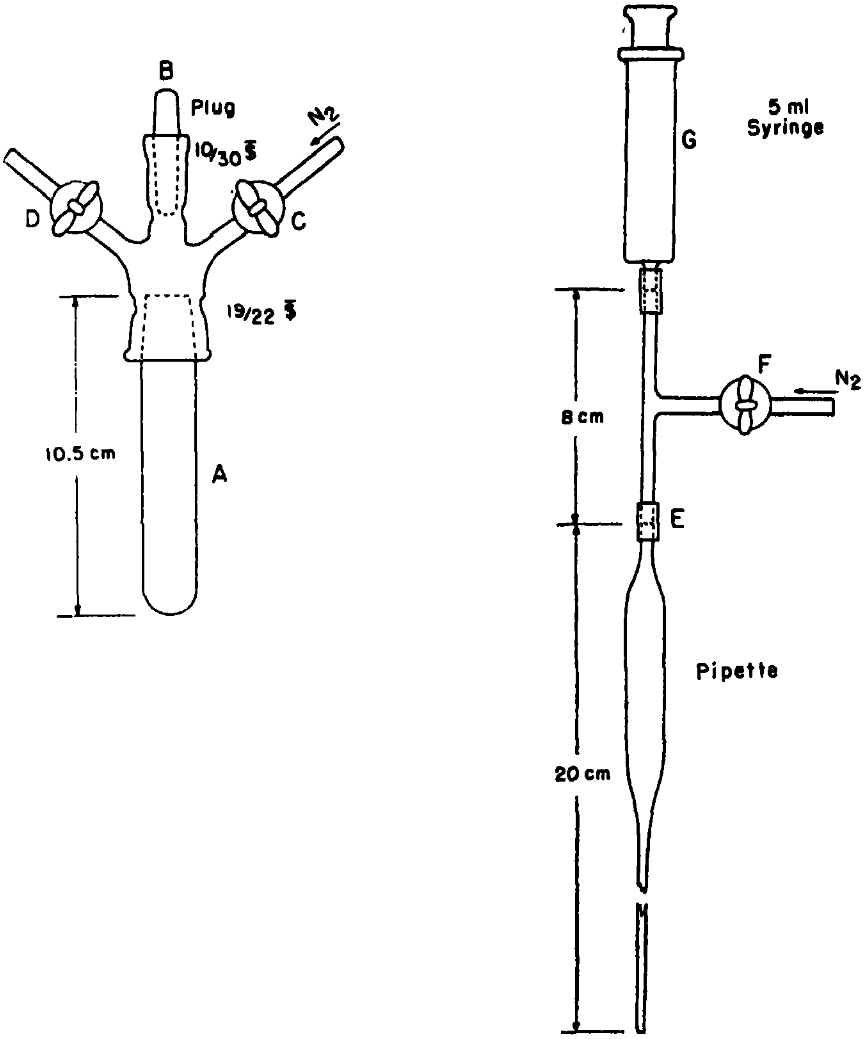

Fig. 1.—Apparatus for the study of tracer-level Eu(II).

The stabilization with respect to oxidation of Eu(II) at tracer scale concentrations (~ 10^{-10} M) during a liquid–liquid extraction was achieved by the following technique: (1) the solid reducing agent (amalgamated zinc) was placed in the extraction vessel and mixed with the aqueous and organic phases during equilibration, (2) high purity N_2 (99·95 per cent) was used to exclude air, and (3) the aqueous phase before equilibration was made 1–10 millimolar in Cr(III).

The solid zinc amalgam reduced both Cr(III) and Eu(III) to their divalent forms. The high purity N_2 excluded essentially all but traces of oxygen gas. The purpose of Cr(II), which was partially extracted into the organic phase during equilibration, was to scavenge as much as possible of dissolved and gaseous oxygen from the system. Since excess zinc amalgam was present, any Cr(II) which was oxidized by traces of oxygen (or any other oxidizing agent) was re-reduced to Cr(II). (If Cr(II) and/or Zn(Hg) is excluded from the solvent extraction system, then tracer Eu(II), added externally if Zn(Hg) is excluded, will be partially oxidized.)

Table 1 shows the distribution ratio of Eu(II), together with the separation factors of several tri-positive lanthanides and Am(III), for the system 0·40 F HEH[ϕP] in toluene, vs. aqueous 0·05 M HCl.

α-active ^{341}Am was used as an internal standard, and β-active $^{152, 154}$Eu was used to measure the *K* for europium radio-metrically. Two types of extractions were performed; a forward extraction in which Eu(III) and Am(III) were introduced into the aqueous phase prior to reduction, and a reverse extraction in which Eu(III) and Am(III) were present in the organic phase prior to reduction.

TABLE 1.—COMPARATIVE EXTRACTION DATA FOR M(III) AND Eu(II)

Organic: 0·40 F HEH[ϕP] in Toluene.
Aqueous: 0·05 M HCl, 0·001 M Cr(II), 0·5 g Zn (0·5% Hg)/ml Aq.
Equilibration time: 5 min.

Conc. of Eu in aq. phase	Type of extn.	$K_{Am(III)}$	$K_{Eu(II)}$	β, $K_{M(III)}/K_{Eu(II)}$
Tracer	Forward	1×10^2	$2{\cdot}6 \times 10^{-3}$	Am, $4{\cdot}2 \times 10^4$
10^{-4} *M*	Forward	1×10^2	$2{\cdot}0 \times 10^{-3}$	Pm, $9{\cdot}6 \times 10^4$
Tracer	Reverse	1×10^2	$3{\cdot}0 \times 10^{-3}$	Eu, $7{\cdot}5 \times 10^5$
10^{-4} *M*	Reverse	1×10^2	$2{\cdot}0 \times 10^{-3}$	Gd, $1{\cdot}5 \times 10^6$
			($2{\cdot}4 \times 10^{-3}$ av.)	

The large separation factors for lanthanide(III)/Eu(II) indicate the probable effectiveness of this system applied to separations.

Extractant and acid dependencies of Eu(II)

The Hn–O[ClMP] (in xylene) extractant and the HDOϕP (in xylene) extractant were used for the study of the acid and extractant dependencies of the distribution ratio of Eu(II), because they give much higher *K* values than either HEH[ϕP] or HDEHP. A relatively high distribution ratio of Eu(II) is essential in a dependency study, because it minimizes the error introduced by a small amount of Eu(III) in the Eu(II). For example, with a β value of $7{\cdot}5 \times 10^5$ for Eu(III)/Eu(II) and a *K* of $2{\cdot}4 \times 10^{-3}$ for Eu(II), only one part of Eu(III) in 10^3 parts of Eu(II) causes a 40 per cent error in the distribution ratio of Eu(II). However, if the *K* for Eu(II) is raised to $2{\cdot}4 \times 10^{-2}$, by use of a different extractant, then one part of Eu(III) in 10^3 parts of Eu(II) causes only a 4 per cent error in the distribution ratio of Eu(II).

The extractant and acid dependencies were measured using aqueous solutions of constant ionic strength and containing 0·001 M Cr(II) and 0·5 g Zn(0·5% Hg)/ml Aq. Figs. 2 and 3 show that, under the conditions studied, the distribution ratio is directly third-power dependent upon the concentration of extractant in the organic phase

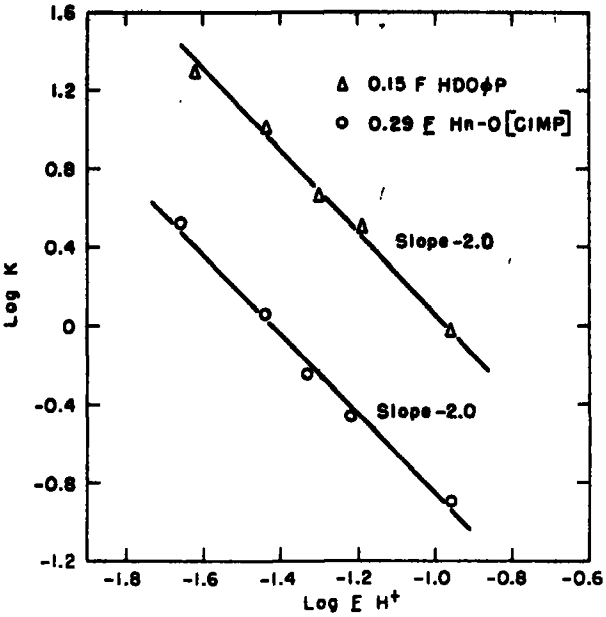

FIG. 2.—Hydrogen ion dependency of the extraction of Eu(II) into xylene solutions of HDOϕP and Hn–O[ClMP] from aqueous HCl+NaCl, 1 F Cl$^-$.

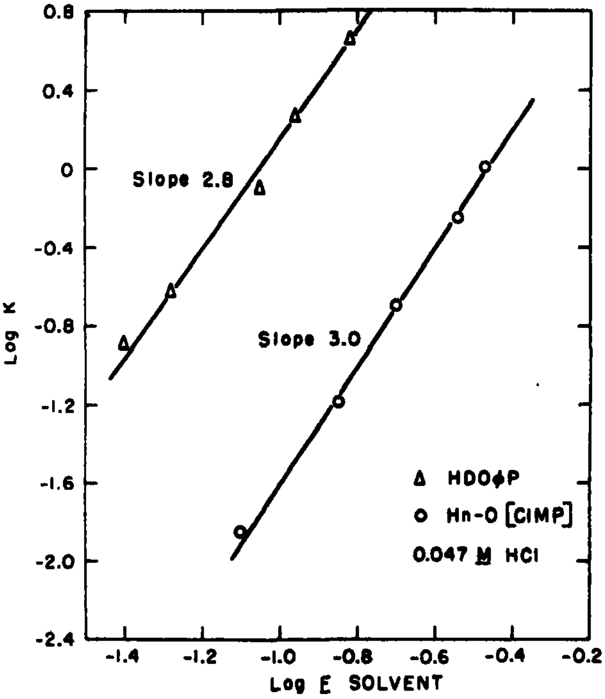

FIG. 3.—Extractant dependency of the extraction of Eu(II) into xylene solutions of HDOϕP and Hn–O[ClMP] from aqueous HCl+NaCl, 1 F Cl$^-$.

and inversely second-power dependent upon the concentration of H^+ in the aqueous phase. Thus, the mode of extraction is postulated as:

$$Eu^{2+}_A + 3(HY)_{2_o} \rightleftharpoons Eu(HY_2)_2(HY)_{2_o} + 2H^+_A \tag{1}$$

The distribution ratio is thus:

$$K_1 = k_1[(HY)_2]^3_o/[H^+]^2_A \tag{2}$$

where $(HY)_2$ represents a dimer of Hn–O[ClMP] or HDOϕP and HY_2^- represents a singly-ionized dimer of Hn–O[ClMP] or HDOϕP. A similar mode of extraction has been postulated for Ba(II).(4)

All of the above compounds have been studied previously as extractants for lanthanides(III).(2, 3) The K for a given lanthanide(III) was found to be directly third-power dependent upon the concentration of extractant, $(HY)_2$, in the organic phase and inversely third-power dependent upon the concentration of hydrogen ion in the aqueous phase. Thus, the mode of extraction was postulated as:

$$M^{3+}_A + 3(HY)_{2_o} \rightleftharpoons M(HY_2)_{3_o} + 3H^+_A \tag{3}$$

the distribution ratio being expressed as:

$$K_3 = k_3[(HY)_2]^3_o/[H^+]^3_A \tag{4}$$

It can be seen from Equations (2) and (4) that the separation factor M(III)/Eu(II), (K_3/K_1), is the following:

$$\beta M(III)/Eu(II) = K_3/K_1 = (k_3/k_1)/[H^+]$$

Thus, as the hydrogen ion concentration decreases, the separation factor increases. However, from a separations standpoint the hydrogen ion concentration must be adjusted so that the Ln(III) ion reports largely to the organic phase and the Eu(II) reports largely to the aqueous phase.

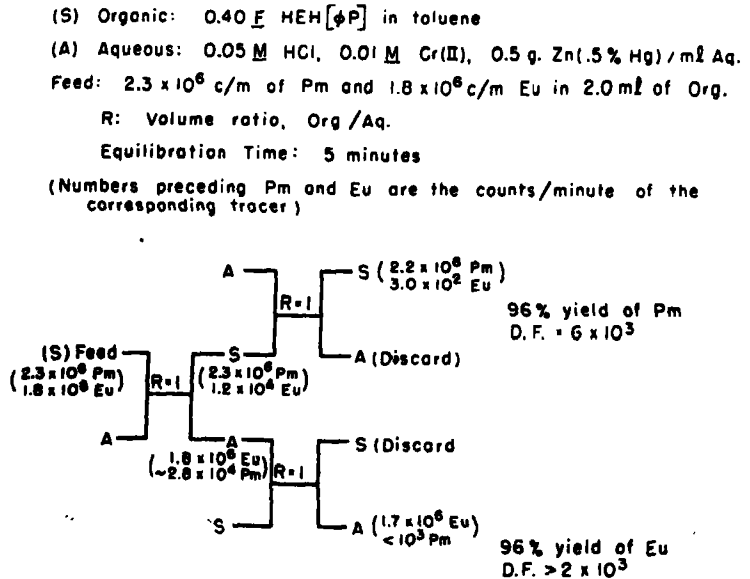

(S) Organic: 0.40 F HEH[ϕP] in toluene

(A) Aqueous: 0.05 M HCl, 0.01 M Cr(II), 0.5 g. Zn(.5% Hg)/ml Aq.

Feed: 2.3×10^6 c/m of Pm and 1.8×10^6 c/m Eu in 2.0 ml of Org.

R: Volume ratio, Org/Aq.

Equilibration Time: 5 minutes

(Numbers preceding Pm and Eu are the counts/minute of the corresponding tracer)

A
S (2.2 x 10⁶ Pm / 3.0 x 10² Eu)
R = 1
96% yield of Pm
D. F. = 6 x 10³
(S) Feed (2.3 x 10⁶ Pm / 1.8 x 10⁶ Eu)
R = 1
S (2.3 x 10⁶ Pm / 1.2 x 10⁴ Eu)
A (Discard)
A
A (1.8 x 10⁶ Eu / ~2.8 x 10⁴ Pm)
R = 1
S (Discard
S
A (1.7 x 10⁶ Eu / < 10³ Pm)
96% yield of Eu
D.F. > 2 x 10³

FIG. 4.—Flow sheet showing the separation of $^{152, 154}$Eu and ^{147}Pm.

Separation of $^{152,\,154}$Eu and ^{147}Pm

Fig. 4 shows the flow sheet employed and the results of the separation of $^{152,\,154}$Eu and ^{147}Pm. The volumes employed were 2 ml. of feed and 2 ml. each of organic and aqueous phases. Because of the lower energy of the β-radiation of ^{147}Pm as compared to that of $^{152,\,154}$Eu, it was possible to determine a small amount of $^{152,\,154}$Eu activity in a large amount of ^{147}Pm activity. However, the reverse of this, determination of a small amount of Pm activity in a large amount of Eu activity was not feasible. Thus, the degree of Eu contamination in Pm may be determined more accurately than may the degree of Pm contamination in Eu. Nevertheless, the results shown in Fig. 4 give ample evidence of the effectiveness of this separation technique.

Another separation of ^{147}Pm and $^{152,\,154}$Eu was carried out with the object of obtaining a high degree of purification of ^{147}Pm with respect to $^{152,\,154}$Eu. Two millilitre portions of feed and of aqueous and organic phases were employed. A flow sheet and the results of this separation are shown in Fig. 5. In the last stage of the separation, the Eu concentration was reduced to such a level that it became impossible to detect the Eu activity in the large amount of ^{147}Pm. By omitting the ^{147}Pm in the second stage, a smaller limit of Eu concentration could be detected.

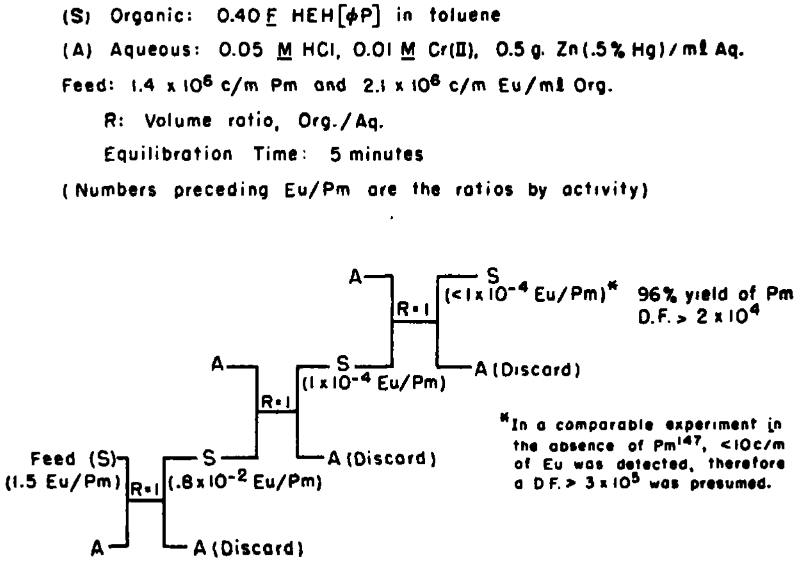
(S) Organic: 0.40 $\underline{F}$ HEH[ϕP] in toluene

(A) Aqueous: 0.05 $\underline{M}$ HCl, 0.01 $\underline{M}$ Cr(II), 0.5 g. Zn(.5% Hg)/ml Aq.

Feed: 1.4×10^6 c/m Pm and 2.1×10^6 c/m Eu/ml Org.

R: Volume ratio, Org./Aq.

Equilibration Time: 5 minutes

(Numbers preceding Eu/Pm are the ratios by activity)

*In a comparable experiment in the absence of Pm^{147}, <10c/m of Eu was detected, therefore a D.F. > 3×10^5 was presumed.

FIG. 5.—Flow sheet showing the purification of ^{147}Pm with respect to $^{152,\,154}$Eu.

It is interesting to note from the results shown in Figs. 4 and 5 that europium was maintained as Eu(II) during the scrubbings of the organic phase, even though the actual concentration of Eu(II) was below 10^{-12} M in the organic phase.

The enrichment of europium from a commercial rare earth oxide

Fig. 6 gives a flow sheet and the results of a separation which illustrates the enrichment, concentration, and recovery in high yield of europium from an admixture with other lanthanides.

The HDEHP extractant was used because of solubility difficulties encountered with HEH[ϕP] in the preparation of a 0·1 M lanthanide organic feed. A commercial rare earth oxide which contained 0·1 % Eu by weight (a complete analysis is given in Fig. 6) was dissolved in HCl and extracted with sufficient 1·6 F HDEHP in toluene to give a 0·1 M lanthanide(III) solution in the organic phase. This organic feed was scrubbed once with an equal volume of 0·3 M HCl to remove the small amounts of La, Ce, and Pr. The resultant organic phase was the feed shown in Fig. 6.

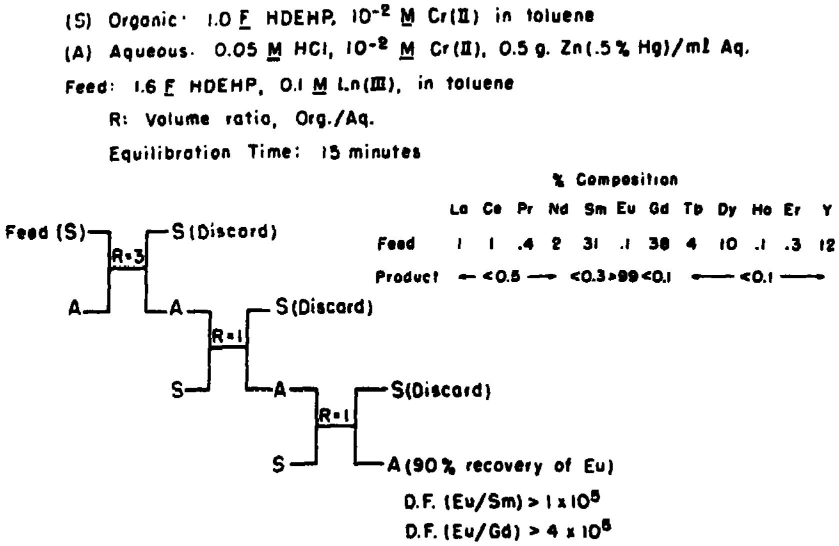
(S) Organic· 1.0 F HDEHP, 10⁻² M Cr(II) in toluene
(A) Aqueous· 0.05 M HCl, 10⁻² M Cr(II), 0.5 g. Zn(.5% Hg)/ml Aq.
Feed: 1.6 F HDEHP, 0.1 M Ln(III), in toluene
R: Volume ratio, Org./Aq.
Equilibration Time: 15 minutes
Feed (S)
R=3
S (Discard)
A
A
R=1
S (Discard)
S
A
R=1
S(Discard)
S
A (90% recovery of Eu)
D.F. (Eu/Sm) > 1 x 10⁵
D.F. (Eu/Gd) > 4 x 10⁶

% Composition

	La	Ce	Pr	Nd	Sm	Eu	Gd	Tb	Dy	Ho	Er	Y
Feed	1	1	.4	2	31	.1	38	4	10	.1	.3	12
Product	← <0.5 →				<0.3	>99	<0.1	← <0.1 →				

Fig. 6.—Flow sheet showing the separation of europium from admixture with other lanthanides.

In order to concentrate europium in the aqueous phase, a volume ratio of three to one (organic to aqueous) was used. The second extraction of the aqueous phase involved the use of 1·0 F HDEHP which contained ~ 10^{-2} M Cr(II). This was necessary, because the first extraction removes the majority of the Cr(II) present in the initial aqueous phase. The 1·0 F HDEHP containing ~ 10^{-2} M Cr(II) was prepared by extracting an equal volume of an aqueous phase 0·04 M in HCl and 0·015 M in Cr(II) in contact with Zn(Hg).

Final purification of Eu(III) *and* Pm(III) *from* Zn(II) *and* Cr(III)

The promethium and europium products shown in Figs. 4, 5, and 6 are contaminated with various amounts of Zn(II) and Cr(II). These contaminants are readily removed by first exposing the aqueous and/or organic phases to the air in order to oxidize Eu(II) and Cr(II). The oxidation product of Cr(II), which is probably $CrCl_2^+$ in the aqueous phase but of uncertain composition in the organic phase, behaves irreversibly and is neither extractable from the aqueous phase with 1·0 F HDEHP nor extractable from the organic phase with 2·5 M HCl. Thus, contaminant Cr(III) is removed when Pm(III) is stripped from the organic phase with 2·5 M HCl and when Eu(III) is extracted from the aqueous phase with 1·0 F HDEHP. The Pm(III) in 2·5 M HCl is extracted successively with 100% TBP to remove Zn(II). The Eu(III) in 1·0 F HDEHP is stripped with 2·5 M HCl and successively extracted with 100% TBP to remove Zn(II).

When the final product is gross europium, a further concentration can be effected while removing the Cr(III) by the proper adjustment of volume ratios.

Possible applications

From a separations viewpoint, possible important applications of these liquid–liquid extraction techniques involving Eu(II) and lanthanides(III) include:

(1) Up-grading of europium from natural material (Fig. 6):

(2) purification of europium (Fig. 6):

(3) separation of europium from mixed fission products, for example purification of Eu from Pm (Figs. 4 and 5):

(4) determination of fission yield for europium:

(5) effecting parent daughter separations such as $^{155}\mathrm{Sm} \xrightarrow[\beta]{23\ \mathrm{min}} {}^{155}\mathrm{Eu}$:

(6) effecting general mutual separations of submicrogram quantities of Eu–Sm, Eu–Gd (Fig. 6):

(7) separating Eu(III) from Eu(II) in exchange work.

From a basic viewpoint, the fact that both Eu(II) and Eu(III) show a third-power extractant dependency suggests that the co-ordination number of these two species is the same. By analogy with the Ca, Sr, and Ba extraction work,$^{(4)}$ it seems likely that the co-ordination number is six.

J. Inorg. Nucl. Chem., 1962, Vol. 24, pp. 441 to 459. Pergamon Press Ltd. Printed in England

THE DEVELOPMENT AND APPLICATION OF A PROCESS FOR THE RECOVERY OF OVER 100g OF PROTACTINUM-231 FROM A URANIUM REFINERY WASTE MATERIAL

D. A. COLLINS, J. J. HILLARY, J. S. NAIRN and G. M. PHILLIPS
Research and Development Branch, U.K.A.E.A., Windscale, and
Calder Works, Sellafield, Seascale, Cumberland

(*Received* 28 *August* 1961; *in revised form* 29 *October* 1961)

Abstract—This paper describes the development of a process for the recovery of protactinium-231 and uranium from a residue known as ethereal sludge that was produced during uranium refining at the U.K.A.E.A. Springfields Works. The process is suitable for operation on a large scale and involves the following stages:

1. Leaching protactinium and uranium from the sludge with cold 4N HNO_3 in the presence of fluoride.
2. Recovering uranium by extraction into 20 per cent TBP–OK.
3. Adding aluminium chloride to the aqueous raffinate and separating a precipitate that carries protactinium.
4. Treating the precipitate with cold NaOH solution and then dissolving it in concentrated hydrochloric acid.
5. Recovering protactinium by extraction into di-isobutylketone.

In laboratory operations the process proved capable of recovering 98–99 per cent of the uranium and 65–70 per cent of the protactinium originally present in the ethereal sludge.

The above process was successfully applied to the recovery of over 100 g of protactinium and of nearly 12 tons of uranium with an efficiency of 63 per cent for protactinium and 99·4 per cent for uranium.

A KNOWLEDGE of the chemistry of protactinium is of technical importance in connection with the chemical processing of irradiated thorium and of fundamental importance because it is the first actinide element for which a sharp distinction between ordinary group properties and actinide properties is possible. Protactinium-231, an α-emitter with a half-life of about $3{\cdot}4\times 10^4$ years, is the longest-lived isotope of protactinium and is the most suitable for chemical studies.

Protactinium-231 occurs naturally as a member of the $4n+3$ radioactive series. It is found in uranium ores to the extent of about 0·2–0·3 p.p.m. of the amount of uranium present. During the refining of the ores, protactinium is separated from the uranium and distributes itself among the various waste streams of the refinery process. ^{231}Pa can also be made artificially by neutron irradiation of ^{230}Th, but ^{232}Th is nearly always present with the ^{230}Th and leads to the production of ^{233}Pa, ^{233}U and fission products, which complicate the separation. Recovery from natural sources is therefore the more favourable approach for the production of gram quantities of ^{231}Pa.

During the processing of rich pitchblende ores, significant quantities of protactinium entered the U.K.A.E.A. uranium refining plant at Springfields, but, more recently, low-grade ore concentrates have been processed which have received a preliminary highly-selective concentration treatment (in which protactinium almost certainly does not follow uranium) before entering the refinery. Thus, only waste streams arising during the processing of pitchblende ores were likely to constitute useful sources of protactinium.

The uranium extraction process operated at Springfields for the treatment of pitchblende ores was surveyed by MADDOCK(1) who concluded that the best source of protactinium yielded by this process was the "ethereal sludge." This material probably originated in the very low acid conditions that existed during the dissolution of uranium peroxide in nitric acid which encouraged the separation of silica and other readily hydrolysed impurities that could carry the protactinium. Some batches of sludge arose during the recovery of uranium from calcium fluoride slags. These picked up significant quantities of fluoride, which later became distributed throughout the sludge stocks during a re-drumming operation. A typical analysis of the material is shown in Table 1. The average protactinium content was reported to be about 3 p.p.m.(2) and, since some 40 tons of sludge (on a dry-weight basis) were available, more than 100 g of protactinium-231 were involved. The sludge also contained a total of about 12 tons of uranium.

A.E.R.E. Harwell sponsored a project for the recovery of the protactinium from this residue. This paper describes the development of the process for recovering both the uranium and protactinium. Subsequently, production operations were carried out at Springfields and Windscale prior to final purification at A.E.R.E.

TABLE 1.—COMPOSITION OF TYPICAL SAMPLE OF ETHEREAL SLUDGE

Analysis of sample dried at 100° C (water content 25–30%)		Analysis of sample dried at 100° C (water content 25–30%)	
Constituent	%	Constituent	%
Uranium	28·3	Aluminium	0·27
Iron	7·7	Phosphorus	0·15
Silica	6·4	Strontium	0·09
Barium	$\sim$ 3	Niobium	< 0·1
Zirconium	2·7	Tantalum	
Molybdenum	2·7	Magnesium	< 0·01
Fluoride	1·8	Nickel	
Ammonium	1·7	Chromium	
Calcium	1·5	Cobalt	
Vanadium	0·9	Manganese	
Titanium	0·44	Tin	
Lead	0·4	Protactinium	$3{\cdot}7 \times 10^{-4}$

---

(1)* J. GOLDEN and A. G. MADDOCK, *Protactinium extraction studies. Part I S.E.R.L.* Technical Report M1 (1954).

(2)* Minutes of meeting held at St. Giles' Court on 6.11.56. IGC–PASG/M5.

* References marked thus, are not available in the general literature but are included to establish the origins of the process described.

REVIEW OF METHODS

An initial selection of possible processes, was based on published information summarized in reviews by ELSON,(3) HYDE,(4) WELCH(5) and KATZ and SEABORG.(6) MADDOCK at Cambridge had already developed a successful process for protactinium recovery from ethereal sludge(7) and had operated this process on a scale involving some hundreds of kilograms of the sludge. SALUTSKY and others(8) had also recently reported successful recovery from a somewhat similar source. MCKAY and others at A.E.R.E. had carried out small-scale separations by anion-exchange methods.(9)

The selected processes that appeared to be the most promising are shown in Fig. 1.

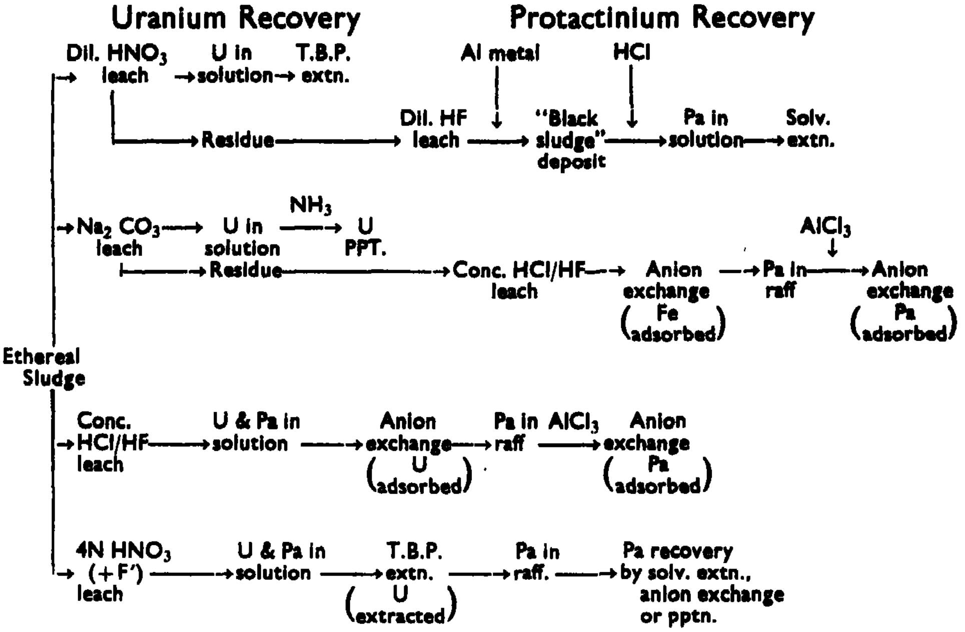

FIG. 1.—Outlines of alternative processes for uranium and protactinium recovery from ethereal sludge.

(3) R. E. ELSON, *The Chemistry of protactinium. Chap. 5. The actinide elements* (Edited by G. T. SEABORG and J. J. KATZ), N.N.E.S. Div. IV, Vol. 14A. McGraw-Hill, New York (1954).

(4) E. K. HYDE, *Proceedings of the International Conference on the Peaceful Uses of Atomic Energy, Geneva*, 1955, Vol. 7, p. 281, P/728. United Nations (1956).

(5) G. A. WELCH. Thesis, University of London (1956).

(6) J. J. KATZ and G. T. SEABORG, *The chemistry of the actinide elements.* Methuen, London (1957).

(7) A. G. GOBLE, J. GOLDEN, A. G. MADDOCK and D. J. TOMS, *The extraction of protactinium from refinery residues. Process Chemistry*, Vol. 2. *Progress in Nuclear Energy, Series III* (Edited by F. R. BRUCE, J. M. FLETCHER and H. H. HYMAN. Pergamon Press, Oxford (1960).

(8) M. L. SALUTSKY, *et al*, *J. Inorg. Nucl. Chem.* 3, 289 (1956).

(9)* H. A. C. MCKAY, AERE C/M 286 (1956); Also H. A. C. MCKAY, N. JACKSON and A. C. FOX. Private communications (1956/57).

* References marked thus, are not available in the general literature but are included to establish the origins of the process described.

The methods were divided into two classes:

(1) Differential leaching techniques, in which uranium was leached out of the sludge completely, leaving all the protactinium in the residue.

(2) Total leaching techniques, in which both uranium and protactinium were leached from the sludge, with subsequent separation of the two elements in solution.

EXPERIMENTAL

The fate of protactinium in the experiments was determined by making analyses for ^{231}Pa. A rather lengthy chemical separation procedure was used for ^{231}Pa analysis. For more rapid assessment of experimental results, simple α-counting was frequently used with adequate accuracy and results were later confirmed by the chemical method. Analytical results on the ethereal sludge and other solids are expressed as percentages by weight on a dry-weight basis.

The determination of protactinium–231

The sample is digested with hydrofluoric acid, and insoluble material filtered off. An aliquot of the filtrate, after addition of protactinium–233, which acts as an isotopic tracer, and aluminium chloride, to complex fluoride, is added to a boiling solution of sodium hydroxide. The precipitated hydroxides are washed and dissolved in a mixture of nitric and hydrofluoric acids, and zirconium and barium carrier solutions are added. The precipitate of barium fluozirconate and the corresponding protactinium compound is washed and dissolved in 8 M hydrochloric acid with the addition of aluminium chloride. The solution is extracted with di-isobutylketone (or di-isopropylketone) and the protactinium back-extracted with 8 M hydrochloric acid containing some fluoride. Aliquots are mounted on platinum discs and counted for α- and β-activity.

For more rapid analysis in the full scale production operations a method based on α-pulse analysis(10 11) was used. In this method, the α disintegration rate of the sample is measured in a Simpson α-proportional counter fitted with a 1049 A head and main amplifier and scaler and followed by α-pulse analysis using a six position gridded ion chamber together with a Wilkinson analyser 1414 A, with head and main amplifier type 1430.

Actual samples of the ethereal sludge, or solutions derived therefrom, were used in all of the experiments reported.

The experimental work was carried out in well-draughted fume hoods, with precautions appropriate to a relatively low level of α-activity. Most of the solutions were handled in polythene vessels in deference to the reported tendency of protactinium to deposit on glass and steel,(1) but some use was also made of both glass and stainless steel apparatus, where suitable, without loss of efficiency. Tests showed that the concentration of protactinium in the leach and leach raffinate solutions remained stable during prolonged contact with stainless steel. The likelihood of loss of protactinium by deposition on plant vessels was therefore considered to be small.

RESULTS AND DISCUSSION

At an early stage, trials were made of two processes that employed the preferential leaching of uranium from the ethereal sludge as an initial step. The first of these was based on results obtained by Jackson of A.E.R.E.(9) and used a solution of hot 3·5 M sodium carbonate to extract the uranium. After washing with water, the residue containing protactinium was dissolved in 8 N HCl–0·5 N HF, and the solution was loaded on to a column of De-Acidite FF anion-exchange resin to absorb iron and any residual uranium. The raffinate from this column was then treated with aluminium chloride to complex the fluoride, followed by sorption of the protactinium on a second column of De-Acidite FF resin, whence it was eluted with 8 N HCl–0·1 N HF.

(10) N. Jackson, F. J. G. Rogers and J. F. Short, AERE/R–3377 (1960).

(11) K. M. Glover (Mrs.) and F. J. G. Rogers, AERE/R–2971 (1959).

Four tests of this procedure were carried out on two different samples of ethereal sludge. The results were not encouraging. None of the four yielded complete recovery of either uranium or protactinium in the desired fractions. Losses of protactinium occurred at various stages; by extraction into the sodium carbonate solution, by sorption on the first anion-exchange column, and by failure to absorb on the second anion-exchange column. Because of these results the method was not pursued. It would also have entailed large-scale operations with HCl–HF solutions (about 10 m^3 being required per ton of ethereal sludge) and the practical sorption capacity of protactinium on De-Acidite FF resin from these solutions proved to be unacceptably low ($< 5 \mu g$ Pa/g resin) for the recovery of protactinium in gram amounts.

The second method was that used by MADDOCK(12) in which 1 N HNO_3 was used to extract the uranium from the sludge, leaving the protactinium in the residue. Attempts to reproduce this separation met with failure to extract all the uranium and to leave all the protactinium unextracted.

This failure to leach uranium preferentially was presumed to be due to the presence in the sludge of fluoride, which was responsible for taking part of the protactinium into solution. It was decided, therefore, to seek conditions in which both uranium and protactinium would be dissolved and, subsequently, to separate the two elements in solution. A nitric acid system was preferred, so as to simplify the recovery of uranium. Tributyl phosphate (TBP) could then be used to extract the uranium, and it was anticipated that the presence of fluoride would prevent the protactinium from being extracted.

The use of moderately concentrated nitric acid to leach the sludge was investigated (see Table 2). Cold 4 N HNO_3 resulted in the dissolution of about 90 per cent of both uranium and protactinium in 4 hr. Only fractionally better results were obtained with cold 8 N HNO_3. Further tests showed that the application of a second 4 N HNO_3 leach to the residue from the first provided recovery of essentially all the uranium and over 95 per cent of the protactinium. This method of leaching was therefore developed with the following results:

(1) A single 8 hr leach together with a brief wash gave an efficiency comparable to that obtained by two 4 hr leach stages.

(2) The acid; sludge ratio could be reduced to 2 l. acid; 1 kg (undried) sludge thus minimizing the total volume of liquor to be processed.

(3) The efficiency of protactinium recovery was not impaired by working with stainless steel vessels.

(4) There was no significant difference in the behaviour of the different samples of sludge.

(5) The addition of aluminium nitrate to the leaching solution reduced the protactinium recovery efficiency by half, thus illustrating that the presence of fluoride was essential for efficient protactinium recovery.

---

(12)* J. GOLDEN and A. G. MADDOCK, *Protactinium extraction studies.* Part II S.E.R.L. Technical Report M2 (1954).

* References marked thus, are not available in the general literature but are included to estalish the origins of the process described.

(6) The sludge could be leached with 4 N HNO_3+0·1 M F′ (to cope with possible fluoride-deficient batches of sludge) without adversely affecting efficiency in respect of those batches that already contained fluoride.

Table 2.—Leaching of ethereal sludge with cold nitric acid in polythene vessels: effect of nitric acid concentration and stirring time

Leaching solution				Distribution of Pa and U				
HNO_3 Conc. (N)	Vol (ml)	Wt. of undried sludge (g)	Stirring time (hr)	In leach solution (%)		In residue (%)		Wt. of residue (g)
				Pa	U	Pa	U	
1	400	100	2	—	40			
			4	—	52			
			48	1·5	60	98·5	40	47·4
4	400	100	2	80	77			
			4	85	89			
			24	90	94			
			48	93	96·4	7	3·6	12·3
8	400	100	2	95	90			
			4	95	90			
			24	95	95			
			48	97	97·1	3	2·9	12·4

Uranium was quantitatively recovered from this solution by conventional solvent extraction into 20 per cent TBP in odourless kerosene (OK) from which it could be subsequently back extracted by cold N/100 HNO_3 and precipitated as pure ammonium diuranate. The amount of protactinium extracted with the uranium was negligible.

Attempts were made to extract protactinium directly from the residual aqueous solution (the "leach raffinate") by means of ion-exchange resins and organic solvents. But, although nitric acid concentration was varied over a wide range and aluminium nitrate was added to complex the fluoride present in solution, the results (Table 3) showed little promise and shed no light on the nature of the protactinium species existing in this solution.

A large number of precipitates was formed experimentally in the leach raffinate solution (Table 3), but only the hydroxide provided reproducibly complete carrying of the protactinium. The carrying efficiency was > 99 per cent, but the greater part of the impurities in the solution also precipitated which resulted in a precipitate of about the same wet bulk as the original ethereal sludge (dry weight was about one fifth of that of ethereal sludge) and thus provided little concentration or purification of the protactinium.

It was found possible to dissolve the hydroxide precipitate in either HCl, H_2SO_4 or HNO_3. In most cases an insoluble residue was left, but this did not normally carry much protactinium. Experiments were carried out on small samples of each of these solutions to see whether protactinium could be extracted simply by ion-exchange or solvent-extraction techniques. In almost every case, negligible amounts of protactinium were recovered (Table 4).

Aluminium chloride added to the solution of the hydroxide precipitate in dilute HCl produced a white precipitate which carried a high proportion of the protactinium. Initial results showed that about 95 per cent of the protactinium could be carried by making the solution 0·5 M in aluminium chloride. In larger-scale experiments, the average efficiency dropped to 77 per cent but the bulk of the precipitate (approximately one eighth of that of the original sludge, when wet) was considerably smaller than that of the hydroxide precipitate and provided a possible route for the concentration of the protactinium.

TABLE 3.—ATTEMPTED RECOVERY OF PROTACTINIUM FROM NITRIC ACID SOLUTION OF ETHEREAL SLUDGE AFTER EXTRACTION OF URANIUM

Pa separation technique	Conditions			Pa removed from solution (%)
	HNO_3 (M)	$Al(NO_3)_3$ (M)	Temp. (° C)	
Solvent extraction				
20% TBP–OK	4	0·5	20	0
0·5 M TTA–benzene	4	0·5	20	3
0·5 M TTA–benzene	8	0·5	20	7
Ion exchange				
Cation resin (Zeo-Karb 225)	0·1	—	20	0–20
Anion resin (De-Acidite FF)	4	0·5	20	0–30
„ „ „ „	8	0·5	20	0–50
„ „ „ „	12	0·5	20	0–40
Precipitation				
Manganese dioxide	3	—	90	12
„ „	3	0·5	90	78
„ „	8	—	90	0
„ „	8	0·5	90	70
Calcium fluoride	4	—	20	5–50
Barium fluoride	4	0·5	90	73
Hydroxide	—	—	20	> 99
Bismuth phosphate	4	0·5	90	66
Sodium silicate	1	—	20	5
„ „	1	0·5	20	24
„ „	1	—	90	7
„ „	1	0·5	90	65
Silica (pre-formed)	4	0·5	20	0
„ „ „	4	0·5	90	30
Titania (pre-formed)	4	0·5	20	4
„ „ „	4	0·5	90	26
Aluminium nitrate	4	0·5	90	21–43 (after 15 min)
„ „	4	1·0	90	22 „ „ „
„ „	4	0·5	20	62 (after 24 hr)
„ „	4	0·5	20	72 (after 70 hr)
„ „	4	1·0	20	68 (after 70 hr)

The precipitate could not be dissolved directly in either concentrated HCl or concentrated HNO_3, but if it was first digested with caustic soda (which would remove alumina and silica) it could be readily dissolved in either acid to yield a stable solution containing all the protactinium.

TABLE 4.—ATTEMPTED RECOVERY OF Pa FROM DISSOLVED "HYDROXIDE PRECIPITATE" BY ANION-EXCHANGE AND SOLVENT EXTRACTION

Extraction technique	Solution conditions	Pa extracted (%)
Anion exchange using De-Acidite FF resin	8 N HCl	0
	8 N HCl + 0·5 M $AlCl_3$	0
	8 N HCl–0·5 N HF + 0·5 M $AlCl_3$	0
	8 N HNO_3	0
	12 N HNO_3	0
	8 N HNO_3 + 0·5 M $Al(NO_3)_3$	95
	,,	30
	8 N HNO_3 + 0·1 M HBO_3	10
	8 N H_2SO_4	0
	12 N H_2SO_4	0
Solvent extraction with 100% TBP	8 N HCl	90
	8 N HCl	23
Solvent extraction with 0·5 M TTA/benzene	6 N HNO_3	0
	6 N HNO_3 + 0·5 M $Al(NO_3)_3$	0

The above steps, namely:

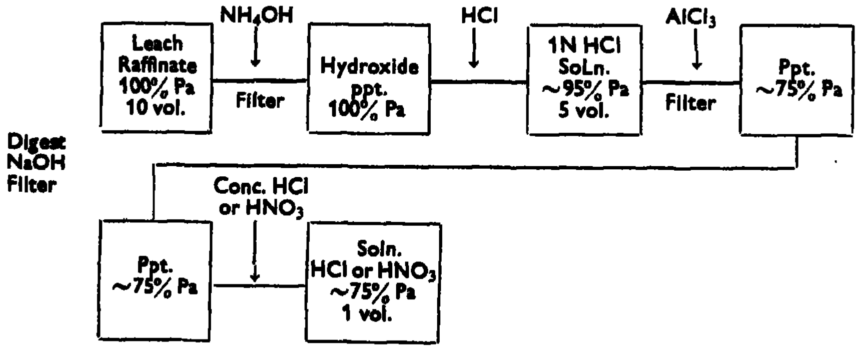

provided a route to a stable solution of protactinium in concentrated HCl or concentrated HNO_3, from which further concentration of protactinium should be feasible, but there were certain disadvantages for large-scale application:

(a) Three major filtration steps were involved, the precipitates being slow to filter and the hydroxide being an exceptionally bulky precipitate.

(b) The use of HCl was required at an early stage in the process, at which the scale of operations had been reduced only by a factor of two.

A much simpler route became possible when it was shown that the addition of aluminium chloride directly to the leach raffinate gave rise to a precipitate in the cold that carried down most of the protactinium (Table 5). This step served to concentrate the protactinium by a factor of about tn. Corrosion tests showed that the use of a 0·5 M concentration of aluminium chloride could safely be accepted in stainless steel plant.

The precipitate consisted essentially of hydrated zirconia and zirconium phosphate with silica, alumina and some titania. Its formation was thought to result from hydrolysis and the precipitation of insoluble phosphates following the release of protactinium and zirconium from fluoride complexes by the competitive action of the aluminium.

TABLE 5.—RECOVERY OF PROTACTINIUM FROM "LEACH RAFFINATE" BY CARRYING ON A PRECIPITATE PRODUCED BY ADDITION OF ALUMINIUM CHLORIDE

Aluminium chloride conc. in leach raffinate (M)	Time allowed for precipitation (hr)	Pa carried on precipitate (%)
0·5	¼	No ppt.
	½	43
	1	74
	2	85
	6	95
	20	95
1·0 Solution corrosive to stainless steel	2	97
0·5	2	80–95 (Result of approx. 50 experiments)

The precipitate could not be re-dissolved directly in hydrochloric or nitric acid but, after treatment with caustic soda, it could be dissolved in either of these acids to yield a stable solution of protactinium (Table 6). Besides removing silica and alumina, the caustic soda appeared to promote the metathesis of the insoluble phosphates, converting them to soluble sodium phosphate, which could then be removed by washing. (Analysis of a precipitate before and after caustic soda treatment showed a very significant reduction in the proportion of phosphate it contained.)

This treatment proved to be the key step in the process. Provided phosphate had been thoroughly removed, the precipitate could be readily dissolved in concentrated hydrochloric or nitric acid. If leaching was inadequate, a precipitate consisting essentially of zirconium phosphate rapidly re-formed on addition of acid and much of the protactinium failed to go into solution (Table 6). This behaviour accounted for the poor recovery of protactinium in many early experiments, where the importance of thorough leaching of the phosphate was not properly appreciated. It was shown, however, that, when the protactinium failed to go into solution and was deposited on a final solid residue, it could be recovered by recycling this residue through the caustic soda leaching and washing stages.

In a number of cases, low protactinium recovery appeared to be associated with ageing of the precipitates, but these results may have been due to inadequate treatment with caustic soda, since, in later experiments, precipitates aged for 3 days were sometimes successfully dissolved. It was, however, considered inadvisable to allow the precipitates to age for more than 24 hr.

TABLE 6.—DEVELOPMENT OF SUITABLE CONDITIONS FOR THE RECOVERY OF PROTACTINIUM FROM THE "$AlCl_3$ PRECIPITATE"

Wt. of '$AlCl_3$ ppt.', (g)	Age of ppt.	Leaching and washing conditions applied					Acid used for final dissolution	Pa taken into solution (%)
		1st NaOH leach	1st water wash	2nd NaOH leach	2nd water wash	Stirred thoroughly throughout		
12·5	3 days	—	—	—	—	—	HCl	25 (Pa on solid residue)
12·3	3 days	150 ml 30% NaOH hot	100 ml cold	not done	not done	no	HCl	90
12	~ 16 hr	150 ml 30% NaOH hot	2 × 50 ml cold	"	"	"	HNO_3	90
50	3 days	100 ml 30% NaOH hot	2 × 50 ml cold	"	"	"	HNO_3	< 1 (Pa on solid residue)
14	~ 2 hr	100 ml 30% NaOH hot	2 × 50 ml cold	"	"	"	HNO_3	95
70	~ 2 hr	150 ml 30% NaOH hot	2 × 50 ml cold	"	"	"	HNO_3	2 (Pa on solid residue)
30	~ 2 hr	100 ml 30% NaOH hot	2 × 100 ml cold	"	"	"	HNO_3	90
32	~ 16 hr	"	2 × 50 ml cold	"	"	"	HNO_3	90
90	2½ days	"	"	"	"	"	HNO_3	< 2 (Pa on solid residue)
7	~ 2 hr	50 ml 30% NaOH hot	"	"	"	"	HNO_3	95
230	~ 16 hr	150 ml 30% NaOH hot	3 × 80 ml cold	"	"	"	HNO_3	3 (Pa on solid residue)
110	~ 2 hr	100 ml 10% NaOH cold	100 ml cold	100 ml 10% NaOH cold	100 ml cold	Yes	HNO_3	90
159	~ 2 hr	"	"	"	"	"	HNO_3	90
95	~ 2 hr	100 ml 20% NaOH cold	100 ml cold	100 ml 20% " "	2 × 100 ml cold	"	HNO_3	95
1000	~ 2 hr	400 ml 20% NaOH cold	400 ml cold	400 ml 20% " "	400 ml cold	"	HNO_3	80
280	~ 16 hr	300 ml 10% NaOH cold	300 ml cold	300 ml 10% " "	300 ml cold	"	HNO_3	65
117	~ 16 hr	50 ml 26% NaOH cold	50 ml cold	50 ml 26% " "	2 × 50 ml cold	"	HCl	95
100 (mean of 20 expts.)	~ 16 hr	50 ml 26% NaOH cold	2 × 100 ml cold	50 ml 26% " "	2 × 100 ml cold	"	HCl	80–95

A satisfactory procedure for the re-dissolution of the precipitate (see Table 6) consisted of two successive treatments with an excess of caustic soda solution, with intermediate and final washing with water. At each stage, really intimate mixing of the liquid with the precipitate was found to be essential.

The solution of the treated precipitate contained protactinium in $\frac{1}{10}$th the volume of the original leach solution. The chief remaining impurities were iron and zirconium, both present at more than 1000 times the concentration of the protactinium. Further purification and concentration were therefore required.

Attempts were first made to concentrate the protactinium in nitric acid medium so as to delay the employment of hydrochloric acid, with its attendant corrosion problems, until the volumes had been reduced to the laboratory scale.

Sixty to 80 per cent of the protactinium could be extracted into 20 per cent TBP–OK from 5 to 8 N HNO_3, but zirconium is also strongly extracted under these conditions and therefore no separation of protactinium and zirconium could be expected (Fig. 2). In some cases the experiments were complicated by the occurrence of a solid zirconium-organic complex, which made phase separation more difficult and tended to carry protactinium.

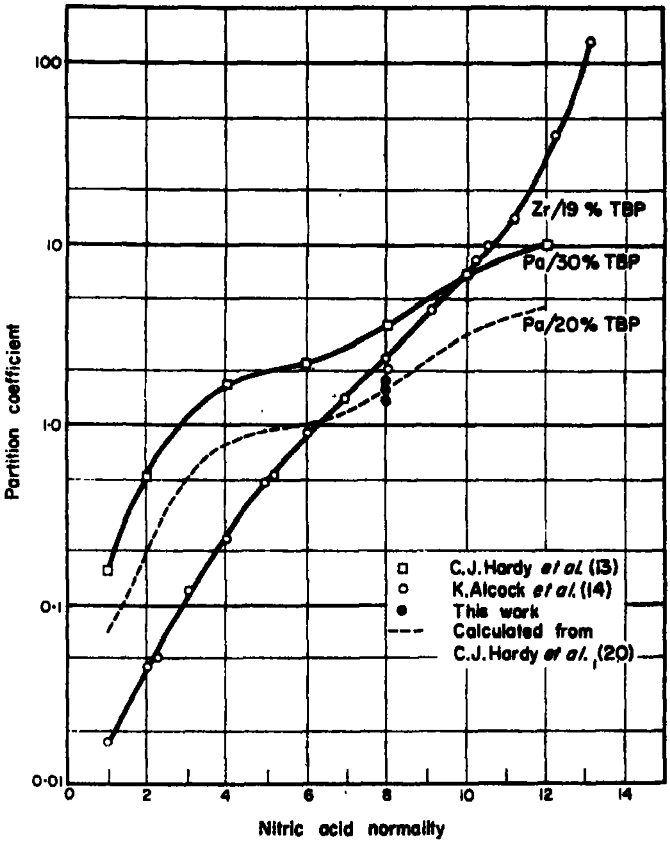

FIG. 2.—Comparative extraction of protactinium and zirconium by TBP from nitric acid solution.

Sorption of the protactinium on an anion-exchange resin could be achieved by increasing the acidity to 12 N HNO_3. The resin capacity of ~ 5 μg Pa/g resin was, however, much too low to afford any hope of concentrating the protactinium by this technique.

Manganese dioxide has frequently been used as a carrier precipitate for protactinium in nitric acid solutions,(15) although MADDOCK(7, 12) has commented upon the unreliability of this technique as a general separation procedure. It was found necessary with this solution to use a Mn/Pa ratio of about 1000 to achieve 85 per cent carrying efficiency:

Mn/Pa ratio	50	150	500	1000
% Pa carried	52	67	79	86

There was little separation from zirconium (DF 2·5) and the precipitate proved difficult to filter and redissolve. A concentration factor of only about five resulted.

These attempts were therefore abandoned and further work was restricted to the hydrochloric acid system.

Solvent extraction with di-isobutylketone was ultimately chosen for this stage, but the application of anion-exchange procedures was first examined.

Anion-exchange

Sorption of both protactinium and iron (ferric) on anion resins takes place from strong hydrochloric acid, but the presence of HF in the hydrochloric acid prevents the sorption of protactinium without affecting that of iron.(16) The two are thus readily separated. The separation from zirconium depends upon a difference in the distribution coefficient for these two elements, which allows a separation at 6–8 N HCl.(17) Between these acidities protactinium is strongly absorbed whereas zirconium is substantially unabsorbed. Two possible procedures for the required separation are then:

Procedure 1

(1) Sorption of iron and protactinium on resin from 6 to 8 N HCl. No sorption of zirconium.

(2) Elution of protactinium with 8 N HCl containing HF. Iron not eluted.

Procedure 2

(1) Sorption of iron on resin from 8 N HCl containing HF. No sorption of protactinium and zirconium.

(2) Complexing of the fluoride by addition of $AlCl_3$. Sorption of protactinium on resin from 6 to 8 N HCl. No sorption of zirconium.

(3) Elution of protactinium from resin with 8 N HCl containing HF.

---

(13) C. J. HARDY, D. SCARGILL and J. M. FLETCHER, *J. Inorg. Nucl. Chem.* **7**, 257 (1958).

(14) K. ALCOCK, F. C. BEDFORD, W. H. HARDWICK and H. A. C. MCKAY, *J. Inorg. Nucl. Chem.* **4**, 100 (1957).

(15) L. I. KATZIN and R. W. STOUGHTON, *J. Inorg. Nucl. Chem.* **3**, 229 (1956).

(16) K. A. KRAUS and G. E. MOORE, *J. Amer. Chem. Soc.* **77**, 1383 (1953).

(17) A. G. MADDOCK and W. PUGH, *J. Inorg. Nucl. Chem.* **2**, 114 (1956).

Neither procedure proved satisfactory for use with the solution in question. A high proportion of the zirconium was absorbed together with the protactinium under the circumstances of procedure (1) (Fig. 3), and the capacity of the resin (De-Acidite FF) for protactinium proved to be rather low, about 50 μg Pa/g resin at a loading rate of 1 ml min^{-1} cm^{-2}. The persistence of hydrolysed species of protactinium and zirconium (following the caustic soda treatment) may have been responsible for this behaviour. In procedure (2) the separation of protactinium, iron and zirconium was satisfactory (Fig. 3), but the resin capacity for protactinium on the second column was still very low. In both procedures about five column volumes were required for elution of the protactinium, which, coupled with the low capacity

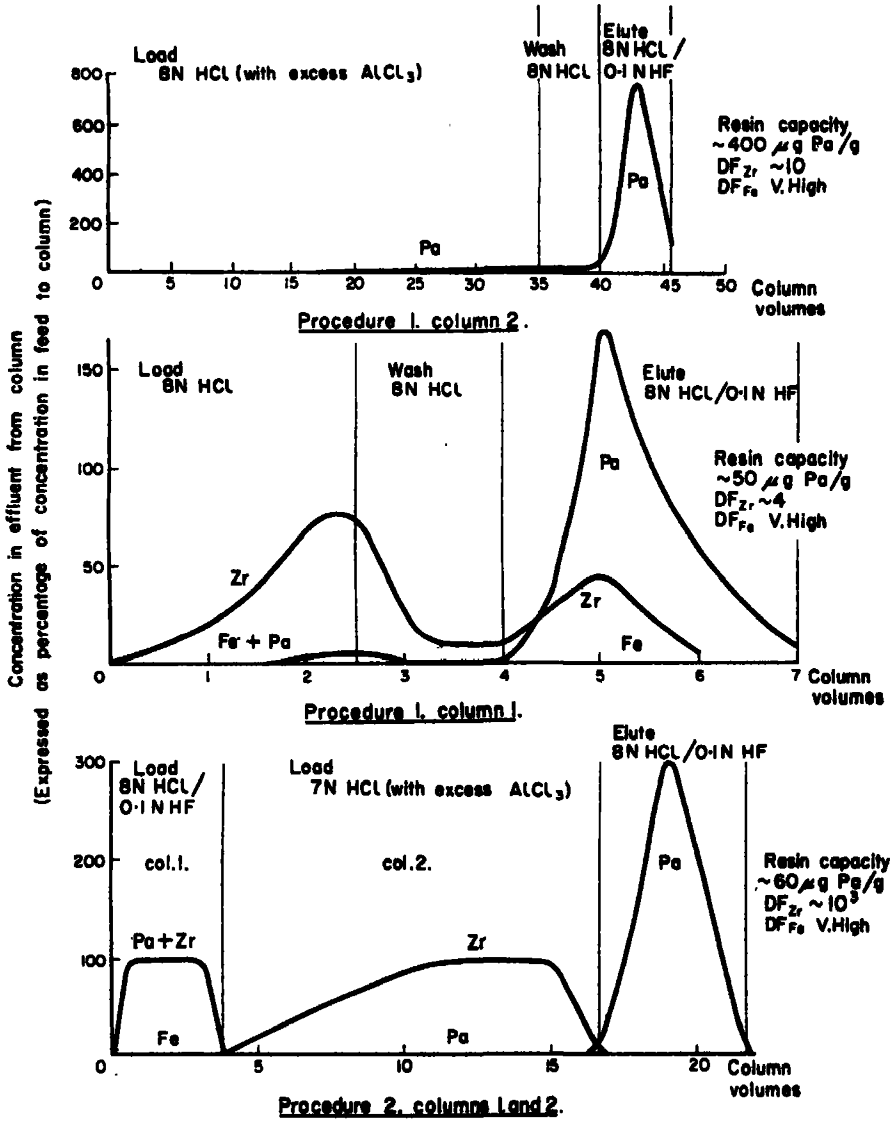

Fig. 3.—Separation of Pa from Zr and Fe by anion exchange.

of the columns, severely limited the degree of concentration obtainable. Appreciably higher resin capacities (up to 0·4 mg Pa/g resin) were obtainable when the protactinium eluate was recycled through a second anion column (after re-complexing the fluoride), but about five column volumes were still required for elution.

Solvent extraction

A large number of solvents have been found to extract protactinium from hydrochloric acid solutions, but certain alkyl ketones and alcohols appear to be reasonably specific. The extraction of protactinium by these solvents is illustrated in Fig. 4. Di-isopropylketone (D.I.P.K.) has generally been preferred in work reported in the literature(18) but, more recently, increasing use has been made of di-isobutylketone (DIBK)(19) because of the unavailability of DIPK. No quantitative data appear to have been published on the extraction of iron and zirconium from hydrochloric acid by DIBK, but it was assumed (cf. DIPK)(18) that iron would be extracted and would remain in the solvent when protactinium was backwashed with HCl–HF and that zirconium would be extracted to a considerably smaller extent than protactinium.

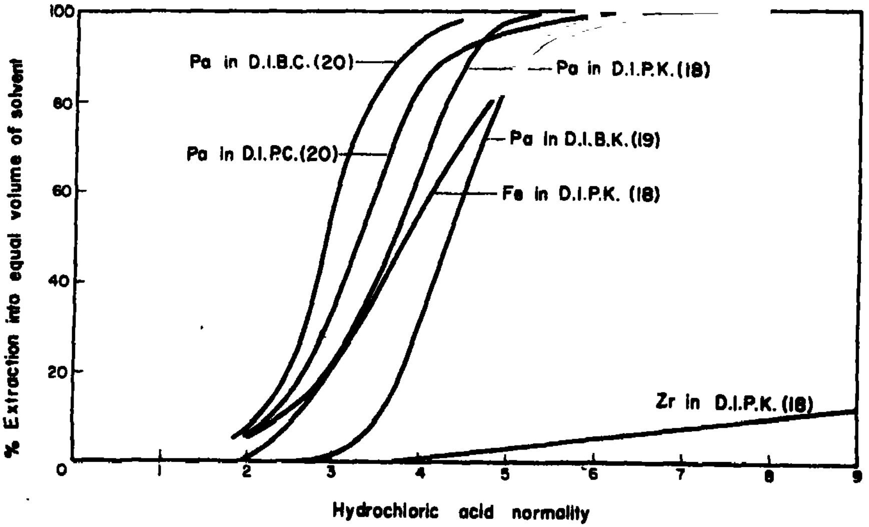

Fig. 4.—Extraction of Pa, Fe and Zr from hydrochloric acid solution by some alkyl ketones and alcohols.

Dalton and Sinclair(21) have shown that zirconium-95 is extracted increasingly strongly from hydrochloric acid as the acidity is increased above 6 N, and rather more strongly by DIBK than by DIPK. At and below 6 N HCl both solvents extract only negligible amounts of zirconium-95.

For efficient extraction of protactinium it is essential that hydrolysed forms, or traces of fluoride, which would complex the protactinium should be absent.

(18) J. Golden and A. G. Maddock, *J. Inorg. Nucl. Chem.* **2**, 46 (1956).

(19) A. G. Goble, J. Golden and A. G. Maddock, *Canad. J. Chem.* **34**, 284 (1956).

(20) A. G. Maddock. To be published.

(21)* J. C. Dalton and J. M. Sinclair. Report IGO–TM/W1050 (1958).

* References marked thus, are not available in the general literature but are included to establish the origins of the process described.

Preliminary experiments carried out by shaking together equal volumes of DIBK and a protactinium concentrate in 7–8 N HCl showed that between 95 and 99 per cent of the protactinium could be extracted and quantitatively recovered by backwash with 0·1–1 N HF solution. When attempts were made to concentrate the protactinium by shaking with a smaller volume of solvent, equilibration was found to result in emulsification, with a tendency for solid material to appear at the solvent/aqueous interface. This threatened to condemn the technique, since protactinium tended to concentrate in the solid phase (which was rich in zirconium) and phase separation was almost impossible. The solution to this difficulty (which had also been experienced by MADDOCK)[22] was to keep the phase-mixing conditions as mild as possible. A decrease in extraction efficiency resulted, but this could be made up by repetition of the extraction stage. A simple column contactor was used in which the solvent formed a stationary phase and the aqueous phase was allowed to drop through. Phase-mixing was provided either by packing the column with glass helices or by using an unpacked column and dispersing the aqueous phase into droplets by a distributor at the top of the column. The solvent phase was finally run out of the column and backwashed by normal shaking or stirring.

This technique was first tried out with the product from a previous ion-exchange experiment used as starting material. This solution, in 8 N HCl–0·1 N HF, was made 0·5 M in $AlCl_3$ and cycled three times through the column (~ 60 cm in length and packed with glass helices). The protactinium was then backwashed from the solvent phase with 1 N HF, an overall volume reduction of ten being achieved. The results were:

Protactinium in raffinate (%)			Protactinium in backwash (%)
1st cycle	2nd cycle	3rd cycle	
41	13	5	95

When an attempt was made to extract the protactinium directly from the caustic-soda-leached precipitate dissolved in 7 N HCl, zero extraction was observed after the first cycle. It was assumed that hydrolysed species of protactinium (persisting from the caustic soda treatment) were interferring with the extraction, and the solution was therefore made 0·1 N in HF and allowed to stand for 1 hr before $AlCl_3$ was added and the conditioned solution circulated through the solvent a second time. Fifty-five per cent of the protactinium was extracted in the second cycle and it was concluded that solution of the caustic-soda-leached precipitate would have to be made in HCl/HF, rather than in HCl alone, and the HF complexed with $AlCl_3$ immediately before solvent extraction, in order to ensure a satisfactory form of protactinium for extraction.

Further experiments were made to develop the technique for large-scale application and to establish the performance that could be expected under operational conditions. After the extraction cycles (in a glass column), the solvent phase was washed with 8 N HCl to remove traces of $AlCl_3$ and to assist in zirconium removal.

[22] A. G. MADDOCK. Verbal information (1957).

TABLE 7.—RESULTS OF EXPERIMENTS CARRIED OUT TO DEVELOP DIBK EXTRACTION STEP FOR PROTACTINIUM PURIFICATION AND CONCENTRATION

Feed to solvent extraction column				Solvent extraction conditions						Product of back-extraction		
Pa content (mg)	HCl (N)	HF (N)	AlCl$_3$ (M)	Ht. of solvent column (cm)	Packed or unpacked	No. of cycles	$\frac{\text{Vol. feed}}{\text{Vol. solvent}}$	Feed flowrate (ml/hr)	Extraction efficiency (%)	Pa content (mg)	Overall recovery (%)	Overall concn. factor
1·38	8	0·1	0·5	60	Packed	3	2·3	600	95·2	1·01	70·3	22
1·16	7	0·2	0·5 for first 3 cycles then 1·0	60	,,	9	3·3	600	83·7	0·86	74·1	31
2·59	8	0·1	0·8	70	,,	4	2·8	500	99·3	1·96	75·7	27
2·8	7	0·1	0·8	70	Unpacked	4	2·5	500	96·0	2·38	80	22
3·76	7	0·1	0·8	68	,,	4	2·8	600	97·8	2·80	74·5	25
7·53	7	0·1	0·8	138	,,	2	2·8	600	92·8	5·89	78·2	25
2·7	7	0·05	0·7	70	,,	4	2·8	600	93·2	2·04	75·6	25
2·4	7	0·1	0·8	75·5	Packed	4	3·8	600	89·8	1·83	(1 backwash) 76·2	34
2·4	7	0·1	0·8	75·0	Unpacked	4	3·0	600	86·4	1·90	(1 backwash) 79·2	27
4·9	7	0·05	0·7	70	,,	4	5·5	600	90·8	4·35	(1 backwash) 89	50
12·26	7	0·05	0·7	183	,,	2	5·2	2000	96·7	11·0	89·7	48

The protactinium was then backwashed with two successive fractions of 8 N HCl–0·1 N HF in a polythene vessel. Ninety to 95 per cent of the protactinium appeared in the first fraction and, to maintain a high concentration factor, the second fraction was used as the first backwash for the succeeding run. The solvent was finally washed with water to remove iron. Results are reported in Tables 7 and 8 from which the following main conclusions may be drawn:

(1) No significant advantage was to be gained by using a packed column.

(2) Increasing the height of the solvent column resulted in increased extraction efficiency, but not in direct proportion to the height increase. Greater extraction was obtained from four cycles through a 68 cm column than from two cycles through a 138-cm column. This suggested that a time-dependent equilibrium between inextractable and extractable protactinium species might be involved.

(3) It was desirable to keep the Al:F mole ratio above five for efficient extraction of protactinium. An HF concentration of 0·05 N in the hydrochloric acid solution of the caustic-soda-leached precipitate appeared to be adequate for the destruction of hydrolysed protactinium species.

(4) A concentration factor of fifty was readily obtainable.

(5) The efficiency of protactinium back-extraction with 8 N HCl–0·1 N HF was generally less than 100 per cent. (There was a possibility of discrepancies in protactinium determinations at low levels in the raffinate and at high levels in the backwash, and these might give rise to misleading backwash efficiencies.)

(6) In practice, an overall protactinium recovery of 80–90 per cent would be expected for this purification cycle.

TABLE 8.—EXTRACTION OF PROTACTINIUM BY DIBK: EFFECT OF COLUMN HEIGHT AND NUMBER OF CYCLES

Ht. of solvent column (cm)	Pa extracted after (%)			
	1st cycle	2nd cycle	3rd cycle	4th cycle
68	56·4	88·6	95·7	97·8
138	73·6	92·8	—	—

In the laboratory trials of this stage the volume of final product was very small and the protactinium was required for further experiments, so that, in general, only diluted samples of the final product were available for chemical analysis. In almost every case the iron and zirconium content of the diluted samples was below the limit of detection. It was therefore impossible to quote decontamination factors for these elements. A later experiment provided sufficient product for accurate determination of the iron and zirconium content and gave decontamination factors of $\sim 7 \times 10^3$ for zirconium and $\sim 6 \times 10^2$ for iron. Further purification can be accomplished by a second cycle of DIBK extraction and backwash, which yields a product of ~95 per cent chemical purity.

A final laboratory test of the process was carried out on a scale of ~10 mg protactinium, starting from ethereal sludge and performing each stage in conditions approximating as closely as possible to those of the full-scale plant. The main features of this test are recorded in Table 9. An overall protactinium recovery of 67·9 per cent was obtained.

Table 9.—Results of process trial on a scale of ~ 10 mg protactinium

Process stage	Weight or volume	Pa content (mg)
Ethereal sludge	7·5 kg	16·2
Leach raffinate	15·9 l.	14·3
Solution of "$AlCl_3$ precipitate"	1·15 l. (increased to 2·5 l. before DIBK stage so as to provide reasonable volume of feed solution)	12·26
DIBK stage:		
1st cycle product	50 ml	11·0

FULL-SCALE OPERATIONS

The protactinium recovery process which had been developed in the laboratory was not an easy one to apply on the large scale, involving, as it did, several filtration steps and also operations with concentrated hydrochloric acid. The process had, however, been developed so as to be thoroughly chemically reproducible on the large scale, and this has not always been the result when attempts have been made to recover protactinium by apparently more elegant techniques.(4)

The stages up to and including dissolution of the carrier precipitate in HCl/HF were carried out at the Springfields factory of the U.K.A.E.A. in a combination of stainless steel and rubber or plastic-lined plant. The purification and concentration by solvent extraction was carried out in specially constructed polythene plant at Windscale. The product of this process was transported to A.E.R.E. Harwell where it was further concentrated and converted to a state of high chemical purity by anion exchange.(23)

In practice, the chemical efficiency of the process anticipated from laboratory-scale experience was very closely achieved. From a total of 59·5 tons of sludge containing an estimated 172 g protactinium and 11·65 tons uranium, 108·2 g protactinium and 11·5 tons uranium were recovered in pure form, which represents an overall efficiency of 63·0 per cent for protactinium and 99·4 per cent for uranium. (The protactinium figures are based on the chemical method of analysis. The α-pulse method gives higher figures at all stages and credits the process with the overall recovery of 126 g protactinium).

The principal results of the full-scale operations are summarized in Table 10. The product of the process described in this paper consisted of 52·4 l. of 8 N HCl/

---

(23) N. Jackson, F. J. G. Rogers and J. Short. AERE/R-3311 (1960).

0·5 N HF containing 108·2 g protactinium, 3·25 g zirconium and 1·42 g iron. The anion exchange step at A.E.R.E. reduced the impurities to the following;

Al	Pb	Fe	Mg	Cu	Na	B	Ca	Mn
1500	250	50	20	100	300	400	400	10

p.p.m. with respect to Pa giving a final chemical purity of > 99·7 per cent and an α-purity of 99·5±0·5 per cent.

TABLE 10.—PRINCIPLE RESULTS OF FULL-SCALE APPLICATION OF THE PROTACTINIUM RECOVERY PROCESS

		Pa content			
Process stage	Wt. or vol.	(g)	α-pulse fig.	Fe content (g)	Zr content (g)
Ethereal sludge	59,542 kg	172·0	(204·74)	⩾ 1·19 × 10⁶	⩾ 1·49 × 10⁵
Solution of carrier precipitate in HCl/HF	15,386 l.	137·2	(143·65)	8·55 × 10⁴	1·16 × 10⁴
DIBK stage:					
1st cycle product	387·7 l.	108·8		205·5	205·5
2nd cycle product	52·4 l.	108·2	(126·75)	1·42	3·25

Acknowledgements—The authors wish to acknowledge the valuable assistance received from Chemical Services Department, Windscale, in the chemical analysis of many hundreds of samples; from Dr. A. G. MADDOCK and his colleagues at Cambridge University and Mr. H. A. C. MCKAY and his colleagues at A.E.R.E. in useful discussions contributing to the process development; from Dr. R. SPENCE in the loan of staff to assist in the practical development of the process.

The production operations were carried out by the U.K.A.E.A. Operations Branch at Springfields Factory with an analytical service provided by Chemical Services Department, Springfields, and by an A.E.R.E. team under Mr. N. JACKSON. (Who also undertook the final purification—not reported here.) Valuable assistance was also given by U.K.A.E.A. Operations Branch in the concentration and purification stages carried out at Windscale.

J. Inorg. Nucl. Chem., 1962, Vol. 24, pp. 461 to 468. Pergamon Press Ltd. Printed in England

THE NITROUS OXIDE RADIATION DOSIMETER

G. R. A. Johnson
Department of Chemistry, Kings College, University of Durham, Newcastle upon Tyne

(*Received* 27 *September* 1961)

Abstract—The initial yield of nitrogen from nitrous oxide (1 atm, 20° C) irradiated with ^{60}Co γ-rays was $G_{N_2} = 12{\cdot}8 \pm 0{\cdot}4$ molecules per 100 eV. The energy absorption was determined by ionization current measurements. Determination of the energy absorbed by the Fricke dosimeter gave $G_{N_2} = 12{\cdot}0 \pm 0{\cdot}4$.

The initial G_{N_2} was independent of the pressure of N_2O between 200 and 760 mm Hg and of dose-rate between 0·73 and $3{\cdot}0 \times 10^{14}$ eV ml^{-1} min^{-1}. G_{N_2} was not independent of total dose but decreased at doses greater than about $2{\cdot}4 \times 10^{17}$ eV ml^{-1}, having a value of 9·3 at $2{\cdot}5 \times 10^{18}$ eV ml^{-1}.

The yields of nitrite, formed when the irradiated gas was extracted with sodium hydroxide solution, and of oxygen have been determined.

It has become common practice to use chemical dosimetry to measure the energy absorbed in liquids irradiated with ionizing radiation; in particular, the ferrous sulphate (Fricke) dosimeter has been generally adopted. While there is no comparable accepted chemical dosimeter for gaseous systems, several reactions have been used for this purpose. These include the polymerization of acetylene,(1, 2) the hydrogen-oxygen reaction,(3) the formation of carbon dioxide from carbon monoxide and oxygen,(3) and the decomposition of nitrous oxide.(4) Of these systems, the latter appears to be the most suitable having, according to Harteck and Dondes,(4) most of the requirements of an ideal dosimeter.

A number of determinations of the energy-yields of the radiolysis products from nitrous oxide have been reported but considerable differences are found in the values obtained by different workers.(4–12) In view of the possible importance of this system as a dosimeter, a redetermination of the energy-yields seemed desirable.

The products from nitrous oxide, at pressures up to one atmosphere and at room temperature, in a glass vessel irradiated with ^{60}Co γ-rays have been determined as a function of the radiation dose. The absorbed energy was measured by two methods: (a) ionization current measurements, (b) the Fricke dosimeter.

(1) S. C. Lind, *Chemical effects of α-particles and electrons.* Chem. Catalogue Co., New York (1928).
(2) F. W. Lampe, *J. Phys. Chem.* **61**, 1015 (1957).
(3) S. C. Lind and D. C. Bardwell, *J. Amer. Chem. Soc.* **51**, 2751 (1929).
(4) P. Harteck and S. Dondes, *Nucleonics* **14**, 66 (1956).
(5) E. Wourtzel, *Radium*, 289 (1919).
(6) G. Gedye, *J. Chem. Soc.* 3016 (1931).
(7) H. Essex and A. D. Kolumban, *J. Chem. Phys.* **8**, 450 (1940).
(8) L. Dolle, *Proceedings of the Second International Conference on the Peaceful Uses of Atomic Energy, Geneva*, 1958, Vol. 20, p. 367. United Nations (1958).
(9) B. P. Burtt and J. F. Kircher, *Radiation Research*, **9**, 1 (1959).
(10) M. Steinberg, BNL 612 (T-182) (1960).
(11) F. Moseley and A. E. Truswell, AERE/R-3078 (1960).
(12) J. A. Hearne and R. W. Hummel, *Radiation Research* **15**, 254 (1961).

EXPERIMENTAL

Nitrous oxide

Medical nitrous oxide from a cylinder (British Oxygen Gases) was condensed at −183° C in a trap previously evacuated to below 10^{-3} mm Hg. The condensed gas was sublimed into another trap, the middle fraction only being collected. Keeping the second trap at −196° C the N_2O was pumped, using a three-stage mercury diffusion pump backed by an oil pump, until the pressure was below 10^{-3} mm Hg. The nitrous oxide was then allowed to liquify. This freezing, pumping, thawing cycle was repeated several times. By this means nitrous oxide was obtained with less than 10^{-3} mole per cent of impurities non-condensable at −196° C. At all stages mercury vapour was excluded by maintaining two traps at −80° C between any mercury (manometers and diffusion pump) and the nitrous oxide.

Irradiation procedure

Source *A* was a lead-shielded ^{60}Co source$^{(13)}$ of approximateley 200 c designed to give a uniform dose-rate over a specified volume; the irradiations were carried out within this volume. Source *B* was approximately 700 c of ^{60}Co shielded by concrete.

The irradiation vessels (borosilicate glass) were evacuated to below 10^{-3} mm Hg then filled with nitrous oxide to a known pressure measured by a mercury manometer, three traps at −80° C being present between the manometer and the vessel to exclude mercury vapour. After filling, the vessels were closed by a stopcock, Apiezon L grease being used.

Gas analysis

After irradiation, the nitrous oxide was condensed at −196° C and the non-condensable gases transferred to a gas burette by means of a one-stage mercury diffusion pump and a Toepler pump. After pressure and volume measurement, the gases were analysed mass-spectrometrically. Where necessary, the non-condensable gas present in the nitrous oxide before irradiation was measured and allowed for.

Nitrite analysis

The irradiated gas was allowed to expand into a previously evacuated bulb of known volume. To the sample thus obtained, 0·1 N aqueous sodium hydroxide solution was added via a break-seal. Nitrite ion was determined spectrophotometrically in the solution by means of α-naphthylamine-sulphonilic acid reagent; two procedures were used$^{(14, 15)}$ identical results being obtained in each case.

Ionization current measurements

An ionization chamber was constructed in which the products from nitrous oxide could be determined (Fig. 1). It consisted of a cylindrical borosilicate glass vessel, provided with a stopcock for filling with gas, tungsten rods (1 mm diameter) being sealed into the vessel as electrodes. One electrode passed down the central axis of the cylinder. Four rods parallel to this and adjacent to the wall of the cylinder were joined outside of the vessel to form the other electrode. The electrodes were soldered to coaxial screened cable; the space between the cable and the vessel being filled with Apiezon "W" wax. The insulation between the electrodes was better than $10^{18}\Omega$.

Voltage was applied to one electrode either from dry batteries (0–500 V) or from a stabilized voltage supply (500–2000 V). The other electrode was connected to earth via a known high resistance ($10^{6}\Omega$) and the voltage developed across this was measured on a "Vibron" d.c. amplifier (Electronic Instruments Ltd.; Model 33B). Normally, the chamber was used with the central electrode positive with respect to the outer electrodes; reversing the polarity did not change the value of the saturation current.

Measurement of absorbed energy by means of ionization current measurements

The suitability of the vessel as an ionization chamber was investigated by measuring the ionization current at different applied voltages. From Fig. 2, which shows measurements at three different gas pressures, it is seen that a good plateau was obtained. As is usual when precise measurements of ionization currents are made, in the saturation region the current was not quite independent of the applied voltage.(16) The value of the saturation current was obtained by plotting the measured current against the reciprocal of the applied voltage and extrapolating the linear portion of the curve to infinite applied voltage. The saturation current per unit pressure of the gas was independent of the pressure over the range studied (6·0–400·0 mm Hg).

---

(13) J. A. Ghormley and C. J. Hochanadel, *Rev. Sci. Instrum.* **22**, 473 (1951).

(14) T. Rigg, G. Scholes and J. Weiss, *J. Chem. Soc.* 1952, 3034.

(15) B. F. Rider and M. G. Mellon, *Industr. Engng. Chem., Analyt. Ed.* **18**, 96 (1946).

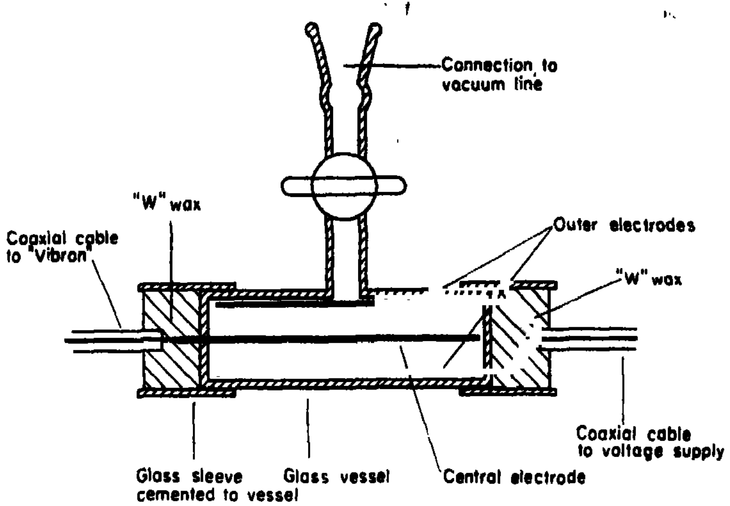
Connection to vacuum line
"W" wax
Coaxial cable to "Vibron"
Outer electrodes
"W" wax
Coaxial cable to voltage supply
Glass sleeve cemented to vessel
Glass vessel
Central electrode

Fig. 1.—Glass ionization chamber.

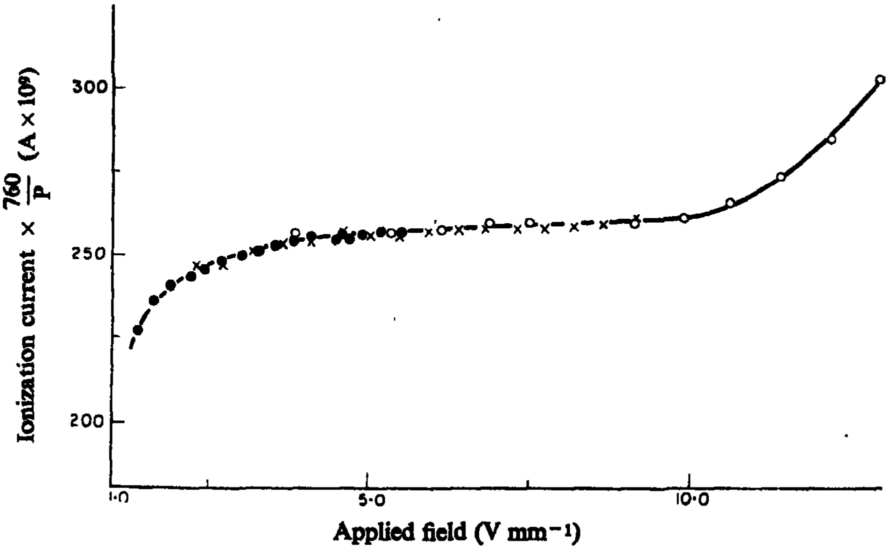

Fig. 2.—Dependence of ionization current on applied voltage at different nitrous oxide pressures.

●, pressure = 368·3 mm. ○, pressure = 131·5 mm. ×, pressure = 220·5 mm.

The saturation current in air was obtained in the same way as that for nitrous oxide.

(16) J. W. Boag, *Radiation Dosimetry* (Edited by G. J. Hine and G. L. Brownell), p. 153. Academic Press, New York (1956).

The saturation current measurements gave the ratio of the mean energies required to produce an ion pair in N_2O and air, W_{N_2O}/W_{air}, = 0·944. Using the value W_{air} = 33·7 eV per ion pair(17) this gives W_{N_2O} = 31·8 eV per ion pair. A value of W_{N_2O} = 31·2 eV per ion pair has been reported for 5 MeV α-particles.(18)

The dose rate in N_2O (E_g) was calculated from $E_g = JW_{N_2O}$ electron volts per min where J, the number of ion pairs formed per minute, is given by $J = 60\,I\,\overline{N}/\overline{F}$, where I is the saturation current in amps, $\overline{N}$ is the Avagadro number and $\overline{F}$ the Faraday in coulombs per mole.

Measurement of absorbed energy by means of the Fricke dosimeter

Under the conditions used, the radiation energy absorbed in the gas is due almost entirely to secondary electrons produced by γ-ray absorption in the glass vessel wall. The energy absorbed in the gas is related to that absorbed in the wall by the Bragg–Gray relationship (cf. reference 19) which gives:

$$E_g = \frac{E_w Z_g S_g}{Z_w S_w} \tag{1}$$

where E_g and E_w are the energies absorbed per cm³, Z_g and Z_w are the number of electrons per cm, and S_g and S_w are the stopping powers per electron in the gas and the wall respectively. The necessary conditions for this to be applicable are:(19) (a) the wall thickness must be greater than the range of the most energetic secondary electron, (b) the proportion of γ-ray attenuation in the wall and the gas must be negligible, (c) the secondary electrons must lose only a negligible fraction of their energy in crossing the gas, (d) the vessel must be in a homogenous radiation field.

The experimental arrangements were adopted to fulfill these conditions as far as possible. The vessel was constructed of glass about 2 mm thick and was cylindrical in shape, the internal diameter being 1·5 cm. The length of the vessel was varied from 5 to 10 cm. The radiations were carried out in a homogenous field (Source *A*—see experimental section). Furthermore, the yield was directly proportional to gas pressure over the range 200–760 mm Hg, showing condition (c) to hold.

Since for ^{60}Co γ-rays and materials of low atomic number the energy absorption is proportional to atomic number, the energy absorbed in the vessel wall (E_w) was assumed to be given by:

$$E_w = \frac{E_s Z_w}{Z_s} \tag{2}$$

where E_s is the energy absorbed per ml in a Fricke dosimeter solution inside the vessel and Z_s is the number of electrons per ml in this solution. However, this assumption is not strictly correct since the measured energy in the Fricke dosimeter is the average energy absorbed over the whole volume of the solution whereas we require the energy absorbed in the vessel wall when a gas is present. Attenuation of the radiation by the solution will result in the apparent value of E_w, calculated according to equation (2), being smaller than the real value of E_w. On the other hand, scattering by the solution will make the apparent value greater than the real value. It is extremely difficult to make an allowance for the error introduced by these two effects and, for the present purposes, it has been assumed that equation (2) is valid.

From equations (1) and (2) we obtain:

$$E_g = E_s \frac{Z_g S_g}{Z_s S_w} = 1{\cdot}76\times10^{-3} E_s \tag{3}$$

from which the energy absorbed in the gas can be obtained. The value of the stopping power ratio is not known but a value calculated from an empirical relationship between stopping power and atomic number(20) indicates that S_g/S_w is not greater than 1·04 and, for the present purposes, it has been assumed to be unity.

---

(17) W. B. REID and H. E. JOHNS, *Radiation Res.* **14**, 1 (1961).

(18) W. RIEZLER and A. RUDLOFF, *Ann. Phys.* **15**, 224 (1955).

(19) F. W. SPIERS, *Radiation Dosimetry* (Edited by G. J. HINE and G. L. BROWNELL), p. 23. Academic Press, New York (1956).

(20) N. A. BAILY and G. C. BROWN, *Radiation Res.* **11**, 745 (1959).

RESULTS

Nitrogen formation

The yields of nitrogen are plotted against total radiation dose in Fig. 3. There is good agreement between values based on ionization current measurements and on Fricke dosimetry, mean G_{N_2} values of 12·8±0·4 and 12·0±0·4 being obtained respectively. The initial G_{N_2} is independent of dose-rate over the range used ($7{\cdot}3\times10^{13}$ to $3{\cdot}0\times10^{14}$ eV ml^{-1} min^{-1}) and of the pressure of nitrous oxide between 200 and 760 mm.*

The yields of nitrogen from nitrous oxide irradiated in the ionization chamber were linear with dose up to the highest dose used ($6{\cdot}2\times10^{17}$ eV ml^{-1}); however, in the experiments using the vessel calibrated by the Fricke dosimeter, a decrease in G_{N_2} was apparent when the dose exceeded $2{\cdot}4\times10^{17}$ eV ml^{-1}. The results are given in Table 1, together with values obtained in a further series of experiments in which a higher dose-rate ($5{\cdot}6\times10^{14}$ eV ml^{-1} min^{-1}) was used. In the latter experiments an annular vessel (volume = 400 ml), which fitted closely around source *B*, was used. The dose-rate in this vessel was calculated from the initial nitrogen yield, assuming $G_{N_2} = 12{\cdot}8$.

TABLE 1.—IRRADIATION OF N_2O AT 760 MM AND 20° C. DEPENDENCE OF THE YIELDS OF NITROGEN AND OXYGEN ON TOTAL RADIATION DOSE

Dose rate (eV ml^{-1} min$^{-1}\times10^{-14}$)	Total dose (eV ml$^{-1}\times10^{-17}$)	Yield of N_2 (mole ml$^{-1}\times10^{8}$)	G_{N_2} (molecules/100 eV)	$\frac{G_{N_2}}{G_{N_2}}$
2·90	0·77	1·51	11·8	0·194
2·90	1·81	3·52	11·7	0·187
2·90	2·18	4·23	11·6	0·172
2·40	2·41	4·98	12·3	—
2·90	2·62	4·95	11·3	0·190
2·90	2·64	5·00	11·35	0·188
2·40	9·50	16·12	10·1	0·153
5·60	4·18	7·40	10·6	—
5·60	5·20	9·10	10·5	0·192
5·60	5·34	8·95	10·1	0·209
5·60	22·10	34·2	9·3	0·098

Oxygen formation

The values obtained for the ratio of the yields of oxygen and nitrogen, O_2/N_2, at different total doses are given in Table 1. The O_2/N_2 ratio was constant and equal to 0·19±0·01 at doses up to 5×10^{17} eV ml^{-1} but lower values were obtained at higher doses, a value $O_2/N_2 = 0{\cdot}098$ being observed at the highest dose used.

---

* It was reported in a note⁽²¹⁾ that very high G_{O_2} values were obtained when N_2O was irradiated at low pressures with a 200 kV X-ray set and it was thought that a chain-reaction must occur under these conditions. It has since been found that the high conversions of N_2O in fact resulted from the existence of an a.c. field from the X-ray tube, in the position where the vessels were irradiated, which presumably produced a discharge in the gas leading to chemical change. The effect disappeared when an earthed gauze screen was placed around the vessel during irradiation. An extensive decomposition of nitrous oxide, qualitatively similar to the radiation-induced decomposition, was found to occur when the gas was subjected to a mains-frequency (50 c/s) field of about 300 V cm^{-1} mm Hg^{-1}.

⁽²¹⁾ G. R. A. JOHNSON, *Proc. Chem. Soc.* 213 (1960).

Nitrate formation

Nitrite was found when the irradiated gas was extracted with 0·1 N sodium hydroxide.[22] The nitrite obtained at total doses up to 6×10^{17} eV ml^{-1} are plotted against total dose in Fig. 4. The yield was linear with dose in this region and corresponded to $G_{NO_2} = 2{\cdot}3\pm0{\cdot}2$.

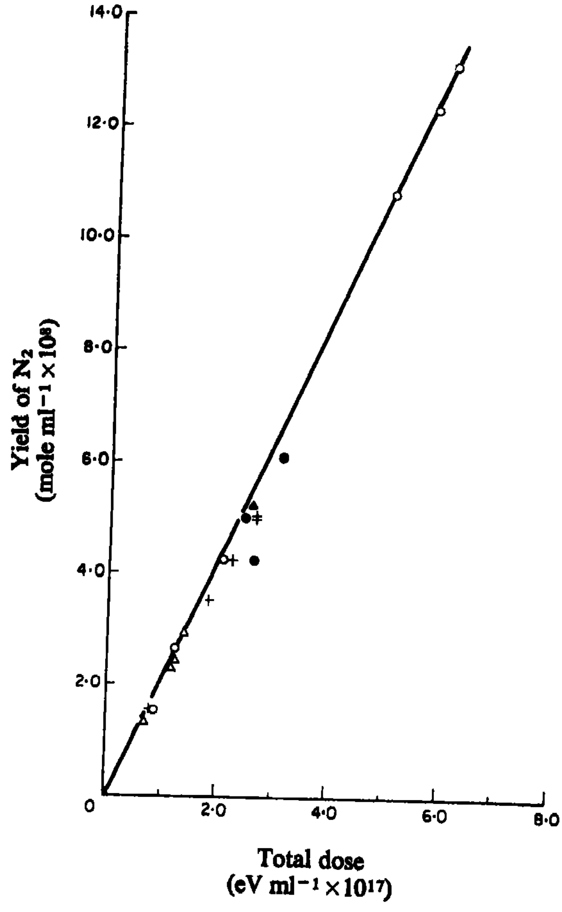

Fig. 3.—Irradiation of nitrous oxide. Dependence of N_2 yield on total dose.
○, dose rate measured by ionization current method = $7{\cdot}3\times10^{13}$ eV ml^{-1} min^{-1}, pressure = 760 mm Hg, vessel volume = 40 ml.
+, dose rate measured by Fricke dosimeter = $2{\cdot}9\times10^{14}$ eV ml^{-1} min^{-1}, pressure = 760 mm, vessel volume = 70 ml.
●, dose rate measured by Fricke dosimeter = $2{\cdot}4\times10^{14}$ eV ml^{-1} min^{-1}, pressure = 760 mm, vessel volume = 58 ml.
△, dose rate measured by Fricke dosimeter = $1{\cdot}21\times10^{14}$ eV ml^{-1} min^{-1}, pressure = 380 mm, vessel volume = 58 ml.
▲, dose rate measured by Fricke dosimeter = $6{\cdot}5\times10^{13}$ eV ml^{-1} min^{-1}, pressure = 200 mm, vessel volume = 58 ml.

---

[22] G. R. A. Johnson and G. A. Salmon, *J. Phys. Chem.* **65**, 177 (1961).

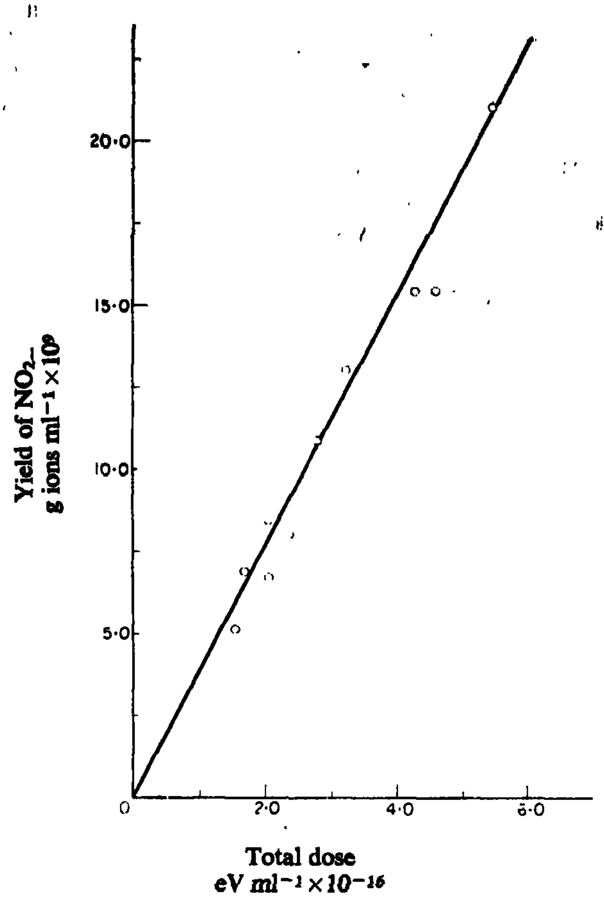

FIG. 4.—Irradiation of nitrous oxide at 760 mm Hg and 20° C. Dependence of nitrite ion yield on total radiation dose.
Dose rate = $2{\cdot}9 \times 10^{14}$ eV ml^{-1} min^{-1}.

DISCUSSION

Values of the initial G_{N_2} based on ionization current measurements and on Fricke dosimetry were $12{\cdot}8 \pm 0{\cdot}4$ and $12{\cdot}0 \pm 0{\cdot}4$ respectively. The small discrepancy between these values may well be due to the uncertainties, involved in calculating the dose-rate in the gas from dose-rate in solutions, which have been mentioned in the experimental section. It is therefore considered that the figure based on ionization current measurements is more likely to be correct.

At conversions of N_2O as low as 0·04 per cent (total dose = $2{\cdot}4 \times 10^{17}$ eV ml^{-1}) a fall-off in G_{N_2} from the initial value was observed (Table 1); thus G_{N_2} decreased from the initial value of 12·8 to a value of 9·3 at a dose of $2{\cdot}2 \times 10^{18}$ eV ml^{-1}. This is in agreement with STEINBERG(10) who, using dose-rates and gas pressures approximately twice those used in the present work, obtained values of G_{N_2} = 12·1, 10·5, 9·2, 8·0 and 6·9 at total doses of 2×10^{16}, 2×10^{17}, 2×10^{18}, 2×10^{19} and 2×10^{20} eV ml^{-1} respectively. HEARNE and HUMMEL(12) obtained an initial G_{N_2} = $11{\cdot}0 \pm 0{\cdot}4$ *and state that the yield is not linear with dose above* 5×10^{17} *eV ml*$^{-1}$. *The initial*

G_{N_2} found in the present work is in reasonable agreement with that of BURTT and KIRCHER⁽⁹⁾ who found $G_{N_2} = 11{\cdot}7$. The lower values of $G_{N_2} = 9{\cdot}7$ and $9{\cdot}4$ reported by HARTECK and DONDES⁽⁴⁾ and MOSELEY and TRUSWELL⁽¹¹⁾ are apparently not initial values.

In the ionization chamber experiments the yield of nitrogen was linear with dose up to the highest dose used, $6{\cdot}2\times10^{17}$ eV ml^{-1}, i.e., up to a dose more than twice that at which a fall-off in the value of G_{N_2} was apparent in the other experiments described above. The dose-rate used in the ionization chamber experiments ($7{\cdot}3\times10^{13}$ eV ml^{-1}) was somewhat lower than the dose-rate ($\nless 3\times10^{14}$ eV ml^{-1} min^{-1}) used in the other experiments and it is possible that the different behaviour may be due this.

Assuming that the primary products are N_2, O_2 and NO and that the reaction

$$2NO+O_2 \rightarrow 2NO_2 \qquad (1)$$

occurs as a trap reaction under the conditions used in the analysis,⁽⁹⁾ the measured yield of oxygen ($G_{O_2}{}^{\text{measured}}$) will be less than the actual yield ($G_{O_2}{}^{\text{actual}}$). Representing the radiation-induced decomposition:

$$N_2O \rightarrow a\,N_2+b\,O_2+c\,NO \qquad (2)$$

we have $2a = 4b+c$. Since $G_{N_2} = a = 12{\cdot}8$ and $G_{O_2}{}^{\text{measured}} = b-\frac{1}{2}c = 2{\cdot}4$ we have $G_{O_2}{}^{\text{actual}} = 5{\cdot}1$ and $G_{NO} = 5{\cdot}4$. This calculated value of G_{NO} is slightly higher than the value $G_{NO} = 4{\cdot}6\pm0{\cdot}4$ derived from the measured $G_{NO_2^-} = 2{\cdot}3\pm0{\cdot}2$ by assuming that reaction (1) proceeds quantitatively in solution and that the NO_2 formed leads to nitrite according to $2NO_2+2OH^- \rightarrow NO_2^-+NO_3^-+H_2O$.

The yields of oxygen previously reported⁽⁴, ⁹⁻¹²⁾ are lower than the value $G_{O_2}{}^{\text{actual}} = 5{\cdot}1$ obtained in the present work. It is suggested that the lower values may be attributable to either the analytical procedures used, or, in some cases, to the fact that the dose has been in excess of that required to give the initial yield.

The nitrous oxide system appears to be of value as a dosimeter but caution must be exercised in its use. It is clear that it is preferable to measure the nitrogen rather than the other products since it is formed with a higher yield and its determination is less subject to analytical difficulties. Care must be taken to ensure that the *initial* yield is measured if the energy absorption is calculated from the value $G_{N_2} = 12{\cdot}8$. For the measurement of low total doses (up to 2×10^{17} eV ml^{-1}) determination of nitrite ion as described may prove to be convenient since the method is sensitive and avoids gas analysis.

Acknowledgement—I thank Professor J. J. WEISS for his encouragement. The mass spectrometric analysis were carried out by Mr. P. KELLY.

J. Inorg. Nucl. Chem., 1962, Vol. 24, pp. 469 to 474. Pergamon Press Ltd. Printed in England

THE CRYSTAL STRUCTURE OF TRIMERIC PHOSPHONITRILIC BROMIDE

P. DE SANTIS, E. GIGLIO and A. RIPAMONTI
Istituto Chimico, Centro di Studio per la Chimica Fisica,
del Consiglio Nazionale delle Ricerche, University of Naples

(*Received* 19 *July* 1961)

Abstract—The results of an X-ray two-dimensional analysis of the crystal structure of trimeric phosphonitrilic bromide are reported.

The compound is isomorphous with trimeric phosphonitrilic chloride, as found by BODE. The refinement of the structure has been carried out by means of Fourier differential synthesis on the projections (100) and (001). On the basis of the results obtained the most important aspects of the molecular geometry are discussed with reference to the other phosphonitrilic halides thus far investigated.

RECENT X-ray studies on the structure of cyclic phosphonitrilic halide polymers provide strong evidence that P–N bond lengths and NPN and PNP bond angles as well as the molecular conformations of these molecules vary with the nature of the substituent groups attached to the phosphorus atoms, and with the size of the ring.

Previously reported results(1) of an X-ray three dimensional analysis of trimeric phosphonitrilic chloride carried out in our laboratory, have shown that the $(PN)_3$ ring has a slight chair conformation and that the P–N bond lengths are considerably shorter than those derived for this compound by BROCKWAY and BRIGHT(2) on the basis of electron diffraction data.

KETELAAR and DE VRIES(3) in an X-ray diffraction study of tetrameric phosphonitrilic chloride have found an average P–N bond length of 1·67 Å and a puckered ring conformation. This structure which cannot be considered very accurate has been refined by Miss A. Vos (private communication). The bond distances are considerably shorter than those of KETELAAR. Recently MCGEACHIN and TROMANS(4) have found in tetrameric phosphonitrilic fluoride a molecular symmetry D_{4h} with values of PN bond length of 1·51 Å and PNP and NPN bond angles of 147° and 123° respectively. On the other hand the results of an X-ray two-dimensional analysis of tetrameric phosphonitrilic dimethylamide carried out by BULLEN(5) show that the $(PN)_4$ ring has a P–N bond length of 1·59 Å and NPN and PNP bond angles of 121° and 129° respectively and a puckered conformation different from that found by KETELAAR and DE VRIES(3) for $(NPCl_2)_4$.

Furthermore an investigation of the molecular conformation of linear polyphosphonitrilic chloride,(6) carried out in our laboratory, has led to the conclusion that the P–N bond lengths and the PNP and NPN bond angles of backbone chain should be significantly different from those found for $(NPCl_2)_3$.

---

(1) F. POMPA and A. RIPAMONTI, *Ric. Sci.* **29**, 1516 (1959); E. GIGLIO, *Ibid.* **30**, 721 (1960).

(2) L. O. BROCKWAY and W. M. BRIGHT, *J. Amer. Chem. Soc.* **65**, 1551 (1943).

(3) J. A. A. KETELAAR and T. A. DE VRIES, *Rec. Trav. Chim.* **58**, 1081 (1939).

(4) H. McD. MCGEACHIN and F. R. TROMANS, *Chem. Industr.* 1131 (1960).

(5) G. J. BULLEN, *Proc. Chem. Soc.* 425 (1960).

(6) E. GIGLIO, F. POMPA and A. RIPAMONTI, *J. Polymer Sci.* In press. (1962).

BODE(7) was the first to investigate the crystal structure of trimeric phosphonitrilic bromide, but was not able to localize the nitrogen atoms on the Fourier projection. The bond angles and bond lengths were derived from the parameters of the Br and P atoms, assuming a planar $(PN)_3$ ring on the basis of the data obtained by BROCKWAY and BRIGHT for $(NPCl_2)_3$.

In order to obtain a clear picture on the molecular structure of phosphonitrilic halides it appeared to us advisable to reconsider the earlier work. A preliminary account of an accurate X-ray structure determination of trimeric phosphonitrilic bromide will therefore be given here.

DETERMINATION OF THE STRUCTURE

Crystals suitable for X-ray analysis were prepared by slow evaporation of solutions of trimeric phosphonitrilic bromide in benzene.

Since the compound sublimes slowly at room temperature the X-ray photographs were taken using crystals enclosed in sealed thin-walled glass capillaries.

The unit cell dimensions determined from measurements on oscillation and precession photographs, are; $a = 6{\cdot}63\ (\pm 0{\cdot}01)$ Å: $b = 13{\cdot}36\ (\pm 0{\cdot}02)$ Å: $c = 14{\cdot}43\ (\pm 0{\cdot}02)$ Å: in good agreement with those found by BODE.(7)

The orthorhombic unit cell contains four molecules, corresponding to a calculated density of $3{\cdot}18$ g cm^{-3}.

The reflexions $0kl$ and $hk0$ were recorded on Weissenberg photographs using Cu$K\alpha$ radiation with a multiple film technique. In this way 83 per cent of the $0kl$ and 65 per cent of the $hk0$ reflexions were recorded up to a value of $(\sin\theta)/\lambda$ of 0·64 and 0·60 respectively. All the intensities were estimated visually with the aid of a calibrated scale and corrected in the usual way for Lorentz and polarization factors. Since the size of our crystals was very small, it was not considered necessary to make a correction for absorption.

The systematic absences in the reflexions and the absence of a piezoelectric effect indicate a very close similarity with the trimeric phosphonitrilic chloride which is orthorhombic with:(8)

$$a = 6{\cdot}17\ \text{Å}: b = 12{\cdot}91\ \text{Å}: c = 14{\cdot}03\ \text{Å}:$$

space group D_{2h}^{16}, $Z = 4$.

Therefore for the first stage of the structure determination, it seemed reasonable to assume for the phosphorus atoms and nitrogen atoms the same co-ordinates as established for $(NPCl_2)_3$. The co-ordinates of the bromine atoms were derived from those of the chlorine atoms assuming a P–Br bond lengths of 2·2 Å.

The atomic parameters were then refined by means of several two dimensional Fourier differential synthesis on the projections (100) and (001), using the SHIONO's programmes for an IBM 650 electronic computer.(9)

When the refinement gave no further improvement, the reliability factor

$$R = \frac{\sum \big||F_{\text{obs}}| - |F_{\text{calc}}|\big|}{\sum |F_{\text{obs}}|}$$

was 0·21 and 0·17 for the F_{0kl}'s and F_{hk0}'s respectively, using a mean isotropic temperature factor $\exp[-3{\cdot}0\,(\sin\theta/\lambda)^2]$.

---

(7) H. BODE, *Angew. Chem.* 61, 438 (1949); *Structure Reports*, Vol. 12, p. 227 (1949). N. V. A. Oosthoek's Uitgevers Mij, Utrecht (1952).

(8) E. CIPOLLINI, F. POMPA and A. RIPAMONTI, *Ric. Sci.* 28, 2055 (1958).

(9) R. SHIONO, *IBM 650 program for differential Fourier Synthesis in X-ray crystal structure analysis*, Technical Report No. 2. University of Pitsburgh (1957).

The Fourier projections of the electron density on (100) and (001) are shown in Figs. 1 and 2.

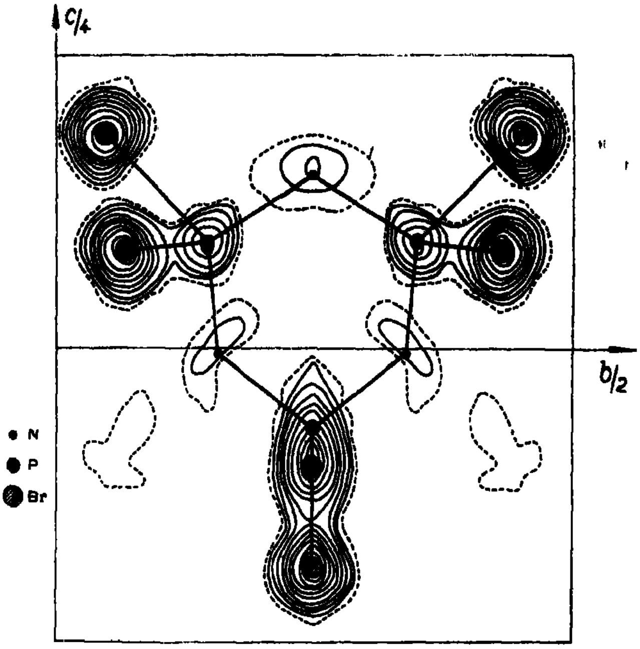

FIG. 1.—Projection of the electron density along (100). Contour are at 6, 8, 11, 16, 21, 26 . . . exÅ^{-2}. The lowest contour line is broken.

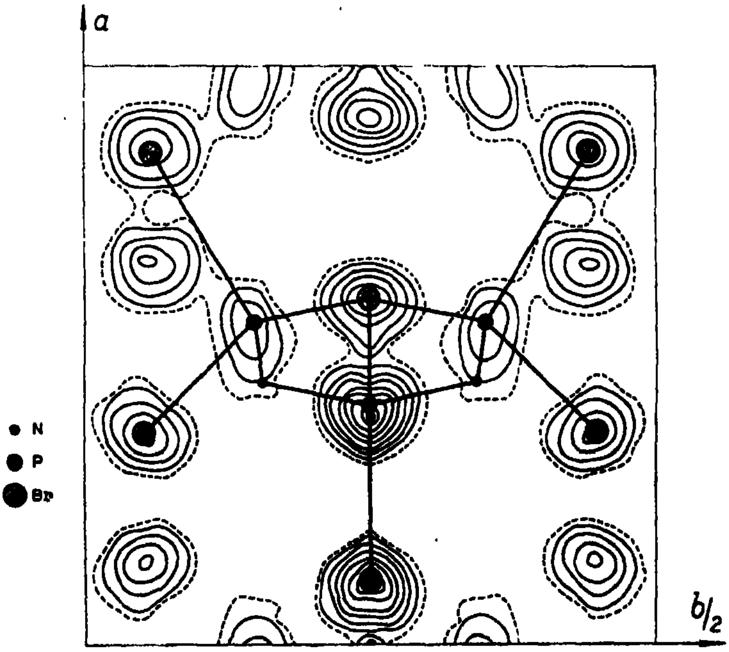

FIG. 2.—Projection of the electron density along (001). Contours are at 12, 16·5, 21, 30, 39 . . . exÅ^{-2}. The lowest contour line is broken.

Table 1 lists the co-ordinates of the atoms contained in the asymmetric unit of structure expressed as fractions of unit cell edges. The labelling of the atoms is indicated in Fig. 3. The atoms N_1, P_1, Br_1 and Br_2 lie on a mirror plane.

TABLE 1.

	x/a	y/b	z/c
N_1	0·580	0·250	0·137
N_2	0·453	0·152	−0·005
P_1	0·413	0·250	−0·058
P_2	0·557	0·150	0·090
Br_1	0·574	0·250	−0·190
Br_2	0·111	0·250	−0·098
Br_3	0·851	0·071	0·082
Br_4	0·380	0·050	0·180

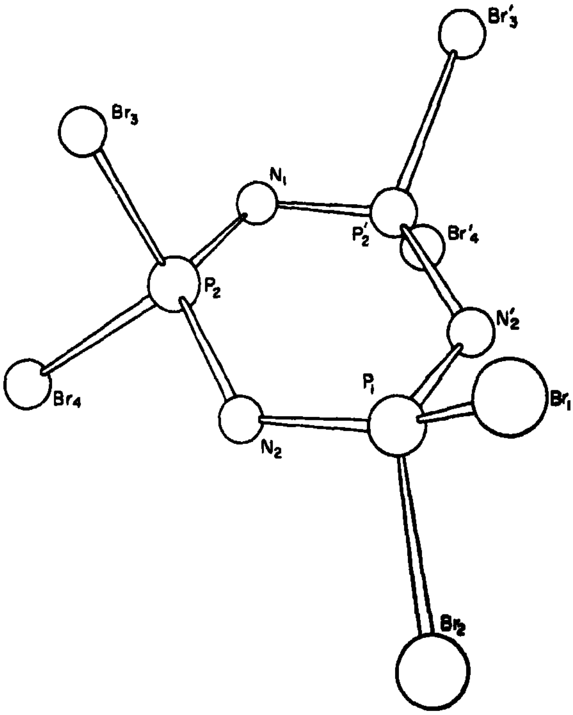

FIG. 3.—Trimeric phosphonitrilic bromide, showing the numbering system used.

DISCUSSION OF THE STRUCTURE

A drawing of the unit cell showing the molecular packing and the closest intermolecular contacts is reported in Fig. 4.

Intermolecular distances correspond to normal Van der Waals interactions.

The values of the bond lengths and bond angles calculated from the co-ordinates of Table 1, are shown in Table 2.

At this stage of the refinement the accuracy is not very high, but it is sufficient to show the most important aspects of the molecular geometry.

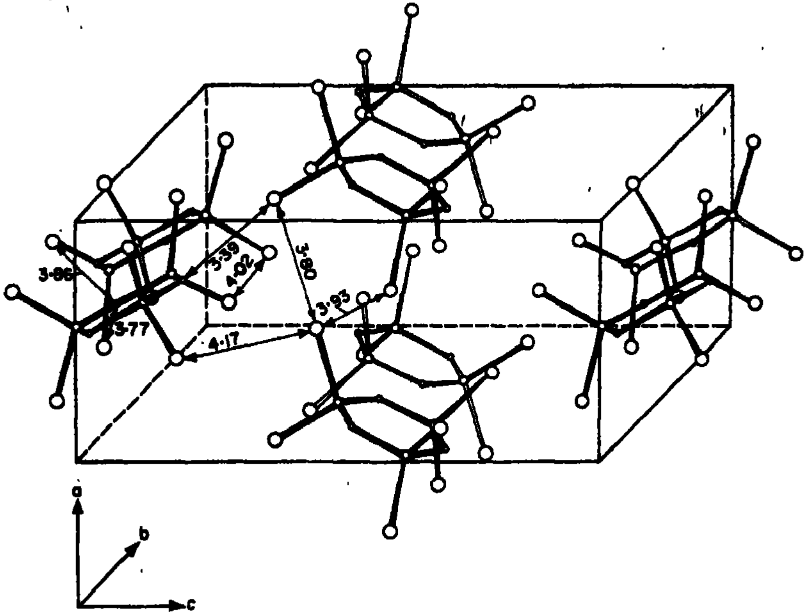

Fig. 4.—Drawing of the unit cell, showing the molecular packing and the closest intermolecular contacts.

Table 2.

$\overline{N_1P_2} = 1{\cdot}51$ Å

$\overline{N_2P_2} = 1{\cdot}53$ Å

$\overline{N_2P_1} = 1{\cdot}54$ Å

$\overline{P_1Br_1} = 2{\cdot}08$ Å

$\overline{P_1Br_2} = 2{\cdot}14$ Å

$\overline{P_2Br_3} = 2{\cdot}22$ Å

$\overline{P_2Br_4} = 2{\cdot}20$ Å

$N_2\widehat{P_1}N_3 = 117°$

$P_2\widehat{N_1}P_3 = 126°$

$N_1\widehat{P_2}N_2 = 116°$

$P_1\widehat{N_2}P_2 = 122°$

$Br_1\widehat{P_1}Br_2 = 103°$

$Br_3\widehat{P_2}Br_4 = 102°$

The best plane of the $(PN)_3$ ring calculated by the least-squares method, using the atomic co-ordinates of Table 1, is defined by the equation:

$$-0{\cdot}326\,x+0{\cdot}140\,z+1 = 0$$

the distance from this plane to the origin of the unit cell being 2·82 Å. The mean deviations of the nitrogen and phosphorus atoms from this plane is small (0·05 Å). However, since the nitrogen atoms lie above and the phosphorus atoms systematically below the best plane, the molecular ring has a slight chair conformation similar to that found for trimeric phosphonitrilic chloride.

This might be taken as an evidence that the deviation from a planar structure which appears to be systematic for the trimeric phosphonitrilic ring is not produced by the crystal forces as suggested by WILSON and CARROLL(10) for the trimeric phosphonitrilic chloride.

The mean P—N bond length of 1·53 Å is smaller than that reported by BODE(7) (1·58 Å) and the average values of PNP and NPN angles are significantly different. A comparison with $(NPCl_2)_3$ again emphasizes the influence of the substituents on the phosphorus atoms on bond lengths and bond angles in the ring. Finally it may be noted that the bond angles on the nitrogen atoms of the molecular ring in all the compounds of the series thus far investigated are significantly larger than those on the phosphorus atoms.

In view of the important theoretical implications involved in the above mentioned effects, the three-dimensional refinement, in progress, of the structure of trimeric phosphonitrilic bromide can be of particular interest.

Acknowledgements—The authors wish to express their gratitude to Professor A. M. LIQUORI for his interest and very helpful discussions, and to Dr. R. A. SHAW for the supply of trimeric phosonitrilic bromide.

This work has been financially supported by the Consiglio Nazionale delle Ricerche.

(10) A. WILSON and D. F. CARROLL, *J. Chem. Soc.* 2548 (1960).

J. Inorg. Nucl. Chem., 1962, Vol. 24, pp. 475 to 482, Pergamon Press Ltd. Printed in England

INFRA-RED SPECTRA OF SEVERAL SALTS OF ACIDIC ORGANOPHOSPHORUS COMPOUNDS*

J. R. Ferraro
Chemistry Division, Argonne National Laboratory, Argonne, Illinois

(*Received* 13 *October* 1961; *in revised form* 10 *November* 1961)

Abstract—The infra-red spectra of several sodium salts of acidic organophosphorus compounds $(GO)_2PO(OH)$, $(GO)G'PO(OH)$† are discussed. It is observed that the salt spectra are sharper than the acid spectra. The phosphoryl absorption $(P \rightarrow O)$ in the acids is replaced by two new peaks—the POO^- asymmetric vibration (1210–1283 cm^{-1}), which is at a higher frequency when the G group is aryl, and the POO^- symmetric vibration (which appears to remain constant for the phosphates at about 1100 cm^{-1}). The position of the POO^- asymmetric vibration for the salts of *p*-substituted aryl phosphoric acids appears to shift to higher frequency as the Hammett function σ_p decreases. In the aryl phosphoric acids and the aryl hydrogen phosphonates, the region of about 960–1000 cm^{-1} attributed to the [P–O]-aryl vibration disappears on salt formation, and a new region at 900–930 cm^{-1} appears.

In the alkali, alkaline earth, Co(II) and Sc(III) salts of bis-(2-ethylhexyl)-phosphoric acid, there appears to be a trend toward lower values of Δ (where Δ is ν_{poo^-} asymmetric $-\nu_{poo^-}$ symmetric) as ϕ (charge/ionic radii) increases.

In the course of previous investigations⁽¹⁾ it was necessary to prepare the sodium salts of several acidic organophosphorus compounds $[(GO)_2PO(OH)$ and $(GO)(G')PO(OH)]$ as an aid in identifying the phosphoryl asymmetric stretching vibration $(P \rightarrow O)$. The purpose of this paper is to discuss the infra-red spectra of these salts, which are presumed to be new.

EXPERIMENTAL

The salts were prepared from the acids by titration of an alcoholic solution with 0·1 N base to a phenolphthalein end point. (The acids (> 99 per cent purity) were prepared and purified as described in a previous publication(1, 2) and their infra-red spectra reported.)(1, 2) The solutions were evaporated slowly and the salts filtered off. Several of these salts were also prepared using a Precision-Dow titrimeter. Both methods gave identical products. Sodium phenyl phosphinate was prepared from phenyl phosphinic acid (ΦHPOOH), obtained from Victor Chem. Works (m.p. 81° C; equivalent weight 142). Sodium di-*p*-nitrophenyl phosphate was prepared from di-*p*-nitrophenyl phosphoric acid, obtained from the Aldrich Chem. Co., Milwaukee, Wisconsin.

The infra-red spectra were obtained with a Beckman infra-red-4 spectrophotometer. The spectra were made on KBr disks and Nujol mulls for checks.

---

* Based on work performed under the auspices of the U.S. Atomic Energy Commission.

† G can be aryl, alkyl or mixed alkyl–aryl or a substituted variant thereof.

(1) D. F. Peppard, J. R. Ferraro and G. W. Mason, *J. Inorg. Nucl. Chem.* **16**, 246 (1961).

(2) D. F. Peppard, J. R. Ferraro and G. W. Mason, *J. Inorg. Nucl. Chem.* **12**, 60 (1959).

DISCUSSION AND RESULTS

As has been previously indicated(1) in forming the salts of acidic organophosphorus compounds, the expectation is to observe two new frequencies corresponding to the POO^- asymmetric and POO^- symmetric absorption. The original P → O absorption, present in the acid, is no longer to be found, for in the salt, the oxygens are indistinguishable (analogous to the situation in salts of monocarboxylic acids). It is observed from the spectra of these salts that the original P → O absorption has disappeared, and is replaced by two peaks corresponding to the POO^- asymmetric and symmetric absorption. In Figs. 1–2 the spectra of two of the acids and their sodium salts in the region 1000–1300 cm^{-1} are compared. The spectra in this region of the other acids and their salts are similar and therefore have been omitted. The asymmetric vibration is located anywhere from 1210–1283 cm^{-1}, and is at higher frequency when the G group is aryl. The symmetric vibration in the sodium salts of the phosphoric acids remains fairly constant at about 1100 cm^{-1}. In the salts of the hydrogen phosphonates, this vibration appears to vary over a larger range. STIMSON(3) found that the COO^- symmetric vibration also remained fairly constant in the salts of substituted benzoic acids. Both (POO^-) peaks are strong and sharp as compared to the rather broad P → O peaks in the acid. In general, the salt spectra are sharper

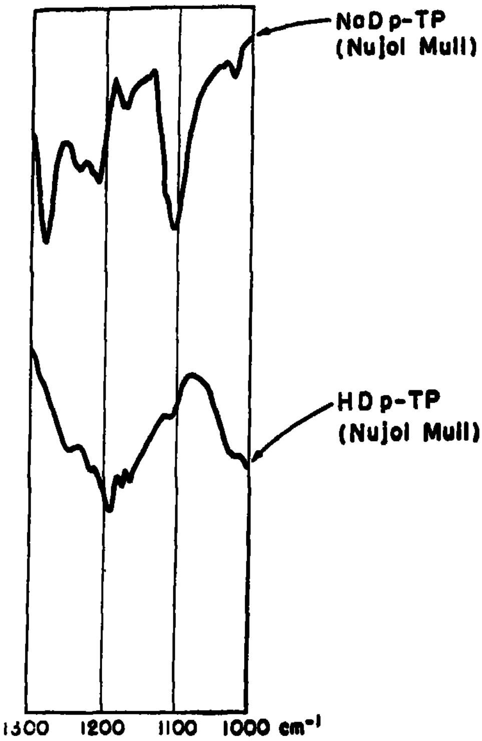

FIG. 1.—Infra-red spectra of bis-(*p*-tolyl)-phosphoric acid and its sodium salt in the 1000–1300 cm^{-1} region.

---

(3) M. STIMSON, *J. Chem. Phys.* **22**, 1942 (1954).

than the acid spectra. This can be a consequence of the hydrogen bonding existing in the acids, which tends to broaden the phosphorus associated vibrations. In the salt spectra, the bonded OH regions disappear as expected. Other regions of absorption in the spectra of these salts are the —CH stretching vibrations occurring at about 2800–3100 cm^{-1}; the —C = C— skeletal in-plane vibrations in the aryl rings at about 1500–1600 cm^{-1}; the —CH bending mode in alkyl groups at about 1350–1480 cm^{-1}; and the out-of-plane —C–H vibrations in the aryl groups at about 700–840 cm^{-1}.

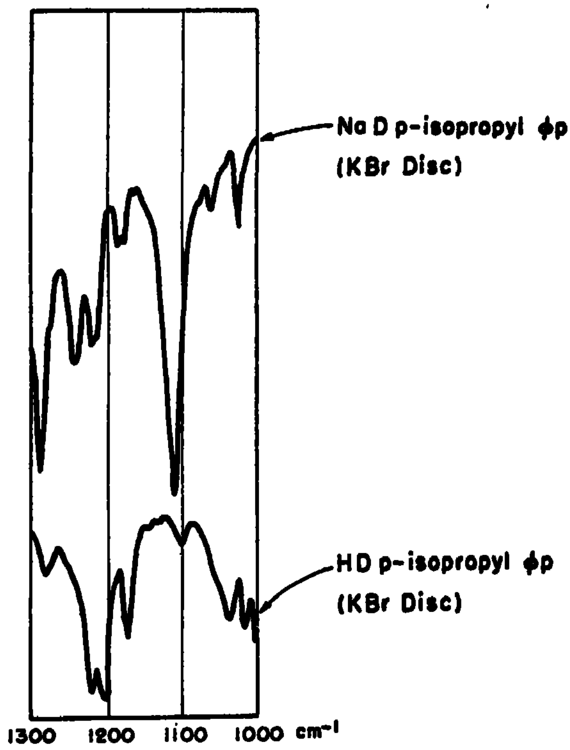

FIG. 2.—Infra-red spectra of bis-(*p*-isopropylphenyl)-phosphoric acid and its sodium salt in the 1000–1300 cm^{-1} region.

The POO$^-$ asymmetric and symmetric absorptions in the sodium salts prepared from fourteen organophosphoric acids and three hydrogen organophosphonates are recorded in Table 1. It is observed that the difference between these absorptions is greater where G is aryl than where G is alkyl, and must be related in part to the electronegativity of the G group. Fig. 3 illustrates the plot for the sodium salts of *p*-substituted aryl phosphoric acids (Hammett σ_p functions vs. POO$^-$ asymmetric vibrations), and it is observed that the POO$^-$ asymmetric vibration shifts to higher frequency as the σ_p function decreases.

BELLAMY[(4)] has called attention to the observation that in two aryl phosphoric acids the absorption at about 1000 cm^{-1} vanishes on salt formation or is much reduced in intensity. This band is presumably the [P–O]-aryl vibration. From this

---

(4) L. J. BELLAMY and L. BEECHER, *J. Chem. Soc.* 728 (1953).

TABLE 1.—THE POO$^-$ ASYMMETRIC AND SYMMETRIC ABSORPTIONS IN THE SODIUM SALTS OF ACIDIC ORGANOPHOSPHORUS COMPOUNDS

Sodium salt of phosphoric acids	ν (cm^{-1}) POO$^-$ asymmetric (1)	ν (cm^{-1}) POO$^-$ symmetric (2)	Δ (1–2)	Nature of G group
p-isopropylphenyl	1282	1105	175	Aryl
p-tolyl	1282	1105	177	Aryl
Phenyl	1278	1110	168	Aryl
p-phenylphenyl	1277	1102	175	Aryl
p-(1, 1, 3, 3-tetramethylbutyl)phenyl	1283	1108	175	Aryl
β-naphthyl	1273	1102	171	Aryl
Phenylethyl	1270	1110	160	Alkyl
o-tolyl	1250	1100	150	Aryl
Cyclohexyl	1250	1105	145	Alkyl
p-nitrophenyl	1235	1090	145	Aryl
Ethylhexyl	1243	1100	143	Alkyl
Butoxyethyl	1250	1115	135	Alkyl
γ-phenyl propyl	1240	1095	145	Alkyl
Butyl	1220	1070	150	Alkyl
Sodium salt of hydrogen phosponates				
Phenyl phenyl	1240	1065	175	Aryl
Benzyl phenyl	1245	1074	171	Aryl
Butyl butyl	1210	1090	120	Alkyl

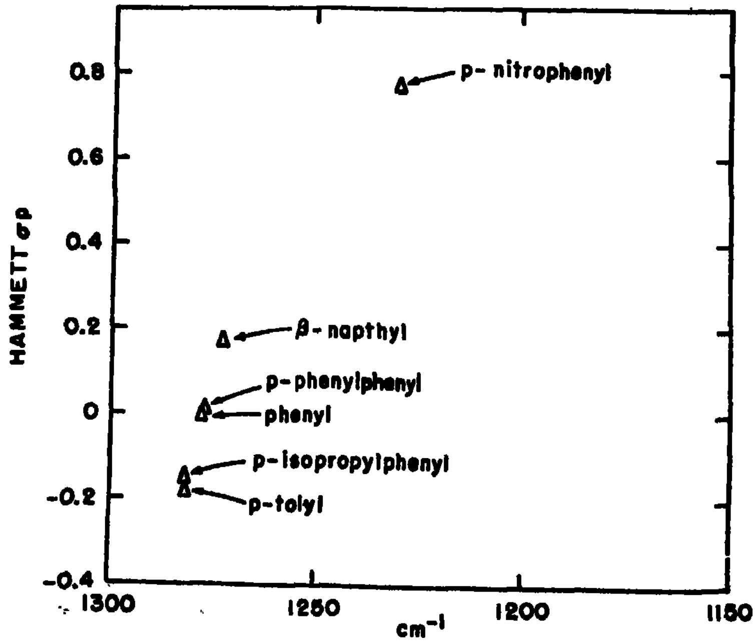

FIG. 3.—The POO$^-$(asymmetric) frequency of several para-substituted aryl phosphoric acids vs. the Hammett σ_p function.

study, it is observed that this is a general behaviour for the salts of the aryl phosphoric acids and may be general for all salts containing an [P–O]-aryl link. The band in the 960–1000 cm^{-1} region disappears on salt formation, and is replaced by a new band at 900–930 cm^{-1}. In some cases, the new band is very sharp and intense. If the new peak is still associated with the [P–O]-aryl vibration, it would represent a weakening of this bond and a consequential shift toward lower frequencies. With the salts of the alkyl phosphoric acids, the region between 1000–1050 cm^{-1}, is apparently maintained, although sharpened up, and several fine peaks replace the one very strong broad peak present in the acid. Sodium phenyl phenylphosphonate, having one [P–O]-aryl group, behaves very much like the aryl phosphoric acids in losing the absorption in the 960–1000 cm^{-1} region on salt formation with new absorptions occurring at lower frequency. Sodium benzyl phenylphosphonate and sodium phenyl phosphinate (ϕHPOONa), lacking the [P–O]-aryl group fail to demonstrate a shift to lower frequency on salt formation. This lends support to the supposition that the absorption in the 960–1000 cm^{-1} region in the acids is associated with the [P–O]-aryl group. Figs. 4–5 illustrate the comparison between the acid and salt spectra in the region 800–1200 cm^{-1}.

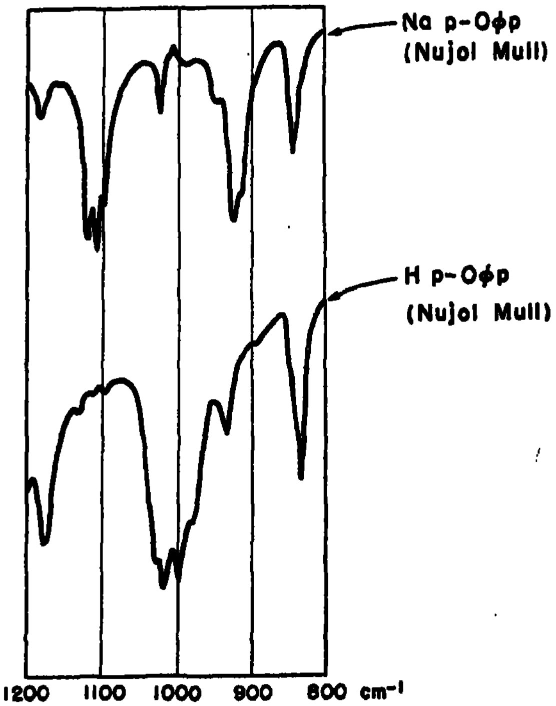

FIG. 4.—Infra-red spectra of Bis-[(p-1, 1, 3, 3-tetramethylbutyl)phenyl]-phosphoric acid and its sodium salt in the 800–1200 cm^{-1} region.

The cation effect on the POO^- asymmetric and symmetric vibrations of the salts of bis-(2-ethylhexyl)-phosphoric and bis-(1, 1, 3, 3-tetramethylbutyl)-phosphoric acids was investigated. The alkali and alkaline earth salts of these acids were prepared and their infra-red spectra obtained. The spectra of the salts $Co(en)_3(DEHP)_3$ and

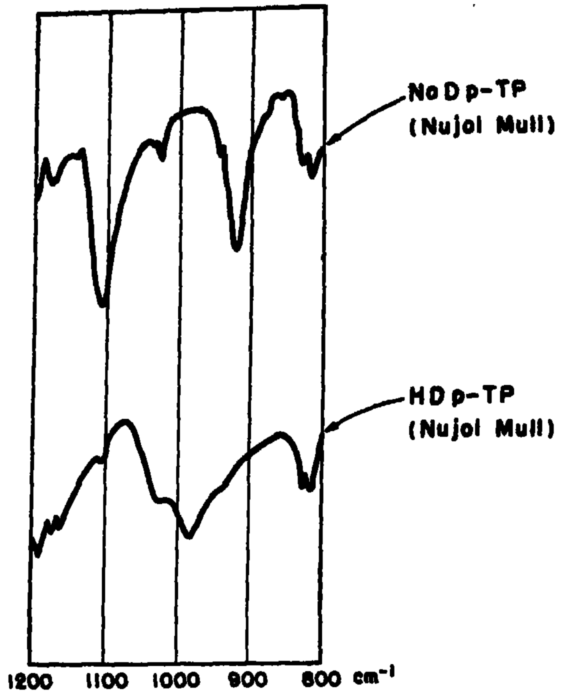

Fig. 5.—Infra-red spectra of bis-(*p*-tolyl)-phosphoric acid and its sodium salt in the 800–1200 cm^{-1} region.

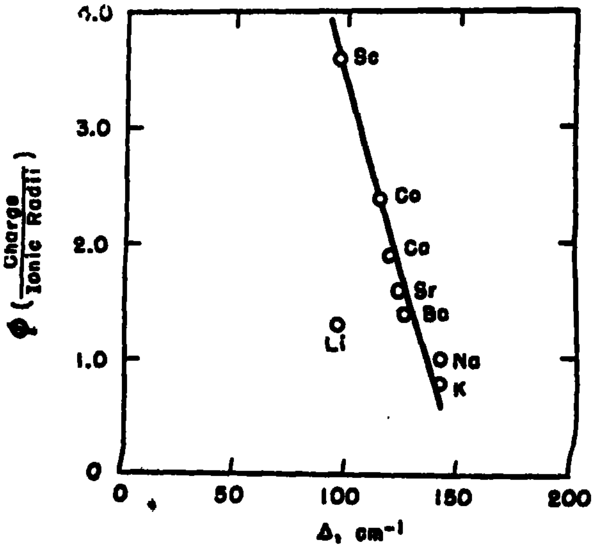

Fig. 6.—Cation effect on the POO$^-$ asymmetric and symmetric frequencies for various salts of bis-(2-ethylhexyl)-phosphoric acid.

TABLE 2.—CATION EFFECT ON THE POO^- ASYMMETRIC AND SYMMETRIC FREQUENCIES FOR VARIOUS SALTS OF BIS-(2-ETHYLHEXYL)- AND BIS-(1, 1, 3, 3-TETRAMETHYLBUTYL)-PHOSPHORIC ACIDS

Bis-(2-ethylhexyl)-phosphoric acid				Bis-(p-1,1,3,3-tetramethylbutyl)phosphoric acid			
Salt	ν_{POO^-} (asymmetric) (1)	ν_{POO^-} (symmetric) (2)	Δ (1–2) (cm^{-1})	Salt	ν_{POO^-} (asymmetric) (1)	ν_{POO^-} (symmetric) (2)	Δ (1–2) (cm^{-1})
Li (KBr disk)	1196	1102	94	Li (Nujol)	1273	1098	175
Na (KBr disk)	1243	1100	143	Na (Nujol)	1283	1108	175
K (KBr disk)	1238	1098	140	K (liquid film)	1250	1095	155
Ca (liquid film)	1220	1103	117	Ca (Nujol)	1248	1110	138
Sr (liquid film)	1222	1100	122	Sr (liquid film)	1252	1100	152
Ba (liquid film)	1220	1095	125	Ba (liquid film)	1252	1090	162
Co (KBr disk)	1203	1093	113				
Sc (KBr disk)	1201	1104	97				

$Sc(DEHP)_3$ were reported in a previous publication.[5] The tabulated results appear in Table 2. Fig. 6 illustrates a plot of charge/ionic radii (ϕ) versus Δ (where Δ is $[\nu_{poo-(asymmetric)} - \nu_{poo-(symmetric)}]$), for various salts of bis-(2-ethylhexyl)-phosphoric acid. Generally there appears to be a trend toward lower values of Δ as the value of ϕ increases (and roughly as the electronegativity of the metal increases). These relationships appear to hold for the salts of organophosphoric acids of high ionic character, such as those presented in Fig. 6. Where a high degree of covalency is introduced in the metal to phosphate bond, the position of $\nu_{poo\ (asymmetric)}$ - appears to shift toward higher frequency.[5] In addition, in the complexes involving metals with high charge (e.g. Th^{4+}, Zr^{4+}, Hf^{4+}, etc.) there is a strong tendency to form polymeric complexes, and this would affect the absorption in this region.[5]

Comparative results with the salts of the carboxylic acids are available. KAGARISE[6] has found for the salts of monocarboxylic acids that the COO^- asymmetric frequency increases as the electronegativity of the metal increases. STIMSON[3] found a tendency for the COO^- asymmetric frequency, in salts of substituted benzoic acids, to increase as the electronegativity of the cation decreased.

Acknowledgement—The author wishes to thank Mr. G. W. MASON of Argonne National Laboratory for purifying the acids from which these salts were prepared.

---

[5] D. F. PEPPARD, J. R. FERRARO and G. W. MASON, *J. Inorg. Nucl. Chem.* **10**, 275 (1959).
[6] R. E. KAGARISE, *J. Phys. Chem.* **59**, 271 (1955).

J. Inorg. Nucl. Chem., 1962, Vol. 24, pp. 483 to 490. Pergamon Press Ltd. Printed in England.

INFRA-RED SPECTRA AND VIBRATION ASSIGNMENT OF PHOSPHONITRILIC HALIDES—I

TRIMERIC PHOSPHONITRILIC CHLORIDE

S. Califano
Istituto Chimico, Via Mezzocannone, 4, Napoli, Italy

(*Received* 19 *July* 1961)

Abstract—The infra-red spectra of $(NPCl_2)_3$, have been measured in the vapour phase, in solution and in KBr pellets, between 3000 and 300 cm^{-1}.

Using the Raman spectra given in the literature, a new vibrational assignment is given on the basis of a D_{3h} molecular symmetry.

The assignment of the infra-red active modes is confirmed from the measurement of their dichroic ratios in the crystal.

Despite the considerable amount of work recently published on the crystal structure⁽¹⁾ and on the electronic configuration⁽²⁾ of the trimeric phosphonitrilic halides, their molecular spectra have received until now relatively limited attention.

The Raman and infra-red spectra of $(NPF_2)_3$ were recently reported by Becher and Seel.⁽³⁾ The Raman spectrum of $(NPCl_2)_3$ was investigated some years ago by Fiequelmont, Magat and Ochs⁽⁴⁾ and later by Daasch.⁽⁵⁾ The latter also determined the infra-red spectrum in solution and proposed a partial assignment assuming a planar structure with D_{3h} symmetry. Scattered information are also available in the literature on the infra-red spectra of the mixed chloro-bromo⁽⁶⁾ and chloro-fluoro⁽⁷⁾ halides, but they are generally of a qualitative nature and limited to the identification of the ring frequency at about 1300 cm^{-1}.

A systematic study of the spectra of the phosphonitrilic halides in the different states of aggregation has therefore been undertaken with the hope of obtaining a more complete and satisfactory picture of the normal modes of vibration of this interesting class of inorganic compounds.

In this first paper we will report on the vibrational assignment of $(NPCl_2)_3$. A detailed analysis of the crystal spectrum in polarized light will be published shortly. We shall however, whenever necessary, make use of the results of the polarization measurements in the discussion of the vibrational assignment, because they are often the only available criteria of choice, the rotational envelope of the vapour bands not being resolved.

---

(1) L. O. Brockway and W. M. Bright, *J. Amer. Chem. Soc.* **65**, 1551 (1943); A. Wilson and D. F. Carrol, *Chem. & Ind.* 1558 (1958); E. Cipollini, F. Pompa and A. Ripamonti, *Ric. Sci.* **28**, 2055 (1958).

(2) D. P. Craig and N. L. Paddock, *Nature, Lond.* **181**, 1052 (1958); M. J. S. Dewar, E. A. C. Lucken and M. A. Whitehead, *J. Chem. Soc.* 2423 (1960).

(3) H. J. Becher and F. Seel, *Z. Anorg. Chem.* **305**, 148 (1960).

(4) A. Fiequelmont, M. Magat and L. Ochs, *C.R. Acad. Sci., Paris* **208**, 1900 (1939).

(5) L. W. Daasch, *J. Amer. Chem. Soc.* **76**, 3403 (1954).

(6) R. G. Rice, L. W. Daasch, J. R. Holden and E. J. Kohn, *J. Inorg. Nucl. Chem.* **5**, 190 (1958).

(7) A. C. Chapman, D. H. Paine, H. T. Searle, D. R. Smith and R. F. M. White, *J. Chem. Soc.* 1768 (1961).

EXPERIMENTAL

The phosphonitrilic chloride trimer used was kindly supplied by the Albright and Wilson Co. and purified by several crystallizations from benzene.

The spectra were obtained in the vapour phase, in KBr pellets as well as in solution (CS_2) with the aid of a Perkin Elmer double beam spectrograph model 13 C equipped with NaCl, KBr and KRS-5 optics.

The vapour phase spectra were obtained by using a cell of 9 cm path, electrically heated to a temperature of about 150° C. The observed frequencies, together with the Raman data taken from the literature are collected in Table 1.

TABLE 1.—INFRA-RED AND RAMAN SPECTRA OF $(NPCl_2)_3$

Infra-red		Raman	
Vapour	Solid	Reference (5)	Reference (4)
		100 *vw* *P*	100 (5) *P*
		162 (4) *dp*	162 (5) *dp*
		173 (3) *dp*	177 (5) *dp*
		210 (3) *dp*	206 (4) —
			312 *vw* —
336 *m*	340 *m*	340 (1) *dp*	339 (3) *dp*
		365 (10) *P*	366 (8) *P*
533 *vs*	526 *vs*	523 (0·5)—	533 (1) *dp*
552 *s*	542 *s*		
584 *vw*		575 (1) *dp*	585 (6) *P*
619 *vs*	} 603 *vs* 613	610 (0·5)—	614 (1) —
636 *m*			
	670 *w*	670 (4) *P*	672 (6) *P*
	700 *vw*		
			707 *vw* —
	739 *vw*		
	785 *w*	785 (2) *P*	
	823 *vw*		
	848 *vw*		
	864 *w*		
	875 *m*		
			885 *vw* —
			940 *vw* —
997 *vw*	991 *vw*		
1037 *vw*	1037 *vw*		
1074 *vw*			
	1094 *vw*		
1125 *w*	1125 *w*		
1150 *w*	1150 *w*		
1202 *s*	1196 *s*		
1226 *vs*	1218 *vs*		
			1230 *vw* —
	1251 *s*		
1266 *m*			
1298 *m*	1310 *m*		
1368 *w*	1368 *w*		1368 *vw* —
1758 *w*	1758 *w*		
1888 *w*	1880 *w*		
1976 *w*	1975 *w*		
1998 *m*	1998 *m*		
2068 *w*	2075 *w*		

The spectra in the vapour phase and in KBr pellet are shown in Figs. 1 and 2. The solution spectrum is not shown being already published in reference (5).

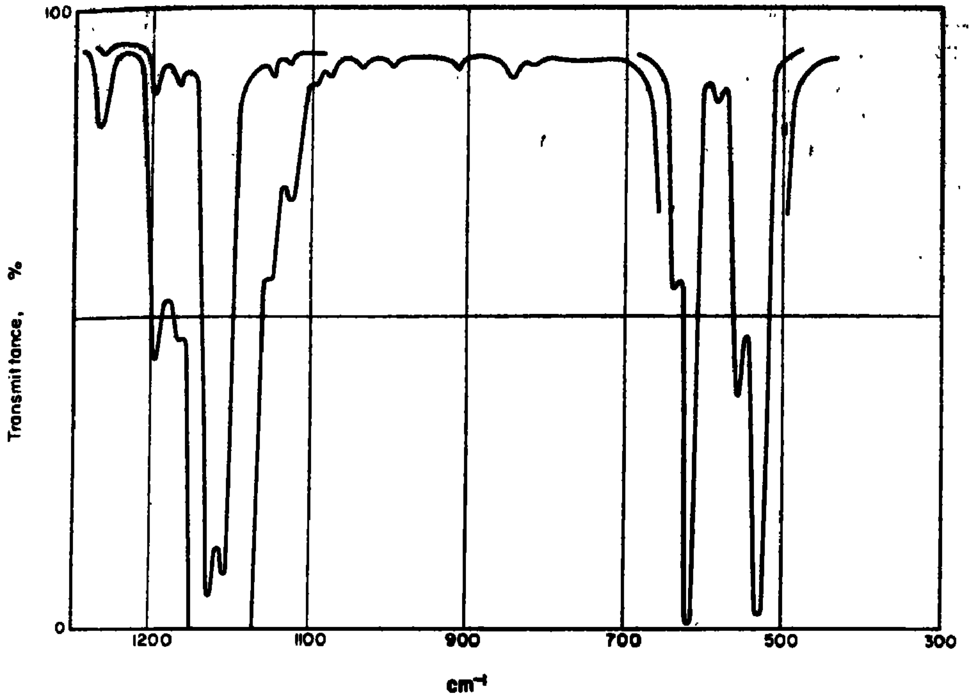

Fig. 1.—Infra-red spectrum of $(NPCl_2)_3$ in the vapour phase. Temperature about 150° C.

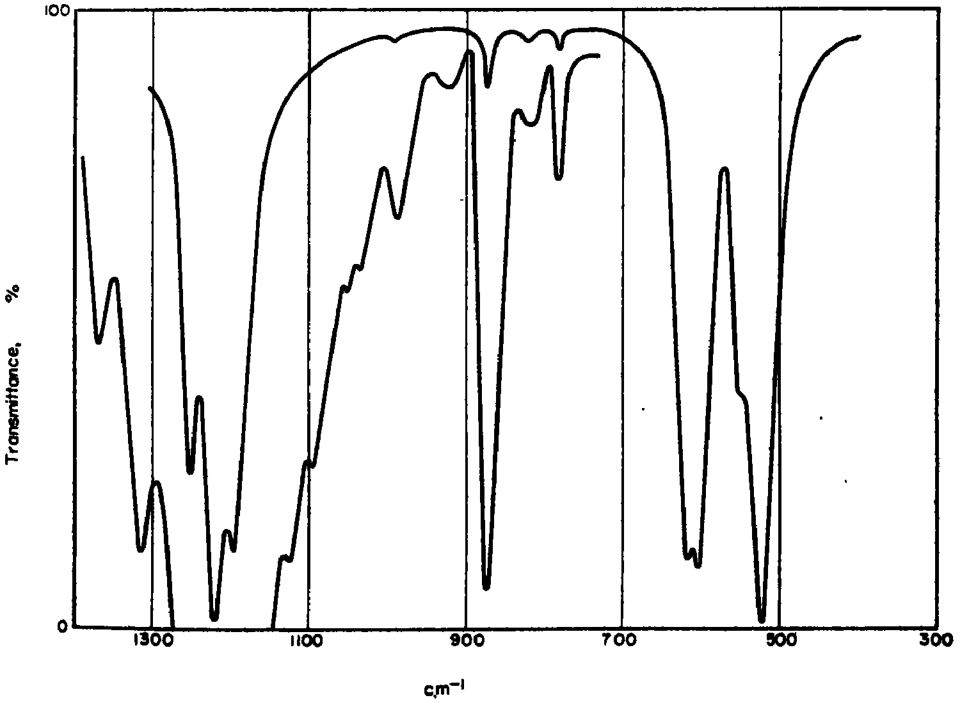

Fig. 2.—Infra-red spectrum of $(NPCl_2)_3$ in KBr pellet.

THE MOLECULAR SYMMETRY

A recent tridimensional Fourier analysis(8) has shown that $(NPCl_2)_3$ exists in the crystal as slightly non-planar six-membered rings with a chair structure. The ring puckering is however so small that the assumption of a planar structure with D_{3h} symmetry seems adequate for the interpretation of the spectra in the vapour phase and in solution. As a matter of fact the Raman spectrum, as pointed out by DAASCH,(5) is consistent only with the D_{3h} molecular symmetry; only four polarized lines appear and no more than five coincidences are observed above 300 cm^{-1}, where the infra-red spectrum is available. The selection rules for the C_{3v} point group (chair structure) would instead require seven polarized Raman lines and all infra-red active bands to be active also in the Raman spectrum.

The selection rules for the D_{3h} point group as well as for the C_{3v} point group are shown in Table 2.

TABLE 2.—SELECTION RULES FOR THE PLANAR AND PUCKERED CONFIGURATION OF $(NPCl_2)_3$

D_{3h}				C_{3v}			
Species	No.	Infra-red	Raman	Species	No.	Infra-red	Raman
A_1'	4	*ia*	*p*	A_1	7	M_z	*p*
A_2''	3	M_z	*ia*				
E'	6	(M_xM_y)	*dp*	E	10	(M_xM_y)	*dp*
E''	4	*ia*	*dp*				
A_1''	1	*ia*	*ia*	A_2	3	*ia*	*ia*
A_2'	2	*ia*	*ia*				

VIBRATIONAL ASSIGNMENT

A_1' species

Three A_1' fundamentals are easily identified in the polarized Raman lines at 100, 365 and 670 cm^{-1}. There is a disagreement in the Raman spectra of references (4) and (5) on the depolarization ratio of the fourth line. FIEQUELMONT *et al.* reported a strong polarized line at 575 cm^{-1}, while DAASCH has found the same line depolarized and has detected a new polarized line at 785 cm^{-1}.

The infra-red spectra do not furnish any conclusive evidence in favour of one or other of the two possibilities. The measurements in polarized light can be better interpreted on the basis of FIEQUELMONT's choice, but, on the other hand, the assignment of the 785 and 670 cm^{-1} bands to A_1' fundamental modes, agrees better with the assignment of other known molecules.

Both arguments are however not decisive and a new Raman spectrum is therefore highly desiderable. If the 785 cm^{-1} band is taken as an A_1' fundamental, then the 575 cm^{-1} line should be assigned to the E'' species, while if the 575 cm^{-1} line is assumed as an A_1' fundamental, then the 785 cm^{-1} band can only be explained as one of the combination bands:

---

(8) F. POMPA and A. RIPAMONTI, *Ric. Sci.* **29**, 1516 (1959); E. GIGLIO, *Ric. Sci.* **30**, 721 (1960).

$$613+173 = 786\ (E')$$
$$575+210 = 785\ (E'').$$

Both assignments are given in Table 3, but a slight preference is given to the first one.

Table 3.—Vibrational assignment of $(NPCl_2)_3$

Symmetry	N	ν I	ν II	Type of vibration
A_1'	1	785	670	Ring stretching
	2	670	575	Ring in pl. def.
	3	365		PCl_2 symm. stretch.
	4	100		PCl_2 symm. bending
A_2''	5	619		Ring out of pl. def.
	6	552		PCl_2 asymm. stretch.
	7	...		PCl_2 rocking
A_1''	8	...		PCl_2 twisting
A_2'	9	875 ?		Ring stretching
	10	...		PCl_2 wagging
E'	11	1226		Ring stretching
	12	1202	875	Ring stretching
	13	533		Ring def. in pl.
	14	336		PCl_2 symm. stretching
	15	(150)		PCl_2 wagging
	16	...		PCl_2 bending
E''	17	575	610	PCl_2 asymm. stretching
	18	210		Ring out of pl. def.
	19	173		PCl_2 twisting
	20	162		PCl_2 rocking

Daasch has assigned the two bands at 785 and 365 cm^{-1} to ring motions and the band at 670 cm^{-1} to a PCl_2 stretching vibration. The comparison with the assignment of PCl_5,(9) for which the symmetric PCl stretching mode occurs at 394 cm^{-1} and the symmetric bending mode at 100 cm^{-1}, suggests however that this assignment should be revised, assigning the 785 and 670 cm^{-1} bands to the ring vibrations and the 365 and 100 cm^{-1} bands to the PCl_2 motions.

There are a few other arguments to support this assignment. Once the 575 cm^{-1} band has been assigned to the E'' species, it can only correspond to the PCl_2 asymmetrical stretching mode. It would seem rather strange to find the corresponding symmetrical vibration at a higher frequency, namely at 670 cm^{-1}, when they are known to occur usually at lower frequencies.

---

(9) H. Gerding and H. Houtgraaf, *Rec.* 74, 5 (1955); J. K. Wilmshurst and H. J. Bernstein, *J. Chem. Phys.* 27, 661 (1957).

Furthermore we would expect ring vibrations to follow the same frequency pattern as other known ring molecules like cyclohexane or benzene. The comparison with their assignment indicates that the 670 cm^{-1} band fits a ring frequency much better than the 365 cm^{-1} band, which falls considerably outside the possible frequency range.

E'' species

The three depolarized and rather strong lines at 162, 173 and 210 cm^{-1} have been ascribed by DAASCH to this species. Owing to the fact that the infra-red spectrum is not available below 300 cm^{-1}, at least, two of them could possibly be assigned also to the E' species. However all the higher frequency bands, which definitely belong to the E' species, are very strong in infra-red, but extremely weak in Raman. For this reason DAASCH's assignment seems quite unquestionable. The 210 cm^{-1} line has been assigned to the ring out of the plane deformation, while the other two at 162 and 173 cm^{-1} correspond to the rocking and twisting modes at the PCl_2 groups.

As fourth E'' fundamental we have chosen the 575 cm^{-1} line in agreement with DAASCH's depolarization measurements. This band, although forbidden by the selection rules, appears also in the infra-red spectrum of the vapour as an extremely weak band at 584 cm^{-1}. Its appearance in the vapour spectrum is explained as due to Coriolis coupling with the strong E' band at 533 cm^{-1}. This hypothesis is substantiated by the fact that the band disappears in solution where the molecular rotations are hindered. From Jahn's rule one can deduce that the 575 cm^{-1} band belongs to the E'' species, and therefore corresponds to the asymmetrical PCl_2 stretching mode. This frequency agrees very nicely with the value of 594 cm^{-1} found for the asymmetrical stretching vibration of PCl_5.

E' species

The assignment of the E' vibrations is rather more difficult. The first complication arises from the fact that they are all strong in the infra-red spectrum, but very weak in Raman. Owing to their weakness in the Raman spectrum, two modes, which, being PCl_2 deformations, occur at frequencies below 250 cm^{-1}, cannot be identified.

The second difficulty is due to the possibility of a confusion with A_2 vibrations, which are also strong in infra-red and, although forbidden in the Raman spectrum, could give rise to weak Raman lines in the spectrum of the liquid, where the selection rules no longer hold strictly.

Nevertheless three E' bands are easily recognized in the medium intensity band at 340 cm^{-1} and in the two very strong bands at 533 and 1226 cm^{-1}. The first two are clearly Raman depolarized while the third corresponds to a very weak Raman line.

On the basis of the assignment given for the A_1' species, there is no difficulty in assigning the 336 cm^{-1} band to the out of phase symmetrical PCl_2 stretching vibration. The 1226 cm^{-1} band clearly corresponds to the ring stretching mode while the one at 533 cm^{-1}, can be the in plane ring deformation.

The assignment of the second ring stretching mode is quite a puzzle. In the infra-red spectrum a very strong band occurs at 619 cm^{-1}, with a very weak counterpart in the Raman spectrum, which has been assigned by DAASCH to an E' vibration. The value of 619 cm^{-1} seems however too low for a ring stretching mode. Owing to the fact that the other *ring stretching mode occurs at 1226 cm^{-1}, one would predict a frequency not lower than about 800 cm^{-1}.*

Although its presence in the Raman spectrum is an argument in favour of the assignment to the E' species, it should be taken into account that Raman forbidden lines can appear as weak lines in the spectrum of the liquid, because of the breaking of the selection rules due to the molecular interactions.

The spectrum of the crystal in polarized light is of great help in clarifying this point. As will be seen in the next paper of this series, the 619 cm^{-1} band shows the type of polarization corresponding to A_2'' vibration and therefore its appartenence to the E' species is definitely ruled out.

If, however, the Raman line at 575 cm^{-1} is assigned to the A_1' species, as FIEQUELMONT's polarization measurement would require, then the appearance of the 610 cm^{-1} line in the Raman spectrum could be explained in a completely different way. We would in fact have an E'' vibration missing and therefore the 610 cm^{-1} line could easily be assigned to this vibration.

We then have to look for another band suitable for an E' ring stretching mode. A band at 875 cm^{-1} of medium intensity, in the solution spectrum was also assigned by DAASCH(5) to the E' species. The band corresponds to a very weak Raman line in the spectrum of Reference (4) and in the crystal spectrum shows the type of polarization expected for E' vibrations. On the other hand it is practically absent in the vapour spectrum and this latter is certainly a stronger piece of evidence against DAASCH's assignment than the first two arguments in its favour. An alternative assignment is available, namely the choice of the strong vapour band at 1202 cm^{-1}, which in the solid spectrum shows also the right type of polarization for an E' vibration. Neither of these two assignments can be taken as conclusive. The second is certainly more consistent with the selection rules, but still does not explain the intensity of the 875 cm^{-1} band in solution. The possibility that this latter could correspond to the A_2' ring stretching mode seems fairly remote, this vibration being inactive for both the D_{3h} and the C_{3v} point groups and it would be the only case, in all the spectra of $(NPCl_2)_3$, of an inactive band made active by solvent interaction. On the other hand, both bands can be reasonably well explained as combination tones. In conclusion we have selected the 1202 cm^{-1} band as E' ring stretching mode, without however claiming any conclusive evidence.

A_2'' species

The three vibrations of this species should be active only in the infra-red spectrum. Only two of them are expected in the region above 300 cm^{-1}, namely a ring deformation and a PCl_2 asymmetric stretching vibration. The third one, corresponding to a PCl_2, rocking vibration should occur at much lower frequency.

The two strong bands at 619 and 552 cm^{-1} in the spectrum of the vapour have been chosen as fundamentals of this species, and assigned respectively to the ring bending and to the PCl_2 asymmetric stretching vibration. In the crystal spectrum in polarized light both show the right type of polarization.

Inactive vibration and combinations bands

The A_1'' and the two A_2' vibrations are inactive both in the infra-red and in the Raman spectrum.

In the solid state, however, the molecules are located on a C_s site symmetry and therefore will gain infra-red activity. The possibility of finding them is of course limited only to one of the A_2' modes, which is a ring stretching vibration. The other two are PCl_2 deformation modes and are expected below 300 cm^{-1}.

Although a few weak bands appear in the spectrum of the solid which are absent in the vapour spectrum, no conclusive evidence for a band identifiable as the A_2' fundamental has been found.

The majority of the weak bands which appear in the spectrum of the vapour and of the solution can be easily explained as combinations of the fundamentals already identified. There are however a few of them that defeat any plausible assignment in this way and call for a more detailed discussion.

The most critical are those at 312 and 1368 cm^{-1}, which require for explanation a fundamental to occur at 150 cm^{-1}. The symmetry species of this fundamental is not unequivocally determined, both the E' and the A_2' species being possible. The assignment of the overtone and combination bands is given in Table 4.

TABLE 4.—ASSIGNMENT OF OVERTONES AND COMBINATION BANDS

ν obs	Assignment	ν calc.
312	(150)+162 (E'')	312 (E'')
636	100 (A_1')+533 (E')	633 (E')
700	162 (E'') +173 (E'') +365 (A_1')	700 (E')
707	533 (E') +173 (E'')	706 (E'')
823	210 (E'') +619 (A_2'')	829 (E')
848	575 (E'') +173 (E'') +100 (A_1')	848 (E')
940	365 (A_1')+575 (E'')	940 (E'')
997	100 (A_1')+365 (E_1') +533 (E')	998 (E')
1074	162 (E'') +336 (E') +575 (E'')	1073 (E')
1094	2×552	1104 (A_1')
1125	785 (A_1')+340 (E')	1125 (E')
1150	2×575 (E'')	1150 (E')
1266	336 (E') +150 (E') +785 (A_1')	1271 (E')
1298	?	?
1368	1218 (E') +150 (E')	1368 (E')
1758	1226 (E') +533 (E')	1759 (E')
1888	1226 (E') +670 (A_1')	1896 (E')
1975	575 (E'') +619 (A_2'')+785 (A_1')	1979 (E')
1998	1226 (E') +785 (A_1')	2011 (E')
2068	533 (E') +670 (A_1') +875 (E')	2078 (E')

Acknowledgement—The author wishes to acknowledge Professor A. M. LIQUORI for having drawn to his attention the problem and for many valuable discussions.

J. Inorg. Nucl. Chem., 1962, Vol. 24, pp. 491 to 497. Pergamon Press Ltd. Printed in England

VIBRATIONAL SPECTRA OF PHOSPHONITRILIC HALIDES—II

THE CRYSTAL SPECTRA OF $(NPCl_2)_3$ IN POLARIZED LIGHT

S. CALIFANO and A. RIPAMONTI
Istituto di Chimica dell'Università di Napoli,
Via Mezzocannone, 4, Napoli, Italia

(*Received* 19 *July* 1961; *in revised form* 20 *November* 1961)

IN the preceding paper by one of us,$^{(1)}$ the infra-red spectra of $(NPCl_2)_3$ in different states of agregation have been discussed.

The assignment of many of the observed bands to the proper symmetry species was however not unambiguous, due to the unresolved rotational shape of the vapour phase bands. In addition to this, the solid phase spectrum shows some interesting features which point out the existence of appreciable crystal field effects. In order to investigate these effects and to furnish more definitive evidence for the vibrational assignment, the crystal spectra in polarized light have been studied. Some of the results obtained have been already anticipated in the first paper of this series and will be discussed in detail.

EXPERIMENTAL

The phosphonitrilic chloride trimer used, was kindly supplied by the Albright and Wilson Co. and was purified by several crystallizations from benzene.

The spectrograph used was a Perkin Elmer double beam spectrograph Model 13 C equipped with NaCl, KBr and KRS-5 optics.

The spectra were obtained both on KBr pellets and on polycrystalline orientated samples. These polycrystalline orientated films were prepared allowing a thin layer of molten substance to crystallize between two alkali halide windows. Following the experimental technique described by GREINACHER and MECKE,$^{(2)}$ full orientation of the crystallites was achieved.

To determine the orientation of the crystal axes in the film, an X-ray precession diagram was run on a sample obtained in this way. The X-ray photograph showed that the crystallographic (*ac*) plane was orientated parallel to the window's surfaces.

The spectra in polarized light were then measured with the electric vector of the incident light parallel to the axes *a* and *c*, using standard Perkin-Elmer AgCl polarizers. X-ray powder photograph of mechanical mixtures and of mixed crystals of $(NPCl_2)_3$ and $(NPBr_2)_3$ were recorded by means of a Debye-Scherrer camera of radius 57·3 mm.

SELECTION RULES AND BAND POLARIZATION

Trimeric phosphonitrilic chloride $(NPCl_2)_3$ crystallizes in the orthorombic system, space group $Pnma-D_{2h}^{16}$, with four molecules in the unit cell.$^{(3)}$ Each molecule is located on a C_s site symmetry. A general view of the unit cell is shown in Fig. 1.

---

(1) S. CALIFANO, *J. Inorg. Nucl. Chem.* **24**, (1962).

(2) R. MECKE and E. GREINACHER, *Z. Elektrochem.* **61**, 530 (1957).

(3) A. WILSON and D. F. CARROLL, *Chem. & Ind.* 1558 (1958); E. CIPOLLINI, F. POMPA and A. RIPAMONTI, *Ric. Sci.* **28**, 2055 (1958).

It has been recently shown by means of a tridimensional X-ray analysis that the $(NPCl_2)_3$ molecules are slightly non-planar[4] and possess a C_{3v} symmetry in the crystalline state. The infra-red spectrum of the vapour and the Raman spectrum of the liquid are however consistent only with a D_{3h} symmetry corresponding to the planar structure.

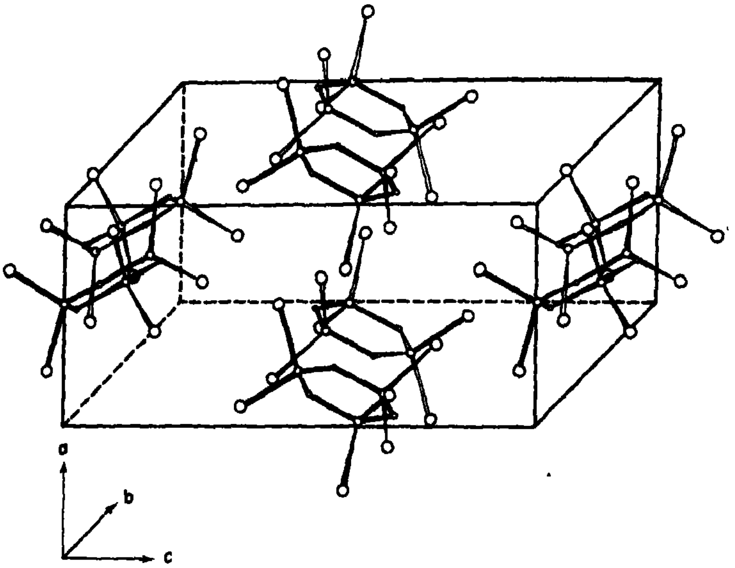

FIG. 1.—General view of the unit cell of $(NPCl_2)_3$.

Although this discrepancy could be due to the fact that the molecule is actually planar in the gaseous state and in solution but slightly distorted from the planarity in the crystal, it is more likely that, the distortion being extremely small, the difference is not enough to invalidate the selection rules for the higher D_{3h} symmetry.

As a matter of fact the crystal spectra can also be completely accounted for on the basis of the D_{3h} symmetry. It is true that some of the bands inactive for the D_{3h} symmetry appear in the crystal spectrum but their appearance can be easily explained as due to the crystalline field. Actually all bands inactive for the D_{3h} point group and active for the C_{3v} point group become infra-red active for the C_s symmetry which is the site symmetry of the molecules in the unit cell. These new crystal bands are all very weak, as one would expect from the fact that their intensity is due only to the dipole moment variation induced from the crystal field.

The selection rules for the solid spectra as well as the number and the symmetry of the vibrations which originate from the coupling between the four molecules in the unit cell are collected in Table 1. This coupling gives rise to four crystal modes for each normal mode of the isolated molecule. These conclusions are reached from the correlation diagram of Table 1, between the irreducible representations of the D_{3h} molecular group, those of the C_s site group and those of the D_{2h} factor group.[5]

---

[4] F. POMPA and A. RIPAMONTI, *Ric. Sci.* **29**, 1516 (1959); E. GIGLIO, *Ric. Sci.* **30**, 721 (1960).

[5] R. S. HALFORD, *J. Chem. Phys.* **14**, 8 (1946); D. F. HORNIG, *J. Chem. Phys.* **16**, 1063 (1948); H. WINSTON and R. S. HALFORD, *J. Chem. Phys.* **17**, 607 (1949); T. H. WALNUT, *J. Chem. Phys.* **20**, 58 (1952).

This latter is isomorphous with the D_{2h}^{16} space group and has the same table of characters.

TABLE 1.—SELECTION RULES FOR THE CRYSTAL OF $(NPCl_2)_3$

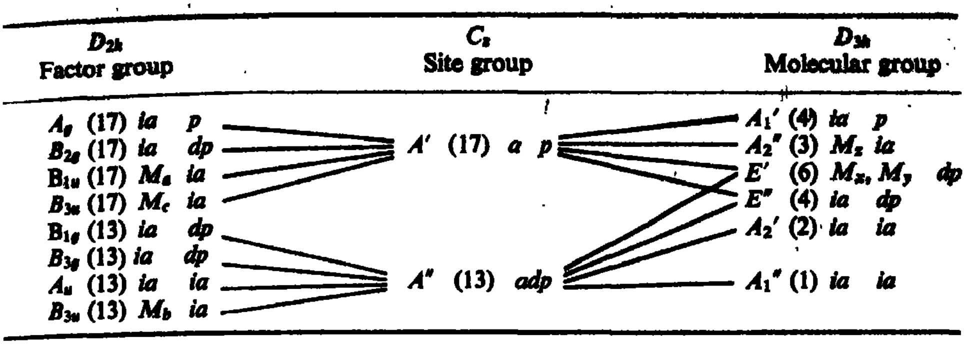

Not all the four crystal modes corresponding to a single normal mode of the free molecule, will be active in infra-red. Vibration of A_1' and A_2'' species give rise in the crystal to two infra-red active modes for which the dipole moment vibrates along the crystallographic axes a and c respectively, while A_2'' and A_2' vibrations give rise to only one infra-red active mode with dipole moment variation along the b crystal axis.

For degenerate vibrations a further complication is due to the site group splitting of the degeneracy, so that for each degenerate mode of the free molecule, we will have two non-generate modes in the crystal.

The first of these vibrations will have a factor group splitting like the vibrations of A_1' and A_2'' species, while the second one will behave like A_2' and A_1'' vibrations. In conclusion each normal mode of E' and E'' species will split into three infra-red active modes with dipole moment variations along the three crystal axes.

The pseudo molecular plane (see Fig. 1) makes an angle of 67° with the crystallographic axis a. In the orienated gas model approximation, the square of the components on the crystal axes a, b and c of unit vectors oriented along the molecular axes x, y and z, summed on all molecules in the unit cell, will be proportional to the absorption intensity along the crystal axes for each vibrational band. Of course these considerations only apply to molecular vibrations associated with an intrinsic dipole variation, namely to vibrations of E' and A_2'' species. However, the effect of the crystalline field being quite appreciable, the induced dipole moment will contribute largely to the absorption intensity. This predominant factor, as well as the known experimental difficulties will spoil the quantitative agreement between the experimental and the calculated dichroic ratios. Nevertheless it is still possible to use the prediction of the orientated gas model as a qualitative basis for the interpretation of the polarized spectra. As a matter of fact the experimental dichroisms are extremally marked and therefore the possibility of misinterpretation is vanishingly small.

These "orientated gas model" predictions are as follows. A_2'' vibrations possess an intrinsic dipole variation perpendicular to the ring plane and therefore the absorption intensity along the a crystal axis (see Fig. 1) should be greater than along the c crystal axis, with a dichroic ratio of $\sin^2 67/\cos^2 67 = 4{\cdot}6$. E' vibrations have intrinsic dipole variation in the molecular plane and therefore the dichroic ratio relative to the crystal axis a and c will be reversed.

DISCUSSION OF THE POLARIZED SPECTRA

The infra-red spectrum of $(NPCl_2)_3$ in polarized light, between 1600 and 400 cm^{-1} is shown in Fig. 2. The solid line represents the spectrum obtained with the electric vector of the light orientated parallel to the *c* crystal axis, while the dotted line corresponds to the orentation of the light vector parallel to the *a* axis. The observed peak frequencies are collected in Table 2. The type of polarization is referred to the *a* crystal axis and is indicated by means of the symbols (‖) parallel and (⊥) perpendicular.

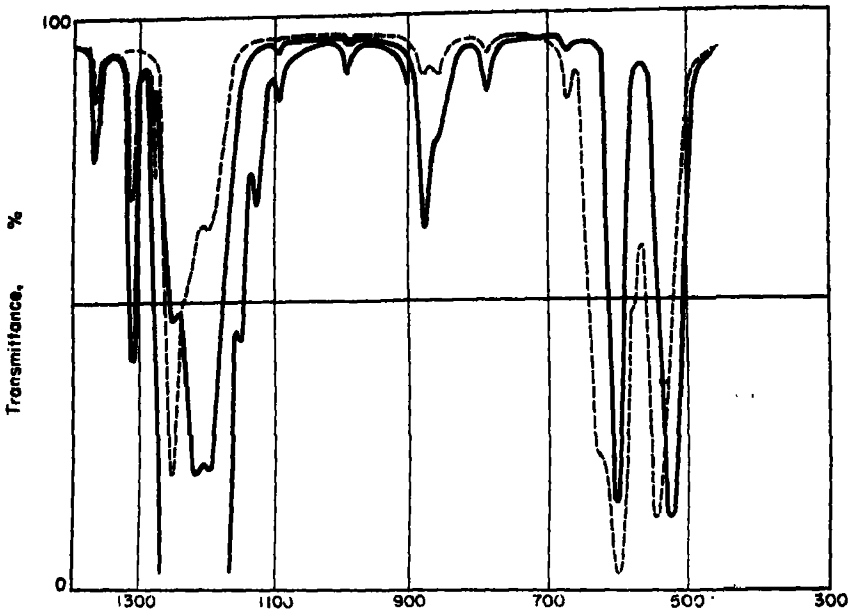

FIG. 2.—Infra-red spectrum in polarized light of $(NPCl_2)_3$. Solid line: electric vector orientated parallel to the *c* crystal axis. Dotted line: electric vector orientated parallel to the *a* crystal axis.

As stated before, vibrations of A_2' species give rise to bands which are of the (‖) type. The two strong bands at 613 and 542 cm^{-1} have this type of polarization and therefore their assignment to the vibrations υ_5 and υ_6 is confirmed.

The band at about 600 cm^{-1} shows an appreciable factor group splitting, being resolved into two components which peaks at 613 and 600 cm^{-1}. In the parallel type spectrum the band is extremly intense and broad while in the perpendicular spectrum the 613 cm^{-1} band practically disappears and only the 600 cm^{-1} component is observable.

The proof that this splitting is due to the coupling of the vibration υ_5 of the four molecules in the unit cell, has been obtained by means of the mixed-crystal technique.(6)

Fortunately the trimeric phosphonitrilic bromide $(NPBr_2)_3$, which is isomorphous with the chloride, is completely transparent in this region. Therefore a diluted solid solution of the chloride in a bromide matrix (molecular ratio about 1:8) was examined in the 600 cm^{-1} region, in KBr pellet.

(6) G. L. HIEBERT and D. F. HORNIG, *J. Chem. Phys.* **20**, 918 (1952).

The formation of mixed crystals in this ratio was proved by means of their X-ray powder photographs. The X-ray diagram of crystals prepared by evaporation of a benzene solution of the components shows the occurrence of single Debye-Scherrer lines, where the X-ray diagram of the mechanical mixture shows the presence of doublets which in turn correspond to the spectra of the single compounds.

TABLE 2.—INFRA-RED SPECTRA IN POLARIZED LIGHT OF $(NPCl_2)_3$

	Polarization	Assignment	Species
526 *vs*	⊥	ν_{13} in pl. ring deformation	E'
542 *s*	∥	ν_6 PCl_2 as. stretching	A_2''
575 *vw*	∥	ν_{17} PCl_2 as. stretching*(.)	E;
603 *vs* }	⊥	ν_5 out of pl. ring deformat.	A_2''
613 *vs* }	∥		
670 *w*	∥	ν_2 in pl. ring deformat.*(.)	A_1''
700 *vw*			
785 *w*	⊥	ν_1 ring stretching	A_1'
823 *vw*	∥		
848 *vw*	∥		
860 *w*	⊥		
875 *m*	⊥		
991 *vw*			
1037 *vw*			
1094 *vw*	⊥		
1125 *w*	⊥		
1150 *w*	⊥		
1198 *vs*	⊥	ν_{12} ring stretching ?	E'
1208 *vs*	⊥	ν_{11} ring stretching	E'
1251 *vs*	∥		
1310 *m*	⊥		
1368 *m*	⊥		
1758 *w*	⊥		
1880 *w*	⊥		
1975 *w*	⊥		
1998 *m*	⊥		
2075 *w*	⊥		

* For alternative assignment see Reference (1).

Although the ratio used is not so large as to ensure that each molecules of chloride is surrounded only by bromide molecules, the dilution of the chloride–chloride contacts was found to be enough to assume an average distribution of isolated chloride molecules.

The vibrational frequencies of the bromide being different from these of the chloride, the coupling of the molecular vibrations of the molecules in the unit cell disappears. The spectrum of Fig. 3 illustrates this effect. The spectrum of pure $(NPCl_2)_3$ (solid line) shows the presence of the 613–600 cm^{-1} doublet, which disappears in the spectrum of the mixed-crystals (dotted line) and is replaced by a single band at 609 cm^{-1}.

The factor group splitting of the 542 cm^{-1} band has not been observed, due to the strong overlap with the nearest (⊥) band at 526 cm^{-1}.

Vibrations of E' species give rise to bands of the ($\perp$) type. The bands at 1208, 1198 and 526 cm^{-1} clearly belong to this species. The infra-red band at 875 cm^{-1} has also a ($\perp$) type of polarization, like E' vibrations. However, being absent in the vapour spectrum its choice as E' fundamental cannot be accepted without a serious straining of the selection rules, and for this reason the 1198 cm^{-1} band has been prefered as E' ring stretching mode. The 1208–1198 cm^{-1} doublet has a complex behaviour in the solid spectrum. With light polarized parallel to the c-axis, both bands are very strong and give a characteristic doublet pattern.

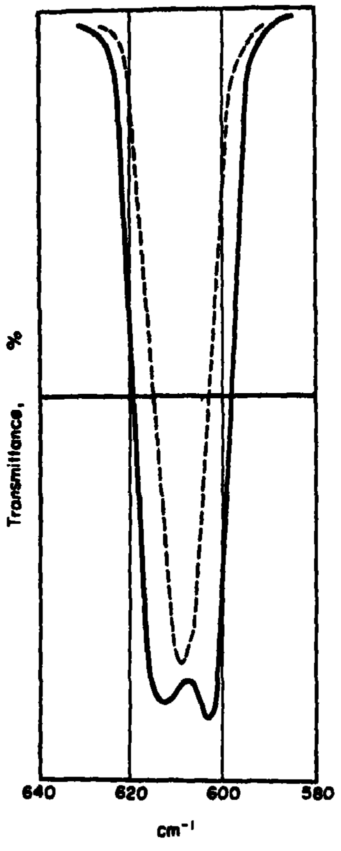

FIG. 3.—The ν_5 band of $(NPCl_2)_3$ at about 600 cm^{-1}. The solid line shows the spectrum of pure $(NPCl_2)_3$ while the dotted line shows the spectrum of a solid solution of $(NPCl_2)_3$ in $(NPBr_2)_3$.

With light polarized parallel to the a axis, both bands practically disappear and a new, much narrower band appears at 1251 cm^{-1}. The hypothesis that this band corresponds to the ($\parallel$) component of the 1208 cm^{-1} fundamental cannot be proved directly the mixed crystal spectrum being of no help due to the strong absorption of $(NPBr_2)_3$ in this region.

It should however be noted that a similar splitting has also been observed in the crystal spectrum in polarized light of $(NPBr_2)_3$.(7)

(7) S. CALIFANO. To be published.

Another convenient explanation of the presence of the 1251 cm^{-1} band is the assignment to a combination band of the 1208 cm^{-1} fundamental with a lattice vibration. It is well known that combination bands of fundamental modes with lattice vibration, can display strong infra-red activity even if the molecular modes are themselves inactive.

In the absence of definitive evidence in favour of one of these two explanations we prefer to assume the second is correct, simply because a splitting factor of about 43 cm^{-1} seems too large if compared to the splitting of 13 cm^{-1} observed for the A_2'' fundamental at 613 cm^{-1}.

The five bands at 1208, 1198 (or 875), 610, 542 and 526 cm^{-1} are the only infra-red active fundamentals which appear above 400 cm^{-1}. In addition to these, some of the modes inactive in the case of the vapour spectrum (D_{3h} symmetry) gain infra-red activity in the crystal spectrum. The orientated gas model gives no prediction on the type of polarization of such vibrations, because they are not associated with an intrinsic dipole variation.

The direction of vibration of the dipole moment induced from the crystalline field can even be different for vibrations of the same symmetry species, and a general theory able to predict these directions has not yet been achieved.

It is however at least surprising to observe that the two bands at 785 and 670 cm^{-1} assigned by DAASCH to the A_1' species show different types of polarization in the infra-red spectrum of the crystal. The one at 785 cm^{-1} has the ($\perp$) type of polarization, while the band at 670 cm^{-1} has the ($\parallel$) type of polarization. This situation is even more puzzling if the results of the Raman depolarization measurements are considered. We have already discussed(1) the discrepancy between the two Raman spectra of $(NPCl_2)_3$ existing in the literature.(8) The fact that the Raman polarization measurements are in disagreement just in the case of the 785 cm^{-1} band which has a type of polarization in the infra-red inconsistent with that of the 670 cm^{-1} band, assigned to the same symmetry species, needs to be taken into consideration. For the reasons discussed before the infra-red polarization measurements are not decisive in this case and only a new Raman spectrum can definitely settle the question.

(8) A. FIEQUELMONT, M. MAGAT and L. OCHS, *C.R. Acad. Sci., Paris* **208**, 1900 (1939); L. W. DAASCH, *J. Amer. Chem. Soc.* **76**, 3403 (1954).

J. Inorg. Nucl. Chem., 1962, Vol. 24, pp. 499 to 510. Pergamon Press Ltd. Printed in England

OBSERVATIONS ON THE RARE EARTHS—LXXV(1)

THE STABILITIES OF DIETHYLENETRIAMINEPENTAACETIC ACID CHELATES

T. Moeller and L. C. Thompson*
Noyes Chemical Laboratory, University of Illinois, Urbana, Illinois

(*Received* 22 *September* 1961)

Abstract—The interaction between diethylenetriaminepentaacetic acid (H_5DTPA or H_5Z) and rare-earth metal ions (Ln^{3+}) has been investigated. The acid formation constants of the hydrogen chelates ($LnHZ^-$) and the formation constants of the normal chelates (LnZ^{2-}) have been obtained at 10, 20 and 30° C, and an ionic strength of $0{\cdot}1(KNO_3)$, the former by a titration technique and the latter by a mercury indicator electrode technique. The data have been treated by a least-squares method for evaluation of $\Delta H°$ and $\Delta S°$. Although errors in these functions are substantial, the functions have been related to observed trends in stability. The dissociation constants for the last three protons of diethylenetriaminepentaacetic acid have been measured as a function of temperature at ionic strength $0{\cdot}1(KNO_3)$ and converted to thermodynamic functions by least squares analysis. These functions have been compared with corresponding values for related chelating agents.

On the basis of many well established instances of ionic bonding in rare-earth metal compounds, it has been quite generally concluded that the stabilities of complexes derived from the tripositive cations of these metals should increase with decreasing cation radius or increasing atomic number. An examination of stability constant data for a number of complexing agents(1–12) quite generally bears out this expectation but reveals that in all instances there is a larger discontinuity at gadolinium than the corresponding discontinuity in radii(13) would suggest and that with some reagents stabilities fail to increase regularly or even at all for ions higher than gadolinium in the series.

No complete explanation for these variations has been offered.(1, 12) Recently, however, the "gadolinium break" for chelates with ethylenediaminetetraacetic acid

---

* Present address University of Minnesota-Duluth, Duluth, Minnesota.

(1) For the preceding paper in this series, see T. Moeller and R. Ferrús, *Inorg. Chem.* **1**, 49 (1962).

(2) E. J. Wheelwright, F. H. Spedding and G. Schwarzenbach, *J. Amer. Chem. Soc.* **75**, 4196 (1953).

(3) G. Schwarzenbach, R. Gut and G. Anderegg, *Helv. Chim. Acta*, **37**, 937 (1954).

(4) G. Schwarzenbach and R. Gut, *Helv. Chim. Acta*, **39**, 1589 (1956).

(5) F. H. Spedding, J. E. Powell and E. J. Wheelwright, *J. Amer. Chem. Soc.* **78**, 34 (1956).

(6) R. Harder and S. Chaberek, *J. Inorg. Nucl. Chem.* **11**, 197 (1959).

(7) M. A. Hiller, Doctoral dissertation, Iowa State University (1959).

(8) A. Sonesson, *Acta Chem. Scand.* **12**, 165, 1937 (1958); **13**, 998, 1437 (1959); **14**, 1495 (1960); **15**, 1 (1961).

(9) B. F. Freasier, A. G. Oberg and W. W. Wendlandt, *J. Phys. Chem.* **62**, 700 (1958).

(10) I. Grenthe and W. C. Fernelius, *J. Amer. Chem. Soc.* **82**, 6258 (1960).

(11) I. Grenthe, *J. Amer. Chem. Soc.* **83**, 360 (1961).

(12) T. Moeller and R. Ferrús, *J. Inorg. Nucl. Chem.* **20**, 261 (1961).

(13) D. H. Templeton and C. H. Dauben, *J. Amer. Chem. Soc.* **76**, 5237 (1954).

(H_4EDTA) has been ascribed to a change in the number of co-ordinating positions occupied by the ligand on the basis of the observation that the partial molal entropy of the ions, $Ln(EDTA)^-$, has one constant value from lanthanum through europium and another, but different, constant value from terbium through lutetium.(14) It has been of interest to test this conclusion by evaluating and comparing partial molal entropy data for other structurally related chelating agents, particularly those that form complexes of varying stability in the terbium to lutetium region. Results reported for N-hydroxyethylethylenediaminetriacetic acid(12) and nitrilotriacetic acid(1) support a gradual loosening of a bond with a resulting significant configurational entropy contribution rather than a sudden change in number of positions occupied. The present extension of this approach to diethylenetriaminepentaacetic acid(6) is in agreement with this point of view.

The formation constants of a number of $Ln(DTPA)^{2-}$ complexes have been determined using the tren exchange method.(6) We have minimized the difficulties in this method(2, 15) by utilizing the mercury indicator electrode approach developed by SCHWARZENBACH and ANDEREGG.(16) As an essential to evaluation of formation constants by this procedure, dissociation constants for the last three acidic protons of diethylenetriaminepentaacetic acid were determined as a function of temperature. Thermodynamic functions were then evaluated from these data.

EXPERIMENTAL

Materials. Yttrium and rare-earth metal oxides (except cerium) of 99^+–$99{\cdot}9^+$ per cent purity were kindly supplied by the Lindsay Chemical Division of the American Potash and Chemical Co. Cerium(III) nitrate 6-hydrate was obtained from the G. F. Smith Chemical Co. Diethylenetriaminepentaacetic acid from Geigy Industrial Chemicals was recrystallized twice from water to a product analysing to 99·6 per cent purity by potentiometric titration with potassium hydroxide in the presence of a slight excess of copper(II) chloride. Hydrochloric acid and carbonate-free potassium hydroxide solutions, prepared from Acculate standards, were titrated potentiometrically against sodium carbonate and potassium hydrogen phthalate, respectively. Mercury was purified by the nitric acid–mercury(I) nitrate-air oxidation procedure.(17) All other chemicals were of analytical reagent grade. Freshly-boiled distilled water was used at all times.

Solutions. An approximately 10^{-3} M solution of diethylenetriaminepentaacetic acid was prepared by direct weighing and standardized by potentiometric titration with carbonate-free potassium hydroxide in the presence of copper(II) chloride and then again in the presence of neodymium chloride. Solutions of mercury(II) and rare-earth metal nitrates were obtained by dissolving weighed quantities of the oxides in slight excesses of standard nitric acid. The mercury(II) nitrate solution was standardized against standard potassium thiocyanate, using iron(III) as indicator.(18) The rare-earth metal nitrate solutions were titrated complexometrically, using Eriochrome Black T.(19) Cerium(III) nitrate solution was prepared by dissolving the solid in water, adding 100-volume hydrogen peroxide and boiling. Standardization was then effected complexometrically. All solutions were ca. 5×10^{-3} M in metal ion and 10^{-3} M in excess nitric acid. Solutions of the mercury(II) and rare-earth metal ion (except cerium) chelates were obtained by dissolving weighed quantities of the oxides and diethylenetriaminepentaacetic acid in known excess quantities of nitric acid. The cerium(III) chelate solution was obtained by adding the requisite amount of the chelating acid to the cerium(III) nitrate solution. All such solutions were ca. 5×10^{-3}M in the chelated species and 3×10^{-2}M in total hydrogen ion concentration.

---

(14) R. H. BETTS and O. F. DAHLINGER, *Canad. J. Chem.* **37**, 91 (1959).

(15) G. ANDEREGG, P. NÄGELI, F. MÜLLER and G. SCHWARZENBACH, *Helv. Chim. Acta*, **42**, 827 (1959).

(16) G. SCHWARZENBACH and G. ANDEREGG, *Helv. Chim. Acta*, **40**, 1773 (1957).

(17) F. DANIELS, J. H. MATHEWS, J. W. WILLIAMS, P. BENDER and R. A. ALBERTY, *Experimental Physical Chemistry*, p. 467. McGraw-Hill, New York (1956).

(18) I. M. KOLTHOFF and E. B. SANDELL, *Textbook of Quantitative Inorganic Analysis* (3rd Ed.), p. 546. Macmillan, New York (1957).

(19) G. SCHWARZENBACH, *Complexometric Titrations* (Translated by H. IRVING), p. 73. Interscience, New York (1957).

Apparatus. All pH measurements were made with a Beckman Model G pH Meter, using a saturated calomel reference electrode and an all-purpose glass electrode. Titrations were carried out in a 200 ml Berzelius beaker equipped with a rubber stopper containing holes for electrodes, a microburette, and gas-inlet and -outlet tubes. Temperature was controlled to ±0·03° C with a Sargent Model S–84805 bath. For measurements at 10° C, cooling water was first circulated through a coil in an ice-water bath. Potentials were measured with a Rubicon potentiometer and galvanometer. The cell used was a large tube fitted with a platinum wire sealed in the bottom and an appropriate side-arm for electrical contact. Glass and saturated calomel electrodes were inserted at the top through a rubber stopper. The calomel electrode was surrounded by a glass tube equipped at the bottom with a glass frit covered with a thin layer of agar gel containing 0·1000 M potassium nitrate. This tube was filled with 0·1000 M potassium nitrate.

Procedure. The stoicheiometry of the reaction between a rare-earth metal ion and the chelating agent was determined by potentiometric titration of mixtures of reactants in various ratios, using 0·1 M carbonate-free potassium hydroxide. Ionic strength was maintained at 0·1 by addition of 1·000 M potassium nitrate.

The acid dissociation constants of diethylenetriaminepentaacetic acid were determined by potentiometric titration with carbonate-free hydroxide at constant ionic strength (0·1 KNO_3). During titration, the solution was stirred with nitrogen that had been presaturated with vapour from a potassium nitrate solution of ionic strength 0·1 at the same temperature. Acid formation constants for metal-hydrogen chelates were determined in the same way. All pH readings from the meter, standardized against NBS-scale buffers, were converted to hydrogen ion concentrations by using the difference between the pH reading of a 10^{-3} M hydrochloric acid solution ($\mu = 0{\cdot}1$ KNO_3) and the known stoicheiometric quantity of hydrogen ion. It was assumed that this correction is valid over the entire pH range.

Stability constants for the rare-earth metal–DTPA chelates were determined by an adaptation of the mercury indicator electrode procedure of SCHWARZENBACH and ANDEREGG.(16) For each measurement, known volumes of standard solutions of the mercury(II)— and rare-earth metal–DTPA chelate and of the rare-earth metal nitrate, a sufficient volume of 1·000 M potassium nitrate to make the ionic strength 0·1, and a small drop of mercury were placed in a stoppered 300 ml flask and shaken mechanically for 2 hr for equilibration of the mercury species. The mixture was then transferred to the cell, sufficient mercury was added to cover the platinum contact, the cell was placed in the thermostat, and presaturated nitrogen was bubbled through the solution. After thermal equilibrium had been established, the electrodes were inserted, and the potential of the mercury electrode and the pH were determined.

CALCULATIONS AND RESULTS

Titration curves. Data for the titration of diethylenetriaminepentaacetic acid and its mixtures with neodymium ion, as summarized in Fig. 1, are typical of those obtained for all the rare-earth metal systems. Such curves indicate clearly the formation of a one-to-one chelate of considerable stability and the presence of protonated species ($LnHZ^-$) but give no indication of the presence of species containing more than one metal ion per chelating anion. This interpretation is in agreement with the observations of HARDER and CHABEREK.(6)

Stabilities of protonated chelates. Acid formation constants for these chelates ($LnHZ^-$ and $HgHZ^{2-}$) were obtained from data between four and five moles of base added per mole of the acid (= *a*) in the titration of 1 : 1 mixtures of the metal ion and diethylenetriaminepentaacetic acid. In this region, the important equilibrium is:

$$LnHZ^- \rightleftharpoons LnZ^{2-} + H^+ \qquad (I)$$

The values listed in Table 1 were obtained using equations previously developed.(15)

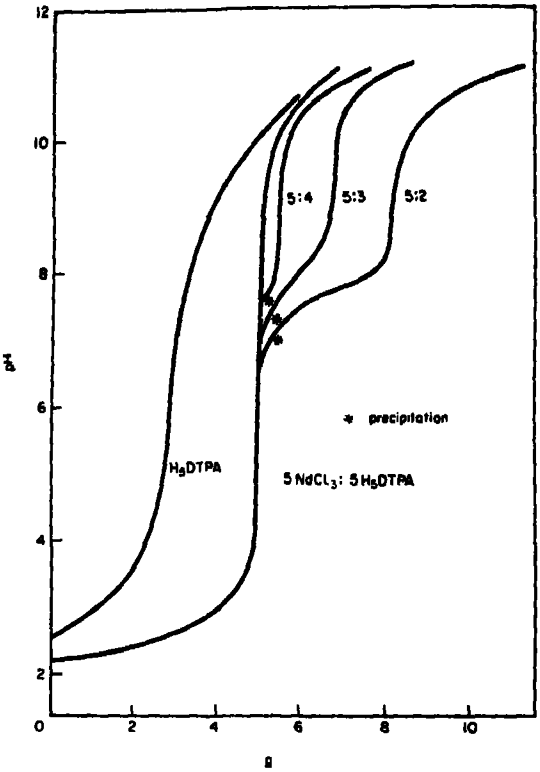

Fig. 1.—Titration curves for diethylenetriaminepentaacetic acid and certain of its mixtures with neodymium chloride.

Inasmuch as all these chelates are strong acids, the values obtained are only approximate. Since the values for the rare-earth metal complexes are virtually independent of temperature, only those at 20°C are included. Values for the mercury (II) complex show greater temperature dependence.

Dissociation constants for H_5DTPA. Values for the dissociation constants of the free acid, as calculated by the method of Ryskiewich,(20) are summarized for various temperatures in Table 2. For these calculations, necessary hydroxyl ion concentrations were obtained from measured p_cH values in terms of the expression.(21)

$$K_a w = \frac{\gamma H^+ \gamma OH^-}{{}^a H_2O} M_{H^+} M_{OH^-} \qquad (1)$$

A value of 0·60 was used for the activity coefficient function.(22)

---

(20) D. P. Ryskiewich. Doctoral dissertation, New York University (1956).

(21) H. S. Harned and B. B. Owen, *The Physical Chemistry of Electrolytic Solutions* (2nd Ed.), p. 482. Reinhold, New York (1950).

(22) H. S. Harned and B. B. Owen, *The Physical Chemistry of Electrolytic Solutions* (2nd Ed.), p. 578. Reinhold, New York (1950).

TABLE 1.—ACID FORMATION CONSTANTS FOR Hg(II)- AND Ln(III)-DTPA CHELATES
$\mu = 0{\cdot}1$, KNO_3

M^{n+}	$\log K_H$ MHZ		
	10° C	20° C	30° C
Hg^{2+}	4·14	4·10	4·12
La^{3+}		2·60	
Pr^{3+}		2·38	
Nd^{3+}		2·39	
Sm^{3+}		2·20	
Eu^{3+}		2·15	
Gd^{3+}		2·39	
Tb^{3+}		2·14	
Dy^{3+}		2·19	
Ho^{3+}		2·25	
Er^{3+}		2·00	
Tm^{3+}		1·90	
Yb^{3+}		2·30	
Lu^{3+}		2·18	
Y^{3+}		1·91	

TABLE 2.—DISSOCIATION CONSTANTS FOR DIETHYLENETRIAMINEPENTAACETIC ACID
$\mu = 0{\cdot}1$ (KNO_3)

	10° C	20° C	30° C	40° C
pK_1	—	1·80	—	—
pK_2	—	2·55	—	—
pK_3	4·39	4·33	4·30	4·27
pK_4	8·72	8·60	8·46	8·37
pK_5	10·63	10·58	10·34	10·23

It is significant that the dissociation constants of diethylenetriaminepentaacetic acid obtained (Table 2) agree closely with those previously reported.(23–27)

Values of the third, fourth and fifth dissociation constants for the acid were fitted by a least squares analysis to the relationship:

$$pK_i = \frac{\Delta H i^{\circ}}{2{\cdot}303\,RT} + \text{constant} \qquad (2)$$

where subscript i refers to a particular dissociation step. Values of ΔH_i° obtained were combined with ΔF_i° to yield ΔS_i° for each step. These thermodynamic functions are summarized in Table 3, where the ± values represent the 95 per cent confidence intervals.

---

(23) E. J. DURHAM and D. P. RYSKIEWICH, *J. Amer. Chem. Soc.* **80**, 4812 (1958).

(24) G. ANDEREGG, P. NÄGELI, F. MÜLLER and G. SCHWARZENBACH, *Helv. Chim. Acta* **42**, 827 (1959).

(25) E. WANNINEN, *Acta Chem. Fenn.* **28 B**, 146 (1955).

(26) H. KROLL, G. PINCHING and F. BUTLER, *Abstr. 122nd American Chemical Society Meeting*, p. 6. Atlantic City, N.J., Sept. 14–19, 1952.

(27) A. E. FROST, *Nature* (*Lond.*), **178**, 322 (1956).

Stability constants of chelates. The mercury electrode was standardized by measuring its potential in solutions of known mercury(II) concentration and varying nitric acid concentration, but always at ionic strength (0·1 KNO_3). Inasmuch as these solutions were shaken with mercury, reduction of the bulk of the mercury(II) to mercury(I) occurred, and mercury (II) concentrations had to be evaluated from the onstant (K_{eq}) for the equilibirum:(30)

TABLE 3.—THERMODYNAMIC FUNCTIONS FOR THE DISSOCIATION OF DIETHYLENETRIAMINE-PENTAACETIC ACID, ETHYLENEDIAMINETETRAACETIC ACID,(29) AND DIETHYLENETRIAMINE (DEN)(30)

Dissociation step	ΔF° (kcal/mole)	ΔH° (kcal/mole)	ΔS° (e.u./mole)	μ	t (° C)
H_5DTPA					
3rd	5·88 ± 0·03	1·49 ± 0·70	—14·7 ± 2·2	0·1	25
4th	11·64 ± 0·03	4·86 ± 0·70	—22·7 ± 2·4	(KNO_3)	
5th	14·23 ± 0·02	5·44 ± 0·42	—29·5 ± 1·4		
H_4EDTA					
3rd	8·26	4·39	—13·2	0·1	20
4th	13·76	5·69	—27·5	(KCl)	
den					
1st	5	7·6	+8	0·1	25
2nd	11	12·2	+1	(KCl)	
3rd	13	11·1	—8		

$$Hg^{2+} + Hg(l) \rightleftharpoons Hg_2{}^{2+} \tag{II}$$

and the expression:

$$(1+K_{eq})\,[Hg^{2+}] = [Hg^{2+}]_t \tag{3}$$

where $[Hg^{2+}]_t$ is the total quantity of mercury(II) added initially. The cell employed can be represented as*

$$\mathrm{Hg_2Cl_2,\ Hg{:}\ KCl(sat.)} \underset{E_j}{\Big\|} \mathrm{0{\cdot}1M\,KNO_3} \underset{E_j}{\Big\|} \begin{array}{l}\text{Equilibrium solution: Hg or glass electrode}\\ \mu = 0{\cdot}1(\mathrm{KNO_3})\end{array}$$

The potential of this cell is given by:

$$E_{\text{cell}} = E_{\text{sat. calomel}} - E_{Hg} \tag{4}$$

and that of the mercury electrode by:

$$E_{Hg} = E^\circ_{Hg} - \frac{2{\cdot}303RT}{2F}\log\,[Hg^{2+}] \tag{5}$$

---

* The Latimer convention is employed in the cell designation for the mercury electrode For consistency, the reverse designation should be used for the cell for pH measurement.

(28) G. SCHWARZENBACH and G. ANDEREGG, *Helv. Chim. Acta* **37**, 1289 (1954).

(29) M. J. L. TILLOTSON and L. A. K. STAVELEY, *J. Chem. Soc.* 3613 (1958).

(30) G. H. MCINTYRE, JR., B. P. BLOCK and W. C. FERNELIUS, *J. Amer. Chem. Soc.* **81**, 529 (1959).

Values of E^{0}_{Hg} so determined contain the two junction potentials, E_j' and E_j. Readings from the pH meter were again converted to p_cH-values by use of correction factors.

In solutions obtained by mixing the species HgZ^{3-}, LnZ^{2-}, and Ln^{3+}, the equilibrium:

$$HgZ^{3-} + Ln^{3+} \rightleftharpoons Hg^{2+} + LnZ^{2-} \qquad \text{(III)}$$

is established. For a specific determination, this equilibrium was evaluated by duplicate runs for each of four separate samples in which $[HgZ^{3-}]$ varied from 5×10^{-4} to 2×10^{-4} M, $[LnZ^{2-}]$ varied from 1×10^{-3} to $1{\cdot}2\times10^{-3}$ M. $[Ln^{3+}]$ remained constant at 2×10^{-4} M, and p_cH varied from 3 to 3·5. Somewhat wider concentration ranges were investigated for lanthanum and praseodymium without significant alteration in results. Cerium(III) solutions were studied only at 20°C because of their ease of oxidation. The conditions outlined avoided the difficulties inherent in this procedure,(16) namely precipitation of mercury (I and II) with the species HgZ^{3-} if equilibrium III is displaced too far to the right and precipitation of mercury(II) oxide if p_cH is too high. A further complication, however, could result from formation of mixed chelates of the type HgLnZ. However, it has been shown(24) that the ion HgZ^{3-} has little tendency to form such mixed species. Furthermore, titration of a mixture of $HgHZ^{2-}$ and Ln^{3+} with potassium hydroxide gave an upper limit of 10^3 for the formation of such complexes. A value of this magnitude would have no effect on the subsequent calculations.

The equilibrium constant for reaction III:

$$K_{\mathrm{III}} = \frac{[Hg^{2+}]\,[LnZ^{2-}]}{[Ln^{3+}]\,[HgZ^{3-}]} = K_{\mathrm{LnZ}}/K_{\mathrm{HgZ}} \qquad (6)$$

can be calculated from p_cH, the experimentally determined concentration of Hg^{2+} ion, the initial concentrations of Ln^{3+}, HgZ^{3-} and LnZ^{2-} ions, and the stoicheiometric equations:

$$[\mathrm{HgDTPA}]_t = [\mathrm{HgZ}]+[\mathrm{HgHZ}] = [\mathrm{HgZ}]\,(1+[\mathrm{H}]K_{\mathrm{HgHZ}}) \qquad (7)$$

$$[\mathrm{LnDTPA}]_t = [\mathrm{LnZ}]+[\mathrm{LnHZ}] = [\mathrm{LnZ}]\,(1+[\mathrm{H}]K_{\mathrm{LnHZ}}) \qquad (8)$$

$$[\mathrm{Ln}]_t = [\mathrm{Ln}] \qquad (9)$$

where ionic charges are omitted for simplicity and subscript t refers to total concentration of the species initially added. Since K_{HgZ} can be evaluated from p_cH and $[Hg^{2+}]$ in solutions of HgZ^{3-} and H_5DTPA (equation 7), and the relationship

$$[H_5DTPA] = [Z]\{1+[H]10^{pK_5}+[H]^2 10^{pK_5+pK_4}+[H]^3 10^{pK_5+pK_4+pK_3}+ \text{----}\} \qquad (10)$$

the value of K_{III} can be used to obtain K_{LnZ}

In total, twelve values for log K_{HgZ} were obtained at each temperature (10, 20, 30°C), and eight values for log K_{LnZ} at each temperature for each rare-earth metal ion except cerium(III). The experimental results are given in Table 4. These constants were fitted to the relationship:

$$\log \underset{\mathrm{MZ}}{K_{\mathrm{M}}} = \frac{-\Delta H^{\circ}}{2{\cdot}303\,RT} + \text{constant} \tag{11}$$

by least squares analysis. Data resulting from this analysis and application of the following relationship are given in Table 5:

$$\log \underset{\mathrm{LnZ}}{K_{\mathrm{Ln}}} = \log K_{\mathrm{III}} + \log \underset{\mathrm{HgZ}}{K_{\mathrm{Hg}}} \tag{12}$$

$$\Delta F^{\circ}_{\mathrm{MZ}} = -2{\cdot}303\,RT \log \underset{\mathrm{MZ}}{K_{\mathrm{M}}} \tag{13}$$

$$\Delta H^{\circ}_{\mathrm{LnZ}} = \Delta H^{\circ}_{\mathrm{III}} + \Delta H^{\circ}_{\mathrm{HgZ}} \tag{14}$$

$$\Delta S^{\circ}_{\mathrm{LnZ}} = \frac{\Delta H^{\circ}_{\mathrm{LnZ}} - \Delta F^{\circ}_{\mathrm{LnZ}}}{T} \tag{15}$$

The ± variations represent 95 per cent confidence intervals. Values for $\log \underset{\mathrm{LnZ}}{K_{\mathrm{Ln}}}$ at 25°C are given graphically in Fig. 2.

TABLE 4.—EXPERIMENTAL VALUES OF LOG $\underset{\mathrm{Hg}}{K_{\mathrm{Hg}}}$ AND —LOG K_{III}

$\mu = 0{\cdot}1\ \mathrm{KNO_3}$

M^{n+}	log K 10·00° C	 19·90° C	 29·90° C
Hg^{2+}	27·11	26·59	25·99
La^{3+}	7·432	7·003	6·600
Pr^{3+}	5·791	5·363	5·035
Nd^{3+}	5·303	4·875	4·479
Sm^{3+}	4·506	4·133	3·801
Eu^{3+}	4·427	4·042	3·719
Gd^{3+}	4·386	3·966	3·648
Tb^{3+}	4·138	3·702	3·409
Dy^{3+}	4·010	3·595	3·297
Ho^{3+}	4·075	3·643	3·339
Er^{3+}	4·117	3·703	3·369
Tm^{3+}	4·208	3·727	3·367
Yb^{3+}	4·300	3·844	3·461
Lu^{3+}	4·530	4·016	3·646
Y^{3+}	4·899	4·376	4·042

DISCUSSION

Previously cited agreement between the measured acid dissociation constants of diethylenetriaminepentaacetic acid and those previously reported supports the accuracy of the experimental approach. The location of the protons in molecules of this substance has been discussed previously.⁽²⁴⁾ Values of the thermodynamic functions associated with pK_3, pK_4 and pK_5 can be compared with profit with corresponding values for diethylenetriamine (Table 3). The usual observations that ΔH_f° for the polyamine is larger than for the corresponding amine polycarboxylic acid and that the reverse is true for ΔS_f⁽³¹⁾ are also apparent in this case.

---

(31) N. E. Ockerbloom and A. E. Martell, *J. Amer. Chem. Soc.* **78**, 267 (1956).

TABLE 5.—FORMATION CONSTANTS AND VALUES OF THE THERMODYNAMIC FUNCTIONS FOR Ln-DTPA AND Hg(II)-DTPA CHELATES AT 25° C
$\mu = 0{\cdot}1\ KNO_3$

M_n^+	$-\log K_{III}$	ΔH°_{III}	$\log K^{M}_{MZ}$	$-\Delta F^\circ_{MZ}$ (kcal/mole)	$-\Delta H^\circ_{MZ}$ (kcal/mole)	ΔS°_{MZ} (e.u./mole)	$(\Delta S^\circ_{LnZ} - S^\circ_{Ln})^*$
Hg^{2+}	—	—	26·27 ±0·07	35·85 ±0·09	22·1 ±1·0	46·1 ±3·3	
La^{3+}	6·80 ±0·05	16·4 ±2·1	19·48 ±0·08	26·57 ±0·12	5·7 ±2·3	70·0 ±7·7	35·3
Ce^{3+}			*ca.* 20·5				
Pr^{3+}	5·20 ±0·05	15·0 ±2·1	21·07 ±0·08	28·74 ±0·12	7·1 ±2·3	72·0 ±7·7	34·5
Nd^{3+}	4·67 ±0·03	16·3 ±1·3	21·60 ±0·08	29·47 ±0·12	5·8 ±1·6	79·4 ±5·4	40·9
Sm^{3+}	3·93 ±0·02	13·9 ±0·9	22·34 ±0·07	30·48 ±0·10	8·2 ±1·3	74·7 ±4·4	34·4
Eu^{3+}	3·88 ±0·04	14·0 ±1·5	22·39 ±0·08	30·55 ±0·12	8·1 ±1·8	75·3 ±6·0	34·2
Gd^{3+}	3·81 ±0·03	14·6 ±1·3	22·46 ±0·07	30·65 ±0·10	7·5 ±1·6	77·6 ±3·4	35·8
Tb^{3+}	3·56 ±0·03	14·4 ±1·2	22·71 ±0·07	30·99 ±0·10	7·7 ±1·5	78·1 ±5·0	36·4
Dy^{3+}	3·45 ±0·03	14·1 ±1·1	22·82 ±0·07	31·14 ±0·10	8·0 ±1·5	77·6 ±5·0	34·0
Ho^{3+}	3·49 ±0·03	14·5 ±1·4	22·78 ±0·07	31·08 ±0·10	7·6 ±1·7	78·7 ±5·7	34·2
Er^{3+}	3·53 ±0·04	14·8 ±1·7	22·74 ±0·08	31·02 ±0·12	7·3 ±2·0	79·6 ±6·7	34·3
Tm^{3+}	3·55 ±0·02	16·6 ±1·0	22·72 ±0·07	31·00 ±0·10	5·5 ±1·4	85·5 ±4·7	39·4
Yb^{3+}	3·65 ±0·03	16·6 ±1·1	22·62 ±0·07	30·87 ±0·10	5·5 ±1·5	85·1 ±5·0	38·3
Lu^{3+}	3·83 ±0·03	17·5 ±1·0	22·44 ±0·07	30·61 ±0·10	4·6 ±1·4	87·2 ±4·7	40·7
Y^{3+}	4·22 ±0·03	16·9 ±1·0	22·05 ±0·07	30·08 ±0·10	5·2 ±1·4	83·4 ±4·7	36·2

* Values of $\bar{S}^\circ_{Ln}$ taken from reference 14.

It is also of interest to compare the thermodynamic functions associated with pK_4 and pK_5 of H_5DTPA with the corresponding values for pK_3 and pK_4 for H_4EDTA (Table 3). On the basis of a calorimetric investigation of the steps in the dissociation of H_4EDTA, Tillotson and Staveley[29] suggested that the structure of the H_2EDTA^{2-} ion in aqueous solution is:

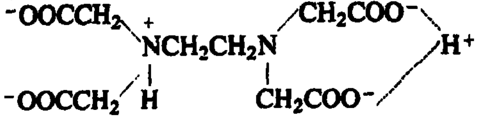

rather than the more commonly accepted completely zwitter-ion arrangement:

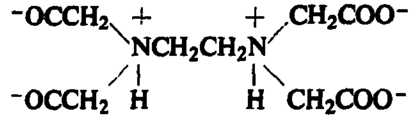

and that the second structure becomes increasingly important for acids of this type as the number of methylene groups between the two nitrogen atoms increases. This corresponds to an observed increase in magnitude of pK_3.[32] That pK_4 for H_5DTPA is larger than pK_3 suggests that the second type of structure is important for the ion H_2DTPA^{3-}. The smaller differences in $\Delta H°$ and $\Delta S°$ for pK_4 and pK_5 for H_5DTPA over those for pK_3 and pK_4 for H_4EDTA then are the result of close similarity between the dissociation steps for H_5DTPA.

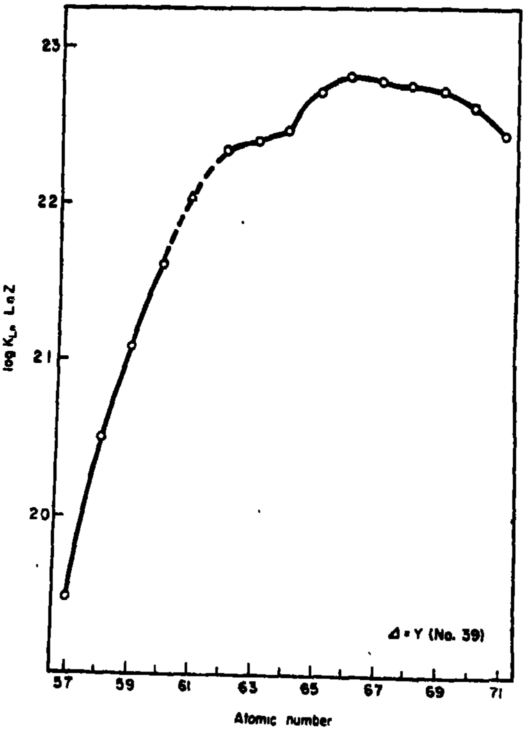

Fig. 2.—Variation in log K_{LnZ} for DTPA chelates with atomic number at 25° C and μ = 0·1 (KNO_3).

---

[32] G. Schwarzenbach and H. Ackermann, *Helv. Chim. Acta*, 31, 1029 (1948).

Values for the acid formation constants of the chelates LnHZ^- (Table 1) are somewhat larger than the p*K* value of 2·8 reported by **Harder** and **Chaberek**(6) for the lanthanum and ytterbium species. However, since all these materials are reasonably strong acids, the agreement is satisfactory. For the mercury chelate, the value log K_{Hg} = 26·59 (20°C: μ = 0·1 KNO_3) agrees quite well with the reported value of 26·70 (20°C: μ = 0·1, NaNO_3).(24)

Although, for the reasons previously outlined, values obtained for log K_{La} are
Lnz
believed to be more accurate than those previously reported,(6) they are of the same general order of magnitude. It has been suggested that the particularly large stabilities of the chelates indicated by these values may be due to the ability of the rare-earth metal ions to be 8-co-ordinate.(24) However, these data do not permit proof or disproof of this postulate. It is of interest though that a correlation between log K_{Ln} for the light rare-earth metal chelates with ethylenediaminetetraacetic acid,
Lnz
N-hydroxyethylenediaminetriacetic acid, and diethylenetriaminepentaacetic acid and the sum the last three or last two or the average of the last two pK values for the chelating groups exists (Fig. 3). Since the curves obtained all deviate only slightly from straight lines, it is reasonable to conclude that each chelating agent forms the

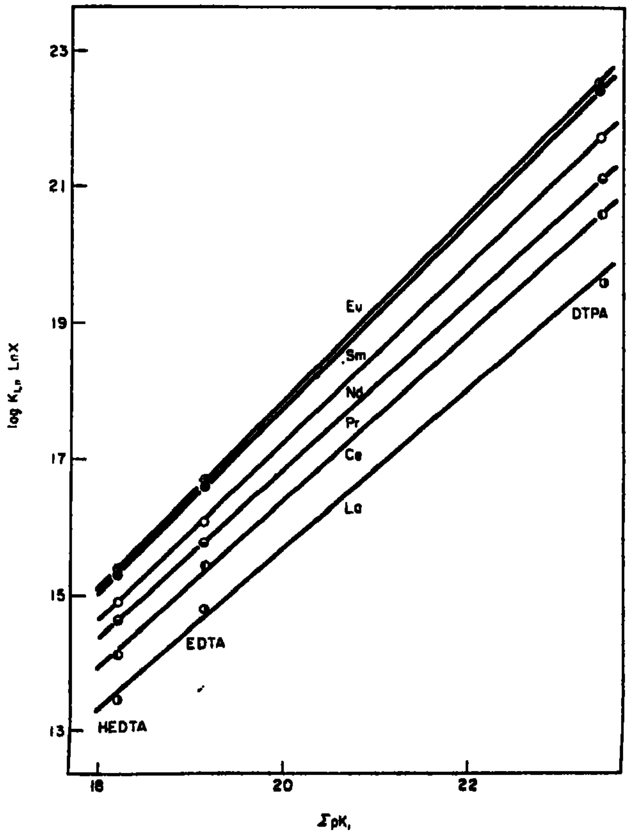

Fig. 3.—Correlation of stability constants of certain rare-earth metal chelates with summation of dissociation constants for last three protons of the ligand.

same number of rings. This is consistent with earlier observations that linear relationships between pK_1 values and stability constants result for ligands that give the same number of rings.(33)

Variations in stability with atomic number and the position of yttrium are essentially those reported by Harder and Chaberek.(6) It was at first believed that thermodynamic data, following the approach of Betts and Dahlinger,(14) would permit a choice among possible explanations for the somewhat unexpected order of stability (Fig. 2) among the chelates of the heavier cations. It was found, however, that errors associated with ΔH°_{LnZ} and ΔS°_{LnZ} are too large to make quantitative comparisons possible. Although the 95 per cent confidence limits associated with ΔH°_{HgZ} and ΔH°_{III} (Table 5) are of the order of 5–15 per cent of the values themselves, such limits climb to 20–40 per cent when ΔH°_{LnZ} is determined. Values of ΔS°_{LnZ} then have 95 per cent confidence limits of ± 7 e.u. and cannot be used to detect small differences between adjacent rare-earth metal ions.*

Some general observations are possible, however. Values obtained for ΔH°_{LnZ} are larger than those found for the EDTA—(34) and HEDTA—(12) chelates. This is to be expected since Care and Staveley(35) have found that the ΔH° values for EDTA-chelates are largely determined by the co-ordination between the nitrogen atoms and the metal ion. Inasmuch as the DTPA grouping contains one more nitrogen donor than either the EDTA or HEDTA, larger changes in enthalpy should characterize the formation of its chelates.

For the rare-earth metal chelates, ΔH°_{LnZ} remains nearly constant through dysprosium and then drops consistently from holmium through lutetium. If the bonding is essentially ionic in these compounds and the same number of atoms is co-ordinated, a reasonably regular increase in ΔH°_{LnZ} with decrease in crystal radius (or increase in nuclear charge) might be expected. However, in no series of rare-earth metal chelates thus far investigated has this trend been found.(1, 12, 34) Rather, a reasonable constancy or slight increase in $-\Delta H^\circ_{LnZ}$ appears to characterize the lanthanum-through-europium region, with subsequent decreases for species derived from the heavier elements. Similarly, measures of S°_{LnZ} vary widely for complexes derived from the lighter elements but increase substantially for those of the heavier elements.(1, 12) If the number of donor atoms utilized by the metal ion does indeed change at gadolinium, as has been suggested for the EDTA chelates,(2, 14) differences in these functions between the first and second half of the series might be expected. Within the limits of experimental error, therefore, it seems reasonable to conclude that the data for the DTPA complexes further support the assumption that both translational and configurational contributions to stability are important(12) and that the latter becomes increasingly important as cation size decreases and the bond holding a chelating group is thereby progressively weakened.

Acknowledgement—Grateful appreciation is expressed both to the Graduate College of the University of Illinois and to the United States Rubber Company for fellowship support given to the junior author.

* It should be noted, however, that for internal comparisons the part of the error associated with the formation constant of the mercury chelate is constant throughout the series and the relative errors would be somewhat less than cited above.

(33) A. E. Martell and M. Calvin, *Chemistry of the Metal Chelate Compounds*, p. 156. Prentice-Hall, Englewood Cliffs, N.J. (1952).

(34) L. A. K. Staveley (Private communication).

(35) R. A. Care and L. A. K. Staveley, *J. Chem. Soc.* 4571 (1956).

J. Inorg. Nucl. Chem., 1962, Vol. 24, pp. 511 to 517. Pergamon Press Ltd. Printed in England

THE STABILITY CONSTANTS OF SEVERAL COPPER(II) COMPLEXES WITH AROMATIC CARBOXYLIC ACIDS AND THEIR CORRELATION WITH THE HAMMETT RELATIONSHIP

W. R. MAY and M. M. JONES
Department of Chemistry, Vanderbilt University, Nashville, Tennessee

(*Received* 16 *October* 1961; *in revised form* 31 *October* 1961)

Abstract—The first and second stability constants of seventeen copper(II) complexes with aromatic carboxylic acids have been determined at 25° in a 50 per cent by volume water/dioxane solvent with four of these systems being extended to 30 and 35°. The corresponding thermodynamic values have been calculated. The first stability constants have been fitted to the Hammett equation using σ values obtained from the dissociation constants of the parent acids in this solvent.

An inverse relationship is found which can be attributed to either of two possible causes. The first is the formation of strong π-bonds by back-donation of electrons from the copper(II) to the ligand. The second possible cause is the fortuitous cancellation of a direct relationship by some inverse relationship involving the polymerization of the carboxylic acid. In this second case both processes would be governed by a Hammett type relationship but would be dependent upon variations in the σ constants in an opposite manner.

WHILE a large number of correlations between acid or base strength of ligand and stability constants of metal complexes have been reported, no attempt has previously been made to relate such correlations *directly* with the large body of data on organic compounds which is correlated with the Hammett equation. This paper presents such an attempt, using as ligands some of those aromatic carboxylic acids whose ionization constants have already been correlated with structural parameters with this equation. If the factors governing the interaction of the carboxylate anions with the hydrogen ion are similar to, or identical with, the factors governing the interaction of the carboxylate anions with the Cu(II) ion, then the instability constants of the complexes of the substituted anions should be related to that for benzoic acid through an equation of the type:

$$\log\left(\frac{k}{k_0}\right) = \sigma\rho.$$

Here k and k_0 are the instability constants of the complexes with the substituted and unsubstituted acids, respectively, σ should be a constant characteristic of the substituent group (very near to the value it assumes in the similar equation relating the ionization constants) and ρ will be a constant characteristic of the reaction (especially of the metal ion).

That such a correlation is a reasonable expectation may be seen from such correlations of base or acid strength and stability constants as have appeared in the literature to date.(1-7) There have also been several reports in which such a direct and simple correlation have definitely not been found.(8, 9) Perhaps the most closely related study which failed to reveal a direct correlation between proton attracting ability and complex stability is that reported for a series of complexes of anthranilic acid and its derivatives with divalent cobalt, nickel, copper, zinc and cadmium.(10) The complexes of cadmium with aromatic sulphonates were also found *not* to give a correlation.(11)

It is fairly well established that the exchange of ligand species leads to a very small enthalpy change if the atom forming the donor group is of the same type in both species.(12) In the present work, a direct test of the Hammett type relation for copper complexes of aromatic carboxylic acids, a complexation reaction was examined which involved the replacement of one type of co-ordinated oxygen by another. This means the testing of such a correlation in an oxygen donor solvent may require the use of data on reactions in which the net enthalpy change is either very small or zero.*

EXPERIMENTAL

The experimental procedure used was based upon the method of CALVIN and WILSON(15) and the corrections to it suggested by VAN UITERT and HAAS.(16) The titrations were carried out using a Beckmann Model GS pH meter or a Radiometer PHM-4 pH meter with a Radiometer combination electrode GK 202 A-G. The solutions were placed in a jacketed beaker through whose jacket was circulated water from a constant temperature bath regulated to within ±0·02° C. Stirring of the solution was accomplished by a magnetic stirrer. The pH meters were standardized prior to each run with a phthalate buffer solution (pH 4·01).

A solvent of 50 per cent by volume water/dioxane was employed. The dioxane was commercial reagent (Mathieson, Coleman and Bell) or C. P. (Fisher) and was redistilled before use. The fraction with b.p. 100–101° C was used in preparing the solutions.

---

* Those correlations involving Hammett substituent constants or their equivalent which have been previously reported are of the type in which a donor atom of the solvent is replaced by a different donor atom of the ligand. Reference (4) and ARMEANU and LUCA.(13) The data given by these authors for mono substituted aniline complexes of Ag(I) reveals a Hammett type relation between the substituent constants and the stability constants. In this system, co-ordinated oxygen is replaced by co-ordinated nitrogen.(14)

(1) A. E. MARTELL and M. CALVIN, *The Chemistry of the Metal Chelate Compounds*, p. 151–160. Prentice-Hall, New York (1952).
(2) S. CHABEREK and A. E. MARTELL, *Organic Sequestering Agents*, p. 130–133. J. Wiley, New York (1959).
(3) W. W. BRANDT and D. K. GULLSTROM, *J. Amer. Chem. Soc.* **74**, 3532 (1952).
(4) V. KLEMENCIC and I. FILIPOVIC, *Croat. Chim. Acta* **30**, 99 (1958); *Chem. Abstr.* **54**, 1127 f.
(5) J. O. EDWARDS, *J. Amer. Chem. Soc.* **76**, 1541 (1954).
(6) H. KIDO, W. C. FERNELIUS and C. G. HAAS, JR., *Analyt. Chim. Acta* **23**, 116 (1960).
(7) L. SACCONI and G. LOMBARDO, *J. Amer. Chem. Soc.* **82**, 6266 (1960).
(8) W. F. HARRIS and T. R. SWEET, *J. Phys. Chem.* **60**, 509 (1956).
(9) J. R. JOY and M. ORCHIN, *J. Amer. Chem. Soc.* **81**, 310 (1959).
(10) A. YOUNG and T. R. SWEET, *J. Amer. Chem. Soc.* **80**, 800 (1958).
(11) J. F. TATE and M. M. JONES, *J. Amer. Chem. Soc.* **83**, 3024 (1961).
(12) J. M. HOLLOWAY. Thesis, University of North Carolina (1959).
(13) L. ARMEANU and C. LUCA, *Z. Phys. Chem.* **214**, 81 (1960).
(14) P. ELLIS, R. HOGG and R. G. WILKINS, *J. Chem. Soc.* 3308 (1959).
(15) M. CALVIN and K. WILSON, *J. Amer. Chem. Soc.* **67**, 2003 (1945).
(16) L. G. VAN UITERT and C. G. HAAS, JR., *J. Amer. Chem. Soc.* **75**, 451 (1953).

The aromatic carboxylic acids used were selected to give a large range of σ constants. They were obtained from Eastman Organic Chemicals, Aldrich Chemical Co. and the Vanderbilt University Chemistry Department. Each was purified by vacuum sublimation before use. The following melting points were obtained: benzoic acid, 122°; *m*-fluorobenzoic acid, 125°; *m*-chlorobenzoic acid, 152°; *m*-bromobenzoic acid, 154°; *m*-iodobenzoic acid, 183°; *p*-fluorobenzoic acid, 182–3°; *p*-chlorobenzoic acid, 239–41°; *p*-bromobenzoic acid, 249°; *p*-iodobenzoic acid, 269–70°; *p*-*t*-butylbenzoic acid, 152–154°; *p*-hydroxybenzoic acid, 213–4°; *m*-hydroxybenzoic acid, 199–200°; *m*-nitrobenzoic acid, 141°; *p*-nitrobenzoic acid, 238–9°; *p*-toluic acid, 178°; and *p*-anisic acid, 180–1°.

The copper(II) was added as $Cu(ClO_4)_2 \cdot 6\,H_2O$ which was obtained from the G. F. Smith Chemical Co. The titrations were carried out using standard sodium hydroxide solution with a concentration in the neighbourhood of 1 M.

The solutions were prepared for titration in the following way. Enough aromatic carboxylic acid was weighed out to make 100 ml of solution about 0·01 M. Then 50 ml of distilled dioxane was added and the acid dissolved. Next, 50 ml of a previously prepared 0·002–0·003 M solution of $Cu(ClO_4)_2$ was added which yielded a solution 0·001–0·0015 M in Cu(II). Then 0·25 ml of 11·68 M $HClO_4$ was added to lower the initial pH to about 1·6. The solutions were found to become cloudy with a precipitate at pH above 5·5 and no values in this range or higher were used in the calculations. The solution was then placed in the jacketed beaker and titrated with the 1 M NaOH. The sodium hydroxide was added in 0·05 ml increments from a calibrated buret obtained from the Corning Glassware Co., Corning, New York.

TABLE 1.

Ligand (acid)	p*ki*	log K_1	log K_2	$-\log\frac{K_1}{K_{1_0}}$	σ	$-\Delta F$ (kcal/ mol)	ΔH (kcal/ mol)	ΔS (cal/ mol^{-1}°C^{-1})
Determinations at 25°								
1. Benzoic	5·79	3·91	3·65	0	0	5·33	0·0	17·9
2. *m*-F-benzoic	5·40	4·14	3·78	−0·23	0·39	5·65		
3. *m*-Cl ,,	5·48	4·08	3·76	−0·17	0·31	5·56	10·9	55·2
4. *m*-Br ,,	5·32	4·11	3·85	−0·20	0·47	5·60	21·4	90·6
5. *m*-I ,,	5·40	4·15	3·81	−0·24	0·39	5·66	24·4	100·9
6. *p*-F ,,	5·42	4·15	3·81	−0·24	0·37	5·66		
7. *p*-Cl ,,	5·19	4·20	3·90	−0·29	0·60	5·73		
8. *p*-Br ,,	5·59	4·00	3·70	−0·09	0·20	5·45		
9. *p*-I ,,	5·28	4·23	3·90	−0·32	0·51	5·77		
10. *p*-*t*-butyl	5·63	4·11	3·78	−0·20	0·16	5·60		
11. *m*-*t*- ,,	5·67	4·00	3·65	−0·09	0·12	5·45		
12. *p*-OH ,,	6·03	3·78	3·48	+0·13	−0·24	5·15		
13. *m*-OH ,,	5·85	3·88	3·57	+0·03	−0·06	5·09		
14. *m*-nitro ,,	4·92	4·40	4·11	−0·49	0·87	6·00		
15. *p*-nitro ,,	4·78	4·43	4·11	−0·52	1·01	6·04		
16. *p*-toluic ,,	6·12	3·78	3·48	+0·13	−0·33	5·15		
17. *p*-anisic ,,	6·12	3·71	3·42	+0·20	−0·33	5·06		
Determinations at 30°								
18. Benzoic	5·73	4·04	3·74	0	0	5·51	0·0	18·2
19. *m*-Cl-benzoic	5·33	3·88	3·52	−0·22	0·40	5·29	10·9	53·4
20. *m*-Br ,,	5·16	3·72	3·46	−0·44	0·57	5·07	21·4	87·4
21. *m*-I ,,	5·43	3·88	3·54	−0·22	0·30	5·29	24·4	98·0
Determinations at 35°								
22. Benzoic	5·80	3·92	3·61	0	0	5·35	0·0	17·4
23. *m*-Cl-benzoic	5·57	3·82	3·52	−0·14	0·23	5·21	10·9	52·3
24. *m*-Br ,,	5·51	3·60	3·30	−0·44	0·29	4·91	21·4	85·4
25. *m*-I ,,	5·54	3·54	3·15	−0·52	0·26	4·83	24·4	94·9

No apparent difficulties were encountered in obtaining reproducible, steady values of pH. However, the electrode did require "conditioning" in the water/dioxane solution for about 15 min after removal from the aqueous buffer before the readings became steady. The pH meter responded instantly when the sodium hydroxide was added and the pH reading could be taken after each addition. This pH value was found to remain constant with time on the numerous occasions when this constancy was tested.

The stability constants were determined at 25° for each system and also at 30 and 35° for a few of them. Several of the systems were examined for reproducibility and average values are reported in these cases. The spread in these cases was of the order of 0·1 log unit in the stability constant. The values at 25, 30 and 35° were used to estimate the enthalpy changes in the complexation reaction.

The dissociation constants of the substituted benzoic acids in the water/dioxane mixture are required for the calculation of the stability constants. These were obtained by the titration of known amounts of the acids with standard sodium hydroxide solution, using the pH meter to determine the pH after each addition of base. From these titration curves the dissociation constants were obtained by use of the relation $pK = pH$ at the half-titrated point. Each of the dissociation constants listed in Table 1 is the average of two or more such determinations.

CALCULATIONS

Expressions were needed for $\bar{n}$, the average number of ligands bound to the central metal ion and [A], the concentration of the free ligand species in solution.

$\bar{n}$ may be expressed as:

$$\bar{n} = \frac{C_a - [A]}{C_m} = \frac{T_{bb}}{C_m}$$

where C_a is the total concentration of ligand (the benzoate anion in this case) and C_m is the total concentration of metal ion (the copper(II) ion in this case). T_{bb} is the total bound benzoate. A form of this equation which can be applied to the experimental data may be obtained by solving for T_{bb} and [A] in the following conservation equations. The total aromatic acid present is given by: $T_{HA} = [HA]+[A^-]+[CuA^+]+2[CuA_2]+3[CuA_3^-]+4[CuA_4^{2-}]$, the total copper present by $T_{Cu} = [Cu^{2+}]+[CuA^+]+[CuA_2]+[CuA_3^-]+[CuA_4^{2-}]$, the total bound benzoate by $T_{bb} = [CuA^+]+2[CuA_2]+3[CuA_3^-]+4[CuA_4^{2-}]$, the electrical neutrality condition by $[CuA^+]+2[Cu^{2+}]+[Na^+]+[H^+] = [ClO_4^-]+2[CuA_4^{2-}]+[OH^-]+[A^-]$, and the dissociation of the aromatic acid by $k_d = \frac{[H^+][A^-]}{[HA]}$. From these relations, the following expressions are obtained:

$$\bar{n} = \frac{1}{C_m}\{[Na^+]+[H^+]-[P^-]-[OH^-]-\frac{k_d}{[H]}([P^-]-[Na^+]-[H^+]+[OH^-]+T_{HA})\}$$

$$[A] = \frac{k_d}{[H]}([P^-]-[Na^+]-[H^+]+[OH^-]T+_{HA})$$

where $[P^-]$ is the concentration of the ClO_4^- ion contributed by the $HClO_4$ only.

A preliminary set of stability constants was obtained from a plot of $\bar{n}$ vs. pA and selecting the pA values at $\bar{n} = \frac{1}{2}, \frac{3}{2}, \frac{5}{2}$, and $\frac{7}{2}$ as approximate values of K_1, K_2, K_3 and K_4. However, a consideration of the validity of such a method in the present case showed such values to be rather poor approximations. Following BJERRUM(17) the spreading factor x, defined as $K_1/K_2 = 4x^2$, was calculated and found to be quite small. Since under these conditions, this commonly used method for determining the stability constants is invalid, the alternative method of POULSEN *et al.*(18) was used. This is a graphical method which introduces no special assumptions and is perfectly adequate for treating data where the successive constants do not differ greatly in magnitude. The resultant $\bar{n}$ and [A] values were then used with the graphical method to obtain K_1 and K_2.

---

(17) J. BJERRUM. Thesis, p. 24 ff. Haase, Copenhagen (1957).

(18) K. G. POULSEN, J. BJERRUM and J. POULSEN, *Acta Chem. Scand.* 8, 921 (1954).

A typical set of data, to demonstrate how the constants were obtained, is one of the titrations used in determining an average value for K_1 and K_2 for the Cu(II)–benzoate complex at 25°. Inspection of the relationship for $\bar{n}$ and [A] reveals that only a small portion of the curve will yield reasonable results. These are just before the sodium ion concentration becomes so large an impossible $\bar{n}$ is computed. The following concentrations of species were present in the solution: 0·009966 M benzoic acid, 0·01153 M $Cu(ClO_4)_2$, 0·02921 mole of $HClO_4$ added and a 50 per cent by volume water/dioxane solvent with a total volume of 100·25 ml. It was then titrated with 1·008 M NaOH. The following data was obtained: ($F = \bar{n}/[A]$)

NaOH (ml)	pH	[A]	$\bar{n}$	F
2·9	3·354	$3{\cdot}40\times10^{-5}$	0·295	$8{\cdot}68\times10^{3}$
3·0	3·792	$8{\cdot}69\times10^{-5}$	0·859	$9{\cdot}88\times10^{3}$
3·1	4·077	$1{\cdot}48\times10^{-4}$	1·613	$1{\cdot}09\times10^{4}$
3·2	4·345	$2{\cdot}41\times10^{-4}$	2·377	$9{\cdot}86\times10^{3}$
3·3	4·492	$2{\cdot}91\times10^{-4}$	3·190	$1{\cdot}10\times10^{4}$
3·4	4·637	$3{\cdot}38\times10^{-4}$	4·101	$1{\cdot}20\times10^{4}$

From an extrapolation of the plot of F vs. [A] to [A] = O and an analysis of the slope, the following constants were obtained: $K_1 = 9{\cdot}2\times10^3$ and $K_2 = 5{\cdot}0\times10^3$.

RESULTS AND DISCUSSION

The stability constants, related thermodynamic constants, and dissociation constants of the parent acids are presented in Table 1. The stability constants are in most cases the average of two or more runs, in which a reproducibility of about ±0·1 log units was found. The graphical method of Poulsen *et al.* involves the extrapolation of the curve of F vs. [A] which yields K_1 at [A] = O. Then, K_2 is obtained from the slope of the curve, or slope = $K_1(2K_2-K_1)$. If the slope is small, K_2 will approach one-half of K_1, which is statistically the expected result. Most of the lines used had a small negative slope which resulted in a K_2 slightly less than $\frac{1}{2}K_1$. The value for the stability constant of benzoic acid and copper(II) is considerably higher than that found by Yamasaki and Ohtaki(19) in water. However, different solvents and ionic strength, among other conditions, may be expected to account for this difference.

The principal objective of this work was to test the application of a correlation used with compounds of organic nature to related inorganic compounds. This was done with the Hammett equation. An initial attempt was made using σ values from the compilation of Jaffe.(20) This was found to give a fair fit. However, it may be recalled that these values were obtained from a great variety of data and have, in some cases, a rather large probability spread. In addition, the dissociation constants of the acids in the water/dioxane solvent were found to give only a fair plot using these σ values. A new set of σ values was set up using the dissociation constants of the parent acids as a basis. The plot of $-\log K_1/K_{1_0}$ vs. the new σ values is seen in Fig. 1 which gives an excellent fit within ±0·1 log units.

(19) K. Yamasaki and H. Ohtaki, *Bull. Chem. Soc. Japan* **33**, 1067 (1960).

(20) H. H. Jaffe, *Chem. Rev.* **53**, 191 (1953).

There are two possible explanations for the correlation obtained here. The first is based upon the fact that there are copper(II) complexes known which contain weak σ bonds and strong π bonds, the latter arising from the back donation of electrons from the metal to the ligand.(21) The curve has a negative slope which indicates that an electron withdrawing group such as the nitro group, instead of pulling an electron away from the proton as it does in the parent acid (resulting in a weaker bond and a larger dissociation constant) pulls electrons from the Cu(II) ion, and increases back donation and the stability of the complex.* In a similar fashion, a group such as the hydroxy group, which is expected to release electrons and increase the bond stability between the acid anion and the proton, will decrease the back donation between the anion and the Cu(II) ion resulting in a less stable complex.

The reaction constant ρ, or the slope of the Hammett plot, is a measure of the susceptibility of the reaction to the influence of the substituents on the parent acid. These influences are of three general types:

(1) the transmission of electrical effects to the reaction site, (2) the effect the electron density at the reaction site has on the reactions, and (3) the effect of other conditions (temperature, solvent, etc.) influencing the reaction.(20)

The important factor effecting ρ in this case is the electron density at the reaction site. A negative ρ indicates the reaction is favoured by a high electron density.(23) The ρ value for the plot in Fig. 1 was found to be $-0{\cdot}58$. This indicates the reaction is favoured by a high electron density at the reaction site which is to be expected if back donation from the Cu(II) ion is taking place.

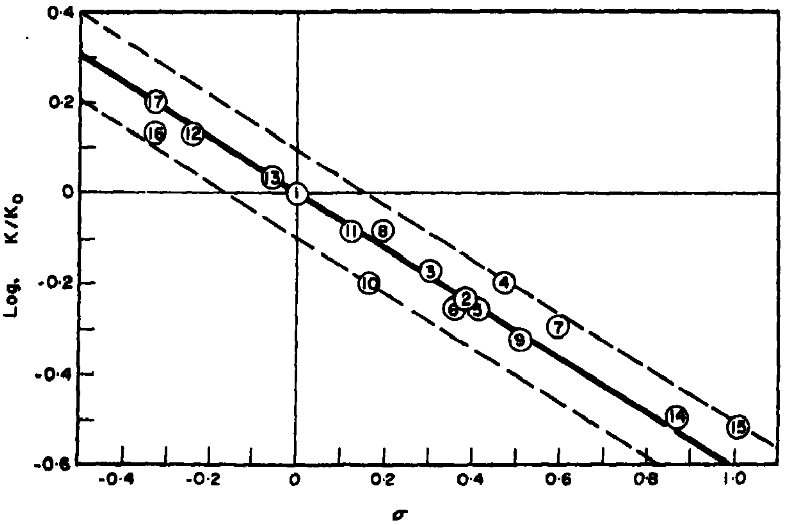

---

* A similar situation was found with the pyridine complexes of Ag(I) in which electron attracting groups on the pyridine ring were found to pull electrons from the Ag(I) ion into the ring (when resonance conditions permitted) and increase the stability of the complex.(22)

(21) B. R. McGarvey, *J. Phys. Chem.* **60**, 71 (1956).

(22) R. K. Murmann and F. Basolo, *J. Amer. Chem. Soc.* **77**, 3484 (1955).

(23) A. E. Remick, *Electronic Interpretations of Organic Chemistry* (2nd Ed.), p. 47. J. Wiley, New York (1949).

An alternative possibility is that the observed correlation is the result of the fortuitous cancellation of two concurrent processes, both of which are governed by a Hammett-type relationship. If the carboxylic acid is present in some sort of polymerized form it is possible that the breakdown of the polymers is favoured by the presence of electron withdrawing groups in the benzene ring. If this is so, then there will be a more favourable situation for the formation of complexes of the more extensively dissociated species. This could lead to an effect which could completely overshadow a correlation of the more normal sort. The fact that Fig. 1 presents a reasonably good fit would seem good evidence that both such processes are correlated by the Hammett equation, though possibly with different signs for ρ. An explanation of this sort seems less likely than the first in view of the recent work of CARSON and ROSSOTTI,(24)* but cannot be completely dismissed.

Acknowledgement—This work has been supported by a grant from the National Science Foundation (G-9919) for which we wish to express our gratitude.

* These workers found that such polymerization equilibria would result in *slight* errors in literature values for stability constants of monocarboxylate-metal ion complexes in water.

(24) J. D. E. CARSON and F. J. C. ROSSOTTI, *Advances in the Chemistry of the Co-ordination Compounds* (Edited by S. KIRSCHNER), p. 180. Macmillan, New York (1961).

J. Inorg. Nucl. Chem., 1962, Vol. 24, pp. 519 to 524. Pergamon Press Ltd. Printed in England

TERNARY COMPOUNDS BETWEEN THORIUM MONOCARBIDE AND THORIUM DIHYDRIDE*

D. T. Peterson and J. Rexer
Institute for Atomic Research and Department of Chemistry,
Iowa State University, Ames, Iowa

(*Received* 10 *February* 1961; *in revised form* 30 *October* 1961)

Abstract—The thorium–hydrogen–carbon system was studied by measuring hydrogen equilibrium pressures at various compositions and temperatures. Two compounds, $ThC{\cdot}ThH_2$ and $ThC{\cdot}2ThH_2$, were found and characterized. $ThC{\cdot}ThH_2$ has a hexagonal closest-packed lattice with $a_0 = 3{\cdot}816$ Å and $c_0 = 6{\cdot}302$ Å. $ThC{\cdot}2ThH_2$ has a monoclinic lattice with $a_0 = 6{\cdot}50$ Å, $b_0 = 3{\cdot}80$ Å, $c_0 = 10{\cdot}91$ Å and $\beta = 119°$. The enthalpies of formation for each compound were determined.

An investigation of the solid solubility of thorium dihydride in thorium by Peterson and Westlake⁽¹⁾ indicated that this solubility was increased by carbon dissolved in the thorium. The thorium-hydrogen-carbon system was investigated to determine whether this apparent increase in solubility was due to an interaction between carbon and hydrogen in solution which decreased the activity of hydrogen or whether it was due to the formation of a compound containing carbon and hydrogen. Measurement of the equilibrium-hydrogen pressure over thorium specimens containing varying amounts of carbon as a function of hydrogen concentration was chosen as the experimental method because it would clearly distinguish between these two cases and would give valuable thermodynamic data.

EXPERIMENTAL METHODS AND MATERIALS

Materials. The thorium specimens were prepared from calcium-reduced thorium identical to that used by Peterson and Westlake.⁽¹⁾ This metal was arc melted with spectrographic graphite to obtain the desired carbon content. The specimens, cut from the arc-melted buttons, were cylinders about 6 mm in diameter and 15 mm long which weighed ~ 5 g. The carbon content of the specimens was determined by the combustion method. Pure hydrogen was obtained by thermal decomposition of uranium hydride as described by Spedding *et al.*⁽²⁾

Apparatus. The apparatus is shown in Fig. 1. The furnace tube was 8 mm inside diameter and extended into the stainless steel block in the centre of the furnace. The temperature was measured by a thermocouple between the furnace tube and the stainless steel block. The temperature for an axial distance of 5 cm within the block was uniform within 1° C. The specimen was centred in this region and, consequently, the existence of an appreciable thermal gradient in the specimen was unlikely. The temperature of the furnace was held constant to within 2° C by an autotransformer and a constant voltage transformer.

---

* Contribution No. 985. Work was performed in the Ames Laboratory of the U.S. Atomic Energy Commission.

⁽¹⁾ D. T. Peterson and D. G. Westlake, *Trans. Amer. Inst. Min. (Metals) Engrs.* **215** 444 (1959).

⁽²⁾ F. H. Spedding, A. S. Newton, J. C. Wharf, O. Johnson, R. W. Nottorf, I. B. Johns and A. H. Daane, *Nucleonics* **4**, 4 (1949).

The volumes of the various portions of the gas system were determined so that the gas system could be used to measure the amount of hydrogen added to or taken from the specimen. The amount of gas in the furnace tube at constant pressure decreased with increasing furnace temperature so an effective volume was determined at several furnace temperatures. The amount of hydrogen in the specimen was the difference between the known total quantity of hydrogen in the system and the amount of hydrogen in the gas phase. The mercury manometer could be read to ±0·3 mm and the McLeod gauge, to ±6 μ up to 900 μ. The pressure was measured at a given temperature and composition after it had been constant within 3 mm for at least 12 hr. This often required several days at the lower temperatures because the attainment of equilibrium required diffusion of carbon as well as the diffusion of hydrogen.

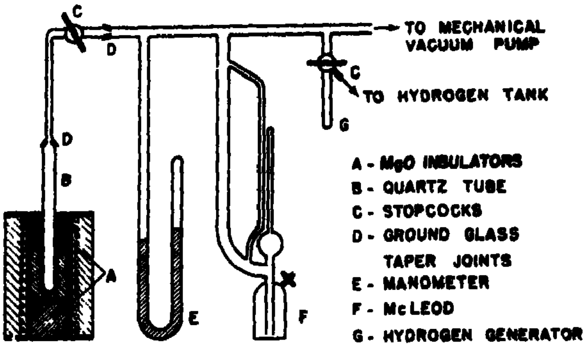

FIG. 1.—Schematic diagram of the apparatus.

RESULTS

The pressure–composition isotherms showed that two compounds of thorium, hydrogen and carbon were formed which were more stable than thorium dihydride. The equilibrium hydrogen pressures over a sample with a 0·46 atomic ratio of carbon to thorium is shown in Fig. 2. As the hydrogen content of the sample was increased the hydrogen first went into solid solution in both the metal and carbide phases. Formation of the ternary compound started at a fixed pressure at each temperature and continued at a constant pressure until the metal or the carbide phase disappeared. Subsequently, the hydrogen content of the ternary compound increased as the hydrogen pressure increased. This compound is not of fixed composition but apparently exists from $ThC\cdot ThH_{1\cdot 8}$ to $ThC\cdot ThH_{2\cdot 0}$ This variation in hydrogen content is quite similar to that observed in thorium dihydride.

The formation of a second ternary compound is shown in Fig. 3 which is a pressure–composition isotherm at 851° for a specimen with a 0·24 carbon to thorium ratio. $ThC\cdot ThH_2$ was formed first as the hydrogen content increased. At a higher hydrogen content and pressure, the $ThC\cdot ThH_2$ reacted with thorium metal and hydrogen to form $ThC\cdot 2ThH_2$. Because there was thorium metal in excess of the amount required to combine with all of the carbon, ThH_2 was formed when the hydrogen pressure became high enough for this compound to be stable. This specimen initially consisted of ThC and thorium metal saturated with ThC and finally consisted of ThH_2 and $ThC\cdot 2ThH_2$. Consequently, all of the equilibrium phases between ThC and ThH_2 should be shown by this isotherm.

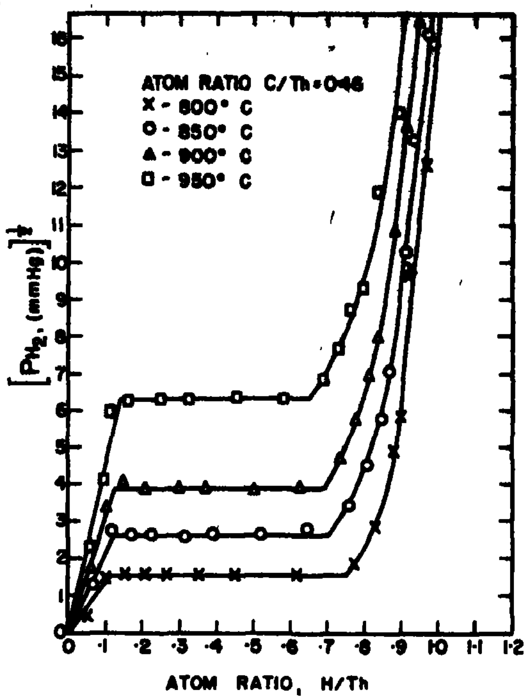

FIG. 2.—Pressure–composition isotherms for a specimen with a 0·46 C/Th ratio.

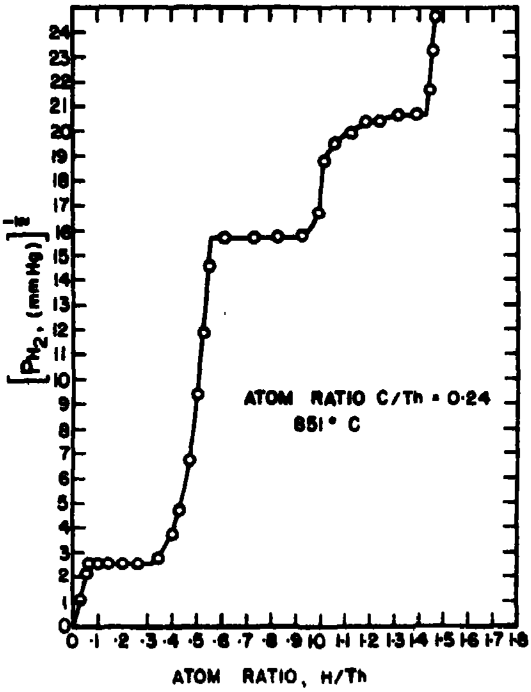

FIG. 3.—Pressure–composition isotherm for a specimen with a 0·24 C/Th ratio.

Specimens of each compound were prepared by equilibrating a sample having the proper carbon to thorium ratio with hydrogen at one atmosphere and 850° C. These compounds were quite brittle and −200 mesh powder for X-ray diffraction examination was prepared by crushing in a diamond mortar. Powder diffraction patterns were taken on a 11·46 cm Debye–Scherrer camera. ThC·ThH$_2$ was found to be hexagonal with $a_0 = 3{\cdot}816$ Å and $c_0 = 6{\cdot}302$ Å. The thorium atoms were arranged in a hexagonal closest-packed structure but the positions of the carbon and hydrogen atoms could not be established by X-ray methods. The compound ThC·2ThH$_2$ had a more complex structure. Examination of a single crystal showed the lattice to be monoclinic with $a_0 = 6{\cdot}50$ Å, $b_0 = 3{\cdot}80$ Å, $c_0 = 10{\cdot}91$ Å and $\beta = 119°$. The arrangement of the thorium atoms was a slightly distorted hexagonal closest-packed array.

The activity of hydrogen in specimens below the solubility limit⁽³⁾ of ThC in thorium was determined. A pressure-composition isotherm at 800° for two carbon compositions below the solubility limit are shown in Fig. 4 with the data of Mallet and Campbell⁽⁴⁾ for pure thorium. The equilibrium hydrogen pressure over all the specimens fell on the same straight line until the hydrogen pressure at which ThC·ThH$_2$ began to form was reached. This pressure in the specimen with a 0·060 carbon-to-thorium ratio was only slightly above the pressure for formation of ThC·ThH$_2$ from ThC and thorium because this specimen was nearly saturated with

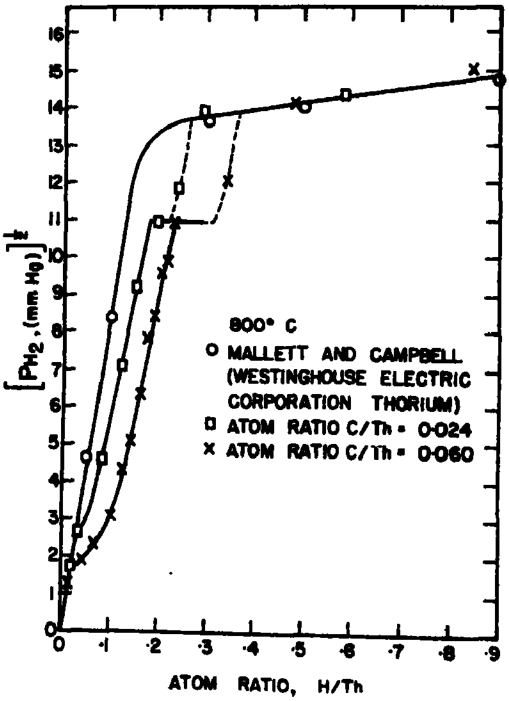

Fig. 4.—Pressure-composition isotherms for specimens with carbon contents below saturation.

---

(3) R. Mickelson and D. T. Peterson, *Trans. Amer. Soc. Metals* **50**, 340 (1958).

(4) M W. Mallet and I. E. Campbell, *J. Amer. Chem. Soc.* **73**, 4850 (1951).

ThC. The pressure at which ThC·ThH_2 began to form in a specimen with a 0·024 carbon-to-thorium ratio was higher, as would be expected from the law of mass action. As the hydrogen pressure increased further, the hydrogen concentration in solid solution in the thorium increased and ThC·ThH_2 also continued to precipitate. At a fixed higher pressure both specimens showed the formation of ThC·$2ThH_2$, and finally the formation of ThH_2 appeared at essentially the same pressure as for thorium with a very low carbon content.

A ternary section at 850° C for the Th–ThC–ThH_2 system, shown in Fig. 5, has been constructed. The ternary section allows a more accurate estimate of the composition ranges of the ternary compounds to be made. The effect of the stability of ThC·ThH_2 in limiting the solid solubility of both hydrogen and carbon in thorium is quite striking. Due to this restricted solubility, ThC·ThH_2 is the first phase to appear on adding hydrogen to thorium unless the carbon content is extremely low. A calculation based on constant activity co-efficients for carbon and hydrogen in thorium indicated that at 800° C ThC·ThH_2 would be formed if the carbon content were above 40 p.p.m. The ternary section also shows that thorium and hydrogen together dissolve to a significant extent in ThC. The absorption of hydrogen by pure ThC was found to be very small but when thorium metal was present ThC would dissolve more than 20 a/o hydrogen.

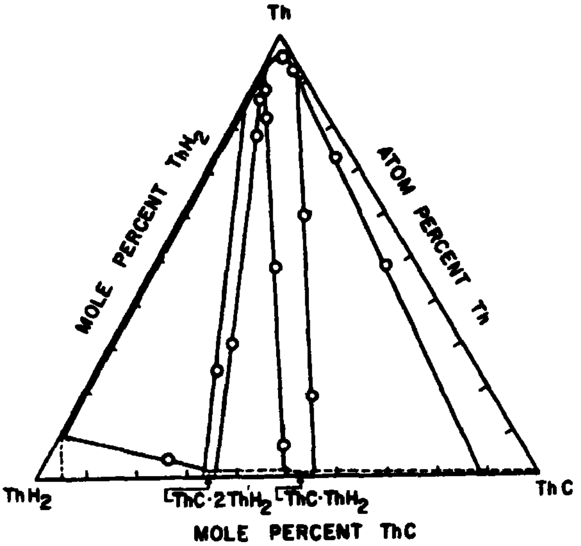

Fig. 5.—Ternary section at 850° of the Th–ThC–ThH_2 system.

The enthalpy of formation of these compounds was calculated from the variation of the equilibrium hydrogen pressure with temperature. The plot of the logarithm of the equilibrium pressure against reciprocal temperature is shown in Fig. 6. The data were treated by a least squares method to obtain the constants for the linear equations. The reactions for the respective equations given below are:

$$\left[\text{Log}\, P_{(\text{mm Hg})} = \frac{-10{,}580}{T} + 10{\cdot}20 \text{ and } \text{Log}\, P_{(\text{mm Hg})} = \frac{-8{,}365}{T} + 9{\cdot}84\right].$$

The reaction for the formation of ThC·ThH_2 is $Th_{(s)} + ThC_{(s)} + H_2 \rightleftharpoons ThC{\cdot}ThH_{2(s)}$ and for ThC·$2ThH_2$ is $Th_{(s)} + ThC{\cdot}ThH_{2(s)} + H_{2(g)} \rightleftharpoons ThC{\cdot}2ThH_2$. The enthalpy of formation of $ThC \cdot ThH_2$ by the reaction given above is $-48 \cdot 4$ kcal per mole. The enthalpy of formation of $ThC \cdot 2ThH_2$ by the reaction given above is $-38 \cdot 3$ kcal per mole.

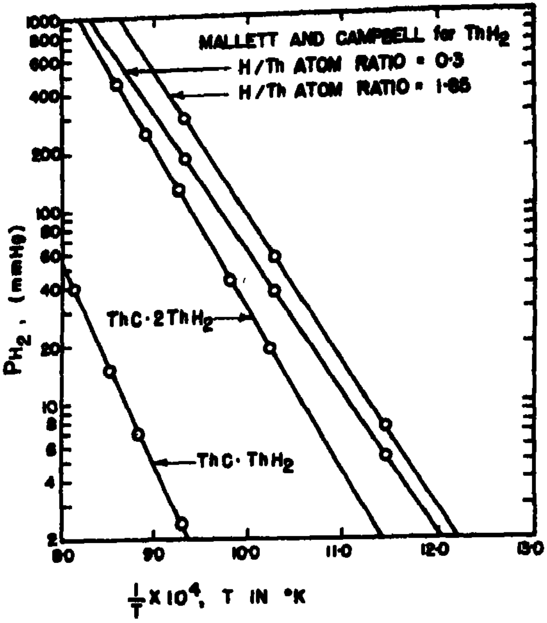

Fig. 6.—Logarithm of equilibrium hydrogen pressure vs. reciprocal temperature.

DISCUSSION

The positions of the carbon and hydrogen atoms in the $ThC \cdot ThH_2$ structure have not been determined and, consequently, the bonding in this compound can not be deduced from the bond distances and arrangement. However, the bonding in this compound is probably quite similar to the bonding in ThC and ThH_2. The volume of $ThC \cdot ThH_2$ is very nearly equal to the sum of the volumes of the ThC and ThH_2 that it contains. The volume of one $ThC \cdot ThH_2$ unit cell is 79·5 Å^3 and the sum of one fourth of the face-centred-cubic(5) ThC unit cell and one half of the body-centred tetragonal(6) ThH_2 unit cell is 79·3 Å^3. The metallic lustre and relatively high electrical conductivity of ThC and ThH_2 are also shown by $ThC \cdot ThH_2$.

The hexagonal closest-packed γ-phase reported in the zirconium–hydrogen system by Hagg(7) may have been an analogous compound formed by zirconium. It is interesting that the volume of the unit cell reported for this compound is 52·94 Å^3 and the sum of the volumes of ZrC and ZrH_2 is 52·83 Å^3. The presence of carbon in the specimens examined by Hagg is supported by his observation in a sample containing 9 a/o hydrogen of a face-centred-cubic phase with a lattice constant of 4·669 Å which is very nearly equal to the lattice constant of ZrC in equilibrium with zirconium metal. It appears quite likely that the β-phase reported by Hagg was zirconium carbide and the γ-phase was a ternary zirconium-hydrogen–carbon compound rather than non-equilibrium phases formed by zirconium and hydrogen. The similarity of the hydrides and carbides of Ti and Hf to those of Zr and Th makes the formation of similar compounds with these metals likely.

(5) H. A. Wilhelm and P. Chiotti, *Trans. Amer. Soc. Metals* **42**, 1925 (1950).

(6) R. E. Rundle, C. G. Shull and E. O. Wollan, *Acta Cryst.* **5**, 22 (1952).

(7) G. Hagg, *Z. Phys. Chem.* Vol. B 11, 433 (1931).

J. Inorg. Nucl. Chem., 1962, Vol. 24, pp. 525 to 534. Pergamon Press Ltd. Printed in England

THE CHEMICAL NATURE OF SODIUM BERYLLATE SOLUTIONS

D. A. EVEREST, R. A. MERCER, R. P. MILLER and G. L. MILWARD
National Chemical Laboratory, Teddington, Middlesex

(*Received* 30 *November* 1961)

Abstract—In sodium beryllate solutions of low Na_2O/BeO ratios, polymeric beryllate anions are present and range from ionic to colloidal dimensions. At high Na_2O/BeO ratios simple beryllate anions are probably present. Addition of silicon (as Na_2SiF_6 or Na_2SiO_3) to beryllate solutions of low Na_2O/BeO ratio causes precipitation of the beryllium as an X-ray-amorphous phase. Addition of calcium or strontium salts under similar conditions results in the precipitation of crystalline complexes which, it is believed, are derived from polyberyllate anions.

THERE has long been controversy in the literature on the nature of the species formed when amphoteric oxides dissolve in alkali. In general, when the Na_2O/BeO ratio is low, such solutions are unstable, many show colloidal properties and only at relatively high Na_2O/oxide ratios is true ionic solution considered to exist. This has been shown for aluminium,(1) zinc,(2) chromium,(2) silicon,(3) tin(4) and scandium.(5) In the last instance the Tyndall effect was evident until the Na_2O/Sc_2O_3 ratio was greater than five, showing that particles of colloidal dimensions were present up to this value.

The existence of cationic polynuclear beryllium species in the pH range 3–5 (i.e. prior to precipitation) has been demonstrated by KAKIHANA and SILLEN(6) who postulated an olated complex, $Be_3(OH)_3^{3+}$, i.e. the Be atoms are linked by hydroxyl bridges. THOMAS(7) has suggested the existence of larger olated complexes in the colloidal particles formed prior to precipitation of gelatinous $Be(OH)_2$ from acidic solution and in the hydroxide itself. It is further suggested here that similar anionic polynuclear species are formed on dissolution of $Be(OH)_2$ in alkali and a plausible picture of the dissolution can be obtained on the basis of olation.(8, 9) Addition of alkali to the uncharged, gelatinous beryllium hydroxide first displaces the water molecules at the end of the olated units to give negatively-charged colloidal beryllate particles: at higher alkali concentrations it is postulated that the hydroxyl bridges are progressively broken down by the reaction

---

(1) P. LANASPEZE and C. EYRAUD, *Bull. Soc. Chim. France* 2, 313 (1960); C. BROSSET, *Acta Chem. Scand.* 6, 910 (1952).

(2) H. B. WEISER, *The Hydrous Oxides.* Chap. 3 and 6. McGraw-Hill, New York (1926).

(3) W. EITEL, *The Physical Chemistry of the Silicates.* Univ. Chicago Press (1954).

(4) J. S. JOHNSON and K. A. KRAUS, *J. Amer. Chem. Soc.* 81, 1569 (1959).

(5) B. N. IVANOV-EMIN and E. A. OSTROUMOV, *J. Inorg. Chem.* (*U.S.S.R.*), (English translation), 1, 27 (1959); *Zh. Neorg. Khim.* 4, 71 (1959).

(6) H. KAKIHANA and L. G. SILLEN, *Acta Chem. Scand.* 10, 985 (1956).

(7) A. W. THOMAS and H. S. MILLER, *J. Amer. Chem. Soc.* 58, 2526 (1936).

(8) F. BASALO and R. G. PEARSON, *Mechanisms of Inorganic Reactions*, p. 388. J. Wiley, New York (1958).

(9) J. C. BAILAR, JR. (Editor), *Chemistry of the Co-ordination Compounds*, Monograph Series No. 131, Chapt. 13. Reinhold, New York (1956).

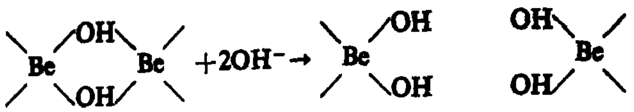

Such a reaction results in the formation of progressively smaller polymers with increased charge/beryllium ratios. The eventual limit of this reaction is the formation of the mononuclear beryllate ion, $[Be(OH)_4]^{2-}$, sometimes expressed as BeO_2^{2-}. It appears probable that complete conversion of polynuclear beryllate to the mononuclear species requires high alkali concentrations. For example, Brintzinger(10) claims, from the results of diffusion experiments, that even in a solution in which the ratio of Na_2O/BeO was 14:1 the predominant beryllate species contained ten beryllium atoms.

The beryllate system seems, therefore, to resemble other isopolyacid systems in that increasing concentration of alkali on the negative side of the isoelectric point decreases the degree of polymerization of the system. It must be emphasized that although the experimental results recorded here are in accord with the above suggestion that beryllate solutions are an alkali-dependent polymerization system they give no information concerning the actual bonding of the beryllate species.

EXPERIMENTAL

(a) *Tyndall effect.* A comparison between the intensities of the Tyndall beam produced in beryllate solutions was made by measuring the intensity of light scattered at an angle of 90° to the incident beam by means of a fluorimetric attachment to a Unicam spectrophotometer.

The solutions were prepared by precipitating beryllium from sulphate solutions of known strength by addition of NaOH to pH 12; the $Be(OH)_2$ was centrifuged before adding the amount of NaOH solution appropriate to the desired excess (expressed in terms of the Na_2O/BeO molar ratio). Each solution was centrifuged before readings were taken.

In the absence of a suitable standard, arbitrary units of light-scattering were employed. The solution in each series (i.e. at each BeO concentration studied) with the most intense scatter was taken as the reference solution (100 per cent scatter) for that series and the scatter from any other was expressed as a percentage of it. For this reason the results for different concentrations of BeO cannot be rigidly compared.

The scatter from a pure NaOH solution of strength equivalent to the highest NaOH concentration used in each series (i.e. at $Na_2O/BeO = 10$) was taken as the "blank" level.

(b) *Stability to heat.* Beryllate solutions were prepared as in (a), CO_2 was excluded by the use of Sofnolite traps and each solution was heated for 2 hr at 95°C. The beryllium precipitated was separated by centrifuge and the amount determined.

(c) *The effect of silicon, calcium and strontium on beryllate stability.* The effect of silicon was studied by addition of varying amounts of (i) Na_2SiF_6 and (ii) freshly-prepared Na_2SiO_3 solutions to a series of beryllates prepared as in (a). The effect of calcium and strontium was studied by direct addition of the respective chlorides. After adjustment to the required concentration, the solutions were protected from CO_2, heated for 1 hr at 50° C (at which temperature a pure beryllate solution is stable but insoluble hydroxides will coagulate) and any precipitates centrifuged and analysed.

The result of calcium addition to beryllium sulphate solutions prior to precipitation was also studied.

A Philips camera (36 cm circumference) with iron-filtered Co*Kα* radiation was used for X-ray diffraction photographs.

---

(10) H. Brintzinger and H. Osswald, *Z. Angew. Chem.* **47**, 61 (1934).

RESULTS AND DISCUSSION

Tyndall effect. Two series of beryllates were prepared with beryllium concentrations of 1·56 g BeO/l. and 3·13 g BeO/l. in which the Na_2O/BeO ratios were varied between 2·0 and 10·0. The results are plotted graphically in Fig. 1. They demonstrate the marked Tyndall effect observed for beryllate solutions of low Na_2O/BeO ratio when these are compared with pure NaOH solutions: at both beryllium concentrations it is evident that the light-scattering falls off markedly as the Na_2O/BeO ratio increases, thus indicating that the species in solution diminish in size as the alkali concentration increases.

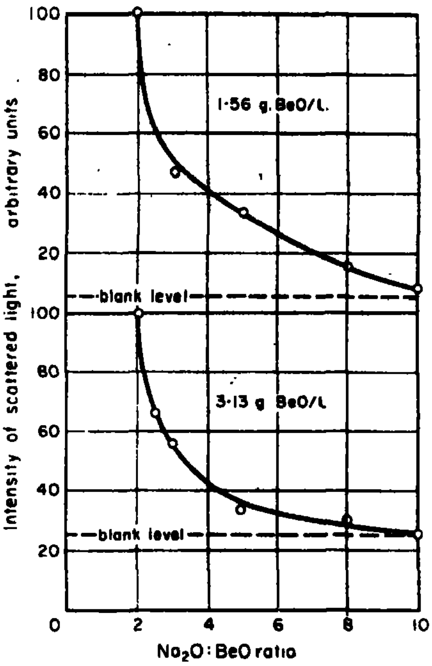

FIG. 1.—Light-scattering from beryllate solutions.

The stability of beryllate solutions on heating. Beryllium is normally recovered from a beryllate solution by heating it at, or near, its boiling point to precipitate granular beryllium hydroxide. The effects of changing the ratio of Na_2O/BeO and the initial beryllium concentration on the recovery of beryllium on heating are shown in Figs. 2 and 3. Both sets of results demonstrate that the amount of beryllium precipitated on heating decreases with increase in the concentration of alkali in solution. Such behaviour would be expected as the large polymeric beryllate species present at lower alkali concentrations can more readily coalesce because of their lower charge/beryllium ratio than can simple mononuclear $[Be(OH)_4]^{2-}$ ions.

The effect of silicon on beryllate solutions. It was found that quite small amounts of silicon (as silicate) could greatly reduce the solubility of beryllium hydroxide in alkali or cause precipitation of beryllium from a beryllate solution. This was investigated by the addition of silicon to a beryllate solution ($Na_2O/BeO = 2$; 10·25 M in Be) to determine whether a quantitative relationship existed between the

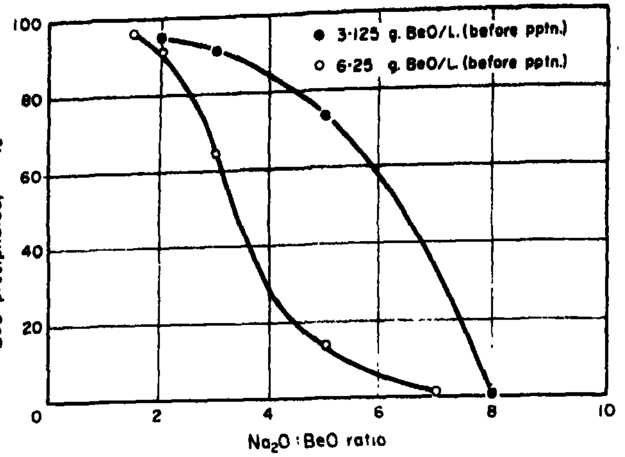

Fig. 2.—Stability of beryllate solutions at 95°C (after 2 hr heating). Effect of Na$_2$O:BeO ratio.

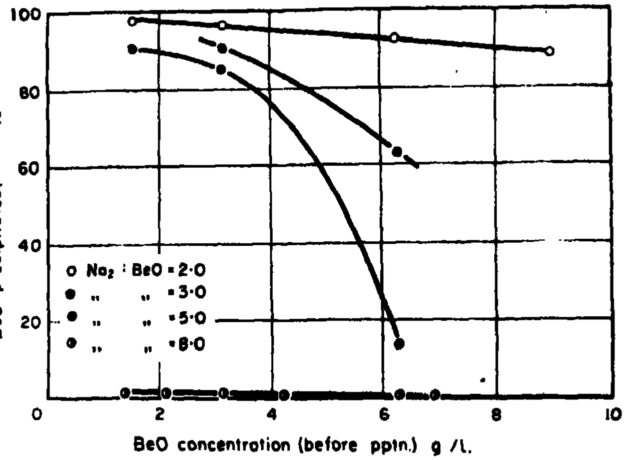

Fig. 3.—Stability of beryllate solutions at 95°C (after 2 hr heating). Effect of BeO concentration.

amount of silicon added and the amount of beryllium precipitated. A comparison was made between the behaviour of sodium silicate (Na_2SiO_3) and sodium fluosilicate (Na_2SiF_6); these sources of silicon were regarded as two which would be likely to rapidly establish equilibrium, with respect to the silicate species present, in solutions of high concentrations of alkali. The results (Tables 1 and 2) show that no simple beryllium-silica species is precipitated. It was possible, however, to apply the classical adsorption isotherm;

$$\frac{x}{m} = mc^{1/n}$$

where x = amount adsorbed, m = mass of adsorbent, c = equilibrium concentration of species being adsorbed, and k and n are constants, assuming that only the precipitated beryllium presented an adsorbing surface (Fig. 4).

The precipitation of an amorphous, non-stoicheiometric silica-beryllium species is consistent with a picture of polymeric beryllate species of colloidal dimensions having a random distribution of terminal OH groups, their number depending on the degree of polymerization. By equating these with the active centres involved when unimolecular adsorption is considered, a type of heteropoly cross-linking which results in insolubility is easily envisaged: this concept is supported by the isotherm relationship.

TABLE 1.—PRECIPITATION OF BERYLLIUM FROM BERYLLATES BY ADDITION OF SILICON AS Na_2SiF_6

Original beryllate			Precipitate		
BeO (mg)	SiO_2 (mg)	BeO/SiO_2 mole ratio	BeO (mg) [m]	SiO_2 (mg) [x]	BeO/SiO_2 mole ratio
62·5	nil	—	nil	—	—
,,	1·0	1:0·0067	8·5	0·38	1:0·018
,,	4·0	1:0·0268	16·5	2·03	1:0·051
,,	5·0	1:0·0335	19·6	2·83	1:0·060
,,	10·0	1:0·067	30·7	6·40	1:0·087
,,	20·0	1:0·134	35·5	10·10	1:0·120

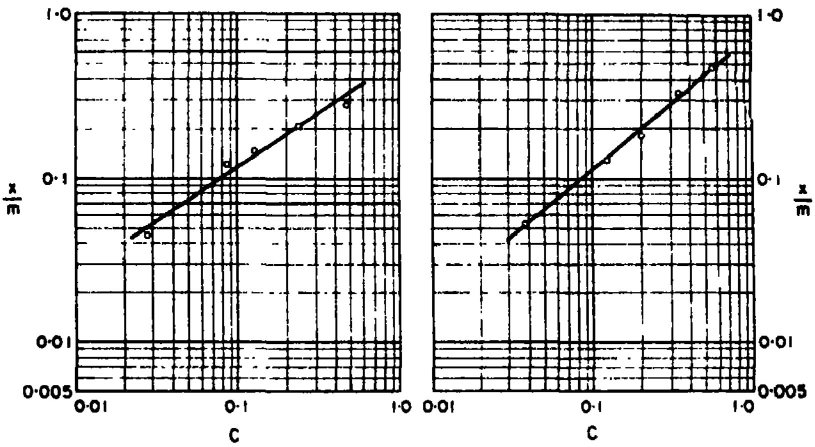

FIG. 4.—(a) Addition of Na_2SiF_6 to sodium beryllate solution.
(b) Addition of Na_2SiO_3 to sodium beryllate solution.
SiO_2 adsorbed on precipitated beryllium.

Confirmation that the larger beryllate species were reacting with the silicate ions was obtained when the above experiments were repeated in the presence of a greater excess of NaOH($Na_2O/BeO = 10$). Under these conditions the beryllium is probably mainly present as beryllate ions of low molecular weight (cf. Tyndall effect and stability to heat of such solutions). Such solutions always remained indefinitely stable on addition of silicon.

TABLE 2.—PRECIPITATION OF BERYLLIUM FROM BERYLLATES BY ADDITION OF SILICA AS Na_2SiO_3

Original beryllate			Precipitate		
BoO (mg)	SiO_2 (mg)	BeO/SiO_2 mole ratio	BeO (mg) [*m*]	SiO_2 (mg) [*x*]	BeO/SiO_2 mole ratio
62·5	nil	—	nil	—	—
,,	1·0	1:0·0067	7·3	0·38	1:0·022
,,	5·0	1:0·0335	19·2	2·5	1:0·054
,,	10·0	1:0·0670	29·0	5·3	1:0·076
,,	20·0	1:0·134	37·0	12·8	1:0·144
,,	40·0	1:0·268	49·5	24·5	1:0·206

It is of interest to note that this effect of silicon on beryllate solutions of low Na_2O/BeO ratio is similar to those observed for solutions of both aluminate and zincate (0·125 M-Al_2O_3 and ZnO respectively) when the ratio of Na_2O/oxide was two. The addition of sodium silicate solution produced immediate precipitation.

THE COMPLEX CALCIUM AND STRONTIUM HYDROXY-COMPOUNDS OF BERYLLIUM

It was shown by the results of studies in another context that beryllate formation, when another Group II metal was present, was restricted, and, under certain conditions was almost entirely prevented.

A series of beryllates ($Na_2O:BeO = 2:1$; 0·25 M-BeO) was prepared and equimolar amounts of the chlorides of Mg, Ca, Sr and Ba were added to give an arbitrary ratio of oxide to BeO of 1:14. The amount of beryllium precipitated was determined and the results are shown graphically in Fig. 5.

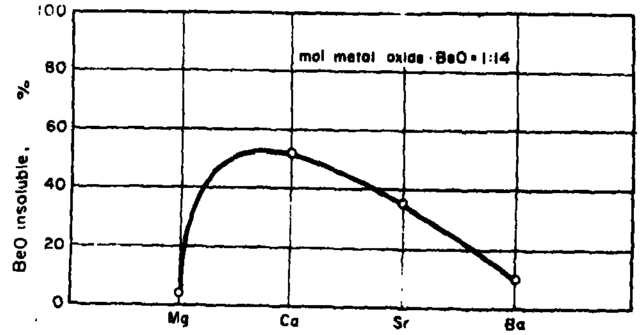

FIG. 5.—Effect of equimolar amounts of Group IIa hydroxides on stability of beryllates ($Na_2O/BeO = 2$).

Calcium and strontium can be seen to have the greatest influence and subsequent investigation was concentrated on the extent of beryllate decomposition caused by the presence of these elements and the nature of the compounds precipitated.

Table 3 demonstrates the marked decrease in solubility of $Be(OH)_2$ in 4 N sodium hydroxide solution ($Na_2O/BeO = 2·0$) when co-precipitated with increasing amounts of $Ca(OH)_2$.

The washed and air-dried solids were clearly microcrystalline and gave very similar X-ray photographs, the lines of which could not be assigned to any known phase. A strong line at about $d = 8$ Å was particularly characteristic.

The direct addition of calcium chloride solution to stable beryllate solutions resulted in the immediate precipitation of the identical complex.

TABLE 3.—EFFECT OF CALCIUM ON THE SOLUBILITY OF $Be(OH)_2$ IN NaOH

Mol. ratio $Ca(OH)_2$/ $Be(OH)_2$ in pptd. hydroxides	0:1	0·054:1	0·058:1	0·097:1	0·105:1	0·165:1
BeO insoluble after 1 hr at 50°C (%)	nil	45·5	41·0	74·5	75·5	89·0
CaO/BeO (mol) in pptd. solid		1:8·3	1:7·2	1:7·7	1:7·2	1:5·6

A systematic study of the degree of precipitation from beryllates of varying Na_2O/BeO ratio on the addition of a constant amount of calcium chloride was made. From the results shown in Table 4, it can be seen that in test 1 almost complete precipitation of beryllium occurred and no lines of the powder photograph related to any phase other than the characteristic complex. In test 2 the stability of the beryllate was slightly increased and the strong lines of $Ca(OH)_2$ were discernible among those of the complex. This was the only change in the X-ray spectrum. In test 3 and particularly test 4 the lines of $Ca(OH)_2$ clearly predominated but line intensity was the only change noted in the pattern associated with the complex. The presence of $Ca(OH)_2$ in the precipitates from solutions with the higher Na_2O/BeO ratio is also shown by the increased CaO/BeO ratio in the precipitate.

TABLE 4.—PRECIPITATION OF BERYLLIA FROM BERYLLATE SOLUTIONS ON ADDITION OF 3·6 M MOLE. CaO AS $CaCl_2$ TO 40 ML 0·25 M-BERYLLATE SOLUTION (I.E. 10 M MOLE BeO)

Test no.	Na_2O:BeO (mole)	BeO pptd. (%)	CaO:BeO in ppt. (mole)
1	2	95·8	1:4·1
2	4	92·9	1:3·1
3	6	34·8	1:0·82
4	8	8·9	1:0·05

The improved stability that followed an increase of the Na_2O/BeO ratio parallels that found on addition of silicon. This confirms the significance of the ratio in defining the equilibrium state.

When strontium chloride was added to beryllates an analogous complex was precipitated and a more detailed study of these two compounds was undertaken.

TABLE 5.—ANALYSIS OF COMPLEX CALCIUM AND STRONTIUM HYDROXY BERYLLATES

	Vacuum-desiccated				Oven-dried (110°C)			
Calcium complex	CaO (%)	BeO (%)	H_2O* (%)	Mole ratio, $Ca(OH)_2/Be(OH)_2/H_2O$	CaO (%)	BeO (%)	H_2O* (%)	Mole ratio, $Ca(OH)_2/Be(OH)_2/H_2O$
	18·0	34·8	47·2	1:4·3:2·8	20·7	40·0	39·3	1:4·3:0·6
Strontium complex	SrO (%)	BeO (%)	H_2O* (%)	Mole ratio, $Sr(OH)_2/Be(OH)_2/H_2O$	SrO (%)	BeO (%)	H_2O* (%)	Mole ratio, $Sr(OH)_2/Be(OH)_2/H_2O$
	28·7	30·7	40·6	1:4·4:2·7	32·2	34·3	33·5	1:4·4:0·5

* By difference.

The respective preparations were made by direct addition of an arbitrarily chosen amount of the chlorides to a beryllate (1 mole MCl_2:5·6 mol. BeO; 2·5 M-BeO solution, $Na_2O/BeO = 2$). Microscopic examination of the vacuum-dried products revealed that both compounds consisted of ill-defined hexagonal plates. No change in crystal habit was apparent on drying at 110°C. The analytical results shown in Table 5 are typical of several, all of which were in close agreement and which point to deviation from simple stoichieometry. It can be seen that the further drying at 110°C resulted in the expulsion of approximately 2 mole H_2O.

Within analytical error both calcium and strontium are represented in identical ratios to beryllium in these crystals and interpretation of the X-ray data by the usual graphical and numerical methods showed that the higher hydrates had identical unit cells (Table 6).

TABLE 6.—LATTICE PARAMETERS AND DENSITIES OF CALCIUM AND STRONTIUM COMPLEXES

	Crystal class	a (Å)	c (Å)	Density (g/cm³)
Calcium hydroxy beryllate (vacuum-dried)	Hexagonal	14·9	16·6	1·83
Calcium hydroxy beryllate (dried at 110°C)	„	14·6	13·1	2·23
Strontium hydroxy beryllate (vacuum-dried)	„	14·9	16·6	2·08
Strontium hydroxy beryllate (dried at 110°C)	„	14·6	13·5	2·29

Several aspects of interest arise from these observations which should repay a more detailed investigation. The data are consistent with complexes of hexagonal layer lattice structure: absence of the odd order (*ool*) reflexions show them to be of the *ABAB* type common to many hydroxy salts precipitated from both acid and alkaline solutions. Several other cations of high ionic potential (e.g. Bi^{3+}, Al^{3+}, UO_2^{2+}) which have been claimed(11, 12, 13) to undergo condensation reactions which produce hydroxy-bridged complex ions in solution also form sheet structures on precipitation.

The high field strength of beryllium may be expected to exert a strong attraction on the OH groups and it is of interest to note that, unlike most hydroxides, granular $Be(OH)_2$ does not form a layer lattice(14) but is a structure based upon the OH groups arranged tetrahedrally around the Be^{2+} ions in an orthorhombic cell. This is the stable form of $Be(OH)_2$ into which the gelatinous form passes on standing or boiling, and the form generated by boiling a beryllate solution.

The hypothesis of hydroxy bridging already suggested would also presumably involve Be^{2+} in fourfold co-ordination and models show that since this demands a

(11) L. G. SILLÉN, *Naturwissenschaften*. **30**, 318 (1942).

(12) C. BROSSETT, *Acta Chem. Scand.* **6**, 910 (1952).

(13) S. AHRLAND, *Acta Chem. Scand.* **3**, 374 (1949).

(14) VON A. SEITZ *et al.*, *Z. Anorg. Chem.* **261**, 94 (1950).

sharing of the edges of tetrahedra, the Be^{2+} ions are closer than in the other arrangement. The tendency to form sheets on this basis is only possible if the terminal OH groups are shared, thus;

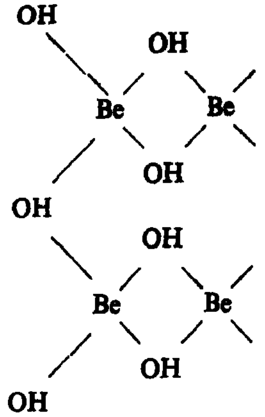

A lateral extension of this arrangement seems unlikely.

The simplest unit would therefore be a tetramer and attention is drawn to the ideal formula for the complexes which suggests that the tetramer is the unit laid down in the lattice. Consideration of the densities indicates that twelve such units occupy the unit cell but confirmation of these implications requires more refined studies.

The contraction along the *C* axis when about two moles of water are expelled on drying the solids at 110°C indicates that these are intercalated between the layers, analogous to the behaviour of the clay minerals. It was also noted that these compounds, particularly the higher hydrates, absorbed carbon dioxide but whether this, too, became intercalated or assumed a constitutional role was not investigated.

Other results (on the products of the experiments recorded in Table 3) have suggested that variations in the preparative procedure modify the Ca:Be ratio without making marked changes in the cell size. This parallels work of Brandenberger(15) for the system:

$$x\, Ca(OH)_2\, y\, Al(OH)_3\, z\, H_2O$$

in which variations of x, y and z had little influence on the diffraction patterns.

These results and observations are important for those hydrometallurgical processes which depend upon the attainment of stable alkaline solutions of the metal, for example beryllium or aluminium. Indeed, it appears from the work of Malyshev and Drozdov(16, 17) that the chemistry of aluminates bears a strong resemblance to that of beryllates with respect to their reactions with calcium hydroxide and silica.

Acknowledgement—This paper describes work undertaken on behalf of the United Kingdom Atomic Energy Authority and is published by their permission and by that of the Director of the National Chemical Laboratory.

(15) E. Brandenberger, *Schweiz, Min. Petr. Mitt.* **13**, 569 (1933).
(16) B. V. Drozdov and M. F. Malyshev, *Zh. Priklad. Khim.* **30**, 1600 (1957).
(17) B. V. Drozdov and M. F. Malyshev, *Zh. Priklad. Khim.* **33**, 20 (1960).

J. Inorg. Nucl. Chem., 1962, Vol. 24, pp. 535 to 540. Pergamon Press Ltd. Printed in England

KINETICS OF THE REDUCTION OF NEPTUNIUM(V) WITH IODIDE ION

N. K. SHASTRI, J. O. WEAR and E. S. AMIS
The Chemistry Department, University of Arkansas, Fayetteville, Arkansas

(*Received* 22 *May* 1961; *in revised form* 10 *August* 1961; *in final form* 10 *November* 1961)

Abstract—The rate law for the reaction, $NpO_2^+ + I^- = Np^{4+} + \frac{1}{2}I_2$, may be expressed as $d\,Np^{4+}/dt = k[NpO_2^+][I^-]^{1.5}[H^+]^{2.5}$. At 25° and in 3·29 M HCl, the rate constant is $10{\cdot}27 \times 10^{-2}$ l.^{4} mole^{-4}min^{-1}. The apparent activation energy is 28,300 cal mole^{-1}. A possible mechanism is suggested.

IN the case of the actinide elements, reactions between different valence forms of the same element are said to be similar. The reactions between different valence forms of the same element also resemble and obey the same kinetic forms as the ionic reactions of the actinides with various cations and anions.(1) Thus, the reduction of neptunium(V) by neptunium(III)(2) has the same rate law and follows a similar mechanism as the neptunium(V)–iron(II)(3) reaction. Iodide ion in hydrochloric acid solutions has a greater reducing potential and thus offers a more complete reduction than iron. Neptunium(V) is very stable under a wide range of conditions and no disproportionation is reported to occur in acid concentrations below five molar.(4, 5) Consequently, reduction of neptunium(V) with iodide ion becomes very interesting from a kinetic standpoint. So far only a qualitative study of the neptunium(V)–iodide reaction has been reported.(6) The following paper presents a systematic investigation of the rate law and a probable mechanism for the kinetics of the neptunium(V)–iodide reaction.

EXPERIMENTAL

A neptunium(V) stock solution was prepared by electrolytic reduction(7) of a ^{237}Np sample furnished by the AEC and its purity in 1 M acid was ascertained by observing the neptunium(V) peaks to the exclusion of others on a Beckman DK-1 spectrophotometer. The neptunium concentrations were determined by alpha particle counting on the basis of 790 α-counts min^{-1} μg^{-1} specific counting yield on a Nuclear Chicago gas flow counter.(8)

All solutions were prepared in distilled water which was previously run through an ion-exchange column and boiled to remove oxygen. A standard stock solution of sodium iodide was made by weighing out the required amount of A.R. grade (Mallinckrodt) sodium iodide and dissolving it in oxygen-free water in a volumetric flask.

(1) J. C. HINDMAN, *Proceedings of the Second International Conference on Peaceful Uses of Atomic Energy, Geneva*, 1958, Vol. 28, p. 349. United Nations (1958).

(2) J. C. HINDMAN, J. C. SULLIVAN and D. COHEN, *J. Amer. Chem. Soc.* **80**, 1812 (1958).

(3) L. B. MAGNUSSON, J. C. HINDMAN and T. J. LACHAPPELLE, *Transuranium Elements*, Pt. II, *NNES*. Div. IV, Vol. 14 B, 1143. McGraw-Hill, New York (1949).

(4) J. R. HUIZENGA and L. B. MAGNUSSON, *J. Amer. Chem. Soc.* **73**, 3202 (1951).

(5) R. SJOBLOM and J. C. HINDMAN, *J. Amer. Chem. Soc.* **73**, 1744 (1951).

(6) L. B. MAGNUSSON, J. C. HINDMAN and T. J. LACHAPPELLE, *Transuranium Elements*, Pt. II, *NNES*. Div. IV, Vol. 14 B, 1146. McGraw-Hill, New York (1949).

(7) D. COHEN and J. C. HINDMAN, *J. Amer. Chem. Soc.* **74**, 4679, 4682 (1952).

(8) L. B. MAGNUSSON and T. J. LACHAPPELLE, *J. Amer. Chem. Soc.* **70**, 3534 (1948); *Transuranium Elements*, Pt. I, *NNES*. Div. IV, Vol. 14 B, 39. McGraw-Hill, New York (1949).

The stock solution of hydrochloric acid was standardized against a standard sodium hydroxide solution using phenolphthalein as an indicator.

A 0·5 M solution of TTA (thenonyltrifluoroacetone) was prepared in reagent grade benzene.

The course of the reaction was followed by extracting the Np^{4+} ion with TTA at different intervals of time and determining its concentration by α-particle counting. To eliminate the reverse reaction, reduction of Np(V) was carried out in a two phase system, with carbontetrachloride as a carrier of iodine. No evidence of a photochemical reaction was found when parallel runs were made in blackened vessels.

The reaction was carried out in an atmosphere of nitrogen. The nitrogen used was freed from oxygen by passing it through gas wash-bottles containing pyrogallol and sulphuric acid, respectively. Finally, it was saturated with the solvent by passing it through the solvent contained in a gas wash bottle placed in the thermostat bath.

The reaction vessel was a 70 ml flat bottomed flask (Fig. 1) with a side-arm opening at the base, which served as an inlet for nitrogen to bubble through the solution. The cap of the vessel had both an inlet as well as an outlet for nitrogen. The vessel was air-tight when both the parts were joined together and clasped with rubber bands. Both the inlets for nitrogen were provided with stop-cocks, and nitrogen could be passed through either of them at will. The outlet at the top was a 7 mm glass tube with a piece of rubber tubing attached to it. The height of the tubing was so adjusted that when the bulb of a one ml pipette was pressed against it, the tip of the pipette dipped into the solution. A sample could be withdrawn in this way by opening the upper nitrogen inlet and forcing the solution into the pipette.

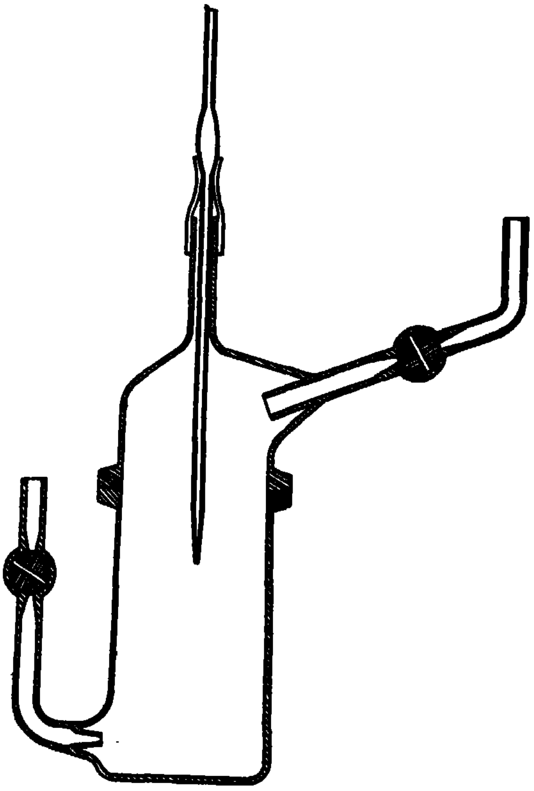

FIG. 1.—Reaction vessel with inserted pipette.

Appropriate amounts of HCl and water with about 50 ml of CCl_4 were placed in the reaction vessel and put in the thermostated bath. The other two reactants were also placed separately in the bath. Presaturated nitrogen was bubbled through all the three solutions long enough to attain constant temperature and complete deoxygenation. When thermal equilibrium was attained, the required amount of sodium iodide was added to the reaction vessel. No decomposition of sodium iodide was observed in the runs made. The reaction was started by adding the neptunium(V) solution. The start of the reaction was timed when half of the neptunium solution had drained out of the pipette. Nitrogen was kept bubbling through the solution for a thorough mixing of the reactants. The temperature of the bath was kept constant within ±0·2°. The thermometer used was calibrated against a National Bureau of Standards thermometer.

One ml samples were withdrawn at different measured intervals of time and poured into 10 × 75 mm test tubes containing one ml of water and one ml of 0·5 M TTA in benzene. As the reaction is dependent upon a large acid concentration, dilution with water quenched the reaction. The mixture was shaken for 3 min for complete extraction. The aqueous and benzene layers were separated by a centrifuge. Fifty λ samples of benzene layer were spotted on platinum planchettes in triplicate, evaporated under a lamp, heated to red heat over a flame, cooled, and counted for α-particle activity of neptunium(IV). The background count of the planchettes was subtracted and a statistical average of three counts was taken as a point on the rate plot.

Order of the reaction

The rate data obtained at equimolar concentrations of Np(V) and iodide ions failed to satisfy the bimolecular or simpler expressions. Consequently, the procedure adopted was to first determine the orders with respect to various reaction ions and then to obtain a rate expression. Orders were determined by making a number of runs in which the concentration of only one reactant was varied. The initial rate was determined graphically from concentration vs. time plots. The logarithms of initial rates when plotted against the logarithms of initial concentrations gave a straight line, the slope of which was equal to the order with respect to the ion the concentration of which was varied.

Orders were determined from the slopes of plots of log dc/dt as ordinates vs. log c as abscissae. The data showed good precision and gave slopes of 0·86, 1·55 and 2·61 for NpO_2^+, I^- and H^+ ions, respectively. The fifth column in Table 1 contains the values of k as calculated by substituting the orders in the rate law. The values agree with the average value within ±3·9 per cent.

TABLE 1.—INITIAL RATES AND SPECIFIC VELOCITY CONSTANTS WITH VARIOUS NpO_2^+, I^- AND H^+ ION CONCENTRATIONS AT 25°; μ = 3·0

$[NpO_2^+] \times 10^2$ M	$[I^-] \times 10^2$ M	$[H^+]$M	$\frac{dc}{dt} \cdot \frac{10^6}{6\cdot84}$	$k \times 10^2$
0·423	1·229	3·29	3·26	9·93
0·307	1·229	3·29	2·42	9·70
0·265	1·229	3·29	2·20	9·86
0·614	1·229	3·29	4·45	10·05
0·614	1·229	3·29	4·47	9·97
0·423	0·988	3·29	2·36	10·28
0·423	1·474	3·29	4·23	9·91
0·423	1·474	3·76	6·67	10·79
0·565	2·000	2·88	6·72	10·77
1·224	0·800	3·28	4·26	10·27
1·379	1·200	3·06	7·33	10·57
0·608	3·000	2·48	9·53	11·24

Average $10\cdot27 \times 10^{-2} \pm 0\cdot40$
$l.^4\ mole^{-4}\ min^{-1}$

Effect of ionic strength

The ionic strength, μ, in this reaction changes with time during the course of the reaction. To observe the effect of a neutral electrolyte on the reaction rate, runs were made with the addition of sodium chloride. Data in Table 2 indicates no perceptible effect on the rate with changing μ.

Table 2.—Effect of ionic strength on the rate of reaction of neptunium(V) and sodium iodide at 25°

$[NpO_2^+]\times10^2$ M	$[I^-]\times10^2$ M	$[H^+]$ M	μ	$k\times10^2$
0·423	1·474	2·820	2·84	10·64
0·565	2·000	2·884	3·00	10·77
0·565	2·000	2·884	3·32	11·21
0·565	2·000	2·884	3·63	11·09
0·423	1·474	4·230	4·25	9·95

The energy of activation

The energy of activation was determined by carrying out the reaction at three temperatures and plotting the values of log k against $1/T$. A straight line was obtained, as illustrated in Fig. 2. From the slope of the line, the energy of activation is calculated to be 28·3 kcal mole^{-1}.

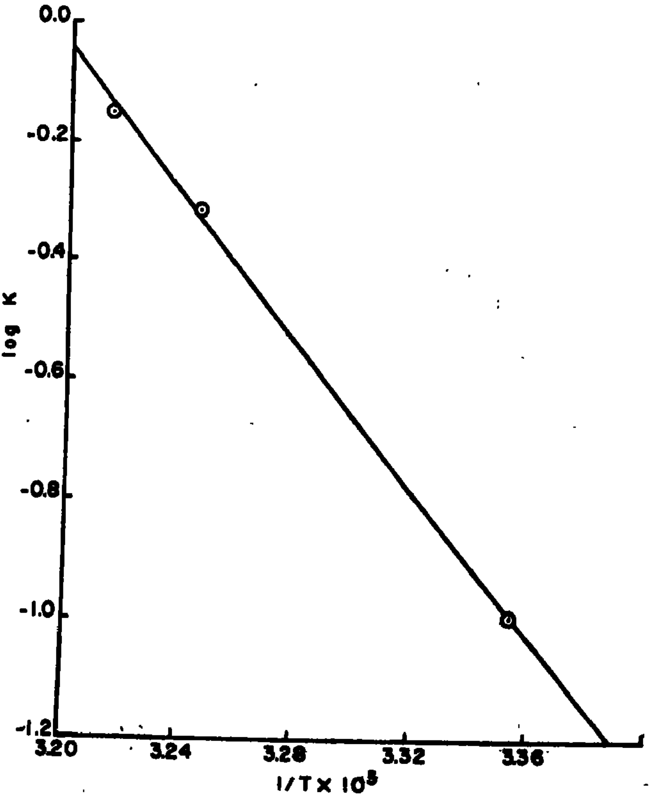

Fig. 2.—A plot of log K against $1/T\times10^3$.

DISCUSSION AND MECHANISM

Assuming the orders to be either whole numbers or half-fractions, the stoicheiometry of the neptunium(V) and sodium iodide reaction is satisfied by the following mechanism:

$$NpO_2^+ + 2H^+ + I^- \rightarrow Np(OH)_2I^{2+} \qquad (3)$$

$$NpO_2^+ + 3H^+ + 2I^- \rightarrow Np(OH)I_2^{2+} + H_2O \qquad (4)$$

An average of these two steps would give a rate which would depend on $[NpO^+]$ to the first power: $[I^-]$ to the 1·5 power and $[H^+]$ to the 2·5 power. This mechanism leads to the following rate law:

$$\frac{-d[NpO_2^+]}{dt} = k_1[NpO_2^+][H^+]^2[I^-] + k_2[NpO_2^+][H^+]^3[I^-]^2 \qquad (5)$$

or

$$\frac{\text{Rate}}{[NpO_2^+][H^+]^2[I^-]} = k_1 + k_2[H^+][I^-] \qquad (6)$$

Equation (6) can be tested against the experimental results. Rate values, as given in Table 1, column 4, when divided by the concentrations of the reactant ions raised to appropriate powers, are plotted against the product $[H^+][I^-]$, a straight line is obtained (Fig. 3) as demanded by the rate law. The intercept of this line gives the value of k_1, which is $1{\cdot}82 \times 10^{-2}$: and the slope gives the value of k_2, which is $5{\cdot}41 \times 10^{-1}$.

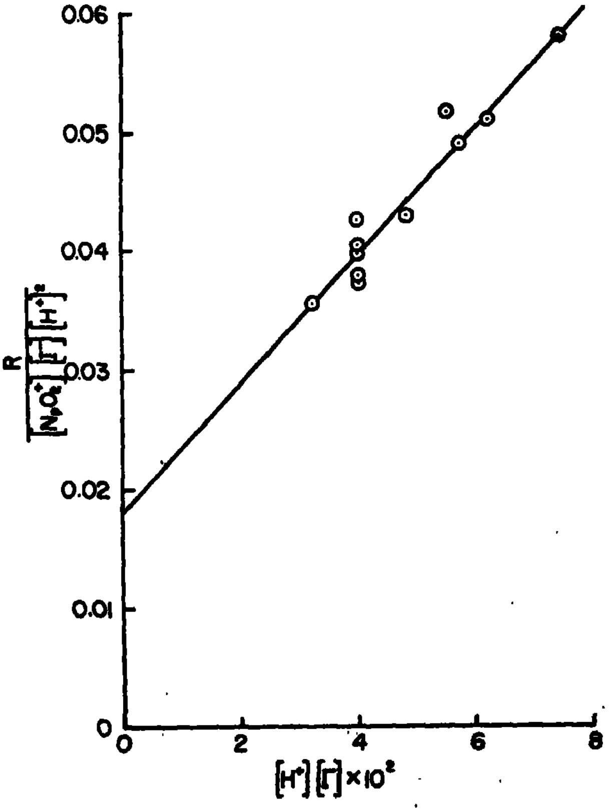

FIG. 3.—Plot of differential Rate expression from the mechanism.

The integrated form of Equation (5), assuming H^+ to be constant, is:

$$\frac{1}{2Kk_3}\log\left[\frac{z^2}{k_4z^2+(k_4K+k_3)z+Kk_3}\right]-\frac{(k_4K+k_3)}{k_3K[(k_4K+k_3)^2-4k_4Kk_3]^{\frac{1}{2}}}\cdot$$

$$\log\left[\frac{2k_4z+(k_4K+k_3)-[(k_4K+k_3)^2-4k_4Kk_3]^{\frac{1}{2}}}{2k_4z+(k_4K+k_3)+[(k_4K+k_3)^2-4k_4Kk]_3{}^{\frac{1}{2}}}\right]=L=-Kk_3t+\mathrm{I} \qquad (7)$$

where $k_3 = k_1[H^+]^2$, $k_4 = k_2[H^+]^3$, $K = (a-b)$, $z = (b-x)$, $a = [NpO_2^+]_o$, $b = [I_-]_o$, and I is an integration constant. By substituting the various values in Equation (7) and using the values of k_1 and k_2 obtained from Fig. 3, a plot of the integrated expression, L, against t gives a straight line (Fig. 4), which is in good agreement with the proposed mechanism.

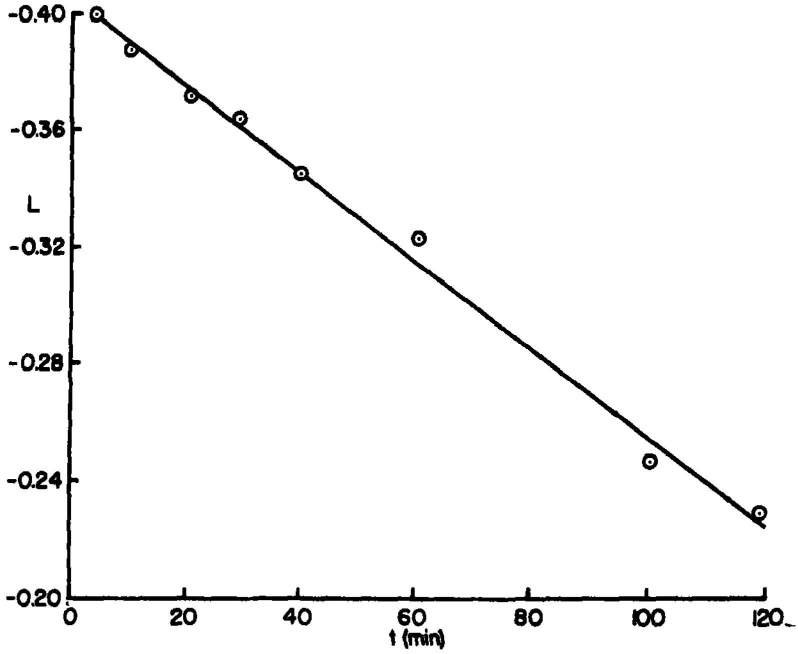

Further reactions after the steps signified in Equations (3) and (4) may be as follows:

$$Np(OH)_2I_2^+ + Np(OH)_2I^{2+} \rightarrow [X]^* \rightarrow NpO^{2+} + Np(OH)I^{2+} + I_2 + H_2O \qquad (8)$$

It should be emphasized that the rate-law only implies a formula for the activated complex and gives no information concerning subsequent reactions.

At this stage, with the paucity of data regarding neptunium chemistry, the mechanism suggested is not meant to imply the structures of ions involved. Other mechanisms involving complex polynuclear ions or chlorocomplexes can be written and the choice of any would be a matter of personal preference.

Acknowledgements—The authors wish to thank the Atomic Energy Commission for Contract AT-(40-1)-2069 which supported this reasearch financially. One of us (J.O.W.) wishes to thank the National Science Foundation for a Co-operative Fellowship.

J. Inorg. Nucl. Chem., 1962 Vol. 24, pp 541 to 544. Pergamon Press Ltd. Printed in England

THE EXTRACTION OF Pu(IV) NITRATE BY LONG CHAIN TERTIARY AMINES NITRATES

F. Baroncelli, G. Scibona and M. Zifferero

C.N.E.N., Laboratorio Trattamento Elementi Combustibili, Rome

(*Received* 14 *November* 1961)

Abstract—The acid dependence of the partition coefficient of Pu(IV) nitrate into organic solutions of long chain tertiary aliphatic amine nitrates is attributed to the different extraction behaviour of the Pu complexes which are formed in the aqueous phase at different nitric acid concentration.

Of the several possible plutonium nitrate complexes only $Pu(NO_3)_4$ and $Pu(NO_3)_8^{2-}$ can undergo extraction to a useful extent.

Spectrophotometric data, ion exchange absorption and solid $Pu(NO_3)_4$ solubility experiments support this interpretation. The plutonium species predominating in the organic phase has been confirmed to be $(R_3N)_2$ $Pu(NO_3)_6$ under a wide variety of experimental conditions.

The possibility to recover plutonium values by solvent extraction with tertiary amines was first reported by Sheppard.(1) Successive works on this subject dealt mainly with the possible application in irradiated fuel processing(2) and with the comparative extraction behaviour of actinides elements(3, 4) but only limited attempts were made to give an interpretation of the extraction behaviour.

Published data seem to agree on the existence, in the amine organic phase, of a plutonium hexanitrato complex,(3) also in the case of secondary amine extraction.(5) The purpose of this work is to provide additional information on the extraction behaviour of Pu(IV) in tertiary amine nitrates solutions and to afford an explanation of the extraction mechanism.

The existence of only one hexanitrato complex of Pu in the organic phase been confirmed: the dependence of the plutonium partition coefficient from the nitric acid molarity in the aqueous phase can be explained if two different extraction reactions are considered:

$$Pu(NO_3)_4 + 2R_3NHNO_3 \rightleftharpoons (R_3N)_2\,Pu(NO_3)_6 \qquad (1)$$

$$Pu(NO_3)_6^{2-} + 2R_3NHNO_3 \rightleftharpoons (R_3N)_2\,Pu(NO_3)_6 + 2NO_3^-. \qquad (2)$$

---

(1) J. C. Sheppard, HW 51958 (1957).

(2) A. S. Wilson, *Proceeding of the Second International Conference on the Peaceful Uses of Atomic Energy, Geneva*, 1958, P/544, Vol. 17, p. 348. United Nations (1958).

(3) W. E. Keder, J. C. Sheppard and A. S. Wilson, *J. Inorg. Nucl. Chem.* **12**, 327 (1960).

(4) B. Weaver and D. E. Horner, *J. Chem. Engng. Data* **5**, 260 (1960).

(5) J. A. Brothers, R. G. Hart and W. G. Mathers, *J. Inorg. Nucl. Chem.* **7**, 85 (1958).

TABLE 1.—CHEMICAL COMPOSITION OF TERTIARY AMINES*

Amine	Eq MW	Tertiary (%)	Secondary (%)	Primary (%)
TLA	522	98	< 2	< 0·3
TOA	350	94·7	~ 5	"
TIOA	381	93·4	~ 6	"
TCA	414	97·5	2·2	"

* The composition is given in terms of moles per cent.

EXPERIMENTAL

Reagents: source and purity

The following tertiary amines were used as extractants:

Trilaurylamine (TLA) supplied by Rhone and Poulenc in a special high purity batch: a straight chain tridodecylamine

Triisooctylamine (TIOA) supplied by Union Carbide. Aliphatic chains are a mixture of dimethylhexyls and methylheptyls, principally 3–5, 4–5 and 3–4 dimethylhexyl

Tri-n-octylamine (TOA) supplied by Fluka AG

Alamine 336 or Tricaprilylamine (TCA) supplied by General Mills. Aliphatic chains are a mixture of n-octyls (predominating) and n-decyls.

Data on the equivalent molecular weights and on the secondary and primary amine content as it results from differential non aqueous titration are collected in Table 1.

Tertiary amines were used as such, without further purification. Solvesso 100, an industrial aromatic naphta, was used as a diluent. Amines nitrates were prepared by contacting the amine–diluent solution with a tenfold volume of nitric acid of the desired concentration: the phase disengagement, usually very rapid, was improved by centrifugation. Freshly prepared solutions were employed each time to avoid ageing effects.

Plutonium–239 nitrate, as received from USAEC, was unsuitable for extraction experiments due to the presence of interfering amounts of ^{241}Am. An anionic exchange purification procedure(6) was used and a concentrated plutonium nitrate solution in 1 M HNO_3 was stored with 0·05 M sodium nitrite to keep plutonium in the tetravalent state. Suitable aliquots of the stock solution were diluted with a nitric acid solution of the desired concentration. The values of the partition coefficient were checked at random by back extracting the plutonium from the organic into a fresh aqueous phase.

Extraction procedure

A constant plutonium concentration of 0·1 g/l. was used. In extraction experiments 5 ml of the plutonium solution were contacted at constant temperature (25 ± 0·1° C) with an equal volume of the organic phase. After centrifugation suitable aliquots of both phases were α counted on a proportional flow counting system.

Spectrophotometry

All spectra were recorded with a Beckman Model DK apparatus equipped with 1 cm glass cells. The plutonium concentration in the organic phase was approximately 2·5 mg/ml.

RESULTS AND DISCUSSION

The extraction data for the four amines tested are plotted in Fig. 1. The plutonium partition coefficient is maximum at 3–4 M aqueous nitric acid for all the amines. The absolute values of the partition coefficient are related with the amine concentration: organic solutions 10 v/o in Solvesso were employed in the experiment but the values of the partition coefficients would be sensibly the same if equal molar concentration of the amine were used.

(6) J. L. RYAN and E. J. WHEELWRIGHT, *Industr. Engng. Chem.* 51, 60 (1958).

TABLE 2.—SLOPES OF LOG–LOG PLOTS OF E_{Pu} VS. AMINE NITRATE CONCENTRATION

Amine	Aq. HNO_3 (M)	Slope
TLA	1	2·05
TLA	2	2·05
TLA	4	1·97
TLA	8	1·96
TCA	4	2·00
TOA	4	2·01
TIOA	4	1·95

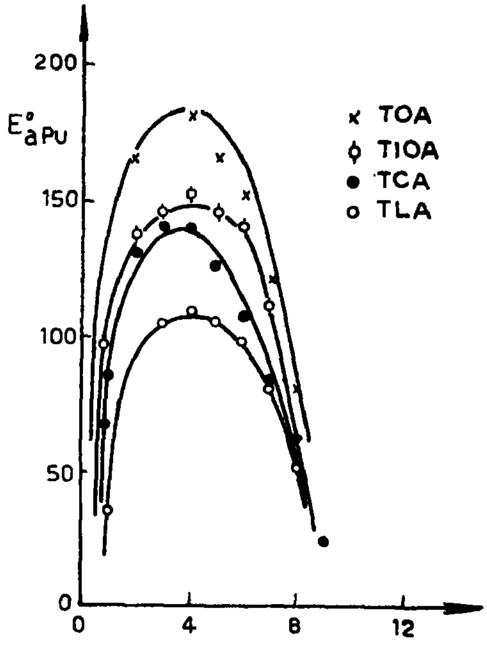

FIG. 1.—The extraction of Pu(IV) by 10 v/o tertiary aliphatic amine nitrates in Solvesso 100.

The slope of a log–log plot of E^0_{aPu} versus the amine concentration is a measure of the amine-to-plutonium ratio in the organic phase. Fig. 2 gives an example of these plots applied to the TLA case. In Table 2 the values of the slope of log–log plots of E_{Pu} vs. the amine concentration are collected for the different amines at different values of the aqueous nitric acid concentration.

The fact that the slope is constant for all the amines and in a wide range of nitric acid concentration indicates that only one complex of plutonium is present in the organic phase having an amine to metal ratio of two.

This result is confirmed by the absorption spectra of the plutonium bearing amine phases obtained by the extraction of aqueous solutions 1–14 M in nitric acid.

All spectra provide strong evidence (Fig. 3) for the existence of one single complex $(R_3NH)_2\ Pu(NO_3)_6$; they are not affected by increasing nitric acid concentration in the organic phase and their analogy with the well known⁽⁷, ⁸⁾ absorption spectrum of the aqueous hexanitrato complex $Pu(NO_3)_6^{2-}$ can be easily verified.

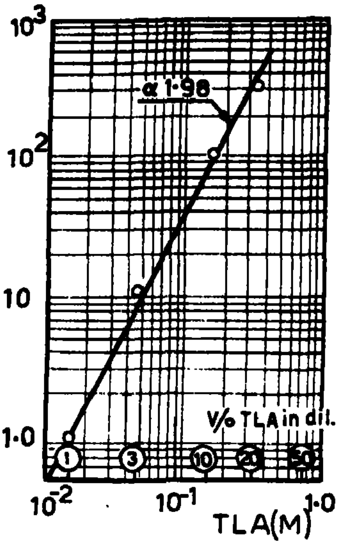

FIG. 2.—The extraction of Pu(IV) in TLAHNO₃ from 4 M HNO₃.

Since no substantial change related to the plutonium species is detectable in the organic phase at increasing HNO_3 concentration in the aqueous and hence in the organic phase, the acid dependence of E_{Pu} is most likely due to the plutonium(IV) complex chemistry in the aqueous phase. Existing information on this subject⁽⁵, ⁷, ⁸⁾

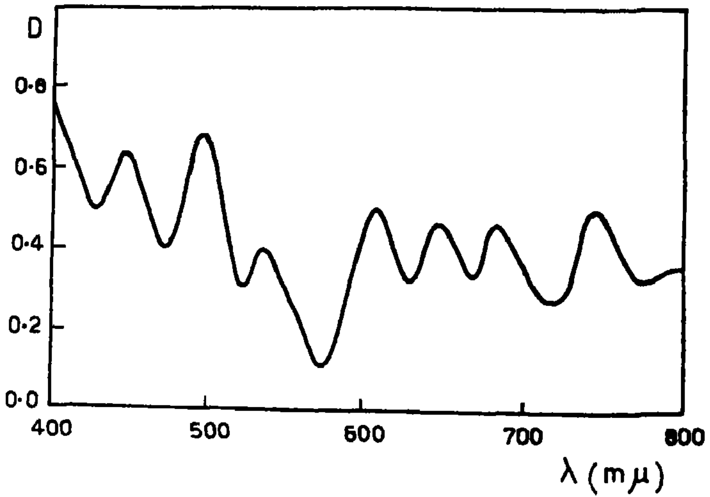

FIG. 3.—The absorption spectra of Pu(IV) extracted in 10 v/o TLA nitrate in Solvesso 100.

---

(7) G. T. SEABORG, J. J. KATZ and W. M. MANNING, *The Transuranium Elements, NNES*, Plutonium Project Record, Vol. 4–14 B. McGraw-Hill (1949).

(8) J. L. RYAN, *J. Phys. Chem.* 64, 1375 (1960).

is based on absorption spectra modifications at increasing acidity. Accordingly the variations of the spectral behaviour can be divided into two classes depending on the acidity range. From 0 to 5 M nitric acid spectral changes are due to the presence of positive or neutral plutonium nitrate complexes: above 5 M nitric acid the formation of anion complexes $Pu(NO_3)_6^{2-}$, $Pu(NO_3)_5^-$, $HPu(NO_3)_5$ and $H_2Pu(NO_3)_6^-$ is responsible *for further spectral modifications.* The *neutral* form $Pu(NO_3)_4$ is predominating in the nitric acid range 2–4 M.⁽⁵⁾

Comparing the anion exchange absorption with spectrophotometric data RYAN⁽⁸⁾ has established that the decrease of the resin absorption at 7·6–7·8 M HNO_3 is due to the formation of HPu $(NO_3)_5$ and $H_2Pu(NO_3)_6$. No decrease in fact is noticed if $Ca(NO_3)_2$ is used instead of nitric acid.

A plot of the plutonium partition coefficient into 10v/o TLA–Solvesso vs. nitrate ion concentration at constant low acidity is given in Fig. 4. E_{Pu} increases at increasing nitrate ion concentration as in the case of anion resin absorption.⁽⁸⁾

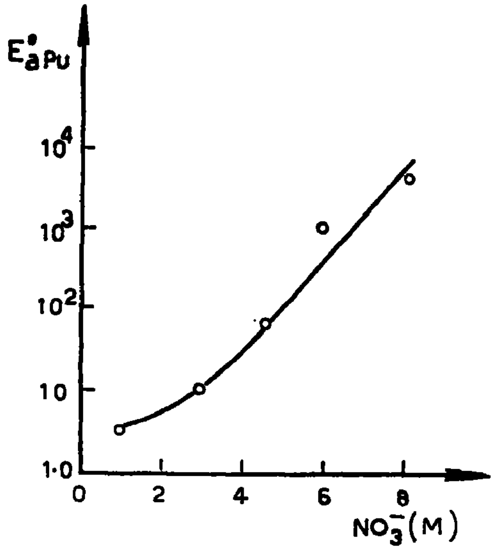

FIG. 4.—The extraction of Pu(IV) in $TLAHNO_3$ from $Ca(NO_3)_2$ solutions (0·3 M HNO_3).

The analogy between resin absorption and amine extraction is limited to the above experimental conditions; actually when nitric acid is used instead of calcium nitrate the position of the E_{Pu} maximum is ~4 M HNO_3 for the amines and ~8 M for anion resins.

The extraction behaviour of Pu(IV) nitrate can be interpreted by admitting that plutonium(IV) is extracted from aqueous solutions into organic solutions of tertiary amines nitrates under two different forms, namely $Pu(NO_3)_4$ and $Pu(NO_3)_6^{2-}$ according to the following equilibria:

$$Pu(NO_3)_4+2R_3NHNO_3 \rightleftharpoons (R_3NH)_2\,Pu(NO_3^-)_6$$

and

$$Pu(NO_3)_6^{2-}+2R_3NHNO_3 \rightleftharpoons (R_3NH)_2\,Pu(NO_3)_6+2NO_3^-$$

if this is the case:

$$E_{Pu} = E_{Pu}(NO_3)_4+E_{Pu}(NO_3)_6^{2-}$$

In the hypothesis that the $Pu(NO_3)_6^{2-}$ species is less extractable than $Pu(NO_3)_4$ the decrease of E_{Pu} above 4M HNO_3 may be attributed to the increase of the plutonium anion complex. Around 8M the plutonium extraction falls rapidly (the formation of the non extractable acid form $H_2Pu(NO_3)_6$ may be responsible for this). In agreement with this picture the absorption spectra in the 2–4 M HNO_3 range show the existence of the predominant $Pu(NO_3)_4$ neutral form; above 4 M HNO_3 an increasing formation of $Pu(NO_3)_6^{2-}$ is verified.

Furthermore a 10v/o TLA–Solvesso solution is capable to dissolve at room temperature sizeable amounts of solid $Pu(NO_3)_4$. The absorption spectra of the resulting organic phase is identical with that obtained in extraction condition. This fact shows the capacity of an amine nitrate to interact with neutral plutonium species, as already reported for uranium.(9)

The extraction of a neutral Pu complex by amine type solvents could provide an explanation for the different positions of Pu absorption maxima vs. nitric acid concentration between tertiary amines and anion exchange resins. In the resin case only the negatively charged Pu complex is most like to undergo extraction. It must be pointed out however that also other factors can be responsible for this difference; this possibility deserves further investigation, now in progress.

Acknowledgement—Authors are indebted to Professor G. Giacomello for a critical review of the manuscript, to Messrs. G. B. Biondi and D. Filoni for the experimental work. Plutonium absorption spectra in the organic phase were made by Dr. G. Valentini whose co-operation is gratefully acknowledged.

(9) F. Baroncelli, G. Scibona and M. Zifferero, *J. Inorg. Nucl. Chem.* To be published.

J. Inorg. Nucl. Chem., 1962, Vol. 24, pp. 547 to 559. Pergamon Press Ltd. Printed in England

THE EXTRACTION OF HEXAVALENT URANIUM FROM NITRIC ACID SOLUTIONS BY TRI-*n*-DODECYLAMINE NITRATE

F. Baroncelli, G. Scibona and M. Zifferero
C.N.E.N., Laboratorio Trattamento Elementi Combustibili, Rome

(*Received* 9 *November* 1961)

Abstract—Solutions of tertiary amines nitrates behave like liquid anion exchangers in the extraction of uranyl nitrate from aqueous solutions. The extraction mechanism is based on the formation of anionic uranium complexes in the aqueous phase which undergo extraction:

$$UO_2(NO_3)_{2+n}^{n-} + n[R_3NH^+NO_3^-]^0 \rightleftarrows [(R_3NH^+)_nUO_2(NO_3)_{2+n}^{n-}]^0 + nNO_3^-$$

The uranium partition coefficient increases at increasing nitric acid molarities in the aqueous phase, reaches a maximum at approximately 6 M HNO_3, then decreases. This behaviour is explained as due to the presence of different types of uranium complexes in the aqueous phase. Below 6 M HNO_3 the extractable species $UO_2(NO_3)_{2+n}^{n-}$ is predominating; above 6 M HNO_3 the inextractable $HUO_2(NO_3)_3$ complex prevails as indicated by absorption spectra and ion exchange behaviour.

Different values of *n*, ranging from 1 to 1·7 were found depending on salting strength, uranium and nitric acid concentration. The influence of the organic phase composition was studied by directly dissolving solid uranyl nitrate in the amine solvent. No difference was detected in the absorption spectra and ion exchange behaviour between the uranium loaded organic phase obtained by extraction and the one obtained by solid UNH solubilization. Results of solubility experiments seem to exclude an extraction mechanism based on the stepwise complex formation of an amine polinitrate.

In previous works the extraction of nitric acid into benzene solutions of long chain aliphatic amines has been investigated; simple equations were given to compute the amount of nitric acid extracted in the organic phase⁽¹⁾ and the nature and the stability range of the R_3N–HNO_3 system were studied by means of infra-red absorption and ion exchange techniques.⁽²⁾ The aim of the present work is to provide information on the nature of the system R_3N–HNO_3–$UO_2(NO_3)_2$.

The extraction of uranium and other elements from nitric acid solutions by long chain tertiary amines has lately received increasing attention. Several and some times conflicting hypothesis have been made by different authors. According to Wilson *et al.*⁽³⁾ the species formed upon equilibration of an amine solution with nitric acid is thought to be $R_3NH^+NO_3^-$; this species when in contact with a metal ion solution extracts a metal anion which replaces the nitrate ion.

---

(1) F. Baroncelli, G. Scibona and M. Zifferero, *J. Inorg. Nucl. Chem.* Submitted.
(2) G. Klotz, G. Scibona and M. Zifferero, CNEN 107 (1961).
(3) W. E. Keder, J. C. Sheppard and A. S. Wilson, *J Inorg. Nucl. Chem.* **12**, 327 (1960).

Similar mechanisms have been suggested by other authors;[4] they do not however explain why a decrease in the extraction coefficients is verified at higher acidities of the aqueous phase. This behaviour has been in one case[5] interpreted as due to the competitive extraction of the nitric acid, in analogy with the tributylphosphate case.

A somewhat different explanation has been recently proposed by TALAT-ERBEN;[6] accordingly the amine nitrate should form with nitric acid a series of successive complexes, $R_3N{\cdot}HNO_3$, $R_3N{\cdot}2HNO_3$, $R_3N{\cdot}3HNO_3$ etc. At increasing acidities the molar fraction of the mononitrate (which is responsible for the metal extraction) decreases exponentially and the extraction coefficients consequently decreases. In this theory the formation of a uranium complex $(R_3N)_2UO_2(NO_3)_4$ is assumed, implying a dependency of the extraction coefficient on the square of the amine concentration.

None of these works has taken into account the modifications induced in the aqueous phase by an increase of the nitric acid concentration. Actually the formation of ion pairs in the organic phase is responsible for the extraction; in this sense the structural variation of the organic phase must influence the extraction behaviour. But since the ionic species which are present in the aqueous solution strongly depend on the nitric acid concentration, it is felt that the extraction behaviour must be also interpreted in terms of composition of the aqueous solution.

For this reason the variation of the aqueous phase composition has been investigated in this work with ion exchange and spectrophotometrical techniques. The influence of the organic phase composition has also received attention and interesting results have been obtained by directly dissolving solid uranyl nitrate into the organic solvent.

EXPERIMENTAL

(a) *Chemicals*

Tri-n-dodecylamine or Trilaurylamine (TLA)* was used without further purification. A potentiometric titration gave an equivalent weight within 1 per cent of the theoretical value. Other chemicals were reagent grade. Pure ^{233}U nitrate was used in most cases and uranium concentration was determined directly by α-counting. Where uranium concentration in excess of 10^{-2} M was needed, ^{233}U was used as tracer, after dilution with natural uranium. When the aqueous phase contained high salt concentration, α-counting was limited to the organic phase and aqueous phase concentration obtained indirectly.

(b) *Extraction procedure*

Extractions were conducted with equal volumes of aqueous and organic phase at constant temperature (25° ± 0·1° C). Phase separation after contacting was improved by centrifugation. Unless specified a 0·5 g U/l. concentration was used.

(c) *Solubility determination*

The solubility of solid UNH in the organic phase was determined as follows: uranyl-233 nitrate and natural uranyl nitrate (1:100) were dissolved in ethyl ether. The solvent was removed at reduced pressure at room temperature. The tracer containing solid UNH was subsequently contacted with the organic phase to obtain a saturated solution. Aliquots of the organic were α-counted for uranium content.

---

* Supplied by Rhone and Poulenc in a special high purity batch.

[4] G. E. BOYD and Q. V. LARSON, *J. Phys. Chem.* **64**, 988 (1960).

[5] M. ZIFFERERO and F. BARONCELLI, CNC 41 (1960).

[6] M. TALAT-ERBEN. Private communication (1960); See also *Eurochemic Technical Report*, ETR No. 83, 88, 90 (1960), Eurochemic Company, Mol (Belgium).

(d) *Ion exchange procedure*

Five ml of the aqueous or organic solution to be tested were thoroughly shaken at room temperature with 0·5 g of nitrate form Dowex 1×4 (200–400 mesh) resin. After centrifugation an aliquot of the solution was α-counted for uranium content.

(e) *Spectrophotometry*

A Beckman DU spectrophotometer was used. All determinations were made at constant temperature (25 ±0·1° C).

RESULTS AND DISCUSSION

In Fig. 1 the partition coefficient of uranium(VI), E^a_{oU}, is plotted vs. nitric acid aqueous molarity. The two curves refer to TLA nitrate extraction and to ion exchange with a strong anion exchanger. The analogy of the two curves and the close position of the maxima give credit to an extraction mechanism based on the formation of anionic complexes in the aqueous phase which are subsequently extracted:

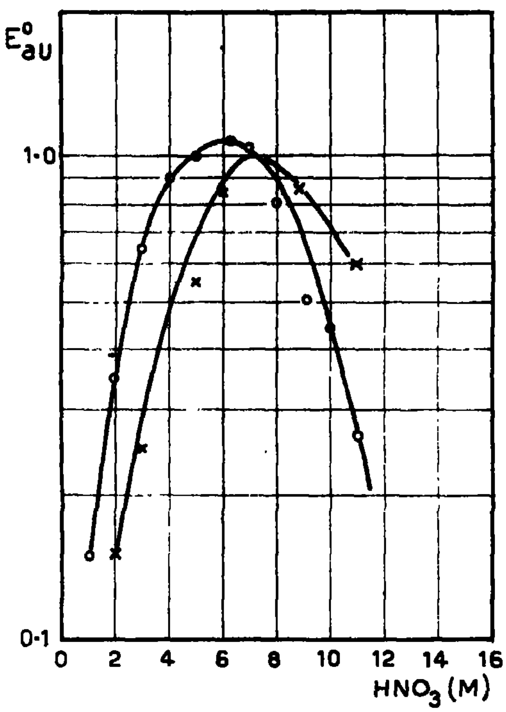

FIG. 1.— —O— The extraction of U(VI) by 10 v/o TLA in xilene;
—×— The extraction of U(VI) by Dowex 1 (see experimental for conditions).

$$UO_2(NO_3)_{2+n}^{n-} + n\,[R_3NH^+NO_3^-] \overset{\circ}{\rightleftharpoons} [(R_3NH^+)\,UO_2(NO_3)_{2+n}^{n-}]^{\circ} + nNO_3^- \qquad (1)$$

with an equilibrium constant K and with $n = 1$.

The existence of an organic trinitratouranyl complex $UO_2(NO_3)_3^-$ has been shown by KAPLAN.(7) The complex formation constants of $UO_2NO_3^+$, $UO_2(NO_3)_2$ and $UO_2(NO_3)_3^-$ in the aqueous phase at ionic strength 1 (32° C) have been calculated.(8)

---

(7) L. KAPLAN, R. A. HILDEBRANDT and M. ADER, *J. Inorg. Nucl. Chem.* **2**, 153 (1956).

(8) D. BANERJEA and K. K. TRIPATHI, *J. Inorg. Nucl. Chem.* **18**, 199 (1961).

The absorption spectra of uranyl nitrate solutions in a wide range of aqueous nitric acid concentration (Fig. 2) show substantial variation at increasing acidity. Above 6 M nitric acid some new absorption bands appear at 422, 434, 450 and 466mμ and they become sharper at increasing acidity. This means that at nitric acid concentration above 6 M the formation of another uranium complex is promoted. The existence of this complex is conditioned by the presence of nitric acid; in fact uranyl nitrate

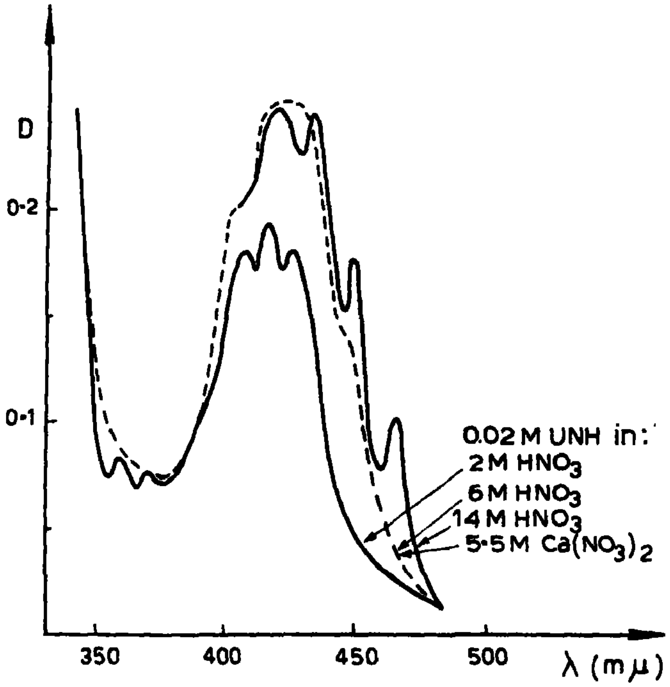

FIG. 2.—Effect of nitric acid and nitrate ions conc. on the absorption bands of uranyl nitrate.

solutions in 10·5 N $Ca(NO_3)_2$ (0·5 M HNO_3) show spectra substantially analogous to those obtained in 6 M nitric acid. Furthermore the absorption of uranium on solid anion exchange resin shows no maximum at increasing calcium nitrate concentration. This behaviour is attributed to the formation of the $HUO_2(NO_3)_3$ in nitric acid solution above 6 M. $HUO_2(NO_3)_3$ is not extracted by amine solvents. This interpretation has some analogies with that given by RYAN[9] for the resin absorption of $Pu(NO_3)_4$. Therefore for a nitric acid solution of uranyl nitrate the following equilibria can be written:

$$UO_2^{2+} + NO_3^- \rightleftharpoons UO_2NO_3^- \quad \text{(equilibrium constant } K_1) \quad (2)$$

$$UO_2NO_3^- + NO_3^- \rightleftharpoons UO_2(NO_3)_2 \quad (\quad " \quad " \quad K_2) \quad (3)$$

$$UO_2(NO_3)_2 + NO_3^- \rightleftharpoons UO_2(NO_3)_3^- \quad (\quad " \quad " \quad K_3) \quad (4)$$

$$UO_2(NO_3)_3^- + H^+ \rightleftharpoons HUO_2(NO_3)_3 \quad (\quad " \quad " \quad K_4) \quad (5)$$

---

[9] J. L. RYAN, *J. Phys. Chem.* 64, 1375 (1960).

Taking now into account the concentration of nitrate ions in a nitric acid solution (Fig. 3)(10) and the related formation of undissociated nitric acid at increasing acid concentration (Fig. 4)(11) an additional equilibrium yielding $HUO_2(NO_3)_3$ can be conceived:

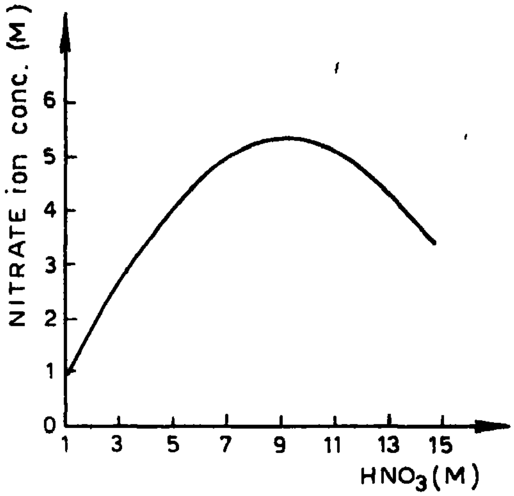

Fig. 3.—Concentration of nitrate ion in nitric acid solutions.

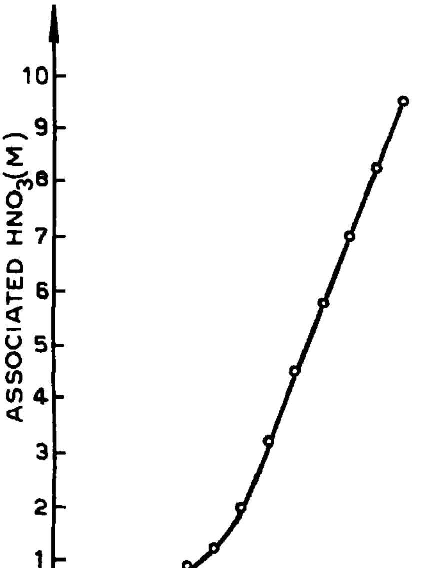

Fig. 4.—Concentration of associated nitric acid in aqueous nitric acid solutions.

(10) G. C. Hood, O. Redlich and C. A. Reilly, *J. Chem. Phys.* 22, 2067 (1954).

(11) T. J. Collopy and S. H. Cavendish, *J. Phys. Chem.* 64, 1328 (1960).

$$UO_2(NO_3)_2 + HNO_3 \rightleftharpoons HUO_2(NO_3)_3 \text{ (equilibrium constant } K_5) \qquad (6)$$

Reactions (5) and (6) are important at high nitric acid concentration and they lead to the formation of a scarcely extractable uranium complex: in this way the behaviour of E°_{aU} in Fig. 1 can be explained.

If this is correct, one should expect no decrease of the uranium partition coefficient when E°_{aU} is plotted vs. the nitrate ion concentration at constant (low) aqueous acidities. Actually (Fig. 5) this expected behaviour is verfiied both for the amine and for the resin extraction when calcium nitrate is the source of nitrate ions.

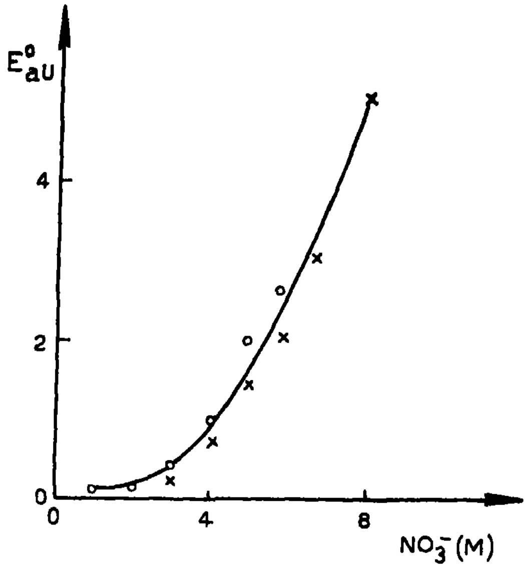

FIG. 5.— —O— The extraction of U(VI) by 10 v/o TLA in xylene with $Ca(NO_3)_2$ as salting agent (0·9 M HNO_3).
—×— The extraction of U(VI) by Dowex 1 with $Ca(NO_3)_2$ as salting agent (0·9 M HNO_3). See experimental for conditions.

A less qualitative explanation of the uranium extraction behaviour can be given if the two different cases are considered: metal nitrates or nitric acid as a source of nitrate ions.

(a) $Ca(NO_3)_2$ *as a source of nitrate ions*

The uranium partition coefficient E°_{aU} = U org/U aq, when reactions (5) and (6) are negligible can be easily derived:

$$E_U = kc^2_{NO_3^-} \downarrow c^{n}_{R_3NHNO_3} \, {}_{\gamma l} \Pi A \qquad (7)$$

where $k = K \cdot K_1 K_2 K_3$ and

$$1/A = 1 + K_1 c_{NO_3^-} (\Pi_{\gamma l})_2 + K_1 K_2 c^2_{NO_3^-} (\Pi_{\gamma l})_3 + K_1 K_2 K_3 c^3_{NO_3^-} (\Pi_{\gamma l})_4$$

where $(\Pi \gamma i)j$ with $j = 2, 3, 4$ are the products of the activity coefficients of the species involved in equilibria (2), (3) and (4).

From reference (8) $K_1 = K_2 = 0 \cdot 04$ and $K_3 = 0 \cdot 32$ and assuming that these values do not change substantially at different ionic strength, the role played by A in equation (7) can be neglected since its value approaches one.

A log-log plot of E_U vs. $c_{NO_3^-}$ yields a straight line (Fig. 6) whose slope is 2 in agreement with equation (7), supposing $y_i = 1$. A log-log plot of E_U vs. the amine concentration (Fig. 7) gives another straight line, the slope being 1·1.

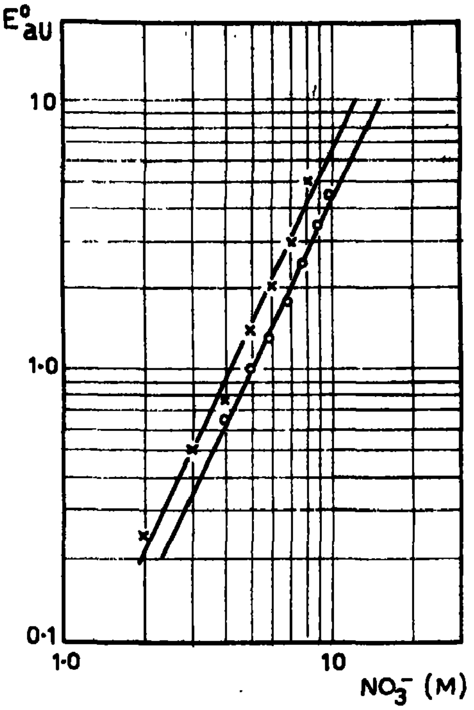

Fig. 6.— —O— The extraction of U(VI) by 10 v/o TLA in xylene. $Ca(NO_3)_2$ as salting agent (0·5 M HNO_3)
—×— The extraction of U(VI) by Dowex 1: $Ca(NO_3)_2$ as salting agent (0·5 M HNO_3). See experimental for condition.

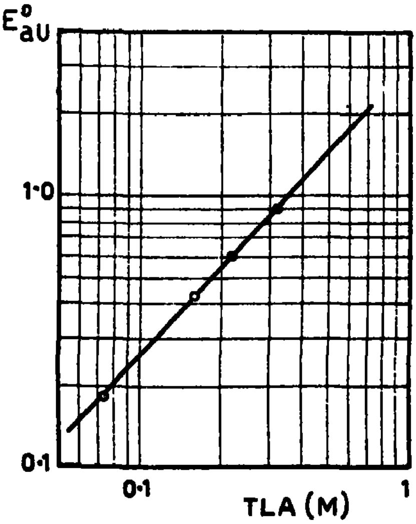

Fig. 7.—The extraction of U(VI) from 4 M HNO_3.

This means (equations 1 and 7) that uranium is extracted as $UO_2(NO_3)_3^-$ and n of equation (7) is equal to one. In addition, the plot in Fig. 7 allows to compute k by extrapolation at $c_{R_3N} = 1$; this value is affected by the lack of information on the activity coefficients and by the uncertainty on the variation of K_1, K_2 and K_3 at different ionic strength. For this reason we prefer to consider k as an experimental value depending on uranium and nitrate ion concentration.

(b) HNO_3 *as a source of nitrate ions*

When the source of nitrate ions is nitric acid equation (7) is valid only below 6 M, when reactions (5) and (6) are negligible. Above 6 M nitric acid reactions (5) and (6) cannot be neglected and a corrective coefficient which takes care of equilibria (5) and (6) must be introduced into equation (7) to re-establish its validity.

A log–log plot of E_U vs. the amine concentration at different aqueous nitric acid concentration gives straight lines whose slope are collected in Table 1. Since the slope is n number of amine molecules per mole of uranium present in the organic phase, Table 1 shows that, within the experimental error, this number decreases at increasing acidity in the range 0–4 M and levels off above 4 M. Data in Table 1 were obtained with 2×10^{-3} M uranium. If the uranium concentration is increased at constant (6 M) nitric acid, a further decrease of the slope is noticed on the same log–log plot. Data are collected in Table 2.

Table 1.—Slopes of log–log plots of E_U vs. the amine concentration at different aqueous HNO_3 concentration (2×10^{-3} M U)

Aqueous HNO_3 (M)	Slope
0·5	1·73 ± 0·1
1·0	1·54 ± 0·1
4·0	1·38 ± 0·1
6·0	1·43 ± 0·1
8·0	1·38 ± 0·1
11·0	1·45 ± 0·1

Table 2.—Slopes of log–log plots of E_U vs. the amine concentration at different aqueous uranium concentration (6 M HNO_3)

Aqueous U (M)	Slope
2×10^{-3}	1·43 ± 0·1
0·1	1·46 ± 0·1
0·5	1·24 ± 0·1
1·0	1·15 ± 0·1

The effect of the acidity and uranium concentration on the value of n are the following: for uranium concentration below 0·1 M n is about 1·4; along this range a decrease of the acidity promotes an increase of n, probably due to the formation of hydrolysed uranium compounds. The fact that n is 1·4 suggests an extraction mechanism based on the exchange of one or more complexes whose average charge is 1·4. The existence of these anion complexes is related to the value of NO_3^-/U ratio. A decrease of this ratio reduces *n* to one, as requested by the exchange reaction:

$$UO_2(NO_3)_3^- + [R_3NH^+NO_3^-]^0 \rightarrow [R_3NH^+UO_2(NO_3)_3^-]^0 + NO_3^-.$$

The effect of uranium and nitric acid concentration on E_U is shown in Figs. 8 and 9. In the range of low uranium molarities, E_U is constant and its value depends only on the nitric acid concentration (Fig. 8).

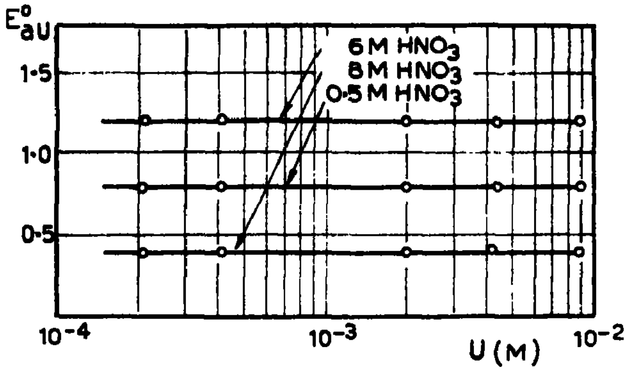

FIG. 8.—Extraction isotherms of U(VI) by 10 v/o TLA in xylene in a low uranium conc. range.

At higher uranium concentration E_U decreases probably due to the variation in the activity coefficients. This behaviour of E_U is related to the acidity as shown in Fig. 9, in agreement with other results.(5) The progressive disappearance of the

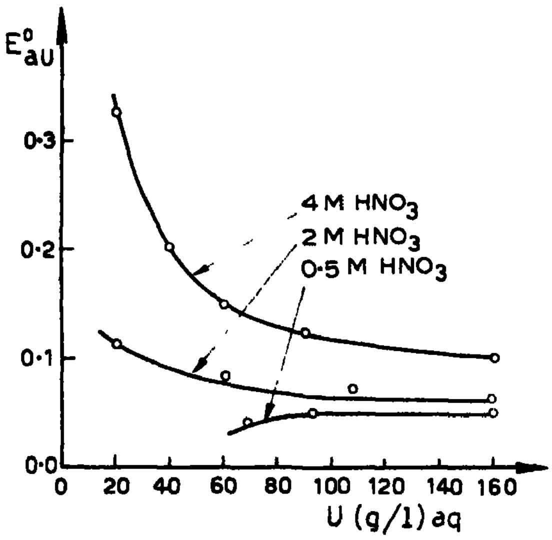

FIG. 9.—Extraction isotherms of U(VI) by 10 v/o TLA in xylene for different values of aqueous HNO_3 conc.

maximum of E_U at high U concentration (Fig. 10) indicates a solvent saturation for an amine/uranium ratio of approximately two.

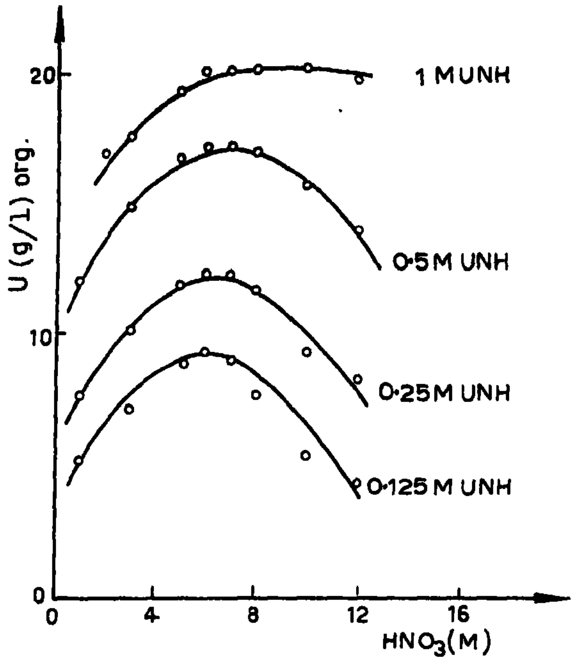

FIG. 10.—Uranium(VI) extraction by 10 v/o TLA in xylene. Different curves refer to different values of initial uranium aqueous conc.

When uranium enters the organic phase, some nitric acid is displaced from the organic into the aqueous. This is shown by the nitric acid extraction isotherms at different U concentration in Fig. 11. Since the decrease of HNO_3 in the organic

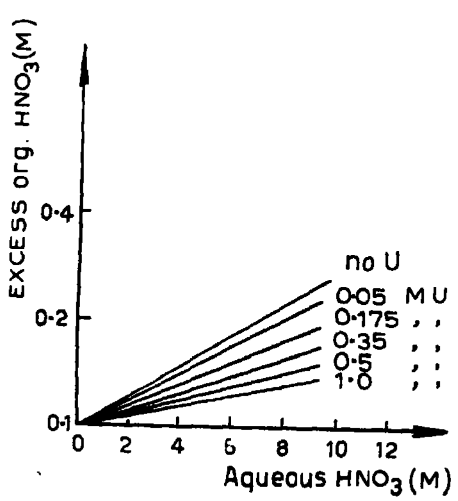

FIG. 11.—The effect of uranium aqueous concentration (initial) on the HNO_3 extraction by 10 v/o TLA in xylene.

phase is not balanced by a parallel increase of uranium there is no direct competition between uranium and nitric acid in the extraction. This is shown by the variation of $E^0_{a\,HNO_3}$ at increasing uranium concentration (Fig. 12).

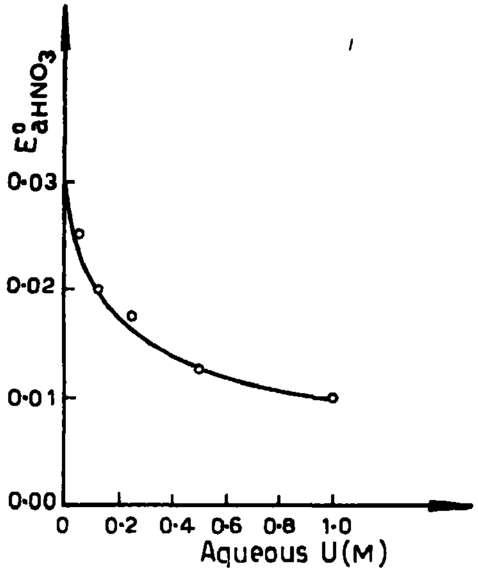

FIG. 12.—The effect of uranium aqueous concentration (initial) on the HNO_3 extraction by 10 v/o TLA in xylene.

Some interesting facts have merged in an investigation on the absorption spectra of the uranium extracted in the organic phase. The trinitrato uranyl complex of TLA shows well defined absorption peaks at 426, 440, 454 and 470 mμ (Fig. 13). The molar extinction coefficients ε are collected in Table 3; they are not influenced by even large variation of nitric acid concentration in the organic phase.

If solid uranyl nitrate hexahydrate is dissolved in a $TLAHNO_3$ solution, the spectrum and the ε values show exactly the same behaviour (Fig. 13). Also in this case no frequency modification arises in the spectra if the acidity of the organic solution is largely increased.

In both cases the presence of an anionic type uranium complex is certified by the exchange of organic uranium on solid anion exchange resins. This fact supports the hypothesis that solid UNH is dissolved in the amine phase with the following reaction:

$$UO_2(NO_3)_{2\ org} + n[R_3NH^+NO_3^-]^\circ \rightleftharpoons [(R_3NH^+{}_n)UO_{2+n}^{n-}]^\circ \qquad (8)$$

where $UO_2(NO_3)_{2\ org}$ is supplied by the solubility of UNH in the organic phase.

The following equilibrium relation (K_s including the solubility of UNH) applies to reaction (8):

$$\log [(R_3NH^+)_n\, UO_2(NO_3)_{2+n}^{n-}]^\circ = \log K_s + n \log [R_3NH^+NO_3^-]^\circ$$

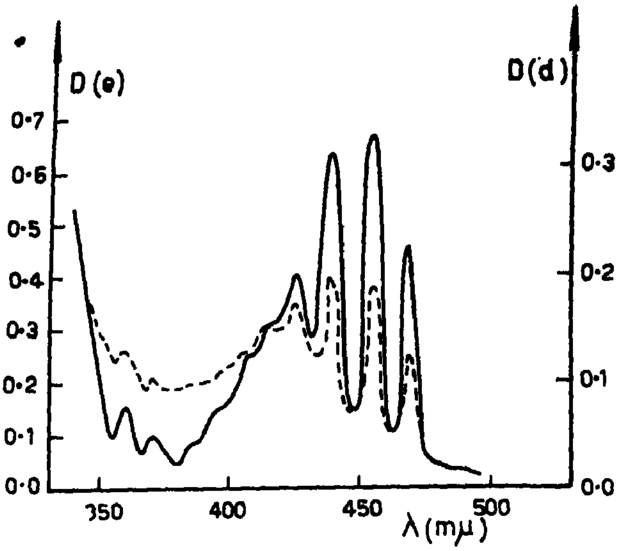

Fig. 13.—The absorption spectra of U(VI) solution in 10 v/o in xylene.
The dotted line refers to an organic phase loaded in uranium by extraction.
The full line refers to an organic phase in which solid UNH has been dissolved.
The corresponding optical densities are respectively under *D*(e) and *D*(d).

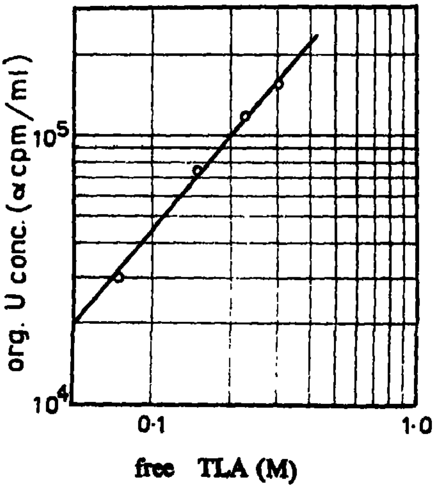

Fig. 14.—Solubility of solid UNH in xylene solutions of TLA. Organic phase was previously treated with 6 M HNO_3.

A log–log plot of the organic uranium concentration vs. amine concentration yields a straight line (Fig. 14) whose slope *n* is the number of negative charges of the $UO_2(NO_3)_{2+n}^{n-}$ anion. To obtain the organic uranium concentration the α-activity due to added ^{233}U tracer was measured; *n* resulted 1·1±0·1.

In conclusion the solubility of solid UNH in an amine solvent yields an organic uranium system identical to the one obtained by the extraction of uranium from aqueous solutions. Therefore a solubility investigation affords a suitable way to obtain first hand information on the effect of the organic phase composition on uranium extraction. The plot in Fig. 15 shows clearly that the presence of nitric acid in excess in an organic solution of TLA nitrate has negligible effect on the uranium extraction. This result contributes further evidence to minimize the rôle plaid by the presence of free nitric acid in the organic phase on the behaviour E_U; this is principally determined by the aqueous complex chemistry of uranium.

TABLE 3.—MOLAR EXTINCTION COEFFICIENTS OF U IN 10% $TLAHNO_3$ IN XILENE

λ (mμ)	ε (mole/l.)
426	15·0
440	18·5
454	26·0
470	13·0

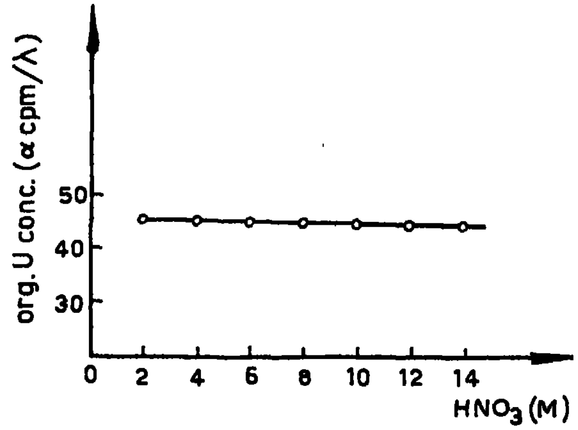

FIG. 15.—Solubility of solid UNH in 5 v/o TLA in xylene. The organic solution has been previously equilibrated with increasing concentration of aqueous nitric acid.

Acknowledgement—We are indebted to Prof. GIACOMELLO for helpful discussions. The contribution of Messrs. P. SUSINI and S. ILARDI to the experimental is gratefully acknowledged.

J. Inorg. Nucl. Chem., 1962, Vol. 24, pp. 561 to 570. Pergamon Press Ltd. Printed in England

EXTRACTION OF TETRA- AND HEXAVALENT ACTINIDES FROM HYDROCHLORIC ACID BY TRI-*n*-OCTYLAMINE IN XYLENE*

W. E. KEDER
Hanford Laboratories Operation, General Electric Company, Richland, Washington

(*Received* 2 *October* 1961)

Abstract—Distribution data for extraction of the tetra- and hexavalent actinides from hydrochloric acid by tri-n-octylamine (TOA) solutions are reported and the spectra of the extracted complex ion species are shown. The hexachloro complexes of the tetravalent metals are found to extract. The data also indicate the extraction of the tetrachloro actinyl ions, but the identity of these ions is not fully established.

THE extraction of metal ions from acid solutions by trialkylamines has received considerable attention in the past few years, and has been used in various separation processes and analytical techniques. This work has been reviewed recently in a monograph by MOORE.(1) Several studies have considered the mechanism of this extraction and attempted to identify the extracted metal complexes.(2–15) The extraction process appears to occur by a mechanism similar to that of the absorption of metal ions by anion exchange resins and can be considered the replacement of the anion of the trialkylammonium salt by a complex anion containing the metal. The complex ion species extracted by the amine has sometimes been found to be different from that absorbed from the same aqueous solutions by anion exchange resins, however.(16)

Attempts to identify extracted metal ion species have usually been made either by determination of metal to amine loading ratios or by measurement of amine concentration dependence of extraction and results have not always agreed or been reasonable. In previous work in this laboratory actinide ion species which extract from nitric acid solutions into tri-n-octylamine were identified by comparison of absorption spectra of their amine solutions with spectra of salts containing known anions.(10-12) Good and Bryan(9) have demonstrated the extraction of tetrachloro ferrate(III) into amine solutions from hydrochloric acid by spectral measurements, also. This technique appears to be reliable in the cases of ions whose absorption spectra are not greatly affected by environment outside the first co-ordination sphere.

---

* Work performed under contract No. AT(45-1)-1350 for the U.S. Atomic Energy Commission.

(1) F. L. MOORE, NAS-NS-3101 (1960).

(2) W. J. MCDOWELL and C. F. BAES, JR., *J. Phys. Chem.* **62**, 777 (1958).

(3) C. F. COLEMAN, K. B. BROWN and J. G. MOORE, *Proceedings of the Second International Conference on the Peaceful Uses of Atomic Energy, Geneva*, 1958, P/510, Vol. 28, p. 278, United Nations (1959).

(4) U. SCHINDEWOLF, *Z. Elektrochem.* **62**, 335 (1958); CEA-TR-A-529 (French); NP-TR-254 (English).

(5) C. BOIRIE, *Bull. Soc. Chim. France*, 980, 1088 (1958).

(6) J. BIZOT and B. TREMILLON, *Bull. Soc. Chim. France*, 122 (1959).

(7) D. J. CARSWELL and J. J. LAWRANCE, *J. Inorg. Nucl. Chem.* **11**, 69 (1959).

(8) V. B. SHEVCHENKO, U. S. SHMIDT and E. A. MEZHOV, *Russ. J. Inorg. Chem.* **5**, 929 (1960).

(9) M. L. GOOD and S. E. BRYAN, *J. Amer. Chem. Soc.* **82**, 5636 (1960).

(10) W. E. KEDER, J. C. SHEPPARD and A. S. WILSON, *J. Inorg. Nucl. Chem.* **12**, 327 (1960).

(11) A. S. WILSON and W. E. KEDER, *J. Inorg. Nucl. Chem.* **18**, 259 (1961).

(12) W. E. KEDER, J. L. RYAN and A. S. WILSON, *J. Inorg. Nucl. Chem.* **20**, 131 (1961).

(13) J. M. WHITE, P. KELLY and N. C. LI, *J. Inorg. Nucl. Chem.* **16**, 337 (1961).

(14) K. VAN IPENBURG, *Rec. Trav. Chim.* **80**, 269 (1961).

(15) W. KNOCH, *Z. Naturforschg.* **16 a**, 525 (1961).

(16) J. L. RYAN, *J. Phys. Chem.* **65**, 1099 (1961).

In the present paper a study of the extraction of the tetra- and hexavalent actinides from hydrochloric acid is reported. Spectra of the chloro complexes extracted have been measured and are compared with the spectra of known species when these are available.

Amine extraction of metals from hydrochloric acid has been variously studied in the past.(1) Coleman *et al.*(3) have shown the extraction of uranyl chloride and they mention that the amine extraction of many other metals from HCl solutions parallels their sorption by anion exchange resins. Other studies of extraction of the actinides from HCl have been made by Bizot and Tremillon(6) on uranium(VI); by Shevchenko *et al.*(8) on plutonium(III) and (IV), and by Moore(17) on uranium(VI), plutonium(VI), and protactinium(V). Cerrai and Testa(18) have described the separation of zirconium and hafnium from HCl by TOA, while the extraction of iron(III) in the same system has been studied by Good and Bryan(9) and by White *et al.*(13) Nakagawa has reported studies of extraction of a large number of metals from HCl by a long chain secondary amine.(19)

EXPERIMENTAL

Amine solutions for extraction experiments were prepared volumetrically from the same amine used previously(10) and Baker's reagent grade xylene. These solutions were contacted three times before use with equal volumes of appropriate concentrations of hydrochloric acid. The TOA used in preparation of solutions for absorption spectra measurements was purified by Wogman and Wilson(20) and was very nearly colourless.

Distribution experiments were carried out in the manner described previously and most extractions were followed by one or more back extractions to eliminate extraneous, non-extractable α-emitters and to check oxidation state purity. Neptunium(VI) and plutonium(VI) were prepared by ozone oxidation in chloride solution. Uranium(IV)-238 was prepared by zinc amalgam reduction in hydrochloric acid solution and uranium(IV) was determined spectrophotometrically. All other analysis were by α-counting ^{233}U, ^{237}Np or ^{239}Pu. Extractions of Np(VI) and Pu(VI) were performed as rapidly as possible to avoid the necessity of correcting for reduction. Absorption spectra of TOA solutions which were extracted from 4 M HCl showed that appreciable reduction of neptunium(VI) took place in one day's time and noticeable reduction of plutonium(VI) took place in two weeks' time.

Spectrophotometric measurements were made with a Cary Model 14 spectrophotometer and the spectra reported are photographs of the curves obtained.

RESULTS AND CONCLUSIONS

The extraction of a metal anion by organic-soluble trialkylammonium salts can be represented by the equation:

$$\underline{zR_3NH\cdot A}+M^{y+}+yA^- \rightleftharpoons \underline{(R_3NH)_z\cdot M(A)_{y+z}} \qquad (1)$$

---

(17) F. L. Moore, *Analyt. Chem.* 27, 70 (1955); 29, 1660 (1957); 30, 908 (1958).

(18) E. Cerrai and C. Testa, *Energia Nucleare* 6, 707, 768 (1959).

(19) G. Nakagawa, *Nippon Kagaku Zasshi* 81, 444, 446, 747, 750, 1258, 1533, 1536 (1960).

(20) A. S. Wilson and N. Wogman, *J. Phys. Chem.* In press.

where the underlines species are those present in the organic phase, M is the actinide ion whose charge is *y* when uncomplexed, and A^- is the anionic ligand. The equilibrium constant *K* is given by the following expression:

$$K = \frac{[\underline{(R_3NH)_z \cdot M(A)_{y+z}}]}{[M^{y+}][A^-]^y[\underline{R_3NH \cdot A}]^z} \cdot J = K'J \tag{2}$$

where the quantities in brackets represent concentrations and *J* represents the corresponding activity co-efficient quotient. Assuming that *J* is constant, it is possible to write the following expression which relates the distribution ratio *D* (the ratio of organic to aqueous metal concentrations) to the equilibrium quotient *K'*:

$$D = K' \frac{[\underline{R_3NH \cdot A}]^z[A^-]^y}{\sum_{n=0}^{y+z} \beta_n[A^-]^n} \tag{3}$$

where *n* is the number of ligands associated with the metal ion in each aqueous species present and β_n denotes their respective cumulative formation constants. If ligand concentration is held constant, *D* will vary only as the *z*th power of the free amine concentration and the charge on the extracted metal complex will equal $-z$, provided *J* remains constant. In the previous work the MO_2^{2+} species extracted from nitric acid could not be identified from the amine dependence in this way.(10–12) In fact, amine dependencies varying from 0·5 to 1·5 have been found for extraction of uranium(VI) from nitric acid, depending on the diluent used for the amine.(10, 15, 21) Others have found a similar discrepancy in the case of extraction of iron(III) from hydrochloric acid.(9, 13) Whether or not changes in the activity coefficient quotient are responsible has not been established. In the present work amine dependencies for extractions from HCl solutions have been determined and comparison of the results with spectra of the extracted ions has again been made.

Extraction of tetravalent actinides

The results of experiments in which tetravalent uranium, neptunium, and plutonium were distributed between TOA–xylene and varying concentrations of hydrochloric acid are shown in Table 1 and Fig. 1. The extractability of plutonium(IV) is seen to be much greater than that of uranium(IV) and neptunium(IV). This would be expected from the work in which RYAN(22) found from absorption spectra that the hexachloro complexes of uranium(IV) and neptunium(IV) are not detectable in 12 M HCl while plutonium(IV) is probably 75% $PuCl_6^{2-}$ in the same solution.

In Table 2 and Fig. 2 distribution ratios are shown for extractions of these metals from constant HCl concentrations at varying TOA concentrations. The slope of the log *D* vs. log (% TOA) plot is very nearly two in each case, which indicates that the extracted species are MCl_6^{2-} ions, as discussed earlier. Figs. 4–6 show photographs of absorption spectra of these metals in TOA solutions extracted from 6 or 9 M HCl. The extracted species may be identified as MCl_6^{2-} in each case by comparison of these spectra with those of the solid tetraethylammonium salts of the hexachloro metal(IV) complexes obtained by RYAN(22) and by GRUEN and MCBETH.(23)

(12) A. S. WILSON. Private communication (1960).

(22) J. L. RYAN, *J. Phys. Chem.* **65**, 1856 (1961).

(23) D. M. GRUEN and R. L. MCBETH, *J. Inorg. Nucl. Chem.* **9**, 290 (1959).

TABLE 1.—DISTRIBUTION RATIOS FOR EXTRACTION FROM HCl WITH TOA IN XYLENE

HCl (M)	Distribution ratios					
	U(IV)*	Np(IV)*	Pu(IV)†	U(VI)†	Np(VI)†	Pu(VI)†
1·0				0·031		0·032
2·1				0·29		0·22
3·1	0·02	0·009	0·017	1·43		2·4
4·2	0·02	0·13	0·89	7·1	9·1	14
5·6	0·26	2·8	19	15	19	48
6·3	0·78	18	55	21	22	82
7·7	5·6	40	150		18	92
8·7	16	110	300	17	13	44
10·0	45		350	7·5	9	15

* 10% TOA † 1·0% TOA

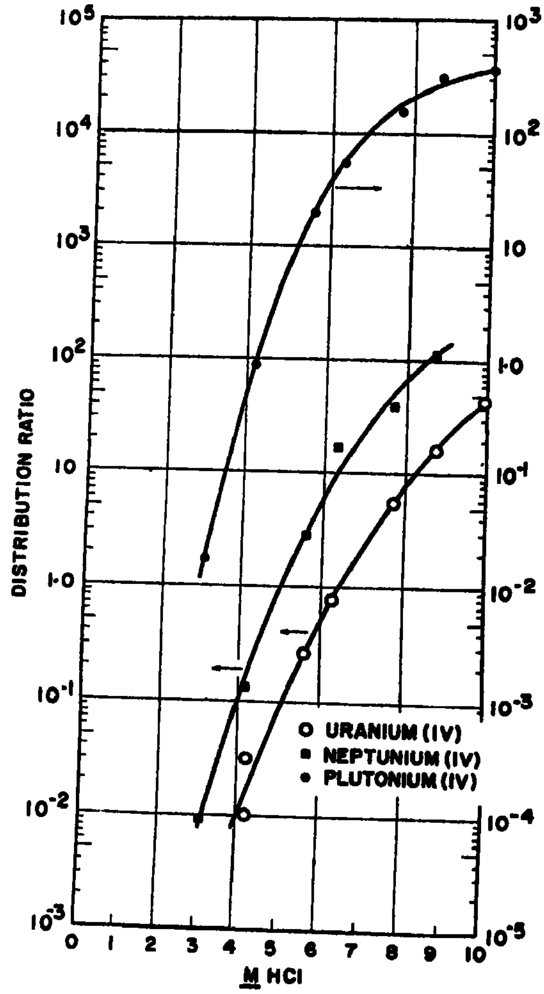

FIG. 1.—Extraction of U(IV) and Np(IV) by 10% TOA and Pu(IV) by 1·0% TOA from HCl solutions. Note: Ordinates are adjusted two orders of magnitude apart on the basis of the results shown in Fig. 2.

TABLE 2.—EXTRACTION FROM 4·2 M HCl WITH TOA IN XYLENE

TOA (%)	Distribution ratio					
	U(IV)	Np(IV)	Pu(IV)	U(VI)	Np(VI)	Pu(VI)
0·10			0·0022	0·037		0·094
0·30			0·044	0·36	1·3	1·00
0·50				0·97	3·2	3·20
1·00			0·72	4·56	2	14
2·5		0·042	5·3	38	62	
5·0		0·042	19	148	125	84
7·5			28			
10	0·02	0·13	33	305	280	110
20	0·14	0·80		450		
30	0·29	1·75				
40	0·68	3·5				
50	1·37	6·2				
100	2·1					

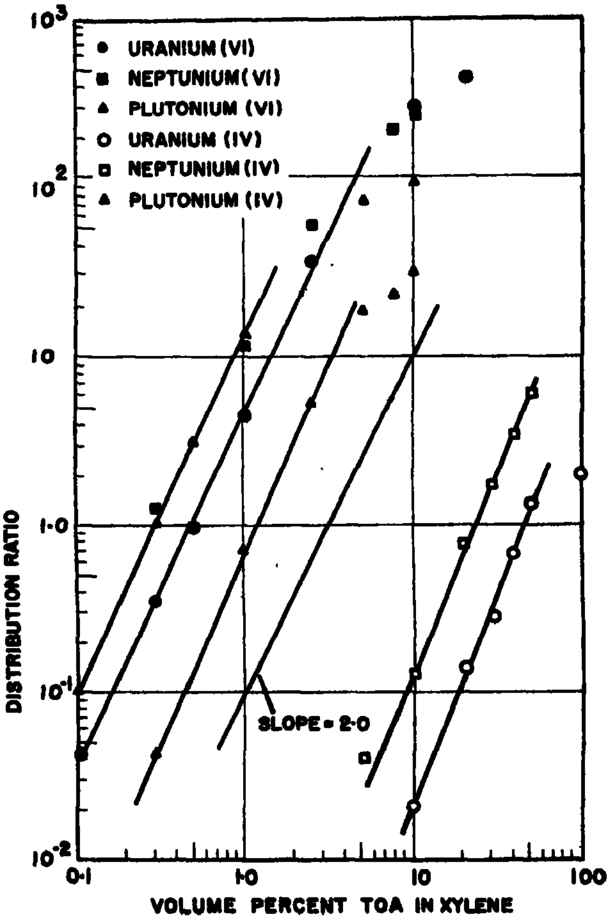

FIG. 2.—Extraction of tetra- and hexavalent uranium, neptunium, and plutonium from 4 M HCl as a function of TOA concentration.

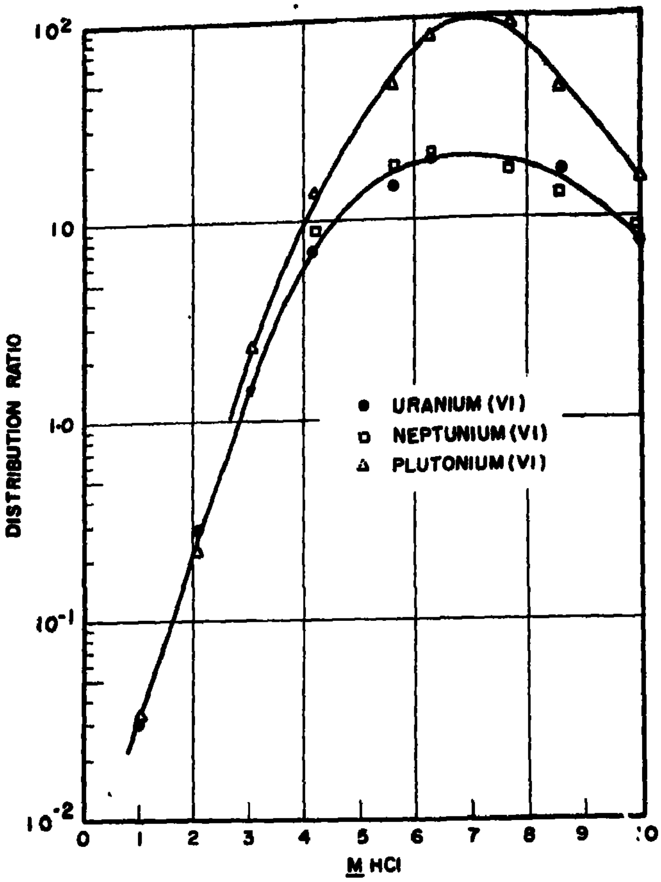

FIG. 3.—Extraction of hexavalent uranium, neptunium, and plutonium from HCl solutions with 1·0% TOA in xylene.

When extractions were made from high metal ion concentrations a second organic phase formed which contained most of the extracted metal. No detectable difference was found between the absorption spectra of the two organic phases in the case of uranium(IV). Third phase formation is rather common in extraction of metals by amine solutions, particularly when straight chain hydrocarbons are used as solvents, but apparently the fact that both organic phases contain the same metal ion species has not been previously established.

Extraction of the hexavalent actinides

The distribution ratios obtained for extraction of the hexavalent actinide metals into TOA from hydrochloric acid are shown in Tables 1 and 2 and in Figs. 2 and 3. The extractabilities of the hexavalent actinides were found to be much greater than those of the corresponding tetravalent metals under the same conditions. At the low HCl concentrations the *D* values are very near to each other for this oxidation state and are about sixth order in HCl concentration. Distribution ratios of the hexavalent actinides show a second order dependence on amine concentration, again indicating extraction of the negative two ions. Extraction of a doubly charged anion of uranium(VI) chloride is also indicated by experiments in which the ratio TOA/U was found to approach a value of two when aqueous uranium concentrations are large.(6, 21)

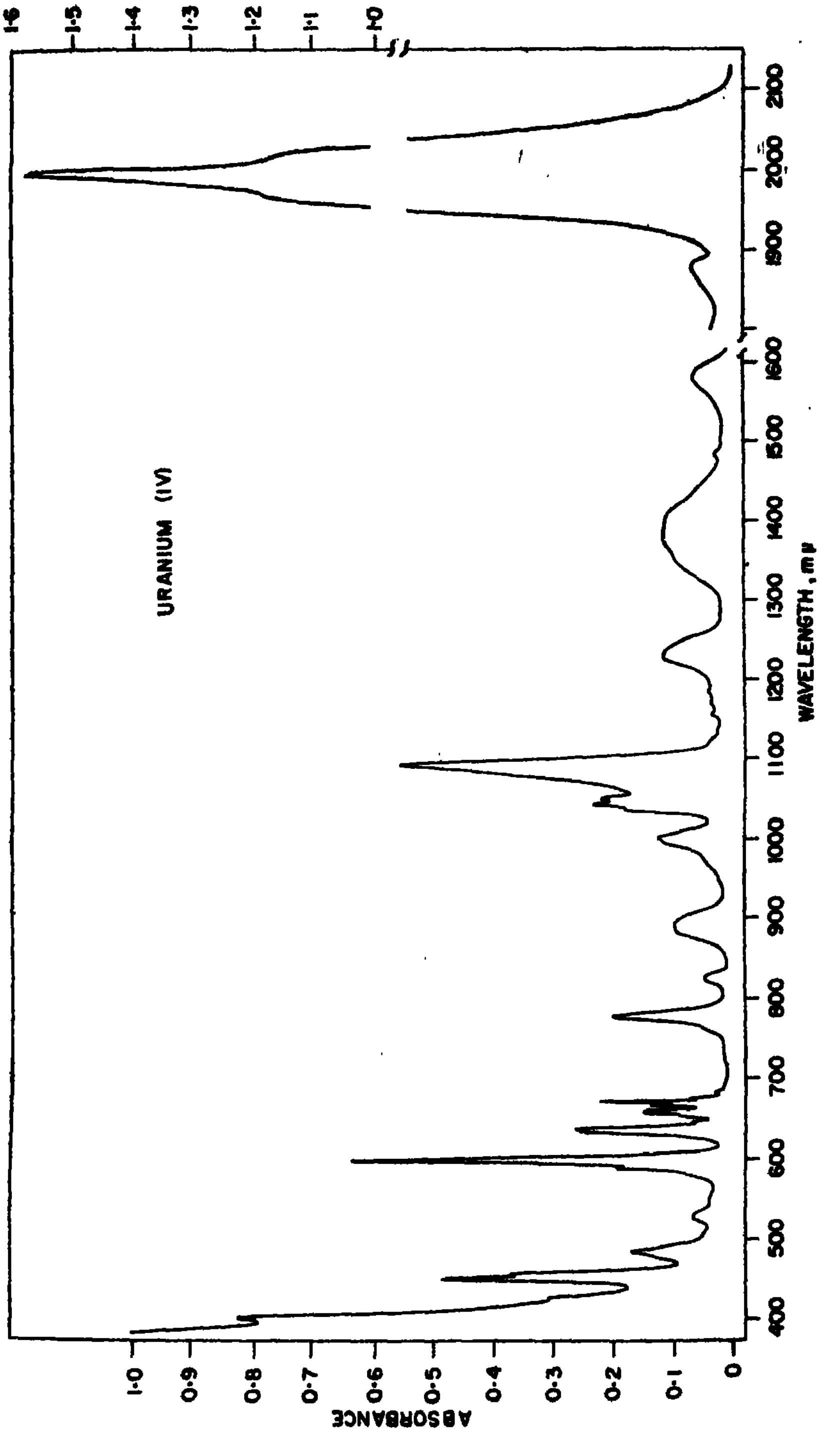

FIG. 4.—6·0 × 10^{-2} M uranium(IV) in 10% TOA solution extracted from 6 M HCl.

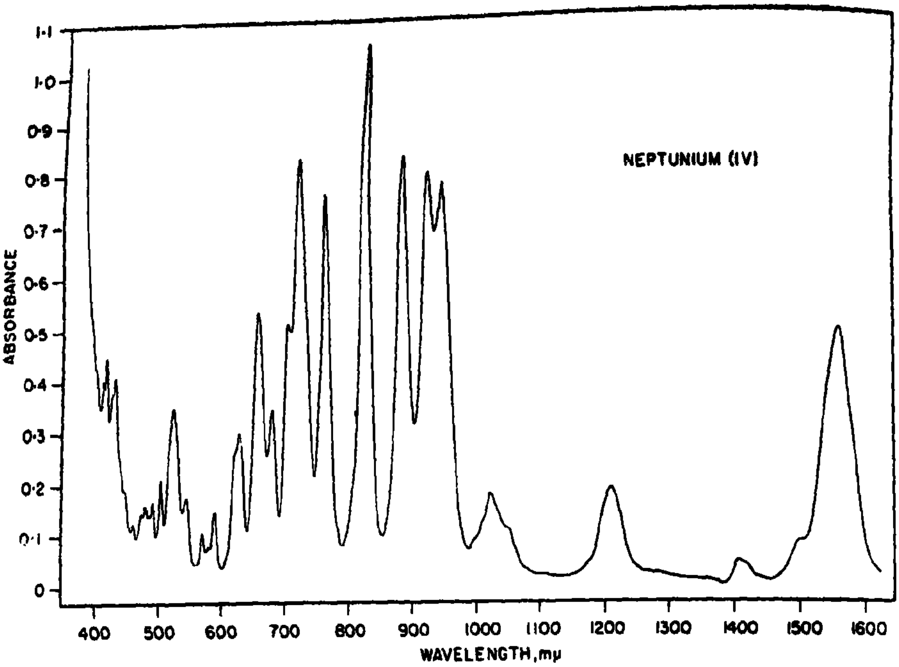

FIG. 5.—7·4 × 10^{-2} M neptunium(IV) in 10% TOA solution extracted from 6 M HCl.

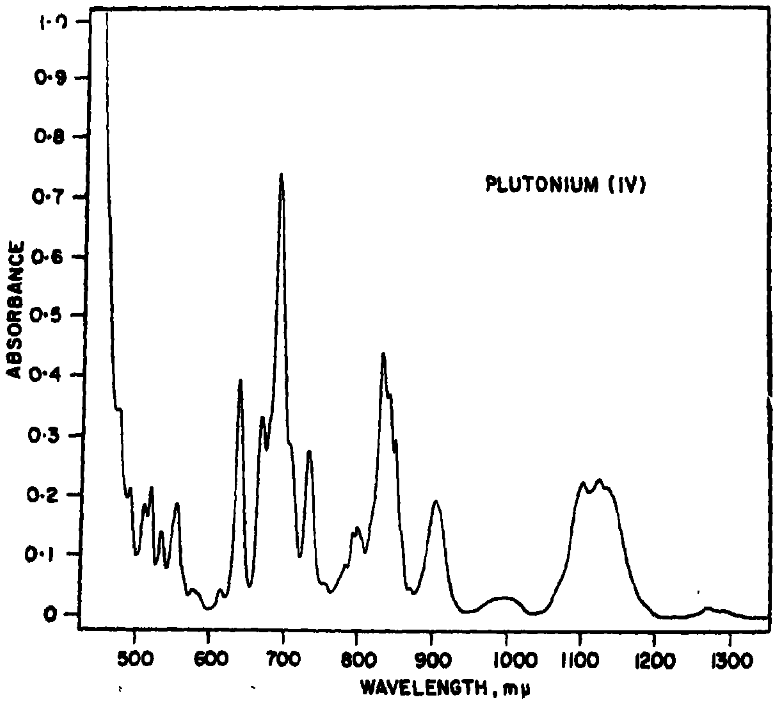

FIG. 6.—4·2 × 10^{-2} M plutonium(IV) in 10% TOA solution extracted from 9 M HCl.

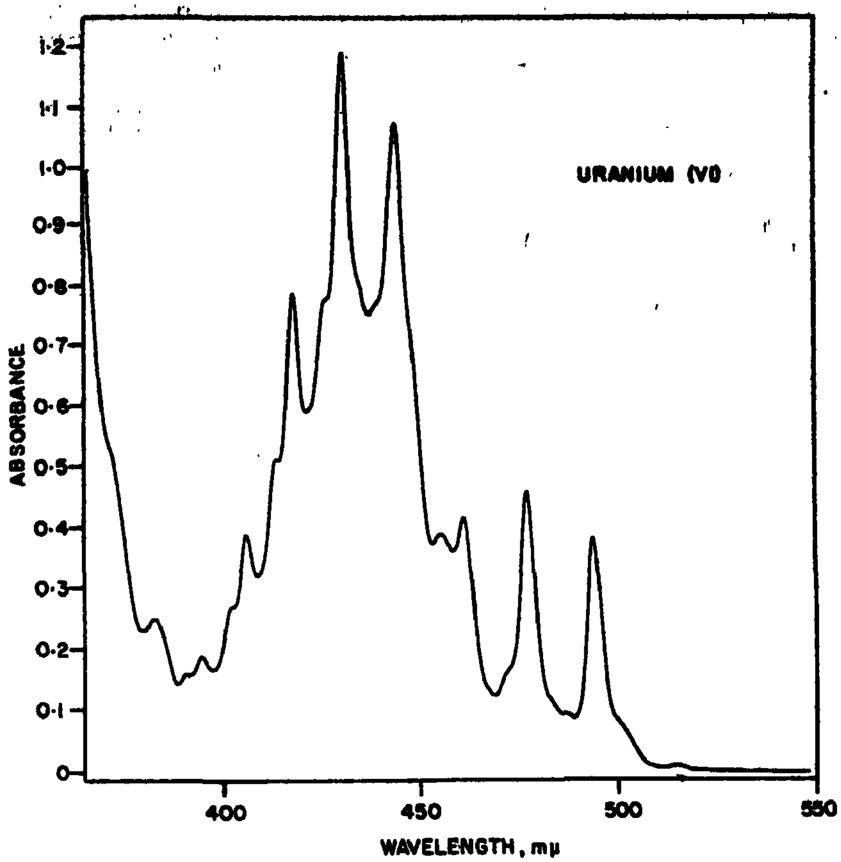

FIG. 7.—7·2 × 10⁻² M uranium(VI) in 10% TOA solution extracted from 4 M HCl.

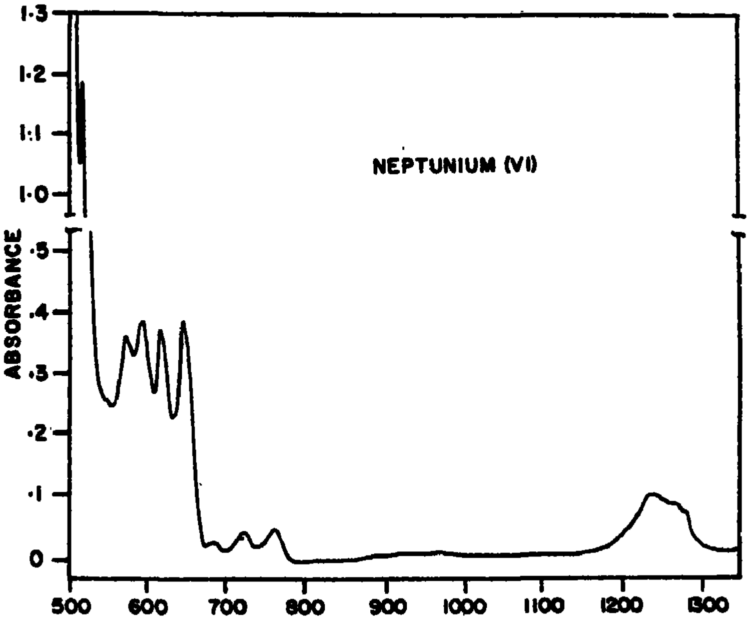

FIG. 8.—3·5 × 10⁻² M neptunium(VI) in 10% TOA solution extracted from 4 M HCl.

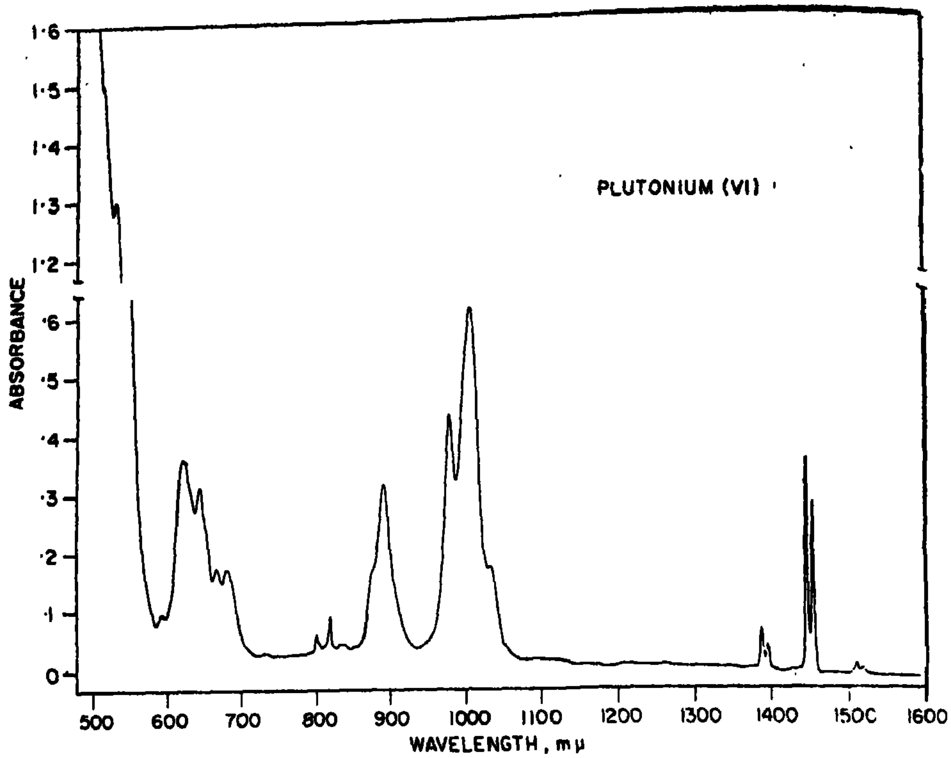

FIG. 9.—$3 \cdot 9 \times 10^{-2}$ M plutonium(VI) in 10% TOA solution extracted from 4 M HCl.

Absorption spectra of the hexavalent actinides in TOA solutions extracted from 4 M HCl are shown in Figs. 7–9, but a spectrum that would provide identification of any of these ions by direct comparison has not been published. That of uranium(VI) chloride in TOA has been reported previously by BIZOT and TREMILLON(6) and attributed by them to the $UO_2Cl_4^{2-}$ ion on the basis of a TOA/U ratio of two, obtained on extraction from concentrated uranium solutions. The spectrum of a petrolatum mull of solid anhydrous $Cs_2UO_2Cl_4$ is quite different from that of the TOA solutions though, which might be taken to indicate incorrect identification of the species in amine solutions. RYAN has found recently, however, that both of these spectra are due to the anhydrous $UO_2Cl_4^{2-}$ ion. He has studied the alkylammonium salts of uranyl chloride extensively in connection with his ion exchange studies and will discuss the two spectral species of $UO_2Cl_4^{2-}$ in a forthcoming publication.(24) All evidence then indicates that the tetrachloro complexes of the hexavalent actinides are the species extracted by TOA from hydrochloric acid.

Acknowledgement—The author wishes to thank J. L. RYAN who prepared some of the actinide stock solutions and adjusted their valence states and Mrs. W. G. ARTMAN who performed most of the distribution experiments.

(24) J. L. RYAN, *J. Phys. Chem.* To be published.

J. Inorg. Nucl. Chem., 1962, Vol. 24, pp. 571 to 586. Pergamon Press Ltd. Printed in England

THE EXTRACTION OF LANTHANONS WITH ALKALI METAL AMALGAMS—I

SAMARIUM AND YTTERBIUM

M. F. Barrett, D. Sweasey and N. E. Topp
National Chemical Laboratory, Teddington, Middlesex

(*Received* 10 *October* 1961)

Abstract—The extraction of samarium and ytterbium from solutions of lanthanon concentrates with sodium amalgam has been studied, using a dropwise extraction procedure. The reproducibility of the method has been established. Extraction of these elements depends on the samarium or ytterbium content of the lanthanon concentrate used, and also on the pH of the solution. Under certain conditions marginal quantities of other lanthanons are extracted.

Mechanisms of the reaction are discussed.

About thirty years ago, rare earth amalgams were carefully studied as a route for the isolation of the rare earth metals. They were prepared by the electrolysis of aqueous solutions of lanthanons, using a mercury cathode. Only a limited number of amalgams could be prepared in this way (e.g. La, Nd, Sm), although the range could be extended by using anhydrous ethanol as a solvent.⁽¹⁾ McCoy was the first to show that alkali metal amalgams would react with aqueous lanthanon solutions⁽²⁾ and he was able to extract europium and ytterbium from mixed lanthanons by treatment with a potassium amalgam. This observation was followed up by Marsh, who developed important methods for extracting samarium, europium and ytterbium from lanthanon solutions by reaction with sodium amalgam.⁽³⁻⁶⁾

If sodium amalgam was shaken with a neutral lanthanon solution, hydroxides were precipitated. However, by making controlled additions of acid to the solution, it was possible to prevent precipitation of the hydroxides and also to extract significant quantities of lanthanons to the amalgam phase. Control was simplified by using a buffered system.

The preferred method was to shake together in a separating funnel sodium amalgam and a lanthanon acetate solution. Short contact periods were used (e.g. 1–5 min), and acetic acid was added periodically to prevent hydroxide precipitation. At the end of the extraction period the amalgam phase was separated and any extracted lanthanons recovered by treatment with hydrochloric acid. Marsh showed that samarium and europium were preferentially extracted from mixed light earths under these conditions. However, if an excess of amalgam was employed, then some of the neighbouring elements tended to be extracted (e.g. La, Pr, Nd). Ytterbium was

---

(1) E. Jukkola, L. Audrieth and B. Hopkins, *J. Amer. Chem. Soc.* **36**, 303 (1934).
(2) H. N. McCoy, *J. Amer. Chem. Soc.* **63**, 1622 (1942).
(3) J. K. Marsh, *J. Chem. Soc.* 398 (1942).
(4) J. K. Marsh, *J. Chem. Soc.* 523 (1942).
(5) J. K. Marsh, *J. Chem. Soc.* 8 (1943).
(6) J. K. Marsh, *J. Chem. Soc.* 531 (1943).

similarly extracted preferentially from its neighbouring elements, but, unlike the light earths, these could not be extracted by using an excess of amalgam. During the extraction process, sodium ions accumulated in the aqueous phase. These were found to reduce the efficiency of the extraction process to a point at which sodium elimination became necessary.

Batchwise extraction is not easy to control, and has been found to give widely divergent results in the hands of different operators. The evidence suggests that the reaction is controlled by the area of the amalgam–solution interface, and large differences have been found in the rate and extent of extraction under differing conditions. Thus, while MARSH recommended short extraction times and vigorous shaking, MOELLER and KREMERS found a maximum extraction of ytterbium in 15–20 min when solution and amalgam were stirred together.(7)

This lack of reproducibility is a serious handicap in studying the reaction quantitatively. There are certain similarities in technique between extraction with amalgams and with organic solvents. A dropwise method of extraction has therefore been examined, and its reproducibility established. Initially, the extraction of samarium and ytterbium from a number of lanthanon concentrates has been examined. This work forms the first part of an investigation into the mechanism of amalgam extraction. While some features of the extraction process have been clarified, it is evident that the systems used here are too complex for elucidating the detailed mechanism, and a further study is being made of simplified model systems.

EXPERIMENTAL

Preliminary examination. When a dilute sodium amalgam (0·3 per cent) was dropped through a 50 cm layer of neutral lanthanon solution (chloride, nitrate or acetate), hydroxides were precipitated. Precipitation was prevented by adding the appropriate acid, but this caused considerable hydrogen evolution through direct reaction of acid with the amalgam. The most suitable compromise was the use of acetate salts and acetic acid. When varying quantities of a sodium amalgam were dropped through constant volumes of an acidified lanthanon acetate solution (Ln_2O_3 55 g/l.; Sm_2O_3 20·0 per cent; initial pH 4·0), lanthanons were extracted by the amalgam in proportion to the quantity of amalgam employed.

Materials. Six lanthanon fractions were examined. Four of these (A, B, C, and F) were isolated from more complex mixtures by ion-exchange chromatography. Sample D was isolated from a xenotime mineral by caustic fusion, leaching the melt until free from phosphate, and dissolving the residual hydroxide in hydrochloric acid. This solution was boiled and filtered, and the mixed lanthanons were isolated as the oxalates. The remaining material (E) was obtained from the xenotime extract by repeated sulphate precipitation from boiling solution; this treatment is stated to remove the light lanthanons.(8) Analysis of these materials is summarized in Table 1.

Neutral acetate solutions were prepared by heating a small excess of oxide with acetic acid overnight and filtering off the excess. Solutions were standardized gravimetrically by oxalate precipitation, followed by ignition to the oxide at 850° C.

Sodium amalgam. Concentrated amalgams (0·5–1% Na) were prepared by direct addition of mercury to molten sodium protected by a layer of medicinal paraffin. The paraffin was washed off by light petroleum, followed by acetone. After dilution with mercury, further washing was given in alcohol, water and finally a second alcohol wash. The product was stored in polythene containers.

All mercury was purified by aeration under acid ferrous sulphate solution. It was washed in nitric acid (1·5 N) followed by water, and was finally vacuum distilled. After use in a lanthanon extraction experiment, the acid and water washing steps were repeated.

(7) T. MOELLER and H. E. KREMERS, *Analyt. Chem.* 17, 798 (1945).

(8) V. SHAW, D. BAUER and J. GOMES, *U.S. Bureau of Mines*, R/I 5521 (1959).

TABLE 1.—ANALYSIS OF LANTHANON FRACTIONS

No.	CeO_2	Pr_6O_{11}	Nd_2O_3	Sm_2O_3	Eu_2O_3	Gd_2O_3	Tb_4O_7	Dy_2O_3	Ho_2O_3	Er_2O_3	Tm_2O_3	Yb_2O_3	Lu_2O_3	Y_2O_3	Total Ln_2O_3 g/l.
A*		—	—	13·95	1·45	19·5	1·35	13·5	1·0						55·8
B		0·9	5·0	26·5	0·7	62·5	—								59·6
C		—	19·9	75·7	—		—								59·8
D	0·6	0·1	0·5	1·0		2	1	14·5	2·5	12·5	2	17·2	3	45	59·8
E	—	—	—	—		0·5	0·1	10	1·5	10	1	20·7	2·5	50	48·7
F	—	—	—	—		—	—	—	—	—	—	90·3	10	—	62·8

* The remainder of this fraction was assumed to be yttria.

Amalgam concentrations were determined by shaking a known weight of amalgam with an excess of standard hydrochloric acid and back-titrating the excess acid with caustic soda.

Lanthanon analysis. The composition of a number of the materials was determined spectrophotometrically, using a Beckman model D.U. instrument with a photomultiplier attachment. The instrument was calibrated with chloride solutions of pure earths (> 99·9 per cent), using the slit-widths and wavelengths recommended by BANKS and KLINGMAN.⁽⁹⁾ Gadolinium and terbium were determined on a Carey spectrophotometer.⁽¹⁰⁾ Europium and ytterbium were estimated polarographically, using a cathode ray instrument (Southern Instruments); the method employed was essentially that of LAITINEN and TAEBEL.⁽¹¹⁾ A number of amalgam extracts were examined spectrographically, using a Jarrell-Ash grating instrument. The methods used were those of FASSEL⁽¹²⁾ and the "iron-flux" method.⁽¹³⁾

Extraction apparatus (Fig. 1). The extraction columns were 100 cm long and 2 cm in diameter, terminating in 2 mm diameter capillary U-tube, which formed a syphon. A side-arm and tap was provided above the syphon to admit nitrogen for stirring. In most of the work, the extraction column was filled with glass beads (6 mm diameter); this minimized mixing at the amalgam–solution interface at the bottom of the column, and considerably increased the amalgam–solution contact time.

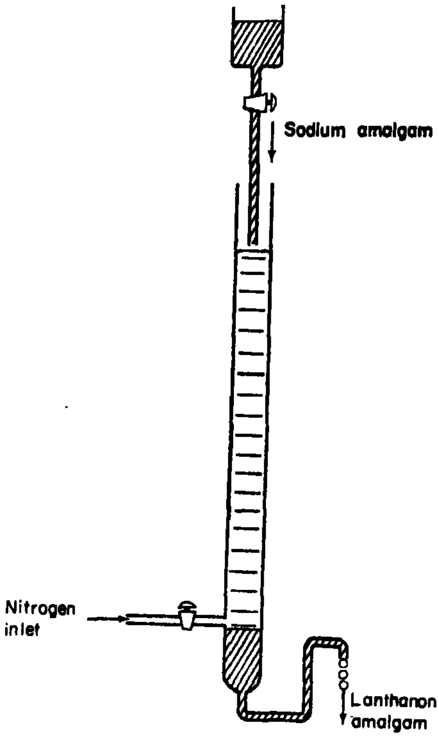

FIG. 1.—Extraction apparatus.

---

(9) C. V. BANKS and D. W. KLINGMAN, *Analyt. Chim. Acta* **15**, 356 (1956).

(10) E. I. ONSTOTT and C. J. BROWN, *Analyt. Chem.* **30**, 172 (1958).

(11) H. A. LAITINEN and W. A. TAEBEL, *Industr. Engng. Chem.* (Analyt. Ed.), **13**, 825 (1941).

(12) V. A. FASSELL, H. D. COOK, L. C. KROTZ and P. W. KEHRES, *Spectrochim Acta* **5**, 201) (1952).

(13) Springfields Chemical Services, Method No. 357 (1954).

Sodium amalgam from a reservoir flowed from a capillary into the column of solution. The flow-rate was controlled by inserting a length of nichrome wire into the upper part of the capillary. For investigating the effect of amalgam drop size on the extraction, capillaries of varying diameter could be attached to the end of the control tube with a P.V.C. sleeve. Before use, the reservoir was carefully cleaned and dried. To prevent blockage of the capillary with sodium oxides, the surface of the amalgam was kept covered with a small volume of dry alcohol. This was very effective, and tests showed that a negligible amount of sodium (< 0·5 per cent) was consumed during an experiment.

Procedure. The syphon of the extraction tube was filled with purified mercury, and a measured volume of lanthanon solution, of the required pH, was transferred to the extraction column. Nitrogen for stirring was admitted through the side-arm. A weighed quantity of sodium amalgam was dropped through the solution at a controlled rate. The rare earth amalgam formed was syphoned off from the extraction column and passed through a small water wash column (15 cm deep), also fitted with a syphon, to a receiver. At the end of an experiment, pure mercury was discharged rapidly through both columns to displace the remaining rare-earth amalgam.

Lanthanons in the amalgam phase were recovered by heating overnight on a hot-plate with 2 N hydrochloric acid. After removing traces of mercury as sulphides, the lanthanons were recovered as oxalates by adding an excess of oxalic acid and adjusting the pH of the solution to 2·0. The pH of the extracted solution was determined, and material balance was checked by recovering the residual lanthanons as oxalates; two precipitations were made to minimize sodium occlusion.

Examination of amalgam drop sizes. Drop sizes of sodium amalgams were examined over a range of flow-rates, and using a series of jets of varying diameter. These were determined by direct observation, using a microscope with an eyepiece graticule. An interrupted light source was provided by a Strobotorch (Dawe Instruments Ltd.). The apparatus was calibrated with pure mercury.

RESULTS AND DISCUSSION

Amalgam extraction technique

1. *The reaction of sodium amalgam with hydrogen ions.* Preliminary experiments had shown that there was some evolution of hydrogen during the extraction of samarium solution with sodium amalgam. Quantitative data were obtained by treating acid and buffer solutions in the extraction apparatus with varying quantities of dilute (0·1–0·2% Na) amalgams.

In water or 1 N electrolyte solutions, reaction was slight, and the caustic soda concentration, after passage of amalgam, rarely exceeded 0·005 N. Hydrochloric and acetic acids were completely neutralized with evolution of hydrogen, and the final solutions again contained approximately 0·005 N sodium hydroxide. Buffer solutions in the pH range from 3 to 5 were not neutralized unless a large excess of amalgam was used. When less than stoicheiometric quantities of sodium were used, the sodium consumption varied with the pH of the solution.

If the extraction column was not packed, and a similar depth of liquid used, less reaction was observed under comparable conditions. Thus, strong acids were not neutralized unless a large excess of amalgam was used. Reaction of the sodium thus depended on the hydrogen ion concentration of the solution and on the residence time of the amalgam in the extraction column. In a packed column containing 100 ml of solution, the drop residence time was 5 sec, and less than one tenth of this in absence of packing.

2. *Reproducibility of extraction procedure.* A variety of tests was made of the method of extraction.

(a) **Extraction of samarium acetate; effect of column packing.** A solution of the samarium concentrate B was adjusted to pH 3·9 by adding 10 N acetic acid. Fifty ml or 100 ml portions of this solution were extracted with varying quantities of a 0·204 per cent sodium amalgam, which was added at 100 g/min from a 1·17 mm diameter jet. Extraction was compared using either a packed column or free fall; the liquid depths in the four cases were 45, 71, 19 and 42 cm, respectively. Results are summarized in Fig. 2, scaled to a common solution volume.

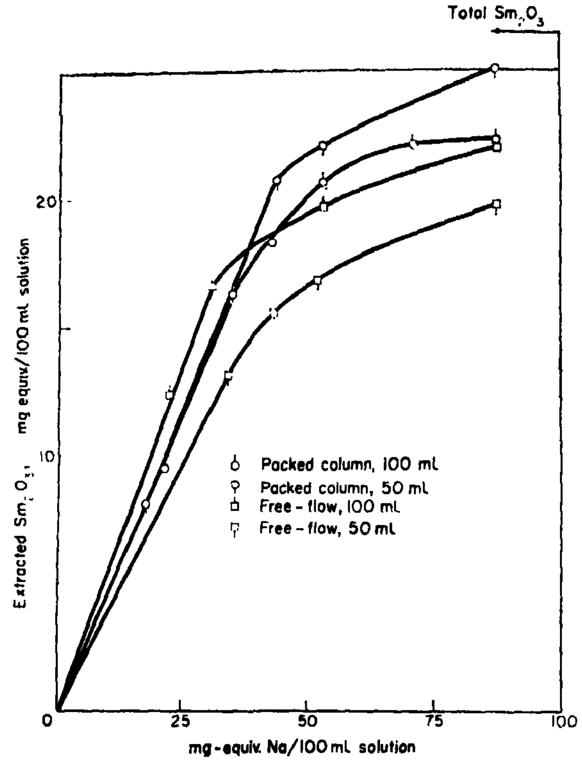

FIG. 2.—Extraction of samarium under varying conditions.

When packed columns were used, the extraction was linear with quantity of amalgam until 70 per cent of the samarium had been extracted, but beyond that point proportionately more samarium was extracted from the smaller quantity of solution. No sodium was found in the column effluent until 75 mg-equivs of sodium/100 ml of solution had been used for extraction.

If free-fall conditions were used, extraction varied with the depth of liquid. With the smaller liquid column, less samarium was extracted than in a corresponding experiment with a packed column, but with a 100 ml sample the initial extraction was somewhat greater. After 60 per cent of the samarium had been extracted the extraction became less efficient, and beyond this point less samarium was extracted under free-fall conditions. Some sodium was found in the samarium amalgam in these experiments.

(b) Flow-rate and amalgam dispersion. A number of extraction experiments were carried out at a fixed solution–sodium ratio. A volume of solution B, either 50 ml or 100 ml, was extracted at a range of flow rates (50 g/min to 250 g/min) using either free fall or a packed extraction column. Under fixed conditions individual extraction experiments were duplicated to within 1 per cent.

Results obtained under free-fall conditions confirmed the behaviour shown in Fig. 2. In general, extraction was decreased if the amalgam flow-rate increased, or if a smaller liquid volume was used. Thus, the amount of samarium extracted from 100 ml of solution decreased by 20 per cent when the flow-rate was increased from 100 to 250 g/min. These effects were clearly due to a reduction of the contact time in the extraction column. If a packed extraction column was used these variations were smaller and in the opposite sense. Extraction was increased either by using a smaller extraction volume or by increasing the amalgam flow-rate; a similar change in flow-rate increased the samarium extraction by 10 per cent.

The effect of amalgam dispersion was studied using a range of capillaries to form the amalgam drops. The capillaries varied in diameter from 0·4 mm to 2 mm, and gave amalgam drops varying from 0·7 to 2·9 mm in diameter. Little variation was observed in the quantity of samarium extracted, and within this range the dispersion of the amalgam was not an important factor.

(c) Stability of the samarium amalgam. Samarium amalgam, prepared in the manner described above, was dropped through 50 ml or 100 ml of 1 N sodium acetate buffer solution (pH approx. 4·0), and the samarium content of the solution was then determined. Under free-fall conditions 2·5 per cent of the samarium was recovered from solution. Appreciably more samarium was recovered if a packed column was used, varying from 5 per cent with a 50 ml solution volume to 11 per cent with a 100 ml volume. This difference was sufficient to account for the higher extraction observed initially under free-fall conditions (Fig. 2), and must be due to back-extraction of samarium from the amalgam by reaction with hydrogen ions in solution.

The extraction of samarium by sodium amalgam can be explained by the following reactions:

$$\mathrm{Sm}^{3+} + 3\mathrm{Na} \rightarrow \mathrm{Sm} + 3\,\mathrm{Na}^{+} \qquad (1)$$

$$\text{or } \mathrm{Sm}^{3+} + \mathrm{Na} \rightarrow \mathrm{Sm}^{2+} + \mathrm{Na}^{+} \xrightarrow{2\mathrm{Na}} \mathrm{Sm} + 3\,\mathrm{Na}^{+} \qquad (2)$$

The direct reaction of sodium with hydrogen ions and the back extraction of the samarium amalgam must also be considered, viz.

$$2\,\mathrm{Na} + 2\,\mathrm{H}^{+} \rightarrow 2\,\mathrm{Na}^{+} + \mathrm{H}_2 \uparrow \qquad (3)$$

$$2\,\mathrm{Sm} + 6\,\mathrm{H}^{+} \rightarrow 2\,\mathrm{Sm}^{3+} + 3\,\mathrm{H}_2 \uparrow \qquad (4)$$

Clearly, the free-fall technique is unsatisfactory unless impracticably long extraction columns are used. Extractions in a packed column represent a compromise, since up to 10 per cent of the samarium can be back-extracted by reaction (4) above. However, if the technique is carefully standardized closely reproducible results can be obtained, and it appears to be the best compromise. In subsequent work, the amalgam flow-rate was standardized at 100 g/min, using a 1·17 mm diameter jet, and a packed extraction column was used. Under these conditions, the amalgam drop size was 2·5 mm.

The extraction of samarium

1. *The effect of acidity on extraction.* The two materials A and C were used for this investigation. Hundred ml portions of solution A were adjusted to pH's of 4·0, 3·75 and 3·3 by the addition of 8, 16 and 24 ml respectively of 10 N acetic acid. These were extracted with varying quantities of a 0·31 per cent sodium amalgam in the manner already described.

Samarium and europium determinations were carried out on the extracted residues. There was a decrease in the content of both elements as increasing quantities of amalgam were used, and over 90 per cent of these elements were extracted. Spectrographic analysis showed the amalgam extract to contain only samarium and europium. Only small variations were found in the europium content, showing that there was no separation from samarium. The sodium content of both the residual solution and the amalgam was determined with a flame photometer. Results are summarized in Table 2 and Fig. 3 (lower curves).

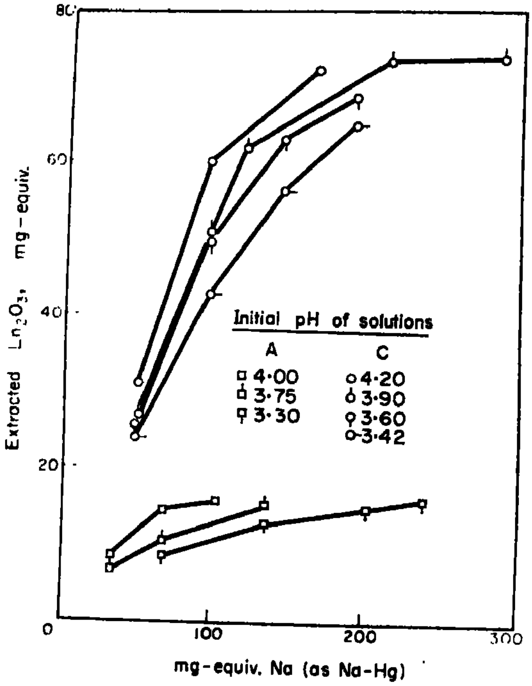

Fig. 3.—Extraction of samarium solutions with sodium amalgam.

Lanthanon extraction was found to increase with amalgam quantity, although the relation was not linear. The most efficient extraction was obtained in solutions of lowest acidity, but in each case the efficiency decreased rapidly after 70–80 per cent of the samarium had been extracted. At this point in the extraction appreciable quantities of sodium were found in the amalgam phase. This was readily detected, since sodium amalgam is appreciably more reactive than lanthanon amalgams.

There was an increase in pH of all extracted solutions. This was due to the evolution of hydrogen during extraction, so that samarium and europium ions were replaced by more than an equivalent quantity of sodium ions. Thus, in the solution of initial pH 4·0 (final pH 5·63), the final sodium content was 0·85 N, while in a more acidic solution (initial pH 3·30, final pH 5·65) it became 2·2 N.

TABLE 2.—EXTRACTION OF SOLUTION A WITH 0·31 PER CENT SODIUM AMALGAM

Initial pH	Final pH	Na (as NaHg) (mg-equivs.)	Extracted Ln_2O_3 (mg-equivs.)	Na in amalgam (mg-equivs.)	Eu_2O_3 in extract (%)
4·0	4·40	33·7	8·66	0·1	8·0
	5·06	67·4	14·7	1·1	8·2
	5·63	101·1	15·67	15·4	9·1
3·75	4·09	33·7	6·63	0·1	8·1
	4·50	67·4	10·68	0·4	8·5
	5·31	134·8	15·27	4·2	8·7
3·30	4·25	67·4	8·49	0·5	9·1
	4·82	134·8	12·78	0·2	9·1
	5·44	202·2	14·92	2·4	9·8
	5·65	238·9	15·97	15	9·3

Similar extraction experiments were carried out with solution C. In this case, the pH's of the solutions were adjusted to 4·2, 3·9, 3·6 and 3·4 before extraction. Solid lanthanon amalgams were obtained upon extraction with a 0·31 per cent amalgam, so a more dilute amalgam was used (0·11 per cent). Spectrographic analysis of the amalgam extracts showed them to contain only samarium and trace quantities of europium (< 0·1 per cent). The results are summarized in Fig. 3 (upper curves).

Lanthanon extraction was again found to increase with the quantity of amalgam, and over the initial part of the extraction a linear relation was found. The extraction became progressively less efficient as the initial pH of the solution decreased, and in each case there was a decrease in efficiency when about 75 per cent of the samarium had been extracted. In no case was it possible to recover more than 95 per cent of the samarium present, although several extractions were continued to a point at which slight lanthanon hydroxide precipitation was observed.

It appeared possible that the incomplete samarium extraction might be due to the increase in pH of the lanthanon solution during extraction. This was tested by periodically re-acidifying the solution after treatment with 2 Kg portions of amalgam, and then continuing the extraction. In Table 3, the results of two experiments are compared with examples where no pH adjustment was made.

TABLE 3.—EFFECT OF RE-ACIDIFYING SOLUTIONS USED IN SAMARIUM EXTRACTION (100 ML SOLUTION C, 0·11 PER CENT SODIUM AMALGAM)

Initial pH	Na (as NaHg) (mg-equivs.)	Extracted Ln_2O_3 (mg-equivs.)	Total extract (mg-equivs.)	Ln_2O_3 in continuous expt. (mg. equivs)
3·60	95·6	49·9	65·45	68·7
	95·6	15·55		
3·90	95·6	50·85	71·85	73·8
	95·6	19·5		
	95·6	1·5		

The samarium extraction obtained was slightly but significantly lower than that where no pH adjustment had been made. A similar decrease in extraction efficiency was found when most of the samarium had been removed. In both types of experiment, no significant quantity of sodium was found in the extract until more than 200 mg-equivs. of amalgam had been used.

The reactions taking place in the extraction column have already been described. *The results in Fig. 3 show that the effect of increasing the acidity of the solution is to* increase the consumption of sodium in the side reaction (3). However, a compromise is necessary since the buffering of lanthanon acetate solutions is very small above pH 5.

There was a remarkable difference in the ease with which samarium was extracted from the three materials. This can be expressed quantitatively as the ratio of lanthanon extracted to sodium consumed. Taking comparable experiments from Figs. 2 and 3, the efficiencies over the initial part of the extraction curves were: A, 22; B, 47; C, 63 per cent.

2. *The effect of solution concentration on extraction.* Extraction of the two materials A and C was compared at lanthanon concentrations of 0·5 N and 0·25 N. The lanthanon acetate:acetic acid ratio used was 1:0·8 (pH's A 4·0; C, 3·90), and 100 ml portions were extracted with a 0·11 per cent sodium amalgam. The results are shown in Fig. 4.

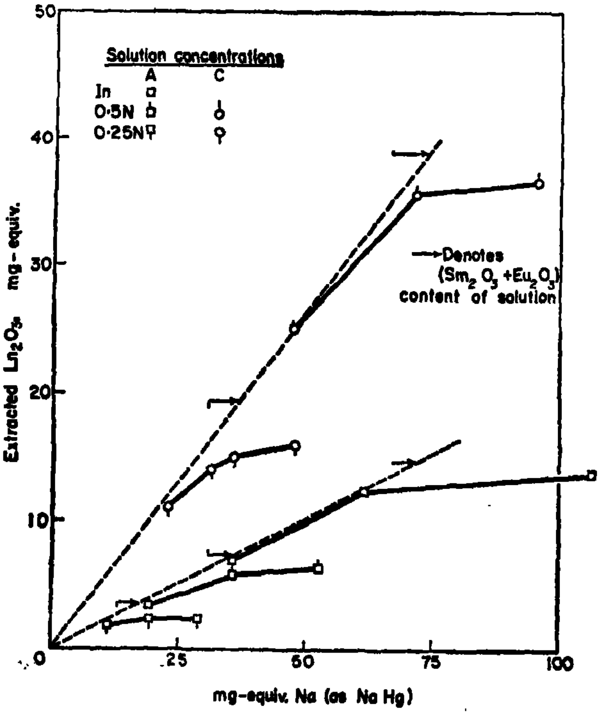

FIG. 4.—Effect of solution concentration on samarium extraction.

The initial part of the extraction curve appeared to be characteristic for each material, over a fourfold range of concentration. However, the point at which the extraction efficiency diminished rapidly was affected by the solution concentration, and it became more difficult to extract a high percentage of the samarium from dilute solutions. A material balance showed the unextracted samarium, with material A to be about 1 mg-equiv., and 5 mg-equiv. for material C, at each concentration.

The extracts from material A contained samarium and europium only. Some neodymium was found in the C extracts; 3 per cent was present in the extracts from the 0·5 N solutions, and 10 per cent with the 0·25 N solutions. None was found when 1 N solutions were used.

In these experiments, the samarium content of the solutions was varied by a factor of 20 (from 0·75 N to 0·037 N). The highest samarium concentration used with material A was similar to the lowest concentration with material C. It appears, therefore, that the efficiency with which a samarium concentrate is extracted depends upon the composition of the concentrate, and not on the concentration of samarium in solution.

3. *The effect of amalgam concentration on extraction.* Normal solutions of materials A and C were extracted at a fixed initial pH (3·90) with identical quantities of sodium; the amalgam concentration was varied from 0·3 to 0·05 per cent. Where fluid amalgams were formed, no significant trends were observed in the quantity of samarium extracted. If semi-fluid amalgams were formed, appreciably lower quantities of samarium were extracted. In such cases, flow of the amalgam through the column was slow, and it was observed that some of the amalgam droplets were coated, presumably with lanthanon hydroxide.

Owing to the variation of extraction efficiency with composition, the choice of a suitable sodium amalgam concentration must be determined by experiment. However, the results showed that amalgams containing more than the equivalent of 2 grams Sm_2O_3 per kilogram of amalgam were semi-fluid or solid.

4. *The effect of sodium ion concentration.* Varying quantities of sodium chloride were added to 100 ml samples of solution A (1 N) and solution C. (0·5 N). These were extracted with similar quantities of sodium amalgam. The results are summarized in Table 4.

TABLE 4.—EXTRACTION OF SAMARIUM FROM SODIUM-CONTAINING SOLUTIONS

	A; 67·4 mg-equivs. Na		C; 47·8 mg-equivs. Na	
NaCl (mole/l.)	Extracted Ln_2O_3 (mg-equivs)	Extract, as Na-free soln. (%)	Extracted Ln_2O_3 (mg-equivs)	Extract, as Na-free soln. (%)
0	14·7		25·7	
0·5	14·5	98	26·55	103
1	13·9	94	26·85	104
2			28·15	109

The observed effect was small, and appeared to depend upon the composition of the solution. It will be recalled that samarium and europium only were extracted from material A, while neodymium was extracted with samarium from dilute solutions of material C. In the presence of sodium chloride, extracts from material A contained only samarium and europium; when 1 N or 2 N sodium chloride was used, no neodymium was detected in extracts from material C.

The extraction of ytterbium

1. *The effect of acidity on extraction.* Fifty ml portions of the solution F were adjusted to pH's of 3·9 or 3·6, which required the addition of 5 ml or 10 ml respectively of 10 N acetic acid. Extraction was carried out with a 0·103 per cent sodium amalgam, at a flow-rate of 100 g/min. The results are shown in Table 5 and Fig. 5 (upper curve).

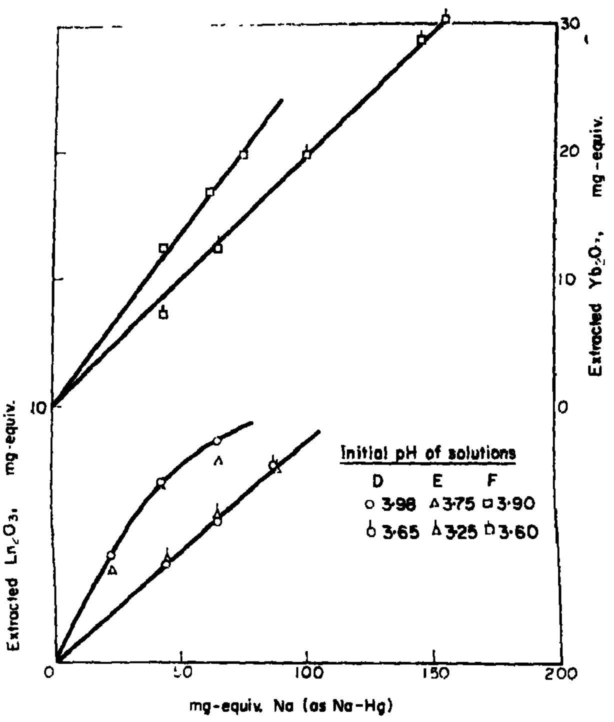

Fig. 5.—Extraction of ytterbium solutions with sodium amalgam.

Table 5.—Extraction of solution F with 0·103 per cent sodium amalgam

Initial pH	Final pH	Na (as Na-Hg) (mg-equivs)	Extracted Yb_2O_3 (mg-equivs)
3·90	5·19	44·8	12·4
	5·91	62·7	16·7
	7·25	76·1	19·73
3·60	4·65	44·8	7·25
	5·13	67·2	12·47
	5·81	101·8	19·6
	8·01*	147·8	28·65
	8·10*	156·7	30·5

There was a vigorous evolution of hydrogen during extraction, due to the direct reaction of some of the sodium with hydrogen ions in solution. The pH of the extracted solution increased with the quantity of amalgam used, and some hydroxide precipitation was observed in the two examples marked with an asterisk. (Table 5). This set an upper limit to the amount of ytterbium that could be extracted, which was 45 per cent in the solution of initial pH 3·9 and 70 per cent with the more acidic solution. These extractions were linear with amalgam quantity. An attempt was made to obtain a more complete extraction of the ytterbium by repeatedly re-acidifying the solution to pH 3·9, and then continuing the extraction with a further quantity of amalgam. The result of one such experiment is shown in Table 6.

TABLE 6.—REPEATED EXTRACTION OF SOLUTION F WITH 0·103 PER CENT SODIUM AMALGAM

Initial pH	Final pH	Na (as Na-Hg) (mg-equivs)	Extracted Yb_2O_3 (mg-equivs)
3·90	7·20	73·9	22·17
3·90	7·05	67·2	13·8
3·90	7·25	44·8	2·8
		Total Na 185·9	Total Yb_2O_3 38·77

A considerably increased ytterbium extraction was obtained. Although it was possible to extract 90 per cent of the ytterbium from solution, the final extraction step required a fifteenfold excess of sodium amalgam, and the residual material still contained 3·8 mg-equivs of ytterbia. A spectrographic examination showed the amalgam extracts from material F to be pure ytterbium.

Batch extraction experiments were also carried out on solutions D and E. Fifty ml portions were used, and these were acidified with the same quantities of acetic acid used in the previous experiments. Results are summarized in Fig. 5 (lower curves).

With both materials, it was possible to extract about 90 per cent of the ytterbium present, but in neither case was pure ytterbium extracted. With material D, polarographic examination showed the ytterbia content of the extracts to be about 85 per cent. A spectrographic examination revealed the presence of $>$ 10 per cent of samarium, together with small quantities ($<$ 0·5 per cent) of La, Nd and Eu. These light elements were present in all of the fractions. Extracts from material E contained none of the light elements, but all of the fractions contained about 1 per cent of samarium.

The extraction of all of these materials was most efficient in solutions of the lowest acidity. The most efficient extraction of material F was 26 per cent, which was the reason for the small ytterbium extraction. The samarium concentrate C extracted at over 50 per cent efficiency under comparable conditions. However, the two lower ytterbium content materials D and E were extracted at 15 per cent efficiency, which is only slightly lower than that found with the low samarium content material A.

A bright orange-yellow colour developed during the extraction of material F. If the amalgam flow was stopped, the colour faded slowly and the solution again became colourless after several minutes. This effect was not observed when the other two lanthanon concentrates were extracted, but in these cases the colour could have been masked by other lanthanons present in solution. This colour was shown to be due to the formation of the ytterbous ion. Ytterbous chloride was prepared by reduction of the trichloride with hydrogen.[14] A $YbCl_2$ solution, and the extracted lanthanon solution F, both absorbed light strongly in the region 320–480 mμ, whereas tervalent ytterbium does not absorb in this region. Both solutions were oxidized by iodine.

2. *The effect of solution concentration on extraction.* Extractions were carried out with 0·103 per cent sodium amalgam on dilutions of the solutions D and F, at total lanthanon concentrations of 0·5 N and 0·25 N. The lanthanon acetate:acetic acid ratio employed was 1:1. (Initial pH's; D, 3·98; F, 3·90.) The results are shown in Fig. 6. With material F, it was possible to obtain a high ytterbium extraction before any hydroxide precipitation took place. Approach to complete extraction was shown by a fading of the colour of the ytterbous ion. At the same point some sodium was carried through with the lanthanon amalgam. The amalgam extracts were pure ytterbium. A comparison with similar results obtained with samarium (Fig. 3) showed the extraction of ytterbium to be linear with sodium quantity over a greater range than was the case with samarium. It was also possible to extract a higher proportion of the ytterbium from solution.

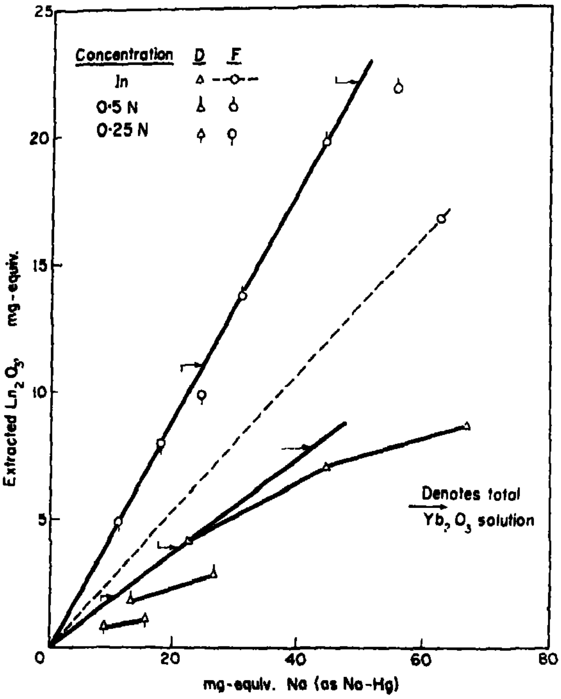

FIG. 6.—Effect of solution concentration on ytterbium extraction.

With the crude xenotime material (D), the efficiency of the initial extraction was not altered substantially by diluting the solution. The extracted material was again found to contain about 15 per cent lanthanons other than ytterbium. However, it became increasingly difficult to obtain a high ytterbium extraction from the more dilute solutions.

---

(14) W. Klemm and W. Schüth, *Z. Anorg. Chem.* **184**, 352 (1929).

When the ytterbium-rich material F was diluted to 0·5 N, the extraction became considerably more efficient. (44 per cent, compared with 26 per cent in a 1 N solution). The 0·5 N and 0·25 N solutions were extracted at the same efficiency. This dilution effect was not observed with samarium concentrates or with the xenotime concentrate D.

The results in Fig. 6 show a considerable difference in the efficiency with which the two materials were extracted; extraction from the high grade material was more than twice as efficient as that from the xenotime concentrate.

3. *The effect of sodium ion concentration.* Some quantitative comparisons were made of the effect of adding sodium ions to the ytterbium concentrate F. Fifty ml aliquots of 0·5 N lanthanon solution were prepared containing various additions of sodium chloride. These were extracted with identical quantities of sodium amalgam, with the results summarized in Table 7.

TABLE 7.—EXTRACTION OF YTTERBIUM FROM SODIUM-CONTAINING SOLUTION
44·8 MG-EQUIVS Na (AS NaHg) PER 50 ML SOLUTION

Added NaCl (mole/l.)	Extract Yb_2O_3 (mg-equivs)	Extract, as Na-free solution (%)
—	18·67	—
0·5	17·83	95
1	15·08	80
2	13·8	74

A significant decrease in extraction was found when 1 N or 2 N sodium chloride was added to the ytterbium solution. During extraction, the sodium ion content of these solutions increased by 0·9 N.

When the xenotime material D was extracted under similar conditions, the ytterbium extraction also decreased if sodium chloride was present. Quantitatively, the effect was smaller than with the high-grade material F. In the original extract, samarium and europium were found together with small quantities of lanthanum and neodymium. The two latter materials were eliminated by extracting in presence of sodium chloride, but all of the extracts contained samarium and europium as well as ytterbium.

CONCLUSIONS

It has been established that the dropwise method of extracting samarium and ytterbium with sodium amalgam is capable of giving closely reproducible results, although the amount of lanthanon extracted is somewhat arbitrary. The extraction of both elements is mainly controlled by the samarium or ytterbium content of the concentrates used, and to a lesser extent by the acidity of the solutions used for extraction. An idealized form of extraction curve is linear up to 70–80 per cent samarium or ytterbium extraction, and then becomes progressively less efficient with increasing extraction. Over the linear portion of the curve, the hydrogen ion concentration of the solution decreases by a factor of about 10^2, the sodium ion concentration increases from zero to 0·5–1·0 N, and the extractable lanthanon content falls to 20–30 per cent of its initial value. It is somewhat easier to extract samarium than ytterbium, but a more complete extraction of the latter element can be made. Europium, if present, is extracted with samarium.

It is known that the potential of sodium amalgams of similar concentrations to those used in this work is of the order of 2 volts. (15, 16) Reactions such as (1) or (2) are thermodynamically feasible if the potentials of the electrodes Sm/Hg and Yb/Hg are smaller than the corresponding sodium potential. Taking a mean sodium amalgam drop size of 2·5 mm, and assuming complete reaction of the sodium in 1 sec, the current density in a typical case would be of the order of 1–2 A/cm². Clearly, the sodium electrode is functioning under conditions of very high hydrogen overpotential, where the surface contains a layer of adsorbed hydrogen atoms.(17) The important electrode processes would be

$$\begin{aligned} &\mathrm{Na}+\mathrm{H}^{+} \rightarrow \mathrm{Na}^{+}+\mathrm{H} \\ &\mathrm{Ln}^{3+}+\mathrm{H} \rightarrow \mathrm{Ln}^{2+}+\mathrm{H}^{+} \xrightarrow{2\mathrm{H}} \mathrm{Ln}+2\,\mathrm{H}^{+} \\ \text{or } &\mathrm{Ln}^{3+}+3\mathrm{H} \rightarrow \mathrm{Ln}+3\mathrm{H}^{+} \\ &\mathrm{H}+\mathrm{H} \rightarrow \mathrm{H}_2 \end{aligned}$$

It is not established whether reduction of samarium or ytterbium proceeds via the bivalent or tervalent states, although divalent ytterbium is certainly formed during extraction. Eu^{2+} and Yb^{2+} would form readily in the boundary layer, since the redox potentials are 0·43 and 1·15 V respectively. The extraction of marginal quantities of other lanthanons is very sensitive to the concentration of sodium ions in solution. This suggests that the potentials of their amalgam electrodes must be considerably closer to the sodium electrode than is the case with Sm, Eu and Yb. To explain the effect of the "non-extractable" lanthanons in depressing the extraction of samarium or ytterbium it is necessary to assume that the potentials of their electrodes Ln/Hg are *greater* than that of the sodium electrode, and also that they will catalyse the reaction $\mathrm{H}+\mathrm{H} \rightarrow \mathrm{H}_2$. The formation of hydride intermediates has been suggested by Halpern to explain certain hydrogenation reactions.(18) Similar mechanisms may apply to this case.

Diffusion of sodium in the amalgam is rapid. This is shown by complete reaction of amalgam droplets in a packed column with hydrochloric or acetic acids; in the initial part of an extraction, all of the sodium remains in the extraction column, and a change of amalgam concentration from 0·3 to 0·05 per cent had no significant effect on the quantity of samarium extracted from two lanthanon solutions. These facts suggest that the decrease in extraction efficiency observed when the samarium or ytterbium concentration has diminished is due to a change in kinetic mechanism to one controlled by film diffusion. More rigorous experiments than those described here are needed to confirm this.

Acknowledgements—Thanks are due to D. Reichenberg for the sodium determinations, and to G. Giles and F. H. Howie for preparing the xenotime extracts. This work forms part of the research programme of the National Chemical Laboratory, and is published by permission of the Director.

(15) G. N. Lewis and C. A. Kraus, *J. Amer. Chem. Soc.* **32**, 1459 (1910).
(16) E. R. Smith and J. K. Taylor, *J. Res. N.B.S.* **25**, 731 (1940).
(17) A. Hickling and F. W. Salt, *Trans. Faraday Soc.* **38**, 474 (1942).
(18) J. Halpern, G. Stein, *et al.*, *Nature, Lond.* **186**, 629 (1960).

J. Inorg. Nucl. Chem., 1962, Vol. 24, pp. 587 to 588. Pergamon Press Ltd. Printed in England

NOTE

On the nature of the solvated 8-quinolinol and 2-methyl-8-quinolinol chelates of thorium (IV)

(*Recieved* 5 *October* 1961; *in revised form* 20 *November* 1961)

THE composition and structure of the 8-quinolinol and 2-methyl–8-quinolinol chelates of thorium (IV) has been the subject of a number of investigations.(1) Two metal chelates are known for each complexing agent; the "normal" compounds, $Th(Ox)_4$ and $Th(MeOx)_4$ (where Ox^- is the 8-quinolinolate ion and $MeOx^-$ is the 2-methyl–8-quinolinolate ion), and the solvated compounds, $Th(Ox)_4 \cdot HOx$ and $Th(MeOx)_4 \cdot MeOxH$. The chemical composition of the solvated 8-quinolinol complex has been well established by conventional methods;(2, 3, 4) however, the composition of the 2-methyl–8-quinolinol complex is still in doubt. PHILLIPS, EMERY and PRICE(5) found that only the normal chelate was precipitated while VAN TASSEL and WENDLANDT(6) reported the preparation of the stoichioemetric solvated metal chelate. However, CORSINI and GRAHAM(7) reported that only the normal chelate could be prepared. To ascertain whether or not the solvated complexes are true compounds, all of the compounds were prepared and subjected to X-ray diffraction analysis.

EXPERIMENTAL

The normal and solvated metal chelates were prepared as previously described.(4, 5, 6)

The X-ray studies were carried out on a Norelco high–low angle diffractometer using Cu K α radiation. The unit cell dimensions were calculated using Ito's method.(8)

RESULTS

The results of the X-ray studies are given in Table 1 and 2.

Previous studies(4, 9, 10) have shown that the solvated 8-quinolinol chelate is a different species in the solid state than a physical mixture of $Th(Ox)_4$ and 8-quinolinol. In this study, it is seen that the *d*-spacings for the normal and solvated 2-methyl–8-quinolinol are similar, differing by only 0·01–0·03 A for each *h k l* position. Thus, it can be concluded that the solvated and the normal chelate structures are the same and that the solvated chelate is merely a mixture of $Th(MeOx)_4$ and 2-methyl–8-quinolinol.

Department of Chemistry
Texas Technological College
Lubbock, Texas

W. W. WENDLANDT
G. R. HORTON

(1) W. W. WENDLANDT and G. R. HORTON, *J. Inorg. Nucl. Chem.* In press (previous literature references cited).
(2) F. FRERE, *J. Amer. Chem. Soc.* **55**, 4362 (1933).
(3) F. HECHT and W. EHRMANN, *Z. Anal. Chem.* **100**, 98 (1935).
(4) T. MOELLER and M. V. RAMANIAH, *J. Amer. Chem. Soc.* **75**, 3946 (1953).
(5) J. P. PHILLIPS, J. F. EMERY and H. P. PRICE, *Anal. Chem.* **24**, 1033 (1952).
(6) J. H. VAN TASSEL and W. W. WENDLANDT, *J. Amer. Chem. Soc.* **82**, 4821 (1960).
(7) A. CORSINI and R. P. GRAHAM, *Anal. Chim. Acta*, **23**, 248 (1960).
(8) T. ITO, "X-ray Studies on Polymorphism", Maruzen, Tokyo, 1949, pp. 187–228.
(9) J. H. VAN TASSEL, W. W. WENDLANDT and E. STURM, *J. Amer. Chem. Soc.* **83**, 810 (1961).
(10) J. H. VAN TASSEL, Ph.D. Thesis, Texas Technological College (1959).

TABLE 1.—X-RAY LINES OF THE THORIUM CHELATES[b]

$Th(Ox)_4 \cdot HOx$		$Th(MeOx)_4$		$Th(MeOx)_4 \cdot MeOxH$	
d (A) spacing	h k l	d (A) spacing	h k l	d (A) spacing	h k l
10·99	100	9·60	100	9·61	100
10·15	010	8·85	010	8·80	010
9·67	a	7·56	001	7·55	001
8·15	$00\bar{1}$	6·87	a	6·86	a
7·47	110	6·07	$10\bar{1}$	6·07	$10\bar{1}$
7·18	a	5·83	110	5·83	110
6·46	101	4·94	a	4·95	a
6·01	$11\bar{1}$	4·78	200	4·81	200
5·85	a	4·41	020	4·39	020
5·45	200	4·12	$20\bar{1}$	4·13	$20\bar{1}$
5·14	020	3·98	201	4·00	201
4·65	120	3·83	002		
4·15	012	3·77	$2\bar{2}0$	3·78	$2\bar{2}0$
4·05	002	3·42	$21\bar{1}$	3·42	$21\bar{1}$
3·86	021	3·29	$3\bar{1}0$	3·31	$3\bar{1}0$
3·65	121	3·22	112		
3·50	$12\bar{2}$	3·12	a	3·12	a
3·45	310	3·02	311	3·02	311
3·25	202	2·89	220	2·88	220
3·06	222	2·74	031	2·75	031
2·97	320	2·66	$2\bar{2}2$		
2·79	$01\bar{3}$	2·62	130		
2·66	$23\bar{2}$	2·47	131	2·48	131
		2·39	400	2·39	400
		2·33	032	2·34	032

(a) unassigned.
(b) d-spacings for $Th(Ox)_4$ previously given.(9, 10)

TABLE 2.—UNIT CELL DIMENSIONS OF METAL CHELATES

Compound	a (Å)	b	c	α	β	γ	V, Å^3
$Th(Ox)_4$(9)	11·74	10·77	7·42	90°	96°27′	90°′	932
$Th(Ox)_4 \cdot HOx$	10·92	10·64	8·40	105°36′	90°	90°	940
$Th(MeOx)_4$	9·91	9·13	7·66	88°52′	92°17′	105°6′	670

Acknowledgments—The helpful assistance of Dr. E. STURM is gratefully acknowledged This work was supported by the U.S. Atomic Energy Commission through Contract No. AT-(40-1)-2482.

J. Inorg. Nucl. Chem., 1962, Vol. 24, pp. 589 to 592. Pergamon Press Ltd. Printed in Northern Ireland

NEW NEUTRON DEFICIENT BARIUM ISOTOPES*

I. L. Preiss and P. M. Strudler
Yale University, New Haven, Connecticut

(*Received* 10 *January* 1962)

Abstract—New barium activities, produced by heavy ion bombardments of indium and tin, were assigned on the basis of chemistry and their decay to cesium daughters. They are: ^{123}Ba, 2 ± 0·5 min; ^{125}Ba, 6·5 ± 0·5 min; and ^{127}Ba, 10·0 ± 0·5 min. In addition the following half-lives are proposed for previously assigned nuclides: ^{126}Ba, 103 ± 5·0 min, ^{123}Cs, 8·0 ± 0·5 min; ^{125}Cs, 49 ± 5·0 min; and ^{123}Xe, 1·85 ± 0·1 hr.

The availability of high intensity heavy ion beams (having energies of up to 10·5 MeV per nucleon) at the Yale University Heavy Ion Accelerator, facilitates the production of extremely neutron deficient isotopes. The mechanism by which these isotopes are formed is generally recognized as the evaporation of several nucleons from compound nuclei which are themselves neutron deficient and have high excitation energies. For example, the compound system formed in a reaction of ^{14}N and ^{115}In is ^{129}Ba, which itself is seven neutrons removed from the line of beta stability.

The present study was undertaken in order to gain information concerning the half-lives and mass assignments of the neutron deficient isotopes ^{123}Ba through ^{127}Ba not presented in studies of this mass region previously reported.(1,2,3)

The heavy ion reactions used to produce the isotopes of interest were:

^{113,115}In(^{16}O;p,xn)^{123}Ba through ^{129}Ba,
^{113,115}In(^{14}N;xn)^{123}Ba through ^{129}Ba,
Natural Sn(^{16}O;α,xn)^{123}Ba through ^{135}Ba and
Natural Sn(^{12}C;xn)^{123}Ba through ^{135}Ba.

EXPERIMENTAL

Targets of metallic foils of In and Sn (42–60 mg/cm^2) were irradiated with heavy ion beams of ^{16}O, ^{14}N and ^{12}C (10·5 MeV/nucleon) for periods ranging from 1 to 10 min.

In all instances, barium was separated chemically by precipitating either $Ba(NO_3)_2$ from 6 N HCl solution using fuming HNO_3, or as $BaSO_4$ using 1 N H_2SO_4. Suitable hold back as well as Ba carriers were added to the HCl solutions used to dissolve the target material. The extent of decontamination of the Ba fraction, with respect to other radio nuclides produced, was estimated through observation of the characteristic *K* X-rays resulting from the decay of the Ba isotopes. The X-ray spectra were taken using a large gas-flow side window proportional counter, and the peak resolution and energies compared to that found for chemically pure ^{133}Ba (20 per cent at 32 keV). This comparison demonstrates that impurities (such as La, Cs, Xe, I, etc.) *constitute not more than 5 per cent of the observable* activity in the Ba fraction immediately following the chemical separation. Resolution change of the spectra, as well as a shift in the energy peak was noted with time, and hence was an additional confirmation of the growth of Cs daughter activities.

The gross β-decay of the barium fraction was followed using an end window gas-flow proportional counter. The gross decay curves could be resolved into the component half-lives for Ba isotopes listed on Table 1. Because of the growth of the daughter activities, these values represent only an approximation of the true half-lives of the individual Ba activities.

---

* This work was supported by the United States Atomic Energy Commission.

(1) H. B. Mathur and E. K. Hyde, *Phys. Rev.* **95**, 708 (1954).
(2) M. I. Kalkstein and J. M. Hollander, *Phys. Rev.* **96**, 730 (1954).
(3) M. Lindner and R. Osborne, *Phys. Rev.* **88**, (1952).

TABLE 1.—Ba HALF-LIVES RESOLVED FROM GROSS DECAY OF CHEMICALLY SEPARATED Ba (In–^{14}N SYSTEM) AND Cs MILKING

Isotope	Half-life observed (min)		Literature[(4)] half-life (min)
	Gross decay	Cs Milking	
^{123}Ba	1·5–3·5	2·0 ± 0·5	—
^{125}Ba	5–8	6·5 ± 0·5	—
^{126}Ba	103 ± 5		97
^{127}Ba	9·5–11	10·0 ± 0·5	12

TABLE 2.—Cs HALF-LIVES RESOLVED FROM GROSS DECAY CHEMICALLY OF SEPARATED Cs (In–^{12}C SYSTEM)

Isotope	Half-life observed	Literature[(4)]
^{123}Cs	8·0 ± 0·5 min	~6 min
^{125}Cs	49 ± 5 min	45 min
^{127}Cs	6·2 hr	6 hr

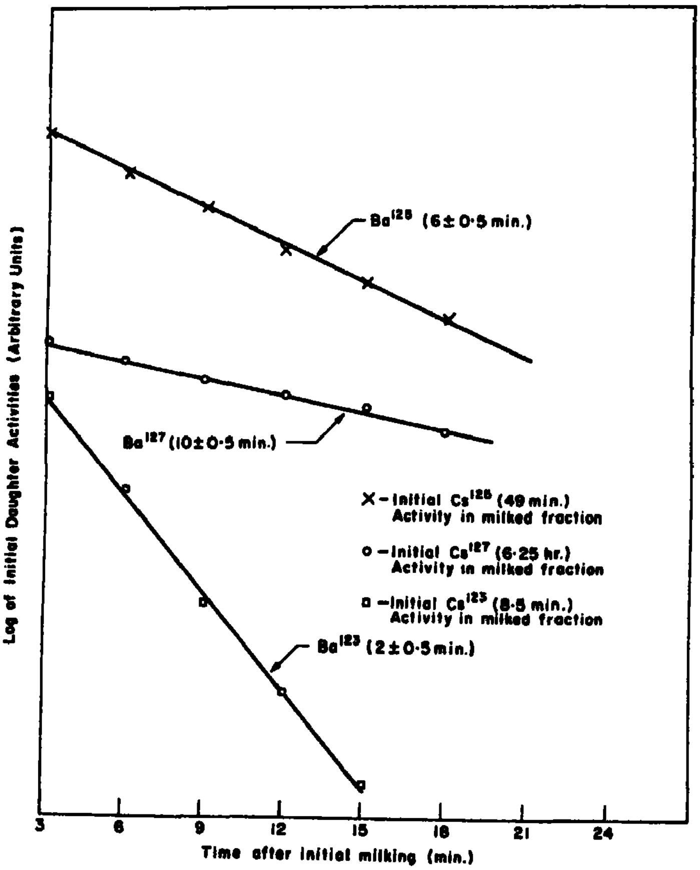

FIG. 1.—Initial activity of cesium isotopes milked from barium chemical fraction vs. time of milking. (In + ^{14}N System).

[(4)] Values from Nuclear Data Sheets (National Academy of Sciences, National Research Council); W. H. SULLIVAN, *Trilinear Chart of Nuclides* (*USAEC*); and D. STROMINGER, J. M. HOLLANDER and G. T. SEABORG, *Rev. Mod. Phys.* 30 (1958).

In order to establish mass assignments for the new barium activities observed, cesium was milked at regular time intervals from Ba separated chemically in other experiments. The barium was precipitated as $Ba(NO_3)_2$, redissolved and cesium precipitated from alcohol solution as Cs_2PtCl_6. The purity of the Cs precipitate was confirmed using X-ray counting as previously described, and the gross β-decay of each milking followed. Each of the gross-decay curves could be resolved into the components listed in Table 2.*

The decrease in the initial activity of each component, then, is a measure of the half-lives of the parent radio nuclides. Typical milking results are shown in Figs. 1 and 2.

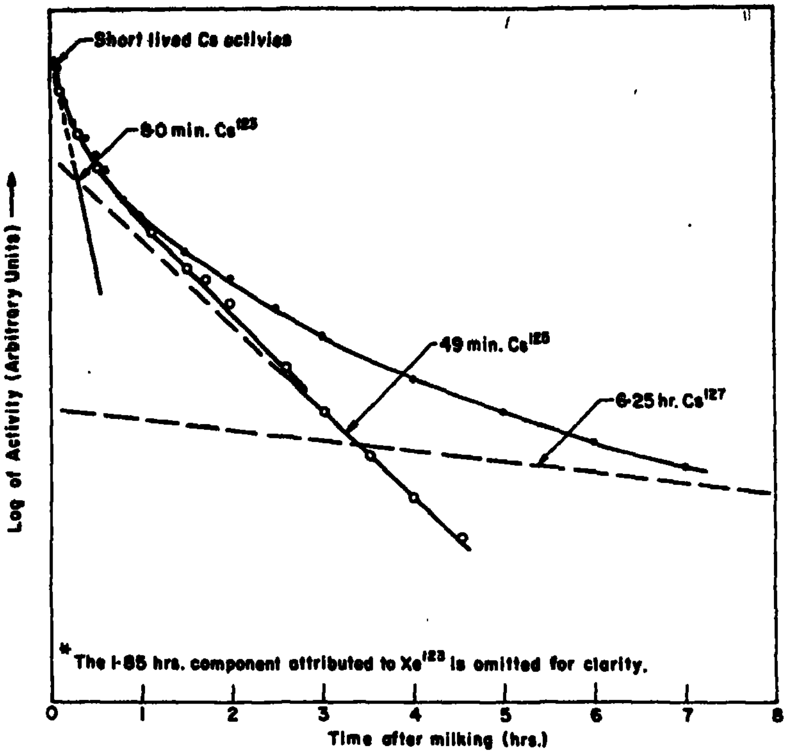

FIG. 2.—A typical 8 hr portion of the gross decay of the cesium milked from a barium chemical fraction. (In–^{14}N System).

In order to confirm the half-lives of the cesium daughters, indium foils were irradiated with 120 MeV carbon, the Cs products separated chemically, and the gross beta decay followed. The gross curves could be resolved into the component half-lives listed in Table 2, and γ-ray spectra, found using a 3 × 3 in. NaI(Tl) crystal and 400 channel pulse-height analyser, demonstrated the presence of known γ-rays resulting from Cs decay. These spectra were found to contain the same energy peaks observed in the Cs samples milked from the barium chemical fraction.

The presence of the chain, ^{123}Ba, ^{123}Cs, ^{123}Xe was confirmed in a separate experiment. Indium targets were irradiated for 1–1·5 min periods with 10·5 MeV per nucleon ^{14}N. The Ba fraction was separated chemically, and Cs daughter activities subsequently separated from the parents following a 4 min growth period (the time of maximum 8 min activity resulting from the decay of a 2 min parent). The decay of the γ-ray spectra of the Cs fraction was followed (using the equipment described above). It was found that the 0·125 MeV γ-ray associated with ^{123}Xe grew in with a period corresponding to the decay of a 7·5–8·5 min parent, and subsequently decayed with a half-life of 1·85 ± 0·05 hr.

The results obtained using both Sn or In, as targets, and ^{16}O, ^{14}N or ^{12}C, as incident heavy ions, were identical within experimental error and demonstrate that the products are not peculiar to the target or heavy ion beam employed.

---

* Although ^{123}Xe (1·85 hr) grows into the Cs fraction, the relative magnitude of the activities, and the time after separation required to establish equilibrium is such that it does not affect the extrapolated initial activities of the Cs components of interest.

CONCLUSIONS

Mass assignments for the new Ba activities were based on the parent daughter genetics using Cs half-lives and γ-ray energies previously reported and/or found in the present study. The proposed half-lives and mass assignments are: ^{123}Ba, 2 ± 0·5 min; ^{125}Ba, 6·5 ± 0·5 min; and ^{127}Ba, 10·0 ± 0·5 min. In addition the following half-lives for ^{126}Ba, ^{123}Xe and the Cs isotopes are proposed: ^{126}Ba, 103 ± 5·0 min; ^{123}Cs, 8·0 ± 0·5 min and ^{125}Cs, 49 ± 5·0 min; ^{123}Xe, 1·85 ± 0·1 hr.

Acknowledgements—The authors wish to thank Professor R. Wolfgang and Dr. I. M. Ladenbauer-Bellis for their interest in this study, and the operating crew of the Heavy Ion Accelerator for their co-operation.

J. Inorg. Nucl. Chem., 1962, Vol. 24, pp. 593 to 600. Pergamon Press Ltd. Printed in Northern Ireland

INFRA-RED SPECTRA AND STRUCTURE OF SOME PHENYLTIN COMPOUNDS

R. C. Poller
Chemistry Department, Queen Elizabeth College, Campden Hill Road,
London, W.8

(*Received 9 November* 1961; *in revised form* 2 *February* 1962)

Abstract—Infra-red spectra of twenty phenyltin compounds have been measured, mainly in the 4000–670 cm^{-1} region. The absorptions are discussed in terms of various structural features in the compounds. Variations in the positions of the benzene ring vibrations have been noted together with some analytically useful bands.

An increasing interest in the chemistry of organotin compounds has become apparent in the last few years, though generally, more emphasis has been placed on synthetic methods than on physical–chemical studies. This was reflected by the absence until recently of any detailed information on the infra-red spectra of organotin compounds, the only exceptions being tetramethyltin(1–5) and tetraphenyltin.(6–8) Within the last year, however, absorptions have been reported for a fairly wide range of alkyltin derivatives(9,10) and Griffiths and Derwish(11) have published a detailed analysis of the absorptions shown by tetraphenyltin and the phenyltin chlorides. Henry and Noltes(12) have examined the spectra of some phenylallyl- and phenylvinyltin compounds and have shown that a band at 1065 cm^{-1} is characteristic of the phenyltin group since it underwent a shift in the analogous silicon, germanium and lead compounds.

It was felt that it would be useful to measure, under identical conditions, the spectra of a wide range of phenyltin compounds of general formula $(C_6H_5)_xSnA_{4-x}$ in which A represented a diversity of chemical types. The measurements were made mainly in the 4000–670 cm^{-1} range and the spectra were examined to determine the effects of the various groups attached to tin on the positions of the phenyl bands and particularly on the position of the characteristic phenyltin band at 1065 cm^{-1}. It will be shown that the results also give information on certain structural problems and that all the spectra show sufficient differences for differentiation between otherwise similar compounds to be possible.

---

(1) H. Siebert, *Z. Anorg. Chem.* **263**, 82 (1950).
(2) W. F. Edgell and C. H. Ward, *J. Amer. Chem. Soc.* **77**, 6486 (1955).
(3) C. F. Kettering and W. W. Sleator, *Physics* **4**, 39 (1933).
(4) N. G. Pai, *Proc. Roy. Soc.* A **149**, 29 (1935).
(5) D. N. Walters and L. A. Woodward, *Proc. Roy. Soc.* A **246**, 119 (1958).
(6) R. D. Kross, V. A. Fassel and M. Margoshes, *J. Amer. Chem. Soc.* **78**, 1332 (1956).
(7) V. A. Fassel and M. Margoshes, *Spectrochim. Acta* **7**, 14 (1955).
(8) C. N. R. Rao *et al.*, *Nature, Lond.* **183**, 1475 (1959).
(9) R. Okawara, D. E. Webster and E. G. Rochow, *J. Amer. Chem. Soc.* **82**, 3287 (1960).
(10) M. P. Brown, R. Okawara and E. G. Rochow, *Spectrochim. Acta*, **16**, 595 (1960).
(11) V. S. Griffiths and G. A. W. Derwish, *J. Mol. Spectrosc.* **2**, 148 (1960).
(12) M. C. Henry and J. G. Noltes, *J. Amer. Chem. Soc.* **82**, 555 (1960).

EXPERIMENTAL

Infra-red measurements

The spectra were measured in the sodium chloride region using a Perkin Elmer Model 137 spectrophotometer; the KBr disk technique was used for all the compounds except phenyltin trichloride which was examined as a liquid film. The spectra of triphenyltin hydroxide, hexaphenyldistannoxane and diphenyltin oxide were also measured in the potassium bromide region, as Nujol mulls, using a Grubb-Parsons G. S. 2A (Series 14) spectrophotometer.

In the tables of absorption frequencies the following abbreviations are used, *w* = weak intensity, *m* = medium intensity, *s* = strong intensity, *sh* = shoulder, *b* = broad.

Preparation of compounds

Compounds 1–14 (see Table 1) were made by standard published procedures and had characteristic melting or boiling points in agreement with the reported values.

Analyses are quoted for the following compounds which do not have characteristic melting points. Diphenyltin oxide, m.p. above 360° (Found C, 49·9; H, 3·7. Calc. for $C_{12}H_{10}OSn$: C, 49·9; H, 3·5%). Triphenyltin fluoride, m.p. above 360° (Found C, 58·65; H, 4·3. Calc. for $C_{18}H_{15}FSn$: C, 58·6; H, 4·1%).

Triphenyltin hydroxide was prepared by the hydrolysis of triphenyltin iodide in ether using 2N sodium hydroxide solution. The product was removed by filtration and purified by two crystallizations from 96 per cent ethanol, after air-drying at slightly above room temperature it had m.p. 120–122°. The melting point of this compound is not particularly characteristic and previous workers have experienced difficulties due to contamination with water and with hexaphenyldistannoxane.⁽¹³⁾ The present product was considered to be pure both from its analysis and its spectrum (see below). (Found C, 58·6; H, 4·6; Sn, 32·0. Calc. for $C_{18}H_{16}OSn$: C, 58·9; H, 4·4; Sn, 32·3%).

Phenyltin triiodide was made by the action of iodine on tetraphenyltin in the absence of a solvent. The product was a yellow solid which, after crystallization from light petroleum (b.p. 40–60°), had m.p. 33–34°; this compound is reported as an oil by previous workers.⁽¹⁴⁾ (Found C, 12·7; H, 0·9. Calc. for $C_6H_5I_3Sn$: C, 12·5; H, 0·9%).

Triphenyltin *p*-nitrophenoxide was prepared by treating hexaphenyldistannoxane with a solution of *p*-nitrophenol (2 mole) in ether and evaporating the mixture in a vacuum desiccator over concentrated sulphuric acid (cf. Reference 15). The crude product was crystallized from cyclohexane to give bright yellow crystals of triphenyltin *p*-nitrophenoxide m.p. 106–108° (D'Ans and Gold⁽¹⁶⁾ give m.p. 101–102°). (Found C, 58·5; H, 3·7; N, 3·05. Calc. for $C_{24}H_{19}O_3NSn$: C, 59·05; H, 3·9; N, 2·9%).

Triphenyltin *p*-toluenesulphonate (this compound has not previously been reported) was prepared by adding silver *p*-toluenesulphonate (1·35 g) to a solution of triphenyltin chloride (2·00 g) in absolute ethanol (40 ml) and boiling the mixture under reflux for 45 min. The silver chloride was filtered off the filtrate evaporated to dryness. The crude product was crystallized from a mixture of chloroform and light petroleum (b.p. 60–80°) to give colourless crystals (1·51 g) m.p. 229–231°, unchanged on further crystallization. (Found C, 57·4; H, 4·2. Calc. for $C_{25}H_{22}O_3SSn$: C, 57·6; H, 4·3%).

DISCUSSION

Benzene ring absorptions (see Table 1)

The spectra of a large number of monosubstituted benzenes have recently been examined by Katritzky and Lagowski⁽¹⁷⁾ who have recorded frequency ranges for a number of phenyl bands. These workers did not examine any compounds with metal atom substituents and it is therefore of interest to compare the present results where, usually, more than one monosubstituted benzene ring is present and, in all cases, the substituent is a heavy one.

The C—H stretching vibrations centred around 3030 cm⁻¹ and the overtone and combination bands in the 2000–1650 cm⁻¹ region were, in general, not well resolved and the discussion here is restricted to the 1500–670 cm⁻¹ range, this includes all the strong intensity absorptions associated with the benzene ring.

---

(13) R. West, R. H. Baney and D. L. Powell, *J. Amer. Chem. Soc.* **82**, 6270 (1960).

(14) A. Tchakirian, M. Lesbre and M. Lewinsohn, *C. R. Acad. Sci., Paris* **202**, 138 (1936).

(15) J. G. A. Luijten and G. J. M. van der Kerk, *Investigations in the Field of Organotin Chemistry*, p. 101. Tin Research Institute (1955).

(16) J. D'Ans and H. Gold, *Ber. Dtsch. Chem. Ges.* **92**, 3076 (1959).

(17) A. R. Katritzky and J. M. Lagowski, *J. Chem. Soc.* 4155 (1958).

(a) *The* 1475 cm^{-1} *band.* A medium to strong intensity band within the range 1480–1468 cm^{-1} was shown by all the compounds except one (No. 15, see Table 1) where it was masked. This band is assigned to a C—C stretching mode by GRIFFITHS and DERWISH(11) who quote the range 1487–1479 cm^{-1} for their four phenyltin compounds. In the purely organic compounds examined by KATRITZKY and LAGOWSKI(17) the range was 1511–1477 cm^{-1} and these authors noted that with heavier substituents in the benzene ring the band was found at the lower frequency end of the range.

(b) *The* 1425 cm^{-1} *range.* With the exception of the C—H out-of-plane vibrations (at 750–670 cm^{-1}) the most intense of the benzene ring bands occurs in the range 1430–1420 cm^{-1} (masked in compound No. 4). This band is assigned to another C—C stretching mode by GRIFFITHS and DERWISH(11) who found corresponding absorptions at 1435–1434 cm^{-1}. KATRITZKY and LAGOWSKI(17) quote the range 1447–1446 cm^{-1} for monosubstituted benzenes with a "heavy" atom substituent. This band was originally quoted(18) at 1429 cm^{-1} for phenylsilicon compounds and has been shown(18) to occur at the same frequency in corresponding germanium and lead compounds.

(c) *The* 1330–1250 cm^{-1} *region.* Three bands, usually of weak or medium intensity, were found in almost all cases around 1300 cm^{-1}. The observed ranges were 1330–1320 cm^{-1} (masked in No. 4), 1302–1290 cm^{-1} (masked in No. 15) and 1258–1250 cm^{-1} (missing or masked in Nos. 11, 12, 13, 15, 19 and 20). It is difficult to quote with certainty the corresponding ranges observed by GRIFFITHS and DERWISH(11) since the higher resolution instrument used by these workers detected other weak bands in this region but the ranges for their compounds are probably 1337–1334, 1305–1304 and 1267–1262 cm^{-1}. No mention is made by BELLAMY(19) or by KATRITZKY and LAGOWSKI(17) of benzene ring absorptions in this region.

(d) *The* 1200–1100 cm^{-1} *region.* Two bands, usually of weak intensity, occur in this region, at 1188–1178 cm^{-1} (masked in Nos. 15 and 20, missing in No. 17) and at 1160–1145 cm^{-1} (all compounds). Of the compounds examined by KATRITZKY and LAGOWSKI(17) generally only those compounds with electron donating substituents absorbed in this region and the ranges quoted are 1181–1170 cm^{-1} and 1160–1150 cm^{-1}. Both of these bands are assigned to C—H in-plane deformations.(20)

(e) *The* 1070 cm^{-1} *band.* There is a very sharp, strong intensity, band occurring in the range 1076–1062 cm^{-1} for all the compounds except phenyltin triiodide where the effect of the heavy SnI_3 group is to displace the absorption to 1055 cm^{-1}. HENRY and NOLTES(18) have shown that a band at 1065 cm^{-1} is characteristic of the phenyltin group and undergoes displacement in compounds where the phenyl group is attached to other Group IV elements. While this band is undoubtedly of great value in recognizing the phenyltin group the present results show that substituents on the tin atom cause variations in the frequency of this band so that overlapping with the phenylgermanium band (1080 cm^{-1}) and the phenyllead band (1052 cm^{-1}) could occur. This band has been noted in the spectra of monosubstituted benzenes by a number of workers and assigned to a C—H in-plane deformation vibration;(11,20) the absorption is much more intense when the substituent in the benzene ring is a metal atom.

(18) C. W. YOUNG *et al.*, *J. Amer. Chem. Soc.* **70**, 3758 (1948).

(19) L. J. BELLAMY, *The Infra-red Spectra of Complex Molecules* (2nd Ed.), Chapt. 5. Methuen, London (1958).

(20) R. R. RANDLE and D. H. WHIFFEN, *Report on Conference of Molecular Spectroscopy*, Paper No. 12. Institute of Petroleum (1954).

Table 1.—List of compounds and melting points.

	Compound	m.p. (°C)	Literature m.p. (°C)	1475 cm^{-1} band	1425 cm^{-1} band	The 1330–1250 cm^{-1} region		
1.	Tetraphenyltin	228–9	225–6[21]	1477 *m*	1424 *s*	1328 *w*	1300 *w*	1255 *w*
2.	Hexaphenylditin	239–241	232·5[22]	1472 *m*	1420 *s*	1325 *m*	1292 *m*	1250 *w*
3.	Hexaphenyldistannoxane	123–4	124[23]	1475 *m*	1422 *s*	1325 *w*	1295 *w*	1255 *w*
4.	Triphenyltin acetate	120–1	121–2[24]	1480 *s*	—	1328 *m*	1302 *m*	1255 *w*
5.	Triphenyltin thiophenoxide	102–4	103[25]	1472 *m*	1422 *s*	1328 *w*	1298 *m*	1255 *w*
6.	*bis*(Triphenyltin) sulphide	145–6	141·5–143[26]	1478 *m*	1426 *s*	1328 *w*	1296 *w*	1255 *w*
7.	Triphenyltin benzoate	84–85·5	82·5–84[27]	1477 *m*	1425 *s*	—	1300 *s*	1252 *m*
8.	Triphenyltin chloride	105–6	106[28]	1471 *m*	1420 *s*	1325 *w*	1295 *w*	1255 *w*
9.	Triphenyltin bromide	120–1	120·5[29]	1475 *m*	1424 *s*	1328 *w*	1294 *w*	1258 *w*
10.	Triphenyltin iodide	122–4	121[29]	1477 *m*	1426 *s*	1328 *m*	1298 *w*	1258 *w*
11.	Diphenyltin dichloride	40–41·5	42[28]	1473 *m*	1426 *s*	1326 *m*	1292 *w*	—
12.	Diphenyltin diiodide	72–3	71–2[30]	1473 *m*	1426 *s*	1322 *m*	1292 *w*	—
13.	Diphenyltin sulphide	184–185·5	183–4[31]	1472 *m*	1424 *s*	1325 *m*	1292 *m*	—
14.	Phenyltin trichloride	120–125/4·5 mm†	142–3/25 mm†[32]	1478 *s*	1430 *s*	1330 *s*	1300 *w*	1258 *w*
15.	Triphenyltin *p*-nitrophenoxide*	106–8	101–2[16]	—	1425 *s*	1320 *s*	—	—
16.	Diphenyltin oxide*	—	—	1475 *m*	1420 *s*	1320 *w*	1290 *w*	1250 *w*
17.	Triphenyltin fluoride*	—	—	1479 *m*	1424 *s*	1328 *w*	1300 *w*	1255 *w*
18.	Triphenyltin hydroxide*	120–2	118[33]	1475 *m*	1420 *s*	1325 *w*	1292 *w*	1255 *w*
19.	Phenyltin triiodide*	33–34	—	1468 *m*	1422 *s*	1320 *m*	1290 *m*	—
20.	Triphenyltin *p*-toluenesulphonate	229–231	—	1477 *m*	1424 *s*	1325 *w*	1295 *w*	—

* Further details for these compounds are given in the Experimental section.

† Boiling point.

(f) *The* 1025–900 cm^{-1} *region.* Three and sometimes four bands occur in this region All the compounds show a band, usually of medium intensity, in the range 1025–1014 cm^{-1} which is assigned to a C—H in-plane deformation mode.[11,20] All the compounds except one show strong to medium intensity absorption within the narrow range 999–996 cm^{-1}, in phenyltin triiodide the SnI_3 group causes a shift in the position of absorption to 992 cm^{-1}. This band is due to a ring vibration[11,20] and it is

---

[21] A. Polis, *Ber. Dtsch. Chem. Ges.* **22**, 2915 (1889).

[22] E. Krause and R. Becker, *Ber. Dtsch. Chem. Ges.* **53**, 173 (1920).

[23] O. Schmitz-Dumont, *Z. Anorg. Chem.* **248**, 289 (1941).

[24] G. J. M. van der Kerk and J. G. A. Luijten, *J. Appl. Chem.* **6**, 49 (1956).

[25] D. Blake, G. E. Coates and J. M. Tate, *J. Chem. Soc.* 622 (1961).

[26] J. G. Noltes and G. J. M. van der Kerk, *Chem. and Industr.* 294 (1959).

[27] H. Gilman and J. Eisch, *J. Org. Chem.* **20**, 763 (1955).

[28] B. Aronheim, *Ann.* **194**, 145 (1878).

[29] E. Krause, *Ber. Dtsch. Chem. Ges.* **51**, 912 (1918).

[30] R. H. Bullard and W. B. Robinson, *J. Amer. Chem. Soc.* **49**, 1368 (1927).

[31] I. T. Eskin, A. N. Nesmeyanov and K. A. Kocheshkov, *J. Gen. Chem.* (*U.S.S.R.*) **8**, 35 (1938).

[32] K. A. Kocheshkov, *J. Russian Phys-Chem. Soc.* **61**, 1385 (1929).

[33] K. A. Kocheshkov *et al.*, *J. Gen. Chem.* (*U.S.S.R.*) **6**, 1672 (1936).

FREQUENCIES OF BENZENE RING ABSORPTIONS

The 1200–1100 cm⁻¹ region		1070 cm⁻¹ band	The 1025–900 cm⁻¹ region				730 cm⁻¹ band	700 cm⁻¹ band
1178 *w*	1150 *w*	1072 *s*	1025 *w*	999 *m*	979 *w*	914 *w*	736 *s*	703 *s*
1185 *m*	1152 *w*	1068 *s*	1018 *m*	996 *s*	985 *sh*, 968 *w*	910 *w*	730 *s*	700 *s*
1185 *w*	1150 *w*	1072 *m*	1020 *w*	996 *m*	—	918 *w*, 912 *w*	732 *s*, 725 *s*	700 *sh*, 696 *s*
1186 *w*	1152 *w*	1062 *m*	1025 *m*	998 *m*	—	918–910 *w,b*	735 *sh*, 732 *s*	699 *s*
1188 *w*	1150 *w*	1070 *s*	1022 *m*	996 *m*	985 *sh*, 975 *w*	920 *w*, 909 *w*	750 *m*, 733 *s*	701 *s*, 691 *s*
1185 *w*	1150 *w*	1070 *s*	1020 *m*	996 *m*	970 *w*	915 *w*	732 *sh*, 728 *s*	699 *s*
1185 *w*	1150 *w*	1062 *s*	1025 *m*	997 *m*	—	913 *w*	732 *s*, 723 *s*	698 *s*
1185 *w*	1152 *w*	1072 *s*	1020 *m*	997 *m*	974 *w*	925–915 *w,b*	733 *s*	698 *s*
1185 *w*	1152 *w*	1070 *s*	1020 *m*	996 *m*	975 *w*, 970 *w*	919 *w*	732 *s*	698 *s*
1185 *w*	1155 *w*	1072 *m*	1022 *m*	999 *m*	973 *w*	920 *w*	737 *sh*, 732 *s*	698 *s*
1185 *w*	1155 *w*	1068 *m*	1020 *w*	996 *m*	—	—	730 *s*	693 *s*
1185 *w*	1155 *w*	1065 *m*	1018 *m*	996 *m*	—	918 *w*, 907 *w*	736 *s*. 727 *s*	694 *sh*, 689 *s*
1182 *w*	1150 *w*	1065 *s*	1020 *m*	996 *s*	—	920–910 *w,b*	736 *sh*, 729 *s*	695 *s*
1188 *w*	1160 *w*	1065 *s*	1020 *m*	997 *s*	985 *w*, 970 *w*	918 *w*	731 *s*	689 *s*
—	1155 *s*	1072 *m*	1022 *m*	996 *m*	—	—	732 *s*	698 *s*
1182 *w*	1148 *w*	1075 *m*	1022 *w*	997 *m*	985 *w*, 960 *w*	907 *w*	726 *sh*, 732 *s*	694 *s*
—	1154 *w*	1076 *s*	1022 *m*	997 *m*	986 *w*, 970 *w*	920 *w*	736 *s*, 727 *s*	700 *s*
1185 *w*	1145 *w*	1075 *s*	1020 *m*	997 *m*	978 *w*, 967 *w*	—	735 *s*, 725 *s*	695 *s*
1182 *m*	1150 *w*	1055 *s*	1014 *s*	992 *s*	980 *w*, 962 *w*	900 *w*	729 *s*	685 *s*
—	1150 *m*	1070 *s*	1025 *s*	996 *s*	—	922–910 *w,b*	731 *s*	697 *s*

noteworthy that not all the compounds examined by KATRITZKY and LAGOWSKI(17) absorbed in this region and that the variation in frequency was much greater (1007–990 cm^{-1}).

Weak absorptions were also noted at 986–960 cm^{-1} (12 compounds only, band often split) and at 925–900 cm^{-1} (17 compounds only, band often split). These bands have been attributed to C—H out-of-plane deformation modes.(11,30)

(g) *The* 750–670 cm^{-1} *region.* The two strong intensity C—H out-of-plane deformation vibrations are centred around 730 and 700 cm^{-1}. In a number of cases splitting of one or other of these bands occurs and this, together with differences in the frequency, intensity and shape of these bands, makes them particularly suitable for distinguishing between different phenyltin compounds.

Bands associated with the Sn—O *group*

To obtain an approximate value for the Sn—O stretching frequency an estimate of the force constant was made using GORDY'S rule.(34) Taking electronegativity values of 1·9 for tin and 3·5 for oxygen and an Sn—O bond length of 2·02 Å (from the sum of the covalent radii corrected for the electronegativity difference(35)) a force constant of 2·7 × 10^{5} dyn/cm was obtained. This gave a stretching frequency of 570 cm^{-1}. Although this figure must be regarded as a first approximation, it is in good agreement with the range 643–580 cm^{-1} found by ROCHOW *et al.*(10) for methyltin compounds containing the Sn—O—Sn group.

---

(34) W. GORDY, *J. Chem. Phys.* **14**, 305 (1946).

(35) L. PAULING, *The Nature of the Chemical Bond* (3rd Ed.) p. 229. Cornell University Press, Ithaca (1960).

Infra-red measurements on triphenyltin hydroxide, hexaphenyldistannoxane and diphenyltin oxide were extended to cover most of the KBr range down to about 475 cm^{-1}. The results were somewhat surprising and the frequencies for the bands tentatively assigned to the Sn—O group are shown in Table 2 together with some results for other organotin compounds.

TABLE 2.—ABSORPTION FREQUENCIES FOR BANDS ASSOCIATED WITH THE Sn—O GROUP

Compound	Frequency (cm^{-1})	Reference
(1) Triphenyltin hydroxide	912 *s*, 898 *s*	
(2) Triethyltin hydroxide*	855 *s*	36
(3) Hexaphenyldistannoxane	777 *s*	
(4) Hexapropyldistannoxane	780–765 *s,b*, 500 *s*	37
(5) Hexabutyldistannoxane	787–763 *s,b*, 500 *s*	37
(6) Diphenyltin oxide	571 *s*, 553 *sh*	
(7) Dimethyltin oxide	580 *s*	10
(8) $[Cl(CH_3)_2Sn{\cdot}O{\cdot}Sn(CH_3)_2Cl]_2$	600 *s*, 572 *sh*	10
(9) $MeSnO_{\frac{3}{2}}$	643 *s*	10

* The spectrum of this compound was measured in the NaCl region only; the frequency was read from the published absorption curve.

The results in Table 2 show that the pattern of absorption in the organotin oxides is very different from that found in the corresponding silicon compounds. The asymmetric Si—O—Si stretch frequency in simple disiloxanes occurs in the range 1100–1000 cm^{-1} and although the complexity of this band increases with increasing chain length the organopolysiloxanes absorb at essentially the same frequency.(38) The compounds quoted in Table 2 fall into two groups with compounds 6–9 absorbing in the KBr range at 643–553 cm^{-1} and compounds 1–5 absorbing in the NaCl range at much higher frequencies. It may be significant that compounds 6–9 all show coordination from oxygen to tin. The disubstituted tin oxides R_2SnO are usually described as linear polymers but their physical properties, particularly their general insolubility and infusibility, indicate that the Sn·O·Sn·O chains in those compounds are cross-linked by co-ordination from an oxygen atom in one chain to a tin atom in another chain. The compound $CH_3SnO_{\frac{3}{2}}$ is interesting in that it appears to be the first example of a dehydrated stannonic acid. This material will possess a cross-linked polymeric structure which, it is considered, will be stabilized by co-ordination. Compound 8 was originally formulated(10) as the monomer but it has since been shown(39) that it is dimeric and that in this type of dimeric distannoxane the two molecules are coupled by coordination from oxygen to tin.

Of the high frequency absorptions shown by compounds 1–5 the strong bands around 900 cm^{-1} shown by the trisubstituted tin hydroxides are the most remarkable. While an assignment of these high frequency bands to the Sn—O stretching vibration

(36) L. DOMANGE, and J. GUY, *Ann. Pharm. Franc.* **16**, 161 (1958).

(37) R. C. POLLER, Unpublished results.

(38) A. L. SMITH, *Spectrochim. Acta* **16**, 101 (1960).

(39) (a) R. OKAWARA, *Proc. Chem. Soc.* 383 (1961). (b) D. L. ALLESTON, A. G. DAVIES and B. N. FIGGIS, *Ibid.* 457 (1961).

seems very unlikely it should be noted that, except for one very weak intensity band, triphenyltin hydroxide does not appear to absorb in the KBr region. A partial explanation for the higher frequency absorptions shown by compounds 1–5 may be that, in these compounds, some overlap between the oxygen *p*-orbitals and the *d*-orbitals on tin occurs. The resulting higher bond order would cause an increase in the force constant leading to a higher vibration frequency. It has been predicted(40) that *dπ–pπ*-bonding of this nature should be as well developed in tin as in silicon compounds. This was found(41) to be the case for π-bonding between aromatic carbon and tin and silicon, though from acidity studies West *et al.*(18) concluded that there was no significant π-bonding between tin and oxygen in triphenyltin hydroxide. In compounds 6–9 the oxygen *p*-electrons are involved in coordination and are less available for π-bonding.

The existence of these characteristic strong intensity peaks at 777 cm^{-1} for hexaphenyldistannoxane and at 912 and 898 cm^{-1} for triphenyltin hydroxide is experimentally very useful since these compounds have similar melting points and are readily interconvertible. In addition to the analytical data the absence of any absorption at 777 cm^{-1} in the spectrum of triphenyltin hydroxide showed that the material was free from the distannoxane. (*Cf.* West *et al.*(18) who concluded that their specimens of the hydroxide contained considerable quantities of hexaphenyldistannoxane.)

The spectrum of triphenyltin *p*-nitrophenoxide was too complex for a band to be assigned to the Sn—O group with any certainty but it was considered that a strong intensity composite band at 868–862 cm^{-1} was probably due to an overlap of an Sn—O band with the C—N band which usually occurs near 850 cm^{-1} in aromatic nitro-compounds(42).

Triphenyltin-acetate, benzoate and p-toluenesulphonate

The C—O stretching vibrations for the triphenyltin carboxylates are shown in Table 3.

Table 3.—C—O stretching frequencies in cm^{-1}

Compound	Sym. stretch	Asym. stretch	Separation
Triphenyltin acetate	1425 *s*	1530 *s*	105
Triphenyltin benzoate	1335 *s*	1620 *s*	285

The strong absorption associated with the C=O stretching mode in esters is absent in these compounds although it is present in the analogous silicon compounds.(43) The absorptions for triphenyltin acetate are similar to those obtained by Okawara *et al.*(9) for a number of methyltin acetates and these authors concluded that their compounds were essentially ionic and that the absorption bands were those of the acetate ion. It has recently been pointed out,(44) however, that an acetate group which was acting as a chelate, or bridging group, would be expected to show C—O stretching frequencies very similar to those of an ionic acetate. From the available evidence no firm decision can be made between these two alternatives but since triphenyltin acetate and benzoate (like the alkyltin acetates) have relatively low melting points and are soluble in warm petroleum ether it seems probable that they are essentially covalent compounds containing bidentate carboxyl groups. The significance of the degree of separation of the two C—O stretching frequencies in this type of compound, has been discussed(45,46) but it is difficult to explain why, in the present work, the benzoate should show a much greater separation than the acetate. This is the reverse of the situation in the six trimethyltin carboxylates examined by Okawara *et al.*(9) where the separation increases with the strength of the carboxylic acid (a plot of the C—O band separations taken from Okawara's paper against the pK values for the acids gives a straight line for all the compounds except trimethyltin formate).

---

(40) D. P. Craig *et al.*, *J. Chem. Soc.* 332 (1954).

(41) J. Chatt and A. A. Williams, *J. Chem. Soc.* 4403 (1954).

(42) R. R. Randle and D. H. Whiffen, *J. Chem. Soc.* 4153 (1952).

(43) A. L. Smith, *Spectrochim. Acta* **16**, 97 (1960).

(44) I. R. Beattie and T. Gilson, *J. Chem. Soc.* 2585 (1961).

Esters of sulphonic acids show a strong absorption in the range 1420–1330 cm^{-1}(47) and triphenyltin *p*-toluenesulphonate does not absorb at, or close to, this region. Strong intensity absorptions are shown at 678, 1040 and 1188 cm^{-1} which are consistent with an ionic sulphonate but the alternative of a tridentate sulphonate grouping cannot be ruled out.

Miscellaneous

All the compounds examined have the general formula $(C_6H_5)_nSnA_{4-n}$ and in twelve of them (Nos. 1, 2, 6, 8–14, 16, 17 and 19, see Table 1) the group A does not absorb in the sodium chloride region so that all of these compounds show only benzene ring absorptions and their spectra, except for the minor variations already discussed, are essentially the same. It follows that, as expected, absorptions associated with the tin–halogen and tin–sulphur groups occur at frequencies below 670 cm^{-1}.

The structures of these twelve compounds are straightforward with two exceptions. Triphenyltin fluoride is usually described as an ionic compound in view of its infusibility, but Beattie and Gilson(44) have shown that, for trisubstituted tin fluorides, a polymeric structure containing five-co-ordinate tin and bridging fluorine atoms may be preferred.

The structures of the disubstituted tin sulphides have not been widely investigated but Harada(48) has shown that dimethyltin sulphide and diethyltin sulphide are trimers with, presumably, a cyclic structure. The molecular weight of diphenyltin sulphide was measured cryoscopically in benzene and the results (Found 916, 923: required for trimer 914·9) showed that the correct formulation for this compound is $[(C_6H_5)_2SnS]_3$ so that the structure is similar to that of the corresponding alkyl compounds.

Acknowledgements—The author thanks Dr. A. G. Davies for helpful discussion, Dr. M. D. Johnson for making available the Grubb-Parsons spectrophotometer, and Mr. A. Sarsfield for experimental assistance.

(45) K. Nakamoto *et al.*, *J. Amer. Chem. Soc.* **79**, 4904 (1957).

(46) J. Lewis and R. G. Wilkins, *Modern Co-ordination Chemistry*, p. 369. Interscience, New York (1960).

(47) L. J. Bellamy, *The Infra-red Spectra of Complex Molecules* (2nd Ed.) p. 364. Methuen, London (1958).

(48) T. Harada, *Bull. Chem. Soc. Japan* **17**, 283 (1942).

J. Inorg. Nucl. Chem., 1962, Vol. 24, pp. 601 to 608. Pergamon Press Ltd. Printed in Northern Ireland

INFRA-RED SPECTRA OF METAL COMPLEXES OF RIBOFLAVIN

J. T. SPENCE and E. R. PETERSON
Department of Chemistry, Utah State University, Logan, Utah

(*Received* 6 *November* 1961; *in revised form* 17 *January* 1962)

Abstract—The infra-red spectra of solid Cu(II), Co(II), Mn(II), Fe(II), Ni(II) and Ag(I) complexes of riboflavin and the Cu(II) complexes of 6,7-dimethylalloxazine (lumichrome) and 2,4-dihydroxypteridine have been examined. The spectra indicate dipolar-ion chelates involving the 4-carbonyl group of riboflavin are formed with the divalent metals in the solid state.

RIBOFLAVIN has been reported by ALBERT⁽¹⁾ to form 1:1 and 2:1 complexes with divalent metal ions in aqueous solution. Using potentiometric titration techniques he evaluated stability constants for these complexes, although the results were hampered somewhat by precipitation. FOYE and LANGE⁽²⁾ isolated solid divalent metal-ion complexes of riboflavin containing two metal ions per riboflavin molecule. They reported that when a solution of metal salt was added to a solution of riboflavin, initially at pH 9, a substantial drop in pH occurred, and a coloured precipitate was formed immediately. Furthermore, until two equivalents of metal ion had been added, tests for metal ion in solution by means of dithizone and ferricyanide were negative. In addition, paper chromatograms indicated two spots, one for riboflavin and one for the complex until two equivalents of metal ion had been added, at which time the spot for riboflavin disappeared leaving only the spot for the complex. This work has been questioned by various authors⁽³,⁴,⁵⁾ HEMMERICH and FALLAB⁽³⁾, on the basis of an analysis of potentiometric titration curves, have concluded that riboflavin forms only very weak complexes in solution, and that the curves may be explained by the formation of $Cu(OH)^+$. Their work, however, was done in dioxane–water mixtures, while ALBERT worked in aqueous solution. These authors also reported that the precipitate, isolated at pH 6, obtained in the titration of the riboflavin–copper (II) complex gave unreproducible amounts of copper upon analysis and they suggested the precipitate may be $Cu(OH)_2$ containing adsorbed riboflavin. However, this precipitate was obtained at a pH different from that used by FOYE and LANGE and was not purified by extensive extraction with acetone, a procedure reported by FOYE and LANGE to be necessary in order to obtain pure compounds.

In connection with other studies on biochemical complexing agents, solid metal complexes of riboflavin and related compounds have been prepared in this laboratory and it seemed of interest to examine their infra-red spectra to determine if this could contribute to the solution of the problem. In the present work, the infra-red spectra of the complexes of riboflavin with Cu(II), Fe(II), Ni(II), Co(II), Mn(II) and Ag(I),

⁽¹⁾ A. ALBERT, *Biochem. J.* **54**, 646 (1953).
⁽²⁾ W. V. FOYE and W. E. LANGE, *J. Amer. Chem. Soc.* **76**, 2199 (1954).
⁽³⁾ P. HEMMERICH and S. FALLAB, *Helv. Chim. Acta* **41**, 498 (1958).
⁽⁴⁾ T. R. HARKINS and H. FREISER, *J. Phys. Chem.* **63**, 309 (1959).
⁽⁵⁾ D. E. METZLER and I. F. BAARDA, *Biochem. Biophys. Acta* **50**, 463 (1961).

and the Cu(II) complexes of 6,7-dimethylalloxazine (lumichrome) and 2,4-dihydroxypteridine are reported and discussed.

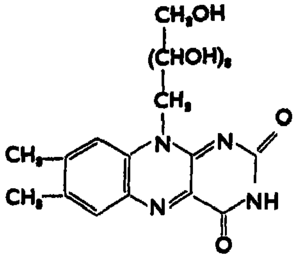

Riboflavin

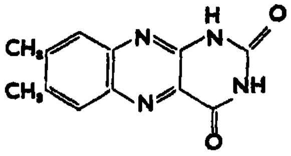

6,7-dimethylalloxazine
(lumichrome)

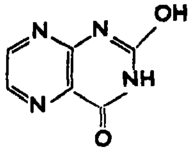

2,4-dihydroxypteridine

EXPERIMENTAL

Riboflavin was purchased from Nutritional Biochemicals Corp. and its purity checked by paper chromatography. The divalent metal complexes of riboflavin were prepared according to the method of Foye and Lange.[3] The Ag(I)–riboflavin complex (RAg) was prepared as described by Metzler and Baarda[5] and the Ag(I)–(riboflavin)$_2$ [(R$_2$Ag)Na] complex as described by Hemmerich and Bamberg.[6] The 2,4-dihydroxypteridine was synthesized and purified according to the procedure of Weijlard *et al.*[7] Lumichrome was synthesized as described by Stern and Holiday[8] and purified by recrystallization from ethanol.

The copper (II) complex of 2,4-dihydroxypteridine was prepared by dissolving 1·64 g (0·01 mole) in 100 ml of water and adjusting the pH to 6·5. A solution of 1·21 g (0·005 moles) of $Cu(NO_3)_2 \cdot 3H_2O$ was added slowly with stirring and the pH was kept in the range of 6·5–7 by simultaneous addition of 10 per cent sodium hydroxide. With the addition of the metal the pH drops and a light green precipitate forms. After the addition was complete, the precipitate was filtered with suction, washed with water and dried *in vacuo* over P_2O_5 at 75°C for 8 hr. (Found: C, 32·44; H, 2·77; N, 24·54; Cu (polarographically), 14·3. Calc. for $(C_6H_3O_2N_4)_2Cu \cdot 3H_2O$: C, 32·47; H, 2·73; N, 25·25; Cu, 14·32%).

The copper(II) complex of lumichrome was prepared by mixing 0·24 g (0·001 mole) of lumichrome in 100 ml of water and adjusting the pH to 9, centrifuging the suspension to remove the very small amount of undissolved material and adding 0·096 g (4 × 10^{-4} mole) of $Cu(NO_3)_2 \cdot 2H_2O$ to the supernatant. The pH of the solution was kept constant by simultaneous addition of dilute NaOH. As the metal ion was added, a dark green precipitate formed. After addition of the metal ion, the precipitate was filtered with suction, washed with water and extracted for 2 hr in a soxhlet extractor with ethanol. It was then dried *in vacuo* over P_2O_5 at 75° for 5 hr. (Found: C, 40·50; H, 3·95; Cu (polarographically), 16·9. Calc. for $C_{12}H_8N_4O_2 \cdot Cu \cdot 3H_2O$: C, 40·27; H, 3·94; Cu, 17·75%.)

Infra-red spectra were obtained on a Perkin-Elmer Model 21 double beam recording spectrophotometer equipped with sodium chloride optics, using the potassium bromide disc technique. Approximately 10^{-4} moles of each compound were mixed thoroughly with 400 mg of potassium bromide and pressed. Spectra were recorded under identical conditions and regions of particular interest were obtained at slow scanning speeds.

RESULTS AND DISCUSSION

Fig. 1 shows the infra-red spectra of riboflavin and its complexes in the region of 2000–1000 cm^{-1}. Riboflavin undoubtedly exists with the four oxygen in the keto form.

---

(6) P. Hemmerich and P. Bamberg, *Helv. Chim. Acta* **44**, 1001 (1961).

(7) J. Weijlard, M. Tishler and A. Frickson, *J. Amer. Chem Soc.* **67**, 804 (1945).

(8) K. G. Stern and R. Holiday, *Ber. Dtsch. Chem. Ges.* **67**, 1442 (1934).

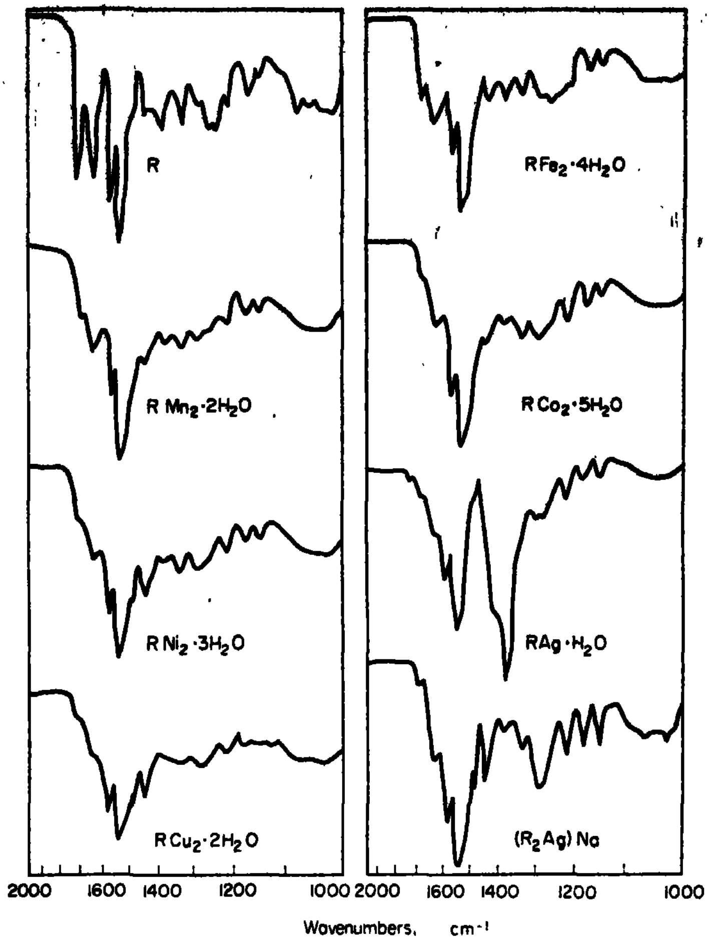

FIG. 1.—Infra-red spectra of riboflavin (R) and riboflavin metal complexes (R_xM_y) in KBr.

BROWN and MASON(9), in a study of hydroxypteridines, concluded that 4-hydroxypteridine exists in the keto form, and riboflavin has a similar structure. This conclusion is supported by the work of HEMMERICH and co-workers on the chemical properties of riboflavin.(10) Furthermore, MASON and BROWN noted that the 4-keto group absorbs at a wavelength near 1710 cm^{-1}. On this basis, the peak at 1725 cm^{-1} can be assigned to the 4-carbonyl group.(11) This assignment is substantiated by HEMMERICH *et al.*, who reported the infra-red spectra of derivatives of riboflavin.(12) This assignment is further strengthened by the work of SHORT and THOMPSON(13) on substituted uracils, and by the spectrum of lumichrome and 2,4-dihydroxypteridine (discussed below). The peak at 1645 cm^{-1} is more difficult to identify. It may be due to the 2-carbonyl group, although the carbonyl group of 2-hydroxypteridine absorbs at 1681

(9) D. J. BROWN and S. F. MASON, *J. Chem. Soc.* 3443 (1956).

(10) P. BAMBERG, P. HEMMERICH and H. ERLENMEYER, *Helv. Chim. Acta* 43, 395 (1960).

(11) L. J. BELLAMY, *The Infra-red Spectra of Complex Molecules* (2nd Ed.), p. 203. J. Wiley, New York (1959).

(12) P. HEMMERICH, B. PRIJS and H. ERLENMEYER, *Helv. Chim. Acta* 43, 372 (1960).

(13) L. N. SHORT and H. W. THOMPSON, *J. Chem. Soc.* 168 (1952).

cm^{-1}. Again, it may be due to —C=N— absorption which overlaps this region[11]. The peaks at 1578 cm^{-1} and 1545 cm^{-1} are undoubtedly amide II bands, arising from —C=N— absorption.

It will be noted that in all the complexes the 4-carbonyl absorption at 1725 cm^{-1} has almost completely disappeared, the absorption at 1645 cm^{-1} is greatly reduced and the amide II bands are relatively unaffected except for a general broadening. The almost complete disappearance of the peak at 1725 cm^{-1} in the metal complexes can be ascribed to the bonding of a metal ion at the four position in an oxinate-like chelate structure, converting the keto form to the enol form with the subsequent loss of the carbonyl absorption.

Silver (I) forms two complexes with riboflavin. The first (RAg) is obtained at a pH of 7 from a solution equal molar in riboflavin and silver. It is apparent from recent work[5,6] that this complex is somewhat different from those of the divalent metals. It is brilliant red in solution, with an electronic absorption spectrum similar to that of the semiquinone radical, rhodoflavin. It has been proposed by HEMMERICH[6] that it is best represented as a Ag(II)-riboflavin semi-quinone chelate in which the silver ion has transferred an electron to riboflavin:

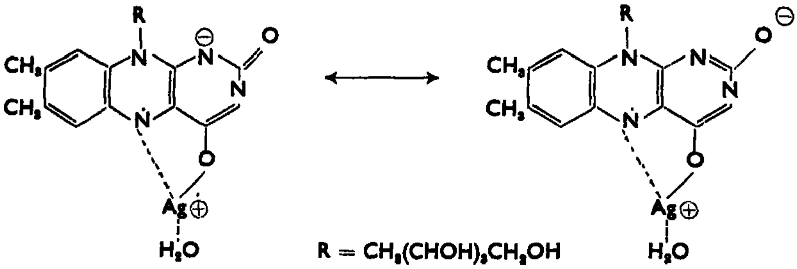

The infra-red spectrum of this complex is similar to that of the divalent metal complexes. Again, the 4-carbonyl absorption has disappeared and the absorption at 1645 cm^{-1} is lost. The complete absence of any absorption in the carbonyl region indicates the second resonance structure is preferred. In addition, a new, very strong peak has appeared at 1380 cm^{-1}. It is possible that this peak is due to the new —C—N— bond or perhaps it represents some absorption peculiar to the semi-quinone form. A definite assignment of this peak is not possible. In any case, the spectrum of RAg indicates a structure similar in the carbonyl region to that of the divalent metal complexes.

The second silver complex [(R_2Ag)Na] is obtained at a pH of 10 from a solution in which the riboflavin/silver ratio is 2/1. This complex appears to be quite similar to the divalent metal complexes. It is deep orange in colour and very insoluble in water. HEMMERICH has proposed the following structure for this compound.[6]

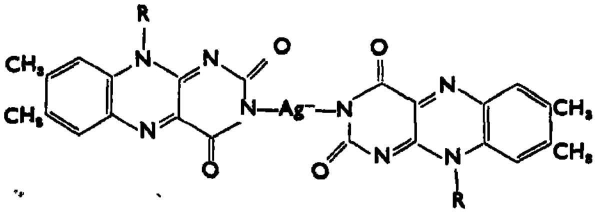

This structure seems unlikely. The spectrum is identical in the carbonyl region to that of RAg, and again indicates loss of the 4-carbonyl group and severe diminution of the 1645 cm^{-1} absorption. It is distinguished from the spectrum of RAg only by the loss of the strong peak at 1380 cm^{-1} and some small differences in the 1100 cm^{-1}–1000 cm^{-1} region.

Lumichrome and 2,4-dihydroxypteridine were also studied since they have structures quite similar to riboflavin. In addition, they do not have the polyol side chain and therefore provided an opportunity to evaluate the effect of this group on the structure of the riboflavin complexes. The pteridine forms a copper(II) complex that has a pteridine/metal ion ratio of 2/1, while the lumichrome–copper(II) complex has a 1/1 ratio. The reason for this difference is that the methylene group of the benzene ring of lumichrome, being "*ortho*" to the nitrogen taking part in co-ordination offers considerable steric hindrance to the approach of a second lumichrome molecule in a planar structure. This has been demonstrated by HEMMERICH and FALLAB[8] with similar compounds, all of which form 1 : 1 complexes. This hindrance is not present in the case of the pteridine.

Fig. 2 gives the spectra of lumichrome, 2,4-dihydroxypteridine and their copper(II) complexes. Lumichrome has two peaks close together at 1727 and 1700 cm^{-1}. There is a broad peak at 1574 cm^{-1} with a shoulder at 1560 cm^{-1}. According to MASON and BROWN[9], 4-hydroxypteridine has two peaks at 1710 and 1697 cm^{-1}. On this basis, the two peaks at 1727 and 1700 cm^{-1} are due to the 4-carbonyl group. It is not possible to determine from the spectrum if the 2-oxygen is in the keto form. Since 2-hydroxypteridine has a strong carbonyl absorption at 1681 cm^{-1}, it would appear that the 2-oxygen may be in the enol form. However, a medium peak at 1681 cm^{-1} could be obscured by the strong 4-carbonyl absorption. The peak at 1574 cm^{-1} is most likely due to —C=N— absorption (amide II band).

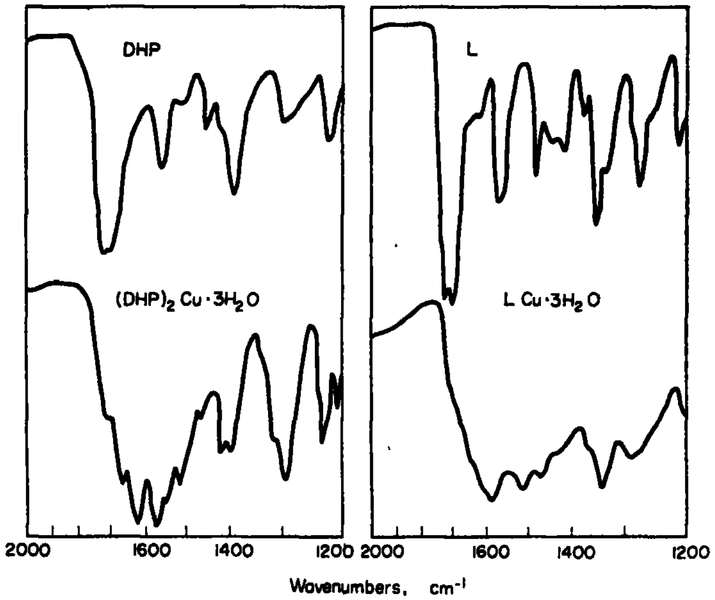

FIG. 2.—Infra-red spectra of 2,4-dihydroxypteridine (DHP), its copper(II) complex [(DHP)$_2$·Cu·3H$_2$O], lumichrome (L) and its copper(II) complex (L·Cu·3H$_2$O) in KBr.

The spectrum of 2,4-dihydroxypteridine is very similar to that of lumichrome, with a peak at 1718 cm^{-1} and a shoulder at 1698 cm^{-1} which can be assigned to the 4 carbonyl group. There is no apparent evidence for 2-carbonyl absorption.

The spectrum of the copper(II) complex of 2,4-dihydroxypteridine indicates that the peak at 1718 cm^{-1} has disappeared, leaving a broad shoulder near 1690 cm^{-1}. The rest of the spectrum is quite similar to that of the pteridine with the exception of a new peak appearing at 1610 cm^{-1}. This peak may be due to the new —C=N— bond formed when the complex is formed. The disappearance of the 4-carbonyl absorption is due to the enolization of this group when the chelate structure is formed and is analogous to the change in the spectrum when the riboflavin–divalent metal complexes are formed.

The spectrum of the copper(II) complex of lumichrome shows similar changes. In general, however, the peaks are not as well defined. The strong carbonyl absorption at 1727 and 1700 cm^{-1} has disappeared, again leaving a broad shoulder. As with the pteridine, this loss of the 4-carbonyl absorption is no doubt due to the formation of the chelate.

These studies support the work of Foye and Lange[2] on the solid metal complexes of riboflavin. The evidence obtained from the infra-red spectra indicate chelates are formed in the solid state involving enolization of the 4-carbonyl group of riboflavin:

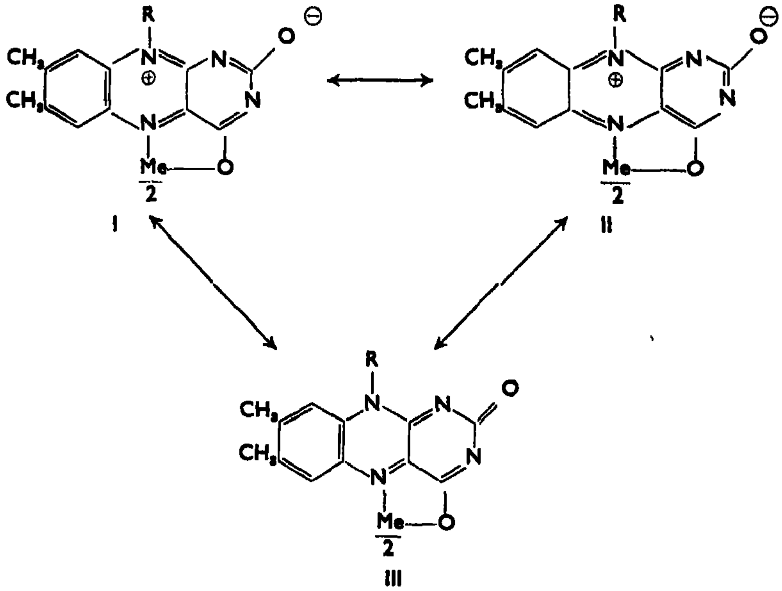

Since the spectra indicate the complete absence of 4-carbonyl absorption and almost complete loss of absorption in the 2-carbonyl region, they are best represented as dipolar ion complexes, with resonance structures I and II (first suggested by Hemmerich *et al.*[10]). Resonance structure III, and other possible structures in which the negative charge is found on the 1- or 3-nitrogen must be of minor importance.

Further evidence for complex formation is obtained from a study of 2,4-dihydroxypteridine, lumichrome and their copper(II) complexes. Solutions of these compounds are pale yellow in colour. Immediately upon addition of copper nitrate the solutions turn green and a substantial drop in pH occurs. Upon further addition of metal salt, a green precipitate of the complex is formed. All of these observations indicate chelate formation.(14) The changes in the infra-red spectra of these compounds upon chelate formation are quite similar to those with riboflavin and indicate that the solid complexes formed when divalent metal ions are added to solutions of riboflavin have similar structures.

Finally, the chelate structure of the solid divalent metal riboflavin complexes is supported by the spectra of the silver riboflavin complexes. There can be little doubt, from the work of Hemmerich(6) and Metzler(5) that RAg has an oxinate-type structure in solution. Since the infra-red spectra of the solid divalent metal complexes of riboflavin are very similar in 4-carbonyl region to the spectrum of the solid RAg, they very likely have similar structures.

As the spectrum indicates, $(R_2Ag)Na$ must also have a similar structure, contrary to that proposed by Hemmerich and Fallab(6). In view of the absence of carbonyl absorption it is best represented:

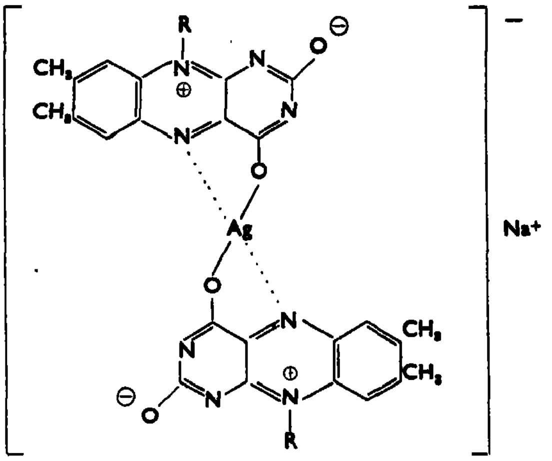

Although silver(I) ordinarily has a co-ordination number of two, it sometimes forms tetrahedral complexes in which it exhibits a co-ordination number of four, as with oxine(15) and thioacetamide.(16) It is likely that the larger size of the silver(I) ion, as compared with the divalent ions studied, makes it possible for two riboflavin molecules to chelate with one silver ion without steric hindrance, particularly since silver(I) forms tetrahedral structures, while those of the other metals are primarily planar or octahedral.

The position of the second metal ion in the divalent metal complexes is not known. There is some evidence from the spectra that changes in the 1000–1100 cm^{-1} region occur when the complexes are formed. Absorption in this region is due either to —C—O— stretching or —O—H deformation bands,(17) mainly of the ribitol side chain. Kanzawa states that compounds having the ribitol side chain show changes in this region upon deuteration.[18] In fact he uses absorption in this region as evidence for the presence of the polyol side chain in flavin type compounds. Ribitol itself shows absorption similar to riboflavin in this region. Furthermore, it is known that polyols form solid complexes with many metal ions.[19] Moreover, lumichrome, with a similar structure to that of riboflavin, except for the absent polyol side chain, forms a 1:1 copper(II) complex, as contrasted with the 1:2 riboflavin–metal complexes, thus suggesting the side chain as the site of complexing of the second metal ion. The changes in the spectra in this region upon complex formation (Fig. 2) are quite similar for all the metal complexes (with the exception of R_2Ag) and can be described as a loss of fine structure and general diminution of absorption. It is possible these changes may be due to loss of the —OH deformation frequencies which could be ascribed to co-ordination of a second metal ion with the oxygen atoms of the side chain. However, similar changes occur in this region for RAg, which contains only one metal ion per riboflavin molecule. This may be due to polymerization in this case, with the silver ion co-ordinating with a second riboflavin molecule through the side chain (METZLER and BAARDA have reported RAg appears to be at least partially polymerized[5]). It is perhaps significant that $[R_2Ag]Na$, which cannot involve the side chain, has a spectrum in this region very similar to that of riboflavin.

---

(14) A. E. Martell and M. Calvin, *Chemistry of the Metal Chelates*. Prentice-Hall, New York (1952).

(15) F. Hein and H. Regler, *Ber. Dtsch. Chem. Ges.* 69 B, 1692 (1936).

(16) E. G. Cox, W. Wardlaw and K. C. Webster, *J. Chem. Soc.* 139, 775 (1936).

(17) L. J. Bellamy, *The Infra-red Spectra of Complex Molecules*, (2nd Ed.) p. 108. J. Wiley, New York (1958).

These studies on the solid complexes cannot, of course, be applied directly to the work of ALBERT on aqueous systems. It can be said with some certainty, however, that divalent metal ions form oxinate-like chelates with riboflavin in the solid state.

Acknowledgement—This investigation was supported by the Research Council of Utah State University and by PHS research grant, RG-8347, Division of General Medical Sciences, Public Health Service.

[18] T. KANZAWA, T. KUNOSUKA and T. MATSUDA, *Pharm. Bull. (Tokyo)* 4, 316 (1956).

[19] W. TRAUBE and F. KUHBIER, *Ber. Dtsch. Ges.* 65, 187 (1932).

J. Inorg. Nucl. Chem., 1962, Vol. 24, pp. 609 to 618. Pergamon Press Ltd. Printed in Northern Ireland

CHARGE-TRANSFER SPECTRA OF CERTAIN METAL CHELATES OF PYRAZYLMETHYL KETONES

N. NAQVI, E. L. AMMA and Q. FERNANDO
Department of Chemistry, University of Pittsburgh, Pittsburgh 13, Pennsylvania

(*Received* 30 *October* 1961; *in revised form* 2 *February* 1962)

Abstract—The ultra-violet and visible spectra of copper (II), nickel (II), and cobalt (II) chelates of 2-, 3-, and 4-pyridyl pyrazylmethyl ketones and phenacylpyrazine have been examined in various solutions and the results related to the empirical assignments made for the parent compounds. Strong evidence has been found for the formation of two types of chelates with copper (II) and 2-pyridyl pyrazylmethyl ketone. One type of chelate consists of a six-membered chelate ring in which the pyrazine nitrogen is bonded to the copper (II), and the second type consists of a five-membered chelate ring in which the pyridine nitrogen is bonded to the copper (II).

Certain of these pyrazylmethyl ketone chelates could be protonated in acid solutions and were therefore isolated as perchlorate salts. From the spectral behaviour of these chelates in solution it was possible to predict the presence of the protonated chelates. Furthermore, somewhat surprising information about the stability and dissociation of these chelates in methanol solution, was obtained from the ultra-violet spectra.

IN a previous study of the ultra-violet and visible spectra and the acid dissociation constants of a series of pyrazylmethyl ketones, it was found that these compounds showed a remarkable selectivity in their reactions with metal ions.(1) It was decided to examine in as much detail as possible, the visible and ultra-violet charge-transfer spectra of certain transition metal chelates of pyrazyl-methyl ketones, in order to obtain information on the nature of the bonding in the metal chelates and on the solution behaviour of these chelates.

Another aspect of this investigation was concerned with the type of chelate that was formed with 2-pyridyl pyrazylmethyl ketone. There are two possibilities for chelate formation with this compound: (1) chelation with the pyridine nitrogen and the carbonyl oxygen forming a five-membered chelate ring, and (2) chelation with the pyrazine nitrogen and the carbonyl oxygen forming a six-membered chelate ring, I. One would undoubtedly predict that the five-membered ring would be formed exclusively because of the generally greater stability of five-membered chelate rings, and particularly since the pyridine nitrogen is far more basic than the pyrazine nitrogen.(2) However, this work has shown that both types of chelates were formed with copper (II) and 2-pyridyl pyrazylmethyl ketone.†

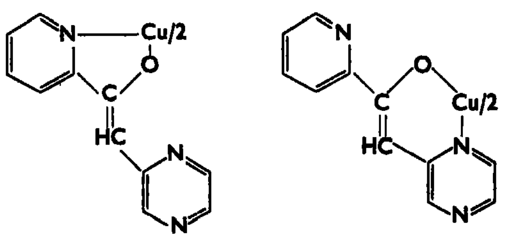

I

---

† Presented in part 140th American Chemical Society Meeting, Chicago, September, 1961.

(1) N. NAQVI, E. L. AMMA, Q. FERNANDO and R. LEVINE, *J. Phys. Chem.* **65**, 218 (1961).

(2) F. J. C. ROSSOTTI, *The Thermodynamics of Metal Ion Complex Formation in Solution, in Modern Co-ordination Chemistry* (Edited by J. LEWIS and R. G. WILKINS) Interscience, New York (1960).

TABLE 1.—ANALYSES OF METAL CHELATES OF THE PYRAZYLMETHYL KETONES

Metal	Compound†	Formula of chelate	C (%)	H (%)	N (%)	Metal (%)
Cu^{2+}	I	$CuC_{24}H_{18}N_4O_2$	63·01 (62·94)‡	3·97 (4·15)‡	12·33 12·24‡	13·34 13·81‡
Ni^{2+}	I	$NiC_{24}H_{18}N_4O_2$	63·37 (63·61)	4·20 (4·01)	12·28 (12·36)	12·72 (12·96)
Cu^{2+}	II	$CuC_{22}H_{16}N_6O_2$	57·45 (57·45)	3·65 (3·51)	—	14·07 (13·81)
Ni^{2+}	II	$NiC_{22}H_{16}N_6O_2$	58·03 (58·06)	3·69 (3·54)	—	13·38 (12·90)
Co^{2+}	II	$CoC_{22}H_{18}N_6O_2 \cdot ClO_4 \cdot 2H_2O$	39·02 (38·17)	3·89 (3·21)	11·35 (12·14)	8·30 (8·50)
Cu^{2+}	III	$CuC_{22}H_{17}N_6O_2 \cdot ClO_4$	48·27 (47·15)	3·60 (3·04)	14·32 (14·99)	11·19 (11·26)
Ni^{2+}	III	$NiC_{22}H_{16}O_2 \cdot 4H_2O$	50·65 (50·12)	4·07 (4·58)	14·06 (15·94)	11·02 (11·13)
Co^{2+}	III	$CoC_{22}H_{17}N_6O_2ClO_4$	47·22 (47·61)	2·97 (2·91)	15·88 (15·15)	10·97 (10·63)
Cu^{2+}	IV	$CuC_{22}H_{17}N_6O_2ClO_4$	45·74 (45·68)	3·69 (3·23)	12·65 (11·07)	10·07 (10·98)
Ni^{2+}	IV	$NiC_{22}H_{16}N_6O_2$	58·08 (58·06)	4·44 (3·54)	17·23 (18·47)	—
Co^{2+}	IV	$CoC_{22}H_{16}N_6O_2 \cdot H_2O$	54·92 (55·82)	3·89 (3·83)	18·30 (17·76)	12·71 (12·46)

† I = Phenacylpyrazine
II = 2-Pyridyl pyrazylmethyl ketone
III = 3-Pyridyl pyrazylmethyl ketone
IV = 4-Pyridyl pyrazylmethyl ketone

‡ Values given in parenthesis are calculated values.

EXPERIMENTAL

Preparation and purification of compounds

The pyrazylmethyl ketones used in this work were kindly supplied by Professor R. LEVINE. The methods of preparation of these compounds have been published.(8)

The compounds were purified as follows: Phenacylpyrazine was dissolved in 20 per cent sodium hydroxide solution and rapidly neutralized to a pH of 7. The freshly precipitated enol form was dissolved in benzene, the solution shaken with Florisil, filtered and cooled. The crystal obtained had a melting point of 82–83°C. The 2- and 3-pyridyl pyrazylmethyl ketones were recrystallized from a mixture of ether and petroleum ether. The pure products had melting points of 87–88°C and 129–130°C respectively. The 4-pyridyl compound was recrystallized from a mixture of benzene and petroleum ether and the pure compound had a melting point of 142–143°C.

Preparation of metal chelates

The copper (II), nickel (II) and cobalt (II) chelates of the four pyrazylmethyl ketones were prepared by the slow addition of 50 ml of 0·01 M metal perchlorate solution in water to 250–300 ml of 90 per cent methanol solution containing 0·3 g of the chelating agent. The pH of the solution was maintained between 4 and 6 by the addition of appropriate quantities of perchloric acid or sodium hydroxide. The resulting solutions were warmed on a water-bath until the precipitates coagulated. The solutions were filtered, and the precipitates were washed with water and with methanol repeatedly to remove any free reagent. The chelates were finally washed with benzene and with ether and dried at 110°C. During the preparation of the cobalt (II) chelates, a current of nitrogen was passed through the solution to prevent any oxidation. The C, H, N and metal analyses of the chelates are given in Table 1. Chelates with a 1:2 metal:ligand ratio were obtained with copper (II) and nickel (II) and phenacylpyrazine and 2-pyridyl pyrazylmethyl ketone, and also with nickel (II) and cobalt (II) and 4-pyridyl pyrazylmethyl ketone. All the other chelates were obtained as perchlorate salts in which the cation consisted of the reagent molecule in which the pyridine nitrogen was protonated.

Ultra-violet and visible spectra

All the chelates were difficult to dissolve in common solvents. Spectrograde methanol was chosen as the best solvent for these chelates. The concentrations of the solutions used in this work ranged from 1 to 10 mg of chelate per liter. The spectra of all the solutions were recorded on a Cary Model 14 spectrophotometer using a pair of 1 cm silica cells or a pair of 10 cm silica cells. The spectra obtained are shown in Figs. 1–4 and Figs. 6–8.

The ethanol soluble and the ethanol insoluble portions of the copper (II) chelate of 2-pyridyl pyrazylmethyl ketone were separated and their spectra obtained on a Beckman Model DB Recording Spectrophotometer (Fig. 5).

RESULTS

The ultra-violet and visible spectra of copper (II), nickel (II), and cobalt (II) chelates with phenacylpyrazine, 2-, 3- and 4-pyridyl pyrazylmethyl ketones II, are

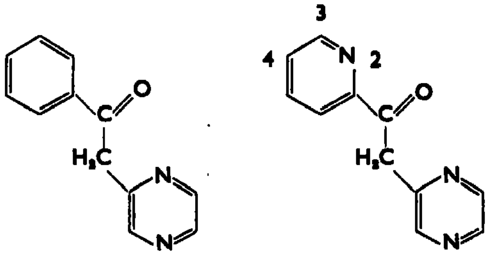

II

summarized in Table 2 and Figs. 1–4. The general features of the copper (II) and nickel (II) chelate spectra resemble those of the parent compounds. Four principal regions of absorption are found in the chelate spectra as well as in the ligand spectra, ~400, ~330, ~260, and ~240 mμ. The 400 mμ and the 330 mμ bands are shifted ~40 mμ upon chelation. From the variation in intensity and position of the long wavelength bands with acid concentration, the dissociation of the metal chelate is readily observable. The behaviour of the 240 mμ and the 260 mμ bands depends on the ligand that is present in the metal chelate. Furthermore, the existence of the protonated pyridine cation is directly observable from the characteristics of the 240 and 260 mμ bands.

---

(8) J. D. BEHUN and R. LEVINE, *J. Amer. Chem. Soc.* **81**, 5157 (1959).

The spectral evidence for the existence of two types of chelates of copper (II) and 2-pyridyl pyrazylmethyl ketone, is discussed below.

TABLE 2.—CHARGE-TRANSFER SPECTRA OF METAL CHELATES OF PYRAZYLMETHYL KETONES IN METHANOL

Metal	Phenacylpyrazine†	2-Pyridyl	3-Pyridyl	4-Pyridyl
Cu(II)		245 (4·23)†		
	260 (4·04)†	263 (4·17)	263 (4·33)†	255 (4·06)†
	320 (3·94)		313 (4·26)	325 (3·92)
	403 (3·91)	398 (4·60)	400 (4·33)	400 (4·09)
		~410 *sh*§	430 *sh*	~430 *sh*
Ni(II)		242 (4·03)		
	265 (4·13)	263 (4·03)	268 (3·89)	264‡
	322 (3·88)		~340 (3·80)	355‡
	408 (3·83)	400 (4·14)	~415 (3·79)	~410 *b sh*
Co(II)		230 (4·19)		
		270 (4·26)	265 (4·15)	265‡
		313 (4·12)		
		358 (4·22)	~350 (3·96)	348‡
		~410 (4·04)	412 (3·92)	~410 *b sh*

† The values in parenthesis are log molar extinction coefficients.
‡ log molar extinction coefficients could not be determined to any accuracy.
§ *b* = broad band; *sh* = shoulder

DISCUSSION

Spectra of 2-pyridyl pyrazylmethyl ketone chelates

The ultra-violet spectra of the copper (II) chelate and the free chelating agent are very similar in methanol solution,(1) Fig. 2. Four principal regions of intense absorption are observed ~400, ~330, ~260, and ~240 mμ, Table 2. Empirical band assignments for the free chelating agent have been made in a previous paper.(1) In dilute acid solution the spectrum of the copper (II) chelate varies with increasing acid concentration as does the spectrum of the free ligand, particularly the 240 mμ band. This band decreases in intensity with decreasing pH and appears to be shifted to the blue, Fig. 2, 6. In our previous work we have deduced that this effect is caused by the protonation of the pyridine nitrogen. Hence, the nitrogen atom in the pyridine ring is free, and can be protonated in the chelate and therefore chelation with copper (II) must occur with the far less basic pyrazine nitrogen, forming a six-membered ring.

The absorption band at ~260 mμ in 2-pyridyl pyrazylmethyl ketone is hardly affected if at all in going from methanol to 0·1 M acid, but is completely removed in strongly basic solution.(1) This band is made up of a composite of the $\pi - \pi_1^*$ pyridine absorption and the $\pi - \pi^*$ pyrazine absorption and hence on formation of the enolate anion it is shifted to 380 mμ.(1) It is noteworthy that in acid solutions of the parent compound the band at 240 mμ is essentially completely removed, but it is always present in the spectrum of the copper (II) chelate and is somewhat shifted

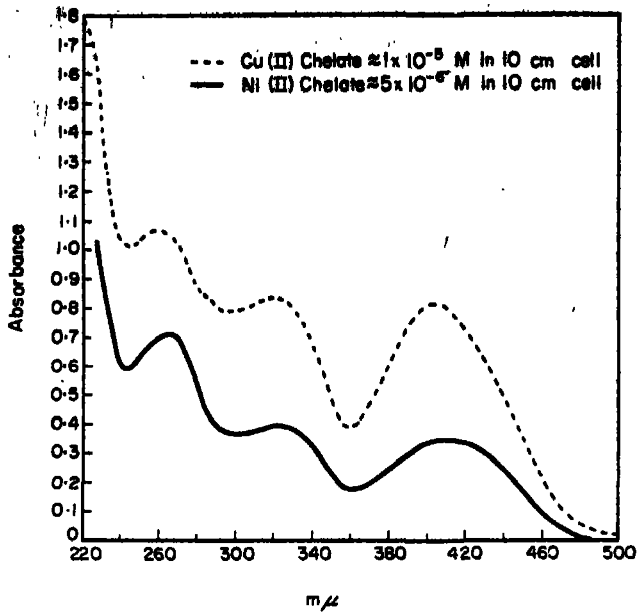

FIG. 1.—Ultra-violet and visible spectra of the metal chelates of phenacylpyrazine in methanol.

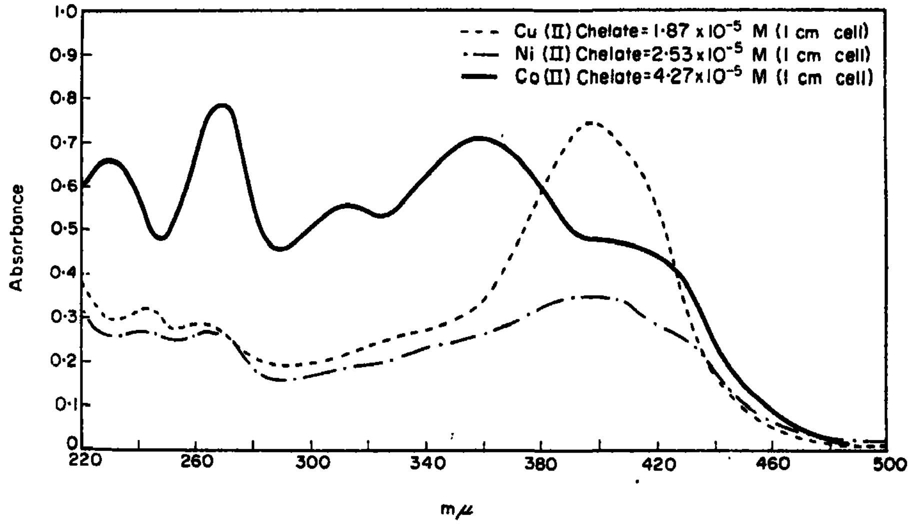

FIG. 2.—Ultra-violet and visible spectra of the metal chelates of the 2-pyridyl compound in methanol.

to the red with respect to the parent compound. This implies that in the copper (II) chelate not all of the pyridine nitrogen atoms are tied up by chelation. Hence, the copper (II) chelate was extracted with ethanol, and the ratio of the absorbances at 260 and 240 mμ were measured for a series of extracts. The more soluble fraction had a lower ratio. By continued extraction it was found possible to isolate two different fractions that were distinctly different in colour. The fraction with the lower 260 mμ/240 mμ absorbance ratio is rich in the chelate in which a six-membered ring is present,

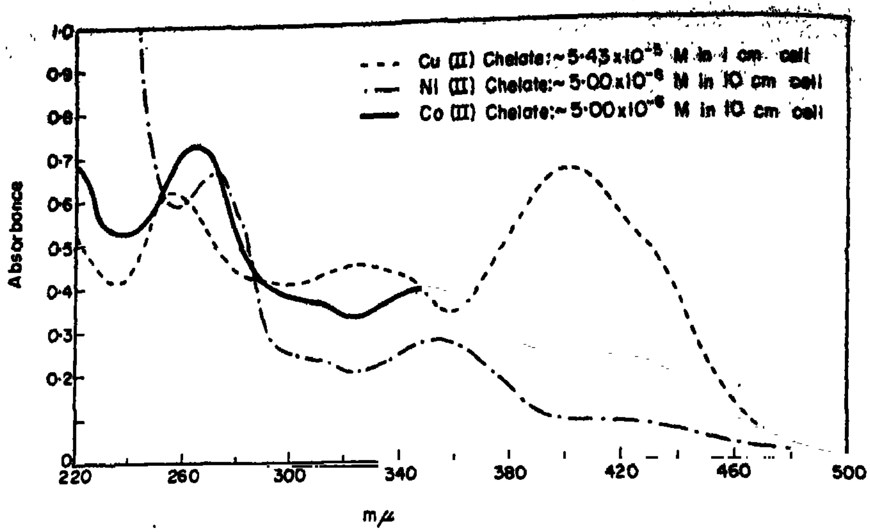

FIG. 3.—Ultra-violet and visible spectra of the metal chelates of the 4-pyridyl compound in methanol.

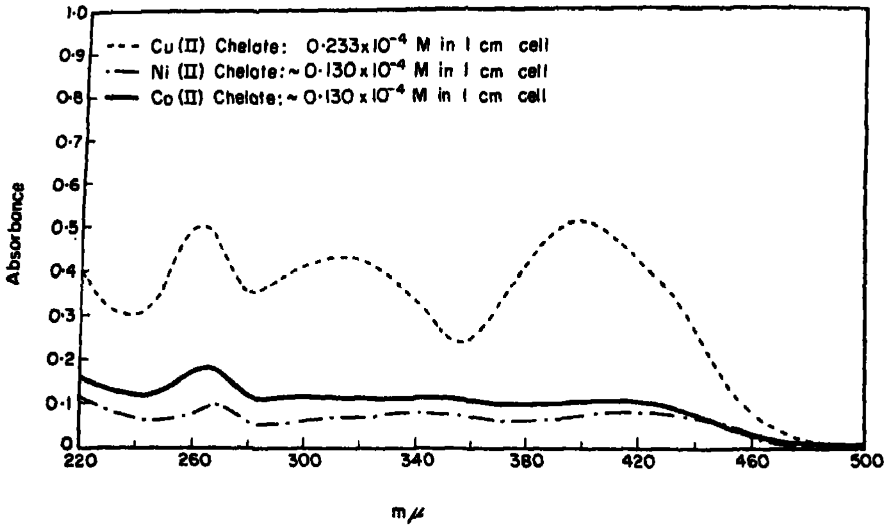

FIG. 4.—Ultra-violet and visible spectra of the metal chelates of the 3-pyridyl compound in methanol.

and the pyrazine nitrogen is bonded to the metal atom. The fraction with the higher absorbance ratio has a five-membered chelate ring in which the pyridine nitrogen is bonded to the metal. In these two types of chelates a fine energetic balance is achieved between the greater basicity of the pyridine nitrogen and the five-membered ring stability as against the very much lower basicity of the pyrazine nitrogen and the six-member ring stability. The compensating factor is most likely the greater π-bonding tendency of the pyrazine system as is indicated by its lower π excitation energy.(4) If the metal symmetry is assumed to be essentially D_{4h}, then the ligand π

---

(4) Preliminary report on the spectra of this compound, N. NAQVI, E. L. AMMA and Q. FERNANDO, *Spectrochim. Acta* 17, 1288 (1961).

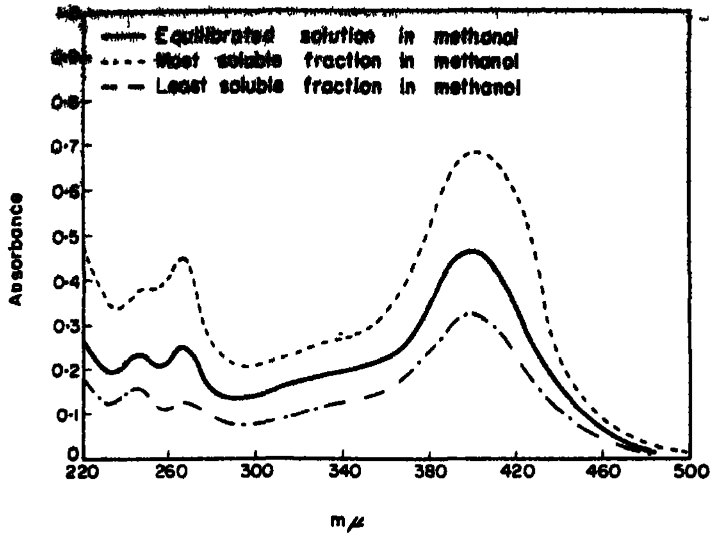

Fig. 5.—Ultra-violet and visible spectra of methanol extracted fractions of the Cu (II) chelate of the 2-pyridyl compound.

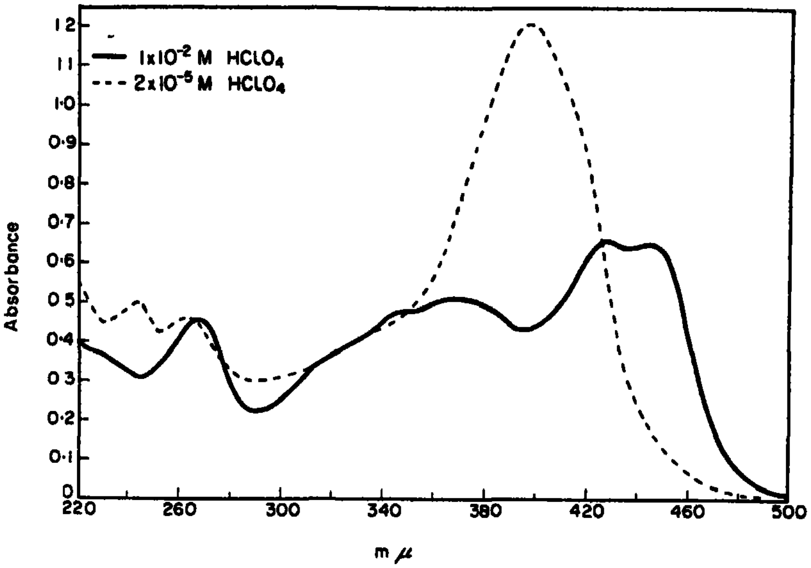

Fig 6.—Ultra-violet and visible spectra of the Cu (II) chelate of the 2-pyridyl compound in acidic solutions of 90 per cent methanol.

electrons can mix with either the metal $4p_z(a_{2u})$ or the $3d_{xz}$, $3d_{yz}(e_g)$ orbitals. One might expect greater overlap and greater interaction between the metal a_{2u} orbital and the ligand π-system than between metal e_g and ligand π in spite of the greater energy separation between the ligand π orbitals and the e_g and a_{2u} orbitals. This is not only intuitively appealing and in line with the intense spectral bands, but is supported by indirect evidence in other systems.(5)

(5) R. E. Rundle, *J. Phys. Chem.* 61, 45 (1957).

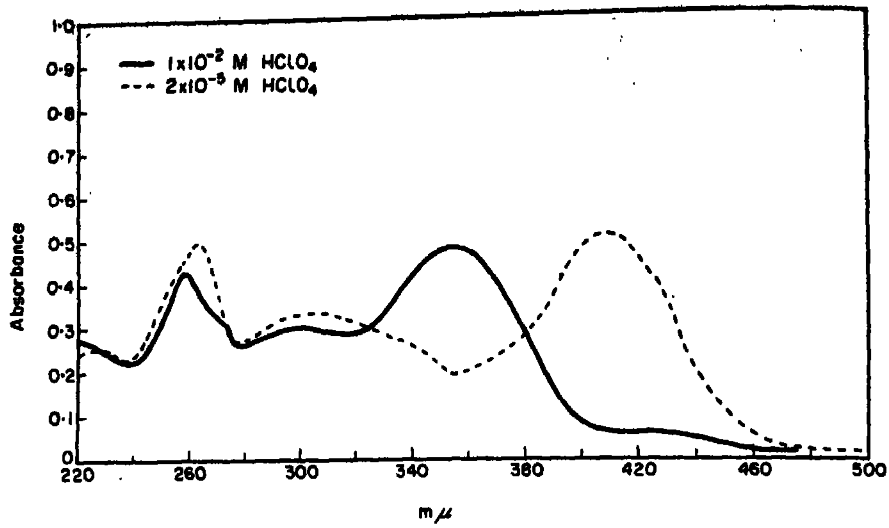

FIG. 7.—Ultra-violet and visible spectra of the Cu (II) chelate of the 3-pyridyl compound in acidic 90 per cent methanol solution.

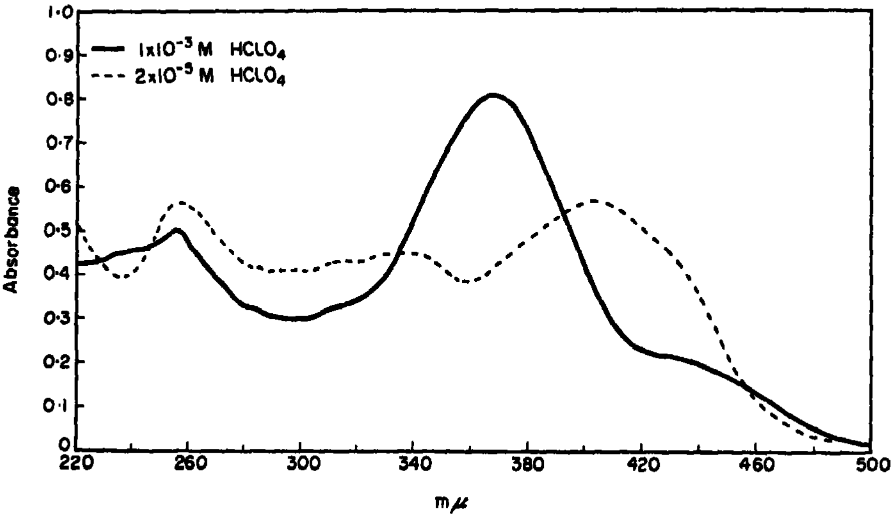

FIG. 8.—Ultra-violet and visible spectra of the Cu (II) chelate of the 4-pyridyl compound in acid solutions of 90 per cent methanol.

Since it was shown the pyridine nitrogen is available for protonation in the copper (II) chelate of 2-pyridyl pyrazylmethyl ketone, it was decided to investigate the spectral behaviour of the chelate in acid solutions. Several features of the long wavelength bands at ~360 mμ and ~400 mμ correlate well with the measured p*K* values of the chelating agent.⁽¹⁾ In acid concentrations of ~10^{-5} M the spectrum is unchanged from that of the copper (II) chelate in methanol solution, but in acid solutions between 10^{-5} and 10^{-4} M the band at 400 mμ decreases monotonically in intensity (Fig. 6). In 10^{-3} M this acid solution band splits into a doublet due to the protonation of the pyridine nitrogen. In an acid solution which is 10^{-2} M the chelate begins to dissociate; this can be readily seen from the absorption band at 360 mμ ($\pi - \pi^*_{ea}$)(1) which is the intense enol band in acid solution.

It has been stated in the literature that there is no explanation for the red and/or blue shifts that are observed upon chelation of absorbing molecules.(6) We feel that in our systems we can at least rationalize the band shifts we observe on chelation. The red shift of the 230 mμ band on chelation with copper (II) is due to the increased conjugation of the pyridine system with the copper $4p_z$ orbital (charge-transfer). This is similar to what we observed in the case of the enolate anion.(1) The blue shift that the 270 mμ band undergoes on chelation is due to some of the pyrazine rings being bonded on chelate formation and thus affecting the π-system of the pyrazine ring.

TABLE 3.—CHARGE-TRANSFER SPECTRA OF Cu(II) CHELATES OF PYRAZYLMETHYL KETONES IN ACID 90 PER CENT METHANOL SOLUTIONS

Acid Strength	2-Pyridyl	3-Pyridyl	4-Pyridyl
1×10^{-3} M	230 *sh*†	230 *sh*	238
	265	258	256
	365	300	310 *b sh*
		355	368
	$\left.\begin{matrix}425\\445\end{matrix}\right\}$ doublet	425 *b sh*	430 *b sh*
2×10^{-5} M	244	230 *sh*	
	263	264	257
		310	330
	398	410	405
	415 *sh*	430 *sh*	425 *sh*

† *b* = broad; *sh* = shoulder

The nickel (II) chelate spectral band maxima occur at approximately the same positions as in the copper (II) chelate of 2-pyridyl pyrazylmethyl ketone. However, it is to be noted that the log ϵ values are generally smaller perhaps due to the fact that copper (II) is a better electron acceptor than nickel (II). Further, the broad absorption at ~360 mμ indicates that the nickel chelate probably dissociates in methanol and is therefore less stable than the copper (II) chelate. This lower stability of the nickel (II) chelate compared with that of the copper (II) chelate precluded the search for the two types of nickel (II) chelates analogous to the two types of chelates found with copper (II).

The cobalt (II) chelate of 2-pyridyl pyrazylmethyl ketone appears to be appreciably dissociated in methanol solution from the presence of the strong band at 360 mμ. The analysis of the cobalt (II) chelate (Table 1), shows that this compound was isolated as a perchlorate salt. As will be discussed later, in the case of the 3-pyridyl and 4-pyridyl pyrazylmethyl ketone chelates, the presence of perchlorate salts can be unambiguously determined from the spectra, but due to the dissociation of the cobalt (II) chelate the relevant bands are obscured.

Spectra of 3-pyridyl pyrazylmethyl ketone chelates

The spectral behaviour of the copper (II) chelate of 3-pyridyl pyrazylmethyl ketone is very similar to that of the copper (II) chelate of the 2-pyridyl compound in the ~400 mμ, ~330 mμ and ~260 mμ regions, but it is markedly different in the 240 region. In our previous work it was shown that in the parent compound, the 240 mμ band is invariant in solutions of pH 7–11 and in methanol, but in contrast it is decreased considerably in intensity and shifted to the blue (~10 mμ) in acid solutions. This, of course, is due to the protonation of the pyridine nitrogen and it is clear that the copper (II) chelate of the 3-pyridyl compound that was dissolved in the methanol solution was a perchlorate salt. This feature in the spectra of these chelates can therefore be used in determining the presence of perchlorate salts of these compounds. The 240 mμ band is present in the copper (II) chelate of 2-pyridyl pyrazylmethyl ketone for two reasons: (1) the perchlorate ion cannot readily form a salt with the 2-pyridyl compound due to a steric effect, and (2) the pyridine nitrogen is less basic in this system.

---

(6) A. E. MARTELL and M. CALVIN in *Chemistry of the Metal Chelate Compounds*. Prentice-Hall (1952).

In acid solutions of concentration less than 10^{-4} M, the copper (II) chelate of the 3-pyridyl compound is stable; however, in more concentrated acid solutions, the chelate dissociates as can be seen from the appearance of the enol band at 360 mμ ($\pi - \pi^*_{e2}$) and the $\pi - \pi_1{}^*$ band at 230 mμ (Fig. 7).

The nickel (II) chelate of the 3-pyridyl compound shows almost a continuous absorption with essentially no characteristic features and little can be said concerning its spectra.

The analytical results show that the cobalt (II) chelate of the 3-pyridyl compound was isolated as a perchlorate salt but as in the case of the nickel (II) chelate the spectrum is broad and almost featureless.

Spectra of 4-pyridyl pyrazylmethyl ketone chelates

The spectrum of the copper (II) chelate of the 4-pyridyl compound is very much like that of the copper (II) chelate of the 3-pyridyl compound, including the behaviour of the short wavelength band. Hence, this compound also exists as the perchlorate salt in methanol solution and this fact is further supported by the analytical results obtained for the chelate.

In a 10^{-5} M acid solution of the copper (II) chelate of the 4-pyridyl compound, the spectrum differs very little from the spectrum in methanol, but in an acid solution of concentration 10^{-4} M the chelate dissociates and the band at 360 mμ, characteristic of the enol form of the protonated molecule, appears. In 10^{-3} M acid solutions, the chelate appears to be completely dissociated (Fig. 8).

The nickel (II) chelate of the 4-pyridyl compound is appreciably dissociated in methanol solution as evidenced from the 310 mμ and 360 mμ bands and is not as stable a chelate as the corresponding copper (II) chelate.

The cobalt (II) chelate of the 4-pyridyl compound is similar to the corresponding copper (II) chelate and is considerably dissociated in methanol solution.

Spectra of phenacylpyrazine chelates

The only important feature in the spectra of these compounds is the red shifts of the long wavelength bands on chelation. This is due to an increased delocalization of the π-electrons in the ring with the metal atoms. The absence of the 360 mμ band for the nickel (II) chelate indicates that it is the most stable of the nickel (II) chelates studied and does not dissociate in methanol solution.

Acknowledgement—This work was supported by a research grant, G-9736, from the National Science Foundation, and a grant from the National Institute of Health.

J. Inorg. Nucl. Chem., 1962, Vol. 24, pp. 619 to 631. Pergamon Press Ltd. Printed in Northern Ireland

ABSORPTION SPECTRA OF URANIUM (VI) COMPLEXES IN SOLUTIONS

Z. Libuś
Department of Electrochemistry, Institute of Physical Chemistry
Polish Academy of Sciences, Warszawa

(*Received* 9 *November* 1961; *in revised form* 9 *February* 1962)

Abstract—Absorption spectra of the complex $[UO_2(NO_3)_2(TBP)_2]$ in various organic solvent solutions and that of $[UO_2(CH_3COO)_3]^-$ in water solutions of various acetates have been determined. The stepwise formation of uranyl acetate complexes has been followed spectrophotometrically. Characteristic features of spectral effects accompanying solvent exchange, outer-sphere association and ligand exchange involving the uranyl ion are discussed. Conclusions are drawn from the spectral effects observed regarding the interpretation of the absorption band of the uranyl ion between 370 and 480 mμ.

The standard spectrophotometric methods of identification of complexes in solutions (continuous variations method, mole ratio method, method of corresponding solutions, etc.) and the spectrophotometric methods of establishing the stability constants, involve the supposition that every single complex has its own characteristic spectrum independent of changes taking place outside its co-ordination sphere. This supposition, however, does not hold in general, and in doubtful cases should be verified before the methods, mentioned above are applied.

The opinion prevails, that the *d-d* bands of transition metal complexes of the $3d^n$ series are determined by the composition of first co-ordination sphere and are only slightly influenced by the outer-sphere association(1,2,3) or by exchange of the solvent.(4) The opinion is also often advanced, that the charge transfer spectra of such metal complexes are dependent not only on the composition of their first co-ordination spheres, but also, to a high extent, on outer-sphere association of ions. Smithson and Williams have suggested that this difference in the properties of the two kinds of absorption bands may serve as basis for experimental differentiation between complexes and ion-pairs, provided that both kinds of bands are present in the spectrum of the system investigated.(1)

In investigations of uranyl complex compounds measurements of light absorption, chiefly in the range of characteristic absorption band situated in the transition region between the visible and the ultra-violet (370–480 mμ), have been used extensively. However, in the case of this spectrum the validity of the assumption of the absence of influence of the medium on the spectra of individual complexes has not been proved so far. The analysis of this problem seems to be particularly necessary as the band in question is supposed to be of charge-transfer type. According to Jørgensen(5) it must be due to the transfer of an odd electron from the ligand to the empty 5*f*-shell of the central ion. Provided that this interpretation is correct, we might expect a rather significant effect of medium changes on the spectra of individual uranyl complexes.

(1) J. M. Smithson and R. J. P. Williams, *J. Chem. Soc.* 457 (1958).

(2) J. F. Duncan and D. L. Kepert, in *The Structure of Electrolytic Solutions*, pp. 395–399. Hamer, New York (1950).

(3) H. Taube and F. A. Posey, *J. Amer. Chem. Soc.* 75, 1463 (1953).

(4) J. Bjerrum, A. W. Adamson and O. Bostrup, *Acta Chem. Scand.* 10, 329 (1956).

(5) Chr. K. Jørgensen, *Acta Chem. Scand.* 11, 175 (1957).

The character of the spectral changes accompanying the stepwise complex formation by the uranyl ion has likewise not been investigated systematically so far. In the case of transition metals, often mere changes of the spectrum corresponding to gradually changing concentration of the complex forming agent in solution provide essential information on the character of complex formation.(6,7) It might be hoped that a detailed investigation of these relations for the uranyl ion would enable some conclusions to be drawn regarding the processes occurring in solution with changing concentrations.

The present work was undertaken with the object of determining the changes in the absorption spectrum of the uranyl ion in solution, owing to:

(1) changes of the medium (solvent, electrolyte) without change of composition of the light-absorbing complex.
(2) changes of the composition of the first co-ordination sphere.

The absorption band in the range 370–480 mμ has been studied.

EXPERIMENTAL

Uranyl nitrate and sodium acetate were purified by recrystallization. Uranyl perchlorate was prepared by repeated evaporation of recrystallized uranyl nitrate with perchloric acid, followed by crystallization. The $[UO_2(NO_3)_2(TBP)_2]$ complex was prepared as described by Healy and McKay(8). Lithium, potassium, calcium and barium acetates were prepared by the action of acetic acid respectively on lithium carbonate, potassium hydroxide, calcium oxide and barium hydroxide. After evaporation the acetates were recrystallized. All the reagents used were of reagent grade quality.

Solutions of known concentrations of uranium (VI) were prepared by weighing of $[UO_2(NO_3)_2(TBP)_2]$ or $UO_2(NO_3)_2.2H_2O$. The water content in $UO_2(NO_3)_2.2H_2O$ was controlled by Karl Fischer titrations.

The concentrations of the acetates were determined by drying of weighed samples at 115–120°C.

The solvents—n-butyl alcohol, benzene, isoamyl acetic ester and cyclohexanone were distilled through a thirty plate column, and the proper fractions were collected. Tri-n-butyl phosphate was purified by vacuum distillation followed by heating with 0·5 per cent solution of NaOH in water, during several hours and repeated washing with distilled water. Carbon tetrachloride, iso-octane, cyclohexane, n-butyl ether and chloroform were purified by simple distillation. Undecane (L. Light & Co. Ltd.) and n-decane (BDH) were used without previous purification.

For dehydration of the uranyl nitrate solution in n-butyl alcohol, half of the primary volume of butyl alcohol was removed from the solution by distillation under vacuum. After this operation the water content in the solution did not exceed 0·05 per cent. The tri-n-butyl phosphate was dried by heating (40–60°C) during several hours under vacuum. Special dehydration of the other solvents was not necessary. In the hydrocarbons the water content was below 0·03 per cent, in carbon tetrachloride and in n-butyl ether below 0·08 per cent. In butyl alcohol it was ca 0·03 per cent.

The water content in solvents and in solutions was controlled by Karl Fischer titration.

All operations with uranium solutions in organic solvents were performed in a dark room with orange light, as they proved to be photosensitive.

The absorption spectra were measured by means of a Unicam SP 500 spectrophotometer, at room temperature varying between 18–23°C.

RESULTS AND DISCUSSION

Effect of the medium on the spectra of individual uranyl complexes

The effect of the medium on the spectra of individual complexes can be relatively easily investigated in the case of inert complex-forming systems, but in labile systems such as those involving uranyl, the only possibility is to investigate the limiting (i.e. the most highly complexed) complex.

---

(6) W. Libuś, *Roczniki Chem.* 33, 931 (1959); 33, 951 (1959); 35, 411 (1961).

(7) W. Libuś, A. Ugniewska and S. Minc, *Roczniki Chem.* 34, 29 (1960).

(8) T. V. Healy and H. A. C. McKay, *Trans. Faraday Soc.* 52, 633 (1956).

1. *Effect of solvent on the spectrum of* $[UO_2(NO_3)_2(TBP)_2]$ *complex.* It was particularly convenient to investigate the effect of the solvent on the spectrum of the $[UO_2(NO_3)_2(TBP)_2]$ complex because of its sufficiently high stability and solubility in non-donor or slightly donor organic solvents,

Absorption spectra of this complex in tri-n-butyl phosphate, carbon tetrachloride, benzene, cyclohexane, isooctane, n-decane, undecane, n-butyl ether and chloroform were determined. The results are presented in Fig. 1, ε being the molar extinction coefficient. The spectra of the complex in tri-n-butyl phosphate, benzene and carbon tetrachloride solutions are shown as one common curve, because they are identical within the limits of experimental error. The absorption spectrum of the complex in butyl ether is also closely similar to that for tri-n-butyl phosphate solution. On the other hand the extinction maxima in the spectra of the $[UO_2(NO_3)_2(TBP)_2]$ complex in isooctane, cyclohexane, n-decane and undecane are lower than those in the spectra corresponding to the other solvents, though their locations remain the same, as also do the intensity ratios of component bands.

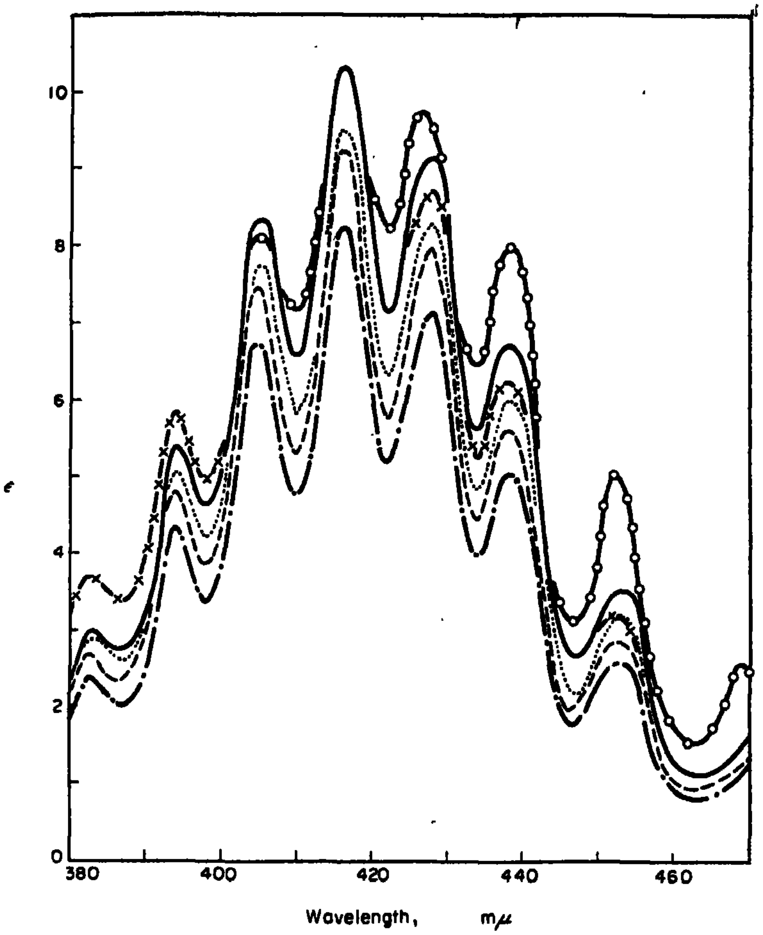

FIG. 1.—Absorption spectra of $UO_2(NO_3)_2(TBP)_2$ in various solvents: —— tri-n-butyl phosphate, benzene, carbon tetrachloride, · · · · cyclohexane, – – – isooctane, — · — n-decane and undecane, — × — n-butyl ether, — ○ — chloroform.

The extinction curve of the complex in chloroform differs from the others by relatively high values of the extinction coefficients and by markedly more diffuse vibrational structure. These facts may in some way be related to the formation of hydrogen bonds between uranyl ions and chloroform. Among the solvents used in the present experiments chloroform is the only one possessing hydrogen atoms capable of forming hydrogen bonds.

It is difficult to perceive any simple relation between the properties of the investigated solvents and the magnitude of the extinction coefficients of the $[UO_2(NO_3)_2(TBP)_2]$ complex. Roughly speaking it can be stated, that the values of molar extinction coefficients of the complex decrease with the decreasing dielectric constant of the solvent.

Reference should be made at this point to the work of Kaplan, Hildebrandt and Ader(9), who reported a much weaker effect of the solvent on the spectrum of $[UO_2(NO_3)_3]^-$. They found that the spectrum of this complex was essentially the same independently of whether the complex was formed by addition of ammonium nitrate to a solution of uranyl nitrate in acetone or by additions of a number of ammine nitrates to solutions of uranyl nitrate in methylisobutyl ketone or cyclohexanone. The differences in the positions of absorption maxima observed by these authors were about 1–2 mμ; the differences of extinction coefficient values at constant wavelengths did not exceed 2–3 per cent, whereas we observed a change from $\varepsilon = 8{\cdot}25$ to $\varepsilon = 10{\cdot}3$ at 416 mμ on changing from n-decane to tri-n-butyl phosphate as solvent.

2. *Effect of ionic medium on the spectrum of* $[UO_2(CH_3COO)_3]^-$. The triacetate uranyl complex $[UO_2(CH_3COO)_3]^-$ has been selected for examination of the effect of an ionic medium on the spectrum of a single uranyl complex. As may be seen from the shape of the formation curve in Ahrland's paper,(10) the triacetate is the limiting complex in relation to the acetate ion. Moreover, it is quite stable in aqueous solutions, so that even at moderate concentrations of acetate ions all the uranium (VI) exists in the form of this complex.

The absorption spectra of $[UO_2(CH_3COO)_3]^-$ were determined in aqueous solutions of the buffers containing Li, Na, K, Ca or Ba acetates. The average mole ratio of acetic acid to the acetate was 2·5. The concentrations of acetates in solutions were 0·322–0·375 N. The experiments described below confirm the supposition that in solutions of this composition all uranyl ions occur in the form of triacetate complexes. Spectrophotometric measurements at higher concentrations of acetates have been performed only in the case of lithium and calcium salts. When sodium, potassium or barium acetates were used, a precipitate was formed at higher concentrations of the corresponding buffers.

The absorption curves of the $[UO_2(CH_3COO)_3]^-$ complex in the solutions under discussion are presented in Fig. 2. For the sake of clarity only two extreme extinction curves have been drawn. The remaining ones lie between them. Two almost equally high absorption maxima appear at 420 and 432 mμ in every case. As may be seen the nature of the cation does not affect the absorption spectrum of the uranyl complex. Neither do we observe an effect of lithium acetate concentration, provided the minimal value necessary for the complete formation of $[UO_2(CH_3COO)_3]^-$ has been exceeded (Fig. 4). It is worth stressing, however, that the system investigated did not provide a possibility of any stronger interaction between the uranyl complex ion and the other ions present in solution, because of the isolating action of methyl groups. Other uranyl complexes might permit stronger interaction.

---

(9) L. Kaplan, R. A. Hildebrandt and M. Ader, *J. Inorg. Nucl. Chem.* **2**, 153 (1956).

(10) S. Ahrland, *Acta Chem. Scand.* **5**, 199 (1951).

In the paper already cited[9] it has been demonstrated that the spectra of the trinitrate uranyl complex are closely similar, whatever the organic cation present in solution. These results suggest, that in this case too the effect of the ionic medium on the spectrum is insignificant.

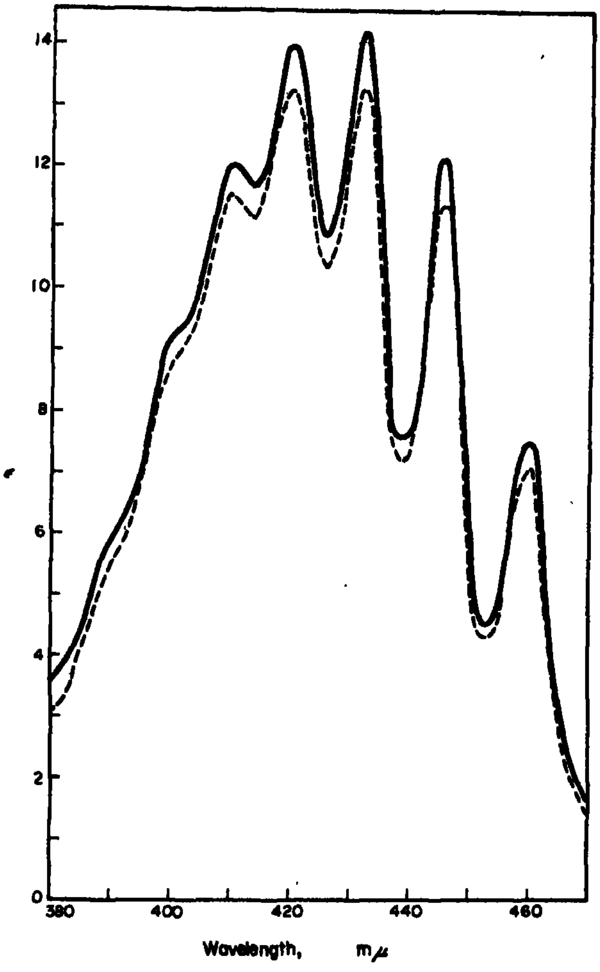

FIG. 2.—Absorption spectra of $[UO_2(CH_3COO)_3]^-$ in water solutions of various acetate buffers: - - - 0·349 N CH_3COONa, —— 0·735 N CH_3COOLi. The remaining absorption curves of $[UO_2(CH_3COO)_3]^-$ in solutions of 0·351 N CH_3COOLi, 0·375 N CH_3COOK, 0·342 N and 1·09 N $(CH_3COO)_2Ca$ and 0·322 N $(CH_3COO)_2Ba$ lie between the two curves shown in the figure.

The concentration of uranium (VI) in all solutions was kept within the limits 0·0212–0·0213 M.

Spectral effects resulting from ligand exchange in uranyl complexes

1. *The exchange of co-ordinated water molecules for acetate ions.* It might be expected that on introduction of acetate into an aqueous solution of uranyl perchlorate,

a stepwise substitution of co-ordinated water molecules by acetate ions would take place. This might therefore be expected to occur according to the scheme:

$$[UO_2(H_2O)_6]^{2+} \rightarrow [UO_2(CH_3COO)(H_2O)_4]^{+} \rightarrow [UO_2(CH_3COO)_2(H_2O)_2]$$
$$\rightarrow [UO_2(CH_3COO)_3]^{-}.$$

The acetate complexes would then be similar to the nitrate complexes.[11]

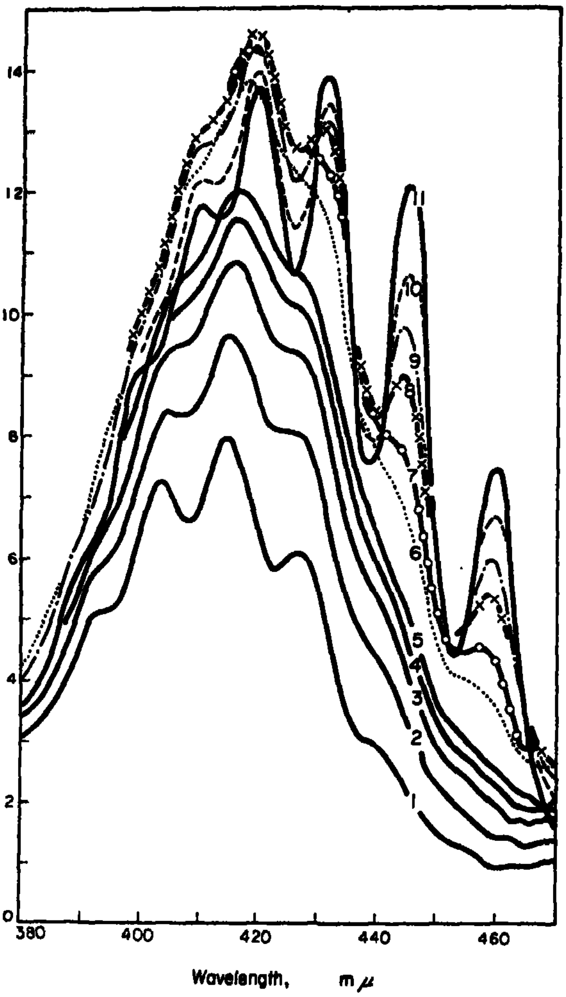

Fig. 3.—Absorption spectra of $UO_2(ClO_4)_2$ in water solutions in the presence of lithium acetate buffer, the concentration of acetate being: 1—0·0 N, 2—0·00332 N, 3—0·00792 N, 4—0·0112 N, 5—0·0144 N, 6—0·0279 N, 7—0·0400 N, 8—0·0581 N, 9—0·0727 N, 10—0·102 N, 11—0·351 N.
The concentration of uranyl perchlorate was 0·0210–0·0213 M.

Although the formation of acetate uranyl complexes in water solutions has been studied in detail by Ahrland, only a few spectra have been determined. The determination of a complete set of absorption curves corresponding to gradually increasing concentrations of acetate seemed therefore to be of interest. The acetate ions were introduced by addition of buffer consisting of acetic acid and lithium acetate in the mole ratio of 2·52. According to the data in AHRLAND's paper it is believed that very little, if any, hydrolysis of the uranyl ion should occur in the presence of such a buffer.

---

[11] S. Minc and Z. Libuš, *Radiokhimiya* 2, 643 (1960).

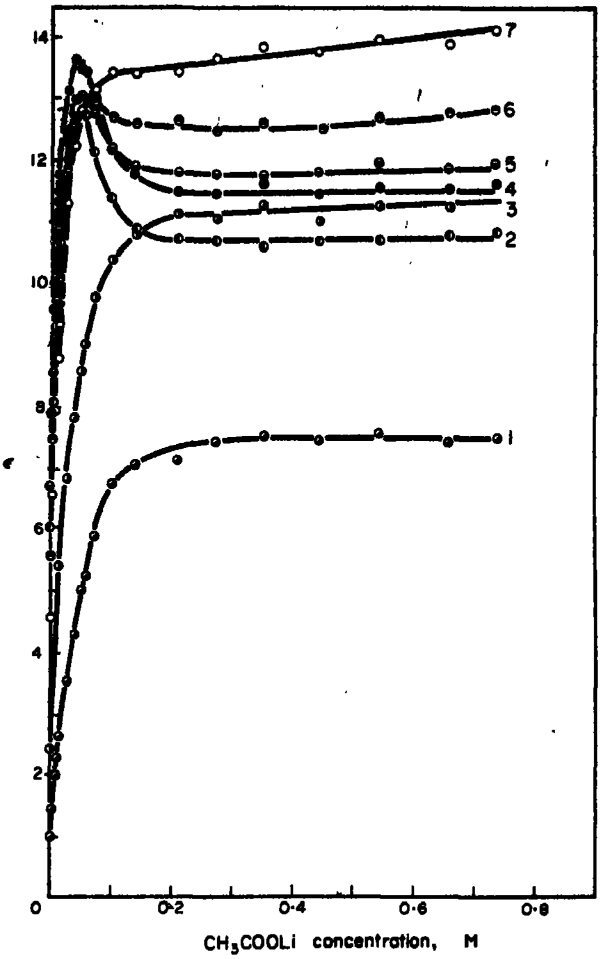

FIG. 4.—Dependence of extinction coefficients of uranium (VI) on the concentration of lithium acetate for various wavelengths: 1—460 mμ, 2—426 mμ, 3—444 mμ, 4—414 mμ, 5—410 mμ, 6—430 mμ, 7—432 mμ.

As may be seen from Fig. 3 and 4 the changes of the uranyl ion absorption spectrum taking place on increasing the concentration of acetate ions are rather surprising. In the range of lower concentrations of acetate ions up to 0·0279 N there is only a very small and gradual shift of the absorption band towards longer wavelengths, accompanied by a significant increase of extinction coefficient values and some diffusion of the vibrational structure. The difference in the position of the band for a solution at lithium acetate concentration 0·0279 N and that for a water solution of uranyl perchlorate without acetate amounts to 3 mμ. In this range of acetate ion concentration the formation of consecutive $[UO_2(CH_3COO)(H_2O)_4]^+$ and $[UO_2(CH_3COO)_2(H_2O)_3]$ complexes might be expected. Much more pronounced spectral changes are observed at concentrations of lithium acetate within the range 0·0400–0·209 N. At these concentrations the evolution of the limiting spectrum may be seen, which afterwards remains unaffected by further increase of the acetate ion concentration in solution. There is no doubt that the limiting spectrum is due to the limiting complex $[UO_2(CH_3COO)_3]^-$. The component vibration bands in this spectrum are very distinct and the absorption maxima are displaced towards longer wavelengths by about 5 mμ in comparison with the spectrum of the hydrated complexes. In the range of lower concentrations, close to those corresponding to the limiting spectrum, several isosbestic points are observed. In this concentration range, therefore, only two kinds of complexes can exist: probably the limiting triacetate complex and the diacetate.

It is important to note that the disappearance of the vibrational structure observed in the spectrum at 0·0279 N concentration of lithium acetate (curve 6 in Fig. 3) obviously results from a superposition of the spectrum of the triacetate complex and that of a lower complex, the maxima of which are displaced to each other by several mμ. From the above example it becomes evident that the prominence of vibrational bands in the spectrum of a uranyl complex of a given composition on the one hand, and the development or disappearance of vibrational bands in the spectra of solutions usually containing a mixture of two or more different complexes on the other, present two entirely different problems. It may easily be seen, that a distinct vibrational structure is characteristic of the spectra of uranyl complexes having only a small possibility of intermolecular interaction with the medium, e.g.

$$[UO_2(CH_3COO)_3]^-,\quad [UO_2(NO_3)_3]^-,\quad [UO_2(NO_3)_2(TBP)_2].$$

Uranyl complexes containing water are characterized, on the other hand, by a much less distinct vibrational structure, obviously as a result of the formation of hydrogen bonds between the coordinated water molecules and molecules or ions outside the co-ordination sphere. This observation is in agreement with the theory of Bayliss and McRae which explain the blurring of vibrational structure in solution spectra in terms of the s.c. cage effect.[12] Almost complete disappearance of the vibrational bands (e.g. as in curve 6, Fig. 3) can probably occur only as a result of the superposition of the spectra of two or more different complexes. Such situations have been met when investigating the spectra of the systems: $UO_2(NO_3)_2 + TBP + C_4H_9OH$[11] and $UO_2(NO_3)_2 + LiCl + H_2O$.[13]

The formation of the lower uranyl acetate complexes manifests itself only by relatively small spectral effects. It may indeed be said that their formation results only in a deformation of the spectrum of the hydrated uranyl ion. This can be explained by assuming that, in the region of lower concentrations of acetate ions in solution, only outer-sphere association of acetate ions with the hexahydrated uranyl ions takes place, and that displacement of water molecules co-ordinated by the uranium does not occur until the limiting complex $[UO_2(CH_3COO)_3]^-$ begins to form. This interpretation involves the assumption that the outer-sphere association of the complex ion $[UO_2(H_2O)_6]^{2+}$ with CH_3COO^- anions results in a relatively significant change of its spectrum. This assumption is not necessarily in contradiction with the observations discussed in the previous section, because the possibility exists of hydrogen bond formation between the associating ions in this case, whereas such interactions were impossible for $[UO_2(CH_3COO)_3]^-$. On the other hand it is difficult to understand why in a certain concentration range only outer-sphere association should take place and the displacement of water molecules by anions should be possible only after some boundary conditions have been exceeded. Further investigations directed to a solution of this problem will be undertaken in the near future.

---

[12] N. S. Bayliss and E. G. McRae, *J. Phys. Chem.* **58**, 1002 (1954).

[13] M. Siekierska, Unpublished results (1959).

It is important to note that the character of the spectral changes observed for the UO_2^{2+}–CH_3COO^- system is not exceptional. Closely similar spectral effects have been observed in the work of MINC and UGNIEWSKA[14] for the system UO_2^{2+}–NO_3^-. In this system, however, even in the most concentrated nitrate solutions, the trinitrate complex $[UO_2(NO_3)_3]^-$ did not form.

2. *The exchange of co-ordinated organic solvent molecules for water molecules.* It seemed to be of interest, in addition to the experiments described in the previous sections, to study also the character of spectral changes accompanying the exchange of electrically neutral ligands in uranyl complexes. Ligand exchange of this kind has already been dealt with in a previous paper[11] where the system $UO_2(NO_3)_2$–TBP–C_4H_9OH was investigated. In the present work we have investigated the exchange of several organic solvents for water in the co-ordination sphere of the uranyl ion. This kind of ligand exchange is of some practical importance as it usually takes place in solutions of uranyl salts in organic solvents.

In the first place the spectra of solutions of uranyl nitrate in n-butyl alcohol at varying concentration of water have been determined. This is one of the few organic solvents apart from tri-n-butyl phosphate for which nearly anhydrous solutions of uranyl nitrate can be prepared relatively simply.

All solutions in this series of experiments were acidified with nitric acid, its concentration varying between 0·012–0·025 M. This concentration proved to be necessary to avoid the errors due to hydrolysis. Nonacidified solutions showed higher extinction values.

Assuming a stoichiometric exchange of ligands we should expect the following series of complexes to be formed on increasing the concentration of water in the solutions:

$$[UO_2Bu_2(NO_3)_2] \dashrightarrow [UO_2(NO_3)_2BuH_2O] \dashrightarrow [UO_2(NO_3)_2(H_2O)_2] \dashrightarrow$$
$$\dashrightarrow \dots\dots\dots\dots \longrightarrow [UO_2(H_2O)_6]^{2+}$$

There is little doubt that in the region of lowest concentrations of water in the solutions a displacement of alcohol molecules rather than of nitrate ions by water will take place.

Several of the extinction curves determined are presented in Fig. 5. As may be seen from the figure the exchange of butyl alcohol molecules for water in the co-ordination sphere of the uranyl ion is accompanied by a considerable change of the absorption band, its position being shifted towards shorter wavelengths. Also in this series of experiments a range of concentrations may be observed, within which the corresponding absorption curves lose their vibrational fine structure (e.g. the curve corresponding to a water concentration of 6·69 M). From Fig. 5 it is evident that this effect results from a superposition of the spectra of different species.

---

[14] S. MINC and A. UGNIEWSKA, *Radiokhimiya* 3, 137 (1961).

Further examples of spectral changes due to penetration of water into the co-ordination sphere of the uranyl ion are given by the absorption curves presented in Fig. 6. They represent the spectra of solutions of uranyl nitrate dihydrate in anhydrous and nearly water saturated solvents of different chemical constitution, viz.: cyclohexanone, n-butyl ether and isoamyl acetic ester. In this case even solutions with the lowest water content probably contained water in the co-ordination sphere of the uranyl ion. Although it is difficult to define more closely the ligand exchange process taking place in this case it may be seen that the corresponding changes of the spectrum are of the same magnitude as those observed in other processes of ligand exchange involving the uranyl ion.

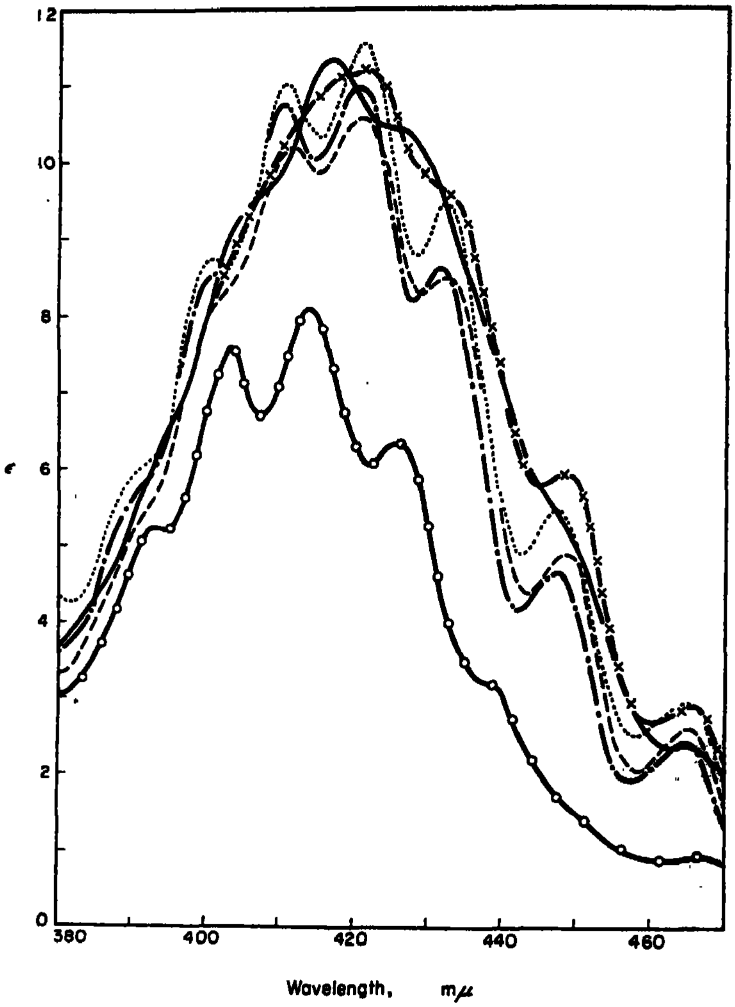

FIG. 5.—Absorption spectra of $UO_2(NO_3)_2$ in n-butyl alcohol at various concentrations of water: —·— 0·05 M, - - - 0·94 M, — × — 3·47 M, — 6·69 M, · · · · 0·02 M, non-acidified solution, — ○ — water solution.
The concentration of uranyl nitrate was 0·0727–0·0749 M.

From the experiments above the conclusion may be drawn that uranyl nitrate in organic solvent solutions containing small quantities of water may exist in the form of various complexes possessing different spectra. This fact must be taken into consideration in all spectrophotometric investigations of the formation of uranyl complexes in organic media.

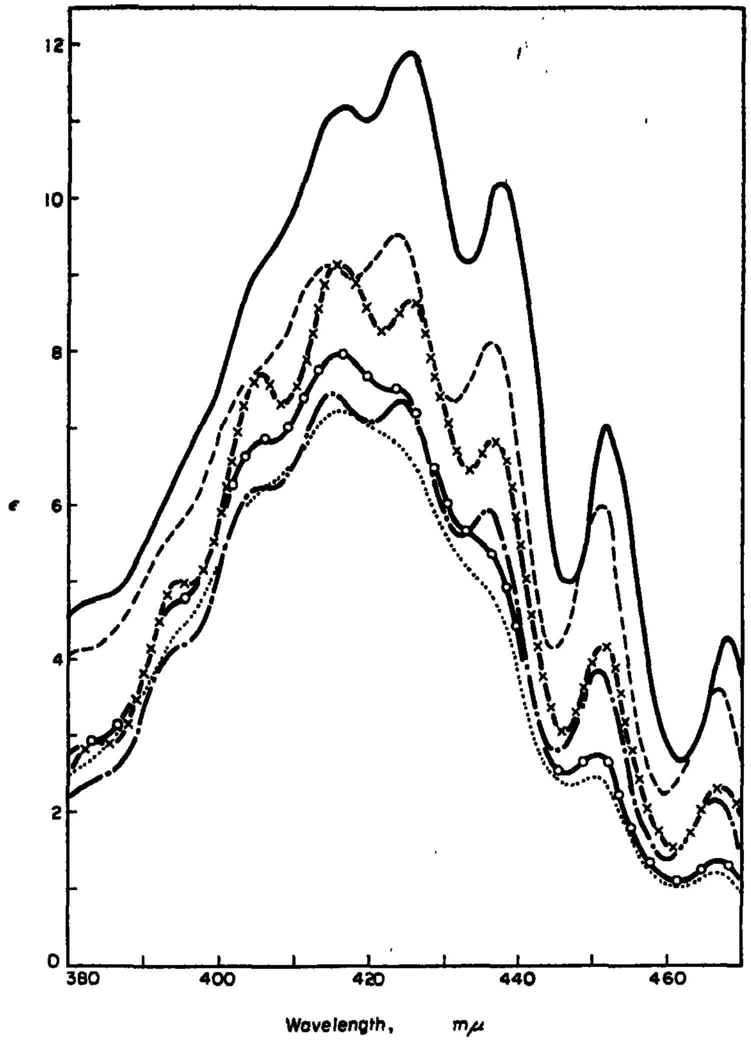

Fig. 6.—Absorption spectra of $UO_2(NO_3)_2 \cdot 2H_2O$ in different organic solvents at various concentrations of water: — ○ — 0·33 M in n-butyl ether, · · · · 0·60 M in n-butyl ether, — × — 0·27 M in isoamyl acetic ester, — · — 1·27 M in isoamyl acetic ester, —— 0·19 M in cyclohexanone, - - - 2·16 M in cyclohexanone. The concentration of uranyl nitrate was 0·0731–0·129 M.

On the interpretation of the absorption band of the uranyl ion

According to Jørgensen[5] the characteristic absorption band of the uranyl ion, usually located between 370 and 480 mμ, is due to the transfer of an odd electron from a ligand to the empty 5*f*-shell of a uranium atom. Our work introduces some new considerations in the interpretation of this band.

In typical electron-transfer spectra the displacement of water molecules of hydrated cations by other ligands of lower ionization potentials results in the appearance of new absorption bands in the range of longer wavelengths in comparison with the positions of absorption bands of hydrated cations. Thus the formation of chloro complexes of lead(II) in water solution manifests itself by the appearance of a new band ca. 3800 cm^{-1} distant from the absorption band of the hydrated cation and displaced towards longer wavelengths(15). The corresponding difference in the case of cupric chloro complexes amounts to ca. 10,000 cm^{-1},(16) and in the case of ferric chloro complexes to 16,000 cm^{-1}.(17) Moreover the lower halogeno complexes of the above mentioned metals possess at the same time the charge transfer bands characteristic of hydrated cations as well as the bands corresponding to the other ligand.(18) None of these characteristic features of charge transfer spectra are observed among the spectral effects accompanying complex formation by the uranyl cation. The appearance of new absorption bands on introduction of new ligands into the co-ordination sphere of this ion have not been observed, and the differences in the positions of the absorption band for different complexes are not obviously related to the ionization potentials of the corresponding ligands. Even the formation of chloro complexes in aqueous solution only manifests itself in the spectrum of the uranyl ion by a shift of about 790 cm^{-1} towards the red.(13)

The author believes that these facts may be understood by assuming that the band in question is due to an electron process localized within the UO_2^{2+} group, and does not correspond to the transfer of an electron from a ligand co-ordinated by this ion to the uranium atom. Possibly it might correspond to an electron transfer from O^{2-} to U^{6+} in the UO_2 group. The rather large dependence of the band on the properties of the solvent supports the charge-transfer interpretation of JØRGENSEN, with the limitation formulated above.

CONCLUSIONS

(1) The differences in intensity of the absorption band between 370 and 480 mμ of the same uranyl complex when dissolved in different solvents may amount to several score per cent. At the same time the position of the absorption band and the distribution of intensities among the component oscillation bands remains practically unaffected.

(2) The magnitude of the effect of ionic medium (and of eventual outer-sphere association) on the absorption band of uranyl complexes depends on their structure. It is rather small in the case of complexes "well isolated" from outer interactions. In the case of uranyl complexes possessing water in their co-ordination spheres the effect of outer-sphere association on the spectrum seems to be marked. It consists of a significant increase of intensity, accompanied by some diffusion of the oscillation structure and small change of the position of the band.

(3) Ligand exchange in the co-ordination spheres of uranyl ions is accompanied by a displacement of the absorption band of several millimicrons and a change of intensity distribution among component oscillation bands. The magnitude of the displacement contradicts the interpretation of the band by an electron-transfer between ligands of

---

(15) H. FROMHERZ and KUN-HOU LIH, *Z. Phys. Chem.* A **153**, 321 (1931).

(16) E. DOEHLEMANN and H. FROMHERZ, *Z. Phys. Chem.* A **171**, 353 (1934).

(17) G. A. GAMLEN and D. O. JORDAN, *J. Chem. Soc.* 1453 (1953), D. E. METZLER and R. MYERS, *J. Amer. Chem. Soc.* **72**, 3776 (1950).

(18) W. LIBUŚ. To be published.

the uranyl ion and the empty 5*f*-shell of the uranium atom. The conclusion is that the absorption band corresponds to an electron process localized in the UO_2 group.

(4) Complete, or almost complete disappearance of component oscillation bands in the spectrum of solutions results from the superposition of spectra of different complexes present. The oscillation bands in the spectra of individual complexes are the better developed, the less is the possibility of interaction of co-ordinated ligands with the medium.

(5) Owing to the significant effect of the medium on the spectra of individual uranyl complexes, the possibility of application of light absorption measurements in the range 370–480 mμ in investigations of complex forming equilibria is rather limited. Nevertheless the observation of spectral changes with gradually changing concentrations may lead to important conclusions regarding the character of the processes undergone by the uranyl ion in the corresponding solutions.

Acknowledgement—The author wishes to express her sincere thanks to Professor S. Minc, for his continued interest and for helpful discussions.

Inorg. Nucl. Chem., 1962, Vol. 24, pp. 633 to 636. Pergamon Press Ltd. Printed in Northern Ireland

COMPOUND FORMATION IN THE SYSTEM CADMIUM OXIDE-BORIC OXIDE

P. B. Hart and E. G. Steward*
The General Electric Company Limited, Central Research Laboratories,
Hirst Research Centre, Wembley, England

(*Received* 14 *October* 1961)

Abstract—Compound formation has been investigated in the $CdO\text{-}B_2O_3$ system. From X-ray examination, differential thermal analysis, and high temperature microscopy, it is concluded that three compounds can be prepared by ceramic techniques; $3CdO.B_2O_3$, $2CdO.B_2O_3$, and $2CdO.3B_2O_3$. In contrast with the findings of other workers, the $2CdO.B_2O_3$ compound was not found to be metastable below 780°C, nor could a $3CdO.2B_2O_3$ compound be prepared.

The first investigators to make a full study of the $CdO\text{-}B_2O_3$ system were Subbarao and Hummel(1) who in 1956 reported fully on the thermal, optical and X-ray diffraction characteristics of the four compounds they obtained, $3CdO.B_2O_3$, $2CdO.B_2O_3$, $3CdO.2B_2O_3$ and $2CdO.3B_2O_3$. From partial studies of the system, earlier workers(2,3) had described 2:1, 1:1 and 2:3 $CdO.B_2O_3$ compounds but Subbarao and Hummel could find no evidence for the existence of a 1:1 compound.

In connection with other investigations, some cadmium borate compounds were needed, and an attempt was made to prepare the four reported by Subbarao and Hummel. Three of the compounds were readily obtained, but a number of attempts to prepare the fourth compound, $3CdO.2B_2O_3$, were not successful. To investigate this apparent discrepancy further, a more detailed study of the system was made.

EXPERIMENTAL METHODS

Laboratory grade boric acid, cadmium oxide and cadmium carbonate were used. The various preparations were made by thoroughly mixing and grinding the starting materials in appropriate proportions, firing and then regrinding before a final heat treatment. Platinum vessels were used throughout. The details of the treatment for each preparation are given in Table 1.

Compositions were checked by the weight loss which occurred on firing and also by chemical analyses, and always agreed closely with the nominal compositions as listed in Table 1. X-ray diffraction patterns were obtained using a Philips 11·46 cm diameter camera, with Ni-filtered Cu-radiation. More accurate intensity measurements were also made with a Philips High-Angle diffractometer, and a proportional counter.

Differential thermal analysis (D.T.A.) was used to examine a number of the preparations. One gramme samples were placed in a platinum crucible, and an identical crucible was filled with a dried α-alumina. The two crucibles, placed in a ceramic holder, were heated to 1000°C in a horizontal tube furnace at a rate of 10°C/min. The temperature difference between the sample and standard was measured using a differential Pt/Pt 13% Rh/Pt thermocouple, the output from which was fed through a d.c. amplifier to a pen recorder. The temperature of the standard was obtained with another Pt/Pt 13% Rh thermocouple and recorded on the same chart.

Melting points were also determined with an apparatus similar to that described by Welch(4). A small specimen is observed, through a microscope, at the tip of a thermocouple junction, and is heated by passing an electric current through the thermocouple wire. A rapid switching device enables the thermal e.m.f. to be measured as the sample is heated.

---

* Now at Northampton College of Advanced Technology, London.

(1) E. C. Subbarao and F. A. Hummel, *J. Electrochem. Soc.* **103**, 29 (1956).

(2) Th. P. J. Botden and F. A. Kroger, *Physica* **13**, 261 (1947).

(3) C. Mazetti and F. deCarli, *Gass. Chim. Ital.* **56**, 19 (1926).

(4) J. H. Welch, *J. Sci. Instrum.* **31**, 458 (1954).

Sodium chloride [m.p. 800·4°C(5)] was used as a standard substance for melting point determinations. These were found to be reproducible within ±5°C, both by D.T.A. and by microscopy methods.

RESULTS AND DISCUSSION

Table 1 lists the preparations examined and gives details of heat treatment and the phases detected by X-ray examination. Three compounds were found in the system, $3CdO.B_2O_3$, $2CdO.B_2O_3$ and $2CdO.3B_2O_3$ and X-ray powder diffraction data for them are listed in Table 3. SUBBARAO and HUMMEL also found these three compounds, and their X-ray data are in fair agreement with those of the present investigation. In neither study was a $CdO.B_2O_3$ compound detected. However, a $3CdO.2B_2O_3$ compound was found by SUBBARAO and HUMMEL, who also reported that the $2CdO.B_2O_3$ compound was unstable below 780°C. Neither of these two findings could be confirmed.

TABLE 1.—MOLAR COMPOSITIONS OF PREPARATIONS, MATERIAL USED, HEAT TREATMENT AND COMPOUNDS DETECTED BY X-RAY EXAMINATION

	$CdO:B_2O_3$ ratios	Materials used	Heat treatment	Compounds detected
1	3:1	Boric acid and cadmium oxide	16 hr at 850°C	$3CdO.B_2O_3$
2	2:1	Boric acid and cadmium oxide	16 hr at 850°C	$2CdO.B_2O_3$
3	3:2	Boric acid and cadmium oxide	16 hr at 850°C	A mixture of $2CdO.B_2O_3$ and $2CdO.3B_2O_3$
4	5:4	Boric acid and cadmium oxide	16 hr at 850°C	A mixture of $2CdO.B_2O_3$ and $2CdO.3B_2O_3$
5	1:1	Boric acid and cadmium oxide	16 hr at 850°C	A mixture of $2CdO.B_2O_3$ and $2CdO.3B_2O_3$
6	2:3	Boric acid and cadmium oxide	16 hr at 850°C	$2CdO.3B_2O_3$
7	4:9	Boric acid and cadmium oxide	16 hr at 800°C	$2CdO.3B_2O_3$ and 'glassy' B_2O_3
8	2:1	Further heat treatment of preparation 2	40 hr at 725°C	$2CdO.B_2O_3$
9	2:1	Boric oxide and cadmium oxide	16 hr at 725°C	$2CdO.B_2O_3$
10	2:1	Boric oxide and cadmium carbonate	16 hr at 725°C	$2CdO.B_2O_3$

In a careful study of the region between $2CdO.B_2O_3$ and $2CdO.3B_2O_3$, no evidence was found for the existence of a $3CdO.2B_2O_3$ compound and mixtures of the 2:1 and 2:3 compounds were always formed. The X-ray diffraction patterns shown in Fig. 1 illustrate this for the $3CdO.2B_2O_3$ composition. These findings were supported by D.T.A. and high temperature microscope studies. Liquidus temperatures for several compositions were measured by both these methods, and results in good agreement were obtained. Comparison with the earlier data is made in Table 2 and it will be seen that for the $3CdO.2B_2O_3$ composition, the two results differ substantially. The lower value of the present investigation is consistent with the presence of a mixture.

---

(5) H. S. ROBERTS, *Phys. Rev.* 23, 386 (1924).

(6) P. B. HART and S. E. F. SMALLWOOD, Paper in preparation.

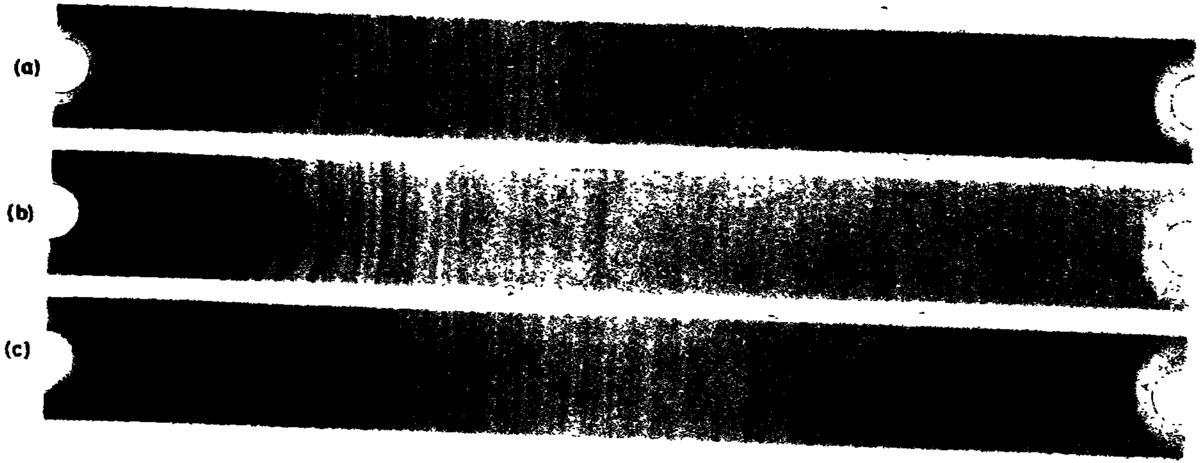

FIG. 1.—X-ray diffraction patterns of (a) the $2CdO.B_2O_3$ compound (b) a $3CdO:2B_2O_3$ composition. Faint lines of the 2:3 compound can be seen. (c) the $2CdO.3B_2O_3$ compound.

Subbarao and Hummel also reported that below 780°C the 2:1 compound ed to decompose into the 3:1 and 3:2 compounds, various 2CdO:B_2O_3 composi- made from different starting materials were fired at 725°C. It was found that the pound was as readily formed at 725°C as at 780°C, and no decomposition was d after heating for over 40 hr at 725°C.

2.—Melting temperatures determined by D.T.A. and high temperature microscopy

No.	CdO:B_2O_3 Ratio	m.p. (°C) D.T.A.	m.p. (°C) microscopy	m.p. (°C) (Subbarao and Hummel)
2	2:1	974	977	980 ± 5
3	3:2	952	960	1005 ± 5
6	2:3	972	975	980 ± 5

Estimated error in both D.T.A. and microscopy methods ±5°C.

Table 3.—X-ray diffractometer data

3CdO.B_2O_3		2CdO.B_2O_3		2CdO.3B_2O_3	
d	I/I_0	*d*	I/I_0	*d*	I/I_0
4·21	30	6·11	20	5·51	65
3·71	20	5·92	30	5·37	100
3·60	10	4·62	100	4·62	40
3·40	20	4·37	15	4·15	50
3·23	25	3·20	45	4·10	25
2·98	35	3·06	35	3·72	65
2·90	25	3·00	25	3·59	50
2·86	100	2·96	40	3·55	35
2·81	15	2·83	100	3·20	90
2·78	20	2·76$_8$	60	2·98	20
2·67	80	2·75$_6$	40	2·92	50
2·43	75	2·71	25	2·56	90
2·38	20	2·58	25	2·28	50
1·86	20	2·56	15	2·01	35
1·81	20	2·40	15	1·97	50
1·78$_8$	40	2·38	5	1·84	15
1·77$_7$	20	2·33$_2$	10	1·83	20
1·70	20	2·32$_6$	15	1·82	25
1·68	15	2·25	15	1·78	20
1·66	15	2·22	15	1·73	20
1·49$_2$	15	2·09	50		
1·48$_8$	10	2·02	20		
1·46	25	1·73$_0$	25		
		1·72$_6$	20		
		1·72$_2$	15		
		1·63$_8$	20		
		1·63$_6$	15		
		1·59	20		

The conclusions from our own work are reinforced by some of the observations of Subbarao and Hummel. Their sets of X-ray data for the 3:2 and 2:1 compounds have many strong lines in common, and both sets contain additional lines when compared with our own data. In optical properties there is a marked similarity; both the 2:1 and the 3:2 compounds form highly birefringent crystals, with refractive indices surprisingly close in view of the difference in cadmium oxide content. Taken alone, these properties of the 3:2 composition would certainly suggest that the 2:1 compound was the major constituent, with smaller amounts of another material also present.

From the structural viewpoint, a $3MO.2B_2O_3$ compound is possible; the simplest anion would have the formula $(B_4O_9)^{6-}$ and a possible structure would be a chain of four boron atoms linked by oxygens. However, no such compound or anion has yet been reported in other divalent metal borate systems. In a study of borate anions and their structures by infra-red methods⁽⁵⁾ a $3CdO:2B_2O_3$ composition was examined, and the spectrum obtained was clearly that of a mixture of the $2CdO.B_2O_3$ and the $2CdO.3B_2O_3$ compounds.

Three compounds only have been identified in the $CdO–B_2O_3$ system in this work; these are $3CdO.B_2O_3$ and $2CdO.3B_2O_3$. No evidence has been found for either a $CdO.B_2O_3$ or a $3CdO.2B_2O_3$ compound.

J. Inorg. Nucl. Chem., 1962, Vol. 24, pp. 637 to 639. Pergamon Press Ltd. Printed in Northern Ireland

PREPARATION OF ANHYDROUS LANTHANON ACETATES BY DESOLVATION*

J. R. WITT† and E. I. ONSTOTT
University of California, Los Alamos Scientific Laboratory, Los Alamos, New Mexico

(*Received* 2 *May* 1961; *in revised form* 14 *June* 1961)

Abstract—Anhydrous acetates of Y, La, Eu, Gd, Tb, Dy, Ho, Er, Tm, Yb and Lu were prepared by desolvation of the acetates in vacuum at 150°C after dissolution of the oxides in 50 per cent acetic acid and evaporation to dryness. Acetates of Pr and Nd did not reach constant composition before decomposition occurred. A hemihydrate of Sm acetate was formed which decomposed at temperatures above 150°C without converting to the anhydrous acetate. Hemihydrates of Tb and Ho were formed at about 75°C.

THE anhydrous acetates of the heavy lanthanons are particularly useful for studying the electrochemical separation of these lanthanons in methanol electrolytes.(1) It was therefore of interest to find an easy method of synthesis and to characterize the resulting preparations.

It was found that acetates of the heaviest lanthanons, prepared by evaporation to dryness of the aqueous acetic acid solutions, are easily desolvated to give the anhydrous salts. Consequently this method was extended to include a study of the entire series except for Ce and Pm.

Methods of preparing the anhydrous acetates of some of the lanthanons have been reviewed by SEATON, *et al.*,(2) who prepared anhydrous acetates of La, Nd and Sm by refluxing the oxides with acetic anhydride.(2) We were able to confirm their results. More recently, MOELLER, GALASYN and XAVIER(3) described preparation of anhydrous acetates of La, Dy, Ho, Er, Yb and Y by treatment with N,N-dimethylformamide and benzene with subsequent azeotropic distillation. Anhydrous acetates of Ce, Pr, Nd, Sm, Eu, and Gd were prepared by the same workers(3) by vacuum desolvation of N,N-dimethylformamide monosolvates of these lanthanon acetates.

EXPERIMENTAL

Lanthanons. The oxides were recently purchased from commercial suppliers and specified to be of 99·9 per cent or better purity.

Method. Ten grammes of the oxide were dissolved in about 500 ml of 50 per cent acetic acid on a steam plate and the resulting solution was evaporated to dryness with the temperature of the crystallizing salt kept at about 75°C until most of the solvent was removed.‡ The dried salt was then transferred to a weighing bottle and placed in a Pyrex vacuum desiccator containing NaOH (Ascarite) and $Mg(ClO_4)_2$. After evacuation with a vacuum pump the entire desiccator was heated in an oven at the desired temperature (See Table 2) until the salt reached a constant weight.

---

* Work was done under the auspices of the Atomic Energy Commission. Reprint requests should be sent to the Los Alamos Scientific Laboratory, P.O. Box 1663, Los Alamos, New Mexico.

† Present address: Department of Chemistry, The University of Minnesota, Minneapolis, Minn.

‡ Pr, Nd and Sm form a viscous polymeric glass on evaporation.

(1) E. I. ONSTOTT, Division of Inorganic Chemistry, 138th Meeting, ACS, New York, N.Y., 1960.

(2) J. A. SEATON, F. G. SHERIF and L. F. AUDRIETH, *J. Inorg. Nucl. Chem.* 9, 222 (1959).

(3) T. MOELLER, V. GALASYN and J. XAVIER, *J. Inorg. Nucl. Chem.* 15, 259 (1960).

Oxides of the lighter lanthanons were generally easily dissolved, but the heavy lanthanons were much more slowly dissolved. For example, the Lu_2O_3 sometimes required a week of heating on a steam plate for complete dissolution. Hydrogen peroxide was used to aid the dissolution of Pr_6O_{11} and Tb_4O_7.

Analyses. The metal was determined by the classic method of ignition to the oxide. Carbon and hydrogen analyses were done in the conventional manner. Samples of about 200 mg were burned in a stream of dry oxygen so that the weighed CO_2 and H_2O samples would be large enough to give good precision. The precision on carbon determinations was better than five parts per 1000 and the precision on hydrogen determinations was ten parts per 1000 or better.

Analytical results on prepared acetates are given in Table 1.

TABLE 1.—ANALYTICAL DATA ON ANHYDROUS ACETATES AND HEMIHYDRATES

Lanthanon acetate	Calculated			Found		
	H (%)	C (%)	Ln (%)	H (%)	C (%)	Ln (%)
$Y(OAc)_3$	3·41	27·09	33·42	3·42	26·96	33·7
$La(OAc)_3$	2·87	22·80	43·96	2·83	22·74	43·8
$Eu(OAc)_3$	2·76	21·89	46·18	2·74	21·81	46·3
$Gd(OAc)_3$	2·71	21·55	47·03	2·69	21·47	47·2
$Tb(OAc)_3$	2·70	21·44	47·29	2·68	21·31	47·1
$Dy(OAc)_3$	2·67	21·22	47·85	2·63	21·10	48·0
$Ho(OAc)_3$	2·65	21·07	48·22	2·63	20·89	48·4
$Er(OAc)_3$	2·63	20·92	48·57	2·61	20·77	48·7
$Tm(OAc)_3$	2·62	20·82	48·82	2·62	20·73	48·8
$Yb(OAc)_3$	2·59	20·58	49·42	2·57	20·41	49·6
$Lu(OAc)_3$	2·58	20·46	49·70	2·57	20·43	49·8
$Sm(OAc)_3{\cdot}0{\cdot}5\ H_2O$	3·00	21·41	44·68	2·95	21·27	45·0
$Tb(OAc)_3{\cdot}0{\cdot}5\ H_2O$	2·92	20·87	46·02	2·90	20·90	46·0
$Ho(OAc)_3{\cdot}0{\cdot}5\ H_2O$	2·86	20·43	46·77	2·86	20·51	47·1

Infra-red observations. Some of the anhydrous acetates were examined with a Baird Model B spectrophotometer by incorporating the acetates in potassium bromide pellets. Absence of hydroxy salts, hydrates and acetic acid solvates were indicated by the low absorption at the wavelengths where OH normally strongly absorbs.

DISCUSSION OF RESULTS

The conditions required to obtain acetates of definite composition are listed in Table 2.

Pr and Nd are included in the table but do not reach a constant composition before decomposition occurs. Sm forms a hemihydrate at 150°C which decomposes at higher temperatures before the remaining solvent is removed. Tb and Ho likewise form hemihydrates, but at a lower temperature of about 75°C. Desolvation of the latter two salts takes place completely at 150°C and the anhydrous acetates are formed. We made no attempt to prepare hemihydrates other than those listed.

The behaviour of Y is expected since it normally behaves more like the middle and heavy lanthanons than like Pr, Nd and Sm. The behaviour of Pr, Nd and Sm in not forming anhydrous acetates by the same desolvation procedure that anhydrous acetates of Eu and heavier lanthanons are formed seems to indicate an effect of ion size on crystal structure. However, La with the largest cation radius is perhaps unusual in forming the anhydrous acetate by desolvation. The crystal structure of anhydrous La and Eu acetates would not be expected to be similar, but anhydrous

TABLE 2.—COMPOSITION OF ACETATE SALTS

Lanthanon	Desolvation temp. (°C)*	Acetate salt
Y	150	$Y(OAc)_3$
La	150	$La(OAc)_3$
Pr	175	Uncertain†
Nd	175	Uncertain†
Sm	150	$Sm(OAc)_3 \cdot 0{\cdot}5\ H_2O$
Eu	150	$Eu(OAc)_3$
Gd	150	$Gd(OAc)_3$
Tb	75	$Tb(OAc)_3 \cdot 0{\cdot}5\ H_2O$
Tb	150	$Tb(OAc)_3$
Dy	150	$Dy(OAc)_3$
Ho	75	$Ho(OAc)_3 \cdot 0{\cdot}5\ H_2O$
Ho	150	$Ho(OAc)_3$
Er	120	$Er(OAc)_3$
Tm	120	$Tm(OAc)_3$
Yb	75	$Yb(OAc)_3$
Lu	75	$Lu(OAc)_3$

* Constant composition generally reached in 24 hr.
† Decomposed without reaching constant weight.

Eu and Gd acetates could possibly be isostructural. A cursory examination of X-ray powder photographs of anhydrous acetates of La, Eu and Gd showed that the patterns differed so much from each other that any isostructuralism seems highly improbable.

Although the anhydrous acetates of Er, Tm, Yb and Lu can be prepared at temperatures below 150°C, these acetates are stable at 150°C. Thus all of the lanthanons which form anhydrous acetates by desolvation can be prepared at 150°C.

This method complements the method of SEATON *et al.*[2] and the method of MOELLER, GALASYN and XAVIER for preparing anhydrous lanthanon acetates. Anhydrous Pm acetate which has not been prepared probably could be obtained by both of the above mentioned methods since both Nd and Sm anhydrous acetates can be synthesized,[2,3] but it is uncertain whether a hemihydrate or indefinite composition would be obtained by the method used in this work.

Measurements with a thermobalance would have given more information than we obtained, but our main interest was in a method of preparation. We do not anticipate further studies on this problem.

Acknowledgement—The authors wish to thank F. H. ELLINGER for the X-ray photographs and the interpretation.

J. Inorg. Nucl. Chem., 1962, Vol. 24, pp. 641 to 644. Pergamon Press Ltd. Printed in Northern Ireland

THE VAPOUR-PRESSURE AND TRANSITION POINTS OF TcF_6*

H. Selig and J. G. Malm
Argonne National Laboratory, Argonne, Illinois

(*Received* 12 *January* 1962)

Abstract—The vapour-pressure and transition points of TcF_6 have been measured. The vapour-pressure is represented by the following equations: Solid I ($-16{\cdot}32$ to $-5{\cdot}3°$) $\log_{10}p = -(3564{\cdot}8/T) - 10{\cdot}787 \log_{10} T + 41{\cdot}1252$; Solid II ($-5{\cdot}3$ to $37{\cdot}4°$) $\log_{10}p = -(2178{\cdot}0/T) - 2{\cdot}295 \log_{10} T + 15{\cdot}33427$; Liquid ($37{\cdot}4$–$51{\cdot}67°$) $\log_{10}p = -(2404{\cdot}9/T) - 5{\cdot}8036 \log_{10} T + 24{\cdot}8087$. TcF_6 undergoes a solid–solid transition at $-4{\cdot}54°$ and melts at $37{\cdot}4°$.

THE THIRD transition group elements from tungsten through platinum form a series of volatile hexafluorides which are remarkable for the regularity they exhibit in their physical properties, such as vapour-pressures and transition points.(1–3)

Until recently molybdenum was the only element known to form a volatile hexafluoride in the second transition group. This has recently been augmented by the preparation and identification of additional hexafluorides in this series, those of technetium,(4) ruthenium,(5) and rhodium.(6)

A study of the properties of the hexafluorides of this series has been undertaken at this laboratory. We report here our measurements of the vapour-pressure and transition points of technetium hexafluoride.

EXPERIMENTAL

Technetium hexafluoride was prepared by the reaction of pure distilled fluorine gas on Tc metal at 400°. It was purified by sublimation at reduced pressures as described elsewhere.(7) The purity was checked by inspection of the infra-red spectrum(8) and the intercomparison of numerous samples prepared in different batches as well as different cuts from the same batch. A convenient check-point for this purpose is the vapour pressure at 0°. The absence of extraneous infra-red peaks and the constancy of the ice-point from sample to sample attested to the purity of the TcF_6.

Vapour-pressure measurements on 1 g samples were made with a quartz differential Bourdon gauge used as a null instrument. A description of this apparatus and its mode of operation is given elsewhere.(9) The over-all sensitivity of the gauge was $\pm 0{\cdot}02$ mm Hg. The thermostated bath was regulated to $\pm 0{\cdot}01°$ as measured with a copper-constantan thermocouple which had been calibrated against a Bureau of Standards platinum resistance thermometer.

The triple point and solid–solid transformation temperature of TcF_6 were measured by the thermal arrest method. The procedure was similar to that described elsewhere,(9) except that the glass bulb was replaced by an all-nickel welded bulb.

* Based on work performed under the auspices of the U.S. Atomic Energy Commission.

(1) G. H. Cady and G. B. Hargreaves, *J. Chem. Soc.* 1563 (1961).
(2) J. G. Malm and H. Selig, *J. Inorg. Nucl. Chem.* **20**, 189 (1961).
(3) B. Weinstock, J. G. Malm and E. E. Weaver, *J. Amer. Chem. Soc.* **83**, 4310 (1961).
(4) H. Selig, C. L. Chernick and J. G. Malm, *J. Inorg. Nucl. Chem.* **19**, 377 (1961).
(5) H. H. Claassen, H. Selig, J. G. Malm, C. L. Chernick and B. Weinstock, *J. Amer. Chem. Soc.* **83**, 2390 (1961).
(6) C. L. Chernick, H. H. Claassen and B. Weinstock, *J. Amer. Chem. Soc.* **83**, 3165 (1961).
(7) B. Weinstock and J. G. Malm, *J. Inorg. Nucl. Chem.* **2**, 380 (1956).
(8) H. H. Claassen, H. Selig and J. G. Malm, *J. Chem. Phys.* In Press.
(9) B. Weinstock, E. E. Weaver and J. G. Malm, *J. Inorg. Nucl. Chem.* **11**, 104 (1959).

RESULTS

The vapour-pressure data for the two solid and the liquid phases of TcF_6 are given in Table 1. Temperatures are given in degrees Kelvin and pressures in mm Hg at 0° and standard gravity. The following equations which were derived by the method of least squares summarize the results:

Solid I (−16·32 to −5·3°)

$$\log_{10} p = -\frac{3564\cdot8}{T} - 10\cdot787 \log_{10} T + 41\cdot1252 \tag{1}$$

Solid II (−5·3 to +37·4°)

$$\log_{10} p = -\frac{2178\cdot0}{T} - 2\cdot295 \log_{10} T + 15\cdot33427 \tag{2}$$

Liquid (+37·4–51·67°)

$$\log_{10} p = -\frac{2404\cdot9}{T} - 5\cdot8036 \log_{10} T + 24\cdot8087 \tag{3}$$

Each point was weighted by its observed vapour-pressure, since the reading of the pressure was considered to be the major uncertainty in the measurement.

The calculated solid-solid transition point from simultaneous solution of equations (1) and (2) is −4·54° in comparison to the measured value of −5·3°. The calculated triple point from the simultaneous solution of equations (2) and (3) is 37·36° compared to a measured value of 37·4°. The boiling point of TcF_6 calculated using equation (3) is 55·3°.

Thermodynamic calculations. The heats of sublimation and vaporization of TcF_6 were derived from the vapour-pressure equations using the Clausius-Clapeyron relation. The heat of sublimation at 37·4° is 8555 cal $mole^{-1}$ and the heat of vaporization at this temperature is 7427 cal $mole^{-1}$. The heat of fusion is 1128 cal $mole^{-1}$ and the entropy of fusion is 3·63 e.u. The heat of sublimation of solid I at −5·3° is 10,577 cal $mole^{-1}$. The heat of sublimation of solid II is 8750 cal $mole^{-1}$ at this temperature. The heat of transition calculated from the heats of sublimation at the transition point is 1827 cal $mole^{-1}$ and the entropy of transition is 6·82 e.u. The Trouton constant for liquid TcF_6 is 22·0 cal $mole^{-1}$ $°C^{-1}$.

DISCUSSION

Extensive surveys of the vapour-pressures and transition points of the "5*d*" hexafluorides as well as of MoF_6 have been completed recently.(1,3) The volatilities of the "5*d*" hexafluorides decrease regularly in going across the series while the solid–solid transition temperatures and triple points increase in a regular fashion. The present work combined with the MoF_6 data as well as some preliminary data for RuF_6(5) and RhF_6(6) confirm that a similar regularity exists in the "4*d*" series.

This may possibly be explained qualitatively in the following way. The M-F distances from WF_6 to IrF_6 are practically constant.* By analogy the same situation probably obtains in the "4*d*" series. However, the cell constants of the solid phases in both series decrease regularly in going across the series.(11) It is reasonable therefore

---

* Preliminary results by Kimura *et al.*(10)

(10) Kimura, Weinstock and Schomaker, *Proceedings of the Second International Conference on the Peaceful Use of Atomic Energy, Geneva,* 1958, P/942 United Nations (1958).

(11) D. Northrop and S. Siegel. Private communication.

TABLE I.—VAPOUR-PRESSURE OF TcF_6

T(°K)	Observed pressure (mm Hg)	$P_{obs} - P_{calc}$ (mm Hg)
Solid I		
256·83	17·90	0·02
257·95	19·60	0·00
258·97	21·24	−0·05
259·74	22·64	−0·01
260·77	24·62	0·03
261·85	26·62	−0·15
262·03	27·24	0·08
263·00	29·39	0·10
263·19	29·76	0·03
264·06	31·76	−0·03
264·19	32·11	0·00
265·17	34·54	−0·07
265·68	35·94	−0·03
266·24	37·40	−0·12
266·29	37·75	0·08
266·69	38·97	0·16
267·68	41·73	−0·06
Solid II		
268·32	43·96	−0·03
268·71	44·95	−0·10
269·88	48·35	−0·01
269·98	48·62	−0·03
272·00	54·85	−0·05
272·20	55·70	0·14
273·15	58·79	0·03
274·08	62·17	0·12
274·54	63·42	−0·32
275·12	65·93	0·01
275·69	68·50	0·37
276·12	69·79	−0·05
277·31	75·13	0·37
278·52	80·50	0·44
279·25	83·20	−0·22
280·08	87·34	−0·04
281·32	93·45	−0·15
282·17	97·89	−0·20
284·16	109·24	−0·07
286·12	121·21	−0·22
286·49	123·81	−0·03
288·12	134·75	−0·21
289·12	142·13	−0·07
290·10	149·29	−0·33
291·05	157·05	−0·07
293·06	173·88	−0·18
294·59	188·19	0·22
296·05	202·6	0·4
297·53	217·8	0·4
297·79	220·3	0·1
298·19	224·2	−0·3
299·22	236·8	0·4
299·96	244·2	−0·4
300·51	251·8	0·6
301·98	270·1	0·7
302·60	276·9	−0·5
302·64	277·8	−0·1
302·71	278·4	−0·4
302·72	278·6	−0·3
303·44	289·3	0·8
304·10	297·4	−0·2
304·19	298·0	−0·8
304·28	299·9	−0·2
304·96	310·4	0·7
305·90	323·1	−0·4
305·93	323·3	−0·6
306·92	340·6	1·6
308·16	358·9	0·2
309·16	374·1	−1·2
310·03	390·6	0·4
Liquid		
311·11	407·9	−0·2
312·05	323·5	0·4
313·15	440·5	−0·7
313·94	454·6	−0·1
314·07	457·4	0·6
315·33	478·1	−0·8
316·11	494·3	1·3
317·17	511·9	−0·8
318·04	530·4	1·1
319·19	550·9	−1·0
319·19	551·6	−0·2
320·08	571·1	1·3
321·20	591·9	−1·2
322·19	614·2	−0·1
322·26	615·1	−0·7
323·16	635·8	0·1
323·81	651·4	1·2
324·82	673·2	−0·3

that the intermolecular distances decrease, and therefore the Van der Waals forces in the crystals increase in going across both series. The observed changes in vapour pressures and transition points agree with this view.

The "4*d*" hexafluorides are considerably less volatile than their "5*d*" counterparts. The reason for this is not understood at present.

Finally, it should be pointed out that the vapour-pressure data and infra-red spectra of TcF_6 did not show any evidence for the existence of TcF_7. Discrepancies in similar data on the volatile fluorination products of Re metal led to the first identification of ReF_7.(12)

(12) J. G. MALM, H. SELIG and S. FRIED, *J. Amer. Chem. Soc.* **82**, 1510 (1960).

J. Inorg. Nucl. Chem., 1962, Vol. 24, pp. 645 to 661. Pergamon Press Ltd. Printed in Northern Ireland

EFFECT OF SULPHUR TRIOXIDE ON THE ANATASE–RUTILE TRANSFORMATION*

W. F. SULLIVAN and J. R. COLEMAN
National Lead Company, Titanium Division, Research Department, South Amboy, N.J.

(*Received* 25 *September* 1961)

Abstract—Hydrous titanium dioxide prepared from titanium sulphate solution contains adsorbed sulphur trioxide which has been reported to inhibit the transformation of anatase to rutile at elevated temperatures. Samples of hydrous titanium dioxide were prepared containing sulphur-35 as a tracer for sulphur trioxide. The kinetics of sulphur trioxide release on heating and the concentration of sulphur trioxide at levels down to 0·003 per cent were determined by a radiochemical technique. Sulphur trioxide was found to be distributed on the titanium dioxide at two positions and to be released from each position according to first order kinetics. The temperature distribution between positions was found to follow a modified exponential function. Transformation of anatase to rutile was studied by X-ray diffraction, and, following an induction time, was also found to follow first order kinetics. Comparison of the kinetics of sulphur trioxide release and the kinetics of the transformation showed no correlation, nor was any correlation found between the concentration of sulphur trioxide and the concentration of rutile.

EARLY work on the transformation of anatase to rutile was mostly performed with natural crystals of anatase and was culminated in 1928 by SCHRÖDER's(1) value of 915°C for the transition temperature. Recent work(2–5) has, however, been largely concerned with synthetic anatases prepared by hydrolysis, particularly the hydrolysis of titanium sulphate solution. These anatases are characterized by their very small crystal size and the large amounts of bound water and sulphur trioxide which they contain. Further, it has been noted that they transform to rutile at temperatures which vary widely and which are generally lower than that reported by SCHRÖDER.

As a generality it has been suggested by PARRAVANO and CAGLIOTI(6,7) and SCHOSSBERGER(8) that sulphur trioxide is a stabilizer for anatase. Since small amounts of sulphur trioxide were found to persist in anatase samples in the neighbourhood of the transformation, it was assumed that sulphur trioxide occupies certain stabilizing sites in the anatase lattice and that the degree of stabilization increases with the number of sites occupied. Removal of sulphur trioxide by heating allows rutile to form.

Attempts(8,9,10) to correlate the sulphur trioxide content with the ease of transformation of anatase to rutile have not been successful, presumably because the amount of sulphur trioxide present in stabilizing sites was below the amount determinable by the standard gravimetric method of analysis. With the availability of radio-sulphur, a tracer method for determining small amounts of sulphur trioxide in titanium dioxide appeared feasible, and provided the basis for a detailed study of the effect of sulphur trioxide on the transformation.

---

* Paper presented at the *XVIIIth International Congress of Pure and Applied Chemistry*, Montreal, Canada, August 6–12, 1961 and submitted for publication in the *Journal of Inorganic and Nuclear Chemistry*.

(1) A. SCHRÖDER, *Z. Krist.* **67**, 485 (1928).

(2) W. F. SULLIVAN and S. S. COLE, *J. Amer. Cer. Soc.* **42**, 127 (1959).

(3) C. N. R. RAO, A. TURNER and J. M. HONIG, *J. Phys. Chem. Solids* **11**, 173 (1959).

(4) W. KNOLL and U. KÜHNHOLD, *Naturwissenschafts* **44**, 394 (1957).

(5) A. W. CZANDERNA, C. N. RAMACHANDRA RAO and J. M. HONIG, *Trans. Faraday Soc.* **54**, 1069 (1958).

(6) N. PARRAVANO and V. CAGLIOTI, *Gazz.* **64**, 703 (1934).

(7) N. PARRAVANO and V. CAGLIOTI, *Gazz.* **64**, 429 (1934).

(8) F. SCHOSSBERGER, *Z. Krist.* **104**, 358 (1942).

(9) A. V. PAMFILOV and J. G. IVANCHOVA, *J. Gen. Chem. USSR*, **10**, 736 (1940).

(10) T. KUBO, K. SHINRIKI and M. KOTO, *J. Chem. Soc. Japan, Industr. Chem. Sect.* **56**, 149 (1953).

Hydrous titanium dioxide containing radio-sulphur

A. *Pure titanium sulphate solution.* Titanyl sulphate dihydrate crystals ($TiOSO_4 \cdot 2H_2O$) were the starting point in this investigation. Commercial titanyl sulphate* was dissolved in water, the solution filtered and crystallized three times from boiling 45% H_2SO_4 solution, following the procedure developed by HIXSON and PLECHNER(11) and HIXSON and FREDRICKSON.(12) Analysis of the acetone-washed crystals is given in Table 1 and agrees closely with the theoretical. The crystals were dissolved in water, the solution adjusted in acidity with H_2SO_4 to a weight ratio of total H_2SO_4 to TiO_2 of 2·00 and the solution concentrated at 35°C under vacuum, using a dry-ice trap, to yield a final, clear solution analysing 260 g/l. TiO_2 and 520 g/l. H_2SO_4.

TABLE 1.—ANALYSIS OF TITANYL SULPHATE DIHYDRATE CRYSTALS

Chemical analysis

Batch Number	TiO_2(%)		H_2SO_4(%)	
1	39·8	40·1	49·7	50·2
2	40·6		50·9	
3	40·1		49·8	
4	39·7		50·2	
Theoretical for $TiOSO_4 \cdot 2H_2O$	40·8		50·0	

Spectrographic analysis

SiO_2(%)	Fe_2O_3(%)	Al_2O_3(%)	Sb_2O_3(%)	SnO_2(%)	Mg(%)	Nb(%)	
0·10	0·008	0·003	<0·001	<0·001	0·0007	0·01	
Cu(%)	Pb(%)	Mn(%)	W(%)	V(%)	Cr(%)	Na_2O(%)	CaO(%)
<0·0003	0·003	0·00008	<0·005	<0·001	<0·001	<0·01	0·004

Radio-sulphur (S-35), as received from Oak Ridge National Laboratory, was converted to radioactive H_2SO_4 by adding a small amount of non-radioactive H_2SO_4 and distilling out the HCl. A volume of 3·0 ml was added per litre of titanium sulphate solution, so that the specific activity of the final solution was $7·5 \times 10^{-3}$ mc/ml. The mixture was stirred for 48 hr at 25°C to allow exchange equilibrium to be reached. Tests indicated that exchange equilibrium was rapid. An isotope effect, due to the difference in mass of the sulphur isotopes, was expected to be negligible.

B. *Hydrolysis of titanium sulphate solution.* The hydrolysis procedure was similar to one developed originally by BLUMENFELD and various modifications have been described.(13,14) In this study 2500 ml of the above titanium sulphate solution at 25°C was added at a rate of 57·0 ml/min through a nozzle to 250 ml of boiling water. The mixture was stirred vigorously during solution addition and the mixture temperature allowed to fall at a rate of 2·0°C/min until it reached 80°C. The mixture was held at 80°C for 30 min and then heated to the boiling point (108°C) at a rate of 0·6°C/min. After boiling for 10 min a sufficient volume of water was added rapidly to decrease the TiO_2 concentration to 200 g/l. The mixture temperature was allowed to fall to 95°C over an 8 min interval. Hydrolysis was continued at 95°C for 1480 min.

---

* Available from Titanium Pigment Corporation, 111 Broadway, New York, N.Y.

(11) A. W. HIXSON and W. W. PLECHNER, *Industr. Engng. Chem.* **25**, 262 (1933).

(12) A. W. HIXSON and R. E. C. FREDRICKSON, *Industr. Engng. Chem.* **37**, 678 (1945).

(13) *Gmelins Handbuch der Anorganischen Chemie*, System No. 41, Titan, 8th Ed., Verlag Chemie G.m.b.H., Weinheim/Bergstrasse Germany (1951).

(14) R. E. KIRK and D. F. OTHMER, *Encyclopedia of Chemical Technology, Vol.* 14, *Titanium Compounds*, p. 213. Interscience, New York (1955).

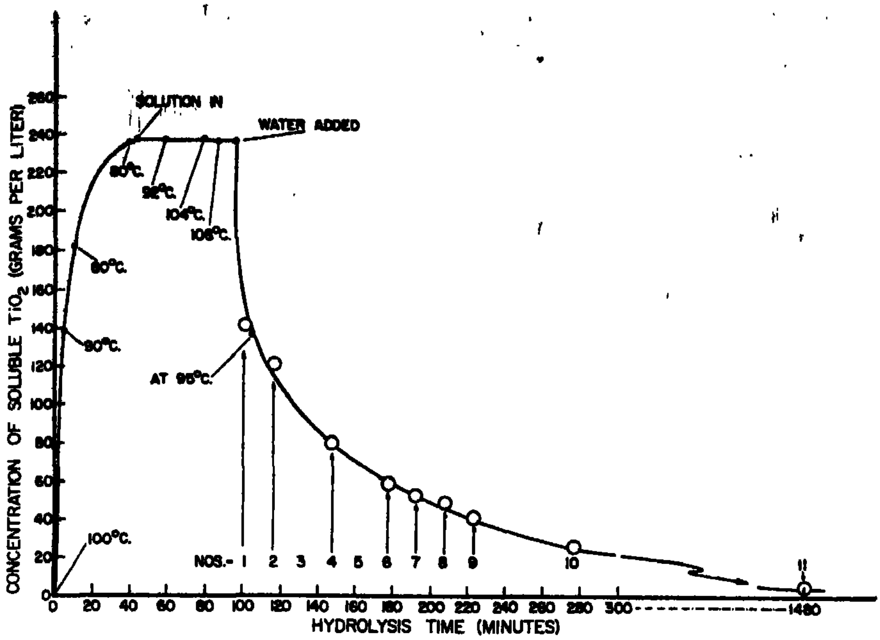

FIG. 1.—Hydrolysis of titanium sulphate solution.

Samples of hydrolysis liquor were removed at the times indicated in Fig. 1, quenched in ice-water, filtered and TiO_2 concentrations of the filtrates determined. The filter cakes were washed with water until the filtrates gave no test for sulphate ion. Approximately 50 g of TiO_2 were removed with each of eleven samples of hydrolysis liquor. For convenience the hydrous titanium dioxide samples were labeled No. 1 through 11 respectively.

This method of preparing hydrous titanium dioxide is a convenient one, since a wide range in physical properties may be encompassed by performing only a single hydrolysis. Extensive X-ray and electron diffraction analyses, as well as other methods of analysis,(2) have shown that hydrous oxides of this type consist of flocculates of small anatase crystals having large amounts of adsorbed water and sulphur trioxide. The approximate chemical analysis of the filter cakes was TiO_2, 35; H_2O, 62; SO_3, 3%.

Radiochemical technique for determining sulphur trioxide

A. "*Infinite Thickness*" *of titanium dioxide.* Since sulphur-35 is a β-emitter with a maximum energy of 0·167 MeV, self absorption occurs. A technique(15) was therefore developed in which "infinite thicknesses" of titanium dioxide were counted. All radioassay work was performed with standard scalers and a 1·9 mg/cm^2 end-window Geiger-Müller tube. To insure good counting statistics a minimum of 10,000 counts was recorded in all cases. The activity, defined as the number of counts per minute, was determined by dividing the total number of counts, after subtraction of background, by the counting time in minutes. Corrections were made for radioactive decay (half-life 87·1 days), coincidence losses and counting system variations according to the usual procedures.(15)

After heating samples of hydrous titanium dioxide to 300°C or higher to remove substantially all water, the titanium dioxide samples were ground in a small Alundum mortar and a known weight added to a planchet one inch in diameter. A volume of 1·0 ml of 0·5 per cent potassium phosphate solution was added, the titanium dioxide dispersed by swirling and the slurry centrifuged for 2 min at 3600 rev/min. The planchet with sample was then baked for 2 hr under infra-red lamps to evaporate the water and leave a smooth coating of titanium dioxide on the bottom of the planchet.

Fig. 2 shows several "infinite thickness" curves obtained for Sample No. 1. Similar curves were obtained for other samples and show that 80 mg is a sufficient sample weight to insure "infinite thickness". Based on these data a sample weight of 100 mg was selected for radioassay purposes.

---

(15) R. E. LAPP and H. T. ANDREWS, *Nuclear Radiation Physics.* Prentice-Hall, New York (1948).

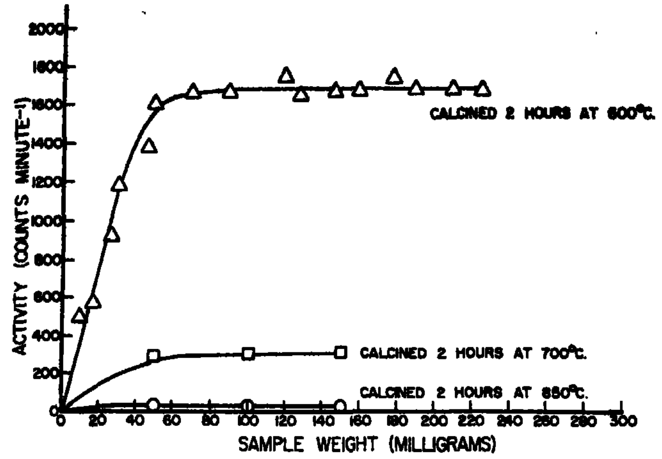

FIG. 2.—"Infinite thickness" curves of sample No. 1.

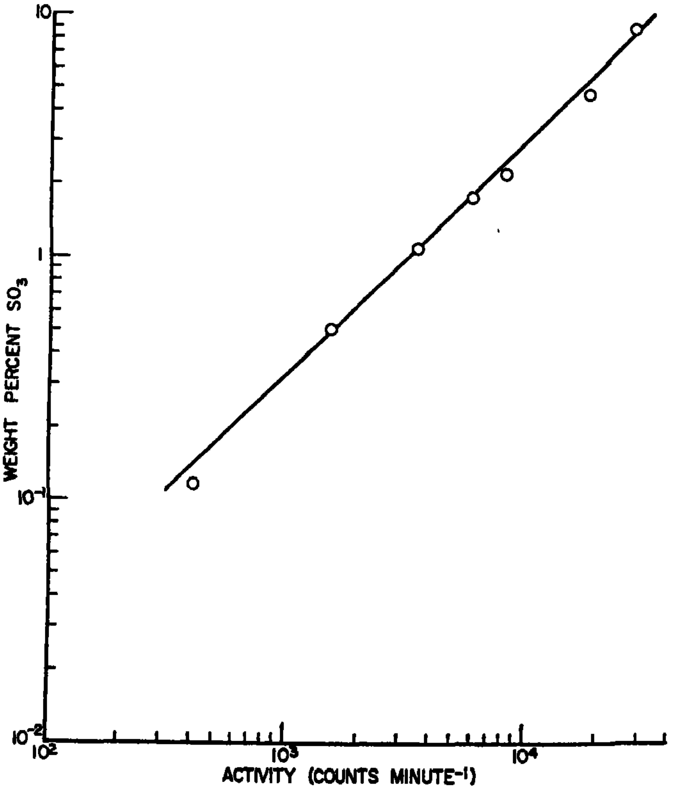

FIG. 3.—Sulphur activity and weight per cent SO_3.

B. *Sulphur activity and weight per cent sulphur trioxide.* It may be expected that direct proportionality exists between sulphur activity and weight per cent sulphur trioxide, so that

$$c = KA \tag{1}$$

where c = concentration of sulphur trioxide in weight per cent,
A = activity in counts per minute, and
K = a proportionality constant,

may be written. Fig. 3 is a log-log plot of experimental data obtained by calcining randomly selected samples over a temperature range of 300–850°C, determining sulphur activities by the previously described technique and sulphur trioxide analyses by a standard gravimetric procedure.(10) From the straight line, K was calculated to be $3{\cdot}00 \times 10^{-4}$. Since reasonable counting precision can be obtained at rates as low as 10 counts/min, the concentration of sulphur trioxide was determined to the 0·003 per cent level. It is obvious that lower levels could be determined by increasing the specific activity of the titanium sulphate solution. The lower limit of the gravimetric procedure is about 0·1 per cent.

Kinetics of sulphur trioxide release

A. *Experimental data.* Hydrous titanium dioxide samples containing approximately 1 g of titanium dioxide were heated in air for times up to 24 hr at temperatures ranging from 300–900°C. To minimize temperature gradients the calcinations were performed in a small, firebrick chamber located at the centre of an electric muffle. Chromel–alumel thermocouples in conjunction with a Whellco Controller were used to control and record temperatures which were held to within less than ±15°C of the designated values. Frequent temperature checks were made with a second thermocouple and potentiometer, and thermocouples were changed weekly to prevent false readings due to chemical attack by sulphur trioxide.

The weight per cent sulphur trioxide was determined in duplicate for all samples by the radiochemical technique previously described. Results for four of the eleven samples are presented in Figs. 4, 5, 6 and 7, the remaining samples exhibiting a similar behaviour. The circles, triangles, etc. represent the experimental points, whereas the solid line curves were calculated on the basis of a first order kinetic theory.

B. *Theory of sulphur trioxide removal.* A theory leading to satisfactory agreement with experimental results may be developed on the basis of the following assumptions.

(1) Sulphur trioxide is distributed on the titanium dioxide at two positions, where a position is defined as a collection of sites in which almost all molecules have approximately the same energy.

(2) The loosely bound position (I) contains molecules in second, third and higher adsorbed layers and may contain capillary-condensed sulphur trioxide.

(3) The tightly bound position (II) contains molecules in the first layer. Since substantially all water is removed from hydrous titanium dioxide at 300°C, only adsorbed sulphur trioxide is considered present on the surface.

(4) On heating at temperatures above 300°C sulphur trioxide is released from position I according to first order kinetics, and from position II at a rate dependent upon the fraction θ of the surface covered.

(5) The temperature distribution among sites is established at times very short compared to times necessary for appreciable evaporation to occur, and follows a modified Boltzmann exponential function.

(6) The reaction rate constants have a temperature dependence given by the Arrhenius equation.

At constant temperature we may therefore write

$$-\frac{dc}{dt} = k_{\mathrm{I}}c_{\mathrm{I}} + k_{\mathrm{II}}c_{\mathrm{II}} \qquad (2)$$

where c_{I}, c_{II} = concentration of sulphur trioxide at I, II,

k_{I}, k_{II} = reaction rate constants, and t = time.

---

(10) M. Codell, *Analytical Chemistry of Titanium Metals and Compounds*. Interscience, New York (1959).

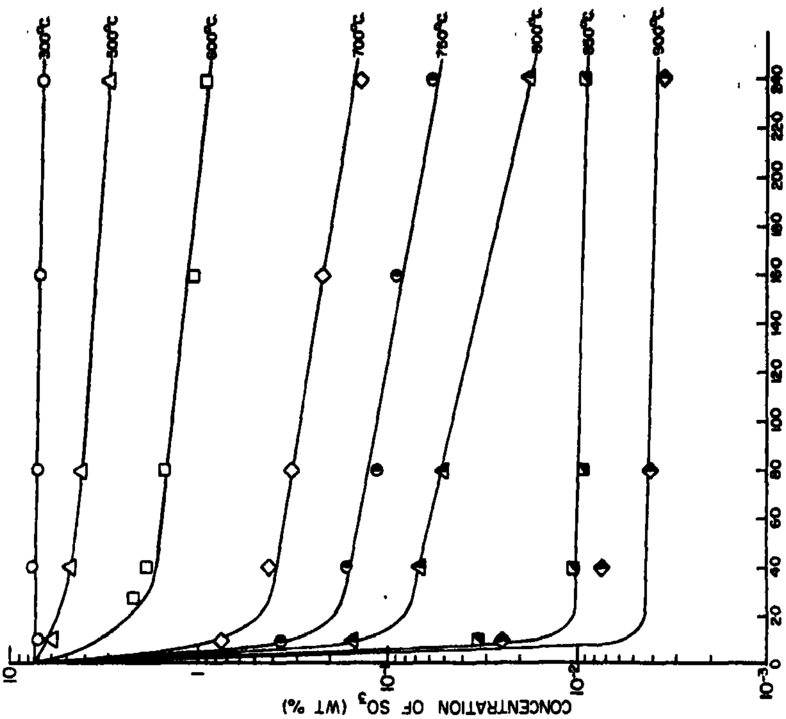

FIG. 5.—Sulphur trioxide release from sample No. 3.

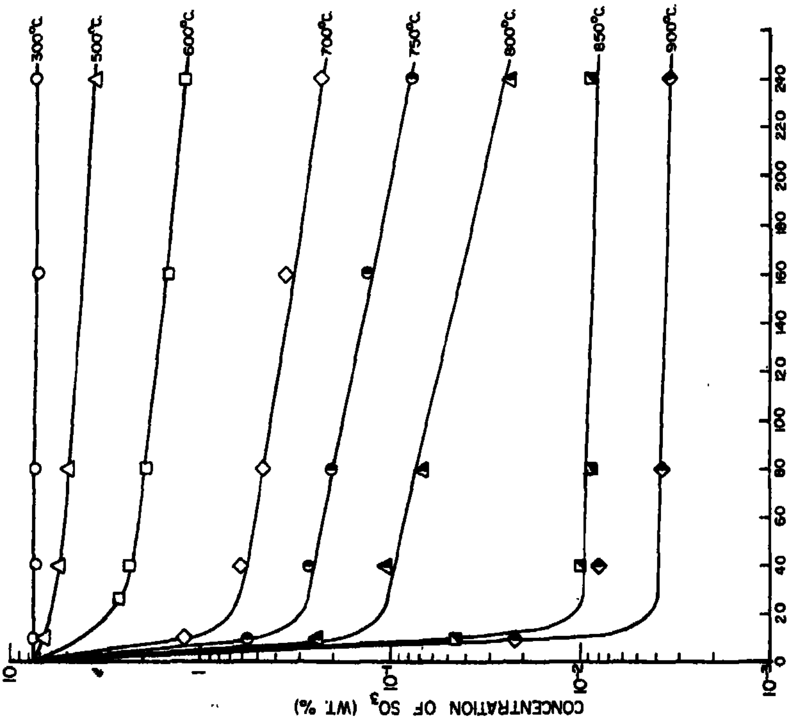

FIG. 4.—Sulphur trioxide release from sample No. 1.

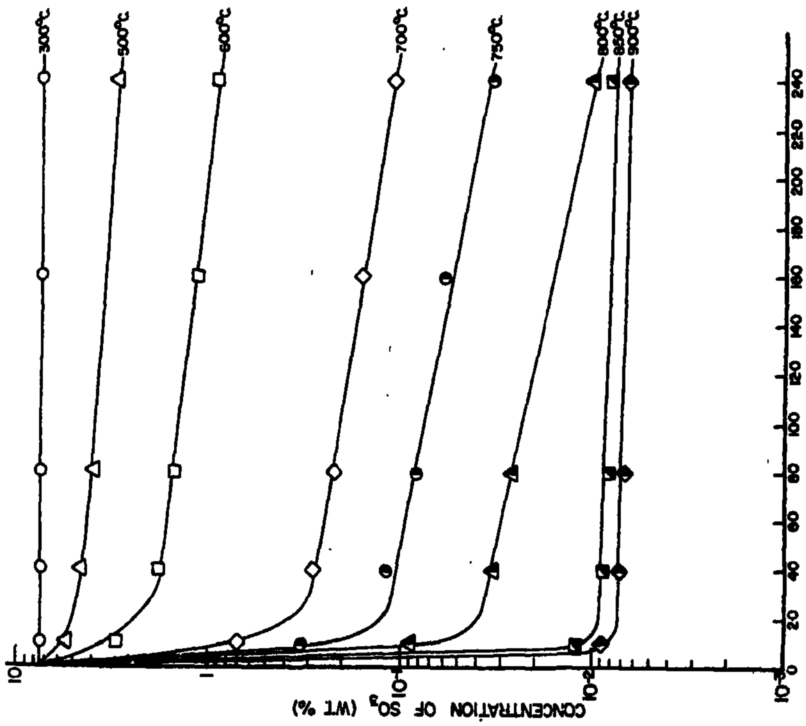

FIG. 6.—Sulphur trioxide release from sample No. 10.

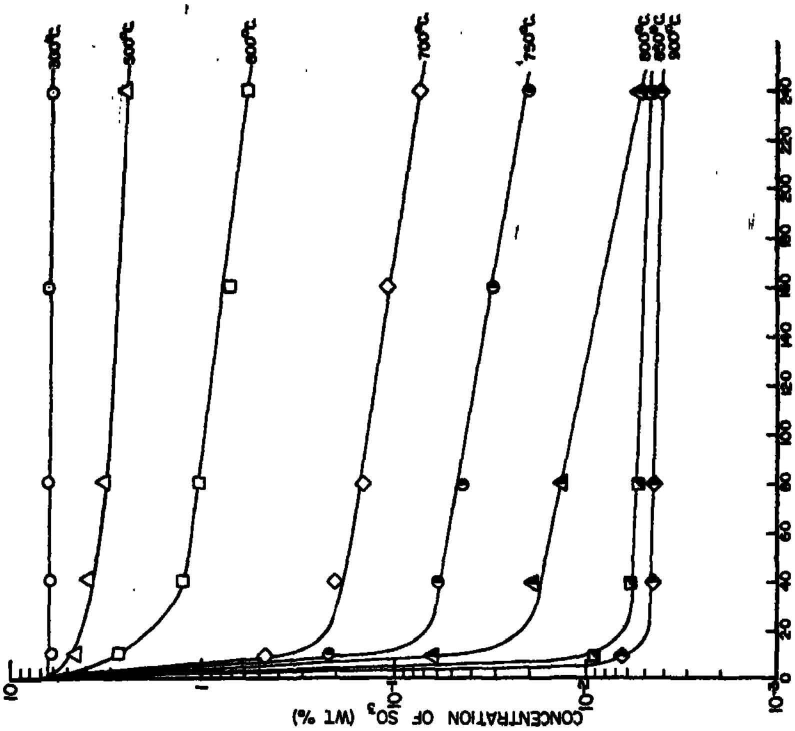

FIG. 7.—Sulphur trioxide release from sample No. 11.

The Arrhenius equations may be written as

$$k_{\rm I} = B_{\rm I} \exp(-\Delta H_{\rm I}/RT) \tag{3}$$

$$k_{\rm II} = B_{\rm II} \exp(-\Delta H_{\rm II}/RT) \tag{4}$$

where $B_{\rm I}$, $B_{\rm II}$ = frequency factor associated with I, II,
$\Delta H_{\rm I}$, $\Delta H_{\rm II}$ = activation energy associated with I, II, and
T = absolute temperature.

In general $B_{\rm II}$ and $\Delta H_{\rm II}$ depend on the fraction of the surface covered,(17,18) so that

$$-\frac{dc}{dt} = k_{\rm I}c_{\rm I} + B_{\rm II}c_{\rm II} \exp(-\Delta H_{\rm II}/RT) \tag{5}$$

cannot be integrated unless the functional relation is known or assumed.

Inspection of the experimental data of Figs. 4, 5, 6 and 7 shows that at temperatures up to 800°C, $B_{\rm II}$ and $\Delta H_{\rm II}$ may be taken as independent of concentration, so that Equation (5) may be integrated to give the simplified expression

$$c = c_{\rm I}{}^{\circ}e^{-k_{\rm I}t} + c_{\rm II}{}^{\circ}e^{-k_{\rm II}t} \tag{6}$$

where $c_{\rm I}{}^{\circ}$, $c_{\rm II}{}^{\circ}$ = concentrations of sulphur trioxide at I, II at zero time.

The constants $c_{\rm I}{}^{\circ}$ and $c_{\rm II}{}^{\circ}$ may be obtained directly from the experimental data by a method similar to the one employed in analysing a composite, radioactive decay curve.(15) The frequency factors and activation energies giving satisfactory agreement with experimental data at temperatures of 300 through 800°C are

$$B_{\rm I} = 3{\cdot}20 \times 10^{3}\ \text{hr}^{-1} \qquad \Delta H_{\rm I} = 14{\cdot}2\ \text{kcal mole}^{-1}$$

$$B_{\rm II} = 1{\cdot}65\ \text{hr}^{-1} \qquad \Delta H_{\rm II} = 6{\cdot}9\ \text{kcal mole}^{-1}$$

Table 2 contains numerical values to be used in conjunction with Equation (6) in drawing the curves of Figs. 4, 5, 6 and 7.

C. *Effect of temperature on distribution.* The Boltzmann exponential function

$$\frac{N_{\rm I}{}^{\circ}}{V_{\rm I}} = \frac{N_{\rm II}{}^{\circ}}{V_{\rm II}} \exp(-E_p/RT) \tag{7}$$

where $N_{\rm I}{}^{\circ}$, $N_{\rm II}{}^{\circ}$ = number of sulphur trioxide molecules at I, II at zero time,
$V_{\rm I}$, $V_{\rm II}$ = the "free volume" available at I, II and
E_p = the potential energy difference per mole of sulphur trioxide between I and II,

may be written, following the methods described by EUCKEN(19), as

$$\frac{N_{\rm I}{}^{\circ}}{V_{\rm I}} = \frac{N_{\rm II}{}^{\circ}}{(A_{\rm II} - N_{\rm II}{}^{\circ}\sigma)X} \exp(-E_p/RT) \tag{8}$$

At I it is assumed that an infinite volume is available for the molecules, whereas at II the volume occupied by the molecules is subtracted from the total volume. $A_{\rm II}$ is the

---

(17) A. W. ADAMSON, *Physical Chemistry of Surfaces*, Interscience, New York (1960).

(18) C. H. PITT and M. E. WADSWORTH, Report, AECU-3759 (1958).

(19) A. EUCKEN, "*Grundriss der Physikalischen Chemie*," Akademische Verlagagesellschaft m.b.H. (1934).

TABLE 2.—INITIAL CONCENTRATIONS AND REACTION RATE CONSTANTS

Temp. (°C)	k_I(hr^{-1})	k_{II}(hr^{-1})	No. 1		No. 3		No. 10		No. 11	
			c_I°	c_{II}°	c_I°	c_{II}°	c_I°	c_{II}°	c_I°	c_{II}°
300	$1·50 \times 10^{-2}$	$3·75 \times 10^{-3}$	0	7·60	0	7·35	0	7·65	0	6·30
500	$4·00 \times 10^{-1}$	$1·85 \times 10^{-2}$	1·75	5·85	2·40	4·95	3·15	4·50	2·70	3·60
600	1·18	$3·08 \times 10^{-2}$	4·96	2·64	5·49	1·86	5·65	2·00	4·98	1·32
700	2·75	$4·55 \times 10^{-2}$	6·94	$6·60 \times 10^{-1}$	6·88	$4·65 \times 10^{-1}$	7·34	$3·15 \times 10^{-1}$	6·07	$2·25 \times 10^{-1}$
750	4·00	$5·05 \times 10^{-2}$	7·29	$3·06 \times 10^{-1}$	7·14	$2·10 \times 10^{-1}$	7·52	$1·32 \times 10^{-1}$	6·23	$7·20 \times 10^{-2}$
800	5·40	$6·45 \times 10^{-2}$	7·48	$1·20 \times 10^{-1}$	7·26	$8·55 \times 10^{-2}$	7·61	$4·05 \times 10^{-2}$	6·28	$2·25 \times 10^{-2}$
850	7·20	$7·73 \times 10^{-3}$	7·59	$1·00 \times 10^{-2}$	7·34	$1·08 \times 10^{-2}$	7·64	$9·20 \times 10^{-3}$	6·29	$6·10 \times 10^{-3}$
900	9·30	$7·73 \times 10^{-3}$	7·60	$4·10 \times 10^{-3}$	7·35	$4·50 \times 10^{-3}$	7·65	$7·50 \times 10^{-3}$	6·30	$4·70 \times 10^{-3}$

TABLE 3.—VARIATION OF DISTRIBUTION COEFFICIENT WITH TEMPERATURE

Temp. (°C)	No. 1				No. 3			
	$N_I°/m$	$N_{II}°/m$	$N_I°/N_{II}°$	D	$N_I°/m$	$N_{II}°/m$	$N_I°/N_{II}°$	D
500	1.34×10^{20}	4.67×10^{20}	2.86×10^{-1}	2.10×10^{-1}	1.85×10^{20}	3.90×10^{20}	4.74×10^{-1}	3.17×10^{-1}
600	4.00×10^{20}	2.04×10^{20}	1.96	1.73	4.37×10^{20}	1.42×10^{20}	3.06	2.69
700	5.61×10^{20}	4.99×10^{19}	1.12×10^{1}	1.09×10^{1}	5.55×10^{20}	3.51×10^{19}	1.58×10^{1}	1.53×10^{1}
750	5.91×10^{20}	2.31×10^{19}	2.56×10^{1}	2.52×10^{1}	5.78×10^{20}	1.58×10^{19}	3.65×10^{1}	3.60×10^{1}
800	6.08×10^{20}	9.03×10^{18}	6.72×10^{1}	6.69×10^{1}	5.89×10^{20}	6.43×10^{18}	9.15×10^{1}	9.11×10^{1}
850	6.17×10^{20}	7.52×10^{17}	8.21×10^{2}	8.21×10^{2}	5.96×10^{20}	9.02×10^{17}	6.60×10^{2}	6.59×10^{2}
900	6.18×10^{20}	3.01×10^{17}	2.05×10^{3}	2.05×10^{3}	5.97×10^{20}	4.13×10^{17}	1.44×10^{3}	1.44×10^{3}
	No. 10				No. 11			
500	2.45×10^{20}	3.54×10^{20}	6.90×10^{-1}	1.70×10^{-1}	2.07×10^{20}	2.81×10^{20}	7.43×10^{-1}	1.52×10^{-1}
600	4.50×10^{20}	1.53×10^{20}	2.93	1.98	3.94×10^{20}	1.01×10^{20}	3.92	2.80
700	5.96×10^{20}	2.36×10^{19}	2.50×10^{1}	2.38×10^{1}	4.86×10^{20}	1.70×10^{19}	2.86×10^{1}	2.73×10^{1}
750	6.11×10^{20}	9.37×10^{18}	6.15×10^{1}	6.02×10^{1}	4.99×10^{20}	5.42×10^{18}	9.22×10^{1}	9.08×10^{1}
800	6.19×10^{20}	3.05×10^{18}	2.03×10^{2}	2.02×10^{2}	5.04×10^{20}	1.69×10^{18}	2.97×10^{2}	2.96×10^{2}
850	6.22×10^{20}	7.52×10^{17}	8.26×10^{2}	8.26×10^{2}	5.05×10^{20}	4.51×10^{17}	1.12×10^{3}	1.12×10^{3}
900	6.23×10^{20}	5.64×10^{17}	1.10×10^{3}	1.10×10^{3}	5.05×10^{20}	3.57×10^{17}	1.41×10^{3}	1.41×10^{3}

* Calculated from the data of Table 3 by use of $N_I°/m = 7.518 \times 10^{21} \dfrac{c_I°}{100 - c_I°}$

surface area, σ the cross-sectional area of the sulphur trioxide molecule and X the thickness of the first layer. By dividing both sides of Equation (8) by the mass m of titanium dioxide and introducing the ratio

$$S = \frac{A_{\mathrm{II}}/m}{\sigma} \tag{9}$$

we may write

$$N_{\mathrm{I}}{}^{\circ}/m = \frac{N_{\mathrm{II}}{}^{\circ}/m}{1 - \dfrac{N_{\mathrm{II}}{}^{\circ}/m}{S}} \frac{V_{\mathrm{I}}}{A_{\mathrm{II}}X} \exp(-E_p/RT) \tag{10}$$

If a distribution coefficient D is defined as

$$D = \frac{N_{\mathrm{I}}{}^{\circ}/m}{N_{\mathrm{II}}{}^{\circ}/m}\left(1 - \frac{N_{\mathrm{II}}{}^{\circ}/m}{S}\right) \tag{11}$$

then

$$\log D = \frac{E_p}{2{\cdot}303\,RT} + \log \frac{V_{\mathrm{I}}}{A_{\mathrm{II}}X} \tag{12}$$

Table 3 contains numerical data necessary to evaluate Equation (12). For each sample of titanium dioxide a value of S has been arbitrarily selected which insures optimum agreement with Equation (12). Table 3 shows that only the data at 500 and 600°C are significantly changed by this "free volume" correction. The results are represented graphically in Fig. 8 which shows that, over the temperature range of 500–800°C, good straight lines are obtained as required by Equation (12). The change in slope at 850 and 950°C is presumably due to an increase in the energy term with decreased surface coverage.

Values of S, used in calculating D, as well as surface areas, are contained in Table 4. The surface areas of titanium dioxide were calculated from Equation (9) on the basis of 17Å^2 for the cross-sectional area of the sulphur trioxide molecule, a value calculated in the usual way from the density of sulphur trioxide.(20) The surface areas are in good agreement with values obtained by observations with the electron microscope and with values previously reported(2) for crystallite size measured by X-ray diffraction line broadening. Thus anatase with a diameter of 60Å is equivalent to a surface area of 260 m^{2}g^{-1}.

D. *Surface coverage*. Although sufficient data are not available to map out the $\log k_{\mathrm{II}}$, $\frac{1}{T}$, θ-space, it is apparent that at values of θ less than 0·01, $\log k_{\mathrm{II}}$ decreases markedly. This indicates that at low surface coverages the activation energy ΔH_{II} increases and the frequency factor B_{II} probably decreases. On the reasonable assumption that, at short times, $V_{\mathrm{I}}/A_{\mathrm{II}}X$ is independent of temperature, it is also possible to estimate the behavior of E_p with surface coverage. The data, averaged over four titanium dioxide samples, are given in Table 5. Values of θ were calculated from

$$\theta = \frac{N_{\mathrm{II}}{}^{\circ}/m}{S} \tag{13}$$

and hence do not depend on an assumed cross-sectional area of the sulphur trioxide molecule. The data show that about one site in a hundred on the titamium dioxide surface is characterized by high binding energy of sulphur trioxide. Since the heat of

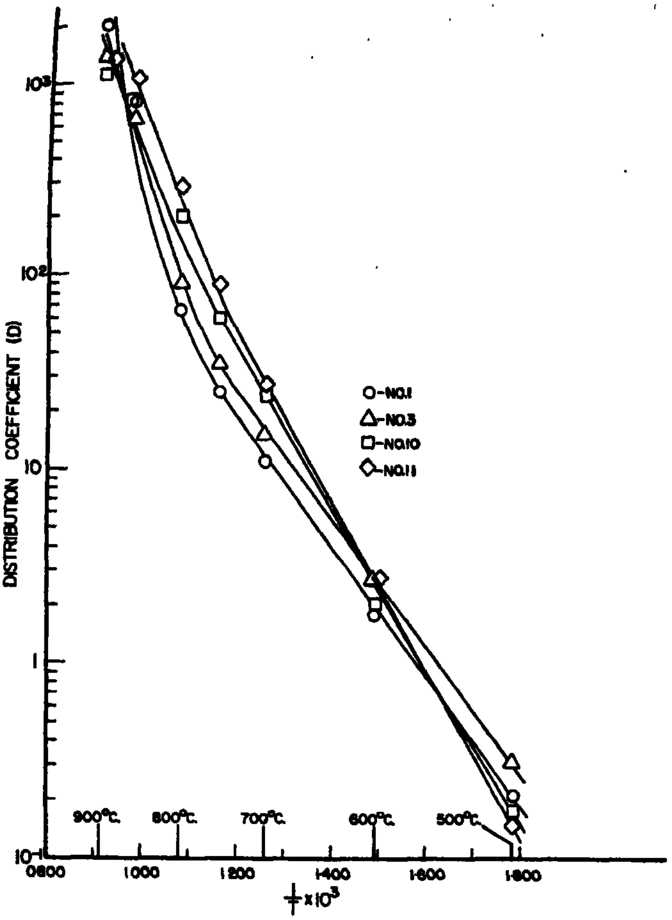

FIG. 8.—Effect of temperature on distribution coefficient.

TABLE 4.—SURFACE AREAS OF TITANIUM DIOXIDE

Sample no.	S	$A_{II/m}$ (m^2g^{-1})
1	$1{\cdot}76 \times 10^{21}$	300
3	$1{\cdot}18 \times 10^{21}$	200
10	$4{\cdot}71 \times 10^{20}$	80
11	$3{\cdot}53 \times 10^{20}$	60

TABLE 5.—SURFACE COVERAGE OF TITANIUM DIOXIDE

Temp. (°C)	θ	log k_{II}	ΔH_{II} (kcal mole^{-1})	B_{II} (hr^{-1})	E_p (kcal mole^{-1})
500	$5{\cdot}35 \times 10^{-1}$	$\bar{2}{\cdot}2071$	6·9	1·65	17·2
600	$2{\cdot}11 \times 10^{-1}$	$\bar{2}{\cdot}4885$	6·9	1·65	17·2
700	$3{\cdot}91 \times 10^{-2}$	$\bar{2}{\cdot}6580$	6·9	1·65	17·2
750	$1{\cdot}57 \times 10^{-2}$	$\bar{2}{\cdot}7032$	6·9	1·65	17·2
800	$5{\cdot}41 \times 10^{-3}$	$\bar{2}{\cdot}8096$	6·9	1·65	26·4
850	$9{\cdot}73 \times 10^{-4}$	$\bar{3}{\cdot}8881$	>6·9	<1·65	34·2
900	$6{\cdot}22 \times 10^{-4}$	$\bar{3}{\cdot}8881$	>6·9	<1·65	34·2

sublimation of sulphur trioxide varies between 11·9 and 16·3 kcal mole^{-1},(20) the adsorption may be classified as chemisorption.

Anatase–rutile transformation

Time–temperature curves for the transformation of anatase to rutile are shown in Figs. 9, 10, 11 and 12. The standard X-ray diffraction method(21) of analysing powder mixtures was used for determining the amounts of each phase. Precision was determined to be ±3·0 per cent for 95 per cent confidence limits. As previously found(2) the kinetics obey the first order equation

$$c_a = c_a{}^{\circ} e^{-\lambda t} \tag{14}$$

where c_a = concentration of anatase in weight per cent at time t,

$c_a{}^{\circ}$ = concentration of anatase in weight per cent at zero time, and

λ = the reaction rate constant,

following an induction time which is presumably due to a nucleation process. Activation energies ΔH_t and frequency factory B_t also obey the Arrhenius equation. The kinetic data are summarized in Table 6 and the Arrhenius parameters in Table 7. The variations in activation energies and frequency factors and comparison with previously published values(2,5) emphasize the dominant effect of the method of preparation on the transformation.

Relationship between sulphur trioxide and the transformation

A. *Anatase and sulphur trioxide concentrations.* To test the hypothesis(6–10) that anatase is stabilized by the presence of sulphur trioxide at certain sites, the concentration of anatase was compared with the concentration of sulphur trioxide at corresponding times. The data were taken directly from Figs. 4 through 7 and Figs. 9 through 12. Examination of these results, presented in Fig. 13, show that the concentration of anatase is a multivalued function of the sulphur trioxide concentration.

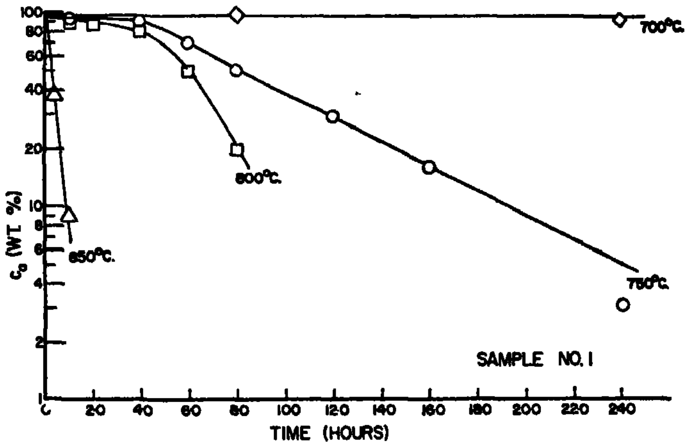

FIG. 9.—Transformation of sample No. 1.

---

(20) R. E. KIRK and D. F. OTHMER, *Encyclopedia of Chemical Technology, Vol.* 13, *Sulphur Trioxide,* p. 501. Interscience, New York (1955).

(21) H. P. KLUG and L. E. ALEXANDER, *X-ray Diffraction Procedures for Polycrystalline and Amorphous Materials.* J. Wiley, New York (1954).

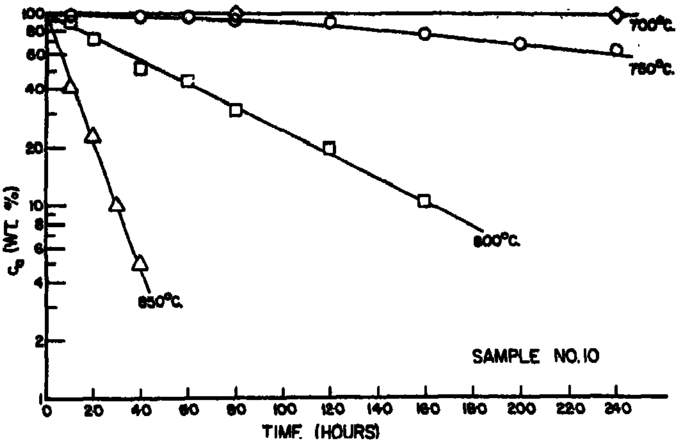

FIG. 10.—Transformation of sample No. 3.

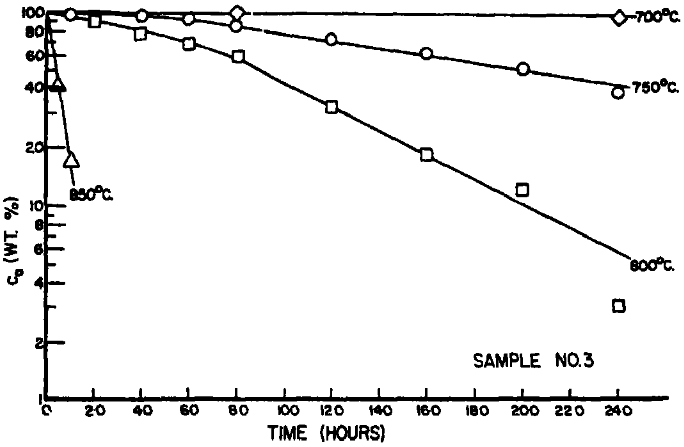

FIG. 11.—Transformation of sample No. 10.

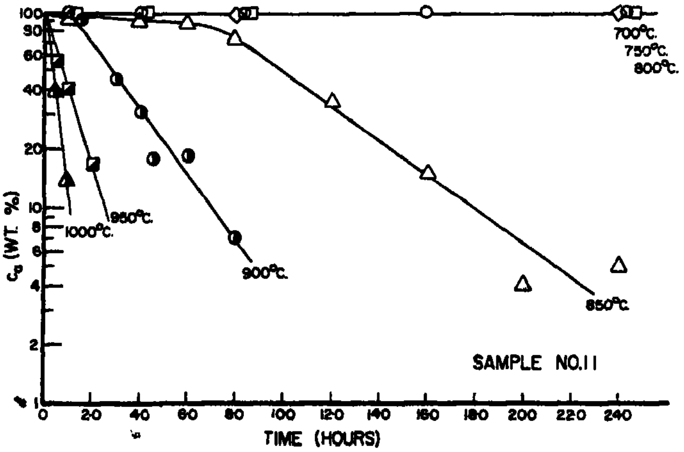

FIG. 12.—Transformation of sample No. 11.

TABLE 6.—KINETIC DATA FOR THE TRANSFORMATION OF ANATASE TO RUTILE

Temp. (°C)	No. 1		No. 3		No. 10		No. 11	
	Induct. time (hr)	λ (hr^{-1})	Induct. time (hr)	λ (hr^{-1})	Induct. time (hr)	λ (hr^{-1})	Induct. time (hr)	λ (hr^{-1})
700	>8·0	$4{\cdot}3 \times 10^{-3}$	>8·0	$4{\cdot}3 \times 10^{-3}$	>8·0	$4{\cdot}3 \times 10^{-3}$		
750	4·0	$1{\cdot}47 \times 10^{-1}$	6·4	$4{\cdot}40 \times 10^{-2}$	8·0	$3{\cdot}00 \times 10^{-2}$		
800	4·0	$5{\cdot}23 \times 10^{-1}$	6·0	$1{\cdot}53 \times 10^{-1}$	0·5	$1{\cdot}46 \times 10^{-1}$		
850	0	2·30	0	1·76	0	$7{\cdot}80 \times 10^{-1}$	7·6	$2{\cdot}10 \times 10^{-1}$
900							1·2	$4{\cdot}26 \times 10^{-1}$
950							0	$9{\cdot}21 \times 10^{-1}$
1000							0	1·77

TABLE 7.—ACTIVATION ENERGIES AND FREQUENCY FACTORS

Sample no.	ΔH_t (kcal mole^{-1})	B_t (hr^{-1})
1	66	$1{\cdot}6 \times 10^{13}$
2	85	$5{\cdot}6 \times 10^{18}$
3	76	$5{\cdot}6 \times 10^{14}$
4	41	$2{\cdot}5 \times 10^{8}$

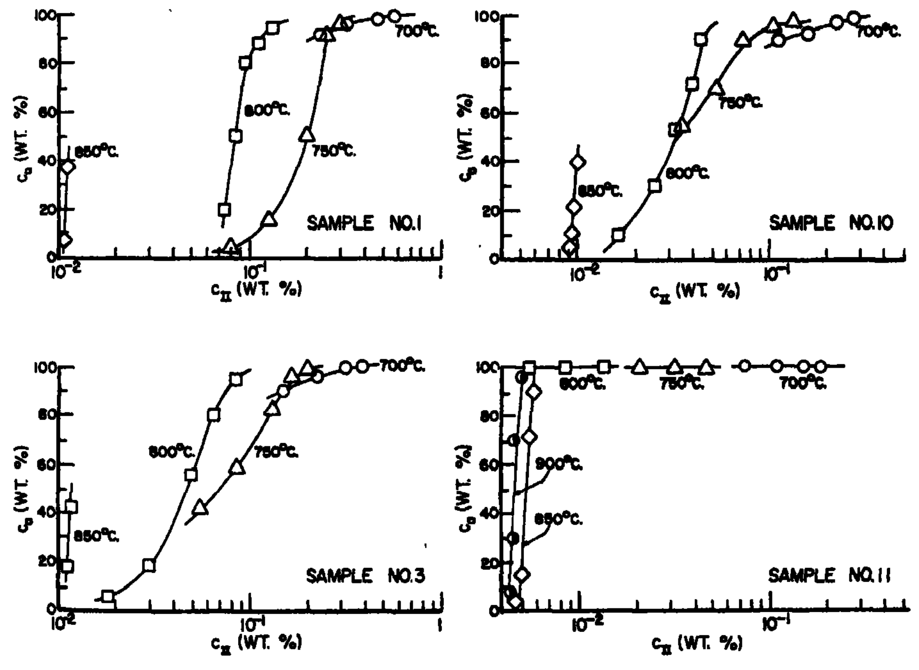

FIG. 13.—Anatase and sulphur trioxide concentrations.

Thus mixtures of anatase and rutile, or the single phases, may be prepared having a wide range of sulphur trioxide concentrations. For a given sample the sulphur trioxide concentration at the start of the transformation also varies widely, depending on the time and temperature of calcination. Further, Sample No. 11 which requires the highest temperature for transformation to rutile has the lowest concentration of sulphur trioxide. These results show that there is no obvious correlation between the anatase and sulphur trioxide contents.

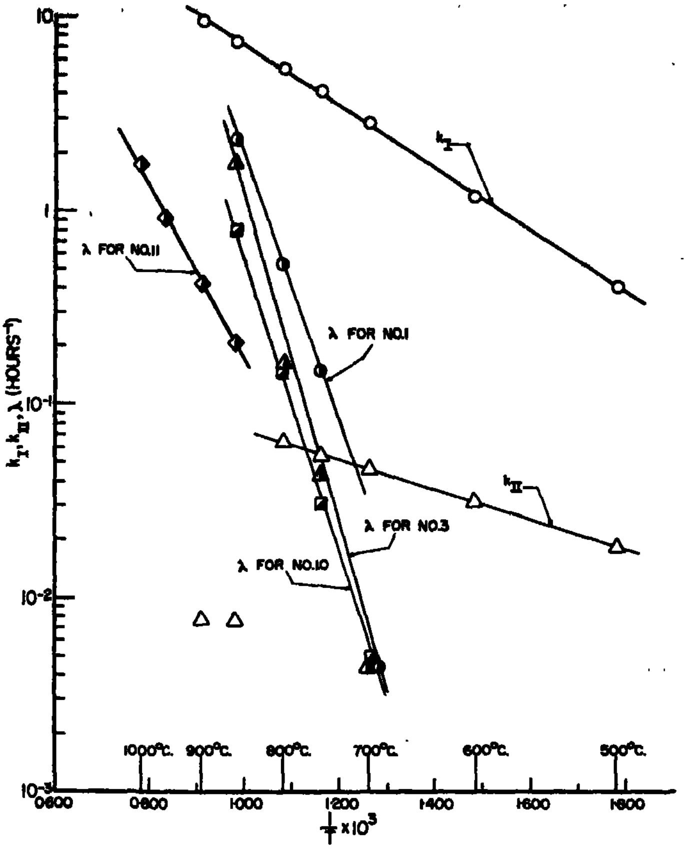

FIG. 14.—Effect of temperature on reaction rate constants.

B. *Activation energies and frequency factors.* The kinetic data for sulphur trioxide release and for the transformation may also be compared. Values taken from Tables 2 and 6 were used to make the Arrhenius-type plot in Fig. 14. Inspection shows that there is no obvious relationship between the rate constants, nor between the activation energies and frequency factors.

The low values of k_{II} at 850 and 900°C have been previously ascribed to the presence of a small fraction of sites on the titanium dioxide surface having high binding energy. It has not been possible to relate these sites with anatase stabilizing sites. Thus, the transformation to rutile begins at a surface coverage of about $\theta = 2 \times 10^{-2}$ where there is no noticeable effect on the activation energy or frequency factor (Table 5). The increase in ΔH_{II} at very low coverages does not appear sufficient to reach values above 40 kcal mole^{-1}, such as are characteristic of the transformation.

Conclusion

It has not been possible to confirm the hypothesis that anatase is stabilized by the presence of sulphur trioxide at certain lattice sites. Further, there is no evidence down to a level of 0·003 per cent for the validity of the assumption⁽⁸⁾ that a small amount of sulphur trioxide is present within the anatase lattice, but rather the experimental data are satisfied by the reasonable assumption of chemisorbed sulphur trioxide with a small fraction of the surface sites being highly active.

It seems probable that the transformation depends basically on such factors as crystallite size, the defect structure of the anatase lattice and solid state nucleation. The data of Tables 4 and 6 show, as expected, that anatases with high surface area are easier to transform to rutile than those with low areas. The concentration and kinetics of sulphur trioxide release also appear to depend basically on structural differences and are therefore not the primary factors associated with the transformation. Stabilizing anions appear to be important only in the transition between solution and solid phases, and not in the transition between the two solid phases.

J. Inorg. Nucl. Chem., 1962, Vol. 24, pp. 663 to 671. Pergamon Press Ltd. Printed in Northern Ireland

A SPECTROPHOTOMETRIC STUDY OF THE DIMERIZATION OF PENTAVALENT MOLYBDENUM IN HYDROCHLORIC ACID

G. P. HAIGHT, JR.
Chemistry Department, Swarthmore College, Swarthmore, Pennsylvania

(*Received* 5 *March* 1961; *in revised form* 12 *December* 1961)

Abstract—The hydrolysis of $MoOCl_5^{2-}$ in 5–6 M hydrochloric acid is shown to involve dimerization with the production of hydrogen ions and chloride ions according to the equation

$$MoOCl_5^{2-} + H_2O \rightleftharpoons [MoOCl_4]_2O^{4-} + 2H^+ + 2Cl^-.$$

This equilibrium has been studied by observing the absorbance of solutions at 450 mμ where the molar extinction changes from 12·6 for $MoOCl_5^{2-}$ to 2200 for the dimer at this wavelength. The absorption curve for the dimer is characterized by enhanced absorbance over the whole visible region with the same wave lengths of maximum absorption as obtained for monomer.

Futher hydrolysis in more dilute acid involves no futher polymerization; however, the absorption bands in the visible region virtually disappear in dilute acid (1·0–3·0 M).

The dimer formed in 5·0–6·0 M hydrochloric acid appears to have characteristics similar to other dimeric complex ions containing oxygen or hydroxide bridges.

THE addition of water to green Mo(V) solutions in concentrated hydrochloric acid produces enhanced colour(1,2,3) and reduced paramagnetism.(4) Such behaviour is often characteristic of the formation of oxygen bridges between paramagnetic ions.(5,6,7) Observation that the enhancement of the absorbance at the 450 mμ band maximum was proportional to the square of the Mo(V) concentration in 6 M hydrochloric acid led the author to use this enhancement to study the dimerization hydrolysis of $MoOCl_5^{2-}$. (The spectrum of Mo(V) in 9–12 M hydrochloric acid is virtually identical with the reflectance spectrum K_2MoOCl_5.(8))

EXPERIMENTAL

Mo(V) solutions were prepared by reduction with mercury of sodium molybdate dissolved in 1·0 molar hydrochloric acid. Solutions had to be stored over mercury and under nitrogen to prevent air oxidation. A Beckman model D.U. spectrophotometer was used for all measurements. Cell spacers which reduced the light path to 1 mm were employed for solutions of high absorbancy. The cell compartment was thermostated at 25°C except during studies of temperature dependence of equilibria.

Solutions of 0·1 molar Mo(V) (measured as if Mo(V) were monomeric) were diluted with previously standardized hydrochloric acid solutions. Equilibrium was established in the time required to make measurements.

OBSERVATIONS

The effect of changing concentration of hydrochloric acid on the spectrum is illustrated in Fig. 1. As 12 molar acid is diluted the visible spectrum is enhanced without shifting wave lengths of maxima and minima in the absorbance curve. As

---

(1) C. F. HISKEY and V. W. MELOCHE, *J. Amer. Chem. Soc.* **62**, 1819 (1940); **63**, 964 (1941).

(2) H. K. EL-SHAMY and A. M. EL-AGGAN, *J. Amer. Chem. Soc.* **75**, 1187 (1953).

(3) C. KLIXBÜLL-JORGENSEN, *Acta Chem. Scand.* **11**, 73 (1957).

(4) L. SACCONI and R. CINI, *J. Amer. Chem. Soc.* **76**, 4239 (1954).

(5) J. D. DUNITZ and L. E. ORGEL, *J. Chem. Soc.* 2594 (1953).

(6) W. K. WILMARTH, H. GROFF and S. T. GUSTIN, *J. Amer. Chem. Soc.* **78**, 2683 (1956).

(7) L. N. MULAY and P. W. SELWOOD, *J. Amer. Chem. Soc.* **77**, 2693 (1955).

(8) H. GRAY. Private communication (1961).

the acid is diluted below 5·0 molar, the visible peaks disappear. Changes in the ultraviolet spectrum also occur, but the high absorbance made it necessary to study solutions containing concentrations of Mo(V) so low that dimerization in the range 5·0–6·0 molar acid was not significant. Fig. 2 shows the change of absorbance with hydrochloric acid concentration at the wavelengths of maximum absorbance, together with the change in paramagnetism observed by Sacconi and Cini.[(4)] The different patterns of change all occurring in the region of 5·0–6·0 molar acid is striking. The spectrum changes due to changing concentration of hydrochloric acid can be effected by changing either hydrogen ion or chloride ion concentrations independently. In 6·0 molar hydrochloric acid the enhancement of the 450 mμ peak was observed to be directly proportional to the square of the Mo(V) concentration. This led to a postulate of a monomer-dimer equilibrium on the high acid side of the curves with peaks in Fig. 2. On the low acid side of the peaks, Beer's law is obeyed, indicating that the extent of polymerization is not changed further.

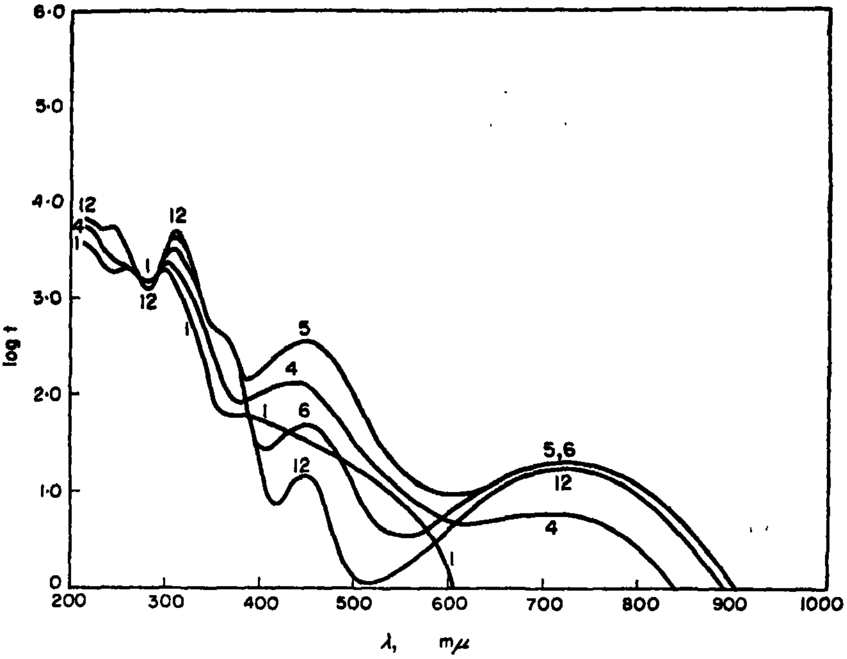

Fig. 1.—Absorption spectra of Mo(V) in various concentrations of hydrochloric acid. ε is the molar extinction coefficient for Mo(V) taken as monomer. [Mo(V)] = 0·005 M for measurements between 350 mμ and 900 mμ. [Mo(V)] = 10^{-4} M for measurements from 220 mμ to 350 mμ. The numbers adjacent to the curves indicate the molarity of the hydrochloric acid.

THEORY

In order to obtain information about the dimer giving the enhanced visible spectrum it has been assumed that equilibrium between monomer and all dimeric forms exists on the high acid side of enhancement curves, as follows:

$$2\,\mathrm{M} \overset{K_1}{\rightleftharpoons} \mathrm{D}_1 \overset{K_2}{\rightleftharpoons} \mathrm{D}_2 \overset{K_3}{\rightleftharpoons} \text{etc.}$$

where M is monomer and D_1, D_2, etc. are various dimeric species, and the *K*'s are equilibrium constants.

If [D] is the concentration of all dimeric forms, a dissociation constant $K = [M]^2/[D]$ should exist for any given concentration of hydrogen and chloride ions. It should now be possible to test the absorption spectrum for the existence of such equilibria.

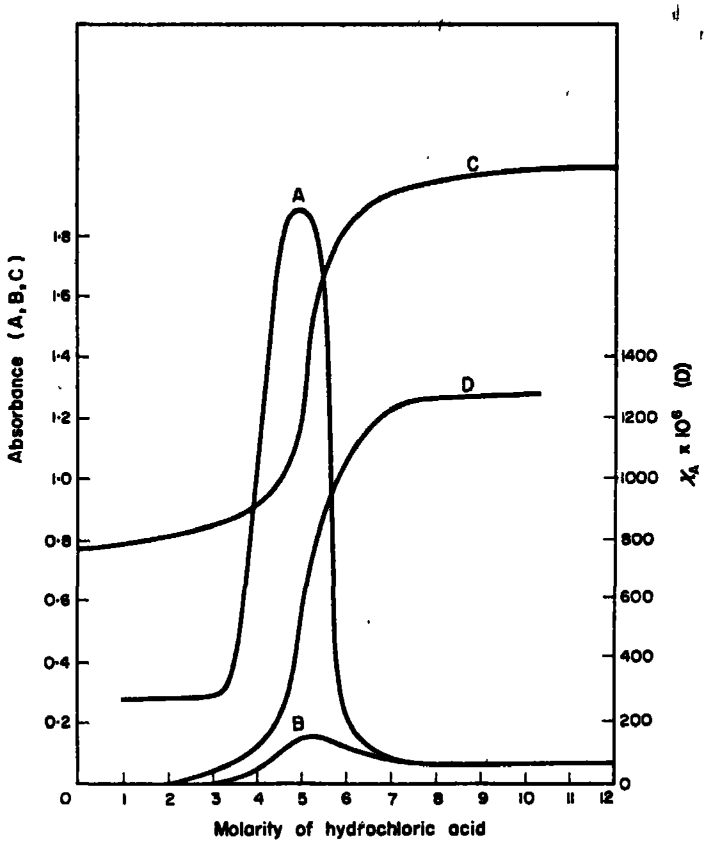

FIG. 2.—Effects of changing concentrations of hydrochloric acid on absorbance of Mo(V) solutions at 450 mμ (*A*); at 730 mμ (*B*); and at 310 mμ (*C*); and on the paramagnetic susceptibility (*D*). Concentrations of Mo(V) are 0·005 molar in curves *A* and *B* and light path 1·0 cm. In curve *C*, Mo(V) was 0·004 molar and the light path 1·0 mm. Curve *D*, taken from Reference 4, was determined by measurements on 0·426 molar Mo(V) solution.

Definitions of terms

A_D = observed absorbance due to the dimer(s).

ϵ_D = molar absorbance of the dimer(s).

C = total Mo(V) concentration, measured as monomer.

[M] = concentration of Mo(V) monomer.

[D] = concentration of Mo(V) dimer(s).

K = dissociation constant of dimer(s).

$$K = [M]^2/[D] \qquad C = [M] + 2[D] \qquad A_D = [D]\epsilon_D \tag{1}$$

$$K = \frac{(C - 2[D])^2}{[D]} = \frac{\left[C - \frac{2A_D}{\epsilon_D}\right]^2}{A_D/\epsilon_D} = \frac{(\epsilon_D C - 2A_D)^2}{\epsilon_D A_D} \tag{2}$$

$$\epsilon_D C - 2A_D = \sqrt{A_D \epsilon_D K}$$

$$\frac{\epsilon_D}{2} - \frac{A_D}{C} = \frac{\sqrt{A_D \epsilon_D K}}{2C} \tag{3}$$

A plot of A_D/C vs. $\sqrt{(A_D)}/C$ should give a straight line of slope $-\sqrt{(\epsilon_D K)}/2$ and intercepts of $\epsilon_D/2$ and $\sqrt{(\epsilon_D/K)}$.

RESULTS

The absorbance due to dimer (A) had to be obtained by successive approximations from the data in Table 1. The molar absorbance of monomer obtained in 9·0 to 12·0 molar acid is 12·4 at 450 mμ, while that of the dimer will be shown to be over 2000. As a first approximation A_D was found by subtracting 12·4 C from the observed absorbance. Once ϵ_D had been estimated, K could also be estimated, A_D could be improved by successive approximations of the term to be subtracted, only one further approximation ever being necessary. Tests of Equation (3) are shown by the plots in Fig. 3. Extrapolation of the results in 6·0 molar acid is not feasible, but two separate plots in different media give good straight lines with a common intercept representing $\epsilon_D/2$. This common intercept could be obtained only if there were a single dimeric species in equilibrium with monomer. It was thus possible to anchor the lines for the results in 6·0 molar acid on this intercept and evaluate equilibrium constants. Given this value of $\epsilon_D = 2200$ (or 1100 per Mo atom in absorbing species) equilibrium constants could be obtained from the absorbance of Mo(V) solutions wherever enhancement was observed. Using the constants one can construct an absorption curve in the visible region for the dimer causing the enhancement. Results of these studies are found in Tables 2, 3 and 4. The calculated absorption curve for the dimer

TABLE 1.—DEVIATIONS FROM BEER'S LAW AT 450 mμ IN SOLUTIONS OF Mo(V)

(Mo(V)) (m/l.)	Absorbance	Absorbance if $MoOCl_5^{2-}$ were only species	Medium
0·0010	0·070	0·012	5 M HCl
0·0028	0·385	0·035	
0·0040	0·785	0·050	
0·0055	1·297	0·068	
0·0100	3·03	0·124	
0·0400	25·80	0·496	
0·00642	0·450	0·080	6 M HCl
0·0107	0·975	0·133	
0·0214	3·12	0·266	
0·0263	4·48	0·326	
0·00137	0·392	0·017	0·5 M HCl
0·00274	1·121	0·034	+
0·00411	1·980	0·051	5·5 M $HClO_4$
0·00549	2·870	0·068	
0·00823	5·010	0·102	

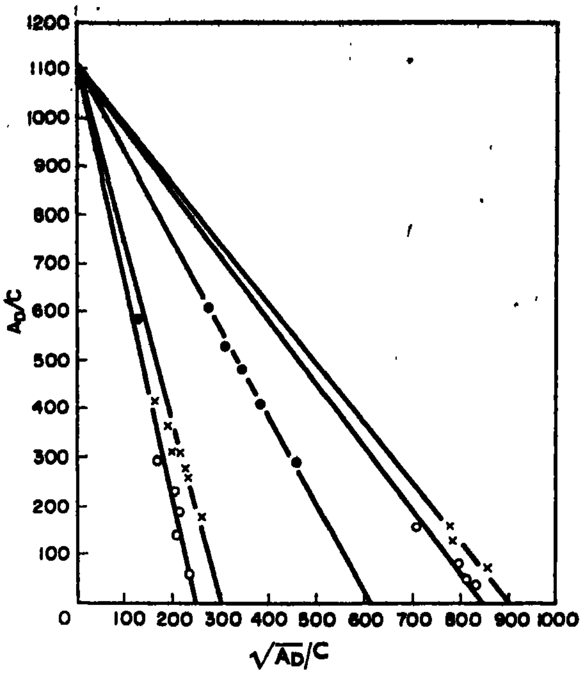

Fig. 3.—A plot of the variables in Equation (3) at different concentrations of hydrogen and chloride ions.

○ 5·00 molar hydrochloric acid, abscissa full scale. Left.
6·00 molar hydrochloric acid, abscissa one-tenth scale. Right.
× 5·05 molar hydrochloric acid, abscissa full scale. Left.
6·15 molar hydrochloric acid, abscissa one-tenth scale. Right.
● 5·5 molar perchloric acid, 0·5 molar hydrochloric acid.
Abscissa full scale.
Absorbance measured at 450 mμ.

Table 2.—Effect of (H^+) on monomer-dimer equilibrium constants (25°C)

Ion Strength = 6·0

[Mo(V)] = 0·005 M as monomer

A	A_D	K (m/l.)	[HCl] (m/l.)	[LiCl] (m/l.)	$[K]/[H^+]^2 \times 10^3$
0·268	0·208	0·241	6·0	0	6·7
0·304	0·245	0·207	5·0	1·0	8·3
0·402	0·344	0·142	4·5	1·5	7·0
0·548	0·490	0·093	4·0	2·0	5·8
0·702	0·647	0·066	3·5	2·5	5·4
0·810	0·756	0·055	3·0	3·0	6·1
1·000	0·950	0·0397	2·5	3·5	6·3
1·441	1·396	0·0217	2·0	4·0	5·4

TABLE 3.—EFFECT OF (Cl^-) ON MONOMER-DIMER EQUILIBRIUM CONSTANTS (25°C)
Ion Strength = 6·0
[Mo(V)] = 0·005 M as monomer.

A	A_D	K (m/l.)	[HCl] (m/l.)	[$HClO_4$] (m/l.)	$[K]/[Cl^-]^2 \times 10^3$
0·268	0·208	0·241	6·0	0·0	
0·257	0·197	0·24	5·0	1·0	
0·256	0·196	0·24	4·0	2·0	15*
0·288	0·226	0·23	3·0	3·0	25*
0·372	0·314	0·157	2·0	4·0	39
0·885	0·830	0·048	1·0	5·0	48
1·470	1·435	0·0216	0·7	5·3	44
2·110	2·072	0·0107	0·55	5·45	37
2·110	2·072	0·0107	0·40	5·6	70†

* Activity effects cause deviations.

† More than one dimer present. $K/[Cl^-]^2$ calculated as if dimer giving the enhancement and monomer were the only species.

TABLE 4.—VARIATION OF DIMER-MONOMER DISSOCIATION CONSTANTS WITH THE MOLAL ACTIVITY OF HYDROCHLORIC ACID

K (m/l.)	Molarity HCl	Molality HCl	a_{HCl}	K/a^4
0·0243	5·00	5·60	16·4	$3·4 \times 10^{-7}$
0·035	5·05	5·67	17·1	$4·2 \times 10^{-7}$
0·243	6·00	6·80	28·9	$3·5 \times 10^{-7}$
0·265	6·00	6·80	28·9	$3·7 \times 10^{-7}$
0·394	6·15	7·02	31·6	$4·0 \times 10^{-7}$

is given in Fig. 4. The dimer spectrum indicates a general breakdown of the structure of the spectrum during the enhancement. Maxima are still at the same wave lengths but are much less clearly defined. The general absorbance in the visible is reflected in the fact that if one adds water to green Mo(V) in concentrated hydrochloric acid or hydrogen chloride to brown Mo(V) in dilute acid the solution at first becomes opaque—dark brown or black—before changing finally to the high or low acid form. The opacity is undoubtedly due to the intermediate formation of the dimer under discussion.

Effect of hydrogen and chloride ions on dimer dissociation. Because lithium ion fits into water structure so well it is feasible to substitute LiCl for HCl even at an ion normality of 6·0. Dissociation constants for the dimer show a clear cut dependence on the square of the hydrogen ion concentration indicating two hydrogen ions are consumed when the dimer dissociates. The effect of chloride ion is not so easily determined. Substitution of perchloric acid for hydrochloric acid at ion strength 6·0 introduces activity effects which are difficult to assess quantitatively. Almost no change in the spectrum is observed in changing from 6·0 molar hydrochloric acid to 3·0 molar hydrochloric and 3·0 molar perchloric acids. The activity of perchloric acid is considerably higher than that of hydrochloric acid in 6·0 molar concentration.(9) The increase in activity of hydrogen ions and chloride ions caused by the added perchloric acid apparently compensates for the decrease in chloride ion concentration.

---

(9) R. A. ROBINSON and R. H. STOKES, *Electrolyte Solutions*, Appendix 8, 10, Table 9 p. 476. Butterworths, London (1955).

A rough dependence of the dissociation constant on the square of the chloride ion concentration over the rising portion of the curve (Table 3) plus the dependence of the constant on the fourth power of the molal activity of hydrochloric acid (Table 4) leads to the conclusion that the chemical equation for the dissociation of the dimer is:

$$\text{Mo(V)—O—Mo(V)} + 2H^{+} + 2Cl^{-} \rightarrow 2\text{Mo(V)Cl} + H_2O \tag{4}$$

Two hydroxide groups might be used instead of the single oxygen bridge.

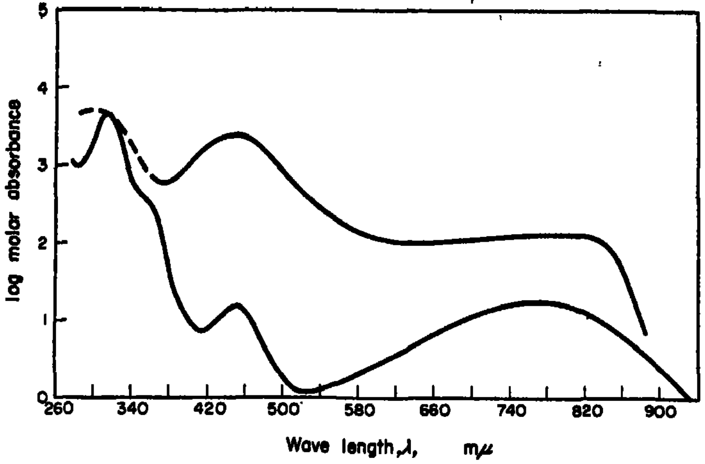

Fig. 4.—Calculated absorption spectrum for the dimer giving enhanced absorbance in the visible region. Dotted portion indicates great uncertainty because calculations are based on differences which are comparable with the uncertainty of measurements. Upper curve is Mo(V) dimer. Lower curve is $MoOCl_5^{2-}$ monomer.

TABLE 5.—EFFECT OF TEMPERATURE ON THE DISSOCIATION CONSTANT OF Mo(V) DIMER
5·0 M HCl
0·00372 M Mo(V)

Temperature (°C)	A	$K \times 10^3$ (m/l.)
14·0	1·048	1·72
15·5	1·026	1·78
19·5	0·942	2·07
20·5	0·923	2·14
23·2	0·868	2·38
24·5	0·848	2·47
25·0	0·842	2·50
22·5	0·875	2·36
16·6	0·939	1·93
17·6	0·962	1·98
20·7	0·910	2·18
22·2	0·882	2·33
23·3	0·862	2·41
20·5	0·935	2·10

$\Delta H = 6·0 \pm 0·2$ kcal.
$\Delta S = 12 \pm 2$ e.u.

Temperature dependence of dimer dissociation. Table 5 shows the effect of temperature on the monomer-dimer equilibrium. The reaction is endothermic with $\Delta H_{298} = 6·0 \pm 0·2$ kcal per mole of dimer and $\Delta S_{298} = 12 \pm 2$ entropy units.

Further hydrolysis of dimer. Dilution of 5 molar hydrochloric acid causes a sharp decrease in the enhancement of the 450 mμ peak and a shift of the peak to shorter wavelengths. The same behaviour is noted on the peak at 310 mμ over the entire acid concentration range. This represents the gradual substitution of water, hydroxyl ion, and/or oxide ion for chloride. The equilibria are many and overlap one another so that no effort has been made to sort them out. The strict adherence to Beer's law for the dilute solutions of Mo(V) (10^{-3} to 10^{-4} molar) employed in observations at 310 mμ over the entire concentration range of acid suggests that dimerization may not occur appreciably in such dilute solutions, or if it does, dimers and monomers have identical ultraviolet absorption spectra.

DISCUSSION

Species of Mo(V). It seems certain that the species in concentrated acid is the $MoOCl_5^{2-}$ ion. WARDLAW has prepared green salts of this ion the appearance of which is very similar to the green solutions. If the dimer enhancing the spectrum of this ion is produced with the production of two chloride and two hydrogen ions as in the reverse of Equation (4) we have the choice of introducing one oxo- or two hydroxo-bridges between the Mo(V) atoms after removing one chloride from each. The choice of most likely structure for the dimer must be

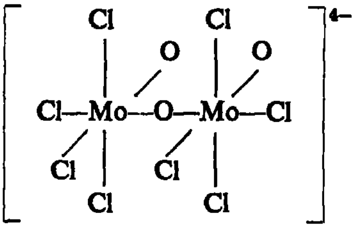

Two hydroxo-bridges would raise the co-ordination number to seven which is unlikely. It is suggested that the oxygen bridge is substituted for one of the four equatorial chloride ions in $MoOCl_5^{2-}$ to destroy the symmetry without severely changing the crystal field. This would change the band associated with the d orbital in the plane of the chloride to an allowed band without changing the energy of the transition. It is also known that in oxy-anions such as VO^{2+} very weak binding occurs trans to the metal oxygen bond, thus the trans position is the least likely point for a bridging oxygen to bind.

Effect of dimerization on paramagnetism. The fact that oxygen bridge formation in other systems is accompanied by decrease in paramagnetism(5,6,7) makes it tempting to correlate this work with the magnetic study of SACCONI and CINI.[4] However their work employed 0·5 M Mo(V) which had large and indeterminate effects on the concentrations of [H^+] and [Cl^-]. One cannot say if the dimer causing enhanced absorbance in the visible is paramagnetic or diamagnetic by comparing their data with that presented here. Electron paramagnetic resonance measurement at Columbia University have recently shown that the monomer, $MoOCl_5^{2-}$, is not the only paramagnetic species.(8) Other paramagnetic species are present in maximum concentration where the dimer under discussion is also present in maximum concentration strongly indicating that $[OCl_4Mo{-}O{-}MoCl_4O^{4-}]$ is paramagnetic. It is evident that the hydrolysis and aquation of $MoOCl_5^{2-}$ involves the production of a complicated sequence of dimers, the first of which is involved in this study. Undoubtedly some of the compounds prepared by JAMES and WARDLAW(10) from dilute hydrochloric acid contained dimeric Mo(V) anions. For instance JAMES and WARDLAW showed the compound $Mo(OH)_3Cl_2py$ first prepared by SAND and BURGER(11) to be a pyridinium salt. A dimer structure such as

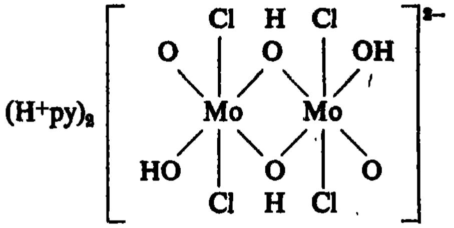

would be required to preserve co-ordination number six.

Acknowledgements—The author wishes to thank the Office of Ordnance Research, U.S. Army, for support of this investigation; Miss J. WEGMAN, Mrs. J. HEALD, and Mr. F. MCKNIGHT who measured some of the spectra; and Mr. C. SCHAEFFER and Prof. J. BJERRUM for valuable discussions.

The author is also indebted to Dr. H. GRAY and Mr. I. BERNAL for communicating preliminary results of electron paramagnetic resonance studies recently obtained.

(10) R. G. JAMES and W. WARDLAW, *J. Chem. Soc.* 2145 (1927).

(11) J. SAND and O. BERGER, *Ber. Dtsch. Chem. Ges.* 39, 1971 (1906).

J. Inorg. Nucl. Chem., 1962, Vol. 24, pp. 673 to 677. Pergamon Press Ltd. Printed in Northern Ireland

POLAROGRAPHY OF HEXAVALENT MOLYBDENUM IN HYDROCHLORIC ACID*

G. P. Haight, Jr.†
Inorganic Chemistry Laboratory, Oxford; the Chemistry Department of
the University of Kansas

(*Received* 5 *March* 1961; *in revised form* 12 *December* 1961)

Abstract—Solutions containing hydrochloric acid in concentrations less than 1·0 molar and molybdate ions in concentrations less than 10^{-4} molar give polarograms containing one or three waves. The single wave observed in 0·5–0·7 M hydrochloric acid and the middle wave of the three observed in more dilute acid have reversible two electron characteristics. The half-wave potential of this wave is given by the equation:

$$E_{\frac{1}{2}} = -0{\cdot}080 + 0{\cdot}12 \log (H^+) + 0{\cdot}035 \log (Cl^-)$$

corresponding to the electrochemical equation:

$$Mo(VI) + 4H^+ + Cl^- + 2e \rightarrow Mo(IV)$$

Evidence that the chemically unstable Mo(IV) is the primary reduction product is discussed.

This study was undertaken in an effort to explain the complete lack of correspondence between waves observed when molybdate at concentrations less than 10^{-4} molar is polarographed in hydrochloric acid and waves reported by Carritt[1] for solutions containing molybdate in concentrations greater than 10^{-3} molar in the same acid. Polarograms of 10^{-4} molar molybdate solutions can be obtained only when the hydrochloric acid concentration is kept below 1·0 molar. At high acid concentrations the reduction potential for molybdate becomes more positive than the potential for the anodic dissolution of mercury. In the more concentrated solutions studies by Carritt[1], waves are shifted to more negative potentials and multiple waves, maxima, and discontinuities very much complicate the observations.

EXPERIMENTAL

Polarograms were made in a conventional manner using a Tinsley Recording Polarograph at Oxford University and a Sargent Model XXI Polarograph at the University of Kansas. Reagent grade chemicals were used without further purification. An H-cell was employed with one arm containing a saturated calomel electrode for reference. For accurate measurement of half-wave potentials an external potentiometer was used and readings obtained manually. Temperature of the cell was regulated at 30 and 25°C.

OBSERVATIONS AND RESULTS

Polarograms of $8{\cdot}75 \times 10^{-5}$ molar Mo(VI) in 0·1 and 0·3 molar solutions of hydrochloric acid are shown in Fig. 1. The single wave observed in 0·3 molar (and more concentrated) acid has reversible two-electron characteristics. An ill-defined early wave and a later wave both appear in the more dilute acid, the later wave corresponding to a wave observed when Mo(V) is polarographed in dilute hydrochloric acid.[2] Since no wave for Mo(V) is observed in 0·3 molar hydrochloric acid following the wave for Mo(VI), it is suggested that the product of reduction of Mo(VI) must be a

---

* From a paper presented before the Division of Physical and Inorganic Chemistry at the 131st Meeting of the American Chemical Society, Miami, Florida, 1957.

† Present address: Department of Chemistry, Swarthmore College, Swarthmore, Pennsylvania.

[1] D. Carritt, Ph.D. Thesis, Harvard University (1947).

[2] C. E. Worsham. Unpublished results.

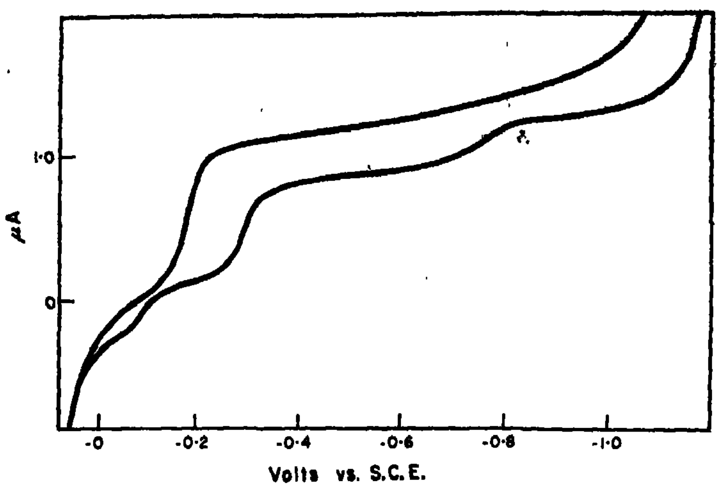

FIG. 1.—Polarograms of 8·75 × 10^{-5} molar Mo(VI) in 0·3 molar HCl (upper curve) and in 0·1 molar HCl (lower curve). The lower curve has been lowered on the diagram to prevent interference. $m^{2/3}t^{1/6}$ is 2·30 mg$^{2/3}$sec$^{-1/2}$. T = 30°C.

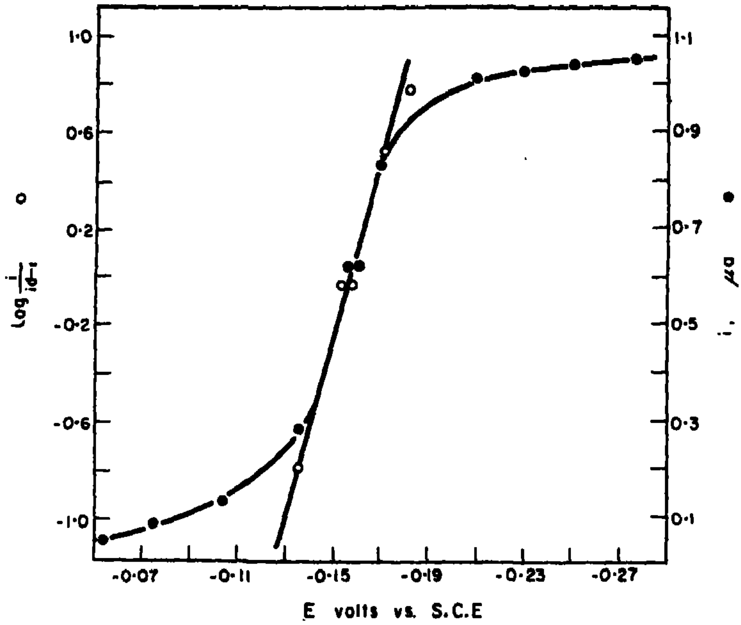

FIG. 2.—Polarogram of 8·75 × 10^{-5} molar Mo(VI) in 0·3 molar HCl (solid dots). Upper plateau continues until hydrogen ion is reduced. Slope of E vs. log $i/(i_d - i)$ plot is 0·030 (open circles). T = 30°C.

lower oxidation state, presumably Mo(IV) in light of the two-electron character of the wave. Figure 2 shows the conventional log $i/(i_d - i)$ vs. E plot for this wave with a slope of 0·030.

The slope of 0·030 for the log $i/(i_d - i)$ vs. E plot is necessary but insufficient evidence for a two electron reduction. The number of electrons taking part in the

(8) KOLTHOFF and LINGANE, *Polarography*, 2nd Ed., Interscience, New York (1952).

TABLE 1.—CHARACTERISTICS OF THE SINGLE WAVE FOR Mo(VI) IN HCl
(Mo(VI)) = 10^{-4} molar*

(HCl) mole/l.	$E_{\frac{1}{2}}$	$\frac{i_d}{(\text{Mo(VI)})m^{2/3}t^{1/6}}$ 25°C	$\frac{i_d}{(\text{Mo(VI)})m^{2/3}t^{1/6}}$ 30°C	D (cm^2/sec) 25°C
0·3	−0·161			
0·5	−0·127	413	443	$1{\cdot}0 \times 10^{-5}$
0·7	−0·104			

* Diffusion currents for a given (Mo(VI)) concentration were the same within experimental error in all solutions showing only one wave for Mo(VI). D is given assuming a two electron reduction.

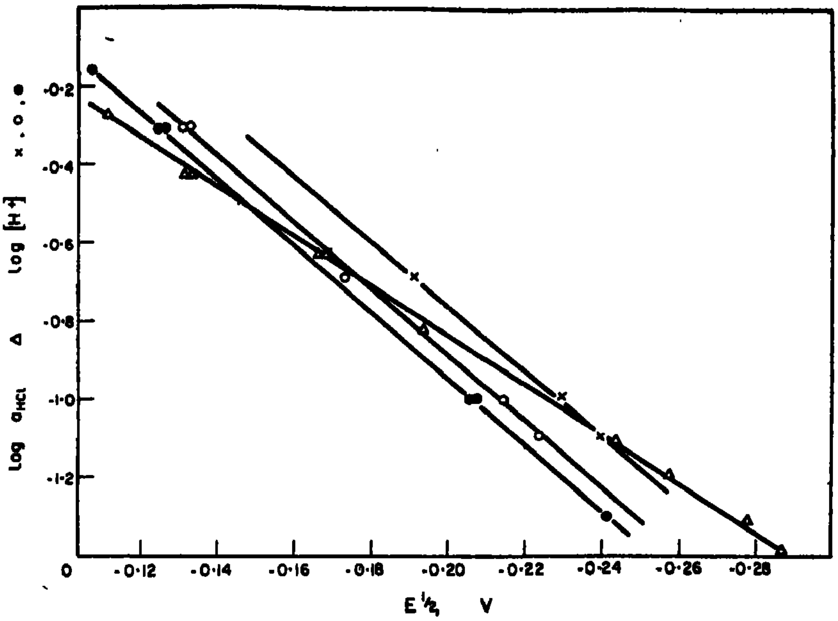

FIG. 3.—Effect of changing concentrations of hydrogen ion and chloride ion on half-wave potential.

× Log [H$^+$] vs. $E_{\frac{1}{2}}$ in 0·7 M -(HCl) + (NaCl)-
○ Log [H$^+$] vs. $E_{\frac{1}{2}}$ in 0·5 M -(HCl) + (NaCl)-
● Log [H$^+$] vs. $E_{\frac{1}{2}}$ in 0·3 M -(HCl) + (NaCl)-
△ Log activity of HCl vs. $E_{\frac{1}{2}}$.

reduction is also a factor in the Ilkovic equation(3) for the different current. To measure n the diffusion coefficient of the reducible species must be known. The results of JANDER *et al.*(4) when corrected to 25°C suggests a diffusion coefficient, D, of 10×10^{-6} cm^2/sec for mononuclear molybdate and 5×10^{-6} cm^2/sec for polynuclear (presumably heptameric(5,6)) species. The higher of the two diffusion coefficients is consistent with a two-electron reduction, the lower is consistent with a three-electron reduction. Since polymerized molybdate gives *stepwise* polarographic waves

(4) G. JANDER, K. F. JAHR and W. HEUCKESHOVEN, *Z. Anorg. Chem.* **194**, 383 (1930).
(5) G. SCHWARZENBACH and J. MEIER, *J. Inorg. Nucl. Chem.* **8**, 302 (1958).
(6) Y. SASAKI, L. G. SILLEN and I. LINDQUIST, *J. Inorg. Nucl. Chem.* **9**, 93 (1959).

in other media with diffusion coefficients of about 5×10^{-6} cm²/sec, it will be assumed that the single wave here observed is due to a monomeric species undergoing reversible two-electron reduction. Furthermore Carritt(1) has found evidence for Mo(IV) as a product of constant potential electrolyses of molybdate solutions considerably more concentrated than those employed in this study. The characteristics of the reversible two-electron wave for the reduction of Mo(VI) in hydrochloric acid are summarized in Table 1.

Effect of changing hydrochloric acid concentration on the half wave potential of the reversible wave. Fig. 3 shows the effect of variation of hydrogen ion and chloride ion concentrations on the half-wave potential. At three different values of ion strength a plot of log [H⁺] vs. $E_{\frac{1}{2}}$ gives straight lines with slope of 0·12 indicating that four hydrogen ions per molybdate ion participate in the reduction. It proved impossible to study chloride ion dependence at constant ion strength since all other common anions affect the polarographic behaviour of molybdate. For instance, perchlorate and nitrate are catalytically reduced, and sulphate completely alters the nature of the polarograms observed. The dotted line in Fig. 3 shows the effect of changing hydrochloric acid activity on the half-wave potential. From the slope of this line and the dependence on hydrogen ion, the following equation for the reduction of molybdate is deduced.

$$E_{\frac{1}{2}} = -0{\cdot}080 + 0{\cdot}12 \log [\mathrm{H^+}] + 0{\cdot}035 \log [\mathrm{Cl^-}] \text{ volts vs. S.C.E.}$$

This equation corresponds approximately to the electrochemical reaction

$$\mathrm{Mo(VI)} + 4\mathrm{H^+} + \mathrm{Cl^-} + 2e \rightarrow \mathrm{Mo(IV)}$$

Presumably one more chloride is attached to Mo(IV) than to Mo(VI) and either two oxygens or four hydroxide ions attached to Mo(VI) are converted to water.

DISCUSSION

The nature of Mo(VI) *in dilute hydrochloric acid.* The work of Jander, *et al.*(4) indicates that polymolybdates depolymerize at acidities greater than 0·1 molar hydrogen ion. Kinetic studies by Schwarzenbach and Meier(5) indicate that monomeric molybdate is diprotonated at acidities greater than millimolar [H⁺]. They suggest $\mathrm{Mo(OH)_6}$ as the probable form of mononuclear molybdic acid and have evaluated K_1K_2 for diprotonation of $\mathrm{MoO_4^{2-}}$. Sillen *et al.*(6) have studied the polymerization of molybdate from monomer to heptamer. Using the value of K_1K_2 of Schwarzenbach and Meier(5) and the polymerization equilibrium constants of Sillen *et al.*(6) it is found that the equilbirium

$$18\mathrm{H_2O} + \mathrm{H_2Mo_7O_{24}^{4-}} + 4\mathrm{H^+} \rightleftarrows 7\mathrm{H_6MoO_6}$$

lies far to the right for 10^{-4} M Mo(VI) in 0·5 M hydrochloric acid. It must be pointed out that Schwarzenbach and Meier's data do not describe equilibrium conditions, but they do give information concerning equilibria between monomeric Mo(VI) species. The calculation does not take into account possible higher polymers suggested by the data of Sillen, Lindquist and Sasaki for acidities greater than millimolar [H⁺]. It does seem likely that the formation of new species with different polarographic characteristics at Mo(VI) concentrations greater than millimolar(1) is brought about by polymerization of monomeric Mo(VI) as its concentration increases. If this interpretation is correct the equation for the reversible two-electron polarographic wave becomes:

$$Mo(OH)_6 + 4H^+ + Cl^- + 2e \rightarrow Mo(OH)_2(OH_2)_3Cl^+ + H_2O$$

(A spectrophotometric study by NEUMANN and COOK(17) on chloro molybdate species merely indicates that less than two chloride ions are bound to each molybdate ion in 0·5 molar hydrochloric acid).

Evidence for Mo(IV) *as the primary reduction product.* Since Mo(IV) is incapable of direct identification, supporting evidence for its formation is required, and other possible explanations for the reversible two-electron wave must be considered. The possibility that a dimer of Mo(VI) is reversibly reduced to a dimer of Mo(V) is ruled out by the absence of a Mo(V) wave and by the failure of SASAKI *et al.*(6) to find intermediate polymers between monomer and heptamer during acidification of solutions of MoO_4^{2-}.

HAIGHT and SAGER(8) have offered evidence that Mo(IV) is the catalytic species responsible for the molybdate catalysed reduction of perchlorate. This catalysis is observed in conjunction with the reversible two-electron wave(9) indicating that Mo(IV) must be produced during the reduction of Mo(VI) in the polarograms now in question.

In conclusion it is interesting that the known pentavalent state of molybdenum is apparently bypassed in this electrochemical process. If one assumes that electrons are transferred one at a time the implication follows that monomeric Mo(V) is much more susceptible of reduction than the dimeric form normally found in dilute hydrochloric acid. This is confirmed in the recent observation that monomeric Mo(V) which is formed in hydrochloric acid of concentration greater than 8 molar(10) is reduced by stannous chloride, whereas the dimeric form present in dilute acid is not.(11)

Acknowledgement—The author wishes to acknowledge with thanks the encouragement of Dr. M. N. H. IRVING and financial assistance from the Rhodes Trust and the Office of Ordnance Research, U.S. Army.

(7) H. M. NEUMANN and N. COOK, *J. Amer. Chem. Soc.* **79**, 3026 (1957).
(8) G. P. HAIGHT, JR. and W. F. SAGER, *J. Amer. Chem. Soc.* **74**, 6056 (1952).
(9) G. P. HAIGHT, JR. Unpublished work, *Analyt. Chem.* **23**, 1505 (1951).
(10) L. SACCONI and R. CINI, *J. Amer. Chem. Soc.* **76**, 4239 (1954).
(11) A. BERGH, Ph.D. Thesis, University of Pennsylvania (1959).

J. Inorg. Nucl. Chem., 1962, Vol. 24, pp. 679 to 688. Pergamon Press Ltd. Printed in Northern Ireland

COMPLEXING BEHAVIOUR OF KOJIC ACID WITH METAL IONS—II

Fe(III) CHELATES*,†

Y. MURAKAMI
Department of Organic Synthesis, Faculty of Engineering, Kyushu University,
Fukuoka, Japan

(*Received* 6 *July* 1961; *in revised form* 11 *September* 1961)

Abstract—Kojic acid forms a stable chelate with Fe(III) ion at 1:1 molar ratio in weakly acidic media. In the absence of enough ligand, Fe(III)–kojate chelates tend to hydrolyse to an appreciable extent as a pH value of the solution goes up. At 1:1 molar ratio of ligand to metal ion four hydrolysed species; $Fe(OH)A$, $Fe(OH)_2A$, $\{Fe(OH)A\}_2$ and $\{Fe(OH)_2A\}_2$; are formed. In comparison with the 1:1 chelate, hydrolytic tendency of the 2:1 chelate decreases, and $Fe(OH)A_2$ and $\{Fe(OH)A_2\}_2$ are the only hydrolysed products. Furthermore, in the case where more than three moles of ligand per mole of metal ion are present, such hydrolysis reactions do not proceed to a significant extent and stable chelate species formed are FeA_2 and FeA_3. All the measurements were carried out at $t = 25°$ and $\mu = 0{\cdot}10$ M, and the corresponding equilibrium and stability constants were estimated.

IN the previous work,(1) kojic acid as one of β-diketones was found to form the metal chelates with Mg(II) and Mn(II) ions whose stabilities were nearly equal to the corresponding metal chelates of β-diketones of the same acidity in aqueous media as far as available data are concerned.

It has been known that Fe(III) chelates exhibit great tendency toward hydrolytic polymerization in aqueous media(2) when some of the co-ordinating sites of Fe(III) are not occupied with donor atoms of great chelating ability. In order to provide a comparison in hydrolytic tendencies between those chelates previously reported and the kojate chelates, potentiometric measurements were carried out at different molar ratios of ligand to metal ion. On the other hand, kojic acid has been used as a metal indicator(3) for the chelatometric titration of Fe(III) ion because of its profound coloration with the metal ion in weakly acidic media. However, studies on the Fe(III)–kojate system have not been conducted so far to obtain stability constants of such chelates. Thus, it is the purpose of the present work to clarify the interaction between Fe(III) ion and kojic acid and pursue the hydrolytic tendencies of partially chelated Fe(III) ion in aqueous media.

---

* Contribution No. 20 from the Department of Organic Synthesis, Faculty of Engineering, Kyushu University.

† Presented in part at the 14th Annual Meeting of the Chemical Society of Japan held in Tokyo, April, 1961.

(1) Y. MURAKAMI, *Bull. Chem. Soc. Japan* **35**, 52 (1962).

(2) (a) C. F. RICHARD, R. L. GUSTAFSON and A. E. MARTELL, *J. Amer. Chem. Soc.* **81**, 1033 (1959); (b) R. L. GUSTAFSON and A. E. MARTELL, Annual Progress Report from the Department of Chemistry, Clark University, U.S.A.E.C. AT(30-1) 1823, p. 21 (1960).

(3) L. SOMMER and Z. KOLARIK, *Chem. Listy* **50**, 1323 (1956); *Coll. Czech. Chem. Comm.* **21**, 1645 (1956).

EXPERIMENTAL

Reagents. Kojic acid was purchased from the Tokyo Kasei Kogyo Co., Ltd. and was purified by sublimation *in vacuo*: m.p. 156–156·6°; reported 154–156°(4); 154°(5). This purified material was used to prepare an aqueous stock solution which was standardized by potentiometric titration with standard base.

Reagent grade $Fe(NO_3)_3 \cdot 9H_2O$ was purchased from the Wako Pure Chemical Industries, Ltd and used to prepare stock solutions which were standardized by chelatometric titration(6) with Variamin blue B (N-(*p*-methoxyphenyl)-*p*-phenylenediamine) as a metal indicator.

Potentiometric measurements. An HRL Model P pH meter of the Horiba Instruments Inc., Kyoto equipped with extention glass and calomel electrodes was used to measure hydrogen ion concentration directly. Calibration of the pH meter was performed by the aid of acetic acid buffer as well as standard HCl and NaOH. Measurements were carried out at 25·0 ± 0·1° in a jacketed titration cell fitted with a magnetic stirrer, nitrogen inlet and outlet tubes, microburet delivery tube and electrodes. All the titrating solutions whose ionic strength was maintained at approximately 0·10 M with KNO_3, were kept under a nitrogen atmosphere throughout titrations.

Spectrophotometric measurements. The method of continuous variations(7) was applied to the determination of the formula of the chelate formed in the lower pH region. Total concentration, $T_A + T_M$, (where T_A and T_M represent total concentrations of kojate and metal species, respectively) was maintained constant at $1{\cdot}28 \times 10^{-3}$ M and the mole fraction of kojate, $T_A/(T_A + T_M)$, varied from 0·00 to 1·00. Samples were allowed to equilibrate for five days and optical density measurements were performed with a Hitachi EPS-2 type recording spectrophotometer. Hydrogen ion concentration and ionic strength of sample solutions were adjusted at 0·1097 N with HNO_3. The increase in optical density caused by chelate formation was determined at several wavelengths in accordance with the equation:

$$\delta D = l \cdot D - l \cdot (\varepsilon_1 T_M + \varepsilon_2 T_A) \tag{1}$$

where ε_1 = extinction coefficient of Fe(III)
ε_2 = extinction coefficient of kojic acid.
D = optical density measured
l = length of light path

The stability constant of a 1:1 Fe(III)-kojate chelate which formed in the low pH region was estimated spectrophotometrically with the same recording spectrophotometer. pH value of the solution was adjusted at appropriate value with HNO_3 and also the ionic strength was maintained at approximately 0·10 M in nitrate concentration. Temperature range of the sample solutions lay between 14·0° and 16·0°. The amount of the red chelate formed in such low pH region where any other side reaction may be reasonably neglected, was estimated.

MATHEMATICAL TREATMENT

In the iron(III) chelate systems which contain equimolar concentrations of ligand and metal ion, five species may be considered to exist: a normal aquo chelate, FeA^{2+}; a monohydroxo species, $Fe(OH)A^+$; a dihydroxo species, $Fe(OH)_2A$; a monohydroxo dimer, $\{Fe(OH)A\}_2^{2+}$; and a dihydroxo dimer, $\{Fe(OH)_2A\}_2$. The solution equilibria may be expressed in terms of the equations:

$$HA \rightleftharpoons H^+ + A^- \qquad K_D = \frac{[H^+][A^-]}{[HA]} \tag{2}$$

$$Fe^{3+} + HA \rightleftharpoons FeA^{2+} + H^+ \qquad K'_1 = \frac{[FeA^{2+}][H^+]}{[Fe^{3+}][HA]} \tag{3}$$

$$FeA^{2+} + H_2O \rightleftharpoons Fe(OH)A^+ + H^+ \qquad K_{M(OH)A} = \frac{[Fe(OH)A^+][H^+]}{[FeA^{2+}]} \tag{4}$$

---

(4) B. E. BRYANT and W. C. FERNELIUS, *J. Amer. Chem. Soc.* **76**, 5351 (1954).

(5) F. CHALLENGER, T. KLEIN and T. K. WALKER, *J. Chem. Soc.* 1498 (1929).

(6) K. UENO, *Chelatometric titration* (in Japanese) p. 259. Nankodo, Tokyo (1960).

(7) (a) P. JOB, *Ann. Chem.* **11**, 97 (1936); (b) W. C. VOSBURGH and G. R. COOPER, *J. Amer. Chem. Soc.* **63**, 437 (1941).

$$2\mathrm{FeA}^{2+} + 2\mathrm{H_2O} \rightleftharpoons \{\mathrm{Fe(OH)A}\}_2^{2+} + 2\mathrm{H}^+ \quad K_{\{\mathrm{M(OH)A}\}_2} = \frac{[\mathrm{Fe(OH)A}_2^{2+}][\mathrm{H}^+]^2}{[\mathrm{FeA}^{2+}]} \tag{5}$$

$$\mathrm{FeA}^{2+} + 2\mathrm{H_2O} \rightleftharpoons \mathrm{Fe(OH)_2A} + 2\mathrm{H}^+ \quad K_{\mathrm{M(OH)_2A}} = \frac{[\mathrm{Fe(OH)_2A}][\mathrm{H}^+]^2}{[\mathrm{FeA}^{2+}]} \tag{6}$$

$$2\mathrm{FeA}^{2+} + 4\mathrm{H_2O} \rightleftharpoons \{\mathrm{Fe(OH)_2A}\}_2 + 4\mathrm{H}^+ \quad K_{\{\mathrm{M(OH)_2A}\}_2} = \frac{[\{\mathrm{Fe(OH)_2A}\}_2][\mathrm{H}^+]^4}{[\mathrm{FeA}^{2+}]^2} \tag{7}$$

The amount and distributing ratio of the various chelate species formed under varying conditions of pH and total concentrations of Fe(III) and kojate may be calculated from the above equilibrium relationships which are to be discussed in the forthcoming paragraphs.

Since chelate forming reaction whose equilibrium is expressed by equation (3) was completed before hydrolytic reactions proceeded to an appreciable extent, stoicheiometric relationships corresponding to those equilibrium relations shown above may be represented as follows:

$$T_A = T_M = [\mathrm{FeA}^{2+}] + [\mathrm{Fe(OH)A}^+] + [\mathrm{Fe(OH)_2A}] + 2[\{\mathrm{Fe(OH)A}\}_2^{2+}] + 2[\{\mathrm{Fe(OH)_2A}\}_2] \tag{8}$$

$$[\mathrm{H}^+] + T_{\mathrm{OH}} = [\mathrm{FeA}^{2+}] + 2[\mathrm{Fe(OH)A}^+] + 3[\mathrm{Fe(OH)_2A}] + 4[\{\mathrm{Fe(OH)A}\}_2^{2+}] + 6[\{\mathrm{Fe(OH)_2A}\}_2] \tag{9}$$

It is quite reasonable to assume that the reactions yielding dihydroxo, $\mathrm{Fe(OH)_2A}$, and dimeric dihydroxo species, $\{\mathrm{Fe(OH)_2A}\}_2$ proceed through those yielding monohydroxo, Fe(OH)A, and dimeric monohydroxo species, $\{\mathrm{Fe(OH)A}\}_2$. Thus, contribution of equations (6) and (7) is not significant and may be neglected in the pH region of adequately low values. Combination of equilibrium relations (4), (5) and stoicheiometric relationships (8) and (9) results in the following equations:

$$[\mathrm{FeA}^{2+}] = (2 - m)\, T_M - [\mathrm{H}^+] \tag{10}$$

$$\frac{[\mathrm{H}^+] + (m-1)T_M}{[\mathrm{FeA}^{2+}]/[\mathrm{H}^+]} = K_{\mathrm{M(OH)A}} + 2K_{\{\mathrm{M(OH)A}\}_2}\frac{[\mathrm{FeA}^{2+}]}{[\mathrm{H}^+]} \tag{11}$$

where m represents moles of base added per mole of total metal species present in solution. Therefore, if hydrolysis reactions represented by equations (4) and (5) occur, a straight line is to be obtained when $[\mathrm{H}^+] + (m-1)T_M/\{[\mathrm{FeA}^{2+}]/[\mathrm{H}^+]\}$ is plotted against $[\mathrm{FeA}^{2+}]/[\mathrm{H}^+]$, the slope of which is equal to $2K_{\{\mathrm{M(OH)A}\}_2}$ and the intercept at $[\mathrm{FeA}^{2+}]/[\mathrm{H}^+] = 0$ is equal to $K_{\mathrm{M(OH)A}}$.

When the pH value of the solution climbs up higher, further hydrolysis reactions which yield dihydroxo species come into play and equilibrium relationships (6) and (7) should be taken into consideration. $K_{\mathrm{M(OH)A}}$ and $K_{\{\mathrm{M(OH)A}\}_2}$ being obtained in accordance with equation 11 in the preceding pH region, $K_{\mathrm{M(OH)_2A}}$ and $K_{\{\mathrm{M(OH)_2A}\}_2}$ may be evaluated by the combination of equilibrium relations (4)–(7) and equations (8) and (9) which gives the relationships shown below:

$$[\mathrm{FeA}^{2+}] = \frac{-b + \sqrt{(b^2 + 4ac)}}{2a} \tag{12}$$

where

$$a = \frac{2K_{\{M(OH)A\}_2}}{[H^+]^2}\ ; \qquad b = 2 + \frac{K_{M(OH)A}}{[H^+]}\ ; \qquad c = (3-m)T_M - [H^+]$$

and

$$R = K_{M(OH)_2A} + 2K_{\{M(OH)_2A\}_2}\frac{[FeA^{2+}]}{[H^+]^2} \tag{13}$$

where

$$R = \frac{T_M[H^+]^2}{[FeA^{2+}]} - [H^+]^2 - K_{M(OH)A}[H^+] - 2K_{\{M(OH)A\}_2}[FeA^{2+}]$$

Equation (13) means that R may be plotted as a linear function of $[FeA^{2+}]/[H^+]^2$ and the slope is equal to $2K_{\{M(OH)_2A\}_2}$ while the intercept at $[FeA^{2+}]/[H^+]^2 = 0$ is equal to $K_{M(OH)_2A}$.

In the presence of enough ligand co-ordinating tendency of metal species seems to be much greater than hydrolytic tendencies. Thus, all the hydrolytic reactions mentioned above for the 1:1 chelate system may be neglected in the presence of more than three moles of ligand per mole of metal ion when a proper range of pH value is selected. In this instance following two reactions may proceed simultaneously:

$$FeA^{2+} + HA \rightleftharpoons FeA_2^+ + H^+ \qquad K_2' = \frac{[FeA_2^+][H^+]}{[FeA^{2+}][HA]} \tag{14}$$

$$FeA_2^+ + HA \rightleftharpoons FeA_3 + H^+ \qquad K_3' = \frac{[FeA_3][H^+]}{[FeA_2^+][HA]} \tag{15}$$

In a similar manner described in the preceding paper⁽¹⁾ following equations may be derived from equations (14) and (15) as well as the corresponding stoicheiometric relations which make the evaluation of K_2 and K_3 possible.

$$[HA] = T_A - \{T_{OH} + [H^+]\} \tag{16}$$

$$\frac{1}{(F-1)[HA]/[H^+]} = K_2' + K_2'\,K_3'\,\frac{(2F-1)\,[HA]}{(F-1)\,[H^+]} \tag{17}$$

where

$$F = \frac{T_M}{T_A - T_M - [HA]}$$

Equation (17) indicates the linear relationship between

$$\frac{1}{(F-1)\,[HA]/[H^+]} \quad \text{and} \quad \frac{(2F-1)}{(F-1)}\frac{[HA]}{[H^+]} \quad \text{and} \quad K_2',\ K_2'\,K_3'$$

values may be estimated from the intercept at

$$\frac{(2F-1)}{(F-1)}\frac{[HA]}{[H^+]} = 0$$

and the slope of the straight line, respectively. Equilibrium constants; K_1', K_2' and K_3'; may be converted into the corresponding stability constants; K_1, K_2 and K_3; as follows:

$$K_1 = K_1'/K_D;\ K_2 = K_2'/K_D;\ K_3 = K_3'/K_D.$$

RESULTS AND DISCUSSION

1:1 *Chelate*. Dark reddish colour observed when both iron(III) and kojic acid solutions were mixed at arbitrary molar ratio in the lower pH region indicates the formation of stable Fe(III)-kojate chelate species. The colour was found to be most deep in the pH range between 2·0 and 3·0 and diminished slightly as a pH value deviated from this range. The method of continuous variations was employed to determine the composition of the Fe(III)-kojate chelate formed in such a low pH region. To avoid any appreciable hydrolysis reaction of metal ion and metal chelate species, a pH value of the sample solution was maintained at 0·960. Maximum increase in optical density in accordance with equation (1) was observed for solutions containing equivalent amounts of ligand and metal ion at all wavelengths studied as shown in Fig. 1, indicating the presence of a 1:1 chelate.

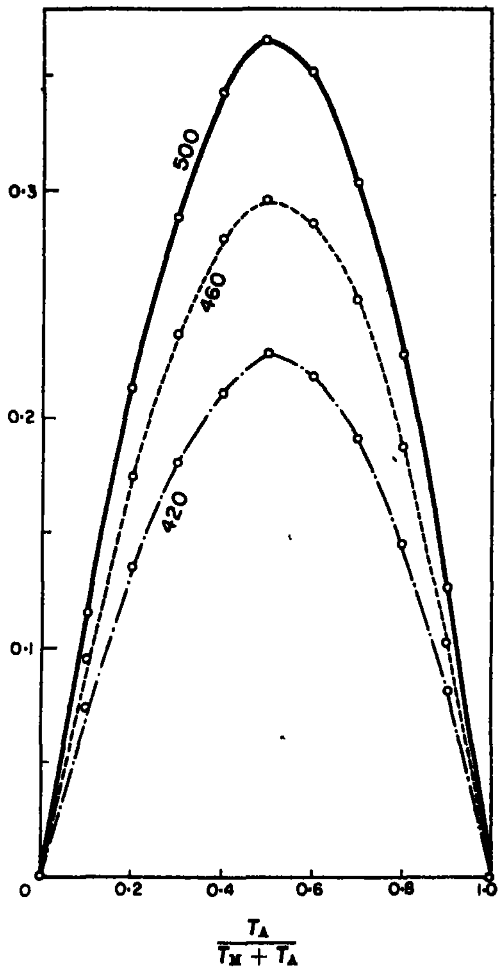

Fig. 1.—Method of continuous variations applied to the Fe(III)-kojate system at a hydrogen ion concentration of 0·1097 N in HNO$_3$. $T_M + T_A = 1{\cdot}28 \times 10^{-3}$ M. Numbers refer to wavelengths measured in mμ.

Analysis of the titration data shown in Fig. 2 for 1:1 ratio of ligand to metal ion

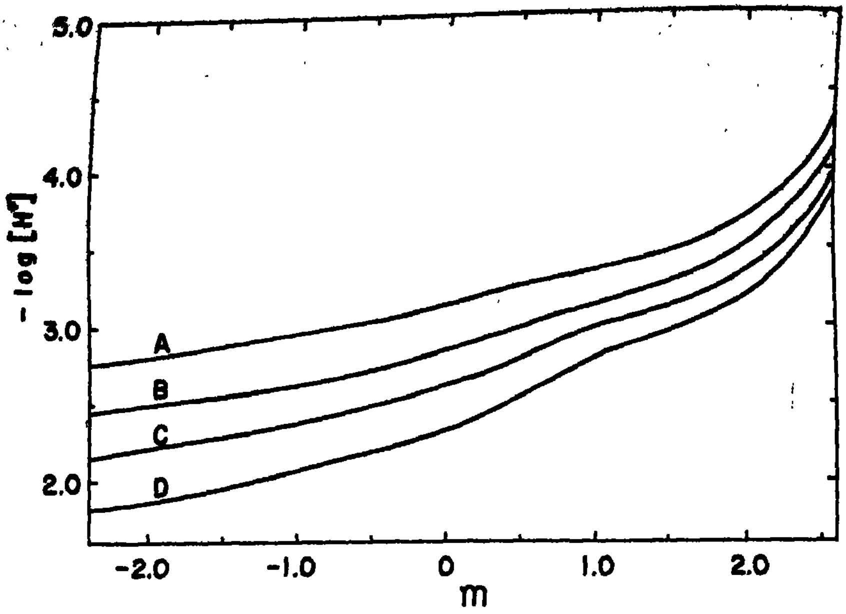

FIG. 2.—Potentiometric titration of 1:1 Fe(III)–kojate chelate system at concentrations: A, $5\cdot53 \times 10^{-4}$ M; B, $1\cdot10 \times 10^{-3}$ M; C, $2\cdot21 \times 10^{-3}$ M; D, $4\cdot42 \times 10^{-3}$ M. $t = 25°$; $\mu = 0\cdot10$ (KNO_3); m = moles of base added per gramme-ion of metal present.

TABLE 1.—EQUILIBRIUM CONSTANTS FOR THE INTERACTION OF Fe(III) ION WITH VARIOUS LIGANDS

Ligand	log K_1	log K_2	log K_3	p$K_{M(OH(A}$	p$K_{\{M(OH)A\}_2}$	p$K_{M(OH)_2A}$	p$K_{\{M(OH)_2A\}_2}$	Ref.
Kojic acid	10·20[d]	8·78	7·53	3·16	3·92	7·40	9·92	
8-Quinolinol-5-sulphonate[a]	11·6	11·2	—	3·06	—	7·00	—	2a
NTA[b]	—	—	—	4·08	—	11·85	—	8
NTA[c]	—	—	—	5·0	6·0	—	—	2b
EDTA[b]	—	—	—	7·52	—	16·96	—	9
EDTA[c]	—	—	—	7·58	12·21	—	—	2b
CDTA[c]	—	—	—	9·32	17·62	—	—	2b
HEDTA[c]	—	—	—	4·11	5·84	12·80	—	2b

(a) $\mu = 0\cdot10$ M; $t = 25°$.
(b) $\mu = 0\cdot1$ M; $t = 20°$
(c) $\mu = 1\cdot0$; $t = 25°$
(d) accuracy, $\pm 0\cdot13$; $t = 14 \sim 16°C$.

Dissociation constant (K_D) of kojic acid determined in the present work: p$K_D = 7\cdot68$.

over a eight fold concentration range demands that the 1:1 chelate is already completely formed even at a *m* value of as low as $-2\cdot7$. The correct value of molar extinction coefficient of the 1:1 chelate is needed to evaluate its stability constant. Visible absorption spectra of the solutions containing equimolar amount of ligand and metal ion do not change their shapes and their absorption maximum at 500 mμ in the pH range up to at least those corresponding to a m value of $-2\cdot7$. This phenomenon can be said with assurance in the concentration range below those shown in Fig. 2. In addition to this fact, the absorption maximum is shifted toward lower

---

(8) G. SCHWARZENBACH and I. HELLER, *Helv. Chim. Acta* **34**, 1889 (1951).
(9) G. SCHWARZENBACH and J. HELLER, *Helv. Chim. Acta* **34**, 576 (1951).

wavelength at $m = 0$ possibly due to hydrolysis of the chelate. Thus the extinction coefficient of the 1:1 chelate is established from the spectrum of the solution which contains equimolar amount of ligand and metal ion and whose m value is $-2{\cdot}7$. The estimated K_1 value is shown in Table 1.

A family of titration curves provide information about the hydrolytic behaviour of the 1:1 Fe(III)–kojate chelate. Titrating solutions reached their equilibria immediately below $m = 1{\cdot}0$ while it took some time to reach them above $m = 1{\cdot}0$ and dark reddish precipitates tended to appear beyond inflection region around $m = 3{\cdot}0$. Under the assumption that reactions (4) and (5) took place in the region

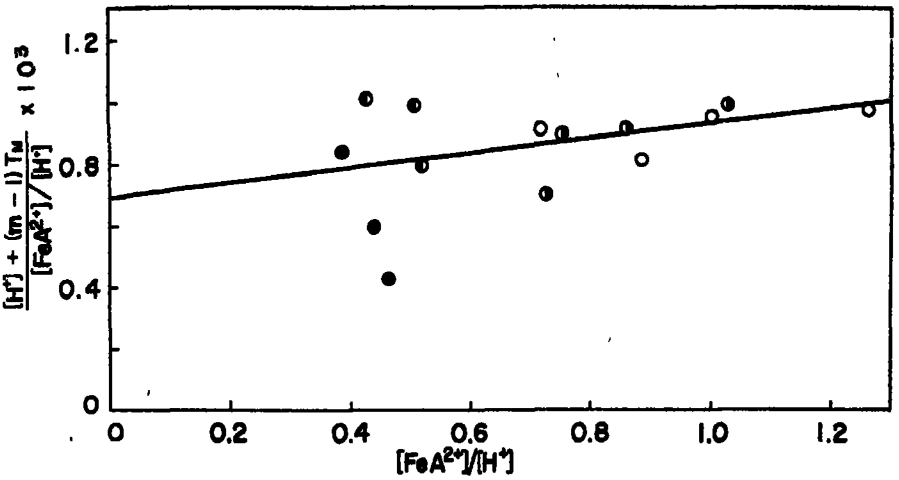

FIG. 3.—Graphical evaluation of the equilibrium constants for hydrolysis reactions of the 1:1 Fe(III)–kojate chelate forming monohydroxo species at 25° in accordance with equation(11). Total concentration of metal species; ○, $4{\cdot}42 \times 10^{-3}$ M; ◑, $2{\cdot}21 \times 10^{-3}$ M; ◐, $1{\cdot}10 \times 10^{-3}$ M; ●, $5{\cdot}53 \times 10^{-4}$ M.

between $m = 0$ and $1{\cdot}0$, equation (11) was employed and data were plotted as shown in Fig. 3. In spite of scattering of the data for the lower concentrations, satisfactory hydrolysis constants $K_{M(OH)A}$ and $K_{\{M(OH)A\}_2}$ may be obtained from the straight line. This result indicates that reactions yielding monohydroxo and binuclear monohydroxo chelate species are taking place predominantly in this region. The distinctive inflection region around $m = 3{\cdot}0$ suggests that not only monohydroxo-forming reactions but also dihydroxo-forming reactions occur in the region lying before the inflection region. Thus, the assumption was made that all the four hydrolysis reactions represented by equilibrium relationships (4), (5), (6) and (7) were proceeding simultaneously beyond m values of $1{\cdot}0$ and titration data corresponding to m values between $1{\cdot}0$ and $2{\cdot}2$ were taken for the evaluation of equilibrium constants. Equation (13) was employed for this purpose and reasonably good linear relationship (Fig. 4) approves the above assumption. The evaluated equilibrium constants are summarized in Table 1.

Fe(III) chelates with bidentate ligands such as kojic acid and 8-quinolinol-5-sulphonate show approximately the same magnitude of hydrolytic tendencies between them, which are greater than those of the chelates with polydentate ligand such as NTA(nitrilotriacetic acid), EDTA(ethylenediaminetetraacetic acid), CDTA(trans-1,2-diaminocyclohexanetetraacetic acid), and HEDTA(N-hydroxyethylethylenediaminetriacetic acid). This is quite a self-evident matter according to the following reasons:

(1) Hydroxide ion replaces aquo group easily while donor groups of strong affinity with metal ion in a polydentate ligand may not be replaced so easily even in the relatively high pH range.

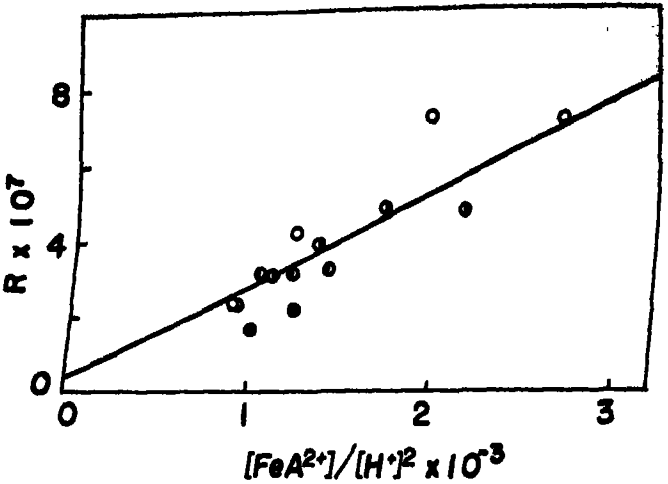

FIG. 4.—Graphical evaluation of the equilibrium constants for hydrolysis reactions of the 1:1 Fe(III)–kojate chelate forming dihydroxo species at 25° in accordance with equation (13). Total concentration of metal species: ○, 4·42 × 10^{-3} M; ◑, 2·21 × 10^{-3} M; ◐, 1·10 × 10^{-3} M; ●, 5·53 × 10^{-4}. M.

(2) A ligand part of a metal chelate interfers with the approaching hydroxide ion. Thus, when a metal ion is well enclosed with a polydentate ligand molecule, significant steric hindrance seems to occur against coming hydroxide ion due to exposed ligand part.

(3) Acidic property of a central metal ion decreases as number of the co-ordination sites with negatively charged donor groups increases.

Stepwise hydrolysis reactions of the 1:1 Fe(III)–kojate chelate are shown in Chart 1.

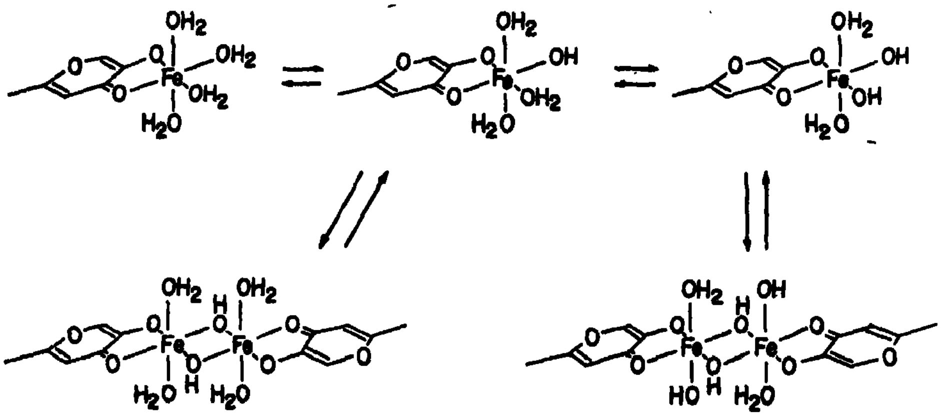

CHART 1.—Stepwise hydrolysis reactions of the 1:1 Fe(III)–kojate chelate.

2:1 *Chelate.* A titration curve for 2:1 molar ratio of ligand to metal ion is shown in Fig. 5. A steep inflection at $m = 3{\cdot}0$ suggests that the chelate forming reactions and hydrolysis reactions shown in Chart 2 are occurring in the preceding buffer region.

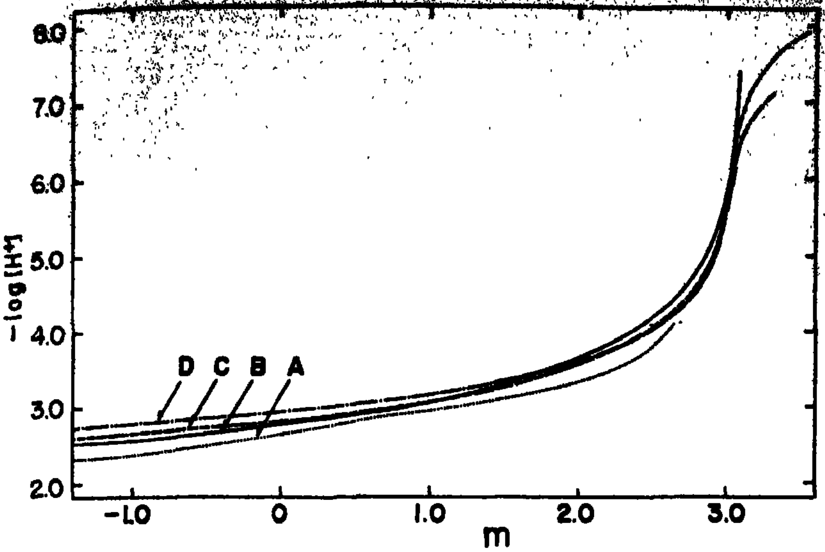

FIG. 5.—Potentiometric titration of Fe(III)-kojate chelate system at total kojate concentration of 2·21 × 10^{-3} M, with these molar ratios of ligand to metal ion: A, 1:1; B, 2:1; C, 3:1; D, 4:1; m = moles of base added per gramme-ion of metal present; μ = 0·10 M(KNO$_3$); t = 25°.

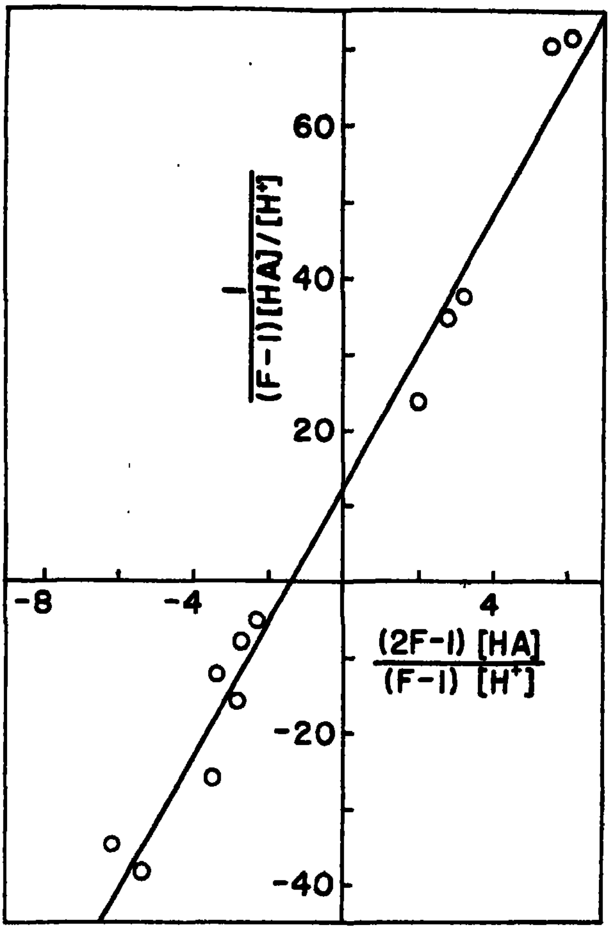

FIG. 6.—Graphical evaluation of the formation constants for the 1:2 and 1:3 Fe(III)-kojate chelates in connection with equation (17).

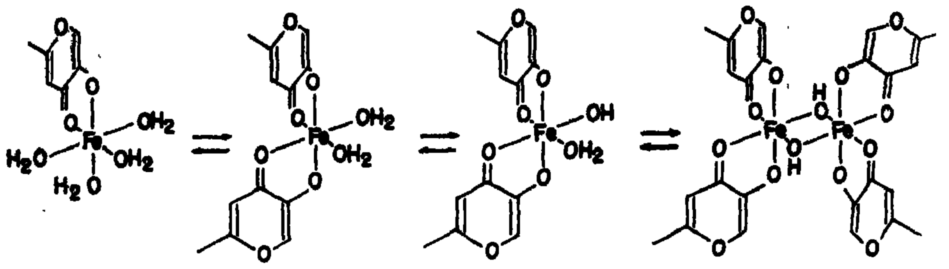

CHART 2.—Stepwise hydrolysis reactions of the 1:2 Fe(III)-kojate chelate.

3:1 *Chelate.* Titration curves for more than three moles of ligand per mole of metal ion show steep inflection at $m = 3{\cdot}0$, suggesting that the 3:1 Fe(III)-kojate chelate is formed without any significant contribution of hydrolysis reactions in the buffer region preceding to the inflection range. In addition, the titration data approve that the co-ordination number of Fe(III) is and not more than six. Stability constants for the 2:1 and 3:1 chelates were estimated by the aid of equation (17) and plotting the data as shown in Fig. 6. These constants thus determined are summarized in Table 1. Oxygen atom is generally said to be profound donor atom toward iron(III) ion. This is approved in the case of Fe(III)-kojate chelates and kojic acid is an excellent chelating agent for iron(III) ion.

Beyond the inflection region at $m = 3{\cdot}0$ the pH value of the solution did not reach equilibrium in a short period of time and precipitates started to appear. This precipitation is possibly due to either disproportionation reaction or further hydrolysis reaction, both of which yield hydrolysed species of Fe(III)-kojate chelates.

Acknowledgment—The author wishes to express his gratitude to the Ministry of Education for the Scientific Research Grant which supported this work in part.

J. Inorg. Nucl. Chem., 1962, Vol. 24, pp. 689 to 692. Pergamon Press Ltd. Printed in Northern Ireland

THE DETERMINATION OF ION ASSOCIATION* CONSTANTS FROM CATION EXCHANGE MEASUREMENTS—I

THE CADMIUM CHLORIDE AND CADMIUM BROMIDE SYSTEMS

O. D. BONNER, H. DOLYNIUK†, C. F. JORDAN‡ and G. B. HANSON
Chemistry Dept. University of South Carolina, Columbia, South Carolina.

(*Received* 5 *December* 1961; *in revised form* 23 *January* 1962)

Abstract—Studies of ion association reactions involving cadmium bromide and cadmium chloride have been made using cation exchange equilibrium measurements over the temperature range 0–98°. The cadmium chloride ion pair formation constants increase with temperature over the entire temperature range while those of cadmium bromide initially decrease and then increase at temperatures above about 60°. This results in a change in sign of the value of ΔH° for the bromide ion association constant as the temperature is increased. Values of both the formation constants and enthalpies of formation for those ions agree with those found in the literature at 25°.

MANY measurements of ion association constants have been made in both aqueous and non-aqueous media. NANCOLLAS has recently treated the thermodynamics of ion association in aqueous solutions.(1) Among the most interesting results reported have been those for the ion pairs $CdCl^+$ and $CdBr^+$ since near room temperature $CdCl^+$ becomes more stable and $CdBr^+$ becomes less stable as the temperature is elevated. AUSTIN *et al.* have made a critical survey of measurements on the $CdCl^+$ system and have contributed further data on the $CdBr^+$ system.(2) Ion association constants calculated for the reaction

$$M^{2+} + X^- = MX^+ \tag{1}$$

are reported to 91 ± 5 for $CdCl^+$ and 142 ± 7 for $CdBr^+$. The value for $CdCl^+$ was calculated from e.m.f. measurements,(3) although consideration was given to conductance(4) and potentiometric titration(5,6) data. The value for $CdBr^+$ was that calculated from spectrophotometric data by the authors. Values of ΔH° calculated for the above reactions are reported to be 980 ± 200 for the formation of $CdCl^+$ and −320 ± 100 for the formation of $CdBr^+$. These values were calculated from the measurements of heats of dilution by ROBINSON and WALLACE.(7)

---

* This research programme in the field of Ion Exchange Equilibria is supported by a contract with the Atomic Energy Commission.

† National Science Foundation Summer Participant.

‡ National Science Foundation Undergraduate Research Participant.

(1) G. H. NANCOLLAS, *Chem. Soc. Quart. Rev.* 14, 402 (1960).

(2) J. M. AUSTIN, R. A. MATHESON, and R. N. PARTON, *Some Thermodynamic Properties of Solutions of Salts of Bivalent Metals* in *The Structure of Electrolyte Solutions* (Edited by J. HAMER) J. Wiley, New York (1959).

(3) H. S. HARNED and M. W. FITZGERALD, *J. Amer. Chem. Soc.* 58, 2624 (1936).

(4) E. C. RIGHELLATO and C. W. DAVIES, *Trans. Faraday Soc.* 151, 2029 (1931).

(5) H. L. RILEY and V. GALLAFENT, *J. Chem. Soc.* 2029 (1931).

(6) C. E. VANDERZEE and H. J. DAWSON, *J. Amer. Chem. Soc.* 75, 5659 (1933).

(7) A. L. ROBINSON and W. E. WALLACE *Chem. Revs.* 30, 1195 (1942).

Ion association constants from cation exchange equilibria

KRAUS and co-workers[8] have estimated ion pair (or complex) formation constants for many systems using anion-exchange data. These studies involved the use of mixed electrolyte solutions containing a sufficiently high concentration of the complexing anion to form an anionic complex of the type MX_n^{z-}. If, however, the investigation of a cationic complex of the type MX^+ is desired, one may use a cation-exchanger and somewhat more dilute solutions noting the effect of the variation of the anion (co-ion) on the exchanger-solution equilibrium.

The exchange of calcium ion for cadmium ion by an ion exchanger may be represented by the equation

$$Ca^{2+} + CdRes = Cd^{2+} + CaRes \tag{2}$$

The equilibrium quotient for this exchange would be

$$k = \left(\frac{c_{Cd}^{2+}}{c_{Ca}^{2+}}\right)_{soln.} \left(\frac{X_{Ca}}{X_{Cd}}\right)_{resin} \tag{3}$$

where c represents concentration in moles per litre and X represents mole fraction. In dilute solutions, where the ionic strength principle might be expected to apply, this quotient is a function of the resin loading and ionic strength only and is independent of the co-ion used. Any apparent deviations from constancy may be attributed to ion association in the aqueous solution since the virtual exclusion of the co-ion from the resin phase makes the possibility of ion association in the resin almost negligible.

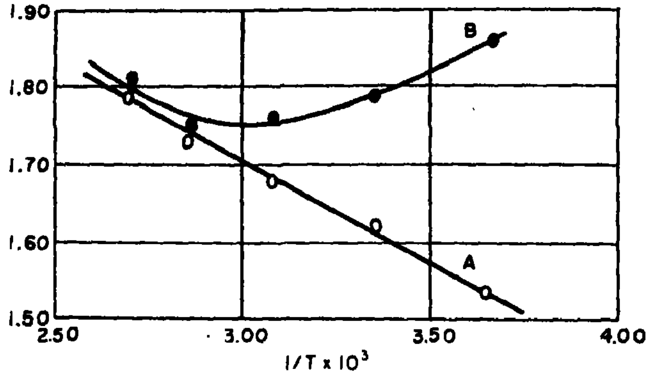

FIG. 1.—Ion association constants at various temperatures
A, CdCl, $\Delta H^\circ_{25^\circ} = +1100$ cal; B, CdBr, $\Delta H^\circ_{25^\circ} = -770$ cal.

The calculation of ion association constants

$$K = \left(\frac{MX^+}{M^{2+}\,X^-}\right) = K'\left(\frac{\gamma_{MX}{}^{+}}{\gamma_{M}{}^{2+}\gamma^{M-}}\right) \tag{4}$$

corresponding to the reaction shown in equation (1) may be performed using ion exchange data from experiments involving salts containing the anion in question and comparing these data with those where a non-associating anion such as perchlorate is used. For example, at a resin loading corresponding to equal amounts of calcium and cadmium ion ($X_{Ca} = X_{Cd} = 0{\cdot}5$), the equilibrium quotient, k, is equal to the experimentally determined solution concentration ratio $\left(\frac{[\mathrm{Cd}]}{[\mathrm{Ca}]}\right)$ total, when perchlorates are used. When the experiment is repeated using chloride salts, the concentration of calcium ion is still equal to the experimentally determined total calcium concentration but the total cadmium concentration is now equal to the cadmium ion concentration plus the amount of $CdCl^+$ ion which is formed. The apparent equilibrium quotient, k_{obs}, for this exchange is still equal to the ratio $\left(\frac{[\mathrm{Cd}]}{[\mathrm{Ca}]}\right)$ total. The actual Cd^{2+} ion concentration is then calculated to be the product of the total cadmium concentration and the quotient of the observed equilibrium quotients for the exchanges using solutions of chloride and perchlorate salts. The concentration of $CdCl^+$ is the difference between the total cadmium concentration and the calculated concentration of Cd^{2+} ion.

---

[8] KRAUS and co-workers have published many results of studies of a metal complexes. A summary of much of their work appears in K. A. KRAUS and F. NELSON, *Anion Exchange Studies of Metal Complexes*, in *The Structure of Electrolyte Solutions* (Edited by W. J. HAMER). J. Wiley, New York (1959).

Experimental. Approximately 0·5 g of 8 % DVB ion exchange resin which had been previously converted to either the calcium of cadmium form was placed along with 100 ml of a solution 0·033M in calcium and cadmium perchlorate in a jacketed flask equipped with a stirrer. The ratio of the concentration of calcium to cadmium in the 0·033M metal perchlorate solution was adjusted so as to yield the desired resin loading at equilibrium. A liquid having the desired boiling point was refluxed through the jacket of the equilibrium vessel maintaining a constant temperature. Convenient liquids with their boiling points are cyclopentane, 50°; carbon tetrachloride, 77·5°; n-heptane, 98°. The same apparatus was used at lower temperatures by circulation of water through the jacket or by packing it with ice.

After equilibrium was attained (2–4 hr), the phases were separated by withdrawing the liquid phase through a glass frit (while maintaining the apparatus at the temperature of the experiment. The resin phase was then washed with distilled water and eluted with 2 molar KCl solution. The eluate as well as the equilibrium solution were analysed for both calcium and cadmium concentration by compleximetric titration with a standard solution of the disodium salt of ethylenediaminetetraacetic acid (EDTA). Both calcium and cadmium are complexed in alkaline solution while only cadmium is complexed in acidic solutions.

Results. Ion association constants and enthalpies of association may be calculated at various temperatures since ion exchange equilibrium measurements are easily made at temperatures other than room temperature. The results of ion exchange experiments at five temperatures are reported in Table 1. Although equilibrium quotients were measured at several resin loadings, those measured at equal calcium and cadmium loading were felt to be most accurate and values at this point were taken from smoothed plots and used in the calculations. Uncorrected ion association constants, K', were calculated from the raw data. Activity coefficient corrections which were applied at 25° in order to calculate values of K for comparison with values reported by AUSTIN *et al.* are those reported by KLOTZ(9). No attempt was made to correct the experimental constants at other temperatures because of the unavailability of activity coefficient data. The raw data were used directly in the calculation of enthalpy values since the activity coefficient corrections at each temperature would be largely compensatory.

(9) I. M. KLOTZ, *Chemical Thermodynamics*, p. 332. Prentice-Hall, New York (1950).

Although no calculations were attempted, the data for the nitrate salts indicate agreement with the reported value of 2·5 for the ion pair formation constant for Cd NO_3^+.

The ion association constants as calculated from ion exchange measurements at 25° are in satisfactory agreement with those reported by AUSTIN and co-workers. The value of $\Delta H°$ at 25° for the formation of CdCl^+, as calculated from ion exchange experiments by means of the vant Hoff equation, is in agreement within the limits of reliability of the method (±10 per cent), with that reported by AUSTIN. The value for CdBr^+ is somewhat more negative than that reported by AUSTIN. It is believed, however, that this value is probably somewhat more reliable than that calculated from heats of dilution. It is of interest to note that although the values of $\Delta H°$ for the ion association reactions involving the chloride and bromide ions have opposite signs at lower temperatures, they are both positive at higher temperatures.

TABLE 1.—CALCULATION OF ION ASSOCIATION CONSTANTS FOR CADMIUM SALTS

Temperature	Counter-ion	Ion-exchange equilibrium quotient at $X_{Cd} = 0·5$	Ion association constants K'	K
0°	ClO_4^-	2·46		
	NO_3^-	2·50		
	Cl^-	6·50	34	
	Br^-	10·20	72	
25°	ClO_4^-	1·97		
	NO_3^-	2·00		
	Cl^-	5·95	42	95
	Br^-	7·50	61	133
50°	ClO_4^-	1·74		
	NO_3^-	1·75		
	Cl^-	5·65	48	
	Br^-	6·40	58	
77°	ClO_4^-	1·60		
	Cl^-	5·60	54	
	Br^-	5·85	57	
98°	ClO_4^-	1·50		
	Cl^-	5·65	60	
	Br^-	5·90	65	

J. Inorg. Nucl. Chem., 1962, Vol. 24, pp. 693 to 697. Pergamon Press Ltd. Printed in Northern Ireland

ISOTOPIC EXCHANGE IN THE COBALTOUS-COBALTIC SYSTEM IN PERCHLORIC ACID—II

HEATS AND ENTROPIES OF EXCHANGE

J. SHANKAR and B. C. DE SOUZA
Chemistry Division, Atomic Energy Establishment Trombay, Bombay

(*Received* 20 *November* 1961)

Abstract—Thermodynamic data have been evaluated for the two paths through which exchange takes place in the cobaltous-cobaltic aquo system in perchloric acid. For the acid-independent path $\Delta H^{\ddagger}$ and $\Delta S^{\ddagger}$ have been found to be 12·6 ± 0·5 kcal mole^{-1}, and −14 ± 2 e.u. respectively, while the values for the acid-dependent path were 11·6 ± 2·5 kcal mole^{-1} and −7 ± 5 e.u. The temperature was varied from 0 to 20°C while the ionic strength was maintained at 1·0 throughout.

IN a previous paper,[1] the authors have reported the results of a study of the exchange in the Co(II)aq–Co(III)aq system at 0°C. The exchange was found to proceed via two paths: (A) an acid independent path and (B) an acid dependent one. In this paper an attempt has been made to evaluate some of the thermodynamic quantities for these two paths.

EXPERIMENTAL

The experimental details were the same as those described previously.[1] The ionic strength (μ) was maintained at 1·0 using sodium perchlorate while the perchloric acid concentration was varied from 0·3F to 1·0F. The desired temperatures were maintained constant within ±0·2°C with water in Dewar flasks. At the concentrations of acid used, the decomposition of Co(III) was negligible during the experiment (~1 hr). Since the concentrations of the reactants were small, Co^{2+} and [Co(NH$_3$)$_6$]$^{3+}$ were added as carriers (~3 × 10^{-3}F) during the chemical separation.

RESULTS AND DISCUSSION

The plots of the velocity constant k against $1/[\mathrm{H}]^+$ (where [H$^+$] is the hydrogen ion concentration) at $\mu = 1$ at different temperatures are given in Fig. 1. The accuracy of the values of k is ±5 per cent. From the slopes of the straight lines and the intercepts were obtained the constants k_2 and k_1K_h in the relation

$$k = k_2 + \frac{k_1K_h}{[\mathrm{H}^+]} \dots \quad (1)$$

(where K_h is the hydrolysis constant), and these are given in Table 1.

TABLE 1.—THE INTERCEPTS (a) AND SLOPES (b) OBTAINED FROM FIG. 1

Temperature (°C)	0.0 ± 0·2	7·0 ± 0·2	14·0 ± 0·2	20·0 ± 0·2
$a = k_2$(F^{-1}min^{-1})	29 ± 2	50 ± 3	90 ± 6	150 ± 12
$b = k_1K_h$(min^{-1})	13 ± 2	37 ± 3	85 ± 6	205 ± 12

Plots of log a and log b versus $1/T$ are shown in Fig. 2, from which the values of activation energy have been calculated. A consideration of Table 1 shows that even at (H$^+$) = 1·0 E, the contribution of the acid-dependent path to the overall k is

---

(1) J. SHANKAR and B. C. DE SOUZA, *J. Inorg. Nucl. Chem.* **24**, 187 (1962).

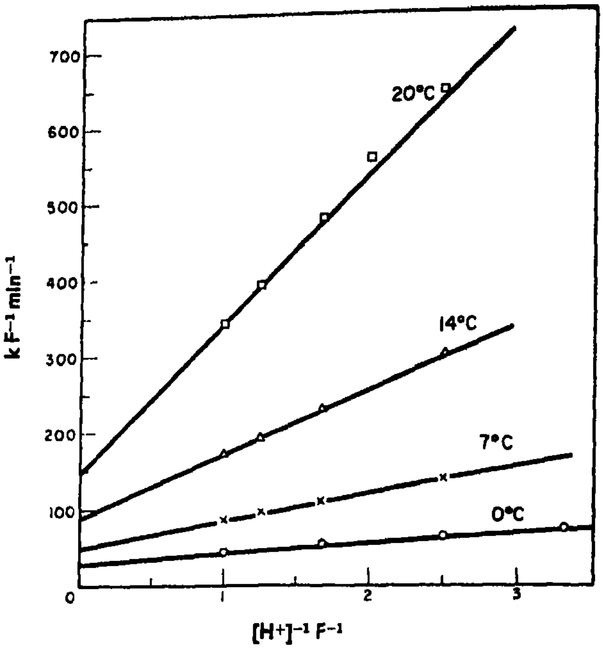

FIG. 1.—Effect of H^+ on exchange rate at different temperatures and $\mu = 1{\cdot}0$.

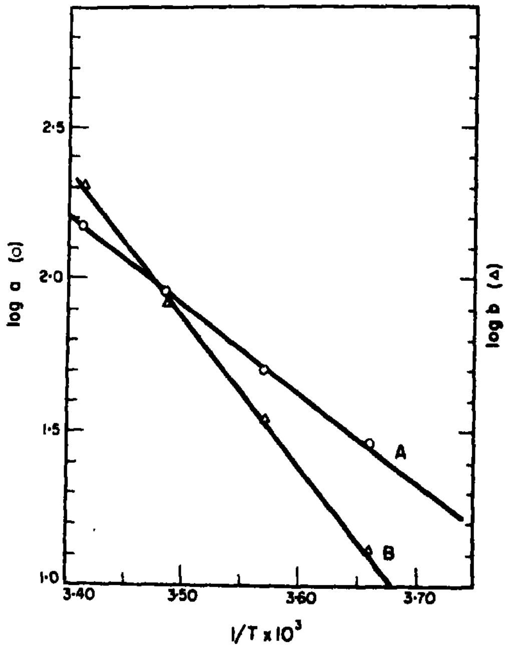

FIG. 2.—Arrhenius plots for the acid independent (*A*) and acid dependent path (*B*).

appreciable (~30 per cent at 0°C). As such the overall E value of 16 kcal obtained by us and that of 13·2 kcal obtained by HUNT and BONNER⁽²⁾ are not of much significance. In the present work the linear Arrhenius plots (Fig. 2) show that the activation energies are constant over the range of temperatures studied. The value of E_a, the activitation energy for the acid-independent path, is obtained directly from the plot A of Fig. 2 as 13·2 ± 0·5 kcal mole^{-1}, from which $\Delta H^{\ddagger}$ can be calculated as 12·6 ± 0·5 kcal mole^{-1} and $\Delta S^{\ddagger}$, as −14 ± 2 e.u. The value of 21·6 ± 0·6 kcal mole^{-1} and +18 ± 2 e.u. for the acid-dependent path include ΔH and ΔS for the hydrolysis of Co^{3+} ion. A knowledge of these is thus necessary to evaluate the true activation energy and entropy for the acid-dependent path.

SUTCLIFFE and WEBER⁽³⁾ have reported values of 10 ± 2 kcal mole^{-1} and 25 ± 7 e.u. for ΔH and ΔS in the hydrolysis reaction, but in a later paper⁽⁴⁾ they consider that the values may be in error due to interference by dimer formation in the spectrophotometric measurements on which the above results are based. A survey of the literature⁽⁵⁻¹⁰⁾ shows that among metallic ions the hydrolysis of which has been studied, ΔH for the reaction $M^{n+} + H_2O \leftrightharpoons MOH^{(n-1)+} + H^+$ lies close to 10 kcal mole^{-1}, especially for those elements which in size and charge resemble Co^{3+} aq. Furthermore, using the emperical equation of COBBLE⁽¹¹⁾ ΔS° for the reaction Co^{3+} aq + $H_2O \leftrightharpoons CoOH^{2+} + H^+$ is calculated as 25 ± 5 e.u., suggesting that the values of ΔH and ΔS reported by SUTCLIFFE and WEBER⁽³⁾ may not be greatly in error.

Using these values $\Delta H^{\ddagger}$ and $\Delta S^{\ddagger}$ for the acid-dependent path become 11·6 ± 2·5 kcal mole^{-1} and −7 ± 5 e.u. respectively.

The difference in values of E_a for the acid-independent paths in the systems Co(II)aq–Co(III)aq and Fe(II)aq–Fe(III)aq is ~4 kcal mole^{-1}. It is interesting to note that a similar energy value was proposed by FRIEDMAN⁽¹²⁾ *et al.* for the preliminary conversion of the $d\varepsilon^6$ configuration of Co^{3+} aq to one of $d\varepsilon^4\, d\gamma^2$, the latter facilitating isotopic exchange. The corresponding rearrangement energy in the system $Fe(III)^{2+,3+}$ aq would appear to be negligible.

STRANKS⁽¹³⁾ and coworkers, who have studied the variation in the exchange rate in aqueous solution between a series of redox pairs of the formula $Co(NH_3)_{6-n}(H_2O)_n^{3+,2+}$, where n varies from 1 to 6, find that when n is varied from 1 to 3, the activation energy for the exchange remains almost constant at 13·5 kcal, while the entropy becomes steadily less negative with the introduction of each OH group (the exchange proceeds through the hydroxy form). From this they concluded that the exchange in the $Co(H_2O)_6{}^{3+,2+}$ system (presumably through the acid-dependent path) will be characterized by values of E_a = 13·5 kcal mole^{-1} and $\Delta S^{\ddagger}$ = −13 e.u. Due to the rather large experimental error, the predicted values apparently agree with the

---

⁽²⁾ N. A. BONNER and J. P. HUNT, *J. Amer. Chem. Soc.* **82**, 3826 (1960).

⁽³⁾ L. H. SUTCLIFFE and J. R. WEBER, *Trans. Faraday. Soc.* **52**, 1225 (1956).

⁽⁴⁾ L. H. SUTCLIFFE and J. R. WEBER, *J. Inorg. Nucl. Chem.* **12**, 281 (1960).

⁽⁵⁾ F. BASALO and R. G. PEARSON, *Mechanism of inorganic reactions*, p. 66. J. Wiley, New York (1958).

⁽⁶⁾ R. M. MILBURN, *J. Amer. Chem. Soc.* **79**, 537 (1957).

⁽⁷⁾ G. N. BJERRUM, *Z. Phys. Chem.* **59**, 336 (1907).

⁽⁸⁾ S. C. FURMAN and C. S. GARNER, *J. Amer. Chem. Soc.* **72**, 1785 (1950).

⁽⁹⁾ K. A. KRAUS and F. NELSON, *J. Amer. Chem. Soc.* **77**, 3721 (1955).

⁽¹⁰⁾ G. HARBOTTLE and R. W. DODSON, *J. Amer. Chem. Soc.* **73**, 2442 (1951).

⁽¹¹⁾ J. W. COBBLE, *J. Chem. Phys.* **21**, 1446 (1953).

⁽¹²⁾ H. L. FRIEDMAN, J. P. HUNT, R. A. PLANE and H. TAUBE, *J. Amer. Chem. Soc.* **73**, 4028 (1951).

⁽¹³⁾ D. R. STRANKS, *Disc. Faraday. Soc.* **29**, 73 (1960).

experimentally determined ones. However, the extrapolation is not entirely justified, since preliminary conversion of the electronic configurations into these favourable for exchange will be easier in the case of the aquo redox pair, due to the difference in the ligand field strengths of the $-OH_2$ and the $-NH_3$ groups. This difference in the rearrangement energy should be reflected in the E_a values.

The authors have already suggested⁽¹⁾ that for the acid-dependent path, an atom-transfer mechanism appears more attractive, while true electron transfer would probably obtain for the acid-independent path. A comparison with other systems suspected of undergoing exchange through similar mechanisms would be interesting. Table 2 gives data for systems that exchange though atom transfer while Table 3 contains data for some systems that exchange most probably by direct electron transfer.

In Table 3, the complexes have been arranged in order of decreasing ligand field strength, which will also affect the difference in the bond distance $(r_2 - r_1)$ in the various redox pairs. Both in the case of a strong ligand field and a weak one, the difference $(r_2 - r_1)$ is small and hence exchange is facilitated. For intermediate field

TABLE 2.—THERMODYNAMIC DATA FOR SOME SYSTEMS IN WHICH EXCHANGE PROBABLY PROCEEDS THROUGH H ATOM TRANSFER

System	E_a(kcal)	$\Delta S^\ddagger$ (e.u.)	$\Delta F^\ddagger$ (kcal)	μ	Temp range (°C)	Ref.
Tl^{3+}–$TlOH^{2+}$	14·7	−33	23	6·0	25–41	10
VOH^{2+}–VO^{2+}	10·7	−24	17	2·5	25–40	14
Fe^{2+}–$FeOH^{2+}$	10·0*	−28*	18*	0·55	0–20	15
Co^{2+}–$CoOH^{2+}$	12·2	−7	14	1·0	0–20	This paper

* Calculated using the values of ΔH and ΔS for the hydrolysis of Fe^{3+} aq obtained by MILBURN⁽⁶⁾.

TABLE 3.—THERMODYNAMIC DATA FOR SOME SYSTEMS IN WHICH TRUE ELECTRON TRANSFER IS PROBABLE

System*	r_2–r_1†	E_a(kcal)	$\Delta S^\ddagger$(e.u.)	μ	Temp range (°C)	Rate of exchange	Ref.
$Co(phen)^{3+,2+}$	Large	17	+4	0·1	0–13	Slow	16
$Co(en)_3^{3+,2+}$	Very large	14·3	−33	0·98 1·98	25–45	Very slow	17
$Co(NH_3)_6^{3+,2+}$	Very large	13·5	−41	–	–	Very slow	18
$Co(EDTA)^{1-,2-}$	Very large	22	−17	0·1	60–85	Very slow	19
$Co(H_2O)_6^{3+,2+}$	Small	13·2	−14	1·0	0–20	Fast	This paper
$Fe(H_2O)_6^{3+,2+}$	Small	9·9	−25	0·55	0–20	Fast	15
$NpO_2^{1+,2+}$	Small	8·3	−24	1·0	0–10	Fast	20
$Ce(aq)^{4+,3+}$	Small	7·7	−40	6·18	−10–25	Fast	21

* phen = o-phenanthrolene EDTA = ethylene diamine tetraacetic acid en = ethylene diamine.
† r_2,r_1 are the bond distances in the reduced and oxidized states.

(14) C. S. GARNER and S. C. FURMAN, *J. Amer. Chem. Soc.* **74**, 2333 (1952).
(15) J. SILVERMAN and R. W. DODSON, *J. Phys. Chem.* **56**, 846 (1952).
(16) B. R. BAKER, F. BASALO and H. N. NEUMANN, *J. Phys. Chem.* **63**, 371 (1959).
(17) W. B. LEWIS, C. D. CORYELL and J. W. IRVINE, *J. Chem. Soc.*, S.386, (1949).
(18) N. S. BIRADAR, D. R. STRANKS, M. S. VAIDHYA, G. J. WESTON and D. J. SIMPSON, *Trans. Faraday Soc.* **55**, 1268 (1959).
(19) A. W. ADAMSON and K. S. VORRES, *J. Inorg. Nucl. Chem.* **3**, 206 (1956).
(20) D. COHEN, J. C. SULLIVAN and J. C. HINDMAN, *J. Amer. Chem. Soc.* **76**, 352 (1954).
(21) J. W. GRYDER and R. W. DODSON, *J. Amer. Chem. Soc.* **73**, 2890 (1951).

strengths, $(r_2 - r_1)$ is larger and exchange is not favoured. Thus, the experimentally determined value of $(r_2 - r_1)$ for $Co(NH_3)_6{}^{3+,2+}$ (intermediate ligand field) is 0·45 Å,(22,23) and for $Co(H_2O)_6{}^{3+,2+}$ (weak field) is 0·17 Å.(5) The rate of exchange observed for the system $Co(H_2O)_6{}^{3+,2+}$ is thus in good agreement with these concepts.

(22) T. WATANABE, M. ATOJI and C. OKAZAKI, *Acta. Cryst.* 3, 405 (1950).

(23) H. C. BROION, *J. Phy. Chem.* 56, 868 (1952).

J. Inorg. Nucl. Chem., 1962, Vol. 24, pp. 699 to 706. Pergamon Press Ltd. Printed in Northern Ireland

THE EXTRACTION OF URANIUM (VI) FROM SULPHURIC ACID SOLUTIONS BY DI-(2-ETHYLHEXYL)-PHOSPHORIC ACID

TAICHI SATO

Government Chemical Industrial Research Institute, Honmachi, Shibuya-ku, Tokyo, Japan

(*Received* 11 *September* 1961)

Abstract—The partition of uranium (VI) between sulphuric acid solutions and solutions of di-(2-ethylhexyl)-phosphoric acid (DEHPA) in kerosene has been investigated at varying concentrations of sulphuric acid, solvent and uranium at different temperatures. Changes in acidity of the organic solutions have been examined, and infra-red data have been obtained; the mechanism of uranium extraction is discussed on the basis of these results.

TRIBUTYL phosphate (TBP), which is used in many extraction processes, is not effective for the extraction of uranium from sulphuric acid solution, and di-(2-ethylhexyl)-phosphoric acid (DEHPA) plays an important rôle in this system. The extraction of uranium from acid solutions by DEHPA has been studied by many investigators,(1) but observations on the extraction mechanism are limited.(2) This study has been made to present some information on the mechanism of uranium (VI) extraction from sulphuric acid solution by DEHPA.

EXPERIMENTAL

DEHPA (Virginia Carolina Chemical Corporation) was purified by washing several times successively with 10 per cent sodium carbonate solution, 6 N hydrochloric acid and water.

Extractions were carried out as follows: 20 ml of DEHPA diluted with kerosene and an equal volume of uranyl sulphate solution containing sulphuric acid were shaken for 5 min in a 50 ml stoppered conical flask in a water bath at the required temperature. Uranium in the organic phase was then back-extracted with 6 N hydrochloric acid and the partition coefficient was determined as described previously.(3) Uranium was determined(4) by adding an excess of EDTA and ascorbic acid to form the uranium (IV)–EDTA complex in boiling solution, the free EDTA being back-titrated with thorium nitrate solution using xylenol orange as indicator at pH 2–3.

The acidity of the organic phase was determined by adding 2 ml to 25 ml of 75 per cent ethyl alcohol containing 2 per cent sodium oxalate solution(5) titrating with 0·01 N sodium hydroxide solution using phenolphthalein as indicator.

Infra-red spectra were measured after separation from the aqueous phase in a cell with thallium halide windows, using a Shimazu IR recording infra-red spectrophotometer with sodium chloride prisms.

RESULTS AND DISCUSSION

(a) *Dependence on acid and solvent concentration*

The extraction of uranyl sulphate solution (4·5 g/l) containing sulphuric acid by DEHPA in kerosene at 20°C was measured at varying sulphuric acid concentration with the results shown in Fig. 1.

(1) E.g., C. A. BLAKE, K. B. BROWN and C. F. COLEMAN, U.S.A.E.C., ORNL 1903 (1955); C. A. BLAKE D. J. CROUSE, C. F. COLEMAN, K. B. BROWN and A. D. KELMERS, U.S.A.E.C., ORNL 2172 (1956); C. A. BLAKE, JR., C. F. BAES, JR., K. B. BROWN, C. F. COLEMAN and J. C. WHITE, *Proceedings of the Second International Conference on the Peaceful Uses of Atomic Energy, Geneva*, 1958. Vol. 28, p. 289. United Nations (1958).

(2) C. F. BAES, JR., R. A. ZINGARO and C. F. COLEMAN, *J. Phys. Chem.* **62**, 129 (1958).

(3) T. SATO, *J. Inorg. Nucl. Chem.* **6**, 334 (1958).

(4) J. KINNUNEN and B. WENNERSTRAND, *Chemist-Analyt.* **46**, 92 (1957).

(5) T. SATO, *J. Inorg. Nucl. Chem.* **9**, 188 (1959).

According to BAES *et al.*(2), DEHPA extracts uranium (VI) from acid perchlorate solutions by the ion-exchange mechanism

$$UO_2^{2+}(a) + 2(HX)_2(o) \rightleftarrows UO_2H_2X_4(o) + 2H^+(a) \qquad (1)$$

where X represents the anion $(RO)_2PO_2^-$ and (a) and (o) represent the aqueous and organic phases respectively. If the extraction of uranium (VI) from sulphuric acid solutions by DEHPA also follows this mechanism then the following relationship must hold:

$$\log 4\,E_a^0 = \log K + 2\log (C_s - 4C_U)/C_H \qquad (2)$$

in which E_a^0 is the partition coefficient, K the equilibrium constant, C_s the total DEHPA concentration, C_U the organic phase uranium concentration and C_H the aqueous acidity. In order to investigate the dependence of partition coefficient on solvent concentration, values of $\log E_a^0$ were taken form Fig. 1 and plotted vs. $\log (C_s - 4C_U)/C_H$ at constant sulphuric acid concentration with the results shown in

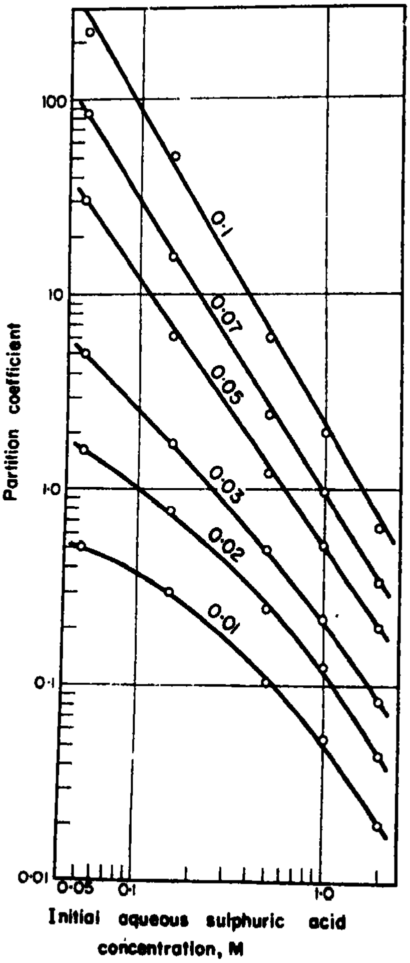

FIG. 1.—Effect of sulphuric acid concentration upon the extraction of uranium (VI) by DEHPA in kerosene (figures on curves are DEHPA concentrations, M)

Fig. 2. The slope of this curve shows that equation (2) is satisfied except in 0·05 and 0·15 M H_2SO_4. Thus, although the extraction of uranium (VI) from sulphuric acid solutions by DEHPA generally occurs via the formation of 1:4 uranium–DEHPA

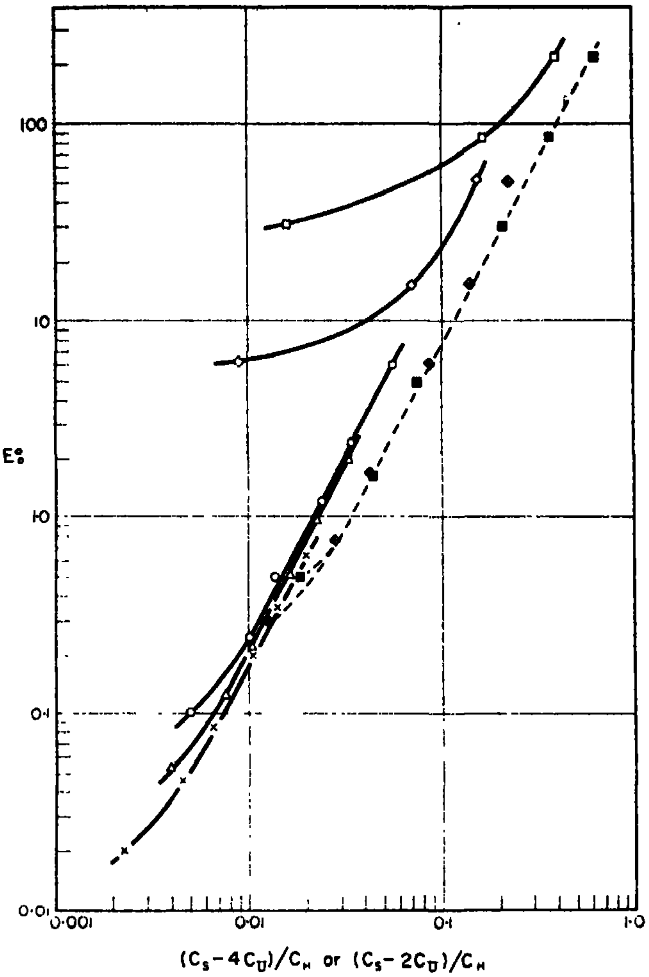

FIG. 2.—Partition coefficients for DEHPA concentrations between 0·01 and 0·1 M in kerosene (values of log E_a° vs. log $(C_s - 4C_U)/C_H$ at 0·05 (□), 0·15 (◇), 0·5 (○), 1·0 (△) and 2·0 (×) M sulphuric acid values of log E_a° vs. log $(C_s - 2C_U)/C_H$ at 0·05 (■) and 0·15 (◆) M sulphuric acid)

complex, at low sulphuric acid concentrations equation (1) is not obeyed. Under these conditions a polymeric uranium-DEHPA complex⁽²⁾ may be formed by the following reaction in addition to that in equation (1):

$$UO_2X_4H_2(o) + UO_2^{2+}(a) + (HX)_2(o) \rightleftarrows (UO_2)_2X_6H_2(o) + 2H^+ \qquad (3)$$

i.e.

$$2UO_2^{2+} + 3(HX)_2 \rightleftarrows (UO_2)_2X_6H_2(o) + 4H^+ \qquad (4)$$

This leads to the following relationship:

$$\log 4E_a^\circ = \log K_1 + 2\log (C_s - 2C_U)/C_H \qquad (5)$$

where K_1 is a constant. When values of log E_a° vs. log $(C_s - 2C_U)/C_H$ were plotted for sulphuric acid concentrations of 0·05 and 0·15 M it was observed that equation (5) is satisfied under those conditions. Hence it is presumed that at low sulphuric acid concentrations extraction takes place via the formation of a polymeric uranium-DEHPA complex according to equation (4).

In order to investigate the acid dependence of the partition coefficient, values of log E_a° were plotted vs. log $(C_s - 4C_U)/C_H$ at constant DEHPA concentration between 0·5 and 2·0 M acid with the results shown in Fig. 3. This shows that equation (2) is not satisfied at DEHPA concentrations below 0·03 M. From these results it is inferred that as the organic phase uranium concentration exceeds that corresponding to the formation of the 1:4 uranium-DEHPA complex the polymeric uranium-DEHPA complex may be formed at low DEHPA concentration.

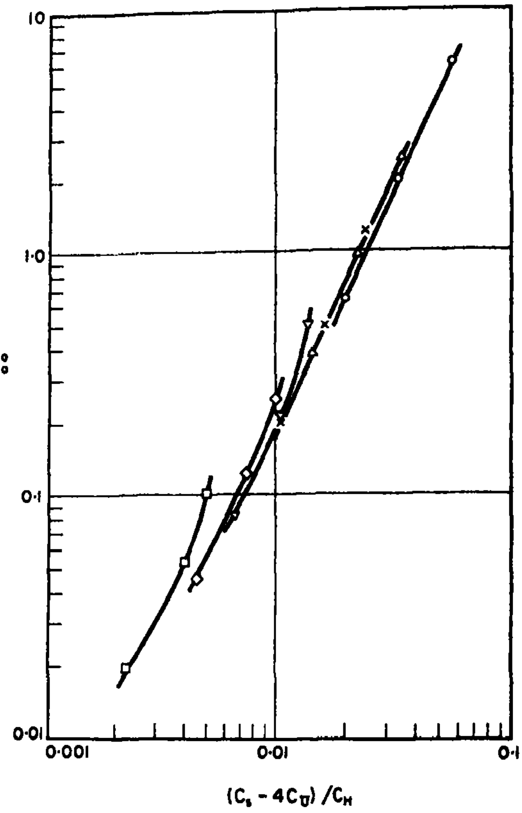

FIG. 3.—Partition coefficients in sulphuric acid between 0·5 and 2·0 M (values of log E_a° vs. log $(C_s - 4C_U)/C_H$ at 0·01 (□), 0·02 (◇), 0·03 (▽), 0·05 (×), 0·07 (△) and 0·1 (○) M DEHPA in kerosene)

(b) *Dependence on uranium concentration*

Extractions were carried out with 0·1 M DEHPA in kerosene at 20°C at concentrations of uranyl sulphate between 0·45 and 45 g/l., with the results shown in Fig. 4. Below 0·025 M initial aqueous uranium concentration the organic phase concentration increases linearly with increasing initial aqueous concentration, but less rapidly above 0·025 M. This suggests that the 1:4 uranium–DEPHA complex is formed at low uranium concentrations, and the polymeric complex may be formed at higher uranium concentration.

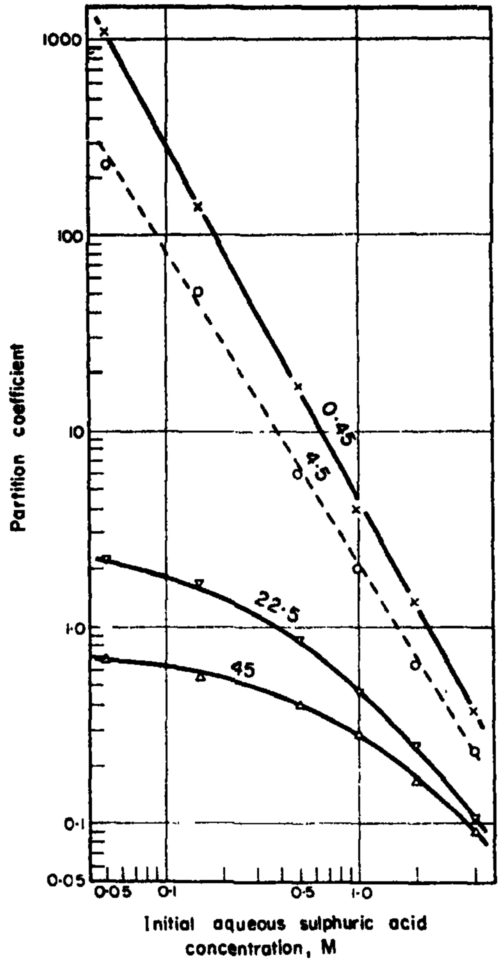

FIG. 4.—Effect of uranium concentration upon the extraction of uranium (VI) by 0·1 M DEHPA in kerosene (figures on curves are uranyl sulphate concentrations, g/l)

(c) *Dependence on organic phase acidity*

In order to clarify the ion-exchange behaviour of DEHPA in the extraction of uranium, uranyl sulphate solutions (4·5 g/l) containing sulphuric acid of various concentrations were extracted with 0·1 M DEHPA in kerosene at 20°C, followed by measurement of the acidity of the organic phase. Similar experiments were carried out with sulphuric acid solutions in the absence of uranium.

Fig. 5 shows that in the absence of uranium the acidity remains approximately constant, but in the presence of uranium the acidity diminishes with diminishing sulphuric acid concentration. The increase in acidity of the organic phase corresponds to the hydrogen ion released on exchange, assuming an ion-exchange mechanism of the type shown in equations (1) and (4).

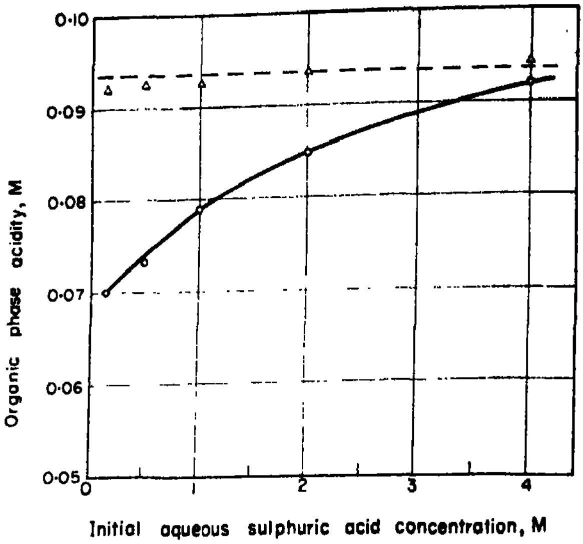

FIG. 5.—Change in acidity of the organic phase on extraction of uranium (VI) with 0·1 M DEHPA in kerosene (○ in the presence of uranium, △ in the absence of uranium)

(d) *Temperature effects*

Extractions of uranyl sulphate solution (4·5 g/l.) containing 0·15 and 1·0 M sulphuric acid with 0·1 M DEHPA in kerosene at temperatures between 10 and 50° gave the results shown in Fig. 6.

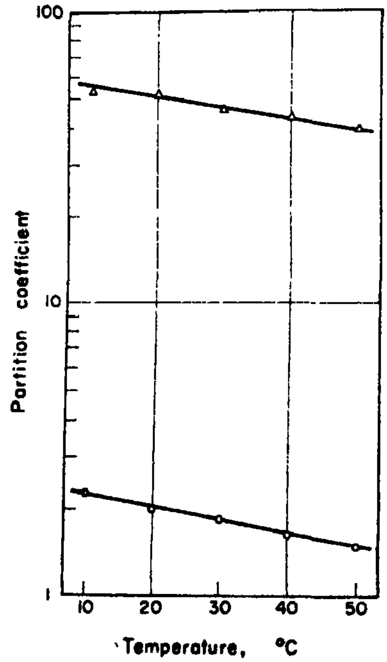

FIG. 6.—Effect of temperature upon the extraction of uranium (VI) by 0·1 M DEHPA in kerosene (△ and ○ represent 0·15 and 1·0 M sulphuric acid respectively)

The partition coefficient is large when the extraction temperature is low, and decreases with increasing temperature. The heat of reaction (i.e. the value of the enthalpy change) (1) was estimated to be 1·71 kcal/mol in 0·15 M H_2SO_4 and 2·42 kcal/mol in 1·0 M H_2SO_4.

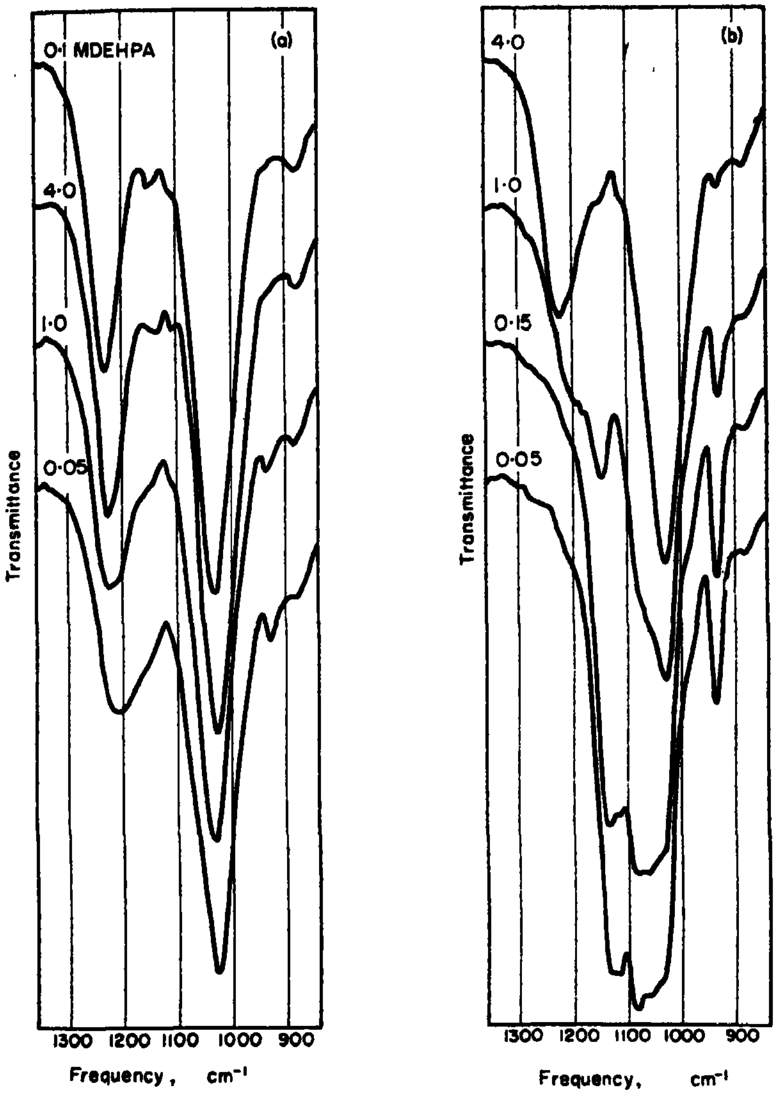

Fig. 7.—Infra-red spectra of the organic solutions involved in the extraction of 4·5(a) and 45(b) g/l uranyl sulphate solutions containing sulphuric acid of various concentrations by 0·1 M DEHPA in kerosene (figures on curves are sulphuric acid concentrations, M)

(e) *Infra-red spectra*

Infra-red spectra of the organic phases were examined after extraction of uranyl sulphate solutions (4·5 and 45 g/l.) containing sulphuric acid of various concentrations with 0·1 M DEHPA in kerosene at 20°C; the spectra are given in Figs. 7(a)–(b).

In the infra-red spectra of DEHPA in kerosene (Fig. 7a), the absorption band at 1230 cm^{-1} is assigned to the P → 0 frequency,(6) and OH stretching bands at 2680 and 2350 cm^{-1}, which are attributed to the formation of dimer, and the OH bending band at 1690 cm^{-1} also appear. In the extraction of uranyl sulphate solutions at 4·5 g/l. (Fig. 7a), the following results are observed: with diminishing sulphuric acid concentration, the band at 930 cm^{-1} assigned to the uranyl group,(7) becomes stronger and the P → 0 absorption band is gradually shifted from 1230 to 1200 cm^{-1}, while the intensities of the OH stretching and bending bands decrease. In the more concentrated solution (Fig. 7b), the uranyl band at 930 cm^{-1} is sharper, due to the increased uranium concentration in the organic phase. Simultaneously, with diminishing sulphuric acid concentration the OH stretching and bending bands almost disappear, and the P → 0 frequency at 1230 cm^{-1} is progressively shifted as follows: 1220 cm^{-1} (4·0 M H_2SO_4), 1145 cm^{-1} (1·0 M H_2SO_4), 1135 cm^{-1} (0·15 and 0·05 M H_2SO_4). In the last two cases however, the bands at 1085 and 1060 cm^{-1}, of uncertain assignment, appear in addition to the [P—O]—C stretching vibration at 1030 cm^{-1}.

Moreover, the spectra of the organic phases from 0·2 M DEHPA extraction are analogous to those from 0·1 M DEHPA. Formation of the uranium-DEHPA complex is thus accompanied by a shift of the P → O absorption band at 1230 cm^{-1} to lower frequencies, confirming that the cation-exchange reaction affects the P → O bond.

Acknowledgements—The author wishes to thank Mr. T. GOTO for assistance with experimental work and also thanks Atomic Fuel Corporation for a gift of di-(3-ethylhexyl)- phosphoric acid.

---

(6) D. F. PEPPARD and J. R. FERRARO, *J. Inorg. Nucl. Chem.* **15**, 365 (1960).

(7) E.g., B. M. GATEHOUSE and A. E. COMYNS, *J. Chem. Soc.* 3965 (1958); G. L. CALDOW, A. B. VAN CLEAVE and R. L. EAGER, *Canad. J. Chem.* **38**, 772 (1960).

J. Inorg. Nucl. Chem., 1962, Vol. 24, pp. 707 to 720. Pergamon Press Ltd. Printed in Northern Ireland

THE EXTRACTION OF METALLIC SPECIES BY DIALKYLPHOSPHORIC ACIDS*

C. F. Baes, Jr.
Reactor Chemistry Division, Oak Ridge National Laboratory
Oak Ridge, Tennessee, U.S.A.

(*Received* 22 *January* 1962)

Abstract—Of the organophosphates, the mono-acidic dialkylphosphates—$(RO)_2P(O)OH$—have not only proven valuable solvent extraction reagents for the separation of metallic species, they have also proven a rewarding subject for the investigator interested in solvent extraction mechanisms. Studies of extraction behaviour, osmotic behaviour, and infra-red spectra have shown that these reagents are usually present in organic solvents as hydrogen-bonded dimers H_2X_2 which, at low loadings, extract metal cations M^{z+} to form complexes of the type $M(X_2H)_z$. The demonstrated wide occurrence of this simple cation exchange mechanism—free of complicating extensive association and electrolyte extraction—offers an excellent opportunity to examine the effects of ion charge, size, and coordination properties on extraction. In contrast, systems at high loadings have shown more varied and complicated behaviour involving polynuclear complex formation and anion extraction. The pronounced and selective "synergistic" enhancement of extraction found when the dialkylphosphoric acids are used in combination with the neutral organophosphorous compounds has aroused considerable interest and deserves continued study.

While solvent extraction has been increasingly applied in chemical analysis and chemical separations for many years, progress toward an adequate understanding of its basic chemistry has been relatively slow. This is not surprising since the physical chemistry of the organic solutions used as extractant media is relatively less familiar than that of aqueous solutions, and the chemical nature of the extraction products formed is still less familiar.

In studying the extraction chemistry of a given class of reagents, it is important to examine separately, insofar as possible, each of the many variables such as solvent, reagent structure, and the size, charge and bonding properties of the extracted species. In many cases this task has proven especially difficult because the extractants (and their extraction products) are often extensively associated, they may distribute appreciably to the aqueous phase, and besides extracting the metallic species of interest they may extract acids, water and other aqueous solutes.

The dialkylphosphoric acids, $(RO)_2P(O)OH$, offer a rewarding subject for the investigator of solvent extraction mechanisms because their chemistry is often relatively free of these complications. At low loadings they extract cations by a simple hydrogen ion exchange (often free of water, acid and anion extraction) and the extraction products are usually mononuclear.

In the early investigations of these extractants it was noted that the extraction coefficient E for various cations varied as the $-z$th power of the acidity (where z is the cation charge) and the $+z$th power of the reagent concentration, and that often the saturation mole ratio of metal to reagent (either in solution or as a precipitate) corresponded to the formula $MX_z(X = (RO)_2PO_2^-)$. This of course suggested the general extraction reaction to be

$$M_{aq}^{z+} + zHX_{org} \rightleftharpoons MX_{z\,org} + zH_{aq}^{+}. \tag{1}$$

---

* Presented at The 140th Annual Meeting of The American Chemical Society, Chicago, Illinois, September, 1961.

It was subsequently found, however, that in non-polar solvents (wherein extraction coefficients were the highest) these reagents were present as stable hydrogen-bonded dimers

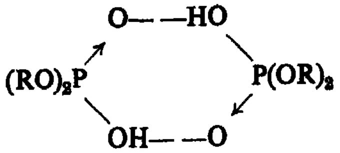

Thus it was concluded that the general extraction reaction is instead

$$M_{aq}^{z+} + z(H_2X_2)_{org} \rightleftharpoons MX_{2z}H_{z\,org} + zH_{aq}^{+} \qquad (2)$$
$${}^{z}K = E([H^+]_{aq}/[H_2X_2]_{org})^{z}$$

at low loadings. While additional extraction complexes are usually formed as the loading is increased (complexes which are often polynuclear and which can contain water and anions), at low loadings this reaction, leading to the formation of a complex $MX_{2z}H_z$ in which only half the acidic hydrogen of the extractant is replaced, has been found to be quite common. This has led the author to suggest the following simple chelate structure

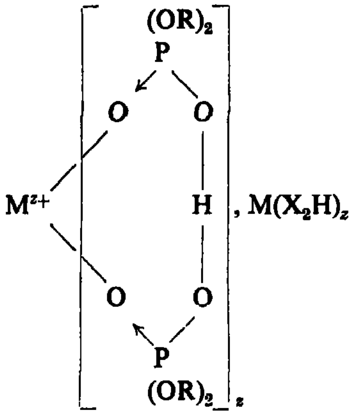

I

(yielding the usual chelate co-ordination number 2*z*, but involving an eight membered, hydrogen bonded ring) for the extraction complex $MX_{2z}H_2$.

The prevalence of reaction (2), and the implied stability of a single structure for the extraction complex makes it profitable to examine the considerable body of information now available for this class of extractants with the object of drawing some conclusions concerning the effect on extraction of solvent, reagent structure, ion charge, ion size and loading.

1. *Solvent effect on reagent association and extraction.* From measurements of the distribution of di(n-butyl) phosphate (DBP) between a given organic solvent and aqueous solutions, Dyrssen and co-workers(1,2) and Hardy and co-workers(3,4) have evaluated the dimerization constant

$$K_2 = [H_2X_2]_{org}/[HX]^2_{org} \qquad (3)$$

---

(1) D. Dyrssen, *Acta Chem. Scand.* **11**, 1771 (1957).

(2) D. Dyrssen and L. D. Hay, *Acta Chem. Scand.* **14**, 1091 (1960).

(3) C. J. Hardy and D. Scargill, *J. Inorg. Nucl. Chem.* **11**, 128 (1959).

(4) B. F. Greenfield and C. J. Hardy, AERE/R-3686 (1961).

and the distribution coefficient of the monomer

$$K_d = [HX]_{org}/[HX]_{aq} \tag{4}$$

From their results they have pointed out that the dimerization constant K_2 decreases as the monomer distribution constant K_d increases. This is to be expected, since increasing interaction of the more polar monomer with the solvent should tend to cause increasing dissociation of the dimer. DYRSSEN points out that if log K_2 is plotted vs. log K_d, many solvents fall close to a straight line of slope 2 so that the product

$$K_2K_d^2 = [H_2X_2]_{org}/[HX]_{aq}^2 \tag{5}$$

in these cases is approximately constant (~5 × 10^3).

Such a plot is presented in Fig. 1. It should be noted that, again as expected,

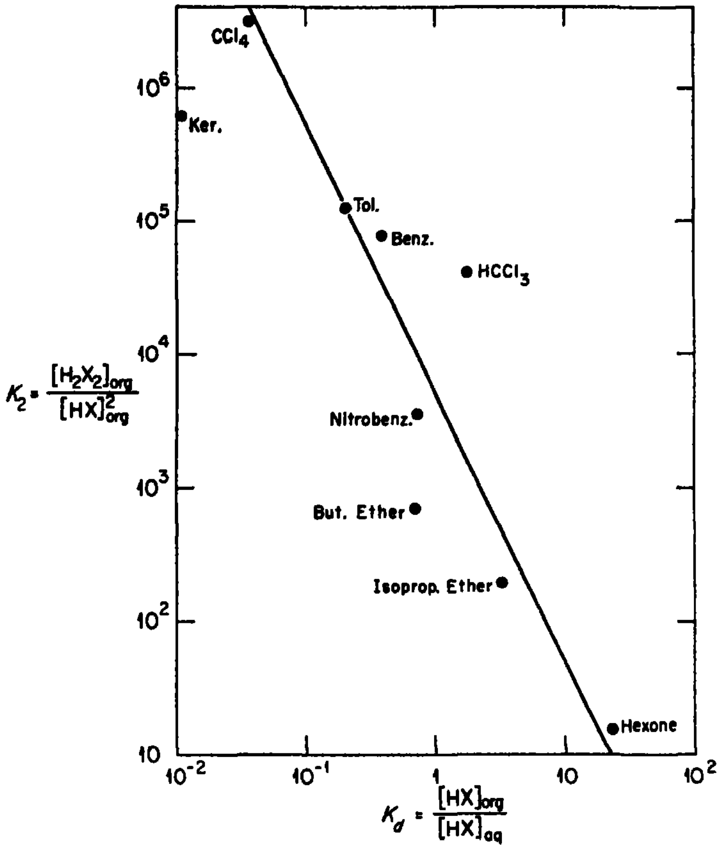

FIG. 1.—Dimerization of DBP in various solvents.

generally K_2 decreases and K_d increases with increasing solvent polarity and hydrogen-bonding power. For the most non-polar solvents (e.g. the hydrocarbons) the dimerization constant is of the order of 10^6, much higher than for carboxylic acid dimerization. For those solvents which do not conform to the relationship $K_2K_d^2 = 5 \times 10^3$, it appears that there is something irregular about the solvation of the dimer, H_2X_2 (the product $K_2K_d^2$ involves only the dimer as an organic phase species). In the cases of kerosene, hexane and butyl ether, $K_2K_d^2$ is lower than the average suggesting less than average dimer solvation. This is not surprising except for butyl ether. Chloroform appears to solvate the dimer relatively strongly, presumably through hydrogen bonding.

While dimerization is the principle mode of association of dialkylphosphoric acids it should be noted that there is good evidence of further association in non-polar solvents at the higher concentrations. Dyrssen and co-workers have noted this in their distribution studies for DBP in hexane above 0·05 M.(2) Similarly, isopiestic results for di(2-ethylhexyl) phosphoric acid in octane suggest partial trimerization,(5) and Fe(III) extraction by this medium showed deviations from third power reagent concentration dependence which could also be explained by partial trimerization.(6) The possibility of such further association becomes especially important in interpreting the observed effect of reagent concentration on the extraction of more highly charged metal ions.

DBP extraction quotients ^{z}K for several divalent(7,8) and trivalent(9,10,11) cations in various solvents are presented in Fig. 2. The solvents are arranged in the order of increasing $K_2K_d^2$ values, i.e., in the order of increasing dimer solvation. It is seen that the ^{z}K values generally decrease with increasing dimer solvation, the effect being greater

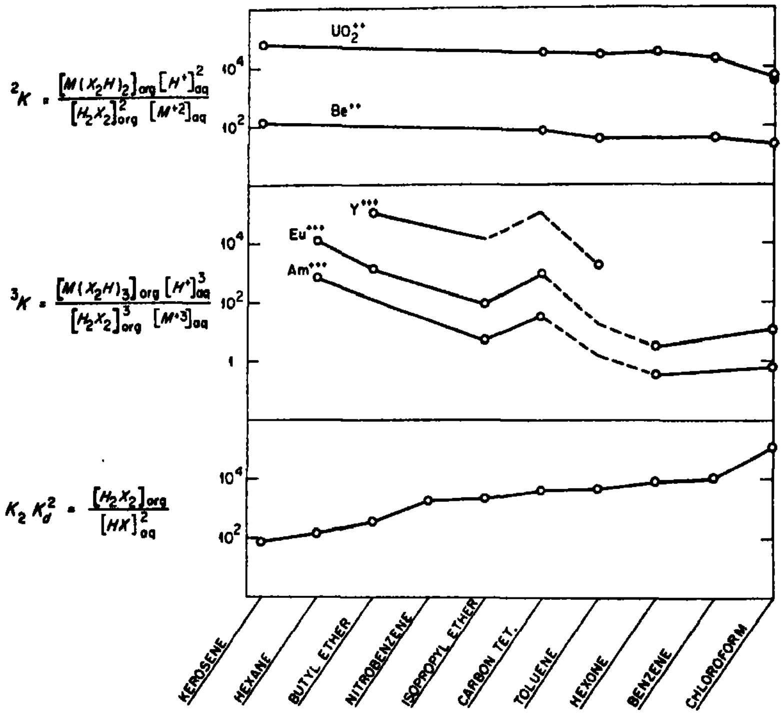

Fig. 2.—Effect of diluent on DBP extractions.

---

(5) C. F. Baes, Jr. Report ORNL-2737 (1959).

(6) C. F. Baes, Jr. and H. T. Baker, *J. Phys. Chem.* **64**, 89 (1960).

(7) C. J. Hardy, B. F. Greenfield and D. Scargill, AERE/R-3316 (1960).

(8) C. J. Hardy, AERE/R-3267 (1960).

(9) D. Dyrssen and L. D. Hay, *Acta Chem. Scand.* **14**, 1100 (1960).

(10) D. Dyrssen, *Acta Chem. Scand.* **11**, 1277 (1957).

(11) G. Duyckaertz, P. Dreze and A. Simon, *J. Inorg. Nucl. Chem.* **13**, 332 (1960).

for trivalent ions than for the divalent ions. Carbon tetrachloride appears a better diluent for trivalent ions than expected.

For these data it is instructive to examine the product ${}^{z}K(K_2K_d^2)^z$, which represents the quotients

$${}^{2}K(K_2K_d^2)^2 = \frac{[\mathrm{MX_4H_2}]_{\mathrm{org}}\,[\mathrm{H^+}]^2_{\mathrm{aq}}}{[\mathrm{M^{2+}}]_{\mathrm{aq}}\,[\mathrm{HX}]^4_{\mathrm{aq}}} \tag{6}$$

$${}^{3}K(K_2K_d^2)^3 = \frac{[\mathrm{MX_6H_3}]_{\mathrm{org}}[\mathrm{H^+}]^3_{\mathrm{aq}}}{[\mathrm{M^{3+}}]_{\mathrm{aq}}[\mathrm{HX}]^6_{\mathrm{aq}}} \tag{7}$$

Since here the extraction product, $\mathrm{MX_{2z}H_z}$, is the only organic phase species involved, the variation of ${}^{z}K(K_2K_d^2)^z$ with solvent should reflect the changing solvation of this species. Fig. 3 presents values of this product for the various solvents. It is seen that for both divalent and trivalent ions, the same trend in solvation noted for the HX dimer is present. This suggests that interaction with the polar core of the extraction complex is the dominant solvation effect. That the effect is no larger for the trivalent complexes than for the divalent complexes could be attributed to their less open structure. The magnitude of the variations in $K_2K_d^2$ (~1000-fold) and ${}^{z}K(K_2K_d^2)^z$ (10^5–10^6-fold) indicate solvation energy variations of ~4 kcal and ~8 kcal, respectively for $\mathrm{H_2X_2}$ and $\mathrm{MX_{2z}H_z}$.

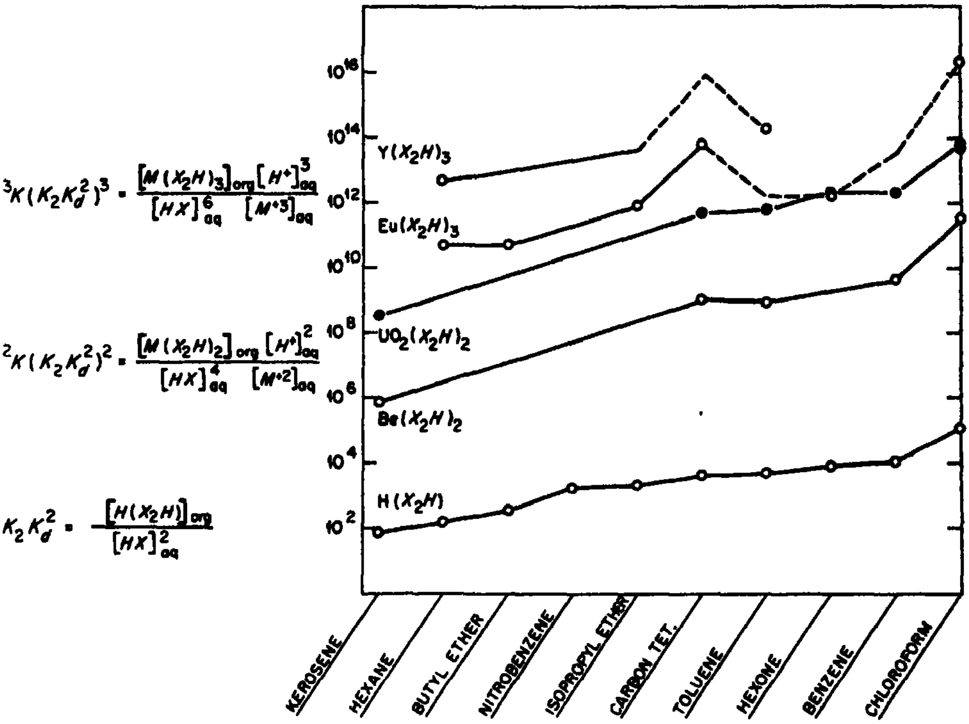

FIG. 3.—Effect of diluent on DBP extractions.

2. *Reagent structure effect.* In Fig. 4, ${}^{z}K$ values for $\mathrm{UO_2}^{2+(8,12)}$, $\mathrm{Be}^{2+(7)}$ and $\mathrm{Y}^{3+(10,11)}$

---

(12) C. A. BLAKE, C. F. BAES, JR., K. B. BROWN, C. F. COLEMAN and J. C. WHITE, *Proceedings of the Second International Conference on the Peaceful Uses of Atomic Energy, Geneva*, 1958, Paper 1550, Vol. 28, p. 289. United Nations, New York (1959).

extraction by a number of dialkylphosphoric acids are plotted. Here the various alkyl groups have been arranged in the order of increasing UO_2^{2+} extraction. Starting with

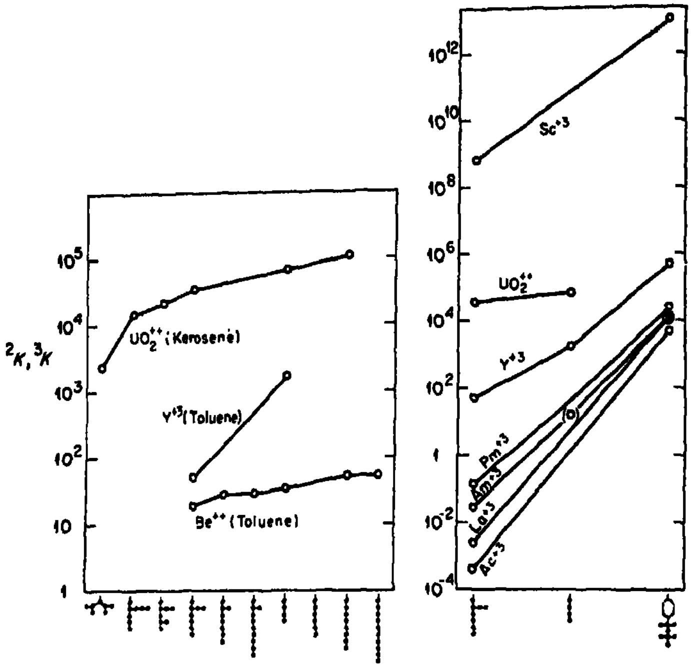

Fig. 4.—Effect of alkyl group on $(RO)_2P(O)OH$ extractions.

the highly branched di-isopropylmethyl and proceeding to 2-propyl, 2-ethyl, 2-methyl and normal alkyl groups it is clear that decreased branching near the ester linkage results in increased extraction. Increased chain length has a similar effect. The effects appear similar in magnitude for both UO_2^{2+} and Be^{2+}. The effect of branching is clearly much greater for the trivalent Y^{3+}.

Perhaps the largest structure effect so far observed in this class of reagents is also shown in Fig. 4. Peppard and co-workers have observed this effect in comparing Groups III lanthanide and actinide metal extractions by di(2-ethylhexyl) phosphoric acid, DEPA, and di(para 1, 1, 3, 3 tetramaethylbutylphenyl) phosphoric acid.(13) In the case of Ac^{3+} the latter reagent gave ^3K values 10^7-fold greater than did DEPA, indicating a difference of ~ 10 kcal in the free energy of extraction complex formation. While large effects of chain branching are to be expected for the trivalent metal complexes, the difference between the n-butyl and the phenyl reagents is surprising. A similar large effect has also been found by Peppard and co-workers in the case of thorium.(14)

3. *Extraction of cations at low loading.* From the extensive work of a number of investigators (principally Dyrssen,(9,10) Peppard,(13,15,16) Hardy,(7,8) Blake,(12)

---

(13) D. Peppard, G. W. Mason, W. J. Driscoll and R. J. Sironen, *J. Inorg. Nucl. Chem.* **7**, 276 (1958).

(14) D. F. Peppard, G. W. Mason and S. McCarty, *J. Inorg. Nucl. Chem.* **13**, 138 (1960).

(15) D. F. Peppard, G. W. Mason, J. L. Maier and W. J. Driscoll, *J. Inorg. Nucl. Chem.* **4**, 344 (1957).

(16) D. F. Peppard, G. W. Mason and S. W. Moline, *J. Inorg. Nucl. Chem.* **5**, 141 (1957).

KIMURA(17,18) and their co-workers) it now appears that a large number of cations are extracted by di-alkylphosphoric acids in accordance with the reaction in equation (2). In Table 1 many of these cations are listed with log ${}^zK$ for extraction by di(2-ethylhexyl) phosphoric acid (DEPA) in toluene. Many of the measurements were made in this medium, the others were made with di(n-butyl) phosphoric acid (DBP) and/or with another solvent. Log ${}^1K$ values for the alkali metal ions are uniformly about one log unit higher in Amsco 80–125(19) than in toluene,(17) and this was taken to be the corresponding solvent correction for all the monovalent ions. Log ${}^2K$ values for divalent ions, estimated from the work of several investigators, involved smaller corrections for extractant and solvent. These corrections were estimated from Figs. 2 and 4. Log ${}^3K$ values for the trivalent ions, with the exception of Fe^{3+} were estimated from the results of PEPPARD *et al.*,(13,15) in DEPA–toluene, and DUYCKAERTZ *et al.*,(11) in DBP–butyl ether. The latter log ${}^3K$ values were corrected by subtracting 3·63, which appears to be the average difference between the two sets of results. This is reasonably consistent with the correction expected from the effects shown by the trivalent ions in Figs. 2 and 4.

Many cations not listed in Table 1 have been reported to extract in accordance with Equation (2). They have not been included here either because there was doubt that extraction equilibrium had not been reached (e.g., Al^{3+}, Ir^{3+}, Ru^{3+}) and/or the ions were extracted from solutions in which strong complex ion formation is to be expected (e.g., Ac^{3+}, Co^{2+}, Cu^{2+}, Ga^{3+} and Ir^{3+} in chloride).(17,18)

Cations found not to conform to Equation (2) include those of Groups IVa, Va, VIa, the second and third transition series, Ge, Sn, As and Sb. In most cases the aqueous chemistry of these metals is complex involving polymer, oxyion and complex ion formation. Much of the available information not included in Table 1 is discussed by KIMURA.(17,18) Th^{4+} has been studied in some detail by PEPPARD,(14) who finds that ThX_6H_2 complexes and $ThX_5(Y)H_2$ (when Y^- is NO_3^- or Cl^-) rather than ThX_8H_4 complexes are formed. This and other tetravalent ions deserve further study. It may be that stearic factors prevent the attachment of eight phosphate groups about these ions.

4. *Ion size and ion charge effect.* It has been pointed out by DYRSSEN(9) that for the trivalent ions of Groups III, the lanthanide and the actinide metals log ${}^zK$ appears to vary inversely as the ion radius. This correlation is clearly apparent in Fig. 5. Here, in a plot of (log ${}^zK$)/z vs. z/r, are also included the monovalent alkali metal ions, Ag^+ and Tl^+; the divalent alkaline earth ions, Cd^{2+} and Zn^{2+}, UO_2^{2+} and NpO_2^{2+}, and Fe^{3+}.

It is seen that all these ions generally show an upward trend in (log ${}^zK$)/z with z/r. The monovalent ions thus show the lowest extractability and the smallest dependence of log ${}^zK$ on r, the range of ${}^1K$ values for the alkali metal ions being only a factor of four. ${}^1K$ values for Ag^+ and Tl^+ are ten-fold higher, suggesting a difference perhaps in the bonding and/or state of hydration of the complex formed here.

The divalent alkaline earth ions yield ${}^2K$ values covering a 10^6-fold range. ${}^2K$ for Mg^{2+} (4×10^{-5}) is surprisingly low. This value is from KIMURA's results,(17,18) which were obtained using relatively short contact times, and so it may not be an equilibrium value. From the trend shown by the other alkaline earths, ${}^2K$ for Mg^{2+} is predicted to

---

(17) K. KIMURA, *Bull. Chem. Soc. Japan* **33**, 1038 (1960).
(18) K. KIMURA, *Bull. Chem. Soc. Japan* **34**, 63 (1961).
(19) E. LAMB, Report ORNL CF-60-6-132, p. 5 (1960).

TABLE 1.—EXTRACTION OF VARIOUS CATIONS AT LOW CONCENTRATIONS BY DIALKYLPHOSPHORIC ACIDS (DBP = DI(n-BUTYL) PHOSPHORIC ACID; DEPA = DI(2-ETHYLHEXYL) PHOSPHORIC ACID)

$$ {}^{s}K = \frac{[MX_{2s}H_s]_{org}[H^+]_{aq}^{s}}{[M^{s+}]_{aq}[H_2X_2]_{org}^{s}} = (2^s)E\left[\frac{[H^+]_{aq}}{M_{HX\,org}}\right]^s $$

Ion	Aq medium	Solvent	Reagent	Log (${}^{s}K$)	Log (${}^{s}K$) DEPA–Toluene	Ion radius (Å)	Reference
Monovalent Ions							
Na^+	Cl^-	Toluene	DEPA		−3·84	0·98	17
	NO_3	Amsco 80–125	DEPA	−2·90	(−3·9)		19
K^+	Cl^-	Toluene	DEPA		−3·88	1·33	17
K^+	NO_3	Amsco 80–125	DEPA	−2·94	(−3·9)		19
Rb^+	Cl^-	Toluene	DEPA		−3·98	1·48	17
	NO_3	Amsco 80–125	DEPA	−2·95	(−4·0)		19
Cs^+	Cl^-	Toluene	DEPA		−4·43	1·67	17
	NO_3	Amsco 80–125	DEPA	−3·25	(−4·4)		19
Ag^+	NO_3	Toluene	DEPA		−1·84	1·26	17
	NO_3	Amsco 80–125	DEPA	−1·69	(−2·7)		19
Tl^+	Cl^-	Toluene	DEPA		−2·58	1·47	17
Divalent Ions							
Be^{2+}	NO_3^-	Toluene	DEPA		1·28	0·30	7
Mg^{2+}	Cl^-	Toluene	DEPA		−4·45	0·65	17
Ca^{2+}		Chloroform	DBP	−2·5	(−2·6)	0·94	9
	NO_3^-	Amsco 80–125	DEPA	−1·2	(−1·8)		19
Sr^{2+}		Chloroform	DBP	−3·7	(−3·8)	1·10	9
	Cl^-	Toluene	DEPA		−3·6		16
	Cl^-	Toluene	DEPA		−4·47		17
	NO_3^-	Amsco 80–125	DEPA	−3·2	(−3·8)		19
Ba^{2+}	Cl^-	Toluene	DEPA		−3·9	1·29	16
	NO_3^-	Amsco 80–125	DEPA	−3·9	(−4·5)		19
	Cl^-	Toluene	DEPA		−4·6		17
Co^{2+}	NO_3^-	Amsco 80–125	DEPA	−3·4	(−4·0)	0·73	19
	Cl^-	Toluene	DEPA		−4·90		17
Cu^{2+}	Cl^-	Toluene	DEPA		−3·52	0·72	17
Zn^{2+}	NO_3^-	Amsco 80–125	DEPA	−1·2	(−1·8)	0·74	19
	Cl^-	Toluene	DEPA		−1·30		17
Cd^{2+}	NO_3^-	Amsco 80–125	DEPA	−1·8	(−2·4)	0·97	19
	Cl^-	Toluene	DEPA		−3·75		17
UO_2^{2+}	ClO_4^-	Toluene	DBP	4·56	(4·4)	(0·83)	8
	ClO_4	Hexane	DEPA	4·60	(4·3)		20
NpO_2^{2+}	ClO_4^-	Toluene	DEPA		4·36	(0·82)	21

TABLE 1 (Cont'd)

Ion	Aq medium	Solvent	Reagent	Log (${}^3K$)	Log (${}^3K$) DEPA–Toluene	Ion radius (Å)	Reference
			Trivalent Ions				
Sc^{3+}	ClO_4^-	Toluene	DEPA		8·8	0·78	13
Y^{3+}	ClO_4^-	Butyl ether	DBP	5·06	(1·4)	0·88	11
	ClO_4	Toluene	DEPA		1·7		13
La^{3+}	ClO_4^-	Butyl ether	DBP	1·23	(−2·4)	1·04	11
	ClO_4	Toluene	DEPA		−2·62		13
Ac^{3+}	ClO_4^-	Toluene	DEPA		−3·4	1.11	13
Ce^{3+}	ClO_4^-	Butyl ether	DBP	2·00	(−1·6)	1·03	11
	Cl^-	Toluene	DEPA		−2·22		15
Pr^{3+}	ClO_4^-	Butyl ether	DBP	2·00	(−1·6)	1·02	11
	Cl^-	Toluene	DEPA		−1·92		15
Pm^{3+}	ClO_4^-	Butyl ether	DBP	2·54	(−1·1)	0·98	11
	ClO_4^-	Toluene	DEPA		−0·83		13
	Cl^-	Toluene	DEPA		−1·10		15
Sm^{3+}	ClO_4^-	Butyl ether	DBP	2·84	(−0·8)	0·96	11
Eu^{3+}	ClO_4^-	Butyl ether	DBP	3·11	(−0·5)	0·94	11
	Cl^-	Toluene	DEPA		−0·44		15
Cd^{3+}	ClO_4^-	Butyl ether	DBP	3·80	(0·2)	0·93	11
Tb^{3+}	ClO_4^-	Butyl ether	DBP	4·10	(0·5)	0.90	11
	Cl^-	Toluene	DEPA		0·56		15
Ho^{3+}	ClO_4^-	Butyl ether	DBP	5·00	(1·4)	0·89	11
Tm^{3+}	ClO_4^-	Butyl ether	DBP	6·20	(2·5)	0·87	11
	ClO_4^-	Toluene	DEPA		2·27		13
	Cl^-	Toluene	DEPA		2·20		15
Yb^{3+}	Cl^-	Toluene	DEPA		2·58	0·86	15
Lu^{3+}	ClO_4^-	Butyl ether	DBP	7·70	(4·1)	0·84	11
	Cl^-	Toluene	DEPA		2·9		15
Am^{3+}	ClO_4^-	Toluene	DEPA		−1·53	0·99	13
Fe^{3+}	ClO_4^-	Octane	DEPA	6·65	(3·6)	0·64	6

be in the range 0·1–1. If the linear relationship found for the trivalent ions is assumed for the heavier alkaline earth ions, then ${}^2K$ for Be^{2+} is many orders of magnitude lower than would be predicted. This of course could be caused by a difference in hydration here compared to the other alkaline earth complexes. It seems more likely, however, that it is the effect of the small size of Be^{2+} which, even with tetrahedral co-ordination of the phosphatic oxygens, should result in oxygen–oxygen contact. Finally, of the divalent ions; UO_2^{2+}(8,20), NpO_2^{2+}(21,22) and PuO_2^{2+}(22) are by far the most strongly extracted. They seem to occupy a position analogous to that of Ag^+ and Tl^+ among the monovalent ions.

The trivalent ions show a remarkably large (nearly 10^{13}-fold) range of ${}^zK$ values. While the results of DUYCKAERTZ, *et al.*,(11) in extractions by DBP in butylether show an upward trend for the heavier rare earths, inverse linear variation of log ${}^3K$ with r for Ac^{3+}, La^{3+}, Y^{3+}, Sc^{3+}, the lanthanides and the actinides is striking. The only other trivalent cation for which equilibrium results free of large aqueous complexing effects are available is Fe^{3+}.(6) It is seen to yield a ${}^3K$ value more than seven orders of magnitude lower than would be predicted by this linear relationship. It is likely that, as in the case of Be^{2+}, this relatively low extractability is caused by the small size of Fe^{3+} (r = 0·64 Å), which approaches the size at which anion–anion contact would occur with octahedrally bonded phosphatic oxygen atoms. It would be of interest to have equilibrium extraction results for the even smaller Al^{3+} ion.

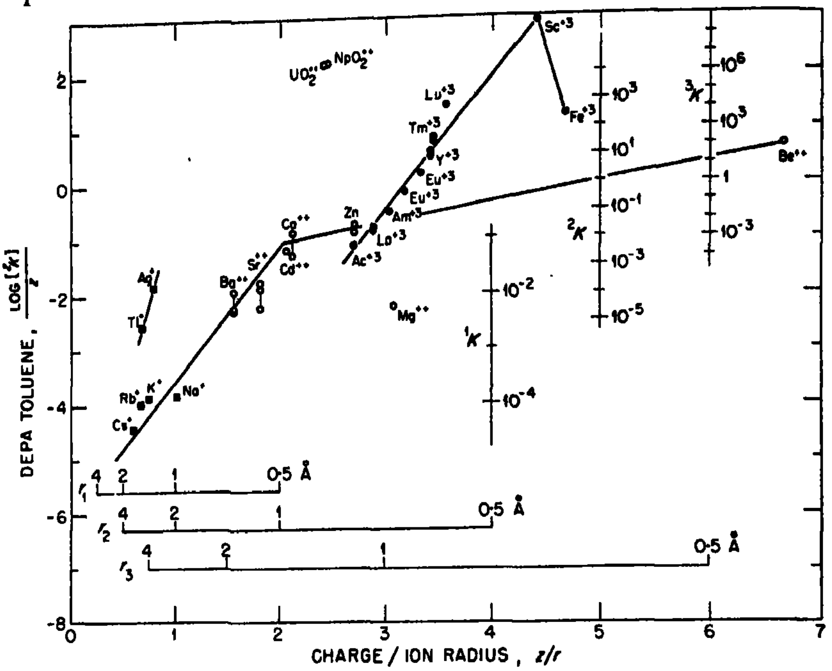

FIG. 5.—*Effect of ion charge and ion size on extraction by dialkylphosphoric acids.*

From the fairly uniform variation of (log ${}^zK$)/z (proportional to the free energy of formation of an M-X_2H linkage in structure I, above), with z/r (roughly proportional to the charge density about the ion) for most of the points in Fig. 5, it seems reasonable to conclude that a single structure such as $M(X_2H)_z$ (structure I, above) involving ionic bonds is fairly generally formed. There is, however, uncertainty about the state of hydration of the extraction complex in many cases and of the effect of a change in hydration on relative extractibility within a series. While from steric considerations it is expected that MX_6H_3 complexes are not hydrated and it is known that $UO_2X_4H_2$

---

(20) C. F. BAES, JR., R. A. ZINGARO and C. F. COLEMAN, *J. Phys. Chem.* **62**, 129 (1958).

(21) E. NAKAMURA, *Bull. Chem. Soc. Japan* **34**, 402 (1961).

(22) B. WEAVER and D. E. HORNER, *J. Chem. Engng. Data* **5**, No. 3, 260 (1960).

is not, there is little direct information available concerning the state of hydration of other MX_4H_2 complexes and, especially, the MX_2H complexes. Since in these latter complexes the cation coordination number is only two if the structure is $M(X_2H)$, hydration may well occur. It is known that at higher loading polymeric, highly hydrated sodium-dialkylphosphate species are formed. In the $(MX_2H)_2$ structure a co-ordination number of four may be sufficient that hydration does not occur, at least for the heavier alkaline earth ions. The observed low ${}^{2}K'$ value of Mg^{2+} (if it is an equilibrium value) and that for Be^{2+} may denote the formation of a hydrated $M(H_2O)_X(X_2H)_2$ species.

Structure I yields a co-ordination number of only 4 for uranyl ion (not counting the uranyl oxygens) instead of the expected value of six. This led Kennedy(23) to propose the following structure for $UO_2X_4H_2$

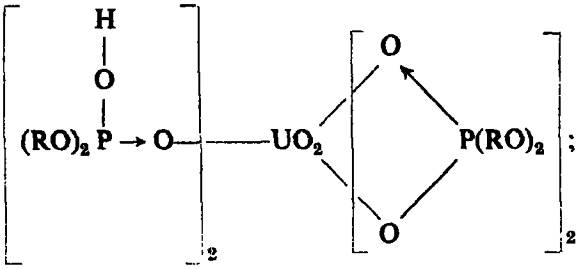

; $UO_2X_2(HX)_2$ II

From subsequent infra-red measurements on $UO_2X_4H_2$ (X = DBP) in carbon tetrachloride, Kennedy and Deane(24) concluded, however, that this was probably incorrect. From their results they suggest, instead, that an entity

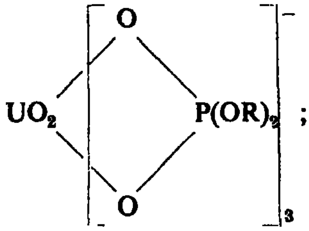

; $UO_2X_3^-$ III

is present in which three dialkylphosphate anions are equivalently bonded. The mode of combination of the remaining HX molecule and the proton is not specified. As noted above, the extractability of UO_2^{2+} (and NpO_2^{2+} and PuO_2^{2+}) is relatively high, possibly because of covalent bonding. It may also be the result of a relatively more stable structure (such as III) in which a higher co-ordination number than four is achieved.

5. *Approach to saturation.* The complex $MX_{2z}H_z$ occurs only in organic solutions in which there is sufficient excess of the dialkylphosphoric acid. With increasing loading it is often found that more of the metal cation is extracted than corresponds to this composition. Only two cases, namely, UO_2^{2+}—HX(20) and Fe^{3+}—HX,(6) have been examined sufficiently to permit identification of the new species formed. In the case of UO_2^{2+}, evidence from the loading isotherm and from isopiestic measurements indicated chain polymer formation as follows,

$$HX_2(UO_2)X_2H \rightarrow HX_2(UO_2)X_2(UO_2)X_2H \rightarrow HX_2[(UO_2)X_2]_n(UO_2)X_2H$$

---

(23) J. Kennedy, AERE/C/M-369 (1958).

(24) J. Kennedy and A. M. Deane, *J. Inorg. Nucl. Chem.* **19**, 174 (1961).

This process proceeds to a limiting composition UO_2X_2. There appeared to be no water or anion (ClO_4^-) extracted. In the case of Fe^{3+}, the isotherm was more complex. Analysis of the organic phase indicated water and anion extraction and isopiestic evidence indicated polymerization. Besides FeX_6H_3 (at low loadings) it appeared that at least two other complexes,

$$[Fe_3X_8(ClO_4)\cdot ca\ 5H_2O]_4$$

followed by

$$Fe_5X_8(ClO_4)(OH)_6\cdot ca\ 7H_2O$$

were formed as saturation is approached. The completely different behaviour of these two systems is striking and suggests that other equally interesting systems await investigation.

PEPPARD and co-workers noted[(15)] in their work on extraction of the rare earths that precipitates of composition MX_3 were formed. In later infra-red studies[(25)] they prepared a number of di(2-ethylhexyl) phosphate salts, including: KX, NaX, LiX, UO_2X_2, ScX_3, ThX_4, ZrX_4, HfX_4. In addition the following mixed nitrate salts were prepared: $Hf(NO_3)X_3$, $Th(NO_3)X_3$, $Ce_2O(NO_3)_2X_4$. They concluded from their infra-red measurements that the nitrate ion is covalently bonded to the metal. Only in the case of Zr^{4+} and Hf^{4+} was there evidence for covalent bonding of the phosphate. It is of course possible that many of these salts in solution are associated and/or hydrated.

It has already been noted that the extraction of Th(IV) can be accompanied by anions[(14)] at very low loadings. Similar behaviour is perhaps to be expected in the extraction of other tetravalent ions, particularly in the presence of nitrate. At high concentrations, mineral acids are extracted by dialkylphosphoric acids[(14)] in a manner analogous to the behaviour of tri(n-butyl) phosphate. Similarly the extraction of anions along with the metal cation quite often occurs at high aqueous acidities.

6. *Synergistic effect.* It was discovered by SCHMITT[(26)] that use of neutral organophosphates ($(RO)_3PO$, $(RO)_2RPO$, $(RO)R_2PO$ or R_3PO) in combination with dialkylphosphoric acids results in a strong (synergistic) enhancement of uranium (VI) extraction. Upon further investigation by BLAKE *et al.*,[(27)] UO_2^{2+} and PuO_2^{2+} were found to be the only ions (of a relatively small number tested) and dialkylphosphoric acids to be the only organophosphorous acids to produce this effect.

In general, a synergistic effect should result if two reagents, A and B, which separately can extract an aqueous species M to form MA_a and MB_b (and if A and B do not react strongly with one another) can together form a mixed complex MA_cB_d. The resulting extraction coefficient, E, is

$$E = \frac{[MA_a] + [MB_b] + [MA_cB_d]_{org}}{[M]_{aq}} \tag{8}$$

$$E = E_A + E_B + \Delta E \tag{9}$$

wherein E_A and E_B are the extraction coefficients expected for each reagent alone.

---

(25) D. F. PEPPARD and J. R. FERRARO, *J. Inorg. Nucl. Chem.* **10**, 275 (1959).

(26) J. M. SCHMITT, reported by K. B. BROWN, C. F. COLEMAN, D. J. CROUSE and A. D. RYON, Progress Reports on Raw Materials, ORNL-2346 (1957).

(27) C. A. BLAKE, D. E. HORNER and J. M. SCHMITT, Report ORNL-2259 (1959).

The magnitude of the increase in extraction, ΔE is determined by the formation constant $K_{cd} = \dfrac{[\mathrm{MA}_c\mathrm{D}_d]}{[\mathrm{A}]^c[\mathrm{B}]^d[\mathrm{M}]_{aq}}$;

$$\Delta E = K_{cd}[\mathrm{A}]^c[\mathrm{B}]^d \qquad (10)$$

In addition, it can easily be shown that

$$\left(\frac{\partial \log \Delta E}{\partial \log [\mathrm{B}]}\right)_{[\mathrm{A}]} = d; \qquad \left(\frac{\partial \log \Delta E}{\partial \log [\mathrm{A}]}\right)_{[\mathrm{B}]} = c \qquad (11)$$

Three things are noteworthy here:

1. A synergistic effect does not necessarily imply that the mixed complex $\mathrm{MA}_c\mathrm{B}_d$ is inherently more stable than MA_a or MB_b, though its stability does determine the magnitude of the effect.
2. In examining extraction behaviour to characterize the mixed complex the variation of ΔE (not E) with [A] and [B], should be studied.
3. In such studies, low loadings of M are usually used and [A] and [B] are assumed equal to the total concentrations of A and B, respectively. If, however, A and B react with each other (as often happens) the concentration of free extractants will of course be lowered as a result.

From their data, Blake *et al.*,(27) proposed the mixed complex was formed by simple addition of the neutral reagent B.

$$\mathrm{UO_2X_4H_2} + \mathrm{B} \rightleftharpoons \mathrm{UO_2X_4H_2B} \qquad (12)$$

This reaction was suggested by the observed approximate second power dependence of E on $[\mathrm{H_2X_2}]$ with [B] constant and by the shape of the loading isotherm. This showed a more pronounced flattening in the vicinity of a uranium(VI)–DEPA mole ratio of 1:4 with [B] present than with [B] absent. They noted also that direct reaction of $\mathrm{H_2X_2}$ and B apparently occurred. Thus with increasing [B] at constant $[\mathrm{H_2X_2}]$ the extraction coefficient rose to a maximum and then decreased. Such a reaction has been reported by Hardy and Scargill,(3) Baker and Baes,(28) and by Dyrssen.(2) It may be written

$$\mathrm{H_2X_2} + 2\mathrm{B} \rightleftharpoons 2\mathrm{XHB} \qquad (13)$$

Baker and Baes,(28) from infra-red and isopiestic measurements, also found evidence for a second interaction product

$$\mathrm{H_2X_2} + \mathrm{B} \rightleftharpoons \mathrm{HX_2HB} \qquad (14)$$

Thus a full interpretation of extraction behaviour in M^{z+}–$\mathrm{H_2X_2}$–B systems should include at least three possible equilibria (Equations 12, 13 and 14) in addition to those which occur in separate M^{z+}–$\mathrm{H_2X_2}$ and M^{z+}–B systems. In view of the number of possible reactions, the mixed complex proposed by Blake *et al.*, could not be conclusively established. Dyrssen,(29) from detailed measurements in the $\mathrm{UO_2}^{2+}$–DBP–TBP system proposed instead the monosubstituted mixed complex $\mathrm{UO_2X_3HB}$

$$\mathrm{UO_2X_4H_2} + \mathrm{B} \rightleftharpoons \mathrm{UO_2X_3HB} + \tfrac{1}{2}\mathrm{H_2X_2} \qquad (15)$$

---

(28) H. T. Baker and C. F. Baes, Jr., Report ORNL-CF-58-5-93 (1958) (In Press).

(29) D. Dyrssen and L. Kuca, *Acta Chem. Scand.* **14**, 1945 (1960).

His treatment of the results did not include consideration of the reaction in Equation (14). In addition, because both DBP and TBP distribute appreciably to the aqueous phase, the interpretation was involved and possibly not conclusive. KENNEDY[23] has argued that a disubstituted complex, $UO_2X_2B_2$ is the most reasonable because its formation from $UO_2X_4H_2$

$$UO_2X_4H_2 + 2B \rightleftharpoons UO_2X_2B_2 + H_2X_2 \qquad (16)$$

would be stabilized by the free energy of dimerization of the two HX molecules released. Subsequently, KENNEDY and DEANE[24] interpreted their infra-red studies of UO_2^{2+}–DBP–tri(n-octyl) phosphine oxide solutions in carbon tetrachloride to indicate that both $UO_2X_2B_2$ and UO_2X_3HB are formed, the latter complex containing the same entity, $UO_2X_3^-$ (structure III, above) suggested by them to occur in $UO_2X_4H_2$. Further investigation is needed, in the author's opinion, to establish which of these proposed mixed complexes is the correct one.

Recently IRVING and EDDINGTON,[30] investigating analogous systems in which the dialkylphosphoric acid is replaced by TTA (thenoyl trifluoroacetone), found strong synergistic effects in uranium (VI) extraction. HEALY[31] further has shown that here synergisism is a general effect, occurring in the extraction of alkaline earth, trivalent lanthanide, trivalent actinide, and thorium (IV) ions as well as with uranyl ion. In his very extensive measurements, HEALY found the mixed complex in every case to be an addition product.

$$M(TTA)_z + cB \rightleftharpoons M(TTA)_zB_c \qquad (17)$$

In TTA systems the direct reaction between the acidic and neutral reagent is evidently less important than in the corresponding dialkylphosphoric acid systems. This weaker competing interaction may account for the generally larger and more widely occurring synergistic effects observed.

Perhaps the most interesting unanswered question is the manner in which the neutral reagent, B, is held in the mixed complex. BLAKE *et al.*,[27] suggested that hydrogen bonding was involved. While this is not yet ruled out in dialkylphosphoric acid systems, it cannot occur in TTA systems unless water molecules are present in the mixed complex. From HEALY's results the equilibrium quotient for the above reaction (Equation 17) can be calculated, yielding bonding free energies in the range of 4–8 kcal per mole of B in $M(TTA)_zB_c$ complexes. This is comparable to the range of variation found for the solvation free energy of $MX_{2z}H_z$ complexes (Fig. 3). In addition, HEALY reports[32] strong dependence of the synergistic effect in the choice of solvent, the order of decreasing effect being essentially the same as the order of increasing solvation free energy for $MX_{2z}H_z$. This tends to suggest that B is present as a solvate in the mixed complex.

---

[30] H. IRVING and D. N. EDDINGTON, *J. Inorg. Nucl. Chem.* **15**, 158 (1960).
[31] T. V. HEALY, *J. Inorg. Nucl. Chem.* **19**, 314 (1961).
[32] T. V. HEALY, *J. Inorg. Nucl. Chem.* **19**, 328 (1961).

J. Inorg. Nucl. Chem., 1962, Vol. 24, pp. 721 to 728. Pergamon Press Ltd. Printed in Northern Ireland

EXTRACTION OF URANIUM FROM SOLUTIONS OF COMPLEX URANYLCARBONATE BY CETYL-DIMETHYL-BENZYL-AMMONIUM CHLORIDE*

M. T. Sardiña, R. F. Cellini and T. Batuecas Rodriguez
Chemistry Division, Junta de Energia Nuclear, Madrid, Spain

(*Received* 28 *December* 1961)

Abstract—The behaviour of the cetyl-dimethyl-benzyl-ammonium chloride (CDMBA) in the extraction of uranium dissolved in a carbonate medium has been studied in laboratory scale.

The effect of a certain number of variables on the extraction factor has been determined. The variables considered included: the amount and concentration of CDMBA, carbonate and bicarbonate concentrations, uranium concentration, temperature, contact time and variations in the composition of the diluent.

It has been found that, in the case of a uranium concentration of 1 g/l., the amount of uranium extracted in a single stage is as high as 94·4 per cent of the total if the concentration of CDMBA is 0·034 M and as 98 per cent if CDMBA 0·050 M is used.

The application of the liquid–liquid extraction process to solutions coming from alkaline leaching of uranium minerals is of interest; nevertheless, there is very little information on methods in which this process might be utilized. Clifford and co-workers⁽¹⁾ have studied the formation of the internal complex uranyloxiquinolate and its use in the extraction of uranium from carbonate solutions. Crouse and Brown⁽²⁾ have reported an experiment in which uranium is extracted from alkaline solutions by dimethyl-didodecenyl-ammonium chloride and, later on,⁽³⁾ they describe the use of a trialkyl-methyl-ammonium chloride with the same purpose.

It was proved in a series of preliminary experiments with extraction agents, that the alkyl-dimethyl-benzyl-ammonium chlorides (alkyl radicals C_{12} to C_{18}) have characteristics which render them suitable for the extraction of uranium from alkaline solutions. Consequently, extensive research has been carried out to establish the conditions for using them as extraction agents, cetyl-dimethyl-benzyl-ammonium chloride (CDMBA) being used as a prototype. In this report, the laboratory scale extraction as a function of the composition of the extraction agent is described. The effect of the variables: temperature, contact time and the volume ratio of both phases is studied, and the CDMBA saturation isotherms are given.

EXTRACTION CONDITIONS AND ANALYTICAL METHODS

The experiments were performed in 150 ml separation funnels by mixing 15 ml of organic phase with the same volume of aqueous phase. After the phases had separated spontaneously and completely, samples of both phases were taken and the amount of uranium determined by colorimetric methods.⁽⁴⁾ Whenever the concentrations of uranium were lower than 0·05 g/l. a fluorimetric method was used.(5) The alkyl-dimethyl-benzyl chloride was determined by a photometric method on the compound which it forms with bromophenol blue.(6)

---

* Presented to the XXXII Congress of Industrial Chemistry, 23–30 October 1960, Barcelona, Spain.

(1) W. E. Clifford, P. Noble and E. P. Bullwinkel, *J. Amer. Chem. Soc.* **80**, 2959–61 (1958).
(2) D. J. Crouse, K. B. Brown, W. D. Arnold and others, Report ORNL-2099 (1956).
(3) D. J. Crouse. Private communication (1959).
(4) J. Rodden, *Analytical Chemistry of the Manhattan Project*, Vol. 8-1, p. 93, McGraw-Hill, New York (1950).

The following reagents have been used: cetyl-dimethyl-benzyl-ammonium chloride, trade mark "Leda", pharmaceutical grade; normal octyl alcohol, trade marks "Schuchardt" and "Fluka", technical grade; kerosene, 160–210°C fraction.

EXPERIMENTAL RESULTS

Effect produced by the contents of octyl alcohol in the diluent

It was proved that in order to get a mixture of CDMBA chloride using kerosene as diluent, it was sufficient to add a long chain alcohol. For that reason, the normal octyl was adopted, which, at the same time, helps avoiding the formation of emulsions. The effect on the extraction factor produced by the addition of n-octyl alcohol was examined by measuring the extent of the extraction from two aqueous phases with different concentrations of uranium and organic phases in which the ratio CDMBA : U was held constant. The concentration of n-octyl alcohol in the diluent was changed within the range 10–40 per cent v/v. The results presented in Table 1 clearly prove that, for fixed quantities of CDMBA and U, the extraction factor decreases when the concentration of n-octyl alcohol increases. For this reason, in all the experiments reported in this paper, the amount of n-octyl alcohol used was the minimum necessary to maintain the CDMBA dissolved in kerosene.

TABLE 1.—EFFECT OF THE CONCENTRATION OF n-OCTYL ALCOHOL IN THE DILUENT ON THE EXTRACTION OF URANIUM WITH CDMBA

Aqueous Phase 15 g of free Na_2CO_3/l.
Group (a): 0·958 g U/l. in aqueous phase and 20·4 g CDMBA/l. in organic phase
Group (b): 0·319 g U/l. in aqueous phase and 6·8 g CDMBA/l. in organic phase
Phase ratio 1:1
Contact time 5 min at 18°C

% v/v of Octyl Alcohol in the organic phase		% Extracted		E_a°	
(a)	(b)	(a)	(b)	(a)	(b)
—	10·7	—	95·3	—	20·3
12·0	—	97·3	—	35·4	—
15·3	15·3	97·1	93·3	33·1	14·0
20·0	20·0	(97·2)	90·6	(34·2)	9·6
25·3	25·3	95·9	85·9	23·8	6·1
30·0	30·0	95·4	80·4	20·9	4·1
35·3	35·3	94·1	75·0	16·0	3·0
40·0	40·0	92·6	67·7	12·5	2·1

Effect of the total amount of CDMBA

The generally admitted similarity between the extraction of uranium from its acid solutions by amines and the fixation of that uranium by weak base ion-exchangers(7) allows to expect that the quaternary ammonium compounds would behave in a similar way to the strong base ion-exchangers and accordingly they would extract through a chemical process analogous to the one by which the uranium, in the form of uranyltricarbonate is extracted from alkaline solutions by ion-exchangers.[8] CDMBA, like other long chain compounds of quaternary ammonium, would form, when in solution, ionic aggregates, micelles, which give place to species soluble in organic liquids. An organic solution of one of these aggregates behaves like an ion-exchanger, therefore, it will interchange antagonic ions with the uranyltricarbonate anion. If the micellar nature of the compound, formed by association of ions of CDMBA and uranyltricarbonate, is admitted, then the effect produced by n-octyl alcohol is clear; the presence of this compound tends to avoid the condensation of ionic pairs, possibly by partly saturating the CDMBA bounds and by making the association in micelles more difficult.

---

(5) F. S. GRIMALDI, U.S. Geological Survey, CIRC 199 (1952).

(6) E. L. COLICHMAN, *Analyt. Chem.* 19, 430 (1947).

(7) C. F. COLEMAN, K. B. BROWN, J. G. MOORE and others, *Proceedings of the Second International Conference on the Peaceful Uses of Atomic Energy, Geneva* 1958, Vol. 28, 278–88. United Nations (1959).

The equilibrium between the ions in the aqueous phase and the undissociated molecules in the organic phase, which is responsible for the uranium extraction by CDMBA, must correspond stoicheiometrically with the following equation

$$4R_4NCl_{(o)} + UO_2(CO_3)_3^{4-} \rightleftarrows (R_4N)_4UO_2(CO_3)_{3(o)} + 4Cl^-$$

where R_4NCl = CDMBA chloride.

Assuming that the law of mass action applies to such an equilibrium, then the ratio of the amount of uranium in the organic phase [chemical form $(R_4N)_4UO_2(CO_3)_3$] to the uranium in the aqueous phase (as $UO_2(CO_3)_3^{4-}$) will depend essentially on the amount of R_4NCl dissolved in the organic phase, and on the concentration of Cl^- anion from the quaternary ammonium compound, in the aqueous phase. The results given in Table 2 agree with the ones obtained from Equation (1), they express the variation of the extraction factor and the per cent extracted when the amount of CDMBA increases. It has been observed that an amount of CDMBA must be used such that the ratio "moles of CDMBA/moles of U" varies within the range 8–10. It can be deduced also that the percentage extracted is proportional to the amount of quaternary ammonium present in the organic phase; this fact seems to indicate that the activity coefficient of CDMBA remains constant instead of being proportional to its concentration in the organic phase, this being in good agreement with the hypothesis that the CDMBA forms micelles which constitute themselves a separate phase.

The results given in Table 2 also indicate that, for low concentrations, the extraction factor varies as the second power of the CDMBA concentration. When the free carbonate in the aqueous phase and the CDMBA chloride are brought together, they must react according to the equation

$$2R_4NCl_{(o)} + CO_3^{2-} \rightleftarrows (R_4N)_2CO_{3(o)} + 2Cl^-$$

CDMBA remaining in the organic phase as a carbonate. It is for this reason that the factor of extraction of uranium should be proportional to the square of the concentration of CDMBA, since

$$2(R_4N)_2CO_{3(o)} + UO_2(CO_3)_3^{4-} \rightleftarrows (R_4N)_4UO_2(CO_3)_{3(o)} + 2CO_3^{2-}$$

At the same time, there must be a strong relationship between the uranium extraction factor and the amount of free carbonate in the aqueous phase.

---

[8] M. URGELL, J. A. PÉREZ BUSTAMANTE, T. BATUECAS RODRÍGUEZ and others, Report JEN-52, Madrid (1959).

Effect produced by the ratio "organic volume:aqueous volume"

We have studied also the effect produced on the extraction of the uranium if, maintaining constant the amounts of the reagents, the volume of the organic phase changes. The results are shown in Table 3. When the volume of the organic decreases, the extraction factor, as expected, increases, but this increase is faster than the one corresponding to the variation of volume, so that the total amount of uranium extracted increases as well. Therefore, a fixed quantity of CDMBA-n-Octyl Alcohol extracts the more uranium the smaller the volume in which it is dissolved.

Table 2.—Effect of the total amount of CDMBA on the extraction of uranium

Aqueous phase: 0·958 g U/l. and 15 g of free Na_2CO_3/l.
Diluent: kerosene with 25 per cent v/v of Octyl Alcohol
Ratio of phases: 1:1
Contact time: 5 min at 20°C

CDMBA (mg)	CDMBA moles:U moles	% Extracted	E_a^o
0	0	—	—
50	2	23·1	0·3
100	4	54·5	1·2
125	5	68·9	1·9
150	6	75·6	3·1
250	10	96·2	25·6
300	12	98·1	52·1
350	14	98·2	56·0
450	18	98·9	91·3
600	24	99·2	134·5
750	30	>99·99	>2000

Table 3.—Effect of CDMBA-octyl alcohol concentrations in kerosene on the extraction of uranium

Aqueous phase: 1 g U/l. and 15 g of free Na_2CO_3/l.
Total amount of CDMBA: 200 mg
Contact time: 5 min at 21·5°C

CDMBA molar concentration	Organic vol.:aqueous vol.	% Extracted	E_a^o
0·097	1:3	93·3	42·2
0·048	2:3	91·9	17·0
0·032	1:1	90·4	9·4
0·016	2:1	87·2	3·4

Table 4.—Effect of free carbonate concentration on the extraction of uranium with 14 g/l. of CDMBA in kerosene with 7 per cent v/v of N-octyl alcohol

Aqueous phase: 1 g/U/l.
Ratio of phases 1:1
Contact time: 5 min at 18°C

Free carbonate at start (M)	Initial pH	% Extracted	E_a^o
0·01	10·60	>99·9	>1000
0·08	10·90	97·8	44·7
0·48	11·20	67·4	2·1
1·00	11·24	40·6	0·68

Effect of the concentration of free carbonate and bicarbonate

To study the effect produced by the free carbonate in the aqueous phase, we have used aqueous solutions with 1 g of U/l. without bicarbonate, and with concentrations in free carbonate within the range 0·01–1·00 M. In Table 4 it is shown that there is a strong relationship between the extraction factor and the concentration in free carbonate. If the initial concentration in free carbonate decreases to 0·01 M, the uranium extraction is practically complete.

Test showing the effects produced by carbonate, that is free from uranyltricarbonate, on CDMBA, confirm that the carbonate anion passes to the organic phase.

The importance of the presence of bicarbonate becomes quite clear from the results given in Table 5. When the relative amount of bicarbonate increases, a point is reached at which the uranyl complex is not exclusively uranyltricarbonate, there being also present products from hydrolysis. It is because of the presence of such products that the extraction factor decreases.

TABLE 5.—EFFECT OF THE RATIO CARBONATE:BICARBONATE, BEING CONSTANT THE CONCENTRATION OF TOTAL CARBONATE, ON THE EXTRACTION OF URANIUM WITH 14 g/l. OF CDMBA IN KEROSENE WITH 7 PER CENT v/v OF N-OCTYL ALCOHOL

Aqueous phase: 0·958 g U/l.
Ratio of phases: 1:1
Contact time: 5 min at 18°C

Free carbonate at start (M)	Free bicarbonate at start (M)	Carbonate:bicarbonate (M:M)	pH initial	% Extracted	E_a°
0·036	0·436	0·083	8·61	40·5	0·68
0·197	0·295	0·668	9·49	51·2	1·05
0·423	0·058	7·293	10·25	68·2	2·14

Effect of pH

The results obtained by changing the concentration of free carbonate, without bicarbonate, and the effects caused by the different ratios carbonate:bicarbonate, do

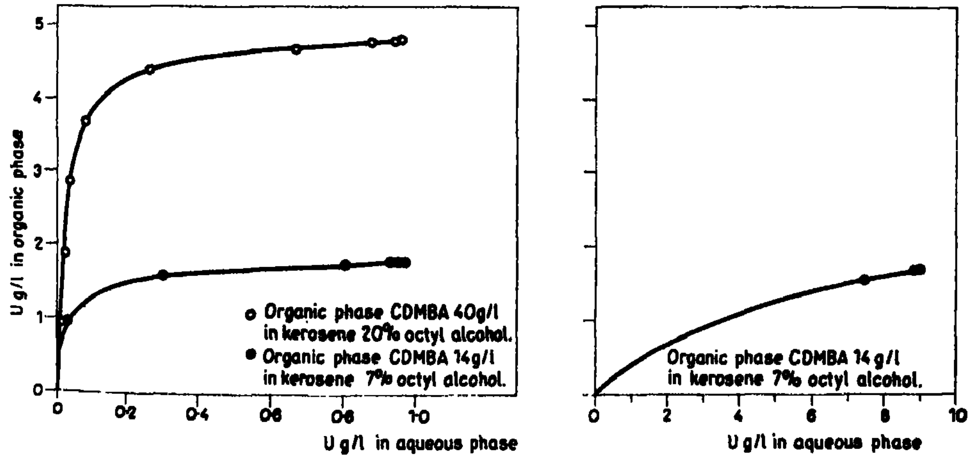

(Aqueous phase 1g U/l and 15g free Na_2CO_3/l) (Aqueous phase 9·2g U/l and 15g free Na_2CO_3/l)

FIG. 1.—Isotherms of uranium extraction.

not indicate a direct effect of the pH on the extraction; the pH seems to act only through the ratio carbonate:bicarbonate in the aqueous phase.

Extraction isotherms

Fig. 1 shows three examples of saturation of CDMBA with uranyltricarbonate. In each case 15 ml of organic phase were treated successively with portions of 15 ml of fresh aqueous phase, until equilibrium was established. From the normal shape of these isotherms it is concluded that the organic complex is a monomer with respect to the uranium. By exploring the two isotherms corresponding to the same concentration of CDMBA in the organic phase, it is deduced that the more diluted the uranium the more complete its extraction; this result is completely logic because the less uranium present the bigger the amount of free CDMBA. The final point on each curve corresponds to the organic phase saturated with uranium and in equilibrium with the aqueous phase; when the concentration of CDMBA is higher the uranium contents of the organic phase at saturation is also higher; thus, the maximum concentration of uranium in the organic solvent is directly proportional to the concentration of CDMBA and therefore it is possible to obtain a uranium saturated organic phase even by using very diluted feeding solutions.

The saturation value of CDMBA on each isotherm corresponds to the association of a fixed number of moles of quaternary ammonium with each mole of uranium, so that the quaternary ammonium is completely bounded and cannot extract more uranium. For the three isotherms the saturation is reached with about four moles or ammonium for each mole of uranium. The saturation values given in Table 6 are in good agreement with the stoicheiometric laws governing the proposed chemical reaction.

TABLE 6.—EFFECT OF THE URANIUM AND CDMBA CONCENTRATION ON THE SATURATION VALUE OF CDMBA

Ratio of phases 1:1
Contact time: 5 min at 19°C

Initial g U/l. in the aqueous phase	Initial g CDMBA/l. in the organic phase	CDMBA moles:U moles in the saturated organic phase
1·0	14	4·47
1·0	40	4·80
9·2	14	4·79

Effect of the diluent

Table 7 shows the results obtained from the extraction of an aqueous solution with the same amount of CDMBA in four different diluents, the n-octyl alcohol contents of all of them was 7 per cent v/v. The highest extraction is obtained with benzene; the lowest value obtained in these tests correspond to the chloroform. Nevertheless, the advantages obtained by using benzene do not compensate the difficulties of handling it and the drawback of its higher cost.

The effect of the contact time

In relation to the effect of the contact time between the phases on the extraction of uranium, it must be noted the high rate of uranium transfer. Table 8 shows the results

TABLE 7.—EFFECT OF THE DILUENT ON THE EXTRACTION OF URANIUM WITH 14 g/l. CDMBA AND 7 PER CENT v/v OF n-OCTYL ALCOHOL

Aqueous phase: 1 g U/l. and 15 g of free Na_2CO_3/l.
Ratio of phases 1:1
Contact time: 5 min at 21°C

Diluent	% Extracted	E_a°
Kerosene 160–210°C	92·9	13·2
White spirit 140–160°C	93·8	15·3
Benzene	94·9	18·5
Chloroform	66·1	1·95

obtained from extractions performed with the same aqueous and organic phases and different contact time. The equilibrium is obtained after 10 sec of shaking; longer times do not appreciably increase the degree of extraction.

TABLE 8.—EFFECT OF THE CONTACT TIME ON THE EXTRACTION OF URANIUM WITH A SOLUTION OF 14 g/l. CDMBA IN KEROSENE 7 PER CENT v/v OF n-OCTYL ALCOHOL

Aqueous phase: 1 g U/l. and 15 g free Na_2CO_3/l.
Ratio of phases: 1:1
Temperature: 21°C

Contact time	% Extracted	E_a°
10 sec	94·9	18·8
20 sec	94·6	17·5
1 min	94·4	17·0
31 min	94·6	17·4

Effect of the temperature

A temperature increase does not produce a marked effect on the extraction. A temperature increase from 16 to 32°C produces only a decrease of a 3 per cent in the extraction. This fact is explained because the solubility of CDMBA in the aqueous phase increases. Nevertheless, extraction of uranium at 60°C is still high. Table 9 gives the results.

TABLE 9.—EFFECT OF THE TEMPERATURE ON THE EXTRACTION OF URANIUM WITH A SOLUTION OF 14 g/l. CDMBA IN KEROSENE 7 PER CENT v/v OF n-OCTYL ALCOHOL

Aqueous phase: 1 g U/l. and 15 g free Na_2CO_3/l.
Ratio of phases: 1:1
Contact time: 5 min

Temperature (°C)	% Extracted	E_a°
16	97·7	43·0
32	94·5	17·1
60	94·0	15·7

Other tests

Finally, the amount of CDMBA lost by transfer to the aqueous phase in each step of extraction, at normalized conditions, has proved to be smaller than 0·048 g/l. equivalent to 0·34 per cent of the initial CDMBA.

Experiments have been started to recuperate the extraction solvent and to re-extract the uranium. Preliminary tests seem to indicate that the sulphuric and nitric acids, as well as some of their salts, are promising.

Emulsion formation

Along the reported work, it was observed that, in some cases, there was a strong tendency toward the formation of a stable emulsion within the organic and aqueous phases. Since the elimination of such emulsions offers a great interest, it has been determined not only the effect of the studied variables on the extraction factor but also the influence of each one of these variables on the separation time of phases has been analysed.

The results show that within the experimented range, the pH has no effect on the phases separation time and that the contact time, if shaking is not violent, only produces weak variations in the separation time. The tendency of a phase to disperse into the other is modified by changing the ratio organic volume/aqueous volume; within certain limits it is convenient that the volume of the organic phase be smaller than that of the aqueous one. On the other hand, if the temperature increases the separation time decreases notably. The separation time can also be modified by changing the type of diluent.

The concentration of CDMBA not bounded to the uranyltricarbonate is decisive and must not be above a certain limit if the formation of emulsions is to be avoided; as a consequence, it is very important to control the concentration of free carbonate in the aqueous phase and that of the n-octyl alcohol in the kerosene. And above all, the intensity of shaking is of capital importance, if it is very small, the separation time of the phases can be small without altering the value of the extraction factor. On the contrary, if the separation time is lowered by changing the temperature or the diluent, then the value of E_a^0 also goes down.

CONCLUSIONS

The CDMBA is an efficient solvent in the extraction of the uranium contents in solutions of alkaline carbonates. Within the parameters which define the extraction conditions it is of great interest the concentration of free carbonate; decreasing that concentration the efficiency of the extraction is increased substantially. It is remarkable the high rate of transfer of uranium when extracted with CDMBA.

In the extraction conditions adopted in the laboratory, i.e. without active shaking, using an aqueous phase with 1 g U/l. and 15 g free Na_2CO_3/l. and an organic phase made out of 14 g/l. CDMBA in kerosene and 7 per cent v/v n-octyl alcohol, the separation time of the phase is less than 5 min at 20°C and it is possible to extract 94·4 per cent of the total uranium in one single contact.

J. Inorg. Nucl. Chem., 1962, Vol. 24, pp. 729 to 737. Pergamon Press Ltd. Printed in Northern Ireland

EXTRACTIONS FROM HCL—I

ADIPONITRILE AS AN EXTRACTION SOLVENT*

G. W. LATIMER, JR.† and N. H. FURMAN‡
Contribution from the Frick Chemical Laboratory, Princeton University
Princeton, N.J.

(*Received* 10 *January* 1961; *in revised form* 8 *February* 1962)

Abstract—Adiponitrile, 1-4 butane dinitrile, extracts both Fe(III) and Mo(VI) from aqueous hydrochloric acid. The extraction curves for this system generally follow the extraction curves for the same metals in ether systems.

The empirical formulae for the species extracted by adiponitrile are $(HFeCl_4)n$ and $(HMoO_2Cl_3)n$.

Adiponitrile also extracts these metal ions from chloride salt solutions containing only enough acid to prevent hydrolysis. The salting order for Fe(III) is Li > Na > NH_4 > Ca and for Mo(VI) is Li ≈ Na ≈ Ca > NH_4.

DESPITE experiments demonstrating that compounds other than those containing oxygen could extract metal complexes of the type HMX_4,⁽¹⁾ no systematic study of any of these compounds has been published. The data available indicate that in systems containing hydrocarbons or their chlorinated derivatives the distribution of the complex greatly favours the aqueous phase.⁽²⁾ Benzonitrile, however, extracts a number of metal ions quite effectively from 7 M HCl.⁽¹·³⁾

Adiponitrile, 1-4 butane dinitrile, also extracts metal ions from aqueous acid.⁽⁴⁾ This paper describes the behaviour of Fe(III) and Mo(VI) in the system HCl–adiponitrile and in similar systems containing chloride salts.

EXPERIMENTAL

1. *Materials and solutions*

Adiponitrile (ADN), Eastman White Label, was used without further purification. The m.p. of this commercial material was 1–3°C; n_d^{20} was 1·4382. The corresponding literature values are 1°C⁽⁵⁾ and 1·4380.⁽⁶⁾

All of the other chemicals and solvents used were of analytical reagent grade.

The stock solutions of metals were prepared by weighing out sufficient $FeCl_3 \cdot 6H_2O$ and ammonium molybdate to give two litres each of a solution approximately 0·20 M in metal ion. The Fe(III) was 0·20 M in HCl and the ammonium molybdate 0·025 M in NaOH.

The cupferron solution was 6 per cent w/v. The reagent was kept cold when not in use.

The necessary solutions of hydrochloric acid were prepared by diluting known amounts of HCl to one litre and standardizing the resulting solutions against NaOH.

Salt solutions were prepared by dissolving weighted amounts of the appropriate chloride in one litre of water. The resulting solutions were analysed for both the cation and for chloride.

---

* This paper represents part of the work submitted by G. W. LATIMER, Jr. to the Graduate School of Princeton University in partial fulfillment of the requirements for the degree of Doctor of Philosophy.

† Present address: Pittsburgh Plate Glass Chemical Division, Corpus Christi, Texas.

‡ Present address: Department of Chemistry, Wake Forest.

⁽¹⁾ H. L. FRIEDMAN, *J. Amer. Chem. Soc.* **74**, 5 (1952).

⁽²⁾ M. MORI and R. TSUCHIYA, *Nippon Kagaku Zasshi* **77**, 1525 (1956).

⁽³⁾ A. G. GOBEL and A. G. MADDOCK, *J. Inorg. Nucl. Chem.* **7**, 94 (1958).

⁽⁴⁾ G. W. LATIMER and N. H. FURMAN, Unpublished work (1960).

⁽⁵⁾ *Lange's Handbook of Chemistry and Physics*, 8th ed., Handbook Publishers Inc., Sandusky, Ohio (1952).

⁽⁶⁾ V. V. KORSHAK and I. I. POKHOMOV, *J. Appl. Chem.* (*USSR*) **14**, 632 (1941).

2. *Apparatus*

The extractions were done in 125 ml separatory funnels possessing short stems carefully shaped to prevent holdup.

Spectra were taken on a Warren Spectracord using 1 cm quartz cuvettes.

Conductometric data were taken using a Serfass Model RCM15 conductance bridge.

3. *Preparation of the extraction curves*

Five ml of metal stock solution, 15 ml of hydrochloric acid of known strength, and 20 ml of ADN were shaken vigorously at room temperature (21–22°C) in 125 ml separatory funnels. Although equilibrium was reached in less than a minute, agitation was carried out for five; then the phases were permitted to separate. Each phase was analysed in its entirety; in all cases, the mass balance was at least 99·5 per cent of that added.

A similar procedure was used to study the extraction of hydrochloric acid by ADN except that 5 ml of water was substituted for the metal stock solution. In one set of experiments the ADN was titrated conductometrically with sodium hydroxide; in a duplicate set, the ADN was analysed for chloride. The hydrochloric acid content calculated from the two sets of analyses was within experimental error.

4. *Formula of the extractable species*

To define the empirical formula of the species extracted by the organic phase, four variables must be known (a) the number of moles of the metal ion present; (b) the number of moles of the chloride present; (c) the total number of moles of acid present; and (d) the number of moles of acid which distribute independently of the extractable complex.

Determination of the metal ion and of chloride ion is straightforward, but determination of acid in the presence of easily hydrolysed metals ions is not.

Traditionally, the acid present is titrated with standard base. Since some base will be consumed in precipitating a metal hydroxide rather than in titrating the acid present, the amount of base required to precipitate a stoicheiometric metallic hydroxide is deducted from the total litre. The amount of acid which distributes independently of the metal is determined in a separate set of experiments. The difference between these two values represents the acid associated with the metal complex.

Recently, methods which require no assumptions concerning the composition of a metallic hydroxide have been developed for the determination of acid in the presence of hydrolysable cations.(7–9) The method developed by DAVID and FURMAN involving conductometric titration of the acid with cupferron(9) was used for the determinations.

A known amount of metal ion was extracted from hydrochloric acid of such strength that the maximum amount of metal ion would be extracted (this HCl value was determined from the previously established extraction curves) by shaking with ADN. The phases were permitted to separate; the aqueous phase was withdrawn and discarded. The ADN was centrifuged and three 5·00 ml aliquots were taken. One aliquot was added to 150 ml of water and titrated conductometrically with 6 per cent cupferron solution. Of the two remaining 5 ml aliquots, one was analysed for chloride using a modified Volhard procedure, while the other was analysed for the metal ion. The amount of acid which distributes independently of the metal ion was found in a separate determination by conductometric titration with standard base.

5. *Salting effects*

To study the effect of different salts on the extraction of these metal ions, extractions were performed in which hydrochloric acid was replaced by an equivalent amount of a metal chloride-lithium, ammonium, sodium, or calcium chloride. Enough acid was present to prevent hydrolysis.

In all other respects the procedure described in section 2 was followed.

RESULTS AND DISCUSSION

1. *The nature of the extraction curves*

Both the basicity of an electron donor and the relative binding energy of its addition complexes decrease with increasing ionization potential.(10) While the ionization

---

(7) F. J. MILLER and P. F. THOMASON, *Analyt. Chem.* **31**, 1498 (1959).

(8) G. L. BOOMAN, *et al.*, *Analyt. Chem.* **30**, 284 (1958).

(9) J. C. DAVID, Thesis, Princeton University (1951).

(10) G. J. JANZ and S. S. DANYLUCK, *Chem. Revs.* **60**, 209 (1960).

potential of ADN has not been measured, the values for nitriles are high—acetonitrile being 11·96 eV[11]. Although the value for ADN should be lower than that for acetonitrile because of the increased inductive effects of the methylene groups as contrasted to the single methyl present in acetonitrile and because of the presence of two functional groups in the molecule, the value should not be comparable to that of diethyl ether (9·7–10·2 eV). Thus, under comparable conditions of acidity, ethers should be capable of extracting more of an ion-pair complex than ADN. That this is not the case is apparent from the extraction curves (Fig. 1 and 2): in the region 1-5 M HCl, ADN extracts significantly more Fe(III) than diethyl or diisopropyl ether and more Mo(VI) than diethyl ether from solutions of equivalent acidity.

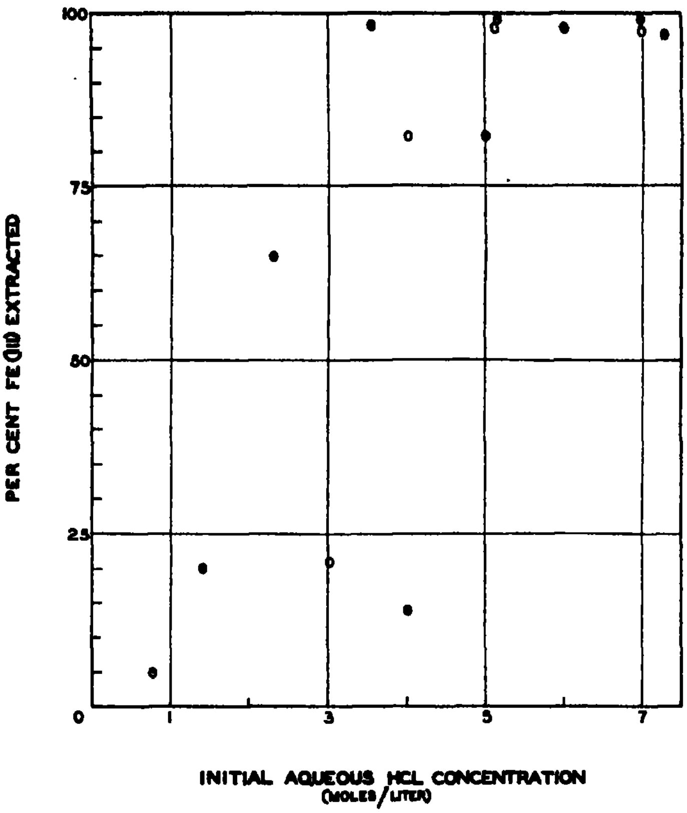

Fig. 1.—The extraction of iron from aqueous HCl.
○ with ADN
○ with diethyl ether[14]
● with diisopropyl ether.[14]

The ADN system shows no tendency to form a three phase system so characteristic of systems involving diisopropyl ether.[12–14] In this respect it behaves more like the analogous diethyl ether systems.

---

[11] G. J. Janz and S. S. Danyluck, *J. Amer. Chem. Soc.* **81**, 3846 (1959).

[12] G. H. Morrison and H. Freiser, *Solvent Extraction in Analytical Chemistry*, J. Wiley, New York (1957).

[13] A. H. Laurene, D. E. Campbell, S. E. Wilberly and H. M. Clark, *J. Phys. Chem.* **60**, 901 (1956).

[14] R. W. Dodson, G. J. Forney and E. H. Swift, *J. Amer. Chem. Soc.* **58**, 2573 (1936).

In other respects, however, the extraction curves for this system follow the classic pattern already established for many other systems: the extraction of the metal ion increases with increasing acid concentration to a maximum value; beyond this value the extraction decreases.

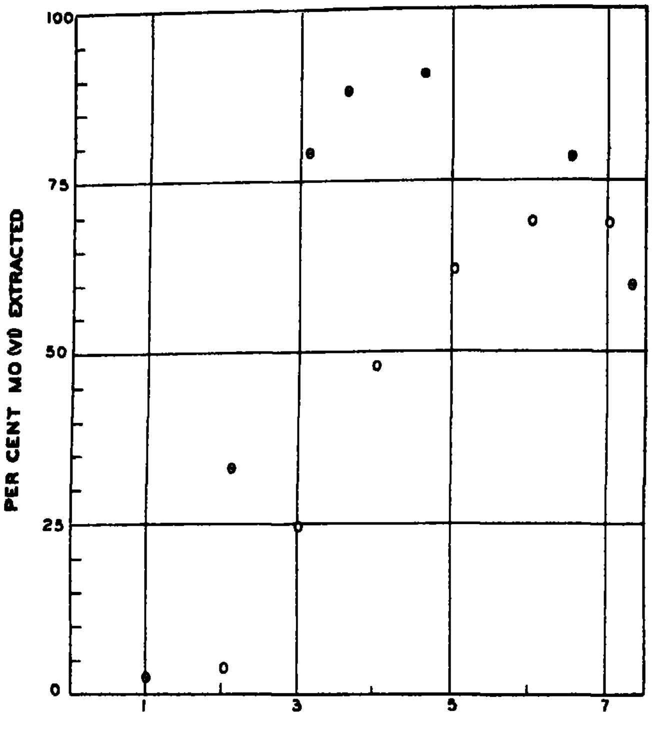

Fig. 2.—The extraction of Mo(VI) from aqueous HCl.
○ with ADN
○ with diethyl ether (calcd. from Reference 19).

Attempts have been made to reduce extraction behaviour to a set of mathematical formulae.(12,15,16) While reasonably accurate at low concentrations of acid, no-one has been capable of explaining the decrease in extraction which occurs above a certain HCl value. To account for this behaviour, the equations require the inclusion of terms which correspond physically to the formation in the aqueous phase of complexes greater than any which have been shown to exist.

Since repeated attempts to find complexes of this type have failed,(1,17) other physical processes not capable of direct mathematical treatment have been examined in an attempt to explain the behaviour of the curves. If the equilibrium HCl value is plotted as a function of the initial aqueous HCl concentration, the equilibrium value for many systems including diethyl and diisopropyl ether passes through a maximum

(15) H. Irving, F. J. C. Rossotti, R. J. P. Williams, *J. Chem. Soc.* 1906 (1955).
(16) R. E. Diamond, *J. Phys. Chem.* 61, 69 (1957).
(17) Y. Marcus, *J. Inorg. Nucl. Chem.* 12, 287 (1960).

describing a curve very similar to that of the metal ion (Fig. 3). These data suggest that the decrease in the concentration of the acid and of the chloride in the aqueous phase is one reason for the decrease in the extraction of the metal.(18,19) The equilibrium aqueous HCl values for the ADN system exhibit the same behaviour (Fig. 3). If the extraction curves for the ADN-HCl system and the ether-HCl systems are compared

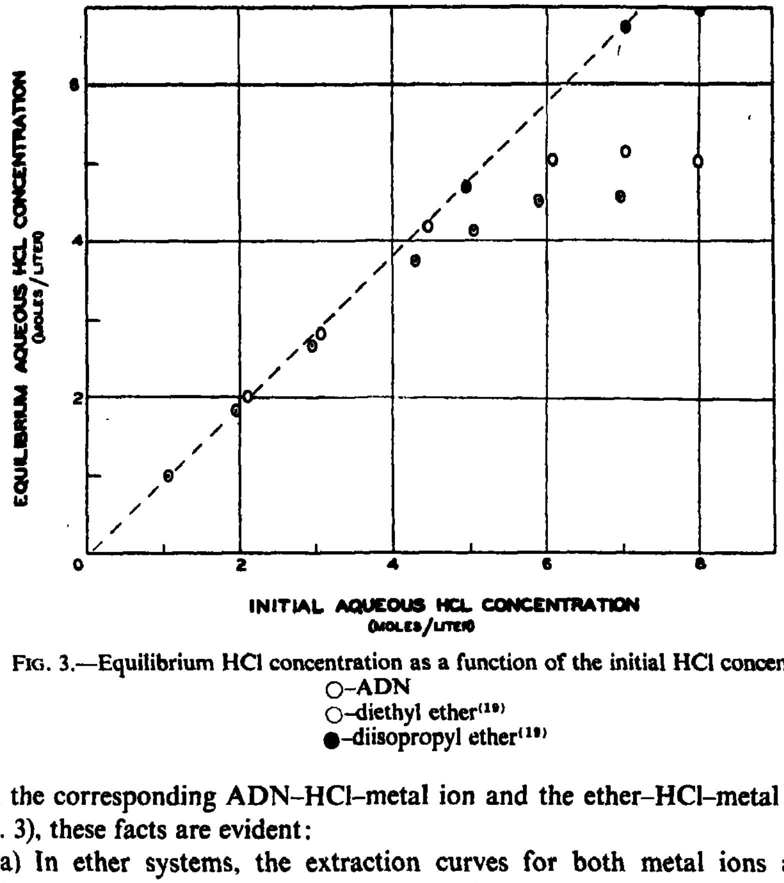

FIG. 3.—Equilibrium HCl concentration as a function of the initial HCl concentration.
○-ADN
○-diethyl ether(19)
●-diisopropyl ether(19)

with the corresponding ADN-HCl-metal ion and the ether-HCl-metal ion systems (Fig. 3), these facts are evident:

(a) In ether systems, the extraction curves for both metal ions and for the equilibrium aqueous HCl value pass through maxima at approximately the same concentration of HCl.

(b) In the ADN system the extraction curves for both metal ions reach their maximum values before the maximum equilibrium HCl value is reached; indeed, the amount of Mo(VI) extracted has passed through its maximum and decreased significantly.

(c) Although the maximum aqueous HCl concentration in the ADN system is lower than in the diethyl ether, the ADN is a significantly better system for the extraction of Mo(VI).

Similar studies made with V(V) show an effect opposite to that described in case (b). In this instance the extraction of vanadium continue to increase even though the maximum aqueous HCl concentration has been reached.(4,14)

All of these results are in accord with previous investigations which conclude that

(18) D. E. METZLER and R. J. MEYERS, *J. Amer. Chem. Soc.* **72**, 3774 (1950).
(19) I. NELIDOW and R. E. DIAMOND, *J. Phys. Chem.* **59**, 710 (1955).

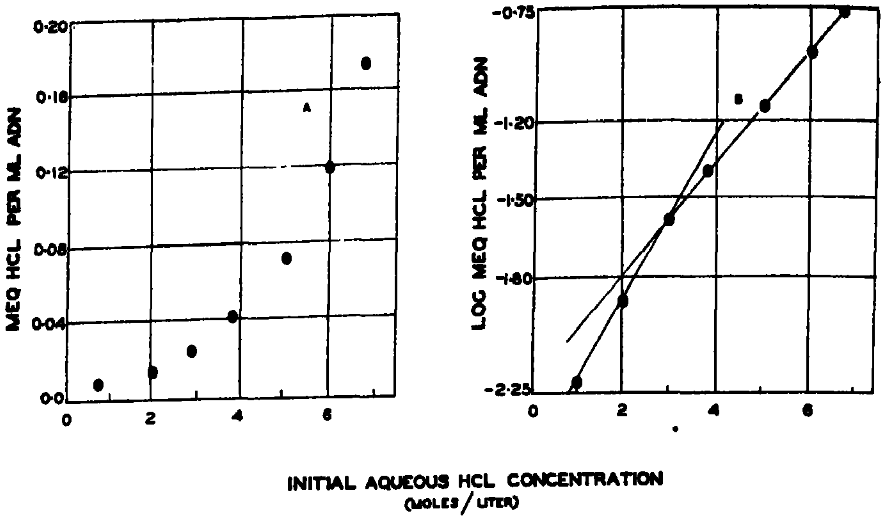

FIG. 4.—The extraction of HCl by ADN.

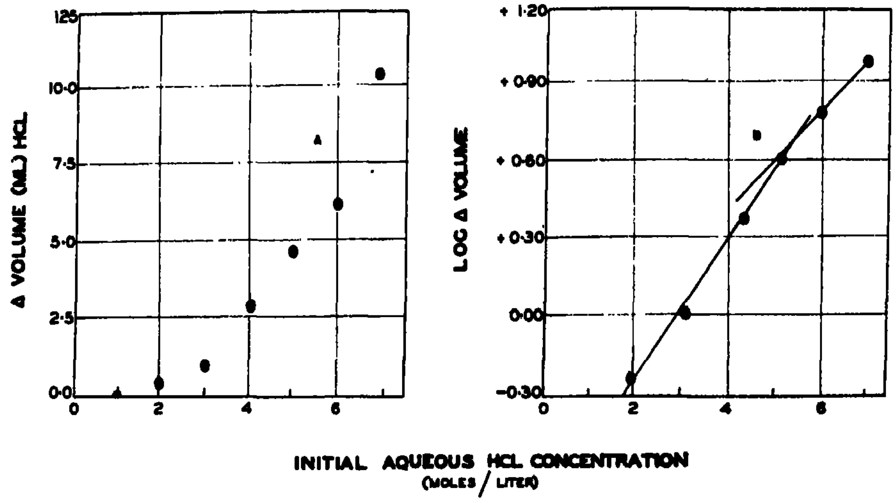

FIG. 5.—The volume of the aqueous HCl phase as a function of the initial HCl concentration.

there is no correlation between the maximum acid concentration attainable and its ability to extract metal complexes of the type HMX_4.(20)

2. *The extraction of hydrochloric acid by* ADN

When concentrated hydrochloric acid (>1 M) is shaken with ADN, the system becomes noticeably cooler although there is little change in the volume of the system.

The amount of HCl extracted by the ADN increases exponentially with the concentration of acid (Fig. 4a and b). An interesting corollary is that the volume solubility of ADN in aqueous HCl also increases exponentially (Fig. 5a and b). The

(20) H. IRVING and F. J. C. ROSSOTTI, *J. Chem. Soc.*, 1946 (1955).

system is miscible above 8·5 M HCl. The breaks in the slopes (Fig. 4b and 5b) appear to be real and not experimental error. An investigation is to be made of their significance.

There was some question whether the extremely acid conditions would induce hydrolysis of ADN to adipic acid. It was for this reason that the titrations of the ADN–HCl extracts which were used to establish the extraction curve in Fig. 4a were done conductometrically. In no case was there any indication that a weak acid was present. The close equivalence between the results for hydrogen ion and the chloride further substantiates this fact.

3. *Nature of the extracted species*

The formulae of the species extracted by ADN are given in Table 1. The empirical formula for the iron complex is in agreement with previously reported values;(1,12,21) that for Mo(VI) agrees with that found by ZHAROVSKII.(22)

TABLE 1.—ANALYSIS OF THE ADIPONITRILE EXTRACTS

System	(mmole)H^+	(mmole)Metal ion	(mmole)Chloride	Ratio H:Metal:Cl
Fe(III)–ADN	0·13	0·122	0·461	1·1:1·0:3·8
	0·10	0·123	0·462	0·82:1·0:3·6
	0·13	0·123	0·482	1·0:1·0:3·9
	0·09	0·120	0·460	0·75:1·0:3·8
Mo(VI)–ADN	0·10	0·077	0·229	1·3:1·0:3·0
	0·07	0·081	0·225	0·9:1·0:2·8
	0·09	0·082	0·222	1·1:1·0:2·7
	0·07	0·083	0·227	0·9:1·0:2·8

Since the available evidence indicates that $HFeCl_4$ is polymerized above 10^{-3},(23) spectra of ADN systems containing Fe(III) concentrations above and below this value were taken.

Although the solutions were diluted to approximately the same final concentration (10^{-4} M), the spectra of extracts from systems in which the initial aqueous iron concentration was less than 10^{-3} M yielded absorption curves similar to that obtained under comparable conditions in ether solutions(24) (Fig. 6a) while the spectra in which the initial iron concentrations were greater than 10^{-3} M were considerably different (Fig. 6bcd). The latter solutions yielded the typical $HFeCl_4$ spectrum only after some time (Fig. 6c) suggesting that this complex was not merely an ion-pair cluster, but a true polymer and that the rate of depolymerization $(HFeCl_4)_n \rightarrow nHFeCl_4$ was relatively slow. Depolymerization is accelerated by acid (Fig. 6d).

Despite agreement between our results and those obtained by ZHAROVSKII for the formula of the extractable molybdenum species, the exceedingly complex nature of acidified molybdenum solutions and the difficulties in analysis of the solution make generalization precarious. The chloride value for iron has been known to vary from 3·5 to 5·4 depending upon the concentration of acid in the system;(21) there is no reason to believe that this could not be the case with Mo(VI). This simple fact may explain the discrepancy between these results and those of DIAMOND.

(21) B. V. NEKRAVSOV and V. V. OVSYANKINA, *J. Gen. Chem.* (*USSR*) **11**, 573 (1941).

(22) F. G. ZHAROVSKII, *Zh. Neorg. Khim.* **2**, 623 (1957). *Chem. Abstr.* **51**, 17345g.

(23) R. J. MEYERS, D. E. METZLER and E. H. SWIFT, *J. Amer. Chem. Soc.* **72**, 3767 (1955).

(24) D. E. METZLER and MEYERS, *J. Amer. Chem. Soc.* **72**, 3776 (1955).

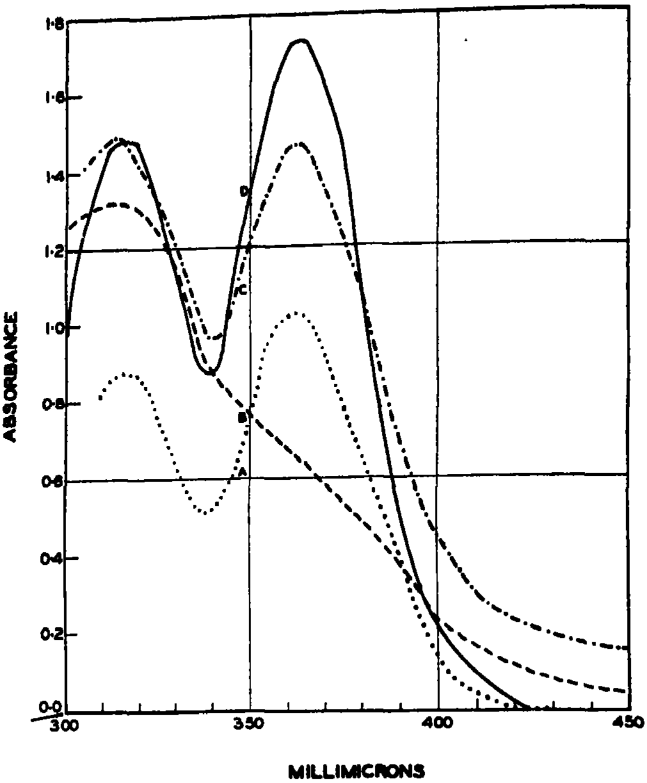

FIG. 6.—Spectra of Fe(III)–ADN solutions.

a. Spectrum of ADN extract 1·5 × 10^{-4} M in Fe(III) (Aqueous solution extracted was 1·9 × 10^{-4} M in Fe(III) and 6·0 M in HCl)

b. Spectrum of ADN extract 1·9 × 10^{-4} M in Fe(III) (Aqueous solution extracted was 1·9 × 10^{-2} M in Fe(III) and 6·0 M in HCl. This ADN extract was diluted 100 fold with ADN)

c. Spectrum of ADN extract (b) after three weeks

d. Spectrum of ADN extract (b) after shaking with 6·0 M HCl.

This formula is not without other verification: a compound having the formula $MoO_2Cl_3 \cdot HCl$ has been prepared as well as salts of the type $KMoO_2Cl_3 \cdot H_2O$.(25,26)

4. *The influence of salts on the* ADN–HCl-*metal ion system*

The salt effects exhibited in these systems (Table 2) differ from those which would have been predicted according to the rule enunciated by MORRISON that at equivalent anion concentrations the cation with the greatest valence should show the largest effect.(27)

For the Fe(III) system the amount of Fe extracted decreases going from LiCl to NH_4Cl. This decrease in extraction is paralleled by a decrease in the order of hydration.(28) The near equivalence of H_3O^+ and Li^+ is not particularly surprising considering that their aqueous activities are very nearly alike.(17,24) The position of

---

(25) J. W. MELLOR, *A Comprehensive Treatise on Inorganic and Theoretical Chemistry*, Vol. 9, pp. 632–633. Longmans, Green, New York (1931).

(26) N. V. SIDGEWICK, *The Chemical Elements and Their Compounds*, Vol. 1 and 2. Clarendon, Oxford (1950).

(27) G. MORRISON, *Analyt. Chem.* **22**, 1388 (1950).

(28) R. M. DIAMOND, *J. Phys. Chem.* **63**, 659 (1959).

TABLE 2.—THE EFFECT OF CHLORIDE SALTS ON THE EXTRACTION OF METAL IONS BY ADIPONITRILE

Salt	Per cent Extracted Fe(III)-ADN*	 Mo(VI)-ADN†
HCl	99‡	90‡
LiCl	96	95
NaCl	88	97
NH_4Cl	75	79
$CaCl_2$	62	91

* Solution 3·89 M in chloride and 0·05 M in H^+.
† Solution 4·90 M in chloride and 1·90 M in H^+.
‡ Values calculated from the extraction curves (Figs. 1 and 2).

the Ca^{2+} in order of effectiveness is the more interesting particularly since the hydration numbers of Ca^{2+} and Li^+ are similar and somewhat greater than Na^+.(30) The fact that the distribution of the Fe(III) complex is not as dependent upon acid concentration as upon the chloride may indicate that $(HFeCl_4)n$ is not a strong acid in every extraction system.

The Mo(VI)-ADN system presents a more complicated picture. The apparent difference between the effectiveness of LiCl and NaCl is within the experimental error, but NH_4Cl is obviously an inferior agent for salting out the Mo(VI). The real problem is why HCl is inferior to NaCl, LiCl, and, possibly, $CaCl_2$. Although the addition of salt decreases the solubility of ADN in the aqueous phase, the solubility of the two phases is so slight at 1·90 M HCl that the equilibrium HCl value is not substantially different from the initial value (Fig. 3). Two other explanations are more probable:

(1) Decreasing the acid strength by substituting a salt for the acid frees solvent molecules which have co-ordinated with hydrogen ion for co-ordination with the extracted species.(28) This would increase the extraction of Mo(VI).

(2) $HMoO_2Cl_3$ is probably a weak acid; therefore, the distribution of the complex is not so dependent upon the acid concentration. This view is supported by literature describing its structure as $MoO(OH)Cl_3$.(25,26)

The nature of these salting effects is not yet understood despite some attempts at suggesting generally comprehensive theories.(16,28) DIAMOND suggests that strong acids extract better than their salts when oxygenated solvents are being considered. From the evidence offered, a more comprehensive statement might be that any acidic species either strong or weak extracts better than its corresponding salt when Lewis base solvents are used. Salts effect the extraction of a complex far more by the addition of an ion in common with the extractable species, by alteration of the structure of the aqueous phase,(17) and by the amount of water which they make available to the distributing species than by any intrinsic tendency to form a different extractable complex.

Acknowledgements—The financial aid (as a McKay Fellow and as an NSF Co-operative Fellow) received by G. W. L. is gratefully acknowledged.

(28) B. CHU and R. M. DIAMOND, *J. Phys. Chem.* **63**, 2021 (1959).
(30) H. REMY, *Treatise on Inorganic Chemistry*, Vol. 1. Elsevier, New York (1955).

J. Inorg. Nucl. Chem., 1962, Vol. 24, pp. 739 to 748. Pergamon Press Ltd. Printed in Northern Ireland

THE TEMPERATURE RANGE OF LIQUID LEAD AND SILVER AND AN ESTIMATE OF THEIR CRITICAL CONSTANTS*

A. V. GROSSE and A. D. KIRSHENBAUM
Research Institute of Temple University, Philadelphia, Pa.

(*Received* 13 *October* 1961)

Abstract—The temperature range diagrams of liquid Pb and Ag are constructed from experimental density data, from their melting points to their normal boiling points, the law of rectilinear diameter and the theorem of corresponding states. From these diagrams or the equations on which they are based, the critical constants are estimated as follows:

	For Pb	For Ag
T_c (°K)	5400	7500
D_c (g/cm^3)	2·2	1·85
V_c (cm^3/g atom)	94	58·3
P_c (atm)	850	(5000)

Liquid densities below the critical range can be calculated with much greater reliability and are as follows:

T (°K)	Pb	Ag
2024	8·801	—
2500	8·167	8·197
3000	7·488	7·741
3500	6·786	7·276
4000	6·061	6·795
4500	5·313	6·295
5000	—	5·771
5500	—	5·223
6000	—	4·652
6500	—	4·060

IT was shown recently$^{(1,2)}$ that the critical constants of metals could be estimated consistently by two independent semi-empirical methods.

Of all the known eighty metals, mercury is the only one whose critical constants have been determined experimentally

$$(T_c = 1733°\mathrm{K};\ P_c = 1587 \pm 50\ \mathrm{atm},\ D_c = 4{\cdot}70 \pm 0{\cdot}20\ \mathrm{g/cm^3}).$$

It was demonstrated that mercury, like all other thermally stable liquids, follows the law of Cailletet and Mathias or the law of rectilinear diameter.$^{(1,2)}$ The average density of liquid mercury and its saturated vapour, i.e. $\frac{1}{2}(D_l + D_v)$, is a straight line function of temperature. This is the basis of the *first method*. A liquid range diagram of the metal obtained by plotting or calculating the *experimental liquid density* and

---

* This research was supported in part by Grant 15540 of the National Science Foundation.

(1) A. V. GROSSE, *J. Inorg. Nucl. Chem.* **22**, 23 (1961).

(2) A. V. GROSSE, "The Liquid Range of Metals and Some of Their Physical Properties at High Temperatures," Research Institute of Temple University, Sept. 5, 1960.

the ideal vapour density vs. temperature. The maximum possible critical temperature (and the minimum critical density) is the point where the ideal vapour density crosses the rectilinear diameter. Actually, the real vapour density is always greater than the ideal, so that the real critical temperature is lower than the one obtained in the above manner. The lower limit of the critical temperature (and conversely the maximum critical density) is set by the fact that the real saturated vapour density has to approach the liquid density near T_c.

The *second method* is based on the theorem of corresponding states. The theorem requires that at corresponding or reduced temperatures, i.e. $T_{red} = T/T_c$, liquid metals have the same entropy of vaporization,

$$\Delta S_{vap} = \Delta H_{vap}/T$$

So far the entropy vs. T function has been established experimentally only for one metal—mercury.(1,2) Since the heats of vaporization of nearly all metals are known at their normal boiling points, or can be reliably extrapolated,(3) one can estimate from the mercury curve and the ΔS value at the temperature T the reduced temperature, and thus the critical temperature, of any metal. Critical temperatures of about 15 metals, together with their ΔS_{vap}, and other data were given before;(1,2) the critical temperatures range from 1733°K for mercury to about 23,000°K for tungsten.

In two recent experimental investigations the liquid densities of lead(4) and silver(5) were determined over a much wider temperature range than heretofore, namely, from their melting points (600·6° and 1234·0°K, respectively) up to their normal boiling points (2024° and 2450°K, respectively). The densities are straight line functions of temperature and are as follows:

for Pb:

$$D_T = 10{\cdot}678\text{-}13{\cdot}174 \times 10^{-4}(T\text{-}600{\cdot}6^\circ),$$

and for Ag:

$$D_T = 9{\cdot}346\text{-}9{\cdot}067 \times 10^{-4}(T\text{-}1234{\cdot}0^\circ),$$

where T is in °K and D in g/cm^3.

Values of the density of liquid lead and silver at their melting and normal boiling points as well as at some set temperatures are given in Table 1.

TABLE 1.—EXPERIMENTAL DENSITIES OF LIQUID LEAD(4) AND SILVER(5) IN G/CM^3

	Pb	Ag
M.P. (°K)	600·6	1234·0
D at M.P. (g/cm^3)	10·678	9·346 ± 0·009
Normal b.p. (°K)	2024	2450
D at normal b.p. (g/cm^3)	8·803 ± 0·009	8·244 ± 0·009
D at 1000°K	10·152	(solid)
1500°K	9·493	9·105
2000°K	8·834	8·652
2500°K	(see Table 2)	8·198

---

(3) D. R. STULL and G. C. SINKE, *Thermodynamic Properties of the Elements*, No. 18 of the *Advances in Chemistry* Series, American Chemical Society, Washington, D.C. (1956).

(4) A. D. KIRSHENBAUM, J. A. CAHILL and A. V. GROSSE, *J. Inorg. Nucl. Chem.* **22**, 33 (1961).

(5) A. D. KIRSHENBAUM, J. A. CAHILL and A. V. GROSSE, *J. Inorg. Nucl. Chem.* In press (1962).

Construction of the temperature range diagrams of liquid lead and silver

The whole temperature range of a liquid metal, i.e., the spread from the melting point to the critical point and an estimate of the critical data are of theoretical and practical importance.

One can now proceed with the construction of the liquid range diagrams of lead and silver. They are shown in Figs. 1 and 2.

From the vapour pressure data of both metals we can calculate the ideal gas density of their saturated vapours. It was demonstrated many years ago by WARTENBERG[6] that the vapours of Pb and Ag are monatomic. The density was determined directly in an iridium flask at a temperature close to the boiling point. In the case of mercury[1,2] it was shown that the ideal gas density equals the experimental saturated vapour density up to ≃85 per cent of the critical point. It is only above a reduced temperature of ≃0·85 that the actual saturated vapour density increases rapidly and of course equals the liquid density at the critical point.

As one will see later the ideal gas density at the normal boiling points (see Table 2) is still so small that it can be neglected. Thus, the rectilinear diameter density:

$$D_{0''} = \tfrac{1}{2} D_{\text{liq.}}$$

and the equation of the rectilinear diameter is, for Pb:

$$D^{\text{Pb}}_{0''} = 5{\cdot}339\text{-}6{\cdot}587 \times 10^{-4}(T\text{-}600{\cdot}6^\circ)$$

or

$$= 5{\cdot}734\text{-}6{\cdot}587 \times 10^{-4} \cdot T$$

and for Ag:

$$D^{\text{Ag}}_{0''} = 4{\cdot}673\text{-}4{\cdot}534 \times 10^{-4}(T\text{-}1234{\cdot}0^\circ)$$

or

$$= 5{\cdot}232\text{-}4{\cdot}534 \times 10^{-4} T,$$

where again D is in g/cm³ and T in °K.

The rectilinear diameter is extrapolated in Figs. 1 and 2 to the critical region. The probable error is indicated by a dotted line "error cone."

Estimate of the critical temperatures of lead and silver from the theorem of corresponding states

The pertinent data are taken from reference 3. The entropy of vaporization curve for mercury is given in references 1 and 2, and permits one to obtain the reduced temperature of Pb and Ag at their normal boiling points.

	Pb	Ag
Heat of vaporization at normal b.p. (cal/g atom)	42,880	60,960
Normal b.p. (°K)	2024	2450
Entropy of vaporization at normal b.p. (cal g atom^{-1} °K^{-1})	21·2	24·9
Reduced temperature ($T_{\text{red.}}$)	0·375	0·327
Critical temperature, T_c (°K)	5400	7500

These critical temperatures are estimated to be accurate to ±10 per cent. This is indicated in Figs. 1 and 2 by the shaded area in the critical region. We will see later that these critical temperatures are bracketed on both the high and low

---

[6] H. V. WARTENBERG, *Z. Anorg. Chem.* **56**, 320–336 (1908).

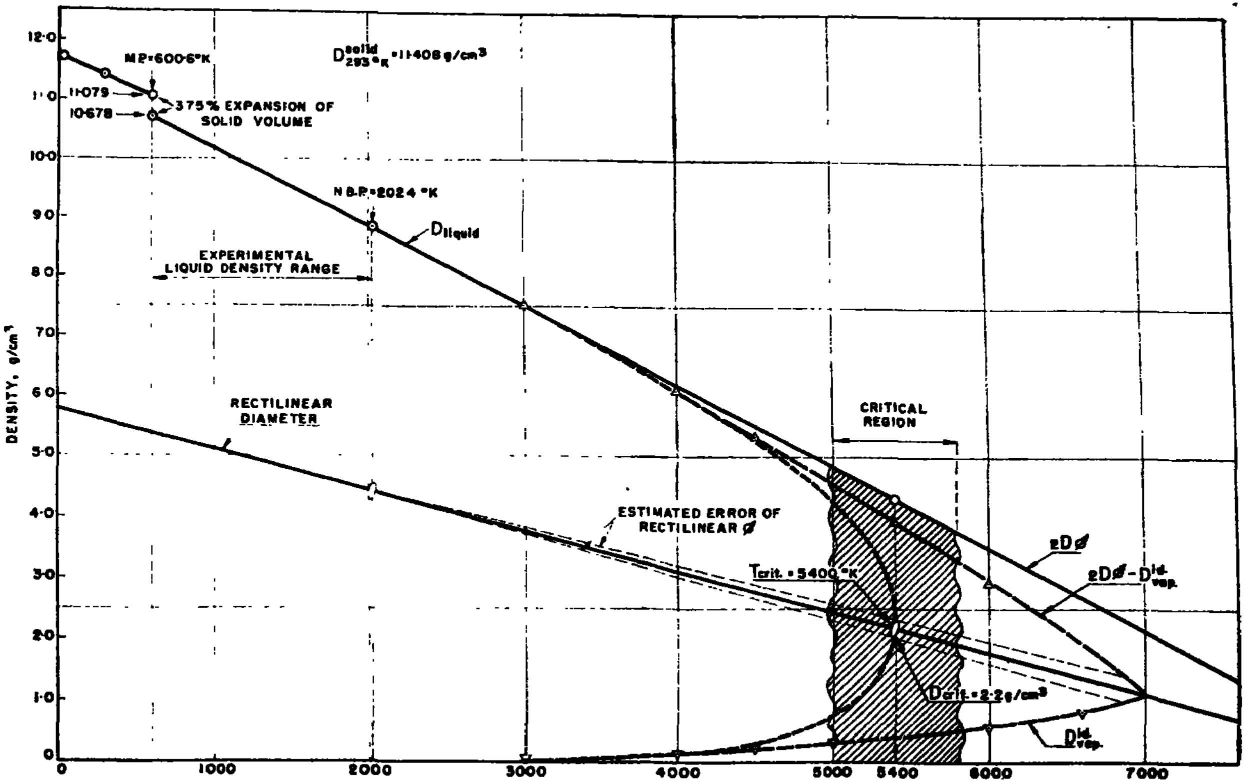

FIG. 1.—Liquid temperature range diagram of lead.

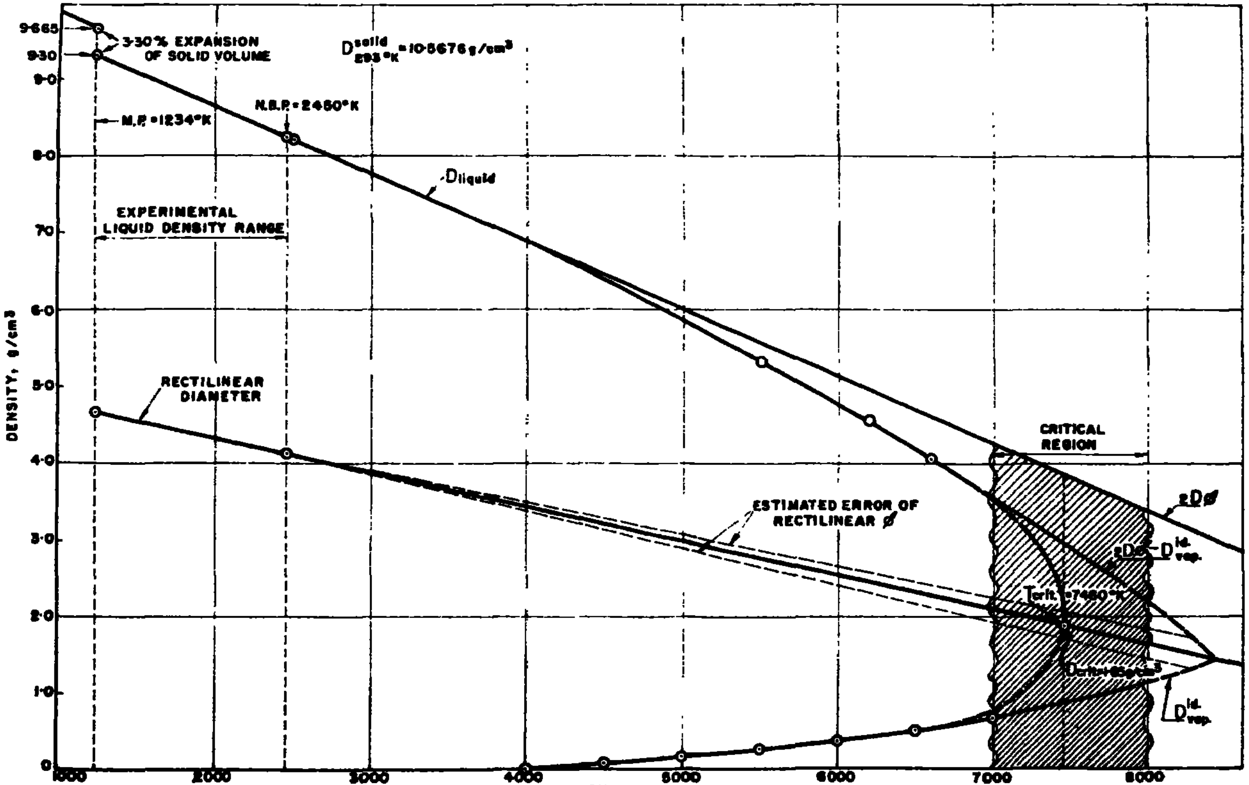

FIG. 2.—Liquid temperature range diagram of silver.

temperature sides by the considerations from the law of rectilinear diameter and the saturated vapour densities of the two metals.

The liquid densities beyond our experimental determinations can be calculated from the law of rectilinear diameter if the saturated vapour densities are known. As mentioned previously, the real densities should be equal to the ideal densities up to about 85 per cent of the critical temperature. The ideal densities can be easily obtained from the vapour pressure data of the two metals.

Saturated vapour densities of Pb *and* Ag

The vapour pressures used in these calculations were the most recent compilation of thermodynamic properties of the elements, tabulated by STULL and SINKE.(3) We have reviewed the original literature, however, particularly in view of our interest in vapour-pressure at atmospheric pressure or above.

The vapour-pressure of lead was determined over fifty years ago by GREENWOOD(7,8) up to 12 atm, far beyond the range of any other experimenters. KELLEY, a very careful worker, failed to notice, in referring to GREENWOOD'S work, in his well known compilation(9) of vapour-pressure data, that the latter had a "self-correcting" temperature scale. He calibrated his Wanner optical pyrometer using pure Pt, Rh and Ir, "specially prepared of a high degree of purity by Messrs. Johnson, Matthey & Co.," and used Holborn & Henning's 1905 black body values of their melting points, i.e., Pt = 1545°C (1818°K), Rh = 1650°C (1923°K), and Ir = 2000°C (= 2273°K). We know now, 55 years later, that the *correct* melting points are: Pt = 2043°K, Rh = 2239°K and Ir = 2727°K. GREENWOOD'S three melting points lie on a straight line; using their true melting points GREENWOOD'S temperature scale can be corrected in a straightforward manner. GREENWOOD'S true temperature, T_{true} in °K.

$$T_{\text{true}} = 1{\cdot}502 \cdot T_{\text{Greenwood}} - 682^\circ,$$

where $T_{\text{Greenwood}}$ are the original temperatures given by GREENWOOD *in* °K.

STULL and SINKE base their selection on KELLEY'S review, who in turn picked Harteck's low temperature data as being the most reliable.

In Fig. 3 we compare STULL and SINKE'S straight line with GREENWOOD'S corrected data which extend to ≃2900 K, and also of BAUR and BRUNNER,(10) RODEBUSH and DIXON,(11) and LEITGEBEL.(12) It can be readily seen that all of the experimental measurements are now in close agreement, except GREENWOOD'S values at 6 and 12 atm. As mentioned by him(8) observations of the boiling lead surface becomes increasingly difficult at higher pressures. From 1·00 atm at 2024°K down to a vapour-pressure of $5{\cdot}6 \times 10^{-8}$ atm at 800°K (measured by EGERTON(13) (800–1000°K)), i.e., over a hundred million-fold pressure range, the log of vapour-pressure is a straight-line function of $1/T$°K. The same observation was made in the case of mercury(1,2) up to the critical point. We are thus justified in making the assumption that the straight line log P vs. $1/T$ relationship can be extended to the critical point also in the case of Pb and Ag.

The data for silver do not extend beyond 1 atm. The only data available at one atmosphere are old measurements of GREENWOOD (corrected), RUFF(14) and

(7) H. C. GREENWOOD, *Proc. Roy. Soc.* **82** A, 396–408 (1909).

(8) H. C. GREENWOOD, *Proc. Roy. Soc.* **83** A, 483–491, particularly p. 488 (1910).

(9) K. K. KELLEY, *U.S. Bureau of Mines, Bull.* 383, 59–60 (1935).

(10) E. BAUR and R. BRUNNER, *Helv. Chim. Acta* **17**, 958 (1934).

(11) W. H. RODEBUSH and A. L. DIXON, *J. Amer. Chem. Soc.* **47**, 1036 (1925).

(12) W. LEITGEBEL, *Z. Anorg. Chem.* **202**, 305 (1931).

(13) A. C. G. EGERTON, *Proc. Roy. Soc.* A **103**, 469 (1923).

(14) O. RUFF and B. BERGDAHL, *Z. Anorg. Chem.* **106**, 91 (1919).

WARTENBERG.(6) They show appreciable scatter around 2400°K, and additional experimental work in this pressure range and above is recommended.

STULL and SINKE's vapour-pressure data lead to the following expressions, for Pb:

$$\log_{10} P_{\mathrm{atm}} = -9{,}596/T + 4{\cdot}74043 \ (T \text{ in } {}^{\circ}\mathrm{K})$$

or in exponential form: $P_{\mathrm{atm}} = 5{\cdot}5009 \times 10^4 . \exp(-22{,}100/T)$, and for Ag:

$$\log_{10} P_{\mathrm{atm}} = -13{,}388/T + 5{\cdot}46223 \ (T \text{ in } {}^{\circ}\mathrm{K})$$

or in exponential form: $P_{\mathrm{atm}} = 2{\cdot}8989 \times 10^5 . \exp(-30{,}827/T)$

Since the density of the ideal saturated vapour, D_{vap}, $= A/V_A$, where A and V_A are atomic weight and volume respectively, it follows, from the ideal gas laws, that:

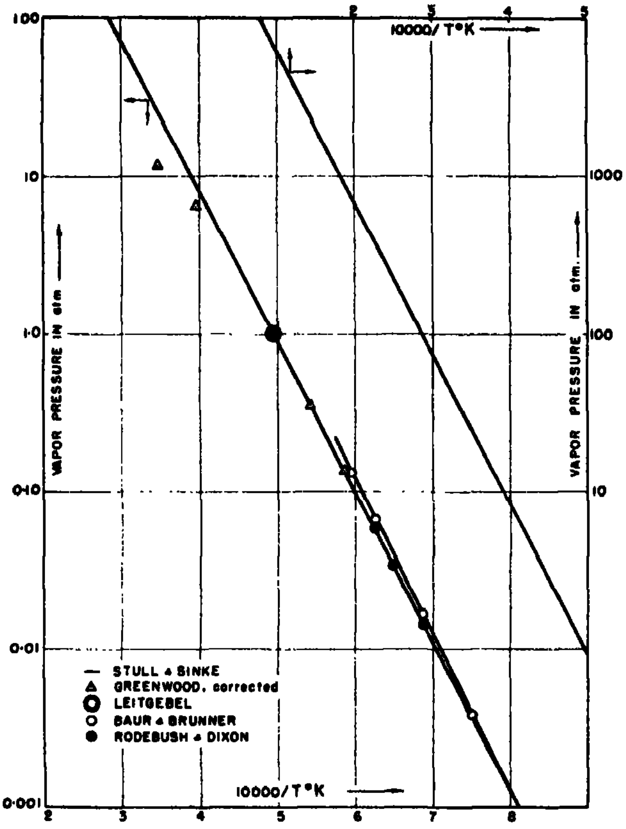

FIG. 3.—Vapour-pressure of lead.

$$D_{\mathrm{vap}} = A . P/R . T$$

thus, D_{vap}, for Pb $= 1{\cdot}38920/T \times 10^5 . \exp(-22{,}100/T)$
and for Ag $= 3{\cdot}8145/T \times 10^5 . \exp(-30{,}827/T)$

The values so obtained for lead and silver are tabulated in Table 2.

TABLE 2.—$D^{\text{id.}}_{\text{vap}}$ IN G/CM³ CALCULATED FROM VAPOUR-PRESSURE EQUATIONS AND IDEAL GAS LAWS

T (°K)	Pb		Ag	
	D (g/cm³)	P (Atm)	D (g/cm³)	P (Atm)
2024	0·00124	1·00	—	—
2500	0·00805	7·97	0·000681	1·28
3000	0·0292	34·7	0·004340	10·00
3500	0·0722	100·1	0·01629	43·4
4000	0·1381	219	0·04286	130·0
4500	0·2276	406	0·08967	307
5000	0·3344	662	0·1601	610
5500	—	—	0·2549	1067
6000	—	—	0·3730	1700
6500	—	—	0·5111	2527
7000	—	—	0·6658	3500

Calculations of the liquid densities of Pb *and* Ag *above their normal boiling point*

From the law of rectilinear diameter it follows that:

$$D_{\text{liq.}} = 2D_{\varnothing}' - D^{\text{id.}}_{\text{vap.}}$$

up to about $T_{\text{red.}} = 0{\cdot}85$, i.e., 4500°K for Pb and 6300°K for Ag. Above these temperatures, as was shown in the case of mercury,(1,2) the *real* saturated vapour density begins to digress appreciably from the ideal density. This can be readily seen from the anticipated liquid and gas densities in the critical and near critical regions of Figs. 1 and 2.

Up to $T_{\text{red.}} = 0{\cdot}85$ and based on the above general equation, the specific and exact equations for the densities of Pb and Ag are respectively:

$D^{T}_{\text{liq.}}$ of Pb, in g/cm³ =

$$11{\cdot}4692 - 13{\cdot}174 \times 10^{-4}T - \frac{1{\cdot}3892}{T} \times 10^{5}\,.\exp(-22{,}100/T)$$

and for Ag =

$$10{\cdot}465 - 9{\cdot}067 \times 10^{-4}T - \frac{3{\cdot}8145}{T} \times 10^{5}\,.\exp(-30{,}827/T)$$

where T is in °K.

In the classical work on the densities of liquids it has been the custom to express the liquid density in power series in T (see for example International Critical Tables, Volumes 1, 2 and 3). Using the method of least squares the following expressions have been obtained for $D_{\text{liq.}}$ of Pb and Ag:

$$D_{\text{liq.}} \text{ of Pb (g/cm}^3) = 11{\cdot}3039 - 1{\cdot}1576 \times 10^{-3}T - 3{\cdot}847 \times 10^{-8}T^2$$

and

$$D_{\text{liq.}} \text{ of Ag (g/cm}^3) = 10{\cdot}1667 - 6{\cdot}9155 \times 10^{-4}T - 3{\cdot}7996 \times 10^{-8}T^2 \;(T \text{ in °K})$$

The calculated liquid densities up to $T_{\text{red.}} = 0{\cdot}85$, using the exact or exponential equations given above, are shown in Table 3 and reproduced in Figs. 1 and 2.

The calculated *ideal* liquid and vapour densities cross the rectilinear diameter at a point which gives a maximum limit of the critical temperature (7000°K for Pb and 8500°K for Ag). The lower limit of critical temperature is a range where the vapour density is about 20–25 per cent of the liquid density, i.e., about 5000°K for Pb and

TABLE 3.—$D_{liq.}$ IN G/CM³ CALCULATED FROM THE RECTILINEAR DIAMETER AND IDEAL GAS DENSITY (SEE TABLE 2), *i.e.* $D_{liq.} = 2D_{\varnothing}' - D^{id.}_{vap.}$

T (°K)	Pb		Ag	
	$D_{liq.}$ (g/cm³)	Estimate of probable error (g/cm³)	$D_{liq.}$ (g/cm³)	Estimate of probable error (g/cm³)
2500	8·17	±0·02	8·20	±0·01
3000	7·49	±0·03	7·74	±0·02
3500	6·79	±0·04	7·28	±0·02
4000	6·06	±0·06	6·80	±0·03
4500	5·31	±0·1	6·30	±0·05
5000	—	—	5·77	±0·06
6000	—	—	4·65	±0·08
6500	—	—	4·06	±0·09
7000	—	—	3·4	±0·1

7000°K for Ag. The errors rapidly increase in the critical range, which is represented by the shaded area in Figs. 1 and 2. This is due both to the inaccuracy of T_c, assumed to be about ±10 per cent, and our experimental error in the rectilinear diameter. We estimate the critical constants of Pb and Ag to be as follows:

	Pb	Ag
T_c (°K)	5400 ± 10%	7500 ± 10%
D_c (g/cm³)	2·2 ± 0·3	1·85 ± 0·3
V_c (cm³/g atom)	$94\begin{pmatrix}+15\\-10\end{pmatrix}$	58·3 (±10)
P_c (atm)	$850\begin{pmatrix}+450\\-250\end{pmatrix}$	5000 (±560)

In order to pin down the critical data further it would be particularly desirable to extend liquid density determinations of lead and silver to about 3500°K (vapour-pressure ≃100 atm for Pb and ≃40 atm for Ag), and extend entropy of vaporization data similarly to those of sodium (see Fig. 2 of reference 2). It will be many years before lead or silver will be observed under critical conditions experimentally.

It is of interest to compare our semiempirical estimates with theory. The theory of liquids, in contrast to the solid and gaseous state is the least developed. Recently EYRING and his associates(15) have calculated some properties of liquid metals, including Hg and Pb, by EYRING's method of significant structures. In general the theory uses two adjustable parameters: n and a to obtain agreement with experimental data. The advantage of the theory is that various properties, such as liquid density, vapour pressure, viscosity, self-diffusion and others are developed from a consistent viewpoint.

A comparison of our results and the experimental data for Hg with those of EYRING's theory are presented in Table 4. Comments on the comparison are as follows:

1. *Critical density.* In the case of Hg, EYRING's value (=3·15) is lower than the experiment, in the case of Pb (=3·04) higher than our estimate.* In either case the

---

* EYRING's calc. *D*-value for Pb at the normal b.p. = 9·59, whereas our experimental density = 8·803.

(15) C. C. CARLSON, H. EYRING and T. REE, *Proc. Nat. Acad. Sci.* 46, 649–659 (1960); see there for earlier literature.

theoretical values seem to be outside the experimental error (see Fig. 1 in citation 1 and Fig. 1 of this paper) of the rectilinear diameter.

TABLE 4.—COMPARISON OF SEMIEMPIRICAL DATA WITH THEORETICAL CALCULATIONS

	Experimental for Hg (see reference 1 and 2) or this paper for Pb and Ag	EYRING'S theoretical calculations[15]	
Hg Parameter n		11	
T_c (°K)	1733 ± 50	1552	
V_c (cm³/g atom)	42·7 ± 3·0	63·7	
D_c (g/cm³)	4·70 ± 0·20	3·15	
P_c (atm)	1587 ± 50	610	
Pb Parameter n	—	11	6
T_c (°K)	5400 + 540	8390	6266
V_c (cm³/g atom)	$94\begin{pmatrix}+15\\-10\end{pmatrix}$	68·2	68·3
D_c (g/cm³)	2·2 ± 0·3	3·04	3·04
P_c (atm)	$850\begin{pmatrix}+450\\-250\end{pmatrix}$	3500	2530
Ag			
T_c (°K)	7500 (±750)		
V_c (cm³/g atom)	58·3 (±10)	No data	
D_c (g/cm³)	1·85 (±0·3)		
P_c (atm)	5000 (±560)		

2. *Critical temperature.* We believe our value for Pb to be closer to the true value of Pb. The theoretical value with $n = 11$ is definitely far outside the maximum shown in Fig. 1; the value with $n = 6$ is closer to our estimate.

3. *Critical pressure.* P_c is the most doubtful of the critical constants. The theoretical values are much lower in the case of Hg and by approximately the same factor higher in the case of Pb.

In comparing the two methods it should be kept in mind that in the case of Pb both represent extrapolations of 3000°K or more beyond the present experimental range. Obviously both methods should be improved.

The critical scientist should remember, however, that in this case we are in a realm of temperatures at which *all* of the few million inorganic and organic compounds cease to exist and that only a few metals exist as liquids, since they are elementary and monatomic substances. The only thermal reaction possible is ionization. The present view on solid and liquid metals is that at room temperature they are already ions surrounded by a sea of electrons. The amount of ionization in the saturated metal vapour can be accurately calculated from the Saha equation and their well known ionization potentials; for metals like Ta and W, even at 20,000°K, the ionization is only a few per cent, due primarily to the high saturation vapour-pressures.

Acknowledgement—Acknowledgement is due to P. J. MCGONIGAL for a number of density equation calculations.

J. Inorg. Nucl. Chem., 1962, Vol. 24, pp. 749 to 753. Pergamon Press Ltd. Printed in England

NEUTRON CAPTURE CROSS-SECTION DATA FOR ^{152}Sm

M. J. Cabell
Chemistry Division, A.E.R.E., Harwell, Berks.

(*Received* 30 *October* 1961)

Abstract—An activation method has been used for the determination of the neutron capture cross-sections of ^{152}Sm for reactor neutrons ($\hat{\sigma}$) and for 2200 m/sec neutrons (σ_0), and for the determination of Σ', its above $1/v$ resonance capture integral. The results obtained i.e. $\hat{\sigma} = 320 \pm 13$ barns (for $r\sqrt{(T/T_0)} = 0{\cdot}0320$), $\sigma_0 = 209 \pm 9$ barns and $\Sigma' = 3070 \pm 100$ barns, are in good agreement with all the current data for this isotope.

Recent neutron transmission measurements using mono-energetic neutrons (1958)(1) and neutron absorption measurements using a pile oscillator (also in 1958)(2) have resulted in a current value of 216±6 barns for the 2200 m/sec neutron absorption cross section of ^{152}Sm.(3) In contrast to this figure the only recorded measurement made by an activation method was reported as long ago as 1947(4) and gave 138±40 barns for the capture cross-section for thermal neutrons. The main purpose of the work described here was to obtain a more precise value for the capture cross section of ^{152}Sm and, if possible, to eliminate this discrepancy.

In addition, at the time this work was started only one measurement with any claim to precision had been made of the resonance absorption integral of ^{152}Sm(5) and an independent check seemed desirable. This situation has improved since the present work was completed. A more reliable value for the ratio of the resonance capture integral to the thermal cross section is now available(6) and, in addition, the resonance parameters for the only known resonance are now known sufficiently well that a lower limit for the resonance capture integral can be calculated precisely.(7)

EXPERIMENTAL METHODS

The method employed was similar to those described in detail elsewhere(8, 9) so only an outline will be given here. The main nuclear reactions involved are,

$$^{152}\text{Sm (stable)} \xrightarrow{n,\gamma} {}^{153}\text{Sm} \xrightarrow[T_{\frac{1}{2}} = 47\text{ hr}]{\beta^-} {}^{153}\text{Eu (stable)}$$

---

(1) N. J. Pattenden, *Proceedings of the Second International Conference on the Peaceful Uses of Atomic Energy, Geneva*, 1958, Paper 11. United Nations (1958).

(2) H. Rose, W. A. Cooper and R. B. Tattersall, *Proceedings of the Second International Conference on the Peaceful Uses of Atomic Energy, Geneva*, 1958, Paper 14. United Nations (1958).

(3) D. J. Hughes, B. A. Magurno and M. K. Brussel. Report, BNL 325, 2nd Ed., Supplement No. 1 (January 1960).

(4) L. Seren, H. N. Friedlander and S. H. Turkel, *Phys. Rev.* **72**, 888 (1947).

(5) R. B. Tattersall, H. Rose, S. K. Pattenden and D. Jowitt, *Reactor Science*, **12**, 32 (1960).

(6) W. H. Walker and R. E. Green, *Canad. J. Phys.* **39**, 1184 (1961).

(7) R. E. Chrien, *Canad. J. Phys.* **39**, 1193 (1961).

(8) M. J. Cabell, *Reactor Science* **12**, 172 (1960).

(9) M. J. Cabell, *J. Inorg. Nucl. Chem.* **21**, 1 (1961).

The target material was enriched ^{152}Sm (98·65 ±0·02 atom per cent ^{152}Sm, 0·76 ±0·01 atom per cent ^{154}Sm) supplied by the Electromagnetic Separation Group of Chemistry Division. Fifty microlitre aliquots (containing approximately 10 μg ^{152}Sm each) of a stock solution of the target material were irradiated in a lattice position of BEPO for between 0·500 and 2·000 hr, (a) unshielded and (b) shielded by 0·071 cm cadmium. Thin gold foils were attached to measure the thermal and epi-cadmium fluxes. After irradiation the samples were allowed to stand for at least three hours to allow the majority of any ^{155}Sm to decay ($T_{\frac{1}{2}}$ = 23 min, produced from ^{154}Sm impurity), then the samarium was purified by cation exchange chromatography and obtained finally in good yield (> 99 per cent) in 5 ml of a 1·2 M solution of nitric acid.

Aliquots were taken as follows. One aliquot (2 ml, containing about 4 μg ^{152}Sm) was mixed with an equal volume, taken with the same pipette, of a solution containing a known concentration of enriched ^{154}Sm (see below) and the resultant atomic ratio of ^{152}Sm to ^{154}Sm in the solution was determined using a mass spectrometer. Further aliquots (50 μl, containing about 0·1 μg ^{152}Sm each) were taken with a calibrated micropipette, evaporated to dryness on thin, gold-coated organic films (total thickness about 50 μg cm^{-2}) and the absolute β-disintegration rates of the sources so obtained were determined using an argon–methane-flow 4π proportional β-counter. The ^{153}Sm content of each source was determined from its absolute β-disintegration rate and the corresponding ^{152}Sm content was determined from the mass spectrometric measurements. With a knowledge of these quantities and the neutron fluxes the capture cross section of ^{152}Sm for reactor and for thermal neutrons and its resonance capture integral can be calculated.

The solution of enriched ^{154}Sm mentioned above was taken from a stock which had been prepared from a sample supplied by the Electromagnetic Separation Group of the Chemistry Division (98·95 ±0·02 atom per cent ^{154}Sm, 0·51 ±0·01 atom per cent ^{152}Sm). Initially the solution was made to contain approximately 2 μg samarium per ml and this quantity was then determined precisely by isotopic dilution analysis using a solution of natural samarium of known concentration. Isotopic analyses in this as in all cases were made by depositing about 1 μg of samarium on the centre of the tantalum filament of a single filament surface ionization source and examining it in an A.E.I. Type M.S.5 mass spectrometer with a filament current of 3·5 A–4·5 A.

The measured disintegration rate for each source was used to calculate the disintegration rate it would have had at the end of the irradiation (A_0). For this purpose the value of 47·1 ±0·1 hr given by CORK *et al.*(10) has been used for the half-life of ^{153}Sm rather than the more recent value of 46·2 ±0·1 hr due to GREEN and WALKER,(11) since the former value was in better accord with our experimental data.

Thus, for example, the decay of one source of ^{153}Sm was followed for thirteen half-lives and no departure from decay with a half-life of 47·1 ±0·1 hr was found during the first nine half-lives (by which time the count was six times the background); residual long-lived activity was less than 0·02 per cent of the initial value. The γ-spectrum of the irradiated ^{152}Sm showed no peaks other than those expected from ^{153}Sm.

RESULTS

The cross section results were calculated by the method which has been described more fully elsewhere.(8, 9, 12, 13).

---

(10) J. M. CORK, M. K. BRICE, R. G. HEIMER and R. M. WOODS, *Phys. Rev.* **110**, 526 (1958).

(11) R. E. GREEN and W. H. WALKER, *Canad. J. Phys.* **39**, 1216 (1961).

(12) T. A. EASTWOOD, A. P. BAERG, C. B. BIGHAM, F. BROWN, M. J. CABELL, W. E. GRUMMITT, J. C. ROY, L. P. ROY and R. P. SCHUMAN, *Proceedings of the Second International Conference on the Peaceful Uses of Atomic Energy, Geneva,* 1958, Paper 203. United Nations (1958).

(13) C. H. WESTCOTT, W. H. WALKER and T. A. ALEXANDER, *Proceedings of the Second International Conference on the Peaceful Uses of Atomic Energy, Geneva,* 1958, Paper 202. United Nations (1958).

The effective capture cross section of ^{152}Sm ($\hat{\sigma}$) was first obtained from the expression:

$$\hat{\sigma}\,(nv_o) = R_E = A_I/N_o\,(1-\text{exp.}\,(-\lambda_I\,t_I)) \tag{1}$$

in which (nv_o) is the 2200 m/sec neutron flux, R_E is the equilibrium rate of conversion of ^{152}Sm into ^{153}Sm, N_o is the number of atoms of ^{152}Sm in the source counted, λ_I is the radioactive decay constant of ^{153}Sm and t_I is the time of irradiation.(9)* The assumption is now made that ^{152}Sm is a $1/v$ absorber for thermal neutrons and it follows that:

$$\hat{\sigma} = \sigma_o\,[1+rs_o\sqrt{(T/T_o)}] \tag{2}$$

in which $r\sqrt{(T/T_o)}$ and s_o are quantities obtained from the cadmium ratio measurements for the gold monitors and for ^{152}Sm respectively, and σ_o is the cross-section of ^{152}Sm for 2200 m/sec neutrons.

The reduced resonance integral i.e. Σ', the usual resonance capture integral with the $1/v$ contribution subtracted, can then be obtained from s_o and the relationship:

$$\Sigma' = \frac{S_o\sigma_o\sqrt{\pi}}{2} \tag{3}$$

and Σ, the resonance capture integral as normally expressed, is equal to $(\Sigma'+0{\cdot}44\sigma_o)$.

A complete set of results for a typical pair of experiments is given in Table 1.

TABLE 1.—COMPLETE RESULTS FOR A PAIR OF EXPERIMENTS

Experiment number	7 (without cadmium cover)	8 (with cadmium cover)
t_I (hr)	1·500	1·500
A_I (disintegrations/sec)	1457·5	535·6
N_o	$3{\cdot}40\times10^{14}$	$3{\cdot}53\times10^{14}$
R_E for ^{152}Sm (sec^{-1})	$1{\cdot}96\times10^{-10}$	$6{\cdot}96\times10^{-11}$
R_E for ^{197}Au (sec^{-1})	$9{\cdot}41\times10^{-11}$	$3{\cdot}45\times10^{-11}$
$r\sqrt{(T/T_o)}$	0·0321	
$\hat{\sigma}$ for ^{197}Au (barns)	154·5	
(nv_o) in neutrons cm^{-2} sec^{-1}	$6{\cdot}09\times10^{11}$	
$\hat{\sigma}$ for ^{152}Sm (barns)	322	
R_{Cd} for ^{152}Sm	2·82	
s_o for ^{152}Sm	16·42	
σ_o for ^{152}Sm (barns)	211	
Σ' for ^{152}Sm (barns)	3070	
Σ for ^{152}Sm (barns)	3163	

Table 2 gives a summary of all the cross-section results.

TABLE 2.—^{152}Sm CROSS-SECTION RESULTS

Experiments	t_I (hr)	$r\sqrt{(T/T_o)}$	$\hat{\sigma}$ (barns)	σ_o (barns)	Σ'/σ_o	Σ'	Σ
1 and 2	0·500	0·0315	312	205	14·68	3011	3101
3 and 4	0·800	0·0322	331	217	14·36	3120	3216
5 and 6	1·000	0·0328	324	210	14·58	3066	3159
7 and 8	1·500	0·0321	322	211	14·55	3070	3163
9 and 10	2·000	0·0311	311	203	15·21	3081	3173
Average		0·0320±0·0003	320±4	209±3	14·68±0·15	3070±18	3162±19

---

* The nomenclature used in the earlier papers is retained here.

The errors quoted for the averages given in Table 2 are their standard errors in each case and arise from random variations in the factors used in the calculations e.g. short term variations in the neutron flux, statistical errors in counting, errors in measuring isotopic ratios, errors in pipetting etc. Systematic errors have been estimated as follows:

(a) 1 per cent in A_I. This was estimated by considering the maximum energies of the β particles emitted by ^{153}Sm,(14) the low superficial densities of the sources (0·1 μg cm^{-2}) and their mode of preparation.(15)

(b) 0·5 per cent in (nv_0). This arises from similar considerations applied to the gold monitors. Although tending to cancel factor (a) the two errors have nevertheless been added.

(c) 1 per cent in N_0. This arises almost entirely from the value assumed for the atomic proportion of ^{152}Sm in natural samarium. We found this to be 0·269± 0·001, in agreement with INGHRAM *et al.*,(16) but have allowed an overall error of 1 per cent in N_0 to take into account possible mass discrimination in our mass spectrometer.

(d) 0·2 per cent in the growth factor, $(1—\exp(-\lambda_1 t_1))$. This arises from the error in λ_1.

When all the errors were taken into account the final values obtained were $\hat{\sigma} = 320\pm13$ barns, $\sigma_0 = 209\pm9$ barns, $\Sigma' = 3070\pm100$ barns and $\Sigma = 3162\pm104$ barns.

DISCUSSION

PATTENDEN(1) has measured the total cross-section of ^{152}Sm for the 2200 m/sec neutrons produced from a crystal spectrometer mounted on the Harwell reactor BEPO. The figure he obtained i.e. 206±6 barns, when corrected for neutron scattering, gave an initial value of 200±6 barns for σ_0(1) which should now be amended to 202±6 barns as a result of more precise scattering data.(17)

ROSE *et al.*,(2) using the oscillator mounted on the Harwell reactor DIMPLE, measured the absorption cross section of ^{152}Sm in a Maxwellian spectrum having a very small epi-thermal content $\left(r = 0{\cdot}0003 \begin{matrix}+0{\cdot}0006\\-0{\cdot}0002\end{matrix}\right)$ and obtained a value of $\sigma_M = \sigma_0 g = 224\pm7$ barns (where g is a measure of the departure of ^{152}Sm from $1/v$ behaviour for thermal neutrons).

A measurement of the capture cross section of ^{152}Sm for the reactor flux in the lattice of BEPO has been described here and the fraction of this quantity due to thermal neutrons alone has been determined. On the assumption that g is unity—and this assumption seems justified both in the light of measurements of the variation of total cross-section with neutron energy(1) and as a result of theoretical considerations(6)—a value of 209±9 barns was obtained for σ_0.

Based on the assumption that $g = 1$ then, the three cross sections i.e. 202±6 barns, 224±7 barns and 209±9 barns can all be equated to σ_0. It will then be noted that the value obtained here is in agreement, within the experimental errors, with both the other values although the other two values are not in agreement with each

(14) D. STROMINGER, J. M. HOLLANDER and G. T. SEABORG, *Rev. Mod. Phys.* **30**, 585 (1958).

(15) J. S. MERRITT, J. G. V. TAYLOR and P. J. CAMPION, *Canad. J. Chem.* **37**, 1109 (1959).

(16) M. G. INGHRAM, D. C. HESS and R. J. HAYDEN, *Phys. Rev.* **73**, 180 (1948).

(17) N. J. PATTENDEN. Private communiaction (1961).

other. None of the three values agree with the original figure i.e. 138±40 barns,(4) obtained by an activation method. The unweighted average of the three results is $\sigma_0 = 212 \pm 7$ barns.

The contribution to σ_0 from the only known resonance of ^{152}Sm (at 8·02 eV) is 224±18 barns.(7) The good agreement between this figure and the result obtained in this work adds further evidence to the conclusion that this resonance determines the neutron capture behaviour of ^{152}Sm in the thermal region.

The value for $\Sigma'\cdot\sigma_0$ obtained in these experiments was 14·68±0·15 (Table 2). This is in excellent agreement with the ratio obtained recently by WALKER and GREEN,(6) i.e. 14·65±0·41.

Using the results obtained in this work resulted in $\Sigma' = 3070 \pm 100$ barns. TATTERSALL *et al.*(5) have measured Σ' (apparent) for solutions of ^{152}Sm showing appreciable self-screening and by extrapolation of their data to infinite dilution, and hence to zero self-screening, obtained Σ' (infinite dilution) = 2850±300 barns. This result is also in good agreement with our figure.

The contribution to Σ' from the 8·02 eV resonance has been calculated to be 3090±220 barns(7) showing that this resonance determines the neutron capture behaviour of ^{152}Sm for $1/E$ neutrons as well as for thermal neutrons.

Acknowledgements—Grateful acknowledgement is made to Messrs N. J. D. PROSSER, D. AVERY and D. TAYLOR for some of the mass spectrometric measurements used in this work.

J. Inorg. Nucl. Chem., 1962, Vol. 24, pp. 755 to 761. Pergamon Press Ltd. Printed in England

THE USE OF ^{129}I AS AN ISOTOPIC TRACER AND ITS DETERMINATION ALONG WITH NORMAL ^{127}I BY NEUTRON ACTIVATION—THE ISOLATION OF IODINE FROM A VARIETY OF MATERIALS*

M. H. STUDIER, C. POSTMUS, Jr., J. MECH, R. R. WALTERS and E. N. SLOTH
Argonne National Laboratory, Argonne, Illinois

(*Received* 25 *June* 1962)

Abstract—In order to make the 1·7 × 10^7 year ^{129}I useful as an iodine tracer a neutron activation procedure was used for its determination. A procedure involving high temperature ignition in a stream of oxygen was devised for the isolation of iodine from a variety of materials. After activation and decontamination a large sodium iodide, well-type crystal was used as a selective detector for the ^{130}I activation product. The normal iodine content of a sample is readily determined at the same time.

EIGHT-DAY ^{131}I is readily available and has been used extensively as an iodine tracer. Its short half-life, however, limits its usefulness for long term experiments such as may be involved in biological studies. The 1·7 × 10^7 year ^{129}I promises to be a useful isotope for such experiments. It does not occur in nature except in minute quantities as a result of fission in uranium ores.[1] Although its specific activity (370 disintegrations per min per μg) is too low for convenient use as a direct radioactive tracer, the neutron activation technique can be used to increase the sensitivity for its detection by a factor of 10^6 or more.

The pertinent reactions in the neutron activation of ^{129}I and ^{127}I are as follows:

$$^{129}\mathrm{I}\,(n,\gamma)\,^{130}\mathrm{I}\xrightarrow[12\cdot5\text{ hr}]{\beta,\,\gamma}{}^{130}\mathrm{Xe}\text{ (stable)} \qquad (1)$$

$$^{127}\mathrm{I}\,(n,\gamma)\,^{128}\mathrm{I}\xrightarrow[25\cdot0\text{ min}]{\beta,\,\gamma}{}^{128}\mathrm{Xe}\text{ (stable)} \qquad (2)$$

Interfering Iodine activities are produced by the following reactions:

$$^{127}\mathrm{I}\,(n,2n)\,^{126}\mathrm{I}\xrightarrow[13\cdot3\text{ days}]{\beta,\,\gamma}{}^{126}\mathrm{Xe}\text{ (stable)} \qquad (3)$$

$$^{127}\mathrm{I}\,(n,\gamma)\,^{128}\mathrm{I}\,(n,\gamma)\,^{129}\mathrm{I}\,(n,\gamma)\,^{130}\mathrm{I} \qquad (4)$$

Since reaction (3) is produced by very energetic neutrons (greater than 9 MeV) only, the use of a well moderated neutron flux is helpful. Although the fission product iodine from as little as 10^{-12} g of natural uranium can limit the sensitivity of the method, this interference can be eliminated by very careful purification from uranium before irradiation.

---

* Based on work performed under the auspices of the U.S. Atomic Energy Commission.

(1) B. C. PURKAYASTHA and G. R. MARTIN, *Canad. J. Chem.* 34, 293 (1956).

$$^{235}\mathrm{U}\,(n,\ \text{fission})\begin{cases} ^{131}\mathrm{I}\ \dfrac{\beta,\gamma}{8\ \text{days}} \\ ^{132}\mathrm{I}\ \dfrac{\beta,\gamma}{2{\cdot}3\ \text{hr}} \\ ^{133}\mathrm{I}\ \dfrac{\beta,\gamma}{21\ \text{hr}}. \\ ^{134}\mathrm{I}\ \dfrac{\beta,\gamma}{52\ \text{min}} \\ ^{135}\mathrm{I}\ \dfrac{\beta,\gamma}{6{\cdot}7\ \text{hr}} \end{cases} \tag{5}$$

The analysis of a sample for ^{129}I and ^{127}I involves the following steps:

(1) Isolation of an iodine fraction from the sample without the addition of carrier, but with ^{131}I tracer for determination of yield.

(2) Packaging in a container suitable for neutron irradiation with a minimum of chemical impurities.

(3) Irradiation of the isolated iodine in a moderated neutron flux.

(4) Irradiation of an ^{127}I monitor containing a known amount of ^{129}I in a separate container adjacent to sample.

(5) Decontamination of the irradiated sample and monitor from extraneous activities.

(6) Measurement and resolution of the various iodine activities which may be present.

(7) Determination of the specific activities of the monitor with respect to the 25 *min* ^{128}I, the 12·5 hr ^{130}I and the 13·3 day ^{126}I. From these data the ^{127}I and ^{129}I content of the sample can be determined by direct comparison with the same activities in the sample, corrected for chemical yield.

The chemical isolation of iodine

A satisfactory procedure that has been devised for the isolation of iodine from many different types of samples involves the following steps:

(1) Ignition of the sample in a stream of oxygen in a quartz apparatus.

(2) Trapping of the iodine in a dilute solution of sulphurous acid.

(3) Carrying of the iodide ion on a precipitate of silver chloride.

(4) Decomposition of the silver chloride by heating with aluminium metal in a vacuum and the distillation of the iodine into a quartz tube.

A quartz ignition apparatus (modifications of an apparatus described by Godfrey *et al.*(2)) coupled to a Pyrex scrubbing tower by means of a semi ball-joint is illustrated in Fig. 1. The apparatus is suitable for samples weighing as much as 100 g. A scaled down version may be used for smaller samples. After insertion of a quartz wool plug into the bottom of the inner quartz tube, the sample is packed in with a glass rod with periodic additions of a solution containing ^{131}I tracer. The apparatus is assembled and initially oxygen is passed between the concentric quartz tubes at a rate of 2000 cm^3 min^{-1}. About 30 ml of water is added to the scrubbing tower and a flow of gaseous sulphur dioxide is started. This gas enters through the side arm of the scrubbing tower. The first step in the burning is a gradual downward destructive distillation of the sample with ignition of the volatile decomposition products in the region of the 2 mm holes using ring burners. For complete combustion of these volatile products the rate of destructive distillation must be sufficiently slow that an excess of oxygen is maintained, but must be sufficiently fast that the flame produced is hot enough to prevent the formation of soot. The area of the 2 mm holes is kept hot at all times. Oxygen enters through these holes and the flame is contained within the inner quartz tube. In this manner the outer tube is protected from extensive strains due to the hot flame and fused salts. After the destructive distillation is complete, the carbonaceous residue is ignited in a stream of oxygen. The oxygen flow between the tubes is reduced by half, and oxygen is passed up the inner tube. The area of the 2 mm holes is heated and then the sample ignited at the bottom. The flow rate of oxygen up the inner tube is gradually increased. The rate is limited by necessity for complete combustion of additional volatile material at the top of the combustion tube. After all combustible material has been burned, the entire quartz apparatus is baked out at a temperature of about 800°C in a stream of oxygen to remove the last traces of iodine.

---

(2) P. R. Godfrey, H. E. Parker and F. Quackenbush, *Analyt. Chem.* 23, 1860 (1951).

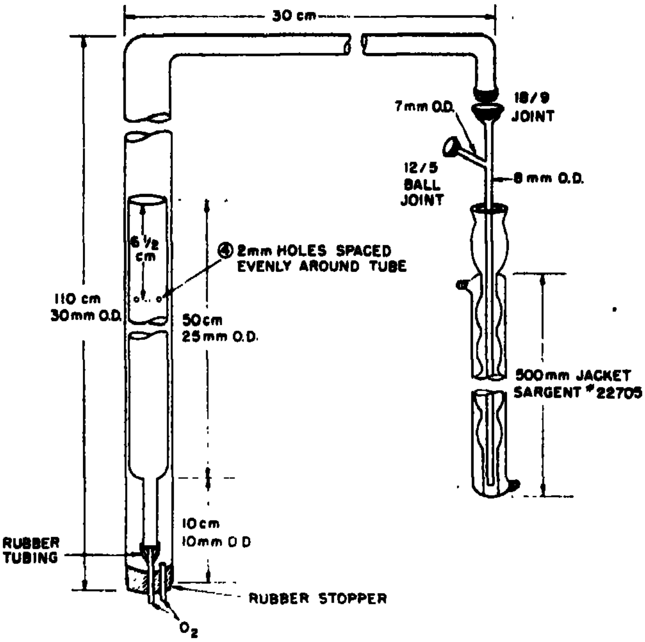

FIG. 1.—Ignition apparatus.

After the scrubbing solution has been transferred to a suitable container and acidified with sulphuric acid, the excess sulphur dioxide is removed by bubbling nitrogen through the solution. Silver chloride is precipitated by the addition of silver nitrate. Usually, enough chlorides distil from the sample so that none need be added; however, if no precipitate forms, hydrochloric acid is added followed by the addition of more silver nitrate. Two or three milligrams of silver are sufficient for adequate carrying of the iodine. After digestion to coagulate the silver chloride, the precipitate is centrifuged, washed with water, and dissolved in a solution of sodium cyanide. At this point any insoluble material (such as traces of soot) is removed by centrifugation and the silver chloride is reprecipitated by acidification. The precipitate is washed with acid and water, and then transferred with acetone to the quartz tube of Fig. 2. After centrifugation, the bulk of the acetone is removed with a transfer pipette and the last traces by evaporation.

After the addition of about 0·3 g aluminium wire the tube is sealed to the quartz distillation apparatus below the quartz frit. The apparatus is evacuated with gentle flaming to a pressure of three microns or less. The U-tube is immersed in liquid nitrogen and the temperature of the aluminium silver chloride mixture raised to a red heat with a small furnace. The iodine distils into the U-tube along with aluminium chloride. Normally the iodine distils in two fractions. The more volatile of these appears in the U-tube as soon as the aluminium melts. The less volatile fraction must be moved into the U-tube by flaming to a temperature of 300–400°C. After sealing off both ends of the U-tube the iodine is moved into the arm opposite the reaction vessel by cooling that end in liquid nitrogen while flaming the rest of the tube. This end is sealed off at a convenient length and irradiated along with an ^{127}I–^{129}I monitor in a separate tube. Before irradiation, it is convenient to check the chemical yield by dropping the quartz tube into the well of a sodium iodide crystal and counting the 0·36 MeV γ-ray of ^{131}I.

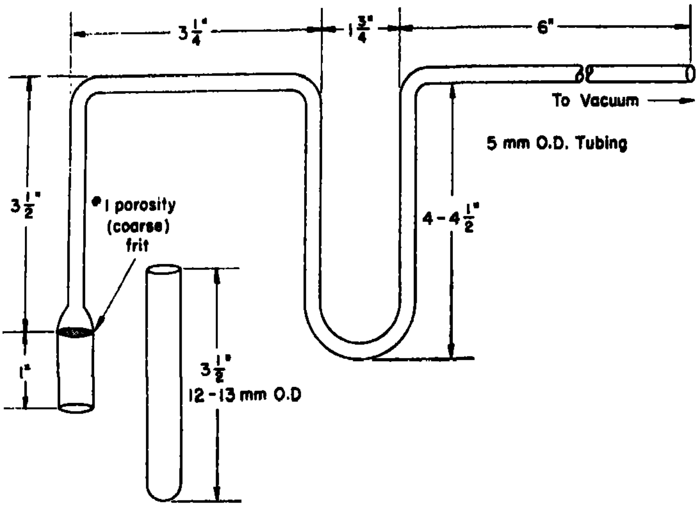

Fig. 2.—Quartz distillation apparatus.

Decontamination procedure

After irradiation the iodine is decontaminated from all extraneous activities. The most troublesome contaminant has been that of the 36 hr ^{82}Br which has a decay scheme similar to that of ^{130}I. Since iodine is not separated from other halogens before irradiation, radiobromine is always produced to some extent. Because of its volatility in the elemental form precautions must be taken to prevent contamination of reagents and apparatus which may result in subsequent recontamination of the iodine fraction. This is particularly troublesome when solvent extraction procedures are used along with oxidation reduction cycles.

The addition of milligram quantities of iodine and bromine improves yields and decontamination factors. If exchange between the radionuclides and the added carriers is complete, adequate yields and decontamination factors can be achieved by a variety of procedures. Frequently, however, poor yields and low decontamination factors resulted when the radiohalogens reacted with traces of organic matter and the resulting organic halides did not exchange with the carriers. The conditions of irradiation in the reactor are particularly favourable for the production of organic halides.(3) The effects were exaggerated by the deliberate addition of organic matter. The problem was solved by the high temperature ignition of the irradiated sample followed by distillation of the iodine. The procedure is as follows:

(1) The irradiated quartz ampule is washed in strong acid to remove surface contaminants.

(2) The ampule is placed in the apparatus of Fig. 3 such that the file scratch is at the edge of the ball-joint. With the furnace at 800°C and a slow constant stream of oxygen following, the semi-ball joint is twisted to break the tube at the scribed mark.

(3) The halogens are distilled from the ampule by heating with a torch. They pass through the hot copper oxide furnace and are absorbed by a solution of 1 N sodium hydroxide containing iodide, iodate, bromide and bromate in the distillation apparatus.

---

(3) E. N. Weber, P. F. Forsyth and R. H. Schuler, *Radiation Research*, 3, 68 (1955).

(4) A few milligrams of sodium peroxide are added to the distillation flask to promote exchange of halogens by oxidation to a common state. Excess peroxide is decomposed by boiling and the solution is acidified with sulphuric acid saturated with sulphur dioxide to reduce the halogens to a common reduced state. Excess sulphur dioxide is removed by boiling in a stream of nitrogen.

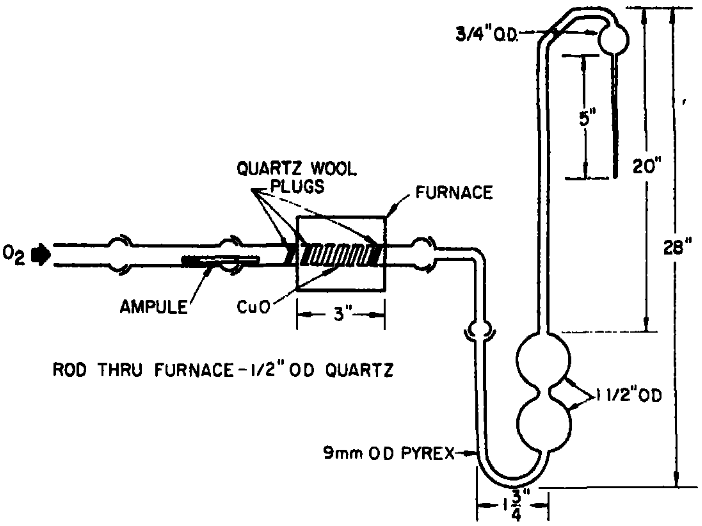

Fig. 3.—Decontamination apparatus.

(5) After cooling the solution to prevent air oxidation, ferric sulphate is added to oxidize iodide to iodine leaving bromide in solution.

(6) The iodine is distilled in a small volume with reflux by vigorous boiling with a slow nitrogen stream.

(7) The iodine is trapped in a small volume of sulphurous acid. The distillation procedure is repeated as often as required. When exchange is complete, the iodine is quantitatively distilled with decontamination from bromine by a factor of 10^4 or more for each distillation. The iodine is finally precipitated as silver iodide in a tube suitable for counting in the well of a sodium iodide scintillator.

(8) The irradiated ^{127}I–^{129}I monitor is decontaminated, precipitated as silver iodide, weighed and counted.

Counting procedure

The use of a γ-ray spectrometer has simplified the measurement and resolution of the iodine activities involved in the determination of ^{129}I by activation. The spectrometer used consists of a well-type sodium iodide scintillator, multiplier phototube, amplifier and a single channel pulse height selector. A one-mil nickel sheath within the well served as a β shield.

In Fig. 4 is illustrated the decay scheme(4) of ^{130}I. Associated with each disintegration is a total γ-energy of 1·9 MeV or greater. Although this energy is liberated by relatively low energy γ-rays in cascade, a large fraction of the events will be recorded as high energy coincidences of the cascade γ-rays when the sample is placed in the centre of a large sodium iodide scintillator. As the size of the crystal is increased, the fraction of the disintegrations which appear at high energies is increased with a consequent decrease in the low energy events. This is illustrated in Fig. 4 where differential curves of counting rates vs. energy for three different size crystals are shown. It seems probable that an integration of all the events observed with the 5 in. crystal represents a counting efficiency approaching 100 per cent.

(4) R. S. Caird and A. C. G. Mitchell, *Phys. Rev.* **94**, 412 (1954).

In addition to ^{130}I three other radioactive isotopes are always present during the counting procedure. They are the eight-day ^{131}I, the 25 min ^{128}I, and the 13 day ^{126}I with maximum γ-decay energies of 0·72, 0·98 and 1·42 MeV (in low abundance), respectively. The ^{131}I is added at the beginning of the isolation procedure as tracer to determine the chemical yield of the iodine. The other two are formed by neutron reactions with normal ^{127}I during the activation. With the 5 in. crystal it is possible to measure the disintegration rate of ^{130}I with a high counting efficiency while discriminating severely against the activities of the other three iodine isotopes. After consideration of backgrounds in addition to counting efficiencies and discrimination against activities other than that of ^{130}I, two operating conditions were chosen for measurements of ^{130}I activity with the 5 in. crystal. When the ^{126}I activity is a serious problem (e.g., when the sample contains large amounts of natural iodine), the ^{130}I is measured in the energy region from 1·6 to 2·5 MeV. Under these conditions the counting efficiency for ^{130}I is ~ 40 per cent and the background is 40 counts per min. When the activity of ^{126}I is low, the ^{130}I measurements are made in the energy band between 1·2 and 2·5 MeV. Under these conditions the counting efficiency is ~ 70 per cent and the background is 90 counts per min. The abundances of the other three activities are determined by measurements in a narrow energy band in the region of low γ-energy (0·25–0·50 MeV).

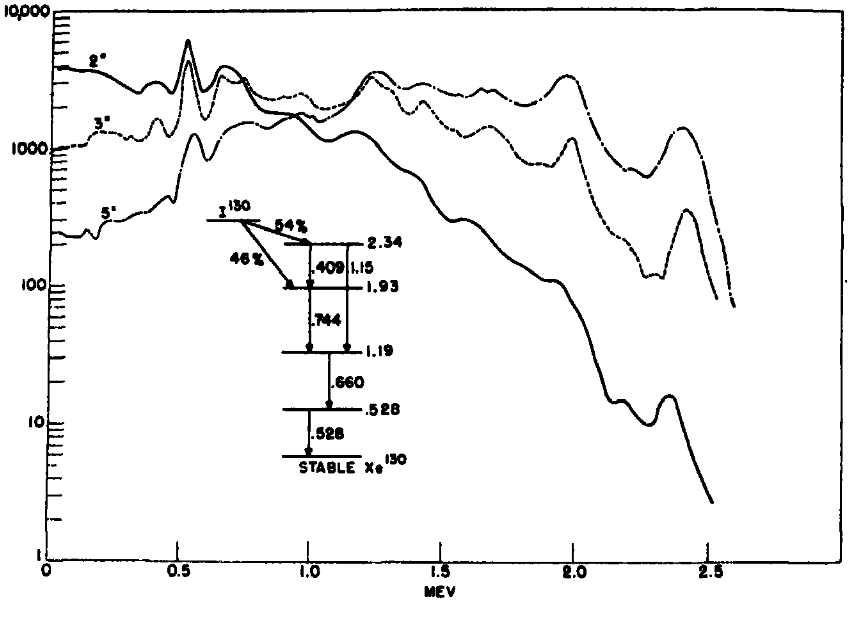

Fig. 4.—γ-spectra of ^{130}I in various size sodium iodide crystals.
———— crystal size = 2 in. × 2 in.
well = $\frac{5}{8}$ in. × 1$\frac{1}{2}$ in.
- - - - - - crystal size = 3 in. × 3 in.
well = $\frac{3}{4}$ in. × 1$\frac{1}{2}$ in.
—— - —— crystal size = 5 in. × 5 in.
well = $\frac{11}{16}$ in. × 2$\frac{1}{2}$ in.
Note.—All curves are normalized to the same disintegration rate.

RESULTS AND DISCUSSION

A variety of biological samples (leaves, grain, soil, roots, bark, twigs, thyroids and other animal tissues) to which ^{129}I had been added in varying amounts were analysed for ^{127}I and ^{129}I to check the procedures as they were developed. Typical chemical yields were about 50 per cent through the entire isolation and decontamination procedures. The ^{127}I content of samples varied from 5 parts per billion for a wheat sample to 2150 parts per billion for a lake weed.

To demonstrate the sensitivity of the method for ^{129}I the iodine from 100 g of leaves was isolated without addition of ^{129}I, activated and measured. An upper limit of 6×10^{-16} g of ^{129}I per gramme of leaf was determined. The same sample was found to contain 143 parts per billion of normal iodine.

Samples were irradiated in Argonne's CP-5 reactor at a flux of 3×10^{13} neutrons cm^{-2} sec^{-1}. At this flux the method can determine as little as 10^{-10} g of ^{127}I and 10^{-13} g of ^{129}I.

J. Inorg. Nucl. Chem., 1962, Vol. 24, pp. 763 to 776. Pergamon Press Ltd. Printed in England

INFRA-RED SPECTRA OF METAL COMPLEX IONS BELOW 600 cm^{-1}—I

THE SPECTRA OF THE TRIS COMPLEXES OF 1, 10-PHENANTHROLINE AND 2, 2'-BIPYRIDINE WITH THE TRANSITION METALS IRON(II) THROUGH ZINC(II)

R. G. INSKEEP*
Department of Chemistry, University of Vermont, Burlington, Vermont,
and
The National Bureau of Standards, Washington, D.C.

(*Received* 16 *March* 1961; *in revised form* 20 *November* 1961)

Abstract—The infra-red spectra of the tris-2, 2'-bipyridine and the tris-1,10-phenanthroline complexes of iron(II), cobalt(II), nickel(II), copper(II), and zinc(II) have been obtained from 250 to 2000 cm^{-1}. These spectra have been correlated with the bonding properties, and a metal–nitrogen bond vibration assignment has been proposed.

RECENTLY an excellent study of the infra-red spectra of 1, 10-phenanthroline metal ion complexes in the rock salt region appeared.(1) However, it was pointed out by INSKEEP and BENSON(2) that the only unique bands, i.e., not merely perturbed ligand absorption bands, are those appearing at frequencies of less than 600 cm^{-1}. In the present work, the spectra of a series of divalent transition element ions with 1, 10-phenanthroline and with 2, 2'-bipyridine have been obtained together with the spectra of the free ligands. To keep the spectra as uncluttered with extraneous elements as possible, the spectra of the complexes were obtained as a low concentration of complex in alkali halide pellets, and the anion of the complexes was the simple chloride ion except in the cases of copper and zinc, where in order to negate the possibility of having the chloride ion in the inner co-ordination sphere, the nitrate ion was used.

EXPERIMENTAL RESULTS

Spectra of the tris-2, 2'-bipyridine complexes of the divalent ions and the spectrum of the pure ligand are shown in Figs. 1–2; while the measured frequencies of the absorption bands are given in Table 1. The spectra of the tris-1, 10-phenanthroline complexes and the spectrum of the hydrate of the free base are shown in Figs. 3–4; and the absorption band frequencies are tabulated in Table 2.

As demonstrated by SCHILT and TAYLOR,(1) the spectra of the various phenanthroline and of the various bipyridine complexes are very similar to one another in the rock salt region: it is only in the low frequency (i.e., CsBr) region that the spectra differ from one another within a given series. In the higher frequency region, the spectra of cobalt(II), nickel(II), copper(II) and zinc(II) complexes in each series are essentially identical once the anion nitrate bands are taken into account in

* Present address: Department of Chemistry, University of Hawaii, Honolulu 14, Hawaii.

(1) A. A. SCHILT and R. C. TAYLOR, *J. Inorg. Nucl. Chem.* **9**, 211 (1959).
(2) R. G. INSKEEP and M. D. BENSON, *J. Inorg. Nucl. Chem.* **20**, 290 (1961).

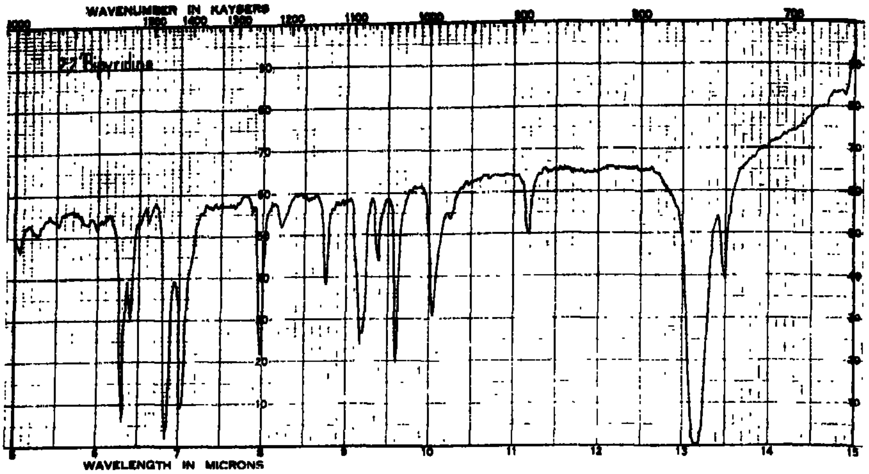
WAVENUMBER IN KAYSERS
2000
1500
1400
1300
1200
1100
1000
900
800
700
2,2' Bipyridine
90
80
70
60
50
40
30
20
10
5
6
7
8
9
10
11
12
13
14
15
WAVELENGTH IN MICRONS

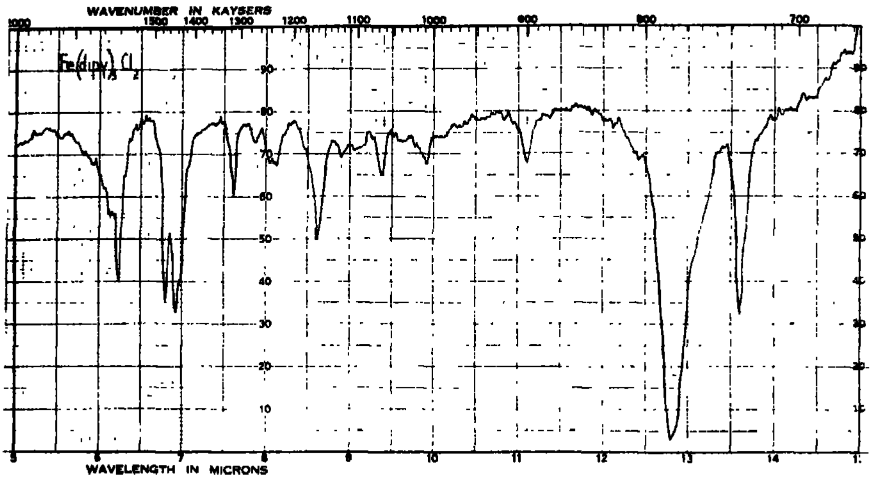
WAVENUMBER IN KAYSERS
2000
1500
1400
1300
1200
1100
1000
900
800
700
Fe(dipy)3 Cl2
90
80
70
60
50
40
30
20
10
5
6
7
8
9
10
11
12
13
14
15
WAVELENGTH IN MICRONS

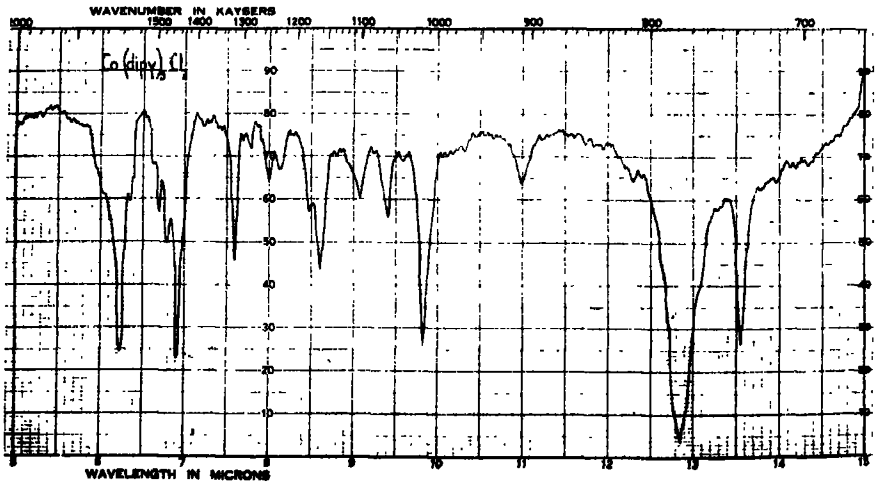
WAVENUMBER IN KAYSERS
2000
1500
1400
1300
1200
1100
1000
900
800
700
Co(dipy)3 Cl2
90
80
70
60
50
40
30
20
10
5
6
7
8
9
10
11
12
13
14
15
WAVELENGTH IN MICRONS

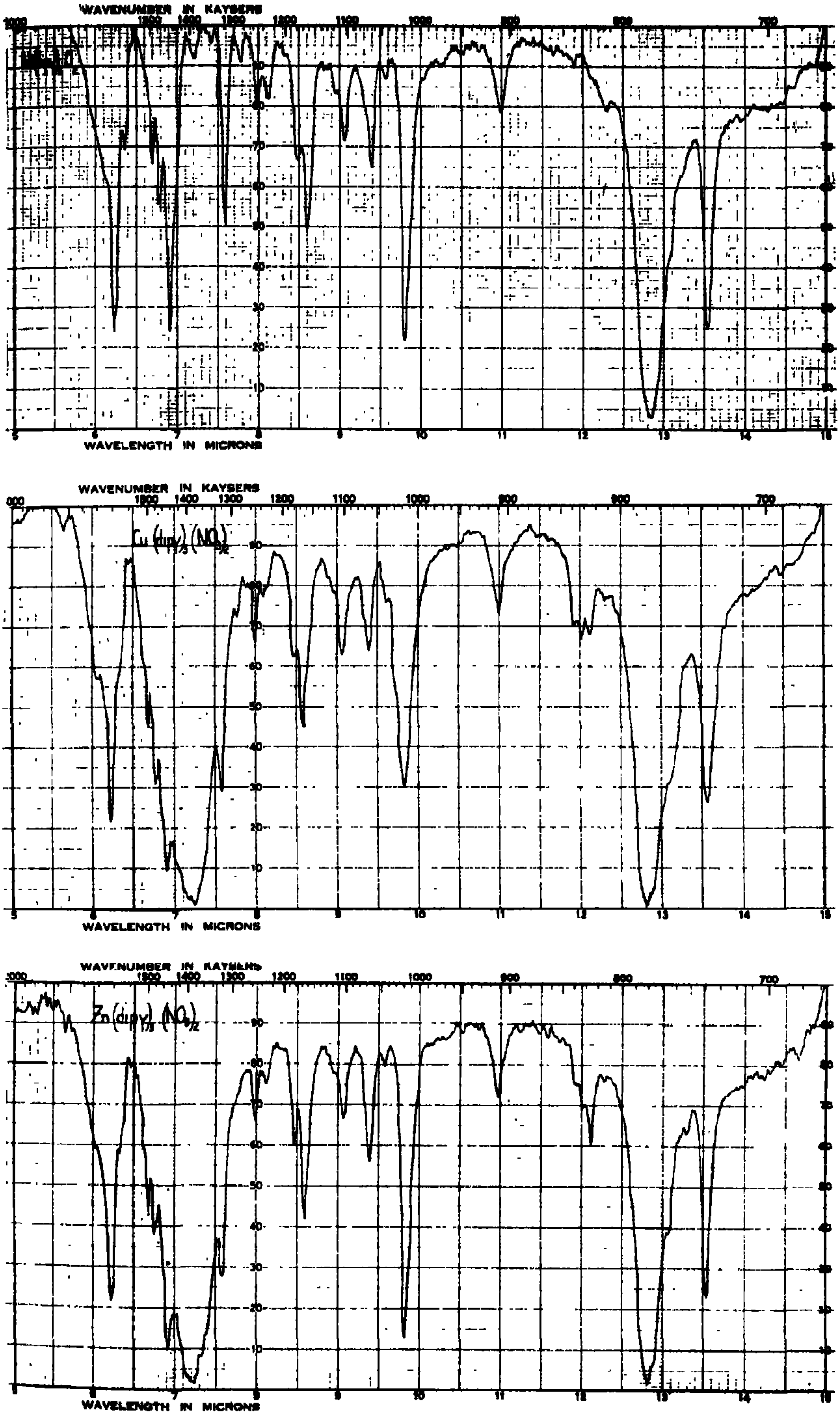

FIG. 1.—The infra-red absorption spectra of the 2,2′-bipyridine complexes from 5 to 15 μ.

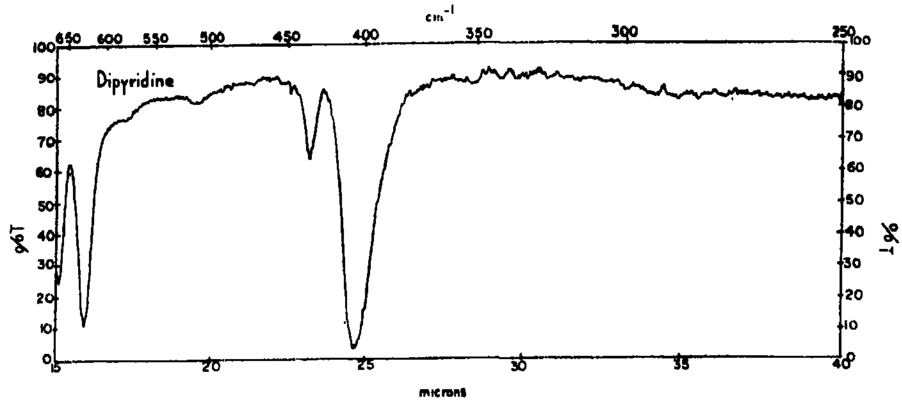
cm⁻¹
650 600 550 500 450 400 350 300 250
Dipyridine
%T
0 10 20 30 40 50 60 70 80 90 100
15 20 25 30 35 40
microns

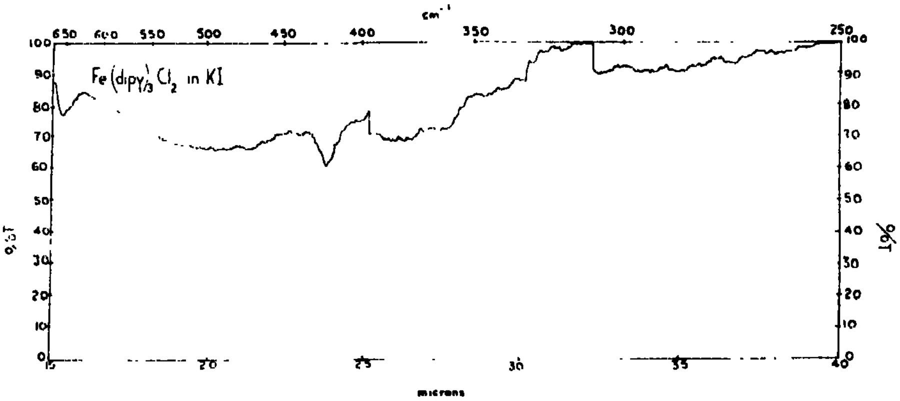
cm⁻¹
650 600 550 500 450 400 350 300 250
Fe(dipy)₃ Cl₂ in KI
%T
0 10 20 30 40 50 60 70 80 90 100
15 20 25 30 35 40
microns

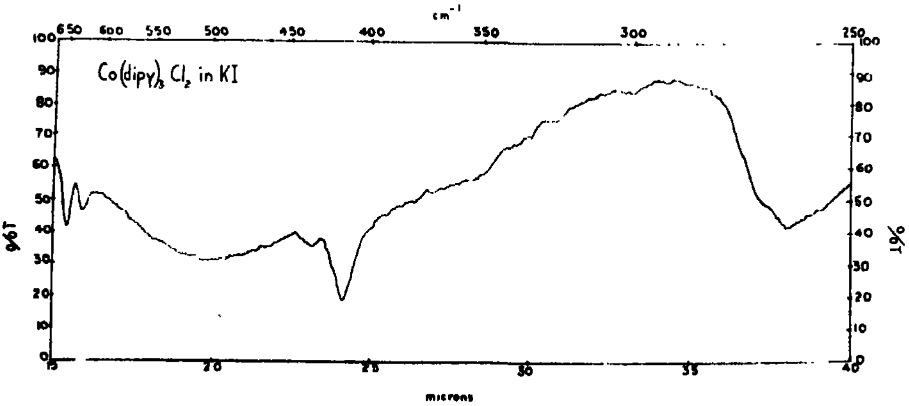
cm⁻¹
650 600 550 500 450 400 350 300 250
Co(dipy)₃ Cl₂ in KI
%T
0 10 20 30 40 50 60 70 80 90 100
15 20 25 30 35 40
microns

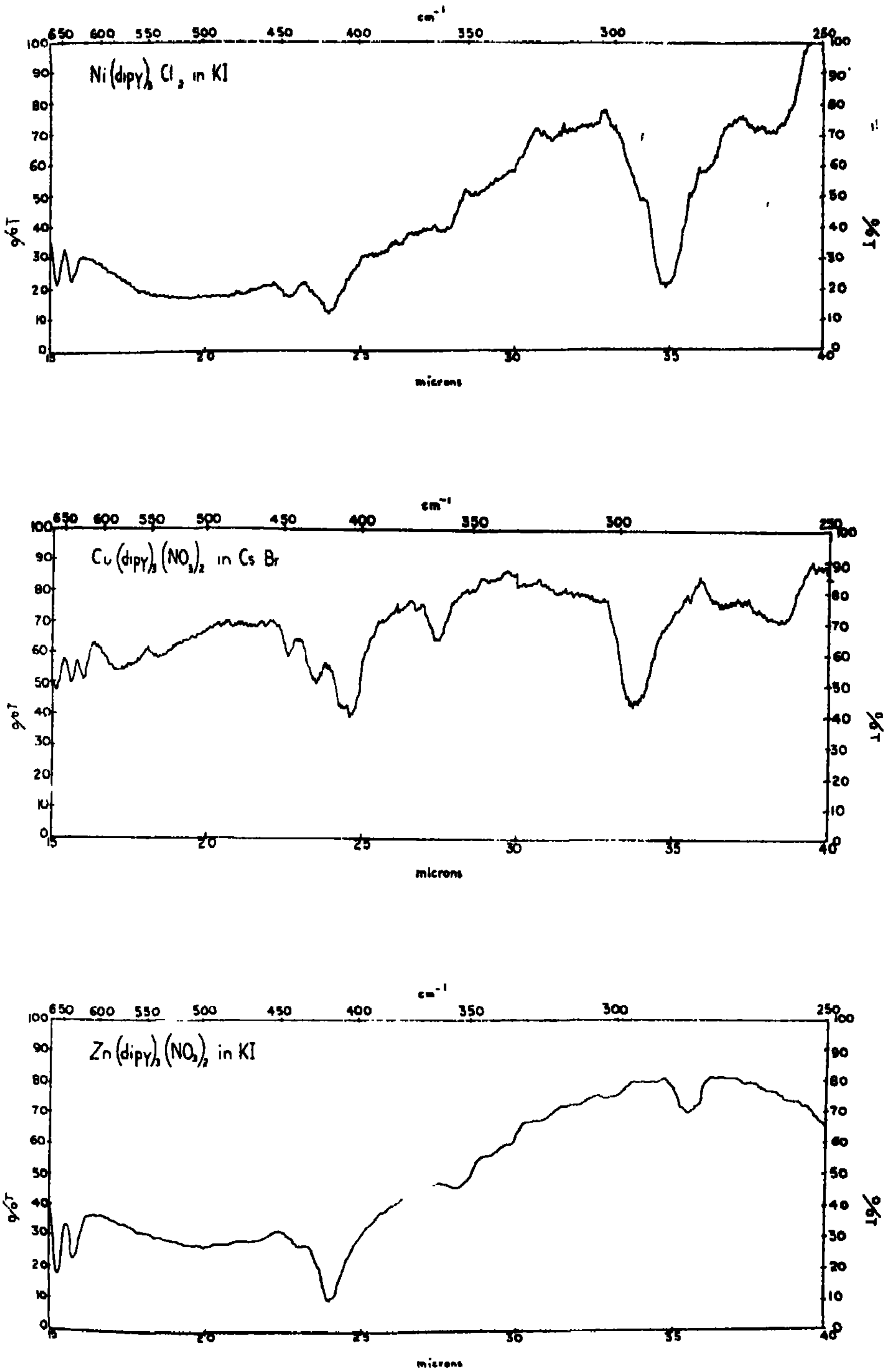

Fig. 2.—The infra-red absorption spectra of the 2,2′-bipyridine complexes from 15 to 40 μ.

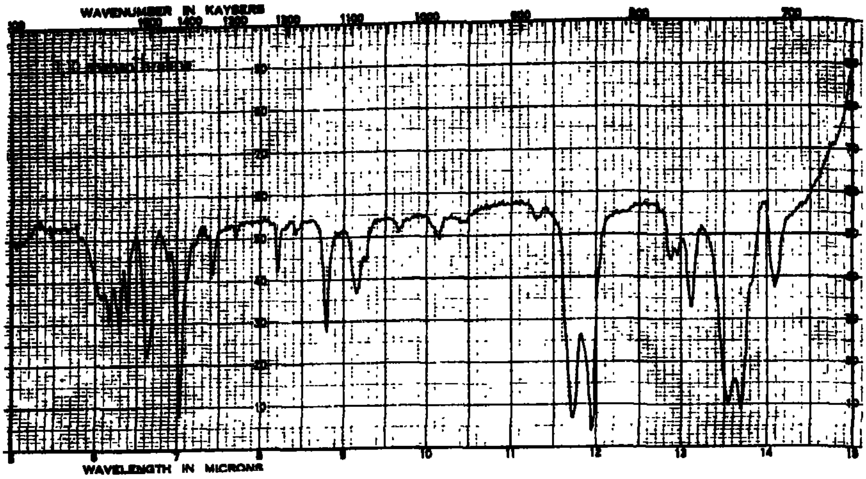
WAVENUMBER IN KAYSERS
1500 1400 1300 1200 1100 1000 900 800 700
90 80 70 60 50 40 30 20 10
6 7 8 9 10 11 12 13 14 15
WAVELENGTH IN MICRONS

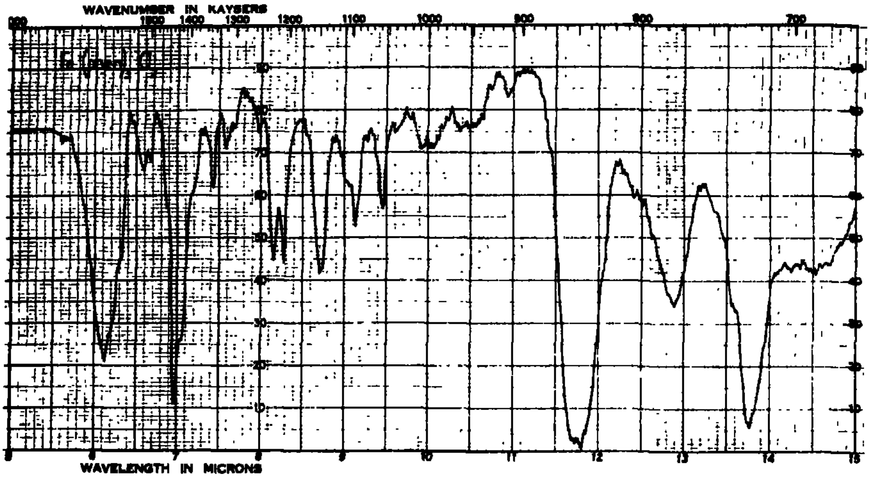
WAVENUMBER IN KAYSERS
1500 1400 1300 1200 1100 1000 900 800 700
Co (phen) Cl
90 80 70 60 50 40 30 20 10
5 6 7 8 9 10 11 12 13 14 15
WAVELENGTH IN MICRONS

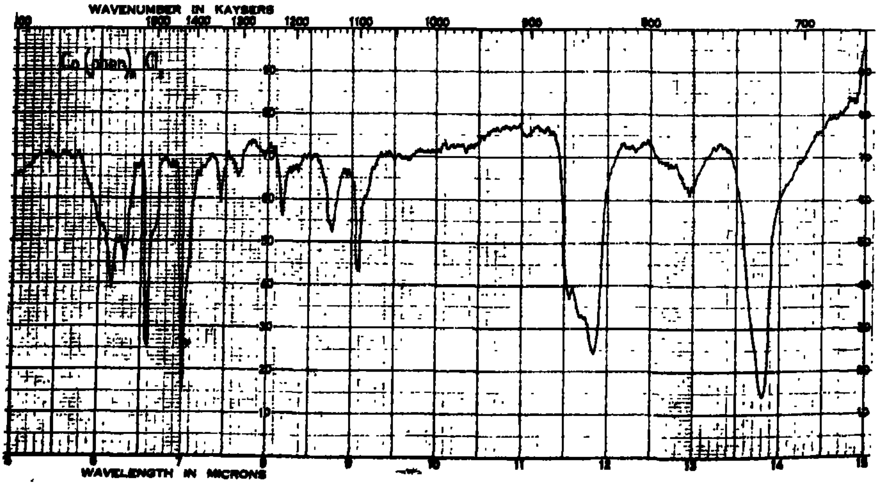
WAVENUMBER IN KAYSERS
1500 1400 1300 1200 1100 1000 900 800 700
Co (phen) Cl
90 80 70 60 50 40 30 20 10
5 6 7 8 9 10 11 12 13 14 15
WAVELENGTH IN MICRONS

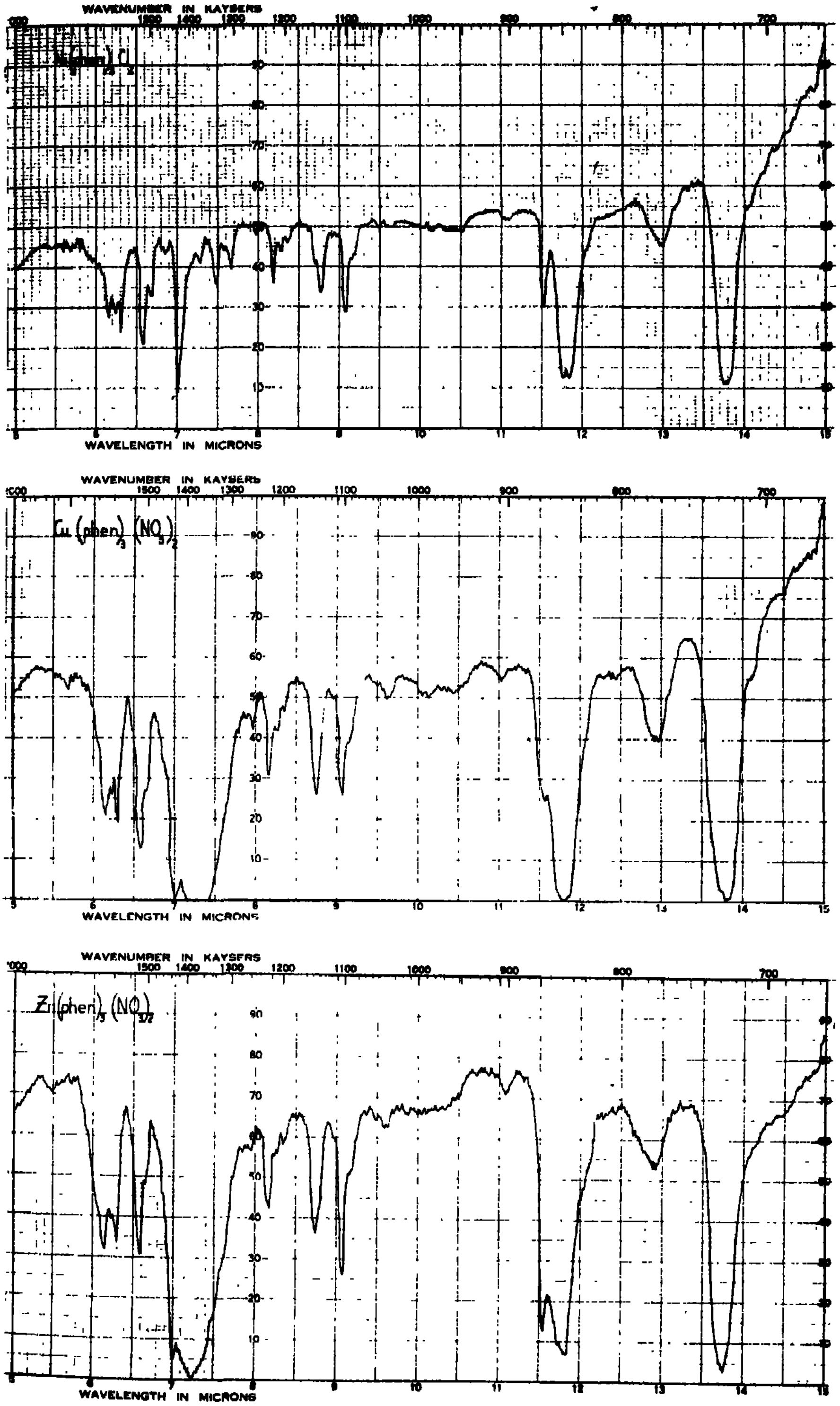

FIG. 3.—The infra-red absorption spectra of the 1,10-phenanthroline complexes from 5 to 15 μ.

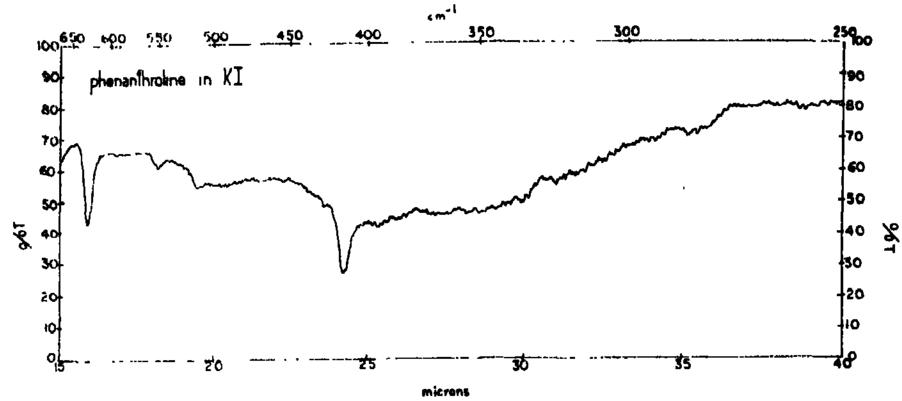
cm⁻¹
650 600 550 500 450 400 350 300 250
phenanthroline in KI
%T
0 10 20 30 40 50 60 70 80 90 100
15 20 25 30 35 40
microns

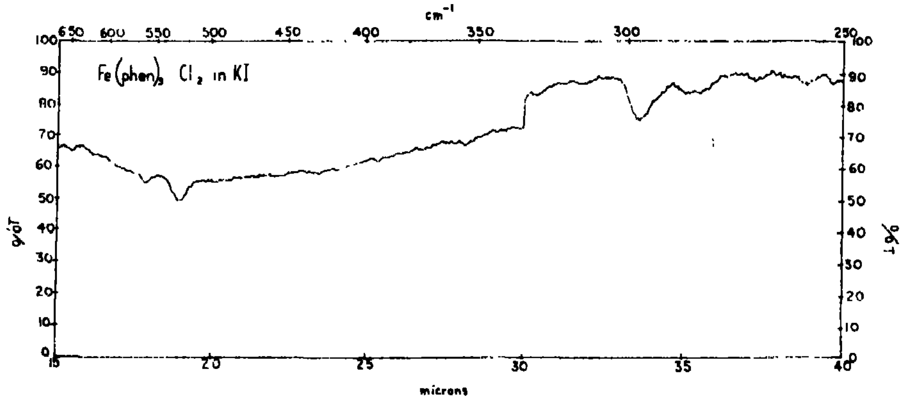
cm⁻¹
650 600 550 500 450 400 350 300 250
Fe(phen)₃ Cl₂ in KI
%T
0 10 20 30 40 50 60 70 80 90 100
15 20 25 30 35 40
microns

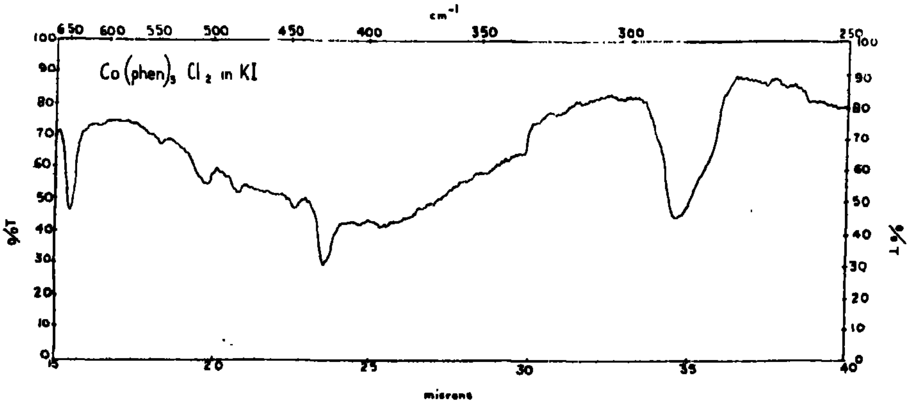
cm⁻¹
650 600 550 500 450 400 350 300 250
Co(phen)₃ Cl₂ in KI
%T
0 10 20 30 40 50 60 70 80 90 100
15 20 25 30 35 40
microns

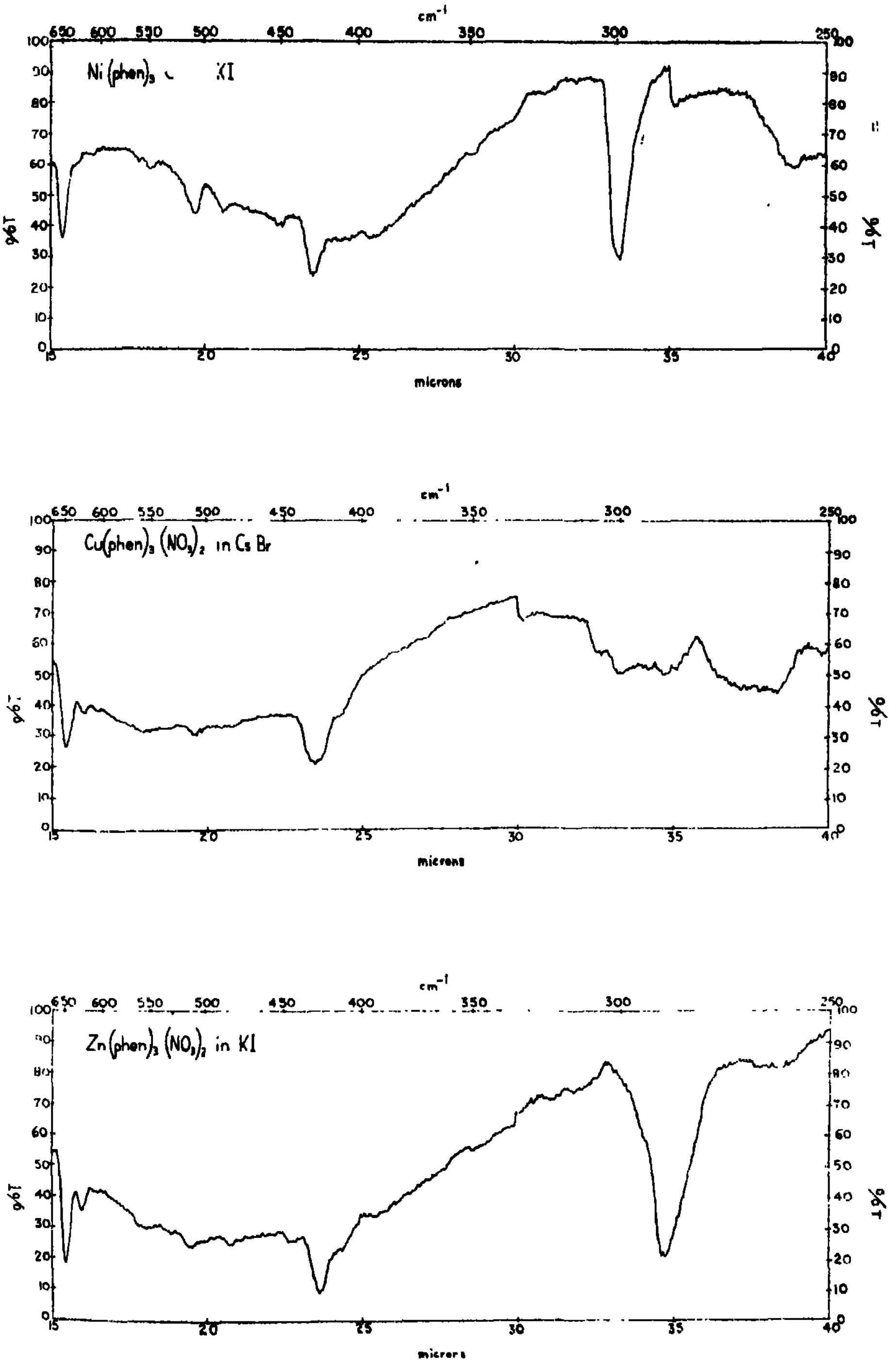

Fig. 4.—The infra-red absorption spectra of the 1,10-phenanthroline complexes from 15 to 40 μ.

TABLE 1.—INFRA-RED FREQUENCIES OF METAL ION 2,2′-DIPYRIDINE COMPLEXES IN KI FROM 2000 CM^{-1} TO 250 CM^{-1}

Dipy	$Fe(dipy)_3Cl_2$	$Co(dipy)_3Cl_2$	$Ni(dipy)_3Cl_2$	$Cu(dipy)_3(NO_3)_2$	$Zn(dipy)_3(NO_3)_2$
	1626 (*sh*)	1650 (*sh*)	1640 (*sh*)	1648 (*sh*)	1658 (*sh*)
1582*	1605*	1600*	1602*	1604*	1607*
1560		1570	1571		
1506		1490	1492	1496	1497
1460*	1470*	1470*	1473*	1467*	1478*
1422*	1443*	1442*	1443*	1447*	1443*
			1385	1375 (NO_3^-)	1380 (NO_3^-)
	1314	1312*	1315*	1319*	1320*
		1284	1285	1288	
1254*	1243	1249	1250	1251	1251
1214		1230	1230	1234	1230
		1179	1180	1179	1180
1140*	1160*	1160*	1160*	1161*	1161*
	1121				
1091*	1101	1100	1102	1101	1100
1065	1065	1062	1063	1062	1062
1040*	1044	1040	1043	1041	1043
995*	1020	1018*	1020*	1017*	1018*
	1008				
976					
891	901	908	910	910	911
				837	837
				830 } NO_3^-	830 } NO_3^-
				824	825
759†	778*	778*	778†	779†	778*
		765 (*sh*)	765 (*sh*)	763 (*sh*)	763 (*sh*)
741	735*	737*	738*	737*	738*
660	660	651	655	659	652
625		630	635	638	630
				623	
				540	
				442	
430	423*	433	440	425	433
405*		415*	415*	408*	415*
				405	
	364			364	355
		264*	286*	297*	280*
			260	258	

* Indicates the more intense bands.

† Indicates very intense bands.

the latter two metal ion cases. The iron(II) complex of each ligand differs very markedly from its homologues. However, all of the spectra of the complexes in this higher frequency range are chiefly spectra of slightly perturbed free ligands. These perturbations were discussed by SCHILT and TAYLOR.(1)

Below 600 cm^{-1}, in the spectra of all of the complexes of both series, new bands appear that are not found in the spectra of the pure ligands. In the region, the spectra of the different homologues within a series differ from one another. This area offers the greatest hope for the correlation of the spectra with other properties of the complexes.

TABLE 2.—INFRA-RED FREQUENCIES OF METAL ION 1,10-PHENANTHROLINE COMPLEXES IN Cl FROM 2000 CM^{-1} TO 250 CM^{-1}

Phen	$Fe(phen)_3Cl_2$	$Co(phen)_3Cl_2$	$Ni(phen)_3Cl_2$	$Cu(phen)_3(NO_3)_2$	$Zn(phen)_3(NO_3)_2$
		1667 (*sh*)			
1642					
1621	1630*	1625*	1620*	1620*	1625*
			1602	1605	
1585	1580 (*sh*)	1588	1578	1585	1588
1565					
1508*	1512	1520*	1520*	1520*	1520*
	1499	1503 (*sh*)	1498 (*sh*)	1497 (*sh*)	1501 (*sh*)
1422*	1435*	1425*	1421*	1421*	1430*
			1370	1380 (NO_3^-)†	1380 (NO_3^-)†
1344	1335	1347	1339	1340 (*sh*)	
	1319	1308	1302		
	1299				
	1254	1258	1252	1255	1255
1217	1222*	1222	1221	1223	1221
			1208	1207	1209
1183	1193*	1200	1200	1200	1199
1135	1143*	1140	1140	1143	1143
	1105 (*sh*)	1102*	1100*	1100	1101
1091	1093		1090 (*sh*)	1091 (*sh*)	1090 (*sh*)
1077	1055				
	1037				
	1007				
985	991				
	943				
	914				904
883		865 (*sh*)	865*	865*	865*
852*		855	850		
837*	845†	845†	842*	847†	848*
776					
772	775*	773*	769*	775*	773*
762					
738*				732	
730*	726†	725†	723†	722†	726†
709					
626*	645*	643*	645*	644*	643*
				620	621
					603
547	559	555	545		548
	530*				
511		508	506	508	511
		478	483		478
		440	444		457
411*		422*	425*	425*	422*
			409	410	407
			393		
				306	
	297*	288*	299*	300	288*
				288	
			256	266	262

* Indicates the more intense bands.

† Indicates very intense bands.

DISCUSSION OF THE RESULTS

For strong crystal field ligands, the maximum crystal field stabilization energy (CFSE) is for the d^6 electronic iron(II) system with a subsequent linear decrease of the CFSE to zero from cobalt(II) through zinc(II) except for the Jahn-Teller stabilized d^9 system of Cu(II). Superimposed on this trend is the increasing electrostatic attraction imposed by the decreasing ionic radii of iron(II) through Cu(II). Table 3 gives the log β_3's (the cumulative formation constants, BJERRUM *et al.*⁽³⁾) for the two homologous series. BUSCH and BAILAR⁽⁴⁾ postulate that the log β_3 of the iron(II) complexes is enhanced by π-bond formation from the metal ion to the heterocyclic aromatic ring ligand; and they cite the changes in the infra-red absorption spectra in the 1500–1700 cm^{-1} region as evidence to support this postulate.

TABLE 3.

Metal ion	Log β_3(dipy)⁽³⁾	Log β_3(phen)⁽⁷⁾
Fe^{2+}	17·1	21·5
Co^{2+}	—	20·1
Ni^{2+}	15	23·9
Cu^{2+}	17·9	20·4
Zn^{2+}	13·5	17·0

It might well be expected that this π-bond formation would be at a maximum when the $d\varepsilon$ triplet is filled and the $d\gamma$ doublet is vacant as is the case in iron(II), and would rapidly diminish in its contribution to the bonding as the $d\gamma$ doublet is filled. This is amply borne out by the spectral evidence in the case of both the $Fe(phen)_3Cl_2$ and the $Fe(dipy)_3Cl_2$ as the spectra of these complexes differ greatly in many respects from the spectra of the other members of the series. The increased stability of the iron(II) complexes on π-bond formation would be partially cancelled by the pairing energy required by the conversion of the electron configuration $d^2d^1d^1d^1d^1$ to that of $d^2d^2d^2d^0d^0$.

The spectra of the cobalt(II) complexes over the entire frequency range studied were quite similar to zinc(II) complexes and differed from the iron(II) complexes. Zinc(II) with its $d\varepsilon^6\,d\gamma^4$ electron configuration would have but a minimum of π-bond contribution to the metal ion–nitrogen bonds; hence, one would predict that the cobalt(II) nitrogen bonds possess little π-bond character. Consistent with this postulate is the measurements of FIGGIS and NYHOLM⁽⁵⁾ and RAGLIA and SIRONI⁽⁶⁾ who find that cobalt(II) in these complexes are high spin complexes rather than low spin complexes. Strong π-bonds in the cobalt(II) complexes would be expected to give low spin complexes.

BANKS and BYSTOFF⁽⁷⁾ suggest that the greater stability of the nickel(II) phenanthroline complexes relative to the copper(II) case occurs because the rigid phenanthroline ligand does not permit the tetragonal distortion required by the

---

⁽³⁾ J. BJERRUM, G. SCHWARZENBACH and L. G. SILLEN, *Stability Constants of Metal Ion Complexes with Solubility Products of Inorganic Substances, Part I. Organic Ligands.* The Chemical Society, London (1957).

⁽⁴⁾ D. H. BUSCH and J. C. BAILAR, *J. Amer. Chem. Soc.* **78**, 1137 (1956).

⁽⁵⁾ Q. FIGGIS and Q. NYHOLM, *J. Chem. Soc.* 338 (1959).

⁽⁶⁾ Q. RAGLIA and Q. SIRONI, *Gazz. Chim. Ital.* **87**, 1125 (1957).

⁽⁷⁾ C. V. BANKS and R. I. BYSTOFF, *J. Amer. Chem. Soc.* **81**, 6153 (1959).

Jahn-Teller stabilization of the d^9 copper(II) system. The spectrum of $Cu(dipy)_3(NO_3)_2$ does indicate some tetragonal distortion (i.e., the 625, 660 cm^{-1} bipyridine doublet is split into a 623, 638, 659 triplet in the copper compound), but the more rigid ligand phenanthroline indicates but little distortion by the evidence of the $Cu(phen)_3(NO_3)_2$ spectrum.

The octahedral complexes would possess D_3 symmetry, and one could as a first approximation regard the complex a seven body system of a metal ion and six nitrogen atoms interconnected pairwise. However, the experimentally covered frequency region would certainly not include all of the metal–ligand bond angle deformation vibrations; hence it does not seem profitable to attempt a complete vibrational assignment of the low frequency region on the basis of even this simplifying assumption.

As the vibration of the ligands and the metal ion against one another would be expected to be the highest energy new absorptions appearing in the spectrum of the complex; the highest frequency new bands should be assigned to the metal ion-nitrogen stretch. The assignment in Table 4 is based on this assumption with the exception of the iron complexes. Because the spectra of the iron complexes differed greatly from the uncomplexed amines and also the other metal–ammine complexes in the NaCl region; the author believes that the bonding of the iron complexes differs from the bonding of the other complexes. The spectral evidence indicates that the degree of π-bonding is greater for the iron complexes and that the iron–nitrogen stretching vibrations are at 423 for the dipyridine complex and 530 for the phenanthroline complex. The fact that the stability constants of the iron complexes do not differ greatly from those of the other complexes can be explained by the fact that the enhanced overall stability due to π-bond formation for these iron complexes is diminished by the energy required to pair the two electrons necessary to form these low-spin complexes.

TABLE 4.—SUGGESTED ASSIGNMENT FOR THE METAL ION–NITROGEN STRETCH VIBRATIONS FROM THIS WORK

Metal ion	ν me-N (dipy) cm^{-1}	ν me-N (phen) cm^{-1}
Fe^{2+}	423	530
Co^{2+}	264	288
Ni^{2+}	286	299
Cu^{2+}	297	(300)*
Zn^{2+}	280	288

* Average of multiple absorption.

Spectroscopic

The infra-red absorption spectra were obtained with a Beckman Model IR-4 spectrometer equipped with NaCl optics and with a Perkin Elmer Model 21 equipped with CsBr optics. All substances were examined as suspensions in KI pellets except for the Cu(II) compounds which oxidized the KI; for these substances KCl and CsBr pelleting materials were used. All substances were also run as Nujol mulls, and the only areas of difference were the relative intensities of the 700–800 cm^{-1} bands.

Analytical

All compounds were analysed for carbon, hydrogen, and nitrogen.* Since most of the compounds undergo decomposition on heating, melting points were not determined. The 1,10-phenanthroline monohydrate and 2,2′-bipyridine were obtained from the Distillation Products Industries and used without further purification.

For each of the following compounds the appropriate metal salt was dissolved in the minimum amount of water, and this solution was heated with a slight stoicheiometric excess of the amine until a single phase system was obtained. Upon cooling, crystals were obtained which were isolated by filtration through a glass fritted funnel, and the substances were recrystallised from hot water and stored over anhydrous sulphuric acid.

Tris-(2,2′-bipyridine)-iron(II) chloride pentahydrate. (Found: C, 52·64; H, 4·97; N, 12·15. Calc. for $Fe(dipy)_3Cl_2 \cdot 5H_2O$: C, 52·55; H, 4·97; N, 12·27%.)

Tris-(2,2′-bipyridine)-cobalt(II) chloride hexahydrate. An aqueous solution of this compound took up oxygen changing colour from yellow-brown to dark brown. The change was reversed upon the addition of an acid. The compound was crystallized from dilute hydrochloric acid and stored *in vacuo*. (Found: C, 51·09; H, 5·53; N, 12·12. Calc. for $Co(dipy)_3Cl_2 \cdot 6H_2O$: C, 50·90; H, 5·09; N, 11·85%.)

Tris-(2,2′-bipyridine)-nickel(II) chloride hexahydrate. (Found: C, 50·94; H, 4·96; N, 12·24. Calc. for $Ni(dipy)_3Cl_2 \cdot 6H_2O$: C, 50·9; H, 5·09; N, 11·90%.)

Tris-(2,2′-bipyridine)-copper(II) nitrate monohydrate. (Found: C, 53·45; H, 4·06; N, 16·32. Calc. for $Cu(dipy)_3(NO_3)_2 \cdot H_2O$: C, 53·45; H, 3·86; N, 16·61%.)

Tris-(2,2′-bipyridine)-zinc(II) nitrate tetrahydrate. (Found: C, 51·41; H, 4·45; N, 15·15. Calc. for $Zn(dipy)_3(NO_3)_2 \cdot 4H_2O$: C, 49·5; H, 4·39; N, 15·38%.)

Tris-(1,10-phenanthroline)-iron(II) chloride heptahydrate. (Found: C, 54·06; H, 4·81; N, 10·95. Calc. for $Fe(phen)_3Cl_2 \cdot 7H_2O$: C, 54·5; H, 4·79; N, 10·60%.)

Tris-(1,10-phenanthroline)-cobalt(II) chloride hexahydrate. This compound also exhibited the oxygen sensitivity described for the tris(dipy) cobalt(II) chloride. This was minimised by crystallisation from dilute hydrochloric acid and storing *in vacuo*. (Found: C, 55·03; H, 4·91; N, 10·93. Calc. for $Co(phen)_3Cl_2 \cdot 6H_2O$: C, 55·6; H, 4·63; N, 10·82%.)

Tris-(1,10-phenanthroline)-nickel(II) chloride heptahydrate. (Found: C, 53·78; H, 4·42; N, 10·45. Calc. for $Ni(phen)_3Cl_2 \cdot 7H_2O$: C, 54·1; H, 4·77; N, 10·51%.)

Tris-(1,10-phenanthroline)-copper(II) nitrate trihydrate. The use of copper(II) chloride in preparation gave a bright green product that was insoluble in water. The use of copper(II) nitrate gave a pale blue product. (Found: C, 56·79; H, 3·93; N, 14·23. Calc. for $Cu(phen)_3(NO_3)_2 \cdot 3H_2O$: C, 55·4; H, 3·83; N, 14·33%.)

Tris-(1,10-phenanthroline) zinc (II) nitrate dihydrate. (Found: C, 56·84; H, 3·55; N, 14·26. Calc. for $Zn(phen)_3(NO_3)_2 \cdot 2H_2O$: C, 56·62; H, 3·66; N, 14·66%.)

Acknowledgement—The author wishes to acknowledge the generous assistance of his NBS colleague Dr. S. C. WATT, JR. in many useful and stimulating discussions.

---

* Carbon, hydrogen, and nitrogen analyses were carried out by the Galbraith Microanalytical Laboratories, Knoxville, Tennessee.

J. Inorg. Nucl. Chem., 1962, Vol. 24, pp. 777 to 789. Pergamon Press Ltd. Printed in England

ECHANGE HETEROGENE D'IONS ISOTOPIQUES SUR COLONNE

APPLICATIONS RADIOCHIMIQUES: SEPARATION DU PHOSPHORE-32 ET DU SOUFRE-35 SUR COLONNE DE SULFATE DE BARIUM

M. Barrachina
División de Química, Junta de Energía Nuclear, Madrid, Espagne

(*Received* 7 *November* 1961)

On sait que les sels inorganiques considérés comme insolubles, mis dans l'eau, se dissolvent partiellement jusqu'à ce que la concentration de leurs ions dans la phase aqueuse atteigne la valeur prévue par leur produit de solubilité. Il s'ensuit que dans ce phénomène il y a un transport de matière au travers de l'interphase solide-liquide, initialement non compensé, par lequel un certain nombre d'ions qui constituent le corps solide passent en solution. Quand les concentrations d'équilibre sont atteintes, le transport des ions entre les deux phases, qui s'opère d'une façon permanente, a la même valeur dans les deux sens. Le système physique ainsi constitué est un exemple d'equilibre stationnaire de transport, analogue à celui existant entre un liquide et sa vapeur à la pression partielle d'équilibre.

Ce transfert d'ions entre les deux phases a été utilisé par Paneth et d'autres chercheurs,(1-4) en employant des indicateurs radiochimiques isotopiques avec les ions qui forment le composé insoluble, pour déterminer les superficies de corps finement divisés, tels que les precipités. On admet pour celà que le radioisotope ajouté à la solution contenant le corps se dilue isotopiquement avec tous ses ions existant dans la phase liquide et tous ceux qui forment la surface de la phase solide.

Ce même phénomène a été appliqué par Kolthoff et d'autres(5, 6) pour étudier l'influence de certains facteurs dans les processus de formation des cristaux qui constituent les precipités d'intérêt analytique.

Recemment, l'échange isotopique hétérogène a été employé par Sunderman, Meinke et d'autres,(7-10) pour séparer un radioisotope déterminé d'une solution qui contient un mélange complexe de radioélèments, par example, séparation de l'iode

---

(1) F. Paneth, *Elektrochem.* **28**, 113 (1922); F. Paneth et W. Vorwerk, *Z. Physik. Chem.* **101**, 445 (1922).

(2) R. M. Stow et J. W. T. Spinks, *Canad. J. Chem.* **33**, 938 (1955).

(3) R. E. Krehbiel et J. W. T. Spinks, *Canad. J. Chem.* **35**, 294 (1957).

(4) W. van den Heuvel, *Proceedings of the Second International Conference on the Peaceful Uses of Atomic Energy, Geneva*, 1958, Vol. 20, p. 145. United Nations (1958).

(5) I. M. Kolthoff et C. Rosenblum, *J. Amer. Chem. Soc.* **55**, 2656 (1933); **56**, 1264, 1658 (1934); **57**, 597, 607, 2573, 2577 (1935); **58**, 116, 171 (1936); I. M. Kolthoff et B. van't Riet. *Ibid.* **63**, 817 (1959).

(6) D. H. Lieser et A. Fabrikanos, *Z. Physik. Chem.* **22**, 246, 278, 398, 406 (1959).

(7) D. N. Sunderman et W. W. Meinke, U.S. A.E.C. Report AECU-3846 (1955).

(8) W. W. Meinke et D. N. Sunderman, *Nucleonics* **13**, No. 12, 58 (1955).

(9) D. N. Sunderman et W. W. Meinke, *Analyt. Chem.* **29**, 1579 (1957).

(10) W. J. Maeck et J. E. Rein, *Analyt. Chem.* **32**, 1079 (1960).

dans les produits de fission(10) et de l'argent-111 du palladium irradié.(8) La technique employé est très simple; elle consiste à introduire dans la solution une maille de platine contenant une pellicule de chlorure d'argent, sur laquelle s'effectue l'échange de ses ions inactifs par les $^{111}Ag^+$ de la solution(8) ou bien de mettre celle-ci en contact avec un précipité formé au préalable d'iodure d'argent.(10)

Dans les applications antérieurement citées, et d'autres que nous ne commentons pas,(11-13) étant moins en rapport avec l'objet de ce travail, la technique opératoire consiste toujours à mettre en contact d'un seul coup la phase liquide avec celle solide; ainsi l'échange de l'isotope actif se vérifie simultanément sur tous les points de la surface du précipité.

Au contraire, les applications décrites de l'échange isotopique employant la technique de "la colonne" sont jusqu' à présent très rares,(3, 4) malgré l'efficacité de fixation supérieure qu'on peut obtenir. Sans doute, cette faute d'applications a été motivée par deux causes: en premier lieu, par les difficultés de manipulation que présente l'emploi de produits finement divisés pour le remplissage des colonnes, et en second lieu, par la grande tendance qu'on suppose que ces corps aient, en raison de leur grande superficie, à présenter des phénomènes d'adsorption.

Le présent travail a pour objet d'initier l'étude des possibilités réelles qu'offre à la radiochimie ce type d'échange opérant sur colonne, de même qu'à la connaissance des facteurs qui jouent un rôle important lors de la fixation.

Il en résulte, d'après les expériences préliminaires réalisées, que des colonnes de précipités de petite hauteur, inférieure à un centimètre, permettent l'élimination complète d'un radioisotope d'une solution; on ne doit donc pas surestimer les difficultés que présente l'emploi de ces corps pour faire le remplissage de colonnes (grande perte linéaire de charge, débits faibles, etc.). Quand aux phénomènes d'adsorption, il est à conseiller d'employer des précipités cristallins envieillis, ceux-ci devant présenter ces phénomènes réduits au minimum. D'accord avec ce critère, le sulfate de barium fut choisi comme premier précipité à étudier.†

PARTIE EXPERIMENTALE

Réactifs

Sulfate de barium pour remplir les colonnes. Pour obtenir 50 g de $BaSO_4$ on part de 52·4 g de $BaCl_2 \cdot 2H_2O$ que l'on dissout dans 800 ml d'eau distillée contenant 5 ml d'acide nitrique concentré; à la solution chauffée presque à ébullition, en agitant continuellement, on ajoute goutte à goutte 100 ml d'une solution aqueuse qui contient 28·3 g de $(NH_4)_2SO_4$. La précipitation terminée on continue d'agiter en chauffant pendant une heure. Une fois le précipité deposé, et la phase liquide décantée, on ajoute 800 ml d'eau distillée et 1 ml d'acide nitrique concentré. Après avoir agité en chauffant pendant une heure on décante à nouveau la phase liquide. On effectue encore trois lavages par décantation en employant la même quantité d'eau distillée. Avant l'emploi, ce précipité est stocké une semaine dans le même recipitent, submergé par une petite quantité d'eau distillée.

---

† On emploie ici l'expression "d'ion isotopique actif ou inactif" pour distinguer le même ion dans le cas ordinaire et dans le cas où celuici comporte des isotopes actifs dans ses éléments constituants.

(11) T. W. OLCOTT, U.S. A.E.C. Report AECU-3372 (1956).

(12) S. IONESCU, I. NEGOESCU et I. GAINOR, *Proceedings of the Second International Conference on the Peaceful Uses of Atomic Energy, Geneva*, 1958, Vol. 20, p. 123. United Nations (1958).

(13) A. LANGER, *J. Chem. Phys.* **10**, 321 (1942); **11**, 11 (1943); *Analyt. Chem.* **22**, 1288 (1950).

Solution neutre de SO_4^{2-} *de 1 mg/ml.* Peser 1·37 g de $(NH_4)_2SO_4$ et dissoudre dans 1 l. d'eau distillée.

Solution neutre de NaCl *de 100 mg/ml.* Peser 10·00 g de NaCl et dissoudre dans 100 ml d'eau distillée.

Acide nitrique concentré; N; 0·1 N; 0·01 N. Tous les reactifs employés sont Merck, pour analyse.

Solution traceur de ^{35}S. Activité approximative 10 μc/ml, pH 2, soufre-35 sous forme sulfate.

Solution traceur de ^{32}P. Activité approximative 5 μc/ml, pH 2, on suppose que tout le phosphore-32 est sous la forme phosphate.

Apparaillage

pH mètre Beckman, modèle G, avec électrode de verre.
Détecteur G.M., Tracerlab, modèle TGC 2.
Echelle de 100, JEN, modèle E-6.
Colection de filtres d'aluminium pour mesures d'adsorption bêta, Tracerlab, modèle E-25.
Balance semimicro Mettler.
Pompe à vide, à membrane, Jouan.
Erlenmeyer à filtration de 1 l.
Feuille flexible de plastique (polyéthylène) de 0·1 mm d'épaisseur.

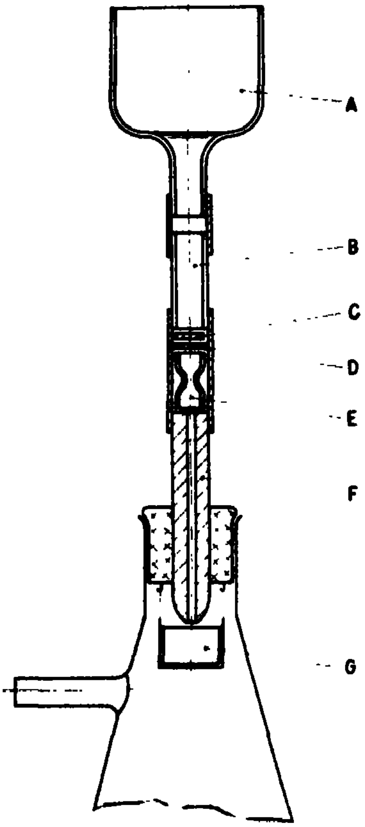

Fig. 1.—Montage des colonnes de precipités.

Méthode

Préparation des colonnes de sulfate de barium. On emploi le dispositif représenté sur la Figure 1, où:

A = récipient destiné à contenir le liquide qui doit passer sur la colonne.
B = tube de verre de 8 mm de diamètre intérieur dans lequel on forme la colonne de $BaSO_4$.
C = papier filtre à pores fins.
D = lamelle de polyéthylène ou de chlorure de polyvinyle avec de nombreux trous de très petits diamètres. On peut employer aussi de la laine de polyéthylène.
E = tube de verre étranglé au centre, sur lequel on fixe la lamelle D. La laine de polyéthylène substitue D et E.
F = tube capillaire.
G = petit récipient pour collecter les fractions.

Pour préparer la colonne on enlève le récipient A et on remplit le tube B avec la quantité nécessaire de la suspension de $BaSO_4$, on évacue l'eau au moyen d'un léger vide effectué dans l'Erlenmeyer, et on entraine le précipité qui adhère aux parois du tube avec de l'eau et en s'aidant d'une petite tige de verre. On lave par l'eau en réglant le débit à 6–8 ml h^{-1} cm^{-2}.

Les colonnes de $BaSO_4$ ainsi préparées ne permettent pas le passage de l'air même si elles manquent de liquide, car l'eau retenue dans le $BaSO_4$ par capilarité agit comme une valve fermant la colonne dans le domaine de dépression nécessaire pour obtenir les débits indiqués.

Caractéristiques des colonnes employées

Hauter du précipité = 1 cm
Section de la colonne = 0·5 cm^2
Densité apparente = 2–2·5 g de $BaSO_4/cm^3$ de colonne
Volume de phase aqueuse dans la colonne = 0·32 ml/g de $BaSO_4$
Débit = 6–8 ml/h cm^2
Superficie du $BaSO_4$ = $1{\cdot}3 \times 10^4$ cm^2/g
Relation des ions SO_4^{2-} en surface des cristaux de $BaSO_4$, au total des ions SO_4^{2-} dans le $BaSO_4$, approximativement, 1 pour 1000.

Expériences realisées avec les colonnes de $BaSO_4$

On a étudié les quatre types de problèmes suivants:

(a) Facteurs qui influent lors de la fixation de l'ion $^{35}SO_4^{2-}$ sur la colonne de $BaSO_4$.
(b) Adsorption sur la colonne des ions non isotopiques ($^{32}PO_4^{3-}$).
(c) Elution des ions $^{35}SO_4^{2-}$ fixés préalablement sur la colonne.
(d) Séparation des ions $^{32}PO_4^{3-}$ et $^{35}SO_4^{2-}$.

Pour étudier la fixation de l'ion $^{35}SO_4^{2-}$ sur la colonne on a fait passer à chaque fois des solutions marquées avec 1 μc de soufre-35 dans un volume total de 4 ml, sauf quand on étudie l'influence du volume; une fois la solution active passée, on á lavé la colonne avec 0·5 ml d'eau distillée. La distribution de l'activité du soufre-35 sur la phase solide de $BaSO_4$ a été déterminée par une technique autochromatographique semblable a celle décrite par KREHBIEL et SPINKS,(3) qui consiste à extraire la colonne de précipité, la couper en fragments de poids adequat selon la distribution de l'activité que l'on prévoit, former une couche d'épaisseur homogène avec chaque fragment dans une coupelle tarée, secher à 130°C à l'étuve, peser, mesurer l'activité et la corriger en tenant compte de l'autoabsorption.

Il en résulte dans ces conditions, loin de la saturation de la capacité de la colonne, que l'activité du soufre-35, exprimée en cpm/mg de $BaSO_4$, à différentes hauteurs de colonne, suit une loi approximativement exponentielle; pour cette raison on a adopté la représentation semi-logarithmique de la Figure 2, qui donne une droite bien définie, dont la pente permet de caractériser l'allure de la fixation sur chaque essai. A partir de la valeur de la pente trouvée, p, on peut calculer la hauteur de colonne qui fixe la moitié de l'activité passé sur colonne:

$$E_{\frac{1}{2}}\,(\text{g/cm}^2) = \frac{-0{\cdot}693}{p}$$

et avec cette valeur on peut prévoir la hauteur nécessaire de colonne qui élimine de la solution le pourcentage désiré.

Pour des conditions expérimentales différentes de celles décrites ci-dessus, on verra que la représentation exponentielle n'est plus valable, Figure 3, et que les courbes de fixation suivent l'allure clasique de celles de saturation dans les phénomènes d'échange ionique.

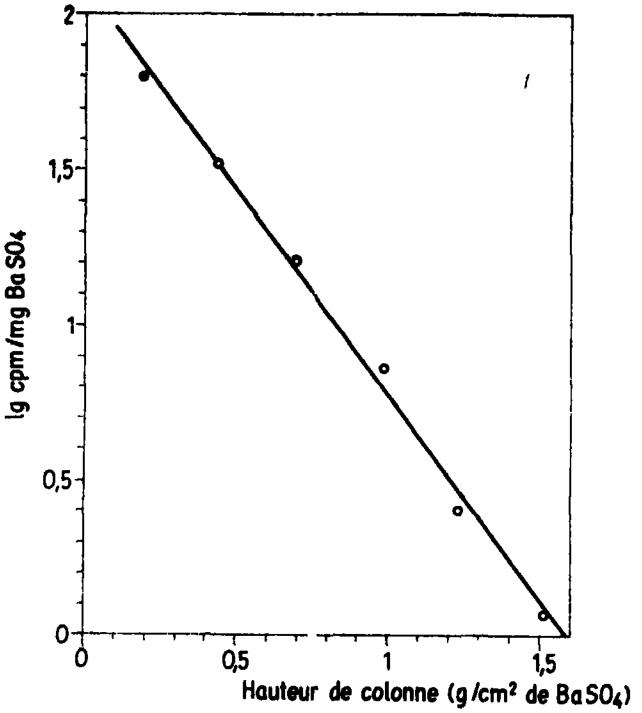

FIG. 2.—Distribution de l'activité du $^{35}SO_4^{2-}$ dans une colonne de $BaSO_4$. pH de fixation = 2, concentration de SO_4^{2-} = 25 μg/ml.

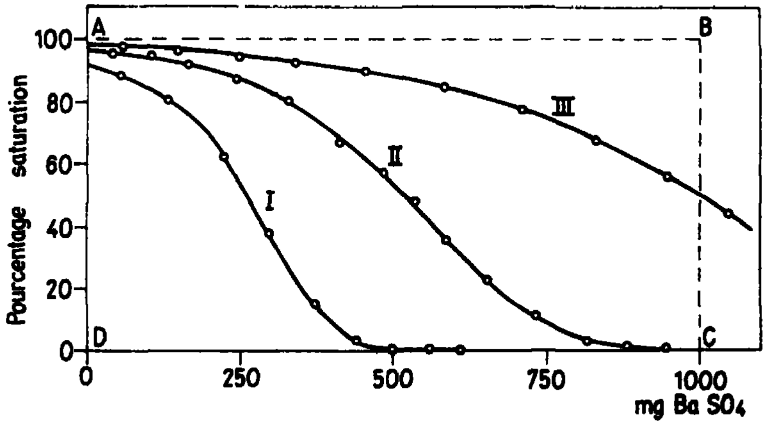

FIG. 3.—Courbes de saturation des colonnes de $BaSO_4$ pour la fixation du $^{35}SO_4^{2-}$ avec entraîneur.

Courbe I: 5 μg SO_4^{2-}/ml
Courbe II: 10 μg SO_4^{2-}/ml
Courbe III: 20 μg SO_4^{2-}/ml

Pour étudier l'adsorption qu'une colonne de ce genre présente pour des ions non isotopiques on a employé des solutions marquées par 0·5 μc de phosphore-32. On a choisi ce radioisotope pour la fréquence avec laquelle il est accompagné du soufre-35 dans les procédés respectifs de production dans un réacteur et parce qu'on a jamais donné une méthode facile pour la purification totale de l'un par rapport à l'autre avec un rendement élevé.

On a jugé qualitativement l'importance de l'adsorption à partir de la forme des courbes d'activité effluant de phosphore-32 en fonction du volume passé. Citons dans ce cas, comme dans celui où on étudie l'élution du $^{35}SO_4^{2-}$, que les solutions passées sur colonne contenaient 10 mg/ml de NaCl, ayant pour objet de déterminer par pesée de l'extrait sec le volume de chacune des fractions collectées. Les fractions recueillies dans le collecteur ont été transférées dans des coupelles tarées, séchées à l'étuve, pesées, et leur activité mesurée. Si le residu sec est grand, on fait la correction due à l'autoabsorption.

DISCUSSION DES RESULTATS

Influence du pH dans la fixation de l'ion $^{35}SO_4^{2-}$ *sur la colonne de* $BaSO_4$

Sur la Figure 4 on a représenté les résultats expérimentaux d'une série d'essais de fixation où l'unique variable est le pH de la solution de passage sur colonne. Pour des pH inférieurs à 2, les valeurs qui figurent en abscisses ont été déduites de la normalité de l'acide nitrique employé pour préparer les solutions.

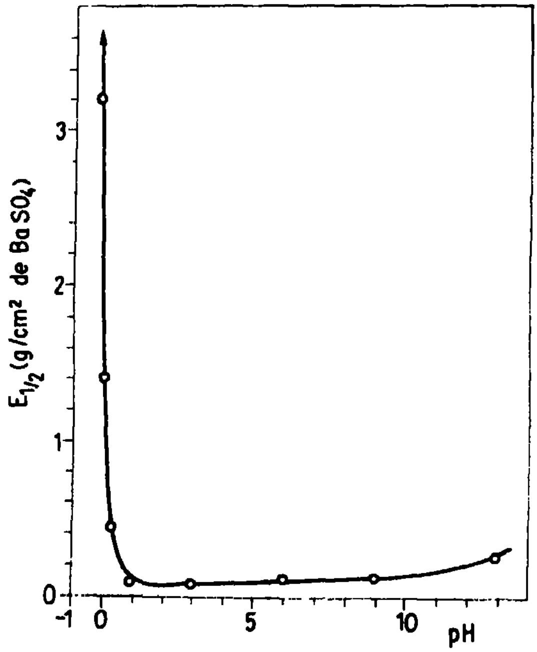

FIG. 4.—Influence du pH dans la distribution du $^{35}SO_4^{2-}$ sur colonne de $BaSO_4$.

Comme on peut le voir, la fixation de l'ion $^{35}SO_4^{2-}$ sur la colonne a lieu tout au long de la zone de pH où le $BaSO_4$ est stable: quand l'acidité est supérieure à 0·1 N, la longueur de la colonne nécessaire pour éliminer le soufre-35 de la solution augmente brusquement, celà est dû à ce que dans ces conditions, le $BaSO_4$ commençant à se dissoudre, il y a une augmentation de la concentration des ions sulfate dans la phase liquide, d'où une diminution de la probabilité d'échange entre les ions sulfate actifs de la solution et les inactifs de la surface de la phase solide. Pour des concentrations d'acide nitrique N ou supérieures on peut considérer, du point de vue de cet échange, que le $BaSO_4$ est instable, puis qu'il y a un certain déséquilibre de transport des ions sulfate, à travers de l'interphase, favorable à la phase liquide. D'autre part, pour des acidités élevées le soufre-35 doit se trouver complètement sous forme d'acide sulfurique, ou, au moins, d'ion SO_4H^-, qui ne serait pas facilement échangeable avec les ions SO_4^{2-} du réseau cristallin.

Influence de la concentration des ions SO_4^{2-} *inactifs dans la fixation des ions* $^{35}SO_4^{2-}$ *sur la colonne de* $BaSO_4$

Sur la Figure 5 on a représenté les résultats expérimentaux d'une série d'essais de fixation à pH 2, où l'unique variable est la concentration des ions SO_4^{2-} dans la solution active de $^{35}SO_4^{2-}$ qui est passée sur la colonne.

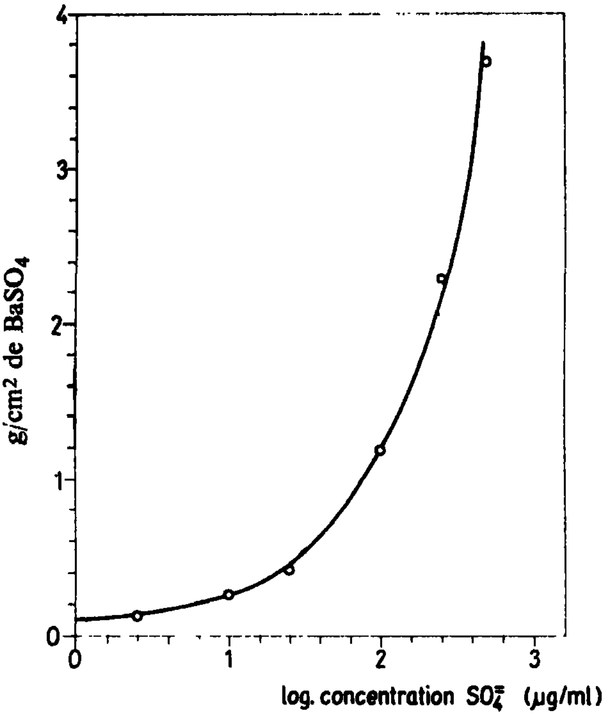

FIG. 5.—Influence de la concentration du SO_4^{-} dans la distribution du $^{35}SO_4^{2-}$ sur colonne de $BaSO_4$.

On s'apperçoit immédiatement du rôle décisif que joue la concentration de l'entraîneur sur la hauteur de colonne nécessaire pour fixer l'activité du soufre-35. Pour des grandes concentrations en entraîneur la colonne se comporte comme si elle était perméable aux ions actifs, ceci est dû à ce que la probabilité qu'ont les ions $^{35}SO_4^{2-}$ d'être échangés lors de leur passage à travers la masse de $BaSO_4$ est petite, et par conséquent dans la solution effluente on peut toujours trouver ceux-ci en quantité.

Au contraire, quand la concentration d'entraîneur est faible, l'efficacité de la colonne pour la fixation augmente rapidement. Etant donné que la concentration minimum d'entraîneur à laquelle on peut faire la fixation est celle du produit de solubilité du $BaSO_4$, la hauteur de colonne pour cette valeur, que l'on peut déduire approximativement de l'ordonnée à l'origine du graphique, sera une donnée importante dans toutes les fixations de soufre-35 sans entraîneur.

A la différence des échangeurs d'ions ordinaires qui ont une capacité définie de fixation, les colonnes de précipités présentent une capacité pour fixer leurs ions isotopiques actifs que dépend de la relation où se trouvent ceux-ci par rapport aux inactifs dans la phase liquide et du nombre total d'ions dans cette phase au total d'ions du même genre formant la surface de la phase solide.

Des essais de fixation réalisés en ajoutant 1 mg/ml d'ion PO_4^{3-} ont démontré que la présence de cet ion n'a aucun effet sur la fixation de l'ion $^{35}SO_4^{2-}$ sur la colonne.

Détermination de la capacité maximum d'une colonne de $BaSO_4$ *pour fixer l'ion* $^{35}SO_4^{2-}$

Sur la Figure 3 on a représenté les resultats de fixation à pH 5 de trois solutions de 25 ml de volume contenant 5, 10 et 20 μg/ml d'ion SO_4^{2-} marqué avec du $^{35}SO_4^{2-}$. Avec ces courbes on peut déterminer graphiquement la capacité de ces colonnes pour fixer l'ion $^{35}SO_4^{2-}$. Il suffit pour celà de mesurer la surface s comprise entre l'une des courbes I ou II, et l'axe d'abscisses et la rapporter à la "surface de saturation" S représentée par le rectangle $ABCD$. La capacité maximum vient donnée par la formule suivante;

$$\text{Capacité max. (c/g BaSO}_4) = \frac{S\,N}{s\,n}$$

où, N est le nombre de μg totaux d'ion SO_4^{2-} passés sur colonne, et n, le nombre de μg d'ion $^{35}SO_4^{2-}$ portant un curie.

Des courbes I et II de la Figure 3 on obtient que 1 g du $BaSO_4$ employé peut éliminer d'une solution 9–10 c de soufre-35 sans entraîneur sous forme sulfate.

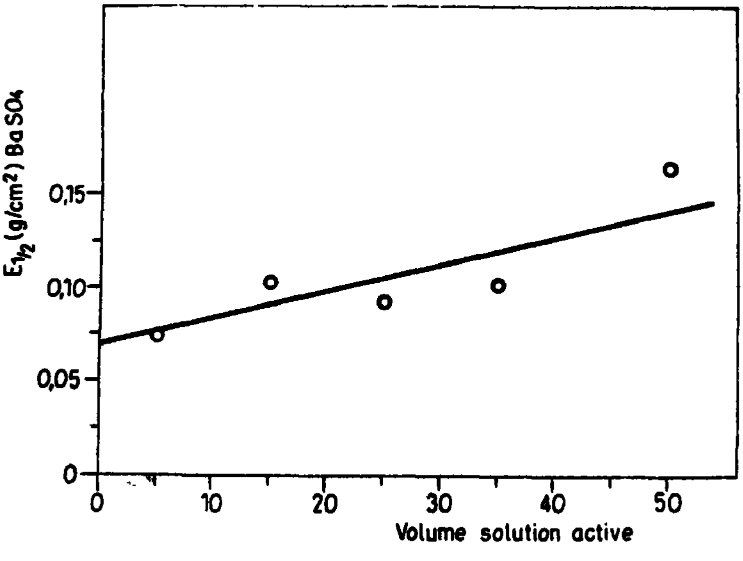

FIG. 6.—Influence du volume de solution active passée sur colonne dans la distribution du $^{35}SO_4^{2-}$. Activité constante.

Influence du volume de solution active passée sur colonne dans la fixation des ions $^{35}SO_4^{2-}$ *sur le* $BaSO_4$

Sur la Figure 6 on a représenté les résultats experimentaux d'une série d'essais de fixation à pH 2 sans entraîneur, où la seule variable est le volume dans lequel on a dilué la solution active. On a observé que lorsque les volumes passés sur colonne sont élevés, les résultats expérimentaux ne satisfont pas correctement la loie exponentielle proposée. Cependant, on peut déduire du graphique que la capacité de fixation de la colonne diminue légèrement à fur et à mesure que le volume dans lequel est contenue la solution est grand. Ceci paraît indiquer que la concentration des ions SO_4^{2-} en équilibre avec le $BaSO_4$ produit un certain effet d'autoélution proportionnel au volume passé.

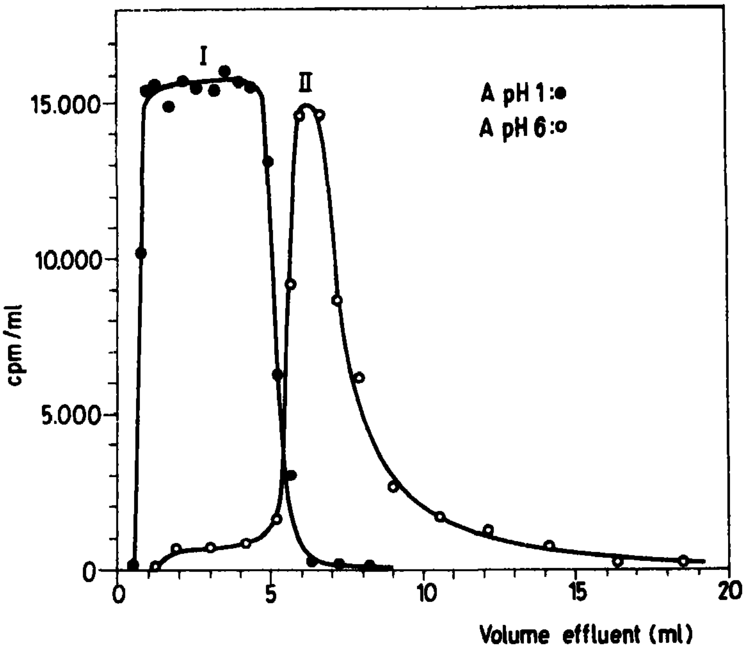

FIG. 7.—Activité du $^{32}PO_4^{3-}$ effluent d'une colonne de $BaSO_4$.

Adsorption des ions $^{32}PO_4^{3-}$ *sur colonne de* $BaSO_4$

Sur la Figure 7 on a représenté les resultats obtenus en faisant passer sur la colonne une quantité totale du ^{32}P de 0·5 μc dans 4 ml, à pH 1, et à pH 6, et en mesurant l'activité des effluents; on emploi comme solution de lavage une solution de NaCl à 10 mg/ml au pH correspondant. Les courbes obtenues aux valeurs du pH comprises entre les deux citées plus haut présentent une évolution graduelle de formes entre les deux représentées.

La courbe I est typique d'un ion actif qui passe sur la colonne sans y subir aucune interaction. La colonne est, dans ces conditions, perméable pour le ^{32}P en tant que phosphate. La courbe II indique, au contraire, qu'à pH 6 la colonne exerce un fort effet cromatographique au passage de l'ion $^{32}PO_4^{3-}$. Ceci implique, pour autant, que l'adsorption des ions PO_4^{3-} augmente progressivement avec le pH. Cependant, on peut considérer que lorsque le pH est inférieur à 3, l'ion $^{32}PO_4^{3-}$ passe quantitativement sur la colonne sans subir une perte apreciable d'activité.

Elution des ions $^{35}SO_4^{2-}$ *fixés sur la colonne de* $BaSO_4$ *avec une solution inactive de* SO_4^{2-} *de* 0·1 *mg/ml*

Sur la Figure 8 on a représenté la courbe d'élution à pH 6 de l'ion $^{35}SO_4^{2-}$ qu'on avait préalablement fixé sur la colonne au même pH.

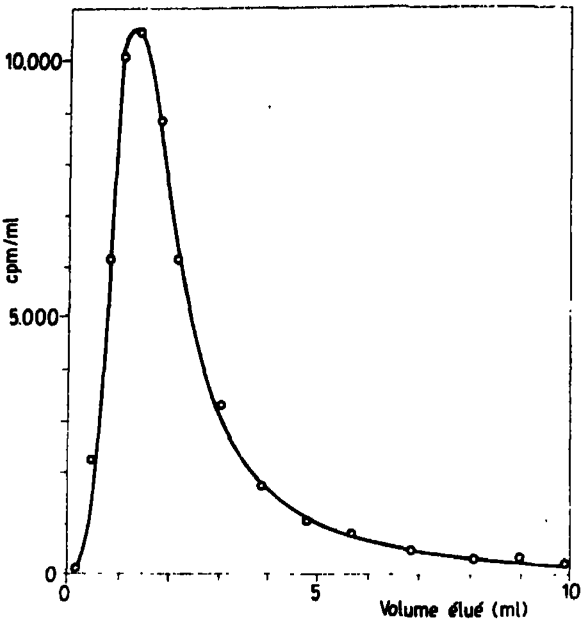

FIG. 8.—Elution du $^{35}SO_4^{2-}$ fixé sur colonne de $BaSO_4$ avec solution de SO_4^{2-} (0·1 mg/ml).

Cette courbe a de l'importance au point de vue du mécanisme de l'échange isotopique hétérogène, car elle démontre que les ions $^{35}SO_4^{2-}$ restent déposés sur la surface des cristaux qui forment la masse de $BaSO_4$, d'où ils peuvent être remplacés par les ions SO_4^{2-} durant l'élution.

La longue queue que ces courbes présentent peut être dûe, pour une part, à la nature purement statistique, même affinité, par laquelle opère la solution éluante, et d'autre part, à la diffusion possible des ions $^{35}SO_4^{2-}$ vers l'intérieur des cristaux de $BaSO_4$, qui seraient alors plus difficiles à éluer. L'effet de la diffusion dépend, naturellement, du temps passé entre la fixation et l'élution.

Importance de la diffusion des ions SO_4^{2-} *dans les cristaux de* $BaSO_4$

On prépare du $BaSO_4$ marqué avec una quantité connue de soufre-35, suivant la méthode de précipitation décrite, et on emploie ce précipité, au lieu de l'inactif, pour former une colonne d'environ 5 mm de hauteur. Sur la colonne ainsi obtenue, après l'avoir lavée avec de l'eau distillée, on fait passer une solution qui contient 1 mg/ml de l'ion SO_4^{2-} et 10 mg/ml de NaCl, à pH 6; l'opération terminée, on lave à nouveau la colonne avec de l'eau distillée. On a représenté sur la Figure 9 la teneur en soufre-35 de la solution effluente.

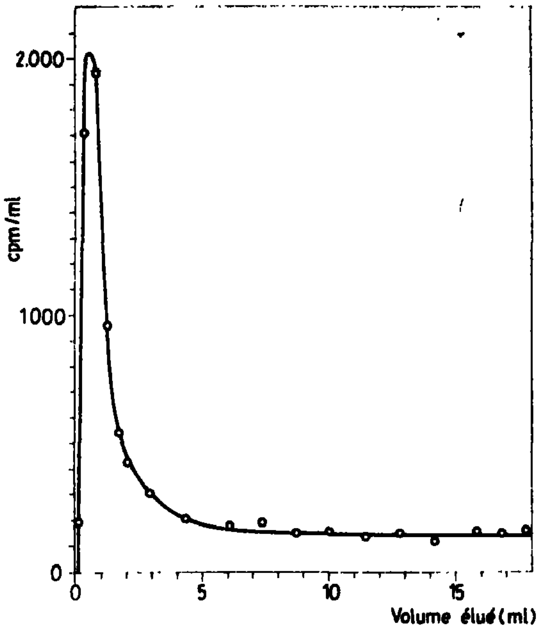

FIG. 9.—Elution du $^{3}{}_{8}SO^{52-}$ du $Ba^{*}SO_4$ avec solution de SO_4^{2-} (1 mg/ml). Hauteur de colonne ≃ 5 mm.

On a répété deux fois sur la même colonne le passage des solutions décrites antérieurement en laissant s'écouler entre chaque opération l'intervalle d'un jour.

Les trois courbes d'élution obtenues ont la même forme et correspondent à la même activité totale que celle repréntée sur la Figure 9. Il est à noter le palier horizontal qu'elles présentent à partir d'un certain volume élué. Ces courbes peuvent s'interpréter de la façon suivante;

(a) Le maximum de la courbe correspond à l'élution des ions $^{35}SO_4^{2-}$ que les cristaux de la masse de $BaSO_4$ possédaient "in situ" formant leur surface.

(b) Le palier horizontal correspond à l'élution des ions $^{35}SO_4^{2-}$ qui diffusent depuis l'intérieur du cristal vers la couche externe du même cristal, d'où ils sont élués.

(c) La colonne laissée en repos un certain temps, la distribution des ions $^{35}SO_4^{2-}$ est homogénéisée à nouveau par diffusion sur la surface et à l'intérieur des cristaux et il est possible de retrouver la courbe d'élution (Figure 9) de l'opération précédente.

Les courbes tracées à la suite de ces essais ont de l'intérêt pour la détermination des coefficients de diffusion. En ce qui nous concerne, les données radiochimiques, les données cristallographiques du $BaSO_4$ et la superficie total de la masse de $BaSO_4$ employée, nous ont permis d'attribuer au coefficient de diffusion des ions SO_4^{2-} dans le $BaSO_4$ une valeur de l'ordre de 10^{-19} cm²/seg.(6, 15) Ainsi, si on laisse s'écouler peu de temps entre la fixation et l'élution, la diffusion a une importance très secondaire.

Séparation des ions $^{32}PO_4$ *et* $^{35}SO_4$ *sur colonne de* $BaSO_4$

Sur la Figure 10 on a représenté l'activité effluente d'une colonne de $BaSO_4$ sur laquelle on a fait passer una solution active qui contenait le mélange d'ions $^{32}PO_4^{3-}$ et $^{35}SO_4^{2-}$, à pH 2.

(14) E. D. McClanahan, U.S. A.E.C. Report HW-47676 (1959).

(15) J. Crank, *The Mathematics of Diffusion*, p. 2. Clarendon Press, Oxford (1956).

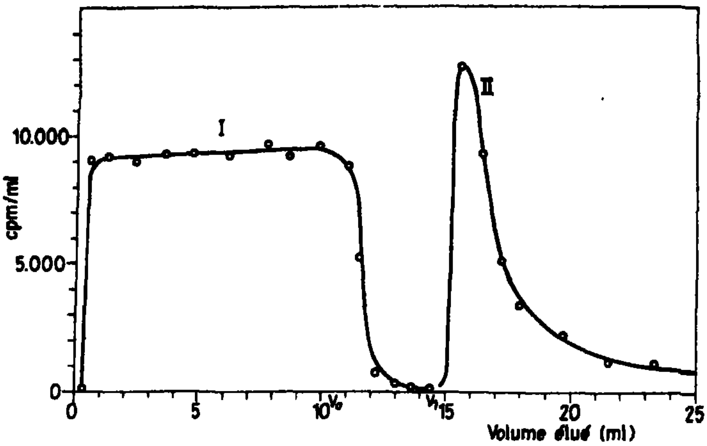

FIG. 10.—Séparation du $^{32}PO^{3}_{4}{}^{-}$ et du $^{35}SO_4{}^{2-}$ sur colonne de $BaSO_4$.

La courbe I, de forme rectangulaire, correspond à l'activité du phosphore-32 que passe sur la colonne sans subir de fixation ni d'adsorption et par conséquent, il en résulte aucune dilution de son activité.

Le volume élué compris entre v_0 et v_1 correspond au lavage avec l'acide nitrique 0·01 N que l'on effectue après avoir passé la solution active.

La courbe II correspond à l'élution de l'activité du soufre-35 fixé sur la colonne, en employant comme solution éluante 0·2 mg/ml de $SO_4{}^{2-}$, à pH 2.

On a vérifié par adsorption bêta et détermination de la période sur diverses fractions collectées que les espèces radiochimiques ainsi séparées ne présentaient aucune contamination mutuelle.

Il faut noter que cette séparation est spécialement intérésante pour déterminer ou purifier le phosphore-32 contenu dans le mélange, car l'élution de soufre-35 ne peut être considérée comme quantitative (longue queue d'élution), et en plus, le produit obtenu a une activité spécifique très basse. Si le but recherché est de déterminer ou de purifier le soufre-35 on doit employer alors une colonne qui soit isotopique avec le $^{32}PO_4{}^{3-}$. Dans ce sens, nous avons employé avec succès des colonnes de $BiPO_4$ et la solution à passer sur colonne étant à pH 10. Dans ces conditions le $^{35}SO_4{}^{2-}$ ne se fixe pas, ni s'adsorbe pas, tandis que tout le $^{32}PO_4{}^{3-}$ est retenu.

CONCLUSIONS

Nous résumons dans ce qui suit les aspects les plus remarquables de l'échange isotopique hétérogène (en abrégé EIH) mis en évidence dans ce qui précède.

(1) L'EIH est un phénomène qui consiste au transport ininterrompu d'ions isotopiques à travers l'interphase du système.

(2) Le nombre total d'ions transportés par unité de temps et unité de superficie de l'interphase controle la cinétique de l'échange d'un ion isotopique actif avec ceux de la colonne.

(3) En employant des précipités cristallins envieillis, la surface des cristaux est la seule partie à jouer un rôle important pour l'EIH. La participation que peut avoir la partie intérieure des cristaux dépend de la valeur qu'à le coefficient de diffusion du cristal pour ses propres ions et du temps du processus.

(4) L'EIH pratiqué sur colonne profite de la dilution qu'opère cet échange sur un ion isotopique actif entre les deux phases du système, et permet de "l'arrêter" de façon la plus effective sur la phase solide, la phase liquide effluente restant exempte de lui.

(5) La spécificité de l'EIH est dûe à la sélection qu'opère le réseau cristallin du précipité sur les ions qui peuvent éventuellement former partie de celui-ci. Des réactions d'autres ions actifs qui conduisent à les fixer sur la colonne peuvent diminuer cette spécificité, tel la formation de composés isomorphiques, la formation de complexes, l'hydrolyse, l'adsorption, la diffusion, etc.

(6) L'intérêt de l'EIH reste limité en principe à la radiochimie, car seulement l'emploi de radioisotopes rend cet échange visible ou profitable.

(7) L'EIH sur colonne peut substituer avantageusement dans quelques cas les précipitations avec entraîneur employées en analyse radiochimique.

(8) L'EIH sur colonne peut être utile dans le champ de production de radioisotopes artificiels pour éliminer des impuretés radiochimiques.

(9) Le grand nombre de composés insolubles qui peuvent s'employer "comme masse de résine" ouvre un champ intérésant de travail dans ce sens à la radiochimie.

———Je tiens à remercier ici le Prof. R. F. Cellini et M. M. G. Dominguez et Fe de la Cruz, par leurs encouragements et leurs conseils, grâce auxquels il nous a été possible de mener à bien ce travail.

J. Inorg. Nucl. Chem., 1962, Vol. 24, pp. 791 to 795. Pergamon Press Ltd. Printed in England

THE CRYSTAL STRUCTURE OF DI-IODODI-(*o*-PHENYLENEBISDIMETHYLARSINE) PLATINUM(II) $Pt(C_6H_4[As(CH_3)_2]_2)_2I_2$

N. C. STEPHENSON
Department of Chemistry, University of New South Wales, Sydney, Australia

(*Received* 11 *July* 1961; *in revised form* 20 *November* 1961)

Abstract—The structure of the compound $Pt(C_6H_4[As(CH_3)_2]_2)_2I_2$ has been determined by X-ray diffraction methods. The substance crystallizes in the monoclinic system, space group $P2_{1/c}$ (C_{2h}^5) with $a = 9{\cdot}68$ Å, $b = 9{\cdot}27$ Å, $c = 17{\cdot}27$ Å, $\beta = 114°30'$ (all to $\frac{1}{4}$ per cent), $Z = 2$. The calculated and observed densities of the compound are 2·25 and 2·26 g cm^{-3} respectively.

The atomic co-ordinates were refined by successive Fourier difference maps using the (*hol*) and (*okl*) data. The structure consists of discrete molecules packed together in the crystal lattice. The central divalent platinum atom is surrounded by four arsenic atoms in a square plane and at distances of 2·38 Å. The two iodine atoms complete a distorted octahedral arrangement with elongated metal iodine bonds of 3·50 Å. The nature of the bonding is briefly discussed.

WHILE investigating the complexes of the chelate group *o*-phenylenebis-(dimethylarsine), denoted by diarsine, the reaction

$$[M(diarsine)_2]^{2+} + X^- \rightarrow [M(diarsine)X_2]^+$$

where X = Cl, Br and I, and M = Pd and Ni, was observed (1) to occur in non-aqueous ionizing solvents such as nitrobenzene. Complexes of the general formula $[M(diarsine)_2X]ClO_4$ were isolated from acetone solutions. The metal apparently exist as five covalentions in nitrobenzene solution, for the perchlorates function as uni-univalent electrolytes in this solvent.

The compound $Pt(diarsine)_2I_2$ also behaves as a uni-univalent electrolyte in nitrobenzene solution, presumably forming the ions $[Pt(diarsine_2I]^+$ and I^-. The usual stereochemistry of divalent platinum is that of a square-planar arrangement and for this reason the structure of di-iododi-(*o*-phenylenebisdimethylarsine) platinum (II) has been investigated.

EXPERIMENTAL

A single crystal of the compound was obtained by slow evaporation from a nitrobenzene solution. An examination of the reciprocal lattice with a Buerger precession instrument revealed a monoclinic cell with dimensions $a = 9{\cdot}68$ Å, $b = 9{\cdot}27$ Å, $c = 17{\cdot}27$ Å, $\beta = 114°30'$ (all to $\frac{1}{4}$ per cent).

The density of the crystals at room temperature was measured by flotation in a methylene iodide–benzene mixture ($\rho_{obs} = 2{\cdot}26$ g cm^{-3}). Two molecules of the diarsine complex per unit cell give a calculated density of 2·25 g cm^{-3}.

The only absent spectra were (*hol*) with *l* odd and (*oko*) with *k* odd. The space group is thus $C_{2h}^5 - P2_1/c$.

(1) C. M. HARRIS. Ph.D. Thesis, Sydney (1955).

Three hundred reflexions were recorded with the Buerger precession camera ($\mu = 30°$, $F = 6{\cdot}000$ cm, $S = 26{\cdot}0$ mm, $\lambda \mathrm{Mo}K\alpha = 0{\cdot}7107$ Å). Ilford G film was utilized in timed exposures for the (*hol*) and (*okl*) levels which gave an interfilm density ratio of 10:1. The intensities were measured photometrically and corrected for the polarization and asymmetric Lorentz factors according to WASER.(2) Square roots were then taken in order to obtain the moduli of the observed structure factors.

DETERMINATION OF THE STRUCTURE

The two platinum atoms in the unit cell were placed in special position 000 and $0\frac{1}{2}\frac{1}{2}$ viz, position *a* of space group No. 14. Their contributions to the structure factors, although always at a positive maximum, were not enough to completely determine phases. Consequently, two dimensional Patterson functions were computed at 6° intervals on the 010 and 100 planes. The very heavy Pt-I vectors enabled the iodine atom to be located and by shifting the origin to the centric I-I vector the co-ordination of the arsenic atoms were obtained.

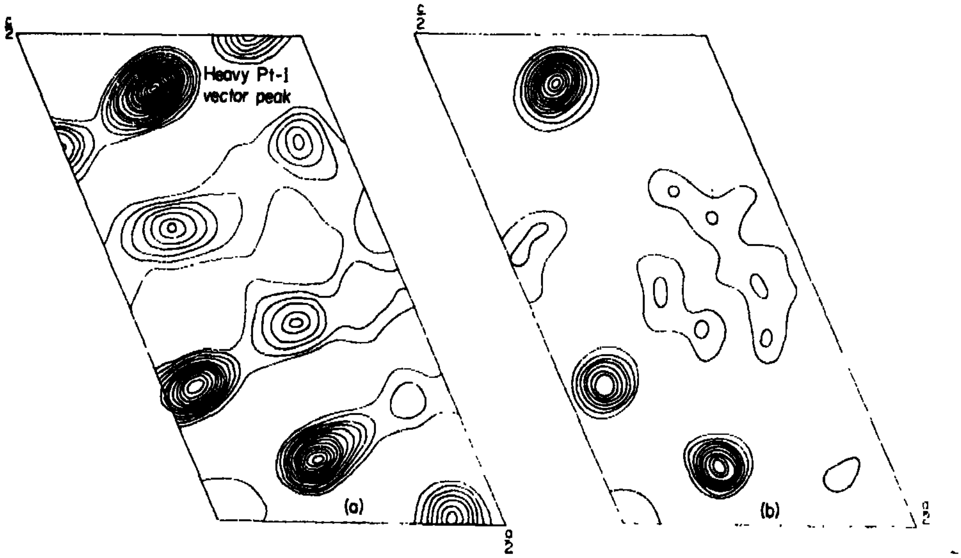

FIG. 1 (a).—The (*hol*) Patterson function, showing the very heavy Pt–I vector peak.

FIG. 1 (b).—The first (*hol*) Fourrier map showing resolution of the arsenic and iodine atoms.

Contours on an arbitrary scale; negative contours omitted.

Further information to assist in assigning phases was obtained from the moduli of the observed (*hol*) and (*okl*) structure factors for the related palladium and nickel compounds. The series of compounds of the formula M(diarsine)$_2$I$_2$ where M = Pt, Pd and Ni, proved to be isomorphous and have the following cell dimensions.

The intensity data for each compound were placed on an approximate absolute scale by the method of WILSON (3) and the resulting sets of structure factors, for corresponding zones, examined. Since the heavy metal atoms (M) are located at the origin their

(2) J. WASER, *Rev. Sci. Instrum.* **22**, 567 (1957).

(3) A. J. C. WILSON, *Nature, Lond.* **150**, 152 (1942).

contributions to the structure factors, viz. $F(\mathrm{M})$ will always be positive and except for very small values of $F(\mathrm{Pt})$ the phase angles of $F(\mathrm{Pt})$ are zero if $F(\mathrm{Pt}) > F(\mathrm{Pd}) > F(\mathrm{Ni})$ or π if $F(\mathrm{Pt}) < F(\mathrm{Pd}) < F(\mathrm{Ni})$.

	Pt(diarsine)$_2$I$_2$	Pd(diarsine)$_2$I$_2$	Ni(diarsine)$_2$I$_2$
a Å	9·68	9·64	9·49
b Å	9·27	9·24	9·25
c Å	17·27	17·23	16·94
β	114°30′	114°0′	114°0′

The information obtained by these methods enabled the signs of a large number of observed structure factors to be determined and the resulting Fourier projection on the 100 and 010 planes yielded co-ordinates for the heavy atoms. The light carbon atoms were located and the co-ordinates of all atoms were then refined by successive difference Fourier projections. The final atomic co-ordinates are listed in Table 1. These co-ordinates were used to compute the final calculated structure factors which are listed in the appendix for comparison with the moduli of the observed structure factors. An overall isotropic temperature factor $B(okl) = 2{\cdot}79$ Å^2 was used in this calculation for the (okl) zone of reflexions. The scattering curve for iodine for the (hol) zone of reflexions was represented by $f = f_0 \exp[-\{\alpha+\beta\sin^2(\phi-\psi)\}S^2]$ where $\alpha = 2{\cdot}7$, $\beta = 3{\cdot}4$, $\psi = 102°$ were determined directly from the difference maps. (4) Isotropic thermal parameters of 2·8, 3·1, and 3·1, were used for platinum, arsenic and carbon respectively.

TABLE 1.—FINAL ATOMIC CO-ORDINATES

	x	y	z		x	y	z
	a	b	c		a	b	c
Pt	0·0000	0·0000	0·0000	C$_4$	0·935	0·930	0·198
As$_1$	0·2083	0·1624	0·0590	C$_5$	0·200	0·029	0·203
As$_2$	0·0715	0·9164	0·1419	C$_6$	0·227	0·025	0·290
I	0·2050	0·7384	0·9451	C$_7$	0·342	0·109	0·347
C$_1$	0·149	0·347	0·031	C$_8$	0·438	0·194	0·328
C$_2$	0·359	0·141	0·021	C$_9$	0·398	0·217	0·234
C$_3$	0·188	0·756	0·171	C$_{10}$	0·267	0·136	0·183

The Reliability Index R, calculated over all reflexions was 0·10.

THE PRECISION OF THE FINAL ATOMIC CO-ORDINATES

An approximate estimate of peak curvature was obtained by making assumptions which are not strictly valid; firstly that the peak shape is given by $\eta_r = \eta_o \exp(-pr^2)$ and secondly that the errors are independent of orientation. The above expression was normalized so that the area under the curve represented the atomic number of the atom concerned and values for the second differential were calculated. Valves of p were obtained for circular, resolved atoms by calculating the one dimensional shape transforms of the appropriate atomic form factors which had been corrected for temperature effects. The values of p for arsenic, iodine and carbon curves are 5·4, 5·4 and 4·6, giving standard deviations in atomic co-ordinates of 0·002 Å, 0·001 Å and 0·03 Å respectively.

(4) W. COCHRAN, *Acta Cryst.* **4**, 81 (1951).

DISCUSSION OF THE STRUCTURE

New co-ordinates were assigned to each atom, referring them to a set of orthogonal axes *a*, *b*, and *c'*, *c'* being taken perpendicular to the *a* and *b* crystal axes. These co-ordinates were expressed in Angstrom units and enabled bond distances and angles to be readily calculated.

The environment of the platinum atom, as it exists in the crystal, is depicted in Fig. 2. The bond lengths and angles are given both in Fig. 2, and Table 2.

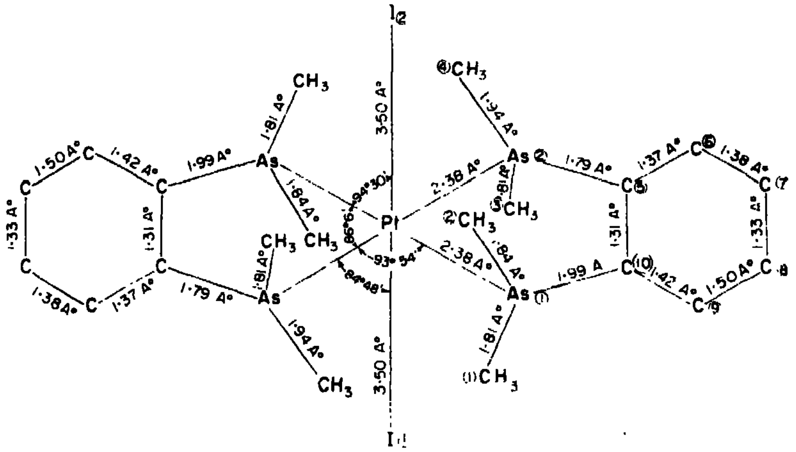

FIG. 2.—Diagram of the di-iododi-(*o*-phenylenebisdimethylarsine)platinum(II) molecule.

TABLE 2.—INTRAMOLECULAR INTERATOMIC DISTANCES AND ANGLES

	Å		Å		Å
Pt–As_1	2·38	As_2–C_3	1·81	C_6–C_7	1·38
Pt–As_2	2·38	As_2–C_4	1·94	C_7–C_8	1·33
Pt–I	3·50	As_2–C_8	1·79	C_8–C_9	1·50
As_1–C_1	1·81	As_1–C_{10}	1·99	C_9–C_{10}	1·43
As_1–C_2	1·84	C_5–C_6	1·37	C_{10}–C_5	1·31

As_1–Pt–As_2	86°6'	As_2–Pt–I	84°48'
As_1–Pt–I	85°30'	As_2–Pt–As_1	93°54'

Deviations of atoms from the plane of the benzene ring $0{\cdot}670\,x-0{\cdot}740\,y+0{\cdot}0692\,z = 0{\cdot}241$

C_5	0·103 Å	C_9	0·049 Å	Pt	0·241 Å
C_6	0·018 Å	C_{10}	0·122 Å		
C_7	0·059 Å	As_1	0·226 Å		
C_8	0·051 Å	As_2	0·269 Å		

It is evident that the configuration around the Pt(II) atom is that of a slightly distorted octahedron; four arsenic atoms in a plane and each at a distance of 2·38 Å from the platinum atom and two iodine atoms at longer distances of 3·50 Å in octahedral sites. The equation of the platinum-arsenic plane is $0{\cdot}721\,x-0{\cdot}680\,y-0{\cdot}132\,z=0$, each atom lying completely in this plane. The As—Pt—As angles have estimated standard deviations of 0·07° and the slight deviations of these angles from 90° are significant. The Pt—I bond is inclined 7° to the normal from the platinum-arsenic plane, this distortion undoubtedly being due to the proximity of the benzene ring of an adjacent molecule. The distances of the C_6 and C_7 atoms of this ring from the iodine are 3·81 Å and 4·10 Å, compared with the sum of the van der Waal's radii for methyl group and iodine atom (2·0+2·15 = 4·15 Å).

The Pt-As bond distances, each at 2·38 Å are less than the sum of the square covalent radius for platinum (II), and the tetrahedral covalent radius for arsenic (1·31+1·18 = 2·49 Å). Although the Pt-I bond distances of 3·50 Å are considerably greater than the covalent sum for these atoms (1·31+1·33 = 2·64 Å), they are less than the non-bonded distance of 4·27 Å. This latter figure is obtained by adding to the ionic radius of the iodide ion (2·20 Å) the van der Waal's radius of the platinum atom, taken as one half of the separation distance of adjacent $PtCl_4$ ions (2·07 Å) in the compound K_2PtCl_4. (5) Also PAULING (6) has observed that the van der Waal's radii of many elements exceed the corresponding single-bond covalent radii by between 0·75 to 0·83 Å which in this case would give platinum a van der Waal's radius of 2·06–2·14 Å.

The plane of the benzene ring is given by the equation $0{\cdot}670x - 0{\cdot}740y + 0{\cdot}069z = 0{\cdot}241$ and inclined to the platinum-arsenic plane by 12°30′. It is doubtful if the positions of the carbon atoms deviate significantly from this plane. The As-C bond lengths indicate normal covalency whilst in the benzene ring the bond lengths are consistent with the aromatic carbon-carbon bond distance of 1·39 Å.

The structure thus consists of discrete molecules of $Pt(diarsine)_2I_2$. A square Pt(II) complex, eg. $[Pt(diarsine)_2][ClO_4]_2$ has a platinum atom which is using the square bonding orbitals $5d6s6p^2$. This leaves a vacant $6p$-orbital normal to the plane of the square through the platinum atom. PAULING (7) has suggested that this vacant p-orbital might possibly give rise to five-covalency in the case of Pr(II). In order to obtain these five-covalent complexes the right type of ligand must be used so as to leave the Pt(II) atom with a residual positive charge and hence the capacity to attract the lone pair of a suitable ligand (eg. the I^- ion) onto the vacant p-orbital. If the ligand involves only nitrogen atoms, as when one uses ethylenediamine as the ligand, single co-ordinate σ-bonds only can be used between the Pt(II) and nitrogen atoms. This leads to a negative charge, on the platinum atom, a situation most unfavourable to the attraction of a negatively charged iodide ion onto the vacant p-orbital. However, the possibility of $d\pi$–$d\pi$-bonding between the Pt(II) and arsenic atoms, involving the use of vacant d orbitals of the latter atom, promotes stability through the formation of bonds with partial double bond character. The platinum is thus enabled to minimise the number of electrons it has accumulated due to co-ordination and to attract an iodide ion. Evidence for this $d\pi$–$d\pi$-bonding is manifested in a shortening of the Pt-As bond to 2·38 Å.

The explanation of the addition of a second iodide ion appears a little more difficult since no further $6p$-orbitals are available. It has been suggested (8) that the two iodine atoms might be held by co-linear $6p6d$ hybrid bonds. These should be elongated-consistent with the observed length 3·50 Å.

(5) W. THEILACKER, *Z. Anorg. Chem.* **234**, 161 (1937).

(6) L. PAULING, *The Nature of the Chemical Bond*, p. 192. Cornell Univ. Press, New York (1948).

(7) L. PAULING, *The Nature of the Chemical Bond*, p. 99. Cornell Univ. Press, New York (1948).

(8) C. HARRIS, R. NYHOLM and N. C. STEPHENSON, *Nature, Lond.* **177**, 1127 (1956).

J. Inorg. Nucl. Chem., 1962, Vol. 24, pp. 797 to 800. Pergamon Press Ltd. Printed in England

THE STRUCTURE OF THE DI-IODODI-(*o*-PHENYLENEBISDIMETHYLARSINE)-PALLADIUM(II) MOLECULE

N. C. STEPHENSON
Department of Chemistry, University of New South Wales, Sydney, Australia

(*Received* 28 *July* 1961; *in revised form* 20 *November* 1961)

Abstract—The crystal structure of the compound $Pd(C_6H_4[As(CH_3)_2]_2)_2I_2$ has been determined by X-ray diffraction methods. The compound is monoclinic, space group $P2_1/c$ (C^5_{2h}) with $a = 9{\cdot}64$ Å, $b = 9{\cdot}24$ Å, $c = 17{\cdot}23$ Å, $\beta = 114°$ (all to ½ per cent), and $z = 2$; specific gravity (calc) = 2·25, (obs) = 2·26.

The palladium(II) atom is surrounded by four coplanar arsenic atoms with two iodine atoms completing a distorted octahedron. The short Pd–As bond lengths suggest some double bond character whilst the elongated Pd–I distances of 3·40 Å are much longer than the usual single bond distances.

The isolation of five covalent palladium(II) complexes has been reported recently by HARRIS and NYHOLM [(1)]. They have examined complexes of the type PdX_2(diarsine)$_2$ where X = Cl, Br, I, CNS, NO_2, ClO_4 and (diarsine) is the chelate group *o*-phenylenebis(dimethylarsine). In particular di-iodi-(*o*-phenylenebisdimethylarsine) palladium(II) and iododi-(*o*-phenylenebisdimethylarsine)palladium(II) perchlorate function as uni-univalent electrolytes in nitrobenzene solution and the existence of the five covalent ion Pd(diarsine)$_2$I$^+$ in solution is inferred.

In view of the large number of compounds in which divalent palladium forms square planar complexes, the crystal structure of the substance Pd(diarsine)$_2$I$_2$ has been examined and preliminary findings reported elsewhere.[(2)] The details of the investigation are reported below.

EXPERIMENTAL

Single crystals of the compound were obtained from a nitrobenzene solution. The crystallography of PdI$_2$(diarsine)$_2$ was determined from Buerger precession photographs made with MoKα radiation. The photographs show monoclinic symmetry and the only systematic absences observed were (*hol*) with *l* odd and (*oko*) with *k* odd. The space group must therefore be $P2_1/c$ (C^5_{2h}). The following unit cell data were obtained: $a = 9{\cdot}64$ Å, $b = 9{\cdot}24$ Å, $c = 17{\cdot}23$ Å, $\beta = 114°$ (all to ½ per cent).

The density of the crystals at room temperature was measured by flotation in a methylene iodide–benzene mixture ($\rho_{obs} = 2{\cdot}26$ g cm^{-3}). Two molecules of the diarsine complex per unit cell give a calculated density of 2·25 g cm^{-3}.

Approximately three hundred reflexions were recorded with the Buerger precession camera ($\mu = 30°$, $F = 6{\cdot}000$ cm, $s = 26{\cdot}0$ mm, λMoK$\alpha_{1,2} = 0{\cdot}7107$ Å). Lorentz and polarization corrections for the intensity data for the (*hol*) and (*okl*) zones were determined by the use of a transparent overlay based upon the chart prepared by WASER.[(3)] Intensities were measured photometrically with an Optica Milano Evaluation Unit which had been calibrated against a standard intensity wedge prepared in the usual manner.

---

(1) C. M. HARRIS and R. S. NYHOLM, *J. Chem. Soc.* 4375 (1956).

(2) C. M. HARRIS, R. S. NYHOLM and N. C. STEPHENSON, *Nature, Lond.* **177**, 1127 (1956).

(3) J. WASER, *Rev. Sci. Instrum.* **22**, 567 (1957).

DETERMINATION OF THE STRUCTURE

The two palladium atoms in the unit cell were placed in special positions 000 and 0, $\frac{1}{2}$, $\frac{1}{2}$ viz. position *a* of space group No. 14. Many of the phases of the structure factors were determined by firstly scaling to approximate absolute values by the method of WILSON(4) and then comparing the resulting sets of structure factors, for separate zones, with the corresponding data for the isomorphous platinum compound.(5) These structure factors were used to calculate Fourier projections on the

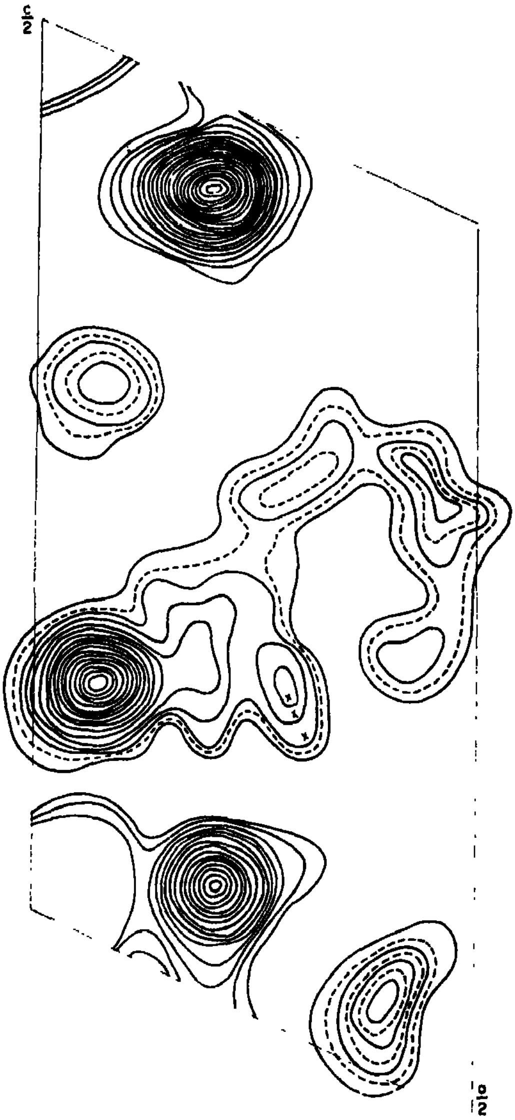

FIG. 1.—The first (*hol*) Fourier map.
Contours are on an arbitrary scale and only the outer contours for the Pd atom are shown.

---

(4) A. J. C. WILSON, *Nature, Lond.* **150**, 152 (1942).
(5) N. C. STEPHENSON, *J. Inorg. Nucl. Chem.* **24**, (1962).

010 and 100 planes (Fig. 1). The resulting co-ordinates and further details of the structure were refined by successive difference Fourier syntheses. The final parameters are given in Table 1. These co-ordinates were used to compute the final calculated structure factors which are listed in the appendix for comparison with the moduli of the observed structure factors. Isotropic thermal parameters of $B(hol) = 3\cdot1$ Å^2 and $B(okl) = 2\cdot7$ Å^2 were used in the calculations.

TABLE 1.—FINAL ATOMIC CO-ORDINATES

Atom	*x/a*	*y/b*	*z/c*	Atom	*x/a*	*y/b*	*z/c*
Pd	0·0000	0·0000	0·0000	C_1	0·208	0·344	0·028
As_1	0·2106	0·1610	0·0613	C_2	0·353	0·196	0·022
As_2	0·0710	0·9130	0·1426	C_3	0·151	0·725	0·138
I	0·1971	0·7416	0·9464	C_4	0·910	0·931	0·190
C_5	0·237	0·043	0·212	C_8	0·486	0·210	0·306
C_6	0·315	0·035	0·302	C_9	0·440	0·233	0·220
C_7	0·448	0·102	0·348	C_{10}	0·297	0·137	0·181

Estimates of the standard deviations in the atomic co-ordinates of isolated iodine, arsenic and carbon atoms were obtained in a manner previously reported(5) for the isomorphous platinum compound $PtI_2As_4C_{20}H_{32}$. These values of 0·001, 0·002 and 0·03 Å respectively are probably a fair estimate for the heavier atoms but not very relevant to the probable accuracy of the carbon co-ordinates, as judged from the variations in carbon–carbon and arsenic–carbon bond lengths. The Reliability Index (R) calculated over all reflections is 0·14.

DISCUSSION OF THE STRUCTURE

New co-ordinates, expressed in Angstrom units, were assigned to each atom referring them to a set of orthogonal axes *a*, *b*, and *c′*, *c′* being taken perpendicular to the *a* and *b* crystal axes. From these co-ordinates the interatomic distances and angles, listed in Table 2, were calculated.

TABLE 2.—INTERATOMIC DISTANCES Å AND ANGLES

Pd–As_1	2·39	As_1–C_{10}	1·90	As_1–Pd–As_2	85°12′
Pd–As_2	2·40	C_5–C_6	1·42	As_1–Pd–I	84°53′
Pd–I	3·40	C_6–C_7	1·35	As_2–Pd–I	85°18′
As_1–C_1	1·78	C_7–C_8	1·37	As_1–Pd–As_1	94°18′
As_1–C_2	1·75	C_8–C_9	1·38		
As_2–C_3	1·92	C_9–C_{10}	1·54		
As_2–C_4	2·04	C_{10}–C_5	1·28		
As_2–C_5	1·96				

Deviations (Å) from the plane $0\cdot690\,x - 0\cdot714\,y - 0\cdot118\,z + 0\cdot118 = O$

C_5	0·01	C_9	0·03	Pd	0·12
C_6	0·04	C_{10}	0·02		
C_7	0·06	As_1	0·05		
C_8	0·08	As_2	0·21		

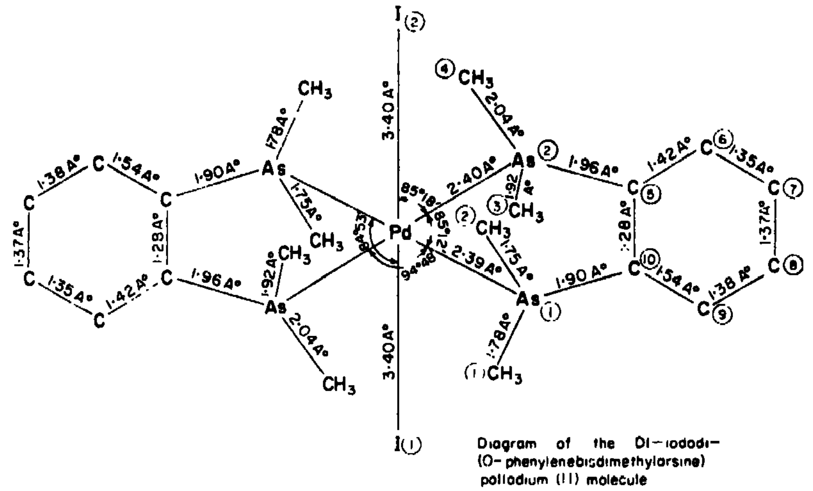

Fig. 2.—Diagram of the di-iododi-(*o*-phenylenebisdimethylarsine)palladium(II) molecule.

The environment of the palladium atom, as it exists in the crystal, is depicted in Fig. 2. The palladium lies in the plane of four arsenic atoms, the co-ordination of these arsenic atoms being that of a slightly but significantly distorted square. The equation of this plane, relative to the orthogonal axes *a*, *b* and *c'*, was determined by the method of least squares, and is $0{\cdot}719\,x - 0{\cdot}679\,y - 0{\cdot}146\,z = 0$. In accordance with the requirements of the centre of symmetry each of the above relevant atoms lies completely in this plane. In octahedral sites and at distances of 3·40 Å are iodine atoms. The Pd-I bond is inclined 6°35′ to the normal from the palladium–arsenic plane, due to the proximity of a neighbouring molecule.

The plane of the benzene ring of the diarsine chelate, referred to the orthogonal axes *a*, *b* and *c'*, is given by the equation $0{\cdot}690\,x - 0{\cdot}714\,y - 0{\cdot}118\,z + 0{\cdot}118 = 0$ and the deviations of the carbon atoms from this plane (listed in Table 2) cannot be regarded as significant. The bond lengths within this plane differ from the aromatic carbon–carbon distance of 1·39 Å because, in the presence of Pd, As and I it is impossible to locate carbon atoms accurately by a simple two-dimensional analysis.

The structure is thus very similar to that of Pt(diarsine)$_2$I$_2$ packed together in the crystal lattice. There appears for the first time direct evidence of the $d\pi$-$d\pi$ bonding between arsenic and palladium. The observed(6) length of the As-Pd bond in $(Me_3AsPdBr_2)_2$ is 2·50 Å, no notable contraction from the normal single covalent bond distance of 2·52 Å. The Pd-As bond distances of 2·39 and 2·40 Å in the diarsine do indicate contraction attributable to double bonding between palladium and arsenic.

The Pd-I bond of 3·40 Å is significantly shorter than the corresponding Pt-I bond (3·50 Å). This is in agreement with the experimental observations of Harris(7) which indicate that palladium(II) tends to form stronger octahedral complexes with *o*-phenylenebisdimethylarsine than platinum(II). This shorter and presumably stronger bond causes less interference with adjacent molecules as the benzene ring is inclined only 2°42′ to the Pd-As plane as compared with 12°30′ in the platinum compound.

---

(6) F. G. Mann and A. F. Wells, *J. Chem. Soc.* 702 (1938).

(7) C. M. Harris, S. E. Livingstone and I. Reece, *J. Chem. Soc.* 1505 (1959).

J. Inorg. Nucl. Chem., 1962, Vol. 24, pp. 801 to 808. Pergamon Press Ltd. Printed in England

THE CRYSTAL STRUCTURE OF DIAMMINE BIS(ACETAMIDINE)PLATINUM(II) CHLORIDE MONOHYDRATE, $Pt(NH_3)_2[CH_3.C.(NH_2).NH]_2Cl_2.H_2O$

N. C. Stephenson
Department of Chemistry, University of New South Wales, Sydney, Australia

(*Received* 11 *July* 1961; *in revised form* 20 *November* 1961)

Abstract—The crystal structure of the compound $Pt(NH_3)_2[CH_3.C.(NH_2).NH]_2Cl_2.H_2O$ has been determined by X-ray diffraction methods. The compound is monoclinic, space group $A2/a$ (C_{2h}^6) with $a = 15{\cdot}940$, $b = 6{\cdot}250$, $c = 17{\cdot}246$, $\beta = 130°23'$, and $Z = 4$; specific gravity (calc) = 2·202, (obs) = 2·21 g cm^{-3}. Intensity data were obtained from integrated equatorial and equi-inclination Weissenberg photographs about the *a* and *b*-axes. No absorption corrections were made. The final atomic parameters were obtained from three-dimensional Fourier difference maps.

The platinum(II) atom exhibits square planar co-ordination; two ammonia molecules, in *trans*-positions, and two acetamidine molecules are co-ordinated to the divalent metal atom. This compound has previously been referred to as one of the rare examples of sexicovalent platinum(II), allegedly containing four ammonia and two acetonitrile molecules co-ordinated to the metal atom. The original name of the compound was bisacetonitriletetrammineplatinum(II) chloride monohydrate $Pt(NH_3)_4(CH_3CN)_2Cl_2.H_2O$.

The structure is held together by ionic forces of attraction and hydrogen bonds from the water molecule to acetamidine molecules and to chloride ions.

It is well known that divalent platinum forms complexes in which four covalent bonds from the metal atom are coplanar and directed towards the corners of a square. The sterochemistry of square complexes has been discussed in detail by Mellor⁽¹⁾ and a large number of structures of this type have been reported by Wells.⁽²⁾

A small number of compounds of bivalent platinum have been listed by Sidgwick⁽³⁾ in which the platinum is alleged to be six-covalent. The structural evidence for six-covalent platinum is limited to two substances,⁽⁴, ⁵⁾ and for this reason the determination of the structure of "bisacetonitriletetrammineplatinum(II) chloride monohydrate", $Pt(NH_3)_4(CH_3CN)_2{\cdot}Cl_2{\cdot}H_2O$, has been undertaken. In this compound it is alleged that the platinum atom is bonded to four ammonia molecules and also to two acetonitrile molecules.

EXPERIMENTAL

Bisacetonitriletetrammineplatinum(II) chloride was prepared by the method described by Tschugaev and Lebedinski⁽⁶⁾ and crystals of the monohydrate were obtained by the slow evaporation of an aqueous solution. Preliminary values of lattice constants were obtained from precession photographs and these were used to index a powder photograph.

---

(1) D. P. Mellor, *Chem. Rev.* **33**, 137 (1943).

(2) A. F. Wells, *Structural Inorganic Chemistry*, p. 645. Oxford Univ. Press, London (1950).

(3) N. Sidgwick, *The Chemical Elements and Their Compounds*, p. 1583. Oxford Univ. Press, London (1950).

(4) C. Brosset, *Ark. Kemi. Min. Geol.* **25**, No. 19 (1948).

(5) C. M. Harris, R. S. Nyholm and N. C. Stephenson, *Nature, Lond.* **177**, 1127 (1956).

(6) L. Tschugaev and W. Lebedinski, *C.R. Acad. Sci., Paris* **161**, 563 (1915).

taken with a Guinier focussing camera, by expressing $\sin^2\theta$ in the form $\sin^2\theta = R_{11}h^2 + R_{13}hl + R_{22}k^2 + R_{33}l^2$. Four normal equations obtained from eighteen of the above expressions were solved to give the following lattice constants:

$$a = 15{\cdot}940\ \text{Å},\ b = 6{\cdot}250\ \text{Å},\ c = 17{\cdot}246\ \text{Å},\ \beta = 130°23'.$$

The observed density (by flotation) = 2·21 g cm^{-3}; calculated density for four molecules per unit cell = 2·202 g cm^{-3}.

Approximately 1200 reflexions were observed on equatorial and equi-inclination Weissenberg photographs taken about the *a* and *b*-axes. Systematic absences of (*hkl*) with $k+l$ odd, *hoo* and *oko* and *ool* with odd values for *h*, *k* and *l* indicate the space group *A*2/*a* or *Aa*. To avoid the "heavy atom" effect,(7) (*hkl*) spectra with *h* odd were utilised for the statistical distribution test of HOWELLS *et al.*(8) The *N*(*z*) test (Table 1) indicated the centric space group *A*2/*a*.

TABLE 1.—THE STATISTICAL DISTRIBUTION OF INTENSITIES

$\sin\theta/\lambda$	*M**	< I >	*N*(10)	*N*(20)	*N*(30)	*N*(40)	*N*(50)	*N*(60)	*N*(70)	*N*(80)
0·05–0·15	neglect									
0·15–0·25	27	2529·3	4	9	10	13½	16	17	18	21
0·25–0·35	40	1732·0	10	17½	23	24	25	26	26	28
0·35–0·45	52	1129·0	7	17	18	22	25	26	30	31
0·45–0·55	58	658·3	8	17	22	24	27	30	34	40
	177		29	60½	73	83½	93	99	108	120
Weighted average *N*(*z*)%			16·4	34·2	41·2	47·2	52·5	55·9	61·0	67·8
Theoretical centric			24·8	34·5	41·8	47·3	52·1	56·1	59·7	62·9
acentric			9·5	18·1	25·9	33·0	39·3	45·1	50·3	55·1

**M* denotes the number of reflexions in a group.

Weissenberg photographs were taken on a Nonius integrating goniometer. The strong reflexions with $h = 0,2,4,6$; $k = 0,1,2,\cdots 6$, were obtained using Mo$K\alpha_{1,2}$ radiation and exposure times of 60 hr per level. The weak reflexions with $h = 1,3,5$ were recorded with Cu $K\alpha_{1,2}$ radiation and exposure times of 160 hr per level. Each 60 hr exposure was taken with a multiple film pack of Ilford G backed by Ilford B and Ilford C films. Density ratios of 5·2: 1 and 3·7: 1 were obtained photometrically. The 120 hr exposures were taken with a pack of four Ilford G films having a density ratio of 2·8 1 for adjacent films. The intensities were measured photometrically with an Optica Milano Evaluation Unit which had been calibrated against a standard intensity scale. Lorentz and polarization connections were applied graphically.

For levels with *h* even, values for F^2 (*hkl*) on a relative scale were approximately placed on an absolute scale and the isotropic thermal parameter determined by the method proposed by WILSON.(9) The values of *B* varied with each level and were made a constant 1·37 Å^2 by applying an artificial temperature factor of a magnitude appropriate to each level. The F^2 (*hkl*) values were then scaled by the use of common sets of reflexions. The *F* (*hkl*) values with *h* odd were very weak and scaling was effected against structure factors calculated from trial models.

(7) A. HARGREAVES, *Acta Cryst.* **8**, 12 (1955).

(8) E. R. HOWELLS, D. C. PHILLIPS and D. ROGERS, *Acta Cryst.* **3**, 210 (1950).

(9) A. J. C. WILSON, *Nature, Lond.* **150**, 152 (1942).

DETERMINATION OF THE STRUCTURE AND REFINEMENT OF THE ATOMIC CO-ORDINATES

The intensities of the general order reflexions with *h* even were very much stronger than those with *h* odd. The platinum atoms were therefore placed at 000, $\frac{1}{2}\frac{1}{2}\frac{1}{2}$, and $\frac{1}{2}00$. The phases of the *F*(*hol*) data were taken as zero and an (*hol*) Fourier projection was calculated. No significant detail, other than the location of the chloride ion, could be obtained from this projection because of the heavy diffraction ripples emanating from the platinum atoms. After suitable scaling of observed data a difference map was computed. In this map the platinum atoms had been removed using the scattering curve of THOMAS and UMEDA(10) which had been modified by an isotropic temperature factor ($B = 1{\cdot}37$ A^2) and corrected for anomalous dispersion.(11) This difference map is drawn in Fig. 1(a). The required number of peaks are present for the light atoms but the positional parameters will necessarily be in error, particularly for N_1 and N_2 due to large anisotropic thermal movement of the platinum and chlorine atoms.

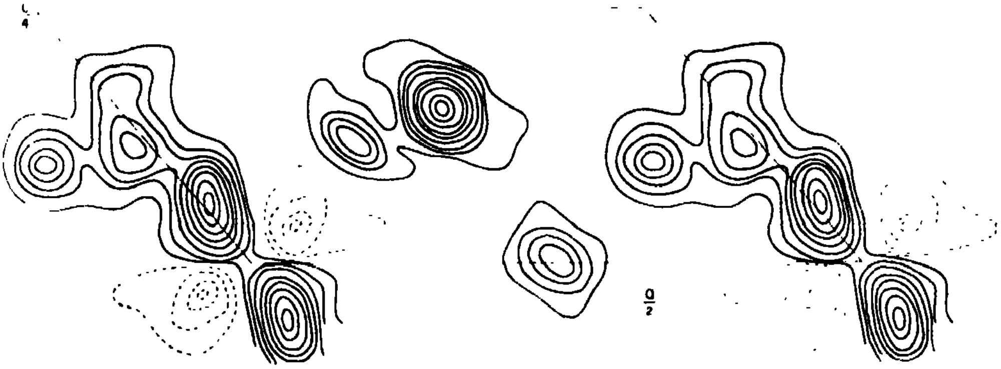

FIG. 1 (a).—The (*hol*) difference Fourier map in which the platinum atom at the origin has been removed. Thermal anisotropy for the platinum atom and chloride ion is indicated.
Contours = 1 eÅ^{-2}. Negative regions dotted.
Contours for the chloride ion = 2 e Å^{-2}.

The refinement of the parameters for the anistropic thermal movement of the heavy atoms was realised using a programme devised by ROLLETT. The computations were carried out on UTECOM.* After seven cycles of refinement the structure factors were used together with the scaled F_o values to compute a second difference map (Fig. 1(b)).

In order to obtain information about the *y* co-ordinates of the atoms a three-dimensional Fourier synthesis was computed using the *F*(*hkl*) data with *h* even. These data were assigned zero phases because of the dominating contributions of the platinum atoms. The location of peak maxima was effected by an analytical method first proposed by CARPENTER and DONOHUE(12) and later modified by SHOEMAKER

---

* Digital computer, University of New South Wales.

(10) L. H. THOMAS and K. UMEDA. *J. Chem. Phys.* **26**, 293 (1957).
(11) C. DAUBEN and D. TEMPLETON, *Acta Cryst.* **8**, 841 (1955).
(12) G. CARPENTER and J. DONOHUE, *J. Amer. Chem. Soc.* **72**, 2315 (1950).

et al.(13) An (010) mirror plane appeared in the Fourier function due to the use of selected data. This made it possible to determine x and z co-ordinates without ambiguity but the parameters were uncertain as to sign. The calculated structure factors $F(hkl)$ with h odd are dependent on the sign of the y co-ordinates of the contributing atoms, for their sign and magnitude. Eight sets of structure factors were calculated involving various combinations of signs for the y co-ordinates and rational molecular models involving accepted interatomic distances. The good agreement between observed and calculated structure factors was only obtained when a divergence from the previously accepted stereochemistry of the compound was made. A trial model involving acetamidine co-ordinated to the platinum atom converged to give the final structure.

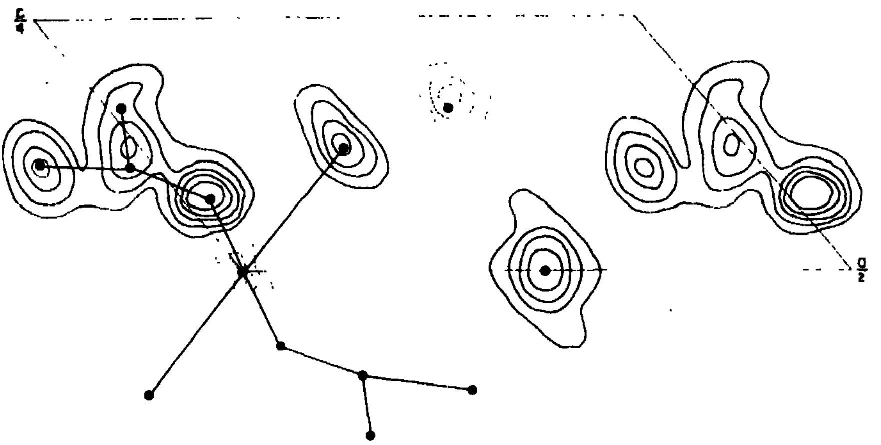

FIG. 1 (b).—The (*hol*) difference Fourier map in which platinum and chlorine atoms have been removed. Allowance has been made for anisotropic thermal movement. The positions of the light atoms, shown as black dots, have been determined from three-dimensional data.

The atomic co-ordinates were refined by successive three-dimensional difference maps. When the accidentally absent reflexions are given values of $\frac{1}{2}(F_o)_{\text{min}}$. for their structure factors the overall R factor calculates at 0·13.

The final values of the atomic parameters are given in Table 2.

TABLE 2.—ATOMIC PARAMETERS

	x/a	y/b	z/c
Pt	0·0000	0·0000	0·0000
C_1	0·0095	0·5474	0·1626
C_2	0·9778	0·3341	0·1059
N_1	0·0225	0·2669	0·0707
N_2	0·1641	0·9573	0·1175
N_3	0·9049	0·2330	0·1054
H_2O	0·7500	0·8440	0·0000
Cl^-	0·2634	0·4408	0·1485

Temperature factor $B = 1{\cdot}67$ Å^2.

(13) D. SHOEMAKER, J. DONOHUE, V. SCHOMAKER and R. COREY, *J. Amer. Chem. Soc.* 77, 77, 2334 (1950).

ESTIMATION OF ACCURACY

The standard deviations of the atomic co-ordinates were estimated by the method of CRUICKSHANK.(14) The curvatures for these calculations were obtained by differentiating the Gaussian functions representing peak shapes. The standard deviations of atomic co-ordinates of atoms in the complex cation are given in Table 3.

TABLE 3.—STANDARD ERRORS OF PARAMETERS FOR ATOMS IN THE COMPLEX CATION

	Peak height $\rho(xyz)$ electrons Å^{-3}	Curvatures $\frac{\partial^2\rho}{\partial x^2}$	$\frac{\partial^2\rho}{\partial y^2}$	$\frac{\partial^2\rho}{\partial z^2}$	Errors Å	r.m.s. Å
C_1 x	5·62	61·99			0·022	
y			50·31		0·028	0·026
z				43·19	0·028	
C_2 x	5·77	47·65			0·028	
y			65·02		0·022	0·023
z				69·65	0·017	
N_1 x	7·03	61·50			0·022	
y			94·19		0·015	0·018
z				77·29	0·015	
N_2 x	7·38	52·35			0·026	
y			90·48		0·015	0·018
z				116·66	0·010	
N_3 x	6·51	70·57			0·019	
y			72·00		0·019	0·021
z				46·79	0·025	
					r.m.s.	0·021

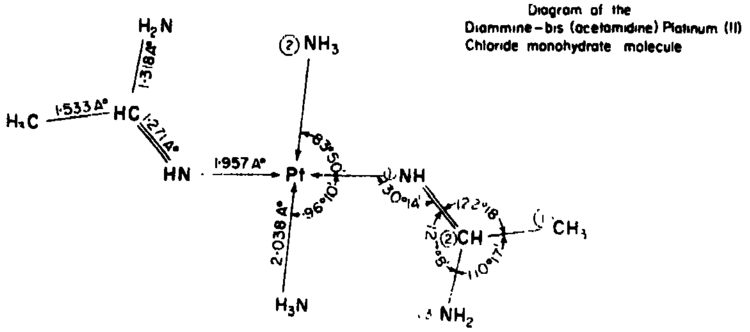

FIG. 2.—Diagram of the diammine-bis(acetamidine)platinum(II) ion.

---

(14) D. CRUICKSHANK, *Acta Cryst.* **2**, 65; **2**, 154 (1949).

DISCUSSION OF THE STRUCTURE

The shape of the complex cation, as it exists in the crystal, is given in Fig. 2. The bond lengths and the bond angles are given both in Table 4 and Fig. 2. It is apparent that the platinum(II) atom is not six-covalent, as hitherto expected, but four-covalent. There are only two ammonia molecules co-ordinated to the platinum atom, the other two being associated with the acetonitrile as acetamidine molecules. It is perhaps significant that acetamidine can be prepared by reacting acetonitrile and ammonia together in the presence of hydrochloric acid. Evidently the last step in the preparation of the substance is:

$$\mathrm{Pt(MeCN)_2Cl_2+4NH_3 \rightarrow Pt(Acetamidine)_2(NH_3)_2Cl_2}$$

and not:

$$\mathrm{Pt(MeCN)_2Cl_2+4NH_3 \rightarrow [Pt(MeCN)_2(NH_3)_4]Cl_2}.$$

TABLE 4.—INTRAMOLECULAR INTERATOMIC DISTANCES AND BOND ANGLES

$Pt–N_1$	2·038 Å	$< N_2–Pt–N_1$	83°50′
$Pt–N_2$	1·957 Å	$< Pt–N_1–C_2$	130°14′
$C_1–C_2$	1·533 Å	$< N_1–C_2–N_3$	127°8′
$C_2–N_1$	1·271 Å	$< N_1–C_2–C_1$	122°18′
$C_2–N_3$	1·318 Å	$< C_1–C_2–N_3$	110°17′

New co-ordinates, expressed in Ångström units, were assigned to each atom, referring them to a set of orthogonal axes a, b and c', c' being taken perpendicular to the a and b crystal axes. Referred to these axes the plane through the platinum and its four co-ordinated nitrogen atoms is given by the equation:

$$0{\cdot}716\,x-0{\cdot}472\,y+0{\cdot}514\,z = 0$$

and these atoms necessarily lie exactly in this plane because of the centre of symmetry. The co-ordination around the platinum atom is not exactly square; the $N_2—Pt—N_1$ angle differs significantly from a right angle ($\Delta/\sigma = 7{\cdot}0$) and the difference between the bond lengths $Pt—N_2$ and $Pt—N_1$ is possibly significant ($\Delta/\sigma = 2{\cdot}7$). The sum of the angle bond and square covalent radii for nitrogen and platinum(II) is $0{\cdot}70+1{\cdot}31 = 2{\cdot}01$ Å.

The acetamidine molecule is not strictly planar. The best fit plane through the atoms C_1, C_2, N_1 and N_3 is $0{\cdot}042\,x-0{\cdot}44\,y+0{\cdot}893\,z = 0{\cdot}402$ and this is inclined 45°28′ to the abovementioned plane through the platinum atom. The atoms C_1 and C_2 lie within 0·04 Å of the plane but the remaining two atoms are significantly displaced from it: N_1 is 0·30 Å towards the Pt atom and N_3 is 0·25 Å towards a water molecule to which it is hydrogen bonded.

The bond lengths and angles in the acetamidine molecule compare very favourably with those observed in similar molecules (see Table 5). The length of the $C_1—C_2$ bond (1·53 Å) agrees well with the accepted normal single bond covalent distance of 1·54 Å. The carbon–nitrogen intramolecular distances lie between the single and double bond covalent distances of 1·48 Å and 1·24 Å given by SCHOMAKER and STEVENSON.⁽¹⁵⁾ The use of Pauling's equation relating bond length with double bond character leads to 65 per cent double bond character in the $C_2—N_1$ bond and 35 per cent double bond character in the $C_2—N_3$ bond.

⁽¹⁵⁾ V. SCHOMAKER and D. STEVENSON, *J. Amer. Chem. Soc.* **63**, 37 (1941).

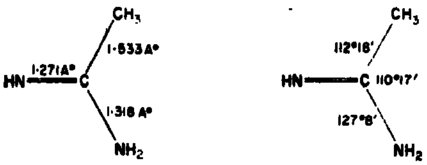

Acetamidine

Acetamide

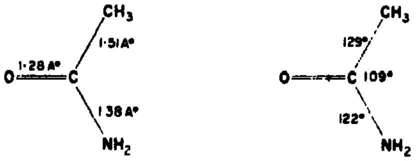

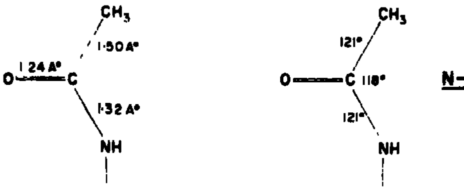

N-acetylglycine

B-glycylglycine

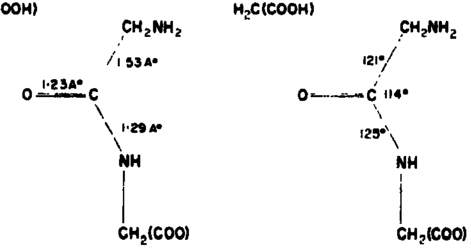

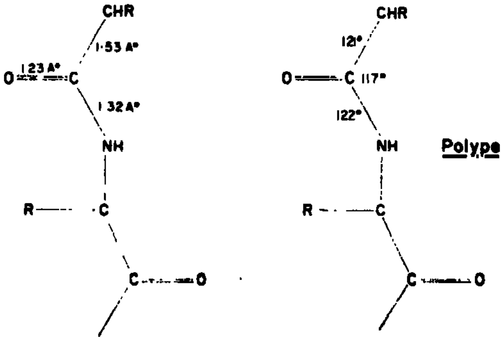

Polypeptide chain

Urea

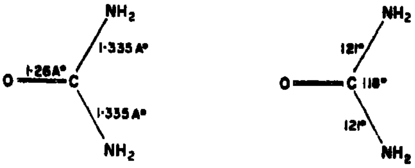

TABLE 5.—A TABLE OF BOND LENGTHS AND ANGLES IN COMPOUNDS SIMILAR TO ACETAMIDINE.

The chloride ion touches its surrounding complex cations at a number of points (see Fig. 3). The non-bonded Cl^-—NH_3, Cl^-—CH_3, Cl^-—O distances as computed from ionic and van der Waal's radii are 3·40, 3·81 and 3·21 Å respectively. The approach distances in the crystal are shown in Fig. 3.

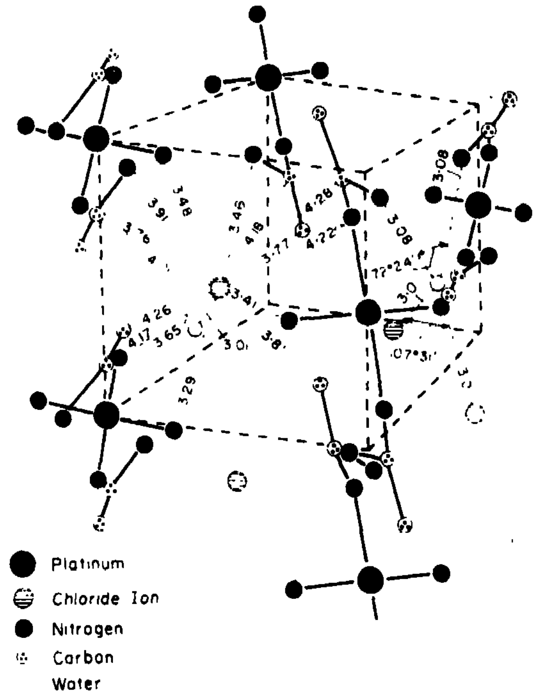

FIG. 3.—Diagram depicting the environment of the chloride ion.

The role of the water molecule in the intermolecular bonding is also illustrated in Fig. 3. It forms two short hydrogen bonds (each 3·01 Å) to two chloride ions, the Cl^-—H_2O—Cl^- angle being 107°31′. In the tetrahedral positions of the oxygen atom are two —NH_2 groups from acetamidine molecules. As in urea,⁽¹⁶⁾ each of the N—H . . . O bonds is practically coplanar with the corresponding acetamidine molecule, which is to be expected in view of the partial double-bond character of the C—N bonds. The N—H . . . O bond distances of 3·08 Å correspond to rather weak bonds since both are considerably larger than the N— . . . O distances of 2·7–2·9 Å found in the amino acids. A similar hydrogen bond exists in urea (N—H . . . O = 3·04 Å). VAUGHAN and DONOHUE⁽¹⁷⁾ explain the relative lengthening as being due to (1) the acceptance of four hydrogen bonds by the oxygen atoms, and (2) the smaller formal charge on the nitrogen atom in (this case) acetamidine; in the amino acids this atom, because of the zwitterion structure, has a charge of +1, whilst in acetamidine, it has a smaller positive charge.

Acknowledgement—I would like to thank Dr. A. D. WADSLEY for taking the powder photographs with his Guinier camera, and Dr. C. M. HARRIS for providing me with the compound.

(16) R. WYCKOFF and R. COREY, *Z. Krist.* **89**, 462 (1934).
(17) P. VAUGHAN and J. DONOHUE, *Acta Cryst.* **5**, 530 (1952).

J. Inorg. Nucl. Chem., 1962, Vol. 24, pp. 809 to 819. Pergamon Press Ltd. Printed in England

USE OF THE METHOD OF CONTINUOUS VARIATIONS WITH MIXED LIGAND COMPLEXES

K. O. WATKINS* and M. M. JONES†
Department of Chemistry, Vanderbilt University, Nashville 5, Tennessee

(*Received* 17 *August* 1961; *in revised form* 13 *November* 1961)

Abstract—An examination of the use of the method of continuous variations with complexes containing two ligand species has been carried out. It is shown that the molar ratio at which the concentration of a mixed complex reaches a maximum is generally different from the molar ratio of the reactants in the complex. The equations for this difference are developed and checked against experimental data for some five mixed complexes. A method for determining the equilibrium constants in some of these systems is given. The equilibrium constants in the systems studied are very close to the values expected for a statistical distribution of the ligands over the available co-ordination sites.

OF the various procedures which can be used for studying complexes in aqueous solution, the method of continuous variations is probably the most treacherous. The vagaries of this method when applied to simple systems, have been examined in some detail.(1, 2, 3) The present work extends the study of these irregularities to systems containing complexes with mixed ligands. In general, when the method is used to study a mixed ligand system either

(1) the measurements are made in such a manner that displacements from stoicheiometric points are not obvious, (2) displacements occur but are ignored, or (3) displacements are recognized, but no theory is given to explain these displacements.

In this study, the application of the method of continuous variations to mixed ligand systems is studied from both a theoretical and an experimental viewpoint.

The use of this method with systems containing two ligands has previously been studied by EICHORN and MARCHAND(4) who used an ingenious graphical method for presenting their results, by SCHILT(5) who studied the mixed cyanide–diamine complexes of iron(II), in studies of the systems; copper(II)-pyridine–salicylate,(6) copper(II)–ethylenediamine–*D* mannosan,(7) copper(II)–ethylenediamine–erythritol anhydride,(8) nickel(II)–ethylenediamine–cyanide, copper(II)–ethylenediamine–

---

* Present address, Adams State College, Alamosa, Colorado.

† To whom communications concerning this paper should be addressed.

(1) F. WOLDBYE, *Acta Chem. Scand.* **9**, 299 (1955).

(2) M. M. JONES and K. K. INNES, *J. Phys. Chem.* **62**, 1005 (1958).

(3) M. M. JONES, *J. Amer. Chem. Soc.* **81**, 4485 (1959).

(4) G. L. EICHORN and N. D. MARCHAND, *J. Amer. Chem. Soc.* **78**, 2688 (1956).

(5) A. A. SCHILT, *J. Amer. Chem. Soc.* **79**, 5421 (1957).

(6) A. K. BABKO and M. M. TANANAIKO, *Zh. Obschei Khim.* **23**, 1459 (1953); *Chem. Abstr.* **48**, 3837 (1954).

(7) L. SEGAL, H. B. JONASSEN and R. E. REEVES, *J. Amer. Chem. Soc.* **78**, 273 (1956).

(8) L. SEGAL, H. B. JONASSEN and R. E. REEVES, *J. Amer. Chem. Soc.* **77**, 2667 (1955).

cyanide,(9) $[PtX_4]^{2-}$ ($X = Cl^-$ or Br^-) and cyanide,(10) and the $[Hg(CN)_3 X]^{2-}$ ($X = Cl^-$, Br^- or SCN^-) systems.(11) A very careful experimental study of several mixed ligand systems involving copper(II) has been carried out by WATTERS and his students using this method to verify the stoicheiometry of the mixed ligand complexes formed.(12-15) In a very recent investigation, KATO used the method to study mixed ligand complexes in the copper(II)-biuret-ethylenediamine system.(16)

SOMMER and HNILICKOVA(17) have used this method to study the formation of mixed ligand complexes in the presence of buffers or added salts which influence the position of the maxima in the continuous variations curves. They derived an equation for the displacement of the maxima which worked well in the TiO^{2+}-chromotropic acid-EDTA system but which gave physically impossible values for the Fe^{3+}-SCN^--F^- system. The limitations responsible for this, as is shown in more detail below, are

(1) neglect of other complexes present in these systems, (2) neglect of the associated protonic equilibria, and (3) identification of the empirical Y function with the concentration of the mixed complex.

Their paper, nevertheless, represents an important step in showing how the method of continuous variations can be used to describe behaviour in a system if enough auxilliary information is available.

It seems reasonable to expect that this method should be capable of furnishing equations which describe the behaviour of a system of complexes just as exactly as those obtained using other methods if the following three conditions are met. Firstly, all the pertinent equilibria are included; secondly, no unrealistic assumptions are made about the concentrations of any of the species and, thirdly, the mathematical manipulations are carried out correctly, in detail, without using any simplifying assumptions. It may happen (as often appears to be the case) that the use of such equations requires data of a much higher order of accuracy than is generally obtained. In this case, the method may be rightly condemned as very inappropriate or inconvenient but not as erroneous. As we shall see below, it is the difficulty of fulfilling all these conditions that results in the frequent disagreement found between the results obtained with this method and those found with less demanding methods.

This paper reports the results obtained in a theoretical and experimental study of the systems: Cu^{2+}-ethylenediamine-pyridine, Cu^{2+}-propylenediamine-pyridine, Cu^{2+}-glycine-pyridine, Cu^{2+} glycine-ethylenediamine, and Cu^{2+}-propylenediamine-glycine.

EXPERIMENTAL

Materials and apparatus. Stock solutions of cupric perchlorate, ethylenediamine, propylenediamine, pyridine and glycine were prepared and analysed. The cupric perchlorate used in these studies was reagent grade material obtained from the G. F. Smith Chemical Co. It was recrystallized from distilled water prior to use. The cupric perchlorate solutions were analysed by electrodeposition of copper. The other materials used were Eastman White Label Grade and their solutions were prepared either by use of exact weights of the reagent or by subsequent dilution of a stock solution standardized volumetrically. The absorption spectra were obtained using a Cary Model 14 Spectrophotometer in an air-conditioned room kept at approximately 25°. Occasional checks were made on a Beckman Model DU instrument in the same room.

---

(9) S. KIDA, *Bull. Chem. Soc. Japan* **32**, 981 (1959).

(10) S. KIDA, *Bull. Chem. Soc. Japan* **33**, 587 (1960).

(11) L. NEWMAN and D. N. HUME, *J. Amer. Chem. Soc.* **83**, 1795 (1961).

(12) J. I. WATTERS and A. AARON, *J. Amer. Chem. Soc.* **75**, 611 (1953).

(13) J. I. WATTERS and E. D. LONGHRAN, *J. Amer. Chem. Soc.* **75**, 4819 (1953).

(14) J. I. WATTERS, J. MASON and A. AARON, *J. Amer. Chem. Soc.* **75**, 5212 (1953).

(15) J. I. WATTERS and R. DE WITT, *J. Amer. Chem. Soc.* **76**, 3810 (1954).

(16) M. KATO, *Z. Phys. Chem.* **23**, 391 (1960).

(17) L. SOMMER and M. HNILICKOVA, *Bull. Soc. Chim. France* **36**, (1959).

RESULTS AND DISCUSSION

The continuous variations curves for the five systems studied are presented in Figs. 1 and 2. As can plainly be seen, each curve possesses a maximum which is displaced from the 5/5 position expected for a system where the complex formed is of the type CuBC or $CuBD_2$ (B and C represent bidentate ligands and D represents a monodentate ligand). In order to analyse the displacements that have been found experimentally, it is necessary to derive equations which show the displacement of the maximum in the concentration of the mixed ligand complex from the true stoicheiometric ratio. The displacement equation for the formation of a mixed ligand complex involving two bidentate ligands is given below. Let the equilibria in such a system be limited to the following:

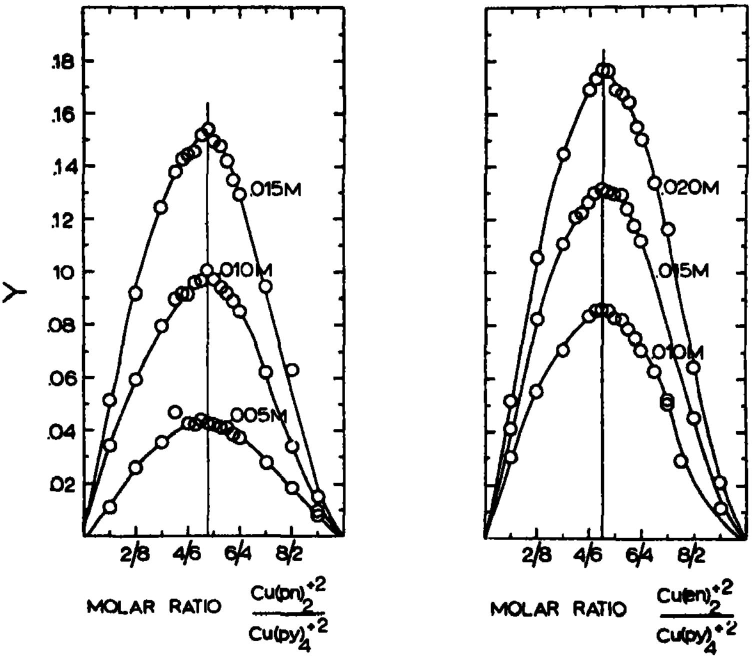

Fig. 1.—Continuous variations curves for the systems $Cu(pn)_2^{2+}$–$Cu(py)_4^{2+}$ and $Cu(en)_2^{2+}$–$Cu(py)_4^{2+}$.

$$2\,ABC \rightleftharpoons AB_2+AC_2 \qquad (1)$$
$$ABC \rightleftharpoons AB+C \qquad (2)$$
$$ABC \rightleftharpoons AC+B \qquad (3)$$
$$AB_2 \rightleftharpoons AB+B \qquad (4)$$
$$AC_2 \rightleftharpoons AC+C \qquad (5)$$

where A is a four co-ordinate metal atom (such as copper) and B and C are bidentate ligands. The concentrations of the various species present are represented by $C_1 = [AB_2]$; $C_2 = [AC_2]$; $C_3 = [ABC]$; $C_4 = [AB]$; $C_5 = [AC]$; $C_6 = [B]$; and $C_7 = [C]$. From the five equilibrium expression, five equilibrium constants can be written.

$$C_1C_2 = K_1C_3^2 \tag{6}$$
$$C_4C_7 = K_2C_3 \tag{7}$$
$$C_5C_6 = K_3C_3 \tag{8}$$
$$C_4C_6 = K_4C_1 \tag{9}$$
$$C_5C_7 = K_5C_2 \tag{10}$$

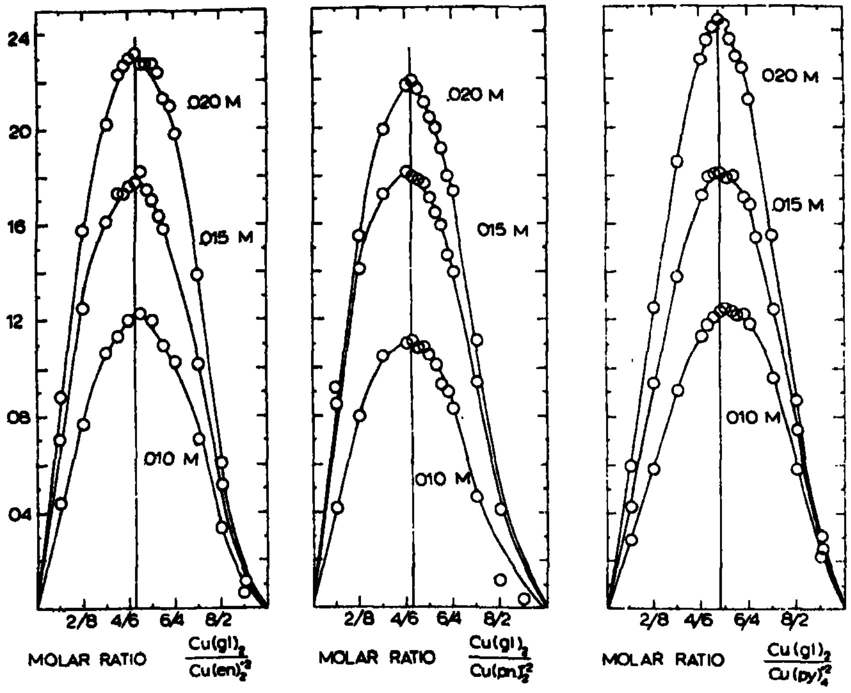

FIG. 2.—Continuous variations curves for the systems $Cu(gl)_2$–$Cu(en)_2^{2+}$, $Cu(gl)_2$–$Cu(pn)_2^{2+}$, and $Cu(gl)_2$–$Cu(py)_4^{2+}$.

If solutions are prepared for a continuous variations study using the customary procedure,(2, 3) mixing (1-x) volumes of a solutions of concentration M in AB_2 with x volumes of a solution M in AC_2, then the concentrations of the complexes AB_2 and AC_2 in the resulting solutions are, respectively:

$$C_1 = M\,(1-x) - C_4 - C_3/2 \tag{11}$$
$$C_2 = M\,x - C_5 - C_3/2 \tag{12}$$

If only the reactions given in equations (1) thru (5) are considered, then the approximation that $C_5 = C_7$ and $C_4 = C_6$ can be used. While these assumptions limit the generality of the results it is felt that they are reasonably valid and allow the detailed examination of the cases studied experimentally. These assumptions are not valid in a *general* sense, however. To determine the conditions under which the concentration of the mixed complex, C_3, is a maximum, C_6 and C_7 are eliminated from the equations above and equations (6) through (12) are differentiated with respect to x.

The condition for a maximum in the mixed complex is $dC_3/dx = 0$. The derivatives of (11) and (12) are substituted into the derivatives of (6) thru (10) and then all the derivatives are eliminated by using simultaneous equations. The values for C_1 and C_2 are substituted into the solution from the simultaneous equations and the result is that the concentration of the complex ABC is a maximum at that value of x for which:

$$\frac{x}{1-x} = 1+\left\{\frac{C_5-C_4}{2M(1-x)}\right\} \tag{13}$$

Thus the point of maximum concentration of ABC will in general be displaced from the position expected if the subsidiary equilibria are not taken into consideration. This displacement is governed by the relative concentrations of the species AB and AC.

Another closely related system is that containing both monodentate and didentate ligands. For such a system consider the following equilibria as sufficient to describe the behaviour:

$$2\,ABD_2 \rightleftarrows AB_2+AD_4 \tag{14}$$
$$ABD_2 \rightleftarrows AB+2\,D \tag{15}$$
$$ABD_2 \rightleftarrows AD_2+B \tag{16}$$
$$AB_2 \rightleftarrows AB+B \tag{17}$$
$$AD_4 \rightleftarrows AD_2+2D \tag{18}$$

Where A is again the central metal ion, B a bidentate ligand and D a monodentate ligand. If the concentrations of the various species are represented by $C_1 = [AB_2]$, $C_2 = [AD_4]$, $C_3 = [ABD_2]$, $C_4 = [AB]$, $C_5 = [AD_2]$, $C_6 = [B]$, $C_7 = [D]$, then the equilibrium constants for reactions (14) through (18) can be written as:

$$C_1C_2 = K_1C_3 \tag{19}$$
$$C_4C_7^2 = K_2C_3 \tag{20}$$
$$C_5C_6 = K_3C_3 \tag{21}$$
$$C_4C_6 = K_4C_1 \tag{22}$$
$$C_5C_7^2 = K_5C_2 \tag{23}$$

For solutions prepared as in the previous example:

$$C_1 = M(1\text{-}x)-C_4\text{-}C_3/2 \tag{24}$$
$$C_2 = Mx-C_5\text{-}C_3/2 \tag{25}$$

If only reactions (14) through (18) are considered then $C_4 = C_6$, and C_6 can be eliminated in these equations. By imposing the condition $dC_3/dx = 0$ after differentiating equations (19) through (25) with respect to x and simplifying the resulting equations as described in the system involving two bidentate ligands, an equation is obtained for the x value at which a maximum in the concentration of the mixed complex occurs, namely:

$$\frac{x}{1-x} = 1+\left\{\frac{C_5-C_4}{2\,M(1-x)}\right\} \tag{26}$$

Once again the maximum will generally not occur at the stoicheiometric point. This equation is identical with the equation developed for a system in which a mixed ligand complex is formed involving two bidentate ligands.

Since this method is always used with a physical property of the solution, such as optical density at a given wave length, it is necessary to examine the deviation of such a measured parameter from the value predicted for it on the basis of no reaction. If the system containing only bidentate ligands is considered, the deviation (Y) is given by equation (27)

$$Y = L\,[\varepsilon_1 C_1 + \varepsilon_2 C_2 + \varepsilon_3 C_3 + \varepsilon_4 C_4 + \varepsilon_5 C_5 - \varepsilon_1\, M(1-x) - \varepsilon_2\, Mx - \varepsilon_4 C_4^{\circ} - \varepsilon_5 C_5^{\circ}]. \quad (27)$$

In equation (27), L represents the length of the path travelled by the light thru the solution and the ε's and C's are extinction co-efficients and concentrations respectively. The superscript ° represents the initial concentrations of C_4 and C_5 before reaction and dilution. After dilution, the equilibrium concentrations of C_4 and C_5 will not equal the original concentrations C_4° and C_5°, therefore, these terms should be included in the Y function. In order to have a simultaneous extremum in the Y function and in the concentration of the complex, the condition that $dY/dx = O$ when $dC_3/dx = O$ must be satisfied. Since the dissociated species will be present regardless of the formation of mixed complexes, the question remains how these affect the behaviour of the Y function. If the concentration of the species AB and AC (i.e. C_4 and C_5) remains constant regardless of the reaction then the derivative of equation (27) with respect to x is:

$$\frac{dY}{dx} = L\left[\varepsilon_2 - \left\{\frac{\varepsilon_1 + \varepsilon_2}{2}\right\}\right]\frac{dC_3}{dx} \qquad (28)$$

It is evident from this equation that $(dY/dx) = O$ when $(dC_3/dx) = O$, if $\varepsilon_3 = (\varepsilon_1 + \varepsilon_2)/2$, and Y will be a maximum when $(dc_3/dx) = O$ if $\varepsilon_3 > (\varepsilon_1 + \varepsilon_2)/2$ and a minimum if $\varepsilon_3 < (\varepsilon_1 + \varepsilon_2)/2$. If these terms *do not* remain constant then (dY/dx) O when $(dc_3/dx) = O$, but rather will have the value:

$$\frac{dY}{dx} = (\varepsilon_4 - \varepsilon_1)\frac{dC_4}{dx} + (\varepsilon_5 - \varepsilon_2)\frac{dC_5}{dx} - \varepsilon_4\frac{dC_4^{\circ}}{dx} - \varepsilon_5\frac{dC_5^{\circ}}{dx} \qquad (29)$$

This is an additional disturbing factor in the use of the method of continuous variations for the study of mixed complexes, as the Y function is ordinarily used in a form that ignores the variations in the terms C_4, C_5, C_4° and C_5°. The influence of the terms C_4, C_5, C_4° and C_5° *becomes greater as one goes to wave-lengths further away from that for which the maximum absorbance occurs in the solution with the correct* $x/(1-x)$ *ratio*. The deviation of the observed maximum in Y from that in C_3 also becomes greater. In the interpretation given below, for the curves obtained here, it is assumed that $C_4 = C_4^{\circ}$ and $C_5 = C_5^{\circ}$. This is not a drastic assumption if the wavelength is carefully chosen.

A. *Systems containing basic ligands*

Copper(II)–ethylenediamine–pyridine system. The absorbance data for this system were obtained over a wavelength range of 400 to 800 mμ. The continuous variations curves for the 0·010, 0·015 and 0·020 M solutions shown in Fig. 1 were derived from measurements at 612·5 mμ, the absorbance maximum for the 5/5 solution. In this system the maximum in the Y function occurs at a ratio of $[Cu(py)_4{}^{2+}]/[Cu(en)_2{}^{2+}]$ of 5·5/4·5 or 1·22. The displacement is related to the difference between the concentrations of $Cu(en)^{2+}$ and $Cu(py)_2{}^{2+}$. An approximate calculation using the stability constants from the literature shows that the dissociation of the pyridine complex is much more extensive than that of the ethylenediamine complex,(18) therefore, the concentration of the $Cu(py)_2^{2+}$, produced (C_5) is greater than that of the $Cu(en)^{2+}$ (C_4) with the result that the predicted ratio should be greater than one. In this case it is 5·5/4·5 or 1·22.

Copper(II)-propylenediamine-pyridine system. The absorption data for this system were obtained over a wave length range of 600 to 800 mμ. The absorption maximum of the 5/5 solution occurred at 612·5 mμ, and the continuous variations curves (Fig. 1) for the 0·005, 0·010 and 0·015 M solutions were constructed from Y values, calculated at this wave length. The extremum in the Y function for this system occurs at the ratio $[Cu(py)_4^{2+}]/[Cu(pn)_2^{2+}] = 5{\cdot}25/4{\cdot}75 = 1{\cdot}15$. The dissociation constant of the tetrapyridrine complex is greater than that of the bis (propylenediamine) complex(19, 20) so the predicted displacement is once again to values of $^x/_{1-x}$ greater than one. The experimental value found for this system is 1·15.

B. *Systems with amphiprotic ligands*

Three systems with an amphiprotic chelating agent (glycine) in admixture with a basic ligand (amine) were examined experimentally to determine how the presence of such a ligand species affects the observed shift in the maximum or minimum of the Y function. These systems also provide a direct indication of how valid it is to ignore the subsidiary protonic equilibria in a continuous variation study involving amphiprotic ligands. This point is of considerable interest in the evaluation of many published studies using such ligands in which these subsidiary equilibria have been ignored.

Copper(II)-glycine-ethylenediamine system. The absorption spectra of this system were obtained over a wavelength range of 600–800 mμ. The continuous variations curves shown in Fig. 2 were constructed from Y functions of the 0·010, 0·015 and 0·020 M solutions at 631 mμ (the absorption maximum for the 5/5 solution). The extremum in the Y function occurs at a value of $[Cu(gl)_2]/[Cu(en)_2^{2+}]$ of 4·25/5·75 or $x = 0{\cdot}74$. The direction of the displacement is contrary to a prediction made solely on the basis of the relative stabilities of the bis(glycinato)(21) and bis(ethylenediamine) complexes involved, since these would lead to the expectation that $[Cu(gl)^+] > [Cu(en)^{2+}]$ (i.e. $C_5 > C_4$). In this case the protonic equilibria are of sufficient importance to reverse the order of the concentrations.

The maximum in the Y function is displaced from the molar ratio of 0·375/0·625 at 600 mμ to 7/3 at 800 mμ. This indicates the affect of wave length when only the simple Y function is considered. At a wavelength of 650 mμ the maximum occurs at the 0·5/0·5 molar ratio; and if wavelengths greater than 650 mμ are chosen, the maximum in the Y value would be shifted according to the prediction of the equation that has been developed.

Copper(II)-glycine-propylenediamine system. The continuous variations curves for the 0·010, 0·015 and 0·020 M solutions were constructed from the Y functions calculated at a wavelength of 628 mμ. The wavelength range of 600–800 mμ was studied. In this system, as in the system above, the maximum occurs at a molar ratio of $[Cu(gl)_2]/[Cu(pn)_2{}^{2+}] = 4{\cdot}25/5{\cdot}75$ or $x = 0{\cdot}74$. Once again, the experimental value is contrary to the prediction based on the dissociation constants of the bis(glycinato) and bis(propylenediamine) complexes. The extremum is displaced from the 3/7 ratio at 600 mμ to the 7/3 ratio at 800 mμ. Above 660 mμ (molar ratio 5/5) the maximum is shifted according to theory. The reason for the deviation is the same as in the case above.

---

(18) J. Bjerrum and E. J. Nielson, *Acta Chem. Scand.* 2, 297 (1948).

(19) F. Basolo, Y. T. Chen and R. K. Murmann, *J. Amer. Chem. Soc.* 76, 956 (1954).

(20) F. Basolo, R. K. Murmann and Y. T. Chen, *J. Amer. Chem. Soc.* 75, 1478 (1953).

(21) F. Basolo and Y. T. Chen, *J. Amer. Chem. Soc.* 76, 953 (1954).

Copper(II)–glycine–pyridine system. The absorption data used to calculate the Y values for this system were obtained over a wavelength range of 550–800 mμ. The absorption maximum of the 0·020 M, 5/5 solution occurred at 678 mμ, and continuous variations curves for the 0·010, 0·015 and 0·020 M solutions were obtained from calculations of the Y values based on absorption data at this wavelength (see Fig. 2). The extremum in this system occurs at a ratio of $[Cu(gl)_2]/[Cu(py)_4{}^{2+}]$ of $0{\cdot}475/0{\cdot}525 = 0{\cdot}905$. A comparison of the stability constants for the tetrapyridine and the bis(glycinato) copper(II) complexes indicates a greater dissociation in the case of the tetrapyridine complex, and, therefore, the maximum in the Y function is shifted as predicted. The maximum in the Y function is displaced from the molar ratio of 4·25/5·75 at 600 mμ to 5/5 at 700 mμ: and at a wavelength of 800 mμ it approaches the 7/3 ratio. The agreement between theory and experiment in this case, in contrast to the other cases of this type, is probably because pyridine is a much weaker base than ethylenediamine and propylenediamine and therefore, the subsidiary protonic equilibria are relatively less important.

Equilibrium constants

One of the greatest shortcomings of the method of continuous variations is the lack of any general method for obtaining equilibrium constants from the type of data such studies provide. Each type of complexation reaction seems to require the development of a special procedure and the present case is no exception. The usual methods for obtaining equilibrium constants from spectrophotometric data(22–28) are not useable here, nor are the methods which have been developed for systems with a single type of ligand.(29–37) The crux of the problem is the lack of a procedure for

---

(22) R. T. FOLEY and R. C. ANDERSON, *J. Amer. Chem. Soc.* **71**, 909 (1949).

(23) P. HAGENMULLER, *Ann. Chim.* [12], **6**, 5 (1951).

(24) J. A. A. KETELAAR, C. VAN DE STOLPE, A. GOUDSMIT and W. DZCUBAS, *Rec. Trav. Chim.* **71**, 1104 (1952).

(25) S. NAKAGURA, *J. Amer. Chem. Soc.* **76**, 3070 (1954).

(26) S. NAKAGURA, *J. Amer. Chem. Soc.* **80**, 520 (1958).

(27) R. M. KEEFER and L. J. ANDREWS, *J. Amer. Chem. Soc.* **74**, 1891 (1952).

(28) H. A. BENESI and J. H. HILDEBRAND, *J. Amer. Chem. Soc.* **71**, 2703 (1949).

(29) L. NEWMAN and D. N. HUME, *J. Amer. Chem. Soc.* **79**, 4571 (1957).

(30) P. JOB, *Ann. Chim.* [10], **9**, 113 (1928).

(31) P. JOB, *Ann. Chim.* [11], **6**, 97 (1936).

(32) P. HAGENMULLER, *C.R. Acad. Sci., Paris* **230**, 2190 (1950).

(33) B. BANERJEE and P. RAY, *J. Indian Chem. Soc.* **35**, 297, 493, 817 (1958).

(34) M. MANDEL and C. DEPOMMIER, *Bull. Soc. Chim. Belges.* **68**, 139 (1959).

(35) N. TANAKA and T. TAKAMURA, *J. Inorg. Nucl. Chem.* **9**, 15 (1959).

(36) H. IRVING and T. B. PRICE, *J. Chem. Soc.*, 2565 (1959).

(37) Y. WORMSER, *C.R. Acad. Sci., Paris* **250**, 3647 (1960).

reducing the data when there are several species absorbing light at the wavelengths used. In the present case, a method was developed for a system in which there are three species absorbing. The treatment is patterned after the procedure used by ROSE and DRAGO[38] for a simpler system. The basic assumptions used in the present development are (1) Beer's law is followed by each of the absorbing constituents, and (2) the activity co-efficients remain constant and therefore concentrations can be used in place of activities. The types of reactions considered are:

$$AB_2+AC_4 \rightleftarrows 2\,ABC \qquad (1)$$
$$\text{or } AB_2+AD_4 \rightleftarrows 2\,ABD_2 \qquad (15)$$

If the concentrations and the extinction co-efficients for these species are the same as used previously, and if these species are considered to be the major constituents of the solution (and the neglect of the others will not introduce a serious error), then the total absorbance A at a given wavelength will be (for $L = 1$)

$$A = \varepsilon_1 C_1+\varepsilon_2 C_2+\varepsilon_3 C_3 \qquad (30)$$

If the relationships between the concentrations and x given earlier in equations (11), (12), (24) and (25) are used in equations (30), the expression for the absorbance is

$$A = C_3\left[\varepsilon_3-\frac{(\varepsilon_1+\varepsilon_2)}{2}\right]+\varepsilon_1 M(1-x)+\varepsilon_2 Mx \qquad (31)$$

the equilibrium constant, K, for the reaction is:

$$K = \frac{[C_3]^2}{[C_1][C_2]} \qquad (32)$$

If equation (30) is solved for C_3, and the values of C_1, C_2 and C_3 are substituted into equation (32), equation (33) is obtained

$$K=\frac{\left\{\dfrac{A}{\varepsilon_3-\dfrac{(\varepsilon_1+\varepsilon_2)}{2}+\varepsilon_1 M(1-x)+\varepsilon_2 Mx}\right\}^2}{\left[\left\{M(1-x)-\left\{\dfrac{A}{2\,\varepsilon_3-\dfrac{(\varepsilon_1+\varepsilon_2)}{2}+\varepsilon_1 M(1-x)+\varepsilon_2 Mx}\right\}\right].\left[Mx-\left\{\dfrac{A}{2\,\varepsilon_3-\dfrac{(\varepsilon_1+\varepsilon_2)}{2}+\varepsilon_1 M(1-x)+\varepsilon_2 Mx}\right\}\right]\right.} \qquad (33)$$

In equation (33), A, ε_1, ε_2, M and x are known and only ε_3 and K are unknown. Since a maximum occurs in the Y function, for these systems, ε_3 must be greater than $(\varepsilon_1+\varepsilon_2)/2$. This requirement sets a lower limit for ε_3. Various values for the extinction co-efficient, ε_3, of the complex are assumed and substituted into equation (33). For each assumed value of ε_3, a corresponding K is calculated.

---

(38) N. J. ROSE and R. S. DRAGO, *J. Amer. Chem. Soc.* **81**, 6138, 6141 (1959).

Since the equilibrium constants obtained are small, their dependence upon the extrapolation of a line is critical. The IBM 650 computer was used to obtain least square values of ε_3. A plot of K against the corrected ε_3 values for various molar ratios of the reacting species (same total molarity) gives several intersecting lines (see Fig. 3). The point of intersection of the lines determines the equilibrium constant and the extinction coefficient for the mixed ligand complex formed.

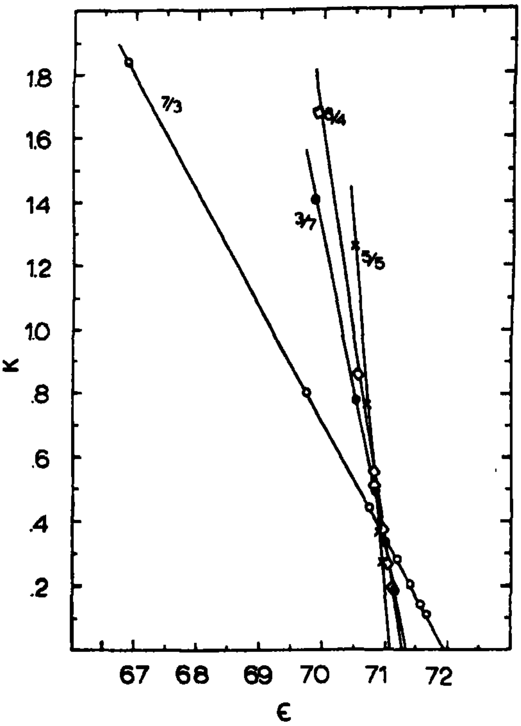

FIG. 3.—Graphical determination of K.

A second method was also used to obtain the equilibrium constants. This method involved the solution of all possible combinations of the linear equation obtained from the IBM 650 computer. The average equilibrium constant, K, obtained from a solution of these equations and the extinction co-efficients, ε_3, corresponding to these constants are given in Table 1. This table also contains the best single point, values of the equilibrium constant, K, and the extinction co-efficient, $\bar{\varepsilon}_3$ chosen from the graphical plots.

TABLE 1.—EQUILIBRIUM CONSTANTS FOR THE FORMATION OF MIXED LIGAND COMPLEXES

Complex	K	$\bar{K}$	$\bar{\varepsilon}_3$	ε_3
$[Cu(en)(py)_2]^{+2}$	0·62	0·30	70	78
$[Cu(pn)(py)_2]^{+2}$	0·63	0·30	75	78
$[Cu(gl)(en)]^{+}$	0·64	0·30	61	62
$[Cu(gl)(pn)]^{+}$	0·68	0·30	59	61
$[Cu(gl)(py)_2]^{+}$	0·52	0·35	67	67·5

The absorbances at different molar ratios, but at the same total molar concentration and the same wavelength, were used in each system studied. These conditions were chosen so that the extinction co-efficients of all absorbing species would remain constant. Consequently, no additional error was introduced in the observed extinction co-efficients due to dilutions. The wavelength chosen in all cases was that at which the mixed ligand complex showed a maximum.

The statistical formation constant for complexes of the type studied here is four. The values obtained are thus reasonably close to those that would be predicted on the basis of a simple random mixing of the ligands on co-ordination sites.(9, 39) This is reasonable in view of the fact that the same numbers of each type of co-ordinate bond are present in both the reactants and products. For such reactions, the enthalpy changes are generally very small or zero leaving the entropy changes paramount in determining the free energy change.(40) Table 2 lists the formation constants of a few mixed ligand complexes similar to those studied in this work. It can be seen that such a simple statistical distribution of ligands is not a general phenomena.

TABLE 2.—FORMATION CONSTANTS OF SOME MIXED LIGAND COMPLEXES

Complex	Formation constant	Reference
$[Cu(C_2O_4)(en)]$	10	15
[Cu(iminodiacetate)(en)]	~ 100	41
$[Cu(P_2O_7)(NH_3)_2]^{2-}$	~ 0·01	14
$[Cu(P_2O_7)(en)]^{2-}$	0·01	13

Acknowledgement—We wish to acknowledge, with thanks, the support for this investigation provided by the Research Corporation and the National Science Foundation.

(39) Y. MARCUS, *Acta Chem. Scand.* **11**, 610 (1957) is a recent discussion of this topic.

(40) J. H. HOLLOWAY. Ph.D. Thesis, University of North Carolina (1959) and the literature cited therein.

(41) W. E. BENNETT, *J. Amer. Chem. Soc.* **79**, 1290 (1957) who also suggested that charge neutralization was responsible, in part, for such a large value.

J. Inorg. Nucl. Chem., 1962, Vol. 24, pp. 821 to 827. Pergamon Press Ltd. Printed in England

STUDY OF CATECHOL DERIVATIVES OF THORIUM

R. P. Agarwal and R. C. Mehrotra*
Chemical Laboratories, University of Gorakhpur, Gorakhpur, U.P. (India)

(*Received* 12 *May* 1961; *in revised form* 13 *November* 1961)

Abstract—Complexing reactions of thorium with catechol have been studied by potentiometric and preparative methods. In acidic solution the formation of the mono-catechollate derivative only was indicated even in the presence of a large excess of catechol. The equilibrium constant K of the reaction:

$$Th^{4+} + C_6H_4(OH)_2 \rightleftharpoons [Th(C_6H_4O_2)]^{2+} + 2H^+$$

was found to be: $K = 2{\cdot}98 \times 10^{-5}$ and the formation constant k of the complex was $5{\cdot}25 \times 10^{17}$. Potentiometric titrations of thorium nitrate in presence of catechol showed a sharp inflexion at four equivalents of alkali per mole of thorium ion, suggesting the possibility of an electrometric estimation method for thorium. New compounds $(NH_4)_2$-$[Th(C_6H_4O_2)_3]C_6H_6O_2$ and $(C_5H_5N)_2Th(C_6H_6O_2)_2$ were isolated.

In view of the interesting results reported^(1, 2)^ on the catechol derivatives of zirconium from our laboratories, it was considered of interest to study similar derivatives of thorium. Although catechol derivatives of thorium have been synthesized by a number of workers, no physico-chemical study appears to have been carried out. In the present investigation, the systems have been investigated by a potentiometric method and formation constant of the thorium mono-catechollate derivative has been determined by calculating the equilibrium constant of the reaction:

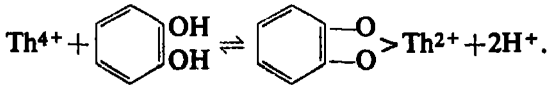

The synthesis of catechol derivatives of thorium has been studied in detail by Rosenheim and co-workers,^(3)^ who prepared well defined derivatives with formulae $(NH_4)_2\ [Th(C_6H_4O_2)_3].\ 7H_2O$ and $(NH_4)_2\ [Th_3(C_6H_4O_2)_6\ (OH)_2].\ 10H_2O$. They have also reported an improved method for the preparation of the tri-catechollate derivative, $(NH_4)_2[Th(C_6H_4O_2)_3].5H_2O$. H. Sperl^(4)^ prepared the pyridine complex $Th(OC_6H_4OH)_4(C_5H_5N)_2$. A similar ammonium compound with the composition $(NH_4)_2H_2\ [Th(C_6H_4O_2)_4]$ was obtained by slightly varying the conditions of preparation as described by Rosenheim.^(3)^ It was found that the above compound was hydrolysed to $(NH_4)_2\ [Th_3(C_6H_4O_2)_6(OH)_2].\ 10H_2O$ by excess of ammonia on boiling. It was also observed that the pyridine complex $Th(OC_6H_4OH)_4(C_5H_5N)_2$, reported earlier by Sperl,^(4)^ was converted into $(C_5H_5N)_2Th\ (C_6H_4O_2)_2$ with excess of pyridine.

---

* Present address: University of Rajasthan, Jaipur.

(1) R. N. Kapoor and R. C. Mehrotra, *Z. Anorg. Chem.* **293**, 92 (1957).

(2) R. N. Kapoor and R. C. Mehrotra, *Z. Anorg. Chem.* **293**, 104 (1957).

(3) A. Rosenheim, B. Raimann and G. Schendel, *Z. Anorg. Chem.* **196**, 173 (1931).

(4) R. Weinland and H. Sperl, *Z. Anorg. Chem.* **150**, 72 (1926).

EXPERIMENTAL

Materials. Thorium nitrate, $Th(NO_3)_4 \cdot 4H_2O$ employed was of B.D.H. reagent grade quality. Catechol was a Merck product. Potassium permanganate, caustic alkalies and acids were reagent grade products of B.D.H.

A stock solution of thorium nitrate was standardized gravimetrically by precipitation with ammonium hydroxide and subsequent ignition of the hydroxide to ThO_2. The solution of catechol was made by direct weighing.

pH measurements were carried out at room temperature with a Phillips pH-meter (P.R. 9400), standardized against a 0·05 M solution of potassium hydrogen phthalate.

Analytical methods. Thorium was estimated as ThO_2 by direct ignition of the compound. The alkaline permanganate method(5) of oxidation of organic compounds was found to oxidize catechol quantitatively to carbon dioxide and water and has been adopted in the present investigation for estimation of catechol.

Preparative studies

1. *Reaction of thorium nitrate with* 3·8 *to* 4·0 *mole of caustic potash in presence of different amounts of catechol*

In order to test the conclusion from potentiometric titrations that thorium monocatechollate is formed in the acidic medium irrespective of the molar ratio of catechol to thorium, thorium nitrate solution was treated with varying amounts of caustic potash (3·8 to 4·0 mole) in the presence of different amounts of catechol. In all the cases a greenish white precipitate having a thorium to catechol ratio approximately equal to one was obtained.

2. *Reaction of thorium nitrate with ammonium hydroxide in presence of excess of catechol*

(2 a) The above experiment was also repeated with ammonium hydroxide (slightly less than 4 mole) instead of caustic potash. In this case as well analysis of the precipitate indicated a thorium to catechol ratio of approximately one.

(2 b) A mixture of thorium nitrate (5·88 g, 0·01 g-mole) and catechol (8·8 g, 0·08 g/mole) was dissolved in water (20 ml) and was treated with ammonium hydroxide until faintly ammonical. A little insoluble material separated and was quickly filtered off. The filtrate was heated on a water bath for 5 min and cooled when a white crystalline compound separated.

(2 c) In another experiment, more ammonium hydroxide was added to the above reaction mixture (2 b) which was boiled for about 2 min and then cooled. A white crystalline compound separated. The compounds were washed several times with dioxane and finally with water and dried in vacuum (1 mm) for about 6 hr at room temperature (30° C).

Analysis. (2a) Th = 52·21, Catechol = 25·34 per cent, Ratio of thorium to Catechol = 0·941.

(2 b). Found: Th = 32·42, Catechol = 61·44, NH_4 = 5·12 per cent. Calcd for $(NH_4)_2H_2[Th(C_6H_4O_2)_4]$ or $(NH_4)_2[Th(C_6H_4O_2)_3] \cdot C_6H_6O_2$: Th = 33·04, Catechol = 61·55, NH_4 = 5·13 per cent.

(2 c) Found: Th = 42·92, Catechol = 40·45, NH_4 = 2·24 per cent. Calculated for $(NH_4)_2[Th_3(C_6H_4O_2)_6(OH)_2] \cdot 10H_2O$: Th = 43·42, Catechol = 40·47, NH_4 = 2·25 per cent.

3. *Reaction of thorium nitrate with pyridine in presence of excess of catechol*

The initial reaction mixture of (2 b) was treated with pyridine, 1·6 and 2·0 ml in experiments (3 a) and (3 b) respectively. Yellow crystalline compounds were obtained. The compounds were washed with water and dried in vacuum (1 mm) at room temperature (30° C).

Analysis. 3(a) Found: Th = 27·90, Catechol = 52·45, N = 3·35 per cent. Calculated for $Th(OC_6H_4OH)_4(C_5H_5N)_2$: Th = 28·0, Catechol = 52·78, N = 3·38 per cent.

(3 b) Found: Th = 38·05, Catechol = 35·89, N = 4·35 per cent. Calculated for $(C_5H_5N)_2Th(C_6H_4O_2)_2$: Th = 38·26, Catechol = 35·65, N = 4·62 per cent.

(5) G. BOTTGER and R. E. OESPER, *Newer Methods of Volumetric Chemical Analysis*, p. 55.

ELECTROMETRIC STUDIES

The potentiometric titration of thorium ion with catechol, shown in curves 1 and 2 (Fig. 1) indicates chelation of the type:

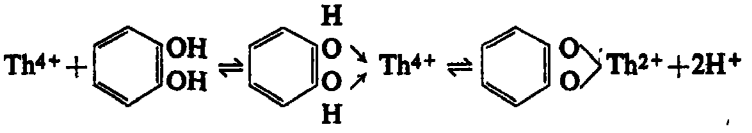

(A) (1)

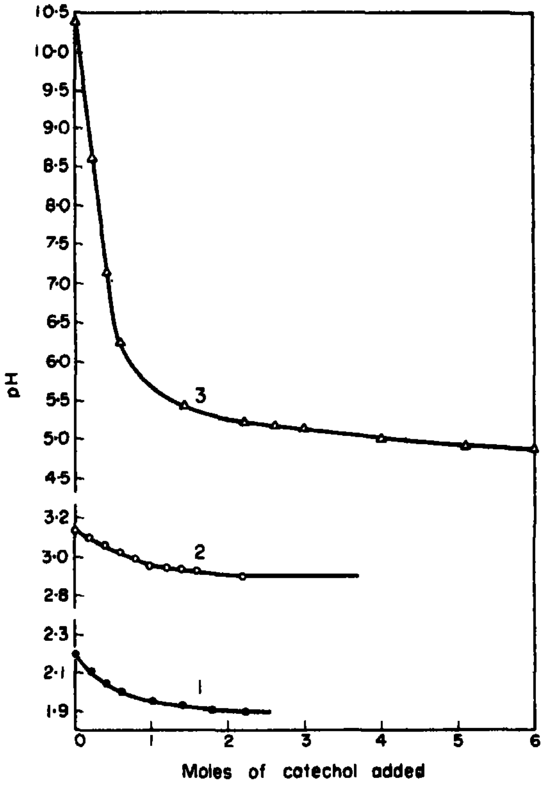

FIG. 1.—Curve (1): Potentiometric titration of thorium nitrate (0·05 M, 20 ml) with molar catechol.

Curves (2) and (3): Above titrations after the addition of 2 and 4 ml of molar caustic potash to the thorium nitrate solution.

This chelation by the donation of a lone pair of electrons from the hydroxy oxygen atoms makes the hydrogen atom more labile and acidic and thus, the lowering of the pH of the system is a direct measure of chelation. The curve (3) (Fig. 1) also supports the above conclusion.

The derivative (A) containing the charged complex cation remains in solution. Addition of alkali to the above reaction mixture neutralizes the hydrogen ions produced by chelation which tends to shift the above equilibrium (1) towards right and thus favours the formation of (A). At higher pH hydrolytic effects in the system also come into play and may be represented:

$$[\text{Cat. Th}]^{2+} \overset{\text{OH}}{\rightleftharpoons} [\text{Cat. Th(OH)}]^{+} \overset{\text{OH}^-}{\rightleftharpoons} [\text{Cat. Th(OH)}_2] \qquad (2)$$

In acidic medium curves 1, 2, 3, 4 and 5 (Fig. 2) for the potentiometric titrations of thorium nitrate with caustic potash in presence of 1, 2, 3, 4 and 5 moles of catechol respectively, are similar to each other with a common point of inflexion at four equivalents of alkali indicating the similarity of reactions. Thus in acidic solution the formation of thorium mono-catechollate was indicated irrespective of the amount of catechol present in the system. This was confirmed by the actual isolation of the precipitates. However, beyond the inflexion point, *m* = 4 where *m* represents

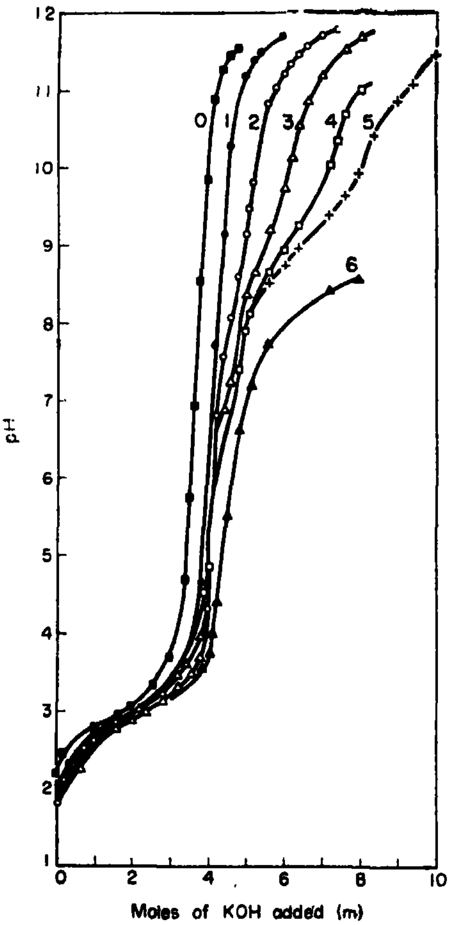

FIG. 2.—Curves (0), (1), (2), (3), (4) and (5) represent potentiometric titrations of thorium nitrate (0·05 M, 20 ml) with caustic potash (1 M) in presence of 0, 1, 2, 3, 4 and 5 ml of catechol (1 M).

Curve (6): same as curve (5) but with ammonium hydroxide in place of caustic potash. *m* = mole of base added per mole of thorium ion.

equivalents of base added per mole of thorium ion, the curves begin to fall short indicating equilibria of the type:

$$[\text{Cat.}\,\text{Th(OH)}_2] \overset{\text{OH}^-}{\rightleftharpoons} [\text{Cat.}\,\text{Th(OH)}_3]^- \overset{\text{Cat.}}{\rightleftharpoons} [\text{Cat.}\,{}_2\text{Th(OH)}]^- \overset{\text{Cat.}}{\rightleftharpoons} [\text{Cat.}\,{}_3\text{Th}]^{2-}$$

The inflexions at $m = 4, 5, 6$ in curves (1), (2) and (3) are easily explained by the above equilibria.

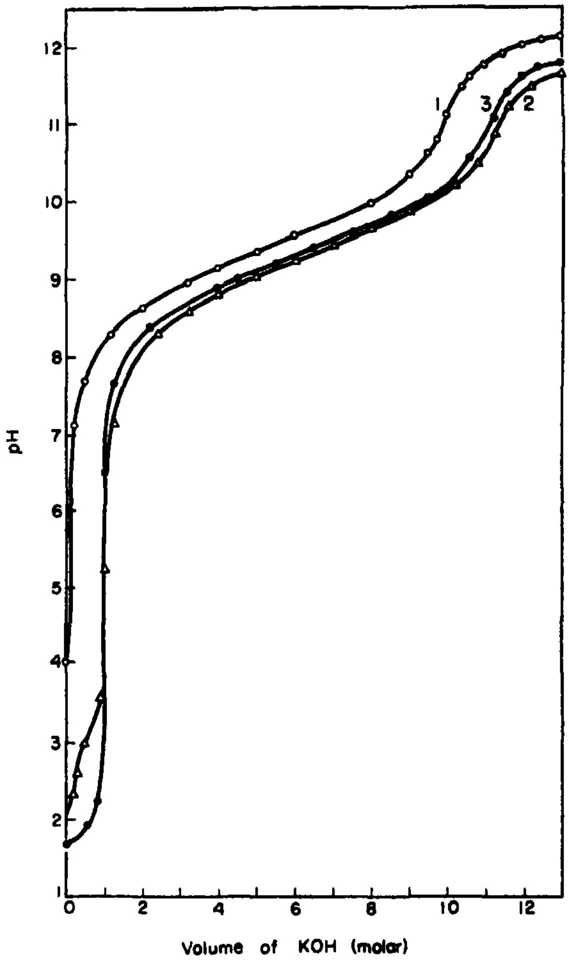

FIG. 3.—Curves (1), (2) and (3) represent potentiometric titrations of catechol (0·5 M, 20 ml) with molar caustic potash in presence of 5 ml of water, thorium nitrate (0·05 M) and nitric acid (0·2 M).

In curves (4) and (5) (Fig. 2) inflexions occur at $m = 7$ and 8 respectively. These appear to be due to the neutralization of free catechol by the extra one or two moles of alkali respectively, but the possibility of further weak chelation by catechol could also be inferred from these observations. To distinguish between these possibilities potentiometric titrations of catechol with caustic potash (curves (1), (2), Fig. 3) in the absence and presence of small amounts of thorium ion were carried out and it was found that the excess alkali consumed to the inflexion point in the experiment shown in curve (2) compared with that in curve (1) was equal to six moles per mole of the metal ion. This fact together with the inflexions at $m = 7$ and 8 in curves (4) and (5) (Fig. 2) indicate the probability of the formation of the tri-catechollate only. A compound having catechol to thorium ratio equal to four could only be isolated (preparation 2b) in the presence of a large excess of catechol. In view of the above, this compound appears to have the formula $(NH_4)_2[Th(C_6H_4O_2)_3]$. $C_6H_6O_2$ rather than $(NH_4)_2H_2[Th(C_6H_4O_2)_4]$.

EQUILIBRIUM AND FORMATION CONSTANTS

As catechol is prone to be oxidized by atmospheric oxygen, particularly in alkaline media, titrations have been repeated in an atmosphere of nitrogen, curves (1′), (2′), (3′) and (4′) (Fig. 4). This also served the purpose of excluding carbon dioxide from the system. In these latter titrations, the ionic strength was maintained relatively constant by using a medium containing 0·1 M potassium nitrate and low concentrations of ligand and metal ion to enable calculations of equilibrium and formation constants.

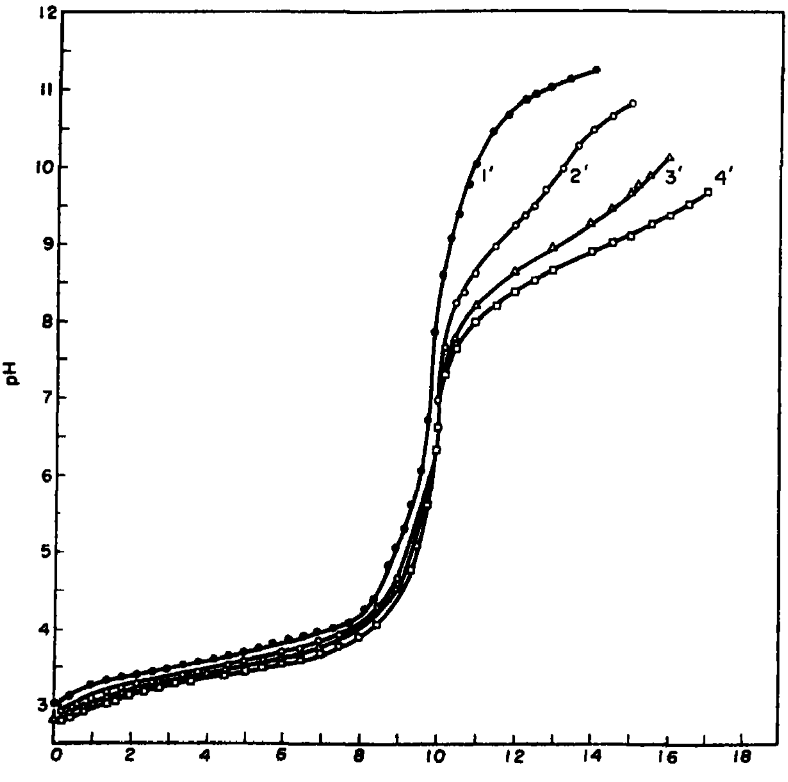

FIG. 4.—Potentiometric titrations of thorium nitrate with caustic potash in presence of catechol at 0·1 M ionic strength in nitrogen atmosphere: Curve (1′), 5×10^{-3} M in thorium nitrate and 5×10^{-3} M in catechol; Curve (2′), 5×10^{-3} M in thorium nitrate and 1×10^{-2} M in catechol; Curve (3′), 5×10^{-3} M in thorium nitrate and $1 \cdot 5 \times 10^{-3}$ M in catechol; Curve (4′), 5×10^{-3} M in thorium nitrate and 2×10^{-2} M in catechol.

(6) C. F. TIMBERLAKE, *J. Chem. Soc.* 4987 (1957).

As the mono-catechollate derivative alone appears to be formed in the acidic range, it was considered of interest to calculate the equilibrium constant of the reaction given by:

$$K = \frac{[\mathrm{ThA}^{2+}][\mathrm{H}^+]^2}{[\mathrm{Th}^{4+}][\mathrm{H_2A}]}$$

K was calculated from the various concentrations of $[\mathrm{ThA}^{2+}]$, $[\mathrm{H}^+]$, $[\mathrm{Th}^{4+}]$ and $[\mathrm{H_2A}]$ present in the equilibrium mixture. Over the pH range studied the concentrations of $[\mathrm{HA}^-]$, $[\mathrm{A}^{2-}]$ and $[\mathrm{OH}^-]$ were negligible compared to the other ionic species present.

The values of pK were calculated at various points on the curves (1′) to (4′) (Fig. 4) from $m = o$ to $m = 1·5$, where m represents moles of base added per mole of the metal ion. It was observed that as the molar ratio of catechol to thorium in the reaction mixture was increased the constancy of the values of pK improved at the greater values of m. This indicated that in the presence of excess of catechol the reaction (1) is pushed towards right and the hydrolytic effects in the system are gradually reduced. Numerical data obtained for curve (4′) are shown below.

Ml. KOH	0·2	0·4	0·6	0·8	1·0	1·4	1·8	2·4
pH	2·82	2·86	2·89	2·93	2·96	3·03	3·11	3·18
pK	4·542	4·544	4·524	4·533	4·523	4·526	4·559	4·490

Mean pK = 4·526.

After determining the equilibrium constant of the reaction (1), the formation constant k of the complex ThA^{2+} was determined from:

$$k = \frac{K}{K_{a1}\,K_{a2}},$$ where K_{a1} $(3·7\times10^{-10})$ and K_{a2} $(1·5\times10^{-13})$[6]

represent dissociation constants of catechol. Thus the value of log $k = 17·72$ was obtained.

Attempts were also made to calculate the equilibrium and formation constants for other equilibria indicated in the electrometric studies. However, on the alkaline side the hydrolytic effects cause too much disturbance for anything beyond very approximate values to be obtained.

Although not investigated from that view point, the titration curves indicate that it would be possible to estimate thorium ions electrometrically with caustic potash when a pronounced inflexion at four equivalents of alkali is obtained.

Acknowledgement—Thanks of the authors are due to the Council of Scientific and Industrial Research authorities for providing a junior research fellowship to one of them (R.P.A.)

J. Inorg. Nucl. Chem., 1962, Vol. 24, pp. 829 to 838. Pergamon Press Ltd. Printed in England

FLUORESCENCE OF METAL CHELATE COMPOUNDS OF 8-QUINOLINOL—III

THE MONO-(8-QUINOLINOL)-ALUMINIUM SPECIES IN ABSOLUTE ETHANOL

W. E. Ohnesorge and A. Capotosto, Jr.
Department of Chemistry, University of Rhode Island, Kingston, Rhode Island

(*Received* 9 *October* 1961; *in revised form* 13 *November* 1961)

Abstract—Fluorometric, absorptiometric, and potentiometric data have confirmed the existence of a fluorescent species formed between aluminium ion and 8-quinolinol having a ligand-to-metal molar ratio of one. This species in absolute ethanol is probably a polynuclear complex and has a formation constant estimated to be in the order of 10^9. The nature of the chelation reaction is discussed; it apparently proceeds via replacement by oxine of a solvated ethoxide ion and a solvated ethanol molecule from the co-ordination sphere of the aluminium ion.

The anomalous increase in the fluorescence intensity and the shift of the wavelength of maximum emittance which accompany the partial decomposition upon addition of acid to or by exposure to ultra-violet radiation of aluminium oxinate solutions prepared by dissolving the solid in ethanol (or in chloroform) has been attributed to the formation of a lower complex between the metal and the ligand.(1) It is hardly surprising that the lower complex(es) might exist or that such species would be capable of fluorescence. Irving had previously suggested the existence of an aluminium-oxine chelate having a ligand-to-metal ratio of one or of two.(2) A one-to-one fluorescent species between aluminium ion and morin was postulated by Szambo and Beck.(3) These species would meet the generally accepted (necessary, but not sufficient) requirements for fluorescence: a closed ring and, in the case of the monoligand species, a planar structure.(4, 5)

In the present work absorbance and fluorescence data obtained using the Molar Ratio Method confirm the existence of a one-to-one aluminium–oxine complex species in absolute ethanol. The formation constant was estimated from the same data and from other data obtained by titration. The titration data also show that the formation of the lower complex in slightly acidic, neutral, or slightly alkaline absolute alcohol proceeds by a mechanism in which the ligand molecule replaces a solvated ethanol molecule and a solvated lyate ion which takes up the phenolic proton from the 8-quinolinol.

---

(1) W. E. Ohnesorge and L. B. Rogers, *Spectrochim. Acta* 41 (1959).
(2) H. Irving, E. J. Butler and M. F. Ring, *J. Chem. Soc.* 1489 (1949).
(3) Z. G. Szambo and M. T. Beck, *Acta Chim. Acad. Sci. Hung.* 4, 211 (1954).
(4) W. West, *Chemical Applications of Spectroscopy*, Chap. 6, *Technique of Organic Chemistry*, Vol. 9 (Edited by A. Weissberger). Interscience, New York (1956).
(5) T. Förster, *Fluoreszenz Organischer Verbindungen*, Chap. 22. Vandenhöck and Ruprecht, Göttingen (1951).

EXPERIMENTAL

All solutions were prepared from reagent-grade chemicals. The 8-quinolinol (Eastman, White label) was assayed by the standard bromination technique,(6) found to be sufficiently pure, and was used as obtained.

Solutions of aluminium ion in absolute ethanol were prepared by dissolving the hydrated nitrate or the anhydrous chloride salt. The salts were analysed gravimetrically by precipitation and weighing of aluminium oxinate.(6) Working solution concentrations were made sufficiently dilute to avoid fluorometric errors due to attenuation(7) which occurred if the absorbance of the solution (in 1·0 cm cells) exceeded 0·6 at the wavelength used to excite fluorescence.

The apparent-pH measurements were made with a Beckman Zeromatic pH Meter using a saturated calomel electrode and a glass electrode. The meter was "standardized" against absolute ethanol before beginning each experiment by adjusting the asymmetry control to obtain a meter reading of 1·0, 3·0, 7·0 or 11·0 depending on the composition of the experimental solution and on the acidity changes expected in the experiment. The data were converted for comparison purposes to a common base of 11·0. The conversion of experimental pH data to the common base was validated by running replicate titrations using different standardization values. The reproducibility of measurements varied, but not sufficiently to affect interpretation of the results, which are based only on rather large changes in apparent-pH.

Absorbance data were obtained on a Beckman Model DK-2 recording spectrophotometer and on a Coleman Model 14 spectrophotometer; cells with an effective path length of 1·1 cm were used with the latter instrument. Radiation at the wavelength selected for absorbance measurements (365 mμ), which was used also to excite fluorescence, is absorbed by the aluminium-oxine species, protonated oxine (8-quinolinium ion), and the oxinate ion, but is not absorbed appreciably by oxine.(8)

Fluorescence intensity measurements were made on a modified Farrand Model 104243 spectrofluorometer; 5 mμ slits were used in both monochromators. The instrument was modified by substituting a low-pressure mercury lamp (General Electric UA-2) for the xenon source supplied with the fluorometer. Fluorescence intensity measurements were made at 498 mμ near the apparent maximum in the emission spectrum of the aluminium–oxine species as determined on solutions prepared by dissolving solid aluminium oxinate in absolute ethanol.

Fluorescence intensity and absorbance measurements have been corrected for dilution; fluorescence data were also corrected for background as determined with pure solvent. All fluorescence intensity measurements were made with reference to a quinine standard (7). The instrument was calibrated daily with 3·0 p.p.m. solution of quinine sulphate in 0·1 N sulphuric acid. The fluorometer sensitivity was set to give an emittance reading at 495 mμ of 0·2 μA when the standard was excited with 365 mμ radiation.

RESULTS AND DISCUSSION

An equilibrium diagram showing amounts of three oxine species in absolute ethanol solution as a function of the apparent-pH (based on the pure solvent having a value of 11·0) is shown in Fig. 1. The diagram was constructed using molar absorbance values obtained with oxine solutions which contained a large excess of acid or of base and from absorbance and apparent-pH data obtained when ethanolic oxine solutions were titrated with standard hydrochloric acid or with standard sodium hydroxide solutions in the same solvent, Figs. 2 and 3. Fluorescence was not observed and was not expected in these systems.(8)

---

(6) I. M. KOLTHOFF and E. B. SANDELL, *Textbook of Quantitative Inorganic Analysis* (3rd Ed.). p. 321. MacMillan, New York (1955).

(7) [illegible] COLLAT and L. B. ROGERS, *Analyt. Chem.* 27, 961 (1955).

(8) [illegible] OHNESORGE and L. B. ROGERS, *Spectrochim. Acta* 27 (1959).

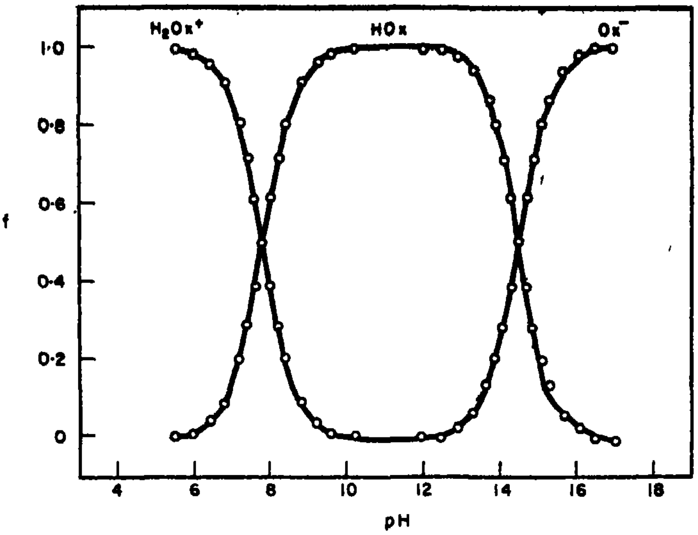

Fig. 1.—Equilibrium diagram for oxine in absolute ethanol, showing the fraction, *f*, of oxine present as:

H_2Ox^+ = 8-quinolinium ion
HOx = 8-quinolinol
Ox^- = 8-quinolinolate ion.

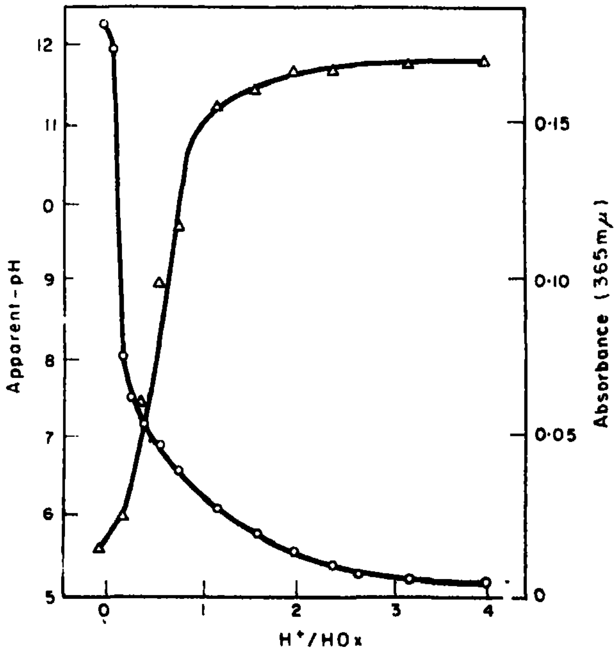

Fig. 2.—Variation of apparent-pH and absorbance at 365 mμ during the titration of 50 ml of 0·10 mM oxine with 1·98 mM HCl. Solvent: absolute ethanol, O: apparent-pH Δ: absorbance (1·1 cm cells).

The equilibrium diagram shows that whenever the apparent-pH is less than 6 no significant amounts of oxine, i.e. less than one per cent, will exist in solution and the protonated species, 8-quinolinium ion, will predominate. Between an apparent-pH of 9 and 13 the molecular form will be the important species in solution, but above 15 the 8-quinolinolate ion will predominate.

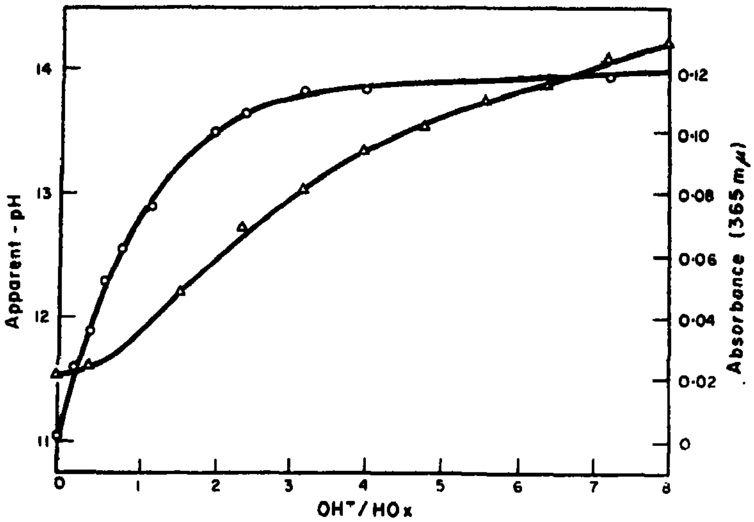

Fig. 3.—Variation of apparent-pH and absorbance at 365 mμ during the titration of 50 ml of 0·10 mM oxine with 2·0 mM NaOH. Solvent: absolute ethanol, O: apparent-pH Δ: absorbance (1·1 cm cells).

From the equilibrium diagram the pK_b for oxine in absolute ethanol is estimated to be approximately 13. The pK_a of the 8-quinolinium ion is equal to the (true) pH at which the amounts of this ion and its conjugate base, oxine, are equal. This occurs (Fig. 1) at an apparent-pH of 7·8. Considering that the autoprotolysis constant for absolute ethanol, K_S, is $10^{-19\cdot5}$,⁽⁹⁾ i.e. neutral absolute ethanol has a true-pH of 9·75, not 11·0, equal amounts of oxine and its conjugate acid would exist at a true-pH of 6·6. Because the sum of the pK_a for an acid and the pK_b of its conjugate base is equal to the pK_S of the solvent, the pK_b of oxine is (19·5–6·6) or about 13. An estimate for the pK_a of 14 is similarly obtained. Agreement with values predicted by the pertinent equation of Grunwald and Berkowitz⁽⁹⁾ (pK_b = 13·5, pK_a = 15·5) is satisfactory. Another estimate for pK_b made from the rounding near the stoicheiometric point of the absorbance titration curve of oxine with acid gave a value of 13.

The apparent-pH titration curves observed when solutions of aluminium ion were titrated with alcoholic sodium hydroxide are shown as a function of the solvent composition in Fig. 4. Only one break was observed; in absolute ethanol it occurred when the molar amount of added hydroxide was equal to two and one-half times the molar amount of aluminium present. When the amount of water in the solvent was increased, the hydroxide-to-aluminium molar ratio at the endpoint also increased but the magnitude and the sharpness of the break in the curve decreased.

Aluminium hydroxide precipitates were observed in aqueous and in 50 per cent ethanol solutions, but not in 95 per cent or in absolute ethanol solutions even upon standing for 1 hr after titration. No measurable absorption at 365 mμ and no fluorescence was detected during these titrations.

(9) E. [illegible]runwald and B. J. Berkowitz, *J. Amer. Chem. Soc.* **73**, 4939 (1951).

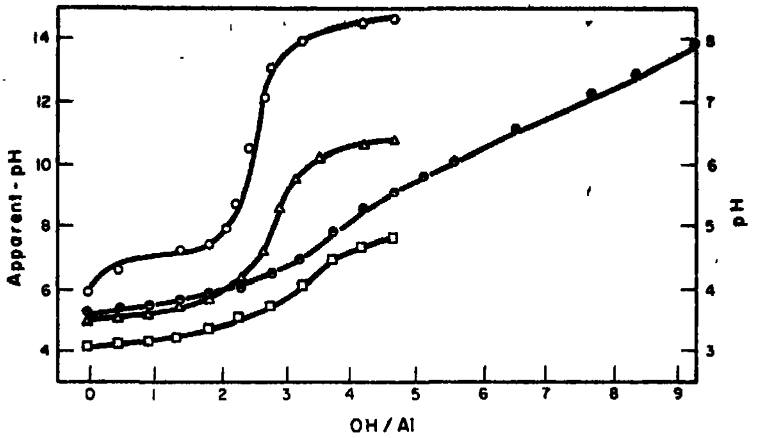

Fig. 4.—Variation of apparent-pH for non-aqueous systems and pH for aqueous systems during the titration of 50 ml of 0·077 mM $AlCl_3$ with 1·85 mM NaOH as a function of the solvent. O: absolute ethanol, Δ: 95 per cent ethanol, □: 50 per cent ethanol, ●: H_2O.

The hydrated aluminium ion behaves as a weak acid in water, pK_a of about 5.(10) Titration with aqueous hydroxide produces a precipitate of hydrated aluminium hydroxide and an end-point break is observed when approximately three moles of hydroxide ion have been added for each mole of aluminium.(11, 12) The existence and

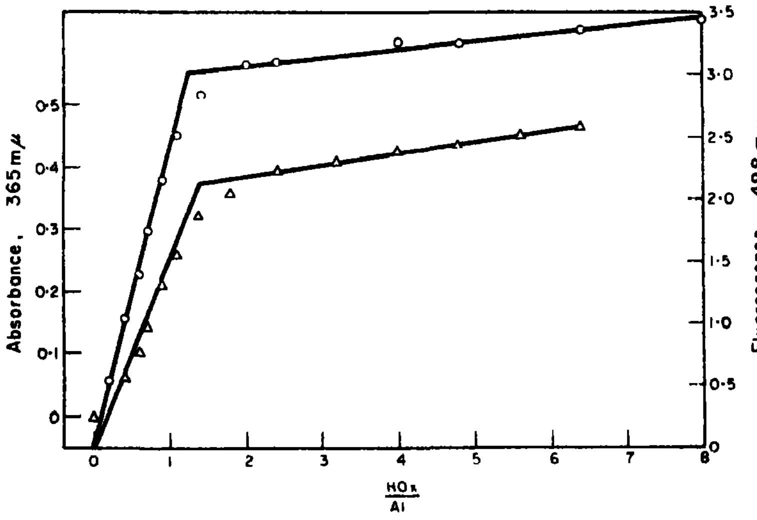

Fig. 5.—Variation of absorbance at 365 mμ and fluorescence intensity at 498 mμ (365 mμ excitation) with amount of 2·0 mM oxine added to 40 ml 0·12 mM $AlCl_3$ in 0·75 mM NaOH. Solvent: absolute ethanol, Δ: absorbance (in 1·10 cm cells), O: fluorescence (arbitrary units).

---

(10) J. Bjerrum (Editor), *Stability Constants*, Pt. II, pp. 20, 21. The Chemical Society, London (1957).

(11) I. M. Kolthoff and V. A. Stenger, *Volumetric Analysis*, Vol. 2, pp. 183–186. Interscience, New York (1947).

(12) S. LaCroix, *Anal. Chim. Acta* 1, 3 (1947).

stability of polynuclear complexes in aqueous solution has been verified and some of these species have a molar ratio of hydroxide to aluminium of 2·5.(10, 13, 14)

One would expect the solvated aluminium ion in absolute ethanol to be acidic. The exact nature of the species cannot be predicted with certainty. It appears, however, that traces of water would not displace the solvated ethanol. BJERRUM and JORGENSEN(15, 16) have shown that increasing the alcohol content of methanol- or ethanol–water solutions of trivalent neodymium, divalent copper, nickel or cobalt results in gradual replacement of solvated water molecules with the alcohol. Similar titration curves were observed when ethanolic solutions prepared from anhydrous aluminium chloride and those prepared from the nitrate nonahydrate were titrated with alcoholic sodium hydroxide.

The acid dissociation constant of solvated aluminium ion in absolute alcohol would be expected to be smaller than the corresponding value for aquated aluminium ion in water because ethanol is both a weaker acid and a weaker base than water. One would also expect polynuclear complex species to be found in absolute ethanol solutions. Thus, near the break in the titration curve for aluminium with hydroxide, the predominant metallic species in absolute ethanol solution written in its simplest, though perhaps incorrect,(13) form would be:

$Al_2(OC_2H_5)_5\,(C_2H_5OH)_4^+$:

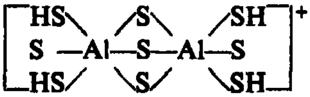

where $S = C_2H_5O^-$.

A Molar Ratio study was made by adding different amounts of oxine to solutions which contained a given amount of aluminium chloride. Sodium hydroxide was also present in sufficient quantity to neutralize any protons released during solvolysis and complexation and to maintain the apparent-pH at a value, near 10, such that nearly all uncomplexed oxine would exist in the molecular form. Absorbance and emittance measurements were made ten minutes after preparation. Both the absorbance and the emittance were found to increase during the first 8 min after preparation, but then remained constant for at least 1 hr. Typical results are shown in Fig. 5 and indicate that a one-to-one complex species is formed between the aluminium ion and oxine.

The slight rise in the fluorescence curve beyond the stoicheiometric point is attributed to the very slight amount of oxinate ion which is formed at this apparent-pH. The oxinate ion will force the formation of more complex by mass-action. A similar but somewhat greater rise in the absorbance curve is probably due to the same effect plus the effect of the absorbance of the excess oxine and the oxinate ion, the latter absorbs appreciably at 365 mμ.

Only the chloride band (near 200 mμ) appeared in the absorption spectrum of the original solution. Addition of oxine resulted in the appearance of bands near 310 mμ and near 375 mμ. The "310 mμ" band appears in the spectra of oxine and of aluminium oxinate: the "375 mμ" band is characteristic of the complex.(8) Both bands increased in intensity until the ligand-to-metal ratio was one; beyond this

(13) C. BROSSET, G. BIEDERMANN and L. G. SILLEN, *Acta Chem. Scand.* **8**, 1917 (1954).

(14) W. D. TREADWELL and M. ZURCHER, *Helv. Chim. Acta* **15**, 980 (1932).

(15) J. BJERRUM and C. K. JORGENSEN, *Acta Chem. Scand.* **7**, 951 (1953).

(16) C. K. JORGENSEN, *Acta Chem. Scand.* **8**, 1475 (1954).

point only the "310 mμ" band continued to increase in intensity with increased amounts of 8-quinolinol. The fluorescence spectra were identical for all solutions, a broad structureless band with a peak at 508 mμ which very strongly suggests that the same fluorescent species exists in each of these solutions.

The formation of the complex ion was also followed by titrating solutions which contained both aluminium chloride and oxine with standard ethanolic sodium hydroxide. The titrations were followed by measuring the apparent-pH, absorbance, and fluorescence intensity as before. Readings were made immediately after the addition of each increment of base; no kinetic effect was noted and the measured quantities remained constant for at least 20 min.

The apparent-pH titration curves showed a single endpoint break when the hydroxide-to-aluminium molar ratio was about 2·5. With the exception of the initial apparent-pH values all curves were identically shaped and similar to those obtained when aluminium ion alone was present in the titrated solution.

All absorbance titration curves showed two breaks. The final break occurred when 2·5 times the molar amount of hydroxide ion (to aluminium ion) had been added. The other break was more clearly defined and occurred when the same ratio was about 2·0. Most curves had similar shape, except those obtained with solutions having an oxine-to-metal molar ratio less than about 1·5, and in these cases an initial flat portion was observed as in Fig. 6. The absorbance of the original solutions was proportional to the amount of oxine present except for those with large ligand-to-metal ratios, Table 1.

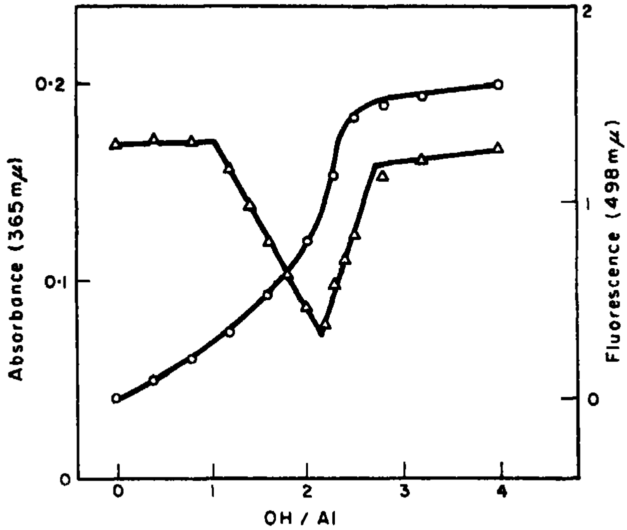

Fig. 6.—Variation of absorbance at 365 mμ and fluorescence intensity at 498 mμ (365 mμ excitation) with added 1·85 mM NaOH. Initial solution: 50 ml, 0·10 mM in oxine and 0·10 mM in AlCl$_3$. Solvent: absolute ethanol, Δ: absorbance (1·10 cm cells), O: fluoerscence (arbitrary units).

Variation of the emittance with the amount of base added is shown for a typical case in Fig. 6. All curves were similar except as noted below. No appreciable emittance was observed from solutions as originally prepared. Addition of base caused an increase in fluorescence, at first rather slowly then more rapidly as indicated

Table 1.—Summary of data obtained in the titration of Al^{3+} and oxine solutions with hydroxide

Total (Al^{3+}) (mMole)	Ligand-to-metal molar ratio	Initial		At "endpoint" when (OH^-/Al^{3+}) = 2·5	
		Apparent-pH	Absorbance 365 mμ	Absorbance 365 mμ	Emittance at 495 mμ
0·10	0·30	5·7	0·05	0·05	0·5
0·067	0·75	6·2	0·07	0·07	1·2
0·10	0·50	6·1	0·08	0·08	0·9
0·10	0·80	6·1	0·14	0·10	1·3
0·10	1·0	4·8	0·16	0·14	1·4
0·10	2·0	5·2	0·29	0·16	1·5
0·10	3·0	6·7	0·36	0·21	1·6
0·15	1·0	4·6	0·23	0·19	1·8

by the increasing slope of the fluorescence titration curve. The maximum emittance was first observed when the hydroxide-to-aluminium molar ratio was approximately 2·5.

When the ligand-to-metal molar ratio was one or above, the final absorbance and fluorescence intensity values were almost directly proportional to the amount of aluminium present, but did depend to a small extent on the ligand-to-metal ratio, probably due to a mass-action effect of excess ligand. However, if this ratio was less than one, the amount of oxine effectively determined the final absorbance and emittance values, although mass action effects due to excess aluminium were noticeable. These results are summarized in Table 1.

It is evident from these data that the formation of the monoligand complex proceeds as a replacement reaction in which the oxine, a bidentate, displaces a solvated ethoxide ion and a solvated ethanol molecule. The displaced ethoxide ion is converted to ethanol using the phenolic proton of oxine, e.g.

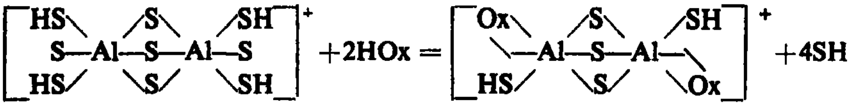

(1)

where S = $C_2H_5O^-$ and Ox^- =

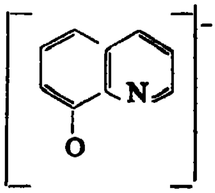

If the oxinate ion displaced two solvated ethanol molecules, the amount of acid consumed in these titrations would be larger than 2·5 times the molar amount of aluminium, i.e. larger than the quantity of base used to neutralize solutions containing only the metallic ion, and the amount of base consumed would increase proportionally with the amount of ligand entering into complexation.

Absorption and fluorescence spectra were recorded on several solutions during the course of these titrations. The absorption spectrum of the initial solution is essentially that of the 8-quinolinium ion showing bands at 315, 330 and 365 mμ.⁽⁸⁾ The addition of hydroxide ion causes a decrease in absorbance at 365 mμ and the maximum near 315 mμ blue-shifts. When the added base is about two times the molar amount of aluminium (minimum in the absorbance titration curve) the band near 370 mμ has almost disappeared and the band near 315 mμ has blue-shifted to 308 mμ. The spectrum is essentially that of oxine.⁽⁸⁾ Further addition of base causes a red-shift of the 310 mμ band to 315 mμ again, and the reappearance of a band near 370 mμ, but now the peak is at 375 mμ (365 mμ before). This spectrum is similar to those obtained on solutions prepared by dissolving solid aluminium oxinate in ethanol.⁽⁸⁾ The fluorescence spectra obtained from these solutions were identical in shape: a structureless band with the apparent wavelength of maximum emission at 506 mμ.

Further examination of these titration curves reveals that there is virtually no complexation in these solutions as originally prepared. In most cases, except those in which the ligand-to-metal ratio is larger than about three, most of the ligand is protonated and there are free hydrogen ions, i.e. protonated ethanol, as evidenced by the initial apparent-pH readings less than about 6.

The introduction of base neutralizes the free-acid or deprotonates the 8-quinolinium ions:

$$C_2H_5OH_2^+ + OH^- = H_2O + C_2H_5OH \tag{2}$$

$$H_2Ox^+ + OH^- = H_2O + HOx \tag{3}$$

These reactions may be assumed, as a first approximation, to go to completion. The equilibria of importance are then:

$$H_2Ox^+ = H^+ + HOx \tag{4}$$

$$[Al(III)] + H_2Ox^+ = [Al(III)Ox] + SH_2^+ \tag{5}$$

where Al(III) = solvated aluminium ion.

As more base is introduced these equilibria shift toward the right, fluorescence intensity increases with formation of more of the complex, but the absorbance decreases because of oxine formation. With increased oxine concentration the complexation equilibrium (6) becomes more important:

$$[Al(III)] + HOx = [Al(III)Ox] + SH \tag{6}$$

Because the equilibrium represented by reaction (6) would favour the right hand side more than would reaction (5), the rise in emittance is more rapid as the quantity of free oxine increases and eventually the absorbance will increase due to complexation of the oxine. Beyond the endpoint a small amount of oxine is neutralized with an attendant small increase in the amounts of the complex species and the oxinate ion which result in a slight increase in fluorescence and a slightly larger increase in absorbance at 365 mμ as stated previously.

Numerical analysis of these titration data also substantiate the reaction sequence outlined above. The amount of complex at any point during the titration can be calculated from the emittance. The absorbance due to the complex was then calculated and subtracted from the observed absorbance. The residual absorbance was used to calculate the amount of 8-quinolinium ion or the amount of oxinate ion depending on the observed apparent-pH. The amount of free 8-quinolinol was then determined by difference from the known total ligand in the solution. The expected apparent-pH was found from the equilibrium diagram using the calculated ratio of oxine to its conjugate acid or base and compared with the observed value. The extent of agreement is shown for one case in Table 2.

Table 2.—Results of numerical analysis of data obtained in titrating a solution 0·10 mM in $AlCl_3$ and 0·30 mM in oxine with 2·00 mM NaOH

	Concentration of				Apparent-pH	
$\left(\frac{OH^-}{Al^{3+}}\right)$	[AlOx] (mMole)	H_2Ox^+ (mMole)	HOx (mMole)	Ox^- (mMole)	Calc.	Obs.
0·2	0·007	0·25	0·04	—	7·0	7·0
0·6	0·017	0·20	0·08	—	7·4	7·2
1·0	0·029	0·15	0·12	—	7·7	7·5
1·4	0·044	0·09	0·17	—	8·1	7·7
1·8	0·061	0·04	0·20	—	8·5	8·1
2·2	0·078	—	0·22	—	10–12	9·4
2·6	0·10	—	0·19	0·01	13·2	12·5
3·0	0·11	—	0·18	0·01	13·3	13·3
3·4	0·11	—	0·18	0·01	13·3	13·7
4·0	0·11	—	0·17	0·02	13·6	14·1

The equilibrium constant for reaction (1) was estimated from these data and also from the data obtained in the Molar Ratio study. Although the stoicheiometry of the true formation reaction is uncertain and probably varies with the acidity of the solution, reaction (1) would appear to provide the most reasonable basis in view of the present work for such calculations applied to nearly neutral solutions. Calculations using fluorescence and absorbance data from the Molar Ratio study and titration data in nearly neutral solutions gave an average value of the formation constant of about 10^9; agreement among individual values was only fair.

Acknowledgements—The Authors gratefully acknowledge the financial support of the Research Corporation and are also indebted to Mr. A. L. Burlingame for some preliminary experimental data.

J. Inorg. Nucl. Chem., 1962, Vol. 24, pp. 839 to 845. Pergamon Press Ltd. Printed in England

THE SYSTEM Cr_2O_3–UO_2–O_2*

E. J. FELTEN,† E. F. JUENKE and S. F. BARTRAM

Nuclear Materials and Propulsion Operation, Flight Propulsion Laboratory Department,
General Electric Company, Cincinnati 15, Ohio

(*Received* 16 *October* 1961; *in revised form* 14 *November* 1961)

Abstract—Three phases were identified in the Cr_2O_3–UO_2–O_2 system between 1200 and 1600° C; namely, Cr_2O_3, U_3O_8, and a mixed oxide of the composition $CrUO_4$. The mixed-oxide phase has orthorhombic symmetry and the lattice constants: $a_0 = 4{\cdot}86_8$ Å, $b_0 = 5{\cdot}04_8$ Å and $c_0 = 11{\cdot}78_5$ Å. It is probably isostructural with the mineral pucherite which has the composition $BiVO_4$.

$CrUO_4$ was found to volatilize at elevated temperatures, probably dissociating into UO_3 and CrO_3. The activation energy for this process is 97 kcal/mole.

A NUMBER of trivalent metal oxide–uranium oxide systems have been investigated. In the UO_2–Al_2O_3 system there is no evidence for solid solution or compound formation.(1, 2, 3) However, in the rare earth oxide systems such as lanthanum oxide, neodymium oxide, samarium oxide and ytterbium oxide with U_3O_8, mixed crystals having the fluorite structure have been prepared.(4) Yttrium oxide(5) and scandium oxide(4) also form mixed crystals of the fluorite type. In addition the rare earth oxides react with U_3O_8 to form a mixed oxide phase having rhombohedral symmetry.(6)

Information concerning the uranium oxide–chromium oxide system is limited. In the course of Cr–U_3O_8 reaction studies, BORCHARDT(7) showed that Cr_2O_3 and U_3O_8 react to form a new phase. This phase was assumed to contain three moles of Cr_2O_3 to two of U_3O_8. X-ray data for the new phase was presented. In reactions between UO_2 and Cr_2O_3 no new phases were found. This is the extent of the information on the uranium oxide–chromium oxide system.

The purpose of the work reported here was to explore more extensively the U_3O_8–Cr_2O_3 system in order to determine the phases present. In addition, data is presented concerning the structure of the phase originally observed by BORCHARDT.(7)

---

* Work performed under AEC Contract AT(11-1)-171.

† Presently associated with the Advanced Materials Research and Development Laboratory, Pratt and Whitney Aircraft, North Haven, Connecticut.

(1) S. M. LANG, F. P. KNUDSEN, C. L. FILLMORE and R. S. ROTH, *High Temperature Reactions of Uranium Oxide with Various Metal Oxides*, NBS Circular 568 (1956).

(2) H. R. HOEKSTRA and S. SIEGEL, *Proceedings of the International Conference on the Peaceful Uses of Atomic Energy, Geneva*, 1955, A/Conf. 8/P/737. United Nations (1956).

(3) W. A. LAMBERTSON and M. H. MUELLER, *J. Amer. Chem. Soc.* **36**, 329 (1953).

(4) F. HUND and U. PEETZ, *Z. Anorg. Chem.* **271**, 6–16 (1952).

(5) F. HUND, U. PEETZ and G. KOTTENHAHN, *Z. Anorg. Chem.* **278**, 184–191 (1955).

(6) E. F. JUENKE. To be published.

(7) H. C. BORCHARDT, *J. Inorg. Nucl. Chem.* **12**, 113–21 (1959).

EXPERIMENTAL

The starting materials used in this investigation were high-purity Cr_2O_3 and UO_2 or U_3O_8. It should be noted that no effort was made to attain stoicheiometric $UO_{2.0}$. Thermogravimetric analysis indicated the oxygen–uranium ratio of the starting material to be nearer 2·10.

The powders were blended by grinding in an agate mortar, and were reacted in platinum cups in a muffle furnace in stagnant air. For several experiments the powders were reacted in sealed quartz tubes in vacuum. The phases present in the reacted powders were determined by standard X-ray diffraction powder techniques. Both film and diffractometer methods were employed.

To determine the chemical composition of the intermediate phase in the system, mixtures on the urania-rich side were prepared and the excess U_3O_8 removed by leaching with dilute nitric acid. The undissolved powder was analysed by wet chemical techniques for uranium and chromium.

In order to determine the crystal symmetry of the intermediate phase, single crystals of the phase were grown. The crystals were grown in the solid state using boric oxide as a fluxing agent. Sufficient boric oxide was added so that one atom of boron was present for each cation in the urania–chromium oxide phase. The powders were mixed in a high speed blender and heated in a platinum dish for about 100 hr at 1370° C. Single crystals suitable for X-ray structural analysis were isolated from the reaction product.

For studies of the volatility of the intermediate compound between urania and chromium oxide, the loose powder was heated in platinum buckets for varying lengths of time between 1350 and 1550° C. The buckets were weighed before and after heating with allowance made for loss of platinum.

RESULTS AND DISCUSSION

1. *Phase studies*

The initial experiments involved the reaction of UO_2 and Cr_2O_3, in varying proportions, in air at 1200, 1400 and 1600° C. The weight changes observed during firing were noted and the phases present after firing determined by X-ray powder methods. The results obtained are found in Table 1. At each of the temperatures three phases were found; namely, chromium oxide (Cr_2O_3), uranium oxide (U_3O_8), and a dark grey mixed oxide phase. As indicated by the X-ray results, the mixed oxide phase was identical to that reported by BORCHARDT.(7) At Cr_2O_3 compositions greater than 27 w/o, the two phases present were the mixed oxide and Cr_2O_3. At Cr_2O_3 compositions below 20 w/o, the mixed oxide phase was found to co-exist with U_3O_8. Preparations containing about 22 w/o Cr_2O_3 showed only the mixed oxide phase to be present. Examination of the data indicated that the mixed oxide contained uranium and chromium in equi-atomic amounts. This will be discussed in a later section.

To determine whether the reaction occurs between UO_2 or U_3O_8 and Cr_2O_3, mixtures of each of the oxides with Cr_2O_3 in the proper proportions were prepared. The mixed oxides were sealed into evacuated quartz tubes and fired at 1200° C for 24 hr. No reaction between UO_2 and Cr_2O_3 was detected. However, the U_3O_8 and Cr_2O_3 were completely converted to the mixed oxide phase. This confirms the results reported by BORCHARDT.(7)

2. *Determination of mixed oxide composition*

a. *Thermogravimetric analysis.* The results of the thermogravimetric analysis of the reaction between $2UO_2$ and Cr_2O_3 tend to show that U_3O_8 is the active uranium oxide species. As seen in Fig. 1, the initial weight gains are due to the transformation of $UO_{2.19}$ to $UO_{2.36}$ and then to $UO_{2.67}$. These results are in agreement with data obtained by JUENKE for the oxidation of UO_2.[8] Between 855 and 1020° C the oxygen to uranium ratio decreases to about 2·50 and remains at that level to about 1400° C.

TABLE 1.—X-RAY DATA FOR Cr_2O_3–UO_2 MIXTURES HEATED IN AIR AT 1200, 1400 AND 1600° C

Original composition	Cr_2O_3 (w/o)	Temperature (° C)	Time (hr)	Phases found
$3Cr_2O_3+UO_2$	62·8	1200	24	Cr_2O_3 + mixed oxide*
$2Cr_2O_3+UO_2$	52·8	1200	24	Cr_2O_3 + mixed oxide
$Cr_2O_3+UO_2$	36·0	1200	24	Cr_2O_3 + mixed oxide
$2Cr_2O_3+3UO_2$	27·2	1200	24	Cr_2O_3 + mixed oxide
$Cr_2O_3+2UO_2$	21·9	1200	24	Mixed oxide
$4Cr_2O_3+9UO_2$	20·1	1200	24	Mixed oxide + U_3O_8
$2Cr_2O_3+5UO_2$	18·1	1200	24	Mixed oxide + U_3O_8
$Cr_2O_3+3UO_2$	16·4	1200	24	Mixed oxide + U_3O_8
$2Cr_2O_3+UO_2$	36·0	1200	64	Cr_2O_3 + mixed oxide
$Cr_2O_3+UO_2$	52·8	1200	64	Cr_2O_3 + mixed oxide
$Cr_2O_3+2UO_2$	21·9	1200	64	Mixed oxide
$2Cr_2O_3+UO_2$	52·8	1400	24	Cr_2O_3 + mixed oxide
$2Cr_2O_3+3UO_2$	27·2	1400	24	Cr_2O_3 + mixed oxide
$Cr_2O_3+2UO_2$	21·9	1400	24	Mixed oxide
$4Cr_2O_3+9UO_2$	20·1	1400	24	Mixed oxide + U_3O_8
$2Cr_2O_3+5UO_2$	18·1	1400	24	Mixed oxide + U_3O_8
$Cr_2O_3+UO_2$	36·0	1600	4	Cr_2O_3 + mixed oxide
$2Cr_2O_3+3UO_2$	27·2	1600	4	Cr_2O_3 + mixed oxide
$Cr_2O_3+2UO_2$	21·9	1600	4	Mixed oxide
$4Cr_2O_3+9UO_2$	20·1	1600	4	Mixed oxide + U_3O_8
$2Cr_2O_3+5UO_2$	18·1	1600	4	Mixed oxide + U_3O_8

* Mixed oxide assumed to be $CrUO_4$.

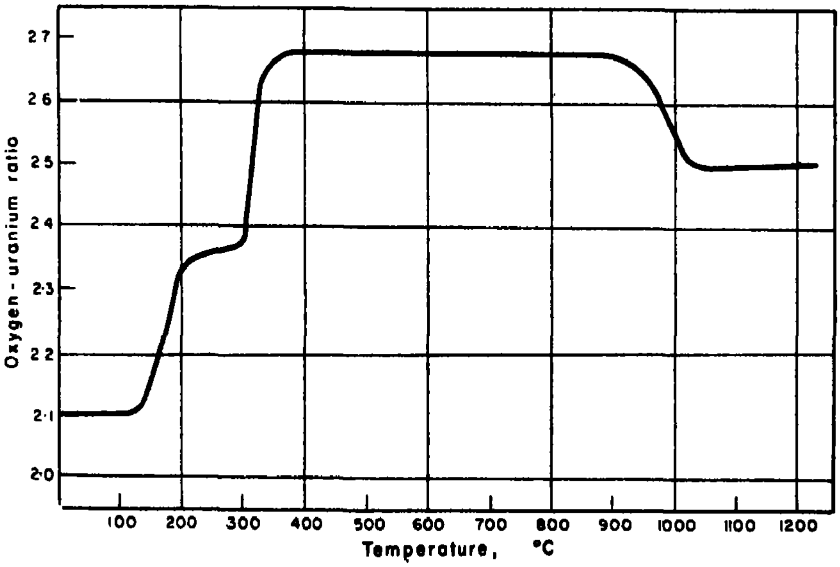

FIG. 1.—Thermogravimetric analysis of the reaction between 2 UO_2 and Cr_2O_3 in air.

---

[8] E. F. JUENKE. To be published.

This behaviour indicates that the reaction between U_3O_8 and Cr_2O_3 occurs in the temperature region from 855 to 1020° C. U_3O_8 alone does not show such a marked decrease in oxygen–uranium ratio in this region. The oxygen–uranium ratio for the U_3O_{8-x} phase at 1020° C is approximately 2·63.(8) If we assume that uranium and chromium are present in equi-atomic proportions then the equation for the reaction is given by:

$$2UO_2+Cr_2O_3+\tfrac{1}{2}O_2 \rightarrow 2CrUO_4$$

b. *Chemical analysis.* The metal atom concentrations in the mixed oxide phase were determined from two-phase mixtures where U_3O_8 was the second phase. The U_3O_8 was removed from the mixture by treatment with hot 1:1 nitric acid. X-ray patterns of the oxide insoluble in HNO_3 showed only the mixed oxide phase to be present, while solid obtained from the nitric acid by evaporation proved to be uranyl nitrate.

In addition, both the insoluble and soluble materials were analysed by standard techniques for both chromium and uranium. The results obtained are found in Table 2 and support the contention that uranium and chromium are present in equi-atomic proportions. In addition the sum of the U_3O_8 content of the two portions and Cr_2O_3 in the HNO_3 insoluble portion is 100·3 per cent.

TABLE 2.—ANALYTICAL RESULTS OF THE HNO_3-SOLUBLE AND INSOLUBLE PORTIONS OF A U_3O_8–MIXED OXIDE POWDER

	Cr_2O_3 (%)	U (%)	U_3O_8 (%)	$\frac{U}{Cr_2O_3}$ Found	$\frac{U}{Cr_2O_3}$ For $CrUO_4$
HNO_3 insoluble	14·62	46·22	54·50	3·16	3·13
HNO_3 soluble	Nil	26·45	31·19		

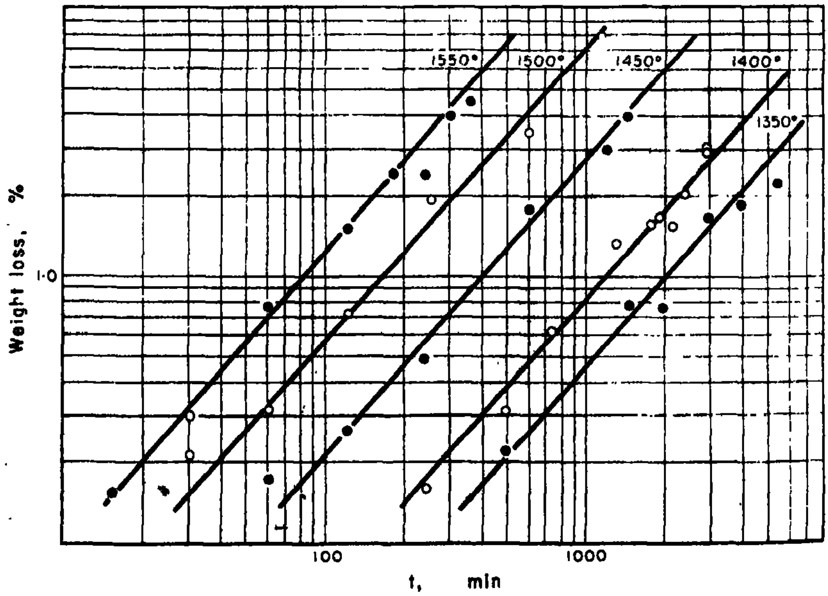

FIG. 2.—Weight loss vs. time for $CrUO_4$ between 1350° and 1550° C.

3. *Volatility of* $CrUO_4$

The volatility of the $CrUO_4$ phase was determined between 1350 and 1550° C. The powder used in this experiment had been previously reacted for 50 hr at 1200° C. The results obtained are presented in Fig. 2, where the logarithm of the weight loss is plotted against the logarithm of the time. The results indicate a nearly linear relationship between weight loss and time. A 5 g powder sample of $CrUO_4$, prepared at 1200° C, was heated for 115 hr at 1450° C in air. A total weight loss of 18·6 per cent was observed. Chemical analysis, however, revealed that the relative proportions of uranium and chromium remained unchanged throughout the experiment (Table 3).

TABLE 3.—ANALYTICAL RESULTS—$CrUO_4$ HEATED 115 HR IN AIR AT 1450° C

	U (w/o)	Cr (w/o)
Initial composition	66·17	14·32
After heat treatment	66·13	14·82

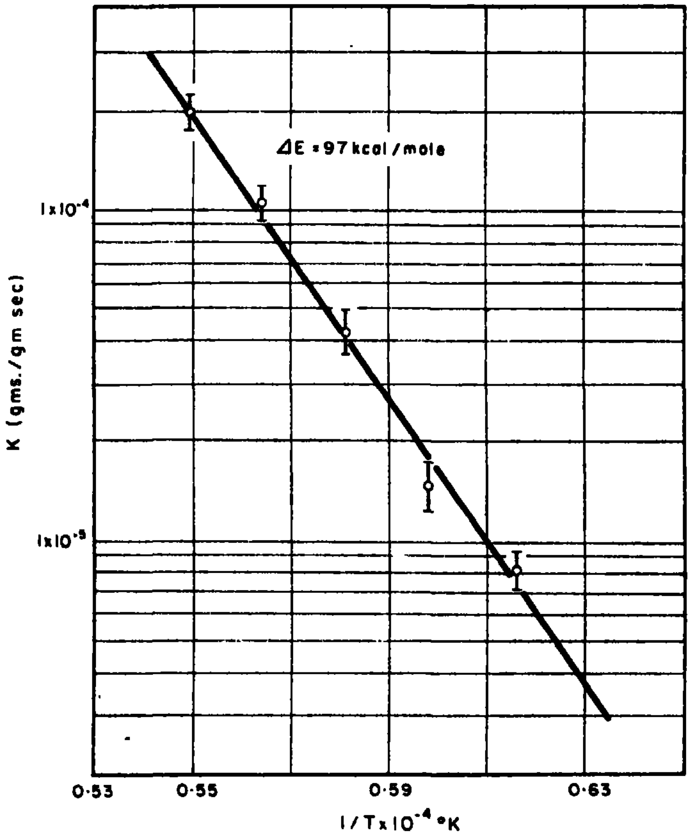

FIG. 3.—Arrhenius plot for volatilization of $CrUO_4$.

It is therefore assumed that at these temperatures decomposition of $CrUO_4$ takes place to form the two volatile oxides UO_3 and CrO_3.

The relationship between the reaction rate constant and temperature is presented in the usual manner in Fig. 3. The activation energy for the process was found to be 97 kcal/mole.

Table 4.—Powder diffraction pattern of $CrUO_4$

hkl	*d* (Å)	Relative intensity	Sin² *θ* observed	Sin² *θ* calculated
002	5·84	13	0·0174	0·0171
101	4·47	8	0·0297	0·0294
012	3·82	33	0·0407	0·0404
111	3·345	100	0·0531	0·0527
103	3·045	45	0·0641	0·0636
004	2·939	5	0·0688	0·0685
113	2·609	5	0·0873	0·0869
014	2·539	23	0·0922	0·0918
020	2·520	15	0·0936	0·0933
200	2·428	18	0·1008	0·1003
022	2·319	4	0·1105	0·1104
202	2·247	5	0·1178	0·1174
121	2·198	5	0·1228	0·1225
105	2·116	6	0·1325	0·1318
212	2·050	16	0·1412	0·1405
006	1·959	7	0·1546	0·1538
115	1·951	25	0·1559	0·1551
123	1·943	30	0·1572	0·1566
024	1·914	4	0·1620	0·1615
204	1·873	10	0·1691	0·1685
214	1·757	21	0·1922	0·1917
220	1·752	21	0·1933	0·1933
222	1·678	3	0·2107	0·2104
125	1·6226	10	0·2253	0·2250
032	1·6179	10	0·2267	0·2267
301	1·6051	8	0·2303	0·2296
107	1·5894	4	0·2349	0·2343
131	1·5767	10	0·2386	0·2389
026	1·5487	4	0·2474	0·2469
311	1·5304	12	0·2533	0·2529
206	1·5269	12	0·2545	0·2539
117	1·5159	14	0·2582	0·2576
224	1·5048	5	0·2620	0·2616
303	1·4981	20	0·2643	0·2638
216	1·4614	4	0·2778	0·2772
313	1·4369	3	0·2874	0·2870
018	1·4132	10	0·2971	0·2967
321	1·3554	3	0·3229	0·3227
232	1·3478	15	0·3266	0·3268
127	1·3447	10	0·3281	0·3275
305	1·3362	3	0·3323	0·3321
135	1·3186	6	0·3412	0·3414
226	1·3074	8	0·3471	0·3471
315	1·2915	4	0·3557	0·3554
323	1·2891	8	0·3570	0·3569
028	1·2722	2	0·3666	0·3665
109	1·2646	5	0·3713	0·3710
234	1·2532	11	0·3778	0·3781
218	1·2223	5	0·3971	0·3968
400	1·2171	2	0·4005	0·4006
307	1·1680	5	0·4349	0·4346
331	1·1630	5	0·4386	0·4392
044	1·1601	5	0·4408	0·4409
137	1·1569	5	0·4433	0·4439
317	1·1382	9	0·4580	0·4579
129	1·1307	2	0·4641	0·4642
228	1·1280	4	0·4663	0·4667
240	1·1216	3	0·4716	0·4727
038	1·1091	2	0·4823	0·4830
414	1·0981	4	0·4920	0·4922

Orthorhombic unit cell

$a = 4{\cdot}86_8$ Å $b = 5{\cdot}04_8$ Å $c = 11{\cdot}78_5$ Å

Probable space group—*Cmmc*

$\rho_{obs} = 7{\cdot}72$ g/cm³ $\rho_{calc} = 8{\cdot}12$ g/cm³ $Z = 4$

4. *Structure of* $CrUO_4$

Single crystals of $CrUO_4$ suitable for structure analysis were obtained by the boric acid flux method previously described. Moving-film single-crystal photographs taken with a Weissenberg camera showed that $CrUO_4$ has orthorhombic symmetry with $a_0 = 4{\cdot}86_8$, $b_0 = 5{\cdot}04_8$ and $c_0 = 11{\cdot}78_5$ Å. The pycnometric density of $CrUO_4$ was found to be 7·72 g/cm^3, which gives 3·8 formula weights of $CrUO_4$ in the unit cell. It can be assumed, therefore, that the cell contains four $CrUO_4$ units. These results indicate that this new compound is isostructural with the rare mineral pucherite which has the composition $BiVO_4$. The X-ray data reported by DEJONG and DELANGE⁽⁹⁾ for pucherite gives an orthorhombic unit cell containing four $BiVO_4$ units with $a_0 = 5{\cdot}38$, $b_0 = 5{\cdot}04$ and $c_0 = 11{\cdot}98$ Å.

The possible space groups, as determined from the systematic absences on the single crystal photographs, are $C222_12$, $Cm2_1c$, and $Cmmc$. Space group $Cmmc$ is most probably correct, since this would permit the sixteen oxygen atoms to be placed in a general position. A complete crystal structure determination is presently being carried out by SMITH *et al.*⁽¹⁰⁾ at Lawrence Radiation Laboratory. Their preliminary results have shown $CrUO_4$ to crystallize in the unique space group Pbnc with pseudo-symmetry $Cmmc$.

The X-ray powder diffraction pattern of $CrUO_4$ was indexed on the basis of the single-crystal photographs. These results are presented in Table 4, the intensities given were obtained from the diffractometer record.

CONCLUSION

At temperatures between 1200 and 1600° C, three phases are present in the Cr_2O_3–UO_2–O_2 system, namely: Cr_2O_3, U_3O_8, and a mixed oxide phase. This compound is the result of reaction between U_3O_8 and Cr_2O_3 but not between UO_2 and Cr_2O_3.

Thermogravimetric analysis of the reaction between $2UO_2$ and Cr_2O_3 in air and chemical analysis of the mixed oxide phase indicate the chemical formula of the phase to be $CrUO_4$. Although there is no evidence that this compound is a uranate of chromium, the formula $CrUO_4$ has been assigned by analogy with other well established compounds such as $MgUO_4$ and Ca_2UO_4. In these compounds the uranium is known to exist only in the tetravalent or hexavalent state. $CrUO_4$, however, is highly unusual in this respect because the presence of pentavalent uranium is definitely indicated and the chemical formula of its composition could be written $Cr_2O_3 \cdot U_2O_5$. Equal quantities of U^{4+} and U^{6+} ions would be just as satisfactory an explanation; the crystal structure analysis may prove whether or not there are two kinds of uranium ions present. As another approach to the solution of the controversial question regarding the existence of U^{5+} ions in solid compounds, magnetic susceptibility measurements on $CrUO_4$ should be carried out.

Volatilization of $CrUO_4$ takes place as a result of dissociation of mixed oxide to UO_3(g) and CrO_3(g). The activation energy of this process was found to be 97 kcal/mole.

X-ray analysis of $CrUO_4$ single crystals show that this compound crystallizes in an orthorhombic cell containing four $CrUO_4$ units. The lattice parameters are $a_0 = 4{\cdot}86_8$, $b_0 = 5{\cdot}04_8$ and $c_0 = 11{\cdot}78_5$ Å.

Acknowledgement—The authors wish to thank E. A. AITKEN for suggesting the problem and to G. CHASE for some of the X-ray diffraction work.

⁽⁹⁾ W. F. DE JONG and J. J. DE LANGE, *Amer. Mineralogist* **21**, 809 (1936).

⁽¹⁰⁾ D. K. SMITH, C. F. CLINE and D. E. SANDS, *Nature, Lond.* **192**, 861 (1961)

J. Inorg. Nucl. Chem., 1962, Vol. 24, pp. 847 to 850. Pergamon Press Ltd. Printed in England

PREPARATION AND PROPERTIES OF CHROMYL BORATE

S. Z. Haider, M. H. Khundkar and K. De

Department of Chemistry, Dacca University, Dacca, Pakistan

(*Received* 25 *October* 1961; *in revised form* 28 *November* 1961)

Abstract—The reaction between chromyl chloride and silver borate has been investigated. Little reaction occurred when gaseous chromyl chloride was bubbled through a suspension of silver borate in carbon tetrachloride. Reaction between liquid chromyl chloride and silver borate led to the formation of a solid product from which brown crystals $CrO_2(BO_2)_2$ could be separated. This decomposed rapidly in the presence of moisture and the aqueous solution contained free boric and chromic acids. The density of the solid was found to be 1·8 and the refractive index in acetone solution was determined. The thermal decomposition of the substance has been studied from 50° to 500°. The acetone solution of chromyl borate absorbed strongly around 335, 350, and 360 mμ.

Chromyl chloride, CrO_2Cl_2, is the only well known chromyl compound. Recently Krauss(1) prepared chromyl acetate, $CrO_2(CH_3COO)_2$ in the form of red crystals having m.p. 30·5 by shaking chromium trioxide with acetic anhydride in carbon tetrachloride for 5 hr in the absence of light and moisture. The compound is soluble in inert organic solvents, has absorption maxima at 283 and 400 mμ (CCl_4) and fumes in air with the separation of a solid hydrolysis product. Forbes and Anderson(2) described the methods of preparation and properties of chromyl cyanates and thiocyanates. Chromyl isocyanate, $CrO_2(CNO)_2$ was found to be stable in solution in carbon tetrachloride only. Chromyl thiocyanate, $CrO_2(SCN)_2$, existed only for a short time in solution when chromyl chloride was reacted with silicon thiocyanate, the brown solid which first separated decomposing with feeble explosions.

Ruff and Braun(3) described the preparation of chromyl fluoride, CrO_2F_2, by mixing calcium fluoride and lead chromate with sulphuric acid or with fluorosulphuric acid. Wartenberg(4) showed it to be a brown gas condensing to a brown solid which ultimately polymerized to a white solid. Hellwege(5) found the absorption spectrum of the gas to be remarkably similar to that of chromyl chloride. The researches of Cristol and Eiler(6) and of Palmer(7) regarding the reactions and structure of chromyl chloride lead to the conclusion that the bonding nature of Cl in the tetrahedral chromyl chloride molecule is more covalent than in the salt UO_2Cl_2, which is ionic. Chromyl chloride, therefore, may not react readily with silver salts.

(1) H. L. Krauss, *Angew. Chem.* **70**, 502 (1958).

(2) G. S. Forbes and H. H. Anderson, *J. Amer. Chem. Soc.* **65**, 2273 (1943).

(3) O. Ruff and H. J. Braun, **47**, 658 (1914).

(4) H. V. Wartenberg, *Z. Anorg. Chem.* **247**, 135 (1941).

(5) K. H. Hellwege, *Z. Phys.* **117**, 596 (1941).

(6) S. J. Cristol and K. R. Eiler, *J. Amer. Chem. Soc.* **72**, 4353 (1950).

(7) K. Palmer, *J. Amer. Chem. Soc.* **60**, 2360 (1938).

Silver borate has been used in this laboratory for the preparation of acetyl and benzyl borates and also for complexes such as metal ammino borates.(8) In the present work reactions between chromyl chloride and silver borate have been carried out and a new chromyl metaborate has been isolated.

Preparations of the samples

Silver borate. This was prepared by mixing together saturated solutions of borax and silver nitrate quickly in one portion, filtering under suction and washing the white precipitate with 1 per cent boric acid solution. The precipitate was dried in a vacuum desiccator over calcium chloride in the dark. The composition conformed closely to $AgBO_2$ on analysis.

Chromyl borate. In the course of preliminary investigations, it was observed that prolonged bubbling of freshly prepared chromyl chloride vapour through a suspension of silver borate in carbon tetrachloride at ordinary temperature was not a satisfactory method for the preparation of chromyl borate. The reaction did not proceed to completion, as was indicated by the yield of silver chloride formed. When dry silver borate was added to liquid chromyl chloride much heat was evolved and a series of experiments was performed to determine the conditions for the completion of the reaction. For this purpose the brown solid reaction product, isolated after thoroughly washing with carbon tetrachloride, was decomposed by warming with dilute nitric acid (4 N), filtering and weighing the precipitate of silver chloride formed. Under the most suitable conditions the yield of silver chloride was almost quantitative. The results of two such runs are shown in Table 1.

TABLE 1.—YIELD OF AgCl SHOWING COMPLETION OF REACTION

Amount of $AgBO_2$ taken (g)	Chromyl chloride added (ml)	AgCl found (g)	AgCl calculated (g)
1·992	20·0	1·883	1·894
1·002	12·5	0·946	0·953

The final procedure adopted for the preparation of chromyl borate in a typical case is as follows: A known amount of silver borate (10 g) was added to excess of liquid chromyl chloride (50 ml) in a dark-coloured, stoppered bottle and shaken for 2 hr. The bottle was then warmed up to 60–70° in a bath and kept at that temperature for 1 hr with occasional shaking. The excess of unreacted liquid chromyl chloride was decanted off and the solid product washed thoroughly with carbon tetrachloride. The brown product was admixed with a large quantity of silver chloride. Attempts were made to extract the brown product by means of various organic solvents. Only acetone successfully extracted the brown product completely giving a dark brown solution, which on evaporation produced a brown crystalline product. This was stored in a desiccator over calcium chloride (Yield about 4·2 g).

Analysis of the brown crystalline product isolated from acetone indicated the formation of chromyl dimetaborate $CrO_2(BO_2)_2$. The substance was dissolved in water or in 4 N hydrochloric acid and from the solution chromium was determined iodometrically and boric acid by a method developed in this laboratory.(9) Results of two typical analysis are summarized in Table 2.

TABLE 2.—COMPOSITION OF CHROMYL BORATE

Amount of substance (g)	H_2CrO_4 found (g)	H_3BO_3 found (g)	Molar ratio H_3BO_3/H_2CrO_4
0·7042	0·4704	0·4826	1·95
0·5350	0·3624	0·3946	2·08

[illegible]M. H. KHUNDKAR and S. Z. HAIDER, *Z. Anorg. Allgem. Chem.* 284, 312 (1956).

[illegible] Z. HAIDER, *Analyst.* 79, 454 (1954).

Properties of chromyl borate

This chromyl borate was found to be hygroscopic and to possess oxidizing properties such as liberating sulphur from hydrogen sulphide in solution. It is readily dissolved in water, forming a mixture of chromic and boric acids. It is also decomposed by alcohol but is insoluble in ether, petroleum ether, benzene and chloroform. It is highly soluble in acetone, from which it can be recrystallized. The density of solid chromyl borate was found to be 1·8 at 30° by the liquid displacement (CCl_4) method. The refractive index of an acetone solution containing 1·5 g of chromyl borate per 100 ml was 1·3605.

The thermal decomposition of the crystalline chromyl borate has been studied within a temperature range of 50–500° at intervals of 50°, the temperature variation at each stage being approximately ±5°. At each temperature the time of heating was about 4 hr in two steps: the weight was measured after an initial heating of 3 hr and again after heating for another hour or so. The two weights were almost the same. The maximum loss in weight was observed at a temperature of about 390°. The effect of heat is recorded in Table 3 and the variation of weights with temperature is shown in Fig. 1.

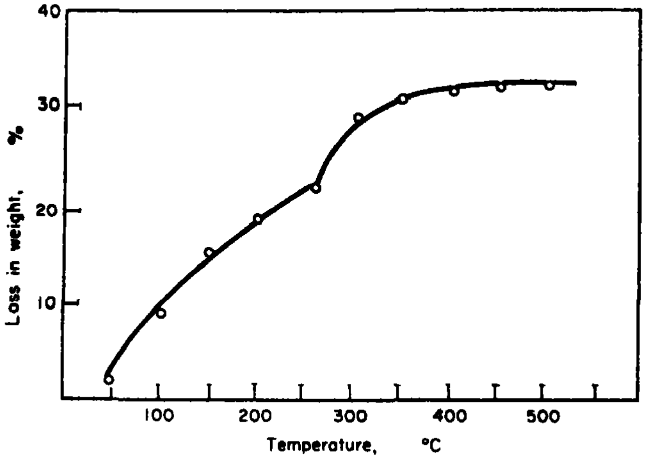

FIG. 1.—Thermal decomposition of chromyl borate.

TABLE 3.—EFFECT OF HEAT ON CHROMYL BORATE

Temperature (°C)	Loss in wt. (%)
50	1·0
100	8·1
150	16·0
200	19·4
250	23·1
300	29·3
350	30·7
400	31·8
450	31·9
500	32·0

After ignition, the substance was coloured dark green and possibly contained Cr_2O_3 and B_2O_3 in a chemically combined form since no boric acid could be leached out by hot water. Concentrated hydrochloric acid only partially dissolved the ignited mass giving a green coloured solution, indicating the presence of trivalent chromium. Complete dissolution was brought about by means of alkali fusion. The reduction of hexavalent chromium to the trivalent state during the thermal treatment is not very well understood. The analysis of the ignited residue indicated lower values of chromium and boron contents than were present in the original chromium borate, and conformed to no definite composition. The curve in Fig. 1 shows that, as the temperature is gradually increased, two different processes occur. In order to account for the lowering of chromium and boron contents in the ignited product and the reduction of hexavalent chromium to the trivalent state, it may be assumed that the substance volatilizes as such with slight decomposition at the start of the ignition process but the decomposition becomes rapid after the temperature of about 250° has been reached. The decomposition terminates at about 390° and this might have taken place with the evolution of oxygen and consequent formation of trivalent chromium. However, chromium and boron remain chemically combined and the probable formation of a polymer may not be altogether ruled out. Modern techniques such as X-ray diffraction may be applied to arrive at some definite conclusion regarding these changes.

The ultra-violet absorption spectrum of chromyl borate in acetone solution (0·01 g in 100 ml) was also studied with the help of a Unicam Sp. 500 photoelectric spectrophotometer. The absorption curve is shown in Fig. 2. The maximum absorptions take place around wavelengths of 335, 350 and 360 mμ.

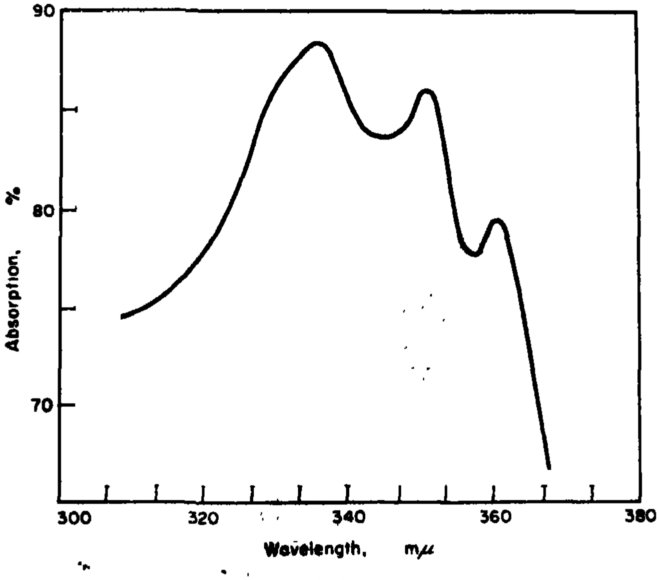

FIG. 2.—U-V absorption curve of chromyl borate in acetone solution.

J. Inorg. Nucl. Chem., 1962, Vol. 24, pp. 851 to 861. Pergamon Press Ltd. Printed in England

PROPERTIES OF ALUMINIUM ETHOXIDE*

R. C. WILHOIT, J. R. BURTON, FU-TIEN KUO, SUI-RONG HUANG and A. VIQUESNEL
Department of Chemistry, New Mexico Highlands University, Las Vegas, New Mexico

(*Received* 2 *November* 1961; *in revised form* 4 *December* 1961)

Abstract—Methods of preparation, melting point, solubility, molecular weight and infra-red spectra of aluminium ethoxide have been studied. Contrary to previous reports pure aluminium ethoxide was found to exist in only one form which melts at about 140° C and is only slightly soluble in non-polar organic solvents at room temperature. Impure forms, which result from the partial decomposition or hydrolysis of aluminium ethoxide, are very complex in nature and are much more soluble than is pure aluminium ethoxide. Properties of these materials depend to some extent on the method of preparation. Some assignments of vibrational frequencies have been made for aluminium ethoxide.

THE physical and chemical properties of aluminium alkoxides have been under investigation for over eighty years and a considerable volume of information is now available. However, poor quantitative agreement is often found among the physical properties reported by various authors and there is still much which is not understood about the molecular structure of the aluminium alkoxides in the solid state and in solution. Except for aluminium methoxide, which does not seem to be similar in properties to the other alkoxides, aluminium ethoxide is the simplest member of this series. Any progress made in the understanding of the properties of aluminium ethoxide should be helpful in the study of the higher alkoxides. The aluminium alkoxides have a strong affinity for water and must be prepared and stored under rigorously anhydrous conditions if they are to be kept pure. It seems likely that failure to maintain these conditions accounts for many of the discrepancies found in the literature.

Aluminium ethoxide was first prepared by GLADSTONE⁽¹⁾ by the reaction of aluminium with absolute ethanol catalysed by iodine. Further studies on the properties of aluminium alkoxides were made by GLADSTONE and TRIBE⁽²⁾ who reported that aluminium ethoxide melts at 130° C, is easily distilled under reduced pressure, is insoluble in ethanol but moderately soluble in benzene, and that it has a density of 1·147 g ml^{-1}. Improved methods of preparation were later devised by WISLICENUS and KAUFMAN,⁽³⁾ HILLYER and CROOKER,⁽⁴⁾ BERGER,⁽⁵⁾ and HENLE.⁽⁶⁾ Over the years melting point determinations have ranged from 123 to 151°(7–11). Numerous boiling point measurements have been reported although comparison among different investigators is difficult because different pressures were used in the measurements. Vapour-pressure–temperature curves have been determined by Mehrotra(12) using a distillation method and by Wilhoit(13) using an isoteniscope method. Agreement between these two sets of data is within experimental error of the pressure measurements in the range of 140–190° C but becomes worse above 190° C. Aluminium ethoxide has been found to be associated when dissolved in non-polar organic solvents. The degree of association is 4·41[*] in freezing benzene,(9) 3·8[*] in freezing naphthalene(10) and 4·1[*] in boiling benzene.(12) The concentrations used by Ulich and Nespital range from 1·88 to 7·62 g of aluminium ethoxide per 100 g of benzene while the concentrations used by Mehrotra range from 0·14 to 1·0 g per 100 g of benzene. No appreciable dependence of degree of association on molecular weight was found. Robinson and Peak(10) give the parachor of aluminium ethoxide as 340·8 and Ulich and Nespital(9) report a value of 1·35 e.s.u. as the dipole moment of aluminium ethoxide in benzene. Studies of compounds of the type $Al_xO_y(OEt)_z$ which are formed by the partial decomposition or hydrolysis of aluminium ethoxide have been carried out by Henle,(6) Adkins,(8) Malatesta and Magnani,(11) and Child and Adkins.(14) Compounds of the type $Al(OEt)_xR_y$ where R is an alkyl radical or halide atom were studied by Ullich and Nespital,(9) and Bonitz.(15) Meerwein and Bersin(16) have prepared several compounds of the class $M[Al(OEt)_4]_x$ and $M_x[Al(OEt)_6]_y$, where M is a Group I or II metal. Child and Adkins(17) studied the catalytic activities of compounds such as $MCl_x{\cdot}nAl(OEt)_3$. Whitaker(18) has recently written a review of certain aspects of aluminium alkoxide chemistry, especially the possible industrial applications.

---

* Taken from portions of the following M.S. thesis: FU-TIEN KUO, March (1959), SUEI-RON HUANG, August (1959), and A. VIQUESNEL, August (1961), all of New Mexico Highlands University, and J. R. BURTON, Texas Technological College, August (1957).

(1) J. H. GLADSTONE, *J. Chem. Soc.* **29**, 158 (1876).
(2) J. H. GLADSTONE and A. TRIBE, *J. Chem. Soc.* **39**, 1 (1881).
(3) H. WISLICENUS and L. KAUFMAN, *Ber. Dtsch. Chem. Ges.* **28**, 1323 (1895).
(4) H. W. HILLYER and O. E. CROOKER, *J. Amer. Chem. Soc.* **19**, 37 (1897).
(5) C. BERGER, *C.R. Acad. Sci., Paris* **157**, 717 (1914).
(6) F. HENLE, *Ber. Dtsch. Chem. Ges.* **53**, 719 (1920).

The possibility that aluminium ethoxide exists in two or more modifications in the solid state has been considered by several investigators, but the preparation and properties of these forms, as well as the reasons advanced for the existence of the modifications, differs. Child and Adkins(14) explain the differences in terms of two "allotropic" crystalline modifications. The α-form solidifies from the liquid at a little above room temperature and is soluble in xylene, while the β-form melts at 140° C and is insoluble in xylene. Distillation of the α-form partly converts it into the β-form while heating of the β-form in a sealed tube at 275° C for 15 hr completely converts it into the α-form. It seems difficult to reconcile these statements with the interpretation that the two forms are polymorphic crystalline modifications. MEERWIN(19) mentions soluble and insoluble forms and states that the difference is due to the presence or absence of solvated alcohol in the solid crystals. MALATESTA and MAGNANI(11) also discuss preparation and properties of soluble and insoluble forms of aluminium ethoxide. They believe that the two forms differ in type of co-ordination existing between the ethoxide group and the aluminium atom. The insoluble form, which is prepared by the reaction of aluminium with an excess of pure ethanol, is some sort of polymer of $Al(OEt)_3$ and may be more accurately represented by the formula $[Al(OEt)_4]_3Al$. The soluble form exists as $Al(OEt)_3$ monomer and is prepared by the reaction of aluminium with ethanol in the presence of boiling xylene as a solvent. The alcohol is added slowly so that its concentration is always kept low. The soluble form melts at 123° and the insoluble form at 136°. Once prepared the soluble and insoluble forms cannot be interconverted.

---

[*] The "degree of association" will be taken to mean the value of n in the formula $[Al(OEt)_3]_n$.

(7) W. Tischtschenko, *J. Soc. Physl-Chim. Russ.* **31**, 694 (1899).
(8) H. Adkins, *J. Amer. Chem. Soc.* **44**, 2175 (1922).
(9) H. Ulich and W. Nespital, *Z. Phys. Chem.* A **165**, 294 (1933).
(10) R. A. Robertson and D. A. Peak, *J. Phys. Chem.* **39**, 1125 (1935).
(11) L. Malatesta and E. Magnani, *Gazz. Chim. Ital.* **80**, 113 (1950).
(12) R. C. Mehrotra, *J. Indian Chem. Soc.* **30**, 585 (1953).
(13) R. C. Wilhoit, *J. Phys. Chem.* **61**, 114 (1957).
(14) W. C. Child and H. Adkins, *J. Amer. Chem. Soc.* **45**, 3013 (1923).
(15) E. Bonitz, *Ber. Dtsch. Chem. Ges.* **88**, 742 (1955).
(16) H. Meerwein and T. Bersin, *Ann.* **476**, 113 (1929).
(17) W. C. Child and H. Adkins, *J. Amer. Chem. Soc.* **47**, 798 (1925).
(18) G. C. Whitaker, *Metal-Organic Compounds*, p. 184–189. American Chemical Society (1959).

EXPERIMENTAL

For convenience in discussion the following three general methods of preparation will be identified.

Method of Wislicenus. Aluminium foil or shavings are placed in an excess of absolute ethanol and a small quantity of mercuric chloride added. The mixture is refluxed, under anhydrous conditions, until all the aluminium has dissolved. This requires from 1 to 3 hr. Alcohol is removed first by distillation at atmospheric pressure, and finally by distillation under reduced pressure. The residue is distilled at pressures of 1–4 mm of mercury and at temperatures in the range of 145–180° C.

Method of Meerwein. Aluminium foil or shavings are placed in a large quantity of xylene which acts as an inert solvent, and small quantities of mercuric chloride and iodine added. Absolute ethanol is slowly added to the refluxing xylene solution in such a manner that it reacts as fast as it is added. Any remaining insoluble material is removed by filtration and the aluminium ethoxide recovered from solution by evaporation of the solvent.

Method of Maletesta and Magnani. Twenty-five grammes of aluminium foil are placed in 100 ml of xylene. The aluminium is either amalgamated in advance or a small quantity of mercuric chloride is added. This procedure uses less xylene than does the method of Meerwein. One hundred and thirty-five grammes of absolute ethanol are added while the mixture is refluxing. The aluminium should be completely dissolved at the end of one half hour. The solution is filtered while hot and the aluminium ethoxide recovered by crystallization on cooling. The product is recrystallized from a mixture of xylene and ligroin.

We have prepared a large number of samples of aluminium ethoxide by these three methods as well as by numerous variations of them. Those samples which we believe to be the most nearly pure were prepared under rigorously anhydrous conditions. Either the final recovery of product or the complete preparation was carried out in a dry-box. Absolute ethanol was generally prepared by distillation from an ethanol solution of aluminium ethoxide. Distillation of aluminium ethoxide was done at as low a temperature as possible to reduce the possibility of thermal decomposition. In a few cases the product was purified by sublimation at around 120° C.

Quantitative analysis was carried out by dissolving a weighed quantity of aluminium ethoxide in hydrochloric acid solution. The aluminium was precipitated with 8-hydroxyquinoline and weighed as the chelate. The amount of ethanol produced from the ethoxide was determined by oxidizing an aliquot of the hydrochloric acid solution with standard dichromate under controlled conditions, and back-titrating with thiosulphate.

Melting points were obtained by two methods. In the capillary tube method 1–2 mg of sample were sealed in a melting-point tube which was totally immersed in an oil bath fitted with electrical heaters and with a circulating pump which permitted close temperature control. The melting temperatures were determined by means of a mercury thermometer graduated in 0·1° intervals. This thermometer had been compared to one calibrated by the National Bureau of Standards. Stem corrections were applied to the readings. Melting ranges of 1–3° C were generally observed by this method. The cooling curve method was accomplished by melting a 10 g sample in a glass tube and allowing it to cool through the melting range in about one half hour. Temperature–time curves were obtained with a small iron–constantan thermocouple and an automatic recorder. If left undisturbed during the cooling the shape of the curve indicates considerable supercooling before crystallization begins. The supercooling can be prevented by adding a small seed crystal of aluminium ethoxide at the appropriate time. Melting points obtained in this way cover a 1–2° C range.

---

(19) H. MEERWEIN, *Ger. Pat.* 475557 (1925); *Chem. Abstr.* **23**, 3718 (1929).

Some preliminary measurements have been made on the vapour-pressure depression observed in solutions of aluminium ethoxide in benzene. Two similar Washburn-Cottrell boiling point apparatuses(20) were connected to a regulated pressure system and manometer. Pure benzene was placed in one apparatus and the solution in the other. The difference in pressure needed to cause the two solutions to boil and the same temperature was then determined. Temperature equality was established through the use of a ten junction copper-constantan thermopile and potentiometer. Sensitivity was 0·001° C. A system for withdrawing samples of the boiling solution for analysis was also included. Tests with known compounds showed that molecular weights calculated from the pressure difference, assuming Raoult's law, were accurate to 1 or 2 per cent in range of concentrations used.

Infra-red spectra were observed with a Beckman Infra-red-4 spectrophotometer using sodium chloride optics for the 1–14 μ region and potassium bromide optics for the 10–25 μ region. In most cases several different instrument settings were used to bring out all of the features of the spectra. Preparation of the purer samples for observation was generally done in the dry-box. Solid samples were examined in the form of KBr pellets, Nujol mulls, and as a slurry of finely powdered material suspended in xylene. The pellets were prepared by compressing a powdered mixture of sample and infra-red grade potassium bromide in a pellet press in the usual manner. Nujol mulls were prepared by grinding a mixture of solid sample and Nujol in an agate mortor to form a thick paste. The paste was placed between two sodium chloride (or potassium bromide) windows for examination. A sodium chloride (or potassium bromide) window equal to the combined thickness of the two windows was placed in the reference beam. Since the thickness of the sample was not accurately controlled no attempt was made to compensate for the absorption of the Nujol by placing Nujol in the reference beam. Examinations of the slurry and also of solutions of aluminium ethoxide in benzene and xylene were made by placing them in a standard liquid cell, with a similar cell containing the solvent in the reference beam. The spectra observed for the Nujol mulls includes the effect of both the oil and the sample. These spectra were interpreted with the aid of Table 1, which lists the absorptions observed for the Nujol alone.

TABLE 1.—ABSORPTION SPECTRA OF NUJOL

Observed frequency (cm^{-1})	Intensity*	Observed frequency (cm^{-1})	Intensity
2930	*s*	1080	*w*
1700	*w*	1000	*w*
1630	*w*	940	*w*
1470	*s*	885	*w*
1390	*s*	827	*w*
1300	*w*	760	*w*
1220	*w*	736	*w*
1178	*w*	614	*w*
1123	*w*	569	*w*

* *s* = strong, *w* = weak.

---

(20) E. W. WASHBURN and J. W. READ, *J. Amer. Chem. Soc.* 41, 729 (1919).

RESULTS

Pure aluminium ethoxide consists of 16·64 per cent aluminium and 83·36 per cent ethoxide. Samples whose composition deviate from this contain impurities of the type $Al_xO_y(OEt)_z$ or $Al_x(OH)_y(OEt)_z$ which result from partial hydrolysis or decomposition during the preparation. However quantitative analysis is not always a very sensitive or reliable indication of purity. Thus, for example, $Al_3(OH)(OEt)_8$ contains 17·66 per cent Al and $Al_3O(OEt)_7$ contains 19·63 per cent Al. Appreciable quantities of either of these compounds could be present with $Al(OEt)_3$ without having much effect on the proportion of aluminium present. Furthermore, the effect of absorption of moisture from the air by an ethoxide sample without loss of the alcohol produced by the hydrolysis would be to lower the proportion of aluminium present. Therefore, a sample could analyse very close to the theoretical proportion of aluminium even though it had undergone an appreciable hydrolysis. Analysis of samples of aluminium ethoxide which we have prepared range from 16·5 to 29·8 per cent aluminium and from less than 70 to 83·5 per cent ethoxide.

The melting points of five samples of aluminium ethoxide prepared by the method of WISLICENUS were determined by the cooling curve method. Although these samples were prepared carefully their purity is somewhat uncertain because of some exposure to the atmosphere during the experiment. Melting points of these samples range from 120 to 130° C. Melting points of thirty samples, prepared by the three methods described and by variations of them, have been taken by the capillary tube method. There seems to be no correlation between melting point and method of preparation, but there is a rough correlation between melting point and per cent aluminium. These results are summarized in Table 2.

TABLE 2.—MELTING POINTS OF ALUMINIUM ETHOXIDE SAMPLES OF VARYING PURITY

Al (%)	Range of melting points (° C)
16·7–16·8	137–143
16·9–17·0	146–151
17·2–17·3	150–153
17·7–17·9	158–161
> 19·0	infusible

No correlation could be detected between method of preparation and solubility. Solubilities of samples judged most likely to be pure ranged between 8 and 12 g per 100 ml in ethanol and 0·4 and 1·5 g per 100 ml in xylene at room temperature. We observed that the solubility in xylene increased rapidly with an increase in temperature, although no quantitative measurements were made at higher temperatures. There was a marked correlation of solubility with per cent aluminium. Those samples having a high proportion of aluminium were much more soluble than samples having an aluminium content corresponding to pure aluminium ethoxide. The conclusion that the solubility of aluminium ethoxide samples increases as the degree of hydrolysis increases is supported by the results of the following experiment which is typical of several that we have done. Aluminium ethoxide, sample number 1, was stirred with

100 ml of dry benzene in a closed flask for several hours. The solution was separated from the solid residue and the solvent removed by evaporation leaving solid sample number 2. The insoluble residue was extracted again in a similar manner with 100 ml of benzene producing a soluble portion, sample number 3, and an insoluble residue. This insoluble portion was extracted a third time producing the soluble portion, sample number 4, and the final insoluble material, sample number 5. Properties of these samples are summarized in Table 3. It can be seen that the melting points of samples 2 and 4 are less than samples of the same composition shown in Table 2, while the melting point of sample 5 is similar to that previously found. Some samples prepared by the evaporation of benzene or xylene solutions of aluminium ethoxide have been found to be amorphous with no definite melting point at all. This indicates that samples of partially hydrolysed aluminium ethoxide may differ in properties when prepared by different methods even though the stoicheiometric composition remains the same.

Table 3.—Extraction of aluminium ethoxide with benzene

Sample number	Weight (g)	Al (%)	OEt (%)	m.p. (° C)
1	10·0	17·67	80·7	
2	2·28	19·16	78·0	105–108
3	0·59	19·64	78·6	
4	0·20	17·96	80·6	112–114
5	6·97	16·89	82·9	146–149

Our measurements on the solubility of pure aluminium ethoxide in non-polar solvents throw some doubt on the validity of previous molecular weight determinations of aluminium ethoxide. The concentrations used by Ulich and Nespital(9) in their molecular weight measurements are much greater than we have found for the solubility of pure aluminium ethoxide in benzene. Since it is probable that their solutions were prepared at room temperature, their samples must have been impure. Mehrotra(12) used a lower range of concentrations, but the higher concentrations still exceed the solubility of aluminium ethoxide at room temperature. Table 4 shows the degree of association calculated from our preliminary measurements on the vapour-pressure depression of benzene solutions of aluminium ethoxide. These data all apply to a temperature of 78°. Using a similar method it was also found that the degree of association of aluminium *n*-propoxide varied from 1·0 at a concentration of 0·11 g/100 g of benzene to 2·8 at 1·65 g/100 g of benzene, while the association of aluminium sec-butoxide remained constant at 2·4 in the concentration range of 4·65–23·8 g/100 g benzene. The data shown in Table 4 were obtained by withdrawing samples of the boiling solutions, analysing for aluminium, and basing the calculations on the assumption that aluminium ethoxide consists of 16·64 per cent aluminium. If the aluminium ethoxide had not been completely pure this assumption would introduce some error into the calculations of molecular weight, but, since all measurements were made on the same sample the conclusion that the degree of association increases with increasing concentration would not be altered. The fact that the solubility of the aluminium ethoxide sample used in these measurements was low enough so that the final solution could be prepared only by heating the benzene to boiling indicates at least a fair degree of purity.

TABLE 4.—DEGREE OF ASSOCIATION OF $Al(OEt)_3$ IN BOILING BENZENE

g $(Al(OEt)_3$ per 100 g of benzene	Average degree of association
0·42	2·6
0·78	2·9
1·14	3·1
7·85	4·4

Because of the time dependence previously found in the properties of aluminium iso-propoxide(13) we have also searched for a time dependence in the properties of aluminium ethoxide. No time dependence was found in the vapour-pressure of aluminium ethoxide at temperatures of 157° or higher. However, any delay in the attainment of equilibrium should be more pronounced at lower temperatures and therefore more readily observed. We found that 2–4 hr of boiling were required to attain a steady temperature for the aluminium ethoxide solutions, while ½–1 hr was sufficient, in the same apparatus, for solutes such as naphthalene, benzil and azobenzene. It therefore seems probable that some appreciable time is needed for aluminium ethoxide to reach a constant degree of association in solution. If the calculations had been based on data taken after only ½ hr of boiling the degree of association would have been about 4·0 for all concentrations. It is not certain whether the data in Table 4 represent states of final equilibrium or not, and therefore any attempt to calculate an equilibrium constant is not justified at this time.

GUERTIN *et al.*(21) and BELL *et al.*(22) have reported the infra-red spectra of several of the aluminium alkoxides other than the ethoxide. SCOTT *et al.*(23) and LUDKE *et al.*(24) have studied spectra of some aluminium soaps which may contain bonds similar to those present in the aluminium alkoxides. The pertinent conclusions reached by these investigators may be summarized as follows.

(1) Absorption bands typical of compounds containing ethoxide groups occur at 1160 cm^{-1} and 1090 cm^{-1}.

(2) Vibrations arising from the $\text{Al}-\overset{|}{\text{O}}\rightarrow\text{Al}$ co-ordinate bond occur in the vicinity of 990 cm^{-1}. This absorption peak is found in aluminium oxide, aluminium soaps and in some aluminium alkoxides.

(3) Vibrations in the Al–O–C bonds give rise to absorptions at 1033 cm^{-1} in aluminium isopropoxide, at 1058 cm^{-1} in aluminium secbutoxide and at 1070 cm^{-1} in aluminium 2-pentoxide.

(4) An absorption peak which occurs at 3700 cm^{-1} in aluminium soaps has been assigned to an O-H stretching frequenty present in polymeric structures such as

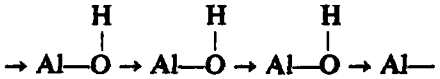

$$\rightarrow \text{Al}-\overset{\overset{\text{H}}{|}}{\text{O}} \rightarrow \text{Al}-\overset{\overset{\text{H}}{|}}{\text{O}} \rightarrow \text{Al}-\overset{\overset{\text{H}}{|}}{\text{O}} \rightarrow \text{Al}-$$

---

(21) D. G. GUERTIN, S. E. WIBERLEY, W. H. BAUER and J. GOLDENSON, *J. Phys. Chem.* **60**, 1018 (1956).

(22) J. V. BELL, J. HEISLER, H. TANNENBAUM and J. GOLDENSON, *Analyt. Chem.* **25**, 1720 (1953).

(23) F. A. SCOTT, J. GOLDENSON, S. E. WIBERLEY and W. H. BAUER, *J. Phys. Chem.* **58**, 61 (1954).

(24) W. O. LUDKE, S. E. WIBERLEY, J. GOLDENSON and W. H. BAUER, *J. Phys. Chem.* **59**, 222 (1955).

We have observed the infra-red spectra of a large number of samples of aluminium ethoxide in the range from 1–14 μ and of a few samples in the range 10–25 μ. These samples have been prepared by the methods previously described and include samples of varying aluminium content. In addition we have observed the spectra of aluminium iso-propoxide, aluminium n-butoxide, aluminium n-propoxide and several examples of the alkoxo-salts $[Al(OEt)_n]_xM_y$ where M is calcium or magnesium. Table 5 lists the absorption peaks of the purest samples of aluminium ethoxide obtained from the examination of the Nujol mulls. Assignments are based either upon well known absorptions or by comparison with assignments previously made on similar materials.(21–24)

TABLE 5.—ABSORPTION SPECTRA OF "PURE" ALUMINIUM ETHOXIDE, 1–25 μ

Observed frequency (cm^{-1})	Intensity	Assignment
6250	*w*	
4250	*m*	
3340	*w*	O—H stretching vibration in $(-Al-\overset{H}{O}-Al-)$ polymer chains
2740–1520 (21 equally spaced bands)	*w*	
1460	*s*	$-CH_2-$ deformation
1382	*s*	$-CH_3$ deformation
1350	*w*	—OH bending
1178	*m*	ethoxide skelatal vibration
1105	*m*	ethoxide skelatal vibration
1059	*s*	Al—O—C stretching vibration
935	*w*	Al—O→Al stretching vibration
896	*s*	
707	*s*	
650	*s*	
515	*s*	
465	*w*	

s = strong, *m* = intermediate, *w* = weak

Table 5 lists only those absorption peaks which can definitely be ascribed to aluminium ethoxide. Other weak bands may also be present which are masked by the absorption of the Nujol. If the assignments made for the 3340 and 1350 cm^{-1} bands are correct, they must be the result of a small amount of hydrolysis. Most of the bands in Table 5 were confirmed by the examination of the slurries suspended in xylene but the spectra obtained from the KBr pellet technique showed significant variation from the data of Table 5. Because of the possibility of exchange of bromide and ethoxide ions and of the increased possibility of hydrolysis of samples it is felt that the spectra of the KBr pellets is not typical of pure aluminium ethoxide

The spectra of partially hydrolysed samples of aluminium ethoxide depends primarily upon the proportion of aluminium present. As the degree of hydrolysis increases the following changes have been found to take place.

(1) The intensity of all absorption bands except those at 3340 and 935 cm^{-1} decreases.

(2) The 3340 cm^{-1} peak becomes sharper, more intense, and shifts to slightly higher frequencies.

(3) The 935 cm^{-1} peak becomes broader and shifts to slightly lower frequencies.

We have confirmed the absorption observed by GUERTIN *et al.*(21) at 1033 cm^{-1} in aluminium iso-propoxide and have also observed corresponding peaks in the n-propoxide and the n-butoxide. All of the presently available data on the Al-O-C vibration are given in Table 6 in order of increasing frequencies.

TABLE 6.—ABSORPTION FREQUENCIES FOR THE Al—O—C VIBRATION IN ALUMINIUM ALKOXIDES

Alkoxide group	Frequency (cm^{-1})
n-propoxide	1015
iso-propoxide	1033
n-butoxide	1048
sec-butoxide	1058
ethoxide	1059
2-pentoxide	1070

There seems to be no obvious correlation of the order of alkoxides in this list with any simple property of the alkoxy groups. Table 7 lists the Al-$\overset{|}{\mathrm{O}}\rightarrow$ Al frequencies for several aluminium alkoxides and soaps as compiled from the data of BELL *et al.*(22) and SCOTT *et al.*(23) and our observations.

TABLE 7.—ABSORPTION FREQUENCIES FOR THE Al—$\overset{|}{\mathrm{O}}\rightarrow$Al VIBRATION IN ALUMINIUM ALKOXIDES AND SOAPS

Alkoxide group	Frequency (cm^{-1})
n-propoxide	898
Ethoxide	935
iso-propoxide	950
Al soaps	983
n-butoxide	995

Table 8 shows our results on the infra-red spectra of several of the alkoxo-salts. It seems likely that the 1080 cm^{-1} band in these compounds originates in the Al-O-C vibration and the 918 cm^{-1} band in the $[Al(OEt)_4]_2$ M compounds and the 918 cm^{-1} in $[Al(OEt)_6]_2Mg_3$ originates in the Al-$\overset{|}{\mathrm{O}}\rightarrow$ Al vibration.

Observations on the infra-red spectra of solutions of aluminium ethoxide were much less satisfactory than were those made on the solid samples. Since our purest samples were not sufficiently soluble in benzene or xylene at room temperature to permit observation of the spectra the results are confined to those samples showing a greater degree of hydrolysis. An additional difficulty was introduced by the formation of a thin film on the salt windows of the liquid cells after two or three fillings with the ethoxide solutions. This film contributed a spectra of its own and it was necessary to dismantle the cells and clean and polish the windows frequently. Many minor variations were found in the spectra of different samples. There were some systematic differences between samples prepared by the method of WISLICENUS and those prepared by the method of MEERWEIN; and also between solutions in benzene and solutions in xylene. Table 9 lists those absorptions which were common to all solutions. Additional absorption peaks were observed in particular samples. Table 9 also indicates the qualitative effect of concentration on the intensity of the bands.

TABLE 8.—ABSORPTION SPECTRA OF THE ALUMINIUM ALKOXO-SALTS

Observed frequency (cm^{-1})	Intensity of bands $[Al(OEt)_4]_2M$ (M = Ca or Mg)	 $[Al(OEt)_6]_2Mg_3$
6250	*w*	*w*
4250	*m*	*m*
1470	*m*	*m*
1400	*m*	*m*
1120	*s*	absent
1080	*s*	*w*
926	absent	*s*
918	*s*	absent
730	absent	*s*

TABLE 9.—ABSORPTION SPECTRA OF SOLUTIONS OF PARTIALLY HYDROLYSED ALUMINIUM ETHOXIDE IN BENZENE AND XYLENE

Observed frequency (cm^{-1})	Intensity	Effect of concentration	Observed frequency (cm^{-1})	Intensity	Effect of concentration
3570	*w*	—	1110	*s*	O
2900	*m*	O	1080	*s*	O
2750	*w*	O	915	*s*	O
1390	*s*	O	810	*m*	—
1370	*w*	O	775	*m*	—
1320	*w*	—			
1190	*s*	+			

As the concentration of the solute is decreased all of the bands decrease in intensity but they decrease at different rates. The bands could be grouped into three classes. Within each class the changes in absorbancies are proportional. Those marked — changed the least, those marked o changed more rapidly and the one marked + changed at the greatest rate. This suggest that the solute molecules exist in two or more polymeric forms with at least partial equilibrium among the different species. If this is the case, then the absorption bands marked — probably originate in the monomeric forms, those marked o probably originate in all of the forms, and the one marked + probably originates in the polymeric forms. It is difficult to make an unequivocal correlation between the data of Table 5 and the data of and the data of Table 9.

DISCUSSION

It is not easy to account for all of our data on any consistent picture of molecular structure of aluminium ethoxide and its hydrolysed or decomposition products. Nor is it possible to explain certain discrepancies among our findings and those of previous investigators. However, some conclusions do emerge from our studies.

(1) Preparation of highly pure samples of aluminium ethoxide is difficult. Many of the discrepancies in physical properties found in the literature are probably due to the use of impure materials.

(2) Pure aluminium ethoxide exists in only one form, irrespective of the method of preparation, which is only slightly soluble in non-polar organic solvents at room temperature. Soluble forms of aluminium ethoxide previously reported probably consist of materials containing products of hydrolysis or decomposition of aluminium ethoxide. A consistent interpretation of the data of CHILD and ADKINS(14) can be made on the assumption that the β-form is relatively pure aluminium ethoxide and the α-form is the soluble impure form of aluminium ethoxide.

(3) Materials resulting from the partial hydrolysis of aluminium ethoxide are very complex in character and probably consist of mixtures of many molecular species, supposing that definite molecules can be identified in such materials at all. Properties of samples having the same stoicheiometric composition may vary widely when prepared by different procedures.

(4) Solutions of partially hydrolysed or decomposed samples of aluminium ethoxide are also very complex in character. Equilibrium, if attained at all, is reached slowly in these solutions.

Acknowledgement—Financial assistance was received for part of this work from the National Science Foundation under grant no. NSF-G7304.

J. Inorg. Nucl. Chem., 1962, Vol. 24, pp. 863 to 867. Pergamon Press Ltd. Printed in England

ALKOXIDES OF URANIUM (IV)

D. C. BRADLEY*, R. N. KAPOOR† and B. C. SMITH
Department of Chemistry, Birkbeck College (University of London),
Malet Street, London, W.C.1

(*Received* 28 *November* 1961)

Abstract—Lower alcohols form addition compounds with uranium tetrachloride, and uranium tetraalkoxides are prepared by the action of alkali metal alkoxides on uranium tetrachloride. The preparation of dichlorobis(diethylmethylsilyloxy)uranium(IV) is reported. The uranium tetra-alkoxides, which are oxidized extremely readily, have physicochemical properties which are typical of polymeric metal alkoxides.

ANHYDROUS uranium tetrachloride reacts vigorously with methyl, ethyl, and isopropyl alcohols to give alcoholates of formula $UCl_4,4ROH$. These compounds are non-volatile green solids which are oxidized readily in air. They may be recrystallized from the parent alcohols, but they are insoluble in benzene and other non-polar organic solvents. Similar addition compounds of thorium tetrachloride have been reported previously⁽¹⁾ and in these and other 1:4 addition compounds of uranium (IV) and thorium (IV) which are listed by COMYNS⁽²⁾ it is likely that the metals exhibit the co-ordination number eight. The butyl alcohols also react with uranium tetrachloride but replacement of chloride increases in the order $Bu^n < Bu^s < Bu^t$. This type of solvolysis occurs also with titanium and zirconium tetrachlorides, and the possible mechanism has been discussed by BRADLEY *et al.*⁽¹⁾

The reaction of sodium ethoxide and sodium i-propoxide with uranium tetrachloride was investigated by ALBERS *et al.*⁽³⁾ and the preparation of uranium tetramethoxide, tetraethoxide, and tetra-t-butoxide has been reported by GILMAN and his co-workers.⁽⁴⁾ The preparation of uranium tetra-n-propoxide and tetra-i-propoxide from uranium tetrachloride and sodium alkoxides in dimethylcellosolve is now described, and the preparation of uranium methoxide and uranium ethoxide has been repeated using reactions involving uranium tetrachloride and the appropriate lithium alkoxide. All attempts to prepare uranium tetra-t-butoxide were unsuccessful. GILMAN and his co-workers⁽⁴⁾ reported that the compound was soluble in petroleum

---

[*] Present address: Department of Chemistry, University of Western Ontario, London, Ontario, Canada.

[†] Present address: Department of Chemistry, Gorakhpur University, Uttar Pradesh, India.

(1) D. C. BRADLEY, M. A. SAAD and W. WARDLAW, *J. Chem. Soc.* 2002 (1959).
(2) A. E. COMYNS, *Chem. Revs.* **60**, 115 (1960).
(3) H. ALBERS, M. DEUTSCH, W. KRASTINAT and H. VON OSTEN, *Ber. Dtsch. Chem. Ges.* **85**, 267 (1952).
(4) R. G. JONES, C. KARMAS, G. A. MARTIN and H. GILMAN, *J. Amer. Chem. Soc.* **78**, 4285 (1956).

ether and comparatively stable to oxidation, but sublimation or oxidation in solution⁽⁵⁾ gave a red crystalline product to which the formula $UO_2(OBu^t)_2, 4Bu^tOH$ was assigned.

Alkoxides of uranium(IV) are oxidized very readily, and the action of ammonia on uranium tetrachloride–alcohol addition compounds gave derivatives of uranium(V). During attempted preparations of uranium tetra-t-butoxide in the absence of air, oxidation always occurred. A grey-brown quinquevalent solid was formed from which a brown sublimate of uranium penta-t-butoxide could be obtained. Oxidation and evaporation of a petroleum ether solution of the original quinquevalent compound gave red crystals of uranium hexa-t-butoxide whose infrared spectrum showed no peaks corresponding to hydroxyl groups. It seems likely that the red compound reported by GILMAN⁽⁵⁾ was uranium hexa-t-butoxide, which has also been prepared⁽⁶⁾ by disproportionation of $UO(OBu^t)_4, Bu^tOH$ during the attempted preparation of uranyl-t-butoxide, $UO_2(OBu^t)_2$. The ease of oxidation of uranium(IV) alkoxides compared with the relative stabilty of hydrated U^{4+} ions is worthy of comment. In view of the precautions taken to exclude oxygen we are tempted to suggest that uranium(IV) alkoxides actually reduce alcohols with liberation of hydrogen by analogy with the reaction between an alkali metal and alcohol. It is significant that uranium(IV) alkoxides obtained in this research were all insoluble compounds and it may well be that insolubility lowers the reactivity of these compounds. Uranium is not alone in showing this behaviour since vanadium(III) alkoxides⁽⁷⁾ and cerium(III) alkoxides⁽⁸⁾ are also extremely readily oxidized to quadrivalent compounds under comparable conditions, and niobium(IV) alkoxides⁽⁹⁾ are similarly oxidized to quinquevalent niobium alkoxides.

Attempts to prepare uranium tetrakistrialkylsilyloxides were unsuccessful. Reaction of uranium tetrachloride with the lithium salt of diethylmethylsilanol gave $UCl_2(OSiEt_2Me)_2$, a distillable green solid which oxidized on exposure to air.

Uranium tetra-alkoxides are less volatile than corresponding titanium or zirconium alkoxides but more volatile than cerium and thorium alkoxides (see Table 1). Uranium tetramethoxide did not sublime even on heating to 300°C/ca. 10^{-4} mm and uranium tetraethoxide was regarded previously as non-volatile.⁽¹⁰⁾ Volatility in metal alkoxides is determined largely by the radius of the metal atom and the size and shape of the alkyl groups and from the atomic radii of these elements (see Table) it would be expected that uranium(IV) alkoxides would be very similar in volatility to zirconium alkoxides and more volatile than cerium(IV) or thorium alkoxides. However, it has been pointed out previously⁽¹¹⁾ that the relative volatilities of cerium(IV) and thorium tertiary alkoxides are less consistent with atomic radii than with the radii of tetrapositive ions in octahedral co-ordination.

---

(5) R. G. JONES, E. BINDSCHADLER, G. A. MARTIN, J. R. THIRTLE and H. GILMAN, *J. Amer. Chem. Soc.* **79**, 4921 (1957).

(6) D. C. BRADLEY, A. K. CHATTERJEE and A. K. CHATTERJEE, *Proc. Chem. Soc.* 260 (1957); *J. Inorg. Nucl. Chem.* **12**, 71 (1959).

(7) D. C. BRADLEY and M. L. MEHTA. Unpublished results (1960).

(8) D. C. BRADLEY and A. K. CHATTERJEE. Unpublished results.

(9) D. C. BRADLEY and I. M. THOMAS. Unpublished results.

(10) R. G. JONES, W. BINDSCHADLER, G. KARMAS, F. A. YOEMAN and H. GILMAN, *J. Amer. Chem. Soc.* **78**, 4287 (1956).

(11) D. C. BRADLEY, A. K. CHATTERJEE and W. WARDLAW, *J. Chem. Soc.* 2600 (1957).

TABLE 1.—VOLATILITIES (°C/MM) OF TETRA-ALKOXIDES

M	Atomic radius(19) (Å)	M^{4+} radius(20) (Å)	$M(OMe)_4$	$M(OEt)_4$	$M(OPr^n)_4$	$M(OPr^i)_4$
Ti	1·32	0·64	170/0·1*(18)	103/0·1(13)	124/0·1(13)	49/0·1(12)
Zr	1·45	0·87	280/10^{-5}*(17)	180/0·1*(13)	208/0·1(13)	160/0·1(12)
U	1·42	1·05	> 300/*ca.* 10^{-4}	220/0·01*	240/0·01*	160/0·01*
Ce	1·65	1·02	> 200/*vac.*(15)	> 200/*vac.*(15)	> 200/*vac.*	160 – 170/0·05*(16)
Th	1·65	1·10	> 300/0·05(14)	> 300/0·05(14)		200 – 210/0·05–0·1*(16)

* Sublimation temperature.

---

(12) D. C. BRADLEY, R. C. MEHROTRA and W. WARDLAW, *J. Chem. Soc.* 5020 (1952).
(13) D. C. BRADLEY, R. C. MEHROTRA, J. D. SWANWICK and W. WARDLAW, *J. Chem. Soc.* 2025 (1953).
(14) D. C. BRADLEY, M. A. SAAD and W. WARDLAW, *J. Chem. Soc.* 1091 (1954).
(15) D. C. BRADLEY, A. K. CHATTERJEE and W. WARDLAW, *J. Chem. Soc.* 2260 (1956).
(16) D. C. BRADLEY, A. K. CHATTERJEE and W. WARDLAW, *J. Chem. Soc.* 3469 (1956).
(17) D. C. BRADLEY and M. M. FAKTOR, *Nature, Lond.* **184**, 55 (1959).
(18) D. C. HANCOCK. Personal communication.
(19) T. MOELLER, *Inorganic Chemistry*, p. 135. J. Wiley, London (1952).
(20) T. MOELLER, *Inorganic Chemistry*, p. 141. J. Wiley, London (1952).

Consideration of the M^{4+} radii (see Table 1) would suggest that uranium compounds should be less volatile than cerium compounds and more volatile than thorium compounds. In view of the uncertainty in the values of atomic or ionic radii and of the lack of precision in the volatility data it would be pointless to attempt a more detailed interpretation of these properties, but it appears that ionic radii afford a more reasonable correlation with volatilities than "covalent" radii. Although we could not determine the molecular weights of the uranium(IV) alkoxides, there can be little doubt from their volatilities that they are polymeric and involve uranium in a co-ordination number of six or higher. In particular, the striking increase in volatility caused by chain branching in the propoxides is characteristic of the behaviour of polymeric metal alkoxides.

EXPERIMENTAL

Reactions were carried out in the absence of oxygen, and products for analysis were sealed in evacuated tubes.

Preparation of alcoholates

Anhydrous uranium tetrachloride reacted vigorously with methyl, ethyl, and i-propyl alcohols to give the following green solid addition compounds: *uranium tetrachloride-tetrakismethanol* (Found: U, 46·7; Cl, 27·6; MeO, 22·6. Calc. for $C_4H_{16}Cl_4O_4U$: U, 46·8; Cl, 27·9; OMe, 24·4%); *uranium tetrachloride-tetrakisethanol* (Found: U, 41·7; Cl, 24·8; EtO, 31·7. Calc. for $C_8H_{24}Cl_4O_4U$: U, 42·1; Cl, 25·1; OEt, 31·9%); and *uranium tetrachloride-tetrakisisopropanol* (Found: U, 38·5; Cl, 21·8; Pr^{i}O, 38·2. Calc. for $C_{12}H_{32}Cl_4O_4U$: U, 38·4; Cl, 22·8; Pr^{i}O, 38·1%). Similar reactions with n-, s-, and t- butyl alcohols gave green solids in which Cl : U ratios were respectively 2·9, 2·5 and 0·4.

Reactions of alcoholates

Ammonia was bubbled through a solution of uranium tetrachloride–tetrakisethanol in benzene–ethanol. Ammonium chloride was removed by filtration, and analysis of the brown tarry residue obtained on evaporation corresponded to *triethoxyoxouranium*(V)-*ethanol*, $UO(OEt)_3,EtOH$. (Found: U, 54·4; OEt, 39·9; valency, 5·2. Calc. for $C_8H_{21}O_5U$: U, 54·7; OEt, 41·6%.) Distillation at 160°–180°C/0·1 mm gave uranium pentaethoxide(10, 21) (Found: U, 51·7; OEt, 46·8; valency, 5·0. Calc. for $C_{10}H_{25}O_5U$: U, 51·4; OEt, 48·6%.) A similar reaction of ammonia with uranium tetrachloride–tetrakisisopropanol gave a light brown solid which recrystallized from i-propanol to form golden crystals of uranium penta-i-propoxide.(21, 22) (Found: U, 44·7; OPr^i, 55·2; valency, 5·0. Calc. for $C_{15}H_{35}O_5U$: U, 44·6; OPr^i, 55·4%.)

Preparation of alkoxides

Uranium tetramethoxide was prepared by filtration of the green precipitate formed on mixing methanolic solutions of lithium methoxide and uranium tetrachloride–tetrakismethanol. (Found: U, 65·2; OMe, 38·8. Calc. for $C_4H_{12}O_4U$: U, 65·7; OMe, 34·2%.) Ethanolic solutions of lithium ethoxide and uranium tetrachloride-tetrakisethanol formed a green precipitate of uranium tetraethoxide, which sublimed at 220° C/0·01 mm. (Found: U, 57·0; OEt, 42·8; valency, 4·0. Calc. for $C_8H_{20}O_4U$: U, 56·9; OEt, 43·0%.) Lithium n-propoxide in dimethylcellosolve reacted vigorously with uranium tetrachloride to form a green precipitate. The solvent was removed and *uranium tetra-n-propoxide* sublimed at 240° C/0·1 mm. (Found: U, 50·6; valency, 4·1. Calc. for $C_{12}H_{28}O_4U$: U, 50·2%.) Lithium-i-propoxide and uranium tetrachloride reacted similarly to form *uranium tetra-i-propoxide* which sublimed at 160° C/0·01 mm. (Found: U, 50·5; OPr^i, 49·2; valency, 4·0. Calc. for $C_{12}H_{28}O_4U$: U, 50·2; OPr^i, 49·8%.)

Attempted preparation of uranium tetra-t-butoxide

(a) Uranium tetramethoxide was heated under reflux with benzene-t-butanol, and methanol was removed slowly as an azeotrope with benzene. The solution became red and a brown solid formed. Impure uranium penta-t-butoxide(21, 22) was isolated from the reaction mixture.

(b) Anhydrous uranium tetrachloride and t-butanol were added to a solution of potassium amide in liquid ammonia. Evaporation of ammonia and extraction of the residue with dry petroleum ether gave grey-brown crystals of a quinquevalent uranium compound. (Found: U, 45·8; valency, 5·0. Calc. for $UO(OBu^t)_3,Bu^tOH$: U, 43·5%.) A brown sublimate of uranium penta-t-butoxide was obtained at 130°C/0·1 mm. (Found: U, 40·2; valency, 5·0. Calc. for $C_{20}H_{45}O_5U$: U, 39·5%.) The grey-brown colour of a solution of $UO(OBu^t)_3,Bu^tOH$ in petroleum ether changed to red on standing in air for three days. Evaporation gave red crystals of uranium hexa-t-butoxide which sublimed at 100°C/0·1 mm. (Found: U, 35·6. Calc. for $C_{24}H_{54}O_6U$: U, 35·2%.)

Silyloxide reaction

Uranium tetrachloride reacted with lithium diethylmethylsilyloxide in dimethyl cellosolve–benzene to form a green precipitate. Distillation yielded *dichlorobis(diethylmethylsilyloxy)uranium(IV)*, b.p. 260°C/0·01 mm. (Found: U, 43·0; Cl, 13·05; Si, 10·4; valency 4·0. Calc. for $C_{10}H_{26}Cl_2O_2Si_2U$: U, 43·8; Cl, 13·1; Si, 10·3%.)

Materials

Anhydrous uranium tetrachloride was prepared from uranium trioxide and hexachloropropene.(23) Organic solvents, of "Analytical Reagent" grade when possible, were dried carefully by conventional methods before passing through columns packed with molecular-sieve.

Analysis

Chloride was determined gravimetrically as silver chloride. Uranium was oxidized and precipitated as the trioxide, and weighed as U_3O_8 after ignition at 800°C in a platinum crucible. The valency of uranium was established volumetrically.(21) Alkoxy groups were estimated by the method of Bradley *et al.*(24)

Acknowledgement—This work was supported by the United Kingdom Atomic Energy Research Establishment, Harwell, and the authors thank Mr. F. Hudswell for his interest and encouragement.

(21) D. C. Bradley, B. N. Chakravarti and A. K. Chatterjee, *J. Inorg. Nucl. Chem.* 3, 367 (1957).

(22) R. G. Jones, G. Karmas, G. A. Martin, J. R. Thirtle, F. A. Yoeman and H. Gilman, *J. Amer. Chem. Soc.* **78**, 4289 (1956).

(23) J. A. Hermann and J. F. Suttle, *Inorg. Synth.* **5**, 143 (1957).

(24) D. C. Bradley, F. M. Abd-el Halim and W. Wardlaw, *J. Chem. Soc.* 3450 (1950).

J. Inorg. Nucl. Chem., 1962, Vol. 24, pp. 869 to 879. Pergamon Press Ltd. Printed in England

THE THERMAL DECOMPOSITION OF THE RARE-EARTH SULPHATES

THERMOGRAVIMETRIC AND DIFFERENTIAL THERMAL ANALYSIS STUDIES UP TO 1400°C*

M. W. NATHANS
Lawrence Radiation Laboratory, University of California, Livermore, California
and
W. W. WENDLANDT
Department of Chemistry, Texas Technological College, Lubbock, Texas

(*Received* 23 *August* 1961; *in revised form* 4 *January* 1962)

Abstract—The thermal decomposition of the anhydrous rare-earth sulphates was studied by thermogravimetric analysis (TGA) and differential thermal analysis (DTA) up to a temperature limit of 1400° C. TGA curves showed that the thermal decomposition reaction took place in two steps. The first step corresponded to the formation of metal oxysulphates, $M_2O_2(SO_4)$, the second step corresponded to the formation of the metal oxides. DTA studies also revealed this decomposition pattern, giving as evidence two endothermic peaks. The heats of decomposition to the metal oxysulphates and sulphates were determined by quantitative DTA methods. Preliminary information was obtained on the kinetics of the decomposition reactions.

THE rare-earth sulphate hydrates thermally decompose according to the following transitions: Rare-earth sulphate hydrates $\xrightarrow{I}$ metal sulphate $\xrightarrow{II}$ metal oxysulphate $\xrightarrow{III}$ metal oxide. The dehydration reaction(I) has been studied previously by ignition and thermogravimetric analysis (TGA) studies(1–8) and by differential thermal analysis (DTA).(8, 9) TGA data revealed that the first weight-loss temperatures ranged from 40 to 110° C, while the minimum temperatures for the complete dehydration ranged from 155 to 295°C.(7) In the DTA studies(9) the dehydration reactions were found to be complete below 350°C. The heats of dehydration for the metal–sulphate hydrates, as determined by quantitative DTA studies,(9) ranged from 68 kcal mole^{-1} for $Ce_2(SO_4)_3 \cdot 5H_2O$, to 152 kcal mole^{-1} for $Yb_2(SO_4)_3 \cdot 11H_2O$.

---

* This work was done under the auspices of the U.S. Atomic Energy Commission.

(1) J. W. MELLOR, *A Comprehensive Treatise on Inorganic and Theoretical Chemistry*, Vol. 5, Chap. 28. Longmans, Green, London (1924).
(2) G. R. HALL and T. L. MARKIN, *J. Inorg. Nucl. Chem.* **4**, 137 (1957).
(3) C. DUVAL, *Inorganic Thermogravimetric Analysis*, pp. 403–412. Elsevier, Amsterdam (1953).
(4) S. H. KATZ and C. JAMES, *J. Amer. Chem. Soc.* **36**, 779 (1914).
(5) J. J. PITHA, A. L. SMITH and R. WARD, *J. Amer. Chem. Soc.* **69**, 1870 (1947).
(6) B. BRAUNER and F. PAVLICEK, *J. Chem. Soc.* **81**, 1243 (1902).
(7) W. W. WENDLANDT, *J. Inorg. Nucl. Chem.* **7**, 51 (1958).
(8) L. A. ALEKSEENKO, A. F. LEMENKOVA and V. V. SEREBRENNIKOV, *Zh. Neorg. Khim.* **4**, 1382 (1959).
(9) W. W. WENDLANDT and T. D. GEORGE, *J. Inorg. Nucl. Chem.* **9**, 245 (1961).

The decomposition of the metal sulphates to metal oxysulphates(II) and metal oxides(III) has been reported to take place in the 650 to 1400°C temperature range.(1, 5, 7, 10, 11) The lower limit is the minimum decomposition temperature for the $Ce_2(SO_4)_3 \rightarrow CeO_2$ transition(7) while the upper limit applies to lanthanum. In this study, the thermal decomposition of all of the rare-earth metal sulphates was investigated by the methods of TGA and DTA up to a temperature of ~ 1400°C. In addition the heats of decomposition to the metal oxysulphates and the metal oxides were evaluated and some preliminary data obtained on the kinetics of the decomposition reactions.

EXPERIMENTAL

Rare-earth metal sulphates

All of the metal sulphates, except the cerium salt, were prepared from the metal oxides as previously described.(7) The cerium salt was obtained as cerium sulphate 9-hydrate. The composition of the metal sulphates was determined by weight-loss after heating to 400°C in a muffle furnace, and by residue weight after ignition to 1400°C.

Thermobalance

The automatic recording instrument has previously been described.(12) It was further modified in that the nichrome-wound furnace assembly was replaced by a Kanthal-wound unit of similar dimensions. The temperature of the Kanthal furnace was detected by a chromel–alumel thermocouple placed near the sample crucible, and recorded on a potentiometric strip-chart recorder. Sample sizes of the anhydrous metal sulphates ranged in weight from 90 to 100 mg. A static air atmosphere was maintained in the furnace during the pyrolysis reactions.

The DTA apparatus used has previously been described.(13) It was modified slightly in that a platinum wire was welded to the platinum junction of the differential thermocouple so that the sample temperature could be measured with an external potentiometer at any given instant, the precision being about ±2°C. The liquid sample holder was employed so that the samples could be weighed before as well as after a run. Moreover, it was believed that the technique of introducing and distributing the sample in the chamber would be more reproducible.

Standard conditions for each DTA run were 100–105 mg of sample and a heating rate of 10°C min^{-1} (nominal) in a dynamic atmosphere of argon at atmospheric pressure. Kinetic data were obtained for lanthanum, europium, and ytterbium sulphates by varying the heating rate. In several instances, the sample size was also varied.

RESULTS AND DISCUSSION

TGA results

The TGA curves for all of the metal sulphates except cerium are given in Figs. 1–3 with arbitrary temperature axes. In general, the temperatures at which the reaction

$$M_2(SO_4)_3 \rightarrow M_2O_2(SO_4)+2SO_2+O_2 \qquad (1)$$

becomes noticeable range from 855 to 946°C. The trend appeared to be that this temperature increased slightly with an increase in atomic number of the metal ion. For the reaction

$$M_2O_2(SO_4) \rightarrow M_2O_3+SO_2+\tfrac{1}{2}O_2 \qquad (2)$$

---

(10) L. WOHLER and M. GRUNZWEIG, *Ber. Dtsch. Chem. Ges.* **46,** 1726 (1913).

(11) L. WOHLER and K. FLICK, *Ber. Dtsch. Chem. Ges.* **67 B,** 1679 (1934).

(12) W. W. WENDLANDT, *Analyt. Chem.* **30,** 56 (1958); **32,** 848 (1960).

(13) M. W. NATHANS, *J. Inorg. Nucl. Chem.* **22,** 231 (1961).

(with the exception of praseodymium and terbium) the minimum decomposition temperature ranged from 1090° to ~ 1250°C. In the case of ytterbium and lutetium, the decomposition process appeared to be a single step giving the metal oxides directly. The decomposition temperatures of the $M_2O_2(SO_4)$ compounds were definitely more dependent upon the atomic number of the metal ion than the initial decomposition of the anhydrous metal sulphates appeared to be. As the atomic number of the metal ion increased, the weight levels corresponding to the $M_2O_2(SO_4)$ compounds became shorter, indicating that the compounds became less stable. This stability was much less in the case of ytterbium and lutetium in that instead of a horizontal weight-level in the curve, a slight inflexion point was observed which indicated the transient existence of probably $M_2O_2(SO_4)$ compounds.

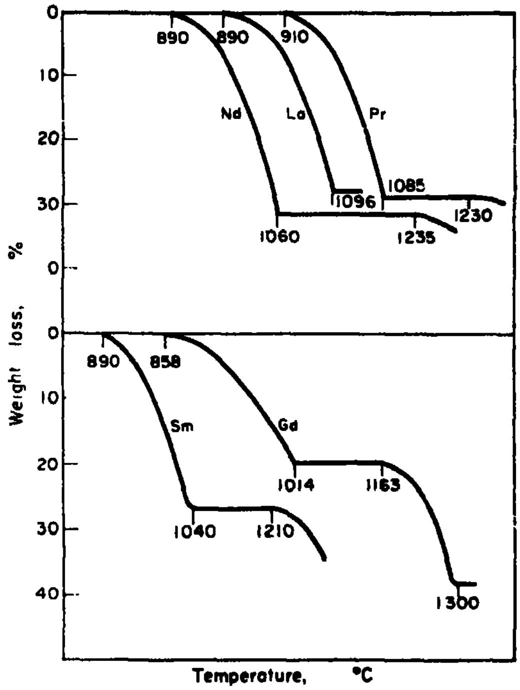

Fig. 1.—Thermogravimetric analysis curves of the sulphates of La, Pr, Nd, Sm, Gd.

DTA results

Since all of the rare-earth DTA curves were quite similar to each other, only four of them are reproduced in Fig. 4. The DTA curves all exhibited two endothermic peaks.* The first peak was due to the reaction in Equation (1) while the second was for the reaction illustrated by Equation (2). As the atomic number of the metal ion increased, the two endothermic peaks became closer together although still indicating the two reaction decomposition sequence. Cerium sulphate was an exception from this general behaviour of thermal decomposition.

* It was observed that between 350° and 450°C the sulphates of Pr, Nd, Sm, Eu, and Gd gave a small exothermic peak. X-ray diffraction of appropriate samples of the Sm salt showed that the dehydration of these salts leaves an amorphous material which transforms into a crystalline material at the above temperatures. The crystalline anhydrous samarium sulphate is isostructural with the lanthanum sulphate. An unsuccessful attempt was made to index the powder pattern. It appears that the structure is either monoclinic or triclinic.

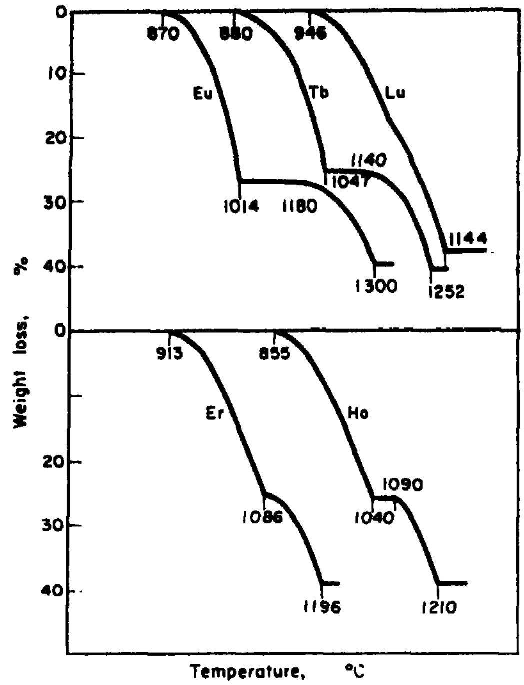

FIG. 2.—Thermogravimetric analysis curves of the sulphates of Eu, Tb, Ho, Er, Lu.

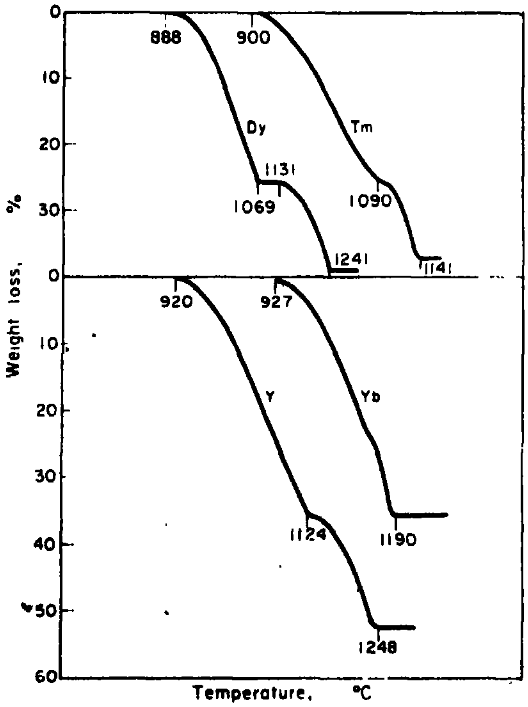

FIG. 3.—Thermogravimetric analysis curves of the sulphates of Dy, Tm, Yb, Y.

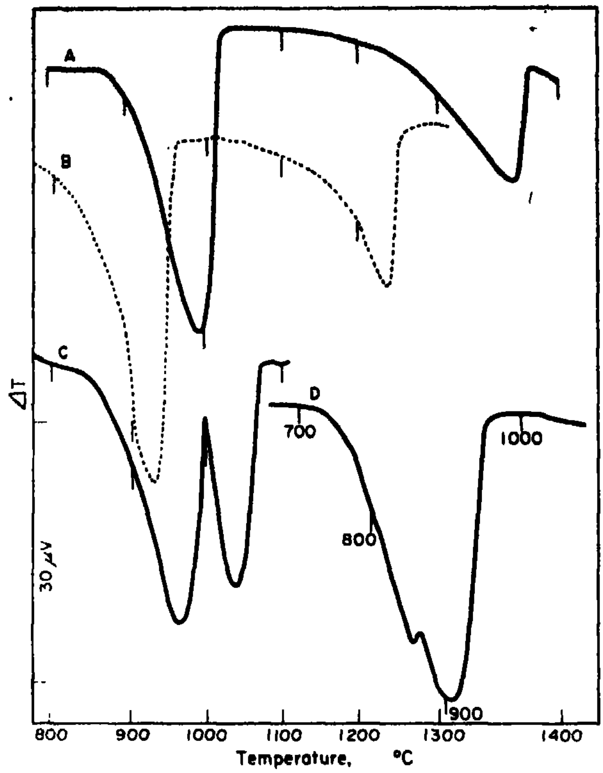

FIG. 4.—Differential thermal analysis curves of some rare-earth sulphates. A–La; B–Eu; C–Yb; D–Ce.

A qualitative agreement between TGA and DTA is apparent. It would appear, however, that in DTA the reaction starts at a much lower temperature than in TGA. Some of this difference may be caused by the greater sensitivity of the DTA equipment. The main reason seems to lie in the conditions used. When a stationary air atmosphere was employed the DTA curves of the lanthanum sulphate were shifted to considerably higher temperatures, the first peak from 960 to about 1040°C. The same was observed at LRL with calcium carbonate powders. In this case it was established that the diffusion of product gas through the sample to the surrounding atmosphere was rate determining. We suggest a similar phenomenon here.

Fig. 5 shows a plot of the peak temperature vs. atomic number. The plot shows a behaviour which does not have as complete a regularity as might be expected.

Heats of reaction

The heats of reaction for equations (1) and (2) were determined from the DTA curves by use of the relationship:

$$\Delta H = C\int_{t_1}^{t_2} \Delta T\, dt$$

where t_1 and t_2 are the times at the beginning and at the end of the reaction, ΔT is the differential temperature, and C is the proportionality constant which not only contains an instrument-dependent factor but also a factor which depends upon the particle size, sample packing, and sample thermal conductivity.(14) The integral is the area under the peak. The problem in this technique is the determination of the constant C. Of the various methods available (none of which has as yet attained a high degree of accuracy), the use of $CaCO_3$ was decided upon as the reference compound since it undergoes a decomposition reaction to CaO and CO_2 in a temperature range not too far from that under study.

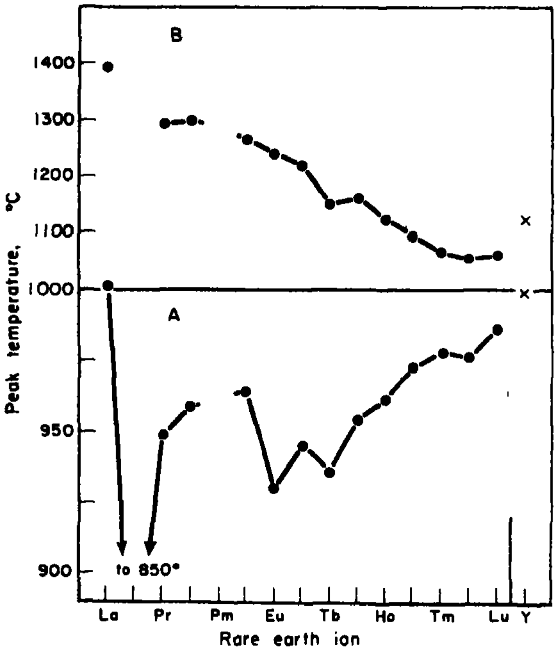

Fig. 5.—Differential thermal analysis peak temperatures for: *A*, sulphate decomposition; *B*, oxysulphate decomposition. All at 10°C/min heating rate.

The heat of decomposition was taken as 37 kcal/mole, a value obtained from the slope of the en p vs. $1/T$ curve.(15)

The heats of reaction for the metal sulphates were determined by use of the above method. It was felt necessary, however, to investigate first the effect of some of the factors which may have an influence on the peak area determination.

The peak areas for a given sample size of lanthanum sulphate, europium sulphate, and ytterbium sulphate were independent of the upheat rate, except for heating rates below 3°C/min. This is shown in Table 1 for two of the cases investigated. The deviation at low heating rates can be explained by the condition that the heat absorbed by the reaction must be *measurably* greater than the heat supplied by the furnace and sample block assembly. The effect of sample size is less clear. This was not further investigated than is indicated in Table 1 because it was apparent that 100 mg was a suitable sample size.

---

(14) S. Speil, L. H. Berkelhamer, J. A. Pask and B. Davis, *U.S. Bureau of Mines, Tech. Paper* 664 (1945).

(15) (a) F. H. Smith and L. H. Adams, *J. Amer. Chem. Soc.* **45**, 1167 (1923).
(b) G. C. Kennedy. Private communication (July, 1961).
(c) R. L. Stone and M. W. Nathans. Unpublished data.

TABLE 1.—PEAK AREAS FOR RARE EARTH SULPHATE DECOMPOSITION AT VARIOUS HEATING RATES

$La_2(SO_4)_3 \rightarrow La_2O_2SO_4 + 2SO_2 + O_2$		$Yb_2O_2SO_4 \rightarrow Yb_2O_3 + SO_2 + \frac{1}{2}O_2$	
Heating rate (°C/min)	Peak area*	Heating rate (°C/min)	Peak area*
22·0	1280†	19·5	500†
10·0	1220	9·7	510
9·7	1029	7·4	490
8·0	1246	5·1	440
7·8	1290		
5	1410		
3·5	760		
1	0		
10·0	970‡		
9·6	1312§		

* Arbitrary units, per 1000 mg sample.

† Sample size: 100–105 mg in this series.

‡ Sample size: 31 mg.

§ Sample size: 197 mg.

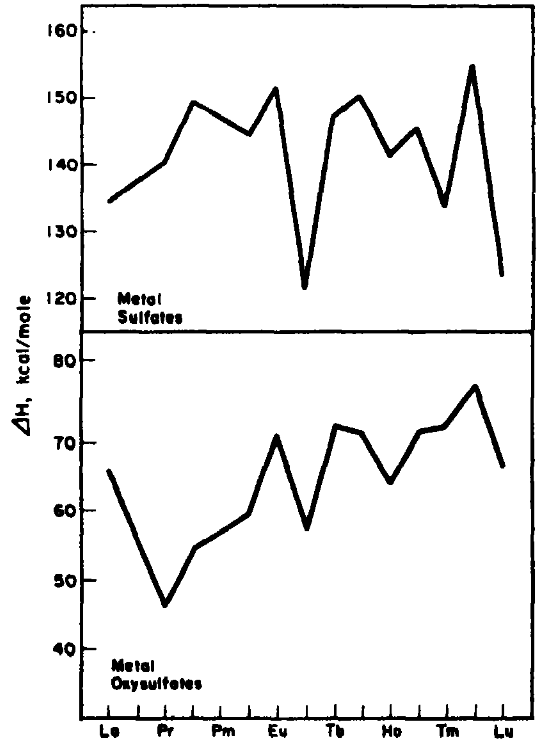

FIG. 6.—Heats of decomposition of rare-earth sulphates and oxysulphates.

The results of the measurements are shown graphically in Fig. 6. The 95 per cent confidence limits calculated from a series of results for lanthanum, europium, and ytterbium sulphate is about ±8 per cent. The method used for this calculation is the one suggested for small numbers of observations by DEAN and DIXON.(16) The precision is not high enough to try to establish any correlations. It does seem, however, that there is a regular increase in the heat of reaction for the oxysulphate decomposition from praseodymium to lutetium, and that its value is less for the decomposition of the gadolinium and lutetium salts compared to that of the others.

Kinetic studies

The constants for the kinetics of the decomposition reactions as shown in Equations (1) and (2) were determined by the method of KISSINGER.(17, 18) The constants are evaluated from the equation

$$\frac{d\,\ln(\phi/T_m^2)}{d(1/T_m)} = -\frac{E'}{R}$$

where ϕ is dT/dt, the heating rate, T_m is the peak maximum temperature, and E' is the activation energy. From a plot of log ϕ/T_m^2 vs. $1/T_m$, the slope is $E'/2{\cdot}3\,R$, from which E' can be obtained. The frequency factor, A, was calculated from the relationship

$$A = (E'\,\phi/RT_m^2)\exp(-E'/RT_m)$$

Activation energies were determined for the decomposition of La, Eu and Yb sulphates. Figs. 7 and 8 show plots of log ϕ/T_m^2 vs. $1/T_m$. Table 2 lists the kinetic constants obtained from a least-square fit. The limits on E' are standard deviations. It is believed that several additional points would have considerably reduced the error in E'.

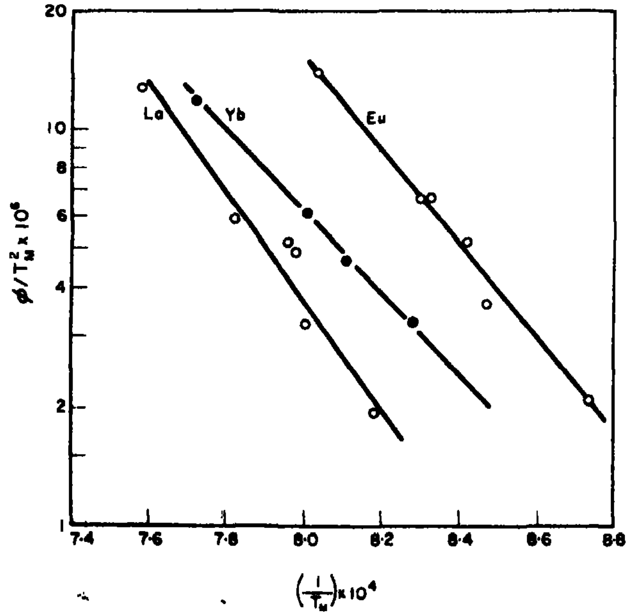

FIG. 7.—Kinetics plot for the rare-earth sulphate decomposition.

---

(16) R. B. DEAN and W. J. DIXON, *Analyt. Chem.* 23, 636 (1951).

(17) H. E. KISSINGER, *J. Research Nat. Bur. Standards* 57, 217 (1956).

(18) H. E. KISSINGER, *Analyt. Chem.* 29, 1702 (1957).

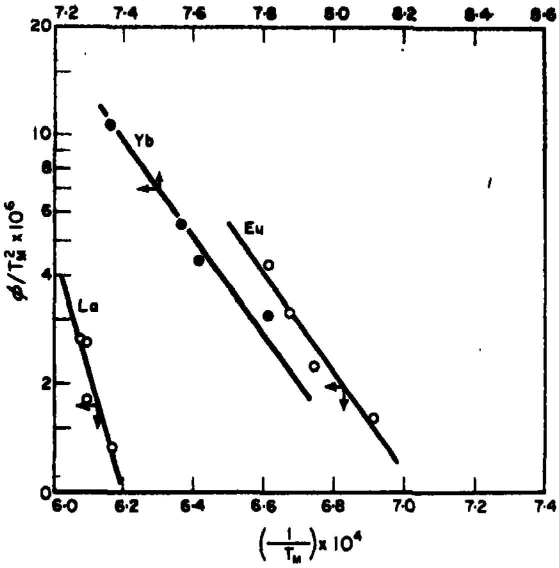

FIG. 8.—Kinetics plot for the rare-earth oxysulphate decomposition.

TABLE 2.—ARRHENIUS CONSTANTS FOR SOME RARE-EARTH SULPHATE AND OXYSULPHATE DECOMPOSITIONS*

	Sulphate		Oxysulphate	
	A	E′	*A**	E′
La	$1 \cdot 2 \times 10^{10}$	62·2 ± 6·5†	$2 \cdot 3 \times 10^{24}$	185 ± 33
Eu	$7 \cdot 1 \times 10^{9}$	58 ± 26	$2 \cdot 8 \times 10^{8}$	65 ± 12
Yb	$4 \cdot 4 \times 10^{6}$	46 ± 4	$3 \cdot 6 \times 10^{10}$	64 ± 19

* Rate constant = $A \exp(-E'/RT)$, with A in min^{-1}, E† in kcal/mole.
† Standard deviation.

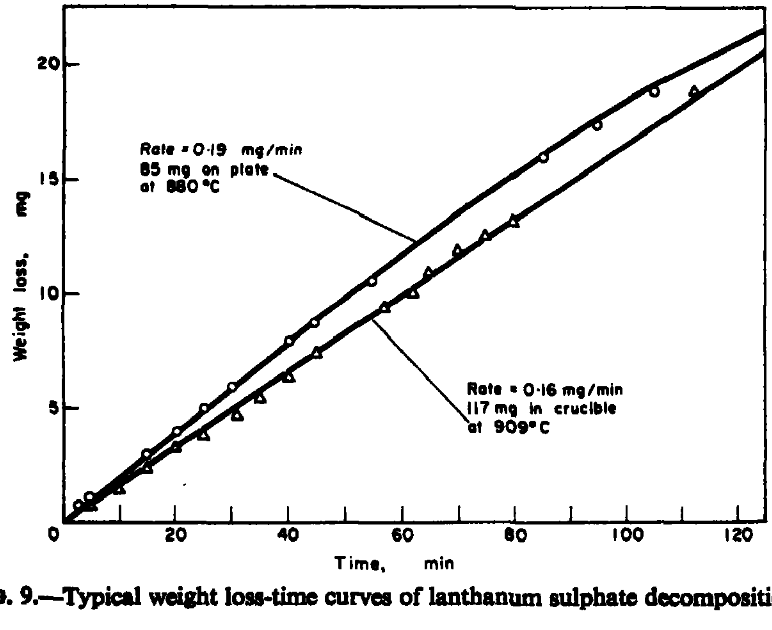

FIG. 9.—Typical weight loss-time curves of lanthanum sulphate decomposition.

The reaction order, n, was calculated with the formula $n = 1{\cdot}26\ S^{\frac{1}{2}}$ where S is the shape index of the DTA peak. With very few exceptions, all of the peaks were quite asymmetric, and S was difficult to determine with any degree of precision. The apparent order was estimated to be about 0·3; the oxysulphate decomposition of ytterbium and lutetium showed an apparent order of about 0·75. The meaning of these numbers needs to be investigated further.

At present there is insufficient evidence that DTA experiments give the correct values of the calorimetric and kinetic properties. An attempt was made to check the heats of decomposition by determining the difference in the heats of solution of anhydrous lanthanum sulphate and lanthanum oxysulphate. The attempt failed because of the slow rate of dissolution of the oxysulphate in the acid solvents used.

The kinetic data for reaction (1) were checked by isothermal experiments of two kinds. One hundred milligram samples were spread out on a small piece of gold foil. The weight loss was determined as a function of time at various temperatures by suspending the sample from a balance in a suitable manner in a furnace. In another series the sample was located in a small porcelain crucible to determine the effect of geometry. One typical curve of each series is shown in Fig. 9. It is clear that straight lines, hence zero order reactions, are obtained over a large extent up to at least 40 per cent reacted. The behaviour of the curves is in general agreement with

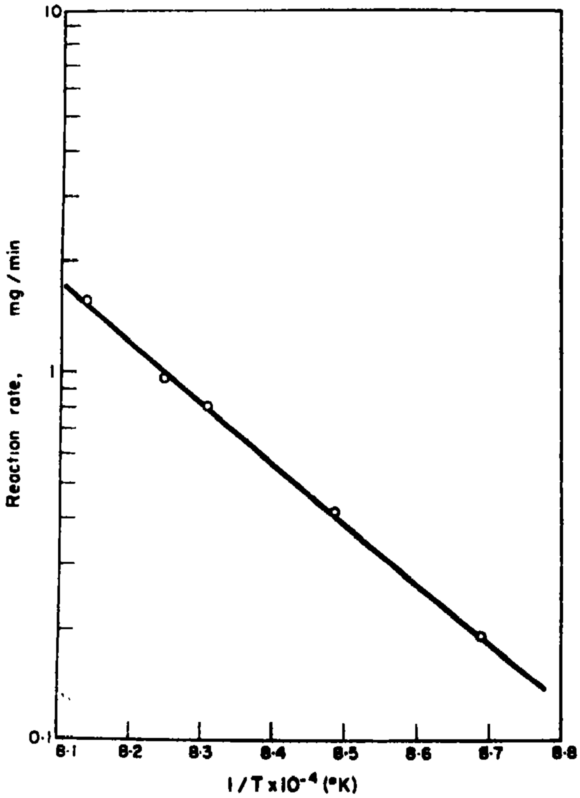

FIG. 10.—Arrhenius plot for the lanthanum sulphate decomposition.

the DTA results. The slope of the straight line portion, the rate constant, was found to be dependent on the sample size, but not proportional to it. This was not investigated further.

Fig. 10 shows a plot of the ln (rate) vs. $1/T$ for a constant sample size. The slope gives an activation energy of 74 kcal/mole, considerably higher than that determined by DTA.

Acknowledgements—The authors wish to acknowledge the valuable help of Mr. F. MacMurphy in obtaining the DTA curves, and of Mr. V. Silveira for obtaining the X-ray diffraction patterns. Mr. G. Rynders, who was kind enough to review a portion of the manuscript, made some helpful suggestions which have been incorporated.

J. inorg. Nucl. Chem., 1962, Vol. 24, pp. 881 to 888. Pergamon Press Ltd. Printed in England

STABILITY CONSTANTS OF CERTAIN LANTHANIDE(III) AND ACTINIDE(III) CHLORIDE AND NITRATE COMPLEXES*

D. F. PEPPARD, G. W. MASON and I. HUCHER
Argonne National Laboratory, Argonne, Illinois

(*Received* 15 *November* 1961; *in revised form* 29 *December* 1961)

Abstract—By means of acid-dependency studies, the extractant di[para(1,1,3,3-tetramethyl butyl)phenyl] phosphoric acid, HDOΦP, in toluene as a carrier diluent has been shown to extract M(III) lanthanides and actinides from aqueous perchlorate, chloride and nitrate media as species containing none of the anions present in the aqueous phase. Consequently, extraction of M(III) lanthanides and actinides from mixed perchlorate-chloride and from mixed perchlorate-nitrate aqueous phases may be used to determine the stability constant, k_c, for MCl^{2+} and $M(NO_3)^{2+}$. The k_c values, at 22 ± 1° C, $\mu = 1{\cdot}0$, so determined are: MCl^{2+}, La (0·9 ± 0·3), Ce(0·9 ± 0·3), Pr(0·9 ± 0·3), Eu(0·9 ± 0·3), Tm(0·8 ± 0·3), Yb(0·6 ± 0·2), Lu(0·4 ± 0·2), Am(0·9 ± 0·2); $M(NO_3)^{2+}$, La(1·3 ± 0·3), Ce(1·3 ± 0·3), Pr(1·7 ± 0·3), Eu(2·0 ± 0·3), Tm(0·7 ± 0·2), Yb(0·6 ± 0·2), Lu(0·6 ± 0·2), Am(1·8 ± 0·3).

IN general, the aqueous M^{b+}, $MX^{(b-1)+}$ and X^- systems may be studied by measuring a property of either M^{b+} or of $MX^{(b-1)+}$ as a function of the concentration of X^-, if the sum of the concentrations of M^{b+} and $MX^{(b-1)+}$ is known and if no other M-containing species is present. Consequently, a liquid–liquid extraction system involving mutually equilibrated sensibly immiscible aqueous and organic phases, in which M^{b+} is extractable and $MX^{+(b-1)}$ is non-extractable from the aqueous phase into the organic phase, may be used in the determination of the stability constant of $MX^{+(b-1)}$. This technique, which has found wide application, has been reviewed by ZOZULYA and PESHKOVA.⁽¹⁾

Specifically, a monoacidic ester of orthophosphoric acid in toluene as a carrier diluent has been used to extract M(III) from an aqueous phase one molar in combined $HClO_4$ plus HX, where HX is HCl or HNO_3. The variation of K with X^- was then used in computing the value of the stability constant for MX^{2+}.

EXPERIMENTAL

Nomenclature

The "type" extractant, $(GO)_2PO(OH)$,⁽²⁾ is a monoacidic "di-ester" of orthophosphoric acid in which G represents a generalized organic group. Continuing previous usage of symbolic formulae,⁽²⁾ this extractant may also be represented as HDGP where H signifies a theoretically ionizable hydrogen and D, G and P respectively signify the prefix di-, a generalized organic group, and phosphoric ester. For example $(n\text{-}C_4H_9O)_2PO(OH)$ is represented as HDBP, i.e. dibutyl phosphoric acid.

---

* Based on work performed under the auspices of the U.S. Atomic Energy Commission.

⁽¹⁾ A. P. ZOZULYA and V. M. PESHKOVA, *Russ. Chem. Rev.* (Eng. Transl.) **2**, 101 (1960), i.e. *Uspekhi Khimii* **2**, 234 (1960).

⁽²⁾ D. F. PEPPARD, G. W. MASON, W. J. DRISCOLL and R. J. SIRONEN, *J. Inorg. Nucl. Chem.* **7**, 276 (1958).

The extractant employed in the present study, di[para(1,1,3,3-tetramethyl butyl)phenyl] phosphoric acid, is referred to as di octyl-phenyl phosphoric acid and is symbolized as HDOΦP. It should be remembered that these symbolic formulae are used without regard to molecular complexity.

The distribution ratio, *K*, is defined as the concentration of a given nuclide in the "organic" phase divided by the concentration in the "aqueous" phase following mutual equilibration of these phases. Specifically, the counting rate, alpha or beta, associated with a given aliquot of a phase is taken as a direct measure of the concentration of the pertinent nuclide.

Sources of materials

Di[para(1,1,3,3-tetramethyl butyl)phenyl]phosphoric acid, $[p\text{-}(C_8H_{17})(C_6H_4O)]_2PO(OH)$, HDOΦP, was isolated and purified as described previously,(3) using the mixture obtained from Victor Chemical Works, except that the procedure for eliminating pyro contaminants was modified. Stirring with 6 M HCl at 80° C was extended from the previously described 8-hr period to a 48-hr period. Reagent grade toluene was used as carrier diluent. The $NaClO_4$ and $NaNO_3$ and the corresponding acids used in preparing the constant μ solutions were purified as described previously.(4)

The β-active nuclides 40·2 hr ^{140}La (with parent 12·8 day ^{140}Ba), 285 day ^{144}Ce (with daughter 17 min ^{144}Pr) and (13, 16) year $^{152,154}Eu$ were obtained from the Isotopes Division of the Oak Ridge National Laboratory. Daughter ^{140}La(5) was isolated from its parent, and the other nuclides(5, 6) were subjected to further purification cycles, by application of liquid–liquid extraction techniques. The β-active nuclides 129 day ^{170}Tm, (32, 4·2) day $^{169,175}Yb$ and 6·8 day ^{177}Lu were prepared by neutron irradiation of the highly-purified corresponding gross lanthanides. β-active 13·8 day ^{143}Pr was isolated from a neutron-irradiated sample of highly-purified gross cerium.(5)

Determination of distribution ratios, general

The distribution ratio, *K*, was determined as previously described(6) with the following modifications. The two phases (2 ml portions of each) were mixed in 15 ml polypropylene conical centrifuge cones fitted with hollow stoppers, obtained from The Nalge Co., Inc., Rochester 2, N.Y. All of the experiments corresponding to the points of a given curve were performed simultaneously, the stoppered cones being placed as a bundle in a straight-wall screw-cap glass jar in such a way as to be fixed rigidly in place. The assembly was then shaken manually for a 6 min period. Following gravity phase disengagement, approximately 1·5 ml portions of the phases were transferred individually to fresh centrifuge cones and centrifuged at full speed for a 1 min period in an International Clinical Centrifuge, Model CL and the assay made as described.(6) All of the data were obtained at 22 ± 1° C. Aqueous phases with salt content were analysed by the "octyl pyrophosphate" extraction technique.(7)

Determination of complexity constants

For determination of chloride complexity constants, the members of a series of solutions 1·0 M in H^+ and 1·0 M in combined perchlorate and chloride ions were used as aqueous phases against a solution of HDOΦP in toluene as the opposing organic phase. The concentration of HDOΦP, so chosen that the measured *K* values fell between 0·1 and 10, was kept fixed throughout the determinations for a given curve. The *K* values were determined by both "direct" and "reverse" procedures, i.e. an aqueous phase containing radioactive M(III) was contacted with barren organic phase ("direct") and an organic phase containing radioactive M(III) was contacted with barren aqueous phase ("reverse"). Duplicate assays of each phase were made. The average of these four determinations was used in calculating the *K* values.

In a similar fashion, a series of aqueous solutions 1·0 M in H^+ and 1·0 M in combined perchlorate and nitrate ions was used in the determination of nitrate complexity constants.

(3) D. F. Peppard, J. R. Ferraro and G. W. Mason, *J. Inorg. Nucl. Chem.* **7**, 231 (1958).

(4) D. F. Peppard, G. W. Mason and S. McCarty, *J. Inorg. Nucl. Chem.* **13**, 138 (1960).

(5) D. F. Peppard, G. W. Mason and S. W. Moline, *J. Inorg. Nucl. Chem.* **5**, 141 (1957).

(6) D. F. Peppard, G. W. Mason, J. L. Maier and W. J. Driscoll, *J. Inorg. Nucl. Chem.* **4**, 334 (1957).

(7) D. F. Peppard, G. W. Mason and I. Hucher, *J. Inorg. Nucl. Chem.* **18**, 245 (1961).

RESULTS AND CONCLUSIONS

The extraction of M(III) lanthanides and actinides in the HDOΦP (in toluene diluent) vs. an aqueous perchlorate phase system has been represented[(2)] as:

$$M^{3+}_{A}+3(HDO\Phi P)_{2_0} \rightleftharpoons M[H(DO\Phi)_2]_{3_0}+3H^{+}_{A} \qquad (1)$$

In this previous study,[(2)] Expression (1) was proved applicable to aqueous perchlorate phases and specifically to La, Pm, Y, Sc, Ac and Am. The distribution ratio, *K*, for M(III) is thus expressed[(2)] as:

$$K = k_1[(HDO\Phi P)_2]^3_0/[H^+]^3_A \qquad (2)$$

The present work extends the investigation to aqueous chloride and nitrate phases and to other lanthanides(III). The absolute *K* values are not in complete agreement with previous data,[(2)] but the dependencies remain unchanged.

Since all points used in determination of a given stability constant were obtained at a fixed extractant concentration, knowledge of the extractant dependency is not necessary in interpreting the data. Consequently, although extraction dependency data were obtained for Pr and Tm in 1 M $HClO_4$, 1 M HCl and 1 M HNO_3 and the extraction dependency shown to be third-power, the curves are not presented here. However, it is imperative that an inverse third-power hydrogen ion dependency be proved in order to establish the absence of ClO_4^-, Cl^- or NO_3^- in the M(III) extracted

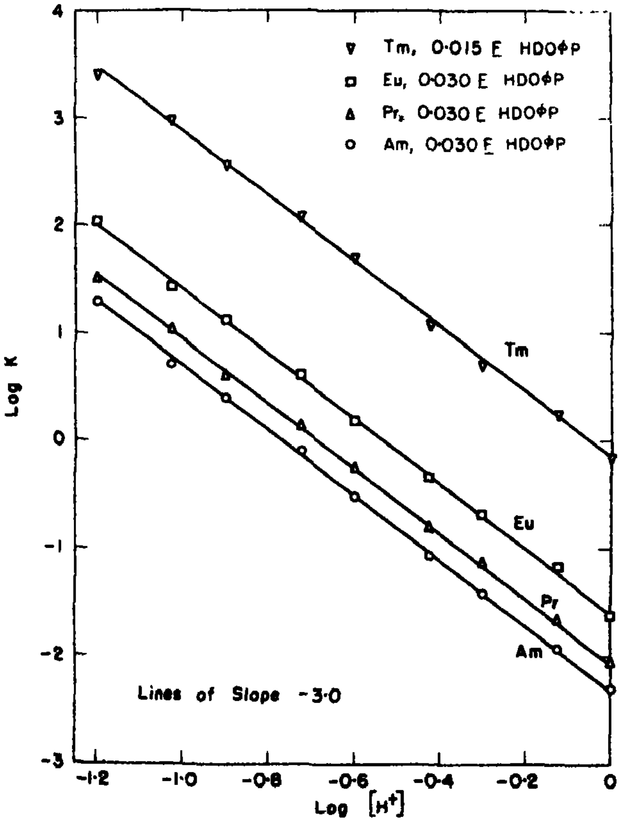

FIG. 1.—Hydrogen ion dependency of the extraction of M(III) into HDOΦP (toluene) from HCl + NaCl, $\mu = 1{\cdot}0$.

species. Therefore, acid-dependency data were obtained for each of the M(III) elements studied in ClO_4^-, Cl^- and NO_3^- aqueous phases, using the appropriate sodium salt to maintain unit ionic strength. In each case, the expected inverse third-power hydrogen ion dependency was observed throughout the range 0·063–1·00 *M* H^+. The data for Pr, Eu, Tm and Am are considered typical and are presented in Figs. 1 and 2 for the chloride and nitrate systems, respectively.

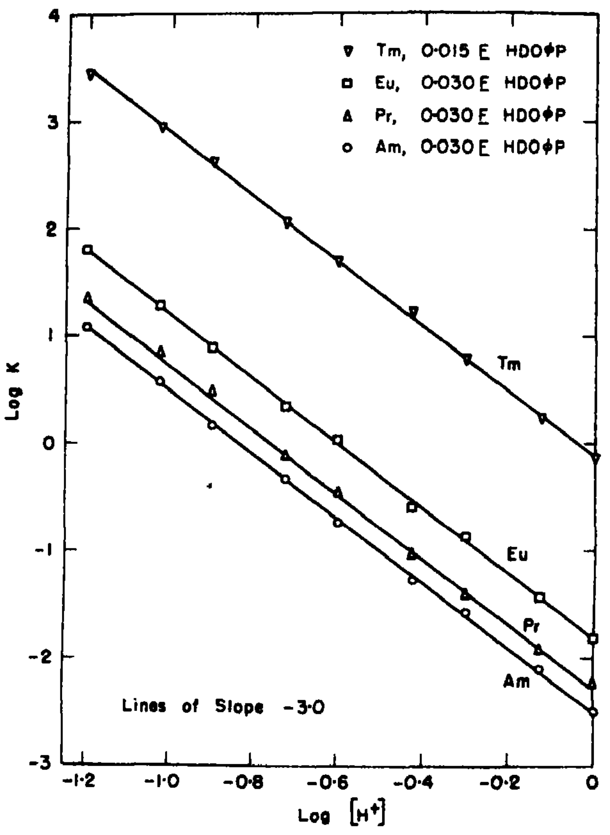

Fig. 2.—Hydrogen ion dependency of the extraction of M(III) into HDOΦP (toluene) from $HNO_3 + NaNO_3$, $\mu = 1·0$.

The variation of *K* with concentration of X^- in an HDOΦP (fixed concentration in toluene) vs. 1·00 M ($HClO_4 + HX$) system was then determined for each M(III) element studied. The Pr, Eu, Tm and Am data are considered representative and are presented in Figs. 3 and 4 for the perchlorate–chloride and perchlorate–nitrate systems, respectively. The plot of $1/K$ vs. M of X^- is represented acceptably well by a straight line, and from the slope and zero intercept the value of the stability constant of MX^{2+} may be calculated. In practice, k_c in each instance was obtained by a least-squares analysis of the data.

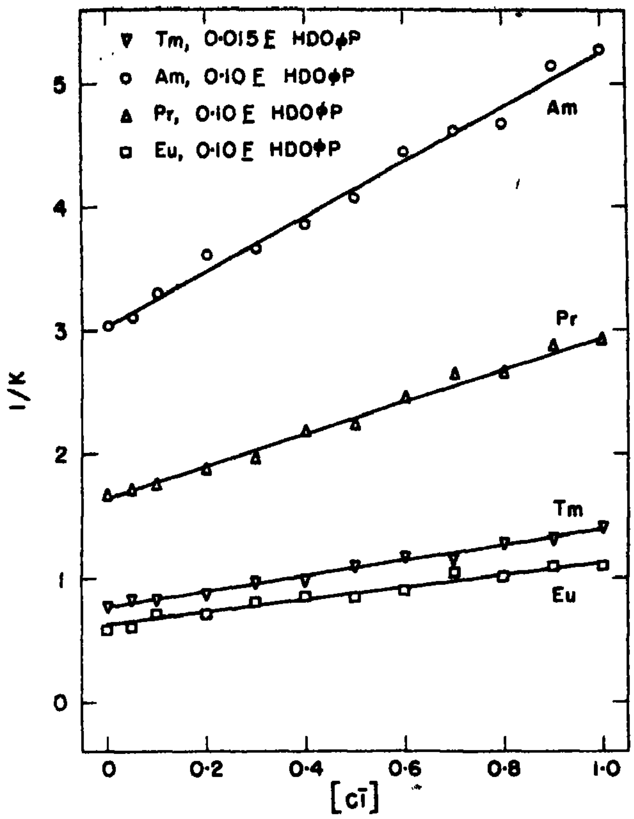

FIG. 3.—Variation of $(1/K)$ for M(III) with $[Cl^-]$ in $HClO_4 + HCl$, $\mu = 1·0$.

The calculated stability constants, k_c, for the MX^{2+} ions are presented in Table 1. Comparative data from other sources are given in Table 2.

TABLE 1.—STABILITY CONSTANTS FOR MX^{2+}, $\mu = 1·00$, 22 ± 1° C

	k_c for MX^{2+}	
M(III)	$X^- = Cl^-$	$X^- = NO_3^-$
La	0·9 ± 0·3	1·3 ± 0·3
Ce	0·9 ± 0·3	1·3 ± 0·3
Pr	0·9 ± 0·3	1·7 ± 0·3
Eu	0·9 ± 0·3	2·0 ± 0·3
Tm	0·8 ± 0·3	0·7 ± 0·2
Yb	0·6 ± 0·2	0·6 ± 0·2
Lu	0·4 ± 0·2	0·6 ± 0·2
Am	0·9 ± 0·2	1·8 ± 0·3

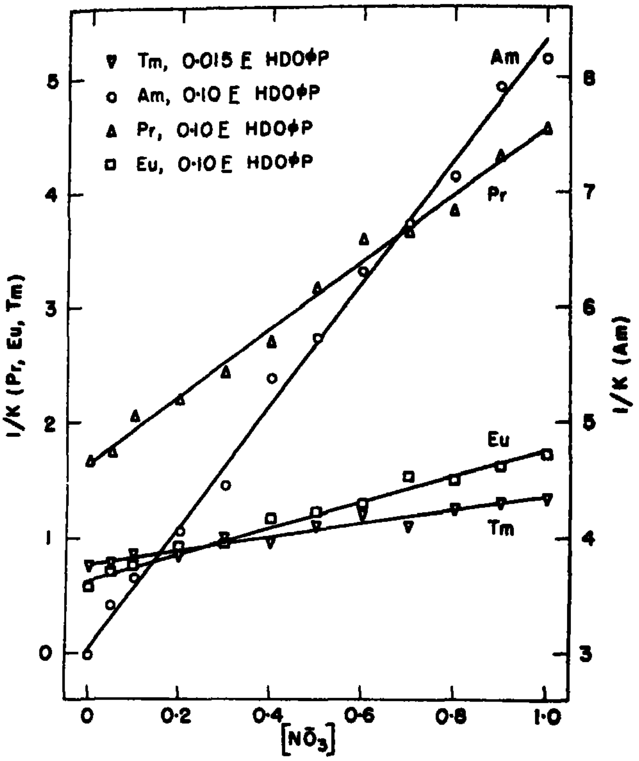

Fig. 4.—Variation of (1/*K*) for M(III) with [NO_3^-] in $HClO_4 + HNO_3$, $\mu = 1{\cdot}0$.

Table 2.—Comparative stability constants for MX^{2+} from other studies*

M(III)	X^-	μ	k_c for MX^{2+}	Reference
Pu	Cl^-	0·5	1·7	8
	Cl^-	1·0	0·9	8
Am	Cl^-	0·5	1·7	8
	NO_3^-	1·0	4·0	9
Ce	Cl^-	0·6	1·25	10
	Cl^-	1·0	1·73	10
	NO_3^-	~ 0·9	1·4	10
	NO_3^-	?	11 ± 2·5	11
Lu	Cl^-	0·1	28	12

* References 8, 9, 11: no temperature given, so "room temperature" is assumed. References 10 and 12: 25 ± 0·5° C and 20° C, respectively.

---

(8) M. Ward and G. A. Welch, *J. Inorg. Nucl. Chem.* **2**, 395 (1956).

(9) I. A. Lebedev, S. V. Pirozhkov and G. N. Yakovlev, *Akad. Nauk. S.S.S.R.*, Ordena Lenina Institut Atomnoi Energii. United States Atomic Energy Commission Translation, AEC-Tr-4275.

(10) R. E. Connick and S. W. Mayer, *J. Amer. Chem. Soc.* **73**, 1176 (1951).

(11) V. V. Fomin, R. E. Kartushova and T. I. Rudenko, *Zh. Neorg. Khim.* **3**, 2117 (1958); Quoted from *Chem. Abstr.* **53**, 11953 g.

(12) E. J. Wheelwright, F. H. Spedding and G. Schwarzenbach, *J. Amer. Chem. Soc.* **75**, 4196 (1953).

DISCUSSION

As has been pointed out by investigators utilizing the thenoyl trifluoroacetone (HTTA) extraction technique in determining ThX^{3+} stability constants[13] if only the "first" complex is of importance a simple relationship between K and $[X^-]$ exists and the k for the complex may be obtained by graphical or equivalent procedures. For the M(III) extraction, the K of Expression (1) becomes;

$$K = k_1[(HDO\Phi P)_2]^3/\{[H^+]^3(1+k_c[X^-])\} \tag{3}$$

Setting $[X^-]$ equal to zero, dividing the resulting expression for K_O (i.e. only perchlorate, no X^-) by Expression (3) and rearranging terms yields;

$$1/K = 1/K_O+(k_c/K_O)[X^-] \tag{4}$$

Consequently, from a plot of $1/K$ vs. $[X^-]$ the slope plus the intercept serve to evaluate k_c.

In considering the k_c values of Table 1 it should be remembered that concentration, not activities, have been employed and that $[H^+]^3$, which does not appear in Expression (4) because it was cancelled in the derivation, may be cancelled legitimately only if "1·00 M H^+" has the same effect upon the extraction mechanism in the presence of 1·00 M ClO_4^-, 1·00 M X^-, and the various 1·00 M $(ClO_4^-+X^-)$ mixtures.

It is doubtful whether the cancellation of the $[H^+]^3$ term may be justified completely. However, in comparing results obtained by this technique with those obtained by an ion-exchange technique it should be realized that the same cancellation of "hydrogen ion dependency" is involved in the two approaches. In the ion exchange method, CONNICK and MAYER[10] found it necessary to correct for the adsorption of $CeCl^{2+}$ by the resin. No analogous correction for extraction of MX^{2+} was required in the present study.

The extraction of neutral MX_3 may also be used in the determination of the stability constant of MX^{2+}, etc., the stoicheiometry of extraction of Ce(III) from an aqueous nitrate phase into a tributyl phosphate (TBP) in carrier diluent phase being represented as:

$$Ce^{3+}_A+3NO^-_{3A}+3TBP_0 \rightleftharpoons Ce(NO_3)_3(TBP)_{30} \tag{5}$$

$$Ce^{3+}_A+NO^-_{3A} \rightleftharpoons Ce(NO_3)^{2+}_A \tag{6}$$

$$K = k_5[NO_3^-]^3_A[TBP]^3_0(1+k_c[NO_3^-])^{-1} \tag{7}$$

in the NO_3^- concentration range in which $Ce(NO_3)^{2+}$ is the only complex of importance. A plot of $(1/K)[NO_3^-]^3_A[TBP]^3_0$ vs. $[NO_3^-]$ then serves to evaluate k_c. In this instance, the major concerns are whether the extrapolation to zero concentration of NO_3^- is sufficiently precise and whether "mixed species", for example $Ce(ClO_4)(NO_3)_2(TBP)_3$ etc., may be extracting from solutions of constant μ. Further, if appreciable concentrations of HNO_3 are employed the tendency of HNO_3 to extract into the TBP phase, thereby lowering the concentration of free TBP, must also be considered and suitable corrections made.

---

[13] (a) R. A. DAY, JR. and R. W. STOUGHTON, *J. Amer. Chem. Soc.* **72**, 5662 (1950);
(b) E. L. ZEBROSKI, H. W. ALTER and F. K. HEUMANN, *J. Amer. Chem. Soc.* **73**, 5646 (1951); and
(c) W. C. WAGGENER and R. W. STOUGHTON, *J. Phys. Chem.* **56**, 1 (1952).

It is evident that each of these three techniques for determining k_c for MX^{2+}: ion exchange, extraction of M^{3+} and extraction of MX_3 is inherently incapable of yielding extremely trustworthy values from a thermodynamic viewpoint. However, the method presently employed serves to fix the k_c values within reasonable limits upon the assumption that the activity of 1·0 M H^+ is unaffected as perchlorate ion is replaced by an equivalent amount of nitrate (or chloride) ion in a 1·0 μ solution.

From a comparison of the WARD and WELCH(8) data of Table 2 for $PuCl^{2+}$ and $AmCl^{2+}$, the k_c for $AmCl^{2+}$ at $\mu = 1·0$ may be estimated as 0·9 with which the value of Table 1 is in agreement. The LEBEDEV *et al.*(9) value of 4·0 for the k_c of $Am(NO_3)^{2+}$, obtained by an ion exchange method, is to be compared with 1·8 of Table 1. The k_c for $CeCl^{2+}$ of Table 1 is smaller by a factor of 1·7 than that reported by CONNICK and MAYER,(10) Table 2, but that for $Ce(NO_3)^{2+}$ is in essential agreement with that of these investigators. However, the value of k_c for $Ce(NO_3)^{2+}$ reported by FOMIN *et al.*,(11) presumably not determined at constant μ, is considerably higher than the value presently reported. The value of twenty-eight reported for the stability constant of $LuCl^{2+}$ ($\mu = 0·1$) by WHEELWRIGHT *et al.*(12) can not be compared directly with the value of Table 1 ($\mu = 1·0$).

It is suggested that the technique of extraction by HDOΦP, or similar phosphates or analogous phosphonates and phosphinic acids may be applied to the determination of stability constants of MX^{b+} etc. under conditions such that application of ion exchange techniques or of other liquid–liquid extraction techniques might not prove applicable due to hydrolysis difficulties, adsorption of complex species, extraction of "mixed species", etc.

J. Inorg. Nucl. Chem., 1962, Vol. 24, pp. 889 to 897. Pergamon Press Ltd. Printed in England

AQUEOUS SYSTEMS AT HIGH TEMPERATURE—VI
INVESTIGATIONS ON THE SYSTEM NiO–SO_3–H_2O AND ITS D_2O ANALOGUE FROM 10^{-4} TO 3 m SO_3, 150–450° C*†

WILLIAM L. MARSHALL, JAMES S. GILL and RUTH SLUSHER

Reactor Chemistry Division, Oak Ridge National Laboratory, Oak Ridge, Tennessee

(*Received* 24 *November* 1961)

Abstract—The condensed system NiO-SO_3-H_2O and its D_2O analogue were investigated at concentrations of SO_3 from 10^{-4} to 3 molal and at temperatures from 150 to 450° C. Liquid phase compositions and temperatures were established over which $NiSO_4 \cdot H_2O$ or its D_2O analogue, some partially identified nickel-oxy-sulphates, and $Ni(OH)_2$ were stable solids. Concentrations of NiO as high as 0·2 molal in 2·0 molal SO_3 were observed at temperatures above 374° in the super-critical fluid SO_3-H_2O.

Combined results showed that all solids increased in solubility upon increasing the concentration of SO_3 in the liquid phase but exhibited negative temperature-coefficients of solubility at constant molality of SO_3. Stoicheiometric solutions of $NiSO_4$ were unstable. These solutions precipitated either one or two solids—nickel-oxy-sulphates, $Ni(OH)_2$, or $NiSO_4 \cdot H_2O$—in order to reach equilibrium conditions.

At temperatures between 250° and 350°, $NiSO_4 \cdot D_2O$ showed between 5 and 25 per cent higher solubilities in D_2SO_4-D_2O solutions of moderately high acid concentrations than the corresponding hydrate in H_2SO_4-H_2O solutions. To the best of our knowledge, the reverse relation always has been observed for stoicheiometric salts dissolved only in the solvent.

AT temperatures between 100° and 350°, $NiSO_4$ appears in aqueous homogeneous reactor fuels of UO_2SO_4, D_2SO_4, and D_2O⁽²⁾ as a corrosion product of stainless steel used as a container material. In order to have a broad knowledge of the phase behaviour of separate reactor fuel components it was desirable to investigate the system NiO–SO_3–H_2O and its D_2O analogue at some temperatures between 100° and 450° and at widely varying concentrations of SO_3.

The system $NiSO_4$–H_2SO_4–H_2O was studied previously by others at temperatures up to 100°.(3, 4, 5) For the range 100–205°, BENRATH reported temperatures for the start of precipitation, upon heating, from solutions of various concentrations of nickel sulphate;⁽⁶⁾ the observations defined an "aufscheidungskurve" which, according to BENRATH, is distinctly above the (unknown) true solubility curve.

---

* This paper is based upon work performed at Oak Ridge National Laboratory, which is operated by Union Carbide Corporation for the Atomic Energy Commission.

† Previous paper in series: "Distribution of CuO and NiO Components in the Two-Liquid Phase Region of the System UO_3-SO_3-H_2O and its D_2O Analogue, 300–350° C."(1)

(1) E. V. JONES and W. L. MARSHALL, *J. Inorg. Nucl. Chem.* 23, 295–303 (1961).

(2) H. F. MCDUFFIE, *Properties of Aqueous Fuel Solutions* in *Fluid Fuel Reactors* (Edited by J. A. LANE, H. G. MACPHERSON and F. MASLON), Chap. 3, pp. 85–127. Addison-Wesley, Reading, Mass. (1958).

(3) R. ROHMER, *Ann. Chim.* 11, 611–725 (1939).

(4) A. W. BABAJEWA and E. I. DANILUSCHKINA, *Z. Anorg. Chem.* 226, 338–40 (1936).

(5) C. MONTEMARTINI and L. LOSANA, *L'Industria Chimica*, 4, 199–205 (1929).

This paper presents solubilities obtained by the direct sampling procedure of solids in the system $NiO–SO_3–H_2O$, as well as some comparative solubilities in the system $NiO–SO_3–D_2O$, at solution concentrations between 10^{-4} and 3 molal SO_3 and at temperatures between 150 and 350°. Some concentrations of NiO soluble in the supercritical fluid $SO_3–H_2O$ above 374° are presented.

EXPERIMENTAL PROCEDURES

The experimental procedures were generally the same as described previously⁽⁷⁾ although in this study, C.p. $NiSO_4·7H_2O$ rather than $NiSO_4·H_2O$ was used as a starting material. Also, another reagent, $Ni(OH)_2$, was prepared by precipitation from a $NiCl_2$-H_2O solution (made from C.p. $NiCl_2$) using NH_4OH as the precipitating agent. The precipitate was washed extensively with "CO_2-free" distilled water until all chloride was removed. In the preparation of D_2O solutions the addition of H_2O_2 increased the H_2O content of the solvent from 0·3 per cent (value obtained by an improved analysis of the D_2O; previously reported in paper IV as 2 per cent) to approximately 5 per cent.

The pressure vessels were of an advanced design and were capable of being used at temperatures up to 500°. These are described in detail elsewhere.⁽⁸⁾ Eight of these vessels, each containing different solution and solid mixtures, were sealed and placed in the furnace. After the control temperature was reached these vessels containing the mixtures were rocked for periods varying from 2 to 36 hr before sampling. Equilibration was allowed to continue at the same temperature or at higher or lower temperatures for later samplings. After these procedures the vessels were cooled and the solids removed in the manner described previously.⁽⁷⁾

Equilibration was substantiated by: (1) observing approximate rates of approach to equilibrium in sealed tubes using the synthetic method,⁽⁹⁾ (2) duplicating results on subsequent samplings at constant temperature, and (3) observing reversal of equilibrium upon reaching constant temperature from both lower and higher temperatures. Reversibility of equilibrium was observed to occur within 2 hr at concentrations in the region of stability for $NiSO_4·H_2O$ provided that no induction period for precipitation of solids was involved in the process. An induction period was sometimes observed when only a solution phase was added initially to a pressure vessel.

Some critical temperatures (at which the meniscus between vapour and liquid phases disappears) and some exploratory boundary limits of temperature and composition for precipitation of $NiSO_4·H_2O$ were determined using the synthetic method described previously.⁽⁹⁾ Fused silica capillary tubes containing approximately 50 per cent volume filling of solution at 25° and 60 to 80 per cent filling at the temperature of phase disappearance or transition were used for these experiments. Considerable super-saturation by $NiSO_4·H_2O$ was observed upon increasing the temperature, but upon slowly lowering the temperature after the solid phase had appeared approximate limits of solubility were established.

Analyses of the solutions for NiO and SO_3 components were made either by acid–base titration or by direct measurements of pH on volumetric samples. The use of the particular method depended on the range of concentration of the component. As a rule, acid–base titrations were used for determining concentrations of components above 0·05 molal. Preliminary titrations on mixtures of $NiSO_4$ and H_2SO_4 in H_2O solution showed that $NiSO_4$ would not affect appreciably the sharpness of the endpoint for excess H_2SO_4. Excess acid was determined in that manner. All nickel was removed from a second sample by washing the

---

⁽⁶⁾ A. BENRATH, *Z. Anorg. Chem.* **247**, 147–60 (1941).

⁽⁷⁾ W. L. MARSHALL and J. S. GILL, *J. Inorg. Nucl. Chem.* **22**, 115–132 (1961).

⁽⁸⁾ J. S. GILL and W. L. MARSHALL, *Rev. Sci. Instrum.* **32**, 1060 (1961).

⁽⁹⁾ C. J. BARTON, G. M. HEBERT and W. L. MARSHALL, *J. Inorg. Nucl. Chem.* **21**, 141–151 (1961).

sample through a cation exchanger column containing Dowex-50.(10) The eluent was titrated for SO_3. The molar concentration of the NiO component was determined by difference.

A vibrating-reed electrometer in conjunction with a Rubicon potentiometer was used to make direct measurements of pH (at 25°) for concentrations below 0·05 molal.(11) Control curves were determined by measuring the pH of NiO-SO_3-H_2O solutions at constant molar or molal ratio, m_{NiO}/m_{SO_3}, as a function of the concentration of excess H_2SO_4 (Table 1). At molal ratios, m_{NiO}/m_{SO_3}, of 0·8 or lower, the pH curves drawn from the data corresponded closely to the pH curve for H_2SO_4 in H_2O. A pH measurement was made on the original sample which, by the use of the curves, thus gave an approximate concentration of excess H_2SO_4. Nickel was removed from another sample of the same solution by means of the cation exchanger column and the eluent was diluted to a known volume. A pH measurement of the diluted sample now containing only H_2SO_4 and H_2O gave the concentration of H_2SO_4 which upon using the aliquot factor gave the concentration of total SO_3 in the original sample. An approximate molal ratio, m_{NiO}/m_{SO_3}, was then found which, by means of the curves, was used to obtain a better value for the concentration of excess H_2SO_4 and subsequently for the molal ratio. It was only necessary to repeat this procedure one or two times to get a constant value for the NiO and SO_3 concentrations as low as 10^{-4} molal which were reproducible to ±1 per cent.

TABLE 1.—THE pH AT 25° C OF H_2O SOLUTIONS OF $NiSO_4$ AND H_2SO_4

M_{NiO}/M_{SO_3}: H_2SO_4 (M)	0·000	0·500	0·800	0·870	0·907	0·950
0·1022	1·000	1·083	1·185			
0·0337	1·414	1·477	1·598			
0·01022	1·858	1·907	2·006	2·049	2·075	2·134
0·00337	2·277	2·308	2·375			
0·001022	2·757	2·771	2·811	2·834	2·855	2·896
0·000337	3·211	3·223	3·250			
0·0001022	About 3·75					

In order to convert molar to molal concentrations, densities (at 25° C) were determined for two series of solutions, one series containing 1·5 molar excess sulphuric acid and another series containing 0·75 molar excess acid, both for H_2O and D_2O solutions (Table 2—densities of D_2O solutions corrected slightly for H_2O impurity). With molal:molar ratios calculated from these densities, these ratios were plotted against the excess molarity of sulphuric acid. The curves showed a major dependency on $M_{H_2SO_4}$ but a minor dependency on M_{NiSO_4}, and with these curves it was relatively easy to make the conversion.

RESULTS AND DISCUSSION

General. All solubility data obtained by the direct sampling procedure for the system NiO–SO_3–H_2O are plotted in Fig. 1 as the saturation molal ratio, m_{NiO}:m_{SO_3}, defined as R_{Ni} and equal to the number of moles of NiO component present for each mole of SO_3 component, against the logarithm of the SO_3 molality.

Curves for solubilities at temperatures from 150 to 350° are shown. The concentration of the NiO component at saturation is obtained by multiplying R_{Ni} by the selected molality of SO_3. Values of R_{Ni} lower than those along a curve at constant temperature represent unsaturated solutions. The solubility of solid phases decreases as the temperature increases at constant molality of SO_3. It is likely that this general behaviour may apply to the solubility of many metallic sulphates and metallic oxide solids in aqueous sulphate systems at high temperature.

---

(10) H. O. DAY, E. V. JONES, J. S. GILL and W. L. MARSHALL, *Analyt. Chem.* **26**, 611 (1954).
(11) W. L. MARSHALL, *Analyt. Chem.* **27**, 1923 (1955).

Table 2.—The densities and m/M ratios at 25° ± 1° C for H_2O and D_2O solutions of $NiSO_4$ in sulphuric acid

H₂O solutions				D₂O solutions			
$M_{H_2SO_4}$	M_{NiSO_4}	Density (g/cm³)	m/M	$M_{D_2SO_4}$	M_{NiSO_4}	Density (g/cm³)	m/M
1·491	1·254	1·270$_5$	1·076	1·488	1·254	1·371$_3$	0·975
1·491	1·148	1·256$_0$	1·074	1·496	1·148	1·356$_1$	0·974
1·494	1·045	1·241$_2$	1·073	1·496	1·045	1·342$_1$	0·972
1·488	0·918	1·224$_3$	1·070	1·496	0·918	1·323$_8$	0·970
1·488	0·808	1·208$_6$	1·068	1·494	0·808	1·308$_3$	0·969
1·491	0·660	1·187$_5$	1·066	1·491	0·660	1·287$_0$	0·967
1·491	0·548	1·170$_9$	1·065	1·491	0·548	1·271$_4$	0·966
0·745	0·627	1·141$_9$	1·029	0·744	0·627	1·242$_2$	0·935
0·745	0·574	1·134$_4$	1·029	0·748	0·574	1·233$_6$	0·935
0·747	0·522	1·126$_6$	1·029	0·748	0·522	1·226$_6$	0·935
0·744	0·459	1·116$_7$	1·029	0·748	0·459	1·217$_1$	0·935
0·744	0·404	1·109$_5$	1·027	0·747	0·404	1·211$_2$	0·932
0·745	0·330	1·098$_6$	1·027	0·745	0·330	1·200$_9$	0·931
0·745	0·274	1·089$_5$	1·027	0·745	0·274	1·192$_3$	0·931

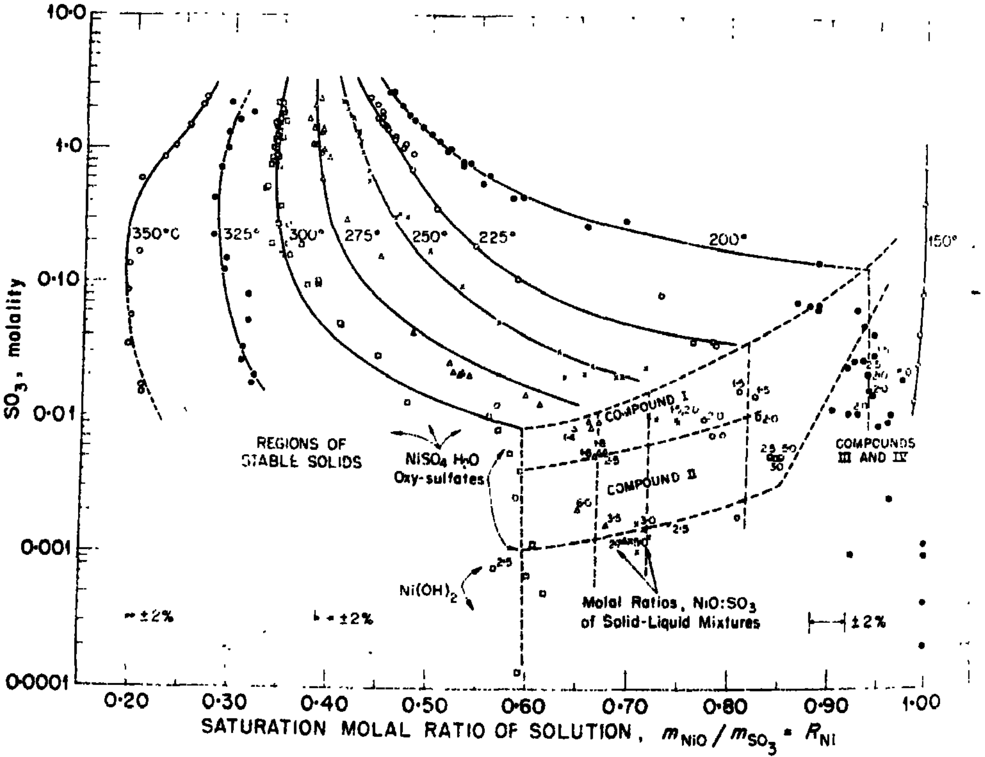

Fig. 1.—The system NiO-SO_3-H_2O, 150–350° C.

Regions of stability of solid phases. The solids, $NiSO_4 \cdot H_2O$ and $Ni(OH)_2$, specified as stable phases in Fig. 1, were identified by comparison of X-ray diffraction patterns of the solids removed from the pressure vessels after a run with those known for these compounds. Powder-pattern, X-ray diffraction data were obtained (Table 3) for other solids, I, II, III, and IV, but these data could not be matched with any published values for nickel compounds. Presumably these other solids in the intermediate range of solution SO_3 concentrations were nickel-oxy-sulphates. In an attempt to determine approximate compositions of stable oxy-sulphates and to locate isothermal, ternary $L+2S$ points, several runs were made at temperatures from 200 to 300° with 0·3 to 3·0 g amounts of solid mixtures of molal ratios, $NiO:SO_3$ varying from 1:1 to 6:1. These mixtures were shaken with 25 ml of H_2O at constant temperature. The gramme amounts of solid for each run were chosen in order that the relative change in the molal ratio of each solid mixture would be very small and negligible after attainment of equilibrium; but the X-ray examination of the residual solids showed that complete equilibrium with respect to solid transformations had not always been reached. Nevertheless, at temperatures between 225° and 300° an examination of the relative solution-composition groupings (see Fig. 1), as well as the X-ray diffraction data, with respect to the initial composition of mixtures, favoured

TABLE 3.—DEBYE-SCHERRER POWDER PATTERNS FOR SOLIDS I, II, III, AND IV (CuK$_{\alpha}$ RADIATION)

I		II		III		IV	
*i**	*d*	*i**	*d*	*i**	*d*	*i**	*d*
s^{-}	7·10	*f*	10·00	*s*	10·10	*f*	7·75
f	6·30	*s*	5·25	*vf*	6·20	*s*	6·70
m	5·70	*vvf*	3·42	*f*	5·40	*m*	5·05
f	4·70	*vf*	3·20	s^{-}	5·10	m^{-}	3·82
f^{+}	4·33	*vvf*	2·85	f^{+}	4·65	*f*	3·37
s	4·00	*m*	2·74	*f*	4·05	f^{+}	2·93
f	3·80	m^{+}	2·62	f^{-}	3·80	*f*	2·73
vf	3·60	*f*	2·42	*m*	3·40	*vvf*	2·62
vf	3·52	*f*	2·27	*vf*	3·28	*f*	2·56
f^{+}	3·39	*vvf*	2·18	*f*	3·09	f^{-}	2·49
f^{+}	3·22	m^{-}	2·09	*vvf*	2·92	f^{-}	2·42
f	3·07	*vvf*	1·90	*m*	2·70	m^{+}	2·22
m^{+}	2·92	*f*	1·75	m^{-}	2·62	*vvf*	2·05
m^{+}	2·86	m^{-}	1·60	*f*	2·55	f^{+}	1·98
f	2·80			*m*	2·50	f^{+}	1·96
f^{+}	2·76			*f*	2·43	f^{-}	1·86
m^{-}	2·64			*f*	2·38		
m^{-}	2·47						

where

*i** = Relative Intensity
s = Strong
m = Medium
f = Faint
vf = Very Faint
vvf = Very, Very Faint

two oxy-sulphates having a molal ratio, NiO:SO_3, near 1·5 for solid I and a ratio near 2·5 for solid II. For the 150° data the solid phases observed ranged from solid I for the two highest concentrations through III, IV and $Ni(OH)_2$ for the others.

Low precision in solubility data and in the identity of solid phases was evident in the regions of composition and temperature where $Ni(OH)_2$ and oxy-sulphates were the solids. It is possible, although the solution phases appeared to be saturated in less than 2 hr at constant temperature, that metastable nickel-oxy-sulphates or $Ni(OH)_2$ were incompletely converted to stable oxy-sulphates or $Ni(OH)_2$ thus resulting in low precision of the solubility data. Furthermore, the extreme dilution of the liquid phases and the fact that the solids, other than $NiSO_4 \cdot H_2O$, were not visibly crystalline made the collection of precise data difficult.

Solubility of $NiSO_4 \cdot H_2O$ *in* H_2SO_4–H_2O. Upon inspection of Fig. 1, it is apparent that stoicheiometric $NiSO_4$ is not stable in H_2O solution at temperatures of 200° and above, at least in the concentration ranges of this study, but hydrolyses to precipitate either an oxy-sulphate and insoluble $NiSO_4$, or one or two of an oxy-sulphate and $Ni(OH)_2$, depending upon the initial concentration. Excess H_2SO_4 must thus be in solution to prevent hydrolytic precipitation of solid phases.

If the compositions of liquid phases over which $NiSO_4 \cdot H_2O$ is a stable solid are expressed in terms of $NiSO_4$, H_2SO_4 and H_2O as the components, then the solubilities of $NiSO_4 \cdot H_2O$ may be plotted against the concentration of excess H_2SO_4. Such plots on linear scales are shown in Fig. 2 and define solubility curves at various

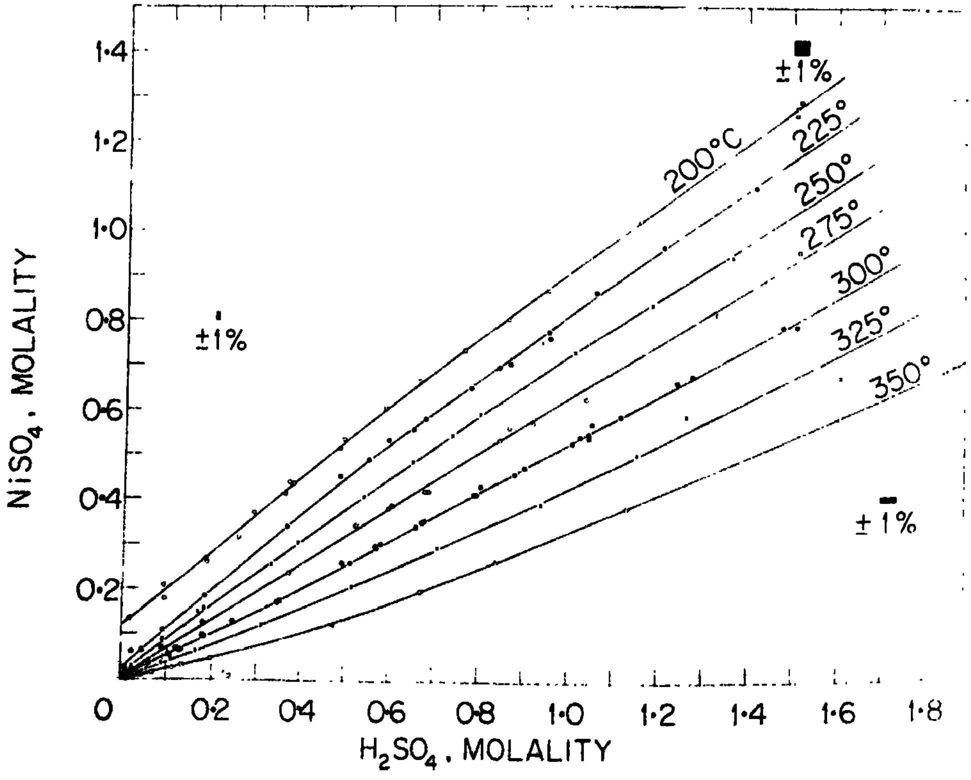

FIG. 2.—The solubility of $NiSO_4 \cdot H_2O$ in H_2SO_4-H_2O solutions, 200–350° C.

temperatures between 200 and 350°. The hypothetical solubility of $NiSO_4 \cdot H_2O$ in H_2O may be obtained by extrapolating these curves to zero concentration of excess H_2SO_4.

The solubility data for $NiSO_4 \cdot H_2O$ in H_2SO_4–H_2O solutions were treated by a computer technique involving a method of least squares and are expressed by an empirical equation. This equation is given in Table 4 together with the values for the coefficients, the number of observations, and the standard error of fit, defined as

$$\sqrt{\left[\frac{\sum(X_{\text{obs}}-X_{\text{calcd.}})^2}{n-(1+\text{no. of coefficients})}\right]}$$

at the different temperatures. The experimental precision of the data can be compared to the calculated curves in Fig. 2.

TABLE 4.—EQUATION AND COEFFICIENTS FOR THE SOLUBILITY OF $NiSO_4 \cdot H_2O$ IN H_2O_4-H_2O SOLUTION, 200–350° C
(APPLICABLE FOR RANGES OF DATA SHOWN IN FIG. 2)

$$m_{NiSO_4} = a_0 + a_1(m_{H_2SO_4}) + a_2(m_{H_2SO_4})^2 + a_3(m_{H_2SO_4})^3$$
where m = molality

T(° C)	$a_0 \times 10^3$	$a_1 \times 10$	$a_2 \times 10^2$	$a_3 \times 10^2$	Std. error of fit, molal units	No. of observations, n
200	+116·5	+8·513	−5·518	0	0·0100	21
225	+ 29·18	+8·680	−8·272	0	0·0106	21
250	+ 15·53	+7·647	−6·027	0	0·00519	17
275	+ 8·497	+6·113	+0·3607	0	0·00946	21
300	+ 4·109	+5·040	+1·773	0	0·00634	43
325	+ 1·181	+3·934	−0·7614	+3·899	0·00233	14
350	+ 2·085	+1·892	+18·61	−4·766	0·00222	15

Solubility of $NiSO_4 \cdot D_2O$ *in* D_2SO_4–D_2O. Solubilities of $NiSO_4 \cdot D_2O$ in D_2SO_4–D_2O solutions as a function of the concentration of excess D_2SO_4, as well as the comparative solubility curves for the H_2O system, are presented in Fig. 3. The solubilities are given in 100 per cent D_2O solvent, and were obtained by a linear extrapolation from the values in H_2O and those in D_2O solvent containing the 5 per cent H_2O impurity. The same empirical equation applies for these solubilities as for the analogous values in H_2O but the coefficients are different (Table 5).

The marked effect of sulphuric acid on the solubility of the monohydrate, both in H_2O and in D_2O, may be due in part to general ionic effect and in part to formation of HSO_4^- (as in Ag_2SO_4).(12) At the temperatures above 200°, a larger solubility (by about 5 to 25 per cent, depending upon concentration of excess acid and temperature) was found in D_2O–D_2SO_4 solutions. To the best of our knowledge, reported solubilities of stoicheiometric salts at low temperature are always lower in D_2O than in H_2O due to the effect of solvent. The interaction of ionic reactant and solvent effects may be observed in this study by comparison of the hypothetical solubility in water, represented approximately by the coefficient, a_0 (Tables 4 and 5).

(12) M. H. LIETZKE and R. W. STOUGHTON, *J. Phys. Chem.* **63**, 1188 (1959).

At constant temperature, this coefficient for the H_2O system is always larger than for the D_2O system. Thus, at the temperatures above 200° (Fig. 3), as the concentration of excess sulphuric acid approaches zero, there is a cross-over in the curves and the solubility in H_2O solution becomes larger than in D_2O solution.

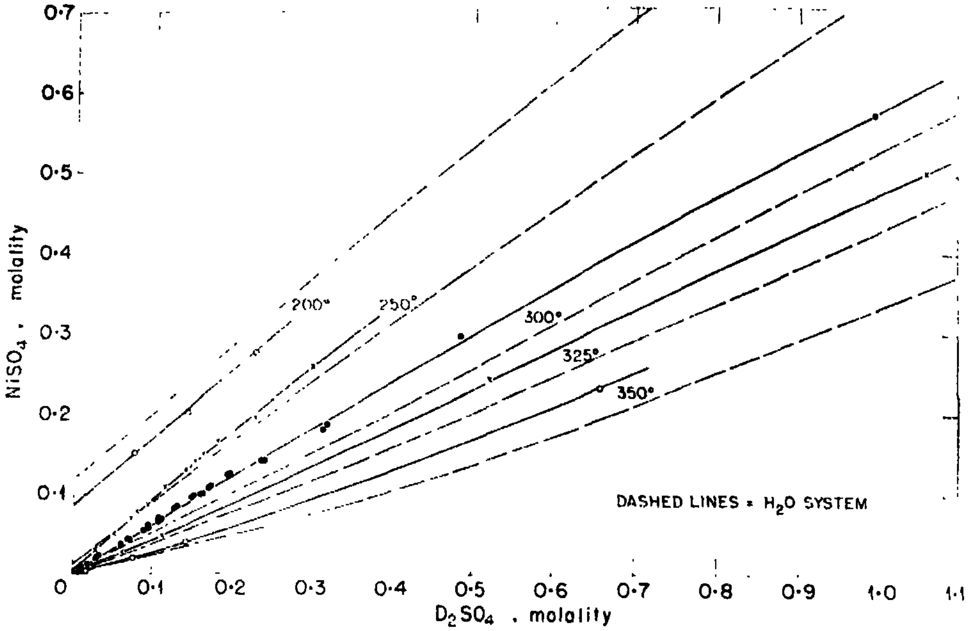

FIG. 3.—The solubility of $NiSO_4{\cdot}D_2O$ in D_2SO_4-D_2O solutions, 200–350° C.

TABLE 5.—EQUATION AND COEFFICIENTS FOR THE SOLUBILITY OF $NiSO_4{\cdot}D_2O$ IN D_2SO_4-D_2O SOLUTION, 200–350° C (APPLICABLE FOR RANGES OF DATA SHOWN IN FIG. 3)

$$m_{NiSO_4} = a_0 + a_1\,(m_{D_2SO_4}) + a_2\,(m_{D_2SO_4})^2$$
where m = molality

T(° C)	$a_0 \times 10^3$	$a_1 \times 10$	$a_2 \times 10^2$	Std. error of fit, molal units	No. of observations, n
200	+84·57	+8·182	0	0·00293	3
250	+ 4·040	+9·484	−35·54	0·00236	12
300	+ 3·232	+6·039	− 2·916	0·00374	31
325	+ 0·1710	+4·480	+ 2·620	0·00161	7
350	+ 0·9630	+2·453	+15·91	0·000476	6

Concentrations of NiO *in the supercritical fluid* SO_3–H_2O. In a study carried out with F. J. Smith,[*] concentrations of NiO were observed to be stable above 375° in supercritical SO_3–H_2O fluids. Also some phase-composition boundaries in the system NiO–SO_3-H_2O were determined by another method—the synthetic method—rather than the direct sampling method. In this exploration it was established that a region of liquid–liquid immiscibility did not exist, at least over the range

[*] Oak Ridge National Laboratory, Summer, 1960.

of concentration and temperature investigated. This finding was of interest since some other systems involving $SO_3(UO_2SO_4\text{-}H_2O,$[13] $UO_2F_2\text{-}H_2O,$[14] $UO_2SO_4\text{-}CuSO_4\text{-}H_2SO_4\text{-}H_2O,$[15] $UO_3\text{-}CuO\text{-}NiO\text{-}SO_3\text{-}H_2O$[1]) were found to show liquid-liquid immiscibility at temperatures between 285 and 375°.

In Fig. 4 temperatures at which a solid phase appeared or at which the meniscus between liquid and vapour phase disappeared (the critical temperature) are plotted against R_{Ni}. The concentration of SO_3 is constant along each curve. Critical temperatures at $R_{Ni} = 0$ were obtained by SECOY and STUCKEY.[16] The curves for solutions 0·5, 1·0, 2·0 and 3·0 molal in SO_3, drawn at temperatures up to 350° and extrapolated to higher temperatures, were derived from the solubility curves shown in Fig. 1. These values obtained by direct sampling are considered best since there is no possibility for supersaturation of the solution phase when solid is present and no assumption has to be made for the loss of components to the vapour phase.

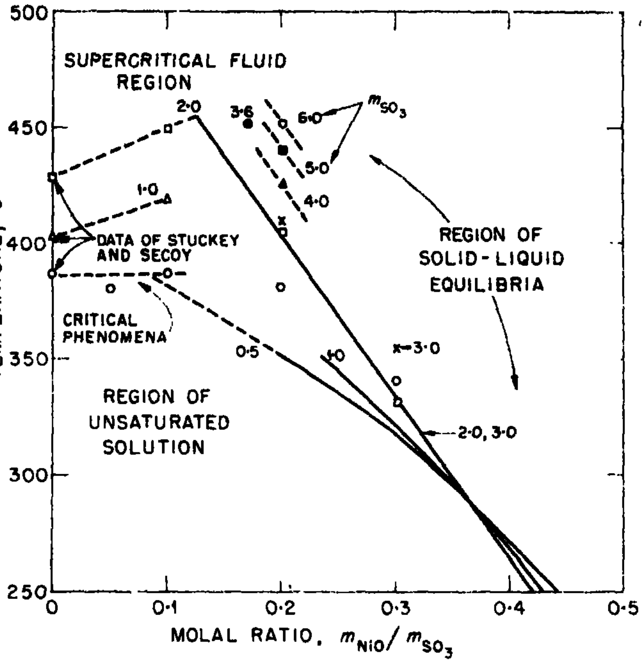

FIG. 4.—Solid-liquid phase boundaries and critical phenomena; system $NiO\text{-}SO_3\text{-}H_2O$.

Acknowledgements—The authors thank Professor J. E. RICCI, New York University, for his critical suggestions and advice during the course of this research and during the preparation of the manuscript. The help of M. H. LIETZKE, Chemistry Division, in applying computer techniques to the representation of the data is acknowledged. R. L. SHERMAN, Analytical Chemistry Division, obtained the X-ray diffraction data and differentiated the patterns for the various solid phases.

[13] C. H. SECOY, *J. Amer. Chem. Soc.* 72, 3343 (1950).

[14] W. L. MARSHALL, J. S. GILL and C. H. SECOY, *J. Amer. Chem. Soc.* 76, 4279 (1954).

[15] F. E. CLARK, J. S. GILL, R. SLUSHER and C. H. SECOY, *J. Chem. Engng. Data*, 4, 12 (1959).

[16] J. E. STUCKEY, Ph.D. Dissertation. The University of Oklahoma Graduate College, Norman, Oklahoma (1957).

J. Inorg. Nucl. Chem., 1962, Vol. 24, pp. 899 to 902. Pergamon Press Ltd. Printed in England

SOLUBILITY OF NEPTUNIUM(IV) PEROXIDE*

E. K. Dukes and G. A. Burney
Savannah River Laboratory, E. I. du Pont de Nemours & Co.,
Aiken, South Carolina

(*Received* 11 *September* 1961; *in revised form* 13 *December* 1961)

ALTHOUGH the properties of plutonium peroxide have been thoroughly studied, only a meager amount of data are available for neptunium peroxide. LA CHAPELLE *et al.*(1) report that a colourless to white flocculent precipitate of neptunium(IV) with a solubility of 100 mg per litre was formed in a 0·08 M HNO_3–3·0 M H_2O_2 solution. To our knowledge no systematic study has been published on the solubility or crystalline form of neptunium peroxide.

This paper describes the preparation of two crystalline forms of neptunium peroxide and presents data for the solubility of neptunium(IV) peroxide in nitric acid–hydrogen peroxide solutions.

EXPERIMENTAL

Reagents

Neptunium(IV) solution. A stock solution of pure neptunium(IV) was prepared by anion exchange. A 200 ml aliquot of 0·5 M nitric acid containing 5 g of neptunium was adjusted to 8·0 M nitric acid. The solution was made 0·05 M in ferrous sulphamate to reduce neptunium to the (IV) valence. The anionic nitrate complex of neptunium(IV) was absorbed on "Dowex" 1-X4 anion resin. The resin was washed with 8·0 M nitric acid and neptunium(IV) was eluted at about 35 g/l. with 0·35 M nitric acid containing 0·05 M hydrazine to maintain neptunium in the (IV) valence. The absence of other actinides was verified by an alpha energy analysis with an RCL 256 channel analyser, and the presence of neptunium(IV) was verified by spectrophotometric examination.(2)

Neptunium(IV) peroxide. Precipitates of neptunium(IV) peroxide were prepared in the following manner. An aliquot of the pure neptunium(IV) stock solution was added to a mixture of nitric acid and hydrogen peroxide to give a final composition of 2·0 M nitric acid–4·6 M peroxide. The mixture was agitated for 1 hr, then the peroxide precipitate was removed by filtration. The precipitate was washed with a solution of 2 M nitric acid–4·6 M hydrogen peroxide followed by an alcohol wash and air drying at 23°C.

Hydrogen peroxide. A 30 per cent solution of reagent-grade hydrogen peroxide that was stabilized with sodium stannate was used for all experiments.

Hydrazine. The hydrazine was a 35 per cent aqueous solution produced by Betz Laboratories and marketed under the trade name "Hyzeen".

Other reagents. All other reagents were prepared from reagent-grade chemicals.

---

* The information contained in this article was developed during the course of work under contract AT(07-2)-1 with the U.S. Atomic Energy Commission.

(1) T. J. LA CHAPELLE, L. B. MAGNUSSON and J. C. HINDMAN, *Radiochemical Studies: The Transuranium Elements* (Edited by G. T. SEABORG, J. J. KATZ and W. M. MANNING), NNES, Div. 14, Vol. 14 B, Paper 15.6, McGraw-Hill, New York (1949).

(2) R. SJOBLOM and J. C. HINDMAN, *J. Amer. Chem. Soc.* 73, 1744–51 (1951).

Procedures

Solubility. An aliquot of pure neptunium(IV) solution or a portion of solid neptunium peroxide was added to a small plastic bottle that contained a mixture of nitric acid and hydrogen peroxide of the desired concentrations. In each determination enough neptunium was added to ensure an excess of neptunium peroxide at equilibrium. The plastic bottle was placed on a mechanical shaker and agitated at 23°C and at regular intervals an aliquot of the sample was withdrawn for analysis. This aliquot was centrifuged and the concentration of neptunium was determined from the α-activity in the supernate. The concentration of nitric acid was determined by titration with standard sodium hydroxide, and the concentration of peroxide was determined by titration with standard potassium permanganate. Analyses were continued until the system reached equilibrium.

Crystalline structure. Determination of the crystalline structures was made from X-ray diffraction patterns. Precipitates were prepared by the method previously described except that each precipitate was prepared separately to obtain the desired variation in concentration for nitric acid and peroxide in the supernatant.

Peroxy-oxygen content. The peroxy-oxygen content of the neptunium peroxide was determined by titrating the I_2 produced in the reaction, peroxy-oxygen–iodide, with standard $Na_2S_2O_3$.

Samples of approximately 100 mg were dissolved in duplicate in 25 ml of 3 M $HClO_4$ containing 2 g of NaI. After 2 hr at room temperature the iodine produced was titrated with 0·1 N $Na_2S_2O_3$ to the starch endpoint. Examination of the absorption curve obtained with a Carey Model 11M spectrophotometer confirmed that the neptunium was in the (IV) valence state at the endpoint.

The titrated solution was then diluted in a volumetric flask and the neptunium concentration was determined by alpha counting.

RESULTS AND DISCUSSION

Preliminary studies showed that the neptunium(IV) peroxide precipitate was greyish purple and did not progress through the highly coloured, soluble peroxy complexes encountered in the precipitation of plutonium peroxide;⁽³⁾ however, two crystalline forms of neptunium peroxide were prepared that were quite similar to the two forms of plutonium peroxide found under similar conditions.⁽⁴⁾ The crystalline form found in solutions of low acidity (1·0 M HNO_3) was face-centered cubic ($a = 17$ Å), while that formed at higher acidity (3·0 M HNO_3) was nearly identical with the hexagonal form of plutonium peroxide. The hexagonal form, when added to dilute solutions of nitric acid, was not converted to the cubic form. When the cubic form was added to solutions of high acidity, it was converted to the hexagonal form.

The peroxy-oxygen to neptunium ratio in the two crystalline modifications was 2·9 for the cubic form and 3·3 for the hexagonal form, which compares to 3·04 and 3·34 reported for the two forms of plutonium peroxide.⁽⁴⁾

The solubility of neptunium peroxide at 23°C varied as a function of the concentration of nitric acid and hydrogen peroxide. Solubilities decreased with an inverse power dependence of approximately two on the concentration of hydrogen peroxide (Fig. 1). The solubility curve as a function of acid concentration divides into three parts (Fig. 2). In 0·08–0·5 M nitric acid, the solubilities were erratic but decreased with approximately an inverse first power dependence on acid concentration. Between 1·0 and 2·5 M nitric acid the solubility varied comparatively little with acid concentration, while at acid concentrations greater than 3 M the solubility increased with an approximate fourth power dependence.

⁽³⁾ R. E. CONNICK and W. H. MCVEY, *J. Amer. Chem. Soc.* **71**, 1534–42 (1949).

⁽⁴⁾ J. A. LEARY, Report, LA-1913 (1954).

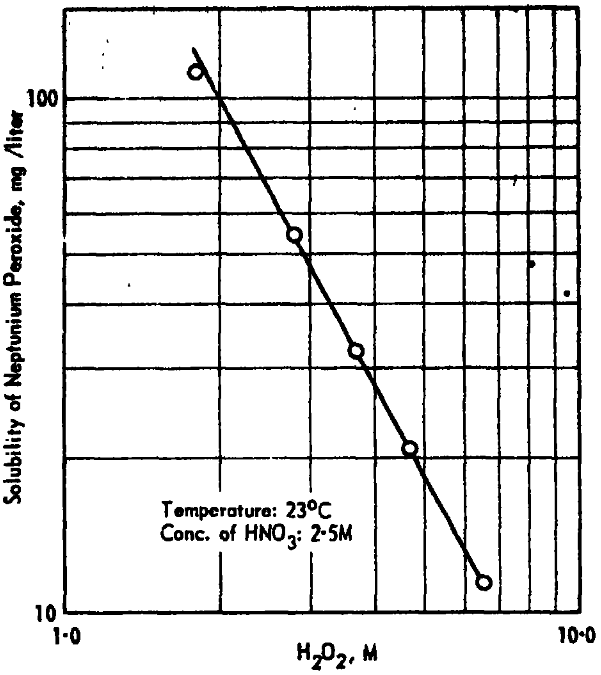

FIG. 1.—Solubility of neptunium peroxide as a function of hydrogen peroxide concentration.

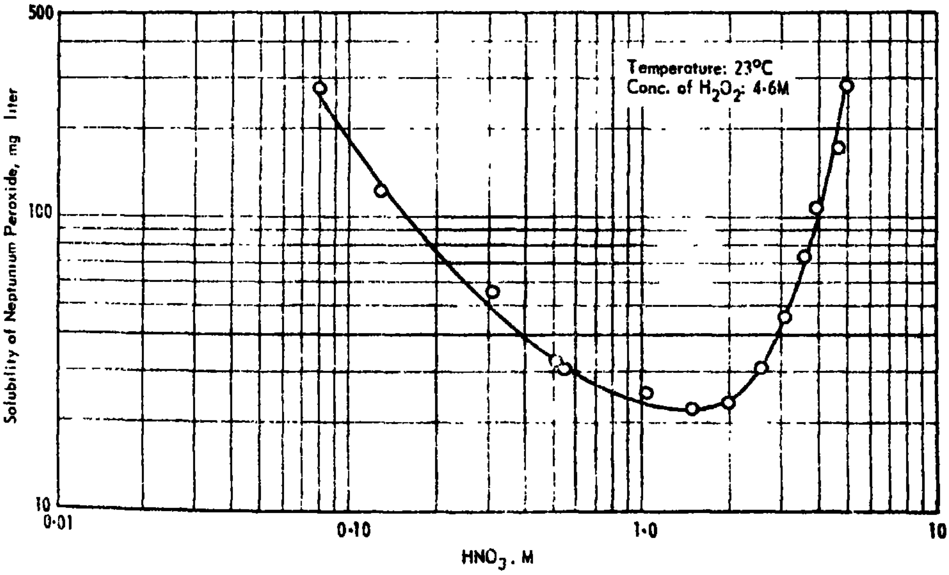

FIG. 2.—Solubility of neptunium peroxide as a function of nitric acid concentration.

Solubilities were reproducible only at acid concentrations greater than 2·5 M. In the range of 3–5 M acid the experimental data can be fitted reasonably well with the expression:

$$S = 9{\cdot}93 \frac{[H^+]^4}{[H_2O_2]^2}$$

where S is the neptunium concentration in mg per litre, and hydrogen ion and hydrogen peroxide are expressed in molar concentration. In fact, the fit obtained was much better than expected since activity coefficients were not considered.

A comparison of experimental and calculated solubilities is shown in Table 1.

TABLE 1.—SOLUBILITY OF NEPTUNIUM PEROXIDE AT 23°C

		Solubility (mg/l.)	
HNO_3 (M)	H_2O_2 (M)	Experimental	Calculated
2·6	4·6	30	21
3·1	4·6	46	43
3·6	4·6	72	79
3·8	4·6	108	98
4·7	4·6	218	229
5·0	4·6	282	293
2·5	1·8	113	120
2·5	2·8	54	49
2·5	3·7	32	28
2·5	4·7	21	18
2·5	6·5	11	9

The solubility data shown in Fig. 2 in the acid range 0·1–2·5 M are minimum values. Experimental solubilities in this range were erratic and often were two or three times greater than the values shown. The failure to obtain reproducible results may have been due to the presence of mixtures of oxidation states of neptunium, mixtures of the crystalline forms of the peroxide precipitate, or to variations in the composition of the crystals.

Acknowledgement—The authors wish to thank W. R. Cornman for the X-ray diffraction studies, and R. M. Wallace for helpful advice and suggestions.

J. Inorg. Nucl. Chem., 1962, Vol. 24, pp. 903 to 911. Pergamon Press Ltd. Printed in England

A STUDY OF TRANSFERENCE AND SOLVATION PHENOMENA—VII

A DETERMINATION OF TRUE TRANSFERENCE NUMBERS AND RELATIVE SOLVATION NUMBERS IN MIXED SOLVENTS

J. O. WEAR and E. S. AMIS
Department of Chemistry, University of Arkansas, Fayetteville, Arkansas

(*Received* 6 *October* 1961; *in revised form* 12 *December* 1961)

THIS paper is a part of the programme of study of transference and solvation phenomena carried out by AMIS and co-workers(1-6) in water, water–ethanol and ethanol solvents. The present paper is the first attempt at making a semi-theoretical use of the accumulated data.

Since true transference numbers are used in electrochemical calculations, it seemed to be important to obtain true transference numbers in mixed solvents. A logical approach appeared to be the method used by WASHBURN(7) for determining true transference numbers in aqueous solutions.

Washburn's equation is:

$$T-t = \Delta N_{sol}^{F} \frac{n_s}{n_{sol}} \tag{1}$$

where T and t are true and Hittorf transference numbers, respectively, ΔN_{sol}^{F} is the moles of solvent transferred per faraday, n_s the equivalents of solute in n_{sol} moles of solvent. By using the relations:

$$\Delta N_{sol}^{F} = \frac{\Delta G_{sol}^{F}}{M_{sol}} \text{ and } n_{sol} = \frac{g_{sol}}{M_{sol}} \tag{2}$$

where ΔG_{sol}^{F} is the grammes of solvent transferred per faraday, g_{sol} the grammes of solvent, and M_{sol} the molecular weight of solvent, the following equation is obtained:

$$T-t = \Delta G_{sol}^{F} \frac{n_s}{g_{sol}} \tag{3}$$

whereby the true transference numbers may be obtained from Hittorf transference numbers without having a knowledge of the molecular weight of the solvent mixture.

---

(1) D. M. MATHEWS, J. O. WEAR and E. S. AMIS, *J. Inorg. Nucl. Chem.* **13**, 298 (1960).
(2) W. V. CHILDS and E. S. AMIS, *J. Inorg. Nucl. Chem.* **16**, 114 (1960).
(3) J. O. WEAR, C. V. MCNULLY and E. S. AMIS, *J. Inorg. Nucl. Chem.* **18**, 48 (1961).
(4) J. O. WEAR, C. V. MCNULLY and E. S. AMIS, *J. Inorg. Chem.* **19**, 278 (1961).
(5) J. O. WEAR, C. V. MCNULLY and E. S. AMIS, *J. Inorg. Nucl. Chem.* **20**, 100 (1961).
(6) J. O. WEAR, J. T. CURTIS, JR. and E. S. AMIS, *J. Inorg. Nucl. Chem.* **24**, 93 (1962).
(7) E. W. WASHBURN, *J. Amer. Chem. Soc.* **31**, 322 (1909).

With true transference numbers the following two relations can be written for a two component solvent, A+B:

$$\Delta G^{F}_{(sol)A} = M_{(sol)A}N^{c}_{(sol)A}T^{c} - M_{(sol)A}N^{a}_{(sol)A}T^{a} \tag{4}$$

$$\Delta G^{F}_{sol} = [M_{(sol)A}N^{c}_{(sol)A} + M_{(sol)B}N^{c}_{(sol)B}]T^{c} - [M_{(sol)A}N^{a}_{(sol)A} + M_{(sol)B}N^{a}_{(sol)B}]T^{a} \tag{5}$$

where $\Delta G^{F}_{(sol)A}$ and ΔG^{F}_{sol} represent the grammes of solvent A and grammes of total solvent, respectively, transferred from the anode to the cathode per faraday: $M_{(sol)A}$ and $M_{(sol)B}$ the molecular weights of solvent components A and B, respectively: $N^{c}_{(sol)A}$ and $N^{c}_{(sol)B}$ the moles of solvent components A and B solvating the cation, respectively: $N^{a}_{(sol)A}$ and $N^{a}_{(sol)B}$ the moles of solvent components A and B solvating the anion, respectively: and T^{c} and T^{a} the true transference numbers of the anion and the cation.

Equation (4) is the same equation obtained for a pure solvent and can be written as:

$$\Delta N^{F}_{(sol)A} = N^{c}_{(sol)A}T^{c} - N^{a}_{(sol)A}T^{a} \tag{6}$$

where $\Delta N^{F}_{(sol)A}$ is the number of moles of solvent A transferred from the anode to the cathode per faraday. Equation (6) has an infinite number of solutions: but these can be readily reduced with the assumption that $N^{c}_{(sol)A}$ and $N^{a}_{(sol)A}$ must be integers and by placing upper and lower limits on $N^{c}_{(sol)A}$ and $N^{a}_{(sol)A}$.

If nothing is known of the system as far as the solvation, which is usually the case, the lower limit must be assumed to be zero. Now the upper limit will be the maximum possible number of molecules of solvent A that could solvate one ion assuming the other ion is not solvated by solvent A. The total number of moles of solvent A solvating the ions must not exceed the number of moles of solvent component A in the solvent. This leads to the relation:

$$N^{c}_{(sol)A} + N^{a}_{(sol)A} \leq \frac{N_{(sol)A}}{n_{s}} \tag{7}$$

where $N_{(sol)A}$ is the total moles of solvent A in the solution and n_{s} is the equivalent of solute. With these restrictions Equation (7) can be programmed and solved for all possible solutions in the integers, provided one has the necessary transference and solvation data.

Equation (5) can be expanded and Equation (4) substituted into it to obtain the following equation:

$$\frac{\Delta G^{F}_{sol} - \Delta G^{F}_{(sol)A}}{M_{(sol)B}} = N^{c}_{(sol)B}T^{c} - N^{a}_{(sol)B}T^{a} \tag{8}$$

Equation (8) has the same form as Equation (7) and can be solved in the same manner.

In the present paper true transference numbers in water, and water–ethanol are calculated for LiCl, NaCl, and KCl. Also relative solvation is calculated for NaCl and KCl in water and LiCl in water–ethanol.

EXPERIMENTAL

All data for the NaCl and KCl calculations are from the literature(4, 5) as well as a portion of the LiCl data.(3) The LiCl data presented here was obtained as described in a previous paper (1).

RESULTS AND DISCUSSION

True transference numbers were calculated by the use of Equation (3) which permitted their calculation in mixed solvents. The results of the calculations for LiCl, NaCl, and KCl are recorded in Tables 1–3. Solvation data to be used in other calculations are also included in these tables.

TABLE 1.—TRUE TRANSFERENCE NUMBERS AND MOLES OF WATER TRANSPORTED FROM THE ANODE TO THE CATHODE FOR NaCl

EtOH (%)	Concentration (Moles per 1000 g of solution)	T_c	$\Delta N^F_{H_2O}$
0	0·1519	0·389	−0·80
0	0·1863	0·393	0·66
0	0·2195	0·400	0·66
0	0·3435	0·380	1·1
0	0·3435	0·381	1·1
0	0·4891	0·382	1·4
0	0·4891	0·377	2·0
12	0·1826	0·396	
12	0·1870	0·409	
25	0·1875	0·445	
25	0·1875	0·440	
32	0·1889	0·413	
40	0·1872	0·407	
40	0·1872	0·398	
55	0·1879	0·404	
55	0·1879	0·372	
63	0·1914	0·398	
63	0·1914	0·386	
71	0·1886	0·417	
71	0·1886	0·418	

The values for NaCl and KCl in water agree reasonably well with the work of WASHBURN and MILLARD.(8)

The data for the transference number and grammes of ethanol transferred from anode to cathode per faraday at various weights per cent ethanol for LiCl are recorded in Table 4. With this data and interpolated values of grammes of solvent transferred from the anode to the cathode per faraday from previous work,(3) Equations (4) and (8) can be applied. These calculations were made on an I.B.M. 650 computor.

From error analysis a per cent of error of ±25 per cent was placed on the data.

In Table 5 are tabulated the maxima and minima values for moles of water or ethanol per anion and cation in the various ethanol mixtures. The trends indicated in this table are in agreement with each other and what is expected, except for the maximum number of moles of water around the anion. Either the value at 80 wt. per cent ethanol is too low or the value at 90 wt. per cent ethanol is too high.

By looking at Table 5 it can be seen that the maxima and minima number of moles of water on the cation and anion decrease or remain about the same with decrease in per cent water in the solvent. The maxima and minima number of moles of ethanol on the cation and anion increase or remain about the same with increasing weight per cent ethanol.

---

(8) E. W. WASHBURN and E. B. MILLARD, *J. Amer. Chem. Soc.* 37, 694 (1915).

TABLE 2.—TRUE TRANSFERENCE NUMBERS AND MOLES OF WATER TRANSPORTED FROM THE ANODE TO THE CATHODE FOR KCl

EtOH (%)	Concentration (Moles per 1000 g of solution)	T_c	$\Delta N^F_{H_2O}$
0	0·1004	0·485	—2·4
0	0·1559	0·478	—0·67
0	0·1559	0·494	—1·1
0	0·1786	0·495	0·22
0	0·1786	0·487	0·03
0	0·3624	0·491	1·4
0	0·4870	0·465	1·3
0	0·4870	0·465	0·96
10·9	0·1432	0·501	
10·9	0·1519	0·516	
10·9	0·1522	0·499	
24·8	0·1456	0·494	
24·8	0·1529	0·507	
44·1	0·1522	0·508	
44·1	0·1547	0·519	
53·6	0·1589	0·462	
53·6	0·1589	0·453	
53·6	0·1538	0·479	
74·3	0·1564	0·490	
74·3	0·1564	0·501	

TABLE 3.—TRUE TRANSFERENCE NUMBERS FOR LiCl

EtOH (%)	Concentration (Moles per 100 g of solution)	T_c
26·8	0·3282	0·320
26·8	0·4771	0·319
26·8	0·4771	0·316
55·0	0·3723	0·342
55·0	0·4271	0·288
55·0	0·4271	0·307
68·9	0·3524	0·349
68·9	0·3811	0·333
79·5	0·3801	0·318
79·5	0·3801	0·317
84·5	0·3645	0·345
84·5	0·3645	0·333
84·5	0·4320	0·302
84·5	0·4320	0·296
94·0	0·2476	0·349
94·0	0·3651	0·352

TABLE 4.—TRANSFERENCE AND SOLVATION DATA ON LiCl IN ETHANOL–WATER SOLVENTS*

P_s^a	1·44626	1·54548	1·33518
P_s^m	1·50605	1·61162	1·39199
d_d^a	0·978688	0·975162	0·977538
d_d^m	0·977604	0·985370	0·978155
W_{ss}^a	19·1136	19·0909	13·7056
W_{ss}^m	25·3743	12·5290	14·4959
W_d^a	95·5335	111·2830	99·7882
W_d^m	119·4109	135·0483	109·2932
P_{ed}^a	11·08590	13·83623	12·34429
P_{ed}^m	14·67583	7·38109	11·98948
P_e^a	58·0000	79·92813	89·8765
P_e^m	57·8373	79·55942	90·3958
$N^a \times 10^4$	3·411	3·645	3·146
$N^m \times 10^4$	3·552	3·801	3·283
W	182·9750	174·4057	169·7400
W_s	180·3287	171·7003	167·4737
$F \times 10^3$	8·146	8·954	7·467
t	0·322	0·309	0·315
t	0·678	0·691	0·685
ΔG_{EtOH}^F	− 62·0	− 89·0	129·0

* Symbols are as previousley used (1).

TABLE 5.—MAXIMUM AND MINIMUM VALUES FOR MOLES OF WATER AND ETHANOL SOLVATION OF CATIONS AND ANIONS OF LiCl IN VARIOUS WEIGHTS PER CENT OF ETHANOL

Weight per cent ethanol	58	80	90
LiCl Moles per 1000 g of solution	0·3552	0·3801	0·3283
$N_{H_2O}^c$ (max)	50	28	8
$N_{H_2O}^a$ (max)	18	4	10
$N_{H_2O}^c$ (min)	11	15	0
$N_{H_2O}^a$ (min)	0	0	5
N_{EtOH}^c (max)	22	29	43
N_{EtOH}^a (max)	13	17	17
N_{EtOH}^c (min)	0	0	7
N_{EtOH}^a (min)	2	3	0

In order to eliminate some of the possible calculations it has been assumed that solvation, especially in water, occurs in multiples of four. This is reasonable since the primary solvation of the lithium ion is four molecules in both water⁽⁹⁾ and

---

⁽⁹⁾ O. YA. SAMOILOV, *Izvest. Akad. Nauk. S.S.S.R. Otdel Khim. Nauk.* 398 (1952).

ethanol(10) and the primary solvation of the chloride ion(11) is eight molecules of water. The hydrogen ion combines with four waters to form the pyramidal $H_9O_4^+$ complex stable up to 100°C.(12) Also it has been found that much hydration is a geometric build up on tetrahedrons.(13) The most common geometric build up appears to be a dodecahedron, which is five tetrahedrons. This appears on a sound basis since the structure of water is tetrahedral and secondary solvation is probably greatly influenced by water structure as well as electrostatics. On the assumption that solvation is in multiples of four Table 6 is made up, applying Equations (4) and (8) to pertinent transference and solvation data.

Table 6 shows the same trends as are shown in Table 5; therefore, no further discussion is needed.

In order to qualitatively study the hydration of the ions of sodium and potassuim chlorides, the following equations were solved on the I.B.M. 650 computer:

$$-0{\cdot}80 \pm 0{\cdot}1 = [0{\cdot}389]N^{c}_{H_2O} - [0{\cdot}611]N^{a}_{H_2O} \tag{9}$$

TABLE 6.—SOLUTIONS TO THE FOLLOWING EQUATIONS CONSIDERING SOLVATION IN MULTIPLES OF FOUR AT 58 WEIGHT PER CENT ETHANOL FOR LiCl

$$(1)\quad 4{\cdot}78 \pm 1{\cdot}20 = N^{a}_{H_2O}[0{\cdot}331] - N^{c}_{H_2O}[0{\cdot}669]$$

$$(2)\quad -1{\cdot}35 \pm 0{\cdot}34 = N^{a}_{EtOH}[0{\cdot}331] - N^{c}_{EtOH}[0{\cdot}669]$$

$N^{c}_{H_2O}$	$N^{a}_{H_2O}$	N^{c}_{EtOH}	N^{a}_{EtOH}
48	16	20	12
44	16	12	8
40	12	4	4
36	12		
32	8		
28	8		
24	4		
20	4		
16	0		
12	0		

SOLUTIONS TO THE FOLLOWING EQUATIONS CONSIDERING SOLVATION IN MULTIPLES OF FOUR AT 80 WEIGHT PER CENT ETHANOL FOR LiCl

$$(1)\quad 6{\cdot}28 \pm 1{\cdot}57 = N^{c}_{H_2O}[0{\cdot}318] - N^{a}_{H_2O}[0{\cdot}682]$$

$$(2)\quad -1{\cdot}93 \pm 0{\cdot}48 = N^{c}_{EtOH}[0{\cdot}318] - N^{a}_{EtOH}[0{\cdot}682]$$

$N^{c}_{H_2O}$	$N^{a}_{H_2O}$	N^{c}_{EtOH}	N^{a}_{EtOH}
24	4	28	16
24	0	20	12
20	0	12	8
		4	4

---

(10) Q. OSAKA, *Bull. Chem. Soc. Japan* **12**, 177 (1937).

(11) K. P. MISHCHENKO. *Zh. Fiz. Khim.* **26**, 1736 (1950).

(12) M. EIGEN and L. DE MAEYER, *Hydrogen Bond Structure, Proton Hydration, and Proton Transfer in Aqueous Solution* in *The Structure of Electrolytic Solutions* (Edited by W. J. HAMER), Chap. 5. J. Wiley, New York (1959).

(13) *Chem. Engng. News.* **39**, No. 7, 40 (1961).

SOLUTIONS TO THE FOLLOWING EQUATIONS CONSIDERING SOLVATION IN MULTIPLES OF FOUR AT 90 WEIGHT PER CENT ETHANOL FOR LiCl

$$(1)\quad -4{\cdot}00\pm1{\cdot}00 = N^{c}_{H_2O}[0{\cdot}334]-N^{a}_{H_2O}[0{\cdot}666]$$

$$(2)\quad 2{\cdot}80\pm0{\cdot}70 = N^{c}_{H_2O}[0{\cdot}334]-N^{a}_{H_2O}[0{\cdot}666]$$

$N^{c}_{H_2O}$	$N^{a}_{H_2O}$	N^{c}_{EtOH}	N^{a}_{EtOH}
4	8	40	16
		32	12
		24	8
		16	4
		8	0

$$0{\cdot}66\pm0{\cdot}1 = [0{\cdot}393]N^{c}_{H_2O}-[0{\cdot}607]N^{a}_{H_2O} \tag{10}$$

$$1{\cdot}1\pm0{\cdot}2 = [0{\cdot}380]N^{c}_{H_2O}-[0{\cdot}620]N^{a}_{H_2O} \tag{11}$$

$$1{\cdot}7\pm0{\cdot}2 = [0{\cdot}380]N^{c}_{H_2O}-[0{\cdot}620]N^{a}_{H_2O} \tag{12}$$

$$-2{\cdot}4\pm0{\cdot}3 = [0{\cdot}485]N^{c}_{H_2O}-[0{\cdot}515]N^{a}_{H_2O} \tag{13}$$

$$-0{\cdot}9\pm0{\cdot}2 = [0{\cdot}488]N^{c}_{H_2O}-[0{\cdot}512]N^{a}_{H_2O} \tag{14}$$

$$1{\cdot}4\pm0{\cdot}2 = [0{\cdot}491]N^{c}_{H_2O}-[0{\cdot}509]N^{a}_{H_2O} \tag{15}$$

$$1{\cdot}1\pm0{\cdot}2 = [0{\cdot}465]N^{c}_{H_2O}-[0{\cdot}535]N^{a}_{H_2O} \tag{16}$$

Equations (9) through (12) are for NaCl and the data for them are recorded in Table 1. In Table 2 are recorded the data for Equations (13) through (16) which are for KCl.

TABLE 7.—MAXIMUM AND MINIMUM VALUES FOR MOLES OF WATER HYDRATING CATIONS AND ANIONS OF NaCl AND KCl

NaCl moles per 1000 g of solution	0·1519	0·1863	0·3435	0·4891
$N^{c}_{H_2O}$ (max)	224	181	102	73
$N^{a}_{H_2O}$ (max)	144	116	61	42
$N^{c}_{H_2O}$ (min)	1	3	3	4
$N^{a}_{H_2O}$ (min)	2	1	0	0
KCl moles per 1000 g of solution	**0·1004**	**0·1559**	**0·3624**	**0·4870**
$N^{c}_{H_2O}$ (max)	283	188	74	62
$N^{a}_{H_2O}$ (max)	271	181	69	52
$N^{c}_{H_2O}$ (min)	0	0	3	2
$N^{a}_{H_2O}$ (min)	5	2	0	0

In Table 8 is tabulated the maxima and minima number of moles of water that could hydrate the cations and anions of KCl and NaCl at various salt concentrations. By comparing similar salt concentrations it can be seen that the sodium ion has a larger maximum than the potassium ion. It is also seen that the maxima for the potassium ion and chloride ion are about the same in KCl solutions, especially below 0·2 moles per 1000 g of solution Looking at minima it can be seen that in the more dilute solutions the chloride ion can be more solvated than either the potassium or sodium ion.

Using the same assumption of multiples of four as used in connection with Table 6, Tables 8 and 9 are justified. In Table 8 it is seen that the sodium ion always has more hydration than the chloride ion, which is what would be expected.(14) There is also the indication that hydration is much greater in dilute solutions, which is also expected.(15) Also from Table 8 it can be seen that the hydration of the chloride ion might decrease faster than that of the sodium ion.

TABLE 8.—SOLUTIONS TO EQUATIONS (7)–(10) CONSIDERING HYDRATION IN MULTIPLES OF FOUR FOR NaCl

Equation	7		8		9		10	
Conc. moles per 1000 g of solution	0·1519		0·1863		0·3435		0·4891	
	$N^c_{H_2O}$	$N^a_{H_2O}$	$N^c_{H_2O}$	$N^a_{H_2O}$	$N^c_{H_2O}$	$N^a_{H_2O}$	$N^c_{H_2O}$	$N^a_{H_2O}$
	224	144	156	100	88	52	44	24
	180	116	144	92	68	40	24	12
	136	88	88	56	36	20	4	0
	92	60	76	48	16	8		
	48	32	20	12				
			8	4				

From looking at Table 9 one can see that most probably the potassium and chloride ions have the same amount of hydration in solutions below 0·2 mole per 1000 g of solution. This agrees well with other work.(15) At higher concentrations the potassium ion is more hydrated than the chloride ion which would be expected since t_c decreases at 0·4870 mole per 1000 g of solution.(4)

The results obtained from Equations (3), (7) and (8) are significant and could be treated quantitatively if the data were more accurate. Two ways to make the data more accurate would be to use an ultraviolet lamp on the polarimetry, which can increase specific rotation, especially for colourless compounds,(16) and determine solvent composition with an interferometer.

---

(14) S. Glasstone, *Textbook of Physical Chemistry*, p. 921. Van Nostrand, New York (1948).

(15) H. Ulich, *A. Physik. Chem.* A 168, 141 (1934).

(16) C. Djerassi, *Optical Rotatory Dispersion*. McGraw-Hill, New York (1960).

TABLE 9.—SOLUTIONS TO EQUATIONS (11)–(14) CONSIDERING HYDRATION IN MULTIPLES OF FOUR FOR KCl

Equation	11		12		13		14	
Conc. moles per 1000 g of solution	0·1004		0·1559		0·3624		0·4870	
	$N^c_{H_2O}$	$N^a_{H_2O}$	$N^c_{H_2O}$	$N^a_{H_2O}$	$N^c_{H_2O}$	$N^a_{H_2O}$	$N^c_{H_2O}$	$N^a_{H_2O}$
	280	268	128	124	44	40	48	40
	276	264	124	120	40	36	44	36
	224	216	120	116	36	32	16	12
	220	212	116	112	32	28	12	8
	216	208	44	44	28	24		
	212	204	40	40				
	208	200	36	36				
	156	152	32	32				
	152	148						
	148	144						
	144	140						
	140	136						
	88	88						
	84	84						
	80	80						
	76	76						
	72	72						
	20	24						
	16	20						
	12	16						
	8	12						
	4	8						

Acknowledgement—The authors wish to thank the Atomic Energy Commission for Contract AT-(40-1)-2069 which supported this research financially. One of us (J.O.W.) wishes to thank the National Science Foundation for a Co-operative Fellowship.

J. Inorg. Nucl. Chem., 1962, Vol. 24, pp. 913 to 917. Pergamon Press Ltd. Printed in England.

THE NATURE OF ZIRCONYL CHLORIDE IN STRONG HYDROCHLORIC ACID: LIGHT SCATTERING†

R. L. Angstadt and S. Y. Tyree
Department of Chemistry, University of North Carolina, Chapel Hill, North Carolina

(*Received* 25 *September* 1961; *in revised form* 15 *December* 1961)

Abstract—The degree of aggregation of zirconyl ion in strong hydrochloric acid solutions is estimated from light scattering data. The principle species in 2·800 M HCl is a trimer with a charge of plus three. In 0·750 M HCl the predominant species is apparently a hexamer with a charge between plus five and plus six.

Other papers⁽¹, ²⁾ have reviewed the early literature concerning the hydrolysis and polymerization of zirconium(IV) in aqueous solution. More recently low angle X-ray studies on two molal zirconyl and hafnyl chlorides and bromides were carried out by Muha and Vaughn.⁽³⁾ The assumption of the existence of a complex $[M_4(OH)_8(H_2O)_{16}]X_8$ and construction of a model along the lines of the structure developed for the crystal⁽⁴⁾ gave good agreement between the found and calculated intensities for the hafnyl halides. For the zirconyl halide solutions, however, the agreement was not so good. They suggest that more highly polymerized species might be present in the latter solutions.

Ultra-centrifugation of 0·023–0·052 M zirconyl chloride in solutions 1 M in HCl and 1 M in NaCl led Johnson and Kraus⁽², ⁵⁾ to the conclusion that only one principle species, either a trimer or tetramer with a charge per zirconium atom of less than one, is present. At higher and lower acidities, 3 M HCl and 0·1 M HCl, apparent degrees of polymerization of 2–2·6 and 4–5·4 respectively were indicated.

In many respects the application of light scattering to the study of such systems parallels that of the ultracentrifuge. Recently we outlined a method⁽⁶⁾ for applying the techniques of light scattering to the investigation of the polymerization in inorganic electrolytes. The equation relating the degree of polymerization of the zirconyl cation solute to the excess turbidity (the turbidity of the solution less that due to the solvent and the supporting electrolyte) is:

$$\frac{1}{Nz'} = \frac{H''\phi\psi'M'}{\tau^*} - \frac{Z'^2M'}{2(M_3+M_5)} \tag{1}$$

$$H'' = \frac{32000\pi^3n^2}{3N\lambda^4}$$

---

† From a thesis submitted by R. L. Angstadt to the Graduate School of the University of North Carolina in partial fulfillment of the requirements for the Ph.D. degree, 1961.

⁽¹⁾ R. E. Connick and W. H. Reas, *J. Amer. Chem. Soc.* **73**, 1171 (1951).
⁽²⁾ J. S. Johnson and K. A. Kraus, *J. Amer. Chem. Soc.* **78**, 3937 (1956).
⁽³⁾ G. M. Muha and P. A. Vaughn, *J. Chem. Phys.* **33**, 194 (1960).
⁽⁴⁾ P. A. Vaughn and A. Clearfield, *Acta Cryst.* **9**, 555 (1956).
⁽⁵⁾ K. A. Kraus and J. S. Johnson, *J. Amer. Chem. Soc.* **75**, 5769 (1953).
⁽⁶⁾ R. S. Tobias and S. Y. Tyree, Jr. *J. Amer. Chem. Soc.* **81**, 6385 (1959).

N_z' = degree of polymerization
ϕ = volume fraction of solvent
τ^* = excess turbidity
n = refractive index of solution
N = Avogadro's number
λ = 435·8 mμ
M_3 = molar concentration of HCl
M_5 = molar concentration of NaCl
M' = molar concentration of zirconium
Z' = charge/zirconium atom
ψ' = differential refractive index of polymer/zirconium atom.

It is necessary to correct ψ' for ionization since we are interested in characterizing only the polymeric component. It is assumed that ψ' for the polymeric component can be approximated by
where

$$\psi' = \left(\frac{\partial n}{\partial M_{Zr}}\right) - \frac{z'M_3}{2(M_3+M_5)}\left(\frac{\partial n}{\partial M_3}\right) - \frac{z'M_5}{2(M_3+M_5)}\left(\frac{\partial n}{\partial M_5}\right)$$

where $\left(\frac{\partial n}{\partial M_{Zr}}\right)$, $\left(\frac{\partial n}{\partial M_3}\right)$, and $\left(\frac{\partial n}{\partial M_5}\right)$ are the measured differential refractive indices of zirconyl chloride, hydrochloric acid and sodium chloride respectively.

The present study was conducted in rather high concentrations of HCl to suppress any further hydrolysis of the zirconyl ion or to swamp out any increase in the acid concentration due to such hydrolysis. In addition, we sought to duplicate the conditions of the most recent previous investigations,(2, 3) so that a meaningful comparison could be made between previously reported results and those obtained from the light scattering data.

EXPERIMENTAL

$ZrOCl_2 \cdot 8H_2O$ obtained from the Titanium Alloy Manufacturing Division of the National Lead Company was purified by several recrystallizations from aqueous HCl. A stock solution of this material was prepared and was analysed for zirconium with EDTA utilizing a back titration with iron(III).(7) Chloride was determined potentiometrically. The concentration of free acid present as HCl was taken as the difference between the molar chloride concentration and twice the molar zirconium concentration.

Two series of solutions were prepared for study. In series (a) the total acid concentration was held at $[H^+]$ = 2·800 M, and the total chloride concentration $[Cl^-]$ = 3·000 M, the difference between total chloride and that from both HCl and $ZrOCl_2$ being made up by NaCl. The zirconium concentration varied from 0·02224 M to 0·1001 M. In series (b) $[H^+]$ = 0·750 M, $[Cl^-]$ = 1·000 M, and [Zr(IV)] varied from 0·01112 M to 0·1112 M.

Refractive index increments were determined at 4358 Å with a Brice-Phoenix differential refractometer calibrated with sucrose solutions.(8)

---

(7) G. Schwarzenbach, *Complexometric Titrations*, p.74 Interscience, New York. (1957)

(8) C. A. Brown and F. W. Zerban, *Physical and Chemical Methods of Sugar Analysis* (3rd Ed.), p. 1206. J. Wiley, New York (1941).

Measurements of the turbidity were made with unpolarized 4358 Å light using a modified Brice photometer.⁽⁹⁾ The photometer and cells were calibrated using reagent grade benzene dried over $CaCl_2$ as the secondary standard. The value selected for the absolute turbidity of benzene is that of KUSHNER⁽¹⁰⁾ and of STAMM and BUTTON.⁽¹¹⁾ The calibration was checked by determining the molecular weight of raffinose. Value found: 500 ± 10; Calc. value: 504.

RESULTS

The differential refractive indices determined in this investigation are given below. The differential refractive index of NaCl was determined in both 2·800 M HCl and in 0·750 M HCl. Actually $\Delta n/M$ increments were measured and found to be constant over the concentration ranges covered. $\Delta n/M$ values are assumed to be equal to the corresponding partial values.

$$\left(\frac{\partial n}{\partial M_{\mathrm{HCl}}}\right) \sim \left(\frac{\partial n}{\partial M_3}\right) = 8{\cdot}49 \times 10^{-3}\ \mathrm{l.\ moles}^{-1}$$

Series (a)

$$\left(\frac{\partial n}{\partial M_{\mathrm{NaCl}}}\right) \sim \left(\frac{\partial n}{\partial M_5}\right) = 9{\cdot}29 \times 10^{-3}\ \mathrm{l.\ moles}^{-1}$$

$$\left(\frac{\partial n}{\partial M_{\mathrm{Zr}}}\right) = 4{\cdot}07 \times 10^{-2}\ \mathrm{l.\ moles}^{-1}$$

Series (b)

$$\left(\frac{\partial n}{\partial M_{\mathrm{NaCl}}}\right) \sim \left(\frac{\partial n}{\partial M_5}\right) = 10{\cdot}05 \times 10^{-3}\ \mathrm{l.\ moles}^{-1}$$

$$\left(\frac{\partial n}{\partial M_{\mathrm{Zr}}}\right) = 4{\cdot}04 \times 10^{-2}\ \mathrm{l.\ moles}^{-1}$$

The excess turbidities, τ^*, for the zirconyl chloride solutions are given in Table 1. The values tabulated are the result of drawing a smooth curve through experimental points (each of which is the average of several measurements) and reading smoothed values from the curve.

TABLE 1.—EXCESS TURBIDITIES, τ^*

Molar conc. Zr	$\tau^* \times 10^5$ (cm^{-1})	
	Series (a)	Series (b)
0·01112		2·31
0·02224	2·23	4·55
0·03333	3·34	6·66
0·04447	4·51	8·65
0·05561	5·63	10·50
0·06671	6·61	12·35
0·07785	7·66	13·83
0·1001	9·56	16·52
0·1112		17·8

---

(9) A. W. GRAHAM, III. *Dissertation*, University of North Carolina (1954).

(10) L. M. KUSHNER, *J. Opt. Soc. Amer.* **44**, 155 (1954).

(11) R. F. STAMM and P. A. BUTTON, *J. Chem. Phys.* **23**, 2456 (1955).

The volume fractions, ϕ, for the two series of solutions was taken to be approximately that in solutions 3·000 M and 1·000 M in HCl. *The Handbook of Chemistry and Physics*, lists the density of a solution 3·000 M in HCl as 1·05 g/ml and that of a solution 1·000 M in HCl as somewhat less than 1·02 g/ml. Assuming the partial molar volume of water in these solutions to be 18·0 ml/mole this value would correspond to $\phi = 0{\cdot}93$ and $\phi = 0{\cdot}97$ for series (a) and series (b) respectively.

The procedure followed in applying Equation (1) is to consider the charge z' to be a parameter. A plot of $1/N_z'$ vs. M' is made for the various values assumed for Z'. The value of Z' for which $1/N'$ is independent of M' will be the correct value for the charge and the corresponding value of $1/N_z'$ will yield the proper degree of polymerization. Figs. 1 and 2 are such plots for series (a) and series (b) respectively. In 2·800 M HCl a value of $Z' = 1{\cdot}0$ gives values of $1/N_z'$ which appear to vary around $1/N_z' = 0{\cdot}33$ independently of M'. The indication is then that the predominant species in these solutions is a trimer with a total charge of plus three. In series (b) a value of $Z' = 0{\cdot}8$ comes closest to determining a line of slope equal to zero for small values of M' and $1/N_z' = 0{\cdot}17$.

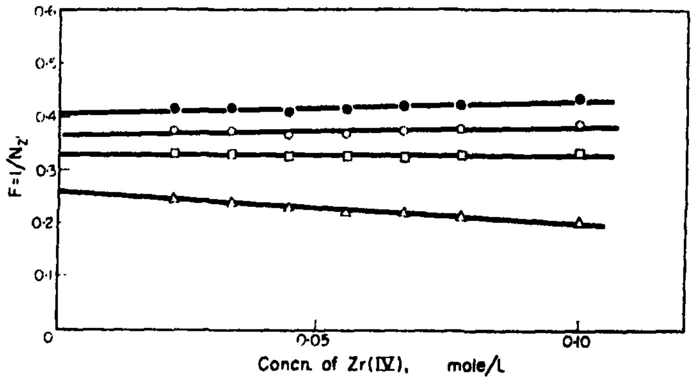

FIG. 1.—● $Z' = 0{\cdot}0$; ○ $Z' = 0{\cdot}5$; □ $Z' = 1{\cdot}0$; Δ $Z' = 2{\cdot}0$.

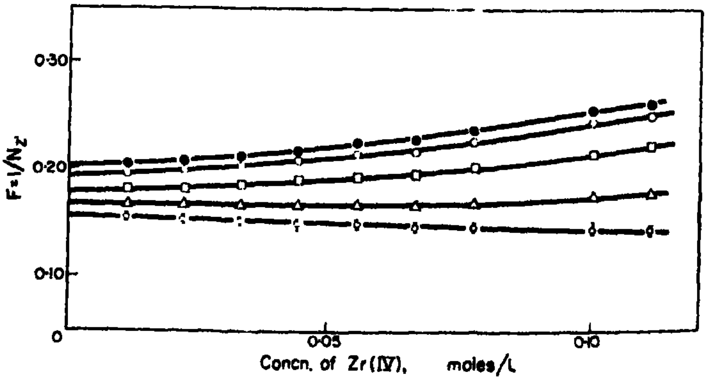

FIG. 2.—● $Z' = 0{\cdot}0$; ○ $Z' = 0{\cdot}2$; □ $Z' = 0{\cdot}5$; Δ $Z' = 0{\cdot}8$; ϕ $Z' = 1{\cdot}0$.

DISCUSSION

In evaluating the data two sources of error are important. First there is the difficulty of obtaining accurate light scattering data on such low molecular weight species. We estimate that the uncertainty in the turbidity of the solutions is less than 5 per cent. The uncertainty is held so low by eliminating bad random errors through plots of τ^* vs. M'.

The second possible source of error is introduced through the use of benzene as a secondary standard in calibrating the light scattering photometer. The various values for the absolute turbidity of benzene have been discussed thoroughly by Carpenter and Krigbaum.(12) Using the highest value our values for $1/N$ become 0·31 and 0·16 for the (a) and (b) series respectively.

Different values for the refractive index increments for both $ZrOCl_2$ and NaCl were found for series (a) and series (b). In the case of $ZrOCl_2$ the difference is within experimental error. It is not thought that the values for the differential refractive indices of NaCl in 0·750 M HCl and 2·800 M HCl differ by the amount reported. However, the error involved changes the value of ψ' in Equation (1) by no more than 1 per cent.

In developing this treatment the assumption was made that the fluctuations in activity coefficients due to changes in ionic strength can be reduced by keeping the gegenion concentration constant and at a rather high level, ~ 3 M. This curvature of the lines in Fig. 2 is taken as an indication of the breaking down of this assumption for the higher zirconium concentrations when the gegenion concentration is held at a somewhat lower level. The lower the gegenion concentration: however, the more sensitive is the slope of the lines of the $1/N_z'$ vs. M' plots to the value assumed for Z', and the more easily can the proper value of the charge be determined.

The results of this investigation as to the degree of polymerization in acidic solutions of zirconyl chloride tend to reaffirm the conclusions of the more recent investigations in this area.(2, 3, 5, 14) In highly acidic solutions the number of zirconium atoms per aggregate is small. Compare the approximate degree of polymerization of three found in this work in solutions 2·8 M in HCl and that of 2–2·6 in 3 M HCl reported by Kraus and Johnson.(5) As the acid concentration is lowered; however, there is a small, but very real, increase in polymerization. The value of six zirconium atoms per aggregate in solutions 0·75 M in HCl found in this work is somewhat higher than the trimers or tetramers reported by Johnson and Kraus for solutions 1·0 M in HCl or even the 4–5·4 zirconium atoms per aggregate reported by these same investigators for solutions 0·1 M in HCl.

The charge per zirconium atom in the systems studied here appears in both cases to be either about or somewhat less than one. This also agrees well with the conclusions reached by Johnson and Kraus.

Acknowledgement—The work reported herein was supported in part by a grant from the Titanium Alloy Manufacturing Division of the National Lead Company.

(12) D. K. Carpenter and W. R. Krigbaum, *J. Chem. Phys.* **24**, 1041 (1956).
(13) R. S. Tobias, *J. Chem. Educ.* **35**, 592 (1958).
(14) A. J. Zielen and R. E. Connick, *J. Amer. Chem. Soc.* **78**, 5785 (1956).

J. Inorg. Nucl. Chem., 1962, Vol. 24, pp. 919 to 923. Pergamon Press Ltd. Printed in England

METAL-DINITROGEN TETROXIDE REACTIONS IN ACETONITRILE AND DIMETHYLSULPHOXIDE

D. K. Straub, H. H. Sisler and G. E. Ryschkewitsch
Department of Chemistry, University of Florida, Gainesville, Florida

(*Received* 24 *November* 1961)

Abstract—Magnesium and bismuth react with dinitrogen tetroxide in acetonitrile solution to give acetonitrile adducts of magnesium and bismuth nitrates. With excess dinitrogen tetroxide, bismuth reacts to form a bismuth nitrate adduct which can be decomposed to give anhydrous bismuth nitrate. Many metals which do not react with dinitrogen tetroxide in acetonitrile do react in dimethylsulphoxide, probably as a consequence of the greater co-ordinating ability of dimethylsulphoxide toward both dinitrogen tetroxide and the metal cation formed in the reaction. Antimony gives a white, deliquescent substance having the composition expressed by the formula $SbO(NO_3)\cdot(CH_3)_2SO$, bismuth, a colourless crystalline substance with a composition expressed by the formula $Bi(NO_3)_3\cdot 3(CH_3)_2SO$. Molybdenum is oxidized to the +6 oxidation state, and a yellow crystalline compound of unknown structure having the unusual stoicheiometry $4MoO_3\cdot 5(CH_3)_2SO$ is formed. Lead reacts readily to give lead nitrate. Aluminium, titanium, iron, nickel, chromium, tin, arsenic, silicon and selenium show little or no tendency to react with dinitrogen tetroxide in dimethylsulphoxide.

In their work on the reaction of metals with dinitrogen tetroxide in various solvents, Addison and co-workers$^{(1, 2)}$ have found that the rate of reaction depends upon (1) the ionizing power of the solvent, (2) the donor properties of the solvent toward dinitrogen tetroxide, and (3) the co-ordinating ability of the solvent toward the metal ion formed in the reaction.

A solvent with a high dielectric constant and strong donor properties favours the ionic dissociation of the tetroxide: $N_2O_4 \rightleftharpoons NO^+ + NO_3^-$:$^{(3)}$ and one with good co-ordinating ability solvates the metal cation (formed by oxidation of the metal by NO^+ or N_2O_4) adsorbed on the surface of the metal. This decreases the electrostatic attraction between the cation and the metal, and helps to remove the cation from the surface of the metal. In a comparison of the rates of reaction of copper metal with dinitrogen tetroxide in nitromethane and acetonitrile, Addison *et al.*$^{(1)}$ found the rate to be greater in acetonitrile. Although these solvents have high and almost equal dielectric constants (approximately 37), acetonitrile solvates the Cu(II) formed, whereas nitromethane does not.

It was of interest to us to investigate the reactions of dinitrogen tetroxide in acetonitrile with a number of metals whose ions might be expected to be solvated by acetonitrile. It was also of interest to investigate reactions in ethylene carbonate, a solvent of very high dielectric constant (89·6),$^{(4)}$ probably with poor donor properties toward dinitrogen tetroxide, and poor co-ordinating ability to the metal ion, and dimethylsulphoxide, a solvent of high dielectric constant (46),[5] with excellent donor properties toward dinitrogen tetroxide,[6] and with excellent co-ordinating ability toward metal ions. It was expected that metals would be most reactive with dinitrogen tetroxide in dimethylsulphoxide. Of the metals tested, vanadium, cobalt, copper, molybdenum, cadmium, antimony, silver, bismuth, mercury and lead reacted with the dinitrogen tetroxide solutions in dimethylsulphoxide, whereas aluminium, titanium, iron, chromium, nickel, tin, arsenic, silicon and selenium showed little or no tendency to react. Some of the metals which reacted in dimethylsulphoxide (e.g. antimony, molybdenum, and lead) did not react in ethylene carbonate, despite its high dielectric constant, and further work with this solvent was discontinued. This supports the belief that the co-ordinating ability of the solvent toward the metal ions formed is an important consideration.

---

(1) C. C. Addison, J. C. Sheldon and N. Hodge, *J. Chem. Soc.* 3900 (1956).

(2) C. C. Addison and J. C. Sheldon, *J. Chem. Soc.* 1937 (1957).

(3) J. D. S. Goulden and D. J. Millen, *J. Chem. Soc.* 2620 (1950).

(4) R. F. Kempa and W. H. Lee, *J. Chem. Soc.* 100 (1961).

EXPERIMENTAL

Materials

The dimethylsulphoxide and ethylene carbonate were commercially obtained and were at least 99 per cent pure. All other solvents were reagent grade. The dinitrogen tetroxide was dried by passing it through a 30 cm tube packed with phosphorus(V) oxide and sand before use. The metals were reagent grade and in powder form. Care was taken throughout to avoid contamination by moisture.

The infra-red spectra were obtained on a Perkin-Elmer Infracord from mulls prepared in both Nujol and hexachlorobutadiene. The X-ray diffraction powder patterns were obtained with a diffractometer using Ni-filtered Cu-$K\alpha$ radiation.

Reactions in acetonitrile

(a) *Magnesium.* A mixture of excess dinitrogen tetroxide, 0·5 g magnesium, and about 15 ml acetonitrile was allowed to react at room temperature until complete solution of the metal had taken place. The colourless gum obtained after removal of nitrogen oxides and most of the acetonitrile under reduced pressure was treated with methylene chloride, stirred until the mass was completely broken up, and the methylene chloride removed under reduced pressure. A repetition of this treatment gave a white, deliquescent powder. The infra-red spectrum of this compound indicated an acetonitrile adduct of magnesium nitrate. The acetonitrile was not removed by heating to 52° C and 1·0 mm for 20 hr. The material still contained some acetonitrile after 20 hr at 100° C and 0·5 mm, but some decomposition had taken place. Anhydrous magnesium nitrate is, therefore, not conveniently prepared in this way.

(b) *Bismuth.* A mixture of dinitrogen tetroxide, about 13 g bismuth (a stoicheiometric excess), and 20 ml acetonitrile was allowed to react at room temperature. After completion of the reaction, the viscous, deep green liquid was centrifuged to remove unreacted metal, then evaporated under reduced pressure. A frothy, white mass was formed. This was treated with methylene chloride and stirred until it was transformed into a heavy white powder. Most of the methylene chloride was removed by decantation. The deliquescent powder was dried *in vacuo* several hours at room temperature.

(Found: C, 5·12; H, 0·96; N, 11·25. Calc. for $Bi(NO_3)_3 \cdot CH_3CN$: C, 5·51; H, 0·69; N, 12·85%.)

Five grammes of bismuth in 15 ml acetonitrile was treated with a large excess of dinitrogen tetroxide. The reaction was allowed to proceed for 48 hr with occasional stirring. After about 24 hr fine, needle-like crystals had formed in the solution. The liquid was decanted, and the large amount of precipitate dried *in vacuo* for 2 hr at room temperature. A deep yellow, highly deliquescent, crystalline mass was obtained. (Found: C, 1·34; H, 0·88; N, 11·24. Calc. for $Bi(NO_3)_3 \cdot 0{\cdot}25\,N_2O_4 \cdot 0{\cdot}25\,CH_3CN$: C, 1·40; H, 0·18; N, 12·15%.)

---

(5) H. L. SCHAFER and W. SCHAFFERNICHT, *Angew. Chem.* **72**, 618 (1960).

(6) C. C. ADDISON and J. C. SHELDON, *J. Chem. Soc.* 2705 (1956).

The compound, when kept at 100° C and 0·5 mm for 40 hr gave white, anhydrous bismuth nitrate. (Found: Bi, 52·40; N, 10·35. Calc. for $Bi(NO_3)_3$: Bi, 52·91; N, 10·63%.) Principle lines in the X-ray powder pattern of this substance occurred at 3·40, 3·10, 2·85, 2·70, 2·55, 2·37, 2·19, 2·11, 1·78 and 1·69. The infra-red spectrum showed peaks at 2290, 1275, 1025 (shoulder), 990, 795 (shoulder) and 735 cm^{-1}.

Reactions in dimethylsulphoxide

(a) *Antimony*. A mixture of excess dinitrogen tetroxide, 5 g antimony and 15 ml of dimethylsulphoxide was allowed to react at room temperature. After the reaction had gone to completion, the remaining nitrogen oxides were removed under reduced pressure, and a little dimethylsulphoxide was added to dissolve the residue. A small amount of an insoluble impurity was removed by centrifugation. Addition of a 4:1 mixture of methylene chloride and carbon tetrachloride precipitated a white solid. This was collected, washed with methylene chloride, and dried *in vacuo* for 1 hr at room temperature. The substance is highly deliquescent. (Found: C, 8·62; H, 2·33; N, 4·83; Sb, 43·6. Calc. for $SbONO_3\cdot(CH_3)_2SO$: C, 8·63; H, 2·16; N, 5·04; Sb, 43·8%.) The infra-red spectrum showed peaks at 1370, ca. 1050 (shoulder), ca. 1010 (broad), ca. 930 (broad), 835 and 720 cm^{-1}.

(b) *Bismuth*. Five grammes of bismuth in 10 ml of dimethylsulphoxide was treated with dinitrogen tetroxide at room temperature for about 24 hr. The bismuth was in excess. After removal of unreacted metal, about 10 ml of acetonitrile was added to the clear, almost colourless syrup; then a 4:1 mixture of methylene chloride and carbon tetrachloride was added. Upon standing, large colourless crystals were deposited from the solution. These were removed, washed with a very little acetonitrile (in which the crystals are quite soluble), then dried *in vacuo* at room temperature for 1 hr. (Found: C, 11·57; H, 2·77; N, 6·85. Calc. for $Bi(NO_3)_3\cdot3(CH_3)_2SO$: C, 11·45; H, 2·86; N, 6·68%.)

(c) *Molybdenum*. Five grammes of molybdenum was treated with excess dinitrogen tetroxide in about 15 ml of dimethylsulphoxide at room temperature until it had completely dissolved. The nitrogen oxides were removed under reduced pressure. The semi-solid residue was collected, washed with dimethylsulphoxide, then dissolved in a large quantity of hot acetonitrile. The acetonitrile solution was filtered and evaporated to a small volume under reduced pressure. Small, transparent yellow, irregularly formed crystals appeared. These were collected and dried *in vacuo* for 30 min at room temperature. (Found: C, 12·44; H, 2·82; Mo, 40·0. Calc. for $4MoO_3\cdot5(CH_3)_2SO$: C, 12·44; H, 3·15; Mo, 39·8%.) The molybdenum was determined gravimetrically as lead molybdate. All of the molybdenum is present in the +6 oxidation state. It melts to a frothy liquid at 163–165° C; at 204° C the yellow-orange liquid becomes deep green (reduction of Mo(VI) by dimethylsulphoxide) and at about 220° C it chars.

The infra-red spectrum of this compound had a peak at 1035 cm^{-1} and a shoulder at about 1000 cm^{-1} in the S-O stretching region.

(d) *Lead*. An excess of lead, about 1 g, was allowed to react with dinitrogen tetroxide in 20 ml dimethylsulphoxide at room temperature for 24 hr. The excess of unreacted metal was removed, and methylene chloride was added to the solution. The oil which initially precipitated quickly solidified, giving white crystals. These were washed with methylene chloride and dried *in vacuo* at room temperature for 2 hr.

The infra-red spectrum of a hexachlorobutadiene mull of this compound showed no CH peaks. The X-ray powder pattern of the solid indicated that it was pure lead(II) nitrate.

Other reactions in dimethylsulphoxide

The reactivities of a number of additional metals toward dinitrogen tetroxide in dimethylsulphoxide were investigated by allowing about 0·1 g samples of the powdered metals to react with 3 ml portions of a dimethylsulphoxide solution of dinitrogen tetroxide for 24 hr at room temperature. Reaction took place with vanadium, cobalt, copper, cadmium, silver and mercury. Aluminium, titanium, chromium, iron, nickel, tin, arsenic, silicon and selenium did not react.

Reactions in ethylene carbonate

A mixture of about 0·1 g powdered antimony and 3 ml of a solution of dinitrogen tetroxide in ethylene carbonate was allowed to stand for 24 hr. At the end of this time, no reaction had taken place. Similarly, it was found that molybdenum and lead do not react with dinitrogen tetroxide in this solvent.

DISCUSSION

Reaction between magnesium and dinitrogen tetroxide in acetonitrile takes place readily. The product is an acetonitrile adduct of magnesium nitrate. It is very difficult to remove the acetonitrile and attempts to obtain anhydrous magnesium nitrate from the adduct were unsuccessful.

Bismuth exhibits very interesting behaviour toward dinitrogen tetroxide in acetonitrile. The products of the reaction depends upon which reactant is in excess. With excess bismuth, an acetonitrile adduct of bismuth(III) nitrate is formed, $Bi(NO_3)_3 \cdot CH_3CN$. However, when the dinitrogen tetroxide is in excess, a deliquescent, yellow crystalline product which is an adduct of bismuth(III) nitrate with dinitrogen tetroxide and acetonitrile is obtained. The dinitrogen tetroxide does not appear to be attached very strongly to the bismuth nitrate, since, upon solution in acetonitrile (in which the compound is very soluble), an appreciable vapour-pressure of N_2O_4 or NO_2 is produced above the solution.

When the above adduct is kept at 100° C *in vacuo* for 40 hr, white, anhydrous bismuth(III) nitrate is obtained. The nitrate and bismuth appear to be covalently bonded rather than existing as ions, since the infra-red spectrum has peaks at about 2290 (a combination band), 1275 (V_1 of $-ONO_2$), 1025 (shoulder), 990 (both due to V_2 of $-ONO_2$, which is usually split), 795 (V_6 of $-ONO_2$), 755 and 735 cm^{-1} (V_3 and V_5 of $-ONO_2$).(7) The X-ray powder pattern of the material indicates the absence of Bi_2O_3.

Several metals which show little or no reaction with dinitrogen tetroxide in acetonitrile react readily in dimethylsulphoxide. Among these metals are lead, molybdenum and antimony. Dimethylsulphoxide appears to be the best solvent so far investigated for promoting reaction between dinitrogen tetroxide and metals. This reasonably may be assumed to result from the strong co-ordination tendency of dimethylsulphoxide toward dinitrogen tetroxide which tends to enhance the tendency of dinitrogen tetroxide molecules to ionize to NO^+ and NO^- ions. The co-ordination reactions of dimethylsulphoxide toward various metal ions likewise favour this process. The final products usually contain co-ordinated dimethylsulphoxide.

It is interesting to compare the reactivities toward dinitrogen tetroxide of arsenic, antimony and bismuth in both acetonitrile and dimethylsulphoxide. Arsenic shows no reaction with dinitrogen tetroxide in either solvent, antimony reacts only in dimethylsulphoxide and bismuth reacts readily in both solvents. This is in accord with the order of increasing metallic character, viz. As < Sb < Bi. Another point of difference between antimony and bismuth concerns the final reaction product when the reaction is carried out in dimethylsulphoxide. Antimony gives the compound $SbONO_3 \cdot (CH_3)_2SO$. The infra-red spectrum of this compound shows co-ordinated sulphoxide (broad band about 1010 cm^{-1}) and free nitrate (bands at 720 cm^{-1}, 835 cm^{-1}, 1370 cm^{-1} and shoulder at about 1050 cm^{-1}, due to the V_4, V_2, V_3 and V_1 vibration modes, respectively).(7) Bismuth, however, gives the compound

---

(7) C. C. Addison and B. M. Gatehouse, *J. Chem. Soc.* 613 (1960).

$Bi(NO_3)_3 \cdot 3(CH_3)_2SO$.* The formation of an oxynitrate in the case of antimony, and the normal nitrate in the case of bismuth, is in keeping with the lesser metallic character of antimony than of bismuth.

Molybdenum reacts readily with dinitrogen tetroxide in dimethylsulphoxide, and is completely oxidized to the +6 state. From the reaction mixture a yellow crystalline compound can be isolated which has the unusual stoicheiometry, $4MoO_3 \cdot 5(CH_3)_2SO$. This compound is very slightly soluble in acetonitrile. Its infra-red spectrum shows co-ordinated sulphoxide.

Lead reacts readily in dimethylsulphoxide to form lead nitrate, which is probably solvated in dimethylsulphoxide solution, but is precipitated as the unsolvated compound.

Acknowledgements—This work was supported in part by the Office of Naval Research through a contract with the University of Florida. Thanks are due to Mr. P. MORRISETT and Mr. H. LATZ for the infra-red spectra, and to Mr. R. W. GOULD for the X-ray diffraction data. Analysis were performed by Galbraith Laboratories, Knoxville, Tennessee.

* The physical properties and structure of this compound, prepared by a different route, will be given in a later paper.

J. Inorg. Nucl. Chem., 1962, Vol. 24, pp. 925 to 934. Pergamon Press Ltd. Printed in England

NOTES

Reductive carbonylation synthesis of metal carbonyls—VI

A sodium-naphthalene complex route to Group VI-B metal carbonyls(1)

(*Received* 2 *November* 1961)

RECENT publications have described the use of sodium metal as a reducing agent for the preparation of chromium hexacarbonyl in the presence of complexing solvents, such as pyridine and diglyme.(2, 3) However, it has not been known heretofore that the alkali metal complexes with aromatic hydrocarbons might similarly be capable of the synthesis of Group VI–B metal carbonyls. We now wish to report a demonstration of the usefulness of such complexes in the synthesis of chromium carbonyl.

The general technique employed has been previously described.(3) A mixture of 0·020 mole of anhydrous $CrCl_3$ and 120 ml of a diglyme solution containing 0·12 mole of a 1:1 sodium-naphthalene complex (prepared from 8 ml of a 40 per cent dispersion of sodium in Nujol and 16·4 g naphthalene) was added at 25° to a 1 :l. Parr autoclave. The autoclave was sealed and pressurized to 3500 p.s.i. with carbon monoxide. After being stirred for 18 hr the reaction mixture was quenched and hydrolised with 6 M HCl, and steam distilled. A 10 per cent yield of chromium carbonyl was recovered. When the same quantities of reactants were heated during the reaction period, lower yields of chromium carbonyl were obtained For example, a 3 per cent yield of chromium carbonyl resulted at a reaction temperature of 100°.

It is felt that the yield of Group VI–B metal carbonyl obtained through this alkali metal-aromatic hydrocarbon complex route could be considerably improved. The complexes appear to have two important advantages in carbonylation reactions. One is that the reducing agent may be handled in solution and pumped into the metal salt-carbon monoxide solution. Alkali metals, on the other hand, are difficult to pump under pressure. Also, the use of metal-hydrocarbon complexes allows the reagent to be mixed at room temperature without excessive reduction of metal salt to free metal.

The actual reducing agent in the subject experiments is probably the naphthalene radical carbanion of Na^+,

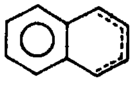

and not Na°, as might be indicated by the work of PAUL *et al.*(4) on the sodium complexes. It is to be expected that the naphthalene carbanion, on oxidation, would yield naphthalene, which could be recycled. In the presence of diglyme as a solvent the probable intermediate is $2[(\text{diglyme})_2Na]^+ [Cr(CO)_5]'^{-2}$.

---

(1) This constitutes paper VI in the series, "Reductive Carbonylation Synthesis of Metal Carbonyls". For paper V, see H. E. PODALL and A. P. GIRAITIS, *J. Org. Chem.* **26**, 2587 (1961).

(2) A. N. NESMEYANOV, E. P. MIKHEEV, K. N. ANISIMOV and N. P. FILIMONOVA, *Russ. J. Inorg. Chem.* **4**, 889 (1959).

(3) H. E. PODALL, H. B. PRESTRIDGE and H. SHAPIRO, *J. Amer. Chem. Soc.* **83**, 2057 (1961).

(4) D. E. PAUL, D. LIPKIN and S. I. WEISMAN, *J. Amer. Chem. Soc.* **78**, 116 (1956).

Presumably, other polycyclic aromatic hydrocarbons could be used to complex the alkali metal instead of naphthalene, such as biphenyl, anthracene, or phenanthrene. Also, other hydrocarbon, amine, and ether solvents in which the metal-hydrocarbon complex is soluble, such as toluene, pyridine, dimethyl ether, tetrahydrofuran, and anisole, should be useful instead of diglyme.

HYMIN SHAPIRO
H. E. PODALL*

Research and Development Department
Ethyl Corporation
Baton Rouge, La.

* Present address: Melpar, Inc., Physical Sciences Laboratory, Falls Church, Virginia.

Preparation and structure of ruthenium tetracarbonyldiiodide

(*Received* 17 *November* 1961)

ALTHOUGH iron tetracarbonyldiiodide(1, 2, 3) and osmium tetracarbonyldiiodide(4) have been prepared and characterised, the analagous ruthenium compound has not been previously reported. In fact no tetracarbonyldihalides of ruthenium have been reported to date,(5) but it has been pointed out(9, 10, 11) that ruthenium *di*-carbonyldiiodide combines with σ-bonding nitrogen bases and π-bonding ligands to form substituted derivatives of the hitherto unknown ruthenium tetracarbonyldiiodide.

We have isolated ruthenium tetracarbonyldiiodide from reactions undertaken to prepare triruthenium dodecacarbonyl for single crystal structure analysis.(12, 13) A mixture of ruthenium triiodide powder and finely divided copper was placed in a glass liner which was sealed in a copper gasketed stainless steel autoclave. The autoclave was pressurized to about 200 atmospheres with carbon monoxide, and heated to 170° for 24 hr. Prior to the reaction the copper powder was cleaned of oxide film by washing with dilute hydrochloric acid, followed by drying with acetone. After the reaction with carbon monoxide, the ruthenium tetracarbonyldiiodide was isolated by sublimation.

Ruthenium tetracarbonyldiiodide forms golden yellow crystals which are soluble in non-polar organic solvents. The crystals sublime at 126° at atmospheric pressure; at temperatures above 140° the crystals decompose. Elemental analysis;(14) found: Ru, 20·9%; C, 11·3%; I, 53·2%; calculated for $Ru(CO)_4I_2$: Ru, 21·65%; C, 10·3%; I, 54·4%.

The infra-red spectrum of this compound was taken with a Perkin-Elmer Model 112 single beam double pass spectrometer equipped with a calcium fluoride prism. The sample was studied as a saturated solution in carbontetrachloride in a 0·1 mm cell. Five peaks.

(1) W. HIEBER and G. BADER, *Ber. Dtsch. Chem. Ges.* **61**, 1717 (1928); *Z. anorg. u. allgem Chem.* **190**, 193, 215 (1930); **201**, 329 (1931).

(2) W. HIEBER, *Z. Elektrochem.* **43**, 390 (1937).

(3) W. HIEBER and H. LAGALLY, *Z. Anorg. Chem.* **245**, 295, 305 (1940).

(4) W. HIEBER and H. STALLMAN, *Ber. Dtsch. Chem. Ges.* **75 B**, 1472 (1942).

(5) $Ru(CO)_2X_2$ (X = Cl, Br, I)[6, 7] and $Ru(CO)Br$[8] have been prepared.

(6) W. MANCHOT and J. KÖNIG, *Ber. Dtsch. Chem. Ges.* **57**, 2130 (1924).

(7) W. MANCHOT and W. J. MANCHOT, *Z. Anorg. Chem.* **226**, 385 (1936).

(8) W. MANCHOT and E. ENK, *Ber. Dtsch. Chem. Ges.* **63**, 1635 (1930).

(9) R. J. IRVING, *J. Chem. Soc.* 2879 (1956).

(10) W. HIEBER and H. HEUSINGER, *J. Inorg. Nucl. Chem.* **4**, 179 (1957).

(11) H. J. EMELIUS and J. S. ANDERSON, "Modern Aspects of Inorganic Chemistry", 266. Van Nostrand, Princeton, New Jersey, 1960.

(12) E. R. COREY and L. F. DAHL, *J. Amer. Chem. Soc.* **83**, 2203 (1961).

(13) L. F. DAHL, E. R. COREY and E. R. DEGIL, to be published.

(14) Analysis performed by Schwarzkopf Microanalytical Laboratory, New York.

were observed in the carbonyl stretching region: 2068 cm^{-1} (s), 2097 cm^{-1} (s), 2106 cm^{-1} (vs), 2119 cm^{-1} (w), and 2161 cm^{-1} (m), and no significant absorption was observed in the 2000–1700 cm^{-1} region. This large number of peaks is inconsistent with a *trans*-configuration for an octahedral monomeric complex of point group symmetry D_{4h}. However, the observed spectrum is not inconsistent with a *cis*-octahedral configuration of point group symmetry C_{2v}. Four infra-red active CO stretching fundamentals are expected, if it is assumed that there is coupling between the stretching vibrations of the individual carbonyl groups; this coupling has been demonstrated in the spectra of analogous metal carbonyl compounds.(15) The weak 2119 cm^{-1} band may be a combination band.

Confirmation of the above infra-red interpretation in terms of a *cis*-octahedral configuration has been made by a single crystal X-ray investigation.(16) Our results also are completely consistent with the proposed *cis*-form for iron tetracarbonyldiiodide based on a dipole moment study.(17)

Acknowledgement—We wish to thank the Petroleum Research Advisory Board (Fund No. 471A) for financial support of this work and Professor W. F. EDGELL for his advice concerning the interpretation of the infra-red spectrum.

E. R. COREY
M. V. EVANS
L. F. DAHL

Department of Chemistry
University of Wisconsin
Madison 6, *Wisconsin*

(15) W. F. EDGELL, private communication.

(16) L. F. DAHL and D. L. WAMPLER, Acta Cryst. 15, (1962).

(17) W. HIEBER and E. WEISS, *Z. Anorg. Chem.* 287, 223 (1956).

Chemical effects of nuclear recoil: metal phthalocyanines

(*Received* 12 *October* 1961; *in revised form* 7 *December* 1961)

IN a former paper(1) the retention in zinc, copper and cobalt phthalocyanines was related to the energy of the recoil atom in the radiative neutron capture reaction. The present paper gives some complementary information. The retention is shown insensitive to ionizing radiation to which the crystals are exposed before neutron activation. The effect of the energy of the incident neutrons on the retention has also been investigated.

1. *Effect of ionizing radiation*

Having shown that the phthalocyanines are inert towards radiation annealing,(1) it seems interesting to observe the retention as a function of the dose absorbed on preirradiation. The results are given in Tables 1 and 2. The samples were treated as previously described but before irradiation in the BR1 reactor at a flux of 2×10^{11} neutrons/cm^2 sec the samples were exposed to the γ-rays of a cobalt source at a dose rate of $4{\cdot}7 \times 10^5$ rads/hr. The data in Tables 1 and 2 show a negligible effect.*

* While in the earlier work the retentions of ^{65}Zn and ^{69}Zn in non pretreated crystalline zinc phthalocyanines were found to be 28·9 and 41·6 respectively, the present values are 25·4 and 37·5. This slight discrepancy might be attributed to the fact that the present material is obtained from a different preparation, so involving small differences in the crystal size. Indeed, it has been emphasized already that the retention is influenced by the physical state of the material (see retentions in crystalline and powdered material).(1) To eliminate this source of error all samples should come from a same preparation. Corrections can, however, be applied when results from different series of experiments have to be compared.

(1) D. J. APERS and P. C. CAPRON, *Symposium on the Chemical Effects of Nuclear Transformations*, I.A.E.A., Prague, October, 1960.

TABLE 1.—PREIRRADIATION OF ZINC PHTHALOCYANINE

Thermal neutron flux: 2 × 10^{11}/cm^2 sec.
Fast neutron flux: 2 × 10^{10}/cm^2 sec.
Reactor Gamma flux: 3·5 × 10^4 rads/h.
Temperature: below 50° C.
Irradiation time: 24 hr.

Dose in Mrads	Ret. ^{65}Zn	Ret. ^{69}Zn
0	25·4 ±0·7	37·5 ±1·2
4·7	23·5 ±0·2	36·8 ±0·9
9·4	25·6 ±0·1	36·0 ±0·5
23·5	24·3 ±1·1	31·1 ±0·5
47·0	22·5 ±2·1	32·1 ±3·0
94·0	21·4 ±0·5	30·9 ±0·7

TABLE 2.—PREIRRADIATION OF COPPER PHTHALOCYANINE

Thermal neutron flux: 2 × 10^{11}/cm^2 sec.
Fast neutron flux: 2 × 10^{10}/cm^2 sec.
Reactor Gamma flux: 3·5 × 10^4 rads/h.
Temperature: below 50° C.
Irradiation time: 24 hr.

Dose in Mrads	Ret. ^{64}Cu
0	22·3 ±0·8
4·7	22·8 ±0·7
9·4	24·7 ±0·8
23·5	25·1 ±1·3
47·0	25·1 ±0·4
92·5	24·0 ±0·6

2. *Influence of the energy of the incident neutrons*

As no neutron velocity selector is available, it has only been possible to compare retentions in uncovered samples and in samples wrapped in cadmium foil. For these experiments an irradiation site was chosen which is rich in fast neutrons (near the heart of the reactor). (Table 3). Each result is the average of four experiments.

TABLE 3.—INFLUENCE OF NEUTRON ENERGY

Irradiation in a water loop at the center of the reactor.
Thermal neutron flux: 5 × 10^{12}/cm^2 sec.
Flux of neutrons from 1 e V to 1 MeV: 3·5 × 10^{12}/cm^2 sec.
Flux of neutrons above 1 MeV: 0·5 × 10^{12}/cm^2 sec.
Reactor gamma flux: 10^6 rads/hr.
Temperature: 25° to 33° C.

Irradiation time	Uncovered		Cadmium wrapped	
	^{65}Zn	^{69}Zn	^{65}Zn	^{69}Zn
24 hours	22·8 ±1·0	29·5 ±1·3	22·2 ±0·9	27·8 ±1·7
15 hours	22·7 ±1·9	32·1 ±2·3	19·8 ±3·2	25·9 ±0·5
3 hours	21·7 ±0·5	33·1 ±1·9		28·0 ±3·6

From this table the following conclusions may be drawn:

1. The irradiation time has no influence on either of the two zinc isotopes.
2. It seems that, while ^{65}Zn is not affected, ^{69}Zn is slightly sensitive to the influence of the neutron energy, although the relatively large errors do not permit a certain conclusion.

One is thus inclined to suppose that the recoil of ^{69}Zn takes place in a different way on fast neutron irradiation. Indeed, a larger recoil energy could be caused by the de-excitation of the compound nucleus which is formed in a more energetic level. As a consequence of this interpretation, the ^{69}Zn recoil atom would be ejected over a longer distance and would be removed further away from the zone where recombination remains possible.

This hypothesis is confirmed in some thermal annealing experiments. The results are given in Table 4 (a, b, c, d).

TABLE 4.—THERMAL ANNEALING RELATED TO THE NEUTRON ENERGY

Same irradiation conditions as Table 3.

a. Uncovered; annealing temperature 160° C.

Heating time	Ret. ^{65}Zn	Ret. ^{69}Zn
0	21·1	29·5
3 hours	22·3	33·0
7 hours	23·4	35·3
15 hours	19·6	31·2
1 day	22·9	32·8
3 days	22·3	31·3
4 days	22·9	
10 days	20·7	
11 days	22·4	

b. Cadmium wrapped; annealing temperature 160° C.

Heating time	Ret. ^{65}Zn	Ret. ^{69}Zn
0	21·3	27·5
3 hours	23·5	28·4
15 hours	23·0	29·4
18 hours	22·8	27·2
1 day	21·8	29·2
4 days	24·0	
5 days	22·7	
7 days	23·5	
10 days	20·9	
12 days	22·4	

c. Uncovered; annealing temperature 308° C.

Heating time	Ret. ^{65}Zn	Ret. ^{69}Zn
0	24·1	29·5
5 hours	26·6	38·2
1 day	24·8	32·7
2 days	23·9	
5 days	19·8	36·3
7 days	26·1	

d. Cadmium wrapped; annealing temperature 308° C.

Heating time	Ret. ^{65}Zn	Ret. ^{69}Zn
0	23·2	26·7
5 hours	26·5	24·6
1 day	24·5	27·6
2 days	19·2	23·0
5 days	21·3	

It has already been observed that the retention of ^{65}Zn is not affected by thermal annealing after thermal neutron bombardment. This fact was explained by the considerable recoil energy of this isotope. It is violently ejected from its molecule and all return or recombination becomes impossible. For similar reasons ^{69}Zn, formed by fast neutron capture, does not undergo thermal annealing.

D. J. Apers
F. G. Dejehet
B. S. van Outryve d'Ydewalle
P. C. Capron

Institut Interuniversitaire des Sciences Nucléaires
Centre de Physique Nucléaire
Université de Louvain, Belgium

Preparations of nitrides and phosphides of rare-earth metals

(*Received* 1 *December* 1961)

Relatively pure nitrides and phosphides of the rare-earth metals have always been difficult to prepare in quantity. Preparation of the nitrides usually necessitates the reaction of a gas with a solid, a reaction fraught with difficulties. The phosphides, prepared from the solid elements, often react explosively and thus shatter the sealed quartz tubes or react with or fuse to the quartz or other ceramic containers which may be used in metal bombs. The methods described below overcome many of these difficulties.

NITRIDES

The metal is cut into approximate cubes, 0·5 cm on edge, under an inert atmosphere in a glove box. The cuttings are saved for the preparation of the phosphide. The cubes are removed from the box and buffed on a wire wheel. Most of the rare-earth metals are stable toward air oxidation; lanthanum, cerium, and europium are somewhat sensitive.

The metal is first converted to the hydride in the apparatus sketched in Fig. 1. It is contained in an alundum boat in quartz tube *A*. The system is flushed out several times

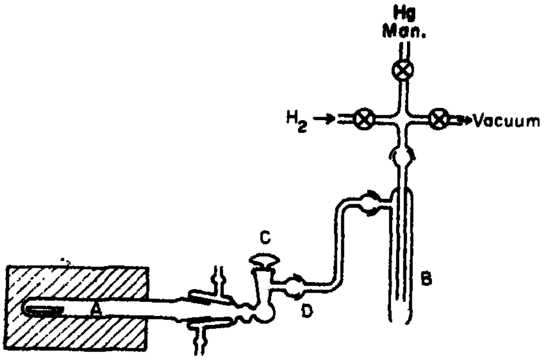

Fig. 1.—Apparatus for the preparation of hydrides.

with catalytically purified hydrogen and is then evacuated. The quartz tube is out-gassed by increasing the temperature to 150° C. The trap *B* is then cooled in liquid nitrogen, and hydrogen is admitted to the system. Sometimes the rare-earth metal begins to react immediately, causing the contents of the boat to become red hot. Stopcock *C* is used to shut off the hydrogen and thus to control the reaction. Usually reaction begins at 300°–400° C and then only after an induction period of 10–20 min. Sometimes a temperature of 600° C is required to start the reaction. When the reaction has moderated, hydrogen is admitted to the system as it is needed, the pressure being kept a few centimeters above atmospheric. When the manometer indicates that hydrogen is no longer being taken up, the charge is allowed to cool slowly to room temperature. The system is then evacuated, stopcock *C* is closed, the apparatus is disconnected at *D*, and the material is transferred to the glove box. The hydride that results is ground to 100 mesh. (The hydrides of the rare-earth metals react moderately with atmospheric moisture but not with dry air.)

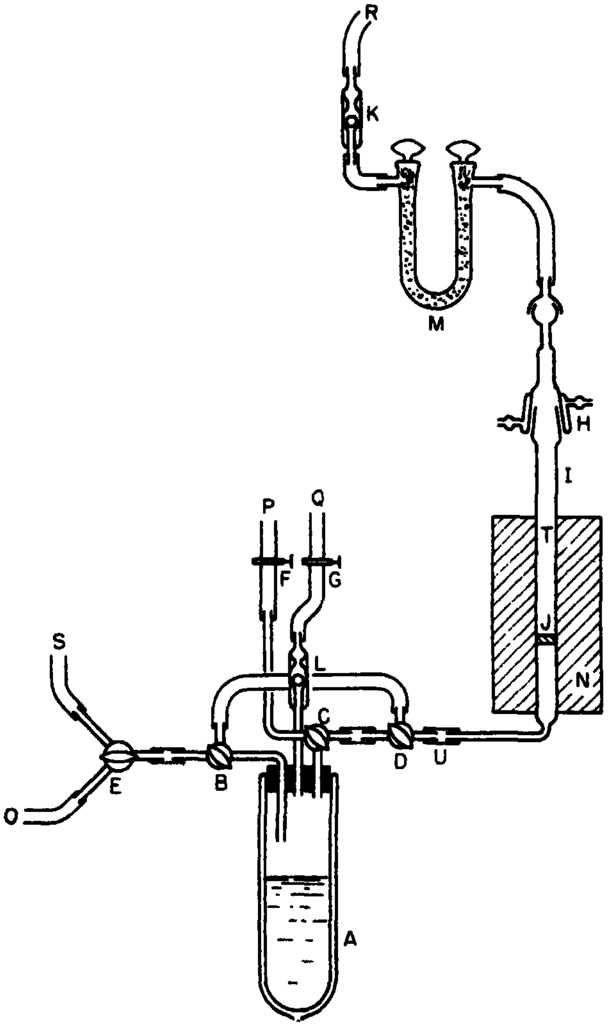

Fig. 2.—Apparatus for the preparation of nitrides.

Conversion of the hydride to the nitride is carried out in the apparatus sketched in Fig. 2. Neoprene tubing is required. Stopcocks *B*, *C*, and *D* are three-way; *E* is a 120° stopcock. Flow of ammonia is controlled with pinch clamps *F* and *G*. A water-cooled joint *H* surmounts quartz reaction tube *I* into which is sealed the fused-silica fritted disk *J*. (The fritted disks may be obtained from either the Thermal American Fused Quartz Co. or the Amersil Division of Englehard Industries.) Each of the check values *K* and *L* consists of a ground-glass ball resting on a ground seat, thus allowing gas to flow in one direction only. The U-tube *M* contains NaOH pellets. *N* is an ordinary tube furnace. The tubes *O*, *P*, *Q*, and *S* lead to bubble counters. The bubble counter *O* contains water; bubble counters *P*, *Q*, and *R* contain concentrated NH_4OH. High-purity nitrogen enters at *S*. The unsilvered Dewar flask *A* contains liquid ammonia. The flask is attached loosely to the system, and all the lines are flushed out with nitrogen. The rubber stopper that holds the entrance tubes to the Dewar flask is then loosened, and pieces of sodium metal are dropped in. Reaction occurs until the impurities in the liquid ammonia are used up; then the solution becomes blue. More sodium is added until 20 or 30 pieces the size of a pea are contained in the flask. The stopper is then seated firmly in the Dewar flask, and all the lines are again flushed out with nitrogen. During these operations, ammonia gas escapes through check valve *L*. Next, the water-cooled joint is removed from the reaction tube *I*, and a funnel having a stem long enough to reach almost to the fritted disk is inserted into the tube. With nitrogen passing up through and around the funnel, the hydride is poured into the funnel and down onto the fritted disk. A piece of quartz wool may be placed at position *T* in order to keep fine particles from being carried out of the hot zone. The system is flushed thoroughly with nitrogen. Pinch clamp *G* is then tightened to divert ammonia through the charge. The nitrogen is diverted out through *O* by means of stopcock *E*. The temperature of the furnace is increased to 800° C and is maintained for 3 hr. (Rare-earth metals begin to react with quartz at about 700° C; the hydrides of the rare-earth metals begin to react at a somewhat higher temperature, that is, 800° to 900° C.) The charge is cooled and is flushed with nitrogen. The quartz tube is detached from the system at *U* and *H*. Since the surface of the particles is now covered by the more insensitive nitride, the material can be poured into a container for removal to the glove box where it is ground to 200 mesh. In this more finely divided state, it is treated again with ammonia, this time at 800° C for ½ hr and then at 900° C for 2 hr. This treatment should practically complete the conversion of the rare-earth-metal hydride to the nitride.

In order to determine the completeness of the reaction, the product is analysed for nitrogen. In view of original impurities, 96–97 per cent of the theoretical nitrogen content can be considered to indicate complete reaction. If the result is as low as 94 per cent, the product may be ground to 270 mesh and treated at 950° C for 1 hr; however, a point of diminishing returns due to reaction with the quartz must now be considered.

Nitrogen is determined by the Kjeldahl method, but certain precautions must be observed. Previously tared weighing bottles are brought into the glove box, and three test portions of 200 to 300 mg size are taken from the product and put into the weighing bottles. The bottles are removed from the glove box, and if helium had been the atmosphere in the glove box, the weighing bottles are placed in a desiccator for 1 hr in order to allow the helium to diffuse out and to be replaced by dry air. The portions are then weighed. A portion is dissolved by dumping it quickly into a clean dry iodine flask, stoppering the flask quickly, and pouring 1:4 HCl around the stopper. The HCl is allowed to seep into the flask a little at a time, and the hydrogen to escape upward through the remaining HCl. Caution: If fine particles of original metal or hydride are present, sparks may occasionally occur which will cause the evolving hydrogen to explode. (The hydrides of the rare-earth metals are remarkably stable and some may remain even after treatment at 900° C.)

PHOSPHIDES

The phosphide of a rare-earth metal can be produced in quantities of 20 g or more by ignition of the reactant elements in a metal cylinder between snugly fitting plungers under an inert atmosphere. The preparation of holmium phosphide, which is one of the more difficult rare-earth-metal phosphides to prepare, is described below.

Red phosphorus is stirred as a slurry with 7 per cent NaOH in a platinum dish for several hours in order to remove oxides. The slurry is filtered, and the phosphorus is extracted with water overnight in a Soxhlet extractor, after which it is vacuum desiccated over P_2O_5 for several days. Holmium metal, in the form of shavings or filings, is treated with a magnet to remove traces of iron. Equal volumes of holmium and phosphorus are mixed together; such a mixture gives an excess of phosphorus equivalent to about three times the stoichiometric ratio.

The reaction is carried out in a stainless steel cylinder that is fitted at each end with movable plungers—an apparatus similar to that used in powder metallurgy for the compression of metal powders or other charges. The apparatus used for 15 g of holmium metal was a cylinder of $\frac{3}{16}$ in. wall thickness, $\frac{3}{4}$ in. i.d. and 3 in. length; each plunger was about $1\frac{1}{2}$ in. long. The charge is placed in this apparatus and is compressed moderately in a vice; a small amount of a mixture of molybdenum sulphide and graphite is used on the plungers as a lubricant. The apparatus is then placed in the clamp arrangement, sketched in Fig. 3, which is constructed of carbon steel. The entire apparatus rests in the furnace, a sketch of which is shown in Fig. 3. At *A* is the bottom part of a desiccator $\frac{1}{2}$–$\frac{2}{3}$ filled with crushed dry ice. The tube *B* enters through metal plate *C* to admit argon; carbon dioxide and argon exit through a centre hole in the metal plate. The Marshall type furnace rests on a large ceramic cylinder *D* (or metal cylinder wrapped with asbestos), which separates it from the desiccator. A narrower and longer ceramic cylinder *E* rests on the metal plate and supports the reaction apparatus in the center of the furnace. Wet asbestos paper is used on both rims of cylinder *D* to minimize leakage.

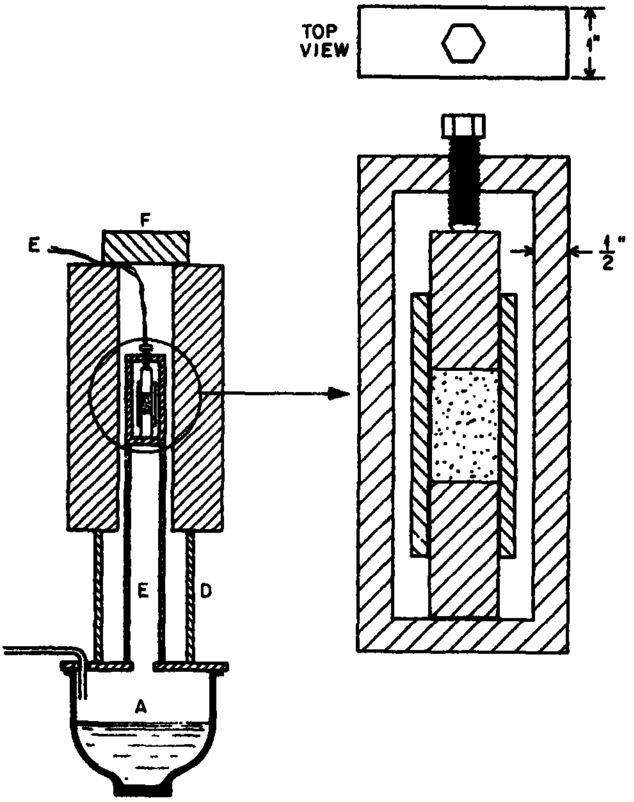

Fig. 3.—Apparatus for the preparation of phosphides.

In an operation of this nature, the approximate temperature of the incidence of reaction must be known. Heating small amounts of the reactant elements in sealed quartz tubes to different temperatures furnishes this information either by the resulting explosion or on examination of the contents after heating. The rare-earth metals react with phosphorus in the temperature range from 700° to 800° C. The charge must be brought to reaction temperature within a short time.

Accordingly, the temperature of the furnace is first increased to 1000° C; the flow of argon is adjusted so that the interior is flushed with inert gas at the same time. The charge is then lowered into the furnace by means of nichrome wire *E* attached to the bolt on the reaction apparatus, and the firebrick *F* is replaced. The temperature decreases immediately to 800° C, and almost at once phosphorus begins to burn at the top of the furnace. The temperature is constant for a minute or two and then increases fairly rapidly to about 850° C, thus indicating that the reaction has occurred. The excess phosphorus escapes around the plungers and either burns at the top of the furnace or condenses at the bottom.

After a few minutes during which the excess phosphorus is allowed to escape, the reaction apparatus is removed and is placed in a can that contains crushed dry ice. The can is covered, and the apparatus is allowed to cool. The apparatus is transferred to the glove box where the reaction product is removed, crushed, and placed in a quartz-tube apparatus similar to that used in preparing the hydrides. It is then heated to 600° C in vacuum to remove any remaining excess phosphorus.

Phosphide phosphorus in the product is determined by the method of WHITE and BUSHEY.(1) The purity is usually about 99 per cent. Spectroscopic analysis showed that the metal contamination from the cylinder is less than 100 ppm. Caution must be observed in disposing of phosphide residues. Their reaction with moisture produces poisonous phosphine.

D. E. LAVALLE

Analytical Chemistry Division
Oak Ridge National Laboratory
Oak Ridge, Tennessee

---

(1) W. E. WHITE and A. H. BUSHEY, *J. Amer. Chem. Soc.* 66, 1666 (1944).

J. Inorg. Nucl. Chem., 1962, Vol. 24, pp. 935 to 936. Pergamon Press Ltd. Printed in England

BOOK REVIEWS

R. C. Koch. **Activation Analysis Handbook:** x + 219 pp. Academic Press Inc., New York and London, 1960. 64s.

The increasingly wide-spread recognition of the virtues of activation analysis, particularly as a method for the determination of trace constituents, has led to the production of this book whose purpose, the author states, is "to present a tabulation of the pertinent published data".

The book is divided into four chapters. The first three chapters (15 pages) give a description of the technique and deal briefly with the considerations involved in selecting the most suitable reaction, the advantages and disadvantages of the various methods of irradiation, and the interpretation of results. The treatment of these subjects is adequate considering the space allowed but tends to be repetitive and several mistakes in elementary English have remained uncorrected, e.g. alternate is used when alternative is meant, referencing instead of references, radiochemistry instead of radiochemical, etc.

Chapter 4, however, is the main body of the book and consists of 166 pages of tabulated information. The elements are arranged in order of atomic number and each is dealt with on two facing pages. The left hand page is devoted to data relevant to neutron activation and the corresponding right hand page lists similar data for charged particle and photon activation. This arrangement, whilst convenient for reference purposes, is very wasteful in space; thus 16 pages are left completely blank whilst 46 pages are less than half full.

The data for neutron activation includes isotopic abundances, thermal cross sections and resonance capture integrals, half-lives of the product nuclei and the energies of the principal β- and γ-radiations they emit, possible interfering reactions, a "standard" sensitivity for each reaction under fixed conditions and references to published applications. The data for particle and photon activation includes threshold energies and references to measurements of excitation functions.

Whilst it has not been possible to check all the data, some mistakes have been noticed. Thus, for example, in referring to a paper describing the determination of rubidium and caesium (of which the reviewer was an author), the reactions involved and the sensitivities quoted have both been incorrectly reported for both elements.

To the non-specialist who requires an idea of the capabilities and limitations of activation analysis, this book may be useful. It will be of less use to the experienced analyst, however, since he requires up-to-date information on applications (and new applications are published at the rate of about 100 each year), a detailed knowledge of decay schemes, and can obtain a large part of the information given in the book from an intelligent use of the General Electric "Chart of the Nuclides".

M. J. Cabell

C. B. Monk. **Electrolytic Dissociation:** 320 pp. Academic Press, London and New York, 1961.

It is now clear that very few electrolytes are fully dissociated in solution and this book, volume VIII of a series of monographs in physical chemistry, deals with the important problem of characterizing the ionic species in such solutions. The determination both of thermodynamic dissociation constants and quotients at constant ionic strength is discussed in detail although only mononuclear species are considered. This selection is a natural one for an author who has for many years been active in this field; polynuclear species have been very fully covered in other recent works.

The first part of the book (130 pp) is more in the nature of a general electrochemistry textbook and deals in a logical fashion with experimental and theoretical aspects of conductance, transference numbers, reversible cells, activity co-efficients, partial molal quantities and diffusion. Throughout the theoretical sections there are a number of worked examples taken from original papers which form a particularly valuable feature of the book.

The second part, with extensive bibliography, deals with all the most important methods for determining dissociation constants. In each, both the theory and essential experimental methods are described and again there are a number of useful worked examples. This is a very considerable field to cover in only 127 pages and as a result, some of the descriptions are very condensed. In polarography a worker would be confused by a recommended drop time given as 2–4 drops/sec instead of sec/drop. Quite apart from this, however, the large number of techniques which have been used extensively by the author are very well and critically discussed and his intimate knowledge of possible sources of error etc. make the descriptions all the more valuable.

The book is aimed at a level between the elementary texts and the more mathematical treatises and is strongly recommended for Honours students in chemistry and for research workers interested in ionic equilibria. It provides an excellent and up-to-date summary and should find a place on the bookshelf of every Chemist who uses solutions of electrolytes. It is well printed and illustrated and contains few typographical and bibliographical errors.

G. H. Nancollas

R. Choppin. **Experimental Nuclear Chemistry.** Prentice-Hall Inc., Englewood Cliffs, New Jersey, U.S.A. (1961). $ 6.95 and $ 9.25.

This book is intended to be used by practising Chemists who need to acquire a knowledge of the techniques of nuclear chemistry, and of the essential theoretical background to them. It is also intended for University students who are taking a course in nuclear chemistry, and for the instructors who are conducting the course.

The general layout of the book follows a simple and effective pattern. Each chapter begins with a discussion of the subject matter of the chapter, copiously illustrated. This is then followed by a number of practical experiments and theoretical problems on the particular subject.

The experiments are very well designed and illustrated, and are laid out step by step in full detail. This is an important point for any instructor intending to present an experiment to his students, since it will not be necessary for him to waste time in working out small practical details.

The subject matter of the book covers all that is needed for a preliminary course in nuclear chemistry. Anyone who has conscientiously worked through it will be well equipped to use radioactive isotopes in his normal research work, or to proceed further into basic nuclear chemical research itself. Radiation protection is covered early in the book, and the essential precautions are adequately stated, without being over-emphasized. It is, however, surprising to note that wooden glove boxes are still apparently used in the U.S.A.

One criticism which must be made from the point of view of European readers concerns Appendices B and D. Appendix B deals with American regulations on the use of radioactivity and American suppliers of isotopes. Appendix D lists suitable American counting equipment for the course. It would not seem to be very difficult for the publishers to substitute European versions of these two Appendices for the benefit of their European readers. To a lesser extent the same criticism applies to references to equipment in the text of the book, but it would clearly be a big task to try to Europeanize these too.

Apart from this minor complaint, it must be said that this book fulfils its purpose extremely well, and may be highly recommended as the most suitable one on this aspect of nuclear chemistry at the present time. It ought also to be on the shelves of all practising research nuclear chemists, since it is a useful first reference for a wide variety of practical matters not always to be found easily in the general literature.

J. G. Cuninghame

J. Inorg. Nucl. Chem., 1962, Vol. 24, pp. 937 to 952. Pergamon Press Ltd. Printed in Northern Ireland

VALENCE-STATES OF BORON, CARBON, NITROGEN AND OXYGEN

G. Pilcher and H. A. Skinner
Chemistry Department, University of Manchester

(*Received* 4 *November* 1961; *in revised form* 15 *February* 1962)

Abstract—Empirical values of the parameters in the Slater-Condon theory of atomic spectra are evaluated from experimental atomic energy levels for B, C, N and O, and for their unipositive ions. From extrapolations through isoelectronic series, parameter values for the uninegative ions are also obtained. The parameters are used to calculate energies of excitation from ground states to defined valence states.

Ionization potentials and electron affinities of specified hybrid atomic orbitals are listed, and the relative electronegativites of the orbitals are evaluated.

The effect of charge on the ionization potential of an electron from certain defined atomic orbitals is examined. By comparing the ionization potentials of OH_2, NH_3 and $\cdot CH_3$ with those calculated for O, N and C atoms of the same orbital geometry, we obtain maximum values for the degree of charge transfer to the central atoms in these molecules, and maximum values for the percentage ionic character of O—H, N—H and C—H bonds: the correlation with electronegativity difference between bonded atoms is examined.

The theory of atomic spectra, developed by Slater(1), Condon and Shortley(2), and Racah(3), provides approximate expressions for the energy levels of an atom in terms of certain exchange and coulombic integrals (represented by the parameters G and F in Slater's formulation), which may be determined empirically provided the spectrum of the atom is sufficiently well investigated. In view of the approximations in Slater's theory, the parameters do not have unique values, and "best values" for them are normally determined by least squares fitting of the available spectroscopic data to the theoretical equations. The evaluation of the parameters may be based on directly observed spectroscopic energy levels, as was done, e.g., by Jaffé(4) in the case of the carbon atom, and by Skinner and Sumner(5) for the atoms vanadium through to copper. Atomic states of a given configuration are, however, perturbed in certain cases by near-lying states from a different configuration, and to make more refined evaluations of parameters correction for configuration interactions should be made, as described, e.g., by Rohrlich(6).

The first part of this paper gives a re-evaluation of spectral parameters for the atoms (and ions) of Be, B, C, N, O and F, special attention being paid to boron, carbon and nitrogen. The evaluation is based on empirical spectral data tabulated by Moore(7), with allowance for the displacements of certain levels due to configuration interactions s^2p^{n-2}–p^n.

Evaluation of spectral parameters

(a) C(I), N(II). The centres of gravity of the *observed* term values belonging to the configurations s^2p^2, sp^3 and p^4 of C(I) and N(II) are listed in columns 1, 2 of Table 1.

---

(1) J. C. Slater, *Phys. Rev.* **34**, 1293 (1929).

(2) E. U. Condon and G. H. Shortley, *Theory of Atomic Spectra*. Cambridge Univ. Press (1935).

(3) G. Racah, *Phys. Rev.* **62**, 438 (1942).

(4) I. J. Goldfarb and H. H. Jaffé, *J. Chem. Phys.* **30**, 1622 (1959).

(5) H. A. Skinner and F. H. Sumner, *J. Inorg. Nucl. Chem.* **4**, 245 (1957).

(6) F. Rohrlich, *Phys. Rev.* **101**, 69 (1956).

(7) C. E. Moore, *Atomic Energy Levels* Vol. 1. Nat. Bur. Stands. Washington, Circular 467 (1948).

TABLE 1.—OBSERVED AND CALCULATED TERM VALUES

		Observed		"Adjusted"		Calculated	
		C(I)	N(II)	C(I)	N(II)	C(I)	N(II)
s^2p^2	^3P	30	89	*2890*	*3640*	*2975*	*3774*
	^1D	10194	15316	*13420*	*19060*	*13275*	*18925*
	^1S	21648	32687	—	—	*28800*	*41650*
sp^3	^5S	33735	46785	33510	47170	29260	43570
	^3D	64091	92245	64210	92060	65650	93840
	^3P	75256	109219	75480	108800	76000	108990
	^1D	(97878)	144189	(102210)	144380	107380	148930
	^3S	105800	155130	113440	155000	112720	153750
	^1P	(119878)	166766	(119780)	165760	117730	164080
p^4	^3P	(154500)	(219200)	(*151640*)	(*215650*)	*151635*	*215645*
		B(I)	C(II)	B(I)	C(II)	B(I)	C(II)
s^2p	^2P	11	43	*4720*	*6300*	*4720*	*6300*
sp^2	^4P	28812	43033	28620	43000	28659	43182
	^2D	47857	74932	48510	74690	51013	77175
	^2S	63561	96494	63430	97040	60382	93951
	^2P	72543	110653	76500	111200	76983	111609
p^3	^4S	97037	142024	97060	141910	91985	136760
	^2D	—	150465	(98380)	150625	101354	153536
	^2P	—	168744	(*105500*)	*162480*	*101600*	*164720*
		Be(I)	B(II)	Be(I)	B(II)	Be(I)	B(II)
s^2	^1S	0	0	*6180*	*8580*	*6180*	*8580*
sp	^3P	21981	37344	22180	37210	22550	37520
	^1P	42565	73397	46120	74280	45750	73970
p^2	^3P	59697	98924	60150	98590	59610	98330
	^1D	56433	102362	*58240*	*104460*	*62610*	*106490*
	^1S	71499	127662	*66570*	*118480*	*67110*	*118730*
sd	^3D	62055	150649	—	—	—	—
	^1D	64428	154687	*62620*	*152590*	—	—
		N(I)	O(II)	N(I)	O(II)	N(I)	O(II)
s^2p^3	^4S	0	0	0	0	500	810
	^2D	19223	26817	19990	26810	20570	27900
	^2P	28840	40468	*35040*	*47870*	*33950*	*45960*
sp^4	^4P	88135	119933	87750	120000	85210	119130
	^2D	—	165991	(122360)	166090	123225	168550
	^2S	—	195710	(140000)	196900	143295	195640
	^2P	—	212616	(160720)	213510	159115	213210
p^5	^2P	(234200)	([illegible])	(*228000*)	(*310600*)	*228000*	*310600*

(i) Uncertain or estimated term values are given in brackets.
(ii) Italicized term values are adjusted for the configuration interaction shifts, s^2p^{n-2}–p^n: they are the levels of the "pure" configurations.

Columns 3, 4 give "*adjusted*" values of these same spectroscopic terms. The last two columns give *calculated* term values, using the spectral parameters now proposed and listed in Table 2.

The configurations s^2p^2 and p^4 both give rise to states ^3P, ^1D and ^1S, and each pair of states of like designation interacts: the wave function describing an observed state belonging to s^2p^2 or p^4 will thus be a combination of those describing separately a

TABLE 2.—SPECTRAL PARAMETER VALUES (IN CM⁻¹)

	Be(I)	B(II)		Be⁻	B(I)	C(II)
$A(s^2)$	6180	8580	$A(s^2p)$	3140	4720	6300
$A(sp)$	34150	55745	$A(sp^2)$	34040	66080	98120
$A(p^2)$	62110	105130	$A(p^3)$	50480	106500	164720
F_2^{pp}	500	1360	F_2^{pp}	218	1041	1864
G_1^{sp}	11600	18225	G_1^{sp}	9407	16108	22809
Δ_0^{sp}	−10	2220	Δ_0^{sp}	−5053	−3732	−2411

	B⁻	C(I)	N(II)		C⁻	N(I)	O(II)
$A(s^2p^2)$	6700	11550	16400	$A(s^2p^3)$	21940	33950	45960
$A(sp^3)$	71380	117730	164080	$A(sp^4)$	94360	145630	196900 19 500
$A(p^4)$	92250	160260	228270	$A(p^5)$	145400	228000	310600
F_2^{pp}	915	1725	2525	F_2^{pp}	1460	2230	3010
G_1^{sp}	14190	20865	27545	G_1^{sp}	17910	24635	31360
Δ_0^{sp}	−6280	−4670	−3150	Δ_0^{sp}	−3470	−4675	−5884

	N⁻	O(I)	F(II)
$A(s^2p^4)$	9570	13610	17650
$A(sp^5)$	114000	158070	202140
$A(p^6)$	214100	296870	379640
F_2^{pp}	2080	2820	3560
G_1^{sp}	22500	29500	36500
Δ_0^{sp}	−4330	−5660	−6990

(i) The A parameters of an atom are evaluated with respect to the observed ground-state, taken as the zero of energy: they may be expressed explicitly in terms of core-integrals I_s, I_p, and coulomb and exchange integrals F_0, F_2 and G_1 (e.g., MOFFITT[(9)]).

The A parameters for each configuration are defined in the following Slater formulae;

$$
\begin{aligned}
{}^1S,\, s^2 &= A(s^2)\\
\tfrac{1}{2}({}^1P,\, sp + {}^3P,\, sp) &= A(sp)\\
{}^3P,\, p^2 &= A(p^2) - 5F_2^{pp}\\
{}^2P,\, s^2p &= A(s^2p)\\
{}^4P,\, sp^2 &= A(sp^2) - 5F_2^{pp} - 2G_1^{sp}\\
{}^2P,\, p^3 &= A(p^3)\\
{}^3P,\, s^2p^2 &= A(s^2p^2) - 5F_2^{pp}\\
{}^5S,\, sp^3 &= A(sp^3) - 15F_2^{pp} - 3G_1^{sp}\\
{}^3P,\, p^4 &= A(p^4) - 5F_2^{pp}\\
{}^4S,\, s^2p^3 &= A(s^2p^3) - 15F_2^{pp}\\
{}^4P,\, sp^4 &= A(sp^4) - 5F_2^{pp} - 2G_1^{sp}\\
{}^2P,\, p^5 &= A(p^5)\\
{}^3P,\, s^2p^4 &= A(s^2p^4) - 5F_2^{pp}\\
\tfrac{1}{2}({}^1P,\, sp^5 + {}^3P,\, sp^5) &= A(sp^5)\\
{}^1S,\, p^6 &= A(p^6)
\end{aligned}
$$

In most cases, several equations are available for deriving a single A parameter (e.g. there are six terms involving $A(sp^3)$, and the *mean* value obtained from the available equations has been accepted. (ii) $\Delta_0^{sp} = F_0^{ss} - 2F_0^{sp} + F_0^{pp}$ This is not an independent spectral parameter, but is useful to simplify the writing down of valence-state equations (see Appendix). Δ_0^{sp} is defined in terms of the other parameters by:

$$
\begin{aligned}
\Delta_0^{sp} &= A(s^2) + A(p^2) - 2A(sp)\\
\Delta_0^{sp} &= A(s^2p) + A(p^3) - 2A(sp^2) + G_1^{sp}\\
\Delta_0^{sp} &= A(s^2p^2) + A(p^4) - 2A(sp^3) + 2G_1^{sp} + 10F_2^{pp}\\
\Delta_0^{sp} &= A(s^2p^3) + A(p^5) - 2A(sp^4) + G_1^{sp}\\
\Delta_0^{sp} &= A(s^2p^4) + A(p^6) - 2A(sp^5).
\end{aligned}
$$

---

(8) R. F. BACHER, *Phys. Rev.* 43, 264 (1933).

(9) W. MOFFITT, *Proc. Roy. Soc.* 202 A, 534 (1950).

"pure" s^2p^2 state and a "pure" p^4 state. As a result of the interaction, the observed s^2p^2 states are depressed, and the observed p^4 states correspondingly elevated with respect to the levels of the "pure" states. The displacements may be calculated from equations given by ROHRLICH(6).

Calculated s^2p^2–p^4 displacements for O(III), F(IV), Ne(V) and Na(VI), in cm^{-1}, are listed below:

		O(III)	F(IV)	Ne(V)	Na(VI)
s^2p^2–p^4	^{3}P	4244	4994	5640	6315
	^{1}D	4339			5962
	^{1}S	16741			

The shifts in C(I) and N(II) were estimated by linear extrapolation of the above data (direct calculations cannot be made as the p^4 states have not been spectroscopically located. We have, however, estimated the positions of $^3P(p^4)$ in N(II) and C(I) by extrapolation through the ^3P levels of higher members of the isoelectronic series). The "adjusted" term values for ^3P, $^1D(s^2p^2)$ and $^3P(p^4)$ states of N(II) and C(I) given in Table 1 are the expected positions of the "pure" states.

The configuration sp^3 gives rise to six states, $^{5,3}S$, $^{3,1}D$ and $^{3,1}P$. The perturbations of these levels by higher-lying states are considered by ROHRLICH to be small relative to the s^2p^2–p^4 interactions. The configurational shifts of the "pure" sp^3 states would be difficult to calculate, and have been ignored in the present analysis.

The centres of gravity of each of the six states deriving from the sp^3 configuration for the elements C(I) to Si(IX) inclusive, plotted against atomic number, give satisfactory straight line plots. The "adjusted" term values for the sp^3 states of C(I) and N(II) in Table 1 were read off from the "best" straight lines.

The spectral parameters G_1^{sp} and F_2^{pp} were calculated from the observed sp^3 term values for each element of the isoelectronic series C(I)–Si(XI) inclusive. These values, plotted against atomic number, also gave satisfactory straight lines. The chosen values in Table 2 were read off from the "best" straight line plots.

The parameters $A(sp^3)$, $A(s^2p^2)$ and $A(p^4)$ were calculated from the "adjusted" term values, assuming the parameters F_2^{pp} and G_1^{sp} to retain their values unchanged in each configuration.

(b) B(I) *and* C(II). The observed term values of the configurations s^2p, sp^2 and p^3 are listed in Table 1. Adjustments to these values have been made,

(i) to allow for the displacement of the ^2P levels due to the p^3–s^2p configuration interaction, and

(ii) to give conformity with the term values of the isoelectronic series B(I)–Al(IX) inclusive.

(c) Be(I) *and* B(II). Table 1 lists the observed term values belonging to the configurations s^2, sp, p^2 and $2s3d$ of Be(I) and B(II). Adjustments were made,

(i) to allow for the configuration interaction s^2–p^2 displacing the ^1S states of these configurations;

(ii) to allow for the displacement of the ^1D states due to the configuration interaction p^2–sd. The shifts were calculated by the method of BACHER(8): Slater orbitals were used to evaluate the off-diagonal matrix elements;

(iii) to give conformity with term values of elements in the isoelectronic series C(III) to Mg(IX) inclusive.

(d) N(I) *and* O(II). The observed term values belonging to s^2p^3, sp^4 and p^5 are listed in Table 1. The "adjusted" term values make allowance for the configuration interaction s^2p^3–p^5, displacing the ^2P levels. Minor adjustments were also made to give conformity with term values of elements in the isoelectronic series extending to P(IX).

(e) O(I) *and* F(II). Term values have been observed for states belonging to s^2p^4 and sp^5 for all elements in the isoelectronic series, from O(I) to Si(VII). Values of the parameters G_1^{sp} and $A(sp^5)$ were calculated from the spectral data, and gave straight line plots against atomic number.

The term $^1S, p^6$ has not been located for any member of the series, so that the extent of the configuration interaction s^2p^4–p^6, displacing ^1S states, cannot be calculated directly. We have thus been obliged to deduce $A(p^6)$ and F_2^{pp} indirectly by extrapolation.

The parameters G_1^{sp} plotted through Be(I), B(I), C(I), N(I) and O(I) give a straight line with respect to atomic number: the plot of F_2^{pp} is linear from Be(I) to N(I), and we have accepted the value for O(I) obtained by extending this line.

The parameters $A(s^2p^4)$ were evaluated from the observed s^2p^4 levels, ^3P and ^1D (the level ^1S being ignored), and $A(sp^5)$ from the mean of the sp^5 levels, ^1P and ^3P. $A(p^6)$ was evaluated by an extrapolation procedure based on examination of the form of the A parameters when written out fully in terms of the core-integrals, and the parameters F_0, F_2 and G_1.*

Valence states excitation energies

The valence state formulae were derived following the procedure described by Van Vleck(10). They are presented separately in the Appendix.

The excitation energies of chosen valence states relative to ground state atoms were calculated by substituting the parameter values of Table 2 into the appropriate valence state formulae. The calculated values (in eV) are listed in Table 3. Atomic orbitals of designation s, p_x, p_y, p_z are represented s, x, y, z, and hybrid orbitals are symbolized T(= tetrahedral, sp^3), t(= trigonal, sp^2) and d(= digonal, sp).

Calculated ionization potentials (I.P.) and electron affinities (E.A.) of selected orbitals of valence states of Be, B, C, N and O are listed in Table 4. These values were derived using the excitation energies of Table 3, the experimental ionization potentials (from ground state atoms) recommended by Moore(7), and the electron affinities estimated by Edlén(11), viz:

	I.P.(eV)	E.A.(eV)
Be	9·320	−0·19
B	8·296	0·33
C	11·256	1·24
N	14·53	0·05
O	13·614	1·47

---

* The quantities $A(sp) - A(s^2)$; $A(sp^2) - A(s^2p) - G_1$; $A(sp^3) - A(s^2p^2) - 2G_1$; $A(sp^4) - A(s^2p^3) + 10F_2 - 2G_1$; and $A(sp^5) - A(s^2p^4) + 10F_2 - 2G_1$ were evaluated from Table 2 and plotted against atomic number, and a smooth curve drawn through the points. The quantities $A(p^2) - A(sp)$; $A(p^3) - A(sp^2)$; $A(p^4) - A(sp^3) + 10F_2$; $A(p^5) - A(sp^4) + 10F_2 - G_1$; and $A(p^6) - A(sp^5) + 10F_2 - 2G_1$ plotted against atomic number should give a curve essentially similar to the first one: hence, the position of the point dependent upon $A(p^6)$ was estimated.

(10 J. H. Van Vleck, *J. Chem. Phys.* 2, 22 (1934).

(11) B. Edlén, *J. Chem. Phys.* 33, 98 (1960).

TABLE 3.—VALENCE STATE EXCITATION ENERGIES

Be^-		Be(I)		Be(II)	
s^2x	0·39	sx	3·51	x	3·96
sx^2	3·16			s	0·00
$d_1^2d_2$	1·78	d_1d_2	2·83	d_2	1·98
$t_1^2t_2$	3·82	t_1t_2	4·53	t_2	2·64
$T_1^2T_2$	4·65	T_1T_2	5·36	T_2	2·96
$t_1t_2t_3$	2·09				
B^-		**B(I)**		**B(II)**	
s^2xy	0·43	sxy	5·74	xy	12·47
$d_1^2d_2x$	3·15	d_1d_2x	4·75	d_2x	9·11
d_1^2xy	7·58	d_1xy	8·86		
$t_1^2t_2t_3$	3·65	$t_1t_2t_3$	4·42	t_2t_3	7·55
$T_1^2T_2T_3$	6·03	$T_1T_2T_3$	6·56	T_2T_3	8·86
$d_1d_2x^2$	4·96			d_1d_2	4·77
d_1xy^2	8·45				
sxy^2	5·87			sx	5·78
$t_1t_2t_3z$	3·79				
$T_1T_2T_3T_4$	3·64				
$sxyz$	5·02				
C^-		**C(I)**		**C(II)**	
s^2xyz	0·82	$sxyz$	8·47	xyz	17·99
$d_1^2d_2xy$	4·83	d_1d_2xy	7·21	d_2xy	13·26
$t_1^2t_2t_3z$	5·69	$t_1t_2t_3z$	6·79	t_2t_3z	11·09
$T_1^2T_2T_3T_4$	6·03	$T_1T_2T_3T_4$	6·58	$T_2T_3T_4$	9·89
sx^2yz	8·84			sxy	8·53
$d_1d_2xy^2$	7·77			d_1d_2x	7·19
$t_1t_2t_3z^2$	7·41			$t_1t_2t_3$	6·75
		$t_1^2t_2t_3$	6·38		
N^-		**N(I)**		**N(II)**	
s^2x^2yz	0·28	sx^2yz	14·03	x^2yz	27·20
$d_1^2d_2^2xy$	0·28	$d_1^2d_2xy$	7·67	d_1^2xy	17·26
$d_1d_2^2x^2y$	6·51	$d_1d_2x^2y$	12·56	d_1x^2y	20·74
$t_1^2t_2t_3z^2$	7·99	$t_1t_2t_3z^2$	12·08	$t_2t_3z^2$	17·87
$T_1^2T_2^2T_3T_4$	6·18	$T_1^2T_2T_3T_4$	9·75	$T_1^2T_3T_4$	14·57
sx^2y^2z	12·74			sx^2z	14·28
$d_1d_2x^2y^2$	11·40			$d_1d_2x^2$	12·68
				$d_1^2d_2x$	7·61
		$t_1^2t_2t_3z$	9·14	$t_1^2t_2t_3$	9·12
				d_1d_2xy	10·33
				$t_1t_2t_3z$	9·80
				$T_1T_2T_3T_4$	9·53
O^-		**O(I)**		**O(II)**	
$s^2x^2y^2z$	0·00	sx^2y^2z	17·76	x^2y^2z	38·50
$d_1^2d_2x^2y^2$	7·68	$d_1d_2x^2y^2$	16·02	$d_2x^2y^2$	30·25
$t_1^2t_2t_3^2z^2$	5·12	$t_1^2t_2t_3z^2$	11·22	$t_1^2t_2z^2$	23·34
$T_1^2T_2^2T_3^2T_4$	3·84	$T_1^2T_2^2T_3T_4$	8·68	$T_1^2T_2^2T_4$	19·26
$sx^2y^2z^2$	15·37			sx^2y^2	22·01
				$t_1t_2t_3z^2$	16·75
				$T_1^2T_2T_3T_4$	13·47
		$t_1^2t_2^2t_3z$	6·23	$t_1^2t_2^2t_3$	9·87
				$t_1^2t_2t_3z$	12·58

TABLE 4.—VALENCE-STATE IONIZATION POTENTIALS AND ELECTRON AFFINITIES (IN eV)

(i) Be → Be⁺	I.P.	Process	Be → Be⁻	E.A.	Process
$sx \rightarrow x$	9·76	$-s$	$sx \rightarrow s^2x$	2·94	$+s$
$d_1d_2 \rightarrow d_1$	8·47	$-d$	$d_1d_2 \rightarrow d_1^2d_2$	1·93	$+d$
$t_1t_2 \rightarrow t_1$	7·43	$-t$	$t_1t_2 \rightarrow t_1^2t_2$	0·52	$+t$
$T_1T_2 \rightarrow T_1$	6·92	$-T$	$T_1T_2 \rightarrow T_1^2T_2$	0·53	$+T$
$sx \rightarrow s$	5·81	$-p$	$sx \rightarrow sx^2$	0·16	$+p$
			$d_1d_2 \rightarrow t_1t_2t_3$	0·55	$+p$
(ii) B → B⁺			**B → B⁻**		
$sxy \rightarrow xy$	15·02	$-s$	$sxy \rightarrow s^2xy$	5·64	$+s$
$d_1d_2x \rightarrow d_2x$	12·66	$-d$	$d_1d_2x \rightarrow d_1^2d_2x$	1·93	$+d$
$d_1xy \rightarrow xy$	11·91	$-d$	$d_1xy \rightarrow d_1^2xy$	1·61	$+d$
$t_1t_2t_3 \rightarrow t_1t_2$	11·43	$-t$	$t_1t_2t_3 \rightarrow t_1^2t_2t_3$	1·10	$+t$
$T_1T_2T_3 \rightarrow T_1T_2$	10·59	$-T$	$T_1T_2T_3 \rightarrow T_1^2T_2T_3$	0·86	$+T$
$d_1d_2x \rightarrow d_1d_2$	8·32	$-p$	$d_1d_2x \rightarrow d_1d_2x^2$	0·12	$+p$
$d_1xy \rightarrow d_1x$	8·55	$-p$	$d_1xy \rightarrow d_1xy^2$	0·74	$+p$
$sxy \rightarrow sx$	8·33	$-p$	$sxy \rightarrow sxy^2$	0·20	$+p$
			$t_1t_2t_3 \rightarrow t_1t_2t_3z$	0·96	$+p$
			$t_1t_2t_3 \rightarrow T_1T_2T_3T_4$	1·11	$+p$
			$sxy \rightarrow syxz$	1·05	$+p$
(iii) C → C⁺			**C → C⁻**		
$sxyz \rightarrow xyz$	20·78	$-s$	$sxyz \rightarrow s^2xyz$	8·89	$+s$
$d_1d_2xy \rightarrow d_1xy$	17·30	$-d$	$d_1d_2xy \rightarrow d_1^2d_2xy$	3·62	$+d$
$t_1t_2t_3z \rightarrow t_1t_2z$	15·56	$-t$	$t_1t_2t_3z \rightarrow t_1^2t_2t_3z$	2·34	$+t$
$T_1T_2T_3T_4 \rightarrow T_1T_2T_3$	14·57	$-T$	$T_1T_2T_3T_4 \rightarrow T_1^2T_2T_3T_4$	1·79	$+T$
$t^2t_2t_3 \rightarrow t_1t_2t_3$	11·63	$-t$			
$sxyz \rightarrow sxy$	11·31	$-p$	$sxyz \rightarrow sx^2yz$	0·87	$+p$
$d_1d_2xy \rightarrow d_1d_2x$	11·24	$-p$	$d_1d_2xy \rightarrow d_1d_2xy^2$	0·68	$+p$
$t_1t_2t_3z \rightarrow t_1t_2t_3$	11·22	$-p$	$t_1t_2t_3z \rightarrow t_1t_2t_3z^2$	0·62	$+p$
(iv) N → N⁺			**N → N⁻**		
$sx^2yz \rightarrow x^2yz$	27·70	$-s$	$sx^2yz \rightarrow s^2x^2yz$	13·80	$+s$
$d_1^2d_2xy \rightarrow d_1^2xy$	24·12	$-d$	$d_1^2d_2xy \rightarrow d_1^2d_2^2xy$	7·44	$+d$
$d_1d_2x^2y \rightarrow d_1x^2y$	22·70	$-d$	$d_1d_2x^2y \rightarrow d_1d_2^2x^2y$	6·11	$+d$
$t_1t_2t_3z^2 \rightarrow t_1t_2z^2$	20·32	$-t$	$t_1t_2t_3z^2 \rightarrow t_1^2t_2t_3z^2$	4·14	$+t$
$T_1^2T_2T_3T_4 \rightarrow T_1^2T_2T_4$	19·35	$-T$	$T_1^2T_2T_3T_4 \rightarrow T_1^2T_2^2T_3T_4$	3·63	$+T$
$d_1^2d_2xy \rightarrow d_1d_2xy$	17·19	$-d$			
$t_1^2t_2t_3z \rightarrow t_1t_2t_3z$	15·19	$-t$			
$T_1^2T_2T_3T_4 \rightarrow T_1T_2T_3T_4$	14·31	$-T$			
$sx^2yz \rightarrow sx^2y$	14·78	$-p$	$sx^2yz \rightarrow sx^2yz^2$	1·34	$+p$
$d_1d_2x^2y \rightarrow d_1d_2x^2$	14·65	$-p$	$d_1d_2x^2y \rightarrow d_1d_2x^2y^2$	1·20	$+p$
$d_1^2d_2xy \rightarrow d_1^2d_2x$	14·47	$-p$	$d_1^2d_2xy \rightarrow d_1^2d_2xy^2$	1·21	$+p$
$t_1^2t_2t_3z \rightarrow t_1^2t_2t_3$	14·51	$-p$	$t_1^2t_2t_3z \rightarrow t_1^2t_2t_3z^2$	1·20	$+p$
$t_1t_2t_3z^2 \rightarrow t_1t_2t_3z$	12·25	$-p$			
(v) O → O⁺			**O → O⁻**		
$sx^2y^2z \rightarrow x^2y^2z$	34·35	$-s$	$sx^2y^2z \rightarrow s^2x^2y^2z$	19·24	$+s$
$d_1d_2x^2y^2 \rightarrow d_1x^2y^2$	27·84	$-d$	$d_1d_2x^2y^2 \rightarrow d_1^2d_2x^2y^2$	9·81	$+d$
$t_1^2t_2t_3z^2 \rightarrow t_1^2t_3z^2$	25·73	$-t$	$t_1^2t_2t_3z^2 \rightarrow t_1^2t_2^2t_3z^2$	7·57	$+t$
$T_1^2T_2^2T_3T_4 \rightarrow T_1^2T_2^2T_3$	24·20	$-T$	$T_1^2T_2^2T_3T_4 \rightarrow T_1^2T_2^2T_3^2T_4$	6·31	$+T$
$t_1^2t_2t_3z^2 \rightarrow t_1t_2t_3z^2$	19·14	$-t$			
$T_1^2T_2^2T_3T_4 \rightarrow T_1^2T_2T_3T_4$	18·40	$-T$			
$t_1^2t_2^2t_3z \rightarrow t_1^2t_2^2t_3$	17·25	$-p$			
$sx^2y^2z \rightarrow sx^2y^2$	17·86	$-p$	$sx^2y^2z \rightarrow sx^2y^2z^2$	3·87	$+p$
$t_1^2t_2t_3z^2 \rightarrow t_1^2t_2t_3z$	14·97	$-p$			

Electroaffinities of specified atomic orbitals

The electroaffinity of an atomic orbital of an atom was defined by Mulliken(12) as the mean of the "valence state" ionization potential and electron affinity of the orbital. Calculated electroaffinities for *p*, tetrahedral (*T*), trigonal (*t*), and digonal (*d*) orbitals, and for *s*-orbitals are listed in Table 5. The valence state of the neutral atom is given in brackets in cases where the orbital involved requires specification.

Table 5.—Electroaffinities, ½(I + E) in eV

Atom	Orbitals				
	p	*T*	*t*	*d*	*s*
Be	2·93 (sx)	3·72	3·98	4·67	6·35 (sx)
B	4·22 $(d\pi\pi)$	5·73	6·26	6·76 $(d\pi\pi)$	10·33 (sxy)
	4·27 (sxy)			7·29 $(dd\pi)$	
	4·64 $(dd\pi)$				
C	5·92 $(t_1t_2t_3\pi)$	8·18	8·95	10·46	14·84 $(sxyz)$
	5·96 $(d_1d_2\pi\pi)$				
	6·09 $(sxyz)$				
N	7·84 $(d_1^2d_2\pi\pi)$	11·49	12·23	14·41 $(d_1d_2\pi^2\pi)$	20·75 (sx^2yz)
	7·85 $(t_1^2t_2t_3\pi)$			15·88 $(d_1^2d_2\pi\pi)$	
	7·93 $(d_1d_2\pi^2\pi)$				
	8·06 (sx^2yz)				
O	10·86 (sx^2y^2z)	15·25	16·65	18·83	26·79 (sx^2y^2z)

The electroaffinities may be related to the Pauling scale of electronegativities by dividing them by a suitable factor.(12,13) The values listed below are based on the factor 3·27—chosen to make the calculated electronegativity of tetrahedral carbon = 2·50, as in Pauling's scale.

Calculated electronegativity values

	p	*T*	*t*	*d*	*s*
Be				1·43	
B			1·91		
C		2·50	2·74	3·20	
N	2·46	3·51	3·74	4·40(—N═) 4·86(N≡)	
O	3·32	4·66			
H					2·19

DISCUSSION

The calculated orbital electronegativities of C, N and O increase sharply with increasing degree of *s*-character. The effect is shown quantitatively in Fig. 1, in which the electronegativity of the bonding orbitals of trivalent N (forming three *equivalent* bonds) is plotted as a function of theoretical bond-angle (from 90°, pure *p*-bonding, to 120°, sp^2-bonding). The figure also shows the calculated ionization potential for removal of one electron from the lone-pair occupying the non-bonding orbital of N as a function of bond-angle.

Fig. 2 similarly shows the variation of the orbital electronegativity of divalent O with bond-angle, and the corresponding dependence of the ionization potential for

---

(12) R. S. Mulliken *J. Chem. Phys.* 2, 782 (1934).

(13) H. O. Pritchard and H. A. Skinner, *Chem. Rev.* 55, 745 (1955).

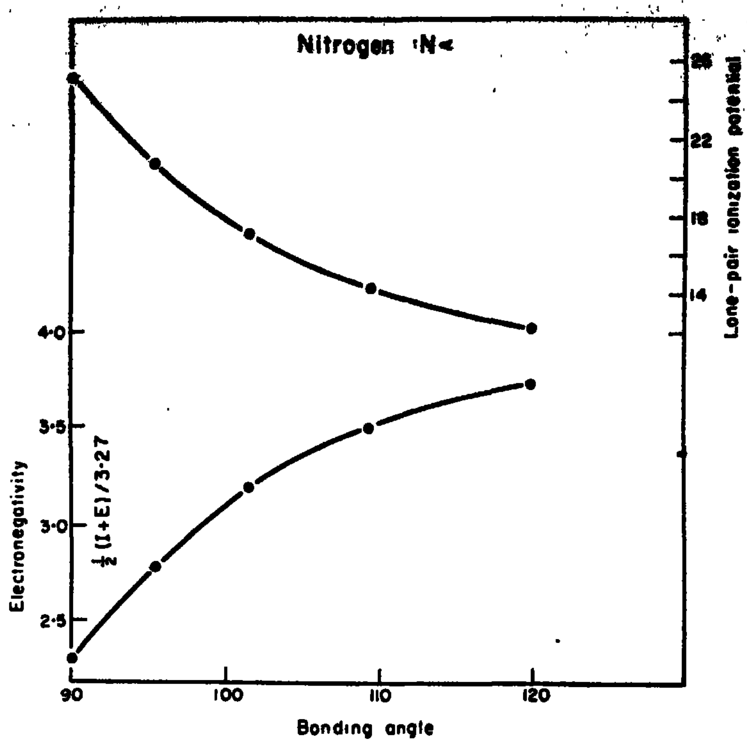

FIG. 1

removal of an electron from one of the equivalent lone-pairs of the divalent O atom.

The bond-angle[14] in NH_3 is 107°, and the ionization potential[15] is reported to be 10·15 eV: in the H_2O molecule, the bond-angle[14] is 104½°, and the ionization potential[15] is 12·59 eV. The ionization potentials of the free atoms, *hybridized to give the same orbital geometry* as in NH_3 and OH_2, are decidedly larger than those of the molecules. The same is true, to a lesser degree, of the π-electron ionization potential of sp^2-hybridized C (Table 4) relative to the ionization potential[16] of the CH_3 radical; the data are summarized below:

Molecule	Bond angle	I.P.(eV)	Atom	I.P.(eV)	Bond-orbital electronegativity
NH_3	107°	10·15	:N<	15·12	3·42
OH_2	104½°	12·59	:O<	19·30	4·38
$\cdot CH_3$	120°	9·84	C	11·22	2·74

These data suggest a correlation between the electronegativity of an atom and the change in ionization potential in passing from the free atom to molecules. To pursue this further, we have calculated the valence state ionization potentials of the neutral atoms of C, N and O, and of their positive and negative ions, in order to obtain a

---

[14] G. HERZBERG, *Infra-red and Raman Spectra*. Van Nostrand, New York (1945).
[15] K. WATANABE, *J. Chem. Phys.* **26**, 542 and 1772 (1957).
[16] G. HERZBERG and J. SHOOSMITH *Canad. J. Phys.* **34**, 523 (1956).

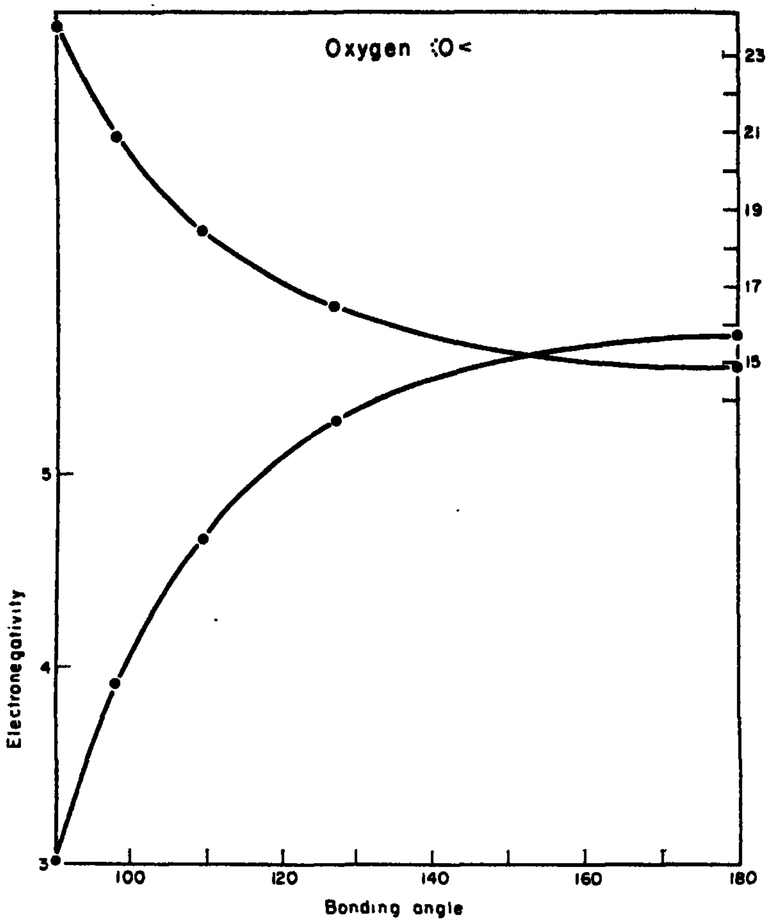

FIG. 2

quantitative measure of the effect of charge on ionization potential. The results are shown graphically in Fig. 3: smooth curves were drawn through the points listed below:

Nitrogen (bond-angle 107°)	Ionization potential (eV)	
N^-, $h_1^2h_2^2h_3h_4 \rightarrow N$, $h_1h_2^2h_3h_4$	4·24	($q = -1$)
N, $h_1^2h_2h_3h_4 \rightarrow N^+$, $h_1h_2h_3h_4$	15·12	($q = 0$)
N^+, $h_1^2h_2h_3 \rightarrow N^{2+}$, $h_1h_2h_3$	28·85	($q = +1$)
(h_1 = lone-pair orbital)		
Oxygen (bond-angle 104½°)		
O^-, $h_1^2h_2^2h_3^2h_4 \rightarrow O$, $h_1h_2^2h_3^2h_4$	6·29	($q = -1$)
O, $h_1^2h_2^2h_3h_4 \rightarrow O^+$, $h_1h_2^2h_3h_4$	19·30	($q = 0$)
O^+, $h_1^2h_2^2h_3 \rightarrow O^{2+}$, $h_1h_2^2h_3$	32·93	($q = +1$)
(h_1h_2 are lone-pair orbitals)		
Carbon (bond-angle 120°)		
C^-, $t_1^2t_2t_3\pi \rightarrow C$, $t_1^2t_2t_3$	1·93	($q = -1$)
C, $t_1t_2t_3\pi \rightarrow C^+$ $t_1t_2t_3$	11·22	($q = 0$)
C^+, $t_1t_2\pi \rightarrow C^{2+}$, t_1t_2	23·86	($q = +1$)

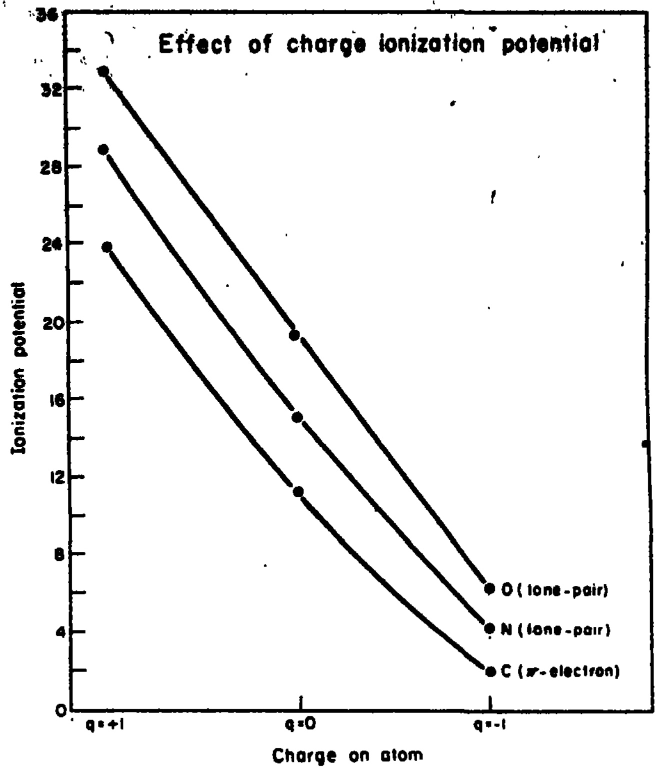

FIG. 3

From Fig. 3, the ionization potential of O, when carrying a negative charge of 0·48 e ($q = -0{\cdot}48$) becomes equal to that of the H_2O molecule: correspondingly the ionization potential of N, $q = -0{\cdot}42$, is the same as that of NH_3, and the ionization potential of C, $q = -0{\cdot}12$, the same as in CH_3. Thus if we attribute the *entire* difference between the ionization potentials of neutral atom and molecule to charge transfer within the molecule, it follows that the O—H bonds in H_2O have 24 per cent ionic character and that the N—H bonds in NH_3 and the C—H bonds in CH_3 have 14 and 4 per cent ionic character respectively.

These values for percentage ionic character may be plotted against the differences in orbital electronegativity of the bonded atoms (the H atom is assumed to use the 1*s*-orbital, electronegativity = 2·19). The resultant curve is similar in general shape to that proposed by PAULING[17], but gives smaller degrees of ionic character for a given electronegativity difference.

This plot probably *overestimates* the degree of ionic character of bonds, since it is unlikely that changes in ionization potential from atom to molecule are entirely due to charge transfer. The values given for O—H and N—H bonds require that the lone-pairs in H_2O contribute *ca.* 0·5 *D* to the total dipole moment, and that the lone-pair in NH_3 contributes *ca.* 0·8 *D*.

The main conclusions of this paper were presented at the 18th Congress of I.U.P.A.C., in Montreal, in August, 1961: at the same meeting, JAFFÉ, *et al.*[18] gave a similar paper on orbital electronegativity and valence state dependence. The methods of calculation differed slightly, but the results of the two independent investigations in general agree rather closely.

---

[17] L. PAULING, *The Nature of the Chemical Bond.* Cornell Univ. Press (1939).

[18] H. H. JAFFÉ, M. A. WHITEHEAD and J. HINZE, Abstract A1-4, 18th I.U.P.A.C. Congress, Montreal, August 1961. Also J. HINZE and H. H. JAFFE, *J. Amer. Chem. Soc.* **84**, 540 (1962).

APPENDIX

Valence state formulae

The valence state formulae given below were obtained by VAN VLECK's procedure.⁽¹⁰⁾ Atomic orbitals of the types s, p_x, p_y, p_z are represented by s, x, y, z.

(i) Valence state of atomic orbitals

V_2,	sx	$A(sp) - \frac{1}{2}G_1^{sp}$
V_1,	sx^2	$A(sp^2) + 4F_2^{pp} - G_1^{sp}$
V_3,	sxy	$A(sp^2) - 3\frac{1}{2}F_2^{pp} - G_1^{sp}$
V_2,	sx^2y	$A(sp^3) - 3F_2^{pp} - 1\frac{1}{2}G_1^{sp}$
V_4,	$sxyz$	$A(sp^3) - 10\frac{1}{2}F_2^{pp} - 1\frac{1}{2}G_1^{sp}$
V_1,	sx^2y^2	$A(sp^4) + 4F_2^{pp} - G_1^{sp}$
V_3,	sx^2yz	$A(sp^4) - 3\frac{1}{2}F_2^{pp} - G_1^{sp}$
V_2,	sx^2y^2z	$A(sp^5) - \frac{1}{2}G_1^{sp}$
V_1,	$sx^2y^2z^2$	$A(sp^6)$
V_1,	s^2x	$A(s^2p)$
V_0,	s^2x^2	$A(s^2p^2) + 4F_2^{pp}$
V_2,	s^2xy	$A(s^2p^2) - 3\frac{1}{2}F_2^{pp}$
V_1,	s^2x^2y	$A(s^2p^3) - 3F_2^{pp}$
V_3,	s^2xyz	$A(s^2p^3) - 10\frac{1}{2}F_2^{pp}$
V_2,	s^2x^2yz	$A(s^2p^4) - 3\frac{1}{2}F_2^{pp}$
V_0,	$s^2x^2y^2$	$A(s^2p^4) + 4F_2^{pp}$
V_1,	$s^2x^2y^2z$	$A(s^2p^5)$

V_0,	x^2	$A(p^2) + 4F_2^{pp}$
V_2,	xy	$A(p^2) - 3\frac{1}{2}F_2^{pp}$
V_3,	xyz	$A(p^3) - 10\frac{1}{2}F_2^{pp}$
V_2,	x^2yz	$A(p^4) - 3\frac{1}{2}F_2^{pp}$
V_1,	x^2y^2z	$A(p^5)$

(ii) Regular tetrahedral orbitals

$$\begin{cases} T_1 = \frac{1}{2}[s + x + y + z] \\ T_2 = \frac{1}{2}[s + x - y - z] \\ T_3 = \frac{1}{2}[s - x + y - z] \\ T_4 = \frac{1}{2}[s - x - y + z] \end{cases}$$

V_2,	T_1T_2	$\frac{1}{4}[A(sp) + A(p^2)] - \frac{13}{8}F_2^{pp} - \frac{3}{8}G_1^{sp} + \frac{1}{32}\Delta_0^{sp}$
V_2,	$T_1T_2T_3$	$\frac{1}{4}[3A(sp^2) + A(p^3)] - \frac{33}{8}F_2^{pp} - \frac{3}{8}G_1^{sp} + \frac{3}{32}\Delta_0^{sp}$
V_4,	$T_1T_2T_3T_4$	$A(sp^3) - \frac{33}{4}F_2^{pp} - \frac{3}{4}G_1^{sp} + \frac{3}{16}\Delta_0^{sp}$
V_2,	$T_1^2T_2T_3T_4$	$\frac{1}{4}[A(s^2p^3) + 3A(sp^4)] - \frac{33}{8}F_2^{pp} - \frac{3}{8}G_1^{sp} + \frac{3}{32}\Delta_0^{sp}$
V_2,	$T_1^2T_2^2T_3T_4$	$\frac{1}{4}[A(s^2p^4) + A(sp^5)] - \frac{13}{8}F_2^{pp} - \frac{3}{8}G_1^{sp} + \frac{1}{32}\Delta_0^{sp}$
V_1,	$T_1^2T_2^2T_3^2T_4$	$\frac{1}{4}[3A(s^2p^5) + A(sp^6)]$
V_1,	$T_1^2T_2$	$\frac{1}{4}[3A(sp^2) + A(p^3)] - F_2^{pp} + \frac{1}{8}\Delta_0^{sp}$

V_2,	$T_1^2T_2T_3$	$\frac{1}{4}[A(s^2p^4) + 2A(sp^5) + A(p^6)] - \frac{9}{4}F_2^{pp} - \frac{3}{4}G_1^{sp} - \frac{1}{16}\Delta_0^{sp}$
V_1,	$T_1^2T_2^2T_3$	$\frac{1}{4}[A(s^2p^5) + 3A(sp^6)] - F_2^{pp} + \frac{1}{4}\Delta_0^{sp}$

(iii) Regular trigonal orbitals

$$\begin{cases} t_1 = \dfrac{1}{\sqrt{3}}s + \sqrt{\dfrac{2}{3}}x \\ t_2 = \dfrac{1}{\sqrt{3}}s - \dfrac{1}{\sqrt{6}}x + \dfrac{1}{\sqrt{2}}y \\ t_3 = \dfrac{1}{\sqrt{3}}s - \dfrac{1}{\sqrt{6}}x - \dfrac{1}{\sqrt{2}}y \\ z \end{cases}$$

V_2,	t_1t_2	$\frac{1}{3}[2A(sp) + A(p^2)] - \frac{17}{18}F_2^{pp} - \frac{5}{9}G_1^{sp} + \frac{1}{18}\Delta_0^{sp}$
V_1,	$t_1^2t_2$	$A(sp^2) - \frac{1}{9}F_2^{pp} - \frac{2}{9}G_1^{sp} + \frac{2}{9}\Delta_0^{sp}$
V_2,	$t_1t_2z^2$	$\frac{1}{3}[2A(sp^3) + A(p^4)] - \frac{53}{18}F_2^{pp} - \frac{11}{9}G_1^{sp} + \frac{1}{18}\Delta_0^{sp}$
V_1,	$t_1^2t_2^2t_3$	$\frac{1}{3}[2A(s^2p^3) + A(sp^4)] - \frac{2}{3}F_2^{pp} - \frac{1}{3}G_1^{sp}$
V_4,	$t_1t_2t_3z$	$A(sp^3) - \frac{59}{6}F_2^{pp} - \frac{13}{6}G_1^{sp} + \frac{1}{6}\Delta_0^{sp}$
V_3,	t_1t_2z	$\frac{1}{3}[2A(sp^2) + A(p^3)] - \frac{101}{18}F_2^{pp} - \frac{8}{9}G_1^{sp} + \frac{1}{18}\Delta_0^{sp}$
V_3,	$t_1t_2t_3$	$A(sp^2) - \frac{17}{6}F_2^{pp} - \frac{5}{3}G_1^{sp} + \frac{1}{6}\Delta_0^{sp}$
V_3,	$t_1^2t_2t_3z$	$\frac{1}{3}[2A(s^2p^3) + A(p^5)] - \frac{101}{18}F_2^{pp} - \frac{5}{9}G_1^{sp} - \frac{5}{18}\Delta_0^{sp}$
V_3,	$t_1t_2t_3z^2$	$A(sp^4) - \frac{17}{6}F_2^{pp} - \frac{5}{3}G_1^{sp} + \frac{1}{6}\Delta_0^{sp}$
V_2,	$t_1^2t_2t_3z^2$	$\frac{1}{3}[A(s^2p^4) + 2A(sp^5)] - \frac{17}{18}F_2^{pp} - \frac{5}{9}G_1^{sp} + \frac{1}{18}\Delta_0^{sp}$
V_2,	$t_1^2t_2t_3$	$\frac{1}{3}[2A(s^2p^2) + A(p^4)] + \frac{7}{18}F_2^{pp} - \frac{5}{9}G_1^{sp} - \frac{5}{18}\Delta_0^{sp}$
V_2,	$t_1^2t_2^2t_3z$	$\frac{1}{3}[2A(s^2p^4) + A(sp^5)] - \frac{7}{3}F_2^{pp} - \frac{1}{3}G_1^{sp}$
V_1,	$t_1^2t_2z^2$	$A(sp^4) - \frac{1}{9}F_2^{pp} - \frac{2}{9}G_1^{sp} + \frac{2}{9}\Delta_0^{sp}$
V_1,	$t_1^2t_2^2t_3z^2$	$\frac{1}{3}[2A(s^2p^5) + A(sp^6)]$

(iv) Digonal orbitals

$$\begin{cases} d_1 = \dfrac{1}{\sqrt{2}}(s + z) \\ d_2 = \dfrac{1}{\sqrt{2}}(s - z) \\ x, y \end{cases}$$

V_4,	d_1d_2xy	$A(sp^3) - 10F_2^{pp} - 2G_1^{sp} + \frac{1}{6}\Delta_0^{sp}$
V_3,	d_1xy	$\frac{1}{2}[A(sp^2) + A(p^3)] - 7F_2^{pp} - \frac{1}{2}G_1^{sp}$
V_3,	d_1d_2x	$A(sp^2) - 3F_2^{pp} - \frac{3}{2}G_1^{sp} + \frac{1}{6}\Delta_0^{sp}$
V_3,	$d_1^2d_2xy$	$\frac{1}{2}[A(s^2p^3) + A(sp^4)] - 7F_2^{pp} - \frac{1}{2}G_1^{sp}$
V_3,	$d_1d_2x^2y$	$A(sp^4) - 3F_2^{pp} - \frac{3}{2}G_1^{sp} + \frac{1}{6}\Delta_0^{sp}$
V_2,	$d_1d_2x^2y^2$	$A(sp^5) + \frac{1}{2}F_2^{pp} - G_1^{sp} + \frac{1}{6}\Delta_0^{sp}$
V_1,	$d_1x^2y^2$	$\frac{1}{2}[A(sp^4) + A(p^5)] + 2F_2^{pp} - \frac{1}{2}G_1^{sp}$
V_1,	$d_1^2d_2x^2y^2$	$\frac{1}{2}[A(s^2p^5) + A(sp^6)]$

V_2,	d_1x^2y	$\frac{1}{2}[A(sp^3) + A(p^4)] - \frac{13}{4}F_2^{pp} - \frac{3}{4}G_1^{sp}$
V_2,	$d_1^2d_2x^2y$	$\frac{1}{2}[A(s^2p^4) + A(sp^5)] - \frac{7}{4}F_2^{pp} - \frac{1}{4}G_1^{sp}$
V_2,	d_1x	$\frac{1}{2}[A(sp) + A(p^2)] - \frac{7}{4}F_2^{pp} - \frac{1}{4}G_1^{sp}$
V_2,	$d_1^2d_2x$	$\frac{1}{2}[A(s^2p^2) + A(sp^3)] - \frac{13}{4}F_2^{pp} - \frac{3}{4}G_1^{sp}$
V_2,	d_1d_2	$A(sp) + \frac{1}{5}F^{pp} - G_1^{sp} + \frac{1}{6}\Delta_0^{sp}$
V_1,	$d_1^2d_2$	$\frac{1}{2}[A(s^2p) + A(sp^2)] + 2F_2^{pp} - \frac{1}{2}G_1^{sp}$
V_2,	d_1^2xy	$A(sp^3) - \frac{13}{2}F_2^{pp} + \frac{1}{4}\Delta_0^{sp}$
V_2,	$d_1d_2x^2$	$A(sp^3) - \frac{5}{2}F_2^{pp} - 2G_1^{sp} + \frac{1}{6}\Delta_0^{sp}$
V_2,	$d_1^2d_2^2xy$	$A(s^2p^4) - \frac{7}{2}F_2^{pp}$

Valence states of Boron

$$\text{Orbitals}\begin{cases} h_2 = \dfrac{1}{\sqrt{3}}[(\cos\alpha)s - (\sin\alpha)z] + \sqrt{\dfrac{2}{3}}\,x \\ h_3 = \dfrac{1}{\sqrt{3}}[(\cos\alpha)s - (\sin\alpha)z] - \dfrac{1}{\sqrt{6}}x + \dfrac{1}{\sqrt{2}}y \\ h_4 = \dfrac{1}{\sqrt{3}}[(\cos\alpha)s - (\sin\alpha)z] - \dfrac{1}{\sqrt{6}}x - \dfrac{1}{\sqrt{2}}y \end{cases}$$

These orbitals range from trigonal hybrids ($\alpha = 0$) to pure p-orbitals $\left(\alpha = \dfrac{\pi}{2}\right)$

B, V_3, $h_2h_3h_4$: $A(p^3)\sin^2\alpha + A(sp^2)\cos^2\alpha - 7F_2^{pp}(\frac{1}{2} + \sin^2\alpha)$
$\qquad - G_1^{sp}\cos^2\alpha + \frac{1}{6}[\Delta_0^{sp} + 4F_2^{pp} - 4G_1^{sp}]\cos^4\alpha$

B⁺, V_2, h_2h_3 : $\frac{1}{3}A(p^2) + \frac{2}{3}[A(p^2)\sin^2\alpha + A(sp)\cos^2\alpha] - \frac{7}{6}F_2^{pp}(1 + 2\sin^2\alpha)$
$\qquad - \frac{1}{3}G_1^{sp}\cos^2\alpha + \frac{1}{18}[\Delta_0^{sp} + 4F_2^{pp} - 4G_1^{sp}]\cos^4\alpha$

B⁻, V_2, $h_2^2h_3h_4$: $A(p^4)\sin^2\alpha + \frac{1}{3}[A(s^2p^2) + 2A(sp^3)]\cos^2\alpha$
$\qquad - \frac{1}{6}F_2^{pp}(19 + 62\sin^2\alpha) - \frac{1}{9}G_1^{sp}(19 + 15\sin^2\alpha)$
$\qquad + \frac{1}{18}[\Delta_0^{sp} + 4F_2^{pp} - 4G_1^{sp}][1 - 8\sin^2\alpha + 7\sin^4\alpha]$

see N⁺ [illegible] see

B⁻, V_4, $h_1h_2h_3h_4$: see N⁺, V_4, $h_1h_2h_3h_4$

Valence states of Nitrogen

$$\text{Orbitals}\begin{cases} h_1 = (\sin\alpha)s + (\cos\alpha)z \\ h_2 = \dfrac{1}{\sqrt{3}}[(\cos\alpha)s - (\sin\alpha)z] + \sqrt{\dfrac{2}{3}}\,x \\ h_3 = \dfrac{1}{\sqrt{3}}[(\cos\alpha)s - (\sin\alpha)z] - \dfrac{1}{\sqrt{6}}x + \dfrac{1}{\sqrt{2}}y \\ h_4 = \dfrac{1}{\sqrt{3}}[(\cos\alpha)s - (\sin\alpha)z] - \dfrac{1}{\sqrt{6}}x - \dfrac{1}{\sqrt{2}}y \end{cases}$$

h_2, h_3 and h_4 are equivalent orbitals

The bond angles $\theta(h_1h_2)$ and $\theta(h_2h_3)$ for different values of α, and the "bonding power" of the orbitals $S(h_1)$ and $S(h_2)$ are listed below (bonding power is defined by PAULING(17))

$\pi\ h_1 h_2$

α	$\theta(h_1h_2)$	$\theta(h_3h_4)$	$S(h_1)$	$S(h_3)$
0	90°	120°	1·73	1·99
$\pi/6$	109°28′	109°28′	2·00	2·00
$\pi/4$	116°34′	101°32′	1·93	1·99
$\pi/3$	121°29′ ?	95°15′	1·73	1·93
$\pi/2$	$\boxed{125°16′}$	90°	1·00	1·73

N, V_3, $h_1^2h_2h_3h_4$: $A(s^2p^3)\sin^2\alpha + A(sp^4)\cos^2\alpha - \overset{7}{\cancel{7}}F_2^{pp}(\frac{4}{5} + \sin^2\alpha)$
$- G_1^{sp}\cos^2\alpha + \frac{1}{6}[\Delta_0^{sp} + 4F_2^{pp} - 4G_1^{sp}]\cos^4\alpha$

N$^+$, V_2, $h_1^2h_2h_3$: $A(s^2p^2)\sin^2\alpha + \frac{1}{3}[2A(sp^3) + A(p^4)]\cos^2\alpha$
$+ F_2^{pp}(6\frac{1}{18} + 3\sin^2\alpha) - G_1^{sp}\cos^2\alpha$
$+ \frac{1}{18}[\Delta_0^{sp} + 4F_2^{pp} - 4G_1^{sp}][1 - 8\sin^2\alpha + 7\sin^4\alpha]$

N$^-$, V_2, $h_1^2h_2^2h_3h_4$: $\frac{2}{3}A(s^2p^4) + \frac{1}{3}[A(s^2p^4)\sin^2\alpha + A(p^6)\cos^2\alpha]$
$- F_2^{pp}(\frac{22}{3} + \frac{49}{9}\sin^2\alpha) - \frac{5}{3}G_1^{sp}\cos^2\alpha$
$+ \frac{1}{18}[\Delta_0^{sp} + 4F_2^{pp} - 4G_1^{sp}][\sin^4\alpha + 4\sin^2\alpha - 5]$

N$^+$, V_4, $h_1h_2h_3h_4$: $A(sp^3) - 10\frac{1}{2}F_2^{pp} - 1\frac{1}{2}G_1^{sp}$
$+ \frac{1}{6}[\Delta_0^{sp} + 4F_2^{pp} - 4G_1^{sp}][1 + \sin^2\alpha - 2\sin^4\alpha]$

N^{++}, V_3, $h_1h_2h_3$: $\frac{2}{3}A(sp^2) + \frac{1}{3}[A(sp^2)\sin^2\alpha + A(p^3)\cos^2\alpha]$
$- F_2^{pp}[\frac{25}{6} - \frac{7}{3}\sin^2\alpha] - G_1^{sp}[\frac{2}{3} + \frac{1}{3}\sin^2\alpha]$
$+ \frac{1}{18}[\Delta_0^{sp} + 4F_2^{pp} - 4G_1^{sp}][1 + 4\sin^2\alpha - 5\sin^4\alpha]$

N, V_3, $h_1h_2^2h_3h_4$: $A(sp^4)\sin^2\alpha + \frac{1}{2}[A(s^2p^3) + 2A(sp^4)]\cos^2\alpha$
$- F_2^{pp}[\frac{25}{6} - \frac{7}{3}\sin^2\alpha] - G_1^{sp}[\frac{2}{3} + \frac{1}{3}\sin^2\alpha]$
$+ \frac{1}{18}[\Delta_0^{sp} + 4F_2^{pp} - 4G_1^{sp}][1 + 4\sin^2\alpha - 5\sin^4\alpha]$

Valence states of Oxygen

$$\text{Orbitals}\begin{cases} h_1 = \dfrac{1}{\sqrt{2}}[(\sin\alpha)s + (\cos\alpha)x + z] \\ h_2 = \dfrac{1}{\sqrt{2}}[(\sin\alpha)s + (\cos\alpha)x - z] \\ h_3 = \dfrac{1}{\sqrt{2}}[(\cos\alpha)s - (\sin\alpha)x + y] \\ h_4 = \dfrac{1}{\sqrt{2}}[(\cos\alpha)s - (\sin\alpha)x - y] \end{cases}$$

h_1 and h_2 are equivalent orbitals: so are h_3 and h_4
The bond angles $\theta(h_1h_2)$ and $\theta(h_3h_4)$ for different values of α, and the bonding power of the orbitals, $S(h_1)$ and $S(h_3)$ are listed below:

α	$\theta(h_1h_2)$	$\theta(h_3h_4)$	$S(h_1)$	$S(h_3)$
0	90°	180°	1·73	1·93
$\pi/6$	98°12′	126°52′	1·97	1·98
$\pi/4$	109°28′	109°28′	2·00	2·00
$\pi/3$	126°52′	98°12′	1·98	1·97
$\pi/2$	180°	90°	1·93	1·73

O, V_2, $h_1^2h_2^2h_3h_4$: $A(s^2p^4)\sin^2\alpha + A(sp^5)\cos^2\alpha - \frac{7}{3}F_2^{pp}\sin^2\alpha - \frac{1}{3}G_1^{sp}\cos^2\alpha$
$+ \frac{1}{6}[\Delta_0^{sp} + 4F_2^{pp} - 4G_1^{sp}]\cos^4\alpha$

O^+, V_1, $h_1^2h_2^2h_3$: $A(s^2p^3)\sin^2\alpha + \frac{1}{2}[A(sp^4) + A(p^5)]\cos^2\alpha + F_2^{pp}(2 - 5\sin^2\alpha)$
$- \frac{1}{2}G_1^{sp}\cos^2\alpha - \frac{1}{2}[\Delta_0^{sp} + 4F_2^{pp} - 4G_1^{sp}]\sin^2\alpha\cos^2\alpha$

O^-, V_1, $h_1^2h_2^2h_3^2h_4$: $A(s^2p^5)\sin^2\alpha + \frac{1}{2}[A(s^2p^5) + A(sp^6)]\cos^2\alpha$

O^+, V_3, $h_1^2h_2h_3h_4$: $\frac{1}{2}[A(s^2p^3) + A(sp^4)]\sin^2\alpha + A(sp^4)\cos^2\alpha - \frac{7}{8}F_2^{pp}(1 + \sin^2\alpha)$
$- G_1^{sp}(1 - \frac{1}{2}\sin^2\alpha) + \frac{1}{8}[\Delta_0^{sp} + 4F_2^{pp} - 4G_1^{sp}][1 - \sin^4\alpha]$

O^{2+}, V_2, $h_1^2h_2h_3$: $\frac{1}{2}[A(sp^3) + A(p^4)] + \frac{1}{2}[A(s^2p^2) - A(p^4)]\sin^2\alpha$
$- F_2^{pp}(\frac{12}{4} + 8\sin^2\alpha) - \frac{3}{4}G_1^{sp}$
$- \frac{1}{8}[\Delta_0^{sp} + 4F_2^{pp} - 4G_1^{sp}]\sin^2\alpha\cos^2\alpha$

O, V_2, $h_1^2h_2h_3^2h_4$: $\frac{1}{2}[A(s^2p^4) + A(sp^5)] - \frac{7}{4}F_2^{pp} - \frac{1}{4}G_1^{sp}$
$+ \frac{1}{8}[\Delta_0^{sp} + 4F_2^{pp} - 4G_1^{sp}]\sin^2\alpha\cos^2\alpha$

J. Inorg. Nucl. Chem., 1962, Vol. 24, pp. 953 to 960. Pergamon Press Ltd. Printed in Northern Ireland

THE PREPARATION AND CHARACTERIZATION OF TRI-N-PROPYL-, TRI-ISOPROPYL- AND TRIVINYLGALLIUM*

J. P. OLIVER and L. G. STEVENS†
Department of Chemistry, Wayne State University
Detroit 2, Michigan

(*Received* 4 *January* 1962; *in revised form* 12 *February* 1962)

Abstract—The preparation of three triorganogallium compounds is described in detail. The reaction of divinyl- and diallylmercury with gallium metal has been found to occur readily at room temperature unlike dialkylmercury compounds which require elevated temperatures before reaction occurs.

The compounds prepared have been characterized by their infra-red spectra, vapour-pressures, and melting points; and also, by the reactions with acid solution, iodine, trimethylamine, and ammonia.

Cryoscopic measurements show trivinylgallium exists as the dimer and a structure is postulated for this molecular species. The two tripropylgallium compounds are shown to be monomeric in the vapour state.

THE preparation of trialkylgallium compounds was first reported in 1932 by DENNIS[1] and by RENWANZ[2]. Trimethyl- and triethylgallium etherates were obtained from the reaction of the appropriate Grignard reagent on a solution of gallium trichloride in ether. Two methods were soon devised for the preparation of the ether free compounds; these methods are described by the following equations:

$$3HgR_2 + 2Ga \rightarrow 2GaR_3 + 3Hg$$
$$2GaCl_3 + 3ZnR_2 \rightarrow 2GaR_3 + 3ZnCl_2.$$

Both reactions were originally reported to form trialkylgallium compounds only when heated to reflux temperatures.[1,3] Recently divinylmercury has been reported to react with gallium metal at room temperature to produce ethylene and a vinylmetallic compound[4] A more complete study has shown that trivinylgallium is produced by this reaction.[5]

The exchange reaction

$$3AlR_3 + GaCl_3 \rightarrow GaR_3 + 3AlR_2Cl$$

has also been used for the preparation of trialkylgallium compounds but has not been described in detail.[6]

---

* This work was supported by the National Science Foundation Grant, N.S.F.-G-15829, and by a Fredric-Gardner Cottrell Grant from the Research Corporation; it was presented in part at the 140th National Meeting of the American Chemical Society.

† This work was taken in part from the Ph.D. Thesis of L. G. Stevens, Wayne State University, 1962.

[1] L. M. DENNIS, and W. PANTODE, *J. Amer. Chem. Soc.* **54**, 182 (1932).
[2] G. RENWANZ, *Ber. Dtsch. Chem. Ges.* **65 B**, 1208 (1932).
[3] C. A. KRAUS and F. E. TOONDER, *Proc. Nat. Acad. Sci.* **19**, 292 (1933).
[4] F. E. BRINCKMAN and F. G. A. STONE, *J. Inorg. Nucl. Chem.* **11**, 24 (1959).
[5] J. P. OLIVER and L. G. STEVENS, *J. Inorg. Nucl. Chem.* **19**, 378 (1961).
[6] J. EISCH and H. GILMAN, *Advances in Inorganic Chemistry and Radiochemistry*, (Edited by H. J. EMELEUS and A. G. SHARPE) Vol. 2, pp. 61–103. Academic, New York (1960).

The work so far cited provides several excellent procedures for the preparation of organogallium compounds, there is, however, little information concerning the physical and chemical properties of compounds other than trimethyl- and triethylgallium.[7-9]

The current interest in the catalytic activity of the Group III trialkyls, i.e., those of boron and aluminium, has lead us to undertake an exploration of the physical and chemical properties of simple triorganogallium compounds in the hope that they may prove useful in this area of research. This paper constitutes a report on the preparation of two previously unreported compounds, tri-n-propyl- and tri-isopropylgallium and a brief characterization of them by some of their physical and chemical properties, as well as a more complete discussion of the preparation and properties of trivinylgallium.

EXPERIMENTAL AND RESULTS

Apparatus. All reactions were carried out in standard high vacuum apparatus or under a nitrogen atmosphere being kept free of oxygen and water as required by the reactivity of these compounds. Further, this was required when handling trivinylgallium because of its vile and clinging odour and by the toxicity of the organomercury compounds.

Materials. The gallium and gallium trichloride used were reagent grade obtained from Fairmount Chemical Company. The di-n-propylmercury, di-isopropylmercury, and divinylmercury were synthesized by the reaction of an excess of the appropriate Grignard reagent with mercuric chloride.

A minor modification of this procedure found useful in this laboratory was to dissolve the mercuric chloride in tetrahydrofuran. The solution was then added through a dropping funnel to the Grignard reagent; thus eliminating the soxhlet extractor normally used. This procedure was found useful in the preparation of these mercury compounds. The mercury compounds were purified by repeated fractional distillation and identified by vapour-pressure. The infra-red spectra were taken and showed that no ether was retained in the mercury compounds.

Tri-n-propylgallium. The reaction of di-n-propylmercury with gallium metal was carried out using 11·1 mmole of $Hg(n\text{-}C_3H_7)_2$ with 7·43 mmole of gallium metal. This provided a very small excess of gallium metal. The reaction mixture was sealed into a glass tube and heated on a steam bath for 3 days, then cooled in ice-water with resultant solidification of the metal indicating that the reaction had not proceeded to a great extent. The reaction mixture was then heated at 150°C for 15 hr. The reaction products were transferred to the vacuum line for analysis and separation.

A small amount of gas which was noncondensable in liquid nitrogen was found, most likely, hydrogen. In addition, substantial amounts of propane and propylene were obtained. The remaining heavy material was used without further purification in the following experiments and constituted a yield of approximately 80 per cent.

The reaction of n-propylmagnesium bromide on gallium trichloride was also used to prepare tri-n-propylgallium.* This reaction proved less satisfactory, however, yielding a product difficult to separate from the ether which was used as a solvent. The acid hydrolysis, of the partially purified product, carried out as described below, gave a propane to gallium ratio of 2·9:1 for this product.

---

* This method for the preparation of tri-n-propylgallium has recently been reported in the literature, but no details of preparation were included.[10]

[7] G. E. COATES, *J. Chem. Soc.* 2003 (1951).

[8] G. E. COATES and R. G. HAYTER, *J. Chem. Soc.* 2519 (1953).

[9] G. E. COATES, *Organometallic Compounds* (2nd Ed.). J. Wiley, New York (1960).

[10] H. HARTMANN and H. LUTSCHE, *Naturwissenschaften* **48**, 601 (1961).

Tri-isopropylgallium. Due to the success of the metal exchange used in the preparation of the tri-n-propylgallium, this was the only procedure used in the preparation of tri-isopropylgallium. In a reaction tube 2·26 mmole of gallium metal was placed and 1·45 mmole of di-isopropylmercury was distilled into the tube. This was sealed off and heated in an oil bath at 150°C for 8 hr. The tube was then reattached to the vacuum line and products transferred into it for separation and analysis.

A considerable amount of hydrocarbons, consisting largely of propane and propylene were removed by fractional distillation. The purified product represented a 75 per cent yield of tri-isopropylgallium.

Trivinylgallium. Three different methods have been tried for the preparation of trivinylgallium. The first, the reaction of sodium vinyl and dimethylgallium chloride proved to give complex reaction products containing trace amounts of volatile gallium compounds. The second, the reaction of vinylmagnesium chloride with gallium trichloride in ether, provided small amounts of volatile gallium compounds which upon hydrolysis yielded ethylene. The low yields of these reactions, however, made them impractical.

The third method for the preparation of trivinylgallium was the reaction of divinylmercury with gallium metal. In this case divinylmercury was distilled into a reaction vessel containing an excess of gallium metal and the reaction carried out at room temperature. Best results were obtained when the reaction mixture was allowed to stand for 12 hr and then stirred with a magnetic stirrer in the presence of broken glass for approximately 4 hr. A typical reaction was carried out using 1·20 g of gallium metal and 3·86 g of divinylmercury. The purified product from this reaction weighed 1·31 g which represents a yield of 87 per cent based on the divinylmercury used in the reaction.

It should also be pointed out that when very carefully purified divinylmercury is used and all air and moisture is rigorously excluded, no ethylene is evolved during the course of the reaction as had previously been found.(6)

The product was purified by downward flow of the vaporized reaction products through a trap designed for fractional crystalization. This trap was maintained at −23°C allowing the trivinylgallium to crystallize on the sides of the tube, while, the divinylmercury drained into the bottom of the trap and could then be distilled away. Material purified in this manner contained no impurities detectable by mass spectrometry and was used in the subsequent reactions.

Triallylgallium has also been obtained by the reaction of diallylmercury under the conditions used for the preparation of trivinylgallium.* The details of this preparation and the properties of triallylgallium will be discussed in a subsequent paper.

Analysis. Samples of the gallium compounds were distilled from the vacuum line into weighted tubes, equipped with stopcocks and standard tapper joints, which were then reweighed providing an accurate method for determination of the sample size. Then the tube was reattached to the vacuum line and approximately 1 ml of either water or 6N hydrochloric acid was distilled into the vessel to hydrolyse the sample.

---

* Triallylgallium has also been prepared in this laboratory by the reaction of allyl Grignard reagent on gallium trichloride.

It was found that the aqueous hydrolysis was quite slow and did not go to completion in a reasonable time unless the lower portion of the reaction vessel was heated in a bath maintained at 100°C causing the reaction to take place under reflux conditions. Even then, it required 48 hr for complete hydrolysis of a sample of trivinylgallium. The acid hydrolysis is considerably more rapid in all cases, but required heating to drive the reaction to completion in less than a day. The complete reaction proceeds according to the equation:

$$GaR_3 + xH_2O + 3H^+ \rightarrow Ga(H_2O)_x^{3+} + 3RH.$$

The hydrolysis of tri-n-propyl- and tri-isopropylgallium was even more difficult to drive to completion requiring prolonged periods of heating in acid solution. The gas evolved during the hydrolysis was transferred to the vacuum line and its quantity determined in a standard volume. The results of the hydrolysis experiments are given in Table 1. The gallium analysis(11) was carried out by titration with potassium ferrocyanide while the evolved gases were identified by their infrared spectra.(12) Ethylene was produced on the hydrolysis of trivinylgallium and propane was obtained from the two propyl derivatives. In all cases, the purity of the gas was determined by use of gas–liquid chromatography.

TABLE 1.—PRODUCTS FROM THE HYDROLYSIS OF THE ORGANOGALLIUM COMPOUNDS

Sample	Evolved gas (mmole) Calc.	Evolved gas (mmole) Found	Gallium (mmole) Calc.	Gallium (mmole) Found
Trivinylgallium				
23·4 mg (HCl)	0·465	0·461	0·155	0·146
42·5 mg (H_2O)	0·842	0·835	0·281	0·257
Tri-n-propylgallium				
72·5 mg (HCl)	1·092	1·105	0·364	0·356
Tri-isopropylgallium				
119·5 mg (HCl)	1·803	1·751	0·601	0·564

Reactions with halogens. In addition to the above analysis, samples of the tri-n-propyl- and tri-isopropylgallium were reacted with iodine and chlorine in an effort to further substantiate their structures by the production of the corresponding halogenated alkyls.

The reaction with iodine was performed by distilling a sample of either tri-n-propyl- or tri-isopropylgallium into a tube which was then attached to an apparatus containing iodine. This was so arranged that the iodine could readily be sublimed into the reaction vessel which was immersed in liquid nitrogen. When a known quantity of iodine had been sublimed into the reaction vessel, it was allowed to warm to room temperature and tipped so that the gallium compound could come in contact with the solid iodine. The gallium compounds dissolved the iodine giving a brown solution which was decolourized in 5–10 min when an excess of the gallium compound was present.

The resulting alkyl iodides which were produced in nearly quantitative yield were identified by their infra-red spectra and shown to be n-propyl iodide from tri-n-propylgallium and isopropyl iodide from tri-isopropylgallium, substantiating the formulation of the compounds.

---

(11) R. BELCHER, A. J. NUTTEN and W. L. STEPHEN, *J. Chem. Soc.* 2438 (1952).

(12) R. H. PIERSON, A. N. FLETCHER and E. GANTZ, *Analyt. Chem.* **28**, 1218 (1956).

Chlorine was also reacted with tri-isopropylgallium, but in this case the reaction did not proceed quantitatively to produce gallium trichloride and isopropyl chloride but produced isopropyl chloride as well as some other chlorinated products and a black residue. The reaction proceeded in this general fashion even when stoichemetric amounts of chlorine were added to tri-isopropylgallium, cooled with liquid nitrogen, and allowed to warm very slowly to room temperature.

Physical properties. The melting points of trivinyl- and tri-n-propylgallium and triallylgallium have been determined by the Stock method and are given in Table 2 with melting points of trimethyl- and triethylglallium for reference. The melting point of tri-isopropylgallium is below −100°C, but was not determined precisely.

TABLE 2.—MELTING POINTS OF SEVERAL TRISUBSTITUTED GALLIUM COMPOUNDS

Compound	m.p. (°C)
Trivinylgallium	$-9{\cdot}0 \pm 1°$
Trimethylgallium(13)	$-15{\cdot}70$—$-15{\cdot}9°$
Triallygallium	$-72{\cdot}0° \pm 1°$
Triethylgallium(13)	$-82{\cdot}3°$
Tri-n-propylgallium	$-85{\cdot}2 \pm 1°$
Tri-isopropylgallium	Below $-100°$

The vapour-pressure of tri-n-propyl-, tri-isopropyl-, and trivinylgallium were determined over the temperature range 25–100°C and are given by the equation $\log_{10} P_{\mathrm{mm}} = -A/T + B$. The values for A and B are given in Table 3; the calculated heats of vaporization are also included. The two tripropylgallium compounds were found to be stable over the temperature range used, however, trivinylgallium started to decompose at approximately 60°C to a brown oil and a mixture of hydrocarbons.

TABLE 3.—VAPOUR-PRESSURE AND HEATS OF VAPORIZATION FOR TRIVINYL-, TRI-N-PROPYL-, AND TRI-ISOPROPYLGALLIUM FOR THE EQUATION ($\log_{10} P_{\mathrm{mm}} = -A/T + B$)

	A	B	ΔHvap. kcal/mole
Trivinylgallium	3790	12·12	17·4
Tri-n-propylgallium	2567	8·510	11·7
Tri-iso-propylgallium	2560	8·637	11·7

Molecular weights. The gas phase molecular weights of tri n-propyi- and tri-isopropylgallium were determined and found to be within experimental error of the molecular weight of the monomer, calc. 198·99. Repeated efforts to determine the gas phase molecular weight of trivinylgallium resulted in failure due to its low vapour-pressure and its tendency to undergo polymerization. Cryoscopic measurements in cyclohexane, however, clearly show that this compound exists as a dimer in solution, calc. mol. wt. 301·72. The average molecular weight determined from three independent experiments was 302.

Infra-red spectra. The infra-red spectra of trivinyl-, tri-n-propyl- and tri-isopropylgallium are recorded in Table 4. These spectra were taken in carbon tetrachloride solution using a Beckman I.R. 4 Spectrophotometer.

---

(13) E. WIBERG, T. JOHANNSEN and O. STECHER, *Z. Anorg. Chem.* **251**, 114 (1943).

TABLE 4.—INFRA-RED SPECTRA OF SEVERAL ORGANOGALLIUM COMPOUNDS

$Ga(C_2H_3)_3$ (cm^{-1})		$Ga(nC_3H_7)_3$ (cm^{-1})		$Ga(iC_3H_7)_3$ (cm^{-1})	
3013	*m*	2936	*s*	2935	*s*
2935	*m*	1464	*m*	2857	*s*
2909	*m*	1425	*w*	1468	*m*
1394	*s*	1379	*w*	1385	*m*
1264	*w*	1333	*w*	1162	*w*
1042	*m*	1063	*s*	1122	*m*
1017	*s*	1022	*w*	1063	*w*
981	*m*	982	*m*	988	*w*
952	*s*			959	*m*
				875	*w*

Reaction with air. The 5 per cent carbon tetrachloride solutions used for the infra-red measurements were opened to the air. No immediate reaction appeared to take place, however, between 30 and 60 min later the solutions of the tripropylgallium compounds became cloudy. After standing overnight a white crystalline precipitate formed. Trivinylgallium reacted more slowly requiring several hours of exposure to the atmosphere before any cloudiness appeared and one to two days for complete precipitation of a white crystalline material. These products are now under investigation but have not yet been rigorously identified.

Reactions with ammonia and Trimethylamine. A known amount of ammonia or trimethylamine was distilled into tubes containing weighted samples of the gallium compounds. The tubes were then closed off, warmed to room temperature for several minutes and cooled with a dry-ice–acetone bath. The tubes were then reopened to the vacuum line and the excess reactant distilled away and measured. In all cases, the initial uptake of amine corresponds to the formation of 1 : 1 addition compound. All of these products were liquid at room temperature and the vapour pressures were less than 1 mm at 25°C.

The trimethylamine compounds were quite stable toward hydrolysis or reaction with the atmosphere, as were the ammonia adducts. However, the ammonia addition compounds slowly decomposed at room temperature with evolution of hydrocarbon and the formation of a new gallium compound.

DISCUSSION

All of the physical and chemical data support the assignment of the formulas of tri-n-propylgallium and tri-isopropylgallium. In particular these structures are supported by the formation of the corresponding iodides from the reaction of iodine with the compound in question. Also the infra-red spectra of the parent compounds are compatible with this assignment.(14) The considerable amount of decomposition which occurred in the preparation of both tri-propylgallium compounds leads one to suspect that rearrangement might have occurred and the infra-red spectrum does not rule out this possibility. However, as noted earlier, the essentially quantitative formation of the corresponding alkyl iodides from these compounds demonstrates that little rearrangement took place.

(14) L. J. BELLAMY, *The Infra-red Spectra of Complex Molecules*, J. Wiley, New York (1954).

The trivinylgallium has been characterized from its infra-red spectrum which clearly indicates the vinyl substituent[14,15] and from its quantitative hydrolysis to ethylene and Ga^{3+}. In addition, the nuclear magnetic resonance spectrum has been obtained and indicates that the three vinyl groups are equivalent.* A complete analysis of this spectrum will be given at a later date.

It is suggested from several different physical measurements that trivinylgallium exists as a dimer or higher polymer in liquid phase, in solution, and in the solid state. The evidence supporting this is as follows:

(1) Trivinylgallium has a very high melting point (−9°C) compared to triethylgallium (−82·3) but quite similar to that of trimethylgallium (−15·8).

(2) The vapour-pressure of trivinylgallium is considerably lower (0·8 mm ± 0·1 at 25°C) than that of triethylgallium (6·8 mm at 25°C).

(3) Cryoscopic measurements in cyclohexane indicate that the molecular weight is 302.

These data show conclusively that trivinylgallium exists as a dimer in solution and suggest that in the pure liquid and in the solid state it occurs as a dimer or more highly associated species. Unfortunately, little information is avaliable on the molecular structures of gallium compounds except that there is some evidence for association of trimethylgallium in the liquid state[17] and for the association of triethylgallium in benzene solution.[1] Comparing vapour-pressures and melting points of these two compounds with trivinylgallium provides strong circumstantial evidence for molecular association in both liquid and solid trivinylgallium.

The structure of the dimer is most likely similar to that known for the aluminium alkyls with the bridge bonding carbon atom

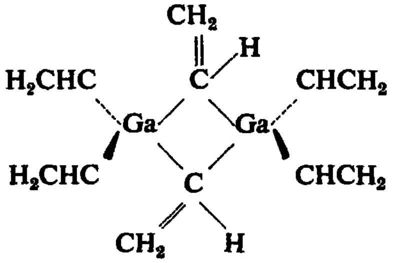

however, the possibility exists for the bonding to occur between the vacant *p*-orbital on the gallium and the π-electrons in the vinyl group. The present data does not allow a distinction to be made between these two possibilities.

---

* The equivalence of the three vinyl groups as demonstrated by n.m.r. is not anticipated from the proposed dimeric structure. However, this can be explained on the basis of a rapid equilibrium involving the exchange of the vinyl bridge groups with the terminal groups regardless of whether this equilibrium is inter- or intra-molecular. A similar equivalence of bridging and terminal alkyl groups has been demonstrated for the dimer of trimethylaluminum at ambient temperature.[18]

[15] (a) H. D. Kaesz and F. G. A. Stone, *Spectrochim. Acta* **15**, 360 (1959); (b) H. D. Kaesz and F. G. A. Stone, *Organometallic Chemistry*, *Amer. Chem. Soc.* Monograph No. 147 (Edited by H. Zeiss, p. 88–149 Reinhold, New York (1960).

[16] N. Muller and D. E. Pretchard, *J. Amer. Chem. Soc.* **82**, 248 (1960); S. Brownstein, B. C. Smith, G. Erlich and A. W. Lambengayer, *Ibid.* **82**, 1000 (1960); M. P. Groenewege, J. Smidt and H. de Vries, *Ibid* **82**, 4425 (1960).

[17] L. H. Long and J. F. Sackman, *Trans. Faraday Soc.* **54**, 1797 (1958).

Furthermore, it should be noted that there is a great disparity in the ease of preparation of the triorganogallium compounds from the corresponding mercury derivatives. In the case of the saturated hydrocarbons the reaction takes place only at elevated temperatures, while for the vinyl and allyl compounds reaction occurs readily at room temperature.

There are two possible explanations for this depending upon the mechanism of reaction. In the event of a radical reaction the ease of formation of the hydrocarbon free radical will be the determining step. This appears quite reasonable since the thermal decomposition of the mercury compound produces the corresponding free radical and reaction of the mercury compounds with gallium occurs near the decomposition point. The lack of radical rearrangement products makes this explanation somewhat dubious.

The second explanation can be given assuming that the reaction occurs between an electrophilic gallium atom and the carbon–mercury bond. In this case the polarity of the bond will influence the ease of reaction. This will increase greatly between the saturated mercury compounds and the unsaturated derivatives again providing a qualitative explanation in agreement with experiment. This explanation is further supported by work on other metal exchange reactions in which retention of configuration is observed, indicating a substitution mechanism.(15b) Neither of these explanations can be eliminated, however, until further work is carried out on gallium–mercury systems.

Acknowledgements—The authors wish to thank Mr. C. M. SMITH for the preliminary work on the preparation of tri-n-propyl- and tri-isopropylgallium, and Dr. M. T. EMERSON of Florida State University for the determination of the n.m.r. spectrum of trivinylgallium.

J. Inorg. Nucl. Chem., 1962, Vol. 24, pp. 961 to 966. Pergamon Press Ltd. Printed in Northern Ireland

STUDIES IN HEAVY METAL SOAPS—II(1)

MOLECULAR WEIGHTS OF ALUMINIUM SOAPS

R. C. MEHROTRA and A. K. RAI,
Chemical Laboratories, University of Gorakhpur, Gorakhpur, India

(*Received* 8 *December* 1961)

Abstract—The molecular weights of some aluminium soaps have been measured in various organic solvents. The tri-soaps were found monomeric mono, the alkoxy soaps dimeric and the mono and di-chloride soaps tri-meric in solution. Probable structures have been suggested for the compounds.

THE aluminium soaps prepared by metathetic reactions between aluminium salts and sodium soaps in water are hydrolysed products and are characterized by their strong gelling tendency in hydrocarbon solvents. It was believed(2,3,4) that the gel structure arose from hydrogen bonding,(5,6,7) but infra-red(8) absorption studies have shown that no such bonds are present in hydrolysed aluminium soaps. The aluminium tri-soaps and also mono and di-isopropoxide aluminium soaps have been successfully synthesized recently by PANDE and MEHROTRA(9). In a recent communication,(10) the preparation of aluminium chloride soaps by the reaction between anhydrous aluminium chloride and fatty acids in organic solvents has also been described. Not only the tri-soaps but the alkoxide as well as chloride soaps have been found to give mobile solutions in benzene, showing a low degree of molecular association. This is in agreement with the actual observations of GILMOUR *et al.*(11) on the cryscopic molecular weights of aluminium tri-laurate and tri-stearate in benzene:

Aluminium	Conc.	0·16	0·35	0·58	0·94	1·27	1·77	2·39
Tri-laurate 624 (Calc.)	Mol. wt.	652	702	730	692	726	802	954
Aluminium	Conc.	0·56	1·0	1·46	1·82	2·23		
Tri-stearate 877 (Calc.)	Mol. wt.	1547	1214	1525	1566	1427		

However, these data do show some degree of dimerization which is marked much more in the case of aluminium stearate. From purely steric considerations and the observed behaviour of alkoxides,(12) the tendency to association should decrease with increase in the alkyl chain length.

In view of the above, it was considered worthwhile to reinvestigate the degree of molecular association shown by the aluminium tri-soaps and the chloride and isopropoxide products.

---

(1) R. C. MEHROTRA and A. K. RAI, *J. Inorg. Nucl. Chem.* In Press.
(2) S. B. ELLIOT, *Alkaline Earths and Heavy Metal Soaps*. Reinhold., New York (1946).
(3) R. G. BOSSERT, *J. Chem. Educ.* **27**, 10 (1950).
(4) F. J. LICATA, *Metallic Soaps*. Metasap Chemical Company, New Jersey (1940).
(5) T. S. MCROBERTS and J. H. SCHULMAN, *Proc. Roy. Soc.* A **200**, 136 (1950).
(6) J. W. MCBAIN and W. L. MCLATCHIE, *J. Amer. Chem. Soc.* **54**, 3266 (1932).
(7) V. R. GREY and A. E. ALEXANDER, *J. Phys. Colloid Chem.* **53**, 23 (1949).
(8) A. E. LEGER, R. L. HAINES, C. E. HUBLEY, J. C. HYDE and H. SHEFFER, *Canad. J. Chem.* **35**, 799 (1957).
(9) R. C. MEHROTRA and K. C. PANDE, *J. Inorg. Nucl. Chem.* **2**, 60 (1956).
(10) R. C. MEHROTRA and A. K. RAI, *J. Ind. Chem. Soc.* In press.
(11) GILMOUR, JOBLING and NELSON, *J. Chem. Soc.* 1972 (1956).
(12) R. C. MEHROTRA, *J. Ind. Chem. Soc.* **30**, 585 (1953).

In the Table 1 are given the results of the observed molecular weights in benzene, carbon tetrachloride and n-hexane. From approximate straight lines (Figs. 1, 2 and 3) obtained on plotting resistance against the weight of the solute (up to about 0·6 g of the compound per 16 ml of the solvent) added, it can be concluded that molecular association is independent of the concentration in the range studied. The tri-soaps are all monomeric, whereas the isopropoxide and chloride soaps show dimeric and trimeric association respectively in all the three solvents:

TABLE 1

Name of the compound	Molecular formula	Molecular weight calc.	Molecular weight found		
			Benzene	Carbon tetra chloride	n-Hexane.
Aluminium tri-laurate.	$Al(C_{11}H_{23}COO)_3$	624	618	628	—
Aluminium tri-palmitate.	$Al(C_{15}H_{31}COO)_3$	792	772	800	816
Aluminium tri-behnate.	$Al(C_{21}H_{43}COO)_3$	1044	—	1085	—
Aluminium mono-isopropoxy Di-behnate.	$Al(OPr^i)(C_{21}H_{43}COO)_2$	764	1535	1532	1524
Aluminium di-isopropoxy mono-behnate.	$Al(OPr^i)_2(C_{21}H_{43}COO)$	484	958	980	—
Aluminium di-chloride mono-behnate.	$AlCl_2(C_{21}H_{43}COO)$	437	1342	1305	1322
Aluminium mono-chloride di-palmitate.	$AlCl(C_{15}H_{31}COO)_2$	572·5	1782	1791	—
Aluminium mono-chloride di-laurate.	$AlCl(C_{11}H_{23}COO)_2$	460·5	1332	1366	—

In view of the above results, following structures may be suggested for the isopropoxide (1 and 2), chloride (3 and 4) and tri-soaps (5).

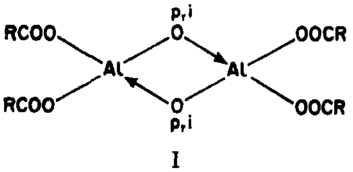

I

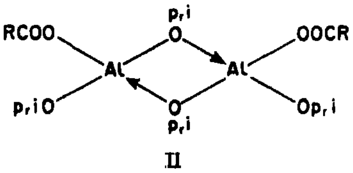

II

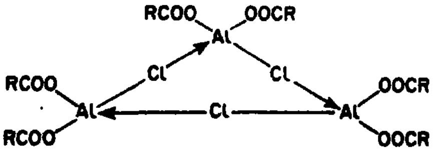

III

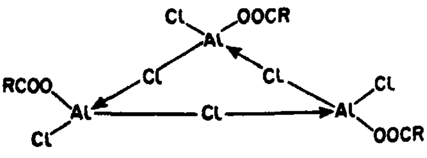

IV

$Al(OOCR)_3$

V

The above structures also explain the observation that in the reaction of aluminium isopropoxide and chloride with excess fatty acids, two isopropyl radicals or chlorine atoms are removed with much greater ease than the third. This is confirmed by the heat changes observed in the reaction of aluminium secondary butoxide with fatty acids, when the reaction is known to be exothermic up to the addition of two moles of the fatty acids to per mole of the butoxide.(7)

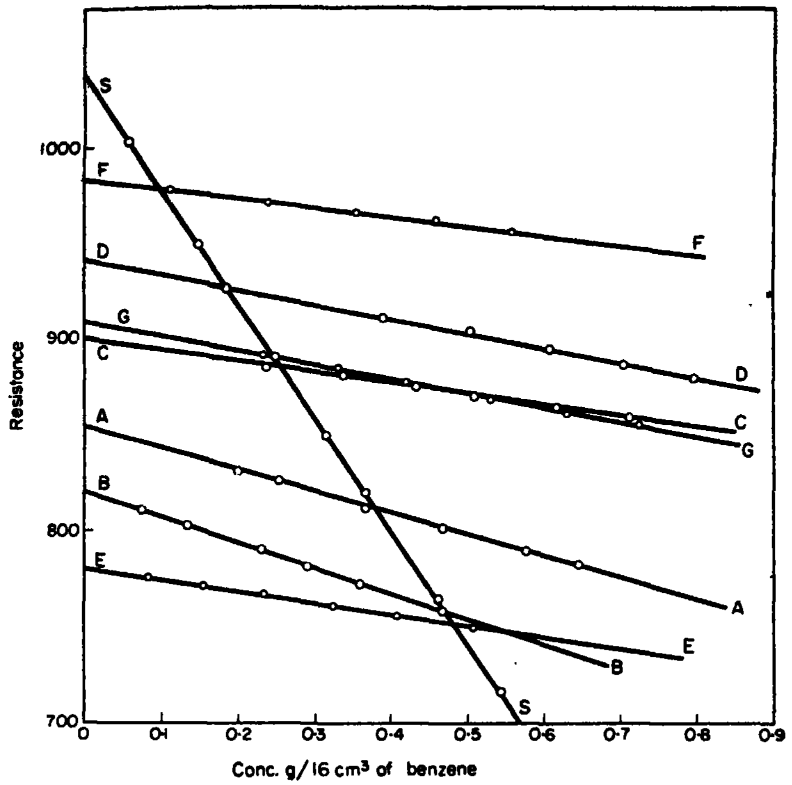

FIG. 1.—AA—$Al(C_{15}H_{31}COO)_3$ SS—Naphthalene
BB—$Al(C_{11}H_{23}COO)_3$ EE—$AlCl(C_{11}H_{23}COO)_2$
CC—$Al(Opr^i)(C_{21}H_{43}COO)_2$ FF—$AlCl(C_{15}H_{31}COO)_2$
DD—$Al(Opr^i)_2(C_{21}H_{43}COO)$ GG—$AlCl_2(C_{21}H_{43}COO)$

In all the above structures, aluminium has achieved co-ordination number four. Alternative structures could be written in which aluminium would have coordination number five or six. For example, the structure of mono-isopropoxy aluminium dialkanoates could be represented as:

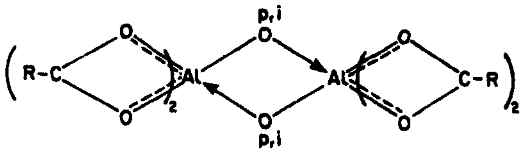

The chelating properties of alkanoate radicals were suggested by SIDGWICK(13), but were discarded due to the strain involved in a four membered ring. Evidence for the

---

(13) N. V. SIDGWICK, *The Chemical element and their compounds* Vol. 1, pp. 524.

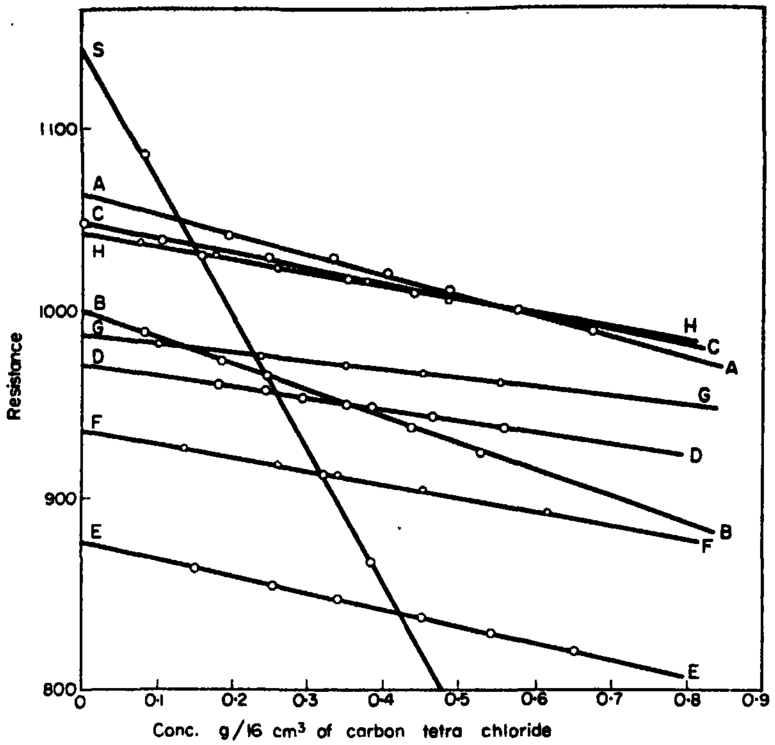

FIG. 2.—AA—$Al(C_{15}H_{31}COO)_3$
BB—$Al(C_{11}H_{23}COO)_3$
CC—$Al(C_{21}H_{43}COO)_3$
DD—$Al(Opr^i)(C_{21}H_{43}COO)_2$
EE—$Al(Opr^i)_2(C_{21}H_{43}COO)_2$
SS—Naphthalene
FF—$AlCl(C_{11}H_{23}COO)_2$
GG—$AlCl(C_{15}H_{31}COO)_2$
HH—$AlCl_2(C_{21}H_{43}COO)$

presence of these chelate rings have been found by LACOMTE and coworkers$^{(14)}$ from infra-red studies in formates, acetates and other fatty acid soaps. Similar evidence has been found by HONIG and SINGLETERRY$^{(15)}$ in alkali and alkaline earth phenyl stearates and by KUNTZEL$^{(16)}$ in chromium-fatty acid complexes. SHEFFER and coworkers$^{(8)}$ have also assumed such chelation in aluminium soaps. A possible explanation for the monomeric nature of aluminium tri-soaps has to be sought in a structure of the type:

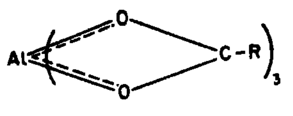

In the alkoxides$^{(12)}$ and β-diketone derivatives,$^{(17)}$ of aluminium, the predominance of four-co-ordinate aluminium in determining the properties of these compounds is quite evident. For example, derivatives like the dichloride or diethoxide monoacetyl-

---

(14) C. DUVAL, J. LACOMETE and F. DOUVILLE, *Ann. Phys.* 17, 5 (1942).

(15) J. C. HONIG and C. R. SINGLETERY, *J. Phys. Chem.* 60, 1114 (1956).

(16) A. KUNTZEL, H. ERDMANN and H. SPAHRKAS, *Das Leder*, 4, 73 (1953); 3, 30 (1952). cf. *Chem. Abstr.* 47, 12087f (1953).

(17) R. K. MEHROTRA and R. C. MEHROTRA, *Canad. J. Chem.* 39, 795 (1961).

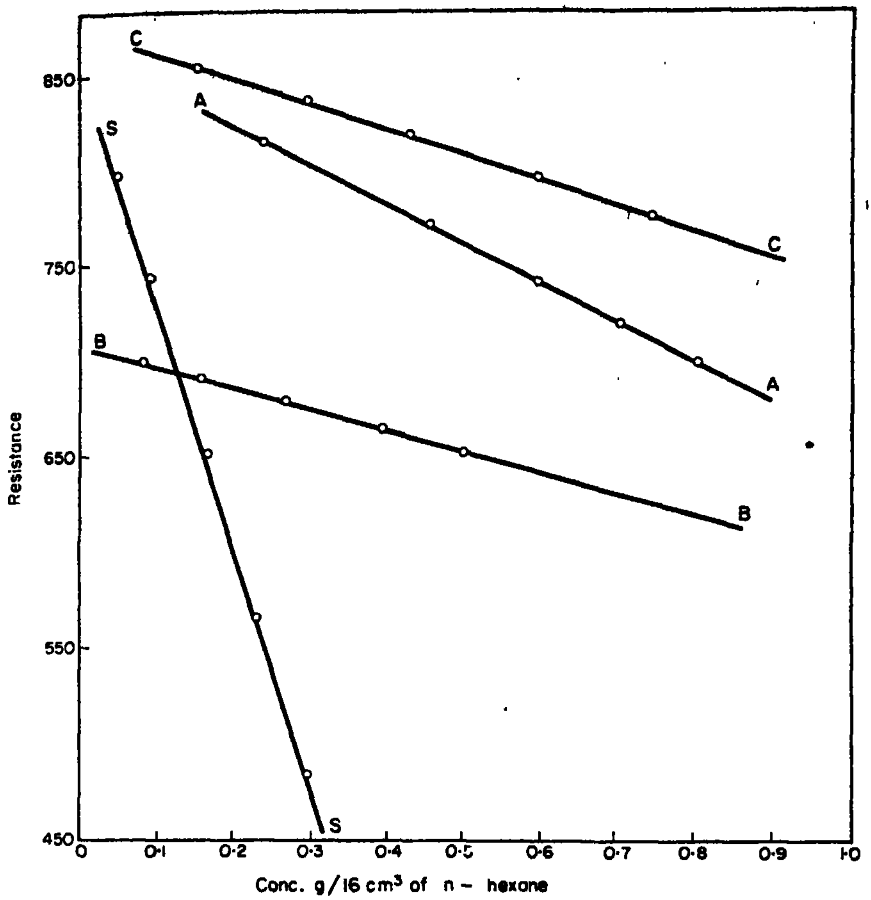

FIG. 3.—AA—Al($C_{15}H_{31}COOH)_3$ CC—Al$Cl_2(C_{21}H_{43}COO)$
BB—Al(Opr^i)$(C_{21}H_{43}COO)_2$ SS—Naphthalene

acetonate of aluminium have been shown to be monomeric and given the structure:

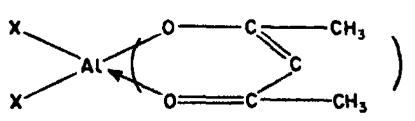

Any tendency to association of such derivatives would be due to six four-co-ordinate changing to six-co-ordinate aluminium. It is possible that even in aluminium tri-acetylacetonate and tri-alkanoate only tetravalency is achieved by partial chelation of the three attached groups. However, a final picture can be reached only after structural analysis.

EXPERIMENTAL

Aluminium tri-palmitate, tri-laurate, tri-behnate, mono-chloride di-laurate, mono-chloride di-palmitate and di-chloride mono-behnate have been prepared by the reaction of aluminium chloride (Judex) with the various fatty acids (Lauric acid, B.D.H., distilled at 140 ± 0·5°/0·2 mm, palmitic acid, B.D.H., distilled at 182 ± 1°/3·0 mm and behnic acid, L. Light and Co. Ltd.), dried at 80°/

0·2 mm in different stoicheiometric ratios. The reactions proceed as follows:

$$AlCl_3 + RCOOH \rightarrow AlCl_2(RCOO) + HCl$$
$$AlCl_3 + 2RCOOH \rightarrow AlCl(RCOO)_2 + 2HCl$$
$$AlCl_3 + 3RCOOH \rightarrow Al(RCOO)_3 + 3HCL$$

or

more

The chloride soaps are very reactive to moisture, so extra precautions were taken to exclude moisture from the reaction mixtures. The soaps were analysed for aluminium and chlorine by standard methods. The lower percentage of chlorine in the compounds have been discussed previously.(10)

TABLE 2

Name of the compound	Molecular formula	Al(%)		Cl(%)	
		Found	Calc.	Found	Calc.
Aluminium tri-laurate	$Al(C_{11}H_{23}COO)_3$	4·36	4·33	—	
Aluminium tri-palmitate	$Al(C_{15}H_{31}COO)_3$	3·39	3·41	—	—
Aluminium tri-behnate	$Al(C_{21}H_{43}COO)_3$	2·57	2·59	—	—
Aluminium mono-chloride di-laurate	$AlCl(C_{11}H_{23}COO)_2$	5·79	5·86	6·96	7·71
Aluminium mono-chloride di-palmitate	$AlCl(C_{15}H_{31}COO)_2$	4·67	4·71	5·46	6·20
Aluminium di-chloride mono-behnate	$AlCl_2(C_{21}H_{43}COO)$	6·44	6·41	15·62	16·25

Aluminium mono-isopropoxy di-behnate and di-isopropoxy mono-behnate were prepared by the reaction of aluminium isopropoxide and behnic acid in stoicheiometric ratios.(9) The isopropoxy content in the azeotrope and the compounds are determined by oxidation with chromic acid.(18) The compounds gave on analysis

TABLE 3

Name of the compound	Molecular formula	Al(%)		Isopropoxy (%)	
		Found	Calc.	Found	Calc.
Aluminium mono-isopropoxy di-behnate.	$Al(Opr^i)(C_{21}H_{43}COO)_2$	3·58	3·55	7·05	7·85
Aluminium di-isopropoxy mono-behnate.	$Al(Opr^i)_2(C_{21}H_{43}COO)$	5·52	5·58	22·8	24·4

The molecular weights of the lower alkoxy soaps were not measured because of their viscous nature.

The molecular weights were determined with a semi-micro ebulliometer (Gallenkamp) using a thermistor. The experimental techniques have been described previously.(11) Sixteen ml of solvent was taken in the ebulliometer bulb. A regular decrease in resistance with increase of solute concentration in the solvent was observed (Figs. 1, 2 and 3). Since the molecular weights are high, a graphical method was employed for the calculation of molecular weights. The general formula $M = K.W/R$ (where K is the constant for the solvent, W is the weight of the solute added and R is the decrease in resistance due to addition of solute W) reduces to $M = Km$ (where m is the slope of the straight line) The constant (K) for benzene, carbon tetra-chloride and n-hexane was taken to be 77200, 91060 and 167600, after several determinations, using napthalene as solute.

Acknowledgement—The authors are grateful to the Council of Scientific and Industrial Research, New Delhi, for a research fellowship to one of them (A. K. R.) during the tenure of which the present investigations were carried out.

J. Inorg. Nucl. Chem., 1962, Vol. 24, pp. 967 to 977 Pergamon Press Ltd. Printed in Northern Ireland

SYNERGISTIC EFFECTS IN THE EXTRACTION OF SELECTED METALLIC CATIONS BY MONO (2-ETHYL HEXYL) PHOSPHORIC ACID*

G. W. MASON, S. McCARTY and D. F. PEPPARD
Argonne National Laboratory, Argonne, Illinois

(*Received* 9 *January* 1962)

Abstract—The effect of synergistic agents upon the extraction of M(III) lanthanides, Y(III), Am(III), Cm(III), Th(IV), and U(VI) by H_2MEHP, mono 2-ethyl hexyl phosphoric acid, in a carrier diluent from aqueous HCl has been investigated as a function of carrier diluent, synergistic agent, concentration of H_2MEHP and Z of M(III) lanthanides. It was found that a plot of log K vs log (r-0·5) or log (r-2), depending upon the synergist, is more meaningful than a plot of log K vs F or log F of the synergist, where r is the ratio, (F of synergist/F of H_2MEHP). For some elements as r increases from zero, K rises to a maximum (region of positive synergism); in others no positive synergism is noted. In each instance in which a maximum is found, the maximum becomes progressively more pronounced as the synergist is varied from n-decanol to TBP, tri-n-butyl phosphate, to TOPO, tri-n-octyl phosphine oxide. In the negative synergism range, the limiting slope of the log K vs log (r-0·5) plot for all of the M(III) examples studied (TBP synergist, cyclohexane and toluene diluents) is -3. Similarly, the limiting slope of the log K vs log (r-2) plot (n-decanol synergist, cyclohexane diluent) is -3 for M(III), -4 for Th(IV) and -2 for U(VI). The extractant dependency for Eu(III) and Am(III) by H_2MEHP in the absence of synergist is shown to be first power in toluene diluent and third power in n-decanol diluent. Z-studies in the diluents toluene, cyclohexane and n-decanol are included. Tentative explanations of the negative synergistic effects are proposed in terms of assumed chemical interaction between synergist and H_2MEHP; and possible applications of these effects are suggested.

THE extraction of M(III) cations from an aqueous mineral acid phase into an opposing phase consisting of a $(GO)PO(OH)_2$ extractant in a carrier diluent has been reported by two sets of investigators, employing two different diluents, with widely different interpretations. PEPPARD, *et al.*[1] using toluene as diluent (G:2-ethyl hexyl and para (1,1,3,3-tetramethyl butyl) phenyl), reported the extractant dependency for Am(III) and Pm(III) as first-power. WARREN and SUTTLE[2], using n-amyl alcohol as diluent (G:n-butyl, n-amyl, n-hexyl, and n-octyl), reported the extractant dependencies (as deduced from the suggested extraction powers) for Sc(III) and for Y(III) and La(III) as third-power and fourth-power, respectively.

This discrepancy, coupled with the observations that the distribution ratio, K, for Pm(III) in a specific $(GO)PO(OH)_2$ vs. mineral acid system is 300 times greater in a system employing toluene than in a system employing 2-ethyl hexanol as diluent[3] and that the K for Np(IV) in a specific $(GO)PO(OH)_2$ vs. H_2SO_4 system may be decreased by a factor in excess of 10^4 by addition of tributyl phosphate,[4] led to an investigation of synergistic interactions involving mono(2-ethyl hexyl) phosphoric acid, H_2MEHP, and hydrogen bond acceptor and donor molecules.

---

* Based on work performed under the auspices of the U.S. Atomic Energy Commission.

[1] D. F. PEPPARD, G. W. MASON, W. J. DRISCOLL and R. J. SIRONEN, *J. Inorg. Nucl. Chem.* **7**, 276 (1958).

[2] C. G. WARREN and J. F. SUTTLE, *J. Inorg. Nucl. Chem.* **12**, 336 (1960).

[3] D. F. PEPPARD, G. W. MASON, W. J. DRISCOLL and S. McCARTY, *J. Inorg. Nucl. Chem.* **12**, 141 (1959).

[4] D. F. PEPPARD, G. W. MASON and R. J. SIRONEN, *J. Inorg. Nucl. Chem.* **10**, 117 (1959).

EXPERIMENTAL

Nomenclature

Mono(2-ethyl hexyl) phosphoric acid, the primary extractant used throughout this study, is symbolized as H_2MEHP in accordance with previous usage.(1,4) The symbols H, M, EH and P respectively indicate: a theoretically ionizable hydrogen, the prefix mono-, the 2-ethyl hexyl group, and phosphorus in an ortho phosphate. In this representation the molecular complexity of the extractant and extractant-diluent interactions are ignored. Similarly, TBP symbolizes tri n-butyl phosphate, $(n\text{-}C_4H_9O)_3PO$, and TOPO symbolizes tri n-octyl phosphine oxide, $(n\text{-}C_8H_{17})_3PO$.

The distribution ratio, *K*, of a specific nuclide is defined as the concentration of nuclide in the upper divided by the concentration of nuclide in the lower of two mutually-equilibrated sensibly-immiscible liquid phases.

The ratio of the concentrations, expressed in formality units, of synergist to H_2MEHP is symbolized as *r*.

Sources of materials

A mixture of mono- and di(2-ethyl hexyl) phosphoric acids was obtained from Victor Chemical Works. The mono ester, H_2MEHP, was isolated as previously described,(5) except that the procedure for eliminating pyro contaminants was modified, the contacting with 6M HCl at 80°C being extended from an 8 hr to a 48 hr period.

Tributyl phosphate, $(n\text{-}C_4H_9O)_3PO$, TBP, was obtained from Commercial Solvents Corporation and further purified as described previously(6) with the following modifications: the number of scrubs was doubled and water was removed from the product TBP by evaporation at room temperature at reduced pressure using the rotating evacuated flask technique previously described in the purification of acidic organophosphorus compounds.(5)

Tris n-octyl phosphine oxide, $(n\text{-}C_8H_{17})_3PO$, TOPO, was obtained from Eastman Organic Chemicals Department of Distillation Products Industries. It was purified in a manner similar to that employed in the purification of TBP. A 0·1F solution of TOPO in benzene was stirred with an equal volume of 6M HCl at 40°C in a sealed flask for 48 hr. This benzene solution was then successively given (using equal-volume portions): two water scrubs, three 5% Na_2CO_3 scrubs, and six water scrubs. The benzene and water were then removed under reduced pressure at room temperature.

Toluene, cyclohexane and n-decyl alcohol were obtained from Eastman Organic Chemicals Department of Distillation Products Industries.

The β-active nuclides, 40·2 hr ^{140}La (with parent 12·8 day ^{140}Ba), 285 day ^{144}Ce, 2·6 year ^{147}Pm, (13, 16) year ^{152,154}Eu and 58 day ^{91}Y were obtained from the Isotopes Division of the Oak Ridge National Laboratory. Daughter ^{140}La was separated from parent ^{140}Ba (and from contaminant ^{90}Y daughter of parent ^{90}Sr present in the ^{140}Ba sample) and ^{144}Ce was separated, as Ce(IV), from contaminant ^{147}Pm by the liquid-liquid extraction techniques previously described.(7) Liquid–liquid extraction was also employed in purifying ^{147}Pm from residual quantities of ^{144}Ce(7) and ^{91}Y(8) and in purifying ^{91}Y(8) with respect to ^{147}Pm contaminants.

The other β-active lanthanides employed were prepared by neutron irradiation of samples of highly purified stable normal isotopic mixtures with the exception of Pr and Ho. In the preparation of ^{143}Pr, highly purified natural cerium (as the ignited nitrate) was subjected to neutron bombardment to form ^{143}Ce, disintegrating to ^{143}Pr. The 13·8 day β-active ^{143}Pr was isolated from the bombarded samples by a liquid–liquid extraction technique based upon the differences in extraction between Ce(IV) and Pr(III).(7) In the preparation of Dy tracer, secondary neutron capture by Dy led to the formation of 82 hr ^{166}Dy which has a 27·2 hr ^{166}Ho daughter. By differential counting, both Dy and Ho data were obtained in a single experiment as described in the section entitled *Determination of distribution ratios*. No studies of Nd and Gd were made.

The α-active nuclides 470 year ^{241}Am, $8{\cdot}0 \times 10^4$ year ^{230}Th (^{230}Th/^{232}Th mass ratio ~ 11) and $1{\cdot}6 \times 10^5$ year ^{233}U were obtained from Argonne stocks and 18 year ^{244}Cm was obtained from P. R. FIELDS (Argonne).

Determination of distribution ratios

The distribution ratio, *K*, for a given nuclide was obtained radiometrically by allowing the nuclide to distribute, at equilibrium, between the two mutually equilibrated liquid phases, and then determining the radioactivity, in terms of counts per minute, alpha or beta, associated with a given aliquot of each phase as described previously.(8) Equilibrium distribution of radionuclides was accomplished by 3 min manual shaking in stoppered vials. All data were obtained at 22 ± 1°C.

---

(5) D. F. PEPPARD, J. R. FERRARO and G. W. MASON, *J. Inorg. Nucl. Chem.* **7**, 231 (1958).

(6) D. F. PEPPARD, G. W. MASON and J. L. MAIER, *J. Inorg. Nucl. Chem.* **3**, 215 (1956).

(7) D. F. PEPPARD, G. W. MASON and S. W. MOLINE, *J. Inorg. Nucl. Chem.* **5**, 141 (1957).

(8) D. F. PEPPARD, G. W. MASON, J. L. MAIER and W. J. DRISCOLL, *J. Inorg. Nucl. Chem.* **4**, 334 (1957).

Each of the points on the extractant dependency curves of Fig. 9 is the average of "direct" and "reverse" extraction data, i.e., radio-nuclide in the aqueous phase with the organic phase barren initially and radio-nuclide in the organic phase with the aqueous phase barren initially, respectively. At least two random points on each of the other curves were checked with direct and reverse extraction data. In each case, the variation between direct and reverse data was within the expected random variation.

In the Dy experiment, Ho data were obtained also by differential counting. An aliquot of each phase was evaporated on a platinum disc immediately following phase disengagement after equilibration. These samples were then assayed by beta counting through an aliminum absorber (100 mg), the absorber serving to screen out essentially all of the Dy activity. Approximately seven days later, the plates were assayed by β-counting without absorber at which time the 82 hr ^{166}Dy parent and 27·2 hr ^{166}Ho daughter were essentially at secular equilibrium. From these two sets of data, both Ho and Dy *K* values were calculated.

Establishment of Z-curves

Since the *Z*-effect in some portions of the curves is very small and since not all of the lanthanides available for study had been studied in the detailed synergistic investigation, the data for a given curve of Fig. 10 were obtained as a single experiment. In no case were these data in serious conflict with those obtained in the synergistic study.

RESULTS AND CONCLUSIONS

In Figs. 1–3, the effects upon the extractive power of H_2MEHP in toluene diluent produced by the synergists n-decanol, TBP and TOPO are shown. Similarly, Figs. 4 and 5 treat the effect of the synergists n-decanol and TBP upon the extractive power of H_2MEHP in cyclohexane diluent. In order best to delineate this region of low concentration of synergist (as well as small *r*, i.e. *F* synergist:*F* H_2MEHP) these plots are semilogarithmic.

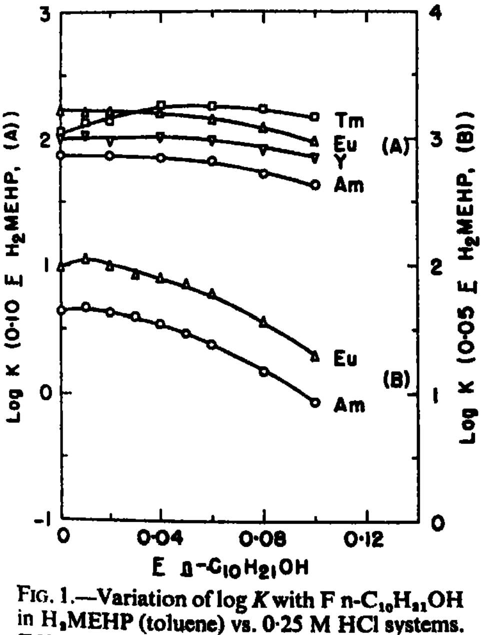

FIG. 1.—Variation of log *K* with F n-$C_{10}H_{21}OH$ in H_2MEHP (toluene) vs. 0·25 M HCl systems. F H_2MEHP: (A), 0·10; (B), 0·05. M(III): Eu, Tm, Y, Am.

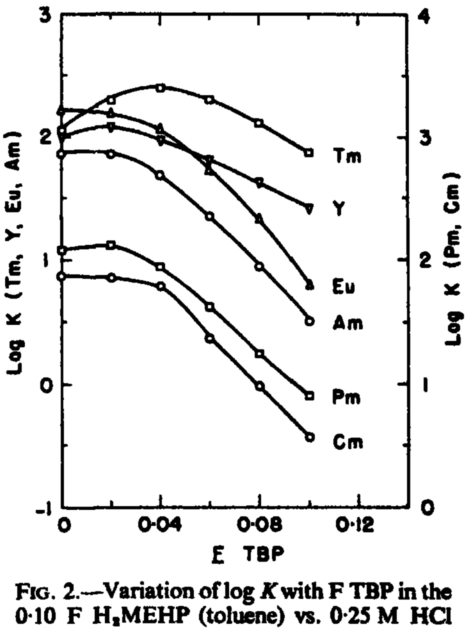

FIG. 2.—Variation of log *K* with F TBP in the 0·10 F H_2MEHP (toluene) vs. 0·25 M HCl system. M(III): Pm, Eu, Tm, Y, Am, Cm.

In the "A" section of Fig. 1, the plot for Tm rises to a flat maximum, the value of *K* at 0·1 F n-decanol being higher than that for no synergist. The corresponding Am curve has no maximum, and the value of K at 0·1 F n-decanol is approximately 0·6 that for no synergist.

The "B" section of Fig. 1 illustrates the effect of r, the value of K for Am at 0·1 F n-decanol being approximately 0·2 that for no synergist.

By comparison of the "A" section of Fig. 1 with Fig. 2, TBP is seen to be a more effective antisynergist than n-decanol, the K for Am being depressed a factor of approximately 22 by 0·1 F TBP as compared to approximately 1·7 by 0·1 F n-decanol. Further, TBP produces a more pronounced maximum in the Tm curve, and the value of K at 0·1 F synergist is below that for no synergist. A slight maximum is also noted in the Y curve.

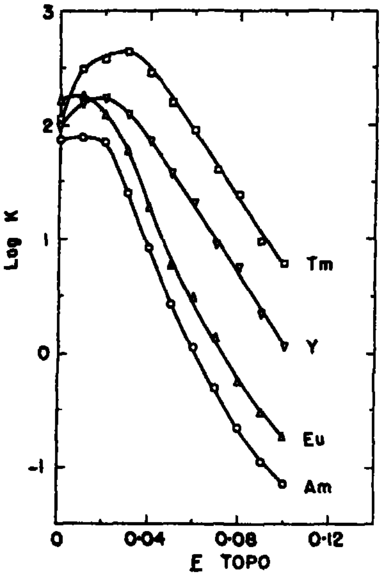

FIG. 3.—Variation of log K with F TOPO in the 0·10 F H_2MEHP (toluene) vs. 0·25 M HCl system. M(III): Eu, Tm, Y, Am.

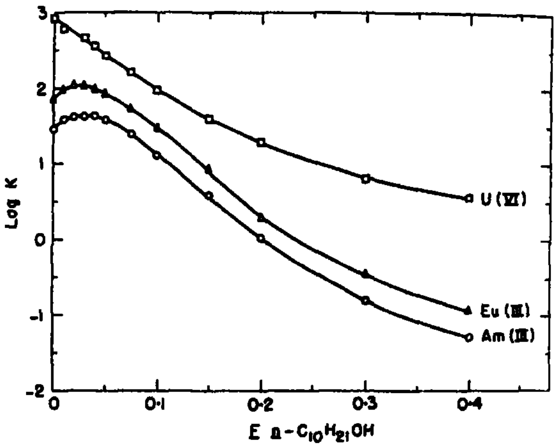

FIG. 4.—Variation of log K with F n-$C_{10}H_{21}OH$ in the 0·05 F H_2MEHP (cyclohexane) vs. 0·25 M HCl system: Eu(III), Am(III), U(VI).

In Fig. 3, the curves for Eu and Am show slight maxima and those for Tm and Y quite pronounced maxima. With respect to Tm, the maximum enhancement factor, a measure of positive synergism, as read from Fig. 1(A), Fig. 2 and Fig. 3 are: 1·6 (n-decanol), 2·2 (TBP) and 3·9 (TOPO). With respect to Am, the depressant factor, a measure of negative synergism, (calculated fron the base point of no synergist) at 0·1 F synergist as read from Fig. 1(A), Fig. 2 and Fig. 3 are: 1·7 (n-decanol), 22 (TBP) and 1,000 (TOPO).

The effect of diluent is seen by mutual comparison of Figs. 1 and 4 and of Figs. 2 and 5. In Figs. 4 and 5 (cyclohexane diluent), the Am and Eu values rise to a maximum for the two synergists, n-decanol and TBP. In Fig. 4 the data for U(VI) are included to show that for this solute, negative synergism obtains throughout the range studied. (Studies involving TBP and TOPO were not made with U(VI), since the K for extraction by the synergist (in the absence of H_2MEHP) is quite high.)

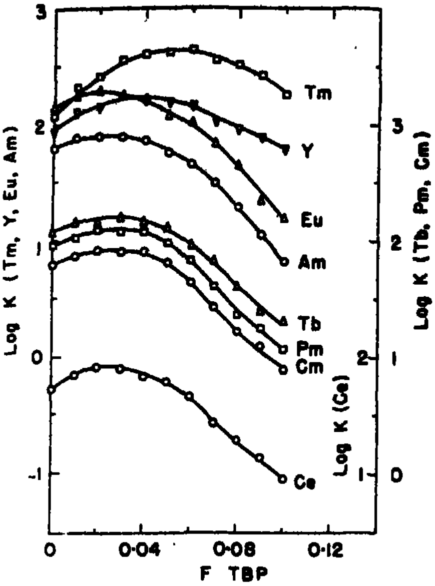

FIG. 5.—Variation of log K with F TBP in the 0·10 F H_2MEHP (cyclohexane) vs. 0·25 M HCl system. M(III): Ce, Pm, Eu, Tb, Tm, Y, Am, Cm.

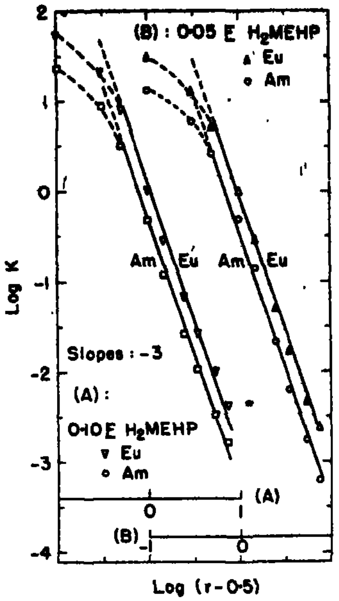

FIG. 6.—Variation of log K with log (r-0·5), TBP, in H_2MEHP (toluene) vs. 0·25 M HCl systems. F H_2MEHP: (A), 0·10; (B) 0·05. Eu(III), Am(III).

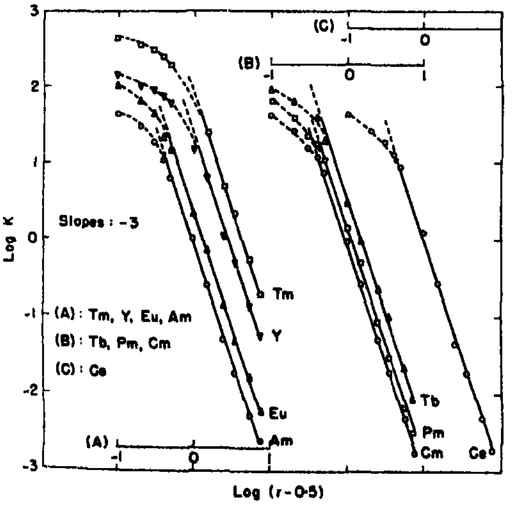

FIG. 7.—Variation of log K with log (r-0·5), TBP, in the 0·10F H_2MEHP (cyclohexane) vs. 0·25 M HCl system. M(III): Ce, Pm, Eu, Tb, Tm, Y, Am, Cm.

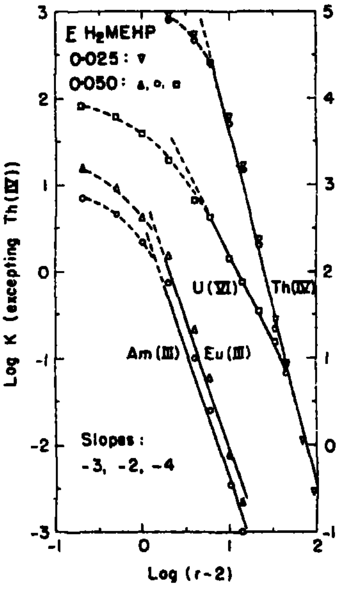

FIG. 8.—Variation of log K with log (r-2), n-$C_{10}H_{21}OH$, in H_2MEHP (cyclohexane) vs. HCl systems. M HCl: 0·25, Eu(III), Am(III); 1·00, Th(IV), U(VI).

By comparison of sections "A" and "B" of Fig. 1, it appears that a plot of log K vs. r or some function of r might be more meaningful than a plot of log K vs. F synergist. Consequently, Figs. 6, 7 and 8, extending over a wide range of F synergist and of values of r, are log K vs. log (r — 0·5) and log K vs. log (r — 2) plots. The rationale for the use of (r-0·5) and (r-2) in preference to r is given in the discussion section.

In Figs. 6 and 7, the limiting slopes are —3 for the M(III) examples shown, using TBP as synergist and toluene and cyclohexane as diluents.

In Fig. 8, involving cyclohexane as diluent and n-decanol as synergist, the limiting values are —2, for UO_2^{2+}; —3, for Am^{3+} and Eu^{3+}; and —4, for Th^{4+}. The limiting negative slope has the same absolute value as the charge on the metal extracted.

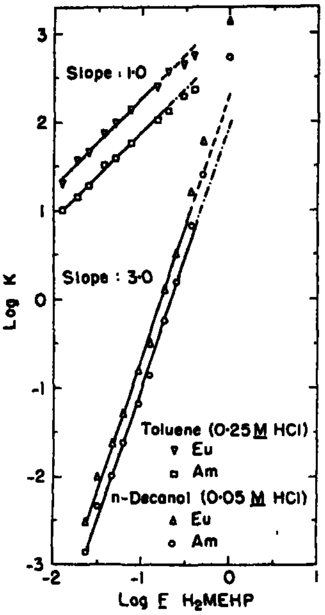

Fig. 9.—Extractant dependencies for Eu(III) and Am(III) in H_2MEHP (diluent) vs. HCl systems. Diluents: toluene, n-decanol.

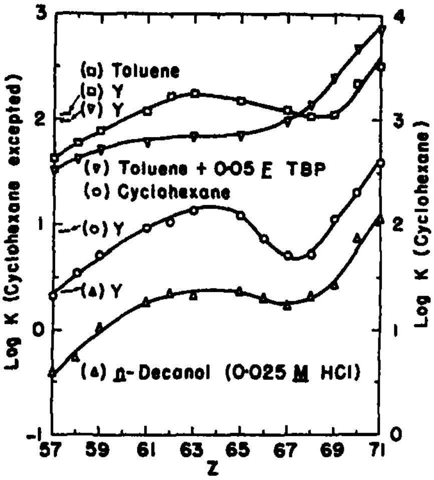

Fig. 10 —Variation of log K with Z of lanthanides (III) in the 0·1F H_2MEHP (diluent) vs. 0·25 M HCl (n-decanol excepted) systems. Diluents: □, toluene; ▽, toluene plus 0·05 F TBP; ○, cyclohexane; △, n-decanol.

A study of n-decanol as a diluent is presented in Fig. 9. Throughout the left-hand portion of the range studied, it is seen that a third-power extractant dependency for the extraction of Am(III) and Eu(III) may be derived from the data. At higher concentrations of H_2MEHP, departures from this curve, in the direction of rendering the curve steeper, are incurred. In the same figure, a first-power extractant dependency is seen to apply to the extraction of the same two elements if toluene is the diluent. (*The toluene data were obtained at 0·25 M HCl rather than at 0·05 M HCl so that the K value would be more easily determined, since the hydrogen ion dependency for K is inverse third-power.*[1,2] However, less extensive data obtained at 0·05 M HCl also indicate a first-power extractant dependency.)

In Fig. 10, log K vs. Z curves for H_2MEHP in three pure diluents, toluene, cyclohexane and n-decanol, and in one composite diluent, toluene which is 0·05 F in TBP, are presented. The three pure diluent curves are mutually similar in general shape. However, both the maximum and minimum are more pronounced in the cyclohexane curve than in the others. The cyclohexane and toluene curves differ from each other by a factor less than three at all points, whereas the n-decanol curve, as presented, is a factor of 30–100 lower than the toluene curve. Noting that the n-decanol curve was obtained in a system employing 0·05 M HCl as opposed to 0·25 M HCl, it is concluded, assuming an inverse third-power hydrogen ion dependency, that for identical systems with respect to HCl and H_2MEHP concentrations, the n-decanol curve should be a factor of (3·7–12·5) × 10^3 lower than the toluene curve, the exact factor being a function of Z.

The curve for the composite diluent, toluene which is 0·05 F in TBP, lies below the pure toluene curve in the 57–67 atomic number region and above it in the 68–71 region. In contrast to the curve for pure toluene, it has no maximum or minimum.

DISCUSSION

The general conclusions, with respect to synergistic effects, to be correlated and reconciled with a theoretical interpretation are:

(1) In some instances there exists a region of enhanced extraction (Figs. 1–5);
(2) In each instance there exists a region of decreased extraction;
(3) Each of the foregoing effects is a function of the nature of the synergistic agent;
(4) The effects differ as a function of Z for M(III) lanthanides;
(5) The effects differ markedly for M(III), Th(IV), and U(VI);
(6) The limiting plot of log K vs. log r, or better (r–0·5) or (r–2) for specific cases, approaches a straight line of negative slope numerically equal to the charge on the cation, i.e., −2 for UO_2^{2+}, −3 for M(III) and −4 for Th(IV).

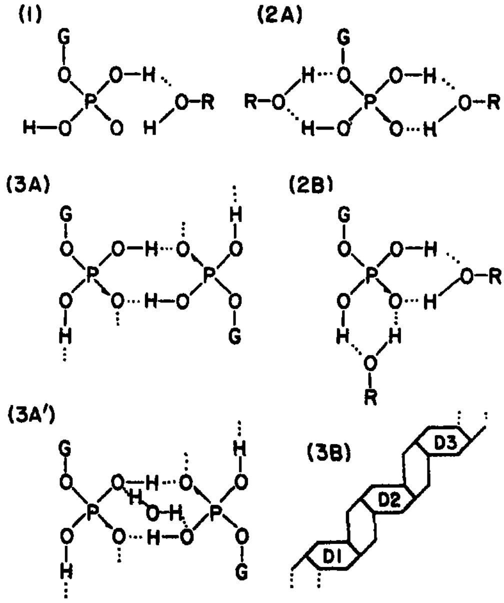

Fig. 11.—Possible hydrogen-bonded structures of $(GO)PO(OH)_2$: (1) and (2), with ROH; (3), with itself and with H_2O. Except for (2A), applicable to $(G)PO(OH)_2$ also.

It is postulated that the original extractant, $(H_2MEHP)_x$, A, of which a possible structure is shown as (3B) in Fig. 11, is converted by the synergist into an adduct B which is in turn converted by further interaction with synergist into adduct C, as follows:

$$(A), (H_2MEHP)_x \xrightarrow{\text{Syn.}} B \xrightarrow{\text{Syn.}} C \qquad (1)$$

It is further considered that, as an extractant, C is by far the least efficient of the three and that B may be more or less effective than A. If B is sufficiently effective, as compared with A, then a region of enhanced extraction will exist. Since there is no *a priori* reason to expect the Z-curve to be the same for B as for A, it seems logical that the curves for some elements should display this positive region while others should not. (In Fig. 10, the log K vs. Z plots for lanthanides (III) in 0·1 F H_2MEHP (toluene) and in 0·1 F H_2MEHP + 0·05 F TBP (toluene) systems are seen to cross mutually).

The terminal adduct, C, since it is assumed to be a highly inefficient extractant, is considered to contain H_2MEHP with all of its reactive sites inactivated through strong hydrogen bonding.

Since H_2MEHP has been demonstrated to exist as a monomer in methyl alcohol⁽⁹⁾ it is assumed that C contains only one unit of H_2MEHP in the n-decyl alcohol systems. Considering both theoretically-ionizable hydrogen atoms to be inactivated the formulation is given as (H_2MEHP) (n-decanol)$_2$, and possible structures are shown as 2A and 2B in Fig. 11.

Since H_2MEHP has been shown to be reduced to a dimer, but not to a monomer, by acetone,⁽⁹⁾ which, like TBP, can accept but cannot contribute a hydrogen atom in hydrogen bond formation, it is postulated that C contains a dimeric unit in the TBP systems. Considering all theoretically ionizable hydrogen atoms to be inactivated, the formulation is given as $(H_2MEHP)_2$ TBP; and a possible structure is derived from 3A or 3A′ of Fig. 11, if the dimer has one of the two pictured terminal acidic H atoms bonded internally to one of the sterically available O atoms and the other bonded to the unique O of TBP, $(n\text{-}C_4H_9O)_3PO$.

Assuming the formulations of C as given in Table 1, the concentration of free synergist in the region in which essentially all of the H_2MEHP is in the C form may be calculated. Hence, log K is plotted as a function of log (r–2) and of log (r-0·5), respectively, in the n-decanol and the TBP systems.

TABLE 1.—POSTULATED FORMULATIONS OF B AND C OF EXPRESSION (1)

Synergist	B	C
$n\text{-}C_{10}H_{21}OH$, DOH	$(H_2MEHP)(DOH)$	$(H_2MEHP)(DOH)_2$
$(n\text{-}C_4H_9O)_3PO$, TBP	$(H_2MEHP)_2(TBP)_2$	$(H_2MEHP)_2(TBP)$

Since the plot of log K vs. (r–2) in the n-decanol systems approaches, as a limit, a straight line of negative slope numerically equal to the charge of the cations extracted, it is assumed that B is functioning as a mono-ionized extractant equivalent to B^-. Therefore, using the simplest interpretation, B is formulated as monomeric H_2MEHP combined with one molecule of n-decanol, i.e., (H_2MEHP) (n-decanol), Table 1. The

---

(9) J. R. FERRARO, G. W. MASON and D. F. PEPPARD, *J. Inorg. Nucl. Chem.* **22**, 285 (1961).

extraction of M^{p+} and the K in the limiting region are thus represented as:

$$M_A^{p+} + p(H_2MEHP)(DOH)_0 \rightleftharpoons M[(HMEHP)(DOH)]_{p_0} + pH_A^+ \qquad (2)$$

$$(H_2MEHP)(DOH)_0 + DOH_0 \rightleftharpoons (H_2MEHP)(DOH)_{2_0} \qquad (3)$$

$$K_{M^{p+}} = k_4/[DOH]_0^p \qquad (4)$$

Similarly, it is assumed that B in the TBP systems functions as a mono-ionized extractant equivalent to B^-. From the established interaction of TBP and H_2MEHP, in the absence of water, in the ratio of 1:3 by formula weights$^{(10)}$ and the formulation of the product as an adduct, $(H_2MEHP)_6(TBP)_2$$^{(10)}$ it is postulated that B is an adduct of hexameric H_2MEHP and two molecules of TBP, probably containing water, Table 1. The extraction of M^{p+} and the K in the limiting range are thus represented as:

$$M_A^{p+} + p(H_2MEHP)_6(TBP)_{2_0} \rightleftharpoons M[H_{11}(MEHP)_6(TBP)_2]_{p_0} + pH_A^+ \qquad (5)$$

$$(H_2MEHP)_6(TBP)_{2_0} + TBP_0 \rightleftharpoons 3(H_2MEHP)_2(TBP)_0 \qquad (6)$$

$$K_{M^{p+}} = k_7/[TBP]_0^p \qquad (7)$$

Presumably the action of TOPO, $(n\text{-}C_8H_{17})_3PO$, whose sole oxygen is analogous to the unique oxygen of TBP, is similar to that of TBP and differs only in magnitude.

Before discussing the extraction of M^{p+} by H_2MEHP in toluene or cyclohexane in the absence of synergist, it is necessary to consider the nature of the polymeric species. Although a considerable body of data concerning such polymers has been reported,$^{(9-11)}$ it must be remembered that the structure and nature of the species may differ widely in wet and dry diluents.

A possible structure of polymeric $(GO)PO(OH)_2$, and of the analogous $(G)PO(OH)_2$, is shown in 3A and 3B of Fig. 11. Assuming, as in 2B of Fig. 11, that an oxygen atom may exhibit a co-ordination number of three in such a polymer, the fundamental "dimeric unit", an 8-membered ring, may be represented by the structure 3A. A second "dimeric unit" may be placed above (in two-dimensional parlance) the first unit with its left end above the right end of the first in such a way that the two units may join and in so doing create a new 8-membered ring indistinguishable in characteristics from the first two.

This polymeric structure is represented as 3B, Fig. 11, the section shown being a hexamer composed of three dimers, D_1, D_2 and D_3. It is apparent that through flexion this hexamer might be joined, end to end, to form a cyclic hexamer of six 8-membered rings. Alternatively, a polymer of "dimeric units" might be linear and have two terminal "unbonded" OH groups.

If such a polymer, cyclic or otherwise, loses, by ionization, a proton involved in polymer formation, then the resultant anion should be less stable in a dry diluent. However, in a wet diluent it seems likely that the polymer contains water molecules as structural units.$^{(9)}$ A possible mode of attachment is illustrated in (3A′) of Fig. 11.

Presumably, a large polymer composed of units such as represented by (3A′) should be capable of losing several protons by ionization, thereby acquiring a net negative charge of several units. However, a small polymer, such as a hexamer, might well suffer greatly in stability by acquiring a negative charge numerically greater than unity.

---

(10) J. R. Ferraro and D. F. Peppard, *J. Phys. Chem.* **65**, 539 (1961).

(11) D. F. Peppard, J. R. Ferraro and G. W. Mason, *J. Inorg. Nucl. Chem.* **4**, 371 (1957).

Consequently, it appears that in the absence of a synergist the extraction of M^{p+} by H_2MEHP in a nonhydrogen-bonding diluent proceeds by the mechanism previously reported:⁽¹⁾

$$M_A{}^{p+} + (H_2Y)_{x_0} \rightleftharpoons [M(H_{2x-p}Y_x)]_0 + pH_A{}^+ \tag{8}$$

$$K_{M^{p+}} = k_8[(H_2Y)_x]_0/[H^+]_A{}^p \tag{9}$$

where $(H_2Y)_x$ represents the polymeric form of the extractant, probably containing water molecules, 3A′, Fig. 11. The mechanism is presumably applicable to other $(GO)PO(OH)_2$ and to $(G)PO(OH)_2$ extractants as well. A first-power extractant dependency, implicit in Expression (9), was reported by PEPPARD *et al.*⁽¹⁾ for the extraction of M(III) using H_2MEHP and mono[*p*-(1,1,3,3-tetramethyl butyl)phenyl] phosphoric acid, the latter symbolized as $H_2MO\phi P$, as extractants in toluene diluent.

In an alcohol diluent, ROH, it is assumed that $(GO)PO(OH)_2$ (and presumably $(G)PO(OH)_2$ is monomeric, possibly with two molecules of ROH bonded directly to each unit, 2A or 2B, Fig. 11. This monomer, without regard to the ROH of constitution, is represented as H_2Y and the extraction of M^{p+} represented as:

$$M_A{}^{p+} + pH_2Y_0 \rightleftharpoons M(HY)_{p_0} + pH_A{}^+ \tag{10}$$

$$K_{M^{p+}} = k_{10}[H_2Y]_0{}^p/[H^+]_A{}^p \tag{11}$$

The third-power extractant dependency for M(III) implicit in Expression (11) is observed for the extraction of Eu(III) and Am(III) by H_2MEHP in n-decanol, Fig. 9.

However, it was observed that at concentrations appreciably greater than 0·4 F (Fig. 9) the plot of log K vs. log F H_2MEHP departed from a straight line and became progressively steeper. This effect is to be expected if the monomerization to the final interacted H_2MEHP + ROH species is not complete. Conversely, at concentrations sufficiently below the lowest concentration reported in Fig. 9, it is expected that double ionization of the monomer to form Y^{2-} might become relatively important with respect to single ionization to form HY^-. Consequently, for the extraction of M^{p+}, the plot of log K vs. F H_2MEHP might approach a slope of $0{\cdot}5p$ as a limit as the concentrations of H_2MEHP become sufficiently small.

It may be noted that Expression (10) with $p = 3$, is equivalent to the expression for the extraction of Sc(III) given by WARREN and SUTTLE⁽²⁾ who reported a third-power extractant dependency for Sc(III) but a fourth-power for La(III) and Y(III). A possible explanation for the fourth-power extractant dependency is based on the fact that the La(III) and Y(III) data were obtained in a higher $(GO)PO(OH)_2$ concentration range than the Sc(III) data, the lowest concentration of the former study being larger than the highest concentration of the latter.

A comparative study of the extraction of Eu(III) and Am(III) in H_2MEHP (diluent) vs. aqueous HCl systems is shown in Fig. 9 in which toluene and n-decyl alcohol are the diluents. For both elements, the extractant dependency is first-power in toluene and third-power in n-decyl alcohol. (It should be noted for Figs. 9 and 10 that in systems involving the same concentration of HCl in the aqueous phase the K for M(III) at a fixed total F of H_2MEHP is much greater in toluene than in decyl alcohol).

It appears likely, therefore, that Expressions (8) and (9) represent extractions employing toluene and other diluents which do not greatly decrease the degree of polymerization of the extractant while Expressions (10) and (11) represent extractions employing alcohol, and presumably certain other diluents, which monomerize the extractant.

Although positive synergistic effects were noted which gave increased β-values for a given pair of elements (beta $= K_A/K_B$ for elements A and B), see the Z curves of Fig. 10, the effects are of no practical importance, since other extractive systems with superior β-values are available.(1,8) However, negative synergistic action appears to be of great practical importance.

For example, an element such as Tm(III) may be extracted into H_2MEHP in toluene (or cyclohexane, etc.) as a concentration and preliminary purification step; but, in order to transfer the Tm(III) to an aqueous phase, a high concentration of mineral acid (or a suitable complexing agent) is necessary. (Nothing is accomplished by diluting the pregnant organic phase with toluene since the extractant dependency is first-power). However, the removal to an aqueous phase is easily accomplished through addition of a synergistic agent which greatly decreases the K.

The techniques of adding a negative synergist to decrease the K of $M^{\nu+}$ and thereby render it transferable to an aqueous phase is especially valuable in the case of elements with extremely high K values, for example: Th(IV), U(IV), U(VI), Np(IV), etc. Since these cations tend to extract reasonably well into TBP also, the major effort was expended upon the n-decyl alcohol systems. In Fig. 8, it is seen that the K values for UO_2^{2+}, M^{3+} and Th^{4+} are reduced by addition of n-decyl alcohol in a manner consistent with Expression (10), the log K vs. log (r–2) plots approaching limiting slopes of -2, -3 and -4, respectively. It is apparent, then that M(III), M(IV) and M(VI) may be extracted with a toluene (or cyclohexane) solution of H_2MEHP with high K values and that they may be returned to an aqueous mineral acid phase by adding n-decyl alcohol, as a negative synergist, to the pregnant extract.

J. Inorg. Nucl. Chem., 1962, Vol. 24, pp. 979 to 988. Pergamon Press Ltd. Printed in Northern Ireland

EXTRACTION OF Th(IV) AS A MIXED COMPLEX, NITRATE OR CHLORIDE, BY 2-ETHYLHEXYL HYDROGEN 2-ETHYLHEXYL PHOSPHONATE*

D. F. Peppard, M. N. Namboodiri† and G. W. Mason
Argonne National Laboratory, Argonne, Illinois

(*Received 26 January 1962; in revised form 20 February 1962*)

Abstract—The extraction of Th(IV) from aqueous perchlorate, chloride and nitrate aqueous phases into a solution of an acidic phosphonate, generally represented as (GO)(G)PO(OH); dissolved in a carrier diluent is reported for the first time. Specifically, 2-ethylhexyl hydrogen 2-ethylhexyl phosphonate, (EHO)(EH)PO(OH), dissolved in toluene has been employed as the extractant phase.

From a nitrate phase, Th(IV), in tracer level concentration, is extracted as two mono-nuclear species containing one and two nitrate groups per atom of Th(IV), respectively. The extraction of the two-nitrate entity is favoured, with respect to that of the one-nitrate entity, as the acidity of the aqueous phase increases. The *K* for each of these species appears to be third-power dependent upon the concentration of the (EHO)(EH)PO(OH), which is dimeric in the diluent employed. The extraction of a nitrate-free entity is negligible under the conditions of the investigation. In saturation experiments, the empirical composition of the extract, as determined by gross analyses, is $Th(NO_3)_{1\cdot9}(EH[EHP])_{2\cdot2}$.

From a chloride phase, the extract in tracer-level studies contained a chloride-free and a one-chloride species. The *K* values for these two species are third-power and 2·5-power extractant dependent, respectively. In saturation experiments, the empirical composition of the extract, as determined by gross analyses, is $Th(Cl)_{0\cdot9}(EH[EHP])_{2\cdot9}$.

The perchlorate behaviour parallels that of the chloride system, except that the extractant dependency is third-power. The empirical composition of the extract, in saturation experiments, is $Th(ClO_4)_{0\cdot4}(EH[EHP])_{2\cdot7}$.

Bis 2-ethylhexyl phosphoric acid (symbolized as HDEHP), a representative of the $(GO)_2PO(OH)$ type of extractant, dissolved in a carrier diluent, has been shown to extract M(III) lanthanides from an aqueous nitrate phase, as $M[H(DEHP)_2]_3$ and as $M(DEHP)_3$, respectively, at "far below saturation" and at "saturation" of the organic phase.⁽¹,²⁾ In an extension of the study to Th(IV), it was found that the extracted entity contained one nitrate group per thorium atom, both at levels far below saturation⁽³⁾ and at saturation.⁽⁴⁾

The closely analogous 2-ethylhexyl hydrogen 2-ethylhexyl phosphonate (symbolized as HEH[EHP]), a representative of the (GO)(G)PO(OH) type of extractant, dissolved in a carrier diluent has recently been shown to extract tracer-level Pm(III) and Cm(III) from an aqueous nitrate phase as $M\{H(EH[EHP])_2\}_3$,⁽⁵⁾ i.e., an entity containing no nitrate. The corresponding Th(IV) study has now demonstrated both one-nitrate and two-nitrate species in the extract.

---

* Based on work performed under the auspices of the U.S. Atomic Energy Commission.

† Affiliate of the International Institute of Nuclear Science and Engineering at the Argonne National Laboratory and representative of the Laboratories of the Indian Atomic Energy Establishment—Trombay, Bombay.

(1) D. F. Peppard, G. W. Mason, J. L. Maier and W. J. Driscoll, *J. Inorg. Nucl. Chem.* 4, 334 (1957).

(2) D. F. Peppard, G. W. Mason, W. J. Driscoll and R. J. Sironen, *J. Inorg. Nucl. Chem.* 7, 276 (1958).

(3) D. F. Peppard, G. W. Mason and S. McCarty, *J. Inorg. Nucl. Chem.* 13, 138 (1960).

(4) D. F. Peppard and J. R. Ferraro, *J. Inorg. Nucl. Chem.* 10, 275 (1959).

(5) D. F. Peppard, G. W. Mason and I. Hucher, *J. Inorg. Nucl. Chem.* 18, 245 (1961).

EXPERIMENTAL

Nomenclature

The nomeclature employed in the study of acidic esters of phosphonic acid as extractants for M(III)(6) cations is employed throughout. Hence, (GO)(G)PO(OH) is the general formulation; and (EHO)(EH)PO(OH) represents 2-ethylhexyl hydrogen 2-ethylhexyl phosphonate, symbolized as HEH[EHP]. The bracketed grouping represents the phosphorus atom and the 2-ethylhexyl group attached by a C-P bond. Similarly, $(GO)_2PO(OH)$ is the general formulation of the analogous phosphate; and the specific example utilized, bis[para (1,1,3,3-tetramethyl butyl) phenyl] ortho phosphoric acid, for convenience called di octyl phenyl phosphoric acid, is symbolized as HDOϕP.

The distribution ratio, *K*, for Th(IV) is defined as the concentration of Th(IV) in the organic phase divided by the concentration of Th(IV) in the aqueous phase, the two sensibly-immiscible liquid phases having been mutually equilibrated and the Th(IV) "concentrations" being represented by alpha-emitting rates per unit volume.

Sources of materials

The HEH[EHP],(5,6) and the mineral acids(3) and their corresponding salts(3) were prepared and purified as described previously. α-active 8×10^4 year Th^{230} (Th^{230} to Th^{232} in the ratio of 10:1) was obtained from A.N.L. stocks and was freshly purified with respect to daughter activities before use.

Determination of distribution ratios

The distribution ratio, *K*, was determined as described previously,(3,5) using toluene as the carrier diluent. The absence of a Th(IV) concentration effect, at tracer-levels, upon *K* was established by varying the equilibrium concentration of Th(IV) in the aqueous phase over a range of 100 under otherwise identical conditions. It has been established that in each of the systems the concentration of mineral acid, HX, in the equilibrated organic phase was less than 6×10^{-4}F, a maximum value for the 1·0F HX systems.

Extractant and acid dependency studies

Both extractant and acid dependency studies were made at a constant ionic strength in the aqueous phase.

Anion dependency studies

Since preliminary experiments indicated the probable presence of mixed nitrate–perchlorate and chloride–perchlorate extracted species in studies involving constant ionic strength, maintained with $HClO_4$ or $NaClO_4$, in the nitrate and chloride studies, these studies were restricted to the use of a single anion and varying ionic strength.

*Determination of gross anion-to-*Th *ratios*

The extracts were prepared, in general, as described previously.(3,4) In a specific chloride experiment, a 1,200 ml portion of 0·10F HEH[EHP] in toluene was contacted with a 500 ml portion of aqueous 0·10M HCl, 0·90M NaCl, and approximately 2×10^{-3}M $ThCl_4$ phase. Following centrifugation, two 500 ml aliquots of the organic extract were withdrawn. (a) One aliquot was contacted successively with four 50 ml portions of 2·5M HNO_3. The resulting aqueous phases were combined and washed with benzene. The chloride content was determined by precipitation of AgCl. (b) The remaining aliquot was diluted to 2,000 ml with toluene and contacted successively with four 75 ml portions of 4·0M HCl. The combined aqueous phase was washed with benzene and evaporated to a small volume. The Th content was determined by precipitation of $Th(OH)_4$ and ignition to ThO_2.

In experiments involving nitrate and perchlorate, similar procedures were followed. The anion, in these instances, was determined by precipitation with nitron.(7)

"Saturation" experiments were performed as described previously.(3,4) In these studies, the technique for re-extraction of Th was modified in that each re-extract was scrubbed with two 100 ml portions of benzene, in sequence. The depleted organic extract and the two benzene phases were then scrubbed, in sequence, with five 100-ml portions of water to remove all mineral acid. These three organic phases were then combined and an aliquot titrated with standard NaOH to determine the HEH[EHP] content.

In a specific chloride experiment, a 100 ml portion of 0·1F HEH[EHP] solution was contacted successively with three 20-ml portions of a 1·5M $ThCl_4$ + 0·2M HCl solution and then shaken with solid $ThCl_4 \cdot xH_2O$ in the presence of the final aqueous phase for two hours. Following centrifugation, aliquots were treated as described above.

---

(6) D. F. PEPPARD, J. R. FERRARO and G. W. MASON, *J. Inorg. Nucl. Chem.* **12**, 60 (1959).

(7) (a) M. BUSCH, *Ber. Dtsch. Chem. Ges.* **38**, 861 (1905);
A. GUTBIER, *Z. Angew. Chem.* **18**, 494 (1905).

RESULTS AND CONCLUSIONS

Acid dependencies

From Fig. 1, it is seen that the hydrogen ion dependency of the *K* for Th(IV) into $9{\cdot}4 \times 10^{-3}$F HEH[EHP] from a 1·0F ($NaNO_3$ + HNO_3) solution is less steep than inverse third-power throughout the range studied, approaching inverse third-power and inverse second-power respectively in the low and high acidity regions. Assuming that two extracted species, respectively, containing the equivalent of $Th(NO)_3^{3+}$ and $Th(NO_3)_2^{2+}$, are involved, the two broken lines of Fig. 1 representing plots of log K_1 and log K_2 are drawn. The solid line, which is a plot of log (K_1 + K_2), is seen to represent the experimental data satisfactorily.

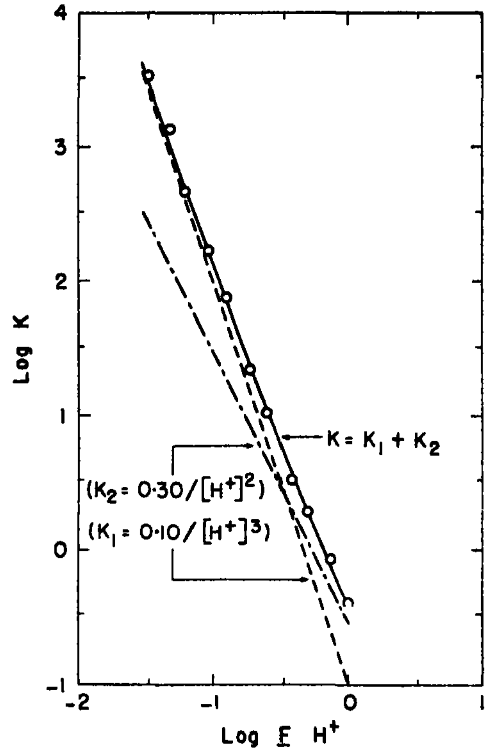

FIG. 1.—Hydrogen ion dependency of the extraction of Th(IV) into $9{\cdot}4 \times 10^{-3}$F HEH[EHP], toluene diluent, from a 1·0F ($NaNO_3$ + HNO_3) solution.

In Fig. 2, the hydrogen ion dependencies for the corresponding 1·0F chloride and perchlorate solutions are seen to be third-power in the high acid region but greater in the low. These data are considered to indicate a mixed mechanism involving the equivalent of ThX^{3+} and Th^{4+} in the extracted species. It should be noted that the perchlorate and chloride data were obtained in systems involving 0·075F and 0·0375F HEH[EHP], respectively, whereas the nitrate data were obtained in systems involving 0·0094F HEH[EHP]. It is evident, from comparison of Figs. 1 and 2, that the tendency for the $Th(NO_3)^{3+}$ and $Th(NO_3)_2^{2+}$ containing species to extract is much greater than that of the $ThCl^{3+}$ and $Th(ClO_4)^{3+}$ containing species.

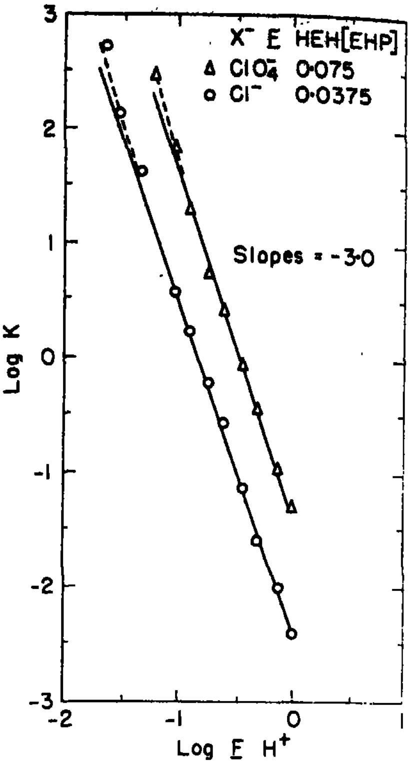

FIG. 2.—Hydrogen ion dependency of the extraction of Th(IV) into HEH[EHP], toluene diluent, from a 1·0F (NaX + HX) solution; $X^- = ClO_4^-, Cl^-$.

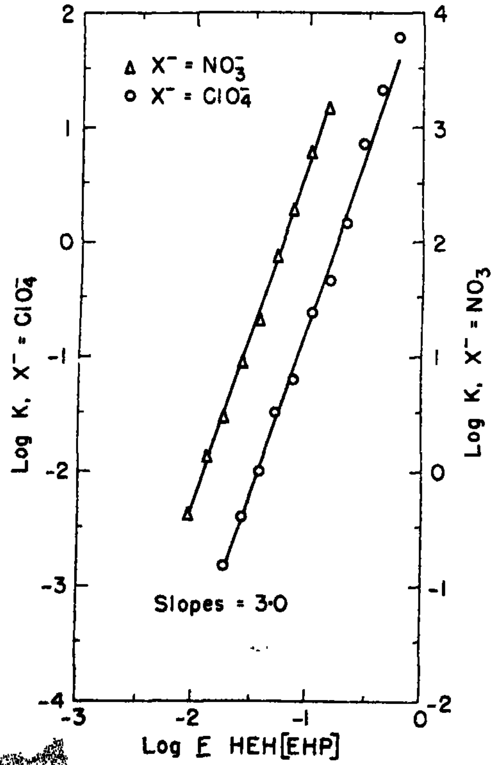

FIG. 3.—Extractant dependency of the extraction of Th(IV) into HEH[EHP], toluene diluent, from a 1·0F HX solution; $X^- = NO_3^-, ClO_4^-$.

Extractant dependencies

From Fig. 3, the extractant dependencies of the K for Th(IV) is seen to be third-power in systems involving 1·0F HNO_3 or 1·0F $HClO_4$ up to an extractant concentration of 0·15F.

The data of Fig. 4 for the chloride systems are adequately fitted by lines of slope 2·5 and 3·0 in the regions of low and high extractant concentration, respectively. In the 1·0F HCl system, the 2·5-power extractant dependency law holds through the 0·15F HEH[EHP] point.

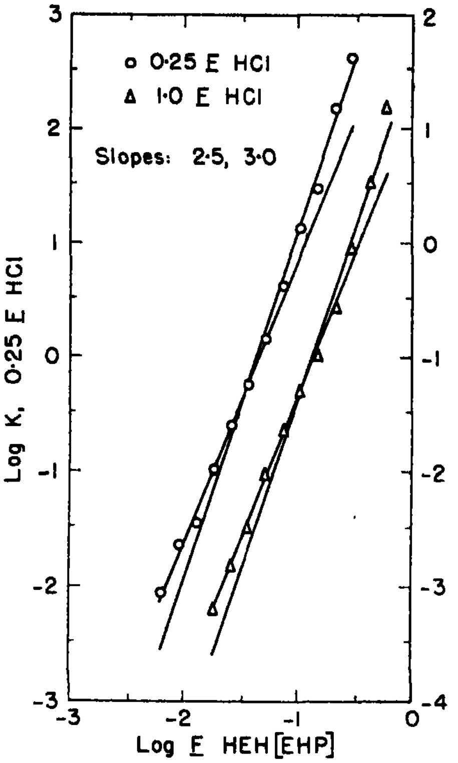

FIG. 4.—Extractant dependency of the extraction of Th(IV) into HEH[EHP], toluene diluent, from 0·25F and 1·0F HCl solutions.

From a comparison of Figs. 3 and 4, the respective K values for Th(IV) into 0·1F HEH[EHP] from 1·0F HX are: HNO_3, $4·9 \times 10^2$; $HClO_4$, $1·9 \times 10^{-1}$; and HCl, $4·4 \times 10^{-2}$.

Anion dependencies

The plot of log K for Th(IV) into $4·7 \times 10^{-3}$F HEH[EHP] from a ($NaNO_3$ + 0·3F HNO_3) solution vs. log F NO_3^-, Fig. 5, is a slightly concave downward curve of positive slope throughout. In the same figure is a plot of log K for Th(IV) vs. log F NO_3^- in a system employing 7×10^{-4}F HDOφP. (This latter extractant, di[para-(1,1,3,3-tetramethyl butyl) phenyl] ortho phosphoric acid, has been shown to extract Th(IV) from aqueous perchlorate, chloride or nitrate phases as an entity containing no perchlorate, chloride or nitrate, respectively.(8))

The HDOφP plot is a concave downward curve of negative slope, throughout, the departure from a horizontal line being attributed to the combined μ-effect and nitrate-complexing of Th^{4+} in the aqueous phase. Since the aqueous phases employed in this study were of the same composition as those used in the HEH[EHP] investigation, the HDOϕP data were used in making a point-for-point correction of the HEH[EHP] data to yield the broken curve of Fig. 5. (The addition of 0·30 log unit is made for the purpose of raising the plot for greater clarity in presentation.)

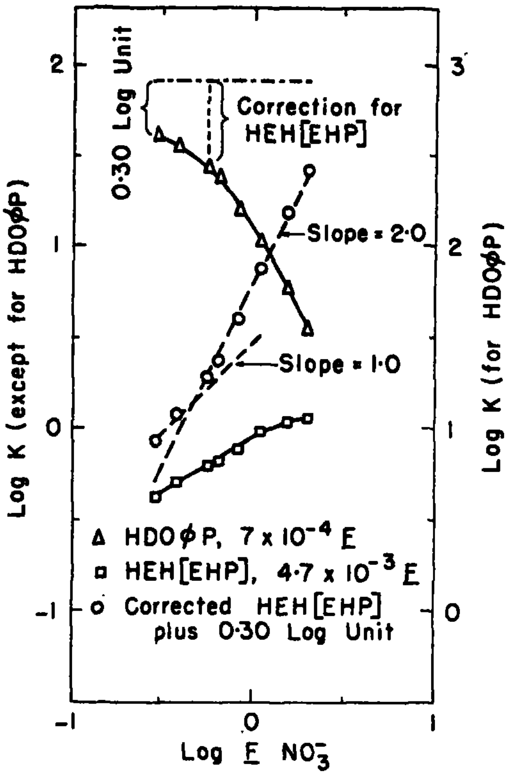

FIG. 5.—Nitrate dependency of the extraction of Th(IV) into HEH[EHP], toluene diluent, from (NaNO$_3$ + 0·30F HNO$_3$) solutions.

In making the corrections to the HEH[EHP] data, a horizontal line is drawn 0·30 log units above the highest HDOϕP point. The vertical distance (absolute) from this horizontal line to a given HDOϕP point is then added above the corresponding HEH[EHP] point (for the same F NO$_3^-$) to give a corrected point indicated by a circle in Fig. 5. Straight lines of slopes 1·0 and 2·0 through these corrected points indicate first-power and second-power nitrate dependencies, respectively. It must be remembered that these are dependencies determined under varying ionic strength conditions.

In Fig. 6, the plot of log K for Th(IV) into 3·7 × 10^{-2}F HEH[EHP] from a (NaCl + 0·25F HCl) solution vs. log F Cl$^-$ is a slightly concave downward curve of negative slope throughout. The point-for-point corrections, as determined by HDOϕP extraction data, are made as described for Fig. 5. The limiting slope of 0·80 as drawn is in sensible agreement with the assumption of the equivalent of ThCl^{3+} in the extracted entity considered in Figs. 2 and 4.

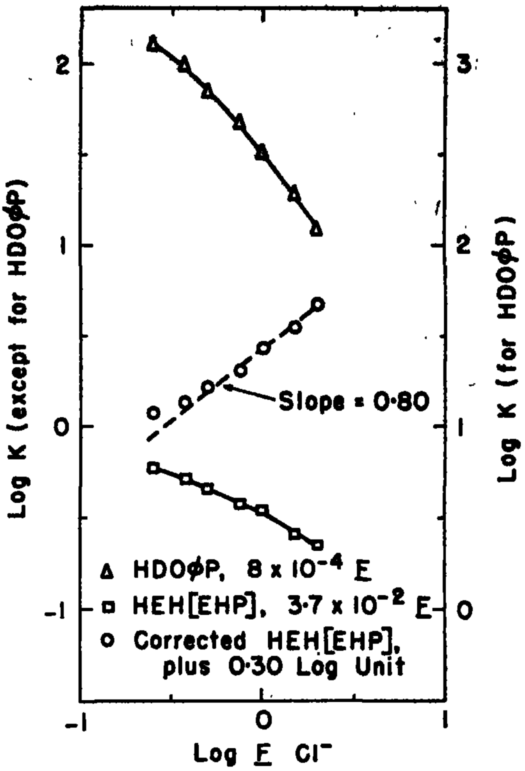

FIG. 6.—Chloride dependency of the extraction of Th(IV) into HEH[EHP], toluene diluent, from (NaCl + 0·25F HCl) solutions.

Gross data

The gross extraction data of Tables 1 and 2 confirm the existence of "mixed" extracted species. Table 1 represents "nonsaturation" experiments in which, in general, less than 7 per cent of the extractant is utilized in forming the extracted species, calculated on the basis of three dimers of extractant per Th atom.

In comparing the "saturation" data of Table 2 with the date of Table 1, it should be recalled that at saturation, a "monomer" mechanism, with respect to the extractant, is involved. (This does not preclude the possibility of polynuclear species with respect to Th.) Conversely, under conditions far removed from saturation, a dimer mechanism, with respect to the extractant, is involved. Consequently, saturation data do not necessarily bear any easily demonstrable relationship to tracer-level data.

DISCUSSION

The extraction of tracer-level M(III) lanthanides and actinides by $(GO)_2PO(OH)$ extractants dissolved in toluene as carrier diluent, from aqueous mineral acid phases has been shown(2,8–10) to be represented by the over-all equilibrium:

$$M_A^{3+} + 3(HY)_{2O} \rightleftharpoons M(HY_2)_{3O} + 3H_A^+ \qquad (1)$$

(8) (a) D. DYRSSEN, *Acta Chem. Scand.* 11, 1277 (1957);
(b) D. DYRSSEN and L. D. HAY, *Acta Chem. Scand.* 14, 1100 (1960).

(9) (a) K. KIMURA, *Bull. Chem. Soc. Japan* 33, 1038 (1960);
(b) K. KIMURA, *Bull. Chem. Soc. Japan* 34, 63 (1961).

(10) G. DUYCKAERTS, P. DREZE and A. SIMON, *J. Inorg. Nucl. Chem.* 13, 332 (1960).

Table 1.—Gross data on composition of Th(IV) extract (toluene diluent) in equilibrium with various aqueous phases*

X^-	Equilibrated Aqueous Phase	Organic extract X^-/Th	HEH[EHP]/Th
NO_3^-	0·1F HX + 0·9F NaX	1·24	*G*100
	1·0F HX	1·65	*G*100
Cl^-	0·1F HX + 0·9F NaX	0·30	*G*100
	0·25F HX + 0·75F NaX	0·44	*G*70
	1·0F HX	0·83	*G*50
ClO_4^-	1·0F HX	0·5	*G*100

* The ratios are by formula weight; and *G* signifies "greater than".

Table 2.—Gross data on composition of Th(IV) extracts (toluene diluent) prepared under saturation conditions*

X^-	Organic extract	
	X^-/Th	EH[EHP]$^-$/Th
NO_3^-	1·87	2·2
Cl^-	0·91	2·9
ClO_4^-	0·4	3·7

* The ratios are by formula weight, the EH [EHP]$^-$ being calculated as a monomer

where the subscripts A and O refer, respectively, to mutually equilibrated aqueous and organic phases and $(HY)_2$ refers to the extractant, which is dimeric(11,12) in toluene.

Although HDOϕP, bis[para(1,1,3,3-tetramethyl butyl) phenyl] orthophosphoric acid, in toluene as carrier diluent, extracts M(III) lanthanides and actinides according to Expression (1), the expected analogous extraction of Th(IV) is not found. Although the hydrogen ion dependency is inverse fourth-power, the extractant dependency is not fourth-power, but third-power. The extraction is thus represented(3) by:

$$Th_A^{4+} + 3(HDO\phi P)_{2O} \rightleftharpoons Th(DO\phi P)_2[H(DO\phi P)_2]_{2O} + 4H_A^+ \qquad (2)$$

However, HDEHP, bis 2-ethylhexyl phosphoric acid, in toluene diluent which extracts M(III) lanthanides and actinides according to Expression (1)(1,2) and which extracts Th(IV) according to Expression (2) throughout a wide range of conditions from aqueous chloride(3) or perchlorate(3) solutions, extracts Th(IV) from aqueous nitrate solutions according to a different stoicheiometry.(3) The corresponding extraction equilibrium is thus represented as:

$$Th_A^{4+} + NO_{3A}^- + 3(HDEHP)_{2O} \rightleftharpoons Th(NO_3)[H(DEHP)_2]_{3O} + 3H_A^+ \qquad (3)$$

It is obvious that if the concentration of nitrate ion is varied, both Expressions (2) and (3) must be modified by a correction for nitrate complexing of Th(IV) to obtain the

---

(11) D. Dyrssen, *Acta Chem. Scand.* 11, 1771 (1957).

(12) (a) D. F. Peppard, J. R. Ferraro and G. W. Mason, *J. Inorg. Nucl. Chem.* 4, 371 (1957).
(b) D. F. Peppard, J. R. Ferraro and G. W. Mason, *J. Inorg. Nucl. Chem.* 7, 231 (1958).

hydrogen and extractant dependencies indicated. The distribution ratio, K, derived from Expression (3) is:

$$K = k_3[NO_3^-]_A[(HDEHP)_2]_O^3/[H^+]_A^3 \tag{4}$$

and the observed K is essentially first-power dependent upon the aqueous nitrate concentration, following correction for nitrate complexing in the aqueous phase.

In the present study, the extractant HEH[EHP], (EHO)(EH)PO(OH), differs from HDEHP, $(EHO)_2PO(OH)$, only in the absence of one oxygen atom so that the compound contains one C—P bond. (Both extractants are dimeric in toluene.[6,11,12]) However, the extraction behaviour differs radically.

In perchlorate systems, two co-existing mechanisms are assumed, HY representing HEH[EHP]:

$$Th_A^{4+} + 3(HY)_{2O} \rightleftharpoons ThY_2(HY_2)_{2O} + 4H_A^+ \tag{5}$$

$$Th_A^{4+} + ClO_{4A}^- + 3(HY)_{2O} \rightleftharpoons Th(ClO_4)(HY_2)_{3O} + 3H_A^+ \tag{6}$$

The corresponding K expressions being, respectively:

$$K_5 = k_5[(HY)_2]_O^3/[H^+]_A^4 \tag{5a}$$

$$K_6 = k_6[ClO_4^-]_A[(HY)_2]_O^3/[H^+]_A^3 \tag{6a}$$

In chloride systems, the corresponding Expressions for the co-existing mechanisms are considered to be:

$$Th_A^{4+} + 3(HY)_{2O} \rightleftharpoons ThY_2(HY_2)_{2O} + 4H_A^+ \tag{7}$$

$$Th_A^{4+} + Cl^-_A + 2{\cdot}5(HY)_{2O} \rightleftharpoons Th(Cl)(Y)(HY_2)_{2O} + 3H_A^+ \tag{8}$$

$$K_7 = k_7[(HY)_2]_O^3/[H^+]_A^4 \tag{7a}$$

$$K_8 = k_8[Cl^-]_A[(HY)_2]_O^{2.5}/[H^+]_A^3 \tag{8a}$$

In nitrate systems, the mechanism corresponding to Expressions (5) and (7) is unimportant, its contribution being below detection under the conditions of the study. The two important stoicheiometries may be represented as:

$$Th_A^{4+} + NO_{3A}^- + 3(HY)_{2O} \rightleftharpoons Th(NO_3)(HY_2)_{3O} + 3H_A^+ \tag{9}$$

$$Th_A^{4+} + 2NO_{3A}^- + 3(HY)_{2O} \rightleftharpoons Th(NO_3)_2(HY_2)_2(HY)_{2O} + 2H_A^+ \tag{10}$$

(Throughout this discussion, the total number of Y and H groups in an extracted entity is obtained from considerations of stoicheiometry. No knowledge of the mode of attachment is implied. For example, in the light of present knowledge, $ThY_2(HY_2)_2$ of Expression (7) might equally well be represented as $ThY_4(HY)_2$.) Therefore, the corresponding Expressions for K are:

$$K_9 = k_9[NO_3^-]_A[(HY)_2]_O^3/[H^+]_A^3 \tag{9a}$$

$$K_{10} = k_{10}[NO_3^-]_A^2[(HY)_2]_O^3/[H^+]_A^2 \tag{10a}$$

(The stoicheiometry with respect to $(HY)_2$ is deduced from the third-power dependence shown in Fig. 3, representing conditions under which the extracted entity containing two nitrate groups presumably predominates, and from analogy with Expression (3).)

Under the specific conditions represented in Fig. 1, the ratio of K_{10} to K_9 at 1·0F

H^+ is assumed to be 3·0, the corresponding specific K expressions being given as K_2 and K_1 for the acidity range shown. From Expressions (9a) and (10a), it is apparent that the extraction stoicheiometry involving two nitrate groups becomes relatively more important at the expense of the one-nitrate mechanism as the hydrogen ion concentration is increased. This variation is confirmed both by the radiometric tracer data of Fig. 1 and by the gross extraction data of Table 1.

Since both Cl^- and ClO_4^- extract in the form of mixed complexes, Tables 1 and 2 and Figs. 2 and 6, it was deemed likely that extracted species simultaneously containing both nitrate and perchlorate and both chloride and perchlorate would be encountered if constant ionic strength solution, maintained by $NaClO_4$ and/or $HClO_4$, were used in the nitrate and chloride studies. Consequently, a study analogous to that reported for the extraction of Th(IV) by HDEHP in which the nitrate concentration of a 1·0F (HNO_3 + $HClO_4$) aqueous phase was varied in order to establish the nitrate dependency was not feasible. As a substitute, the studies represented by Figs. 5 and 6 were made.

Since the HDOϕP data serve to correct for aqueous phase nitrate complexing of Th(IV) and for general μ-effects, assumed to be the same for the two extractants, the corrected HEH[EHP] data of Figs. 5 and 6 should represent the nitrate and chloride dependencies, respectively.

From the K_2 and K_1 values at 0·10F and 1·0 F H^+ of Fig. 1, it may be calculated that the relative concentrations of the two-nitrate and one-nitrate extracted entities at 0·10F and 1·0F H^+ ($\mu = 1{\cdot}0$) should be, respectively, 3:10 and 3:1. Therefore, the corresponding total NO_3:Th ratios should be 1·23 and 1·75, values which agree very closely with the respective experimental values of 1·24 and 1·65 of Table 1.

The Cl^-:Th ratios of Table 1 are not so readily correlated with the chloride data of Fig. 2, since the extractant dependency of the chloride containing entity is not the same as that of the chloride-free entity and the concentrations of extractant employed in the gross studies were much greater than that of Fig. 2. However, the Cl^-:Th ratio does decrease with decreasing acidity, as expected from consideration of Expressions (7) and (8) and Expressions (7a) and (8a).

The gross data of Table 2 can not be compared directly with those of Table 1, since the extractions of Table 2 are necessarily interpreted in terms of a "monomer" mechanism of extraction, i.e. the (X^- + EH[EHP]$^-$)/Th ratio is, within experimental error, 4:1 indicating saturation of the extractant. It seems likely that all of the species represented in Table 2 are polynuclear,⁽⁴⁾ with phosphonate groups acting as bridges. Conversely, the species of Table 1 are mono-nuclear, as demonstrated by the fact that K is independent of the concentration of Th(IV) in the aqueous phase in tracer-level studies.

J. Inorg. Nucl. Chem., 1962, Vol. 24, pp. 989 to 994. Pergamon Press Ltd. Printed in Northern Ireland

BENZENE EXTRACTION OF STANNIC IODIDE

D. D. GILBERT* and E. B. SANDELL
School of Chemistry, University of Minnesota, Minneapolis 14, Minnesota

(*Received* 8 *January* 1962; *in revised form* 12 *February* 1962)

Abstract—The extractability of tin (IV) iodide by benzene from aqueous solution has been determined as a function of acidity, iodide concentration, and tin concentration. Anionic iodo tin (IV) species are not evident up to 5 M iodide. The extractability of tin decreases with increasing tin concentration in the aqueous phase. The partition coefficient $[SnI_4]_{benzene}/[SnI_4]_{H_2O}$ has a value of 2000 ± 150 at an ionic strength of 5 M.

IN connection with the development of an extraction method for the analytical separation of tin,(1) the effects of various factors on the benzene extractions of SnI_4 from aqueous solution were investigated. Because no equilibrium constants for the hydrolysis in tin (IV) solutions are available, the results cannot be interpreted quantitatively at the present time although general trends can be explained.

HILDEBRAND and DORFMAN(2) determined the solubility of stannic iodide in a number of organic solvents. At 25° the solubility of SnI_4 is 15·17 g in 100 g of benzene. The weight per cent solubility in benzene is greater than in any other solvents used with the exception of carbon disulphide, and, accordingly, benzene was selected as the extracting solvent in the present work.

EXPERIMENTAL

Stannic iodide was prepared by heating granulated tin metal with iodine in carbon tetrachloride.(3) The product, recrystallized from carbon tetrachloride, had a melting point of 143–144° (literature value 143·5°) and contained 81·25 %I as determined by Volhard titration (theoretical value 81·03 %I).

A standard stock solution of stannic tin (1 mg/ml) was prepared by dissolving tin metal in hot concentrated sulphuric acid, fuming to expel SO_2 and diluting, after cooling, to an acidity of 3 M sulphuric acid. This solution showed no evidence of hydrolytic precipitation after 8 months.

The distribution of tin between the aqueous and benzene phases was studied in either (or both) of two ways. In the first, the aqueous solution containing tin (IV), sodium iodide, sodium perchlorate (to adjust the ionic strength), and sulphuric acid (sometimes perchloric acid) was shaken for 1·5 min with reagent-grade benzene. This period of shaking was found to be sufficient for attainment of equilibrium; additional shaking for 30–60 min in some experiments produced no significant change in distribution. In the second method, a freshly prepared solution of stannic iodide in dry benzene was shaken with an aqueous solution of the desired composition. The introduction of sulphuric acid with an aqueous standard tin solution was thus avoided and complexing of tin (IV) with sulphate ion was eliminated. All extractions were carried out at 25°.

Tin was determined spectrophotometrically with phenylfluorone in the phase having the lower tin concentration.(1) Tin in the benzene phase was transferred to an acidic aqueous solution before determination.

Molar absorptivities of stannic iodide in benzene were determined with a Cary Model 10–11 recording spectrophotometer whose wave length scale had been calibrated against mercury, sodium, nickel, and potassium emission lines.

---

* California Research Corporation, Richmond, California

(1) D. D. GILBERT and E. B. SANDELL, *Microchem. J.* 4, 491 (1960).

(2) J. H. HILDEBRAND and M. E. DORFMAN, *J. Amer. Chem. Soc.* 49, 729 (1927).

(3) D. EDWARDS and T. MOELLER, *Inorganic Syntheses*, Vol 6, p. 119 McGraw-Hill New York (1953).

DISCUSSION

The extracted species

Spectra of a benzene extract of tin (IV) from an aqueous phase and of a benzene solution of SnI_4 (Fig. 1) are identical, with SnI_4 molar absorptivities of 9120 and 8620 l. mole^{-1} cm^{-1} at 365 and 300 mμ, respectively.* A molecular weight determination of stannic iodide in benzene (0·5 g and 1·0 g SnI_4 in 25 ml) by freezing point depression gave the values 613 and 629; the formula weight of SnI_4 is 626. No significant polymerization of stannic iodide in benzene is indicated.

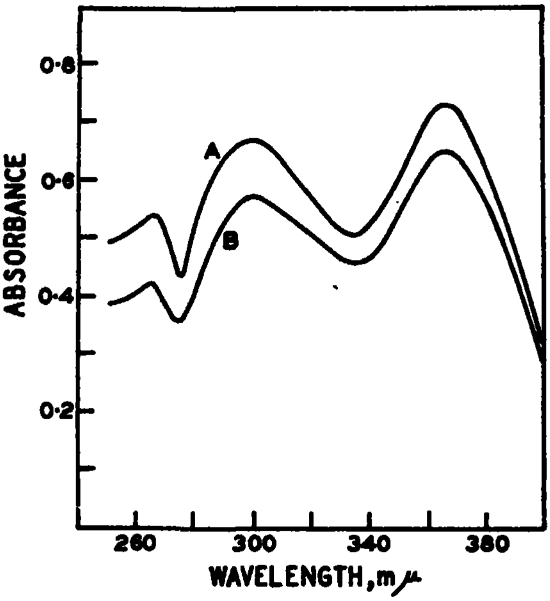

FIG. 1.—Absorption spectra of stannic iodide in benzene and of a benzene extract of tin (IV) from an acidic, aqueous iodide solution.
A. 0·5 mg SnI_4/ml C_6H_6; B. Extract of Sn(IV) from an aqueous phase 0·025 M in NaI, 3·0 M in $HClO_4$, ionic strength 5·0 M. 1 cm Vycor cells with 0·904 cm silica spacers. Beckman Model DU spectrophotometer.

Partition coefficient of stannic iodide

The partition coefficient $[SnI_4]_o/[SnI_4]_w$ (o = benzene, w = aqueous phase) was estimated at an ionic strength of 5·0 M by seeing whether the *extraction* coefficient of tin, $E = [SnI_4]_o/\sum[Sn]_w$, could be made to approach a constant value at high iodide and hydrogen-ion concentrations (anionic iodo tin complexes have little tendency to be formed). As seen from Table 1, the extraction coefficient of tin increases only from 1940 to 2100 (±150) as the iodide concentration is increased from 1·0 to 2·5 M. However, to maintain the ionic strength constant at 5·0 M, the perchloric acid concentration must be decreased from 4·0 to 2·5 M as the iodide concentration is increased, so that an increase in hydrolysed tin species may contribute to a slowing down in the increase of the extraction coefficient. Moreover, the salting out effects

---

* The absorption curve of SnI_4 in benzene is very similar to that in chloroform and *t*-butyl alcohol, as determined by Katzin.[(4)]

[(4)] L. I. KATZIN, *J. Chem. Phys.* 23, 2057 (1955).

TABLE 1.—EXTRACTION COEFFICIENT OF TIN (IV) AT HIGH ACIDITIES AND IODIDE CONCENTRATION*

$HClO_4$ (M)	NaI (M)	Sn (Total) (μg)	$[SnI_4]_o$ ($M \times 10^6$)	$\Sigma[Sn]_w$ ($M \times 10^6$)	$[SnI_4]_o/\Sigma[Sn]_w$
1·0	1·5†	950	1600	4·2	380
1·0	4·0†	1030	1740	1·7	1020
4·0	1·0	1500	2530	1·3	1940
2·5	2·5	2856	4800	2·3	2100

* Ionic strength 5·0M ($NaClO_4$ where necessary), 25·0 ± 0·2°.

† $V_o = V_w = 5$ ml. In other experiments, $V_o = 5$ ml, $V_w = 20$ ml.

of $HClO_4$ and NaI on stannic iodide are not likely to be the same. Nevertheless, it can be said that ~2000 is the lower limit of $[SnI_4]_o/[SnI_4]_w$ for an aqueous solution of the above composition. The true value may not be far from this.

Effect of iodide concentration on stannic iodide extraction

In Fig. 2 the extractability of tin in terms of percentage extraction and of log $([SnI_4]_o/\sum[Sn]_w)$ is plotted against the iodide concentration in the aqueous phase for ionic strengths of 3·2 and 5·2 M at a low acidity (0·15 M sulphuric acid). The salting out effect of sodium perchlorate is marked. Thus, at 2·0 M I^-, the extraction coefficients are respectively 15·6 and 158 for ionic strengths of 3·2 and 5·2 M. At the higher ionic strength, the extraction coefficient of tin reaches a virtually constant value in the range 3–5 M iodide. There is no evidence for the formation of an appreciable amount of anionic iodo tin (IV) species under these conditions, although rubidium and

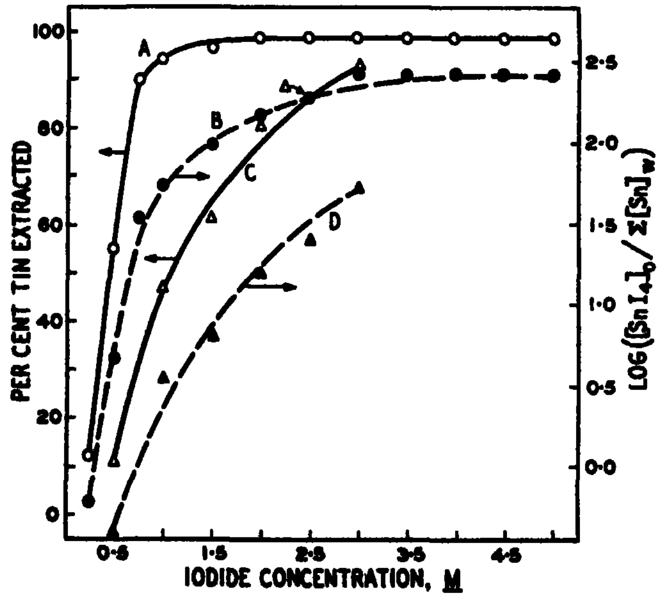

FIG. 2.—Extractability of tin as iodide at two ionic strengths.
—— Per cent tin extracted; ---- Log E = Log $([SnI_4]/_o\Sigma[Sn]_w)$. ○ Per cent extracted at ionic strength 5·2 M ● Log E at ionic strength 5·2 M △ Per cent extracted at ionic strength 3·2 M ▲ Log E at ionic strength 3·2 M. 25·0 ± 0·2°, 1256 μg total tin, 0·15 M H_2SO_4, $V_w = 20$ ml, $V_o = 5$ ml

cesium iodostannates have been prepared by mixing alcoholic HI solutions of stannic iodide with an HI solution of the alkali iodide.(5) The slight tendency to form anionic iodo species is in accord with the relatively small size of tin (IV) ion.

A series of extraction experiments were run in 2·0 M perchloric acid at low iodide concentrations (0·015–0·15 M), with two concentrations of tin (initially 1 and 10 mg in 20 ml of aqueous phase). Under these conditions, the logarithm of the extraction coefficient of tin increases linearly with the logarithm of the iodide concentration up to about 0·10 M iodide, above which it begins to fall off (Fig. 3). The variation of the logarithm of the extraction coefficient of tin with the logarithm of the total equilibrium iodide concentration in the aqueous phase is given by the following expression, in which the charges of the species have been omitted:

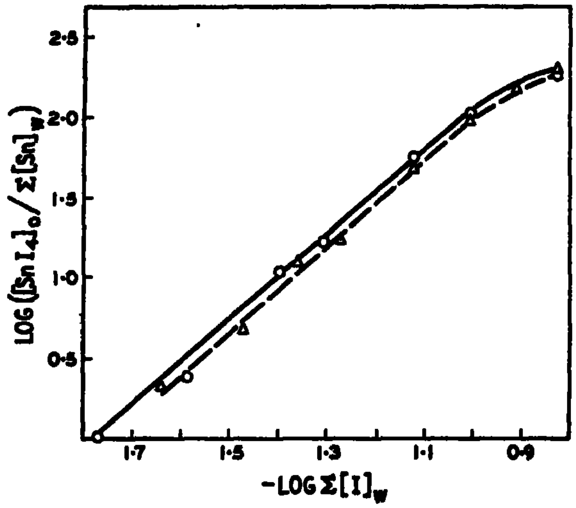

FIG. 3.—Extraction coefficient of stannic iodide as a function of iodide concentration.
—○—○— 1 mg total tin; - -△- -△- -. 10 mg total tin
25·0 ± 0·2°, ionic strength 5·0 M, 2·0 M HClO$_4$, $V_w = 20$ ml, $V_o = 5$ ml

$$\frac{\partial \log E}{\partial \log \sum [\mathrm{I}]_w} = \left\{\left(4 - \frac{\sum\limits_i i[\mathrm{SnI}_i] + \sum\limits_{kl} l[\mathrm{Sn(OH)}_k\mathrm{I}_l] + \sum\limits_{xyz} zx[\mathrm{Sn}_x\mathrm{(OH)}_y\mathrm{I}_z]}{\sum\limits_i [\mathrm{SnI}_i] + \sum\limits_j [\mathrm{Sn(OH)}_j] + \sum\limits_{kl} [\mathrm{Sn(OH)}_k\mathrm{I}_l] + \sum\limits_{xyz} x[\mathrm{Sn}_x\mathrm{(OH)}_y\mathrm{I}_z]}\right) \times \left(\frac{[\mathrm{I}] + \sum\limits_i i[\mathrm{SnI}_i] + \sum\limits_{kl} l[\mathrm{Sn(OH)}_k\mathrm{I}_l] + \sum\limits_{xyz} z[\mathrm{Sn}_x\mathrm{(OH)}_y\mathrm{I}_z]}{[\mathrm{I}] + \sum\limits_i i^2[\mathrm{SnI}_i] + \sum\limits_{kl} l^2[\mathrm{Sn(OH)}_k\mathrm{I}_l] + \sum\limits_{xyz} z^2[\mathrm{Sn}_x\mathrm{(OH)}_y\mathrm{I}_z]}\right)\right\}$$

where $\sum\limits_i [\mathrm{SnI}_i]$ represents the sum of the equilibrium aqueous concentrations of Sn^{4+} SnI^{3+}, SnI_2^{2+}, SnI_3^{+}, and SnI_4; and similarly with $\sum\limits_j [\mathrm{Sn(OH)}_j]$ except $j \neq 0$, and with $\sum\limits_{kl} [\mathrm{Sn(OH)}_k\mathrm{I}_l]$ except k and $l \neq 0$; $x > 1$ in $\sum\limits_{xyz} [\mathrm{Sn}_x\mathrm{(OH)}_y\mathrm{I}_z]$. If the free iodide concentration is markedly greater than the sum of concentrations of the aqueous iodo-tin species, Equation (1) can be written:

---

(5) W. WERKER, *Rec. Trav. Chim.* 58, 257 (1939).

$$\frac{\partial \log E}{\partial \log \sum [\mathrm{I}]} \cong \frac{\partial \log E}{\partial \log [\mathrm{I}]} = 4 - (\sum_i i f_{\mathrm{SnI}_i} + \sum_{kl} l f_{\mathrm{Sn(OH)}_k\mathrm{I}_l} + \sum_{xyz} z f_{\mathrm{Sn}_x(\mathrm{OH})_y\mathrm{I}_z})$$

or,

$$\frac{\partial \log E}{\partial \log \sum [\mathrm{I}]} \cong 4 - \bar{n},$$

where f_{SnI_i}, $f_{\mathrm{Sn(OH)}_k\mathrm{I}_l}$, and $f_{\mathrm{Sn}_x(\mathrm{OH})_y\mathrm{I}_z}$ are fractions of tin present as the various iodo-tin species in the aqueous phase at equilibrium and $\bar{n}$ is the average number of iodide ligands per tin (IV) species.

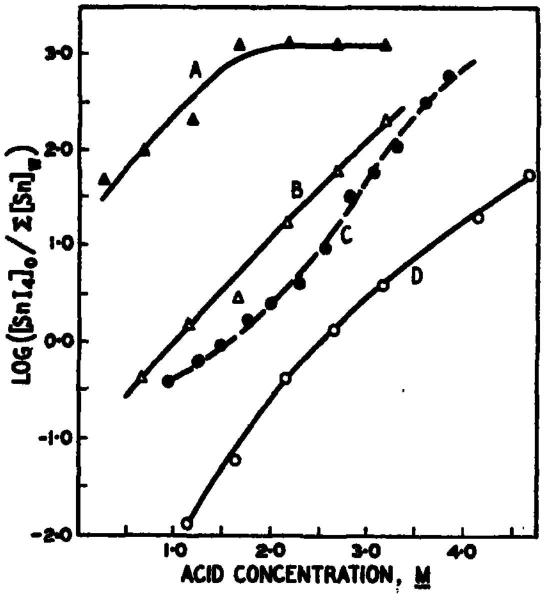

FIG. 4.—Extraction coefficient of stannic iodide as a function of acidity.
A. 0·50 M NaI, *B*. 0·061 M NaI, *C* and *D*. 0·025 M NaI. (All initial concentrations.)
Sulphuric acid present in *A*, *B*, and *D*, but absent in *C*. 1 mg total tin in each case.
25·0 ± 0·2°, ionic strength 5·0 M (*C*) and 5·2 M (*A*, *B*, *D*), V_w = 20 ml, V_o = 5 ml

Thus, a linear variation of log E with log $\sum[\mathrm{I}]_w$ is to be expected if (1) the free iodide concentration is markedly greater than the concentrations of the aqueous iodo-tin species and (2) the average number of iodide ligands per tin (IV) species remains approximately constant. The slope of the linear portion of Fig. 3 gives a value of 1·4 for $\bar{n}$. With a value of 2000 for the partition coefficient of stannic iodide, no more than 10 per cent of the tin in the aqueous phase at equilibrium can be present as SnI_4 at the highest iodide concentration (0·15 M) in the series.

Effect of acidity and temperature

The extraction coefficient of tin at various iodide concentrations is plotted as a function of the acidity in Fig. 4. At low iodide concentrations, the extraction of tin is still increasing in 3·5–4 M perchloric acid, indicating appreciable hydrolysis at these high acidities. The complexing of tin (IV) by sulphuric acid is incidentally demonstrated in this figure (cf. C and D).

The extractability of tin is unaffected if a solution prepared by dilution of a standard tin solution in sulphuric acid to 1·0 M in perchloric acid (μ = 5·2 M) is allowed to stand 20 hr before addition of iodide and subsequent extraction, instead of being extracted immediately after dilution.

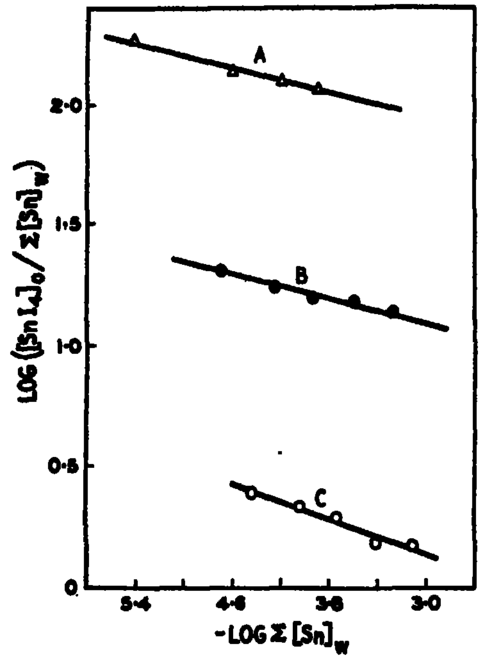

Fig. 5.—Extraction coefficient of stannic iodide as a function of total tin concentration. *A*. 0·100 M NaI, 2·0 M $HClO_4$; *B*. 0·100 M NaI, 1·0 M $HClO_4$; *C*. 0·050 M NaI, 1·0 M $HClO_4$. (Equilibrium iodide and initial perchloric acid concentrations are given.) 25·0 ± 0·2°, ionic strength 5·0 M, V_w = 20 ml, V_o = 5 ml.

At constant acidity (above 1·7 M perchloric acid) and iodide concentration (0·025 M), the extractability of tin increases with a rise in temperature. Thus, in the range 2–4·5 M perchloric acid, the extraction coefficient E increases by approximately 150 per cent from 25° to 30°.

Effect of tin concentration

At constant acidity and iodide concentration, the extraction coefficient of tin decreases with increasing tin concentration. A plot of log E against the negative logarithm of the aqueous tin concentration, $-\log \sum[\mathrm{Sn}]$, gives a linear relation or a close approach to it (Fig. 5). In these runs the iodide concentration was adjusted so that it was constant for any one series at equilibrium. The formation of polynuclear tin species is indicated, although it is not possible to interpret the results on the basis of a model in which one or more mononuclear tin species is in equilibrium with a single predominant polynuclear tin species.

Acknowledgement—One of us (D. D. G.) wishes to thank the Shell Companies Foundation, Inc., and the Procter and Gamble Company for fellowships held during the 1958–1959 academic year and the summer of 1959.

J. Inorg. Nucl. Chem., 1962, Vol. 24, pp. 995 to 1000. Pergamon Press Ltd. Printed in Northern Ireland

AQUEOUS SYSTEMS AT HIGH TEMPERATURE—VII

LIQUID-LIQUID IMMISCIBILITY AND CRITICAL PHENOMENA IN THE SYSTEMS UO_3–SO_3–H_2O, UO_3–SO_3–D_2O AND CuO–SO_3–D_2O, 270–430°C*(1)

WILLIAM L. MARSHALL, ERNEST V. JONES, G. M. HEBERT and F. J. SMITH
Reactor Chemistry Division Oak Ridge National Laboratory Oak Ridge, Tennessee

(*Received* 1 *February* 1962)

Abstract—In the condensed systems UO_3–SO_3–H_2O, UO_3–SO_3–D_2O and CuO–SO_3–D_2O boundary limits of liquid–liquid immiscibility were extended to compositions at which $L_1 = V =$ supercritical fluid at several fixed concentrations of SO_3. These (isothermal) critical end points were found at temperatures between 374 and 430°C with solutions having molal ratios, $m_{\text{metallic oxide}}: m_{SO_3}$, between 0·20 and 0·50 depending upon the concentration of SO_3 in the systems. A second liquid phase was not observed at lower molal ratios. Instead, critical phenomena (in this paper used to designate the disappearance of the meniscus between liquid and vapour phases and not to specify the appearance of a second liquid phase) revealed concentrations of UO_3 or of CuO as high as 0·25 molal in a supercritical fluid SO_3–D_2O, 1·0 molal in SO_3. These observations coincided with those made previously which showed an appreciable solubility of the NiO component in the supercritical fluid SO_3–H_2O.

PREVIOUS investigations of liquid–liquid immiscibility in the systems UO_3–SO_3–H_2O and UO_3–SO_3–D_2O at high temperature have disclosed (1) boundary limits of temperature and composition for stoicheiometric UO_2SO_4 in H_2O and D_2O,(2,3) (2) some boundary limits for solutions of molal ratio, $m_{UO_3}:m_{SO_3}$, varying from 0·33 to 1·2,(3) and (3) compositions of the heavy and light liquid phases in equilibrium.(4) Another investigation has disclosed boundary limits of liquid–liquid immiscibility for the systems

$$UO_2SO_4\text{–}H_2SO_4\text{–}H_2O,\ CuSO_4\text{–}H_2SO_4\text{–}H_2O,\ \text{and}\ UO_2SO_4\text{–}CuSO_4\text{–}H_2SO_4\text{–}H_2O$$

at molal ratios, $(m_{UO_3} + m_{CuO}):m_{SO_3}$, varying from 0·72 to 1·00.(5) In earlier work, SECOY observed a solubility of UO_2SO_4 in super-critical H_2O containing low concentrations of H_2SO_4.(6)

The purpose of this present investigation was to extend the determination of phase boundaries in the condensed systems to a wider range of SO_3 concentration and to molal ratios, $m_{UO_3}:m_{SO_3}$ or $m_{CuO}:m_{SO_3}$, designated R_U and R_{Cu}, respectively, as low as 0·1 at temperatures from approximately 300° to critical temperatures (where $L_1 = V$). From the observations of SECOY and from extrapolations of earlier two-liquid phase data to temperatures near 400°, it was expected that compositions at which $L_1 = V =$

---

* This paper is based on work performed at Oak Ridge National Laboratory, which is operated by Union Carbide Corporation for the Atomic Energy Commission.

(1) Previous paper in series: "*Investigations on the System* NiO–SO_3–H_2O *and its* D_2O *Analogue from* 10^{-4} *to* 2 m SO_3, 150–400°C." W. L. MARSHALL, J. S. GILL and R. SLUSHER, *J. Inorg. Nucl. Chem.* In press (1962).

(2) C. H. SECOY, *J. Amer. Chem. Soc.* **72**, 3343 (1950).

(3) H. F. MCDUFFIE, Review in *Fluid Fuel Reactors* (Edited by J. A. LANE, H. G. MACPHERSON, F. MASLAN) pp. 85–127 Addison-Wesley Reading, Mass. (1958).

(4) E. V. JONES and W. L. MARSHALL, *J. Inorg. Nucl. Chem.* **23**, 287 (1961).

(5) F. E. CLARK, J. S. GILL, R. SLUSHER and C. H. SECOY, *J. Chem. Engng. Data*, **4**, 12 (1959).

(6) C. H. SECOY, Report ORNL-607, pp. 33–38 (1949).

super-critical fluid would be found indicating appreciable solubility of UO_3 and CuO in supercritical fluids SO_3–H_2O and SO_3–D_2O.

In addition to being of fundamental interest, the phase boundary information on the systems containing uranium would be useful in specifying operating limits of temperature and composition for aqueous homogeneous reactor fuels. Information on systems containing copper would be useful since copper has been included in fuel compositions as a catalyst for the recombination of radiolytic H_2 and O_2.(3) The operating temperatures of aqueous homogeneous reactors might be extended above 370° by using fuels of compositions showing critical phenomena but no phase changes at considerably lower temperatures. The vapour phase could be eliminated at all temperatures by maintaining a hydrostatic pressure on the system greater than the critical pressure.

This paper presents some liquid–liquid immiscibility limits of temperature and composition as well as some temperatures for critical phenomena in the systems UO_3–SO_3–H_2O, UO_3–SO_3–D_2O, and CuO–SO_3–D_2O.

EXPERIMENTAL PROCEDURES

The preparation of stock solutions of UO_3 or of CuO dissolved in H_2SO_4—H_2O or D_2SO_4—D_2O, and the chemical analyses for UO_3, CuO and SO_3 were performed in the manner described previously.(4,7) The source of the $UO_3 \cdot H_2O$, H_2SO_4, and D_2O reagents was the same as for the previous work although the D_2O was found by an improved analysis to contain only 0·3% H_2O instead of 2% reported previously.

Experimental runs by the synthetic method were carried out in the type of apparatus described elsewhere(8) using quartz capillary tubes which contained solutions of known compositions. Supersaturation by the heavy liquid phase was not observed. The absence of supersaturation in experiments conducted previously(2,4,8) indicated that no supersaturation was to be expected in these experiments. Appearance of immiscibility or critical phenomenon was instantaneous at temperatures defining the phase boundary limits. The tubes containing solutions were filled 40–50 per cent full at 25° and at final temperatures were from 50–90 per cent full.

RESULTS AND DISCUSSION

Experimental data given in Tables 1, 2 and 3 are shown graphically in Figs. 1, 2 and 3 for the systems UO_3–SO_3–H_2O, UO_3–SO_3–D_2O, and CuO–SO_3–D_2O, respectively.

TABLE 1.—TEMPERATURES (°C) FOR THE APPEARANCE OF LIQUID–LIQUID IMMISCIBILITY AND CRITICAL PHENOMENA IN THE SYSTEM UO_3–SO_3–H_2O;

Molal ratio	SO_3 (molality)			
m_{UO_3}/m_{SO_3}	0.2000	0.1000	0.0500	0.0200
1·000	298·0*L**	308·9*L*	321·0*L* + *S*	<350*S*
0·950	301·5*L*	312·2*L*	—	—
0·900	306·8*L*	316·3*L*	327·0*L* + *S*	<350*S*
0·800	316·0*L*	324·8*L*	333·6*L*	—
0·750	—	—	—	351·8*L*
0·700	325·0*L*	331·5*L*	340·6*L*	—
0·600	334·2*L*	340·0*L*	348·2*L*	357·8*L*
0·500	344·6*L*	348·8*L*	356·0*L*	362·8*L*
0·400	357·5*L*	358·3*L*	363·0*L*	368·4*L*
0·300	370·0*L*	368·5*L*	370·4*L*	375*LC*(?)
0·250	—	—	—	374*C*
0·2000	380*C*	377*LC*(?)	378*C*	—
0·1000	—	—	377*C*	—
0·0000	380*C*	379*C*	—	—

* *L* = liquid–liquid immiscibility, *C* = critical phenomena, *S* = solid phase (presumably UO_3 hydrate)

---

(7) E. V. JONES and W. L. MARSHALL, *J. Inorg. Nucl. Chem.* **23**, 295 (1961).

(8) C. J. BARTON, G. M. HEBERT and W. L. MARSHALL, *J. Inorg. Nucl. Chem.* **21**, 141 (1961).

TABLE 2.—TEMPERATURES (°C) FOR THE APPEARANCE OF LIQUID–LIQUID IMMISCIBILITY AND CRITICAL PHENOMENA IN THE SYSTEM UO_3–SO_3–D_2O;

Molal ratio	SO$_3$ (molality)							
m_{UO_3}/m_{SO_3}	1.000	0·800	0·600	0·364	0·2000	0·1000	0·0500	0·0200
1·000	277·5L*	277·8L	278·5L	281·0L	287·8L	297·4L	313·0L	311S
0·800	306·3L	299·2L	301·2L	302·6L	306·8L	315·5L	328·0L	337·7L
0·600	341·8L	332·7L	331·0L	328·2L	329·2L	332·5L	343·3L	352·0L
0·500	360·5L	355·5L	—	—	—	—	352·3L	358·7L
0·400	378·7L	375·8L	367·8L	358·7L	359·3L	354·5L	362·5L	365·0L
0·300	396C	378C	383·6L	375·2L	—	—	374C	373C
	(0·59)†	(0·62)	—	—	—	—	(0·48)	(0·47)
0·2000	399C	396C	392C	383C	380C	375C	373C	373C
	(0·61)	(0·52)	(0·50)	(0·49)	(0·44)	—	(0·48)	(0·48)
0·1000	402C	399C	395C	383C	377C	—	373C	374C
	(0·61)	(0·51)	(0·43)	(0·49)	(0·53)	—	(0·52)	(0·50)
0·0000	408C	400C	392C	384C	379C	376C	373C	372C

* *L* = liquid–liquid immiscibility, *C* = critical phenomena, *S* = solid phase (presumably UO_3 hydrate),

† Value in parentheses = density of supercritical fluid at temperature.

TABLE 3.—TEMPERATURES (°C) FOR THE APPEARANCE OF LIQUID–LIQUID IMMISCIBILITY AND CRITICAL PHENOMENA IN THE SYSTEM CuO–SO_3–D_2O;

Molal ratio m_{CuO}/m_{SO_3}	SO$_3$ (molality)							
	1·000	0·800	0·600	0·364	0·2000	0·1000	0·0500	0·0200
1·000	S*	S	S	S	S	S	S	S
·800	326L	325L	S	S	S	S	S	S
·700	347L	341L	350L	336L	334L	S	S	S
·600	367L	363L	361L	352L	354L	360L	S	S
·500	384L	381L	373L	367L	372L	378L	374C	S
·400	408L	400L	385L	381L	381C	377C	374C	373C
·300	428L	419L	397L	389C	380C	376C	373C	373C
·2000	422C	411C	393C	387C	379C	376C	373C	373C
·1000	415C	406C	391C	385C	379C	376C	373C	372C

* *L* = liquid–liquid immiscibility, *C* = critical phenomena, *S* = blue–green solid (presumably $2CuO \cdot CuSO_4 \cdot 2D_2O$)

The symbol (+*S*) used in Table 1 indicates a small amount of solid forming at temperatures somewhat below those reported for liquid–liquid immiscibility. The combined symbols *LC*(?) designate an apparently simultaneous appearance of second liquid phase and critical phenomenon. Where only the symbol *S* is given but no temperature is reported a solid phase appeared at temperatures considerably below those for liquid–liquid immiscibility or critical phenomenon. Also included in Fig. 1 are some liquid–liquid immiscibility temperatures interpolated from the data of CLARK *et al.*(5) Each curve represents phase boundary conditions of temperature and composition expressed as molal ratios R_U and R_{Cu} for initial compositions containing a fixed concentration of SO_3, specified for each curve. There are two phase boundary regions shown for each system—that of liquid–liquid immiscibility and that of critical phenomenon. For a fixed concentration of SO_3 the two curves representing these boundaries intersect at an (isothermal) critical endpoint where the composition of the light-liquid phase (L_1) = vapour phase (V) = supercritical fluid. The compositions of heavy liquid phases (L_2) which first appear in the systems UO_3–SO_3–H_2O and

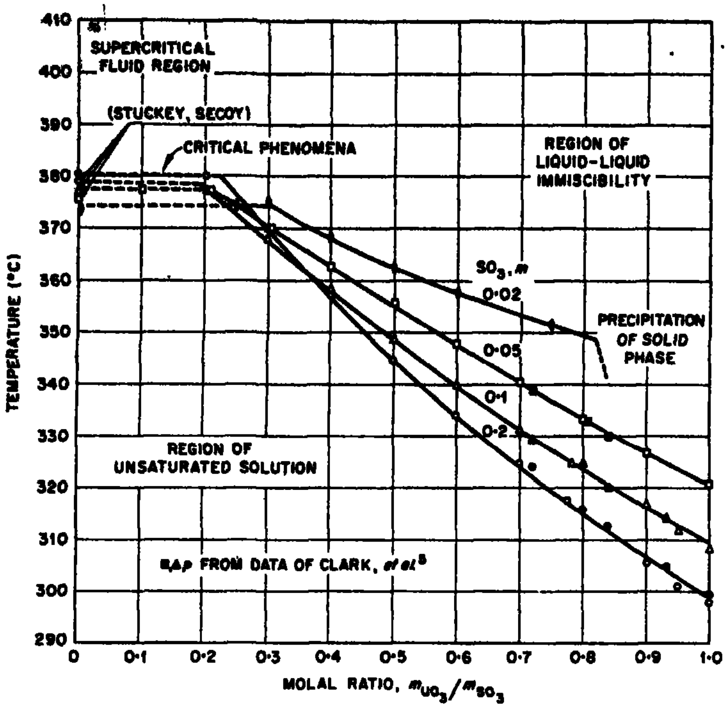

Fig. 1.—System UO_3–SO_3–H_2O, liquid-liquid immiscibility and critical phenomena.

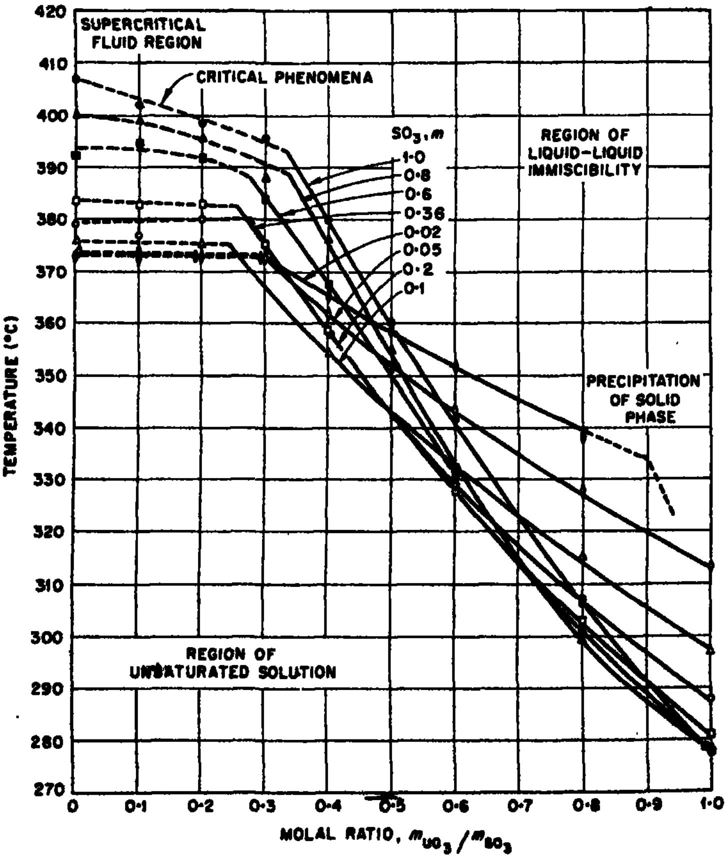

Fig. 2.—System UO_3–SO_3–D_2O, liquid-liquid immiscibility and critical phenomena.

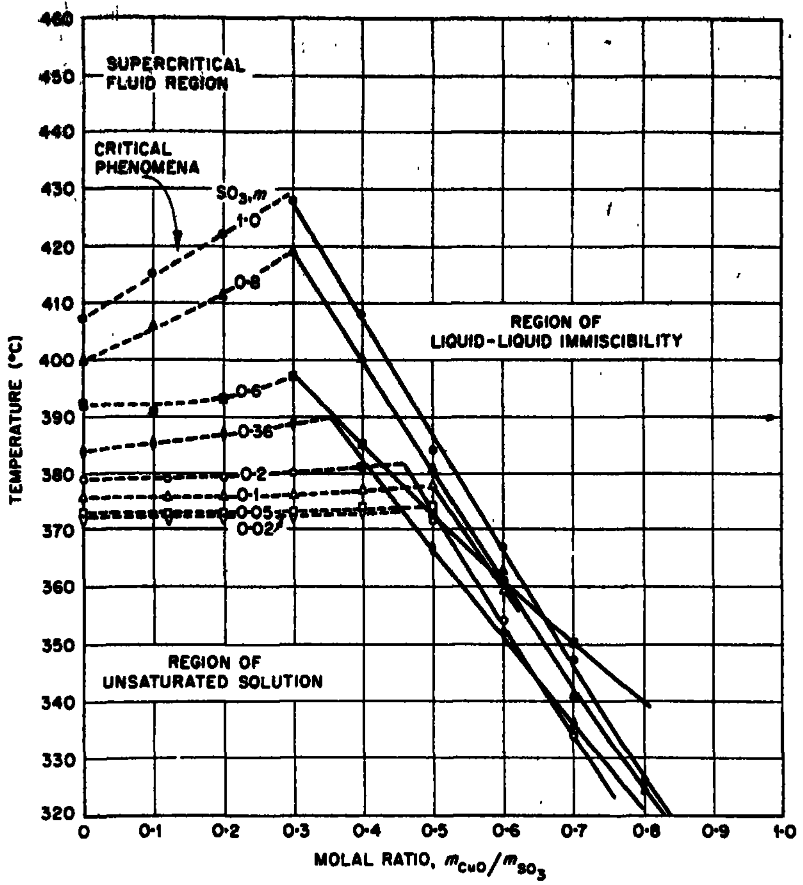

FIG. 3.—System CuO–SO_3–D_2O, liquid–liquid immiscibility and critical phenomena.

UO_3–SO_3–D_2O as the temperature is raised can be estimated from the data previously reported on equilibrium compositions with light-liquid phases.(4)

In Figs. 1–3 the molalities are the molalities of the solutions introduced into the tubes, these solutions being L_1. For the dashed curves, which report the temperatures of the critical phenomenon of L_1 and V, the molalities represent also the molalities of L and V at the reported, apparent critical temperature. However, the true critical temperature (where $L = V$) can be determined only at a volume filling of L_1 of 50 per cent at temperature. The actual fillings at final temperatures in most instances were larger than 50 per cent. But upon comparing some densities of the supercritical fluids in Table 2 (obtained from the densities at 25° and the liquid: total-volume ratios) with those of pure D_2O near its critical temperature,(9) and considering the higher densities of the solutions, the reported temperatures are believed to approximate rather closely the true values. Fig. 1 shows, in addition, some interpolations from critical temperatures obtained by SECOY and STUCKEY for solutions of H_2SO_4–H_2O at $R_U = 0$ and at a final liquid-volume filling of 50 per cent.(10)

For the curves representing the appearance of L_2 the composition of L_1 at the recorded temperature will vary somewhat from the initial composition with variation in the percentage of filling. It was shown previously, however, that in the system UO_3–SO_3–H_2O the immiscibility temperature was little affected by moderate changes in this percentage of filling.(8)

---

(9) G. M. HEBERT, H. F. MCDUFFIE and C. H. SECOY, *J. Phys. Chem.* **62**, 431 (1958).

(10) J. E. STUCKEY, Ph.D. Dissertation, The University of Oklahoma Graduate College, Norman, Oklahoma (1957).

At high concentrations of SO_3 the addition of UO_3 *lowers* the critical temperature. This may arise from a higher degree of association of UO_2SO_4 than of H_2SO_4; thus as UO_3 is added a decrease in concentration of ionic species lowers the critical temperature. As more UO_3 is added R_U increases sufficiently that upon raising the temperature of the system liquid–liquid immiscibility rather than a critical phenomenon ($L = V$) is observed. For the system CuO–SO_3–D_2O at constant molality of SO_3 the addition of CuO component invariably *raises* the critical temperature (Fig. 3). Therefore $CuSO_4$ at these temperatures may dissociate to a greater extent than D_2SO_4 and thus raise the critical temperature.

From Figs. 2 and 3 it is seen that UO_3 and CuO are soluble up to a concentration near 0·3 molal in a supercritical SO_3–D_2O fluid which is 1·0 molal in SO_3. These observations and a similar one on the system NiO–SO_3–H_2O (but near 0·1 molal NiO in 1·0 molal SO_3)(1) indicate that other metallic oxides may show high solubilities in the supercritical fluids SO_3–H_2O and SO_3–D_2O.

Acknowledgement—The authors thank Professor J. E. RICCI, New York University, for his constructive review of the manuscript.

J. Inorg. Nucl. Chem., 1962, Vol. 24, pp. 1001 to 1006. Pergamon Press Ltd. Printed in Northern Ireland

THE AMMONOLYSIS OF VANADIUM (III) BROMIDE

D. Nicholls
Department of Inorganic, Physical and Industrial Chemistry,
The University, Liverpool

(*Received* 16 *October* 1961; *in revised form* 1 *December* 1961)

Abstract—Tensimetric and liquid ammonia extraction studies on the system VBr_3–NH_3 show that the overall ammoniate $VBr_3.7NH_3$, formed at −36° is a mixture of $VBr_2NH_2.5NH_3$ and NH_4Br. The ammonobasic vanadium (III) bromide is soluble in liquid ammonia solutions of ammonium bromide so that VBr_3 is largely soluble in ammonia. Reaction with alkali metal in ammonia solutions yields the inside $M^IV(NH)_3$ and the alkali metal amide. The thermal decomposition of the reaction products has been studied.

While vanadium (IV) chloride is extensively ammonolysed in liquid ammonia(1) it is to be expected that the vanadium (III) halides will be considerably less, or even not at all, ammonolysed in view of their more polar nature. Thus several workers report the formation of ammoniates by the vanadium (III) halides. Meyer and Backa(2) found that vanadium (III) chloride and bromide add approximately six molecules of ammonia, forming the hexammines $[V(NH_3)_6]X_3$, at the boiling point. Ephraim and Amman(3) confirmed these results and found that no ammonobasic products were formed in liquid ammonia. More recently, Jantsch *et al.*(4) have reported ammoniates $V(NH_3)_xCl_3$ where $x = 12, 7, 6, 5, 3$ and 2; the 7-ammoniate being the stable phase at −40° and the 6-ammoniate at 10°. None of these workers have found any ammonolysis of the vanadium (III) halides and consequently vanadium (III) bromide was chosen as a starting material for synthetic reactions in liquid ammonia. The discovery that it was ammonolysed led us to investigate the reaction further in order to discover its extent.

The initial reaction of ammonia with vanadium (III) bromide appears to be the co-ordination of six molecules of ammonia to the vanadium atom to give the latter the octahedral symmetry analogous to that found in the hydrates $[V(H_2O)_6]X_3$:

$$VBr_3 + 6NH_3 \rightarrow [V(NH_3)_6]Br_3$$

This is followed by ammonolysis:

$$[V(NH_3)_6]Br_3 + NH_3 \rightarrow [VNH_2(NH_3)_5]Br_2 + NH_4Br \qquad (2)$$

at least in liquid ammonia, so that an insoluble ammonobasic bromide is obtained upon filtration of the reaction mixture. However, some interaction between the ammonobasic vanadium (III) bromide and ammonium bromide occurs in liquid and the resultant solution probably contains complex vanadium anions:

$$VBr_2NH_2 + NH_4Br \rightarrow NH_4[VBr_3NH_2]$$

This accounts for the large solubility of vanadium (III) bromide in ammonia; some 25 per cent (approximately) of the vanadium not being dissolved. As would be

(1) G. W. A. Fowles and D. Nicholls, *J. Chem. Soc.* 1687 (1958).
(2) J. Meyer and R. Backa, *Z. Anorg. Chem.* **135**, 177 (1924).
(3) E. Epharaim and E. Amman, *Helv. Chim. Acta* **16**, 1273 (1933).
(4) G. Jantsch, K. Bergmann and H. Rupp, *Z. Anorg. Chem.* **262**, 223 (1950).

expected, addition of extra ammonium bromide results in complete solution of the insoluble product. Similar effects were observed in other systems$^{(1,5)}$ and in the TiI_4–NH_3 system$^{(5)}$ the titanium could be extracted from solution upon an anion exchange resin. That the complex vanadium anion is stable only in solution is shown by the tensimetric detection of ammonium bromide.

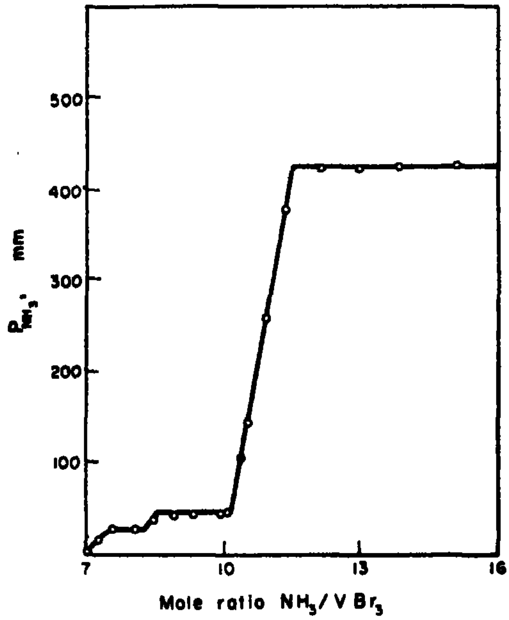

FIG. 1.—Vapour-pressure-composition isotherm for the system VBr_3–NH_3 at −36°.

The initial reaction of the alkali metals with vanadium (III) bromide in ammonia is that with the ammonium bromide produced by ammonolysis:

$$VBr_2NH_2 + NH_4Br + K \rightarrow VBr_2NH_2 + KBr + NH_3 + \tfrac{1}{2}H_2$$

Large quantities of hydrogen are evolved and it is plain that a vanadium compound catalyses the rapid decomposition of the alkali metal solutions even at −63°. No evidence is available to suggest that the catalyst is the finely divided metal, as it often is, e.g. $NiBr_2$ reduction.$^{(6)}$ The result of this decomposition is that vanadium (III) amide $V(NH_2)_3$ formed (either by base catalysed ammonolysis of VBr_2NH_2 or direct nucleophilic attack on VBr_2NH_2 by amide ion from decomposed alkali metal solution) behaves as an amphoteric amide and reacts with e.g. potassamide to give potassium tetra-amidovanadate (III). A multiplicity of amide groups around the vanadium atom is expectedly unstable so that the final product is potassium iminovanadate (III).

$$K[V(NH_2)_4] \rightarrow K[V(NH)_2] + 2NH_3$$

The sodium salt of similar composition can be isolated only in admixture with the insoluble sodamide. Attempts to remove sodamide from this mixture with a liquid ammonia solution of ammonium nitrate yielded a product only crudely corresponding to $NaV(NH)_2$. These salts are readily hydrolysed in moist air and give green solutions in acids indicating that they contain trivalent vanadium. These salts appear to be identical with those obtained by SCHMITZ-DUMONT and BROJA⁽⁷⁾ who treated the complex vanadium (III) thiocyanate $K_3[V(SCN)_6]$ with potassamide in ammonia.

---

(5) G. W. A. FOWLES and D. NICHOLLS, *J. Chem. Soc.* 990 (1959).

(6) G. W. WATT and D. D. DAVIES, *J. Amer. Chem. Soc.* 70, 3753 (1948).

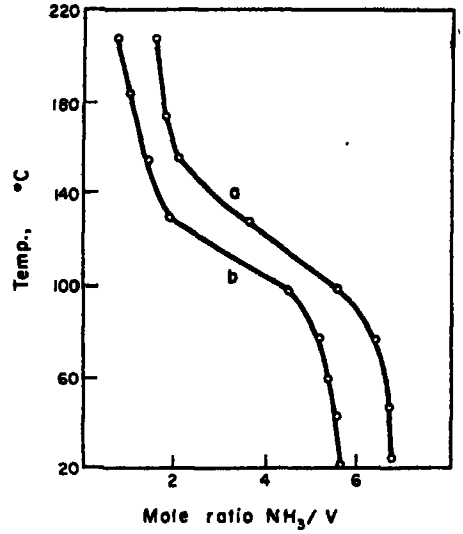

FIG. 2.—Thermal decompositions of (a) $VBr_3.7NH_3$ and (b) $VBr_2NH_2.5NH_3$.

The tensimetric study of the VBr_3–NH_3 reaction shows that at −36° an average of one-third of the V–Br bonds are broken since one mole of ammonium bromide per mole of vanadium (III) bromide is detected by means of the characteristic dissociation pressures of its ammoniates. Since the thermal decomposition of the ammonia insoluble product (Fig. 2, plot *b*) closely parallels that of the ammonolytic mixture (Fig. 2, plot *a*) at least up to 100°, it is seen that no interaction is occurring between NH_4Br and $VBr_2NH_2.5NH_3$ below this temperature. Above 100° rapid decomposition of the pentammine sets in and the composition $VBr_3.2NH_3$ reached at 155° (Fig. 2, plot *a*) probably represents a mixture of NH_4Br with polymeric VBr_2NH_2. This mixture evidently interacts to some extent since a yellow sublimate containing 4–7 per cent of the vanadium, appears with ammonium bromide above 174°. Although this vanadium compound could not be isolated it seems likely that it has the empirical formula $VBr_3.2NH_3$ since deduction of this composition from the sublimate analysis (Table 2) leaves the 1:1 ratio required for ammonium bromide. A similar sublimate has been found in the

$$VBr_2NH_2 + NH_4Br \rightarrow VBr_3 + 2NH_3 \xrightarrow[\text{surface}]{\text{cold}} VBr_3.2NH_3$$

reaction of vanadium (III) chloride with gaseous ammonia at 325°⁽⁸⁾ and the compound $VCl_3.2NMe_3$ which is purified by vacuum sublimation has been shown to be five-coordinate.⁽⁹⁾

At 208°, sublimation of ammonium bromide from the ammonolytic mixture is complete and the residue has the composition $VBr_{2\cdot04}N_{0\cdot85}$. Above 270° and up to

---

(7) O. SCHMITZ-DUMONT and G. BROJA, *Z. Anorg. Chem.* 255, 299 (1948).

(8) G. W. A. FOWLES, P. G. LANIGAN and D. NICHOLLS, *Chem. and Indutr.* 1167 (1961).

(9) G. W. A. FOWLES and C. M. PLEASS, *J. Chem. Soc.* 1674 (1957).

400°, 0·5 mole HBr/g. atom V are evolved and the residue is $VBr_{1\cdot 65}N_{0\cdot 35}$. While the violet solutions obtained upon hydrolysis of these thermal decomposition products indicate that some divalent vanadium is present, the magnetic moment of the 400° product is 2·06 B.M. This low magnetic moment must arise through removal of the ammonia ligands, (i.e. the magnetic dilution around the vanadium atoms) with the resultant spin–spin coupling giving interaction of the anti-ferromagnetic type. The thermal decompositions are obviously complex but the major reactions appear to be illustrated by the scheme (monomeric formulae written for simplicity);

$$\begin{array}{ccccc}
VBr_2NH_2.5NH_3 + NH_4Br & \rightarrow & VBr_2NH_2 & + & NH_4Br + 5NH_3 \\
(VBr_3.7NH_3,\ -37^\circ) & & & (VBr_3.2NH_3,\ 155^\circ) & \\
 & & & \downarrow & \\
VBrNH + HBr & \leftarrow & VBr_2NH_2 & + & NH_4Br \\
 & & \text{residue} & & (VBr_3.2NH_3) \\
 & & \searrow & & \text{sublimate} \\
HBr + VBr_2NVBr & \leftarrow & VBr_2NHVBr_2 & + & NH_3 \\
(VBr_{1\cdot 5}N_{0\cdot 5}) & & & &
\end{array}$$

The simultaneous decomposition of VBr_2NH_2 by two paths i.e. giving NH_3 and HBr, is necessary to account for the formation of the ammonium bromide sublimate in the decomposition of the insoluble product.

EXPERIMENTAL

Materials

Vanadium (III) bromide was prepared by the reaction of bromide with pure vanadium in a nitrogen atmosphere at 550°. The product sublimed from the hot zone and was collected in glass bulbs which were sealed off *in situ*. Oxybromide impurities were removed from the black flakes by vacuum sublimation. The product was stored in sealed ampoules under dry nitrogen (Found, V, 17·7; Br 82·1; VBr_3 requires V, 17·5; Br 82·5%). Liquid ammonia was dried over sodium.

Analyses and magnetic susceptibilities

These were carried out by methods previously described.(1,8)

Reactions

These were studied under rigorously anhydrous conditions in all glass vacuum apparatus.

Tensimetric study of the VBr_3–NH_3 *reaction at* −36°

This was performed in the usual way(10) and the vapour-pressure–composition isotherm obtained is recorded in Fig. 1.

Thermal decomposition of $VBr_3.7NH_3$

The results of this decomposition are presented in Table 1 and Fig. 2 (plot *a*) shows the residual compositions at each temperature. The analytical data for residues and sublimates is recorded in Table 2. The percentage of the original vanadium that volatilized in these decompositions was 4·3 at 200° and 6·8 at 400°. The residues were pyrophoric in air and gave deep violet solutions in moderately strong sulphuric acid. The magnetic moment of the 400° residue was 2·06 B.M. at 25°.

Reaction of VBr_3 *with liquid ammonia followed by extraction of the soluble product*

When an excess (100 ml) of ammonia was distilled on to VBr_3 (1–2g) at −78° and the mixture then allowed to warm to the boiling point (−33°); a brown solution and an insoluble brown product resulted. The mixture was filtered through a glass sinter and the insoluble product washed with several portions of liquid ammonia. Analyses of the insoluble and soluble products after excess of ammonia had been removed at room temperature are presented in Tables 3 and 4.

---

(10) G. W. A. FOWLES and F. H. POLLARD, *J. Chem. Soc.* 4938 (1952).

TABLE 1.—THERMAL DECOMPOSITION OF $VBr_3.7NH_3$

Temp. (°C)	Mole ratio gas evolved/ V(g.atom)	Molecular weight of evolved gas	Colour		Stoichiometry of involatile products:		
			Residue	Sublimate	V	Br	N
−36			Fawn		1	3	6·97
0	0·21		Fawn		1	3	6·76
23	0·10		Fawn		1	3	6·66
45	0·10		Fawn		1	3	6·56
77	0·24		Brown		1	3	6·32
100	0·84	16	Grey-brown		1	3	5·48
129	1·95		Grey		1	3	3·53
155	1·51		Grey		1	3	2·02
174	0·31	15	Grey	Yellow	1	3	1·71
208	0·23	16	Black	Yellow + white	1	3	1·48
270	0·17	80	Black	Yellow + white	1	2·83	1·48
320	0·26	84	Black	Yellow + white	1	2·57	1·48
350	0·04		Black	Yellow + white	1	2·53	1·48
400	0·06	82	Black	Yellow + white	1	2·47	1·48

Both products were readily hydrolysed in moist air and gave green solutions upon hydrolysis in dilute sulphuric acid. Although *insoluble in organic solvents* (C_6H_6, $CHCl_3$, CCl_4), *the insoluble* product dissolved readily in liquid ammonia solutions of ammonium bromide. The magnetic moment of the insoluble product was 2·96 B.M.

TABLE 2.—ANALYSIS OF THERMAL DECOMPOSITION PRODUCTS OF $VBr_3.7NH_3$

Temp. (°C)	Residue				Sublimate			
	V	Br	N	V:Br:N	V	Br	N	V:Br:N
200	22·2	71·0	5·21	1:2·04:0·85	2·44	80·4	13·5	1:21·01:20·12
400	24·9	72·4	1·75	1:1·85:0·26	3·00	80·1	13·2	1:17·03:15·99

TABLE 3.—ANALYSIS OF THE INSOLUBLE PRODUCT

Run	No. of extractions	Period of final evacuation (hr)	V	Br	N	Total	V:Br:N
1	13	3	17·0	52·5	25·9	95·4	1:1·97:5·55
2	4	14	17·0	52·2	25·6	94·8	1:1·96:5·48
3	6	6	16·8	52·6	26·1	95·5	1:2·00:5·65

TABLE 4.—ANALYSIS OF THE SOLUBLE PRODUCT

Run	V	Br	N	Total	V:Br:N	Residue on the assumption that all the vanadium is present as $VBr_2NH_2 4.3NH_3$
1	11·7	60·7	21·3	93·7	1:3·31:6·62	$N_{1·32}Br_{1·31}$
2	12·1	60·2	21·6	93·9	1:3·17:6·49	$N_{1·19}Br_{1·17}$
3	11·6	62·0	21·4	95·0	1:3·41:6·71	$N_{1·41}Br_{1·41}$

Thermal decomposition of the insoluble product

The brown insoluble product (0·6056 g) was heated *in vacuo* at 20° intervals, for 2 hr at each temperature, and the plot *b* Fig. 2 obtained. Up to 207° ammonia only was evolved; on heating to 400°, some HBr was evolved (found M = 76) and the overall composition of the non-gaseous products ($VBr_{1·91}N_{0·70}$) represented a mixture of a black residue (0·3529g) and a yellow and white sublimate (0·0693g). The sublimate was largely ammonium bromide (Found Br, 81·3; NH_4Br requires Br, 81·6%) but gave a positive test for vanadium although the latter was not present in large enough quantities to be estimated quantitatively. Comparison of the weight of vanadium originally introduced as $VBr_3N_{3\cdot 68}$ (0·1017g) with that recovered in the residue (0·0989g) indicated that a small amount of vanadium had sublimed in some form. The black residue gave a deep violet solution in dilute sulphuric acid and had the composition $VBr_{1\cdot 56}N_{0\cdot 40}$ (Found V, 28·0; Br, 68·6; N, 3·07%).

Reaction of VBr_3 *with alkali metal in ammonia solutions*

(a) *Potassium.* A large excess of liquid ammonia was condensed on to weighed quantities of VBr_3 and potassium (excess) at −78°, and the mixture allowed to equilibrate at −63° for 2 hr. Hydrogen evolution (Toepler pump) was found to be continuous, not ceasing until decolorization of the alkali metal solution was complete. The mixture was filtered at the boiling point and the black insoluble product obtained was washed several times with liquid ammonia in order to remove any soluble substances. This material was kept *in vacuo* for several hours at room temperature before being removed from the vacuum system under dry oxygen-free nitrogen. It was pyrophoric in moist air and gave green solutions in dilute sulphuric acid (Found V, 41·8; N, 23·8; K, 32·6; Br, nil; V:N:K = 1·00:2·07:1·02). A tensimetric study of this compound $KV(NH)_2$ in liquid ammonia at −63° showed that it formed no ammoniates at this temperature and that it contained no free potassamide. It dissolved to a brown solution upon treatment with a liquid ammonia solution of ammonium bromide. Upon thermal decomposition, the black solid lost ammonia gradually until at 200° the composition of the residue was $VN_{1\cdot 14}K_{1\cdot 04}$ (Found V, 47·4; N, 14·9%). The soluble portion from the reaction of VBr_3 with potassium contained largely potassium amide and bromide.

(b) *Sodium.* When an excess of sodium reacted with VBr_3 in ammonia, hydrogen was once again copiously evolved and sodamide precipitated. The insoluble product appeared to be a mixture of sodamide with sodium iminovanadate (III), (Found V, 7·80; N, 35·2; Na 54·5%, V:N:Na = 1·00:16·41:15·47). When the mixture was treated with an excess of ammonium nitrate in ammonia at −33°, considerable solution took place ($NaNH_2 \rightarrow NaNO_3$) but the vanadium remained largely insoluble (Found V, 53·5; N, 23·4% NO_3^- absent; V:N:Na = 1·00:1·59:0·87).

Acknowledgements—The author wishes to express his thanks to Dr. G. W. A. FOWLES of the University of Southampton for the use of the Gouy balance and to Mr. R. SWINDELLS of this department for some experimental assistance.

J. Inorg. Nucl. Chem., 1962, Vol. 24, pp. 1007 to 1020. Pergamon Press Ltd. Printed in Northern Ireland

NOTES

Preparation of stoichiometric UO_2 by thermal decomposition of UO_2I_2*

(*Received* 2 *October* 1961; *in revised form* 19 *December* 1961)

In the course of an investigation of the system UO_2-U_4O_9, it was necessary to have stoichiometric UO_2 as a control. A great deal of work has been done on the preparation of UO_2. It has been demonstrated that most preparative methods lead to nonstoichiometric products. Comprehensive reviews of its preparation and physical properties are given by Neely(1), Clayton and Aronson(2), and Belle(3). There are many contradictions on the physical properties of the oxide and is evidence we are dealing with a system which is characteristically nonstoichiometric. This is most clearly illustrated by the difference in lattice constants observed by numerous workers over a long period of time. The preparational methods for UO_2 can be reduced to several categories: oxidation of uranium metal and uranium halides, reduction of higher oxides, thermal decomposition and reduction of diuranates and uranyl compounds, and electrolysis of uranyl halides. Of course, there are many variations of these reactions, and the composition and physical characteristics of the product appear to be largely dependent upon the chemical and thermal history during preparation.

Thermal decomposition of uranyl iodide, UO_2I_2, produces stoichiometric UO_2 according to the reaction:

$$UO_2I_2 \rightarrow UO_2 + I_2$$

The iodide is the least stable of the uranyl halides but can be prepared very simply in aqueous solution by the metathesis reaction between uranyl sulphate and barium iodide(4).

Thermal decomposition of uranyl fluoride(5), chloride(6,7) and bromide(8) has been studied by other investigators and has shown a tendency to form higher oxides. Differences in composition and physical properties of the oxides formed from thermal decomposition of uranyl halides are presumably due to large differences in stabilities of the halides. Thermal decomposition of uranyl fluoride produces U_3O_8 and uranium fluorides. Uranyl chloride and bromide decompose to form a nonstoichiometric product.

EXPERIMENTAL

Starting materials

A barium iodide solution was prepared by neutralizing analytical reagent grade barium hydroxide with freshly distilled hydriodic acid. The solution was boiled to expel any CO_2 coming from traces of barium carbonate. Commercial reagent grade hydriodic acid was distilled to remove hypophosphorous acid, H_3PO_2, used as a preservative against oxidation. The distillation was performed under helium and the constant boiling mixture (B.P. 125°–126°/740 mm Hg, 57% HI, sp.gr. 1·7) was used for the neutralization. (Commercial barium iodide contains this phosphorus impurity.) Specially purified anhydrous uranyl sulphate was obtained from Mallinckrodt.

Preparation of uranyl iodide

An aqueous solution of uranyl sulphate was titrated with freshly prepared iodide solution until no further precipitate of barium sulphate was formed. It was necessary to remove the precipitate by filtration or centrifuging several times near the end point to improve visibility. The clear reddish solution of uranyl iodide was transferred to a round bottom flask, attached to a Rinco film evaporator and the water was removed slightly below room temperature at reduced pressure by continuous pumping. The solvent and liberated iodine (25 per cent of the total iodine based on UO_2I_2) were collected in a cold trap at −196°C. The dried dark-brown partially decomposed uranyl iodide was amorphous to X-rays.

---

* This work was performed under contract to the U.S. Atomic Energy Commission.

(1) J. J. Neely, *Uranium Dioxide*, AEC Report NEPA-355 (1948).

(2) J. C. Clayton and S. Aronson, *Some Preparation Methods and Physical Characteristics of* UO_2 *Powders*, AEC Report WAPD-178 (1958).

(3) J. Belle (editor), Uranium Dioxide: *Properties and Nuclear Applications*, U.S. Government Printing Office, Washington, D.C., 1961.

(4) H. Truttwin, German Patent D.R.P. No. 420,391, from A. Brauer and J. D'Ans, *Fortschritte in der anorganisch-chemischen Industrie*, III: 1327 (1924–1927).

(5) L. M. Ferris and F. G. Baird, *J. Electrochem Soc.*, **107**, 305–308 (1960).

(6) C. A. Kraus, AEC Report N-1789, July, 1943.

(7) O. Johnson, AEC Report CC-1781, October, 1944.

(8) W. Oeschsner de Coninck, *Ch. Acad. Sci.* **135**, 900–901 (1902).

Thermal decomposition

The partially decomposed iodide was transferred to a quartz reaction tube connected to a high vacuum system through a cold-finger trap. A resistance furnace was placed around the lower half of the reaction tube and thermal decomposition was accomplished by slowly increasing the temperature under constant pumping until a temperature of 1100°C was attained. This temperature was maintained for a few hours after iodine evolution had ceased. Violent evolution of iodine was observed at 150°C necessitating careful programming of the rate of temperature increase. After complete decomposition the reaction tube was sealed-off from the trap and transferred into an inert atmosphere glove box where the product was handled. For a 36 g product a 50 hr heating period was sufficient for complete decomposition.

X-Ray

A Debye-Scherrer powder pattern of the final product showed a face centred cubic structure belonging unambiguously to UO_2. A Norelco symmetrical focusing back reflection camera was used for precise determination of the lattice constant. Samples were ground to a fine powder, mixed with a small quantity of Dow Corning Silicone grease and applied to the sample target in a thin film in an inert gas glove box.

Lattice constants were calculated by the method of MUELLER, HEATON and MILLER(9), adapted for the IBM-7090 by KORST *et al.*(10) The lattice constant was found to be 5·4703 ± 0·0002 Å at 20°C, using GRØNVOLD's(11) data to correct for thermal expansion. This is in excellent agreement with GRØNVOLD's value of 5·4704 ± 0·0008 Å at 20°C.

Analyses

A standard polarographic technique(12) was used to determine the O/U ratio by detection of U^{+6} formed by the presence of excess oxygen. A value of 2·001 ± 0·0005 was obtained for two samples chosen at random. Chemical analysis for percentage of uranium metal as a basis for calculating O/U ratios cannot produce this kind of accuracy or precision due to the large differences in molecular weight and the inherent errors of the methods. Emission spectrographic analysis showed impurities at low levels: Ba 0·1 %, Al 0·005 %, Ca 0·004 %, Fe 0·005 % and Si 0·015 %. Other impurities were insignificant. A substantial reduction of these impurities was obtained by heating the product in a degassed tungsten crucible at 1940°C and 10^{-5} mm for 30 min in an induction furnace under constant pumping. Emission spectrographic analysis then showed: Ba 0·0025 % and Ca 0·002 %. Other impurities were below the lower limit of detection. The polarographic O/U ratio was 2·001 ± 0·0005 showing no detectable change as a result of additional heating. The lattice constant was 5·4704 ± 0·0002 Å at 20°C.

Reduction of U_3O_8

For comparison, two experiments were performed using U_3O_8 obtained from the National Bureau of Standards. In each of these experiments the U_3O_8 was reduced at 1000°C by a slow flow of purified hydrogen for t_1 hr, cooled under hydrogen for 24 hr, analysed polarographically, examined by X-ray diffraction, sealed under vacuum in a degassed quartz tube, heated to 1150°C for t_2 hr, quenched rapidly in water and again analysed and examined by X-ray diffraction. The diffraction lines were not as sharp as the lines produced by "iodide" UO_2. The results are given in Table 1. The fact that subsequent heating and quenching causes an increase in the lattice constant (corrected to 25°C) suggests the presence of defect structures; possibly a partial retention of an "out-of-step" structure observed by SATO *et al.*(13).

---

(9) M. H. MUELLER, L. HEATON and K. T. MILLER, *Acta Cryst.* **13**, 828 (1960).

(10) W. L. KORST, I. R. TANNENBAUM, K. T. MILLER, private communication (Research Division, Atomics International).

(11) F. GRØNVOLD, *J. Inorg Nucl. Chem.* **1**, 359 (1955).

(12) R. M. BURD and G. W. GOWARD, AEC Report WAPD 205 (1959).

(13) R. SATO, H. DOI, B. ISHII and H. UCHIKOSHI, *Acta Cryst.* **14**, 763 (1961).

Table 1.—Lattice constant for hydrogen reduced U_3O_8

		First sample	Second sample
t_1	(hr)	31	63
a_0	(±0·0002 Å)	5·4695	5·4680
O/U	(±0·0005)	2·003	2·008
t_2	(hr)	66	1
a_0	(±0·0002 Å)	5·4701	5·4694
O/U	(±0·0005)	2·004	2·007

DISCUSSION

It has been demonstrated that thermal decomposition of uranyl iodide produces UO_2 which is stoichiometric within the limits of experimental detection. Although the dissociation of uranyl iodide in solution changes during dehydration both water and iodine are removed without disturbing the O/U ratio. The oxygen bearing solvent, in this case water, was completely removed at low temperatures eliminating the possibility of further oxidation during thermal decomposition at elevated temperatures. Sharpness of the diffraction lines in the high angle regions indicates good crystallinity in the product produced at 1100°C and also after heating at 1940°C.

The hydrogen reduction of U_3O_8 gives nonstoichiometric products with varying O/U ratios as well as inconsistent lattice constants. The fact that subsequent heating and quenching causes an increase in the lattice constant requires the application of discretion in using the cell dimension as a criterion for the attainment of a particular composition(11,14,15).

Acknowledgments—The author wishes to express his gratitude to Dr. W. L. Korst for assistance with the X-ray work and computations. He also wishes to thank Dr. G. G. Libowitz and W. A. Young for their helpful suggestions and interest.

Atomics International
Division of North American Aviation
P.O. Box 309, Canoga Park, California

Lahmer Lynds

(14) B. E. Schaner, *J. Nucl. Materials*, **2**, 110 (1960).
(15) R. E. Rundle, N. C. Baenziger, A. S. Wilson and R. A. McDonald, *J. Amer. Chem. Soc.* **70**, 99 (1948).

Neutron capture cross-section of 36 hr ^{105}Rh*

(*Received* 11 *May* 1961)

During the course of an investigation in which mass-spectrometric thermal fission yields of ^{239}Pu were measured, the authors found that the yield of ^{105}Pd relative to those of ^{107}Pd, ^{108}Pd and ^{110}Pd was anomalously low (factor of two). Similarly, the yield of ^{106}Pd was anomalously high.

These phenomena indicate a large neutron capture cross section for 36 hr ^{105}Rh in the fission decay chain as follows:

$$\begin{tikzcd}
4{\cdot}5\text{ hr }^{105}\text{Ru} \arrow[r, "\beta^-"] & 36\text{ hr }^{105}\text{Rh} \arrow[r, "\beta^-"] \arrow[d, "\text{n}, \gamma"] & ^{105}\text{Pd} \\
1{\cdot}0\text{ year }^{106}\text{Ru} \arrow[r, "\beta"] & 30\text{ sec }^{106}\text{Rh} \arrow[r, "\beta^-"] & ^{106}\text{Pd}
\end{tikzcd}$$

In order to make an estimate of the value of this cross-section, it is necessary to know the flux to which the ^{239}Pu was subjected. This was calculated by three different methods:-

(a) The total number of fissions in the 168 mg of ^{239}Pu irradiated was calculated from the experimental results and found to be $\sim 1{\cdot}1 \times 10^{20}$. Taking the thermal fission cross-section for ^{239}Pu to be 750 barns, and knowing the irradiation period to have been 14 days, a value of $\sim 3 \times 10^{14}$ neutrons $cm^{-2}\ sec^{-1}$ is obtained for the flux.

(b) Having measured the $^{134}Cs/^{133}Cs$ ratio and found it to be 0·006, and assuming the capture cross-section for ^{133}Cs to be 30 barns, the flux was calculated and again found to be $\sim 3 \times 10^{14}$ neutrons $cm^{-2}\ sec^{-1}$.

---

* Based on work performed under the auspices of U.S. Atomic Energy Commission.

(c) The flux was also calculated from the ^{135}Cs/^{133}Cs ratio (= 0·066). Assuming the capture cross-section of ^{135}Xe to be 3·1 × 10^6 barns, a value of ~1 × 10^{14} neutrons cm^{-2} sec^{-1} is found for the flux. However, this method is heavily dependent on the flux having been constant during the irradiation, since it makes use of the short-lived (9·2 hr) ^{135}Xe. The discrepancy between this calculation of the flux and the other two methods suggests that the initial flux during the irradiation of the ^{239}Pu was high, but that it dropped to a value of ~1 × 10^{14} neutrons cm^{-2} sec^{-1} towards the end of the irradiation.

Using a maximum value of 3 × 10^{14} neutrons cm^{-2} sec^{-1} for the flux, the (*n*, γ) cross-section for ^{105}Rh is found to be ≥1·8 × 10^4 barns. Experiments are in progress to measure this cross-section more accurately by neutron irradiation of ^{104}Ru and mass-spectrometric measurement of the ^{105}Pd/^{106}Pd ratio in Pd separated from the Ru.

J. G. Cuninghame†
L. E. Glendenin
A. L. Harkness

Argonne National Laboratory
Argonne, Illinois

† Exchange scientist from A.E.R.E., Harwell, England.

The Nernst law in concentrated sodium perchlorate solutions

(*Received* 2 *January* 1962; *in revised form* 23 *January* 1962)

In many instances successive stability constants have been measured in aqueous solutions in the presence of a large excess of an inert salt. The inert salt is added in the expectation that the common solution laws may be applied in terms of concentrations rather than activities.(1) The Nernst law governing electrode potentials is a law of this type and has been subjected to a preliminary test by Leden.(2) We have carried out a further test of this using concentration cells patterned after those of Vanderzee and his students.(3,4,5,6) The chief advantage of such cells is that only the potentials due to the concentration difference and the very small liquid junction potential are measured.

The measurements were obtained on cells with three concentric compartments. The solution initially present in all three compartments was 0·001 M in $Cd(ClO_4)_2$, 0·01 M in $HClO_4$, and 2·98 M in $NaClO_4$. A 1% cadmium amalgam electrode was present in the innermost and outermost compartments; the middle compartment served as a salt bridge. The entire cell was contained within a hollow jacket through which water held at 25·00° ± 0·01° was circulated. The preparation of the various solutions was effected by standard methods described elsewhere.(7,8) In a run, the outermost

Table 1.—Test of Nernst law in its concentration form in 3 M sodium perchlorate

Volume of solution in outermost compartment (ml)	Run #1			Run #2		
	ΔE(mv)	$x/[Cd^{+2}]$	$(x' - Cd^{+2})\cdot 10^3$	ΔE(mv)	$x/[Cd^{+2}]$	$(x' - [Cd^{+2}])\cdot 10^3$
400	0	1·0000	0	0	1·0000	0
420	0·6265	1·0500	0·0000	0·6266	1·0500	0·0000
440	1·2232	1·1000	0·0000	1·2267	1·1003	0·0003
460	1·7950	1·1501	0·0001	1·7959	1·1502	0·0002
480	2·3415	1·2002	0·0001	2·3426	1·2003	0·0002
500	2·8648	1·2501	0·0001	2·8769	1·2513	0·0008
520	3·3680	1·3001	0·0000	3·3689	1·3002	0·0001
540	3·8520	1·3501	0·0000	3·8524	1·3501	0·0000

---

(1) G. Biedermann and L. G. Sillén, *Ark. Kemi* **5**, 426 (1953) contains most of the earlier literature and a careful study of several systems containing appreciable liquid junction potentials.

(2) I. Leden, *Z. Phys. Chem.* **188**, 160 (1941).

(3) C. E. Vanderzee and D. E. Rhodes, *J. Amer. Chem. Soc.*, **74**, 3552 (1953).

(4) C. E. Vanderzee, *ibid* **74**, 4806 (1953).

(5) C. E. Vanderzee and H. J. Dawson, Jr., *ibid* **75**, 5659 (1954).

(6) C. E. Vanderzee and W. E. Smith, *ibid* **78**, 721 (1956).

(7) J. F. Tate and M. M. Jones, *J. Amer. Chem. Soc.* **83**, 3024 (1961).

(8) J. F. Tate and M. M. Jones, *J. Phys. Chem.* **65**, 1661 (1961).

compartment was diluted with successive portions of 20 ml of 3 M sodium perchlorate solution. Measurements of the cell potential were made after each addition by means of a Leeds and Northrup K-3 potentiometer. The outer compartment was stirred with a magnetic stirrer. The results of two such runs are presented in Table 1.

In the table, ΔE is the change in potential after the addition of the diluent, x is the concentration of the cadmium (II) ion determined from the known initial concentration of cadmium (II), and $[Cd^{+2}]$ is the concentration of cadmium (II) in the diluted solution determined from the Nernst (this decreases continuously so the ratio $x/[Cd^{+2}]$ increases continuously). The quantity x' represents the concentration of free cadmium (II) as calculated from the initial concentration x and the known initial and final volumes. The difference, $(x' - [Cd^{+2}])$. 10^3 represents the error introduced by this procedure. The error is in no case greater than 1 per cent in the metal ion concentration and is generally much less than this. Obviously, under the present circumstances, the Nernst law does hold hold in terms of concentrations, and holds remarkably well. Although cells such as these must, in principle, have liquid junction potentials, these must be very small in the present case.

Acknowledgement—We wish to thank the National Science Foundation for financial assistance.

Department of Chemistry
Vanderbilt University
Nashville 5, Tennessee

J. F. Tate
M. M. Jones

Concerning acid-base theories

(*Received* 12 *January* 1962)

The recent appearance of a paper by Meek and Drago(1) prompts the following discussion in the hope of clarifying what may become a semantic tangle in the description of acid-base phenomena. It is felt that both the proponents and antagonists of the solvent system concept have failed to examine critically its weak and strong points, respectively.

The interested reader is referred to the above paper(1) as well as previous ones by Gutmann, *et al.*(2) for a complete discussion of the experimental procedures and theoretical interpretations, but the situation may be summed up briefly as follows. Iron(III) chloride is found to behave as an acid in phosphoryl solvents (i.e. phosphorus oxychloride and triethyl phosphate). In the case of phosphorus oxychloride, there is a limited conductivity of the pure solvent suggesting the following autoionization:(3)

$$OPCl_3 \rightleftharpoons OPCl_2^+ + Cl^-$$

Gutmann described acid-base behaviour in terms of a somewhat specialized solvent system approach:

$$OPCl_3 + FeCl_3 \rightleftharpoons OPCl_2^+ + FeCl_4^-$$

Thus iron(III) chloride is an acid because it produces $OPCl_2^+$ ions (or reduces the Cl^- concentration).

Meek and Drago found that in triethyl phosphate, iron(III) chloride dissolved yielding some tetrachloroferrate(III) ions. Since no chloride can come from the solvent in this case, part of the iron must exist in a cationic species (e.g. dichloroiron(III) solvate):

$$2FeCl_3 \rightleftharpoons FeCl_4^- + FeCl_2^+$$

By analogy, they argue that the most likely situation obtaining in phosphorus oxychloride is a similar one. They would attribute the acid character of the iron(III) chloride solutions (e.g. the ability to neutralize R_4NCl) to the solvated dichloroiron(III) cation which accepts chloride ions.

Although the two interpretations seem to differ widely, they are actually quite similar. One point which has not been sufficiently stressed in the past is that in a given solvent undergoing autoionization:

$$AB \rightleftharpoons A^+ + B^-$$

(1) D. Meek and R. S. Drago, *J. Amer. Chem. Soc.* **83**, 4322 (1961).

(2) V. Gutmann, *J. Phys. Chem.* **63**, 378 (1959); V. Gutmann and M. Baaz, *Angew. Chem.* **71**, 57 (1959), *Z. Anorg. Chem.* **298**, 121 (1959), *Monatsh. Chem.* **90**, 271, 729 (1959); M. Baaz, V. Gutmann and L. Hübner, *ibid.* **91**, 537 (1960), *J. Inorg. Nucl. Chem.*, **18**, 276 (1961).

(3) It is assumed throughout that all charged species will be solvated; for the sake of simplicity the solvating molecules have been omitted from the equations. It must be remembered, however, that such solvation is undoubtedly important especially in the case of the cations, $OPCl_2^+$ and $FeCl_2^+$.

there is nothing "typical" or "characteristic" about the acid A^+ or base B^- except that they are the strongest acid and base which can exist in appreciable concentrations in the solvent AB. A stronger acid A^{*+} reacts with the solvent (leveling effect):

$$\mathrm{A^{*+} + AB \rightleftharpoons A^+ + A^*B}$$

as, in converse fashion, does a stronger base, B^{*-}. Thus the solvent system concept merely indicates the strongest possible acid-base pair and points out that their neutralization reaction will form solvent molecules. Attempts to make the system predict more, e.g. "characteristic" acids or bases are unreasonable.

With the above in mind it is readily seen that a further equilibrium can be set up in phosphorus oxychloride:

$$\mathrm{OPCl_2^+ + FeCl_3 \overset{k}{\rightleftharpoons} OPCl_3 + FeCl_2^+}$$

Now the value of k will be determined by the relative strengths of the acids $OPCl_2^+$ and $FeCl_2^+$. If the latter is the stronger, it will accept a chloride ion (base) from the solvent. If it is weaker, it will solvolyse to form only a limited amount of the dichlorophosphoryl cation and will therefore act as a typical weak acid. If the solvent is such that chloride ion transfer cannot take place (e.g. triethyl phosphate) the iron must be content with a less basic species (the phosphoryl group).

The difference between the solvent system concept and the Lewis theory is not that they are mutually exclusive explanations of acid-base phenomena, but that they are ways of looking at these phenomena from different viewpoints. In the same way that the energetics of reactions may be viewed macroscopically (thermodynamics) or microscopically (statistical dynamics), so too can acid-base phenomena be interpreted in terms of bonding (Lewis and Usanovich theories) or in terms of equilibria and concentrations (solvent system theory), where applicable. The solvent system concept does not preempt the Lewis theory. GUTMANN for example defines an acid as a substance which accepts chloride ions. Obviously this acceptance must occur through some sort of coordination. The Lewis theory can explain certain phenomena inexplicable by the solvent system approach, but then too, the USANOVICH theory(4) is more comprehensive than either, so this aspect cannot be the sole criterion of usefulness.

The "essence" of the acidity of iron(III) chloride lies in its tripositive ion of rather small radius and high charge which is compensated only in part by three coordinated chloride ions and which seeks elsewhere for electrons to reduce its positive character. It is thus an acid irrespective of solvent chosen and will accept the strongest base available to it. If the basicity of the phosphoryl group is sufficient (as it must of necessity be in triethyl phosphate or if the chloride ion concentration in phosphorus oxychloride is too low), then iron(III) chloride is less acidic than if it is capable of abstracting a chloride ion from the solvent (where possible). At present it is impossible to predict the inherent relative acidities of the dichlorophosphoryl and dichloroiron(III) ions, but this may be accomplished when more is learned about the electron distribution within these ions.

The importance of the work of MEEK and DRAGO lies in the proof of the existence of $FeCl_4^-$ in non-chloride solvents. One might have supposed that in a non-ionizing solvent iron(III) chloride would exist as a simple solvate. It should be pointed out even under these circumstances the iron(III) would still be acting as an acid since it would be capable of neutralizing R_4NCl. It is probable that as more solvents are investigated by spectroscopy, more examples of such "disproportionation" of solutes will be found. Autoionization of solvents may be looked upon as a specialized example of this phenomenon.

J. E. HUHEEY

Department of Chemistry and Chemical Engineering
Worcester Polytechnic Institute
Worcester, Massachusetts

(4) M. USANOVICH, *Zh. Obshch. Khim.* 182 (1939). *C.A.* 33, 6688 (1939).

The liquid range density, observed normal boiling point and estimated critical constants of indium(1)

(*Received* 18 *January* 1962)

THE density of liquid indium was measured from its melting point, 429·3°K., to its normal boiling point, 2286°K., by the immersed sinker method. A mercury-filled glass sinker suspended by a molybdenum wire was used at the lower temperatures and a graphite sinker with a thin stem was used at

(1) This work was supported by the National Science Foundation under Grant 15540.

the higher temperatures. Volumes of the sinkers were corrected to the operating temperature. Corrections for surface tension effects were made using published data(2) extrapolated as necessary.

Temperature measurements was accomplished by calibrated chromel-alumel thermocouples and an optical pyrometer. The liquid indium was maintained in an argon atmosphere at all times. The indium used was 99·97+ % pure with iron as the principal impurity. Several runs were made covering overlapping temperature ranges and a total of twenty-four density measurements was obtained.

Least squares treatment of the experimental data yielded the following equation:

$$D\ \text{g/cm}^3 = 7{\cdot}315 - 6{\cdot}798 \times 10^{-4}\ T\ (^\circ\text{K.}).$$

The probable error is ±0·023 g/cm³. Smoothed density values calculated from the equation are about 0·15 per cent lower than the data of Williams and Miller(3) over their experimental range (429·32–573°K) and the single value (at the melting point) reported by Gamartsfelder.(4) The data of Schneider and Heymer(5) average about 0·2 per cent higher over their experimental range (504–694°K.). The slope of our line, $-6{\cdot}798 \times 10^{-4}$ g/cm³deg, is smaller than that reported by Williams and Miller ($-8{\cdot}13 \times 10^{-4}$ g/cm³deg.) and the slope calculated from the data of Schneider and Heymer ($-8{\cdot}112 \times 10^{-4}$ g/cm³deg.) but the temperature range over which it was determined is much greater.

The expansion on fusion calculated from our data for liquid density and the solid density data of Williams and Miller is 2·59 per cent of the solid volume. Smoothed densities, atomic volumes and coefficients of cubical expansion are shown in Table 1.

TABLE 1.—SMOOTHED DENSITIES, ATOMIC VOLUMES AND COEFFICIENTS OF CUBICAL EXPANSION OF INDIUM

(T°K)	Density (g/cm³)	Atomic volume cm³/g.at.	Coef. of cubical expansion, (°K⁻¹ × 10⁶)
429·3 m.p.	7·023	16·349	96·80
600	6·907	16·624	98·42
800	6·771	16·958	100·40
1000	6·635	17·305	102·46
1200	6·499	17·667	104·60
1400	6·363	18·045	106·84
1600	6·227	18·439	109·17
1800	6·091	18·851	111·61
2000	5·955	19·281	114·16
2286 b.p.	5·763	19·924	117·96

The boiling point of indium established by direct observation with a calibrated optical pyrometer is 2286 ± 10°K corrected to a pressure of 760 mm Hg. This is in good agreement with the value of 2273 ± 10°K reported by Kohlmeyer and Spandau(6) but is somewhat lower than the value of 2320°K preferred by Stull and Sinke.(7)

The critical constants of indium, estimated according to a procedure described elsewhere(8) are: $T_c = 6680 \pm 670^\circ$K, $P_c = 2400^{+1000}_{-900}$ atm, $V_c = 83{\cdot}0^{+160}_{-120}$ cm³./gat, $D_c = 1{\cdot}39 \pm 0{\cdot}23$ g/cm³. The errors in Pc, Vc and Dc are based on the arbitrary error of 10 per cent assigned to Tc.

Acknowledgement—We wish to thank the Indium Corporation of America for their generous donation of the indium used in this work.

Research Institute
of Temple University
Philadelphia 44, Pennsylvania

P. J. McGonigal(9)
J. A. Cahill
A. D. Kirshenbaum

(2) D. A. Melford and T. P. Hoar, *J. Inst. Metals* **85**, 197 (1956).

(3) D. D. Williams and R. R. Miller, *J. Amer. Chem. Soc.* **72**, 3821 (1950).

(4) C. Gamartsfelder, *J. Chem. Phys.* **9**, 450 (1941).

(5) A. Schneider and G. Heymer, *Z. Anorg. Chem.* **286**, 118 (1956).

(6) E. J. Kohlmeyer and H. Spandau, *Z. Anorg. Chem.* **253**, 37 (1945).

(7) D. R. Stull and G. C. Sinke, *Thermodynamic Properties of the Elements*, American Chemical Society, Advances in Chemistry Series, No. 18, 1956.

(8) A. V. Grosse, "The Temperature Range of Liquid Metals and an Estimate of the Critical Constants," *J. Inorg. Nucl. Chem.* **22**, 23 (1961).

(9) A report of this work will constitute a portion of a dissertation to be submitted by P. J. McGonigal to the Graduate Council of Temple University in partial fulfillment of the requirements for the degree of Doctor of Philosophy.

Solubilities of metal trichloracetates in polar and nonpolar liquids

(*Received* 23 *January* 1962)

DURING a search for salts soluble in widely differing liquids, it was found that many trichloracetates showed the remarkable property of dissolving in both water and heptane. A group of approximate solubilities was determined, and comparison was made with the solubilities of corresponding acetates.

Results are presented in Table 1. Solubilities of a few of these or similar (trifluoracetate) salts have been reported⁽¹⁾, but a list covering metals from a representative sample of the periodic table and covering a variety of solvents was not previously available from the literature.

TABLE 1.—SOLUBILITY LIMITS*

	Trichloracetate salt					Acetate salt
	H_2O	Methanol or ethanol (same results)	Ether or CCl_4 (same results)	Benzene	*n*-heptane	*n*-heptane
Li	s	s	i	i	i	i
K	s	s	i	i	i	i
Cs	s	s	i	i	i	i
Be	s	s	p	p	s	p
Ca	s	s	s	s	s	i
Fe(II)	s	s	s	s	s	i
Fe(III)	s	s	s	s	s	i
Co(II)	s	s	s	s	s	p
Cu(II)	s	s	s	s	s	s
Ag	s	s	p	s	p	i
Zn	s	s	s	s	s	i
Hg(I)	s	s	s	s	i	i
Hg(II)	s	s	s	s	s	s
Al	s	i	i	i	i	i
Pb	s	s	p	i	i	i
Bi	s	s	p	p	p	i

* Solubilities are in 100 ml of solvent at 25°C.

Symbols: s indicates that 1 gm of salt dissolves;
p indicates that 0·1 gm of salt dissolves;
i indicates that less than 0·1 gm of salt dissolves.

EXPERIMENTAL

The hydroxide of each metal was weighed, the amount being equivalent to the desired weight of salt. The hydroxides were washed twice with water, twice with absolute ethanol, and twice in the solvent being studied. The hydroxide was then stirred into a hot solution of the solvent and the acid, the quantity of the acid being twice the quantity needed to form the desired weight of salt. The solution was cooled to 25°C and a seed of hydroxide was added. After 30 min the observer noted whether all of the hydroxide was dissolved. Ferrous and mercurous carbonates were used instead of their hydroxides.

The 1:1 excess of acid was used because it was found necessary for dissolution in some instances. In all cases where most of the hydroxide did not dissolve, the suspension was heated long enough for the hydroxide to change its appearance. The solvent and acid were then drained off, and pure solvent was added and heated with the converted salt. In none of these cases did the converted salt then visibly dissolve in the pure solvent. Also, a few salts were prepared by other means, and the original results were confirmed.

DANIEL SHANEFIELD

Department of Chemistry
Rutgers University
New Brunswick, N.J.

---

(1) *Beilsteins Handbuch der organischen Chemie*, **1**, 208; **I**, 92; **II**, 198. F. SWARTS, *Bull. Soc. Chim. Belg.* **48**, 176 (1939).

The solubility of plutonium(VI) carbonate in lithium acid carbonate

(*Received* 19 *January* 1962)

SOLUBLE plutonium compounds, which have small neutron cross-sections and are stable to radiation, are of interest as fuel materials in nuclear power reactors of the aqueous homogeneous type(1). Plutonium carbonate compounds fulfill these two requirements to a large extent. Preliminary investigations showed that plutonium(III), plutonium(IV) and plutonium(VI) carbonates are sparingly soluble(2); however, a plutonium(VI) carbonate compound is soluble in lithium acid carbonate solutions. Since such a system would be acceptable if lithium-7 were used, a study was undertaken to determine the solubility of plutonium(VI) carbonate in various concentrations of lithium acid carbonate solutions at 24°C.

EXPERIMENTAL

Lithium plutonate was prepared from a plutonium(VI) sulphate solution by precipitation with solid lithium hydroxide. The precipitate was washed several times with dilute lithium hydroxide. It was then slurried in water, and carbon dioxide was bubbled through the slurry until the dark brown precipitate changed to a light buff plutonium carbonate. Portions of the plutonium carbonate were added to lithium acid carbonate solutions of various concentrations and mixed. The solutions were equilibrated with occasional agitation for the indicated times at 24 ± 1°C and centrifuged to remove the undissolved material. An aliquot of the dark-red supernatant liquid was dried on a stainless steel slide and alpha counted to determine the concentration of plutonium in the solution.

The original concentrations of the lithium acid carbonate solutions were determined by titrations with standard hydrochloric acid solution. The carbonate solutions were boiled vigorously near the end point.

RESULTS

The solubilities of plutonium in the various solutions of lithium acid carbonate are given in Table 1. In all cases the solubility is less than that found on 0·5 molar sodium carbonate(3). When the solubility reaction is written

$$PuO_2CO_{3(s)} + xLiHCO_{3(aq)} = Li_xPuO_2(CO_3)(HCO_3)_{x(aq)} \quad (1)$$

TABLE 1.—SOLUBILITY OF Pu(VI) IN $LiHCO_3$

$LiHCO_3$ (M/l. re)		Pu(VI) (g/l. re)
	Equilibrated 16 hr	
0		0·043
0·05		1·12
0·10		3·01
0·24		10·2
0·25		11·4
0·50		14·6
0·94		24·2
	Equilibrated 10 days	
0·05		1·37
0·75		22·3

then the equilibrium constant, K, is

$$K = \frac{[Li_xPuO_2(CO_3)(HCO_3)_x]}{[LiHCO_3]^x} \quad (2)$$

or written in logarithmic form it takes on the straight line form $y = mx + b$

$$\log [Li_xPuO_2(CO_3)(HCO_3)_x] = x \log [LiHCO_3] + \log K. \quad (3)$$

---

(1) H. F. MCDUFFIE, C. H. SECOY, C. J. HOCHANADEL and J. P. MCBRIDE, *Reactor Handbook* **1**, (Materials) Chap. 16, p. 363. Interscience, New York (1960).

(2) B. C. BLANKE, E. N. BOUSQUET, R. H. STEINMEYER, The Solubility of Plutonium Salts in Aqueous Solutions up to 300°C. In press.

(3) B. B. CUNNINGHAM, *National Nuclear Series*, 14 A, Chap. 10, p. 418–419. McGraw-Hill, New York (1949).

In Fig. 1, log $[Li_xPuO_2(CO_3)(HCO_3)_x]$ is plotted versus log $[LiHCO_3]$, where the concentration is used for the activity of each soluble substance. The slope of the line is the x term of equation (3) and the intercept is log K. Since the experimental values lie close to the line which has been drawn with a slope of 1·0, one molecule of lithium acid carbonate appears to be associated with each plutonium ion in solution and the equilibrium constant for these corresponding points is 0·13.

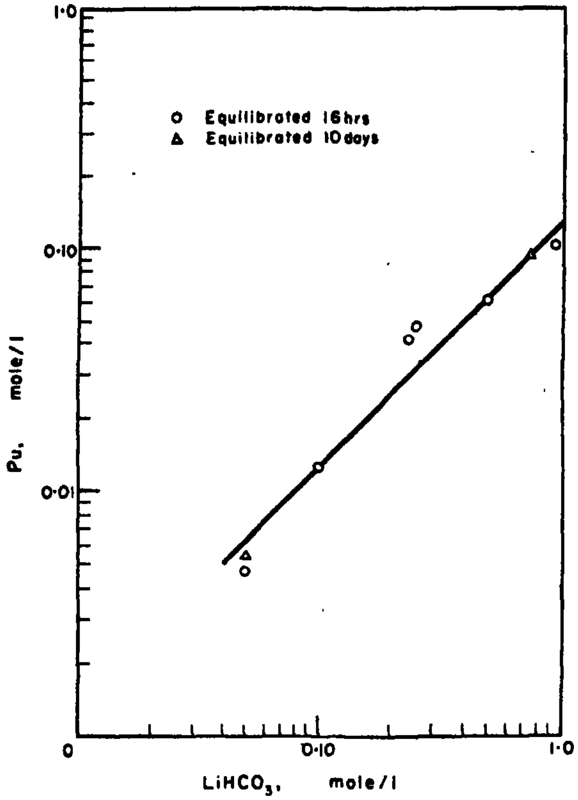

FIG. 1.—Solubility of Pu vs. concentration of $LiHCO_3$.

As an additional experiment each saturated solution of plutonium(VI) carbonate in lithium acid carbonate was sealed in heavy-walled quartz capillary tubes with carbon dioxide at approximately 1000 lb/in^2. pressure and equilibrated at 24°C. In all cases, a light pink precipitate slowly formed which quantitatively removed the plutonium from the solution. This reaction demonstrated the need for lithium carbonate in the solubility reaction given in equation (1) and not merely the addition of CO_2.

L. J. WITTENBERG
R. H. STEINMEYER

Monsanto Chemical Company,
Mound Laboratory,
Miamisburg, Ohio, U.S.A.

Preparation of molybdenum(III) acetylacetonate

(*Received* 25 *January* 1962)

THE synthesis and properties of molybdenum(III) acetylacetonate have not been described in the literature though measurements of its paramagnetic resonance have been published.(1)

Molybdenum(III) acetylacetonate, $Mo(C_5H_7O_2)_3$, is a benzene-soluble, recrystallizable, red-brown solid that is quite different from the canary yellow acetylacetonate reported by GACH(2) and later

(1) H. S. JARRETT, *J. Chem. Phys.* **27**, 1298 (1957).
(2) F. GACH, *Monatsch. Chem.* **21**, 112 (1900).

correctly identified by MORGAN and CASTELL(3) as MoO$_2$(C$_5$H$_7$O$_2$)$_2$. Since molybdenum(III) acetylacetonate oxidizes on exposure to air, it must be prepared, recrystallized, and stored in the complete absence of air.

EXPERIMENTAL

Diammonium pentachloroaquomolybdate(III), (NH$_4$)$_2$[MoCl$_5$·H$_2$O], prepared as described below, was used as the source of trivalent molybdenum. The desired acetylacetonate precipitated when ammonium hydroxide (1·9 normal, 520 ml) was added dropwise over a 6 hr period to a mechanically stirred solution of freshly distilled acetylacetone (125·4 g, 25% excess) and diammonium pentachloroaquomolybdate(III), (NH$_4$)$_2$[MoCl$_5$·H$_2$O], (109·4 g), in deaerated water (1 l.). The mixture was stirred overnight and filtered, and the precipitate was washed with four 500 ml portions of deaerated water and dried *in vacuo* at room temperature. The precipitation, filtration, and washing were conducted under nitrogen in a flask fitted with an attached fritted glass filter assembly. The product was chlorine-free, weighed 113·8 g (86·7 per cent yield based on Mo), and corresponded to Mo(C$_5$H$_7$O$_2$)$_3$ in analysis. Calc.: Mo, 24·40; C, 45·81; H, 5·38 per cent. Found: Mo, 24·52; C, 45·40; H, 5·41 per cent. It could be further purified by recrystallization from boiling 2:1 cyclohexane:benzene.

The diammonium pentachloroaquomolybdate(III) was prepared by a variation of the method of FOERSTER and FRICKE.(4) A diaphragm cell (air excluded) was used with a platinum cathode, a graphite anode, a catholyte 0·143 molar in ammonium paramolybdate and 10 normal in hydrochloric acid, and an anolyte of 12 normal hydrochloric acid. Some brick-red (NH$_4$)$_2$[MoCl$_5$·H$_2$O] crystallized during electrolysis, but the major part was recovered by adding ammonium chloride (8 moles per mole of ammonium paramolybdate) and concentrating to half-volume at 180 mm pressure.

Central Research Department
Experimental Station
E.I. du Pont de Nemours & Company,
Wilmington 98, *Delaware, U.S.A.*

J. H. BALTHIS

(3) G. T. MORGAN and R. A. S. CASTELL, *J. Chem. Soc.* 3252 (1928).

(4) F. FOERSTER and E. FRICKE, *Z. Angew. Chem.* 36, 458 (1923).

The anhydrous hydrochloride salts of dichlorobis (ethylenediamine)cobalt (III) chloride

(*Received* 2 *February* 1962)

A RECENT publication(1) states that hydrochloride salts of *trans*-dichlorobis(ethylenediamine)cobalt (III) chloride probably do not exist in the anhydrous form. A phase study of the system [Co (en)$_2$ Cl$_2$] Cl$_{(s)}$ + HCl$_{(g)}$ has shown that the monohydrochloride does form with both the *trans* and the *cis* isomers of this compound.

Examination of the phase diagrams (Fig. 1) shows the existence of the monohydrochloride at 0°C. An attempt was made to obtain a heat of reaction by a study of the system at various temperatures, but was unsuccessful due to extensive solid solution formation. The higher temperature studies however do suggest the formation of other lower hydrochlorides of these compounds.

EXPERIMENTAL

The *cis* and *trans* isomers of the compound were prepared and dried by standard methods.(2) The compounds were further dried on the vacuum system by heating to 100°C while under vacuum (ca. 10^{-6} mm of Hg). (Found: *trans* salt; Cl-37·2%, Co-20·6%—*cis* salt; Cl-37·4%, Co-20·4%.

---

(1) N. F. CURTIS, *J. Inorg. Nucl. Chem.* 19, 208 (1961).

(2) *Inorganic Synthesis* Vol. II, p. 222, (ed. W. C. Fernelius), McGraw-Hill, New York (1946).

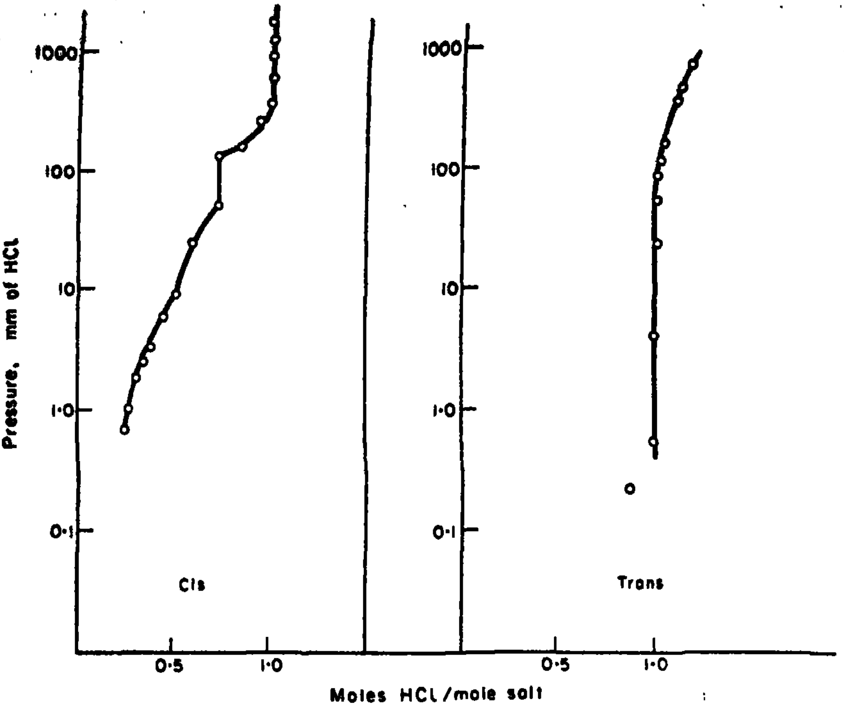

FIG. 1.—Pressure-composition phase diagrams for the systems *cis* and *trans* [Co (en)$_2$ Cl$_2$]Cl$_{(s)}$ + HCl$_{(g)}$

Calc. for [Co (en)$_2$ Cl$_2$]Cl: Cl-37·26%, Co-20·64%.) The λ max in the 6μ region were 6·43μ and 6·26μ for the *cis* and *trans* salts respectively (reported(3) —6·48μ and 6·30μ for the *cis* and *trans* salts respectively).

Acknowledgement—Many helpful suggestions by Dr. T. B. CAMERON are gratefully acknowledged. This work was supported by a National Science Foundation Grant.

Chemistry Department
University of Cincinnati
Cincinnati, Ohio, U.S.A.

R. E. VALLEE
D. H. MCDANIEL

(3) P. MERRITT and S. E. WIBERLY, *J. Phys. Chem.* **59**, 55 (1955).

Amphoterism of hydrous thorium oxide and the adsorption of fuchsine by the hydrous oxide

(*Received* 30 *January* 1962)

A NUMBER of communications(1–4) describe the precipitation of hydrous thorium oxide and it has been observed that its properties are markedly influenced by the conditions of precipitation. The difference observed between the adsorption capacities of the hydrous oxide towards inorganic cations and anions(5,6) arises from the amphoteric character of the hydrous oxide, the properties of which may be controlled by regulating the amount of alkali employed for precipitation.

(1) R. PRASAD and A. K. DEY, *Proc. Nat. Acad. Sci. India*, **27 A**, 350 (1959).
(2) R. PRASAD and A. K. DEY, *J. Indian Chem. Soc.* **37**, 747 (1960).
(3) R. PRASAD and A. K. DEY, *Vijnana Pari. Anu. Patrika*, **3**, 155 (1960).
(4) R. PRASAD and A. K. DEY, *Kolloidzschr.* **174**, 155 (1961): **175**, 53 (1961).
(5) R. PRASAD and A. K. DEY, *J. Sci. Industr. Res.* **20 B**, 230 (1961).
(6) A. K. DEY and S. GHOSH, *Proc. Indian Sci. Congr.* IV, Abstracts, *Chem. Sec.* (1951).

In view of the well-known use of hydrous oxides as mordants, the association of dyes with hydrous thorium oxide is of interest and the adsorption of Congo Red has already been reported(7). The present paper records our observations on the adsorption of the basic dye Fuchsine under different conditions.

EXPERIMENTAL

Aqueous solutions of thorium chloride (BDH Laboratory reagent), sodium hydroxide (BDH AnalaR) and fuchsine (E. Merck) were prepared and standardised. Absorptiometric measurements were made with a Unicam S.P. 500 spectrophotometer, using 10 mm glass cells, to determine optimum conditions, after which further measurements were made with a Klett-Summerson photoelectric colorimeter and colour filter no. 54 (transmission 520–600 mμ). It was found that λ_{max} is at 540 mμ between pH 2·25 and 8·9. The absorbance of a 0·002% Fuchsine solution was found to be 2·00 cm^{-1} at 540 mμ in the pH range 4·20–8·9, and in subsequent colorimetric measurements, the pH was adjusted to 6·8 with a sodium acetate-acetic acid buffer. Beer's Law was obeyed over a range of dye concentrations between 1·8 and 3·4 ppm and the colorimetric determinations were carried out within this range by suitable dilution.

Four samples of the hydrous oxide (A, B, C, D) were precipitated by adding definite volumes of a standard solution of sodium hydroxide to 500 ml of 0·25 M thorium chloride solution at 25°:

A: 10% deficient sodium hydroxide
B: equivalent sodium hydroxide
C: 5% excess sodium hydroxide
D: 10% excess sodium hydroxide.

The samples were freed from thorium (where present), hydroxyl and chloride ions by washing with water, and were then shaken with water in a Microid Flask Shaker for 2 hr to ensure homogeneity of the suspension. The suspensions were finally diluted to 10 g/l. ThO_2. Adsorption experiments were carried out by adding to 5 ml of the suspension (0·05 g ThO_2), varying amounts of the dye making up to 100 ml and equilibrating for 24 hr at 55°C. The concentration of Fuchsine was estimated colorimetrically in the supernatant liquid.

RESULTS

From the amphoteric nature of hydrous thorium oxide we might expect the adsorption of Fuchsine, a basic dye, to follow the order shown below for the different samples:

$$D > C > B > A.$$

The results, however, show the order to be $D > B > A > C$, sample C having least adsorptive capacity. A similar result was found for the acid dye Congo Red and the same hydrous oxide.(7) This suggests that the conditions for preparation of this correspond to the isoelectric point.

Acknowledgment—The authors thank the Council of Scientific and Industrial Research, India, for financial assistance and for the grant of a Senior Research Fellowship to one of them (R. P.).

Chemical Laboratories
University of Allahabad
Allahabad, India

Rameshwar Prasad
Arun K. Dey

(7) R. Prasad and A. K. Dey, *J. Phys. Chem.* **65**, 1272 (1961).

J. Inorg. Nucl. Chem., 1962, Vol. 24, pp. 1021 to 1022. Pergamon Press Ltd. Printed in Northern Ireland

LETTER TO THE EDITOR

The relationship between retention and chemical constitution

(*Received* 19 *January* 1962)

THE lack of a suitable model to explain the behaviour of the recoil atoms resulting from nuclear reactions has led to the development of models which take into account the chemical reactions during the slowing down of these hot atoms. In the particular case of neutron-irradiated crystalline compounds, HARBOTTLE and SUTIN's hot zone model(1) proposes chemical reactions that have a high probability of occurring at the temperature reached in the relatively small hot zone in the crystal. Thus a correlation should exist between the retention and the chemical constitution of the target compound, but obviously specific chemical effects should also appear owing to the unusual conditions under which these reactions occur in the hot zone, even after cooling. The investigation of the retention for a series of salts of oxyanions, for example for the iodates(2), permanganates(3) or chromates and dichromates(4) did not reveal such correlations. On the contrary certain anomalies have indicated specific chemical effects, such as the apparent reduction by the ammonium ion(2,4,5) or by hydration water(3,6).

We have studied the radiocobalt retention in different crystalline cobaltic ammines, varying the anion or the ligand. All the samples were irradiated in the I. F. A. reactor under the same conditions, at the hole temperatture, in air. ($\phi_{th} = 6 . 10^{11}$ cm^{-2} sec^{-1}; $\phi_f = 2 . 10^{11}$ cm^{-2} sec^{-1}; $\delta_{gamma} = 1 . 10^7$ rhr^{-1}; t = 40 hr). The retention was determined by solvent extraction, ion exchange and precipitation with carriers. The activity measurements were made in some cases by gamma spectrometry. The retention was considered as the percentage of the activity not extractable as Co^{++}. The results for some of the compounds investigated are shown in Table 1.

TABLE 1.—RETENTION FOR SOME COBALTAMMINES

Chemical formula	Retention (%)	Chemical formula	Retention (%)
$[Co(NH_3)_6]Cl_3$	83·4	$[Co(NH_3)_6]PO_4 \cdot 4H_2O$	84·3
$[Co(NH_3)_6]Br_3$	89·7	$[Co(NH_3)_6]_2(PO_4H)_3 \cdot H_2O$	73·7
$[Co(NH_3)_6]J_3$	95·4	$[Co(NH_3)_6]_2(PO_4H)_3 \cdot 4H_2O$	67·3
$[Co(NH_3)_6](NO_3)_3$	74·4	$[Co(NH_3)_5NO_2](NO_3)_2$	88·2
$[Co(NH_3)_6](NO_2)_3$	90·3	cis$[Co(NH_3)_4(NO_2)_2]NO_3$	85·8
$[Co(NH_3)_6](MnO_4)_3$	9·6	trans$[Co(NH_3)_4(NO_2)_2]NO_3$	75·4
$[Co(NH_3)_6]_2(CO_3)_3 \cdot 7H_2O$	83·9	$[Co(NH_3)_3(NO_2)_3]$	76·0
$[Co(NH_3)_6]_2(C_2O_4)_3 \cdot 4H_2O$	21·2	$NH_4[Co(NH_3)_2(NO_2)_4]$	72·4
$[Co(NH_3)_6]PO_4$	75·5	$Na_3[Co(NO_2)_6] \cdot H_2O$	40·1

As may be seen the halides show some regularity, the retention increasing approximately linearly with the ionic radius and the mass of the halogen; this would follow from a mechanical model, but at the same time it contradicts a chemical model since the retention increases with the electropositivity of the halogen. The larger retention in nitrite relative to the retention in nitrate is hard to understand with either reducing or oxidizing character for the hot zone. Permanganate, also a strong oxidizing agent, is characterized by a very low retention, which can be explained only by the tendency of the radiolysis fragments of the anion to reach the stable form MnO_2. Perhaps the cobaltammine cationic species, left without the anionic partner, may decompose eventually on dissolution in water. The radiation stability criterion may also explain the low retention in oxalate relative to that found in carbonate. As to the reducing action of the hydration water, the experimental results found for the phosphates and mono-hydrogen phosphates are contradictory. Nor does the ammonium ion in $NH_4[Co(NH_3)_2(NO_2)_4]$ seem to exhibit reducing action. The retention in the cobaltic nitro-ammines decreases with the increase in the number of the acid ligands. At first sight one might apply a mechanical model to the variation of retention but for the fact that chemical isomers show different retentions(6).

---

(1) G. HARBOTTLE and N. SUTIN, *J. Phys. Chem.* **62**, 1344 (1958).
(2) R. E. CLEARY, W. H. HAMILL and R. R. WILLIAMS, *J. Amer. Chem. Soc.* **74**, 4675 (1952).
(3) K. J. MCCALLUM and A. G. MADDOCK, *Trans. Faraday Soc.* **49**, 1150 (1953).
(4) G. HARBOTTLE, *J. Chem. Phys.* **22**, 1083 (1954).
(5) N. GETOFF and M. NISHIKAWA, *Nature, Lond.* **192**, 61 (1961).
(6) T. COSTEA and I. DEMA, *Nature, Lond.* **189**, 478 (1961).

No close relation between retention and chemical constitution may be drawn at the present stage of experiments, owing to the unknown behaviour of the chemical entities in the special conditions of the damaged zone. However, the radiation and thermal stabilities of the compounds are undoubtedly important.

T. Costea
I. Dema.

Laboratory of Radiochemistry,
Institute of Atomic Physics,
Bucharest, Roumania

J. Inorg. Nucl. Chem., 1962, Vol. 24, p. 1023. Pergamon Press Ltd. Printed in Northern Ireland

ERRATA

S. AMDURSKI, C. EDEN and H. FEILCHENFELD: The reaction between triethyl aluminium and water, *J. Inorg. Nucl. Chem.* **23**, 133–134 (1961).

Page 133, Figure 1. The illustration is incorrect and should be:

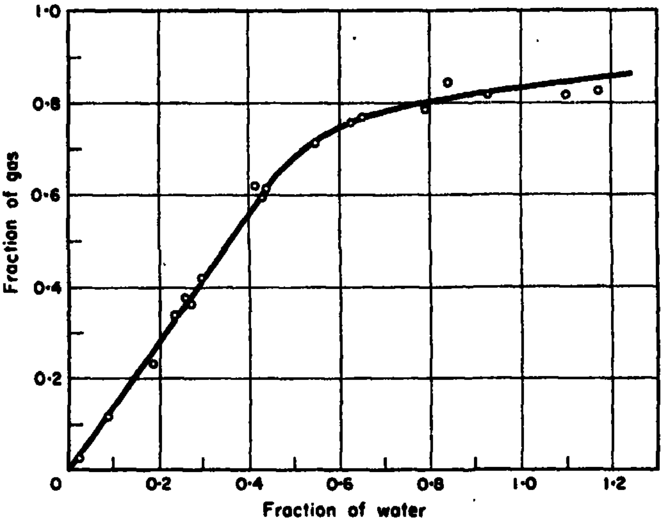

FIG. 1

A. N. BHAT and B. D. JAIN: Spectrophotometric studies of uranium(VI)-3-acetyl-4-hydroxycoumarin complex in ethanol, *J. Inorg. Nucl. Chem.* **23**, 136–139 (1961).

Page 137, following line 23 the structure

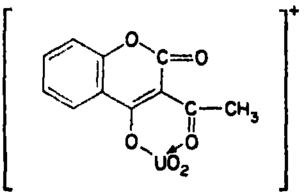

should be inserted.

Page 137, following line 27 the structures

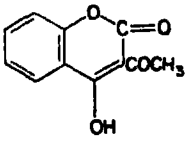

I

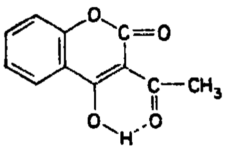

II

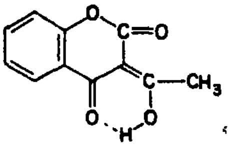

III

should be inserted.

J. Inorg. Nucl. Chem., 1962, Vol. 24, pp. 1025 to 1038. Pergamon Press Ltd. Printed in England

CRYSTAL STRUCTURE, THERMAL EXPANSION AND MELTING POINT OF AMERICIUM METAL*

D. B. McWhan†, B. B. Cunningham and J. C. Wallmann

Department of Chemistry and Lawrence Radiation Laboratory,
University of California, Berkeley, California

(*Received* 12 *March* 1962)

Abstract—The methods for preparing milligram quantities of pure, well crystallized americium metal are discussed in detail. A versatile high and low temperature X-ray powder camera for small radioactive samples is presented.

Americium metal prepared by the reduction of americium trifluoride with barium vapour has been indexed as hexagonal close-packed with $a = 3{\cdot}4681 \pm 0{\cdot}0008$ Å and $c = 11{\cdot}241 \pm 0{\cdot}003$ Å at 20°C. The proposed structure type is that of lanthanum metal ($P6_3$/mmc with metal atoms in 2 (a) 000; 00 $\frac{1}{2}$ and 2 (c) $\frac{1}{3}, \frac{2}{3}, \frac{1}{4}; \frac{2}{3}, \frac{1}{3}, \frac{3}{4}$). Americium metal condensed on a tantalum wire or quartz fibre from the vapour phase was found to be face-centred cubic ($a = 4{\cdot}894 \pm 0{\cdot}005$ Å) with a density similar to the dhcp structure. Evidence for the existence of a face-centred cubic form of americium metal above 600°C, is presented.

The following physical properties of americium metal have been determined:

(1) Melting point: 994 ± 7°C.
(2) Density (X-ray): 13·671 ± 0·005 g/cm^3 (20°C).
(3) Metallic radius (CN 12): 1·730 Å.
(4) Coefficient of thermal expansion: (20°C)
$\alpha_a = 7{\cdot}5 \pm 0{\cdot}2 \times 10^{-6}$°C^{-1}
$\alpha_c = 6{\cdot}2 \pm 0{\cdot}4 \times 10^{-6}$°C^{-1}

In the metallic state uranium, neptunium and plutonium exhibit unusual crystal structures which as yet have received no satisfactory theoretical explanation.

It is not unreasonable to suppose that the exceptional structures are related in some manner to the tendency of these same elements to exhibit multiple valencies in their ordinary chemical behaviour. It has been of interest, therefore, to extend the study of the properties of the actinide metals to americium, which forms positive oxidation states of III, IV, V and VI, like the three preceding elements, but which exhibits a notably greater tendency toward univalency in the sense that oxidation to the higher states is considerably more difficult, and the intermediate states are less stable toward disproportionation.

The existence of a double hexagonal close-packed structure, space group $P6_3$/mmc, with americium atoms in: 2(a)000;00$\frac{1}{2}$ and 2(c) $\frac{1}{3}, \frac{2}{3}, \frac{1}{4}; \frac{2}{3}, \frac{1}{3}, \frac{3}{4}$, with $a = 3{\cdot}642 \pm 0{\cdot}005$ Å and $c = 11{\cdot}76 \pm 0{\cdot}01$ Å was reported by Graf *et al.*(1) several years ago.

---

[*] Taken in part from a thesis submitted by D. B. McWhan to the Graduate Division of the University of California in partial fulfilment of the requirements for the degree of Doctor of Philosophy.

[†] Present address: Department of Inorganic Chemistry, Royal Institute of Technology, Stockholm 70, Sweden.

(1) P. Graf, B. B. Cunningham, C. H. Dauben, J. C. Wallmann, D. H. Templeton and H. Ruben, *J. Amer. Chem. Soc.* 78, 2340 (1956).

The same structure and lattice constants were found for six separate preparations (one made from ^{243}Am) of americium metal, all of which exhibited typical metallic lustre and malleability. In the series of preparations carried out by Graf a technical failure occurred in one of the runs leading to an abnormally short reduction time. A diffraction pattern of the product was obtained, but it was not then calculated. During the course of the present work this film was measured and the values of the a and c parameters were found to be considerably smaller than in Graf's other preparations.

In the original work the less dense hexagonal form was taken to be the room temperature-stable modification of the metal.

More recently, McWhan *et al.*,(2) published crystallographic data on a double-hexagonal close packed phase of americium having lattice parameters $a = 3{\cdot}474 \pm {\cdot}005$ Å and $c = 11{\cdot}25 \pm {\cdot}02$ Å, similar to the metal obtained in Graf's exceptional preparation and suggested that americium, like cerium, may exist in two phases having the same structure, but quite different densities.

The present work represents a continuation of the investigation of the structure and properties of americium metal, in which much effort was devoted toward improving the purity of the preparations.

EXPERIMENTAL

Reagents

Water was prepared by redistilling ordinary distilled water in quartz, and was stored in quartz or polyethylene containers which had been pre-leached for several days in concentrated HCl and rinsed in redistilled water. All aqueous solutions were prepared from this specially purified water and these two were stored in pre-leached polyethylene or quartz containers, since it was found that pure HCl solutions stored in Pyrex showed a rapid accumulation of Ca, Mg, Al and Fe to the extent of several parts per million. This was especially noticeable when Pyrex pipettes were used to withdraw samples of pure HCl solutions for spectrographic analysis. Even momentary contact with Pyrex resulted in significant contamination of the acid.

Hydrochloric acid solutions were prepared from pure water and gaseous hydrogen chloride.

Hydrofluoric acid solutions were made by vapour equilibration of commercial 48 per cent solutions with a small volume of water.

An americium chloride stock solution in 6 M HCl was obtained by purification of an americium nitrate solution* initially containing about two weight per cent each of calcium and aluminium, using the ion exchange procedure of Naito.(3) The resin was packed in a polyethylene column and the eluate collected in polyethylene containers. The americium stock solution prepared in this way was analysed for cationic impurities by emission spectrography, using copper spark excitation. The only impurities detected in a typical analysis† were as follows (expressed in mole per cent impurities): Ca, 0·075; Mg, 0·25.

* Furnished by the A.E.C. Research Materials Pool, Oak Ridge National Laboratory, Oak Ridge, Tennessee.

† The limits of spectrographic detection for common impurities, expressed in micrograms, are as follows

0·01 μg Al, Be, Ca, Cr, Eu, Fe, La, Mg, Mn, Mo, Nb, Si, Sr, Ti, Yb, Y, Zr
0·05 μg Bi, Co, Ge, In, Ni, Sm, V
0·1 μg Ce, Nd, Pb, Pt, Sn, U, W, Zn
0·5 μg Cd, Ir, Sb, Th
1 μg K, Li, Na, Np, Pu.

---

(2) D. B. McWhan, J. C. Wallmann, B. B. Cunningham, L. B. Asprey, F. H. Ellenger and W. H. Zachariasen, *J. Inorg. Nucl. Chem.* **15**, 185 (1960).

(3) K. Naito, Report UCRL-8748 (1959).

Americium trifluoride was prepared by adding enough 24 M hydrofluoric acid to an aliquot of the americium trichloride solution in a polyethylene cone to make the solution ~ 2 M in hydrofluoric acid. The trifluoride precipitate was centrifuged, the supernatant removed and the precipitate washed twice with about twenty times its volume of water. The washed fluoride was dried for a minimum of fourteen days in a vacuum desiccator over phosphorous pentoxide. The fluoride so prepared was obtained in the form of a few "chunks" of very compact, hard, and translucent material readily susceptible to mechanical handling without loss, and yielding well agglomerated metal on reduction.

Americium dioxide was made by igniting americium(III) oxalate in air at 600°C for about 30 min. The oxalate was precipitated from the americium stock solution by adding a slight stoicheiometric excess of 1 M oxalic acid solution made by dissolving reagent grade oxalic acid in water. After removal of the supernatant solution the oxalate precipitate was dried and then transferred to a platinum container for ignition.

Barium used to reduce trifluoride to the metal was of a special grade of purity. Mole per cent impurities detected by spectrographic analysis were as follows: Ca, 0·18; Si, 0·06, or less.

Lithium metal, also used as a reductant, contained: Ca, 0·007 atom per cent.

Impurities detected in the lanthanum metal used to reduce americium dioxide to metal were (in atom per cent impurities): Ca, 0·21; Mg, 0·35; Be, 3.

Metal preparation

By reduction of americium trifluoride. Well agglomerated metal in good yield could be obtained only by reduction in the neighbourhood of 1500°K. The choice of reductant metals was restricted, of course, so those having a favourable free energy of reaction at this temperature, and additionally to those which could readily be separated from americium by reason of their markedly different volatility.

Lithium, calcium and barium satisfy these requirements, as shown in Table 1, the calculated values being based on data tabulated by Glassner.(4)

TABLE 1.—THERMODYNAMICS OF AmF_3 REDUCTIONS

Reductant	ΔF_T (kcal/gramme-atom AmF_3)	Vapour-pressure of MF_x(5) (mm)	T°K, where vapour-pressure of $MF_x = 10^{-3}$ atm	
	1500°K	1500°K		
Li	−30	400	1304	
Ca	−43	170	1690	
Ba	−41	80	1870	
T (in °K)		1000	1250	1500
Vapour-pressure of Am (mm)(6)		3×10^{-6}	10^{-3}	0·05

Most reductions were made with barium, since this metal was available in very pure form, although lithium was used successfully in several preparations. In order to obtain good metal, it was essential that the trifluoride be completely dehydrated prior to reduction. Failure to dehydrate, or exposure of the dry fluoride to air for several days resulted in metal which was noticeably contaminated with americium monoxide.

The reduction apparatus is illustrated in diagrammatic form in Fig. 1. It consisted of an all-tantalum double crucible system (1b) suspended inside a cylindrical induction shield made of 2 mil tantalum sheet. This assembly was suspended in turn in one arm of a high vacuum line and surrounded by an induction coil.

(4) Estimated from A. Glassner, Report ANL 5750 (1957).

(5) R. E. Honig, RCA Review, 195 (1957).

(6) S. C. Carniglia and B. B. Cunningham, *J. Amer. Chem. Soc.* 77, 1502 (1955).

A typical reduction was performed according to the following schedule: The tantalum assembly was degassed at > 1200°C for 30 min or until the pressure fell to less than 10^{-6} mm of Hg. (Besides degassing, this served to volatilize copper deposited during spot welding of the tantalum components). The system was allowed to cool to room temperature in an atmosphere of argon which had been purified by passage over hot uranium or calcium. The glass joint shown in the lower part of Fig. 1a which usually showed a noticeable film of condensed copper, after the degassing operation, was replaced by a clean joint, and the system re-evacuated. An empirical correlation was then established between the current reading of the power generator and the temperature of the induction shield, as observed with an optical pyrometer through a hole in the shield.

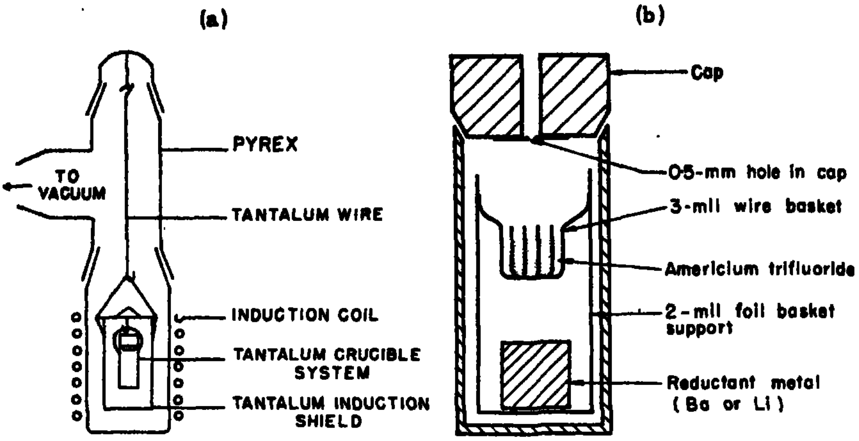

Fig. 1.—Fluoride reduction apparatus.

After cooling, the crucible system was returned to the nitrogen-filled box and the cap and wire basket were removed. A piece of americium trifluoride was added to the basket, and a freshly-cut piece of reductant metal (sufficient to provide about a ten-fold excess over that required for reduction) was dropped into the bottom of the inner crucible. The basket was replaced, the crucible capped and crucible-and-shield assembly returned to the vacuum line.

Pumping was continued until the pressure in the line fell to 10^{-6} mm or less. The temperature of the induction shield was raised slowly to ~ 300°C with further pumping until the pressure again fell to $< 10^{-6}$ mm.

At this stage the power supply was set to give a temperature of 1300°C and held for 30 sec. Twenty of these 30 sec were consumed in bringing the system to the desired temperature. The power was then dropped to the 1100°C level and maintained for 3 min. Generally, this resulted in the removal of almost all of the excess reductant metal, without serious loss of americium by vapourization. From the data of Table 1 it may be calculated that the rates of vapourization of barium and americium, through the 0·5 mm diameter effusion hole at 1100°C were 320 and 0·1 μmole min^{-1}, respectively. The absolute rate of vapourization could not be predicted accurately, in all cases, apparently, because of variable interference with the volatilization due to a coating of barium fluoride slag.

If the metal was intended for X-ray study it was annealed for 4 hr at 760° C and the temperature then reduced to room temperature at a rate of 1·5°C min^{-1}. Otherwise, after the 3 min heating period it was simply allowed to cool in vacuum for several hours.

If the initial reduction temperature of 1300°C was maintained for more than about 10 sec, the metal tended to spread over all of the tantalum wire basket and even onto the walls of the crucible.

Ten seconds at 1300°C (followed by 3 min at 1100°C) usually resulted in the formation of a globule of americium containing only a few embedded tantalum wires, and covered with a glassy coating of slag. The slag was removed by scraping with a scalpel, forceps or tungsten needle in a nitrogen atmosphere, with the aid of a low power binocular microscope.

Pieces of metal weighing less than 100 μg were cut from the clean globule and transferred to X-ray capillaries which were sealed off in vacuum. (Larger samples caused excessive darkening of the X-ray film because of the 40 KeV γ-ray associated with the decay of ^{241}Am).

An analysis of a representative sample of metal (sample No. 22) gave the following result (mol per cent impurities): Al, 0·45; Ba, 1·45; Ca, 0·10; Mg, 0·16.

By reduction of americium dioxide. The preparation of metallic samarium by distillation from a mixture of samarium sesquioxide and lanthanum metal has been described by DAANE *et al.*(7)

ASPREY(8) prepared americium metal by an adaptation of this technique, using a mixture of americium dioxide and lanthanum, and condensing the americium vapour on a quartz fibre.

At 1500°K, the calculated free energies of the reactions

$$AmO_{2(s)} + \tfrac{4}{3}La_{(l)} = Am_{(g)} + \tfrac{2}{3}La_2O_{3(s)},$$

and

$$\tfrac{1}{2}Am_2O_3 + La_{(l)} = Am_{(g)} + \tfrac{1}{2}La_2O_{3(s)}$$

are −44 and −3 kcal/mole Am, respectively.

From the vapour-pressure equations for lanthanum(9) and americium:(6)

$$\log \frac{R_{La}}{R_{Am}} = \frac{-7{,}300}{T} + 1{\cdot}06,$$

where R is the rate of effusion of the metal per unit orifice area under Knudsen conditions. However, as has been shown by CHUPKA *et al.*(10), LaO is comparable in volatility to La. We estimate that at 1500°K

$$\frac{P_{LaO}}{P_{La}} = 2{\cdot}5$$

and hence that the total rate of effusion of lanthanum will be larger than that of La by the factor 3·4 (equal to

$$\frac{P_{LaO}}{P_{La}}\sqrt{\left(\frac{134}{145}\right)}+1).$$

Therefore, at 1500°K:

$$\log \frac{R_{La},\ \text{total}}{R_{Am}} = \frac{-7{,}300}{T} + 1{\cdot}58.$$

The calculated mole percentages of La and oxygen in the americium vapour are 0·05 and ~ 0·03, respectively. The calculation does not take into account the reduction of the vapour pressure of americium owing to its solution in lanthanum and the figures represent minimum contamination of the americium vapour.

The tantalum crucible assembly, consisting of an inner crucible with conical bottom in which a mixture of americium dioxide and lanthanum metal was placed, and an outer crucible with a 20 mil diameter effusion hole in the cap, was heated in high vacuum by electron bombardment.

A 10 mil diameter tantalum wire or quartz fibre was supported one to 2 mm above the effusion hole and served as a condensing surface on which to collect metal. The wire was held in the jaws of a chuck fastened to the end of a tungsten rod which extended into a horizontal side arm. Small pieces of iron fastened to the rod and chuck allowed the rod to be moved and the jaws of the chuck to be released by manipulation with external magnets.

Rotation of the vacuum envelope by 90° about a joint perpendicular to the plane of the drawing moved the chuck to a vertical position directly above a side arm which had been drawn down at the end to capillary dimensions. When the jaws were released the americium-coated wire fell to the bottom of the capillary, which was then sealed off for X-ray work.

---

(7) A. H. DAANE, D. DENNISON and F. H. SPEDDING, *J. Amer. Chem. Soc.* **75**, 2272 (1953).

(8) L. B. ASPREY, Private communication.

(9) A. H. DAANE and F. H. SPEDDING, Abstract of paper presented at American Chemical Society Meeting, Chicago, Ill., Spet. 1958, Paper No. 58, Division of Physical Chemistry.

(10) W. A. CHUPKA, M. G. INGRAM and R. F. PORTER, *J. Chem. Phys.* **24**, 792 (1956).

The apparatus used by us to prepare americium from the dioxide and lanthanum is shown in Fig. 2.

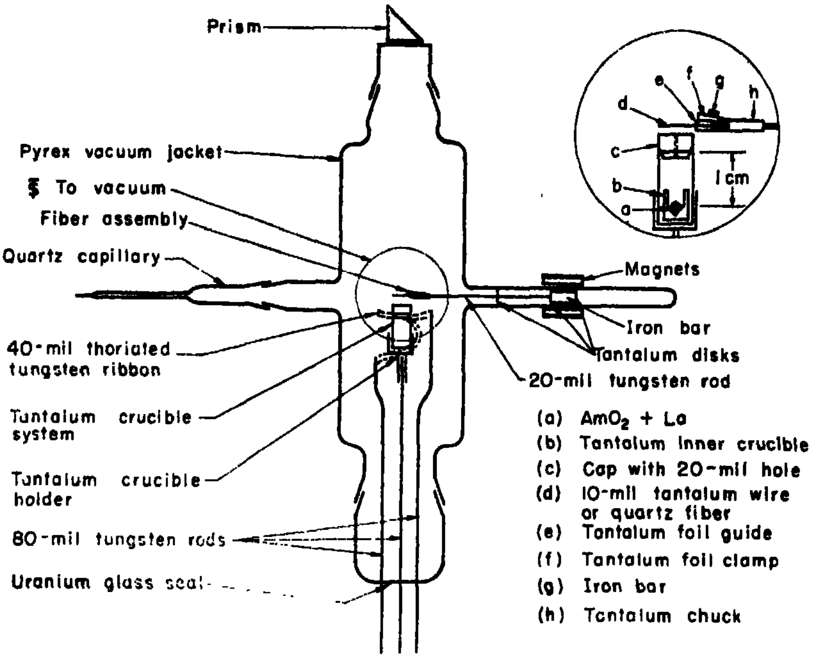

Fig. 2.—Oxide reduction apparatus.

The method and apparatus were tested with samarium, dysprosium and erbium sesquioxides, and in each case metallic coatings showing the crystal structures and lattice parameters reported in the literature were obtained. In one case, a sample of metal prepared by fluoride reduction was vapourized and collected on tantalum in this apparatus. Yields of metal realized by this technique were low, partly because of poor geometry and partly because of incomplete reduction; little or no metal was obtained if the dioxide had been prepared by calcining much above 600°C.

A typical preparation was carried out as follows: about 20 mg of clean lanthanum metal were added to one to five milligrams of americium dioxide in the bottom of the crucible. The apparatus was assembled and pumped down to a pressure of 10^{-6} mm of Hg. The temperature of the inside of the crucible (as read by an optical pyrometer through the effusion hole in the cap) was raised to 1200°C, the collecting wire manipulated in place over the effusion hole and distillation continued for 30–40 min with occasional rotation and fibre released to the capillary. The latter was then sealed off for X-ray examination.

The lanthanum content of a sample of americium made in this way, was ~ 0·4 atom per cent.

X-ray diffraction

Camera and technique. To facilitate the investigation of the crystal structures of americium a special camera was constructed by means of which it was possible to (a) obtain diffraction patterns from −125 to +850°C; (b) obtain two exposures without reloading; (c) accommodate capillaries up to two inches in length; (d) interchange collimators of different sizes so as to secure the optimum ratio of beam diameter to sample diameter. The camera employed vertical suspension of the capillary to prevent the metal pellets from rolling out of the beam. Details of the construction are shown in Fig. 3. The film is mounted in a removable, full-circular cassette using a Straumanis-type film mounting. The camera diameter is 90 mm, a dimension chosen mainly to facilitate comparison with the film file in the Laboratory. The collimator consists of a double pinhole and scatter guard system similar to those used in the commercial Norelco powder cameras and discussed by Parrish and Cisney.(11) The chuck holder is interchangeable with an oven for high-temperature studies and is easily adapted for taking pictures below room temperature.

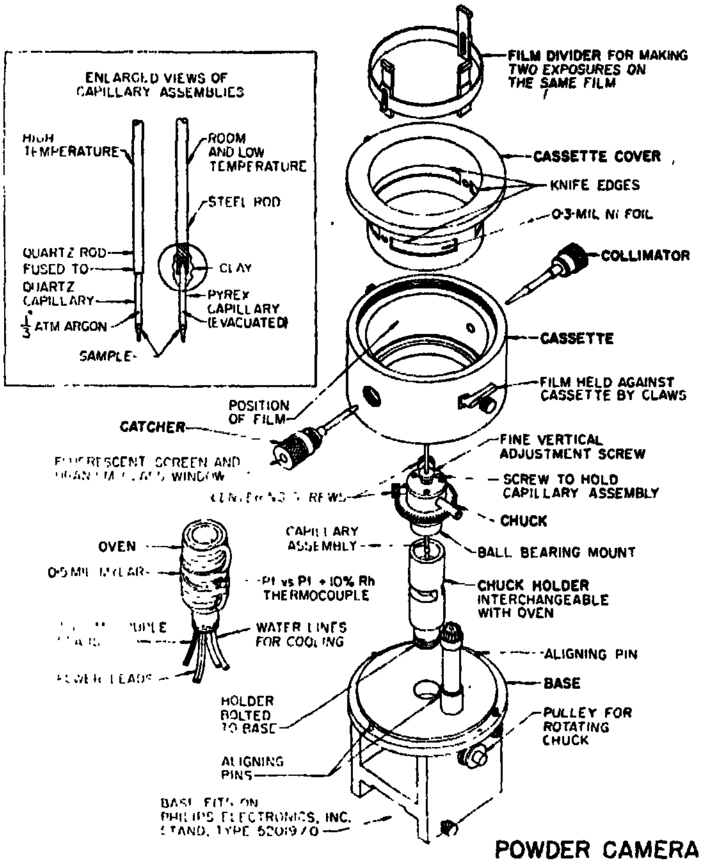
ENLARGED VIEWS OF CAPILLARY ASSEMBLIES
HIGH TEMPERATURE
ROOM AND LOW TEMPERATURE
STEEL ROD
QUARTZ ROD FUSED TO QUARTZ CAPILLARY
CLAY
PYREX CAPILLARY (EVACUATED)
$\frac{1}{3}$ ATM ARGON
SAMPLE
FILM DIVIDER FOR MAKING TWO EXPOSURES ON THE SAME FILM
CASSETTE COVER
KNIFE EDGES
0·3-MIL Ni FOIL
COLLIMATOR
CASSETTE
FILM HELD AGAINST CASSETTE BY CLAWS
POSITION OF FILM
CATCHER
FLUORESCENT SCREEN AND URANIUM GLASS WINDOW
CENTERING SCREWS
FINE VERTICAL ADJUSTMENT SCREW
SCREW TO HOLD CAPILLARY ASSEMBLY
CHUCK
CAPILLARY ASSEMBLY
BALL BEARING MOUNT
OVEN
0·5 MIL MYLAR
Pt vs Pt + 10% Rh THERMOCOUPLE
CHUCK HOLDER INTERCHANGEABLE WITH OVEN
THERMOCOUPLE LEADS
WATER LINES FOR COOLING
POWER LEADS
ALIGNING PIN
BASE
HOLDER BOLTED TO BASE
PULLEY FOR ROTATING CHUCK
ALIGNING PINS
BASE FITS ON PHILIPS ELECTRONICS, INC. STAND, TYPE 52019/0
POWDER CAMERA

Fig. 3.—X-ray diffraction powder camera.

The oven contains a small, low heat capacity furnace consisting of a platinum wire coil wrapped on a ceramic form ("Lava A"). The oven has a $\frac{1}{8}$-in. hole for the capillary and a central X-ray gap. The outside of the oven is water-cooled, and, as a radiological safety precaution at temperatures above 600°C, the X-ray gap is covered with 0·1-mil Mylar. Power is supplied by a step-down transformer controlled by a Variac fed from a Sola constant-voltage transformer. The temperature of the thermocouple was monitored continuously by a Brown Recording Potentiometer. The thermocouple and the input current were calibrated against the melting points of standard substances sealed in quartz capillary assemblies. Diffraction patterns have been obtained at temperatures up to 850°C. The temperature control and measurement with the original oven was accurate to ±5° up to 600°C. A second oven used between 800 and 850°C was calibrated to ±15° with an optical pyrometer.

Modification of the camera to take diffraction patterns below room temperature is shown in Fig. 4. Dry nitrogen cooled by passing through liquid nitrogen was blown over the capillary. The temperature was controlled by varying the flow of nitrogen and was measured with a Chromel-Alumel thermocouple placed directly below the capillary. The top of the camera was sealed providing a "dead air" space which reduces icing of the capillary and partially insulates the film. Temperatures of −125 ± 10°C have been obtained.

---

(11) W. Parrish and E. Cisney, *Phillips Tech. Review*, **10**, 157 (1948).

The camera described above minimizes the danger of breaking the capillary and contaminating the camera. Prior to loading, the sample-containing-capillary is checked for external alpha contamination in a gloved box. If clean, or after decontamination, it is then fixed to the support rod with clay, the camera inserted in the box, and the capillary assembly loaded in the chuck. The chuck is placed in a stand and the sample centred. The capillary is then drawn up into the chuck which in turn is placed in the chuck holder. The capillary can now be lowered into position without danger of breaking, and the final adjustment made with the aid of a microscope. The cassette can be removed to change films without disturbing the capillary. The capillary adjustment screws remain exposed, and if desired further adjustment may be made with respect to the X-ray beam as seen on the fluorescent screen. The X-ray source was a standard Norelco unit Type No. 12045, with copper target, operated at 35 kV and a current of 20 mA. The sample was situated approximately 6 cm away from a high intensity port of this unit.

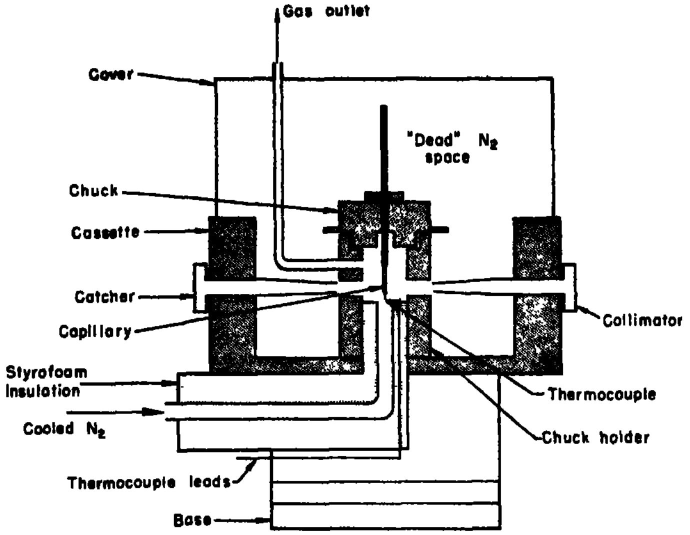

FIG. 4.—Low temperature X-ray diffraction powder camera.

For exposures of 3–8 hr Ilford "Industrial G" film was used, and for longer exposures, Kodak "AA".

Considerable difficulty was encountered in securing high temperature X-ray data because of the volatility and reactive nature of americium. At elevated temperatures, the sample reacts with the quartz capillary, and above approximately 600°C vapourizes onto the walls. By pre-degassing the capillary at 700 to 800°C and sealing the samples in $\frac{1}{3}$–$\frac{1}{2}$ atmosphere of argon, these problems were minimized. (The argon was purified by passing it through anhydrous magnesium perchlorate and then over calcium metal at 600°C). Up to about 600°C only minor reaction of americium with the walls took place, as evidenced by four to eight X-ray diffraction lines of the *fcc* americium monoxide phase which usually appeared at about 400°C.

An attempt was made to obtain X-ray diffraction patterns at 850°C, but even under one atmosphere of argon, the americium vapourized onto the capillary walls before a usable diffraction pattern could be obtained. To reduce the exposure time a shorter film radius was then obtained by wrapping the film directly around the oven. A film holder was made of black paper with nickel foil between the film and the oven to minimize heat transfer to the film. The camera diameter was thus reduced to approximately 38 mm, and diffraction patterns could be obtained in 30–40 min. Although the surface of the film was not accurately cylindrical, tantalum could be used as an internal standard, for correction.

Calculation of lattice parameters. Line positions on each film were measured three times and averaged to minimize random errors. Diffraction angles were then calculated from these measurements.

As is well known, differences between the observed angles and the true Bragg angles may arise because of film shrinkage, divergence and absorption of the X-ray beam and non-central location of the specimen with respect to the film. (The Straumanis method of film mounting eliminates errors due to film shrinkage only if there is no eccentricity in the location of the sample relative to the axis of the cylindrical surface of the film.) The error, $\Delta\theta$, in the true angle θ, from all sources can be related to the plane spacings in the hexagonal system, as follows

$$A(h^2+hk+k^2)+Cl^2 = \sin^2\theta+\Delta\theta\sin 2\theta+\ldots, \tag{1}$$

where

$$\Delta\theta = D\sin 2\theta+E\left(\frac{\cos^2\theta}{\sin\theta}+\frac{\cos^2\theta}{\theta}\right). \tag{2}$$

The error approaches zero as θ approaches 90°. COHEN(12) suggested that in order to obtain the most accurate values for lattice parameters from X-ray data a least-squares fit be obtained for an equation such as (1) and the resulting function extrapolated to infinity.

This problem has been programmed for the IBM 704 computer by MUELLER and HEATON(13) at the Argonne National Laboratory, using Fortran. A Fortran deck, kindly supplied by Dr. MUELLER, was modified and compiled for the Berkeley IBM 709.

All lattice parameters determined in the present work were calculated in this way. The same set of diffraction data was first treated, according to various extrapolation functions, weighting factors and ranges of θ (i.e., all angles or just those > 50°) in order to determine the effect of these variables on the calculated values of the lattice parameters.

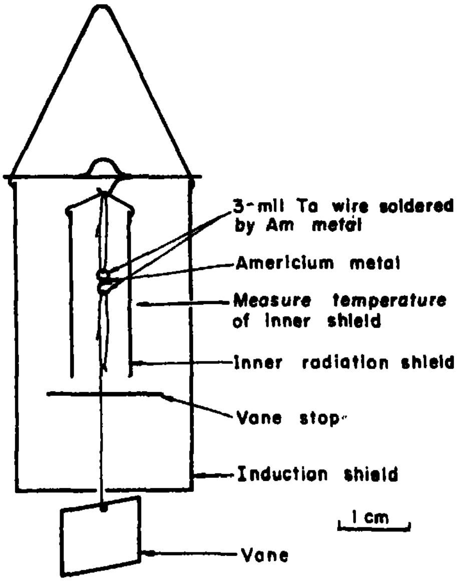

All tantalum components

FIG. 5.—Melting point apparatus.

Regardless of the extrapolation function, weighting factor or angle range the lattice parameters calculated from the same set of data were consistent to ±0·001 Å.

As a final check, the lattice parameter was calculated from the diffraction pattern of a sample of pure gold at 20°C, and found to be $a = 4{\cdot}0779$ Å. WYCKOFF's(14) value of

---

(12) M. U. COHEN, *Rev. Sci. Instrum.* **6**, 68 (1935).

(13) M. H. MUELLER and L. HEATON, Report ANL 6176 (1961); M. H. MUELLER, L. HEATON and K. T. MILLER, *Acta Cryst.* **13**, 828 (1960).

(14) R. W. G. WYCKOFF, *Crystal Structures*. Interscience, New York (1948).

4·07864 Å at 25°, corrects[15] to 4·0783 Å at 20°. The difference is well within our estimated accuracy of measurement of ±0·02 per cent.

Determination of the melting point

Several attempts to determine the melting point of americium have been reported previously,[16] but in no case do the authors claim a reliable result. In the present work the preparation of pieces of metal containing embedded tantalum wires seemed to offer a convenient method of determining the melting point. This was done by suspending the sample from one wire, hanging a light weight on a separate wire and slowly raising the temperature of the "americium soldered" joint in vacuum until the "solder" melted, releasing the weight. A sketch of the apparatus is presented in Fig. 5.

The temperature of the inner radiation shield was observed continuously with an optical pyrometer, through a hole in the outer shield, and the temperature raised in small increments, by induction heating of the outer shield, until the lower vane dropped.

A temperature calibration was established by using this technique to obtain the melting points of samples of gold, cerium and praseodymium, with the results shown in Table 2 below

TABLE 2.—TEMPERATURE CALIBRATIONS FOR MELTING POINT DETERMINATION

Sample	m p	Observed m p	Correction (°C)
Au	1063 ±0·1[17]	1073	−10
Pr	935 ±5[18]	942	− 7
Ce	797 ±3[18]	811	−14
Average correction		−10°C	

RESULTS AND DISCUSSION

Crystal structure of americium

All samples of metal prepared by reduction of the trifluoride could be indexed as double hexagonal close-packed. The structure is like that of lanthanum, $P6_3/mmc$ (D^4_{6h}) with metal atoms in: 2(a), 000;00, ½ and 2(c) ⅓, ⅔, ¼; ⅔, ⅓, ¾.

Diffraction data are listed in Table 3 for a polycrystalline sample containing 1·87 mole per cent cationic impurities (0·45 Al, 1·45 Ba, 0·1 Ca and 0·16 Mg).

Several different assignments for the high angle reflexions were tried, and those listed gave the best fit.

The proposed structure has the general line extinction that for reflexions $(h+2k)/3 = n$, only those with $l/4 = m$ are allowed, and this is in agreement with the lines observed. The intensities of the reflexions calculated from

$$I = F^2 p(1+\cos^2 2\theta)/\sin^2\theta \cos\theta,$$

where F = the structure factor and p = multiplicity, are listed along with the visual estimates of the intensities of the powder pattern lines in Table 3. With a few notable exceptions such as the 00·4, 11·0, 11·4, 0·008, 11·8 and 11·12 lines the calculated intensities are in reasonable agreement with the observed intensities. The discrepancies probably are to be attributed to the presence of stacking faults in the hexagonal layers, leading to abnormal sharpening of some lines. The phenomenon is well known in $CdBr_2$ and has been carefully studied in cobalt.

---

(15) Taking $\alpha = 14{\cdot}3 \times 10^{-6}/°C$ from *Handbook of Chemistry and Physics* (*42nd Ed.*). Chem. Rubber Publ. Co., Cleveland, Ohio (1960).

(16) J. J. Katz and G. T. Seaborg, *The Chemistry of the Actinide Elements*, p. 347. Wiley, New York (0000).

(17) R. L. Weber, *Heat and Temperature Measurement*, p. 264. Prentice Hall, New York (1950).

(18) K. A. Gschneidner, Jr., *Rare Earth Alloys*. Van Nostrand, New York (1961).

WILSON(19) has shown that for this metal lines with $(h-k)/3 = n$ will be sharp and the remaining lines broadened by an amount which is dependent on the average number of stacking faults per N hexagonal layers. More recent work on cobalt indicates that there are several types of faults that can occur and that the *hcp* phase obtained by cooling through the *fcc* phase contains 25–30 per cent of the parent *fcc* phase.(20) The diffraction patterns of americium metal do not show lines that would correspond to the 200 and 331 *fcc* reflexions (the stronger lines which do not superimpose on the *dhcp* reflexions), indicating that very little of the *fcc* phase remains in the *dhcp* phase at room temperature.

For sample No. 22 (purity given in Section—Metal preparation: By reduction of americium trifluoride; diffraction data listed in Table 3) the calculated lattice constants at 20°C are

$$a = 3{\cdot}4681 \pm 0{\cdot}0007\ \text{Å}$$
$$c = 11{\cdot}243 \pm 0{\cdot}003\ \text{Å}$$

and the calculated density is $13{\cdot}671 \pm 0{\cdot}005$ g/cm^3. Each americium has six nearest neighbours at 3·468 Å and six at 3·450 Å, giving a metallic radius for co-ordination number 12 of 1·730 Å. Sample No. 19 (mole per cent impurities

Al, 0·38; Ba, 0·11; Ca, 0·19; and Mg, 0·21)

$$a = 3{\cdot}4680 \pm 0{\cdot}0007\ \text{Å}$$
$$c = 11{\cdot}240 \pm 0{\cdot}002\ \text{Å}$$

also at 20°C.

We take the lattice constants of this phase of americium to be

$$a = 3{\cdot}4681 \pm 0{\cdot}0008\ \text{Å}$$
$$c = 11{\cdot}241 \pm 0{\cdot}003\ \text{Å}$$

at room temperature. The temperature dependence of the lattice constants was investigated for these samples in the range from −120 to +605°C.

The data were fitted to a polynomial of second order by the method of least squares, with the result

$$a_T = 3{\cdot}4672 \pm 0{\cdot}0002 + (2{\cdot}60 \pm 0{\cdot}03) \times 10^{-5}T + (0{\cdot}54 \pm 0{\cdot}02) \times 10^{-8}T^2$$
$$c_T = 11{\cdot}237 \pm 0{\cdot}001 + (6{\cdot}95 \pm 0{\cdot}40)10^{-5}T + (6{\cdot}8 \pm 0{\cdot}5)10^{-8}T^2.$$

At 20°C

$$\alpha_a = (7{\cdot}5 \pm 0{\cdot}2)10^{-6}{}^\circ\text{C}^{-1}$$
$$\alpha_c = (6{\cdot}2 \pm 0{\cdot}4)10^{-6}{}^\circ\text{C}^{-1}$$

Up to 605°C there was no definite indication of any change in the structure.

Diffraction patterns were obtained at 700°C and 850°C by wrapping the film (protected by a nickel foil) directly around the oven, as described earlier. Of twelve lines which could not be attributed to either tantalum or americium monoxide, seven could be indexed as belonging to a *fcc* americium metal phase with a lattice constant about that to be expected from the thermal expansion of this phase (see below). On cooling to room temperature, these lines either disappeared entirely or diminished greatly in intensity. These observations imply that there is a transition to a *fcc* phase between 600 and 700°C, but the evidence is marginal.

Metal prepared by vapour condensation on tantalum or quartz crystallized in a *fcc* phase, with a lattice constant $a = 4{\cdot}894 \pm 0{\cdot}005$ Å at 22°C. A limited study

(19) A. J. C. WILSON, *X-ray Optics*. Methuen, London (1949).

(20) C. R. HONSHA, B. L. AVERBACK and M. COHEN, *Acta Met.* **8**, 81 (1960).

of the thermal expansion of the *fcc* phase (22°–360°C) gave a mean coefficient of thermal expansion of $(9 \pm 3)\ 10^{-6}\,°C^{-1}$.

Two separate determinations of the melting point of americium gave values of 995 and 993°C. We take the melting point to be 994°C, with an uncertainty of ±7°.

On the basis of the present work americium would appear to be a much more "normal" metal than its immediate predecessors in the periodic system. The structure departs only moderately from ideal close packing, and no anomalous behaviour in thermal expansion was found in the temperature range investigated. The melting point is close to that of the early members of the rare earth series (La 920, Ce 797, Pr 935, Nd 1024, Sm 1072°C).

The existence of two similar structures of widely differing density, seen in americium, is an unusual feature in the crystallography of metals although the phenomenon is encountered in metallic cerium.(18)

A disappointing aspect of the present work has been the failure, in over forty preparations, to obtain additional samples of the low density americium observed earlier. The retention of this phase may be quite sensitive to impurities which are difficult to detect at low levels in the small samples of metal which we have prepared. On the other hand, samples with cationic impurities varying from 0·2 to 12·0 mole per cent have shown the phase of higher density.

The development by Markowitz(21) of a sensitive method of activation analysis for oxygen may solve this problem.

We note, finally, that the value of the radius calculated for americium in the more dense form has been interpreted by Zachariasen(22) as indicating that in these structures americium exhibits a metallic valence of four. Magnetic susceptibility data, to be presented in a subsequent paper, do not appear to support this valence assignment.

TABLE 3.—AMERICIUM METAL—DHCP (20°C)—SAMPLE 22

hk. l	$\sin^2\theta_{calc}$	$\sin^2\theta_{obs}$	I (calc)	I (obs)
10·0	0·0659	0·0663	11	*t*
10·1	0·0706	0·0707	62	*s*
00·4	0·0753	0·0754	50	*vs*
10·2	0·0847	0·0847	144	*s*
10·3	0·1082	0·1082	35	*w*
10·4	0·1411	—	8	—
10·5	0·1835	0·1836	16	*vw*
11·0	0·1976	0·1973	37	*m*
10·6	0·2352	0·2352	33	*s*
20·0	0·2635	0·2593	1	*w**
20·1	0·2682	—	9	—
11·4	0·2729	0·2730	45	*s*
20·2	0·2823	0·2821	24	*m*
10·7	0·2964	0·2957	7	*t*
00·8	0·3011	0·3006	6	*m*
20·3	0·3058	—	7	—

* Lines that superimpose on AmO lines (*fcc* $a = 5{\cdot}05$ Å)

---

(21) S. Markowitz and J. Mahony, Report UCRL-9908 (1961).

(22) W. H. Zachariasen, *The Metal Plutonium* (Edited by A. S. Coffinberry and W. N. Miner), Chap. 10. Chicago University Press, Chicago (1961).

TABLE 3 (*continued*).

hk.l	$\sin^2\theta_{calc}$	$\sin^2\theta_{obs}$	I (calc)	I (obs)
20·4	0·3387	—	2	—
10·8	0·3669	—	2	—
20·5	0·3811	0·3792	5	*vw*
20·6	0·4328	0·4330	12	*w*
10·9	0·4469	0·4469	4	*m*
21·0	0·4611	—	1	—
21·1	0·4658	0·4700	7	*vw**
21·2	0·4799	0·4805	21	*w*
20·7	0·4940	—	3	—
11·8	0·4987	0·4983	18	*s*
21·3	0·5034	—	7	—
10·10	0·5363	—	10	—
		0·5361		*w*
21·4	0·5364	—	—	—
20·8	0·5645	0·5651	1	*vw*
21·5	0·5787	0·5787	6	*t*
30·0	0·5028	0·5934	8	*vw*
21·6	0·6304	0·6321	18	*m*
10·11	0·6350	—	3	—
20·9	0·6445	0·6454	3	*t*
30·4	0·6681	0·6676	16	*m*
00·12	0·6774	0·6763	3	*vw*
21·7	0·6916	0·6901	6	*t*
20·10	0·7339	0·7338	9	*vw*
10·12	0·7432	—	1	—
21·8	0·7621	—	2	—
22·0	0·7904	0·7898	9	*vw*
20·11	0·8327	0·8335	4	*t**
21·9	0·8421	0·8420	8	*vw**
31·0α_1	0·8549	0·8553	0·7	*t*
31·0α_2	0·8591	—	0·3	—
10·13α_1	0·8594	0·8598	3	*w*
31·1α_1	0·8596		5	
10·13α_2	0·8637	0·8644	1	*s*
31·1α_2	0·8639		3	
22·4α_1	0·8643		15	
22·4α_2	0·8686	0·8684	8	*t*
11·12α_1	0·8735	0·8730	15	*m*
31·2α_1	0·8737		17	
11·12α_2	0·8779	0·8779	8	*t*
31·2α_2	0·8780		9	
30·8α_1	0·8924	0·8925	17	*m*
30·8α_2	0·8968	0·8971	9	*w*
31·3α_1	0·8972		7	
31·3α_2	0·9016	0·9017	3	*t*
21·10α_1	0·9300	0·9296	25	*m*
31·4α_1	0·9300		3	

* Lines that superimpose on AmO lines (*fcc a* = 5·05 Å)

hk. l	$\sin^2\theta_{calc}$	$\sin^2\theta_{obs}$	*s* (calc)	*s* (obs)
21·10α_2	0·9346	0·9348	13	*vw*
31·4α_2	0·9347		1	
20·12α_1	0·9393	0·9405	1	*t*
20·12α_2	0·9440	0·9448	1	*t*
31·5α_1	0·9723	0·9720	13	*vw*
31·5α_2	0·9771	—	8	—
10·14α_1	0·9862	0·9852	29	*vw*
10·14α_2	0·9911	—	18	—

Acknowledgements—We wish to thank Mr. G. V. Shalimoff for the countless spectrographic analyses which he performed in the course of this investigation and Mr. T. Festin for purification of some of the americium stock solutions. Miss L. Goda assisted in many phases of the work and we wish to acknowledge her contribution. Thanks are due to Mr. B. Watkins and Mr. H. Hagopian for their expert engineering advice and machine work, and to the glass blowing group under Mr. H. Powell. Special thanks are given to the entire Health Chemistry group for providing and maintaining all the radiological protective equipment and to Mrs. G. Bolz, in particular, who gave tireless attention to radiological monitoring.

J. Inorg. Nucl. Chem., 1962, Vol. 24, pp. 1039 to 1045. Pergamon Press Ltd. Printed in England

THE CRYSTAL STRUCTURE OF POTASSIUM CHLORIDE TRICHLOROSTANNITE HYDRATE, KCl, $KSnCl_3$, H_2O

B. KAMENAR
Department of Structural and Inorganic Chemistry, Institute Rudjer Bošković, Zagreb
and
D. GRDENIĆ
Laboratory of General and Inorganic Chemistry, Faculty of Science, University, Zagreb, Yugoslavia

(*Received* 12 *December* 1961; *in revised form* 23 *February* 1962)

Abstract—It has been shown by methods of X-ray crystal structure analysis that the salt formulated previously as K_2SnCl_4, H_2O is actually a hydrated double salt of potassium chloride and potassium trichlorostannite, KCl, $KSnCl_3$, H_2O. The trichlorostannite ion is pyramidal with two Sn-Cl bonds of length 2·54 Å and one of 2·63 Å. The corresponding bond angles are 87·7° and 90·8°. The potassium ion is seven—co-ordinated with two isolated chlorine ions at 3·15 Å and 3·24 Å, four chlorine atoms from two chlorostannite ions at an average distance of 3·25 Å and one water molecule at 2·81 Å.

WE have shown recently ⁽¹⁾ by X-ray structure analysis that stannous chloride dihydrate $SnCl_2$, $2H_2O$ is actually a dichloroaquotin (II) hydrate $Sn(OH_2)\,Cl_2$, H_2O with a pyramidal aquo-complex $Sn(OH_2)\,Cl_2$. Herewith proof is given that the unshared electron pair at the tin atom is stereochemically active according to SIDGWICK and POWELL's rule ⁽²,³⁾ which requires a tetrahedral arrangement of three bonding and one non-bonding pair of electrons.

Following our belief that this rule should be valid for all analogous stannous compounds, we decided to redetermine the crystal structure of the salt known as potassium tetrachlorostannite hydrate K_2SnCl_4, H_2O, since in a previous description of its structure⁽⁴⁾, the presence of an unshared electron pair at the tin atom was not invoked. The chlorostannite ion was described as an infinite chain formed by $SnCl_6$-octahedra sharing two opposite edges. Because the structure was derived from incomplete data, we expected that a more detailed study would reveal an appropriate distortion of the $SnCl_6$-octahedron as a consequence of the presence of an unshared electron pair on the tin atom. Actually, the result of our work confirmed our standpoint in favour of SIDGWICK and POWELL's rule, but the structure came out to be strikingly different from the structure described previously. The compound quoted as K_2SnCl_4,H_2O is in reality a hydrated double salt of potassium chloride with potassium trichlorostannite KCl,$KSnCl_3$,H_2O containing a symmetrical pyramidal $SnCl_3$- ion.⁽⁵⁾

⁽¹⁾ B. KAMENAR and D. GRDENIĆ, *J. Chem. Soc.* 3954 (1961).

⁽²⁾ N. V. SIDGWICK and H. M. POWELL, *Proc. Roy. Soc.* A **176**, 153 (1940).

⁽³⁾ R. J. GILLESPIE and R. S. NYHOLM, *Quart. Rev.* **11**, 339 (1957).

⁽⁴⁾ H. BRASSEUR and A. DE RASSENFOSSE, *Z. Krist.* **101**, 389 (1939).

⁽⁵⁾ D. GRDENIĆ and B. KAMENAR, *Proc. Chem. Soc.* 304 (1961).

Crystallographic and X-ray data

The crystals of potassium tetrachlorostannite hydrate were obtained by cooling a warm saturated aqueous solution of equimolar quantities of stannous and potassium chloride. Orthorhombic prisms, elongated in the *c*-axis direction, were always white and opaque in accordance with previous observations. Our crystallographic data are in good agreement with the data obtained by Brasseur and Rassenfosse. The dimensions of the unit cell, which contains four formula units, are as follows: $a = 8{\cdot}24 \pm 0{\cdot}02$ Å, $b = 12{\cdot}05 \pm 0{\cdot}03$ Å, $c = 9{\cdot}14 \pm 0{\cdot}02$ Å, and were determined from oscillation and Weissenberg photographs. The space group *Pbnm* (D_{2h}^{16}, No. 62), as determined by previous authors, has been confirmed, since the only systematic absences of the reflections were: *Okl* for *k* odd and *hol* for $h+l$ odd.

Intensity measurements

The specimens, cylindrically ground along the *a*- and the *c*-axis, with diameters of 0·58 mm and 0·23 mm, respectively, were used for recording *hkO* and *Okl* reflections on multiple film by means of a "Nonius"-integrating Weissenberg camera. Nickel-filtered Cu*K* radiation was used. The relative intensities of the reflexions were determined from the optical densities which were measured in the centre of each spot by means of a microdensitometer and corrected by means of the characteristic curve of the film. The number of *hkO* and *Okl* reflexions observed was 110 and 68 (out of 129 and 75 possible reflexions), respectively. The absorption correction ($\mu = 399{\cdot}33$ cm^{-1}) was carried out with the help of Tables.⁽⁶⁾ The corrections for polarization and Lorentz factors were made in the usual way. The ratio of the smallest absorption factor to the largest one was 1:15 and 1:34 for *hkO* and *Okl* reflexions, respectively.

Structure determination

The Fourier projections of electron density distribution on (001) and (100) were computed starting from the atomic co-ordinates given by previous authors. The (001) projection was roughly consistent with their description of the structure, while the (100) projection was in a complete disagreement. By using a trial and error procedure we found out that the tin and potassium atoms had been located incorrectly. Four tin atoms should be located in the positions (c) of *International Tables*⁽⁷⁾ but not in the positions (a), while eight potassium ions should be located in general positions (d) but not in special positions (c). The subsequent refinement by repeated computation of both projections on the basis of these new atomic positions has resulted in a complete solution of the structure. The final atomic co-ordinates, evaluated from both (001) and (100) projections by using Booth's method,⁽⁸⁾ are given in Table 1.

Table 1.—Final atomic co-ordinates

	x	*y*	*z*
Sn	0·000	−0·012	$\frac{1}{4}$
K	0·370	0·185	−0·018
Cl (1)	0·112	0·192	$\frac{1}{4}$
Cl (2)	0·207	−0·056	0·448
Cl (3)	0·099	0·266	$\frac{3}{4}$
OH_2 (oxygen)	0·441	0·040	$\frac{3}{4}$

The comparison of observed F_o and calculated F_c structure amplitudes is given in Table 2. For evaluating F_c the corresponding atomic scattering factors from Tables⁽⁹⁾ were used by applying an average temperature factor $\exp(-B\sin^2\Theta/\lambda^2)$ with $B = 2{\cdot}3$ Å^2 and

---

⁽⁶⁾ *International Tables for X-ray Crystallography*, Vol. 2, p. 295. Kynoch Press, Birmingham (1952).

⁽⁷⁾ *International Tables for X-ray Crystallography*, Vol. 1, p. 151. Kynoch Press, Birmingham (1952).

⁽⁸⁾ A. D. Booth, *Fourier Technique in X-ray Organic Structure Analysis*, p. 62. University Press, Cambridge (1948).

⁽⁹⁾ R. Sagel, *Tabellen zur Röntgenstrukturanalyse*, p. 106. Springer Verlag, Berlin (1958).

$B = 2{\cdot}6$ Å^2 for the *hkO* and *Okl* reflexions, respectively. These values of *B*, as well as the values of the scale factor, were obtained from the slope of the straight line defined by points of the plot of $\ln F_o/F_c$ against $\sin^2 \Theta/\lambda^2$. A few near reflexions were corrected for secondary extinction by using PINOCH, TAYLOR and LIPSON's formula.(10) The reliability indices are $R(hkO) = 0{\cdot}12$ and $R(Okl) = 0{\cdot}11$. The accuracy of the atomic co-ordinates is therefore of the same order as that attained for the structure of stannous chloride dihydrate.(1) Consequently, the values of the interatomic distances and bond angles given in Fig. 2 have the standard error of ±0·03 Å and ±1°, respectively.

TABLE 2.—OBSERVED AND CALCULATED STRUCTURE AMPLITUDES

hkO	F_o	F_c	*hkO*	F_o	F_c	*hkO*	F_o	F_c
200	107	120	130	216	206	360	87	−79
400	30	18	230	82	67	460	49	33
600	61	68	330	55	48	560	32	34
800	75	91	430	0	−13	660	74	78
10.0.0	74	68	530	99	109	760	23	23
020	95	106	630	38	41	860	68	78
040	220	220	730	79	85	960	31	−32
060	140	138	830	44	−45	170	103	105
080	42	−43	930	60	62	270	87	89
0.10.0	59	48	10.3.0	0	2	370	108	106
0.12.0	41	23	140	182	176	470	30	−19
0.14.0	0	−6	240	161	148	570	42	25
110	135	167	340	23	10	670	0	−2
210	35	37	440	94	94	770	73	73
310	92	92	540	53	−56	870	0	−9
410	63	−60	640	63	58	970	25	24
510	150	177	740	29	−24	180	0	0
610	0	2	840	52	51	280	122	123
710	38	33	940	0	9	380	39	−34
810	28	25	10.4.0	42	46	480	102	102
910	68	68	150	86	77	580	0	−1
10.1.0	10	17	250	20	−13	680	50	41
120	26	−21	350	177	161	780	0	9
220	102	98	450	61	−47	880	32	17
320	102	−108	550	90	95	980	0	−2
420	243	259	650	68	73	190	76	63
520	43	50	750	47	46	290	38	−31
620	97	107	850	20	−16	390	93	82
720	34	33	950	44	34	490	0	9
820	0	4	10.5.0	0	0	590	29	19
920	27	−33	160	0	6	690	20	22
10.2.0	34	39	260	127	128	790	73	73
890	12	−4	3.11.0	82	78	1.13.0	34	27
1.10.0	28	28	4.11.0	5	20	2.13.0	0	−1
2.10.0	88	80	5.11.0	21	8	3.13.0	30	22
3.10.0	51	50	6.11.0	21	−17	4.13.0	17	16
4.10.0	0	2	7.11.0	23	17	5.13.0	36	26
5.10.0	31	−29	1.12.0	68	−71	1.14.0	0	4
6.10.0	55	40	2.12.0	54	44	2.14.0	21	14
7.10.0	38	−29	3.12.0	32	−27	3.14.0	39	43
8.10.0	43	55	4.12.0	27	19	4.14.0	44	43
1.11.0	53	41	5.12.0	14	19	1.15.0	38	32
2.11.0	0	−6	6.12.0	26	22	2.15.0	17	−24

---

(10) P. R. PINOCH, C. A. TAYLOR and H. LIPSON, *Acta Cryst.* **9**, 173 (1956).

Table 2 (*continued*).

Okl	F_o	F_c	*Okl*	F_o	F_c	*Okl*	F_o	F_c
002	120	−104	022	123	−118	0.10.4	57	57
004	323	338	042	151	−188	0.12.4	34	26
006	137	−138	062	65	−69	0.14.4	0	−5
008	108	106	082	157	−160	025	59	66
0.0.10	82	−88	0.10.2	64	−57	045	80	98
020	132	124	0.12.2	39	−34	065	58	73
040	238	219	0.12.3	43	−50	087	32	−38
060	151	135	0.14.3	49	−49	0.10.7	40	−48
080	38	−41	024	43	44	0.12.7	19	−24
0.10.0	53	45	044	133	153	028	0	0
0.12.0	34	22	064	106	119	048	67	73
0.14.0	0	5	084	0	3	068	67	74
021	0	−26	085	62	79	088	38	36
041	127	143	0.10.5	14	10	0.10.8	58	51
061	44	48	0.12.5	19	26	029	21	22
081	84	96	0.14.5	0	3	049	15	18
0.10.1	40	39	026	112	−108	069	21	25
0.12.1	30	39	046	116	−119	089	27	37
0.14.1	26	24	066	30	−29	0.10.9	0	5
0.14.2	24	−25	086	56	−60	0.2.10	49	−52
023	78	77	0.10.6	22	−14	0.4.10	49	−57
043	50	−74	0.12.6	19	−13	0.6.10	15	−13
063	38	37	027	47	49	0.8.10	15	−14
083	55	−66	047	47	−58	0.2.11	8	11
0.10.3	61	−65	067	30	30	0.4.11	45	−51

DISCUSSION OF THE STRUCTURE

By juxtaposition of both (001) and (100) projections (Fig. 1) one immediately realizes why the (001) projection could be incorrectly interpreted if one lacks the additional data. In this projection overlap tin atoms at $z = \frac{1}{4}, \frac{3}{4}$, as well as Cl(2) atoms at $z = 0{\cdot}448$ and $z = \frac{1}{2}-0{\cdot}448$, by giving double peaks which, together with two Cl(1) peaks, form a rhomb, leading thus to an erroneous conclusion that the peaks arose by projecting $SnCl_6$-octahedra on the (001) plane. Actually, instead of $SnCl_6$-octahedra, there are $SnCl_3$-pyramids which are lined in rows along [001] by a screw axis symmetry operation. Potassium and chlorine ions, as well as water molecules, are located in the channels between these $SnCl_3$-rows. Each $SnCl_3$-ion lies across the mirror plane at $z = \frac{1}{4}, \frac{3}{4}$, so that there are two equal Sn-Cl bonds of length 2·54 Å and one Sn-Cl bond in the mirror plane of length 2·63 Å. Both values are very close to 2·59 Å, the Sn-Cl bond length in the dichloroaquotin-complex.⁽¹⁾ The bond angles Cl-Sn-Cl are 87·7° and 90·8°, which are considerably less than the tetrahedral value and which proves a strong lone-pair–bond-pair repulsion. Such a decrease in bond angles at the tin atom was observed previously for stannous chloride,⁽¹¹⁾ as well as for the $Sn(OH_2)\,Cl_2$-complex in hydrated stannous chloride. The other interatomic

---

(11) M. W. Lister and L. E. Sutton, *Trans. Faraday Soc.* 37, 406 (1941).

and interionic distances tally well with the values expected on the basis of known atomic and ionic radii. The potassium ion is surrounded by two chlorine ions at 3·15 and 3·24 Å, by four chlorine atoms of two different chlorostannite anions at an average distance of 3·25 Å, and by one water molecule at 2·81 Å, exhibiting thus the co-ordination number seven. The co-ordination polyhedron is a distorted octahedron

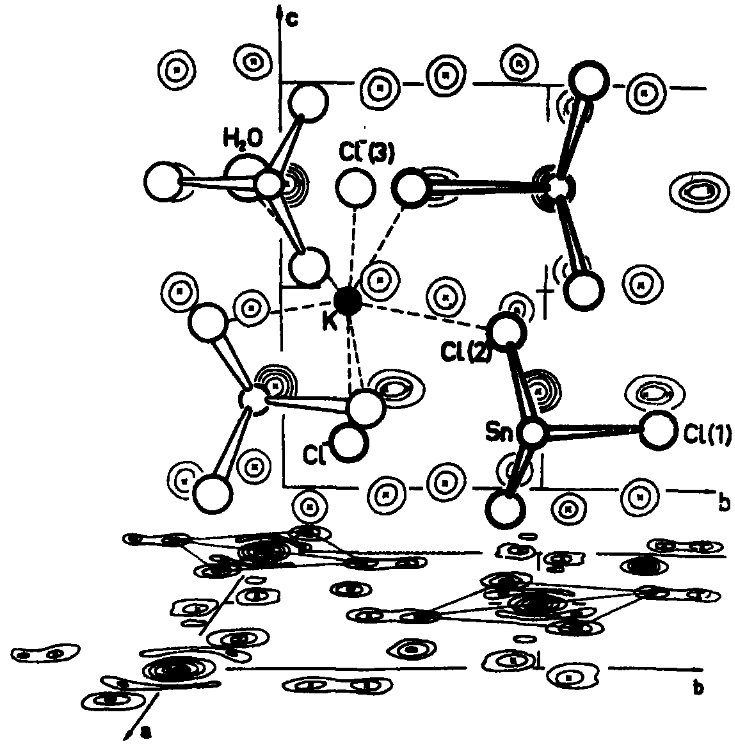

Fig. 1.—The structure of KCl, KSnCl$_3$, H$_2$O as deduced from both (100) and (001) Fourier projections of the electron density distribution. Two pyramidal SnCl$_3$-ions overlap in the (001) projection giving peaks which, without the data of the (100) projection, lead to an erroneous interpretation of the structure in term of SnCl$_6$-octahedra (see Fig. 3).

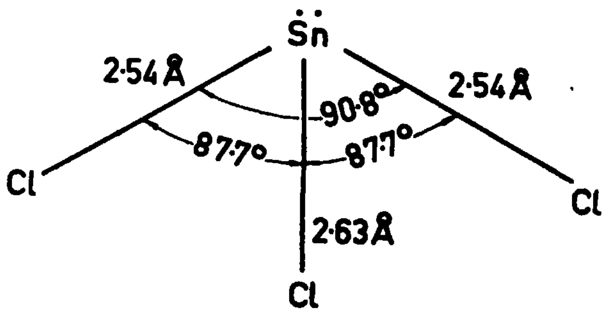

Fig. 2.—(a) Form and dimensions of chlorostannite ion SnCl$_3^-$ as established by crystal structure analysis of KCl, KSnCl$_3$, H$_2$O.

with one additional corner (oxygen atom) above the centre of a face. These $KCl_6(OH_2)$-polyhedra form a row along the *c*-axis direction by sharing two opposite Cl....Cl^- edges. The geometry of the $SnCl_3$-ion as well as the co-ordination around the potassium ion is given diagrammatically in Fig. 2. A view of the structure down a direction which forms an angle of about 6° to the *c*-axis is shown in Fig. 3.

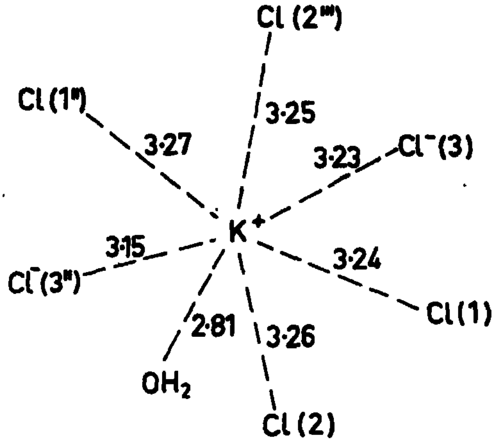

Fig. 2—(b) Co-ordination of potassium ion in KCl, $KSnCl_3$, H_2O (with distances in Å units). The numbering of atoms as in Table 1 (double prime denotes screw axis, triple prime glide-plane symmetry relation to the atom defined by the co-ordinates in Table 1).

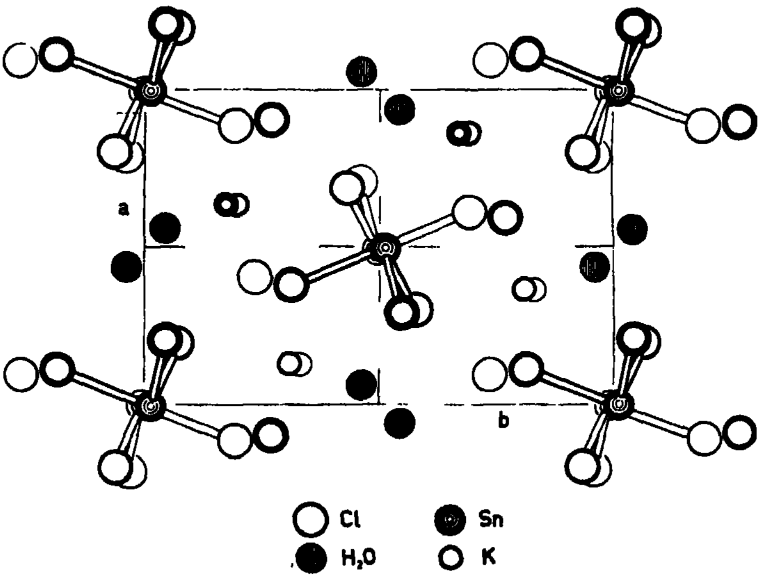

Fig. 3.—The structure of KCl, $KSnCl_3$, H_2O viewed at an angle of about 6° to the *c*-axis so as to avoid overlapping of chlorine and potassium atoms.

In conclusion we want to stress a point of crystallographic interest. Potassium chlorostannite, if formulated K_2SnCl_4,H_2O as previously, and potassium chloromercurate[12] K_2HgCl_4,H_2O have analogous formulae. Moreover, they have very near unit cell dimensions, belong to the same orthorhombic class, give X-ray photographs with the similar distribution of the reflexion intensities, but have different space groups, viz. D_{2h}^{16} and D_{2h}^{9}, respectively. The similarities misled the previous authors[4] to assume the same structural principle, i.e., octahedral co-ordination of the tin. Actually, it follows that the difference between the space groups alone is sufficient evidence for abandoning the supposed analogy.

---

(12) H. C. MACGILLAVRY, J. H. DE WILDE and J. M. BIJVOET, *Z. Krist.* **100**, 212 (1938).

J. Inorg. Nucl. Chem., 1962, Vol. 24, pp. 1047 to 1056. Pergamon Press Ltd. Printed in England

AN EXAMINATION OF THE INFRA-RED SPECTRA OF BORATE ANIONS

P. B. HART* and S. E. F. SMALLWOOD

The General Electric Company Limited, Central Research Laboratories,
Hirst Research Centre, Wembley, England

(*Received* 26 *January* 1962)

Abstract—A range of metal borate compounds has been studied, including a number with unknown structures. The orthoborate ion, $BO_3{}^{3-}$ has been identified in a number of compounds and some force constants have been calculated. The pyroborate ion, $B_2O_5{}^{4-}$ has been found in further compounds, but no assignment of frequencies has been made. The spectra of numbers of metaborates and other compounds have also been obtained, and in some cases structural conclusions have been drawn by comparison with known compounds. It is concluded that in complex compounds inferences about structures and co-ordination must be made with reserve, but that the infra-red spectrum of an inorganic borate is a useful means of identification.

THE study of infra-red spectra for the analysis of organic compounds and the determination of their structures has been well established for a considerable period of time. Similarly, the study of inorganic materials in the gaseous and liquid states has a long history. However, work on the spectra of inorganic solids was severely limited by the need for single crystals specimens, since no satisfactory way of obtaining the spectra of powdered materials was known. Most of the early studies with powdered materials employed the mull technique, in which the powdered sample is dispersed in a suitable liquid such as paraffin. With this method, however, regions of interest can be obscured by the absorption bands of the mulling liquid and, furthermore, consistent results are not readily obtained. Nevertheless, general surveys useful for analytical purposes have been published by MILLER and WILKINS,(1) and by HUNT *et al*(2). In 1952, with the introduction of the potassium bromide pressed disk method,(3, 4) it became possible to examine a wide range of inorganic solids, and in the last decade materials such as ferrite,(5) ferroelectrics,(6) crystalline and vitreous silicates and borates(7, 8, 9) and series of carbonates and orthoborates(10, 11, 12) have been studied.

---

*Present address: Scientific Laboratories, Philco Corporation, Blue Bell, Pa, U.S.A.

(1) F. A. MILLER and C. H. WILKINS, *Analyt. Chem.* **24**, 1253 (1952).
(2) J. M. HUNT, M. P. WISHERD and L. C. BONHAM, *Analyt. Chem.* **22**, 1478 (1950).
(3) M. STIMSON and M. J. O'DONNEL, *J. Amer. Chem. Soc.* **74**, 1805 (1952).
(4) U. SCHIEDT and H. REINWEIN, *Z. Naturf.* 76, 270 (1952).
(5) R. D. WALDRON, *Phys. Rev.* **99**, 1727 (1955).
(6) J. T. LAST, *Phys. Rev.* **105**, 1740 (1957).
(7) H. LEHMANN and H. DUTZ, *Silicates Industriels* **25**, 559 (1960).
(8) J. L. PARSON and M. E. MILBERG, *J. Amer. Cer. Soc.* **43**, 326 (1960).
(9) J. KROGH-MOË, *Ark. Kemi.* **12**, 475 (1958).
(10) C. K. HUANG and F. F. KERR, *Amer. Min.* **45**, 311 (1960).
(11) B. M. GATEHOUSE, S. E. LIVINGSTON and R. S. NYHOLM, *J. Chem. Soc.* 3137 (1958).
(12) C. E. WEIR and E. R. LIPPINCOTT, *J. Res. Natl. Bur. Stds.* 65 A, 173 (1961)

The systematic study of the spectra of inorganic anions in a number of different structural environments could be both of theoretical and of analytical value. It was also expected that an investigation of the infra-red spectra of a range of metal borates might resolve certain problems of structure arising from the synthesis of some hitherto unknown calcium borates. Examinations of the spectra of a number of anhydrous and hydrated metal borates were therefore undertaken and are described in the present paper.

Nomenclature

Throughout the literature a variety of systems of nomenclature is used to describe metal borates. That recommended by the International Union of Chemistry has the advantage of clarity, and it will be used to describe the compounds discussed in this paper. The molar ratios of the component oxides of a compound are explicitly stated, as illustrated by the following examples.

Formula	*Name*
$3CaO \cdot B_2O_3$	calcium 3:1 borate
$Y_2O_3 \cdot B_2O_3$	yttrium 1:1 borate
$K_2O \cdot 5B_2O_3 \cdot 8H_2O$	potassium 1:5 borate octahydrate

However, this system gives no structural information, and in the examples given above it is not immediately clear that the calcium and yttrium compounds both contain the BO_3^{3-} ion, or that part of the water in the potassium compound is structurally bound as hydroxyl groups. For this reason the subdivision of the following discussion is based on the nature of the ion present and not on the oxide ratios in the compound. In borate ions the important factors are the boron–oxygen ratio, the charge, and the hydroxyl groups present. When these factors are known, structural possibilities can be obtained from consideration of bond formation and stereochemistry. The three main types of ion examined in this paper, BO_3^{3-}, $B_2O_5^{4-}$ and $(BO_2)_n^{n-}$, have the names: orthoborate, pyroborate and metaborate.

EXPERIMENTAL

Apparatus

The infra-red spectra shown below were taken on a Hilger H800 recording spectrophotometer using a rocksalt prism covering the spectral range 5000–650 cm^{-1} (2·0–15·4 μ). The control settings were standardised for all the compounds investigated, a scan speed of 25 min being used. The wave number calibration was checked by means of the absorption spectrum of a polystyrene film, and it was found that this calibration never varied by more than 20 wave numbers (produced by a 10°C change in ambient temperature).

In all cases, the compounds investigated were examined as a dispersion in potassium bromide, using the pressed disk technique. One per cent mixtures were generally employed, although in certain compounds with very intense absorption bands, one half per cent mixtures were used (e.g. in the lithium borates). It was found that even the most hygroscopic materials examined, namely the sodium and potassium 1:1 borates, could be made into sample disks which were quite stable for the time needed to obtain the spectra.

Certain of the compounds were re-examined at liquid oxygen temperature to determine whether the absorption peaks became narrower, as is known to occur with very many compounds. A special cell fitted with rock-salt end-windows was used to mount and cool the sample disks. The spectra obtained at liquid oxygen temperature showed little sharpening of the absorption bands when compared with corresponding spectra taken at room temperature. It was concluded that for the compounds investigated, there was no advantage in obtaining the spectra in this way.

Materials

Details of the preparation or source of the various compounds examined are given below. The three new anhydrous calcium borates were prepared by hydrothermal treatment of calcium hydroxide–boric acid mixtures.(13) The other anhydrous calcium borates,(14) and those of magnesium,(15) strontium,(16) barium,(17) cadmium,(18, 19) zinc,(20) and yttrium(21) were prepared from orthoboric acid and the appropriate metal oxide by high temperature solid state reactions. The anhydrous 1:1 borates of sodium and potassium(22) were prepared by dehydration of the hydrated salts, and these in turn were obtained by evaporation of their solutions. The three lithium borates examined were prepared by the methods described by

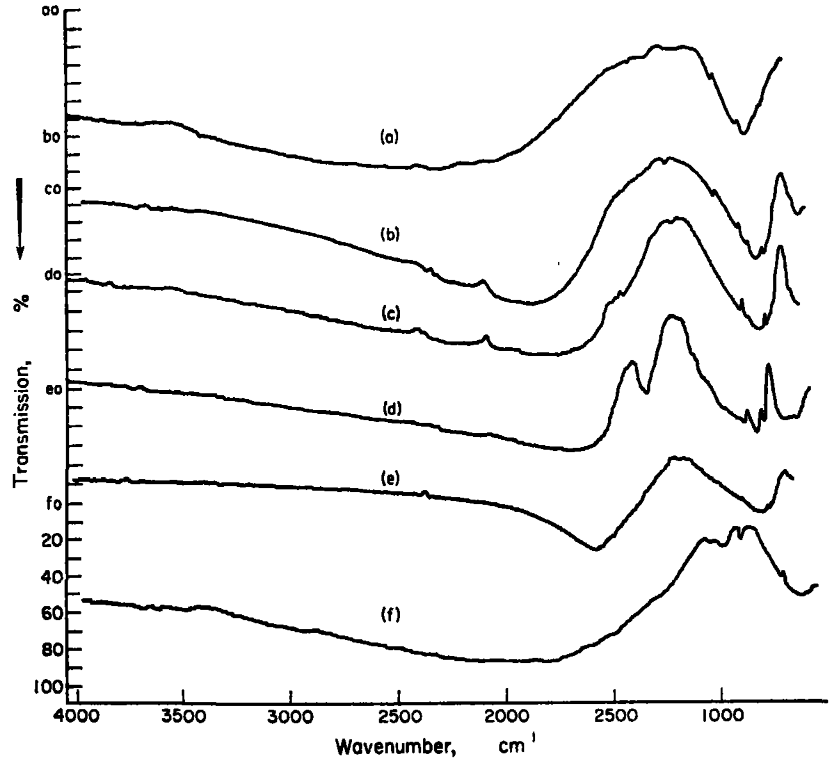

FIG. 1.—Infra-red absorption spectrum of:
(a) magnesium 3:1 borate $3MgO{\cdot}B_2O_3$
(b) calcium 3:1 borate $3CaO{\cdot}B_2O_3$
(c) strontium 3:1 borate $3SrO{\cdot}B_2O_3$
(d) barium 3:1 borate $3BaO{\cdot}B_2O_3$
(e) cadmium 3:1 borate $3CdO{\cdot}B_2O_3$
(f) yttrium 1:1 borate $Y_2O_3{\cdot}B_2O_3$

(13) C. S. BROWN and P. B. HART, *J. Inorg. Nucl. Chem.* **24**, 1057 (1962).

(14) E. T. CARLSON, *J. Res. Natl. Bur. Stds.* **9**, 825 (1932).

(15) H. M. DAVIS and M. A. KNIGHT, *J. Amer. Cer. Soc.* **28**, 97 (1945).

(16) P. B. HART. In preparation.

(17) E. M. LEVIN and H. F. MCMURDIE, *J. Res. Natl. Bur. Stds.* **42**, 131 (1949).

(18) E. C. SUBBARAO and F. A. HUMMEL, *J. Amer. Cer. Soc.* **103**, 29 (1956).

(19) P. B. HART and E. G. STEWARD, *J. Inorg. Nucl. Chem.* **24**, 633 (1962).

(20) D. E. HARRISON and F. A. HUMMEL, *J. Electrochem. Soc.* **103**, 491 (1956).

(21) E. M. LEVIN and R. S. ROTH, Unpublished work referred to in Reference 12.

(22) P. H. KEMP, *The Chemistry of Borates, Part I.* Borax Consolidated, London (1956).

LEHMANN and TIESS.(23) Potassium 1:5 borate octahydrate, $K_2O{\cdot}5B_2O_3{\cdot}8H_2O$, was crystallized from its aqueous solution.(22) Where possible the identity and purity of the compounds were checked by X-ray examination.

DISCUSSION

1. *Compounds of the type* $M_x(BO_3)_y$*–orthoborates*

Six such compounds have been examined; those of magnesium, calcium, strontium, barium, cadmium and yttrium. X-ray determinations of the structures of the magnesium and the yttrium compounds by BERGER(24) and by LEVIN and ROTH(21) have shown that the orthoborate anion BO_3^{3-}, is present in both cases, and it is reasonably certain that this anion also occurs in the other orthoborates. Thus an infra-red study of this range of compounds would be expected to illustrate the effect of different crystal environments on the spectrum of a particular group.

In isolation, the orthoborate anion has a planar and symmetrical structure, arising from the sp^2 hybridization of the boron bonding orbitals. It thus has the symmetry D_3h and three of the four fundamental vibrations would be expected to be infra-red active: ν_2, the out-of-plane bending, ν_3 the doubly-degenerate anti-symmetrical stretching, and ν_4, the doubly-degenerate planar bending.(25) The fourth fundamental vibration, ν_1, the symmetrical stretching, would normally be Raman-active. When such an anion is placed in a crystal structure the symmetry class may be lowered, and degeneracies can be removed and symmetrical vibrations can become infra-red active.

The infra-red spectra of the six orthoborates studied are shown in Fig. 1. Those of calcium, strontium, magnesium and cadmium are very similar to one another, and it has been possible to assign the absorption bands observed to particular vibrations, by comparison with the work of WEIR and LIPPINCOTT(12) on the spectra of carbonates, nitrates and orthoborates. This is done in Table 1, and some force constants for the four compounds are calculated from the observed frequencies. In the spectra of these four compounds a slight splitting of the ν_3 band at about 1250 cm^{-1} is noticeable. In the barium compound this becomes much more marked, and two clearly resolved peaks are observed. The spectrum of the yttrium compound, which has the rather unusual vaterite type structure,(12) is quite different from the other five, and agrees well with that reported by WEIR and LIPPINCOTT, who obtained their spectra by a

TABLE 1.—DATA FOR THE ORTHOBORATE ANION

Compound	Frequency (cm^{-1})				Force constant (dyne cm^{-1} × 10^5)		
	ν_1	ν_2	ν_3	ν_4	K_1	$\frac{K\delta}{l^2}$	$\frac{K\Delta}{l^2}$
$3BaO{\cdot}B_2O_3$	—	885	1215	775			1·35
$3CaO{\cdot}B_2O_3$	1020	905	1240	710	9·76	0·40	1·41
$3CdO{\cdot}B_2O_3$	1010	890	1190	690	9·57	0·37	1·36
$3MgO{\cdot}B_2O_3$	1035	920	1250	725	10·0	0·44	1·46
$3SrO{\cdot}B_2O_3$	—	905	1190	715			1·41

---

(23) H. LEHMANN and D. TIESS, *Chem. Tech.* **11**, 260 (1959).

(24) S. V. BERGER, *Acta Chem. Scand.* **3**, 660 (1949).

(25) G. HERZBERG, *Molecular Spectra and Molecular Structure*, (8th Ed.) Vol 2. Van Nostrand, New York (1959).

rather different method using a diamond pressure cell. It was not possible to assign frequencies for this compound with any certainty.

2. *Compounds of the type* $M_x(B_2O_5)_y$*-pyroborates*

Six of these compounds were examined, those of magnesium, calcium, strontium, barium and cadmium, and a polymorph of the calcium compound, prepared by hydrothermal means. The spectra are shown in Fig. 2. The structure of the magnesium compound has been studied by X-ray methods and the presence of the pyroborate anion, $B_2O_5^{4-}$, has been demonstrated by TAKEUCHI(26). As in the case of the orthoborates, an alternative anion structure with the same charge and boron–oxygen ratio is unlikely.

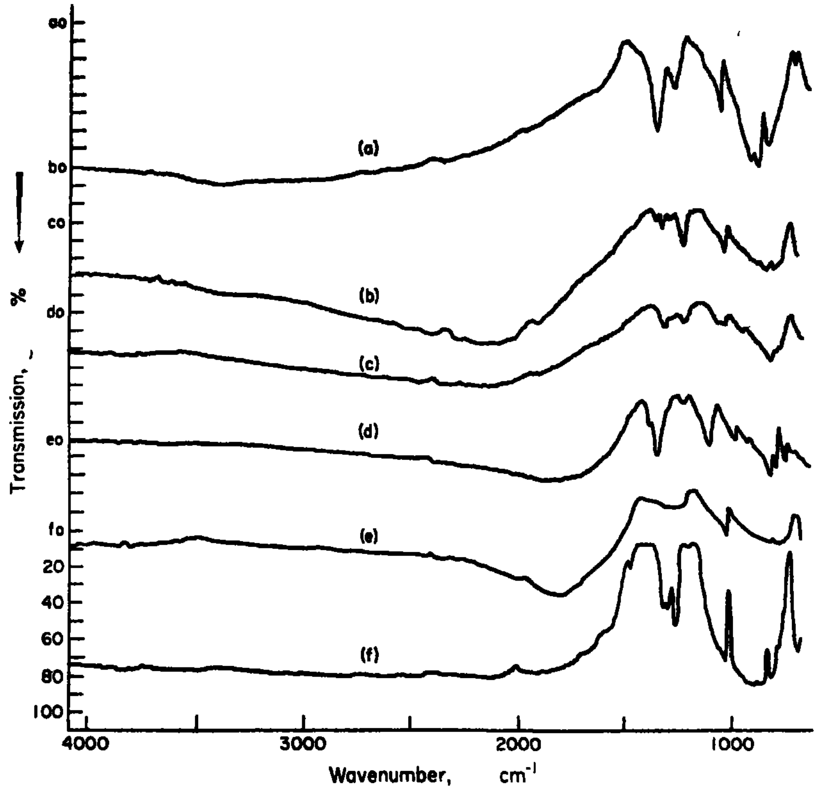

FIG. 2.—Infra-red absorption spectrum of:
(a) magnesium 2:1 borate $2MgO \cdot B_2O_3$
(b) calcium 2:1 borate $2CaO \cdot B_2O_3$
(c) strontium 2:1 borate $2SrO \cdot B_2O_3$
(d) barium 2:1 borate $2BaO \cdot B_2O_3$
(e) cadmium 2:1 borate $2CdO \cdot B_2O_3$
(f) calcium 2:1 borate (hydrothermal preparation) $2CaO \cdot B_2O_3$

The pyroborate ion, containing seven atoms, could have fifteen fundamental frequencies. In an arrangement with the highest degree of symmetry the ion can have two two-fold axes of symmetry, which would reduce the number of non-degenerate vibrations, but in general a fairly complex spectrum would be likely. The spectra

---

(26) Y. TAKEUCHI, *Acta. Cryst.* 5, 574 (1952).

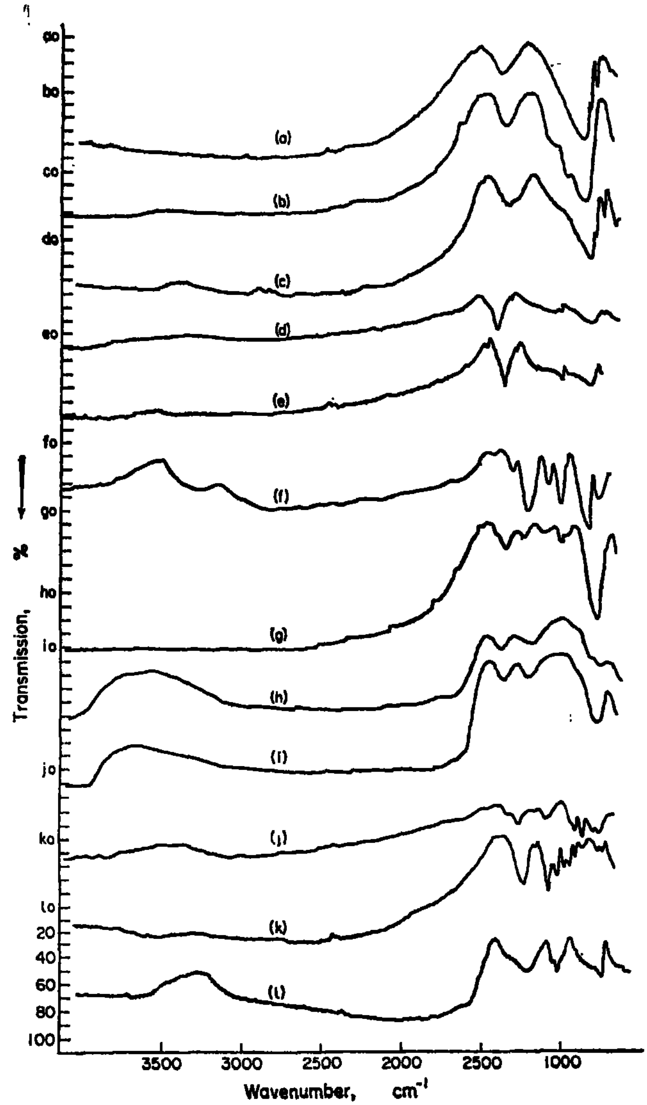

FIG. 3.—Infra-red absorption spectrum of:

(a) calcium 1:1 borate $CaO \cdot B_2O_3$
(b) α lithium 1:1 borate α-$Li_2O \cdot B_2O_3$
(c) strontium 1:1 borate $SrO \cdot B_2O_3$
(d) sodium 1:1 borate $Na_2O \cdot B_2O_3$
(e) potassium 1:1 borate $K_2O \cdot B_2O_3$
(f) potassium 1:5 borate octahydrate $K_2O \cdot 5B_2O_3 \cdot 8H_2O$
(g) β lithium 1:1 borate β-$Li_2O \cdot B_2O_3$
(h) sodium 1:1 borate tetrahydrate $Na_2O \cdot B_2O_3 \cdot 4H_2O$
(i) lithium 1:1 borate hexadecahydrate $Li_2O \cdot B_2O_3 \cdot 16H_2O$
(j) magnesium 1:1 borate $MgO \cdot B_2O_3$
(k) calcium 1:1 borate (hydrothermal preparation) $CaO \cdot B_2O_3$
(l) zinc 1:1 borate $ZnO \cdot B_2O_3$.

obtained experimentally show marked similarities to one another, and in these compounds therefore, the same anion can be clearly identified, although no assignment of vibrations has so far been possible. Of special interest is the hydrothermal calcium compound, since this was first identified as a pyroborate from its infra-red spectrum, when only impure specimens were available.

3. *Compounds of the type* $M_x(BO_2)_y$*–metaborates*

Nine metaborate compounds and three other structurally related compounds have been examined and the spectra are shown in Fig. 3. X-ray methods have so far identified three types of borate ion with the overall formula $(BO_2)_n^{n-}$, and a fourth structure exists as a hydrated form. These structures are a chain anion I, made up of $(-BO_2-)^-$ units, a ring anion II, made from three of the same units,

I

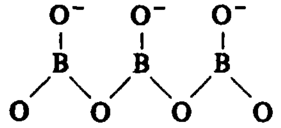

II

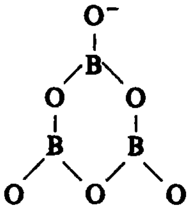

a three dimensional network III, in which all the boron atoms are tetrahedrally co-ordinated, and a double ring structure $B_5O_{10}^{5-}$, IV, in which the two rings are joined by a tetrahedral boron atom.

III

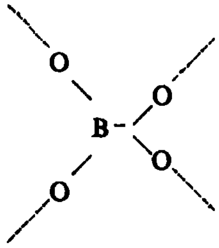

IV

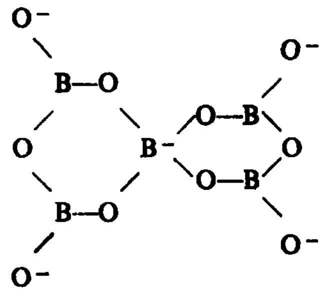

Other structures with larger single and double rings could in theory occur, but none have so far been reported. The four known structure types, already established by X-ray methods, exhibit characteristic infra-red spectra. Further compounds, not yet studied by either method, can thus have structures assigned on the basis of the infra-red spectra, and this has actually been done for three further borates.

The chain anion, I is known to occur in calcium⁽²⁷⁾ and lithium⁽²³⁾ metaborates $CaO{\cdot}B_2O_3$ and α-$Li_2O{\cdot}B_2O_3$, and these and the strontium compound $SrO{\cdot}B_2O_3$ have very similar spectra, whose main features are broad bands at 1470 cm^{-1} and 1125 cm^{-1} and a sharp peak at 730 cm^{-1}. It is evident therefore that the strontium metaborate also contains a chain anion. The sodium and potassium compounds have been shown by ZACHARIASEN⁽²⁸⁾ and by FANG⁽²⁹⁾ to contain the ring anion, II, and their spectra are almost identical, and differ from that of the compound $K_2O{\cdot}5B_2O_3{\cdot}4H_2O$, with

---

(27) W. H. ZACHARIASEN and G. E. ZIEGLER, *Z. Krist.* **83**, 354 (1932).
(28) W. H. ZACHARIASEN, *J. Chem. Phys.* **5**, 919 (1937).
(29) S. M. FANG, *Z. Krist.* **99**, 1 (1938).

the double ring, IV(30)*. The three dimensional structure, III, is found in β-$Li_2O \cdot B_2O_3$(23), and the close similarity of the spectrum of this compound with that of the hydrated compounds $Na_2O \cdot B_2O_3 \cdot 4H_2O$, and $Li_2O \cdot B_2O_3 \cdot 16H_2O$, indicates that the structure of the three compounds are related. X-ray studies by LEHMANN and TIESS(23) suggest that

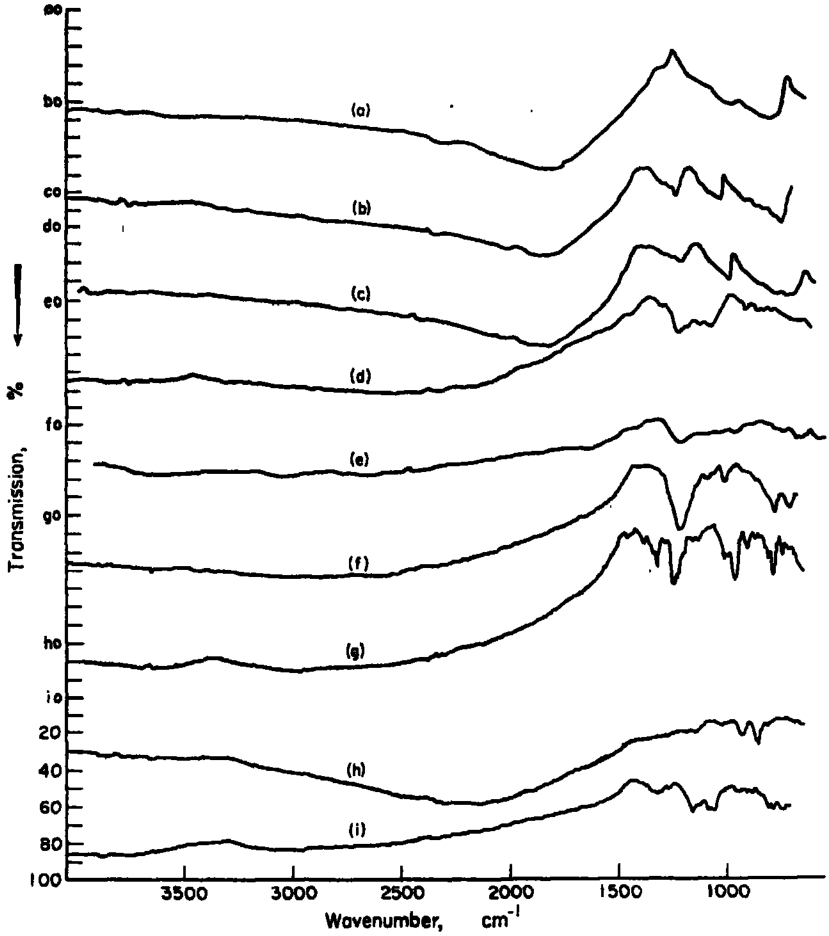

FIG. 4.—Infra-red absorption spectrum of:

(a) zinc 5:2 borate $5ZnO \cdot 2B_2O_3$
(b) supposed cadmium 3:2 borate $3CdO \cdot 2B_2O_3$
(c) mixture 5 parts $2CdO \cdot B_2O_3$ to 1 part $2CdO \cdot 3B_2O_3$
(d) cadmium 2:3 borate $2CdO \cdot 3B_2O_3$
(e) calcium 2:3 borate (hydrothermal preparation) $2CaO \cdot 3B_2O_3$
(f) barium 1:2 borate $BaO \cdot 2B_2O_3$
(g) calcium 1:2 borate $CaO \cdot 2B_2O_3$
(h) strontium 1:2 borate $SrO \cdot 2B_2O_3$
(i) barium 1:4 borate $BaO \cdot 4B_2O_3$.

---

* Comparison of our spectra for $Na_2O \cdot B_2O_3$ with that of MILLER and WILKINS makes it evident that their material was hydrated. The compound is very hygroscopic and on keeping the sample in air, we noted marked changes in the spectrum, which finally became very similar to that reported by MILLER and WILKINS.

(30) W. H. ZACHARIASEN, *Z. Krist.* 98, 266 (1937).

the lithium compound contains the anion $B(OH)_4^-$ and it is deduced that the sodium compound contains the same tetrahedral ion. One further point of interest is that although the spectra of these three compounds are clearly related, and are different from the other metaborates, it is not possible to assign a main metal-oxide stretching frequency and by this means identify the four co-ordinated boron atoms present. This is in contrast with the findings of some other workers[31, 32, 33, 34] who, even when accurate assignments of vibrations were impossible, were able to detect differences in co-ordination number by the shift in frequency of such a main stretching band. Our experience suggests that in complex structures such deductions cannot confidently be made without additional evidence from other sources.

The magnesium metaborate, and the high pressure form of the calcium compound have similar spectra, which differ somewhat from those of the other metaborates, and it is not possible to decide which anion structures are present in these compounds. The zinc metaborate has yet another different spectrum, and again the structure must for the present remain undecided.

4. *Other compounds*

The zinc compound, $5ZnO \cdot 2B_2O_3$ is unusal in that no other compound is known with this ratio of boron–oxygen. From the formula, the simplest single anion possible for this compound is $B_4O_{11}^{4-}$; alternatively, the BO_3^{3-} and $B_2O_5^{4-}$ ions may be present in the compound in equal numbers. It was hoped that the infra-red spectrum would give some information on this point, but the spectrum obtained, Fig. 4(a), although relatively simple, did not appear to be compounded from the spectra of the BO_3^{3-} and $B_2O_5^{4-}$ ions as observed in separate compounds. This could be explained by the differences in crystal symmetries, but the structure remains uncertain.

A $3CdO \cdot 2B_2O_3$ compound has been reported,[18] but in attempts to repeat this preparation, only mixtures of the $2CdO \cdot B_2O_3$, and $2CdO \cdot 3B_2O_3$ compounds were identified by X-ray powder methods.[19] This was confirmed by infra-red examination of the $3CdO \cdot 2B_2O_3$ composition, which had a spectrum identical with that of a mechanical mixture of the $2CdO \cdot B_2O_3$ and $2CdO \cdot 3B_2O_3$ compounds [see Fig. 4(b) and (c).]

The spectrum of the $2CdO \cdot 3B_2O_3$ compound itself shows marked similarities with that of the hydrothermally prepared calcium compound, $2CdO \cdot 3B_2O_3$, [see Fig. 4(d) and (e)] and the same anion structures are probable. Other considerations suggest that this structure is a three-dimensional network with units of six membered boron-oxygen rings,[13] but at present no confirmation of this has been made by assignment of vibrations, or by X-ray means. The spectra of the compounds $BaO \cdot 2B_2O_3$, $CaO \cdot 2B_2O_3$ and $SrO \cdot 2B_2O_3$, have been obtained and also that of the $BaO \cdot 4B_2O_3$ compound, [see Fig. 4(f) to (i)], but no marked similarities have been observed, and hence no conclusions about the structures of the anion groups have, so far, been reached.

---

[31] F. Dachille and R. Roy, *J. Amer. Cer. Soc.* **42,** 78 (1959).

[32] F. Dachille and R. Roy, *Z. Krist.* **111,** 462 (1959).

[33] E. R. Lippincott, A. V. Valkenberg, C. E. Weir and E. N. Bunting, *J. Res. Natl. Bur. Stds.* **61,** 61 (1958).

[34] R. V. Adams, *Phys. Chem. Glasses,* **2,** 101 (1961).

GENERAL DISCUSSION ADD CONCLUSIONS

In the borate compounds examined, anion structures range from the extremely simple to the complex, and even for a simple anion, the spectrum is markedly influenced by environment. In the study of organic compounds, it is found that sharper and more clearly resolved spectra can be obtained by cooling the specimens to low temperatures, and it was hoped that a similar technique would aid the analysis of the spectra reported here. However, no such improvement was obtained by cooling to liquid oxygen temperatures and it is evident that the stronger lattice forces of these inorganic crystals make the spectra relatively insensitive to temperature change. Although in some cases assignment of frequencies has been possible, in others the anion cannot confidently be identified from the spectrum alone, without reference to further structural information. As the complexity increases, so does the difficulty of frequency assignment, and structural conclusions may only be drawn on the basis of the clear similarity of a spectrum with that of a compound of known structure. Even inferences regarding major changes in co-ordination may not be drawn without such comparison. Throughout the range of complexity, however, single compounds may be identified from their previously obtained spectra.

The specific structural conclusions that have been drawn are as follows:—

(1) The BO_3^{3-} ion has been identified in the four compounds: $3CaO{\cdot}B_2O_3$; $3SrO{\cdot}B_2O_3$; $3BaO{\cdot}B_2O_3$; $3CdO{\cdot}B_2O_3$.

Force constants, given in Table 1, have been calculated for the BO_3^{3-} in these and also in the $3MgO{\cdot}B_2O_3$ compound.

(2) The $B_2O_5^{4-}$ ion is present in the compounds: $2CaO{\cdot}B_2O_3$ and its hydrothermal polymorph; $2SrO{\cdot}B_2O_3$; $2BaO{\cdot}B_2O_3$; $2CdO{\cdot}B_2O_3$.

(3) The compound $SrO{\cdot}B_2O_3$ contains a chain anion, $(BO_2)_n^{n-}$.

(4) The compounds $Na_2O{\cdot}B_2O_3{\cdot}4H_2O$ and $Li_2O{\cdot}B_2O_3{\cdot}16H_2O$ both contain tetrahedrally co-ordinated boron.

(5) A supposed $3CdO{\cdot}2B_2O_3$ compound is a mechanical mixture of the compounds $2CdO{\cdot}B_2O_3$ and $2CdO{\cdot}3B_2O_3$.

(6) The $2CdO{\cdot}3B_2O_3$ and $2CaO.3B_2O_3$ compounds have the same anion structure.

J. Inorg. Nucl. Chem., 1962, Vol. 24, pp. 1057 to 1065. Pergamon Press Ltd. Printed in England

THE SYNTHESIS OF NEW CALCIUM BORATE COMPOUNDS BY HYDROTHERMAL METHODS

P. B. HART* and C. S. BROWN

The General Electric Company Limited, Central Research Laboratories,
Hirst Research Centre, Wembley, England

(*Received* 1 *February* 1962)

Abstract—Hydrothermal treatment of calcium hydroxide–boric acid mixtures at temperatures between 200 and 400°C has produced a series of new compounds. These compounds have been characterized by X-ray and chemical examination. Four of the compounds are hydrated; three more anhydrous compounds are of particular interest since they cannot be prepared by normal ceramic methods. One of these compounds has been shown to be a high pressure polymorph of the known compound, $CaO{\cdot}B_2O_3$. In explanation of these syntheses, it is suggested that various complex anions are formed in borate solutions at high temperatures. Possible structures for some of the compounds are suggested, and the petrogenesis of the naturally occurring borates is discussed.

IN the CaO-B_2O_3 system four compounds have been reported⁽¹⁾ $3CaO{\cdot}B_2O_3$, $2CaO{\cdot}B_2O_3$ $CaO{\cdot}B_2O_3$ and $CaO{\cdot}2B_2O_3$. These compounds may be obtained by ceramic techniques and by crystallization from the melt. The $CaO{\cdot}B_2O_3$ compound has been shown⁽²⁾ to contain infinite borate chains with the formula $(BO_2)_n^{n-}$. The structures of the other compounds are not known in detail, but it may be inferred that the anions present in the compounds $3CaO{\cdot}B_2O_3$ and $2CaO{\cdot}B_2O_3$ are $(BO_3)^{3-}$ and $(B_2O_5)^{4-}$, respectively, since these are found in the corresponding magnesium compounds, $3MgO{\cdot}B_2O_3$⁽³⁾ and $2MgO{\cdot}B_2O_3$.⁽⁴⁾

A large number of compounds are known in the hydrated system, CaO-B_2O_3-H_2O; according to a recent review by KEMP⁽⁵⁾ seventeen are well characterized and have been prepared in the laboratory, and of these, some also occur in nature. Few structures are known, though the series $2CaO{\cdot}3B_2O_3xH_2O$ is being studied by CHRIST and CLARK;⁽⁶⁾ in this series the borate anions are complex, being made up from units of six-membered boron-oxygen rings.

Most of the compounds in the hydrated system can be obtained by crystallization from aqueous solutions between 0°C and 100°C, and in general, the higher the temperature of crystallization the less the degree of hydration. This suggests that new compounds might be produced intermediate in the degree of hydration between the known hydrates and the anhydrous system, by crystallization from aqueous solutions above 100°C. This possibility has been investigated, and the results are now reported.

---

* Present address : Scientific Laboratories, Philco Corporation, Blue Bell, Pa., U.S.A.

(1) E. T. CARLSON, *J. Res. Nat. Bur. Stand.* **9**, 825, (1932).

(2) W. H. ZACHARIASEN and G. E. ZIEGLER, *Z. Krist.* **83**, 354, (1932).

(3) S. V. BERGER, *Acta. Chem. Scand.* 3, 660 (1949).

(4) Y. TAKEUCHI, *Acta. Cryst.* **5**, 574 (1952).

(5) P. H. KEMP, *The Chemistry of Borates-Part I*, Borax Consolidated, London (1956)

(6) See C. L. CHRIST and J. R. CLARK, *Amer. Min.* **45**, 334 (1960) for a summary and earlier references.

EXPERIMENTAL

Reagent grade boric acid and calcium hydroxide were used as starting materials for hydrothermal treatment. To confirm that equilibrium was reached in the hydrothermal reactions, some calcium borate minerals and four anhydrous calcium borate preparations were also used as source materials. The minerals, colemanite $2CaO{\cdot}3B_2O_3{\cdot}5H_2O$, meyerhofferite $2CaO{\cdot}3B_2O_3{\cdot}7H_2O$, and inyoite, $2CaO{\cdot}3B_2O_3{\cdot}13H_2O$ were obtained and their identity was checked by comparison of X-ray powder diffraction data with the A.S.T.M. X-ray data file. The anhydrous compounds, $3CaO{\cdot}B_2O_3$, $2CaO{\cdot}B_2O_3$, and $CaO{\cdot}B_2O_3$, and a $CaO{\cdot}2B_2O_3$ glass were obtained by firing appropriate mixtures of calcium hydroxide and boric acid. By reference to X-ray data in the A.S.T.M. file, the identities of the crystalline compounds $3CaO{\cdot}B_2O_3$ and $2CaO{\cdot}B_2O_3$ were confirmed: data obtained in other studies in these Laboratories satisfactorily established the identity of the $CaO{\cdot}B_2O_3$ compound.

The autoclaves used as containers for the hydrothermal reactions were of the type used in earlier studies(7) on the growth of quartz crystals, and had a lens-ring seal. The autoclaves were heated on hot plates in demountable furnaces insulated with vermiculite. Temperatures were measured and controlled using chromel-alumel thermocouples. There was a temperature gradient along the length of the autoclave walls, but previous experience had shown that the temperatures inside the autoclaves were close to those measured externally at a point near the top of the autoclaves. Pressures were calculated from the degree of filling and the estimated temperature, using KENNEDY's P.V.T. data for water.(8) The pressure chosen for the experiments was 500 atm, well within the safety limit of the autoclaves.

Thin walled gold or platinum tubes were used to contain the experimental material inside the autoclaves. These tubes were closed by folding over the ends and compressing them. Some leaks did occur, but a number of tests with cold-welded tubes showed that, in general, such leaks had not altered the results.

At the end of the experiments, the autoclaves were cooled, opened, and the solid products were quickly washed and dried.

Variation of reaction time and of the nature of the source materials did not alter the crystalline materials obtained, and this was taken as good evidence that equilibrium had been reached. The design of the autoclaves and furnaces prevented the use of a rapid quench technique, but the well crystallised products obtained, and the differences resulting from experiments at different temperatures, showed that high temperature equilibria were not significantly altered during the cooling period. In some cases, however, substantial amounts of material were evidently in solution during the experiments, and precipitation of amorphous or poorly crystalline material occurred on cooling, making consistent analytical results difficult to obtain.

X-ray powder photographs were obtained using a Philips 5·76 cm diameter camera, with Ni-filtered Cu-radiation. Accurate *d*-spacings were obtained with a diffractometer unit.

Calcium and boron were determined as their oxides, by dissolution in excess of standard hydrochloric acid, followed by titration with standard, carbonate-free sodium hydroxide, using methyl red indicator, and then phenolphthalein in the presence of glycerol. Water was estimated from the weight loss on heating. X-ray and optical examination showed that in many experiments more than one crystalline species was formed. Samples selected for the determination of composition were the purest available, and analytical results for species (D), (H) and (F) (see Table 1) were sufficiently consistent to give reliable indication of the composition of these phases. Those for (B), (C), (E) and (I) were less so, and the formulae given may require adjustment. The infra-red spectra of the compounds(9) confirmed that (D), (E) and (H) were anhydrous, and the formula $2CaO{\cdot}B_2O_3$ for (E) was initially suggested by comparison with the spectra of other pyroborates.

The compounds were examined by the technique of differential thermal analysis (D.T.A.), by which useful information on dehydration and other thermal transformations can be obtained. One gramme samples, platinum crucibles, and a heating rate of 10°C/min were

(7) C. S. BROWN, R. C. KELL, L. A. THOMAS, N. WOOSTER and W. A. WOOSTER, *Min. Mag.* 29, 858 (1952).

(8) G. C. KENNEDY, *Amer. J. Sci.* 248, 540 (1950).

(9) P. B. HART and S. E. F. SMALLWOOD. *J. Inorg. Nucl. Chem.* 24, 1047 (1962).

employed. As with the chemical analyses, only compounds believed to be pure were examined.

Dry high-pressure experiments were done in uniaxial pressure apparatus similar to that described by MACDONALD.(10)

TABLE 1.

Phase	Composition	Temperature and $CaO:B_2O_3$ ratio for formation	Thermal properties
C	$2CaO{\cdot}B_2O_3{\cdot}H_2O$	200–300°C and 2:1–3:2 $CaO:B_2O_3$	Exothermic D.T.A. peak at 420°C. Dehydrates to $2CaO{\cdot}B_2O_3$
B	$2CaO{\cdot}2B_2O_3{\cdot}H_2O$	200–300°C and 1:1 $CaO:B_2O_3$	Exothermic peaks at 480°, 545°C, endothermic at 660°C. Dehydrates to normal $CaO{\cdot}B_2O_3$
F	$2CaO{\cdot}3B_2O_3{\cdot}H_2O$	200–300°C and 1:2 $CaO:B_2O_3$	Exothermic peaks at 640–655°C, endothermic at 710°C. Dehydrates to give phase H, $2CaO{\cdot}3B_2O_3$; melts at 950°C
E	$2CaO{\cdot}B_2O_3$	400°C and 2:1–1:1 $CaO:B_2O_3$	Exothermic peaks at 525°, 715°, 840°C
D	$CaO{\cdot}B_2O_3$	400°C and 1:1–2:3 $CaO{\cdot}B_2O_3$	Exothermic peak at 800°C with transition to normal $CaO{\cdot}B_2O_3$
H	$2CaO{\cdot}3B_2O_3$	400°C and 2:3–1:2 $CaO:B_2O_3$	Melts at 950°C
I	$3CaO{\cdot}9B_2O_3{\cdot}H_2O$	400°C and 1:2–1:3 $CaO:B_2O_3$	Exothermic peak at 683°C. Dehydrates to give $CaO{\cdot}2B_2O_3$

Analytical results

D. Found: CaO, 44·8; B_2O_3, 55·4. Calc. for $CaO{\cdot}B_2O_3$: CaO, 44·6; B_2O_3, 55·4%.

H. Found: CaO, 34·7; B_2O_3, 65·3. Calc. for $2CaO{\cdot}3B_2O_3$: CaO, 34·9; B_2O_3, 65·1%.

F. Found: CaO, 33·4; B_2O_3, 62·0; H_2O, 5·0. Calc. for $2CaO{\cdot}3B_2O_3{\cdot}H_2O$: CaO, 33·1, B_2O_3, 61·6; H_2O, 5·3%.

RESULTS

By hydrothermal treatment of boric acid–calcium hydroxide mixtures at temperatures between 200 and 400°C, a number of new calcium borate compounds have been obtained. Seven of these compounds have been clearly identified by X-ray and chemical examination. When the compounds were first identified by their X-ray diffraction patterns, they were labelled alphabetically, A-I. Two of the phases so labelled later proved to be mixtures. In a number of experiments, further compounds were obtained but never in good yield, so that they could not be adequately identified. The details of the synthesis, compositions and D.T.A. of the seven compounds are given in Table 1 (for greater clarity, Fig. 1 shows the approximate areas where the compounds occur on a temperature–composition diagram). The X-ray powder data are recorded in Table 2. Some of the compounds formed well defined crystals; compounds (B) and (C) were poorly crystallized and had no readily recognisable habit.

---

(10) G. J. F. MACDONALD, *Amer. Min.* 41, 744 (1956).

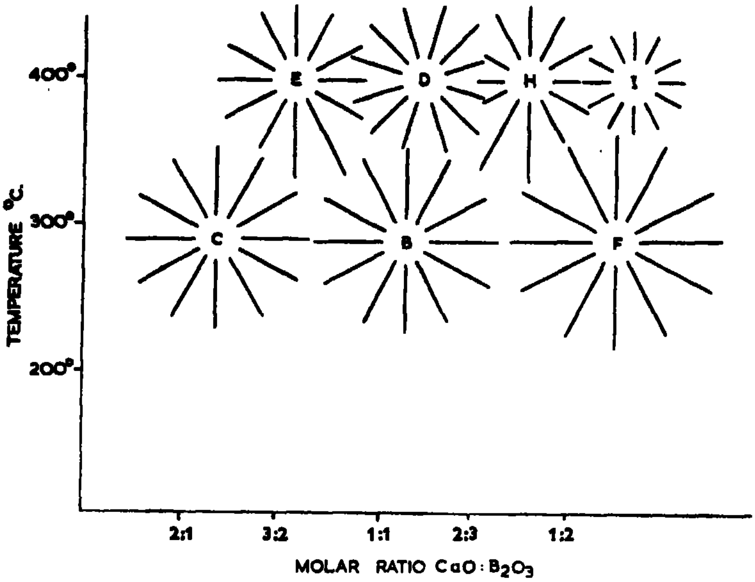

FIG. 1.—Regions of formation of the calcium borate compounds: *B*. $2CaO{\cdot}2B_2O_3{\cdot}H_2O$; *C*. $2CaO{\cdot}B_2O_3{\cdot}H_2O$; *D*. $CaO{\cdot}B_2O_3$; *E*. $2CaO{\cdot}B_2O_3$; *F*. $2CaO{\cdot}3B_2O_3{\cdot}H_2O$; *H*. $2CaO{\cdot}3B_2O_3$; *I*. $2CaO{\cdot}9B_2O_3{\cdot}H_2O$.

Attempts were made to obtain further products by hydrothermal crystallization at 120 °C, but reaction rates were very slow, and only poorly crystalline material was obtained. These products were not analysed, but their water content was determined by heating at 1000 °C. Details are in Table 3.

A series of experiments with uniaxial pressure apparatus showed that compound (D) was a high pressure polymorph of the known $CaO{\cdot}B_2O_3$ compound. Contrary to the experience of MACDONALD, the authors found it impossible to achieve homogeneity of pressure across the sample, and hence quantitative results could not be obtained, but an estimate of the pressure necessary for the conversion was obtained. At approximately 15,000 atm and 650 °C, almost complete conversion was achieved from the known $CaO{\cdot}B_2O_3$ compound to (D). The D.T.A. examination of (D) showed that inversion at atmospheric pressure did not take place until 800 °C was reached, but it is felt that a slow reaction could cause this reading to be in error by large amounts. Compound (H) was also synthesized in the uniaxial device from the stoichiometric mixture of calcium hydroxide and orthoboric acid, at 12,000 atm and 600 °C. Attempts to synthesize compound (E) from the known calcium pyroborate, $2CaO{\cdot}B_2O_3$, as from alcium hydroxide and boric acid, were unsuccessful.

DISCUSSION

The range of new calcium borate compounds formed under hydrothermal conditions is noteworthy in several respects. Limiting temperatures for the formation of the naturally occuring calcium borates are indicated, some interesting structural problems arise, and some light is thrown on the nature of aqueous borate solutions at high temperatures.

TABLE 2.—X-RAY DIFFRACTION DATA

Phase B		Phase C		Phase D		Phase E		Phase F*		Phase H'		Phase I	
d (Å)	I/I_0	d (Å)	I/I_0	d (Å)	I/I_0	d (Å)	I/I_0	d (Å)	I/I_0	d (Å)	I/I_0	d (Å)	I/I_0
4·32	16	6·68	86	7·14	37	6·59	100	6·74	35	4·417	49	8·93	70
3·95	15	4·22	8	6·875	11	6·385	12	6·17	16	4·014	22	8·20	100
3·61	23	3·347	12	4·028	12	5·62	18	3·775	30	3·929	19	6·38	20
3·58	49	2·97	100	3·578	27	4·035	9	3·710	39	3·758	28	6·195	5
3·57	44	2·91	6	3·455	100	3·829	12	3·676	31	3·735	10	5·51	5
3·45	100	2·853	19	2·735	5	3·58	12	3·578	23	3·54	100	5·26	30
3·25	20	2·755	33	2·663	24	3·458	76	3·478	100	3·358	73	4·96	30
3·14	44	2·719	18	2·625	12	3·288	9	3·366	82	3·329	63	4·77	30
3·12	36	2·71	7	2·470	1	3·015	38	3·25	13	3·256	12	4·60	50
2·865	18	2·495	10	2·404	3	2·91	15	3·09	66	3·213	20	4·43	70
2·826	28	2·489	10	2·386	3	2·803	9	3·034	16	3·16	9	4·255	25
2·794	41	2·377	3	2·303	12	2·735	11	2·862	16	3·03	10	4·075	80
2·713	48	2·235	27	2·093	10	2·665	15	2·751	8	3·022	33	3·915	30
2·666	9	2·230	19	2·002	5	2·628	8	2·675	52	2·954	31	3·715	<5
2·644	16	2·071	9	1·973	4	2·304	7	2·529	9	2·877	7	3·565	<5
2·303	9	2·036	7	1·964	3	2·093	9	2·516	10	2·775	50	3·455	20
2·131	14	1·84	5	1·922	4	2·067	7	2·496	12	2·721	23	3·36	<5
2·093	10	1·825	6	1·866	4	1·791	10	2·286	8	2·661	30	3·31	95
2·023	50	1·82	5	1·791	17			2·248	23	2·639	21	3·19	10
1·907	15	1·79	7	1·728	6			2·194	29	2·601	16	3·04	60
								2·183	19	2·583	14	2·95	80
								2·121	9	2·533	18	2·89	20
								2·089	2	2·504	15	2·835	10
								2·049	36	2·422	28	2·77	20
								2·026	20	2·415	18	2·718	15
								2·000	23	2·369	14	2·658	40
								1·923	19	2·307	16	2·595	25
								1·890	46	2·263	30	2·554	15
								1·865	9	2·239	12	2·477	15
								1·84	5	2·229	13	2·443	25
								1·76	20			2·343	15
								1·716	4			2·315	30

* Note: Apart from some differences in relative intensities, this set of data agrees well with that just published for the compound $2CaO{\cdot}3B_2O_3{\cdot}H_2O$, by CLARK *et al.*(11)

Mineral Formation. Of the seven new compounds reported, three are anhydrous and four are hydrated. It is notable that the hydrated compounds are intermediate in water content between the naturally occurring minerals such as colemanite, $2CaO{\cdot}3B_2O_3{\cdot}5H_2O$ and meyerhofferite $2CaO{\cdot}3B_2O_3{\cdot}7H_2O$, and the anhydrous compounds of the CaO–B_2O_3 system, and that the degree of hydration decreases as the temperature of formation is raised. These facts, coupled with the production of a poorly crystallized material at 120°C, also less hydrated than colemanite, suggest that the naturally occurring minerals must have been formed at quite low temperatures, probably below 100°C.

---

(11) J. R. CLARK, C. L. CHRIST, and D. E. APPLETON, *Acta Cryst.*, 15, 207 (1962).

TABLE 3.—EXPERIMENTS AT 120°C

Initial ratio $CaO:B_2O_3$	Water loss at 1000°C (%)	X-ray examination
2:3	19·5	At least two poorly crystalline phases J and K present
1:2	18·8	At least one poorly crystalline phase J present
2:5	18·1	At least one poorly crystalline phase J present

* Colemanite, $2CaO\cdot3BaO_3\cdot5H_2O$, contains 28·0 per cent water and phase C, $2CaO\cdot B_2O_3\cdot H_2O$ has only 8·5 per cent water.

Structures. Two of the new anhydrous compounds, $2CaO\cdot B_2O_3$ and $CaO\cdot B_2O_3$, have polymorphs,(1) while the third, $2CaO\cdot3B_2O_3$ was hitherto unknown. It is almost certain that the $2CaO\cdot B_2O_3$ compound must contain the $B_2O_5{}^{4-}$ pyroborate anion, since there is no simple alternative structure in which boron retains either tervalency or tetravalency. Magnesium pyroborate $2MgO\cdot B_2O_3$, is known to contain the $B_2O_5{}^{4-}$ ion,(4) and infra-red studies have shown that the spectrum of the magnesium compound is very similar to those of the two $2CaO\cdot B_2O_3$ polymorphs.(9) Hence it is deduced that all three contain the same anion, and the two calcium compounds must differ only in their arrangements of the same structure units. It is possible that the hydrothermal compound is in fact a high pressure polymorph of the known compound. However, no satisfactory evidence for this view could be obtained from experiments made with the uniaxial pressure apparatus.

Such experiments did show that the hydrothermal compound, $CaO\cdot B_2O_3$, is indeed a high pressure form of the known $CaO\cdot B_2O_3$ compound. However, at this composition the structural possibilities are greater, since a number of different anion structures are known. For instance a chain type anion, $(BO_2)_n^{n-}$, occurs in the $CaO\cdot B_2O_3$ compound made by solid state methods, a ring anion, $(B_3O_6)^{3-}$ is found in the compounds $Na_2O\cdot B_2O_3$,(12) and $K_2O\cdot B_2O_3$,(13) and in β-$Li_2O\cdot B_2O_3$(14) a three-dimensional structure is found, in which all the boron atoms are 4-co-ordinated. It is possible that larger ring anions could also be formed, and the presence of the double ring structure $(B_5O_6(OH)_4)^{4-}$ in the hydrated compound $K_2O_5\cdot B_2O_5\cdot4H_2O$(15) suggests a further alternative, an anhydrous double ring, $B_5O_{10}{}^{5-}$. Infra-red studies of some of these compounds have been made,(9) but it was not possible to decide whether the

(12) W. H. ZACHARIASEN, *J. Phys. Chem.* **5**, 919 (1937).

(13) S. M. FANG, *Z. Krist.* **99**, 1 (1938).

(14) H. LEHMANN and D. TIESS, *Chem. Tech.* **11**, 260 (1959).

(15) W. H. ZACHARIASEN, *Z. Krist.* **98**, 266 (1938).

pressure-induced transition of the $CaO{\cdot}B_2O_3$ compounds involves merely the rearrangement of structure units or an alteration of the whole anion structure.

A variety of structures also seems possible for the $2CaO{\cdot}3B_2O_3$ compound, but its ready production by the dehydration of the new compound, $2CaO{\cdot}3B_2O_3{\cdot}H_2O$ indicates that the two structures are closely related. This hydrated compound has also been reported by CLARK and CHRIST,(16) who have made preliminary structure studies, and find a relation to the structures of other members of the series $2CaO{\cdot}3B_2O_3{\cdot}xH_2O$.(6) The structure unit of this series is a six-membered ring, $[B_3O_3(OH)_5]^{2-}$, present in meyerhofferite, where $x = 7$, in inyoite, where $x = 13$, and in a synthetic compound where $x = 11$. In colemanite, $x = 5$, the structure units are joined together into an infinite chain, with the formula $(O\text{-}B_3O_3(OH)_3)_n^{2n-}$. In the monohydrate it appears that sheets are formed by the further elimination of water between neighbouring chains, and it therefore seems probable that the anhydrous compound contains a three-dimensional anion structure formed by the linking of the six-membered boron–oxygen rings.

The structures of the other new hydrated borates are as yet unknown, and infra-red studies do not give any guide to them, except to indicate that the water is structurally bound as hydroxyl groups. It is possible that the compound $2CaO{\cdot}B_2O_3{\cdot}H_2O$ is a relatively simple one, containing the anion $(BO_2{\cdot}OH)^{2-}$; the two others are likely to contain complex anions.

Borate solutions at high temperatures. Even at room temperature, the structure of concentrated metal borate solutions is incompletely understood, and in the absence of accurate physico-chemical measurements, it is only possible to speculate on the detailed nature of hydrothermal borate solutions. However, both aqueous borate solutions and molten borate salts are known to be ionic,(5, 17) and the hydrothermal solutions are likely to be the same. Further, some of the more unusual properties of the aqueous solutions and the melts have been correlated with the presence of complex ions, and it is probable that the compounds formed under hydrothermal conditions are associated with the concentration and stability of such ions.

Recent examination of hydrolytic equilibria in concentrated aqueous solutions has shown that polynuclear anions can occur under certain conditions.(18) The presence of the anion $[B_3O_3(OH)_5]^{2-}$ has been demonstrated in borate solutions at 25°C; as mentioned earlier this is the structural unit of the $2CaO{\cdot}3B_2O_3xH_2O$ series of compounds. The hydrolytic studies showed that the concentration of polynuclear ions is often critically affected by the basicity and total concentration of the solutions, and it seems possible that the pronounced effect of temperature and base concentration on the formation of the various hydrothermal compounds is related to the presence of ions needed for their crystallization. The synthesis of the compounds $2CaO{\cdot}3B_2O_3{\cdot}H_2O$, and $2CaO{\cdot}3B_2O_3$ at high temperatures further suggests that the $[B_3O_3(OH)_5]^{2-}$ or a related structure is very stable; the effect of change in temperature may be explained by the thermodynamics of the crystallization process.

(16) J. R. CLARK and C. L. CHRIST, Abstract given in *Acta Cryst.* **13**, 1018 (1960).

(17) J. O'M. BOCKRIS, (Editor), *Modern Aspects of Electrochemistry*, p 249 Butterworths, London (1956).

(18) L. G. SILLÉN, *Quart. Rev.* **13**, 146 (1959).

Another unusual property of some borate solutions may be explained on a similar basis. It is known that some crystalline borates are formed very slowly from solution, an extreme example being the reported crystallization of colemanite from calcium hydroxide/boric acid solutions held at 83 °C for two months.[19] Such a slow reaction would be explained if the anions in colemanite were present in the solution only in very low concentration; suitable adjustment of conditions might lead to the relatively rapid formation of the compound.

A number of factors must influence the stability of complex ions in aqueous solution. Thus structures with unusually long or distorted bonds are unlikely to be formed. Another important consideration is the equilibrium represented by the equation:

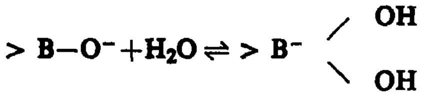

$$> B{-}O^- + H_2O \rightleftharpoons \; > B^- \begin{matrix} \diagup \; OH \\ \diagdown \; OH \end{matrix} \qquad (1)$$

EDWARDS and ROSS[20] have concluded that in borate solutions at 25 °C, in which water has a reasonable activity, this equilibrium lies far to the right. They thus predict that metal borates formed from such solutions will have anions containing tetrahedrally co-ordinated boron atoms, equal in number to the charges of the cations. Their survey of the known borate structures confirms this prediction. The implication of this is that anhydrous metal borates will not crystallize from aqueous solutions at room temperature unless $> B{-}O^-$ groups are absent from their structure.

Examining again the possible structures for the hydrothermal compounds, it is evident that the $2CaO{\cdot}B_2O_3$ compound must contain such a $> B{-}O^-$ group, as must the $CaO{\cdot}B_2O_3$ compound unless the three dimensional anion structure be accepted. The compounds $2CaO{\cdot}3B_2O_3$ and $2CaO{\cdot}3B_2O_3{\cdot}H_2O$ appear to agree with Edwards and Ross's rule, but it is difficult to envisage an anion for the compound $2CaO{\cdot}B_2O_3{\cdot}H_2O$ that does. Thus it is probable that the equilibrium represented by Equation (1) moves to the left under hydrothermal conditions. A contributory factor could be the decreasing density of water at constant pressure as temperature is raised; at 400 °C and 500 atm it is only 0·788 g/cm^3. However, experiments have shown that in general, pressure, and hence solvent density, is not an important variable in these hydrothermal syntheses, at least in the range up to 2000 atm. These considerations also indicate that the naturally occurring minerals have been produced at relatively low temperatures. If some of them had been formed at 400 °C, the $> B{-}O^-$ group would be expected to occur.

CONCLUSIONS

Three anhydrous compounds, $2CaO{\cdot}B_2O_3$, $CaO{\cdot}B_2O_3$ and $2CaO{\cdot}3B_2O_3$, and four hydrated compounds, $2CaO{\cdot}B_2O_3{\cdot}H_2O$, $2CaO{\cdot}2B_2O_3{\cdot}H_2O$, $2CaO{\cdot}3B_2O_3{\cdot}H_2O$, and $3CaO{\cdot}9B_2O_3{\cdot}H_2O$, have been crystallized from hydrothermal solutions. Two compounds, $2CaO{\cdot}B_2O_3$ and $CaO{\cdot}B_2O_3$ have polymorphs, and the latter compound and $2CaO{\cdot}3B_2O_3$ have also been synthesized by high pressure methods.

The syntheses suggest that the hydrated calcium borate minerals were not formed above 100 °C. Structures are proposed for some of the new compounds, and the nature of borate solutions at high temperatures are discussed. It is thought that

---

(19) P. H. KEMP, *The Chemistry of Borates-Part I*, p. 70. Borox Consolidated, London (1956).
(20) J. O EDWARDS and V. ROSS, *J. Inorg. Nucl. Chem.* **15**, 329 (1960).

complex ions are present, and that the hydration equilibria differ from those at room temperature.

Further information on the nature of hydrothermal borate solutions would most readily be derived from physico-chemical measurements on the solutions themselves, and from more detailed knowledge of the structures of the materials produced in such solutions.

Acknowledgements—The authors wish to thank members of the Crystal Analysis Group, who took many of the X-ray photographs, and contributed in discussions on the work.

J. Inorg. Nucl. Chem., 1962, Vol. 24, pp. 1067 to 1072. Pergamon Press Ltd. Printed in England

AMMINES OF IRIDIUM(O)*

G. W. Watt, E. P. Helvenston and L. E. Sharif
Department of Chemistry, The University of Texas, Austin 12, Texas

(*Received* 17 *November* 1961)

Abstract—The reduction of hexammineiridium(III) ion with potassium in ammonia at -33·5° has been shown to provide pentammineiridium(O); this confirms the existence of the ammine previously reported to result from the reduction of bromopentammineiridium(III) ion. The reduction of potassium hexabromoiridate(III) and the corresponding chloro compound has been shown most probably to result in lower ammines of iridium(O). Under the same conditions, potassium hexacyanoiridate(III) is not reduced. An efficient and convenient procedure for the recovery of iridium is described.

It was reported earlier that the reduction of bromopentammineiridium(III) bromide with potassium in liquid ammonia provides pentammineiridium(O),(1) which is analogous to the ammines of platinum(O)(2) and osmium(O).(3) Such species are unusual in that they represent zerovalent transitional metals in combination with (only) sigma bonding ligands. Accordingly, it was considered worthwhile to confirm independently the existence of $[Ir(NH_3)_5]^\circ$. In the course of this work, evidence for the existence of unstable lower ammines of iridium(O) has been obtained.

We report here also data relating to the reduction of certain other iridium complexes with potassium in ammonia. These experiments were carried out with a view to producing the corresponding or related complexes of iridium(II), iridium(I), and/or iridium(O).

EXPERIMENTAL

Materials and methods

With the exceptions noted below, all materials employed in this work were reagent grade chemicals that were used without further purification. All reactions in liquid ammonia were carried out under strictly anhydrous oxygen-free conditions using equipment and procedures that have been described previously.(2, 3, 4)

Hexammineiridium(III) iodide. This compound was prepared by the following modification of the method of Palmaer.(5) Thus, 5·0 g of $Na_3(IrCl_6)\cdot x\ H_2O$ (where $x \cong 2$) and 50 ml of 25 per cent aqueous ammonia were placed in a Pyrex glass tube of dimensions such that the solution occupied at least 80 per cent of the volume of the sealed tube. The tube was heated in an autoclave (containing 25 per cent aqueous ammonia for pressure equalization) at 145° for 36–48 hr. After cooling to room temperature, the tube was opened and the contents evaporated to dryness. From the white solid residue, $[Ir(NH_3)_6]Cl_3$ was leached with four successive 5 ml portions of cold water; the combined extracts were heated to boiling, treated dropwise with 10 ml of 57% HI, cooled, and filtered. The resultant white crystals were dissolved in a minimum of hot water, filtered, treated with 7 ml of 57% HI, cooled to room temperature and filtered. The solid product was dried for 1 hr at 110°; the yield was 4·0 g or 61 per cent. X-ray diffraction data are given in Table 1. (Found: Ir, 28·5; I, 56·1. Calc. for $[Ir(NH_3)_6]I_3$: Ir, 28·55; I, 56·35%.)

---

* This work was supported in part by the U.S. Atomic Energy Commission, Contract AT-(40-1)-1639, and by the Robert A. Welch Foundation.

(1) G. W. Watt and P. I. Mayfield, *J. Amer. Chem. Soc.* **75**, 6178 (1953).

(2) G. W. Watt, M. T. Walling, Jr. and P. I. Mayfield, *J. Amer. Chem. Soc.* **75**, 6175 (1953).

(3) G. W. Watt and E. M. Potrafke. Unpublished work.

(4) G. W. Watt, *et al.*, *J. Inorg. Nucl. Chem.* **9**, 311 (1959); *J. Electrochem. Soc.* **98**, 1 (1951); **102**, 46, 454 (1955); *J. Amer. Chem. Soc.* **76**, 4742 (1954).

(5) W. Palmaer, *Z. Anorg. Chem.* **10**, 320 (1895).

Potassium hexachloroiridate(III). In a typical case, 21·33 g of $(NH_4)_2(IrCl_6)$ was placed in 200 ml of water in a 500 ml flask, heated to boiling and reduced to Ir(III) by dropwise addition of 3·42 g of $(NH_4)_2C_2O_4$ in 100 ml of water over 1 hr. The solution was filtered and passed (at a flow-rate of 1 ml/min) through a cation exchange column consisting of 91 g of Dowex-50W resin in the hydrogen form and contained in an 18 mm i.d. tube. The column was finally washed with distilled water until the washings were neutral. The original (H_3IrCl_6) solution and washings were treated with 12 g of KCl and evaporated to incipient crystallization at a temperature just short of the boiling point of the solution. When the resulting solution was cooled to 0°, dark green plates of $K_3(IrCl_6)\cdot H_2O$ crystallized; this was filtered, washed with two 4 ml portions of cold water, and dried at 110° for 2 hr. The yield of the anhydrous salt was 24·1 g or 95 per cent. X-ray diffraction data are included in Table 1. (Found: Ir, 36·5; Cl/2, 20·0%. Calc. for K_3IrCl_6: Ir, 36·8; Cl/2, 20·4%.)

Potassium hexabromoiridate(III). Iridium(III) chloride 2-hydrate (3·77 g) in 10 ml of water was heated just to boiling, treated with 20 ml of 48% HBr, and evaporated to near dryness. Addition of 15 ml portions of 48% HBr followed by evaporation to near dryness was repeated six times except that the final evaporation was to a volume of 5 ml. To this solution, 5 g of KBr in 20 ml of water was added; this solution was evaporated to 10 ml and cooled at 0° for 2 hr. The resulting olive-green crystals were filtered, washed three times with 5 ml portions of cold water, dried for 30 min at 110° and finally *in vacuo* over $MgClO_4$ for 24 hr. The yield was 8·65 g or 82 per cent; X-ray diffraction data are listed in Table 1. (Found: Ir, 25·2; Br, 60·4. Calc. for K_3IrBr_6: Ir, 25·04; Br, 60·7%.)

TABLE 1.—X-RAY DIFFRACTION DATA*

$[Ir(NH_3)_6]I_3$		K_3IrCl_6		K_3IrBr_6		$K_3Ir(CN)_6$		$[Ir(NH_3)_5]^\circ$	
d (Å)	I/I_0	*d* (Å)	I/I_0	*d* (Å)	I/I_0	*d* (Å)	I/I_0	*d* (Å)	I/I_0
6·39	0·15	5·97	1·00	6·04	1·00	6·84	0·50	6·65	1·00
5·55	0·10	5·16	0·40	5·14	1·00	6·51	0·20	5·87	0·20
3·92	1·00	4·92	0·10	3·08	0·10	5·28	0·40	5·74	0·80
2·76	0·30	3·63	0·30	2·92	0·10	4·17	1·00	5·25	0·05
2·26	0·40	3·50	0·40	2·86	0·10	4·05	0·60	4·09	0·30
1·96	0·10	3·11	0·20	2·75	0·10	3·11	0·60	4·03	0·05
1·87	0·10	2·58	0·10	2·56	0·15	2·98	0·20	1·85	0·05†
1·75	0·10	1·99	0·20	2·31	0·10	2·67	0·60		
1·48	0·10†	1·76	0·10	2·15	0·10†	2·21	0·20		
		1·73	0·10†			2·11	0·50		
						1·90	0·20		
						1·49	0·20†		

* Cu$K\alpha$ radiation, Ni filter, 35 kV tube voltage, 15 mA filament current, 6–8 hr exposure, samples diluted 1:1 with starch, relative intensities estimated visually.

† Less intense lines not included here.

Potassium hexacyanoiridate(III). Although this salt(6) has been made during the present studies by fusion of a number of iridium compounds with KCN, these conversions are accompanied by extensive deposition of elemental iridium. It was found that use of K_3IrCl_6 results in < 2 per cent reduction to iridium and that this is by far the best starting material for the formation of $K_3Ir(CN)_6$, as follows.

An intimate mixture of finely ground K_3IrCl_6 (5·0 g) and KCN (5·0 g) was added *carefully and in very small portions* to 5 g of KCN heated to a temperature just sufficient to keep it molten. Upon completion of the strongly exothermal reaction, the melt was cooled, leached with hot water and filtered. The filtrate was carefully acidified with dilute HCl, warmed to expel HCN, and evaporated to dryness on a steam cone *under reduced pressure* as a precaution against decomposition of the cyanoiridate. The residue was dissolved in 100 ml of water and passed through 100 g of Dowex-50W (hydrogen form) at a rate of 1 ml/min. The resulting solution was evaporated nearly to dryness, redissolved in 100 ml of water and passed (as above) through another 100 g of Dowex-50W to insure complete removal of all cations except hydrogen. Finally, this solution was neutralized with dilute KOH, evaporated to 7 ml, and $K_3Ir(CN)_6$ was precipitated by addition of 40 ml of ethanol. The mixture was cooled to O°, filtered, the solid recrystallized from water-ethanol, as above, and dried for 1 hr at 110°. The yield was 3·64 g or 81 per cent; X-ray diffraction date are given in Table 1. (Found: K, 25·07; $[Ir(CN)_6]^{3-}$, 74·8. Calc. for $K_3Ir(CN)_6$: K, 25·15; $[Ir(CN)_6]^{3-}$, 74·8 %.)

---

(6) See for example, C. A. MARTIUS, *Ann.* 117, 357 (1861).

Recovery of iridium

Owing to the high cost of iridium and its compounds, procedures were devised for the recovery of iridium from accumulated solutions and residues. After consideration of several possibilities, it was concluded that a convenient form for the recovered material (from the standpoint of ease of conversion to other iridium salts) was ammonium hexachloroiridate(IV). Recovery schemes were devised for both HNO_3-soluble and HNO_3-insoluble residues.

To recover HNO_3-soluble iridium, the solution and/or solid was treated with concentrated nitric acid and evaporated nearly to dryness five times to remove halides ions and oxidize combined iridium to iridium(IV), and finally with sulphuric acid to remove nitric acid. The solution was filtered and diluted fifty fold with water; the residue was treated as described below. The pH of the solutions was adjusted to 4–5 and the resulting precipitate of hydrous iridium(IV) oxide was digested for 2 hr on a steam bath. The solid was separated by filtration through a fine porosity filter crucible; the clear colourless filtrate was discarded. The oxide was washed once with water, dissolved in concentrated hydrochloric acid and heated until the solution assumed a deep red colour. The volume was reduced by evaporation to ca. 30 ml, 100 ml of water was added, followed by a five fold excess of ammonium chloride (based on the estimated iridium content of the solution). The resulting $(NH_4)_2IrCl_6$ was digested on a steam cone for 2 hr, cooled to O°, filtered, washed once with a small volume of ice-water and dried *in vacuo* over concentrated sulphuric acid for 24 hr.

Dry solid HNO_3-insoluble residues were fused with 20 parts by weight of sodium peroxide in a silver crucible for 10 min. The melt was cooled, leached repeatedly with water, and filtered. The residue was leached with concentrated nitric acid; the resulting solution was discarded and the solid residue was retained for repeated fusion with sodium peroxide. The water leach was treated with dilute hydrochloric acid until precipitation of AgCl was complete. This was filtered, the pH of the solution was adjusted to 4–5 with dilute sulphuric acid, and the resulting hydrous iridium(IV) oxide precipitate was treated as described above.

As applied to the recovery of iridium from materials of widely diverse origin, the foregoing procedures generally resulted in the recovery of 80–90 per cent of the estimated iridium present. The only iridium-containing species that did not respond readily to the above treatment was the very stable hexacyanoiridate(III) ion.

Ammonolysis tests

In order to insure that reduction of the four compounds listed in Table 1 would not be complicated by solvolysis of the starting materials, each was treated separately as follows.

Hexammineiridium(III) iodide. This salt dissolved readily in ammonia at −33·5°; the solubility was of the order of 30 g/100 ml of solution. Upon complete removal of the solvent, the residue gave an X-ray diffraction pattern identical with that which led to the data given in Table 1 for $[Ir(NH_3)_6]I_3$ and which included no lines attributable to NH_4I.

Potassium hexachloroiridate(III). This substance is virtually insoluble in ammonia at −33·5°. Treatment of a 725 mg sample with successive 150 ml portions of ammonia for several hours, followed by filtration, provided an ammonia-insoluble residue which gave an X-ray diffraction pattern identical with that for pure K_3IrCl_6 (Table 1). The ammonia-soluble fraction consisted of only ca. 5 mg of white solid; an X-ray diffraction pattern provided an unequivocal identification of NH_4Cl.

Potassium hexabromoiridate(III). This salt exhibits only slight solubility in ammonia at −33·5°. Treatment of a 622 mg sample with successive 150, 50 and 30 ml portions of ammonia over 15 hr, followed by filtration, gave ca. 10 mg of ammonia-soluble material. Both the insoluble and soluble fractions gave X-ray diffraction patterns characteristic of K_3IrBr_6 (Table 1) and showed no evidence of the presence of NH_4Br.

Potassium hexacyanoiridate(III). A 65 mg sample of the salt was exposed to excess ammonia at −33·5° for 4 hr; the solubility was estimated to be of the order of 15 g/100 ml of solution. After evaporation of the solvent, the residue gave a negative test for free cyanide ion and an X-ray diffraction pattern characteristic of (only) $K_3Ir(CN)_6$ (Table 1).

Reduction of hexamminiridium(III) iodide with potassium

Preliminary experiments, including potentiometric titrations, showed that $[Ir(NH_3)_6]I_3$ is reduced by ammonia solutions of potassium without formation of water-insoluble gases and that an initial two-electron reduction (presumably leading to $[Ir(NH_3)_6I)$ is followed by a one-electron reduction to form $[Ir(NH_3)_5]^0$. The ammonia-insoluble product of the relatively rapid initial reaction is a white solid; experiments designed to permit isolation of this substance in pure form were unsuccessful. The second stage in the reduction was quite slow and apparently provided mixtures of $[Ir(NH_3)_6]I$ and $[Ir(NH_3)_5]^0$ unless provision was made for long reaction times; the final product was a pale yellow diamagnetic solid.

In a typical experiment leading to complete reduction, 0·6083 g of the iodide in 150 ml of ammonia was treated with an ammonia solution containing exactly three molar equivalents of potassium over a period of 8 hr. After addition of 2·9 equivalents of potassium, the solution assumed a permanent blue colour. After digestion for 12 hr at −33·5° without change in the intensity of this colour, the mixture was filtered and the pale yellow solid was washed six times with 30 ml portions of ammonia. Following complete removal of the solvent, the product was transferred to the dry box for removal of samples. (Found: Ir, 70·1; NH_3, 29·9. Calc. for $[Ir(NH_3)_5]^0$: Ir, 69·3; NH_3, 30·7%.) X-ray diffraction data are included in Table 1. The foregoing analytical data were obtained by thermally decomposing a 0·1196 g sample of the yellow solid *in vacuo*, measuring the volume of ammonia liberated (largely at 90 ± 2°), and weighing the elemental iridium (identified by X-ray diffraction pattern) remaining both at 135° and after treatment with hydrogen (without loss of weight) at 800°.

In separate experiments conducted as described above, the total iridium accounted for as elemental iridium remaining after thermal decomposition represented 98·6 per cent of that used as $[Ir(NH_3)_6]I_3$. Similarly, analysis of the combined ammonia filtrate and washings accounted for 98·3 per cent of the iodine.

Reduction of potassium hexachloroiridate(III) with potassium

Despite the foregoing evidence for slow ammonolysis of this salt, its reduction with potassium at −33·5° was demonstrated as follows:

A 0·706 g sample of K_3IrCl_6 was slurried in 50 ml of ammonia and treated dropwise with a solution of 0·1586 g (3 equivalents) of potassium in 20 ml of ammonia. The resulting brown ammonia-insoluble product was filtered and washed with ammonia until the washings were chloride ion-free. Thereafter, the solvent was removed under reduced pressure; the resulting pyrophoric solid was analysed by thermal decomposition. (Found: Solid residue, 83·0%; NH_3/Ir, 1·5; Cl, 1·3%.)

Reduction of potassium hexabromoiridate(III) with potassium

Treatment of 0·6227 g of K_3IrBr_6 in 150 ml of ammonia with 0·1027 g of potassium in 22 ml of ammonia resulted in the formation of a brown ammonia-insoluble solid without evolution of water-insoluble gases. The solution assumed a permanent blue colour after addition of 3·1 equivalents of potassium. After digestion for 3 hr at −33·5°, the mixture was filtered and the brown solid was washed five times with 50 ml portions of ammonia. Analysis of the combined solution and washings accounted for 98·5 per cent of the bromine used as K_3IrBr_6.

Upon removal of the residual solvent at −33·5° and warming to room temperature, the bromine-free brown solid appeared to be stable. When, however, the pressure was lowered to 10^{-3} mm, ammonia was evolved slowly and the solid darkened. A 442 mg sample was decomposed thermally by heating *in vacuo* to provide only iridium and ammonia, but the volume of the latter was too small to measure accurately. Iridium was identified by an X-ray diffraction pattern.

Attempted reduction of potassium hexacyanoiridate(III)

Treatment of 1·268 g of $K_3Ir(CN)_6$ in 50 ml of ammonia with an excess of potassium (0·5308 g; 5 equivalents) in 18 ml of ammonia resulted in a low rate of utilization of potassium; hydrogen was evolved continuously. After 5·5 hr, the blue reaction mixture was back-titrated with 1·9690 g of NH_4I in 18 ml of ammonia and the resultant hydrogen was also collected. The total hydrogen amounted to 147·5 cm^3 as compared with 148·3 cm^3 equivalent to the total potassium used. Upon complete removal of the solvent, the residual solid gave an X-ray diffraction pattern characteristic (only) of $K_3Ir(CN)_6$ and a negative test for free cyanide ion.

DISCUSSION

The data given above show that the over-all reduction of hexammineiridium(III) iodide proceeds in accordance with the equation,

$$[Ir(NH_3)_6]I_3 + 3K^+ + 3e^- \rightarrow [Ir(NH_3)_5]^0 + 3K^+ + 3I^- + NH_3$$

thus providing an independent confirmation of the existence of the previously reported(1) pentammineiridium(O). Furthermore, the properties of the product formed in the present work are in all respects virtually identical with those of the product formed by the reduction of bromopentammineiridium(III) bromide.(1) The only difference is that the present product gave a good X-ray diffraction pattern; this presumably is attributable to larger crystal size resulting from a lower rate of formation. Results obtained in the course of these studies were strongly suggestive of an intermediate reduction of $[Ir(NH_3)_6]I_3$ to $[Ir(NH_3)_6]I$, but conclusive confirmatory evidence could not be obtained.

The reduction of K_3IrCl_6 was complicated by a slow competing solvolytic reaction as well as by the insolubility of the chloro complex. Since the ammonia-insoluble product was washed free of KCl, retention of chlorine in the ammonia-insoluble product is most likely due to unreacted K_3IrCl_6; hence, incomplete reduction is indicated. In the case of the corresponding bromide, however, complete removal of bromine was demonstrated and in this case as well as in that of the chloride, it seems most likely that the primary reduction product was an ammine of iridium(O) of the type $[Ir(NH_3)_x]^0$ where $x < 5$. However, since it has not been possible to demonstrate integral NH_3/Ir ratios, the possibility of ammonia absorbed on finely divided metal cannot be eliminated.

The reduction of $K_3Ir(CN)_6$ was expected to lead to potassium hexacyanoiridate(O), or intermediate reduction products, analogous to the corresponding zerovalent species previously observed for other transitional metals.(7–11) The results reported above, however, show that $K_3Ir(CN)_6$ is not reduced by potassium in ammonia at −33·5°.

(7) J. W. Eastes and W. M. Burgess, *J. Amer. Chem. Soc.* **64**, 1187 (1942).

(8) J. J. Burbage and W. C. Fernelius, *J. Amer. Chem. Soc.* **65**, 1484 (1943).

(9) V. J. Christensen, J. Kleinberg and A. W. Davidson, *J. Amer. Chem. Soc.* **75**, 2495 (1953).

(10) W. Hieber and C. Bartenstein, *Naturwissenschaften* **13**, 300 (1952).

(11) G. W. Watt, J. L. Hall, G. R. Choppin and P. S. Gentile, *J. Amer. Chem. Soc.* **76**, 373 (1954).

Although the number of cases studied thus far is limited, it appears that iridium complexes characterized by moderate to large crystal field stabilization energies are resistant to acceptance of electrons even under extreme conditions of reduction. This is illustrated by the CN^- and en(12) ligands. In combination with weak field ligands such as halide ions or NH_3, however, reduction of Ir^{3+} occurs much more readily and in at least two cases it has been shown conclusively that a product that can be interpreted as pentammineiridium(O) results.

Finally, this and earlier papers relating to ammines of transitional metals have not been concerned with detailed structures except for the suggestion that the central metal atom may be in the zero oxidation state. However, several structures have been considered, including ones involving hydride ions. It is hoped that nuclear magnetic resonance studies now in progress will provide information useful in making a choice among different possible structures.(13)

(12) G. W. Watt, L. E. Sharif and E. P. Helvenston, *Inorg. Chem.* 1, 6 (1962)
(13) Cf., J. Chatt and G. A. Rowe, *Nature, Lond.* 191, 1191 (1961).

J. Inorg. Nucl. Chem., 1962, Vol. 24, pp. 1073 to 1081. Pergamon Press Ltd. Printed in England

ORGANOPHOSPHORUS COMPOUNDS—V

A NEW SYNTHESIS OF TERTIARY PHOSPHINES AND ARSINES, PHOSPHONIC AND THIOPHOSPHONIC AS WELL AS PHOSPHINIC AND THIOPHOSPHINIC HALIDES[1]

L. Maier*

Monsanto Chemical Company, Research Department, Inorganic Chemicals Division,
St. Louis, Missouri

(*Received* 22 *January* 1962; *in revised form* 6 *March* 1962)

Abstract—The alkylation of dialkylhalophosphines and arsines with organic lead compounds produces in excellent yields tertiary phosphines and arsines. Since the alkylation can be done stepwise, this represents a simple method for the preparation of tertiary phosphines and arsines containing three different organic groups. Furthermore, phosphoryl and thiophosphoryl halides can also be alkylated and arylated with organic lead and tin compounds to give phosphonic, phosphinic, thiophosphonic, and thiophosphinic halides, respectively. Aminophosphines, phosphite and phosphate esters do not react with organic lead compounds even upon extensive heating at high temperatures.

In a previous paper[2] we showed that tetravinyllead is an excellent vinylating reagent for the preparation of vinyl halogene compounds of the Group V elements. This method has now been extended to show that quadruply connected phosphorus compounds (such as $PSCl_3$, $POCl_3$ and many others) can also be alkylated or arylated with tetraalkyl or tetraaryllead compounds. Organic tin compounds may also be used in this reaction.

RESULTS AND DISCUSSION

Kharasch *et al.*[3] in his studies demonstrated that tetraethyllead reacts with PCl_3 upon heating to give ethyldichlorophosphine. Higher temperatures effect further alkylation and dialkylchlorophosphines are produced.[4,5] We found that dialkyl and arylhalophosphines react further with tetra-alkyl and tetra-aryllead to give tertiary phosphines. Since the alkylation can be done stepwise:

$$3PCl_3 + PbR_4 \rightarrow 3RPCl_2 + PbCl_2 + RCl \quad (1)$$

$$3RPCl_2 + PbR'_4 \rightarrow 3RR'PCl + PbCl_2 + R'Cl \quad (2)$$

$$3RR'PCl + PbR''_4 \rightarrow 3RR'R''P + PbCl_2 + R''Cl \quad (3)$$

this represents an excellent method for the preparation of tertiary phosphines, containing three different organic groups.

Quadruply connected phosphorus halogen compounds do not react as easily as triply connected phosphorus halogen compounds. However, upon heating for longer periods and at higher temperatures similar exchange reactions were observed:

---

* On leave of absence from Monsanto Research S.A., Zurich, 3/45, during 1960.

(1) Part IV of this series, *J. Inorg. Nucl. Chem.* **24**, 275 (1962).

(2) L. Maier, *Tetrahedron Letters*, No. 6, 1 (1959).

(3) M. S. Kharasch, E. V. Jensen and S. Weinhouse, *J. Org. Chem.* **14**, 429 (1949).

(4) M. H. Beeby and F. G. Mann, *J. Chem. Soc.* 411 (1951).

(5) (a) B. Bartocha, C. M. Douglas and M. Y. Gray, *Z. Naturforsch.* **14 b**, 809 (1959); (b) M. Green and R. F. Hudson, *Proc. Chem. Soc.* 145 (1961).

$$3PXCl_3+PbR_4 \rightarrow 3RPXCl_2+PbCl_2+RCl \quad (X = O, S) \qquad (4)$$

$$3RPXCl_2+PbR'_4 \rightarrow 3RR'PXCl+PbCl_2+R'Cl \qquad (5)$$

$$3RR'PXCl+PbR''_4 \rightarrow 3RR'R''PX+PbCl_2+R''Cl \qquad (6)$$

The reaction is catalysed by aluminium trichloride. Many thiophosphonyl halides give a quantitative yield of the alkylated product, but the phosphonyl halides react more sluggishly and only after heating for much longer periods. It is interesting to note that phosphorus thiotrichloride gave, even when used in excess, with organic lead and tin compounds in addition to the thiophosphonic halide appreciable amounts of the dialkylated product, thiophosphinic halide. An explantion for this is that thiophosphonic halides are alkylated about as fast as phosphorus thiotrichloride. By heating various phosphorus compounds with organolead compounds at the same temperature for various time intervals and analysing the mixture by ^{31}P nuclear magnetic resonance, the following approximate series of reactivities were found:

1. Reactivity series of phosphorus compounds:

$$PBr_3 \approx CH_3PBr_2 > PCl_3 > CH_3PCl_2 \approx C_6H_5PCl_2 > (CH_3)_2PCl \approx (C_6H_5)_2PCl > PSCl_3 \approx C_6H_5PSCl_2 \approx CH_3PSCl_2 > ClCH_2PSCl_2 > (CH_3)_2PSCl > POCl_3 \approx C_6H_5POCl > ClCH_2POCl_2$$

2. Reactivity series of organolead compounds:

$$Pb(CH_3)_4 \approx Pb(C_2H_5)_4 > Pb(C_4H_9)_4 > Pb(C_6H_5)_4$$

The results with tetramethyllead, tetraethyllead and tetraphenyllead as alkylating agents and various phosphorus compounds are summarized in Tables 1, 2 and 3.

TABLE 1.—ALKYLATION OF PHOSPHORUS COMPOUNDS WITH $Pb(CH_3)_4$, DISSOLVED IN TOLUENE (85% solution)

P-compound	Ratio P-comp. :$Pb(CH_3)_4$	Heating time at 125°C (hr)	Products	Yield (%)	Chemical shift in p.p.m (ref. 85% H_3PO_4)
PCl_3	2·1:1	20	CH_3PCl_2	100*	−192**
CH_3PCl_2	2·2:1	4	$(CH_3)_2PCl$	12†	−92††
CH_3PBr_2	2·5:1	1 (22°C)	$(CH_3)_2PBr$	13‡	−87·9
$C_6H_5PSCl_2$	2·3:1	120	$C_6H_5(CH_3)PSCl$	90	−81·0
CH_3PSCl_2	2·5:1	200	$(CH_3)_2PSCl$	81	−87·3
$(CH_3)_2PSCl$	2·5:1	200	$(CH_3)_3PS$	12	−59·1
$C_6H_5POCl_2$	2·3:1	200	$C_6H_5(CH_3)POCl$	19	−52·0

* After 4 hrs heating at 122°C, 86% CH_3PCl_2 had formed.

† After additional heating of the tube for 16 hrs at 125°C only $(CH_3)_2PCl$ was detected in the n.m.r. spectra. But the peak intensity had decreased strongly (indication of extensive decomposition of $(CH_3)_2PCl$).

‡ The content of the tube turned solid after one hour standing at room temperature, probably caused by formation of phosphonium type $(R_3PBr^+)Br^-$ compounds.

** Reported −191·2 p.p.m.(6)

†† Reported −93·0 p.p.m.(7)

---

(6) C. STUEBE, W. M. LESUER and G. R. NORMAN, *J. Amer. Chem. Soc.* **77**, 3526 (1955).

(7) G. W. PARSHALL, *J. Inorg. Nucl. Chem.* **12**, 372 (1960).

TABLE 2.—ALKYLATION OF PHOSPHORUS COMPOUNDS WITH $Pb(C_2H_5)_4$

P-compound	Ratio P-comp. :$Pb(C_2H_5)_4$	Heating time at 125°C (hr)	Products	Yield (%)	Chemical shift in p.p.m. (ref. 85% H_3PO_4)
PBr_3	2·79:1	19 (22°C)	$C_2H_5PBr_2$	60[a]	−194·0
CH_3PBr_2	2·71:1	2	$CH_3C_2H_5PBr$	100[a]	− 98·5
PCl_3	2·56:1	4	$C_2H_5PCl_2$	100	−196·3
PCl_3	1·87:1	4	$C_2H_5PCl_2$	89	−196·3
			$(C_2H_5)_2PCl$	11	−119·0
CH_3PCl_2	1·84:1	4[b]	$CH_3C_2H_5PCl$	100	−105·2
$C_6H_5PCl_2$	1·96:1	4	$C_2H_5(C_6H_5)PCl$	100	− 97·0
$(CH_3)_2PCl$	1·85:1	66	$(CH_3)_2C_2H_5P$	83·5	+ 48·5[g]
			$(CH_3)(C_2H_5)_2P$	8·5[c]	+ 34·0[h]
			$(CH_3)_3P$	8·5[c]	+ 61·0[i]
$(C_6H_5)_2PCl$	2·07:1	66	$(C_6H_5)_2C_2H_5P$	90	+ 13·5[k]
			$C_6H_5(C_2H_5)_2P$	5[d]	+ 15·1[l]
			$(C_6H_5)_3P$	5[d]	+ 5·9[m]
$PSCl_3$	2·734:1	39	$C_2H_5PSCl_2$	92	− 94·0[n]
			$(C_2H_5)_2PSCl$	8	−108·3
CH_3PSCl_2	1·94:1	66 (115°C)	$CH_3C_2H_5PSCl$	77[e]	− 98·0
$C_6H_5PSCl_2$	1·92:1	66 (115°C)	$C_2H_5(C_6H_5)PSCl$	70[f]	− 93·7
			$(C_2H_5)_2(C_6H_5)PS$	20	− 52·0
$(CH_3)_2PSCl$	1·89:1	130	$(CH_3)_2C_2H_5PS$	84	− 57·0
$POCl_3$	2·64:1	90	$C_2H_5POCl_2$	40	− 52·5[o]
			$(C_2H_5)_2POCl$	20	− 76·7
$ClCH_2POCl_2$	1·87:1	160	$C_2H_5(ClCH_2)POCl$	42	− 43·8
$C_6H_5POCl_2$	1·77:1	120	$C_2H_5(C_6H_5)POCl$	50	− 59·0

[a] It is better to carry out this reaction in an open flask, since the formation of phosphonium salts can be avoided in this way.

[b] Further heating of the tube for 17 hr at 125°C caused strong decomposition of the product.

[c] Products formed by reorganization of $(CH_3)_2C_2H_5P$ to give $CH_3(C_2H_5)_2P$ plus $(CH_3)_3P$. Additional heating for 117 hr at 125°C gave 67% $(CH_3)_2C_2H_5P$, 16·5% $CH_3(C_2H_5)_2P$ and 16·5% $(CH_3)_3P$. $PbCl_2$ might act as a catalyst in this reorganization reaction. This will be investigated further.

[d] Products formed by reorganization of $(C_6H_5)_2C_2H_5P$ to give $C_6H_5(C_2H_5)_2P$ plus $(C_6H_5)_3P$ (see *c*).

[e] Additional heating of the tube for 70 hr at 125°C gave 58% $CH_3C_2H_5PSCl$ and 35% $CH_3(C_2H_5)_2PS$.

[f] Additional heating of the tube for 70 hr at 125°C gave 47% $C_2H_5(C_6H_5)PSCl$ and 44% $(C_2H_5)_2C_6H_5PS$.

[g] Reported +51 p.p.m.(8)

[h] Reported +34 p.p.m.(8)

[i] Reported +61 p.p.m.(9)

[k] Reported +12 p.p.m.(8)

[l] Reported +16 p.p.m.(8)

[m] Reported +5·88 p.p.m.(9, 10)

[n] Reported −94·3 p.p.m.(9, 10)

[o] Reported −53·0 p.p.m.(9)

(8) W. A. HENDERSON JR. and S. A. BUCKLER, *J. Amer. Chem. Soc.*, **82**, 5794 (1960).

(9) H. FINEGOLD, *Ann. N.Y. Acad. Sci.* **70**, 875 (1958).

(10) N. MULLER, P. C. LAUTERBUR and J. GOLDENSON, *J. Amer. Chem. Soc.* **78**, 3557 (1956).

TABLE 3.—ARYLATION OF PHOSPHORUS COMPOUNDS WITH $Pb(C_6H_5)_4$

P-compound	Ratio P-comp. :$Pb(C_6H_5)_4$	Heating time at 180°C(hr)	Products	Yield (%)	Chemical shift in p.p.m. (ref. 85% H_3PO_4)
PBr_3	3·01:1	180	$C_6H_5PBr_2$	68	−152·0
			$(C_6H_5)_2PBr$	21	− 70·8
CH_3PBr_2	4·63:1	180	$C_6H_5PBr_2$	54[a]	−152·0
			$CH_3C_6H_5PBr$	7	− 77·0
PCl_3	3·03:1	180	$C_6H_5PCl_2$	93	−161·5[d]
			$(C_6H_5)_2PCl$	2	− 81·5
CH_3PCl_2	2·01:1	39 (165°C)	$C_6H_5PCl_2$	55[b]	−161·5[d]
			$CH_3(C_6H_5)PCl$	20	− 83·4
$C_6H_5PCl_2$	3·0:1	83	$(C_6H_5)_2PCl$	90	− 81·5
$(CH_3)_2PCl$	2·03:1	39 (165°C)	$CH_3(C_6H_5)_2P$	50[c]	+ 28·0
			$(CH_3)_2C_6H_5P$	50	+ 47·0[e]
$(C_6H_5)_2PCl$	2·98:1	180	$(C_6H_5)_3P$	95	+ 5·9[f]
$PSCl_3$	3·0:1	180	$C_6H_5PSCl_2$	35	− 74·8[g]
			$(C_6H_5)_2PSCl$	32	− 79·6
CH_3PSCl_2	1·9:1	66	$CH_3C_6H_5PSCl$	100	− 81·0
$C_6H_5PSCl_2$	2·1:1	136	$(C_6H_5)_2PSCl$	94	− 79·6
			$(C_6H_5)_3PS$	6	− 42·6
$ClCH_2PSCl_2$	1·9:1	180	$ClCH_2(C_6H_5)PSCl$	46	− 77·0
$POCl_3$	3·01:1	180	$C_6H_5POCl_2$	29	− 33·7[h]
			$(C_6H_5)_2POCl$	15·5	− 42·7
$C_6H_5POCl_2$	1·93:1	66	$(C_6H_5)_2POCl$	68	− 42·7
$ClCH_2POCl_2$	2·0:1	180	$ClCH_2(C_6H_5)POCl$	11	− 44·4

[a] CH_3PBr_2 decomposes partly at this temperature to give PBr_3 and other products. PBr_3 then reacts with $Pb(C_6H_5)_4$ to give $C_6H_5PBr_2$. When a tube was kept for 18 hr at 100° C, no $C_6H_5PBr_2$ was formed, but 17% $CH_3C_6H_5PBr$.

[b] CH_3PCl_2 decomposes partly at this temperature to give PCl_3 and other products. PCl_3 then reacts with $Pb(C_6H_5)_4$ to give $C_6H_5PCl_2$. When a tube was kept for 18 hr at 100°C, no reaction occurred.

[c] Could have been formed from CH_3PCl_2, a decomposition product of $(CH_3)_2PCl$.

[d] Reported −162 p.p.m.(9)

[e] Reported +46 p.p.m.(8)

[f] Reported +5·88 p.p.m.(9, 10)

[g] Reported −74·8 p.p.m.(9)

[h] Reported −34·5 p.p.m.(9)

This reaction represents a simple method for the preparation of thiophosphonic and thiophosphinic halides, which are important intermediates for the synthesis of phosphorus-containing insecticides.(11)

---

(11) (a) H. H. SCHLÖR, E. SCHEGK and G. SCHRADER, DPA (German patent application) F 23322, F 24304, F 23321 (1957);

(b) A. I. RAZUMOV, O. A. MUKHACHEWA, I. V. ZAIKONNIKOVA, N. N. GODOVINKA and N. I. RIZPOLOZHENSKII, *Akad. Nauk SSSR*, Trudy 1—oi Konferents, 1955, 205 (*Chem. Abstr.* **52**, 293 (1958));

(c) F. W. HOFFMANN and T. R. MOORE, *J. Chem. Amer. Soc.* **80**, 1150 (1958).

Recently, it was postulated(12) that phosphite and phosphate esters give octane loss in leaded fuel by reaction with the tetraethyllead to form compounds of reduced antiknock activity, e.g.:

$$P(OR)_3+Pb(C_2H_5)_4 \rightarrow C_2H_5P(OR)_2+Pb(C_2H_5)_3(OR) \qquad (7)$$

However, we found that aminophosphines $P(NR_2)_3$, phosphite and phosphate esters do not react with tetra-alkyl or aryllead compounds, even upon extensive heating for long periods. Therefore, the lead antagonism of phosphite and phosphate esters cannot be caused by an exchange reaction as postulated in Equation (7).

A few experiments were carried out with alkylhaloarsines in order to establish the scope of the reaction. Here also, a tertiary arsine was produced, when a dialkylhaloarsine was caused to react with a tetra-alkyllead compound. The results are summarized in Table 4. The reaction proceeds according to Equations (8) and (9):

$$3\ RAsBr_2+PbR'_4 \rightarrow 3RR'AsBr+PbBr_2+R'Br \qquad (8)$$

$$3RR'AsBr+PbR''_4 \rightarrow RR'R''As+PbBr_2+R''Br \qquad (9)$$

TABLE 4.—ALKYLATION OF ALKYLHALOARSINES WITH TETRA-ALKYLLEAD COMPOUNDS

PbR_4 R =	As-compound	Product	Yield (%)	b.p. (°C)	n_D^{20}
CH_3	CH_3AsBr_2	$(CH_3)_2AsBr$	90	126–129	1·5703*
C_2H_5	CH_3AsBr_2	$CH_3(C_2H_5)AsBr$	80	154–155	1·5732
$CH_2 = CH$	CH_3AsBr_2	$CH_3(CH_2 = CH)AsBr$	60·5	144–145	
C_4H_9	CH_3AsBr_2	$CH_3(C_4H_9)AsBr$	57	172–178	1·6368
C_2H_5	$(CH_3)_2AsBr$	$(CH_3)_2C_2H_5As$	56	83–84	

* Reported b.p. 128–130°C, $n_D^{20} = 1{\cdot}5713$.(13)

Two experiments with tetraphenyltin demonstrated that it can also be used as an arylating reagent. Tetraethyltin was shown earlier to give excellent yields of $C_2H_5PBr_2$ when reacted with PBr_3(14).

The results are summarized in Table 5.

TABLE 5.—ARYLATION OF PCl_3 AND $PSCl_3$ WITH TETRAPHENYLTIN

P-compound	Ratio P-compound :$Sn(C_6H_5)_4$	Heating time at 180°C (hr)	Products	Yield (%)	Chemical shift in p.p.m. (ref. 85% H_3PO_4)
PCl_3	3·1:1	350	$(C_6H_5)PCl_2$	65	−161·5
$PSCl_3$	3·09:1	130	$C_6H_5PSCl_2$	58	− 74·8*
			$(C_6H_5)_2PSCl$	36	− 79·6

* Reported −74·8 p.p.m.(9)

---

(12) F. C. GUNDERLOY, JR. and R. F. NEBLETT, presented before the Division of Petroleum Chemistry, Amer. Chem. Soc. Cleveland Meeting, April 1960.

(13) L. MAIER, E. G. ROCHOW, W. C. FERNELIUS, *J. Inorg. Nucl. Chem.*, **16**, 213 (1961).

(14) A. SACCO, *Mem.* Acad. Lincei, 101 (1951).

Contrary to tetraphenyllead, tetraphenyltin reacted much faster with $PSCl_3$ than with PCl_3. Thus, heating a mixture of $PSCl_3$ and $Sn(C_6H_5)_4$ in the ratio of 3·09:1 for 40 hr to 180°C produced 22% $C_6H_5PSCl_2$ and 36% $(C_6H_5)_2PSCl$. However, no $C_6H_5PCl_2$ was formed when a mixture containing PCl_3 and $Sn(C_6H_5)_4$ in the ratio 3·1:1 was heated for 40 hr to 180°C, but the reaction mixture became nearly completely solid when cooled to room temperature consisting probably of a complex of the type $[PCl_2]_2^{2+}$ $[Sn(C_6H_5)_4Cl_2]^{2-}$. Subsequent heating of this solid for additional 310 hr to 180°C decomposed it to give $C_6H_5PCl_2$ and $(C_6H_5)_2SnCl_2$.

EXPERIMENTAL

Most of the experiments were carried out in thick-walled 15 mm Pyrex tubes which, after being flashed with nitrogen, were sealed off and heated at temperatures and for time intervals as indicated in Tables 1, 2, 3 and 5. The mixtures were quantitatively analysed by nuclear magnetic resonance spectroscopy. The measurements were made with a Varian Model V-4300 B high resolution nuclear magnetic resonance spectrometer at a frequency of 16·2 mc/s and a magnetic field of approximately 9395 G. The referencing was done by tube interchange using 85% H_3PO_4 as the reference compound. However, some experiments were repeated in an open flask to demonstrate that the reaction goes also to completion without pressure. All the experiments involving haloarsines were carried out in an open flask and the products isolated by fractional distillation in a spinning band column.

1. *Preparation of phosphonous and phosphinous halides*

a. *Methylphosphonous dibromide* CH_3PBr_2. Sixty-five grammes of PBr_3 (0·24 mole) were placed in a three-necked flask, equipped with a stirrer, reflux condenser and a dropping funnel. Then 13 g of $Pb(CH_3)_4$ (0·048 mole) were added dropwise. After about 7 g of $Pb(CH_3)_4$* had been added, a strong exothermic reaction started and continued with further adding. After 2 hr refluxing, the reaction mixture was distilled under reduced pressure and the distillate collected in a trap, cooled with liquid nitrogen. Residue 13 g of $PbBr_2$ (theor. 17·8 g). Fractional distillation of the condensate yielded three fractions: (1) 120–145°C/720 mm (29 g), (2) 145–165°C/720 mm (9·5 g), (3) 165–175°C/720 mm (8 g). Redistillation of fraction 1 and 2 gave pure CH_3PBr_2, b. p. 139–141°C/720 mm, 21 g (= 72·5 per cent) n_D^{20} = 1·6210 (reported b.p. 139–141°C(15)). The ^{31}P chemical shift agreed with an authentic sample (−184·0 p.p.m.). (Found: C, 5·89; H, 1·46; Br, 77·56. Calc. for CH_3Br_2P: C, 5·83; H, 1·47; Br, 77·65%.)

b. *Methylphenyl phosphinous chloride* $C_6H_5(CH_3)PCl$. Similarly from 0·3 mole $C_6H_5PCl_2$, 0·01 mole $AlCl_3$ and 0·1 mole $Pb(CH_3)_4$; heating time 2 hr at 100°C; yield 61 per cent; b.p. 66–67° C/2 mm.

c. *Ethylphenyl phosphinous chloride* $C_6H_5(C_2H_5)PCl$. From 0·3 mole $C_6H_5PCl_2$, 0·01 mole $AlCl_3$ and 0·1 mole $Pb(C_2H_5)_4$; heating time 4 hr at 120°C; yield 80 per cent; b.p. 73–75°C/2 mm (reported b.p. 76° C/2 mm, Reference 5b).

2. *Preparation of tertiary phosphines*

a. *Ethyldiphenylphosphine* $(C_6H_5)_2C_2H_5P$. From 0·2 mole $(C_6H_5)_2PCl$ and 0·1 mole $Pb(C_2H_5)_4$; heating time 27 hr at 110°C; yield 55 per cent; b.p. 126–130°C/0·5 mm (reported b.p. 184°C/22 mm(16a)). This run was repeated with the addition of 0·01 mole $AlCl_3$. In this case a 59 per cent yield of ethyldiphenylphosphine was obtained after 4 hr heating at 110°C.

---

* Tetramethyllead, tetraethyllead and tetraphenyllead were supplied by the Ethyl Corporation.

(15) L. Maier, *Angew. Chem.* **71**, 574 (1959).

(16) (a) J. Meisenheimer, J. Casper, M. Höring, W. Sauter, L. Lichtenstadt and W. Samuel, *Lieb. Ann.* **449**, 213 (1926);

b. *Diethylphenylphosphine* $C_6H_5(C_2H_5)_2P$. From 0·1 mole $C_6H_5PCl_2$, 0·01 mole $AlCl_3$ and 0·1 mole $Pb(C_2H_5)_4$; heating time 4 hr at 110°C; yield 69 per cent; b.p. 60–65°C/2 mm (reported b.p. 96–98°C/10 mm(16a)). This phosphine was characterized as the phosphonium salt $[C_6H_5P(C_2H_5)_3]I$, m.p. 137–139°C (reported m.p. 139°C(16b)). (Found: I, 39·6. Calc. for $C_{12}H_{20}IP$: I, 39·4%.)

c. *Methylethylphenylphosphine* $C_6H_5(C_2H_5)CH_3P$. From 0·17 mole $C_6H_5CH_3PCl$; 0·005 mole $AlCl_3$ and 0·07 mole $Pb(C_2H_5)_4$; heating time 4 hr at 110°C; yield 62 per cent; b.p. 96–97°C/15 mm (reported b.p. 96–97°C/15 mm(16c)). This phosphine was characterized as the phosphonium salt $[C_6H_5(CH_3)P(C_2H_5)_2]I$, m.p. 104–105°C (reported m.p. 108–109°C(16a)). (Found: I, 41·4%. Calc. for $C_{11}H_{18}IP$: I, 41·2%.)

3. *Preparation of* CH_3PSCl_2 *and* $(CH_3)_2PSCl$

A mixture of 50·8 g of $PSCl_3$ (0·3 mole) and 26·7 g of $Pb(CH_3)_4$ (0·1 mole as an 80 per cent solution in toluene) was refluxed for 37 hr. Then the precipitated $PbCl_2$ was filtered off (15 g $PbCl_2$) and the filtrate fractionally distilled. The yield of CH_3PSCl_2 was only 18 per cent in this experiment. Therefore the experiment was repeated with the addition of aluminium trichloride which increased the rate of reaction considerably. Addition of zinc dichloride or cadmium dichloride had no effect on the reaction rate.

To a two-necked flask, equipped with a refluxing condenser and a stirrer, was added 50·8 g of $PSCl_3$ (0·3 mole) and 26·7 g of pure $Pb(CH_3)_4$. Then 2·6 g of technical $AlCl_3$ was added (*note*: $AlCl_3$ has to be added, while the mixture is still cold (at room temperature). In one experiment, where $AlCl_3$ was added to a refluxing mixture of $PSCl_3$ and $Pb(CH_3)_4$ a nearly explosive reaction occurred). Addition of $AlCl_3$ is accompanied by a weak exothermic reaction. Then refluxing of the reaction mixture was started. The refluxing temperature increased over a period of 15 hr from 117 to 135°C. The precipitation of $PbCl_2$ started after about 1 hr refluxing. After cooling of the reaction mixture to room temperature the precipitated $PbCl_2$ was filtered off, washed several times with CCl_4, and dried in the high vacuum (yield 30·2 g), [theor. 30·4 g (27·8 g $PbCl_2$ + 2·6 g $AlCl_3$)]. The filtrate was fractionally distilled, using a spinning band column, fraction 1, b.p. 120–140°C/725 mm, 7·5 g mostly $PSCl_3$, fraction 2, b.p. 46–48°C/9·5 mm Hg, n_D^{20} 1·5509, 22 g of CH_3PSCl_2 (78·6 per cent). (Found: C, 8·02; H, 2·19. Calc. for CH_3Cl_2PS: C, 8·08; H, 2·02%. Reported: b.p. 44–45°C/9 mm Hg; n_D^{25} 1·5485(11b, 11c, 16d)) Fraction 3, b.p. 65–67° C/9·5 mm Hg; n_D^{20} 1·5460, 6 g of $(CH_3)_2PSCl$ (21·4%). (Found: Cl, 27·41. Calc. for C_2H_6ClPS: Cl, 27·58%. Reported: b.p. 72–75°/12 mm; n_D^{20} 1·5451(16e)). The ^{31}P chemical shift agreed with authentic samples CH_3PSCl_2: −79·8 p.p.m. (reported −79·8 p.p.m.(10)) $(CH_3)_2PSCl$: −87·3 p.p.m. (reported −87·3 p.p.m.(16f)). Eighty per cent of the theoretically available methyl groups of tetramethyllead according to Equations (4) and (5) were isolated as methylthiophosphonic and dimethylthio-phosphinic chloride.

4. *Preparation of* $C_2H_5PSCl_2$ *and* $(C_2H_5)_2PSCl$

A mixture of 100 g of $PSCl_3$ (0·59 mole) and 37 g of $Pb(C_2H_5)_4$ (0·115 mole) was refluxed for 10 hr in a two-necked flask, equipped with a stirrer and a reflux condenser. Then the precipitated $PbCl_2$ was filtered off, washed with carbon tetrachloride (23 g $PbCl_2$) and the filtrate fractionally distilled: (1) 177–181°C/740 mm 41 g $C_2H_5PSCl_2$ (= 87·8 per cent) (reported b.p. 80–82° C/50 mm Hg(17)), (2) 225–227°C/740 mm Hg, 5·7 g $(C_2H_5)_2PSCl$

(16) (b) W. C. Davies and W. P. G. Lewis, *J. Chem. Soc.* 1599 (1934);
(c) L. Horner and A. Mentrup, *Lieb. Ann.* **646**, 65 (1961).
(d) Z. Pelchowicz, *J. Chem. Soc.* 238 (1961);
(e) L. Maier, *Ber. Dtsch. Chem. Ges.* **94**, 3051 (1961).
(f) K. Mödritzer, L. Maier and L. D. C. Groenweghe, *J. Chem. Engng. Data.* **7**, 307 (1962).

(17) Fr. Guichard, *Ber. Dtsch. Chem. Ges.* **32**, 1572 (1899).

(= 12·2 per cent) (reported b.p. 117–120°C/15 mm Hg(18)). The ^{31}P chemical shift agreed with authentic samples $C_2H_5PSCl_2$:–94 p.p.m. (reported –94·3 p.p.m.(9) $(C_2H_5)_2PSCl$: –108·3 p.p.m.*

Ninety-four per cent of the theoretically available ethyl groups of tetraethyllead according to Equations (4) and (5) were isolated as ethylthiophosphonic and diethylthio-phosphinic chloride. An additional 10 g of $PbCl_2$ remained as residue in the distillation flask (isolated $PbCl_2$ altogether 33 g, theoretical 31·8 g).

5. *Preparation of* $C_6H_5PSCl_2$ *and* $(C_6H_5)_2PSCl$

A mixture of 32 g of $PSCl_3$ (= 0·189 mole) and 22 g of $Pb(C_6H_5)_4$ (= 0·042 mole) sealed under nitrogen in a thick-walled Pyrex tube was heated for 160 hr to 180°C. Then, the precipitated $PbCl_2$ was filtered off, washed with CCl_4 (13 g theor. 11·8 g) and the filtrate fractionally distilled: (1) 100°C/1 mm Hg, 5·5 g $C_6H_5PSCl_2$ (= 34 per cent), chemical shift –74·4 p.p.m. (reported –74·8 p.p.m.(10)), (2) 160–163°C/0·5 mm Hg, 10·5 g $(C_6H_5)_2PSCl$ (reported b.p. 160°C/0·3 mm Hg(6)), chemical shift –79·6 p.p.m. Eighty-two per cent of the theoretically available phenyl groups of tetraphenyllead according to Equations (4) and (5) were isolated as phenylthiophosphonic and diphenylthiophosphinic chloride.

6. *Attempted reaction of* $(C_2H_5O)_3PO$, $(C_2H_5O)_3P$ *and* $CH_3P[N(C_2H_5)_2]_2$ *with organic lead compounds*

Mixtures of $(C_2H_5O)_3PO$ and $Pb(C_2H_5)_4$ as well as $P(OC_2H_5)_3$ or $CH_3P[N(C_2H_5)_2]_2$ with $Pb(C_2H_5)_4$ (ratio 1:1, 2:1, 4:1 and 1:2), sealed in thick-walled Pyrex tubes, were heated for various time intervals and analysed by n.m.r.

(a) Tubes were kept for three weeks at room temperature. No exchange reaction could be detected.

(b) Additional heating of the tubes for 140 hr to 90°C did not cause any reaction.

(c) When the tubes were heated for 3 hr to 140°C, large amounts of metallic lead deposited, probably caused by decomposition of $Pb(C_2H_5)_4$. The residual liquid contained only the starting phosphorous compound, and no exchange reaction had occurred.

One could conceive an exchange reaction not involving the breakage of a P-O bond but of a C-O bond, such as:

$$Pb(C_6H_5)_4 + (C_2H_5O)_3PO \rightarrow Pb(C_6H_5)_3C_2H_5 + (C_6H_5O)(C_2H_5O)_2PO$$

However, no such reaction was observed when a tube containing $(C_2H_5O)_3PO$ and $Pb(C_6H_5)_4$ was heated for 250 hr to 150°C.

7. *Preparation of* $(CH_3)_2AsBr$

To 65 g of CH_3AsBr_2 (= 0·26 mole)† was slowly added under stirring 13 g of $Pb(CH_3)_4$ (= 0·05 mole). A strong exothermic reaction ensued. CH_3AsBr_2 came to refluxing. After the addition was completed, refluxing was continued for one hour and then the reaction mixture distilled under reduced pressure and the product collected in a trap, cooled with liquid nitrogen (residue 18 g $PbBr_2$, theor. 17·8 g). Fractional distillation of the condensate yielded: (1) 128–130°C/720 mm, Hg 25 g (= 90 per cent) $(CH_3)_2AsBr$, n_D^{20} = 1·570 (reported b.p. 128–129°C/720 mm, n_D^{20} = 1·5712(13)), (2) 175–183°C/720 mm Hg, 31 g CH_3AsBr_2 (starting material). During the reaction, 4·2 g CH_3Br were isolated (theor. 4·7 g).

---

* Authentic sample was obtained by cleavage of $[(C_2H_5)_2PS]_2$ with chlorine in Cl_4 solution and had the same chemical shift.

† Prepared from As + CH_3Br with Cu powder as a catalyst (Reference 13).

(18) V. M. PLETS, Dissertation, Kazan (1938).

8. *Alkylation of* CH_3AsBr_2 *with* $(C_2H_5)_4Pb$, $(CH_2 = CH)_4Pb$,* $(C_4H_9)_4Pb$.†

All these alkylations as well as alkylation of $(CH_3)_2AsBr$ with $(C_2H_5)_4Pb$ were carried out similarly as that described in experiment 7. The results are summarized in Table 4. The following analytical data were obtained.‡ (Found: C, 18·37; H, 4·11; Br, 40·35. Calc. for $CH_3C_2H_5AsBr$: C, 18·12; H, 4·05; Br, 40·18%. Found: Br, 43·08, Calc. for $(CH_3)_2AsBr$: 43·22%. Found: C, 38·73; H, 8·01. Calc. for $(CH_3)_2C_2H_5As$: C, 38·65; H, 8·93. Found: C, 18·2; H, 3·06. Calc. for $CH_3CH_2 = CHAsBr$: C, 18·3 H, 3·07.

Acknowledgements—This research was supported in part by the United States Air Force under Contract AF 33(616)-6950(1960), monitored by the Materials Laboratory, Wright Air Development Center, Wright Patterson Air Force Base, Ohio, U.S.A.

* Tetravinyllead was prepared from $PbCl_2$ and $CH_2 = CHMgCl$ in tetrahydrofuran(2) Contrary to JUENGE and COOK,(19) we hydrolysed the crude reaction mixture with saturated ammonium chloride solutions (about 90 ml per mole Grignard) and obtained 85 per cent pure tetravinyllead as compared to 34·3 per cent by JUENGE *et al.* We cannot confirm their statement that tetravinyllead shows considerable decomposition on hydrolysis with ammonium chloride after standing for one day. No decomposition was observed after standing for several days. However, after standing for two months in the dark, a small amount of white to pale yellow solid had precipitated. This indicates strongly that some decomposition occurs upon standing for long periods. The statement of BARTOCHA and GRAY(20) that tetravinyllead is stable even upon exposure to light is doubtful.

† Prepared from $PbCl_2$ and C_4H_9MgBr according to established procedures.

‡ Microanalyses were performed by A. PEISKER-RITTER, Brugg, Switzerland.

(19) E. C. JUENGE and S. E. COOK, *J. Amer. Chem. Soc.* **81**, 3578 (1959).

(20) B. BARTOCHA and M. Y. GRAY, *Z. Naturforsch.* **14 b**, 350 (1959).

J. Inorg. Nucl. Chem., 1962, Vol. 24, pp. 1083 to 1087. Pergamon Press Ltd. Printed in England

COMPLEXES OF THE RARE EARTHS—II

N,N′-ETHYLENEDIAMINE-DIACETIC ACID

L. C. THOMPSON
Department of Chemistry, University of Minnesota, Duluth, Minnesota

(*Received* 22 *February* 1962)

Abstract—Step-wise stoicheiometric formation constants have been determined for the rare earths (including yttrium) with N,N′-ethylenediaminediacetic acid. The measurements have been made in aqueous solutions of ionic strength $\mu = 0{\cdot}1$ (KNO_3) and a temperature of 25°C. The data have been interpreted in terms of 1:1 and 2:1 chelates. Trends in the values of log K_1 and log K_2 are discussed and compared with similar values for other aminopolycarboxylate complexes. It is further shown that the values of log K_2 are of such a magnitude as to suggest that the rare-earth ions exhibit a co-ordination number larger than six.

DESPITE the current interest in the rare-earth elements, there have been only a few studies devoted to determining their general co-ordinating tendencies.[(1)] At the present time such a project is underway in this laboratory and the stability constants of the rare-earth chelates of a variety of different types of ligands are being determined.

In this communication the stability constants for the 1:1 and 2:1 ethylenediamine-N,N′-diacetic acid–rare earth chelates are reported.

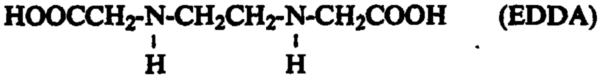

$$\underset{\displaystyle\mathrm{H}}{\overset{}{}}\mathrm{HOOCCH_2\text{-}\underset{\underset{H}{|}}{N}\text{-}CH_2CH_2\text{-}\underset{\underset{H}{|}}{N}\text{-}CH_2COOH}\qquad\text{(EDDA)}$$

Apparently this ligand has been the subject of only one earlier study[(2)] in which the stability constants for the 1:1 chelates with magnesium and several transition metals were reported.

EDDA is of particular interest in view of the recent suggestion[(3)] that the rare-earth ions can expand their co-ordination number beyond the six which is usually assumed. Since one EDDA molecule can only occupy four positions around the rare-earth ion, this leaves at least two, and possibly as many as four, co-ordinating positions unoccupied. The relative magnitudes of the stability constants for the 2:1 chelates compared with the 1:1 chelates should then give some indication as to whether the rare-earth co-ordination number is six or greater than six with this ligand.

EXPERIMENTAL

Solutions. A carbonate-free potassium hydroxide solution was prepared from a Fisher standard and standardized against potassium hydrogen phthalate. The EDDA was purchased from K & K Laboratories, Inc., and purified by two recrystallizations from water. An approximately 0·005 M solution was prepared and standardized by complexometric titration with copper using murexide as the indicator. A 1·000 M potassium nitrate solution was

---

[(1)] For a survey of the literature up to May, 1960, see L. C. THOMPSON, Ph.D. Dissertation, University of Illinois (1960).

[(2)] S. CHABEREK, JR. and A. E. MARTELL, *J. Amer. Chem. Soc.* 74, 6228 (1952).

[(3)] G. ANDEREGG, P. NAGELI, F. MULLER and G. SCHWARZENBACH, *Helv. Chim. Acta*, **42**, 827 (1959).

prepared from the analytical reagent. Solutions of magnesium, cadmium, and copper nitrates were prepared from the reagent grade materials and standardized complexometrically.

Approximately 0·005 M rare-earth nitrate solutions,* with the exception of cerium, were prepared by dissolving a weighed amount of the oxide (99·9 per cent pure) in a known excess of standard nitric acid. The cerium(III) nitrate solution was prepared from cerium(III) nitrate hexahydrate. The rare-earth content of each solution was determined by a complexometric titration using EDTA and Eriochrome Black T.(4) In addition, the cerium, neodymium and samarium solutions were analyzed by precipitating the oxalates, igniting to the oxides and weighing. In all cases the concentrations found experimentally were in good agreement with those calculated from the weight of oxide used. The excess nitric acid was determined by adding an equivalent volume of the rare-earth solution to a standard $Na_2H_2[EDTA]$ solution and titrating the hydrogen ions. The concentration of the excess nitric acid was then found by subtracting the hydrogen ions released upon the formation of $[Ln(EDTA)]^-$ from the total number of hydrogen ions found in the titration. Good agreement between the experimental and calculated values was found.

Experimental procedure. The experimental procedure consisted of a potentiometric titration of EDDA alone and in the presence of the rare-earth ions. Solutions containing a 2:1 or 3:1 ratio of EDDA to rare-earth were used. In all cases the ionic strength was maintained at 0·1 by the addition of potassium nitrate. The measurements were carried out in a constant temperature bath maintained at 25·00 ± 0·02°C. A Beckman model GS pH meter (operated as a model G) equipped with a calomel reference electrode and an all-purpose glass electrode was used to determine the pH values. The titration vessel was a 200 ml Berzelius beaker fitted with a rubber stopper containing holes for the electrodes, microburet, and gas inlet and outlet tubes. Presaturated nitrogen obtained by bubbling commercial water-pumped nitrogen through a 0·1000 M potassium nitrate solution was passed through the solution to effect stirring and maintain an inert atmosphere.

Calculations. Values of pH were converted to concentration values using the correction factor −0·08 pH units found for a dilute solution of nitric acid. This correction factor was assumed to be valid for the pH range 3–10. The concentration of hydroxide ions was determined using a value for K_cW of $1{\cdot}68 \times 10^{-14}$. The acid dissociation constants were calculated by the method outlined by Chaberek and Martell.(5) The stability constants were calculated by solving simultaneous equations as developed by Block and McIntyre.(6)

DISCUSSION

The results obtained for the acid dissociation constants and the rare earth-EDDA stability constants are listed in Table 1. The acid dissociation constants for EDDA can be compared with the literature values of 6·42 and 9·46 (30°C, $\mu = 0{\cdot}1$).(2) The significance of these pK values in terms of the structure of EDDA has been discussed previously.(2) The values for the stability constants can be considered to be reliable within ±0·02 log K_1 units and ±0·05 log A_2 units as determined from the 95 per cent confidence intervals. The possible existence of binuclear chelates of the type $[Ln_2(EDDA)_3]$ was checked in the case of erbium by varying the metal concentration in the titration mixture. It was found that plots of $\bar{n}$ vs. pA coincided within the experimental uncertainty. Moreover, it was found that solutions containing a 2:1 mixture of EDDA and rare-earth ion did not give a precipitate at pH 9, whereas a precipitate was noticed in 3:2 mixtures. Since 1:1 mixtures give precipitates in basic solution, this indicates that in the 3:2 mixtures the rare-earth ions are not co-ordinately saturated.

---

* The rare-earth materials were generously supplied by Lindsay Chemical Division American Potash and Chemical Corporation, West Chicago, Illinois.

(4) G. Schwarzenbach, *Complexometric Titrations*, p. 73. Interscience Publishers, New York (1957).

(5) S. Chaberek, Jr. and A. E. Martell, *J. Amer. Chem. Soc.* 74, 5052 (1952).

(6) B. P. Block and G. H. McIntyre, Jr., *J. Amer. Chem. Soc.* 75, 5667 (1953).

The experimental technique and computational procedure were checked by redetermining the values of the stability constants of the magnesium and cadmium chelates. The values obtained for log K_1 were 3·95 for magnesium and 8·99 for cadmium (25° C, $\mu = 0·1$). These are in good agreement with the values of 3·9 for magnesium and 8·8 for cadmium (30°C, $\mu = 0·1$) reported by CHABEREK and MARTELL.(2)

The stability constants of the 1:1 chelates increase uniformly from lanthanum to europium, decrease to gadolinium and then increase uniformly again to lutetium. It is of interest to note that the gadolinium value is smaller than the samarium value. This is a rather severe example of the "gadolinium break" which is apparently always observed in the stability constants of the rare-earth chelates. The trends which have been noted above for the stability constants of the 1:1 rare earth–EDDA chelates are quite similar to those which have been observed previously for the rare-earth-hydroxyethylethylenediaminetriacetic acid (HEDTA) chelates.(7) Similar trends have also been observed in the glycolate series.(8)

TABLE 1.—FORMATION CONSTANTS FOR EDDA-RARE EARTH CHELATES
$t = 25°C, \mu = 0·10\ (KNO_3)$
$pK_1 = 6·48,\ pK_2 = 9·57$

Metal ion	log K_1*	log K_2*	log β_2*
La^{3+}	7·04	4·73	11·77
Ce^{3+}	7·48	4·92	12·35
Pr^{3+}	7·84	5·23	13·07
Nd^{3+}	8·06	5·63	13·69
Sm^{3+}	8·28	6·07	14·35
En^{3+}	8·38	6·35	14·73
Gd^{3+}	8·13	6·08	14·21
Tb^{3+}	8·18	6·52	14·70
Dy^{3+}	8·31	6·78	15·09
Ho^{3+}	8·42	7·00	15·42
Er^{3+}	8·59	7·45	15·78
Ti^{3+}	8·75	7·64	16·39
Yb^{3+}	8·93	7·92	16·85
Lu^{3+}	9·09	8·48	17·57
Y^{3+}	7·78	6·34	14·12

In view of the marked dissimilarity between HEDTA and EDTA in their behaviour toward the rare earths,(9) this similarity between HEDTA and EDDA is surprising. It has been postulated in the past that both EDTA and HEDTA utilize the same basic chelating structure toward the rare earths(10) (i.e., one carboxyl group unco-ordinated in EDTA and the hydroxyethyl group unco-ordinated in HEDTA). In this connexion it can be noted that the difference between the corresponding log K values ranges

---

$$^{*}K_1 = \frac{[Ln(EDDA)]}{[Ln][EDDA]},\ K_2 = \frac{[Ln(EDDA)_2]}{[Ln(EDDA)][EDDA]},\ \beta_2 = \frac{[Ln(EDDA)_2]}{[Ln][EDDA]^2}.$$

---

(7) F. H. SPEDDING, J. E. POWELL and E. J. WHEELWRIGHT, *J. Amer. Chem. Soc.* **78**, 34 (1956); T. MOELLER and R. FERRUS, *J. Inorg. Nucl. Chem.* **20**, 261 (1961).

(8) A. SONESSON, *Acta Chem. Scand.* **13**, 998 (1959).

(9) T. MOELLER, L. C. THOMPSON and R. FERRUS, in *Rare Earth Research* (Edited by E. V. KLEBER), p. 3. Macmillan, New York (1961).

(10) T. MOELLER and E. P. HORWITZ, *J. Inorg. Nucl. Chem.* **12**, 49 (1959).

from 1·8 to 3·9. The corresponding difference for the divalent metals nickel, zinc, cobalt, cadmium, iron, manganese and calcium is from 1·4 to 3·4 log K units.(11)

The difference between the log K values of the rare earth–HEDTA chelates and the rare earth–EDDA chelates is, however, 6·4–7·1 log K_1 units. For the divalent metal ions listed above, data are available only for nickel, cobalt, zinc and cadmium and this difference is only 3·2–4·2 log K_1 units.(11) The absence of the third carboxyl group, therefore, has a much more pronounced effect on the stability of the rare earth–chelates than upon the divalent metal ions considered here.

A similar comparison can be made between EDDA and nitrilotriacetic acid (NTA). Both ligands contain four donor atoms; two nitrogen atoms and two oxygen atoms in EDDA and one nitrogen atom and three oxygen atoms in NTA. In all cases the rare earth–NTA chelates(12) are much more stable than the corresponding rare earth–EDDA chelates. For the four divalent metals above, the stabilities are either nearly the same or the EDDA chelates are more stable.(11) This difference in behaviour with the two classes of ions can be ascribed to the geometrical arrangement of the donor atoms in the ligands and to the known preference of the rare-earth ions toward oxygen donors and the later transition elements toward nitrogen donors.

The position of yttrium is always of interest since on the basis of size considerations alone, the stability constants of its complexes should fall in the region between dysprosium and erbium. For the 1:1 EDDA chelate, yttrium lies between cerium and praseodymium, corresponding to an "anomolous" behaviour.(9) The similarity between the rare earth–EDDA and –HEDTA chelates is again noted since the yttrium –HEDTA chelate has a stability between praseodymium and neodymium.(7) At the present time, only one other ligand (dipicolinic acid)(13) has been investigated for which yttrium occupies a position so low in the cerium-earth region. The exact cause of this behaviour is not known at the present time, but it is apparent that there are factors involved which are not considered in the simple electrostatic model.

The log K_2 values for the rare earth–EDDA chelates are remarkably large. In fact, log K_2 for each of the last four ions (erbium through lutetium) is larger than log K_1 for lanthanum, a situation which apparently has been encountered previously only in the 8-quinolinol-5-sulphonic acid chelates.(14) With the exception of gadolinium, which has a value quite low in comparison with the values for europium and terbium, the log K_2 values increase consecutively throughout the series. This is to be contrasted to the NTA chelates for which log K_2 increases from lanthanum through dysprosium, decreases through thulium, and then increases for ytterbium and lutetium.(15, 16) The uniform behaviour of log K_2 for EDDA would seem to indicate that other than possibly gadolinium, no steric hindrance is encountered by the second ligand molecule. Yttrium again falls in the cerium-earth region lying between samarium and terbium. The exact position is indeterminate due to the low stability of the gadolinium chelate.

(11) J. BJERRUM, G. SCHWARZENBACH and L. G. SILLEN, *Stability Constants, Part I: Organic Ligands*. The Chemical Society, London (1957).

(12) G. SCHWARZENBACH and R. GUT, *Helv. Chim. Acta*, **39**, 1589 (1956).

(13) I. GRENTHE, *J. Amer. Chem. Soc.* **83**, 360 (1961).

(14) B. F. FREASIER, A. G. OBERG and W. W. WENDLANDT, *J. Phys. Chem.* **62**, 700 (1958).

(15) G. ANDEREGG, *Helv. Chim. Acta*, **43**, 825 (1960).

(16) T. MOELLER and R. FERRUS, *Inorg. Chem.* **1**, 49 (1962).

Since the values of the stability constants for rare earth-glycine complexes are small (log $K \approx 3$),(17) it is highly unlikely that the formation of the 2:1 EDDA complexes involves only one glycine ring from the second ligand molecule. The magnitude of the log K_2 values is also not reasonably explained by assuming that the basic chelating structure involves one oxygen atom and two nitrogen atoms, since the addition of a nitrogen atom should not increase the stability very much over that of the glycinate structure. In view of the relative magnitudes of log K_1 and log K_2 it appears more likely that the second ligand is also utilizing all four donor atoms.

Again it is of interest to compare EDDA with the somewhat similar quadridentate ligand NTA. ANDEREGG(15) has pointed out that the 2:1 rare earth–NTA chelates have remarkably large stability constants when compared to the 1:1 chelates. On this basis he has concluded that the 2:1 chelates are probably eight-co-ordinate. A similar line of reasoning for the EDDA chelates leads to the conclusion that the co-ordination number of the rare-earth ions in this case is also larger than six, presumably eight.

The suggestion that the rare earths may have a co-ordination number of seven or eight in some of their complexes is becoming more widespread. The first such proposal was advanced to explain the large increase in stability of the cerium-diethylenetriaminepentaacetic acid chelate over the corresponding EDTA chelate.(3) This increase is much larger than that observed for the divalent transition metals for which the maximum co-ordination number is six. Structures involving rare-earth ions with co-ordination number seven have recently been proposed for the EDTA complexes and the trisacetylacetonates,(18) each of which in the solid state retains one molecule of water tenaciously. To these can be added the NTA and EDDA complexes. Moreover, recent work in this laboratory on the rare earth-hydroxyethyliminodiacetic acid chelates, and some mixed complexes with HEDTA suggests that a co-ordination number larger than six may be quite common among the chelates formed by the rare earths.

Acknowledgement.—This investigation was supported by a PHS research grant RG-8394 from the Division of General Medical Sciences, Public Health Service and by a research grant from the Graduate School of the University of Minnesota.

(17) A. S. TOMPA. Ph.D. dissertation, Fordham University (1961).

(18) J. L. HOARD, G. S. SMITH and M. LIND, in *Advances in the Chemistry of the Co-ordination Compounds* (Edited by S. KIRSCHNER), p. 296. Macmillan, New York (1961).

J. Inorg. Nucl. Chem., 1962, Vol. 24, pp. 1089 to 1092. Pergamon Press Ltd. Printed in England

METAL COMPLEXES OF PYRONES AND THIOPYRONES

H. B. Gray, E. Billig, R. Hall and L. C. King
Chemistry Departments, Columbia University, New York,
and
Northwestern University, Evanston, Illinois

(*Received* 10 *January* 1962; *in revised form* 8 *March* 1962)

Abstract—The preparation of metal complexes of 2,6-dimethyl-4-thiopyrone (DMTP) and 2,6-dimethyl-4-pyrone (DMP) with the general formulas $M^x(DMTP)_2Cl_x$ and $M^x(DMP)_2Cl_x$ is described. Infra-red evidence suggests metal-sulphur (DMTP) and metal-carbonyl oxygen (DMP) co-ordinate bonds in these complexes. Some physical properties are tabulated and discussed.

The reaction of thioketones and 4-thiopyrones with metal halides, particularly mercuric chloride or bromide, has been known for some time to give adducts which were thought to be of the 1:1 type,⁽¹⁾

$$R_2C{=}S + HgX_2 \rightarrow (R_2C-S-HgX)^+ x^- \qquad (1)$$

Similar 1:1 complexes have been reported for reactions involving pyrones and certain Lewis acids.⁽²⁾

The present investigation involves the preparation of DMTP complexes of transition and non-transition metal chlorides. Some transition metal chloride complexes of DMP have also been prepared. The general reaction is represented by the following equation:

$$M^xCl_x + 2DMP \text{ or } 2DMTP \rightarrow M^x(DMP \text{ or } DMTP)_2Cl_x \qquad (2)$$

Methods of preparation, physical properties and some structural evidence for these complexes are reported in this paper.

EXPERIMENTAL

1. *Preparation of compounds*

DMP and DMTP were prepared as described in the literature.⁽³⁾ Complexes were prepared by mixing hot solutions of reagent grade metal chloride and excess DMP or DMTP. Four different modifications of the general preparative method were used to obtain the complexes. Examples of each of these procedures are the following:

Preparation A—$Ag(DMTP)_2Cl$. To 1·6 g of DMTP in 40 ml of hot alcohol was added 0·845 g (0·005 mole) of $AgNO_3$ in 20 ml of water. A white precipitate formed and was dissolved by heating on a steam bath, after which 10 ml of conc. HCl was added. The yellow crystals which separated on cooling were filtered and dried at 60° *in vacuo*.

Preparation B—$Hg(DMTP)_2Cl_2$. To 1·39 g of $HgCl_2$ in 20 ml of hot alcohol was added 1·5 g of DMTP in hot alcohol. A white precipitate formed which turned yellow after a few minutes. The yellow product was filtered while hot and dried at 60° *in vacuo*.

Preparation C—$Sb(DMTP)_2Cl_3$. To 1·4 g of DMTP in 20 ml of chloroform was added 0·5 g of $SbCl_3$ in 2 ml chloroform. On heating an orange precipitate formed, was separated, recrystallized from alcohol and dried at 60° *in vacuo*.

Preparation D—$Pt(DMTP)_2Cl_2$. An alcoholic solution of K_2PtCl_4 was treated with a solution of DMTP (in excess) in absolute alcohol at 20°. The yellow complex formed immediately, was filtered, washed with cold absolute alcohol and dried at room temperature *in vacuo*. Upon heating this complex decomposes, and a deep red-brown colour appears.

⁽¹⁾ A. Schönberg, M. Elkaschef, M. Nosseir and M. M. Sidky, *J. Amer. Chem. Soc.* **80** 6312 (1958); also references cited therein.

⁽²⁾ D. Cook, *Canad. J. Chem.* **39**, 1184 (1961).

⁽³⁾ L. C. King, F. J. Ozog and J. Moffat, *J. Amer. Chem. Soc.* **73**, 300 (1951).

Analytical data and the physical properties of all the DMP and DMTP metal complexes are tabulated in Table 1.

TABLE 1.—ANALYTICAL DATA AND SOME PHYSICAL PROPERTIES OF METAL DMP AND DMTP COMPLEXES

	Calc.	Found	Colour	Melting pt. (°C)	Prep.*	Λ†
Ag $(DMTP)_2Cl$	C, 39·85	C, 38·82				
	H, 3·82	H, 3·71	Yellow	205 (d)	A (94%)	3
Cu $(DMTP)_2Cl$	C, 44·31	C, 43·43				
	H, 4·22	H, 4·09	Red	240 (d)	A (95%)	3
Hg $(DMTP)_2Cl_2$	C, 30·46	C, 30·54				
	H, 2·92	H, 3·00	White	225 (d)	B(93%)	—
Sb $(DMTP)_2Cl_3$	C, 33·06	C, 33·43		145–		
	H, 3·17	H, 2·96	Orange	150°	C (50%)	8
Bi $(DMTP)_2Cl_3$	C, 28·21	C, 28·45	Yellow-			
	H, 2·70	H, 2·61	orange	230 (d)	A (84%)	8
Co $(DMTP)_2Cl_2$	C, 41·00	C, 42·69		238–		
	H, 3·91	H, 3·90	Green	240	B (90%)	8
Fe $(DMTP)_2Cl_2$	C, 41·29	C, 41·60				
	H, 3·92	H, 3·95	Purple	> 300	A (75%)	4·5
Pt $(DMTP)_2Cl_2$	Pt, 35·8	Pt, 36·12				
	C, 30·7	C, 29·06	Yellow-	218 (d)	D (< 40%)	5
	H, 2·92	H, 2·97	brown	250 (d)	B (91%)	0
Ni $(DMTP)_2Cl_2$	C, 40·99	C, 40·88	Green			
	H, 3·93	H, 3·84				
Pd $(DMTP)_2Cl_2\cdot$	C, 35·30	C, 35·60	Yellow-			
H_2O	H, 3·78	H, 4·55	brown	195 (d)	B (< 40%)	0
Fe $(DMP)_2Cl_2\cdot$	C, 42·7	C, 42·57		180–		
H_2O	H, 4·57	H, 4·46	Orange	183 (d)	B (< 40%)	20
Co $(DMP)_2Cl_2$	C, 44·7	C, 44·44				
	H, 4·23	H, 4·51	Blue	209 (d)	B (< 40%)	4
Mn $(DMP)_2Cl_2\cdot$	C, 42·7	C, 42·95				
H_2O	H, 4·57	H, 5·24	Pink	> 300	B (< 40%)	0

* Capital letters refer to method of preparation given in the experimental section. Yields are in parentheses.

† Molar conductances in $cm^2\ mole^{-1}\ ohm^{-1}$ of the complexes in nitrobenzene solution for the concentration range 1×10^{-4} to 5×10^{-4} M and at 25°.

2. *Spectral measurements*

Infra-red spectra were taken of solid samples using the KBr wafer technique with a Baird spectrophotometer. The results are given in Table 2. Visible and ultra-violet spectra were obtained with a Cary 11 spectrophotometer.

3. *Conductance measurements*

The electrical conductivities of nitrobenzene solutions of the complexes were measured at 25° using a Radiometer Model CDM 2C apparatus. Molar conductances are given in Table 1.

DISCUSSION

In Table 1 are given analytical data supporting the general formulas $M^x(DMTP)_2Cl_x$ and $M^x(DMP)_2Cl_x$ proposed for the complexes. All attempts to add more than two DMTP or DMP molecules per metal ion failed for the metal chlorides. The complexes are stable for months in air, but decompose immediately into free DMTP

TABLE 2.—INFRA-RED SPECTRA OF DMP, DMTP AND DERIVATIVES

Compound	Principal absorption maxima (cm^{-1})
DMP*	1680, 1670, 1612, 1600, 1396, 1372, 1342, 1200, 1161, 1040, 959, 928, 900
Mn $(DMP)_2Cl_2 \cdot H_2O$	1661, 1575, 1563, 1439, 1410, 1333, 1203, 1174, 1033, 962, 910, 871, 886
Fe $(DMP)_2Cl_2 \cdot H_2O$	1653, 1563, 1410, 1370, 1333, 1202, 1170, 1036, 957, 901, 873
Co $(DMP)_2Cl_2$	1649, 1568, 1521, 1445, 1418, 1335, 1204, 1176, 1046, 962, 914, 899, 848
DMTP	1650, 1570, 1446, 1438, 1380, 1281, 1165, 1103, 1038, 1015, 940, 892, 862
2,6-dimethyl-4-mercaptopyrylium chloride	1640, 1635, 1550, 1449, 1290, 1176, 1100, 1042, 1021, 943, 863
$M^x(DMTP)_2Cl_x$†	1650, 1560, 1450, 1288, 1175, 1090, 1038, 1010, 940, 850

or DMP and hydrated metal ion upon dissolution in water. Other complexing groups will also replace DMTP or DMP in the complexes, e.g.

$$Co(DMTP)_2Cl_2 + 2\ \text{pyridine} \xrightarrow{\text{acetone}} Co(py)_2Cl_2 + 2DMTP \qquad (1)$$

$$Co(DMTP_2Cl_2 + 2Cl^-(LiCl) \xrightarrow{\text{acetone}} CoCl_4^{2-} + 2DMTP \qquad (2)$$

Both reactions (1) and (2) are very rapid at 25° as judged by qualitative spectral observations.

The infra-red spectra of DMP, DMTP and their complexes are given in Table 2. The existence of a metal to carbonyl oxygen bond in metal DMP complexes has already been established.(2) The carbonyl stretching frequency is assigned at 1612 cm^{-1} in Nujol for DMP: this band is shifted to lower frequencies as expected for the complexes.

There is a band at 1570 cm^{-1} in the spectrum of DMTP which also shifts to lower frequencies for the metal complexes and for 2, 6-dimethyl-4-methylmercaptopyrylium chloride. This band is tentatively assigned as due to the thiocarbonyl stretching vibration. In addition, it is significant that the bands at 1380 and 892 cm^{-1} in the spectrum of DMTP are not present in the spectra of the metal DMTP complexes and 2, 6-dimethyl-4-methylmercaptopyrylium chloride. These comparisons are convincing evidence for a metal to sulphur bond in the metal DMTP complexes.

In nitrobenzene all the complexes are essentially non-electrolytes as judged by the small Λ values listed in Table 1. Thus the chlorides are complexed in these compounds. The absorption spectrum of the $Co(DMP)_2Cl_2$ complex in nitromethane has maxima at 660 mμ ($\epsilon = 490$) and 578 mμ ($\epsilon = 347$); the $Co(DMTP)_2Cl_2$ complex has absorption maxima at 675 mμ ($\epsilon = 545$) and at 635 mμ ($\epsilon = 755$). Since all tetrahedral Co(II) complexes thus far examined spectroscopically have an absorption band in the 600-800 mμ region with an ϵ in the 400-1600 range(4) the DMP and DMTP complexes of Co(II) are probably pseudo-tetrahedral.

---

* Taken from Reference (2).

† This is the spectrum of Pt $(DMTP)_2Cl_2$. The other DMTP metal complexes have almost identical infra-red spectra.

(4) F. A. COTTON, D. M. L. GOODGAME and M. GOODGAME, *J. Amer. Chem. Soc.* **83**, 4690 (1961); also references cited therein.

The DMP and DMTP complexes of Fe(II) exhibit strong charge transfer bands in the visible and near ultra-violet regions. The absorption maximum for a solution of $Fe(DMP)_2Cl_4.H_2O$ in nitromethane is located at 375 mμ ($\epsilon = 3100$); the maxima for $Fe(DMTP)_2Cl_2$ are at 375 mμ ($\epsilon = 5500$) and 515 mμ ($\epsilon = 2300$). There appear to be no weak bands (inner *d-d* transitions) in the visible region for either complex. Thus these complexes are spectrally similar to the known tetrahedral $FeCl_4^{2-}$(5) and it is reasonable to suggest that $Fe(DMP)_2Cl_2$ and $Fe(DMTP)_2Cl_2$ are pseudo-tetrahedral in nitromethane solution.

The $Pt(DMTP)_2Cl_2$ and $Pd(DMTP)_2Cl_2$ complexes are non-electrolytes in nitrobenzene, and presumably have square planar structures. Aside from this and the above observations, at present nothing further can be said with any degree of certainty about the structures of the DMP and DMTP complexes.

---

(5) N. S. Gill, *J. Chem. Soc.* 3512 (1961).

J. Inorg. Nucl. Chem., 1962, Vol. 24, pp. 1093 to 1103. Pergamon Press Ltd. Printed in England

THE STABILITY OF SOME METAL COMPLEXES INCORPORATING OXYGEN OR SULPHUR AS DONOR ATOMS

K. SUZUKI and K. YAMASAKI

Chemical Institute, Faculty of Science, Nagoya University, Nagoya, Japan

(*Received* 24 *August* 1961; *in revised form* 15 *October* 1961)

Abstract—The stability constants of some bivalent metal complexes were determined which contained ligands incorporating oxygen or sulphur as donor atoms. The strength of the metal–sulphur bond was compared with that of the metal–oxygen bond. The five metals studied here were classified into two groups

(1) larger affinity towards O than S: Zn, Cd, Pb

(2) larger affinity towards S than O: Cu, Ni.

The relative strength of the metal–sulphur bond seems to decrease in the following order:

Cu > Ni > Pb, Cd > Zn.

ONE of the important problems in co-ordination chemistry may be the strength of metal-donor bonds. Many authors contributed to this problem from the various points of view. In 1958, AHRLAND *et al.*[1] classified various acceptors and discussed the relative affinity of donor atoms. According to them, there are two types of acceptors:

(a) those which form the most stable complexes with the first elements of each group in the periodic table, i.e. N, O and F

(b) those which form the most stable complexes with the second or subsequent elements of each group in the periodic table.

Most metals belong to the class (a) and the relative bond strength of their complexes is what would be expected if the complex formation is essentially electrostatic. On the other hand, the strongest acceptors belonging to the class (b) are the elements which form the stable olefine complexes, viz. Cu(I), Rh(I), Pd(II), Ag(I), Pt(II) and Hg(II)[2] and it is pointed out that the class (b) character of a metal appears to depend on the availability of electrons from the lower *d*-orbitals of the metal ion to form a dative π-bonding.[3] In addition to these two classes, there are borderline elements which can show both characters. Since their character depends on the donor groups, it may be interesting to study the stability of the complexes of borderline elements and infer the factors which influence the strength of metal–donor bonds.

---

[1] S. AHRLAND, J. CHATT and N. R. DAVIES, *Quart. Rev.* **12**, 265 (1958); See also H. M. N. H. IRVING, *International Conference on Co-ordination Chemistry*, Chem. Soc. Spec. Publ. No. 13, p. 13 (1959).

[2] I. LEDEN and J. CHATT, *J. Chem. Soc.* 2936 (1955).

[3] J. CHATT, *Nature, Lond.* **165**, 637 (1950); D. P. CRAIG, A. MACCOLL, R. S. NYHOLM, L. E. ORGEL and L. E. SUTTON, *J. Chem. Soc.* 332 (1954); H. H. JAFFÉ, *J. Phys. Chem.* **58**, 185 (1954).

From this point of view, we intended to determine the stability constants of some metal complexes formed with ligands containing oxygen or sulphur as a donor and to compare their affinity towards bivalent metals. As metals copper, nickel, zinc, cadmium and lead were chosen, since the different affinity of sulphur and oxygen to these metals which are classified into separate groups are expected. As the ligands the following compounds were used.

Structure	Name
1. 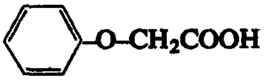	Phenoxyacetic acid
2. 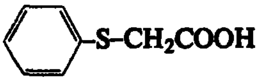	Phenylthioacetic acid
3. 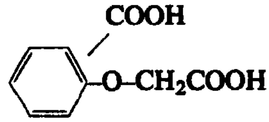	α-Carboxy-*o*-anisic acid
4. 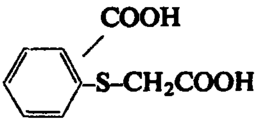	*o*-(Carboxymethylthio)benzoic acid
5. 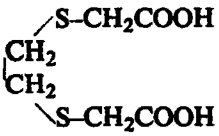	(Ethylenedithio)diacetic acid

These pairs of compounds have analogous structures with oxygen and sulphur as donor atoms. Unfortunately ethylenediglycolic acid which is a partner to (ethylenedithio)diacetic acid was not obtained in a pure state and the stability constants of its complexes could not be determined.

EXPERIMENTAL

Materials. Phenoxyacetic acid commercially obtained was recrystallized twice from water. Phenylthioacetic acid was prepared from thiphenol and monochloroacetic acid.(4) α-Carboxy-*o*-anisic acid was made by the method of Meyer and Duczmal.(5) *o*-(Carboxymethylthio)benzoic acid was made by the method of Friedländer.(6) (Ethylenedithio)diacetic acid was specially prepared by the Katayama Chemical Co. Osaka. The melting points of all these substances were in good agreement with those reported in the literature. Metal perchlorate solutions were prepared from respective metal salt or oxide and perchloric acid and the concentrations were determined by chelatometric titration.

Procedure. The solutions containing metal perchlorate and ligand were prepared, the volume being 50 ml in all cases, and they were titrated with standard NaOH or $HClO_4$ at 25° C. The ionic strength of the solution was kept at 0·1 by adding $NaClO_4$. The volume change accompanying with titration was neglected since added volume of NaOH or $HClO_4$

---

(4) L. Vanino, *Handbuch der präparativen Chemie, Band II*, p. 616. Ferdinand Enke Verlag, Stuttgart (1937).

(5) R. Meyer and C. Duczmal, *Ber. Dtsch. Chem. Ges.* **46**, 3366 (1913).

(6) P. Friedländer, *Liebigs Ann.* **351**, 402 (1907).

was 0·15 ml or less. The pH of the solution was measured by using a Horiba Model P pH meter which was standardized against the standard buffer. The hydrogen ion concentration was calculated from pH values by assuming 0·83 for the activity coefficient of hydrogen ion according to KIELLAND.(7) The concentrations of ligand and metal solutions used were shown in Table 1 in mole/l. The pH range measured is 2·5–4·5.

TABLE 1.

	Ligand	Cu	Ni	Zn	Cd	Pb
1	0·01198–0·01498	0·00829	0·01520	0·00910	0·01036	0·00856
2	0·01198	0·00829	0·01147	0·00911	0·01036	0·00171
3	0·00100–0·00199	0·00165	0·00304	0·00182	0·00207	0·00341
4	0·00100–0·00396	0·00165	0·00304	0·00364	0·00412	0·00171
5	0·00165–0·00199	0·00165	0·00154	0·00182	0·00206	0·00171

1: Phenoxyacetic acid
2: Phenylthioacetic acid
3: α-Carboxy-*o*-anisic acid
4: *o*-(Carboxymethylthio)benzoic acid
5: (Ethylenedithio)diacetic acid

RESULTS

Since phenoxyacetic and phenylthioacetic acids are monobasic acids, their acid dissociation constants were calculated by the algebraic method. For other three dibasic acids the difference of the first and second acid dissociation constants, K_1 and K_2, was too small to allow the separate calculation of them. Therefore, the following equation(8) (1) was used and K_2 values were determined graphically,

$$\frac{\bar{n}_H}{(1-\bar{n}_H)[H]} = \frac{1}{K_2} + \frac{1}{K_1K_2}\,\frac{(2-\bar{n}_H)[H]}{1-\bar{n}_H} \tag{1}$$

$$K_1 = \frac{[AH][H]}{[AH_2]} \text{ and } K_2 = \frac{[A][H]}{[AH]}$$

where $\bar{n}_H$ denotes the average number of hydrogen ion bound to a ligand anion and it corresponds to the BJERRUM's(9) formation function in complex formation. $[AH_2]$ represents concentration of a dibasic acid in mole per litre, A being the ligand anion. The charge of each species is omitted in formulae for the sake of simplicity. These data are shown in Tables 2 and 3 and Fig. 1.

TABLE 2.—p*K* OF *o*-(CARBOXYMETHYLTHIO)BENZOIC ACID

$\frac{\bar{n}_H}{(1-\bar{n}_H)[H]}$	$\frac{(2-\bar{n}_H)[H]}{1-\bar{n}_H}$		$\frac{\bar{n}_H}{(1-\bar{n}_H)[H]}$	$\frac{(2-\bar{n}_H)[H]}{1-\bar{n}_H}$	$\frac{1}{K_1K_2}$	K_1
$(\times 10^4)$	$(\times 10^{-4})$		$(\times 10^3)$	$(\times 10^{-3})$	$(\times 10^6)$	$(\times 10^{-3})$
1·67	9·32		−4·06	−1·56	9·21	1·12
1·54	6·80		−3·41	−1·54	8·90	1·16
1·39	5·23	$\frac{1}{K_2} = 1{\cdot}03 \times 10^4$	−2·96	−1·45	9·13	1·13
1·31	4·04		−2·52	−1·48	8·70	1·18
1·21	3·22	$K_2 = 9{\cdot}72 \times 10^{-5}$	−2·19	−1·48	8·44	1·22
1·20	2·43		−1·92	−1·44	8·50	1·21
				$K_1 = 1{\cdot}18 \times 10^{-3}$		

---

(7) J. KIELLAND, *J. Amer. Chem. Soc.* 59, 1675 (1937).

(8) H. IRVING and H. S. ROSSOTTI, *J. Chem. Soc.* 3397 (1953); F. J. C. ROSSOTTI and H. S. ROSSOTTI, *Acta Chem. Scand.* 9, 1166 (1955).

(9) J. BJERRUM, *Metal Ammine Formation in Aqueous Solution.* P. Haase, Copenhagen (1941).

Table 3.—p*K* of (ethylenedithio)diacetic acid

$\frac{\bar{n}_H}{(1-\bar{n}_H)[H]}$	$\frac{(2-\bar{n}_H)[H]}{1-\bar{n}_H}$		$\frac{\bar{n}_H}{(1-\bar{n}_H)[H]}$	$\frac{(2-\bar{n}_H)[H]}{1-\bar{n}_H}$	$\frac{1}{K_1K_2}$	K_1
$(\times 10^4)$	$(\times 10^{-4})$		$(\times 10^3)$	$(\times 10^{-4})$	$(\times 10^7)$	$(\times 10^{-4})$
2·46	8·80		−3·03	−8·42	1·84	6·79
1·88	5·04		−3·74	−9·68	1·67	7·49
1·60	3·16	$\frac{1}{K_2}=1{\cdot}25\times 10^4$	−4·78	−9·87	1·75	7·14
1·48	1·96		−6·33	−10·54	1·79	6·98
1·43	1·18	$K_2=8{\cdot}00\times 10^{-5}$	−8·78	−11·66	1·83	6·83
			−13·15	−13·75	1·87	6·68
				$K_1=6{\cdot}99\times 10^{-4}$		

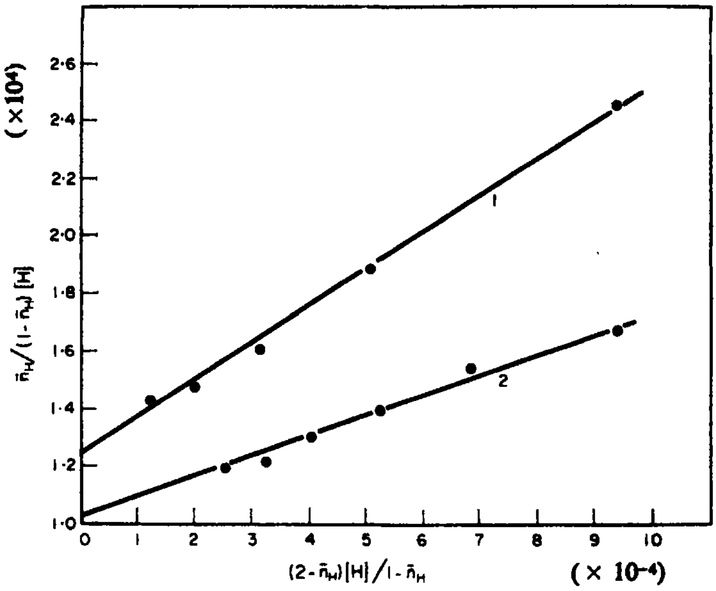

Fig. 1.—p*K* of (ethylenedithio)diacetic and *o*-(carboxymethylthio)benzoic acids
1: (ethylenedithio)diacetic acid
2: *o*-(carboxymethylthio)benzoic acid.

The formation curves are shown in Fig. 2. Except those complexes shown in Fig. 2, that is, the copper complexes of *o*-(carboxymethylthio)benzoic and α-carboxy-*o*-anisic acids and all complexes formed with (ethylenedithio)diacetic acid, $\bar{n}$ values which are sufficient enough to draw the formation curves were not available due to the low stability of complexes. For most of the complexes except the (ethylenedithio)diacetate complex of copper, the ratio of added ligand to the metal ion was kept at 0·3–1·3 and the stability constants were calculated algebraically using $\bar{n}$ values less than 0·5. For phenylthioacetic and phenoxyacetic acids a rather high ratio of ligand to metal was used, but $\bar{n}$ values obtained for these ligand–metal systems were below 0·2 owing to their low stability. Under these conditions it may be reasonable to assume that the predominant species is the 1:1 complex and no 1:2 species is formed. Therefore the following equations for calculating stability constants were used,

$$C_H = [H]+[AH]+2[AH_2]\dagger-[OH]^* \quad (2)$$

$$C_A = [MA]+[A]+[AH]+[AH_2]\dagger \quad (3)$$

$$C_M = [M]+[MA] \quad (4)$$

where C_H, C_A and C_M represent total ionizable hydrogen ion, total ligand and total metal ion concentrations respectively. [M] and [MA] stand for concentrations of free metal ion and the 1:1 complex. The copper complex formed with (ethylenedithio)diacetic acid is very stable and shows the $\bar{n}$ value of 0·84 at pH as low as 2·5. As clearly shown in the formation curve, however, only the formation of the 1:1 complex is expected under the conditions studied here. Therefore, its stability constant was calculated using the same equations (2), (3) and (4).

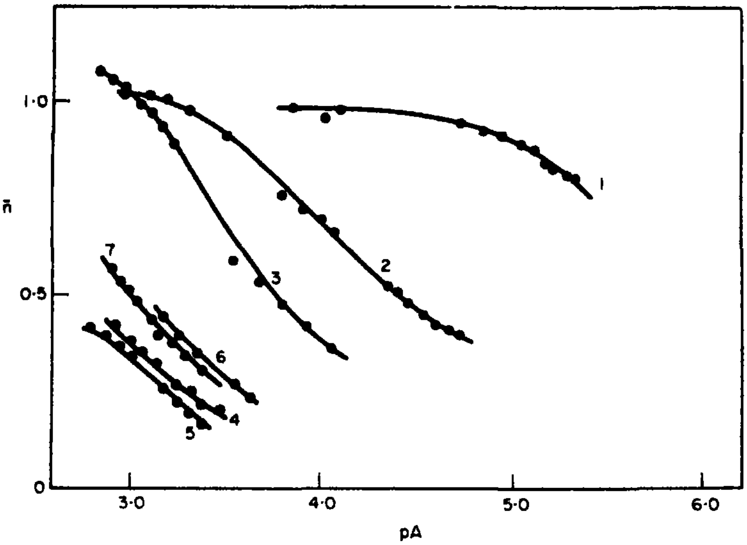

Fig. 2.—Formation curves

Curves (1) ~ (5): (ethylenedithio)diacetic acid complexes.

(1): Cu, (2): Ni, (3): Pb, (4): Cd, (5): Zn

Curve (6), the copper complex of α-carboxy-*o*-anisic acid

Curve (7), the copper complex of *o*-(carboxymethylthio)benzoic acid.

As the examples of the titration data, those of the copper-*o*-(carboxymethylthio)-benzoic acid and the nickel-(ethylenedithio)diacetic acid systems are given in Tables 4 and 5.

The stability and the acid dissociation constants obtained are summarized in Table 6.

---

* The concentration of OH is negligible in the pH range 2·5–4·5.

† For monobasic acids AH_2 is omitted.

TABLE 4.—TITRATION DATA OF THE COPPER-*o*-(CARBOXYMETHYLTHIO)BENZOIC ACID SYSTEM

pH	C_{Cu}	C_A	C_H	$\bar{n}$	pA	log *k*
3·66	0·00165	0·00396	0·00318	0·44	3·11	3·02
3·72	„	„	0·00295	0·47	3·08	3·02
3·78	„	„	0·00272	0·50	3·03	3·03
3·85	„	„	0·00250	0·52	2·99	3·02
3·92	„	„	0·00227	0·54	2·94	3·01
3·99	„	„	0·00205	0·57	2·90	3·03
3·69	„	0·00198	0·00159	0·28	3·43	3·01
3·80	„	„	0·00136	0·30	3·35	2·98
3·92	„	„	0·00114	0·34	3·27	2·97
4·05	„	„	0·00091	0·37	3·20	2·97
4·23	„	„	0·00068	0·39	3·12	2·94

TABLE 5.—TITRATION DATA OF THE NICKEL-(ETHYLENEDITHIO)DIACETIC ACID SYSTEM

pH	C_{Ni}	C_A	C_H	$\bar{n}$	pA	log *k*
2·85	0·00154	0·00199	0·00399	0·41	4·74	4·58
2·90	„	„	0·00376	0·42	4·66	4·53
2·94	„	„	0·00354	0·44	4·60	4·49
2·98	„	„	0·00331	0·46	4·53	4·45
3·03	„	„	0·00309	0·48	4·48	4·45
3·07	„	„	0·00286	0·52	4·42	4·45
3·12	„	„	0·00263	0·55	4·37	4·45

TABLE 6.

Ligand*	p*K*		log *k*†				
	pK_1	pK_2	Cu	Ni	Zn	Cd	Pb
1	2·93		1·3	~ 0·3	~ 0·5	1·0	1·4
2	3·37		1·5	~ 0·7	~ 0·8	1·2	1·8
3	2·51	4·36	3·1	2·0	2·6$_5$	2·0	~ 2·6‡
4	2·93	4·01	3·0	1·9	1·8	2·0	~ 2·5‡
5	3·16	4·10	6·0	4·5	2·7	2·8	3·8

* 1: Phenoxyacetic acid
2: Phenylthioacetic acid
3: α-Carboxy-*o*-anisic acid
4: *o*-(Carboxymethylthio)benzoic acid
5: (Ethylenedithio)diacetic acid

† The stability constant of the 1:1 complex is defined as follows:

$$k = \frac{[MA]}{[M][A]}$$

‡ Less accurate owing to precipitation.

For the copper complexes of α-carboxy-*o*-anisic and *o*-(carboxymethylthio)benzoic acids and all the complexes formed with (ethylenedithio)diacetic acid, the stability constants were also obtained from the formation curve ($\bar{n} = 1/2$), and these values were in good agreement with those given in Table 6.

DISCUSSION

1. *Acid dissociation constants*

Phenylthioacetic and phenoxyacetic acids have only ionizable hydrogen atoms in the $-CH_2COOH$ groups and by comparing p*K* values of these two acids with those of α-carboxy-*o*-anisic and *o*-(carboxymethylthio)benzoic acids, it can be readily understood that the latter two acids dissociate in the following way:

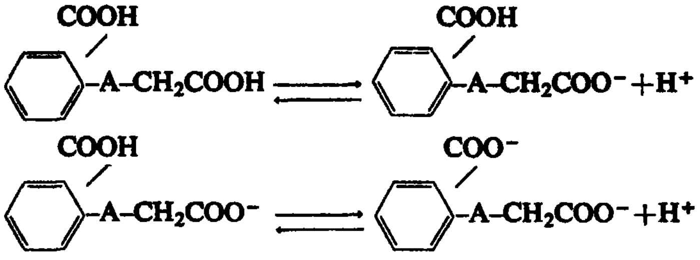

where A represents either oxygen or sulphur.

2. *Stability constants*

a. *Phenoxyacetic and phenylthioacetic acids*

The stability of metal complexes formed with ligands, phenoxyacetic and phenylthioacetic acids, decrease in the following order:

$$Pb > Cu > Cd > Zn > Ni.$$

This order is the same as shown by the carboxylic acids which form seven-membered or larger chelate rings.(10) If phenoxyacetic and phenylthioacetic acids act as bidentate ligands, that is, O or S participates in co-ordination, the formed complexes have five membered chelate rings and thus a different stability order from that mentioned above is expected. Therefore, sulphur and oxygen of these two ligands are perhaps not involved in co-ordination and these ligands are acting as the monodentate.*

For all the metals studied here the stability is larger for complexes of phenylthioacetic acid than for those of phenoxyacetic acid, but it may not be possible to attribute this order directly to the different affinity of O and S towards metals since these two ligands have different p*K* values which affect considerably the stability of the complex formed.(11, 12)

---

* The copper complexes of phenylthioacetic and *o*-(carboxymethylthio)benzoic acids are green, while complexes of other ligands are blue. The spectrophotometric study of these complexes and the relationship between colour and structure of complexes will be published elsewhere.

(10) M. Yasuda, K. Yamasaki and H. Ohtaki, *Bull. Chem. Soc. Japan* 33, 1067 (1960).
(11) M. Yasuda, K. Suzuki and K. Yamasaki, *J. Phys. Chem.* 61, 229 (1957).
(12) H. Irving and H. Rossotti, *Acta Chem. Scand.* 10, 72 (1956).

b. *α-Carboxy-o-anisic and o-(carboxymethylthio)benzoic acids*

These two acids have similar acid dissociation constants, but the stability order for Zn complexes is:

α-carboxy-*o*-anisic acid > *o*-(carboxymethylthio)benzoic acid

This order is in agreement with the classification(1) of AHRLAND *et al.* that zinc shows a larger affinity to oxygen than to sulphur. Usually the oxygen atom in ether bonding has a very weak co-ordinating power. If, however, the oxygen of ether-bonding is a part of the ligand which has other stronger co-ordinating groups, its co-ordinating power will be enhanced.(13) Therefore, in the Zn complex it will be possible that α-carboxy-*o*-anisic acid acts as a tridentate ligand with one oxygen atom and two carboxylic groups in co-ordination and the stability difference may indicate that the affinity of oxygen to zinc is larger than that of sulphur.

For other metals, the stability constants of complexes formed with α-carboxy-*o*-anisic and *o*-(carboxymethylthio)benzoic acids are nearly the same. This result is different from the complexes of diglycolic and thiodiglycolic acids,(10, 14) for which a rather large difference exists in the stability.

TABLE 7.

Ligand	pK_1+pK_2	Cu	Ni	Zn	Cd	Pb
α-Carboxy-*o*-anisic acid	6·87	3·1	2·0	2·6$_5$	2·0	~ 2·6
o-(Carboxymethylthio)-benzoic acid	6·94	3·0	1·9	1·8	2·0	~ 2·5
Diglycolic acid(10)	6·69	3·9	2·6	3·6	3·3	4·4
Thiodiglycolic acid(10)	7·28	4·3	4·0	2·9	2·6	3·6

For all metals studied the stability constants of the complexes formed with α-carboxy-*o*-anisic and *o*-(carboxymethylthio)benzoic acids are small compared with those of diglycolic and thiodiglycolic acid complexes. There may be two factors responsible for these results. The first one is that α-carboxy-*o*-anisic and *o*-(carboxymethylthio)benzoic acid complexes have one five and one six membered rings, when O or S atom co-ordinates to metal, while diglycolic and thiodiglycolic acid complexes have two five membered chelate rings. The second one is the structural restriction that benzene ring makes a part of the chelate ring. Probably both factors may affect the stability in addition to the fact that thiodiglycolic acid has a little larger p*K* value than other three acids.

c. *(Ethylenedithio)diacetic acid*

As ethylenediglycolic acid which is the partner to (ethylenedithio)diacetic acid containing oxygen instead of sulphur, was not obtained in a pure state and the stability of its complexes could not be determined, the stability of the complexes was compared with those of diglycolic and thiodiglycolic acid complexes. If it is assumed that the bonds between carboxylate and metal ions have nearly equal strength in these complexes, the comparison of the stability will give some information about the relative affinity of sulphur and oxygen to the same metal, although the p*K* value of diglycolic acid is a little smaller than those of other two ligands.

---

(13) G. SCHWARZENBACH, *Angew. Chem.* **70**, 451 (1958).

(14) R. M. TICHANE and W. E. BENNETT, *J. Amer. Chem. Soc.* **79**, 1293 (1957).

As is clear from Table 8, the metals studied are divided into three groups by the values of their stability constants.

TABLE 8.

Ligand	pK_1+pK_2	Cu	Ni	Zn	Cd	Pb
(Ethylenedithio)diacetic acid	7·26	6·0	4·5	2·7	2·8	3·8
Diglycolic acid	6·69	3·9	2·6	3·6	3·3	4·4
Thiodiglycolic acid	7·28	4·3	4·0	2·9	2·6	3·6

(i) *Copper and nickel.* Of the three ligands, diglycolic, thiodiglycolic and (ethylenedithio)diacetic acids, these two metals form the most stable complexes with the last one. As reported previously(12) the stability decreases with the increased size of chelate ring. If sulphur atom does not co-ordinate to the metal, the chelate ring formed is a twelve membered ring and the stability will be reduced greatly. The copper complex is stabilized by 1·7 in log k unit than the complex of thiodiglycolic acid. Therefore this large stability may indicate the quadridentate character of this ligand with two sulphur atoms in co-ordination. The formation curve of this complex (Fig. 2) shows that $\bar{n}$ values have a nearly constant value of one over a considerably wide pA range. This fact also supports the quadridentate nature of the complex. In 1959 SAINI and OSTACOLI(15) reported the values of acid dissociation of this ligand and stability of the copper complex to be $pK_1 = 3{\cdot}14$, $pK_2 = 4{\cdot}18$ and $\log k \doteq 6{\cdot}2$ at 20°C and the ionic strength of 0·1 and they confirmed by the spectrophotometric-titration that this ligand formed only the 1:1 complex with copper. Their results are in good agreement with our data.

In the nickel complexes of (ethylenedithio)diacetic and thiodiglycolic acids, the difference of their stability constants is 0·5 and smaller than that for copper complexes. This may indicate that the affinity of sulphur to nickel is smaller than that to copper.

The stability constants of copper and nickel complexes formed with thiodiglycolic and (ethylenedithio)diacetic acids are larger than those of diglycolic acid complexes of the respective metals. This fact may suggest that Cu–S and Ni–S bonds are stronger than Cu-O and Ni-O bonds. MCINTYRE *et al.*(16) and LOTZ *et al.*(17) studied the stability of copper complexes formed with various diamines containing sulphur or oxygen and reported that the Cu-S bond strength was about 2 kcal/mole, while oxygen did not form the bond of measurable strength with copper. Recently SANDELL(18) reported the stability constants of copper complexes of ethoxyacetic and (ethylthio)-acetic acids. His results also showed that the Cu-S bond is stronger than the Cu-O bond. These results agree with ours.

(ii) *Cadmium and lead.* The (ethylenedithio)diacetate complexes of cadmium and lead are slightly more stable than the thiodiglycolate complexes of the respective metals (only 0·2 in log k), but less stable than the diglycolate complexes. These results

(15) G. SAINI and G. OSTACOLI, *International Conference on Co-ordination Chemistry*, p. 142. Chem. Soc. Spec. Publ. No. 13 (1959).

(16) G. H. MCINTYRE, JR., B. P. BLOCK and W. C. FERNELIUS, *J. Amer. Chem. Soc.* **81**, 529 (1959).

(17) J. R. LOTZ, B. P. BLOCK and W. C. FERNELIUS, *J. Phys. Chem.* **63**, 541 (1959).

(18) A. SANDELL, *Acta Chem. Scand.* **15**, 190 (1961).

may indicate that the M-O bond is stronger than the M-S bond in these two metals. Since Ag(I) forms a stronger bond with sulphur than oxygen and Cd(II) is isoelectronic with Ag(I), it is expected that Cd(II) forms a stronger bond with sulphur than oxygen. The stability constants of Cd(II) complexes, however, appear to indicate the opposite tendency as shown above. SCHWARZENBACH *et al.*(19) studied the Cd(II) complexes formed with the following ligands;

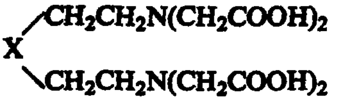

$$X\begin{cases}CH_2CH_2N(CH_2COOH)_2\\CH_2CH_2N(CH_2COOH)_2\end{cases}$$

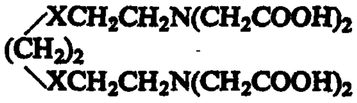

$$(CH_2)_2\begin{cases}XCH_2CH_2N(CH_2COOH)_2\\XCH_2CH_2N(CH_2COOH)_2\end{cases}$$

where X is O or S. Their data also showed that Cd(II) had a larger affinity to oxygen than to sulphur. This may be due to the higher charge of Cd(II) compared with Ag(I) as already pointed out by AHRLAND *et al.*(20)

In the complexes of diglycolic and thiodiglycolic acids, lead forms a more stable complex with the former than the latter. The same tendency has been reported for the lead complexes of $H_3COCH_2CH_2N(CH_2COOH)_2$ and $H_3CSCH_2CH_2N(CH_2COOH)_2$ by SCHWARZENBACH *et al.*(21)

(iii) *Zinc.* Among the (ethylenedithio)diacetate complexes of five metals studied, the stability of zinc complex is the smallest. Its stability constant is also smaller than those of thiodiglycolic and diglycolic acid complexes of the same metal (Table 8). This result is the same as that of α-carboxy-*o*-anisic and *o*-(carboxymethylthio)benzoic acid complexes and shows also that the affinity of sulphur to zinc may be smaller than that of oxygen.

From all the results obtained above, the five metals studied are divided into two classes.

(1) Larger affinity towards O than S: Zn, Cd, Pb

(2) larger affinity towards S than O: Cu, Ni.

The relative affinity of sulphur to metal seems to be:

$$Cu > Ni > Pb, Cd > Zn$$

for the ligands containing neutral sulphur. This order is of course different from that for charged sulphur. For the latter, LEUSSING(22) and FERNANDO *et al.*(23) reported the following orders:

$$Zn > Ni > Co > Fe > Mn$$

for $HSCH_2COOH$ and:

$$Zn > Ni$$

for $HSCH_2CH_2COOH$ respectively. SCHWARZENBACH *et al.*(21) obtained the following order:

$$Pb > Cd > Zn > Ni > Fe > Mn$$

for $HSCH_2CH_2N(CH_2COOH)_2$. Further, CHENY *et al.*(24) reported the following order:

$$Pb > Zn > Co > Ni$$

for the complexes of 6-mercaptopurine.

---

(19) G. SCHWARZENBACH, H. SENN and G. ANDEREGG, *Helv. Chim. Acta* **40**, 1886 (1957).

(20) S. AHRLAND, J. CHATT, N. R. DAVIES and A. A. WILLIAMS, *J. Chem. Soc.* 1403 (1958).

(21) G. SCHWARZENBACH, G. ANDEREGG, W. SCHNEIDER and H. SENN, *Helv. Chim. Acta* **38**, 1147 (1955).

(22) D. L. LEUSSING, *J. Amer. Chem. Soc.* **80**, 4180 (1958).

(23) Q. FERNANDO and H. FREISER, *J. Amer. Chem. Soc.* **80**, 4928 (1958).

(24) G. E. CHENY, H. FREISER and Q. FERNANDO, *J. Amer. Chem. Soc.* **81**, 2611 (1959).

One of the interesting points in these results is the order of nickel and zinc. For charged sulphur zinc appears to have a larger affinity than nickel, while the order is reversed for neutral sulphur. As pointed out by WILLIAMS,(25) these two orders—Ni > Zn for neutral sulphur and Zn > Ni for charged sulphur—seems to be general, at least, in the 1:1 complexes formed with the ligand which contains neutral or charged sulphur. According to LEUSSING(26) the Ni-S bond appears to be predominantly sigma in the nickel complex formed with $HSCH_2CH(SH)CH_2OH$. Therefore, if the affinity of sulphur or oxygen to a metal depends on the formation of a dative π-bonding,(1) the reversal of the stability order of zinc and nickel may suggest a different kind of bonding between the metal and neutral sulphur, although nothing definite is known yet.

(25) R. J. P. WILLIAMS, *Annual Reports on the Progress of Chemistry* **56**, 87 (1959).
(26) D. L. LEUSSING, *J. Amer. Chem. Soc.* **81**, 4208 (1959).

J. Inorg. Nucl. Chem., 1962, Vol. 24, pp. 1105 to 1109. Pergamon Press Ltd. Printed in England

TETRAHYDROFURAN COMPLEXES OF TRANSITION METAL CHLORIDES

R. J. Kern

Monsanto Chemical Company, St. Louis 66, Missouri

(*Received* 14 *February* 1962; *in revised form* 16 *March* 1962)

Abstract—Tetrahydrofuran complexes of $TiCl_3$, VCl_3, $VOCl_2$, $CrCl_3$, $CrCl_2$, $MnCl_2$, $FeCl_2$, $CoCl_2$, $NiCl_2$, $CuCl_2$ and $ZnCl_2$ were isolated and their compositions determined. In general the anhydrous metal chlorides complexed easily. Ferric chloride cleaved the ring predominantly and $CrCl_3$ required a zinc catalyst to react. Nickelous chloride would not react directly at all but a tetrahydrofuranate was prepared via a ligand exchange reaction. Titanium tris-tetrahydrofuran trichloride disproportionates readily several hundred degrees lower than $TiCl_3$ by itself.

Recent advances in polymerization catalysis have employed transition metal complexes to obtain a truly remarkable array of new polymers. The combinations of monomers which may be copolymerized, their distribution in the polymeric chain and polymer stereospecificity are among the properties strongly influenced by the exact nature of these co-ordination catalysts. One not engaged in polymerization chemistry can hardly appreciate the number of property-determining structural variables in macro-molecules which are affected by the catalyst. Evidence, much of it unpublished, accumulates that the control over structural variables exerted by a co-ordination catalyst is related to a delicate balance between transition metal, vinyl group and complexing group.

Complexes of transition metals with a wide variety of ketones, esters, amines, sulphoxides and the like have been described.(1, 2) Quite naturally the more polar organic ligands have been studied in most detail since they form more stable complexes. However, in the design of polymerization catalysts weaker complexing agents are also of interest. For this reason complexes of ethers, a less polar type of ligand, were examined. This communication describes the isolation and composition of tetrahydrofuran complexes along with some of their properties.

Preparation

Tetrahydrofuranates of metal chlorides appreciably soluble in hot tetrahydrofuran ($TiCl_4$,(3) VCl_3,(4) $ZnCl_2$) were prepared simply by dissolving the metal halide and allowing crystallization to occur.

Many metal chlorides were only sparingly soluble in tetrahydrofuran ($TiCl_3$,(5) $CrCl_2$, $FeCl_2$, $CoCl_2$ and $CuCl_2$). Their complexes were concentrated by extraction

---

(1) J. C. Bailar, *Chemistry of Co-ordination Compounds*. Reinhold, New York (1956).

(2) F. Feigl, *Chemistry of Specific, Selective and Sensitive Reactions*. Academic Press, New York (1949).

(3) P. Hamilton, R. McBeth, W. Bekebrede and H. Sisler, *J. Amer. Chem. Soc.* **75**, 2881 (1953).

(4) E. Kurras, *Naturewissenshaften*, **46**, 171 (1959).

(5) G. Pregaglia, G. Mazzanti and D. Morero, *Ann. chim.* (*Rome*), **49**, 1784 (1959).

in a Soxhlet apparatus. $CrCl_3$ is completely insoluble in tetrahydrofuran. As found by HERWIG and ZEISS[(6)] we confirmed that in the presence of zinc it readily forms a soluble tetrahydrofuranate.

Nickel chloride did not react with pure tetrahydrofuran either in the presence or absence of zinc. A $NiCl_2$–tetrahydrofuran complex, $NiCl_2.2THF$ may be prepared, however, by displacement of nitrile from a nickel chloride–acetonitrile complex. The latter may be prepared directly from $NiCl_2$.[(7)]

Manganous chloride is unique among the chlorides in this series. Neither it nor its complex is soluble in tetrahydrofuran. The cyclic ether appears to react directly with solid $MnCl_2$ without an intermediate dissolution-crystallization process.

Ring-opening of tetrahydrofuran by $FeCl_3$ was extensive. This reaction could not be inhibited and no tetrahydrofuranate could be isolated. No reaction between VCl_2 and tetrahydrofuran could be induced. The complex $VOCl_2{\cdot}2THF$ was prepared by the air oxidation of $VCl_3{\cdot}3THF$ in the presence of moisture (equation 1).

$$4VCl_3{\cdot}3THF+O_2+2H_2O \rightarrow 4VOCl_2{\cdot}2THF+4HCl+4THF \qquad (1)$$

Compositions of all tetrahydrofuranates prepared are presented in Table 1.

Properties

The only practical solvent for tetrahydrofuranates is tetrahydrofuran itself. When dissolved in other solvents, the solvent molecules exchange for tetrahydrofuran in the co-ordination sphere. Thus, these tetrahydrofuranates may not be recrystallized from alcohols, ketones, esters and the like. Because of their pronounced tendency to hydrate the tetrahydrofuranates must be prepared and stored out of contact with the atmosphere. The tetrahydrofuranates are insoluble in aromatic and aliphatic hydrocarbons except that the zinc chloride derivative is somewhat soluble in benzene.

Weight losses at temperatures up to 250° were determined for the tetrahydrofuranates of $TiCl_3$, VCl_3, $CrCl_3$, and $ZnCl_2$. Stability (resistance toward losing the first two organic ligands) decreases in the order Cr^{3+}, V^{3+}, Ti^{3+}, Zn^{2+}. Over the range 75–150°, the tetrahydrofuranates of Ti^{3+}, V^{3+}, and Cr^{3+} lose two organic groups recoverable as pure tetrahydrofuran. In the range 150–250°C the third organic group is lost. Four additional minor unidentified components were observed via gas chromatography in volatiles condensed over this 150–250°C range.

Disproportionation of $TiCl_3{\cdot}3THF$ proceeds markedly after two groups are lost. Bright-yellow $TiCl_4{\cdot}2THF$ sublimes from the

$$TiCl_3{\cdot}3THF \xrightarrow{25\text{–}100^{\circ}C} TiCl_3{\cdot}THF \xrightarrow{150\text{–}200^{\circ}C} TiCl_4{\cdot}2THF+TiCl_2$$

pyrolysis tube above 150°. It is noteworthy that complexed $TiCl_3$ disproportionates at an appreciable rate several hundred degrees lower than does uncomplexed $TiCl_3$.[(8)] Analyses showed the non-volatile solids remaining from these pyrolyses to be the original metal chloride in each instance except with the $TiCl_3$ complex.

The 909 and 1069 cm^{-1} bonds in tetrahydrofuran, presumably associated with the C-O-C group,[(9)] shift to lower frequencies in the complexes (see Table 2). This is evidence that co-ordination occurs through the oxygen atom.

[(6)] W. HERWIG and H. ZEISS, *J. Org. Chem.* **23**, 1404 (1958).

[(7)] R. J. KERN, *J. Inorg. Nucl. Chem.* In press.

[(8)] G. B. SKINNER and R. A. RUEHRWEIN, *J. Phys. Chem.* **59**, 113 (1955).

[(9)] L. J. BELLAMY, *The Infra-red Spectra of Complex Molecules* (2nd Ed.), p. 119. J. Wiley, New York (1958).

TABLE 1.—TETRAHYDROFURAN (THF) COMPLEXES

Empirical formula	Colour	Physical form	Solubility relative in THF*	Metal (%)		Cl (%)		Remarks
				Calc.	Found	Calc.	Found	
$TiCl_3 \cdot 3THF$	Sky-blue	Platelets	4	13·0	12·9	28·7	28·9	
$TiCl_4 \cdot 2THF$	Yellow	Waxy	5	14·31	14·35	42·5	42·5	m.p. 118°, See Ref. 1
VCl_2								No complex formed
$VCl_3 \cdot 3THF$	Brick-red	Cubes	3	13·6	13·6	28·5	28·5	Xg = $8{\cdot}3 \times 10^{-6}$; $\mu = 2{\cdot}80$
$VOCl_2 \cdot 2THF$	Green	Needles	4	18·1	18·1	25·2	25·1	Xg = $4{\cdot}7 \times 10^{-6}$; $\mu = 1{\cdot}76$
$CrCl_2 \cdot 2THF$	Pale green	Sandy	2	19·5	19·8	26·6	26·8	Xg = $34{\cdot}3 \times 10^{-6}$; $\mu = 4{\cdot}71$
$CrCl_3 \cdot 3THF$	Violet	Irregular	3					See Ref. 6
$MnCl_2(THF)_{1\cdot5}$	White	Pulp	1	23·5	22·9	30·4	30·6	†
$FeCl_2(THF)_{1\cdot5}$	Tan	Sandy	2	23·8	23·6	30·2	29·7	Xg = $54{\cdot}0 \times 10^{-6}$; $\mu = 5{\cdot}50$
$FeCl_3$						Predominantly ring-opening		
$CoCl_2(THF)_{1\cdot5}$	Blue	Needles	4	24·8	24·6	29·8	29·1	
$NiCl_2 \cdot 2THF$	Yellow	Cubes	4	21·5	21·2	26·0	26·4	
$CuCl_2(THF)_{0\cdot8}$	Ochre	Powder	2	33·2	34·0	37·0	36·1	†
$ZnCl_2 \cdot 2THF$	White	Crystals	5	23·6	23·6	25·3	25·0	Soft, low melting

* Scale 1 to 5, insoluble to highly soluble estimated.

† Composition particularly sensitive to drying conditions.

Xg = Gm magnetic susceptibility, c.g.s. units.

μ = Permanent magnetic dipole moment, Bohr magnetons.

Fig. 1 shows that the shift per unit positive oxidation state of the metal goes through a minimum at $MnCl_2$.

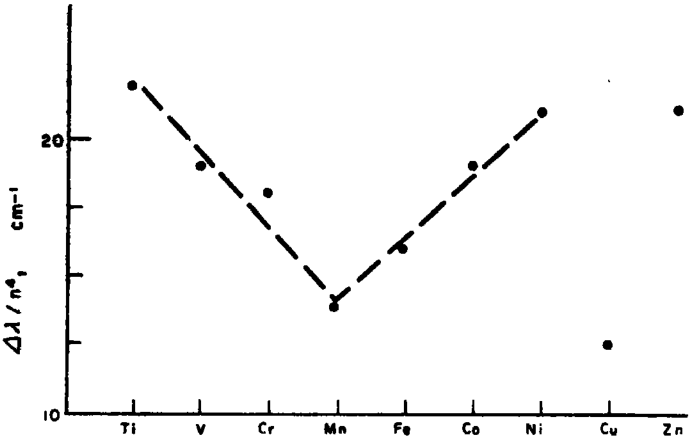

FIG. 1.—Frequency shift of 909 cm^{-1} bond in THF complexes (per unit positive oxidation state of metal atom).

TABLE 2.—FREQUENCY SHIFTS IN THE COMPLEXES OF TETRAHYDROFURAN

THF complex of	Negative frequency shift (cm^{-1})	
	909 cm^{-1} band	1069 cm^{-1} band
THF	0	0
$TiCl_3$	66	60
VCl_3	57	64
$VOCl_2$	45	51
$CrCl_3$	54	57
$MnCl_2$	28	33
$FeCl_2$	33	45
$CoCl_2$	38	40
$NiCl_2$	42	42
$CuCl_2$	25	25
$ZnCl_2$	42	50

General

Operations were carried out under dry nitrogen. This was done either in a dry box or in glass apparatus connected to a nitrogen manifold under a head of about 10 mm Hg pressure above atmospheric. Generally, the anhydrous metal chloride was extracted from a baked paper Soxhlet thimble using tetrahydrofuran which had been freshly distilled from $LiAlH_4$. Dry sand or talc was admixed with the powdered metal chlorides to reduce caking difficulties.

$NiCl_2$-tetrahydrofuranate. Blue crystals of $NiCl_2$-acetonitrile complex(7) (2 g) were placed in a dry nitrogen filled 50 ml flask. Tetrahydrofuran (20 ml) was added whereupon a yellowish-green solution formed. The solvent was carefully removed under mechanical-pump vacuum through a nitrogen manifold. Fresh tetrahydrofuran was again added and the process repeated four times. A yellow residue of flakes remains which may be crystallized from a small amount of tetrahydrofuran in the form of canary-yellow cubes.

If the initial solution of acetonitrile complex in tetrahydrofuran is allowed to stand, green crystals of $NiCl_2(THF)\ (CH_3CN)$ form.

$VOCl_2 \cdot 2THF$. $VCl_3 \cdot 3THF$ crystals (10 g) were dissolved in 200 ml of tetrahydrofuran *and stirred magnetically in the open-air at room temperature. The initial* red solution soon turned green, then blue with noticeable evolution of HCl fumes. Volume was reduced to 100 ml by evaporation, 100 ml hexane added and the solution filtered. On standing green crystals of the compound $VOCl_2 \cdot 2THF$ separated. These crystals dissolve instantly in water forming a clear sky-blue solution typical of vanadyl ion.

Pyrolysis. Weight losses were gravimetrically determined after 15 min exposure at 1 mm pressure at 25° intervals.

J. Inorg. Nucl. Chem., 1962, Vol. 24, pp. 1111 to 1118. Pergamon Press Ltd. Printed in England

COMPLEXES OF OXOVANADIUM (IV)*

J. Selbin and L. H. Holmes Jr.

Coates Chemical Laboratories, Louisiana State University, Baton Rouge, Louisiana

(*Received* 1 *February* 1962; *in revised form* 12 *March* 1962)

Abstract—The preparation and partial characterization of a number of new complexes of the oxovanadium(IV) ion are reported. Cationic, neutral and anionic complexes in which the vanadium(IV) is either five- or six-co-ordinated are included. Conductivity studies have generally allowed the assignment of groups to the first co-ordination sphere and the presence of the vanadium–oxygen multiple bond in each compound has been established by infra-red spectra.

MONONUCLEAR oxycations of the types MO^{n+} and MO_2^{n+} are found mainly among the lighter transition elements (in their high oxidation states) of a given period, e.g., in Groups IV, V, and VI. They are almost non-existent with the later-group metals, although exceptions, such as OsO_2^{2+} and RuO^{2+}, may be noted. The most extensively studied and best characterized oxycation is the dioxouranium (VI) or uranyl ion, UO_2^{2+}.(1,2)

The next best characterized and most studied oxycation is the oxovanadium (IV) or vanadyl ion, VO^{2+}.(3–12)

The strongly bound oxygens of such species present additional means for studying the complexes of the oxycations beyond those normally available with transition metal complexes. Thus, for example, vibrational motions of the "central (polyatomic) ion" can be studied as they are perturbed by the additional ligated species. Indeed it has been shown(1, 13) that a ligand series strikingly similar to the spectrochemical series may be established from the shifts observed in the symmetric and antisymmetric vibrations of the O-U-O entity in a series of uranyl complexes. A similar study of vanadyl complexes[9, 14] has utilized the V-O stretching vibration as the probe to establish certain ligand series and has uncovered a very interesting correlation between infra-red spectral data and electronic spectral data[14]. The oxygen(s) attached to the central metal produce one (or more) additional electronic (electron transfer) absorption bands, which, again, are perturbed to varying degrees by the particular set of ligands. Information from this source is more difficult to unravel and interpret, but, in principle, it should provide independent data concerning the nature of the complexes.[14]

---

* Based in part upon a thesis submitted in partial fulfilment of the requirements for the Ph.D. degree at Louisiana State University, 1961.

(1) S. P. McGlynn, J. K. Smith and W. C. Neely, *J. Chem. Phys.* **35**, 105 (1961), and references contained therein.

(2) R. L. Belford and G. Belford, *J. Phys. Chem.* **34**, 1330 (1961).

(3) F. J. C. Rossotti and H. S. Rossotti, *Acta Chem. Scand.* **9**, 1177 (1955).

(4) M. M. Jones, *Z. Naturforsch*, **12 b**, 595 (1957).

(5) Q. Trujillo *et al.*, series of papers in *Anales real. soc. espan. fiz, y quim* (Madrid), 1956–1958.

(6) C. K. Jorgensen, *Acta Chem. Scand.* **11**, 73 (1957).

(7) C. Furlani, *Ricerca Sci.* **27**, 1141 (1957).

(8) M. B. Palma-Vittorelli, M. U. Palma, D. Palumbo and F. Sgarlata, *Nuovo cimento* **3**, 718 (1956).

(9) J. Selbin, L. H. Holmes, Jr. and S. P. McGlynn, *Chem. and Industry*, 746 (1961).

(10) C. J. Ballhausen and H. B. Gray, *Inorg. Chem.* **1**, 111 (1962).

(11) R. D. Feltham. Thesis, University of California, U.S. A.E.C. Report UCRL-3867 (1957).

(12) R. P. Dodge, U.S. A.E.C. Report UCRL-8225 (1958).

(13) B. Shamburger and J. Selbin. Unpublished results.

In order to have a wide variety of complexes available for such studies as mentioned above, we have prepared and partially characterized a large number of complexes of the oxovanadium(IV) cation. These include cationic, neutral and anionic complexes in which the vanadium is either five-or six-co-ordinated. Complex types in which the vanadium is five-co-ordinated include [VO(AAAA)]*, [VO(ABBA)], $[VO(AA)_2]$, [VO(AA) (BB)] and $[VO(AA)a_2]$. Complex types in which the vanadium is six-co-ordinated include $[VOa_5]$, $[VOa_4b]$, $[VOa_3b_2]$, $[VO(AA)a_3]$ and $[VO(AA)_2a]$.

Conductivity studies of many of these complexes in nitrobenzene generally allowed the assignment of groups to the first co-ordination sphere and the determination of a definite co-ordination number. For example, with $VO(AA)_2X_2$ compounds (where AA=*o*-phen or dipy) the formulation as $[VO(AA)_2X]X$ is found for X=Cl or Br, whereas the formulation $[VO(AA)_2]X_2$ holds for $X=ClO_4$. If $X_2=SO_4$, an intermediate conductivity value is observed, indicating, perhaps, ion-pair association in this case. The infra-red spectrum of this compound indicates that in the solid state the sulphate ion is co-ordinated as a unidentate ligand. Two complexes having empirical formulas $VO(AA)_{1.5}(NCS)_2$ (where AA=*o*-phen or dipy) are formulated as $[VO(AA)_2NCS]$ $[VO(AA)(NCS)_3]$ on the basis of their mode of formation, conductivity data and infra-red spectra.

The assignment of the absorption bands due to the V-O (vanadyl) stretching vibration has been made for over fifty complexes, including a few vanadium (V) compounds.[9,14] They are found to fall in the range 932–1035 cm^{-1}. Several ligand series may be deduced from these results, and the series have been interpreted in terms of ligand σ and π bonding.[14]

The persistence of the vanadium–oxygen multiple bond in all of the complexes may be considered to be established from the infrared spectra of the compounds. Barraclough, *et al.*[15] have concluded that the presence of a metal–oxygen multiple bond can be correlated with a stretching frequency in the range 900–1100 cm^{-1}. We have verified this conclusion with a large number of compounds of MoO^{3+}, MoO_2^{2+} and WO_2^{2+} as well as VO^{2+} and UO_2^{2+}, although we could find no evidence for a TiO^{2+} or a ZrO^{2+} mononuclear species in certain so-called titanyl or zirconyl compounds.

The formation of multiple bonds to oxygen by metals in this region of the periodic table has been explained theoretically for UO_2^{2+}[1], VO^{2+}[10, 14] and MoO^{3+} and CrO^{3+}[16] However, qualitatively this situation may be traced to the ability or tendency for oxygen to delocalize its $p\pi$- electrons away from its highly compact valence sheell, forming π-bonds by this means. GILLESPIE[17] has accumulated a great deal of stereochemical evidence to support the hypothesis that oxygen (and fluorine) will form multiple bonds with atoms or groups which can readily accept π-bonding electrons available in the compact $2p$ level. The early transition elements in their high oxidation states, in which they achieve d^0 or d^1 configurations, are apparently good π-electron acceptors. In fact, it is well known that the metals at the beginning of the transition series form, their most stable complexes with oxygen-donor ligands and that their halide complexes follow the stability order $F \gg Cl > Br > I$. The formation and great stability of multiple bonds with oxygen by the metals in this region of the periodic table is thus not unexpected.

---

* Abbreviations used in this paper are: AAAA = symmetrical quadridentate ligand; AB = unsymmetrical bidentate ligand; a, b = unidentate ligands, etc.; *o*-phen = orthophenanthroline; dipy = dipyridyl; DMSO = dimethylsulphoxide.

[14] J. Selbin, S. P. McGlynn and L. H. Holmes. In preparation for publication.

[15] C. G. Barraclough, J. Lewis and R. S. Nyholm, *J. Chem. Soc.* 3552 (1959).

[16] H. B. Gray and C. R. Hare. *Inorg. Chem.* 1, 363 (1962).

EXPERIMENTAL

A. *Preparation of Compounds*

The starting vanadium materials included $VOSO_4 \cdot 5H_2O$, V_2O_5, and $VOCl_2$(syrupy), all commercial reagent grade products, and $VO(ClO_4)_2 \cdot xH_2O$, prepared as described below.

Vanadyl perchlorate

Three methods were found to be satisfactory for obtaining pure aqueous solutions of this compound.

(a) $VOSO_4$ is treated with sodium hydroxide and the precipitated $VO(OH)_2$ is filtered and washed until free of sodium sulphate. An excess of alkali should be avoided due to the amphoterism exhibited by the VO^{2+} ion. Ammonia may be used, providing all of the ammonia is washed from the precipitated hydroxide. The hydroxide is then dissolved in perchloric acid to give a vanadyl perchlorate solution which is stable for many days at room temperature or below. Heating causes show oxidation of the vanadyl to V_2O_5 by the perchlorate.

(b) Vanadium pentoxide is suspended in perchloric acid and electrolysed at a constant potential of 0·55 V (vs. Ag-AgCl electrode). Complete dissolution and reduction is slow; the solution is then filtered, yielding a vanadyl perchlorate solution.

(c) Perchloric acid is added to a solution of $VOCl_2$ and the resulting solution heated on a steam bath to drive off HCl. Oxidation of the vanadyl ion by the perchlorate ion can be reversed by adding small amounts of ethanol to the solution. Ethanol in acid solution will reduce vanadium pentoxide to VO^{2+}. A blue solution is finally obtained which gives a negative test for chloride ion with silver nitrate. Filtration improves the purity of the solution, but this is the least satisfactory of the three methods.

Solid hydrated vanadyl perchlorate may be obtained as large clear blue crystals by slow vacuum evaporation of the above solutions at room temperature. The crystals are extremely hygroscopic, making precise analysis difficult. (Found: VO, 18·5; ClO_4, 27·2. Calc. for $VO(ClO_4)_2 \cdot 5H_2O$: VO, 18·8; ClO_4, 27·9 and for $VO(ClO_4)_2 \cdot 6H_2O$: VO, 17·9; ClO_4, 26·6%).

Vanadyl chloride and vanadyl bromide

These compounds are prepared in aqueous solution by heating a mixture of vanadium pentoxide, ethyl alcohol, water and the appropriate acid until all of the vanadium pentoxide has reacted. Evaporation yields syrupy liquids and the vanadyl halides contain an indeterminate amount of water. Continued heating results in partial hydrolysis.

Vanadyl fluoride

(a) An aqueous solution of vanadium pentoxide and HF is electrolysed at constant potential and the filtered solution is evaporated to a blue solid: $VOF_2 \cdot xH_2O$; (b) a solution of $VOCl_2$ is treated with a solution of AgF in HF (prepared from silver oxide and HF) and the AgCl removed by filtration. Evaporation of the filtrate yields $VOF_2 \cdot xH_2O$. (Found: VO, 40·1. Calc. for $VOF_2 \cdot 3H_2O$: VO, 42·1, and for $VOF_2 \cdot 4H_2O$: VO, 37·8%).

[17] R. J. GILLESPIE, *J. Amer. Chem. Soc.* **82**, 5978 (1960).

Pentacyano-oxovanadate(IV) ion

(a) *Tetraethylammonium salt.* $VOSO_4 \cdot 5H_2O$ is dissolved in ca. 6M NaCN; the initial precipitate of hydroxide dissolves with stirring. The dark green solution is cooled in ice and filtered. The clear green filtrate is mixed with an aqueous solution of Et_4NBr and the mixture evaporated in an air stream at room temperature. After several hours, green crystals separate and they are filtered, washed with alcohol and ether and dried *in vacuo*. Acetone cannot be used as wash solution since it appears to cause decomposition of the product. The product is insoluble in organic solvents and dissolves with decomposition in water. (Found: VO, 12·25; CN, 22·2. Calc. for $[(C_2H_5)_4N]_3[VO(CN)_5]$: VO, 11·41; CN, 22·2%).

The analysis for vanadyl was made by precipitating the cyanide with an equivalent amount of silver nitrate and titrating the filtrate with permanganate. The high analysis for vanadyl may perhaps be explained as due to some soluble $Ag(CN)_2^-$ which would be oxidized by permanganate.

(b) *Tetramethylammonium salt.* $VOSO_4 \cdot 5H_2O$ is dissolved in ca. 6M NaCN solution and a hot aqueous solution of Me_4NI is added. A precipitate forms immediately and after cooling in ice, a light green powder is filtered and washed with alcohol and ether and vacuum-dried. (Found: VO, 16·80; CN, 32·2. Calc. for $[(CH_3)_4N]_3[VO(CN)_5]$: VO, 16·00; CN, 31·25%).

(c) *Cesium salt.* To a solution of $VOSO_4 \cdot 5H_2O$ dissolved in ca. 6M NaCN is added a solution of CsCl. An aqua coloured precipitate forms which is cooled in ice and filtered. It is washed with ca. 6M NaCN in order to remove Na_2SO_4 which may be coprecipitated. The cyanide solution is used for washing because the cyano complexes are unstable in water but stable in excess cyanide. Finally alcohol and ether are used to wash the product and it is air-dried. (Found: VO, 20·70; CN, 21·07. Calc. for $Cs_3[VO(CN)_5]$: VO, 20·36; CN, 21·80%).

Pentaisothiocyanato–oxovanadate(IV) ion

(a) *Tetraethylammonium salt.* Vanadyl sulphate is dissolved in ca. 8 M NH_4NCS. An aqueous solution of Et_4NBr is added, yielding an immediate precipitate. The solution is heated and the precipitate dissolves; on cooling slowly to ice temperature the solution yields blue needles. They are recrystallized from absolute alcohol, filtered, washed with alcohol and ether and vacuum-dried. (Found: NCS, 40·70; C, 42·39, 42·01; H, 7·25, 7·27; N, 14·48, 14·50. Calc. for $[(C_2H_5)_4N]_3[VO(NCS)_5]$: NCS, 38·90; C, 46·50; H, 8·08; N, 16·05%. Found: C/H, 5·68; C/N, 2·92. Calc. C/H, 5·75; C/N, 2·90.)

It is possible that this compound was not fully decomposed in the analysis for C, H and N, as the ratios would indicate. The crystals recrystallize nicely and are well formed. They appear to be quite pure under a microscope and the analysis for NCS run in this laboratory is satisfactory. There is also the possibility that some bromide ion (from the Et_4NBr) is present: it would lower the C, H and N percentages and raise the thiocyanate percentage which was determined as AgNCS. This last possibility finds support in the superior analysis found with the tetramethylammonium compound prepared from $(CH_3)_4NI$ and described below.

(b) *Tetramethylammonium salt.* Vanadyl sulphate is dissolved in ca. 8 M NH_4NCS and a hot aqueous solution of Me_4NI is added. On cooling, a precipitate of sparkling blue crystals is obtained. These crystals are filtered, recrystallized from absolute alcohol, washed with alcohol and ether and air-dried. A hot solution of the Me_4NI is used here as previously because of the lower solubility of this compound at lower temperatures. (Found: NCS, 49·50; C, 34·53; 34·20; H, 6·51, 6·66; N, 19·00, 19·21. Calc. for $[(CH_3)_4N]_3[VO(NCS)_5]$: NCS, 50·01; C, 34·61; H, 6·26; N, 20·50%).

Sulphatodipyridyloxovanadium(IV)

Vanadyl sulphate is dissolved in warm dimethylformamide (DMF) and then added to a solution of α,α'-dipyridyl in DMF. A green solution is obtained at first, but upon further addition of vanadyl sulphate, a green powder deposits. The powder is refluxed in absolute ethanol, filtered, washed with ether and dried *in vacuo*. (Found: VO, 21·40; SO_4, 31·0. Calc. for $[VO(C_{10}H_8N_2)SO_4]$: VO, 21·00; SO_4, 30·10%).

Sulphato(orthophenanthroline)oxovanadium(IV)

Vanadyl sulphate is dissolved in DMF and added to *o*-phen dissolved in DMF. A yellow solid forms immediately which on further addition of vanadyl sulphate dissolves to produce a green solution. When this solution is heated just below the boiling point, a greenish powder precipitates. It is refluxed in absolute ethanol, filtered, washed with ether and dried *in vacuo*. (Found: VO, 19·35; SO_4, 28·70. Calc. for $[VO(C_{12}H_8N_2)SO_4]$: VO, 19·50; SO_4, 28·00%).

Bis(orthophenanthroline)–oxovanadium(IV) sulphate

Vanadyl sulphate is dissolved in ethanol (containing enough water to cause dissolution) and added in a one to two mole ratio to *o*-phen dissolved in ethanol. A gummy precipitate is obtained which dissolves if the solution is heated. Upon cooling, a yellow-brown powder is deposited which is not very soluble in ethanol after drying. It is washed with acetone and ether and dried *in vacuo*. (Found: VO, 14·20; SO_4, 18·20. Calc. for $VO(C_{12}H_8N_2)_2SO_4$: VO, 12·80; SO_4, 18·35%).

Tetramethylammonium tetrachloro–oxovanadate(IV) monoethanolate

Syrupy vanadyl chloride is mixed with a very concentrated solution of $(CH_3)_4NCl$ and ethanol is added. Upon addition of acetone and ether to this solution a blue oil separates. This oil is washed with successive portions of absolute ethanol–acetone mixtures (enough acetone to prevent redissolving the oil) and then dissolved in a small volume of absolute ethanol. Acetone addition to this solution gives a greenish-blue gummy solid which is washed repeatedly with acetone. The product can then be recrystallized from absolute ethanol by dissolving it and then evaporating some of the solvent, followed by cooling. An aqua coloured powder is obtained which is ether-washed and dried *in vacuo*. (Found: VO, 16·42; Cl, 35·00. Calc. for $[(CH_3)_4N_2][VOCl_4(C_2H_5OH)]$: VO, 16·62; Cl, 35·25%).

Bis(dipyridyl)–oxovanadium(IV) perchlorate

Vanadyl perchlorate (aqueous or solid) is dissolved in acetone and added to α,α'-dipyridyl dissolved in acetone. A greenish-brown solution results which is evaporated to dryness in a vacuum at room temperature. The solid obtained is washed several times with a 1:1 mixture of acetone–ether and again evaporated to dryness under vacuum at room temperature. Washing with acetone–ether mixtures may produce an oil. The final product is a greenish-brown powder which is washed with ether and dried *in vacuo*. (Found: VO, 11·24; C, 42·48; H, 3·38; N, 9·60. Calc. for $[VO(C_{10}H_8N_2)_2](ClO_4)_2$: VO, 11·58; C, 41·60; H, 2·80; N, 9·69%).

Bis(orthophenanthroline)–oxovanadium(IV) perchlorate

Vanadyl perchlorate in acetone is added to *o*-phen dissolved in acetone. After the solution is stirred for several minutes a green precipitate begins to appear and precipitation is complete after cooling in ice. It is filtered, washed with ether and vacuum-dried. (Found: VO, 10·75; C, 45·82; H, 2·98; N, 8·45. Calc. for $[VO(C_{12}H_8N_2)_2](ClO_4)_2$: VO, 10·70; C, 46·00; H, 2·58; N, 8·96%).

Bromobis(orthophenanthroline)–oxovanadium(IV) bromide 1-hydrate

Aqueous vanadyl bromide in acetone is added dropwise with stirring to *o*-phen dissolved in acetone. A chartreuse precipitate appears at once and increases in amount as the $VOBr_2$ is added. The solution above the precipitate is nearly colourless as long as excess *o*-phen is present; if excess $VOBr_2$ is added it becomes greenish. The precipitate is refluxed for some minutes in a 1:1 ethanol–acetone mixture and filtered, washed with ether and vacuum-dried. (Found: Br, 26·4; C, 46·44; H, 2·96; N, 9·10. Calc. for $[VO(C_{12}H_8N_2)_2Br]Br\cdot H_2O$: Br, 26·40; C, 48·00; H, 3·00; N, 9·33%).

Bromobis(dipyridyl)–oxovanadium(IV) bromide 1-hydrate

A solution of hydrated $VOBr_2$ in acetone is added dropwise with stirring to a solution of dipy dissolved in acetone. A green precipitate separates at once, increasing in quantity as $VOBr_2$ is added. The solution remains colourless if an excess of dipy is present, greenish, if not. The precipitate is filtered and dissolved in a 1:1 ethanol-acetone mixture. Upon cooling for several hours in ice the solution deposits a dark green powder, which is washed with ether and vacuum-dried. (Found: Br, 28·20; C, 42·38; H, 3·56; N, 10·08. Calc. for $[VO(C_{10}H_8N_2)_2Br]Br\cdot H_2O$: Br, 28·70; C, 43·20; H, 3·24; N, 10·09%).

Chlorobis(orthophenanthroline)–oxovanadium(IV) chloride

Syrupy $VOCl_2$ dissolved in acetone is added dropwise with stirring to *o*-phen dissolved in acetone. A light greenish-yellow fluffy precipitate forms at first, but on further addition of $VOCl_2$ the precipitate becomes green and heavier, settling out very readily. When the supernatant liquid becomes green the addition is stopped and the mixture heated to boiling for several minutes, filtered and the green powder washed with ether and vacuum-dried. (Found: VO, 13·98; Cl, 14·08. Calc. for $[VO(C_{12}H_8N_2)_2Cl]Cl$: VO, 13·42; Cl, 14·24%).

Chlorobis(dipyridyl)–oxovanadium(IV) chloride

Syrupy $VOCl_2$ dissolved in acetone is added dropwise with stirring to dipy dissolved in acetone. A green precipitate is obtained immediately and $VOCl_2$ addition is stopped when the solution turns green. The mixture is boiled for several minutes, the solid filtered and refluxed in fresh acetone for several more minutes, then filtered, washed with ether and dried *in vacuo*. (Found: VO, 15·01; Cl, 14·51. Calc. for $[VO(C_{10}H_8N_2)_2Cl]Cl$: VO, 14·12; Cl, 14·95%).

$VOC_2O_4 \cdot H_2C_2O_4 \cdot 3H_2O$

Aqueous $VOCl_2$ is mixed with excess oxalic acid and the solution is heated on the steam bath for several hours, water being added as it evaporates. Finally the mixture is evaporated to dryness, leaving a blue solid. This solid is broken up and heated with 95 per cent ethanol. It is filtered hot, yielding a blue powder, which is repeatedly washed with hot 95 per cent ethanol until a negative test for chloride ion is obtained when the powder is dissolved in water. Then the product is washed with ether and dried in vacuo. The vanadyl and oxalate were analysed by titrating a sample with permanganate and calculating the per cent VO using $\frac{1}{5}$ of the volume and the C_2O_4 using $\frac{4}{5}$ of the volume required. (Found: VO, 22·20; C_2O_4, 58·40; C, 16·26; H, 2·00. Calc. for $VOC_2O_4 \cdot H_2C_2O_4 \cdot 3H_2O$: VO, 22·38; C_2O_4, 58·90; C, 17·05; H, 2·67%).

Oxalato(dipyridyl)–oxovanadium(IV)

The product just described, $VOC_2O_4 \cdot H_2C_2O_4 \cdot 3H_2O$, is dissolved in ethanol (containing just enough water to effect dissolution) and added dropwise with stirring to dipy dissolved in alcohol. The solution immediately turns yellow, then darkens to green, and finally a green precipitate deposits. The vanadyl solution is added until there is a 2:1 mole ratio (VO:dipy) present. The mixture is boiled for several minutes, cooled, filtered and the green product washed with acetone and ether and air-dried. (Found: VO, 20·65; C_2O_4, 27·10; C, 43·95; H, 3·17; N, 8·51; C/N, 5·18. Calc. for $[VO(C_{10}H_8N_2)C_2O_4]$: VO, 21·60; C_2O_4, 28·30; C, 46·40; H, 2·58; N, 9·00; C/N, 5·16%).

Oxalato(orthophenanthroline)–oxovanadium(IV)

$VOC_2O_4 \cdot H_2C_2O_4 \cdot 3H_2O$ is dissolved in warm dimethylformamide and added dropwise with stirring to *o*-phen dissolved in ethanol. Immediate precipitation of a yellow-green solid occurs and the addition is stopped when the mole ratio (VO:*o*-phen) is near 2:1. The mixture is boiled for several minutes, cooled in ice, filtered and the product washed with acetone and dried *in vacuo*. (Found: VO, 19·10; C_2O_4, 26·40; C, 47·36; H, 3·22; N, 9·49. Calc. for $[VO(C_{12}H_8N_2)C_2O_4]$: VO, 20·00; C_2O_4, 26·25; C, 50·20; H, 2·39; N, 8·38%).

Difluoro(orthophenathroline)–oxovanadium(IV)

An aqueous solution of vanadyl fluoride (or solid vanadyl fluoride) is dissolved in a 1:1 ethanol–water mixture and then added dropwise with stirring to *o*-phen dissolved in ethanol. A green powder is obtained which, after boiling in the mother liquor for a few minutes, is filtered, washed with several portions of 95 per cent ethanol, acetone and then vacuum-dried. (Found: VO, 23·50; C, 41·85; H, 3·85; N, 7·36; C/N, 5·67. Calc. for $[VO(C_{12}H_8N_2)F_2]$: VO, 23·45; C, 50·60; H, 2·91; N, 10·01%; C/N, 5·05).

The reasons for the poor agreement on the C, H and N analyses are unknown; however the compound appears to be pure (e.g., under the microscope) and our own analysis for vanadyl is quite satisfactory. The C, H and N were determined by a commercial laboratory.

Difluoro(dipyridyl)–oxovanadium(IV)

A solution of vanadyl fluoride in a 1:1 water–ethanol mixture is added dropwise with stirring to dipy dissolved in ethanol. The green precipitate obtained is heated to boiling in the mother liquor for several minutes then filtered. It is then refluxed in acetone for several minutes, filtered, washed with ether and vacuum-dried. (Found: VO, 27·18; C, 45·35; H, 3·63; N, 10·76. Calc. for $[VO(C_{10}H_8N_2)F_2]$: VO, 25·63; C, 46·00; H, 3·07; N, 10·72%).

$(VO)_2(o\text{-phen})_3(NCS)_4$

A solution of vanadyl thiocyanate in ethanol is prepared as follows. Syrupy $VOCl_2$ is dissolved in absolute ethanol and treated with about 3 moles of NH_4NCS for each mole of $VOCl_2$. The solution is heated on a hot plate for about 30 min and then cooled for several hours in ice. The precipitated NH_4Cl is filtered off, leaving vanadyl thiocyanate (and some NH_4NCS) in solution. This is added dropwise with stirring to a solution of *o*-phen in ethanol. A chartreuse precipitate separates out and the mixture is boiled for several minutes. After cooling in ice, it is filtered, washed with acetone and vacuum-dried. (Found: C, 52·30; H, 2·73; N, 14·68. Calc. for $VO(C_{12}H_8N_2)_{1.5}(NCS)_2$: C, 53·00; H, 2·65; N, 15·45%).

$(VO)_2(dipy)_3(NCS)_4$

This compound is prepared by the same procedure used to obtain the previous compound. It is a green powder, which is refluxed in acetone for several minutes, filtered and washed with ether and air-dried. (Found: C, 48·79; H, 2·70; N, 17·00. Calc. for $VO(C_{10}H_8N_2)_{1.5}(NCS)_2$: C, 48·99; H, 2·16; N, 16·79%).

Bis(8-hydroxyquinolinate)–oxovanadium(IV)

This compound is prepared by the method of BIELIG and BAYER.(18) Vanadyl sulphate and oxine are heated in water solution for an hour or so on a steam bath. The brown vanadyl oxinate separates as a solid and is filtered, washed free of SO_4 with hot water and dried *in vacuo*. It is anhydrous.

Ammonium pentafluoro–oxovanadate(IV)

This compound is prepared by the method of MUETTERTIES.(19) Ammonium bifluoride is added to an aqueous solution of vanadyl fluoride and a light blue powder precipitates. It is recrystallized from water and air-dried. It is anhydrous. The same compound can be obtained using vanadyl sulphate in aqueous HF to which ammonium bifluoride is added. (Found: VO, 30·90. Calc. for $(NH_4)_3[VOF_5]$: VO, 31·00%).

Vanadyl phthalocyanine

This compound was prepared from V_2O_5 and phthalonitrile according to the method of BARRETT *et al.*(20)

Pentakis(dimethylsulphoxide)–oxovanadium(IV) perchlorate

An aqueous solution of $VO(ClO_4)_2$ is added to pure dimethylsulphoxide (DMSO): the solution becomes hot and subsequently blue crystals are deposited. The $VO(ClO_4)_2$ must be added to the DMSO; addition of DMSO to a $VO(ClO_4)_2$ solution did not yield a crystalline product. The crystals are washed with ether and vacuum-dried. (Found: ClO_4, 31·0; C, 18·55; H, 4·64. Calc. for $[VO\{(CH_3)_2SO\}_5](ClO_4)_2$: ClO_4, 30·4; C, 18·65; H, 4·57%).

Sulphatotris(dimethylsulphoxide)-oxovanadium(IV)

$VOSO_4 \cdot 5H_2O$ in pure DMSO is heated to dissolution of the salt, then cooled, yielding blue crystals. These are filtered, washed with acetone and ether and vacuum-dried. (Found: SO_4, 25·4; C, 18·38; H, 4·78. Calc. for $[VO\{(CH_3)_2SO\}_3SO_4]$: SO_4, 24·2; C, 18·15; H, 4·54%).

(18) H. J. BIELIG and E. BAYER, *Ann.* **584**, 96 (1953).

(19) E. MUETTERTIES, *J. Amer. Chem. Soc.* **82**, 1082 (1960).

(20) P. A. BARRETT, C. E. DENT, R. P. LINSTEAD, *J. Chem. Soc.* 1719 (1936).

Dichlorotris(dimethylsulphoxide)–oxovanadium(IV)

Syrupy $VOCl_2$ is dissolved in DMSO with the liberation of heat. On cooling, the solution becomes syrupy and it does not yield a precipitate. It is heated to remove some of the DMSO, then added to ethanol. To this solution at its boiling point, acetone is added and then the mixture is cooled in ice. A light blue powder is obtained. It is recrystallized from a 1:1 ethanol–acetone mixture, filtered, washed with ether and vacuum-dried. (Found: Cl, 19·39; C, 19·48; H, 5·34. Calc. for $[VO\{(CH_3)_2SO\}_3Cl_2]$: Cl, 19·20; C, 19·35; H, 4·88%).

Pentakis(dimethylsulphoxide)–oxovanadium(IV) bromide

(a) Aqueous $VOBr_2$ and DMSO are mixed in acetone and ether is added to precipitate a green-blue solid. The product is recrystallized from absolute ethanol, filtered, washed with ether and dried *in vacuo*.

(b) Aqueous $VOBr_2$ is dissolved in pure DMSO and after cooling to 0°C, blue crystals are deposited. They are recrystallized as described in (a). (Found: Br, 26·03; C, 19·24; H, 4·95. Calc. for $[VO\{(CH_3)_2SO\}_5]Br_2$: Br, 25·93; C, 19·49; H, 4·87%).

Vanadyl bis(acetylacetonate)

This compound was obtained as a commercial product from K and K Laboratories.

B. *Physical Measurements*

1. *Conductance*

Equivalent conductances of the vanadyl complexes were obtained in nitrobenzene. Concentrations ranged from 10^{-4} to 10^{-3} M. According to previously published data(21) for the conductances of complexes in nitrobenzene, the range for equivalent conductances in ohm^{-1} cm^2 were taken as follows: four ions, 70–90; three ions, 40–60; two ions, 20–30. In Table 1 the conductance data are collected. These data allow the assignment of ligands to the first co-ordination sphere in all but three of the compounds listed. (That some of the compounds may be polymeric with ligands other than the oxygen acting as bridging groups cannot be completely ruled out at the present time; however, molecular weight determinations have proven $VO(acac)_2$ and $VO(oxine)_2$ to be monomeric in benzene.) The low value (7·6) for the equivalent conductance of $VO(o\text{-phen})_2SO_4$ may result from partial dissociation of the sulphate ion or from strong ion-pair interaction between the divalent cation and anion. A value of ten was obtained for the equivalent conductance of the compounds having empirical formulas of $VO(dipy)_{1.5}(NCS)_2$ and $VO(o\text{-phen})_{1.5}(NCS)_2$. If these formulas are doubled a value of twenty is obtained, which is in the range for a one to one electrolyte. We tentatively suggest that these compounds should be formulated as $[VO(dipy)_2NCS]$-$[VO(dipy)(NCS)_3]$ and $[VO(o\text{-phen})_2NCS][VO(o\text{-phen})(NCS)_3]$. The method of preparation of these compounds is such that it would not be unreasonable to anticipate these products. Thus the addition of the chelating agent (AA) to a solution containing the $[VO(NCS)_5]^{3-}$ species would be expected to form $[VO(AA)(NCS)_3]^-$ initially. This species would then react with additional (AA) to give $[VO(AA)_2NCS]^+$, which may then be precipitated by the anionic complex species to yield $[VO(AA)_2NCS][VO(AA)(NCS)_3]$, a uni-univalent electrolyte. Attempts to get NCS^- to add to $[VO(AA)_2]^{2+}$ to give the cationic complex or to add and displace an AA group to give the anionic complex were unsuccessful.

2. *Infra-red spectra*

The infra-red spectra of the vanadyl complexes were obtained in the 4000–650 cm^{-1} region using a Perkin–Elmer Model 21 spectrophotometer and a Beckman IR-7 spectrophotometer* each equipped with NaCl optics. Nujol mulls were employed since some of the compounds appeared to have been altered in the preparation of KBr pellets. The spectra of all of the ligands were obtained so that ligand bands could be more easily identified in the spectra of the complexes. Generally there was no difficulty in identifying the strong band

---

* The Beckman IR-7 infra-red spectrophotometer was purchased with funds obtained in part from the National Science Foundation, grants numbers NSF-15242 and NSF-16724 and in part from a grant to one of us (J. S.) by the Research Corporation.

(21) F. A. COTTON and D. GOODGAME, *J. Chem. Soc.* 5267 (1960).

(or bands) due to the vanadium-oxygen multiple bond in the infra-red spectra. The frequencies of the V-O stretching vibration ranged from 1020 cm^{-1} to 932 cm^{-1}, depending upon the particular set of ligands which surrounded the VO^{2+} entity.

TABLE 1.—EQUIVALENT CONDUCTANCES OF VANADYL COMPLEXES IN NITROBENZENE

Compound	Equiv. cond. Ω^{-1} cm^2	No. of ions indicated
1. $VO(DMSO)_5(ClO_4)_2$	48·5	3
2. $VO(DMSO)_5Br_2$	18·4	2
3. $VO(DMSO)_3Cl_2$	0	0
4. $VO(DMSO)_3SO_4$	0	0
5. VO(dipy)SO_4	0	0
6. VO(*o*-phen)SO_4	0	0
7. VO(dipy)(ox)	0	0
8. VO(*o*-phen)(ox)	0	0
9. VO(dipy)F_2	0	0
10. VO(*o*-phen)F_2	0	0
11. VO(oxine)$_2$	0	0
12. VO(*o*-phen)$_2Br_2\cdot H_2O$	26·2	2
13. VO(dipy)$_2Br_2\cdot H_2O$	25·2	2
14. VO(*o*-phen)$_2Cl_2$	23·7	2
15. VO(dipy)$_2Cl_2$	18·2	2
16. VO(*o*-phen)$_2SO_4$	7·6	0–2
17. $(VO)_2$(dipy)$_3(NCS)_4$	20	2
18. $(VO)_2$(*o*-phen)$_3(NCS)_4$	20	2
19. VO(*o*-phen)$_2(ClO_4)_2$	56·5	3
20. VO(dipy)$_2(ClO_4)_2$	56	3
21. $(Et_4N)_3VO(NCS)_5$	69·1	4
22. $(Me_4N)_3VO(NCS)_5$	86	4
23. VO(acac)$_2$	0	0

Acknowledgement—The authors are grateful to the National Science Foundation for financial support received under a grant number NSF-G15242.

J. Inorg. Nucl. Chem., 1962, Vol. 24, pp. 1121 to 1127 Pergamon Press Ltd. Printed in England

EVIDENCE FOR A PENTACYANONITROSYL COMPLEX OF MOLYBDENUM*

R. F. Riley and L. Ho†

Department of Chemistry, Polytechnic Institute of Brooklyn

(*Received* 15 *January* 1962; *in revised form* 11 *April* 1962)

Abstract—Evidence is presented for the existence of diamagnetic $K_4Mo(CN)_5NO$. The substance has been reported previously as either a dihydrate or an octa-co-ordinate dihydroxo complex. The present compound is formulated as containing formally zerovalent Mo and NO^+. The low frequency NO stretching fundamental (1455 cm^{-1}) is interpreted as evidence for substantial $d_\pi \rightarrow p_\pi$ bonding in the Mo-N bond.

A number of transition metals form anionic pentacyanonitrosyl complex ions of general formula $[M(CN)_5NO]^{n-}$. These include, Fe ($n = 2, 3$),^(1, 2) Mn ($n = 2, 3$),^(3, 4) Cr ($n = 3$),^(5) V ($n = 4$),^(6) Co ($n = 3$),^(7) Mo ($n = 4$)^(8) and Ru ($n = 2$).^(9) The first members of this class which were prepared are relatively stable, diamagnetic compounds, but more recently both stable and unstable paramagnetic members have been reported.^(3, 5) Interest in this series of compounds arises primarily because (a) the formal charges on the central element and the NO group are not unambiguously defined by the charge on the anion, and (b) the possible ways of linking the NO group to the metal atom are numerous.

A review of probable bonding arrangements for the co-ordinated NO group and a classification, according to this scheme, of existing nitrosyl compounds on the basis of their infra-red spectra has been made recently by Wilkinson and coworkers.^(10) Their compilation shows that the NO groups in the nitrosyl complexes studied absorb in the 1940–1045 cm^{-1} region which they interpret in terms of a change from a predominently triply bonded NO link to one in which the bond order approaches one. Although some degree of metal–NO π-bonding has been assumed in pentacyanonitrosyl complexes, experimental evidence is largely lacking.

---

* Presented at the American Chemical Society Meeting-in-Miniature, New York City, February, 1960.

† Present address: General Telephone Co., Bayside, N.Y.

(1) N. V. Sidgewick, *The Chemical Elements and Their Compounds*, p. 1360. Oxford University Press, Oxford (1950).

(2) N. V. Sidgewick, *The Chemical Element and Their Compounds*, p. 1344 ff. Oxford University Press, Oxford (1950).

(3) F. A. Cotton, R. R. Monchamp, R. J. M. Henry and R. C. Young, *J. Inorg. Nucl. Chem.* **10**, 28 (1959).

(4) W. Manchot and H. Schmid, *Ber. Dtsch. Chem. Ges.* **59**, 2360 (1926): W. Hieber, R. Nast and E. Proeschel, *Z. Anorg. Chem.* **256**, 159 (1948); A. A. Blanchard and F. S. Magnusson, *J. Amer. Chem. Soc.* **62**, 2236 (1941).

(5) W. P. Griffith, J. Lewis and G. Wilkinson, *J. Chem. Soc.* **872** (1959).

(6) W. P. Griffith, J. Lewis and G. Wilkinson, *J. Chem. Soc.* 1632 (1959).

(7) R. Nast and M. Rohmer, *Z. Anorg. Chem.* **285**, 271 (1956).

(8) W. Hieber, R. Nast and G. Gehring, *Z. Anorg. Chem.* **256**, 169 (1948).

(9) W. Manchot and J. Dusing, *Ber. Dtsch. Chem. Ges.* **63**, 1226 (1930).

(10) J. Lewis, R. J. Irving and G. Wilkinson, *J. Inorg. Nucl. Chem.* **7**, 32 (1958).

Purple potassium pentacyanonitrosyl molybdate was first prepared by VAN DER HEIDE and HOFMAN(11) who erroneously formulated it as a double salt. More recently, HIEBER, NAST and GEHRING,(8) utilizing hydroxylamine to reduce basic, cyanide-containing molybdate solutions, reported isolation of a dihydrate, $K_4[Mo(CN)_5NO]\cdot 2H_2O$. They also report being unable to remove the hydration water at 180°C *in vacuo* and suggest the salt is better formulated as an eight-co-ordinate complex. In their formulation the NO group is formally positive, having transferred an unpaired electron to the metal orbitals, which makes the molybdenum formally zerovalent. HIEBER and JAHN,(12) studying the infra-red spectra of this and related compounds, assigned an absorption between 1400 and 1500 cm^{-1} to the NO stretching vibration. Most recently, GRIFFITH *et al.*(5) prepared this compound using the HIEBER and co-workers(8) procedure and on the basis of analyses and infra-red spectra formulated it as eight-co-ordinate $K_4[Mo(OH)_2(CN)_5NO]$ containing a formally divalent molybdenum atom. A strong absorption at 1595 cm^{-1} was assigned to the N-O stretching fundamental by the same authors.

In a study of a number of nitrosyl containing complex ions, it became necessary for us to prepare this pentacyanonitrosyl complex. Our analytical and infra-red spectral results convinced us of the lack of hydrated, co-ordinated or constitutional water in this substance and in what follows we report the results of these and other studies on this rather unstable material

EXPERIMENTAL*

Potassium pentacyanonitrosylmolybdate was prepared by the method of HIEBER *et al.*(8) It was recrystallized several times by dissolving the compound in a minimum amount of hot water and filtering into a saturated solution of potassium hydroxide. After standing at ice temperature for several hours, the crystalline precipitate was filtered, washed with absolute ethanol and ether and stored under nitrogen in a desiccator. All filtration and washing operations were carried out under a nitrogen atmosphere. (Found: K, 37·90, 37·70, 37·80; Mo, 22·70; C, 14·43, 14·62; N, 20·30, 19·90. Calcd. for $K_4[Mo(CN)_5NO]$: K, 37·92; Mo, 23·26; C, 14·55; N, 20·37%.)

Owing to the instability of potassium pentacyanonitrosylmolybdate in air, all nujol and "perfluorolube" mulls for infra-red analysis were prepared in a glove box filled with dry nitrogen and examined immediately after preparation on either a Perkin-Elmer 21 or Perkin-Elmer 112 spectrophotometer. Spectral results from the P-E 21 are shown in Fig. 1 and Table 1. Table 1 also gives the absorption maxima positions for bands in the 1950–2300 cm^{-1} region as recorded on the P-E 112 equipped with a CsBr prism-grating monochromator. The resolution of the P-E 112, so equipped, is 1 cm^{-1}. An instrument calibration was effected by scanning the absorption peaks of carbon monoxide and using the data of MAGOON *et al.*(15)

---

* All carbon and nitrogen analyses performed by the Schwarzkopf Microanalytical Laboratory, Woodside, N.Y. Potassium was analysed by the method of RAFF and BROTZ.(13) Molybdenum analyses were made using the Jones Reductor method outlined in Reference (14).

(11) K. VAN DER HEIDE and K. A. HOFMAN, *Z. Anorg. Chem.* **12**, 282 (1896).

(12) W. HIEBER and A. JAHN, *Z. Naturforsch.* **13 b**, 194 (1958).

(13) P. RAFF and W. BROTZ, *Z. Analyt. Chem.* **133**, 241 (1951).

(14) W. F. HILLEBRAND, G. E. F. LUNDELL, H. A. BRIGHT and J. I. HOFFMAN, *Applied Inorganic Analyses*, (2nd Ed.), pp. 108-112. J. WILEY, New York (1953).

(15) A. R. DOWNIE, M. C. MAGOON, T. PURCELL and B. CRAWFORD, JR., *J. Optical Soc. Amer.* **43**, 941 (1953).

TABLE 1.—INFRA-RED SPECTRAL ABSORPTIONS OF $K_4[Mo(CN)_5NO]$ UNDER MODERATE AND HIGH RESOLUTION

Instrument	Spectral absorptions					
	Cyanide region				NO region	
P-E 21	2108 *w, sp*	2080 *w, sp*	2060 *m, sp*		1470 *s*	1455 *vs, b*
	2040 *vs, sp*	2023 *s, sp*			1430 *s*	1397 *m*
P-E 112	2121	2106	2081	2058		
	2036	2022	2009			

w = weak; *sp* = sharp; *m* = medium; *vs* = very strong; *s* = strong; *b* = broad

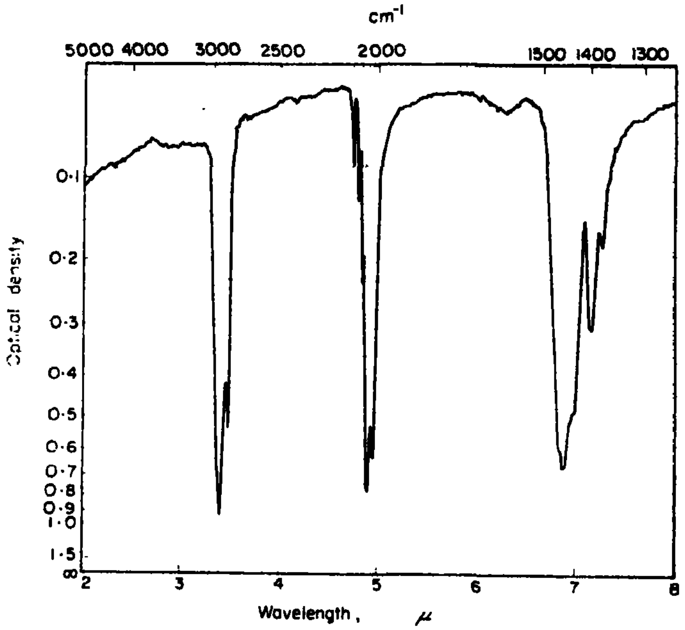

FIG. 1.

The ultra-violet and visible absorption spectrum of this compound was taken on a Cary, Model 11, spectrophotometer. All solution media were carefully deoxygenated by bubbling helium into them before use and solutions of the compound in these media were prepared under a continual sweep of the same gas. Although it was possible to scan the visible peaks without evident decomposition, the dilute aqueous solutions required to see absorption maxima in the ultra-violet region changed colour before scanning was complete. Attempts to stabilize the compound in dilute base (in which preparative work has shown the compound to be more stable) or potassium cyanide solution failed. The reported results are for saturated solutions of the compound in dimethylformamide in which no colour change was evident for several hours. The data is shown in Table 2.

TABLE 2.—VISIBLE AND ULTRA-VIOLET ABSORPTIONS OF $K_4[Mo(CN)_5NO]$

Solvent	Concn. (moles/l.)	Absorption maxima (mμ)	Extinction coefficient (l./mole cm)
H_2O	$7{\cdot}2\times10^{-3}$	544	208
Dimethylformamide	Saturated	298, 270	

HIEBER *et al.*(8) reported that their compound released nearly quantitative amounts (based on the NO group) of nitric oxide and nitrogen when boiled with a 25 per cent sulphuric acid solution of vanadium pentoxide and of nitric oxide, nitrous oxide and nitrogen when boiled with a 25 per cent sulphuric acid solution of $[Ag(C_5H_5N)_2]S_2O_8$. We have tried a variety of oxidizing agents and acids to accomplish the same end and the results are shown in Table 3. In each case the evacuated tube containing the decomposition mixture, after standing the time and temperature specified, was connected to a vacuum system and the gaseous products separated into fractions. The volume of each fraction was measured and its components identified by infra-red examination in a 10 cm gas cell. Previous to volume measurement, the gas condensable with liquid nitrogen was further dried and the majority of its carbon dioxide removed by allowing it to stand briefly at room temperature over powdered barium oxide.

In each case above parallel experiments were carried out to find the extent to which oxidation had occurred. The decomposing reagent was allowed to react at the appropriate temperature and then the excess of oxidizing agent or the reduction products of the reagent were titrated. The results are shown in Table 4. Several runs were made for each of the four reagents shown and, except for potassium hexacyanoferrate(III), the oxidation equivalents depend upon the contact time, becoming greater as the time becomes longer. In each case the results for the maximum contact time are shown.

TABLE 3.—VOLUME MEASUREMENT AND IDENTIFICATION OF GASEOUS DECOMPOSITION PRODUCTS*

Decomposition medium	Decomposition time	Temp.	Moles gas/mole comp. Not cond. —195°	Not cond. —80°	Gas composition
1 M H_2SO_4	24	R.T.	0	0	HCN and N_2O
$Fe_2(SO_4)_3$ in 2 M H_2SO_4	3	R.T.	0	0	HCN and N_2O
NaOCl in 0·5 M NaOH	1	R.T.	0·04	0·08	NH_3, N_2O
V_2O_5 in 25% H_2SO_4	6	95°	0·03	0·6	HCN, CO_2, approx. 5% N_2O

* Each decomposition and volume measurement was repeated twice.

TABLE 4.—QUANTITATIVE OXIDATION OF $K_4[Mo(CN)_5NO]$

Decomposition medium	Titrating agent	Decomposition temperature and time	Oxidation equivalents per mole of $K_4[Mo(CN)_5NO]$
$Fe_2(SO_4)_3$ in 2 M H_2SO_4	Ce^{IV} in 2 M H_2SO_4	R.T. 1 day	1·3
V_2O_5 in 25% H_2SO_4	Ce^{IV} in 2 M H_2SO_4	100°C 7 hr	6·6
NaOCl in 0·5 NaOH	As_2O_3 in 0·5 M NaOH	R.T. 15 min	5·4
$K_3Fe(CN)_6$ in 0·5 M NaOH	As_2O_3 in 0·5 M NaOH	R.T. 10 min	0·5

The chemical change occurring when aqueous solutions of potassium pentacyanonitrosylmolybdate turn yellow on exposure to air is at least partly reversible. Treatment of a weighed portion in solution, which had been allowed to change, with solid KOH afforded a 49 per cent recovery of the original purple material (identified by the identity of its infra-red spectrum with the starting material).

Electron spin resonance measurements on undiluted, powdered potassium pentacyanonitrosylmolybdate and approximately 10^{-3} M solutions by careful scanning over a large spectral range did not yield an observable resonance attributable to the compound. A very small peak due to paramagnetic impurities was noticed, however. For several theoretical reasons one would not expect spin quenching in this compound, so we conclude that the compound is diamagnetic. Recently, a sharp resonance has been studied in paramagnetic $K_3[Cr(CN)_5NO]\cdot H_2O$⁽¹⁶⁾ and the authors report little delocalization of the unpaired spin onto the NO group.

As an aid in establishing the identity of the material we have prepared, its powder diffraction pattern is given in Table 5.

TABLE 5.—X-RAY POWDER PATTERN DATA

d Spacing (Å)	
7·02	3·53
6·65	3·52
6·55	3·16
5·64	3·12
5·01	3·02
4·25	2·87
4·04	2·22
3·64	2·15

DISCUSSION

It is clear from the analyses that the compound prepared by us has a simplest formula in agreement with a six-co-ordinate, unhydrated, pentacyanonitrosyl Mo complex. The absence of infra-red absorptions in the 3300–3600 cm^{-1} and 1600 cm^{-1} regions (Fig. 1) further supports the unhydrated nature of this compound. This formulation is at variance with previous workers who found either co-ordinated water or hydroxide.

Difficulty was encountered in taking an accurate infra-red spectrum of our preparation, since reaction with air and moisture occurs, unless the precautions outlined above were rigidly followed. In Fig. 2 the spectrum of a "perfluorolube" mull of the compound is shown (decomposition was always noted in these thinner mulls even when full precautions were taken) to illustrate the spectral effects of partial exposure to the atmosphere. It can be seen that a weak band between 3300–3500 cm^{-1}, a stronger band at 1580–1590 cm^{-1} (assigned as the NO stretching fundamental by WILKINSON *et al.*) and one or two bands (unobservable in Fig. 2 as only the 5000–1000 cm^{-1} spectral region is reproduced) between 850 and 900 cm^{-1} are characteristic of the partially decomposed material. Analysis of a number of spectra has shown the intensity of these bands to be a function of exposure time of the mulls to the atmosphere. As these are the same regions in which WILKINSON and co-workers⁽⁵⁾ found absorptions it is likely that these workers reported on a partially decomposed sample of the compound reported here.

The compound reported by HIEBER *et al.*⁽⁸⁾ for which complete elementary analyses yield the formula, $K_4[Mo(CN)_5NO]\cdot 2H_2O$ is also likely to be the partially hydrolysed pentacyanonitrosyl complex, since we have found it relatively easy to remove hydrate water from various cyano complex ions and the pentacyanonitrosyl complexes of iron and manganese⁽¹⁷⁾ (see also References 3, 5 and 9).

⁽¹⁶⁾ I. BERNAL and S. E. HARRISON, *J. Chem. Phys.* **34**, 102 (1961).

⁽¹⁷⁾ Unpublished data.

Supposing that the $[Mo(CN)_5NO]^{4-}$ ion exists, it has C_{4v} symmetry so the compound should exhibit three CN stretching modes ($2A_1$, E) and one NO (A_1) stretching fundamental which are active in the infra-red. Wilkinson and co-workers

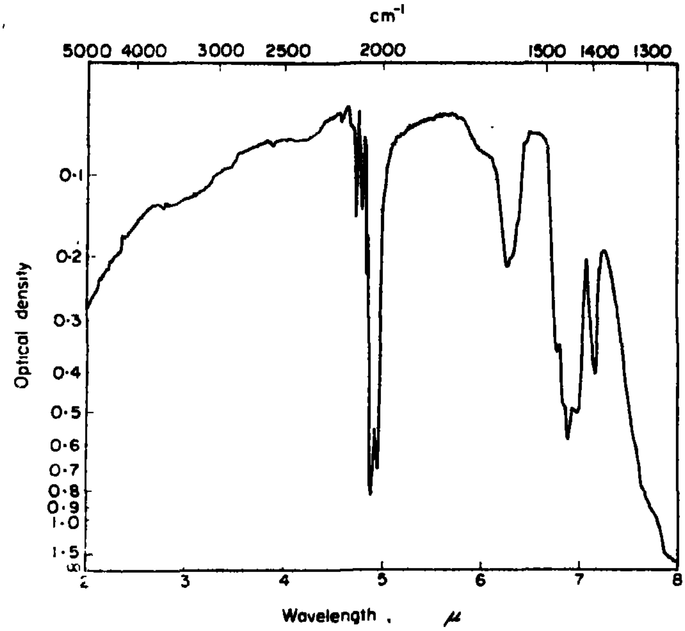

FIG. 2.

report five absorptions in the 2000–2150 cm^{-1} region which we have confirmed (Table 1). However, under higher resolution the splitting is actually more complex as seven absorptions are observed. The three strongest absorptions at 2058, 2036 and 2022 cm^{-1} we assign to the cyanide stretching vibration as their pattern is characteristic of what we have observed in the cyanide region of anhydrous iron and manganese pentacyanonitrosyl complexes.(17) The broad and intense absorption observable at 1455 cm (Fig. 2) shows two satellite peaks, one on either side, which are narrower but almost intense as the central peak. This group we assign to the NO stretching fundamental. The splitting of the NO fundamental is possibly due to solid state effects which have been noted previously for $Na_2[Fe(CN)_5NO]{\cdot}2H_2O$ and $K_3[Mn(CN)_5NO]$.(3, 18) The extreme splitting of the CN peaks may be in part due to the same effects but possibly include some combination frequencies as well. The origin of the moderately intense peak at 1397 cm^{-1} is obscure.

The impossibility of a simple assignment of the infra-red peaks and the occurrence of only a single broad and symmetric absorption, attributable to a *d-d* transition, in the electronic spectrum led us to look for confirmatory evidence for the presence of a simple pentacyanonitrosyl unit.

HIEBER *et al.* reported that most of the oxidizing agents reacted with the complex did not release gaseous nitrogen-containing products. The latter being released quantitatively only with vigorous oxidizing agents under extreme conditions (see Experimental). We have tried a variety of chemical agents known to attack co-ordinated NO groups and release gaseous nitrogen-containing products from this type

(18) G. BOR, *J. Inorg. Nucl. Chem.* 17, 174 (1961).

of complex.(4, 7, 9, 19) The results in Tables 3 and 4 show that although a significant amount of oxidation of the compound occurs, little of the expected gaseous products are produced in accord with the findings of these authors. The lack of significant amount of these products when vanadium pentoxide in 25% sulphuric acid was used (in which case HIEBER *et al.* found a nearly quantitative yield of nitric oxide and nitrogen) is presumed to be due to the difference in decomposition temperature. Our volume measuring techniques did not permit the use of decomposition temperatures above 100°C. However, to partially compensate for this temperature difference the decomposition time was made twice the reported value. That some of the co-ordinated cyano groups were oxidized in these experiments is shown by the carbon dioxide and ammonia found in the gaseous products. The latter arise by oxidation of the cyanide ion to cyanate and the subsequent hydrolysis of the cyanate.

Linkage of NO (for a linear Mo-N-O arrangement) may be through a NO^-, NO or NO^+ group. The probable chemical reactivity of NO^-(12) and the paramagnetic nature of the resultant complex ion (dependent however on the details of the splitting among the non-bonding metal orbitals) make this possibility unlikely. NO linked as a neutral group would lead to paramagnetism and so may be excluded. If NO is linked as a positive species, Mo is then formally zerovalent and, since Mo(O) is a d^6 ion, the non-bonding t_{2g} metal orbitals would be fully occupied. This leads to a diamagnetic species as found experimentally.

The rather low NO stretching frequency observed in this compound (~2300 cm^{-1} in $NOClO_4$(12) and 1944 cm^{-1} in $Na_2Fe(CN)_5NO$(3)) is understandable if back donation ($d_\pi \rightarrow p_\pi$) of the non-bonding t_{2g} electrons (orbitals of the proper symmetry are available(20)) is assumed. Electron release, which should be a function of charge on the metal ion, should be strongly favoured by Mo(O). This possibility is shown schematically below:

$$[(CN)_5Mo{-}N \equiv 01]^{4-} \longleftrightarrow [(CN)_5Mo = N = \bar{0}1]^{4-}$$

The added π-electron density in the Mo-N bond also helps explain the difficulty noted above in removing co-ordinated NO from the complex ion.

(19) W. MANCHOT, E. MERRY and P. WORINGER, *Ber, Dtsch. Chem, Ges.* **45**, 2869 (1912).

(20) L. E. ORGEL, *Proceedings of the Tenth Solvay Conference*, Brussels (1956).

J. Inorg. Nucl. Chem., 1962, Vol. 24, pp. 1129 to 1137. Pergamon Press Ltd. Printed in England

CATALYTIC OXIDATION OF GRAPHITE*

G. R. Hennig
Argonne National Laboratory, Argonne, Illinois

(*Received* 15 *January* 1962; *in revised form* 2 *March* 1962)

Abstract—Colloidal metal particles placed on graphite single crystals catalyse the oxidation of graphite. The catalysis occurs only at the metal–carbon interface. Spreading of catalytically active fragments from the particles was not observed for colloids of platinum, gold, iron or nickel. The particles produce characteristic etch patterns which are indicative of the crystal perfection. On crystals relatively free of defects, the catalysts attack parallel to cleavage surfaces to produce channels, and occasional pits on prismatic surfaces, but are inactive on the cleavage surfaces. On crystals containing lattice defects or substitutional boron impurities, the catalysts may also attack perpendicular to the cleavage surface and produce pits on it. The channels and pits are often oriented along preferred crystallographic directions. Activation energies for catalysis were estimated from the etch patterns and are about 10 kcal/mole parallel and 56 kcal/mole perpendicular to the cleavage surface. Some details of the mechanism of catalytic action have been deduced. Vanadium is an exceptionally active catalyst for graphite oxidation; it behaves differently from other metals because it forms a liquid pentoxide.

The reactions of graphite with gases, particularly with oxygen or carbon dioxide, are strongly affected by various catalytic agents. The action of such catalysts has been investigated by microscopic studies of the surfaces of graphite single crystals.

It was anticipated that catalysts would produce pits on the surfaces of graphite crystals during reaction with oxygen or carbon dioxide. Such pits usually of hexagonal shape are in fact often present on partly reacted crystals; frequently they are found to have penetrated the whole crystal and resulted in hexagonal holes. The presence of such holes has been reported by Hofmann(1) and has been attributed by Greer and Topley(2) to preferential oxidation of incorporated foreign particle or to catalytic action of impurities. Bach and Levitin(3) studied the shape of such holes after reacting impure crystals with carbon dioxide. They observed round holes after reaction with pure CO_2 and hexagonal holes after reaction with CO_2 containing hydrogen chloride.

In preliminary reports it was shown(4) by us that on carefully handled crystals metallic impurities usually do not produce catalytic pits. Special pretreatments such as particle irradiation, quenching or extensive mechanical deformation were required to induce pitting. These pretreatments probably introduced excess vacancies or vacancy clusters into graphite. Pitting was therefore attributed to attack of the catalyst at the vacancies.

* Based on work performed under the auspices of the U.S. Atomic Energy Commission.

(1) U. Hofmann, *Ber. Dtsch. Chem. Ges.* **65 B**, 1821 (1932).

(2) E. N. Greer and B. Topley, *Nature, Lond.* **129**, 904 (1932).

(3) N. Bach and I. Levitin, *Kolloid Z.* **68**, 152 (1924).

(4) G. R. Hennig, *Proceedings of the First and Second Conferences on Carbon*, p. 112. Wiley, Buffalo (1956); *Proceedings of the Third Conference on Carbon*, p. 265. Pergamon Press, New York (1958).

Pretreatment of the crystals by heating was originally carried out to remove residual impurities. However, heat treatment below 2700°C may sometimes convert an inactive impurity to a more active form.

It is intended to confine the present report to a description of the details of the catalytic effects. The application of these observations to quantitative studies of quenching, of vacancy motion,(5) and of impurity diffusion, which have been carried out jointly with Dr. M. A. KANTER, will be published in a separate report.

EXPERIMENTS

Materials. Natural graphite crystals were obtained at Ticonderoga, New York. We collected these crystals in their natural matrix of limestone from which they were separated in the laboratory by hydrochloric acid. The crystals were purified by boiling alternately in HCl and HF and by floatation. The crystals were nearly exclusively non-pitting. Their behaviour was indistinguishable from crystals purified further by heating in chlorine to 900°C or heating in helium to 3000°C and cooling slowly. Some experiments were carried out with commercial "Superflake" crystals which had been purified at 3000°C and cooled slowly.

Colloidal metal suspensions were prepared by rotating a rod of the desired metal against a wire contact of the same material. The contact was submersed in acetone and caused to arc by applying about 30 V a.c. across the contact. The resulting suspensions were light gray to brown. A few drops placed on the crystal added of the order of one metal atom to 10^5 carbon atoms. Colloidal gold solutions in water were also prepared(6) by reduction of the chloride with citric acid and dialysis but did not spread well on the crystals and were not sufficiently free of salts to yield unambiguous results.

Oxidation. To study the effects of catalysts, particularly on pitting graphite, crystals were cleaved to expose fresh internal surfaces containing only a few irregularities and surface steps. The catalyst was then applied and the crystals were transferred to silica or platinum plates and reacted on these supports in dry or wet oxygen. Wet oxygen had been saturated with water at 20°C. Dry oxygen had been passed through a column, at least 12 inches long, of magnesium perchlorate.

To study conditions of very dry oxidation, the crystals were heated to 950°C in helium which had been passed through perchlorate and through a trap cooled with liquid nitrogen. After cooling the crystals to the desired temperature of combustion, oxygen was added to the helium stream.

Microscopy. All microscope and electron microscope examinations were confined to the cleavage surfaces of the crystal and to those steps and edges visible by examination parallel to the *c*-axis. To examine the crystals in the electron microscope, a carbon replica was prepared. The crystal was either pre-shadowed with chromium, or the replica shadowed after separation from the crystal. The separation was accomplished by strengthening the replica with a heavy layer of evaporated gold, reacting the crystal with sulphuric acid containing 10 per cent of nitric acid which caused the crystal to peel off the replica and floating the replica on *aqua regia* to dissolve the gold backing. The replicas were examined in an RCA E.M.-3 electron microscope.

RESULTS

Non-pitting catalysis. Since the crystals were destroyed during replication for electron microscopy, the action of the catalysts had to be inferred from their distribution after a measured period of oxidation. Fig. 1 shows a typical arrangement. Some of the catalyst particles (*A*) were found at the tip of channels in the crystal surface. The channel sides were nearly perpendicular to the cleavage surface. The channel diameter increased with distance from the particle. All channels started at steps (*B*) running irregularly across the crystal surface. The length of the channels was variable. Many catalyst particles (*C*) were located on the cleavage surface some distance from the steps, these particles have not produced channels. The observations are interpreted as showing that catalysts remained inactive on the cleavage surface, until they came in contact with steps which moved along the surface due to uncatalysed oxidation. Once undermined by a step, a particle descended partly or completely to the bottom of the step and commenced to catalyse the oxidation along its contact with the "riser" of the step. This contact area became the tip of a channel which resulted from the accelerated oxidation at the contact area.

---

(5) G. HENNIG and M. KANTER, *Proceedings of the Fourth Conference on Carbon*, p. 141. Pergamon Press, New York (1960).

(6) J. TURKEVITCH, J. HILLIER and P. C. STEVENSON, *Discussions Farad. Soc.* No. 11, 55 (1951).

The channels produced by iron particles were usually curved and irregular (Fig. 2); those produced by gold were nearly straight. The orientation of straight channels after oxidation in moist oxygen was preferentially along $\{2\bar{1}\bar{1}0\}$ and equivalent directions, whereas it tended to $\{10\bar{1}0\}$ in dry oxygen after drying the crystals. It had been observed(7) that uncatalysed oxidation of graphite in moist oxygen causes preferential orientation of surface steps to $\{10\bar{1}0\}$ and in dry oxygen to $\{2\bar{1}\bar{1}0\}$; therefore the direction of the catalytic channels is perpendicular to and the orientation of the walls of the channel is parallel to the preferred orientation of uncatalysed steps.

Reactivity of non-pitting catalysts. The width of the channel at the active tip was equal to the diameter of the catalyst particle. The width increased with distance from the catalyst due to uncatalysed oxidation of the channel sides. Therefore, the difference in half-width between base and tip of a channel divided by the channel length equals the reactivity ratio of uncatalysed to catalysed surface atoms. This ratio was found to increase with temperature as shown by the channels of Fig. 1 and Fig. 3. An Arrhenius plot of this ratio yielded an apparent activation energy difference of about 36 kcal. Since the activation energy for the uncatalysed oxidation of these crystals was 46 kcal,(4) the activation energy of the catalysed reaction was 10 kcal. This value constitutes an average for measurements on many different channels. The value is far from exact because at any given temperature the channel dimensions varied between wide limits. Part of this variation in catalyst activity was found to be due to particle size. Very small and very large particles were less active than particles of several hundred Angstrom diameter. The catalytic activity of particles of comparable size depended also upon the channel depth which was determined from the shadow on the replica. The activity was highest for shallow channels. This correlation of channel depth and catalytic activity is apparent from the data of Table 1, which are, however, further complicated by particle size effects. The correlation was also apparent from visual examination of bent channels. Bends in channel direction often occurred when the active particle at the tip of the channel encountered a surface step. The particle was deflected away from ascending steps because they retarded the particle and towards descending steps which accelerated the motion.

Channels of depth exceeding the particle radius have never been observed. When a particle interacted with a step higher than its own radius, its catalytic action produced one of three different features, a channel with a ledge, a pit or a serrated step. Usually only one of these features predominated but the conditions favouring each are not known. A ledge at the base of the channel indicated that the particle had activated the oxidation of only the top of the step. The uncatalysed portion of the step advanced at the uncatalysed rate and remained as a ledge at the base of the channel. Several such ledges are present in Figs. 1–4. The catalyst sometimes produced pits originating on the step and extending parallel to the cleavage plane. They probably would not be detected by electron microscopy but on rare occasions were seen in the optical microscope. Pits of this type produced interference colours which are shown by contrast in Fig. 5. Such features were found occasionally on cleaved crystals, principally on steps originating at screw dislocations. In Fig. 5, the dislocation has been etched away leaving a large hole. The pits of Fig. 5 are situated at various depths as shown by the differences in contrast and confirmed by careful cleaving. The most frequently observed mode of action of catalysts at high steps was serration. The particle remained attached to the step and accelerated the oxidation parallel to the step (Fig. 6). The catalyst activity decreased with the age of the catalyst suspension. The activation energy for an aged solution of colloidal gold was measured to be 30 kcal. After extensive oxidation, the catalyst particles tended to coagulate (Fig. 4).

---

(7) G. R. Hennig, *Proceedings of the Fifth Conference on Carbon.* Pergamon Press, Oxford (1962).

TABLE 1.—CATALYTIC ACTIVITY

d*	d/c*	r*
1450	5·2	70
660	4·4	80
330	3·5	18
300	3·5	26
180	2·1	19
210	2·0	15

*d = particle diameter in Angstrom
c = channel depth
r = ratio of catalytic to uncatalysed burning rate

Pitting catalysis. Various treatments were found to modify graphite crystals so that they pitted during subsequent catalytic oxidation. These treatments are irradiation with high energy neutrons or electrons, mechanical deformation, or suitable heat treatment. Heating to temperatures above 2700°C followed by quenching usually induced subsequent pitting behaviour probably because excess lattice vacancies were introduced. In crystals which had not previously been oxidised or heat treated, pitting could also be induced by heating for several hours to temperatures between 2400° and 2600°. The rate of subsequent cooling had no influence if it exceeded one degree per minute but very slow cooling rates removed the pitting tendency. Heat treatment below 2700° caused a gradual penetration of this tendency into the crystal. As an example, Fig. 7 shows a cleaved and catalytically oxidised section of a crystal heated for one hour at 2600°. Pitting occurred in a region paralleling the outer surface of the crystal and also along a linear source crossing the crystal which may have been a twin line or low angle boundary present before cleaving. Screw dislocations were also observed to act as sources for the pit forming tendency. This pitting induced below 2700° is probably associated, not with excess lattice vacancies, but with a diffusing impurity. The effect could be enhanced by heating the graphite between 2400 and 2600°C with boric acid but was not enhanced by heating with silica or vanadium chloride. The pitting tendency induced in this temperature range

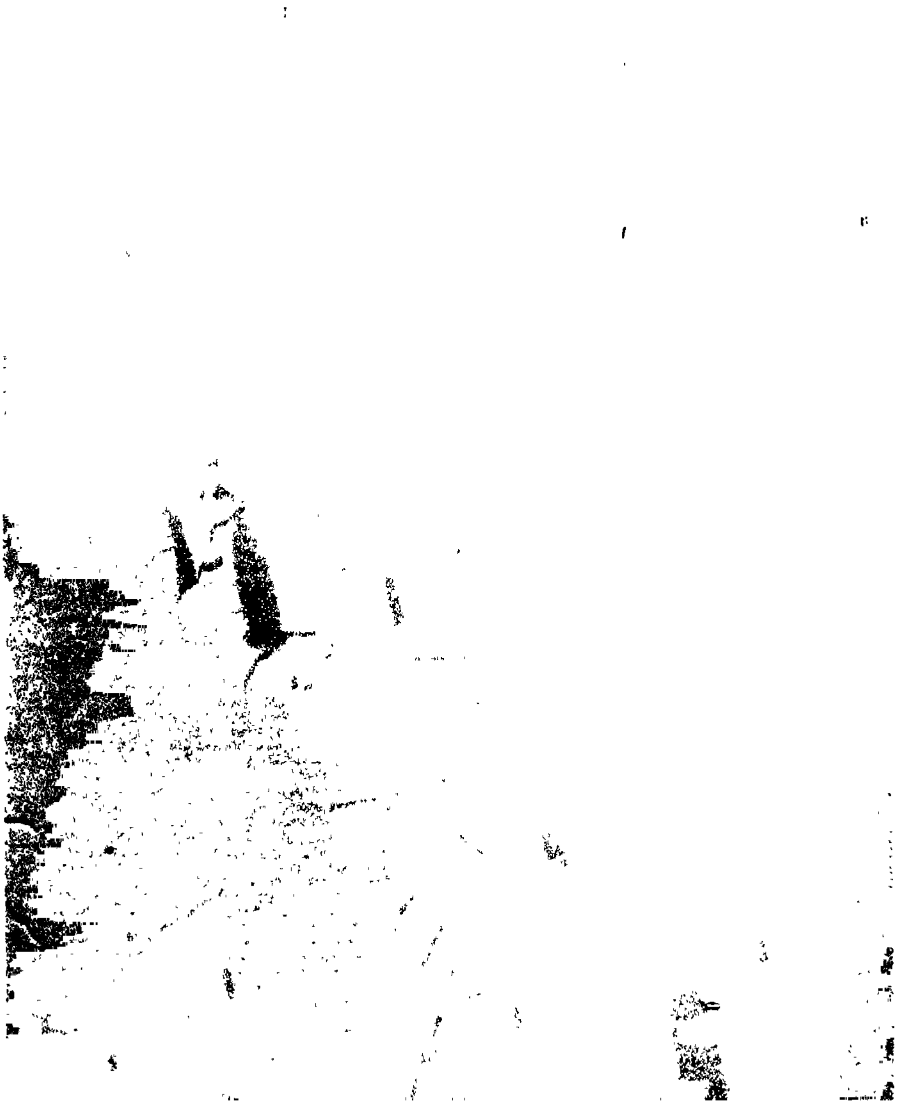

FIG. 1.—Colloidal gold on graphite. One hour oxidation at 550°. A, active catalyst; B, step; C, inactive catalyst; D, crystal bent due to $\{2\bar{1}\bar{1}l\}$ twin.

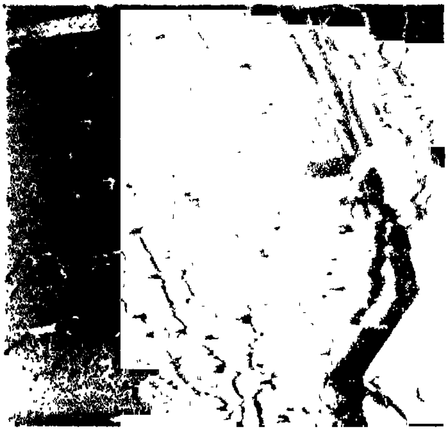

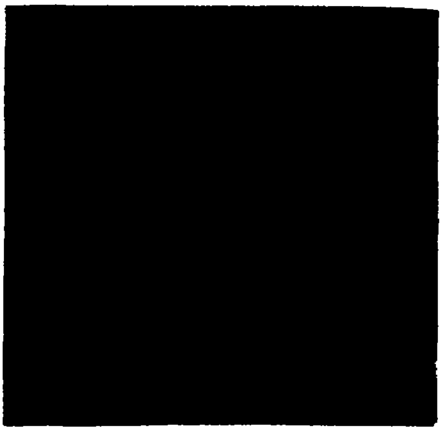

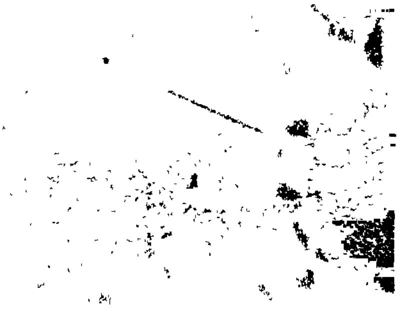

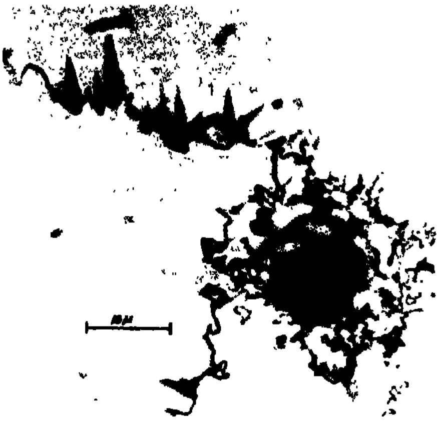

FIG. 2.—Colloidal iron on graphite. One hour wet oxidation at 500°.

FIG. 3.—Colloidal gold on graphite. One quarter hour wet oxidation at 650°.

FIG. 4.—Coagulation of colloid particles. Gold on graphite.

FIG. 5.—Pitting along *a*-axis. Colloidal gold on graphite. Wet oxygen at 700°C. Optical micrograph.

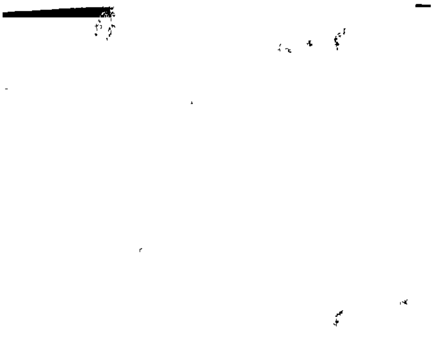

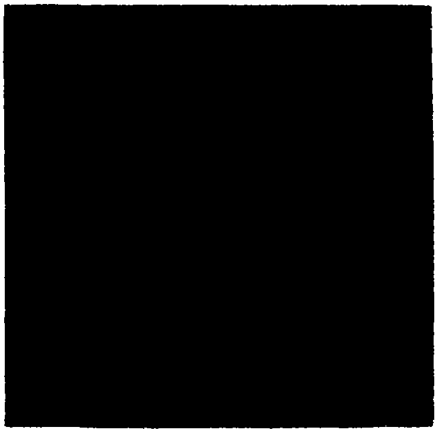

Fig. 6.—Serrated step. Colloidal gold on graphite. One half hour wet oxygen at 650°.

Fig. 7.—Pitting tendency partly diffused into graphite. Colloidal gold catalyst. Optical micrograph.

Fig. 8.—Initial channelling on pitting graphite. Colloidal gold. One hour low pressure oxygen at 700°.

Fig. 9.—Pitting by colloidal gold. Two and a half hours low pressure oxygen at 750°. Twin line showed that pit edges are $\{10\bar{1}0\}$.

Fig. 10.—Irregular hexagonal pit. Colloidal gold. One hour oxygen at 650°. Shadowed after replication.

Fig. 11.—Apparent spiral pit. Two hours oxygen 650°.

Fig. 12.—Islands of vanadium catalyst on pitting graphite. Extensive oxidation.

Fig. 13.—Same material as in Fig. 12, washed and burned ½ hour at 600°.

is therefore probably due to boron impurities present on the crystal surface and diffusing, presumably substitutionally. No distinction will be made in the following between pitting due to boron or due to quenched-in vacancies since no qualitative differences in pitting behaviour had been noted and since quantitative measurements are still in progress. Pitting due to irradiation or mechanical deformation will not be described here.

When metallic catalysts were not added, the oxidation of crystals which had been pretreated to induce pitting behaviour resulted in the development of only a small number of random pits on the cleavage surfaces. In wet oxygen this spontaneous pit formation was more pronounced than in dry oxygen.

Oxidation of pitting crystals which had been contaminated with suspensions of colloidal metal caused very extensive pitting. The progress of this pitting was followed by replicating crystals after progressively increased periods of oxidation. Initially the catalyst particle produced a channel on the surface similar to the channels formed on non-pitting crystals; however, nearly every catalyst particle produced such a channel (Fig. 8), whereas on non-pitting crystals only those particles which were in contact with steps produced channels. Furthermore, on pitting crystals, the channels became progressively deeper; the rate of penetration increased with the defect (boron or vacancy) concentration. When the channel depth was about equal to the radius of the particle, lateral motion became restricted and actual pit formation commenced (Fig. 9).

Temperature effects on pitting catalysis. The length of the initial channel decreased as the temperature of oxidation increased. The crystals did not pit at 600°, unless heavily doped with boron, but at 800° the initial channel was very short and steep. The shape of the pits produced after extensive oxidation was also found to be a function of the temperature, being steeper, the higher the temperature of oxidation. The activation energy for catalytic oxidation parallel to the c-axis can be estimated from the pit shape. The burning rate at the rim of a pit is uncatalysed and should therefore show the activation energy of 46 kcal measured for uncatalysed burning of these crystals. The depth of the pit, determined from the shadow length and shadow angle of replicas, is an index of the rate of catalytic penetration. The ratio of width to depth was of the order of ten but was temperature dependent. An Arrhenius plot of this ratio yielded a value of -10 kcal for the difference between the activation energies of uncatalysed and catalysed oxidation. The activation energy of catalysed penetration is therefore 56 kcal/mole.

The pits produced by colloidal gold or iron in wet oxygen consisted of rather high (> 500 Å) steps oriented $10\bar{1}0$ or equivalently (Fig. 9). At low pressures of oxygen, the pits became perfectly hexagonal in shape. Oxidation at high oxygen pressures and low temperatures resulted in less regular pits which were, however, still bounded by steps consisting of straight sections of preferred orientation (Fig. 10). Near the bottom of the pit the steps were often of lower height and closer together than at the top.

In dry oxygen the burning behaviour usually did not vary appreciably unless an effort was made to remove residual moisture from the crystals by outgassing in dry helium at 950°C. Such dried crystals usually showed less tendency to pit than moist crystals. An appreciable fraction of catalyst particles was found to remain inactive on the surface, the fraction depending also on the boron or defect concentration of the crystal. The pits which were produced under very dry conditions were usually oriented so that their sides were $\{2\bar{1}\bar{1}0\}$. Some of the steps were not parallel to the $\vec{c}$ axis but were high index pyramidal surfaces. The proportion of such pyramidal surfaces increased with the temperature of oxidation.

Spiral pits. Occasional pits appeared, particularly in the optical microscope, to be spiral shaped. Such apparent spirals were always found to be actually pyramidal, the spiral appearance being due to a local crowding of steps which was probably caused by oscillations of the catalyst particle (Fig. 11).

Reactivity of pitting catalysts. The dependence of the catalyst reactivity on moisture and on temperature has already been described. Some differences were noted between various metals. Colloidal gold and iron appeared equally active under moist conditions of oxidation. In dry oxygen, iron was considerably more active than gold in forming pits. Both substances appeared to sinter at 900° into more uniformly round particles which initiated more symmetrical pits or straighter channels. Nickel, platinum, and silver appeared to show catalytic activity comparable to gold. Aluminium appeared to be less active. Colloidal suspensions of vanadium produced a very much larger enhancement of oxidation rate than other metals tested. Occasional vanadium catalyst particles were seen on these crystals at the tip of catalytic channels, but, in addition, the reactivity of all steps on non-pitting crystals and of all surfaces on pitting crystals seemed to be considerably enhanced. Irregular channels indicating excess reactivity were often observed which did not carry visible catalyst particles at their tip. Furthermore those particles which could be found at channel tips appeared to wet the graphite surface and conform to the channel shape. The vanadium catalyst was apparently present as a liquid which wetted and flowed over the graphite surface. This suggests that the catalyst was present as the low melting pentoxide. Frequently, residues of less active catalyst remained in isolated positions, possibly as vanadium carbide (Fig. 12). Water at 25°C reactivated such particles; they retained their shape below 600° but melted above this temperature (Fig. 13). The melting point of bulk vanadium pentoxide is 680° but apparent melting of very small particles due to sintering, surface flow, etc. may occur at lower temperature.

DISCUSSION

The observations demonstrate several details of the mechanism of catalytic oxidation. All the metals studied except vanadium produced catalytic effects only at the interface of a rather sizeable metal particle and the substrate. No evidence was found for any catalysis by individual metal atoms separating from the colloid, the particles did not become smaller, but actually often increased in size by coalescing. In a few experiments, solutions of metal salts were placed on graphite. After brief oxidation, these metals were again found to have coagulated into active colloidal particles.

The metallic particles did not cause catalysis by action at a distance, as for instance by altering the Fermi level of conduction electrons in the graphite. The shape of the channels produced on the graphite surface showed that uncatalysed oxidation occurred up to the immediate vicinity of a catalyst particle.

What caused the motion of the colloidal particles which produced the observed channels? Brownian motion would cause a 200 Å particle to be displaced 0·05 mm/second at 500° in air unless retarded by friction against the crystal surface. However, this friction or bonding of the particle to the cleavage surface appears to prevent

Brownian motion nearly completely since the colloid particles remain randomly distributed instead of moving to surface steps and becoming catalytically active. The forces between the particle and the cleavage surface are probably van der Waals forces. The motion of a particle along its catalytic channel is probably due to additional attractive forces to the carbon atoms along the edge of the channel tip. Since these carbon atoms are constantly being oxidised, only the leading surface of the catalyst particle can be in contact with edge atoms. Thus the attractive forces are unbalanced and cause motion of the particle along the channel direction. Motion by this mechanism rather than by Brownian motion is also deduced from the observation that active particles are always located in the tip of the channels. Particles located elsewhere in the channel are inactive.

The straightness and preferential orientation of the channels can be caused by anisotropic reactivity. If the catalysed oxidation at the interface is faster in certain crystallographic directions, the resulting motion which maintains maximum contact area between particle and graphite, and thus the channel direction, will be perpendicular to one of the directions of fastest oxidation (Fig. 14). It should be noted that these directions of fastest catalysed oxidation coincide with the directions of fastest uncatalysed oxidation since the orientation of the channel sides is usually parallel to the orientation of surface steps in uncatalysed burning, even when this preferred orientation is altered by the action of water.

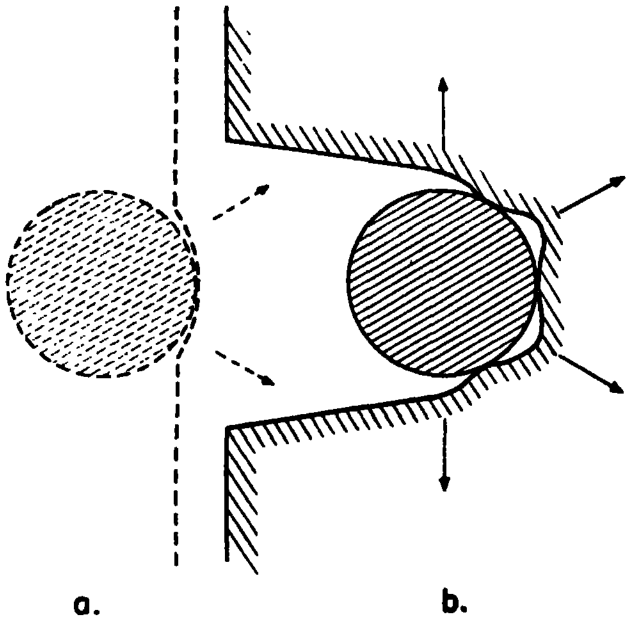

FIG. 14.—Motion of catalyst. Dashed lines: position near beginning of catalysis. Solid lines: position when channel has formed. Arrows denote directions of highest reactivity. Burning along these directions is highly exaggerated in drawing.

The catalytic activity of colloidal particles of a given size is lower in deep than in shallow channels. Since the depth of a channel in non-pitting crystals is determined by the height of the step at which catalysis commenced, this correlation cannot be due to inherent differences between particles but may be due to differences in the area of the particle-graphite interface. The diffusion length of oxygen or reaction products in this interface increases with the channel depth, thus slowing the reaction. When the step height exceeds the particle radius, the particle usually does not form a catalytic channel but moves parallel to the surface step. In this case, the accumulation of reaction products probably prevents the formation of three lines of attachment required for channel formation (Fig. 14). When attached to the step as in Fig. 6, the particle probably changes its area of attachment constantly thereby facilitating the release of reaction products from the contact area.

Mechanism of catalysis. Three sets of observations on non-pitting crystals yield information on the mechanism of catalysis. These are the preferred direction of catalytic attack, the motion of the catalyst particles, and the measured activation energies.

The uncatalysed oxidation of graphite proceeds in several steps which probably include adsorption of oxygen, activation and dissociation of the oxygen, formation of mobile or immobile surface oxide complexes, activation and rupture of carbon bonds between complexes and interior carbon atoms, and removal of adsorbed reaction products. Of these partial reactions, the step which determines the crystallographic orientation of the oxidised surface is probably the rupture of carbon–carbon bonds. It is likely that this particular step in the reaction is not affected by metal catalysis because the preferred orientation is insensitive to catalysis as described earlier.

The observed motion of the catalyst particles demonstrates that bonds are formed between the catalyst and a large number of reactive carbon atoms at the metal–carbon interface. Since this bonding may be incidental to the catalytic action, it does not reveal which of the reaction steps is affected or by-passed by the catalytic action. If the bonding were concomitant with the catalytic action, activation of adsorbed oxygen to form metal–oxygen–carbon bridges would be a likely mechanism of catalytic action.

The measured activation energies for non-pitting catalysis demonstrate that the catalysts cause a pronounced change in the pre-exponential term of the Arrhenius rate equation. The observed reactivity ratio of catalysed to uncatalysed oxidation of carbon atoms was measured to be about 50 at 550°C (Table 1). The activation energy was reduced by catalysis from 46 to about 10 kcal/mole. Therefore the pre-exponential term was reduced by a factor of 10^8 due to catalysis. Such a large change suggests that the catalyst does not merely accelerate one of the reaction steps of oxidation but affects several steps, or bypasses the normal reaction sequence possibly by the formation of metal–oxygen–carbon bridges.

Pit formation appears to be initiated by the accelerated oxidation at those vacancies and/or boron atoms which are present in the initial contact region between catalyst and graphite. This attack is followed by catalytic oxidation of edge atoms until the hole in the surface layer of the crystal is large enough to expose additional vacancies or boron atoms in the next layer. As these are oxidized in turn, the particle gradually penetrates into the crystal while producing a surface channel. When the channel depth has increased to the particle radius, lateral motion is slowed but penetration continues resulting in a pit. The stepped geometry of the pits is not due to periodic bursts of catalytic activity but to excessive reactivity of pyramidal faces initially produced. Even in the absence of metallic catalysts, such pyramidal faces are nearly always converted to prismatic faces. The reason for this preferential burning to prismatic (i.e. "vertical") steps on graphite is not understood but is believed to be due to catalysis by traces of water.

The temperature dependence of the catalytic penetration yielded an apparent activation energy of 56 kcal. It is not surprising that this value is higher than the activation energy of uncatalysed oxidation because the penetration reaction involves oxidation of carbon atoms adjacent to vacancies or boron atoms which may be more tightly bonded than carbon atoms at edges of layer planes.

The conclusions do not apply to vanadium catalysts which melt and wet the surface.

Acknowledgements—The author is indebted to J. Baldwin, P. Roach and C. Kazmierowicz for help in sample preparations. The author gratefully acknowledges the co-operation of the electron microscope group of the Biology Division and particularly O. T. Minick in making the instrument available for these studies.

J. Inorg. Nucl. Chem., 1962, Vol. 24, pp. 1139 to 1144, Pergamon Press Ltd. Printed in England.

EXCHANGE PROPERTIES OF AMMONIUM SALTS OF 12-HETEROPOLYACIDS—IV

Cs EXCHANGE ON AMMONIUM PHOSPHOTUNGSTATE AND PHOSPHOMOLYBDATE

J. Krtil
Institute of Nuclear Research, Czechoslovak Academy of Sciences,
Řež u Prahy, Czechoslovakia

(*Received* 15 *January* 1962)

Abstract—Functional relations have been established describing caesium sorption on ammonium phosphotungstate (NH_4PW) and ammonium phosphomolybdate (NH_4PMo) as a function of the concentrations of nitric acid, ammonium nitrate and caesium in the solution, and on the amount of sorbent.

The use of ammonium salts of heteropolyacids as selective ion exchangers for the isolation of 137 Cs from fission product solutions requires a knowledge of the behaviour of these substances under the conditions obtaining in the reprocessing of nuclear fuel, viz. the strongly acid medium (usually nitric acid) and the presence of high concentrations of sodium and ammonium salts. A study of Cs extraction under these conditions and of the mathematical representation of the sorption phenomena is therefore necessary. The aim of this work was to study the exchange of Cs in micro and macro-amounts on ammonium phosphotungstate and phosphomolybdate in the presence of nitric acid and ammonium nitrate, to find how these factors influence the exchange, and to establish the rules governing the exchange.

There is little published information concerning the mechanism of sorption of alkali metals on ammonium salts of heteropolyacids. Smit *et al.*(1). measured the distribution coefficients of alkali metals in 0·1 NNH_4NO_3 solutions on ammonium salts of various heteropolyacids, and the validity of the mass-action law has been checked for the sorption of Rb on NH_4PMo and of Cs on NH_4PW(2,3).

EXPERIMENTAL

Experiments were carried out at room temperature under static conditions with acid ammonium salts of phosphotungstic and phosphomolybdic acids having the compositions $(NH_4)_{2\cdot 2}H_{0\cdot 8}[PW_{12}O_{40}]\cdot 15\ H_2O$ and $(NH_4)_{2\cdot 38}\ H_{0\cdot 62}[PMo_{12}O_{40}]\cdot 9\cdot 3\ H_2O$. Preparation and analysis of these salts are described elsewhere.(4) The ammonium salts (0·1 g) were weighed into 2·5 ml glass tubes and 2 ml of ammonium nitrate solution containing micro-amounts of ^{137}Cs (10^{-7} mole/l.) was added. In other experiments nitric acid of varying concentrations, or a mixture of nitric acid and ammonium nitrate, containing a micro-amount of ^{137}Cs as tracer was added to the weighed amount. After shaking until equilibrium was attained the solution was centrifuged and the distribution of Cs between the phases was determined radiometrically. The distribution coefficient for Cs, defined as

$$\frac{\text{activity of Cs in 0.1 g of NH}_4\text{PW}}{\text{activity of Cs in 2 ml of solution at equilibrium}} = K_d,$$

was then calculated.

Analytical grade chemicals were used throughout.

---

(1) J. van R. Smit, J. J. Jacobs and W. Robb, *J. Inorg. Nucl. Chem.* 12, 95 (1959).
(2) J. van R. Smit, J. J. Jacobs and W. Robb, *J. Inorg. Nucl. Chem.* 12, 104 (1959).
(3) J. Krtil, *J. Inorg. Nucl. Chem.* 19, 298 (1961).

RESULTS AND DISCUSSION

The percentage of Cs in the solid will be determined by the equilibrium concentrations of ammonium salts and of hydrogen ions present in the solution, since it has been shown (4,5) that the alkali metal (Cs) is exchanged isomorphously into the lattice partly for ammonium and partly also for the acid hydrogen of the sorbent. It has also been shown that in an acid medium the composition of the sorbent(4) is changed. The sorption of Cs or another alkali metal on the ammonium salts of heteropolyacids is thus a complex process, and to express it mathematically it is necessary to simplify the system. This may be fulfilled by examining the sorption of micro-amounts of Cs under suitable conditions of ammonium salt concentration and/or nitric acid concentration and for an amount of sorbent such that Cs is a micro-component relative to ammonium or acid hydrogen; its distribution between the phases will then obey simple laws.

The overall exchange may be regarded as a result of three separate phenomena, viz. exchange of Cs for NH_4 and/or for acid hydrogen, and of acid hydrogen for NH_4. We may express the individual equilibrium constants as follows

$$K_{Cs/NH4} = \frac{[Cs]_S\,[NH_4]_L}{[Cs]_L\,[NH_4]_S} \qquad (1)$$

$$K_{Cs/H} = \frac{[Cs]_S\,[H]_L}{[Cs]_L\,[H]_S} \qquad (2)$$

$$K_{H/NH4} = \frac{[NH_4]_L\,[H]_S}{[NH_4]_S\,[H]_L} \qquad (3)$$

(3), L indicating the solution, and S the precipitate

The value of K_{H/NH_4} is not constant over the range of HNO_3 concentration studied (0·1–10 M), varying by as much as one order of magnitude(4) this is due to the fact that only exchangeable ammonium and not total ammonium concentration in the solid phase should be substituted into Equation (3), since changes in the sorbent composition occur at lower acidities. In 3 M and higher concentration of nitric acid the composition of the acid salt is practically constant. An accurate determination of the amount of exchangeable ammonium is rather difficult, but it may be shown from the experiments which were carried out that this process will not be the determining one for obtaining sorption dependences.

The exchange of Cs for NH_4 at constant acidity was first investigated. Equation (1) may be modified to give $\log K_d = \log A - \log [NH_4]_L$,

$$\text{where} \frac{[Cs]_S}{[Cs]_L} = K_d$$

$$\text{and } K_{Cs/NH_4} \cdot [NH_4]_{LS} = A$$

---

(4) J. KRTIL and V. KOUŘIM, *J. Inorg. Nucl. Chem.* **12**, 367 (1960).

(5) H. BUCHWALD and W. P. THISTLETHWAITE, *J. Inorg. Nucl. Chem.* **5**, 341 (1957).

Thus if (1) is valid we will obtain a linear dependence of log K_d on log $[NH_4]_L$, and this is confirmed by the results shown in Fig. 1. The slope of curve *A* equal 1, showing that one Cs ion replaces one ammonium ion. The amount of hydrogen replaced is constant and negligible within the range of NH_4 concentrations investigated.

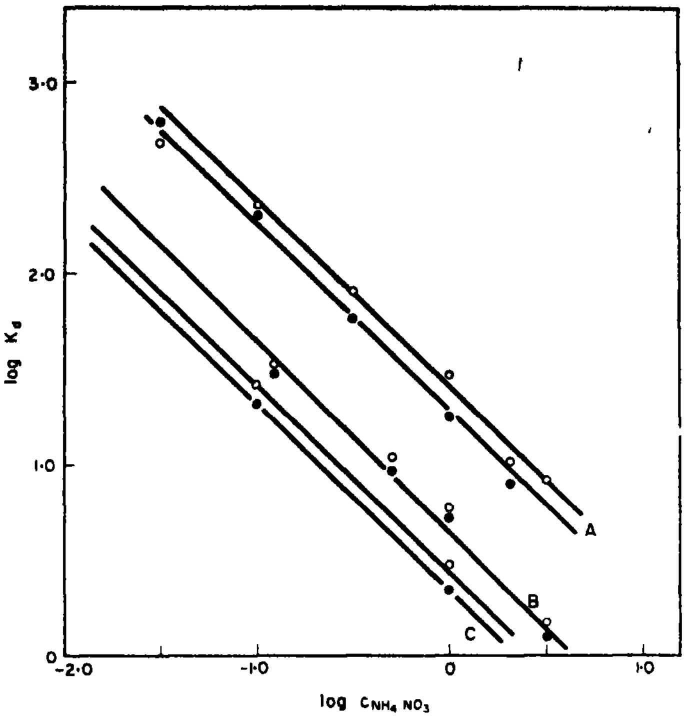

Fig. 1.—Dependence of the distribution coefficient for Cs on ammonium ion concentration in solution at equilibrium.
A, 0·001 M HNO_3 *B*, 5 M HNO_3 *C*, 10 M HNO_3
○ NH_4PMo ● NH_4PW

The distribution coefficient for Cs is higher on NH_4PMo than on NH_4PW (for equal amounts of sorbent) over the whole range of ammonium salt concentrations investigated, but the corresponding equilibrium constants in 0·001M.HNO_3 are $5 \cdot 5 \times 10^2$ for NH_4PW and $4 \cdot 18 \times 10^2$ for NH_4PMo concentration in moles l^{-1}) the latter having a lower value in conformity with the solubilities of the caesium and ammonium salts. The difference between the values of K_d for NH_4PW and NH_4PMo disappears with increasing acidity of the solution. The constant K_{Cs/NH_4} is, of course, valid only for a certain hydrogen ion concentration and decreases with increasing acidity, as may be seen from the other lines in Fig.1. The value of A depends on acidity, and if we suppose that the ammonium concentration in the solid phase varies only slightly (if Cs is present in micro-amounts) we can plot log *A* ($= K_d . [NH_4]_L$) against nitric acid concentration as in Fig. 2. The value of *A* varies only slightly at HNO_3 concentrations less than 3 M, and for $[HNO_3] > 3$ M we obtain a linear dependence of log *A* on log $[H]_L$. Putting $A = f(H)$ we obtain

$$\log K_d . [NH_4]_L = -\log [H]_L + \log (\text{const}).$$

$$K_d . [NH_4]_L [H]_L = 25$$

or $$1/K_d = 0 \cdot 04 [H]_L . [NH_4]_L$$

This relation holds well both for NH_4PW and NH_4PMo.

This empirical dependence may be explained on the basis of the sorbent acting as an ion exchanger. The acid ammonium salt of a heteropolyacid may be regarded as a strong acid ion exchanger, in agreement with the relationship $A = f(H)$. If we treat the sorbent as a mixture of an ammonium salt and a free heteropolyacid, the ammonium salt being completely dissociated and the free heteropolyacid partly dissociated, then the dissociation may be written in the form

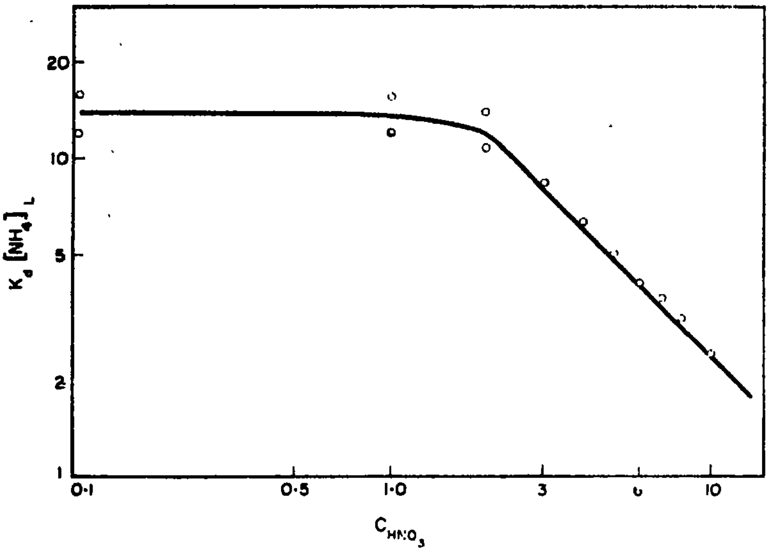

FIG. 2.—Relationship between $K_d[NH_4]_L$ and nitric acid concentration.

$NH_4R \rightleftharpoons NH^+_4 + R^-$ (a) $\qquad HR \rightleftharpoons H^+ + R^-$ (b)

Assuming complete dissociation of the ammonium salt we may approximate as follows

$$[NH_4^+] \doteq [R^-]$$

For (b) the following expression is valid at equilibrium

$$K' = \frac{[H^+]_s [R^-]_s}{[HR]_s} \qquad (c)$$

Substituting (c) into (1) where, $[NH_4]_s$ corresponds to that fraction of ammonium ion which is exchangeable for acid hydrogen, and supposing Donnan's concept of equilibrium to hold, when the concentration of hydrogen ions in the ion exchanger is proportional to the concentration of H ions in the solution, i.e., $[H]_s = k[H]_L$,

$$\text{we obtain } K_{Cs/NH_4} = K_d \frac{[H]_L [NH_4]_L\, C'}{[HR]_s},$$

$$\text{where } C' = \frac{k}{K'} \qquad (4)$$

For low H^+ concentrations the ratio $[H^+]_s/[HR]_s$ will be constant, and therefore K_d will also be constant. For a higher acidity the relation $[HR]_s$ = const. must be valid, as we have obtained the limiting acid salt and then the relationship (4) will be simplified into the form

$$\text{Const.} = K_d[\text{NH}_4^+]_L \cdot [\text{H}^+]_L$$

in agreement with the results obtained.

The results for Cs sorption as a function of HNO_3 concentrations at constant ammonium salt concentration agree with previous data (Fig. 3). A slow decrease in Cs sorption with increasing HNO_3 concentration changes abruptly near $[HNO_3]$ $\sim$3 M, beyond which there is a linear variation with slope $\sim$ 1. Thus at acidities $>$ 3 M HNO_3 the sorption properties of NH_4PW and NH_4PMo change, and the acid hydrogen and Cs may replace each other.

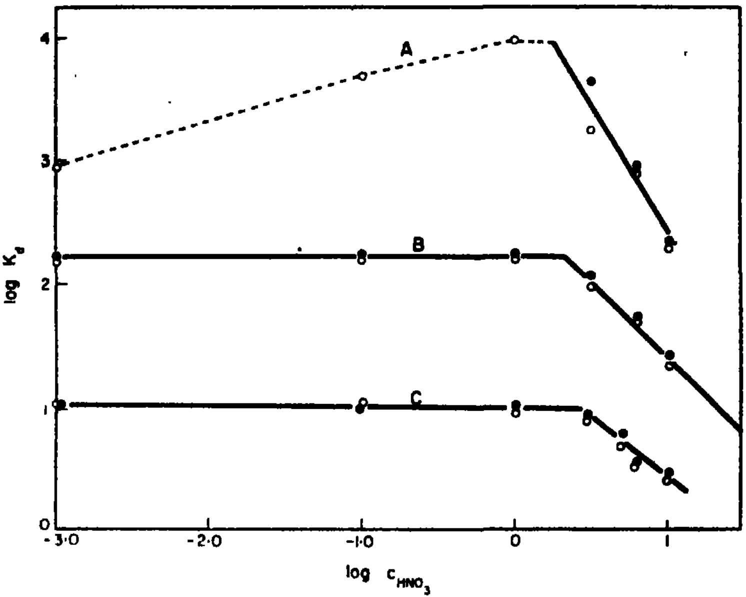

FIG. 3.—Dependence of the distribution coefficient for Cs on nitric acid concentration.

A, without NH_4NO_3 · *B*, 0·1 M NH_4NO_3 *C*, 1·2 M NH_4NO_3
○ NH_4PMo ● NH_4PW

The variation in sorption properties of NH_4PW and NH_4PMo could be due to variation in the sorbent structure. A study of the infra-red spectra of samples of NH_4PW and NH_4PMo which were obtained by shaking the salts with HNO_3 in various concentrations to equilibrium showed no change as the concentration of acid was varied. This can be explained by assuming that there is no substantial change in either the heteropolyanion bonding or in the water of crystallization. As was previously shown analytically(4), exchange of NH_4 for H occurs in an acid medium, the salt becoming more acid and at an acidity $>$ 3 M HNO_3 we obtain the limiting salt $(NH_4)_2HPW$. Under our conditions we may also suppose this acid salt to be formed and it should be further enriched with H^+ or Cs^+. As our experiments show, Cs^+ and H^+ are equivalent. We may conclude from this that the acid hydrogen ions are not equivalent in their bond strength, and undergo substitution by Cs or by another alkali metal in stages. The equilibrium constant $K_{Cs/H}$ reaches a constant value at $>$ 3 M HNO_3; below 3 M HNO_3 it is not constant, due to the fact that the content of acid hydrogen in the NH_4PW molecule changes considerably.

It is necessary, of course, to know the range of Cs concentrations over which these relationships are valid. It may be seen from the dependence of the distribution coefficient K_d(Cs) on the initial concentration of Cs (Fig. 4) that they may be applied up to $[Cs^+] = 10^{-3}$ M. Above this concentration K_d falls sharply, since the amount of exchangeable hydrogen and ammonium ions is limited by the capacity of the exchanges.

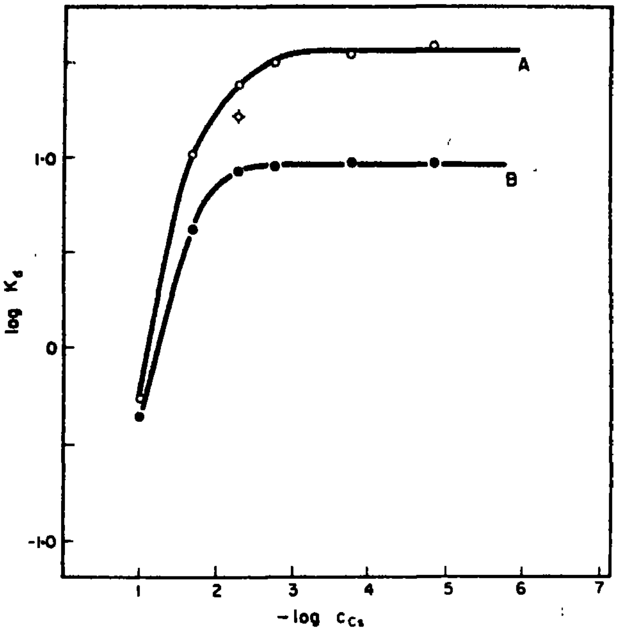

Fig. 4.—Dependence of distribution coefficient for Cs on the initial Cs concentration.
(sorbent: NH_4PW)
A, 0·43 M NH_4NO_3 *B*, 0·5 M NH_4NO_3 + 5 M HNO_3
-◇- Previous results(3)

J. Inorg. Nucl. Chem., 1962, Vol. 24, pp. 1145 to 1151. Pergamon Press Ltd. Printed in England

THE SEPARATION FACTOR OF LITHIUM ISOTOPES WITH ION EXCHANGERS

H. KAKIHANA, T. NOMURA and Y. MORI
Laboratory of Nuclear Chemistry, Tokyo Institute of Technology, Meguro, Tokyo, Japan

(*Received* 12 *December* 1961; *in revised form* 14 *February* 1962)

Abstract—Fundamental equations for the isotopic ion exchange reaction were derived with various degrees of approximation considering the various kinds of external solutions and ion exchangers.

The separation factors of lithium isotopes $S_7^6(\mathrm{Li})$ in ethanol (or acetone)–water mixtures were determined with differently cross-linked sulphonated polystyrene-divinylbenzene copolymers and synthetic inorganic ion exchanger Ionite C (zirconium phosphate type).

LiOH system gave higher separation factors than LiCl systems. The highly cross-linked resins and synthetic inorganic ion exchanger are also favourable for the higher separation factor.

The highest value 1·022 was obtained for the system of 0·1 M LiOH 20 per cent acetone–water mixture using synthetic inorganic ion exchanger.

These experimental results were analysed by fundamental equations.

SINCE TAYLOR and UREY claimed to have observed a separation factor of 1·022 with zeolites, many studies have been done for the ion exchange separation of Li isotopes especially in the system of aqueous LiCl solution on sulphonated exchanger, However, as summarized in Table 1, only very low separation factors 1·001–1·006 were observed. In view of the fact that Li ions are in very nearly the same state both in the aqueous LiCl solution phase and in the sulphonated exchanger phase, these low separation factors may not be surprising.

In the case discussed here, choosing the system containing LiOH and a synthetic inorganic ion exchanger, the similarity of chemical binding in the two phases is effectively avoided and the separation factors obtained are much larger.

FUNDAMENTAL

The separation factor of isotopes A and B between the exchanger of high cross-linkage and the external solution phase of low concentration is expressed as follows:

$$S_{\mathrm{A}}^{\mathrm{B}}=\frac{\text{(Total amount of B in the exchanger)}}{\text{(Total amount of A in the exchanger)}}\times\frac{\text{(Total amount of A in the external solution)}}{\text{(Total amount of B in the external solution)}}$$

$$=\frac{\bar{m}_{\mathrm{B}^+}+\bar{m}_{\mathrm{EB}}}{\bar{m}_{\mathrm{A}^+}+\bar{m}_{\mathrm{EA}}}\cdot\frac{m_{\mathrm{A}^+}+m_{\mathrm{AX}}}{m_{\mathrm{B}^+}+m_{\mathrm{BX}}} \tag{1}$$

or

$$\ln S_{\mathrm{A}}^{\mathrm{B}}=\ln\frac{\bar{m}_{\mathrm{B}^+}\cdot m_{\mathrm{A}^+}}{\bar{m}_{\mathrm{A}^+}\ m_{\mathrm{B}^+}}+\ln\frac{\bar{m}_{\mathrm{B}^+}+\bar{m}_{\mathrm{EB}}}{\bar{m}_{\mathrm{A}^+}+\bar{m}_{\mathrm{EA}}}\cdot\frac{\bar{m}_{\mathrm{A}^+}}{\bar{m}_{\mathrm{B}^+}}+\ln\frac{m_{\mathrm{A}^+}+m_{\mathrm{AX}}}{m_{\mathrm{B}^+}+m_{\mathrm{BX}}}\cdot\frac{m_{\mathrm{B}^+}}{m_{\mathrm{A}^+}} \tag{2}$$

$$=\ln\frac{\bar{m}_{\mathrm{B}^+}\cdot m_{\mathrm{A}^+}}{\bar{m}_{\mathrm{A}^+}\cdot m_{\mathrm{B}^+}}-\ln\frac{\bar{m}_{\mathrm{B}^+}\cdot\bar{m}_{\mathrm{EA}}}{\bar{m}_{\mathrm{A}^+}\cdot\bar{m}_{\mathrm{EB}}}+\ln\frac{m_{\mathrm{B}^+}\cdot m_{\mathrm{AX}}}{m_{\mathrm{A}^+}\cdot m_{\mathrm{BX}}}$$

TABLE 1.

Ion exchanger	Separation factor (S_7^6)	Researchers
Decalso	1·022	TAYLOR, UREY(1)
Zeo-Karb H. I.	> 1	GLUECKAUF *et al.*(2)
Dowex 50-X 10	1·0065	GROSS, JULY(3)
Decalso	1·0058	SESSIONS *et al.*(4)
Dowex 50W	1·0027	BLANCO *et al.*(5)
Dowex 50	1·0025	STADIER *et al.*(6)
Zeo-Karb 225	> 1	DAVIES *et al.*(7)
Dowex 50-X 12	1·001 ~	MÉNÈS *et al.*(8)
Amberlite IRC 50	1·002	
Dowex 50-X 12	1·002	PERRET *et al.*(9)
Zeolithe "Prolabo"	1·004	
Dowex 50-X2 ~ X 24	1·0006 ~ 1·0038	LEE, BEGUN(10) (GLUECKAUF(11))
Dowex 50-X 16	1·0023 ~ 1·005	LEE(12, 13)
Ionac C-100	1·0049	LINDNER, BERGDAHL(14)
Diaion SK 1-X 35	1·006 (LiCl) 1·012 (LiOH)	KAKIHANA *et al.*(15)
Ionite C	1·015 (LiCl) 1·022 (LiOH)	KAKIHANA *et al.*(15)

(1) T. I. TAYLOR and H. C. UREY, *J. Chem. Phys.* **5**, 597 (1937); **6**, 429 (1938).

(2) E. GLUECKAUF, K. H. BARKER and G. P. KITT, *Disc. Faraday Soc.*, No. 7, 199 (1949).

(3) J. H. GROSS, AECD–2952 (1950).
S. H. JURY, ORNL Report CF-52-8-218 (1952).

(4) R. I. SESSIONS, A. H. KIBBEY, J. T. ROBERTS and R. E. BLANCO, ORNL Report CF-53-6-241 (1953).

(5) R. E. BLANCO, A. H. KIBBEY, J. I. LAND and J. T. ROBERTS, ORNL Report CF-53-11-47 (1953).

(6) M. H. STADIER, J. K. BRODY and J. I. MECH, Summary Report of Chemistry Division, p. 23. July 1, 1953–March 31, 1955, ANL-5450 (1955).

(7) C. W. DAVIES and B. D. R. OWEN, *J. Chem. Soc.* 1676 (1956).

(8) F. MÉNÈS, E. SAITO and E. ROTH, *Proceeding of the International Symposium on Isotope Separation*, p. 227. North Holland Publishing Co., Amsterdam (1958).

(9) L. PERRET, L. ROZAND and E. SAITO, *Proceedings of the Second International Conference on Peaceful Uses of Atomic Energy, Geneva*, 1958, A/Conf. 15/P/1267. United Nations (1958).

(10) D. A. LEE and G. M. BEGUN, *J. Amer. Chem. Soc.* **81**, 2332 (1959).

(11) E. GLUECKAUF, *J. Amer. Chem. Soc.* **81**, 5262 (1959).

(12) D. A. LEE, *J. Phys. Chem.* **64**, 187 (1960).

(13) D. A. LEE, *J. Amer. Chem. Soc.* **83**, 1801 (1961).

(14) R. LINDNER and T. BERGDAHL, *Z. Elektrochem.* **64**, 919 (1960).

(15) H. KAKIHANA, T. NOMURA and Y. MORI, *J. Atomic Energy Soc. Japan*, **3**, 849 (1961).

$$+\ln\frac{(1+\bar{m}_{B^+}/\bar{m}_{EB})}{(1+\bar{m}_{A^+}/\bar{m}_{EA})}-\ln\frac{(1+m_{B^+}/m_{BX})}{(1+m_{A^+}/m_{AX})} \tag{3}$$

where m_{A^+}, m_{B^+}, m_{AX} and m_{BX} denote the molalities of the ions A^+ and B^+, and those of the molecules or ion associations AX and BX in the external solution phase, and $\bar{m}_{A^+}$, $\bar{m}_{B^+}$, $\bar{m}_{EA}$ and $\bar{m}_{EB}$ denote the molalities in the exchanger phase analogously.

In a solution of the ions A^+ and B^+, and the molecules or ion associations AX and BX, at isotopic equilibrium with the ions adsorbed on a cation exchanger having some possibility of forming molecules or ion associations EA and EB, the equilibria involved are tentatively described by the equations:

(a) Ion exchange reaction

$$(A^+)_{\text{exchanger}}+(B^+)_{\text{external solution}} \rightleftharpoons (B^+)_{\text{exchanger}}+(A^+)_{\text{external solution}}$$

$$K^{B^+}_{A^+}=\frac{\bar{m}_{B^+}\cdot m_{A^+}}{\bar{m}_{A^+}\cdot m_{B^+}} \tag{4*}$$

(b) Isotopic exchange reaction in the exchanger

$$(A^+)_{\text{exchanger}}+EB \rightleftharpoons (B^+)_{\text{exchanger}}+EA$$

or

$$EB \rightleftharpoons (B^+)_{\text{exchanger}}+E^-$$
$$EA \rightleftharpoons (A^+)_{\text{exchanger}}+E^-$$

$${}^{B}_{A}\bar{K}_{E}=\frac{\bar{m}_{B^+}\cdot\bar{m}_{EA}}{\bar{m}_{A^+}\cdot\bar{m}_{EB}} \tag{5}$$

(c) Isotopic exchange reaction in the external solution

$$(A^+)_{\text{external solution}}+BX \rightleftharpoons (B^+)_{\text{external solution}}+AX$$

or

$$BX \rightleftharpoons (B^+)_{\text{external solution}}+X^-$$
$$AX \rightleftharpoons (A^+)_{\text{external solution}}+X^-$$

$${}^{B}_{A}K_{X}=\frac{m_{B^+}\cdot m_{AX}}{m_{A^+}\cdot m_{BX}} \tag{6}$$

Substituting Equations (4), (5) and (6) in Equation (3) and rearranging

$$\ln S^{B}_{A}=\ln \bar{K}^{B^+}_{A^+}-\ln {}^{B}_{A}K_{E}+\ln {}^{B}_{A}K_{X}$$
$$+\ln\left(1+\frac{{}^{B}_{A}\bar{K}_{E}-1}{1+(\bar{m}_{EA}/\bar{m}_{A^+})}\right)-\ln\left(1+\frac{{}^{B}_{A}K_{X}-1}{1+(m_{AX}/m_{A^+})}\right) \tag{7}$$

With the isotopes A and B, the values for ${}^{B}_{A}\bar{K}_{E}$ and ${}^{B}_{A}K_{X}$ are to be quite near to one except in very special cases (e.g. H and D). Hence with good approximation Equation (7) becomes

$$\ln S^{B}_{A}=\ln K^{B^+}_{A^+}-\ln {}^{B}_{A}\bar{K}_{E}+\ln {}^{B}_{A}K_{X}+\frac{{}^{B}_{A}\bar{K}_{E}-1}{1+(\bar{m}_{EA}/\bar{m}_{A^+})}-\frac{{}^{B}_{A}K_{X}-1}{1+(m_{AX}/m_{A^+})} \tag{8}$$

When both the external solution and the exchanger phase contain very small amounts of the ions compared to the amounts of the molecules or ion associations ($m_{AX}\gg m_{A^+}$ and $\bar{m}_{EA}\gg\bar{m}_{A^+}$), Equation (8) is reduced approximately to

$$\ln S^{B}_{A}=\ln K^{B^+}_{A^+}+\ln {}^{B}_{A}K_{X}-\ln {}^{B}_{A}\bar{K}_{E} \tag{8'}$$

When the exchanger phase contains no appreciable amount of the molecules or ion associations ($\bar{m}_{A^+}\gg\bar{m}_{EA}$), the following equation is obtained instead of Equation (7).

$$\ln S^{B}_{A}=\ln K^{B^+}_{A^+}+\ln {}^{B}_{A}K_{X}-\ln\left(1+\frac{{}^{B}_{A}K_{X}-1}{1+(m_{AX}/m_{A^+})}\right) \tag{7'}$$

---

* For the rigorous thermodynamical consideration of $K^{B^+}_{A^+}$, please refer to (16) and (23).

With good approximation,

$$\ln S_{\mathrm{A}}^{\mathrm{B}} = \ln K_{\mathrm{A}^+}^{\mathrm{B}^+} + \ln {}_{\mathrm{A}}^{\mathrm{B}}K_{\mathrm{X}} - \frac{{}_{\mathrm{A}}^{\mathrm{B}}K_{\mathrm{X}}-1}{1+(m_{\mathrm{AX}}/m_{\mathrm{A}^+})} \tag{9}$$

If the external solution has very small amounts of the ions compared with the amounts of the molecules or ion associations ($m_{\mathrm{AX}} \gg m_{\mathrm{A}^+}$), an approximation gives

$$\ln S_{\mathrm{A}}^{\mathrm{B}} \simeq \ln K_{\mathrm{A}^+}^{\mathrm{B}^+} + \ln {}_{\mathrm{A}}^{\mathrm{B}}K_{\mathrm{X}} \tag{9'}$$

Similarly the following equations are obtained for the system consisting of a strong-electrolyte external solution phase ($m_{\mathrm{A}^+} \gg m_{\mathrm{AX}}$) and an exchanger phase having some possibility of forming molecules or ion associations

$$\ln S_{\mathrm{A}}^{\mathrm{B}} = \ln K_{\mathrm{A}^+}^{\mathrm{B}^+} - \ln {}_{\mathrm{A}}^{\mathrm{B}}\overline{K}_{\mathrm{B}} + \ln\left(1+\frac{{}_{\mathrm{A}}^{\mathrm{B}}\overline{K}_{\mathrm{B}}-1}{+(\bar{m}_{\mathrm{BA}}/\bar{m}_{\mathrm{A}^+}}\right) \tag{7''}$$

$$\ln S_{\mathrm{A}}^{\mathrm{B}} = \ln K_{\mathrm{A}^+}^{\mathrm{B}^+} - \ln {}_{\mathrm{A}}^{\mathrm{B}}\overline{K}_{\mathrm{B}} + \frac{{}_{\mathrm{A}}^{\mathrm{B}}\overline{K}_{\mathrm{B}}-1}{1+(\bar{m}_{\mathrm{BA}}/\bar{m}_{\mathrm{A}^+})} \tag{10}$$

$$\ln S_{\mathrm{A}}^{\mathrm{B}} = \ln K_{\mathrm{A}^+}^{\mathrm{B}^+} - \ln {}_{\mathrm{A}}^{\mathrm{B}}\overline{K}_{\mathrm{B}} \tag{10'}$$

For a system consisting of a strong-electrolyte external solution phase and a strongly ionized ion exchanger phase:

$$\ln S_{\mathrm{A}}^{\mathrm{B}} = \ln K_{\mathrm{A}^+}^{\mathrm{B}^+} \tag{11}$$

These fundamental equations for the separation factor of isotopes indicate how a larger separation factor might be obtained.

(1) A system containing molecules or ion associations in the exchanger phase or in the external solution phase may have chance of giving a larger separation factor than a system containing only strong electrolytes in both phases. [Equation (9), (9'), (10) and (10')].

(2) In the case mentioned above, the larger the amounts of molecules or ion associations, the larger the separation factor that may be obtained. [Equation (9) and (10)].

(3) A system containing molecules or ion associations both in the exchanger phase and in the external solution phase may not give a larger separation factor because of the cancellation of ${}_{\mathrm{A}}^{\mathrm{B}}K_{\mathrm{X}}$ and ${}_{\mathrm{A}}^{\mathrm{B}}\overline{K}_{\mathrm{B}}$. [Equation (8) and (8')].

However, if we choose an exchanger having the ability to form a different type of chemical binding with the isotopes from that in the external solution, the cancellation may be avoided and a larger separation factor may be obtained. Again the larger the amounts of molecules or ion associations both in the exchanger phase and in the external solution phase, the larger the separation factor that can be expected. [Equation (8)].

EXPERIMENTAL

Stock solution of lithium chloride was prepared from lithium carbonate of high purity (99·8 per cent or better) and hydrochloric acid of analytical grade. The stock solution was diluted with a suitable amount of ethanol (or acetone) and water to prepare the sample solution for the equilibrium experiments in the case of LiCl systems.

Lithium hydroxide solutions were prepared just before each of the equilibrium experiments of LiOH systems by passing a solution of lithium chloride through a column of the strongly basic anion exchange resin Diaion SA # 100* in the hydroxide form. Besides the commercially supplied cation exchange resins Dowex 50-X4, X8 and X16, sulphonated highly cross-linked polystyrene resins Diaion SK # 1-X24* and X35* (the figures after X indicate the nominal percentage of divinylbenzene in the copolymer) and a synthetic inorganic ion exchanger Ionite C† (zirconium phosphate type) were used.

About 800 ml of the sample solution was passed very slowly through a small column containing about 0·5 ml of the exchanger in the hydrogen form. The lithium ion adsorbed on the column was recovered by eluting with 1 M hydrochloric acid. After evaporating the excess hydrochloric acid, the lithium chloride was dissolved in a water-ethanol mixture containing 40 per cent ethanol, and converted to lithium iodide on a column of the anion exchange resin Diaion SA # 100 in the iodide form. Just before placing the sample into the mass spectrometer, the lithium iodide solution was evaporated to dryness with the addition of hydroiodic acid. The lithium chloride in the original sample solution was also converted to lithium iodide by a similar procedure. The isotopic ratios of lithium were determined both for the lithium adsorbed on the exchanger and the lithium in the original sample solution with a Nier-type 60 degree mass spectrometer Atlas CH 4 using the thermionic method. Although details of the experimental techniques were described in other paper,‡ a comparison of two different series of measurement for the same sample is shown in Table 2.

TABLE 2.—EXAMPLE OF MASS SPECTROMETRIC ANALYSIS

	isotopic ratio $\frac{^7\mathrm{Li}}{^6\mathrm{Li}}$	
Peak No.	Measurement No. 1	Measurement No. 2
1	$12{\cdot}27_9$	$12{\cdot}32_7$
2	$12{\cdot}30_2$	$12{\cdot}26_3$
3	$12{\cdot}30_6$	$12{\cdot}27_7$
4	$12{\cdot}27_7$	$12{\cdot}25_1$
5	$12{\cdot}28_7$	$12{\cdot}28_3$
6	$12{\cdot}27_4$	$12{\cdot}31_9$
7	$12{\cdot}28_5$	$12{\cdot}29_4$
8	$12{\cdot}28_1$	$12{\cdot}29_9$
9	$12{\cdot}28_8$	$12{\cdot}31_2$
10	$12{\cdot}32_9$	$12{\cdot}33_1$
11	$12{\cdot}32_6$	$12{\cdot}29_1$
Mean	$12{\cdot}29_4 \pm 0{\cdot}02$	$12{\cdot}29_5 \pm 0{\cdot}02$

RESULTS AND DISCUSSION

The value obtained for systems containing LiCl in the external solution are summarized in Table 3, 4 and 5. It is well known from ion exchange studies that the separation factor is dependent upon the size of the solvated ion and also upon the degree of cross-linking in ion exchange resin. The influence of the degree of cross-linking on the separation factor of the isotopes that was found by LEE and BEGUN for lithium isotopes(10) and by us for nitrogen isotopes(16) seems to be reconfirmed by the values

---

* Products of Mitsubishi Chemical Ind. Ltd., Japan.

† Our laboratory name.

‡ Submitted to "Mass Spectrometry" (Japan).

(16) H. KAKIHANA, T. NOMURA and K. KODAIRA, *J. Atomic Energy Soc. Japan*, **1**, 433 (1959).

TABLE 3.
S_7^6 (0·1 M LiCl)

Ethanol (vol %)	Exchanger X4	X8	X16	X24	X35
0	1·001	1·001	1·004	1·004	1·005
60	1·003	1·004	1·006	1·006	1·006

TABLE 4.
S_7^6 (30% ethanol)

LiCl (M)	Exchanger X4	X8	X16
0·1	1·001	1·003	1·005
0·3	1·000	1·002	1·005
1·0	1·000	1·003	1·004

shown in Table 3 and 4 even considering the possible error of the isotopic mass analysis. The very small influence of the addition of ethanol on the separation factor is apparent in Table 3, as in the case of nitrogen isotopes(16,17) and sodium isotopes.(18,19,20) The influence of the concentration of lithium chloride in the external solution can not be confirmed in Table 4 within our experimental accuracy.

While the values of the separation factor with sulphonated cross-linked polystyrene resins lie between 1·000 and 1·006, larger values up to 1·015 shown in Table 5 were obtained with the synthetic inorganic ion exchanger Ionite C. In the case of the systems of lithium chloride with sulphonated resins, both the ion exchanger phase and the external solution phase can be considered to be strongly ionized or scarcely having molecules or ion associations. Therefore, the separation factor for such systems can be simply expressed by Equation (11). On the other hand some kinds of phosphoric acids in the synthetic inorganic ion exchanger may have some possibility of forming a slightly ionized species with lithium. Therefore the separation factor with the synthetic inorganic ion exchanger in lithium chloride solution can be more reasonably expressed by Equation (7'), (10) or (10').

TABLE 5.
Ionite C (0·1 M LiCl)

Ethanol (vol %)	0	20	40	60
S_7^6	1·013	1·015	1·013	1·014

(17) H. KAKIHANA, T. NOMURA and K. KODAIRA, *J. Atomic Energy Soc. Japan*, 3, 519 (1961).

(18) H. KAKIHANA, T. NOMURA, H. FUKUTOMI, H. OHTAKI and K. YAMASAKI, *J. Atomic Energy Soc. Japan*, 1, 46 (1959).

(19) H. OHTAKI, H. KAKIHANA and K. YAMASAKI, *Z. Phys. Chem.* 21, 224 (1959).

(20) H. OHTAKI, *Z. Phys. Chem.* 27, 209 (1961).

The values obtained for the systems containing LiOH in the external solution are summarized in Table 6. As shown in Table 6 the system of the sulponated cross-linked polystyrene resins in 0·1 M lithium hydroxide aqueous solution gave values between 1·005 and 1·008. These slightly higher values may be attributed to the presence of small amounts of undissociated species LiOH in the external solution(21,22) and can be explained by Equation (7′) or (9). The systems of the same resins in 0·1 M lithium hydroxide acetone-water mixture gave higher values 1·012 and 1·011.

TABLE 6.
S_7^6 (0·1 M LiOH)

Acetone (vol %)	Exchanger X24	X35	Ionite C
0	1·005	1·008	1·016
20	1·012	1·011	1·022

It is evident that the addition of acetone results in the increase of the concentration of undissociated species LiOH. Therefore, absolute values for the third term of the right hand side of Equation (9) should be smaller for the acetone–water mixture systems than for the aqueous solution systems, and the cancellation of the second term with the third term can be better avoided in the case of the acetone-water mixture systems. This may be the reason why the higher values were obtained for the acetone–water mixture systems. The separation factor with the synthetic inorganic ion exchanger in lithium hydroxide solution can be reasonably expressed by Equation (7) or (8). The high values obtained for the systems may be attributed to the good combination of the three constants $K_{\mathrm{A}^+}^{\mathrm{B}^+}$, ${}^{\mathrm{B}}_{\mathrm{A}}\overline{K}_{\mathrm{E}}$ and ${}^{\mathrm{B}}_{\mathrm{A}}K_{\mathrm{X}}$ (in this case $K_{7^+}^{6^+}$, ${}^{6}_{7}\overline{K}_{\mathrm{E}}$ and ${}^{6}_{7}K_{\mathrm{OH}}$). Again the preferable effect of the addition of acetone was observed obviously.

CONCLUSION

As the fundamental Equation (8), (9) and (10) predict, the higher values for the separation factors of the lithium isotopes are obtained in the following systems.

(1) 1·013–1·015 for the system of strong electrolyte, LiCl, in the external solution with the weakly acidic inorganic cation exchanger, Ionite C (zirconium phosphate type).

(2) 1·005–1·008 for the system of a weaker electrolyte, LiOH, in the external solution with the strongly acidic organic cation exchange resin. The separation factor reaches 1·012 when acetone is added to the system to reduce the dissociation constant of LiOH.

(3) 1·016 for the system of LiOH in the aqueous solution with the weakly acidic inorganic cation exchanger (Ionite C). The value 1·022 is obtained by adding acetone.

Very low separation factors (1·000–1·006) were obtained for the system of strong electrolyte, LiCl, in the external solution with the strongly acidic (sulphonic acid) cation exchange resins.

(21) H. S. HARNED and H. R. COPSON, *J. Amer. Chem. Soc.* **55**, 2206 (1933).

(22) R. A. ROBINSON and H. S. HARNED, *Chem. Rev.* **28**, 419 (1941).

(23) H. KAKIHANA, T. NOMURA and H. OHTAKI, *Bull. Tokyo Inst. Tech.*, Series-B, No. 1, p. 1 and p. 14.

J. Inorg. Nucl. Chem., 1962, Vol. 24, pp. 1153 to 1157. Pergamon Press Ltd. Printed in England

HIGHER OXIDATION STATES OF SILVER—II
REACTION OF OZONE WITH SILVER (I) COMPLEXES IN NON-AQUEOUS SOLVENTS*

J. Selbin and B. Shamburger

Coates Chemical Laboratories, Louisiana State University, Baton Rouge, La.

(*Received* 7 *February* 1962; *in revised form* 26 *February* 1962)

Abstract—The ozonization of bis(orthophenanthroline)-silver(I) nitrate has been investigated in thirteen non-aqueous solvents both with and without the addition of several Lewis acids. The solvents included (1) dimethylsulphoxide, (2) dimethylformamide, (3) chloroform, (4) carbon tetrachloride, (5) benzene, (6) acetonitrile, (7) n-heptane, (8) ethyl acetate, (9) tetrahydrofuran, (10) acetic anhydride, (11) glacial acetic acid, (12) nitromethane, (13) nitroethane. The Lewis acids included anhydrous aluminium chloride, anhydrous iron(III) chloride, boron trifluoride and silver(I) ion. The oxidation of the silver(I) complex to the silver(II) complex occurred only in the protonic acid solvents, (11), (12) and (13), but the silver(II) complex could be isolated only from acetic acid. Mechanisms of ozonization are proposed which involve the enhancement of the electrophilic character of the ozone molecule by the proton of the particular solvent.

Several complexes of silver (I)† may be oxidized to the corresponding silver (II) complexes either electrolytically or with oxidizing agents such as ozone, peroxydisulphate ion, cerium (IV) ion, lead dioxide or silver (II) oxide.⁽¹⁾ The use of ozone as the oxidant for silver (I) complexes has been limited to aqueous solutions⁽²·³⁾ and moreover, these solutions must be acidic or the reaction will not proceed.

Noyes and co-workers⁽⁴⁾ have made an extensive investigation of the oxidation of Ag^+ by O_3 in nitric acid solution. From their rate data they have postulated the intermediate formation of Ag(III) according to the equations:

$$Ag^+ + O_3 \rightarrow AgO^+ + O_2 \text{ (slow)}$$

$$AgO^+ + Ag^+ + 2H^+ \rightarrow 2Ag^{2+} + H_2O \text{ (fast)}$$

The reaction does not go to completion, but results in the establishment of a steady state, because of the reduction of the dipositive state by water with the evolution of oxygen:

$$4Ag^{2+} + 2H_2O \rightarrow 4Ag^+ + 4H^+ + O_2$$

It is of interest to note that the Noyes *et al.* mechanism indicates that the oxidation rate does not depend appreciably upon the H^+ concentration. However, it should also be pointed out that their studies were carried out in very strong nitric acid solutions, rendering indeterminable the exact role played by the H^+.

---

* Taken in part from a thesis submitted in partial fulfillment of the requirements for the Master of Science degree at Louisiana State University, 1961.

† It is interesting to note that except for porphyrins, all ligands which have been found to stabilize silver(II) contain a pyridine or pyridine-like nitrogen donor atom.

(1) J. A. McMillan, *Chem. Revs.* **62**, 65 (1962).

(2) A. Malaguti, *Atti accad. nazl. Lincei, Rend. classe sci. fis., mat. e. nat.* **9**, 349 (1950); *Chem. Abstr.* **45**, 4596 (1950).

(3) A. Malaguti, and T. Labianca, *Gazz. chim. ital.* **84**, 976 (1954).

(4) A. A. Noyes, J. L. Hoard and K. S. Pitzer, *J. Amer. Chem. Soc.* **57**, 1221 (1935); A. A. Noyes, C. D. Coryell, F. Stritt and A. Kossiakoff, *Ibid.* **59**, 1316 (1937).

WIBAUT and co-workers(5) have observed the electrophilic nature of the ozone molecule in the ozonization of organic molecules. They have also demonstrated that the electrophilic activity may be catalysed by Lewis acids.(6) We may picture this enhancement of the electrophilic character in the following way:

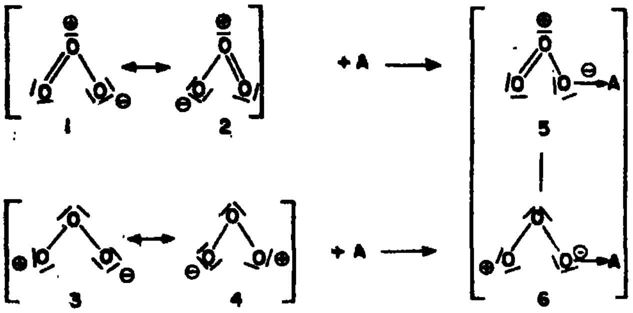

The structures 1, 2, 3 and 4 are the resonance forms generally accepted for the ozone molecule, with 1 and 2 expected to be of slightly lower energy than 3 and 4 (since the charge separation is about 0·90 Å greater in the latter two). The Lewis acid is represented by A and the Lewis acid-base adduct may be pictured as a resonance hybrid of structures 5 and 6, and with 5 being of lower energy.

It appeared likely to us that the necessity for acidic conditions for the effective ozonization of silver(I) complexes in aqueous solutions might be related to the enhancement of the electrophilic nature of the ozone molecule by the Lewis acid, the hydronium ion. (It might be pointed out that the oxidation of several Pt(II) complexes to Pt(IV) complexes(7) as well as the oxidation of Am(III) to Am(VI)(8) and the oxidation of Pu(IV) to Pu(VI)(9) occur in aqueous acid solution.) In order to test the possible generallity of this mechanistic proposal, we have investigated the ozonization of bis (orthophenanthroline)-silver(I) nitrate in a number of non-aqueous solvents, both with and without the addition of several well-known Lewis acids. The choice of this particluar compound was based upon its known behaviour toward ozonization in aqueous solution (in which it is quantitatively and rapidly oxidized to the silver(II) complex), its partial solubility in several non-aqueous solvents and the clear-cut colour change, from pale yellow to dark maroon, which takes place upon oxidation. The solvents employed included (1) dimethylsulphoxide, (2) dimethylformamide (both of which were readily attacked by the ozone), (3) chloroform, (4) carbon tetrachloride, (5) benzene, (6) acetonitrile, (7) n-heptane, (8) ethyl acetate, (9) tetrahydrofuran, (10) acetic anhydride, (11) glacial acetic acid, (12) nitromethane and (13) nitroethane. The solvents were saturated with sodium nitrate prior to the

(5) J. P. WIBAUT and H. BOER, *Rec. Trav. Chim.* 74, 241 (1955), and earlier papers, especially, J. P. WIBAUT, F. L. J. SIXMA, L. W. F. KAMPSCHMIDT and H. BOER, *Ibid.* 69, 1355 (1950).

(6) F. L. J. SIXMA, H. BOER and J. P. WIBAUT, *Ibid.* 70, 1005 (1951).

(7) L. CHUGAEV and V. KLOPIN, *Z. Anorg. Chem.* 151, 253 (1926).

(8) M. WARD and G. A. WELCH, *J. Chem. Soc.* 4038 (1954).

(9) D. W. GRANT, *J. Inorg. Nucl. Chem.* 6, 69 (1958).

reaction in order to effect precipitation of the silver(II) complex should it form in solution. The Lewis acids used included anhydrous alumimum chloride, anhydrous iron(III) chloride, boron trifluoride and silver(I) ion.

EXPERIMENTAL

A. *Materials*

Bis(orthophenanthroline)–silver(I) nitrate and perchlorate were prepared by bringing together aqueous solutions of the ligand and the particular silver salt. The yellow products were washed with ethanol and dried in a vacuum desiccator over magnesium perchlorate for two days. (Found: Ag, 20·56; C, 54·02; H, 3·21; N, 13·08. Calc. for $Ag(C_{12}H_8N_2)_2NO_3$: Ag, 20·35; C, 54·36; H, 3·03; N, 13·21%) and (Found: Ag, 19·51; C, 51·09; H, 3·09; N, 9·57. Calc. for $Ag(C_{12}H_8N_2)_2ClO_4$: Ag, 19·00; C, 50·77; H, 2·83; N, 9·87%).

The silver(II) complexes were prepared by ozonizing acidic solutions of the silver(I) complexes. The solutions were saturated with the sodium salt of the particular anion. The resulting maroon products were washed with water and dried in the same way as the silver(I) complexes. (Found: Ag, 18·5; C, 49·02; H, 3·02; N, 13·92. Calc. for $Ag(C_{12}H_8N_2)_2(NO_3)_2$: Ag, 18·22; C, 48·67; H, 2·71; N, 14·19%) and (Found: Ag, 15·9; C, 43·47; H, 2·66; N, 8·21. Calc. for $Ag(C_{12}H_8N_2)_2(ClO_4)_2$: Ag, 16·17; C, 43·20; H, 2·40; N, 8·39%).

Ozone was obtained from a Welsbach Model T-23 laboratory ozonizer utilizing tank oxygen which was predried by passage through columns packed with magnesium perchlorate. The gaseous stream had a flow rate of approximately 0·3 l./min and contained 2 to 3 per cent ozone in oxygen. The reactions were carried out in a gas adsorption bottle fitted with a course sintered glass filter.

B. *Procedures*

The general procedure was as follows. The particular solvent was saturated with sodium nitrate, the silver(I) complex was added and the mixture ozonized for approximately two hours. If the desired reaction failed to occur (a colour change from yellow to maroon is indicative of this reaction), fresh solutions were prepared separately for each of the Lewis acids: anhydrous Al_2Cl_6, anhydrous Fe_2Cl_6, BF_3 and, in some cases, $AgNO_3$. Ozonization of each mixture was then carried out for the same length of time. If the complex and/or the Lewis acid was insoluble in the particular solvent, the reaction vessel was shaken on a Burrell Wrist-Action shaker during the course of the reaction. All reactions were carried out at room temperature (25–27°C) and at 0°C and −8°C. Other experiments involved premixing the ozone gas stream with gaseous BF_3 prior to its introduction into the reaction vessel. In certain cases, when BF_3 was employed as the catalyst, a white precipitate formed. This was found to occur even in the absence of ozone or the silver complex. Although we did not identify the white precipatate, it may most likely be attributed to a reaction between BF_3 and the nitrate salt. Baumgarten and Bruns(10) showed that boron oxyfluoride and the corresponding metal fluoride or fluoborate may form under these circumstances. When the precipitate appeared, sodium nitrate was added to the reaction vessel periodically throughout the ozonization.

RESULTS AND DISCUSSION

The ozonization of $[Ag(o\text{-}phen)_2]\ NO_3$ to $[Ag(o\text{-}phen)_2]\ (NO_3)_2$ occurred in only three of the thirteen non-aqueous solvents investigated. These were glacial acetic acid, nitromethane and nitroethane. No Lewis acid was necessary in these solvents and in none of the other solvents did the addition of a Lewis acid bring about the oxidation of the silver complex. It is significant that these three solvents are the only protonic acid solvents which were tried.

---

(10) P. Baumgarten and W. Bruns, *Ber. Dtsch. Chem. Ges.* **72**, 1753 (1939).

The silver(I) complex was quite soluble in acetic acid. Within two minutes after ozonization was begun in this solvent the solution turned a maroon colour, and after one hour a maroon precipitate had collected. It was shown to be the silver(II) complex in every way including its infra-red spectrum (which is very slightly different from that of the silver(I) complex) and its visible-ultra-violet spectrum in glacial acetic acid (which is quite different from that of the silver(I) complex).

The silver(I) complex is very soluble in both nitromethane and nitroethane and the experimental results were identical in both of these solvents. The colour of the silver(II) complex appeared within one minute after ozonization began. At the end of 2 hr of ozonization the solution was deeply coloured, but no solid product had settled out as was the case with the acetic acid solution. Furthermore, after ozonization was terminated and the reaction vessel swept free of ozone, the solution became colourless within 2-3 min at room temperature. It was found that the decomposition of the maroon product was greatly retarded by lower temperatures and at dry-ice temperature the colour could be maintained a full day. The visible spectrum of the ozonated nitroalkane solution, obtained by circulating ice-water through a thermostatic cell holder, agreed exactly with that obtained from a nitroalkane solution of the silver(II) complex. However, the maroon product could not be isolated from the nitroalkane solution by addition of sodium nitrate, water, ethanol or dilute perchloric acid. It should be noted at this point that the silver(II) complex (which had been prepared in aqueous solution) dissolved in nitromethane shows no tendency to decompose in the above manner and is stable for weeks in this solvent.

Several additional observations of the ozonated nitroalkane solutions were made. If the perchlorate salt of the silver(I) complex ion were substituted for the nitrate salt, nitrate ion would still be found in the ozonated solution. Formic acid was detected in the nitromethane solution and acetic acid in the nitroethane solution at the end of the reaction. Also, we established that both formaldehyde and acetaldehyde will reduce the silver(II) complex dissolved in the nitroalkanes in a moderately slow reaction which is retarded by lower temperatures.

All of these qualitative results have led us to some tentative suggestions concerning the mechanisms of the reactions which are occurring in the non-aqueous systems. In the following series of reactions Ag(I) and Ag(II) represent the silver(I) and silver(II) complexes, respectively.

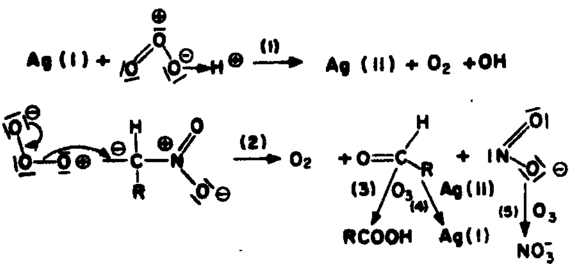

We propose that in reaction (1) the proton from the acidic solvent molecule enhances the electrophilic character of the ozone molecule by forming the adduct shown. This enables the ozone to effectively attack the silver(I) complex and the products are oxygen, the silver(II) complex and the hydroxyl radical (which may react with another radical to produce hydrogen peroxide, but this is pure speculation). Ozone may then attack the negative ion of the solvent by the mechanism shown in reaction (2), which is analogous to the well-known β-elimination reactions. The products of this reaction would be molecular oxygen, aldehyde and nitrate ion, as indicated. Ozone would attack the nitrate ion (reaction 5), oxidizing it to the nitrate ion, which was found in the reaction products. Ozone would also slowly oxidize the aldehyde to peroxyacid (reaction 3). However, this reaction may well be in competition with (reaction 4), the reduction of the silver(II) complex by the aldehyde. This could account for the observed strongly temperature dependent instability of the silver(II) complex in the nitroalkane solutions which have been subjected to ozonization.

The proposals made above must be considered quite tentative at the present time and we are investigating further the nature of the ozonization of silver(I) complexes in both aqueous and non-aqueous solvents.

Acknowledgements—The authors are grateful to the Research Corporation for financial support of part of this research and to Professor J. G. TRAYNHAM for helpful discussions.

J. Inorg. Nucl. Chem., 1962, Vol. 24, pp. 1159 to 1162. Pergamon Press Ltd. Printed in England

HEAT OF ISOMERIZATION OF PEROXYNITRITE TO NITRATE AND KINETICS OF ISOMERIZATION OF PEROXYNITROUS ACID TO NITRIC ACID*

J. D. RAY
School of Chemistry, Georgia Institute of Technology, Atlanta 13, Georgia

(*Received* 13 *November* 1959; *in revised form* 22 *February* 1962)

Abstract—The reaction between hydrogen peroxide and nitrous acid at 0° results in high yields of the rapidly formed intermediate peroxynitrous acid which isomerizes to nitric acid at a slower rate. By stopping the reaction with the addition of base at various times and measuring the total heat evolved in a calorimeter it was possible to determine the rate constant for isomerization to be $0{\cdot}099\ \mathrm{sec}^{-1}$ at 1°. The heat of isomerization of the peroxynitrite ion to the nitrate ion was deduced to be $-38{\cdot}8 \pm 2$ kcal/mole in dilute aqueous solution at 1°.

KINETIC studies of the reaction between nitrous acid and hydrogen peroxide(1, 2, 3) at low concentrations of the latter reagents are in agreement that the rate expression is predominately expressed by:

$$\frac{-d(H_2O_2)}{dt} = k(H_2O_2)(HONO)(H^+). \qquad (1)$$

Results of the present study are in agreement with (1) and the following mechanism:

$$\begin{aligned} H^+ + HONO + H_2O_2 &= HOONO + H_2O + H^+ && k_1 \\ HOONO &= HON^{O}_{O} && k_2 \\ NO_2^- + HOONO &= HON^{O}_{O} + NO_2^- && k_3 \\ HOONO &= HO + NO_2 && k_4 \end{aligned}$$

The present study differs from the kinetic studies in having concentrations of reagents adjusted so as to obtain a concentration of the intermediate peroxynitrous acid that is nearly quantitative with respect to conversion of nitrous acid to peroxynitrous acid. The present experiments thus are similar to those carried out by GLEU and HUBOLD(4).

Materials and methods. "Baker's Analysed" 31·9 per cent hydrogen peroxide was used in all experiments. Du Pont nitric acid of 70 per cent concentration was used. The sodium hydroxide was obtained from a bottle of its concentrated aqueous solution in which it had been standing for several days so as to settle the carbonate. All of these reagents were pipetted from their concentrated solutions. The potassium nitrite was part of a preparation previously used.(5)

---

*Presented at the Southeastern Regional Meeting of the American Chemical Society, Birmingham, Ala., Nov. 3–5, 1960.

(1) E. HALFPENNY and P. L. ROBINSON, *J. Chem. Soc.* 928 (1952).

(2) M. ANBAR and H. TAUBE, *J. Amer. Chem. Soc.* 76, 6243 (1954).

(3) E. A. SHILOV, A. A. RYBAKOW and H. A. PAL, *Chem. Zbl.* II, 377 (1931).
E. A. SHILOV and Z. S. STEPANOVA, *Zh. Fiz. Khim.* 24, 820 (1950); *Chem. Abstr.* 45, 4121 (1951).
E. A. SHILOV, *Zh. Fiz. Khim.* 27, 1103 (1953); *Chem. Abstr.* 49, 5937a.

(4) K. GLEU and R. HUBOLD, *Z. Anorg. Chem.* 223, 305 (1935).

(5) J. D. RAY and R. A. OGG, JR., *J. Phys. Chem.* 60, 1599 (1956).

The calorimeter solutions after reaction were analysed by potentiometric titration of excess H_2O_2 with hypochlorite at pH 12 using platinum and normal calomel electrodes. The nitrite was determined with permanganate.

The calorimeter and its calibration by using the heat of water vapourization as the energy standard have been described previously.(6) The calorimeter was placed in a container of crushed ice so as to minimise temperature drift. All calorimeter reactions reported in this article were carried out with all of the reagents at about 0°. The defined thermochemical calorie was used for calculations.

Heat of isomerization of peroxynitrite to nitrate. Fig. 1 is a plot of observed temperature rise of the calorimeter as a function of the number of seconds between addition of acid followed by base to the calorimeter. Inasmuch as the rate of decomposition of peroxynitrite ion is very slow, it is possible to trap peroxynitrous acid in the form of peroxynitrite by the addition of a strong base. Since the reactions being studied are much too rapid to be followed by means of the temperature change as registered on a Beckman thermometer, the observed temperature changes shown on Fig. 1 correspond to those involving both acid and subsequent base addition. In all cases represented by plotted points except that at zero time the calorimeter contained 500 ml of a solution containing 3·000 g of potassium nitrite and 5·00 ml of 31·9 per cent hydrogen peroxide. The point at zero time involved only the acid and base but no nitrite or peroxide. Solutions of 4·00 ml of 70 per cent nitric acid and 5·00 ml of 46 per cent sodium hydroxide both of which had been diluted to 50 ml were added to the calorimeter in a manner to effect rapid mixing. The acid and base solutions were put in 100 ml beakers which were placed in a container of crushed ice next to the calorimeter. The beakers of acid and base were stirred with thermometers having

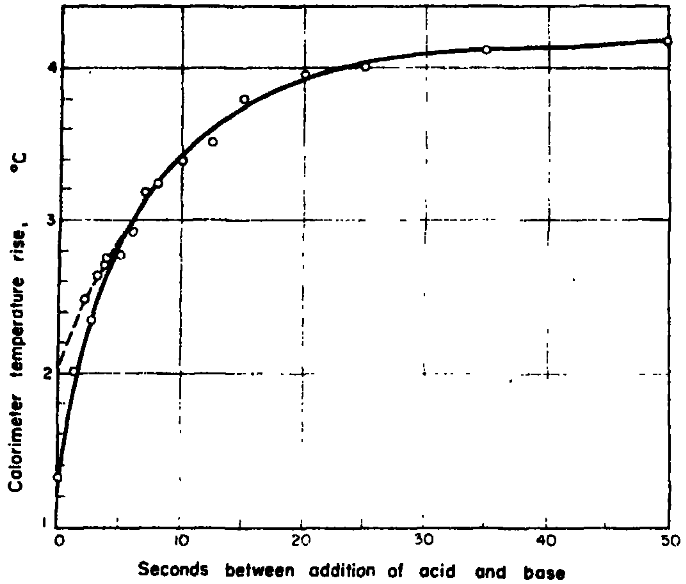

FIG. 1.—Observed temperature rise of calorimeter as a function of the number of seconds between addition of acid and base. The dashed line intersects the temperature axis to indicate the temperature rise associated with quantitative peroxynitrite formation. The shape of the curve is due to the first order reaction $HOONO = HONO_2$.

---

(6) J. D. RAY, *Rev. Sci. Instrum.* **26**, 863 (1956).

0·1° graduations so that temperature drifts could be followed. The acid and base solutions were not just poured in but rather literally "thrown" downward out of the beakers into the calorimeter so that mixing was effected in approximately one second. The two low points near zero time on Fig. 1 indicate some time lag in mixing. The stirring paddle was very effective so that the limiting factor in mixing time was simply getting the solutions out of the beakers.

In the present study the reaction of peroxynitrous acid to form nitric acid can be represented as a first order process. Thus, after the first 2 or 3 sec, all of the nitrite ion has been consumed in making peroxynitrous acid. Therefore, step k_3 is not active beyond the first short period of time that it takes nitrous acid to be formed from nitrite. SHILOV and STEPANOVA(3) suggest that the isomerization may proceed through an acid catalysed step. But the data of Fig. 1 were plotted as the logarithm of the calorimeter temperature rise at infinite time between addition of acid and base minus the temperature rise corresponding to actual time intervals to obtain a straight line between about 3½ sec and 50 sec. The derived rate constant may actually be pseudo first order and include the hydrogen ion concentration.

When the data of Fig. 1 are plotted on log paper as described above, the data extrapolate as indicated by the dashed line of Fig. 1 with intercept 2·03° rather than extending down to intersect the temperature rise axis at 1·35°. The 1·35° intercept represents the observed temperature rise associated with just the heat of acid-base neutralization and dilution effects in the absence of KNO_2 and H_2O_2. The calculated value for this rise, 1·38°, based on the energy equivalent of the calorimeter, 640 cal/°C is within the precision of the calorimeter and reflects a small amount of acid retained in the beaker. The difference between the 1·35° intercept and the extrapolated intercept at 2·03° represents the temperature change associated with the formation of peroxynitrite plus hydroperoxide ion and negligible dilution effects. The temperature rise, 0·22°, due to hydroperoxide formation was calculated from JOYNER's(7) data. The temperature rise, 0·46° due to the reaction

$$H_2O_2(\text{soln})+NO_2^-(\text{soln}) = OONO^-(\text{soln})+H_2O(\text{soln})$$

corresponds to a molar heat of reaction of −8·3 kcal and a heat of formation of peroxynitrite ion from the elements in the solution at 1° of −11·4 kcal, and a heat of isomerization of peroxynitrite to nitrate of −38·1 kcal.

The difference between the intercept at 2·03° and the temperature change 4·21° associated with infinite time elapsed between addition of acid and base is proportional to the heat of isomerization of peroxynitrite ion to nitrate ion, −39·4 kcal. This value corresponds to −10·1 kcal for the heat of formation of peroxynitrite ion from the elements at 1°. The difference in the two values for the heat of formation of peroxynitrite ion, −11·4 and −10.1 reflects neglect of concentration effects on standard heats of formation of the reaction species, uncertainty in the heats of formation of the species, and experimental precision. The average values are ΔH°_{274} $OONO^-$ = −10·8 kcal and $\Delta H^\circ_{274\,OONO^- = NO_3^-}$ = −38·8 kcal. The precision is estimated as ± 2 kcal for both values.

Rate of isomerization of peroxynitrous acid to nitric acid. The half-life of the isomerization of peroxynitrous acid to nitric acid deduced from Fig. 1 and from a plot of the data on log paper is 7·0 sec which corresponds to a rate constant of 0·099 sec^{-1} at a temperature of about 1°.

---

(7) R. A. JOYNER, *Z. Anorg. Chem.* **77**, 103 (1912).

Acknowledgements—This research was supported in part by the United States Air Force under Contract No. AF 49(638)-286 monitored by the AF Office of Scientific Research of the Air Research and Development Command, the Research Corporation and the National Science Foundation (NSF G-15560).

J. Inorg. Nucl. Chem., 1962, Vol. 24, pp. 1163 to 1169. Pergamon Press Ltd. Printed in England

SOME PHYSICAL PROPERTIES OF BORON TRICHLORIDE-PHOSPHINE

P. A. Tierney, D. W. Lewis and D. Berg
Westinghouse Materials Research Laboratories, Pittsburgh 35, Pennsylvania

(*Received* 20 *October* 1961; *in revised form* 16 *March* 1962)

Abstract—Vapour density measurements on $Cl_3B{:}PH_3$ indicate the complex is not 100 per cent dissociated in the gas phase at room temperature. Further evidence of association in the gas phase is obtained from the infra-red spectrum of the gases. The dipole moment of $Cl_3B{:}PH_3$ in benzene solution is $5{\cdot}2 \pm 0{\cdot}1$ D. X-ray diffraction data for this addition compound and for $Br_3B{:}PH_3$ are reported.

The phosphine addition compound of boron trichloride was first prepared by Besson(1) from the reaction of equal volumes of boron trichloride and phosphine below 20°C. Gamble and Gilmont(2) prepared this compound from $B_2H_6{\cdot}2PH_3$ by the reaction:

$$B_2H_6{\cdot}2PH_3+6HCl \longrightarrow 2BCl_3{:}PH_3+6H_2 \qquad (1)$$

They reported that the compound is largely dissociated in the gas phase and that the pressure follows the relationship:

$$\log P = 11{\cdot}137 - \frac{2810}{T}$$

In connection with an investigation of the preparation of boron phosphide we have confirmed the work of Gamble and Gilmont and have obtained additional information about this compound.

EXPERIMENTAL

Materials

BCl_3 was obtained from the Matheson Co. and purified through its nitrobenzene addition compound.(3) Phosphine was prepared from aluminium phosphide and water(4) and fractionated on the vacuum line. Boron tribromide was prepared from aluminium bromide and boron trifluoride according to the procedure of Gamble.(5) Benzene was distilled over sodium on the vacuum line.

Apparatus and techniques

The vapour density measurements and pressure–temperature measurements were carried out in an all glass vacuum system using common techniques.(6)

Preparation of $BCl_3{:}PH_3$ *and* $BBr_3{:}PH_3$

Equal volumes of phosphine and the appropriate boron halide were condensed into a reaction flask cooled to —196°C. A rapid reaction took place as the flask was allowed to warm to room temperature. The excess reactants were removed by opening the reaction flask to the vacuum line for a short time. Because of its high dissociation pressure at room temperature, $BCl_3{:}PH_3$ could be transferred on the vacuum line quite easily. $BBr_3{:}PH_3$ could also be transferred on the line, but because of its low dissociation pressure (less than 1 mm at 25°C) it was more convenient to prepare this compound in situ.

(1) A. Besson, *C.R. Acad. Sci., Paris* 110, 516 (1890).

(2) E. L. Gamble and P. Gilmont, *J. Amer. Chem. Soc.* 62, 717 (1940).

(3) H. C. Brown and R. R. Holmes, *J. Amer. Chem. Soc.* 78, 2173 (1956).

(4) W. E. White and A. H. Bushey, *J. Amer. Chem. Soc.* 66, 1666 (1944).

(5) Inorganic Synthesis, Vol. 3, p. 27. McGraw-Hill, New York (1950).

(6) R. T. Sanderson, *Vacuum Manipulations of Volatile Compounds.* J. Wiley, New York (1948).

Thermal decomposition of $BCl_3{:}PH_3$ *and* $BBr_3{:}PH_3$

Equal volumes of phosphine and the corresponding boron halide were condensed into quartz tubes. The tubes were sealed and heated for 16 hr at 950°C in an electric furnace. X-ray powder patterns obtained on the gray to yellow solid products present in the tube after heating corresponded to those reported(7) for boron phosphide.

Diffraction patterns

X-ray diffraction patterns of the addition compounds were obtained in the following way. The reactants were condensed into a Pyrex tube 10 cm long by 1 cm diameter. The tube was constricted near the top and had a side arm which lead through a Pyrex–quartz graded glass seal to a 0·5 mm diameter quartz capillary tube. The Pyrex tube contained 7 or 8 Pyrex glass beads. The tube was sealed at the top constriction. After reaction had taken place, the white solid product was pulverized by shaking the glass beads. Then the pulverized solid was vibrated into the quartz capillary. The capillary was sealed off in a small flame and placed in the X-ray camera. Diffraction patterns were obtained using $CuK\alpha$ radiation.

Infra-red spectra

Infra-red spectra were obtained with a Perkin-Elmer double beam infra-red spectrophotometer, Model 221, using a sodium chloride optic system. The gas cell contained sodium chloride windows and had a path length of 5·5 cm. The gases were introduced directly into the gas cell from the vacuum line. Benzene solutions of boron trichloride-phosphine and boron trichloride were prepared on the vacuum line. The solutions were transferred to a 0·5 mm sodium chloride cell by means of a hypodermic syringe. The benzene peaks were blanked out by placing a variable spaced cell containing pure benzene in the reference beam.

Dipole moment measurements

Capacitance measurements were made in a Balsbaugh cell fitted with a side arm which allowed attachment to the introductory system of the vacuum line. Weighed amounts of benzene and $Cl_3B{:}PH_3$ were condensed directly into the cell from the vacuum line. The cell was sealed, removed from the vacuum line and placed in a constant temperature bath thermostatically controlled to 25 ±0·1°C.

The cell was calibrated both with air and benzene. A General Radio Co. Type 716-AS1. Capacitance Bridge was used with a General Radio Co. Type 684A oscillator at 1 kc/s. The detector was a tunable Rhode and Schwartz indicating amplifier, type VBM, B1Y12125. The measurements were performed by the substitution method using a General Radio Standard Capacitor Type 722-0.

RESULTS AND DISCUSSION

Mixtures of boron trichloride and phosphine react on warming to room temperature from −196°C forming a simple 1:1 addition compound according to the Equation(3)

$$Cl_3B_{(g)}+PH_{3(g)} \rightleftharpoons Cl_3B{:}PH_{3(s)} \qquad (3)$$

A white solid material forms initially, but on standing at room temperature for a few days large clear crystals, approximately 4 mm on an edge, appear.

The apparent molecular weight of the gas as determined by vapour density measurements was 79±2 g/mole at 31°C. The molecular weight that would be expected if 100% dissociation into boron trichloride and phosphine occurred is 75·6 g/mole. For mol. wt. = 81 the dissociation is 85 per cent, for mol. wt. = 77 the dissociation is 97 per cent. Hence, it appears that the complex is about 90 per cent dissociated at 31°C.

The pressure temperature data for the compound, $BCl_3{:}PH_3$, is summarized in Table 1. From a plot of $\log P$ vs. $1/T$ the relationship:

$$\log P = 11{\cdot}22 - \frac{2{\cdot}81 \times 10^3}{T}$$

was obtained. This agrees with the data of GAMBLE and GILMONT (cf. Equation 2). If

(7) [illegible]PPER and T. A. INGLES, *Nature, Lond.* **179**, 1075 (1957).

the partial pressure of the complex is small compared to the partial pressure of the BCl_3 in the vapour phase, (true at 31°) then the enthalpy of the reaction shown Equation (3), obtained from the vapour-pressure vs. temperature plot, is 26 kcal/mole.

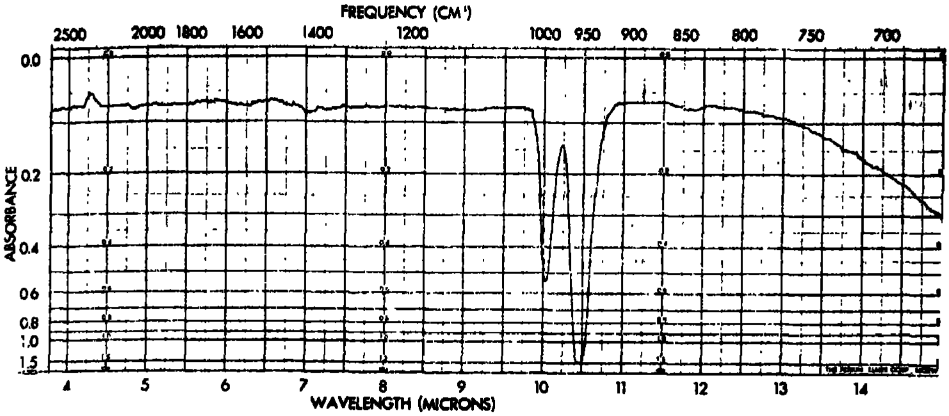

BCl_3 gas

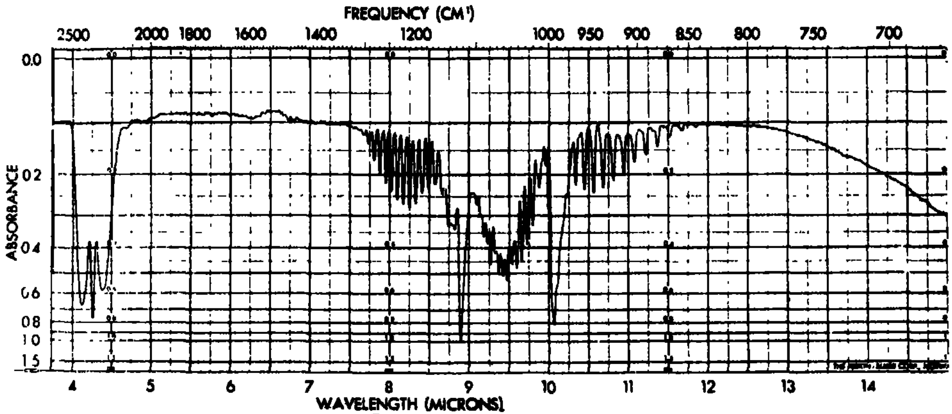

PH_3 gas

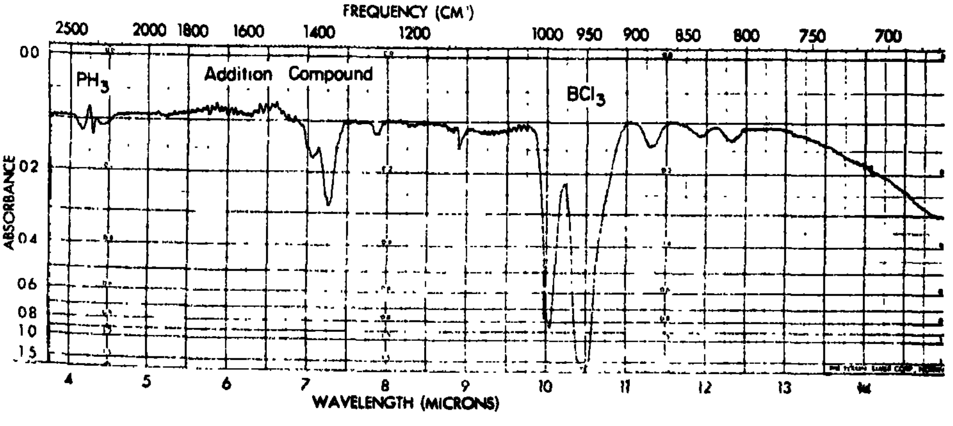

$Cl_3B{:}PH_3$ gas

FIG. 1a.

TABLE 1.—PRESSURE-TEMPERATURE DATA FOR $Cl_3B:PH_3$

Temp. (°C)	Pressure (mm Hg)
23	53
22	50
15	30
0	8·5
—12	2·5
—19	1·5

As a further check on the association of boron trichloride-phosphine in the gas phase, infra-red spectra were obtained on boron trichloride gas, phosphine gas, and the vapours in equilibrium with solid $BCl_3:PH_3$. The spectra are shown in Fig. 1a. In Fig. 1b are the infra-red spectra of benzene solutions of $Cl_3B:PH_3$ and boron trichloride. The presence of absorption peaks in the 7–7·5μ region on the spectrum of $PH_6:BCl_6$, which are not present in the spectrum of phosphine or boron

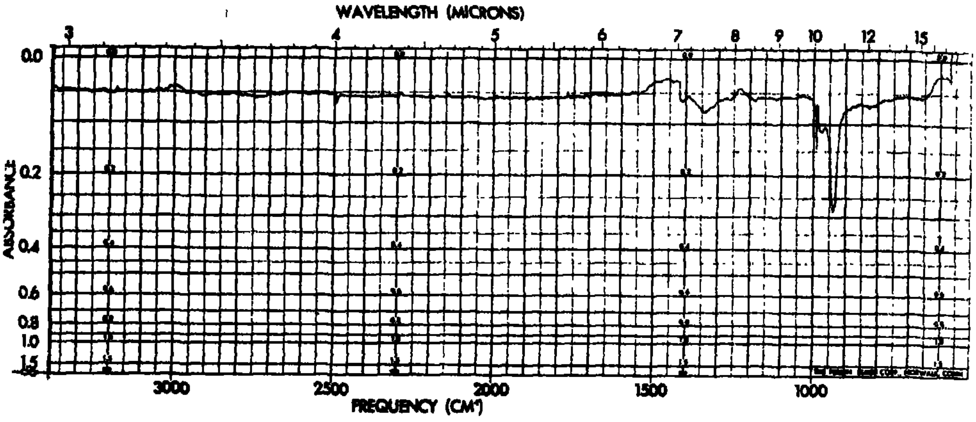

BCl₃ in Benzene

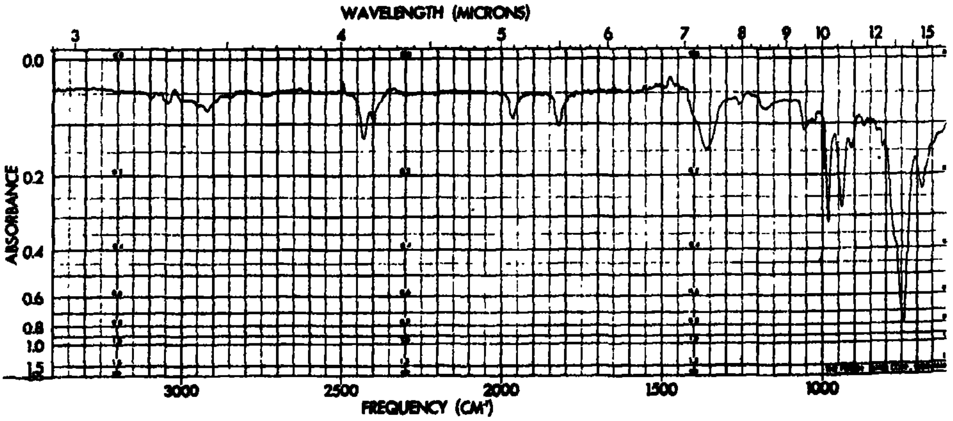

$Cl_3B:PH_3$ in Benzene

FIG. 1b.—Infra-red spectra of BCl_3 and $Cl_3B:PH_3$ in benzene.

trichloride, may be attributed to the complex. Note too that in benzene the intensity of the BCl_3 absorption for the band at about 10·1μ is less than the band at about 10·5μ while for the complex in benzene the opposite is true. In the gas phase the concentration of complex is too low and the unchanged BCl_3 spectrum results at 10·1 and 10·5μ. Also in benzene there are absorption peaks at 5·1, 5·5 and 13·4μ which may be attributed to the complex. However, these absorption peaks do not appear in the gas phase.

The X-ray diffraction pattern for solid $Cl_3B:PH_3$ is summarized in Table 2.

TABLE 2.—X-RAY DIFFRACTION DATA FOR PHOSPHINE ADDITION COMPOUNDS OF BORON TRICHLORIDE AND BORON TRIBROMIDE

$Cl_3B:PH_3$		$Br_3B:PH_3$	
d-spacing (Å)	Intensity	*d*-spacing (Å)	Intensity
6·11	*m*	5·6	*ww*
4·80	*ms*	4·95	*m*
4·30	*m*	4·40	*vvw*
3·75	*vw*	4·20	*vvw*
3·39	*m*	3·50	*vw*
3·29	*w*	3·40	*vw*
3·05	*s*	3·30	*vw*
2·90	*m*	3·15	*m*
2·86	*w*	2·99	*s*
2·75	*m*	2·85	*vvw*
2·70	*m*	2·79	*w*
2·60	*vvw*	2·65	*vvw*
2·45	*vvw*	2·49	*w*
2·40	*w*	2·40	*vvw*
2·27	*w*	2·30	*vw*
2·24	*vw*	2·26	*vw*
2·19	*vw*	2·20	*vw*
2·14	*vw*	2·13	*vw*
2·05	*w*	2·04	*w*
1·97	*w*	1·95	*wm*
1·94	*w*	1·86	*wm*
1·90	*w*	1·78	*vvw*
1·87	*vw*	1·74	*vw*
1·81	*w*	1·71	*vw*
1·73	*vvw*	1·68	*vw*
1·67	*vvw*	1·62	*vw*
1·62	*vvw*	1·60	*vw*
1·57	*vvw*	1·58	*vw*
1·53	*vw*	1·55	*vvw*
1·45	*vvw*	1·52	*vvw*
1·35	*vvw*	1·40	*vvw*
1·30	*vvw*	1·360	*vvw*
1·255	*vvw*	1·345	*vvw*
1·225	*vvw*	1·250	*vvw*
1·180	*vvw*	1·220	*vvw*
1·050	*vvw*	1·200	*vvw*
0·97	*vvw*		

Included in this table are the *d*-spacings for the addition compound of boron tribromide and phosphine.

The boron trichloride-phosphine complex readily dissolves in benzene. In early experiments it was established that the vapour-pressure of the benzene solution was less than the sum of the vapour-pressure of benzene and the vapour-pressure of $BCl_3:PH_3$. The dipole moment of $BCl_3:PH_3$ determined in benzene was $5{\cdot}2\pm0{\cdot}1$D., assuming no dissociation of the complex in solution.

The polarization of the solution, P_{12}, was calculated from the equation:(8)

$$P_{12} = \frac{\epsilon'-1}{\epsilon'+2}\cdot\frac{X_1M_1+X_2M_2}{d} \qquad (4)$$

where ϵ' is the dielectric constant of the solution, X_1 is the mole fraction of the solvent, X_2 is the mole fraction of the solute, M_1 is the molecular weight of the solvent, M_2 is the molecular weight of the solute, and d is the density of the solution.

The polarization of the solute, P_2, was calculated from the equation,

$$P_2 = \frac{P_{12}-P_1}{X_2}+P_1 \qquad (5)$$

where P_1 is the polarization of the solvent and the other symbols are the same as in Equation (4).

The polarization of the solute at infinite dilution, P_2^{∞}, was obtained by extrapolation of the plot of P_2 against X_2 as shown in Fig. 2. The value of P_2^{∞} lies in the range 600–640 cm^3.

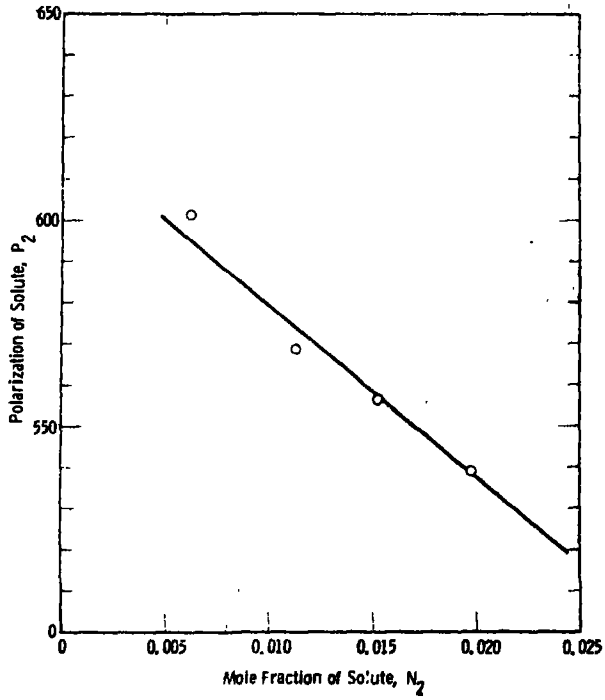

Fig. 2.—Polarization of solute vs. mole fraction of solute for benzene solutions of Cl_3 $B:PH_3$

---

(8) R. J. W. Le Fevre, *Dipole Moments*, p. 28. J. Wiley, New York, (1953).

The dipole moment, μ, was calculated from the equation:(9)

$$P_2^{\infty} = P_E + P_A + \frac{4\pi N\mu^2}{9kT} \tag{6}$$

where N is Avagadro's number, P_E and P_A are the electronic and atomic polarization, k is the Boltzmann constant, and T is the absolute temperature. The contribution of P_A and P_E to the total polarization, P_2^{∞}, was estimated frpm the relationship:

$$P_E = \frac{n^2-1}{n^2+1} \times \frac{M_2}{d} \tag{7}$$

using approximate values for n, the refractive index, d, the density, and assuming that the complex is monomeric in dilute benzene solutions. It was also assumed that the value of P_A was 15 per cent of P_E. The value of P_A+P_E so obtained was 50 cm³.

The electronic and atomic polarizations are small compared to the orientation polarization of the dipole. Since large errors in P_2^{∞} affects the value of μ only slightly, the estimation of the atomic and electronic contributions is reasonable.

The high value of the dipole moment obtained argues strongly that the complex, $Cl_3B{:}PH_3$, is monomeric in dilute benzene solutions. Since the total pressure of the gases in equilibrium with benzene solution of $Cl_3B{:}PH_3$ is less than the sum of the dissociation pressure of $Cl_3B{:}PH_3$ and the vapour-pressure of pure benzene, the complex is not significantly dissociated in benzene. The change in intensity of absorption at 10·1 and 10·5μ in the benzene solution of the complex as compared to pure BCl_3 in benzene also argues for greater association of the complex in benzene as compared to the vapour.

According to PHILIPS *et al.*(10) the dipole moment of triphenyl phosphine–boron trichloride is 7·01 ± 0·06 D. and the moment of trimethyl phosphine–boron trichloride is 7·03 ± 0·01 D.

Acknowledgements—The authors wish to thank Dr.F. MILLERof Mellon Institute of Industrial Research for aid in interpretation of the infra-red spectra. Appreciation is also expressed to Miss B. KAGLE of Westinghouse Research who obtained the X-ray diffraction patterns.

(9) C. P. SMITH, *The Determination of Dipole Moment* in *Physical Methods of Organic Chemistry*, (2nd Ed.) Vol 1. Interscience, New York (1949).

(10) G. M. PHILIPS, J. S. HUNTER and L. E. SUTTON, *J. Chem. Soc.* 146 (1945).

J. Inorg. Nucl. Chem., 1962, Vol. 24, pp. 1171 to 1174. Pergamon Press Ltd. Printed in England

NOTES

Investigation of isopolyacids by a new conductometric technique

(*Received* 22 *January* 1962; *in revised form* 23 *February* 1962)

Complex equilibria existing in solutions of isopolyacids have been studied extensively by the conductometric method and experimental results often interpreted on the basis of the number of protons added. This procedure is incorrect since the position of inflexions in conductometric titrations varies with concentration and, hence, cannot be used directly in the formulation of equations. Below, a new graphical method for the evaluation of the number of protons consumed by a complex system is applied to accurate conductivity measurements for the hydrolysis of ammonium metavanadate with perchloric acid.

The number of protons consumed by each vanadium atom can be calculated from the difference between the conductivity of the solution after it has reached equilibrium and the conductivity if no reaction had taken place. In Fig. 1, the line AB (experimental line) indicates the variation of conductivity with hydrogen ion concentration for solutions whose vanadium concentrations are the same, but whose perchloric acid concentrations differ. The line OC shows the variation of conductivity with concentration for solutions of perchloric acid. If no

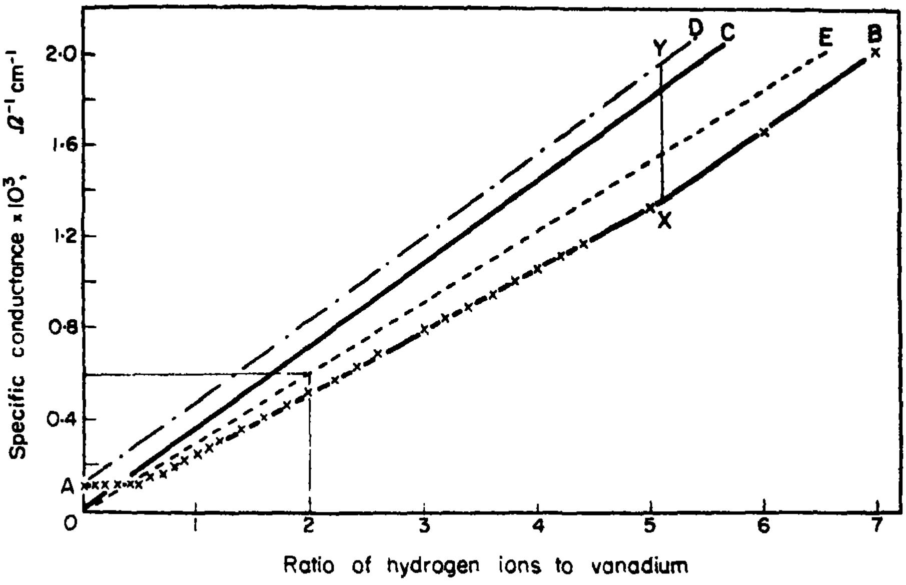

Fig. 1—Variation of specific conductance -x with hydrogen ion concentration for solutions containing ammonium metavanadate and perchloric acid at 25 ± 0·001°. Concentration 0·00088 g atom vanadium/l.

———————— conductivity line for perchloric acid;

– – – – – – – – conductivity line for hydrogen ions;

———·——— constructed conductivity line if no reaction had occurred between metavanadate and perchloric acid.

reaction had occurred between the perchloric acid and the vanadium (v) solution, the conductivity curve would be denoted by AD (constructed line). The difference between the constructed and experimental lines (fall in conductivity) at any point can be equated to the removal of protons. The number of protons removed can be directly obtained from the line OE, which is the proton contribution of the conductivity; this line is calculated knowing the individual ionic conductivities of the hydrogen and perchlorate ions.(1) From this construction, we can determine the number of protons consumed when a given number of protons have been added. The assumption made is that the fall in conductivity due to the removal of protons is large compared with the change in conductivity of vanadium (v) species. As an example, let us consider point X on the curve which denotes the end of the reaction since the line beyond X becomes parallel to the constructed. The number of protons added at this point is 5·1 (abscissae). The number of protons consumed is found as follows: the conductivity at point X is $1{\cdot}33 \times 10^{-3}$ ohm $^{-1}$cm^{-1}, the corresponding value on the constructed line (point Y) being $1{\cdot}93 \times 10^{-3}$ ohm^{-1} cm^{-1}, indicating a fall in conductivity of $0{\cdot}60 \times 10^{-3}$ ohm^{-1} cm^{-1}. The latter value applied to the line OE shows the number of protons consumed to be two, which is precisely the value expressed by the equation

$$\{VO_3^-\}^* + 2H^+ = VO_2^+ + H_2O.$$

Accurate resistance measurements were made with a Jones and Bollinger type cell(4), thermostated in a Townson and Mercer S 200 thermostat containing Puremor 210 light oil. The bridge consisted of Muirhead decade resistance boxes, the null point was detected on a Cossor oscilloscope, the alternating current supply was obtained from an Airmec oscillator at 1500 c/s.

Perchloric acid: 60% w/w "Analar". Ammonium metavanadate solution: prepared from the "Analar" salt.

The ammonium metavanadate solution (20 ml) was placed in a 250 ml beaker together with the required volume of perchloric acid to give a fixed hydrogen ion - vanadium atom ratio. The solution was boiled gently in order to attain equilibrium, allowed to cool, transferred quantitatively to a 100ml graduated flask, and the volume of the solution was made up to 100 ml with conductivity water, giving a final concentration of 0·00088 g atom vanadium/l. Several solutions were prepared containing different amounts of perchloric acid.

* The brackets indicate that the metavanadate is polymerized, probably trimerized (2, 3).

Each solution was in turn placed in the conductance cell, and its resistance measured after it had attained a constant value at 25 ± 0·001°C.

Department of Chemistry,
College of Science and Technology,
Manchester, 1.

G. Kakadadse
H. J. Wilson

(1) R. A. Robinson and R. H. Stokes, *Electrolyte Solutions*, 454. Butterworths Scientific Publications (1955).

(2) R. U. Russell and J. E. Salmon, *J. Chem. Soc.* 4708 (1958).

(3) S. Block, *Nature, Lond.* **186**, 540 (1960).

(4) G. Jones and G. M. Bollinger, *J. Amer. Chem. Soc.* **53**, 411 (1931).

Pentacarbonylacrylonitriletungsten

(*Received* 21 *February* 1962)

X-ray analysis has recently shown tetracarbonylacrylonitrileiron to have a structure in which the metal atom is bonded to the π - system of the carbon-carbon double bond(1). Evidence presented here shows that acrylonitrile may in certain cases alternatively act as a donor molecule via the cyanide group in a similar manner to acetonitrile(2).

(1) A. R. Luxmore and M. R. Truter, *Proc. Chem. Soc.* 466, 1961.

(2) W. Strohmeier and K. Gerlach, *Z. Naturf.* **15 b**, 622 (1960).

On refluxing a large excess of acrylonitrile in strong ultra violet radiation with 2 g of tungsten hexacarbonyl for many hours it is possible to isolate a few mg of pentacarbonylacrylonitriletungsten, I, as one of the products. (Found: C, 25·63; H, 0·76; N, 3·55; M (Cryoscopic in benzene) 385; 397. Calc. for I; C, 25·5; H, 0·80; N, 3·77; M, 377). Unchanged tungsten hexacarbonyl can only be removed from the pale yellow crystals of I by repeatedly passing an ether solution through an alumina column.

I was exceedingly soluble in all the solvents tried, except water. It could be precipitated out of the petroleum ethers by cooling but remained in other solvents to their freezing points. Solutions in carbon tetrachloride and chloroform deteriorated rapidly on standing. It melted at 74–75° and decomposed at a slightly higher temperature in high vacuum without subliming. A sample of I (0·28 m moles) yielded 0·10 m moles of carbon monoxide and 0·09 m moles of acrylonitrile on heating to 120° for 3 hr: the dark brown product evolved a further 0·16 m moles of carbon monoxide at 200°. The final residue afforded 0·35 m moles of carbon monoxide when treated with nitric acid.

The infra red spectrum of I is shown in the Table. In sharp contrast to other acrylonitrile complexes this compound shows bands in the regions of the spectrum associated with the $C=C$ stretching and $=CH_2$ bending modes; the $C\equiv N$ band has also moved to higher frequencies which might be expected if the cyanide group were co-ordinated to the metal atom(3). Furthermore, the region 650–1300 cm^{-1} in the tungsten complex is similar to that of acrylonitrile itself and bears little resemblance to the spectrum of tetracarbonylacrylonitrileiron. The proton magnetic resonance spectrum of the sample dissolved in benzene (Fig. 1), though complex, is remarkably similar to that obtained for free acrylonitrile(4), except the whole spectrum has moved about 0·6 p.p.m. to higher field. This, again, is consistent with a relatively unperturbed vinyl skeleton in the compound, which one would not expect to be the case in structure B.

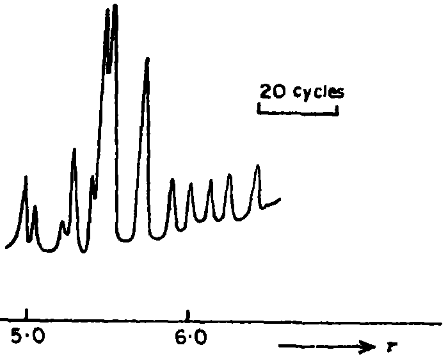

FIG. 1. Proton Magnetic Resonance Spectrum of Pentacarbonylacrylonitriletungsten in benzene at 40 Mc/s.

$CH_2=CHC\equiv N\rightarrow W(CO)_5$

A

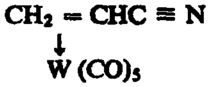

$$\begin{array}{c} CH_2=CHC\equiv N \\ \downarrow \\ W(CO)_5 \end{array}$$

B

Thus all the evidence to hand points strongly to structure A in which the cyanide group is coordinated to the tungsten. It may well be significant that I is the most stable of the acrylonitrile - metal carbonyl derivatives.

Acknowledgements—I wish to thank Imperial Chemical Industries Ltd., for a Fellowship and Dr. M. L. H. GREEN and Dr. N. SHEPPARD for valuable discussion.

A. G. MASSEY,

University Chemical Laboratory
Lensfield Road, Cambridge

(3) D. A. DOWS, A. HAIM and W. K. WILMARTH, *J. Inorg. Nucl. Chem.* 21, 33 (1962); H. A. BRUNE and W. ZEIL, *Z. Naturf.* 16 a, 1251 (1961).

(4) C. N. BANWELL, Ph.D. Thesis, Cambridge.

TABLE—INFRA RED SPECTRA: MAIN PEAKS
(Frequencies in cm^{-1}.)

$(CH_2CHCN)W(CO)_5$ in Nujol	CH_2CHCN film	$(CH_2CHCN)Fe(CO)_4$ in Nujol	Assignments
2255 w	2214 m	2210 m	C ≡ N Stretch
2089 m	—	2112 m	C ≡ O Stretch
1957 s	—	2050 sh	C ≡ O Stretch
1938 s	—	2038 s	C ≡ O Stretch
1900 m	—	2015 s	C ≡ O Stretch
1607 w	1608 w	—	C = C Stretch
—	—	1467 w	
1417 m	1417 m	—	= CH_2 bend
—	—	1362 w	
1288 m	—	—	
—	—	1186 m	
—	—	1017 w	
975 sh	986 sh	—	
963 s	967 v.s.	—	= CH_2 out of plane wag.
948 sh	—	—	
—	—	952 w	
—	—	890 w	
—	—	787 w	
665 m	677 m	—	

s, strong; m, medium; w, weak; sh, shoulder.

J. Inorg. Nucl. Chem., 1962, Vol. 24, pp. 1175 to 1179. Pergamon Press Ltd. Printed in Northern Ireland

THE NEUTRON-DEFICIENT YTTRIUM ISOTOPES ^{82}Y, ^{83}Y AND ^{84}Y*

V. Maxia†, W. H. Kelly‡ and D. J. Horen
Lawrence Radiation Laboratory, University of California, Berkeley, California

(*Received 5 March* 1962)

Abstract—The neutron-deficient yttrium isotopes ^{82}Y, ^{83}Y and ^{84}Y have been produced by irradiations with the Berkeley heavy-ion linear accelerator. Where possible, identifications were made by establishing genetic relationships with known daughter or granddaughter activities. The half-life of ^{84}Y determined by direct decay is 39 ± 2 min. By a series of timed chemical separations, the following half-lives have been established: ^{82}Y, 9 ± 3 min; ^{83}Y, 8 ± 2 min. No information pertaining to the radiations emitted in the decay of these yttrium isotopes, other than ^{84}Y, has been obtained. The γ-ray spectra of ^{84}Y and ^{83}Sr are shown.

Early attempts to study the decay of ^{82}Y revealed that its half-life was much shorter than the 70 min previously reported by Caretto and Wiig.(1) These authors also reported the half-life of ^{85}Y as 5 hr. From other work at this laboratory, in which ^{85m}Sr was chemically separated from yttrium at regular intervals, it was found that ^{85}Y has a 3 hr half-life.(2) The apparent disagreement in the half-life for ^{85}Y as found by Caretto and Wiig(1) and Kim *et al.*(2) has been resolved by the discovery of a 5 hr isomeric state in ^{85}Y.(3) The present work was undertaken in order to clarify the situation pertaining to the neutron-deficient yttrium isotopes with $A < 84$. In this paper we report on the identification of ^{82}Y, ^{83}Y and ^{84}Y.

1. EXPERIMENTAL METHOD

The Berkeley heavy-ion linear accelerator (Hilac) was used to produce neutron-deficient yttrium isotopes by the reactions ^{75}As(^{12}C, xn)$^{87-x}$Y and ^{69}Ga(^{16}O, xn)$^{85-x}$Y. For convenience, most of the data were obtained from bombardments of thick targets of powdered arsenic metal with about 120 MeV carbon ions, while other reactions were mainly used for corroborative purposes. The irradiation times varied from 5 min to 2 hr, depending upon the particular activities being studied. The yttrium activities reported here were also produced by spallation of natural strontium with 240 MeV protons in the Berkeley 184 in. cyclotron. To aid in the identification of ^{84}Y, a few milligrams of enriched ^{84}Sr§ were irradiated with 5- and 15 MeV deuterons in the Crocker 60 in. cyclotron.

The half-lives of ^{82}Y and ^{83}Y were determined by establishing their genetic relationships to known strontium and rubidium isotopes by means of timed chemical separations of daughter activities. Photon spectra were examined with a 7·62 cm × 7·62 cm NaI(Tl) crystal mounted on a Dumont 6363 photomultiplier coupled to a multichannel pulse-height analyser. Positron spectra were measured with a 2·5 cm diam. × 1·25 cm plastic scintillator, and gross β-counting was done with an end-window, flowing-methane proportional counter.

---

* Work done under the auspices of the U.S. Atomic Energy Commission.

† Permanent address: Laboratorio di Radiochimica, Universitá di Pavia, Pavia, Italy.

‡ On leave from the Department of Physics and Astronomy, Michigan State University, East Lansing, Michigan.

§ Obtained from separated Isotopes Division, Oak Ridge National Laboratory, Oak Ridge Tennessee.

(1) A. A. Caretto, Jr. and E. O. Wiig, *J. Amer. Chem. Soc.* 74, 5235 (1952).

(2) Y. E. Kim, D. J. Horen and J. M. Hollander. Unpublished data (1960).

(3) D. J. Horen and W. H. Kelly, *Bull. Amer. Phys. Soc.* 7, 341 (1962); *Bull. Amer. Phys. Soc.* 7, 419 (1962).

2. CHEMICAL PROCEDURES

After irradiation, the arsenic targets were dissolved in hot *aqua regia* and boiled to dryness. The residue was dissolved in 5 ml of 0·1 N HCl from which the yttrium was extracted into a 10-ml solution of 1·5 M di-2-ethyl-hexyl phosphoric acid (i.e., HDEHP) and toluene.(4) The organic phase, containing the yttrium activities, was washed several times with 0·1 N HCl, after which timed chemical separations (milks) of the daughter strontium and rubidium activities were conducted by washing with 0·1 N HCl. The "milk" intervals were varied from 5 to 17 min in different experiments.

In some experiments the strontium and rubidium fractions were separated by using the standard techniques of coprecipitation of $Sr(NO_3)_2$ with $Ba(NO_3)_2$ by the addition of fuming nitric acid and chilling.(5)

3. EXPERIMENTAL RESULTS

3·1 *Yttrium*-82

After an irradiation of powdered arsenic metal with 120 MeV carbon ions, the genetic relationship of ^{82}Y to its daughter ^{82}Sr was established by a series of timed chemical separations (milkings). In these experiments yttrium was extracted into a solution of toluene and HDEHP while strontium was back-extracted into 0·1 N HCl.

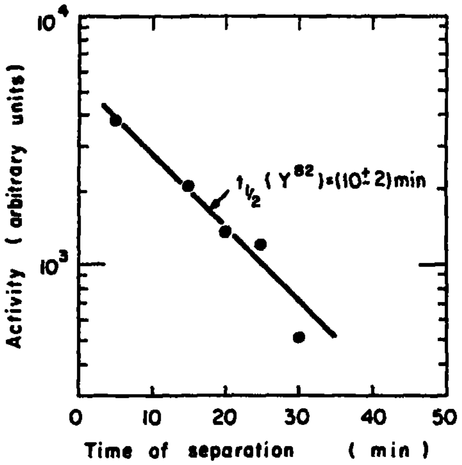

FIG. 1.—Yields of 2·0–3·0 MeV positrons of ^{82}Sr–^{82}Rb decay as a function of time of chemical separation of strontium from yttrium parent.

Several days after the milking experiments were preformed, the strontium fractions were chemically isolated and measured with the scintillation spectrometer and proportional counter. From these measurements it was found that annihilation radiation, a weak 770 keV photon, and approximately 3 MeV positron branch decayed with about a 25 day half-life. These data are attributable to the decay of ^{82}Sr–^{82}Rb–^{82}Kr, since it is known that 25 day ^{82}Sr decays by electron capture to 1·3 min ^{82}Rb, which in turn decays to ^{82}Kr with the emission of 3·1 MeV and 2·3 MeV positron branches and a weak 777 keV photon.(6) By counting the positrons with energies between 2 and 3 MeV, the yield of ^{82}Sr as a function of the time of the chemical separation of strontium from yttrium was obtained. Typical results are shown in Fig. 1. From a number of such experiments, the average value obtained for the half-life of ^{82}Y is 9 ± 3 min.

---

(4) D. F. PEPPARD, G. W. MASON and S. W. MOLINE, *J. Inorg. Nucl. Chem.* **5**, 141 (1957).

(5) D. N. SUNDERMAN and C. W. TOWNLEY, NAS-NS 3010 January (1960).

(6) *Nuclear Data Sheets*, National Academy of Sciences—National Research Council, NRC 59-1-67 (National Research Council, Washington, D.C.)

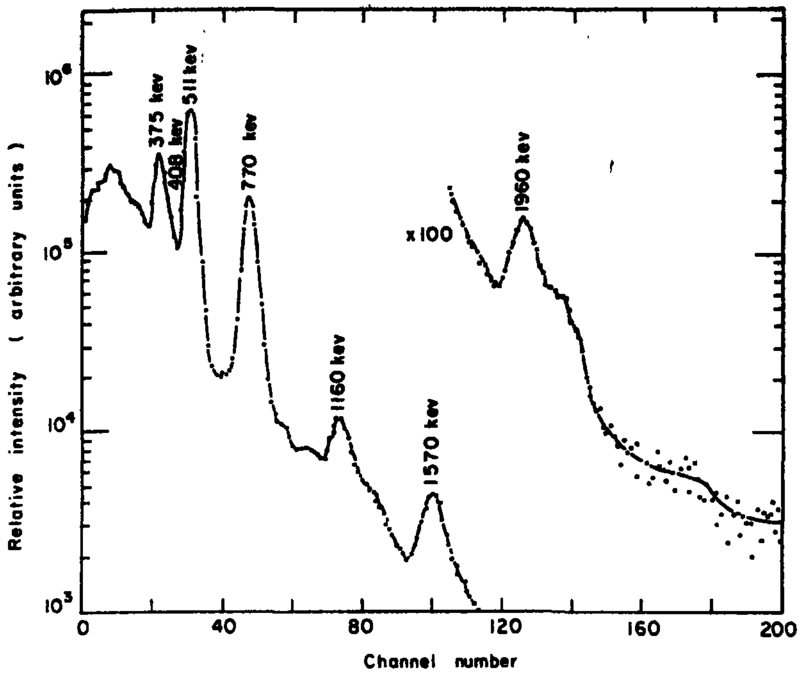

FIG. 2.—γ-ray spectrum of 34 hr ^{83}Sr taken with a 7·6-cm × 7·6-cm NaI(Tl) crystal. A 0·75 cm carbon absorber was placed between the source and crystal to reduce bremmstrahlung and annihilation-in-flight photons caused by the positrons.

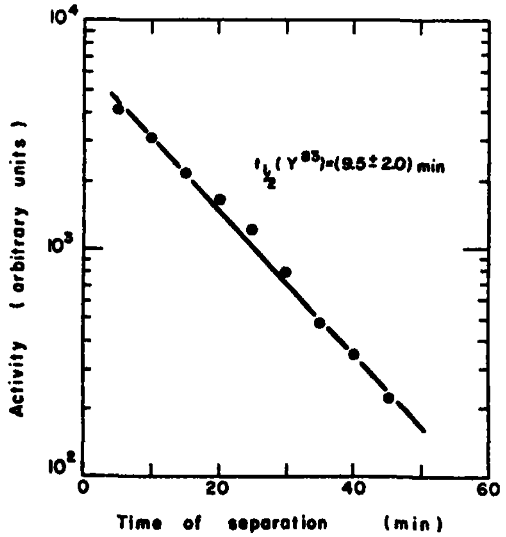

FIG. 3.—Yields of the 375 keV γ-ray of ^{83}Sr as a function of time of chemical separation of strontium from the parent yttrium.

3.2 *Yttrium*-83

The γ-ray spectra of the strontium fractions milked from yttrium contained prominent peaks at 38, 375, 511, 770, 1160 and 1520 keV which decayed with a 34 hr half-life. This activity is assigned to ^{83}Sr, since the latter is known to decay with a similar half-life with the emission of a 1·2 MeV positron branch.[7] A typical γ-ray spectrum of ^{83}Sr is shown in Fig. 2. Fig. 3 shows the yield of the 375 keV peak as a function of the time of the chemical separation of strontium from yttrium. Consideration of the data from several experiments utilizing different production modes of yttrium and different milk times leads to an average value of 8 ± 2 min for the half-life of ^{83}Y.

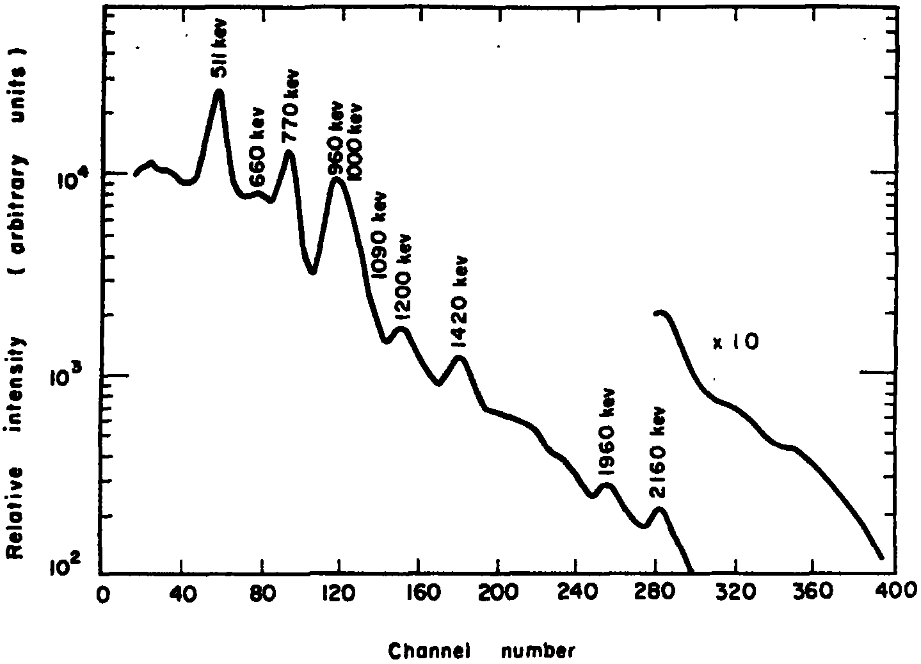

Fig. 4.—Collimated photon singles spectrum of 39 min ^{84}Y taken with a 7·6 cm × 7·6 cm NaI(Tl) crystal.

3.3 *Yttrium*-84

When the yttrium fraction obtained from the bombardment of arsenic with C^{12} ions was chemically repurified approximately 2 hr after the irradiation, the gamma-ray spectrum decayed with 39 ± 2 min (see Fig. 4). Strontium fractions chemically separated from the yttrium activity at fixed time intervals (40 min) contained only 150 and 235 keV photons arising from the decay of ^{85m}Sr and a very weak 513 keV photon from the decay of ^{85}Sr. The half-life of ^{85}Y determined in this way is 3·0 ± 0·2 hr, in good agreement with the results of Kim *et al.*[8] The 39 min yttrium activity was also produced by irradiating strontium enriched in ^{84}Sr with 15 MeV deuterons, but not with 5 MeV deuterons. These data are consistent only with the assignment of the 39 min activity to ^{84}Y. This half-life is in good agreement with that obtained by Yamazaki *et al.*[9]

---

[7] S. V. Castner and D. H. Templeton, *Phys. Rev.* **88**, 126 (1952).

[8] T. Yamazaki, H. Ikegami, M. Sakai, K. Saito, Y. Hashimoto, M. Fujioka, H. Ohnuma, E. Takekoshi, J. Matsumoto and A. Hashizume. Unpublished data; M. Sakai. Private communication (1961).

DISCUSSION

In this work, the neutron-deficient yttrium isotopes with mass numbers 82, 83 and 84 have been synthesized and their half-lives found to be considerably shorter than those previously reported. Owing to lack of time, no information has been obtained concerning the radiations emitted in the decay of these isotopes, with the exception of ^{84}Y.

Acknowledgements—One of us (V. M.) wishes to acknowledge the Conference Board of Associated Research Councils, Washington D.C., for a fellowship, and to thank Professor I. PERLMAN for the hospitality accorded her while a guest at the Lawrence Radiation Laboratory. We wish to thank Drs. S. S. MARKOWITZ, R. M. DIAMOND and J. M. HOLLANDER for many helpful discussions. We wish also to thank Mr. J. A. HARRIS for his assistance in one of the chemical separations, and the operating crews of the Hilac and the 60 in. and 184 in. cyclotrons for providing the irradiations.

J. Inorg. Nucl. Chem., 1962, Vol. 24, pp. 1181 to 1184. Pergamon Press Ltd. Printed in Northern Ireland

RELATIVE CROSS-SECTIONS FOR THE ^{127}I(d,p) REACTION

D. J. Silvester
Medical Research Council, Cyclotron Unit,
Hammersmith Hospital, Ducane Road, London, W.12

and

G. C. Jack
Queen Elizabeth Hospital for Children,
Hackney Road, London, E.2

(*Received* 25 *March* 1962; *in revised form* 17 *April* 1962)

Abstract—Yields of ^{128}I from the ^{127}I(d,p) reaction have been measured for deuteron energies up to 14·8 MeV relative to the yield at 9·98 MeV. In agreement with calculation, the results indicate that the cross-section for this reaction reaches a maximum value at about 11 MeV.

In the course of an investigation into the usefulness of the external deuteron beam of the Medical Research Council's cyclotron as a tool for activation analysis, we have measured the relative cross-sections for the ^{127}I(d,p)^{128}I reaction for deuteron energies up to 15 MeV.

A previous measurement by Balestrini,[1] with deuteron energies up to 18 MeV, suggested that the cross-section reaches a maximum value at about 11 MeV, and remains essentially constant at higher energies. This was unexpected, since calculation showed that for deuteron energies above about 11 MeV, the compound nucleus resulting from an Oppenheimer-Phillips (d,p) process may be left with sufficient energy to emit a neutron, which would lead to a drop in the measured cross-section. The present results show closer agreement with this expectation.

EXPERIMENTAL PROCEDURE

Sample preparation

Samples were prepared for deuteron bombardment by absorbing known weights of standardized potassium iodide solution (each containing about 1 mg I$^-$) on small filter-paper disks (Whatman No. 542, 20 mm diam.) which were then dried in a vacuum desiccator. Each filter-paper disk was subsequently completely enclosed in a 1 in. square envelope made of 0·001 in. 99·999 per cent aluminium foil, in such a fashion that only one thickness of the foil was interposed between the filter-paper and the deuteron beam, unless further thickness of aluminium were deliberately added to reduce the beam energy. This method of sample preparation resulted from our initial interest in the "deuteron activation analysis" of iodine-containing fractions from biological specimens which had been separated by paper-chromatography. When subsequent experiments indicated that iodine was not lost from such samples in the course of bombardment, the method, which is a conveniently simple one, was continued.

Deuteron irradiations

The aluminium envelopes, up to nine at a time, were separately fixed around the face of a 10 in. diameter aluminium wheel, all at the same radius, by screws, the heads of which just overlapped the edge of each envelope without shielding the filter-paper disk inside. This wheel could be set up with its axis parallel to the deflected deuteron beam, and at a fixed distance from the foil window through which the beam emerges from the cyclotron. Immediately in front of the wheel, a collimator reduced the spread in width of the beam from about 4 to 2 in.; the vertical spread was not more than about 0·25 in., and no attempt was made to collimate the beam in this direction. On rotating the wheel (at 13 rev/sec) each sample passed in turn rapidly across the centre of the partially collimated deuteron

---

(1) S. J. Balestrini, *Phys. Rev.* **95**, 1502 (1954).

beam, so that in the course of an irradiation each was exposed to the same number of incident deuterons. The main fluctuations in the deuteron beam were essentially slow compared with the speed of rotation of the sample wheel.

Ten irradiations were carried out after preliminary work had established the reproducibility of the method. The duration of each was 30–45 min, and the beam currents reaching the rotating wheel varied from 10–25 μA. In each irradiation, three samples were covered with an additional 0·015 in. of aluminium, reducing the incident beam energy to 9·98 MeV. Additional samples, three at a time, were exposed to different incident beam energies by varying the thickness of aluminium absorbers used. Thus, all cross-section measurements were made relative to that for 9·98 MeV deuterons.

Estimation of the ^{128}I yield

About 30 min after irradiation, each envelope was removed from the wheel and was immersed completely, without opening, in 5 ml 3M NaOH to which a known weight (~10 mg) of additional iodide carrier had been added. On warming, the aluminium foil dissolved completely and a clear solution was obtained. (After a few minutes of irradiation the filter-paper disks disintegrate: the residue is soluble in hot NaOH.) Addition of excess NH_4Cl solution precipitated the aluminium as $Al(OH)_3$, and the excess ammonia was boiled off. The solution was acidified and oxidized with HNO_3 and $NaNO_2$, and the liberated iodine extracted into 5 ml CCl_4. This was followed by back-extraction into 3 ml of aqueous bisulphite, and a repeated oxidation and extraction into 2 ml CCl_4. After carefully washing the organic phase, the iodine was finally back-extracted into 2 ml of standard (0·1N) sodium arsenite solution. The latter, with a further 2 ml of water used in washing the organic phase, was carefully recovered and transferred to a small polythene tube in which it was made up to 5 ml. This tube was then sealed, and placed in a well-type scintillation counter for measurement of the ^{128}I activity. Samples were ready for counting in 60–90 min after the end of bombardment.

The samples decayed with the expected 25 min half-life(2) and were counted for about 5 hr, or until their activities were no longer distinguishable from background. Traces of long-lived activity were found in samples bombarded at above 10 MeV; these may have been due to 13·3 day ^{126}I, resulting from ($d,p2n$) or ($n,2n$) reactions, but were at such a low level that identification was not possible.

After counting, the recovered iodine was estimated by titration of the excess arsenite: yields of about 50 per cent were customarily obtained. The measured activities were then corrected for decay and chemical recovery, and the activity per mg of iodine bombarded was calculated.

Preliminary irradiation

After numerous experiments had shown the reproducibility of the chemical procedures, it was important to establish that the "spinning-wheel" technique ensured that the samples were uniformly exposed to the deuteron beam. To do this, a preliminary run was carried out in which five samples were irradiated at the same energy, 14·8 MeV. The recovery and counting procedures were carried out as described above, and the corrected activities showed a standard deviation of $\pm 2{\cdot}5$ per cent from the mean.

In subsequent irradiations, where there were always three samples bombarded at any one energy, the resulting activities were again found to agree to within a few per cent. This close agreement, coupled with the result of the preliminary irradiation described above, was considered good evidence that no iodine was lost from the samples in the course of bombardment.

DEUTERON BEAM ENERGY

No direct measurement of the beam energy has been made, but the results of previous experiments with the M.R.C. cyclotron indicated that the maximum energy of the deflected deuteron beam was $16{\cdot}2 \pm 0{\cdot}2$ MeV.(3) The error quoted is the probable error in the measurements, and not the spread in beam energy which is believed to be very small over the region through which the samples were passed. The energy of the deuteron beam when it reached the inside of the aluminium sample envelopes was computed from the range-energy relations for protons in air and aluminium evaluated by Sternheimer(4). The energy widths of the plotted points in Fig. 1 reflect the uncertainty in the initial beam energy.

(2) D. Strominger, J. M. Hollander and G. T. Seaborg, *Rev. Mod. Phys.* **30** (Part 2), 706 (1958).

(3) J. F. Fowler, *Private communication* (1961).

(4) R. M. Sternheimer, *Phys. Rev.* **115**, 137 (1959).

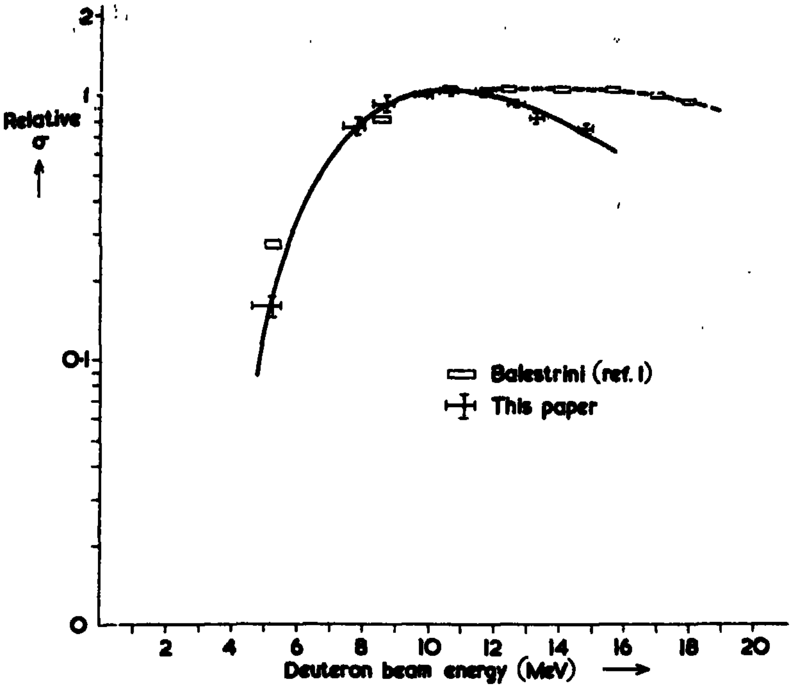

FIG. 1.—Relative cross-sections for the $^{127}I(d,p)^{128}I$ reaction.

An additional uncertainty in the beam energy values results from the thickness of the original filter-paper samples, but as these rapidly disintegrate in the deuteron beam, and as the iodine is distributed throughout their thickness, this cannot be accurately evaluated. However, an upper limit for this uncertainty can be estimated by considering a hypothetical case where the iodine inside the aluminium envelope is covered by a layer of Melinex ($C_{10}H_8O_4$), for which range-energy data are available,[5] of similar surface density, 9·5 mg/cm^2, to the filter-paper ($C_6H_{10}O_5$). The energy losses would be about 2 per cent at 15 MeV, 4·5 per cent at 10 MeV and 15 per cent at 5 MeV, but the shape of the curve in Fig. 1 would not be altered significantly as a result.

RESULTS AND DISCUSSION

A summary of the results is given in Table 1. The error shown at each energy is the standard deviation from the mean of the experimental results. At energies up to 11·7 MeV, the relative cross-sections were found to be in good agreement with BALESTRINI's, but as can be seen in Fig. 1, where the two sets of results are plotted for comparison, they differ significantly at higher energies.

It can be shown[6] that the (d,pn) reaction may compete with the (d,p) reaction when the deuteron energy, ϵ_d, is greater than

$$\epsilon_d^* = (Ze^2/R) + B$$

where R is the interaction distance for the deuteron with the target nucleus, of charge

---

[5] J. F. FOWLER and D. N. SLATER. To be published.

[6] J. M. BLATT and V. F. WEISSKOPF, *Theoretical Nuclear Physics*, Chap. 9. J. Wiley, New York (1952).

Z and mass A, e is the electronic charge, and B is the binding energy of the deuteron (2·23 MeV).

If, following SHAPIRO(7), we adopt for deuteron reactions the interaction distance $R = (r_0 A^{\frac{1}{3}} + 1{\cdot}21) \times 10^{-13}$ cm, then when $r_0 = 1{\cdot}3$, we compute $\epsilon_d{}^* = 12{\cdot}1$ MeV, and when $r_0 = 1{\cdot}5$, $\epsilon_d{}^* = 10{\cdot}9$ MeV. The shape of the curve in Fig. 1 suggests that $r_0 = 1{\cdot}5$ is favoured.

TABLE 1.—VALUES OF THE CROSS-SECTION FOR THE ^{127}I$(d,p)^{128}$I REACTION.

Beam energy (MeV)	Relative σ
5·26	0·158 ± 0·015
7·87	0·757 ± 0·053
8·76	0·932 ± 0·059
9·93	1·000
10·74	1·024 ± 0·024
11·70	1·021 ± 0·038
12·70	0·932 ± 0·022
13·34	0·825 ± 0·035
14·84	0·745 ± 0·029

Acknowledgements—The authors wish to acknowledge with thanks the skilled technical assistance of Miss N. D. WHITE, and the help of the M.R.C. cyclotron crew with the irradiations, and to thank the Director of the Cyclotron Unit, Mr. D. D. VONBERG, for permission to publish this work.

---

(7) M. M. SHAPIRO, *Phys. Rev.* **90**, 171 (1953).

J. Inorg. Nucl. Chem., 1962, Vol. 24, pp. 1185 to 1189. Pergamon Press Ltd. Printed in Northern Ireland

FISSION OF ^{232}Th BY 9·5 MeV DEUTERONS: YIELD-MASS CURVE*

M. V. RAMANIAH† and ARTHUR C. WAHL
Department of Chemistry, Washington University, St. Louis, Missouri

(*Received* 8 *December* 1961)

Abstract—Relative yields for sixteen fission products from fission of ^{232}Th induced by 9·5 MeV deuterons are reported. The yield-mass curve drawn to fit these yields is double humped, has a trough-to-peak ratio of 0·15, and is symmetrical about $A = 115$. The heavy mass peak is in essentially the same position on the A-axis as the heavy mass peak for thermal-neutron fission of ^{235}U; the position of the light mass peak is 2 to 3 mass units lower in A than that of the ^{235}U light mass peak. An analysis of the curve indicates that most fissions result from capture of the entire deuteron and that the average number of prompt neutrons emitted is 4 ± 1.

THE results of yield measurements carried out during 1954–1956 are reported in this paper. Relative yields were determined by comparison of fission-product radioactivities from ^{232}Th fission induced by 9·5 MeV deutrons with those from ^{235}U thermal-neutron fission, for which fission yields are known.(1) Approximate absolute yields for ^{232}Th fission products were estimated by normalization of a symmetrical yield-mass curve drawn to fit the relative yields.

The energies of the deuterons inducing fission in a 2 mil target-foil varied from 8·5 to 9·9 MeV, one-half of the fissions being produced by deuterons with energies $>9·5$ MeV. Less than 0·5 per cent of the fissions were induced by neutrons. These conclusions were drawn from the results of experiments with stacked target foils, from the excitation function determined by JUNGERMAN(2), and from the maximum deuteron energy of 9·9 ± 0·1 MeV in the deflected beam of the Washington University Cyclotron. Water cooling of the target and limitation of the beam current to $<100\,\mu$A prevented loss of volatile fission products.

Uranium with normal isotopic composition was irradiated in the Los Alamos Homogeneous Reactor in a thermal-neutron flux of 5×10^{11} cm^{-2} sec^{-1}. Because of its 2·3 hr half-life ^{83}Br was produced in uranium exposed to thermal neutrons near the cyclotron.

Uranium and thorium metals supplied by A. D. MACKAY were used as targets. Irradiated targets were dissolved in hydrochloric acid, and aliquots of the solutions were taken for radiochemical analysis. After addition of carriers and promotion of exchange between carrier and fission product, purification was accomplished with modifications of standard radiochemical procedures.(3,4,5) Purified samples were weighed, covered with Scotch tape (6·1 mg/cm^2), and measured for radioactivity with a flow-type β-proportional counter.

---

* Abstracted from a dissertation submitted by M. V. RAMANIAH in partial fulfillment of the requirements for the Ph.D. Degree, Washington University, 1956. The work was supported in part by the United States Atomic Energy Commission.

† Present address: Radiochemistry and Isotope Division, Atomic Energy Establishment, Trombay, Bombay-73, India.

(1) S. KATCOFF, *Nucleonics* 18, No. 11, 201 (1960).
(2) J. JUNGERMAN, *Phys. Rev.* 79, 632 (1950).

Irradiated thorium metal was dissolved with difficulty, two steps being required. The target was refluxed with 6 F HCl containing SiF_6^{2-} catalyst, and then the residue from this treatment was again refluxed with fresh 6 F HCl and SiF_6^{2-}. Gases escaping from the reflux condenser were trapped in 2 F NaOH, which was subsequently acidified and added to the HCl solutions. Solutions were filtered before aliquots were taken. It was found that the ratios of fission-product radioactivities in the residue from the first refluxing were the same as those in the first HCl solution. It was also found that recoveries of bromine, iodine and zirconium fission products were incomplete unless carrier was present during the dissolution process. Therefore, these carriers were added before dissolution.

RESULTS

The experimentally determined "R values", the ratio of yield from ^{232}Th($d_{9.5}, f$) to yield from ^{235}U(n_{th}, f) relative to the ratio for ^{99}Mo ($R = 1{\cdot}00$), are listed in column 2 of Table 1. Except for ^{153}Sm and ^{156}Eu, the values are averages of determinations from two or more irradiations. All determinations were made from measurements on two, three or four samples.

Relative values of fission yields for the ^{232}Th($d_{9.5}, f$) reaction were obtained by multiplying the R values by the known fission yields(1) from the ^{235}U(n_{th}, f) reaction. These relative yields were then used to construct a smooth, symmetrical yield-mass curve. This curve was normalized to give a total yield of 200 per cent. The result is shown in Fig. 1 as the solid line. The normalized "absolute" fission yield values from the ^{232}Th($d_{9.5}, f$) reaction are shown in Fig. 1 as filled circles and are listed in the third column of Table 1.

Many sources of uncertainty are inherent in this treatment. Probably the largest is contributed by the assumption of a smooth, symmetrical yield-mass curve. This assumption is justified only to the extent that it is the simplest way of fitting the limited data that are available. However, the assumption affects only the accuracy of the absolute values; the relative yield values are as accurate as the measurements and the values of the yields from the ^{235}U(n_{th}, f) reaction. Uncertainties or irregularities in the ^{235}U yields are, of course, reflected in the ^{232}Th yields. This is illustrated by the fluctuation in the relative yields of ^{111}Ag, ^{112}Pd and ^{115}Cd fission products for which the R values change smoothly.

Another possible source of uncertainty is the assumption that the genetic history of a fission product is the same for the two fission reactions. For the products determined deviations from this assumption could cause appreciable errors only for ^{83}Br and ^{133}I. If all of the ^{83}Br were derived from 25 min ^{83}Se in the ^{232}Th($d_{9.5}, f$) reaction instead of 44 per cent as occurs in the ^{235}U(n_{th}, f) reaction, the yield would be in error by about

(3) C. D. CORYELL and N. SUGARMAN (Editors), *Radiochemical Studies: The Fission Products*, NNES, Plutonium Project Record, Div. IV, Vol. 9, McGraw-Hill, New York (1951).

(4) J. KLEINBERG (Editor), *Collected Radiochemical Procedures*, Los Alamos Scientific Laboratory Report LA-1721 (1954). (Unpublished).

(5) M. LINDNER (Editor), *Radiochemical Procedures in Use at the University of California Radiation Laboratory*, University of California Radiation Laboratory Report UCRL-4377 (1954). (Unpublished).

(6) E. YELLIN. Ph.D. Thesis, Massachusetts Institute of Technology, Cambridge, Mass. (1960).

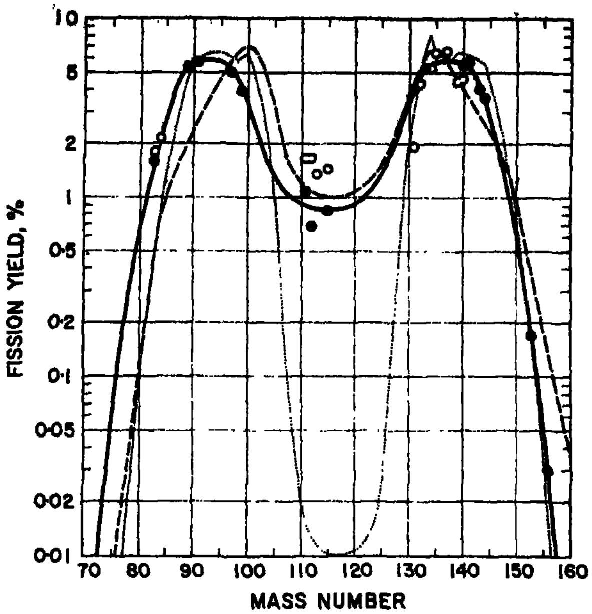

FIG. 1.—Fission yields and yield-mass curves.
—●— ^{232}Th($d_{9\cdot5}$, f) (This article)
○ ^{232}Th($d_{13\cdot6}$, f) (Ref. 7)
· · · · ^{235}U(n_{th}, f) (Ref. 1)
— — — ^{238}U(d_{10}, f) (Ref. 11)

TABLE 1.—YIELDS FROM 9·5 MEV DEUTERON FISSION OF ^{232}Th

Fission product	R value*	Fission yield (%)
^{83}Br	4·44 ± 0·07	1·6
^{89}Sr	1·70 ± 0·02	5·4
^{91}Sr	1·50 ± 0·03	5·8
^{97}Zr	1·27 ± 0·02	5·0
^{99}Mo	"1·00"	4·0
^{111}Ag	86 ± 2	1·1
^{112}Pd	103 ± 4	0·68
^{115m}Cd	123 ± 3	0·06 } 0·84
^{115}Cd	122 ± 4	0·78
^{131}I	2·13 ± 0·06	4·1
^{133}I	1·22 ± 0·04	5·3
^{140}Ba	1·30 ± 0·04	5·5
^{141}Ce	1·37 ± 0·04	5·8
^{143}Ce	1·02 ± 0·02	4·0
^{144}Ce	0·99 ± 0·04	3·7
^{153}Sm	1·56	0·17
^{156}Eu	3·24	0·03

* Ratio of yield from ^{232}Th($d_{9\cdot5}$, f) to yield from ^{235}U(n_{th}, f) relative to the ratio for ^{99}Mo.

10 per cent. If no ^{133}I were derived from 63 min ^{133}Te in the ^{232}Th($d_{9\cdot5}$, f) reaction, instead of 90 per cent as in the ^{235}U(n_{th}, f) reaction, the yield would be in error by about 4 per cent.

As is true for any yield-mass curve determination, there is some uncertainty in equating the fission-product yield and the total chain yield. There is little direct information on the point. YELLIN(6) determined the fractional independent yield of ^{112}Ag to be 0·044 for ^{232}Th fission by 13·6 MeV deuterons, and the independent yield should be smaller at lower energies. ALEXANDER and CORYELL(7) measured independent yields for several products from the ^{232}Th($d_{13\cdot6}$, f) reaction and concluded that these were adequately represented by the equal-charge-displacement (*ECD*) postulate.(8) Application of the postulate to the fission reaction with 9·5 MeV deuterons indicates that the fractional cumulative yields are $> 0\cdot98$ for all products listed in Table 1 except for ^{97}Zr and ^{140}Ba, for which the predicted yields are 0·92 and 0·91–0·98, respectively.* Application of a recent empirical charge-distribution treatment,(9) developed for ^{235}U(n_{th}, f), to the ^{232}Th($d_{9\cdot5}$, f) reaction indicates that fractional cumulative yields are $>0\cdot98$ for all fission products listed in Table 1 except for ^{97}Zr, for which the predicted yield is 0·96. Since these corrections are small and uncertain, none were made.

DISCUSSION

The ratio of valley to peak yields for the yield-mass curve is 0·15. Comparison of this value with empirical correlations(10,11) between valley-to-peak ratios and excitation energies of compound nuclei indicates that the excitation energy of the compound nucleus involved in the ^{232}Th($d_{9\cdot5}$, f) reaction is about 17 MeV. If the whole deuteron were captured the excitation energy of ^{234}Pa is calculated from atomic masses(12) to be 17·8 MeV. If only the neutron were captured and the proton carried away no kinetic energy, the calculated excitation energy of ^{233}Th is 12·2 MeV. More probably the proton would carry away considerable kinetic energy; the most probable excitation energy of ^{233}Th is estimated to be 3 ± 2 MeV,(13) which is less than the fission threshold of about 6·4 MeV.(14) Thus most fission reactions must pass through the compound nucleus ^{234}Pa. This conclusion concerning capture of the deuteron agrees with that of SUGIHARA *et al.*(11) for deuteron induced fission of ^{238}U.

The yield-mass curve is symmetrically about $A = 115$, which implies an average loss of four neutrons during or prior to fission. Shifts in the symmetry point of > 1 mass unit give curves with appreciable deviations from the experimental data. We conclude, therefore, that $\bar{\nu} = 4 \pm 1$.

The open circles in Fig. 1 represent the relative yields from the ^{232}Th($d_{13\cdot6}$, f) reaction determined by ALEXANDER and CORYELL(7) and normalized to our data at the ^{89}Sr yield of 5·4 per cent. As can be seen the yields in the valley are larger at the higher energy as is expected. The ALEXANDER-CORYELL yield for ^{131}I is about a factor of two lower than our value; also, their ^{131}I yields for ^{238}U(d, f) reactions at several energies are nearly a factor of two lower than the Clark University values.(11) If the

---

* The value of $\bar{\nu} = 4$ was used; see the Discussion.

(7) J. M. ALEXANDER and C. D. CORYELL, *Phys. Rev.* **108**, 1274 (1957).

(8) A. C. PAPPAS, *Proceedings of the International Conference on the Peaceful Uses of Atomic Energy, Geneva*, 1955, Vol. 7, pp. 3–14. United Nations (1956).

(9) A. C. WAHL, R. L. FERGUSON, D. R. NETHAWAY, D. E. TROUTNER and K. WOLFSBERG, *Phys. Rev.* **126**, 1112 (1962).

(10) A. TURKEVICH, J. B. NIDAY and A. TOMPKINS, *Phys. Rev.* **89**, 552 (1953).

(11) T. T. SUGIHARA, P. J. DREVINSKY, E. J. TROIANELLO and J. M. ALEXANDER, *Phys. Rev.* **108**, 1264 (1957).

(12) B. M. FOREMAN, JR. and G. T. SEABORG, *J. Inorg. Nucl. Chem.* **7**, 305 (1958).

(13) J. M. BLATT and V. F. WEISSKOPF, *Theoretical Nuclear Physics*, p. 509. J. Wiley, New York (1952).

(14) E. K. HYDE, *A Review of Nuclear Fission: Part One-Fission at Low Energy*, p. 32. University of California Radiation Laboratory Report UCRL-9036 (1960). (Unpublished).

ALEXANDER-CORYELL value is in error, as we believe it to be, the principal evidence for the very broad valley in the yield-mass curve(7) for the ^{232}Th($d_{13\cdot 6}$, f) reaction is eliminated.

Fig. 1 also shows the yield-mass curves for the ^{235}U(n_{th}, f) and ^{236}U(d_{10}, f) reactions. As has been noted in comparison of yield-mass curves for other fission reactions, the position on the *A*-axis of the heavy mass peak is nearly constant, especially the position of the low-*A* side of the peak. The position of the light mass peak shifts with the *A* of the fissioning nucleus.

Acknowledgements—We wish to express our appreciation for numerous thermal-neutron irradiations to members of the Radiochemistry Group at Los Alamos and to the staff of the Los Alamos Homogeneous Reactor. Also, we wish to thank members of the Washington University Cyclotron crew for numerous deuteron irradiations.

J. Inorg. Nucl. Chem., 1962, Vol. 24, pp. 1191 to 1195. Pergamon Press Ltd. Printed in Northern Ireland

THERMODYNAMICS OF $PuCl_4$ FROM TRANSPIRATION DATA*

R. BENZ
Los Alamos Scientific Laboratory, University of California,
Los Alamos, New Mexico

(*Received* 26 *March* 1962; *in revised form* 2 *May* 1962)

Abstract—The free energy change for the reaction $PuCl_{3(s)} + \frac{1}{2}Cl_{2(g)} = PuCl_{4(g)}$ in the temperature range 400–750° was determined from transport in chlorine carrier gas. The molar free energy of reaction may be represented by the relation $\Delta F = 37700 - 28{\cdot}3\,T$(cal.), where T denotes degrees Kelvin. The standard free energy, enthalpy and entropy of formation of $PuCl_4$ are estimated.

THE stability of the III-oxidation-state actinide chlorides increases while that of the IV and higher oxidation states decrease with increasing atomic number. Thus UCl_4 and $NpCl_4$ are stable toward decomposition at room temperatures(1,2) but, although Pu(IV) has been reported(3,4) to exist in double salt chlorides with alkali elements, attempts to prepare pure $PuCl_4$ were unsuccessful.(5) A lower limit for the partial pressure of $PuCl_4$ (postulated compound) in chlorine gas has been determined(5) and, based upon analogy with UCl_4, the thermodynamic properties were estimated.(6)

In this investigation, the transpiration technique was used to study the reaction

$$PuCl_{3(s)} + \tfrac{1}{2}Cl_{2(g)} = PuCl_{4(g)} \tag{1}$$

for which the equilibrium constant may be written

$$K = \frac{p_{PuCl_4}}{p_{Cl_2}^{\frac{1}{2}}} \tag{2}$$

where p_{PuCl_4} and p_{Cl_2} denote respectively the partial pressures of $PuCl_4$ and Cl_2. Basically the method is to pass a stream of chlorine gas or chlorine-argon gas mixture (the carrier gas) over $PuCl_4$ crystals at a selected rate of flow. The equilibrated gas mixture is collected and the chemical composition determined. In order that the transpiration data be significant, it is required that the carrier gas flow be slow enough to saturate the gases with the reaction products but fast enough that diffusion effects be negligible. Wagner and Stein,(7) Merten,(8) and Hofmeister *et al.*(9) have discussed the design for apparatus which favours these conditions. Chlorine and argon gases were considerably above their normal boiling points (238 and 87°K, respectively). Thus, provided the partial pressure of the volatile reaction product $PuCl_4$ is sufficiently low, the ideal gas law and Dalton's law of partial pressure may be used to calculate the partial pressures of each component in the gas mixture.

---

* Work done under the auspices of the U.S. Atomic Energy Commission.

(1) L. BREWER, L. BROMLEY, P. W. GILLES and N. L. LOFGREN, *The Transuranium Elements*, NNES., Div. IV, Vol. 14B, p. 1111. McGraw-Hill, New York (1949).

(2) J. J. KATZ and E. RABINOWITCH, *The Chemistry of Uranium*, NNES., Div. VIII, Vol. 5, p. 450 McGraw-Hill, New York (1951).

(3) H. H. ANDERSON, *The Transuranium Elements*, NNES., Div. IV, Vol. 14B p. 793. McGraw-Hill, New York (1949).

(4) R. BENZ and R. DOUGLAS, *J. Inorg. Nucl. Chem.* 23, 134 (1961).

(5) B. M. ABRAHAM, B. B. BRODY, N. R. DAVIDSON, F. HAGEMANN, I. KARLE, J. J. KATZ and M. J. WOLF, *The Transuranium Elements*, NNES, Div. IV, Vol. 14B, p. 740. McGraw-Hill, New York (1949).

(6) L. BREWER, L. BROMLEY, P. W. GILLES and N. L. LOFGREN, *The Transuranium Elements*, NNES, Div. IV, Vol. 14B, p. 861. McGraw-Hill, New York (1949).

In what follows, it is shown that the reaction involved is

$$n\mathrm{PuCl}_{3(s)} + \frac{n}{2}\mathrm{Cl}_{2(g)} = (\mathrm{PuCl}_4)_{n(g)} \qquad (3)$$

for which one may take $n = 1$ since the analogous gaseous UCl_4 shows no association.(10)

EXPERIMENTAL

Materials. $PuCl_3$ was prepared by hydrochlorination of pure Pu(III) oxalate. It was vacuum distilled and stored as large crystals in a vacuum desiccator. Tank chlorine gas (Matheson and Co., 98·5 per cent) was used without treatment. Argon gas was dried and passed over uranium chips at 600°. Ambient atmospheric pressures were determined with an absolute mercury manometer.

Equipment. The 12 mm quartz reaction tube 35 cm long was closed at one end and provided, at the other end, with a tapered joint at the base of which was a side inlet for the carrier gas. The tapered joint served to receive and centre the condenser tube within the reaction tube. The condenser tube was fabricated from 6 mm quartz tubing and reduced to 1·5 mm tubing over the last 8 cm of length which, in its normal position, was located in the closed end of the horizontally positioned reaction tube. During a run, 10 cm length at the closed end of the reaction tube was charged with fine crystals of $PuCl_3$. This section, containing the $PuCl_3$, will be called the "reaction zone". The section of 1·5 mm tubing extended to within 5 mm of the closed end and was off-centred so as to rest in the upper part of the reaction zone, thus permitting a greater charge of $PuCl_3$ beneath. Carrier gas passed from the side inlet tube, over the $PuCl_3$ crystals and into the 1·5 mm opening of the condenser tube. Transported plutonium chloride was collected as $PuCl_3$ in the larger 6 mm section at the cool end of the condenser tube ($PuCl_4$ on cooling decomposes to $PuCl_3$). With the dimensions described above, effects of diffusion in the carrier gas were verified to be negligible by the determination of the rate of transport in chlorine under static conditions.

The reaction tube was heated in a wire-wound furnace controlled to a constant temperature (±2°C). The temperature was measured with a calibrated Pt–Rh thermocouple located adjacent to the reaction tube and near the entrance of the condenser tube. The temperature adjacent to the reaction tube at the reaction zone was found to be uniform to within 3°. Glass joints and stopcocks were lubricated and sealed with a heavy Fluorocarbon oil. The furnace and gas train were contained in a standard type stainless steel glove-box to protect personnel from hazards of radioactive decay (α-decay of Pu).

Procedure. To begin an experiment, the condenser provided with a reversed flow of carrier gas was positioned in the reaction tube charged with $PuCl_3$ crystals and the reaction tube was then introduced into the furnace. After temperature equilibrium was attained, the reversed gas flow was disconnected and the metered gas flow in the forward direction was begun. The carrier gas at ambient pressure was metered by displacement with concentrated H_2SO_4 from a calibrated two-litre flask. The H_2SO_4 was previously saturated with a gas of the same composition. Ar–Cl_2 mixtures were prepared by, first, introducing Ar into the two litre flask to a selected pressure as indicated on a Hg manometer. Then Cl_2 gas was added until the pressure was equal to the ambient pressure as indicated on a Halocarbon-oil differential manometer. After completion of a run, the $PuCl_3$ collected in the condenser was dissolved in dilute HNO_3 and determined by radioassay (α-decay of ^{239}Pu).

---

(7) C. Wagner and B. Stein, *Z. Physik. Chem.* **192**, 129 (1944).

(8) U. Merten, *J. Phys. Chem.* **63**, 443 (1959).

(9) H. K. Hofmeister, R. V. Haeseler and O. Glemser, *Z. Elektrochem.* **64**, 513 (1960).

(10) J. J. Katz and E. Rabinowitch, *The Chemistry of Uranium*, NNES, Div. VIII, Vol. 5, p. 479. McGraw-Hill, New York (1951).

RESULTS

The partial pressure of $PuCl_4$ was calculated by substitution in the equation

$$p_{PuCl_4} = \frac{n_{Pu}}{n_{Ar} + n_{Cl_2} + \frac{1}{2}n_{Pu}} P_t \qquad (4)$$

where P_t denotes the total pressure, n_{Pu} denotes the number of moles of Pu collected in the condenser, and n_{Ar} and n_{Cl_2} denote, respectively, the number of moles of Ar and Cl_2 displaced by the H_2SO_4. The results are given in column 5 of Table 1. The flow rate, quantity of $PuCl_3$ transported and the partial pressure of chlorine in the saturated carrier gas are tabulated in columns 2, 3, and 4, respectively, of the same table. The equilibrium constants which were computed by substitution into Equation (2) are tabulated in column 6. The values of the "constant" defined by Equation (2) are essentially independent of the Cl_2 partial pressure at 600, 650, 700 and 750°. This substantiates the choice of reaction 1 over the other possible reactions such as that involving the formation of condensed $PuCl_4$ or chlorides of Pu in higher oxidation states.

TABLE 1.—PARTIAL PRESSURE DATA AS A FUNCTION OF TEMPERATURE FROM 400 TO 750° FOR THE EQUILIBRIUM $PuCl_{3(s)} + \frac{1}{2}Cl_{2(g)} = PuCl_{4(g)}$

Temperature, (°K)	Flow-rate (cm^3/min.)	$PuCl_3$ transported, (mg)	P_{Cl_2}, (mm)	P_{PuCl_4}, (mm)	$K \times 10^3$ ($atm^{\frac{1}{2}}$)
1024	21	365	581	9·48	14·3
1024	33	273	288	7·12	15·2
1023	16	188	144	4·92	14·9
1024	5	111	58	2·91	13·9
1024	14	83·5	29	2·19	14·8
1024	7	55·2	11	1·49	16·1
974	30	143	585	3·73	5·59
974	35	104	294	2·72	5·75
974	15	72·6	146	1·91	5·73
974	19	43·9	59	1·16	5·45
974	18	30·8	30	0·81	5·42
973	18	20·3	12	0·54	5·70
925	35	46·7	598	1·22	1·80
925	24	30·0	296	0·86	1·81
875	35	14·5	598	0·379	0·562
875	24	10·0	293	0·261	0·553
824	19	3·91	582	0·102	1·53
774	18	0·683	587	0·024	0·0352
724	18	0·174	592	0·0044	0·00656
698	18	0·0649	589	0·0017	0·00254
674	35	0·0226	588	0·00060	0·000895

The free energy change for reaction 1 was calculated with the aid of the equation

$$\Delta F_1 = -RT \ln K. \qquad (5)$$

The results which are tabulated in column 2 of Table 2 may be represented by the equation

$$\Delta F_1(\text{cal}) = 37\,700 - 28{\cdot}3\,T. \qquad (6)$$

The entropy and enthalpy change for reaction (1) may be computed respectively by substitution of Equation 6 into the equations

$$\Delta S_1(\text{e.u.}) = -\left(\frac{\delta \Delta F_1}{\delta T}\right) \tag{7}$$

and

$$\Delta H_1(\text{cal}) = \Delta F_1 + T\Delta S_1. \tag{8}$$

It has been pointed out that the data show $PuCl_4$ exists only in the gaseous state rather than a condensed state under the conditions investigated. If the chlorine pressure had been sufficiently high, standard condensed $PuCl_4$ would have been formed. In order to refer the quantities ΔF_1, ΔS_1 and ΔH_1 to the standard condensed state of $PuCl_4$, the heats and entropies of fusion and of vaporization of $ThCl_4$, $NpCl_4$(11) and UCl_4(12) were used to estimate for $PuCl_4$ the heat of fusion,

$$\Delta H_f = 12\,000\ \text{cal}, \tag{9}$$

the entropy of fusion,

$$\Delta S_f = 14\ \text{e.u.}, \tag{10}$$

the heat of vaporization,

$$\Delta H_v = 30\,000\ \text{cal}, \tag{11}$$

and the entropy of vaporization,

$$\Delta S_v = 27\ \text{e.u.} \tag{12}$$

These values are approximately the same as those estimated by Brewer *et al.*(6) except that a slightly lower value of entropy of vaporization has been chosen. From these data, the normal melting point and boiling point are calculated respectively to be 857 and 1111°K and the free energies of vaporization and sublimation are respectively

$$\Delta F_v(\text{cal}) = 30\,000 - 27T \tag{13}$$

and

$$\Delta F_s(\text{cal}) = 42\,000 - 41T \tag{14}$$

In addition, the standard free energy, entropy and enthalpy for the formation of solid $PuCl_3$ at elevated temperatures are available from emf data.(13) Jette(14) has summarized data on the fusion of Pu. These data may be combined with Equation (6) to calculate the standard free energy (ΔF°), entropy (ΔS°) and enthalpy (ΔH°) for the formation of $PuCl_4$. The results may be summarized in the following equations:

(a) the standard free energy of formation of gaseous $PuCl_4$,

$$\Delta F^\circ_{(g)} = -182\,000 + 23{\cdot}3T\,(\text{above } 1111^\circ\text{K, extrapolated}) \tag{15}$$

(b) the standard free energy of formation of liquid $PuCl_4$,

$$\Delta F^\circ_{(liq)} \begin{array}{l} = -212\,000 + 50{\cdot}3T(913\text{–}1111^\circ\text{K}) \\ = -210\,000 + 47{\cdot}8T(857\text{–}913^\circ\text{K}) \end{array} \tag{16}$$

and

(c) the standard free energy of formation of solid $PuCl_4$,

$$\Delta F^\circ_{(s)} = -222\,000 + 61{\cdot}8T(674\text{–}857^\circ\text{K}). \tag{17}$$

---

(11) J. J. Katz and G. T. Seaborg, *The Chemistry of the Actinide Elements*, p. 48. Methuen, London, (1957).

(12) J. J. Katz and E. Rabinowitch, *The Chemistry of Uranium*, NNES Div. VIII. Vol. 5, p. 475–7. McGraw-Hill, New York (1951).

(13) R. Benz and J. A. Leary, *J. Phys. Chem.* **65**, 1056 (1961).

(14) E. Jette, *J. Chem. Phys.* **23**, 365 (1955).

TABLE 2.—THE FREE ENERGY OF THE REACTION $PuCl_{3(s)} + \frac{1}{2}Cl_{2(g)} = PuCl_{4(g)}$, ΔF_1, AND THE STANDARD FREE ENERGY OF FORMATION OF $PuCl_{4(s)}$, $\Delta F^{\circ}_{(s)}$, AND OF $PuCl_{4(liq)}$, $\Delta F^{\circ}_{(liq)}$.

Temperature (°K)	ΔF_1 (kcal)	$\Delta F^{\circ}_{(s)}$ (kcal)	$\Delta F^{\circ}_{(liq)}$ (kcal)
1024	$+8{\cdot}6 \pm 0{\cdot}3$		
974	10·0	-163 ± 6	
925	11·6	−166	
875	13·0	−168	
824	14·4		-171 ± 6
774	15·8		−174
724	17·2		−177
698	17·9		−179
674	18·6		−180

Some values of the standard free energy of formation of $PuCl_4$ are listed in columns 3 and 4 of Table 2.

DISCUSSION

An important criterion for the evaluation of the reliability of the data obtained from transpiration experiments is independence of the calculated partial pressure and the flow-rate. An appreciable dependence would reflect effects such as non-equilibrium, diffusion and thermal diffusion. In the present experiments, no systematic dependence of the $PuCl_4$ partial pressure on the flow-rate was observed. Pressure drop through the system due to the finite rate of gas flow was estimated to be less than 2 mm/Hg. In order to reduce effects of absorption of chlorine gas, the sulfuric acid was saturated with a gas mixture of the appropriate composition before each run. The dissociation of Cl_2 gas is negligible.(15) The chlorine partial pressure in Ar–Cl_2 mixtures is accurate to within 1 mm Hg. The vapour pressure of $PuCl_3$(16) is negligible. The uncertainty in the volume of the metered gas is less than 0·5 per cent. The temperature readings are estimated to be within ±4° corresponding to an uncertainty of 0·12 kcal in the free energy of reaction. Radioassays corrected for ^{241}Am contamination give the Pu transported accurate to within 2 per cent. The maximum uncertainty in the free energy change for reaction (1) is estimated to be 0·3 kcal or about 4 per cent. The estimated uncertainty in the enthalpy and entropy are respectively 2 kcal and 2 cal/degree.

The uncertainties in the standard quantities of formation of $PuCl_4$ are somewhat greater because the data for $PuCl_3$ have been extrapolated and, principally, because of the uncertainty in the free energies of condensation, Equations (13) and (14). The molar free energy, enthalpy and entropy are estimated to be reliable to within 6 kcal, 9 kcal and 9 cal/degree, respectively.

The free energy of formation of liquid $PuCl_4$ at 700°, -163 ± 6 kcal, may be compared with −160 kcal which has been estimated by BREWER *et al.*(8)

Acknowledgements—The author wants to thank R. L. NANCE for the preparation of distilled $PuCl_3$ and G. MATLACK and C. F. METZ of the Analytical Group for radioassays.

(15) W. H. EVANS, T. R. MUNSON and D. D. WAGMAN, *J. Res. National Bur. Standards* **55**, 147 (1955).

(16) T. E. PHIPPS, G. W. SEARS, R. L. SEIFERT and O. C. SIMPSON, *J. Chem. Phys.* **18**, 713 (1950).

J. Inorg. Nucl. Chem., 1962, Vol. 24, pp. 1197 to 1204. Pergamon Press Ltd. Printed in Northern Ireland

PHASE AND EQUILIBRIUM PRESSURE STUDIES OF THE ZIRCONIUM-TITANIUM-HYDROGEN SYSTEM

V. Y. Labaton,* E. V. Garner*, and E. Whitehead†
United Kingdom Atomic Energy Authority (Reactor Group),
Reactor Technology Branch, Capenhurst, Chester

(*Received* 18 *December* 1961; *in revised form* 6 *April* 1962)

Abstract—Equilibrium pressure curves have been determined for the ternary zirconium–titanium–hydrogen system, based on the 55 atomic per cent alloy, between 550 and 650°C, and a tentative phase diagram has been constructed for the addition of hydrogen to the alloy. A room-temperature X-ray study has identified the expected phases in the ternary system isomorphous with those in the zirconium and titanium systems, and in addition a new hexagonal phase has been partially characterized.

The reaction of hydrogen with a zirconium-titanium alloy was studied in connection with the use of the alloy as a "getter" for hydrogen, in an inert gas stream. Preliminary experiments, using heated zirconium as a getter for hydrogen, showed that reaction was rapid at about 550°C, and that the hydrogen equilibrium pressure was low. These experiments confirmed the work of previous experimenters regarding the variable reactivity of zirconium, depending on the surface pretreatment. Because of this variable reactivity and the possibility of surface film and dust formation, it was decided to investigate the use of a zirconium alloy for removing hydrogen. It was known that Pascard and Fabre(1) had successfully used a 50 atomic per cent zirconium-titanium alloy at 800°C for removing oxygen from argon, and this alloy and the 55 atomic per cent alloy were studied as hydrogen getters.

A study was made of the kinetics of reaction.(1) However, of fundamental importance to the use of such a getter is the equilibrium pressure of hydrogen above the metal, since the reaction is reversible: the metal when heated in hydrogen reaches an equilibrium value which depends on the temperature and pressure of hydrogen in the surrounding atmosphere. It was therefore necessary to determine equilibrium hydrogen pressures with varying concentrations of hydrogen in the alloy at different temperatures. At the same time it was considered valuable to extend the studies by using X-ray diffraction to characterize the phases found at room temperatures and to relate these, where possible, to those found in the three binary systems Zr-Ti, Zr-H and Ti-H.

The ternary system zirconium-titanium-hydrogen has been examined by McQuillan(2) in the course of a study of the fundamental relationships between zirconium and titanium, e.g., the effect of substituting titanium for zirconium in alloys. Equilibrium pressure measurements were made at higher temperatures than those used in the present study, and some X-ray investigations were made on saturated hydrides.

---

* Present address: U.K.A.E.A. (Reactor Group), Risley, Warrington, Lancs.
† Present address: U.K.A.E.A. (Production Group), Springfields, Salwick, Lancs.

(1) V. Y. Labaton, S. G. Donn, R. H. Watson and E. Whitehead. To be published.
(2) A. D. McQuillan, Birmingham University. Private communication (1959).

The related zirconium–hydrogen and titanium–hydrogen systems have been extensively studied.

Absorption isotherms of the equilibrium concentrations of hydrogen in zirconium have been determined over a wide range of temperature by Hall *et al.*,(3) Edwards *et al.*(4) and Gulbransen and Andrew.(5) Hall *et al.*(3) were among the first to realize the importance of the surface condition of the zirconium and the large inhibiting effect of surface oxide contamination. The effect of oxygen on the reaction between zirconium and hydrogen has been studied by Edwards and Levesque,(6) Gulbransen and Andrew,(7) and Pemsler.(8)

The constitutional diagram of the zirconium–hydrogen system has been studied by Gulbransen and Andrew,(5) Edwards *et al.*,(4) Ells and McQuillan(9) and Libowitz(10) by measuring hydrogen equilibrium pressures over wide ranges of temperature and hydride composition. Vaughan and Bridge(11) determined the phase diagram over the range 0–65 atomic per cent hydrogen by high-temperature X-ray methods, while most recently Espagno *et al.* used high-sensitivity dilatometry(12,13) and X-ray methods(14) to establish the diagram, in particular the characteristics of the eutectic change. The related ternary system zirconium–oxygen–hydrogen has been studied by Hall *et al.*,(3) Edwards and Levesque,(6) and Ells and McQuillan,(9) and partial ternary phase diagrams have been proposed.

Isotherms for the absorption of hydrogen by titanium have been determined by a number of workers including McQuillan.(15) McQuillan and others have noted that surface contamination has a considerable effect on absorption of hydrogen by titanium in a similar way to zirconium. A constitutional diagram for the titanium–hydrogen system was derived by McQuillan from experimental absorption curves, and phase relationships at temperatures below the range investigated by McQuillan have been studied using conventional metallographic techniques by Lenning *et al.*(16)

1. EQUILIBRIUM PRESSURE STUDIES

1.1 *Experimental*

The apparatus shown in Fig. 1 was used to obtain equilibrium pressure composition curves for the zirconium–titanium–hydrogen system, and to study the kinetics of reaction between the alloy and hydrogen at constant pressure.(1) It consisted essentially of two sections connected by a pressure-regulating valve *F*. Samples of zirconium–titanium of known hydrogen content were prepared by admitting a measured amount of hydrogen from the storage section *B* to the alloy heated to the desired temperature. The alloy sample contained in a silica tube *C* was heated in the furnace *G* which was controlled to ±3°C by a Keat Multilec control system. The sample was taken to be at equilibrium when the hydrogen pressure above it, which was measured on the McLeod gauge *D*, remained constant

(3) M. N. A. Hall, S. L. A. Martin and A. L. G. Rees, *Trans. Faraday Soc.* **15**, 306 (1945).

(4) R. K. Edwards, P. Levesque and D. Cubicciotti, *J. Amer. Chem. Soc.* **77**, 1307 (1955).

(5) E. A. Gulbransen and K. F. Andrew, *Trans. Amer. Inst. Min. (Metall.) Engrs.* **203**, 136 (1955).

(6) R. K. Edwards and P. Levesque, *J. Amer. Chem. Soc.* **77**, 1312 (1955).

(7) E. A. Gulbransen and K. F. Andrew, *Rev. Metall.* **51**, 101 (1954).

(8) J. P. Pemsler, *J. Electrochem. Soc.* **105**, 315 (1958).

(9) C. E. Ells and A. D. McQuillan, *J. Inst. Met.* **85**, 89 (1956).

(10) G. G. Libowitz, *Atomics International*, Report NAA-SR-5015 (1960).

(11) D. A. Vaughan and J. R. Bridge, *J. Metals (N.Y.)* **8**, 528 (1956).

(12) L. Espagno, P. Azou and P. Bastien, *C.R. Acad. Sci., Paris*, **247**, 1199 (1958).

(13) L. Espangno, P. Azou and P. Bastien, *C.R. Acad. Sci., Paris*, **248**, 2003 (1959).

(14) R. Espangno, P. Azou and P. Bastien, *C.R. Acad. Sci., Paris*, **249**, 1105 (1959).

(15) A. D. McQuillan, *Proc. Roy. Soc.* A **204**, 309 (1950).

(16) G. A. Lenning, C. M. Craighead and R. I. Jaffee, *Trans. Amer. Inst. Min. (Metall.) Engrs* **200**, 367 (1954).

over a period of 1 hr. A series of equilibrium experiments were made at temperatures between 550 and 650°C.

The 55 atomic per cent zirconium–titanium alloy used for the majority of the investigation was manufactured by Imperial Chemical Industries, Ltd. (Metals Division) from 70 atomic per cent zirconium sponge and 30 per cent titanium granules by melting *in vacuo*.(1) The 50 atomic per cent alloy also used was prepared by argon-arc melting of iodide zirconium and titanium sponge.

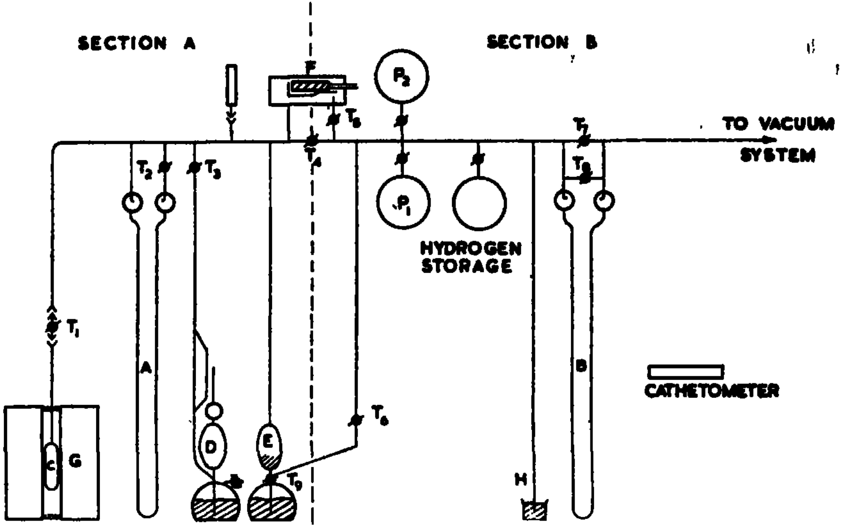

FIG. 1.—Apparatus for equilibrium pressure measurements.

1.2 *Discussion of results*

The results of equilibrium pressure measurements are plotted logarithmically in Fig. 2. From the phase rule, in such plots a change in slope indicates a phase change. It is deduced that, in the temperature region investigated, the first change in slope represents a change in phase from β to $(\beta + \gamma)$, and the second change in slope the transformation from $(\beta + \gamma)$ to γ phase. Here β and γ have the normal connotations i.e. β is the body-centred phase and γ the face-centred cubic phase.

For the 55 atomic per cent alloy the hydrogen contents of the alloy at which the phase changes occur vary only slightly with temperature. The fact that the equilibrium pressure curve at 550°C for the 50 atomic per cent alloy is higher than that for the 55 atomic per cent alloy agrees with the fact that titanium hydrides have higher equilibrium pressures than zirconium hydrides at the same temperature. From the experimental points obtained for the $\beta \rightarrow (\beta + \gamma) \rightarrow \gamma$ transitions and published phase diagrams for the systems zirconium–hydrogen (VAUGHAN and BRIDGE(11)), titanium–hydrogen (MCQUILLAN(16)) and zirconium–titanium (FAST(17)), a three dimensional phase structure was assembled. The phase relationships at 750°C were based on results of MCQUILLAN;(2) at other temperatures the phase relationships were constructed by using literature values for the two-component systems, results from the present study where available, and (where necessary) interpolations based on relative areas and the known effect of temperature on the phase changes. From this tentative three-dimensional phase structure a provisional phase diagram for the 55 atomic per cent alloy and hydrogen was constructed by taking the appropriate plane through the structure; this is shown in Fig. 3. The α-phase is the hexagonal close-packed phase.

(17) J. D. FAST, *Rec. Trav. chim. Pays-Bas* **58**, 973 (1939).

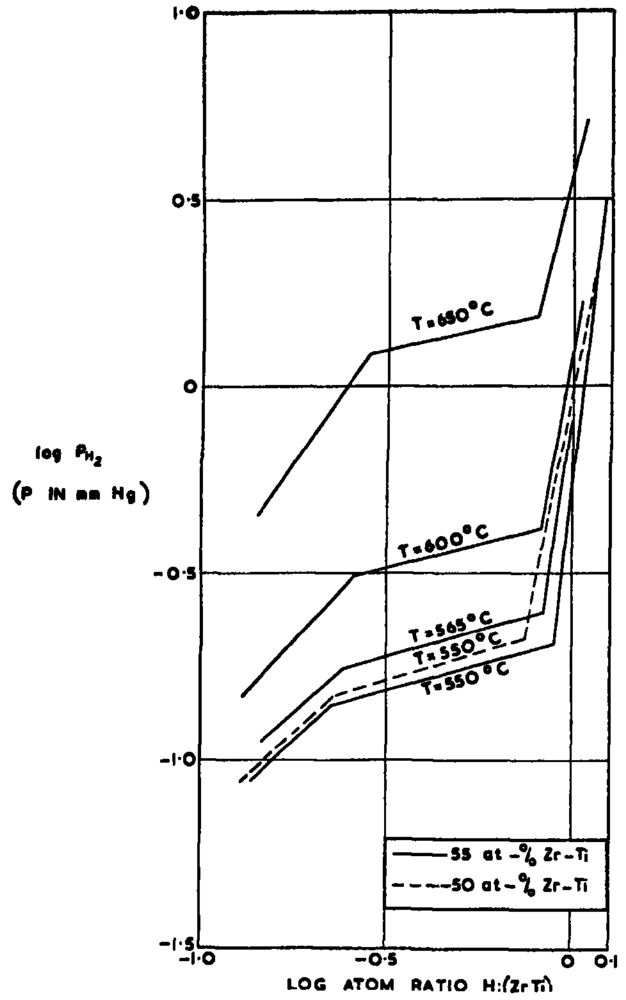

FIG. 2.—Equilibrium pressure curves for the hydrogen zirconium-titanium system.

The phase diagram presented is tentative, being based on limited experimental results, and is incomplete, particularly in the low-temperature range.

Results of an X-ray study (discussed in Sub-section 2.2) of samples prepared in the temperature range 600–700°C and subsequently cooled slowly to room temperature show the presence of phases rich in zirconium and titanium. These results cannot therefore be compared with Fig. 3, which shows the phases present on the 55 atomic per cent zirconium-titanium plane, the assumption being made there that the phases in the ternary system would be intermediate between those of the binary systems.

2. X-RAY STUDIES OF ZIRCONIUM-TITANIUM HYDRIDES

2.1 *Experimental*

All the samples examined, with one exception, were hydrides of alloy containing 55 atomic per cent zirconium; one sample was prepared from 50 atomic per cent alloy. The samples were prepared by allowing the alloy to take up a measured amount of hydrogen at 600°C in the apparatus shown in

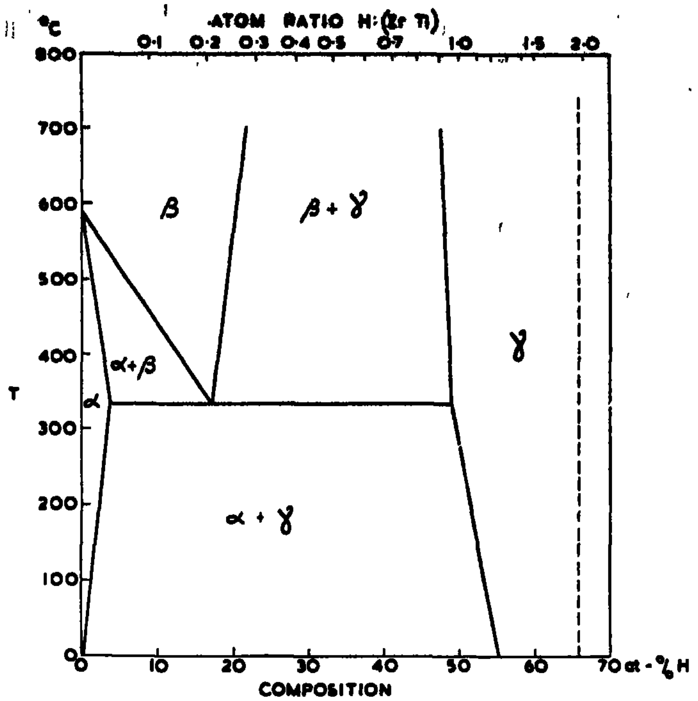

Fig. 3.—Provisional phase diagram for 55 atomic per cent zirconium–titanium alloy and hydrogen.

Fig. 1. They were normally allowed to cool slowly over a period of 2 hr, but in two instances were quenched by plunging the reaction tube into oil at room temperature. Samples with hydrogen contents greater than that represented by the composition $(ZrTi)H_{0\cdot 05}$, was first fully dehydrided by degassing to 0·05 μ at 850°C. This powdered sample of the pure alloy was then treated with the desired amount of hydrogen as described above.

The X-ray diffraction photographs were taken on a Nonius Guinier quadruple-focusing camera of effective diameter 22·9 cm. Since the object of the investigation was only phase identification, lattice parameters were not refined.

2.2 *Discussion of results*

Four major crystalline phases were identified:

(i) A hexagonal phase, α_1, isomorphous with α-Zr and α-Ti and having intermediate lattice dimensions. This phase, which has a hexagonal close-packed structure, has been observed previously by a number of workers investigating the zirconium–titanium system (Fast(17); Hayes *et al.*(18); Duwez(19)). The lattice dimensions found here for alloy with zero hydrogen content agree well with those of Fast.

(ii) A body-centred cubic phase β, isomorphous with β-Zr and β-Ti having intermediate lattice dimensions. This has also been found in the zirconium–titanium system as a high-temperature phase which can be retained at room temperature by quenching. It is not normally found in slowly cooled samples, since transition to the α_1-phase takes place on cooling. The presence of small amounts of hydrogen in solid solution presumably retards the rate of transformation of the high-temperature to the

(18) E. T. Hayes, A. H. Robertson and D. G. Paasche, *Rep. Invest. U.S. Bur. Min.* no. 4826 (1951).
(19) P. Duwez, *J. Inst. Met.* **80**, 525 (1952).

low-temperature phase. Hatt and Williams(20) conclude in a recent study that the β-phase in not retained in the 50 atomic per cent alloy even at fast quenching rates, unless impurities are present. The lattice dimensions found in the present work agree with those of Duwez for alloy of composition 55 atomic per cent.

(iii) A face-centred cubic phase, γ, whose cell side is very close to that of the face-centred cubic phase found in the zirconium–hydrogen system at high hydrogen contents, i.e. at about 60 atomic per cent H. Although this phase appears over a range of composition from $(ZrTi)H_{1\cdot25}$ to $(ZrTi)H_{1\cdot95}$, no systematic variation in cell side has been observed. Accurate estimates of the cell side have not been possible, because of the diffuse nature of the reflections and of coincidences of a number of reflexions with those of other phases. However, differences have been observed between one sample and another which are outside the limits of experimental error. Values of the cell side lie between 4·75 and 4·77 Å. That of γ-ZrH_2 containing 61·8 atomic per cent H is 4·76 Å (Sof'ina *et al.*(21)). γ-Titanium hydride which occurs over the range 50–72 atomic per cent H has a value of *a* lying between 4·395 and 4·45 Å.(15,16,22,23,24)

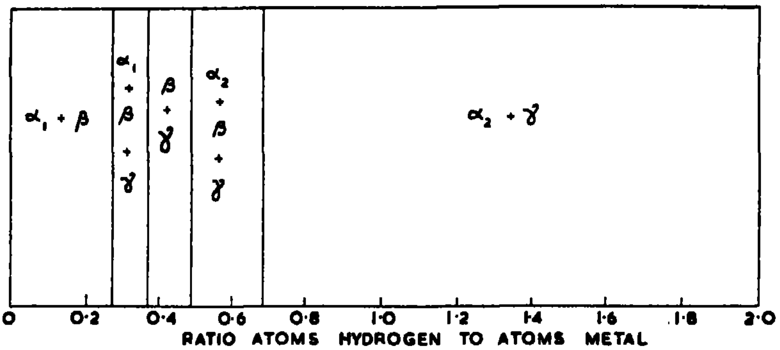

Fig. 4.—Phases found in the Zr–Ti–H system.

Confirmation that this is a zirconium-rich phase also comes from the fact that, in the one instance where this phase was found together with the α_1-phase, the lattice dimensions of the latter were lower than those of the 55 atomic per cent zirconium alloy. Its zirconium content must be lower and hence that of the co-existing γ-phase higher that 55 atomic per cent.

(iv) A hexagonal phase, α_2, quite distinct from the α_1-phase. The *c*-axis is smaller and the *a*-axis larger than in the α_1-phase. The lattice dimensions increase with increasing hydrogen content while the axial ratio remains constant within the limits of experimental error.

The phases found at different hydrogen contents are represented diagrammatically in Fig. 4. This is in no sense a phase diagram since, with one exception, all the samples were examined after cooling slowly to room temperature; they could therefore contain a mixture of high- and low-temperature phases, the proportions depending on the rates of cooling and rates of transition of one phase to another. In the instance where a sample of composition $(ZrTi)Y_{0·58}$ was cooled rapidly by quenching in oil and compared with the slowly cooled one, a marked difference was found in the ratios of the phases, the quenched sample showing an increased proportion of the α_2- and β-phases. This suggests that the α_2-phase might be a high-temperature one. The β-phase is already known to be a high-temperature one from work in the Zr-H and Zr-Ti systems.

---

(20) B. A. Hatt and G. I. Williams, *Acta. Met.* 7, 682 (1959).
(21) V. V. Sof'ina, Z. M. Azarkh and N. N. Orlova, *Kristallographiya* 3, 539 (1958).
(22) G. Hagg, *Z. Phys. Chem.* B 11, 433 (1931).
(23) P. Erlich, *Z. Angew. Chem.* 59, 163 (1947).
(24) T. R. P. Gibb and H. W. Krushwitz, *J. Amer. Chem. Soc.* 72, 5365 (1960).

TABLE 1.—X-RAY POWDER DATA FOR $(ZrTi)H_{1·68}$

d (Å)	Intensity	α_2-phase, *hkl*	γ-phase, *hkl*
4·77	*vvw*	001	
2·91	*s*	100	
2·758	*s*		111
2·480	*vs*	101	200
2·372	*m*	002	
1·676	*w*	110	220
1·579	*m*	111	
1·453	*mw*	200	
1·376	*vvw*	103, 201	222
1·238	*vw*	202	

α_2-phase has $a = 3·354$ Å; $c = 4·74$ Å

TABLE 2.—X-RAY POWDER DATA FOR $(ZrTi)H_{0·67}$

d (Å)	Intensity	α_2-phase, *hkl*	γ-phase, *hkl*	β-phase *hkl*
2·85	*m*+	100		
2·746	*m*		111	
2·471				110
2·425	*s*	101		
2·320	*w*+	002		
1·684	*vw*		220	
1·641	*w*+	110		
1·547	*m*	111		
1·422	*m*-diffuse	200		

α_2-phase has $a = 3·285$ Å; $c = 4·64$ Å

The existence of a new phase (α_2) in the mixed hydride system is of some interest, and although its exact identity cannot be deduced on the basis of the scanty survey made here, a few conclusions can be drawn. It is clear that the hexagonal α_2-phase is quite distinct from the hexagonal close-packed α_1-structure found at low hydrogen contents, for the following reasons. Firstly, the α_1-phase disappears at a hydrogen content of about 28 atomic per cent and the α_2-phase is first observed at a hydrogen content of about 36 atomic per cent. Secondly, the axial ratio ($c/a = 1·413$) is well outside the limits (1·57–1·64) for hexagonal close-packing. Thirdly, the presence of reflexions *hhl* in the diffraction pattern completely rules out the space group P6 *mmc* which is that of hexagonal close-packed structures.

Since the α_2-phase is always found together with the γ-phase, which has a composition close to ZrH_2, it must contain less than 55 atomic per cent of zirconium (the average composition). An examination of hydrides of alloys containing less than 55 per cent of zirconium would undoubtedly throw some light on the composition of this phase. The X-ray patterns of two compositions showing the α_2-phase are given in Tables 1 and 2.

Acknowledgement—This paper is published by permission of Mr. R. V. Moore, Managing Director of the Reactor Group of the United Kingdom Atomic Energy Authority.

J. Inorg. Nucl. Chem., 1962, Vol. 24, pp. 1205 to 1210. Pergamon Press Ltd. Printed in Northern Ireland

THE HEAT STABILITIES OF SOME POLYMERIC METAL COMPLEXES*

Edward J. Friihauf† and **John C. Bailar, Jr.**
The William Albert Noyes Chemical Laboratory, University of Illinois, Urbana, Illinois

(*Received* 9 *April* 1962)

Abstract—Heat stability data are reported for a series of polymeric complexes of bis-(2-pyridinal)-biphenylene-4,4′-diimine. The salts which have been shown to give polymers are nickel(II) sulphate, zinc(II) nitrate and the following divalent metal chlorides and nitrates: iron, cobalt, nickel, copper, cadmium and mercury. In general, the metal nitrate polymers do not lose weight below 200°, the metal chloride polymers below 250°, and nickel(II) sulphate polymer below 300°C.

To date, most efforts to prepare coordination polymers have involved the use of organic chelating agents which simultaneously satisfy charge and fill the coordination positions of the metal ion. This study was undertaken to examine the heat stabilities of some coordination polymers in which the organic chelating agent does not neutralize the charge on the metal ion. bis-(2-Pyridinal)-biphenylene-4,4′-diimine(I) was chosen as the chelating agent because

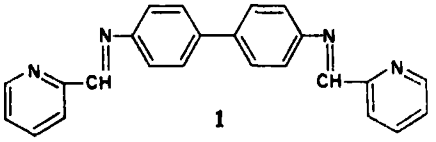

1

(1) It can satisfy acceptor sites on metal atoms but it cannot satisfy their charge. Linear polymeric metal complexes of this chelating agent have the structure shown in II.

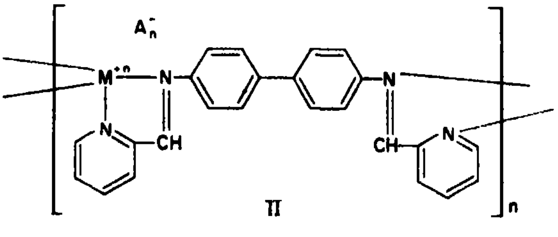

II

Here M represents a metal atom having a positive charge $+n$ and A is some monovalent anion which is not part of the chelating agent. Since the chelating agent does not neutralize charge, an anion must be present to neutralize the positive charge of the metal ions.

(2) Molecular models show that there is little possibility of forming a cyclic chelate as shown in III. Bond angles and steric requirements are such that the cyclic structure shown in III seems less likely than the polymeric structure shown in II. Molecular

---

* This paper represents part of the work submitted by Edward J. Friihauf to the University of Illinois for the degree of Doctor of Philosophy.

† Firestone Tire and Rubber Company Fellow 1959–60; National Science Foundation Fellow 1960–61. Present Address: J. T. Baker Chemical Co., Phillipsburg, N.J.

models also show that there is little evidence for expecting a cross-linked polymer when a hexa-co-ordinate metal such as Fe(II) or Co(II) is used. When three of these chelating groups approach a metal ion, each group prevents the other two from closely approaching the metal ion. However, the models show that two of these chelating groups can closely approach a metal ion having octahedral, tetrahedral or planar stereochemistry.

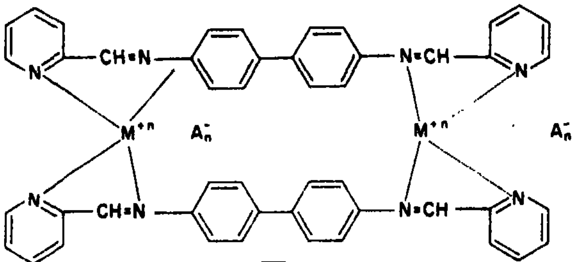

III

(3) The use of the biphenylene functional group avoids the thermal instability of saturated carbon chains. It also imposes a steric situation which lessens the possibility of forming a cyclic chelate as shown in III.

(4) The use of the pyridinal group allows conjugation in the five-membered chelate ring and possible double bonding with the metal atom. The presence of this conjugation or π-bonding may lead to greater heat stability. Since the (C=N) azomethine linkage is a member of a chelate ring, the presence of resonance in this chelate ring can be determined from the magnitude of the C=N stretching frequency. Any π-bonding in this five-membered ring tends to lower the C=N stretching frequency as compared to that of the free base.

The metal sulphates, chlorides and nitrates used in conjunction with (I) to form polymers are listed in Table 2. It was realised that polymers containing the nitrate ion would not be thermally stable. However, it seemed desirable to compare the chloride and nitrate polymers to see whether the same relative order of heat stabilities was displayed by both series. The chloride and nitrate ions were chosen because the former is a good donor and the latter is a bad donor. The heat stability data (Table 2) show the effect of different anions in polymers which contain the same chelating agents and metal ions.

DISCUSSION

1. *Preparation of compounds*

The polymeric complexes were prepared by bringing together methanol solutions of the chelating agent and the appropriate metal salt. In some instances, solid formed during the addition of metal salt and in other instances [$NiCl_2$, $Fe(NO_3)_2$, $Co(NO_3)_2$, $Ni(NO_3)_2$, $Cu(NO_3)_2$], the polymer remained in solution even after all of the salt had been added. Evaporation of the reaction mixtures to dryness led to solid polymeric products which were washed with acetone in a Soxhlet extractor, dried, and analysed.

When acetone or ethanol were used as reaction solvents, solids formed immediately after the metal salt was first added to the chelating agent. Chemical analysis for these solids agree well with those calculated for complexes showing metal to ligand ratios between 4:3 and 3:2.

All of the polymeric products prepared for this study are coloured, hygroscopic solids. This hygroscopic nature accounts in part for the differences between the analytical values calculated and those found. In general, hydrogen values are high and carbon and metal values are low. Chemical analyses for the polymeric complexes of copper(II)chloride and nickel(II)sulphate show that one molecule of water is associated with the repeating unit in the polymer.

A polymeric zinc(II) chloride complex could not be obtained by using the procedure which led to the other polymers. Attempts to prepare the zinc chloride polymer in methanol gave a complex having a metal to ligand ratio of two to one (empirical formula: $C_{24}H_{18}N_4.2ZnCl_2$).

The copper(II) nitrate polymer can be pulled into threads and the nickel(II) chloride polymer forms a putty-like solid just before the respective reaction mixtures are freed of methanol. After the methanol has evaporated, a glassy brittle solid is left in the case of the copper(II) nitrate polymer and a powder in the case of the nickel(II) chloride polymer. When the methanol reaction mixtures of the other polymers are freed of methanol, brittle glasses or finely divided solids remain. After drying, all of the glassy solids can be reduced to fine powders by grinding. The adhesive properties are temporary and depend on the presence of a small amount of methanol which acts as a plasticizer.

TABLE 1.—POLYMER SOLUBILITY*

Polymer	Water	Dimethyl-formamide	Dimethyl-Sulphoxide	Pyridine	Benzene	Tetrahydrofuran	Methanol
$FeCl_2$	*p*	*s*	*s*	*s*	*i*	*p*	*p*
$CoCl_2$	*s*	*s*	*s*	*s*	*i*	*i*	*p*
$NiCl_2$	*s*	*p.m.*	*s*	*s*	*i*	*i*	*p*
$CuCl_2$	*p.m.*	*p.m.*	*p.m.*	*s*	*i*	*i*	*p*
$CdCl_2$	*p.s.*	*p*	*s*	*s*	*i*	*p.s.*	*p*
$HgCl_2$	*i*	*s*	*s*	*s*	*p.s.*	*p*	*p*
$Fe(NO_3)_2$	*p*	*s*	*s*	*p*	*i*	*p*	*p*
$Co(NO_3)_2$	*p*	*s*	*s*	*s*	*i*	*i*	*p*
$Ni(NO_3)_2$	*s*	*s*	*s*	*p.m.*	*i*	*i*	*p*
$Cu(NO_3)_2$	*p*	*p*	*s*	*p*	*i*	*i*	*p*
$Zn(NO_3)_2$	*p*	*s*	*s*	*s*	*p.s.*	*p.s.*	*p*
$Cd(NO_3)_2$	*p*	*p*	*s*	*s*	*i*	*i*	*p.s.*
$Hg(NO_3)_2$	*p*	*p.m.*	*s*	*s*	*i*	*i*	*p*
$NiSO_4$	*s*	*p*	*p*	*p*	*i*	*i*	*p*

* Abbreviations
s—soluble *i*—insoluble *p*—partly soluble
p.m.—partly soluble (almost all is soluble) *p.s.* —partly soluble (very little is soluble)

Qualitative solubility data for the polymers that were tested for heat stability are listed in Table 1. Each determination involved about 3 mg of polymer per 3 ml of solvent.

2. *Infra-red study*

STRATTON and BUSCH have studied the infra-red spectra obtained for metal complexes of 2-pyridinaldazine and 2-pyridinalmethylimine and assigned modes to all bands in the 1400–1700 cm^{-1} region of the spectra.(1) The C=N stretching frequencies displayed by the iron complexes are lower than for the uncomplexed ligands. This lowering of the C=N stretching frequency for the iron complexes is attributed to π-bonding in the chelate ring. Resonance in the chelate ring is expected to lead to a lower C=N stretching frequency because the bond order of the carbon-nitrogen bond is lowered. Possible π-bonding in the polymeric complexes was likewise studied by examining the infrared spectra in the 1500–1700 cm^{-1} region. The polymers show strong bands in the 1600 cm^{-1} region, slightly stronger bands in the 1500 cm^{-1} region and weak bands in the 1560 cm^{-1} region. These bands are attributed to aromatic ring vibrations of the pyridine and benzene rings.(2) The bands of medium intensity above 1625 cm^{-1} are due to the C=N stretching mode. With the exception of the iron(II) nitrate polymer, for which a C=N bond is not observed, all of the polymers display increased C=N stretching frequencies when compared to metal-free bis-(2-pyridinal)-biphenylene-4,4′-diimine. The C=N stretching frequency for the iron(II) nitrate polymer is possibly superimposed on the band at 1600 cm^{-1}. These results indicate some π-bonding in the chelate rings of the iron(II) nitrate polymer and no similar π-bonding for the other polymers.

---

(1) W. T. STRATTON and D. H. BUSCH, *J. Amer. Chem. Soc.* **82**, 4834 (1960).

3. *Heat stability determinations*

The thermogravimetric balance used for this study is similar to the one described by Winslow and Matreyek.(3) The polymeric products were dried for 12 hours at 140° in the balance and tested for heat stability in a nitrogen atmosphere. The data are reported in Table 2 as per cent weight loss over successive twelve hour periods at a

Table 2.—Heat stability data for polymeric metal complexes of bis-(2-pyridinal)-biphenylene-4,4′-diimine, (PBD).

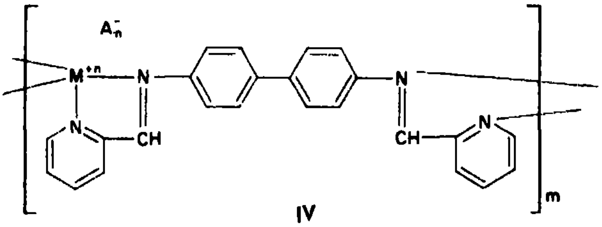

IV

Metal M	Anion A	% Decomposed after Successive 12 hr periods at Designated Temperatures 250°	300°	350°	400°
Fe(II)	Cl	10·7	58·0		
Co(II)	Cl	0·58	8·80	46·0	
Ni(II)	Cl	1·70	5·50	34·5	
Cu(II)	Cl	3·06	12·5	44·0	
Cd(II)	Cl	0·00	5·30	34·0	
Hg(II)	Cl	3·70	11·0	46·0	
Fe(II)	NO_3	43·0			
Co(II)	NO_3	1·48	12·5		
Ni(II)	NO_3	2·0	27·0		
Cu(II)	NO_3	43·0			
Zn(II)	NO_3	2·4	50·0		
Cd(II)	NO_3	0·00	0·25	4·93	70·0
Hg(II)	NO_3	9·50	36·0		
Ni(II)	SO_4	2·50	2·50	7·10	20·4
Metal Free	PBD	0·70	3·00	17·0	

---

[2] L. J. Bellamy, *The Infra-red Spectra of Complex Molecules*, p. 64–73. J. Wiley, New York (1958).

[3] F. H. Winslow and W. Matreyek, *J. Poly. Sci.* **22**, 315 (1956).

TABLE 3.—ANALYTICAL AND OTHER DATA FOR POLYMERIC COMPLEXES OF BIS-(2-PYRIDINAL)-BIPHENYLENE-4,4′-DIIMINE

Divalent cation	Anion	Analysis calc. for	C Calc.	C Found	H Calc.	H Found	Metal Calc.	Metal Found	*m.p.** (°C)	Yield (%)	Drying procedure†	Colour
Fe	Cl	$[C_{24}H_{18}N_4{\cdot}FeCl_2]_n$	59·0	58·5	3·68	3·99	11·4	11·4	>350°	—	1	Green
Co	Cl	$[C_{24}H_{18}N_4{\cdot}CoCl_2]_n$	58·5	58·0	3·66	3·99	12·0	10·0	>350°	80	1	Orange-yellow
Ni	Cl	$[C_{24}H_{18}N_4{\cdot}NiCl_2]_n$	58·6	57·9	3·66	3·84	11·9	10·9	>350°	93	2	Yellow-brown
Cu	Cl	$[C_{24}H_{18}N_4{\cdot}CuCl_2{\cdot}H_2O]_n$	56·0	55·3	3·89	3·88			212°	63	2	Yellow-brown
Cd	Cl	$[C_{24}H_{18}N_4{\cdot}CdCl_2]_n$	52·8	52·2	3·30	3·51			>350°	80	2	Yellow
Hg	Cl	$(C_{24}H_{18}N_4HgCl_2)_3HgCl_2$	43·2	43·0	2·70	2·65			243°d.	73	2	Yellow
Fe	NO_3	$[C_{24}H_{18}N_4{\cdot}Fe(NO_3)_2]_n$	53·2	52·7	3·32	3·15	10·3	8·16	200°d.	88	1	Lavender
Co	NO_3	$[C_{24}H_{18}N_4{\cdot}Co(NO_3)_2]$	52·8	53·1	3·30	3·47	10·8	9·8	>350°	86	2	Red-brown
Ni	NO_3	$[C_{24}H_{18}N_4{\cdot}Ni(NO_3)_2]$	52·8	52·7	3·30	3·51	10·8	9·8	>350°	89	3	Red-brown
Cu	NO_3	$[C_{24}H_{18}N_4{\cdot}Cu(NO_3)_2]$	52·3	52·5	3·28	3·38	11·5	11·5	>350°	—	3	Dark-brown
Zn	NO_3	$[C_{24}H_{18}N_4{\cdot}Zn(NO_3)_2]$	52·3	51·7	3·26	3·55	11·9	11·4	310°d.	86	3	Yellow
Cd	NO_3	$[C_{24}H_{18}N_4{\cdot}Cd(NO_3)_2]$	48·2	49·3	3·01	3·17			>350°	82	2	Yellow
Hg	NO_3	$[C_{24}H_{18}N_4{\cdot}Hg(NO_3)_2]$	41·0	40·4	2·84	2·83			>350°	71	2	Yellow
Ni	SO_4	$[C_{24}H_{18}N_4{\cdot}NiSO_4{\cdot}H_2O]_n$	53·8	54·3	3·36	4·11			>350°	—	2	Orange

* Abbreviations: d. decomposition.

† Abbreviations: 158° *in vacuo* (0.2 mm Hg).
2. 100° *in vacuo* (2·0 mm Hg).
3. 110° in the oven.

designated temperature (constant within $\pm 3^\circ$). The data show many of these polymers to be stable at 250° and the nickel(II) sulphate and cadmium(II) nitrate polymer polymers to temperatures above 300°. Unfortunately, most of the polymers are less heat-stable than the metal-free chelating agent. Many of these polymers retain water after drying for four hours at 100° *in vacuo* (0·3 mm Hg); a weight loss of up to two per cent at 250° is probably due to loss of water. The heat stability of the cadmium nitrate polymer is certainly not expected when one considers the poor heat stability of the other nitrate containing ploymers,

The order of heat stability for the chloride containing polymers is Cd(II) $\simeq$ Ni(II) $>$ Cu(II) $\simeq$ Co(II) $\simeq$ Hg(II) $\gg$ Fe(II) and the order of heat stability for the nitrate containing polymers is Cd(II) $\gg$ Co(II) $>$ Ni(II) $>$ Hg(II) $>$ Zn(II) $\gg$ Cu(II) $\simeq$ Fe(II). The order of heat stability for the nickel polymers is $SO_4^{2-} > Cl^- > NO_3^-$. The data show that the relative orders of stability differ in the nitrate and chloride series. The presence of π-bonding in the chelate rings of the iron(II) nitrate polymer has no significant effect on the thermal stability of the polymer. The data also show that the anion strongly affects the stability of the nickel polymers.

EXPERIMENTAL

Bis-(2-Pyridinal)-biphenylene-4,4′-diimine

A warm solution of benzidene (m.p. 129–130°)(25·7 g, 0·1395 mole) in 200 ml of absolute ethanol was slowly added with stirring to a warm solution of pyridine 2-aldehyde* (30·0 g, 0·280 mole) in 50 ml of absolute ethanol. A yellow solid formed immediately. The reaction mixture was stirred for one half hour. Yield of crude solid after washing with ethanol and drying in air, 52·0 g (100 per cent). Yield of yellow needles after recrystallization from acetone, 23·3 g (46 per cent) m.p. 177–179°. Found: C, 79·4; H, 5·02. Calc. for $C_{24}H_{18}N_4$: C, 79·6; H, 4·98%).

Polymeric metal complexes of bis-(2-pyridinal)-biphenylene-4,4′-diimine (PBD)

All of the polymeric complexes were prepared by essentially the following procedure. Those which were tested for heat stability were prepared in methanol. Reagent grade metal salts were used without further purification. Chemical analyses and other pertinent data are listed in Table 3.

A warm solution of iron(II) chloride tetrahydrate (0·2740 g, 0·00138 mole) in approximately 40 ml of methanol was slowly added with vigorous stirring to a refluxing solution of bis-(2-pyridinal)-biphenylene-4,4′-diimine (PBD)(0·5000 g, 0·00138 mole) in 200 ± 10 ml of methanol. The ferrous chloride solution was added dropwise in four separate portions and the reaction mixture was allowed to reflux on the steam bath for 1–2 min after each portion of salt solution had been added. After all of the salt was added, the reaction mixture was evaporated to dryness on a steam bath to yield a green solid. This solid was dried in the oven at 110°C, and then extracted with acetone. The extracted product was dried in air and then *in vacuo*.

* Pyridine-2-aldehyde (Aldrich Chemical Company) was used without further purification.

J. Inorg. Nucl. Chem., 1962, Vol. 24, pp. 1211 to 1213. Pergamon Press Ltd. Printed in Northern Ireland

Hg–Se SYSTEM

A. J. STRAUSS and L. B. FARRELL
Lincoln Laboratory,* Massachusetts Institute of Technology, Lexington 73, Massachusetts

(*Received* 8 *January* 1962; *in revised form* 16 *April* 1962)

Abstract—The portion of the Hg–Se system between 50 and 100 atomic % Se has been investigated by thermal analysis. The melting point of HgSe is 799°C. A region of two immiscible liquid phases extends from approximately 71–85 atomic % Se at the monotectic temperature (686°C). Within experimental error, the eutectic temperature is the same as the melting point of Se (220°C).

MERCURY and selenium form the compound HgSe (tiemannite), which crystallizes in the zincblende structure with lattice constant $a = 6{\cdot}08$ Å.(1) The only other information published on the Hg–Se system is a report that the HgSe–Se eutectic probably lies very close to pure Se.(2) In the present study, the portion of this system between 50 and 100 atomic % Se has been investigated by thermal analysis.

EXPERIMENTAL

Each sample was prepared by placing Hg and Se (99·999% purity) totaling 200 g in a quartz tube which was then evacuated and sealed off. The thermocouple for measuring sample temperatures was inserted into a re-entrant tube at the bottom of the sample tube. A chromel–alumel thermocouple was used for about half the measurements, and a Pt–(Pt-13% Rh) thermocouple was used for the rest. Each thermocouple was calibrated at the melting point of antimony (630·5°C). The difference between the observed and tabulated voltages at this point was added as a correction term to all voltages measured with the thermocouple. In no case did the temperature difference corresponding to this correction exceed 1°C. In order to reduce thermal gradients within the sample, the sample tube was placed in a heavy-walled stainless steel cylinder. The reference thermocouple for differential measurements was inserted into a hole in the cylinder wall. The sample and cylinder were heated in a vertical resistance furnace to a maximum temperature at least 25°C above the estimated liquidus point. Although the temperature was raised slowly, several sample tubes exploded during heating, presumably because of the presence of free Hg. The Hg-rich portion of the system was not investigated because explosions would probably have occurred even more frequently in this region.

After the sample had remained at the maximum temperature for 12 or more hours, it was cooled at a rate between 1 and 3°C/min until any thermal arrests above 600°C had been observed. If a heating curve or a repetition of the cooling curve was desired, the furnace was then reheated. Otherwise, the furnace was turned off. With the power off, the cooling rate was satisfactory for determining cooling curves in the vicinity of the Se melting point.

In order to measure the sample temperature with high precision, most of the thermocouple signal was bucked out with a d.c. microvolt potentiometer, and the remaining voltage was amplified with a Leeds and Northrup d.c. microvolt amplifier whose output was recorded with a recording potentiometer. The sensitivities of the amplifier and recorder were generally chosen so that the full width of the recorder chart was equal to 100 μV, which corresponds to 2·5°C for the chromel–alumel thermocouple and 8–10°C for the Pt–(Pt-13% Rh) thermocouple. For differential measurements, the difference in voltage between the sample and reference thermocouples was amplified with a second d.c. amplifier whose output was also recorded with a recording potentiometer.

RESULTS AND DISCUSSION

The thermal arrests determined experimentally and the phase diagram deduced from them are shown in Fig. 1. While cooling and heating curves gave consistent

---

* Operated with support from the U.S. Army, Navy and Air Force.

(1) W. B. PEARSON, *A Handbook of Lattice Spacings and Structures of Metals and Alloys*, Chap. 11, p. 688. Pergamon Press, New York (1958).

(2) M. HANSEN, *Constitution of Binary Alloys*, (2nd Ed.), p. 836. McGraw-Hill, New York (1958).

results, the temperature values adopted were generally obtained from the cooling curves, which could be analysed more precisely. The compositions indicated are the nominal values calculated from the weights of Hg and Se used to prepare the samples. Since the vapour within the dead space of the sample tube was relatively richer in Hg than the liquid phase, in each case the percentage of Se in the liquid was greater than the nominal value. The difference between actual and nominal compositions was quite small, however; for example, it is estimated that the percentage of Se was no greater than 50·5 atomic per cent in nominal 50 per cent samples.

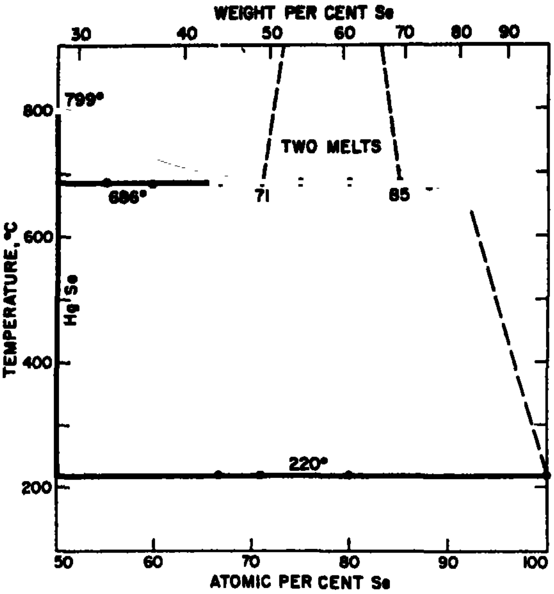

FIG. 1.—Hg–Se system between 50 and 100 atomic % Se.

TABLE 1.—THERMAL ARRESTS OBSERVED IN THE Hg–Se SYSTEM

Atomic % Se	Liquidus (°C)	Monotectic (°C)	Eutectic* (°C)
50	799, 799		
55	765	687	
60	718, 720	684	
66·7	694	687	220
70	688	687	
71	---†	685	220
75	---‡	685	
80	---‡	687	220
85	---‡	687	
88	679		
90	673		
92	647		
100	220		

* Attempts made to observe eutectic arrest only in cases indicated.
† Liquidus and monotectic arrests could not be distinguished.
‡ Arrest due to separation into two liquid phases not detected.

The phase diagram for the Se-rich portion of the Hg–Se system is found to be similar to the corresponding portion of the Pb–Se system.(3) The principal features are a congruently melting equiatomic compound, a region of two immiscible liquid phases, and a eutectic between the compound and Se which occurs at a composition close to pure Se. The melting point of HgSe is 799°C, as determined from cooling curves for two different samples. Monotectic arrests at (686 ± 2)°C were observed for all nominal compositions between 55 and 85 atomic per cent Se. These arrests cannot be associated with an eutectic between HgSe and a second compound of Hg with Se, since eutectic arrests at 220°C—the melting point of Se—were observed in heating curves for all three compositions whose low temperature behaviour was investigated. Furthermore, no evidence for a second compound was obtained in X-ray diffraction measurements. At the monotectic temperature, the region of two immiscible liquid phases extends from approximately 71–85 atomic per cent Se. The boundaries of the two-phase region are indicated schematically in Fig. 1, since the thermal arrests resulting from separation of a single liquid into two separate phases could not be detected. The liquidus between 92 and 100 atomic per cent Se is also indicated schematically.

Although eutectic arrests were observed at 220°C in heating curves for Hg–Se samples, corresponding arrests were not obtained in cooling curves for these samples. It was found that pure Se exhibits similar behaviour, which can be explained on the basis of observations(4,5) that amorphous Se readily transforms into the crystalline hexagonal form at temperatures above about 100°C. A freezing plateau is not obtained when liquid Se is cooled slowly, because the solid formed under these conditions is amorphous. On slow heating this material changes into the hexagonal form below the melting point of the latter, and the melting plateau characteristic of crystalline solids is therefore observed. Apparently the Hg–Se eutectic behaves in the same manner.

No attempt has been made in the present investigation to determine the solubility of Hg in Se or of Hg and Se in HgSe. A study of the electrical properties of HgSe indicates that this compound is always slightly Hg-rich.(6) The concentration of excess Hg is about 10^{17} atoms/cm^3 for samples equilibrated with Se-rich liquid and about 10^{18} atoms/cm^3 for samples equilibrated with Hg-rich liquid.

Acknowledgement—The authors are grateful to T. C. Harman and Professor D. R. Mason for valuable discussions.

(3) M. Hansen, *Constitution of Binary Alloys*, (2nd Ed.), pp. 1104–1106, McGraw-Hill, New York, (1958).

(4) T. Sato and H. Kaneko, *Tech. Reports Tohoku Univ.* 14, 45 (1950).

(5) P. H. Keck, *J. Opt. Soc. Amer.* 42, 221 (1952).

(6) T. C. Harman and A. J. Strauss (to be published).

J. Inorg. Nucl. Chem., 1962, Vol. 24, pp. 1215 to 1219. Pergamon Press Ltd. Printed in Northern Ireland

SPECTROPHOTOMETRIC STUDIES OF ION-PAIR FORMATION

T. WILLIAMS.
The Chemistry Department, Welsh College of Advanced Technology, Cardiff.

(*Received* 19 *February* 1962; *in revised form* 11 *April* 1962)

Abstract—Thermodynamic dissociation constants for $CoCNS^+$ and $NiCNS^+$ have been determined from ultra-violet absorption measurements at 25°C. The results, together with some other literature values, have been used to calculate the distances of closest approach of the ions concerned.

ACCORDING to IRVING and WILLIAMS[1] the stability data of all the complexes of the bivalent metals of the first transition series, with the exception of the cyanides and sulphates, follow the order $Mn < Fe < Co < Ni < Cu > Zn$. This order is generally independent of the nature of the co-ordinating ligand or the number of ligands involved. The thiocyanate complexes of Co(II),[2,3] Ni(II),[4] Cu(II)[5] and Zn(II),[6,7] have already been investigated but the results cannot be compared since each system was investigated under different experimental conditions. The thermodynamic dissociation constant of $CuCNS^+$ has been determined by TANAKA and TAKAMURA[5] using spectrophotometry, and in the present work, the shifts to longer wavelengths of the CNS^- spectrum by Co^{2+} and Ni^{2+} ions have been used to obtain the thermodynamic dissociation constants of $CoCNS^+$ and $NiCNS^+$.

Unfortunately manganese and zinc ions have very little effect on the thiocyanate absorption band and therefore, similar investigations involving these ions were not possible.

EXPERIMENTAL

Optical measurements were made using a Hilger Uvispek and one centimetre quartz cells kept at 25°C by means of a constant temperature cell holder.

Cobalt perchlorate and nickel perchlorate were prepared from the corresponding A.R. chloride and perchloric acid, while recrystallized technical grade sodium perchlorate was used to keep the ionic strength constant. The concentrations of the cobalt and nickel stock solutions were determined by precipitation of cobalt as tetra-pyridine cobalt dithiocyanate and nickel as nickel dimethylglyoxime. Sodium perchlorate solutions were standardized by converting the sodium salt to the corresponding acid (by means of an ion-exchange resin) and titrating with a standard sodium hydroxide solution.

The absorptions of the ion-pairs were found to be unaffected by changes in pH roughly below 4·5 and consequently all measurements were made at pH lower than this.

RESULTS

The method adopted to obtain the dissociation constants is very similar to that reported elsewhere.[8] The optical density, D, in a cell of unit length, for a system such as

$$M^{n+}_{aq.} + L^{m-}_{aq.} \rightleftharpoons ML^{(n-m)+}_{aq.} \qquad (1)$$

---

[1] H. IRVING and R. J. P. WILLIAMS, *J. Chem. Soc.* 3192 (1953).
[2] M. LEHNE, *Bull. Soc. Chim. France.* 76 (1951).
[3] P. SENISE and M. PERRIER, *J. Amer. Chem. Soc.* **80**, 4195 (1958).
[4] S. FRONAEUS, *Acta Chem. Scand.* 7, 21 (1953).
[5] N. TANAKA and T. TAKAMURA, *J. Inorg. Nucl. Chem.* **9**, 15 (1959).
[6] R. E. FRANK and D. N. HUME, *J. Amer. Chem. Soc.* **75**, 1736 (1953).
[7] E. FERRELL, J. M. RIDGION and H. L. RILEY, *J. Chem. Soc.* 1121 (1936).
[8] W. D. BALE, E. W. DAVIES and C. B. MONK, *Trans. Faraday Soc.* **52**, 816 (1956).

involving an ion-pair and its two constituent ions, is given by

$$D = \epsilon x + \epsilon_1(a - x) + \epsilon_2(b - x) \tag{2}$$

where a is the total molarity of $M^{n+}_{aq.}$, b the total molarity of $L^{m-}_{aq.}$, x the concentration of the ion-pair formed and ϵ, ϵ_1 and ϵ_2 the molar absorption coefficients of $ML^{(n-m)+}_{aq.}$, $M^{n+}_{aq.}$ and $L^{m-}_{aq.}$ respectively. If the experimental conditions are such that the only absorbing constituent present is the ion-pair, then equation (2) reduces to

$$D = \epsilon x \tag{3}$$

Combining Equation (3) with the expression for the dissociation constant K, which is given by

$$K = (a - x)(b - x)f_1 f_2/f_3 x \tag{4}$$

where f_1, f_2 and f_3 represent ion activity coefficients, the following relationship is obtained:

$$K/\epsilon = b(a - x)f_1 f_2/f_3 D - (a - x)f_1 f_2/f_3 \epsilon \tag{5}$$

Assuming that x is small compared with a and that $f_1 f_2/f_3$ is constant when the ionic strength is constant, then a plot of ab/D against a is a straight line the slope of which gives a first value of $1/\epsilon$. This value of the molar absorption coefficient is used to determine the first value of x, which is then used in Equation (5) to determine a second value of $1/\epsilon$; by a series of approximations the true value of $1/\epsilon$ is obtained.

In this determination it is assumed that $1/\epsilon$ is independent of salt concentration, but this is not necessarily so.⁽⁹⁾ Thus in the present work $1/\epsilon$ was determined at a relatively low but constant ionic strength in order to eliminate, as far as possible, large differences in the salt concentrations between the different solutions measured.

A second set of determinations, where $M^{n+}_{aq.}$ and $L^{m-}_{aq.}$ are mixed together to give solutions of varying ionic strengths, will yield a range of K values provided $1/\epsilon$ and f_1, f_2 and f_3 are known. $1/\epsilon$ was obtained as explained above, while the activity coefficients were calculated from the DAVIES equation⁽¹⁰⁾

$$-\log f_1 = 0{\cdot}5 z_1^2[I^{\frac{1}{2}}/(1 + I^{\frac{1}{2}}) - 0{\cdot}2I] \tag{6}$$

which has been shown to be satisfactory for 1:1 and 2:1 electrolytes in water at 25°C up to $I = 0{\cdot}1$.

Cobalt thiocyanate

LEHNE has stated⁽²⁾ that the difference between the molar extinction coefficients of the $CoCNS^+$ ion-pair and the Co^{2+} ion in the visible range of the spectrum is too small to give reliable results. In this investigation of the $Co^{2+}-CNS^-$ system, use was made of the shift of the CNS^- ion band, found in the near ultra-violet, to longer wavelengths. Co^{2+} ions do not absorb in this region, and further, it is possible to choose conditions such that the only absorbing ion is $CoCNS^+$.

The formation of $CoCNS^+$ has been demonstrated⁽³⁾ by the method of continuous variations;⁽¹¹⁾ this was confirmed and some indications were obtained of the formation

---

⁽⁹⁾ W. D. BALE, E. W. DAVIES, D. B. MORGANS and C. B. MONK, *Trans. Faraday Soc.* **53**, 94 (1957).

⁽¹⁰⁾ C. W. DAVIES, *J. Chem. Soc.* 2093 (1938).

⁽¹¹⁾ P. JOB, *Ann. Chim.* **9**, 113 (1928).

of higher complexes. In view of this, the ratio of Co^{2+} to CNS^- concentration was kept to more than 1:1.

The addition of varying concentrations of sodium perchlorate showed no effect on the visible spectrum of cobalt perchlorate. This was taken as proof that no complexing took place between cobalt ions and perchlorate ions and thus justified the use of sodium perchlorate for keeping the ionic strength constant.

Table 1 gives the data for the determination of the molar extinction coefficient of $CoCNS^+$, where $a = Co(ClO_4)_2$, $b = KCNS$, $c = NaClO_4$ and $x = CoCNS^+$ molarities. D is the observed absorption (with solvent as reference) of $CoCNS^+$. The slope of the plot of $b(a - x)/D$ against $(a - x)$ was determined by the method of least mean squares and this gave a value of $1/\epsilon = 0{\cdot}00330$.

TABLE 1.—MOLAR EXTINCTION COEFFICIENT OF $CoCNS^+$
$10^4b = 4{\cdot}795$, $I = 0{\cdot}1614 \pm 0{\cdot}0007$, 272 mμ, 1 cm. cells.

10^3a	10^3c	D	10^4x	$10^6b(a - x)/D$
5·340	0·00	0·679	2·171	3·618
4·806	1·60	0·649	2·074	3·400
4·272	3·20	0·600	1·918	3·260
3·738	4·80	0·548	1·755	3·116
3·204	6·40	0·496	1·585	2·944
2·670	8·00	0·445	1·422	2·724

Table 2 contains the results for the determination of the thermodynamic dissociation constant of $CoCNS^+$. The average of the K values given in the table is 0·0191 ± 0·0001.

TABLE 2.—DATA FOR $K(CoCNS^+)$
272 mμ, 1 cm cells.

10^3a	10^4b	10^2I	D	10^4x	f_1f_2/f_3	10^2K
2·670	9·590	8·356	0·929	3·066	0·3844	1·93
2·670	4·795	8·167	0·490	1·617	0·3874	1·91
2·136	9·590	6·822	0·825	2·727	0·4102	1·92
1·940	2·062	6·000	0·191	0·630	0·4272	1·82
1·602	9·590	5·590	0·693	2·287	0·4363	1·91
1·522	10·31	4·360	0·760	2·508	0·4700	1·90
1·068	9·590	3·814	0·529	1·746	0·4877	1·96
1·068	4·795	3·502	0·291	0·960	0·4996	1·94

Nickel thiocyanate

It was observed that Ni^{2+} has a similar effect to Co^{2+} on the CNS^- spectrum, and hence the same method and techniques were adopted to investigate the Ni^{2+}—CNS^-

TABLE 3.—MOLAR EXTINCTION COEFFICIENT OF $NiCNS^+$
$10^4b = 9{\cdot}590$, $I = 0{\cdot}4165 \pm 0{\cdot}0015$, 273 mμ, 1 cm cells.

10^3a	c	D	10^4x	$10^6b(a - x)/D$
4·507	0·2780	0·572	3·884	6·906
4·506	0·2915	0·539	3·660	6·565
3·605	0·3050	0·495	3·361	6·333
3·153	0·3188	0·450	3·056	6·067
2·704	0·3320	0·403	2·736	5·783
2·253	0·3456	0·355	2·411	5·435

system. Table 3 shows the data obtained, where this time a = Ni(ClO$_4$)$_2$ and x = NiCNS$^+$ molarities. $1/\epsilon$ for the nickel thiocyanate ion-pair was determined from the slope of the plot $b(a - x)/D$ against $(a - x)$ and was found to be 0·00679.

Table 4 contains the data for the determination of the thermodynamic dissociation constant of NiCNS$^+$. The average of the K values is 0·0173 ± 0·0002.

TABLE 4.—DATA FOR K(NiCNS$^+$)
273 mμ, 1 cm cells.

10^2a	10^3b	10^2I	D	10^3x	f_1f_2/f_3	10^2K
2·253	19·18	7·601	0·792	5·378	0·3966	1·75
2·253	9·59	7·110	0·440	2·988	0·4030	1·74
1·803	9·59	5·844	0·386	2·621	0·4305	1·77
1·352	9·59	4·568	0·331	2·248	0·4636	1·70
0·901	9·59	3·320	0·253	1·718	0·5070	1·70

The method of calculation of the present paper has been used to recalculate the data of TANAKA and TAKAMURA[(5)] in the hope of obtaining more precise values of K and $1/\epsilon$ for CuCNS$^+$ (Tables 5 and 6). The average K for CuCNS$^+$ at 25°C is thus 0·00470 ± 0·00007

TABLE 5.—DATA FOR K(CuCNS$^+$) AT I = 0·05
10^4b = 1·000, 343 mμ, $10^3/\epsilon$ = 2·05

10^2a	10^2D	10^5x	$10^5b(a - x)/D$	10^3K
0·800	2·07	4·24	3·844	4·88
1·000	2·36	4·84	4·216	4·78
1·200	2·55	5·23	4·686	4·92
1·400	2·73	5·60	5·106	4·95
1·600	2·92	5·99	5·459	4·81

TABLE 6.—DATA FOR K(CuCNS$^+$) AT I = 0·10
10^4b = 1·000, 343 mμ, $10^3/\epsilon$ = 2·11

10^2a	10^2D	10^5x	$10^5b(a - x)/D$	10^3K
0·800	1·84	3·88	4·327	4·55
1·000	2·14	4·52	4·649	4·38
1·400	2·45	5·17	5·694	4·73
1·800	2·82	5·95	6·362	4·43
2·000	2·92	6·16	6·829	4·51

DISCUSSIONS

The K values for CoCNS$^+$, NiCNS$^+$, CuCNS$^+$ and ZnCNS$^+$ are 0·0191, 0·0173, 0·00470 and 0·014[(12)] respectively, the latter being only an approximate value but considered sufficiently accurate to include for comparison purposes. Inspection of the series shows that they follow the IRVING and WILLIAMS pattern. This suggests that the irregularity observed with the cyanide and sulphate complexes is not entirely due to the acidity effect,[(13)] since, as mentioned elsewhere,[(14)] the CNS$^-$ ion has a comparably strong acidity.

---

(12) B. B. OWEN and R. W. GURRY, *J. Amer. Chem. Soc.* **60**, 3074 (1936).

(13) A. E. MARTELL, *J. Phys. Chem.* **59**, 308 (1955).

(14) G. S. LAURENCE, *Trans. Faraday Soc.* **52**, 236 (1956).

Working from the dissociation constants obtained and Bjerrum equation,(15) the distances of closest approach have been calculated, Table 5. These values are extremely small suggesting that the cations do not retain their primary solvation sheath in the associated form. The bond between the interacting ions is probably covalent in character and such ions as $CoCNS^+$, $NiCNS^+$, $CuCNS^+$ are simply first stages in the formation of higher thiocyanate complexes.

$CoSO_4$, $NiSO_4$, $CuSO_4$ and $ZnSO_4$ have the following K values 0·0034, 0·0040,(15) 0·0047,(7) and 0·0049,(16) so the order of stability is $CoSO_4 > NiSO_4 > CuSO_4 > ZnSO_4$. The distances of closest approach calculated for the first three species are very much larger than those of the corresponding thiocyanates. These '*a*' values suggest ionic association between the ions with the cations retaining their primary solvation sheath in the associated form.

On the above evidence, it must be concluded that the interaction between the metal ions concerned and the CNS^- ion is different to that found with the SO_4^{2-} ion. Whether this affords an explanation of the irregularity observed with the sulphates, it is difficult to say.

TABLE 7.—BJERRIUM DISTANCES OF CLOSEST APPROACH

Anion	Co^{2+}	Ni^{2+}	Cu^{2+}
CNS^-	1·69	1·64	1·25
SO_4^{2-}	3·8	4·1	4·4

The rates of formation of $MCNS^+$(17) and MSO_4(18) where M represents Co^{2+} and Ni^{2+} ions, have been recently determined, and it is interesting to observe that the reaction rates follow, in both cases, the order Co > Ni. These results suggest that the velocity at which an ion-pair is formed is independent of its stability.

It seems worth noting that Senise and Perrier, during their work on $CoCNS^+$, obtained a value of 0·00273 for $1/\epsilon$ at $I = 1{\cdot}0$. This is considerably lower than the present value of 0·00330 obtained at an ionic strength of 0·161. On this evidence, the constant I method must be used with caution and every effort should be made to determine this constant at low ionic strengths, in order to eliminate as far as possible, the errors due to salt effects.

Acknowledgements—The author wishes to thank Dr. C. B. Monk for some stimulating discussions.

(15) N. Bjerrum, *Kgl. Danske Vidensk. Selskab.* **7**, No. 9 (1926).
(16) R. W. Money and C. W. Davies, *Trans. Faraday Soc.* **28**, 609 (1932).
(17) A. G. Davies and W. MacF. Smith, *Proc. Chem. Soc.* 380 (1961).
(18) M. Eigen, *Z. Electrochem.* **64**, 115 (1960).

J. Inorg. Nucl. Chem., 1962, Vol. 24, pp. 1221 to 1224. Pergamon Press Ltd. Printed in Northern Ireland

THE REACTIONS OF METAL COMPLEXES WITH ALKYL HALIDES—II

THE REACTIONS OF HALO(TRIPHENYLPHOSPHINE)-CADMIUM(II) COMPLEXES[1]

G. B. Deacon
Department of Physical and Inorganic Chemistry
University of Adelaide

(*Received* 13 *March* 1962, *in revised form* 20 *April* 1962)

Abstract—Dibromo- and di-iodobis(triphenylphosphine)cadmium(II) complexes are converted by ethyl bromide to bis(triphenylethylphosphonium) tetrabromocadmate(II). Reaction of each with methyl iodide gives bis(triphenylmethylphosphonium) tetraiodocadmate(II).

THE conversion of the complexes $(Ph_3P)_nHgX_2$ (where *n* is 1 and 2, and X, is Cl, Br and I) to Group V quaternary iodomercurate(II) complexes by alkyl iodides was described in Part I. It was also found that the complexes $(Ph_3P)_nHgX_2$ (where *n* is 1 and 2, and X is Br and I) would not react with ethyl bromide.[1] Reaction does occur however between the complexes $(Ph_3P)_2CdX_2$ (where X is Br and I) and ethyl bromide. These reactions and those of the same complexes with methyl iodide are now reported. Earlier workers were unable to achieve reaction between di-iodobis-(aryldialkylphosphine)cadmium(II) complexes and methyl iodide.[2]

EXPERIMENTAL

Preparation of dihalobis(triphenylphosphine)cadmium(II) complexes

The complexes were precipitated on mixing ethanol solutions containing the stoicheiometric amounts of the cadmium halide and triphenylphosphine.

1. *Dibromobis(triphenylphosphine)cadmium(II).* This compound was recrystallized from ethanol, gave white needles, m.p. 225–226° (lit.[3] 225–226°), (Found: C, 54·3; H, 4·1. Calc. for $C_{36}H_{30}P_2CdBr_2$: C, 54·2; H, 3·8%). The same complex was precipitated, m.p. 224–225°, mixed m.p. 225–226° (after recrystallization from ethanol), (Found: C, 54·7; H, 3·9%), in an attempt to prepare the complex $(Ph_3P.CdBr_2)$ by mixing ethanol solutions of the stoicheiometric amounts of triphenylphosphine and $CdBr_2.4H_2O$.

2. *Di-iodobis(triphenylphosphine)cadmium(II).* This compound was fine white needles, m.p. 241·5–242° (lit.[3] 243°, with preliminary softening) (Found: C, 48·45; H, 3·6. Calc. for $C_{36}H_{30}P_2CdI_2$: C, 48·5; H, 3·4%).

Preparation of bis(triphenylalkylphosphonium) tetrahalocadmate(II) complexes

1. *Bis(triphenylethylphosphonium) tetrabromocadmate(II).* The compound was precipitated on mixing ethanol solutions of stoicheiometric amounts of triphenylethylphosphonium bromide and $CdBr_2.4H_2O$, and, recrystallized from ethanol, had m.p. 108·5–109° (Found: C, 46·8; H, 4·3. Calc. for $C_{40}H_{40}P_2CdBr_4$: C, 47·3; H, 3·9%).

2. *Bis(triphenylmethylphosphonium) tetraiodocadmate(II).* This compound was similarly prepared, and recrystallized from acetone, had m.p. 173·5–174° (Found: C, 39·9; H, 3·55; Cd, 9·6. Calc. for $C_{38}H_{36}P_2CdI_4$: C, 38·8; H, 3·1; Cd, 9·6%). Further recrystallization failed to improve the purity of the compound (as indicated by the C, H analytical data). The compound is only sparingly soluble in boiling acetone and is less soluble in other suitable solvents, and is thus difficult to purify by recrystallization.

---

[1] Part I, G. B. Deacon and B. O. West, *J. Inorg. Nucl. Chem.* **24**, 169 (1962).

[2] R. C. Cass, G. E. Coates and R. G. Hayter, *J. Chem. Soc.* 4007 (1955).

[3] R. C. Evans, F. G. Mann, H. S. Peiser and D. Purdie, *J. Chem. Soc.* 1209 (1940).

Reactions of dihalobis(triphenylphosphine)cadmium(II) complexes with alkyl halides

Reactions with ethyl bromide. (1) $(Ph_3P)_2CdBr_2$ (0·91 g., 1·14 mmole) was refluxed with ethyl bromide (20 ml) in acetone (20 ml). After 5 hr heating, all the complex had dissolved and after 10 hr precipitation of product began. This was filtered off after 12·5 hr, and consisted of bis(triphenylethylphosphonium) tetrabromocadmate(II) (0·52 g, 0·51 mmole, 43 per cent), which, recrystallized from ethanol, had m.p. 108·5–109·5, mixed m.p. 109–109·5° (Found: C, 47·3; H, 4·4%). The filtrate was evaporated and gave 0·56 g of white solid. This gave m.p. 130–155° (Found: C, 50·15; H, 4·1%) after two recrystallizations from ethanol, and is probably a mixture of the reactant and the product, the solubility properties of which are similar.

(2) $(Ph_3P)_2CdI_2$ (0·93 g, 1·05 mmole) similarly reacted with ethyl bromide in acetone. Solution of the reactant complex was complete in 6 hr, and precipitation of the product commenced after 10 hr. This was filtered off after 14 hr, and consisted of bis(triphenylethylphosphonium) tetrabromocadmate(II) (0·57 g, 0·57 mmole, 54 per cent), which, recrystallized from ethanol, had m.p. 107·5–108°, mixed m.p. 108° (Found: C, 47·0; H, 4·4%). The filtrate was evaporated and gave 0·39 g of white solid, which, on recrystallization from ethanol, yielded bis(triphenylethylphosphonium) tetrabromocadmate(II), m.p. 105–106·5°, mixed m.p. 107–107·5° (Found: C, 46·9; H, 4·2%). The mother liquor was evaporated and gave a cream glue, which was iodine free.

Reactions with methyl iodide

The complexes $(Ph_3P)_2CdX_2$ (where X is Br and I) were refluxed with methyl iodide, either alone or in the presence of added solvent (acetone or ethanol). After the reactions the volatiles were removed and a pale brown residue was obtained in each case. The product was recrystallized to constant melting point from acetone/ethanol, and consisted primarily of bis(triphenylmethylphosphonium) tetraiodocadmate(II). In each instance the product contained a small amount of an ether soluble fraction, which was shown to contain free iodine. Some details of two typical experiments are given.

(1) $(Ph_3P)_2CdI_2$ (0·54 g.) was refluxed with methyl iodide (20 ml) in acetone (20 ml) for 1 hr and 0·76 g of product was obtained, which, on recrystallization, gave m.p. and mixed m.p. 173–174°, (Found: C, 40·1; H, 3·6%). The theoretical weight of product for the formation of $[Ph_3PMe]_2CdI_4$ alone is 0·72 g.

(2) $(Ph_3P)_2CdBr_2$ (0·52 g.) similarly reacted with methyl iodide and 0·80 g of product was obtained, which, on recrystallization, gave melting point 170·5–171·5°, mixed m.p. 171·5–172·5°, (Found: C, 40·2; H, 3·7%). Theoretical weight for formation of $[Ph_3PMe]_2CdI_4$ alone; 0·77 g.

Although it was not possible to purify the product adequately by recrystallization, the formation of $[Ph_3PMe]_2CdI_4$ was established by infra-red spectroscopy. $[Ph_3PMe]_2CdI_4$ has the following bands in the region 2000–667 cm^{-1}: 1709(*w*); 1623(*w*); 1587(*w*); 1486(*w*); 1441(*vs*); 1339(*w*); 1316(*w*); 1226(*w*); 1189(*w*); 1159(*w*); 1111(*vs*); 995(*w*); 905(*vs*); 851(*w*); 784(*w*); 750(*vs*); 718(*s*); 689(*s*). In addition, the formation of the triphenylmethylphosphonium cation was confirmed by reaction of the product in acetone with mercuric iodide (2 moles/mole of product assumed to be $[Ph_3PMe]_2CdI_4$), when triphenylmethylphosphonium tri-iodomercurate(II) could be crystallized in greater than 80 per cent yield after the addition of ethanol to lower the solubility. For example, this method was used to characterize the product from reaction (1) (above). The tri-iodomercurate was recrystallized from acetone/ethanol, and gave m.p. 146–146·5° (lit.⁽⁴⁾ 146–146·5°), mixed m.p. 146·5–147°, (Found: C, 26·3; H, 2·1. Calc. for $C_{19}H_{18}PHgI_3$: C, 26·55; H, 2·1%).

As the weight of crude product in the reactions with methyl iodide was generally greater than that required for the formation of the tetraiodocadmate alone (e.g. reactions (1) and (2) above), the following experiments were performed in an attempt to elucidate which reaction competes with the main reaction.

(1) Bis(triphenylmethylphosphonium) tetraiodocadmate(II) (0·30 g) was refluxed with methyl iodide (10 ml) in acetone (20 ml) for 5 hr. No increase in weight was observed, and the compound was recovered unchanged.

(2) Triphenylphosphine was recovered unchanged after refluxing with acetone for 15 hr. The ultra-violet spectrum of the phosphine in methanol after heating was essentially the same as that of the reactant. (The spectrum of triphenylphosphine in methanol is very similar to that in ethanol.⁽⁵⁾ In methanol there is a maximum at 260 $m\mu$, ε_{max} being $1{\cdot}1 \times 10^4$.)

(3) When a suspension of $(Ph_3P)_2CdI_2$ in acetone was treated with a solution of iodine in the same solvent, the colour of the iodine was discharged and the suspended complex dissolved. Further work is intended with this reaction.

⁽⁴⁾ G. B. DEACON and B. O. WEST, *J. Chem. Soc.* 5127 (1961).

⁽⁵⁾ F. G. MANN, J. T. MILLAR and B. B. SMITH, *J. Chem. Soc.* 1130 (1953).

Microanalyses were by the C.S.I.R.O. Microanalytical Laboratories, Melbourne. The infra-red spectra were measured with a Grubb-Parsons DB 1 Spectrophotometer, fitted with sodium chloride optics, and the ultra-violet spectra were measured with a Unicam SP 500 Spectrophotometer.

RESULTS AND DISCUSSION

Dibromo- and di-iodobis(triphenylphosphine)cadmium(II) complexes react with ethyl bromide with the formation of bis(triphenylethylphosphonium) tetrabromocadmate(II).

$$(Ph_3P)_2CdBr_2 + 2EtBr \rightarrow [Ph_3PEt]_2[CdBr_4]$$

$$(Ph_3P)_2CdI_2 + 4EtBr \rightarrow [Ph_3PEt]_2[CdBr_4] + 2EtI$$

It is considered that the reactions proceed via dissociation of the complexes to free triphenylphosphine, which reacts with ethyl bromide. An alternative mechanism involving preliminary weak co-ordination of ethyl bromide to cadmium (similar to one discussed for the reactions of analogous mercury complexes with alkyl iodides(1)) seems less likely. This mechanism postulates the intermediate

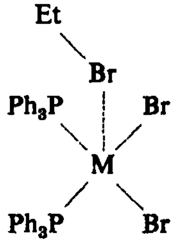

in the reactions of the complexes $(Ph_3P)_2MBr_2$ (where M is Cd, Hg) with ethyl bromide. The formation of this intermediate is more favoured thermodynamically when M=Hg, as mercury complexes have larger stability constants than the corresponding cadmium complexes.(6) (In particular the tribromomercurate ion is more stable than the tribromocadmate ion.(7,8)). As $(Ph_3P)_2HgBr_2$ does not react with ethyl bromide,(1) it is unlikely that the reaction of $(Ph_3P)_2CdBr_2$ with ethyl bromide proceeds by this mechanism, hence the dissociation mechanism probably operates. As cadmium complexes are less stable than those of mercury,(6) it is expected that $(Ph_3P)_2CdBr_2$ would dissociate into free triphenylphosphine more extensively than $(Ph_3P)_2HgBr_2$. Similar arguments favour a dissociation mechanism for the reaction of $(Ph_3P)_2CdI_2$ with ethyl bromide.

Di-iodo- and dibromobis(triphenylphosphine)cadmium(II) react with methyl iodide with the formation of bis(triphenylmethylphosphonium) tetraiodocadmate(II).

$$(Ph_3P)_2CdI_2 + 2MeI \rightarrow [Ph_3PMe]_2[CdI_4]$$

$$(Ph_3P)_2CdBr_2 + 4MeI \rightarrow [Ph_3PMe]_2[CdI_4] + 2MeBr$$

The reactions are similar to those of the corresponding mercury complexes.(1)

In the reactions with methyl iodide, the weight of the crude product consistently exceeded that required for the formation of the tetraiodocadmate alone. It has been shown that this was not caused by subsequent reaction of the tetraiodocadmate with methyl iodide, and, in the reactions which were performed with added acetone, it was not caused by reaction between triphenylphosphine, produced by dissociation of the complexes, and acetone. Free iodine is certainly present in the crude product, but this may not account for all of the excess. A further possibility is that iodine, formed by decomposition of the methyl iodide, may compete in reacting with the halo(triphenylphosphine)cadmium(II) complexes. This would result in the formation of a triphenyliodophosphonium iodocadmate, which may react further. Preliminary experiments have shown that di-iodobis(triphenylphosphine)cadmium(II) does react with iodine. Iodomercurate complexes of Group VB quaternary cations, containing P–I bonds, are known.(9)

---

(6) F. Basolo and R. G. Pearson, *Mechanisms of Inorganic Reactions*, p. 16., J. Wiley, New York (1958).

(7) L. Eriksson, *Acta Chem. Scand.* 7, 1146 (1953).

(8) L. G. Sillén, *Acta Chem. Scand.* 3, 539 (1949).

Acknowledgement—The author is grateful to Dr. B. O. WEST for helpful discussions, to Dr. R. A. JONES of the Department of Organic Chemistry, University of Adelaide, for measurement of the infra-red spectra, and to the Imperial Chemical Industries of Australia and New Zealand for the award of a Fellowship.

(9) K. ISSLEIB and W. SEIDEL, *Z. Anorg. Chem.* **288**, 201 (1956).

J. Inorg. Nucl. Chem., 1962, Vol. 24 pp. 1225 to 1234. Pergamon Press Ltd. Printed in Northern Ireland

SOME CO-ORDINATION POLYMERS PREPARED FROM BIS-(β-DIKETONES)*

J. S. OH and JOHN. C. BAILAR JR.
Noyes Chemical Laboratory, University of Illinois, Urbana, Illinois

(*Received* 12 *February* 1962; *in revised form* 18 *April* 1962)

Abstract—A series of metal ion–bis-(β-diketone) polymers containing beryllium, copper(II), nickel(II), zinc(II) or cobalt(II) have been prepared by four different methods. Three types of structures are postulated on the basis of elementary analysis of the polymers.

The thermal stability of the polymers was studied by a relatively simple method, utilizing a thermogravimetric balance. It was found that, in general, the order of thermal stabilities is Be(II) > Cu(II) > Ni(II) > Zn(II) > Co(II). The polymers derived from bis-(benzoylacetones) and bis-(dibenzoylmethanes) are thermally more stable than those derived from the corresponding bis-(acetylacetones). Similarly, the polymers derived from bis-(β-diketones) containing no connecting link between the diketone groups are thermally more stable than the polymers derived from the corresponding bis-(β-diketones) which contain a connecting link. The stabilities depend upon this connecting link in the following order: 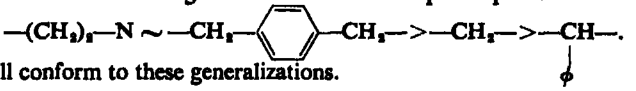 $-(CH_2)_2-N \sim -CH_2-C_6H_4-CH_2- > -CH_2- > -\underset{\phi}{CH}-$. The beryllium polymers do not all conform to these generalizations.

RECENTLY much attention has been paid to inorganic elements as possible units for new polymers. One promising group of compounds consists of coordination polymers, in which metal ions are linked together by di- or poly-functional organic ligands. Co-ordination polymers occupy an intermediate position between organic and inorganic compounds, and it is hoped that their study will lead to the production of polymers which are both thermally stable and useful as fabricating materials.

The preparative methods used for coordination polymers may be classified as follows: (1) the linking of polyfunctional ligands with metal ions, (2) the incorporation of metal ions into existing organic polymer chains and (3) polymer formation by reactions of metal-containing monomeric chelates containing functional groups. This paper is concerned with polymers of bis-β-diketones formed by the first method.

DISCUSSION

Synthesis of bis-(β-diketones)

Bis-(β-diketones) suitable for polymer formation are of two types:

(i) $RCOCH_2CO\text{-}Y\text{-}COCH_2COR'$, in which the two β-diketones residues are linked through the terminal carbon atoms, and

(ii) 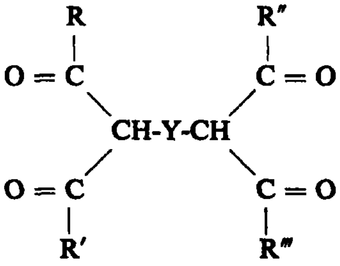

---

* The work described in this paper is taken from the doctoral thesis of J. S. OH, University of Illinois, 1961. It was supported chiefly by a grant from the Socony Mobil Oil Co., to whom our thanks are extended, and in part by Contract AF 33(616)-5486 with the Materials Laboratory of the Wright Air Development Division, Air Research and Development Command, U.S. Air Force.

in which the linkage is between the methylene carbon atoms. Thus, in choosing compounds of type (ii) for this study, two structural variables need be considered: (i) the nature of the connecting link Y, and (ii) the nature of the end groups R and R′.

From the view-point of preparation, bis-(β-diketones) of type (ii) may be divided into three classes:

Type A: bis-(β-diketones) linked between the two methylene carbon atoms but without a bridging atom or group.

Type B: bis-(β-diketones) joined by a chain of two or more carbon atoms.

Type C: bis-(β-diketones) possessing the structure of 1,1,3,3-tetra-acetyl-propane.

The compounds prepared in this study are listed in Tables 1, 2 and 3.

TABLE 1.—COMPOUNDS OF THE TYPE $[(RCO)(R'CO)CH]_2$: TYPE A

R	R′	m.p. °C	Yield (%)	Ref.
CH_3	CH_3	191	70·0	1
CH_3	C_6H_5	176	20·0	2
C_6H_5	C_6H_5	205·5*	4·5	3

* Reported(5) m.p.: 153–154·5

TABLE 2.—COMPOUNDS OF THE TYPE (RCO)(R′CO)CH—Y—CH(R′CO)(RCO): TYPE B

R	R′	Y	m.p. °C	Yield (%)	Ref.
CH_3	CH_3	—$(CH_2)_2$—	b.p. 83/3 mm Hg	23·0	5
CH_3	CH_3	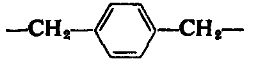	111	68·2	6
CH_3	CH_3	—S—	104 ~ 105	51·0	7

TABLE 3.—COMPOUNDS OF THE TYPE

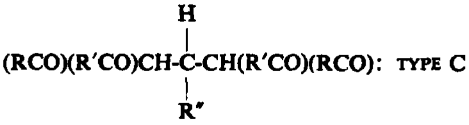

$$(RCO)(R'CO)CH\text{-}\underset{\displaystyle R''}{\overset{\displaystyle H}{C}}\text{-}CH(R'CO)(RCO)$$

: TYPE C

R	R′	R″	m.p. (°C)	Yield (%)	Ref.
CH_3	CH_3	H	84	57·5	8
CH_3	C_6H_5	H	72–73	24·0	9
C_6H_5	C_6H_5	H	177	67·5	10
CH_3	CH_3	C_6H_5	186	36·0	11
CH_3	C_6H_5	C_6H_5	223	50·0	12

---

(1) S. P. MULLIKEN, *Amer. Chem. J.*, **15**, 530 (1890).

(2) E. FISCHER, and C. BÜLOW, *Ber. Dtsch. Chem. Ges.* **18**, 2133 (1885).

(3) R. D. ABELL, *J. Chem. Soc.*, **101**, 989 (1912).

(4) W. C. FERNELIUS *et al.*, WADC Technical Report, 56–203, Part III, p. 29. February (1958).

(5) G. T. MORGAN, and C. J. A. TAYLOR, *J. Chem. Soc.* 43 (1926).

(6) D. F. MARTIN, W. C. FERNILIUS and M. SHAMMA, *J. Amer. Chem. Soc.* **81**, 130 (1959).

(7) A. ANGELI, and MAGNANI, *Gazz. Chim. Ital.*, **24**, I, 342 (1894).

(8) E. KNÖVENAGEL, *Ber. Dtsch. Chem. Ges.* **36**, 2136 (1903).

(9) K. BODENDORF and G. KORALEWSKI, *Arch. Pharm.* **271**, 101 (1933).

(10) S. V. LIEBERMAN and E. C. WAGNER, *J. Org. Chem.* **14**, 1001 (1949).

(11) R. SCHIFF, Ann. **309**, 206 (1899).

(12) E. KNÖVENAGEL and A. ERLER, *Ber. Dtsch. Chem. Ges.* **36**, 2131 (1903).

1,1,3,3-Tetra-acetylpropane has been synthesized by condensing acetylacetone with paraformaldehyde in the presence of diethylamine as a catalyst. It was found that when piperidine was used as a catalyst, crystals did not separate from the reaction mixture even after several months. Similar results were observed in the preparation of 1,3-diacetyl-1,3-dibenzoyl propane and 1,1,3,3-tetrabenzoylpropane. The condensation of paraformaldehyde with β-diketones can be effected in greater than 50 per cent yield. However, in the reaction of benzoylacetone with paraformaldehyde, the yields have been poor.

Metal ion-bis-(β-diketone) polymers

Four methods were used to prepare coordination polymers of divalent metal ions with bis-(β-diketones).

1. *Reaction in aqueous solution* (*method A*). This consists of mixing the ketones and a soluble metal salt in the proper proportions in a water–organic solvent mixture, and adjusting the pH until the chelate precipitates. It is necessary to add an organic solvent such as alcohol, dioxane or dimethylformamide because of the insolubility of the ligand in water. The success of this method depends upon pH, rate of addition of the base, rate of stirring, temperature and reaction time.

In some cases polymers were obtained simply by the addition of an excess of an aqueous solution of metal acetate to a dioxane solution of the bis-(β-diketone). The highly insoluble precipitate was purified by extraction with water followed by an organic solvent such as alcohol, acetone or benzene.

In the cases in which immediate precipitation did not occur, the pH was adjusted by addition of ammonia or urea. When no precipitation occurred in the reaction mixture even after standing for a long time, the reaction mixture was evaporated slowly *in vacuo* and the residue was collected. The residue was purified by extraction with water followed by organic solvent.

2. *Melt polymerization* (*method B*). This is analogous to many organic polymerizations. A mixture of metal acetylacetonate and bis-(β-diketone) was heated under a nitrogen atmosphere, and then *in vacuo*. Volatile by-products were collected in a trap. In order to prevent the condensation of volatile by-products in the reaction vessel, the upper section was heated by means of a resistance wire operated through a Variac. A distinct disadvantage is the formation of metallic oxide due to the decomposition of the metal acetylacetonate. The decomposition can be minimized by controlling the reaction time and temperature.

3. *Reaction in non-aqueous solvents* (*method C.*) A modification of method B was found to be suitable in some instances. A solution of bis-(β-diketone) in a solvent such as decalin or xylene was refluxed with metal acetylacetonate. When equivalent amounts of the metal acetylacetonate and bis-(β-diketone) were refluxed in a non-aqueous solvent, acetylacetonate was produced and distilled *in vacuo*. The polymers precipitated from the solution or were recovered by evaporation of the solution.

4. *Interfacial polymerization* (*Method D*). This method utilizes interfacial systems which consist of an aqueous phase containing the metal salt and an immiscible organic phase containing the bis-(β-diketone). Only one polymer was prepared by this method.

The physical properties and proposed types of structure of the metal ion–bis-(β-diketone) polymers prepared are summarized in Tables 4A–13A.

TABLE 4A.—METAL ION-1,1,2,2-TETRAACETYLETHANE

Metal ion	Method of preparation	m.p. °C	Description	Solubility in common organic solvents	Type of proposed structure
Be(II)	C	>250	White powder	Insoluble	I
Cu(II)	C	>250	Green powder	Insoluble	II
Ni(II)	B	>250	Gray brownish powder	Insoluble	I
Zn(II)	A	decompose at 240	White powder	Insoluble	II
Co(II)	C	250	Purple powder	Insoluble	III

TABLE 5A.—METAL ION-1,2-DIACETYL-1,2 DIBENZOYLETHANE

Metal ion	Method of preparation	m.p. (°C)	Description	Solubility in common organic solvents	Type of proposed structure
Be(II)	B	Soften at 150	Light rose resinous	Insoluble	III
Cu(II)	A	>250	Greenish brown	Insoluble	III
Ni(II)	B	>210	Brown powder	Insoluble	III
Zn(II)	B	>250	Brown powder	Soluble	III

TABLE 6A.—Metal ion-1,1,4,4-tetraacetylbutane

Metal ion	Method of preparation	m.p. (°C)	Description	Solubility in common organic solvents	Type of proposed structure
Be(II)	C	>300	White powder	Insoluble	III
Cu(II)	A	>250	Green powder	Insoluble	I
Ni(II)	C	>250	Brown powder	Soluble	III

TABLE 7A.—METAL ION-1,4-BIS-(2,2-DIACETYLETHYL)-BENZENE

Metal ion	Method of preparation	m.p. °C	Description	Solubility in common organic solvents	Type of proposed structure
Be(II)	C	>250	White powder	Insoluble	I
Cu(II)	A	>250	Gray powder	Insoluble	II
Ni(II)	D	>250	Light green powder	Insoluble	III
Co(II)	C	>250	Purple powder	Insoluble	III

TABLE 8A.—METAL ION-BIS-(DIACETYLMETHYL)-SULPHIDE

Metal ion	Method of preparation	m.p. (°C)	Description	Solubility in common organic solvents	Type of proposed structure
Cu(II)	A	decompose at 123°	Green powder	Insoluble	I

TABLE 9A.—METAL ION-1,1,3,3-TETRA-ACETYLPROPANE

Metal ion	Method of preparation	m.p. (°C)	Description	Solubility in common organic solvents	Type of proposed structure
Be(II)	C	Soften at 100	Light rose, resinous	Soluble	II
Cu(II)	A	Soften at 140	Brown, resinous	Soluble	II
Ni(II)	B	Soften at 140	Green, resinous	Soluble	II

TABLE 10A.—METAL ION-1,3-DIACETYL-1,3-DIBENZOYLPROPANE

Metal ion	Method of preparation	m.p. (°C)	Description	Solubility in common organic solvents	Type of proposed structure
Be(II)	C	Soften at 150	Orange, resinous	Soluble	II
Cu(II)	C	Soften at 120	Green, resinous	Soluble	II
Ni(II)	B	Soften at 200	Brown, resinous	Soluble	II

TABLE 11A.—METAL ION-1,1,3,3-TETRABENZOYLPROPANE

Metal ion	Method of preparation	m.p. (°C)	Description	Solubility in common organic solvents	Type of proposed structure
Be(II)	B	Soften at 150	Light yellow resinous material	Soluble	III
Cu(II)	B	>250	Light green powder	Insoluble	III
Ni(II)	B	>270	Brown powder	Insoluble	III

TABLE 12A.—METAL ION-2-PHENYL-1,1,3,3-TETRAACETYLPROPANE

Metal ion	Method of preparation	m.p. (°C)	Description	Solubility in common organic solvents	Type of proposed structure
Be(II)	B	Soften at 170	Light rose resinous material	Soluble	II
Cu(II)	A	>200	Greenish brown powder	Insoluble	II
Ni(II)	B	>250	Greenish brown powder	Insoluble	III

TABLE 13A.—METAL ION-2-PHENYL-1,3-DIACETYL-1,3-DIBENZOYLPROPANE

Metal ion	Method of preparation	m.p. °C	Description	Solubility in common organic solvents	Type of proposed structure
Be(II)	B	Soften at 150	orange resinous material	Soluble	III
Cu(II)	C	>260	green powder	Insoluble	III
Ni(II)	B	>230	yellowish brown powder	Insoluble	III

On the basis of elementary analysis, three types of structures are postulated for the polymers obtained:

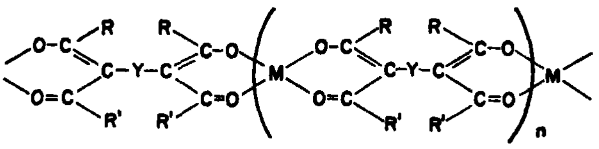

I

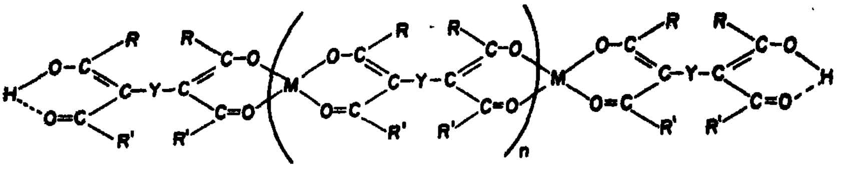

II

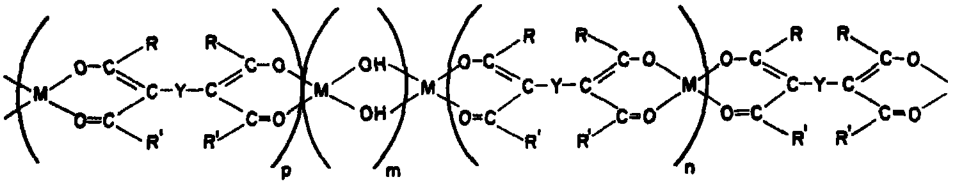

III

where R and R′ represent alkyl or aryl groups, Y a connecting group and M a divalent tetracoordinate metal ion.

All of the polymers of type I are insoluble in organic solvents, probably because they have high molecular weights. Similarly, those of type III, which contain co-ordinated hydroxo groups, are insoluble. The solubility of the type II polymers shows reasonably good correlation with the molecular weight of the polymer, those of low molecular weight dissolving readily. It should be pointed out that on polymers of type II, the number of bis-diketone groups must exceed the number of metallic ions by one, so the analytical data indicate the molecular weights of these polymers. As might be expected, the polymers of type II generally have lower melting points than those of type I and type III. In most cases, the melting points are not at all sharp.

The beryllium polymers prepared by the method of melt polymerization or evaporation of solvent as in methods A and C, generally have a glassy appearance, and are resinous when melted. Similar characteristics were observed in the polymers derived from 1,1,3,3-tetraacetylpropane and 1,3-diacetyl-1,3-dibenzoylpropane shown in Tables 9 and 10, all of which are of type II.

Determination of thermal stability

A relatively simple thermogravimetric balance[13] was used for a study of thermal stability of the polymers prepared. The tests were run on about 200 mg samples. The weight loss was measured after successive heating periods of ten hours at each temperature. The thermal stabilities are summarized in Tables 4B–13B. In general, the order

TABLE 4B.—METAL ION-1,1,2,2-TETRA-ACETYLETHANE (% WEIGHT LOSS)

Metal ion	200°C	250°C	300°C	350°C	400°C
Be(II)	1·18	7·59	8·55	29·20	75·90
Cu(II)	3·10	11·18	36·40	71·20	—
Ni(II)	5·82	13·10	29·50	72·20	—
Zn(II)	8·70	18·88	51·00	—	—
Co(II)	10·02	40·00	62·40	—	—

---

[13] M. L. JUDD, Thesis, Doctor of Philosophy, University of Illinois, (1958).

Table 5B.—Metal ion-1,2-diacetyl-1,2-dibenzoylethane (% weight loss)

Metal ion	200°C	250°C	300°C	350°C	400°C
Be(II)	3·05	8·05	15·70	35·65	60·25
Cu(II)	2·04	11·45	25·25	39·75	79·50
Ni(II)	3·82	16·70	38·80	61·50	—
Zn(II)	5·36	19·47	25·30	49·50	73·50

Table 6B.—Metal ion-1,1,4,4-tetra-acetylbutane

Metal ion	200°C	250°C	300°C	350°C	400°C
Be(II)	3·25	10·75	20·65	40·75	70·65
Cu(II)	4·75	16·95	42·25	69·75	—
Ni(II)	4·95	20·25	41·50	68·75	—

Table 7B.—Metal ion-1,4-bis-(2,2-diacetylethyl) benzene (% weight loss)

Metal ion	200°C	250°C	300°C	350°C	400°C
Be(II)	1·96	6·71	20·00	33·20	79·20
Cu(II)	3·78	32·40	63·20	—	—
Ni(II)	7·66	28·20	70·20	—	—
Zn(II)	9·50	22·30	62·30	—	—
Co(II)	11·50	54·90	63·90	—	—

Table 9B.—Metal ion-1,1,3,3-tetraacetylpropane (% weight loss)

Metal ion	200°C	250°C	300°C	350°C	400°C
Be(II)	8·62	21·72	34·65	42·75	—
Cu(II)	9·50	26·70	40·52	62·72	—
Ni(II)	7·80	25·70	38·50	71·72	—

Table 10B.—Metal ion-1,3-diacetyl-1,3-dibenzoylpropane (% weight loss)

Metal ion	200°C	250°C	300°C	350°C	400°C
Be(II)	9·65	18·45	32·27	40·65	71·80
Cu(II)	8·74	20·37	34·85	62·75	—
Ni(II)	6·07	13·90	29·50	72·30	—

Table 11B.—Metal ion-1,1,3,3-tetrabenzoylpropane (% weight loss)

Metal ion	200°C	250°C	300°C	350°C	400°C
Be(II)	3·02	13·52	25·72	36·72	56·52
Cu(II)	3·12	15·02	31·72	49·65	—
Ni(II)	4·52	17·52	36·92	62·05	—

Table 12B.—Metal ion-2-phenyl-1,1,3,3-tetraacetylpropane (% weight loss)

Metal ion	200°C	250°C	300°C	350°C	400°C
Be(II)	5·52	23·61	35·60	61·80	—
Cu(II)	21·90	39·00	53·50	72·50	—
Ni(II)	17·52	36·72	55·47	78·79	—

Table 13B.—Metal ion-2-phenyl-1,3-diacetyl-1,3-dibenzoylpropane (% weight loss)

Metal ion	200°C	250°C	300°C	350°C	400°C
Be(II)	3·04	19·65	32·54	59·50	—
Cu(II)	6·75	20·65	37·95	65·40	
Ni(II)	10·35	29·65	43·75	69·25	—

of thermal stabilities is Be(II) > Cu(II) > Ni(II) > Zn(II) > Co(II), which loosely parallels the order found in the β-diketone chelates.[14–16] Korshak and coworkers[17] have reported that the hydrolytic stabilities of bis-β-diketone coordination polymers (pK) show a certain parallelism with their thermal stabilities, but the number of cases studied is too small to establish this with any certainty. Generally, the polymers derived from bis-(benzoylacetones) and bis-(dibenzoylmethanes) are thermally more stable than the polymers derived from the corresponding bis-acetylacetones. Similarly, the polymers derived from bis-(β-diketones) containing a connecting group such as $—CH_2—$, $—(CH_2)_2—$, $—CH(C_6H_5)—$ or $—CH_2—$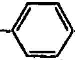$—CH_2—$are thermally less stable than the polymers derived from the corresponding bis-(β-diketones) which have no connecting group; the order of thermal stabilities of such polymers is $—(CH_2)_2— \sim —CH_2—$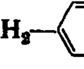$—CH_2— > —CH_2— >$ 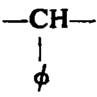 $\underset{\phi}{\underset{|}{—CH—}}$. The beryllium polymers do not always conform to these generalizations.

EXPERIMENTAL

Synthesis of bis-(β-Diketone)

Bis-(β-Diketones) were synthesized according to the methods referred in Tables 1, 2 and 3.

Metal ion-bis-(β-diketones) polymers

1. *Reaction in aqueous solution* (*method A*). To a solution of bis-(diketone) (0·005–0·01 mole) in 75–100 ml of dioxane or methyl alcohol was slowly added an equivalent amount of metal acetate or ammoniacal metal acetate in 25–50 ml of solution over a period of 30–60 min. In the cases in which no precipitate formed, the solution was refluxed for several hours and evaporated to dryness *in vacuo*. The precipitate or residue was washed well with water and extracted with acetone, alcohol or benzene in a Soxhlet extractor.

2. *Melt polymerization* (*method B*). After heating equivalent amounts of the metal acetylacetonate and bis-(β-diketone) at 150–200°C for 2 hr under a nitrogen atmosphere, the melted material was heated *in vacuo* for another 2–3 hr; volatile material was thereby removed. The remaining material was purified by extraction with organic solvents; those which were soluble in organic solvents were not purified.

3. *Reaction in non-aqueous solvents* (*method C*). Solutions of the metal acetylacetonate and bis-(β-diketone) (0·005–0·01 mole) were mixed in 100 ml of decalin or xylene; the mixture was refluxed for five hr and then concentrated to half of its volume under vacuum. If no precipitate came out of the solution on cooling, the product was obtained by evaporating the solution to dryness *in vacuo*. The polymers were purified as described above.

4. *Interfacial polymerization* (*method D*). A 0·005 molar solution of the bis-(β-diketone) in methylene chloride and an equivalent volume of 0·005 molar ammoniacal solution of the metal acetate or bromide were stirred together slowly for 2 hr. A scum formed at the interface of the two layers. The product was filtered, washed well with water, and extracted with organic solvents.

The analytical data and preparative methods are summarized in Tables 4C–13C.

(14) R. G. Charles and M. A. Pawlikowski, *J. Phys. Chem.* **62**, 440 (1958).

(15) J. van Hoene, R. G. Charles and W. M. Hickam, *J. Phys. Chem.* **62**, 1098 (1958).

(16) E. W. Berg and J. T. Truemper, *J. Phys. Chem.* **64**, 487 (1960).

(17) V. V. Korshak, E. S. Krongauz, A. M. Sladkov, V. E. Sheine and L. K. Luneva, *Vysokomolekulyarnyl Soedineniya* **1**, 1765 (1959).

TABLE 4C.—METAL ION-1,1,2,2-TETRA-ACETYLETHANE

Metal ion	Proposed formula	Analytical data					
		Carbon (wt. %)		Hydrogen (wt. %)		Metal (wt. %)	
		Found	Calc.	Found	Calc.	Found	Calc.
Be(II)	$(C_{10}H_{12}O_4Be)n$	59·43	58·52	6·10	5·85	4·29	4·39
Cu(II)	$(C_{10}H_{12}O_4)_{11}Cu_{10}$	48·72	47·3	5·02	4·73	24·20	22·75
Ni(II)	$(C_{10}H_{12}O_4Ni)n$	46·88	47·12	4·94	4·75	20·76	23·02
Zn(II)	$(C_{10}H_{12}O_4)_7Zn_8(H_2O)_{12}$	41·42	42·42	5·00	5·40	19·69	19·90
Co(II)	$(C_{10}H_{12}O_4)_{20}(OH)_2Co_{21}$	46·58	46·12	5·18	4·65	24·60	23·82

TABLE 5C.—METAL ION-1,2-DIACETYL-1,2-DIBENZOYLETHANE

Metal ion	Proposed formula	Analytical data					
		Carbon (wt. %)		Hydrogen (wt. %)		Metal (wt. %)	
		Found	Calc.	Found	Calc.	Found	Calc.
Be(II)	$(C_{20}H_{16}O_4)_{12}(OH)_{14}Be_{19}$	67·50	67·70	5·19	4·88	3·84	4·02
Cu(II)	$(C_{20}H_{16}O_4)_{13}(OH)_2Cu_{14}$	60·94	61·17	4·19	4·16	17·68	17·48
Ni(III)	$(C_{20}H_{16}O_4)_{13}(OH)_2Ni_{14}$	60·23	62·20	4·60	4·21	15·82	16·37
Zn(II)	$(C_{20}H_{16}O_4)_{13}(OH)_4Zn_{15}\cdot 14H_2O$	57·34	57·14	4·31	4·39	17·82	17·95

TABLE 6C.—METAL ION-1,1,4,4-TETRAACETYLBUTANE

Metal ion	Proposed formula	Analytical data					
		Carbon (wt. %)		Hydrogen (wt. %)		Metal (wt. %)	
		Found	Calc.	Found	Calc.	Found	Calc.
Be(II)	$(C_{12}H_{16}O_4)_4(OH)_6Be_7$	55·29	54·27	6·93	6·64	7·17	5·94
Cu(II)	$(C_{12}H_{16}O_4Cu)n$	49·64	50·10	5·74	5·56	21·42	22·08
Ni(II)	$(C_{12}H_{16}O_4)_{11}(OH)_{10}Ni_{16}\cdot 6H_2O$	43·19	43·02	5·37	5·38	24·74	25·50

TABLE 7C.—METAL ION-1,4-BIS(2,2-DIACETYLETHYL) BENZENE

Metal ion	Proposed formula	Analytical data					
		Carbon (wt. %)		Hydrogen (wt. %)		Metal (wt. %)	
		Found	Calc.	Found	Calc.	Found	Calc.
Be(II)	$(C_{18}H_{20}O_4Be\cdot 1/2\ H_2O)n$	67·83	67·92	6·51	6·60	2·70	2·83
Cu(II)	$(C_{18}H_{20}O_4)_5Cu_4$	61·33	61·48	5·81	5·85	14·65	14·46
Ni(II)	$(C_{18}H_{20}O_4)_7(OH)_2Ni_8\cdot 16H_2O$	52·06	52·28	6·37	6·01	16·40	16·32
Co(II)	$(C_{18}H_{20}O_4)_8(OH)_{12}Co_{11}\cdot 7H_2O$	39·97	40·27	4·88	4·69	24·17	24·16

TABLE 8C.—METAL ION-BIS-(DIACETYLMETHYL) SULPHIDE

Metal ion	Proposed formula	Analytical data					
		Carbon (wt. %)		Hydrogen (wt. %)		Metal (wt. %)	
		Found	Calc.	Found	Calc.	Found	Calc.
Cu(II)	$(C_{10}H_{12}O_4SCu)n$	41·79	41·79	5·12	4·12	—	—

TABLE 9C.—METAL ION-1,1,3,3-TETRAACETYLPROPANE

Metal ion	Proposed formula	Analytical data					
		Carbon (wt. %)		Hydrogen (wt. %)		Metal (wt. %)	
		Found	Calc.	Found	Calc.	Found	Calc.
Be(II)	$(C_{11}H_{14}O_4)_2Be$	64·46	61·54	6·49	6·52	1·78	2·09
Cu(II)	$(C_{11}H_{14}O_4)_2Cu\cdot 2H_2O$	50·28	50·82	6·17	6·16	12·54	12·22
Ni(II)	$(C_{11}H_{14}O_4)_3Ni_2$	53·19	53·01	5·08	5·62	15·98	15·71

TABLE 10C.—METAL ION-1,3-DIACETYL-1,3-DIBENZOYLPROPANE

Metal ion	Proposed formula	Analytical data					
		Carbon (wt. %)		Hydrogen (wt. %)		Metal (wt. %)	
		Found	Calc.	Found	Calc.	Found	Calc.
Be(II)	$(C_{21}H_{18}O_4)_2Be$	73·30	74·44	5·86	5·32	1·43	1·33
Cu(II)	$(C_{21}N_{18}O_4)_6Cu_5\cdot 18H_2O$	56·94	57·16	5·96	5·44	12·23	12·00
Ni(II)	$(C_{21}H_{18}O_4)_5Ni_4\cdot 4H_2O$	64·18	63·73	5·13	4·95	11·81	11·87

TABLE 11C.—METAL ION-1,1,3,3-TETRABENZOYLPROPANE

Metal ion	Proposed formula	Analytical data					
		Carbon (wt. %)		Hydrogen (wt. %)		Metal (wt. %)	
		Found	Calc.	Found	Calc.	Found	Calc.
Be(II)	$(C_{31}H_{22}O_4)_{13}(OH)_{10}Be_{18}$	77·08	76·91	5·43	4·74	2·85	2·57
Cu(II)	$(C_{31}H_{22}O_4)_{13}(OH)_6Cu_{16}$	69·37	68·37	4·49	4·15	14·59	14·36
Ni(II)	$(C_{31}H_{22}O_4)_{14}(OH)_2Ni_{15}.2H_2O$	71·16	70·74	4·60	4·26	12·05	11·95

TABLE 12C.—METAL ION-2-PHENYL-1,1,3,3-TETRA-ACETYLPROPANE

Metal ion	Proposed formula	Analytical data					
		Carbon (wt. %)		Hydrogen (wt. %)		Metal (wt. %)	
		Found	Calc.	Found	Calc.	Found	Calc.
Be(II)	$(C_{17}H_{18}O_4)_4Be_3$	69·18	69·6	6·38	6·15	2·30	2·30
Cu(II)	$(C_{17}H_{18}O_4)_4Cu_3$	61·45	61·04	5·70	5·57	13·36	14·24
Ni(II)	$(C_{17}H_{18}O_4)_4(OH)_{10}Ni_9$	44·97	44·29	4·62	4·48	26·68	28·66

TABLE 13C.—METAL ION-2-PHENYL-1,3-DIACETYL-1,3-DIBENZOYLPROPANE

Metal ion	Proposed formula	Analytical data					
		Carbon (wt. %)		Hydrogen (wt. %)		Metal (wt. %)	
		Found	Calc.	Found	Calc.	Found	Calc.
Be(II)	$(C_{27}H_{22}O_4)_5(OH)_4Be_7$	73·78	74·24	5·10	5·26	2·54	2·90
Cu(II)	$(C_{27}H_{22}O_4)_4(OH)_{10}Cu_9$	57·63	54·41	4·28	4·14	25·02	23·99
Ni(II)	$(C_{27}H_{22}O_4)_5(OH)_{14}Ni_{12}\cdot 11H_2O$	50·99	50·77	4·32	4·57	22·01	22·07

J. Inorg. Nucl. Chem., 1962, Vol. 24, pp. 1235 to 1239. Pergamon Press Ltd. Printed in Northern Ireland

A GENERALIZED FORMULATION OF THE METHOD OF CONTINUOUS VARIATIONS FOR MIXED LIGAND COMPLEXES

K. O. WATKINS and M. M. JONES*
Department of Chemistry, Vanderbilt University, Nashville, Tennessee

(*Received* 6 *December* 1961; *in revised form* 23 *April* 1962)

Abstract—Equations are developed which describe the method of continuous variations for the case of a single complex with an arbitrarily large number of types of ligands. The restrictions which apply to the use of the absorption of light in the study of such a case are also developed. When any other complex is present, the maximum concentration of the principal complex will be found in a solution which contains the reactants in a mole ratio other than that in which they enter the complex. Such displacements have been found in a large number of systems reported in the literature and may be expected to be an inevitable, but not necessarily obvious, feature of such studies.

The wide use of the method of continuous variations has resulted in its application to a large number of systems for which there is no corresponding complete theoretical treatment. The purpose of this paper is to present a general continuous variations solution for the case of a single complex containing an arbitrarily large number of ligands. The results of the examination of this general case can then be applied to the examination of some typical cases from the literature.

THE general chemical equation for the formation of a single complex from metal ions, A, and various ligands, B, C, D, etc., can be expressed as:

$$\alpha_1 A + \alpha_2 B + \alpha_3 C + \alpha_4 D + \ldots \alpha_N Z = A\alpha_1 B\alpha_2 C\alpha_3 D\alpha_4 \ldots Z\alpha_N \qquad (1)$$

where the α's represent the integral amounts of A, B, C, D, etc., used to form the complex.

If the activities and concentrations are assumed to be equal, and if C_1 represents the concentration of A, C_2 that of B, etc., then the instability constant can be written as:

$$KC_c = C_1^{\alpha_1} C_2^{\alpha_2} C_3^{\alpha_3} C_4^{\alpha_4} \ldots C_N^{\alpha_N} \qquad (2)$$

where C_c represents the concentration of the complex.

If solutions of the reactants in which the total molarity is constant are prepared, and if the original contributions of A, B, C, D, etc., to the constant molarity are represented as x_1, x_2, x_3, x_4 respectively, then the concentrations of these species after reaction will be:

$$C_N = M\left(1 - \sum_{i=1}^{N-1} x_i\right) - \alpha_N C_c. \qquad (3)$$

In order to show the conditions for a maximum in the concentration of the complex more readily, equation (2) is written

$$\log K + \log C_c = \sum_{i=1}^{i=N} \alpha_i \log C_i \qquad (4)$$

---

* To whom correspondence concerning this paper should be addressed.

The conditions for an extremum in C_c (13) are simply that:

$$\frac{\delta \log C_c}{\delta x_1} = \frac{\delta \log C_c}{\delta x_2} = \frac{\delta \log C_c}{\delta x_3} = \frac{\delta \log C_c}{\delta x_4} = \dots \frac{\delta \log C_c}{\delta x_N} = 0. \tag{5}$$

If equation (4) is differentiated with respect to x_1, then x_2, etc., equation (5) can be used to give a series of equations which must be satisfied simultaneously if an extremum in log C_c (and hence C_c) is to occur. These equations are:

$$\frac{\delta \log C_c}{\delta x_{N-1}} = \alpha_{N-1} \frac{\delta \log C_{N-1}}{\delta x_{N-1}} + \dots\dots \alpha_N \frac{\delta \log C_N}{\delta x_{N-1}} = 0. \tag{6}$$

Substitution of the derivatives of the logarithmic form of equations (3) into equations (6) (setting $dC_c/dx = 0$) gives:

$$\alpha_{N-1}\left(\frac{M}{Mx_{N-1} - \alpha_{N-1}C_c}\right) - \alpha_N \frac{M}{M\left(1 - \sum_{i=1}^{N-1} x_i\right) - \alpha_N C_c} = 0 \tag{7}$$

Equation (7) may be written:

$$\frac{\alpha_1}{Mx_1 - \alpha_1 C_c} = \frac{\alpha_2}{Mx_2 - \alpha_2 C_c} = \frac{\alpha_3}{Mx_3 - \alpha_3 C_c} = \dots = \frac{\alpha_N}{M\left(1 - \sum_{i=1}^{N-1} x_i\right) - \alpha_N C_c} \tag{8}$$

or in pairs such as

$$\alpha_1(Mx_2 - \alpha_2 C_c) = \alpha_2(Mx_1 - \alpha_1 C_c) \text{ etc.} \tag{9}$$

Equation (9) can be satisfied when:

$$\frac{\alpha_1}{x_1} = \frac{\alpha_2}{x_2} \tag{10}$$

and hence equations (8) can be written as:

$$\frac{\alpha_1}{x_1} = \frac{\alpha_2}{x_2} = \frac{\alpha_3}{x_3} = \frac{\alpha_4}{x_4} = \dots = \frac{\alpha_N}{1 - \sum_{i=1}^{N-1} x_i} = \frac{\alpha_N}{x_N}. \tag{11}$$

Equation (11) gives the condition for an extreme value of C_c as one in which the initial molar fractions are the same as the ratios in which the materials enter the complex. This is a maximum, as can be shown by a Taylor series expansion, utilizing the fact that the first derivatives vanish at certain values of x_1 given by equation (11). The values of the variables which satisfy equation (11) are denoted $x_1^{(0)}$, $x_2^{(0)}$, etc. This procedure is analogous to that given by HANCOCK.⁽¹⁾ Let x_1, x_2, etc., be another set of positive values of the variables for which

$$M\left(1 - \sum_{i=1}^{N-1} x_i\right) - \alpha_N C_c$$

is positive, and substitute the value $x_1^{(0)} + u(x_1 - x_1^{(0)}) \dots x_N^{(0)} + u(x_N - x_N^{(0)})$ where $0 < u < 1$ for the variables in log C_c. The Taylor series expansion for log $C_c^{(0)}$

---

(1) H. HANCOCK, *Theory of Maxima and Minima*, Chap. V, Ginn, Boston (1917).

then gives: (observing that the first derivative vanishes)

$$\log C_c^{(0)} = \log C_c - \frac{1}{2}\left[\alpha_1 \frac{(x_1^{(1)} - x_1^{(0)})^2}{(x_1)^2} + \ldots \alpha_N \frac{(\sum x_1^{(1)} - \sum x_1^{(0)})^2}{\left(1 - \sum_{i=1}^{N-1} x_i\right)^2}\right], \quad (12)$$

where $x_1 \ldots x_N$ are variables of the form:

$$x_1^{(0)} + \theta(x_1 - x_1^{(0)}), \ldots x_N^{(0)} + \theta(x_N - x_N^{(0)}) \text{ with } 0 < \theta < 1. \quad (13)$$

Since the bracketed expression is always positive and different from zero for $x_1 \neq x_1^{(0)}$, etc., then $\log C_c > \log C_c^{(0)}$ or $C_c > C_c^{(0)}$, and hence C_c is a *maximum*. If two complexes are present, these conditions are no longer satisfied and it is then more profitable to make a detailed examination of the specific case under consideration.

For a system of mixed ligands, it is imperative that the range of the variables x_1, x_2, ..., x_N be such that only a single complex forms within this range. It is then possible to examine the effect of higher and lower complexes on the position of the maximum by the use of methods similar to those used by Vosburgh[2,3] and Katzin[4].

EXAMINATION OF THE *Y* FUNCTION

The condition for an extreme value in the physical property, in this case the absorption of monochromatic light, for the general case of a complex with many ligands is $dY/dx = 0$.

If ϵ_0, ϵ_1, ϵ_2, ϵ_3, ϵ_4, ..., ϵ_N represent the respective extinction coefficients of compounds A, B, C, D, E, F, ..., Z and C_1, C_2, C_3, C_4, ..., C_N represent the respective concentrations of these compounds, the general expression for the extinction A_r, of the reaction solution for equation (1) can be written

$$A_r = L\left[\left(\sum_{i=1}^{i=N} \epsilon_1 C_i\right) + \epsilon_c C_c\right], \quad (14)$$

where N is the number of compounds involved in the complex and L is the length of the light path. The general expression for the extinction A_{nr}, of the solution assuming no reaction is:

$$A_{nr} = L\left[M\left(1 - \sum_{i=1}^{N-1} x_i\right)\epsilon_N + M \sum_{i=1}^{N-1} x_i \epsilon_i\right]. \quad (15)$$

The Y function is equal to $A_r - A_{nr}$ or

$$Y = L\left[\sum_{i=1}^{i=N} \epsilon_i C_i + \epsilon_c C_c - M\left(1 - \sum_{i=1}^{N=1} x_i\right)\epsilon_N - M \sum_{i=1}^{N=1} x_i \epsilon_i\right]. \quad (16)$$

The condition for Y to show an extreme value is that $dY/dx_1 = dY/dx_2 = dY/dx_3 = \ldots dY/dx_N = 0$. The condition to satisfy for a simultaneous maximum in the

---

[2] W. C. Vosburgh and G. R. Cooper, *J. Amer. Chem. Soc.* **63**, 437 (1941).

[3] R. K. Gould and W. C. Vosburgh, *J. Amer. Chem. Soc.* **64**, 1630 (1942).

[4] L. I. Katzin and E. Gebert, *J. Amer. Chem. Soc.* **72**, 5455 (1950).

physical property and the concentration is $dY/dx_i = dC_c/dx_i = 0$. The expanded Y function from equation (16) is

$$Y = L\Bigg[\epsilon_1 C_1 + \epsilon_2 C_2 + \epsilon_3 C_3 + \ldots \epsilon_N C_N + \epsilon_c C_c - M\left(1 - \epsilon_N \sum_{i=1}^{N-1} x_i\right) - \epsilon_1 M x_1 - \epsilon_2 M x_2 - \epsilon_3 M x_3 - \ldots \epsilon_N M x_N\Bigg]. \tag{17}$$

The derivatives of Y with respect to $x_1, x_2, x_3, \ldots, x_N$ are

$$\frac{dY}{dx_N} = L\left[\epsilon_1 \frac{\delta C_1}{\delta x_N} + \epsilon_2 \frac{\delta C_2}{\delta x_N} + \epsilon_3 \frac{\delta C_3}{\delta x_N} + \ldots \epsilon_N \frac{\delta C_N}{\delta x_N} + \epsilon_c \frac{\delta C_c}{\delta x_N} + \epsilon_N M \frac{\delta\left(\sum_{i=1}^{N-1} x_i\right)}{\delta x_N} - M \frac{\delta\left(\sum_{i=1}^{N-1} \epsilon_i x_i\right)}{\delta x_N}\right]. \tag{18}$$

Substitution of the derivative forms of equations (3) into the equations given above gives the following equations respectively:

$$\frac{dY}{dx_N} = L\Bigg[\epsilon_1\left(M \frac{\delta x_1}{\delta x_N} - \alpha_1 \frac{\delta C_c}{\delta x_N}\right) + \epsilon_2\left(M \frac{\delta x_2}{\delta x_N} - \alpha_2 \frac{\delta C_c}{\delta x_N}\right) + \epsilon_3\left(M \frac{\delta x_3}{\delta x_N} - \alpha_3 \frac{\delta C_c}{\delta x_N}\right) + \ldots \epsilon_N\left\{\left(-M \frac{\delta \sum_{i=1}^{N-1} x_i}{\delta x_N}\right) - \alpha_N \frac{\delta C_c}{\delta x_N}\right\} + \epsilon_c \frac{\delta C_c}{\delta x_N} + \epsilon_N M \frac{\delta \sum_{i=1}^{N-1} x_i}{\delta x_N} - M \frac{\delta \sum_{i=1}^{N-1} \epsilon_i x_i}{\delta x_N}\Bigg]. \tag{19}$$

The general expression dY/dx_N for the formation of a mononuclear complex from many ligands can be written

$$dY/dx_N = L[dC_c/dx_N(\epsilon_c - \alpha_1\epsilon_1 - \alpha_2\epsilon_2 - \alpha_3\epsilon_3 - \ldots \alpha_N\epsilon_N)]. \tag{20}$$

The condition for an extremum in dY/dx_N that coincides with an extremum in dC_c/dx_N is $\epsilon_c \neq \alpha_1\epsilon_1 + \alpha_2\epsilon_2 + \alpha_3\epsilon_3 + \ldots \alpha_N\epsilon_N$.

If $\epsilon_c > \alpha_1\epsilon_1 + \alpha_2\epsilon_2 + \alpha_3\epsilon_3 + \ldots \alpha_N\epsilon_N$, then a maximum occurs in dC_c/dx_N. If $\epsilon_c < \alpha_1\epsilon_1 + \alpha_2\epsilon_2 + \alpha_3\epsilon_3 + \ldots \alpha_N\epsilon_N$, a minimum occurs in dC_c/dx_N.

The most probable way to satisfy the maximum condition is to pick a wavelength so that all the ϵ's except ϵ_c will be zero. In this circumstance, Y will show an extreme value when C_c does, and the extreme value will be a maximum.

It has thus been demonstrated that it is possible to obtain a simultaneous extremum in the concentration of the complex and in the physical property, and this is sufficient proof that the method of continuous variations can be theoretically extended to the formation of any single mixed ligand complex.

The conditions required for this extension are so severe however, that it will be impractical in all but a very few cases. It should be noted that if more than one complex is present, as is almost always the case, then the concentration of even a predominant mixed complex will no longer reach maximum value at the stoicheiometric mole ratios of the reactants. Such displacements are determined by the relative amounts of the principal complex and other complexes present. These displacements can be seen in many of the studies already published which use this method where they may be seen to vary from displacements which are barely perceptible to ones of the order of 0·10 units on x.(5–13)

Acknowledgements—We wish to acknowledge with thanks the financial assistance for this work provided by grants from the Research Corporation and the National Science Foundation.

(5) G. L. Eichhorn and J. W. Dawes, *J. Amer. Chem. Soc.* **76**, 5666 (1954).

(6) G. L. Eichhorn and N. D. Marchand, *J. Amer. Chem. Soc.* **78**, 2691 (1956).

(7) L. Segal, H. B. Jonassen and R. E. Reeves, *J. Amer. Chem. Soc.* **78**, 274 (1956).

(8) A. A. Schildt, *J. Amer, Chem. Soc.* **79**, 5423 (1957).

(9) L. Newman and D. N. Hume, *J. Amer. Chem. Soc.* **79**, 4581 (1952).

(10) L. Somer and M. Hnilickova, *Bull. Soc. Chim. France* 36 (1959), also present a theory which is capable of accounting for some of their observed displacements, but not all. They did not consider the general case.

(11) J. I. Watters, J. Mason, and A. Aaron, *J. Amer. Chem. Soc.* **75**, 5212 (1953).

(12) R. de Witt and J. I. Watters, *J. Amer. Chem. Soc.* **76**, 3810 (1954).

(13) L. Newman and D. N. Hume, *J. Amer. Chem. Soc.* **83**, 1795 (1961).

J. Inorg. Nucl. Chem., 1962, Vol. 24, pp. 1241 to 1250. Pergamon Press Ltd. Printed in Northern Ireland

ACID CATALYSIS OF THE HYDROLYSIS OF ACETATO-PENTAMMINE COMPLEXES OF COBALT(III), RHODIUM(III) AND IRIDIUM(III)*†

F. MONACELLI, F. BASOLO and R. G. PEARSON
Department of Chemistry, Northwestern University, Evanston, Illinois

(*Received* 29 *March* 1962; *in revised form* 23 *April* 1962)

Abstract—The syntheses of $[M(NH_3)_5(RCOO)](ClO_4)_2$ where M = Rh(III) or Ir(III) and $RCOO^-$ = CH_3COO^-, $(CH_3)_3CCOO^-$ or CF_3COO^- are described. The rates of hydrolysis of these complexes as well as the corresponding Co(III) systems were determined in acid, $[H^+] = 0{\cdot}01–0{\cdot}1$ M. In all cases the rates of hydrolysis increase with increase of acid concentration. The mechanism of acid hydrolysis of these systems is discussed.

KINETIC studies of the hydrolysis of acetato and substituted acetatopentamminecobalt (III) ions,

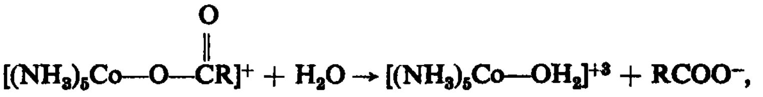

$$[(NH_3)_5Co—O—\overset{\overset{\displaystyle O}{\|}}{C}R]^+ + H_2O \rightarrow [(NH_3)_5Co—OH_2]^{+3} + RCOO^-, \qquad (1)$$

were reported earlier.(1) The rates of hydrolysis were found to be the same, within experimental error, at H^+ concentrations of 0·004 and 0·008 M. It was concluded that in this acid region there was no detectable acid catalysis. Yet it is known that the hydrolysis of certain types of complexes are acid catalysed. These complexes seem to fall into either one or the other of two different categories. (1) Complexes containing ligands that are strongly basic or have a large tendency to hydrogen bond, e.g. $[Co(NH_3)_5CO_3]^+$(2), $[Co(en)_2F_2]^+$(3) and $[Fe(CN)_6]^{4-}$,(4). (2) Complexes containing flexible multidentate basic ligands, e.g. $[Fe(bipy)_3]^{2+}$,(5), $[Fe(EDTA)]^-$,(6), $[Ni(EDTA)]^{2-}$,(7), and $[Cr(C_2O_4)_3]^{3-}$,(8).‡

This paper reports the results of a kinetic investigation on hydrolysis reactions of type (1) where the metals are cobalt (III), rhodium (III), and iridium (III) and the negative ligands are CH_3COO^-, and $(CH_3)_3COO^-$, and CF_3COO^-. In all cases the rates

---

* This research was supported by the United States Air Force through the Air Force Office of Scientific Research of the Air Research and Development Command, under Contract No. AF 49(638)-315. Reproduction in whole or in part is permitted for any purpose of the United States Government.

† This paper was presented by F. M. at the meeting of the Italian Chemical Society in Naples in May, 1962.

‡ The symbols used are: en = ethylenediamine, bipy = 2,2′-bipyridine, EDTA = ethylenediaminetraacetate ion.

(1) F. BASOLO, J. G. BERGMANN and R. G. PEARSON, *J. Phys. Chem.* **56**, 22 (1952).
(2) A. B. LAMB and K. J. MYSELS, *J. Amer. Chem. Soc.* **67**, 468 (1945).
(3) F. BASOLO, W. R. MATOUSH and R. G. PEARSON, *J. Amer. Chem. Soc.* **78**, 4883 (1956).
(4) A. W. ADAMSON, J. P. WELKER and W. B. WRIGHT, *J. Amer. Chem. Soc.* **73**, 4789 (1951).
(5) J. H. BAXENDALE and P. G. GEORGE, *Trans. Faraday Soc.* **46**, 736 (1950).
(6) S. S. JONES and F. A. LONG, *J. Phys. Chem.* **56**, 25 (1952).
(7) D. W. MARGERUM, *J. Phys. Chem.* **63**, 336 (1959).
(8) K. V. KRISHNAMURTY and G. M. HARRIS, *J. Phys. Chem.* **64**, 346 (1960).
(9) A. WERNER and N. GOSLINGS, *Ber. Dtsch. Chem. Ges.* **36**, 2380 (1903).

depend on the concentration of H+ between acid concentrations of 0·01–0·10 M. A tentative mechanism for hydrolysis is discussed.

EXPERIMENTAL

Preparation of complexes. The complexes of Co(III) were prepared by the reaction of [Co(NH$_3$)$_5$CO$_3$]NO$_3$ with the desired acid according to the methods described previously(1,9). The only difference was that the desired complexes, [Co(NH$_3$)$_5$(RCOO)]$^{2+}$, were isolated as the perchlorate salts by the dropwise addition of conc. HClO$_4$ to the reaction mixture surrounded by an ice-bath. The aquo complexes, [M(NH$_3$)$_5$H$_2$O](ClO$_4$)$_3$, of Co(III),(10) Rh(III)(11) and Ir(III)(12) were also prepared by the methods described in the literature.

No report was found for the synthesis of salts of [Ir(NH$_3$)$_5$(RCOO)]$^{2+}$. The compound [Rh(NH$_3$)$_5$(CH$_3$COO)] Br$_2$.H$_2$O is described as being prepared by grinding the hydroxo compound in a suspension of acetic anhydride.(13) Our results by this method were not satisfactory so that the methods described here were used. The Rh(III) and Ir(III) complexes were prepared by the reaction

$$[M(NH_3)_5H_2O]^{3+} + RCOO^- \rightarrow [M(NH_3)_5(RCOO)]^{2+} + H_2O \qquad (2)$$

This is essentially the same reaction as that used for the synthesis of the Co(III) complexes but the experimental conditions are different. Since the Rh(III) and Ir(III) compounds had not been prepared previously, the methods of synthesis are described. However, it should be remembered that the primary purpose was to obtain the pure compounds so that no attempt was made to find the optimum conditions for maximum yields. Detailed procedures are given only for the preparation of the acetato complexes of Rh(III) and Ir(III). The trifluoroacetato complexes were prepared in the same way whereas slight modifications were necessary for the pivalato systems. These modifications, due to the insolubility of pivalic acid in water, are described.

[Rh(NH$_3$)$_5$(CH$_3$COO)](ClO$_4$)$_2$. An excess (~3 g) of Ag$_2$O was added to a hot (~70°C) solution of 2·25 g of [Rh(NH$_3$)$_5$Cl]Cl$_2$(14) contained in 150 ml of water. The mixture was stirred for a few (~5) minutes and then filtered. The filtrate, which is perhaps largely [Rh(NH$_3$)$_5$Cl](OH)$_2$, was refluxed for one hour. At this point a second excess of Ag$_2$O was added and the mixture was again stirred for a few minutes. The insoluble material was removed on a filter and the filtrate was refluxed for one hour. This same procedure was repeated a third time. Such a tedious procedure was used because prolonged refluxing of [Rh(NH$_3$)$_5$Cl] Cl$_2$ in an aqueous suspension of Ag$_2$O—AgCl results in the apparent loss of NH$_3$ and some decomposition of the complex.

The final filtrate containing [Rh(NH$_3$)$_5$OH] (OH)$_2$ was acidified with 25 ml of CH$_3$COOH and the solution was evaporated to dryness on a steam-bath. Care must be taken to remove the solid residue from the steam bath as soon as it becomes dry in order to prevent decomposition. The solid residue was then dissolved in 50 ml of water and conc. HClO$_4$ was added dropwise (~10 ml) with constant stirring. Small white crystals of the desired product, [Rh(NH$_3$)$_5$(CH$_3$COO)](ClO$_4$)$_2$ separated. These were collected on a filter, washed with alcohol and ether, then air dried at room temperature. The compound prepared in this way was sufficiently pure but further purification was possible by recrystallization from a minimum amount of water.

The pivalato complex was prepared in the same way also starting with 2·25 g of [Rh(NH$_3$)$_5$Cl]Cl$_2$. The final filtrate containing [Rh(NH$_3$)$_5$OH](OH)$_2$ was heated on a steam bath and 5 g of (CH$_3$)$_3$CCOOH was added along with sufficient (10 ml) ethanol to put it in solution. The reaction mixture was then concentrated to about 50 ml and 3 g of (CH$_3$)$_3$CCOOH was added plus enough ethanol to dissolve it. After heating on the steam-bath for an additional hour, the solution was cooled to room temperature and transferred to a separatory funnel. The solution was twice extracted with 50 ml of ether to remove the excess acid. The water solution was then cooled in an ice-bath and conc. HClO$_4$ was added (~10 ml) dropwise. The desired crystalline salt was collected on a filter, washed with alcohol and ether, and air dried at room temperature. Since the salt is very soluble in water, it was recrystallized from boiling ethanol to which was added just enough water to dissolve the solid.

[Ir(NH$_3$)$_5$(CH$_3$COO)](ClO$_4$)$_2$. The Ag$_2$O procedure described above was not used for the Ir(III) system which is known(12) to generate the hydroxo complex by reaction with NaOH. A solution of 2 g of [Ir(NH$_3$)$_5$Cl] Cl$_2$(15) in 70 ml of 1M NaOH was refluxed for 8 hr. The reaction mixture was then acidified by the addition of 30 ml of conc. CH$_3$COOH after which it was evaporated to 2 ml on a steam bath. Another 20 ml of conc. CH_3COOH was added and heating was continued for 1 hr. Enough water was added to give a volume of about 50 ml and the solution was cooled in an ice-bath. The addition of conc. $HClO_4$ (~10 ml) dropwise with stirring yielded the desired white crystalline product. This was collected on a filter washed with ethanol and ether, and then air dried at room temperature. Further purification by recrystallization from an ethanol–water mixture was possible.

---

(10) Gmelins' *Handbuch der Anorganischen Chemie*, **58** B, 94 (1932).

(11) Gmelins' *Handbuch der Anorganischen Chemie*, **64**, 109 (1938).

(12) Gmelins' *Handbuch der Anorganischen Chemie*, **67**, 144 (1939).

(13) B. E. Dixon, *J. Chem. Soc.* 781 (1935).

(14) Gmelins' *Handbuch der Anorganischen Chemie*, **64**, 134 (1938).

(15) Gmelins' *Handbuch der Anorganischen Chemie*, **67**, 157 (1939).

The pivalato complex was prepared by refluxing 1·9 g of $[Ir(NH_3)_5H_2O](ClO_4)_3$ with 40 ml of a saturated solution at room temperature of $(CH_3)_3CCOONa$ for 10 hr. This reaction mixture was then cooled to room temperature and 12 ml of conc. $HClO_4$ was slowly added. After transferring to a separatory funnel the mixture was extracted with 150 ml of diethyl ether. The solid containing the desired compound contaminated with pivalic acid was collected on a filter. This solid mixture was then dissolved in 10 ml of hot water and extracted again with 50 ml of ether. The water layer was then cooled in an ice-salt bath and conc. $HClO_4$ (~5 ml) was added dropwise. The crystalline product which separated was collected and recrystallized from absolute ethanol.

The analyses of all of these compounds are reported in Table 1. The microanalysis determinations of C, H and N were made by Miss H. Beck. The percentage of anion, either ClO_4^- or NO_3^-, was determined by the replacement of Cl^- from an anion resin. Approximately 50 mg of the complex salt was dissolved in about 5 ml of water and this solution was passed through IRA-400 in the chloride form. The chloride ion eluted was then titrated with 0·01 M $AgNO_3$ using K_2CrO_4 as an indicator. For the aquo complexes it was necessary to first remove the complex on a cation resin, IR-120 in the sodium form. Unless this is done there is apparently an interaction between the aquo complex and chromate ion which makes it difficult to get reliable results. It was also necessary to remove all Co(III) complexes in this manner, since the pink colored solutions make it difficult to see the visual end point. Analytical data for all of these compounds are reported in Table 1.

TABLE 1.—ANALYSES OF THE $[M(NH_3)_5(RCOO)](ClO_4)_2$ COMPOUNDS

Compound	Per cent calculated C	H	N	ClO_4^-	Per cent found C	H	N	ClO_4^-
$[Co(NH_3)_5H_2O](ClO_4)_3$	—	—	—	64·8	—	—	—	64·5
$[Co(NH_3)_5CH_3COO](NO_3)_2$	7·37	5·50	30·0	37·9*	7·02	5·66	30·3	38·0*
$[Co(NH_3)_5(CH_3)_3CCOO](ClO_4)_2$	13·5	5·40	—	44·8	13·9	5·84	—	45·6
$[Co(NH_3)_5CF_3COO](ClO_4)_2$	5·25	3·28	—	43·6	5·35	3·54	—	43·6
$[Rh(NH_3)_5H_2O](ClO_4)_3$	—	—	13·8	59·2	—	—	13·8	59·5
$[Rh(NH_3)_5CH_3COO](ClO_4)_2$	5·36	4·03	—	44·6	5·36	4·21	—	44·4
$[Rh(NH_3)_5(CH_3)_3COO](ClO_4)_2$	12·3	4·90	14·3	40·8	11·7	5·15	14·0	40·8
$[Rh(NH_3)_5CF_3COO](ClO_4)_2$	4·80	3·00	14·0	39·8	4·70	3·74	14·3	39·7
$[Ir(NH_3)_5H_2O](ClO_4)_3$	—	—	11·9	50·2	—	—	12·1	49·6
$[Ir(NH_3)_5CH_3COO](ClO_4)_2$	4·46	3·35	13·0	37·1	4·93	3·79	13·3	37·3
$[Ir(NH_3)_5(CH_3)_3CCOO](ClO_4)_2$	10·4	4·15	12·1	34·4	9·91	4·09	12·2	34·5
$[Ir(NH_3)_5CF_3COO](ClO_4)_2$	4·06	2·54	11·8	33·7	4·03	2·91	12·0	33·6

* This is % NO_3^-.

Kinetic studies. The rates of reaction were followed spectrophotometrically. In all cases the wavelength used was that known to give a large change in optical density during hydrolysis. These wavelengths (shown for each system in Table 2) were determined by a comparison of the spectra of the acetato complexes, $[(NH_3)_5(RCOO)]^{2+}$, with the corresponding aquo complex, $[M(NH_3)_5(H_2O)]^{3+}$. These spectra were measured using a Beckman DK-2 recording spectrophotometer. The spectra for M = Rh(III) are shown in Fig. 1. Those for Co(III) and Ir(III) are similar except that they are shifted towards longer and shorter wavelengths, respectively.

Except for the very slow reactions of the Ir(III) complexes, the experimental procedure used to follow the rates of hydrolysis was always the same. In general aqueous solutions were prepared containing approximately 1–1·5 mg/ml of complex, 0·01–0·1 M $HClO_4$ and sufficient $NaClO_4$ to give an ionic strength of 0·100 ± 0·005. Some of the solution was placed in a 1 cm stoppered quartz cell which was then inserted in a Beckman DU cell compartment. This was maintained at constant temperature, ±0·1°, by circulating water from a thermostatic bath. Because very high temperatures were required, it was necessary to separate the heated spacers from the rest of the instrument. This was done by placing a half inch insulator layer next to the heated spacers and then water cooled spacers between the insulator and the instrument. In this way it was possible to maintain temperatures as high as 90° in the cell compartment whilst keeping the rest of the instrument at room temperature. The quartz cell containing the reaction mixture was positioned in the light path only during the time of actual measurements of optical density. The reference cell contained either water or a $NaClO_4$–$HClO_4$ solution.

TABLE 2.—RATES OF HYDROLYSES OF $[M(NH_3)_5RCOO]^{2+}$ COMPLEXES*

Complex	λ (mμ)	Temp. (°C)	[H+] (M)	k_{obs} (sec^{-1})	k_{H_2O} (sec^{-1})	k_{H^+} (sec^{-1} M^{-1})
$[Co(NH_3)_5CH_3COO]^{2+}$	292	55·0	0·0485	9·8 × 10^{-6}	1·4 × 10^{-6}	1·7 × 10^{-4}
		69·9	0·0480	5·4 × 10^{-5}	8·0 × 10^{-6}	9·3 × 10^{-4}
		78·8	0·0097	4·3 × 10^{-5}		
		78·7	0·0194	7·1 × 10^{-5}		
		78·8	0·0291	9·6 × 10^{-5}		
		78·8	0·0485	1·4 × 10^{-4}	2·0 × 10^{-5}	2·5 × 10^{-3}
$[Co(NH_3)_5(CH_3)_3CCOO]^{2+}$	310	70·9	0·0480	1·7 × 10^{-5}	5·2 × 10^{-6}	2·5 × 10^{-4}
		78·6	0·0097	2·6 × 10^{-5}		
		78·6	0·0485	5·0 × 10^{-5}		
		78·6	0·0730	6·4 × 10^{-5}		
		78·6	0·0970	7·7 × 10^{-5}	2·1 × 10^{-5}	5·8 × 10^{-4}
		88·3	0·0465	1·6 × 10^{-4}	7·7 × 10^{-5}	1·6 × 10^{-3}
$[Co(NH_3)_5CF_3COO]^{2+}$	268	60·0	0·0192	1·8 × 10^{-5}	1·8 × 10^{-5}	
		70·0	0·0096	5·7 × 10^{-5}	5·7 × 10^{-5}	~3 × 10^{-5}
		78·8	0·0097	1·5 × 10^{-4}		
		78·9	0·0485	1·6 × 10^{-4}		
		78·9	0·0960	1·7 × 10^{-4}	1·5 × 10^{-4}	~1 × 10^{-4}
$[Rh(NH_3)_5CH_3COO]^{2+}$	230	53·8	0·099	2·0 × 10^{-5}		2·0 × 10^{-4}
		62·7	0·096	5·2 × 10^{-5}		5·3 × 10^{-4}
		78·8	0·0194	5·5 × 10^{-5}		
		78·9	0·0291	8·2 × 10^{-5}		
		78·7	0·0485	1·3 × 10^{-4}	~4 × 10^{-6}	2·6 × 10^{-3}
$[Rh(NH_3)_5(CH_3)_3CCOO]^{2+}$	245	68·6	0·098	3·2 × 10^{-5}		3·3 × 10^{-4}
		78·4	0·0194	1·9 × 10^{-5}		
		78·6	0·0485	4·6 × 10^{-5}		
		78·6	0·0970	8·8 × 10^{-5}	~2 × 10^{-6}	8·9 × 10^{-4}
		87·6	0·0470	1·1 × 10^{-4}	~6 × 10^{-6}	2·1 × 10^{-3}
$[Rh(NH_3)_5CF_3COO]^{2+}$	223	64·0	0·0195	3·3 × 10^{-5}	3·1 × 10^{-5}	~8 × 10^{-5}
		72·8	0·0190	8·4 × 10^{-5}	8·2 × 10^{-5}	~1 × 10^{-4}
		78·9	0·0097	1·5 × 10^{-4}		
		78·9	0·0485	1·6 × 10^{-4}	1·5 × 10^{-4}	~1·5 × 10^{-4}
$[Ir(NH_3)_5CH_3COO]^{2+}$	230	79·9	0·0194	1·6 × 10^{-6}		
		79·9	0·0485	4·1 × 10^{-6}		
		80·0	0·0776	5·9 × 10^{-6}		
		80·0	0·0970	7·2 × 10^{-6}	<1 × 10^{-6}†	7·7 × 10^{-5}
		91·5	0·0465	1·1 × 10^{-5}	<1 × 10^{-6}†	2·4 × 10^{-4}
$[Ir(NH_3)_5(CH_3)_3CCOO]^{2+}$	225	80·6	0·0388	3·9 × 10^{-7}		
		80·6	0·0582	6·2 × 10^{-7}		
		80·6	0·0873	8·4 × 10^{-7}	<1 × 10^{-7}†	1·0 × 10^{-5}
		95·5	0·055	3·6 × 10^{-6}	<1 × 10^{-7}†	6·0 × 10^{-5}
$[Ir(NH_3)_5CF_3COO]^{2+}$	240	74·0	0·0475	7·3 × 10^{-6}	1·8 × 10^{-6}	1·2 × 10^{-4}
		80·7	0·0194	6·3 × 10^{-6}		
		80·7	0·0388	1·0 × 10^{-5}		
		80·7	0·0680	1·5 × 10^{-5}		
		80·7	0·0970	2·0 × 10^{-5}	3·1 × 10^{-6}	1·8 × 10^{-4}
		92·5	0·0185	1·7 × 10^{-5}	1·1 × 10^{-5}	3·5 × 10^{-4}

* Ionic strength of 0·10 ($NaClO_4$).

† These values are so small that only limiting values can be assigned.

For the slow reactions of the Ir(III) complexes, the reacting solutions in aluminum foil covered volumetric flasks, were kept in a thermostatic bath. Aliquots of the solutions were removed at various times and the reaction was quenched by cooling to room temperature. The optical densities were determined for each aliquot.

Both techniques gave good results. The data used for kinetic plots were those obtained after equilibrium temperature had been reached, which required about 10 min. From the optical densities observed and the known initial concentrations and the molar absorbancy of the aquo and acetato species, it was possible to calculate the extent of reaction at various times. Fig. 2 shows that good first order plots of the data were obtained over a period of approximately one half-life. The values of k_{obs} have a precision of ±5 per cent or better. The absorption spectra of the reaction mixture of

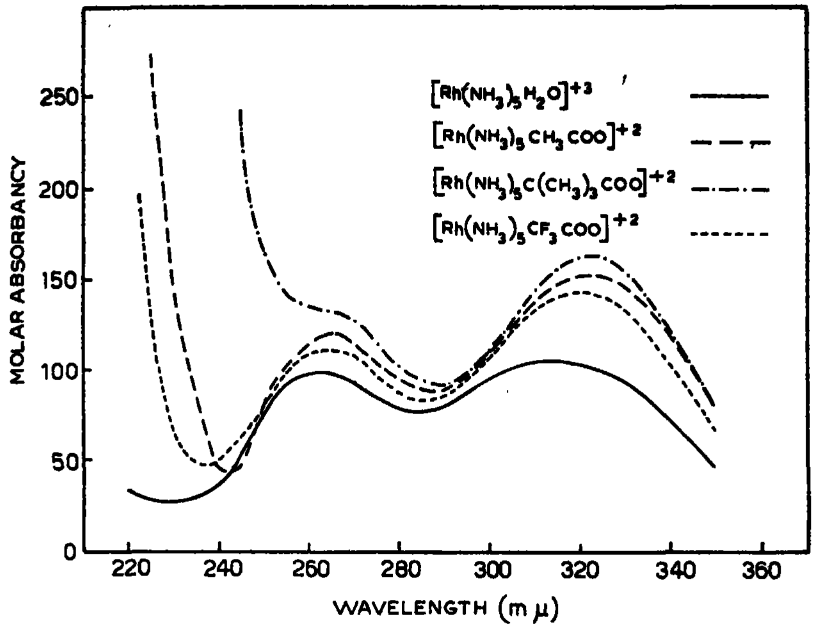

FIG. 1.—The absorption spectra of rhodium(III) complexes.

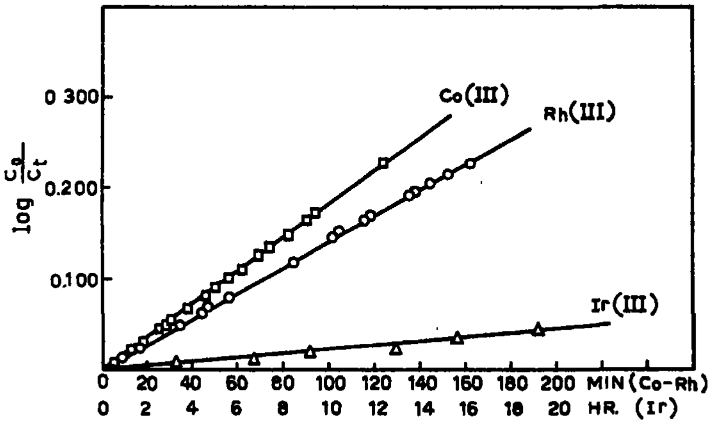

FIG. 2.—The rates of hydrolyses of $[M(NH_3)_5CH_3COO]^{2+}$. Temperatures: Co, 78·7°; Rh, 78·8°; Ir, 79·9°. Acid concentration of 0·0197 M H^+.

$[Rh(NH_3)_5CH_3COO]^{+2}$ at infinite time was the same as that of the corresponding aquo complex. Determinations for Co(III) and Rh(III) were made at three different temperatures in order to estimate the enthalpies and entropies of activation. Only two temperatures were used for the slowest reactions of the Ir(III) complexes.

Oxygen-18 *studies*. The method used to determine the $^{18}O/^{16}O$ ratio in the aquo product $[Rh(NH_3)_5H_2O]\,Br_3$ was the same as that described by ANBAR and GUTTMANN(16). We are indebted

---

(16) M. ANBAR and S. GUTTMANN, *J. Appl. Rad. Isotopes* 5, 233 (1959).

to Professor H. TAUBE for permitting us to perform these experiments in his laboratory. We wish also to thank Mr. J. B. HUNT for his assistance with some of the experimental details.

The general procedure was to dissolve ~0·2 g of $[Rh(NH_3)_5(CH_3COO)](ClO_4)_2$ in 10 ml of 1 M $HClO_4$, of water of approximately 1·8 per cent oxygen-18, which was at 80°. After 20 min. (±95 per cent reaction), the solution was transferred to a centrifuge tube contained in an ice-bath. The mixture was centrifuged and the mother liquor decanted from the crystalline solid. This was then dissolved in 7 ml of normal water and 5 ml of conc. HBr was added. The mixture was cooled in an ice-bath and then centrifuged. The bromide salt was collected and dried in a vacuum desiccator over $CaCl_2$ for 5 hr. A yield of approximately 80 per cent was obtained. The salt had the correct ultra-violet spectrum, bromide analysis and weight loss when heated at 100° for the compound $[Rh(NH_3)_5H_2O]Br_3$. In a control experiment the same procedure was followed starting with 0·2 g of $[Rh(NH_3)_5H_2O](ClO_4)_3$.

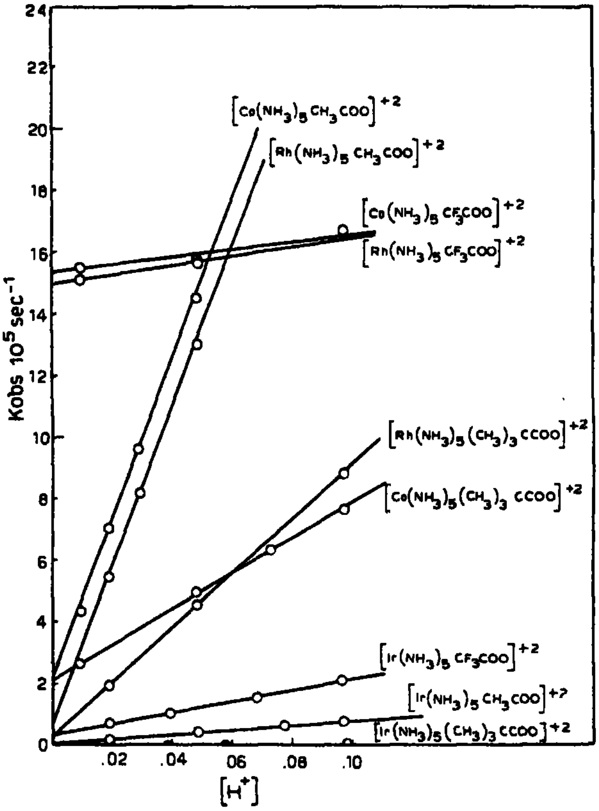

FIG. 3—Rates of hydrolyses of $[M(NH_3)_5(RCOO)]^{+2}$ vs. $[H^+]$ at ~80° and $\mu = 0{\cdot}10$.

RESULTS

The observed rate constants k_{obs}, for the hydrolyses of $[M(NH_3)_5(RCOO)]^{2+}$ as a function of $[H^+]$ are given in Table 2. From plots of k_{obs}vs. $[H^+]$ as shown in Fig. 3, it is possible to estimate the uncatalysed rate constants, k_{H_2O}, as well as the acid catalysed rate constants, k_{H^+} (see Equation 3). The apparent independence of the rate at low $[H^+]$ reported in Reference (2) is not in disagreement with Fig. 3. The variation in rate expected is so small as to be within experimental error. The rate constants at various temperatures are, also included in Table 2. Some of the values of k_{H_2O} are so very small that only a rough approximation is possible. Similarly the k_{H^+} values for $[M(NH_3)_5(CF_3COO)]^{2+}$ of Co(III) and Rh(III) are only given as an order of magnitude. Table 3 contains the available enthalpies and entropies of activation.

Oxygen-18 experiments show that the aquo product obtained by the hydrolysis of $[Rh(NH_3)_5(CH_3COO)]^{+2}$ has an O^{18}/O^{16} ratio corresponding closely to that of the heavy water solvent. Under the same conditions there is complete water exchange with the complex $[Rh(NH_3)_5H_2O]^{3+}$.

TABLE 3.—HEATS AND ENTROPIES OF ACTIVATION

Complex	k_{H_2O}		k_{H^+}	
	kcal/mole	e.u.	kcal/mole	e.u.
$[Co(NH_3)_5CH_3COO]^{2+}$	25	−8	25	+2
$[Co(NH_3)_5C(CH_3)_3COO]^{2+}$	—		26	+6
$[Co(NH_3)_5CF_3COO]^{2+}$	26	−2	—	—
$[Rh(NH_3)_5CH_3COO]^{2+}$	—	—	23	−4
$[Rh(NH_3)_5C(CH_3)_3COO]^{2+}$	—	—	23	−6
$[Rh(NH_3)_5CF_3COO]^{2+}$	25	−6	—	—
$[Ir(NH_3)_5CH_3COO]^{2+}$	—	—	25*	−8
$[Ir(NH_3)_5CF_3COO]^{2+}$	24	−14	14	−36

* Calculated from rate constants at only two temperatures.

DISCUSSION

The results given in Table 1 and shown graphically in Fig. 3, demonstrate that the rates of hydrolysis of $[(NH_3)_5M—O—\overset{\overset{\displaystyle O}{\|}}{C}R]^{2+}$ complexes depend on the H^+ concentration. Under the conditions of these experiments the observed pseudo first-order rate constant, k_{obs}, is found to fit the two term expression

$$k_{obs} = k_{H_2O} + k_{H^+}[H^+] \tag{3}$$

where k_{H_2O} is the extrapolated rate constant for the uncatalysed rate and k_{H^+} is the acid catalysed rate constant. This suggests that two reaction paths are involved and the results can be explained by the reactions

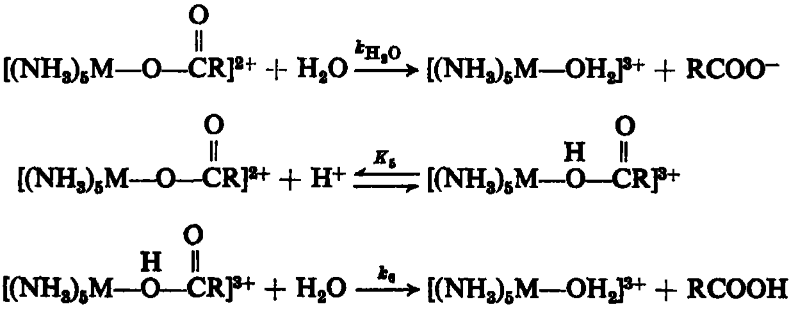

$$[(NH_3)_5M—O—\overset{\overset{\displaystyle O}{\|}}{C}R]^{2+} + H_2O \xrightarrow{k_{H_2O}} [(NH_3)_5M—OH_2]^{3+} + RCOO^- \tag{4}$$

$$[(NH_3)_5M—O—\overset{\overset{\displaystyle O}{\|}}{C}R]^{2+} + H^+ \underset{}{\overset{K_5}{\rightleftharpoons}} [(NH_3)_5M—\overset{H}{O}—\overset{\overset{\displaystyle O}{\|}}{C}R]^{3+} \tag{5}$$

$$[(NH_3)_5M—\overset{H}{O}—\overset{\overset{\displaystyle O}{\|}}{C}R]^{3+} + H_2O \xrightarrow{k_6} [(NH_3)_5M—OH_2]^{3+} + RCOOH \tag{6}$$

$$k_{H+} = K_5k_6$$

The same scheme was used to account for the acid catalysis of the replacement of monodentate ligands from other systems.(2,3,4) This requires that the protonated species be more liable than if it were not protonated, that reaction (6) be faster than (4). Of course it must be noted that only at high acid concentrations will there be enough of the protonated species for it to make an appreciable contribution to the overall rate of hydrolysis. Evidence for the protonation of $[Co(NH_3)_5CH_3COO]^{2+}$ was recently reported by VLČEK.(17)

The acid catalysis observed for the hydrolysis of these complexes containing monodentate carboxylate ligands is of interest with regards to the acid catalysed dissociation of certain metal chelates, e.g. $[Fe(EDTA)]^-$ and $[Cr(C_2O_4)_3]^{3-}$. For such systems containing multidentate carboxylate ligands, it was suggested that the acid catalysis may be due to protonation of the freed carboxylate ion.(6,7,8) This in turn could prevent its returning to the metal and reclosing the opened chelate ring. Kinetic evidence alone does not distinguish between this mechanism and an electrophilic attack by hydrogen ion on a coordinated carboxylate in the chelate,(7) as proposed in (5) and (6). It is not known which process is involved. However the electrophilic attack path is the only one available to systems containing monodentate carboxylate ligands. Thus this path may well be responsible for or at least make a contribution to the acid catalysed dissociation of certain metal chelates.

Previous studies on various acetatopentamminecobalt(III) complexes showed that at low acid concentrations their rates of hydrolyses are almost independent of the steric requirements of the carboxylate ligands, but the rates increase with decreasing base strength of the ligands anions.(1) The present investigation was initiated in order to determine whether the analogous rhodium(III) and iridium(III) systems have the same behaviour. The values of k_{H_2O} for the uncatalysed hydrolysis in Table 2 show that the rates for the acetate and pivalate complexes of Rh(III) and Ir(III) respectively seem to be of the same order of magnitude. Furthermore they are approximately one or two orders of magnitude slower than the rates for the analogous trifluoracetate complexes. Unfortunately the rates are so small that the extrapolated values, except for the trifluoroacetate systems, can only be given to an order of magnitude. However the results do show that the Rh(III) and Ir(III) complexes follow the same general pattern as was observed previously for the complexes of Co(III).

The values for the acid catalysed hydrolysis constants, k_{H^+}, in Table 2 show again that the three metal systems seem to behave in a similar manner. In each case the rate decreases by a factor of approximately five in going from the acetate to the pivalate complexes, whereas a decrease of about twenty occurs in going from acetate to trifluoroacetate for the Co(III) and Rh(III) systems. The slower rate for the trifluoroacetate complexes can be explained in terms of a lower concentration of the protonated species. Thus equilibrium (5) is not so far to the right, due to the trifluoroacetate ion being the weakest base. Since pivalate ion is only a slightly stronger base than acetate ion, the slower rates of hydrolysis of the pivalate complexes are due to steric effects. It is not clear why the value of k_{H^+} for the trifluoroacetate complex of Ir(III) is larger than for the corresponding acetato complex.

These complexes have at least a formal relationship to organic esters, the difference being that the pentamminemetal(III) in essence takes the place of the alkyl group derived from the alcohol in the ester. Various techniques have been used to demonstrate that in the acid hydrolysis of esters, acyl-oxygen bond cleavage,

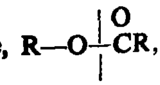

$R{-}O\,\vdots\,\overset{O}{C}R$,

---

(17) A. A. VLČEK, *Advances in the Chemistry of Coordination Compounds* (Edited by S. KIRSCHNER) pp. 590–603. Macmillan, New York (1961).

occurs instead of the alkyl-oxygen bond.(18) With this formalism in mind, it is of interest to consider whether the hydrolysis of these complexes proceeds by metal-oxygen (7) or acyl-oxygen (8) bond fission.

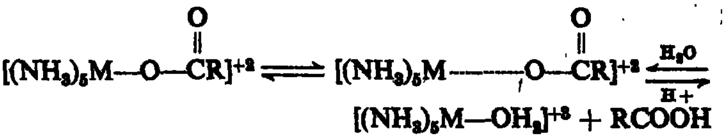

$$[(NH_3)_5M{-}O{-}\overset{\overset{O}{\|}}{C}R]^{+2} \rightleftharpoons [(NH_3)_5M \cdots O{-}\overset{\overset{O}{\|}}{C}R]^{+2} \xrightleftharpoons[H+]{H_2O} [(NH_3)_5M{-}OH_2]^{+3} + RCOOH \qquad (7)$$

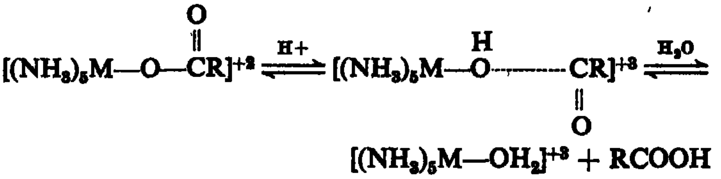

$$[(NH_3)_5M{-}O{-}\overset{\overset{O}{\|}}{C}R]^{+2} \xrightleftharpoons{H+} [(NH_3)_5M{-}\overset{H}{O} \cdots \underset{\underset{O}{\|}}{C}R]^{+3} \xrightleftharpoons{H_2O} [(NH_3)_5M{-}OH_2]^{+3} + RCOOH \qquad (8)$$

Bunton and Llewellyn(19) have performed oxygen-18 experiments, at low acid concentration (pH ~ 4), on the hydrolysis of the cobalt(III) complexes $[Co(NH_3)_5 RCOO]^{2+}$. Using oxygen-18 water as the solvent, they found no isotropic enrichment in the reaction product CH_3COOH, but CF_3COOH contained oxygen-18. For the acetato complex this establishes that the uncatalysed hydrolysis path (4) proceeds by metal-oxygen bond cleavage (7). The result for the trifluoroacetato complex suggests acyl-oxygen bond fission. However this was somewhat inconclusive because under the same experimental conditions there is extensive oxygen exchange between CF_3COOH and water.

In an attempt to determine the position of bond rupture for the acid catalysed path (6), oxygen-18 experiments were performed on $[Rh(NH_3)_5CH_3COO]^{2+}$. Isotopic enrichment was found in the product $[Rh(NH_3)_5H_2O]^{3+}$ but under the same experimental conditions, water in this complex was observed to exchange with the solvent. Therefore the isotopic enrichment found does not provide information as to the position of bond fission during hydrolysis. That the rate of water exchange of the aquo complex is similar to the rate of acid catalysed hydrolysis of the acetato complex may at first seem unexpected. Since the protonated acetate ligand, CH_3COOH, is a weaker base than H_2O, it is expected to be replaced more readily than water. However one must remember that the concentration of the protonated acetato species (5) even in 1 M H^+ is small, whereas the aquo complex is present in 100 per cent concentration. No attempt was made to examine the oxygen-18 content of the hydrolysis product CH_3COOH, because at these conditions of high acid concentration it would appear(20) that there will be extensive oxygen exchange between acetic acid and water.

Although appropriate oxygen-18 experiments have not yet been designed to establish the position of bond fission for the acid catalysed hydrolysis, the kinetic data in Table 2 provide some basis for speculation. First it should be noted that the rates of reaction for complexes of these metals are generally known to decrease in the order Co(III) > Rh(III) > Ir(III). Thus the estimated[21] relative rates of hydrolysis for the complexes $[M(NH_3)_5Br]^{2+}$ are 4,000:1000:1, respectively. This is definitely not the case for the acid catalysed hydrolysis of $[M(NH_3)_5RCOO]^{2+}$. The values of k_{H^+} for corresponding Co(III) and Rh(III) complexes are very nearly the same and those for analogous Ir(III) systems are only about fifty times smaller. It is further important to note that this is also the case for the k_{H_2O} values of the trifluoroacetato complexes. These results suggest an acyl-oxygen bond fission path in which the metal ion, one atom removed from the position of bond rupture, has a small effect.

---

(18) J. Hine, *Physical Organic Chemistry*, Chap. 12. McGraw Hill, New York (1956).

(19) C. A. Bunton and D. R. Llewellyn, *J. Chem. Soc.* 1692 (1953).

(20) I. Roberts and H. C. Urey, *J. Amer. Chem. Soc.* **61**, 2580 (1939); I. Roberts, *J. Chem. Phys.* **6**, 294 (1938); M. L. Bender, R. R. Stone and R. S. Dewey, *J. Amer. Chem. Soc.* **78**, 319 (1956).

(21) F. Basolo and R. G. Pearson, *Mechanisms of Inorganic Reactions*, pp. 121–122. J. Wiley, New York (1958).

For a reaction path involving metal–oxygen bond cleavage, a larger effect of the metal ion on the rate of reaction is expected. On the basis of the available data (Table 2), this appears to be the case for the water reaction, k_{H_2O}, of the acetato and pivalato complexes. Such a result is in agreement with the oxygen-18 experiments of BUNTON and LLEWELLYN.(19)

Additional support that the acetato and pivalato complexes undergo uncatalysed hydrolysis by metal–oxygen bond cleavage is afforded by the observation that the k_{H_2O} values for the two complexes of the same metal ion are approximately the same. Instead some steric retardation is observed for the rates of acid catalysed hydrolysis, k_{H^+}, which appear to involve acyl–oxygen bond fission. These observations are consistent with the expected results, since the pivalato group offers essentially no steric hindrance at the metal ion but does hinder attack at the acyl carbon atom.

That the hydrolyses of trifluoroacetato complexes may proceed by acyl–oxygen bond rupture was suggested earlier on the basis that the more positive acyl carbon atom is more susceptable to nucleophilic attack than it is in the corresponding acetato systems.(19) Likewise a protonated acetato ligand contains a more positive acyl carbon atom than does the parent acetato group. This then may be responsible for the preferred acyl–oxygen bond cleavage in the acid catalysed process.

Although the conclusions reached with regard to the position of bond rupture in these reactions are in accord with all of the present experimental facts, there is as yet no direct proof that these conclusions are correct.

Acknowledgement—F. M. wishes to thank the Consiglio Nazionale delle Ricerche for a travel grant to return to the University of Rome.

J. Inorg. Nucl. Chem., 1962, Vol. 24, pp. 1251 to 1256. Pergamon Press Ltd. Printed in Northern Ireland

THE EXTRACTION OF HYDROCHLORIC ACID AND SOME METAL CHLORIDES BY TRI-n-BUTOXYETHYL PHOSPHATE*

M. Halpern†, T. Kim and N. C. Li
Duquesne University, Pittsburgh 19, Pa.

(*Received* 8 *January* 1962; *in revised form* 23 *April* 1962)

Abstract—The physical chemistry of the extraction of HCl from aqueous solution by tributoxyethyl phosphate (TBEP) has been studied. In addition to the conventional distribution and water content determination, physical–chemical measurements of electrical conductivity, density and viscosity of the organic layer were carried out. The results indicate the formation of a monosolvate, HCl·TBEP. The extraction of chlorides of Zn^{2+}, In^{3+} and Cr^{3+} from aqueous hydrochloric acid into undiluted TBEP and into mixtures of TBEP and benzene has been studied using radioactive tracers. The extraction behaviour of TBEP has been compared with that of tri-n-butyl phosphate.

The extraction of HCl and of several metal chlorides by tri-n-butyl phosphate (TBP) has been studied by several investigators.(1–5) Since tri-n-butoxyethyl phosphate, $(C_4H_9OC_2H_4O)_3Po$, (TBEP), differs from TBP in possessing additional ether linkages, it was thought of interest to study the extraction behaviour of TBEP and compare it with that of TBP. This paper presents the results obtained.

EXPERIMENTAL

Materials. High activity ^{114}In, ^{65}Zn and ^{51}Cr were obtained from Oak Ridge National Laboratory in the form of indium, zinc and chromic chloride, respectively, each in hydrochloric acid solution. A sample of pure TBEP was obtained from the Food Machinery and Chemical Corp., as a gift.

Procedure. The swelling of the TBEP phase, due to the solubility of aqueous hydrochloric acid in it, was measured by introducing 5 ml of both aqueous solution and TBEP into 10 ml graduated (0·1 ml) centrifuge tubes, in the manner described by Kertes(1). It was shown by separate experiments that 15 min shaking periods were sufficient to establish equilibrium. The room temperature was 20 ± 2° and the effect of temperature within this range was within the error of the determinations. The acid contents in the aqueous and TBEP phases were also determined in the manner previously described(1).

Density, viscosity and electrical conductivity of the TBEP layers were measured in the usual manner in a thermostat at 25°. Water determinations in the TBEP layers were carried out by means of Karl Fischer reagent(1).

Kertes and Halpern(6) have demonstrated the hydrolytic degradation of TBP in the presence of hydrochloric acid, and we have observed the same phenomenon for TBEP. For this reason, all solvent equilibrations were made immediately prior to use.

In studies on the extraction of In(III), Cr(III) and Zn(II)-chloride, the aqueous phase normally was prepared to contain metal ion (radioisotope) in concentration of the order of 10^{-7} M and varying concentrations of hydrochloric acid. The organic phase was either undiluted TBEP or TBEP dissolved in benzene. In order to eliminate the volume change, the organic phase was pre-equilibrated with an equal volume of the aqueous solution to be used, without the radioisotope. In carrying out

---

* This investigation was supported by U.S. Atomic Energy Commission through Contract No. AT (30-1)-1922.

† On leave of absence from the Department of Inorganic and Analytical Chemistry, The Hebrew University, Jerusalem, Israel.

(1) A. S. Kertes, *J. Inorg. Nucl. Chem.* 14, 104 (1960).

(2) E. Hesford and H. A. C. McKay, *J. Inorg. Nucl. Chem.* 13, 156 (1960).

(3) H. Irving and D. N. Edgington, *J. Inorg. Nucl. Chem.* 10, 306 (1959).

(4) D. F. Peppard, G. W. Mason and M. V. Gergel, *J. Inorg. Nucl. Chem.* 3, 370 (1957).

(5) D. F. Peppard, G. W. Mason and J. L. Maier, *J. Inorg. Nucl. Chem.* 3, 215 (1956).

(6) A. S. Kertes and M. Halpern, *J. Inorg. Nucl. Chem.* 16, 308 (1961).

the experiment, 5 ml of the aqueous and organic phases were mixed, shaken mechanically for 15 min, and then centrifuged. Aliquots of both phases were removed, and the activity of the metal in each phase was measured with a γ-ray scintillation well counter in the manner described by WHITE *et al.*(7) The distribution coefficient K_d, is defined by the equation

$$K_d = \frac{\text{total M concn. in organic phase}}{\text{total M concn. in aqueous phase}} \qquad (1)$$

RESULTS

(A) *Distribution of hydrochloric acid*

Table 1 shows the molar concentrations of hydrochloric acid in the initial aqueous solutions, and in the equilibrium aqueous and TBEP layers. For solutions no. 1–4, inclusive, a plot of log $(\mathrm{HCl})_{\mathrm{TBEP}}$ vs. log $(\mathrm{HCl})_{\mathrm{aq}}$ is linear, with a slope close to unity.

TABLE 1.—THE DISTRIBUTION OF HCl BETWEEN AQUEOUS AND UNDILUTED TBEP AS A FUNCTION OF THE ACID CONCENTRATION IN THE INITIAL AQUEOUS SOLUTION. INITIAL PHASE VOLUMES 5 ml (12·8 mmole TBEP)

	Molarity of HCl				Extracted into the organic phase (mmole)	
No. of soln.	Initial aqueous soln.	Equil. aqueous phase	Equil. TBEP phase	Swelling of the TBEP phase, (ml)	HCl	H_2O
1	0·104	0·109	0·005	0·35	0·03	21·6
2	0·203	0·216	0·008	0·35	0·04	18·9
3	0·502	0·529	0·025	0·35	0·14	22·8
4	1·009	1·051	0·057	0·35	0·30	22·1
5	2·033	2·033	0·203	0·35	1·09	24·1
6	3·040	2·924	0·433	0·40	2·34	29·1
7	4·047	3·843	0·735	0·50	4·04	31·9
8	5·078	4·685	1·116	0·65	6·31	43·0
9	6·061	5·544	1·593	1·00	9·56	52·1
10	7·096	6·394	2·092	1·35	13·28	61·2
11	8·057	7·230	2·724	1·95	18·93	87·4
12	8·616	7·461	3·116	2·15	22·28	
13	9·092	7·897	3·695	2·60	28·08	118·1
14	9·540	8·156	3·992	3·00	31·93	
15	10·090	8·445	4·465	3·90	39·74	152·4
16	10·418	8·723	4·768	4·00	42·91	

This is expected if we consider the equilibrium

$$\mathrm{H^+_{aq}Cl^-_{aq}} = \mathrm{H^+Cl^-{\cdot}TBEP} \qquad (2)$$

and indicates that when HCl in the TBEP layer is below 0·05 M, it is appreciably ionized.

Fig. 1, curves 1, 2, 3, show the variation in density, viscosity and conductivity of the organic layer, respectively, with the mmoles of HCl extracted into undiluted TBEP (initial phase volumes, 5 ml). For each curve there is one intersection, at approximately 12·8 mmole of HCl in the organic phase. Since the total amount of TBEP in 5 ml corresponds to 12.8 mmoles of the ester (neglecting the extremely low solubility in water, 0·1 per cent), the break therefore may be ascribed to the formation of a mono-solvate, HCl·TBEP.

---

(7) J. M. WHITE, P. KELLY and N. C. LI, *J. Inorg. Nucl. Chem.* **16**, 337 (1961).

Numerical values for the distribution of water in TBEP are given in the last column of Table 1. Initially, about 1¼ mmoles of water are associated with each mmole of TBEP. Beginning with solution no. 5, a plot of the extracted H_2O vs. the extracted HCl, both in mmoles, is almost linear, with a slope approaching four. This indicates that each hydrochloric acid molecule is accompanied by four water molecules on passing from the aqueous phase into TBEP.

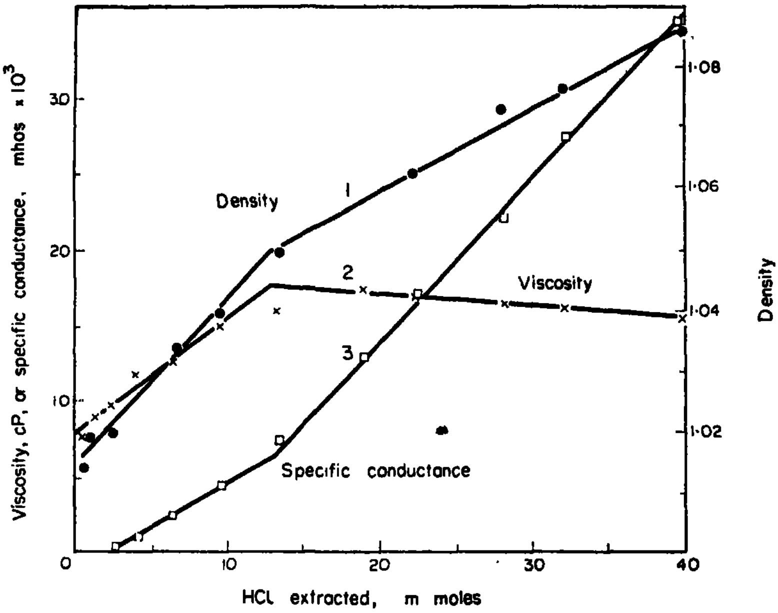

FIG. 1.—Density, viscosity, specific conductance of the equilibrium organic phases as a function of their HCl content.

(B) *Extraction of metal chlorides into* TBEP

Table 2 summarizes the results obtained with extraction of $^{114}InCl_3$, $^{65}ZnCl_2$ and $^{51}CrCl_3$ by undiluted TBEP from aqueous hydrochloric acid solutions. For Cr(III), it was necessary to use HCl solutions above 5 M, because at lower acidities K_d becomes too small to measure.

TABLE 2.—EXTRACTION WITH UNDILUTED TBEP

$(HCl)_{aqueous}$	$(HCl)_{TBEP}$	K_d		
		^{114}In	^{65}Zn	^{51}Cr
1·069 M	0·058 M	1·19	4·48	
1·260	0·073	1·66	5·50	
1·446	0·097	2·43	9·45	
1·655	0·126	3·43	11·51	
1·830	0·162	4·60	20·19	
1·957	0·182	5·76	19·73	
5·204	1·439			0·008
6·238	1·951			0·012
6·933	2·711			0·019
7·686	3·412			0·027
8·258	4·140			0·050

Several experiments were carried out in which the acidity of the equilibrium aqueous phase was kept constant, and the organic phase consisted of solutions of TBEP in benzene of varying concentrations. The results obtained for Zn(II) and In(III) are summarized in Table 3.

TABLE. 3.—EXTRACTION OF METAL IONS BY SOLUTIONS OF TBEP IN BENZENE OF DIFFERENT CONCENTRATION AT CONSTANT ACIDITY IN THE AQUEOUS PHASE

Concn. of TBEP in benzene, M	K_d			
	1 M HCl (aq.)		2 M HCl (aq.)	
	^{65}Zn	^{114}In	^{65}Zn	^{114}In
0·509	0·01	0·00	0·02	0·00
0·764	0·03	0·00	0·09	0·01
1·018	0·07	0·01	0·25	0·05
1·273	0·13	0·03	0·56	0·15
1·528	0·29	0·08	1·05	0·44
1·783	0·56	0·19		1·24

Plots of log K_d vs. log $(\text{TBEP})_{\text{in benzene}}$, at constant 1 M and 2 M HCl in the aqueous phase, yield straight lines with the same slope 3·1, for Zn(II). We would like to propose as a mechanism of extraction the following equation:

$$M^{n+}Cl_n^- + 3TBEP = MCl_n{\cdot}3TBEP + 3H^+Cl^- \qquad (3)$$

At constant acidity in the aqueous phase and using tracer level of metal, Equation (3) suggests that K_d would be proportional to the third power of the concentration of TBEP in benzene. The data of Table 3 for Zn(II) therefore support the proposed mechanism of extraction. Corresponding plots for the extraction of In(III), at constant 1 M and 2 M HCl in the aqueous phase, yield straight lines of slope which is closer to five. No explanation for the unusually high slope for indium can be given at present.

From the data of Table 2, it can be seen that in order to obtain measurable values of K_d for Cr(III) and to obtain the variation of K_d for Cr with concentration of TBEP in benzene, at constant equilibrium acidity in the aqueous phase, it would be advantageous to work with about 8 M HCl solutions. Table 1 shows that below 2 M HCl, the initial aqueous and the equilibrium aqueous phase hydrochloric acid concentrations are approximately the same, whereas they deviate at higher acidities. Hence, in order to maintain the acidity of the equilibrium aqueous phase constant at 8·0 M HCl while varying the concentration of TBEP in benzene, it is necessary to know which initial aqueous solution to use. A series of experiments were therefore carried out in the high acid region for the purpose of determining the relationship between initial aqueous acid and equilibrium aqueous acid concentrations for a given concentration of TBEP in benzene. The results are shown in Fig. 2, from which one can determine the initial HCl concentration required to give an equilibrium aqueous phase HCl concentration of 8·0, for a given TBEP concentration in benzene. Fig. 3 is a plot of log K_d vs. log (TBEP) in benzene at a constant equilibrium aqueous acid content of 8·0 M HCl. The slope is 3·0, indicating that the mechanism of extraction of Cr(III) is the same as that represented by Equation (3).

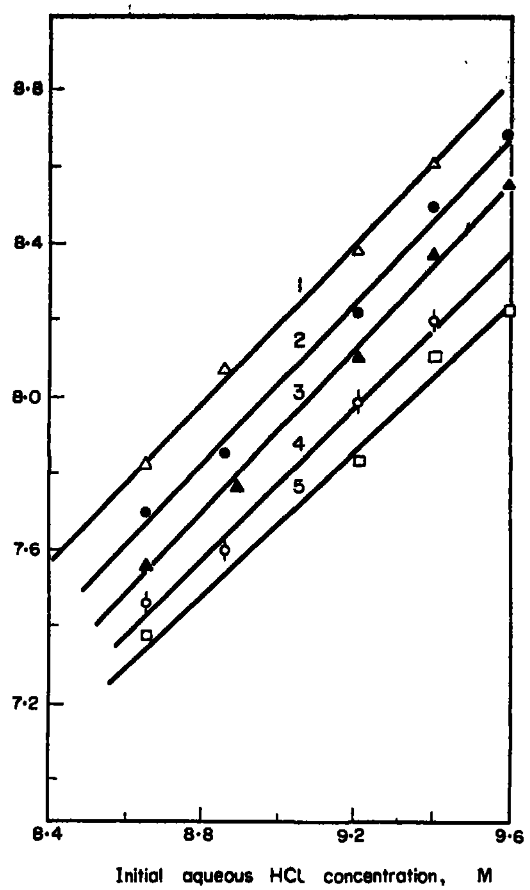

FIG. 2.—Equilibrium aqueous HCl concentration vs. initial aqueous HCl concentration for the following TBEP concentrations in benzene: 1, 1·02 M; 2, 1·27 M; 3, 1·53 M; 4, 1·78 M; 5, 2·04 M.

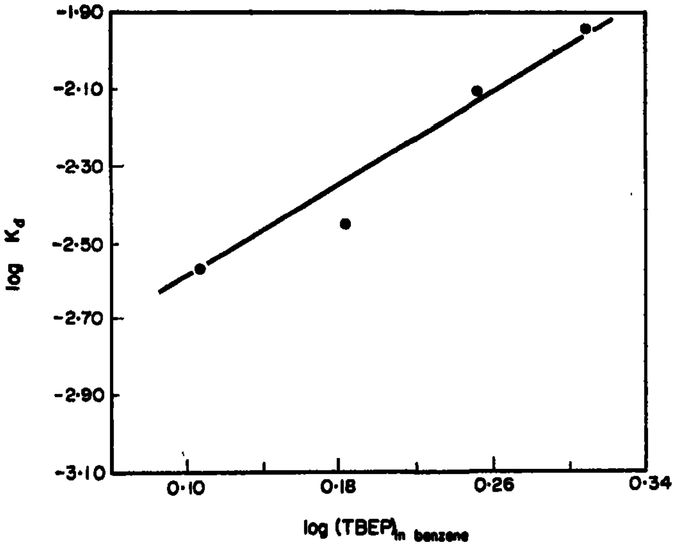

FIG. 3.—Log–log plot of K_d for Cr(III) vs. molarity of TBEP in benzene, at constant equilibrium aqueous hydrochloric acid concentration of 8·0 M.

DISCUSSION

At aqueous phase acidities up to 1 M HCl, the behaviour of the aqueous HCl·TBEP system is very similar to that of the aqueous HCl–TBP system. In this region the water content of the organic phase remains practically unchanged, with a H_2O/TBEP ratio of about 1·5 (the H_2O/TBP ratio is 1·0$^{(1,3)}$). The HCl species in the TBEP phase is appreciably ionized, and this is found to be the case for aqueous HCl–TBP$^{(1)}$ and aqueous HCl–ether.$^{(8)}$ The systems have a common feature in that they all involve oxygen–donor solvents. The swelling of the TBEP phase is equal to the swelling caused by its equilibration with water, and there is little change in the physical chemical properties of the organic layer.

When the acidity of the equilibrium aqueous phase lies in the region 2 M to 8 M, the extraction of one mole of HCl into TBEP is accompanied by four moles of water. A hydration number of four in aqueous solution of mineral acids has been found and discussed by several authors.$^{(9,10)}$ KERTES and HALPERN$^{(1)}$ observed the same phenomenon of TBP, except that when the acidity of the equilibrium aqueous phase goes above 6 M, the amount of water in the organic phase becomes constant, the H_2O/TBP ratio being 3·0. They find two species: $(TBP)_2{\cdot}HCl{\cdot}(H_2O)_6$, (I) and $TBP{\cdot}HCl{\cdot}(H_2O)_3$, (II) and postulate the reaction

$$(\mathrm{I})_{\mathrm{org.}} + \mathrm{H_{aq}}^{+} + \mathrm{Cl_{aq}}^{-} = 2\,(\mathrm{II})_{\mathrm{org}} \tag{4}$$

For the aqueous HCl–TBEP system, we have found only the mono-solvate, HCl·TBEP, and there is no evidence of the disolvate, HCl·2TBEP. It will be noted also that the swelling of the organic phase is much greater for TBEP than for TBP. Thus, starting with initial phase volumes of 5 ml, a change in the equilibrium aqueous acidity from 5·5 M to 8·7 M, produces an increase in volume of the TBEP phase from 1·0 to 4·0 ml (see Table 1), whereas the corresponding increase in volume of the TBP phase is only from 0·9 to 1·3 ml.$^{(1)}$

Tables 2 and 3 show that in the acidity region 1 M to 2 M, Zn^{2+} is extracted more readily by TBEP than In^{3+}. This may appear surprising; however, it is in line with the results for TBP. The extraction of the chlorides of Zn^{2+} and In^{3+} from aqueous hydrochloric acid into TBEP has been studied using radioactive tracers.$^{(3)}$ When the acidity in the aqueous phase is above 2 M, the distribution coefficient of In^{3+} is greater than that of Zn^{2+}, but the reverse is true in solutions less acid than 2 M. Moreover, Zn^{2+} is extracted by TBP much more readily than the other divalent metals. Thus at an acid strength of 3·10 M^3, the values of K_d for Ni^{2+}, Mn^{2+}, Co^{2+} and Zn^{2+} are 0·0030, 0·014. 0·0055 and 34·22 respectively.

Table 2 also shows that Cr^{3+} is much less extractable by TBEP than In^{3+}. Since there is considerable variations in the values of K_d of the divalent metal ions using TBP as extractant, it perhaps is not surprising to see considerable variations among the trivalent metal ions when TBEP is used as extractant. Some challenging problems of interpretation are thus presented.

---

(8) D. E. CHALKY and R. J. P. WILLIAMS, *J. Chem. Soc.* 1920 (1955).

(9) K. N. BASCOMBE and R. P. BELL, *Disc. Faraday Soc.* 24, 158 (1957).

(10) I. NELIDOV and R. M. DIAMOND, *J. Phys. Chem.* 59, 710 (1955).

J. Inorg. Nucl. Chem., 1962, Vol. 24, pp. 1257 to 1265. Pergamon Press Ltd. Printed in Northern Ireland

SOLVENT EXTRACTION STUDIES OF THIOCYANATE COMPLEX OF THE LANTHANIDES

H. YOSHIDA
Japan Atomic Energy Research Institute,
Tokai, Ibaraki, Japan

(*Received* 22 *March* 1962)

Abstract—The extraction behaviours of thiocyanate complex of the lanthanides have been studied for the system $M^{3+}/NH_4SCN/TBP$/diluent. The distribution ratios have been measured as a function of pH, temperature, NH_4SCN and TBP concentration. The distribution ratios of the lanthanides decrease with increase of hydrogen ion in the aqueous phase because of the extraction of thiocyanate ion into the organic phase. The composition of europium thiocyanate complex extracted into the organic phase is probably Eu $(SCN)_3(TBP)_4$ under the conditions studied. The extraction sequence as a function of the atomic number is compared with the ion exchange sequence for all the lanthanides except Pm.

IN contrast to the extensive studies concerning the solvent extraction of the lanthanides from their mineral acid solutions,(1,2) little has been published of other ion association extraction systems. Recent advances in solvent extraction suggest that the difference in the solvation energy of anion in water and organic solvent may be one of the important factors for the partition of salt between water and organic solvent. Considering only hydration energy of the anion, a high partition of thiocyanate complex is expected because of the specially low hydration energy of thiocyanate ion.

Although the ion exchange behaviour of the lanthanides in thiocyanate solution has been reported by SURLS, Jr.,(3) mechanism of solvent extraction of the lanthanides in thiocyanate solution is not known.

Only for practical purposes, APPLETON and SELWOOD(4) studied on the separation of some of the lanthanides based on the slightly different solubilities of their thiocyanates in butanol.

In the present paper, the tri-*n*-butyl phosphate (TBP) extraction of thiocyanate complex of the lanthanides has been studied. The effect of the following factors on the distribution ratios of the lanthanides is described: the concentrations of H^+, NH_4SCN and TBP, temperature and diluent in the organic phase. The distribution of HSCN as a function of pH and TBP concentration was also investigated. From the results obtained, the composition of the extracted species is discussed.

EXPERIMENTAL

Reagents

Purification of TBP was carried out by washing three times with 0·2 N HNO_3, 0·2 N NaOH and water, respectively. Then, the TBP phase was distilled under vacuum, the fraction of b.p. 118–123°C at about 0·1 mm Hg being used. All the isotopes except $^{152+154}$Eu were obtained by neutron irradiation of the spectrographically pure oxides (from Johnson, Matthey) in JRR-1 Reactor. $^{152+154}$Eu was supplied by the Radiochemical Centre, Amersham. These radioactive isotopes were tested for radiochemical purities by means of half-life measurement or γ-ray pulse height analysis.

(1) F. H. SPEDDING and A. H. DAANE, *The rare earths* pp. 38–54. J. Wiley, New York (1961).

(2) P. C. STEVENSON and W. E. NERVIK, NAS-NS-3020 pp. 86–113 (1961).

(3) J. P. SURLS, JR. UCRL-3209 (1956).

(4) D. B. APPLETON and P. W. SELWOOD, *J. Amer. Chem. Soc.* 63, 2029 (1941).

All other materials used were of analytical grade and suitable purifications were carried out when necessary.

Measurements

Determination of the distribution ratio (*D*). The experiments were carried out by equilibrating 10 ml of the aqueous phase with 10 ml of the organic phase (TBP diluted with kerosene), the former contained 10^{-7} mole of the lanthanides labelled with the corresponding radioactive isotopes and various concentrations of NH_4SCN. Although an equilibrium was attained in less than 1 min., shaking was usually continued for 3 min. Unless otherwise stated, all equilibrium experiments were carried out at 25 ± 0·2°C in a thermostat. After centrifuging, two phases were separated and the radioactivity of each phase was measured with a γ-ray scintillation counter.

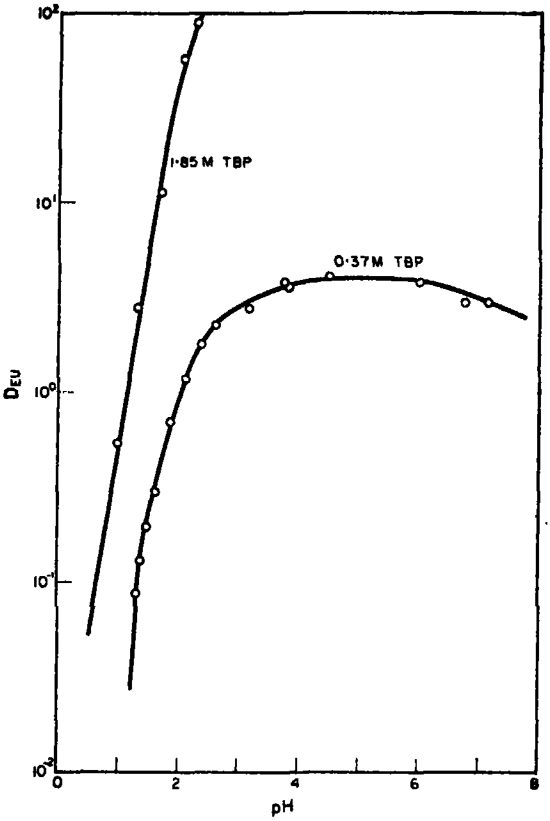

FIG. 1.—Variation of D_{Eu} with pH (Initial concentration of NH_4SCN 2·0 M)

Determination of pH. The pH of the aqueous phase was roughly adjusted to the expected value by addition of dilute HCl or NH_4OH solution. Precise measurements were made with a glass electrode pH meter after an equilibrium of the two phases was attained.

RESULTS AND DISCUSSION

Variation of D_{Eu} *with* pH

Two series of results obtained at various pH values but at constant TBP and NH_4SCN concentrations are shown in Fig. 1. In these experiments, aqueous phases containing Eu and NH_4SCN(2·0 M) were adjusted to various pH values by addition of HCl or NH_4OH solution before extraction. As the pH values increased slightly after extraction, the points plotted in Fig. 1 were obtained just after an equilibrium of the two phases was attained. D_{Eu} increases markedly with increasing pH value. When the extractions were carried out by 1·85 M TBP (2·0 M NH_4SCN), D_{Eu} was greater than 10^3 over the range of 4–8 pH.

Variation of D_{SCN^-} *with pH and* TBP *concentration*

As shown in Fig. 1, hydrogen ion seems to take part in the extraction. However, as will be discussed later, the extraction reaction is independent of the concentration of hydrogen ion in the aqueous phase. The role of hydrogen ion in the extraction system was investigated by distribution studies of thiocyanate ion as a function of pH and TBP concentration. Table 1 shows thiocyanate ion is extracted into the organic phase in the low pH range. The variation of D_{SCN^-} with TBP concentration over the range of 0·15–0·93 M TBP is shown in Fig. 2. In this experiment, although the initial concentration of hydrogen ion in the aqueous phase was held constant, the equilibrium concentration in the aqueous phase decreased with the increase of TBP concentration because of the extraction of acid into the organic phase. In order

TABLE 1.—EXTRACTION OF THIOCYANATE ION BY TBP (INITIAL CONCENTRATIONS OF NH_4SCN AND TBP ARE 2·0 M AND 0·37 M, RESPECTIVELY, VOLUME RATIO = 1/1)

pH*	NH_4SCN* (M)		
	Aqueous	Organic	Total
0·96	1·69	0·24	1·93
1·43	1·78	0·19	1·97
1·98	1·86	0·11	1·97
3·03	2·00	0·02	2·02
5·70	2·00	0·00	2·00

* Equilibrium values

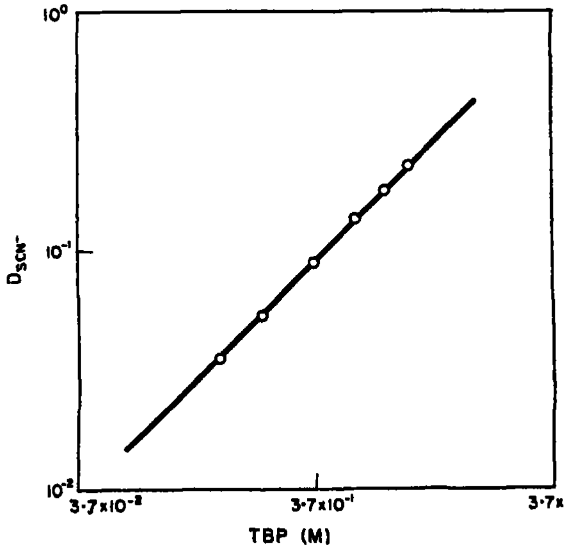

FIG. 2.—TBP dependency for NH_4SCN/TBP/Kerosene system (Initial concentration of NH_4SCN 2·0 M)

to obtain the result of logarithmic plot of D_{SCN^-} vs. TBP concentration at constant equilibrium acidity, D_{SCN^-} obtained at various acidities was calculated by correction for this effect. The result gives a slope of one, indicating the extracted species to be HSCN · TBP.

Variation of D_{Eu} with temperature

The effect of temperature (5–40°C) on D_{Eu} was studied at constant NH_4SCN (2·0 M) and TBP (0·37 M) concentrations. A separatory funnel containing the solution was placed in a thermostat for about 30 min., then shaken for 3 min. The results are shown in Fig. 3. Measurements of the equilibrium concentration of NH_4SCN and pH in the aqueous phase were carried out also. The results indicated that a small amount of thiocyanate ion was extracted into the organic phase at low temperature.

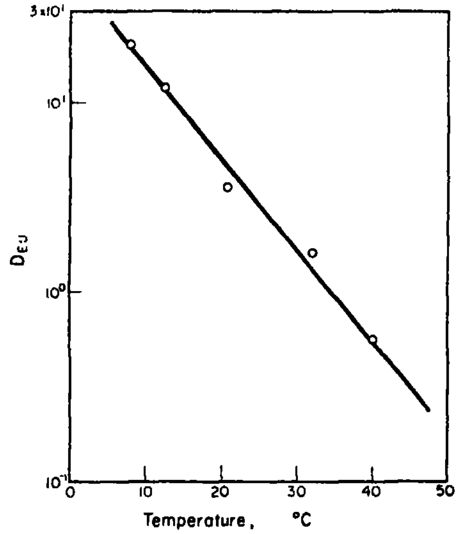

FIG. 3.—Variation of D_{Eu} with temperature (Initial concentrations of NH_4SCN and TBP are 2·0 M and 0·37 M, respectively. Equilibrium pH 2·6–3·0)

Variation of D_{Eu} with the nature of the diluent

Variation of D_{Eu} with the nature of the diluent in the organic phase was studied at constant TBP (0·37 M) and NH_4SCN (2·0 M) concentrations. Table 2 gives some representative extraction data for various diluents, in addition to the dielectric constants of the solvents and solubilities of water in solvents. Cyclohexane, hexane and kerosene give the nearly same value of D_{Eu}, however, carbon tetrachloride, benzene and chloroform cause a considerable decrease of D_{Eu}. The decrease of extractability with the increase of diluent concentration is shown in Fig. 4. It is seen in Table 2 that the smaller the dielectric constants of solvents and the solubilities of water in pure solvents, the higher the distribution ratio of europium.

Although it is difficult to correlate the extractability to the nature of the diluent, the effect of diluent may be due to the diluent structure and to the dipole interaction between the complex and the diluent.

TABLE 2.—EXTRACTION OF Eu BY TBP IN VARIOUS DILUENTS (INITIAL CONCENTRATIONS OF NH_4SCN AND TBP ARE 2·0 M AND 0·37 M, RESPECTIVELY. ACETATE BUFFER, EQUILIBRIUM pH VALUE IS ABOUT 4)

Diluent	D_{Eu}	Solvent dielectric constant*(5)	Solubility of H_2O per 100 g of solvent(6)
Cyclohexane	1·84	2·02	0·01
n-Hexane	1·75	1·89	0·01
Kerosene	1·72		ca. 0·004
Xylene	0·035	2·3	0·03
Carbon tetrachloride	0·021	2·24	0·011
Benzene	0·002	2·28	0·054
o-Dichloro benzene	0·002	9·93	Almost insoluble
Chloroform	<0·001	4·81	0·072
Dichloromethane	<0·001	9·08	0·198
Cyclohexanol	0·466	15·0	11·27
Methyl isobutyl ketone	0·073	13·1	3·7
Butyl acetate	0·037	5·0	2·4

Attention has been given to the above notion recently by other workers.(7–9) The characteristic behaviours of diluents are useful in the practical separation of some metals. For example, the lanthanides were separated completely from thorium by this extraction system using benzene or carbon tetrachloride as diluent.(10)

Variation of D_{Eu} with NH_4SCN and TBP concentration

Variation of D_{Eu} with the concentration of NH_4SCN from 0·05 to 4·0 M at the TBP concentrations of 0·19. 0·37 and 1·85 M was studied. As shown in Fig. 5, the slopes of the logarithmic plot of D_{Eu} vs. NH_4SCN concentration were 3·2, 2·9 and 3·0 for 0·19, 0·37 and 1·85 M TBP, respectively. These results indicate that three moles of SCN^- are associated with each europium ion under these conditions.

The variation of D_{Eu} with TBP concentration from 0·15 M to 1·11 M TBP at 2·0 M NH_4SCN is shown in Fig. 6. The plot has a slope of four over a wide range of TBP concentrations, indicating that four moles of TBP are associated with the extracted species.

Variation of the distribution ratios of lanthanum, europium and ytterbium with NH_4SCN and TBP concentrations

The distribution ratios of lanthanum, europium and ytterbium at various NH_4SCN and TBP concentrations are given in Table 3. The pH values of the aqueous phase after an equilibrium were 4·2–5·2. The separation factor (ratio of distribution ratios of the elements) is almost independent of NH_4SCN concentration over the range 0·5–4·0 M, but it increases gradually as the concentration of TBP is decreased, from 1·85

---

(5) A. WEISSBERGER and S. PROSKAUER, *Technique of Organic Chemistry*, Vol. 8, *Organic Solvents* (2nd Ed.). Interscience, New York (1955).

(6) SEIDELL, *Solubilities of organic compounds* (3rd Ed.). Van Nostrand, New York (1941).

(7) M. TAUBE, *J. Inorg. Nucl. Chem.* **12**, 174 (1959).

(8) T. V. HEALY, *J. Inorg. Nucl. Chem.* **19**, 328 (1961).

(9) N. SUZUKI and T. WAKABAYASHI. Presented at the 10th Annual Meeting of the Japan Society for Analytical Chemistry, October, 1961.

(10) H. YOSHIDA. Paper in preparation.

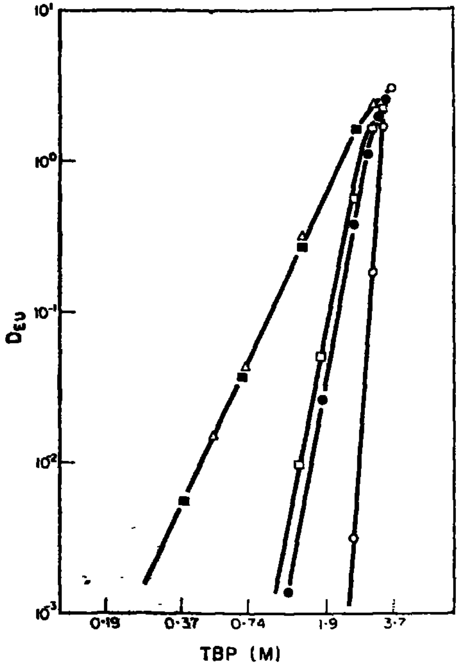

FIG. 4.—Effect of various diluents on D_{Eu} (Eu/NH_4SCN/TBP/diluent system, Equilibrium pH 4·0, initial concentration of NH_4SCN 0·2 M) ○ Chloroform, ● Benzene, □ Carbon tetrachloride, ■ Kerosene, △-n-Hexane.

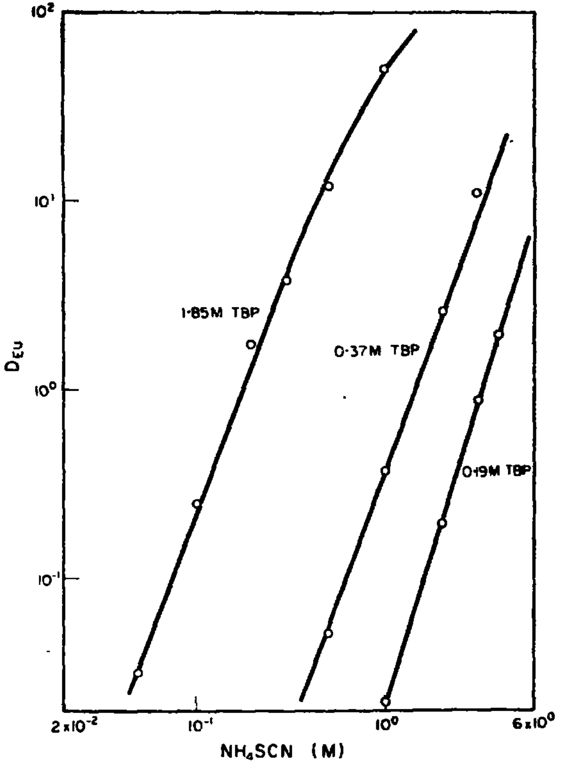

FIG. 5.—NH_4SCN dependency in Eu/NH_4SCN/TBP/kerosene system (Equilibrium pH 4·0)

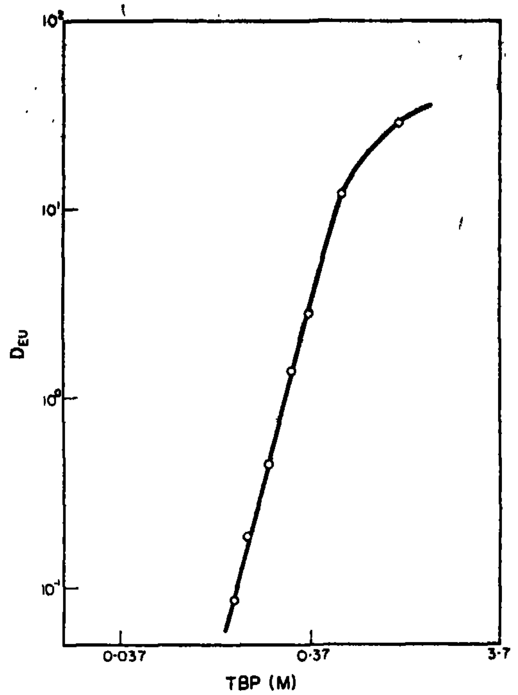

FIG. 6.—TBP dependency in Eu/NH_4SCN/TBP/kerosene system (Initial concentration of NH_4SCN 2·0 M, equilibrium pH 4·0)

TABLE 3.—SEPARATION FACTORS FOR La, Eu AND Yb AS A FUNCTION OF NH_4SCN AND TBP CONCENTRATION (EQUILIBRIUM pH 4·2–5·2)

Concentration (M)		Distribution ratio			Separation factor*		
NH_4SCN	TBP	La	Eu	Yb	Eu/La	Yb/Eu	Yb/La
0·5	1·85	4·52	12·2	16·1	2·69	1·32	3·56
0·3	1·85	1·41	4·69	4·93	3·33	1·05	3·49
0·2	1·85	0·74	1·77	3·40	2·39	1·92	4·59
3·0	0·370	3·96	11·2	15·7	2·83	1·40	3·96
2·0	0·370	0·96	2·60	4·79	2·72	1·83	4·99
1·0	1·370	0·095	0·375	0·71	3·88	1·92	7·47
4·0	0·185	0·565	2·02	5·83	3·58	2·89	10·3
3·0	0·185	0·213	0·887	2·14	4·16	2·41	10·0
2·0	0·185	0·030	0·202	0·33	6·78	1·63	11·1
4·0	0·148	0·202	0·773	2·19	3·83	2·83	10·8

* Ratio of distribution ratios of the elements.

to 0·15 M. Relatively high separation factors as well as high distribution ratios were obtained at low TBP and high NH_4SCN concentrations.

Extraction sequence of the lanthanides as a function of atomic number

The distribution ratios of all the lanthanides except Pm were measured at 3·0 M NH_4SCN and 0·19 M TBP. The experiments were carried out three times for each element. In Fig. 7, the distribution ratios obtained are compared with the elution sequence of the lanthanides with 2 M NH_4SCN and 10 M LiCl from Dowex-1 anion exchange resin. It is observed that the extraction order does not follow the progressive order of the atomic number, and the disorder obtained is nearly analogous to that *found for the elution sequence of the lanthanides with 2 M NH_4SCN or 10 M LiCl from Dowex-1 anion exchange resin.*

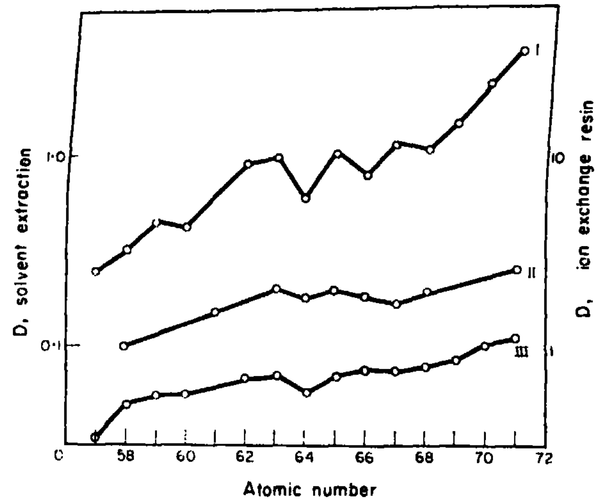

FIG. 7.—Ion exchange and solvent extraction sequence of the lanthanides as a function of atomic number

I. Solvent extraction—NH_4SCN/TBP/kerosene system. Initial concentrations of NH_4SCN and TBP are 3·0 M and 0·19 M, respectively. Equilibrium pH 4·0.
II. Ion exchange resin—Elutions with 2 M NH_4SCN from Dowex-1, 8 % DVB at 33°C(8).
III. Ion exchange resin—Elutions with 10 M LiCl from Dowex-1, 8 % DVB at 87°C(8,12).

GENERAL DISCUSSION

Solvent extraction experiments with a tracer concentration of europium indicated that three thiocyanate ions and four TBP molecules are associated with each europium ion in the organic phase of the $Eu^{3+}/NH_4SCN/TBP$/diluent system. When extraction was carried out in a relatively high acidity range, D_{Eu} decreased because of the extraction of thiocyanate ion into the TBP phase according to the following equation.

$$H^+ + SCN^- + TBP \rightleftarrows HSCN{\cdot}TBP$$

If D_{Eu} in a high acidity range is corrected for this effect, D_{Eu} is independent of hydrogen ion in the aqueous phase. This indicates that the mechanism of extraction of europium under the conditions investigated is represented as follows, even in a relatively high acidity range.

$$Eu^{3+} + 3\ SCN^- + 4TBP \rightleftarrows Eu(SCN)_3(TBP)_4$$

Equilibrium constant for the above equation obtained at 1·98 M NH_4SCN and 0·37 M TBP (pH = 4·50) is 27.5.

The distribution ratios of the lanthanides increases with the atomic number as a whole, although the increase of the distribution ratios is not continuous. In general, the stability of complexes of the lanthanides formed with small ionic ligands, highly charged unidentate ligands, or with multidentate ligands increases as the size of the metal ion decreases. The sequence of stability constants La < — < Gd < —Lu(III) has been established with many ligands. However, the reverse trend of extractability has been observed for the extraction system of the lanthanides/$HClO_4$/TBP.(11) This is probably due to the weak complex-forming tendency of the perchlorate ion. In the perchlorate extraction system, dehydration energy of the metal ion may be a more important factor for the partition of the metal between the aqueous and the organic phase. Also, the disorder of the extractability observed in the extraction system of the lanthanides/NH_4SCN/TBP/diluent is probably due to the disorder of the dehydration energy of the lanthanides.

Acknowledgements—The author wishes to express his thanks to Dr. K. Motojima for his advice and to Drs. K. Naito and H. Natsume for their useful discussions.

(11) S. Siekierski, Polish Academy of Science, Institute of Nuclear Research, 130/V (1960).

(12) E. K. Hulet, R. G. Gumacher and M. S. Coops *J. Inorg. Nucl. Chem.* 17, 350 (1961).

J. Inorg. Nucl. Chem., 1962, Vol. 24, pp. 1267 to 1276. Pergamon Press Ltd. Printed in Northern Ireland

THE EXTRACTION OF URANIUM (VI) FROM SULPHURIC ACID SOLUTIONS BY TRI-n-DODECYLAMINE

TAICHI SATO
Government Chemical Industrial Research Institute, Honmachi, Shibuya-ku, Tokyo, Japan

(*Received* 1 *January* 1962; *in revised form* 16 *April* 1962)

Abstract—The partition of uranium (VI) between sulphuric acid solutions and solutions of tri-n-dodecylamine (TDA) in benzene has been investigated by varying the sulphuric acid concentration, aqueous uranium concentration, solvent concentration and temperature; the extraction of sulphuric acid by TDA in benzene has also been examined. Infra-red spectra have been obtained of the organic solutions involved.

The mechanism of uranium extraction is discussed in the light of these results.

HIGH molecular weight amines in organic diluents have recently been used to extract various metal ions from acidic aqueous solutions. In particular they play an important rôle in the solvent extraction of uranium from sulphuric acid solutions, and the extraction of uranium from acid solutions by various amines has therefore been studied by several investigators;[1] however, observations on the extraction mechanism are few.[2] The present study was therefore made to obtain information on the mechanism of extraction of uranium (VI) from sulphuric acid solution by tri-n-dodecylamine (TDA).

EXPERIMENTAL

TDA was supplied by the Kao Soap Co., Ltd. Extractions were carried out by the following procedure: 20 ml each of TDA solution diluted with benzene and uranyl sulphate solution containing sulphuric acid were placed in 50 ml stoppered conical flasks and shaken for 10 min in a water bath thermostated at the required temperature. Uranium in the organic phase was then back-extracted with 1 N hydrochloric acid solution, and the partition coefficient was determined. Uranium was determined gravimetrically.[3]

The acidity of the organic phases was determined as follows: 2 ml samples of the equilibrated organic phase were added to 25 ml of 75 per cent ethyl alcohol, which was then titrated with 0·05 N sodium hydroxide solution, using phenolphthalein as indicator.

For infra-red measurements the organic phase, after separation from the aqueous phase, was placed in a cell with thallium halide windows and the spectrum was determined using a Shimazu infra-red type recording spectrophotometer equipped with sodium chloride prisms. Spectra were determined relative to benzene as reference or, in wavelength regions where the presence of TDA caused a change in the spectrum, relative to 0·1 M TDA in benzene.

RESULTS AND DISCUSSION

Extraction of sulphuric acid

In order to investigate the reaction between benzene solutions of TDA and aqueous sulphuric acid solutions, the solution of 0·1 M TDA in benzene was shaken with sulphuric acid solutions of various concentrations at 20°C, and the acidities of the organic phases were checked. The extraction of sulphuric acid from 0·5 and 0·2 M sulphuric acid solutions by solutions of TDA in benzene was also examined at different TDA concentrations.

---

[1] E.g., C. F. COLEMAN, K. B. BROWN, J. G. MOORE and K. A. ALLEN, *Proceedings of the Second United Nations International Conference on the Peaceful Uses of Atomic Energy, Geneva*, 1958, Vol. 28, p. 278, United Nations (1958); C. F. COLEMAN, K. B. BROWN, J. G. MOORE and D. J. CROUSE, *Industr. Engng. Chem.*, **50**, 1756 (1958).

[2] E.g., K. A. ALLEN, *J. Amer. Chem. Soc.* **80**, 4133 (1958); W. J. MCDOWELL and C. F. BAES, *J. Phys. Chem.* **62**, 777 (1958); CH. BOIRIE, *Bull. Soc. Chim. France* 1088 (1958).

[3] T. SATO, *J. Inorg. Nucl. Chem.* **6**, 334, (1958).

Fig. 1 shows that the organic phase acidity increases linearly with increasing initial aqueous acidity below ~0·05 M, but its increase is more gradual above this concentration. Fig. 2 shows that the slopes of log (sulphuric acid distribution ratio) vs. log (initial TDA concentration) are very nearly unity. From these results we infer that

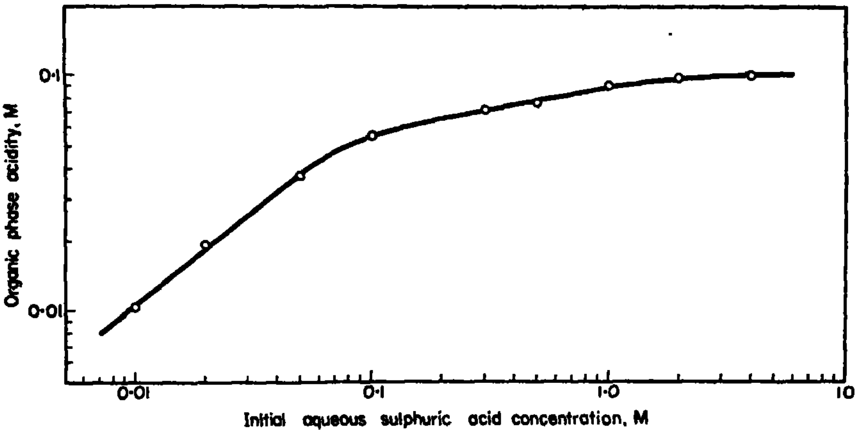

FIG. 1.—Equilibrium acidity of organic solutions (0·1 M TDA in benzene) shaken with sulphuric acid solutions of various concentrations.

the amine sulphate is first formed and additional acid is then extracted to form the amine bisulphate, i.e.

$$H_2SO_4(a) + 2R_3N(o) \rightleftarrows (R_3NH)_2SO_4(o) \qquad (1)$$

$$(R_3NH)_2SO_4(o) + H_2SO_4(a) \rightleftarrows 2(R_3NH)HSO_4(o) \qquad (2)$$

where R represents $C_{12}H_{25}$, (a) and (o) are indicative of aqueous and organic phases respectively.

Variation of uranium concentration

Uranium (VI) was extracted into 0·1M TDA in benzene at 20°C, the concentrations of uranyl sulphate in the aqueous phase being varied between 1 and 25 g/l. Fig. 3 shows that when uranium(VI) is extracted from sulphuric acid solutions of varying acidity, the partition coefficient at first rises steeply, passes through a maximum and then falls markedly again. The maximum partition coefficient appears at ~0·05 M initial sulphuric acid concentration for the extraction from 5 g/l uranyl sulphate, and becomes indeterminate for extractions from 12·5 and 25 g/l uranyl sulphate. The shape of the curve may be interpreted as follows: at low acidities the increase in the partition coefficient arises from the formation of a uranium-amine sulphate complex, while at higher acidities the decrease in the partition coefficient is attributed either to competition between uranium and sulphuric acid for association with the amine or to the formation of less readily extracted complexes.(4)

If the results shown in Fig. 3 are plotted to show the variation of the organic phase uranium concentration as a function of the initial aqueous uranium concentration at constant sulphuric acid concentration, it is seen that the organic phase uranium concentration attains an equilibrium value (~0·025 M) for the extraction of uranium from the sulphuric acid solution in the initial concentration range between 0·05 and 0·3 M. This suggests that four amine molecules are associated with each uranium ion at these sulphuric acid concentrations.

---

(4) D. J. CARSWELL and J. J. LAWRANCE, *J. Inorg. Nucl. Chem.* 11, 69 (1959).

Solvent dependence

The extraction of 5 g/l uranyl sulphate containing sulphuric acid was carried out with solutions of TDA in benzene at 20°C and varying sulphuric acid concentrations.

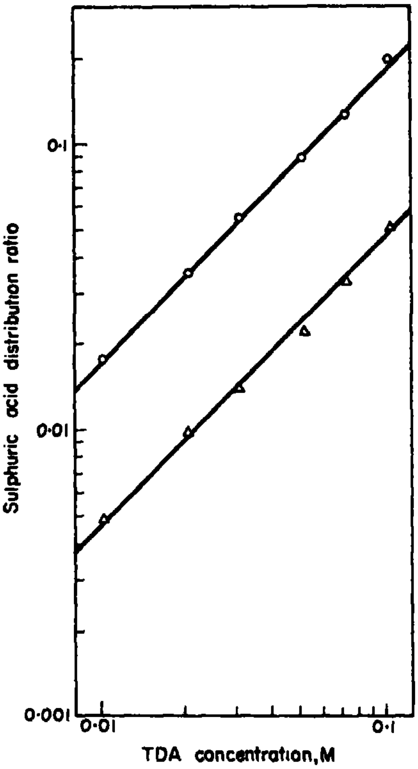

Fig. 2.—Variation of the distribution ratio of sulphuric acid with amine concentration for the extraction of sulphuric acid solution by TDA in benzene (○ and △ refer to 0·5 and 2·0 M sulphuric acid solutions respectively).

Fig. 4 shows that although the maximum partition coefficient appears at ~0·05 M initial acidity for >0·05 M [TDA], the maximum is indistinct for [TDA] <0·03 M.

In order to clarify the solvent dependence at higher acidities, values of log E_a° were plotted vs. log $(C_A - nC_U)$, in which E_a° is the partition coefficient, C_A is the total amine concentration, C_U is the organic phase uranium concentration, and n is an association number ($n = 4$ at constant sulphuric acid concentration). Fig. 5 shows that although the slopes have different values at the different acid concentrations (2·1 in 0·5 M H_2SO_4, 1·6 in 1·0 M H_2SO_4, 1·0 in 2·0 M H_2SO_4), the partition coefficients vary linearly with the concentration of the amine which is present as the bisulphate form uncomplexed with uranium. The slope decreases with increasing sulphuric acid

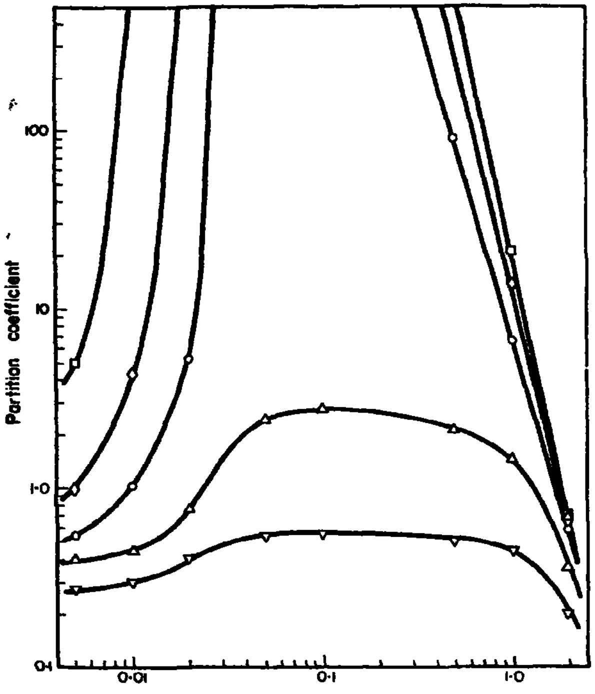

FIG. 3.—Effect of uranium concentration upon the extraction of uranium(VI) from sulphuric acid solutions of various concentrations by 0·1 M TDA in benzene (□, ◇, ○, △ and ▽—uranyl sulphate concentrations 1, 2·5, 5, 12·5 and 25 g/l respectively).

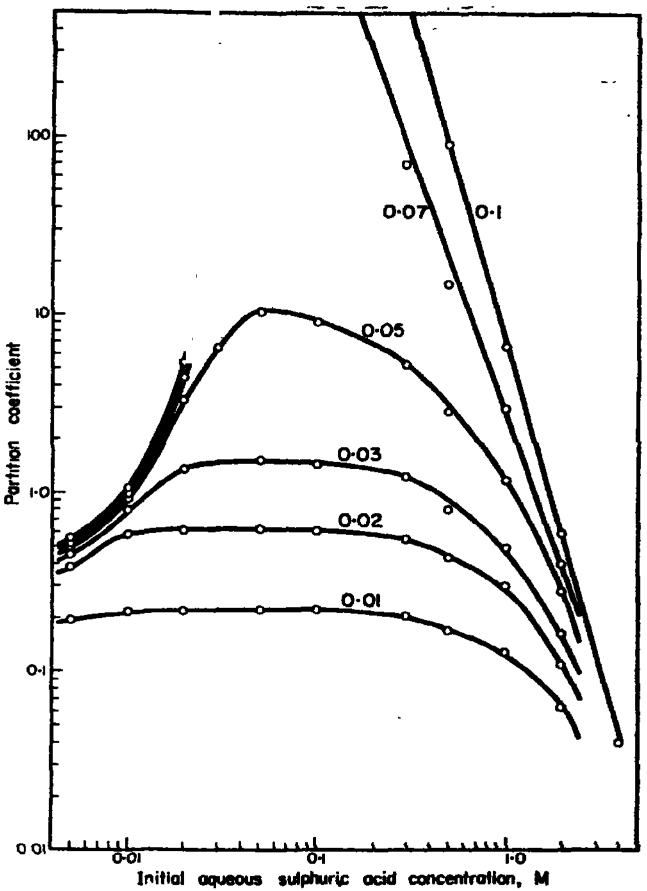

FIG. 4.—Effect of solvent concentration upon the extraction of uranium (VI) from sulphuric acid solutions of various concentrations by TDA in benzene (figures on curves are TDA concentrations, M).

concentration because of the decreased uranium loading. These curves indicate that each uranium ion is associated with four amine molecules at higher acidities also.

At low acidities however, a fraction of the amine which is not complexed with uranium is present as the free amine. Values of C_U and C_A were therefore determined at 0·01 and 0·02 M sulphuric acid concentrations and are plotted in Fig. 6. This shows tha

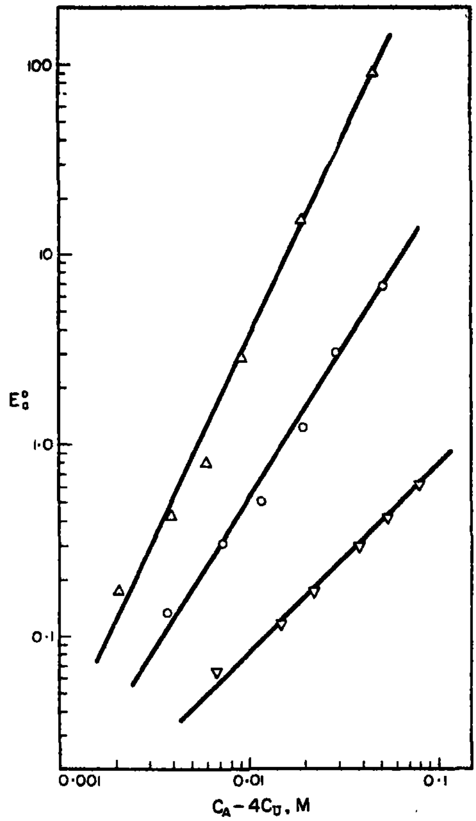

Fig. 5.—Solvent dependence of partition coefficient for the extraction of uranium(VI) from sulphuric acid solutions of higher acidities by TDA in benzene (values of log E_a° vs. log (C_A—$4C_{\bar{U}}$) at 0·5 (△), 1·0 (○) and 2·0 (▽) M sulphuric acid).

the organic phase concentration increases linearly with increasing initial amine concentration below ~0·02 M amine in 0·01 M H_2SO_4 or 0·04 M in 0·02 M H_2SO_4, but the increase in the organic phase concentration is less above these amine concentration. This suggests that when the aqueous sulphuric acid concentration is too low, the concentration of the available amine which is present as the sulphate is restricted by the aqueous phase acidity. In such a case, the value of the association number is presumably less than four, increasing with the aqueous acidity to four at 0·05 M initial sulphuric acid concentration.

Variation of temperature

Extractions of uranyl sulphate solutions containing 0·02 and 1·0 M sulphuric acid were carried out with 0·1 M TDA in benzene at temperatures between 10 and 50°C.

Fig. 7 shows that although the partition coefficient decreases with rising temperature, the decrease is greater for extraction from 1·0 M sulphuric acid than from 0·02 M acid.

Infra-red spectral study

Extractions from 5 and 25 g/l. uranyl sulphate solutions containing sulphuric acid at various concentrations were made with 0·1 M TDA in benzene at 20°C, and the organic phases were examined by infra-red spectroscopy. In the same way the organic solutions were examined from the extraction of sulphuric acid solutions in the absence of uranium. The results are shown in Figs. 8 and 9.

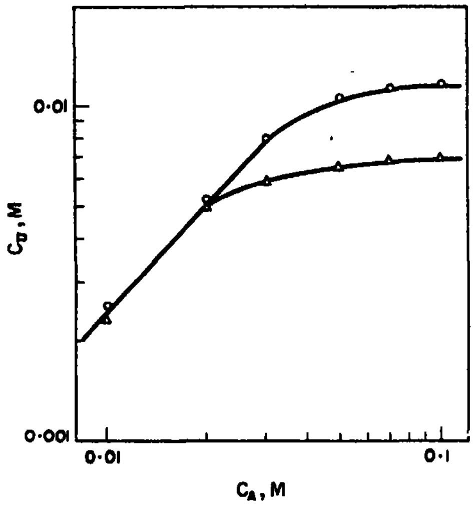

Fig. 6.—Organic phase uranium concentration plotted against total amine concentration for the extraction of uranium (VI) from sulphuric acid solutions at low acidities by TDA in benzene (△ and ○ denote 0·01 and 0·02 M sulphuric acid respectively).

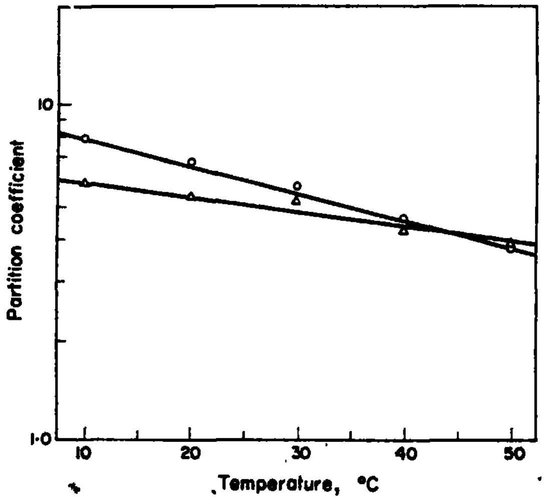

Fig. 7.—Effect of temperature upon the extraction of uranium (VI) from sulphuric acid solution by 0·1 M TDA in benzene (△ and ○ represent the sulphuric acid concentrations of 0·02 and 1·0 M respectively).

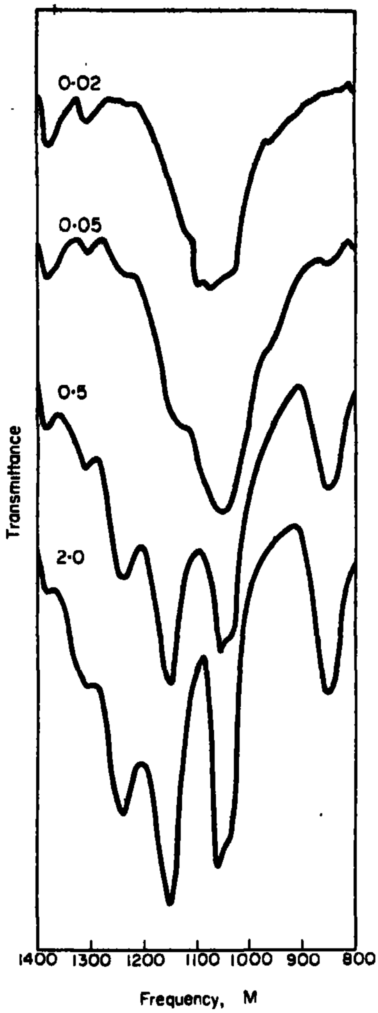

FIG. 8.—Infra-red spectra of organic solutions from the extraction of sulphuric acid solutions with 0·1 M TDA in benzene (figures on curves are sulphuric acid concentrations, M).

In the extraction of sulphuric acid, the following results were observed (Fig. 8) with increasing acidity:

(i) for 0·02 M sulphuric acid, the bands assigned to sulphate ion vibrations[5,6] were observed at 1120 (shoulder), 1095 ∼ 1030 (strong and broad) and 970 cm^{-1} (weak);

(ii) for 0·05 M sulphuric acid, the above bands were more intense, and were accompanied by weak absorption bands at 1240, 1150, 1055 and 850 cm^{-1} which are assigned to the vibrations of the bisulphate ion;[5,6]

(iii) for 0·5 and 2·0 M sulphuric acid, the bands due to the bisulphate ion show a progressive increase in intensity, whereas those of the sulphate ion become weaker.

[5] F. A. MILLER and C. H. WILKINS, *Analyt. Chem.* **24**, 1253 (1952).

[6] G. E. WALRAFEN and D. M. DODD, *Trans. Faraday Soc.* **57**, 1286 (1961).

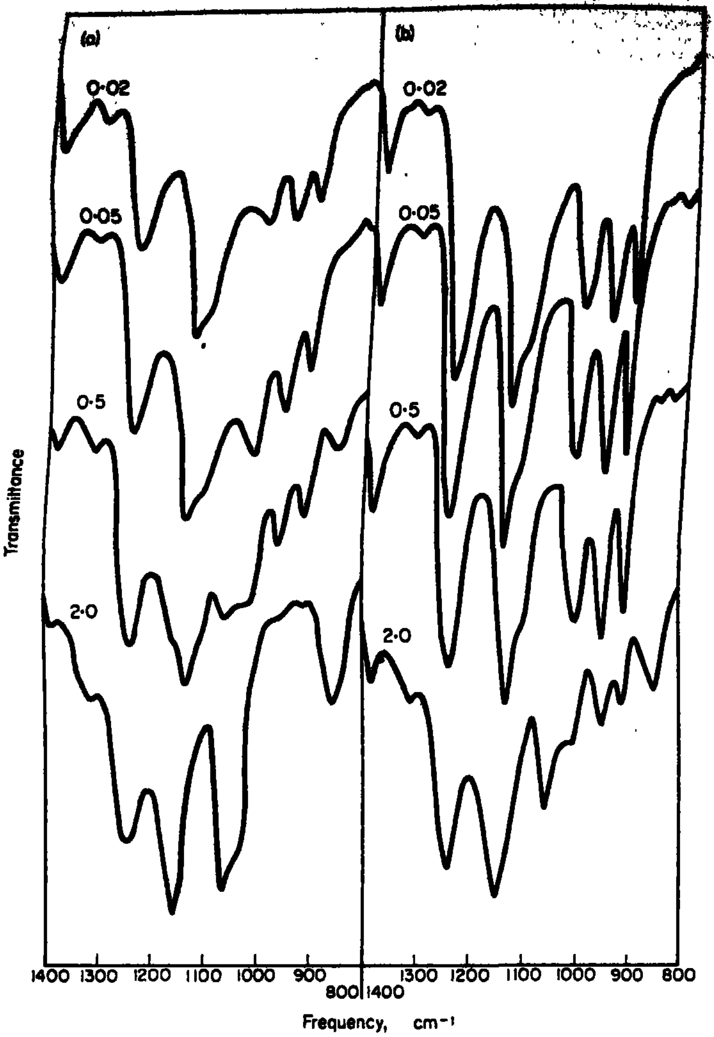

FIG. 9.—Infra-red spectra of organic solutions from the extraction of uranyl sulphate solutions containing sulphuric acid of various concentrations with 0·1 M TDA in benzene (figures on curves are sulphuric acid concentrations, M).
(a) 5 g/l uranyl sulphate
(b) 25 g/l uranyl sulphate

It follows, therefore, that when sulphuric acid solutions are extracted by TDA in benzene the following sequence occurs:

(a) at low acidities, the amine sulphate is formed according to the reaction (1), and

(b) at higher acidities, the amine bisulphate is formed according to reaction (2).

The spectra of the solvent phases from the extraction of uranyl sulphate at an initial aqueous concentration of 5 g/l in sulphuric acid solutions of varying acidity (Fig.9a) show the following bands:

(1) for 0·02 M sulphuric acid, 1235 (strong), 1125 (strong), 1110 (shoulder), 995 (medium), 950 (medium) and 905 cm^{-1} (medium);

(2) for 0·05 M sulphuric acid, the above bands appear with increased intensity, the

increase being roughly proportional to the increase in the amount of uranium in the organic phase (from 0·012 to 0·014 M).

Besides the band at 950 cm^{-1}, assigned to the asymmetric stretching frequency of the uranyl group,(7) some or all of the remaining bands may be assigned to the vibrational frequencies of the sulphato group, indicating a lower symmetry (C_{3v} or C_{2v})* than the sulphate ion (T_d) due to covalent bonding to the uranyl ion. These bands are therefore characteristic of the amine-uranyl sulphate complex formed by extraction of uranyl sulphate;

(3) for 0·5 M sulphuric acid, bands due to the bisulphate ion appear in addition to the absorption bands of the amine-uranyl sulphate complex;

(4) for 2·0 M sulphuric acid, the absorption bands are mainly due to the bisulphate ion, in agreement with the amount of uranium in the organic phase (~0·005 M), indicating that uranyl sulphate is displaced from the amine complex by the bisulphate ion.

The spectra of the solvent phases from the extraction of aqueous solutions containing 25 g/l of uranyl sulphate (Fig. 9b) show stronger absorption bands due to the amine-uranyl sulphate complex for initial aqueous acidities of 0·02, 0·05 and 0·5 M sulphuric acid, consistent with the higher concentration of uranium in the solvent phases compared with the previous solutions (~0·02, 0·025 and 0·023 M respectively). At 2·0 M sulphuric acid in the aqueous phase, however, strong absorption bands due to the bisulphate ion are present in the spectrum superimposed on weaker bands of the amine-uranyl sulphate complex, in agreement with the lower uranium concentration in the solvent phase (~0·011 M). This again indicates that bisulphate ion is displacing the uranyl sulphate from the amine complex, although at a higher acidity than before due to the increased concentration of uranium in the aqueous phase. The absence of bands due to either sulphate ion or bisulphate ion vibrations for 0·5 ~0·02 M sulphuric acid is in agreement with the 4:1 ratio of amine to uranyl sulphate in the complex, since if this were not so these ions would be extracted by the excess amine.

Confirmation was obtained for the formula of the amine-uranyl sulphate complex as follows. The solvent phase from the extraction by 0·1 M TDA in benzene of 25 g/l uranyl sulphate in 0·0 5 M sulphuric acid solution was analysed, since the data obtained indicate that this solution is ~100 per cent pure complex (0·025 M uranium and 0·1 M TDA). The organic phase was found to contain uranium, sulphate, amine and water in the proportions 1:3:4:3†, indicating the stoicheiometry of the amine–uranyl sulphate complex to be $(R_3NH)_4UO_2(SO_4)_3(OH_2)_3$, i.e. $[(R_3NH)_2SO_4]_2 \cdot UO_2SO_4(OH_2)_3$.

From the above results therefore, the extraction of uranium(VI) from sulphuric acid solution by TDA may be expressed as follows:

(a) at low acidities

$$UO_2SO_4(a) + 2(R_3NH)_2SO_4(o) \rightleftarrows (R_3NH)_4UO_2(SO_4)_3(o), \tag{3}$$

and (b) at high acidities

$$UO_2SO_4(a) + 4(R_3NH)HSO_4(o) \rightleftarrows (R_3NH)_4UO_2(SO_4)_3(o) + 2H_2SO_4(a). \tag{4}$$

---

* In comparison with the spectrum of solid uranyl sulphate determined by the Nujol mull method, the bonding of the ligand was expected to be bidentate rather than unidentate.

† Water determination was made by Karl Fischer titration.

(7) E.g., B. M. Gatehouse and A. E. Comyns, *J. Chem. Soc.* 3965 (1958); G. L. Caldow, A. B. Van Cleave and R. L. Eager, *Canad. J. Chem.* **38**, 772 (1960).

Accepting the assumptions that the amine bisulphate is not formed in the extraction of uranium from 0·02 M sulphuric acid by TDA in benzene, and that the amine which is not complexed with uranium is present as the bisulphate for the extraction of uranium from 1·0 M sulphuric acid, the heats of reaction (change in enthalpy) in equation (3) and (4) were estimated from the data in Fig. 7 to be 1·75 kcal/mole for 0·02 M H_2SO_4 and 9·13 kcal/mole for 1·0 M H_2SO_4. Since these values are close to the values for the energy of hydrogen bonding,(8) the nature of the bonding in the organic phase is considered to be analogous to that of latter. However, as the heat of extraction of uranium by TDA in benzene from 1·0 M sulphuric acid is greater than that from 0·02 M sulphuric acid solution, the bond of the uranium bearing complex in the former case may be stronger than that in the latter.

Acknowledgements—The author wishes to thank Mr. M. KUWA and Mr. H. WATANABE, who carried out much of the experimental work. Thanks are also due to the Kao Soap Co., Ltd. for a gift of tri-n-dodecylamine.

(8) E.g., G. C. PIMENTAL and A. L. MCCLELLAN, *The Hydrogen Bond* pp. 350–363. Freeman, San Francisco (1960).

J. Inorg. Nucl. Chem., 1962, Vol. 24, pp. 1277 to 1286. Pergamon Press Ltd. Printed in Northern Ireland

AN INFRA-RED AND ISOPIESTIC INVESTIGATION OF THE INTERACTION BETWEEN DI(2-ETHYLHEXYL) PHOSPHORIC ACID AND TRI-N-OCTYLPHOSPHINE OXIDE IN OCTANE*

H. T. Baker† and C. F. Baes, Jr.
Oak Ridge National Laboratory, Oak Ridge, Tennessee and Texas Woman's University, Denton, Texas

(*Received* 28 *February* 1962; *in revised form* 26 *April* 1962)

Abstract—Upon the addition of tri-n-octylphosphine oxide (R_3PO), B, to di(2-ethylhexyl)phosphoric acid ($(RO)_2PO_2H$), A, in octane the intensity of the phosphoryl band of A at 1232 cm^{-1} is decreased and a new band at *ca.* 1275 cm^{-1} appears. Detailed study of this change by Job's method of continuous variation and by the addition of B to solutions in which the total concentration of A is held constant has suggested the reactions: $B + \frac{1}{2}A_2 = AB$, $Q_1 = 25 \pm 5\ M^{-\frac{1}{2}}$; $B + A_2 = A_2B$, $Q_2 = 100 \pm 50\ M^{-1}$. (The unreacted dialkylphosphoric acid is present as a dimer A_2 in octane solution). The shift in the phosphoryl band of A is consistent with H-bonded structures for A_2, A_2B and AB. Isopiestic results appear consistent with these reactions.

THE extraction of uranium(VI) by a dialkylphosphoric acid [$(RO)_2PO_2H$] in the presence of increasing amounts of a neutral additive such as a trialkylphosphate [$(RO)_3PO$], a phosphonate [$(RO)_2RPO$], a phosphinate [$RO(R)_2PO$], or a phosphine oxide (R_3PO) is characterized by an initial "synergistic" increase in extraction coefficient, followed by a decrease.(1) From this behaviour it has been assumed that at least two equilibria involving the neutral additive occur: one leads to the formation of a mixed complex, $UO_2A_aB_b$, involving uranyl ion, the dialkylphosphoric acid, A and the neutral additive B, the other is a competing interaction between the dialkylphosphoric acid and the neutral additive which leads to the formation of the A_cB_d species. Attempts have been made to deduce the nature of the mixed complex or complexes formed from extraction behaviour,(1,2) but such cannot be considered conclusive until the nature of the competing interaction between A and B has been more fully investigated. The nature and the extent of this interaction may especially be important in explaining the highly specific character of the synergistic effect in alkylphosphoric acid–neutral phosphate systems, wherein it evidently occurs only in the extraction of MO_2^{2+} actinide ions by dialkylphosphoric acids. Recently HEALY(3) has reported that when the acidic reagent is thenoyl trifluorocetone synergism is quite general, a number of divalent, trivalent and one tetravalent ion showing strongly enhanced extraction in the presence of various neutral organophosphate reagents. An obvious difference between the two systems is that TTA apparently does not show as marked an interaction with B.

---

* Presented in preliminary form at the 134th Meeting of the American Chemical Society, Chicago, September, 1958.

† Summer research participant with the Oak Ridge National Laboratory 1957 and 1958, sponsored by the Oak Ridge Institute of Nuclear Studies, Chemistry Department, Texas Woman's University, Denton, Texas.

‡ Operated by Union Carbide Corporation for the U.S. Atomic Energy Commission.

(1) C. A. BLAKE, D. E. HORNER and J. M. SCHMITT, ORNL-2259, Oak Ridge (1959).

(2) D. DYRSSEN and L. KUCA, *Acta Chem. Scand.* **14**, 1945 (1960).

(3) T. V. Healy, *J. Inorg. Nucl. Chem.* **19**, 314, 328 (1961).

The interaction between a dialkylphosphoric acid and a neutral organophosphorous extractant is expected to occur through hydrogen bonding of the acidic $\rangle$POH to the phosphoryl oxygen of the neutral extractant. Since the acid is usually present as a hydrogen-bonded dimer,(4–6) one possible reaction is

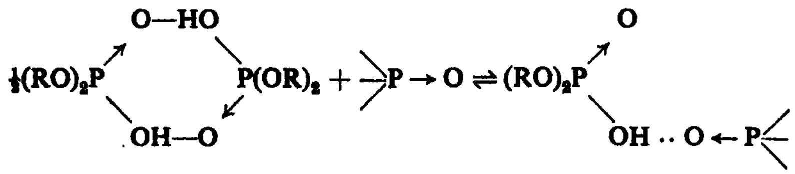
(1)

From measurements of the distribution of di(n-butyl)phosphoric acid to aqueous solutions with added TBP in the organic phase, Dyrssen and Hay(4) and Hardy and Scargill(5) found evidence for the formation of this product AB. From their results the equilibrium quotient for the above reaction is 0·4 in carbon tetrachloride(4) and 0·9 in kerosene.(5)

In the present study, infra-red measurements in the region of phosphoryl stretching (1190–1300 cm^{-1}) were used to examine the nature and extent of such interaction between di(2-ethylhexyl)phosphoric acid (DEPA) A and tri(n-octyl)phosphine oxide (TOPO) B in n-octane solution. Previously reported isopiestic measurements in this solvent(7) have shown that A is dimeric, and that activity coefficients of both A_2 and B decrease appreciably with increasing concentration. Whether or not this non-ideal behaviour of the separate reactants is caused by specific chemical effects (i.e., partial trimerization of A and partial dimerization of B), it may be dealt with adequately here by considering the effect of estimated γ_{A_2} and γ_B variations on the interaction equilibria between A_2 and B.

EXPERIMENTAL

1. *Reagents.* The preparation of tri-n-octylphosphine oxide(8) involved the reaction of $POCl_3$ with excess Grignard reagent, oxidation by dilute neutral permanganate solution at room temperature, treatment with activated alumina, and alkaline extraction. It was purified with special care, the final stage of purification involving repeated recrystallization from petroleum ether. The product contained <0·07 per cent free and combined acid (as di-octylphosphinic and dioctylphosphinous acids). Analysis gave; C 74·9, P 7·85, H 13·2, O 4·05% (by difference). The calculated values are 74·55, 8·01, 13·30 and 4·14%, respectively. The di-(2-ethylhexyl)phosphoric acid reagent was prepared by purification of "Tergitol" Wetting Agent P-28,* a commercially available aqueous solution of sodium di-(2-ethylhexyl)-phosphate. The final product used was 99·5 per cent dioctyl phosphoric acid containing 0·1 per cent mono-octyl phosphoric acid by potentiometric titration with standard sodium hydroxide. The remaining principal impurities were probably 2-ethylhexanol and the tri-octyl-phosphate ester. Their effect on the infra-red results is expected to be less than the experimental uncertainty. The solvent, n-octane, was obtained from the Phillips Petroleum Company, (pure grade, 99 mole per cent minimum) and used without further purification. All experimental solutions were prepared by weight just prior to use.

---

* The purification method involves scrubbing of the impure sodium salt with petroleum ether followed by acidification with hydrochloric acid and extraction of the dialkyl-phosphoric acid into petroleum ether.

(4) D. Dyrssen and Liem-Djiet Hay, *Acta. Chem. Scand.* **14**, 1091 (1960).

(5) C. J. Hardy and D. Scargill, *J. Inorg. Nucl. Chem.* **11**, 128 (1959).

(6) C. F. Baes, Jr., R. A. Zingaro and C. F. Coleman, *J. Phys. Chem.* **62**, 129 (1958).

(7) C. F. Baes, Jr., *J. Phys. Chem.* **66**, 1629 (1962).

(8) W. T. Rainey and J. M. Schmitt, ORNL-2399, pp 7–9, Oak Ridge (1957).

2. *Infra-red measurements*. Measurements of the infra-red spectra of the n-octane solutions of the di(2-ethylhexyl)phosphoric acid and tri-n-octylphosphine oxide were made at 22° ± 1°C with a Perkins Elmer Corporation Model 112 Serial 2 single beam, double pass infra-red instrument with a calcium fluoride prism. The instrument was calibrated by using the CO_2 trough at 2348·6 cm^{-1} and the H_2O peak of 1436·7 cm^{-1}.

Measurements were made alternately on solution samples and solvent in calcium fluoride cells, usually of *ca*. 0·1 mm path length. The absorbancies of solutions relative to the pure solvent were corrected for the usually small effect of replacing part of the solvent by solute as follows

$$D_s = D_t + \left(1 - \frac{c}{100}\right) D_0$$

in which D_s is the corrected solute absorbancy; D_t is observed solution absorbancy vs. pure solvent; D_0 is absorbancy of pure solvent *vs*. an empty cell; *c* is the volume per cent of solvent present in sample.

3. *Isopiestic measurements*. The isopiestic apparatus, incorporating many of the features introduced by SCATCHARD *et al.*(9) has already been described.(6) It contains a mechanism, operated through a bellows, for covering and uncovering the sample cups while the apparatus is sealed.

It was observed in preliminary runs on octane solutions,(7) using the out-gassing procedure previously described,(6) that the time required for isopiestic equilibrium to be reached was generally longer than for hexane solutions and was extremely variable. It was concluded that the distillation rate was critically dependent on the partial pressure of air in the apparatus, the rate being greatly decreased by higher air pressures. Accordingly a more thorough out-gassing procedure was adopted.

RESULTS AND DISCUSSION

1. *Infra-red measurements*. Initial infra-red measurements were made on mixtures of di(2-ethylhexyl)phosphoric acid, A and tri(n-butyl)phosphate, TBP. The results (presented in the upper portion of Fig. 1) were rather disappointing in that they gave little evidence of the interaction which, from the uranium(VI) extraction properties of such mixtures, was thought to have occurred. In contrast, the subsequent measurements on mixtures of A and tri(n-octyl)phosphine oxide B (shown in the lower portion of Fig. 1) not only gave clear evidence of interaction but also indicated the reason for the observed small effect in the case of A–TBP mixtures. It is seen that in mixtures of A and B a new absorption band has appeared with a peak at 1275 cm^{-1}. This band probably arises from the non-hydrogen bonded phosphoryl group in A (cf. reaction (1)). The appearance of this band in A–TBP mixtures would be masked by the disappearance of the TBP band (also associated with a $(-0)_3P \rightarrow 0$ group) in the same region. Similarly, the disappearance of the H-bonded A band (at 1232 cm^{-1}) would be masked by appearance of the H-bonded TBP band. Because the phosphoryl band of the phosphine oxide lies at a lower frequency (< 1200 cm^{-1}) than that of A, pronounced spectral changes occur in A–B mixtures permitting a reasonably quantitative study of the interaction equilibria involved.

These wavelength assignments are generally consistent with the recent observations of KENNEDY and DEANE(10) on DEPA and TOPO in carbon tetrachloride. They assign a 1169, 1195 cm^{-1} peak (mostly below the range of the present measurements) to $P \rightarrow O$ stretching in TOPO, a 1231 cm^{-1} peak to (H–bonded) $P \rightarrow O$ stretching in DEPA, and a 1267 cm^{-1} peak to $P \rightarrow O$ stretching (presumably non H–bonded) in mixtures of the two compounds.

Absorbancy measurements next were made on separate solutions of A and B to test Beer's law for each reactant. Results (Table 1) at three wave numbers in the range 1221–1227 cm^{-1} (near the H-bonded phosphoryl peak of A) and at three wave numbers in the range 1268–1285 cm^{-1} (near the free phosphoryl peak of A) showed no detectable dissociation of the A dimer in the range 0·1–0·001 M A. At the lowest concentra-

(9) G. SCATCHARD, W. J. HAMER and S. E. WOOD, *J. Amer. Chem. Soc.* **60**, 3061 (1938).

(10) J. KENNEDY and A. M. DEANE, *J. Inorg. Nucl. Chem.* **19**, 174 (1961).

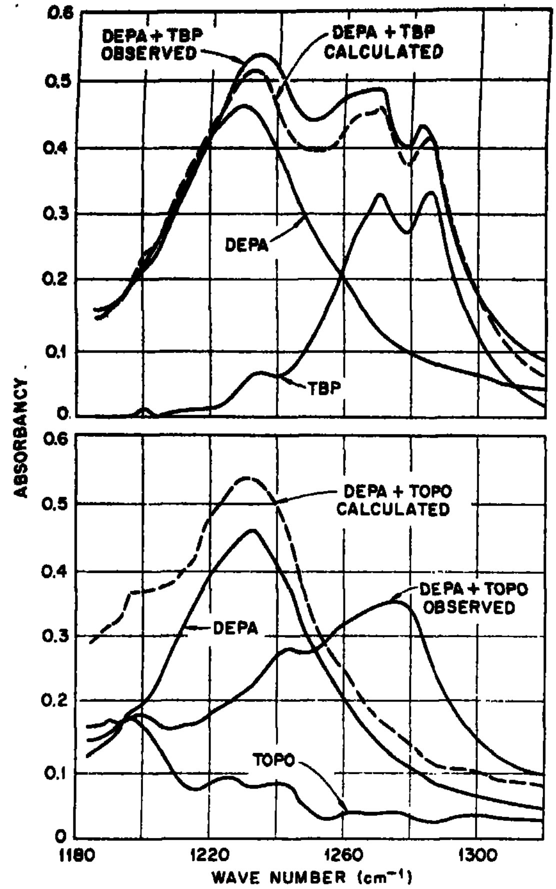

Fig. 1.—Infra-red spectra in the region of phosphoryl stretching. DEPA, TBP, and TOPO are, respectively, di(2-ethylhexyl)phosphoric acid, tri(n-butyl)phosphate, and tri(n-octyl)phosphine oxide. All solutes are 0·5*m* in octane. The broken curves are calculated spectra for mixtures assuring no interaction between the acidic and neutral reagents.

tion, 7×10^{-4} M A_2, it is estimated that less than 10% of the dimer was dissociated. This corresponds to an association constant for the dimer $>3 \times 10^4$, which is consistent with previous estimates in the range 10^5–10^7 for DBP in non polar solvents.(4,5) This however, does not rule out the possible further association of A suggested by the previously reported isopiestic results since such presumably would not change the H-bonded state of the phosphoryl group. Results for B solutions (0·01–0·37 M) at 1192–1198 cm^{-1} also showed Beer's Law behaviour.

Job's method of continuous variations was next applied to mixtures of A and B. In accordance with this method the total concentration of the A dimer C_{A_2} plus C_B was held constant, and the difference D between the observed absorbancy and that calculated assuming no interaction between A and B was determined as a function of the ratio $C_B/(C_{A_2} + C_B)$. If only one interaction product is formed the resulting D vs. $C_B/(C_{A_2} + C_B)$ plot chould have a maximum in the absolute value of D (which may be either positive or negative) at a ratio of C_{A_2} to C_B corresponding to the stoicheiometry of the interaction product. The resulting curves are presented in Fig. 2 for $C_{A_2} + C_B$

TABLE 1.—TEST OF BEER'S LAW FOR DEPA(A) AND TOPO(B) SOLUTIONS IN N-OCTANE

C_A	D/C_A at 1221–1229 cm^{-1}		D/C_B at 1192–1198 cm^{-1}	
	0·45 mm path	0·11 mm path	C	0·45 mm path
0·00145	15·1[a]	—	0·0109	1·778[c]
205	16·2	—	159	1·761
309	15·9	—	209	1·744
399	15·8	—	296	1·713
512	15·8	—	493	1·750
819	16·0	—	707	1·746
992	16·2	3·79[b]	992	1·711
2030	15·8	3·83	1490	1·749
5000	—	3·81	2000	1·737
0·10180	—	3·79	0·3670	1·673
Average	15·9	3·81		1·736
Std. Deviation	±2·2%	±0·5%		±1·5%

[a, b, c] Each of these values is the average of measurements at 2 or 3 different wave numbers (a, b; 1221, 1224, 1229 cm^{-1}: c; 1193, 1196 cm^{-1}) which overlapped because of band width (a, 8·3 cm^{-1}; b, 4·2 cm^{-1}; c, 5·6 cm^{-1}). Standard deviations from Beer's Law for individual sets of measurements were: a, 1·7–4%; b, 0·5–1%; c, 2 and 3·7%.

= 0·1 M and 0·2 M. In each case both the appearance of the 1275 cm^{-1} band (giving positive D values) and the disappearance of the 1232 cm^{-1} band of A (giving negative D values) was followed at the two sets of three wavelengths used in the Beer's Law measurements. The data points plotted are averaged absorbancies for each set of three wavelengths. The appearance plots and the disappearance plots have very nearly the same shape, showing a maximum near $C_B/(C_{A_2} + C_B) = \frac{2}{3}$ (i.e., $C_B/C_A = 1$). This is in agreement with the formation of an interaction product AB predicted by reaction (1) above. However, the observed results are not quite consistent with the formation of AB alone. The discrepancy is indicated by the dashed curve which has been calculated assuming the formation of AB only, taking the formation quotient $Q_1 = [AB]/[A_2]^{\frac{1}{2}}[B]$ to be 25 M$^{-\frac{1}{2}}$ and choosing an appropriate absorbancy parameter in the equation*

$$D = a_1[AB]$$

For a more detailed examination of the interaction between A and B the dependence of D on C_B was determined at the same sets of three wavelengths with C_{A_2} held constant at 0·025 M and at 0·05 M. Again the resulting plots were virtually the same for the appearance of the 1275 cm^{-1} band and the disappearance of the 1232 cm^{-1} band, the ratio of the two averaged D values varying little more than was expected from the experimental error. The results are plotted in Fig. 3.

---

* The calculated absorbancy, D_c, assuming no interaction between A_2 and B is

$$D_c = a_{A_2}C_{A_2} + a_BC_B$$

(where a_{A_2} and a_B are molar extinction coefficients). If one interaction product AB is formed, then the observed absorbancy, D_o, is

$$D_o = a_{AB}[AB] + a_{A_2}[A_2] + a_B[B]$$

Noting that $C_{A_2} = [A_2] + \frac{1}{2}[AB]$ and $C_B = [B] + [AB]$, the difference, $D = D_o - D_c$ is

$$D = (a_B - \tfrac{1}{2}a_{A_2} - a_B)[AB]$$

The quantity in parenthesis is designated a_1.

As in the previous continuous variation results, these results could not be accounted for adequately assuming only the formation of AB. The discrepancy is indicated by curves in the upper part of Fig. 3 labelled $Q_2 = 0$ which have been calculated, as previously, assuming the formation quotient of AB to be 25 $M^{-1/2}$. Variation in the choice of Q_1 did not improve the fit. The choice of a_1 does not enter this comparison since in Fig. 3 the log of [AB] is compared with log D.

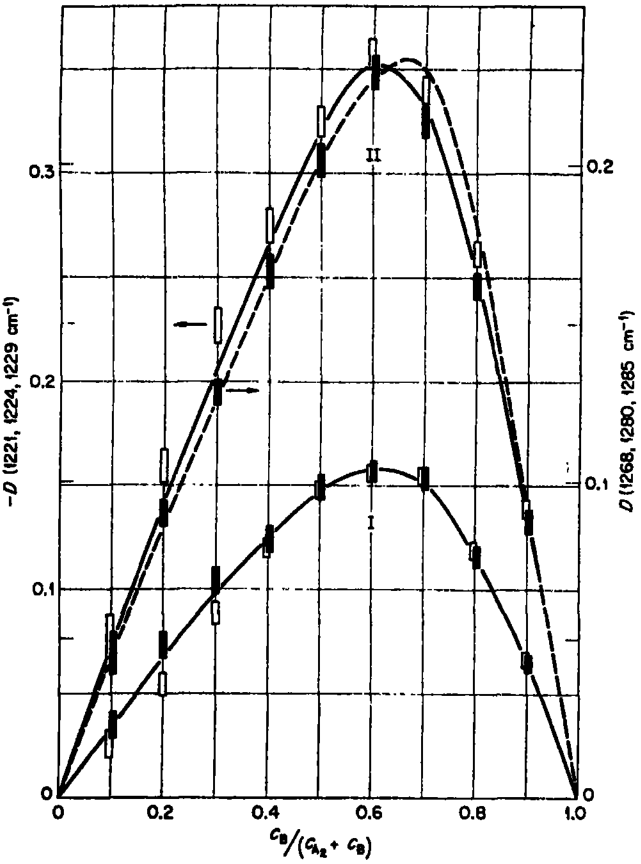

FIG. 2.—Continuous variation results: □, D(1221–1229 cm^{-1}) and ■, D (1268–1285 cm^{-1}) are averaged values of the difference between the observed absorbancy and the calculated absorbancy (assuming no reaction between DEPA dimer A_2 and TOPO B). The vertical bars indicate the range of deviation of the individual D values (normalized to the average) from the average value. For curve I, $C_{A_2} + C_B = 0{\cdot}1$ M; for curve II, $C_{A_2} + C_B = 0{\cdot}2$ M. The dashed curve represents predicted variation of D if only AB is formed ($Q_1 = 25$ $M^{-1/2}$; $C_{A_2} + C_B = 0{\cdot}2$ M).

Of course Q_1 is not expected to remain constant since the activity coefficients of the A dimer and of B are known to fall with increasing concentration.(7) However, in these measurements the activity coefficient product $\gamma_{A_2}{}^{1/2}\gamma_B$ which appears in the relation between Q_1 and the formation constant K_1 were found in trial calculations not to vary widely

$$Q_1 = K_1\gamma_{A_2}{}^{1/2}\gamma_B/\gamma_{AB}$$

since as γ_B decreases with increasing [B], γ_{A_2} increases with decreasing [A_2]. Further, the product $Q_1/\gamma_B\gamma_{A_2}^{\frac{1}{2}}$ (where Q_1 was calculated directly from the observed D values, assuming a reasonable a_1 value) was estimated and plotted vs. the calculated concentration of AB. Since $Q_1/\gamma_B\gamma_{A_2}^{\frac{1}{2}} = K_1/\gamma_{AB}$, the resulting plots of 0·05 M A_2 and 0·025 M A_2 should have been superimposed in a single smooth curve representing the variation of γ_{AB} with [AB]. However the two plots differed widely; both showed maxima at $Q/\gamma_{A_2}^{\frac{1}{2}}\gamma_B = 45$–$55$, but at different values of [AB], then fell sharply to values of 20 at 0·05 *m* [AB] in one case and at 0·1 M [AB] in the other. While variation

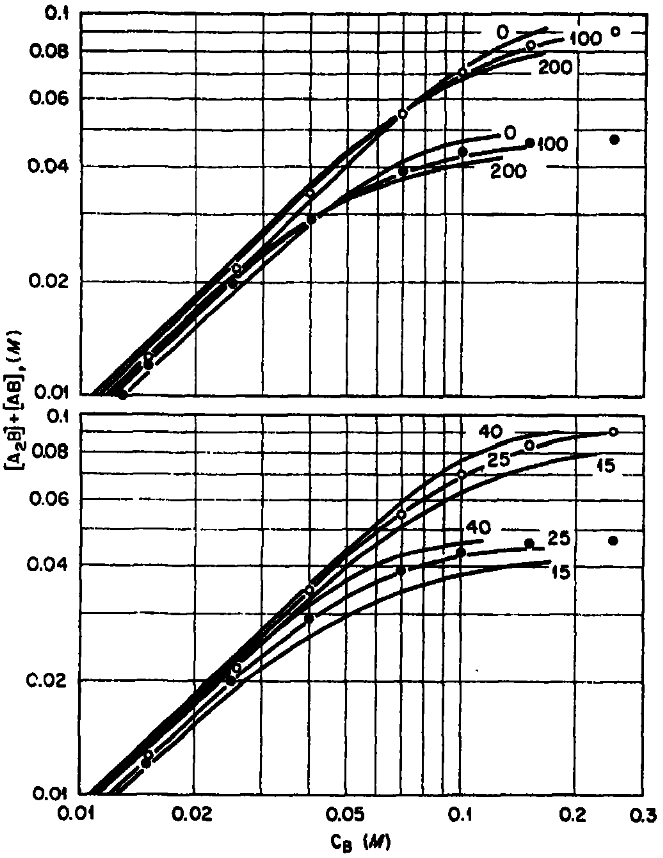

FIG. 3.—Comparison of calculated values of [A_2B] + [AB](curves) with normalized difference (points) between observed absorbancy and calculated absorbancy assuming no reaction between A_2 and B: ○, $C_{A_2} = 0·05$; ●, $C_{A_2} = 0·025$. In the upper plots $Q_1 = 25$ and Q_2 was varied from 0 to 200 as indicated. In the lower plots $Q_2 = 100$ and Q_1 was varied from 15 to 40 as indicated.

in the adjustable parameter a_1 and in the activity coefficients (within the uncertainty of the original estimates(7)) alters the curve, the agreement between the two is not materially improved.

The lack of consistency of the results with the formation of AB alone suggests that in addition to AB at least one other product is formed. Indeed, this is to be expected when it is noted that the formation of AB requires the rupture of both hydrogen bonds of the A dimer; an intermediate product A_2B could be formed upon the rupture of a single H-bond in the A_2 dimer.

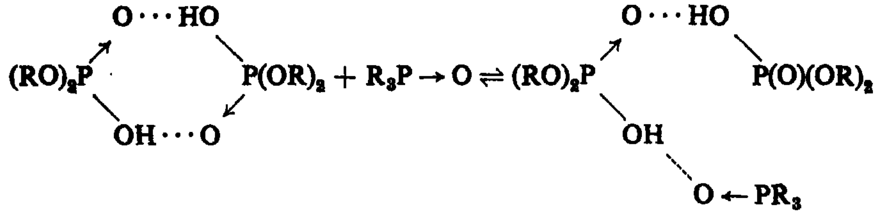
(2)

The results were accordingly re-examined in terms of the formation of A_2B as well as AB. With these interaction products the expression for D becomes ⁽¹³⁾

$$D = a_1[\mathrm{AB}] + a_2[\mathrm{A_2B}]$$

so that the two additional parameters (a_2 and Q_2) are now involved. From the proposed structures of AB and A_2B, however, a_1 and a_2 are expected to be about equal,* so that in treating the results the relation involving only one additional parameter, Q_2, was used.

$$D = a([\mathrm{AB}] + [\mathrm{A_2B}])$$

That $a_1 = a_2$ is indicated by the near proportionality of the D values in the two regions as a function of $C_B/(C_{A_2} + C_B)$ in Fig. 2 and as a function C_B at constant C_{A_2}.

Trial values of Q_1 and Q_2 were chosen and $[A_2B] + [AB]$ (which should be proportional to D) was calculated, assuming for the moment that the formation quotients could be treated as constants. In Fig. 3 two series of log $([A_2B] + [AB])$ vs C_B curves are compared with log D sv. C_B. The set of curves in the lower half of the figure show the effect of varying Q_1 holding Q_2 constant at 100, the best fit being for $Q_1 = 25$. In the upper half of the figure is shown the effect of varying Q_2 while holding Q_1 constant at 25, the best value of Q_2 being *ca.* 100. As expected the fit is less sensitive to the choice of Q_2 than it is for Q_1. It is important to note that for each set of these latter curves there is a cross-over point. This means that if one repeated the calculation choosing Q_1 constant at 15 or 40, the fit to the data in this region would be poorer.

Choosing the values $Q_1 = 25$, $Q_2 = 100$, the effect of possible variations in the activity coefficients γ_{A_2} and γ_B was next tested. Curves corresponding to those in Fig. 3 were calculated introducing the estimated γ_{A_2} and γ_B values.⁽⁷⁾ The resulting curves were found to be very nearly the same shape as previously, except that they were shifted uniformly downward. The experimental data could be superimposed

---

* Using the same procedure as previously (see footnote on page 7) it may be readily shown that

$$D = \underbrace{(a_{AB} - \tfrac{1}{2}a_{A_2} - a_B)}_{a_1}[\mathrm{AB}] + \underbrace{(a_{A_2B} - a_{A_2} - a_B)}_{a_2}[\mathrm{A_2B}]$$

It it is assumed in the region (1232 cm^{-1}) of H-bonded A phosphoryl stretching that a_{AB}, a_{A_2B} and a_{A_2} (all molar extinction coefficients) are proportional to the number of H-bonded A phosphoryl groups in AB (0), A_2B (1) and A_2 (2), then

$$a_1 - a_2 = (a_{AB} - a_{A_2B} + \tfrac{1}{2}a_{A_2}) = 0$$

Similarly, if it is assumed in the region (1275 cm^{-1}) of free A phosphoryl stretching that a_{AB}, a_{A_2B} and a_{A_2} are proportional to the number of free phosphoryl groups in AB (1), A_2B (1) and A_2 (0), then $a_1 - a_2$ is also 0. The fact that the two peaks (arising from H-bonded and non-H-bonded phosphoryl stretching overlap does not alter the conclusion that $a_1 = a_2$, provided the shapes and positions of the peaks are independent of the species in which the bonded or unbonded A phosphoryl group occurs.

on the new curves simply by increasing a from 59 to 63 M^{-1}. It is concluded therefore that the results can be adequately accounted for by the two products AB and A_2B with

$$Q_1 = \frac{[AB]}{[A_2]^{\frac{1}{2}}[B]} = 25 \pm 5\ M^{-\frac{1}{2}}$$

$$Q_2 = \frac{[A_2B]}{[A]\,[B]} = 100 \pm 50M^{-1}$$

TABLE 2.—ISOPIESTIC MEASUREMENTS ON DEPA(A)–TOPO(B) MIXTURES IN OCTANE AT 25°C (ALL CONCENTRATIONS IN MOLALITY)

Reference solution	Test solution		
m_R	m_{A_2}	m_B	$\frac{m_R}{m_{A_2} + m_B}$
	$m_B/m_{A_2} = 0$		
0·0548[a]	0·06	0	0·914[c]
0·0910[a]	0·10	0	0·910[c]
0·1278[a]	0·14	0	0·913[c]
	$m_{A_2}/m_B = 0·5$		
0·0793[a]	0·0731	0·0352	0·751
0·1820[b]	1·1545	0·0777	0·784
	$m_B/m_{A_2} = 1·0$		
0·0794[a]	0·0629	0·0641	0·625
0·0932[a]	0·0691	0·0691	0·674
0·1631[b]	0·1143	0·1142	0·714
	$m_B/m_{A_2} = 1·5$		
0·0932[a]	0·0577	0·0864	0·649
0·1449[b]	0·0835	0·1251	0·695
0·1932[b]	0·1141	0·1709	0·678
0·2607[b]	0·1698	0·2543	0·615
	$m_B/m_{A_2} = 2·0$		
0·0793[a]	0·0385	0·0772	0·685
0·0932[a]	0·0479	0·0957	0·649
0·1541[a]	0·0797	0·1597	0·644
0·1768[b]	0·0869	0·1735	0·679
	$m_B/m_{A_2} = 3·0$		
0·0793[a]	0·0289	0·0865	0·687
	$m_B/m_{A_2} = \infty$[c]		
0·0380[a]	0	0·04	0·949[c]
0·0888[a]	0	0·10	0·888[c]
0·1347[a]	0	0·16	0·842[c]
0·1688[a]	0	0·20	0·844[c]

[a] Reference solute, triphenylmethane.
[b] Reference solute, DEPA dimer.
[c] These are smoothed values taken from a previously reported investigation.(7)

2. *Isopiestic measurements.* Table 2 lists the equilibrium compositions of A_2 — B mixtures in octane which had been equilibrated with reference solutions of triphenylmethane and, at the higher concentrations, A_2. Previously reported smoothed values for the separate components are also included. The isopiestic ratio $m_R/(m_{A_2} + m_B)$ listed in the last column of the table, should be unity if there were no reactions between A_2 and B and if A_2, B, and the reference solute obeyed Raoult's Law. While the isopiestic ratios for the separate components show them to be non-ideal solutes, the

generally much lower ratios observed for the mixtures offer clear evidence of interactions such as Equations (1) and (2) which lead to a reduction in the number of particles in solution.

A portion of the results, those at a roughly constant total concentration of A_2 plus B (0·1 — 0·15 *m*) are plotted according to Job's method in Fig. 4. The dashed lines indicate the ideal behaviour of the isopiestic ratio for three limiting cases; (1) no reaction between A_2 and B, (2) AB only is formed, ($Q_1 = \infty$), (3) A_2B only is formed, ($Q_2 = \infty$). The observed ratios are seen to fall mostly in the region defined by the latter two limiting cases. From this it is concluded that the isopiestic results are consistent with the above assumed formation of both products. A more quantitative analyses of these results to test the above estimated values of Q_1 and Q_2 was not attempted in view of the non-ideal behaviour of solutes A_2 and B.

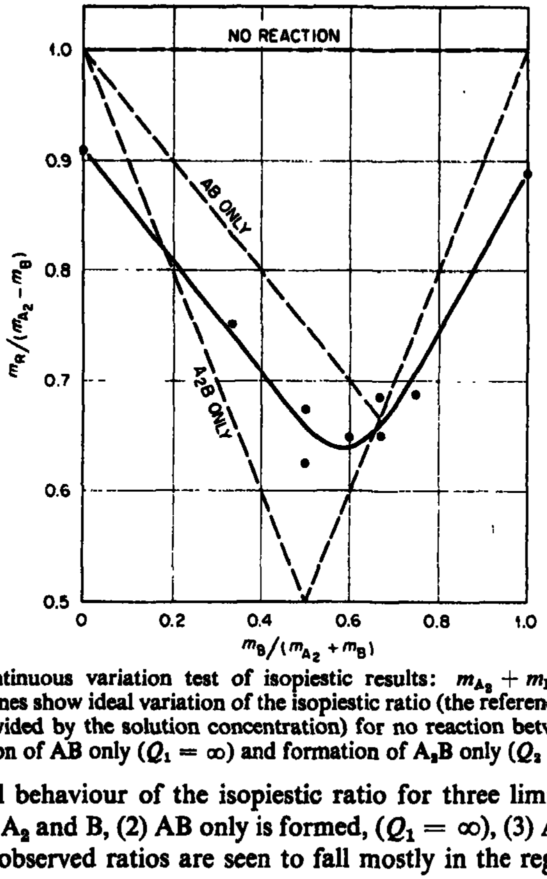

FIG. 4.—Continuous variation test of isopiestic results: $m_{A_2} + m_B = 0{\cdot}1\text{–}0{\cdot}15\ m$. The broken lines show ideal variation of the isopiestic ratio (the reference solution concentration divided by the solution concentration) for no reaction between A_2 and B, formation of AB only ($Q_1 = \infty$) and formation of A_2B only ($Q_2 = \infty$).

3. *Conclusions.* The present value of Q_1 for the DEPA–TOPO, AB product is 25–50 times larger than the corresponding values found for DBP–TBP by DYRSSEN,$^{(4)}$ HARDY$^{(5)}$ and their coworkers. This is the trend expected in view of the more basic character of the phosphoryl oxygen in a phosphine oxide compared to that in a phosphate. The A_2B product has not previously been reported.

The amount of extraction data presently available for MO_2^{2+}–A_2–B systems is insufficient to warrant a detailed test of synergistic behaviour in terms of the formation of AB, A_2B (and a mixed product or products $(MO_2)A_aB_b$); however, the inclusion of these interaction products in the interpretation of future results would appear desirable.

Acknowledgement—The authors are pleased to acknowledge the valuable technical assistance of W. E. OXENDINE in this investigation.

J. Inorg. Nucl. Chem., 1962, Vol. 24, pp. 1287 to 1296. Pergamon Press Ltd. Printed in Northern Ireland

THE DENSITY OF LIQUID NaCl AND KCl AND AN ESTIMATE OF THEIR CRITICAL CONSTANTS TOGETHER WITH THOSE OF THE OTHER ALKALI HALIDES*

A. D. KIRSHENBAUM, J. A. CAHILL, P. J. McGONIGAL† and A. V. GROSSE
Research Institute of Temple University, Philadelphia, Pa.

(*Received* 21 *February* 1962)

Abstract—A procedure for the estimation of the critical constants of salts, provided reliable liquid density data are available, is explained. The method is applied specifically to NaCl and KCl, the liquid densities of which have been determined from the melting point to the normal boiling point The dependence of density on temperature may be expressed by the following equations:

$$D_{\text{NaCl}}\ \text{g/cm}^3 = 2{\cdot}061 - 4{\cdot}759 \times 10^{-4}\ T°\text{K} \pm 0{\cdot}002\ \text{g/cm}^3$$
$$D_{\text{KCl}}\ \text{g/cm}^3 = 2{\cdot}062 - 5{\cdot}350 \times 10^{-4}\ T°\text{K} \pm 0{\cdot}003\ \text{g/cm}^3$$

The estimated critical constants for NaCl are: $T_c = 3400°\text{K} \pm 200°\text{K}$, $D_c = 0{\cdot}22\ \text{g/cm}^3 \pm 0{\cdot}05\ \text{g/cm}^3$, $V_c = 266\ \text{cm}^3\ {}^{-50}_{+70}\ \text{cm}^3$, $P_c = 350\ \text{atm}\ {}^{-120}_{+130}\ \text{atm}$, and for KCl: $T_c = 3200°\text{K} \pm 200°\text{K}$, $D_c = 0{\cdot}175\ \text{g/cm}^3 \pm 0{\cdot}05\ \text{g/cm}^3$, $V_c = 415\ \text{cm}^3\ {}^{-100}_{+200}$, $P_c = 220\ \text{atm},\ {}^{-70}_{+100}\ \text{atm}$.

Estimated critical temperatures are given for the other alkali halides.

IN previous publications$^{(1,2)}$ a procedure for estimating the critical temperature of any metal based on application of the theorem of corresponding states to the entropy of vapourization has been discussed. If density data for the liquid metal are available the law of rectilinear diameters may be used to estimate the critical density and critical volume. Critical pressures may be approximated by extrapolation of ideal gas vapour-pressure data. It has been emphasized$^{(1,2)}$ that in regard to thermal stability the metals form a unique group; since they are elementary monatomic substances the only dissociation process which need be considered is ionization and this is repressed by the high saturation vapour-pressures. Calculations involving the Saha equation indicate that for metallic vapours the degree of ionization is small (of the order of a few per cent) at the critical point, particularly in view of the high vapour-pressure. The critical temperatures of the high-boiling metals, for example, are as follows: Mo–17,000°K, Re–20,500°K, Ta–22,000°K and W–23,000°K.

With molecular species, however, the situation is not so simple and dissociation into atoms, radicals, ions, simpler molecules or a combination of these forms, must be considered, 6000°K may be taken as the upper limit for *real* critical temperatures of

---

* This work was supported by the National Science Foundation under grant 15540.

† Portions of this work will be included in a dissertation to be submitted by P. J. McGONIGAL to the Graduate Council of Temple University in partial fulfillment of the requirements for the degree of Doctor of Philosophy.

(1) A. V. GROSSE, *J. Inorg. and Nucl. Chem.* **22**, 23 (1961).

(2) A. V. GROSSE, Paper No. 2159, A.R.S., Space Flight Report to the Nation, New York, Oct. 9–15, (1961); See also A. V. GROSSE, *The Liquid Range of Metals and Some of their Physical Properties at High Temperatures*, Research Institute of Temple University, Oct. 19, (1960).

molecular substances since above this temperature all chemical bonds will be broken. Many compounds will be substantially dissociated at lower temperatures and it is not always possible to speak of a critical temperature of a compound since it could not exist as such at that temperature. For example, CaO boils at 3800°K and, as a first approximation, would be expected as an ionic compound to have a critical temperature in the neighbourhood of 7600°K. Extrapolation of K_p data for dissociation into the elements as reported by Latimer(3) and vapour-pressure data reported by Bockris *et al.*(4) yield values of 350 and 1860 atm respectively for these quantities at the critical point. The degree of dissociation calculated for CaO at its supposed critical temperature and pressure is 40 per cent. As a more extreme example of a substance which cannot be said to have a critical point we may consider Al_2O_3 which is substantially dissociated into Al_2O, Al_2O_2, O and O_2 at its normal boiling point of 3800°K, which happens to coincide with the flame temperature of the Al-O_2-flame (at 1 atm).(5)

On the other hand calculations based on recent K_p data(6) and linear extrapolation of the vapour-pressure data of Barton and Bloom(7) show that NaCl is only 1·25 per cent dissociated at its estimated critical temperature of 3400°K and critical pressure of 350 atm. The per cent dissociation at the critical point critical temperatures (see Discussion) are given in Table 1. Critical pressures are estimated to be from 200 to 1000 atm, based on available vapour pressure and K_p data. It is, therefore, feasible to speak of critical temperatures for the alkali halides (see Table 9).

Table 1.—Critical temperatures and per cent dissociation of several alkali halides

Salt	T_c(°K)	Dissociation (%)
LiF	4140	0·4
LiCl	3080	0·2
LiBr	3020	0·3
LiI	3250	0·7
NaF	4270	1·7
NaCl	3400	1·2

EXPERIMENTAL

Procedure

The density of sodium and potassium chlorides were determined from their melting points to their normal boiling points by the Archemedian Principle. The procedure used has been described previously in our paper on liquid lead.(8) It was observed previously(9) that graphite did not react with these salts. Therefore, graphite crucibles, sinkers and reflux condensers were used in these experiments. Analyses of the salts after the experiments showed that there was $<$0·02 per cent carbon present in the salts.

(3) W. M. Latimer, *Tables of Free Energy Functions for Elements and Compounds in the Temperature Range 2000–5000°K*, U.S.A.E.C., Oak Ridge, Tenn., 11-18-49-300-A10159 (MDDC-1462).

(4) J. O'M. Bockris, J. L. White and J. D. Mackenzie, *Physico-Chemical Measurements at High Temperatures*, p. 93. Academic Press, New York (1959).

(5) A. V. Grosse and J. B. Conway, *Ind. & Eng. Chem.*, **50**, 663 (1958).

(6) JANAF Interim Thermochemical Tables, Vol. 1 and 2, Prepared under the auspices of the Joint Army-Navy-Air Force Thermochemical Panel, W. H. Jones, Chairman, by the Thermal Laboratory Dow Chemical Co., Midland, Mich., Dec. 1960, with supplements through Sept. 1961.

(7) J. L. Barton and H. Bloom, *J. Phys. Chem.* **60**, 1413 (1956).

(8) A. D. Kirshenbaum, J. A. Cahill and A. V. Grosse, *J. Inorg. Nucl. Chem.*, **22**, 33 (1961).

(9) A. D. Kirshenbaum, J. A. Cahill and C. S. Stokes, *J. Inorg. Nucl. Chem.* **15**, 297 (1960).

The volume of the sinker at 20°C was calibrated in mercury and corrected for surface tension, The volume of the sinkers were always corrected to the operating temperature using the thermal expansion data reported by GOLDSTEIN, *et al.*(10) together with data known for the graphite used.* The volume of the sinker depended upon its depth of immersion in the liquid salts. This was determined by an electric probe, i.e. by the difference between the depth of the liquid salt and the distance of the sinker from the crucible base.(8, 9)

The losses in wt. of the sinkers were corrected for surface tension using the surface tension equations reported by BLOOM *et al.*(11) namely $\gamma_{NaCl} = 190{\cdot}8 - 0{\cdot}093t$ and $\gamma_{KCl} = 155{\cdot}2 - 0{\cdot}073t$ where t is in °C and γ in dynes/cm.

Materials used

The total impurities were 0·027 per cent in the NaCl and 0·020 per cent in the KCl. The main impurities were:

	NaCl	KCl
Bromide	0·005%	0·005%
Chlorate	0·003%	0·003%
Nitrate		0·003%
Iodide	0·002%	0·002%
Sodium	—	0·003%
Potassium	0·002%	—

Thus, the purity of the NaCl was 99·973 per cent and of the KCl was 99·980 per cent.

RESULTS

The experimental data obtained for NaCl and KCl are presented in Table 2. A least squares treatment of the data gave the following linear relationships:

$$D^{\text{liq.}}_{\text{NaCl}} = 2{\cdot}061_0 - 4{\cdot}759 \times 10^{-4} T\,°\text{K} \pm 0{\cdot}002 \text{ g/cm}^3$$

$$D^{\text{liq.}}_{\text{KCl}} = 2{\cdot}062_4 - 5{\cdot}350 \times 10^{-4} T\,°\text{K} \pm 0{\cdot}003 \text{ g/cm}^3.$$

The molar volumes and volume coefficients of expansion of NaCl and KCl are given in Table 3. A comparison of our data with those reported in the literature are

TABLE 2.—EXPERIMENTAL LIQUID DENSITIES

Temperature (°K)	Density (g/cm^3)	Temperature (°K)	Density (g/cm^3)
	NaCl		
1149	1·516	1502	1·347
1162	1·503	1590	1·305
1202	1·486	1552	1·323
1208	1·483	1573	1·312
1404	1·388	1670	1·267
1459	1·367		
	KCl		
1101	1·471$_0$	1317	1·364
1112	1·470$_7$	1410	1·303
1184	1·427$_7$	1420	1·297
1197	1·422$_8$	1507	1·264
1294	1·368$_8$	1607	1·202

---

* Dixon E-821, fine grain petroleum coke base stock with a transverse linear coefficient of expansion from 100 to 600°C of 35 × 10^{-7}/°K and a parallel coefficient of expansion of 20·8 × 10^{-7}/°K.

(10) A. Goldstein, T. E. Waterman and H. J. Hirschhorn, Thermophysical Properties of Solid Materials Vol. 1, p. 59–158. WADC Technical Report 58-476, (1960).

(11) H. Bloom, F. G. Davis and D. W. James, *Trans. Faraday Soc.* **56**, 1179 (1960).

TABLE 3.—MOLAR VOLUMES AND COEFFICIENTS OF EXPANSION OF NaCl AND KCl

Temperature (°K)	Density (g/cm^3)		Molar volume (cm^3/mole)		Cubical Coeff. of Expan. $\times 10^5$ ($°K^{-1}$)	
	NaCl	KCl	NaCl	KCl	NaCl	KCl
1073 (m.p.)	1·5504	—	37·70	—	30·70	—
1063 (m.p.)	—	1·494	—	49·90	—	35·81
1100	1·538	1·473	38·01	50·61	30·94	36·32
1200	1·490	1·420	39·23	52·50	31·94	37·68
1300	1·442	1·366	40·54	54·58	33·00	39·17
1400	1·395	1·313	41·90	56·78	34·11	40·75
1500	1·347	1·259	43·40	59·22	35·33	42·49
1600	1·300	1·206	44·96	61·82	36·61	44·36
1680 (b.p.)	—	1·163	—	64·10	—	46·00
1738 (b.p.)	1·247	—	46·88	—	35·81	—

presented in Tables 4 and 5. There is excellent agreement on the densities of NaCl and KCl at their melting points between our data and those reported in the literature. The literature temperature coefficients, however, do vary slightly for NaCl ($3{\cdot}8$–$6{\cdot}26 \times 10^{-4}$). We give preference to our *dD/dt* values since they cover the whole range of 550°K, from the melting point to the normal boiling point.

TABLE 4.—COMPARISON OF LITERATURE VALUES FOR THE LIQUID DENSITY OF NaCl

Investigator	Temperature range (°K)	Temperature coeff. $\times 10^4$	Density at m.p.	Reference
This work	1150–1700	−4·759	1·5504	
LORENZ, FRIES and JAFS	1125–1225	−3·8	1·521	*Z. phys. Chem.* **61**, 472 (1908)
JAEGER	1100–1450	−6·261	1·549	*Z. Anorg. Chem.* **101**, 180 (1917)
HONDA	1200–1600	−5·07	1·557	*Z. Anorg. Chem.* **154**, 238 (1926)
SAUERWALD	1300–1600	−5·00	1·564	*Z. Anorg. Chem.* **135**, 327 (1924)
ARNDT and GESSLER	1075–1175	−5·4	1·54	*Z. Elektroch.* **14**, 666 (1903)
BRUNNER	1100–1300	−5·4	1·554	*Z. Anorg. Chem.* **38**, 375 (1904)
		avg. =	1·548	

According to BOCKRIS *et al.*(12) the density of solid sodium and potassium chlorides have the following temperature relationships:

$$\text{NaCl:}\quad D_s = 2{\cdot}168 - 1{\cdot}267 \times 11^{-4}t - 1{\cdot}754 \times 10^{-7}t^2(\pm 0{\cdot}002\ \text{g/cm}^3)$$

$$\text{KCl:}\quad D_s = 1{\cdot}985 - 5{\cdot}459 \times 10^{-5}t - 1{\cdot}836 \times 10^{-7}t^2(\pm 0{\cdot}001\ \text{g/cm}^3)$$

where *t* is in °C. The densities and molar volumes of NaCl and KCl at their melting points are:

	D(g/cm^3)	V_M,(cm^3/mole)
NaCl (solid)	1·955	29·90
(liquid)	$1{\cdot}550_4$	37·70
KCl (solid)	1·827	40·81
(liquid)	1·494	49·90

---

(12) J. O'M. BOCKRIS, A. PILLA and J. L. BARTON, *J. Phys. Chem.* **64**, 507 (1960).

TABLE 5.—COMPARISON OF LITERATURE VALUES FOR THE LIQUID DENSITY OF KCl

Investigator	Temperature range (°K)	Temperature coeff. × 10^4	Density at m.p.	Reference
This work	1100–1600°	−5·350	1·494	
NEILHAMER and PEAKE	1075–1300°	−5·8	1·502	*J. Chem. Engng. Data* 6, 197 (1961)
MASHOVETZ and LUNDINA	1075–1400°	−5·7	1·499	Proc. 1st All-Union conf. Non-aqueous solutions 1935, pp. 191–212
PEAKE and BOOTHWELL	1075–1200°	−5·8	1·502	*J. Amer. Chem. Soc.* 76, 2653 (1954)
BRUNNER	1075–1300°	−5·7	1·507	*Z. Anorg. Chem.* 38, 350 (1904)
ARNDT and GESSLER	—	−5·4	1·498	*Z. Elektrochem.* 14, 666 (1903)
JAEGER and KAHN	1075–1225°	−5·95	1·509	*Proc. Acad. Sci. Amster.* 10, 381 (1916)
KLEMM	—	−5·6	1·517	*Z. Anorg. Chem.* 152, 295 (1926)
			avg. = 1·504	

TABLE 6.—VOLUME CHANGE OF NaCl AND KCl ON MELTING

$\Delta V/V_s$ (%)		Reference
NaCl	KCl	
26·06 ± 0·06	22·27 ± 0·08	This paper
25·58 ± 0·07	20·20 ± 0·05	BOCKRIS, PILLA and BARTON, *J. Phys. Chem.* 64, 507 (1960)
—	21·0 ± 0·5	LANDON and UBBELOHDE, *Trans Faraday. Soc.* 52, 647 (1956)
30·0	23·0	EUCKEN, *Z. Angew. Chem.* 55, 163 (1942)
25·0 ± 0·5	17·3 ± 0·5	SCHINKE and SAUERWALD, *Z. Anorg. Chem.* 237, 313 (1956)
22·8 ± 0·7	16·8 ± 0·5	EUCKEN and DANNOHL, *Z. Elektrochem.* 40, 814 (1934)
23·2 ± 2·0	17·5 ± 2·0	BREDIG and JOHNSON, Report ORNL-1940, p. 19

Therefore, the volume change on melting ($\Delta V/V_s$) are 26·06 and 22·27 per cent respectively for NaCl and KCl. A comparison of these values with those reported by previous investigators are given in Table 6.

DISCUSSION

Diagrams covering the entire liquid ranges of NaCl and KCl have been constructed from the experimental liquid density data and vapour densities obtained by extrapolation of the data of BARTON and BLOOM.(7) The general method for the preparation of these diagrams has been previously discussed.(1) Dimeric species were taken into account in the calculations. The amounts were obtained by extrapolation of the data given by DATZ, *et al.*(18) These diagrams are reproduced in Figs. 1 and 2. Densities of vapour and liquid above the normal boiling points of NaCl and KCl are shown in Table 7.

The liquid densities were calculated according to the equation

$$D_{\text{liq.}} = 2D\,\text{♂} - D_{\text{vap.}}$$

where D♂ represents rectilinear diameter. The equations for the rectilinear diameters are:

$$D\text{♂}_{\text{NaCl}} = 1{\cdot}0305 - 2{\cdot}3795 \times 10^{-4}T(°\text{K})$$

$$D\text{♂}_{\text{KCl}} = 1{\cdot}0312 - 2{\cdot}675 \times 10^{-4}T(°\text{K})$$

---

(18) S. DATZ, W. T. SMITH, JR. and E. H. TAYLOR, *J. Chem. Phys.* 34, 558 (1961).

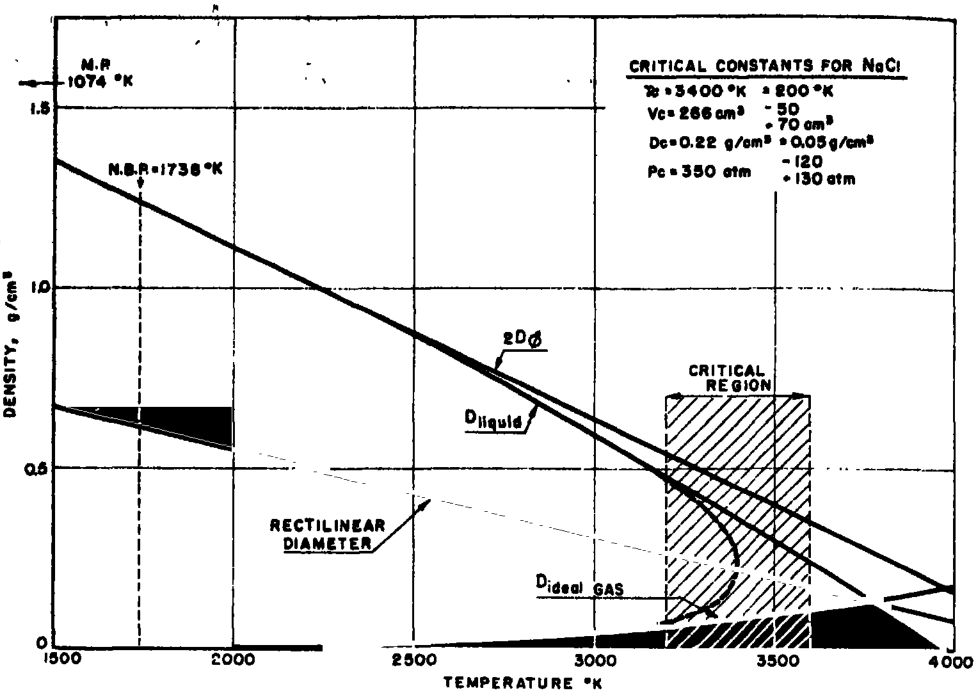

FIG. 1.—Liquid range diagram for NaCl.

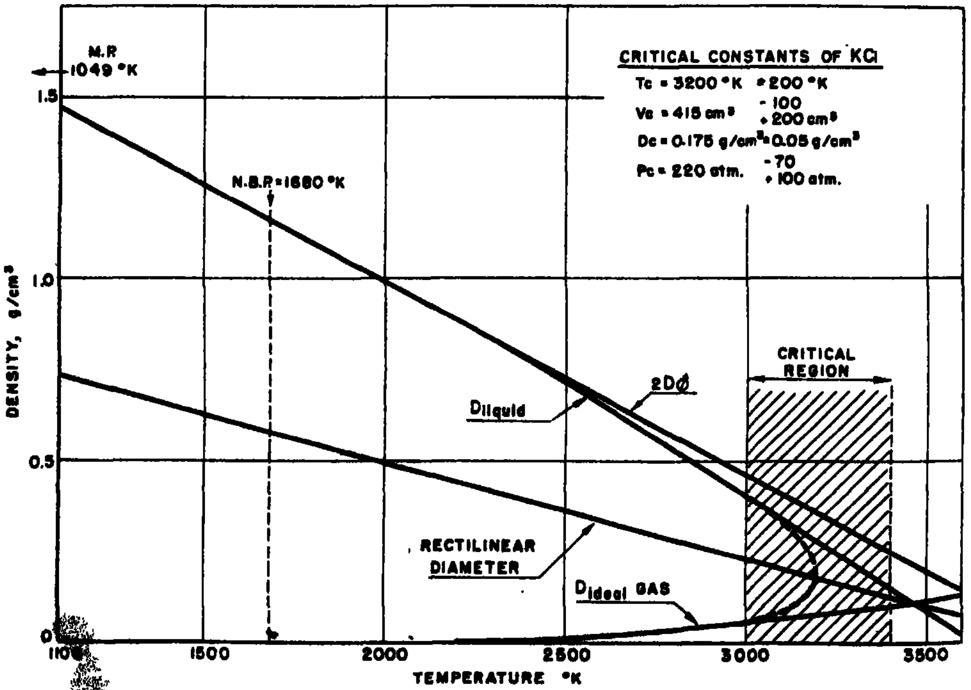

FIG. 2.—Liquid range diagram for KCl.

TABLE 7.—SATURATED VAPOUR AND LIQUID DENSITIES OF NaCl AND KCl ABOVE THEIR NORMAL BOILING POINT

Temperature (°K)	Sat. vapour density (g/cm³)		Liquid densit (g/cm³)	
	NaCl	KCl	NaCl	KCl
1680 (b.p.)	—	0·000595	—	1·162
1738 (b.p.)	0·000577	—	1·233	—
1800	0·000837	0·00117	1·203	1·098
2000	0·00225	0·00290	1·107	0·989
2200	0·00495	0·00636	1·009	0·879
2400	0·0100	0·0125	0·909	0·766
2600	0·0174	0·0208	0·807	0·650
2800	0·041	0·034	0·701	0·530
3000	0·059	0·050	0·622	0·407
3200	0·10	—	0·480	—

The critical temperatures were estimated to be in the centers of the critical regions shown in Figs. 1 and 2. The *upper limit* for the critical region is definitely established by the intersection of the liquid and ideal vapour density curves at the rectilinear diameter. The lower limit is not so well defined but may be taken as that temperature at which the calculated vapour density is one-fifth as great as the calculated liquid density. In the case of NaCl and KCl this temperature is about 400° below the upper limit. The error in the critical temperature in each case is taken to be ±200°K. The critical constants determined from the diagrams are presented in Table 8.

TABLE 8.—CRITICAL CONSTANTS OF NaCl AND KCl

	NaCl		KCl	
	This work	EYRING	This work	EYRING
T_c	3400° ± 200°K	3600°K	3200° ± 200°K	3092°K
D_c	0·22 ± 0·05 g/cm³	0·20 g/cm³	0·18 ± 0·05 g/cm³	0·173 g/cm³
V_c	$266\,{}^{-50\ \mathrm{cm}^3}_{+70}$	293 cm³	$466\,{}^{-100\ \mathrm{cm}^3}_{+200}$	431 cm³
P_c	$350\,{}^{-120\ \mathrm{atm}}_{+130}$	235·5 atm	$220\,{}^{-70\ \mathrm{atm}}_{+100}$	135·5 atm
$\left(\frac{P_cV_c}{RT_c}\right)$	0·332	0·233	0·390	0·230

These constants, obtained on a semiempirical basis, agree reasonably well with those obtained theoretically by EYRING and co-workers[14] who developed a partition function for fused salts based on the concept of significant structures in the liquid state. For purposes of comparison EYRING's data are also shown in Table 8. The molar volumes at the boiling point as calculated by EYRING are 51·15 cm³ for NaCl and 71·20 cm³ for KCl compared to our experimental values of 46·87 cm³ and 64·10 cm³, respectively.

In view of the great similarity of physical and chemical properties of the alkali halides generally we assume that their critical temperatures can be estimated with a fair degree of reliability by application of the law of corresponding states to the entropy of vaporization, $\Delta S_{\mathrm{vap.}}$, vs reduced temperature curve for NaCl. The procedure is similar to that previously described for metals.(1) This curve, which appears in Fig. 3, was constructed from our estimated critical temperature for NaCl and the $\Delta H_{\text{vap.}}$ data of Kelley(16) which, for our purposes, at least are not significantly different from the more recent data of Barton and Bloom.(7)

---

[14] C. M. CARLSON, H. EYRING and T. REE, *Proc. Natl. Acad. Sci.*, **46**, 333 (1960).

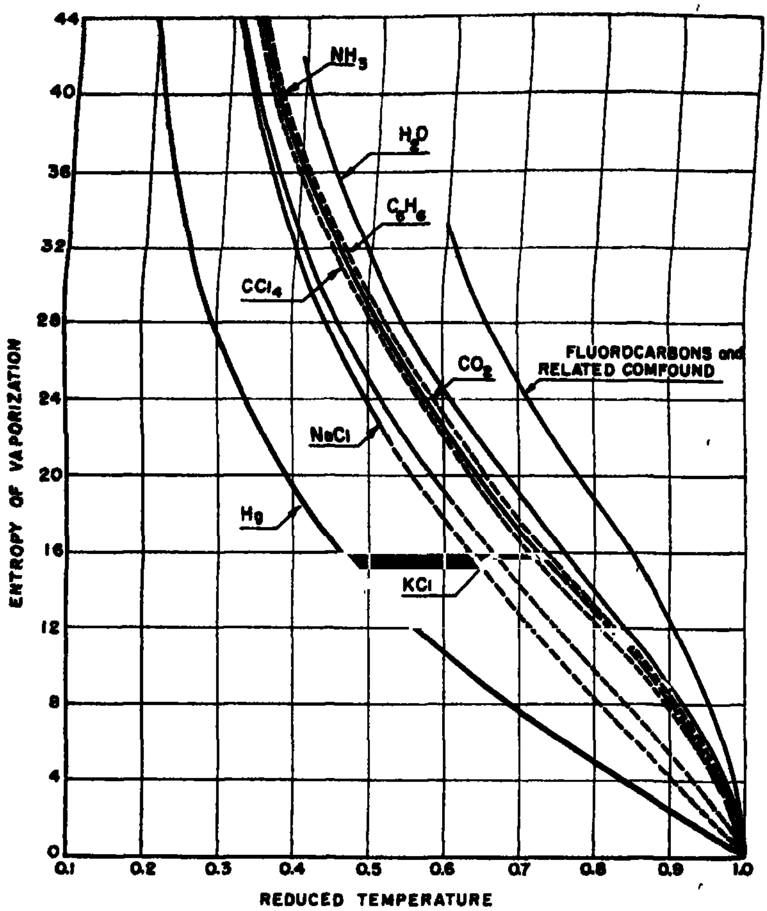

Fig. 3.—ΔS_{vap} vs. reduced temperature.

These estimated critical temperatures are listed in Table 9; the normal boiling points and entropies of vaporization are those reported by Brewer.(15)

Joliet(17) has recently published a procedure for estimating the critical volumes of the alkali halides which involves the assumption that at the critical point each alkali halide molecule occupies a cube whose edge is twice the internuclear distance at room temperature. The critical volumes calculated by this method for NaCl and KCl, 108 cm^3 and 152 cm^3, respectively, are much lower than the values given in Table 8. Joliet's results appear to agree rather well with those of Saslawsky(18) and Lorenz

---

(15) L. Brewer *et al.*, in *The Chemistry and Metallurgy of Miscellaneous Materials, Thermodynamics* (Edited by L. L. Quill) NNES Vol. IV-19B, McGraw-Hill, New York (1950).

(16) K. K. Kelley, *Bureau of Mines Bulletin* 383, (1935).

(17) J. F. Joliet, *C.R. Acad. Sci. Paris* **252**, 719 (1961).

(18) Saslawsky, *Z. Phys. Chem.* **109**, 111 (1924).

TABLE 3.—BOILING POINTS, ENTROPIES OF VAPOURIZATION, REDUCED TEMPERATURES AND CRITICAL TEMPERATURES FOR ALKALI HALIDES

Salt	T_b(°K)	$\Delta S_{vap.}\left(\frac{\text{cal.}}{\text{g. atom. deg.}}\right)$	$T_{red.}$	T_c(°K)
LiF	1954	26·1	0·473	4140
LiCl	1653	21·7	0·537	3080
LiBr	1583	22·4	0·525	3020
LiI	1444	28·2	0·445	3250
NaF	1977	26·9	0·463	4270
NaCl	1738	23·5	0·508	3400
NaBr	1665	22·8	0·520	3200
NaI	1577	24·2	0·498	3160
KF	1775	23·2	0·513	3460
KCl	1680	23·1	0·515	3200
KBr	1656	22·4	0·525	3170
KI	1597	21·7	0·537	2980
RbF	1681	23·5	0·512	3280
RbCl	1654	22·3	0·527	3140
RbBr	1625	22·8	0·520	3130
RbI	1577	22·8	0·520	3035
CsF	1524	22·5	0·523	2915
CsCl	1573	22·7	0·518	3040
CsBr	1573	22·9	0·517	3045
CsI	1553	23·1	0·515	3020

and HERZ.(19) However, it should be noted that SASLAWSKY's values are calculated from an expression which involves the critical temperature which in turn is obtained from the LORENZ relationship, $T_c = T_m/0{\cdot}44$, which cannot be valid for alkali halides since at the critical temperatures this expression yields very low values for the vapour densities. According to the LORENZ equation NaCl and KCl would have about the same critical temperature, 2400°K; at this temperature the vapour densities would be only 0·010 g/cm^3 for NaCl and 0·012 g/cm^3 for KCl.

It would thus seem that JOLIET's assumptions are incorrect.

It is of interest to consider the reduced density vs reduced temperature curve for typical salts as exemplified by NaCl and KCl and to compare it with three other classes of substances, namely, ideal or perfect liquids (argon and other noble gases),(20) metals,(21) and fluorocarbons (and derivatives),(22,23) homopolar liquids with particlarly small intermolecular forces. These curves are shown in Fig. 4. It is apparent that each of the four types of substances has a curve distinct from the others. This is not to say that as the number of examples increases there will not be a band for each type. However, it is to be expected that the *mean* curves will show differences. The reduced density vs reduced temperature behaviour of the substances is not simply related to their structures. However, the similarity of the reduced *vapour* density curves is apparent and is undoubtedly due to the fact that at the large interatomic or intermolecular

(19) LORENZ and HERZ, *Z. Anorg. Chem.* **138**, 330 (1924).
(20) E. A. GUGGENHEIM, *J. Chem. Phys.* **13**, 253 (1945).
(21) P. J. MCGONIGAL, A. D. KIRSHENBAUM and A. V. GROSSE, *J. Phys. Chem.*, **66**, 737 (1962).
(22) R. M. YARRINGTON and W. B. KAY, *J. Chem. Engng. Data*, **5**, 24 (1960).
(23) J. H. SIMONS, *Fluorine Chemistry*, Vol. 1, p. 438. Academic Press, New York (1950).

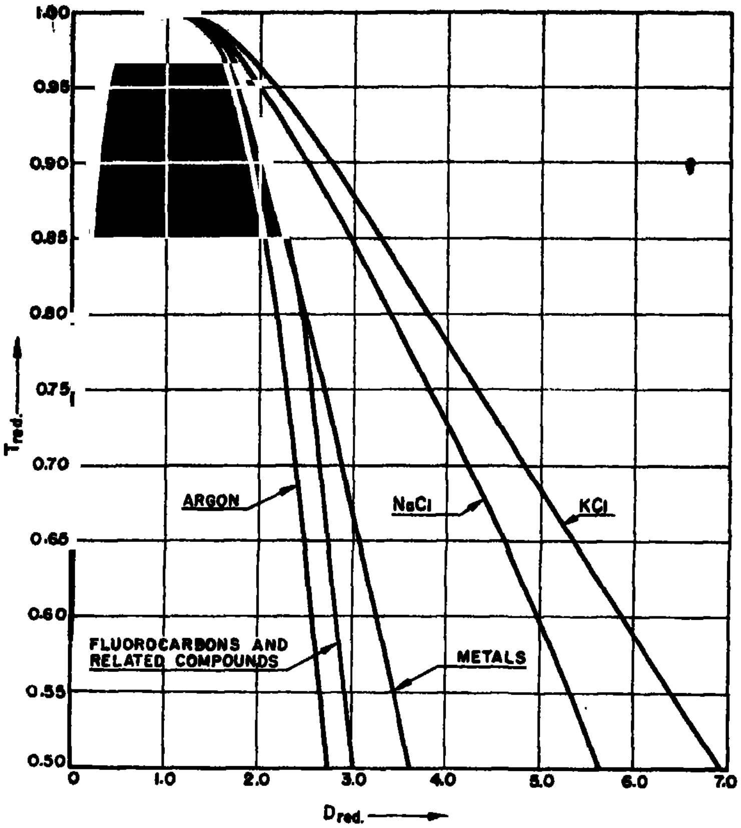

FIG. 4.—Reduced density vs reduced temperature.

distances which exist in the gaseous state the characteristic attractive forces are very much lessened.

A similar and typical separation into classes of substances is shown in Fig. 3 which is a plot of entropy of vapourization vs reduced temperature. It is to be noted that the behaviour of typical homopolar compounds like CCl_4, CO_2 or benzene is essentially the same as that for associated liquids like H_2O and NH_3.

CONCLUSIONS

The method described above allows a reasonable consistent estimation of the critical properties of salts. The agreement of our semi-empirical method with the results of EYRING[14] is encouraging. The greatest discrepancy is in the estimation of the critical pressures. Further experimental work on liquid and vapour densities, especially at high pressures, beyond the normal boiling point, is obviously indicated to extend density data to higher temperatures and to support or narrow down the critical constant estimates presented in this paper. Methods for making such measurements are currently under study at this Institute.

J. Inorg. Nucl. Chem., 1962, Vol. 24, pp. 1297 to 1298. Pergamon Press Ltd. Printed in Northern Ireland

NOTES

Preparation of neptunium targets by electrodeposition

(*Received* 8 *January* 1962; *in revised form* 9 *April* 1962)

NEPTUNIUM has been coated on metal cathodes by the electrolytic deposition of the oxide or hydroxide. The experimental results show that adherent, uniform neptunium sources can be prepared in the range from 0·2 to 4 mg on a nickel cathode area of 7 cm^2. Heavier neptunium sources in the range 0·8–7 mg were also prepared after several successive electrodeposition steps on the same disc. Platinum, stainless steel and tantalum backing discs were found equally suitable for the sources. The electrolytic cell consisted of a polyethylene cylinder and base cap, a nickel plated disc serving as cathode contact, and a platinum ring anode. The cell was kept at 80°C in a water bath, with constant stirring at about 100 rev/min. The cathode discs were treated with carbon tetrachloride and chemically etched immediately before plating. To an electrolyte volume of 15 ml of saturated ammonium oxalate solution, 25–500 μl of 0·5 M HNO$_3$ neptunium solution were added and the pH of the resulting solution adjusted to 7 with ammonium hydroxide. Current densities of 0·043–0·057 A/cm^2 were used in most experiments. At the end of the electrolysis the metal hydroxide deposits were rinsed with distilled water and dried at room temperature. The plate uniformity was determined by means of autoradiographs and densitometic measurements. The maximum density difference ratio {MDDR: (Maximum optical density/Minimum optical density) − 1} varied from 0·16 to 0·40 with an average ratio of 0·28.

Acknowledgements—This investigation has been carried out as part of the programme of the Foundation for the Fundamental Research of Matter (F.O.M.) with the financial support of the Organization for Pure Research (Z.W.O.). Thanks are due to the International Atomic Energy Agency for a fellowship and to the Comisión Nacional de Energía Atómica for giving the necessary leave of absence.

Comisión Nacional de Energía Atómica
Buenos Aires, Argentina

G. A. DUPETIT

Alkylammonium complexes of copper (II)

(*Received* 24 *April* 1962)

THE reaction of copper (II) chloride with amine hydrochlorides to form yellow bis-alkylammonium tetrachlorocuprates (II) has been reported previously.(1,2,3)

As part of another study, we attempted to prepare alkyl diazonium chlorides at low temperatures. We observed, however, that methylamine and ethylamine, in the presence of liquid anhydrous HCl and CuCl$_2$, gave the known(3) corresponding bis-alkylammonium tetrachlorocuprate (II), (RNH$_3^+$)$_2$(CuCl$_4^=$), R = Me and Et.

We found that these complexes are extremely soluble in N-methylpyrrolidone and slightly soluble in γ-butyrolactone, but are precipitated from these solutions on addition of diethyl ether.

The ultraviolet and visible absorption spectra of the two complexes were measured in several solvents and, as reported previously (but without supporting data)(3), we have observed that the results are strongly dependent on the nature of the solvent.

Thus, both complexes exhibited maxima at 475 mμ (ϵ 1500, R = Et) and 316 mμ (ϵ 3570, R = Et) in γ-butyrolactone. The bis-ethylammoniumtetrachlorocuprate (II) (compound A) exhibited maxima at 474 mμ and 344 mμ in acetone and only at 273 mμ in methanol.

(1) H. REMY and G. LAVES, *Ber.* **66B**, 401 (1933).

(2) W. M. DEHN, *J. Amer. Chem. Soc.* **48**, 111 (1926).

(3) R. D. WHEALY, D. H. BIER and B. J. MCCORMICK, *J. Amer. Chem. Soc.* **81**, 5900 (1959).

The influence of a bulky alkyl group in the preparation of such complexes was illustrated by the behavior of tert-octylammonium chloride on treatment with $CuCl_2$ and liquid HCl. The solid, which initially formed, slowly evolved HCl and an aqueous solution of the freshly prepared product possessed a pH of 2. After recrystallization from γ-butyrolactone, the pH of the aqueous solution was 7. The spectrum of this tan-colored tert-octyl ammonium complex was almost identical with that observed for compound A. The analytical data for the crystallized product was fairly consistent with that for tert-octylammoniumtrichlorocuprate (II) (compound B). Calcd: C, 32·02; H, 6·72; N, 4·67; Cl, 35·42%. Found: C, 31·14; H, 6·81; N, 4·46; Cl, 37·09%.

It therefore appears that the initial, unstable product was hydrogen tert-octylammoniumtetrachlorocuprate (II) and it seems likely that during crystallization, γ-butyrolactone served as a proton acceptor. The similarity in spectra of compounds A and B suggests a "pseudo" tetrachlorocuprate (II) structure in B.

Furthermore, methanolic solutions of B reacted with methanolic solutions of $RNH_3{}^+Cl^-$ (R = Me, Et, n-Pr, and n-Bu) to give yellow solids after addition of ether. These products are probably mixed dialkylammoniumtetrachlorocuprate (II) complexes. Their structures are under investigation.

The spectra were determined on a Beckman DK-2 recording spectrophotometer. Microanalysis was carried out by Micro-Tech Laboratories, Skokie, Illinois.

R. Filler
L. Gorelic

Department of Chemistry
Illinois Institute of Technology
Chicago 16, *Illinois, U.S.A.*

J. Inorg. Nucl. Chem., 1962, Vol. 24, pp. 1299 to 1300. Pergamon Press Ltd. Printed in Northern Ireland

BOOK REVIEWS

S. C. LIND. **Radiation Chemistry of Gases.** A. C. S. Monograph No. 151. 313 pp. Reinhold Publishing Company (1961) 100s.

THOSE who for many years have regarded Dr. LIND's monograph ("Chemical Effects of Alpha Particles and Electrons", 1928) as a lucid and penetrating analysis of early work in radiation chemistry will have looked eagerly for a new edition bringing it up to date. The title change is significant; recent studies have used a wider range of radiation sources, and the growing volume of radiation chemical literature makes some restriction of topics inevitable. The behaviour of gases forms the main theme of the earlier monograph and Dr. LIND's own very considerable experimental contributions are in this field.

The first part of the present monograph includes chapters by Dr. C. J. HOCHANADEL on "Absorption of Ionizing Radiations" and by Dr. J. A. GHORMLEY on "Other Sources and Dosimetry". Unfortunately they are in general terms and poorly coordinated with the rest of the book. One looks in vain for any discussion of the special problems of selecting suitable radiation sources for gaseous systems and of measuring or calculating accurately the dose received by gases. That these problems are formidable is clear from the remaining chapters of Part I which deal with the use of radon. The large, some might feel disproportionate, amount of space devoted to radon throughout the book reflects not only the author's special interests but also the large part radon has played in the most thorough of the radiation chemical studies of gases.

The second part of the book describes the experimental data published up to July 1960 and, so far as the reviewer can tell, is comprehensive to the point of being indiscriminate in places. Items such as the radiolysis of $KBrO_3$ are scarcely relevant and others, such as the confusing CO_2-carbon behaviour under radiation, are described with detail which contributes little to our understanding of gas radiolysis. The arrangement of material into "Reactions of One Component", "Oxidation", "Hydrogenation" etc. has little obvious advantage, involves much repetition, and separates related topics (e.g., CO_2 decomposition; CO oxidation; and $CO_2 + H_2$ reaction). Cross-references are, however, abundant and the index and tabular summaries are excellent.

As a reference work summarizing the published data the new monograph is invaluable, but the recent material (often more qualitative and less penetrating than the early work) is not well assimilated. It is not possible therefore to recommend the book as a critical analysis of the data. To a large extent this is a reflection on the state of the subject itself.

J. WRIGHT

Uranium Dioxide: Properties and Nuclear Applications, Edited by J. BELLE, U.S. Government Printing Office, Washington, D.C., 1961, 726 pp. $2.50.

THIS book serves as an excellent illustration of the rapid growth of basic science and technology during the past decade in the field of reactor fuel materials. The extent of the growth is evidenced by the large body of knowledge about uranium dioxide that has been collected and critically examined by forty-two contributing authors. The editor, J. BELLE, deserves special acknowledgement for coordinating the findings of the various disciplines, engineering, ceramics, chemistry, physics, and metallurgy into a valuable sourcebook.

The first four chapters discuss the application of UO_2 to nuclear power reactors and provide a detailed review of the factors that affect the preparation and characterization of UO_2 as a powder and influence its subsequent fabrication into fuel elements. The unirradiated physical properties of UO_2 and the complex solid and vapour phase behaviour in the uranium-oxygen-system are discussed in Chapters 5 and 6, respectively. The extensive compilation and discussion of the thermodynamic and crystallographic data for the uranium oxides, UO_2, U_4O_9, U_6O_{13}, U_3O_8 and UO_3 is most valuable to physical and inorganic chemists because they illustrate the complex phenomena such as polymorph[illegible] deviation from stoichiometry and metastability that one is likely to encounter in a study of a me[illegible] oxygen system wherein the metal exhibits a variety of oxidation states. Binary and a few ternary ox[illegible] systems encountered as reactor fuel materials are also discussed. Chapters 7 and 8 deal principally with the kinetics of self-diffusion (both cation and anion), sintering, oxidation and corrosion phenomena. Finally Chapter 9 devotes over 200 pages to the irradiation behavior of UO_2 and to its performance as a fuel material. Appendix A gives a concise summary of numerical values of the physical, chemical and thermodynamic properties of UO_2. Ceramists and metallurgists will find Appendix B valuable since it deals primarily with the application of light and electron microscopy to the study of microstructures of UO_2 in its various physical forms.

On the whole, the book contains a wealth of bibliographic material which not only serves as factual assistance to present investigators; but will serve to guide more refined and penetrating investigations. The book was prepared and published under the direction of and in cooperation with the Naval Reactors Group of the Atomic Energy Commission.

R. J. ACKERMANN

A. I. VOGEL: **A Text-book of Quantitative Inorganic Analysis, including Elementary Instrumental Analysis.** Third Edition. Pp. xxx + 1216. Longmans, Green, London, 1961. 70s.

THIS is the third edition of a text-book of quantitative inorganic analysis, which was first published in 1939. It has been revised to give, in addition to classical methods of analysis, an introduction to the instrumental methods which have become important in recent years.

Volumetric and gravimetric analysis are dealt with in the first part, roughly half, of the book. After an account of the basic theory there are many practical exercises which illustrate the continued importance of classical methods. Complexometric titration is presented in a new chapter which includes directions for the determination of metals with EDTA. There are gravimetric methods which utilize newer organic precipitants and homogeneous precipitation, and sections on aperiodic balances and thermogravimetry to complete the revision of this part.

The second part, with chapters which are either new or considerably revised, deals with instrumental analysis. A chapter on the analysis of complex materials which utilizes both classical and instrumental methods provides a link between the two parts. There are chapters on electro-analysis comprising, electrogravimetry, using controlled potentials; coulometry; potentiometric titration, including automatic, 'dead-stop' and high-frequency procedures; polarographic analysis and amperometric titration. The chapters on instruments for the measurement of spectra include photoelectric absorptiometry and spectrophotometric methods, including titration; infra-red spectrometry, briefly; fluorimetry, nephelometry and turbidimetry and important chapters on emission spectrography and flame photometry. For each instrumental method, a theoretical introduction is followed by descriptions of commercial instrumentation and suggestions for introductory experiments. References to more specialized texts are given at the end of each chapter. There are also chapters on chromatography, including ion-exchange, and solvent extraction.

The book is comprehensive, well-presented and comparatively cheap. It is intended primarily for use by undergraduate students. The first part of the book will certainly be useful to them. The suggestion that they should also use instrumental methods is at first sight a reasonable one. However, it must be weighed against the need for work which illustrates preparative and structural chemistry. These competing demands on the undergraduates' time may make it desirable to offer courses in instrumental methods at a post-graduate level to those who intend to specialize in Analytical Chemistry. The second part of the book would be more suitable for a course of this kind. It will also be useful to the practising analyst who wishes to acquire new techniques.

J. DALZIEL

J. Inorg. Nucl. Chem., 1962, Vol. 24, pp. 1301 to 1316. Pergamon Press Ltd. Printed in England

A SUMMARY OF THE DECAY OF SOME FISSION PRODUCT TIN AND ANTIMONY ISOTOPES*

B. J. Dropesky and C. J. Orth

Los Alamos Scientific Laboratory, University of California,
Los Alamos, New Mexico

Received 24 *January* 1962, *in revised form* 26 *March* 1962)

Abstract—The mass assignments, half-lives and radiation characteristics of the isobaric pairs ^{126}Sn–^{126}Sb, ^{127}Sn–^{127}Sb, ^{128}Sn–^{128}Sb and ^{129}Sn–^{129}Sb and the isotope ^{130}Sb have been investigated. Samples of tin and antimony chemically separated from reactor-irradiated ^{235}U were examined with β- and γ-scintillation spectrometers and β-proportional counters. The main results of this programme are summarized in the present report.

Considerable disagreement exists in the literature with regard to mass assignments, half-lives and radiation characteristics of some of the tin and antimony isotopes in the fission-product region. The present work was undertaken with the purpose of clarifying the information pertaining to the isobaric pairs ^{126}Sn–^{126}Sb, ^{127}Sn–^{127}Sb, ^{128}Sn–^{128}Sb and ^{129}Sn–^{129}Sb, and the isotope ^{130}Sb. The present paper constitutes a preliminary survey of the properties of these species. A separate report on each of these isobaric pairs will eventually be written. Fig. 1 shows that portion of the Chart of Nuclides representing the species dealt with in this study. The particular nuclides investigated are set off with heavy border lines and the values contained therein are those from the present work. The other nuclide data came from the Nuclear Data Sheets.(1)

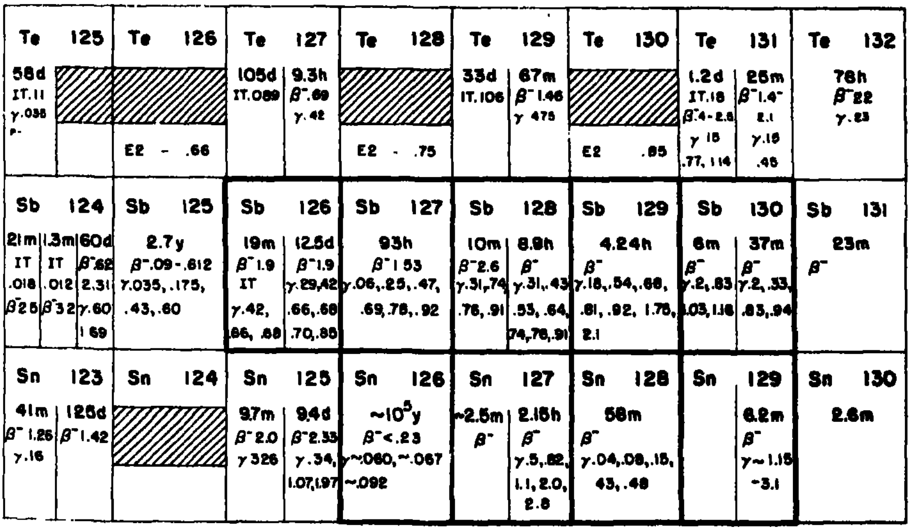

Fig. 1—Portion of the Chart of Nuclides showing the tin-antimony-tellurium nuclides concerned with in this study.

---

* This work done under the auspices of the U.S. Atomic Energy Commission.

(1) C. L. McGinnis *et al.*, *Nuclear Data Sheets*, National Academy of Sciences—National Research Council, Washington, D. C. (1958-1961).

EXPERIMENTAL METHODS

Chemical procedures

Fission-product tin and antimony activities were produced by irradiating 10–50 mg ^{235}U foils with neutrons in the Los Alamos Water Boiler reactor or the Omega West reactor. The number of fissions in these sources ranged from 10^{10} to 10^{14} fissions, produced in irradiations from 30 sec to 30 min duration in neutron fluxes ranging up to 5×10^{12} neutrons cm^{-2} sec^{-1}. The irradiated target was dissolved in a few ml of hot 6 M HCl and a drop of conc. HNO_3. Sn(IV) and Sb(III) carriers (~20 mg each) were added, and the solution was adjusted to give 10–20 ml 5 M in HCl. H_2S was bubbled into the solution, and the resulting mixture was then centrifuged.

When antimony was the element of interest, the supernate, which contained the tin, was discarded. The Sb_2S_3 precipitate was dissolved with hot conc. HCl. Te(IV) carrier was added and then precipitated with H_2S. After centrifugation the antimony in the supernate was precipitated by adjusting the solution to 5 M HCl and then bubbling in more H_2S. The Sb_2S_3 was dissolved with hot HCl, and the solution was poured into a distillation flask containing ~20 ml conc. H_2SO_4 and Mo(VI) and Te(IV) hold-back carriers. The antimony was distilled by the dropwise addition of HBr to the heated solution (~200°C). The distillate was adjusted to 2 M HBr, and Sb_2S_3 was precipitated with H_2S. This precipitate, either mounted on a counting plate or made into a slurry in a plastic vial, constituted the antimony sample for measurement of half-life and radiations.

When tin was the element of interest, the supernate from the original Sb_2S_3 precipitation was adjusted to ~0·5 M HCl by the addition of conc. NH_4OH. The SnS_2 was centrifuged and the supernate was discarded. The SnS_2 was dissolved with hot HCl and was then distilled as described above. When the distillation was complete, remaining traces of antimony activity were removed by adding Sb(III) carrier to the distillate, adjusting the acidity to ~5 M in HBr, and precipitating Sb_2S_3 with the addition of H_2S. The supernate, which contained the purified tin, was usually transferred to a plastic vial for γ-ray measurements. For experiments involving β-counting or coincidence measurements the tin was precipitated as SnS_2 or as the metal and was then mounted on a counting plate.

Instrumentation

The γ-ray spectra were measured with one or more of the following detectors: a 3 in. diam. × 3 in. thick NaI(Tl) crystal coupled to a 5 in. DuMont 6364 photomultiplier, and a 2 in. diam. × 2 in. thick or a 1½ in. diam. × 1½ in. thick NaI(Tl) crystal coupled to DuMont 6292 photomultipliers. These scintillators were used in conjunction with stabilized HV supplies, non-overloading linear amplifiers, and a fast 100-channel pulse-height analyser. In all γ-ray experiments, a β-absorber, usually consisting of 1 cm thick Lucite, was interposed between the crystal and the source. For measuring the decay of selected photopeaks a single channel analyser was employed. A coincidence circuit with a resolving time of ~0·4 μsec was used to observe γ-γ and β-γ coincidences. To record decay data an automatic scaler, on-off timer, and printer were often used. β-spectra were measured with either a 1½ in. diam. × ½ in. thick Pilot "B"* plastic scintillator or a 1½ in. diam. × ¼ in. thick transstilbene crystal coupled to a 6292 photomultiplier and used with the above electronics.

β-emission rates were measured with standard methane- or propane-flow β-proportional counters having 1 mil aluminium windows. Most decay data were analysed by the method of least squares with an IBM 704 computer. The time scale normally used at this laboratory in recording decay data is based on precisely stepped increments of 0·001 day

EXPERIMENTAL RESULTS

^{126}Sn–^{126}Sb *decay*

^{126}Sn, originally reported(2) to have a half-life of 50 min, is now known(3) to be very long-lived ($T_{\frac{1}{2}} \approx 10^5$ years). This species was discovered in Water Boiler reactor ^{235}U solution that had been stored for over 10 years. The predominant

---

* Pilot Chemicals Inc., Watertown, Mass.

(2) J. W. BARNES and A. J. FREEDMAN, *Phys. Rev.* **84**, 365 (1951).

(3) C. J. ORTH and B. J. DROPESKY, *Bull. Amer. Phys. Soc.* **3**, No. 3, 207 (1958).

β-activity in a tin sample from this solution is ^{121m}Sn, which was identified by its 0·42 MeV β-spectrum. A weak β-component of a higher energy was radiochemically identified as that of the known(4, 5) 19 min ^{126}Sb in equilibrium with its long-lived ^{126}Sn parent. The longer-lived ^{126}Sb isomer was also found to be produced in the decay of ^{126}Sn and a remeasurement of the half-life showed it to be $12 \cdot 5 \pm 0 \cdot 1$ day. This value differs considerably from the original 6·2 day half-life measured by Bosch and Munczek(6) and attributed to an isomer of ^{126}Sb by Fränz and Münzel,(5) but it is in fair agreement with Bosch's(7) later value of 11 day. Fig. 2 shows the β-decay curves of the ^{126}Sb isomers separated from ^{126}Sn. The ratio of the β-activity of the 19 min isomer to that of the 12·5 day isomer, in equilibrium with their ^{126}Sn parent, is $6 \cdot 2 \pm 0 \cdot 2$. Since the 19 min isomer grows into equilibrium with ^{126}Sn with a 19 min half-period, it is probably fed directly and is therefore the low-spin isomer.

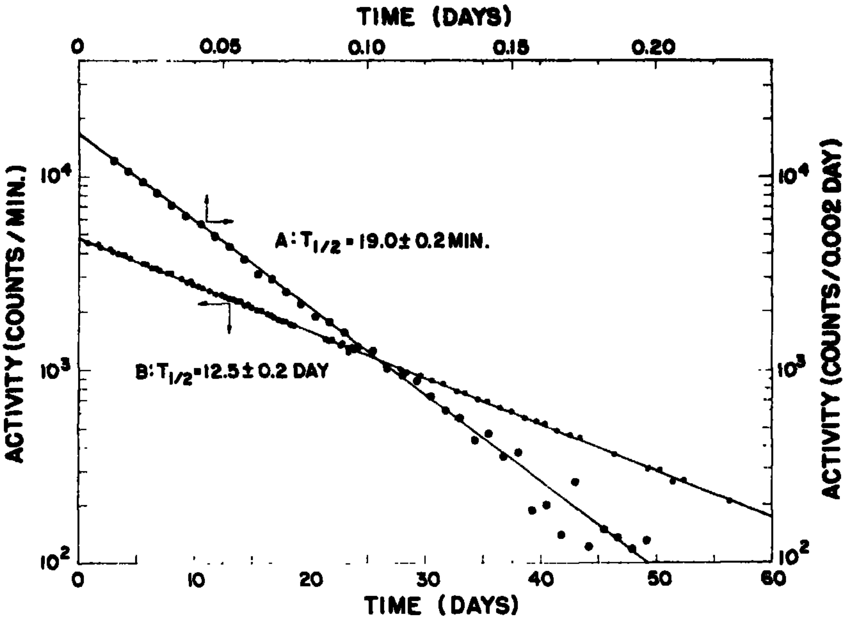

Fig. 2—Decay curves of the ^{126}Sb isomers, separated from ^{126}Sn, as observed with β-proportional counters. Different samples and counters were employed to obtain the two sets of data. Curve A is the β-decay curve of the short-lived ^{126}Sb isomer (top and right scales) and Curve B is the β-decay curve of the long-lived ^{126}Sb isomer (bottom and left scales).

The ^{126}Sn half-life was computed on the basis of the following values: the measured antimony activity in secular equilibrium with the tin sample discussed above; the number of fissions, determined by ^{90}Sr analysis, from which the tin was obtained; and an interpolated fission yield value of 5×10^{-4} for ^{126}Sn.

The highest energy β-groups observed in the decay of both ^{126}Sb isomers have end-points of $1 \cdot 95 \pm 0 \cdot 15$ MeV. γ-ray spectra of the two isomers are shown in Fig. 3.

---

(4) I. Fränz, R. Radicella and J. Rodriguez, *Z. Naturforsch.* **11 A**, 1138 (1956).

(5) I. Fränz and H. Münzel, *Z. Naturforsch.* **13 A**, 53 (1958).

(6) H. Bosch and H. Munczek, *Phys. Rev.* **106**, 983 (1957).

(7) H. E. Bosch, *Bull. Amer. Phys. Soc.* **4**, No. 6, 374 (1959).

The energies of the prominent photopeaks of 12·5 day ^{126}Sb are in fairly good agreement with those reported by BOSCH(7) for the 11 day antimony activity produced by high-energy neutron bombardment of enriched ^{126}Te. The ~0·68 MeV peak results from two γ-rays in the 19 min isomer decay and three γ-rays in the 12·5 day isomer decay. One of the γ-rays contributing to this photopeak is that due to the $E2$ transition from the first excited state to the ground state of ^{126}Te, as measured by several investigators.(8, 9, 10) Shown in the insert of Fig. 3 is the low-energy portion of the γ-spectrum of the ^{126}Sn–^{126}Sb sample. The 60, 67 and 92 keV γ-rays are associated with the decay of ^{126}Sn. The 37 keV γ-rays and the intense Sb K X-rays were found to be in coincidence with the 0·42 MeV β-group. A very similar low energy (< 50 keV) γ-ray spectrum was observed from ^{121m}Sn produced by the (n, γ) reaction on enriched ^{120}Sn. On the basis of this evidence, the 37 keV γ-ray and most of the X-rays are attributed to the decay of ^{121m}Sn. This 37 keV γ-transition is presumed to be from a $g_{7/2}$ excited state to the $d_{5/2}$ ground state in ^{121}Sb. On the basis of preliminary measurements the half-life of ^{121m}Sn is estimated to be ~25 years.

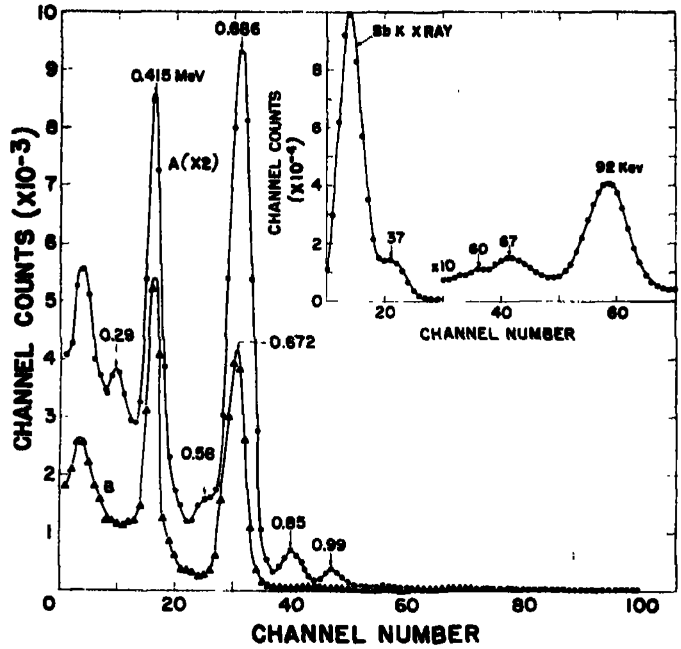

FIG. 3—Scintillation γ-spectra of the ^{126}Sb isomers measured with the 3 in. × 3 in. NaI(Tl) crystal at a distance of 10 cm. Curve A, 12·5 day ^{126}Sb and Curve B, 19 min ^{126}Sb. The insert shows the low energy portion of the γ-spectrum from the ^{126}Sn–^{126}Sb, ^{121m}Sn source measured with 1½ in. × 1½ in. NaI(Tl) scintillator.

---

(8) R. M. SINCLAIR, *Phys. Rev.* **102**, 461 (1956).

(9) G. M. TEMMER and N. P. HEYDENBURG, *Phys. Rev.* **104**, 967 (1956).

(10) P. H. STELSON and F. K. MCGOWAN, *Phys. Rev.* **110**, 489 (1958).

^{127}Sn–^{127}Sb *decay*

2.15 *hr* ^{127}Sn. Half-lives of 1·5 hr,(2) 2·05±0·05 hr(11) and 2·6 hr(12) have been attributed to ^{127}Sn by previous investigators. In the present work, ^{127}Sn samples were prepared for study by following the tin procedure described above and by allowing 12–14 hr of decay, after irradiation, before the final tin–antimony separation was made. These samples contained only a small amount of 10 day ^{125}Sn and most of the 58 min ^{128}Sn and shorter-lived tin isotopes had already decayed away when the measurements were begun. As shown in Fig. 4, the γ-spectrum of ^{127}Sn is very complex and extends to almost 3 MeV. The γ-spectrum of ^{125}Sn is also shown in Fig. 4 to illustrate some interesting similarities to the ^{127}Sn spectrum and to show a previously unreported γ-ray at 2·23 MeV. The ^{127}Sn half-life was measured by observing the decay of that portion of the γ-spectrum between 2 and 3 MeV, where the contribution from ^{128}Sn was completely negligible, and only a slight contribution from ^{125}Sn had to be taken into account. Fig. 5 shows this decay data, which yielded a value of 2·15±0·10 hr for the half-life of ^{127}Sn. The γ-spectrum of the residual activity, after decay of ^{127}Sn, showed the high energy γ-rays to be due only to ^{125}Sn.

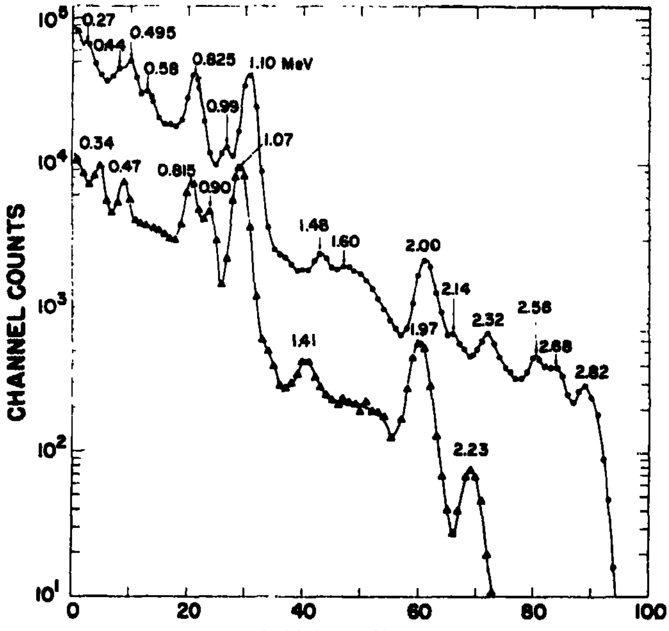

Fig. 4—γ-ray spectrum of 2·15 hr ^{127}Sn (upper curve) measured at 10 cm from the 3 in. × 3 in. NaI(Tl) scintillator. The contribution from 10 day ^{125}Sn has subtracted out. The γ-spectrum of ^{125}Sn (lower curve) is included for comparison.

---

(11) H. Carminatti, I. Fränz, R. Radicella and J. Rodriguez, *Z. Naturforsch.* **11 A**, 419 (1956).

(12) T. Alvager, J. Uhler and O. Melin, *Arkiv för Fysik*, **16**, 482A (1960). In a recent personal communication with Dr. Alvager, one of the authors (B.J.D.) learned that the results reported in this reference were very preliminary and, in fact, were not confirmed by later experiments. The final results of their studies have been submitted for publication in Arkiv för Fysik.

2·5 min ^{127}Sn. Existence of a β-emitting isomer of ^{127}Sn, with a $2{\cdot}5 \pm 1{\cdot}0$ min half-life, was established by making rapid timed separations of antimony from fission-product tin solutions and determining the ^{127}Sb yields. The antimony was separated either by carrying it out of 5 M HCl solution on known quantities of preprecipitated Sb_2S_3 or by stripping the antimony with 0·2 M HCl from a diethyl ether solution of tin complexed with NH_4CNS.(13) If one uses a ^{127}Sb independent fission yield value of 10 per cent(14) of the mass 127 chain, the present experiments show that about half of the remaining 90 per cent of ^{127}Sb comes from each of the two ^{127}Sn isomers.

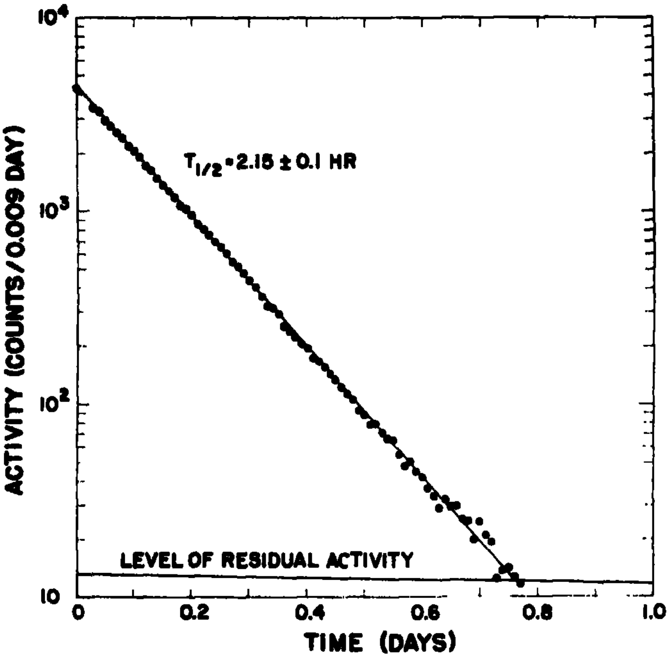

Fig. 5—Decay of the 2–3 MeV portion of the ^{127}Sn γ-spectrum with the source 1 cm from the 3 in. × 3 in. NaI(Tl) scintillator. The residual activity, which was due to 10 day ^{125}Sn, was resolved out.

93 hr ^{127}Sb. The half-life of ^{127}Sb has been commonly quoted to be 93 hr,(15) although somewhat greater values have been reported.(16, 17) Bosch and Munczek,(6) who measured the decay of the γ-spectra of a mixture of antimony isotopes produced in 26 MeV deuteron fission of uranium, reported a half-life of 88 ± 2 hr for ^{127}Sb. A repetition of this type of measurement was performed in the present study on a sample of antimony produced in pile-neutron fission of uranium, in which the independent yield of 12·5 day ^{126}Sb is much lower than in high-energy fission. A half-life for ^{127}Sb of 93–95 hr was obtained. In order to eliminate the influence of ^{126}Sb on the determination of the ^{127}Sb half-life, several careful experiments were performed* which involved the measurement of the yield of 9·3 hr ^{127}Te in transient equilibrium with its ^{127}Sb parent. The antimony fraction from $\sim 2\times 10^{15}$ fissions was separated and purified after the short-lived antimony activities had decayed, and the resulting solution was divided into twelve aliquots. Tellurium carrier was added to each aliquot, and then at two day intervals, starting four days after the original purification, the tellurium activity was chemically separated, mounted, and β-counted. Each of the twelve sets of tellurium decay data was computer-analysed to determine the 9·3 hr ^{127}Te activity at the separation times (corrected for chemical yield and aliquot size). From graphical analysis of the yield data from three experiments an average value of 93·4±1·7 hr was obtained for the half-life of ^{127}Sb. Fig. 6 shows the results of one of these experiments.

---

(13) R. Bock, *Z. Analyt. Chem.* **133**, 110 (1951).

(14) A. C. Wahl, R. L. Ferguson, D. R. Nethaway, D. E. Troutner and K. Wolfsberg, *Nuclear-Charge Distribution in Low Energy Fission*, Washington Univ. (St. Louis). Report, June 1961, *Phys. Rev.* **126**, 1112 (1962).

(15) N. R. Sleight and W. H. Sullivan, *Radiochemical Studies: The Fission Products* (Edited by C. D. Coryell and N. Sugarman), NNES, Plutonium Project Record, Vol. 9, Div. IV, p. 928. McGraw-Hill, New York (1957).

(16) W. E. Grummitt and G. Wilkinson, *Nature, Lond.* **158**, 163 (1946).

(17) A. C. Pappas, MIT LNS Technical Report 63 (1953).

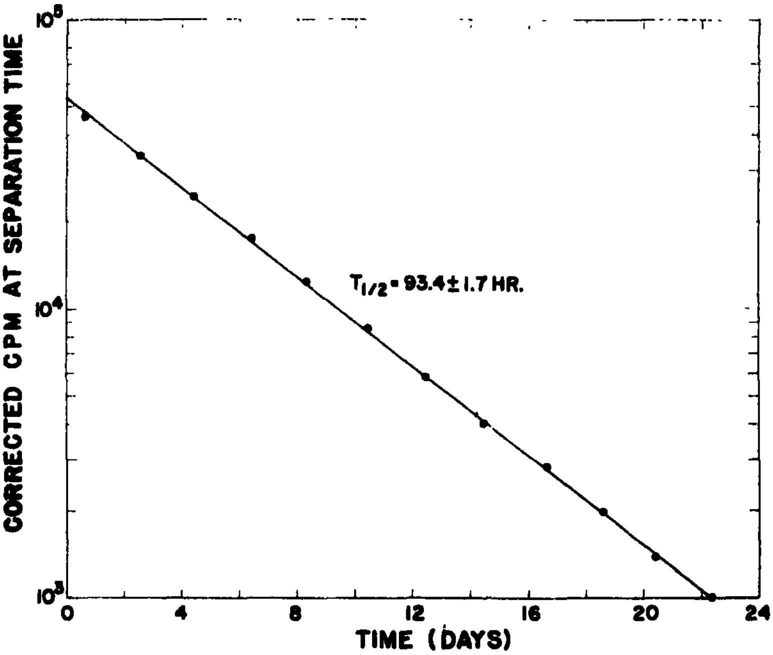

FIG. 6—Yields of 9·3 hr ^{127}Te in transient equilibrium with the parent ^{127}Sb as a function of separation times.

Fig. 7 shows the γ-spectrum of a ^{127}Sb sample measured after all ^{128}Sb had decayed. The sample was grown from its purified tin parent and was thereby free of independently produced ^{126}Sb. Previously reported(6, 18) energy values for the γ-rays of ^{127}Sb resulted from measurements on mixtures of antimony isotopes and are somewhat in disagreement with the present measurements (see Table 1). The insert of Fig. 7 shows the low-energy γ-spectrum of ^{127}Sb.

---

* These experiments were conducted by J. W. BARNES and P. Q. OLIVER.

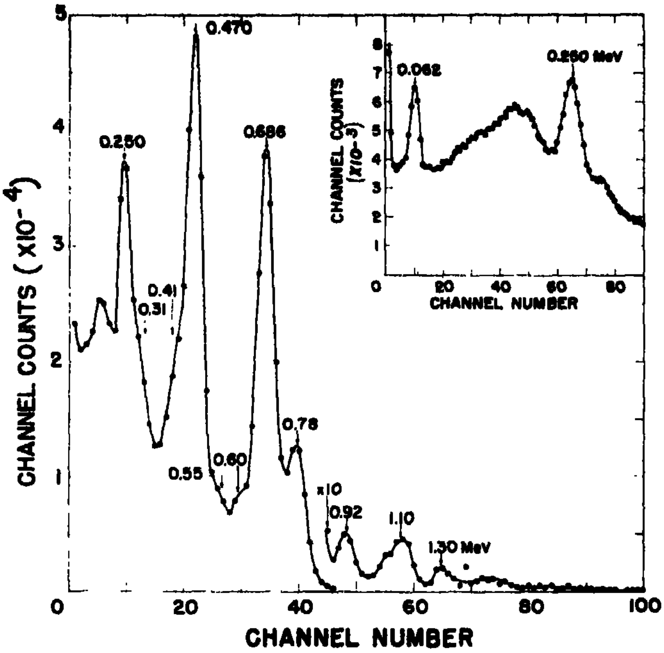

FIG. 7—γ-ray spectrum of ^{127}Sb measured with the 3 in. × 3 in. scintillator at 10 cm distance. The insert shows the low energy portion of the ^{127}Sb γ-spectrum.

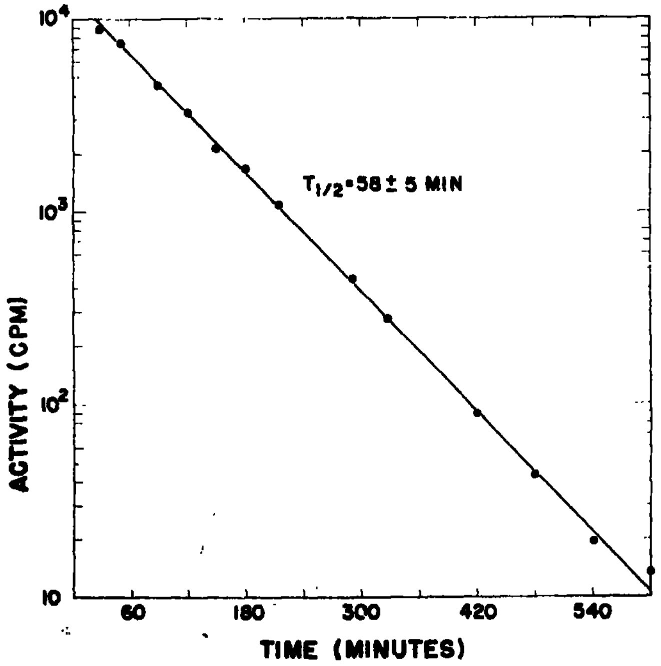

FIG. 8—Decay curve of ^{128}Sn as determined by measuring the decay of the 0·75 MeV γ-rays of 10 min ^{128}Sb in equilibrium with its tin parent.

The end-point of the highest energy β-group of ^{127}Sb, measured with the scintillation spectrometer, is 1·53±0·05 MeV, in agreement with previous values.[18, 19]

^{128}Sn–^{128}Sb *decay*

58 *min* ^{128}Sn. The ^{128}Sn samples were prepared by the method described above in Chemical Procedures. To allow for the decay of the short-lived tin activities of higher mass number, the final tin separation was not performed until 70 min after the end of the irradiation.

The half-life of ^{128}Sn was measured by observation of the decay of the 0·75 MeV γ-rays of 10 min ^{128}Sb which had grown into equilibrium with it. The value obtained was 58±5 min (Fig. 8), in good agreement with a carefully determined value previously reported,[20] but misassigned to mass 130.

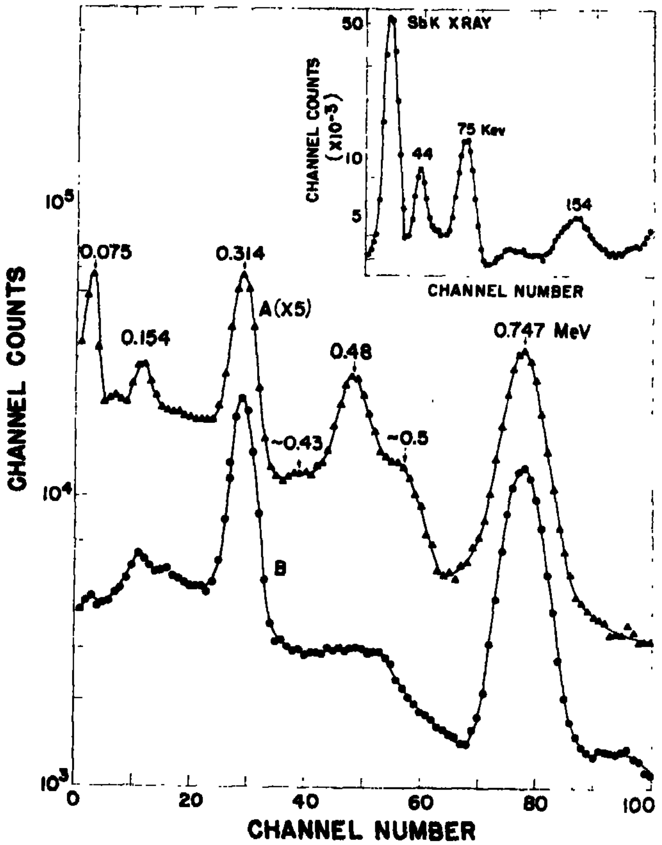

Fig. 9—γ-ray spectra of ^{128}Sn with 10 min ^{128}Sb in equilibrium (Curve A) and 10 min ^{128}Sb only (Curve B) taken at 1 cm from the 3 in. × 3 in. NaI(Tl) scintillator. The insert contains the low energy portion of the γ-spectrum at 1 cm from the 1½ in. × 1½ in. NaI(Tl) scintillator; these photopeaks belong exclusively to ^{128}Sn.

---

(18) M. C. Day, Jr. and A. F. Voigt, *Phys. Rev.* **101**, 1784 (1956).

(19) J. P. Mize, J. D. Knight, J. W. Barnes and J. W. Starner. Private communication.

(20) I. Fränz, J. Rodriguez and H. Caminatti, *Z. Naturforsch.* **10 A**, 82 (1955).

The γ-spectrum of ^{128}Sn, which has not been previously reported, was measured with the 10 min ^{128}Sb isomer in equilibrium. The contribution due to 2·15 hr ^{127}Sn, determined later, was subtracted out. Fig. 9 shows both the composite spectrum of ^{128}Sn–10 min ^{128}Sb and the spectrum of 10 min ^{128}Sb alone. Only the small photopeaks indicated at ~0·43 and ~0·5 MeV and the distinct peak at 0·48 MeV in the high energy spectrum are associated with ^{128}Sn decay, whereas all of the labelled γ-peaks of the low energy spectrum are involved in the decay of ^{128}Sn.

10·1 *min* ^{128}Sb. Samples of the short-lived isomer of ^{128}Sb were grown from purified ^{128}Sn–^{127}Sn, with growth periods of only 10–20 min in order to minimize the production of the longer-lived ^{128}Sb isomer and 93 hr ^{127}Sb. The β-decay curve of such a sample, shown in Fig. 10 (Curve A), yielded a half-life of 10·1±0·2 min for the short-lived ^{128}Sb isomer, in good agreement with previous measurements.(2, 20)

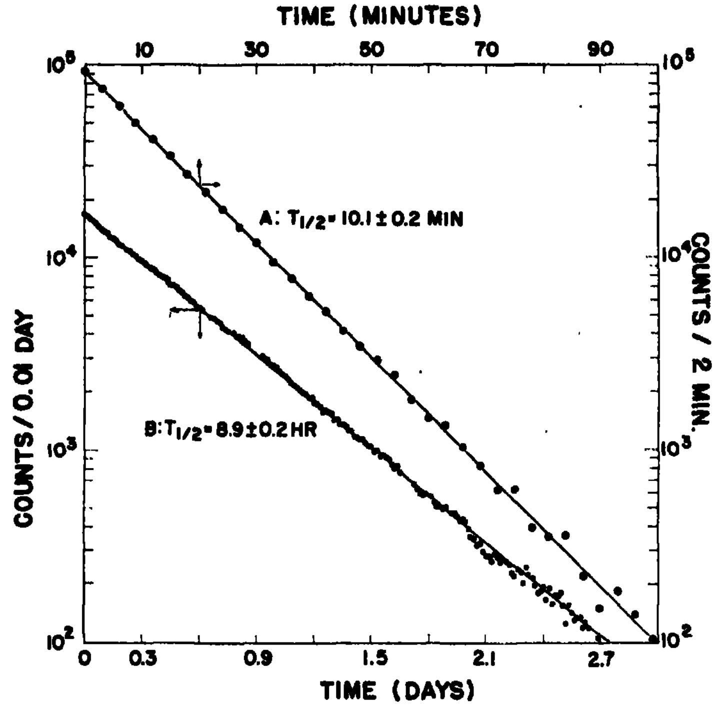

FIG. 10—Decay curves of the isomers of ^{128}Sb. Curve A is the β-decay curve of the short-lived ^{128}Sb isomer (right and top scales). Curve B is the decay curve of the 0·75 MeV photopeak of the long-lived ^{128}Sb isomer (left and bottom scales); the small contribution due to ^{127}Sb has been resolved out.

The γ-spectrum of 10 min ^{128}Sb (Fig. 9, lower curve) is relatively simple, exhibiting only the two photopeaks at 0·314±0·005 and 0·747±0·005 MeV. These energies agree well with those previously reported.(21) However, the 0·747 MeV peak is too broad to be due to a single γ-ray and, indeed, it can be arbitrarily resolved into two photopeaks due to 0·740 and 0·755 MeV γ-rays of equal intensity. An analysis of a scintillation β-spectrum gave a value of 2·6±0·3 MeV for the end-point of the highest energy β-group.

(21) I. FRÄNZ, J. RODRIGUEZ and R. RADICELLA, *Z. Naturforsch.* 11 A, 1037 (1956).

8·9 hr ^{128}Sb. Samples of the longer-lived isomer of ^{128}Sb were grown for a period of ~2 hr from tin purified at about 1 hr after the end of the irradiation. No evidence was found for the presence of ^{129}Sb in these samples.

The half-life of the longer-lived ^{128}Sb isomer was originally measured(2) to be 9 hr, although the activity was thought to be ^{126}Sb. However, more recent measurements give values of 9·6 hr,(21) 9·9 hr(22) and 10 hr(8) for the isomer half-life. In the present study, a remeasurement of this half-life was made by recording the rate of decay of the 0·75 MeV photopeak of the ^{128}Sb γ-spectrum. This technique served to enhance the ratio of ^{128}Sb to ^{127}Sb γ-counts. These measurements were made after 10 min ^{128}Sb had decayed, and corrections were applied for contributions due to the small amount of 93 hr ^{127}Sb present. The average value for the half-life of the longer-lived ^{128}Sb isomer, from several such experiments, is 8·9±0·2 hr. A typical decay curve is shown in Fig. 10 (Curve B).

The γ-spectrum of 8·9 hr ^{128}Sb (Fig. 11, upper curve) is similar to that of the 10 min isomer with the exception of the additional photopeaks at ~0·43, 0·53 and 0·64 MeV. In this spectrum the 0·75 MeV photopeak is also too broad to be due to only one γ-ray.

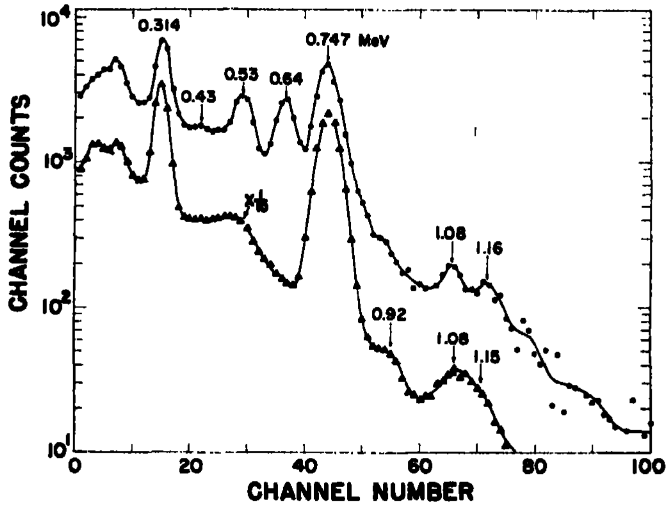

Fig. 11—γ-ray spectrum of 8·9 hr ^{128}Sb (upper curve) as measured 15 cm from the 3 in. ×3 in. NaI(Tl) scintillator. The γ-spectrum of 10 min ^{128}Sb is shown in the lower curve.

The mass assignment of these isomers is well established on the basis of their production by high-energy neutron irradiation of enriched ^{128}Te.(7, 22) Also, one of the γ-rays contributing to the 0·75 MeV photopeak in the ^{128}Sb γ-spectra is undoubtedly due to the $E2$ transition from the first excited state to the ground state of ^{128}Te.(8, 9, 10)

(22) A. C. Pappas. Private communication to National Academy of Science—National Research Council, April 1957.

^{129}Sn–^{129}Sb decay

6 min ^{129}Sn. In the present study, experiments were carried out to determine the half-life of ^{129}Sn(23) by both direct and indirect methods. In the indirect measurement, the yields of ^{129}Sb were determined in samples of antimony separated in rapid succession from a freshly prepared fission-product tin solution. The separations, which employed the Sb_2S_3 method described previously for the determination of the half-life of the short-lived ^{127}Sn isomer, were made at 3 min intervals starting 10 min after the end of a 30 sec irradiation. This measurement yielded a value of 6±1 min for the half-life of ^{129}Sn.

What is presumed to be a direct measurement of the ^{129}Sn half-life was made by recording a series of γ-spectra of a sample of fission-product tin which had been purified rapidly by the distillation method. The final separation of antimony was performed 29 min after the 30 sec pile irradiation of ^{235}U. Analysis of a series of γ-spectra beginning 2 min later and taken at 4 min intervals indicated the presence of an ~6 min activity in addition to a large amount of 58 min ^{128}Sn and its 10 min ^{128}Sb daughter. The γ-spectrum of the ~6 min activity exhibited a prominent photopeak at ~1·15 MeV and a very complex structure extending to over 3 MeV. In a similar experiment in which the recording of the first γ-spectrum was begun at 22 min after the end of the irradiation, additional strong peaks were observed at 0·2 and 0·82 MeV. These two peaks decayed with a short half-life, and, as will be discussed later, are believed to belong to ^{130}Sb. The decay of the high-energy portion (2·8–3·1 MeV) of this spectrum, which is assumed to be associated with ^{129}Sn, was carefully followed. Analysis of

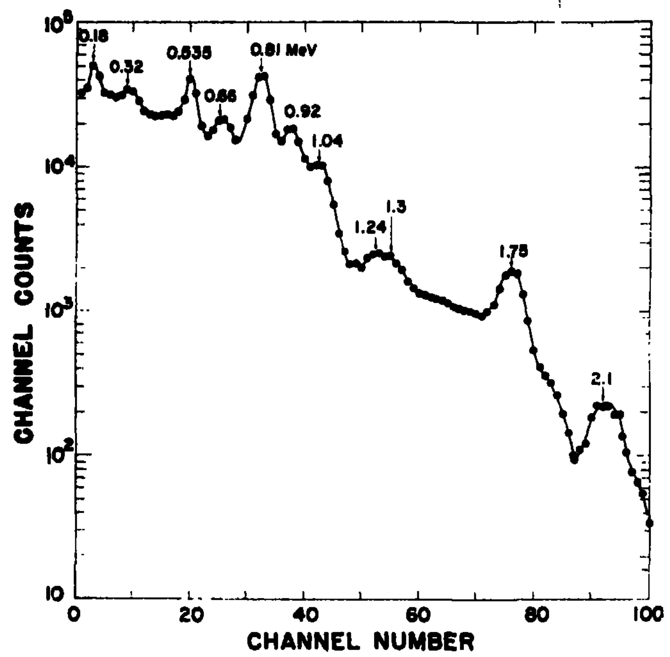

FIG. 12—γ-ray spectrum of 4·24 hr ^{129}Sb measured with the 3 in. × 3 in. NaI(Tl) scintillator at a distance of 5 cm.

---

(23) In a recent personal communication with one of the authors (C.J.O.), PAPPAS reported having observed two isomers of ^{129}Sn with half-lives of 8 min and ~1 hr.

these data yielded a half-life of 6·4±1·0 min. This value, combined with the value from the timed Sb_2S_3 separation method, gives a half-life of 6·2±1·2 min for ^{129}Sn. No evidence was found for a longer-lived isomer of ^{129}Sn in the half-life range 6·2–120 min.(12, 23)

4·24 hr ^{129}Sb. Samples of ^{129}Sb were prepared from fission products by the method described above in Chemical Procedures. To allow time for the decay of the shorter-lived antimony activities, such as ^{130}Sb and ^{131}Sb, which might interfere with radiation measurements, the distillation of the antimony was performed 5 hr after the end of the irradiation. The γ-ray spectrum of ^{127}Sb, as shown in Fig. 12, was recorded when contributions from 8·9 hr ^{128}Sb and 93 hr ^{129}Sb were negligible. The indicated photopeak energies are in fair agreement with those listed by Day and Voigt(18) for ^{129}Sb; however, Day and Voigt reported no γ-rays with energies greater than 0·788 MeV.

The half-life of ^{129}Sb has been reported to be 4·6±0·1 hr(17) and 4·2 hr.(24) In the present study this half-life was remeasured. In order to avoid interference due to ^{126}Sb, ^{127}Sb, ^{127}Te, ^{128}Sb and ^{129}Te which would unavoidably be present or grow in, in small-to-moderate amounts, use was made of the fact that only ^{129}Sb emits γ-rays of energies greater than ~1·3 MeV. The decay of that portion of the ^{129}Sb γ-spectrum between 1·38 and 2·5 MeV was followed with the 3 in.×3 in. NaI(Tl) scintillator and single channel analyser. To eliminate interference from γ-γ summing effects, 15·8 g/cm^2 of Pb was interposed between the source and detector. The resulting decay data from two such experiments yielded a half-life value of 4·24±0·10 hr; a typical set of data, with background subtracted, is shown in Fig. 13.

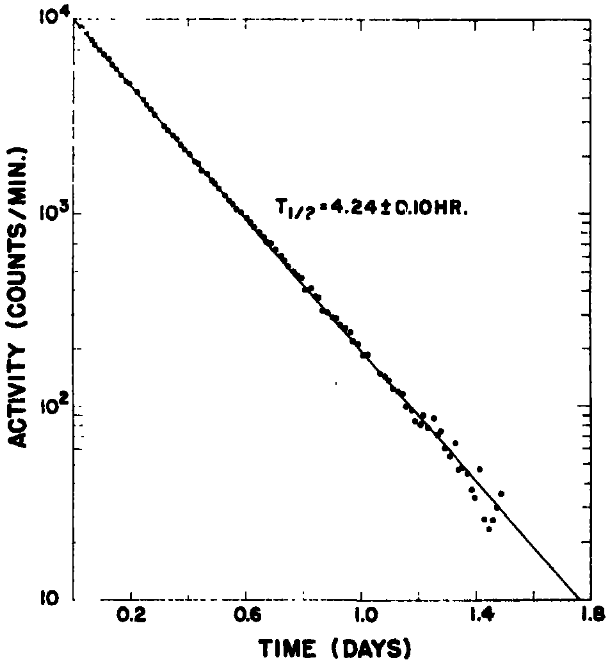

Fig. 13—Decay curve of the 1·38–2·5 MeV portion of the ^{129}Sb γ-spectrum measured through 15·8 g/cm^2 of Pb with the 3 in. ×3 in. NaI(Tl) scintillator

(24) P. H. Abelson, *Phys. Rev.* **56**, 1 (1939).

^{130}Sb *isomers*

37 *min* ^{130}Sb. Two ^{130}Sb isomers with half-lives of 7·1±0·3 min and 33±1 min have been reported by Pappas,(24) who produced these activities by fast-neutron irradiation of enriched ^{130}Te. In the present work a preliminary investigation was made of the decay of these isomers, produced in fission. In a study of the longer-lived isomer, the final antimony purification was performed ~2 hr after the end of the irradiation to allow time for decay of the shorter-lived antimony activities, including 20 min ^{131}Sb. 4·2 hr ^{129}Sb was the predominant interfering activity remaining. The γ-spectrum shown in Fig. 14 is the net ^{130}Sb spectrum obtained by the subtraction of the ^{129}Sb–^{129}Te spectrum. The odd dip in the spectrum at about channel 35 is due to the fact that 67 min ^{129}Te, which emits a 0·475 MeV γ-ray,(25) had not grown into equilibrium with ^{129}Sb when the early gross spectrum was measured. The 0·825 MeV photopeak appears to be due to at least two γ-rays on the basis of its half-width and preliminary γ-γ coincidence measurements. One of the γ-rays contributing to this photopeak is apparently due to the E2 transition from the first excited state to the ground state of ^{130}Te.(8, 9, 10)

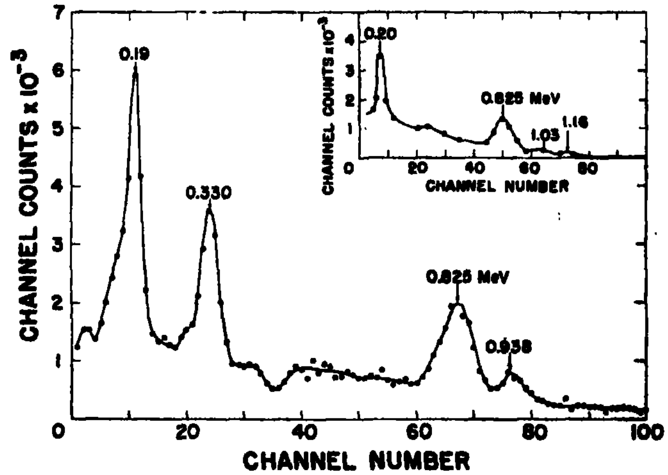

Fig. 14—γ-ray spectrum of 37 min ^{130}Sb obtained after subtraction of the ^{129}Sb–^{129}Te spectrum. Measurements were made at 5 cm from the 3 in. × 3 in. scintillator. The dip in the spectrum at about channel 35 is due to the fact that 67 min ^{129}Te, which emits a 0·475 MeV γ-ray, had not grown into equilibrium with ^{129}Sb when the early gross spectrum was measured. The insert shows the γ-spectrum of 6 min ^{130}Sb measured with a 2 in. × 2 in. NaI(Tl) scintillator at 8 cm distance. A small contribution due to 10 min ^{128}Sb has been removed.

Measurement of the half-life of the longer-lived ^{130}Sb isomer is complicated by the unavoidable presence of a very large amount of ^{129}Sb activity in the samples. Preliminary γ-γ coincidence studies indicated that the 0·33 and 0·825 (complex) MeV γ-rays of ^{130}Sb are in coincidence. An experiment was performed which involved the measurement of the decay of coincidences between the 0·33 MeV pulses in one scintillator and the 0·825 MeV pulses in a second scintillator. The results, shown in Fig. 15, yielded a half-life value of 37±3 min for ^{130}Sb, in fair agreement with Pappas'(22) value.

---

(25) W. E. Graves and A. C. G. Mitchell, *Phys. Rev.* **101**, 701 (1956).

6 min ^{130}Sb. The 0·2 and 0·82 MeV photopeaks observed in the γ-spectrum of the tin sample recorded 22 min after the end of a short irradiation (see Section 6 *min* ^{129}Sn) were not observed in the spectrum of the tin sample that took 9 min longer to separate and purify. This suggested the presence of ^{130}Sb which had grown from a very short-lived (< 3 min) tin parent; PAPPAS reported a half-life of 2·6 min for ^{130}Sn.(26) The 0·2 and 0·82 MeV γ-rays were shown to be associated with the antimony activites grown from a fission-product tin sample during the time interval 12·5–14·5 min after the end of a 30 sec pile irradiation of ^{235}U. Purification of the antimony was started 6·5 min after the end of the growth period. In addition to the 0·20 and 0·825 MeV γ-rays shown in the Fig. 14 insert, the 0·32 and 0·75 MeV γ-rays of 10 min ^{128}Sb were observed but were subtracted out of the spectrum presented. The former

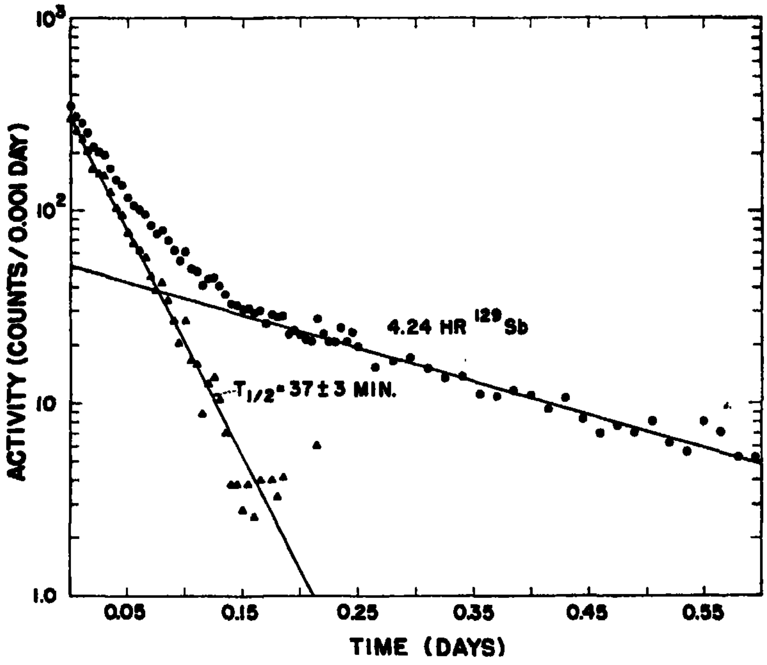

FIG. 15—Decay of 0·33–0·82 MeV γ-γ coincidences of ^{130}Sb in the presence of ^{129}Sb–^{129}Te.

two γ-rays peaks decayed with a 6·0±1·5 min half-life and are assigned to an isomer of ^{130}Sb on the basis of the similarity of the 0·825 MeV peak to that observed in the 37 min ^{130}Sb spectrum. This assignment is in agreement with the work of PAPPAS.(22) Low intensity γ-rays of 1·03 and 1·16 MeV are also attributed to 6 min ^{130}Sb. The 0·2 MeV γ-ray observed from 6 min ^{130}Sb is probably the same as the 0·19 MeV γ-ray observed from 37 min ^{130}Sb. 37 min ^{130}Sb was not observed to grow from ^{130}Sn.

---

(26) A. C. PAPPAS and D. R. WILES, *J. Inorg. Nucl. Chem.* **2**, 69 (1956).

TABLE 1.—SUMMARY OF THE PRESENT WORK

Nuclide	$T\frac{1}{2}$	Principal γ-rays (MeV)	Max. $E\beta$ (MeV)
^{126}Sn	~10^5 years	~0·060, ~0·067, 0·092	<0·225
^{126}Sb	19·0 ±0·2 min	0·415, (0·665, 0·68)	1·95 ±0·15
^{126}Sb	12·5 ±0·2 days	0·29, 0·415, 0·58, (0·665, 0·68, 0·70), 0·85, 0·99	1·95 ±0·15
^{127}Sn	2·15 ±0·10 hr	0·12, 0·27, 0·44, 0·495, 0·58, 0·825, 0·99, 1·10, 1·48, 1·60, 2·00, 2·14, 2·32, 2·58, 2·68, 2·82	
^{127m}Sn	~2·5 min	Spectrum not measured	
^{127}Sb	93·4 ±1·7 hr or 3·89 ±0·07 days	0·062, 0·250, 0·30, 0·41, 0·470, 0·55, 0·60, 0·686, 0·78, 0·92, 1·10, 1·30	1·53 ±0·05
^{128}Sn	58 ±5 min	0·044, 0·075, 0·154, 0·43, 0·48	
^{128}Sb	10·1 ±0·2 min	0·314, (0·740, 0·755), 0·91	2·6 ±0·1
^{128}Sb	8·9 ±0·2 hr	0·314, 0·43, 0·53, 0·64, (0·740, 0·755), 0·91	
^{129}Sn	6·2 ±1·2 min	~1·15, many others to 3·1	
^{129}Sb	4·24 ±0·10 hr	0·18, 0·31–0·36 complex, 0·535, 0·66 complex, 0·81, 0·92, 1·04, 1·24, 1·3, 1·75, 2·1	
^{130}Sb	37 ±3 min	0·19, 0·33, 0·825 (complex), 0·938	
^{130}Sb	6·0 ±1·5 min	0·20, 0·825 (complex), 1·03, 1·16	

Therefore, it is estimated that at least 90 per cent of the ^{130}Sn decays go to the 6 min ^{130}Sb isomer. The lack of evidence for the presence of 23 min ^{131}Sb in the above sample suggests that the half-life of its ^{131}Sn parent is <2 min, in contrast to the reported half-life of 3·4 min.(26)

Acknowledgements—The authors wish to acknowledge the cooperation of the group at the Los Alamos reactor in providing the neutron irradiations. Thanks are also due to Dr. J. D. KNIGHT for many helpful discussions, to C. C. LONGMIRE for assistance with the rapid chemical separations done at the reactor site, and to R. F. CHAVEZ for help in processing the experimental data.

J. Inorg. Nucl. Chem., 1962, Vol. 24, pp. 1317 to 1320. Pergamon Press Ltd. Printed in England

ISOMERIC STATES OF ^{92}Nb*

E. T. Bramlitt and R. W. Fink†

Department of Chemistry, University of Arkansas,
Fayetteville, Arkansas

(*Received* 2 *February* 1962)

Abstract—The literature reports the existence of isomeric states of ^{92}Nb with half-lives of 21·6 hr, 13 hr, 5·9 μsec, and 191 min. Evidence is presented which indicates that all but the 5·9 μsec isomer are in error. In connection with this investigation, the following total activation cross sections for 14·7 MeV neutrons have been measured: ^{92}Mo (n, p) ^{92}Nb (10·1 days + 5·9 μsec), 60 ± 15 mbarns; and ^{92}Mo (n, α) ^{89}Zr (79·0 hr + 4·4 min), 20 ± 8 mbarns.

INTRODUCTION AND DISCUSSION

The literature contains reports of isomeric states of ^{92}Nb with half-lives of 21·6 hr(1), 13 ± 2 hr,(2) 5·9 ± 0·5 μsec,(3) and 191 ± 3 min.(4) Evidence is given in the present work that all but the 5·9 μsec isomer are incorrect.

The 21·6 *hr activity*

Wiedenbeck(1) in 1946 proposed the 21·6 hr half-life on the basis of an experiment in which niobium was bombarded with 10 MeV deutrons to produce the (d,t) reaction. Half-lives of 21·6 hr and 11 days were found and assigned to ^{92m}Nb and ^{92g}Nb, respectively, on the basis that both periods followed similar excitation functions with thresholds of 5–6 MeV and that a 21 hr activity had been found in proton bombardments of zirconium. Radiochemical separation was not done.

It is now known that a similarity in excitation functions is not a valid argument in the assignment of isomeric states; indeed, isomeric yields in nuclear reactions are known to vary with energy.(5) Furthermore, the 21 hr activity from proton bombardment of zirconium is now well established(6) as 23 hr ^{96}Nb.

We have been unable to confirm the 21·6 hr activity by means of the ^{93}Nb $(n, 2n)$ and the ^{92}Mo (n, p) reactions at 14·7 MeV, as reported below. Neither have Silva *et al.*(7) found a 21·6 hr period in studies of (γ, n) and $(\gamma, 2n)$ reactions of niobium.

---

* Supported in part by the U.S. Atomic Energy Commission.

† Present address : Department of Physics, Marquette University, Milwaukee 3, Wisconsin.

(1) M. L. Wiedenbeck, *Phys. Rev.* **70**, 435 (1946).

(2) R. A. James, *Phys. Rev.* **93**, 288 (1954).

(3) R. B. Duffield and S. H. Vegors, *Phys. Rev.* **112**, 1958 (1958).

(4) M. Bocciolini, G. di Caporiacco, L. Foa and M. Mando, *Nuovo Cim.* **16**, 780 (1960).

(5) See, for example, S. M. Bailey, Report UCRL-8710 (1959).

(6) Nuclear Data Cards, National Academy of Science-National Research Council, Washington 25, D. C. (1961).

(7) E. Silva, J. Goldemberg, P. R. Smith and V. L. Marquez, *Nuovo Cim.* **9**, 17 (1958).

The 13±2 *hr activity*

A 13±2 hr activity was reported in 1954 from proton bombardment of niobium to produce the (*p*, *pn*) reaction.(2) The assignment to ^{92m}Nb was supported by radiochemical separation on spectroscopically pure Nb_2O_5 and by the similarity of the 13 hr and 10·1 day ^{92g}(Nb) excitation functions. No positrons or annihilation gammas were found to be associated with the 13 hr activity, which decayed by electron capture (*K* X-rays observed) followed by emission of a 2·35 MeV gamma.

SILVA *et al.*(7) in a study of (*γ*, *n*) and (*γ*, 2*n*) reactions of niobium were unable to detect the 2·35 MeV, 13 hr gamma and placed an intensity limit on it of 0·02 per cent of the intensity of the 0·93 MeV, 10·1 day ^{92g}Nb gamma.

Neither BOCCIOLINI *et al.*(4) nor BRAMLITT and FINK(8) were able to observe the 13 hr activity through the ^{93}Nb (*n*, 2*n*) reaction at 14·7 MeV. BOCCIOLINI *et al.*(4) placed an upper limit on the cross-section ratio for activation of 13 hr ^{92m}Nb/10·1 day ^{92g}Nb activities at 4×10^{-5}, while BRAMLITT and FINK gave an upper limit of 1·2 mbarns for the ^{93}Nb (*n*, 2*n*) reaction leading to 13 hr ^{92m}Nb, assuming that the 2·35 MeV gamma occurs in 100 per cent of the 13 hr decays. Furthermore, MATUSZEK(9) was able to produce only the 10·1 day ground-state of ^{92}Nb in ^{93}Nb (*α*,*α'n*) reactions at 28, 36, and 42 MeV, *α*-spectra of radiochemically separated niobium revealing only the 0·93 MeV, 10·1 day ^{92g}Nb gamma. No 13 hr activity appeared in integral *γ* counting.

The 5·9±0·5 *μsec activity*

In 1958 DUFFIELD and VEGORS(3) found the 5·9 *μ*sec, 88 keV activity in irradiations or niobium with bremsstrahlung from a 22 MeV betatron. The activity was ascribed to ^{92m}Nb on the basis that its threshold is about 88 keV greater than the threshold for the ground-state.

BOCCIOLINI *et al.*(4) did not observe the 5·9 *μ*sec, 88 keV isomeric state in 14 MeV neutron irradiations of niobium. They accounted for this by assuming that the 88 keV state has a lower spin than the ground-state, and that the 191 min "isomer" had a higher spin. Clearly, this argument does not rule out the 5·9 *μ*sec ^{92m}Nb isomer, since the 191 min period does not belong to ^{92}Nb.

Since no isomeric state is known which would feed the 88 keV state, and as no other fast studies have been made, it is reasonable to accept the 5·9 *μ*sec period as an isomer of ^{92}Nb.

The 191±3 *min activity*

BOCCIOLINI *et al.*(4) and BRAMLITT and FINK(8) found the 191 min period in 14·7 MeV neutron bombardments of niobium, but this activity definitely can be ascribed to the newly discovered 3·1 hr ^{90m}Y isomer, which has since been produced by several different methods, including radiochemical separation from 14·7 MeV neutron bombarded niobium.(8, 10, 11)

(8) E. T. BRAMLITT and R. W. FINK, *J. Inorg. Nucl. Chem.* **24**, 1548 (1962).

(9) J. M. MATUSZEK, Jr. Private communication (1961).

(10) L. HASKIN and R. VANDENBOSCH, *Phys. Rev.* **123**, 184 (1961); R. L. HEATH, J. E. CLINE, C. N. REICH, E. L. YATES and E. H. TURK, *Ibid.* **123**, 903 (1961); W. S. LYON, J. S. ELDRIDGE and L. C. BATE, *Ibid.* **123**, 1747 (1961); J. M. FERGUSON, *Nucl. Phys.* **27**, 344 (1961).

(11) W. L. ALFORD, D. R. KOEHLER and L. E. MANDEVILLE, *Phys. Rev.* **123**, 1365 (1961).

EXPERIMENTS AND RESULTS

In attempts to produce the 13 and 21·6 hr activities, we have irradiated both natural molybdenum (as foil, metallic powder and oxide) and 92·1 per cent enriched ^{92}Mo oxide with 14·7 MeV neutrons from the Arkansas 400 kV Cockcroft-Walton accelerator. Bombardments lasting up to 14 hr with neutron outputs ranging between $1{\cdot}1\times10^{11}$ and $5{\cdot}0\times10^{10}$ neutrons/sec were carried out to produce the ^{92}Mo (n,p) reaction. A 3×3-in. NaI(Tl) scintillation spectrometer and RIDL 200-channel transistorized analyser were used to follow the γ-spectra of the irradiated samples. No evidence for a 13 hr, 2·35 MeV gamma could be found with any of the samples. An upper limit on the ^{92}Mo (n,p) cross-section for formation of the 13 hr isomer was set at 600 μbarns at 14·7 MeV, relative to the ^{27}Al $(n, \alpha)^{24}$Na (15 hr) monitoring reaction (114 mbarns). Also, with enriched ^{92}Mo oxide, no gammas (<4 MeV) were observed to decay with a 21·6 hr half-life; furthermore, gross beta counting using an end-window beta proportional counter revealed neither 13 hr nor 21·6 hr activities.

To examine the possibility that a 13 hr acitivity existed in these irradiated samples that does not emit a 2·35 MeV gamma, the K X-ray spectra of both molybdenum and niobium samples bombarded with 14·7 MeV neutrons were followed with a thin (2 mm) NaI(Tl) crystal fitted with a 0·005-in. thick beryllium window in conjunction with the 200-channel analyser. With irradiated niobium, the decay of the K X-rays exhibited half-lives of 6 min [^{94m}Nb from the (n,γ) reaction] and 10 days (^{92g}Nb) only. The irradiated molybdenum samples exhibited some short-lived components which disappeared in about 5 hr, then exhibited no apparent decay in the next 24 hr.

While analysing the γ-spectra of irradiated molybdenum samples, the decay of the 0·934 MeV and 0·915 MeV gammas, associated with 10·1 day ^{92}Nb and 79·0 hr ^{89}Zr, respectively,(6) was followed so that it was possible to determine the total activation cross sections: $^{92}\text{Mo}(n,p)^{92}\text{Nb}$ (10·1 day+5·9 μsec), 60±15 mbarns; and $^{92}\text{Mo}(n,\alpha)^{89}\text{Zr}$ (79·0 hr+4·4 min), 20±8 mbarns. These cross sections represent formation of both isomers since essentially all (93 per cent) of the 4·4 min ^{89}Zr isomer decays to the ground-state(6) while presumably all of the 88 keV 5·9 μsec ^{92}Nb isomer does so as well (no decay scheme for the latter, however, is reported). The counting corrections and techniques used in obtaining these cross sections are the same as reported by BRAMLITT and FINK.(8)

Since the cross-section ratio for formation of 3·1 hr ^{90m}Y/64 hr ^{90g}Y is ~0·3 at 14 MeV from the ^{90}Zr (n,p) reaction,(11, 12) one might expect *a priori* that at the same energy a similar isomeric yield ratio might obtain for the ^{92}Mo (n,p) reaction. Since the ^{92}Mo (n,p) ^{92}Nb (10·1 days+5·9 μsec) reaction cross section as measured in the present work is 60±15 mbarns, a cross-section of about 18 mbarns might be expected for the ^{92}Mo (n,p) reaction leading to 13 hr or 21·6 hr isomers. This is a factor of thirty times larger than the sensitivity limit (600 μbarns) of the present experiments for the detection of a 13 hr, 2·35 MeV gamma (with a similar sensitivity in the K X-ray experiments as well).

These results clearly suggest that the assignments of 13 hr and 21·6 hr periods as ^{92m}Mb are in error.

---

(12) B. P. BAYHURST and R. J. PRESTWOOD, Report LA-2493 (1960); V. L. SAILOR, Ed., U. S. AEC Report, WASH-1021 (1959); J. E. BROLLEY, J. L. FOWLER and L. K. SCHLACKS, *Phys. Rev.* **88**, 618 (1952); C. H. REED. Ph.D. Thesis, University of Utah (1960).

Since the ^{92}Mo (n,p) cross-section to the 10·1 day ^{92m}Nb is no greater than 60-mbarns, considerably smaller than the value of 288 mbarns predicted from systematics of (n,p) reactions at 14–15 MeV,(13) an *independently-decaying* isomer of ^{92}Nb would account for the difference. An as-yet-undiscovered isomer of ^{92}Nb, therefore, might exist. On the other hand, the low (n,p) cross-section may be a result of competition from the (n,np) reaction, which leads to a product nuclide having a closed shell of fifty neutrons. Such an explanation is supported by the data of COLLI *et al.*(14) in which the $(n,p)/(n,np)$ cross-section ratio on ^{92}Mo was found to be very low, namely, 0·277.

Acknowledgements—We are indebted to C. CALDWELL, Jr. and the crew of the Accelerator Laboratory for assisting with the bombardments.

(13) D. G. GARDNER, *Nuclear Phys.* **29**, 373 (1962).

(14) L. COLLI, U. FACCHINI, I. IORI, M. G. MARCAZZAN and A. M. SONA, *Nuovo Cim.* **13**, 730 (1959).

J. Inorg. Nucl. Chem., 1962, Vol. 24, pp. 1321 to 1325. Pergamon Press Ltd. Printed in England

ABSOLUTE ACTIVATION CROSS SECTIONS FOR REACTIONS OF NIOBIUM WITH 14·5 MeV NEUTRONS*

E. T. Bramlitt and R. W. Fink†
Department of Chemistry, University of Arkansas, Fayetteville, Arkansas, U.S.A.

(*Received* 2 *February* 1962)

Abstract—Absolute neutron activation cross sections at 14·5 MeV have been measured for the mono-isotopic nuclide, ^{93}Nb, by means of γ-scintillation spectroscopy and β-proportional counting as well as by the use of chemical separation techniques. The observed reactions, product half-lives, and cross-sections are as follows: ^{93}Nb $(n, 2n)$ ^{92g}Nb, 10·1 days, 499 ±91 mbarns; ^{93}Nb (n, γ) ^{94m}Nb, 6·6 min, 0·44 ±0·25 mbarns; ^{93}Nb (n, α) ^{90g}Y, 64 hr, 8·6 ±2·5 mbarns; ^{93}Nb (n, α) ^{90m}Y, 3·0 hr, 5·9 ±2·0 mbarns; ^{93}Nb $(n, n'\alpha)$ ^{89m}Y, 16 sec, 2·5 ±1·1 mbarns. No activity was observed in the zirconium fraction, the (n, p) product, nor was the 13 hr ^{92m}Nb produced through an $(n, 2n)$ reaction. Half-lives of ^{90m}Y and ^{89m}Y were determined by least squares analysis to be 3·02 ±0·09 hr and 16·3 ±1·3 sec, respectively.

Neutron activation cross-sections of niobium have been measured at 14·5±0·9 MeV as part of a more extensive investigation of the neutron induced nuclear reactions on nuclides Z which lead to the $(Z\text{-}2)$ products. The reactions which are energetically possible at 14 MeV for most nuclides and which are being considered include the $(n, 2p)$, $(n, {}^{3}\text{He})$, (n, α), $(n, n'\alpha)$, and the $(n, {}^{6}\text{He})$.

EXPERIMENTAL

Neutrons of 14·5 ±0·9 MeV are produced by deuteron bombardment (400 keV) of ZrT or TiT targets using the University of Arkansas Cockcroft-Walton accelerator. Total neutron yields, as measured by both a BF_3 "long counter" and an α-counter, were between 10^9 and 10^{11} neutrons/sec.

The niobium samples irradiated were in most cases in the form of spectroscopically pure powder, rod, or the pentoxide; otherwise, niobium foil or potassium hexaniobate of purity greater than 99·9 per cent was used. During irradiation, samples were surrounded with cadmium foil so as to remove any thermal neutrons present in the neutron beam.

Chemical separations were performed on irradiated samples of niobium pentoxide and potassium hexaniobate by first dissolving them in hydrofluoric acid and then adding zirconium and yttrium carriers. The yttrium fluoride precipitate which forms immediately was dissolved in a mixture of boric and nitric acids, precipitated as the hydroxide, and ignited to the oxide in which form it was counted. Zirconium was precipitated as the barium fluorozirconate while niobium was recovered as the hydroxide and then ignited to the oxide.

Gross β-counting was carried out with either an aluminium-walled methane flow proportional counter fitted with a 0·9 mg/cm² aluminized Mylar end-window or a windowless proportional counter. γ-rays were measured with a 3 × 3-in. NaI(Tl) scintillation spectrometer and RIDL 200-channel analyser. For X-ray measurements a 25 × 2-mm NaI(Tl) crystal with beryllium window was used in conjunction with the RIDL analyser. Counting corrections were made as described in a previous paper.(1)

---

*Supported in part by the U.S. Atomic Energy Commission.

†Present address: Department of Physics, Marquette University, Milwaukee 3, Wisconsin.

(1) E. T. Bramlitt, R. W. Fink, D. G. Gardner and A. Poularikas, *Phys. Rev.* **125**, 297 (1962).

The neutron flux passing through each sample was determined by placing thin foils of copper (0·00025 in.) and/or aluminium (0·001 in.), having the same area as the sample, in front and behind of the sample and making use of the reactions ^{63}Cu $(n, 2n)$ ^{62}Cu, ^{62}Cu $(n, 2n)$ ^{64}Cu, and ^{27}Al (n, α) ^{24}Na with cross-sections of 556 ± 28,(2) 954 ± 130,(3) and 114 ± 7 mbarns,(3) respectively. When β counting of these monitors was performed, the 9·9 min(4) Cu^{62} and 15·0 hour ^{24}Na were assumed to be counted with 100 per cent efficiency whereas for the 12·8 hr ^{64}Cu, a 62 per cent efficiency was assumed. To serve as a monitor by means of γ-scintillation spectrometry, the area under the 0·51 MeV annihilation photopeak from ^{62}Cu and ^{64}Cu (98·2 and 19 per cent of decays, respectively) and the 1·37 MeV (100 per cent) photopeak from ^{24}Na was measured (all γ-peak areas were measured with a compensating polar planimeter).

In determining the cross-section for production of 16 sec ^{89m}Y by the $(n, n'\alpha)$ reaction, spectroscopically pure niobium and copper powders were intimately mixed in a ratio of about 10 to 1 (by weight) insuring identical sample and monitor geometry. A newly installed fast transport system was used which permits the sample to be sent from the target to the counting position in less than a half-second.

ERRORS

The errors affixed to cross-section values reported in this work are probable errors based on a propagation of the estimated errors in the various terms used in calculating the cross-section, i.e., the duration of bombardment, activities at the end of bombardment, half-lives, sample and monitor weights, and monitor cross-sections. The errors in the activities include the errors in any terms used in obtaining absolute disintegration rates, e.g., scattering and absorption factors, peak-to-total ratio, internal conversion coefficients, and efficiencies. Errors in weights, half-lives, and duration of bombardment were usually negligible; on the other hand, counting correction factors were estimated to be within 5 per cent correct and photopeak areas and chemical yields within 10 per cent correct. The estimated errors used for the monitor cross sections and conversion coefficients were actually the standard deviations for these values as taken from the literature.

RESULTS

^{93}Nb $(n, 2n)$ ^{92g}Nb

The 0·93 MeV gamma associated with the decay of 10·1 day ^{92g}Nb (98 per cent) was counted to determine the cross section for the $(n, 2n)$ reaction on ^{93}Nb. A value of 499±91 mbarns (Table 1) was obtained from several measurements, using both copper and aluminum foils as flux monitors.

^{93}Nb $(n, 2n)$ ^{92m}Nb

No 13 hr ^{92m}Nb was observed to be produced in bombardments of niobium as indicated by the absence of the 2·35 MeV gamma which occurs in 100 per cent of the decays of this isomer. An upper limit for the reaction of 1·2 mbarns was obtained by drawing in a photopeak corresponding to a 2·35 MeV gamma of such size that it would have been seen if present and after making the usual counting corrections, comparing it to the γ-photopeak of the monitor.

(2) S. Yasumi, *J. Phys. Soc.* (Japan) 12, 443 (1957).

(3) A. Poularikas and R. W. Fink, *Phys. Rev.* **115**, 989 (1959).

(4) Half-lives and other decay information cited in this paper, unless otherwise stated, are taken from *Nuclear Data Cards*, National Academy of Science, National Research Council, U. S. Goverment Printing Office, Washington, D. C.

^{93}Nb (n, γ) ^{94m}Nb

X-ray spectra of irradiated niobium indicated the presence of the 6·6 min ^{94m}Nb isomer which would have to be produced by an (n, γ) reaction. Almost complete absence of a 0·04 MeV gamma in the X-ray spectra implies that the ^{94m}Nb is about 100 per cent converted. The cross-section for its production was thus determined by counting irradiated niobium foils (0·001 inch) in a windowless proportional counter and assuming 100±20 per cent efficiency for counting the conversion electrons and X-rays. A value of 0·44±0·25 mbarns was obtained (Table 1).

^{93}Nb (n, p) ^{93}Zr

The (n, p) product produced from niobium is 9×10^5 year ^{93}Zr which is too long-lived to be observed by the activation methods employed. Chemical separations on irradiated Nb_2O_5 were performed, however, to remove any zirconium activities. No activities followed the zirconium fraction (the time of separation being about 45 min) indicating no short lived ($> \sim10$ min) isomers of ^{93}Zr.

^{93}Nb (n, α) Y^{90g}

The cross-section for production of 64 hr ^{90g}Y was determined by gross β-counting to be 8·6±2·5 mbarns (Table 1) using both copper and aluminium monitors. Several determinations were made with and without chemical separations being performed.

^{93}Nb (n, α) ^{90m}Y

The recently reported 3·1 hr isomer(5–8) of ^{90}Y has been produced in bombardments of niobium through the (n, α) reaction. The isomer decays to the ground state of ^{90}Y through two cascade γ-rays of energy 0·48 and 0·20 MeV. Total conversion coefficients for these two gammas have been measured by HEATH, *et al.*(6) and found to be 0·11±0·02 and 0·03±0·01, respectively. L. HASKIN(5) determined values of 0·10±0·02 and 0·036±0·007. The area under the 0·48 MeV γ-photopeak was measured and compared to that of the 0·93 MeV photopeak from ^{92g}Nb produced by the $(n, 2n)$ reaction. Using an average of the reported values for the conversion coefficient and a value of 499±20 mbarns for the cross-section of the internal monitor, it was possible to determine the (n, α) cross-section to be 5·9±2·0 mbarns (Table 1). Single channel decay of the 0·20 MeV gamma followed a straight line for over seven periods to background with a half life at 3·02 ±0·09 hr as determined by a least squares analysis.

The 3 hr γ-emitter also was observed in gross β-decay of the yttrium fraction from niobium bombardments as a result of its conversion electrons. By assuming that the β-proportional counter detects no gammas, then the true activity of the isomer will equal the observed activity divided by the probability that a gamma is converted. This probability is determined from the following expression:

$$P = \frac{1}{1+\dfrac{1}{\alpha_1+\alpha_2+\alpha_1\alpha_2}}$$

where α_1 and α_2 are the total conversion coefficients for each gamma. The above expression takes into account the possibility that the two gammas are converted simultaneously and counted only as one event. Using the value of 0·12±0·06 for this probability, the cross-section for formation of ^{90m}Y as determined by β-counting was comparable to the results obtained from gamma counting.

---

(5) L. HASKIN, *Phys. Rev.* **123**, 184 (1961).

(6) R. L. HEATH, J. E. CLINE, C. W. REICH, E. C. YATES and E. H. TURK, *Phys. Rev.* **123**, 903 (1961).

(7) W. L. ALFORD, D. R. KOEHLER and C. E. MANDEVILLE, *Phys. Rev.* **123**, 1365 (1961).

(8) W. S. LYON, J. S. ELDRIDGE and L. C. BATE, *Phys. Rev.* **123**, 1747 (1961).

^{93}Nb (n, $n'\alpha$) ^{89m}Y

An activity decaying with a half life of 16·3±1·3 sec was observed in the bombardments of spectroscopically pure niobium rod and powder. The γ-spectra showed only a 0·91 MeV gamma decaying with this period (single channel decay of the 0·91 MeV gamma followed straight for over five periods to background) indicating ^{89m}Y had been formed. Such a nuclide would be produced through the (n, $n'\alpha$) reaction. A cross-section was determined relative to the 9·9 min ^{62}Cu, assuming a negligible amount of conversion of the 0·91 MeV gamma, to be 2·5±1·1 mbarns (Table 1).

Table 1.—Cross-section for reactions of niobium at 14·5 MeV

Reaction	Product half-life	Measured cross-section (mbarns) Present work	Literature
^{93}Nb (n, $2n$) ^{92g}Nb	10·1 days	499 ±91	430 ±70(9) 530 ±60(10)
^{93}Nb (n, $2n$) ^{92m}Nb	13 hr	<1·2	
^{93}Nb (n, γ) ^{94m}Nb	6·6 min	0·44 ±0·25	
^{93}Nb (n, α) ^{90g}Y	64 hr	8·6 ±2·5	9·5 ±5(11) 9·0 ±2·2(12)
^{93}Nb (n, α) ^{90m}Y	3·02 hr	5·9 ±2·0	5 ±2(7)
^{93}Nb (n, $n'\alpha$) ^{89m}Y	16·3 sec	2·5 ±1·1	

* Errors are probable errors based on a propagation of the estimated fractional error in all terms used in calculating the cross sections.

DISCUSSION

The (n, $2n$) and (n, α) cross-sections determined in the present work agree well with those reported in the literature. The (n, α) cross-section for formation of ^{90m}Y was obtained by using experimentally measured conversion coefficients and agrees well with the value reported by Alford, *et al.*(7) which was calculated from theoretical values of the conversion coefficients.

Coleman(13) measured the (n, γ) cross-section for many nuclides at 14 MeV and found values ranging between ~ 1 and 10 mbarns. Wille and Fink(14) have also reported (n,γ) reactions at 14 MeV for several nuclides in the rare earth region. Diven *et al.*(15) have shown that the (n,γ) reaction on niobium is significant (35 mbarns) at 1 MeV. Thus, the fact that it is observed at 14·5 MeV seems reasonable. The cross-section may even be low because of the assumption that the counting efficiency was 100 per cent. Most conversion electrons from ^{94m}Nb will be absorbed by the sample, whereas probably not all of the X-rays are stopped in the sensitive area of the counter chamber.

(9) H. Vonach and H. Münzer, *Österr. Akad. Wiss.*, Nr. **6**, 120 (1959).
(10) V. L. Glagolev and P. A. Yampolskii, *Zh. Eksptl. i Teoret, Fiz.* **40**, 743 (1961).
(11) B. P. Bayhurst and R. J. Prestwood, Report LA-2493 (1960).
(12) H. G. Blosser, C. D. Goodman and T. H. Handley, *Phys. Rev.* **110**, 531 (1958).
(13) R. F. Coleman, *Proc. Phys. Soc.* **72**, 505 (1958).
(14) R. G. Wille and R. W. Fink, *Phys. Rev.* **118**, 242 (1960).
(15) B. C. Diven, J. Terrell and A. Hemmendinger, *Phys. Rev.* **120**, 556 (1961).

The ratio of the (n, α) cross-section to $(n, n'\alpha)$ cross-section is roughly four. Results of the same order of magnitude have been obtained with other nuclides in this laboratory and will be reported at a later date. NEUERT(16) has also observed the $(n, n'\alpha)$ reaction with ^{51}V, ^{69}Ga and ^{65}Cu at 14 MeV with cross-sections about $\frac{1}{3}$ to $\frac{1}{7}$ as large as the (n,α) cross-section.

(16) H. NEUERT. Private communication (1961); M. BORMANN, S. CIERJACKS, R. LANGKAU and H. NEUERT, *Z. Physik*, 166, 477 (1962).

J. Inorg. Nucl. Chem., 1962, Vol. 24, pp. 1327 to 1336. Pergamon Press Ltd. Printed in England

NEUTRON-INDUCED REACTIONS IN IODOBENZENE

J. E. C. Macrae and P. F. D. Shaw

The Clarendon Laboratory, Oxford

(*Received* 13 *February* 1962)

Abstract—The organic yields of radio-iodine produced by neutron irradiation of mixtures containing iodobenzene and iodine have been investigated; they were unaffected by a slow radiolytic exchange reaction and there was little evidence that they are influenced by thermal exchange occurring in the hot zone. The results can be explained by assuming that in such systems, phenyl radicals react to form iodonium radicals by addition to iodobenzene molecules. In the presence of benzene organic yields are reduced, possibly by reaction between phenyl radicals and benzene to form diphenyl compounds. This explanation is consistent with the absence of any self-scavenging effect in solutions of iodine in benzene.

When organic iodides are irradiated with neutrons they undergo the Szilard-Chalmers[(1)] reaction in which part of the radio-iodine produced by neutron capture is found in organic, and part in inorganic, combination. The nature of the primary event responsible for the disruption of the parent molecule is still obscure, but the diversity of the new organic species produced (see, for example, Glückauf and Fay,[(2)] or Evans and Willard[(3)]) indicates that considerable energy from the neutron capture event is available for the chemical disruption of the neighbouring molecules. Some insight into the processes occurring after neutron capture can be obtained from the "scavenger" effect, or the fall in retention (fraction of organically bound radio-iodine atoms) observed when a radical scavenger such as elementary iodine is present during the irradiation.[(3a)] Small concentrations of iodine cause a disproportionately large drop in the retention, thus indicating that the formation of organic radio-iodides proceeds partly by a diffusion-controlled step in which organic radicals produced by the primary event make many collisions before combining with the active iodine atom. As the concentration of free iodine is increased, the retention becomes less sensitive to its variation, and this part of the retention is regarded as arising from recombination or replacement reactions which do not involve diffusive processes, and may be termed "hot" since presumably a considerable amount of energy from the capture event may still be available in the radio-iodine atom or the surrounding molecules.

In the case of some aliphatic bromides, which behave similarly, it has been shown[(4)] that at high bromine concentrations the bromine insensitive part of the scavenger curve falls off linearly with the molar fraction of bromine present and that an extrapolation of this curve to zero bromine concentration affords a convenient way of determining the "hot" retention. No authors have used such high concentrations of iodine in organic iodides, probably because of the limitations imposed by the solubility of iodine.

---

(1) L. Szilard and T. A. Chalmers, *Nature, Lond.* 134, 462 (1934).

(2) E. Glückauf and J. W. J. Fay, *J. Chem. Soc.* 390 (1936).

(3) (a) J. E. Willard, *Ann .Rev. Phys. Chem.* 6, 141 (1955).
(b) J. B. Evans and J. E. Willard, *J. Amer. Chem. Soc.* 78, 2908 (1956).

(4) M. Milman and P. F. D. Shaw, *J. Chem. Soc.* 1303, 1318 (1957).

For most aliphatic iodides, the retentions, in the absence of iodine, lie between 25 and 40 per cent, but in the case of iodobenzene the retention found (about 60 per cent) is much greater. It has been suggested⁽⁵⁾ that phenyl radicals produced by the capture event might be stabilized by addition to iodobenzene to form diphenyl iodonium radicals which could then react diffusively with the active iodine atom; in support of this it was shown that diphenyl iodonium compounds were produced by the action of light, or pile irradiation, upon iodobenzene. Further evidence for the existence of such radicals has been obtained from polarographic data.⁽⁶⁾

However, more recent work has suggested other possible causes for the high retention. A high retention observed in bromobenzene⁽⁷⁾ was found to be due to a radiolytic or photochemical exchange occurring subsequently to the neutron capture event. A preliminary kinetic study showed that the exchange proceeded by the dissociation of bromine molecules, followed by exchange with bromine atoms.

Another exchange which might modify the retention in iodobenzene containing iodine is that observed by LEVINE and NOYES.⁽⁸⁾ This exchange is thermal and proceeds by a dual mechanism; the rate in iodobenzene, or its solution in non-polar solvents, is given by:

$$k_r(\mathrm{PhI})(\mathrm{I_2})^{\frac{1}{2}}+k_p(\mathrm{PhI})^2.$$

The first term describes an exchange between iodobenzene and thermally produced iodine atoms, and the second represents one which proceeds by the formation and subsequent decomposition of a diphenyl iodonium intermediate. Both exchanges have large (> 30 kcal/g mole) activation energies and their effect on the Szilard-Chalmers reaction might therefore be to modify the magnitude of the hot zone retention which occurs before all the energy from the neutron capture event is dissipated.

PRELIMINARY EXPERIMENTS

1. *Radiolytic exchange*

The radiolytic exchange occurring during neutron irradiation using a 500 mc Ra–Be source was extremely small, and barely detectable within the small period allowed for its study by the decay of ^{128}I (half-life 25 min). A few experiments were made with ^{131}I (half-life 8·14 days); these established that a radiolytic exchange occurred and confirmed that its effect on the retention was negligible. For example, an aerobic iodobenzene specimen containing 6×10^{-6} mf I_2 placed 2 cm from a ^{60}Co source of strength 1c, showed a period for half-exchange of 80 hr. The exchange was accompanied by iodine liberation, the rate of which was reduced under anaerobic conditions. No simple dependence of the exchange rate upon the iodine concentration could be established.

Evidence was again found for the presence of diphenyl-iodonium derivatives. After γ-irradiation for 96 hr, an aerobic specimen of iodobenzene which contained initially 10^{-5} mf I_2 was found to have exchanged 34 per cent of the active iodine. On

(5) P. F. D. SHAW, *J. Chem. Soc.* 443 (1951).
(6) H. E. BACHOFNER, F. M. BERINGER and L. MEITES, *J. Amer. Chem. Soc.* **80**, 4269 (1958).
(7) M. MILMAN and P. F. D. SHAW, *J. Chem. Soc.* 2101 (1956).
(8) S. LEVINE and R. M. NOYES, *J. Amer. Chem. Soc.* **80**, 2401 (1958).

warming another aliquot for 5 min at 100 °C in the absence of light or γ-rays, the activity in organic combination rose to 42 per cent. Further heating caused no increase in the exchange; in a separate experiment it was found that such heating led to the complete decomposition of diphenyl iodonium iodide to give iodobenzene. Spectrophotometric examination of the irradiated solution, and a solution of iodobenzene containing diphenyl iodonium iodide together with the appropriate amount of iodine was also consistent with this explanation.

2. *Photochemical exchange*

In view of the slowness of the radiolytic exchange, a brief study was made of the photochemical exchange under aerobic conditions using light from a high pressure mercury lamp. Iodine production was again observed, but when the light was passed through a nitrobenzene filter both iodine production and exchange were stopped. Since the former can only occur by dissociation, or activation, of iodobenzene, it indicates that the exchange also proceeds by a similar mechanism. Since nitrobenzene is transparent to light which corresponds to the absorption maximum of iodine (wavelength 490 mμ) and which is known(9) to cause its dissociation, these results suggest that at room temperature iodine atoms do not exchange with iodobenzene by a direct substitution mechanism and contrast with the photochemical exchange found in bromobenzene.(7)

No evidence was found for the production of diphenyl-iodonium iodide. A solution of this in iodobenzene was found to decompose quickly under the influence of light from the mercury lamp so that its equilibrium concentration would probably be too small to detect.

The exchange occurring was not fast: for example a solution of iodobenzene containing initially 10^{-5} mf iodine showed 50 per cent exchange in eight hours when held 15 cm from a 100W high pressure quartz mercury lamp. In diffuse daylight, and in periods of the order of the half-life of ^{128}I, the exchange was negligible and no corrections for it were necessary in the experiments described below.

THE SZILARD-CHALMERS REACTION IN IODOBENZENE

The scavenger curves shown in Figs. 1 and 2 were determined for iodobenzene and *p*-iodotoluene at 97 °C, and for methyl and ethyl iodides at 67 °C; these temperatures were used in order to increase the iodine solubility. The curves for the aliphatic iodides follow the form found previously for aliphatic bromides(4) being linear when c (the molar fraction of iodine) is greater than 0·2, and extrapolating to zero retention at $c = 1$. By contrast, the curves taken for the aromatic iodides showed no linear portion.

Analysis of ethyl bromide–bromine mixtures(4) showed that the sum of the radioactive organic fractions other than the parent compound fell off linearly with increasing bromine concentration. A crude analysis of the products from iodobenzene was made and is given in Table 1. It can be seen that the di-iodobenzene fraction decreased non-linearly with the iodine concentration, and fell off more rapidly than would be expected had a linear relationship held.

---

(9) See, for example G. Hertzberg *The Spectra of Diatomic Molecules*. Van Nostrand, New York (1950).

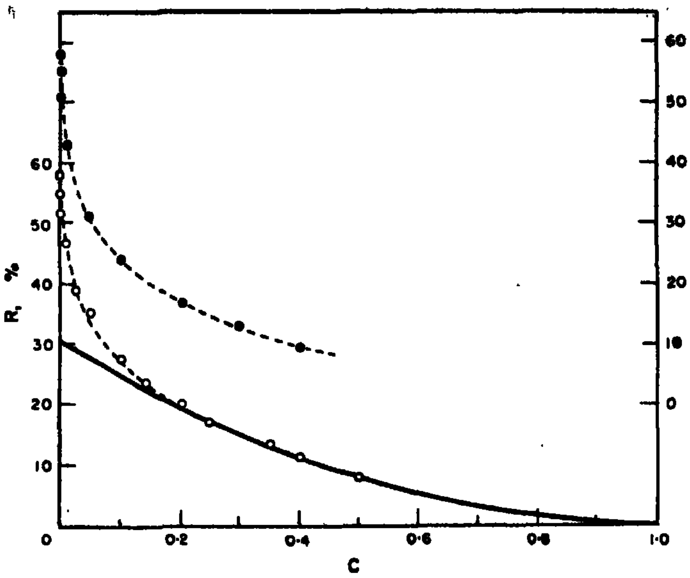

FIG. 1.—The retentions (*R*) of iodobenzene (O) and *p*-iodotoluene (●) at 97°C as a function of the molar fraction of added iodine (c). Left and right hand ordinates refer to iodobenzene and *p*-iodotoluene respectively.

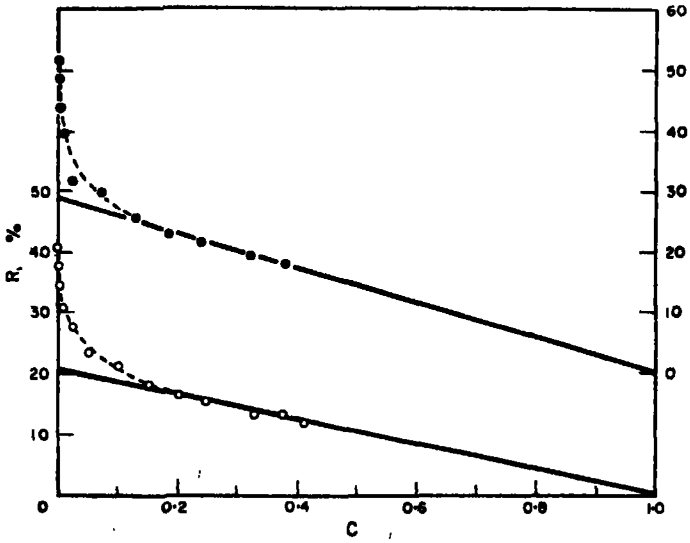

FIG. 2.—The retentions of methyl (●) and ethyl (O) iodides at 67°C as a function of the molar fraction of added iodine (*c*). Left and right hand scales refer to methyl and ethyl iodides respectively.

The iodobenzene scavenger curves are of the form expected if a thermal exchange occurs in the hot zone; under these conditions exchange would tend to distribute the active atoms between the iodobenzene and the iodine molecules in a statistical manner; since the relative numbers of iodine atoms present as iodobenzene and as iodine are $(1-c)$ and $2c$ respectively, the retention should tend to $(1-c)/(1-c+2c)$ or $(1-c)/(1+c)$; such a distribution is non-linear in c, and of the right form.

TABLE 1

Iodine concentration (molar fraction)	C_6H_5I(%)	$C_6H_4I_2$(%)	Retention observed (%)
10^{-4}	43·4 ± 0·4	11·2 ± 0·4	54·2 ± 0·5
0·11	20·2 ± 0·4	8·1 ± 0·4	27·1 ± 0·5
0·25	11·0 ± 0·5	5·7 ± 0·3	16·9 ± 0·7

To test this further, scavenger curves were constructed for equi-molar mixtures of benzene and iodobenzene and of nitrobenzene and iodobenzene at 80°C (Fig. 3).

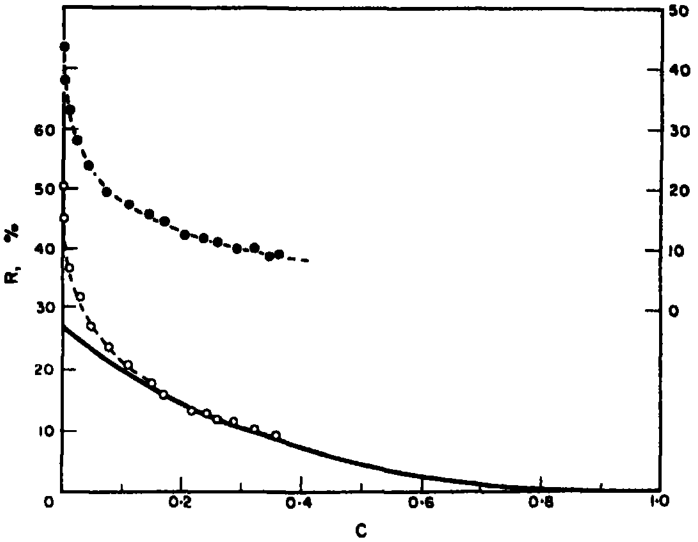

FIG. 3.—The retentions of benzene-iodobenzene (O, left hand scale) and nitrobenzene-iodobenzene (●, right hand scale) mixtures at 80°C as a function of the molar fraction of added iodine (c).

According to the conclusions of LEVINE and NOYES,(8) in the first system the exchange might be expected to proceed by both the mechanisms outlined above, but in the presence of nitrobenzene the exchange proceeding by the formation of the diphenyl iodonium intermediate should be inhibited. If the exchange occurring in the hot zone was reduced by dilution, or partly inhibited, it would be expected that the curvature of the scavenger curves would lessen, and that their intercept on the zero retention axis would be greater than that found in iodobenzene. Unfortunately the limiting solubility of iodine in these systems at 80°C enabled only a small portion of the relevant part of the curves to be determined. The intercepts on the zero retention axis obtained by extrapolating the lines through the retention values at $c = 0{\cdot}25$ and $0{\cdot}35$ are about 0·70, 0·75 and 0·80 respectively for pure iodobenzene and its solution in benzene and nitrobenzene, and are qualitatively in agreement with an explanation based upon exchange. However, the near equality of the retentions for the benzene–iodobenzene and nitrobenzene–iodobenzene curves when c is greater than 0·2 is surprising and suggests that any exchange proceeding by an iodonium intermediate is very small. The inhibition of the exchange in nitrobenzene was ascribed(8) to the interference of the polar nitrobenzene on the nucleophilic attack of one iodobenzene molecule upon another; in the present case, any iodonium intermediate could be produced by the attachment of an aryl radical to an iodobenzene molecule, since the energy provided by the neutron capture event is sufficient to cause the dissociation of many iodobenzene molecules. Under these circumstances the importance of nitrobenzene as an inhibitor of the exchange may be considerably diminished.

The scavenger curve of iodine in benzene

This was determined to assist the interpretation of the above curves. Within experimental error, the retentions were independent of iodine concentration over the range studied (Fig. 4). The independence of the retention upon iodine concentration was confirmed by repeating the curve at a higher temperature (75°C) in order to enhance the iodine solubility. The retentions were considerably lower than those found at the lower temperature (15°C). Change of temperature is known to alter the retention of similar systems by small amounts, and can be accounted for by assuming that the effectiveness of the surrounding molecules in caging radicals and atoms is temperature dependent.(10) The effect observed here is considerably greater than any reported hitherto, and suggests that a different mechanism is operative.

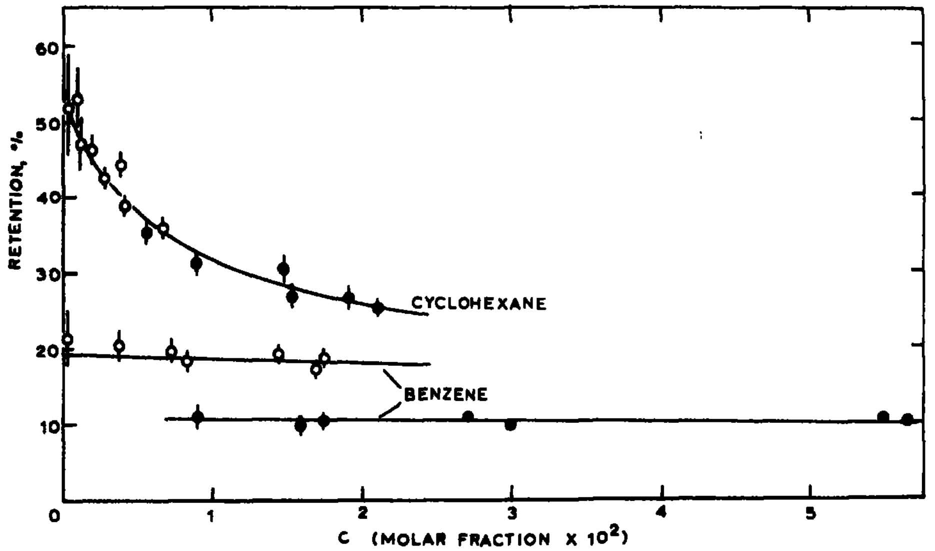

FIG. 4.—Retention of solutions of iodine in cyclohexane and benzene as a function of the molar fraction of iodine (c). Points taken at 15°C, O; at 75°C, ●.

---

(10) S. Aditya and J. E. Willard, *J. Amer. Chem. Soc.* **79**, 3367 (1957).

The constancy of the retentions at a given temperature indicates that there is no "self-scavenging" by the iodine. A self-scavenging effect would have been expected, *a priori*, for, if radicals are produced by a capture event involving one iodine molecule, the other iodine molecules should exhibit a scavenging action by reacting with them in the diffusive stages of the process, so reducing their probability of reaction with the newly formed radioactive atom. Self-scavenging by iodine has been observed in other hydrocarbon solvents by McCauley and Schuler,(11) and has been confirmed in this laboratory. A self-scavenging curve of iodine in cyclohexane is given for comparison in Fig. 4. This differs from the curves for iodine–benzene mixtures since it shows the expected fall with increasing iodine concentration, and also because the points taken at 15 and 75°C fall approximately on the same curve, thus indicating that any temperature dependence is small.

The absence of a self-scavenging effect in the benzene–iodine system indicates that no organic radicals are present in the diffusive stages of the reaction, so that the retention found corresponds to that arising in the hot zone. Further, since a temperature change of 60°C reduces the retention by a factor of two, it seems probable that the reactions governing the retention must have small activation energies.

All these features can be explained if it is assumed that the capture event causes the dissociation of some of the neighbouring molecules of benzene into hydrogen atoms and phenyl radicals which can then combine with the active atom or undergo the reaction.(12)

$$\mathrm{Ph+PhH \rightarrow Ph_2+H}$$

If the latter required a small activation energy, a small increase in temperature would reduce the concentration of phenyl radicals available at any time, and hence lead to a decrease in the retention. If all the phenyl radicals generated in the hot zone reacted to form hydrogen atoms before diffusive recombination occurred, no self-scavenging could be observed since the ensuing recombination reactions would not involve any organic radicals, and would therefore not contribute to the retention.

DISCUSSION

No explanation based upon a thermal exchange occurring in the hot zone accounts satisfactorily for the shape (above $c = 0{\cdot}2$) of the retention curves of the aromatic iodides studied. If an exchange occurred, and proceeded to equilibrium the retention should show a $(1-c)/(1+c)$ dependence. Even in this extreme case, the slope and curvature of such a function are both less than that found.

At iodine concentrations greater than 0·2 mf the curves for iodobenzene, pure and mixed with benzene, are of the form $K(1-c)^2$, K being a constant. This suggests that the retention is primarily dependent on the formation of a diphenyl iodonium intermediate.

A possible explanation of the $(1-c)^2$ dependence can be based on a modified "radical cluster" occurring in the hot zone; providing that the retention is regarded as resulting from a large number of events, the treatment given is valid also for a hot zone such as that postulated for bromoethane,(13) in which there are relatively few dissociated molecules.

---

(11) C. E. McCauley and R. H. Schuler, *J. Phys. Chem.* **62**, 1364 (1958).

(12) For review, see D. R. Augood and G. H. Williams, *Chem. Rev.* **57**, 123 (1957).

(13) B. Knight, G. E. Miller and P. F. D. Shaw, *J. Inorg. Nucl. Chem.* **23**, 15 (1961).

Suppose that initially (stage 1) the energy imparted to the system by the capture event causes the dissociation of a few of the neighbouring molecules; combination of the active atom with one of these may not be immediately possible because the active atom may not be sufficiently "cool". In this case, the radicals and atoms may combine among themselves, or phenylic radicals may undergo one of the reactions (stage 2):

$$\mathrm{Ph+PhI \rightarrow Ph_2I-}, \tag{1}$$

$$\mathrm{Ph+PhH \rightarrow Ph_2+H}, \tag{2}$$

$$\text{or } \mathrm{Ph+I_2 \rightarrow PhI+I} \tag{3}$$

so that by the time that combination with the active atom can occur, the only possible reaction leading to retention is:

$$\mathrm{Ph_2I+I^* \rightarrow (Ph_2I\}I^*) \rightarrow PhI+PhI^*} \tag{4}$$

Quantitatively, let the concentrations of iodobenzene, benzene and iodine be a, b and c respectively, and let the fraction of these dissociated in the vicinity of the newly formed radio-iodine atom be α, β and γ, where α, β and γ are assumed to be small compared with unity. The total concentration of organic radicals at any time will then be $(\alpha a+\beta b)$, that of the atoms being $(\alpha a+\beta b+2\gamma c)$, so that the ratio of organic radicals to the total number of radicals and atoms in stage I is $(\alpha a+\beta b)/2(\alpha a+\beta b+\gamma c)$. If we assume that all the organic radicals react in stage 2 by one of the reactions 1, 2 or 3, the fraction of these available for retentive combination will be given by $K_1a/(K_1a+K_2b+K_3c)$ where K_1 K_2 and K_3 are factors describing the relative probabilities of undergoing 1, 2 or 3. The retention can now be written:

$$f\frac{(\alpha a+\beta b)}{2(\alpha a+\beta b+\gamma c)}\,\frac{K_1a}{K_1a+K_2b+K_3c} \tag{i}$$

where f is the fraction of radio-iodine atoms available for retention in the hot zone.

For iodobenzene–iodine mixtures (b = O) the best fit to the experimental results is with $\gamma/a = 1{\cdot}01\pm0{\cdot}04$, $K_3/K_1 = 0{\cdot}96\pm0{\cdot}03$ and $f = 0{\cdot}60$. The curve obtained using $\gamma/\alpha = 1$, $K_3/K_1 = 1$ and $f = 0{\cdot}60$ is given by the solid line in Fig. 1. It is of interest that with $\gamma/\alpha = 1$, the expression (i) reduces to:

$$\frac{f}{2}(1-c)\left(\frac{K_1a}{K_1a+K_2b+K_3c}\right) \tag{ii}$$

and in the absence of the right-hand bracket the retention shows a linear dependence on c similar to that found in ethyl and methyl iodides (Fig. 2) and in some aliphatic bromides.(4)

In other systems(4, 13) it is found that substitution products are produced almost entirely in the hot zone. If this occurs in iodobenzene, the yield of di-iodobenzene would be expected to follow the hot zone retention (R_E) curve, since the reactions of iodophenyl and phenyl radicals might be expected to be similar; that is:

$$\frac{(\mathrm{C_6H_4I_2})c = 0}{(\mathrm{C_6H_4I_2})c = C} = \frac{R_E(c = 0)}{R_E(c = C)}$$

so that the ratio of the di-iodobenzene yields to the corresponding values of R_E, calculated from (ii) should be constant. The ratios found at 10^{-4}, 0·11 and 0·25 molar fraction of iodine are respectively 37·3±1·3, 34·2±1·7, 33·8±1·8 and appear to be consistent with the formulation.

Using the modified expression (ii), a satisfactory fit to the iodobenzene-benzene curve ($a = b$) is obtained with $K_3/K_1 = 1$, $K_2/K_1 = 0{\cdot}1$ and $f = 0{\cdot}60$, and is given by the solid line in Fig. 3. This formula can have only a limited validity since it predicts zero retention in benzene–iodine mixtures (a = O) so that other processes leading to hot zone retention (for example the replacement of hydrogen atoms by the active iodine atom or by its direct combination with phenyl radicals) must also occur at low iodobenzene concentrations.

The apparent preference of phenyl radicals to form iodobenzene by an iodonium intermediate may be because such intermediates are rapidly formed (within the time taken by the atom to "cool" down) but it is possible that other factors may also be contributory. For example, under the conditions prevailing in the hot zone, where the temperature may be high owing to the incomplete dissipation of the energy from the capture event, the energy obtained from the direct combination of iodine atoms with a phenyl radical may not be easily lost by collisions, so that redissociation may be frequent. Combination with a diphenyl iodonium radical will produce molecules of phenyl iodide which are closer together than their van der Waals' distance of closest approach, so that at least part of the energy of recombination will be lost by imparting kinetic energy to the molecules. The energy of activation for the decomposition of diphenyl iodonium iodide is 26 kcal/g mole(14) so that for reaction (4) to proceed to completion, the heat of recombination of the atom and the radical should be in excess of this.

In this discussion, the possibility of diphenyl iodonium radicals reacting similarly to the phenyl radicals in (2) and (3) has been neglected. Attention has been drawn(5) to the structural similarities between the iodonium radical and diphenyl methyl which is stabilised by about 25 kcal/g mole.(15) The polarographic data of BACHOFNER *et al.*(6) have shown that the formation of the iodonium radical by electron transfer to the ion is reversible, so that at least no immediate decomposition of the radical occurs. Under these circumstances the reactions analagous to (2) and (3), in which phenyl are replaced by iodonium radicals, might have considerably increased activation energies so that their effect may be neglected.

EXPERIMENTAL

All materials were obtained from British Drug Houses Ltd. Iodine, benzene and nitrobenzene were of "Analar" quality and were used without further purification. Iodobenzene was shaken in turn with dilute acid, dilute alkali and water, dried with calcium chloride and allowed to stand for several days after a small quantity of iodine had been admitted; it was then fractionally distilled under reduced pressure, a middle fraction being retained. *P*-iodotoluene was prepared similarly, warm solutions being used for the extraction, and the column of the still being warmed to prevent crystallization. Ethyl and methyl iodides and cyclohexane were allowed to stand over iodine, and were then fractionally distilled. The diphenyl iodonium iodide used in the preliminary experiments was made by the method described by LUCAS, *et al.*(16)

Irradiations were made with a 500 mc Ra–Be source. At temperatures greater than 15°C this was held in a soft glass Dewar vessel onto which the samples for irradiation were clipped; the whole assembly was placed in a thermostat. Under these conditions, irradiations were kept short (30 min) to prevent undue warming of the neutron source.

The retentions were measured and calculated as described elsewhere.(4) When excessive quantities of iodine were present it crystallized out on cooling so that it was necessary to dilute the sample with a known volume of ethyl iodide before extraction; ethyl iodide was chosen since iodine is relatively soluble in it.

No attempt was made to exclude air from the irradiated solutions except in the case of methyl iodide when specimens were frozen in liquid oxygen and sealed off under vacuum. Specimens of methyl iodide containing less than 10^{-5} mf of iodine gave anomalously high

(14) C. J. M. FLETCHER and C. N. HINSHELWOOD, *J. Chem. Soc.* 596 (1935).

(15) G. W. WHELAND, *Resonance in Organic Chemistry*, p. 384. J. Wiley, New York (1955).

(16) H. J. LUCAS, E. R. KENNEDY and C. A. WILMOT, *J. Amer. Chem. Soc.* 58, 157 (1936).

retentions, both at 15°C and 67°C in agreement with the findings of ALIMARIN and SVOBODA;(17) above this concentration the variation of retention with iodine concentration was similar to that found in ethyl iodide and in aliphatic bromides.

The analysis of iodobenzene–iodine mixtures was made by adding 20 g *p*-di-iodobenzene to 25 ml of the extracted iodobenzene. The mixture was then distilled at reduced pressure until all the iodobenzene had been removed. A central fraction of the latter was then purified by slow freezing and used for counting. The residue was assumed to consist of the di-iodobenzene and was dissolved in benzene before counting. The latter assumption was justified by distilling approximately half the residue, and ascertaining that the specific activities of the distilled and undistilled portions were equal. The use of *p*-di-iodobenzene as carrier for *o*-, *m*- and *p*-di-iodobenzene is reasonable because under the conditions used no appreciable separation could be effected by fractional distillation. The results given in Table 1 are the average of two experiments at each iodine concentration.

In view of the difficulty of obtaining reproducible results in the benzene-iodine system,(11) a number of different methods of preparing the starting materials was used. Benzene samples were prepared by distillation, fractional freezing, and were used undried or dried over sodium; iodine was sublimed or used without purification. The retention values obtained were always within those expected from the statistics of counting.

Acknowledgement— The authors express their gratitude to Professor D. H. WILKINSON for his encouragement and for lively interest in this work.

(17) I. P. ALIMARIN and K. F. SVOBODA, *Atomnaya Energiya*, 5. 73 (1958).

J. Inorg. Nucl. Chem., 1962, Vol. 24, pp. 1337 to 1350. Pergamon Press Ltd. Printed in England

EFFECTS OF NEUTRON CAPTURE UPON BENZENE SOLUTIONS OF ORGANIC IODIDES

J. E. C. MACRAE and P. F. D. SHAW
The Clarendon Laboratory, Oxford

(*Received* 13 *February* 1962)

Abstract—An attempt has been made to distinguish between thermal and hot yields of radio-iodine in mixtures of benzene and organic iodides. Mechanisms to explain the general pattern of yields are discussed; the simplest of these involves competitive reactions of phenyl radicals with benzene or the iodides present.

WHEN iodine atoms in organic combination undergo neutron capture a fraction (termed the retention) of the radio-iodine atoms produced is found in organic combination, the remainder being easily extracted by an aqueous reagent. The retention is dependent on the presence of free iodine in the irradiated iodide, and falls extremely rapidly when the iodine concentration (c) is increased from 0 to 0·05 molar fraction; further increase in c still causes a reduction in retention, but the rate at which this decreases is much less. This has been explained by WILLARD and his colleagues(1) who postulated that one of the processes leading to the formation of organically bound radio-iodine was the thermal combination of radicals produced by the capture event with the radio-iodine atoms. If such combination involves the diffusion of the reacting species, small concentrations of iodine can intercept and react with the radicals, so decreasing the chance of their reaction with the active atom. In most cases investigated, the diffusion-controlled reactions have been shown to lead to the formation of the parent compound. For example, LEVEY and WILLARD(2) have shown that the fall in retention when small quantities of iodine are added to methyl iodide is balanced by the reduction in activity of the active methyl iodide present; over the same range of iodine concentration, the activity of other species produced, for example methylene iodide, was unaffected within experimental error.

The part of the retention which is less sensitive to variation of c is assumed to arise from processes in which diffusion plays very little part, such as the recombination of the active atom with a radical without diffusion, or by reactions in which either hydrogen or iodine atoms in the original substance are replaced by the active iodine atom. Empirically it has been found(3) that the retention in this region, which may be termed the hot zone, is approximately proportional to $(1-c)$ in the case of methyl and ethyl iodides, and to $(1-c)^2$ for some aryl iodides. Back-extrapolation of this portion of the curve gives an intercept at $c = 0$, which is assumed to correspond to the total hot-zone retention at very small iodine concentrations.

---

(1) For review see J. E. WILLARD, *Ann. Rev. Nucl. Sci.* 3, 193 (1953); *Ann. Rev. Phys. Chem.* 6, 141 (1955).

(2) G. LEVEY and J. E. WILLARD, *J. Amer. Chem. Soc.* 74, 6161 (1953).

(3) J. E. C. MACRAE and P. F. D. SHAW, *J. Inorg. Nucl. Chem.* 24, 1327, (1962).

Several authors have examined the effects of neutron irradiation upon organic halides dissolved in hydrocarbon or other solvents. Early workers⁽⁴⁾ observed that hydrogen atoms in solvent molecules could be substituted by the active atom. WILLARD and his colleagues⁽⁵⁾ observed increased retentions in aliphatic hydrocarbon solvents, and they were able to ascribe part of this increase to the relative effectiveness of the solvent molecules in caging the products from the neutron capture event. MILLER and DODSON⁽⁶⁾ made a systematic study of carbon tetrachloride dissolved in benzene, and observed that the retention was reduced as the concentration of benzene was increased. Reduced retentions have also been observed by VELJKOVIC⁽⁷⁾ in bromobenzene–benzene mixtures.

The reduction in the retention of iodobenzene dissolved in benzene has been partly explained⁽³⁾ by assuming that phenyl radicals produced by the active atom reacted with the benzene present to form diphenyl and hydrogen atoms. In this way radicals potentially capable of reacting with the active atom to form iodobenzene were removed from the system so that a fall in retention occurred. In support of this, it was shown that elementary iodine dissolved in benzene did not show a sharp fall in retention as its concentration was increased, whereas in cyclohexane–iodine mixtures the expected fall was observed. This indicates that in benzene very few radicals survive to take part in thermal recombination reactions and that the retention observed must therefore correspond to that produced in the hot-zone. A similar, and more striking effect of this sort has been found by MILMAN⁽⁸⁾ in solutions of elementary bromine in benzene, where restrictions imposed by the solubility of the free halogen do not apply, and enable a much greater range of concentrations to be studied. In this case the retention fell linearly with bromine concentration, and was of the form expected if the retention arises entirely in the hot-zone.

The work described in this paper is an extension of that described earlier⁽³⁾ and was undertaken to investigate further the role of benzene when it is used as a solvent for iodides subjected to neutron irradiation.

EXPERIMENTAL

All chemicals were obtained from British Drug Houses Ltd. Analar benzene and iodine were used without purification. Organic iodides were purified by shaking with dilute alkali, drying over calcium chloride to which a small quantity of iodine had been added, and distilling through a column equivalent to four theoretical plates; iodobenzene was distilled under reduced pressure; in all cases a middle 50 per cent fraction was retained for measurement.

Neutron irradiations were made at 15°C with a 500 mc Ra-Be source. Extractions and measurements were made as described earlier.⁽⁹ᵃ⁾ Water was not rigorously excluded from the systems since different methods of drying gave consistent results, and no spurious effects due to the possible formation of phenolic compounds⁽¹⁰⁾ could be detected.

---

(4) See, for example, (a) E. GLUCKAUF and J. W. J. FAY, *J. Chem. Soc.* 390 (1936); (b) A. F. REID, *Phys. Rev.* 69, 530 (1946).

(5) (a) S. GOLDHABER and J. E. WILLARD, *J. Amer. Chem. Soc.* 74, 318 (1952).
(b) S. ADITYA and J. E. WILLARD, *J. Amer. Chem. Soc.* 79, 3367 (1957).

(6) J. M. MILLER and R. W. DODSON, *J. Chem. Phys.* 18, 865 (1950).

(7) S. R. VELJKOVIC, *Bull. Ins. B. Kidrich.* 7, 65 (1957).

(8) M. MILMAN Private communication. (1961)

(9) M. MILMAN and P. F. D. SHAW, (a) *J. Chem. Soc.* 1303 (1957); (b) *J. Chem. Soc.* 1310, 1317 (1957).

(10) M. MILMAN and P. F. D. SHAW, *J. Chem. Soc.* 412 (1956).

A limited number of analyses were made. Owing to the difficulty of separating higher boiling compounds, and to the uncertain nature of some of these, efforts were made to obtain pure fractions of some of the more volatile iodides only. In all cases, methyl, ethyl, methylene iodides and iodobenzene were added as carriers (when necessary) and middle portions of the appropriate fraction obtained by distillation were taken for measurement. In making analyses of benzene–ethyl iodide mixtures it was found difficult to obtain ethyl iodide free from benzene in the available time, which was determined by the half-life of ^{128}I (25 min). In order to obtain the specific activity of ethyl iodide, therefore, a mixture of ethyl iodide and benzene was distilled and counted, and this was subsequently analysed by comparing its density with the densities of a number of standard mixtures.

THE RETENTION CURVES OF IODIDES DISSOLVED IN BENZENE

These are shown in Figs. 1–3; in order to aid their interpretation, retentions of

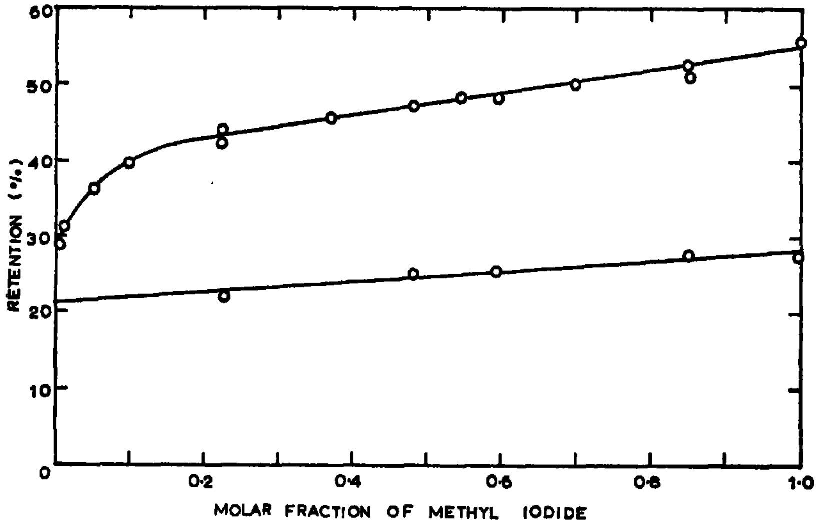

FIG. 1.—The retention of methyl iodide–benzene mixtures as a function of methyl iodide concentration. Upper curve, total retention; lower curve, hot zone retention.

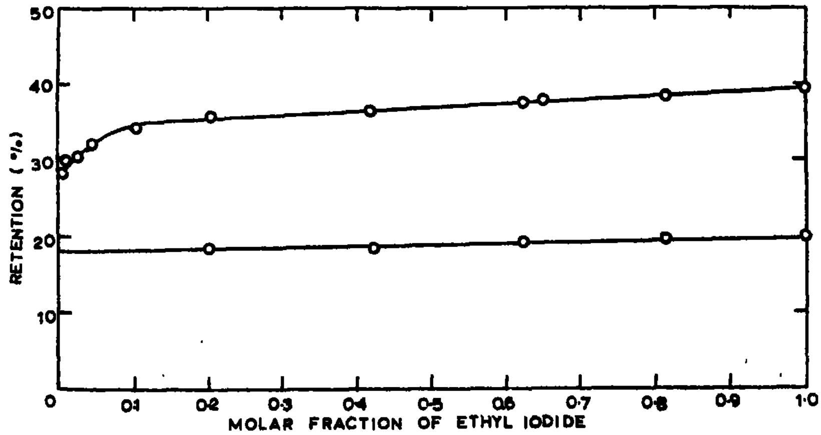

FIG. 2.—The retention of ethyl iodide–benzene mixtures as a function of ethyl iodide concentration. Upper curve, total retention; lower curve, hot zone retention.

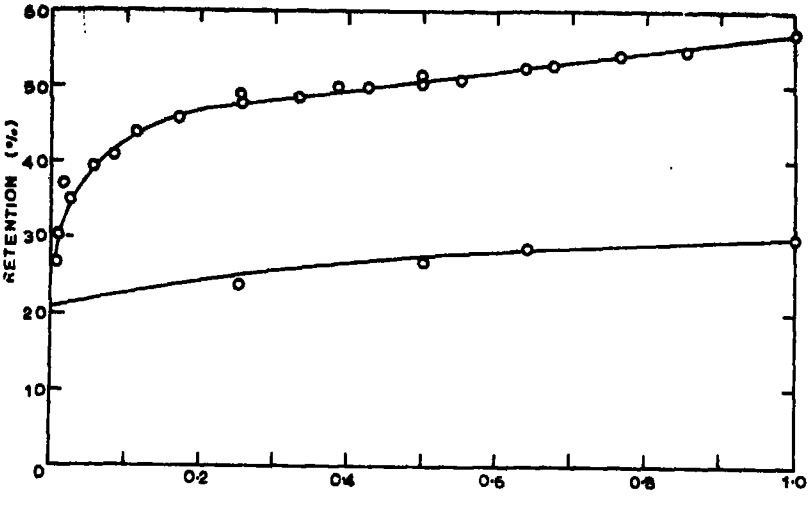

FIG. 3.—The retention of iodobenzene–benzene mixtures as a function of iodobenzene concentration. Upper curve, total retention; lower curve, hot zone retention.

mixtures of both methyl iodide and ethyl iodide in iodobenzene were also determined (Figs. 4 and 5). To reduce the possibility of spurious results arising from small quantities of impurities which might otherwise react with the radio-iodine produced, all samples contained a small constant concentration (10^{-5} mf) of iodine. At such low concentration this does not result in a significant fall in retention, so that the retention obtained can be regarded as arising from both thermal and hot zone processes.

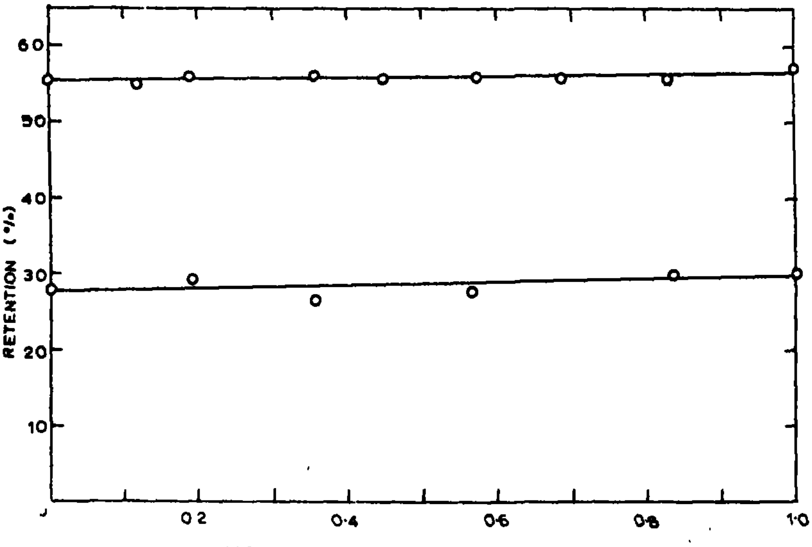

FIG. 4.—The retention of methyl iodide–iodobenzene mixtures as a function of iodobenzene concentration. Upper curve, total retention; lower curve, hot zone retention.

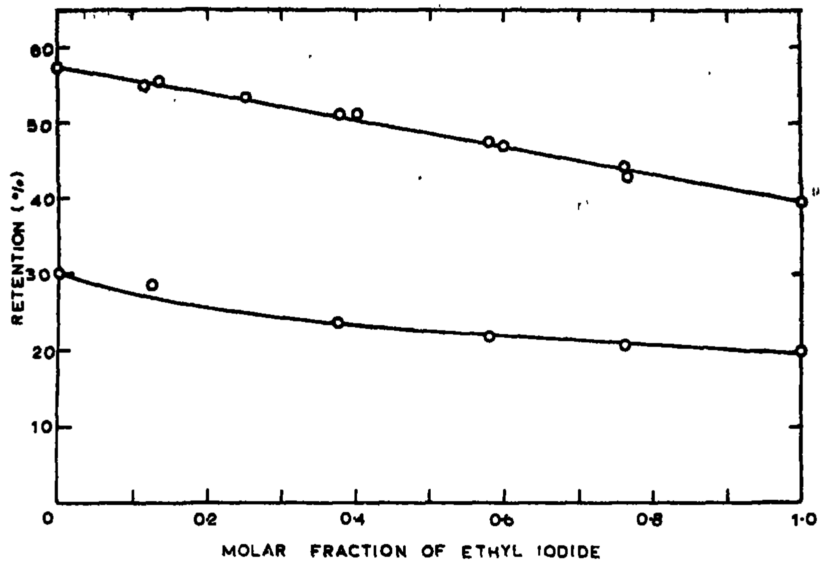

FIG. 5.—The retention of ethyl iodide–iodobenzene mixtures as a function of ethyl iodide concentration. Upper curve, total retention; lower curve, hot zone retention.

For iodide concentrations of less than 10^{-2} mf, the activities obtained were very low, and in this region (Figs. 1–3) the accuracy of the points is poor (approximately ±5 per cent at 10^{-2} mf, and ±2 per cent at 5×10^{-2} mf). This, together with the extremely rapid variation of the retention in this region makes the direct determination of the intercept on the axis of zero iodide concentration uncertain.

To determine whether the factors which are responsible for the general shape of the curves arise in the hot zone or in the thermal region it is necessary to estimate the hot zone retention curves. In principle, this can be done by determining scavenger curves (the retention as a function of iodine concentration) for different mixtures of the components, and by then using a simple back-extrapolation of the curves obtained at higher iodine concentration to determine the intercept on the axis of ($c = 0$). However this is difficult since the limiting solubility of iodine in the systems studied precludes the determination of a proper scavenger curve; the enhancement of iodine solubility by increase of temperature cannot be used, since marked temperature effects occur when the benzene concentration is high.(3) In view of these difficulties, hot zone retentions have been estimated by using a semi-empirical method.

The scavenger curves determined at 67°C(3) for ethyl and methyl iodides were found to agree, within experimental error, with points determined at 15°C, so that the hot zone retentions for pure iodides at 15°C may be taken from these curves. If the retentions obtained for different iodine concentrations are normalized by dividing by the retention obtained at $c = 10^{-5}$ mf, a curve which fits the results for both methyl and ethyl iodides is obtained (Fig. 6); (it is of passing interest that this curve also represents the results found for several aliphatic bromides studied earlier(9)). If it is assumed that the form of the scavenger curve for benzene-iodide mixtures is the same as that given by Fig. 6, it is possible to estimate the hot zone retention (R_H) at $c = 10^{-5}$ mf from the figure, since R_H will bear the same relation to the total retention as the intercept, at $c = 0$, obtained by back-extrapolating the linear portion

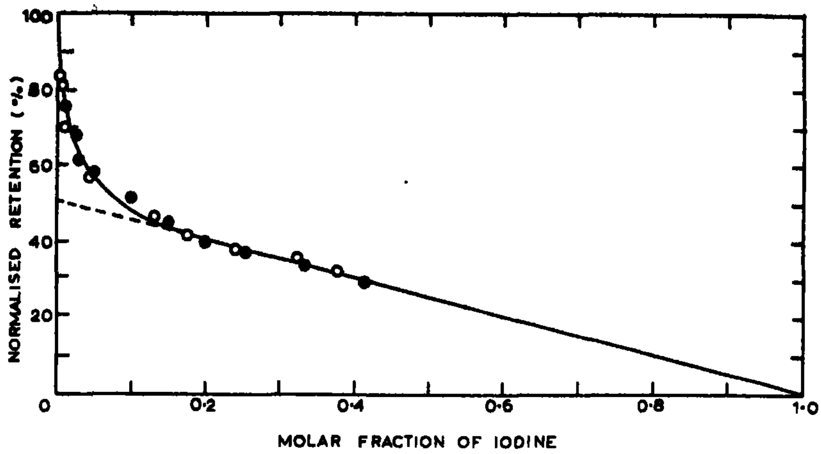

FIG. 6.—The normalized retention ($R_{c=c}/R_{c=0}$) plotted against the molar fraction of iodine (c), for ethyl (○) and methyl (●) iodides.

of the normalized curve. Some justification of this procedure, which is clearly not applicable for small concentrations of iodide in benzene, is given in Table 1. It can be seen that the ratio of the retentions R_1 and R_2 found respectively at low (10^{-5} mf) and high iodine concentrations bear a close relationship to the corresponding ratio found from Fig. 6. In particular the series of results taken to justify the method for methyl iodide (0·595 mf) in benzene give reasonable agreement with those determined

TABLE 1.

Mixture				Retention (R_1) at $C = 10^{-5}$ mf (%)	Iodine concentration C_2 (Molar fraction)	Retention (R_2) at $C = C_2$ (%)	R_2/R_1		Hot-zone retention R_H (%)†
Substance	Molar fraction	Substance	Molar fraction				Observed	Calculated	
MeI	0·228	PhH	0·772	44·0	$3{\cdot}2 \times 10^{-2}$	27·7	0·63	0·63	22·0
	0·483		0·517	47·1	0·111	24·6	0·52	0·49	25·0
	0·595		0·405	48·3	0·121	23·4	0·48	0·47	
					0·114	25·1	0·52	0·49	
					0·091	25·3	0·52	0·51	25·2
					0·057	27·9	0·58	0·56	
					0·025	31·3	0·65	0·65	
	0·851		0·149	51·5	0·132	26·5	0·51	0·47	28·0
	1·0		0	55·1	—	—	—	—	27·4
EtI	0·201		0·799	35·5	0·018	25·8	0·71	0·69	18·2
	0·421		0·579	36·2	0·123	17·4	0·48	0·47	18·5
	0·621		0·379	37·5	0·130	17·8	0·47	0·46	19·3
	0·816		0·184	38·2	0·206	15·7	0·41	0·40	19·6
	1·0		0	39·5	—	—	—	—	20·0

† Calculated from Fig. 6.

from Fig. 6. It can be seen from this figure that the ratio of the hot zone to the total retention is 0·5, and the values of R_H, corrected for possible departures from the "ideal" form, have been taken to be $0{\cdot}5\ R_1(R_2/R_1)_{\text{obs.}} \times (R_1/R_2)_{\text{calc.}}$ The values obtained are plotted in Figs. 1 and 2, and extrapolate reasonably to an intercept of about 20 per cent at zero iodide concentration.

To estimate the hot zone retentions in benzene-iodobenzene mixtures, a number of retentions were determined with large quantities of iodine present, and these are given in Table 2. As shown previously⁽³⁾ the scavenger curves in such systems are not linear at high iodine concentrations, but proportional to $(1-c)^2$. To provide an indication of the hot zone retention, values of R_H have been calculated assuming a scavenger curve of the form given in Fig. 6 (Table 2, column I), and also that of the form found for pure iodobenzene (column II) by using a similar procedure. Column III gives values of R_H calculated from the formula found previously;⁽³⁾ this formula, based on the ability of phenyl radicals to form iodonium radicals or to react with benzene to give diphenyl is of doubtful validity in the present circumstances since it is based on the competitive reactions occurring at 67°C, and also because it does not hold for low concentrations of iodobenzene. It can be seen that the values of R_H found by these methods do not vary greatly, and the mean values of columns II and III have been adopted and plotted in Fig. 3.

TABLE 2.

Mixture		Retention (R_1) at $C=10^{-5}$ mf (%)	Iodine concentration (C_2) (mf.)	Retention (R_2) at $C=C_2$ (%)		I		II		III
PhI (mf)	PhH (mf)				R_2/R_1 (obs.)	R_2/R_1 (calc.)	R_H (calc.)	R_2/R_1 (calc.)	R_H (calc.)	R_H (calc.)
0·254	0·746	48·2	0·058	27·2	0·56	0·55	24·5	0·57	24·7	23·0
0·500	0·500	51·3	0·072	27·3	0·53	0·53	25·6	0·52	26·3	27·3
0·640	0·360	52·6	0·091	27·5	0·52	0·51	26·7	0·49	29·2	28·3
1·0	0	57·2	—	—	—	—	—	—	30·0	30·0

The hot zone retentions of iodobenzene mixed with methyl or ethyl iodides are more easily determined since the solubility of iodine in these systems is much greater. The retentions obtained for mixtures containing varying amounts of iodine are given in Table 3. *A priori*, it would be expected that the scavenger curves would tend to follow the form found for iodobenzene when this is present in large concentrations, and that for aliphatic iodides when the predominant constituent is either methyl or ethyl iodide. Table 3 shows that the values of R_2/R_1 observed are in general closer to those calculated on the basis of the aliphatic scavenger curve (column I) than those found using the form of curve for iodobenzene (column II). The values of R_H calculated also fall more readily onto a smooth curve when the values from column I are adopted, and these have been plotted in Figs. 4 and 5. A possible reason for the tendency of these systems to exhibit an "aliphatic" form of scavenger curve will be discussed later.

TABLE 3

Mixture				Retention (R_1) at $C=10^{-5}$ mf (%)	Iodine concentration C_2 mf	Retention (R_2) at $C=C_2$ (%)		I		II	
Substance	mf	Substance	mf				R_2/R_1 (obs.)	R_2/R_1 (calc.)	R_H (calc.)	R_2/R_1 (calc.)	R_H (calc.)
MeI	0	PhI	1	57·2	—	—	—	—	—	—	30·0
	0·167		0·833	55·6	0·142	26·8	0·48	0·45	29·8	0·41	35·0
	0·435		0·565	56·0	0·187	22·8	0·41	0·41	27·5	0·36	34·4
	0·645		0·355	56·2	0·114	25·6	0·46	0·48	26·5	0·46	30·1
	0·807		0·193	56·0	0·156	25·7	0·46	0·43	29·4	0·39	34·3
	1·0		0	56·0	—	—	—	—	28·0	—	—
EtI	0	PhI	1	57·2	—	—	—	—	—	—	30.0
	0·134		0·866	55·1	0·143	25·4	0·46	0·45	28·2	0·41	32·4
	0·378		0·622	50·7	0·201	18·6	0·37	0·40	23·4	0·34	31·4
	0·579		0·421	47·4	0·223	16·5	0·35	0·38	21·8	0·32	27·2
	0·764		0·236	44·1	0·146	18·2	0·41	0·44	20·6	0·41	23·1
	1		0	39·5	—	—	—	—	20·0	—	—

The hot zone retentions shown in Figs. 1–3 show rather less variation than the curves for the total retention, so indicating that the shapes of the latter may be largely dependent upon processes occurring in the thermal region. For mixtures of methyl or ethyl iodides in benzene, the hot zone retentions show a roughly linear dependence upon the molar fraction of the iodide. Extrapolation to the axis of the unit molar fraction of benzene gives intercepts of 21 and 18·2 per cent for methyl and ethyl iodides respectively which agree roughly with the retention found for solutions of iodine in benzene.(3) The latter system was found to exhibit no self-scavenging effect and it was assumed that the observed retentions arose entirely from reactions occurring in the hot zone, so that the present findings appear to confirm this view.

TABLE 4.

Substance	Retention (%)	Parent compound (%)	Other compounds produced (%)
Iodobenzene(3)	57·2	46·0	11·2 ($C_6H_4I_2$)
Methyl iodide(2, 11)	56·2	47·1	9·1 (CH_2I_2)
Ethyl iodide(2)	40·2	33·5	3·3 (CH_3I) 2·9 (Higher boiling)

In benzene–iodobenzene mixtures the calculated hot zone retentions are not a linear function of the molar fraction of iodobenzene and in Fig. 3 the curve has been drawn to give an intercept of 21 per cent at unit molar fraction of benzene.

---

(11) T. Brustad and J. Baarli, *J. Chem. Phys.* **22**, 1311 (1954).

REACTIONS IN THE THERMAL ZONE

For a mixture of two iodides it seems reasonable to assume that the retention might be represented by an expression of the form

$$R = m_1R_1+m_2R_2$$

where R_1 and R_2 are the retentions of the pure iodides and m_1 and m_2 are their respective molar fractions. Retentions of this linear form are shown by mixtures of iodobenzene both with methyl and with ethyl iodides. If there were no interaction between the radicals produced from iodide (I) with iodide (II) or vice versa, the yields of the parent compounds should be m_1P_1 and m_2P_2, where P_1 and P_2 are the yields obtained in the pure iodides. Table 5 summarizes the known data obtained from analyses of the pure iodides used; for each substance the predominant product of the thermal reactions leading to retention is the parent compound. Results of analyses of the mixed iodides are given in Table 6, and show that the above simple view does not hold in these systems. For example, for the mixture of methyl iodide (0·167 mf) and iodobenzene (0·833 mf) the yield of methyl iodide expected should be 0·167×47·1 per cent or 7·87 per cent, whereas the yield observed is 14·9 per cent, the greater part of which is produced thermally, since the yield is reduced to 5·6 per cent by the presence of 0·142 mf iodine. Similarly the observed yield of methyl iodide (43·1 per cent) exceeds that expected (38·1 per cent) in the mixture containing 0·807 mf methyl iodide.

TABLE 5.

Mixture				Iodine concentration (mf)	Retention (%)	Retention difference	† Aliphatic iodide (%)	Difference in aliphatic iodide yields
Substance	mf	Substance	mf					
MeI	0·167	PhI	0·833	10⁻⁵	55·6	28·8	14·9	9·3
				0·142	26·8		5·6	
	0·807		0·193	10⁻⁵	56·0	30·3	43·1	27·6
				0·156	25·7		15·5	
EtI	0·134	PhI	0·866	10⁻⁵	55·1	29·7	13·2	8·8
				0·143	25·4		4·40	
	0·764		0·236	10⁻⁵	44·1	25·9	32·7	19·6
				0·146	18·2		13·1	

† i.e., methyl iodide in methyl iodide-iodobenzene mixtures, and ethyl iodide in ethyl iodide-iodobenzene mixtures.

TABLE 6.

Mixture								
Sub-stance	mf	Sub-stance	mf	Iodine concentration (mf)	Retention (%)	Retention difference	Aliphatic iodide (%)	Difference in aliphatic iodide yields
MeI	0·228	PhH	0·772	10^{-5}	44·0		30·1	
						16·3		17·0
				0·032	27·7		13·1	
	0·851		0·149	10^{-5}	51·5		39·9	
						25·0		23·5
				0·132	26·5		16·4	
EtI	0·201	PhH	0·799	10^{-5}	35·5		25·7	
						9·7		9·7
				0·018	25·8		16·0	
	0·816		0·814	10^{-5}	38·2		34·8	
						22·5		21·7
				0·206	15·7		13·1	

If the chief processes responsible for the thermal retention of the active iodine atom are:

$$R. + I^* \rightarrow RI^*, \tag{1}$$

$$\text{or } R. + II^* \rightarrow RI^* + I, \tag{2}$$

where R. is the radical formed by dissociation of the parent iodide, the predominant formation of methyl iodide in methyl iodide–iodobenzene mixtures indicates that more methyl, relative to phenyl, radicals are produced in the hot zone. In this system, both the total and the hot zone retentions, and therefore those arising from the thermal region, are approximately constant; this suggests that the total number of radicals available for reaction in the thermal zone is also constant. If these radicals are produced chiefly by collision of an energetic iodine atom, produced by recoil following neutron capture, with the surrounding molecules, it seems improbable that there would be much differentiation between the dissociation of methyl iodide or iodobenzene molecules, since the initial energy of the radio-iodine atom will be greatly in excess of the dissociation energies of the C-I bonds in these molecules. Under these circumstances the relative number of phenyl and methyl radicals produced by the primary event should be in proportion to the amounts of iodobenzene and methyl iodide in the irradiated mixture; to account for the constancy of the number of radicals available for reaction in the thermal zone, and for the preponderance of methyl radicals it is necessary to assume that the reaction

$$Ph. + MeI \rightarrow PhI + Me. \tag{3}$$

occurs in this system, presumably in the hot zone. Reaction (3) is exothermic, and might well proceed by a mechanism involving an iodonium intermediate; in this case a relatively small activation might be required. As an alternative to reaction (3), phenyl radicals could form diphenyl iodonium radicals by addition to iodobenzene:

$$Ph. + PhI \rightarrow Ph_2I. \tag{4}$$

and so be preserved to enable them to undergo subsequent reaction with the active iodine atom in the thermal region.

The same reasoning applied to the ethyl iodide–iodobenzene system, where there is a similar enhancement in the yield of ethyl iodide, indicates that the reaction

$$\mathrm{Ph.+EtI \rightarrow PhI+Et.} \tag{5}$$

might occur in this region. In these mixtures the secondary reactions postulated tend to convert phenyl radicals into methyl or ethyl radicals, so that it is not surprising that these systems tend to exhibit an "aliphatic" rather than an "aromatic" form of scavenger curve.

In the case of iodobenzene–benzene mixtures, the phenyl radicals produced by the capture event can react to form diphenyl iodonium radicals by (4) or undergo the reaction

$$\mathrm{Ph.+PhH \rightarrow Ph_2+H.} \qquad (6$$

The latter has been well studied in other systems,(12) and has been previously postulated to account for the form of the scavenger curve in this system, and in iodine–benzene solutions.(3) If any phenyl radicals produced in the hot zone reacted by (4) or (6) before the onset of the recombination reactions occurring in the thermal region, a fall of retention would be expected as the concentration of benzene was increased, since (6) effectively causes phenyl radicals to be replaced by hydrogen atoms, so that there will be an enhanced yield of hydrogen iodide resulting from the thermal combination of the active atom with the radicals and atoms available. To account for the shape of the retention curve (Fig. 3) it is necessary to assume that the rate constant for (6) is less than that for (4), so that effect of (6) can only be seen at large ($>0{\cdot}8$ mf) concentrations of benzene, where the retention begins to fall off sharply.

An alternative explanation of the fall in retention with increasing benzene concentration is that phenyl radicals can only be produced in this system by the dissociation of iodobenzene so that as the concentration of the latter falls, there will be fewer phenyl radicals available for reaction in the thermal region. This could also account for the independence of the retention on iodine concentration in iodine–benzene mixtures since there could be no self-scavenging effect if no dissociation of benzene molecules occurred; the observed retention could then be the result of reactions in which the activated iodine atom displaced a hydrogen atom in a single step.

Such an explanation does not appear to be tenable for the following reasons:

(i) iodine atoms activated by neutron capture are capable of causing the dissociation of carbon–hydrogen bonds, as shown by the self-scavenging curves observed in cyclohexane,(3) and it seems probable that similar dissociation of benzene molecules can occur;

(ii) it does not account for the strong temperature dependence of the retention in benzene–iodine solutions;

(iii) it does not account for the shape of the iodobenzene–benzene retention curve. At iodobenzene concentrations in excess of 0·2 mf, the retention increases from about 50–56 per cent as the iodobenzene concentration increases from 0·3–1·0 mf and the thermal retention is approximately constant. Using a simple model for the recombination processes taking place when the reactants, initially held in a small spherical volume, diffuse outwards, it has been shown(13) that the thermal retention is a function of the number of radicals per unit "track length" of the recoil atom.

(12) For review, see D. R. Augood and G. H. Williams, *Chem. Rev.* 57, 123 (1957).

(13) M. Milman and P. F. D. Shaw, *J. Chem. Soc.* 1325 (1957).

The approximate constancy of the retention in this region therefore indicates that this quantity is also approximately constant so that at least some of the radicals available for reaction in the thermal region are produced by the dissociation of benzene molecules.

In the following discussion such dissociation will be assumed; by making this assumption it is possible to account for all the main features of the methyl iodide-benzene and ethyl iodide-benzene systems, but the possibility of molecular ions or activated benzene molecules playing a part analagous to that postulated for the phenyl radicals cannot be excluded. Results of the analyses for these systems are given in Table 6. Comparison of the retentions for a given mixture containing different iodine concentrations shows that in all cases studied, the fall in retention is equal, within experimental error, to the reduction in activity of the aliphatic iodide fraction. The parent iodide is therefore the sole product of the thermal reactions which lead to retention, and the amount of iodobenzene resulting from such reactions is very small.

If phenyl radicals are produced in the hot zone they must therefore have disappeared from the system by the time the thermal processes occur, presumably by reacting according to (3) or (5). The methyl or ethyl radicals so produced are then able to react thermally to maintain the relatively large yields of active methyl or ethyl iodides, even when the actual quantity of these substances is relatively small (0·2 mf). At still smaller concentrations, the fall in retention can again be explained by assuming that reaction (6) is effective in competing with (3) or (5) so that the ratio of organic radicals to (inorganic) atoms available for reaction in the thermal region is reduced.

Comparison of the results given in Tables 4 and 6 shows that whereas the thermal retention in mixtures of ethyl or methyl iodides in iodobenzene is made up partly of the parent aliphatic iodide and partly of iodobenzene, in mixtures of the same aliphatic iodides in benzene it is made up almost entirely of the parent iodide. That is, the chance of a phenyl radical surviving for sufficient time to take part in the thermal reactions is dependent on the presence of iodobenzene, and, presumably, on its ability to form an iodonium radical under these circumstances. This conclusion strongly supports the assumption previously made to account for the shape of the scavenger curve in iodobenzene,(3) and provides further evidence that the phenyl radicals produced by the primary event must react by (3)–(6) before the start of the thermal recombination reactions.

In this discussion the rôle of ion–molecule reactions, or the possibility of radical production by ionic mechanisms, has been neglected. Lack of data about the electron affinities of the different molecules considered makes it difficult to discuss adequately the part played by negative ions, but it can be shown that no explanation based solely upon positive ion interactions can give a complete account of the data observed.

If the active iodine atom produced by neutron capture is left with a positive charge,(14) it seems improbable that this could be retained for long in the systems studied, since the first ionization potential of an iodine atom (10·44 eV) is greater than that of any of the liquid components considered; under these circumstances, electron transfer to the iodine ion might be expected, so that any explanation of the effects observed must relate to the formation of the radicals found in the thermal region. In the methyl iodide–iodobenzene system a preponderance of positively charged iodobenzene molecules is to be expected since the ionization potential of methyl iodide (9·67 eV)(15) is greater than that of iodobenzene (9·10 eV);(15) subsequent neutralization of the latter by a free electron or by collision with a negative ion might cause its dissociation and so lead to the production of phenyl radicals in this system. However, it does not seem possible to account for the observed enhanced yield of methyl iodide by an ionic mechanism. Similar arguments apply to the methyl iodide–benzene system where the ionization potentials (9·67 eV and 9·52 eV respectively)(15) again favour the formation of positively charged benzene ions. Although the formation of phenyl radicals might arise from ionic reactions, therefore, there seems to be no ready explanation for the enhanced yield of aliphatic products from the thermal region without invoking reactions of the type postulated.

---

(14) S. WEXLER and T. H. DAVIES, *J. Chem. Phys.* **20**, 1688 (1952).

The data obtained cannot exclude the possibility of activated benzene molecules playing an important rôle in the processes following neutron capture. If such molecules were produced, collision with, for example, methyl iodide molecules might lead to their dissociation, so accounting for the predominant yield of methyl iodide. The fall in retention with decreasing methyl iodide concentration could then be partly explained by an overall decrease in the number of radicals available for reaction with the active iodine atom. However, this explanation cannot account for the observed temperature dependence of the retention of solutions of iodine in benzene, and it therefore seems probable that, if operative, such mechanisms must also be accompanied by others which involve the dissociation of benzene molecules.

REACTIONS IN THE HOT ZONE

The term "hot zone retention" has been used in this paper to describe that part of the retention which is insensitive to small variation of scavenger concentration, and has been used to contrast such behaviour with that of the diffusion-controlled retention which shows a strong dependence upon scavenger concentration. To some extent this appears to be a misnomer; the lack of evidence in iodobenzene(3) for a thermal exchange which is known to occur at high temperatures(16) indicates that the local heating effects which presumably accompany neutron capture have no important bearing upon the final retention. The marked dependence of the retention of iodine–benzene solutions upon relatively small changes of temperature(3) again indicates that reactions occurring at a relatively low temperature influence the "hot zone" retention.

The yields of aliphatic iodide obtained from solutions of methyl or ethyl iodide dissolved in benzene or iodobenzene do not show a linear dependence upon the concentration of iodide and exhibit a similar non-linearity even when the system contains relatively large quantities of iodine. This implies that the reactions postulated to account for the distribution of activity resulting from thermal reactions must also be effective in the hot zone. In particular, it does not seem possible to account for the retention in this zone entirely on the basis of reactions in which the active iodine atom replaces other atoms either by a billiard-ball mechanism or by the epithermal reactions postulated by LIBBY.(17) The retention of solutions of iodine in benzene might arise partly from such reactions, but its strong temperature dependence implies that phenyl radicals, or possibly some complex of a phenyl radical and a benzene molecule (c.f. JAQUISS and SWARC)(18) are involved.

(15) J. D. MORRISON and J. C. NICHOLSON, *J. Chem. Phys.* **20**, 1021 (1952).

(16) S. LEVINE and R. M. NOYES, *J. Amer. Chem. Soc.* **80**, 2401, (1958).

(17) W. F. LIBBY, *J. Amer. Chem. Soc.* **69**, 2523 (1947).

(18) M. T. JAQUISS and M. SWARC, *Nature, Lond.* **170**, 312 (1952).

To reconcile this essentially free-radical picture of the processes occurring in the hot zone with the weak dependence upon iodine concentration it is necessary to assume that the active iodine must often be de-energized in the vicinity of a radical, so that combination occurs before the radical can be intercepted by the scavenger molecules.

In summary, it seems possible to account for the retentions observed in dilute benzene solutions by the following sequence. The activated iodine atom causes the dissociation of some of the surrounding benzene molecules, and in some instances may undergo a replacement reaction to form iodobenzene. The phenyl radicals produced may either react with benzene to form diphenyl molecules and hydrogen atoms, or otherwise react with other molecules of the iodide to form alkyl radicals, or, in the case of iodobenzene, diphenyl iodonium radicals. If the active iodine atom has not undergone a replacement reaction, it may then combine with one of the radicals present to contribute to the total retention. Such combination may, or may not, involve diffusion, so contributing respectively to the "thermal" or the "hot" retention.

Experiments are being performed in order to determine the degree to which non-dissociation of the parent iodide contributes to the retention, and to estimate the mean number of radicals produced in such systems.

Acknowledgements—The authors express their gratitude to Professors B. BLEANEY and D. H. WILKINSON for their encouragement and for the facilities which they have provided.

J. Inorg. Nucl. Chem., 1962, Vol. 24, pp. 1351 to 1353. Pergamon Press Ltd. Printed in England

DIOXANE ADDITION COMPOUNDS OF HYDRATED YTTRIUM, LANTHANUM AND RARE EARTH PERCHLORATES

G. Vicentini, J. V. Valarelli, M. Perrier and E. Giesbrecht

Departmento de Química e Departmento de Mineralogia da Faculdade de Filosofia, Ciencias e Letras da Universidade de São Paulo, Brazil

(*Received* 5 *February* 1962; *in revised form* 3 *April* 1962)

In a previous communication⁽¹⁾ the preparation of addition compounds between dioxane and yttrium, lanthanum, cerium, praseodymium, neodymium, samarium, europium, gadolinium and erbium hydrated perchlorates were reported. It was observed that the thullium, dysprosium, holmium, terbium, ytterbium and lutetium hydrated perchlorates react with dioxane in the same way as the others, forming compounds with the general formula $M(ClO_4)_3{\cdot}9H_2O{\cdot}4C_4H_8O_2$. This note describes the preparation of these compounds together with infra-red data and some isomourphous relations observed by X-ray powder patterns.

Infra-red spectra. The spectra of the yttrium, lanthanum and rare earth complex perchlorates where determined in the infra-red region. In all cases, the dioxane spectrum was observed without essential modification. The peaks at 875 and 1122 cm^{-1}⁽²⁾ appeared in the infra-red spectra of all substances. According to results obtained with similar substances described in previous papers⁽³, ⁴⁾ the binding with dioxane must be relatively weak.

X-ray powder patterns. The X-ray powder procedure showed two series of isomorphous substances:

(a) The first one includes the corresponding yttrium, lanthanum, cerium, praseodymium, neodymium, samarium, europium, gadolinium, terbium and dysprosium compounds.

(b) The second one includes the corresponding holmium, thullium, erbium, ytterbium and lutetium compounds.

The X-ray diffraction data will be published elsewhere.

EXPERIMENTAL

a. *Dioxane addition compounds.* They were prepared by heating on a water bath the corresponding oxides (Tb_4O_7, Dy_2O_3, Ho_2O_3, Tm_2O_3, Yb_2O_3 and Lu_2O_3, reagent grade, Johnson, Matthey E. Co., London) with the appropriate amount of 70 per cent perchloric acid and a few drops of perhydrol added. The solutions were evaporated to near dryness, the residues ground with excess dioxane and the resulting crystals recrystallized from hot dioxane. All compounds were stored in a vacuum desiccator over calcium chloride.

---

(1) G. Vicentini, M. Perrier and E. Giesbrecht, *Ber. Dtsch. Chem. Ges.* **94**, 1153 (1961).

(2) S. C. Burket and R. M. Badger, *J. Amer. Chem. Soc.* **72**, 4397 (1950).

(3) M. Perrier, E. Giesbrecht, W. G. R. de Camargo and G. Vicentini, *Ber. Dtsch. Chem. Ges.* **95**, 257 (1962).

(4) E. Giesbrecht, W. G. R. de Camargo, G. Vicentini and M. Perrier, *J. Inorg. Nucl. Chem.* **24**, 381 (1962).

TABLE 1.—SUMMARY OF ANALYTICAL RESULTS

Compound	Aspect	Formula weight	Analysis					
			Metal		Perchlorate		Water	
			Theor. (%)	Exp. (%)	Theor. (%)	Exp. (%)	Theor. (%)	Exp. (%)
$Tb(ClO_4)_3 \cdot 9H_2O \cdot 4C_4H_8O_2$	Colourless plates	972·1	16·37	16·34	30·69	30·73	16·67	16·91
$Dy(ClO)_4)_3 \cdot 9H_2O \cdot 4C_4H_8O_2$	,, ,,	975·4	16·65	16·42	30·58	30·71	16·62	16·06
$Ho(ClO_4)_3 \cdot 9H_2O \cdot 4C_4H_8O_2$	*	977·9	16·86	16·56	30·51	30·47	16·58	16·26
$Tm(ClO_4)_3 \cdot 9H_2O \cdot 4C_4H_8O_2$	Colourless needles	982·3	17·24	17·27	30·37	30·55	16·50	16·14
$Yb(ClO_4)_3 \cdot 9H_2O \cdot 4C_4H_8O_2$	,, ,,	986·0	17·54	17·27	30·26	30·41	16·44	16·05
$Lu(ClO_4)_3 \cdot 9H_2O \cdot 4C_4H_8O_2$	,, ,,	987·9	17·71	17·68	30·20	30·37	16·41	16·41

* The compound is colourless, with a slight pink or yellow hue.

b. *Analytical data.* The rare earths were determined by the usual oxalate method. Water and perchlorate were determined by methods described in a previous paper.⁽⁵⁾ The analytical results are summarized in Table 1.

c. *Solubilities.* All compounds are very soluble in water, methanol, ethanol, acetone and ethylacetate. They are practically insoluble in chloroform carbon tetrachloride and benzene. All compounds are moderately soluble in hot dioxane and could be recrystallized from this solvent.

d. *Infra-red spectra.* The infra-red spectra were obtained with a Perkin-Elmer Model 137 Double Beam Recording Spectrophotometer, using Nujol suspensions between rock salt plates.

e. *X-ray diffraction patterns.* They were obtained with a NORELCO unit, Buerger powder camera (114·6 mm).

All samples were sealed in 0·5 mm Lindemann glass capillartubes and exposed to Cu-$K\alpha$ radiation (λ = 1·5148 Å) at room temperature, during 18–24 hr.

Acknowledgements—The authors wish to thank the Rockefeller Foundation and Conselho Nacional de Pesquisas (Rio de Janeiro) for financial support.

(5) G. Vicentini, M. Perrier, W. G. R. de Camargo and J. M. V. Coutinho, *Ber. Dtsch. Chem. Ges.* **94**, 1063 (1961).

J. Inorg. Nucl. Chem., 1962, Vol. 24, pp. 1355 to 1363. Pergamon Press Ltd. Printed in England

THE RACEMIZATION OF COMPLEX IONS ON ACTIVATED CARBON—I

THE RACEMIZATION OF POTASSIUM D-ETHYLENEDIAMINETETRA-ACETATOCOBALTATE(III)*

W. C. ERDMAN and B. E. DOUGLAS
Department of Chemistry, University of Pittsburgh, Pittsburgh, Pa

(*Received* 22 *March* 1962)

Abstract—Activated sugar carbon accelerates the racemization of K[Co(EDTA)] without appreciable decomposition of the complex. The rate of racemization using equal weights of complex and carbon was found to follow essentially second order kinetics, first order in complex and first order in carbon. The activation energy of the racemization process was found to be 7·3 kcal/mole. Wood carbon of greater activity gave a pseudo first order reaction.

ACTIVATED carbon is often used as a catalyst in the preparation of cobalt(III) complexes by oxidation of the corresponding cobalt(II) complex using oxygen (in air) as the oxidizing agent. It has been used to help establish equilibrium for determinations of stability constants of cobalt(III) complexes. It has been shown that the rate of racemization of D-tris(ethylenediamine)cobalt(III) ion is greatly accelerated in the presence of activated carbon.(1)

The racemization of tris(ethylenediamine)cobalt(III) ion on carbon has been studied in some detail and other catalysts have been investigated.(2, 3) The racemization of potassium D-ethylenediaminetetra-acetatocobaltate(III) will be discussed first because this was the first case for which a kinetic treatment was worked out. The initial results with D-$[Co(en)_3]^{3+}$ and activated carbon(1) did not follow simple kinetics.

Initial studies of the racemization of K[Co(EDTA)] were made with wood carbon as used for the studies of the racemization of $[Co(en)_3]Cl_3$. However, wood carbon caused the racemization of K[Co(EDTA)] to proceed too rapidly for convenient study under varied conditions. The absorption spectra taken of samples immediately after treatment with wood carbon gave evidence of some concentration loss. The activity of sugar carbon was found to be only about $\frac{1}{5}$ to $\frac{1}{10}$ that of an equal weight of wood carbon. The sugar carbon brought about the racemization of K[Co(EDTA)] at a convenient rate over the temperature range 0–50°C. Its activity was more easily reproducible than that of wood carbon. Since the concentration loss of the complex due to adsorption or reaction on the surface of the active sugar carbon was less than 2 per cent, it was possible to treat the concentration of the complex as constant throughout a run.

---

* This work was supported by grants from the Research Corporation and the U.S. Public Health Service, National Institute of Arthritis and Metabolic Diseases (Grant A-2219). Taken from a thesis submitted to the University of Pittsburgh in partial fulfilment of the requirements for the Ph.D. by W. C. ERDMAN, 1959.

(1) B. E. DOUGLAS, *J. Amer. Chem. Soc.* **76**, 1020 (1954).

(2) W. C. ERDMAN, H. E. SWIFT and B. E. DOUGLAS. *J. Inorg. Nucl. Chem.* **24**, 1365 (1962)

(3) W. C. FERNELIUS and D. SEN, *J. Inorg. Nucl. Chem.* **10**, 269 (1959).

The decreased activity of the sugar carbon was believed to be only partly due to the difference in particle size (200 mesh for wood carbon samples vs. 100 mesh for sugar carbon samples). No attempt was made to determine surface areas of the carbon samples. The accessible internal surface area depends on the size of the adsorbed particle. The surface area determined for some gaseous molecule might not give a reliable estimate of the surface area available for the complex ions. Although it seems certain that the surface area of the wood carbon is considerably greater than that of sugar carbon, it is possible that there are also more active sites per unit surface area of the wood carbon.*

EXPERIMENTAL

Optical rotations were measured with a Rudolph Model 70 Precision Polarimeter using sodium and mercury light sources with appropriate filters. The instrument was fitted with a photoelectric attachment built in this laboratory. Cary Model and Beckman DU spectrophotometers were used for measurements of optical absorption spectra.

The preparation of $K[Co(EDTA)]\cdot 2H_2O$ was accomplished according to the method of DWYER *et al.*(4) The complex was resolved according to DWYER's method.(5) The active complex had a specific rotation of +1000° at 5461 Å as reported by DWYER.

Active wood carbon was prepared directly from Baker and Adamson decolourizing wood carbon by heating 15–20 g of carbon in a porcelain container for one hour at 800°C. The ash layer was removed with a ¼ in. rubber tube connected to an aspirator. The tube was brought close to the surface of the carbon, causing the ash to be pulled away. This procedure avoids mixing the ash with the bulk of the carbon below it. The carbon was stored in a desiccator until ready for use. Sugar carbon was prepared by burning cane sugar. One thousand grammes of sugar was ignited in a porcelain container. The ignition and burning were speeded by heating the container with a Fisher burner from above during the early part of burning. The sugar was added slowly to avoid excessive foaming. The carbonaceous mass was allowed to cool and was ground to a coarse powder in a mortar. The final grinding to a particle size of 100 mesh was accomplished in a ball mill. The sugar carbon was ignited for 1 hr at 800°C in a muffle furnace. Smaller samples were activated in a similar manner to that used for wood carbon by heating in the furnace for another hour within a few days of use. A determination of ash content gave a value of 8 per cent ash for wood carbon and 0·2 per cent for sugar carbon. The ash residue from sugar carbon samples did not give a basic reaction when leached with water as did wood carbon samples and gave no precipitate with sodium oxalate or silver nitrate.

* The total number of sites must be small in all carbon samples. Compared to the total number of molecules of complex with equal weights of carbon and complex as used in most experiments, there is a ratio of 32 carbon atoms to one complex ion. Assuming a surface area of 3×10^2 cm²/g of carbon for a typical sample of carbon, then the area per atom of carbon would be 6×10^{-5} Å/atom. Since the C-C bond distance in graphite is approximately 1·42 Å, the cross-sectional area per atom is 1·58 Å². Therefore there should be about 3×10^4 atoms of carbon/atom on the surface. For a typical sample of 25 mg of carbon there would be about 4×10^{16} carbon atoms on the surface. However, in 25 mg of $K[Co(EDTA)]\cdot 2H_2O$ there are $3{\cdot}6 \times 10^{19}$ complex ions.

In addition to active sites on the surface of the carbon one might consider sites within the porous structure of the charcoal. Although stirring of the slurry would minimize diffusion effects around the carbon particles, the internal diffusion would remain largely unaffected. Because of the rapidity of complete exchange with the carbon surface as evidenced by the rapid racemization with the very active carbon and the low adsorption, it was assumed that slow diffusion processes must be relatively unimportant.

(4) F. P. DWYER, E. C. GYARFAS and D. P. MELLOR, *J. Phys. Chem.* **59**, 296 (1955).
(5) F. P. DWYER and F. L. GARVAN, *Inorg. Syntheses*, VI, 192 (1960).

The sample container was a 150 ml Erlenmeyer flask. A typical sample contained 25 mg of complex and 25 mg of carbon in 50·00 ml of water. The flask was immersed to the neck in a thermostatted water bath. Samples were stirred with a magnetic stirring-bar to avoid the inconvenience of a stirring shaft through the top of the container. Any such stirring shaft makes removal of samples more difficult. The stirring bar actuator was a bar magnet driven by four coupled right angle drives. This immersible magnetic driving system had the advantage of allowing direct use of the water bath to thermostat the reaction vessel, avoiding the necessity for a jacketed container and circulating system.

The reaction was timed with an electric stop-clock actuated whenever carbon was introduced to the samples in the thermostatted reaction vessel. Since racemization was "frozen" upon removal of the carbon from samples, rapid filtration is an excellent way to stop the progress of the reaction. Ordinary filtration techniques involving several transfers are time consuming and ordinarily require one to two minutes for completion. The method that was adopted uses 7 mm glass tubing packed with Pyrex wool as a filter. The packed tubes were placed, using a fitting prepared for the purpose, on the end of a 10 ml hypodermic syringe. It was found that samples could be filtered and withdrawn in five to ten seconds. The efficiency of this method in removing carbon was tested by withdrawing a sample of D-K[Co(EDTA)] from a carbon slurry through one of the filters. The solution was examined for optical rotation immediately after withdrawal. It was then thermostatted for 1 hr at 50°C and rechecked at the end of this period with no loss of optical activity noted.

RESULTS

The results of racemization of D-K[Co(EDTA)] on wood carbon indicated good agreement with first order kinetics. (See Fig. 1.) The activation energy calculated from wood carbon racemization curves by plotting 1/T vs. log k gave a value of 7·1 kcal/mole.

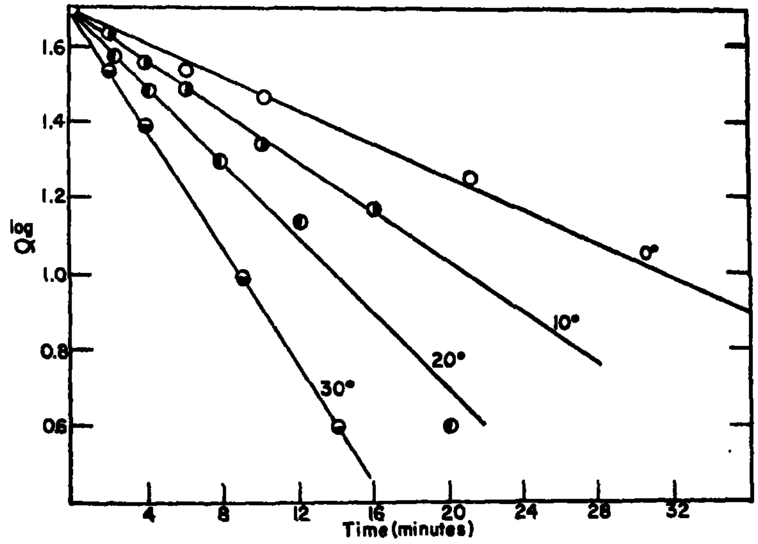

FIG. 1.—First order plots for the racemization of K D-[Co(EDTA)] (25 mg) in the presence of active wood carbon (25 mg) in 50 ml of water.

The racemization using equal weights (25 mg) of complex and sugar carbon did not follow first order kinetics. A plot of $1/\alpha$ vs. time gave a nearly linear plot over the temperature range 10–50°C (see Fig. 2). This result would be expected if the reaction were second order in complex or first order in carbon and first order in complex with the starting concentrations nearly equal. When the amount of carbon or its activity were changed, the $1/\alpha$ vs. time plot was no longer linear, thus eliminating the possibility of a reaction second order in complex. It should be noted that a large excess of carbon or a very active carbon sample should cause the reaction to be pseudo first-order. The high activity of the wood carbon gave an effectively high "concentration" of active sites, so that the observed first order plot using wood carbon is consistent with a second order reaction.

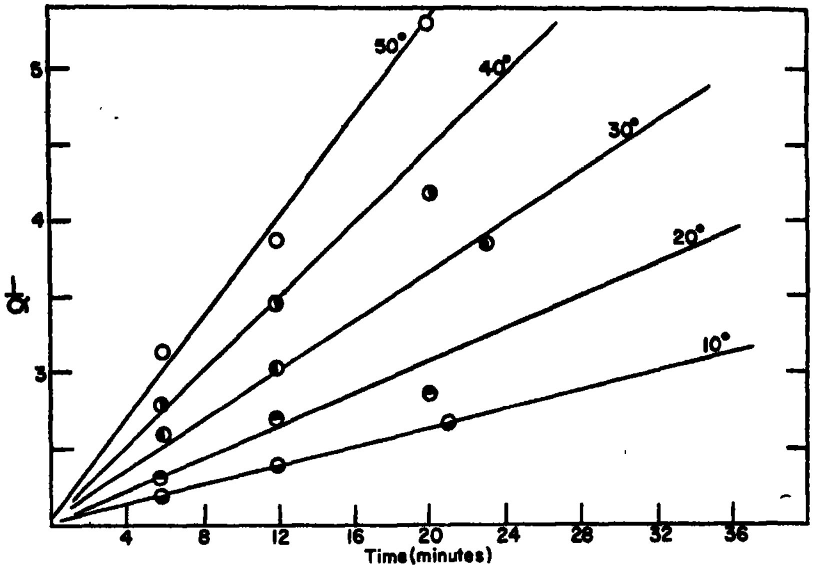

Fig. 2.—Second order plots for the racemization of K D-[Co(EDTA)] (25 mg) in the presence of active sugar carbon (25 mg) in 50 ml of water.

The reaction would be expected to differ from the usual second order reaction in that, although the active carbon sites are apparently depleted during the reaction as expected, the concentration of complex is constant because the active and racemic complex are chemically identical and should compete equally for the active carbon sites. The decrease in optical rotation permits one to follow the course of the reaction although the effective concentration of complex does not change, but is equal to the initial concentration. The reaction may be represented as follows:

$$A+C \xrightarrow{k} BC \tag{1}$$

$$B+C \xrightarrow{k} BC \tag{2}$$

$$BC \longrightarrow B+C' \tag{3}$$

$$[A_0] = [A]+[B]+[BC] \tag{4}$$

where $[A_0]$ is the total concentration of complex, A is the optically active complex, B is the racemic complex, C is the active carbon, C′ is the deactivated carbon, and BC is the complex adsorbed on carbon. Since BC is small as indicated by optical absorption data,

$$[A_0] \cong [A]+[B] \tag{5}$$

The rate of change in "concentration" of carbon is given by:

$$-\frac{d[C]}{dt} = k[A][C]+k[B][C] = k[C][A_0] \tag{6}$$

from which the rate law is found to be:

$$[C] = [C_0]e^{-k[A_0]t} \tag{7}$$

where $[C_0]$ is the initial carbon concentration.

The rate of change in concentration of complex is given by:

$$-\frac{d[A]}{dt} = k[A][C_0]e^{-k[A_0]t} \tag{8}$$

from which Equation (9) is obtained with substitution from Equation (7).

$$\log\left(2{\cdot}3\frac{[A_0]}{[C_0]}\log\frac{[A]}{[A_0]}+1\right) = \frac{-k[A_0]t}{2{\cdot}3} \tag{9}$$

No direct measure of the effective "concentration" of active carbon was available. If the reaction were first order in complex and first order in carbon, the plot of $1/\alpha$ vs. time would be linear only if the initial concentrations of complex and carbon were equal. The effective carbon concentration was interpreted as representing the number of active sites on the carbon surface. Since the value used seemed quite arbitrary, the linearity of the $1/\alpha$ plot was taken as the basis for evaluating the concentrations. The observed rotation of the complex for this plot was used for the "concentration" of complex and of active carbon sites. For the case where the weight of carbon was $\frac{1}{2}$ that of the complex, the "concentration" of carbon was taken as $\frac{1}{2}$ the observed rotation of the complex. Equal weights (25 mg) of carbon and complex gave linear $1/\alpha$ plots for the carbon samples used for the initial study with sugar carbon and for the runs carried out at different temperatures. The carbon used for the studies involving varying ratios of carbon and complex was slightly less active so that the "concentrations" of complex and carbon were taken as equal (linear $1/\alpha$ plot) for a ratio of 24 mg of complex to 25 mg of sugar carbon.

Equation (9) gave excellent agreement with the observed rates over the first 20–30 min of the reaction (Fig. 3). However, for the concentrations used, the difference between a simple second order process and one described by Equation (9) is small for short time intervals. It is only after an appreciable amount of racemic complex has accumulated that deviation from second order kinetics is expected. Unfortunately at long time intervals the reaction departed from both types of kinetics. Higher concentrations of carbon and complex were tried because the predicted difference becomes greater at short time intervals for higher concentrations. The results at high concentrations showed even more marked deviation from both types of kinetics as the time interval increased. Lower concentrations were also tried and gave good agreement (Fig. 4) when plot of: $-\log\left(2{\cdot}3\frac{[A_0]}{[C_0]}\log\frac{[A]}{[A_0]}+1\right)$ vs. time was made.

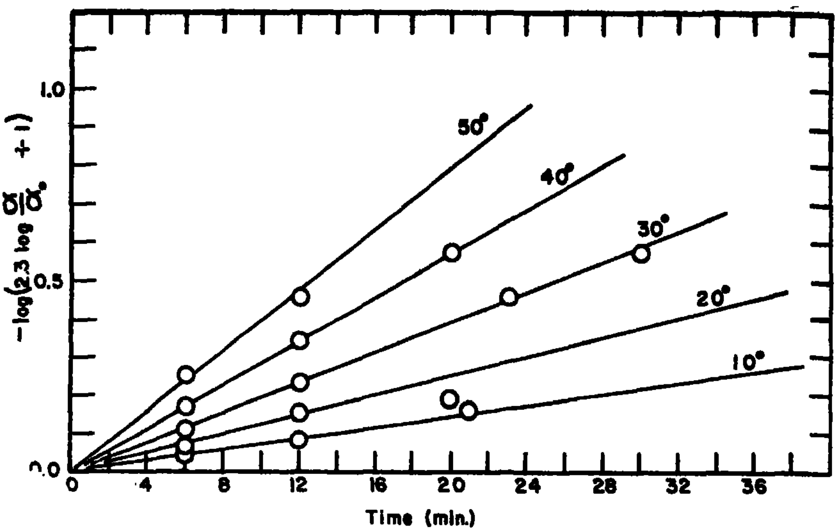

FIG. 3.—Kinetic plots for the racemization of K D-[Co(EDTA)] (25 mg) in the presence of active sugar carbon (25 mg) in 50 ml of water.

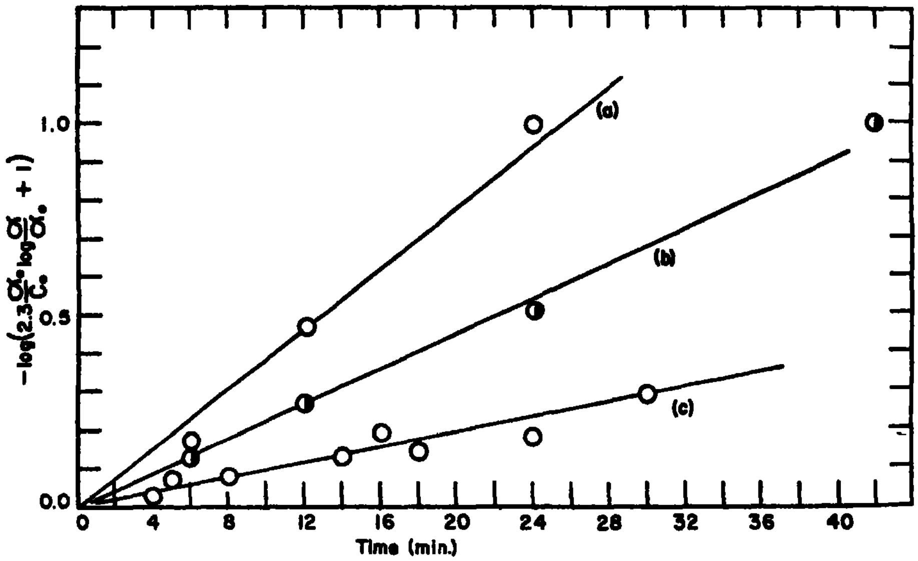

FIG. 4.—Kinetic plots for the racemization of K D-[Co(EDTA)] in the presence of active sugar carbon at 30°C, (a) 48 mg complex and 24 mg carbon in 50 ml water, (b) 24 mg complex and 12 mg carbon in 50 ml water, (c) 12 mg complex and 24 mg carbon in 50 ml water.

No effective way was found to distinguish more clearly between the second order kinetics and the mechanism described by Equation (9). However, it is apparent that the complex must compete equally well for the carbon as does the optically active complex. Any strictly second order process would have to assume the racemic complex inert toward the carbon. This has been shown not to be the case.(2) The rate constants calculated from Equation (9) were slightly more consistent than those calculated for a second order process (Table 1).

TABLE 1.—RATE CONSTANTS FOR THE RACEMIZATION OF K[Co(EDTA)] ON SUGAR CARBON AT 30°C

$[A_0]$ (Complex	$[C_0]$ (Carbon)	k (Product reacts)*	k (Second order)
0·46	0·46	0·10	0·086
0·23	0·46	0·10	0·09
0·46	0·23	0·11	0·10
0·50	0·50	0·092	0·08

* k is obtained from the slope of the straight line in plots of Equation (9) (see Fig. 4). $k = \text{slope} \times \frac{2{\cdot}3}{A_0}$

The observed rotations were in somewhat better agreement with the theoretical curve for Equation (9) than for a strictly second order reaction. The failure to obtain a clear cut choice between the two mechanisms can be attributed, at least partly, to the use of a second order plot ($1/\alpha$) as the basis for adjusting and evaluating the carbon "concentration". However, except for high concentrations and/or long time intervals, the two processes differ only slightly (Fig. 5).

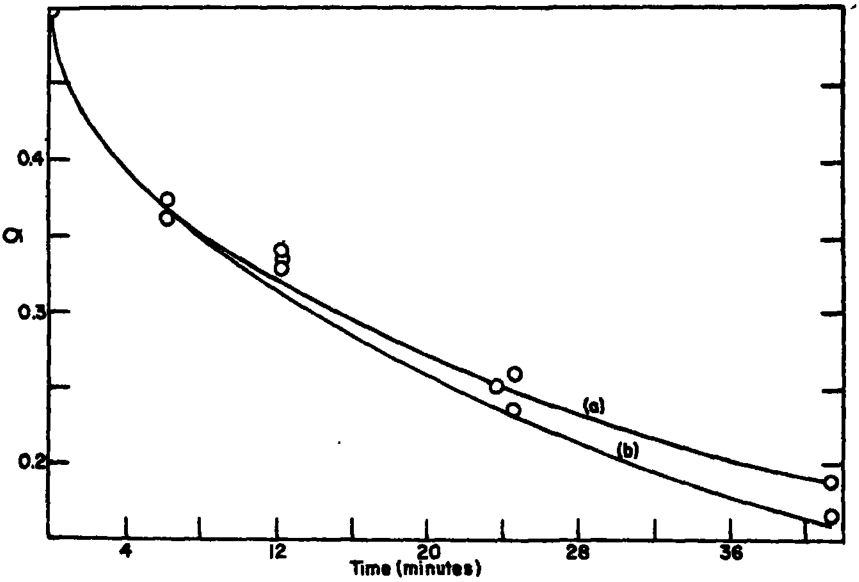

FIG. 5.—Kinetic plots for the racemization of K D-[Co(EDTA)] (25 mg) in the presence of sugar carbon (25 mg) in 50 ml water at 30°C. Circles represent experimental points, (a) is the theoretical curve for Equation (9), (b) is the theoretical curve for a simple second order process.

If, as would be expected, the active carbon sites differ in the number of collisions needed for their deactivation, then deviations in the kinetics at extended time intervals become understandable. With differences in the effective lifetime of the sites in the presence of complex, the persistence of long lived sites would produce a carbon site population that is substantially different from the initial one. Such a site population would make the carbon behave as a more effective reactant than would otherwise be expected if all sites were identical. This was the observed experimental behaviour with deviations always tending to make rotations lower than predicted.

The activation energy for the reaction on sugar carbon using the rate constant from Equation (9) gave a value of 7·3 kcal/mole (see Fig. 6). This is in excellent agreement with the results for wood carbon (7·1 kcal/mole) where an assumption of first order kinetics was made. It is much lower than the activation energy for thermal racemization⁽⁶⁾ (40·6 kcal/mole).

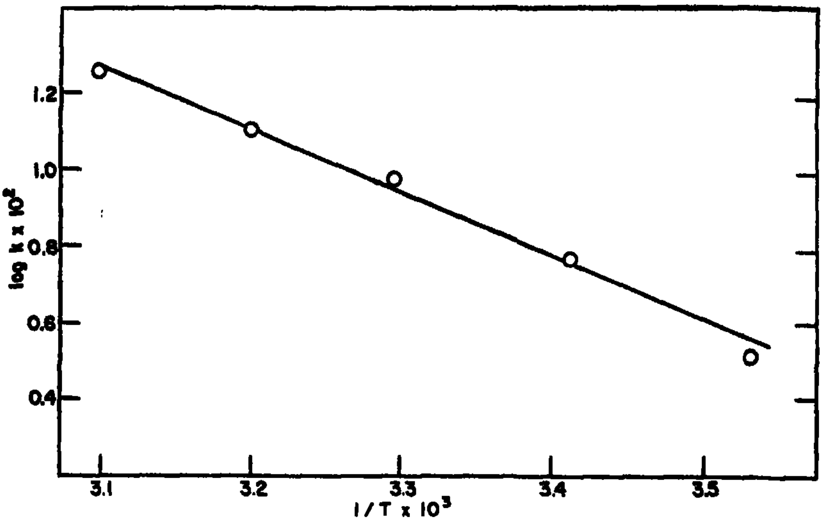

Fig. 6.—Plot for the determination of the activation energy for the racemization of K D-[Co(EDTA)] in the presence of active sugar carbon.

Spectral examination of a solution of K[Co(EDTA)] after treatment with a sample of very active wood carbon for 30 min revealed a concentration reduction (15 per cent) but no indication of the formation of a new compound. These conditions were much more drastic than those used for the racemization studies. When 3 per cent H_2O_2 was added to these samples while in contact with carbon the extent of concentration loss was lessened. The addition of H_2O_2 after removal of the carbon recovered about $\frac{1}{2}$ of the original concentration loss caused by contact with the carbon. The use of H_2O_2 was suggested because this is an oxidizing agent used in the preparation of K[Co(EDTA)]. Apparently the presence of the reduced species is masked by the stronger optical absorption of the $[Co(EDTA)]^-$ ion. Because the oxidation of $[Co(EDTA)]^{2-}$ was found to be much faster in basic solution, the samples were adjusted to pH 9 with KOH after the addition of H_2O_2. After about 5 min the samples were adjusted to pH 2 with dilute HNO_3 and allowed to stand for 30 min before measurement. Any quinquidentate complex that might be present is rapidly converted to sexadentate in acid solution. The effect of electrolytes on the absorption maxima was checked by measurements made in the presence of 0·1 M KCl. No significant change was observed. Similar experiments with sugar carbon, where the concentration loss is much smaller (less than 2 per cent), revealed a recovery of about $\frac{1}{2}$ of the total concentration loss resulting from contact with the carbon. The total concentration loss and extent of reduction were almost temperature independent over the range 10–25°C.

(6) D. W. Cooke, Y. A. Im and D. H. Busch, *Inorg. Chem.* 1, 13 (1962).

INTERPRETATION OF RESULTS

The racemization of K[Co(EDTA)] on active carbon indicates a reaction that is first order in complex and first order in carbon. Although the carbon is commonly referred to as a catalyst, it is obvious that its activity decreases as though it were reacting in stoicheiometric proportions. A comparison of the probable number of active carbon sites with the number of molecules of complex indicates that an active carbon site has a probable lifetime extending over many interactions with molecules of complex.

Although some reduction of the complex is indicated in experiments with wood carbon, the amount of reduction using sugar carbon is very small. Thus the racemization of $[Co(EDTA)]^-$ by electron exchange with the reduced species in solution is probably relatively unimportant. The electron rich carbon surface might be pictured as holding the complex ions during the time they are adsorbed in a *quasi* reduced state, thus aiding the racemization process. If this were so, it would be difficult to understand why the reaction should be first order with respect to carbon.

The activation of carbon will be discussed in a later paper. The activation seems to require the removal of chemi-sorbed oxygen which is removed as CO on ignition. The removal of CO might create active sites by leaving "craters" or regions in which the carbon atoms have unsaturated valences. These high energy sites might give up some of their energy to adsorbed complex ions which are large enough to span the crater and bring about some "healing" of the jagged edges. The complex ions in an activated state could more readily undergo intramolecular racemization. The activity of the carbon is known to be diminished in the presence of racemic complex and more slowly in contact with water alone.(2)

The small number of active sites would require that each site bring about racemization of many complex ions. The activated complex ions which have enough energy for intramolecular racemization might also transfer energy to other complex ions by collision to bring about the racemization of other complexes by a chain reaction, possibly terminated by solvent deactivation. The average number of racemization processes brought about by each site, directly or indirectly, must be reproducible in order to permit the first order dependence on carbon. If this is the correct mechanism the carbon is an unusual reactant which serves merely as a source of energy for the intramolecular racemization.

J. Inorg. Nucl. Chem., 1962, Vol. 24, pp. 1365 to 1371. Pergamon Press Ltd. Printed in England

THE RACEMIZATION OF COMPLEX IONS ON ACTIVATED CARBON—II

THE RACEMIZATION OF D-TRIS(ETHYLENEDIAMINE)COBALT(III) CHLORIDE AND OTHER COMPLEXES*

W. C. Erdman, H. E. Swift and B. E. Douglas
Department of Chemistry, University of Pittsburgh, Pittsburgh, Pa.

(*Received* 22 *March* 1962)

Abstract—Silica gel, activated alumina, platinized asbestos, and partially reduced zinc oxide were found to have no effect on the rate of racemization of several complexes studied. Raney nickel caused the decomposition of $[Co(en)_3]Cl_3$. Activated carbon decomposed $K_3[Co(C_2O_4)_3]$ and $K_3[Cr(C_2O_4)_3]$. It caused some conversion to the *trans* isomer of *cis*-$[Co(en)_2(NO_2)_2]Br_3$, in addition to accelerating the racemization of the complex. Using wood carbon activated at 700°C for 1 hr, the racemization of D-$[Co(en)_3]Cl_3$ was found to be essentially second order, first order in complex and first order in carbon. The activation energy for the racemization process was 17 kcal/mole. Although an electron exchange mechanism for the racemization on carbon cannot be ruled out, an intramolecular process is favoured.

CARBON has been observed to accelerate the racemization of optically active $[Co(en)_3]Cl_3$,(1-3) K[Co(EDTA)],(4) and $[Pt(en)_3]Cl_4$.(5) The optically active $[Rh(en)_3]Cl_3$ complex has been found to be unaffected by activated carbon.(5) It seemed desirable to investigate the effect of activated carbon on other complexes and the effect of other catalysts. The success of the kinetic treatment of the results with K[Co(EDTA)](4) made it seem desirable to investigate further the racemization of $[Co(en)_3]Cl_3$ on carbon.

EXPERIMENTAL

Instrumentation. The apparatus for the racemization studies and for the measurements of optical rotation were the same as described previously.(4)

Preparations. $[Co(en)_3]Cl_3$ was prepared by the method of Work(7) and resolved by Werner's method(7) involving the fractional crystallization of the chloro-D-tartrate salt. The dextro isomer was purified by repeated recrystallization of the chlorotartrate salt and finally converted to the chloride salt by the addition of concentrated HCl and alcohol. The very soluble levo diastereoisomer could not be purified as the chlorotartrate salt. It was converted to the chloride salt with HCl. The active chloride salt was recrystallized several times to improve the resolution of the complex by separating the less soluble racemic complex from the more soluble active complex. The specific rotations obtained for the resolved D and L chloride salts were +165° and −155°, respectively. Werner reported $[\alpha]_D = 152°$, and −154°, respectively.

---

* This work was supported by grants from the U.S. Public Health Service, National Institute of Arthritis and Metabolic Diseases (Grant A-2219) and the Research Corporation. It is based upon portions of doctoral dissertations of W. C. Erdman (1959) and H. E. Swift (1961), The University of Pittsburgh.

(1) B. E. Douglas, *J. Amer. Chem. Soc.* **76**, 1020 (1954).
(2) F. P. Dwyer and A. M. Sargeson, *Nature, Lond.* **187**, 1022 (1960).
(3) H. E. Swift and B. E. Douglas, *Nature, Lond.* **193**, 1173 (1962).
(4) W. C. Erdman and B. E. Douglas, Part I, *J. Inorg. Nucl. Chem.* **24**, 1557 (1962).
(5) D. Sen and W. C. Fernelius, *J. Inorg. Nucl. Chem.* **10**, 269 (1959).
(6) J. B. Work, *Inorg. Syntheses* II, 221 (1946).
(7) A. Werner, *Ber. Dtsch. Chem. Ges.* **45**, 121 (1912).

The preparation of $K_3[Co(C_2O_4)_3]\cdot 3H_2O$ followed the method of Bailar and Jones.(8) It was resolved by Jaeger's method(9) involving the fractional precipitation of the strychnine salt. The specific rotation observed for L-$K_3[Co(C_2O_4)_3]\cdot H_2O$ was $[\alpha]_{5461} = -717°$ as compared to $-140°$ reported by Jaeger.

A sample of *cis*-$[Co(en)_2(NO_2)_2]Br_3$ was prepared by the method of Holtzclaw *et al.*(10) and resolved by Dwyer's method.(11) The specific rotation observed was $[\alpha]_D = 42°$, the same as reported by Dwyer.

A sample of $[Cr(en)_3]Cl_3$ was prepared by the method of Rollinson and Bailar(12) and resolved by Werner's method.(13) The specific rotation of D-$[Cr(en)_3]I_3$ was $[\alpha]_{5461} = 88°$ as compared to 131° reported by Werner. No attempt was made to improve the resolution because of the failure of the complex to undergo racemization with activated carbon.

Potassium tris(oxalato)chromate(III) was prepared by the method of Bailar and Jones.(8) It was not resolved since the complex was decomposed by activated carbon.

The activation of Baker and Adamson wood carbon was described previously.(4) The initial studies were made with carbon activated at 800°C for 1 hr. The carbon used for the kinetic studies and for the determination of the activation energy for racemization was activated at 700° for 1 hr. Silica gel was washed with dilute HCl and then twice with distilled water. It was then dried at 130°C for 6 hr. Catalytic alumina was activated by heating for 6 hr at 160°C. Samples of Raney nickel and platinized asbestos were prepared by standard methods. Zinc oxide was partially reduced by passing H_2 over a sample of zinc oxide at red heat.

The sampling technique was the same as described earlier(4) for some of the work. However, in the kinetic studies of the racemization of $[Co(en)_3]Cl_3$ some difficulty was experienced in completely removing the carbon by filtration through a piece of glass tubing packed with Pyrex glass wool. Consequently, for these runs the sample was removed with a pipette and filtered quickly through a sintered glass funnel using suction. Except for the runs involving varying ratios of complex to carbon, the samples contained 0·500 g $[Co(en)_3]Cl_3$ and 0·500 g carbon in 50 ml water. The runs with the other solid catalysts involved 1:5 ratios of complex to catalyst (by weight).

RESULTS

Raney nickel caused the decomposition of even the robust $[Co(en)_3]Cl_3$ so that it was not investigated further. Silica gel, activated alumina, platinized asbestos, and partially reduced zinc oxide had no effect on the complexes investigated at 50°C. Silica gel and alumina were selected to provide examples of acidic and basic surfaces. The partially reduced zinc oxide was tried as a possible electron source in case the racemization occurred by electron exchange.

Potassium tris(oxalato)chromate(III) and potassium tris(oxalato)cobaltate(III) were decomposed by activated carbon at 40°C. Tris(ethylenediamine)chromium(III) chloride did not undergo racemization at 50°C. There was some decrease in adsorbance (about 5 per cent) caused by decomposition or adsorption of the complex by the carbon. In order to determine whether the activity of the carbon was being destroyed by some decomposition of the complex, the racemization of K[Co(EDTA)] was followed in the presence of $[Cr(en)_3]Cl_3$ and carbon. No greater effect on the racemization of K[Co(EDTA)] was noted than caused by an equivalent amount of KCl.

---

(8) J. C. Bailar, Jr. and E. M. Jones, *Inorg. Syntheses* I, 37 (1942).

(9) F. M. Jaeger, *Rec. Trav. Chim.* 38, 251 (1919).

(10) H. Holtzclaw, D. Sheetz and W. McCarty, *Inorg. Syntheses* IV, 176 (1953).

(11) F. P. Dwyer and F. L. Garvan, *Inorg. Syntheses* VI, 195 (1960).

(12) C. L. Rollinson and J. C. Bailar, Jr., *Inorg. Syntheses* II, 198 (1946).

(13) A. Werner, *Ber. Dtsch. Chem. Ges.* 45, 867 (1912).

The racemization of *cis*-$[Co(en)_2(NO_2)_2]Br_3$ proceeded at a convenient rate at 40 or 50°C using 200 mg of complex and 200 mg of carbon in 50 ml of water. However, an examination of the spectrum of the final solution revealed some conversion to the *trans* isomer, although this conversion was slower than the racemization. The half-life for the racemization is about 4 min at 50°C while the conversion to the *trans* isomer is only about 5 per cent complete in that time. The isomerization was not investigated further because the similarity in the spectra of the *cis* and *trans* isomers made quantitative treatment of the results difficult.

The early studies of the racemization of $[Co(en)_3]Cl_3$ by wood carbon activated at 800°C for 1 hr showed no promise for a kinetic treatment of the data. The data did not follow simple kinetics. DWYER(2) reported that the complex was partially reduced (6 per cent) by boiling with carbon for 3 min. SEN and FERNELIUS(5) noted that decomposition of the complex was extensive after boiling for 5 min with carbon and was essentially complete in 10 min. At 80°C little decomposition was observed in 15 min, although racemization was complete. DOUGLAS(1) found that the absorption spectrum of the complex was not altered appreciably after 5 min at 90°C. However, the experiments were not conducted in such a way as to reveal concentration losses due to adsorption. At the temperatures used in the present study (30–50°) the extent of concentration loss or decomposition was slight (2–3 per cent after 3 min and 4–5 per cent after 30 min at 50° in the presence of the more active carbon). Apparently the diminution of the adsorption peak at 468 mμ was caused by decomposition of the complex with the formation of a new complex, since the peak at 337 mμ increased in intensity. The less active carbon (activated at 700°) used for the kinetic studies gave no significant alteration in the adsorption spectrum after one hour at 40°C.

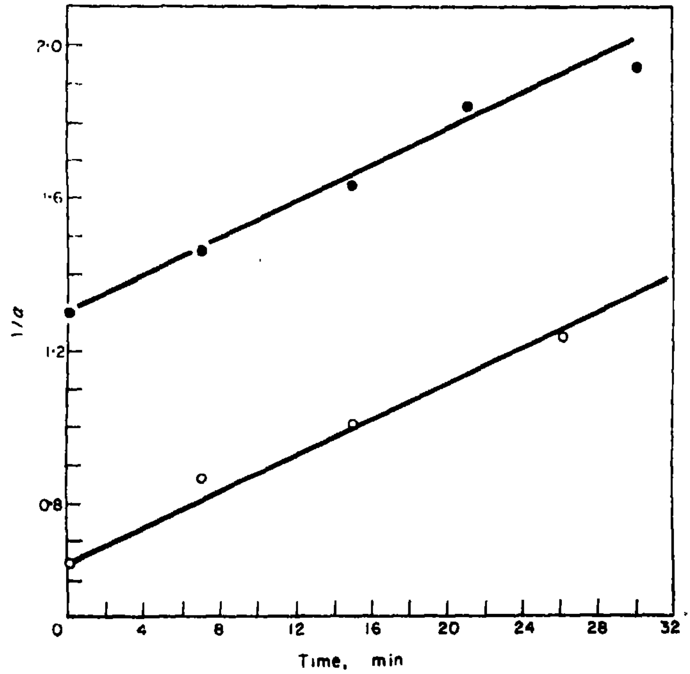

FIG. 1.—Plots of 1/α vs. time for equal weights of D-$[Co(en)_3]Cl_3$ in 50 ml of water at 40°C (O, 0·500 g samples; ●, 0·250 g samples).

Although the racemization of $[Co(en)_3]Cl_3$ using carbon activated at 800°C did not follow simple kinetics, the plots of $1/\alpha$ vs. time were reasonably linear using equal weights of complex and carbon activated at 700° (Fig. 1). As in the case of K[Co(EDTA)],(4) the second order plots were interpreted as indicating a reaction first order in complex and first order in carbon. To check this, second order plots were made using data obtained for runs involving 2:1 and 1:2 ratios of complex to carbon (Fig. 2). These linear plots were obtained by expressing the concentration of active complex as the observed rotation and the "concentration" of carbon as the rotation of an equal weight of complex.(4)

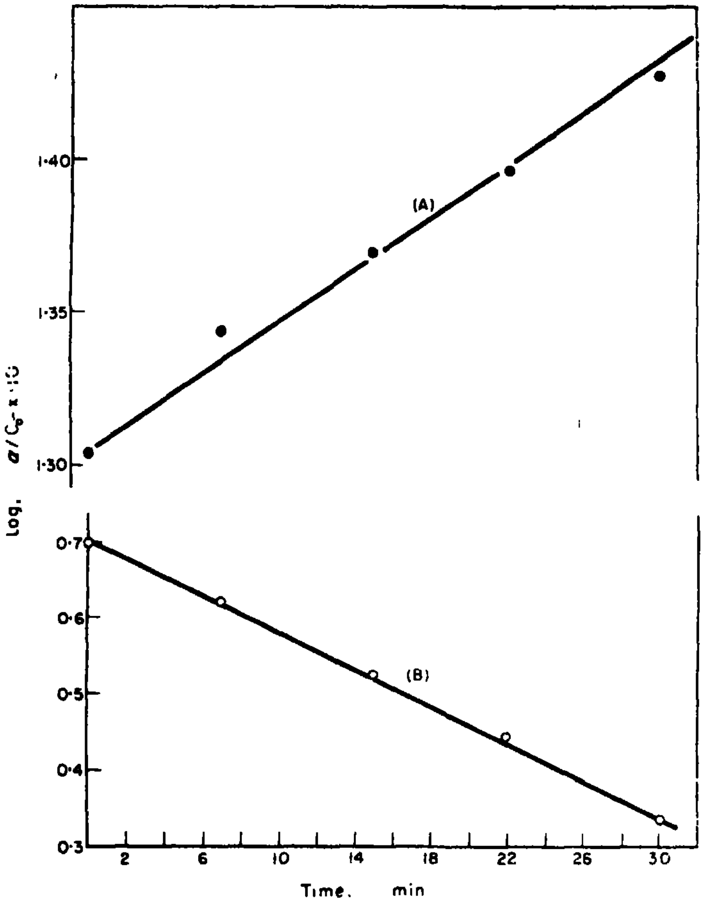

Fig. 2.—Kinetic plots for the racemization of D-$[Co(en)_3]Cl_3$ in the presence of active wood carbon at 40°C, (A) 0·500 g complex and 0·250 g carbon in 50 ml water, (B) 0·250 g complex and 0·500 g carbon in 50 ml water.

It has been pointed out that the reaction would be expected to deviate from a strictly second order process after some racemic complex has accumulated.(4) This is true because the racemic complex and active complex are chemically identical and both can deactivate the active carbon sites. However, the difference between the two mechanisms is slight except for long time intervals. The data obtained for the racemization of $[Co(en)_3]Cl_3$ could be treated satisfactorily assuming a second order reaction. The second order rate constants varied more widely than those for

K[Co(EDTA)], but no improvement was obtained for the mechanism in which the deactivation of carbon by the racemic complex was considered. The second order rate constants are given in Table 1. The activation energy obtained from the plots of log *k* vs. 1/*T* (Fig. 3) was 17·3 kcal/mole. Although there are significant differences in the rate constants given in Fig. 3 (for the same temperature) using different samples of carbon and different concentrations, the activation energies obtained agreed within 0·1 kcal. Because of some variation of the activity of the carbon from one batch to another, a set of similar runs was carried out within a day or two with carbon freshly activated in one batch. The variation in activity results in differences in the observed rate constants since a change in activity changes the number of active sites in a sample of carbon. The constancy of the activation energy gave added confidence in the proposed kinetic treatment.

TABLE 1.—SECOND ORDER RATE CONSTANTS FOR THE RACEMIZATION OF D-$[Co(en)_3]Cl_3$ ON ACTIVATED WOOD CARBON AT 40°C

Weight of complex (g in 50 ml)	Weight of carbon (g in 50 ml)	Second order Rate constant
0·25	0·25	0·025
0·50	0·50	0·025
0·25	0·50	0·033
0·50	0·25	0·014

In typical runs the carbon was added to a solution of the sample of complex in 50 ml of water in a constant temperature bath. In one run the carbon was allowed to stir in the water for 15 min at 40°C before the complex was added to determine the extent to which the carbon is deactivated in contact with water. The racemization of the complex proceeded more slowly using the carbon which had been in contact with water. The 1/α plot was still reasonably linear, giving an apparent second order rate constant of 0·014 compared to 0·025 for normal runs.

In order to verify the deactivation of the carbon by racemic complex, a 0·500 g sample of carbon was added to a solution of 0·025 g of racemic complex in 50 ml of water and allowed to stir for 15 min before 0·250 g of active complex was added. In this case the rate of racemization was decreased markedly and seemed to level off after about 30 min, with the optical rotation reduced by about 30 per cent. The same weight (0·250 g) of active complex in the presence of 0·500 g carbon loses half of its activity in 15 min.

DISCUSSION OF RESULTS

The results with the various catalysts tried do not permit any conclusions to be reached concerning the requirements for a good "catalyst" for the racemization of complexes. Activated carbon seems to be the only "catalyst" suitable for general study.

Obviously only very stable complexes lend themselves to the study of racemization on activated carbon. Since both cationic and anionic complexes undergo racemization in the presence of activated carbon, the charge on the complex cannot be critical. The complexes for which the results have significance are $[Co(en)_3]Cl_3$, K[Co(EDTA)], *cis*-$[Co(en)_2(NO_2)_2]Br_3$, and $[Cr(en)_3]Cl_3$.

The first order dependence on carbon of the racemization of $[Co(en)_3]Cl_3$ and $K[Co(EDTA)]$ suggests that the carbon "reacts" stoichiometrically in both cases. The assumption that each active site must cause many racemization events has already been discussed.(4) The racemization of $[Co(en)_3]Cl_3$ on carbon requires a much higher activation energy than that for $K[Co(EDTA)]$ (7·3 kcal/mole) and the more active wood carbon is needed for the former complex. Apparently many of the active sites on sugar carbon for the racemization of $K[Co(EDTA)]$ cannot supply sufficient energy for the racemization of $[Co(en)_3]Cl_3$.

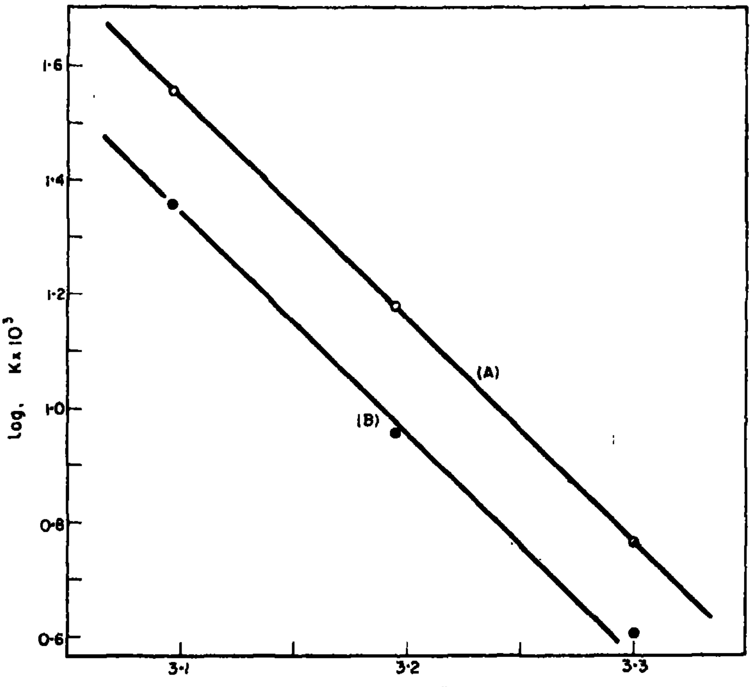

Fig. 3.—Plots for the determination of the activation energy for the racemization of D-$[Co(en)_3]Cl_3$ in the presence of active wood carbon, using equal weights of complex and carbon in 50 ml water, (A) 0·400 g samples, (B) 0·500 g samples.

It is remarkable that such heterogeneous reactions seem to follow simple second order kinetics. Of course arbitrary adjustments have been made in the weight and activity of carbon used in order to obtain linear plots of $1/\alpha$ vs. time. The results obtained in the presence of racemic complex make it apparent that the reaction should deviate from a simple second order process as the racemic complex accumulates. However, second order kinetics seem to describe the process adaquately for the conditions used. The fact that the carbon is deactivated in the presence of water, even though more slowly than in the presence of the complex, indicates that this is another factor not considered in the simple second order mechanism. Apparently this effect is compensated for in the experimental choice of the weight and activity of carbon used.

There is less consistency among the rate constants obtained for the racemization of $[Co(en)_3]Cl_3$ as compared to those for $K[Co(EDTA)]$.(4) The rate constant obtained for a ratio of complex to carbon of 2:1 is lower than that for a 1:1 ratio, while the value of a 1:2 ratio is high. These results might be expected from the deactivation of carbon by water. This deactivation was compensated for by the choice of conditions for the 1:1 ratio. It would be relatively less important in the presence of a high proportion of carbon so that the "extra" carbon would speed up the racemization. It would be relatively more important for a low proportion of carbon, slowing down the racemization.

The failure of $[Cr(en)_3]Cl_3$ to racemize in the presence of carbon was surprising since the chromium oxalato complex undergoes autoracemization more rapidly than the cobalt oxalato complex. This difference between the ethylenediamine complexes on carbon suggests for the racemization of $[Co(en)_3]^{3+}$ an electron exchange mechanism, as proposed by DWYER,(2) since reduction to the 2+ state might be expected to occur more readily for the cobalt complex. However, there is also the possibility that the racemization of $[Co(en)_3]^{3+}$ occurs through an intramolecular process involving an activated state of the complex. Perhaps the corresponding activated state of $[Cr(en)_3]^{3+}$ is less readily accessible.

The report that the racemization process of $[Co(en)_3]^{3+}$ on carbon proceeded through an electron exchange process was based on the observation that the racemization was much slower in the presence of H_2SO_4, presumably because of the destruction of the labile cobalt(II) complex. A preliminary report of the effect of electrolytes on the racemization by carbon has shown that Li_2SO_4 has almost as great an effect on the racemization as does H_2SO_4. A more complete report of the effect of electrolytes will be discussed in Part III.

The racemization of *cis*-$[Co(en)_2(NO_2)_2]^+$ was faster than the conversion to the *trans* isomer in the presence of carbon. The racemization and *cis-trans* isomerization can both occur by the same intramolecular mechanism involving the twisting of one triangular face of the octahedron relative to the opposite face.(14) There are more ways to twist the complex ion to bring about racemization than there are to bring about *cis-trans* isomerization. It is also possible that these processes do not all have the same activation energy.

While an electron exchange mechanism cannot be ruled out, it is felt that an intramolecular mechanism is probably more important. The sites of the carbon are pictured as providing the necessary energy for the intramolecular racemization. Each site must be used many times or else the complex ions which have acquired the necessary energy from the carbon surface must be able to transmit it to other complex ions by collision. A chain reaction involving transfer of vibrational energy from one complex to another would have to be terminated after a number of such events, possibly by the solvent, in order to result in first order dependence on carbon. The proposed mechanism has been discussed more fully elsewhere.(4)

(14) J. C. BAILAR, Jr., *J. Inorg. Nucl. Chem.* **8**, 172 (1958).

J. Inorg. Nucl. Chem., 1962, Vol. 24, pp. 1373 to 1379. Pergamon Press Ltd. Printed in England

SPECTROPHOTOMETRIC STUDY OF THE CHROMIUM(III) AZIDE REACTION

F. G. SHERIF, W. M. ORABY and HUSSEIN SADEK
Faculty of Science, Alexandria University, Alexandria, Egypt

(*Received* 18 *January* 1962; *in revised form* 20 *March* 1962)

Abstract—Conditions for the use of the azide as a spectrophotometric reagent for Cr(III) are investigated. The system obeys Beer's law in the range of 4–320 p.p.m. The colour is affected by acid concentration; maximum colour development is attained in a pH range of 4·2–5·2. Interference due to Cu^{2+}, Fe^{3+} and UO_2^{2+} ions can be reduced by adding a few ml of EDTA. The logarithmic method confirmed the existence of a monoazidochromium(III) ion in dilute solutions. In concentrated solutions, Job's method of continuous variation revealed the existence of a series of complexes between chromium and azide ions varying in composition from 1:1 (green) to 1:6 (violet) chromium to azide.

IN connection with studies entailing the reaction of Cr(III) (violet form) with sodium azide in aqueous solution and the characterisation of the structure of the possible complex ions,(1) it became necessary to study the use of the coloured solutions for the spectrophotometric determination of minute amounts of Cr(III). Only a limited amount of data is available in the literature concerning the determination of Cr(III) by colormetric methods. Other spectrophotometric determinations are generally based on the oxidation to Cr(VI) in aqueous solutions prior to measurement. This is probably due to the slow reaction of the strongly hydrated Cr(III) ions with many ligands. However, oxidation requires severe conditions for accurate results. The azide reaction has been used recently for the determination of a few transition elements, such as Fe^{3+},(2) Cu^{2+}(3) and UO_2^{2+}.(4) The azide ion N_3^-, similar to the thiocyanate, is a member of the pseudohalogenoid group and forms highly intense coloured complexes. Sodium azide, a strong electrolyte, has no absorption in the visible range; this is an advantage in spectrophotometric measurements. In spite of the high sensitivity of this reagent towards Cr(III), its use is limited to weakly acidic solutions. Strong mineral acids decompose the colour owing to the displacement of the weakly dissociated hydrazoic acid. Nevertheless, the determination can always be carried out in solutions with adjusted pH values and traces of chromium can thus be determined. Conditions for this procedure are discussed in the present investigation. The method of continuous variation of JOB(5) was applied to chromium azide in relatively concentrated solutions, so as to indicate the possible formation of different complexed species in the same solution.

(1) F. G. SHERIF and W. M. ORABY, *J. Inorg. Nucl. Chem.* **17**, 152 (1961).
(2) H. K. EL-SHAMY and F. G. SHERIF, *Egypt. J. Chem.* **1**, 35 (1958); **2**, 217 (1959).
(3) G. SAINI and G. OSTOCALI, *J. Inorg. Nucl. Chem.* **8**, 346 (1958).
(4) F. G. SHERIF and A. M. AWAD, *J. Inorg. Nucl. Chem.* **19**, 94 (1961).
(5) P. JOB, *C.R. Acad. Sci., Paris*, **180**, 928 (1925).

EXPERIMENTAL

The preparation and analysis of the different solutions used, together with the experimental procedures are given in a previous article.(1) The hydrated violet form of chromium nitrate was used. Colour intensities were measured by a Unicam spectrophotometer S.P.500. The pH values were measured using a Cambridge pH meter, model G.

RESULTS

Effect of concentration of reagents

The absorbancy of one series of solutions containing 0·008 M Cr(III) and 0·02 N $HClO_4$ and varying amounts of 1 M azide solution (25 ml total volume) was measured at the wavelength 440 mμ. From the data presented in Table 1, it appears that the maximum intensity of the colour was reached when the concentration of the reagent reached 0·2 M. Further addition of azide resulted in turbidity and eventually basic chromium azide was precipitated. However, in concentrated solutions the precipitate dissolved after 48 hr and the solution turned violet. In another series of solutions containing the above concentration of Cr(III) and 0·2 M NaN_3, varying amounts of 1 N $HClO_4$ were added and the total volume adjusted to 25 ml. Maximum absorbancy was reached when the concentration of acid was 0·06 N. Higher concentration of the acid resulted in a decrease in intensity and the solutions smelled strongly of hydrazoic acid. The pH values of this series of solutions were measured.

Table 1.—Effect of reagents on colour intensity Cr(III) = 0·008 M

Concn. of N^- in moles$_3$ (H^+ = 0·02 N)	Absorbancy 440 mμ	Conc. of $HClO_4$ N (N_3^- = 0·2 M)	pH	Absorbancy 440 mμ
0·04	0·27	0·01	5·48	0·64
0·08	0·54	0·02	5·39	0·67
0·12	0·61	0·03	5·22	0·75
0·16	0·65	0·04	5·05	0·81
0·20	0·67	0·06	4·77	0·84
0·24	0·64	0·08	4·46	0·82
		0·10	4·24	0·80
		0·14	3·94	0·58

The results are shown in Table 1. It was found that the optimum pH range for the maximum development of colour for analytical determinations lay between 4·2–5·2. Subsequent measurements were carried out using solutions within this acid concentration. Small changes in acid concentration in this range of pH have negligible effects on the colour, because the solutions are buffered by the HN_3–NaN_3 mixture formed. Acetate and phosphate buffer solutions could not be used to adjust the pH values as the Cr(III) ion forms interfering complexes with them.

When increasing amounts of different acids were added to chromium azide solutions prepared from NaN_3 and chromium perchlorate, nitrate, sulphate, chloride and acetate respectively, the colour intensity decreased irrespective of the anion of the acid.

In order to study the effect of anions, solutions of chromium azide were prepared from different salts of 0·02 M Cr(III) and 0·02 M azide with no adjustment of pH. It was found that the perchlorate solution was the most intense and the acetate was the least. The order of colour intensity was $ClO_4^- > NO_3^- > Cl^- > SO_4^{2-} > Ch_3COO^-$. This is in agreement with the well known fact that the perchlorate ion is the least complexing, giving enough free Cr(III) ions to react with the azide, while the chromium acetate complex is the most stable.

Stability of colour

The absorbancy of a solution which was 0·008 M with respect to Cr(III) and contained the optimum concentrations of reagents was measured periodically at 440 mμ against a reference solution containing the reagents. The temperature of the solution was kept at room temperature (24–28 °C). The rate of the reaction between the chromium and azide ions was found to be very slow. The absorbancy value was doubled in one hour. Then it increased slowly and the deep green colour of the complex seemed to be fully developed after two hours from mixing and did not change for at least 6 hr. The absorbancies of some solutions were found to be unchanged after 2 days.

Effect of temperature and light

Solutions containing excess of azide were found to be stable to temperature changes in a range of 15–45°C. There was a negligible difference between the intensities of solutions at varying temperatures and those kept at room temperature as long as the colour was already fully developed. No difference was found between two solutions containing the same chromium concentration and reagents, one being kept in the dark and the other exposed to daylight over the same period of time (2 days).

Conformity to Beer's law

A number of solutions containing varying amounts of chromium and the optimum amounts of azide and perchloric acid were prepared and their absorbancies measured at 440 mμ after 2 hr from mixing, using a reagent blank. A plot of absorbancy values against Cr(III) concentration gave a straight line passing through the origin, showing that Beer's law is obeyed in a range of 4–320 p.p.m. Cr(III), with a sensitivity of 2 p.p.m. This method has a distinct advantage of providing a wide range of applicability. The lower limit could be extended significantly by the use of longer cells. This is especially promising as the absorption of the reagent itself is negligible.

Effect of diverse ions

In order to study the effect of diverse ions, solutions containing 0·008 M Cr^{3+}, 0·2 M N_3^- and 0·06 N H^+ were prepared and solutions of different ions were then added in a titration fashion. The absorbancy of the mixture was measured after each addition, allowing for colour development of the original solution prior to measurements. The results are corrected for volume changes. A change of $\pm 0{\cdot}01$ of absorbancy unit is considered to be interference. The results are given in Table 2. The interference of Cu^{2+} and UO_2^{2+} ions can be reduced appreciably by the addition of 1 ml of 0·05 M solution of EDTA. Interference of Fe^{3+} ions could only be decreased by the addition of 2 ml of EDTA and measurement at 500 mμ. The phosphate ions form a precipitate after the addition of few fractions of a ml of the solution. Thorium behaves similarly, but suitable increase of acid concentration will prevent precipitation.

TABLE 2.—MAXIMUM TOLERANCE OF INTERFERING IONS
Cr^{3+} = 0·008 M; N_3^- = 0·2 M; H^+ = 0·06 N; λ = 440 μ

Ion	Added as	Maximum tolerance (p.p.m.)
Cu^{2+}	$CuCl_2$	0·3 (35)
UO_2^{2+}	$UO_2(NO_3)_2$	6 (34)
Fe^{3+}	$Fe(NO_3)_3$	0·1 (33)
Th^{4+}	$Th(NO_3)_4$	46
Ni^{2+}	$NiCl_2$	96
Mn^{2+}	$MnCl_2$	130
Ce^{3+}	$Ce(NO_3)_3$	110
NH_4^+	NH_4NO_3	24
Hg^{2+}	$HgCl_2$	240
VO_3^-	$NaVO_3$	12
$Mo_7O_{24}^{6-}$	$(NH_4)_6Mo_7O_{24}$	32
WO_4^{2-}	Na_2WO_4	300
$Cr_2O_7^{2-}$	$K_2Cr_2O_7$	170
PO_4^{3-}	Na_3PO_4	300
F^-	NaF	160

Values in parentheses for Cu^{2+} and UO_2^{2+} are taken in presence of 1 ml of 0·05 M EDTA. The value for Fe^{3+} is in presence of 2 ml of EDTA at λ = 500 μ.

Structure of the chromium azide complex in dilute solutions

It was shown previously that a monoazidochromium(III) ion, CrN_3^{2+}, can be formed in dilute aqueous solutions containing chromium nitrate and sodium azide,⁽¹⁾ that have two absorption maxima at 440 and 605 mμ. The logarithmic method of BENT and FRENCH⁽⁶⁾ was applied here to further confirm these results. In one series of solutions the total concentration of chromium was kept constant at 0·024 M and that of azide was varied from 0·002 to 0·012 M, keeping the ionic strength constant at 0·156 by adding the appropriate amounts of sodium perchlorate solution. The absorbancy was measured at 440 mμ. The logarithm of the absorbancy was a linear function of the logarithm of the N_3^- ion concentration (Fig. 1). In a second series of solutions the concentration of sodium azide was kept constant at 0·012 M and that of chromium was varied from 0·004 to 0·020 M, keeping the ionic strength the same as before. The logarithmic relation was similarly obtained. The reaction between chromium and azide ions can be represented by the equation:

$$m\,Cr^{3+}+n\,N_3^- = [Cr_m(N_3)_n]^{(3m-n)+} \qquad (1)$$

The logarithm of absorbancy will be proportional to log $[Cr_mN_{3n}]$ in the logarithmic expression:

$$\text{Log}\,[Cr_mN_{3n}] = m \log [Cr^{3+}]+n \log [N_3^-]+\log K \qquad (2)$$

The experimental points were found to fall on the theoretical line with the assumption that $m = n = 1$.

⁽⁶⁾ H. E. BENT and C. L. FRENCH, *J. Amer. Chem. Soc.* 63, 568 (1941).

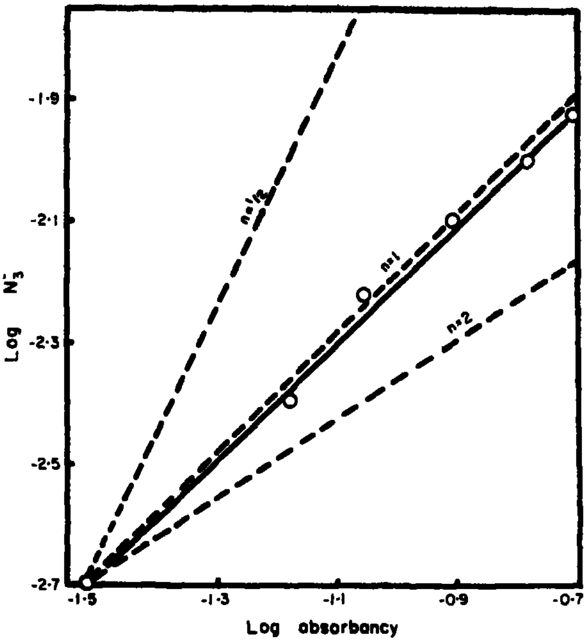

FIG. 1.—Limiting logarithmic method at wavelength 440 mμ. Cr^{3+}: 0·024 M and azide concn. varied from 0·002 to 0·012 M. Ionic strength = 0·156. The circles are the experimental points. The dotted lines represent the theoretical values for n = 0·5, 1 and 2, where *n* is the number of azide ions associated with one Cr^{3+} ion in the complex.

Structure of the complex in concentrated solutions

The method of continuous variations of JOB(5) was applied at different wavelengths and at different total concentrations. The contours of the curves obtained in every case would be indicative of the formation of different coloured species with different stabilities and absorption properties. Deformed curves might be obtained in the stepwise formation of complex ions formed from a metallic ion and the same ligand, if the formation constants and maximum absorptions are not widely separated from each other.

In our work, the observed absorbancy values were plotted against the mole fraction of the metallic ion rather than *Y* values (Y = difference between observed values and those calculated for no reaction) as stated by JOB, since it was found that there is no difference between the contours of the curves in both cases. The blank used was a chromium nitrate solution of the same concentration as that present in the test solution. Three different runs with total concentrations of 0·04, 0·16 and 0·32 M were carried out using equimolar solutions. In our previous report,(1) it was stated that a 1:1 compound, CrN_3^{2+} is formed in dilute solution, at a total concentration of 0·008 M. In Fig. 2, the irregularity of the curves near the maximum can be smoothed to one sharp maximum at a mole fraction of Cr(III) of 0·333 suggesting the formation of a 1:2 complex, $Cr(N_3)_2^+$. When the rules of VOSBURGH and COOPER(7) were applied, the solid curve was obtained, showing one definite maximum at 1:2 molar ratio, assuming that the 1:1 complex was first formed. At a

(7) W. C. VOSBURGH and G. R. COOPER, *J. Amer. Chem. Soc.* 63, 437 (1941).

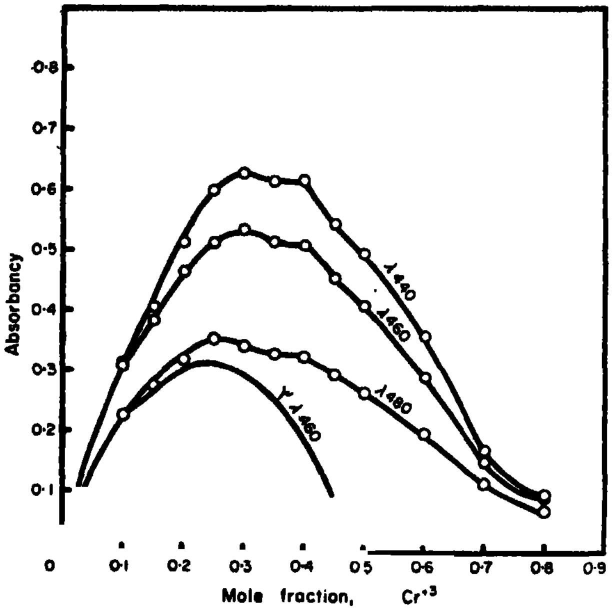

FIG. 2.—Continuous variation method; total concentration of Cr(III) and azide ions is 0·04 M. *Y'* = Observed values minus those calculated for a 1:1 complex.

total concentration of 0·16 M, the results show that the prevailing species in solution are the 1:3 complex. In solutions having a total concentration of 0·32 M (Fig. 3) there is sufficient contribution from the 1:1 form to produce a definite asymmetry

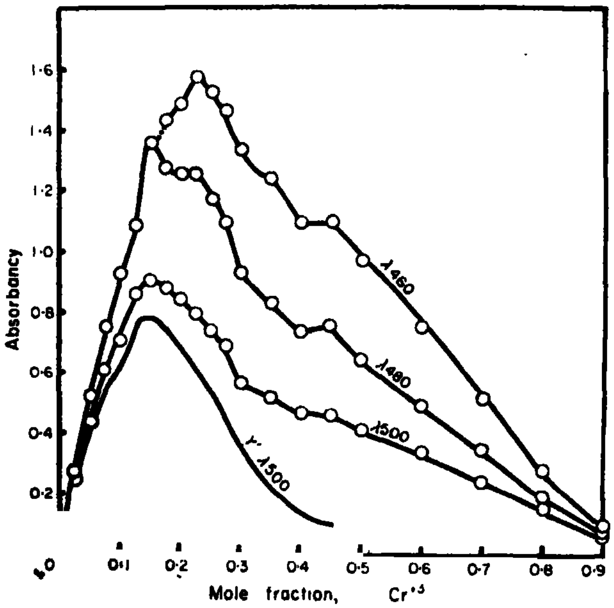

FIG. 3.—Continuous variation method; total concentration of Cr(III) and azide ions is 0·32 M. *Y'* = Observed values minus those calculated for 1:1 Cr:azide.

in the curves, as shown by the shoulder at a mole fraction of Cr(III) of 0·45. However, there is a clear maximum at longer wavelengths, 480 and 500 mμ, indicating the formation of a 1:6 compound $Cr(N_3)_6^{3-}$. As we approach shorter wavelengths, e.g. 460 mμ, the maximum falls at a ratio of 1:4, $Cr(N_3)_4^-$. By applying the rules of VOSBURGH and COOPER and plotting the difference between the observed values and those calculated for 1:1, the interference in the different curves due to the 1:1 form disappears, and a curve with one maximum at a ratio of 1:6 is obtained.

These data show that the increase in concentration of reagents leads to the formation of azide-rich complexes. Higher complexes are easier to identify as we approach longer wavelengths. These results are confirmed by observing a hypsochromic effect produced upon the gradual increase in azide ion concentration with respect to a solution 0·04 M Cr(III). The colour changes gradually from deep green to distinct violet, and the maxima change from 440 and 605 mμ to 490 and 655 mμ respectively.

J. Inorg. Nucl. Chem., 1962, Vol. 24, pp. 1381 to 1386. Pergamon Press Ltd. Printed in England

THE BASICITY AND DISSOCIATION CONSTANTS OF SOME COMPLEX MOLYBDIC ACIDS

E. R. Clark
College of Advanced Technology, Gosta Green, Birmingham 4

(*Received* 9 *January* 1962; *in revised form* 2 *April* 1962)

Abstract—The behaviour of molybdoquinic, molybdocitric, molybdogluconic and molybdotartaric acids during titration with sodium hydroxide in media of approximately constant ionic strength has been investigated. A dilute solution of molybdoquinic acid behaves as a monobasic acid (pK_1 = 1·88 in 0·1 N KCl) and is decomposed at pH 5·0. pK values for molybdocitric and molybdogluconic acids (also in 0·1 N KCl) are pK_1 = 2·18, pK_2 = 5·24 and pK_1 = 2·42, pK_2 = 6·18 respectively. Molybdotartaric acid behaves as a tribasic acid in dilute solution from pH 2·0–6·5 (pK_1 = 2·12, pK_2 = 3·82, pK_3 = 6·22) and is decomposed around pH 6·5. The complex acids are stronger acids than the parent acids from which they are formed.

Reaction between certain α-hydroxy acids and molybdic acid has been reported by many workers,(1–10) using many different methods. Much of the previous work has been carried out using either sodium molybdate, impure molybdic acid or impure molybdenum trioxide. This has been criticized by Richardson(11) who developed a method for the production of pure molybdic acid solutions using a cation exchange resin and used this solution to investigate the reaction between molybdic acid and aqueous solutions of various α-hydroxy acids. The solubility of pure molybdenum trioxide in water and in solutions of polyhydroxyalcohols has also been investigated by Richardson.(12)

The presence of well-defined complexes of molybdic acid with citric, tartaric, quinic and gluconic acids in aqueous solution is well established although different ratios Mo/organic acid have been reported for the tartaric acid complex.

The titration of lactic and tartaric acids by a solution of sodium molybdate has been studied by Rao and Pani.(6) The behaviour of the 1:1 tartaric acid complex during titration has been examined by Britton and Jackson(8) but solutions were prepared from sodium molybdate, tartaric acid and hydrochloric acid, and thus the ionic strength was not kept constant. More recently, the natures of the 1:1 molybdate

(1) E. Rimbach and P. Ley, *Z. Phys. Chem.* **100**, 393 (1922).
(2) A. B. Biswas, *J. Indian Chem. Soc.* **22**, 351–8 (1945).
(3) M. Theodoresco, *C.R. Acad. Sci., Paris*, **204**, 1649–51 (1937).
(4) A. B. Biswas, *J. Indian Chem. Soc.* **23**, 249–57 (1946).
(5) P. Souchay, *Bull. Soc. Chim., France*, 914–24 (1947).
(6) D. V. R. Rao and S. Pani, *Current Sci., India*, **22**, 273–4 (1953).
(7) Y. K. Heng, *J. Chem. Phys.* **33**, 356–413 (1936).
(8) H. T. S. Britton and P. Jackson, *J. Chem. Soc.* 1055 (1934).
(9) M. J. Baillie and D. H. Brown, *J. Chem. Soc.* 3691–95 (1961).
(10) D. H. Brown, *J. Chem. Soc.* 4732–6 (1961).
(11) E. Richardson, *J. Inorg. Nucl. Chem.* **9**, 273–8 (1959).
(12) E. Richardson, *J. Inorg. Nucl. Chem.* **12**, 349–53 (1960).

and tungstate complexes of tartaric acid have been investigated by BAILLIE and BROWN(9) using polarimetric, conductometric and potentiometric methods. These workers investigated the tartrato tungstate complex in detail but report that "the molybdate complexes appear only to exist over a limited, more acid region." The potentiometric titration of the complex acids of molybdenum in media of approximate constant ionic strength has not previously been carried out. A study would be worthwhile to determine not only the basicity of the complex acids but also their dissociation constants and stability at different pH values.

EXPERIMENTAL

Materials

All chemicals used were of Analar quality. The molybdenum trioxide gave no reaction for ammonia. The conductivity water used was prepared by passing distilled water through a mixed bed deionization column consisting of Amberlite Resin IR 120 and IR 400.(14) All samples had a conductivity of $1 \cdot 0$–$1 \cdot 5 \times 10^{-6}$ mhos at 25°C.

Potentiometric titration

Solutions of the complex acids were prepared by dissolving the required amount of MoO_3 in 0·01 or 0·005 M solutions of the hydroxy acid, the solutions being made 0·1 N with respect to KCl. Complete solution was effected by heating on a hot plate for 4–6 hr. with constant stirring by a magnet coated with "Polythene".

Fifty ml aliquots of the complex molybdic acid solutions contained in a special cell(15) were titrated with a standard solution of sodium hydroxide using a Cambridge portable pH meter and glass and silver/silver chloride electrodes standardised with a mixture of 0·01 N HCl and 0·09 N KCl (Veibels solution) which has a pH of 2·10 at 25°C.(16) All pH readings were carried out at 25°C and within 48 hr of preparation of the solutions.

DISCUSSION AND RESULTS

RICHARDSON has investigated the solubility of MoO_3 in aqueous solutions of some polyhydroxy compounds(12) and in certain cases observed enhanced solubility. As a preliminary to the work described in this paper it was found that α-hydroxy acids likewise give enhanced solubility of MoO_3, and the reaction may be followed conductiometrically. Dissolution is rapid at first, especially if agitation and heat are used, but falls off after a time.* Various quantities of MoO_3 and 0·04 M solutions of the α-hydroxy acids were mixed such that the total concentration of Mo and acid was equal to 0·04 M. After 4 hr on a water bath the solutions were cooled and made up to the required volume. The conductivities of these mixtures showed maxima at certain molar ratios indicating that citric, tartaric, quinic and gluconic acids react with molybdic acid in mole ratios MoO_3:organic acid of 1:1, 1:2, 1:2 and 1:2 respectively. These results, except that for the citric acid complex, are in agreement with those observed by RICHARDSON.(13) The method of continuous variations has been criticised(17) but analysis of the potentiometric titration curves of the complex acids as shown below indicates that the assumption that only one species of complex acid is present in solution is justified.

---

* Over 95 per cent of the MoO_3 dissolves in the first hour if water bath temperatures are used.

(13) E. RICHARDSON, *J. Inorg. Nucl. Chem.* **13**, 84–90 (1960).

(14) C. W. DAVIES and G. H. NANCOLLAS, *Chem. and Indust.* **7**, 129 (1950).

(15) E. R. CLARK, *J. Inorg. Nucl. Chem.* **24**, 82, (1962)

(16) R. G. BATES, *Electrometric pH determinations*, pp. 73–4. J. Wiley, New York (1954).

(17) F. WOLDBYE, *Acta. Chem. Scand.* **9**, 299 (1955).

It is difficult to produce 0·04 M solutions of the complex acids using MoO_3 even if heat and agitation are used. A very small quantity of MoO_3 remains undissolved even after long periods. However, more dilute solutions, i.e. 0·01 M or 0·005 M, can be prepared by boiling the required amount of MoO_3 with solutions of the hydroxy acid which must be stirred rapidly. Periods of up to 6 hr were used and in all cases there was no formation of molybdenum blue.†

The potentiometric titration of 0·01 M gluconic and quinic acids and these two acids containing 0·005 M MoO_3 at 25°C in 0·1 N KCl are shown in Fig. 1. Molybdogluconic and molybdoquinic acids become unstable at pH 6·5 and pH 5 respectively (points *A* and *B* on Fig. 1) and the titrations were not continued above these particular values. In fact, steady readings could not be obtained immediately. The pH values of the solutions were initially very high and then gradually dropped to a lower value over a period of 5 min or so. Presumably some type of rearrangement is occurring, possibly with the formation of another complex anion. Analysis of the potentiometric titration curves for these two complex acids by the procedure outlined in a previous

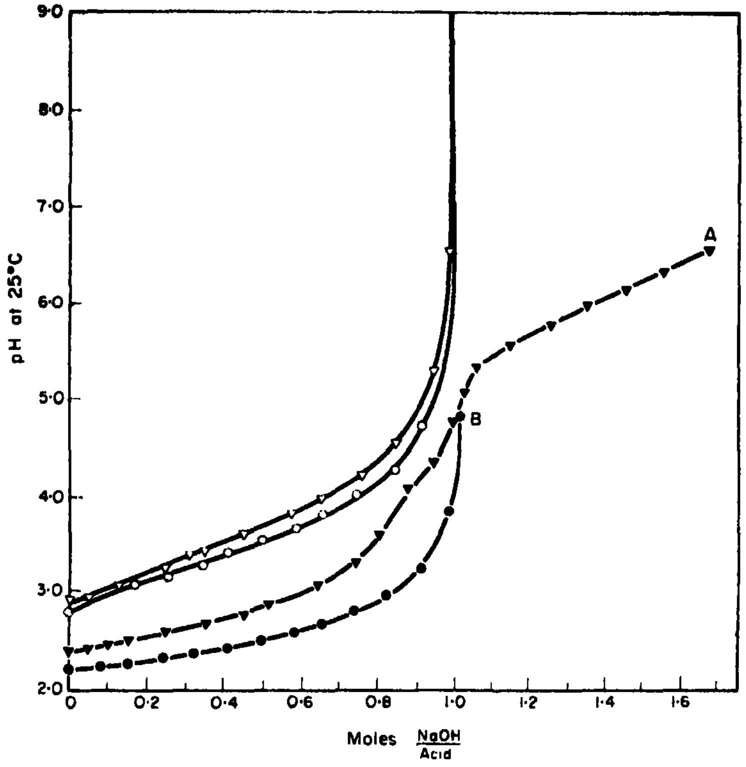

Fig. 1.—Potentiometric titrations at 25°C ○ 0·01 M quinic acid, ● 0·01 M quinic acid containing 0·005 M MoO_3, ▽ 0·01 M gluconic acid, ▼ 0·01 M gluconic acid containing 0·005 M MoO_3.

---

† Similar experiments with MoO_3 and mandelic and malic acids resulted in the formation of pale blue coloured solutions.

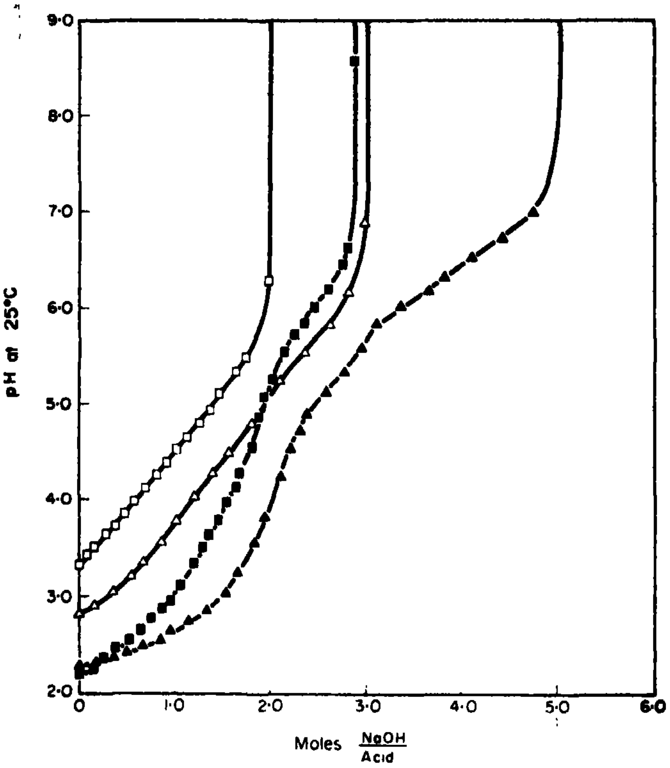

FIG. 2.—Potentiometric titrations at 25°C □ 0·01 M tartaric acid, ■ 0·01 M tartaric acid containing 0·005 M MoO_3, Δ 0·005 M citric acid, ▲ 0·005 M citric acid containing 0·005 M MoO_3.

paper(15) indicates that during titration molybdoquinic acid and molybdogluconic acid behave as monobasic and dibasic acids respectively. The plot of hx against x where h = hydrogen ion concentration and $x = a+h-kw/h$ (a = concentration of added alkali), gives straight line plots (Fig. 3) for both of the complex acids indicating that the Henderson equation is being obeyed. K for molybdoquinic acid is $1{\cdot}33\times10^{-2}$ and K_1 for molybdogluconic acid $3{\cdot}77\times10^{-3}$. K_2 for the latter acid is approximately $6{\cdot}6\times10^{-7}$. Results in this region of pH are not considered as accurate as those at lower pH values. The dissociation constants of the parent acids can also be calculated from the titration curves (Fig. 1). Results (Fig. 4) give K for quinic acid as $3{\cdot}30\times10^{-4}$ (pK = 3·48) and gluconic acid as $2{\cdot}70\times10^{-4}$ (pK = 3·57).

The potentiometric titration of 0·005 M citric acid and 0·005 M citric acid containing 0·005 M MoO_3 is shown in Fig. 2. Analysis of the titration curves shows that molybdocitric acid behaves as a dibasic acid up to pH 5·8 with $K_1 = 6{\cdot}72\times10^{-3}$ (Fig. 3), and $K_2 = 5{\cdot}73\times10^{-6}$.* Deviation from the straight line relationship occurs at pH 5·8 and it is probable that at this pH value hydrogen ions from a third stage are being replaced before those from the second stage have been completely replaced by sodium ions. It seems likely that a third stage exists but the dissociation constants are too close together and although a value of K_3 could be obtained from the titration curve it is not considered to be very accurate and is not reported here. There is no indication of any rearrangement taking place during titration.

* Graph not reproduced.

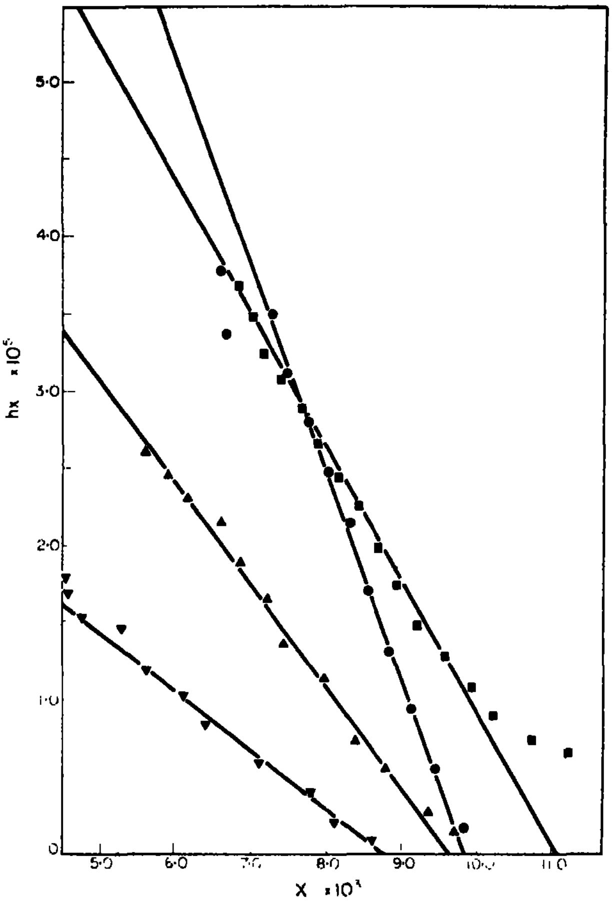

FIG. 3.—Plot of *hx* against *x*. ■ molybdotartaric acid (1st stage), ● molybdoquinic acid (1st stage), ▲ molybdocitric acid (1st stage), ▼ molybdogluconic acid (1st stage).

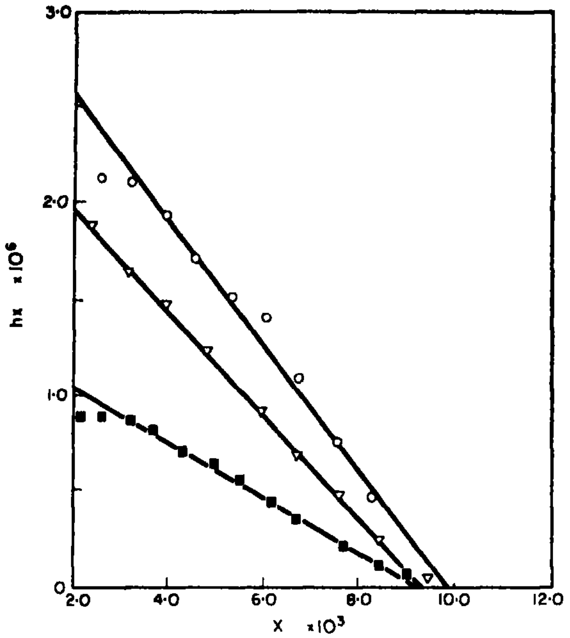

FIG. 4.—Plot of *hx* against *x*. ○ quinic acid, ▽ gluconic acid, ■ molybdotartaric acid (2nd stage).

Analysis of the results of potentiometric titration of 0·01 M tartaric acid and 0·01 M tartaric acid containing 0·005 M MoO_3 (Fig. 2) shows that the complex acid behaves as a tribasic acid up to pH 7·0. $K_1 = 7{\cdot}56 \times 10^{-3}$ (Fig. 3), $K_2 = 1{\cdot}50 \times 10^{-4}$ (Fig. 4) and $K_3 = 6{\cdot}00 \times 10^{-7}$.* pH readings became difficult to observe near pH 6·5 and it is likely that the complex acid is decomposed in this region possibly with the formation of another complex anion of different Mo/acid ratio.

For all the molybdo-acids it is likely that reaction takes place through carboxylic and/or hydroxyl groups. There is no simple relationship between the total number of carboxylic and hydroxyl groups available and the basicity of the complex acid. However, the basicity of molybdoquinic and molybdogluconic acids is smaller than the other two investigated and yet the parent acids contain a large number of hydroxyl groups. Evidently, α-hydroxy groups are the most important as far as complexing is concerned.

---

*Graph not reproduced.

J. Inorg. Nucl. Chem., 1962, Vol. 24, pp. 1387 to 1397. Pergamon Press Ltd. Printed in England

COMPARATIVE EXTRACTION OF U(VI) BY NEUTRAL AND MONO-ACIDIC PHOSPHATES AND PHOSPHONATES*

D. F. Peppard, G. W. Mason, I. Hucher and F. A. J. A. Brandao†
Argonne National Laboratory, Argonne, Illinois

(*Received* 13 *March* 1962; *in revised form* 11 *April* 1962)

Abstract—The extraction of U(VI) by a neutral phosphate extractant, tri 2-ethyl hexyl phosphate, and by the analogous neutral phosphonate extractant, di 2-ethyl hexyl 2-ethyl hexyl phosphonate, in toluene diluent from an aqueous nitrate phase, as expressed by the distribution ratio, K, for α-active ^{233}U, has been shown to be second-power dependent upon the concentration of extractant in the organic phase and second-power dependent upon the concentration of nitrate ion in the aqueous phase. An inhibiting effect is noted at nitrate concentrations in excess of 0·5 F, the K falling below the theoretical curve. Under identical conditions, the phosphonate is approximately thirty-three times more effective in extracting U(VI) than is the phosphate.

The extraction of U(VI) by a mono-acidic phosphate, di 2-ethyl hexyl phosphoric acid, and by the analogous mono-acidic phosphonate, 2-ethyl hexyl hydrogen 2-ethyl hexyl phosphonate, in toluene diluent from an aqueous 1·00 F (HX+NaX) phase, X = ClO_4^-, Cl^-, NO_3^-, has been shown to be second-power dependent upon the concentration of extractant in the organic phase and inversely second-power dependent upon the concentration of hydrogen ion in the aqueous phase. (The extraction of U(VI) by a (GO)GPO(OH) extractant is reported for the first time.) Essentially no difference between the ClO_4^- and NO_3^- data were noted. The difference between the ClO_4^- and Cl^- data is consistent with the assumption of a stability constant of 0·8 ± 0·2 for the UO_2Cl^+ complex, μ = 1·00, 22 ± 1°C. In all of these systems, the acidic phosphonate excels the acidic phosphate by a factor of 1·9 ± 0·2.

The relative phosphonate/phosphate data of U(VI) are compared with those for Th(IV), lanthanides(III) and actinides(III).

The possible difficulties encountered in the use of neutral phosphonates and phosphates as extractants in determining stability constant of M^{b+} nitrate complexes are discussed.

The comparative extraction of U(VI), presumably as $UO_2(NO_3)_2S_2$, where S represents the extractant molecule, from an aqueous nitrate phase by neutral phosphate and phosphonate esters has been studied by a number of investigators(1, 2, 3a, 4) who agree that a given phosphonate is superior to the analogous phosphate. The extraction of selected M(III) cations by mono-acidic phosphonates has been reported recently;(5) and it was noted, in comparison with mono-acidic phosphate data, that the acidic phosphonate is inferior to the analogous acidic phosphate.

---

* Based on work performed under the auspices of the U.S. Atomic Energy Commission.

† Participant, sponsored by the National Nuclear Energy Commission, Rio de Janiero, Brazil, in the Ninth Session of the International School of Nuclear Science and Technology.

(1) L. L. Burger, *J. Phys. Chem.* 62, 590 (1958).

(2) C. A. Blake, Jr., C. F. Baes, Jr., K. B. Brown, C. F. Coleman and J. C. White, *Proceedings of the Second International Conference on the Peaceful Uses of Atomic Energy, Geneva* (1958), 28, 289. Paper P/1550 United Nations (1958).

(3) (a) C. A. Blake, Jr., C. F. Baes, Jr. and K. B. Brown, *Industr. Engng. Chem.* 50, 1763 (1958).
(b) C. F. Baes, Jr., R. A. Zingaro and C. F. Coleman, *J. Phys. Chem.* 62, 129 (1958).

(4) T. H. Siddall, III, *Industr. Engng. Chem.* 51, 41 (1959).

(5) D. F. Peppard, G. W. Mason and I. Hucher, *J. Inorg. Nucl. Chem.* 18, 245 (1961).

Accordingly, a study of the extraction of U(VI) by $(GO)_3PO$ and $(GO)_2GPO$, analogous neutral phosphate and phosphonate extractants respectively, and by $(GO)_2PO(OH)$ and $(GO)GPO(OH)$, analogous mono-acidic phosphate and phosphonate extractants respectively, all in toluene diluent, G = 2-ethyl hexyl, from aqueous nitrate phases was undertaken in order to establish the relative extractive power and the effect of varying nitrate concentration. The acidic extractant studies were extended to include aqueous chloride and perchlorate phases.

EXPERIMENTAL

Nomenclature

In accordance with previous usage(5, 6) in which H represents a theoretically ionizable hydrogen and G a generalized organic group bound at a C atom, the symbolic formulae $(GO)_3PO$ and $(GO)_2GPO$ respectively represent homogeneous neutral phosphates and phosphonates, and the symbolic formulae $(GO)_2PO(OH)$ and $(GO)GPO(OH)$ respectively represent homogeneous monoacidic phosphates and phosphonates. These four classes of compounds are further represented, respectively, as TGP, DG[GP], HDGP and HG[GP], the bracket indicating the grouping joined by a C-P bond. In the present study, G is specifically 2-ethyl hexyl represented as EH. Therefore, the extractants are symbolized and named as: $(EHO)_3PO$, TEHP, tri(2-ethyl hexyl) phosphoric acid; $(EHO)_2(EH)PO$, DEH[EHP], di(2-ethyl hexyl) 2-ethyl hexyl phosphonate; $(EHO)_2PO(OH)$, HDEHP, di(2-ethyl hexyl) phosphoric acid; and $(EHO)(EH)PO(OH)$, HEH[EHP], 2-ethyl hexyl hydrogen 2-ethyl hexyl phosphonate.

Since the two mono acidic extractants are dimeric(7–10) in benzene and cyclohexane, they are assumed to be dimeric in toluene. Therefore, in the interest of brevity in the discussion of extraction mechanisms, both extractants are represented as HY in the theoretical monomeric state, Y representing the aggregate excepting the theoretically ionizable hydrogen atom, and as $(HY)_2$ in the dimeric state. Similarly, in stoicheiometric expressions, the neutral extractants, TEHP and DEH[EHP] are symbolized as N.

The distribution ratio, K, of U(VI) is defined as the concentration of ^{233}U in the upper divided by the concentration of ^{233}U in the lower of two mutually equilibrated sensibly-immiscible liquid phases, the upper phase in this study being a toluene solution of the extractant under study. The quantity K_S is defined by the expressions in which it occurs as is K_N.

Sources of materials

The neutral extractants, tri(2-ethyl hexyl) phosphoric acid, TEHP, and di(2-ethyl hexyl) 2-ethyl hexyl phosphonate, DEH[EHP], were obtained from Union Carbide Chemicals Co. and Virginia-Carolina Chemical Corporation, respectively.

Di-(2-ethyl hexyl) phosphoric acid, HDEHP, was obtained from Virginia-Carolina Chemical Corporation; and 2-ethyl hexyl hydrogen 2-ethyl hexyl phosphonate, HEH[EHP], was prepared by hydrolysis of DEH[EHP] as described previously.(9)

The $HClO_4$, HNO_3 and HCl and their corresponding salts were purified as described previously.(11a)

α-active $1{\cdot}6 \times 10^5$ year ^{233}U (^{238}U:^{233}U mass ratio less than 0·03) was obtained from Argonne National Laboratory stocks and re-purified by extraction and scrubbing using the tri n-butyl phosphate vs. HCl system.(11b)

---

(6) D. F. PEPPARD, G. W. MASON, W. J. DRISCOLL and R. J. SIRONEN, *J. Inorg. Nucl. Chem.* **7**, 276 (1958).

(7) D. F. PEPPARD, J. R. FERRARO and G. W. MASON, *J. Inorg. Nucl. Chem.* **4**, 371 (1957).

(8) D. F. PEPPARD, J. R. FERRARO and G. W. MASON, *J. Inorg. Nucl. Chem.* **7**, 231 (1958).

(9) D. F. PEPPARD, J. R. FERRARO and G. W. MASON, *J. Inorg. Nucl. Chem.* **12**, 60 (1959).

(10) J. R. FERRARO, G. W. MASON and D. F. PEPPARD, *J. Inorg. Nucl. Chem.* **22**, 285 (1961).

(11) (a) D. F. PEPPARD, G. W. MASON and S. MCCARTY, *J. Inorg. Nucl. Chem.* **13**, 138 (1960).
(b) D. F. PEPPARD, G. W. MASON and M. V. GERGEL, *J. Inorg. Nucl. Chem.* **3**, 370 (1957).

Purification of extractants

A modification of the technique reported[12] for the purification of tri n-octyl phosphine oxide, $(n\text{-}C_8H_{17})_3PO$, TOPO, was employed in the purification of the neutral extractants, TEHP and DEH[EHP]. The extractant, as received, was dissolved in benzene to form a solution approximately 0·4 F. This solution was stirred with an equal volume of 6 M HCl, with which it is sensibly immiscible, at approximately 60°C for 8 hr. This benzene solution was then successively contacted (using equal-volume portions) with: two water scrubs, three aqueous 5% Na_2CO_3 scrubs and eight water scrubs. The benzene (and dissolved water) were then removed from the separated organic phase under reduced pressure at room temperature using the rotating evacuated flask technique previously described in the purification of acidic organo-phosphorus compounds.[8] The extractants were stored, excluding moisture and light, until needed, at which time the appropriate solutions were prepared using toluene as carrier diluent.

The purification of HDEHP[6] and of HEH[EHP][9] has been described previously.

Determination of distribution ratios

The distribution ratio, *K*, of U(VI) was determined, in a general way, as described in previous studies,[6, 11] the phases, in a 5 ml stoppered glass cylinder, being mixed by manual shaking. (The values are considered to be correct within ± 5 per cent.) In each instance, the organic and aqueous phases were mutually pre-equilibrated before use. (This was presumably an unnecessary precaution, in the case of the acidic extractants, since the transfer of mineral acid and/or water to the organic phase and the transfer of organic extractant and/or diluent to the aqueous phase were negligible.) All data were obtained using reverse extractions followed by confirmatory direct extractions, i.e., the U(VI) was extracted into the organic phase, the pregnant organic phase contacted with a barren aqueous phase to yield "reverse extraction" data and the resultant pregnant aqueous phase contacted with barren organic

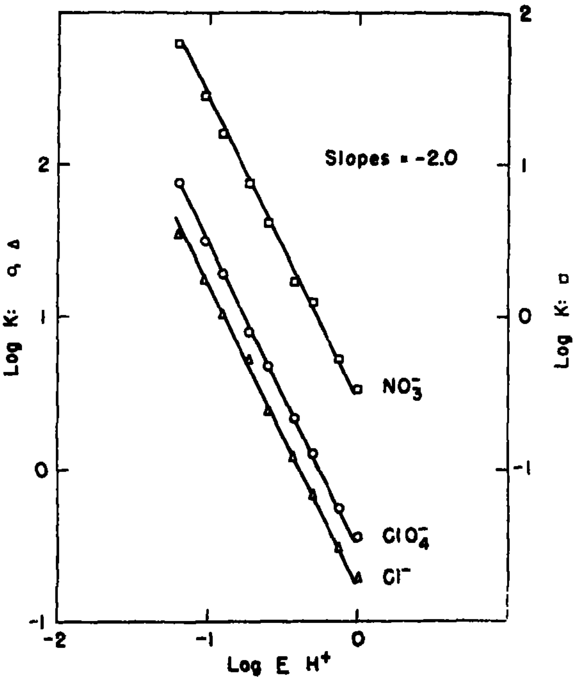

FIG. 1.—Hydrogen ion dependency of the extraction of U(VI) into $1{\cdot}88 \times 10^{-2}$ F HDEHP, toluene diluent, from a 1·00 F (NaX+HX) solution; $X^- = ClO_4^-$, Cl^-, NO_3^-.

---

[12] G. W. MASON, S. MCCARTY and D. F. PEPPARD, *J. Inorg. Nucl. Chem.* **24**, 967 (1962)

phase to yield "direct extraction" data. In each instance, a contact time of three minutes was employed. Suitable aliquots, usually 0·050 ml, were then evaporated on platinum disks, using induction heating, for radiometric assay by α-counting.

In each experiment involving an aqueous phase with salt content, a 1·0 ml portion of the separated aqueous phase, following partition of the metal tracer, was contacted with a 1·0 ml portion of a toluene solution of HEH[EHP] sufficiently concentrated to assure a *K* in excess of 500. An aliquot of the resultant organic phase was then evaporated on a platinum disk. The analysis of this aliquot is equivalent to the analysis of an identical aliquot of the equilibrated aqueous phase.

In all such studies the supporting cation was Na^+.

All data were obtained at 22 ± 1 °C.

The extraction of the mineral acids $HClO_4$, HCl and HNO_3 by a toluene solution of the acidic extractants employed is negligible under the conditions of this study.

RESULTS AND CONCLUSIONS

Acidic extractants

In Figs. 1 and 2, the *K* for U(VI) is seen to vary inversely with the second-power of the concentration of hydrogen ion in the equilibrated aqueous phase at a constant ionic strength of 1·00, the anion being ClO_4^-, Cl^- or NO_3^-. For both the HDEHP (Fig. 1) and HEH[EHP] (Fig. 2) systems, the NO_3^- curve is essentially coincident with the ClO_4^- curve, and the Cl^- curve is below the latter by a factor of approximately 1·9. From these data, it is concluded that no anion of the mineral acid is contained in the extracted species.

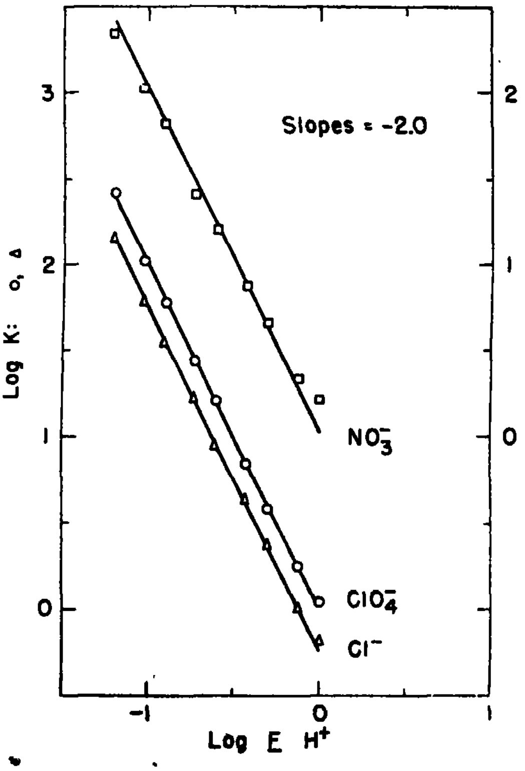

Fig. 2.—Hydrogen ion dependency of the extraction of U(VI) into 2·65 × 10^{-2} F HEH[EHP], toluene diluent, from a 1·00 F (NaX + HX) solution; $X^- = ClO_4^-$, Cl^-, NO_3^-.

In Figs. 3 and 4, the K for U(VI) is seen to vary directly with the second-power of the concentration of extractant in the equilibrated organic phase, the opposing phase being a 1·00 F solution of $HClO_4$, HCl or HNO_3.

The stoicheiometry of the extraction is therefore considered to be:

$$UO_{2A}^{2+} + 2(HY)_{2A} \rightleftharpoons UO_2(HY_2)_{2O} + 2H_A^+ \qquad (1)$$

where $(HY)_2$ represents the dimeric form of HDEHP or HEH[EHP], and the subscripts A and O refer to mutually equilibrated aqueous and organic phases, respectively. This stoicheiometry has been reported previously for HDEHP in a different diluent.(3) The HEH[EHP] extraction of U(VI) is reported for the first time. The corresponding expression for K is:

$$K = k_1[(HY)_2]_O^2/[H^+]_A^2 \qquad (2)$$

where k_1 is the mass law equilibrium constant for Expression (1). By substitution of $K_S F_O^2$ for $k_1[(HY)_2]_O^2$ where F is the number of formula weights of the extractant per litre of equilibrated organic phase, and rearranging, Expression (2) is transformed into:

$$K_S = K[H^+]_A^2/F_O^2 \qquad (3)$$

K_S being interpreted as the hypothetical value of K for a system employing 1·0 F H^+ in the aqueous phase and 1·0 F extractant in the organic phase.(5, 6) It should be noted that K_S is dependent upon the ionic strength of the aqueous phase, upon the anions present and upon the diluent employed.

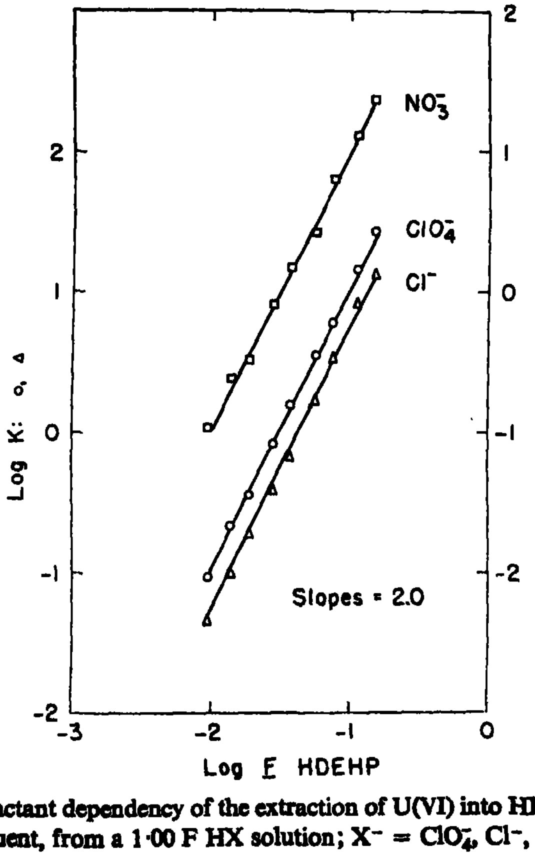

FIG. 3.—Extractant dependency of the extraction of U(VI) into HDEHP, toluene diluent, from a 1·00 F HX solution; $X^- = ClO_4^-, Cl^-, NO_3^-$.

The K_S values as determined from the straight lines of the respective acid and extractant dependency curves differ only slightly, Figs. 1 and 3 for HDEHP and Figs. 2 and 4 for HEH[EHP], the averages being given in Table 1.

Table 1.—Comparison of K_S values for U(VI) in HY (toluene diluent) vs. aqueous 1·00 F (HX+NaX) systems at 22±1 °C

X^-	K_S for HY: HDEHP	K_S for HY: HEH[EHP]	$\frac{K_{S\ HEH[EHP]}}{K_{S\ HDEHP}}$
ClO_4^-	$9{\cdot}5\times10^2$	$1{\cdot}7\times10^3$	1·8
Cl^-	$5{\cdot}2\times10^2$	$9{\cdot}3\times10^2$	1·8
NO_3^-	$9{\cdot}0\times10^2$	$1{\cdot}8\times10^3$	2·0

$(K_{S\ HEH[EHP]}/K_{S\ HDEHP}) = 1{\cdot}9\pm0{\cdot}2$, $K_{ClO_4^-}/K_{Cl^-} = 1{\cdot}8\pm0{\cdot}2$

It is seen, from Table 1, that HEH[EHP] is a somewhat more effective extractant than HDEHP, the ratio of their respective K_S values being 1·9±0·2. In both the HEH[EHP] and HDEHP systems, the ratio of the respective perchlorate and chloride K values is 1·8±0·2.

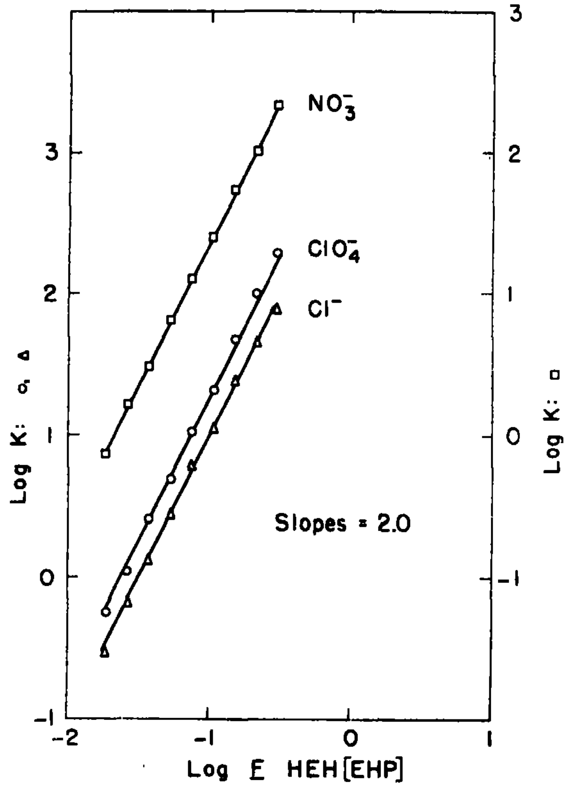

Fig. 4.—Extractant dependency of the extraction of U(VI) into HEH[EHP], toluene diluent, from a 1·00 F HX solution; $X^- = ClO_4^-, Cl^-, NO_3^-$.

In both Fig. 1 and Fig. 2, the 1·00 F H^+ point lies somewhat above the curve as drawn, the 1·00 F HNO_3 point in Fig. 2 being especially noticeable. Presumably, this is an activity coefficient effect. However, the magnitude of this effect for the

1·00 F HNO_3 point of Fig. 2 as compared with that for the other 1·00 F HX points is somewhat surprizing.

Neutral extractants

In Fig. 5, the *K* for U(VI) from an aqueous 1·00 F HNO_3 solution into a toluene solution of TEHP or DEH[EHP] is shown to be second-power dependent upon the concentration of extractant.

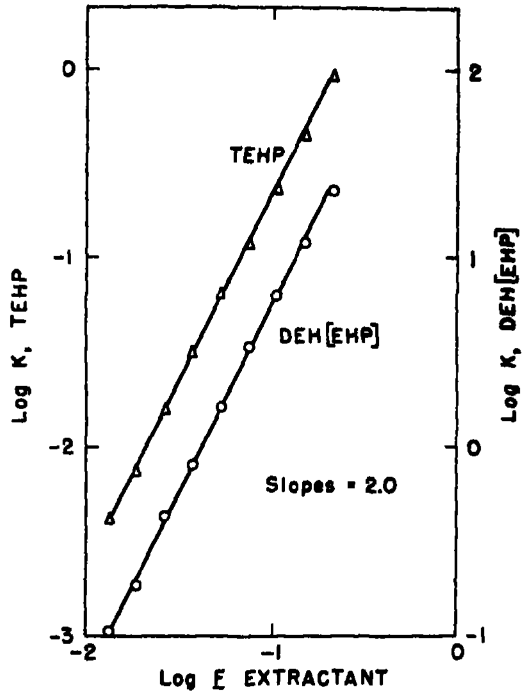

FIG. 5.—Extractant dependency of the extraction of U(VI) from a 1·00 F HNO_3 solution into TEHP, Δ, and into DEH(EHP), O; toluene diluent.

In Fig. 6, the nitrate dependency of the *K* for U(VI) from an aqueous 1·00 F (HNO_3+$HClO_4$) solution into 0·15 F TEHP or 0·05 F DEH[EHP] in toluene is seen to be directly second-power.

In experiments otherwise identical with those represented by the points of Fig. 6, but involving no ^{233}U, the concentration of mineral acid in each equilibrated organic phase was determined. Assuming that each formula weight of the mineral acid present in an organic phase effectually inactivated one formula weight of extractant, the raw data of Fig. 6 were corrected by multiplying the observed *K* by the factor (0·15/*F* "free" extractant)^2 to yield the points represented by the symbol X. This correction is negligible in the range of low nitrate concentrations.

The assumption of the presence of TEHP·HX and DEH[EHP]·HX adducts is based upon the organophosphate plus HNO_3 and $HClO_4$ studies of ALCOCK *et al.*(13)

(13) K. ALCOCK, S. S. GRIMLEY, T. V. HEALY, J. KENNEDY and H. A. C. MCKAY, *Trans. Faraday Soc.* **52**, Part I, 39 (1956).

and Hesford and McKay(14) and upon the organophosphonate plus HNO_3 studies of Siddall.(4)

Since the K for HNO_3 extraction from a given aqueous phase is thus first-power dependent upon the concentration of extractant, the fraction of the total concentration of extractant present in free form is a constant. Therefore, no correction of extractant inactivation has been made in Fig. 5, since the purpose of this plot is to demonstrate the second-power dependence of the K for U(VI).

The two points represented by the symbol + on the left portion of the TEHP curve of Fig. 6 are corrected for the extraction of U(VI) as the perchlorate. (The K from a 1·00 F $HClO_4$ solution is corrected on the assumption of a second-power dependence upon perchlorate ion concentration.) The corresponding corrections for the DEH[EHP] data are neglibible. (The presence of $UO_2(NO_3)(ClO_4)(N)_x$ is not excluded, but this species is certainly not of major importance.)

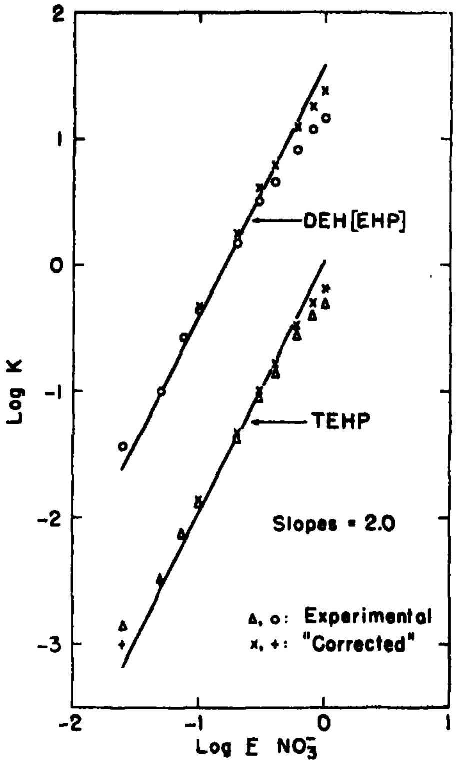

Fig. 6.—Nitrate dependency of the extraction of U(VI) from a 1·00 F ($HClO_4$+ HNO_3) solution into 0·15 F TEHP, Δ, and into 0·15 F DEH[EHP], O; toluene diluent.

The flattening of both curves of Fig. 6, even after correction, in the 0·5–1·0 F NO_3^- region remains unexplained.

The stoicheiometry of the extraction may be represented as:

$$UO_{2A}^{2+} + 2NO_{3A}^{-} + 2N_O \rightleftharpoons UO_2(NO_3)_2N_{2O} \tag{4}$$

where N represents the neutral extractant and the subscripts A and O refer, respectively, to mutually equilibrated aqueous and organic phases. The corresponding representation of K is:

---

(14) E. Hesford and H. A. C. McKay, *J. Inorg. Nucl. Chem.* 13, 156 (1960).

$$K = k_4[\mathrm{NO_3}^-]_A{}^2[\mathrm{N}]_O{}^2 \tag{5}$$

(This expression implies that aqueous phase complexing of U(VI) by nitrate ion under the conditions employed is negligible. The data of Table 1 and the reported(15) stability constant for $UO_2(NO_3)^+$, probably less than 0·25, support this assumption.)

Following substitution of $K_N F_O{}^2$ for $k_4[\mathrm{N}]_O{}^2$ and rearrangement, Expression (5) becomes:

$$K_N = K[\mathrm{NO_3}^-]_A^{-2} F_O{}^{-2} \tag{6}$$

K_N being interpreted as the hypothetical value of K for a system employing 1·0 F NO_3^- in the aqueous phase and 1·0 F extractant in the organic phase. (Like K_S, employed in the treatment of the acidic extractant data, K_N is dependent upon the ionic strength of the aqueous phase, upon the anion present and upon the diluent employed.)

Comparative K_N data are presented in Table 2. The columns headed Fig. 5 and Fig. 6, respectively, pertain to calculations based upon the straight lines, as drawn, in Figs. 5 and 6. The column headed 1·0 F HNO_3 (Fig. 6) pertains to calculations based upon the 1·0 F HNO_3 raw data of Fig. 6.

It is concluded that the values in the column headed Fig. 6 are the most significant of the three sets. Therefore, the ratio of the respective K_N values for DEH[EHP] and TEHP was computed from these data as 33±3.

DISCUSSION

The extraction of U(VI) from an aqueous nitrate phase into an organic phase consisting of a carrier diluent and a neutral organophosphate, $(GO)_3PO$, has been reported by many investigators using a variety of diluents, and a considerable range of variation in G.(1, 2, 4, 16–21) Analogous studies involving a neutral organophosphonate, $(GO)_2GPO$ or $(GO)_2G'PO$, are less numerous.(1, 2, 4, 18, 21, 22)

In general, the stoicheiometry of the extraction is presented as that of Expression (4). From the above studies, it may be concluded that the extractant dependency is, indeed, second-power. However, the second-power nitrate dependency has not been demonstrated for either a phosphate system or a phosphonate system under conditions of constant ionic strength of the aqueous phase. (Bernstrom and Rydberg(17) and Maito(20) have reported nitrate dependency studies under varying ionic strength conditions.)

Whereas it is difficult to visualize an extraction of U(VI) under these conditions as being anything other than second-power dependent upon nitrate ion concentration, still it is instructive to study the plots of Fig. 6. The fact that even the "corrected"

(15) (a) R. H. Betts and R. K. Michels, *J. Chem. Soc.* Supplementary Issue 2, 286 (1949);
(b) S. Ahrland, *Acta Chem. Scand.* **5**, 1271 (1951).
(c) R. A. Day, Jr. and R. M. Powers, *J. Amer. Chem. Soc.* **76**, 3895 (1954).

(16) H. A. C. McKay, *Proceedings of the International Conference on the Peaceful Uses of Atomic Energy, Geneva*, 1955, Vol. 7, 314. United Nations (1956).

(17) B. Bernstrom and J. Rydberg, *Acta Chem. Scand.* **11**, 1173 (1957).

(18) T. V. Healy and J. Kennedy, *J. Inorg. Nucl. Chem.* **10**, 128 (1959).

(19) T. V. Healy, J. Kennedy and G. M. Waind, *J. Inorg. Nucl. Chem.* **10**, 137 (1959).

(20) K. Naito, *Bull. Chem. Soc., Japan*, **33**, 363 (1960).

(21) S. Nomura and R. Hara, *Anal. Chim. Acta*, **25**, 212 (1961).

(22) A. S. Solovkin, M. I. Konarev and D. P. Adaev, *Russ. J. Inorg. Chem.* **5**, 903 (1959). (Chem. Soc. translation.)

points in the region of high nitrate ion concentration fall decidedly below the straight line of slope 2·0 indicates that an inhibitory influence is operative. Since the complexing action of nitrate ion upon U(VI) is far too small to account for this deviation below the line (cf. the ClO_4^- and NO_3^- data of Figs. 1–4 and of Table 1) this inhibitory influence must be considered of unknown origin.

TABLE 2.—COMPARISON OF K_N VALUES FOR U(VI) IN N(TOLUENE DILUENT) vs. 1·00 F ($HNO_3 + NaNO_3$) SYSTEMS AT 22 ± 1 °C

N	K_N from: Straight line of: Fig. 5	Fig. 6	1·0 F HNO_3 (Fig. 6)
DEH[EHP]	$5{\cdot}8 \times 10^2$	$1{\cdot}6 \times 10^3$	$6{\cdot}2 \times 10^2$
TEHP	$2{\cdot}2 \times 10$	$4{\cdot}9 \times 10$	$2{\cdot}1 \times 10$

($K_{N,\,DEH[EHP]}/K_{N,\,TEHP}$) Fig. 6 = 33 ± 3

It seems possible that such an inhibitory effect is operative in any general extraction of a metallic nitrate by neutral organophosphates and organophosphonates represented as:

$$M_A^{b+} + bNO_{3A}^- + cN_O \rightleftharpoons M(NO_3)_b(N)_{cO} \qquad (7)$$

If so, then the assumption that the K for the extraction of M^{b+} is bth-power dependent upon the concentration of nitrate is not valid in all regions.

Since this assumption is implicit in the determination of stability constants of $Th(NO_3)_x^{+(4-x)}$, $Ce(NO_3)_x^{+(3-x)}$, etc. by extraction of the M(IV), M(III), etc. from an aqueous nitrate phase into an organic phase containing a $(GO)_3PO$ or $(GO)_2G'PO$ extractant, it is suggested that the inhibitory phenomenon merits further study. The use of such a liquid–liquid extraction system in determining stability constants of metallic complexes has been discussed by ZOZULYA and PESHKOVA(23) in a review, *Investigation of Complex Formation in Solution by the Distribution Method.*

The method has been used in studying the nitrate complexes of Ce(III),(24) Pu(III),(25) Pu(IV),(26) Th(IV)(27) and Zr(IV)(28). In several of these studies, the reported stability constants are markedly higher than those reported by investigators using other methods. If an inhibitory effect, increasing with increasing concentration of nitrate ion, were operative, the measured values of the stability constants would be too high.

In the straight line region of Fig. 6, presumably this inhibitory effect is negligible. Consequently, the ratio of the K_N value for DEH[EHP] to that for TEHP, Table 2, has been calculated for this region. The value of the ratio, 33 ± 3, employing toluene as a diluent, may be compared with the value of approximately eighteen derived from Figs. 1 and 2 of the study of the same extractants by SIDDALL,(4) employing a 1·09 F extractant in n-dodecane vs. 1·0 F HNO_3. BURGER(1) also found a given neutral

(23) A. P. ZOZULYA and V. M. PESHKOVA, *Russ. Chem. Rev.* **2**, 101 (1960), i.e. *Uspekhi Khimii*, **2**, 234 (1960).

(24) V. V. FOMIN, R. E. KARTUSHOVA and T. I. RUDENKO, *Zh. Neorg. Khim.* **3**, 2117 (1958).

(25) V. B. SHEVCHENKO, V. G. TIMOSHEV and A. A. VOLKOVA, *J. Nucl. Energy*, Part B: Reactor Technology **1**, 211 (1960).

(26) J. A. BROTHERS, R. G. HART and W. G. MATHERS, *J. Inorg. Nucl. Chem.* **7**, 85 (1958).

(27) V. V. FOMIN and E. P. MAIOROVA, *Zh. Neorg. Khim.* **1**, 1703 (1956).

(28) A. S. SOLOVKIN, *Zh. Neorg. Khim.* **2**, 611 (1957).

phosphonate to be more effective in the extraction of U(VI) by a factor of approximately fifteen to twenty than the corresponding neutral phosphate in systems involving carbon tetrachloride as the diluent and a dilute aqueous uranyl nitrate solution as the opposing phase.

The K_S values of Table 1 show that of the two acidic extractants, HEH[EHP] is more effective than HDEHP in the extraction of U(VI), the ratio of their respective K_S values being $1{\cdot}9 \pm 0{\cdot}2$ in systems involving toluene as diluent and a 1·0 F (HX+NaX) aqueous solution as opposing phase.

Conversely, HEH[EHP] is the less effective of the two acidic extractants in the extraction of lanthanides(III) and actinides(III) in similar systems. For example, the K_S values for Pm(III) and Cm(III) for HDEHP are 60–100 times larger than the corresponding values for HEH[EHP] in systems employing toluene as diluent and a 1·0 F ($HClO_4$+$NaClO_4$) aqueous solution as opposing phase.(5) This relative effect is general for lanthanides(III) and for all actinides(III) which have been investigated, the K_S for the HDEHP systems exceeding that for the corresponding HEH[EHP] by a factor of 50–200 for each of the elements for chloride, perchlorate or nitrate systems.(5, 6, 29) Similarly, HDEHP is approximately 100 times more effective than HEH[EHP] in the extraction of Th(IV) from a 0·1 F $HClO_4$+0·9 F $NaClO_4$ aqueous phase in a system employing toluene as diluent.(11, 30)

In recapitulation, the $K_{S,\,\mathrm{HEH[EHP]}}/K_{S,\mathrm{HDEHP}}$ ratio in a 1·0 μ perchlorate, toluene diluent, system has the values: U(VI), 1·9; Th(IV), ~0·01; Actinides(III), ~0·01–0·02; Lanthanides(III), ~0·01–0·02. It will be noted that the ratio of K_S values is somewhat greater than unity for U(VI) and considerably less than unity for Th(IV), whereas the ratio of K_N values for the corresponding neutral extractant is: U(VI), 33 ± 3 (this study) and approximately 18 (a similar study by SIDDALL(4) with a different diluent); and Th(IV), 26 (above quoted study by SIDDALL).(4)

A consideration of the ratio of ratios, i.e. the ratio of $(K_{N,\,\mathrm{DEH[EHP]}}/K_{N,\mathrm{TEHP}})$ to $(K_{S,\,\mathrm{HEH[EHP]}}/K_{S,\,\mathrm{HDEHP}})$ for each element is instructive. This ratio, based upon the foregoing values, is approximately: U(VI), 9–17; and Th(IV), $2{\cdot}6 \times 10^3$. These two ratios differ quite markedly; and the possibility is suggested that steric hindrance due to the branching at the 2-position in 2-ethyl hexyl becomes relatively more important for Th(IV) than for U(VI) in the acidic phosphonate.

In this connection, it may be noted that SIDDALL,(31) studying the extraction from 3·0 F HNO_3 into a n-dodecane solution of a neutral phosphate, found the extraction of U(VI) enhanced by a factor of 1·7 and that of Th(IV) depressed by a factor of 6·4 when tri n-butyl phosphate, TBP, was replaced by the 2-butyl analogue. Presumably, the steric hindrance produced by the secondary alkoxy group seriously interferes with phosphoryl bonding to Th.

The remaining tabular data to be rationalized are the K_S values of Table 1 for perchlorate and chloride systems. The ratio of respective K_S values, $1{\cdot}8 \pm 0{\cdot}2$, if its departure from unity is attributed solely to chloride complexing of U(VI) to form UO_2Cl^+, may be used to deduce a value of $0{\cdot}8 \pm 0{\cdot}2$ for the stability constant of UO_2Cl^+ ($\mu = 1{\cdot}00$, 22 ± 1°C). The literature values are 0·8(15b) ($\mu = 1{\cdot}00$, 20°C) and 0·88(15c) ($\mu = 2{\cdot}00$, 25°C).

(29) D. F. PEPPARD, G. W. MASON, J. L. MAIER and W. J. DRISCOLL, *J. Inorg. Nucl. Chem.* **4**, 334 (1957).

(30) D. F. PEPPARD, M. N. NAMBOODIRI and G. W. MASON, *J. Inorg. Nucl. Chem.* **24**, 979 (1962).

(31) T. H. SIDDALL, III, *J. Inorg. Nucl. Chem.* **13**, 151 (1960).

J. Inorg. Nucl. Chem., 1962, Vol. 24, pp. 1399 to 1404. Pergamon Press Ltd. Printed in England

ÜBER IONENAUSTAUSCHERHARZE MIT KOMPLEXBILDENDEN ANKERGRUPPEN-IV(1)

DIE BINDUNGSVERHÄLTNISSE DER SELTENERD-IONEN AM IDE-AUSTAUSCHERHARZ

R. HERING
Institut fur Anorgonische Chemie der Karl-Marx-Universität, Leipzig

(*Received* 20 *February* 1962)

Abstract—The result of this work, connected with the present knowledge of the structures of the rare earth complexon chelates leads to the conclusion that contrary to the best results in the separation of bivalent metal ions already known, the separation of neighbouring rare earth ions on IDE chelating resin by diluted mineral acid appears to be impossible.

Zusammenfassung—Das Ergebnis dieser Arbeit, verbunden mit der gegenwärtigen Kenntnis über die Struktur der Komplexonato-Komplexe der Seltenerd-Ionen führt zu dem Schluss, dass im Gegensatz zu den bereits bekannten, besten Trennerfolgen an zweiwertigen Metallionen, die Trennung benachbarter Seltenerd-Ionen am IDE-Austauscherharz mit verdünnten Mineralsäuren aussichtslos erscheint.

ZWEIWERTIGE komplexbildende Metallionen sind in einfacher Weise am IDE-Austauscherharz(2) (IDE = Iminodiessigsäure) durch Elution mit verdünnter Mineralsäure(3) wirksam zu trennen. Überraschenderweise ist bei dreiwertigen Metallionen (Pr^{3+}/Nd^{3+}) mit den gleichen Elutionsmitteln eine Auftrennung oder Anreicherung nicht zu erzielen.(4) Dieses gegensätzliche Verhalten zwei- und dreiwertiger komplexbildender Metallionen gab den Anlass, die Bindungsverhältnisse der Seltenerd-Ionen am IDE-Austauscherharz zum Vergleich mit denjenigen zweiwertiger Metallionen genauer zu untersuchen.

Ein Teil dieser Untersuchungen führte u.a. zur Entwicklung eines NTE-Austauscherharzes mit koordinationsfähigem Stickstoff.(1, 2) Die drei am Stickstoff haftenden Essigsäure-Gruppen der NTE verleihen dem Harz ähnliche Eigenschaften gegenüber dreiwertigen Metallionen, wie sie das IDE-Austauscherharz für zweiwertige Metallionen besitzt.

Die hohe Reinheit, Stabilität und Kapazität des durch Umsatz von chlormethyliertem Polystyrol mit Iminodiessigsäurediäthylester dargestellten IDE-Austauscherharzes gestattet dessen stöchiometrische Anwendung. Mehrere Proben von je 1 mMol IDE-Austauscherharz (330 mg in H-Form) wurden im Säulenverfahren bei verschiedenen pH-Werten (Acetatpuffer in 0·5 M KNO_3) mit La^{3+} bzw. Yb^{3+} gesättigt. Nach dem Waschen mit Wasser wurden die Seltenerd-Ionen mit je 10 ml N HCl entfernt, nachgewaschen, der Säureverbrauch potentiometrisch durch Rücktitration mit KOH ermittelt und das Seltenerd-Ion komplexometrisch bestimmt.

---

(1) 3. Mitt.: *J. Prakt. Chem.* **14**, 285 (1961).

(2) L. WOLF und R. HERING, *Chem. Techn.* **10**, 661 (1958).

(3) L. WOLF und R. HERING: unveröff.; Dissertation von R. Hering Leipzig Januar 1960; W.P. 12g/70139 angemeldet.

(4) L. WOLF, R. HERING und R. WAGENER, unveröff.; Diplomarbeit von R. Wagener, Leipzig Juni 1960.

Im pH-Bereich 3–4 liegt für Yb^{3+} (gleiche Befunde gelten bei 0·6 höheren pH-Werten für La^{3+}) die wasserbeständige Kapazität des IDE-Austauscherharzes bei 0·5 mMol Yb^{3+} pro mMol IDE-Austauscherharz. Entsprechend einem Yb:Y-Verhältnis (Y = verankerte IDE) von 1:2 und der zur Dekomplexierung verbrauchten Säure (Gl. 3) stehen 3 mögliche Komplexformen zur Diskussion:

$$\underset{(I)}{[YbYHY]};\qquad \underset{(II)}{[YbY]^+ + [HY]^-};\qquad \underset{(III)}{[YbY_2]H}$$

Die Form III ist nur in stark alkalischem Gebiet in der Salzform $[YbY_2]^-$ beständig. I wird wegen des mit steigendem pH kontinuierlichen Kapazitätsanstiegs unwahrscheinlich, so dass II, die Salzform zwischen einen kationischen 1:1—Komplex und der anionischen Betainform, als existent betrachtet werden kann.

Die zur Dekomplexierung verbrauchte Säure verlangt für Kapazitäten über 0·5 (Dimension wie oben) in Übereinstimmung mit den zugehörigen Dekomplexierungsgleichungen (Gl. 4) die zusätzliche Bindung eines Anions im seltenerd-beladenen IDE-Austauscherharz. Die Differenz der anionischen Betainform $[HY]^-$ reicht hier nicht mehr aus, die überschüssigen positiven Ladungen des kationischen Komplexes $[YbY]^+$ zu kompensieren.

2 Komplexformen werden damit möglich:

$$\underset{(IV)}{2\,[YbY]^+ + [HY]^- + NO_3^-}\ \text{bzw.}\ \underset{(V)}{\{[YbY]_2\overset{(+)}{Y}H\}^+ + NO_3^-}$$

V wird nur dann begreiflich, wenn die tatsächliche Struktur der Salz-Betainform der IDE berücksichtigt wird.

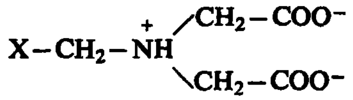

$$X-CH_2-\overset{+}{N}H\begin{cases}CH_2-COO^-\\CH_2-COO^-\end{cases}\qquad (VI)$$

(X = Ankerstelle)

Obwohl IDE als einbasische Säure fungiert, besitzt die Molekel neben positivem Ammoniumstickstoff zwei gleichwertige Acetatgruppierungen. Damit wird, bedingt durch die Koordinationstendenz dieser Acetatgruppen, die Form eines kationischen 2:3—Komplexes wahrscheinlich.

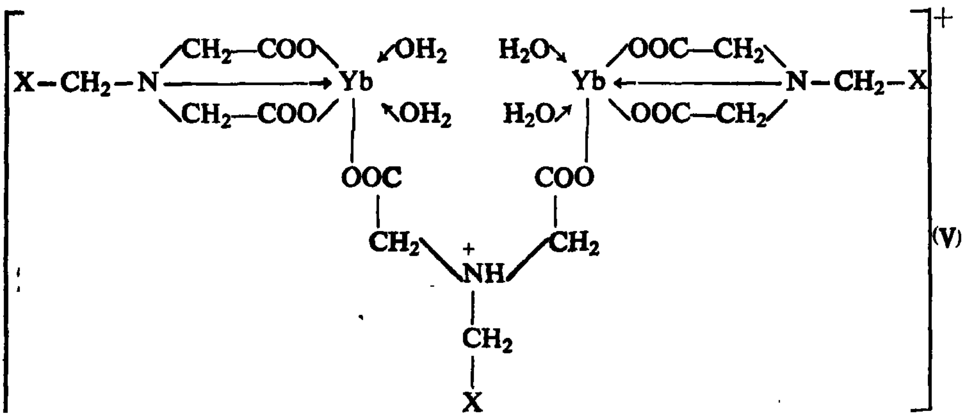

(V)

V zufolge besäße das IDE-Austauscherharz bei Beladung über 0·50 bewegliche Anionen, die unter geeigneten Bedingungen ausgetauscht werden können. Die experimentelle Untersuchung dieser Vermutung ergab, daß Beladungen über 0·50, sowohl in der Lanthan- als auch in der Ytterbiumform anionenaustauschende Eigenschaften aufweisen. Austauschversuche von NO_3^- gegen Cl^- und umgekehrt ergaben bei einem Beladungsgrad von 0·50–0·63 ansteigende Anionenkapazität bis 0·09 mVal NO_3^- bzw. Cl^- pro mMol IDE-Austauscherharz. Theoretische Austauschkapazitäten konnten deshalb nicht erreicht werden, weil jede anionenaustauschfähige Beladungsform bei der Behandlung mit KNO_3— bzw. KCl-Lösung merklich Seltenerd-Ionen abgab.

Beladungen über 0·65 verlieren durch KCl- od. KNO_3-Lösung weniger Seltenerd-Ionen und zeigen geringere Anionenaustauschfähigkeit. Noch höhere Beladungsgrade verlieren völlig diese Eigenschaft. Der Verlust der Anionenaustauschfähigkeit tritt auch dann auf, wenn an Beladungen zwischen 0·50 und 0·63 im alkalischeren Gebiet, als der Beladung 0·63 entspricht, der Austausch versucht wird. Demzufolge ist der Übergang zum alkalischen Gebiet mit einer Umwandlung des kationischen 2:3-Komplexes V in einen nichtionogenen 2:3-Protonen-Hydroxokomplex verbunden. Die Reaktionsbereitschaft zu niederem und höheren pH wird durch folgende Grenzzustände charakterisiert:

$$\begin{tikzcd}[column sep=large] \text{(VIII)}\quad \{[YbY]_2\overset{(+)}{Y}H\}^{+}+OH^- \arrow[r, rightleftharpoons] \arrow[d, shift left] & \{[YbY]_2\overset{(+)}{Y}H,\ \overset{(-)}{OH}\} \arrow[d, shift left] \\ {[Yb_2HY_3]^{+}+OH^-} \arrow[u, shift left] \arrow[r, rightleftharpoons] & {[Yb_2HY_3OH]}\quad \text{(XI)} \arrow[u, shift left] \end{tikzcd}$$

VIII liegt beim Übergang zu niederen pH-Werten vor. Anstelle von OH^- tritt ein austauschfähiges Anion. VIII besitzt bereits die Elemente von II, $[YbY]^+$ und $[HY]^-$, die in niederen pH-Bereichen beständig sind.

Mit steigendem pH lagert sich VIII in die Struktur einer primären komplexen Pseudobase IX um und bildet bei Beladungen über 0·66 ausserdem eine sekundäre komplexe Pseudobase [YbYOH] (X). X ist bereits in IX vorgebildet:

$$[Yb_2HY_3OH] \rightleftharpoons [YbYOH]+[YbY][HY]$$

Höhere Beladungsgrade geben bei der Behandlung mit alkalischen Kaliumacetate-Lösungen (pH 10–13) merklich $Yb(OH)_3$ ab. Dabei zerfällt X, wie zu erwarten, unter Verbrauch von Hydroxylionen in dem anionischen 1:2-Komplex $[YbY_2]^-$ (XI) und Seltenerd-Hydroxyd.

$$2[YbYOH]+OH^- \rightleftharpoons [YbY_2]^-+Yb(OH)_3 \qquad \text{(Gl. 1)}$$

In Übereinstimmung mit dem Experiment verhindert XI, im alkalischen Gebiet den theoretischen Beladungsgrad 1·00 zu erreichen.

Die hier dargelegten experimentellen Ergebnisse und ihre Schlußfolgerungen stimmen im wesentlichen mit der derzeitigen Kenntnis über die Struktur und Bildungsweise der Komplexonato-Komplexe der Seltenerd-Ionen überein. In einer diesbezüglichen umfassenden Arbeit beschreibt Wolf(5) einen experimentell dargestellten 2:3-Komplex $[LaX]_2X.8\ H_2O$ (XII) (X = o-oxycyclohexyliminodiessigsäure), der auch als Salz des kationischen 1:1-Komplexes mit dem anionischen 1:2-Komplex $[LaX][LaX_2]\cdot 8\ H_2O$ oder als neutraler 2:3-Komplex $[La_2X_3]\cdot 8\ H_2O$ auffassbar wäre. Die Nichtexistenz der beiden letzteren Komplexformen konnte von Wolf u. Mitarbeitern eindeutig sichergestellt werden.

---

(5) L. Wolf, *Österr. Chem. Z.* **60**, 99 (1959).

Der im stark alkalischen Gebiet liegende Existenzbereich des in XII formulierten Anions X^{2-} steht im Widerspruch zu dein Existenzbereich des kationischen 1:1-Komplexes $[LaX]^+$, so dass Formulierung XII ebenfalls nicht den stabilen Zustand dieses Komplexes wiederspiegelt.

Eine stabile Form des Komplexes ist aber dann vorhanden, wenn in Analogie zu VIII und IX eine Kristallwassermolekel im dissoziierten Zustand am Aufbau der Komplexverbindung beteiligt ist: $\{[LaX]_2\overset{(+)}{X}H\}^+$, $OH^- \cdot 7\,H_2O$ bzw. $[La_2HX_3OH] \cdot 7\,H_2O$ Die präparative Darstellungsmöglichkeit von XII bestätigt somit einerseits die Komplextypen V, VIII und IX, andererseits erklären die pH- und beladungsabhängigen Kapazitäts- und Austauschverhältnisse die Struktur der Komplexverbindung XII.

Die zur Dekomplexierung der gebundenen Seltenerd-Ionen benötigte Säuremenge hängt von der Bindungsform des Harzkomplexes ab und diente neben den Kapazitätsbestimmungen und der potentiometrischen Titration der Benzyliminodiessigsäure,(6) der monomeren Vergleichssubstanz des IDE-Austauscherharzes, zur Aufklärung der Komplex-Strukturen. In Gl. 2–7 sind die Dekomplexierungs-Reaktionsgleichungen für die erwähnten Stufen mit den zugehörigen Dekomplexierungs-Säureäquivalenten pro Mol IDE-Austauscherharz (H^+/Y) aufgeführt. Für jede Messung wurde der Säureverbrauch aus den gemessenen Kapazitätswerten und den Dekomplexierungsgleichungen zum Vergleich mit dem experimentellen Säureverbrauch errechnet. Der Beladungsgrad 0·50 wurde mit Gl. 3, der Beladungsgrad 0·66 mit Gl. 4 berechnet. Tieferliegende Werte als 0·50 wurden anteilmäßig aus Gl. 2 und Gl. 3, zwischen 0·50 und 0·66 liegende Werte wurden anteilmäßig aus Gl. 3 und Gl. 4, wenig über 0·66 liegende Werte mit Gl. 4 und Gl. 5 bzw. Gl. 5, hohe Beladungsgrade nach Gl. 5 bzw. Gl. 5 und Gl. 6 berechnet. Die berechneten Säuremengen stimmen mit den experimentellen Befunden überein.

$$[HY]^- + H^+ \rightarrow [HY]H \qquad (1\,H^+/Y) \quad (\text{Gl. } 2)$$
$$[YbY]^+ + [HX]^- + 3\,H^+ \rightarrow Yb^{3+} + 2\,[HY]H \qquad (1/5\,H^+/Y) \quad (\text{Gl. } 3)$$
$$\{[YbY]_2{}^{(+)}YH\}^+ + 5\,H^+ \rightarrow 2Yb^{3+} + 3\,[HY]H \qquad (1{\cdot}66\,H^+/Y) \quad \text{Gl. } 4)$$
$$[YbHY_3OH] + 6\,H^+ \rightarrow 2Yb^{3+} + 3\,[HY]H \qquad (2\,H^+/Y) \quad (\text{Gl. } 5)$$
$$[YbYOH] + 3\,H^+ \rightarrow Yb^{3+}\ [HY]H \qquad (3\,H^+/Y) \quad (\text{Gl. } 6)$$
$$[YbY_2]^- + 4\,H^+ \rightarrow Yb^{3+} + 2\,[HY]H \qquad (2\,H^+/Y) \quad (\text{Gl. } 7)$$

TABELLE 1.—FASST ALLE MÖGLICHEN KOMPLEXTYPEN, DEREN EXISTENZ VOM pH-WERT UND VOM BELADUNGSGRAD ABHÄNGT, ZUSAMMEN

	pH—Bereich		
Bindungsform	Yb^{3+}	La^{3+}	Beladungsgrad
$[YbY]^+$; $[HY]^-$; $[HY]H$	< 3·0	< 3·5	0·45
$[YbY]^+$; $[HY]^-$	3·5–3·9	4·1–4·5	0·50
$_3\{[YbY]_2\overset{(+)}{X}H\}^+ + NO_3^-$	5·1–5·5	5·7–6·1	0·67
$_3[Yb_2HY_3OH]$	5·7–6·0	6·3–6·7	0·67
$[YbYOH]$	> 6·0	> 6·6	0·67
$_2[YbY_2]^-$	> 9	> 10	

Der Vergleich des pH-abhängigen Kapazitätsverlaufs zwischen zwei- und dreiwertigen Metallionen verdeutlicht die unterschiedlichen Eigenschaften. Ob die Abweichungen der Seltenerd-Messpunkte vom geradlinigen Kapazitätsanstieg auf Messfehler oder unterschiedliche Komplexstabilitäten der verschiedenen Komplexformen zurückzuführen sind, wurde noch nicht untersucht.

---

(6) R. HERING, W. KRÜGER und G. KÜHN *Zf. Chem.* 2, Dezember 1962.

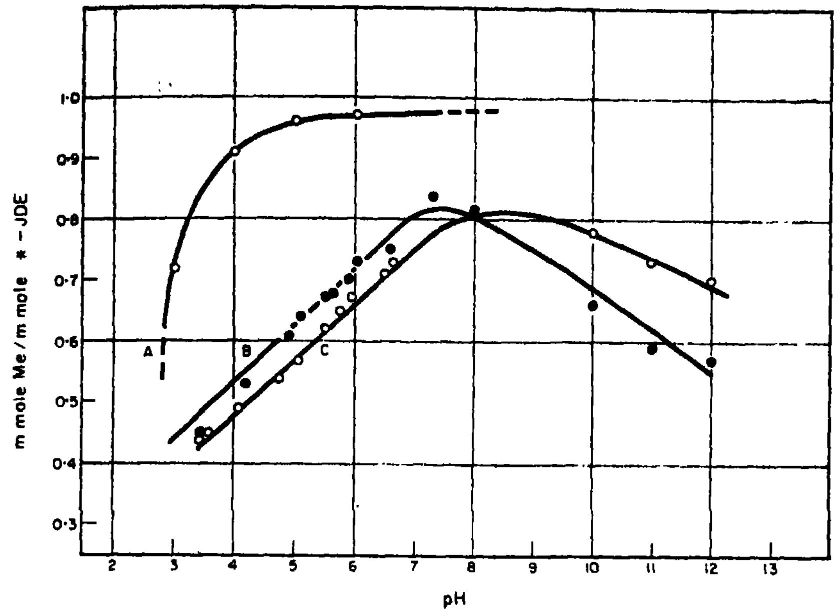

Abb. 1.—Zeigt den pH-abhängigen Kapazitäts-Verlauf für Zn^{2+}(A), Yb^{3+}(B) und La^{3+}(C).

Die Anwendung der bisherigen Erkenntnis auf den Elutionsverlauf bei Trennversuchen begründet sowohl den Trennerfolg bei zweiwertigen als auch den Misserfolg bei dreiwertigen komplexbildenden Metallionen.

Wird eine mit zweiwertigen Metallionen beladene IDE-Austauschersäule mit verdünnter Mineralsäure eluiert,(3) dann stehen nur die neutralen 1:1-Komplexe mit den wandernden Metallionen (bzw. wandernden anionischen Metallkomplexen) *in einfachem und übersichtlichem* Austauschgleichgewicht.(7)

Die IDE-Harzkomplexe werden unter Verbrauch von Wasserstoffionen dekomplexiert, wobei neben Me^{2+} die saure Betainform des IDE-Austauscherharzes gebildet wird.

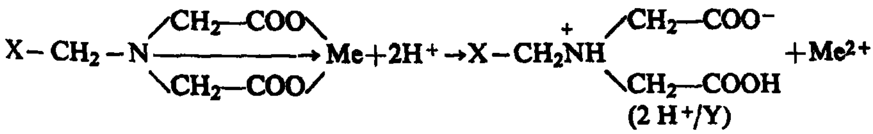

$$X-CH_2-N\begin{matrix}\diagup CH_2-COO\diagdown \\ \\ \diagdown CH_2-COO\diagup\end{matrix}Me+2H^+\rightarrow X-CH_2\overset{+}{N}H\begin{matrix}\diagup CH_2-COO^- \\ \\ \diagdown CH_2-COOH\end{matrix}+Me^{2+} \quad \text{(Gl. 8)}$$
$$(2\,H^+/Y)$$

Die schwächer komplexbildenden Metallionen werden bevorzugt dekomplexiert und wandern somit schneller in der IDE-Austauscher-Säule. Am unteren Rand des Me^{2+}-Zone, der oberen Grenze der Alkali-Betain-Form des Harzes, bilden die wandernden Me^{2+}-Ionen erneut IDE-Komplexe. Dabei werden Wasserstoff-Ionen in Freiheit gesetzt, die von einem Teil der Alkaliform der verankerten IDE abgefangen werden.

(7) R. Hering *Zf. Chem.* 3, Januar und Februar (1963)

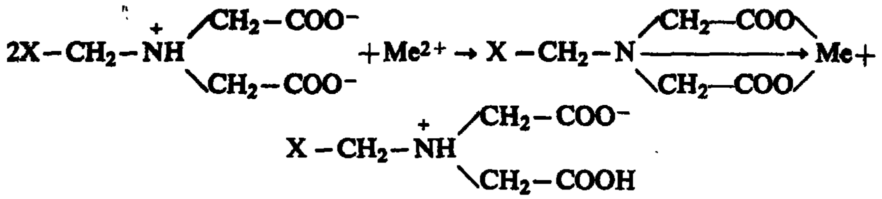

$$2X-CH_2-\overset{+}{N}H\begin{array}{l}\nearrow CH_2-COO^-\\ \searrow CH_2-COO^-\end{array}+Me^{2+}\rightarrow X-CH_2-N\begin{array}{l}\nearrow CH_2-COO\searrow\\ \searrow CH_2-COO\nearrow\end{array}Me+X-CH_2-\overset{+}{N}H\begin{array}{l}\nearrow CH_2-COO^-\\ \searrow CH_2-COOH\end{array}\qquad \text{(Gl. 9)}$$

Damit scheidet ein Teil dieser IDE-Gruppen von der Komplexbildung aus. Bei fortlaufender Elution verwandelt sich die unterhalb der Me^{2+}-Zone befindliche Alkaliform immer stärker in die H-Form. Dieser *Säurevorlaufeffekt* kann zu nachträglichen Störungen des Trenneffektes führen, wenn zu lange Säulen verwendet werden.*

Die zweiwertigen Metallionen erscheinen in Reihenfolgen steigender Komplexstabilität (z.B. Co-Zn-Ni-Cu) mit charakteristischein *Zersetzungs-* oder *Dekomplexsierungs-pH-Wert* im Eluat. Letzterer ist *unabhängig* von der Säurekonzentration des Elutionsmittels.

Demgegenüber sind bei dreiwertigen Metallionen mehrere Komplexformen am Elutionsvorgang beteiligt. Der Zersetzungs-pH-Wert der zu Trennversuchen verwandten Alkali-Form des IDE-Austauscherharzes liegt im neutralen Gebiet, derjenige der Seltenerd-Ionen zwischen pH 2·3 und 2·7.† Bei einem analogen Trennversuch von dreiwertigen Metallionen müssen alle für diesen pH-Bereich zutreffenden Komplex-Formen, auch die anionenaustauschende Form V und die pseudobasischen Formen IX und X, durchlaufen werden. Sämtliche Komplexarten bestitzen, auch wenn dies durch die vorliegenden Messungen nicht zum Ausdruck kommt, unterschiedliche Komplexstabilitäten, d.h. sie wandeln sich bei der Elution nicht völlig kontinuierlich ineinander um. Die ohnehin wenig differenzierten Komplexstabilitäten benachbarter Seltenerd-Ionen ermöglichen damit bei Anwesenheit verschiedener Seltenerd-Ionen eine Überlagerung der Stabilitätsbereiche der möglichen Komplextypen, wodurch eine Auftrennung verhindert wird.

Dem Prorektorat für Forschung der Karl-Marx-Universität Leipzig danke ich für die Bereitstellung von Forschungsmitteln.

---

* Bei Trennungen von zweiwertigen Metallionen, deren Dekomplexierungs-pH-Werte mehr als 0·2–0·3 pH-Einheiten differieren, beeinflußt der Säureverlauf kaum den quantitativen Trenneffekt; andernfalls wird eine Abstimmung der Säulenlänge erforderlich.

† Dreiwertige Metallionen besitzen keinen charakteristischen Dekomplexierungs-pH-Wert.

J. Inorg. Nucl. Chem., 1962, Vol. 24, pp. 1405 to 1415. Pergamon Press Ltd. Printed in England

ON ANION-EXCHANGE RESIN SELECTIVITIES*

B. CHU†
Department of Chemistry, Cornell University, Ithaca, New York
and
D. C. WHITNEY ‡ and R. M. DIAMOND
Department of Chemistry and Lawrence Radiation Laboratory,
University of California, Berkeley, California

(*Received* 20 *December* 1961)

Abstract—The selectivity of anion-exchange resins in contact with very dilute external solutions (negligible resin invasion by non-exchange electrolyte) is considered due in large part to changes in the solvation of the ions, resulting from differences in the properties of the resin-phase solution and the external dilute aqueous solution. The resin-phase solution is a concentrated electrolyte solution with three significant differences from a dilute electrolyte solution: (a) the cationic species is fixed on the resin matrix; (b) electrostatic forces are stronger; (c) the water molecules in the resin phase have less co-operative structure. The tendency of large univalent ions to be forced out of the dilute solution and into the resin phase because of their small degree of hydration and considerable water-structure-breaking character is considered, as well as the effects of specific group hydration.

ALTHOUGH considerable data have now been accumulated on the ion-exchange process, and ion-exchange resins are much used in separation and purification schemes, less success has been achieved in explaining the selectivity of the process. We shall consider only equivalent exchange—that is, exchange with very dilute external solutions—so that there is negligible resin invasion by non-exchange electrolyte. The process may be treated as a chemical equilibrium, so that for univalent ions we have

$$\mathrm{M}^- + \bar{\mathrm{N}}^- = \bar{\mathrm{M}}^- + \mathrm{N}^-,$$

where the superscript bar stands for the resin phase. This leads to the usual equilibrium-constant expression,

$$K = [(\bar{\mathrm{M}})(\mathrm{N})/(\mathrm{M})(\bar{\mathrm{N}})]\,[\bar{\gamma}_{\mathrm{M}}\gamma_{\mathrm{N}}/\gamma_{\mathrm{M}}\bar{\gamma}_{\mathrm{N}}].$$

The parentheses ( ) signify species concentration, and γ the species activity coefficient, and ionic charges have been omitted for simplicity. Choosing the same standard state for the resin phase and the dilute external solution fixes the value of the equilibrium constant at unity. Then the equilibrium quotient or concentration constant, $Q_{\mathrm{N}}^{\mathrm{M}}$, which is what is most readily determined from experiment, becomes

$$Q_{\mathrm{N}}^{\mathrm{M}} = [(\bar{\mathrm{M}})(\mathrm{N})/(\mathrm{M})(\bar{\mathrm{N}})] = [\gamma_{\mathrm{M}}\bar{\gamma}_{\mathrm{N}}/\gamma_{\mathrm{M}}\gamma_{\mathrm{N}}].$$

The responsibility for the specificity of the exchange process is thus placed on the ratios of the activity coefficients, particularly on those of the resin phase, as the external solution can be made so dilute that $\gamma_{\mathrm{M}}/\gamma_{\mathrm{N}}$ is essentially unity or has a known value.

---

* This work was supported in part by U.S. Atomic Energy Commission. Presented in part at 133rd Meeting of the American Chemical Society, San Francisco, California, 1958. Abstracts of the Meeting, Paper 55Q.

† Present address: Chemistry Department, University of Kansas, Lawrence, Kansas.

‡ Present address: Department of Chemistry, University of California at Davis, Davis, California.

From experimentally determined Q_N^Ms and the known values of γ_M/γ_N, ratios of resin-phase activity coefficients can be obtained. Conversely, if the resin-phase activity coefficients for various ions can be estimated, their ion-exchange behaviour can be predicted. This has been done in certain special cases, but requires a considerable amount of experimental data on low-crosslinked resins and on activity coefficients for mixed electrolyte solutions.(1, 2) Obviously it would be most desirable to be able to explain, even qualitatively, the physical reasons behind the resin-exchange specificity.

Toward this goal, several models for the ion-exchange process have been proposed. For example, Gregor has pointed out that an osmotic free-energy term included in the free-energy expression for the exchange would help explain resin specificities from the mechanical swelling properties of the resin and the hydrated volumes of the ions:(3)

$$RT \ln Q_N^M = \pi(\bar{V}_N - \bar{V}_M) + RT \ln (\gamma_M \bar{\gamma}_N/\bar{\gamma}_M \gamma_N),$$

where π is the osmotic swelling pressure and $\bar{V}_N$ and $\bar{V}_M$ are the partial molal volumes of species N and M in the resin phase. Qualitatively, this idea was in agreement with experiment; usually ions that swelled the resin phase the most were least absorbed by the resin. This marked a significant advance in resin theory, but, quantitatively, the pressure-volume term proved too small in magnitude to yield the experimental values of Q under normal conditions.(2, 4) In fact, a more detailed molecular model,(5) which assumes all resin specificity to be based upon ion pairing between the resin groups and the exchanging ions, predicts the change in the resin volume as a result of the exchange, rather than as the cause of the exchange.

The idea of electrostatic ion pairing as the source of resin specificity goes back, perhaps, to the empirical observations that the affinity of cation resins for an ion apparently increases with increasing charge and decreasing hydrated radius. Such an electrostatic model has been used by Pauley for the calculation of Q for some cation-exchange reactions.(6) Interactions of this type may play a part in determining resin selectivity, particularly with highly cross-linked cation resins, but ion pairing, at least as it has been considered, cannot be the main factor in anion exchange. Firstly, strong ion–ion interactions between halide ions and large model resinate ions such as trimethylphenylammonium ion are not expected in aqueous solutions. Secondly, if electrostatic ion pairing were the principal source of resin selectivity, the higher-charged ions would be greatly preferred. Actually, the converse is usually true if one carefully compares anion-exchange constants.* Thirdly, with a simple electrostatic model it is very difficult to account for the great preference shown by anion-exchange resins for SCN^- over CN^-, ClO_4^- over I^-, and $AuCl_4^-$ over ClO_4^-, as the first ion is the larger in each pair and might be expected to have the weaker interaction with the resin ionic group.

* For example, the value of Q_{Cl}^M for ReO_4^- is larger than that for WO_4^{2-} by 10^3, and a similar difference occurs for MnO_4^- and CrO_4^{2-}(7). This situation will be discussed in a subsequent paper.

(1) G. E. Myers and G. E. Boyd, *J. Phys. Chem.* **60**, 521 (1956); G. E. Boyd, S. Lindenbaum and G. E. Myers, *J. Phys. Chem.* **65**, 577 (1961).

(2) E. Glueckauf, *Proc. Roy. Soc.* **214** A, 207 (1952).

(3) H. P. Gregor, *J. Amer. Chem. Soc.* **70**, 1293 (1948); **73**, 642 (1951).

(4) G. E. Boyd and B. A. Soldano, *Z. Elektrochem.* **57**, 162 (1953).

(5) S. A. Rice and F. E. Harris, *Z. Physik. Chem.* **8**, 207 (1956).

(6) J. L. Pauley, *J. Amer. Chem. Soc.* **76**, 1422 (1954).

A third suggestion as to the cause of anion-exchange selectivity has been that the selectivity depends upon the polarizability of the anion in the field of the resin cation.(8, 9) But this scheme also has so many exceptions that it cannot be the determining factor either. For example, the observed sequences of ion-exchange selectivity, $ClO_4^- > I^-$ and $ClO_3^- > BrO_3^- > IO_3^-$ and $MnO_4^- > TcO_4^- > ReO_4^-$, are the reverse of the order expected from the anion polarizability as measured by the ionic refraction.

We would like to suggest that the difference in the local water structure inside and outside the resin and the extent of hydration of the ion play major parts in determining resin selectivity, and that the ion hydration influences resin selectivity by other means than just giving the effective size of the ion as in electrostatic ion pairing considerations.

EXPERIMENTAL

Reagents. The formic, acetic and trichloracetic acids were Baker and Adamson reagent grade. The butyric acid was Baker and Adamson technical grade, 98–100 per cent and the caproic acid was Matheson, Coleman, and Bell, m.p. −5 to −3°C. The valeric and trimethylacetic acids were Eastman White Label. Seventy-three per cent sodium methyldichloroacetate from United Mineral and Chemical Corp. was acidified with 3 M HCl at 0°C, and the methyldichloroacetic acid was extracted into ether and distilled under reduced pressure.

One-molar solutions of the sodium salts of each of the acids were prepared by placing the appropriate weighed amount of each acid in freshly boiled distilled water and adding NaOH pellets (Baker and Adamson reagent grade, 97 per cent minimum) with stirring until a pH of 7·5 was reached, then diluting with boiled distilled water to the final volume. For all these solutions, the final pH was between 7·3 and 7·5. The 1 M solutions of all the salts of acids with $pK \simeq 5$ were titrated with standard HCl using a pH meter; the concentrations of the salts of the stronger acids were determined from the weight of the acid. All lower concentrations were made by dilution of the 1 M solutions with freshly distilled water. The chloride content of the salts was determined to be 1 per cent or less in all cases except for the methyldichloroacetate (3 per cent), and corrections, where significant, were applied. The Dowex AG-1 X10, 100-200 mesh, analytical grade anion-exchange resin was obtained from Bio-Rad Laboratories. The resin was washed alternately with 3 M HCl and water several times and rinsed with water until the rinse water was chloride-free. The washed resin was allowed to air-dry for 3 days, dried over anhydrous $Mg(ClO_4)_2$ in a vacuum desiccator for 8 days, and stored in an airtight bottle. The resin capacity was determined to be 2·692 meq/g by complete elution of the chloride ion from the resin with 3 M $HClO_4$ and titration of the displaced chloride. The volume of water absorbed by the resin when placed in contact with a salt solution was found to be 0·5 ml/g.

Procedure. Exactly 1·000 g resin and 10·00 ml of salt solution were placed in a 30 ml polyethylene bottle with a polyethylene screw top, and shaken for 10–14 hr. Two 4·00 ml samples were removed through fritted glass filters and titrated by the Volhard method(10) to determine the chloride displaced from the resin by the salt. By use of this information plus the initial salt concentration (corrected for the water absorbed by the resin) and the resin capacity, and assuming no resin invasion (no non-exchange electrolyte), the quantities listed in Table 1 were calculated. [Actually, of course, there is some non-exchange electrolyte present in the resin when in contact with the 1·0 M solutions, or even with the 0·02 M solutions. But this leads to less than a 5–10 per cent error in the values of Q and D listed in Table 1 for the 1·0 M solutions, and a progressively smaller error for the more dilute ones.]

---

(7) B. Chu and R. M. Diamond. Unpublished data

(8) H. P. Gregor, J. Belle and R. A. Marcus, *J. Amer. Chem. Soc.* 77, 2713 (1955).

(9) J. Aveston, D. A. Everest and R. A. Wells, *J. Chem. Soc.* 231 (1958).

(10) W. C. Pierce and E. L. Haenisch, *Quantitative Analysis* (3rd Ed.), p. 302. J Wiley, New York (1948).

TABLE 1.—EXPERIMENTAL RESULTS

Sodium salt	M_0	(Cl)	$(\overline{\mathrm{A}})$	(A)	$(\overline{\mathrm{Cl}})$	Q	D	X_{Cl}
Acetate	1·095	0·129	1·225	0·966	1·467	0·112	1·27	0·545
	0·547	0·0993	0·995	0·448	1·737	0·122	2·13	0·645
	0·219	0·0645	0·613	0·155	2·079	0·123	3·98	0·772
	0·1095	0·0443	0·421	0·0652	2·271	0·126	6·46	0·844
	0·0547	0·0293	0·278	0·0254	2·414	0·133	10·9	0·897
	0·0219	0·0150	0·143	0·0069	2·549	0·122	21·0	0·947
Formate	1·054	0·1455	1·382	0·909	1·310	0·170	1·53	0·487
	0·527	0·1135	1·078	0·413	1·614	0·184	2·62	0·600
	0·211	0·0720	0·684	0·139	2·008	0·175	4·96	0·746
	0·105	0·0510	0·487	0·054	2·207	0·208	9·0	0·820
	0·0527	0·0326	0·309	0·0201	2·382	0·210	15·4	0·885
	0·0211	0·0162	0·153	0·0049	2·538	0·20	31	0·943
Butyrate	1·074	0·161	1·530	0·913	1·162	0·232	1·68	0·432
	0·537	0·123	1·169	0·414	1·523	0·228	2·82	0·566
	0·215	0·0798	0·758	0·135	1·934	0·231	5·61	0·718
	0·1074	0·0543	0·516	0·0531	2·176	0·243	9·72	0·808
	0·0537	0·0345	0·328	0·0192	2·364	0·249	17·1	0·878
	0·0215	0·0173	0·164	0·0042	2·528	0·27	39	0·937
Trimethylacetate	1·116	0·180	1·710	0·936	0·982	0·335	1·83	0·365
	0·558	0·142	1·349	0·416	1·343	0·341	3·24	0·499
	0·223	0·0915	0·869	0·132	1·823	0·332	6·61	0·677
	0·1116	0·0623	0·592	0·0493	2·100	0·356	12·0	0·780
	0·0558	0·0390	0·371	0·0168	2·321	0·371	22·1	0·862
	0·0223	0·0185	0·176	0·0038	2·516	0·34	46	0·935
Trimethylacetate (repeat run)	1·116	0·1742	1·655	0·946	1·037	0·293	1·75	0·385
	0·558	0·1355	1·287	0·422	1·405	0·295	3·06	0·522
	0·223	0·0902	0·857	0·133	1·835	0·318	6·47	0·682
	0·1116	0·0612	0·575	0·0504	2·111	0·327	11·3	0·784
	0·0558	0·0388	0·368	0·0170	2·323	0·362	21·7	0·863
	0·0223	0·0185	0·176	0·0038	2·516	0·34	46	0·935
Valerate	1·158	0·193	1·834	0·965	0·858	0·427	1·90	0·319
	0·579	0·155	1·473	0·424	1·219	0·442	3·47	0·453
	0·232	0·1005	0·955	0·132	1·737	0·420	7·26	0·645
	0·1158	0·0685	0·651	0·0473	2·041	0·462	13·8	0·758
	0·0579	0·0433	0·411	0·0146	2·281	0·534	28·2	0·847
	0·0232	0·0198	0·188	0·0034	2·504	0·44	55	0·930
Caproate	1·063	0·207	1·966	0·856	0·726	0·654	2·30	0·270
	0·532	0·175	1·662	0·357	1·030	0·792	4·66	0·383
	0·213	0·117	1·111	0·096	1·581	0·86	11·6	0·587
	0·1063	0·0777	0·738	0·0286	1·954	1·03	25·8	0·726
	0·0532	0·0450	0·427	0·0082	2·265	1·03	52	0·841
	0·0213	0·0193	0·183	0·0020	2·509	0·70	92	0·932
Methyldichloroacetate	1·068	0·212	2·014	0·854	0·678	0·74	2·36	0·252
	0·533	0·203	1·928	0·330	0·764	1·55	5·84	0·284
	0·213	0·144	1·370	0·069	1·322	2·17	19·9	0·491
	0·1068	0·0877	0·833	0·0189	1·859	2·08	44	0·691
	0·0533	0·0478	0·454	0·0055	2·238	1·76	83	0·831
	0·0213	0·0197	0·187	0·0016	2·505	0·9	120	0·931
Trichloroacetate	1·071	0·277	2·631	0·794	0·061	15·1	3·3	0·023
	0·536	0·266	2·527	0·270	0·165	15·1	9·4	0·061
	0·214	0·179	1·700	0·035	0·992	8·8	49	0·369
	0·1071	0·0947	0·900	0·0124	1·792	3·8	73	0·666
	0·0536	0·0485	0·461	0·0051	2·231	2·0	90	0·829
	0·0214	0·0201	0·191	0·0013	2·501	1·2	150	0·929

RESULTS AND DISCUSSION

The resin phase can be considered as a concentrated electrolyte solution, and it has the following significant differences from the dilute electrolyte solution external to the resin:

(1) One species of ion in the resin solution phase, the quaternary ammonium resin cation, is relatively immobile, being fixed on the resin matrix, but this matrix itself can swell and shrink to an extent dependent on the degree of cross-linking.

(2) Electrostatic interactions are stronger in the resin solution (the effective dielectric constant of the resin phase is lower).

(3) The water in the resin phase has less co-operative structure, i.e., the water molecules are, on the average, hydrogen-bonded to fewer other water molecules than in a dilute aqueous solution.

Factor (1) leads to the treatment of the resin as a Donnan membrane. If we consider only very dilute external solutions, the high concentration of resin-fixed ions existing in the usual exchange resin allows a negligible concentration of mobile ions of the same charge type to enter the resin phase. Only equivalent exchange occurs.

Factor (2), more intense electrostatic interactions in the resin phase, owes its origin to several causes, as follows.

(a) The resin–solution phase has a high concentration of ions, and even moderately concentrated salt solutions may have dielectric constant values below fifty because a significant fraction of the water molecules is oriented around the ions.(11) That is, the proportion of "free" water is reduced.

(b) A large proportion of the wet resin volume (about $\frac{1}{2}$ or more, for moderately cross-linked resins) is made of hydrocarbon matrix with a low dielectric constant, similar to that of benzene.

(c) There is a reduction in the co-operative effect of the water dipoles in producing a large moment because of disorganization of the water structure.

Factor (3), the partial disruption of the normal structure of water, is due to the intrusion of the resin matrix into the water structure and to the high concentration of ions in the resin solution. In water at room temperature, each water molecule is hydrogen-bonded, on the average, to about three other water molecules in a pseudotetrahedral short-range structure.(11a, 12, 13, 14) Inside the resin phase, however, this short-range order is disturbed and broken up by the high concentrations of resin ions and counter ions. These ions occupy solution volume and tend, to a greater or lesser extent depending upon their charge and size, to orient the water dipoles around themselves. Furthermore, the hydrocarbon matrix of the resin intrudes into the solution and confines the water and mobile ions to relatively narrow capillary pores and sheets with one, and possibly two, dimensions of the order of magnitude of 10 Å. Thus a water molecule in the resin phase is hydrogen-bonded on the average to fewer other water molecules than in the dilute external solution.

Factor (2), the enhanced electrostatic interactions between ions in the resin phase, cannot be the primary factor leading to the observed anion selectivity orders. For, as mentioned in the introduction, there are too many exceptions to the order of selectivity required by purely electrostatic ion-pairing.

---

(11) (a) G. H. Haggis, J. B. Hasted and T. J. Buchanan, *J. Chem. Phys.* **20**, 1452 (1952); (b) F. E. Harris and C. T. O'Konski, *J. Phys. Chem.* **61**, 310 (1957).

(12) L. Pauling, *Nature of the Chemical Bond*, p. 468. Cornell University Press, Ithaca, New York (1960).

(13) P. Cross, J. Burnham and P. Leighton, *J. Amer. Chem. Soc.* **59**, 1134 (1937).

(14) J. Morgan and B. E. Warren, *J. Chem. Phys.* **6**, 666 (1938).

On the other hand, Factor (3), leading to differences between the ion-water and the water–water interactions in both the resin and the external aqueous phases, must be considered as a possible reason for resin selectivity. The hydration of ions in the resin phase will certainly be reduced below that in the dilute external solution. This is due, as in any concentrated electrolyte solution, to the smaller ratio of water molecules to ions, and to the fact that there is not sufficient room in the resin pores to allow as complete secondary solvation of the ion as in the dilute solution phase. That is, at distances from the ion greater than a few angstroms, there exist in the resin phase relatively nonpolarizable ions and hydrocarbon matrix, while in a dilute aqueous solution essentially only polarizable and orientable water molecules occur in the vicinity of the ion.* A small, highly charged ion will prefer the aqueous phase, as its transfer into the resin requires a loss of hydration energy. However, the larger the ion and the smaller its charge, the smaller its degree of hydration in the aqueous phase and the less hydration energy it can and does lose on passing into the resin phase. Thus, in an exchange process, the larger, less hydrated ion is pushed into the resin phase so that the smaller ion can achieve maximum hydration in the dilute external phase. The value of the equilibrium quotient for the exchange is larger as the disparity in the hydration of the ions is greater.

The idea that the larger the ion is, the less well it is hydrated, and the more strongly it is forced into the resin phase, is not correct if the ion has structural features or groups which are strongly hydrophilic. For anions of similar size and structure, the degree of hydrolysis of the anion, or the strength of the parent acid, is an indication of the strength of the ion's interaction with water. The more strongly an anion picks up a proton (the weaker the parent acid), the more strongly the anion (hydrogen-bonds) to a water molecule, and the more strongly it prefers the dilute external solution phase to the concentrated resin phase.

The difference between the water–water interactions in the two phases must also be considered. The dilute external solution has essentially the hydrogen-bonded structure of pure water. The addition of ions disrupts this structure. Small, highly charged ions reorganize the nearest water molecules into their own hydration shell, and orient and polarize water molecules for some distance. On the other hand, large, low-charged ions break up a large volume of the water structure but do not have a sufficiently high charge density to tightly bind the nearest water molecules. The hydrogen-bonded water structure can be thought of as an elastic framework which tends to oppose the entrance of the intruding large ion. The limiting case is furnished by an uncharged molecule such as CCl_4 which is actually kept out of solution by the water structure. (Large anions such as $FeCl_4^-$, $AuCl_4^-$, etc., are similar to the CCl_4 molecule but with a single negative charge smeared over the chlorine atoms, and so should also be affected by this opposition of the water structure, though to a smaller extent.) In the resin phase, the water structure is already so badly disrupted that it offers much less opposition to the entrance of a large ion. The larger the ion, the more easily it is transferred out of the dilute aqueous solution into the less ordered water structure of the resin phase, yielding the same selectivity order as already indicated above by consideration of the ion-water interactions alone.

---

* Ions that are so strongly hydrated in the external solution as to possess a primary shell co-ordinated water molecules certainly tend to retain this co-ordinated shell in the resin phase, at least for resins of not too high a cross-linking. For example, it has been shown that the hexaquo chromium(III) ion keeps its primary hydration shell in a cation-exchange resin (Cf. BOYD and SOLDANO(15).) But the solvation of this first water shell will be greatly disturbed in the resin phase.

(15) G. E. BOYD and B. A. SOLDANO, *J. Amer. Chem. Soc.* **75**, 6105 (1953).

An obvious limitation on the foregoing is forced by the size of the ion-exchange resin pores. When an ion is too large to fit into the pores without considerable expenditure of energy to expand the resin matrix, it is discriminated against by the resin. Since resins do not have a single pore size, but a distribution of sizes, and the average value decreases with increasing cross-linkage, the pore-size limitation is least important for the lower-cross-linked resins. For the usual anions and for resins of normal cross-linking (8–10% DVB content), and keeping the pore-size limitation in mind, we may state that in an ion-exchange reaction, the less highly hydrated (larger) ion is preferentially ejected by the water structure into the resin phase, and the more highly hydrated (smaller) ion preferentially solvates in the dilute aqueous phase, thus maximizing the water–water and water–ion interactions in the system.

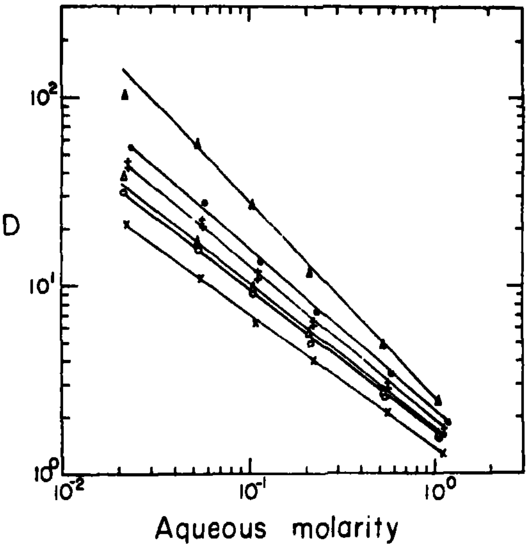

FIG. 1.—Plot of distribution ratio, *D*, against total aqueous molarity for sodium acetate, x——x; sodium formate, o——o; sodium butyrate, Δ——Δ; sodium trimethylacetate, +——+; sodium valerate, ●——●; and sodium caproate, ▲——▲.

The predicted effect of ion size has been tested by determining the order of resin selectivity for the fatty acid anions acetate, butyrate, trimethylacetate, valerate, and caproate against the common ion, chloride. This was done at total aqueous phase concentrations of 1·0, 0·5, 0·2, 0·1, 0·05, and 0·02 M, and the results are shown in Table 1 and Fig. 1. The symbol *Q*, the concentration constant, is defined as $Q = (\bar{A})(Cl)/(A)(\bar{Cl})$ where (¯) means resin phase concentration in millimoles per gram of resin, and ( ) means aqueous phase concentration in millimoles per millilitre of solution. Similarly the distribution ratio *D* is defined as $D = (\bar{A})/(A)$. The charge on these fatty acid anions is concentrated in the carboxylate group, and so this group is the principal source of hydration for the ions. Furthermore, these anions are all derived from weak acids of the same strength, and so the hydration of the carboxylate group in each is comparable, leaving primarily their size as a selectivity factor. In going from acetate to caproate, the increasing size of the hydrocarbon tail must increasingly disturb the hydrogen-bonded water structure of the dilute external solution, so that the larger the tail, the more strongly the anion should be pushed into the less structured resin phase. This leads to the predicted order of resin selectivity acetate < butyrate < valerate < caproate, which is that observed experimentally. Trimethylacetate has a more compact structure than its straight-chain isomer, valerate, and so has a somewhat smaller value of D and Q. These selectivity orders cannot be explained by a simple electrostatic ion pairing model.

Besides the effect of ion size, the effect of specific ion hydration was also tested. The sequence of anions trimethylacetate, methyldichloroacetate, and trichloroacetate was used. In replacing a methyl group with a chloro group, the size of the anion is held substantially constant, but the inductive effect of the chlorine atom transforms the anion into a progressively weaker base. That is, the corresponding acids become progressively stronger, as can be seen in Table 2, where are listed the ionization constants for the similar acids acetic, chloroacetic and trichloracetic. Since the carboxylate of the increasingly chlorine-substituted anion is less basic toward capturing a proton from water, it also interacts less strongly with water molecules.

TABLE 2—LIMITING EQUIVALENT CONDUCTIVITY OF ANION, λ°, AND DISSOCIATION CONSTANT OF PARENT ACID, K_a, AT 25°C(16)

Anion	λ°	K_a of parent acid
F^-	55·4	$6{\cdot}7 \times 10^{-4}$(18)
Cl^-	76·4	Strong
Br^-	78·1	Strong
I^-	76·8	Strong
ClO_4^-	67·4	Strong
HCO_2^-	54·6	$1{\cdot}77 \times 10^{-4}$
$CH_3CO_2^-$	40·9	$1{\cdot}76 \times 10^{-5}$
$CH_3CH_2CO_2^-$	35·8	$1{\cdot}34 \times 10^{-5}$
$CH_3(CH_2)_2CO_2^-$	32·6	$1{\cdot}51 \times 10^{-5}$
$CH_3(CH_2)_3CO_2^-$	—	$1{\cdot}38 \times 10^{-5}$
$CClH_2CO_2^-$	39(17)	$1{\cdot}38 \times 10^{-3}$
$CCl_2HCO_2^-$	38·5(17)	
$CCl_3CO_2^-$	37(17)	Strong
ClO_3^-	64·6	Strong
BrO_3^-	55·7	
IO_3^-	39·4(17)	$1{\cdot}67 \times 10^{-1}$(19)
NO_2^-	62·(17)	$4{\cdot}5 \times 10^{-4}$(18)
NO_3^-	71·5	Strong
ClO^-		$3{\cdot}2 \times 10^{-8}$
BrO^-		$2{\cdot}1 \times 10^{-9}$
IO^-		10^{-11}

---

(16) R. A. ROBINSON and R. H. STOKES, *Electrolyte Solutions*. Butterworths Scientific Publications, London (1955).

(17) *International Critical Tables*, Vol. 6. McGraw-Hill, New York (1929).

(18) W. M. LATIMER, *Oxidation Potentials*. Prentice-Hall, New York (1952).

(19) H. V. HALBAN and J. BRÜLL, *Helv. Chim. Acta.* 27, 1719 (1944).

That is, the anion of the stronger acid is less strongly solvated by water. Thus, it would be expected that trimethylacetate would prefer the dilute external solution more than the weaker base, methyldichloroacetate; and the latter ion, in turn, would prefer the aqueous phase more than the still weaker base, trichloroacetate. This is precisely the experimentally observed order, as given in Table 1 and Fig. 2.

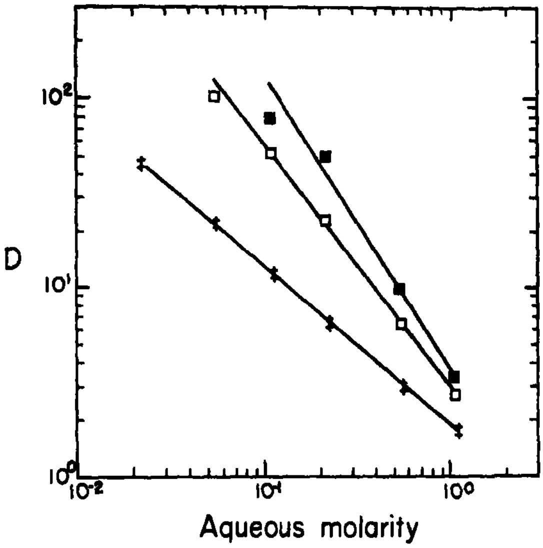

FIG. 2.—Plot of distribution ratio, *D*, against total aqueous molarity for sodium trimethylacetate, +——+; sodium methyldichloroacetate, □—□; and sodium trichloroacetate, ■——■.

The effects of ion size (water-structure-breaking factor) and of specific ion hydration may act in opposite directions. Usually the latter dominates in determining the order of anion selectivity. Formate and acetate ions (Table 1 and Fig. 1) furnish an example. From the argument given above for the larger fatty acid anions, it might be expected that the larger acetate ion would be preferred by the resin over formate. But in the earlier example, all the anions were of the same base strength, whereas formate is a weaker base than acetate (Table 2), so that its carboxylate group interacts more weakly with water than that of the acetate ion. The stronger ion hydration of acetate than of formate holds the former preferentially in the external aqueous phase, giving the observed resin order formate > acetate < butyrate.

In fact, for any series of similar complex anions from a family of the periodic table one should be able to predict the order of resin selectivity from the order of base strength of the anions. For a family in which the elements become more electropositive on going to the heavier members, one would expect a sequence of similar complex anions derived from these elements to become stronger bases on going down the family. Because of the resulting stronger interaction with water one would predict that such a sequence of anions would show a decreasing affinity for the resin. Examples are $MnO_4^- > TcO_4^- > ReO_4^-$, $CrO_4^{2-} > WO_4^{2-}$, and $ClO_3^- > BrO_3^- > IO_3^-$, and these are indeed the observed orders.(7, 9, 20) It can be predicted that the selectivity order $ClO^- > BrO^- > IO^-$ should also occur, as the base strength of these anions similarly increases from ClO^- to IO^- (Table 2). These selectivities cannot be explained by the polarizability of the anions, at least as indicated by their ionic refractions, for such a model leads to the reverse ordering.

On the other hand, if, in going down a family, the elements become less electropositive, their complex anions become less basic and interact with water less strongly. As a result, such a sequence of anions should show increasing selectivity by the resin—the opposite behaviour to that mentioned in the preceding paragraph. Examples of such sequences would be predicted for complexes of the nobler metal elements, e.g., $Ag(CN)_2^- < Au(CN)_2^-$ and $Ni(CN)_4^{2-} < Pd(CN)_4^{2-} < Pt(CN)_4^{2-}$, and these are the experimentally observed orders.(9)

If the effects of both (crystallographic) ion size and specific ion hydration act in the same direction, prediction of the order of resin selectivity for a series of ions is unambiguous. Such is the case for the resin selectivity sequence $F^- < Cl^- < Br^- < I^- < ClO_4^- < AuCl_4^-$.(8, 9, 21-24) The ions get progressively larger and become weaker bases, both factors leading to the actually observed order. For the smaller F^- and Cl^- ions, the effect of better solvation in the dilute aqueous phase is probably the predominant factor (the greater hydration of F^- relative to Cl^- is indicated by the relative strengths of the parent hydrohalic acids and by the smaller limiting equivalent conductivity of F^-). For Cl^-, Br^-, and I^-, both factors probably contribute significantly, and for the larger, less highly hydrated ions I^-, ClO_4^-, and $AuCl_4^-$ the disruption of the water structure is probably the more important factor.

It is difficult to explain this sequence solely on the basis of electrostatic ion pairing of the resin quaternary ammonium ion with the anion. The ions Cl^-, Br^-, and I^- have similar limiting equivalent conductivities (Table 2), indicating approximately the same effective (hydrated) radii, and the limiting equivalent conductivity for ClO_4^- is considerably less, indicating a still larger effective radius in solution. If only electrostatic ion pairing were important in determining anion selectivities, Cl^-, Br^-, and I^- should then be bound to the resin about equally, and all much more strongly than ClO_4^-, in contradiction to the experimental facts. Also, any explanation based solely on anion polarizability fails in the ClO_4^-—I^- case, as I^- has a larger ionic refraction than ClO_4^-.

Another example in which size of the ions and the effect of specific ion hydration, as measured by the strength of the parent acid, combine to give an unambiguous order is furnished by the pair NO_2^- and NO_3^-. The first one is derived from the weaker acid, and so is more highly hydrated. (It shows, in fact, the lower limiting equivalent conductivity (Table 2).) The order of resin selectivity expected then is $NO_2^- < NO_3^-$, and this is the observed sequence.(21) For similar reasons the resin selectivity orders $ClO^- < ClO_3^- < ClO_4^-$, $BrO^- < BrO_3^-$, $IO^- < IO_3^-$, $HSO_3^- < HSO_4^-$, $SO_3^{2-} < SO_4^{2-}$, etc., can be predicted. Except for the sequence $ClO_3^- < ClO_4^-$,(9) these particular sequences have not yet been experimentally determined, but they would provide interesting confirmation of the ideas presented.

In summary, then, it is seen that for anions of weak acids, the specific effect of ion hydration is the predominant one, and the more basic the ion the more it prefers

---

(20) R. W. Atterbury and G. E. Boyd, *J. Amer. Chem. Soc.* **72**, 4805 (1950).

(21) R. M. Wheaton and W. C. Bauman, *Indust. Engng. Chem.* **43**, 1088 (1951).

(22) R. Kunin and F. X. McCarthy, *Indust. Engng. Chem.* **41**, 12 (1949).

(23) K. A. Kraus and F. Nelson, *J. Amer. Chem. Soc.* **76**, 984 (1954).

(24) G. E. Boyd, S. Lindenbaum and G. E. Myers, *J. Phys. Chem.* **65**, 577 (1961).

the dilute external phase. For large anions, or those of strong acids, ion hydration is less important, and the effect of disrupting the hydrogen-bonded water structure of the dilute external solution becomes more important—the more so as the ion becomes larger. That is, in the exchange, the large ion is squeezed out of the solution into the less structured resin phase (pore size permitting), as such behaviour maximizes the ion–water and water–water interactions in the total system. It is suggested that these differences in ion–water (ion hydration) and water–water (water-structure) interactions between the resin and aqueous phases are the principal origins of anion selectivity with the usual synthetic organic resins, rather than any specific resin ion-counter ion or resin matrix-counter ion interaction, as is postulated in any electrostatic ion pairing model or one based solely on anion polarizability.

J. Inorg. Nucl. Chem., 1962, Vol. 24, pp. 1417 to 1428. Pergamon Press Ltd. Printed in England

DISTRIBUTION OF NITRIC ACID BETWEEN WATER AND AMBERLITE LA-1 LIQUID ANION EXCHANGER

A. S. KERTES* and I. T. PLATZNER

Department of Inorganic and Analytical Chemistry,
The Hebrew University of Jerusalem, Jerusalem, Israel

(*Received* 20 *December* 1961)

Abstract—The solute–solvent interaction between Amberlite LA-1, a long-chain secondary amine extractant dissolved in carbon tetrachloride or benzene and aqueous nitric acid solution up to ~ 16 M has been investigated by physical and chemical measurements. The first reaction is an acid–base equilibrium leading to the formation of amine nitrate. The equilibrium constants were evaluated as $K_1 = 3{\cdot}8 \times 10^5$ and $5{\cdot}4 \times 10^5$ in carbon tetrachloride and benzene respectively. The second and third reactions postulated involve amine nitrate and associated nitric acid molecules, leading to the formation of a molecular addition compound identified as $R_2HNHNO_3{\cdot}HNO_3$ and to the physical partition of associated nitric acid between the aqueous and organic phases. The equilibrium concentration product quotients have the values $K_2 = 1{\cdot}85$ for carbon tetrachloride and $K_2 = 2{\cdot}24$ for benzene, and the distribution constant has the value $K_d = 0{\cdot}1 \pm 0{\cdot}02$ for 1 M amine solution in both diluents. The effects of the formation of the amine nitrate aggregates or of the extracted molecular addition compound, or both, are not taken into account. Evidence was obtained that the aggregation of the species in the organic phase is largely a post-equilibrium phenomenon.

IT has been observed$^{(1-7)}$ that the extraction of nitric acid by long-chain amines is not simply a case of an acid-base reaction leading to the formation of amine nitrate, since potentiometric neutralization curves of the acid contained in the equilibrium organic phase give two endpoints. The amount of base consumed from the first to the second endpoint is equivalent to the amount of amine present, and the amount required to reach the first endpoint is a function of the concentration of nitric acid in the aqueous phase at equilibrium. This indicates that the acid is bound in two different ways.

---

* Present address: Department of Chemistry and Laboratory for Nuclear Science, Massachusetts Institute of Technology, Cambridge 39, Mass.

(1) E. A. MASON and V. C. A. VAUGHEN, Report AECU-4631 (1959); Report TID-5720 (1960); V. C. A. VAUGHEN and E. A. MASON, Summary Report, Dept. of Nuclear. Engineering, M.I.T. (1960).

(2) U. BERTOCCI, AERE/R-2933 (1959).

(3) D. J. CARSWELL and J. J. LAWRENCE, *J. Inorg. Nucl. Chem.* **11**, 69 (1959).

(4) D. E. HORNER and C. F. COLEMAN, Report ORNL-3051 (1961).

(5) (a) G. SCIBONA, *Italian Comm. Nucl. Res.*, Report CNC-43 (1960);
(b) G. SCIBONA and M. ZIFFERERO, *Ibid.* CNEN-51 (1961).

(6) V. B. SHEVCHENKO, V. S. SHMIDT, E. A. NENAROKOMOV and K. A. PETROV, *Zh. Neorg. Khim.* **5**, 1852 (1960).

(7) O. I. ZAHAROV-NARCISOV and A. V. OCHKIN, *Zh. Neorg. Khim.* **6**, 1936 (1961).

Several studies have been published in the last two years on the extraction of actinides(2, 3, 4, 8), lanthanides,(9) technetium and rhenium,(10, 11) some fission products(1, 12, 13) and heavy metals(14) from nitrate systems by amines. Some work has also been devoted to the rôle of nitric acid. In MASON's laboratory(1) the extraction of nitric acid in the range 2–10 M by a number of primary, secondary and tertiary amines has been investigated. The nitric acid in the organic phase in excess of that equivalent to the amine concentration was found to be proportional to the concentration of the acid in the equilibrium aqueous phase for the tertiary amines, but a less simple relationship was observed for primary and secondary amines. CARSWELL and LAWRENCE,(3) BERTOCCI(2) and COLEMAN and HORNER(4) provide support for the linear relation with tertiary amines, and according to the work at Oak Ridge the linear relationship appears to hold for all amines, including primary and secondary ones.(4) Thus, the concentration of extracted nitric acid can be related to the concentrations of amine and aqueous acid by the expression

$$(\mathrm{HNO}_{3\,\mathrm{excess}})_{\mathrm{org}}/(\mathrm{Amine})_{\mathrm{org}}(\mathrm{HNO}_3)_{\mathrm{aq}} = \alpha$$

where $(\mathrm{HNO}_{3\,\mathrm{excess}})$ is the organic nitric acid concentration above the stoichiometric ratio 1:1 with the amine. The available results fit this relationship with values of α between 0·16–0·18 for tertiary, 0·10–0·14 for secondary and 0·06–0·11 for primary amines. We have found that Amberlite LA-1, a secondary amine, follows the above relationship in the range between 3 and 12 M nitric acid in the initial aqueous solution, the constant α having a value of 0·13–0·14. Although this relationship is valid for a wide range of acid loadings and amine concentrations it cannot be interpreted as the mechanism of the reaction, and represents only an empirical relationship. SHEVCHENKO *et al.*(6) have studied the extraction of nitric acid by trioctylamine, and propose as the extraction mechanism complex formation between the amine nitrate and excess nitric acid according to the reaction

$$(\mathrm{TOA}\cdot\mathrm{HNO}_3)_{\mathrm{O}} + \mathrm{H}^+_{\mathrm{a}} + (\mathrm{NO}_3^-)_{\mathrm{a}} \rightarrow [(\mathrm{TOA}\cdot\mathrm{HNO}_3)\cdot\mathrm{HNO}_3]_{\mathrm{o}}$$

The calculated equilibrium constants have values of $K = 0{\cdot}09$ and 0·13 for the diluents carbon tetrachloride and xylene respectively. K showed satisfactory constancy in the range of 1–5 M aqueous nitric acid, but was measured for only one

(8) W. E. KEDER, J. C. SHEPPARD and A. S. WILSON, *J. Inorg. Nucl. Chem.* **12**, 327 (1960); J. C. SHEPPARD, Report HW-51958 (1957); A. S. WILSON and W. E. KEDER, Report HW-62908 (1959); A. S. WILSON, Report HW-68207 (1961); W. E. KEDER, J. L. RYAN and A. S. WILSON, *J. Inorg. Nucl. Chem.* In press; F. ICHIKAWA and S. URUNO, *Bull. Chem. Soc. Japan*, **33**, 569 (1960); C. J. HARDY, D. SCARGILL and J. M. FLETCHER, *J. Inorg. Nucl. Chem.* **7**, 257 (1958); K. B. BROTHERS, C. F. COLEMAN, D. J. CROUSE, J. V. DENIS and J. G. MOORE, *J. Inorg. Nucl. Chem.* **7**, 85 (1958); H. G. PETROW, Report TID-6357 (1960); F. R. BRUCE, R. E. BLANCO and J. C. BRESEE, Report CF-58-11-91 (1959); B. WEAVER and D. E. HORNER, *J. Chem. Engng. Data*, **5**, 260 (1960); M. DE TRENTINIAN and A. CHESNE, Report CEA-1426 (1960).

(9) F. ICHIKAVA, *Bull. Chem. Soc. Japan*, **34**, 183 (1961).

(10) G. E. BOYD and G. V. LARSON, *J. Phys. Chem* **64**, 988 (1960); A. S. KERTES and A. BECK, *J. Chem. Soc.* 1926 (1961); A. BECK. Ph.D. Thesis, The Hebrew University, Jerusalem (1961).

(11) F. L. CULLER, Annual Progress Report, ORNL–2993 (1960).

(12) E. A. MASON and V. C. VAUGHEN, Report AECU-4239 (1959); Report AECU-4351 (1959).

(13) V. B. SHEVCHENKO and V. S. SMIDT, *Radiokhimija*, 3, 121 (1961); W. KNOCH and R. LINDER, *Z. Elektrochemie*, **64**, 1020 (1960); W. KNOCH, *Z. Naturforschung*, **16 a**, 525 (1961).

(14) E. A. MASON and R. E. SKAVDALL, Report TID-11196 (1960).

concentration of amine (0·47 M). An unsuccessful attempt was made to fit the results obtained in this study to the above reaction; the calculated values of K were not satisfactorily constant. In a paper published while this report was being completed, ZAHAROV-NARCISOV *et al.*(7) have interpreted the equilibrium data in the system 0·25 M triheptylamine nitrate–aqueous nitric acid (1·3–4 M) by the extraction of undissociated nitric acid, and postulated the existence of the species $(THA \cdot HNO_3)$-HNO_3 with a formation constant $K = 7{\cdot}2 \pm 0{\cdot}2$. These authors also found that in carbon tetrachloride the organic solution of amine or amine nitrate is non-ideal, and constant values for K could not be obtained.

The purpose of this investigation was to ascertain whether the amine nitrate and nitric acid interact, and if so to what extent. In addition to a study of equilibrium data for the acid distribution, this investigation is devoted particularly to the physico-chemical behaviour of the loaded organic layer, its viscosity, density and conductivity. Similar studies with phosphoric acid esters as extractants(15, 16) have been successfully employed in clarifying the heterogeneous equilibria in these solvent extraction processes.

Amberlite LA-1 was chosen as extractant, since it is one of the few organo-nitrogen compounds selected as suitable for process use.(17)

EXPERIMENTAL

Materials. Amberlite LA-1* is a secondary amine, with a molecular weight of 416 as determined in a potentiometric titration using perchloric acid.(18) In the free base form, as supplied by the manufacturer, it is a viscous, amber-coloured liquid, very slightly soluble in aqueous solutions (10–20 p.p.m.). The diluents used were carbon tetrachloride and benzene, both of the highest quality, and they were used without further purification.

Extraction procedure. Equal volumes, usually 5 ml, of the amine solution and the aqueous nitric acid solution were mixed in a 15 ml graduated centrifuge tube and shaken vigorously mechanically for 15 min. Certain experiments in which a different technique was employed are described later. After equilibration with 0·89 M amine solutions when acid solutions of concentration greater than ~ 10 M were used, swelling of the organic phase occurred irrespectively of the diluent. In these systems, prolonged centrifugation at maximum speed was necessary to produce phase separation, in order to enable volume change to be measured. As a precaution against changes observed in the organic phase which are described later, the samples were treated one after another through all stages of the work, and in addition were, in so far as possible, protected from light. Work on each sample took about 30 min. As preliminary experiments had shown only a slight temperature dependence, extractions were performed at room temperature (22–26°C) except where otherwise stated. Colour changes, from light to dark brown, were observed on bringing the amine solution into contact with the more concentrated nitric acid. No attempt was made to investigate this phenomenon.

Analytical procedure. Aliquots of the phases were diluted, the organic phase with an 8:5:1 methanol:acetone:water mixture, and the acid content determined potentiometrically using a Beckman Zeromatic pH-meter. Two endpoints were observed in titrations of amine phases which were in contact with more concentrated nitric acid solutions. Turbidity, which does not interfere with the pH readings, appears just at the point when the excess acid (over the stoicheiometric ratio of 1:1 amine to acid) is neutralized.

---

* We are indebted to Messrs. Rohm and Haas Company for kindly providing a free sample of the amine.

(15) A. S. KERTES, *J. Inorg. Nucl. Chem.* **14**, 104 (1960); A. S. KERTES and V. KERTES, *Canadian J. Chem.* **38**, 612 (1960); *J. Appl. Chem.* **10**, 287 (1960); A. S. KERTES and M. HALPERN, *J. Inorg. Nucl. Chem.* **16**, 308 (1961).

(16) A. S. KERTES, A. BECK and Y. HABOUSHA, *J. Inorg. Nucl. Chem.* **21**, 108 (1961).

(17) C. F. COLEMAN, K. B. BROWN, J. G. MOORE and D. J. CROUSE, *Industr. Engng. Chem.* **50**, 1756 (1958).

(18) CH. BOIRIE, *Bull. Soc. Chim. France*, 980, 1088 (1958); J. BIZOT and B. TÉRMILLON, *Bull. Soc. Chim. France*, 122 (1959).

Blank extractions with the diluents alone indicated that appreciable amounts of nitric acid are extracted into benzene,(5, 19) particularly at the higher acid concentrations (> 10 M). The benzene blank based on the volume percentage of benzene in the organic solution, determined separately, was therefore subtracted from the total acid in the organic phase. The values for organic acid content given in the tables and graphs throughout this work are those for extraction by the amine alone.

Physical chemical measurements. The density, viscosity and conductivity of the homogeneous organic layers were measured immediately after separation, according to the procedure previously described.(15)

Measurement of amine nitrate formation constant. The equilibrium constant for the acid–base reaction leading to the formation of amine nitrate was studied by converting the base into the nitrate, equilibrating the amine nitrate dissolved in the organic phase with water, and measuring the hydrogen ion activity in the aqueous phase.(18, 20)

A pure amine salt solution in benzene or carbon tetrachloride was prepared by converting the base to the nitrate form by shaking it with an aqueous nitric acid solution of slightly greater acidity, and removing excess acid by three washings with aqueous nitric acid solution of slightly lower acidity. The results referred to later in Fig. 5 show that the amine nitrate so obtained in the organic phase contained neither free amine base nor free nitric acid. A series of dilutions of this amine nitrate stock solution with the appropriate diluent was made down to 0·0015 M. Ten ml aliquots of the amine nitrate solutions were equilibrated with equal volumes of triply-distilled water, and the hydrogen ion activity of the aqueous equilibrium phases was determined by pH measurements using a Cambridge pH-meter to an accuracy of 0·01 pH units.

Degree of agitation and "post-equilibrium" changes of the loaded organic phases. ALLEN and MCDOWELL(21) have observed that in amine systems the final distribution of the solute is not entirely independent of the way in which equilibrium is reached. Following the experimental procedure suggested by them, results were obtained for the extraction of nitric acid by both vigorous and gentle agitation at 27° ±0·1°C. The results presented in Table 1 show that the organic acid loading varies with contact time and type of agitation

TABLE 1.—DISTRIBUTION OF NITRIC ACID AT VARIOUS INITIAL CONCENTRATIONS BETWEEN WATER AND 0·45 M AMINE IN CARBON TETRACHLORIDE AS A FUNCTION OF TIME AND TYPE OF AGITATION

Initial aqueous acid (M)	NaOH consumed for 5 ml of the organic phase	Slow equilibration			Violent equilib. 15 mins
		1 day	3 days	7 days	
	ml 0·259 N NaOH for amine nitrate	8·75	8·90	9·05	8·75
2·154	ml 0·259 N NaOH for total acid	9·70	9·80	9·85	9·80
	$[HNO_3]_o$, total organic acid loading	0·504	0·508	0·511	0·508
	ml 0·259 N NaOH for amine nitrate	8·75	8·90	9·40	8·75
4·194	ml 0·259 N NaOH for total acid	11·80	11·95	12·55	12·05
	$[HNO_3]_o$, total organic acid loading	0·613	0·620	0·652	0·633
	ml 0·259 N NaOH for amine nitrate	8·75	9·00	9·45	8·75
6·518	ml 0·259 N NaOH for total acid	14·85	14·95	15·70	15·15
	$[HNO_3]_o$, total organic acid loading	0·772	0·776	0·815	0·784
	ml 0·259 N NaOH for amine nitrate	8·75	9·15	9·45	8·75
8·527	ml 0·259 N NaOH for total acid	17·40	17·50	18·25	17·80
	$[HNO_3]_o$, total organic acid loading	0·904	0·908	0·946	0·923

---

(19) C. J. HARDY, B. F. GREENFIELD and D. SCARGILL, *J. Chem. Soc.* 90 (1961).

(20) L. NEWMAN and P. KLOTZ, *J. Phys. Chem.* **65**, 796 (1961).

(21) K. A. ALLEN and W. J. MCDOWELL, *J. Phys. Chem.* **64**, 877 (1960).

in a manner similar to that observed by ALLEN and McDOWELL. Furthermore, as our results show, the amount of base necessary to neutralize the amine nitrate varies with the time of contact of the two phases. In addition, the loaded organic phase, previously separated from the aqueous layer, and containing nitric acid in concentrations above the 1:1 stoicheiometric ratio, undergoes changes both in density and viscosity; Fig. 1 shows viscosity measurements

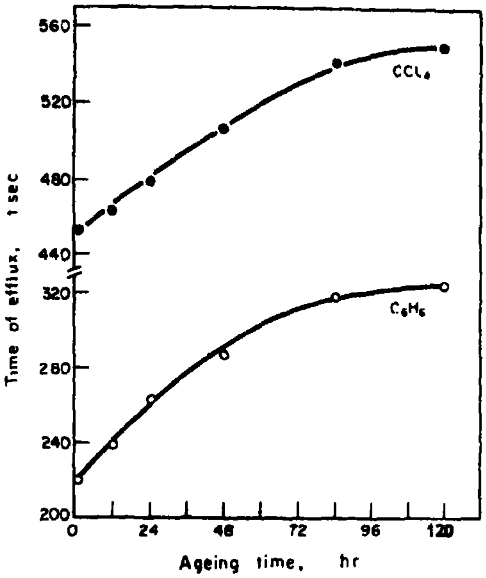

FIG. 1.—Post-equilibrium changes in the viscosity of the loaded organic phase (0·89 M amine equilibrated with 9·24 M nitric acid solution).

carried out on ageing solutions. A plot of time of efflux in an Ostwald viscosity pipette is given rather than true viscosity values, since difficulties were encountered in density determinations using the usual Sprengel type pycnometer.

The cause of change in the organic phase has not been determined. Possible causes are re-arrangements in the organic phase to yield different final amine-nitric acid species, which may be due either to some unknown post-equilibrium aggregation effect(1, 5, 22) or to simpler chemical reactions such as oxidation or reduction. Therefore, we do not feel that the anomalous solvent extraction equilibria are entirely due to violence of agitation, as suggested by ALLEN and McDOWELL.(21) As additional evidence for this view, we point out that neither the time nor the way of mixing was found to be critical in at least two different systems using other amines, viz. amine nitrate–cerium nitrate(1) and tertiary amine-sulphuric acid.(23) In any case, this post-equilibrium change, shown in Table 1 and Fig. 1, raises considerable doubts concerning the applicability of the equilibrium results for aged solutions to an interpretation of extraction mechanism. It was therefore decided that rapid extraction equilibria would be simpler to interpret than those performed under changing conditions. Consequently, 15 min of violent shaking was taken as an adequate and convenient shaking time for valid equilibrium interpretation.

(22) K. A. ALLEN, *J. Phys. Chem.* **60**, 239, 943 (1956); **62**, 1119 (1958); *J. Amer. Chem. Soc.* **80**, 4133 (1958); W. J. McDOWELL and C. F. BAES, *J. Phys. Chem.* **62**, 777 (1958).

(23) J. M. P. J. VERSTEGEN and J. A. A. KETELAAR, *Trans. Faraday Soc.* **57**, 1527 (1961).

RESULTS AND DISCUSSION

Physico-chemical properties of the organic layer. The density and viscosity of the equilibrated organic phases as a function of the ratio $[HNO_3]_0/[R_2HN]_0$ are shown in Figs. 2 and 3. The curves for carbon tetrachloride diluent (0·89 M amine) each

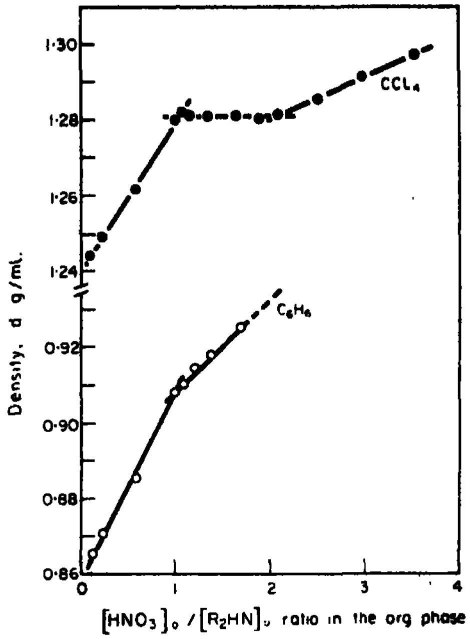

Fig. 2.—Density of the equilibrium organic phase as a function of the nitric acid:amine ratio in the organic phase. Initial amine concentration 0·89 M.

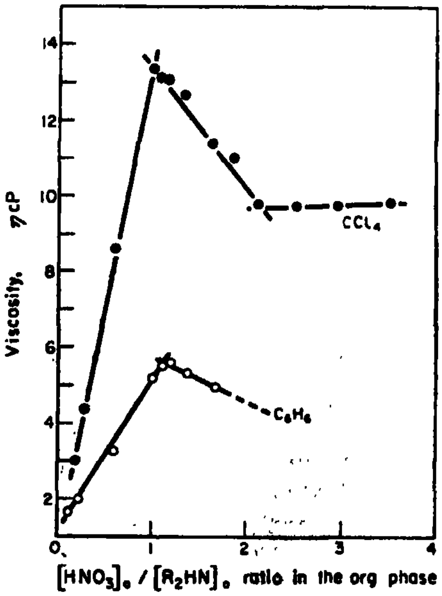

Fig. 3.—Viscosity of the equilibrium organic phase as a function of the nitric acid:amine ratio in the organic phase. Initial amine concentration 0·89 M.

show two intersections between straight lines of different slopes. The first intersection corresponds to the amount of acid necessary to neutralize the amine in the organic phase, producing the amine nitrate, R_2HNHNO_3. The second intersection is at a ratio of 2:1, indicating that the amine nitrate has interacted with more nitric acid to give a molecular addition compound which may be tentatively identified as $R_2HNHNO_3.HNO_3$. The corresponding curves for benzene diluent are only plotted to a ratio of about two, since appropriate corrections could not be made for the benzene blank. Measurements were carried out also with 0·45 and 0·25 M amine solutions in carbon tetrachloride, but the high diluent content in these solutions caused the viscosity and density values to level off.(7) A change in reaction mechanism is also indicated by the conductivity curves in Fig. 4. Both the amine and the amine nitrate solutions showed no detectable conductivity with the equipment available, and the onset of conductivity is believed to be due to formation of a conducting species, such as the addition compound tentatively defined above. This suggests that the extent of ion-pair dissociation in the organic phase is likely to be important. A rough estimate of the acid dissociation as calculated by WALDEN's rule ($\eta\lambda/60$), shows that it does not exceed five per cent at the highest acid and amine concentrations. Partial ionization of tributyl phosphate–nitric acid compounds at the highest nitric acid concentrations, found from infra-red absorption data by TUCK,(24) may be indicative of some similarity between the two systems.

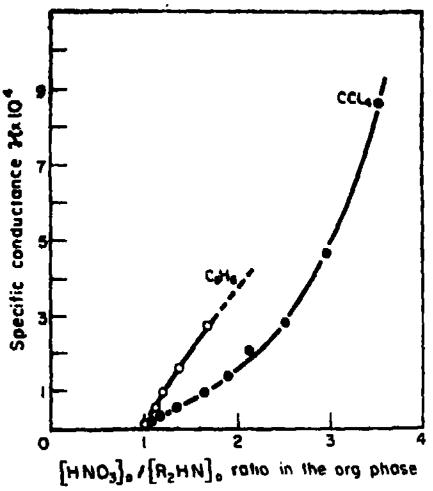

FIG. 4.—Specific conductance of the equilibrium organic phase as a function of the nitric acid:amine ratio in the organic phase. Initial amine concentration 0·89 M.

Formation of amine nitrate. The neutralization reaction between amine and nitric acid up to a $[HNO_3]_o/[R_2HN]_o$ ratio of unity may be represented as

$$(R_2HN)_o + H_a^+ + (NO_3^-)_a \rightleftharpoons (R_2HNHNO_3)_o \qquad (1)$$

where R_2HN stands for the amine base and R_2HNHNO_3 for the amine nitrate, and the subscripts —a— and —o— indicate the aqueous and organic phases respectively.

---

(24) D. G. TUCK, *J. Chem. Soc.* 2783 (1958).

The thermodynamic equilibrium constant for this reaction is:

$$K_1 = \frac{\gamma_{AN}\cdot[R_2HNHNO_3]_o}{\gamma_A.[R_2HN]_o\{H^+\}_a\{NO_3^-\}_a} \tag{2}$$

γ_{AN} is the activity coefficient of the amine nitrate and γ_A is that of the amine base both in the organic phase; their ratio can be taken as unity, since they refer to low concentrations and to species that are relatively alike with respect to the medium. Under the experimental conditions described, $\{H_+\}_a$, the hydrogen ion activity, can be taken as equal to the nitrate ion activity $\{NO_3^-\}_a$, and is also numerically equal to the concentration of free amine base $[R_2HN]_o$. Assuming ideal immiscibility of the phases, $[R_2HNHNO_3]_o$ equals the initial amine nitrate concentration less $\{H^+\}_a$. Thus, transforming (2) into a logarithmic form, we obtain

$$-\log([R_2HNHNO_3]_i-\{H^+\}_a) = 3pH+pK_1 \tag{3}$$

A plot of the left-hand expression vs. the pH readings should give a straight line with a slope of three and an intercept equal to pK_1. Fig. 5 shows such plots, with intercepts $K_1 = 3{\cdot}8\times10^5$ and $K_1 = 5{\cdot}4\times10^5$ for carbon tetrachloride and benzene media respectively.

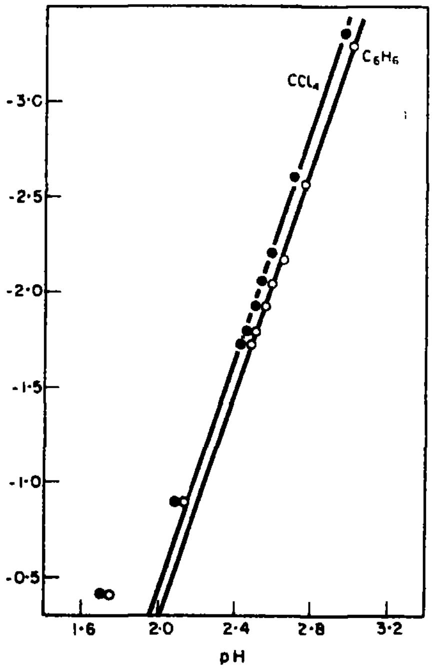

FIG. 5.—Plot of Equation (3) for the determination of K_1.

As seen from the plots, the method of calculation obviously fails when the amine nitrate concentration exceeds 0·05 M. Since deviations from linearity increase gradually with the amine salt concentration in the organic phase, it appears that the limitations are imposed rather by the inability to determine activity coefficients for the organic solutes, than by a change in the mechanism.(20)

Extraction of acid by amine nitrate. The extent of the extraction of nitric acid by amine nitrate as a function of its equilibrium aqueous concentration is shown in Figs. 6 and 7 for carbon tetrachloride and benzene as diluents, respectively.

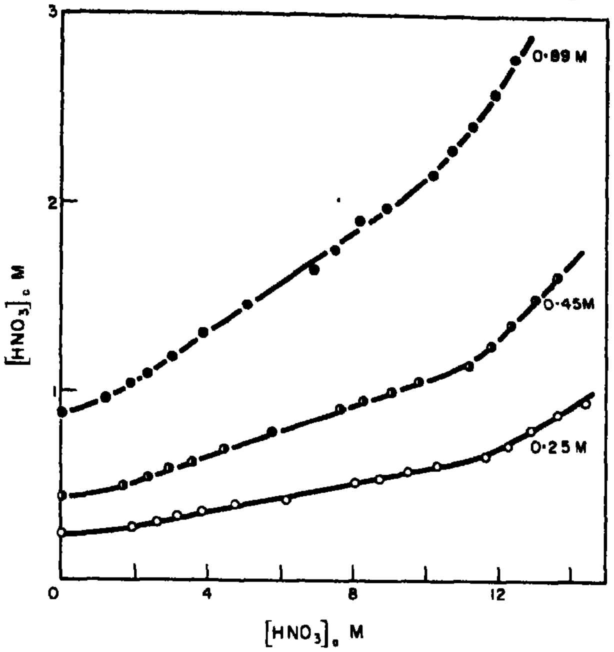

FIG. 6.—Equilibrium distribution of nitric acid between water and carbon tetrachloride solution of the amine.

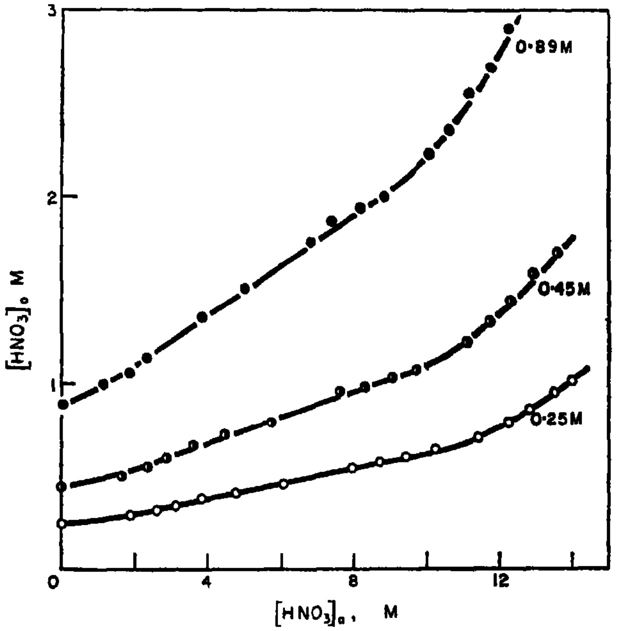

FIG. 7.—Equilibrium distribution of nitric acid between water and benzene solution of the amine.

It was found that 18 M nitric acid is completely miscible with undiluted amine nitrate; this might be taken as evidence for the extraction of associated nitric acid molecules rather than ionized nitric acid. Similar observations and interpretations were made by SHULER(25) and by COLLOPY and co-workers(26) in nitric acid extraction by tributyl phosphate. The amine nitrate forms a molecular addition compound with associated nitric acid and the amine nitrate–nitric acid species formed may be an amine analogue of the tributyl phosphate–nitric acid species $TBP.HNO_3$ or even $TBP.(HNO_3)_2$. The comparable shapes of the isotherms for extraction of nitric acid by TBP and by amine nitrate emphasise this similarity (compare Figs. 6 and 7 with Fig. 2 of reference 25).

The above reasoning implies the existence of the equilibrium

$$(R_2HNHNO_3)_o + (HNO_3)_a \rightleftharpoons (R_2HNHNO_3.HNO_3)_o \qquad (4)$$

with the equilibrium concentration product quotient

$$K_2 = \frac{[R_2HNHNO_3.HNO_3]_o}{[R_2HNHNO_3]_o[HNO_3]_a} \qquad (5)$$

where $[HNO_3]_a$ is the concentration of undissociated, or ion-paired, nitric acid in the equilibrium aqueous phase, which can be calculated from the data of KRAWETZ.(27) Knowing both the total organic acid concentration and the initial concentration of amine in the organic phase, we may write

$$[R_2HNHNO_3.HNO_3]_o = [HNO_3]_o - [R_2HN]_o$$

and

$$[R_2HNHNO_3]_o = [R_2HN]_o - [R_2HNHNO_3.HNO_3]_o = 2[R_2HN]_o - [HNO_3]_o$$

Substituting these values in Equation (5), values for the quotient K_2 have been calculated (Table 2). The constancy of the values of $K_2^{CCl_4} = 1{\cdot}85$ and $K_2^{C_6H_6} = 2{\cdot}24$ is considered remarkable in view of the fact that both ionic strength and the media change markedly as the aqueous nitric acid content increases, and considering that the activity coefficients of the solutes were taken as unity.

The mass-action equilibrium (4) obviously fails to explain the extraction mechanism when the ratio $[HNO_3]_o/[R_2HN]_o$ exceeds two. There are two possible ways in which further nitric acid, exceeding the above ratio of two, can be extracted into the organic phase. The first is by partition of associated nitric acid between its aqueous solution and the amine nitrate-nitric acid complex, and the second by a further complex formation reaction leading to the formation of molecular addition compounds of the type $R_2HNHNO_3.(HNO_3)_x$, with $x \geqslant 2$. It is not possible at present to decide which process is responsible for the phenomenon. This fact is not surprising, in view of the widely contradicting interpretations of solute–solvent interaction in the more thoroughly studied system tributyl phosphate–nitric acid (reference 25, and references therein).

However, since the physico-chemical measurements on the loaded organic phase (Figs. 2 and 3) do not indicate any further compound formation beyond $R_2HNHNO_3.HNO_3$, we believe that nitric acid is extracted by amine nitrate by two

---

(25) W. E. SHULER, Report DP-513 (1960).

(26) T. J. COLLOPY and J. F. BLUM, *J. Phys. Chem.* **64**, 1324 (1960); T. J. COLLOPY and J. H. CAVENDISH, *J. Phys. Chem.* **64**, 1328 (1960).

(27) W. J. HAMER (Editor), *The Structure of Electrolytic Solutions*, p. 43. J. Wiley, New York (1959).

TABLE 2.—CALCULATED EQUILIBRIUM CONCENTRATION PRODUCT QUOTIENT FOR THE REACTION OF ASSOCIATED NITRIC ACID WITH AMINE NITRATE USING EQUATION (5)

	HNO_3 (M)					HNO_3 (M)			
$[R_2HN]_0$ (M)	Initial aqueous	Equil. aqueous	Equil. org.	K_2	$[R_2HN]_0$ (M)	Initial aqueous	Equil. aqueous	Equil. org.	K_2
Carbon tetrachloride diluent									
0·89	2·15	1·20	0·96	2·14	0·45	3·46	2·88	0·59	1·75
	2·90	1·87	1·04	2·18		4·19	3·56	0·63	1·78
	3·46	2·36	1·09	1·93		5·16	4·47	0·70	1·72
	4·19	2·99	1·19	1·88		6·52	5·75	0·77	1·89
	5·16	3·86	1·31	1·77	0·25	2·15	1·88	0·28	1·71
	6·52	5·06	1·46	1·82		2·90	2·58	0·31	1·68
	8·53	6·88	1·64	2·27		3·46	3·12	0·34	1·81
	9·24	7·47	1·76	1·81		4·19	3·83	0·37	1·82
0·45	2·15	1·65	0·51	1·93		5·16	4·76	0·40	1·77
	2·90	2·35	0·55	1·90		6·52	6·08	0·43	1·76
Benzene diluent*									
0·89	2·15	1·16	0·99	3·16	0·45	4·19	3·55	0·66	2·18
	2·90	1·86	1·06	2·36		5·16	4·44	0·72	2·21
	3·46	2·31	1·13	2·30		6·52	5·71	0·79	2·36
	4·19	2·96	1·23	2·29	0·25	2·15	1·87	0·29	2·12
	5·16	3·79	1·36	2·24		2·90	2·58	0·32	2·05
	6·52	4·99	1·50	2·31		3·46	3·12	0·35	2·14
	8·53	6·75	1·76	2·31		4·19	3·82	0·38	2·08
0·45	2·15	1·65	0·51	2·20		5·16	4·74	0·41	2·12
	2·90	2·34	0·56	2·22		6·52	6·06	0·45	2·63
	3·46	2·84	0·60	2·07					

* Corrected for the solubility of the acid in pure benzene.

mechanisms only: the first by the equilibrium (4) and the second by physical distribution without further complex formation. The first mechanism is chiefly operative when the amine is equilibrated with aqueous nitric acid solutions up to about 6·5 M, and the second one takes place virtually only at the highest acid concentrations. Consequently, the equilibrium conditions can be described simultaneously by equation (4) and by the distribution constant of associated nitric acid

$$K_d = \frac{[HNO_3]_{OM}}{[HNO_3]_a} \tag{6}$$

where $[HNO_3]_{OM}$ stands for the amount of associated nitric acid in the organic phase which does not enter into compound formation with the amine and $[HNO_3]_a$ stands for the amount of associated nitric acid in the equilibrium aqueous phase. Assuming ideally immiscible phases, we can write

$$[R_2HN]_o = [R_2HNHNO_3]_o + [R_2HNHNO_3.HNO_3]_o$$

and

$$[HNO_3]_o = [R_2HNHNO_3]_o + 2[R_2HNHNO_3.HNO_3]_C + [HNO_3]_{OM}$$

Solving Equations (4) and (6) for K_d we finally obtain

$$K_d = \frac{[HNO_3]_o}{[HNO_3]_a} - \frac{[R_2HN]_o(1+2[HNO_3]_a K_2)}{[HNO_3]_a(1+[HNO_3]_a K_2)} \tag{7}$$

Calculations according to Equation (7) showed that K_d is proportional to the amine concentration in the diluent, and the distribution constant has a value of $K_d = 0{\cdot}10 \pm 0{\cdot}02$ for 1 M amine in both the diluents employed. The values computed obviously reflect the inaccuracy of K_2 and the non-ideality of the organic phase at high acid loadings. Nevertheless, the facts that K_d is constant for a given amine concentration and proportional to the amine concentration confirm the mechanism postulated for the extraction of nitric acid by amine nitrate.

Acknowledgement—The authors wish to express their appreciation to Dr. Anna Beck for her participation in many valuable discussions concerned with this investigation.

J. Inorg. Nucl. Chem., 1962, Vol. 24, pp. 1429 to 1448. Pergamon Press Ltd. Printed in England

SYNERGISM IN THE SOLVENT EXTRACTION OF DI, TRI AND TETRAVALENT METAL IONS—III

ANTISYNERGISM WITH THENOYL TRIFLUORACETONE*

T. V. Healy†, D. F. Peppard and G. W. Mason
Argonne National Laboratory, Argonne, Illinois

(*Received* 26 *December* 1961; *in revised form* 19 *March* 1962)

Abstract—Greatly enhanced extraction (synergism) of di, tri and tetravalent cations from aqueous solution has previously been reported for the system $H_2O/M^{n+}/HTTA/S/diluent$, where S is a neutral organophosphorus ester and HTTA is thenoyl trifluoracetone. Examples are now given where S contains no phosphorus and is an amide, alcohol or ketone. Complete destruction of this greatly enhanced extraction by addition of excess S whether the neutral additive is a phosphorus ester, an amide, alcohol or ketone is demonstrated. These antisynergic effects are shown to be greater than, but the same type as, the effects due to some so called inert diluents.

This phenomenon of antisynergism is shown to be connected with the water content of the organic phase and the destruction of the anhydrous synergic species $M(TTA)_xS_y$. The HTTA thermodynamic activity is lowered and water probably enters the complex. Absorptiometric measurements demonstrate three different spectra for HTTA/TBP in non-aqueous solution (a) the enolate form in dry TBP, probably hydrogen bonded to the TBP (b) the normal enol form in hexane solution in the presence or absence of low concentrations of TBP and water and (c) the ketohydrate form in water equilibrated TBP. $UO_2(TTA)_2$ or $Th(TTA)_4$ in dry TBP have the HTTA enolate spectra whereas in wet TBP the metal/TTA enol spectra obtains, evidence that water helps to destroy the anhydrous synergic species, causing antisynergism to occur.

The enhancement of the extraction of a cation from aqueous solution by a mixture of acidic and neutral substances, the extraction being better than by either constituent alone was first called synergism by Blake *et al.*⁽¹⁾ They used a mixture of an acidic dialkyl phosphate and certain neutral organophosphorus esters in the extraction of uranium. They also noted that above a certain concentration of ester, synergism no longer occurred and, in fact, a decrease in extraction took place. With some phosphorus acids no synergism occurred, there being an immediate decrease in the extraction in comparison with the acid alone. They considered this to be due to interaction between the acid and the ester. Other workers have noted this phenomenon, now called antisynergism, and Peppard *et al.*⁽²⁾ made use of it in a separation technique. The nature of the interaction has been examined⁽³⁾ and it is considered to be due to the formation of an association product between the acid and the neutral esters, thereby effectively removing these reagents from the solvent extraction system.

* Based on work performed under the auspices of the U.S. Atomic Energy Commission.

† Harwell Exchange Fellow at Argonne National Laboratory.

(1) C. A. Blake, C. F. Baes, K. B. Brown, C. F. Coleman and J. C. White, *Proceedings of the Second International Conference on Peaceful Uses of Atomic Energy, Geneva*, 1958, 15/P/1550. United Nations (1958).

(2) D. F. Peppard, G. W. Mason and R. J. Sironen, *J. Inorg. Nucl. Chem.* **10**, 117 (1959).

(3) J. R. Ferraro, D. F. Peppard, *J. Phys. Chem.* **65**, 539 (1961); H. T. Baker and C. F. Baes, Report ORNL-2443 (1957); 2486 (1957); 2451 (1957); 2737 (1959).

Part I of this series(4) describes the very great enhancement of extraction (synergism) for di, tri and tetravalent cations for the system $H_2O/M^{n+}/HTTA/S$ where HTTA is thenoyl trifluoracetone and S is a neutral organophosphorus ester. The present work shows that large synergistic enhancement of cation extraction may also be obtained if S is an amide, an alcohol or a ketone. The species extracted are discussed in the paper.

Further addition of S, whether it be phosphorus ester, amide, alcohol or ketone, eventually causes the synergistic system to break down and an antisynergism develops. On examination, this phenomenon does not appear to work by the same mechanism as obtains in the phosphorus acid-phosphorus ester antisynergistic system. In this work, antisynergism in the HTTA system is studied both by tracer techniques and by absorption spectrophotometry.

EXPERIMENTAL

The alpha active nuclides 8×10^4 years ^{230}Th, $1{\cdot}6 \times 10^5$ year ^{233}U and the 470 year ^{241}Am were all obtained from ANL stocks. The β-active nuclide 2·6 year ^{147}Pm was obtained from Isotopes Division of the Oak Ridge National Laboratory. All these tracers were subjected to further purification cycles using liquid/liquid extraction techniques. The method of determining distribution ratios and the solvent extraction techniques employed have been previously described.(4)

Tri-n-octyl phosphine oxide (TOPO) was used without further purification. Tributyl phosphate (TBP) received from Commercial Solvents Corporation and dibutyl butyl phosphonate (DBBP) from the Virginia Carolina Chemical Co., were purified as described previously.(5) HTTA received from the Dow Chemical Co., was recrystallized from benzene with a molecular weight of 222·2. N, n-butyl acetanilide (BAA), obtained from the Matheson Co. Inc., and N, N-dibutyl acetamide from Eastman Organic Chemicals, were used without further purification. The alcohols isobutyl, ethyl hexyl and n-decyl were also obtained pure from Eastman.

Absorption spectral measurements were made with a Carey 14 Automatic Recording Spectrophotometer using silica cells of 1 cm or 0·1 cm path length.

RESULTS

Tracer work on the extraction coefficients of three groups (a) trivalent Am/Pm (b) tetravalent Th and (c) divalent UO_2 from aqueous into hexane/HTTA solutions was carried out in the presence of various additives. These added materials varied from very small to very large concentrations and caused both a positive synergism and antisynergism, the extraction coefficients varying over a range as high as 10^8. The additives varied from a number of neutral phosphorus esters, alcohols, ethers, ketones to so called "inert" diluents, such as benzene or chloroform. The absorption spectroscopy of mixtures of HTTA and TBP or TOPO was examined at various concentrations in hexane, both dry and water equilibrated, for evidence of interaction. Uranyl and thorium TTA salts in TBP were also studied spectrophotometrically.

Synergism and antisynergism in Am/Pm tracer studies

It was reported in Part I of this series(4) that addition of a neutral organophosphorus ester increased the extraction of Am/Pm from aqueous solutions into a HTTA/hexane solution by many powers of ten. At a constant acidity and constant HTTA concentration it was shown that the partition coefficient *K* plotted on log/log paper against the neutral additive gave a line of slope +2. This was true up to a concentration of

---

[illegible] T. V. HEALY, *J. Inorg. Nucl. Chem.* **19**, 314 (1961).

[illegible] D. F. PEPPARD, W. J. DRISCOLL, R. J. SIRONEN and S. MCCARTY, *J. Inorg. Nucl. Chem.* 4, [illegible] (1957).

between 10^{-2} and 10^{-1} molar additive. However, more additive causes the slope of the line to decrease gradually, become horizontal and finally turn down in a negative slope. Fig. 1 shows this behaviour in the system H_2O/Am/Pm/HTTA/DBBP/hexane.

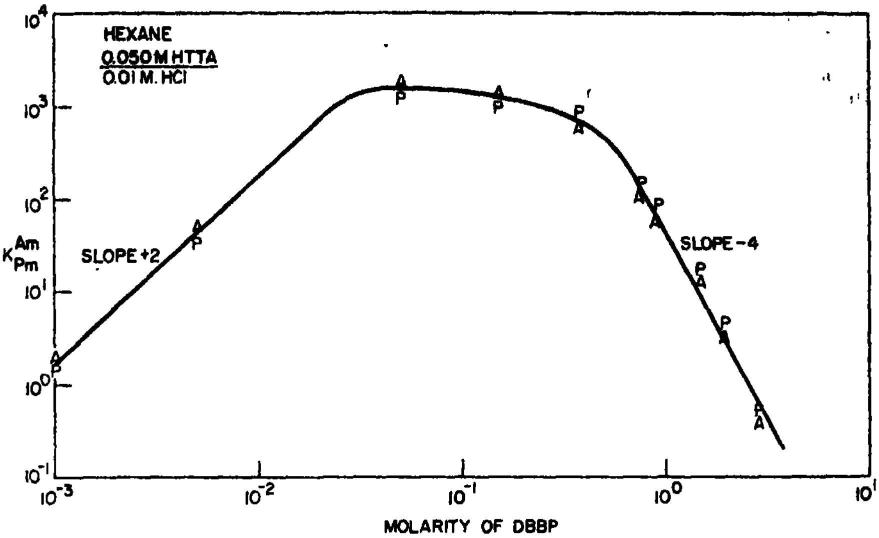

FIG. 1.—Synergism and antisynergism with trivalent complexes.

This starts off with a slope of +2 as in the complex $Am(TTA)_3(DBBP)_2$ for a second power dependency of DBBP. The line then curves round and eventually has a slope of −4. Also, as reported previously,(6) so called "inert" diluents gave varying K values over a range of 10^6, hexane, carbon tetrachloride, benzene and chloroform in that order decreasing the K values obtained in cyclohexane. Fig. 2 shows this effect in

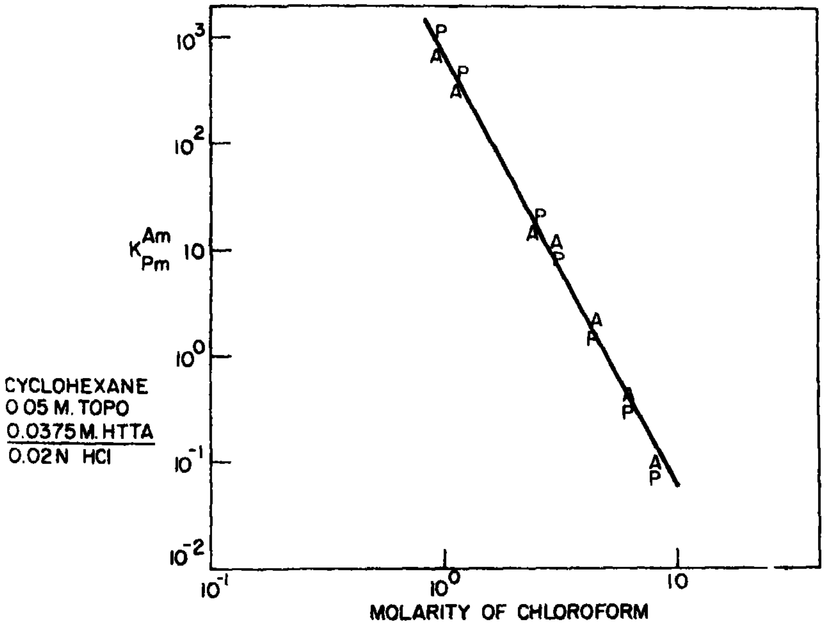

FIG. 2.—Antisynergism with "inert" diluent.

(6) T. V. HEALY, *J. Inorg. Nucl. Chem.* 19, 328 (1961).

the substitution of chloroform for cyclohexane using the system $H_2O/Am/Pm/HTTA/TOPO/cyclohexane$. A log/log plot of *K* vs. the molarity of chloroform produces a

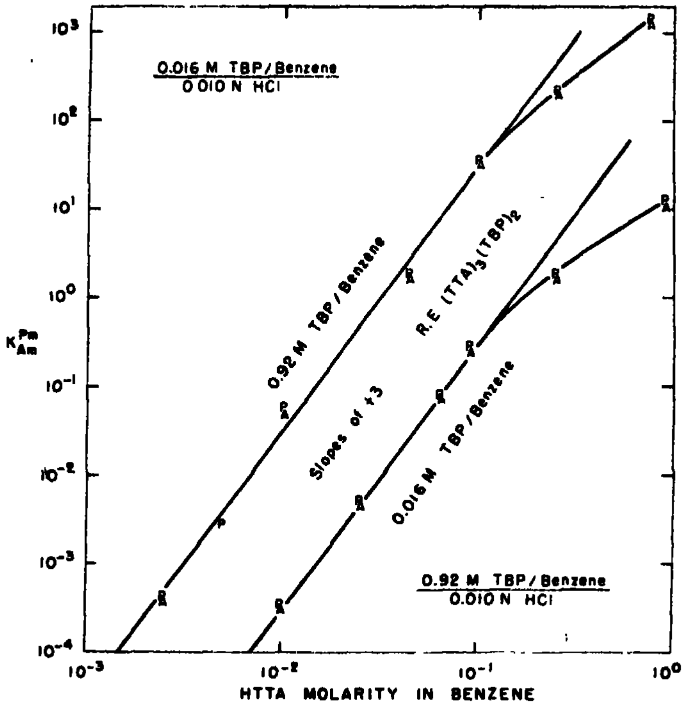

FIG. 3.—HTTA dependency in both synergistic and antisynergistic systems.

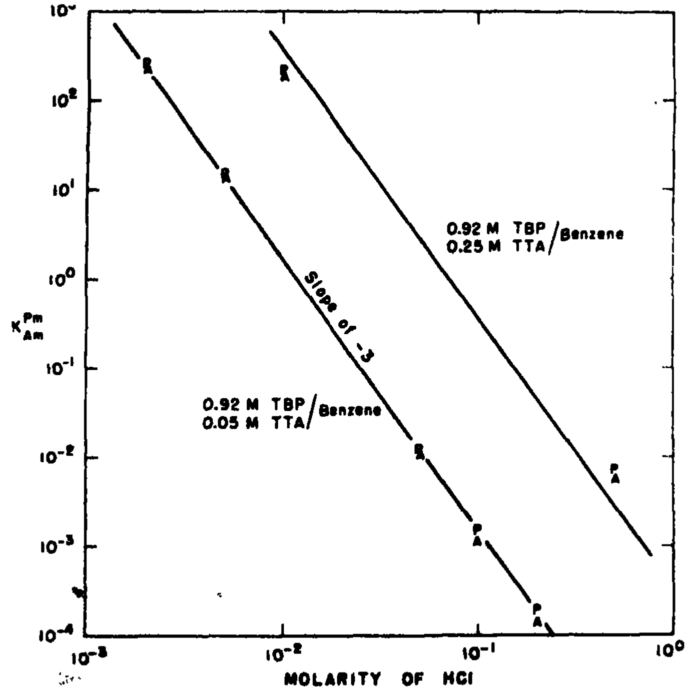

FIG. 4.—[H$^+$] dependency in both synergistic and antisynergistic systems.

slope of —4, the same antisynergistic slope that obtains in excess DBBP (see Fig. 1). Similarly, substitution of benzene for cyclohexane in the system Am/Pm/HTTA/TBP/cyclohexane also furnishes a slope of —4. It has been previously reported$^{(4)}$ that, in the synergistic system H_2O/M^{3+}/HTTA/TBP there was a power dependency of +3 for HTTA and —3 for $[H^+]$. This work was repeated at both low and high TBP concentrations, that is at the middle of the synergistic region and the middle of the antisynergistic region. Figs. 3 and 4 show that, in the two regions, the same power dependency holds both for HTTA and for $[H^+]$.

Synergism had not previously been demonstrated by the two donor solvents, ethyl hexyl alcohol (EHA) and methyl isobutyl ketone (MIK), in combination with HTTA. It is now shown on the same basis as for the HTTA/TBP synergism, that both these non-phosphorus compounds exhibit a power dependency of plus two for trivalent metals (Fig. 5), indicating the species $Am(TTA)_3(EHA)_2$, $Pm(TTA)_3(EHA)_2$, $Am(TTA)_3(MIK)_2$ and $Pm(TTA)_3(MIK)_2$. Their synergistic powers do not match those of the HTTA/TBP system but nevertheless they increase the partition coefficient up to 400 times greater than for either HTTA or the neutral reagent alone. Here again, the difference between two so called "inert" diluents cyclohexane and benzene is demonstrated (Fig. 5), a factor of up to 30 in the partition coefficients being observed. The same synergism and antisynergism are observed in this series also but because of the relatively small effects it is not possible to say with certainty, what the antisynergistic slope or dependency is. Other differences from the phosphorus ester systems are (1) that greater concentrations of EHA and MIK are required before the synergistic effect is really noticeable and (2) the antisynergic effect is not really definite until concentrations of greater than 1 molar EHA or MIK are present.

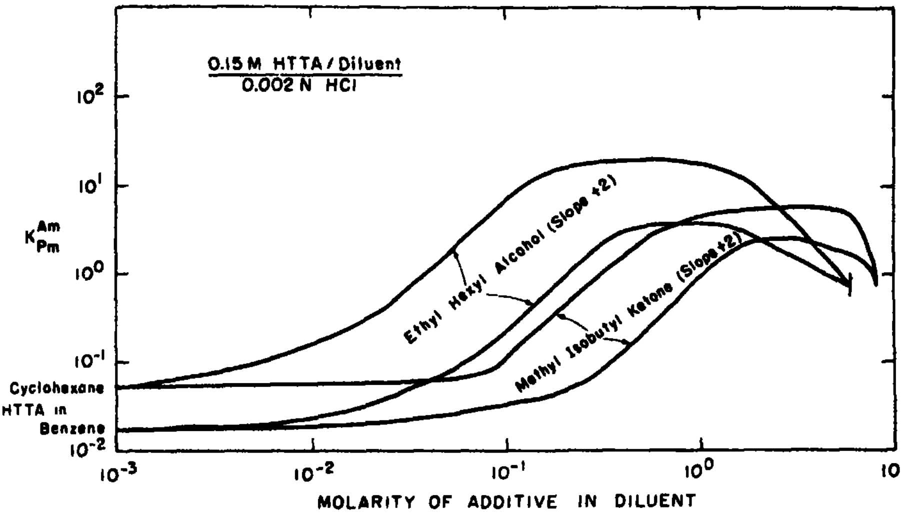

FIG. 5.—Ethyl hexyl alcohol and methyl isobutyl ketone as both synergists and antisynergists.

Synergism and antisynergism in thorium tracer studies

As reported previously,$^{(4)}$ the system H_2O/Th/HTTA/TBP has a power dependency of plus one for TBP concentration as the species $Th(TTA)_4(TBP)_1$ is synergistically extracted into the organic phase. Further increase in the TBP concentration above the 10^{-2}–10^{-1} molar region causes the synergistic extraction system to break down, the power dependency line of slope +1 bends down, becomes horizontal and eventually decreases to a constant slope of −2. Fig. 6 demonstrates this graphically and also shows similar behaviour for two other synergistic reagents which are non-phosphorus containing compounds. Ethyl hexyl alcohol in combination with HTTA has been shown in the previous paragraph to exert a synergistic effect on the trivalent rare earths and actinides. This is also true for thorium where Fig. 6 shows both the synergistic effect with the extraction of the species $Th(TTA)_4(EHA)_1$ and the antisynergistic effect. N, n-butyl acetanilide (BAA) is a donor solvent which one would expect to have some extracting properties for metal salts. It is shown here to have very good synergistic properties in combination with HTTA (Fig. 6), the extracted thorium species being $Th(TTA)_4(BAA)_1$. Like TBP it exerts both synergistic and antisynergistic properties with BAA dependencies also of +1 and −2 respectively. Also, on this composite curve in Fig. 6 is shown the effect produced by addition of BAA or EHA to the synergistic system H_2O/Th/HTTA/TBP containing 0·01 molar HTTA and 0·01 molar TBP. It is interesting to see that addition of the alcohol EHA causes an immediate antisynergistic effect and eventually the extraction is the same as that of the antisynergistic part of the EHA curve itself in the system H_2O/Th/HTTA/EHA which contains no TBP. In this case the initial synergistic effect of the TBP has completely disappeared in excess EHA. Addition of BAA to the previous H_2O/Th/HTTA/TBP system causes a slight initial rise in the thorium partition coefficient, then a gradual fall until the partition line coincides with that of the H_2O/Th/HTTA/BAA system which has a slope of −2.

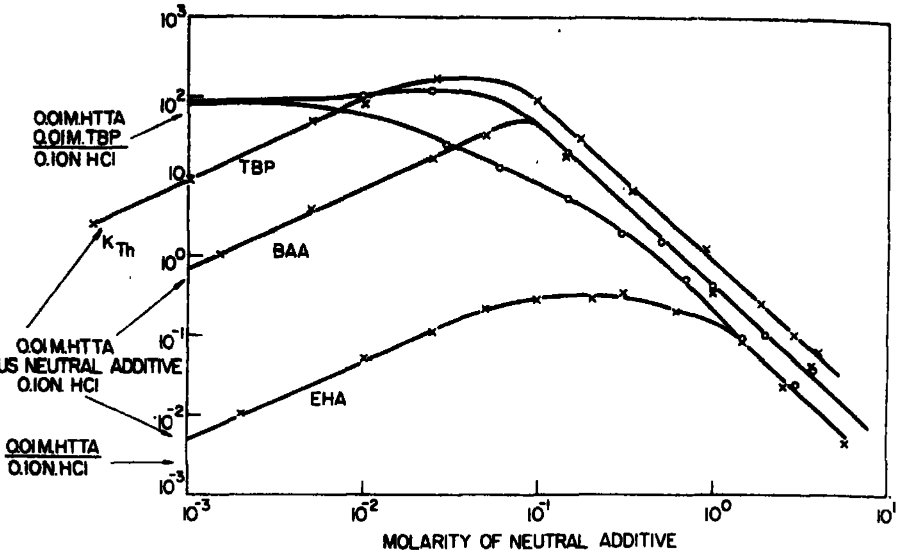

FIG. 6.—A phosphorus ester, an amide and an alcohol as both synergists and antisynergists in Th/HTTA/TBP systems.

The antisynergistic effect of so called "inert" diluents has been commented on in the work on the trivalent metal series above. This is also true for thorium except that the slope of the power dependency of the diluent is changed from −4 to −2. Fig. 7 illustrates the strong antisynergic effect of chloroform additions. Benzene is not shown but has somewhat less of an effect with the same slope of −2. MIK, mesityl oxide and the dibutoxy ether of ethylene glycol, all have a similar antisynergistic effect of slope −2, but only one, MIK, is shown, because the lines are more or less co-incident with each other. BAA and three alcohols, isobutyl, decyl and ethyl hexyl have somewhat greater antisynergistic effects, all with slopes of −2. All the above effects are illustrated in Fig. 7 as part of a composite whole where the Th/HTTA/TBP

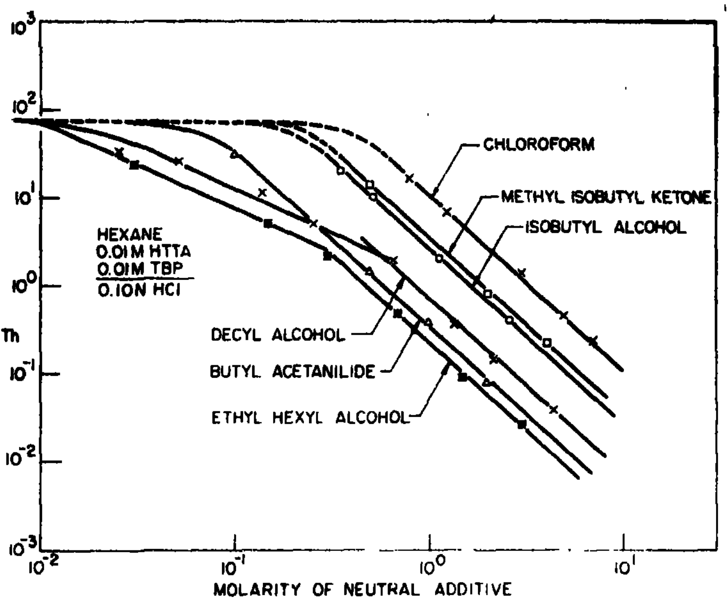

Fig. 7.—Antisynergic effects in Th/HTTA/TBP systems produced by amides, alcohols, ketones and "inert" diluents.

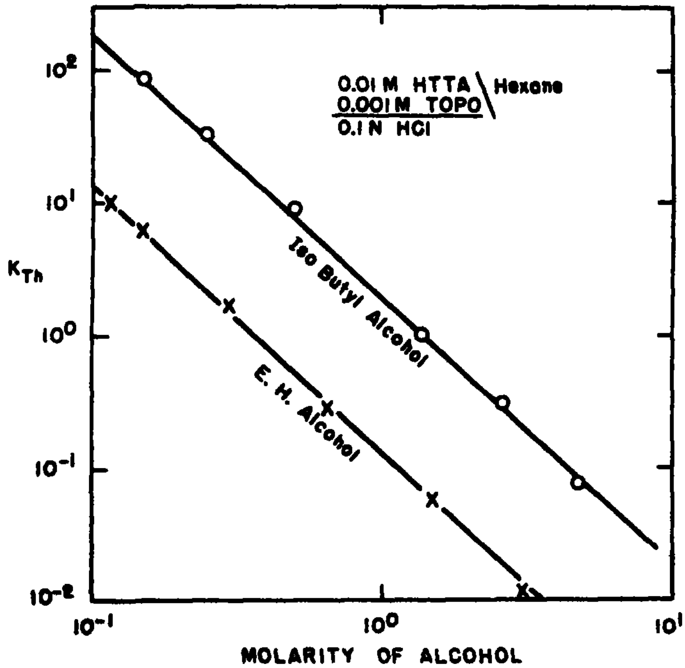

Fig. 8.—Antisynergic effects in Th/TOPO systems produced by alcohols.

synergistic effect is destroyed by different types of solvents and all with a power dependency of −2. TOPO is one of the stronger donor solvents, much stronger than TBP, yet antisynergistic agents like alcohols cause large decreases in the partition coefficients. For example, in the system $H_2O/Th/HTTA/TOPO$, both isobutyl alcohol and ethyl hexyl alcohol have inverse second power dependencies, and slopes of −2 are illustrated in Fig. 8. In an attempt to ascertain if the maximum on the synergistic-antisynergistic curve varied with the relative proportion of HTTA to neutral additive, two curves were obtained for the system $H_2O/Th/HTTA/EHA$, one at 0·01 molar and another at 0·08 molar HTTA. Fig. 9 indicates that, although the system containing the 0·01 molar HTTA had a larger synergistic effect below 0·01 molar EHA than the other system, the maximum occurred in the same region, in both cases. Probably, if a very large HTTA concentration had been used (say 0·5–1 molar), there might have been no visible synergistic effect with EHA at all, only an antisynergistic effect.

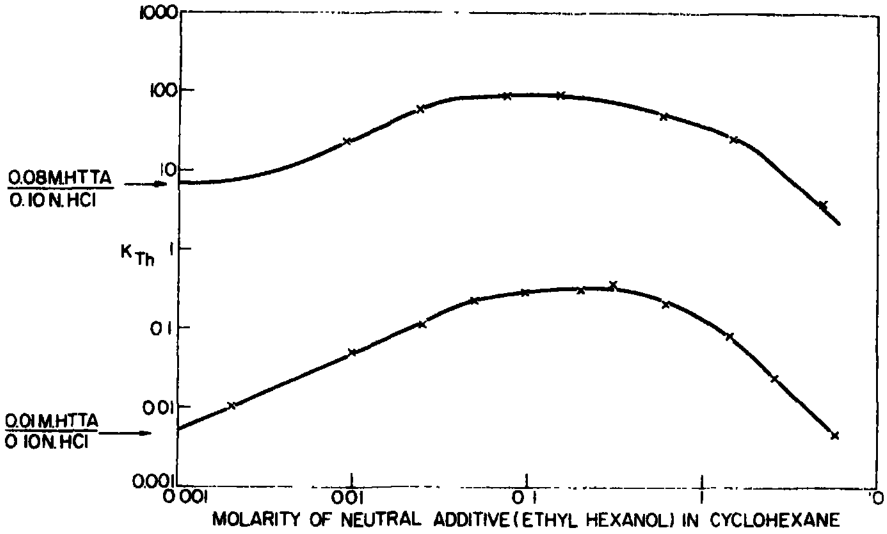

FIG. 9.—Effect of [HTTA] on Th/EHA synergistic and antisynergistic curves.

Synergism and antisynergism in uranyl (II) tracer studies

The uranyl/HTTA/S systems exhibit the same synergistic and antisynergistic effects as shown by the other elements. The difference is in the amount of antisynergism, that is, there is a shift to the right in the maximum of the syn./antisyn. curves. This is illustrated in the $H_2O/UO_2/HTTA/TBP$ system in Fig. 10. The synergistic line has a slope of +1, and the small antisynergistic line has a slope of −2 similar to the thorium system. Also shown on this graph is the synergistic effect produced in the uranyl system by the BAA dependency of +1. The antisynergistic effect of $CHCl_3$ on the $H_2O/UO_2/HTTA/TBP$ system also causes an initial flattening out at the top part of the curve, and the overall antisynergistic effect of $CHCl_3$ is thereby much reduced. The final dependency, however, is still the same, namely −2.

Absorption spectral evidence for water/HTTA/donor solvent interaction

It was initially observed that the absorption spectra of solutions of HTTA in dry and water saturated organic solvents were somewhat different, the dry solution spectra having a peak in the 350–400 mμ region when compared with the wetted solution. This peak position moved toward longer wave length with increasing HTTA concentration. The increasing height of the peak, not surprisingly, did not follow Beer's Law. It was also observed that addition of a donor solvent such as TBP to a dry hexane solution of HTTA similarly increased this peak height when compared with the initial HTTA solution. In contrast, addition of TBP to an aqueous saturated hexane solution of HTTA caused initially an increase followed by a decrease in peak height. This rise and fall in peak height with addition of TBP showed a similar pattern to the synergism followed by antisynergism exhibited in the extraction of metals by HTTA–TBP mixtures from aqueous solution.

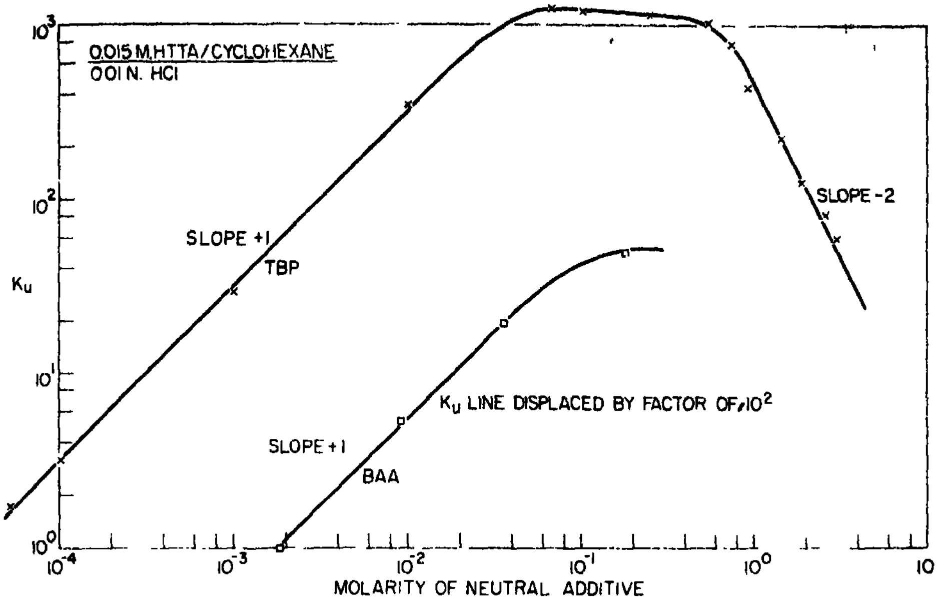

FIG. 10—Synergism and antisynergism with uranyl complexes.

The absorption spectral data of HTTA–TBP mixtures were therefore investigated, solutions being made up with three different concentrations of HTTA in hexane, namely 0·1, 5×10^{-3} and 5×10^{-5} M HTTA respectively. In order to be able to ascertain the species present, the most dilute solution (5×10^{-5} M HTTA) was examined first in the spectrophotometer using hexane as the blank solution. These dilute HTTA solutions contained various concentrations of TBP, one series being dry and the other equilibrated overnight with water. Table 1 gives the spectral peaks, humps or shoulders of importance in the various solutions.

This table shows very clearly that HTTA plus a great excess of TBP in the presence of water gives a spectrum almost identical with that of HTTA hydrate in aqueous solution(7) whereas in the absence of water the spectrum corresponds to the aqueous enolate ion.(7) Neither of these spectra have been obtained in a non-aqueous solution

---

(7) E. L. ZEBROSKI, Report TID-098 (1947).

TABLE 1.—SPECTRAL PEAKS OF HTTA SOLUTIONS (5×10^{-5}M) CONTAINING TBP IN HEXANE

TBP Molarity (M)	Aqueous equilibrated solutions		Dry solutions	
	Wavelength (mμ)	Density (1 cm cell)	Wavelength (mμ)	Density (1 cm cell)
0·000	338 314	0·58 *h* 0·68	338 315	0·65 *h* 0·79
0·001	338 315	0·58 *h* 0·68	338 315	0·64 *h* 0·79
0·10	338 315 265	0·58 *h* 0·64 0·40 *sh*	338 250	0·99 0·49
1·1	360–320 286 262	0·20 *sh* 0·44 0·51	338 250	0·98 0·48
3·6	288 262	0·41 0·53	338 250	0·98 0·48
Aqueous solutions	HTTA hydrate 292 266	pH 1–3 0·40 0·50	Enolate ion 338 262	pH 9 0·89 0·32

previously, but their correspondence with the two aqueous spectra is perhaps shown more clearly in Table 2, where the extinction coefficients of the spectral peaks are given.

TABLE 2.—COMPARISON OF AQUEOUS AND TBP SOLUTIONS OF HTTA

TBP solutions 5×10^{-5}M HTTA in TBP	
Dry	Water equilibrated
E_{338} = 19,600 E_{250} = 9,000	E_{290} = 8,200 E_{262} = 11,000
Aqueous solutions	
Enolate ion	HTTA hydrate
E_{338} = 17,700 E_{262} = 6,250	E_{292} = 7,940 E_{266} = 10,100

This means that in the absence of water HTTA combines with TBP, the basic donor properties of the ester presumably causing hydrogen bonding on to the enolic form of the acid HTTA. In the presence of water this bonding is much weaker than the keto hydrate formation which destroys the enol bond completely. There is also infra-red evidence(8) to support the formation of TBP-hydrate in the water equilibrated TBP solutions of HTTA, the 1260 cm^{-1} waveband moving over to 1270 cm^{-1}. Both the wetted and dry dilute TBP–HTTA solution spectra are similar to those of the pure HTTA in wetted and dry solutions and all have the normal enol structure formed in organic solutions of HTTA.

---

(8) J. R. FERRARO and T. V. HEALY, Unpublished work.

When the addition of TBP to HTTA solution reaches about 0·1 molar TBP, the spectral evidence (Table 1) shows that the usual enol spectrum is changing. This change is either towards that of the keto hydrate (wet) or enolate (dry) spectra and is almost complete at a concentration of 1 molar TBP. In the enolate species the HTTA probably forms a complex with TBP, the ester presumably hydrogen bonding on to the enolate form of the HTTA. The three HTTA spectra are illustrated in Fig. 11, and the probable species are given below.

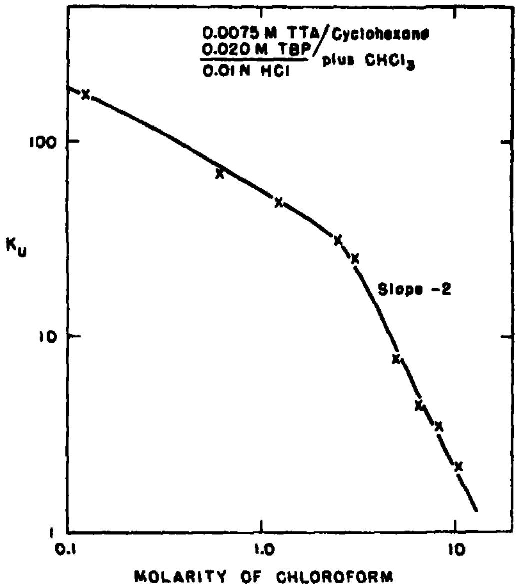

Fig. 11.—Antisynergic effect of chloroform with uranyl complexes.

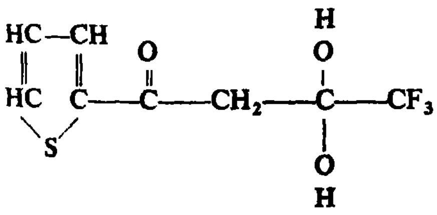

KETOHYDRATE

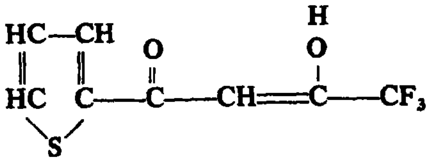

ENOL

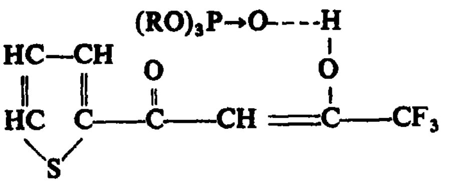

ENOLATE

Addition of TBP to higher concentrations of HTTA in hexane cannot show directly the three spectral species owing to the very high extinction coefficients of HTTA. But these mixtures of TBP–HTTA solutions can be examined spectrally using the HTTA solution alone as blank. In this way the increasing height of a peak can be plotted against an increasing TBP concentration in a constant molarity HTTA solution. The wavelength of the peaks varies with the HTTA concentration and Beer's Law does not apply. This is because the spectrophotometer is really being used beyond its capabilities due to the poor transmission of the more concentrated HTTA solutions. Table 3 illustrates these points by showing the increasing peak wavelength and the small change in peak height (1 cm cells) as the HTTA concentration increases.

TABLE 3.—EFFECT OF TBP ADDITION ON PEAK HEIGHT AND WAVELENGTH OF HTTA/HEXANE

Wet solutions	Sample	vs. Reference solution	Dry solutions
0·16 = D_{396} ←——	10^{-1}M HTTA + 1·1 M. TBP	10^{-1}M HTTA ——→	D_{397} = 3·9
0·12 = D_{387} ←	5×10^{-3}M HTTA + 1·1 M. TBP	5×10^{-3}M HTTA →	D_{385} = 2·2
−0·35 = D_{338} ←	5×10^{-5}M HTTA + 1·1 M. TBP	5×10^{-5}M HTTA →	D_{340} = 0·39
0·44 = D_{286} ←	5×10^{-5}M HTTA + 1·1 M. TBP	5×10^{-5}M HTTA →	D_{338} = 0·98

As shown above, the presence of TBP in dry HTTA solutions increases the peak height at all the HTTA concentrations. Although the peak position has moved toward longer wavelength at increased HTTA molarities, this is undoubtedly a measure of the production of the enolate species. Similarly, the very slight rise and fall of this peak height in the water saturated solutions plus the changing wavelength must also indicate the competition for the HTTA between TBP and water. These data are given below, the dry and wet solutions meaning dry hexane and water equilibrated hexane solutions respectively. Sample A and reference blank A contain 0·1 M HTTA. Similarly B and C contain 5×10^{-3}M and 5×10^{-5}M HTTA respectively.

A similar effect to that of TBP on HTTA solutions can be shown by most electron donor solvents. For instance, the effect of dry TOPO in dry 0·1 M HTTA solution in hexane is shown by the gradual increase in the peak height at a wavelength of 397 mμ using 0·1 M HTTA in a 1 cm reference cell. In this case, the optical density of this peak increases from 0·52 at 0·02 M, 0·95 at 0·04 M, 1·35 at 0·06 M, 1·53 at 0·08 M, 1·88 at 0·1 M to 5·0 at 0·2 M TOPO. This is a greater effect than that produced by the corresponding TBP solution A in Table 4, and indicates that, in dry solution, the HTTA–TOPO interaction is much stronger as would be expected from the very strong electron donor properties of TOPO as compared with TBP. In aqueous equilibrated hexane solutions of HTTA–TOPO, the formation of ketohydrate and TOPO hydrate would also be greater than in the case of TBP for the same reason. The following table gives a few examples of the complexing of HTTA by a donor solvent in the absence of water, and the competition between water and donor solvent for HTTA complexing in the presence of water. The optical density of the 397 mμ peak is used to compare the effect of the donor solvents TOPO, TBP, N-butyl acetanilide (BAA) and dibutyl acetamide (DBA) on 0·1 molar HTTA in hexane.

TABLE 4.—EFFECT OF TBP ON SPECTRA OF WET AND DRY HTTA/HEXANE SOLUTIONS

TBP molarity	⟶	0·005	0·01	0·05	0·10	0·2	0·55	1·1	1·8	2·9	3·6
Dry solution A	Peak height	—	0·1	0·37	0·80	—	3·0	3·9	4·3	—	—
	Wavelength (mμ)	398									398
Dry solution B	Peak height	0·02	0·07	0·10	0·50	0·73	1·6	2·2	2·7	3·2	3·3
	Wavelength (mμ)	385									385
Dry solution C	Peak height	0·01	—	—	0·08	—	—	0·39	—	—	0·42
	Wavelength (mμ)	340									340
Wet solution A	Peak height	—	0·10	0·34	0·40	—	0·26	0·16	0·07	—	—
	Wavelength (mμ)		397	397	396		396	396	396		
Wet solution B	Peak height	0·01	0·05	0·3	0·35	0·36	0·14	(-0·05)	(-0·24)	(-0·83)	(-1·45)
	Wavelength (mμ)	384	384	385	385	385	386	382	382	382	382
Wet solution C	Peak height	0·01			(-0·02)						(-0·35)
	Wavelength (mμ)	338			338						338

TABLE 5.—COMPARISON OF HTTA–SOLVENT INTERACTION PEAKS

Reference blank is 0·1 M HTTA/hexane

Dry solutions		Water equilibrated/ solutions
D_{397}	0·1 M HTTA	D_{397}
1·9	0·1 M TOPO	0·19
0·80	0·1 M HTTA 0·1 M TBP	0·40
0·62	0·1 M HTTA 0·1 M BAA	0·62
0·30	0·1 M HTTA 0·1 M DBA	0·01

This peak height gives a measure in the dry solutions of their donor strengths and also of their possible synergic effect on the formation of metal/TTA/S complexes. The peaks in the wet solutions are less reliable but give a measure of the competition between donor solvent and water in the formation of ketohydrate. A more reliable measure would be the production of a series of absorption spectra from dry and aqueous equilibrated hexane solutions of 10^{-5} molar HTTA with increasing amounts of donor solvents added as illustrated in Table 1. In this way one can assess the amount of enolate and ketohydrate which is formed from initial 90–100 per cent enol form of HTTA normally found in organic solvents. The diluent hexane has been used in all previous experiments with HTTA–donor solvent. But, by varying the diluent, the HTTA solvent interaction peak also varies both in height and in wavelength. The diluent in which water is least soluble produces the least difference between the HTTA–donor solvent interaction peaks when the dry and the aqueous equilibrated solutions are compared spectrophotometrically. The table below bears this out for the solvents cyclohexane (CH), hexane (H), benzene (Bz) and butanol (BuOH). For the donors, hexone (MIK), ethyl hexyl alcohol (EHA) and TBP which bring even more water into the water equilibrated organic phase the differences are even more striking, due to the tendency to enolate formation in dry solutions and ketohydrate in wet solutions. This order in Table 6 is also the order of increasing antisynergism in the metal/TTA/solvent extraction.

TABLE 6.—EFFECT OF DILUENTS ON HTTA–TBP INTERACTION PEAK

0·1 M HTTA+0·1 M TBP.—Dry solution is +ve sample in 1 cm cell
Wet solution is −ve reference in 1 cm cell

	CH	H	Bz	BuOH	MIK	EHA	TBP
Peak height	0·2	0·25	0·35	0·75	2	2·5	5
Wavelength (mμ)	396	397	404	397	401	399	398

Absorption spectral evidence for water/$M(TTA)_x$/TBP *interaction*

The absorption spectra of $UO_2(TTA)_2TBP$ in benzene or hexane is essentially the same as that of $UO_2(TTA)_2$ in these solvents, having two large peaks at 330 and 380 mμ. The only difference is above 400 mμ where the well defined peaks of the $UO_2(TTA)_2TBP$ complex at 426, 440 and 454 mμ are missing from the $UO_2(TTA)_2$ spectrum. These spectra are also very similar in the presence of slight excess TBP and/or in the presence of an aqueous phase. By dissolving a small quantity of the solid $UO_2(TTA)_2$ complex in dry liquid TBP, a new spectrum is formed with peaks at 256 and 336 mμ. This is essentially the spectrum of HTTA dissolved in dry TBP plus a smaller amount of the spectrum of $UO_2(TTA)_2TBP$ in a ratio of about 2:1 (Fig. 12). On saturating this TBP solution of $UO_2(TTA)_2$ with water, the spectrum is changed back to that of $UO_2(TTA)_2$ with peaks at 330 and 377 mμ (Fig. 12). The pronounced peaks above 400 mμ of $UO_2(TTA)_2TBP$ are absent. The sequence above indicates that addition of a little TBP to $UO_2(TTA)_2$ forms the $UO_2(TTA)_2TBP$ complex. Addition of (1) great excess dry TBP breaks it down to form a HTTA-TBP complex and (2) great excess wet TBP breaks it down to form $UO_2(TTA)_2$ which may or may not have a hydrate attached. The following table gives the extinction coefficient obtained in this series.

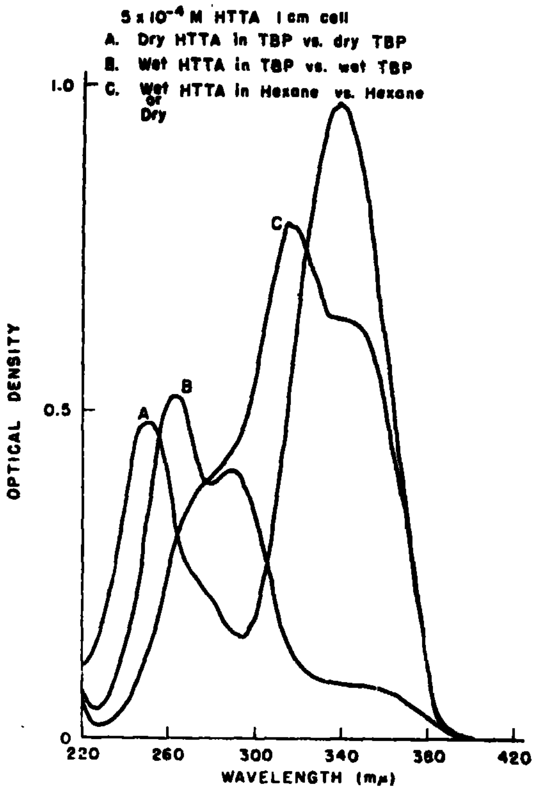

FIG. 12.—Absorption spectra of HTTA in organic solution, (A) enolate (B) ketohydrate and (C) enol.

The spectra of $Th(TTA)_4$ and $Th(TTA)_4TBP$ in benzene are practically the same. Both have one large peak at 350 mμ with an extinction coefficient of about 85,000. It was expected that solutions of $Th(TTA)_4$ in wet and dry TBP would behave similarly to the uranium salts and give different spectra. Actually they gave somewhat similar spectra, as both gave a large peak of E about 80,000. The wavelengths of the peaks differed by about 10 mμ. The peak was at 349 for the spectrum of $Th(TTA)_4$ in water saturated TBP indicating it was practically identical with the $Th(TTA)_4$ and the $Th(TTA)_4TBP$ spectra. By analogy with the uranium species it was probably a $Th(TTA)_4$ hydrate

TABLE 7.—EXTINCTION COEFFICIENTS OF $UO_2(TTA)_2$ COMPLEXES

$UO_2(TTA)_2$ in benzene	—	E_{338} 26,400	E_{384} 21,200	—	—	—
$UO_2(TTA)_2TBP$ in benzene	—	E_{332} 27,500	E_{380} 22,000	E_{430} 1,450	E_{444} 950	E_{458} 500
$UO_2(TTA)_2$ in water sat'd TBP	—	E_{330} 25,000	E_{377} 21,000	—	—	—
$UO_2(TTA)_2$ in dry TBP	E_{256} 16,000	E_{336} 33,000	—	E_{422} 550	E_{435} 400	E_{449} 200
HTTA in dry TBP	E_{262} 6,250	E_{338} 17,700	—	—	—	—

spectra in hydrated TBP. The $Th(TTA)_4$ spectrum in dry TBP had a peak at 340 mμ which is essentially that of HTTA dissolved in dry TBP indicating that the excess dry TBP had broken down the thorium complex liberating the HTTA which then complexed with the dry TBP. Again this behaviour is analogous to that of $UO_2(TTA)_2$ when dissolved in dry TBP.

DISCUSSION

Synergism not confined to HTTA *plus phosphorus esters*

Synergism in metal extraction by HTTA plus phosphorus esters has been demonstrated previously.(4) It is shown in this paper that phosphorus esters can be replaced by ketones, alcohols, and amides, and it should be mentioned that HTTA plus sulphoxides or plus amines also exhibits synergism. Two obvious alternatives to HTTA, namely 8-hydroxy quinolin and cupferron, both exhibited somewhat limited synergism with TBP. Several alcohols plus HTTA exhibit synergism with di, tri and tetravalent metal species. Among the stronger alcohols in this respect are n-decyl alcohol and ethyl hexyl alcohol (EHA). Species apparent from tracer work (Figs. 5 and 9) are $Th(TTA)_4EHA$, $Am(TTA)_3(EHA)_2$ and $Pm(TTA)_3(EHA)_2$.

As an example of this synergism, addition of about 2 per cent of ethyl hexyl alcohol to a solution of 0·15 molar HTTA in cyclohexane increases the partition coefficient of Am or Pm by a factor of 200 to 300. The fact that these alcohols and also ketones plus HTTA exhibit this phenomenon of synergism shows that it is not confined to strong electron donor solvents. Two of the stronger donor ketones are methyl isobutyl (MIK) and methyl isopropyl ketone, the species extracted by MIK being $Am(TTA)_3(MIK)_2$ and $Pm(TTA)_3(MIK)_2$. It has been reported in the literature(8) that extraction of metals with HTTA is greater if hexone (MIK) rather than benzene is used as the solvent, but no reason was given for this. It is now seen that gradual replacement of benzene by MIK solution causes a rise in the partition coefficient of the metal as the $M(TTA)_x(MIK)_y$ species is formed. Eventually, the partition coefficient decreases again by a relatively small amount as benzene is completely substituted by the MIK. N-butyl acetanilide (BAA) plus HTTA together have a large synergistic effect on the extraction of thorium from aqueous solution, increases of greater than 10^4 being obtained (Fig. 6). The species extracted was found, from this tracer work, to be

---

(8) J. R. THOMAS, H. W. CRANDALL, T. E. HICKS, B. RUBIN and J. SALDICK, Report KLX-44 (1949); T. KIBA and S. MIZUKAMI, *Bull. Chem. Soc. Japan*, 31, 1007 (1958).

Th(TTA)$_4$BAA. Other species found from tracer and macro work were UO$_2$(TTA)$_2$ BAA and Nd(TTA)$_3$(BAA)$_2$. Ultra-voilet and visible absorption spectral data to be reported elsewhere[10] also confirm the formulae for these species.

Antisynergism

Antisynergism was first reported as a phenomenon by BLAKE *et al.*[1] and later for separation procedures by PEPPARD *et al.*[2] in the organophosphorus acid–phosphorus ester series. In both cases[3] antisynergism, that is the reverse of synergism, was considered to be due to interaction between the synergistic agents—acid plus ester. On adding TBP in excess to a H$_2$O/metal/HTTA/TBP synergistic system, the system breaks down, the partition coefficient decreases and the phenomenon of antisynergism occurs. At first, it was thought that this antisynergism was likewise due to interaction between the acid (HTTA) and the ester (TBP) to form an association product. An examination of the power dependencies of the metal extractions on TBP or other similar phosphorus ester (S) for the systems H$_2$O/Th/HTTA/S indicated a positive synergistic power dependency for S of +1 followed by a negative antisynergistic power dependency for S of −2 due to excess of S. The same +1 and −2 dependencies were found when the amide BAA and the alcohol EHA were used instead of S. It was also remarkable that if either EHA or BAA were gradually added to the fixed synergistic system H$_2$O/Th/0·01 M HTTA/0·01 M TBP, antisynergism was found to occur (See Fig. 6). These lines, also of slope −2 eventually became coincident with the antisynergistic part of the H$_2$O/Th/0·01 M HTTA/BAA or EHA systems. It was also found (Fig. 7) that other alcohols, amides, ketones and ethers all produced the same antisynergistic slope of −2 when added to the system H$_2$O/Th/0·01 M HTTA/0·01 M TBP/hexane. Furthermore, so called inert diluents such as benzene or chloroform on addition to this system also produced antisynergistic slopes of −2. It appeared from all these data that antisynergism in the case of thorium could hardly be due to direct interaction of the HTTA with either the TBP or the other donor or non-donor solvents. Experiments substituting Am or Pm for thorium in similar systems showed exactly the same results except for the fact that in all cases the synergistic power dependency slope was +2 with a corresponding antisynergistic dependency of −4. It should also be noted that, in both the synergistic and antisynergistic regions, the trivalent elements had the usual power dependency of +3 for the HTTA and −3 for the hydrogen ion dependency. The following table summarizes the synergistic and antisynergistic power dependencies of UO$_2$, Th, Am and Pm systems for both donor and non-donor solvents at constant HTTA and hydrogen ion concentration.

TABLE 8.—SYNERGISM AND ANTISYNERGISM POWER DEPENDENCIES

	Synergism due to phosphorus esters, amides, alcohols and ketones	Antisynergism due to phosphorus esters, amides, alcohols, ketones and inert diluents
Th	+1	−2
Am, Pm	+2	−4
UO$_2$	+1	−2

---

[10] T. V. HEALY and J. FERRARO, Unpublished work

It appears that the only common constituents in the organic phases of these systems is HTTA and the water content. Different donor solvents give the same positive and negative power dependencies while different so called inert diluents give similar negative power dependencies. Also the HTTA and hydrogen ion dependencies are consistently as expected both in the synergistic and antisynergistic regions. This fact indicates that, throughout the system, the $M(TTA)_x$ is an integral part of the extracted species, x being the valency of M. One is led therefore to the assumption that water in the organic phase has an appreciable effect on the breakdown of the anhydrous synergistic complex $M(TTA)_xS_y$.

Spectrophotometric evidence to support this is shown first in the HTTA–TBP system and then in the M/HTTA/TBP system. The absorption spectra of dilute HTTA solutions in hexane whether in the presence or absence of an aqueous phase is very similar to the same solutions also containing small amounts of TBP. These spectra are of the usual enolic form of HTTA in organic solvents. These are also the concentrations used in obtaining synergistic extraction of metals from aqueous solution by HTTA/TBP solutions. However, if a great excess of TBP is added to HTTA in the presence of an aqueous phase i.e. under conditions where antisynergistic extraction of metals occurs, the spectrum is changed to that of HTTA ketohydrate. There is also infra-red evidence of reformation of TBP hydrate and of a shift in the carbonyl peaks.(8) On addition of TBP in increasing quantities to a fixed concentration of HTTA in the absence of water the carbonyl infrared absorption peak at 1600 cm^{-1} shifts gradually to 1650 cm^{-1}. The same TBP addition to HTTA in the presence of D_2O shows initially a shift of the 1600 cm^{-1} peak to 1650 cm^{-1} but further TBP addition appears to shift the peak back towards 1600 cm^{-1}(8) This provides further evidence for the initial HTTA–TBP complexing in the presence and absence of water, followed by the breakdown of the complex on further addition of water saturated TBP. Great excess of TBP plus HTTA, in the absence of water, forms a completely different ultra-violet absorption spectrum, namely one similar to that of the enolate ion seen in aqueous alkaline solution. The gradual increase in peak height of the spectrum as more dry TBP is added to HTTA is a measure of formation of the HTTA-TBP complex. However addition of TBP to HTTA in the presence of an aqueous phase shows the peak height (Table 4) rising through a maximum which corresponds approximately to the synergism and antisynergism concentration regions in the metal/HTTA/TBP systems.

An examination of the absorption spectra of organic solutions of $UO_2(TTA)_2$ and $UO_2(TTA)_2TBP$ in the presence or absence of an aqueous phase shows them to be essentially the same except for the well defined peaks of the latter complex at wavelength of > 400 mμ. Dissolution of either complex in dry TBP furnishes essentially the spectra of dry HTTA in dry TBP, that is the uranyl complex is broken down and the liberated HTTA is hydrogen bonded to the dry TBP. In the presence of an aqueous phase the spectrum is different—it is that of $UO_2(TTA)_2$. This tends to show directly the competition of water with TBP. In the presence of an aqueous phase, addition of TBP to $UO_2(TTA)_2$ in hexane, produces the $UO_2(TTA)_2TBP$ complex. Further addition of excess TBP causes this complex to be broken down back to $UO_2(TTA)_2$. This would also explain the synergism followed by the antisynergism exhibited in the extraction of uranium in this system. Thorium is shown to behave similarly, forming initially the synergistic $Th(TTA)_4TBP$ and then, with antisynergism, returning to

$\mathrm{Th(TTA)_4}$. Confirmatory evidence for this TBP/water competition in the metal/TTA complex system is obtained from infra-red studies.[8] It was observed that addition of dry TBP to solid $\mathrm{UO_2(TTA)_2}$ gives an infra-red spectrum (in the 1600 $\mathrm{cm^{-1}}$ region) similar to that obtained for solid $\mathrm{UO_2(TTA)_2TBP}$. Two equally intense peaks are obtained at 1622 and 1595 $\mathrm{cm^{-1}}$. However, on contacting a dilute solution of $\mathrm{UO_2(TTA)_2}$ in TBP with $\mathrm{D_2O}$, the higher frequency peak becomes a small shoulder relative to the main peak at 1595 $\mathrm{cm^{-1}}$, indicating a shift to the $\mathrm{UO_2(TTA)_2}$ spectrum obtained in wet solution. Similar results were obtained when the $\mathrm{Th(TTA)_4}$ was dissolved in excess TBP both dry and wet. Karl Fischer water content measurements have shown[10] that as one adds Th, $\mathrm{UO_2}$ or Nd to HTTA/TBP mixtures in hexane the water content of the phase gradually decreases until at the stoichiometric quantity of metal to HTTA and TBP the hexane solution is practically free of water. Addition of excess TBP causes the water content of the hexane phase to rise again.

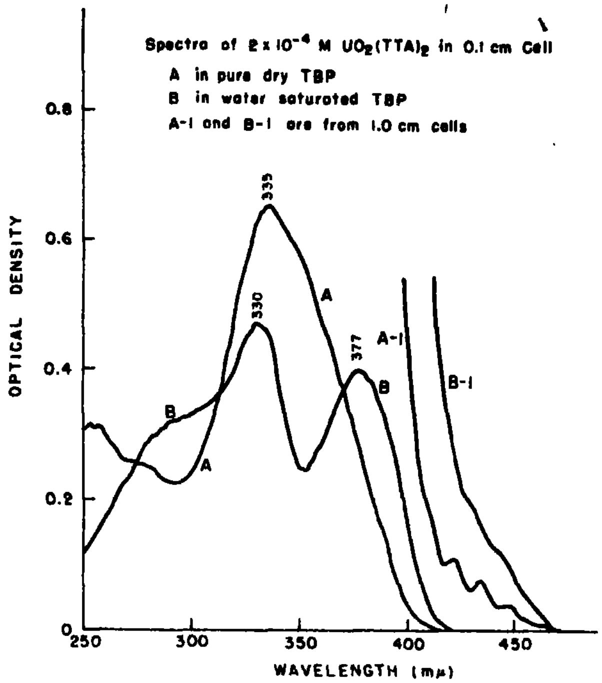

FIG. 13.—Effect of water on absorption spectra of $\mathrm{UO_2(TTA)_2}$ in TBP.

It is interesting to see that the order of bringing about antisynergism in the solvents used is also the same order as the solubility of water in these solvents. For example, cyclohexane, which has the poorest antisynergistic effect and lowest water solubility (0·04 g $\mathrm{H_2O}$ per litre) is followed by hexane (0·07 g/l.), $\mathrm{CCl_4}$ (0·15 g/l.), benzene (0·6 g/l.), $\mathrm{CHCl_3}$ (1·5 g/l.), dibutyl carbitol (14 g/l.), MIK (19 g/l.), decanol (24 g/l.), 2-ethylhexanol (26 g/l.) and TBP (60 g $\mathrm{H_2O}$ per litre). While the mechanism of formation of the synergistic complexes $\mathrm{M(TTA)}_x\mathrm{S}_y$ is relatively well understood through the reaction:

$$\mathrm{M}^{x+} + x\mathrm{TTA_e}^- + y\mathrm{S} \rightarrow \mathrm{M(TTA_e)}_x\mathrm{S}_y$$

$$\text{and the equilibrium } [\mathrm{TTA_e}]^x[\mathrm{S}]_y^{\prime} = \frac{\mathrm{K}[\mathrm{M(TTA_e)}_x\mathrm{S}_y]}{[\mathrm{M}^{x+}]}$$

it appears difficult to interpret the mechanism of antisynergism as enough is not known about it. Addition of more donor solvent will simply cause an increase in the activity of [S] and so the only way to cause antisynergism must be by decreasing the $[TTA_e]$ activity. The subscript e for [TTA] means the enol form as distinct from the ketohydrate or enolate forms.

It has been shown that the HTTA–TBP interaction in the absence of water gives the HTTA enolate structure and this is clearly not involved in the antisynergism. It is also likely that the formation of the ketohydrate structure (TTA_i) is involved. This structure probably contains attached water but in any case it is very much influenced by the presence of water; it may or may not contain S. Formation of a metal/TTA complex containing a hydrate would be expected to give lower partition coefficients because the normal coordination energy of the hydrate water with other water is lost on extraction; the complex is also more hydrophillic. On the other hand, while one possibility is formation of a $M(TTA)_xS_y(H_2O)$ this species would have to be formed at the same aqueous activity as the anhydrous $M(TTA)_xS_y$ and this seems less likely.

Antisynergism caused by addition of another donor solvent to a $M(TTA)_xS_y$ synergistic system such as addition of methyl isobutyl ketone to $Pm(TTA)_3(TBP)_2$ can also be similarly attributed to the lowering of the HTTA activity $[TTA_e]$ and the formation of $[TTA_i]$. Ultra-violet evidence also indicates that changing from one "inert" diluent to another, also causes $[TTA_e]$–$[TTA_i]$ differences, that is changes in the $[TTA_e]$ activity. The reduction of $[TTA_e]$ activity is obviously bound up with the organic water content and water is necessary for formation of the $[TTA_i]$ species.

Versatility of the synergistic–antisynergistic phenomena in metal or group separations

In view of the difference in complexes formed in the synergistic extraction of metals, use could be made of these properties in the separation of metallic species. For example, the rare earths Eu, Pm, with complexes such as $Eu(TTA)_3(TBP)_2$ form different complexes from other rare earths such as thulium which forms a complex $Tm(TTA)_3TBP$. Similarly, separations could be made of certain species by taking advantage of different antisynergistic properties of either the donor or non-donor antisynergists. Altogether, the available scope for variations in extraction procedures opened up by the synergistic and antisynergistic phenomena offers many possibilities for separation techniques and for methods of analysis.

J. Inorg. Nucl. Chem., 1962, Vol. 24, pp. 1449 to 1461. Pergamon Press Ltd. Printed in England

SYNERGISM IN THE SOLVENT EXTRACTION OF DI, TRI AND TETRAVALENT METAL IONS—IV

ABSORPTION SPECTRAL STUDIES OF THE SYNERGISTIC COMPLEXES*

T. V. Healy† and J. R. Ferraro‡

(*Received* 17 *January* 1962)

Abstract—In previous work with radioactive tracers in this series, formulae have been assigned to the metal complexes synergistically extracted from aqueous solution by an organic phase containing thenoyl trifluoracetone (HTTA) and neutral organophosphorous compounds. Stable solid complexes have now been isolated and are shown to have the same formulae. These formulae have been confirmed by ultra-violet and visible absorption spectrophotometric measurements of dilute solutions of uranyl, thorium and neodymium complexes.

In earlier work in this series,(1) formulae were derived for the metal species synergistically extracted from aqueous solution into organic phases containing thenoyl trifluoracetone (HTTA) and neutral organophosphorous esters (S). This enhanced synergic effect has been defined as a definite enhancement of metal extraction by a mixture of an acid and a neutral additive, the resulting mixture giving a better metal extraction than either the acid or the neutral additive alone. Among the formulae suggested for the extracted species on the basis of radioactive tracer work were $UO_2(TTA)_2S_1$, $UO_2(TTA)_2S_3$, $Th(TTA)_4S_1$, and $Pm(TTA)_3S_2$. A number of crystalline solid complexes have now been isolated in the uranyl and thorium series and these have been examined both analytically and by absorption spectrophotometry. The rare earth complexes that were prepared remained as oils and did not solidify. Absorption spectral measurements were carried out in the systems $H_2O/M^{n+}/HTTA/S$ and it was found that by keeping all constituents constant except HTTA or except S a maximum spectral peak height could be obtained. This enabled formulae for the extracted species to be ascertained at concentrations much greater than those used in tracer work. The studies indicated that the same formulae for the species were found at tracer levels, at millimolar levels and in the solids or oils. In this work, S was usually a neutral organophosphorous ester as in the tracer studies.(1, 2) N.n.butyl acetanilide (BAA), shown to give large synergic effects in combination with HTTA(3), was also used in these studies.

Isolation and properties of metal/TTA/S synergic complexes

Uranyl complexes

Two volumes of an aqueous solution of 0·025 molar uranyl nitrate were added to one volume of a hexane solution of 0·10 molar HTTA and 0·05 molar neutral organophosphorous ester. The mixture was shaken vigorously for about 20 min, the aqueous phase removed and the hexane solution allowed to evaporate. Yellow microcrystalline material gradually settled out during the evaporation. When about nine-tenths of the hexane had evaporated the precipitate was filtered off, washed with a little water and a little hexane. Further purification was brought about by recrystallization from one of many organic solvents, such as hexane, cyclohexane or benzene. In this way, solid crystalline components of the formula $UO_2(TTA)_2S$ were obtained, where S is TBP, TOPO or BAA. $UO_2(TTA)_2(TOPO)_3$ was also isolated as a solid by using three to four times the usual concentration of TOPO.

---

* Based on work performed under the auspices of the United States Atomic Energy Commission.

† Harwell Exchange Fellow at Argonne National Laboratory.

‡ Argonne National Laboratory.

(1) T. V. Healy, Part I of this series, *J. Inorg. Nucl. Chem.* **19**, 321 (1961).

(2) T. V. Healy, Part II of this series, *J. Inorg. Nucl. Chem.* **19**, 328 (1961).

(3) T. V. Healy, Part III of this series, *J. Inorg. Nucl. Chem.* **24**, 1429 (1962).

Thorium complexes

These salts were obtained in a manner similar to the above uranyl complexes except that the reagent mole ratio for Th:HTTA:S was 1:4:1. Cream coloured solids were obtained in these thorium salts where S is TBP, TOPO, or BAA and the general formula is $Th(TTA)_4S$.

Neodymium complexes

These were also obtained similarly using the reagent ratio for Nd:HTTA:S of 1:3:2. It was found necessary to raise the pH of the aqueous phase in order to effect complete extraction of Nd into the organic phase. Complexes made with TOPO and BAA were oils at room temperatures.

All the metallic solid complexes isolated were anhydrous. The simple compounds $M(TTA)_x$, where x is the valency of the metal, can be made in exactly the same manner as the M/TTA/S complexes, the only difference being that S is omitted from the preparation. Alternatively, they can be made by the same methods used for preparing the corresponding acetylacetonates$^{(4)}$. Table 1 gives the complexes prepared their melting points and analytical data.

Table 1.—Data on metal/tta/s complexes

Complex	M.P. (°C)	Analysis			
		Theory		Experimental	
		Metal (%)	P (%)	Metal (%)	P (%)
$UO_2(TTA)_2$	212	—	—	—	—
$UO_2(TTA)_2TBP$	112	24·3	3·17	23·8	2·7
$UO_2(TTA)_2TOPO$	57	—	—	—	—
$UO_2(TTA)_2(TOPO)_3$	37	—	—	—	—
$UO_2(TTA)_2BAA$	107	—	—	—	—
$Th(TTA)_4$	226	—	—	—	—
$Th(TTA)_4TBP$	178	16·7	2·26	16·6	2·3
$Th(TTA)_4TOPO$	110	15·5	2·07	16·0	1·9
$Th(TTA)_4BAA$	Oil	—	—	—	—
$Nd(TTA)_3$	155–165	—	—	—	—
$Nd(TTA)_3(TOPO)_2$	Oil	—	—	—	—
$Nd(TTA)_3(BAA)_2$	Oil	—	—	—	—

It can be seen from the above table that introduction of a mole of TBP into a metal/TTA complex lowers the melting point about 50°C, while introduction of a mole of TOPO lowers it about 100°C. The formation of $UO_2(TTA)_2(TOPO)_3$ is demonstrated by lowering of the mixed melting point, by tracer studies$^{(2)}$ and by infra-red studies$^{(5)}$.

(4) W. C. Fernelius, Editor, *Organic Syntheses* Vol. 2, p. 15. McGraw Hill, New York (1946).

(5) J. R. Ferraro and T. V. Healy, Part V of this series. *J. Inorg. Nucl. Chem.* **24**, 1463 (1962).

$UO_2(TTA)_2$ itself, which is anhydrous, has the same m.p. as that given in the literature[(6)] (212°C).

Analyses for uranium and thorium were carried out by standard methods after the metal was washed out of the benzene solution of the complex by strong aqueous acid. Phosphorus was estimated also by standard methods after evaporation of the metal-free organic solvent.

VISIBLE AND ULTRA-VIOLET SPECTRAL RESULTS

A Cary 14 automatic recording spectrophotometer was used throughout this work.

Uranyl solid complexes

The absorption spectra of $UO_2(TTA)_2$ in organic solvents, such as benzene, are well known in the literature.[(6)] Two peaks are observed at about 330 and 380 mμ, the first being somewhat more intense than the second. The absorption spectra of the complexes $UO_2(TTA)_2TBP$and $UO_2(TTA)_2TOPO$ in benzene are reproduced in Fig. 1 and are almost identical with that of $UO_2(TTA)_2$ in the same solvent. In Fig. 1, the spectrum of $UO_2(TTA)_2TBP$ in normal hexane is shown, which is also very similar.

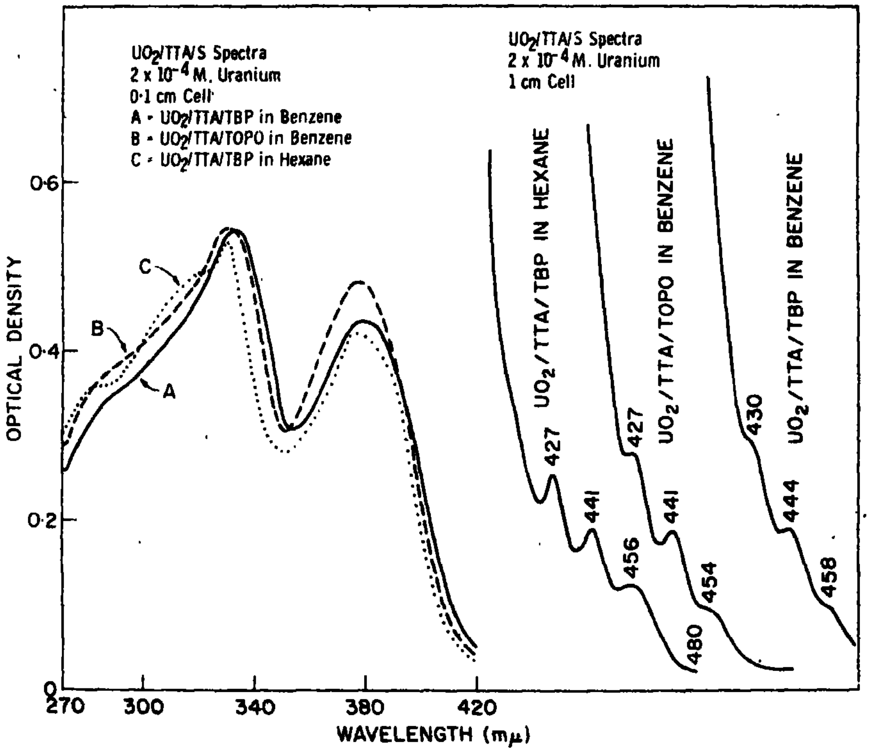

FIG. 1.—Absorption spectra of solid uranyl complexes dissolved in organic diluents.

The big difference between the spectra of $UO_2(TTA)_2TBP$ in benzene and hexane is at the wavelength above 400 mμ. There are well defined peaks at 427, 441 and 456 mμ in hexane whereas, in benzene, these are only humps in the spectra, and are practically invisible in $UO_2(TTA)_2$ alone. This point is illustrated at the right hand side of Fig. 1

[(6)] E. L. ZEBROSKI, T.I.D. 1098 (1947).

where the heights of the spectra are increased by a factor of ten compared with the left hand side. These peaks beyond 400 mμ are characteristic of the uranyl grouping and are present in both aqueous and organic solutions of uranyl nitrate. However, the extinction coefficient in the $UO_2(TTA)_2TBP$ complex at 426 mμ is more than a hundred times greater than it is in most other uranyl salts. The only other relatively high uranyl extinction coefficient is that of the trinitratouranyl nitrate, but even those peak heights are less than one tenth the height of those in the M/TTA/TBP complexes. These high extinction coefficients at above 400 mμ no doubt account for the increase in intensity of the yellow colour of $UO_2(TTA)_2$ solutions upon addition of the synergic agent TBP. Because of these more clearly defined spectra in hexane at above 400 mμ compared with benzene, much of the subsequent ultra-violet work was done using hexane as the organic medium. Although $UO_2(TTA)_2$ is very soluble in benzene, it is almost insoluble in dry hexane. Addition of water to a hexane suspension of $UO_2(TTA)_2$ changes the spectrum of the hexane solution, the spectrum obtained being the normal "enol" spectrum of HTTA. This indicates hydrolysis of the $UO_2(TTA)_2$ in wet hexane, a phenomenon which does not occur in wet benzene. Extinction coefficients (E) for the uranyl complexes are listed in Table 2.

TABLE 2.—EXTINCTION COEFFICIENTS OF ULTRA-VIOLET PEAKS IN THE URANYL COMPLEXES

Complex	Peak (mμ)	E	Peak (mμ)	E	Peak (mμ)	E	Peak (mμ)	E	Peak (mμ)	E
$UO_2(TTA)_2$ in benzene	338	26,400	384	21,200						
$UO_2(TTA)_2TBP$ in benzene	332	27,500	380	22,000	430	1,450	444	950	458	500
$UO_2(TTA)_2TOPO$ in benzene	330	27,000	377	24,000	427	1,400	441	950	454	500
$UO_2(TTA)_2TBP$ in hexane	328	26,000	375	21,000	427	1,350	441	950	456	550

Uranyl complexes extracted into the organic phase

The above spectra were obtained from the dissolved crystalline compounds of known composition. In extremely dilute solutions, that is, solutions of uranyl salts of $< 10^{-5}$ molar, the composition was found by tracer work to be the same, namely, $UO_2(TTA)_2S_1$ where S is a neutral additive such as TBP, DBBP or TOPO. Two species were, however, obtained using the last additive, TOPO, namely $UO_2(TTA)_2(TOPO)_1$ and $UO_2(TTA)_2(TOPO)_3$. An attempt was made, using absorption spectra, to ascertain the formulae of the species in dilute organic solutions of uranium (10^{-3} molar) by using 10^{-3} to 10^{-1} molar HTTA. Owing to the very high extinction coefficients of HTTA and its salts, it proved impossible to compare solution spectra using a diluent such as hexane as a reference in the spectrophotometer. Hexane solutions were therefore made up of known concentrations of HTTA and TBP, and divided into two equal portions, one to be shaken with an aqueous uranium solution and the other with a similar aqueous solution containing no uranium. After equilibrium, the organic phase which had extracted the uranium would be compared spectrophotometrically with the other half of the HTTA–TBP mixtures as a reference.

In this way, absorption spectra could be obtained using HTTA as high as 0·2 molar in solution. In order to find the ratio of U to HTTA or to TBP in the extracted species, two of these would be kept constant, of which one would be present in excess. The third constituent is then gradually increased in concentration until a maximum is obtained in an absorption peak. In all these experiments, uranium was kept constant at 10^{-3} molar. By keeping excess TBP in solution and varying HTTA it was observed that the spectral peaks rose to a maximum at a HTTA concentration of 2×10^{-3} molar indicating that there were 2 TTA moles per uranyl mole in the species $UO_2(TTA)_2TBP$. These spectra are illustrated in Fig. 2. In these experiments, the uranium was increasingly extracted out of the aqueous phase as the HTTA concentration of the organic phase increased. In a similar manner, using 10^{-3} molar aqueous uranium plus an excess of HTTA in the hexane phase, a precipitate of $UO_2(TTA)_2$ was produced. By gradual addition of TBP, the precipitate dissolved and the

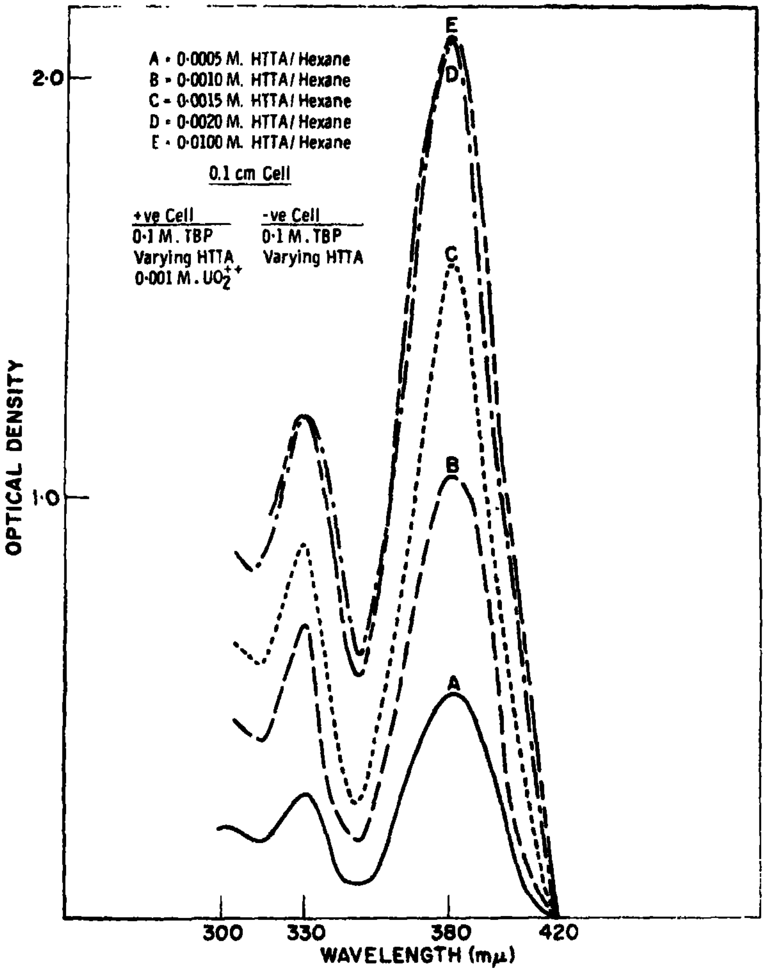

FIG. 2.—Effect of added HTTA or absorption spectral peak heights below 400 mμ in the UO_2/HTTA/TBP system.

absorption peaks increased to a maximum, then remained constant. This occurred when 10^{-3} molar TBP had been added, indicating formation of the species $UO_2(TTA)_2$ (TBP). The following tables show the gradual increase to the maximum peak heights.

TABLE 3.—OPTICAL DENSITY MAXIMA FOR U/HTTA MOLE RATIOS IN U/HTTA/TBP SYSTEMS

	U = 0·001 molar		TBP = 0·1 molar			
	0·1 cm path length		1 cm path length			
HTTA molarity	D_{328}mμ	D_{378}mμ	D_{428}mμ	D_{442}mμ	D_{456}mμ	HTTA/U mole ratio
0·0005	0·32	0·55	0·26	0·17	0·09	0·5:1
0·0010	0·72	1·1	0·55	0·36	0·17	1:1
0·0015	0·91	1·57	0·80	0·57	0·25	1·5:1
0·0020	1·2	2·1	1·01	0·71	0·36	2:1
0·0100	1·2	2·15	1·05	0·72	0·38	10:1

It is interesting to note that the extinction coefficient of the 328 mμ peak is higher than that of the 378mμ peak in the absorption spectral data given in Table 2 for the solid complexes dissolved in hexane, whereas the reverse is true in Table 3. The latter table, however, gives the spectral data for a comparison of U/TTA/TBP against HTTA/TBP in hexane. An examination of the spectra of HTTA/TBP in hexane against hexane alone shows a high peak at 330 mμ and no peak at 380. It is the production of this 330 mμ peak in HTTA/TBP solutions which accounts for the apparent reversal or lowering of the 330 peak relative to the 380 mμ peak in Table 3. An examination of Table 4 not only shows the reversal relative to Table 2, but shows a large shift in these peaks to longer wavelengths. This is because a relatively large constant concentration of HTTA (0·1 molar) is used in the series in Table 4, the shift increasing further to the right as the HTTA molarity is increased. This is undoubtedly due to the poor light transmission of the more concentrated HTTA solutions.

TABLE 4.—OPTICAL DENSITY MAXIMA FOR U/TBP MOLE RATIOS

	U = 0·001 molar		HTTA = 0·1 molar			
	0·1 cm path length		1 cm path length			
TBP molarity	D_{350}mμ	D_{390}mμ	D_{428}mμ	D_{442}mμ	D_{456}mμ	TBP/U mole ratio
0·00025	0·3	0·55	0·26	0·17	0·09	0·25:1
0·00050	0·6	1·1	0·55	0·36	0·17	0·5:1
0·0010	1·1	2·1	1·04	0·71	0·34	1:1
0·0020	1·1	2·1	1·06	0·72	0·36	2:1

In a similar procedure to that given for the UO_2/TTA/TBP systems, the UO_2/TTA/TOPO systems have been examined and it has been ascertained that one mole of uranium complexes with two moles of HTTA and one mole of TOPO to give the complex $UO_2(TTA)_2(TOPO)$. Production of a complex containing more than one mole of TOPO, namely $UO_2(TTA)_2(TOPO)_3$ does not appear to cause any effect on absorption spectrum and yet there is strong evidence for its production both from tracer work and from mixed melting points of the solid complexes $UO_2(TTA)_2$, $UO_2(TTA)_2TOPO$ and $UO_2(TTA)_2(TOPO)_3$. Fig. 3 and Tables 5 and 6 illustrate formation of the species $UO_2(TTA)_2(TOPO)_1$.

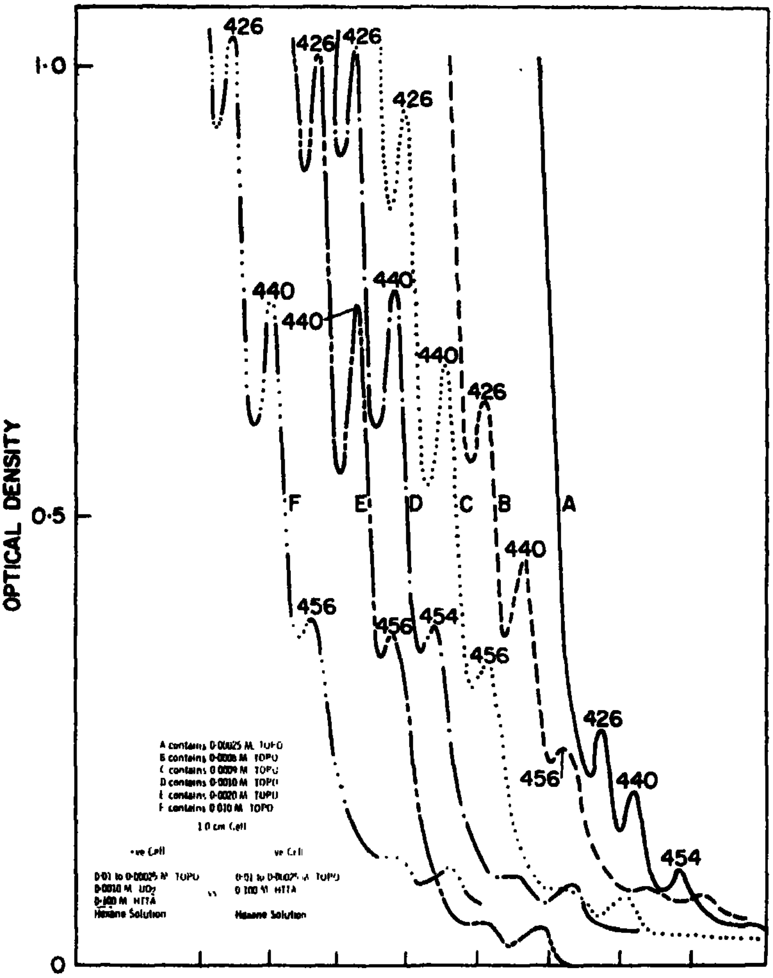

FIG. 3.—Effect of added TOPO on absorption spectral peak heights above 600 mμ in the system UO_2/HTTA/TOPO.

TABLE 5.—OPTICAL DENSITY MAXIMA FOR U/HTTA MOLE RATIOS IN U/HTTA/TOPO SYSTEMS

U = 0·001 molar			TOPO is 0·10 molar		
	0·1 cm cell		1 cm cell path length		
HTTA molarity	D_{325}mμ	D_{378}mμ	D_{426}mμ	D_{440}mμ	D_{456}mμ
0·0005	0·40	0·56	0·25	0·18	0·10
0·0010	0·70	1·1	0·47	0·34	0·18
0·0015	1·0	1·5	0·69	0·46	0·29
0·0020	1·3	2·1	0·94	0·70	0·35
0·0100	1·4	2·2	0·97	0·72	0·37

TABLE 6.—OPTICAL DENSITY MEASUREMENTS FOR U/TOPO MOLE RATIOS IN U/HTTA/TOPO SYSTEMS

U is 0·001 M	1·0 cm path length		HTTA is 0·004 M
TOPO molarity	$D_{426 m\mu}$	$D_{440 m\mu}$	$D_{456 m\mu}$
0·00025	0·27	0·20	0·10
0·00060	0·63	0·45	0·23
0·00090	0·95	0·66	0·33
0·0010	1·02	0·74	0·36
0·0020	1·02	0·74	0·36
0·010	1·04	0·74	0·38

Among the amides which exert a strong synergism on the metal·TTA system, n-butyl acetanilide (BAA) is shown here as an example. Again, it is clear from these spectrophotometric measurements in Table 7 which confirms tracer and macrowork that the synergistic species is $UO_2(TTA)_2(BAA)_1$.

TABLE 7.—OPTICAL DENSITY MAXIMA FOR U/HTTA AND U/BAA MOLE RATIOS IN U/HTTA/BAA SYSTEMS

U is 0·001 M			U is 0·001 M		
1·0 cm cell path length					
BAA is 0·1 molar			HTTA is 0·1 molar		
HTTA molarity	$D_{428 m\mu}$	$D_{442 m\mu}$	BAA molarity	$D_{428 m\mu}$	$D_{442 m\mu}$
0·0005	0·26	0·17	0·00025	0·28	0·19
0·0010	0·49	0·34	0·00050	0·54	0·37
0·0015	0·77	0·50	0·00075	0·81	0·57
0·0020	0·89	0·65	0·00100	1·06	0·73
0·0100	1·06	0·72	0·0050	1·07	0·74

Thorium solid complexes

The absorption spectra of $Th(TTA)_4$ in organic solvents such as benzene are well known(6) and are presumed to consist of the normal "enol" form of chelate. Fig. 4 shows these absorption spectra plus those of $Th(TTA)_4TBP$ and $Th(TTA)_4$ TOPO. The spectra consist mainly of one large peak at 345–350 mμ with an extinction coefficient of 85,000 and in all three instances are more or less identical.

TABLE 8.—OPTICAL DENSITY MAXIMA FOR Th/TBP MOLE RATIOS IN THE Th/HTTA/TBP SYSTEMS

System contains 5×10^{-4} M Th and $2{\cdot}5 \times 10^{-3}$ M HTTA (0·1 cm cell path length)				
TBP molarity	1×10^{-4}	$2{\cdot}5 \times 10^{-4}$	5×10^{-4}	50×10^{-4}
Optical density ($D_{350 m\mu}$)	0·5	1·1	2·2	2·3

Table 9 and Fig. 5 show the ratio of Th to HTTA is 1 to 4 in the system Th/HTTA/TOPO and Table 10 shows the ratio of Th to BAA is 1 to 1 in the system Th/HTTA/BAA.

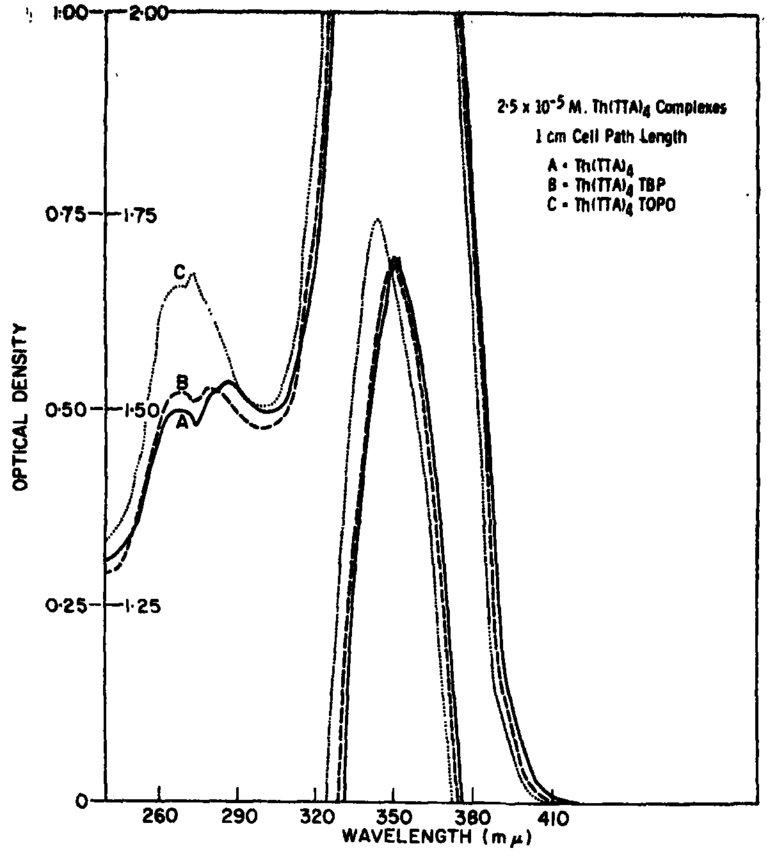

FIG. 4.—Absorption spectra of solid thorium complexes dissolved in benzene.

TABLE 9.—OPTICAL DENSITY MAXIMA FOR Th/HTTA MOLE RATIO IN THE Th/HTTA/TOPO SYSTEM

System contains 5×10^{-4} molar Th 4×10^{-2} molar TOPO in hexane (0·1 cm path length)

HTTA molarity $\times 10^4$	5	10	15	20	50
Optical density (D_{345}mμ)	0·58	1·1	1·58	2·08	2·11

Thorium complexes extracted into the organic phase

Both tracer work in solution and macro analysis of the solid show the formula of the TBP extract to be $Th(TTA)_4(TBP)_1$. Spectrophotometric evidence confirms that there is one TBP mole per mole of Th in the complex. The method used is similar to that carried out with the uranium complexes. At a constant concentration of thorium and HTTA, gradual addition of TBP causes an increase in the height of the 350 mμ peak up to a maximum at a Th/TBP ratio of 1 to 1.

It should be noted that the peak wavelength in Table 10 (388 mμ) is much higher than in the previous tables. In this case, a higher HTTA concentration had to be used and this caused the shift in wavelength. This is undoubtedly due to the poor light transmission of the more concentrated HTTA solutions. As an example of this behaviour, a hexane solution containing 5×10^{-4} molar Th, 10^{-3} molar TOPO and $2{\cdot}5 \times 10^{-3}$ molar HTTA, using 10^{-3} molar TOPO and $2{\cdot}5 \times 10^{-3}$ molar HTTA as reference, has an optical density of 2·1 at 345 mμ when viewed through a 0·1 cm cell.

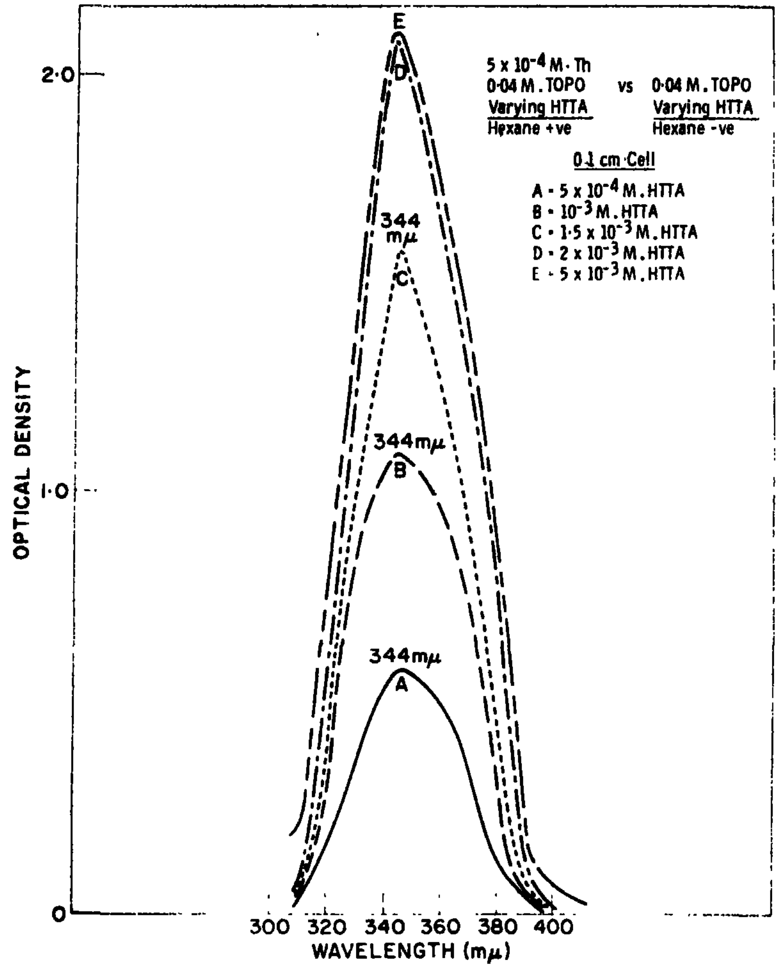

Fig. 5.—Effect of added HTTA on absorption spectral peak heights in the Th/HTTA/TOPO system.

Table 10.—Optical density maxima for Th/BAA mole ratio in the Th/HTTA/BAA system

System contains 5×10^{-4} molar Th, 10^{-2} molar HTTA in hexane
(1 cm path length)

BAA molarity $\times 10^4$	5	10	20	50
Optical density ($D_{388 m\mu}$)	0·55	0·98	1·91	1·95

According to Beers Law, this solution, viewed through a 1 cm cell, should have an optical density of twenty-one. Instead, the optical density is only 2·3 but the wavelength of the peak has increased to 384 mμ.

Neodymium complexes extracted into organic phase

Aqueous neodymium nitrate has a visible spectrum with the largest peaks at 576 ($E = 6{\cdot}90$) and 522 ($E = 4{\cdot}20$). Similarly, the organic solution of neodymium nitrate in TOPO/hexane has peaks at 584 ($E = 48$) and 528 ($E = 8{\cdot}3$). The extinction coefficient at the higher wavelength is about seven times greater for the organic solution than the aqueous solution. $Nd(TTA)_3TOPO$ has practically the same visible spectrum as $Nd(NO_3)_3$ and Nd $(TTA)_3$ in benzene. By using the same spectrophotometric technique as that used above for both uranium and thorium/HTTA complexes it is shown that Nd/HTTA/TOPO exist in the complex as $Nd(TTA)_3(TOPO)_2$ which is in agreement with tracer work.[11] (See Fig. 6 and Table 11). Table 12 indicates formula $Nd(TTA)_3(BAA)_2$.

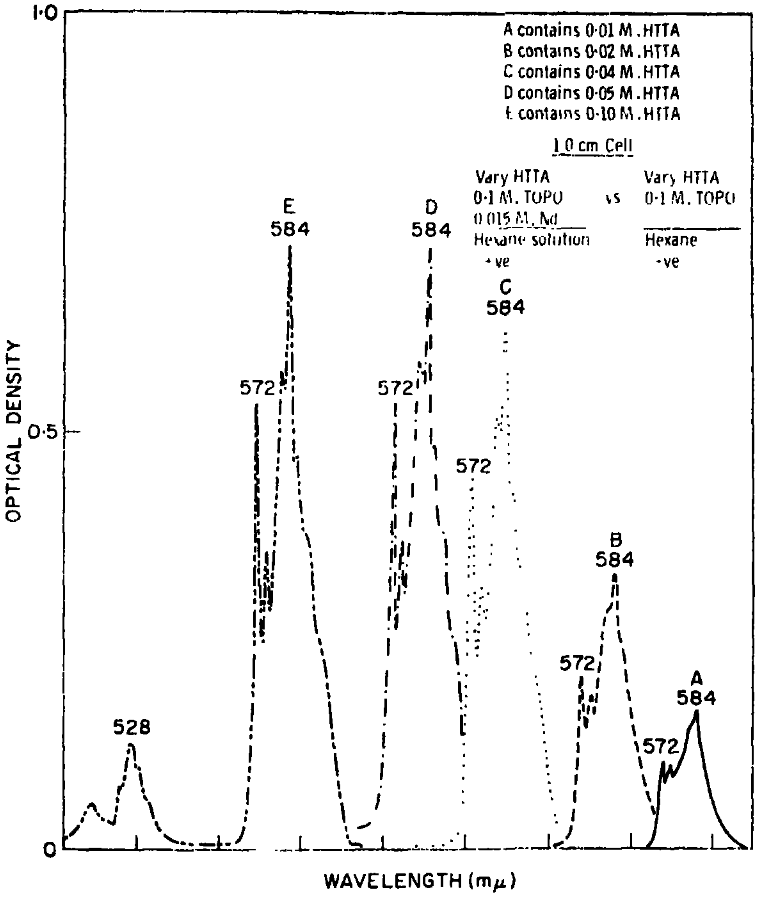

FIG. 6.—Effect of added HTTA on absorption spectral peak heights in the Nd/HTTA/TOPO system.

TABLE 11.—OPTICAL DENSITY MAXIMA FOR Nd/HTTA AND Nd/TOPO IN THE Nd/HTTA/TOPO SYSTEM

Nd is 0·015 molar HTTA is 0·20 molar		1 cm cell path length	Nd is 0·015 molar TOPO is 0·10 molar	
TOPO molarity	$D_{584 m\mu}$		HTTA molarity	$D_{584 m\mu}$
0·005	0·13		0·010	0·17
0·010	0·25		0·020	0·33
0·020	0·50		0·040	0·63
0·030	0·72		0·045	0·72
0·045	0·72		0·050	0·72
0·10	0·72		0·20	0·72

Similarly, it can be shown (Table 12) that the mole ratio of Nd to BAA is 1 to 2.

TABLE 12.—OPTICAL DENSITY MAXIMA FOR Nd/BAA IN THE SYSTEM Nd/HTTA/BAA
System contains 0·015 molar Nd and 0·2 molar HTTA in Hexane

BAA molarity	0·005	0·010	0·015	0·020	0·030	0·050	0·100
$D_{584 m\mu}$	0·12	0·24	0·35	0·47	0·71	0·72	0·72

DISCUSSION

The absorption spectral work discussed does not shed any light on the structural differences between $M_x(TTA)_y$ and $M_x(TTA)_yS$. However, it does substantiate the formulae obtained for the complexes of U, Th and Nd by both tracer work and work with the solid complexes. This indicates that at all concentrations there seems to be the same species present in solution. There is also no differentiation observable spectrophotometrically in the species $UO_2(TTA)_2TOPO$ and $UO_2(TTA)_2(TOPO)_3$.

The spectrum of $M_x(TTA)_y$ has been discussed in the literature⁽⁶⁾ and is considered to be the normal enol chelate form. The synergistic enhancement of the extraction of metals by HTTA plus neutral additives which changes the chelate group into a monodentate ligand⁽⁵⁾ does not appear to affect the visible spectra of the $M_x(TTA)_y$. The only observable difference is the large enhancement of uranyl peaks at 426 to 454 mμ which do indicate an effect on the structure even more marked than the change from uranyl $[UO_2(NO_3)_2]$ to trinitrato uranyl nitrate $[HUO_2(NO_3)_3]$ species.⁽⁷⁾

An attempt was made to observe the formation of $UO_2(TTA)(NO_3)S$ or $UO_2(TTA)(OH)S$ in the presence of insufficient HTTA and an excess of $NaNO_3$ or NaOH. NaOH caused precipitation of U from some solutions otherwise the spectra was normal. On a number of solutions with insufficient HTTA, saturated aqueous $NaNO_3$ did cause a general lowering of the spectrum by a factor of about two, but this was probably due to the salting in of $UO_2(NO_3)_2\cdot 2S$ giving a mixture of this complex with the usual $UO_2(TTA)_2S$. The same situation was true for the $Th(TTA)_4\cdot TBP$ complex, there being no evidence for substitution of TTA by nitrate group.

The use of this spectrophotometric technique for ascertaining the formula of the species in solution is really based on the fact that the $M_x(TTA)_y$ complex (1) has a high extinction coefficient and (2) it has a low solubility in hexane or cyclohexane.

⁽⁷⁾ L. KAPLAN, R. A. HILDEBRANDT and M. ADER, *J. Inorg. Nucl. Chem.* **2**, 153 (1956).

Addition of the neutral donor solvent very greatly increases the solubility of the metal by forming the synergistic complex $M_x(TTA)_yS_z$. Some of these complexes have solubilities in the organic phase greater than 0·1 molar and where the complexes do not form solids, as in most of the rare earths, the solubilities are appreciably higher.

Use could be made of this spectrophotometric technique in analysing solutions for many metals such as thorium, uranium, rare earths or transuranics. The unknown aqueous concentration could be brought to a pH between 1 and 6, then extracted by an equal volume of a mixture of HTTA plus TBP in hexane. The organic extract could be examined spectrophotometrically using as reference solution, part of the original extractant previously wetted. The effect of various aqueous complexing agents and other interfering metals would have to be ascertained. The method has good possibilities for estimating many metals including for example, micrograms of thorium and uranium. The authors, however, do not propose to pursue this analytical method any further.

J. Inorg. Nucl. Chem., 1962, Vol. 24, pp. 1463 to 1474. Pergamon Press Ltd. Printed in England

SYNERGISM IN THE SOLVENT EXTRACTION OF DI-, TRI- AND TETRAVALENT METAL IONS—V

INFRA-RED STUDIES OF THE ISOLATED COMPLEXES*

J. R. Ferraro† and T. V. Healy‡

Chemistry Division, Argonne National Laboratory, Argonne, Illinois

(*Received* 2 *March* 1962; *in revised form* 17 *April* 1962)

Abstract—In the synergistic extractions of metal ions with the systems 1,1,1-trifluoro-3-2′-thenoyl acetone (HTTA) and neutral organophosphorus compounds, stable complexes have been isolated from the organic phase. These have the following formulae: $UO_2(TTA)_2S_1$, $UO_2(TTA)_2S_3$, $Th(TTA)_4S_1$ and Rare Earth $(TTA)_3S_2$, where S = a neutral organophosphorus compound. The infra-red spectra of these complexes have been obtained and are discussed in terms of various possible structures.

RECENTLY, synergistic and anti-synergistic effects in the solvent extraction of various cations have been reported.(1–14) Use of these effects has been made in various separations of metals.(2, 3) BROWN,(6) KENNEDY(7) and DYRSSEN(9) have explained the effects found with the systems $[(GO)_2PO(OH)]_2$ and $(GO)_3PO$ or G_3PO** in terms of mechanisms involving addition or substitution of the neutral phosphorus compound for the acid. The system 1,1,1-trifluoro-3-2′-thenoyl acetone (HTTA)–tri-n-butyl phosphate (TBP), was first reported by CUNNINGHAME and co-workers.(1)

---

* Based on work performed under the auspices of the United States Atomic Energy Commission.

† Argonne National Laboratory, Argonne, Illinois.

‡ Harwell Exchange Fellow at Argonne National Laboratory.

** G = alkyl, aryl or variant thereof.

(1) J. G. CUNNINGHAME, P. SCARGILL and H. M. WILLIS, AERE/C/M-215 (1954).

(2) D. F. PEPPARD, G. W. MASON and R. J. SIRONEN, *J. Inorg. Nucl. Chem.* **10**, 117 (1959).

(3) D. F. PEPPARD. Unpublished data.

(4) H. T. BAKER and C. F. BAES, Jr., U.S.A.E.C. Unclassified Documents, ORNL-2443 (1957); 2486 (1957); 2451 (1957); 2737 (1959).

(5) C. A. BLAKE, D. E. HORNER and J. M. SCHMITT, U.S.A.E.C. Unclassified Document ORNL—2259 (1959).

(6) C. A. BLAKE, C. F. BAES, K. B. BROWN, C. F. COLEMAN and J. C. WHITE, *Proceedings of the Second International Conference on the Peaceful Uses of Atomic Energy, Geneva,* 1958, Vol. 28, p. 289. United Nations (1959).

(7) J. KENNEDY, U.K.A.E.A. Doc. No. AERE/C/M369 (1958).

(8) T. H. SIDDAL, III, *J. Inorg. Nucl. Chem.* **13**, 151 (1960).

(9) D. DYRSSEN and L. KUCA, *Acta Chem. Scand.* **14**, 1945 (1960).

(10) H. IRVING and D. N. EDGINGTON, *Pro. Chem. Soc.* 360 (1959).

(11) H. IRVING and D. N. EDGINGTON, *J. Inorg. Nucl. Chem.* **15**, 158 (1960).

(12) H. IRVING and D. N. EDGINGTON, *Chem. and Industry,* 77 (1960).

(13) T. V. HEALY, *J. Inorg. Nucl. Chem.* **19**, 314 (1961).

(14) T. V. HEALY, *J. Inorg. Nucl. Chem.* **19**, 328 (1961).

Further studies have been made[10, 14] using other types of neutral organophosphorus compounds. For the systems metal–TTA–neutral organophosphorus compound, where the metal is $UO_2(II)$, thorium (IV) or rare earth (III), stable complexes have been isolated from the organic phase. Although the solids isolated may not be directly causing the synergistic effects, it would be of interest to obtain additional information regarding the structural nature of these solids. An infra-red study was therefore carried out on these complexes, and the results are discussed on the basis of various possible structures.

ABBREVIATIONS

There are several abbreviations used throughout the paper for the purpose of brevity, and these are listed below together with the source of the material:

HTTA — neutral 1,1,1-trifluoro-2, 3′-thenoyl-acetone [$COCH_2COCF_3$]. Midcontinent Chemical Co., Chicago, Illinois; and Dow Chem. Co., Midland, Mich., recrystallized from benzene.

TTA — monionized 1,1,1-trifluoro-2, 3′-thenoyl-acetone [$COCHCOCF_3]^-$

TBP — Tri-n-butyl phosphate $[(nC_4H_9O)_3PO]$, from Commercial Solvents Corp., purified, as previously reported.[15]

TMP — Tri-methyl phosphate $[(CH_3O)_3PO]$; Delta Chemical Wks., New York, N.Y.

TOPO — Tri-n-octyl phosphine oxide $[(C_8H_{17})_3PO]$; Eastman Organic Chemicals, Rochester, N.Y.

TEHPO — Tri-2-ethylhexyl phosphine oxide $[(2\text{-}C_2H_5C_6H_{12})_3PO]$; Chemical Procurement Laboratory, College Point, N.Y.

TPPO — Tri-phenyl phosphine oxide $[(C_6H_5)_3PO]$; Aldrich Chem. Co., Milwaukee, Wisc.

DBBP — Di-n-butyl n-butyl phosphonate $[(nC_4H_9O)_2(nC_4H_9)PO]$, from Virginia-Carolina Co., Purified as previously reported.[15]

BAA — N–n-butyl acetanilide $[CH_3CO\text{-}NH\ nC_4H_9]$; Matheson Co., Inc., Joliet, Ill.

EXPERIMENTAL

Preparation of solid complexes

Uranyl complexes. Two volumes of an aqueous solution of 0·025 molar uranyl nitrate were added to one volume of a hexane solution of 0·10 molar HTTA and 0·05 molar neutral organophosphorus ester. The mixture was shaken vigorously for about 20 min; then the aqueous phase was removed and the hexane solution allowed to evaporate. Yellow microcrystalline material gradually settled out during the evaporation. When about nine-tenths of the hexane evaporated, the precipitate was filtered off and washed with a little water and a little hexane. Recrystallization from one of many organic solvents such as hexane, cyclohexane or benzene further purified the solid. In this way, solid crystalline compounds of the formula $UO_2(TTA)_2S$ were obtained where S is TBP, TOPO, TPPO, DBBP, TEHPO, and BAA. Also, by using three to four times the usual concentration of TOPO, a solid compound of the formula $UO_2(TTA)_2(TOPO)_3$ was isolated.

Thorium complexes. These complexes were obtained using the same procedure previously described for the uranyl complexes, except that the reagent mole ratio for Th:HTTA:S was 1:4:1. Cream coloured solids with the general formula $Th(TTA)_4S$ were obtained where S is TBP, TOPO and TPPO.

---

[15] D. F. Peppard, G. W. Mason and J. L. Maier, *J. Inorg. Nucl. Chem.* 3, 215 (1956).

Neodymium and scandium complexes. The complexes of these metals were obtained by the method used for the uranyl complexes, also. The reagent ratios for M:HTTA:S were 1:3:2. In the case of Nd, alkali was added to raise the pH of the aqueous phase in order to affect complete extraction of the Nd into the organic phase. Complexes made with S being TBP, and TOPO were oils, while $Nd(TTA)_3(TPPO)_2$ was a solid.

The simple compounds of general formula $M(TTA)_x$, where x is the valency of the metal, can be made in exactly the same way as the M/TTA/S complexes, except that S is omitted from the preparation.

Melting points

The melting points were made on a Fisher-Johns Melting Point Block. Mixed melting points on mixtures were made similarly after weighing the appropriate amounts of the constituents.

Isopiestic molecular weights

In the isopiestic molecular weights, TBP was used as the standard and the method of SIGNER was followed.(16) Errors were estimated to be in the range of 5–10 per cent.

Analyses of the complexes

Cation analyses in some of these complexes were obtained by standard analytical procedures, after scrubbing the metal out from a benzene solution with strong aqueous acid. The metal-free organic solution was then evaporated and the phosphorus residue determined by standard methods. For the other complexes reported in this paper the TTA/M and S/M ratios were determined by absorption spectrophotometry.(17)

Infra-red studies

All infra-red data were obtained with a Perkin-Elmer Model No. 221 spectrophotometer. The results recorded in this paper were made with KBr disks, checked by Nujol Mulls.

EXPERIMENTAL RESULTS

Physical properties of complexes

Listed in Table 1 are the analytical data, melting points and isopiestic molecular weights for several of the metal complexes of 1,1,1-trifluoro-2, 3′-thenoyl-acetone and various neutral organophosphorus compounds. All of the complexes studied were anhydrous as discussed later, and as shown in Table 2. The complexes had definite melting points and all solids having intermediate compositions gave lower melting points in all systems (e.g. UO_2, Th, Nd complexes) than the definite compounds. It can be noted that the melting point of the complexes containing 1 TBP or 1 TOPO are lower than the simple TTA complex while the melting points of the 1 TPPO complexes are raised. Isopiestic molecular weights in benzene were determined for several of the solids and found to be monomeric. The solids appear to be quite stable as evidenced by the fact that TBP pumped at its melting point under 0·3 mm pressure for several hours showed only a 0·04 per cent loss in weight.

For the uranyl complexes, the ratio of neutral phosphorus ester to metal was always one, except for TOPO, where the compounds $UO_2(TTA)_2 \cdot TOPO$ and $UO_2(TTA)_2 \cdot 3TOPO$ were isolated. The formation of $UO_2(TTA)_2 \cdot 3TOPO$ was previously suggested by tracer studies,(13, 14) and has been confirmed in this investigation by mixed melting points and infra-red data. For thorium, the metal/S ratio was always 1:1, but for the rare earth complexes and probably scandium too, it was 1:2. The studies indicated that the formulae for the synergistic species found at tracer level(13, 14) and

(16) R. SIGNER, *Ann. Chem.* 477, 246 (1930).

(17) T. V. HEALY and J. R. FERRARO, *J. Inorg. Nucl. Chem.* To be published.

TABLE 1.—PHYSICAL PROPERTIES OF THE METALLIC COMPLEXES OF 1,1,1-TRIFLUORO-2,3'-THENOYL-ACETONE/NEUTRAL ORGANOPHOSPHORUS COMPOUNDS

Complex	m.p. (°C)	Molecular weight*		Analytical Data†			
				Calcd.		Found	
		Calcd.	Found	M (%)	P (%)	M (%)	P (%)
$UO_2(TTA)_2$	210–212						
$UO_2(TTA)_2\cdot TBP$	112	978	907	24·3	3·17	23·8	2·7
$UO_2(TTA)_2\cdot TOPO$	57	1099	1070				
$UO_2(TTA)_2\cdot 3TOPO$	37						
$UO_2(TTA)_2\cdot TPPO$	238						
$UO_2(TTA)_2\cdot DBBP$	68						
$UO_2(TTA)_2TEHPO$	60						
$Th(TTA)_4$	224						
$Th(TTA)_4\cdot TBP$	178	1382	1363	16·7	2·24	16·6	2·3
$Th(TTA)_4\cdot TOPO$	110	1502	1500	15·5	2·07	16·0	1·9
$Th(TTA)_4\cdot TPPO$	305			16·8	2·26	17·2	2·3
$Nd(TTA)_3$	155–165						
$Nd(TTA)_3\cdot 2TOPO$	Oil						
$Nd(TTA)_3\cdot 2TPPO$	285	1363	1343	10·7	4·62	10·4	4·5
$Sc(TTA)_3\cdot 2TBP$	Oil						
$Sc(TTA)_3\cdot 2TOPO$	Oil						
$Sc(TTA)_3\cdot 2TPPO$	Oil						

* TBP was used as Standard and the solvent was Spectroscopic Grade benzene (Eastman Organic Co.) in the isopiestic molecular weight determination.

† All of the M/TTA/S complexes were also analysed for TTA/M and S/M ratios by absorption spectrophotometric methods.(17)

spectrophotometrically(17) at millimolar levels are identical to the solids or oils isolated from the organic phase.

Water content of hexane solutions of $M_x(TTA)_yS_z$ complexes

The water content of several hexane solutions was determined using the standard Karl Fischer apparatus. Concentrations of HTTA, TBP and uranium in hexane solutions were prepared separately as well as together. The individual concentrations were in the same ratio as in the complex $UO_2(TTA)_2TBP$; namely, 2 moles of HTTA per mole of U or TBP. After shaking with water overnight, the water content of these hexane solutions was examined. It was found that water was extracted by the hexane solutions containing HTTA or TBP, either separately or together, but when uranium was present in these hexane solutions, the water content dropped considerably. This was also found to be true in the UO_2/HTTA/TOPO system. For example, the water content of a hexane solution containing 0·10 molar HTTA and 0·05 molar TOPO was 0·035 molar, but the addition of 0·05 molar uranyl ion caused the water content to drop by a factor of nearly ten to 0·004 molar, a figure which is about equal to that of the water content of saturated hexane alone. Table 2 shows how the advent of the metal link into the HTTA/ester/hexane system caused the water content to decrease to an almost negligible figure, establishing the fact that the metal/TTA/ester complexes were anhydrous. This has been established for uranium, thorium and neodymium.

TABLE 2.—WATER CONTENT OF H_2O/METAL/HTTA/ESTER/HEXANE SYSTEMS

$UO_2(TTA)_2TBP$ hexane system		$Th(TTA)_4TBP$ hexane system	
Hexane solutions	Water content	Hexane solutions	Water content
0·05 M TBP	0·006 M H_2O	0·05 M TBP	0·006 M H_2O
0·10 M HTTA	0·005 M H_2O	0·20 M HTTA	0·016 M H_2O
0·05 M TBP 0·10 M HTTA	0·010 M H_2O	0·05 M TBP 0·20 M HTTA	0·021 M H_2O
0·05 M TBP 0·10 M HTTA 0·05 M UO_2	0·002 M H_2O	0·05 M TBP 0·20 M HTTA 0·05 M Th	0·003 M H_2O
$UO_2(TTA)_2TOPO$ hexane system		**$Th(TTA)_4TOPO$ hexane system**	
Hexane solutions	Water content	Hexane solutions	Water content
0·05 M TOPO	0·078 M H_2O	0·05 M TOPO	0·028 M H_2O
0·05 M TOPO 0·10 M HTTA	0·035 M H_2O	0·05 M TOPO 0·20 M HTTA	0·042 M H_2O
0·05 M TOPO 0·10 M HTTA 0·05 M UO_2	0·004 M H_2O	0·05 M TOPO 0·20 M HTTA 0·05 M Th	0·001 M H_2O

$Nd(TTA)_3(TOPO)_2$ hexane system	
Hexane solutions	Water content
0·11 M HTTA 0·072 M TOPO	0·058 M H_2O
0·11 M HTTA 0·072 M TOPO 0·036 M Nd	0·005 M H_2O

TABLE 3.—CARBONYL AND C=C FREQUENCIES IN TTA–METALLIC COMPLEXES

Complex	$\upsilon C=O\ldots M$ (cm^{-1})	$\upsilon C-O-M$ (cm^{-1})	$\upsilon C=C$ (cm^{-1})
UO_2(II)	1600	1309	1535
Th(IV)	1601	1312	1542
Nd(III)	1605	1302	1537
Co(II)	1600	1308	1535

TABLE 4.—CARBONYL AND C=C FREQUENCIES IN TTA–ORGANOPHOSPHORUS-METALLIC COMPLEXES (cm^{-1})

Complex	Carbonyl region	$\upsilon C-O-M$	$\upsilon C=C$
$UO_2(TTA)_2TBP$	1622, 1595	1320	1538
$Th(TTA)_4TBP$	1633, 1599	1310	1540
$Sc(TTA)_3\cdot 2TBP$	1630, 1603	1320	1540
$UO_2(TTA)_2\cdot TOPO$	1615, 1597	1310	1538
$UO_2(TTA)_2 3TOPO$	1615, 1597	1309	1537
$Th(TTA)_4\cdot TOPO$	1640, 1598	1310	1538
$Sc(TTA)_3\cdot 2TOPO$	1635, 1607	1320	1540
$Nd(TTA)_3\cdot 2TOPO$	1632, 1610	1300	1532
$UO_2(TTA)_2\cdot TPPO$	1612, 1592	1310	1537
$Th(TTA)_4\cdot TPPO$	1640, 1600	1312	1540
$Sc(TTA)_3\cdot 2TPPO$	1640, 1608	1320	1543
$Nd(TTA)_3\cdot 2TPPO$	1635, 1612	1305	1537

Infra-red spectra

(A) TTA-*metallic complexes.* The infra-red spectra of UO_2(II) and Th(IV) TTA-metallic complexes in the region 1700–1000 cm^{-1} are illustrated in Fig. 1. Although the spectra are complicated, some important features can be cited. For these complexes, an intense peak was observed in the carbonyl absorption region at about 1600 cm^{-1}. A second peak, of less intensity, was found at 1540 cm^{-1}. A third intense peak was found at about 1310 cm^{-1}. The peak at the highest frequency is probably associated with the co-ordinated carbonyl (C = O . . . M) vibration, since it corresponds to the values for this vibration obtained for related complexes.(18)

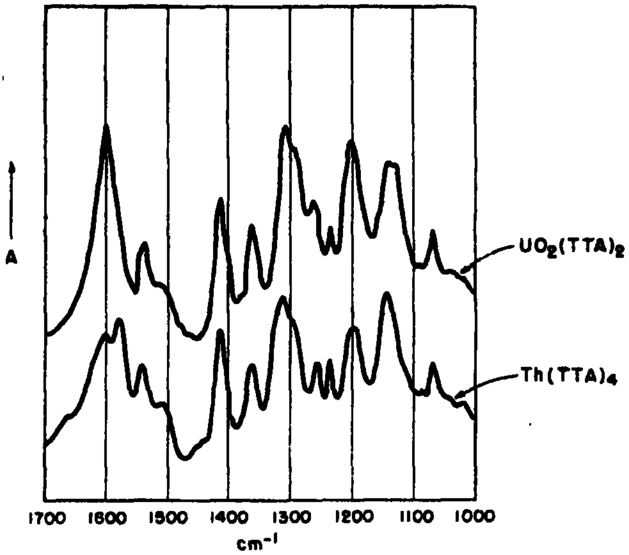

FIG. 1.—Infra-red spectra of $UO_2(TTA)_2$ and $Th(TTA)_4$–KBr disks.

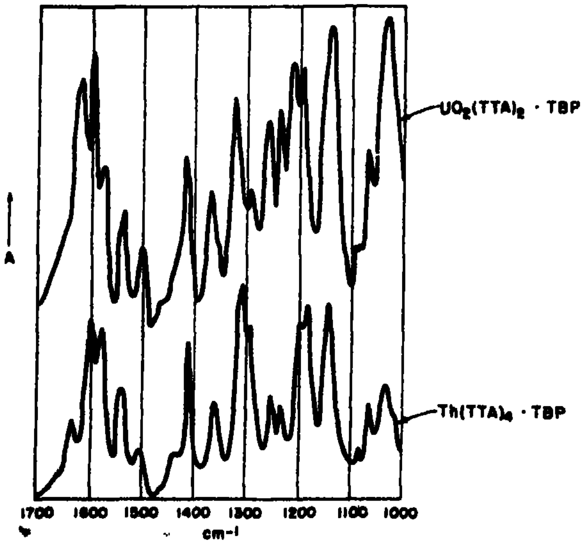

FIG. 2.—Infra-red spectra of $UO_2(TTA)_2$·TBP and $Th(TTA)_4$·TBP–KBr disks.

---

(18) L. J. BELLAMY and R. F. BRANCH, *J. Chem. Soc.* 4491 (1954).

The $\geq$C–O— enolic bond in the complexes is probably located at about 1310 cm^{-1} in agreement with the values found for this vibration in the Cu(II), Co(II), Zn(II) chelates of TTA.(18) The absorption at 1540 cm^{-1} was rather constant from complex to complex, and has been attributed to the C = C vibration.(19) A tabulation of these frequencies appears in Table 3.

(B) TTA-*organophosphorus metallic complexes.* In the spectra of the TTA-organophosphorus metallic complexes, the region at 1600 cm^{-1} showed two peaks, independent of the metal (Figs. 2–4 and Table 4). One peak was at the same position as that found in the TTA–metallic complexes, and the second was located at a higher frequency. The ratio of intensity of the higher frequency peak to the lower frequency peak for the complexes M/TTA/S appeared to increase from Th(IV) to UO_2(II). In the complexes M/TTA/2S this ratio is greater for Sc(III) than for Nd(III) (Table 5). In addition, the position of the higher frequency increased as one goes from UO_2(II) through Sc(III) and Nd(III) to Th(IV) complexes. The second peak at the higher frequency appeared in the spectra upon the first addition of neutral organophosphorus compound.

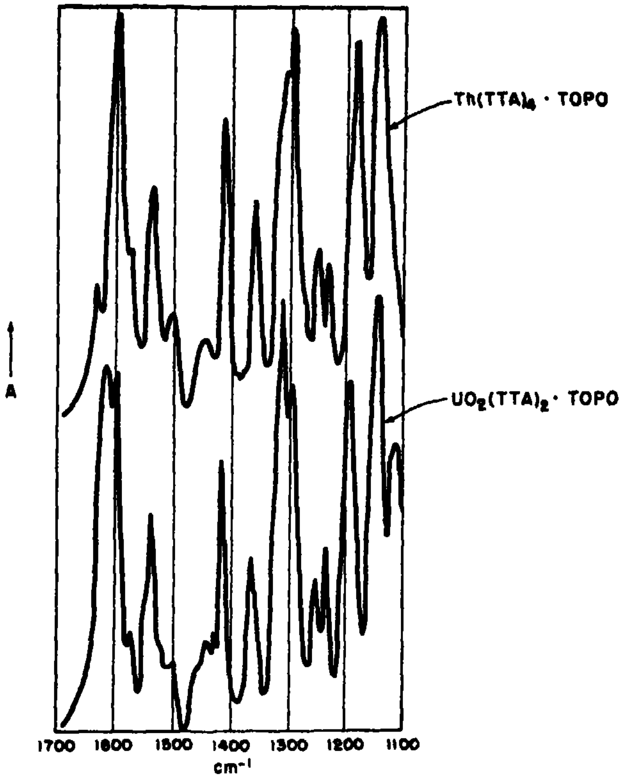

FIG. 3.—*Infra-red spectra of Th(TTA)·TOPO and $UO_2(TTA)_2$·TOPO–KBr disks.*

The P $\rightharpoonup$ O stretching frequency was displaced toward lower frequency in all of the complexes. The shift appeared to be small in the case of TOPO. For the other neutral organophosphorus ligands, this shift appeared to be normal for a P $\rightharpoonup$ O . . . M type of link. Table 6 lists the P → O frequencies found for these complexes, and gives the shift from the P → O frequency observed in the unbonded organophosphorus ligands.

---

(19) J. LECOMTE, *Dis. Faraday Soc.* 9, 125 (1950).

In all of these complexes, the 3500 cm^{-1} region was free of absorption as were the regions of the bonded P—[OH] vibration at about 2700, 2300 cm^{-1}. The =C—H absorption in the complex ring was very weak, and was seldom seen. Whenever it was observed, it appeared at 3070 cm^{-1}.

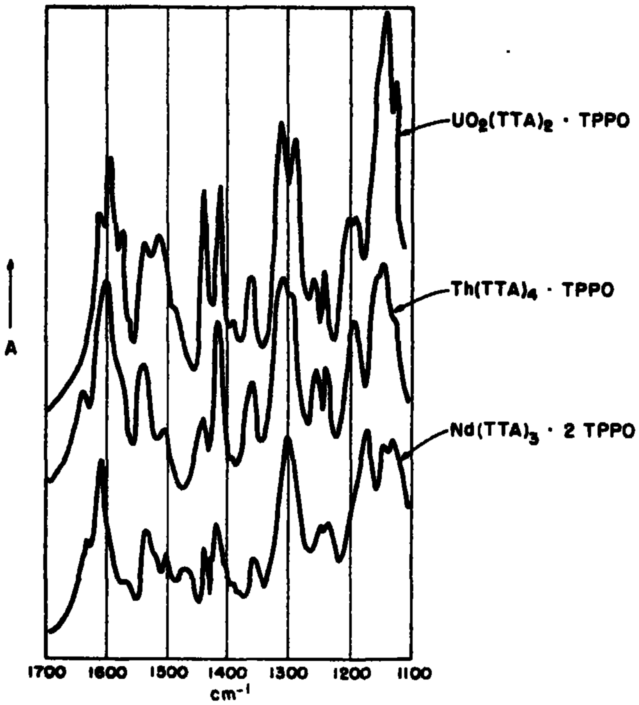

FIG. 4.—Infra-red spectra of $UO_2(TTA)_2$·TPPO, $Th(TTA)_4$·TPPO, and $Nd(TTA)_3$·2TPPO–KBr disks.

TABLE 5.—RATIO OF ABSORBANCES $A_{C=O}/A_{C=O \ldots M}$ FOR VARIOUS TTA–ORGANOPHOSPHORUS–METALLIC COMPLEXES

Complex	A_r*
$UO_2(TTA)_2$TBP	1·0
$UO_2(TTA)_2$·TOPO	1·1
$UO_2(TTA)_2$·3TOPO	1·0
$UO_2(TTA)_2$·TPPO	0·85
$Sc(TTA)_3$·2TBP	0·74
$Sc(TTA)_3$·2TOPO	0·87
$Sc(TTA)_3$·2TPPO	0·76
$Nd(TTA)_3$·2TOPO	0·58
$Nd(TTA)_3$·2TPPO	0·80
$Th(TTA)_4$·TBP	0·74
$Th(TTA)_4$·TOPO	0·40
$Th(TTA)_4$·TPPO	0·77

* A_r = Absorbance (C=O)/Absorbance (C=O . . . M)

In Fig. 5, a comparison of the spectra of NaTTA and $Th(TTA)_4$ and $Th(TTA)_4{\cdot}TBP$ is given.

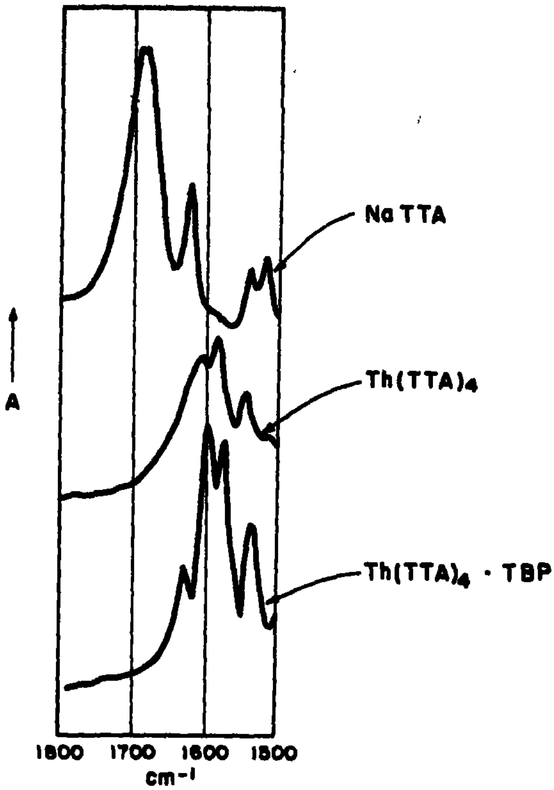

Fig. 5.—Comparison of spectra of TTA ion in NaTTA with the co-ordinated TTA in complexes with thorium (KBr disks).

Table 6.—Phosphoryl frequencies in the TTA-organophosphorus-metallic complexes (cm^{-1})

	$\nu P \rightarrow O$	Shift*
TBP	1285, 1269	—
TOPO	1152	—
TPPO	1195	—
$UO_2(TTA)_2{\cdot}TBP$	1212	−73, −57
$Th(TTA)_4{\cdot}TBP$	1200	−85, −69
$Sc(TTA)_3{\cdot}2TBP$	1192	−93, −77
$UO_2(TTA)_2{\cdot}TOPO$	1145	−7
$UO_2(TTA)_2{\cdot}3TOPO$	1145	−7
$Th(TTA)_4{\cdot}TOPO$	1145	−7
$Sc(TTA)_3{\cdot}2TOPO$	1145	−7
$Nd(TTA)_3{\cdot}2TOPO$	1140	−12
$UO_2(TTA)_2{\cdot}TPPO$	1142, 1152 (*sh*)	−53, −43
$Th(TTA)_4{\cdot}TPPO$	1158	−37
$Sc(TTA)_3{\cdot}2TPPO$	1150	−45
$Nd(TTA)_3{\cdot}2TPPO$	1172	−23

* Defined as the $\nu_{P \rightarrow O}$ in complex $-\nu_{P \rightarrow O}$ in unbonded ligand.

(C) HTTA–TBP *and* HTTA–TBP–D_2O *systems.* In the anhydrous system HTTA–TBP, the addition of increasing amounts of TBP (up to 18 × HTTA concentration) to a fixed concentration of HTTA showed a shift of the infrared absorption peak ($\nu_{C=O}$) from 1600 cm^{-1} in pure HTTA to 1650 cm^{-1}. The TBP peaks ($\nu_{P\rightarrow O}$ at ~1285, 1269 cm^{-1} became a single strong peak at 1280 cm^{-1}.

In the system of HTTA – TBP contacted with D_2O, increasing amounts of TBP up to 5·5 × HTTA concentration) added to a fixed concentration of HTTA showed a shift of the peak at 1600 cm^{-1} to 1650 cm^{-1}. With further increases (up to 18 × HTTA concentration), there appeared to be a shift back toward 1600 cm^{-1} and a shift of the $\nu_{P\rightarrow O}$ in TBP to a strong peak at 1270 cm^{-1} with a shoulder at 1285 cm^{-1}.

In both the anhydrous and D_2O experiments, large excesses of TBP were necessary to show the interaction with HTTA. The solvent used in these experiments was n-hexane (Matheson, Coleman and Bell Co.).

(D) $UO_2(TTA)_2$–TOPO *system.* As illustrated in Figs. 1 and 3, the addition of one mole of TOPO to one mole of $UO_2(TTA)_2$ produced two peaks in the 1600 cm^{-1} region of about equal intensity. The $_{P\rightarrow}\nu_O$ absorption showed a shift from 1152 cm^{-1} to 1145 cm^{-1}. With the addition of two and three moles of TOPO, the intensity of the higher frequency band in the 1600 cm^{-1} region increased slightly as did the peak at 1145 cm^{-1}. When 4–5 moles of TOPO were added, no change in the 1600 cm^{-1} region was noted, but the main peak in the $\nu_{P\rightarrow O}$ region shifted to 1152 cm^{-1} with a shoulder at 1145 cm^{-1}.

Use of TEHPO produced only $UO_2(TTA)_2$·TEHPO. From infra-red data, no evidence for a $UO_2(TTA)_2$·3 TEHPO could be found.

(E) $UO_2(TTA)_2$–TBP, $Th(TTA)_4$–TBP *and* $UO_2(TTA)_2$–TBP–D_2O *and* $Th(TTA)_4$ –TBP–D_2O *systems.* The addition of dry TBP to solid $UO_2(TTA)_2$ gave a spectrum (in the 1600 cm^{-1} region) very similar to that obtained for solid $UO_2(TTA)_2$·TBP. Two equally intense peaks were obtained at 1622 and 1595 cm^{-1}. However, when the solution of $UO_2(TTA)_2$ in TBP was contacted with D_2O, significant changes occurred in the spectrum as the TBP concentration increased. For a 0·10 M solution of $UO_2(TTA)_2$ in TBP, the normal double peak was obtained in the 1600 cm^{-1} region, but as the solution became more dilute in $UO_2(TTA)_2$ the peak at higher frequency began to diminish, and at a 0·003 M solution was present only as a very weak shoulder to the main peak at about 1595 cm^{-1}. There appeared to be a shift to the $UO_2(TTA)_2$ spectrum in the wet solutions, as an excess of TBP was added, versus a $UO_2(TTA)_2$·TBP spectrum in a dry excess of TBP.

Similar results were obtained when the $Th(TTA)_4$ was dissolved in excess TBP both dry and wet.

Deuterium oxide was used rather than water in the wet solution to prevent the complication of the bending mode of vibration in water from interfering with the $\nu_{C=O}$ frequency in the complexes in the region 1600–1650 cm^{-1}.

DISCUSSION

From the infra-red studies, it was observed that the reaction of neutral organophosphorus compounds with TTA–metal complexes to form TTA/S/metal complexes resulted in the splitting of the single peak present in the 1600 cm^{-1} region into two peaks. This splitting is observed not only in the crystal spectra but in the solution spectra, and therefore cannot be entirely due to any crystal effects. One peak was found at higher frequency, and its position varied with the metal. This would indicate the presence of some unco-ordinated (free) TTA carbonyl. The second peak was found approximately at its original position, thus indicating that in the M–TTA–S complexes part of the TTA is still bonded as in the simple TTA compounds.

These results seem to eliminate for the TTA/S/metal compounds, a structure involving only bidentate TTA. The possibility that the structure may be one involving some of the TTA in the ionic form can also be dismissed since the spectrum of ionic NaTTA is entirely different in the region of 1600–1700 cm^{-1} (see Fig. 5) from the spectra of these complexes. A third possible structure involving the solvation of the basic organophosphorus compound, through hydrogen bonding at the ring =CH position, was also dismissed, as this structure would in no way account for the splitting of absorption in the 1600 cm^{-1} region, and in addition P–[OH] vibrations were absent. A fourth possible structure appears to explain most of the experimental data more satisfactorily. This is a structure containing TTA both as a monodentate and bidentate ligand in the complex. Thus UO$_2$(TTA)$_2$·TOPO and UO$_2$(TTA)$_2$·3TOPO could have structures 1 and 2 with co-ordination numbers of 6 and 8, respectively.

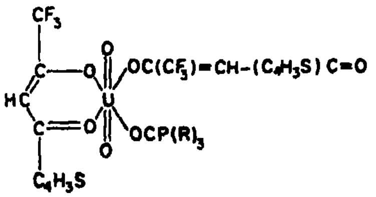

UO$_2$(TTA)$_2$ R$_3$P→O

(1)

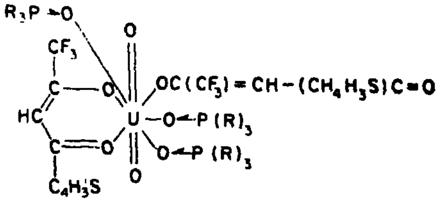

UO$_2$(TTA)$_2$·3R$_3$P→O

(2)

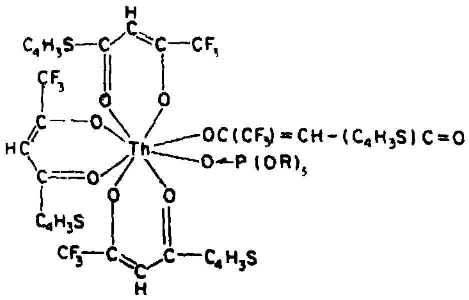

Th(TTA)$_4$·(RO)$_3$P→O

(3)

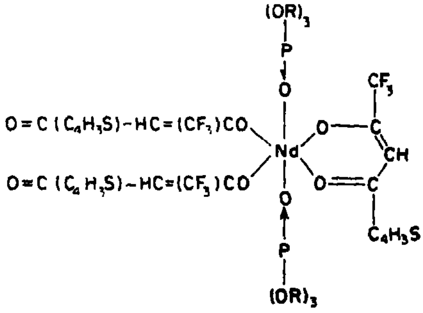
(OR)$_3$
P
O
O=C(C$_4$H$_3$S)-HC=(CF$_3$)CO
O=C(C$_4$H$_3$S)-HC=(CF$_3$)CO
Nd
CF$_3$
CH
C$_4$H$_3$S
P
(OR)$_3$

Nd(TTA)$_3$·2(RO)$_3$P→O

(4)

For the thorium complexes, structure (3) would have a co-ordination number of 8. For the neodymium complexes, structure (4) would have a co-ordination number of 6. These structures account for the observed splitting in the 1600 cm^{-1} region as well as for the lack of absorption due to water and P–[OH], and for the shifting of P → O vibration toward lower frequency.

A postulated structure of this type involves even co-ordination numbers. If a structure involving only monodentate TTA were considered in the complex UO$_2$(TTA)$_2$·3TOPO, then hepta-co-ordination would have to be invoked, such as postulated by SACCONI(20) for $UO_2(AA)_2 \cdot NH_3$. In the case of $UO_2(TTA)_2 \cdot TOPO$, $Th(TTA)_4 \cdot TBP$ or $Nd(TTA)_3 \cdot 2TPPO$, again odd co-ordination would have to be postulated (e.g. 5). In all cases, therefore co-ordinative saturation would not be reached and a molecule of water could co-ordinate. Such species would be very hard to visualize as causing a synergistic effect, since they would probably be less organic soluble than the anhydrous materials. Besides, infra-red and Karl Fisher data point to the fact that only anhydrous species are involved.

It is important to emphasize that these results were obtained with complexes isolated from the organic phase. It is quite possible that in solution, additional species may be involved. In addition, since the infra-red method is only indicative, these complexes should be studied by other physical methods, such as X-ray. Recently an X-ray study(21) of the compound $Th(AA)_4$ indicated that the AA was chelated to thorium. Such X-ray studies might help in determining if the structure of these complexes involves monodentate and/or bidentate TTA.

(20) L. SACCONI and G. GIANNONI, *J. Chem. Soc.* 2368 (1954).
(21) D. GRDENIĆ and B. MATKOVIĆ, *Nature, Lond.* **182**, 465 (1958).

J. Inorg. Nucl. Chem., 1962, Vol. 24, pp. 1475 to 1483. Pergamon Press Ltd. Printed in England

NOTES

The ammono-deliquescence of lithium metal

(*Received* 19 *February* 1962; *in revised form* 8 *March* 1962)

LITHIUM, in contrast to the other common alkali metals, is capable of forming solutions with ammonia through exposure of the metal to dry ammonia gas at ambient conditions of temperature and pressure. This liquefaction phenomenon is interpreted in terms of a general treatment of deliquescence based on the inequality of chemical potential of the solvent component in the gaseous phase and in the saturated solution phase. Thus, lithium metal manifests ammono-deliquescence.

The customary definition of "deliquescence" applies to the absorption of water-vapour by a solid from its surrounding gaseous environment to yield a saturated aqueous solution of the solid(1). It should be pointed out, however, that such solution formation can occur in any system where an imbalance in chemical potential exists between the solvent component in the vapour phase and that volatile component in the solution phase. As a practical consequence, then, for solvent absorption from the vapour phase, the saturated solution must have a partial pressure of the volatile component less than the partial pressure of that component in the atmosphere. Thus, in this more general sense AUDRIETH and KLEINBERG(2) have applied the term "ammono-deliquescence" to the liquefaction behaviour observed in the ammonia solvent system. The salts lithium nitrate, ammonium nitrate, and ammonium thiocyanate tend to go into solution when exposed to ammonia gas near ambient temperature and pressure(3, 4, 5). Accordingly, it is of interest to report that lithium metal itself, quite in contrast to the other common alkali metals, manifests ammono-deliquescence through simple exposure of the metal to an atmosphere of ammonia gas at ambient conditions. The dissolution of the alkali metals in liquid ammonia at its boiling point (−33°) or under elevated pressures at higher temperatures is, of course, well-established.

The ammono-deliquescence of lithium metal can be readily demonstrated by passing a stream of anhydrous ammonia gas over the surface of the metal at room temperature and pressure. After a short period of time, bronze, opaque droplets form and then coalesce. The colour of the solution is characteristic of the high metal concentration in the solvent(6). The solution process for lithium is exothermic(7, 8, 9) and an appreciable temperature rise can be noted in the system.

The physicochemical basis for the absorption of gaseous ammonia by lithium metal may be seen from inspection of the vapour pressure-temperature curves for saturated solutions of various of the alkali metals in liquid ammonia (Fig.1). Clearly, the lithium-containing solutions show the lowest equilibrium vapour-pressures of ammonia within the temperature ranges covered; thus, at 20°, the vapour pressure of ammonia above a saturated solution of

(1) M. M. MARKOWITZ and D. A. BORYTA, *J. Chem. Engng. Data*, **6**, 16 (1961).

(2) L. F. AUDRIETH and J. KLEINBERG, *Non-aqueous Solvents*, p.45. J.Wiley, New York (1953).

(3) R. O. E. DAVIS, L. B. OLMSTEAD and F. O. LUNDSTROM, *J. Amer. Chem. Soc.* **43**, 1575 (1921).

(4) H. HUNT, *J. Amer. Chem. Soc.* **54**, 3509 (1932).

(5) H. HUNT and L. BONCYK, *J. Amer. Chem. Soc.* **55**, 3528 (1933).

(6) W. L. JOLLY, in *Progress in Inorganic Chemistry*, Vol. 1 (Edited by F. A. COTTON), pp. 235–281. Interscience, New York (1959).

(7) C. A. KRAUS and F. C. SCHMIDT, *J. Amer. Chem. Soc.* **56**, 2297 (1934).

(8) F. C. SCHMIDT, F. J. STUDER and J. SOTTYSIAK, *J. Amer. Chem. Soc.* **60**, 2780 (1938).

(9) L. V. COULTER and L. MONCHICK, *J. Amer. Chem. Soc.* **73**, 5867 (1951).

lithium is only 97 mm Hg(10–14), whereas the corresponding sodium (vapour-pressure, 3544 mm Hg(14)), and potassium (vapour-pressure, 1584 mm Hg(14–15) solutions possess vapour-pressures considerably above atmospheric. The vapour-pressure of pure liquid ammonia at 20° is 6428 mm Hg(16). For any partial pressure of ammonia in the atmosphere above an alkali metal greater than the equilibrium vapour-pressure characteristic of the particular metal–ammonia saturated solution, the potential for solution formation will be present. Thus, lithium metal easily manifests ammono-deliquescence at room temperature and relatively low pressures of ammonia.

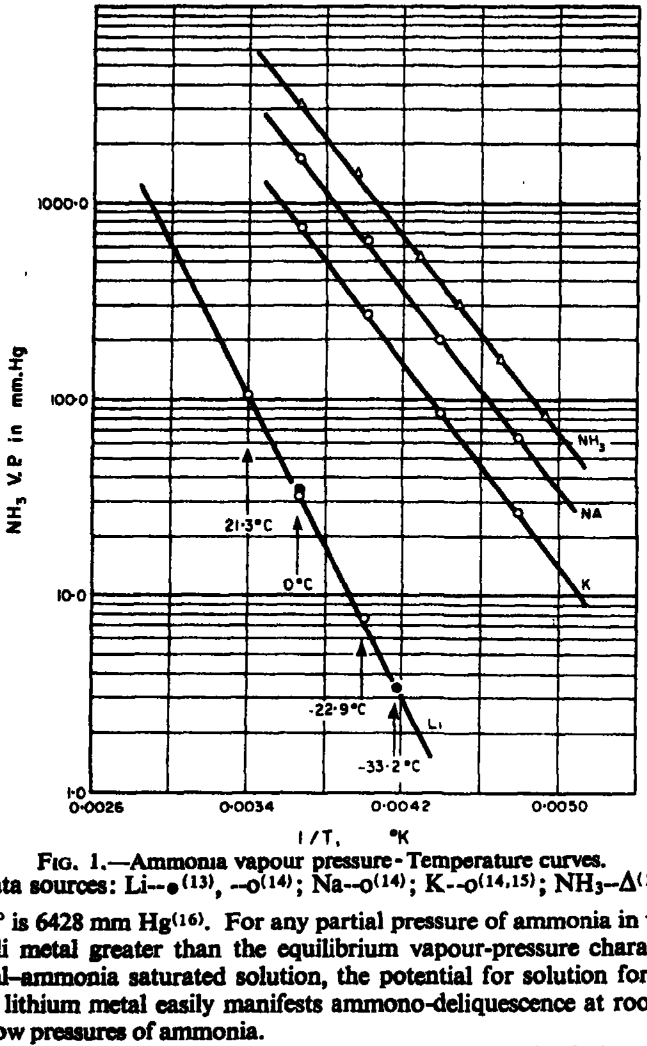

FIG. 1.—Ammonia vapour pressure-Temperature curves.
Data sources: Li--●(13), --o(14); Na--o(14); K--o(14,15); NH_3--Δ(16).

Application of the Clapeyron-Clausius equation to the metal solution curves of Fig. 1 gives the following equations for the vapour-pressures (p, in mm Hg) of these saturated solutions:

$$\text{Li-NH}_3\text{: } \log p = -1894{\cdot}2/T + 8{\cdot}4486$$
$$\text{Na-NH}_3\text{: } \log p = -1280{\cdot}5/T + 7{\cdot}9166$$
$$\text{K-NH}_3\text{: } \log p = -1300{\cdot}3/T + 7{\cdot}6347$$

(10) C. A. KRAUS, *J. Amer. Chem. Soc.* **30**, 651 (1908).

(11) O. RUFF and J. ZEDNER, *Ber. Dtsch. Chem. Ges.* **41**, 1948 (1908).

(12) C. A. KRAUS and W. C. JOHNSON, *J. Amer. Chem. Soc.* **47**, 725 (1925).

(13) W. C. JOHNSON and M. M. PISKUR, *J. Phys. Chem.* **37**, 93 (1933).

(14) P. R. MARSHALL and H. HUNT, *J. Phys. Chem.* **60**, 732 (1933).

(15) W. C. JOHNSON and A. W. MEYER, *J. Phys. Chem.* **33**, 1922 (1929).

(16) W. W[illegible]BURN (Editor), *International Critical Tables*, Vol. 3, p. 234. McGraw-Hill New [illegible]rk (1929).

From the above equations, the temperatures corresponding to a solution vapour-pressure of 760 mm Hg (i.e., the normal boiling point) may be computed for each of these systems. The calculations yield the values of +67·0°, −18·9°, and +0·3° for the saturated solutions of lithium, sodium and potassium, respectively, in liquid ammonia. Experimental determinations of the boiling points for these solutions at 760 mm Hg have been reported by Ruff and Zedner(11) to be +63° (lithium), −19·4° (sodium), and −0·2° (potassium).

Meyer M. Markowitz

Foote Mineral Company
Research and Engineering Centre
Route 100
Exton, Pennsylvania

The solubilities of alkali metal iodides in ethanol

Received 12 *February* 1962)

Several tables of physical constants of inorganic compounds quote high and conflicting figures for the solubility of potassium iodide in ethanol. Examples, at 20°C, are 4 g(1) and 14·3 g(2) solute per 100 g solvent, and 14·3 g(3) solute per 100 ml solvent. The figures for 25°C quoted in the chemical journals are much lower, e.g., 2·16 g(4) and 1·88 g(5) solute per 100 g solvent, and 1·92 g(6) solute per 100 g solution. Due to this very wide disparity between the highest and lowest figures, the solubility of potassium iodide in absolute ethanol has been redetermined and figures for 20°C and 25°C are reported in this communication. The solubilities of rubidium iodide and caesium iodide in ethanol at the same temperatures are also reported.

EXPERIMENTAL

The solubility measurements were carried out in absolute ethanol, for which $d_4^{25} = 0·78501$. This was prepared by distilling the 95 per cent alcohol after standing for several days over freshly burnt quicklime.

Saturated solutions of the iodides were obtained by agitation of the salt-ethanol mixture in a glass-stoppered flask immersed in a water thermostat at the required temperature. Samples of the saturated solution were removed into a previously weighed weighing bottle and the weight of the salt determined after removal of the solvent from the weighed sample.

Many of the dried samples were checked for complete removal of the solvent by estimation of the iodide with potassium iodate by the Andrews procedure using a high concentration of hydrocholric acid and carbon tetrachloride. The titration figures agreed with the weight of dried salt in each case.

The following results were obtained:—

Salt	Potassium	iodide	Rubidium	iodide	Caesium	iodide
Temperature (°C)	20	25	20	25	20	25
Solubility (g per 100 g EtOH)	1·75	1·90	0·95	0·98	0·290	0·331

DISCUSSION

The figure of 1·90 g per 100 g ethanol for the solubility of potassium iodide at 25°C is in agreement with that of 1·88 g found by Larson and Hunt(5). Solubilities greater than 2 g potassium iodide per 100 parts of ethanol (quoted above) have probably been determined in the presence of a trace, and probably more, of moisture. In fact preliminary determinations during the course of the present investigation gave a figure for the solubility of 2.12 g potassium iodide per 100 g ethanol, when the system was exposed to the atmosphere during saturation. Due to this sensitivity towards traces of moisture, Larson and Hunt(5) took stern measures to exclude all traces by carrying out all operations, including sampling, in a closed system.

The decreasing solubility, in ethanol, with increasing cation size, from 251 g per 100 g for lithium iodide(4) and 43·3 g per 100 g for sodium iodide (5) to 0·331 g per 100 g for caesium iodide, all at 25°C, is in contrast to minimal solubilities often observed for alkali metal halides when water is the solvent. This type of pattern has been explained for aqueous solutions (7, 8) and the similar explanation in this case is that there is possibly a decrease in solvation energy with increasing cation size in contrast to little change in lattice energy. The high solubility of lithium iodide is probably partly explained by polarization. Other factors such as the size of the solvent ethanol molecule preventing its entry between the ions in the crystal lattice, also probably contribute towards the observed trend.

(1) N. A. Lange (Ed.), *Handbook of Chemistry*, 6th Edition. Handbook Publishers Inc. (1946).
(2) J. H. Perry (Ed.), *Chemical Engineering Handbook*, 2nd Edition. McGraw Hill, New York (1941).
(3) C. D. Hodgman (Ed), *Handbook of Chemistry and Physics*, 41st Edition. Chemical Rubber Publishing Co. (1959).
(4) W. E. S. Turner and C. C. Bissett, *J. Chem. Soc.* 1904 (1913).
(5) R. G. Larson and H. Hunt, *J. Phys. Chem.* 43, 417 (1939).
(6) P. T. Walden, *Z. Phys. Chem.* 55, 712 (1906).
(7) L. Brewer, *J. Chem. Educ.* 36, 446 (1959).
(8) M. F. C. Ladd and W. H. Lee, *Trans. Faraday Soc.* 54, 34 (1958).

Department of Chemistry and Biology
Welsh College of Advanced Technology
Cathays Park, Cardiff

J. D. R. Thomas

A cryoscopic study in ethylenediamine

(*Received* 22 *February* 1962; *in revised form* 2 *April* 1962)

In connexion with equilibrium studies in ethylenediamine (EDA),(1, 2) it became necessary to determine the state of aggregation of several acids and salts. EDA has a very convenient melting point ~ 11 °C(3), and it was decided to use cryoscopy to obtain the necessary data. A literature search failed to reveal any previous cryoscopic study in this solvent. Preliminary attempts to obtain useable temperature-time cooling curves were unsuccessful. EDA supercools readily, and on freezing large crystals form which adhere to the cryoscopic cell wall. EDA continues to separate on this adherent coating, forming a hollow shell of frozen solvent rather than separating as individual crystals which can be suspended in the solution by agitation. The net result of this type of crystallization is a cooling curve which shows rapid temperature fluctuations, probably as a result of local temperature gradients in the solution. In addition, even brief exposure of the EDA solution to the atmosphere resulted in significant decrease in freezing point. The cell design shown in Fig. 1 proved to be a satisfactory solution to these problems. The temperature sensitive device was a Veco Type 32A83 thermistor in a conventional equal-arm Wheatstone bridge. Using a 1·000 V bridge supply and a 1·00 mV, variable zero, potentiometric recorder, a sensitivity of 3×10^{-4}°C was attainable. The gas-tight construction of the cryoscopic cell allowed indefinite storage of solutions without a detectable change in freezing point. All solutions were saturated with dry nitrogen by introducing a gas bubbler through joint C of Fig. 1. The gas bubbler was then removed and replaced by the assembly shown in joint C of Fig. 1. This assembly consisted of an outer TS 12/18 joint sealed to a short stem of glass tubing of an inside diameter to just pass another glass tube which had a short piece of platinum wire sealed into the bottom. A sleeve of polyethylene tubing allowed the platinum wire to be adjusted in height without exposing the cell contents to the atmosphere. A large paddle type stirrer entered the cell through a water-jacketed glass bearing and was rotated at ~900 rev/min. A cooling curve was obtained by placing the cell

---

([illegible]) S. Bruckenstein and L. M. Mukherjee, *J. Phys. Chem.* 64, 1601 (1960).
(2) L. M. Mukherjee. Ph.D. Thesis, University of Minnesota (1961).
(3) L. Audriath and J. Kleinberg, *Non-aqueous Solvents*, p.119. J.Wiley, New York (1953).

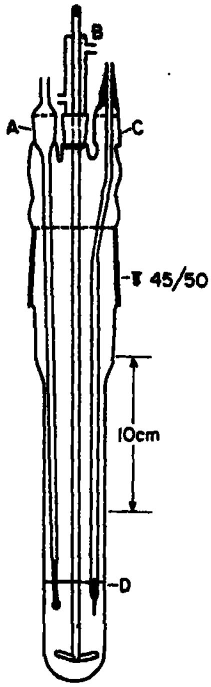

FIG. 1. Freezing Point Cell. A. Ŧ 20/40 joint with Veco Type 32A83 thermistor shown in position; B. Ŧ 20/40 joint with Labglass watercooled, precision ground sleeve bearing stirrer shown in position; C, Ŧ 12/18 joint. Inlet port for nitrogen bubbler (not shown) and platinum (0·010 wire) cold finger (shown in position): D. liquid level. Cell contents 50 ml.

in a water bath held at 9 ±0·02°C. Powdered solid carbon dioxide was dropped inside the tube with the platinum wire, and the wire submerged in the EDA solution as the anticipated freezing point was approached. Crystals of solvent formed on the platinum wire and were distributed through the solution by the vigorous stirring. These crystals greatly reduced supercooling and minimized the tendency of the solvent to solidify as an adherent layer on the cell walls. More than half the cooling curves obtained were satisfactory. On random occasions poor cooling curves were still obtained. In all cases each solution was reexamined until three satisfactory cooling curves were obtained. The average of the three determinations usually agreed to ±0·0015°C.

The thermistor was calibrated by evaluating the constant, B, in the equation $\ln R_{T1}/R_{T2} = B(1/T_1 - 1/T_2)$ from the measured resistances at the melting points of ice and of very pure acetic acid.⁽⁴⁾ This calibration yielded a calculated sensitivity of 0·0954°C/mV of unbalance bridge potential at 10·6° compared to the experimental value of 0·0952°C/mV over the range 9·3–12°C.

The solvent handling techniques and the reagents used have been described elsewhere.(1, 2)

The freezing point of pure ethylenediamine was determined to be 11·3°C, as compared to the previously reported value of 11·0°C.(3)

The molal freezing point depression constant, $K_f°$, was determined using benzene and naphthalene as standards. Using benzene, six solutions in the concentration range 0·05–0·33 molal were studied, yielding $K_f° = 2{\cdot}43 \pm 0{\cdot}04$°C/mole/kg. Three naphthalene solutions, 0·04–0·11 molal, yielded $K_f° = 2{\cdot}44 \pm 0{\cdot}01$°C/mole/kg. The mean value obtained giving equal weight to each individual measurement is 2·43 ±0·02°C/mole/kg. The latent heat of fusion of EDA is calculated to be 64·5 ±0·6 cal/g at 11·3°C, as compared to a calorimetrically determined value of 77 cal/g at 0°C.

(4) K. HESS and H. HUBER, *Ber. Dtsch. Ges.* **70**, 2205 (1937).

Earlier potentiometric studies of silver cyanide(1) were interpreted in terms of the reaction:

$$2AgCN \rightleftharpoons Ag^+ + AgCN_2^-$$

assuming the silver cyanide was nearly completely present in the form of the undissociated monomer. Cryoscopic studies of silver cyanide in the concentration range 0·018–0·16 molal verified that this compound exists quantitatively as undissociated AgCN. (By quantitatively, we mean the molality found cryoscopically was indistinguishable from the analytical concentration within the experimental error.)

Solutions of silver, potassium and sodium iodide were also studied in the concentration range of ~0·02–0·1 *M* and found to be present quantitatively as undissociated monomers.

Silver bromide and chloride, and phenylacetic and acetic acids are not measurably dissociated in EDA in the concentration range of ~0·01–0·09 *M*.

Silver nitrate is measurably dissociated in EDA. The results obtained are given in Table I, m_s is the analytical concentration and Σm the molality calculated from the freezing point depression. The third column lists the value of the dissociation constant of silver nitrate calculated from the freezing point data assuming ideal behavior; i.e., from the expression $K_{AgNO_3} = [(\Sigma m - m_s)]^2/[\Sigma m - 2(\Sigma m - m_s)]$. An estimate of the thermodynamic dissociation constant requires that some relation for the activity coefficient of ions and the ionic strength ($\mu = [Ag^+]$) be assumed. SCHAAP *et al.*(6) have suggested that the Marshall-Grunwald equation would be applicable to EDA solutions. The fourth column in Table 1 gives calculated values of the dissociation constant of silver nitrate ($K_{AgNO_3\,M,G}$) using the latter relation to estimate the single ion activity coefficients. The mean value of (K_{AgNO_3}) equals $3{\cdot}8 \pm 0{\cdot}2 \times 10^{-4}$.

TABLE 1.—CRYOSCOPIC DATA FOR $AgNO_3$ IN EDA

m_s	Σm	K_{AgNO_3}	$(K_{AgNO_3})_{M,G}$
0·0158	0·0230	$(6{\cdot}0 \times 10^{-3})$	$(1{\cdot}2 \times 10^{-4})$
0·0359	0·0441	$2{\cdot}4 \times 10^{-3}$	$4{\cdot}2 \times 10^{-4}$
0·0561	0·0670	$2{\cdot}6 \times 10^{-3}$	$3{\cdot}9 \times 10^{-4}$
0·0809	0·0938	$2{\cdot}5 \times 10^{-3}$	$3{\cdot}4 \times 10^{-4}$
0·1129	0·1305	$3{\cdot}3 \times 10^{-3}$	$3{\cdot}8 \times 10^{-4}$

Mean value $K_{AgNO_3} = 2{\cdot}7 \pm 0{\cdot}5 \times 10^{-3}$
" " $(K_{AgNO_3})_{M,G} = 3{\cdot}8 \pm 0{\cdot}2 \times 10^{-4}$

The dissociation constant of silver nitrate was estimated to be $\sim 6 \times 10^{-4}$ in our previous potentiometric study(1) and $5{\cdot}75 \times 10^{-4}$ by HIBBARD and SCHMIDT(7) using the Fuoss-Kraus method. SIEFKER(8) obtained similar values using a combination of potentiometric and conductometric data.

Finally, an attempt was made to demonstrate the existence of KI·AgI and NaI·AgI by studying mixtures of the alkali and silver iodides. The latter two species have been postulated to interpret data obtained using a silver indicator electrode.(1) As is shown in Table 2, the total molality as found cryoscopically is substantially lower than the sum of the analytical concentrations of the silver and alkali halide.

---

(5) H. HIEBER and A. WOERNER, *Z. Elektrochem.* **40**, 252 (1934).

(6) W. B. SCHAAP, R. E. BAYER, J. R. SIEFKER, J. K. KIM, P. W. BREWSTER and F. C. SCHMIDT, Record of Chemical Progress, **22**, 197 (1961).

(7) B. B. HIBBARD and F. C. SCHMIDT, *J. Amer. Chem. Soc.* **77**, 225 (1955).

(8) J. R. SIEFKER. Ph.D. Thesis, Indiana University (1960).

TABLE 2.—CRYOSCOPIC DATA FOR AgI·KI AND AgI·NaI SOLUTIONS

MI	m_s, MI[(a)]	m_s, AgI[(a)]	Σm[(b)]	$K_{MI.AgI}$
Potassium iodide	0·1127	0·1138	0·2050	2·6
Sodium iodide	0·0803	0·1271	0·1880	3·0

(a) m_s is molal analytical concentration of species indicated by subscript.
(b) Σm is total molal concentration calculated by freezing point depression.

Assuming ideal behavior, the formation constant, $K_{MI.AgI} = [MI \cdot AgI]/[MI][AgI] = [(m_s)_{MI} + (m_s)_{AgI}][\Sigma m - (m_s)_{AgI}] - (m_{AgI}][\Sigma m - (m_s)_{MI}]$, was calculated from the data in Table 2. The results obtained are in fair agreement with the previously obtained values of $K_{KI \cdot AgI} = 1 \cdot 1$ and $K_{NaI \cdot AgI} = 1 \cdot 3$.(1)

Acknowledgment.—This work was sponsored by the Office of Ordinance Research.

L. D. PETTIT*
STANLEY BRUCKENSTEIN

School of Chemistry
University of Minnesota
Minneapolis 14, *Minn.*

* Present address: Department of Inorganic and Structural Chemistry, The University, Leeds.

BOOK REVIEWS

H. H. SISLER: **Chemistry in Non-Aqueous Solvents** vii + 119 pp. Reinhold, New York, 1916. $1.95

THIS monograph appears to be intended for the undergraduate interested in chemistry rather than either the specialist or educated layman. To this end, the author steers a course between dull scholarship and a Sunday supplement popular science approach and,' on the whole, is successful. Current ideas in the chemistry of non-aqueous solutions are given with adequate examples.

The classical approach to non-aqueous chemistry in terms of water analogs is illustrated by liquid ammonia. The section on sulphuric acid emphasizes the more recent work of R. J. GILLESPIE and his colleagues, but fits neatly into acid-base concepts involving proton transfer. The other solvents selected for individual attention are sulphur dioxide and nitrogen dioxide a choice which permits exploration of the range of usefulness and the limitations of the solvent-system ionization concept.

The book, however, has some flaws which may reduce its value for the teacher and the serious student. It is not completely authoritative; for instance, the data given in the various tables are not provided with references, and many of the constants may be out-of-date. The observant reader, for example, will have difficulty in reconciling the ion product constant for liquid ammonia described as being in the neighborhood of 10^{-33}, with a specific conductance greater than 10^{-7} ohm^{-1}. Experimenters (V. F. HNIZDA, C. A. KRAUS, *J. Amer. Chem. Soc.* **71**, 1565–75 1949). have obtained liquid ammonia with a specific electrical conductivity below 10^{-10} ohm $^{-1}$cm^{-1}. It is likely that the pure liquid is even less conducting and that the ion product estimate of PLESKOV which SISLER quotes is a realistic estimate.

Similarly, the electrical conductivity of sulphur dioxide is undoubtedly much lower than the value given in the text and self ionization does not take place to anything like the extent that JANDER believed at the time of his early research. Perhaps the most serious deficiency in this volume is an inadequate treatment of the experimental problems associated with research with non-aqueous solvents. This gives a spurious air of authenticity both to the numbers in the tables and to the ideas expressed. The latter do represent a reasonable consensus of current opinion, which however will be continuously modified, at least in emphasis, as improved experimental procedures are developed, and as a number of additional solvents are investigated in detail.

The failure to suggest to the reader that the accumulation of data and the evolution of ideas are still under way is a serious pedagogical error that all working scientists should deplore.

This series nevertheless represents a pioneering effort which ought to be encouraged. The present volume is readable and recommended for the undergraduate or bright high school senior interested in going a little beyond his general chemistry text.

H. H. HYMAN

Plutonium 1961 Edited by E. GRISON, W. B. H. LORD and R. D. FOWLER. Proceedings of the Second International Conference on Plutonium Metallurgy, Grenoble, France. 19-22 April 1960. xvii 804 pp. Cleaver-Hulme, London, 1961. 189 S.

THE second conference on Atomic Energy, held at Geneva in 1958, was notable for the first release of real information on plutonium. As a result, two further conferences have been held, of which this book represents the proceedings of the second. The information now presented is wider in scope, and presents a balanced picture up to 1960.

Four separate sessions were held at the conference, dividing the subject under the headings of physical properties, alloys, ceramics, and nuclear fuels. The discussion following each group of papers included new material, and this is also included in the book.

One feature of note, which is emphasized throughout the book, is that of purity. In certain cases the actual impurity content is quoted by the authors, but generally the matter is dealt with rather vaguely. Experiments on the allotropic transformations, physical and mechanical properties, are undoubtedly affected by impurity content, and interpretation of results obtained at temperatures in the vicinity of an allotropic change must be extremely difficult.

From the physical standpoint, much new information is presented on the electronic states in plutonium, and the effect on physical properties. The ferromagnetic impurity elements, (inevitably present as a result of the methods of manufacture) have a particular influence, for example on low temperature specific heat, resistivity, and thermal expansion.

The section on alloys is also noteworthy for the concentration on theoretical implications. Considering the emphasis on the utilization of plutonium for practical purposes of nuclear energy which must lie behind this work, it is remarkable to see how far the more practical has not been allowed to subdue the fundamental understanding of the metal.

The chemical metallurgy of plutonium received attention at the Conference in matters ranging from preparation of high purity metal to atmospheric oxidation. The papers dealing with preparation include the use of fused salt electrolysis, the reduction of plutonium hadides by calcium, and the removal of impurities by volatilization. One paper, in French, describes the [illegible] technological difficulties encountered in a "production" process. The work reported on oxidation is brief, but important.

The manufacture of fuel elements containing plutonium as metal or oxides, occupies one third of the book, although mechanical properties are included in this section. One important aspect of the application of this metal is given prominence, that of the cost of development of such a material for a power reactor programme.

Although much remains to be learned about plutonium, the Conference reported in this book did reveal a tremendous amount of information. Any one concerned with power reactor development, or the scientific aspects of the transition metals, will learn much from it. The printing of text and photographs is extremely good, although one or two obvious spelling errors should not have passed the proof-reading. The price is presumably related to the cost of the metal with which the subject matter is concerned.

C. B. TOTTLE

J. Inorg. Nucl. Chem., 1962, Vol. 24, pp. 1485 to 1491. Pergamon Press Ltd. Printed in Northern Ireland

MASS DISTRIBUTION IN THE SPONTANEOUS FISSION OF ^{240}Pu

J. B. LAIDLER and F. BROWN
Atomic Weapons Research Establishment, Aldermaston, Berkshire

(*Received* 25 *April* 1962)

Abstract—The distribution of mass in the spontaneous fission of ^{240}Pu has been investigated radiochemically by measuring the fission yields of fifteen isotopes in the mass range 89–147. Comparisons are made with other published work on spontaneous fission to reveal trends in the yield–mass relationship with increasing mass of the fissioning nucleus.

Since neutron-induced fission of ^{239}Pu is essentially fission of ^{240}Pu in excitation levels above the ground state, a further series of changes in the yield–mass function for fission in various states of excitation of the same nucleus is also presented.

SPONTANEOUS fisson was suggested in 1939 as a theoretical possibility by BOHR and WHEELER in their paper on the liquid drop model of fission.(1) It was first reported by FLEROV and PETRZHAK for natural uranium.(2) They observed a half-life for decay by this process of about 10^{16}–10^{17} years and the spontaneous fission in the uranium was later attributed to ^{238}U.(3)

Spontaneous fission has since been observed in many nuclides and numerous papers have been published on the more physical aspects of the subject. Reviews of available information have been given by BUTLER(4), GHIORSO(5) and PETRZHAK(6).

There is still one aspect of spontaneous fission on which information is limited. This is the distribution of mass between the fission fragments. Mass distribution in spontaneous fission has been studied in ^{238}U(3,7,8,9), in ^{242}Cm(10) and in ^{252}Cf.(11,12,13)

There are two main reasons why information on this subject is so limited:

(a) Nuclides exhibiting spontaneous fission which are readily available have long half-lives and hence relatively low spontaneous fission activity.

(b) Nuclides which have shorter spontaneous fission half-lives are not obtainable in sufficient amounts to make radiochemical investigations of their mass distributions practicable.

---

(1) N. BOHR and J. WHEELER, *Phys. Rev.* **56**, 426 (1939).

(2) G. N. FLEROV and K. A. PETRZHAK, *Phys. Rev.* **58**, 59 (1940).

(3) W. H. FLEMING and H. G. THODE, *Phys. Rev.* **92**, 378 (1953).

(4) J. B. BUTLER, CRP 642A Paper B4 (1956).

(5) A. GHIORSO, A/Conf. 8/P/718. *The Proceedings of the International Conference on the Peaceful Uses of Atomic Energy, Geneva* 1955, *United Nations* (1956).

(6) K. A. PETRZHAK, *Sov. J. Atomic Energy.* Suppl. 1, 101 (1957).

(7) J. MACNAMARA and H. G. THODE, *Phys. Rev.* **80**, 471 (1950); also H. G. THODE *Canad. J. Phys.* **38**, 1 (1960).

(8) G. W. WETHERILL, *Phys. Rev.* **92**, 907 (1953).

(9) F. T. ASHIZAWA and P. K. KURODA, *J. Inorg. Nucl. Chem.* **5**, 12 (1958), also P. L. PARKER and P. K. KURODA, *Ibid.* **5**, 153 (1958).

(10) L. E. GLENDENIN and E. P. STEINBERG, *Phys. Rev.* **95**, (2) 431 (1954).

(11) L. E. GLENDENIN and E. P. STEINBERG, *J. Inorg. Nucl. Chem.* **1**, 45 (1955).

(12) J. G. CUNINGHAME, *J. Inorg. Nucl. Chem.* **6**, 181 (1958).

(13) W. E. NERVIK, *Phys. Rev.* **119**, (5) 1685 (1960).

Information published to date on the spontaneous fission of ^{240}Pu can be summarized as follows:

(1) Half-life for spontaneous fission(14)—1·23 × 10^{11} years.
(2) Specific spontaneous fission activity(15)—(1·61 ± 0·04) × 10^{6} fission g^{-1} hr^{-1}.
(3) Number of prompt neutrons per spontaneous fission—2·2 ± 0·03.(16)
(4) The energy distribution of the fission fragments is a two humped curve which has maxima at about 65 and 95 MeV.(17,18)
(5) A mass distribution curve derived from physical measurement of the energies of the fission fragments.(19)

All these physical measurements have been made on samples of plutonium with fairly low ^{240}Pu contents.

A source of highly enriched ^{240}Pu (about 92 per cent) of sufficient size to attempt a radiochemical investigation of the mass distribution was made available by the U.S.A.E.C. The fission yields of 15 isotopes are reported as well as a re-determination of the spontaneous fission half-life.

EXPERIMENTAL

At the commencement of each run, an inactive isotope of the element to be determined was added to the plutonium stock solution. The fission product activity and the carrier were equilibrated, separated from the plutonium and discarded. The separation time was taken as the zero time for a growth period ranging from a day to several weeks depending on the isotope under consideration. One milligram of carrier was added and at the end of the growth period, equilibrated and separated from the plutonium. The carrier was then removed from the glove box, in which the plutonium stock solution was handled, and rigorously purified from other fission products using standard radiochemical techniques. Particular attention was paid to purification from plutonium to obtain the required decontamination factor of 10^{11}.

The final purified carrier solution was weighed and aliquots taken for source preparation and chemical recovery estimations.

Sources were prepared on "glass fibre disks", described by Vallis and Thomas(20), as this type of source mount eliminates the need for self absorption and self scattering corrections in the sub-milligram region.

The sources were counted in a Van Duuren shielded end-window β-counter which had a background of 1·5 ± 0·5 counts/min. Radiochemical purity was checked by following the decay of the sources over several half-lives. The counter was calibrated prior to this work using the method of Bayhurst and Prestwood(21) and periodically checked using a natural uranium standard.

Before each separation, ^{241}Am was removed from the stock solution by ion exchange and the total α-disintegration rate of the plutonium solution measured by dilution and α-scintillation counting. The α-counting was done in A.E.R.E. Type 1093B scintillation units which were calibrated against a standard low geometry counter. These specific activity measurements were used as comparisons of the amounts of plutonium used in successive runs. The amount of plutonium was estimated chemically in a stock solution of known specific α activity by a method involving reduction with trivalent antimony and back titration with potassium iodate. The weight of plutonium measured in this way agreed to within 0·1 per cent with that calculated from α activity plus mass spectrometric results.

---

(14) O. Chamberlain, G. W. Farwell and E. Segrè, *Phys. Rev.* **94**, 156 (1954).
(15) F. R. Barclay, W. Galbraith and W. Whitehouse. *Proc. Phys. Soc.* **67** A. 646 (1954).
(16) J. E. Hammel and J. E. Kephart, *Phys. Rev.* **100**, 190 (1955).
(17) G. Hanna, B. Harvey, N. Moss and P. Tunnicliffe, *Phys. Rev.* **81**, 466 (1951).
(18) E. Segrè and C. Wiegand, *Phys. Rev.* **94**, 157 (1954).
(19) T. A. Mostovaya, *The Proceedings of the Second International Conference on the Peaceful Uses of Atomic Energy, Geneva* 1958, United Nations (1958). A/Conf. 15/P/2031.
(20) D. G. Vallis and A. O. Thomas, AWRE Report No. 0–25/61.
(21) B. P. Bayhurst and R. J. Prestwood, *Nucleonics* **17**, (3) 82 (1959).
(22) R. G. Monk and J. Herrington, *Analyt. Chim. Acta* **24**, (5) 481 (1961).

RESULTS

The fission yield of any fission product was defined as follows:

$$\text{Fission yield} = \frac{\text{Disintegration rate corrected for chemical recovery and counting efficiency}}{\text{Fission rate of Pu}^{240} \times \text{partial saturation factor.}}$$

Due to the low spontaneous fisson rate of the Pu^{240} (approximately $1{\cdot}6 \times 10^4$ fission/min), growth periods were chosen such that saturation activity of the fission product in question was attained. However, in cases when the fission product had a long half-life it was not practicable to wait until equilibrium conditions were reached and a partial saturation factor had to be applied.

This factor was defined as:

Partial saturation factor $= (1 - e^{-\lambda t})$

where λ = decay constant of fission product

t = growth period in corresponding units to λ

Mass spectrometric analyses were carried out at A.W.R.E. and at A.E.R.E. Harwell and the isotopic composition of the plutonium is shown in Table 1.

TABLE 1

Isotopes	A.W.R.E. result Wt. %	A.E.R.E. result Wt. %
239	6·71 ± 0·04	6·70 ± 0·10
240	91·70 ± 0·04	91·70 ± 0·1
241	1·51 ± 0·01	1·51 ± 0·02
242	0·071 ± 0·004	0·073 ± 0·004

Although the ^{239}Pu and ^{241}Pu contents of the plutonium were low, it was necessary to estimate the proportion of neutron-induced fissions occurring in these isotopes. Fission yields measured in the trough region could be greatly in error if induced fission took place to any appreciable extent. There are two sources of neutrons in the plutonium stock solution during growth periods, spontaneous fission neutrons and neutrons produced by (α, n) reactions on the light elements in the solution. Using diffusion theory it is possible to estimate the number of neutrons being thermalized and subsequently inducing fission in ^{239}Pu or ^{241}Pu. Two group theory with logarithmic boundary conditions in a spherical model was used to show that for solution volumes greater than 30 ml, less than 0·2 per cent of the fissions occurring were neutron induced. The error involved in this method may be considerable, but the order of magnitude should be correct. Since the lower limit of measurement of spontaneous yields is about 0·03 per cent and the yield of trough elements in thermal neutron fission of ^{239}Pu is about 0·05 per cent, the contribution from induced fission to yields in this region must be negligible.

For all isotopes considered in this work, duplicate determinations were carried out and the results quoted in Table 2 are the medians of the determinations. The errors are standard deviations calculated from the range of the observations by the method described by DEAN and DIXON(23).

(23) R. B. DEAN and W. J. DIXON, *Analyt. Chem.* 23, (4) 636 (1951)

Table 2.

Nuclide	No. of determinations	Observed fission yield (%)	Calculated independent yield of daughter (%)	Total chain yield (%)
^{89}Sr	2	0·80 ± 0·32	0	0·80 ± 0·32
^{91}Sr	3	1·51 ± 0·17	0	1·51 ± 0·17
^{97}Zr	2	6·46 ± 0·21	0·02	6·48 ± 0·21
^{99}Mo	3	6·82 ± 0·07	0	6·82 ± 0·07
^{105}Rh	3	7·10 ± 0·55	0	7·10 ± 0·55
^{109}Pd	3	0·94 ± 0·12	0	0·94 ± 0·12
^{111}Ag	2	0·035 ± 0·009	0	0·035 ± 0·009
^{115}Cd*	2	<0·03	0	<0·03
^{131}I	3	2·34 ± 0·05	0	2·34 ± 0·05
^{133}I	3	8·19 ± 0·12	0·01	8·20 ± 0·12
^{135}I	3	6·39 ± 0·67	0·55	6·94 ± 0·67
^{140}Ba	4	5·99 ± 0·22	0	5·99 ± 0·22
^{141}Ce	3	6·02 ± 0·39	0	6·02 ± 0·39
^{143}Pr	2	4·78 ± 0·39	0	4·78 ± 0·39
^{147}Nd	2	1·22 ± 0·37	0	1·22 ± 0·37

* Upper limit based on 2σ statistics of the counter background.

The independent fission yields of the daughter elements were calculated by the method of Glendenin *et al.*,(24) assuming that the equal charge displacement postulate of charge distribution holds in spontaneous fission. This could not be verified as there was insufficient fission activity to measure any independent fission yields. However as charge distribution appears to obey this postulate in most cases of low energy induced fission studied(25,26) and also in the spontaneous fission of ^{242}Cm,(10) the assumption would seem to be valid in this instance.

In conjunction with this work, the spontaneous fission rate of ^{240}Pu was measured using an ionization chamber and coincidence counting techniques. A new value $1{\cdot}340 \pm 0{\cdot}015 \times 10^{11}$ years of the spontaneous fission half life was obtained which was appreciably longer than the previously published values.(27)

DISCUSSION

The experimental results are shown in Fig. 1. Mirror points were obtained by folding the curve about mass 118·9, which is the point of symmetrical mass division found by using Hammel and Kephart's value of 2·2 for the number of prompt neutrons per fission.

It can be seen that spontaneous fission of ^{240}Pu produces a predominantly asymmetric mass distribution with maxima at masses 101 and 137. No symmetric fission is observed as far as the limits of detection allow.

The distribution of mass about the two maxima is quite narrow, peak widths at half height being only about thirteen mass units. There is some evidence of fine structure occurring in the region of the 82 neutron shell. Also, since the fine structure peak is observed in the mirror position, cf. masses 133 and 105, it would appear that enhanced formation of isotopes in the region of the 82 neutron shell is favoured in the fission act itself, rather than by subsequent neutron emission to attain the enclosed shell configuration.

---

(24) L. E. Glendenin, C. D. Coryell and R. R. Edwards, N.N.E.S. IV 9. p. 52.

(25) A. C. Pappas, *The Proceedings of the International Conference on the Peaceful Uses of Atomic Energy, Geneva* 1955, A/Conf. 8/P/881. United Nations (1956).

(26) A. C. Wahl, *J. Inorg. Nucl. Chem.* **6**, 263 (1958).

(27) D. E. Watt, F. J. Bannister, J. B. Laidler and F. Brown, *Phys. Rev.* **126**, (1) 264 (1962).

A comparison of all published spontaneous fission yield mass curves is shown in Fig. 2. Several trends are obvious as the mass of the nucleus undergoing spontaneous fission increases. Most noticeable is the increasing width of the peaks indicating a general broadening of the mass distribution. Although the width of the trough appears to be decreasing, no significant change in the symmetric mode of fission can be seen because fission yields at the bottom of the trough have never been obtained. Fine structure appears in the peaks in three of the nuclides studied, and in the case of ^{238}U insufficient experimental evidence is available to discuss the subject. The results of GLENDENIN and STEINBERG for ^{252}Cf show pronounced fine structure which does not appear in NERVIK's curve for the same nuclide. However, the former workers were forced to place large errors on their results because of the very small amount of ^{252}Cf available for their investigation.

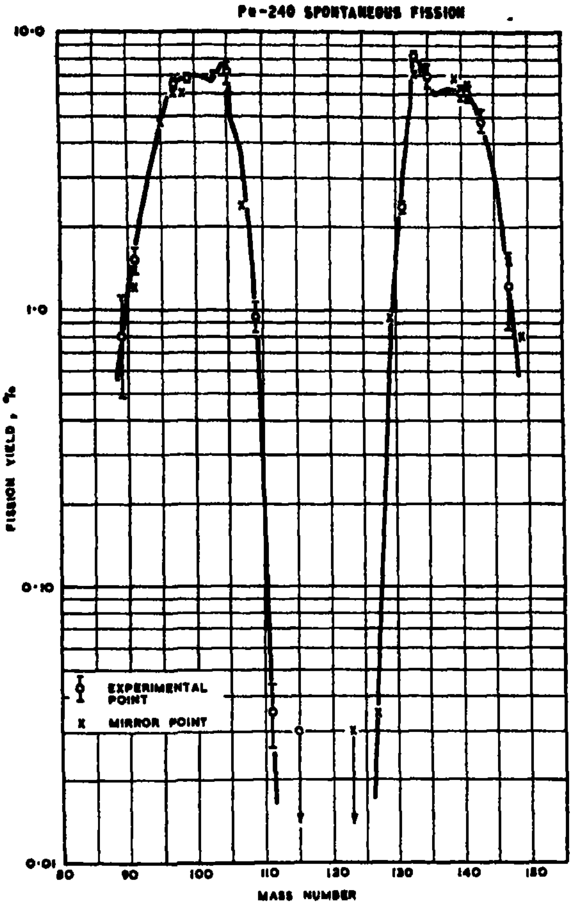

FIG. 1.

Since neutron induced fission of ^{239}Pu produces a compound nucleus which is ^{240}Pu in an excited state, comparison of yield: mass curves for ^{239}Pu (n,f,) and ^{240}Pu (s.f.) should show the variation in fission modes as excitation of the fissioning nucleus in increased from the ground state, Unfortunately, information on high energy neutron induced fission of ^{239}Pu is rather scarce; the available results are shown in Fig. 3.

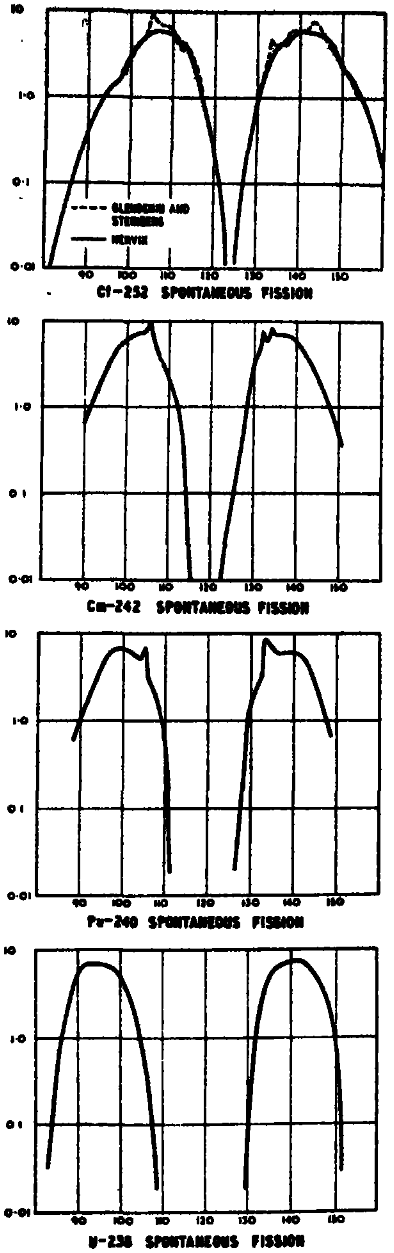

FIG. 2.

(1) Cf^{252} spontaneous fission
- (a) L. E. Glendenin and E. P. Steinberg$^{(11)}$
- (b) J. G. Cuninghame$^{(12)}$
- (c) W. E. Nervik$^{(13)}$

(2) Cm^{242} spontaneous fission
- (a) L. E. Glendenin and E. P. Steinberg$^{(10)}$

(3) U^{238} spontaneous fission
- (a) W. H. Fleming and H. G. Thode$^{(6)}$
- (b) J. MacNamara and H. G. Thode$^{(7)}$
- (c) G. W. Wetherill$^{(8)}$
- (d) F. T. Ashizawa and P. K. Kuroda; P. L. Parker and P. K. Kuroda$^{(9)}$

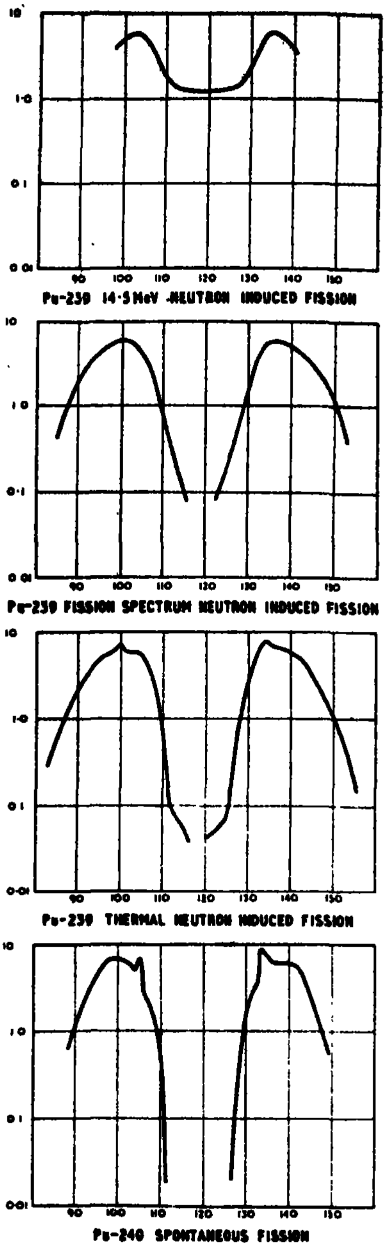

FIG. 3.

(1) Pu^{239} 14·5 Mev fission and fission spectrum neutron fission.
- (a) Y. K. Bonyushkin *et al. Atomnaya Energiya* **10,** (1) 13. (1961)

(2) Pu^{239} thermal neutron fission.
- (a) S. Katkoff, *Nucleonics* **18,** (11) 201 (1960).

Three trends can be observed as the excitation energy of the fissioning nucleus is increased.

Firstly, increasing yields in the trough region indicate increasing preference for the symmetric mode of fission. Secondly, increases in the yields of nuclides on the outside wings of the peaks show that very asymmetric fission also becomes more important at higher levels of excitation. Thirdly, it would appear that fine structure in the region of the 82 neutron shell tends to be smoothed out as excitation energy increases. The third trend is not so marked because of scanty information at higher excitation energies. This type of comparison has already been made, and similar trends observed in neutron induced fission of ^{235}U, although fission in the ground state cannot be measured in this case.(28)

Individual separation and purification methods

(1) *Strontium* ^{89}Sr: $t_{\frac{1}{2}} = 54$ *day* Sr^{91}: $t_{\frac{1}{2}} = 9 \cdot 7$ *hr*. The carrier was separated from plutonium after growth periods of 5–6 weeks for ^{89}Sr, and about one week for ^{91}Sr, by passage through a 20 cm × 2 cm column of Amberlite CG400 anion exchange resin in a constant boiling HCl solution. The plutonium was adsorbed by the resin and recovered later by elution with a 10 per cent solution of hydroxylamine hydrochloride in 2 M HCl.

The strontium was purified by a series of $Sr(NO_3)_2$ precipitations with alternate $Nd(OH)_3$ scavenges followed by $BaCl_2$ scavenges, and a final $SrCO_3$ precipitation.

As most of the final solution was needed for source separation, the chemical recovery measurements were carried out on aliquots containing about 5–10 μg of Sr. The Sr was determined by titration with electrically generated EDTA ion from a solution buffered to pH 10·5 with ammonia. The end point was detected by following the potential across a pair of polarized mercury electrodes until a sharp rise was observed.

(2) *Zirconium* ^{97}Zr, $t_{\frac{1}{2}} = 17$ *hr*. The carrier was separated from the plutonium after growth periods of about 1 week by the same procedure as used for Sr. The carrier was purified by repeated precipitations of barium fluozirconate from dilute HF, with alternate NdF_3 scavenges from solutions containing hydrazine nitrate to reduce any plutonium still present.

The recovery of the Zr carrier was measured spectrophotometrically(22) by comparing the absorbancy of the quercitin complex at 400 mμ with standard Zr solutions made by accurate dilution of the original carrier solution.

(3) *Molybdenum* ^{99}Mo, $t_{\frac{1}{2}} = 67$ *hr*. The carrier was separated from plutonium after growth periods of about 3 weeks by precipitation of the Mo α-benzoin oxime complex from approximately 1 M HCl. The complex was destroyed and the Mo purified by adsorption from 4 M HCl on a 5 cm × 4 cm column of CG 400 anion exchange resin followed by elution in 1 M HCl. This was followed by a series of Mo α-benzoin oxime complex precipitations interspersed with $Fe(OH)_3$ and $Nd(OH)_3$ scavenges.

The chemical recovery of Mo carrier was obtained by measuring the absorbancy of the molybdenumthioglycollate complex at 365 mμ(22).

(4) *Rhodium* Rh^{105} $t_{\frac{1}{2}} = 36$ *hr*. The carrier was separated from plutonium after growth periods of about 10 days by the same procedure as used for Sr. The carrier was purified by adsorption on a 5 cm × 4 mm column of CG400 anion exchange resin from 0·1M HCl followed by elution in 6M HCl. Further purification was afforded by a AgCl scavenge, followed by a repetition of the ion exchange step and finally by precipitation of potassium rhodinitrite.

The chemical recovery of the carrier was determined spectrophotometrically by measuring the absorbancy at 480 mμ of the red colour obtained when Rh Cl_3 is heated with $SnCl_2$ in HCl.(28)

(5) *Palladium* ^{109}Pd, $t_{\frac{1}{2}} = 13 \cdot 6$ *hr*. The carrier was separated from plutonium after growth periods of about 1 week by extraction of the Pd α-furil dioxime complex into $CHCl_3$ from about 2 M HCl. The separated complex was converted to the di-ethyl dithiocarbonate complex which was well washed and then destroyed. The residue was dissolved in 4 M HCl and adsorbed on a 5 cm × 4 mm column of CG400 resin and eluted in 1 M NH_4OH. The eluent was scavenged with $Nd(OH)_3$, acidified and scavenged with AgCl. PdS was then precipitated, washed and destroyed and the residue dissolved in 0·1 M HCl for source preparation and chemical recovery estimations.

The chemical recovery was determined by a spectrophotometric method depending on the colour of the palladium–thioglycollate complex at 360–380 mμ.(22)

---

(28) S. Katcoff, *Nucleonics* **18**, (11) 201 (1960).

The presence of 21 hr ^{112}Pd was not observed in the decay of the sources.

(6) *Silver* ^{111}Ag, $t_{\frac{1}{2}}$ = 7·5 *days*. The carrier was separated from plutonium after two week growth periods by adsorption on a 5 cm × 4 mm column of CG400 resin from 4 M HCl which was then well washed with dilute HCl to remove as much plutonium as possible. The Ag was eluted in 1 M NH_4OH and the eluent scavenged with $Nd(OH)_3$ to remove plutonium. The carrier was further purified by a series of AgCl precipitations with alternate $Nd(OH)_3$ scavenges and finally by several reductions to metallic silver.

The chemical recovery was determined by a potentiometric titration method depending on precipitation of AgI,(22).

(7) *Cadmium* ^{115}Cd $t_{\frac{1}{2}}$ = 54 *hr*. The carrier was separated from plutonium after two week growth periods by the same procedure as used for Ag. The ammoniacal eluent containing the Cd was buffered with ammonium acetate and CdS precipitated. The sulphide precipitations were repeated with alternate PdS and $Nd(OH)_3$ scavenges. The chemical recovery was obtained by the microcoulometric method described for strontium.

(8) *Iodine* ^{131}I, $t_{\frac{1}{2}}$ = 8·05 *day*, ^{133}I, $t_{\frac{1}{2}}$ = 21 *hr*; ^{135}I, $t_{\frac{1}{2}}$ = 6·7 *hr*. In this case very careful precautions were taken to ensure exchange between the inactive carrier and the fission product iodine. The plutonium was precipitated with dilute KOH, the carrier added as KI and allowed to stand in contact with the hydroxide slurry. At the end of growth periods of about 1 week the KI was oxidized to KIO_4 with NaClO and the solution acidified with concentrated HNO_3 to redissolve the plutonium hydroxide. Hydroxylamine hydrochloride was then added to reduce KIO_4 to I_2 which was extracted into CCl_4 to separate it from the plutonium. The carrier was than purified by an oxidation, solvent extraction, reduction, back extraction cycle using $NaNO_2$ as the oxidant and $NaHSO_3$ as the reductant. This stage was repeated several times. The final solution was evaporated with dilute NaOH to remove the Xe daughter products and the source mounted as NaI. It was then possible to remove daughter activities *in situ* simply by wetting the source to redissolve the NaI and re-drying it under an infra-red lamp. By this means a decay curve of all five iodine isotopes from 131–135 was produced without the added complication of growing activities due to Xe.

Graphical resolution of this decay curve could only produce results for the three longest lived isotopes, ^{131}I, ^{133}I and ^{135}I because of the low activity available. Computational analysis on the IBM 7090 was also limited to these three isotopes because of the poor statistics on the early counting results. However agreement on ^{131}I, ^{133}I and ^{135}I, by the two methods of calculation was good and the averaged results are presented in Table 2.

The chemical recovery of the iodide carrier was measured by the reverse of the potentiometric titration method used in the silver analysis.(22)

(9) *Barium* ^{140}Ba, $t_{\frac{1}{2}}$ = 12·8 *days*. The carrier was separated from plutonium after growth periods of 5–6 weeks by the same method as used for strontium. The purification was also similar to the strontium method in that $Ba(NO_3)_2$ precipitations were alternated with $Nd(OH)_3$ scavenges. The final stage was a precipitation of $BaCl_2$ from 1:5 ether:concentrated HCl.

The chemical recovery was determined as with strontium by the microcoulometric method.

(10) *Rare earths* ^{147}Nd, $t_{\frac{1}{2}}$ = 11·6 *days*; ^{143}Pr $t_{\frac{1}{2}}$ = 13·8 *days*; ^{141}Ce $t_{\frac{1}{2}}$ = 32 *days*. The carriers for the three elements were separated from plutonium by the ion-exchange method used for strontium after long growth periods of at least 6 weeks. The separated carriers were purified together through a series of hydroxide and fluoride precipitation stages, and the ion exchange step was repeated using a small 5 cm × 4 cm column. At this point Ce was separated from Nd and Pr by precipitation of $Ce(IO_3)_4$. The cerium was further purified by repeated iodate and hydroxide precipitations and by a final repeated ion exchange step.

The Nd and Pr fraction was found to carry the bulk of the ^{241}Am grown in from ^{241}Pu and this was separated by adsorption *on a column 10 cm × 1 cm of CG400 resin* heated to about 70°C *from* a saturated solution of LiCl in 0·5 M HCl. The rare earth carriers were precipitated from the eluent as hydroxides with gaseous ammonia. Separation of the Nd and Pr was effected by cation exchange on a 20 cm × 6 mm column of Zeocarb 225 cation exchange resin in a trichlorethylene vapour-jacket using α hydroxy iso butyric acid adjusted to pH 4·00 with NH_4OH as the eluent. Nd and Pr oxalates were precipitated from the eluent, the oxalates were destroyed and the residues dissolved in dilute HNO_3 for source preparation.

Chemical recovery of carriers were determined microcoulometrically as with strontium except that the mercury E.D.T.A. electrolyte is buffered to pH5 using sodium acetate for these estimations.

Acknowledgements—This investigation was made possible by the loan of the enriched ^{240}Pu sample from the Tripartite Nuclear Cross-Sections Committee and the U.S.A.E.C. The authors appreciate the guidance of Dr. F. MORGAN and thanks are due to Mrs. R. C. JEFFREY and Mr. K. STEED for assistance in the practical work and to Dr. A. BRICKSTOCK for help in computing the results.

J. Inorg. Nucl. Chem., 1962, Vol. 24, pp. 1493 to 1500. Pergamon Press Ltd. Printed in Northern Ireland

THE RATIO OF NEUTRON CAPTURE TO FISSION FOR URANIUM-235

M. J. Cabell and L. J. Slee
Chemistry Division, Atomic Energy Research Establishment, Harwell, Didcot, Berks.

(*Received* 29 *March* 1962)

Abstract—Alpha (the ratio of neutron capture to fission) for ^{235}U has been measured at nine different points along a flux scanning tube of the reactor PLUTO. Experimental values for $\hat{\alpha}$ varied from 0·178 to 0·189. Correcting all the results to 2200 m/sec neutrons gave a mean value for α_0 of 0·1725 ± 0·0034 (standard error), a result in excellent agreement with present recommended values.

It is of great importance to have precise values for α (the ratio of neutron capture to fission cross-sections) for each of the primary fissile nuclides, since, by means of the relationships $\sigma_A = (1 + \alpha)\sigma_F$ and $\bar{\nu} = (1 + \alpha)\eta$, these either lead to improved precision in other nuclear parameters, or are instrumental in either confirming or disproving the reliability of high precisions which may be already claimed for them. Thus, for example, direct measurements of the thermal fission cross-section of ^{235}U have resulted in a mean value which has a standard error of ±0·85 per cent, whilst direct measurements of the thermal absorption cross-section give a mean value whose standard error is ±0·53 per cent;$^{(1)}$ since, however, α for ^{235}U is about 0·173, it follows that if α is known to better than only 4·5 per cent, a more precise value for the fission cross-section is obtained by means of the expression $\sigma_F = \sigma_A/(1 + \alpha)$ than is obtained by direct measurement.

α for ^{235}U has been measured several times before this present determination. Nearly all such measurements have involved irradiations in a reactor flux of high intensity and, apart from additional errors due to special circumstances, e.g. imprecise determinations of the number of fissions, inadequate "burn-up" of the sample, self-shielding by the sample due to its thickness, contamination of the sample by natural uranium etc., there is an uncertainty common to all these measurements. This is that, since little attempt was made to characterize the neutron spectra in the irradiation positions used, it is not possible to calculate α_0 (the value for 2200 m/sec neutrons) precisely from the experimental values. The main purpose of the present measurements was to determine α for several well-defined neutron spectra in order that errors arising in this way could be reduced. In addition, by carefully choosing the composition of the target material and by ensuring that it was irradiated for a sufficiently long time that its composition was altered appreciably (approximately 20 per cent of the ^{235}U "burnt-up", 3–4 per cent converted to ^{236}U), the measurement of the changes brought about by irradiation was made both simple and precise.

Microgram quantities of a mixture of enriched ^{235}U and enriched ^{238}U, dispersed in an inert powder to minimise neutron self-shielding, were irradiated at several points along an aluminium tube which served as a high-flux irradiation position of the reactor

---

(1) N. G. Sjöstrand and J. S. Story, *Nuclear Data for Reactor Design*, Vol. 1. Pergamon Press. To be published.

PLUTO. Monitors were attached to each sample to measure the integrated neutron flux it received. Immediately after the irradiations had been completed the neutron temperature, i.e. the temperature corresponding to the modal velocity of the Maxwellian component of the neutron flux, and the epi-thermal index (which is a measure of the intensity of the epi-thermal neutron flux to the thermal flux) were measured at several of the irradiation points, and this information, together with a knowledge of the depletion of ^{235}U and the formation of ^{236}U in the samples (both measured relative to ^{238}U by means of a mass spectrometer), was used to calculate $\hat{\alpha}$, the effective alpha for the reactor spectrum and from this, α_0.

CALCULATIONS

Let us suppose that a target material is chosen in which the initial numbers of atoms of ^{234}U, ^{235}U, ^{236}U and ^{238}U are $N_{4,0}$, $N_{5,0}$, $N_{6,0}$ and $N_{8,0}$ respectively, and that, after irradiation in an integrated flux of i neutrons per cm^2 (i is the product of the average conventional flux (nv_0) and the time), the corresponding numbers are N_4, N_5, N_6 and N_8. Let us define R_1, R_2 . . . etc as follows:—

$$R_1 = N_{4,0}/N_{8,0},\ R_2 = N_4/N_8,\ R_3 = N_{5,0}/N_{8,0},\ R_4 = N_5/N_8,\ R_5 = N_{6,0}/N_{8,0} \text{ and}$$
$$R_6 = N_6/N_8.$$

Then it can be shown that

$$R_6 = R_5 \exp(\hat{S}_8 - \hat{S}_6)i + [\hat{\sigma}_5/(\hat{S}_5 - \hat{S}_6)][R_3 \exp(\hat{S}_8 - \hat{S}_6)i - R_4]$$
$$+ [\hat{\sigma}_5/(\hat{S}_5 - \hat{S}_6)][R_1\hat{\sigma}_4/(\hat{S}_4 - \hat{S}_6)][\exp(\hat{S}_8 - \hat{S}_6)i - \exp(\hat{S}_8 - \hat{S}_4)i] \quad (1)$$

in which S_4, S_5, S_6 and S_8 are the *destruction* cross sections of ^{234}U, ^{235}U, ^{236}U and ^{238}U, σ_4 and σ_5 are the *capture* cross sections of ^{234}U and ^{235}U and the circumflexes indicate effective values in the reactor flux chosen. Since, however, the fission cross-sections of ^{234}U, ^{236}U and ^{238}U are negligible compared with their capture cross-sections and, since the radioactive decay constants of all the uranium isotopes which have been referred to are very small, Equation (1) can be simplified to :

$$R_6 = R_5 \exp(\hat{\sigma}_8 - \hat{\sigma}_6)i + [\hat{\sigma}_5/\hat{\sigma}_{A.5} - \hat{\sigma}_6)][R_3 \exp(\hat{\sigma}_8 - \hat{\sigma}_6)i - R_4]$$
$$+ [\hat{\sigma}_5/(\hat{\sigma}_{A.5} - \hat{\sigma}_6)][R_1\hat{\sigma}_4/\hat{\sigma}_4 - \hat{\sigma}_6)]\ [\exp(\hat{\sigma}_8 - \hat{\sigma}_6)i - \exp(\hat{\sigma}_8 - \hat{\sigma}_4)i] \quad (2)$$

in which $\hat{\sigma}_{A.5}$ is the effective neutron absorption cross-section of ^{235}U and all other cross-sections are for neutron capture.

To determine the quantity $\hat{\sigma}_5/(\hat{\sigma}_{A.5} - \hat{\sigma}_6)$ from Equation (2), then, it is necessary to know R_1, R_3, R_4, R_5, R_6, $\hat{\sigma}_4$, $\hat{\sigma}_6$, $\hat{\sigma}_8$ and i. The atomic ratios can all be determined by mass spectrometric measurements and i can be determined by means of a suitable monitor (cobalt was used in this case). The effective capture cross-sections, however, will vary with the neutron spectrum chosen so, in order to calculate these from their 2200 m/sec values and the resonance integrals of the nuclides concerned, it is necessary to know the neutron temperature and epi-thermal index of each irradiation position. We have determined these in the present experiments by the simultaneous irradiation of three monitors, i.e. ^{59}Co (which is most sensitive to the thermal component of the reactor spectrum), ^{238}U (which is most sensitive to the epi-thermal component of the reactor spectrum) and ^{149}Sm (which is sensitive to neutron temperature). The formulae derived by WESTCOTT *et al.*(2) were then applied to obtain the desired results.

Having obtained the quantity $\hat{\sigma}_5/(\hat{\sigma}_{A.5} - \hat{\sigma}_6)$, this can be set equal to $\hat{\alpha}\hat{\sigma}_{A.5}/(1 + \hat{\alpha})(\hat{\sigma}_{A.5} - \hat{\sigma}_6)$ and hence, given $\hat{\sigma}_{A.5}$, $\hat{\alpha}$ can be found. The effective absorption cross-section of ^{235}U can be obtained from the 2200 m/sec value which has been measured precisely and independently of either α_0 or the fission cross-section.

EXPERIMENTAL DETAILS

The experimental techniques used in this work were similar to those which have been described in a previous publication(3) so only an outline will be given here.

1. *Mass spectrometric measurements*

All mass spectrometric measurements were made using an A.E.I. Type M.S.5 mass spectrometer, which is a 90° sector instrument of 12 in. radius. For each isotopic analysis about 10 μg uranium were mounted on one of the side filaments of a tungsten triple-filament surface ionization source and, with centre and side-filament currents of about 6 A and 2·5 A respectively, the mass spectrum was scanned using an eleven-stage Be–Cu electron multiplier detector and a d.c. amplifier. The usual assumption was made that the electron multiplier produces the same number of secondary electrons for ions of equal velocity, and the experimentally observed isotopic ratios were corrected accordingly. CAMPBELL and WHITTEM have shown(4) that such a correction reduces errors arising from electron multiplier discrimination to less than 0·1 per cent per mass unit. Experience in this laboratory supports this conclusion.

2. *Target material*

A stock solution of target material was prepared by mixing 93 per cent ^{235}U with highly enriched ^{238}U (>99·995 per cent) and aliquots were taken for examination in the mass spectrometer. In order to eliminate possible errors arising from source variation, eight different sources were prepared and, for each source, at least twenty consecutive measurements were made of each of the isotopic ratios of interest. The results for each source were then averaged and the averages weighted proportionally to the reciprocal of the square of their standard deviation (usually about one per cent or less) to give final weighted means. In this way R_1, R_3 and R_5 were found to be 0·05978 ± 0·00014, 5·0811 ± 0·0047 and 0·00908 ± 0·00017 respectively, where the error quoted in each case is the standard error of the weighted mean. This particular ratio was chosen for R_3 so that after irradiation R_4 would approximate to $1/R_6$, thus minimizing the random errors which could otherwise arise in the measurement of either very large or very small ratios. Ideally both R_1 and R_5 should be zero but the sample of enriched ^{238}U used for the measurement was the purest available.

The samples for irradiation were prepared as described previously;(3) approximately 100 μg ^{235}U dispersed in about 10 mg magnesium oxide was used in each case.

3. *Irradiations*

The preparation of ^{59}Co, ^{235}U and ^{149}Sm monitors has already been described.(3)

The aluminium flux scanning tube attached to the side of the fuel element number B4 of the enriched-uranium, heavy-water-moderated, high-flux reactor PLUTO was used for irradiations. Ten samples, each with a cobalt monitor attached, were packed in separate irradiation cans, strung together, and lowered into the flux scanning tube. They occupied a total of about 23 in. of the length of the tube and were all below the heavy-water level in the reactor. The samples were irradiated in this position for 47 days.

Immediately the irradiation of the samples had been completed a string of ten cans, some of which contained monitors, were lowered into exactly the same positions the samples had occupied and were irradiated there for two days. Numbering the cans from the top downwards, cans 1, 5 and 9 contained ^{235}U and ^{59}Co monitors and cans 3 and 7 contained ^{149}Sm and ^{59}Co monitors; the other cans

(2) C. H. WESTCOTT, W. H. WALKER and T. K. ALEXANDER, *The Proceedings of the Second International Conference on the Peaceful Uses of Atomic Energy, Geneva* 1958. P/202 United Nations (1959).

(3) M. J. CABELL and L. J. SLEE, *Reactor Science and Technology* **16**, 195 (1962)

(4) B. L. CAMPBELL and R. N. WHITTEM, *J. Sci. Instrum.* **38**, 516 (1961).

were empty. At exactly the same time these monitors were being irradiated, identical irradiations were also being carried out in a similar flux scanning tube of the reactor.

4. *Post-irradiation treatment*

The post-irradiation treatment given to both the samples and the ^{59}Co, ^{238}U and ^{149}Sm monitors was similar to that described elsewhere.[3]

RESULTS

The quantity which is obtained from each monitor is the equilibrium rate of the corresponding neutron capture reaction, e.g. for ^{59}Co this is R_{59}, the number of atoms of ^{60}Co formed per second per ^{59}Co atom irradiated. These reaction rates can be expressed as the product of the 2200 m/sec flux and an effective cross-section and the latter, in turn, can be expressed in terms of each 2200 m/sec cross-section by using WESTCOTT's equation[2]

$$\hat{\sigma} = \sigma_0(g + rs) \tag{3}$$

which, in the case of a $1/v$ absorber, becomes

$$\hat{\sigma} = \sigma_0 + r\,\Sigma'\sqrt{(4T/\pi T_0)} \tag{4}$$

in which Σ' is the reduced resonance integral, i.e. the usual resonance integral with the $1/v$ contribution subtracted, and T is the neutron temperature.

By adjusting all the appropriate literature values relative to the gold and Harwell boron cross-sections and other reference nuclear data recommended by SJÖSTRAND and STORY[1], we have derived the following expressions for the ^{59}Co, ^{238}U and ^{149}Sm reaction rates respectively:

$$R_{59} = (nv_0)\hat{\sigma}_{59} = [(36{\cdot}1 \pm 0{\cdot}5) + (31{\cdot}1 \pm 1{\cdot}3)r\sqrt{(4T/\pi T_0)}](nv_0)10^{-24} \tag{5}$$

$$R_8 = (nv_0)\hat{\sigma}_8 = [(2{\cdot}72 \pm 0{\cdot}04) + (281 \pm 9)r\sqrt{(4T/\pi T_0)}](nv_0)10^{-24} \tag{6}$$

$$R_{149} = (nv_0)\hat{\sigma}_{149} = (4{\cdot}290 \pm 0{\cdot}054)\,10^{-20}\,(g_{149} + rs_{149})(nv_0) \tag{7}$$

In deriving these equations the data quoted by EASTWOOD and WERNER[5] and JOHNSTON *et al.*[6] for the resonance integral of ^{60}Co, by STORY[7] for the thermal cross-section of ^{59}Co, i.e. 37·2 barns, by EASTWOOD and WERNER[8] for the self-shielding factors to be applied to cobalt wires, by WESTCOTT[9] for the thermal capture cross-section and resonance capture integral of ^{238}U and by AITKEN and CORNISH[10] for the effective capture cross-section of ^{149}Sm, have all been taken into account.

By means of equations (5), (6) and (7), and the tables given by WESTCOTT[9] for g and s for ^{149}Sm, the neutron temperature and epi-thermal indices could be obtained for the positions monitored. The neutron temperatures found in this way were 124° and 93° in positions 3 and 7 of the flux scanning tube used for the irradiations, and 107° and 106° in the same positions in a similar tube; in practice the average value, i.e. 108°, was used throughout. The epi-thermal indices determined for positions 1, 5 and 9 are listed in column 2 of Table 1; the other values given there were obtained by interpolation.

---

[5] T. A. EASTWOOD and R. D. WERNER, Atomic Energy of Canada Ltd., Report CI-207 (Unpublished) (1959).

[6] F. J. JOHNSTON, J. HALPERIN and R. W. STOUGHTON, *Reactor Science*, 11, 95 (1960).

[7] J. STORY, Private communication (1962).

[8] T. A. EASTWOOD and R. D. WERNER, *Trans. Amer. Nucl. Soc.* 4, No. 1 61 (1961).

[9] C. H. WESTCOTT, Atomic Energy of Canada Ltd., Report CRRP 960 (3rd Ed. corrected) (1960).

[10] K. L. AITKEN and F. W. CORNISH, *J. Inorg. Nucl. Chem.* 17, 6 (1961).

Table 1 summarizes all the results obtained in this series of experiments (note, sample 6 was lost). The headings A, B and C of columns 6, 7 and 8 of the table stand for the three terms $R_5 \exp(\hat{\sigma}_8 - \hat{\sigma}_6)i$, $[R_8 \exp(\hat{\sigma}_8 - \hat{\sigma}_6)i - R_4]$ and $[R_1\hat{\sigma}_4/(\hat{\sigma}_4 - \hat{\sigma}_6)]$ $[\exp(\hat{\sigma}_8 - \hat{\sigma}_6)i - \exp(\hat{\sigma}_8 - \hat{\sigma}_4)i]$ on the right hand side of equation 2. In computing these terms we used the expressions:

$$\hat{\sigma}_4 = [(105 \pm 4) + (653 \pm 70)r\sqrt{(4T/\pi T)_0}] \text{ barns} \tag{8}$$

and

$$\hat{\sigma}_6 = [(5{\cdot}55 \pm 0{\cdot}3) + (295 \pm 25)r\sqrt{4T/\pi T_0})] \text{ barns} \tag{9}$$

which were derived from the data quoted by Hughes *et al.*(11) and Stoughton and Halperin(12) for the thermal cross-section and resonance integral of ^{234}U and by Cabell *et al.*(13) for the corresponding parameters for ^{236}U; again the literature values were adjusted to recommended values(1) for the cross-sections of reference nuclides.

The values of R_4 and R_6 quoted in the table were obtained by preparing duplicate sources from each sample of purified, irradiated uranium, making at least twenty consecutive measurements of each isotopic ratio of interest for each source, averaging the two sets of results and weighting the averages proportionally to the reciprocal of their standard deviation. Agreement between the duplicate averages was good and differences were usually less than one part in two hundred.

As mentioned previously, to obtain $\hat{\alpha}$ from the factor $\hat{\sigma}_5/(\hat{\sigma}_{A.5} - \hat{\sigma}_6)$ it is necessary to know $\hat{\sigma}_{A.5}$. We have obtained this by using the 2200 m/sec value recommended by Sjöstrand and Story,(1) i.e. 680·5 ± 2·9 barns, and the tables given by Westcott(9). The latter have also been used to calculate α_0 from $\hat{\alpha}$ by means of the expression:

$$\alpha_0 = \hat{\alpha}\frac{(g_f + rs_f)}{(g_\gamma + rs_\gamma)} \tag{10}$$

in which the subscripts f and γ imply fission and neutron capture respectively.

The nine results for α_0 given in Table 1 have a mean value of 0·1725 with a standard error of ±0·0012. This error, which is entirely random in origin, arises largely from variations in the recorded mass spectrometric ratios. Systematic errors are small also since it is clear that very large errors can be tolerated in the cross-section values used in the calculations without affecting the result appreciably. Thus, we have calculated that the errors quoted above in Equations (5)–(9) result in a 50 per cent error in $(\hat{\sigma}_8 - \hat{\sigma}_6)$ and a 5 per cent error in $(\hat{\sigma}_8 - \hat{\sigma}_4)$, but that these, combined with errors in the integrated flux, result in uncertainties of only ±0·07 per cent and ±0·3 per cent in $\exp(\hat{\sigma}_8 - \hat{\sigma}_6)i$ and $\exp(\hat{\sigma}_8 - \hat{\sigma}_4)i$ respectively. The corresponding uncertainties in A, B and C of Table 1 are ±1·9, ±0·4 and ±7 per cent respectively but, of these, the effect of the first and the last on $\hat{\sigma}_5/(\hat{\sigma}_{A.5} - \hat{\sigma}_6)$ is negligible. The corresponding error in $\hat{\sigma}_5/(\hat{\sigma}_{A.5} - \hat{\sigma}_6)$ is ±0·5 per cent, and since that on $\hat{\sigma}_{A.5}/(\hat{\sigma}_{A.5} - \hat{\sigma}_6)$ is ±0·3 per cent, the uncertainty in $\hat{\alpha}/(1 + \hat{\alpha})$ becomes ±0·8 per cent, and that in $\hat{\alpha}$, ±1·0 per cent.

---

(11) D. J. Hughes, B. A. Magurno and M. K. Brussel, BNL 325 (2nd Ed.), Supplement No. 1 (1960).
(12) R. W. Stoughton and J. Halperin, *Nucl. Sci. Engng*. 6, 100 (1959).
(13) M. J. Cabell, T. A. Eastwood and P. J. Campion, *J. Nucl. Energy* 7, 81 (1958).

TABLE 1.—ALPHA FOR A REACTOR FLUX AND FOR 2200 M/SEC NEUTRONS

Irradiation position	Epithermal index	Integrated neutron flux (neutron/cm^2)	R_A	R_e	A	B	C	$\hat{\sigma}_8/(\hat{\sigma}_{A,5} - \hat{\sigma}_e)$	$\hat{\alpha}$	α_0
1	0·0569	3·045 × 10^{20}	4·197	0·1554	0·00907	0·878	0·00273	0·1661	0·1894	0·1782
2	0·0593	3·398 × 10^{20}	4·086	0·1719	0·00907	0·988	0·00307	0·1642	0·1866	0·1753
3	0·0616	3·706 × 10^{20}	3·972	0·1881	0·00907	1·102	0·00338	0·1620	0·1833	0·1720
4	0·0639	4·008 × 10^{20}	3·922	0·1969	0·00907	1·151	0·00370	0·1627	0·1839	0·1722
5	0·0662	4·084 × 10^{20}	3·888	0·2054	0·00907	1·185	0·00381	0·1652	0·1869	0·1748
7	0·0582	4·064 × 10^{20}	3·856	0·2024	0·00907	1·217	0·00364	0·1584	0·1789	0·1682
8	0·0542	3·843 × 10^{20}	3·927	0·1953	0·00907	1·147	0·00337	0·1619	0·1841	0·1736
9	0·0502	3·736 × 10^{20}	3·929	0·1893	0·00907	1·145	0·00321	0·1570	0·1780	0·1683
10	0·0462	3·888 × 10^{20}	3·884	0·1967	0·00907	1·190	0·00326	0·1572	0·1788	0·1695

TABLE 2.—THE CAPTURE TO FISSION RATIO OF ^{235}U FOR SLOW NEUTRONS

Reference	$\hat{\alpha}$	α_0	Weight	Comments
DEUTSCH *et al.*(14)	0·188 ± 0·012	0·173 ± 0·012	0·02	Mass spectrometry, with radio-chemical determinations of no. of fissions. Small burn-up in Oak Ridge reactor. ^{236}U/^{235}U ~ 0·03%
DEUTSCH *et al.*(14)	0·188 ± 0·017	0·172 ± 0·017		As above. Irradiation in Hanford reactor, Washington. ^{236}U/^{235}U ~ 0·2%.
WILLIAMS(15)	0·177 ± 0·006	0·165 ± 0·007	1·0	Similar to this work. Irradiation in Hanford reactor to give ^{236}U/^{235}U ~ 2%.
KANNE *et al.*(16)	0·174 ± 0·026	0·165 ± 0·026	0·1	Irradiation in NRX, Chalk River. No. of fissions estimated crudely by a radio-chemical method.
TINGEY and VANCE(17)	0·184 ± 0·012	0·177 ± 0·012	0·3	Irradiation in MTR, Idaho.
CRAIG *et al.*(18)	0·194 ± 0·002	0·184 ± 0·006	0·7	Sections of fuel elements highly irradiated in NRX. Analyses by mass spectrometry and α-spectrometry.
BIGHAM *et al.*(19)	0·187 ± 0·003			
COCKING(20)	0·172 ± 0·022			Measurement of (1 + α) with nearly monokinetic neutrons of 0·0011 EV.
SAFFORD and MELKONIAN(21)	0·171 ± 0·009	0·159 ± 0·014	0·9	Measurement of (1 + α) with neutrons of 0·00291 eV.
CORNISH(22)	0·200 ± 0·008	0·189 ± 0·008	0·5	Irradiation in DIDO, Harwell ^{235}U burn-up measured relative to low abundance ^{234}U and from gross fission product γ-radiation
Weighted mean		0·1714 ± 0·0077		

(14) M. DEUTSCH, M. KAHN and J. A. MISKEL, Report LA 511 (1946).

(15) D. WILLIAMS, Report LA 512 (1946).

(16) W. R. KANNE, H. B. STEWART and F. A. WHITE, *The Proceedings of the First International Conference on the Peaceful Uses of Atomic Energy, Geneva*, 1955. P/595 United Nations (1956).

(17) F. H. TINGEY and F. P. VANCE, U.S.A.E.C., Report, TID 405 (1955).

(18) D. S. CRAIG, G. C. HANNA, D. G. HURST, S. A. KUSHNERIUK, W. B. LEWIS and A. G. WARD, *The Proceedings of the Second International Conference on the Peaceful Uses of Atomic Energy, Geneva*, 1958. P/205 United Nations (1959).

(19) C. B. BIGHAM, G. C. HANNA and P. R. TUNNICLIFFE, Atomic Energy of Canada Ltd., Report CRR 861 (1959).

(20) S. J. COCKING, *J. Nucl. Energy* **6**, 285 (1958).

(21) G. J. SAFFORD and E. MELKONIAN, *Phys. Rev.* **113**, 1285 (1959).

(22) F. W. CORNISH. Private communication (1960).

A possible error of ±5 per cent in r is reflected as only ±0·2 per cent in the calculation of α_0 from $\hat{\alpha}$. If we allow for this possibility and sum up, we conclude that possible systematic errors in α_0 arise as follows:

from the calculation of $\hat{\alpha}$	±1·0%
from the calculation of α_0 from $\hat{\alpha}$	±0·2%
from mass discrimination in the mass spectrometer	±0·1%
Total	±1·3%

and therefore that α_0 for ^{235}U is 0·1725 ± 0·0034 (the only error not included in this result is any which might arise from using Westcott's tables to obtain α_0 from $\hat{\alpha}$).

CONCLUSIONS

Sjöstrand and Story(1) have collated all reported measurements of alpha for ^{235}U up to early 1961. Their results are reproduced in Table 2, columns 3 and 4 of which give, respectively, the value of α_0 Sjöstrand and Story have computed from each experimental result, and the weighting factor they have applied to these values to obtain a final mean. It will be noted that the reported values for $\hat{\alpha}$ vary considerably (from 0·200 to 0·171) and that this is reflected in the corresponding values for α_0 (0·189–0·159). The weighted mean for α_0 obtained from Table 2 is 0·1714 ± 0·0077, a result which does not take into account the recent values obtained by Jones *et al.*(23) and by Hanna(24), i.e. α_0 = 0·173 ± 0·004 and 0·177 ± 0·004, which were not available at the time.

Taking the data of Table 2 and all the other known data for ^{235}U into account, Sjöstrand and Story arrive at a "recommended" value for α_0 of 0·1734 ± 0·0050; this compares with the present "world consistent set" value of α_0 = 0·174 ± 0·010 quoted by Hughes *et al.*(11)

The value obtained here, i.e. α_0 = 0·1725 ± 0·0034, is in excellent agreement with both the mean obtained from previous determinations, the value recommended by Sjöstrand and Story and the world consistent set value.

Acknowledgement—Grateful acknowledgement is made to N. G. Sjöstrand and J. S. Story for permission to reproduce Table 2, and to D. Avery for his help with the mass spectrometric measurements.

(23) R. W. Jones, M. Lounsbury, G. C. Hanna and R. G. Hart. Private communication (1962).
(24) G. C. Hanna, Private communication (1962).

J. Inorg. Nucl. Chem. 1962, Vol. 24, pp. 1501 to 1515. Pergamon Press Ltd. Printed in Northern Ireland

DEPOSITION OF VARIOUS RADIOACTIVE ELEMENTS ON THE SURFACE OF THE PLATINUM ANODE

I. MÁDI
Physical Chemical Institute, University of Sciences
L. Kossuth, Debrecen

(*Received* 21 *February* 1962; *in revised form* 14 *May* 1962)

Abstract—The anodic deposition of ^{204}Tl, ^{144}Ce, ^{90}Y, ^{175}Yb, ^{143}Pr, ^{147}Pm and ^{166}Ho were investigated as a function of time, with special consideration of ^{204}Tl and ^{144}Ce. These studies show that when these atoms are anodically deposited, a plot of the equilibrium distribution coefficient as a function of the applied voltage passes through a maximum. The number of active centres on the surface of the platinum anode was determined for the anodic deposition of ^{204}Tl and ^{144}Ce by the isotherm method. A plot of the number of active centres as a function of the applied voltage also gave a curve with a maximum. The effect of hydrogen ion concentration was also investigated and a linear relation between the pH and the logarithm of the number of active centres found. Investigation of the deposition of ^{204}Tl on platinum from a solution containing hydrogen peroxide shows that the chemisorbed oxide layer, which develops on the platinum anode, plays an important role in the anodic deposition.

THE theory developed by IMRE(1,2) of the thermodynamic and kinetic behaviour of the transitory layers, which develop at the solid-liquid interface, offers substantial help in the kinetic study of the electro-deposition of radioactive elements. The experience, which we have gained in our Institute during such studies,(3,4) offers the possibility of a better understanding of the complicated process by which the radioactive atoms are anodically deposited.

Radioactive elements are deposited on the surface of platinum anodes in the form of oxides or peroxides and the nascent oxygen, which is formed by the deposition of the hydroxyl ions at the anode, has an important role in the process for two reasons: on the one hand, it can take part in the oxidation of the radioactive element itself, while, on the other hand, it passivates the surface of the platinum anode by forming a chemisorbed oxide layer, which plays an important part in binding the radioactive atoms. In this communication some experience gained during a kinetic and static study of the anodic deposition of some radioactive atoms will be described. An electrochromatographic method(5,6) based on these experiments has been developed and has been applied successfully to the separation of radioactive elements in a carrier-free state.

EXPERIMENTAL RESULTS

Many of the experiments were carried out with preparative ends in view, but they gave results which are also noteworthy from the viewpoint of the general problem of the anodic deposition of radioactive elements. Experiments were carried out with asymmetrically arranged platinum electrodes as used by IMRE.

(1) L. IMRE, *Kolloid Zschr.* 154, 119 (1957).
(2) L. IMRE, *Kolloid Zschr.* 166, 122 (1959).
(3) L. IMRE and G. FEJES, *Acta Univ. Debrecen.* 3, 176 (1955).
(4) L. IMRE and G. FEJES, *Acta Univ. Debrecen.* (In press)
(5) I. MÁDI, *Naturwissenschaften* 48, 155 (1961).
(6) I. MÁDI, *J. Inorg. Nucl. Chem.* 22, 169 (1961).

The method used was described in a previous communication:[(6)] all experiments were carried out under similar conditions. The purity of the radioactive substances used was determined in every case by radioanalytical measurements. The active material was available in each case as a 20 ml nitric acid solution of 0·01 N, 0·001 N or 0·0001 N concentration. The surface of the platinum anode was 3·14 cm^2, the needle cathode had a surface one hundred times smaller. During electrolysis the solution was thoroughly mixed. The voltage applied in the experiments in this paper was so low that no radioactive substance was deposited on the needle cathode.

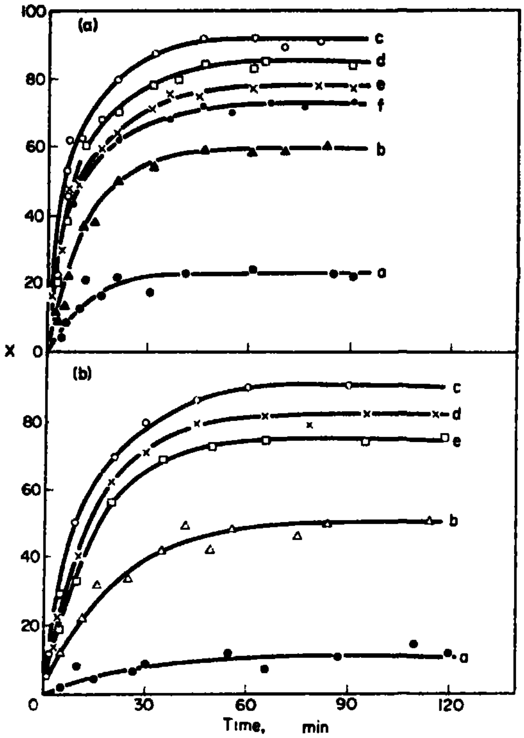

FIG. 1.—(a) Anodic deposition of ^{204}Tl as a function of time at various applied voltages.
(a) 0·8 V, 0·03 mA; (b) 1·0 V, 0·07 mA; (c) 1·2 V, 0·12 mA;
(d) 2·0 V, 0·20 mA; (e) 3·0 V, 0·44 mA; (f) 4·0 V, 0·75 mA.
(b) Anodic deposition of ^{144}Ce as a function of time at various applied voltages.
(a) 0·8 V, 0·12 mA; (b) 1·2 V, 0·50 mA; (c) 3·0 V, 0·9 mA;
(d) 4·0 V, 1·8 mA; (e) 5·0 V, 2·8 mA.

Fig. 1a shows results for the anodic deposition of ^{204}Tl as a function of time for various applied voltages. Each point in Fig. 1a was obtained with a fresh 0·001 N nitric acid solution of ^{204}Tl and regenerated electrodes. The amount of radioactive substance deposited on the anode (x) is expressed as a percentage of the total amount of radioactive substance in the system and presented as a function of the time of electrolysis (t). Fig. 1a shows that the anodic deposition of ^{204}Tl leads to an equilibrium at all voltages. The equilibrium distribution coefficient $(x/1 - x)_\infty$ is a function of the applied voltage showing a maximum.

As shown in Fig. 1b similar results were obtained for the anodic deposition of ^{144}Ce: the distribution coefficient reaches a maximum at a given applied voltage.

(The ^{144}Ce was anodically deposited from a 0·01 N nitric acid solution. Radioactive measurements were always carried out about 180 minutes after the end of the experiment, so that the ^{144}Ce deposited on the anode as well as that left behind in the solution should reach a state of equilibrium with the daughter ^{144}Pr.)

The dissolution of the ^{204}Tl deposited on the surface of the anode was also observed as a function of the time. Electrolysis of 20 ml of 0·001 N nitric acid solution containing the ^{204}Tl was continued until equilibrium (50 min). The electrodes were then removed from the solution and the activity of the anode was measured. The platinum strip used as anode was then immersed in either a 0·0001 N or a 0·001 N nitric acid solution, and the solution thoroughly mixed. After a predetermined time the platinum strip was taken from the solution and its activity measured again. The dissolution of the ^{204}Tl, deposited on the surface of the anode, was determined as a function of time from these experiments. The experimental data of Fig. 2 show that the dissolution of the Tl_2O_3 deposited on the surface of the anode also reached an equilibrium. This state of equilibrium might be regarded as a redox equilibrium according to the equation:

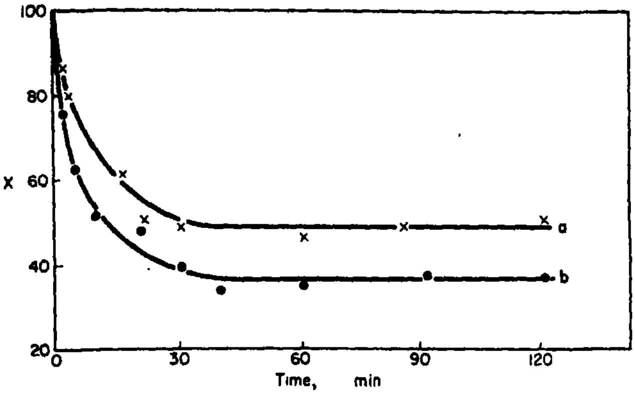

FIG. 2.—Dissolution of ^{204}Tl deposited on the surface of the platinum anode as a function of time, in (a) 0·0001 N, (b) 0·001 N nitric acid solution.

$$Tl_2O_3 + 6H^+ + 4e^- \rightleftharpoons 2Tl^+ + 3H_2O$$

As the ^{204}Tl and ^{144}Ce preparations at our disposal contained small amounts of carrier ($c_{^{204}\text{Tl}} = 1\cdot1 \times 10^{-8}$ N $TlNO_3$; $c_{^{144}\text{Ce}} = 2\cdot1 \times 10^{-8}$ N $Ce_2(SO_4)_3$) we examined the effect of the addition of inactive $TlNO_3$ on the anodic deposition. It was found that if labelled $TlNO_3$ solutions of varying concentration in 0·001 N nitric acid are electrolysed at an applied voltage of 3 V, the relative quantity of thallium deposited on the anode, which is only a fraction of the thallium present in the system, decreased as the concentration increased. The experimental data are shown in Fig. 3a where the amount of Tl deposited from solutions of varying concentrations are shown as a function of the time. From these results the equilibrium distribution coefficients $(1 - x/x)_\infty$ for the anode can be evaluated and an isotherm can be constructed in which values of $c/a = 1/V(1 - x/x)_\infty$ are presented graphically as a function of the equilibrium concentration (c). A linear isotherm is thus derived on the basis of the Langmuir formula:

$$\frac{1}{V}\left(\frac{1-x}{x}\right)_\infty = \frac{1}{z}c + \frac{1}{z}C \quad \text{if } c \rightarrow 0\text{, then} \quad \frac{1}{V}\left(\frac{1-x}{x}\right)_\infty = \frac{1}{z}C \qquad (1)$$

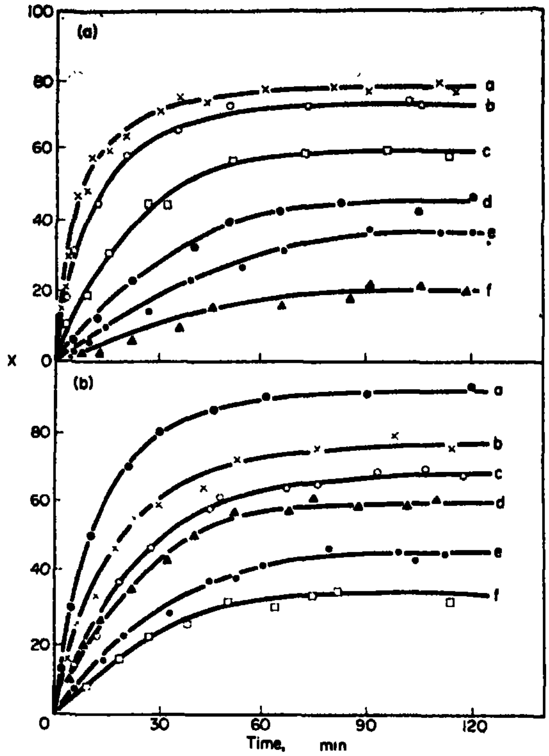

FIG. 3.—(a) Anodic deposition of Tl^+ ions as a function of time during the electrolysis of $TlNO_3$ solutions of varying concentrations. (Deposition process followed with ^{204}Tl.)
(a) $c_0 = 0{\cdot}26 \times 10^{-7}$ N; (b) $c_0 = 0{\cdot}39 \times 10^{-7}$ N; (c) $c_0 = 0{\cdot}79 \times 10^{-7}$ N;
(d) $c_0 = 1{\cdot}30 \times 10^{-7}$ N; (e) $c_0 = 1{\cdot}98 \times 10^{-7}$ N; (f) $c_0 = 4{\cdot}00 \times 10^{-7}$ N;
(b) Anodic deposition of Ce^{3+} ions as a function of time during the electrolysis of $Ce_2(SO_4)_3$ solutions of varying concentrations. (Deposition process followed with ^{144}Ce.)
(a) $c_0 = 0{\cdot}11 \times 10^{-7}$ N; (b) $c_0 = 0{\cdot}40 \times 10^{-7}$ N; (c) $c_0 = 0{\cdot}55 \times 10^{-7}$ N;
(d) $c_0 = 0{\cdot}71 \times 10^{-7}$ N; (e) $c_0 = 1{\cdot}36 \times 10^{-7}$ N; (f) $c_0 = 1{\cdot}84 \times 10^{-7}$ N.

where x_∞ is the quantity of radioactive substance deposited on the surface of the anode, $(1 - x)_\infty$ the quantity of the radioactive substance in solution, V the volume of the solution, c the equilibrium concentration, z the number of active centres on the surface, and C the solution tension of the radioactive substance deposited on the surface of the anode. The straight line d in Fig. 4 is the isotherm constructed with the help of the equilibrium distribution coefficients which were evaluated from the data of Fig. 3a.

Isotherm measurements were carried out for each voltage value in Fig. 1a. The experimental data are presented in Fig. 4. (The electrolyte was 0·001 N in nitric acid in all the measurements.)

Similar results were obtained when the concentration of the solution containing ^{144}Ce was increased by the addition of inactive $Ce_2(SO_4)_3$. These measurements were carried out in 0·01 N nitric acid solution. Fig. 3b shows the experimental data for the anodic electrolysis of $Ce_2(SO_4)_3$ solutions of various concentrations as a function of the time. The isotherm constructed from the equilibrium distribution coefficients

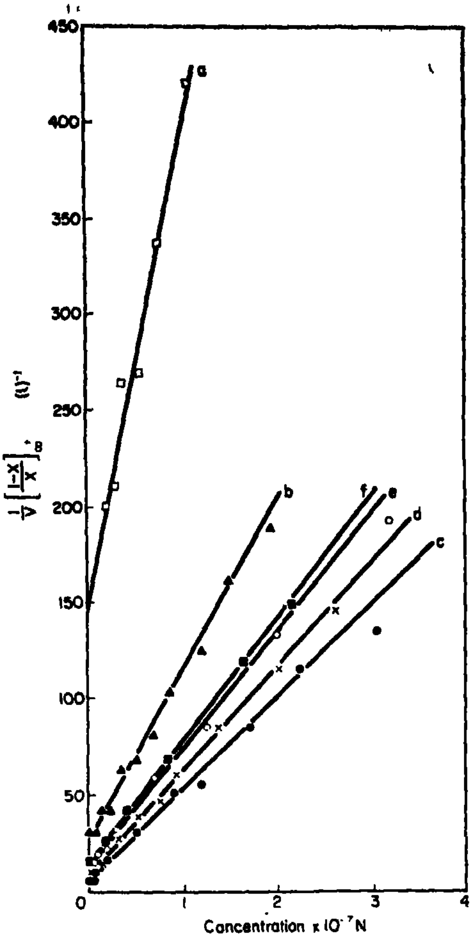

FIG. 4.—Isotherms characteristic of the anodic deposition of Tl^{+} ions at various values of the applied voltage.
(a) 0·8 V; (b) 1·0 V; (c) 1·2 V; (d) 2·0 V; (e) 3·0 V; (f) 4·0 V.

evaluated from the data of Fig. 3B, is the straight line *b* in Fig. 5. Isotherm measurements were also carried out with applied voltages of 1·2, 4 and 5 V. A $Ce_2(SO_4)_3$ solution (0·01 N in nitric acid) of given concentration was electrolysed at a given applied voltage till equilibrium was reached and the isotherms were constructed from the distribution coefficients thus obtained (Fig. 5).

The hydrogen ion concentration of the electrolyte greatly affects the anodic deposition of ^{204}Tl and ^{144}Ce. Therefore the effect of hydrogen ion concentration on the process was carefully examined. The anodic electrolysis of ^{144}Ce was carried out in nitric acid solutions of varying concentrations with an applied voltage of 3 V in such a way that the shift in the equilibrium distribution coefficients, due to the increase in the $Ce_2(SO_4)_3$ concentration of the solution, was examined for solutions of varying pH and isotherms were constructed from these data at the various pH values. The results are shown in Fig. 6.

The anodic deposition of some other radioactive elements where no change of valency can occur was also examined. It appears from the data of Fig. 7 that ^{90}Y,

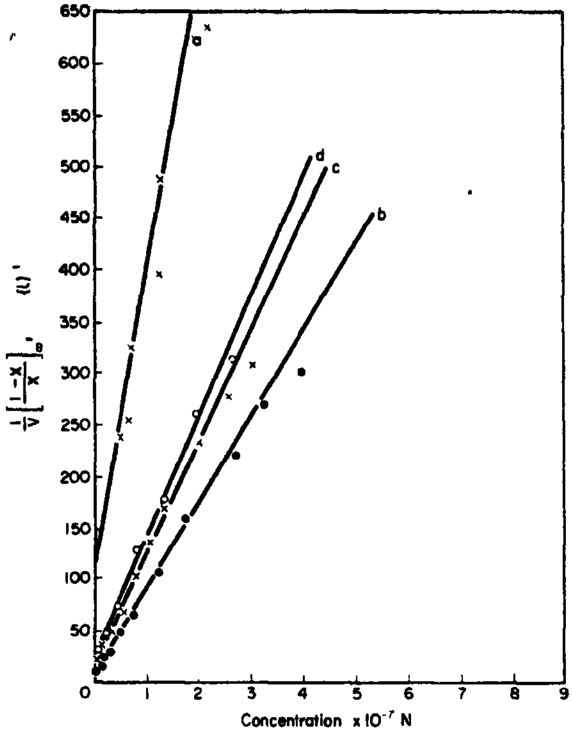

FIG. 5.—Isotherms characteristic of the anodic deposition of Ce^{3+} ions at various values of the applied voltage. (a) 1·2 V; (b) 3·0 V; (c) 4·0 V; (d) 5·0 V.

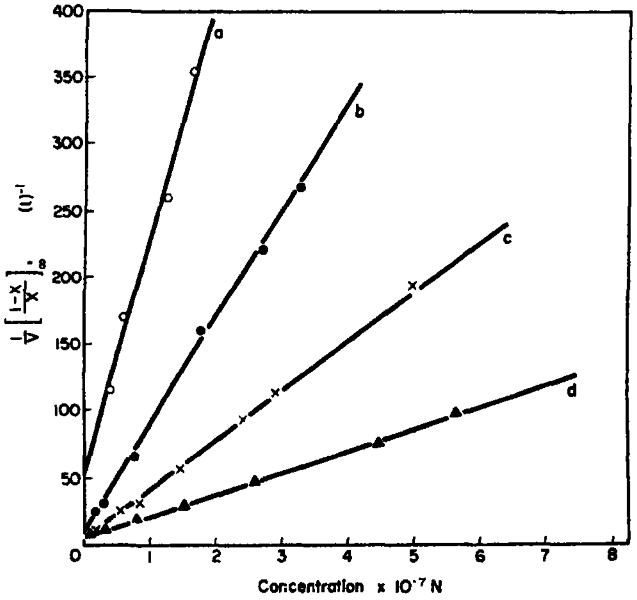

FIG. 6.—*Isotherms characteristic of the anodic deposition of Ce^{3+} ions from solutions* with different hydrogen ion concentration. (Anodic deposition was followed with ^{144}Ce.) (a) pH = 1·06; (b) pH = 2·10; (c) pH = 3·05; (d) pH = 4·02.

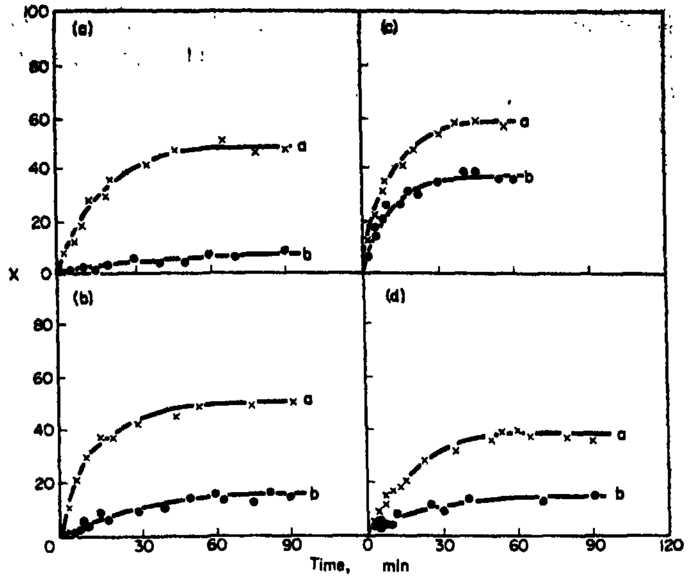

FIG. 7.—(a) Anodic deposition of ^{90}Y as a function of time, in (a) 0·0001 N; (b) 0·001 N nitric acid solution.
(b) Anodic deposition of (a) ^{147}Pm, (b) ^{175}Yb as a function of time in 0·001 N nitric acid solution.
(c) Anodic deposition of ^{143}Pr as a function of time in (a) 0·0001 N, (b) 0·001 N nitric acid solution.
(d) Anodic deposition of ^{166}Ho as a function of time in (a) 0·0001 N, (b) 0·001 N nitric acid solution.

^{166}Ho, ^{147}Pm, ^{175}Yb, ^{143}Pr are also deposited on the surface of the platinum anode. The anodic deposition, both in relation to the time and in its final result is again greatly affected by the hydrogen ion concentration of the solution to be electrolysed. It is possible to explain the anodic deposition of such elements in terms of the effects of the chemisorbed oxide layer, developed on the surface of the platinum anode.

DISCUSSION OF EXPERIMENTAL RESULTS

The experimental results show that for each applied voltage an equilibrium is reached between the radioactive substance deposited on the anode and left in the solution. The system reaches equilibrium as a result of competition between deposition and dissolution. The anodic deposition of the radioactive substance is determined by factors determining the time dependence of these processes. At any given time t the rate of deposition on the surface of the platinum anode is determined by the quantity of radioactive substance still in solution, $(1 - x)$. As in redox processes the transfer of electrons is a slow reaction,(7) not all of the particles reaching the anode will be deposited there, but only a fraction corresponding to $\exp(-E_+/RT)$, where E_+ is the activation energy of the deposition process. The process of deposition can thus be described by the following differential equation:

$$\frac{dx_+}{dt} = k_1(1 - x)\exp\left(-\frac{E_+}{RT}\right) \tag{2}$$

where k_1 is a constant characteristic of the deposition process.

(7) T. ERDEY-GRUZ and M. VOLMER, *Z. Phys. Chem.* **150**, 203 (1930); **157**, 165 (1931).

If the quantity of radioactive substance deposited on the anode is so small that it is not enough to form a monomolecular layer, the rate of dissolution from the surface of the anode will depend on the quantity of radioactive substance deposited on the anode by the time t, (x) and on the activation energy of the dissolution process, according to the following equation:

$$\frac{dx_-}{dt} = k_2 x \exp\left(-\frac{E_-}{RT}\right) \tag{3}$$

where E_- is the activation energy of the dissolution process and k_2 is a constant.

Thus if the anodic deposition of radioactive substances is treated as the sum of the processes and it is noted that

$$\frac{dx_+}{dt} = \frac{dx_-}{dt} \tag{4}$$

at equilibrium, then

$$k_2 = k_1 \left(\frac{1-x}{x}\right)_\infty \exp\left(\frac{E_-}{RT} - \frac{E_+}{RT}\right) \tag{5}$$

and for the overall process:

$$\frac{dx}{dt} = k_1 \exp\left(-\frac{E_+}{RT}\right)\left[1 - x - \left(\frac{1-x}{x}\right)_\infty x\right] \tag{6}$$

Integrating with $x = 0$ at $t = 0$ we obtain

$$\frac{1}{1+K}\ln\left[1 - (1+K)x\right] = -k_1 \exp\left(-\frac{E_+}{RT}\right) t \tag{7}$$

where $[1 - x/x]_\infty = K$, the numerical value of the equilibrium distribution coefficient referring to the anode.

At any given applied voltage and at constant temperature $k_1 \exp(-E_+/RT)$ is a constant the value of which can be determined if the $\ln[1 - (1 + K)x]$ values are plotted as a function of time (Fig. 8). From the slope of the straight line obtained the numerical value of the rate coefficient of the reaction can be determined.

From the data of Fig. 8 0·0498 min^{-1} was obtained for the rate constant characteristic of the deposition of ^{204}Tl at an applied voltage of 3 V, while the rate constant for the anodic deposition of ^{144}Ce under the same conditions is 0·0636 min^{-1}. The value of the activation energy is being determined in experiments on the temperature dependence of the process now in progress.

Our experimental data presented in Figs. 1a and 1b show that the value $[x/1 - x]_\infty$ characteristic of the equilibrium distribution between anode and solution, plotted as a function of the voltage, gives a curve with a maximum as shown in Fig. 9.

Experimental data of Figs. 4 and 5 show further that the number of active centres on the surface of the platinum anode plotted as a function of the applied voltage also results in a maximum. The number of active centres on the surface was calculated from the isotherms in Figs. 4 and 5. On the basis of the Langmuir Equation (1) the slope of the isotherm gives the reciprocal of the number of active centres.

Figs. 10a and 10b record the number of active centres calculated from the data in Figs. 4 and 5 for various applied voltages.

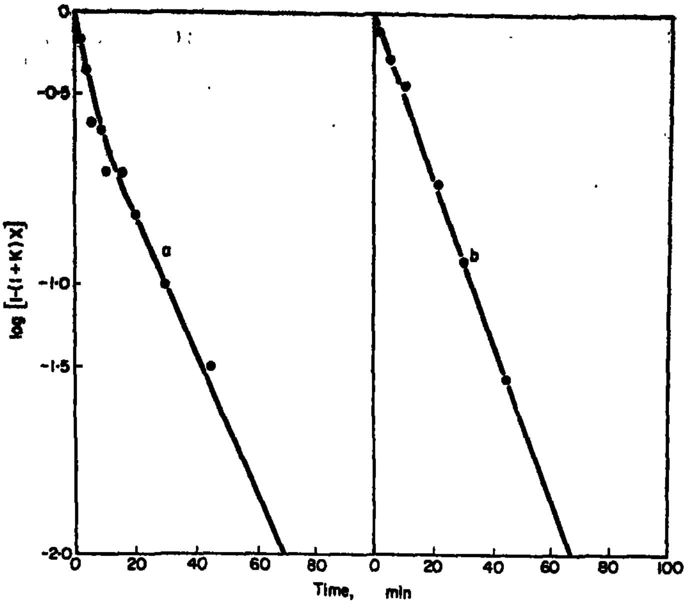

Fig. 8.—Rate curves characteristic of the anodic electrolysis of (a) ^{204}Tl, (b) ^{144}Ce with 3 V applied voltage. (From the data of Fig. 1(A)(e) and 1(B)(c).)

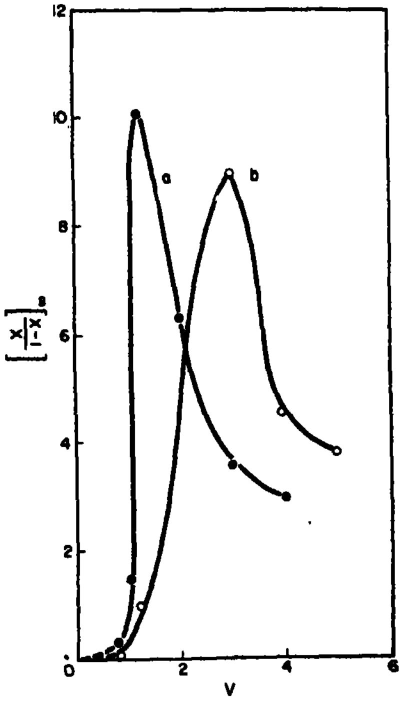

Fig. 9.—Distribution coefficient as a function of the applied voltage by the anodic electrolysis of (a) ^{204}Tl, (b) ^{144}Ce.

Our experimental results can only be interpreted by taking into account the important role played by the chemisorbed oxide layer, developed on the surface of the

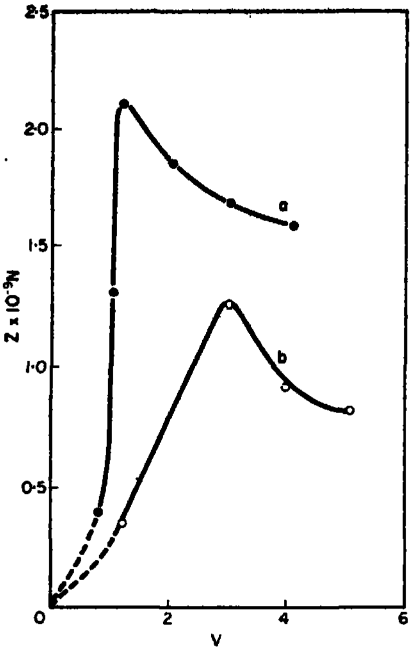

FIG. 10.—The number of active centres on the surface of the anode as a function of the applied voltage during the anodic electrolysis of (a) ^{204}Tl, ^{144}Ce.

platinum anodes. The nascent oxygen atoms, provided by the deposition of the OH^- ions on the surface of the anode, passivate the surface of the platinum and a two dimensional oxide layer develops as a result of the chemisorption of the nascent oxygen atoms. A number of experimental observations prove the existence of this oxide layer and the role which it plays in anodic oxidation. THALINGER and VOLMER(8) were the first to draw attention to these facts. BOWDEN(9) and BUTLER(10) have proved the existence of a surface oxide layer by an oscillographic examination of the potential changes during the transition from cathodic to anodic polarization. The existence of a surface oxide layer has been invoked by several authors(11–16) for the explanation of oxygen overvoltage. The effect of the passive layer developed on anodic oxidation, has also been known for a long time. For instance, the investigation of the electrolysis of sodium sulphide solutions with platinum electrodes has shown(17) that at very low potential values a sulphide layer is deposited on the platinum anode, while at higher potentials polysulphides and, at very high potentials, thiosulphate and sulphate ions are formed on the anode. The same experiments have also proved that nascent oxygen plays a very important role in the formation of thiosulphate and sulphate ions,

(8) M. THALINGER and M. VOLMER, *J. phys. Chem.* D **150**, 401 (1930).
(9) F. P. BOWDEN, *Proc. Roy. Soc.* B **125**, 446 (1929).
(10) F. A. BUTLER, *Trans. Faraday Soc.* **32**, 427 (1936).
(11) A. HICKLING, *Discuss. Faraday Soc.* **1**, 225 (1947).
(12) J. O. M. BOCKRIS, *J. Chem. Phys.* **24**, 817 (1956).
(13) M. BECKER and M. BREITER, *Z. Elektrochem.* **60**, 1080 (1956).
(14) S. ALTMANN and R. H. BUSCH, *Trans. Faraday Soc.* **45**, 720 (1949).
(15) T. ERDEY-GRUZ and I. SAFARIK, *Acta Chim. Hung.* **13**, 159 (1957).
(16) T. ER[illegible]GRUZ and I. VAJASDY, *Acta Chim. Hung.* **29**, 47 (1961).
(17) H. G[illegible]SCHER, *Z. Elektrochem.* **54**, 540 (1950).

because it passivates the surface of the platinum and increases the oxygen over-voltage which favours the formation of higher oxidation products. Therefore it seems probable that the chemisorbed oxide layer, which develops on the surface of the anode, has an effect on the anodic deposition of radioactive substances too. This is further confirmed by some of our own experiments. A platinum strip of 3·14 cm^2 surface, similar to our previous anodes, was heated and coated on one side with paraffin. It was immersed in 20 ml solution of 0·001 N nitric acid containing ^{204}Tl and 1·5% H_2O_2. The solution was thoroughly mixed. After a predetermined time had elapsed, the platinum strip was removed and the activity of the radioactive substance deposited on its surface measured. Each solution was evaporated in a small platinum dish and its activity was measured under geometrical conditions similar to that of the platinum strips. Each measurement was carried out with fresh solutions of identical composition and with regenerated platinum strips. The relative quantity of the radioactive ^{204}Tl deposited on the platinum strip was plotted as a function of time (t). According to curve a in Fig. 11, 56 per cent of the radioactive ^{204}Tl present in the solution at time $t = 0$ is deposited on the surface of the platinum strip from a H_2O_2 solution and this deposition process too leads to an equilibrium. The phenomenon might be explained by assuming that the catalytic decomposition of H_2O_2 on the platinum strip occurs as a combination of electrochemical processes, in the course of which nascent oxygen is formed according to the following equation$^{(18-20)}$:

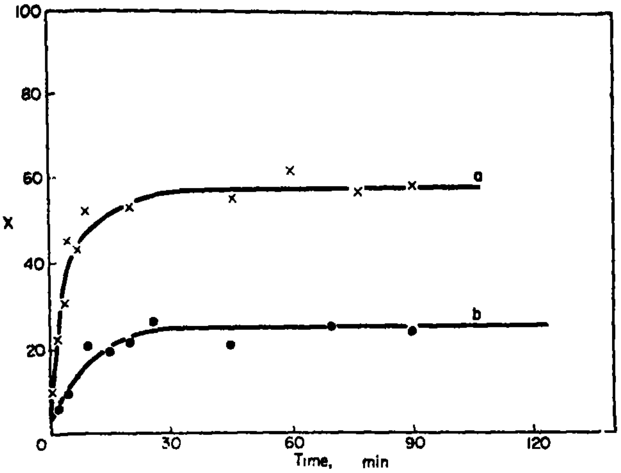

FIG. 11.—Deposition of ^{204}Tl on the surface of the platinum strip as a function of time, (a) in 1·5% H_2O_2 solution, (b) on the surface of a previously anodically polarized platinum strip.

$$H_2O_2 \rightarrow O_2 + 2H^+ + 2e^- \qquad \text{anodic step}$$

$$\left.\begin{array}{l} H_2O_2 \rightarrow H_2O + O_{ads} \\ O_{ads} + 2H^+ + 2e^- \rightarrow H_2O \end{array}\right\} H_2O_2 + 2H^+ + 2e^- \rightarrow 2H_2O \qquad \text{cathodic step}$$

---

(18) R. GERISCHER and H. GERISCHER, *Z. physik. Chm.* (N.F.) 6, 178 (1956).
(19) D. WINKELMANN, *Z. Elektrochem.* 60, 731 (1956).
(20) J. GINER, *Z. Elektrochem.* 64, 491 (1960).

The nascent oxygen formed by the decomposition of H_2O_2 also passivates the surface of the platinum strip. The platinum oxides formed in this way, just like the platinum oxides formed on the anode during electrolysis, are dipoles, the negative ends of which are turned towards the solution and these negatively orientated dipoles are capable of binding the oxidized radioactive ions.

BALASCHOWA's[21] experiments furnished unequivocal proof of the orientation of the platinum oxide dipoles. Her experiments have shown that in the potential range in which the oxide layer is formed a minimum in the anion adsorption occurs, that is to say the chemisorbed oxide layer developed on the surface of the platinum anode, has a retressive effect on the adsorption of the anions.

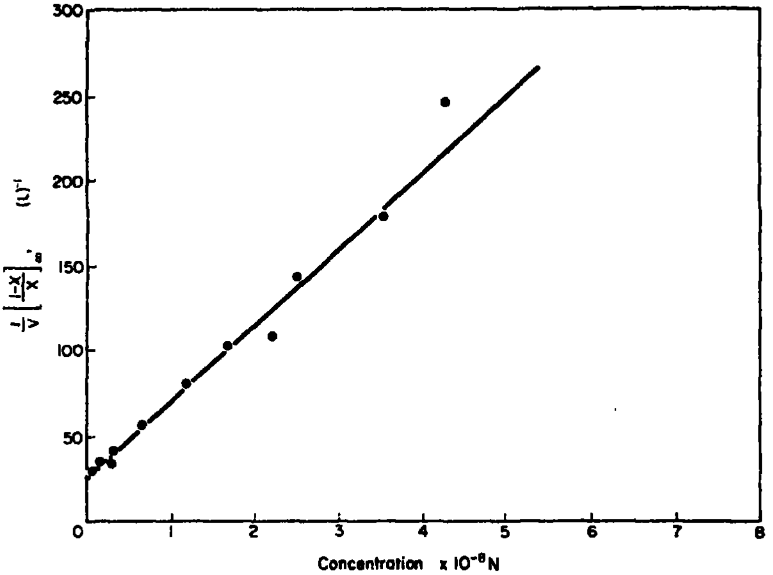

FIG. 12.—Isotherm characteristic of the deposition of Tl^+ ions from a 1·5% H_2O_2 solution. (Deposition process followed with ^{204}Tl).

The isotherm for the deposition of radioactive substances from a H_2O_2 solution onto the surface of platinum was also examined and the number of active centres on the surface of the platinum was determined under these conditions. The results are shown in Fig. 12. The number of active centres determined from the slope of the isotherm is $z = 0{\cdot}22 \times 10^{-9}$ g equivalent.

In addition the role of the chemisorbed oxide layer was confirmed(6) by the electrolysis of 0·001 N nitric acid solution with the platinum electrodes used in anodic electrolysis for 10 min. The circuit was then broken and a quantity of ^{204}Tl was added to the solution. About 26 per cent of the ^{204}Tl was deposited on the surface of the previously anodically polarized surface of the platinum strip (Fig. 11b). Thus this is not an electrolytic deposition, as the circuit was broken prior to the addition of the radioactive substance. Since under similar conditions only one to two per cent of the ^{204}Tl were deposited on the surface of platinum strips if it had not been polarized anodically, this considerable deposition of radioactive substance might be explained by the passivation of the platinum surface during the preceding electrolysis of the nitric

---

(21) N. BALASCHOWA, *Ber. Akad. Wiss. U.S.S.R.* **103**, 639 (1955).

acid solution. The passive layer remained on the surface even when electrolysis was interrupted and then negatively directed dipoles bound the radioactive ^{204}Tl.

These results allow us to interpret the behaviour of those types of radioactive atoms for which no change in valency can be assumed during anodic deposition. According to the data presented in Fig. 7, atoms such as ^{90}Y, ^{175}Yb, ^{166}Ho, ^{147}Pm, ^{143}Pr, are also deposited on the surface of the anode. In then cases we are dealing with simple surface processes without the transfer of electrons. Due to the attraction of the negatively directed dipoles formed by the platinum oxides, the radioactive substances are adsorbed on the surface.

The experimental results showing the value of the distribution coefficient changes so that maximum is found can be interpreted if the different processes (neutralization of OH^- ions, formation of an oxide layer on the surface of the platinum anode, oxygen production) occurring at the surface of the platinum anodes are known. This result can be attributed to the fact that at higher voltages continuous formation of oxygen occurs according to the following equation:(22)

$$\mathrm{Pt} + \mathrm{H_2O} \rightarrow \mathrm{Pt-O} + 2\mathrm{H^+} + 2e^-$$

$$\mathrm{Pt-O} + \mathrm{H_2O} \rightarrow \mathrm{Pt} + \mathrm{O_2} + 2\mathrm{H^+} + 2e^-$$

The oxygen evolved occupies more and more of the active centres on the surface of the passive platinum anode and consequently the anodic deposition of the radioactive substance is suppressed.

Our experiments have shown that the hydrogen ion concentration of the electrolyte has an effect on the anodic deposition as a function of time, on the equilibrium distribution coefficient, and on the number of active centres on the surface of the anode. This is as expected, because on the basis of experiments carried out by a large number of authors(23–26) with other types of radioactive atoms, it must be assumed that the following processes take place in the anode region:

$$2\mathrm{Tl^+} + 3\mathrm{H_2O} \rightleftharpoons \mathrm{Tl_2O_3} + 6\mathrm{H^+} + 4e^-$$

$$\mathrm{Ce^{3+}} + 2\mathrm{H_2O} \rightleftharpoons \mathrm{CeO_2} + 4\mathrm{H^+} + e^-$$

Taking into consideration the effect of the hydrogen ion concentration, the numerical value of the equilibrium potential may therefore be given as follows:

$$E_1 = E_1^0 - \frac{RT}{\nu F} \ln (a_{\mathrm{H}^+})^6 - \frac{RT}{\nu F} \ln \left(\frac{x}{1-x}\right)_{\infty,1} \tag{8}$$

or

$$E_2 = E_2^0 - \frac{RT}{\nu F} \ln (a_{\mathrm{H}^+})^4 - \frac{RT}{\nu F} \ln \left(\frac{x}{1-x}\right)_{\infty,2} \tag{8a}$$

Thus in general the following relation is obtained between the equilibrium distribution coefficient for the deposition of the radioactive substance on the anode and the hydrogen ion concentration of the electrolyte:

---

(22) J. Giner, *Z. Elektrochem.* **63**, 386 (1959).

(23) G. Hevesy and F. Paneth, *Montash.* **36**, 75 (1915).

(24) M. Haissinsky, *J. Chim. Phys.* **30**, 28 (1933).

(25) L. B. Rogers and A. F. Stehney, *J. Elechtrochem. Soc.* **95**, 33 (1949).

(26) M. Haissinsky, *Electrochimie des Substances Radioactives*, Paris (1946).

$$\log\left(\frac{x}{1-x}\right)_{\infty} = K - k\log(a_{H^+}) \tag{9}$$

As shown in Fig. 6 of our previous paper,(6) a linear relation was indeed obtained between the logarithm of the equilibrium distribution coefficient and the pH of the solution in the case of the anodic deposition of ^{144}Ce. Further experiments are however needed for the interpretation of the quantitative relations.

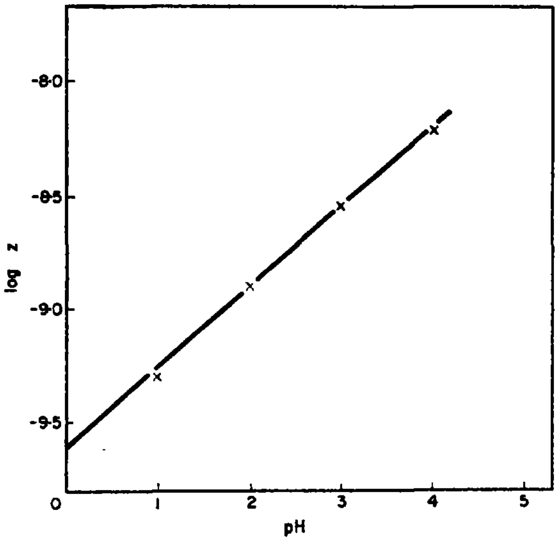

FIG. 13.—Correlation between the number of active centres on the surface of the platinum anode and the hydrogen ion concentration of the electrolyte.

The data of Fig. 6 in the present paper show the effect of the hydrogen ion concentration of the solution on the number of active centres on the surface of the anode.

From the slopes of these plots z may be calculated. Taking into consideration Equations (1), (8) and (8a) the following relation is obtained between the equilibrium potential and the number of active centres on the surface:

$$E_1 = E_1^0 - \frac{RT}{\nu F}\ln(a_{H+})^6 + \frac{RT}{\nu F}\ln C_1V - \frac{RT}{\nu F}\ln z_1 \tag{10}$$

$$E_2 = E_2^0 - \frac{RT}{\nu F}\ln(a_{H+})^4 + \frac{RT}{\nu F}\ln C_2V - \frac{RT}{\nu F}\ln z_2 \tag{10a}$$

The following relation is generally valid:

$$\log z = \text{Const} - \text{const}\log(a_{H+}) \tag{11}$$

Qualitatively this equation is in good agreement with the experimental data as shown in Fig. 13. Further experiments are needed to confirm the quantitative validity of Equation (11).

Our study suggests the possibility of making use of these observations in preparative nuclear chemical work, but, we cannot deal with the possibilities in detail in the present paper. For instance ^{144}Ce can be electrolytically separated from other rare earth type atoms, as about 90 per cent of ^{144}Ce is deposited from a 0·01 N nitric acid solution at 3 V applied voltage on the surface of the platinum anode, while under the same circumstances ^{90}Y, ^{175}Yb, ^{166}Ho for instance are not deposited. Of the radioactive species mentioned only about 10–15 per cent are deposited even from a 0·001 N nitric acid solution.

A combination of chromatography and electrolysis has been worked out and has been applied successfully in a number of cases.

Acknowledgement—The author wishes to express his thanks to Prof. L. IMRE for his valuable help offered in the course of this work.

J. Inorg. Nucl. Chem., 1962, Vol. 24, pp. 1517 to 1526. Pergamon Press Ltd. Printed in Northern Ireland

LOW-TEMPERATURE STUDIES OF RECOIL REACTIONS*

S. R. VELJKOVIĆ† and G. HARBOTTLE
Chemistry Department, Brookhaven National Laboratory,
Upton, Long Island, New York

(*Received* 16 *March* 1962; *in revised form* 10 *May* 1962)

Abstract—The Szilard-Chalmers reaction has been investigated in a number of crystalline compounds with a special effort being made to maintain the temperature at low values during bombardment, storage and dissolution. Evidence of rapid thermal annealing at moderate temperatures is found. The data suggest that it will for this reason be extremely difficult to obtain reliable information on the true yields of the hot-atom processes which occurred before any annealing took place.

IN two recent, short communications[1,2] the authors presented reasons for undertaking the investigation of the Szilard-Chalmers reaction in crystals continuously held at low temperature during the bombardment, storage and dissolution steps. Evidence was presented that annealing reactions were important at, and considerably below, ambient laboratory or reactor temperatures. The influence of thermal annealing, in several cases, was in fact so great as to vitiate entirely any mechanistic interpretations based upon those yields measured at room temperature.

In the present report, more complete data on these systems, and on a variety of others, are presented. The compounds investigated include bromacetic acid, bromacetates, and several oxyanion salts. These data confirm, in general, the fear that many retention figures previously reported in the literature actually represent the sum of two quantities: an unknown "intrinsic" retention,[3] which could only be measured by an experiment carried out *in toto* at an indefinitely low temperature, and an unknown increase in retention above this figure due to thermal (and/or radiation) annealing.

I. EXPERIMENTAL

1. *Preparation of material for bombardment*

Lithium nitrate was recrystallized twice from water, keeping the temperature above 70°C, to avoid formation of the trihydrate. The anhydrous salt was dried at 120°C and vacuum desiccated over Drierite before use. Potassium permanganate was recrystallized twice from hot water, dried and vacuum desiccated over Drierite. Potassium chromate and dichromate, and ammonium chromate, were the best reagent grade, used without further purification. Sodium chromate tetrahydrate was prepared by recrystallization from aqueous solutions kept above 30°C, as higher hydrates form below that temperature. Chromium trioxide was recrystallized from water-conc. nitric acid (1:5) solutions,

---

* Research performed under the auspices of the U.S. Atomic Energy Commission.

† On leave from the University of Belgrade, Yugoslavia.

(1) S. R. VELJKOVIĆ and G. HARBOTTLE, *Nature, Lond.* **191**, 1287 (1961).
(2) S. R. VELJKOVIĆ and G. HARBOTTLE, *J. Inorg. Nucl. Chem.* **23**, 159 (1961).
(3) K. J. MCCALLUM and A. G. MADDOCK, *Trans. Faraday Soc.* **49**, 1150 (1953).

filtered off and vacuum-desiccated over sodium hydroxide pellets: stock-bottle material gave identical results. It was found difficult to recrystallize bromacetic acid, and for this reason, although different lots of crystals gave consistent results, the authors regard these results as possibly subject to systematic error due to impurities. The procedure was to dissolve the bromacetic acid in ether, pass it once through an alumina column and re-evaporate the ether at room temperature, *in vacuo*. Sodium bromacetate was prepared by neutralizing ethanol solutions of bromacetic acid with ethanolic sodium hydroxide to bromthymol blue endpoint, avoiding excess base. The product was recrystallized twice from water and desiccated *in vacuo*. Potassium bromate was recrystallized from water and desiccated.

All solvents were the purest obtainable grade, and were redistilled before use. It was found imperative to purify the acetone used with permanganate from traces of methanol, and this was done by dissolving potassium permanganate in the acetone in excess, standing (dark) 24 hr, filtering and distilling through a column of 8 to 10 plates. Fresh acetone was prepared every two or three days.

The lithium chloride–water eutectic mixture (designated LiCl in the Tables) has been described.[1]

Where irradiated bromacetic acid was dissolved in methanol, an amount of sodium hydroxide calculated to neutralize it was present in the solvent. The same was true when it was dissolved in water. These solvents are designated MeOH—OH^- and H_2O—OH^- respectively in the tables.

2. *Bombardments*

Thermal neutron irradiations were made in the BNL graphite reactor. The positions were the pneumatic tube (PN 4, flux 4·8 × 10^{12} neutron/cm^2 sec, Cd ratio ca. 100, radiation level ca. 10^7 r/hr) for irradiations at ambient (see below) or dry-ice temperatures. The animal or instrument tunnels (flux about 2·9 × 10^9 neutron/cm^2 sec, Cd ratio ~120) were used for irradiations at liquid nitrogen temperature.

Fast neutron irradiations of lithium nitrate to produce the $^{14}N(n,2n)^{13}N$ reaction were made at the BNL 60 in. cyclotron (20 MeV deuterons on beryllium) and of sodium bromacetate to give ^{80m}Br by $^{81}Br(n,2n)$ at the Van de Graaff (800 keV deuterons on tritium). Samples were wrapped in cadmium foil to eliminate thermal neutrons.

A few irradiations of potassium permanganate were made in the 3 GeV internal proton beam of the BNL Cosmotron [$^{55}Mn(p,p3n)^{52}Mn$].

All samples were irradiated in the presence of air, in closed ampoules of appropriate materials.

Since the pneumatic tube PN 4 was employed for so many studies, the temperature conditions at the irradiation site were directly measured with a thermocouple. It was found that the temperature rose in the first 15 secs to ~35°C, in one minute to 48°C, 2 mins to 56°C and from 3·5 minutes onward was about 60°C. It is possible that the temperature of crystal samples in their containers did not rise quite so rapidly as this.

3. *Analytical procedures*

After irradiation, one portion of the lithium nitrate (for a total-activity determination) was weighed directly into a counting vial and dissolved. The vial was kept sealed to prevent loss of active gases. Another portion was dissolved in acetone at −60°C and aliquot portions were (a) evaporated to dryness in a stream of nitrogen and (b) treated with sulphamic acid and then evaporated to dryness. The sulphamic acid treatment converted recoil-produced NO_2 or NO_2^- to gaseous forms which were then removed. After evaporation, samples (a) and (b) were redissolved and counted. Comparison of the total activity and (a) samples gave the percentage of active gaseous species, while comparison of the total and (b) gave the retention, or percentage of ^{13}N present as nitrate. Positrons from ^{13}N were scintillation counted through their annihilation radiations.

Irradiated potassium permanganate was dissolved in acetone at temperatures from +21 to −95°C. The solution was filtered through layers of manganese dioxide on a glass frit. Experimentally it was found that three such filtrations, using fresh layers of aged MnO_2 each time, sufficed to remove all the separable activity. The MnO_2 was then treated with conc. HCl (it was not necessary to dissolve more than the surface layer, which contained all the adsorbed activity), Cl_2 was boiled out of the solution and the activity compared with that of the filtrate by scintillation counting of the ^{56}Mn (2·58 hr). All vessels were checked for ^{56}Mn adsorption on the walls.

Irradiated chromates dissolved in LiCl–H_2O eutectic mixture were analysed by a modification of the lead chromate procedure previously used.[4] Ten-millilitre aliquot portions of the LiCl–chromate solution (which had warmed up to about 0°C) were withdrawn: one was diluted to about 120 ml with water containing carrier Cr(III) and Cr(VI) (inactive) and a pH of 2·5 to 3·5. Lead chromate was precipitated, filtered off and washed, yielding the CrVI fraction of the sample. The second aliquot was diluted with 10 ml of water, made basic with NaOH and oxidized with Na_2O_2, excess peroxide being destroyed on the steam bath. The resultant solution was diluted to 120 ml and precipitated as before, yielding the total chromium fraction. The lead chromate precipitates were dissolved in nitric acid and the ^{51}Cr (27 day) scintillation counted, making use of a single channel analyser with samples of low activity.

---

[4] G. Harbottle, *J. Chem. Phys.* **22**, 1083 (1954).

Sodium chromate tetrahydrate and chromium trioxide which had been dissolved in acetone after bombardment were treated as above, except that the acetone was evaporated from the total chromium fraction before the NaOH–Na_2O_2 oxidation. The glass walls of various vessels were checked for adsorption of ^{51}Cr from acetone solutions: none was found. Irradiated potassium dichromate dissolved in water was analysed by the usual procedure.(4)

No solvent suitable for low-temperature dissolution of potassium bromate was found; therefore, it was dissolved, after irradiation, in water at ice-temperature and analysed by the paper-electrophoresis technique previously employed.(5)

Irradiated sodium bromacetate was dissolved in methanol at low temperatures and a 10 μl portion of the solution directly analysed for bromacetate and bromide activities by an electrophoresis technique.(5b) The percentage of organic bromide (principally CH_2Br_2) activity was determined by extraction with toluene.(6,7) Where $(n,2n)$ reactions were observed, the ^{80m}Br activity was too low for the electrophoresis technique. Here a silver bromide precipitation was employed:(7) the methanol solutions were much diluted with water to avoid reduction of silver ion. When bromacetic acid was dissolved in ether direct electrophoresis could not be used because of the apparent exchange of bromine between bromacetate and bromide. Hence, ether solutions were used only for determination of active CH_2Br_2, which did not exchange. ^{80m}Br activity was determined by either proportional or scintillation counting and ^{82}Br by scintillation counting.

In all radionuclide determinations, appropriate corrections for background, decay, and counting efficiency were applied. Since several of the low-temperature procedures employed novel solvents or reagents, in every case comparisons were made between a standard method for determination of the retention and the low-temperature method, with each applied to the same sample of room-temperature-irradiated and annealed material. For a low-temperature method to be acceptable, it was required that it give a retention for room temperature annealed material close to the conventional value.

II. RESULTS

The experimental results are presented in Tables 1 to 4. Some of these results have been given in our preliminary communications.(1,2) Unless otherwise noted, figures are averages of at least two, and in some cases as many as eight, determinations. The bombardment temperatures are nominal, liquid nitrogen being indicated by -195°C, dry-ice by -78, ambient (room) by $+25$, which also is applied to bombardments in PN 4 for 10 or 15 sec (see "Bombardments" above) and 3 min bombardments in PN 4 by $+50$, nearly the final temperature attained. The "storage" temperature applies from the moment of removal of the sample from the bombardment site and the dissolution temperature should also be considered as subject to variations of a few degrees. Under the heading "Medium" Acet. = purified acetone, LiCl = LiCl—H_2O eutectic mixture, H_2O = water containing inactive carriers, Ether = redistilled diethyl ether, MeOH = redistilled methanol. MeOH—OH^- and H_2O—OH^-, methanol and water made basic with NaOH, see "Experimental" Section 1.

Errors attached to the results in the tables are $\pm 0{\cdot}6$ per cent in the chromate series, $\pm 0{\cdot}3$ per cent in the bromates, bromacetates and permanganates, about $\pm 0{\cdot}8$ per cent in bromacetic acid, ± 1 per cent in lithium nitrate and ± 4 per cent in figures preceded by "ca".

---

(5) a. J. Jach and G. Harbottle, *Trans. Faraday Soc.* **54**, 520 (1958);
b. J. Jach, H. Kawahara and G. Harbottle, *J. Chromatography* **1**, 501 (1958);
c. G. Harbottle, *J. Amer. Chem. Soc.* **82**, 805 (1960).

(6) E. Glueckauf and J. W. J. Fay, *J. Chem. Soc.* 390 (1936).

(7) M. Vlatkovic and A. H. W. Aten Jr., *J. Inorg. Nucl. Chem.* **14**, 134 (1960).

III. DISCUSSION

Comparison with other authors

If our results are compared with those of other authors, reasonable agreement is found where the experimental conditions are strictly comparable. For example, **Vlatković** and **Aten**(7) find 56 ± 4 and 49 ± 1 per cent retention for (presumably) room-temperature thermal neutron irradiations of bromacetic acid, for the isotopes ^{80m}Br and ^{82}Br. We obtain 53·1 and 47·5 per cent. They have slightly lower results than ours for room-temperature sodium bromacetate. Our figures for yield of methylene dibromide agree well with theirs in the case of the sodium salt, but not in the acid.

In the bromates, chromates and permanganates generally good agreement is obtained.(3,4,5c,8,11a) In lithium nitrate **Smith** and **Aten** obtained 51 ± 4 per cent retention;(9) we have 53·1 per cent. In chromium trioxide **Harbottle** and **Maddock**(10) found 79·1 per cent retention against 73·0 here, but the bombardment was much longer in the former case.

Effect of temperature and annealing

If we examine Tables 1 and 2 it may be noted that all compounds studied, except CrO_3, showed the same trend to lower retentions as temperatures were held to lower values during irradiation, storage and dissolution. This trend has been noted previously(11) and appears to be very general. As we mentioned in our preliminary announcements,(1,2) it clearly implies that until much more work is done on bombardments and analyses at very low temperatures, one will not have trustworthy data which can be used to develop or to test theories (like the "billiard-ball",(12) "brush-heap"(13) or "hot-zone"(14) models) which are concerned with the interpretation of recoil-atom product yields in crystals. If we adopt a Vand-Primak(15) picture, i.e. that the annealing processes are distributed over a spectrum of activation energies, these data imply that the spectra are in general so broad that not merely processes which go at or above room temperature ($E_{act} \approx$ 0·7 or 0·8–1·2 eV) but also processes which go at considerably lower temperatures (0·8 eV in activation energy) are present. Potassium permanganate and $Na_2CrO_4 \cdot 4H_2O$ furnish striking examples of this. It is interesting that bromine atoms which have recoiled with very high energies show the same trend ($CH_2BrCOONa$, (*n*, 2*n*) reaction, Table 2).

If in Tables 1 and 2 one compares the results for the completely room-temperature experiments (bombardment temperatures > 25°C and storage temperature 25°C) with the "quenching" experiments (samples quickly transferred to dry-ice after

(8) H. Sano, *Bull. Chem. Soc. Japan* **33**, 1738 (1960).

(9) R. D. Smith and A. H. W. Aten Jr., *J. Inorg. Nucl. Chem.* **1**, 296 (1955).

(10) G. Harbottle and A. G. Maddock, *J. Inorg. Nucl. Chem.* **5**, 249 (1958).

(11) a. J. W. Cobble and G. E. Boyd, *J. Amer. Chem. Soc.* **74**, 1282 (1952);
 b. H. Rauscher and G. Harbottle, *J. Inorg. Nucl. Chem.* **4**, 155 (1957);
 c. L. Lindner and G. Harbottle, *Chemical Effects of Nuclear Transformations*, p. 485, International Atomic Energy Agency, Vienna (1961).
 d. G. Harbottle, *Ibid.* p. 301.

(12) W. F. Libby, *J. Amer. Chem. Soc.* **62**, 1930 (1940).

(13) J. E. Willard, *Ann. Rev. Nucl. Sci.* **3**, 193 (1953).

(14) a. P. E. Yankwich, *Canad. J. Chem.* **34**, 301 (1956);
 b. L. Lindner. Thesis, University of Amsterdam (1958);
 c. G. Harbottle and N. Sutin, *J. Amer. Chem.* **62**, 1344 (1958).

(15) a. V. Vand, *Proc. Phys. Soc.* (London) A **55**, 222 (1943);
 b. [illegible] Primak, *Phys. Rev.* **100**, 1677 (1955).

TABLE 1.—THE INFLUENCE OF THE THERMAL HISTORY OF A SAMPLE UPON ITS MEASURED RETENTION: OXYANION COMPOUNDS

Compound	Nuclear process	Bombardment Temp (°C)	Bombardment Time	Storage Temp (°C)	Storage Time	Dissolution Temp (°C)	Dissolution Time	Medium	Retention (%)
$LiNO_3$	$^{14}N(n, 2n)^{13}N$	−78	15 min	−78	10 min	−60	5 min	Acet	43·9
		+25	15 min	+25	10 min	−60	5 min		53·1
$KMnO_4$	$^{55}Mn(n, \gamma)^{56}Mn$	−195	90 min	−195	1 hr	−95	15 min	Acet	5·1
		−78	15 sec	−78	2 hr	−60	10 min		8·9
		+25	15 sec	−78	2 hr	−60	10 min		15·6
		−78	15 sec	−78	2 hr	+21	2 min		18·2
		+25	15 sec	+25	2 hr	−60	10 min		19·3
		+25	15 sec	+25	2 hr	+2	5 min	H_2O	20·7
$KMnO_4$	$^{55}Mn(p, p3n)^{52}Mn$	+25	15 min-2 hr	+25	5 hr	−60	10 min	Acet	ca. 18
K_2CrO_4	$^{50}Cr(n, \gamma)^{51}Cr$	−195	4 hr	−195	1 day	−55	4 hr	LiCl	ca. 40
		−78	3 min	−78	3 days	−55	4 hr	LiCl	47·2
		−78	3 min	−78	6 days	+2	5 sec	H_2O	50·0
		+50	3 min	+25	6 days	+2	5 sec	H_2O	60·4
		+50	3 min	+25	6 days	−55	4 hr	LiCl	58·6
$K_2Cr_2O_7$	$^{50}Cr(n, \gamma)^{51}Cr$	−78	3 min	−78	1 day	−55	6 hr	LiCl	65·3
		+25	7 day	+25	6 days	+25	15 sec	H_2O	89·9*
$(NH_4)_2CrO_4$	$^{50}Cr(n, \gamma)^{51}Cr$	−78	3 min	−78	1 day	−55	4 hr	LiCl	10·1
		−78	3 min	−78	1 day	+2	5 sec	H_2O	14·5
		+50	3 min	+25	1 day	+25	5 sec	H_2O	17·3
		+50	1 min	+25	1 day	−55	4 hr	LiCl	16·7
$Na_2CrO_4 \cdot 4H_2O$	$^{50}Cr(n, \gamma)^{51}Cr$	−195	4 hr	−195	1 day	−92	4 hr	Acet	32·1
		−195	4 hr	−195	1 day	−55	4 hr	LiCl	35·3
		−78	3 min	−78	6 days	−55	4 hr	LiCl	39·8
		+50	3 min	−78	1 day	−55	4 hr	LiCl	54·8
		+50	3 min	+25	6 days	−55	4 hr	LiCl	88·6
		+50	3 min	+25	6 days	+2	30 sec	H_2O	89·3†
CrO_3	$^{50}Cr(n, \gamma)^{51}Cr$	−78	3 min	−78	2 hr	−80	1 hr	Acet	69·1
		+50	3 min	+25	7 days	−60	30 min	Acet	68·8
		+50	3 min	+25	7 days	+25	5 sec	H_2O	73·0

---

* Thermal-column bombardment, flux 6 × 10^8 n/cm^2 sec, Ref. 4.

† Single determination, in good agreement with previous results, Reference (4).

TABLE 2.—THE INFLUENCE OF THE THERMAL HISTORY OF A SAMPLE UPON ITS MEASURED RETENTION: COMPOUNDS CONTAINING BROMIDE

Compound	Nuclear process	Bombardment		Storage		Dissolution		Medium	Retention (%)	
		Temp (°C)	Time	Temp (°C)	Time	Temp (°C)	Time		^{80m}Br	^{82}Br
$KBrO_3$	$^{79}Br(n, \gamma)^{80m}Br$	−78	3 min	−78	2 hr	+2	1 min	H_2O	10·9	12·2
	and	+25	10 sec	+25	2 hr	+2	1 min	H_2O	12·1	13·2
	$^{81}Br(n, \gamma)^{82}Br$	+50	3 min	−78	2 hr	+2	1 min	H_2O	13·3	13·5
		+50	3 min	+25	2 hr	+2	1 min	H_2O	15·6	16·5
$CH_2BrCOOH$	$^{79}Br(n, \gamma)^{80m}Br$	−195	5 hr	−195	2 hr	−95	45 min	MeOH—OH^-	39·5	34·0
	and	−78	10 sec	−78	2 hr	−60	15 min	MeOH—OH^-	42·5	37·4
	$^{81}Br(n, \gamma)^{82}Br$	+25	10 sec	+25	2 hr	−60	15 min	MeOH—OH^-	53·1	47·5
		−78	10 sec	−78	2 hr	+2	1 min	H_2O—OH^-	42·5	37·4
$CH_2BrCOONa$	$^{79}Br(n, \gamma)^{80m}Br$	−195	4 hr	−195	2 hr	−60	15 min	MeOH	25·0	18·0
	and	−78	3 min	−78	2 hr	−60	15 min	MeOH	25·5	18·1
	$^{81}Br(n, \gamma)^{82}Br$	+25	10 sec	−78	2 hr	−60	15 min	MeOH	26·6	18·3
		+25	10 sec	+25	2 hr	−60	15 min	MeOH	30·5	25·4
$CH_2BrCOONa$	$^{81}Br(n, 2n)^{80m}Br$	−78	1·5 hr	−78	1 hr	−60	15 min	MeOH	19·4	
		+25	10 min	−78	1 hr	−60	15 min	MeOH	19·6	
		+25	1 hr	+25	1 hr	−60	15 min	MeOH	26·4	

bombardment at $T > 25°C$) one can obtain a measure of the room-temperature annealing which follows a hot atom process that also took place at or near room temperature. More direct evidence for rapid room-temperature annealing is given in Table 4.

If one now compares, in Table 2, the retentions in the "quenching" experiment on sodium bromacetate ($R = 26{\cdot}6$ and $18{\cdot}3$ for ^{80m}Br and ^{82}Br) with those for the dry-ice bombardment ($R = 25{\cdot}5$ and $18{\cdot}1$) it is noted that there is little effect of the ambient temperature during bombardment upon the yield. The same is true in the fast neutron bombardment of this salt (Table 2).

Annealing effects similar to those presented in Tables 1 and 2 for the parent species ("retention" measurement) are presented in Table 3 for a radiosynthetic product, CH_2Br_2. Here again yields are found to decrease sharply with decreasing temperature.

The effect of increasing the bombardment time can be seen in the bromacetate yields from the sodium salt, if one compares the samples bombarded for 3 min at −78°, and annealed at room temperature, +25 for 2 hr (retentions 32·3 and 24·0 per cent, Table 4, line 3) with those bombarded for 10 sec at room temperature, and annealed the same period (retentions 30·5 and 25·4 per cent, Table 2, line 12). Presumably the crystal bombarded at dry-ice temperature "stores up" radiation damage, for example trapped electrons, which then increase the annealing in the ^{80m}Br isotope on warming to room temperature. A similar phenomenon has been observed in the hot-atom chemistry of bromine atoms in C_2Br_6(16) and $Ca(BrO_3)_2$,(17) and in K_2CrO_4.(18)

Although mechanisms for annealing reactions of hot atoms must necessarily be speculative, one can imagine that the increases in $BrCH_2COO^-$ and CH_2Br_2 yields in the various samples are the result of recombinations of bromine atoms with radicals such as $\cdot CH_2COO^-$ and $CH_2Br\cdot$. Spin resonance techniques have demonstrated the presence of $\cdot CH_2COOH$ in γ-irradiated crystals of malonic acid.(19) One would expect trapped atoms to become mobile in solids at temperatures T(°K) such that the reduced temperature T/T_m (where T_m is the melting temperature °K) $\approx 0{\cdot}4$–$0{\cdot}6$.(20) For bromacetic acid this would be 130–194°K, both below dry-ice temperature, and for sodium bromacetate around 160–250°K, a range which is certainly in the range of our experiments. By analogy one might envision recombination processes involving oxygen atoms in the oxyanion series.

Isotope effects

The experiments presented in Tables 2 and 4 show clearly that the two isotopes of bromine, ^{80m}Br and ^{82}Br, do not behave identically. JACH and HARBOTTLE have shown(5a) that in the annealing reactions of bromine atoms in crystalline alkali bromates, ^{82}Br annealed more rapidly than ^{80m}Br, coming to a higher plateau. Since the isotopic atoms differ so little in mass, the large differences observed in experiments of the kind reported here must come about as a result of the nuclear process being different,

---

(16) J. E. WILLARD, Progress Report, University of Wisconsin, dated March 1, 1961.

(17) A. G. MADDOCK and H. MULLER, *Trans. Faraday Soc.* **56**, 509 (1960).

(18) A. G. MADDOCK and J. I. VARGAS, *Nature, Lond.* **184**, 1931 (1959).

(19) A. HORSFIELD, J. R. MORTON and D. H. WHIFFEN, *Mol. Phys.* **4**, 327 (1961).

(20) G. C. PIMENTEL, *Formation and Trapping of Free Radicals* (Edited by A. M. BASS and B. P. BROIDA) pp. 75 et seq. Academic Press, New York (1960).

TABLE 3.—THE YIELD OF ORGANIC BROMIDES IN NEUTRON-IRRADIATED BROMACETATES

Compound	Nuclear process	Irradiation Temp (°C)	Irradiation Time	Storage Temp (°C)	Storage Time	Dissolution Temp (°C)	Dissolution Time	Medium	Organic Yield* ^{80m}Br	Organic Yield* ^{82}Br
$CH_2BrCOOH$	(*n*, γ)	−195	5 hr	−195	2 hr	−95	30 min	Ether	16·2	18·3
		−78	10 sec	−78	2 hr	−60	15 min	Ether	18·5	21·3
		+25	10 sec	+25	2 hr	−60	15 min	Ether	31·1	31·2
$CH_2BrCOONa$	(*n*, γ)	−195	5 hr	−195	2 hr	−60	15 min	MeOH	2·9	3·2
		−78	3 min	−78	2 hr	−60	15 min	MeOH	2·9	3·1
		+25	3 min	+25	2 hr	−60	15 min	MeOH	3·8	3·9
$CH_2BrCOONa$	(*n*, 2*n*)	−78	1·5 hr	−78	1 hr	−60	15 min	MeOH	3·1	
		+25	1 hr	+25	1 hr	−60	15 min	MeOH	3·9	

* The organic bromides are mainly CH_2Br_2. The yield of labelled $BrCH_2COO^-$ ion is reported as the "Retention" in Table 2, and is not included in this table.

TABLE 4.—EFFECT OF POST-IRRADIATION ANNEALING UPON THE RETENTION

Compound	Nuclear process	Bombardment Temp (°C)	Bombardment Time	Annealing or storage Temp (°C)	Annealing or storage Time	Dissolution Temp (°C)	Dissolution Time	Medium	Retentions (%) ^{80m}Br	Retentions (%) ^{82}Br
$CH_2BrCOONa$	(*n*, γ)	−195	4 hr	−195	2 hr	−60	15 min	MeOH	25·0	18·0
		−78	3 min	−78	2 hr	−60	15 min		25·5	18·1
		−78	3 min	+25	2 hr	−60	15 min		32·3	24·0
				+45	1 min				31·8	28·8
				+45	3 min				33·1	27·6
				+45	11 min				35·8	30·0
		+50	3 min	−78	2 hr	−60	15 min		30·0	19·5
		+50	3 min	+25	2 hr	−60	15 min		33·5	26·2
		+25	10 sec	+25	2 hr	−60	15 min		30·5	25·4
$CH_2BrCOONa$	(*n*, 2*n*)	−78	1·5 hr	−78	1 hr	−60	15 min	MeOH	19·4	
		−78	1·5 hr	+25	2 hr	−60	15 min		24·0	
				+54	3 min				24·0	
				+54	11 min				39·3	
		+25	10 min	−78	2 hr	−60	15 min		19·6	
		+25	1 hr	+25	2 hr	−60	15 min		26·4	
$(NH_4)_2CrO_4$	(*n*, γ)	−78	3 min	−78	1 day	−55	4 hr	LiCl	10·1	
		−78	3 min	*		+2	5 sec	H_2O	14·5	
$K_2Cr_2O_7$	(*n*, γ)	−78	3 min	−78	1 day	−55	6 hr	LiCl	65·3	
		−78	3 min	−78	1 day	−20	2 hr	LiCl	67·5	
		−78	3 min	*		+2	30 sec	H_2O	71·9	
$Na_2CrO_4 \cdot 4H_2O$	(*n*, γ)	−78	3 min	−78	6 days	−55	4 hr	LiCl	39·8	
		−78	3 min	*, †		+2	30 sec	H_2O	47·3	
				+20	1 min	+2	30 sec	H_2O	54·1	
				+20	3 min				58·9	
				+20	10½ min				58·1	
				+20	35 min				64·2	
				+20	27 hr				79·0	

---

* In this experiment, annealing only occurred during the period of warmup and dissolution: i.e., the sample was transferred from its container at −78°C into water at +2 and dissolved as quickly as possible.

† This, and the following experiments are single determinations, to which an error of about ±2 per cent should be attached.

i.e. in differing internal conversion of capture γ-rays(21) or different recoil energy. Although the errors are large our data suggest that the largest isotopic differences occur in the least-annealed samples. These larger differences would then be related to annealing events having the lowest activation energies, in the Vand-Primak distribution. We are thus led to believe that here the true initial differences in recoil behaviour, i.e. in the environments of the hot-atoms immediately following recoil, with a minimum distortion due to subsequent annealing, are reflected. Clearly more work, involving experiments in which annealing is followed with greater precision at low temperature, is needed.

IV. CONCLUSIONS

It would appear from these results, and from others in which low-temperature annealing has been noted(11) that, for the time being, we must be prepared to get along without any reliable information on the "primitive", or "intrinsic" yields of hot-atom reactions in crystals except, of course, where those yields are essentially zero. This will continue to be the case until new techniques, perhaps utilizing spin-resonance measurements at low temperature, can be brought to bear on the question "What radioactive species are present after recoil, but before annealing, in a solid?" An extension of existing chemical analytical techniques to lower temperatures is also desirable, but it will probably prove difficult to operate at sufficiently low temperatures.

We may, however, continue to study the course of annealing reactions in solids, and hope that these studies can be correlated with experiments and theory from the field of Solid State Physics, to yield information on diffusion, interstitial-vacancy recombination, lattice relaxation, electron traps and related topics.

(21) S. WEXLER and T. H. DAVIES, *J. Chem. Phys.* **20**, 1688 (1952).

J. Inorg. Nucl. Chem., 1962, Vol. 24, pp. 1527 to 1538. Pergamon Press Ltd. Printed in Northern Ireland

RADIATIONS FROM SHORT-LIVED RARE GAS FISSION PRODUCTS*†

M. A. WAHLGREN‡ and W. W. MEINKE
Department of Chemistry, University of Michigan, Ann Arbor, Michigan

(*Received* 15 *February* 1962; *in revised form* 21 *May* 1962)

Abstract—The energies of the primary γ-rays emitted in the decay of 3·2 min ^{89}Kr, 33 sec ^{90}Kr, 1·2 min ^{91m}Rb, 41 sec ^{139}Xe, and 66 sec ^{140}Cs were determined and relative γ-ray intensities measured. Photon per disintegration values were estimated for ^{89}Kr, ^{90}Kr, ^{139}Xe and for 9·5 min ^{139}Cs. β-ray energy endpoints were measured for ^{89}Kr, ^{90}Kr, ^{139}Xe and ^{139}Cs, and lower limits established for the decay energies of these nuclides. A simple and rapid gas chromatographic separation which was developed for these studies is described.

A SYSTEMATIC study of the half-lives of the short-lived ($T_{\frac{1}{2}} < 5$ min) gaseous fission products was made by DILLARD *et al.*,(1) utilizing the collection of the daughter activities on a charged wire in a gas flow tube, with subsequent radiochemical analysis to determine the distribution along the length of the wire. They obtained half-lives for the krypton isotopes of mass numbers 89, 91, 92, 93, 94, 95 and 97, and for the xenon isotopes of mass numbers 139, 140, 141, 143 and 144.

Half-life measurements and β-ray endpoint determinations for the krypton and rubidium isotopes of mass numbers 89, 90 and 91 were made by KOFOED-HANSEN and NIELSEN(2) by means of an isotope separator. They also reported the detection of gamma radiations from ^{90}Rb, ^{91}Rb and ^{91m}Rb.

The nuclear characteristics reported in the literature for the nuclides of interest in the present study are given in Table 1.

In the present work, the radiations of several gaseous fission products and daughters with half-lives in the range of 30 sec to several minutes have been studied by γ- and β-ray spectrometry. These data are of considerable interest in the study of the fission process, in nuclear level systematics, and in reactor shielding calculations.

EXPERIMENTAL

Irradiation and sampling

The gas samples were obtained by irradiation of ~50 mg samples of uranyl nitrate for 10–20 sec in the pneumatic tube facility(8,9) of the 1 MW Ford Nuclear Reactor at the University of Michigan.

---

* This work was supported in part by the Michigan Memorial Phoenix Project and by the U.S. Atomic Energy Commission.

† Based in part on a dissertation by M. A. WAHLGREN, submitted to the University of Michigan in partial fulfillment for the Ph.D. degree in Chemistry.

‡ Present address: Chemistry Division, Argonne National Laboratory, Argonne, Illinois.

(1) C. R. DILLARD, R. M. ADAMS, H. FINSTON and A. TURKEVICH, in Coryell and Sugarman, *Radiochemical Studies; The Fission Products* (Edited by C. D. CORYELL and N. SUGARMAN) NNES Plutonium Project Record p. 624. McGraw-Hill, New York (1951).

(2) O. KOFOED-HANSEN and K. O. NIELSEN, *Phys. Rev.* **82**, 96 (1951).

(8) W. W. MEINKE, *Nucleonics* **17**, No. 9, 86 (1959).

(9) The instrumentation, techniques, and experimental results are described in considerably more detail in the Ph.D. thesis of M. WAHLGREN, University of Michigan, 1961 (unpublished); and U.S. Atomic Energy Commission Report TID-11807 (1961).

TABLE 1.—SUMMARY OF PERTINENT NUCLEAR DATA FROM THE LITERATURE(3,4)

Nuclide	Half-life	E_γ (MeV)	E_β −(MeV)
^{89}Kr	3·2, 2·6 or 2·5 min	—	4·0, 3·9
^{90}Kr	33 sec	—	3·2
^{91}Kr	9·8, 10 or 6 sec	—	3·6
^{89}Rb	15·4, 14·9 or 15·5 min	Several(6)	3·9, 4·5, 3·8
^{90}Rb	2·7 min	Several(6)	5·7
^{91m}Rb	1·67 or 1·2 min(9)	Detected	4·6
^{139}Xe	41 sec	—	—
^{140}Xe	16 or 9·8 sec	—	—
^{139}Cs	9·5, 10 or 7 min	0·630, 1·270(7)	—
^{140}Cs	66 sec	—	—
^{139}Ba	84 or 86 min	0·163, 1·43	2·4, 2·2, 0·8

(3) D. STROMINGER, J. M. HOLLANDER and G. T. SEABORG, *Rev. Mod. Phys.* **30**, 585–904 (1958).

(4) K. WAY (Editor) Nuclear Data Group, *Nuclear Data Sheets*, National Academy of Sciences, National Research Council, Washington.

(5) A. C. WAHL, R. L. FERGUSON, D. R. NETHAWAY, D. E. TROUTNER and K. WOLFSBERG, U.S.A.E.C. Report TID-13127 (1961).

(6) G. D. O'KELLEY, E. EICHLER and N. R. JOHNSON, Paper P/672, Vol. 15, *Proceedings of the Second International Conference on the Peaceful Uses of Atomic Energy, Geneva*, 1958. Paper P/672 Vol. 15 United Nations (1959).

(7) J. WASSON, MIT Laboratory for Nuclear Science, Progress Report, May 31, 1958 (unpublished).

Sample transfer from the irradiation position to a hood in the chemistry laboratory required three seconds.

The inert fission gases which separate from the gross fission products by emanation(10) were drawn from the polyethylene irradiation capsule with the sampling device shown in Fig. 1. Although the emanation from organic uranium salts has been shown to be more quantitative than from the nitrate, the small sample size possible with the nitrate is important in this case because of experimental conditions.

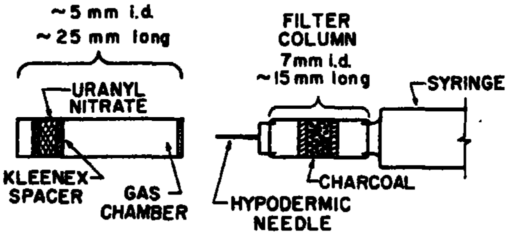

FIG. 1.—System for sampling fission gas.

Preliminary experiments established that the differences in adsorptivity and in effusion rates through the pores of the charcoal were sufficient to accomplish the separation of the submicro amounts of gas into kyrpton and xenon fractions.(9) The krypton was drawn through the column into the syringe while the xenon was retained in the charcoal column. With this system the gas sample could be drawn and separated within 15 sec after the end of irradiation.

The xenon release from a typical column (3–4 mm thick and 7 mm in diameter) left unsealed was studied with 9·1 hr ^{135}Xe tracer. At 25°C and atmospheric pressure the xenon activity decreased by a factor of two each 5 min. Abrupt reduction of pressure by as much as a factor of two across the column in the sampling process was found to lead to carry-through of xenon with the krypton fraction. Pressure reduction sufficient to give a flow rate of carrier gas (air) of 0·1 cm^3 sec^{-1} yielded quantitative separation under the conditions of these experiments, but limited the minimum sampling time to ~5 sec.

By variation of irradiation time, decay time, and by passing the residual gas through paper filters, it was possible to obtain spectra of the various daughter activities as well as those of the longer-lived gaseous nuclides. These spectra are necessary for the analysis of the complex spectra obtained with the short-lived gases.

---

(10) A. C. WAHL and N. A. BONNER, *Radioactivity Applied to Chemistry*, Chap. 9. J. Wiley, New York (1951).

Instrumentation and counting techniques

The dual memory 100-channel pulse-height analyser with associated rapid transfer equipment and detectors used in these studies has been described previously.(8,9) The handling and transfer time from hood to counter (from the midpoint of the sampling period to the start of counting) was 12 sec for γ-ray counting and 24 sec for β-ray counting samples.

All γ-ray spectra were taken at a standard source distance of 10 cm from the 3 in × 3 in. NaI(Tl) crystal using a 2·5 g cm^{-2} Be absorber, with the exception of ^{91m}Rb which was run at 6 cm due to the low counting rate. Sample size was chosen to give at least 75 per cent analyser "live time" to minimize spectral distortion. The resolution of the 3 in. × 3 in. crystal was 7·3 per cent at 0·662 MeV.

The analyser was recycled at 0·5, 5 and 50 min intervals during the decay of the short-lived parent, the daughter, and the longer-lived components respectively. Semi-logarithmic plots of these data readily show the parent-daughter relationships.

For γ-ray spectra of the short-lived xenon fraction the sample was drawn, the charcoal column sealed into a polyethylene "rabbit", and sent by a secondary pneumatic loop to the counting position at the γ-detecting crystal. For the krypton fraction a special polyethylene syringe was used which could be sealed and utilized as a rabbit for transfer to the counter.(9)

A 1 in × 1½ in. right-cylindrical plastic phosphor was used to obtain β-ray spectra. Although subject to distortion from the ampoules, Compton recoil electrons and the general multi-nuclide background, the spectra allow an approximate measurement of the maximum or predominant β-ray endpoint observed in the decay of the short-lived fractions. Energy calibration was based on the known endpoints of ^{89}Rb (3·9 MeV) and ^{138}Cs (3·4 MeV) daughter activities present in the samples. The contribution of Compton electrons was estimated by comparison with a set of similar samples counted through a 1 g cm^{-2} Be absorber. The calibration was checked with $^{90}Sr - ^{90}Y$ and ^{36}Cl sources. Due to the difficulty of reproducing the exact geometry, scattering and absorption of the experimental samples, it was felt that the most reliable calibration was that obtained from known daughter activities in the same samples. The reproducibility of the endpoints measured by this technique is ±0·2 MeV.

Analysis of data

Because of the complexity and possible ambiguity of the β-ray spectra, the quantitative results quoted have been derived from analysis of the gamma-ray spectra in the manner of O'KELLEY *et al.*(10) The pulse height distribution parameters of resolution, Compton continuum, Compton edge, and escape peaks were established from spectra of thirteen nuclides giving essentially monoenergetic γ-ray spectra, for the energy range from 0·191 to 4·1 MeV. From these parameters additional pulse height distributions were synthesized where necessary to provide a reference spectrum at each 0·3 MeV interval in the range from 1 to 4·5 MeV.

Corrections were made where appropriate for the analyser "dead time" and for the time of count, if long compared to the half-life. Subtraction of the contribution of the other nuclides observed in the decay of the sample was then performed if the contribution to the first spectra was significant. The subtraction of each successive gamma ray followed fitting of the top and leading edge from the appropriate reference pulse height distribution. In several cases it was not possible to begin with the highest energy peak observed because of poor statistics. In these cases the first clearly defined peak in order of decreasing energy was used as a starting point.

For the calculation of relative intensities, peak efficiencies based on the data of HEATH(11) and of WOLICKI *et al.*(12) were used. Correction was made for attenuation by the β-absorber based on experimental absorption measurements.

The photon per disintegration rates were derived from analysis of the spectra of the appropriate daughter activity. For this determination neither absolute counting nor intercalibration of counters is required. The geometry of the source is the same for both parent and daughter, and the relative peak efficiencies are well known. The accuracy of the calculation is determined by the accuracy of the half-lives assumed for the calculation, the error in γ-ray spectral analysis, and the validity of the literature values for the decay schemes of the respective daughter activities.

Each of the experiments described in the following section was repeated at least three times. The relative abundances were reproducible to within 5 per cent, and the photon per disintegration values to within 10 per cent, for the primary γ-rays. For precise analysis the coincidence summing should be

---

(11) R. L. HEATH, U.S.A.E.C. Report IDO-16408 (1957).

(12) E. A. WOLICKI, R. JASTROW and F. BROOKS, Naval Research Laboratory Report NRL-4833 (1956).

Table 2.—Summary of experimental data

Nuclide	Half-life (observed)	Irradiation time (sec)	Cooling time (sec)	γ Energy (MeV)	Relative abundance	Photon/dis-integration	β Energy (MeV)	Decay Energy (MeV) (Estimated)	Fig. No.
^{89}Kr	3·2 ± 0·3 (min)	15	240	0·215	80	0·31*	4·0	4·6	2,3
				0·375	35	0·13			
				0·430	33	0·13			
				0·510	49	0·19			
				0·595	100	0·39			
				0·730	39	0·15			
				0·880	58	0·23			
				1·12]	50	0·19			
				1·32	34	0·13			
				1·52	70	0·27			
				1·67	31	0·12			
				1·90	16	0·061			
				2·05	26	0·10			
				2·23	14	0·054			
				2·35	25	0·099			
				2·62	8·0	0·031			
				2·70	5·7	0·022			
				2·85	18	0·071			
				3·00	8·9	0·035			
				3·18	11	0·043			
				3·38	15	0·060			
				3·56	11	0·043			
				3·72	11	0·043			
				3·90	9·6	0·037			
				4·05	3·4	0·014			
				4·16	2·7	0·010			
				4·31	2·7	0·010			
				4·58	1·1	0·005			

^{90}Kr	33 ± 2 sec	10	12–30	0·125	100	0·67†	1·8	3·6	4
				0·240	10	0·07			
				0·540	100	0·67			
				1·10	100	0·67			
				1·54	42	0·28			
				1·78	19	0·12			
^{91m}Rb	1·2 ± 0·1 min	20	30	0·095	100	—	—	—	5
				0·350	47				
^{139}Xe	41 ± 2 sec	15	30	0·170	40	0·20‡	4·6	4·6	6
				0·220	100	0·49			
				0·295	53	0·26			
				0·395	21	0·10			
^{139}Cs	9·5 min§	20	100	1·270	100	0·12‡	3·8	3·8	7
				0·630	18	0·02			
^{140}Cs	66 ± 2 sec	15	40	0·610	—	1·0 (estimated)	—	—	8

---

* Assuming 1250 keV photons in 54 per cent of the disintegrations(6) of ^{89}Rb, and half-lives of 3·2 min and 14·9 min for ^{89}Kr and ^{89}Rb, respectively.

† Assuming 840 keV photons in 61 per cent of the disintegrations(6) of ^{90}Rb, and half-lives of 33 sec and 2·7 min for ^{90}Kr and ^{90}Rb, respectively.

‡ Assuming 165 keV photons in 23 per cent of the disintegrations(13) of ^{139}Ba, and half-lives of 41 sec, 9·5 min, and 85 min for ^{139}Xe, ^{139}Cs and ^{139}Ba, respectively.

§ Accuracy is less than for other nuclides because of an interfering peak at about the same energy.

(18) R. L. MACKLIN. N. H. LAZAR and W. S. LYON, *Phys. Rev.* **107**, 504 (1957).

taken into account. This effect was checked experimentally by comparison of spectra taken at 1 and at 10 cm. The differences, however, were within the experimental error and have been ignored in the data summation which follows.

EXPERIMENTAL RESULTS

The experimental data are summarized in Table 2. A brief discussion of the experiments and the γ-ray spectra obtained are given in the following section. Due to the multi-component nature of some of the spectra and to the poor statistics in counting short-lived samples, low intensity γ rays present may not have been detected.

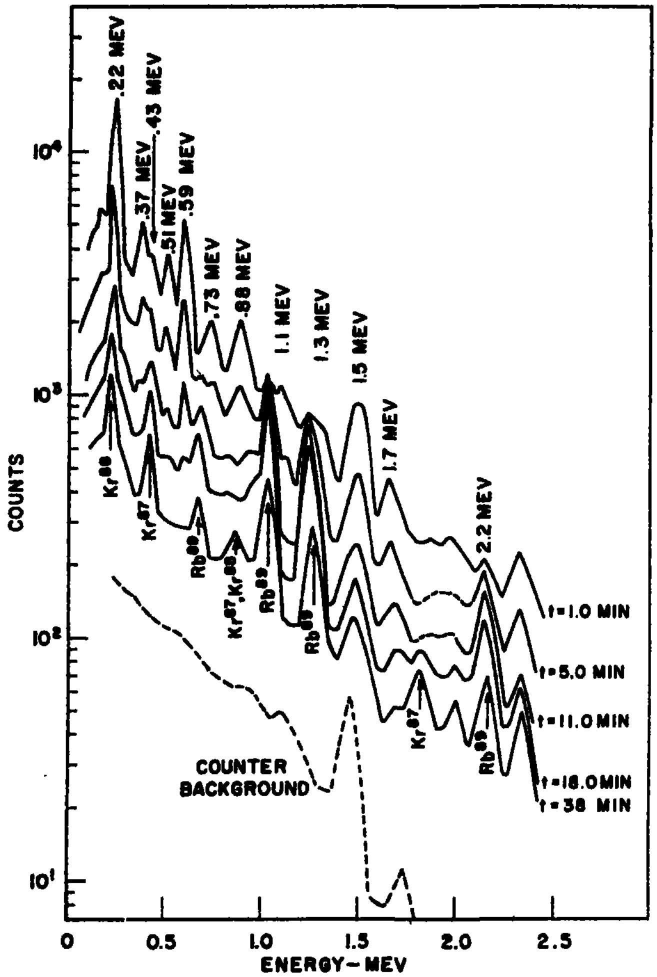

FIG. 2.—Series of γ-spectra of ^{89}Kr separated 4 min after end of 15 sec irradiation. Count length: 2 min.

Mass assignments have been made on the basis of the agreement with the previously reported half-lives, as well as the growth and decay of known daughter activities.

1. *3·2 min* ^{89}Kr

The krypton fraction was allowed to decay for 4 min after the separation to reduce the contribution of 33 sec ^{90}Kr to an insignificant level. It was then filtered to remove the ^{90}Rb and ^{89}Rb formed during the decay period and counted immediately. The 0–2·5 MeV γ-ray spectrum as a function of decay time is shown in Fig. 2.

A limited number of coincidence measurements were made on ^{89}Kr, and γ-γ coincidences were observed between the γ-ray at 215 kev and those at 370, 510, 880 and 1500 keV. No γ-rays were observed in coincidence with the 595 keV γ-ray. This γ-ray was, however, found to be in coincidence with the 4·0 MeV β-ray component. This γ-β coincidence indicates a value of ~4·6 MeV for the decay energy of ^{89}Kr. The detection of γ-rays of energy up to 4·5 MeV established that there is no appreciable β-ray transition to the ground state of ^{89}Rb.

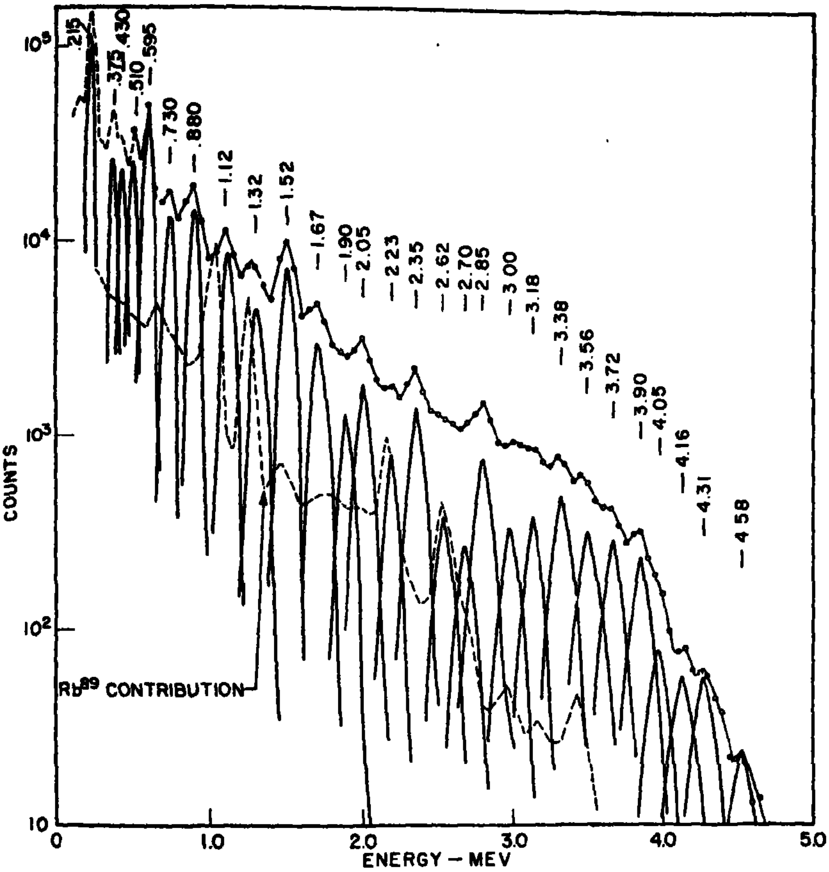

Fig. 3.—Spectrum of ^{89}Kr after subtraction of ^{89}Rb, ^{87}Kr and ^{88}Kr.

The analysis of the complex spectrum into component γ-ray lines is shown in Fig. 3. Due to the large number of γ-rays involved, the analysis is necessary but not sufficient to establish uniquely the energies and intensities of the γ-ray lines of ^{89}Kr. The background correction for 78 min ^{87}Kr and 2·8 hr ^{88}Kr was minimized by utilization of short irradiation and cooling of the sample before the separation. The radiochemical purity of the samples was confirmed by separation of the rubidium daughter after an initial decay period and establishing the absence of detectable amounts of 32 min ^{138}Cs.

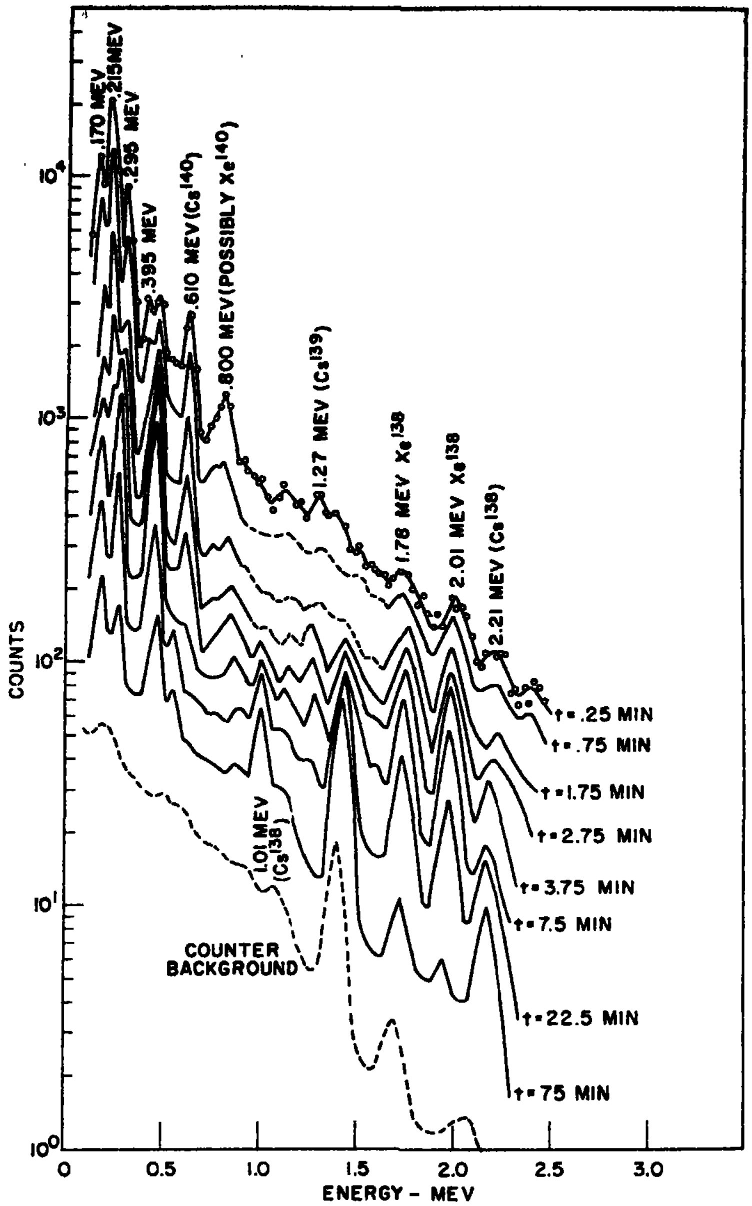

FIG. 6.—Series of γ-spectra of Xe separated 30 sec after end of 15 sec irradiation. Count length: 0·5, 5 and 50 min.

low-lying levels and probably to the ground state of ^{139}Cs. The relative contribution of ^{140}Xe and ^{140}Cs which may have been present should have been negligible under the conditions of the experiment.

5. *9·5 min* ^{139}Cs

The xenon fraction was allowed to decay for 100 sec, and the residual xenon then purged from the charcoal filter with hot air and vacuum. The only γ-rays of ~9·5 min half-life detected were those at 630 and 1270 keV previously reported by WASSON.(7) The relative intensities were resolved from the spectrum taken at 7·5 min, to allow decay of the 66 sec ^{140}Cs peak at 610 keV as shown in Fig. 7. The photon per disintegration values were calculated using the same assumptions as in the case of ^{139}Xe (see Table 2). The Rb activity observed in these spectra results from decay of Kr during the separation step.

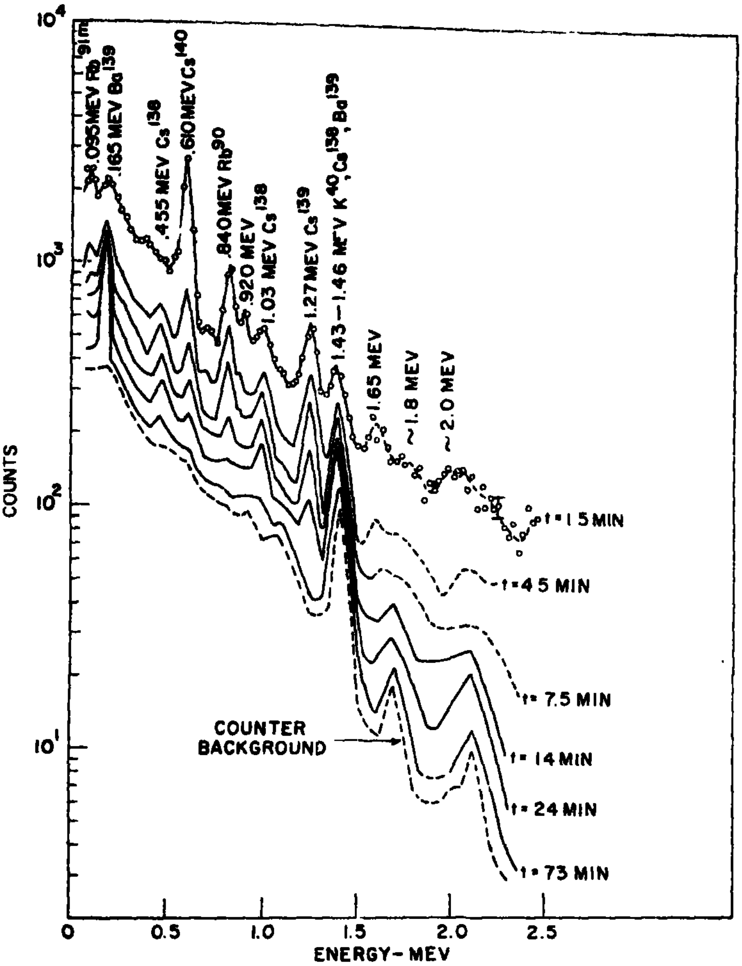

FIG. 7.—Series of γ-spectra of Cs filtered from Xe fraction separated 15 sec after end of 20 sec irradiation and allowed to decay 100 sec. Count length: 3 min.

The maximum β-ray endpoint observed under conditions optimized for the detection of ^{139}Cs was ~3·8 MeV. Because of the low intensity of the observed γ-radiation, this β-ray endpoint is taken as the decay energy.

6. *66 sec* ^{140}Cs

In a similar xenon sample purged after 40 sec cooling, an intense γ-ray of 66 ± 2 sec half-life was observed at 610 keV and is shown in Fig. 8. The presence of higher

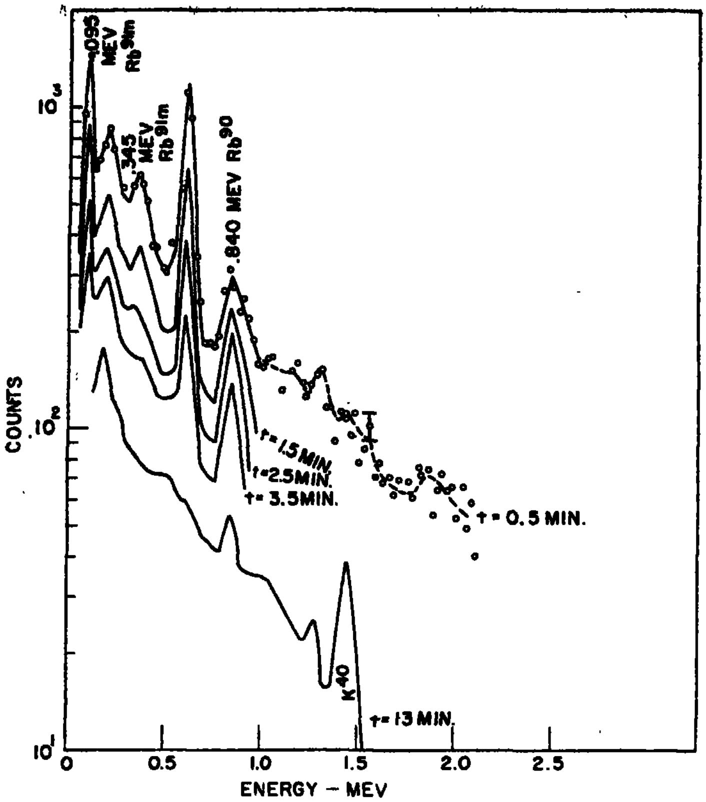

Fig. 8.—Series of γ-spectra of Cs filtered from Xe fraction separated 15 secs after end of 15 sec irradiation and allowed to cool 40 secs. Count length: 1 min.

energy γ-ray radiation of 66 sec half-life was indicated by the gross decay of the higher channels of the spectra. No β-ray spectra of this nuclide were obtained.

CONCLUSIONS

The feasibility of the study of the short-lived fission gases by a simple and rapid gas chromatographic separation has been established. The correlation of the β- and γ-radiations observed in this work into definitive decay schemes will require a considerable amount of further investigation. Extensive coincidence measurements are not practical with the system as set up for these experiments because of the large number of samples necessary to obtain useful statistics. The decay energies given in Table 2 are in fair agreement with those computed by Riddell,(14) but somewhat lower than the revised values quoted by Cameron.(15)

Acknowledgements—The authors wish to thank Professor H. J. Gomberg, C. W. Ricker, W. H. Dunbar, and the staff of the Ford Nuclear Reactor for their cooperation in making available the laboratory and irradiation facilities. The assistance of R. Shideler and H. Nass in many phases of the work is gratefully acknowledged.

(14) J. Riddell, Atomic Energy of Canada Limited, Report CRP-654.

(15) A. G. W. Cameron, Atomic Energy of Canada Limited, Report CRP-690 (1957).

J. Inorg. Nucl. Chem., 1962, Vol. 24, pp. 1539 to 1548. Pergamon Press Ltd. Printed in Northern Ireland

HOT-ATOM CHEMISTRY OF COBALT COMPLEXES—I

HOT-ATOM CHEMISTRY OF NITROAMMINE COBALT (III) COMPLEXES

N. Saito, T. Tominaga and H. Sano
Department of Chemistry, University of Tokyo, Japan

(*Received* 15 *March* 1962; *in revised form* 2 *June* 1962)

Abstract—Nine kinds of nitroamminecobalt (III) complex compounds were irradiated with slow neutrons for 1,5 or 30 hours in JRR-1 reactor. After various storage times the ^{60}Co-labelled recoil species in the irradiated compounds were separated by means of procedures involving paper electrophoresis, paper chromatography, ion exchange, or precipitation.

It was found that the labelled species were composed of the target complex, Co^{2+} ion and the complexes produced through incorporation of outer ions (or molecules) as ligands. The results can be explained by assuming that an electrostatic interaction plays an important role in recoil reactions.

The effects of irradiation and storage time on the distribution of recoil species were also investigated.

A NUMBER of researches have contributed to our knowledge of the hot-atom chemistry of the cobaltammine complexes.(1–8) Most of them, however, have dealt with only a few selected compounds. The present authors are of the opinion that the systematic investigation of a series of closely related compounds might afford clues to the elucidation of the mechanism of the recoil reactions.

In this study, the authors selected, as such a series of compounds, a group of nitroammine cobalt (III) complexes containing different numbers of NH_3 and NO_2 (or NO_3) groups.

These compounds were irradiated with slow neutrons and the resulting recoil species labelled with ^{60}Co were analysed. The distribution of recoil species was compared for all the compounds of the group and the results were explained in terms of their chemical composition. The effects of the period of irradiation and subsequent storage on the distribution of recoil species were also investigated.

EXPERIMENTAL

Target compounds. Nine kinds of crystalline nitroammine cobalt complexes were prepared according to methods found in literature:

1. $[Co(NH_3)_6](NO_2)_3$(9)
2. $[Co(NH_3)_6](NO_3)_3$(10)
3. $[Co(NH_3)_5NO_2](NO_3)_2$(11)

---

(1) P. Süe and G. Kayas, *J. Chim. Phys.* 45, 188 (1948).
(2) G. Kayas and P. Süe, *Bull. Soc. Chim. France* 17, 1145 (1950).
(3) A. Zuber, USAEC Document NYO-6142 BNL (1954).
(4) N. Saito, T. Tominaga and H. Sano, *Bull. Chem. Soc. Japan* 33, 1621 (1960).
(5) G. Harbottle, Chem. Effects Nucl. Transform. Proc. Symp. Prague, 1960, 301 (Pub. 1961).
(6) N. Ikeda, K. Yoshihara and S. Yamagishi, *Bull. Chem. Soc. Japan* 34, 139 (1961).
(7) T. Costea, *J. Inorg. Nucl. Chem.* 17, 20 (1961).
(8) H. E. Rauscher and N. Sutin, *J. Inorg. Nucl. Chem.* 17, 31 (1961).
(9) P. Larisch. Dissertation. p. 95. Zürich (1904).
(10) S. M. Jörgensen, *Z. Anorg. Chem.* 17, 457 (1898).
(11) P. Larisch, Dissertation. p. 96. Zurich (1904); A. Werner, P. Larisch, *Ann.* 386, 29 (1912).

4. $[Co(NH_3)_5NO_2](NO_3)_2$[12]
5. cis-$[Co(NH_3)_4(NO_2)_2]NO_3$[13]
6. trans-$[Co(NH_3)_4(NO_2)_2]NO_3$[14]
7. trans-$[Co(NH_3)_3(NO_2)_3]$[15]
8. $NH_4[Co(NH_3)_2(NO_2)_4]$[16]
9. $K[Co(NH_3)_2(NO_2)_4]$[17]

Some of the nitroammine cobalt complexes prepared as above were found to contain small quantities of other nitroammines of the series as impurities even after they were purified by recrystallization. The quantities of such impurities in the sample were determined beforehand by means of paper electrophoresis and appropriate corrections were made for induced activities arising from such impurities.*

Irradiation and storage conditions. Samples were irradiated in experimental holes in the JRR-1 reactor at pile temperature. The thermal neutron flux was approximately 3×10^{11} neutron/cm² sec. The irradiation times were 1, 5, and 30 hr. All irradiations were made in the presence of air. After irradiation the samples were kept in dry-ice to minimize annealing. A portion of the irradiated sample was analysed immediately and the rest was stored at room temperature for various times (from one month to one year) before analysis.

Procedures of separation. The irradiated samples were dissolved in distilled water after a definite storage time following the completion of irradiation, and the ^{60}Co-labelled recoil species present in the aqueous solutions were separated by means of the chemical procedures described below.

(a) Paper electrophoresis method. It was known that the nitroammine cobalt complexes could be effectively separated from each other by means of a paper electrophoresis procedure using acetate buffer or 0·1 M ammonium oxalate as supporting electrolyte.[18] Small portions (0·05–0·10 ml) of aqueous solutions of the irradiated compounds were placed at a zero-line on the electrophoresis papers. The papers were strips of Toyo No. 50 filter paper cut 2·5 cm or 3·8 cm wide and 60 cm long. The strips were immersed in the electrolyte solution (pH 4·8 acetate buffer or 0·1 M ammonium oxalate) before use. After the sample solution was applied, the central part of the strip was dipped into chlorobenzene contained in a shallow tank and both ends of the strip were dipped into electrolyte tanks. Potentials of 400–800 Vd.c. were applied through platinum electrodes immersed in the electrolyte tanks for 1–3 hr. Then the paper was dried in air and cut athwart into 0·5 or 1 cm pieces. The activity of these strips was counted with a well-type scintillation counter. Macroscopic quantities of cobalt were analysed colorimetrically using α-nitroso-β-naphthol.

(b) Paper chromatography. According to Tsuchida *et al.*,[19] nitroammine cobalt complex compounds with different numbers of co-ordinated NO_2 groups can be separated by means of descending paper chromatography. A solvent mixture containing seven parts methanol, 2·5 parts acetone and one part 30 per cent ammonia solution was reported most effective for the separation, and was employed in the present work.

(c) Ion exchange method. An aqueous solution of the irradiated compound was first passed through a 6 cm × 0·8 cm² column of Dowex 50W, 8 per cent cross-linked, 100–200 mesh in the potassium or sodium form. The effluent was then passed through a 6 cm × 0·8 cm² column of Dowex 1 8 per cent cross-linked, 100–200 mesh in the chloride form. The cation exchanger was then washed with 0·1 M NaCl and the washing was passed through the anion exchanger. By this treatment, all anionic species were adsorbed on the anion exchanger while neutral species remained in the effluent and washings from both columns. Then the cationic species, Co^{2+}, $CoA_4X_2^{+}$, CoA_5X^{2+} and CoA_6^{3+} ($A = NH_3$ and $X = NO_2$ or NO_3, as shown below), were eluted successively from the cation exchange column with 0·5 KCNS, 1 M NaCl, 3 M NaCl and 5 M NaCl. The activity of each fraction was measured with a well-type scintillation counter.

* For example, the sample of trinitrotriamminecobalt(III) was found to contain as impurities small quantities of dinitrotetramminecobalt(III) and tetranitrodiamminecobalt(III) salts, and they could not be removed by recrystallization process. Therefore the quantities of such impurities were determined beforehand and the mixture containing them was subjected to irradiation. The distribution obtained of the ^{60}Co-labelled species was corrected for the contributions by such impurities to induced activities in the mixture.

(12) S. M. Jörgensen, *Z. Anorg. Chem.* 5, 170 (1894); *Ibid.* 17, 464 (1898).
(13) S. M. Jörgensen, *Z. Anorg. Chem.* 17, 473 (1898).
(14) S. M. Jörgensen, *Z. Anorg. Chem.* 17, 469 (1898).
(15) S. M. Jörgensen, *Z. Anorg. Chem.* 17, 463 (1898).
(16) S. M. Jörgensen, *Z. Anorg. Chem.* 17, 477 (1898).
(17) S. M. Jörgensen, *Z. Anorg. Chem.* 7, 304 (1894); 17, 479 (1898).
(18) [illegible] Maki, *Japan Analyst*, 4, 217 (1955).
(19) Y. Yamamoto, A. Nakahara and R. Tsuchida, *J. Chem. Soc.* Japan, Pure Chem. Sec. (Nippon [illegible]aku Zasshi) 75, 114 (1954).

(d) Precipitation method. The radio-cobalt present as Co^{2+} or as forms exchangeable with Co^{2+} in the solution could also be separated by precipitation method. A 0·1 M NaOH solution was added to an aqueous solution of the irradiated compound, containing Co^{2+} carrier, to precipitate the hydroxide of cobalt. The precipitate of the hydroxide was collected, washed and dissolved in diluted HCl; precipitation with NaOH was repeated. Finally, the precipitates were dissolved in HCl and radioactivity was counted with a well-type scintillation counter. On the other hand, the total activity was obtained by measurement of an aliquot of the original solution before NaOH was added.

The "retention", or the fraction of activity in the form identical with the target compound, could also be determined by a recrystallization process. For example, the precentage of the $^{60}Co(NH_3)_6{}^{3+}$ fraction in the irradiated hexammine cobalt compounds was determined by repeated recrystallization as bromide. In order to precipitate $[Co(NH_3)_6]Br_3$, a concentrated NaBr solution was added to a solution of the irradiated compound which might contain if necessary small amounts of the other complexes as hold back carriers. The precipitates were separated, dissolved in water, and recrystallization with NaBr was repeated. At each step of recrystallization, the optical absorbancy of the solution was measured with a spectrophotometer at 480 mμ and the activity was counted with a scintillation counter. The specific activity was calculated from these measurements. The recrystallization process was repeated several times until the specific activity of the purified fraction reached a constant value within the experimental errors. The "retention" value was then obtained by comparison with the specific activity of the original solution before recrystallization.

RESULTS

Four entirely different separation procedures were available for analysis of the recoil species present in solutions of the irradiated compounds. It was found, however, that essentially the same results for the distribution of the recoil species could be obtained for the same sample even if different separation procedures were employed. This fact might imply that the identified recoil species could exist as stable entities in solution in spite of the different conditions involved in these separation procedures.

Therefore, the paper electrophoresis method with pH 4·8 acetate buffer as electrolyte was mainly employed as separation procedure in the present work, because it was the most convenient and reliable of the four methods. Other methods were employed as auxiliary means to confirm the results obtained with the paper electrophoresis method.

Identification of recoil species present in the solution of the irradiated compounds. As a typical example of the electrophoresis pattern, the electrophoresis histogram of the irradiated hexammine cobalt (III) nitrite is shown in Fig. 1.

Six peaks (*a,b,c,d,e,* and *f*) are seen in Fig. 1. Four peaks to the right of the zero-line corresponded to cationic species, while a peak to the left of the zero-line corresponded to an anionic species. The peak *e* remained almost at the zero-line and might be due to a neutral species. As the relative rates of migration were known for all the nitroammine cobalt complexes studied above,(18) these peaks could be identified without much difficulty.

The *a* peak was identified as $CoA_6{}^{3+}$, (A denotes an NH_3 group in most cases) the target ion, because its rate of migration was identical with that of the hexamine cobalt ion, and a macroscopic quantity of cobalt was found only in the *a* peak when no other complexes were present as carriers. This was confirmed by the fact that the percentage of activity in the *a* peak was in good agreement with that of the hexammine fraction obtained by the ion exchange or recrystallization method.

The *b, c, d, e* and *f* peaks were assigned to $[CoA_5NO_2]^{2+}$, Co^{2+}, $[CoA_4(NO_2)_2]^{+}$, $[CoA_3(NO_2)_3]$ and $[CoA_2(NO_2)_4]^{-}$,* respectively on the following evidence: (i) the relative rates of migration of these peaks were compared with those of known samples

---

* "A" denotes an NH_3 group in most cases. However, it is possible that small amounts of species with one or two of the A's being H_2O may also be present in some cases.

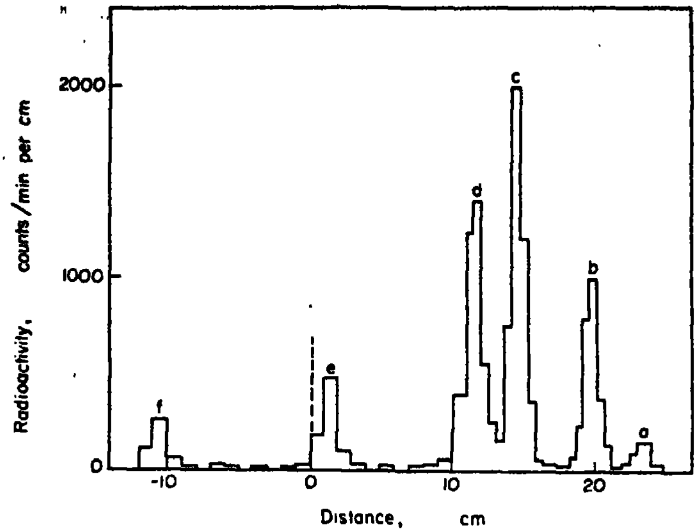

FIG. 1.—Paperelectrophoresis histogram of irradiated [$Co(NH_3)_6$] $(NO_2)_3$ dissolved in water (pH 4·8 acetate buffer used as electrolyte). Cations move right.

of [$Co(NH_3)_5NO_2]^{2+}$, Co^{2+}, *cis*- and *trans*-[$Co(NH_3)_4(NO_2)_2]^+$, [$Co(NH_3)_3(NO_2)_3$], and [$Co(NH_3)_2(NO_2)_4]^-$, (ii) macroscopic quantities of known samples of the above nitroammine complexes were added as carriers to the solution of the irradiated compound†, and the coincidence of the activity peaks with macroscopic quantities of cobalt on the resulting histogram noted, (iii) the distribution of activity amongst the recoil species thus identified was confirmed by comparison with that obtained by means of the ion exchange or precipitation method.

Separation of the *c* and *d* peaks was sometimes incomplete. In such cases the activity of the Co^{2+} fraction corresponding to the *c* peak was determined independently by either the precipitation method or paper electrophoresis with 0·1M ammonium oxalate as electrolyte; the percentage activity of each peak could then be estimated.

Identification of the recoil species was achieved in a similar manner for all the irradiated complex compounds. Tables 1–9 show the results obtained with the samples subjected to various irradiation and storage conditions.

TABLE 1.—PERCENTAGE DISTRIBUTION OF ^{60}CO-LABELLED SPECIES IN IRRADIATED [$Co(NH_3)_6$] $(NO_2)_3$ DISSOLVED IN WATER

Irradiation time (hr)	Storage time	^{60}Co-labelled species (%)					
		CoA_6^{3+}	$CoA_5NO_2^{2+}$	$CoA_4(NO_2)_2^+$	$CoA_3(NO_2)_3$	$CoA_2(NO_2)_4^-$	Co^{2+}
1	1 day*	0·8	5·9	20·3	15·6	4·2	53·2
	2 months	0·8	6·5	16·5	17·5	10·0	48·9
	6 months	1·4	6·7	15·9	14·1	11·0	51·0
5	1 day*	1·4	15·5	34·5	11·1	12·4	24·7
	2 months	1·2	10·9	41·2	9·3	17·9	19·5
	10 months	0·6	13·6	34·0	9·8	19·4	22·5
30	3 days	1·1	2·7	53·5	2·0	5·7	35·0

Probable errors in percentages are: ±0·2 for CoA_6^{3+}; ±3·0 for $CoA_4(NO_2)_2^+$ and Co_2^+; ±0·6-1·4 for other species.

* Stored in dry-ice.

---

† Addition of such carriers did not alter the distribution of the recoil species in the solutions of the irradiated compound.

TABLE 2.—PERCENTAGE DISTRIBUTION OF ^{60}CO-LABELLED SPECIES IN IRRADIATED $[Co(NH_3)_6](NO_3)_3$ DISSOLVED IN WATER

Irradiation time (hr)	Storage time	^{60}Co-labelled species (%)					
		CoA_6^{3+}	$CoA_5NO_{2,3}^{2+}$	$CoA_4(NO_{2,3})_2^+$	$CoA_3(NO_{2,3})_3$	$CoA_2(NO_{2,3})_4^-$	Co^{2+}
1	1 day*	2·8	8·5	20·9	0·7	0·3	66·7
	2 months	2·6	8·7	25·4	1·3	0·7	61·2
	11 months	3·9	9·2	26·7	1·3	0·2	58·6
5	1 day*	4·4	12·1	25·4	1·7	0·5	57·8
	2 months	4·6	10·5	29·5	2·1	0·1	53·5
	6 months	4·5	5·8	29·0	—	—	61·0
	10 months	4·3	7·0	30·5	1·4	0·1	56·6
30	3 days	3·1	4·1	29·1	0·6	0	63·0
	4 months	2·9	3·3	22·2	1·1	0·1	70·4

Probable errors in percentages are: ±0·2 for CoA_6^{3+}; ±0·1–0·7 for other species.
* Stored in dry-ice.

TABLE 3.—PERCENTAGE DISTRIBUTION OF ^{60}CO-LABELLED SPECIES IN IRRADIATED $[Co(NH_3)_5NO_2](NO_2)_2$ DISSOLVED IN WATER

Irradiation time (hr)	Storage time	^{60}Co-labelled species (%)					
		CoA_6^{3+}	$CoA_5NO_2^{2+}$	$CoA_4(NO_2)_2^+$	$CoA_3(NO_2)_3$	$CoA_2(NO_2)_4^-$	Co^{2+}
1	1 day*	<1·0	37·1	11·0	2·5	1·3	47·1
	2 months	—	48·6	8·5	1·5	0·5	41·0
	11 months	—	55·6	10·1	2·0	2·9	29·2
5	1 day*	≤0·3	40·3	17·2	3·3	1·1	38·3
	2 months	—	51·7	9·1	3·3	1·8	34·0
	10 months	—	61·2	9·4	2·0	2·0	25·5
30	3 days	<0·1	47·4	23·4	1·7	1·4	26·0
	4 months	—	49·9	8·2	1·8	1·8	38·3

Probable errors in percentages are: ±1·0 for $CoA_5NO_2^{2+}$ and $CoA_4(NO_2)_2^+$; ±0·1–0·4 for other species.
* Stored in dry-ice.

TABLE 4.—PERCENTAGE DISTRIBUTION OF ^{60}CO-LABELLED SPECIES IN IRRADIATED $[Co(NH_3)_5NO_3](NO_3)_2$ DISSOLVED IN WATER

Irradiation time (hr)	Storage time	^{60}Co-labelled species (%)					
		CoA_6^{3+}	$CoA_5NO_{2,3}^{2+}$	$CoA_4(NO_{2,3})_2^+$	$CoA_3(NO_{2,3})_3$	$CoA_2(NO_{2,3})_4^-$	Co^{2+}
1	1 day*	<0·3	29·1	20·1	4·5	1·6	44·2
	2 months	—	29·0	21·0	5·4	0·7	42·9
	11 months	—	34·1	23·2	3·9	0·7	38·3
5	1 day*	≤0·4	36·3	23·0	3·7	0·8	35·8
	2 months	—	44·8	21·2	4·2	0·3	29·5
	11 months	<0·1	43·8	20·0	3·6	1·1	31·6
30	3 days	—	45·0	29·0	1·5	0·3	24·0
	4 months	—	49·4	15·3	2·0	0·3	33·0

Probable errors in percentages are: ±2·0 for $CoA_5NO_{2,3}^{2+}$; ±1·0 for $CoA_4(NO_{2,3})_2^+$ and Co^{2+}; ±0·2–0·5 for other species.
* Stored in dry-ice.

TABLE 5.—PERCENTAGE DISTRIBUTION OF ^{60}CO-LABELLED SPECIES IN IRRADIATED cis-$[Co(NH_3)_4(NO_3)_2](NO_3)$ DISSOLVED IN WATER

Irradiation time (hr)	Storage time	^{60}Co-labelled species (%)					
		CoA_6^{3+}	$CoA_5NO_{2,3}^{2+}$	$CoA_4(NO_{2,3})_2^+$	$CoA_3(NO_{2,3})_3$	$CoA_2(NO_{2,3})_4^-$	Co^{2+}
1	1 day*	—	<0·3	31·0	4·3	1·1	62·3
	2 months	—	1·0	36·5	3·1	~0	57·7
	11 months	—	1·0	51·7	0·9	—	46·4
5	1 day*	—	1·2	38·4	3·2	1·9	55·3
	2 months	—	0·7	43·3	0·7	0·9	54·4
	10 months	—	0·8	57·8	~0	~0	41·4
30	3 days	—	1·2	56·9	—	—	41·9
	4 months	—	0·6	35·4	—	—	64·0

Probable errors in percentages are: ±0·9 ~ 1·2 for $CoA_4(NO_{2,3})_2^+$, $CoA_3(NO_{2,3})_3$ and Co^{2+}; ±0·2 ~ 0·4 for other species.

* Stored in dry-ice.

TABLE 6.—PERCENTAGE DISTRIBUTION OF ^{60}CO-LABELLED SPECIES IN IRRADIATED trans-$[Co(NH_3)_4(NO_3)_2](NO_3)$ DISSOLVED IN WATER

Irradiation time (hr)	Storage time	^{60}Co-labelled species (%)					
		CoA_6^{3+}	$CoA_5NO_{2,3}^{2+}$	$CoA_4(NO_{2,3})_2^+$	$CoA_3(NO_{2,3})_3$	$CoA_2(NO_{2,3})_4^-$	Co^{2+}
1	1 day*	—	<1·0	31·8	3·7	0·5	62·6
	2 months	—	1·3	45·7	2·5	0·3	50·4
	11 months	—	1·0	61·4	~0	—	37·6
5	1 day*	—	0·8	51·7	2·0	0·2	44·9
	2 months	—	0·7	56·2	1·1	~0	42·3
	10 months	—	0·5	60·4	0·4	~0	38·7
30	3 days	—	0·4	68·2	~0	~0	31·4
	4 months	—	0·2	53·4	~0	~0	46·4

Probable errors in percentages are: ±0·9 for $CoA_4(NO_{2,3})_2^+$; 0·7 for $CoA_3(NO_{2,3})_3$ and Co^{2+}; ±0·1 for other species.

* Stored in dry-ice.

TABLE 7.—PERCENTAGE DISTRIBUTION OF ^{60}CO-LABELLED SPECIES IN IRRADIATED $[Co(NH_3)_3(NO_2)_3]$ DISSOLVED IN WATER

Irradiation time (hr)	Storage time	^{60}Co-labelled species (%)					
		CoA_6^{3+}	$CoA_5NO_2^{2+}$	$CoA_4(NO_2)_2^+$	$CoA_3(NO_2)_3$	$CoA_2(NO_2)_4^-$	Co^{2+}
1	1 day*	—	—	—	29·6	1·0	69·4
	2 months	—	—	0·7	48·3	—	51·0
	11 months	—	—	—	58·0	—	42·0
5	1 day*	—	—	0·4	58·3	0·6	40·7
	2 months	—	—	<1·2	57·0	1·0	40·8
	11 months	—	—	—	68·3	0·3	31·3
30	3 days*	—	—	~0	78·4	~0	21·6

Probable errors in percentages are: ±1·4 for $CoA_3(NO_2)_3$ and Co^{2+}; ±0·2–0·4 for other species.

* Stored in dry-ice.

TABLE 8.—PERCENTAGE DISTRIBUTION OF ^{60}Co-LABELLED SPECIES IN IRRADIATED $NH_4[Co(NH_3)_2(NO_2)_4]$ DISSOLVED IN WATER

Irradiation time (hr)	Storage time	^{60}Co-labelled species (%)					
		CoA_6^{3+}	$CoA_5NO_2^{2+}$	$CoA_4(NO_2)_2^+$	$CoA_3(NO_2)_3$	$CoA_2(NO_2)_4^-$	Co^{2+}
1	1 day*	—	—	0·4	5·4	17·6	76·6
	2 months	—	—	0·3	3·9	36·6	59·3
	11 months	—	—	—	2·8	40·0	57·2
5	1 day*	—	0·1	0·0	7·2	32·9	59·9
	2 months	—	—	$<1·3$	8·1	34·0	56·6
	11 months	—	—	~ 0	7·0	42·7	50·3
30	3 days	—	—	—	3·3	44·6	52·1
	4 months	—	—	—	3·1	43·0	53·9

Probable errors in percentages are: ±0·4 for $CoA_3(NO_2)_3$; ±1·3 for $CoA_2(NO_2)_4^-$ and Co^{2+}; ±0·1 for other species.

* Stored in dry-ice.

TABLE 9.—PERCENTAGE DISTRIBUTION OF ^{60}Co-LABELLED SPECIES IN IRRADIATED $K[Co(NH_3)_2(NO_2)_4]$ DISSOLVED IN WATER

Irradiation time (hr)	Storage time	^{60}Co-labelled species (%)					
		CoA_6^{3+}	$CoA_5NO_2^{2+}$	$CoA_4(NO_2)_2^+$	$CoA_3(NO_2)_3$	$CoA_2(NO_2)_4^-$	Co^{2+}
1	1 day*	—	—	0·2	$<2·7$	31·4	65·7
5	1 day*	—	—	0·2	1·1	34·3	64·6

Probable errors in percentages are: ±0·2 for $CoA_4(NO_2)_2^+$; ±0·5 for $CoA_3(NO_2)_3$; ±1·3 for $CoA_2(NO_2)_4^-$; ±1·1 for Co^{2+}.

* Stored in dry-ice.

DISCUSSION

Effects of irradiation and subsequent storage conditions on the distribution of the recoil species. As shown in Tables 1–9, various kinds of recoil species labelled with ^{60}Co were present in the solution of the irradiated compounds. However, the changes in the distribution of such recoil species due to different irradiation and storage conditions seemed to be quite complex and no simple explanation could be obtained.

Therefore we will discuss the behaviour of only two particular species, viz., the Co^{2+} fraction and the "retention" (fraction in the parent ion or molecule). Annealing or radiation effects on the behaviour of recoil species other than these two will be studied further in future experiments.

Generally speaking, as irradiation time was increased the retention increased while the Co^{2+} fraction decreased. Because of the restrictions on the use of the JRR-1 reactor all irradiations were to be made at pile temperature and cooling of the sample with dry-ice, for example, was not permitted. Based on their experiences of the irradiation of various substances, the present authors estimated that the pile temperature might range from room temperature to as high as 80°C. In a prolonged irradiation, the temperature might rise to 80°C or higher. There was no doubt that such an elevated temperature might cause appreciable thermal annealing in the target compounds even during the irradiation. Thus the increase in retention and the decrease in Co^{2+} fraction with increase in the irradiation time might be attributed to thermal annealing during irradiation. Though concomitant radiations such as gamma rays in the reactor should have some annealing effects on the target compounds the extent of these effects was not fully examined.

Some of the nitroammine cobalt complexes were found to be rather unstable to a prolonged irradiation. As seen in Tables 1 and 2, hexammine cobalt complex salts showed different behaviour from the others: when they were irradiated for 30 hr, the retention was lowered whereas the Co^{2+} fraction was increased by comparison with the values for an irradiation of 5 hours. Such an anomaly was more pronounced in $[Co(NH_3)_6](NO_2)_3$. It seemed that this anomaly might be due to some chemical reactions caused by heat or radiation during the irradiation. After $[Co(NH_3)_6](NO_2)_3$ was irradiated for 5 hr colour of the crystals was somewhat changed, and the wavelength of the maximum in the first absorption band of the solution shifted to a shorter wavelength and approached that of $[Co(NH_3)_4(NO_2)_2]^+$. On irradiation for 30 hours the changes became more distinct and in addition a macroscopic quantity of Co^{2+} (possibly due to partial decomposition of the complex) was detected. The macroscopic changes in $[Co(NH_3)_6](NO_2)_3$ during the prolonged irradiation showed a similarity to the known thermal transformation reactions of the cobaltammine complexes containing NO_2 groups.[20] The present authors thus assume that $[Co(NH_3)_6](NO_2)_3$ might suffer appreciable decomposition under the influence of heat (and possibly radiation) and transformation into $[Co(NH_3)_4(NO_2)_2]^+$ or other nitroammine complexes or into unstable entities which could yield Co^{2+} on dissolution in water during the prolonged period of irradiation (say 5 or 30 hr).

However, no such changes were observed macroscopically when $[Co(NH_3)_6](NO_2)_3$ was irradiated for 1 hr: colour of the crystals remained unchanged, the absorption spectrum of the solution was identical with that of the hexammine cobalt complexes, and no macroscopic quantity of Co^{2+} was detected. For other complex compounds than $[Co(NH_3)_6](NO_2)_3$ no macroscopic changes were observed at all after an irradiation of 1 or 5 hr.

Subsequent storage of the irradiated compounds altered the distribution of the recoil species: for the compounds irradiated for 1 or 5 hr the retention increased while the Co^{2+} fraction decreased with increase in the storage time at room temperature. However, the compounds irradiated for 30 hr showed a different annealing behaviour: most of them gave lower retention values and higher values of the Co^{2+} fraction after storage for four months at room temperature than the freshly irradiated samples. The cause for this anomaly was not known, yet it might be related to chemical reactions involving the damage produced by heat or radiation in the target compounds during such a long period of irradiation. It was also assumed that the radiations (especially beta rays) arising from the decay of ^{60}Co in the irradiated compound might play some role in producing radiation damage or other chemical effects in the crystals. The latter probability will be investigated in future experiments.

Mechanism of recoil reactions. As seen in Tables 1–7, an important feature of the recoil reactions in the nitroammine complexes was that substitution of ligand NH_3 groups by outer anions (NO_2^- or NO_3^-) was observed in most complex compounds whenever the substituted recoil products could exist as reasonably stable entities in aqueous solutions. On the contrary, ^{60}Co-labelled complexes containing less anions as ligands than the target compound were not found except with $NH_4[Co(NH_3)_2(NO_2)_4]$. The products include not only the target compound and Co^{2+} ion but also various ^{60}Co-labelled complexes containing more anionic ligands than the target substance.

In order to clarify the mechanism of such substitution reactions the ratio (S) of radioactivity of the substituted recoil products to the total co-ordinated cobalt was calculated as follows:

---

[20] A. V. ABLOV and N. I. LOBANOV, *Zhur. Obshcheĭ Khim.* **25**, 648 (1955).

$$S = \frac{\text{Sum of percentages of } {}^{60}\text{Co-labelled complexes containing more anionic ligands than the target}}{\text{Sum of percentages of all } {}^{60}\text{Co-labelled complexes}}$$

Calculated values of *S* for all the irradiated compounds are shown in Table 10.

TABLE 10.—VALUES OF SUBSTITUTION RATIO, S

Target	S*		Electric charge on the target complex ion
	S in the sample† irradiated for 1 hr	S in the sample† irradiated for 5 hr	
$[Co(NH_3)_6](NO_3)_3$	0·98 ± 0·01	0·98 ± 0·00	+3
$[Co(NH_3)_6](NO_2)_3$	0·91 ± 0·01	0·89 ± 0·00	+3
$[Co(NH_3)_5NO_2](NO_3)_2$	0·28 ± 0·03	0·35 ± 0·02	+2
$[Co(NH_3)_5NO_2](NO_2)_2$	0·47 ± 0·06	0·43 ± 0·03	+2
Cis-$[Co(NH_3)_4(NO_2)_2](NO_3)$	0·14 ± 0·05	0·11 ± 0·03	+1
Trans-$[Co(NH_3)_4(NO_2)_2](NO_3)$	0·11 ± 0·04	0·05 ± 0·03	+1
$[Co(NH_3)_3(NO_2)_3]$	0·03 ± 0·02	0·02 ± 0·01	0

$$*S = \frac{\text{Sum of percentages of } {}^{60}\text{Co-labelled complexes containing more anionic ligands than target}}{\text{Sum of percentages of all } {}^{60}\text{Co-labelled complexes}}$$

† Storage time: one day in dry ice.

It is worth mentioning that this ratio (*S*) increases with the increase in electric charge on the target complex ion, or with the increase in number of neighbouring outer anions. This fact may be generally explained by assuming that the electrostatic interaction between the outer anions and the more or less fragmented complex ions plays an important role in the recoil reactions. If the recombination reaction between the fragmented complex ion and the neighbouring outer anions is promoted by the electrostatic attraction between them, either an increase in the positive charge on the complex ion or an increase in the number of neighbouring outer anions may favour the recombination reaction which yields recoil species containing more outer anions in ligands than the target complex, and may consequently increase the ratio, *S*.

The two tetranitrodiamminecobaltates(III) in Tables 8 and 9 were quite different in nature from the others because they were salts of complex anions and therefore contained no outer anions. These complex salts contained outer cations (NH_4^+ or K^+) instead. K^+ ions could not be incorporated as ligands whereas NH_4^+ ion might possibly supply NH_3 group on dissociation in hot reactions. For this reason comparison of the recoil species in $K[Co(NH_3)_2(NO_2)_4]$ and $NH_4[Co(NH_3)_2(NO_2)_4]$ might be significant. In this case, however, substitution of NO_2 by NH_3 was of interest, and the ratio (*S′*) was calculated as follows:

$$S' = \frac{\text{Sum of percentages of } {}^{60}\text{Co-labelled complexes containing less anionic ligands (i.e. more } NH_3 \text{ groups) than the target}}{\text{Sum of percentages of all } {}^{60}\text{Co-labelled complexes}}$$

Calculated values of *S′* are given in Table 11.

The substitution ratio (*S′*) was found to be higher for $NH_4[Co(NH_3)_2{\cdot}(NO_2)_4]$ than

Table 11.—Values of substitution ratio, S′

Target	S′*	
	S in the sample† irradiated for 1 hr	S in the sample† irradiated for 5 hr
$NH_4[Co(NH_3)_2(NO_2)_4]$	0·23 ± 0·04	0·18 ± 0·02
$K[Co(NH_3)_2(NO_2)_4]$	<0·08 ± 0·02	0·03 ± 0·01

$$* S' = \frac{\text{Sum of percentages of } {}^{60}\text{Co-labelled complexes containing less anionic ligands than target}}{\text{Sum of percentages of all } {}^{60}\text{Co-labelled complexes}}$$

† Storage time: one day in dry-ice.

for $K[Co(NH_3)_2(NO_2)_4]$ as expected. This fact might confirm that incorporation of the NH_3 group (arising from outer NH_4^+ ions) into the fragmented complex ion occurs during the recoil reactions in $NH_4[Co(NH_3)_2(NO_2)_4]$.

It may be concluded from these results that the mechanism of the recoil reactions occurring in the nitroammine complexes is closely related to their chemical composition, especially, to the nature and number of outer ions. The outer ions which can coordinate as ligands may play an important role in recoil reactions: most recoil species (except the target complex and Co^{2+}) seem to be formed through substitution reactions in which ligands of the target complex are displaced and outer ions (or molecules arising from outer ions) are incorporated in their place.

J. Inorg. Nucl. Chem., 1962, Vol. 24, pp. 1549 to 1554. Pergamon Press Ltd. Printed in Northern Ireland

THE SELF-ASSOCIATION OF HYDROGEN FLUORIDE VAPOUR

J. N. MACLEAN, F. J. C. ROSSOTTI and H. S. ROSSOTTI
Department of Chemistry, University of Edinburgh, Scotland
and
Inorganic Chemistry Laboratory, University of Oxford, England

(*Received* 9 *August* 1961; *in revised form* 16 *April* 1962)

Abstract—Recent curve-fitting methods for obtaining self-association constants have been applied to STROHMEIER and BRIEGLEB's pressure–volume–temperature data for hydrogen fluoride at 26°, 32°, 38°, 44° and 56°C. Definite evidence has been obtained for the existence of HF, $(HF)_2$ and $(HF)_6$, but intermediate and higher oligomers may also be formed. Association constants are reported for monomer–dimer–hexamer, and for extended series models, together with values of the appropriate enthalpy and entropy changes.

THE nature of the hydrogen-bonded associates in hydrogen fluoride vapour is still uncertain. SMITH's analysis(1) of the pressure dependence of the infra-red spectrum appears to indicate that the predominant species are monomer and hexamer, together with small amounts of dimer and tetramer. However, FRANCK and coworkers(2,3) interpret their heat capacity measurements in terms of a stable hexamer and a large sequence of other oligomers. BRIEGLEB and STROHMEIER(4) have deduced from pressure-volume-temperature measurements that a large number of species are present, but that the formation of the hexamer is not particularly favoured. These conflicting views are typical of many that have been published over the last thirty years. In an attempt to resolve this situation, some graphical methods of analysis, which are designed to identify combinations of a few(5,6) or many(6,7) species, have now been applied to STROHMEIER and BRIEGLEB's P–V–T data.(8) These particular measurements were chosen for analysis since there are many data for pressures between 50 and 670 mm Hg at a number of temperatures. Moreover, the interpretation of P–V–T data is not complicated by the necessity for introducing parameters other than equilibrium constants (e.g. extinction coefficients or heat capacities).

PRESENT CALCULATIONS

The measurements lead to pairs of values of the observed vapour pressure.

$$S = \sum_{1}^{Q} p_q = \sum_{1}^{Q} \beta_q b^q \tag{1}$$

and the hypothetical pressure

$$B = \sum_{1}^{Q} q p_q = \sum_{1}^{Q} q \beta_q b^q \tag{2}$$

---

(1) D. F. SMITH, *J. Chem. Phys.* **28**, 1040 (1958).
(2) W. SPALTHOFF and E. U. FRANCK, *Z. Elektrochem.* **61**, 993 (1957).
(3) E. U. FRANK and F. MEYER, *Z. Elektrochem.* **63**, 571 (1959).
(4) G. BRIEGLEB and W. STROHMEIER, *Z. Elektrochem.* **57**, 668 (1953).
(5) F. J. C. ROSSOTTI and H. S. ROSSOTTI, *J. Phys. Chem.* **65**, 926 (1961).
(6) F. J. C. ROSSOTTI and H. S. ROSSOTTI, *J. Phys. Chem.* **65**, 1376 (1961).
(7) F. J. C. ROSSOTTI and H. S. ROSSOTTI, *J. Phys. Chem.* **65**, 930 (1961).
(8) W. STROHMEIER and G. BRIEGLEB, *Z. Elektrochem.* **57**, 662 (1953).

which would be exerted by an ideal unassociated vapour under the same conditions. Here Q is the maximum value of q, p_q is the partial pressure of the species $(HF)_q$ and $b = p_1$ is the partial pressure of the monomer. In the first instance, ideal gas behaviour is assumed at all pressures ($S < 670$ mm Hg) studied. Then the overall stoichiometric self-association constant $\beta_q = p_q b^{-q} = \prod_1^Q K_q$ is the equilibrium constant for the oligomerization

$$q\mathrm{HF} \rightleftharpoons (\mathrm{HF})_q \tag{3}$$

and the stepwise stoichiometric self-association constant $K_q = p_q(p_{q-1}b)^{-1}$ is the equilibrium constant for the association step

$$(\mathrm{HF})_{q-1} + \mathrm{HF} \rightleftharpoons (\mathrm{HF})_q \tag{4}$$

For each point B, S, values of b and of the number average degree of multimerization, $\bar{\nu} = (B - b)(S - b)^{-1}$, of the oligomers were calculated as described previously.(5) At all temperatures, $\bar{\nu}$ is approximately two over a range of low pressures. Hence, the smallest oligomer formed is the dimer. With increasing pressures, $\bar{\nu}$ increases to the maximum values tabulated below:

T°C	26	32	38	44	56
$\bar{\nu}_{\max}$	5·4	5·3	4·4	3·1	2·2

Hence, at least a second oligomer is formed, and this must be the hexamer or a higher species at 26° and 32°.

FEW SPECIES MODELS

The data B, S, b were first treated by curve-fitting methods for systems containing a single oligomer.(5) The measurements can be described very satisfactorily in terms only of dimerization for values of $S \leqslant 200$ mm Hg at 26°, $S \leqslant 400$ mm Hg at 38° and of $S \leqslant 600$ mm Hg at 56°C. Methods(5) for systems containing monomer, dimer and one higher oligomer $(\mathrm{HF})_Q$ were then applied to the data over the entire range of pressures and temperatures. No value of Q other than six gave an acceptable fit.

The possible existence of appreciable concentrations of an intermediate species was tested by comparison of the data with normalised curves calculated for the models $\mathrm{HF} + (\mathrm{HF})_2 + (\mathrm{HF})_q + (\mathrm{HF})_6$, where $q = 3$, 4 or 5. The curve-fitting procedure is analogous to that described elsewhere[5] for the system monomer–dimer–trimer–tetramer. The shapes of the plots of $\log (B - b)b^{-2}$ and $\log (S - b)b^{-2}$ against $\log b$ are now determined by the parameter

$$R_q = \beta_q \beta_2^{(q-6)/4} \beta_6^{(2-q)/4}$$

For all three trial values of q, the best fit was obtained for $R_q = 0$. Hence, there is no evidence for appreciable concentrations of any one intermediate species. The upper limits of $R_q < 0{\cdot}1$ correspond to values of $\log \beta_3 < -7{\cdot}38$, $\log \beta_4 < -9{\cdot}89$ and $\log \beta_5 < -12{\cdot}46$ at 26°C, assuming that only one of the species $(\mathrm{HF})_3$, $(\mathrm{HF})_4$ or $(\mathrm{HF})_5$ coexists with dimer and hexamer.

The values of β_2 and β_6 were checked by substitution into equations (1) and (2) to give $\bar{q}\,(= BS^{-1})$ as a function of S. Excellent agreement was found (see Fig. 1) between the observed and calculated curves at 38°, 44° and 56°, and for lower pressures at 26° and 32°C. The high pressure deviations at the lower temperatures may be due to the presence of one or more oligomers larger than the hexamer, and the data can be fitted over the whole pressure range studied by an extended series model with $q = 1, 2, 6, 7, 8, 9 \ldots$. However, the deviations may be due to non-ideal gas behaviour. Values of β_2 and β_6, together with the upper limits of S and $\bar{q}$ for which the monomer-dimer-hexamer model is valid, are given in Table 1.

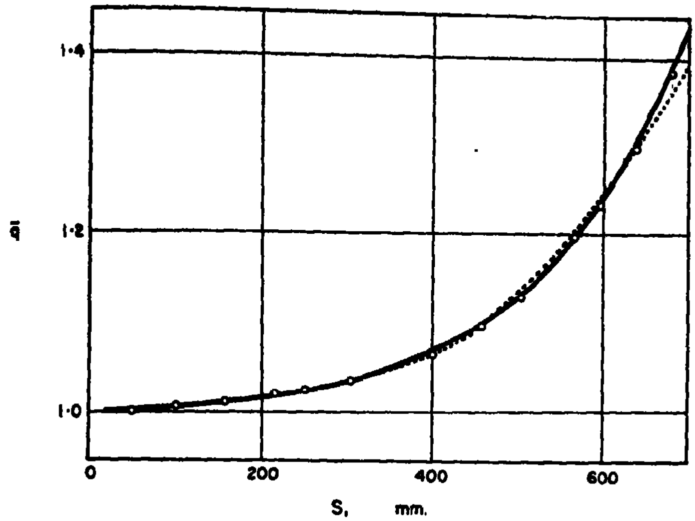

FIG. 1.—The function $\bar{q}(S)$ for 38°C. Open circles: experimental points. Full line: calculated for extended series (Hypothesis I, $R = 0$) with $\log \beta_2 = -4{\cdot}02$ and $\log K = -2{\cdot}95$. Dotted line: calculated for dimer-hexamer model with $\log \beta_2 = -4{\cdot}00$ and $\log \beta_6 = -15{\cdot}05$.

TABLE 1.—ASSOCIATION CONSTANTS FOR DIMER-HEXAMER MODEL (ON MM Hg SCALE)

T(°C)	Log β_2	Log β_6	Range of validity of model	
			Upper limit of S (mm Hg)	Upper limit of $\bar{q}$
26	$-3{\cdot}80 \pm 0{\cdot}02$	$-13{\cdot}94 \pm 0{\cdot}02$	420	1·43
32	$-3{\cdot}92 \pm 0{\cdot}02$	$-14{\cdot}50 \pm 0{\cdot}02$	542	1·41
38	$-4{\cdot}00 \pm 0{\cdot}01$	$-15{\cdot}05 \pm 0{\cdot}02$	636	1·30
44	$-4{\cdot}06 \pm 0{\cdot}01$	$-15{\cdot}62 \pm 0{\cdot}03$	646*	1·14
56	$-4{\cdot}24 \pm 0{\cdot}01$	$-16{\cdot}63 \pm 0{\cdot}03$	646*	1·04

* Highest pressure studied at temperature shown.

Approximate values of the overall enthalpy and entropy changes accompanying dimerization and hexamerization were obtained graphically. The points $\log \beta_2$, T^{-1} and $\log \beta_6$, T^{-1} both fell on very good straight lines, corresponding to:

$$\Delta H_2 = -6{\cdot}_5 \text{ kcal/mole} \qquad \Delta S_2 = -39{\cdot}_2 \text{ e.u.}$$

$$\Delta H_6 = -40{\cdot}_4 \text{ kcal/mole} \qquad \Delta S_6 = -198{\cdot}_5 \text{ e.u.}$$

EXTENDED SERIES MODELS

The data were also analysed by curve fitting methods based on models(6,7) assuming the formation of an extended series of multimers and a number of different relationships between the self-association constants.

The data at each temperature could be described very satisfactorily in terms of three independent parameters β_2, R and K, such that $\beta_3 = \beta_2 RK$ and $\beta_q = \beta_2 K^{q-2}$ for $q > 4$. This model will be referred to as the three parameter Hypothesis I, cf. ref.(7) The data for 26°, 32°, 38° and 44°C could best be represented with $R < 0{\cdot}3$. The measurements at 56°C could not be analysed by assuming extended multimerization on account of the very small contribution of oligomers higher than the dimer ($\bar{\nu}_{\max} =$ 2·2). Less satisfactory fits of the data at 26°, 32°, 38° and 44°C were obtained by using a three parameter model with $\beta_4 = \beta_2 K^2 R$ and $\beta_q = \beta_2 K^{q-2}$ for all other values of q.

The value of $\beta_3 < \beta_2 R$ on Hypothesis I implies that the reaction

$$HF + (HF)_2 \rightleftharpoons (HF)_3$$

occurs less readily than other stepwise associations. A somewhat similar model(7) is the two-parameter Hypothesis II with $\beta_q = \beta_2 K^{q-2}/q - 1$. This model gave a good description of the data for 38° and 44°C, but not for 26° and 32°C. The data could not be represented by two parameter models[7] for which K_q ($q > 3$) is either constant or increases with q.

TABLE 2.—ASSOCIATION CONSTANTS FOR EXTENDED SERIES MODELS (ON MM Hg SCALE)

T(°C)	Hypothesis	log β_2	log K_q
26	I, $R = 0{\cdot}3$	$-3{\cdot}87 \pm 0{\cdot}02$	$-2{\cdot}74 \pm 0{\cdot}01$ ($q > 4$)
32	I, $R = 0{\cdot}2$	$-3{\cdot}97 \pm 0{\cdot}02$	$-2{\cdot}85 \pm 0{\cdot}01$ ($q > 4$)
38	I, $R = 0$	$-4{\cdot}02 \pm 0{\cdot}03$	$-2{\cdot}95 \pm 0{\cdot}01$ ($q > 4$)
44	I, $R = 0{\cdot}3$	$-4{\cdot}12 \pm 0{\cdot}02$	$-3{\cdot}11 \pm 0{\cdot}02$ ($q > 4$)
	II	$-4{\cdot}19 \pm 0{\cdot}02$	$-2{\cdot}91 \pm 0{\cdot}01$ $+ \log (q - 2)/(q - 1)$ ($q > 3$)

The relative merits of the association constants were checked by substitution into Equations (1) and (2). The functions $\bar{q}(S)$ calculated by using the Hypothesis I association constants were in excellent agreement with experimental data at 26°, 38° and 44°C, and in fairly good agreement with those at 32°C. At 38°C, the curve for $R = 0$ gave an appreciably better fit than that for $R = 0{\cdot}3$, indicating that the trimer cannot be detected at this temperature. However, the curve calculated by using the Hypothesis II equilibrium constants represented the primary data less well. At 44°C, the measurements cover a restricted range of values of $\bar{q}$, and no choice can be made between Hypotheses I and II.

Values of the equilibrium parameters are given in Table 2. Approximate values for the enthalpy and entropy changes were calculated by assuming that the Hypothesis I model with $R < 0{\cdot}3$ is valid at 44° as well as at 26°, 32° and 38°C. Acceptable linear plots of log β_2 and log K against T^{-}_{1} gave values of

$$\Delta H_2 = -7{\cdot}_8 \text{ kcal/mole} \qquad \Delta S_2 = -43{\cdot}_7 \text{ e.u.}$$

$$\Delta H = -8{\cdot}_5 \text{ kcal/mole} \qquad \Delta S = -40{\cdot}_9 \text{ e.u.}$$

where ΔH and ΔS refer to the reaction step (4) with $q > 4$. If, however, the data at 44°C are described by Hypothesis II, then $\Delta H_2 = -5{\cdot}_7$ kcal/mole and $\Delta S_2 = -36{\cdot}_0$ e.u. Thus, for any acceptable extended series model, $\Delta H_2 = -6{\cdot}_8 \pm 1$ kcal/mole and $\Delta S_2 = -40 \pm 4$ e.u.

DISCUSSION

The validity of the self-association constants, and even of the formulae proposed for the oligomers, depends on the assumption of ideal gas behaviour. In an earlier analysis of the present data, SMITH(1) has treated BRIEGLEB and STROHMEIER's dimerization constant(4) as a non-ideality parameter, and proceeded to calculate values β_4 and β_6. It is not apparent why the terms $\beta_4 b^4$ and $\beta_6 b^6$ should refer to chemical reactions, if $\beta_2 b^2$ is arbitrarily classed as a physical interaction. On the contrary, deviations from ideality are probably negligible in the pressure range over which the measurements can be described precisely in terms of a single monomer-dimer equilibrium. This situation obtains up to a pressure (S) of 600 mm Hg at 56°C. Since non-chemical forces of interaction are roughly proportional to T^{-3}, behaviour will probably be ideal up to at least 440 mm Hg at 26°C. Moreover, values of the van der Waals constants for water and hydrogen chloride suggest that deviations from ideality in hydrogen fluoride do not exceed 0·5 per cent of the total pressure, even at the lowest temperatures and highest pressures studied.

The present analysis of STROHMEIER and BRIEGLEB's data(8) is based largely on results at the lower pressures. It provides definite evidence for the formation of $(HF)_2$ and $(HF)_6$. The existence of the dimer is supported by infra-red(1,9–11) spectroscopy; that of the hexamer is already well established. Our values of β_2 and β_6 are in rough agreement with those obtained by earlier workers,(12) using less rigorous methods of analysis. The values of ΔH_2 and ΔS_2 obtained from the dimer-hexamer model are in fairly good agreement with those found for the extended series model, and are compatible with a value of $-\Delta H_2 = 6 \pm 1$ kcal/mole calculated from the infra-red spectra.(10) The fact that this value is appreciably greater than the kinetic energy of the gas is further evidence for the reality of the dimer. The values of ΔH_6 and ΔS_6 are roughly independent of the model chosen, and are in good agreement with those of earlier workers.(12) However, it is impossible to deduce from the values of the thermodynamic functions for the dimer and hexamer whether the latter is cyclic or acyclic.

Our results are at variance with SMITH's view(1,10) that $(HF)_2$ is only present in very low concentrations and contributes little to the non-spectroscopic properties of the vapour. Approximate relative partial pressures of $(HF)_2$ and $(HF)_6$ at 26°C, calculated using the dimer-hexamer model, are shown below:

S (mm Hg)	100	200	300	400	520
$100 p_2 S^{-1}$	1	3	4	5	5
$100 p_6 S^{-1}$	10^{-4}	0·3	2	5	13

The relative importance of dimer to hexamer increases at higher temperatures. Thus, at 38°C and $S = 686$ mm Hg, $p_2/p_6 = 1{\cdot}25$ and at 56°C and $S = 650$ mm Hg, $p_2/p_6 = 15$.

The present analysis does not support SMITH's claim(1) that STROHMEIER and BRIEGLEB's data can be reconciled to a monomer–tetramer–hexamer model (with the dimerization constant treated as a non-ideality parameter). Our treatment on the few species model shows that the vapour-pressures give no evidence for significant

---

(9) G. A. KUIPERS, *J. Mol. Spectroscopy* **2**, 75 (1958).

(10) D. F. SMITH, *J. Mol. Spectroscopy* **3**, 473 (1959).

(11) W. F. HERGET, N. M. GAILAR, R. J. LOVELL and A. H. NIELSEN, *J. Opt. Soc. Amer.* **50**, 1264 (1960).

(12) G. C. PIMENTEL and A. L. MCCLENNAN, *The Hydrogen Bond*. Freeman, San Francisco (1960).

concentrations of tetramer. However, if the tetramer is acyclic and the hexamer cyclic, it is feasible that the tetramer has an appreciably larger extinction coefficient and is therefore detectable spectroscopically at extremely low concentrations.

The precision of the data does not warrant BRIEGLEB and STROHMEIER's original analysis[(4)] in terms of nine independent parameters. Nevertheless, an extended series model, such as the three parameter Hypothesis I, gives a good description of the data over the whole pressure range studied. However, this treatment gives no particular evidence for the formation of trimer, tetramer and pentamer, since a good fit can also be obtained using the model $(HF)_2$, $(HF)_6$, $(HF)_7$, $(HF)_8$ .... The extended series models represent the data at low temperatures and high pressures somewhat better than does the monomer–dimer–hexamer model. However, it is under just these conditions that non-ideal behaviour may become appreciable. The present analysis can therefore give no definite information about species larger than the hexamer.

Acknowledgements—We thank Dr. A. D. BUCKINGHAM (Oxford) and Dr. P. GRAY (Leeds) for helpful discussions on gaseous imperfections.

J. Inorg. Nucl. Chem., 1962, Vol. 24, pp. 1555 to 1557. Pergamon Press Ltd. Printed in Northern Ireland

SOME MIXED COMPLEX HALOGEN ACIDS WITH PSEUDOHALOGENS

A. G. GALINOS
Department of Chemistry,
The Polytechnical University, Athens, Greece

(*Received* 2 *April* 1962)

Abstract—The preparation and some properties of the etherated complex halogen acids with pseudohalogens of the formulas $H[Me^{III}X_3X']$, $H[Me^{II}X_2X']$ are reported. The metals contained are Zn, Cd, of Group II and Al, In of Group III.

COMPLEX salts of different metals with pseudohalogen (CN, SCN) are well known and the corresponding free acids are reported in some cases, e.g. $H_3[Co(CN)_6]$, $H[Ag(CN)_2]$, $H[Cu(CN)_3]$, $H_3[Rh(SCN)_6]$, $H_3[Gr(SCN)_6]$, $H_3[Fe(CN)_6]$.(1,2,3) These acids were prepared by the action of mineral acids on the corresponding salts.

We have previously prepared and studied (4–6) many simple complex halogen acids of different metals and also complex mixed halogen acids of the same metals with formulae such as $H[Me^{III}X_3X']H[Me^{II}X_2X']$ where X and X' represent different halogen atoms.(7) These acids were synthesized in an ether medium by addition of dry hydrogen halide to the anhydrous metal salt.

It is interesting to study the mixed halogen acids of the above formulae containing pseudohalogens (CN, SCN, N_3).

The only known compounds of this mixed type are some salts of the $[BiBr_3(CN)_3]^{3-}$, and $[AuI_2(CN)_2]^-$ anions.(8) There are also reported addition compounds of the type MeX_2, HCN or MeX_3, HCN where the metals are Be, Fe, Al, Sn, Ti.(9–12)

In the present paper we report for the first time the preparation of metal complexes of mixed halogen acids with the pseudohalogen thiocyanate.

General method of preparation

For the preparation of these compounds we have employed the method previously described.(7) All reactions were conducted under anhydrous conditions using chemically pure and anhydrous salts. These salts were added little by little with stirring to an excess of absolute ether containing freshly prepared and dried HCNS, cooled to

---

(1) A. BAYER and V. VILLINGER, *Ber. Dtsch. Chem. Ges.* **34**, 2579 (1901).
(2) A. Bayer and V. VILLINGER, *Ber. Dtsch. Chem. Ges.* **35**, 1206 (1902).
(3) J. BRIGANDO, *C.R. Acad. Sci., Paris* **214**, 908 (1942).
(4) E. WIBERG, M. SCHMIDT and A. GALINOS, *Z. Angew. Chem.* **66**, 443 (1954).
(5) E. WIBERG, M. SCHMIDT and A. GALINOS, *Z. Angew. Chem.* **66**, 444 (1954).
(6) A. GALINOS, *Z. Angew. Chem.* **69**, 507 (1957).
(7) A. GALINOS, *J. Amer. Chem. Soc.* **83**, 3032 (1960).
(8) A. VOURNAZOS, *C.R. Acad. Sci.* 172, 535 (1921).
(9) CH. RABAUT, *Bull. Soc. Chim.* (3) **19**, 786 (1898).
(10) G. PERRIER *C.R. Acad. Sci.* 130, 1423 (1898).
(11) G. PATEIN, *Ber. Dtsch. Chem. Ges.* **24**, 734 (1891).
(12) R. FRICKE and O. RODE, *Z. Anorg. Chem.* **152**, 349 (1926).

-10°C. Precautions were taken to use dilute thiocyanate solutions in ether, to exclude decomposition.

The products in the form of heavy oily phases were separated from the ether phase. Excess ether was then pumped off, and the final products dried in a vacuum desiccator. Moisture was rigorously excluded. All these compounds can be obtained as crystals by freezing at -80°, filtering quickly and washing with cold ether.

The compounds were analysed by addition of water yielding a solution containing acidic hydrogen, halide, thiocyanate, metal ions and ether. Standard analytical methods were used to determine the acidic hydrogen, metal and halogen. The thiocyanate anion in the presence of chloride, bromide, and iodide was determined by the method of Volhard,⁽¹³⁾ and the ether content was obtained by difference.

Results are given in the table.

Table

Formula	Analysis	Colour
$H[ZnCl_2SCN]\cdot 2Et_2O$	$H:Zn:Cl:SCN:Et_2O$ 1·03:1·05:2·05:0·90:2·02	Pale yellow
$H[ZnBr_2SCN]\cdot 2Et_2O$	$H:Zn:Br:SCN:Et_2O$ 1:1·02:2·03:0·88:2·1	Deep yellow
$H_2[CdBr_2(SCN)_2]\cdot 3Et_2O$	$H:Cd:Br:SCN:Et_2O$ 1·0:1·03:2·05:1·9:2·9	Orange
$H_2[CdI_2\text{-}SCN)_2]\cdot 3Et_2O$	$H:Cd:I:SCN:Et_2O$ 2·1:1·02:2·1:1·92:3·1	Red
$H[AlCl_3SCN]\cdot 2Et_2O$	$H:Al:Cl:SCN:Et_2O$ 1·02:1·01:3·04:0·90:2·04	Yellow
$H[AlBr_3SCN]\cdot 2Et_2O$	$H:Al:Br:SCN:Et_2O$ 1·01:1·04:3·02:0·91:2·02	Orange yellow
$H[InBr_3SCN]\cdot 2Et_2O$	$H:In:Br:SCN:Et_2O$ 1:1·02:3·1;0·88:2·3	Brownish yellow
$H[InCl_3SCN]\cdot 2Et_2O$	$H:In:Cl:SCN:Et_2O$ 1·1:1·03:3·15:0·85:2·25	Pale yellow

In all cases the monobasic complex halogen acids are formed with two molecules of ether. In the case of the cadmium complex acids $H_2[CdX_2X_2']\cdot 3Et_2O$ a third molecule of ether may be taken up.

General properties

All freshly prepared mixed halogen acids are coloured, their colour varying from pale yellow to red. They are oily liquids, freezing at low temperature. Their freezing points are not sharp. Due to hydrolysis they fume in air.

---

(13) W. D. Treadwell, p. 328. Ibd. F. Dentiene Leipzig-Wien 1930.

They are soluble in many polar (nitrobenzene, chloroform) and insoluble in non-polar solvents. They do not react vigorously with water, but by contrast they react vigorously with organic bases such pyridine, replacing the ether molecules and giving very stable salts.(14)

The formation reaction proceeds more readily from cadmium to aluminium in the order as follows (Cd, <In, <Zn, <Al). Without stirring the reaction is very slow for the cadmium salts requiring up to five days for complete reaction. Stirring speeds up the reaction so that they are generally complete within a few hours.

Solutions in polar media (nitrobenzene) conduct electricity, the acids dissociating into ions.

Stability of the compounds

The compounds were thermally decomposed and the products were collected in a trap cooled by acetone–dry-ice mixture, followed by a trap immersed in liquid nitrogen. The traps were connected to a vacuum pump. In the first trap there were detected HCl, HCN, and ether, in the second, nothing. In the flask there remained beside the metal halide a solid yellow product (isoperthiocyanic acid $H_2C_2N_2S_3$) which is formed in the decomposition together with HCN. These decomposition products refer to the compound $H[ZnCl_2SCN]\cdot 2Et_2O$.

From these observations we conclude that on heating the compounds decomposed according to the reactions used in their formation except that there was also some exchange producing HCl besides HSCN, and the isoperthiocyanic acid.

Attempts were also made to detach the metal from the compounds by precipitation of the metal with H_2S. Passage of H_2S for 15 min into a solution of $H_2[CdBr_2(SCN)_2]\cdot 3\cdot Et_2O$ in nitrobenzene yielded no precipitate of cadmium sulphide. On the other hand similar treatment of the mixture produced by adding an ether solution of the anhydrous cadmium bromide to nitrobenzene yielded yellow CdS immediately.

The stability of these compounds may be ascribed to three types of bonds. (a) homopolar bonds between the central ion of the complex and the halogen ions, (Cl, Br, I, SCN). (b) heteropolar bond between the complex anion and the complex cation. (c) hydrogen bridging between the proton and the oxygen atoms of the ether molecules which increases significantly the volume of the cation, decreases the mobility of the proton, and increases the stability of the molecule. The compounds may be formulated as follows:

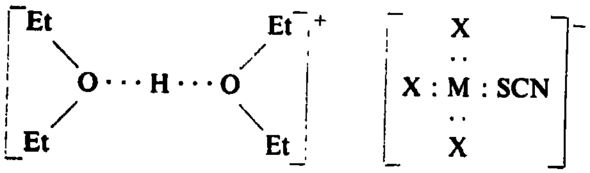

Acknowledgement—This investigation was financially supported by the Royal Hellenic Research Foundation.

---

(14) A. Galinos, *J. Inorg. Nucl. Chem.* **19**, 69 (1961).

J. Inorg. Nucl. Chem., 1962, Vol. 24, pp. 1559 to 1564. Pergamon Press Ltd. Printed in Northern Ireland

THE FORMATION AND COMPOSITION OF SOME METAL 12-MOLYBDOPHOSPHATES

W. P. THISTLETHWAITE and W. T. WATSON
Department of Chemistry, Whitehaven College of Further Education,
Whitehaven, Cumberland

(*Received* 24 *April* 1962; *in revised form* 25 *May* 1962)

Abstract—The insoluble thallium, and the soluble magnesium and zinc salts of 12-molybdophosphoric acid have been prepared and analysed.

The number of thallous ions per anion in the precipitate *below* three is controlled by the ratio pertaining in solution, but *above* three by the acidity of the solution, lending support to the theory of RIPAN that 12-molybdophosphoric acid has three "strong" and four "weak" ionizable hydrogens.

The salts of magnesium and zinc contain respectively 1·82 and 2·32 cation equivalents per anion, independently of the conditions of formation, and are thus acid salts on *any* theory of the ionization of 12-molybdophosphoric acid. In this respect magnesium and zinc resemble potassium and rubidium respectively, but the salts are more soluble.

AMMONIUM 12-molybdophosphate has appeared in the literature practically every year from 1849 to the present time and has been intensively studied from many aspects. By way of contrast, although the 12-molybdophosphates of several metals were prepared during the nineteenth century, for example by FINKENER,(1) they seem to have received little attention in recent years outside this school, with the exception of those of the alkali metals. The salts of potassium, rubidium, caesium and thallium were briefly described by BUCHWALD and THISTLETHWAITE(2) in 1958. It was noted there that thallium appears to be unique in forming a normal salt, even under strongly acid conditions, whereas all other cations so far examined form only acid salts even when the acid concentration is much lower. Some further preparations and analyses of thallous 12-molybdophosphate, and some new preparations of magnesium and zinc salts, are described in the present paper.

The salts of 12-molybdophosphoric acid appear to fall into two rather sharply-defined groups and one intermediate group: those of thallium and ammonium are very insoluble, while those of most other metals (e.g. sodium, magnesium, calcium, strontium, barium, zinc, lanthanum and thorium) are very soluble; it appears that some (e.g. lead, mercurous, bismuth) cannot be isolated by crystallization at all without decomposition. Salts of the larger alkali metals (potassium, rubidium, caesium) are sparingly soluble with solubilities decreasing in that order.

METHODS OF ISOLATION

It necessarily follows that the isolation (and indeed the analysis) of these two groups requires quite different techniques: those of the first group (and of the intermediate group) can be isolated very easily by precipitation; the remainder require much slower evaporation methods. Further limitations, applying in both cases, are the instability of the 12-molybdophosphate ion at pH values above about 4·5 and its extreme sensitiveness to reduction by metals and by many kinds of solid organic material.

---

(1) FINKENER, *Ber. Dtsch. Chem. Ges.* 11, 1638 (1878).
(2) BUCHWALD and THISTLETHWAITE, *J. Inorg. Nucl. Chem.* 7, 292 (1958).

Although the soluble salts carry much more water of crystallization, both kinds can be dried completely by sufficiently prolonged heating at 220–250°C.

In the present study the thallium salt was isolated by both conventional and homogeneous precipitation; those of magnesium and zinc by crystallization in small petri dishes with protection from dust.

Thallium

(a) *Conventional precipitation* (*Series* 1). Thallous nitrate solution (50 ml) was added dropwise from a burette to 12-molybdophosphoric acid solution (100 ml) heated to 50°C in a water-bath, with constant stirring. Although varying amounts of thallium, hetero-acid and nitric acid were used, these volumes were maintained throughout.

The precipitates were then digested with the mother liquor for several hours at 50°C, cooled and filtered on sintered glass crucibles of porosity 5, being washed in and washed six times on the filter with nitric acid (1 per cent).

(b) *Conventional precipitation* (*Series* 2). In this case the order of precipitation was reversed and attempt was made to achieve less acidic conditions. Precipitates were "colloidal" and extremely difficult to filter without loss.

In no. (9), 12-molybdophosphoric acid solution (10 ml) was added dropwise to thallous carbonate solution (50 ml) *in the cold*. Permanent yellow precipitation was deferred until about 0·4 ml had been added. The precipitate was digested with the mother liquor at 50°C for 24 hr, cooled and allowed to stand four weeks before filtration. Further treatment was in as (a) above.

In no. (10), sufficient sodium hydroxide was added to the thallous carbonate to neutralize the nitric acid that had been added in making up the 12-molybdophosphoric acid solution, before mixing: in this case permanent precipitation was delayed till 2–5 ml of the acid had been added. Further treatment was in as (a) above.

(c) *Homogenous precipitation* (*Series* 3). This method was developed from that of Series 2 above, but a much larger amount of sodium hydroxide was added to the thallous carbonate, so that the whole of the 12-molybdophosphoric acid could be added without causing any precipitation.

The mixtures were placed in crystallizing dishes. A "desiccator" was charged with concentrated nitric acid instead of desiccant: in this were placed, for varying periods, the crystallizing dishes so that each solution was gradually acidified by gaseous diffusion of nitric acid, and formation of the heteropoly compound took place as nearly as possible under equilibrium conditions. The acidification process was followed in a crude sort of way by testing with "universal" indicator paper from time to time. In this way a series of values of the ratio Te^+/H_3O^+ varying from 0·0074 to 1·61 was achieved.

Magnesium

Both series were prepared in the same way, the difference lying in the method of analysis and calculation of composition.

Magnesium oxide (1 or 0·667 g) was dissolved in the minimum quantity of 2 N nitric acid and the solution made up to 50 ml. Ten ml portions were added to 12-molybdophosphoric acid solution (20 or 25 ml) containing 7·526 g of the A.R. hydrated acid.

Evaporation was continued until about 5 g of large crystals had appeared; about 5 ml of mother liquor remained. This was drained off and the crystals gently detached and washed with small portions of nitric acid (1 per cent). They were then lightly pressed between filter paper. Efflorescence occurred rapidly, the well-formed crystals soon becoming a spongy mass.

The anhydrous compound was obtained by heating for several hours at 350°C.

Zinc

(a) *Series* 1. The single sample here was obtained in the same way as for the magnesium compounds above, starting from zinc oxide.

(b) *Series* 2. The crystallization method was here modified so as to reduce the volume of solution and hence the period of evaporation. In all cases the same weight of 12-molybdophosphoric acid (7·3 g) was taken and was dissolved in 7–8 ml of water. Zinc nitrate (1 or 2 g) was dissolved in this by gentle warming on a hotplate $\ngtr$ 50°C. The nearly-saturated solutions were set aside, protected from dust. Crystallization was adequate after 3–4 days: the weight of the precipitate varied between 2·5 and 5 g, the residual mother liquor being about 2–3 ml.

The crystals varied a great deal in habit, from a sandy deposit to large well-formed crystals. They were collected in sintered glass crucibles (porosity 3), washed and drained three times with very small portions of water, and air-dried to constant weight prior to heating for several hours at 220°C to produce the anhydrous salt. Estimates of the water of crystallization were made but are low and variable because of varying atmospheric humidity.

(c) *Series* 3. These crystals were obtained in the same way as in Series 2 but were dissolved up in water and recrystallized before recovery.

METHODS OF ANALYSIS

Dissolution of precipitates

The salts of magnesium and zinc dissolve readily in water. That of thallium can be dissolved in ammonia or sodium hydroxide solution but is reprecipitated on acidification (even with acetic acid); since both methods used for molybdenum require acid conditions, molybdenum was not determined in this case.

Determinations

Thallium. A modified version of the method of Rao and Rao(3) was used. The samples of thallous compound were usually about 0·2 g and were dissolved in A.R. sodium hydroxide (0·35 g) with about 50 ml of water. The slightly turbid solution was heated nearly to boiling, conc. HCl (15 ml) added, and the hot solution titrated with ceric sulphate (0·0686 N), using iodine monochloride as catalyst (0·02 M in M HCl, 1 ml) and ferroin as indicator (added near to the end-point).

N.B. Although the addition of acid to the alkaline solution of thallous 12-molybdophosphate reprecipitated some of this compound, it dissolved up gradually as titration proceeded, giving a clear solution before the end-point was reached.

Two results (Nos. 3 and 6) were confirmed by precipitation as TlI.

Zinc. This was determined as pyrophosphate, ignited at 830°C.

Magnesium. This was determined as pyrophosphate, and also in some cases by titration with EDTA, using Eriochrome Black T as indicator. Owing to the very small proportion of magnesium in the 12-molybdophosphate (about 1·3 per cent), aliquots containing not less than 2 g of this had to be used for each gravimetric determination. Reprecipitation was carried out after dissolution of the double phosphate in dilute hydrochloric acid.

Molybdenum. The gravimetric "oxine" method was used for the zinc compound (after determination of zinc) and the Jones reductor method for the magnesium compound (using an aliquot of the original solution).

The filtrate and washings from the zinc determination were made up to 250 ml. Suitable aliquots were taken, and diluted to 100 ml. As the pH was about 7, no buffer was added prior to addition of 8-hydroxyquinoline solution to the hot solution.

For the reductor method, many different models of reductor were tried, and several forms of zinc. Reproducible results were finally obtained with a reductor of total length 70 cm (including a widened upper portion 11 cm long) and a tapped delivery tube 27 cm long. The reducing column was of A.R. zinc pellets, 16–30 mesh (B.D.H.) of length 44 cm. The zinc was amalgamated before packing.

A suitable aliquot was mixed with 2 N sulphuric acid (20 ml) and passed through the "activated" reductor, followed by 2 N sulphuric acid (80 ml). The effluents were collected beneath the surface of ferric alum solution and the resulting ferrous iron titrated with standard potassium permanganate solution (ca. 0·05 N).

Every determination was accompanied by a blank, passing 2 N sulphuric acid (100 ml) through the column and completing the titration in exactly the same way as before.

Reagent

(1) *Standard* EDTA. The disodium salt was carefully heated at 80°C to constant weight ($Na_2H_2C_{10}H_{14}O_8N_2.2H_2O$). 3·721 g were dissolved and made up to 1 l. The solution is 0·01 M.

(2) *Buffer*. Ammonium chloride (70 g) and conc. ammonia solution (570 ml), made up to 1 l.

(3) *Erichrome black T*. The solid indicator (0·2 g), dissolved in triethanolamine (15 ml) + absolute ethanol (5 ml). This solution is stable for a few months.

(4)8 -*hydroxyquinoline*. The solid (2 g) is dissolved in 2 N acetic acid (100 ml); ammonia solution is added dropwise until a slight precipitate is just produced: the precipitate is dissolved by addition of a little acetic acid (2 N).

(3) Rao and Rao, *Z. Anal. Chem.* **168** (2) 83 (1959).

RESULTS

These are shown in Table 1 (thallium), Table 2 (magnesium) and Table 3 (zinc). The symbol PM^{3-} indicates 12-molybdophosphate ion.

TABLE 1

Series	No.	In solution			In precipitate
		(Moles) Tl^+	Ratio $\frac{[Tl^+]}{[PM^{3-}]}$	Ratio $\frac{[Tl^+]}{[H_3O^+]}$	Ratio $\frac{[Tl^+]}{[PM^{3-}]}$
1	1	0·000284	1·76	0·063	1·77*
	2	0·000284	1·76	0·063	2·46
	3	0·000378	2·36	0·084	2·12
	4	0·000378	2·36	0·084	2·20†
	5	0·00165	3·53	0·28	2·98
	6	0·00257	5	0·42	3·10
2	7	0·00146	2·99	0·77	3·25
	8	0·00146	2·99	1·56	3·50
3	9	0·00029	3·00	0·0074	3·03
	10	0·00029	2·99	0·020	3·02
	11	0·00029	2·99	0·042	3·17
	12	0·00029	2·99	0·166	3·08, 3·05
	13	0·00029	2·99	0·66	3·13
	14	0·00029	2·99	0·73	3·45
	15	0·00029	2·99	1·61	3·80

* 1·80 by precipitation as TlCl
† 2·28 by precipitation as TlCl

TABLE 2

Series	no.	In solution		In "precipitate"					
		(Moles) Mg^{2+}	Ratio $\frac{[Mg^{2+}]}{[PM^{3-}]}$	Weight taken for analysis (g)	Mg^{2+} (By $Mg_2P_2O_7$) (g)	Mg^{2+} (By EDTA) (g)	PM^{3-} (By JONES reductor) (g)	Difference (g)	Ratio $\frac{[Mg^{2+}]}{[PM^{3-}]}$
1	1	$0{\cdot}00\dot{3}$	1·09	4·0018	0·044	by difference	3·958		0·83
	2	0·003	1·09	1·4128	0·016		1·397		0·86
	3	0·003	1·09	2·9185	0·026		2·893		0·67
	4	0·003	1·09	3·1082	0·037		3·071		0·70
2	5	$0{\cdot}00\dot{3}$	1·09	2·082	0·0250	—	2·062	+0·005	0·91
	6	0·003	1·09	2·005	0·0194	—	1·988	+0·002	0·73
	7	0·003	1·09	2·029	0·0227	—	2·018	+0·012	0·84
	8	0·003	1·09	1·825	0·0198	—	1·803	−0·002	0·83
	9	0·005	1·55	2·2749	0·0281	0·0292	2·253	+0·060	0·93
	10	0·005	1·55	2·2680	0·0295	0·0325	2·252	+0·014	0·99
	11	0·005	1·55	1·9624	—	0·0248	1·937	(−0·001)*	(0·96)
	12	0·005	1·55	2·7803	0·0359	0·0369	2·750	+0·006	0·98
	13	0·005	1·55	1·8929	0·0261	0·0250	1·872	+0·005	1·05
	14	0·005	1·63	4·4457	0·0504	0·0523	4·468	+0·072	0·86
	15	0·005	1·63	4·7961	0·0560	0·0569	4·710	−0·030	0·89
	16	0·005	1·63	5·0385	0·0600	0·0608	4·909	−0·070	0·90
	17	0·005	1·63	4·7434	0·0557	0·0564	4·670	−0·017	0·91
	18	0·005	1·63	5·1101	0·0616	0·0612	5·110	+0·062	0·91

* Results calculated from EDTA value

TABLE 3

Series	no.	In solution: Zn^{2+} (Moles)	In solution: Ratio $\frac{[Zn^{2+}]}{[PM^{3-}]}$	In "precipitate": Weight taken for analysis (g)	In "precipitate": Zn^{2+} by ($Zn_2P_2O_7$) (g)	In "precipitate": PM^{3-} (by oxine) (g)	In "precipitate": Difference (g)	In "precipitate": Ratio $\frac{[Zn^{2+}]}{[PM^{3-}]}$	In "precipitate": H_2O of cryst. (Moles)
1	1	0·00658	1·49	0·7213	0·0234	0·6948	−0·003	0·95	
		*		0·5065	0·0159	0·4684†	−0·022	0·95	
2	2	0·00329	1·01	2·2107	0·0855	2·114	−0·011	1·27	25·1
	3	0·00329	1·01	2·5940	0·0876	2·491	−0·015	1·15	
	4	0·00329	1·01	2·3411	0·0880	2·257	+0·004	1·04	26·9
	5	0·00329	1·01	3·3567	0·1058	3·227	−0·024	1·12	27·9
	6	0·00329	1·01	1·7961	0·0776	1·691	−0·027	1·28	27·2
	7	0·00329	1·01	1·6130	0·0552	1·363	−0·195	1·13	28·2
	8	0·00658	2·02	1·7840	0·0787	1·714	+0·009	1·28	28·8
	9	0·00658	2·02	1·8872	0·0819	1·805	0·000	1·26	28·4
3	10	0·00494	1·52	2·6370	0·1050	2·540	+0·008	1·15	27·7
	11	0·00494	1·52	3·0907	0·1239	2·966	−0·001	1·17	27·9

* 0·008 moles HNO_3 also present

† By Jones Reductor method.

CONCLUSIONS

1. *Thallium*

Earlier work on the 12-molybdophosphate of this metal(2) demonstrated that under conditions where the larger alkali metal cations and ammonium invariably form acid salts containing 2–2·5 cations per anion, the thallous ion always forms a "normal" salt containing 3 or more cations per anion. However, experiments 1 and 2 of that series, carried out with a much lower ratio of thallous ion to (a) anion (b) hydronium ion in solution gave a ratio 2·2 in the precipate, showing that even thallium may form an acid salt under extreme conditions.

The present series of experiments was designed (a) to investigate the conditions for such acid salt formation and (b) to throw further light on the frequent occurrence of *more* than three thallous ions per anion in precipitates. Conditions for precipitation, whether conventional or homogenous, were quite different from those in the earlier series; in particular, the ratio of thallous ion to anion in solution was much smaller, and only in two cases (numbers 5 and 6) did it exceed the "theoretical" value 3 : 1. However, the ratio of thallous ion to hydronium ion in solution was allowed to range widely.

Conclusions may be stated as follows:

(1) Thallium forms "acid" salts only when the ratio of thallous ion to anion in solution is less than three,

(2) Within this range the ratio in the precipitate is approximately proportional to that in solution and is little affected by hydronium ion concentration.

(3) When the ratio [cation]/[anion] in solution is exactly three, the ratio in the precipitate is > 3 and is controlled by the [cation]/[hydronium] ratio in solution. Number 11 is the only exception to this rule within the "homogenous" series.

(4) Since in the homogenous series the ratio of thallous ion to “the elements of” 12-molybdophosphate ion in *solution* never at any stage exceeds 3, it seems that the *precipitate* ratios >3 do indicate that the basicity of the acid is not limited to three (this has been suggested from time to time in the last 50 years(4–10)). Presumably in the presence of very low concentrations of added mineral acid, more than three hydrogens of the hydrated complex are able to dissociate.(10) For a contrary view see Spitzin.(11)

2. *Magnesium*

With only two exceptions (nos. 3 and 6) the values of the ratio [cation]/[anion] fall within a very narrow range (0·83–1·05, mean 0.91). The differences appear fortuitous and show no correlation with the ratio existing in solution.

Since in all these experiments no added mineral acid was present, it may safely be concluded that magnesium 12-molybdophosphate is an acid salt comparable with that of potassium (i.e. approx. 2 equivalents of cation per anion), though much more soluble.

3. *Zinc*

(1) In series 2 the ratio [cation]/[anion] in the solid compound ranges from 1·04 to 1·28 (mean 1·19). There is no correlation with the ratio in solution. In series 3, involving recrystallization, the two results agree more closely (1·15 and 1·17, mean 1·16). Evidently zinc 12-molybdophosphate is an acid salt containing about 2·30 equivalents of cation and therefore comparable with the rubidium salt, but much more soluble.

(2) The results of series 1 indicate that the presence of additional hydronium ion (mineral acid) depresses the “equivalent” ratio from 2·30 to 1·90, i.e. a still more acid salt is produced.

(3) The values for water of crystallization are probably approaching the value 29 established for the closely-related 12-tungstophosphoric acid.(12)

A final observation is that all these acid salts appear to be nonstoicheiometric, in keeping with the well-known base-exchange properties of the 12-molybdophosphates.

(4) Miolati and Pizzighelli, *J. Prak. Chem.* 77, (ii) 417 (1908).
(5) von Enrédy, *Z. Anorg. Chem.* 194, 239 (1930).
(6) Jander and Witzman, *Z. Anorg. Chem.* 215, 310 (1933).
(7) Jander and Jahr, *Kolloid-Beihefte* 41, 297 (1935).
(8) Santos, *Proc. Roy. Soc.* A 150, 309 (1935).
(9) Nikitina, *Brit. Chem. Abstr.* 298 (1940); 56 (1941); 88 (1941).
(10) Ripan, *C. R. Acad. Sci. Paris* 227, 474 (1948).
(11) Spitzin, *Z. Anorg. Chem.* 304, 196 (1960).
(12) Bradley and Illingworth, *Proc. Roy. Soc.* A 157, 113 (1936).

J. Inorg. Nucl. Chem., 1962, Vol. 24, pp. 1565 to 1570. Pergamon Press Ltd. Printed in Northern Ireland

INTERACTION OF BORANES. THE DIBORANE-PENTABORANE (9) REACTION*

M. Hillman,† D. J. Mangold and J. H. Norman‡
Energy Division, Olin Mathieson Chemical Corporation
New Haven, Connecticut

Abstract—A reinterpretation of existing data reaffirms the conclusion that pentaborane (9) is an intermediate in the formation of decaborane.

During the interval between the time the paper was first presented in a symposium⁽¹⁾ and the time the symposium was finally published,⁽²⁾ objections§ were raised concerning the interpretation of the data. Consequently, we have attempted to reinterpret the data to accommodate the more serious objections while concentrating on the main thesis of the original paper—that in a reaction of diborane and pentaborane (9), half of the boron atoms in decarborane come from pentaborane (9).

It should be noted that in the original paper, the observed isotopic distributions of the decaborane were compared with expected distributions calculated as if neither of the starting boranes underwent any isotopic exchange during the course of the reaction. This criterion was not met in reality. The question is then raised: may the observed distributions be meaningfully compared with the expected distributions in the reported way? They may not, for decaborane, if it does form from a combination of diborane and pentaborane (9) would also be expected to form from these reactants after they have undergone exchange. Furthermore, decaborane is continuously removed from the reaction by reaction with diborane to form polymers. This, in effect, predominantly removes decaborane molecules that might have been formed from the initial reactants since these molecules were in the reaction medium longer, leaving behind decaborane formed later in the reaction. Fortunately, diborane does not exchange borons with decaborane.⁽³⁾ This would complicate the problem even further.¶

Without knowing the rate of change of the boron abundances of diborane and pentaborane (9) and without knowing the rate of formation of decaborane or the rate of reaction of decaborane with diborane, it is impossible to calculate exactly what the isotopic distribution of decaborane is expected to be when formed by any mechanism. However, since the initial and final isotopic distributions of the reactants are known, boundaries can easily be set on the expected isotopic distribution of the

---

* Research supported by Air Force Contract 33(600)-33920.

† Present address: The Hot Laboratory, Brookhaven National Laboratory, Upton, Long Island, New York.

‡ Present address: General Atomic Division, General Dynamics Corp., San Diego, California.

§ The objections were raised by referees.

¶ Since the virtual fate of individual molecules is followed in a tracer experiment, unless an inordinately high isotope effect obtains, it is unimportant to have quantitative yields in a reaction nor is it important to know the yields precisely.

(1) Abstracts of Papers, 133rd National American Chemical Society Meeting, San Francisco, California.

(2) *Borax to Boranes*, Advances in Chemistry Series, p. 151. American Chemical Society, Washington, D.C. (1961).

(3) J. Shapiro and R. E. Williams, *J. Amer. Chem. Soc.* **81**, 4787 (1959).

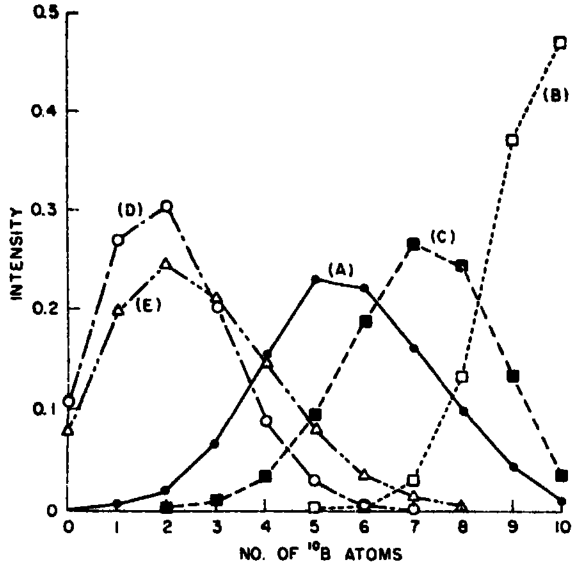

FIG. 1.—Isotopic distributions of decaborane. (A) observed, B_5H_9 + $^{10}B_2H_6$; (B) calculated, all borons from starting $^{10}B_2H_6$; (C) calculated, all borons from final $^{10}B_2H_6$; (D) calculated, all borons from starting B_5H_9; calculated, all borons from final B_5H_9.

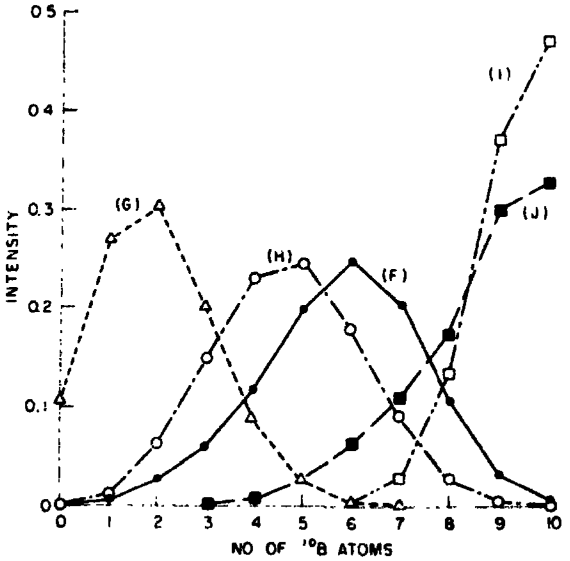

FIG. 2.—Isotopic distributions of decaborane. (F) observed, $^{10}B_5H_9$ + B_2H_6; (G) calculated, all borons from starting B_2H_6; (H) calculated, all borons from final B_2H_6; (I) calculated, all borons from starting $^{10}B_5H_9$; (J) calculated, all borons from final $^{10}B_5H_9$.

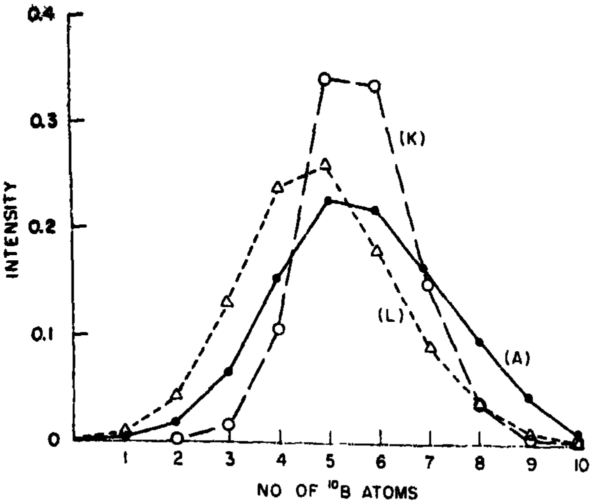

FIG. 3.—Isotopic distributions of decaborane. (A) observed, $B_5H_9 + {}^{10}B_2H_6$; (K) calculated from initial isotopic abundances of $B_5H_9 + \frac{5}{2}\ {}^{10}B_2H_6$; (L) calculated from final isotopic abundances of $B_5H_9 + \frac{5}{2}\ {}^{10}B_2H_6$.

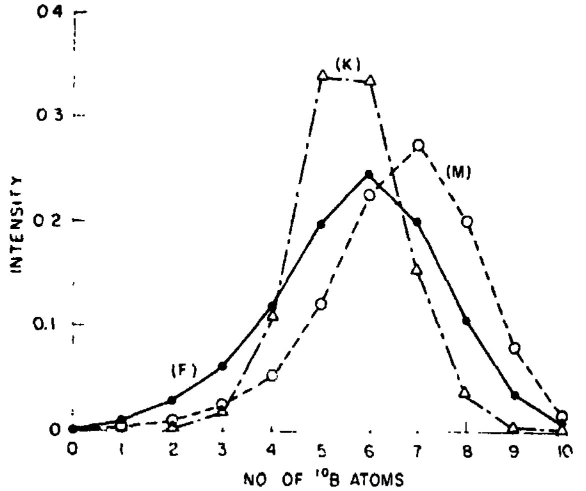

FIG. 4.—Isotopic distributions of decaborane. (F) observed, ${}^{10}B_5H_9 + B_2H_6$; (*K*) calculated from initial isotopic abundances of ${}^{10}B_5H_9 + \frac{5}{2}\ B_2H_6$; (*M*) calculated from final isotopic abundances of ${}^{10}B_5H_9 + \frac{5}{2}\ B_2H_6$.

product. That is, the isotopic distribution of the product can be calculated as if it has been formed from the reactants in their initial condition and again as if it was formed from the reactants in their final condition. The true expected distribution lies somewhere in between.

This technique is illustrated in Figs. 1–6. In these curves the envelopes of expected and observed distributions are plotted, All curves are normalized so that their areas are equal to unity. These curves are interpreted as follows:

The major part of the decaborane was not formed exclusively from either diborane or exclusively from pentaborane (9). Figs. 1 and 2 demonstrate this. In Fig. 1, curve (*A*) represents the experimental distribution of the decaborane obtained from the

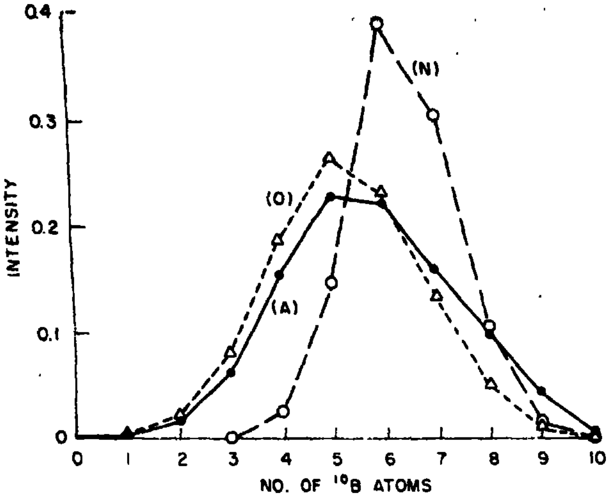

FIG. 5.—Isotopic distributions of decaborane (A) observed, B_5H_9 + $^{10}B_2H_6$ (*N*) calculated from initial isotopic abundances of $\frac{4}{5}$ B_5H_9 + $3^{10}B_2H_6$: (*O*) calculated from final isotopic abundances of $\frac{4}{5}$ B_5H_9 + $3^{10}B_2H_6$.

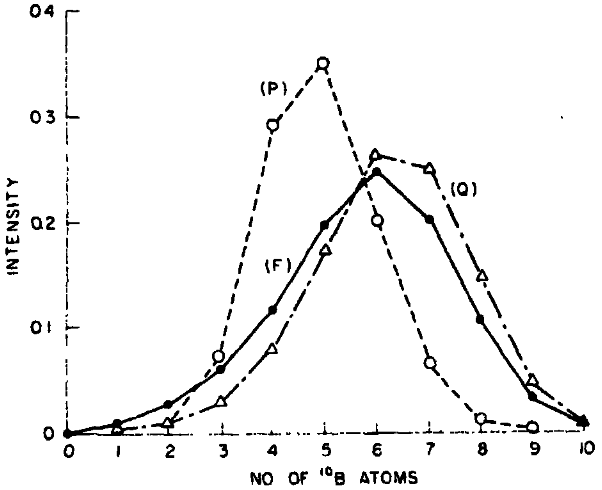

FIG. 6.—Isotopic distributions of decaborane. (*F*) observed, $^{10}B_5H_9$ + B_2H_6; (*P*) calculated from initial isotopic distributions of $\frac{4}{5}$ $^{10}B_5H_9$ + B_2H_6; (*Q*) calculated from final isotopic distributions of $\frac{4}{5}$ $^{10}B_5H_9$ + B_2H_6

enriched diborane and the natural pentaborane (9) experiment. Curves (*B*) and (*C*) represent the expected distributions if the decaborane was formed from the initial diborane and final diborane respectively. Had the decaborane actually been formed exclusively from the diborane the experimental curve would have been expected to fall somewhere between those two curves. The same holds true for the possibility of the formation of decaborane exclusively from pentaborane (9). Curve (*A*) would, in this case, have been expected to fall somewhere between (*D*) and (*E*) which represent the distribution expected for decaborane formed from the initial pentaborane (9) and the final pentaborane (9) respectively.

The nonformation of the decaborane exclusively from either of the reactants was confirmed in the experiment using enriched pentaborane (9) and natural diborane. In Fig. 2, curve (*F*), the experimental distribution does not fall between either pairs of calculated distributions. Here, curves (*G*) and (*H*) represent the expected distributions form the initial and final diborane respectively and (*I*) and (*J*) represent the expected distributions from the initial and final pentaborane (9) respectively.

This evidence demonstrates that decaborane must have been formed from a reaction involving both the diborane and pentaborane (9). Recognizing this, the next step is the determination of the stoicheiometry. Fig. 3 depicts the experimental distribution (*A*) of the decaborane obtained from the enriched diborane reaction compared with the expected distributions (*K*) and (*L*) for decaborane formed from five boron atoms of diborane and five from pentaborane as they existed at the beginning and the end of the experiment. Fig. 4 does the same for the enriched pentaborane (9) experiment. Here, (*K*) is the distribution expected from the initial abundances, (*M*) from the final abundances and (*F*) is the experimental distribution. Generally, except for the fact that they are flatter, the experimental curves fall between pairs of calculated curves.

The lowering of the peak can be accounted for by the formation of decaborane exclusively from diborane in small amounts as a side reaction. This would also account for the excess tailing observed in Fig 3(A) towards the $^{10}B_{10}$ end and in Fig. 4(*H*) towards the $^{11}B_{11}$ end. Curves for the distributions of decaborane formed exclusively from diborane would be expected to fall in the area of the tails and, since all of these curves are plotted so that the total area equals unity, after summing the distributions from the two separate reactions and normalizing, the resultant curve will be of generally lower intensity than either of the original contributions.

This minor side reaction does not necessarily imply that there is a course to decaborane not involving pentaborane (9). Under the conditions of the reaction diborane is converted to pentaborane (9) which, in turn, is converted to decaborane. An alternate minor route to decaborane, however, is by no means eliminated.

We have not at this point established the stoicheiometry of the reaction with certainty although it seems that five boron atoms from each reactant fits fairly well. For the sake of comparison with another conceivable stoicheiometry, in Figs. 5 and 6 the experimental distributions are compared with the calculated distributions from a reaction involving six boron atoms from diborane and four from pentaborane (9). In both figures the experimental distributions fall rather close to the calculated distributions using the reactants as they existed at the end of the reactions. Although they do not seem to fall between the pairs of curves as well as in Figs. 3 and 4, a reaction of this nature cannot be completely ruled out.

The reaction involving six boron atoms from pentaborane (9) and four from diborane is similar to the one above but is not described fully due to the difficulty of conceiving a realistic mechanism whereby this may occur, especially in view of the reported non-self-boron exchange⁽⁴⁾ in pentaborane (9).

DISCUSSION

The evidence presented in the foregoing section reaffirms the conclusion (1,2) that pentaborane (9) is an intermediate in the formation of decaborane from the pyrolysis of

---

(4) I. Shapiro and B. Keilin, *J. Amer. Chem. Soc.* 77, 2663 (1955).

diborane. Whether the route to decaborane through pentaborane (9) is the only possible course has not been established. There is a possibility that other routes may exist.

Evidence has been presented that the stoicheiometry of the reaction between diborane and pentaborane (9) probably involves five boron atoms from diborane and five boron atoms from pentaborane (9). This implies that there is a step wise build up of the pentaborane (9) molecule through higher boranes such as hexaborane, octaborane and nonaborane. The actual steps involved which may be quite complex are still obscure.

Acknowledgements—Indebtedness, inadvertently omitted from the original paper(3), are due Miss D. M. ROBBINS and her staff for infra-red analyses, Mr. L. COLETTA for aid in obtaining the mass spectra and to Mr. R. P. ALEXANDER and Dr. D. S. P. EFTAX for the preparation of the enriched pentaborane (9) and the enriched decaborane.

J. Inorg. Nucl. Chem., 1962, Vol. 24, pp. 1571 to 1585. Pergamon Press Ltd. Printed in Northern Ireland

ABSORPTION SPECTRA OF TRANSITION GROUP COMPLEXES OF SULPHUR-CONTAINING LIGANDS

CHR. K. JØRGENSEN
Cyanamid European Research Institute,
Cologny (Geneva), Switzerland

(*Received* 14 *February* 1962; *in revised form* 1 *May* 1962)

Abstract—Nickel(II), rhodium(III), palladium(II), iridium(III) and other central atoms are combined with diethyldithiophosphate (dtp$^-$) diethyldithiocarbamate (dtc$^-$) 2,2'-di(aminoethyl)sulphide (daes), thiosemicarbazide (tscaz) and other sulphur-containing ligands. The position in the spectrochemical series dtp$^-$ < dtc$^-$ < daes < SO_3^{2-} is related to the number of lone-pair electrons available on the sulphur atom. The nephelauxetic effect is very conspicuous in Rh dtp_3 and Ir dtp_3. The square-planar low-spin Ni dtp_2 and nickel(II) xanthate form high-spin pyridine addition compounds such as $Ni(dtp)_2py_2$, while Ni $daes_2^{2+}$ is high-spin. In dtp_3 and Bi dtp_3 can be precipitated from acid solutions.

THE spectrochemical series of increasing M.O. energy difference (spectroscopic splitting parameter) Δ between the subshells in the complexes of the three transition groups is arranged[1–4] according to decreasing radii of the ligand atoms:

$$I < Br < Cl < F < O < N < C \qquad (1)$$

Hence, it might be expected that S would be ranged somewhere between Cl and F. However, the main purpose of this paper is to show that S has a wide variation of Δ values for a given central ion, going from Cl to well beyond N. It is possible to rationalize this behaviour by reference to the larger π-bonding effects in sulphur ligands with a great quantity of lone-pair electrons, while SO_3^{2-} with a single lone-pair preferably forms a σ-bond to the central atom.

Equation (1) does, of course, not indicate that one single value of Δ is characteristic for each ligand atom, but it allows a certain variation, as is already evident in nickel(II) complexes[5,6] of six N, where Δ varies 13 per cent. SCHÄFFER[7] found that Δ of chromium(III) complexes with six O varies within a range of 26·5 per cent, but suggested rather unusual conditions of bonding in the extreme limits of this series; the main portion of CrO_6 complexes having Δ-values only varying within some 8 per cent. In cases such as the double salts of nickel(II), containing bromide or chloride,[6,8] the variation of Δ ∼ 8 per cent may be ascribed to small differences in the internuclear

---

[1] L. E. ORGEL, *Introduction to Transition-Metal Chemistry*. Methuen, London, (1960).

[2] T. M. DUNN, *Modern Coordination Chemistry*, (Edited by J. LEWIS and R. G. WILKINS): Interscience, New York (1960).

[3] C. K. JØRGENSEN, *Absorption Spectra and Chemical Bonding in Complexes*. Pergamon Press, Oxford (1962).

[4] C. K. JØRGENSEN, *Adv. Chem. Phys.* **5**, 31 (1962).

[5] C. K. JØRGENSEN, *Acta Chem. Scand.* **10**, 887 (1956).

[6] O. BOSTRUP and C. K. JØRGENSEN, *Acta Chem. Scand.* **11**, 1223 (1957).

[7] C. E. SCHÄFFER, *J. Inorg. Nucl. Chem.* **8**, 149 (1958).

[8] R. W. ASMUSSEN and O. BOSTRUP, *Acta Chem. Scand.* **11**, 745 (1957).

distances in the various lattices, comparable to the effects of lower temperature,(8,9) high pressure(10) or solvent effects.(11,12)

Solid sulphides have been studied at low temperature by Pappalardo and Dietz(13) and by Weakliem and McClure.(14) In zinc sulphide and cadmium sulphide, Co(II) and Ni(II) can be incorporated in tetrahedral configuration. Δ is comparable to the values in $CoCl_4{}^{2-}$ and Co(II) in ZnO, and is smaller (probably due to larger internuclear distances, cf. the "ruby compression"(7)) in CdS than ZnS, while the nephelauxetic effect is large and between that of the bromide and the iodide complexes.

We shall find differences in Δ larger than 50 per cent by comparing various types of sulphur-containing ligands.

Diethyldithiophosphates

Various neutral inner-complexes of $dtp^- = (C_2H_5O)_2PS_2{}^-$ have been described in literature. Thus Malatesta and Pizzotti(15) prepared the violet compound Ni dtp_2 and the black Fe dtp_3, whereas Vinogradova and Ivanova(16) report precipitates of Bi dtp_3, As dtp_3, Cd dtp_2, Cu dtp_2 and Pb dtp_2; the latter salt was previously known.(17) Recently, Busev and collaborators have made analytical use of the ligand(18) as also Bode and Arnswald(19) who reported absorption spectra of various of the diethyldithiophosphates extracted in carbon tetrachloride. The preparation of Cr dtp_3 has been reported(20) and Professor W. C. Fernelius was so kind, in a letter of July 1959, as to draw the attention of the present writer to this interesting ligand, and later to send him some samples of Ni dtp_2 and Cr dtp_3. Schäffer(21) also studied these compounds and Co dtp_3.

As discussed in the experimental section, several other transition group ions form rather easily diethyldithiophosphates, which are neutral inner-salts when the co-ordination number is twice the oxidation number. Fig. 1 shows the visible and near-ultra-violet spectra of Rh dtp_3 and Ir dtp_3 which are closely analogous to (22) $RhCl_6{}^{3-}$ and $IrBr_6{}^{3-}$ except for one phenomenon: that the nephelauxetic effect in the hexa-sulphur-co-ordinated complexes is much more pronounced. Actually, the distance between the two spin-allowed transitions, to ${}^1\Gamma_4$ and ${}^1\Gamma_5$, of $\gamma_5{}^5\gamma_3$, is so small as to suggest the following values:

$$\begin{aligned} \text{Rh dtp}_3: \quad & B = 220\ \text{cm}^{-1} \quad \beta = 0{\cdot}29 \\ \text{Ir dtp}_3: \quad & B = 160\ \text{cm}^{-1} \quad \beta = 0{\cdot}25 \end{aligned} \tag{2}$$

(9) D. S. McClure, *Solid State Physics* 9, 399 (1959)

(10) D. R. Stephens and H. G. Drickamer, *J. Chem. Phys.* 35, 427 (1961).

(11) J. Bjerrum, A. W. Adamson and O. Bostrup, *Acta Chem. Scand.* 10, 329 (1956).

(12) C. K. Jørgensen, *J. Inorg. Nucl. Chem.* 24, 1587 (1962).

(13) R. Pappalardo and R. E. Dietz, *Phys. Rev.* 123, 1188 (1961).

(14) H. Weakliem and D. S. McClure, *Suppl. to J. Appl. Phys.* 33, 347 (1962); private communication (1960); H. Weakliem *J. Chem. Phys.* 36, 2117 (1962).

(15) L. Malatesta and R. Pizzotti, *Chimica e industria* 27, 6 (1945).

(16) E. N. Vinogradova and V. A. Ivanova, *Vestnik Moskov. Univ.* 12, *Ser. Mat. Mek. Astron. Fiz. Khim.* No. 3 237 (1957); (*Chem. Abstr.* 52, 4390^{f} (1958)).

(17) T. W. Martin, G. R. Norman and E. A. Weilmünster, *J. Amer. Chem. Soc.* 67, 1662 (1945).

(18) A. I. Busev and M. L. Ivanyutin, *Zh. Anal. Khim.* 11, 523 (1956).

(19) H. Bode and W. Arnswald, *Fresenius' Zeitschr. analyt. Chem.* 185, 99 and 179 (1962).

(20) D. E. Goldberry, W. C. Fernelius and M. Shamma, *Inorganic Syntheses* 6, 142 (1960).

(21) C. E. Schäffer, *Ligand Field Symposium*, 140*th. Amer. Chem. Soc. National Meeting*, Chicago, September (1961).

(22) C. K. Jørgensen, *Acta Chem. Scand.* 10, 500 (1956) and 11, 151 (1957).

It is worth noting that the distance between the spin-forbidden transition to $^3\Gamma_4$, also of $\gamma_5{}^3\gamma_3$, and $^1\Gamma_4$ is 5 kK in Ir dtp$_3$, corresponding to a much smaller nephelauxetic effect. This distance$^{(22)}$ is 5·6 kK in $IrBr_6{}^{3-}$, 6.2 kK in $IrCl_6{}^{3-}$ and 7·1 kK in $Iren_3{}^{3+}$, demonstrating conspicuous deviations from the expanded radial function model in the more covalent complexes$^{(23)}$, though the strong effects of intermediate coupling$^{(24)}$ in Ir(III) are partly responsible for the deviations. It may be remarked that the Pryce-Koide model of $(1 - \varepsilon)B$ diminish the energy differences $^3\Gamma_4 - {}^1\Gamma_4$ and $^1\Gamma_4 - {}^1\Gamma_5$ to the same extent. Table 1 collects wavenumbers of the absorption bands of the octahedral complexes involved.

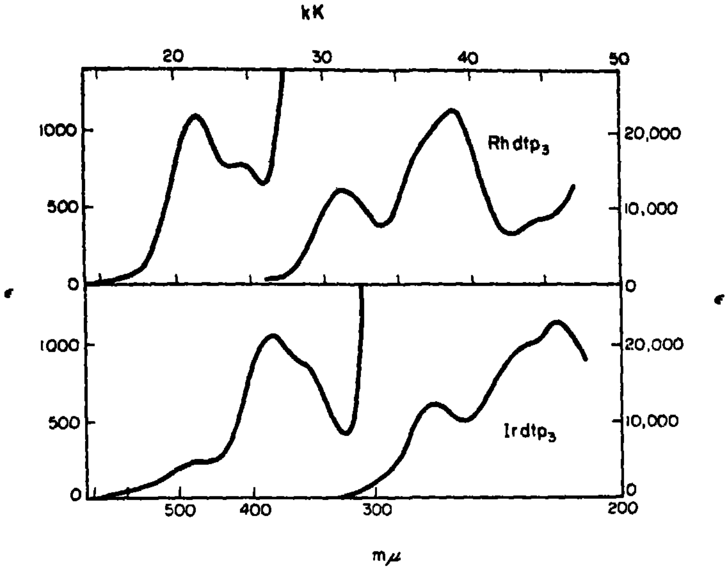

Fig. 1.—Absorption spectra of the two low-spin d^6 complexes rhodium(III) and iridium(III) tris(diethyldithiophosphates) in ethanol.

The colourless In dtp$_3$ is remarkably stable and can even be precipitated from 0·5M nitric acid from $In(NO_3)_3$ and NH_4 dtp. In dtp$_3$ and Cr dtp$_3$ can be syncrystallized, as well as in In dtp$_3$ with Fe dtp$_3$ or Rh dtp$_3$. The iron(III) complex is very unstable, the (greyish-green at lower, dark-purple at higher optical density) solution in ethanol decolourizes rapidly, presumably forming Fe(II) in close analogy to the ephemeric colour reactions of Fe(III) with $S_2O_3{}^{2-}$, cysteine, thiourea, etc., where RSSR frequently is formed. The black crystals of Fe dtp$_3$ deliquesce in air and form brown hydrolysis products. However, the mixed crystals of very little Fe dtp$_3$ and much In dtp$_3$ are stable for a long time and are remarkably dark-violet. The reasons for this strong colour will be discussed in the section on electron transfer bands.

Ni dtp$_2$ is low-spin, square-planar, as seen from the fact (Table 2) that no internal transition in the partly filled shell occurs below 14·5 kK. On the other hand, the green pyridine adduct (which was already prepared by Professor Fernelius), Ni dtp$_2$ py$_2$ is seen to have a band at 9·0 kK and is most certainly hexacoordinated, high-spin.

In aqueous solution, even 0·8 M $NH_4{}^+$ dtp$^-$ does not change the spectrum of

---

(23) C. K. Jørgensen, *Acta Chem. Scand.* 12, 903 (1958).

(24) J. S. Griffith, *Theory of Transition-Metal Ions*. Cambridge University Press (1961).

TABLE 1.—ABSORPTION BANDS OF COMPLEXES WHERE THE CENTRAL ION IS COORDINATED BY SIX SULPHUR ATOMS

		Assignment	λ(mμ)	σ(kK)	ε*
$3d^3$	Cr dtp$_3$	$^4\Gamma_2 \rightarrow {}^2\Gamma_3$	(763)	13·1	(225)
		→ doublets	(732)	13·6	(320)
		$\rightarrow {}^4\Gamma_5$	697	14·3	380
		$\rightarrow {}^4\Gamma_4$ and doublets	536	18·6	270
			523	19·1	265
		Electron transfer	((347))	((28·8))	(5,000)
		$\pi \rightarrow \gamma_5$ and $\pi \rightarrow \gamma_3$	(315)	(31·8)	(9,000)
			280	35·7	15,200
		—	(258)	(38·8)	(6,000)
		—	(238)	(42·0)	(8,000)
	Cr dtc$_3$	$^4\Gamma_2 \rightarrow {}^4\Gamma_5$	643	15·5	380
		$\rightarrow {}^4\Gamma_4$	490	20·4	360
		—	316	31·6	higher
	Cr(S_2CNH_2)$_3$ (KIDA and YONEDA(28))	$^4\Gamma_2 \rightarrow {}^4\Gamma_5$	—	15·5	310
		$\rightarrow {}^4\Gamma_4$	—	20·0	310
		—	—	(~27)	~3,000
		—	—	32	~15,000
$3d^5$	Fe dtp$_3$	Electron transfer	598	16·7	~1,500
			498	20·1	~1,300
			(392)	(25·5)	~4,000
			354	28·3	~5,000
	Fe dtc$_3$	Electron transfer	(586)	(17·1)	~1,200
			509	19·7	~1,700
			(389)	(25·7)	~7,000
			346	28·9	~9,000
$3d^6$	Co(S_2CNH_2)$_3$ (KIDA and YONEDA(28))	$^1\Gamma_1 \rightarrow {}^1\Gamma_4$	—	15·7	280
		$\rightarrow {}^1\Gamma_5$	—	20·7	630
		—	—	26·2	8,000
		—	—	31·8	18,000
	Co exan$_3$ (KIDA and YONEDA(28))	$^1\Gamma_1 \rightarrow {}^1\Gamma_4$	620	16·2	270
		$\rightarrow {}^1\Gamma_5$	480	20·8	360
		—	353	28·3	13,000
		—	285	35·2	32,000
	Co dtc$_3$	$^1\Gamma_1 \rightarrow {}^1\Gamma_4$	645	15·5	~100
		$\rightarrow {}^1\Gamma_5$?	(480)	(20·8)	~600
		—	(393)	(25·4)	~9,000
		—	(360)	(27·8)	~12,000
		—	323	31·0	~20,000
	Co(III)thioglycollate	$^1\Gamma \rightarrow {}^1\Gamma_4$	(613)	(16·3)	~360
		—	483	20·7	~2,200
		—	397	25·2	~2,300
$4d^6$	Rh dtp$_3$	$^1\Gamma_1 \rightarrow {}^1\Gamma_4$	470	21·3	1,090
		$\rightarrow {}^1\Gamma_5$	410	24·4	780
		$\pi \rightarrow \gamma_3$?	321	31·2	12,600
		—	(273)	(36·6)	(18,000)
		—	258	38.8	23,200
		—	((227))	((44·0))	(8,000)
	Rh dtc$_3$	$^1\Gamma_1 \rightarrow {}^1\Gamma_4$	423	23·6	—
		—	282	35·5	—
		—	252	39·7	—
		—	226	44·2	—
$4d^{10}$	In dtp$_3$	—	294	34·0	1,150
		Internal?	244	41·0	8,400
		—	<210	>48	>18,000

TABLE 1 (cont'd)

		Assignment	λ(mμ)	σ(kK)	ε
$5d^6$	Ir dtp$_3$	$^1\Gamma_1 \rightarrow {}^3\Gamma_4$	472	21·2	230
		$\rightarrow {}^1\Gamma_4$	381	26·2	1,070
		$\rightarrow {}^1\Gamma_5$	(350)	(28·6)	890
		$\pi \rightarrow \gamma_3$?	267	37·4	12,280
		—	(232)	(43·1)	(19,500)
		—	219	45·7	23,100
$6s^2$	Bi dtp$_3$	$^1\Gamma_1 \rightarrow {}^3\Gamma_4\,(\Gamma_1)$?	(395)	(25·3)	3,000
		$\rightarrow {}^3\Gamma_4\,(\Gamma_4)$?	329	30·4	13,700
		—	(277)	(36·1)	6,800
		$\rightarrow {}^1\Gamma_1$	233·5	42·9	36,400

* Molar extinction coefficient ε of absorption maxima, and in parentheses, of shoulders.

TABLE 2.—ABSORPTION BANDS OF LOW-SPIN d^8 COMPLEXES COORDINATED BY FOUR SULPHUR ATOMS AND THEIR HIGH-SPIN PYRIDINE ADDITION COMPOUNDS

		Assignment	λ(mμ)	σ(kK)	ε
$3d^8$	Ni dtp$_2$	$^1\Gamma_{t1} \rightarrow {}^1\Gamma_{t2}$	689	14·5	75
		$\rightarrow {}^1\Gamma_{t5}$	524	19·1	90
		$\rightarrow {}^1\Gamma_{t2}$?	383	26·1	800
		$\pi \rightarrow \gamma_{t3}$?	317	31·6	16,400
		—	(280)	(35·7)	4,000
		—	228	43·9	10,000
	Ni dtp$_2$ py$_2$	$^3\Gamma_2 \rightarrow {}^3\Gamma_5$	1,115	9·0	20
		$\rightarrow a^3\Gamma_4$	712	14·0	18
		$\rightarrow b^3\Gamma_4$	(441)	(22·7)	40
	Ni dtc$_2$	$^1\Gamma_{t1} \rightarrow {}^1\Gamma_{t2}$	631	15·8	—
		$\rightarrow {}^1\Gamma_{t5}$	(472)	(21·2)	—
		—	(428)	(23·4)	—
		—	388	25·8	~6,000
		—	327	30·6	~32,000
	Ni(S$_2$CNH$_2$)$_2$ (KIDA and YONEDA(18))	$^1\Gamma_{t1} \rightarrow {}^1\Gamma_{t2}$	—	15·6	63
		$\rightarrow {}^1\Gamma_{t5}$	—	20·4	150
		—	—	(23·5)	1,100
		—	—	26·0	3,300
		—	—	32·1	28,000
		—	—	~40	~15,000
	Ni exan$_2$	$^1\Gamma_{t1} \rightarrow {}^1\Gamma_{t2}$	642	15·5	~50
		—	480	20·8	~1,500
		—	478	23·9	~2,700
		—	(390)	(25·7)	~1,300
		—	316	31·6	~25,000
	Ni exan$_2$ py$_2$	$^3\Gamma_2 \rightarrow {}^3\Gamma_5$	(1,080)	9·3	~15
			980	10·2	~20
		$\rightarrow a^3\Gamma_4$	629	15·9	~50
$4d^8$	Pd dtp$_2$	$^1\Gamma_{t1} \rightarrow {}^1\Gamma_{t2}$	460	21·8	216
		—	(339)	(29·5)	2,600
		$\pi \rightarrow \gamma'_{t3}$?	294	34·0	29,800
		—	259	38·6	5,700
	Pd dtc$_2$	$^1\Gamma_{t1} \rightarrow {}^1\Gamma_{t2}$	449	22·2	—
		—	347	28·8	large
$5d^8$	Pt dtp$_2$	$^1\Gamma_{t1} \rightarrow {}^3\Gamma$	420	23·8	100
		—	282	35·5	2,000
		$\pi \rightarrow \gamma'_{t3}$?	251	39·8	16,800
		—	227	44·0	18,200

Mn(II) measurably, and the spectral change produced by dtp⁻ on $Co(H_2O)_6^{2+}$ is also very small. The 3*d*-elements with the oxidation number +2 (with the possible exception of Cu(II)) seems to form only weak complexes with dtp⁻ (quite in contrast to, say, Rh(III) and Ir(III)). The purple solution of Ni dtp_2 in ethanol is fairly sensitive to water; addition of 20 volume per cent decreases the apparent molar extinction coefficient to a fifth of the original value, but without changing the position of the band maxima. The completely decomposed solution (in above 60 per cent water) is pale-green having maxima (weak, though measured in a 5 cm cell) at the same place as $Ni(H_2O)_6^{2+}$. The only indication of the possible existence of high-spin Ni dtp_2 $(H_2O)_2$ or Ni dtp $(H_2O)_4^+$ in this solution is the slightly higher extinction coefficients than those of the ordinary aquo ion. On the other hand, strong solutions (~0·5 M NH_4^+ dtp⁻) precipitate easily $Ni(H_2O)_6^{2+}$ as the purple crystals of Ni dtp_2 which are not wetted when once dried.

The orange Pd dtp_2 and lemon-yellow Pt dtp_2 were next prepared. It is necessary to add $PdCl_4^{2-}$ or $PtCl_4^{2-}$ to an excess of dtp⁻.

Spectral data for four-co-ordinated complexes are given in Table 2.

Diethyldithiocarbamates

CHATT, DUNCANSON and VENANZI[25] have thoroughly discussed the complexes of dtc⁻ = $(C_2H_5)_2NCS_2^-$. This ligand, well known from the analytical determination of copper(II), actually forms strong complexes of a long series of metals, extractable in chloroform or dichloroethane in the case of neutral inner-complexes, discovered by DELÉPINE.[26] Recent studies have been made by GLEU and SWAB[27] and DELÉPINE.[28]

Cr dtc_3 was independently prepared and measured by Dr. SCHÄFFER and the author; the deep violet crystals and solution in organic solvents are very unstable towards water, hydroxo-complexes being precipitated.

As discussed by REGENASS *et al.*,[29] aqueous solutions of Co(II) and dtc⁻ are immediately oxidized[26] to green Co dtc_3. While the internal transitions in the partly filled shell have higher wavenumbers in M dtc_3 than in M dtp_3, corresponding to a later position in the spectrochemical series, the Laporte-allowed bands in the ultraviolet occur at lower wavenumber[29] in M dtc_3, as will be discussed in the appropriate section below.

Here, Rh dtc_3 was prepared as orange crystals. If $RhCl_6^{3-}$ simply is boiled with Na^+dtc^-, brownish-yellow products are obtained which probably contain chloride and hydroxyl groups. On the other hand, even at room temperature or at 50°C, 10 per cent ethanol + dtc⁻ produces the pure compound. DELÉPINE[30] discovered the spectacular catalysis of alcohols on the reaction between pyridine and $RhCl_6^{3-}$, forming trans-Rh $py_4Cl_2^+$. This catalysis is found, but usually to a smaller degree, in other Rh(III) reactions, e.g. formation of Rh mal_3^{-3} or trans-Rh $py_4Br_2^+$ bromide (the filtrate can be treated with ClO_4^-) in fair yield from the solution[31] of Rh(III) in HBr + Br_2 and pyridine.

---

[25] J. CHATT, L. A. DUNCANSON and L. M. VENANZI, *Suomen Kem.* **29 B** 75 (1956).

[26] M. DELÉPINE, *Bull. Soc. Chim. France* [4] 3, 643 (1908).

[27] K. GLEU and R. SCHWAB, *Angew. Chemie* **62**, 320 (1950).

[28] M. DELÉPINE, *Bull. Soc. Chim. France* 5 (1958).

[29] W. REGENASS, S. FALLAB and H. ERLENMEYER, *Helv. chim. Acta* **38**, 1448 (1955).

[30] M. DELÉPINE, *C.R. Acad. Sci., Paris* **236**, 559 (1953).

[31] L. G. SILLÉN and C. BERECKI-BIEDERMANN, *Research on Characteristics of Transition Elements in Solution*, A.F.61(052)-181, Stockholm (1960), and *Proc. 7. ICCC*, 161 (1962).

The olive-green Ni dtc$_2$ is low-spin[32], and the solution in chloroform does not seem to react with pyridine. Yellow Pd dtc$_2$ was prepared. Spectral data are given in Tables 1 and 2.

KIDA and YONEDA[33] studied Cr(III), Co(III) and Ni(II) complexes of the non-alkylated dithiocarbamate $H_2NCS_2^-$ and of ethylxanthate exan$^-$ = $C_2H_5OCS_2^-$. Since KIDA and YONEDA's paper is not readily accessible in several places, their results have been included for comparison in Tables 1 and 2. Recently, SCHÄFFER[21] has made a profound study of Cr(III) and Co(III) complexes of a large variety of alkylxanthates $ROCS_2^-$ and thioxanthates, $RSCS_2^-$. Hence, we shall not here indulge in the behaviour of xanthates but only remark the rather unusual observations by KREBS *et al.*[34] of the polymeric nature of Ni(II) compounds. The spectral behaviour of Ni exan$_2$ and of Ni exan$_2$ py$_2$ is closely comparable to low-spin Ni dtc$_2$ and high-spin Ni dtp$_2$ py$_2$ (Table 2).

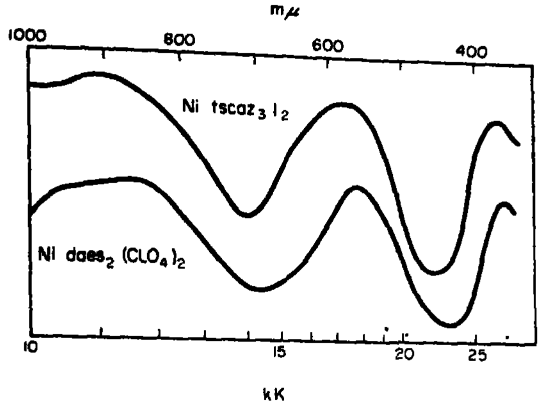

FIG. 2.—Reflexion spectra of crystalline powders nickel(II) tris(thiosemicarbazide)iodide and nickel(II) bis(2,2′-di(aminoethyl)sulphide) perchlorate.

2,2′-di-(aminoethyl)-sulphide complexes

Thio-ethers, R_2S, seem only to form complexes with metals having extreme Chatt-Ahrland B-character, such as Hg(II), Pt(II), Ir(III) and Rh(III). However, the tridentate daes = $NH_2CH_2CH_2SCH_2CH_2NH_2$ bind first transition group ions in virtue of the two amino groups and forces a thio-ether sulphur atom close to the metal atom. GONICK *et al.*[35] demonstrated that Ni(II) forms complexes with one and two molecules daes to approximately the same extent as with tridentate amines and concluded that Ni(II) presumably is high-spin octahedral, quite in contrast to all the low-spin four-coordinated complexes of thioacids and thioamino acids. This conclusion is confirmed by the spectrum, as seen in Table 3 and on Fig. 2. We prepared daes according to MILLS and BOGERT[36] and crystallized a violet perchlorate Ni daes$_2$ $(ClO_4)_2$. This may be compared with the various Ni(II) complexes with the

[32] L. CAMBI and L. SZEGÖ, *Chem. Dtsch. Ges. Ber.* 64, 2591 (1931); 66, 656 (1933).

[33] S. KIDA and H. YONEDA, *J. Chem. Soc. Japan* 76, 1059 (1955).

[34] H. KREBS, E. F. WEBER and H. FASSBENDER, *Z. Anorg. Chem.* 276, 128 (1954).

[35] E. GONICK, W. C. FERNELIUS and B. E. DOUGLAS, *J. Amer. Chem. Soc.* 76, 4671 (1954).

[36] E. J. MILLS and M. T. BOGERT, *J. Amer. Chem. Soc.* 62, 1177 (1940).

Table 3.—Absorption bands of various nickel(II) compounds not included in table 2

		Assignment	λ(mμ)	σ(kK)	ε
Ni daes$_2$(ClO$_4$)$_2$	crystals	$^3\Gamma_2 \rightarrow {}^3\Gamma_5$	(950)	(10·5)	—
		tetragonal splitting	860	11·6	—
		$\rightarrow a^3\Gamma_4$	(665?)	15·0?)	—
		tetragonal splitting	560	17·85	—
		$\rightarrow b^3\Gamma_4$	360	27·8	—
Ni daes$_2^{2+}$	solution in water	$^3\Gamma_2 \rightarrow a^3\Gamma_4$	553	18·1	15
		$\rightarrow b^3\Gamma_4$	354	28·3	19
Ni tscaz$_3$I$_2$	crystals	$^3\Gamma_2 \rightarrow {}^3\Gamma_5$	(1,000?)	(10·0?)	—
		tetragonal splitting	900	11·1	—
		$\rightarrow a^3\Gamma_4$	580	17·25	—
		$\rightarrow b^3\Gamma_4$	370	27·0	—
Ni tscaz$_3^{2+}$	ClO$_4^-$ solution in water	$^3\Gamma_2 \rightarrow a^3\Gamma_4$	588	17·0	26
		$\rightarrow b^3\Gamma_4$	367	27·2	—
Ni(S$_2$O$_2$C$_2$)$_2^{2-}$ (Kida[50])		Internal?	(575)	(17·4)	2,400
		Internal?	501	19·9	4,000
Ni(S$_2$O$_2$C$_3$H$_3$)$_2$ (Deskin[49])		$^1\Gamma_{t1} \rightarrow {}^1\Gamma_{t2}$	575	17·4	167
Ni(S$_2$C)$_2^{2-}$ (Deskin[49])		Internal?	510	19·6	1,600
Ni dmp$_2^{2-}$ (Leussing[45])		$^1\Gamma_{t1} \rightarrow {}^1\Gamma_{t2}$	620	16·2	~100
		$\rightarrow {}^1\Gamma_{t5}$	480	20·9	~100
		—	310	32·2	~12,000
Ni(II) thioglycollate		$^1\Gamma_{t1} \rightarrow {}^1\Gamma_{t2}$	(611)	(16·4)	40
		$\rightarrow {}^1\Gamma_{t5}$	513	19·5	83
		$\rightarrow {}^1\Gamma_{t3}$?	(417)	(24·0)	66

environment NiO$_2$N$_4$ previously reported[5,6] and Δ of the environment NiS$_2$N$_4$ of Ni daes$_2^{2+}$ is seen to be somewhat larger. On the other hand, Ni dtp$_2$ py$_2$, having the environment NiS$_4$N$_2$, has definitely a lower Δ than usual NiO$_4$N$_2$, as expressed on Fig. 3. This is caused by the fundamentally different spectrochemical behaviour of sulphur with three lone-pairs RS$^-$ and with two lone-pairs R$_2$S, while Δ is even larger in Co(III) and Rh(III) sulphite complexes with only one lone-pair SO$_3^{2-}$.

Thiosemicarbazide complexes

tscaz = NH$_2$NHCSNH$_2$ is a bidentate ligand, binding metal ions with the first amino-group and the sulphur atom.[37,38] It is possible to prepare red complexes of nickel(II) Ni tscaz$_2^{2+}$ which were shown by Asmussen[37] to be low-spin, as expected of the environment N$_2$S$_2$, but also blue Ni tscaz$_3^{2+}$ which are ordinary high-spin octahedral complexes. Further on, blue addition compounds Ni tscaz$_2$ (NH$_3$)$_2^{2+}$ are known.[37]

The high-spin form with environment S$_3$N$_3$ is an exception analogous to Ni daes$_2^{2+}$. As seen from Fig. 2 and Table 3, the spectrum is essentially octahedral, but showing strong tetragonal splitting of the first spin-allowed transition to ${}^3\Gamma_5$. This is comparable to(8) (trans-) Ni py$_4$Cl$_2$ and suggests strongly that Ni tscaz$_3{}^{2+}$ has the trans-configuration 1,2,6, while Ni daes$_2{}^{2+}$ is expected to be 1,6 with respect to the two sulphur atoms. An alternative explanation is strong deviations from right-angled L$_1$NiL$_2$ bonding of the ligand atoms L$_1$ and L$_2$.

---

[37] R. W. Asmussen. Thesis, Copenhagen (1944).

[38] K. A. Jensen and E. Ranck-Madsen, *Z. Anorg. Chem.* 219, 243 (1934).

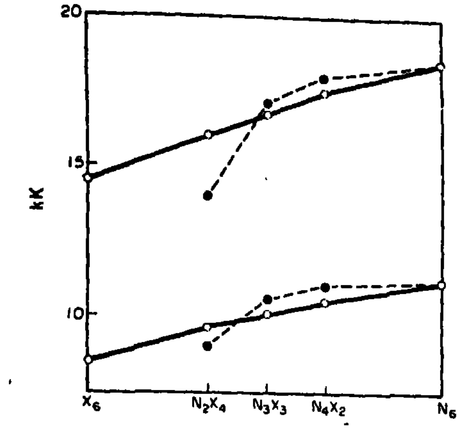

Fig. 3.—Wavenumbers in kK (= 1000 cm^{-1}) of the two transitions to $a^3\Gamma_4$ and $b^3\Gamma_4$ of high-spin octahedral nickel(II) complexes of nitrogen and sulphur (filled circles) or oxygen (empty circles) ligands.

The bond order of CS in tscaz must be intermediate in character between the thio-ethers R$_2$S and the mercaptides RS$^-$, and consequently Δ is somewhat smaller than expected from the N$_4$S$_2$ environment of Ni daes$_2{}^{2+}$ (see Fig. 3).

Spectrochemical position and chemical bonding in low-spin d^8 complexes

After the establishment of the Ni-atom in a compound with the environment NiAs$_3$Br$_2$ being above the plane(39) of the four ligand atoms As$_3$Br, and the existence of square-pyramidal Ni(CN)$_5{}^{3-}$, several authors(40,41) have expressed the opinion that, in low-spin tetra-coordinated d^8 complexes MX$_4$, the central atom M may very well be a little out of the plane formed by the four ligands X. This distortion is, however, so small that, as a first approximation, we may use the group-theoretical quantum numbers Γ_{tn} appropriate for the tetragonal symmetry D_{4h} with a centre of inversion.

If only σ-bonding in the MX$_4$ complex were important, the four non-bonding orbitals constituted primarily of the d-shell of M would be nearly degenerate, and the three transitions from these four orbitals to the empty, σ-antibonding γ_{t3} (consisting of $(x^2 - y^2)$ of M and σ-electrons of X) would approximately coincide. This situation occurs in Pd(NH$_3$)$_4{}^{2+}$. However, if π-bonding of X is also of some importance, the three transitions from the ground-state ${}^1\Gamma_{t1}$ have the order of increasing wavenumber.

$$\begin{aligned}&\to {}^1\Gamma_{t2}\ \gamma_{t4}(xy \text{ and } \pi\text{X}) \to \gamma_{t3}\\ &\to {}^1\Gamma_{t5}\ \gamma_{t5}((xz, yz) \text{ and } \pi\text{X}) \to \gamma_{t3}\\ &\to {}^1\Gamma_{t3}\ \gamma_{t1}(2z^2 - x^2 - y^2) \to \gamma_{t3}\end{aligned} \tag{3}$$

(39) G. A. Mair, H. M. Powell and D. E. Henn, *Proc. Chem. Soc.* 415 (1960).

(40) L. E. Orgel. Private communication (1960).

(41) L. Sacconi, M. Ciampolini, F. Maggio and F. P. Cavasino, *J. Inorg. Nucl. Chem.* **19**, 73 (1961).

as originally found in $PtCl_4^{2-}$ by CHATT *et al.*(42) and supported on M.O. basis by a study of palladium(II) complexes.(3,4) Recently, all three components have been identified by dichroitic studies of nickel(II) biguanide complexes(43) and the yellow(44) $Ni(NH_2CH_2CH_2N(C_2H_5)_2)_2^{2+}$.

LEUSSING(45) studied complexes of dmp^{2-} (where dimercaptopropanol $HSCH_2(HS)CH\,CH_2OH$ is dmp H_2) and dimercaptoethane with Ni(II), having the environment S_4 and low-spin. The spectrum given in Table 3 is clearly analogous to $PdCl_4^{2-}$, demonstrating π-antibonding effects of sulphur (twice(4) the distance between $^1\Gamma_{t2}$ and $^1\Gamma_{t5}$) on the $3d$ shell, corresponding to 9·4 kK (1 kK = 1,000 cm^{-1}). This must be compared with the σ-antibonding effect ($\sim$20·9 + 4·7 $\sim$ 25·6 kK), confirming Leussing's statement that σ-antibonding is considerably more important than π-bonding in his sulphur complexes.* The π-antibonding effects are 9·2 kK in Ni dtp_2 according to Table 2. It may be discussed whether the third, much stronger band of Ni dtp_2 can possibly have $^1\Gamma_{t3}$ as excited state. This is not excluded when considering the admixture of odd $\gamma_{t2}(p_z)$ with γ_{t1} which might become possible with a distortion where the Ni nucleus is outside the plane of the four sulphur nuclei.

The spectrochemical position of a low-spin d^8 complex is closely related to the spectrochemical behaviour of Δ in octahedral complexes, if the first, spin-allowed band is considered,[3] in both cases expressing the difference between the σ- and π-antibonding effects of X on the partly filled shell of M. The nickel(II) complexes described here afford the following spectrochemical series:

$$\text{dtp}^- < \text{exan}^- \sim \text{dtc}^- < \text{dmp}^{2-} < \text{thioglycollate} < \text{dithiomalonate} \lessdot \text{amines} \quad (4)$$

There does not, at present, exist a satisfactory theory for the choice between low-spin and high-spin behaviour in Ni(II). Nearly all sulphur-containing ligands form NiS_4 or NiS_2N_2 environments, but Ni $daes_2^{2+}$ with high-spin is a remarkable exception. While NiN_4 does not seem to form with *o*-phenanthroline and $\alpha\alpha'$-dipyridyl, and with ethylenediamine only under unusual circumstances,[46] Cotton and FACKLER[47] demonstrated that monomeric Ni(II) acetylacetonate has the environment NiO_4 and is low-spin. Of course, a part of the explanation of these anomalies must be found in the delicate balance, where M.O. energy differences (i.e. the spectrochemical position) are compared with the parameters of interelectronic repulsion (and hence the nephelauxetic effect).

Spectrochemical position of sulphur-containing ligands in octahedral complexes

By comparison with previously discussed values(3,4,7) of Δ in Cr(III), Co(III),

---

* However, as Dr. D. L. LEUSSING was so kind to point out, the results of Equation (3) may be changed if the S-atoms are attached to form chelate ligands. Thus, the $3p$-orbital of sulphur in the xy-plane may be predominantly used for σ-bonding of the other atom bound to sulphur, and the $3p_z$ orbital hence have the strongest π-anti-bonding effect on the central ion, i.e. γ_{t5} having higher energy than γ_{t4}. Hence, the identifications of $^1\Gamma_{t2}$ and $^1\Gamma_{t5}$ given in Table 2 may have to be interchanged.

(42) J. CHATT, G. A. GAMLEN and L. E. ORGEL, *J. Chem. Soc.* 486 (1958).
(43) A. CHAKROVORTY and S. BASU, *J. Inorg. Nucl. Chem.* **17**, 55 (1961).
(44) S. YAMADA. Private communication (1960).
(45) D. L. LEUSSING and G. S. ALBERTS, *J. Amer. Chem. Soc.* **82**, 4458 (1960).
(46) K. SONE and M. KATO, *Z. Anorg. Chem.* **301**, 277 (1959).
(47) F. A. COTTON and J. P. FACKLER, *J. Amer. Chem. Soc.* **83**, 2818 (1961).

Rh(III) and Ir(III) complexes, the ligands studied in this paper fell into places in the spectrochemical series:

$$\mathrm{Br}^- < \mathrm{Cl}^- < \mathrm{dtp}^- < \mathrm{F}^- < \mathrm{dtc}^- < \mathrm{exan}^- < \mathrm{H_2O} < \mathrm{R_2S} < \mathrm{NH_3} < \mathrm{SO_3}^{2-} < \mathrm{NO_2}^- \ll \mathrm{CN}^- \quad (5)$$

sulphur showing a much greater spreading than of any other ligand atom known. However, one precedent was discussed by SHIMURA and TSUCHIDA[48], the azide ion N_3^- which is situated between Cl^- and F^- in equation (5). In general, nitrogen-containing anions, such as R_2N^-, have substantially lower values of Δ than the neutral amines. The interpretation of Δ as the *difference* between σ- and π-antibonding effects on the partly filled shell explains these facts satisfactorily: ligands with exactly one lone-pair, such as NH_3, are primarily σ-bonded to the central ion. We neglect here the influence of empty higher orbitals of the ligands, which may increase Δ by π-bonding in the direction from M to X. This neglect seems well-founded in NR_3, but may be much less so in PR_3 and AsR_3. However, there is much chemical, and even some spectroscopical, evidence that the tendency to this π-bonding $M \rightarrow X$ only occurs at low oxidation numbers of M and that the importance, for a given central ion, decreases strongly in the series

$$\mathrm{CO} > \mathrm{dip} > \mathrm{phen} > \mathrm{CNR} \gg \mathrm{CN}^- \ldots \quad (6)$$

and is probably rather weak in the sulphur-ligands discussed here.

The difference between dtp^- on the one hand and dtc^- and $exan^-$ on the other hand is quite illustrative for the idea of the number of available lone-pairs of sulphur determining the (negative) influence of π-bonding $M \leftarrow S$ on Δ. There is much chemical evidence that the bond-order of the P—S bond is very close to 1, i.e. it is a nearly pure σ-bond, while C—S bonds may have somewhat higher bond-orders, probably close to 1·33 in CS_3^{2-}. Therefore, the number of available lone-pair electrons is expected to vary:

$$\begin{array}{ll} \mathrm{dtp}^- & 8 - 2 = 6 \\ \mathrm{dtc}^-, \mathrm{exan}^- & 8 - 2 - x \sim 5{\cdot}5 \\ \mathrm{RCOS}^- & 8 - 3 = 5 \\ \mathrm{R_2S} & 8 - 4 = 4 \\ \mathrm{R_2SO}, \mathrm{SO_3}^{2-} & 8 - 6 - y \sim 2 \end{array} \quad (7)$$

in close correlation with the spectrochemical series, Equation (4) and (5). When $(CH_3)_2SO$ exceptionally binds M with the sulphur end, Δ is expected to be very high. The value for $RCOS^-$ can be derived from the behaviour of nickel(II)-bis-(dithiomalonate)[49] in Equation (4). The much higher absorption bands[49,50] of the complex of dithiooxalate $SOCCOS^{2-}$ are probably caused by internal transitions in the ligand, as discussed in the next section, and they cover completely the weaker transitions in the partly filled shell.

Equation (7) has a less clear significance for solids, such as ZnS and CdS, where each sulphur atom should form σ-bonds alone with the four neighbouring metal

[48] Y. SHIMURA and R. TSUCHIDA, *Bull. Chem. Soc. Japan* 29, 311 (1956).
[49] W. A. DESKIN, *J. Amer. Chem. Soc.* 80, 5680 (1958).
[50] S. KIDA, *Bull. Chem. Soc. Japan* 33, 1204 (1960).

atoms. However, the conditions in the crystals are essentially different, and Δ of cobalt(II) substitutionally included in such a compound may very well still express a mixture of σ- and π-bonding of the cobalt atom. Similar problems arise in oxides(51) where three-, four- and six-co-ordinated oxygen may produce values of Δ scattered around the values found in the hexaquo ion, while monomeric complexes, such as those containing $RCOO^-$ and OH^- ligands, have lower values of Δ, analogous to Equation (7).

Strong absorption bands of sulphur-containing complexes

Usually a condition for occurrence of absorption bands at relatively low wavenumber in a compound outside the transition groups is the existence of bonds with fractional bond-order, e.g. mixed σ- and π-bonds with bond-orders above 1. There are exceptions to this rule, e.g. Cl_2 and I_2, with very weak σ-bonds. However, most sulphur compounds studied here fall in this category. From a group-theoretical point(52) of view, the simplest case is represented by CS_3^{2-} having(53) a rather weak, symmetry-forbidden transition at 22 kK and two much stronger transitions at 29 and 33 kK. As pointed out by McConnell,(54) these transitions are comparable with respect to symmetry-type to the weak band at 32 kK and strong band at 50 kK of NO_3^-. The xanthates and dtc$^-$ are essentially substituted molecules of the CS_3^{2-} type and have accordingly a series of bands in the ultraviolet which are expected to be shifted and multiplied to some extent in complexes, such as is well-known in nitrites,(55) acetylacetonates(56,57) and in complexes(58) such as Co $en_2(SPO_3)_2^{3-}$ and Co $en_2(SSO_3)_2^-$ having spectra closely similar to trans-Co $en_2Br_2^+$.

It is important to distinguish between internal transitions in the ligands and electron transfer bands. It is often useful to compare complexes with a closed *d*-shell with those containing a partly filled shell. Thus, the strong bands(59,60) of Zn dtc_2 occurring at 35·5 and 38·4 kK are most evidently internal transitions and have about the same positions as the solution of the ionic Na^+ dtc$^-$ (34·7 and 38·8 kK). When Cu dtc_2 has a band at 22·9 kK with $\varepsilon \sim 12{,}000$ (cf. also reference 29) it must hence be an electron transfer to the hole in the 3d shell. The strong bands of Ni dtc_2 at 25·8 and 30·6 kK are probably also electron transfer transitions. Kida and Yoneda(33) made similar comparisons between K^+ exan$^-$ (26·2 kK, $\varepsilon = 55$ and 33·2 kK, $\varepsilon = 17{,}000$) and Zn $exan_2$ (29·0 kK, $\varepsilon = 200$ and 34·2 kK, $\varepsilon = 22{,}000$) showing a small blue shift of the internal transitions in the zinc(II) complex.

It is remarkable how high a wavenumber the first band of dtp$^-$ has, viz. 44·5 kK with the half-width $\delta(-) = 2{\cdot}5$ kK. This band can be ascribed to a sort of Rydberg excitation(2) $3p \rightarrow 4s$ of sulphur, in analogy to the $4p \rightarrow 5s$ bands of bromide ions.(61) We would expect electron transfer from dtp$^-$ to the central atom of the complexes to occur at wavenumbers comparable to those of bromide complexes,(63) because it is now realized that a close connection exists between these quantities and the Pauling-Mulliken electronegativity scale.(4,6) Actually, the first strong bands have similar wavenumbers in kK:

---

(51) O. Schmitz-DuMont and D. Reinen, *Z. Elektrochem.* **63**, 978 (1959).

(52) S. P. McGlynn and M. Kaska, *J. Chem. Phys.* **24**, 480 (1956).

(53) H. v. Halban, A. Mackert and W. Ott, *Z. Elektrochem.* **29**, 445 (1923).

(54) H. M. McConnell, *J. Chem. Phys.* **20**, 700 (1952).

(55) M. Linhard, H. Siebert and M. Weigel, *Z. Anorg. Chem.* **278**, 287 (1955).

(56) R. H. Holm and F. A. Cotton, *J. Amer. Chem. Soc.* **80**, 5658 (1958).

(57) D. W. Barnum, *J. Inorg. Nucl. Chem.* **21**, 221 (1961); **22**, 183 (1961).

(58) J. Hidaka, J. Fujita, Y. Shimura and R. Tsuchida, *Bull. Chem. Soc. Japan* **32**, 1317 (1959).

(59) H. P. Koch, *J. Chem. Soc.* 401 (1949).

(60) K. E. Krebs, *Analyt. Chem.* **30**, 433 (1958).

(61) C. K. Jørgensen, *Solid State Physics* **13**, 375 (1962).

Rh dtp_3	31·2	Rh Br_6^{3-}	30·1, 33·9	
Ir dtp_3	37·1	Ir Br_6^{3-}	36·8, 41·1	(8)
Pd dtp_2	34·0	Pd Br_4^{2-}	30·2	

The doublet structure in the hexabromide complexes is connected with strong relativistic effects of intermediate coupling.(62) The assignment $\pi \rightarrow \gamma_3$ for the electron transfer bands in Table 1 uses the symbol π in a somewhat less clear-cut way than in the hexahalides, since only six and not twelve π-similar orbitals are likely to occur in M dtp_3. This problem will be discussed elsewhere.(63)

The band of In dtp_3 at 41·0 kK is probably an internal transition, but the origin of the broad band ($\delta(-)$ = 2·4 kK) at 34·0 kK is much less clear. The two electron transfer bands of $PbCl_6^{2-}$ have similar positions,(62) but a comparison of Sn(IV), Tl(III) and Pb(IV) suggests that indium(III) chloride complexes have their first maximum at 55 kK and In dtp_3 hence at some 46 kK. Possibly, one of the internal transitions is strongly shifted (to 34 kK), similar to the Rh(III) and Ir(III) oxalate complexes,(22) or is a spin-forbidden internal transition in the diethyldithiophosphate group. However, the absence of such a band of Ir dtp_3 becomes even more conspicuous. $4d\gamma_3 \rightarrow 5s\gamma_1$ transitions, which are known in Ag(I), would already be improbable in Cd(II) and frankly phantastic in In(III). On the other hand, linear combinations of empty 4*s*-orbitals of sulphur, bonding between each pair of S atoms in dtp^- and having, in general, no or only a few node-planes in In dtp_3, might have comparatively low energy and be the excited orbital of the 34 kK band. The M.O. without node-plane at all has the same symmetry as 5*s* of the indium atom and may involve a small amount of this contribution.

The rather narrow ($\delta(-)$ = 1·1 kK) first band of Bi dtp_3 is best identified as the first intermediate coupling component of the ${}^1\Gamma_1 \rightarrow {}^3\Gamma_4$ transition (found for $BiBr_6^{3-}$ (or $BiBr_5^{2-}$) at 26·8 kK, having the transition to ${}^1\Gamma_1$ (6*s* 6*p*) at 38·5 kK), and the stronger component of ${}^3\Gamma_4$ occurring at 30·4 kK, whereas ${}^1\Gamma_1 \rightarrow {}^1\Gamma_1$ (6*s* 6*p*) probably occurs at 42.9 kK. It is therefore tempting to ascribe the shoulder at 36·1 kK of Bi dtp_3 to some more or less internal transition.

The electron transfer is nearly certain to be the explanation of the bands in the visible of Fe dtp_3 and Fe dtc_3. An interesting question is whether these species are low-spin γ_5^5 or high-spin $\gamma_5^3\gamma_3^2$. CAMBI and SZEGÖ(32,64) present rather confusing magnetochemical evidence for iron(III) xanthates and Fe dtc_3, which might be interpreted either as a thermic equilibrium between low-spin forms with $S = \frac{1}{2}$ and high-spin forms with $S = \frac{5}{2}$, or as very strong anti-ferromagnetic coupling with large deviations from the Curie-Weiss' law.

From a spectroscopical point of view, the present writer expected that only the low-spin fraction of a given compound participates in the strong visible colour. The reason is that the excited configuration γ_5^6 of a low-spin form has $+\frac{2}{3}D$ more spin-pairing energy(61) than the groundstate, while $\gamma_5^4\gamma_3^2$ has the contribution $+\frac{8}{3}D$.

---

(62) C. K. JØRGENSEN, *Molecular Phys.* 2, 309 (1959).
(63) C. K. JØRGENSEN, *Molecular Phys.* 5, 485 (1962).
(64) L. CAMBI and L. MALATESTA, *Ber. Chem. Dtsch. Ges.* 70, 2067 (1937).

The difference 2 D is sufficient to shift the electron transfer bands from 17–20 kK out in the near-ultra-violet. Actually, the high-spin form *might* have its bands in the visible, but then the expected shift to lower wavenumber by formation of the low-spin forms is not observed.

Dr. C. SCHÄFFER was so kind as to point out to me that Fe exan$_3$ forms nearly colourless solid addition compounds with three molecules of pyridine and that a solution of Fe dtp$_3$ in organic solvents is decoloured by small amounts of pyridine. It might be argued that the ratio Δ/B (e.g. expressed as the competition between 2Δ and $8\ D$) would be higher in a mixed pyridine complex, both because of later spectrochemical position of pyridine and less pronounced nephelauxetic effect. Hence, the threshold-value for high-spin behaviour might be crossed. Rough estimates of $\Delta =$ 12 kK and $D \sim 6{\cdot}5\ B \sim 3$ kK for Fe dtp$_3$ suggest that this compound is indeed low-spin, but close to the lower limit of Δ/B. (Actually, MALATESTA and PIZZOTTI(15) report the molar magnetic susceptibility 14,900 . 10^{-6} for Fe dtp$_3$ at 20°C, indicating $S = \frac{5}{2}$).

Dr. SCHÄFFER also attracted my attention to the fact that Cr dtp$_3$ is highly dichroitic. This must be caused by a trigonal distortion from octahedral symmetry, similar to that studied in the polarization experiments on tris(oxalate) complexes by CARLIN and PIPER.(65) The very strong intensities of the $\gamma_5 \rightarrow \gamma_3$ transitions of Cr dtp$_3$, Rh dtp$_3$ and Ir dtp$_3$ (some ten times higher than in the corresponding hexachlorides) may therefore not only be caused by vibronic interaction with low-lying electron transfer states, but may also, in part, be produced by static distortions without a centre of inversion.

It is expected that diethyldithiophosphate will show up to be as versatile a ligand for formation of inner-salts as acetylacetonate has been shown to be in the literature. The yellow or red colours of platinum-group ions, with their environment consisting entirely of sulphur atoms, are quite surprising: dark-brown colours might have been expected (though, for the reasons outlined above, the sulphite complexes are usually colourless). The somewhat contradictory combination of relatively high wavenumber of the electron transfer bands and very large nephelauxetic effect makes dtp$^-$ a rather unique ligand among those known at present.

Experimental

The colourless crystals of NH_4^+ dtp$^-$ were supplied by American Cyanamid, Stamford, Conn. They are clearly soluble in water or ethanol and keep well in air.

Rh dtp$_3$ was obtained by boiling 7 g Na_3RhCl_6, 12 H_2O (H. DRIJFHOUT and ZOON, Amsterdam) with 50 ml 1 M aqueous NH_4 dtp. After two hours on a vapour-bath, orange-red Rh dtp$_3$ was nearly quantitatively ppt. and was recrystallized from boiling ethanol, producing dark-red crystals. They are too soluble in chloroform or dichloroethane to be readily recrystallized from these solvents, if not mixed with alcohols. (Found: C,21·91, H,4·70, P,15·31, S,31·62. Calc: C,21·88, H,4·65, P,14·11, S,29·21 %).

Ir dtp$_3$ was made in a similar way from 8 g Na_3IrCl_6, 12 H_2O (H. DRIJFHOUT and ZOON). The recrystallized material is yellow. (Found: C,19·44, H,4·24, P,12·45, S,25·38. Calc.: C,19·24, H,4·04, P,12·41, S,25·69 %).

In dtp$_3$ was made from 23 g very pure indium metal (H. DRIJFHOUT and ZOON), dissolved in 100 ml water and 200 ml Merck nitric acid p.a. After all nitrous fumes had been boiled away, the solution was diluted to 1,000 ml and 600 ml 1 M NH_4dtp added. The white precipitate was collected and washed several times with water and showed the characteristic property of all M dtp$_3$ and M dtp$_2$: not to be wetted by water. It was then recrystallized from ethanol and gave rather large crystalline flakes.

---

(65) T. S. PIPER and R. L. CARLIN, *J. Chem. Phys.* 33, 608 (1960).

It is hardly possible to neutralize the excess acid of the strong indium nitrate solution without producing an irreversible, cloudy hydrolysis product.

Bi dtp_3 was precipitated from 0·1 M $Bi(ClO_4)_3$ in 1 M $HClO_4$ and an excess of 1 M NH_4 dtp. The lemon-yellow crystals do not stand a prolonged washing with water, but were directly recrystallized from ethanol.

Fe dtp_3 can be made from anhydrous iron(III) chloride dissolved in anhydrous methanol and an excess of NH_4dtp in the same solvent. The black crystals decompose quickly. For the spectral measurements, solutions were made directly from the reactants, as also in the case of Fe dtc_3.

Ni dtp_2 was precipitated as violet crystals from 100 ml 1 M $NiSO_4$, 6 H_2O (B.D.H.) and 250 ml 1 M NH_4dtp. The pale-green filtrate involves a sensible loss of nickel. The crystals were recrystallized from hot methanol. (Found: C,23·30, H,4·83, S,29·43. Calc. C,22·39, H,4·70, S,29·88 %).

Ni dtp_2 py_2 crystallized from solutions of Ni dtp_2 in ethanol or chloroform by addition of pyridine. The pale-green crystals, when dried, smell only faintly of pyridine.

Pd dtp_2 was obtained by dropwise addition of 3·3 g K_2PdCl_4 (H. DRIJFHOUT and ZOON) dissolved in 20 ml water to 30 ml 1 M NH_4 dtp under stirring. If dtp^- is added to an excess of $PdCl_4^{2-}$, a dark-brown mixture is obtained, probably containing the bridged complex dtp $PdCl_2Pd$ dtp. The orange ppt of Pd dtp_2 is recrystallized from hot ethanol. (Found: C, 20·34, H, 4·19, P, 13·01, S, 26·46. Calc: C, 20·14, H, 4·23, P, 12·98, S, 26·05 %).

Pt dtp_2 was prepared as a lemon-yellow ppt. by boiling 4·15 g K_2PtCl_4 (H. DRIJFHOUT and ZOON) in 50 ml water with 25 ml 1 M NH_4 dtp. (Found: C,17·19, H,3·43, P,10·12, S,25·71, Calc. C, 16·99, H,3·56, P,10·95, S,22·67 %).

Cr dtc_3 was prepared in low yield (due to formation of grey-green hydroxo-precipitates) from 2·6 g Merck green $[CrCl_2(H_2O)_4]Cl,2\,H_2O$ in 200 ml absolute ethanol and slowly heated under magnetic stirring with 4 moles (9 g) Na dtc, 3 H_2O (Merck p.a.). The dark-violet crystals were dissolved in $CHCl_3$, whereas the filtrate was evaporated in vacuo. The chloroform solution is perfectly stable.

Attempts to make Mn dtc_2 resulted in air oxidation to a black product, presumably containing Mn dtc_3.

Dark-green Co dtc_3 was made from 0·05 M $Co(CO_3)_3^{3}$ (from $CoCl_2$, 6 H_2O in saturated $NaHCO_3$ with 30 % H_2O_2) and Na^+ dtc^- and extracted into chloroform. As pointed out by REGENASS, FALLAB and ERLENMEYER(29), cobalt(II) salts form exactly the same Co dtc_3 with dtc^- in aqueous solution.

Ni dtc_2 was precipitated as olive-green crystals from stoichiometric amounts of aqueous $Ni(ClO_4)_2$ and Na dtc, and dissolved in chloroform.

Rh dtc_3 was prepared as discussed on page 1576. Pd dtc_2 was made as a yellow precipitate from K_2PdCl_4 added to an excess of Na dtc.

K exan was crystallized from a mixture of KOH dissolved in absolute ethanol and an excess of redistilled CS_2 was added. This was used for the preparation of orange-brown Ni $exan_2$ (which turns apple-green with pyridine in $CHCl_3$) and yellowish-green Co $exan_3$.

According to DOUGLAS and FERNELIUS(35), daes was made from condensation(36) of monomeric ethyleneimine with H_2S. 1 M nickel(II) perchlorate was added slowly under stirring to a 2 M aqueous solution of the product. The first and last fractions were discarded, because unreacted C_2H_4NH and polymerized ethyleneimine also form violet precipitates with $Ni(ClO_4)_2$. The main product is violet crystals with the analysis: Cl,14·15, C,19·74, H,4·79, N,11·41, S,12·53. Calc. for Ni $daes_2(ClO_4)_2$: Cl,14·23, C,19·29, H,4·85, N,11·25, S,12·88 %).

Aqueous solutions being 0·2 M $Ni(ClO_4)_2$ and 0·8 M thiosemicarbazide (Fluka reinst) are dark-blue. Under vacuum desiccation, a highly hydroscopic, crystalline material can be obtained. However, due to the potentially explosive character of this salt, no extensive study was made. Pale-blue Ni $tscaz_2I_2$ was precipitated from a solution of 0·2 M $NiSO_4$ and 0·8 M thiosemicarbazide with a large quantity of crystalline potassium iodide. The spectrum in Table 3 is of a solution 0·025 M $NiSO_4$ and 1 M thiosemicarbazide. One molar thioglycollic acid $HSCH_2COOH$ was treated with 2 moles of NaOH and used for preparation of a greenish-brown Co(III) solution and a purple Ni(II) solution which is unaffected by ascorbate ions. However, at pH lower than 10, green Ni(II) complexes are precipitated and the supernatant solution has a quite different spectrum.

The spectra of solutions were measured in the region 800–210 mμ on a Cary-11 spectrophotometer, and between 1,100–800 mμ on a Beckman-DU. The latter instrument was also used for reflection spectra of crystalline powders in the region 1,050–340 mμ.

The spectra of dtp^- complexes were generally measured in ethanol, while dtc^- and $exan^-$ complexes were measured in chloroform solutions.

Acknowledgments—I am very much indebted to Professor W. C. FERNELIUS and Dr. C. E. SCHÄFFER for many valuable discussions and for the idea of looking at dtp^- as a ligand. I express my thanks also to my collaborators, Dr. J. W. D. VAN OVERHAGEN and Mr. A. IMGRÜT, for their most useful experimental assistance during this work.

J. Inorg. Nucl. Chem., 1962, Vol. 24, pp. 1587 to 1594. Pergamon Press Ltd. Printed in Northern Ireland

SOLVENT EFFECTS ON THE ABSORPTION BANDS OF IRIDIUM(IV)HEXABROMIDE AND OTHER 5d-HEXAHALIDES

CHR. K. JØRGENSEN
Cyanamid European Research Institute,
Cologny (Geneva), Switzerland

(*Received* 14 *February* 1962)

Abstract—Spectra of di-(tetra(n-butyl)ammonium)-iridium(IV)hexabromide are measured in a variety of organic solvents. Shifts of the electron transfer bands in the visible, amounting to 2–5 per cent to lower wavenumbers, and comparable to the reflexion spectrum of the solid, are related to smaller iridium-bromine internuclear distances, compared to the aqueous solution of $IrBr_6^{2-}$. A rough linear correlation exists between these shifts and the dielectric constant of the solvent. The variation of the shift on the six absorption bands observed is used to support previous identifications of the energy levels involved. Similar effects are observed in $IrCl_6^{2-}$, $OsBr_6^{2-}$ and OsI_6^{2-}.

BJERRUM *et al.*(1) studied the influence of solvents on the position and extinction coefficient of absorption bands caused by internal transitions in the partly filled shell of the central atom and by electron transfer, i.e. transitions from a filled M.O. mainly delocalized in the ligands to the partly filled shell. The low-spin $5d^5$-system $IrBr_6^{2-}$ is particularly suitable for an investigation of solvent effects on electron transfer spectra, since a theoretical interpretation of the energy levels involved would be less complicated than in most other systems.(2,3)

GUTBIER and collaborators prepared a very long series of organic substituted ammonium salts of $5d$-hexahalides, e.g. of iridium(IV)hexachloride(4) and hexabromide.(5) The present author needed a salt which was as lyophilic as possible to organic solvents and he therefore prepared the tetra(n-butyl)ammonium salt $[N(n\text{-}C_4H_9)_4]_2[IrBr_6]$. While $IrBr_6^{2-}$ is violet in aqueous solution, the small crystals are sky-blue and the solutions in organic solvents pure blue. The latter solutions are generally stable for a much longer time than the aqueous solutions, often for several weeks, though the acetone solution has a tendency to reduction to yellow-green Ir(III), and the pyridine solution quickly reacts, during less than half an hour at room temperature, to form yellow-orange Ir(III) complexes, such as $Ir\,py_2Br_4^-$.

Table 1 gives the wavelength shift of the maxima (shoulders in parentheses) relative to water of the various organic solutions measured and in the reflection spectrum of the solid. Fig. 1 shows three characteristic spectra: the solutions in water and in dichloroethane, and the solid. In several cases, the solid could not even be dissolved to the extent of a few milligrams in 10 ml and then solutions in another solvent were made and a greater quantity of the original solvent added. This is the reason why mixtures occur rather often in Table 1. It is seen from the example of 15 per cent ethanol, 85 per cent dichloroethane that no drastic changes are expected on small additions of the more polar solvents, contrary to the case of the Katzin effect, involving

---

(1) J. BJERRUM, A. W. ADAMSON and O. BOSTRUP, *Acta Chem. Scand.* **10**, 329 (1956).
(2) C. K. JØRGENSEN, *Acta Chem. Scand.* **10**, 518 (1956).
(3) C. K. JØRGENSEN, *Molecular Phys.* **2**, 309 (1959).
(4) A. GUTBIER and F. LINDNER, *Z. Phys. Chem.* **69**, 306 (1909).
(5) A. GUTBIER and M. RIESS, *Ber. Chem. Dtsch. Ges.* **42**, 4770 (1909).

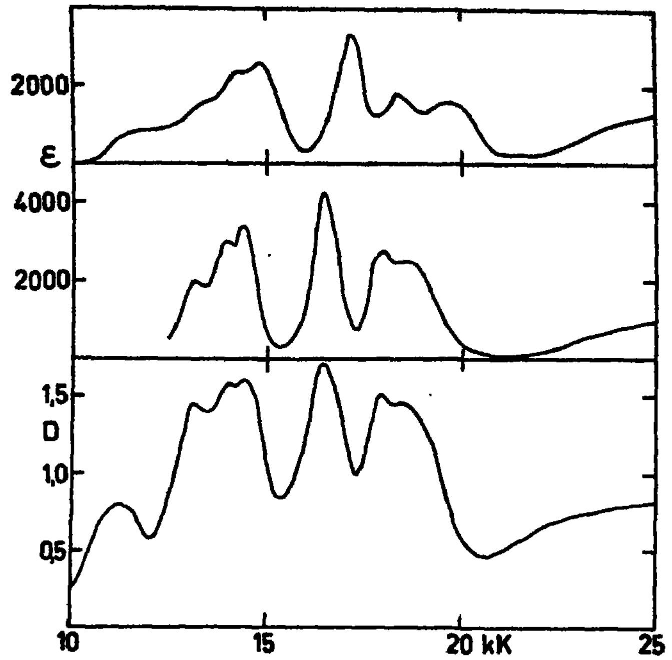

FIG. 1.—Absorption spectra of $[N(n\text{-}C_4H_9)_4]_2[IrBr_6]$ in water and in dichloroethane, and the reflexion spectrum of the solid compound in the form of small crystals. The wavenumber unit is 1 kK = 1000 cm^{-1}.

TABLE 1.—SOLVENT EFFECTS (RED SHIFT IN mμ) ON THE SIX TRANSITIONS OF $IrBr_6^{2-}$ IN THE REGION 800–500 mμ

Transition	IIa	IIb	IIc	III	IVa	IVb
Aqueous solution[8], λ	(745)	(700)	673	583	545	509
50% H_2O, 50% CH_3OH	(−2)	(−2)	+5	+6	+3	+7
CH_3OH	(+3)	+6	+8	+13	+7	+15
2,2,3,3-tetrafluoropropanol	−7	+1	+2	+4	+3	+6·5
CH_3NO_2	+9	+13	+13	+15	+7	+24
88% CCl_4, 12% CH_3OH	(+8)	+10	+12	+17	+9	+19
$CHCl_3$	+12	+16	+15	+19	+11	+25
85% ClH_2CCH_2Cl, 15% C_2H_5OH	+14	+18	+17	+19	+11	+27
ClH_2CCH_2Cl	+15	+18	+18	+21	+10	+28
90% C_6H_6, 10% C_2H_5OH	+13	+17	+19	+21	+15	+25
95% dioxane, 5% C_2H_5OH	+14	+16	+19	+23	+15	(+29)
CH_3COCH_3	+15	+18	+19	+24	+12	(+34)
C_5H_5N, fresh solution	+17	+20	+21	+25	+13	(+35)
75% Cl_2CCCl_2, 25% ClH_2CCH_2Cl	+14	+18	+17·5	+20	+12	+27
90% Cl_2CCCl_2, 10% ClH_2CCH_2Cl (cloudy solution)	+30	+28	+30	+37	+20	+36
90% Cl_2CCCl_2, 10% C_2H_5OH (cloudy solution)	+31	+27	+29	+36	+20	(+35)
Solid $[N(n\text{-}C_4H_9)_4]_2$ $IrBr_6$	+15	+15	+18	+24	+12	+31
Relative wavelength shift Δλ	0·58	0·75	0·79	1·00	0·58	1·29
Wavenumber shift $(\Delta\lambda)/\lambda^2$	1·04	1·53	1·75	2·95	1·96	4·98

solvation and complex formation with anions of metal ions in organic solvents with or without a little water.

The data in Table 1 can be used in two different ways: comparing solvents or comparing the excited energy levels of $IrBr_6^{2-}$. Let us start with the first problem. The six absorption bands seem to shift in a rather regular way, as a function of one parameter *Q* only. This parameter seems to have its extreme values on one side, in water, and on the other side in various, less polar solvents, including acetone and pyridine and the solid salt. Only two exceptions occur: the mixtures of tetrachloroethylene $Cl_2C{=}CCl_2$ with only 10 per cent of ethanol or dichloroethane. The red shift parameter *Q* is here 50 per cent more than the value in the solid. However, these spectra have not been taken on true solutions: the liquid has a dusty appearance, and by filtration on paper wetted with tetrachloroethylene the sky-blue precipitates is removed from an entirely colourless filtrate. This does not readily explain, however, why a dilute suspension of the crystals should have an additional red shift. The clear solution of 75 per cent tetrachloroethylene and 25 per cent dichloroethane has a quite normal "non-polar" spectrum.

Which property of the solvent determines the red shift parameter *Q*? It is most evidently not the availability of hydrogen atoms to form hydrogen bonds with the large anion $IrBr_6^{2-}$, as shown by the small value of *Q* in nitromethane and similar large values of *Q* in chloroform and carbon tetrachloride. This is interesting in view of the common belief that salts containing large cations (as our $N(C_4H_9)_4^+$) and large anions are soluble due to a strong stabilization of the anion rather than the cation. It is especially remarkable that tert-butanol does not dissolve the salt, while on the other hand 1,2-dichloroethane (ethylene chloride) is a very good solvent. It may be compared with nitromethane, often used by NYHOLM *et al.*(6)

Figure 2 shows a certain correlation between *Q* (here measured by the red shift in mμ of the 583 mμ band) and the dielectric constant of the solvent. In some cases (carbon tetrachloride, benzene), *Q* has been extrapolated to the pure solvent. A linear correlation certainly would not obtain e.g. for the reciprocal dielectric constant.*

The physical significance of *Q* can be sought along various lines. Some chemical physicists(7,10) have suggested the difference between the dispersion forces acting on the excited state, as compared to the ground states. These effects should be proportional to the molecular polarizability of the solvent. However, this theory, predicting a red shift, cannot easily be applied in our case, since the dielectric constants of the solvents in general correspond to a blue shift (Fig. 2), as is also the case in the $n \rightarrow \pi^*$ transitions in aromatic systems.(7) The influence of dispersion forces, arising from relatively low excited states of the solvent (corresponding to bands in the near ultraviolet) might be suspected nevertheless to occur as a part of the complete explanation. The high values of *Q* in pyridine (but not in benzene!) and acetone might possibly

---

* The referee was so kind to attract my attention to KOSOWER's concept of *Z*-values which recently has been used for classifying solvent effects on the absorption spectra of organic molecules.(8,9) Our data give a rough correlation with *Z* of the solvent; the correlation is not linear, especially if the value for chloroform is included, and it is inverted for tetrafluoropropanol.

(6) N. S. GILL and R. S. NYHOLM, *J. Chem. Soc.* 3997 (1959).

(7) H. M. MCCONNELL, *J. Chem. Phys.* 20, 700 (1952).

(8) E. M. KOSOWER, *J. Amer. Chem. Soc.* 80, 3253 (1958).

(9) B. D. PEARSON, *Proc. Chem. Soc.* 78 (1962).

(10) H. C. LONGUET-HIGGINS and J. A. POPLE, *J. Chem. Phys.* 27, 192 (1957).

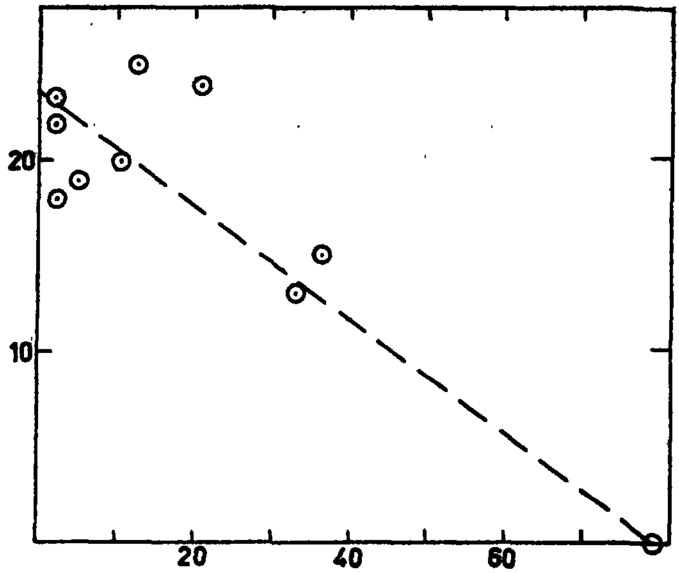

FIG. 2.—Dependence of red shift in mμ of the band in the yellow of $IrBr_6^{2-}$, relative to the position at 583 mμ in aqueous solution, as function of the dielectric constant of the solvent (the value given on the horizontal axis).

suggest this possibility, or some bonding mechanism with double bonds in the solvent, including the unusual behaviour of the tetrachloroethylene suspensions.

However, the present author believes that the main part of the explanation is very simple: it is due to the *variation of the electronic energy differences as a function of the internuclear distances* Ir-Br. In most molecules, the excited electronic states have minima of their potential curves at larger internuclear distances than the equilibrium position of the groundstate. Consequently, the band maxima shift to lower wave-numbers with increasing internuclear distances (e.g. obtaining by heating, involving the anharmonic part of the temperature excitation) while the opposite effect is obtained by increasing the external pressure. In the more primitive models of M^+X^- changed to M^0X^0, where the former state is stabilized by the Madelung energy, this general behaviour is also expected for electron transfer bands. However, STEPHENS and DRICKAMER(11) found that the $\pi Br \rightarrow \gamma_{5g}$ (5*d*, Re) electron transfer bands of K_2ReBr_6 shift to *lower* wavenumber by increasing the pressure, approximately 120 cm^{-1} per 10,000 atm. This is nearly an irrefutable proof that the red shift *Q* occurs at decreasing internuclear distances. Recently, BALCHAN and DRICKAMER(12) have extended these measurements to K_2OsCl_6, K_2OsBr_6, Na_2IrCl_6, K_2IrBr_6, usually up to 100,000 atm., and found invariably a red shift at high pressure.

We have also studied effects of the crystalline state on such ions as $IrCl_6^{2-}$. In some cases, quite remarkable deviations from the principle of additivity of ionic colours occur, such as the dark-green thallium(I) and blue silver(I) salts.(13) These particular effects are probably caused by electron transfer to $IrCl_6^{2-}$ from the 6*s*- and

---

(11) D. R. STEPHENS and H. G. DRICKAMER, *J. Chem. Phys.* 30, 1518 (1959).
(12) A. S. BALCHAN and H. G. DRICKAMER, *J. Chem. Phys.* 35, 356 (1961).
(13) C. K. JØRGENSEN, *Molecular Phys.* 4, 235 (1961).

4*d*-orbitals respectively. In the case of alkali metal salts, the spectral shifts are much less dramatic and are comparable to the effects of high pressure and of organic solvents. Thus, Table 2 shows an additional red shift in the relatively more compressed lattices(13) of Rb_2IrCl_6 and Cs_2IrCl_6 (being dark-red rather than brown), while the reflexion spectrum of $[As(C_6H_5)_4]_2IrCl_6$ is closely comparable to the absorption spectrum of the solution in dichloroethane. Actually, the wavenumbers of the vibrational structure of the band in the visible of $[As(C_6H_5)_4]MnO_4$ in dichloroethane are not distinguishable from the aqueous solution of MnO_4^-.

TABLE 2.—WAVELENGTHS IN mμ OF $IrCl_6^{2-}$ ABSORPTION AND REFLEXION SPECTRA

Transition	I	II	III
$IrCl_6^{2-}$ aqueous solution(3)	590	487	434, 410
$[As(C_6H_5)_4]_2IrCl_6$	588	499 (460)	440
$[As(C_6H_5)_4]_2IrCl_6$ in dichloroethane	586	497 (475)	440
Cs_2IrCl_6 on filter paper	(595)	515	432
Rb_2IrCl_6 alone	580	510	425
$Rb_2IrCl_6 + Al_2O_3$	580	518	~435
Na_2IrCl_6 crystals[10]	—	~515	424

However, the study of reflexion spectra does not necessarily estimate the position of the absorption maxima reliably when the molar extinction coefficients ε are very high. In the latter case, the imaginary part of the refractive index, considered as complex number, is no longer negligible. The variation of the refractive index as a function of the wavelength is very strong close to the strong absorption band and has a discontinuous singularity near the maximum. As JAHODA(14) pointed out, the resulting reflexion spectrum is shifted and distorted compared to the absorption spectrum. Well-known examples are the green reflected light from dried red ink or $KMnO_4$, and the phenomenon may occur even in liquids, such as Br_2. A possible remedy is to measure the reflexion spectrum of the coloured substance, finely powdered and intimately mixed with a larger quantity of a colourless material.(15,16) Actually, some of the data in Table 2 are for such mixtures as $Al_2O_3 + Rb_2IrCl_6$. However, even here it may be difficult to avoid Christiansen filter effects, where the refractive index of the coloured substance passes by that of the colourless material.

Next, we shall attempt to compare the relative values of the red shift for various absorption bands of $IrBr_6^{2-}$ as given in the last line of Table 1. The wavenumber shift $(\Delta\lambda)/\lambda^2$ of the lowest transition (at 860 mμ in aqueous solution and at 895 mμ in the solid, see Fig. 1) corresponds to the value 2·0. Following Reference (3) we call this transition I, while the following transitions have the wavenumber shifts from Table 1: IIa (1·04), IIb (1·53), IIc (1·75), III (2·94), IVa (1·96) and IVb (4·98).

From the groundstate $\pi^{24}\gamma_{5g}{}^5$ (the intermediate coupling component Γ_7 of ${}^2\Gamma_5$) of $IrBr_6^{2-}$, eight transitions to the configurations $\pi^{23}\gamma_{5g}{}^6$ are possible.(3) Of these, four are Laporte-forbidden (to Γ_6, Γ_7, and two Γ_8, all of even parity), one Laporte-allowed but symmetry-forbidden (to odd Γ_6) and three have electric dipole moments (to odd Γ_7 and the two odd Γ_8).

(14) F. C. JAHODA, *Phys. Rev.* **107**, 1261 (1957).

(15) T. R. GRIFFITHS, K. A. K. LOTT and M. C. R. SYMONS, *Analyt. Chem.* **31**, 1338 (1959).

(16) F. KÖNIG and H. L. SCHLÄFER, *Z. Phys. Chem.* **26**, 371 (1960).

There is very little doubt that the lowest transition I has even Γ_8 from $\pi\gamma_{4g} \rightarrow 5d\gamma_{3g}$ as excited level. The size 2·0 of the relative wavenumber shift is easily explained by the increased halogen–halogen antibonding character of the orbitals $\pi\gamma_{4g}$, when the internuclear distances decrease. The six other bonds in the visible have the other seven energy levels to divide between them.

The crucial point is the position of the two odd Γ_8. If it is true that they are represented by III and IVb (rather than IVa, being rather weak, as also the analogous band of $OsBr_6^{2-}$ at 423 mμ, and hence possibly the odd Γ_6), then the rest of the identification becomes much more certain: the odd Γ_7 is IIc, while IIa and IIb must be Laporte-forbidden, and at least one corresponds to $\pi\gamma_{5g}$, the π-bonding component correspondng to the π-antibonding partly filled shell. Woodward and Creighton(17) recently showed that even the stretching frequencies of complexes such as $PtBr_6^{2-}$ and $SnBr_6^{2-}$ hardly are above 210 cm^{-1} and therefore vibrational structure cannot be expected to produce spurious maxima at the distances ~ 1,000 cm^{-1} between adjacent levels found here, if not by a very subtle form of dynamic Jahn-Teller effect.

The relative distances between the energy levels of odd parity, taking into account $\sigma + \pi$ intermixing, can be estimated from Fig. 8 in Reference (3) the variable being the ratio between the Landé parameter of bromine, ζ_{4p}, and the energy difference between the M.O. sets $\pi\gamma_{5u}$ and $\pi\gamma_{4u}$. The degeneracy between the original twelve π-orbitals presumably becomes more and more lifted the smaller the internuclear distances. Balchan and Drickamer(12) thus point out that the III bands have a smaller red shift at high pressure than the I and II bands. However, we find a larger Q of III than of II.

It is less evident what will happen to ζ_{4p} of bromine at small internuclear distances. A somewhat indirect argument may maintain that, since the nephelauxetic effect is more pronounced at high pressure,(18) the effective charges are less positive on the metal atom and less negative on the halogen atom, and therefore by ζ_{4p} larger. However, this tendency might be counteracted by an increasing delocalization of the bonding π-orbitals, drawing electronic density away from the high field-gradients near to the bromine nucleus (but bringing it closer to the even stronger field-gradients of the iridium nucleus). We may, as a provisional guess, assume that $\zeta_{4p}/(E_5 - E_4)$ actually decreases when the internuclear distances are decreased.

We realize that a general shift must be superposed on the diagram (Fig. 8, Reference 3). Actually, the $(\pi + \sigma)\gamma_{4u} \rightarrow 5d\gamma_{3g}$ transitions of K_2PdCl_6, K_2PtBr_6 and K_2PtI_6 show a red shift at high pressure(12) though Δ, the energy difference between $5d\gamma_3$ and $5d\gamma_{5g}$, was expected to increase strongly.(18) An increased value of $(E_5 - E_4)$ combined with a constant value of ζ_{4p} would make this red shift decrease in the order

$$\Gamma_{7u} > a\Gamma_{8u} \gg b\Gamma_{8u} > a\Gamma_{6u} \qquad (1)$$

nearly independently of small shifts of the position $E\sigma$ of the odd $\sigma\gamma_4$ orbital (i.e. variations of $(E_4 - E\sigma)$ of the same size, or the opposite sign but the same order of magnitude as the variation of $(E_5 - E_4)$). Equation (1) seems to be rather in contradiction with the observed order of red shifts

$$\text{II}c < \text{III} > \text{IV}a \ll \text{IV}b \qquad (2)$$

---

(17) L. A. Woodward and J. A. Creighton, *Spectrochim. Acta* 17, 594 (1961).

(18) D. R. Stephens and H. G. Drickamer, *J. Chem. Phys.* 35, 429 (1961).

If the non-diagonal element $\sqrt{2}\zeta_{4p}/2$ between the σ- and π-orbitals with $\omega = \frac{1}{2}$ increased dramatically, strong red shifts of a Γ_{6u}, and to a somewhat smaller extent, of $b\Gamma_{8u}$, could be explained. Another, more plausible idea is that the non-diagonal element of the effective core-field one-electron operator between σ and π orbitals of symmetry type γ_{4u} is much larger at lower internuclear distancs, decreasing both Γ_{8u} in agreement with Equation (2). Hence, the present author is not inclined, at the moment, to attempt a more elaborate explanation without further experimental or theoretical evidence.*

TABLE 3.—RED SHIFT OF $OsBr_6^{2-}$ (WAVELENGTHS IN mμ)

Transition	Aqueous solution	Dichloroethane	$(\Delta\lambda)/\lambda^2$
II a	(528)	(530)	0·7
II b	(506)	(512)	2·3
II c	489·5	498	3·6
III	445	455	5·1
IV a	423	423	0·0
IV b	399	(408)	5·6

Table 3 gives the solvent effect on $[N(C_4H_9)_4]_2OsBr_6$ dissolved in dichloroethane. The wavenumber shifts (in cm^{-1}) are somewhat smaller than of $IrBr_6^{2-}$, but it is interesting to observe that the relative size of the shift of the six transitions has exactly the same order as in the iridium(IV)hexabromide. This supports strongly the idea[3] that the excited states have the same origin in $OsBr_6^{2-}$ and $IrBr_6^{2-}$, the central ion state being approximately $\Gamma_7(\gamma_{5g}^5)$ and $\Gamma_1(\gamma_{5g}^6)$ respectively. On the other hand, Dr. C. S. NAIMAN, M.I.T., was so kind as to inform me that detailed calculations[19] explained the entirely different structure of $\pi^{23}\gamma_{5g}^4$ configurations found as the excited levels of e.g. $ReBr_6^{2-}$.

Recently, two studies have been made of the chloride exchange[20] of $IrCl_6^{2-}$ and $PtCl_6^{2-}$ and of the bromide exchange[21] of $ReBr_6^{2-}$, $OsBr_6^{2-}$, $IrBr_6^{2-}$ and $PtBr_6^{2-}$, with use of radioactive indicators, and spectroscopic measurements have been performed of these systems in acidic aqueous solution, showing essential agreement with Reference (3). These results show that the hexachlorides and hexabromides are quite robust at room temperature, and that it is very improbable that any of the solvent effects discussed here have something to do with a change of the first co-ordination sphere.

Table 4 gives finally the solvent effect on $[N(C_4H_9)_4]_2$-OsI_6 (which is quite difficult to separate from polyiodides such as $[N(C_4H_9)_4]I_3$). The results are closely similar to those in Table 3. The chemistry of osmium(IV)iodides is exceedingly more complicated than that of $OsBr_6^{2-}$. It is suspected that the green hydrolysed species reported by FENN *et al.*[22] might be $I_5OsOOsI_5^{4-}$ in analogy to the ruthenium(IV)oxo-dimers and that the new species found by these authors may be a mixture of $OsICl_5^{2-}$ and $OsCl_6^{2-}$. It is remarkable how rare are the well-identified cases of mixed halogen

---

* An alternative possibility would be a strong participation of 6*p* of the iridium atom in the odd πr_4 orbital, inducing splitting of $b\Gamma_{8u}$ and $a\Gamma_{8u}$ via ζ_{6p}.

[19] C. S. NAIMAN. Private communication (September 1961).

[20] F. BLASIUS, W. PREETZ and R. SCHMITT, *J. Inorg. Nucl. Chem.* 19, 115 (1961).

[21] G. SCHMIDT and W. HERR, *Z. Naturforsch.* 16A, 748 (1961).

[22] E. FENN, R. S. NYHOLM, P. G. OSWTON and A. TURCO, *J. Inorg. Nucl. Chem.* 17, 387 (1961).

TABLE 4.—RED SHIFT OF OsI_6^{2-} (WAVELENGTHS IN mμ)

Transition	Aqueous solution	Dichloroethane	$(\Delta\lambda)/\lambda^2$
I a	(860)	870	1·3
I b	808	826	2·7
II a	(688)	(698)	2·1
II b	653	673	4·7
III a	550	568	5·9
III b	537	553	5·5
$\pi - \gamma_8$ I	373	(387)	10
$\pi - \gamma_8$ II	333	363	—

complexes, with the exception of the type trans-$PtBr_2Cl_4^{2-}$ synthetised by addition of free halogen to platinum(II)tetrahalides.

Experimental

The absorption spectra were measured in 1 cm cells on a Cary-11 recording spectrophotometer, except above 800 mμ where a Beckmann-DU was used. The reflexion spectra were measured with the latter instrument.

$[N(n\text{-}C_4H_9)_4]_2IrBr_6$ was prepared by boiling 1·22 g Na_2IrCl_6, 12 H_2O (H. Drijfhout and Zoon, Amsterdam) with 20 ml AnalaR hydrobromic acid until only some 5 ml were left. This treatment was repeated after addition of 20 ml further HBr. To the cooled brown solution (containing $IrBr_6^{3-}$, etc.) were added 50 ml water and 4 ml saturated bromine water (an excess is to be avoided, since polybromides are next precipitated). Two gramme of tetra-(n-butyl)-ammonium bromide (Fluka) were dissolved in 10 ml H_2O and added to the dark-blue solution. The sky-blue precipitate was kept overnight and filtered, and recrystallized from hot methanol. Yield: 1·1 g (60 per cent). (Found: C, 33·15; H, 6·13; N, 2·45; Br, 41·35; Calc. C, 33·19; H, 6·22; N, 2·42, Br, 41·42%).

$[N(n\text{-}C_4H_9)_4]_2OsBr_6$ was made from 10 g OsO_4 (H. Drijfhout and Zoon, Amsterdam), boiled with 60 ml AnalaR hydrobromic acid until nearly all Br_2 formed was driven off. The resulting solution of H_2OsBr_6 was added to 32 g $N(n\text{-}C_4H_9)_4Br$ (Fluka) in 100 ml ethanol and the red precipitate filtered and recrystallized from hot ethanol.

$[N(n\text{-}C_4H_9)_4]_2OsI_6$ has not been prepared quantitatively in the same way. When OsO_4 is treated with hydroiodic acid, a copious violet-black precipitate is formed, which, according to ROSENHEIM and SATTERATH,(58) simply is anhydrous OsI_4. If sodium iodide is present in great excess, a dark-coloured solution can be filtered off, the free I_2 reduced with ascorbic acid, and $N(n\text{-}C_4H_9)_4I$ (Fluka) then precipitate dark purple crystals. However, they hydrolyse readily and even in dichloroethane the solution turns dark-green after some hours. This reaction can nearly be reversed by addition of tetra-(n-butyl)-ammonium iodide dissolved in dichloroethane.

---

(58) A. ROSENHEIM and E. SASSERATH, *Z. Anorg. Chem.* **21**, 122 (1899).

J. Inorg. Nucl. Chem., 1962, Vol. 24, pp. 1595 to 1599. Pergamon Press Ltd. Printed in Northern Ireland

MIXED COMPLEXES OF COPPER(II) WITH *O*-AZOPHENOL AND ETHANOLAMINE OR ETHYLENEDIAMINE*

E. J. GONZALES and H. B. JONASSEN
Department of Chemistry, Tulane University, New Orleans 18, La.

(*Received* 2 *January* 1962; *in revised form* 30 *April* 1962)

Abstract—The copper(II) ion is known to form a 1:1 complex with *o-o'*dihydroxy azobenzene (abbrev. dye). This complex reacts with ethylenediamine (abbrev. en) or ethanolamine (abbrev. em) to form a 1:1 complex [Cu–dye–en] or [Cu–dye–em] respectively where the copper(II) ion seemingly has a co-ordination number of five. The solid [Cu–dye–em] complex on the other hand is a dimer with a magnetic moment of 1·3 B.M. Hydrogen bonding seems to contribute to dimer stabilization.

ORTHO-azophenol, a dye containing hydroxy groups ortho to the azo group, readily forms a co-ordinatively unsaturated dye complex with transition metal ions.

Previous studies with the Cu(II)-*o*-azophenol complex indicate that the co-ordination number of the Cu(II) ion is unsaturated and can expand to fill its fourth, fifth and possibly even a sixth co-ordination position by using such compounds as pyridine, quinoline(1) and 8-hydroxyquinoline.(2)

A recent investigation(3) of the same metallated dye complex with propylene glycol in basic media also indicates this unsaturation of the Cu(II) co-ordination sphere and formation of a complex having a total ligand co-ordination of five.

In the present study ethylenediamine and ethanolamine have been used to demonstrate this unsaturation. Ethylenediamine almost invariably acts as a bidentate chelating ligand,(4) whereas ethanolamine, possessing one amino and one hydroxy group, may act as a bidentate complexing agent.(5)

If each of these amines reacts as a bidentate ligand, the resulting copper complex with the tridentate dye, *o*-azophenol, should exhibit a total ligand co-ordination of five.

EXPERIMENTAL

A. *Reagents*

Ortho-azophenol (dye) was prepared according to the method of WILLSTATTER and BENZ(6). The melting point determined was 172–173°. Literature value is 172°.

Ethylenediamine (en) was purchased from Union Carbide and Carbon Chemicals, New York. It was purified by distilling at atmospheric pressure over solid NaOH. The anhydrous fraction boiling at 116·5–117·3° was used.

Ethanolamine (em), high purity white label (99 plus per cent), obtained from Eastman, Rochester, New York was used without further purification.

---

* Abstracted in part from a dissertation submitted by Elwood Gonzales to the Tulane University in partial fulfillment of the requirements for the degree of Doctor of Philosophy, 1958. Author is presently with the Southern Utilization Research and Development Division, Agricultural Research Service, U.S. Department of Agriculture, New Orleans, La.

(1) H. D. K. DREW and J. K. LANDQUIST, *J. Chem. Soc.* 292 (1938).

(2) H. B. JONASSEN and J. OLIVER, *J. Amer. Chem. Soc.* **80**, 2347 (1958).

(3) H. B. JONASSEN and E. J. GONZALES, *J. Amer. Chem. Soc.* **79**, 4282 (1957).

(4) A. MARTELL and M. CALVIN, *Chemistry of the Metal Chelate Compounds*, p. 136. Prentice-Hall, New York (1952).

(5) W. HIEBER and E. LEVY, *Z. Anorg. Chem.* **219**, 225 (1934).

(6) R. WILLSTATTER and M. BENZ, *Ber. Dtsch. Chem. Ges.* **39**, 3492 (1906).

Ethanolamine hydrochloride was prepared by dissolving a weighed quantity in chloroform and passing dry HCl into the solution until the hydrochloride was completely precipitated. The product was filtered, washed successively with chloroform and ether, and dried over $CaCl_2$ in a vacuum desiccator. The white waxy crystals were very hygroscopic.

Cu(II)-*o*-azophenol monohydrate was prepared by dissolving 1:1 molar stoichiometric quantities of 95 per cent ethanolic *o*-azophenol and aqueous cupric perchlorate hexahydrate. The redbrown precipitate was filtered, and the filtrate diluted with water to remove the remaining dye complex. The complex was washed thrice with water and dried two hours at 110° giving a 50 per cent yield. Duplicate ash determinations indicated the complex to have a metal:dye:H_2O ratio of 1:1:1. (Found: Ash, 26·87 (as CuO). Calc. for Cu(II)-dye-H_2O: Ash, 27·08% (as CuO)).

All inorganic chemicals used were "Baker's Analysed" C.P. grade.

Alcoholic molar solutions of copper(II)-*o*-azophenol monohydrate and *o*-azophenol were made by accurately weighing the appropriate quantities for a litre of oxygen-free 95 per cent ethanol solution and diluting to volume.

Oxygen-free 95 per cent ethanolic molar solutions of potassium and sodium *o*-azophenolates were prepared by dissolving the accurately weighed amount of dye and measured quantity of the respective base in ethanol and diluting to volume.

Because of the hygroscopic nature of ethanolamine hydrochloride, the salt was roughly weighed and diluted to volume with distilled water. It was standardized potentiometrically with NaOH. All solutions were prepared in solutions using solvents free from oxygen and CO_2.

B. *Spectrophotometric studies*

For visible spectra studies Beckman Models B, DU and DK spectrophotometers using 1 cm matched Pyrex absorption cells were employed. All solutions for visible spectra were diluted with oxygen-free 95 per cent ethanol. This was prepared by passing nitrogen, deoxygenated by a chromous chloride–zinc amalgam column, into ethanol for at least 1 hr.

Infra-red spectra were run on a Beckman IR 4 double beam automatic recording spectrophotometer using NaCl optics and the KBr disk technique.

C. *Conductometric studies*

A Heath oscilloscope and a signal generator were used as a null point indicator in connection with a Leeds and Northrup slidewire potentiometer and decade resistance box. The conductance cell used was a vertical dipping type with platinized platinum electrodes. All conductometric work was carried out at 25–27°, under nitrogen in a constant temperature bath.

D. *pH measurements*

A Beckman Model G pH meter was used in conjunction with a Beckman glass indicator electrode and saturated KCl-calomel reference electrode.

E. *Magnetic studies*

Magnetic susceptibility measurements were made with a Gouy balance. The apparatus was constructed by E. A. Boudreaux and consisted of a Christian Becker analytical balance equipped with an optical system for direct scale reading. The balance was converted so that a sensitivity of 0.02 mg could be maintained. A permanent magnetron magnet having a constant field of 4796 G was employed.

F. *Preparation of complexes*

(1) [Cu–dye–en]. 2·41 g (0·01 mole) $Cu(NO_3)_2 \cdot 3H_2O$ dissolved in 15 ml of distilled water was added to 1·56 g en resulting in a deep purple solution. Two hundred and fifty ml of 95 per cent ethanol was then added followed by 2·14 g (0·01 mole) of dye giving a deep orange-red solution to which water was added until precipitation was complete. The product was filtered through a Buchner, washed with 1 l. of water and dried at 100° for 1 hr. A rust-coloured product, 1·02 g, was obtained. About 0·3 g was dissolved in 25 ml 95 per cent ethanol and 5 ml en was introduced. A rotating vacuum evaporator was then used for 24 hr to evaporate excess en and alcohol. Water was then added to effect precipitation and the precipitate was filtered and washed. The brick red solid was then placed in a vacuum desiccator over $CaCl_2$ for 24 hr. (Found: C, 49·80; H, 5·17; N, 16·78; ash, 21·47 (as CuO). Calc. for [Cu–dye–en]: C, 50·04; H, 4·80; N, 16·68; ash, 23·69% (as CuO)).

(2) $[Cu–dye–em]_2$. Approximately 2·14 g (0·01 mole) of dye was dissolved in the smallest possible volume of 95 per cent ethanol and a solution containing 0·01 mole of $Cu(NO_3)_2$ in 10 ml water was added. One hundred ml more water was then introduced to aid precipitation of the Cu(II)–dye complex. The precipitate was then filtered through a coarse glass filter crucible, washed with 100 ml

water, and dried 1 hr at 110°. Pure em (about 1 mole) added to the dried complex in a 250 ml. beaker changed the colour of the solution from brown to red. After standing for 4 days the precipitate was filtered, washed with cold water (about 15°), dried at 110° for 2 hr, and powdered. 0·7 g of a deep brown complex was obtained. (Found: C, 49·86; H, 4·36; N, 12·31; ash, 22·70 (as CuO). Calc. for [Cu–dye–em]$_2$: C, 49·85; H, 4·50; N, 12·47; ash, 23·61 % (as CuO)).

G. *Molecular weight determination*

The molecular weights of the Cu–dye–en and [Cu–dye–em] complexes were determined by the Rast method. The [Cu–dye–em] was found to be dimeric. (Found: 354. Calc. for [Cu–dye–en]: 335·87. Found: 654. Calc. for [Cu–dye–em]: 336·85).

DISCUSSION OF RESULTS

I. *The Copper(II)–dye–ethylenediamine Complex*

A. *Solution studies*

(1) *Spectral studies.* The spectral shifts observed when various equivalents of en are added to an alcoholic solution of the Cu–dye complex, the concentration of which is kept constant are shown in Fig. 1. Two isosbestic points are shown at 404 and 515 mμ indicative of the formation of a new complex.

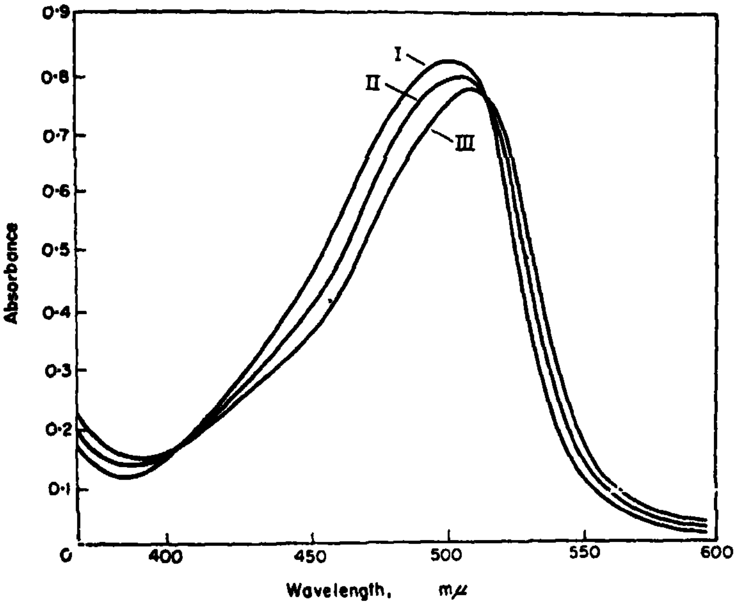

FIG. 1.—Effect of ethylenediamine on Cu–dye at 25°C
(a) Curve I Cu–dye complex
(b) Curve II Cu–dye + one equivalent of en
(c) Curve III Cu–dye + two equivalents of en

Since no further shifts in the absorption characteristics occur after one equivalent of en has been added a coloured complex Cu–dye–en seems to be formed. The absorption maximum shifts from 500 to 510 mμ.

Similar spectra and isosbestic points were obtained when solutions containing the [Cu(en)]$^{2+}$ or [Cu(en)$_2$]$^{2+}$ ions were titrated with either the dye or its sodium salt.

The results of a series of spectrophotometric titrations of [Cu(en)]$^{2+}$ or [Cu(en)$_2$]$^{2+}$ ions with either dye or its sodium salt show the same spectral characteristics. This seems to give additional evidence for the existence of a five co-ordinated [Cu–dye–en] complex.

(2) *Conductometric studies.* This system was also studied by conductometric methods varying the conditions of addition of reagents. In all cases the same spectral changes were observed to occur. All titrations indicated the existence of the stable [Cu–dye–en] complex.

(3) *Continuous variation studies.* Continuous variation studies show breaks or maxima respectively at 1:1 mole ratios. In the reaction of $[Cu(en)_2]^{2+}$ with the dye anion to give [Cu–dye–en] the maximum is shifted slightly when the sodium salt of the dye is used whereas when the free dye is the source of the anion a slight hump precedes the 1:1 maximum. The 1:1 ratio maximum is similarly shifted in the continuous variation of Cu–dye and en. In all instances, the irregularity occurs in the range where the free dye, Na_2 dye or en are in excess. Since the pK of [Cu–dye–H_2O] is 19·8 at 30°(7) and the pK of $[Cu(en_2)]^{2+}$ is about twenty,(8) slow interconversion may be responsible for the shift.

B. *Studies of solid* [Cu–dye–en] *complex*

The infra-red absorption characteristics of this complex reveal several important facts.

The broad band (3500–2500 cm^{-1}) in the spectrum of the dye indicates strong intramolecular hydrogen bonding between the OH groups of the molecule. The Cu–dye complex spectrum shows a nearly complete disappearance of this band and the appearance of a new strong band between 650 and 675 cm^{-1} which has been assigned to metal–ligand vibrations.(9)

The NH_2 stretching frequency which is observed in the amine at 3550 and 3420 cm^{-1} has been shifted in the [Cu–dye–en] complex to 3320 cm^{-1}. Shifts are also observed in the NH_2 bending region around 800 cm^{-1}, but the broadness of the band does not allow assignments of these shifts.

Molecular weight determinations of the complex indicate that the complex is a monomer with a magnetic moment of 1·92 B.M.

II. *The Copper(II)–dye–ethanolamine Complex*

A. *Solution studies*

When an alcoholic solution of the Cu–dye complex, the concentration of which was kept constant, was allowed to react with an aqueous solution of ethanolamine (abbrev. em) no isosbestic point was observed even when an eighty-fold excess of em was added. This would be expected in a much weaker ligand than en.

However, when an excess of pure em was added or when the spectra were observed in pure em the absorption characteristics changed. Again isosbestic points at 404 and 515 mμ were observed.

Conductometric titrations of an equivalent mixture of Cu–dye and em · HCl with NaOH gave slopes different from either the titration of Cu–dye with OH^- ions or that of em · HCl with OH^- ion, indicative of the interaction of the Cu–dye complex present in alcohol with the free em. Similarly, potentiometric titration of the [Cu–dye–em] complex dissolved in ethanol gave a break at one equivalent of HNO_3. The slope again was different than that obtained when either em was titrated with HNO_3 or when the Cu–dye complex was similarly titrated, again indicative of the existence of a [Cu–dye–em] complex.

---

(7) P. E. SLADE, Thesis, Tulane University, New Orleans (1953).

(8) A. MARTELL and M. CALVIN, *Chemistry of the Metal Chelate Compounds*, p. 519. Prentice-Hall, New York (1952).

(9) K. UENO and A. MARTELL, *J. Phys. Chem.* **60**, 1273 (1956).

A 95 per cent alcoholic solution containing the dissolved Cu–dye–em complex to which an additional equivalent of em has been added was titrated with HNO_3. The first break occurred when the free equivalent of em has been neutralized since its slope is the same as that observed above for em alone. The second break occurred when the co-ordinated em was neutralized. Further addition destroyed the Cu–dye complex.

B. *Studies on solid* $[Cu\text{–}dye\text{–}em]_2$

Molecular weight determination of this complex indicates that the complex is a dimer with an unusual moment of 1·32 B.M. indicating the possibility of a δ bond(10) in the dimer possibly stabilized by hydrogen bonding.

The infra-red spectrum of the complex shows a metal–ligand vibrational band at 650–675 cm^{-1},(9) and a broad band around 800 cm^{-1} which seems to be the NH_2 bending region. A broad band from around 3350 to 2400 cm^{-1} with a sharp shoulder at about 3300 cm^{-1} is indicative of intramolecular hydrogen bonding as well as chelation.(11)

The shoulder at 3300 cm^{-1} can be assigned to the NH_2 stretch shifted because of complexing.

The magnetic properties of these complexes will be discussed in a future paper.

Acknowledgements—The financial support of the American Cyanamid Company through a fellowship (E. J. Gonzales) and the assistance of R. T. O'Connor of the Southern Utilization Research and Development Division, United States Department of Agriculture are gratefully acknowledged. Financial support under the Office of Naval Research Contract is gratefully acknowledged for part of this work.

---

(10) H. B. Jonassen, J. Fanning, E. Gonzales, S. Lanoux and J. Oliver, *Unusual Magnetic Properties of Some Dimeric Copper(II) Complexes*, presented at the American Chemical Society Meeting, Chicago, September, 1961.

(11) L. J. Bellamy, *The Infra-red Spectra of Complex Molecules* (2nd Ed.), p. 96. J. Wiley, New York (1957).

J. Inorg. Nucl. Chem., 1962, Vol. 24, pp. 1601 to 1606. Pergamon Press Ltd. Printed in Northern Ireland

COMPLEXES OF LANTHANIDE ELEMENTS WITH MERCAPTO ACETATE LIGANDS

J. L. BEAR, G. R. CHOPPIN and J. V. QUAGLIANO
Department of Chemistry, Florida State University, Tallahassee, Florida

(*Received* 23 *April* 1962)

Abstract—Stability constants have been determined by the Bjerrum method for the complexes of the α-mercaptoacetate ion with yttrium (III) and several trivalent lanthanide ions. The investigation indicates that the α-mercaptoacetate ion acts as a monodentate ligand.

SOLUTIONS of hydroxy carboxylic aicds have been used to separate the trivalent ions of the lanthanide and actinide elements by ion exchange techniques.[1,2,3] With solutions of glycolate, lactate and α-hydroxyisobutyrate ions it was found that the efficiency of separation of the metal ions increases in the order: isobutyrate > lactate > glycolate. In order to explain this trend CHOPPIN and CHOPOORIAN[4] determined the stepwise formation constants of the complexes involved in these systems. These authors found that the order of stability, isobutyrate > lactate > glycolate, holds for each of the complex formation steps, and concluded that the inductive effect arising from methyl group substitution in the α-position is more important than the steric effect caused by the same substitution. In agreement with this interpretation, the stability of the complexes increased with the increase in the atomic number of the metal ions. In all but a few titrations, the experimental value of $\bar{n}$ exceeded three, thus indicating the formation of a fourth complex species, ML_4^-. The existence of this species has been proved independently by other investigations.[5,6]

SONESSON[5,7] has reported values for the stability constants of the acetate and glycolate complexes of a number of the lanthanide elements, He found that the stability constants for the glycolate complexes were about five times larger than the corresponding constants for the acetate system. Since glycolic is a stronger acid than acetic, complexes of gylcolate would be expected to be weaker. The increased stability of the glycolate ligands was attributed to chelation.

In the present investigation, the stepwise formation constants of the complexes of α-mercaptoacetic acid with several trivalent lanthanide ions and yttrium (III) have been determined, in order to study the effect on the stability of the lanthanide complexes of the substitution of the oxygen donor atom by a sulphur atom.

---

(1) D. C. STEWART, *Proceedings of the First International Conference on Peaceful Uses of Atomic Energy, Geneva*, 1955. Vol. 7, paper 837, United Nations (1956).

(2) S. G. THOMPSON, B. G. HARVEY, G. R. CHOPPIN and G. T. SEABORG, *J. Amer. Chem. Soc.* **76**, 6229 (1954).

(3) G. R. CHOPPIN, B. G. HARVEY and S. G. THOMPSON, *J. Inorg. Nucl. Chem.*, **2**, 66 (1956).

(4) G. R. CHOPPIN and J. A. CHOPOORIAN, *J. Inorg. Nucl. Chem.* **22**, 97 (1961).

(5) A. SONESSON, *Acta Chem. Scand.* **13**, 1437 (1959).

(6) G. R. CHOPPIN, D. MOY and L. HOLM, *J. Inorg. Nucl. Chem.* **19**, 251 (1961).

(7) A. SONESSON, *Acta Chem. Scand.* **12**, 165 (1958).

Determination of stability constants

The successive formation constants were calculated by the method of Bjerrum, as previously described by Choppin and Chopoorian for the complexes of the α-hydroxy-carboxylic acids.(4) The method involves the relationship between the average number of ligands bound to a metal ion in the equilibrium mixture, $\bar{n}$, and the total equilibrium concentration of anionic ligand, [L]. The equation which relates $\bar{n}$, [L] and the successive formation constants is:

$$\bar{n} = \frac{\sum_{n=1}^{N} n\beta_n[\mathrm{L}]^n}{1 + \sum_{n=1}^{N} n[\mathrm{L}]^n} \tag{1}$$

where

$$\beta_n = \frac{[\mathrm{ML}_n]}{[\mathrm{M}][\mathrm{L}]^n} \tag{2}$$

The calculation of $\bar{n}$ and [L]

The concentration of the α-mercaptoacetate ion was calculated from hydrogen ion measurements, using a glass electrode.

For a buffer solution of α-mercaptoacetic acid, where the concentration of the protolyzed ligand is designated by C'_{HL} and that of the sodium salt of the acid by C'_{L} the acid equilibrium constant may be expressed as

$$K_a = \frac{[\mathrm{H}]'(C'_{\mathrm{L}} + [\mathrm{H}]')}{C'_{\mathrm{HL}} - [\mathrm{H}]'} \tag{3}$$

where [H]′ is the hydrogen ion concentration of the buffer solution. When lanthanide ions are added to the buffer solution the expression becomes

$$K_a = \frac{[\mathrm{H}][\mathrm{L}]}{C'_{\mathrm{HL}} + C_{\mathrm{H}} - [\mathrm{H}]} \tag{4}$$

where C_{H} is a correction to account for any free acid introduced into the buffer solution along with the lanthanide ions, [H] is the hydrogen ion concentration for the solution containing metal ions, and [L] is the concentration of anionic ligand. Combining Equations (3) and (4) the solution for [L] is

$$[\mathrm{L}] = \frac{[\mathrm{H}]'(C'_{\mathrm{L}} + [\mathrm{H}]')(C'_{\mathrm{HL}} + C_{\mathrm{H}} - [\mathrm{H}])}{[\mathrm{H}](C'_{\mathrm{HL}} - [\mathrm{H}]')} \tag{5}$$

The total concentration of anionic ligand in the solution is equal to $(C'_{\mathrm{L}} + [\mathrm{H}] - C_{\mathrm{H}})$. The concentration of complexed ligand is the difference between this and the free ligand concentration [L]. Therefore,

$$\bar{n} = \frac{C'_{\mathrm{L}} + [\mathrm{H}] - C_{\mathrm{H}} - [\mathrm{L}]}{C_{\mathrm{M}}} \tag{6}$$

where C_{M} is the total metal ion concentration.

By measuring [H] as the acid buffer is added to a solution containing the metal ion and by measuring [H]′ as the buffer is added to another solution not containing metal ion, the values of $\bar{n}$ and [L] may be calculated, since C'_{L}, C_{H} and C'_{HL} are known.

EXPERIMENTAL

Reagents

Lanthanide perchlorate solutions. These were prepared as described previously.[4]

Sodium perchlorate (G. F. Smith Co., anhydrous reagent grade) was used as obtained in adjusting the solutions to 2·0 M ionic strength.

α-Mercaptoacetic acid buffer solution. The aqueous solution of α-mercapto acetic acid (Eastman organic chemicals) was standardized against sodium hydroxide.

The buffer solution was prepared by partially neutralizing the standard acid solution with sodium hydroxide so that the buffer ratio was unity. C'_L varied from 0·7 to 1·0 M.

Equipment

The glass and reference electrodes. The glass electrode was a Beckman Type "42". A silver-silver chloride reference electrode was used.

The pH meter. The meter was a Beckman model G.

The potentiometer. A Leeds-Northrup model K-3 potentiometer was used. A Weston cell was used as the standard cell.

Procedure

The titration procedure involves the titration of a solution containing the metal ion and another solution not containing metal ion with acid buffer so that [H] and [H]′ can be determined. The solution to be titrated is placed in a jacketed cell, through which is circulated water kept at 25 ± 0·1°C. After each addition of α-mercaptoacetic acid buffer the emf is measured on the potentiometer connected to the pH meter.

The hydrogen ion concentration of the titrate solution can be calculated from the Nernst equation using the potential of a pH 7 buffer solution and the potential after each increment of α-mercaptoacetate buffer. For the solution containing metal ions we have the relationship:

$$E - E^s = 59{\cdot}15 \log \frac{[\mathrm{H}]^s}{[\mathrm{H}]}$$

The same expression is used in calculating the hydrogen ion concentration in the solution not containing metal ions.

$$E' - E^s = 59{\cdot}15 \log \frac{[\mathrm{H}]^s}{[\mathrm{H}]'}$$

where

E = potential after each increment of buffer in metal solution.

E' = potential after each increment of buffer in solution not containing metal ions.

E^s = potential of pH 7 buffer.

$[\mathrm{H}]$ = hydrogen ion concentration in metal solution after each increment of buffer.

$[\mathrm{H}]'$ = hydrogen ion concentration in solution without metal ions after each increment of buffer.

$[\mathrm{H}]^s$ = hydrogen ion concentration of pH 7 buffer.

RESULTS

Tables 1 (a–b) list some of the experimental data and the calculated values of [L] and $\bar{n}/[\mathrm{L}]$. The values for $E' - E$ are calculated from the e.m.f.'s measured during the titrations.

The values obtained for the stability constants are listed in Table 2. They were calculated from the $\bar{n}$ and [L] values using an iterative least squares treatment of Equation (1) on an IBM 709 computer.[8] Sets of $\bar{n}$ and [L] values which differed within the determinate error were used to calculate error limits for the stability constants. Errors were found to be of the order of ±10 per cent for K_1 and ±30 per cent for K_2. Random computational errors gave such large fluctuations in the values of K_3 that no values can be confidently reported for it. In order to check the values obtained in this investigation, the successive formation constants of holmium (III) glycolate complexes and lanthanium (III) acetate complexes were determined and compared with the values obtained by CHOPPIN and CHOPOORIAN for the glycolate system and by SONESSON for the acetate system. Both of the earlier investigations used a slightly different potentiometric titration technique. These values are reported in Table 3 and the agreement is satisfactory.

---

[8] J. A. Chopoorian, G. R. Choppin, H. C. Griffith and R. Chandler, *J. Inorg. Nucl. Chem.* **21**, 21 (1961).

TABLE 1.—DETERMINATION OF [L] and $\bar{n}$/L FROM EXPERIMENTAL DATA

(a) Samarium mercaptoacetate system

$C^\circ_H = 0·17$ mM $C^\circ_L = 999·9$ mM

$C^\circ_M = 28·23$ mM $\delta = 1·0$

Volume of titrant (ml)	$(E' - E)$ (mV)	[L] (mM)	$\bar{n}$/[L](M^{-1})
0·10	20·6	4·44	52·73
0·20	18·7	9·53	41·96
0·30	16·9	15·21	35·61
0·40	15·6	21·08	31·94
0·50	14·8	26·95	29·71
0·75	12·9	42·43	25·26
1·00	11·7	57·73	22·89
1·25	10·8	73·12	21·08
1·50	9·9	89·01	19·26
2·00	8·8	118·68	17·40
2·50	7·9	147·61	15·88
3·50	6·8	199·54	14·43
4·00	6·3	223·75	13·84
5·00	5·2	269·12	12·76

b. Gadolinium—α-mercaptoacetate system

$C^\circ_H = 0·19$ mM $C^\circ_L = 999·8$ mM

$C^\circ_M = 24·76$ mM $\delta = 1·00$

Volume of titrant (ml)	$(E' - E)$ (mV)	[L] (mM)	$\bar{n}$/[L] (M^{-1})
0·10	15·3	5·60	37·31
0·20	14·4	5·60	37·31
0·30	13·2	17·61	28·88
0·40	11·7	24·64	26·78
0·50	11·1	31·18	23·31
0·75	9·6	48·32	19·85
1·00	8·7	65·12	18·05
1·25	8·0	81·65	16·71
1·50	7·3	98·72	15·19
1·75	6·7	115·60	13·90
2·50	5·5	162·00	11·99
3·00	5·0	190·31	11·29
4·50	4·1	264·88	10·14
5·00	3·9	286·89	9·94
6·00	3·6	326·62	9·65

A plot of $\bar{n}$/[L] versus [L] for the samarium (III) and gadolinium (III) β-mercaptoacetate systems is shown in Fig. 1.

Fig. 2 shows the first stability constant, K_1, of the acetate, glycolate and α-mercaptoacetate systems as a function of atomic number in the lanthanide series. The values

TABLE 2.—STABILITY CONSTANTS OF THE VARIOUS LANTHANIDE AND YTTRIUM COMPLEXES AT 25·0°C

Ion	K_1	K_2
La	26	5
Ce	27	5
Nd	31	6
Sm	64	8
Eu	56	6
Gd	44	6
Tb	43	6
Y	31	5
Ho	21	7
Er	19	8
Yb	21	8

TABLE 3.—STABILITY CONSTANTS OF THE LANTHANIUM ACETATE AND HOLMIUM GLYCOLATE SYSTEM AT 25·0°C

Lanthanium acetate system			
	K_1	K_2	K_3
Our value	28 ± 3	7 ± 2	~2
SONESSON'S value at 20°C.	36	8·3	3·2
Holmium glycolate system			
	K_1	K_2	K_3
Our value	290	90	18
CHOPPIN'S values	308	109	24

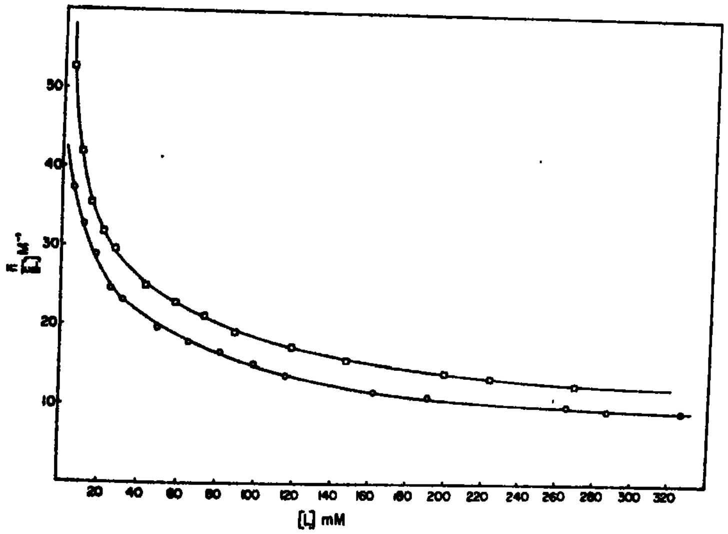

FIG. 1.—Plot of $\bar{n}$/[L] VS [L] for Sm (III) (⊡) and Gd (III) (⊙).

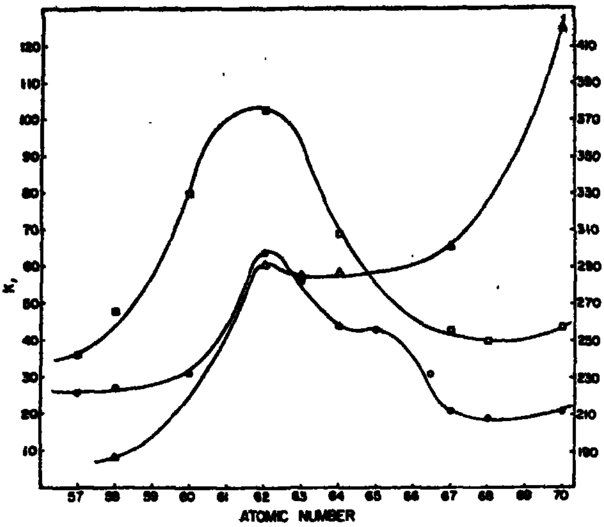

Fig. 2.—Variation of K_1 as a function of atomic number. Scale on the left is for acetate (⊡) and α-mercapto acetate (⊙); the scale on the right is for glycolate (△).

for the acetate and glycolate complexes are those reported by Sonesson and by Choppin and Chopoorian.

DISCUSSION

The greater stability of the glycolate complexes compared to the acetate complexes was attributed by Sonesson to a chelation effect. If both of these anions acted as monodentate ligands with only the carboxylate group involved in the coordination, the glycolate, being the anion of the stronger acid, should form the weaker complexes. The data in Fig. 2 show that K_1 for the α-mercaptoacetate complexes is much smaller than for the glycolate complexes, and comparable to the acetate complexes of the same metal ions. This indicates that in its complexes with trivalent lanthanide ions the α-mercaptoacetate anion is not acting as a chelate ligand. Chelation should result in values of K_1 higher than for the acetate and slightly lower than for the glycolate complexes.

Preliminary studies on the infrared spectra of sodium α-mercaptoacetate and of the complex lanthanum (III) tris-α-mercaptoacetate show no shift in the SH stretching vibration of the lanthanum salt with respect to that of the sodium salt. Although this cannot by itself be considered as conclusive evidence that the mercapto group is not involved in coordination with the lanthanum ions, it does support the conclusion drawn from the values of the stability constants.

Acknowledgements—This research has been supported in part by the United States Atomic Energy Commission. The computer calculations were aided by financial support from the National Science Foundation.

J. Inorg. Nucl. Chem., 1962, Vol. 24, pp. 1607 to 1616. Pergamon Press Ltd. Printed in Northern Ireland

AN EXPERIMENTAL TEST OF A MORE GENERALIZED FORMULATION OF THE METHOD OF CONTINUOUS VARIATIONS

K. O. WATKINS and M. M. JONES*
Department of Chemistry, Vanderbilt University, Nashville, Tennessee

(*Received* 5 *January* 1962; *in revised form* 21 *May* 1962)

Abstract—An analysis of the method of continuous variations is presented for systems containing mononuclear complexes with a single type of ligand. These equations allow the conditions to be determined under which any one of the complexes will reach a maximum concentration for such systems which contain several complexes. A comparison with experimental data shows that this procedure is especially valuable in the treatment of data in which a distinction must be made between several possible complexes AB_n, where *n* is large. The systems examined in detail are the Cu^{2+}–Cl^- system and the Cu^{2+}–SCN^- system.

ALTHOUGH the method of continuous variations has been used to study complexation equilibria in hundreds of systems, there has previously been no attempt to develop and test a generalized theoretical formulation of this method. Earlier studies⁽¹⁾ of the method have been restricted almost exclusively to cases in which the number of complexes which may be present simultaneously is three or less. A general spectrophotometric displacement equation has been presented by YELLIN and PLANE.⁽²⁾ This was derived for use with Raman spectra where the choice of a Raman line due to only one complex is possible. No attempt was made, however, to use it in the *quantitative* interpretation of the data involved. Their general equation is also given in terms of the *total* light intensity (or absorbance) and, strictly speaking, is not set up so that it would reflect the conditions under which *a given complex* would reach its maximum concentration.

The problem is really two-fold: (1) the determination of the composition of the complexes in the system and (2) the determination of the relevant equilibrium constants. It seems reasonable to suppose that if *all* necessary chemical equilibria are considered, the method of relating the point of maximum concentration of the various species present to other parameters should yield equations which are as *valid theoretically* as those methods which follow the complexation reaction in some other way. The resulting method may not be very convenient from an experimental viewpoint,† however. The purposes of this paper are to present a generalized formulation for ligands which are not protonic acids or bases, to show how this governs the shapes of the typical curves obtained experimentally by the method of continuous variations, and to indicate why successive equilibrium constants may not be obtained in practice from such data alone.

---

* To whom correspondence concerning this paper should be addressed.

† The objections raised by WOLDBYE⁽³⁾ are based in part upon an incomplete theoretical analysis of such a system. These objections illustrate the *practical* difficulties associated with the use of the method very well.

(1) The literature on most of this earlier work is collected in M. M. JONES, *J. Amer. Chem. Soc.* **81**, 4485 (1959).

(2) W. YELLIN and R. A. PLANE, *J. Amer. Chem. Soc.* **83**, 2448 (1961).

(3) F. WOLDBYE, *Acta Chim. Scand.* **9**, 299 (1955).

The experimental parameter used with this method is the difference, Y, between the measured physical property (generally light absorption) of an equilibrium mixture of ligand and metal ion in solution and the value this physical property would have if no reaction occurred. The basis of the following treatment of this method is the relation between the mole ratio of the reactants when a given complex species attains its maximum concentration and the values of an experimentally measured property of the solution, such a light absorption. When a system contains more than a single complex present in an appreciable concentration, the concentration of any given complex will reach a maximum at some value of the molar ratio of the reactants that differs from that found in the complex. This has previously been established for systems containing two(4) or three complexes.(5)

The evaluation of this displacement from the stoichiometric point may be carried out using a procedure analogous to that of VOSBURGH and COOPER(4). For a system of four complexes, the concentration of AB reaches a maximum at

$$\frac{x}{1-x} = 1 - \frac{2C_2 + 6C_3 + 12C_4}{M(1-x)} \tag{1}$$

Where $x/1-x$ is the ratio [B] total/[A] total and C_1, C_2, C_3 and C_4 are the concentrations of AB, AB_2, AB_3 and AB_4 respectively. M is the total concentration of A plus B, which is constant. Analogous equations can be developed to express the points at which the higher complexes reach their maximum concentrations. The conditions for the maxima in the concentrations of AB_2, AB_3 and AB_4 are $(dC_2/dx) = 0$, $(dC_3/dx) = 0$ and $(dC_4/dx) = 0$ respectively. It is found that the concentration of AB_2 reaches a maximum at an x value given by

$$\frac{x}{1-x} = 2 + \frac{C_1 - 3C_3 - 8C_4}{M(1-x)}\,; \tag{2}$$

the concentration of AB_3 reaches a maximum when x has the value

$$\frac{x}{1-x} = 3 + \frac{2C_1 + 2C_2 - 4C_4}{M(1-x)} \tag{3}$$

While AB_4 attains its maximum concentration when

$$\frac{x}{1-x} = 4 + \frac{3C_1 + 4C_2 + 3C_3}{M(1-x)} \tag{4}$$

A similar set of equations can be developed for a system containing five or six complexes and presumably for systems containing more than six complexes. A general equation for the displacement of the maximum concentration of a complex AB_i from the stoicheiometric point because of the presence of higher or lower complexes can be written as

$$\frac{x}{1-x} = i + \frac{1}{M(1-x)} \sum_{j=1}^{j=N} (i-j)\,jC_j. \tag{5}$$

[illegible] W. C. VOSBURGH and G. R. COOPER, *J. Amer. Chem. Soc.* 63, 437 (1941).

(5) L. I. KATZIN and E. GEBERT, *J. Amer. Chem. Soc.* 72, 5455 (1950).

Here the complexes present in the system are AB, AB_2, ... AB_N, M is the total molarity, C_j is the concentration of AB_j and x is the value of the mole fraction of B at which AB_i reaches its maximum concentration.

The effect of the presence of the other complexes on the shift of the maximum concentration from the stoicheiometric point can be most readily seen from the general equation. For the case where but a single complex is present (i.e. $C_j \ll C_i$ for all j), the maximum occurs at the stoicheiometric point giving the formal composition ratio for that complex. When this is not the case, it is found that every higher complex present decreases the reagent ratio at which the lower complex reaches its maximum concentration while every lower complex increases the reagent ratio at which a higher complex reaches its maximum concentration. The amount by which the reagent ratio of a complex is increased or decreased depends upon the stoicheiometry and concentration (and hence by implication the formation constants) of the other complexes in the particular system being studied.

A necessary condition for the successful use of the method of continuous variations is that an extremum occur in some function of a physical property of the system at the same value of x at which the maximum occurs in the concentration of the complex being studied. The most suitable physical property is the absorption of monochromatic light and this is the one which will be used for purposes of illustration and for testing the equations derived above.

Let ε_0, ε_w, ε_1, ε_2, ε_3 and ε_4 be the extinction coefficients of A, B, AB, AB_2, AB_3 and AB_4 at a given wavelength and let L be the length of the light path through the solution. Then the absorbance, A, of the solution containing four complexes will be

$$A = L(\varepsilon_0 C_0 + \varepsilon_w C_w + \varepsilon_1 C_1 + \varepsilon_2 C_2 + \varepsilon_3 C_3 + \varepsilon_4 C_4) \tag{6}$$

The absorbance predicted on the basis of no reaction would be

$$A_p = L[\varepsilon_0 M(1 - x) + \varepsilon_w Mx] \tag{7}$$

If the extinction coefficient of B is assumed to be zero, as is usually the case, the absorbance of the solution containing the complexes is

$$A = L[\varepsilon_0 C_0 + \varepsilon_1 C_1 + \varepsilon_2 C_2 + \varepsilon_3 C_3 + \varepsilon_4 C_4] \tag{8}$$

while the absorbance predicted for no reaction is

$$A_p = L[\varepsilon_0 M(1 - x)] \tag{9}$$

The difference function, Y, is the difference between the measured and the predicted values of the absorbance, in this case:

$$Y = L[\varepsilon_0 C_0 + \varepsilon_1 C_1 + \varepsilon_2 C_2 + \varepsilon_3 C_3 + \varepsilon_4 C_4 - \varepsilon_0 M(1 - x)] \tag{10}$$

This is *identified with* the Y function defined by

$$Y = A_{\text{measured}} - A_p, \tag{11}$$

though this identification is valid only if the measured absorbance is defined *exactly* by an equation such as (8).

It is now necessary to examine the Y function to determine whether an extremum in Y occurs simultaneously with a maximum in the concentration of the complex, i.e.

whether $(dC_1/dx) = 0$ is a necessary and sufficient condition that $(dY/dx) = 0$ and $(d^2Y/dx^2) = 0$. Differentiation of Y (Equation 10) with respect to x gives

$$\left(\frac{dY}{dx}\right) = L\left[\varepsilon_0\left(\frac{dC_0}{dx}\right) + \varepsilon_1\left(\frac{dC_1}{dx}\right) + \varepsilon_2\left(\frac{dC_2}{dx}\right) + \varepsilon_3\left(\frac{dC_3}{dx}\right) + \varepsilon_4\left(\frac{dC_4}{dx}\right) + \varepsilon_0 M\right] \quad (12)$$

From Equation (11) one obtains (dC_0/dx) as

$$\left(\frac{dC_0}{dx}\right) = -M - \left(\frac{dC_1}{dx}\right) - \left(\frac{dC_2}{dx}\right) - \left(\frac{dC_3}{dx}\right) - \left(\frac{dC_4}{dx}\right) \quad (13)$$

Using this, (dY/dx) may be written as

$$\left(\frac{dY}{dx}\right) = L\left[(\varepsilon_1 - \varepsilon_0)\left(\frac{dC_1}{dx}\right) + (\varepsilon_2 - \varepsilon_0)\left(\frac{dC_2}{dx}\right) + (\varepsilon_3 - \varepsilon_0)\left(\frac{dC_3}{dx}\right) + (\varepsilon_4 - \varepsilon_0)\left(\frac{dC_4}{dx}\right)\right] \quad (14)$$

In general, the maximum or minimum values of Y will not coincide with maxima in C_1, C_2, C_3 or C_4, since (dY/dx) may be zero when none of the terms (dC_1/dx), (dC_2/dx), (dC_3/dx) or (dC_4/dx) are zero. The value of x at which (dY/dx) is zero may be expected to vary with the species present and therefore with the wavelength of the light used.

By choosing the wavelength carefully, it may be possible to have the maximum in Y correspond to the maximum in the concentration of a given complex. For example, if a maximum in the concentration of the AB complex is considered, it might be possible to choose the wavelength so that $\varepsilon_1 - \varepsilon_0 \neq 0$ while $\varepsilon_2 = \varepsilon_0$, $\varepsilon_3 = \varepsilon_0$, and $\varepsilon_4 = \varepsilon_0$. This would mean that $(dY/dx) = 0$ when $(dC_1/dx) = 0$ and $(d^2Y/dx^2) \neq 0$. Such a situation will arise if only the complex AB absorbs at the wavelength used. As can be seen, a similar restriction holds if Y extrema are to be related to maxima in the concentrations of the other complexes. For systems with five or six complexes, analogous restrictions must be met if extrema in Y are to coincide with maxima in the concentrations of the various complexes present. The general equation for (dY/dx), assuming that the extinction coefficient for B is zero is

$$(dY/dx) = L\sum_{i=1}^{N}(\varepsilon_i - \varepsilon_0)\left(\frac{dC_i}{dx}\right) \quad (15)$$

As can be seen, the conditions for simultaneous maxima in Y and one of the C_i's require conditions on the ε_i's of the same sort as those mentioned for the case with four complexes.

EXPERIMENTAL

In order to test the equations developed here, a study of the displacements in the Cu^{2+}–SCN^- system and the Cu^{2+}–Cl^- system was carried out. Stock solutions of cupric perchlorate, perchloric acid, hydrochloric acid, and sodium thiocyanate were prepared and standardized by analysis.(6) The solutions used in this work were prepared and kept in glass stoppered flasks in an air-conditioned room kept at approximately 25°. The solutions were allowed to equilibrate before the spectrophotometric measurements were made. The absorption spectra were obtained using a Cary Model 14 recording spectrophotometer.

The cupric–thiocyanate systems studied were of total molarity 0·01, 0·02, 0·03, 0·05 (all kept at an ionic strength of 0·2), 0·07 and 0·09 (of ionic strengths 0·25 and 0·30 respectively). The pH of all these solutions was kept below two. The cupric–chloride systems examined were of total molarity 0·010, 0·015, 0·030, 0·050, 0·20 (all of ionic strength 1), 0·50 (ionic strength of 2), 0·60 (ionic strength of 2·2), 0·80 (ionic strength of 2·5) and 1·00 M (ionic strength of 3·1). The ionic strengths of the solutions were maintained by the addition of the appropriate amounts of concentrated perchloric acid. In order to locate the maxima in the $x/(1-x)$ ratios more exactly, several solutions were prepared with fractional molar ratios of reactants between the whole number ratios 5/5 to 7/3. To determine the extinction coefficients of the Cu SCN$^+$ and the Cu(SCN)$_4^{2-}$ complexes, additional solutions were prepared. One of these contained 0·001 M sodium thiocyanate and 0·063 M cupric perchlorate and had an ionic strength of 0·20. It was assumed that the only complex present in this solution was Cu SCN$^+$. Another solution contained 0·001 M cupric perchlorate and 0·158 M sodium thiocyanate (also of ionic strength 0·20) and it was assumed that only the Cu (SCN)$_4^{2-}$ complex was present. By varying the concentrations of these species it was established that Beer's law was obeyed. The results of the continuous variations studies on the Cu^{2+} SCN$^-$ system are presented in Fig. 1; those for the

---

(6) W. J. BLAEDEL and V. W. MELOCHE, *Elementary Quantitative Analysis*, Row, Peterson and Co., Evanston, Ill. (1957).

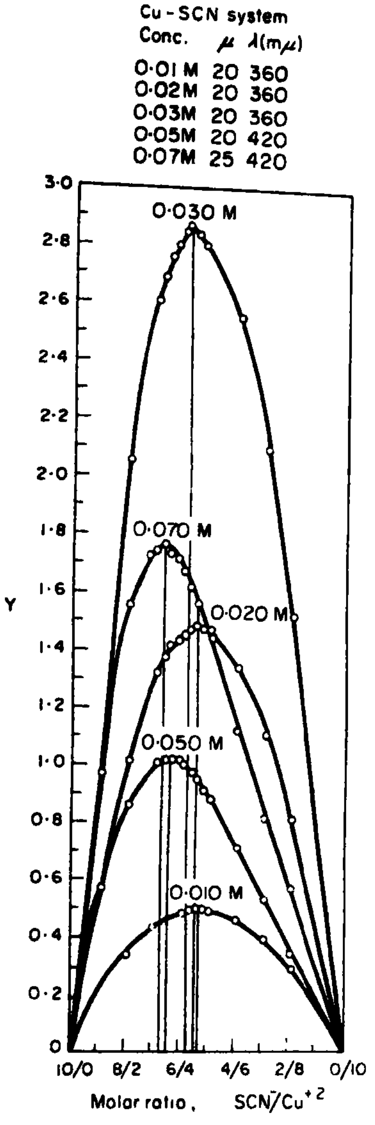

FIG. 1.—Continuous variations curves for the Cu^{2+}–SCN$^-$ system.

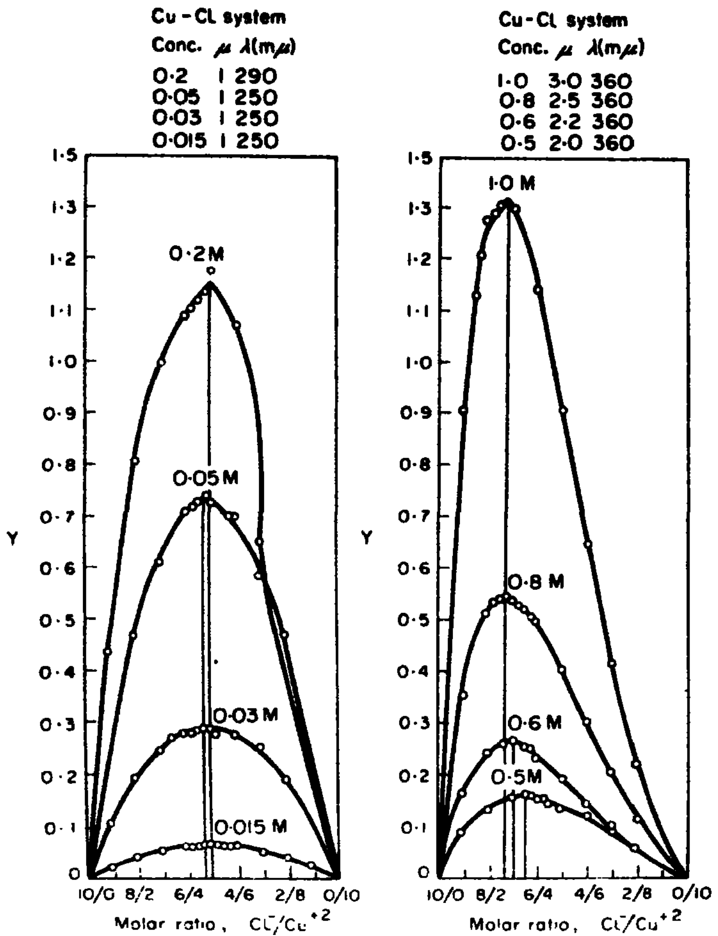

FIG. 2.—Continuous variations curves for the Cu^{2+}–Cl^- system.

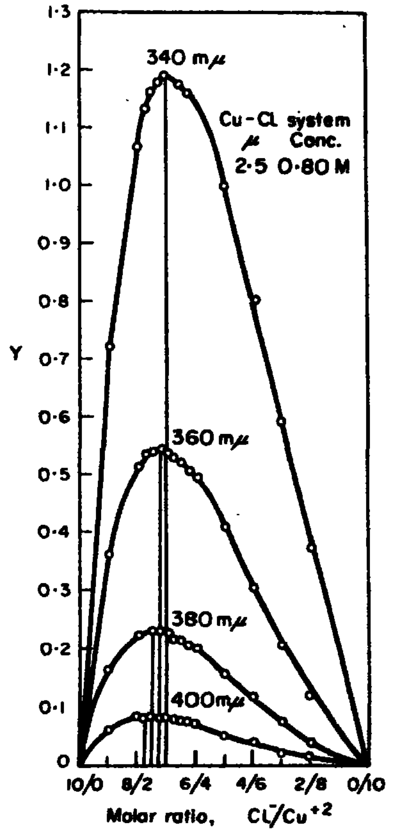

FIG. 3.—Continuous variations curves for the Cu^{2+}–Cl^- system at various wavelengths.

Cu^{2+}–Cl^- system are given in Figs 2 and 3. Fig. 2 gives the data obtained at various concentrations, while Fig. 3 shows the displacements of the Y function for the 0·8 M solutions at various wavelengths where it can easily be seen that the location of the maximum is dependent on the wavelength. For the Cu^{2+}–SCN^- system the measurements must be made soon after preparation of the solutions, especially with those of higher concentration, as precipitation of copper (I) thiocyanate(7) occurs on standing.

DISCUSSION

In order to test the equations developed to describe the displacements it is necessary to know the concentrations of the various complexes which are present in that solution in which one of them attains a maximum concentration. The equilibrium constants required for this may be obtained from the literature. For the Cu^{2+}–SCN^- system the constants reported by TANAKA and TAKAMURA(8) were used. Several spectrophotometric studies have been made on the Cu^{2+}–Cl^- system;(9–16) we have used the results of BJERRUM(9) in our calculations. For the Cu^{2+}–SCN^- system the variation in equilibrium constants with ionic strength has been calculated using the procedure given by VANDERZEE and DAWSON for the Cd^{2+}–halide systems.(17) From the equilibrium constants and the known total concentrations of Cu^{2+} and SCN^-, the concentrations of all the complexes were calculated by an iteration process. Once these were known it was possible to calculate the ratios $x/1 - x$ from equations of the type (1) through (5). In order to determine the exact point at which the concentration of the complex went through a maximum it was necessary to set up a slightly different difference function defined in such a manner that $Y_T = \varepsilon_i C_i$ for each complex AB_i. The extinction coefficients for each of the species present was calculated from a knowledge of the equilibrium constants for solutions of known composition and optical density. Then Y_T values were determined for the 1:1 complex from

$$Y_T = A_{\text{measured}} - L(\varepsilon_2 C_2 - \varepsilon_3 C_3 - \varepsilon_4 C_4) \tag{16}$$

and for the 1:2 complex

$$Y_T = A_{\text{measured}} - L(\varepsilon_1 C_1 - \varepsilon_3 C_3 - \varepsilon_4 C_4) \tag{17}$$

By working at a wavelength of 360 mμ, ε_0 and ε_w may be set equal to zero for the Cu^{2+}–SCN^- system. Several values of Y_T were determined numerically, and the x value at which a maximum occurred was found. The extinction coefficients of Cu SCN^+ and Cu $(SCN)_4{}^{2-}$ were obtained from measurements on solutions that contained an excess of metal ion or thiocyanate respectively. The extinction coefficients for $Cu(SCN)_2$ and $Cu(SCN)_3{}^-$ were obtained by solving two simultaneous equations of the type $A = \varepsilon_1 C_1 + \varepsilon_2 C_2 + \varepsilon_3 C_3 + \varepsilon_4 C_4$. The concentrations were calculated from the equilibrium constants and the A from the absorption spectra. The values obtained at 420 mμ, for example, were $\varepsilon_1 = 4{\cdot}50 \times 10$, $\varepsilon_2 = 3{\cdot}40 \times 10^2$, $\varepsilon_3 = 7{\cdot}76 \times 10^2$ and

---

(7) N. V. SIDGWICK, *The Chemical Elements and Their Compounds*, Vol. 1, page 149. Oxford (1950).
(8) N. TANAKA and T. TAKAMURA, *J. Inorg. Nucl. Chem.* **9**, 15 (1959).
(9) J. BJERRUM, *Kgl. Danske Videns. Sel. Mat. Fys. Medd.*, **22**, No. 18 (1946).
(10) H. MCCONNELL and N. DAVIDSON, *J. Amer. Chem. Soc.* **72**, 3164 (1950).
(11) R. NASANEN, *Acta Chem. Scand.* **4**, 140 (1950).
(12) R. NASANEN, *Suomen Kemistilehti* B **26**, 37 (1953).
(13) E. DOEHLEMANN and H. FROMHERZ, *Z. Phys. Chem.* A **171**, 353 (1934).
(14) E. V. KISELEVA, *Zhr. fiz. Khim* **27**, 443 (1953), *Chem. Abstr.* A **48**, 13363.
(15) R. KRUH, *J. Amer. Chem. Soc.* **76**, 4865 (1954).
(16) T. MOELLER, *J. Phys. Chem.* **48**, 111 (1944).
(17) C. E. VANDERZEE and H. J. DAWSON, *J. Amer. Chem. Soc.* **75**, 5659 (1953).

$\varepsilon_4 = 3{\cdot}00 \times 10^2$. The values at which Y_T reached a maxima are designated x_{max} (theor.) and are listed in Table 1 along with the values at which the other Y functions reach their maximum values. As can be seen from the table, the theoretical equation is in good accord with the actual x values at which the given complexes reach their maximum concentration (i.e. with the x_{max} derived from the Y defined by Equations (16) or (17). It can also be seen that the Y value customarily used, defined by Equation (11) may give a rather poor indication of what is going on in the system. A similar set of calculations comparing the experimental values at which Y defined by Equation (11) reaches a maximum and the values at which the various complexes in the Cu^{2+}–Cl^- system attain a maximum concentration is given in Table 2. The last column gives the values for x_{max} calculated from the known equilibrium constants for this system.

TABLE 1.—COMPARISON OF x_{max} VALUES FOR THE Cu^{2+}–SCN^- SYSTEM

M	μ	λ(mμ)	Complex assumed	x_{max} Y of eqn. (11)	x_{max} Y (eqn. (16 or 17)	x_{max} Theor. (eqn. 5)
0·01	0·2	360	$CuSCN^+$	0·525	0·525	0·498
0·03	0·2	360	$CuSCN^+$	0·575	0·525	0·498
0·03	0·2	360	$Cu(SCN)_2$	0·575	0·687	0·713
0·03	0·2	420	$Cu(SCN)_2$	0·625	0·700	0·713
0·07	0·25	420	$Cu(SCN)_2$	0·675	0·725	0·713

TABLE 2.—COMPARISON OF x_{max} VALUES FOR THE Cu^{2+}–Cl^- SYSTEM

M	μ	(mμ)	Complex assumed	x_{max} (eqn. 11)	x_{max} (eqn. 5)
0·015	1	250	$CuCl^+$	0·500	0·500
0·030	1	250	$CuCl^+$	0·525	0·500
0·050	1	250	$CuCl^+$	0·525	0·500
0·200	1	290	$CuCl^+$	0·500	0·499
0·500	2	360	$CuCl_2$	0·625	0·694
0·600	2·2	360	$CuCl_2$	0·700	0·698
0·800	2·5	340	$CuCl_2$	0·700	0·692
0·800	2·5	340	$CuCl_3^-$	0·700	0·787
0·800	2·5	360	$CuCl_2$	0·725	0·692
0·800	2·5	360	$CuCl_3^-$	0·725	0·787
0·800	2·5	380	$CuCl_2$	0·750	0·692
0·800	2·5	380	$CuCl_3^-$	0·750	0·787
0·800	2·5	400	$CuCl_3^-$	0·775	0·787
0·800	2·5	400	$CuCl_4^{2-}$	0·775	0·848
1·000	3·0	360	$CuCl_2$	0·750	0·705
1·000	3·0	360	$CuCl_3^-$	0·750	0·786
1·000	3·0	400	$CuCl_3^-$	0·775	0·786
1·000	3·0	400	$CuCl_4^{2-}$	0·775	0·856

It is apparent that one of the major sources of difficulty in the use of this method is the fact that the expression customarily used to obtain Y (Equation 11) is blind to the fine points of the chemical behaviour of these systems. This is a defect which becomes progressively worse as the stability of the complexes decreases. It is obvious that the disentangling of the various factors contributing to the customary Y function requires a knowledge of the various terms in an expression such as (10). These concentration terms can only be obtained if the stability constants are known! So, it must be concluded that in the *general case* it will be *impossible* to obtain detailed information on a system containing several successive complexes by the use of this method *alone*. In some special cases where the variation in the different ε's is especially propitious such information may be available and, of course, it will be available where only a single complex is present. Thus the method of continuous variations has as its principal limitation, not the inability to adequately describe these systems as is sometimes stated (3), but rather its requirement of more information for this purpose than it can furnish itself.

Two earlier studies are of interest in showing the requirements for the use of this method. SOMMER and HNILICKOVA(18) studied the displacements that occur when two ligands are competing for the same metal ion. They developed an equation to predict x_{max} values for systems of this type on the basis of a number of simplifying assumptions. The equation was tested on the systems: chromotropic acid–Ti(IV)–EDTA; SCN^-–Fe^{3+}–F^- and kojic acid–Fe^{3+}–F^-. They showed that the ratio found for the continuous variations curves was always greater than the theoretical ratio predicted from their equation. Thus for the second system mentioned, the x values found experimentally varied from 0·458 to 0·233 while their predicted values ranged from 0·397 to the obviously impossible value of —1·88. In this case these authors have neglected the detailed nature of the Y function in their calculations as well as the role of associated protonic equilibria. They also assumed that only one or two complexes were present. Where these assumptions were valid the agreement between their theory and their experimental results was quite satisfactory.

Another example for which our results provide a basis for the rationalization of previously reported data may be seen in the Bi^{3+}–Cl^- system. NEWMAN and HUME studied this system by several methods,(19) including the method of continuous variations. They attempted to use this method to predict the stoichiometry of the higher complexes, but decided that it was unsuitable for this because the maximum in the Y function shifted and appeared to be not well defined. If their data is examined in the light of the equations developed here, an explanation for these displacements can be given. Their Y function defined by Equation (11) passed through maxima for various concentrations at x values corresponding to a range of complexes from $BiCl_5^{2-}$ to $BiCl_8^{5-}$, though other spectrophotomeric evidence indicated no complexes higher then $BiCl_5^{2-}$. We have taken their equilibrium constants and that for $BiCl_6^{3-}$ from the work of AHRLAND and GRENTHE(20) and calculated x_{max} values from the theoretical equations developed here. The x_{max} values calculated in this manner by assuming a maximum in $BiCl_4^-$, $BiCl_5^{2-}$ and $BiCl_6^{3-}$ are 0·768, 0·905 and 1·00 respectively. The theoretical value in best agreement with the experimental data is 0·905, indicating a maximum in the concentration of $BiCl_5^{2-}$ for their systems. From the raw Y function complexes higher than this might erroneously be expected.

Thus, it has been demonstrated that the interpretation of the difference curves obtained by the method of continuous variations may be carried to completion if sufficient information is available on the systems studied. It has also been shown that the usual Y function may lead to false conclusion about the stoichiometry of the complexes and consequently yield a meaningless equilibrium constant. This method is not capable of furnishing all the information required by itself, but must rely to some extent on data obtained using other methods.

---

(18) L. SOMMER and M. M. HNILICKOVA, *Bull. Soc. Chim. France* 36 (1959).

(19) L. NEWMAN and D. HUME, *J. Amer. Chem. Soc.* 79, 4576 (1957).

(20) S. AHRLAND and I. GRENTHE, *Acta Chem. Scand.* 11, 1111 (1957).

Acknowledgements—We wish to thank Dr. M. GINTER for his considerable assistance in recasting the general equation into its present abbreviated form. This work has been supported by grants from the Research Corporation and the National Science Foundation, for which we wish to express our sincere gratitude.

J. Inorg. Nucl. Chem., 1962, Vol. 24, pp. 1617 to 1621. Pergamon Press Ltd. Printed in Northern Ireland

KINETICS OF REACTION BETWEEN PLUTONIUM(III) AND CHLORINE IN CHLORIDE SOLUTIONS

A. S. Ghosh Mazumdar, K. P. R. Pisharody and R. N. Singh
Radiochemistry and Isotope Division Atomic Energy Establishment Trombay, Bombay

Abstract—Oxidation of plutonium(III) to (IV) by chlorine has been shown to follow an apparently first order rate law, with respect to both the reactants, when other conditions are constant. The rate was independent of acidity, but markedly dependent on the chloride ion concentration, and this dependence has been shown to be due to a specific effect of chloride ions rather than to a general effect of anions or ionic strength.

The oxidation of plutonium(III) to (IV) by chlorine is reported to be slow in 0·5 M hydrochloric acid, being only about 10 per cent in 5 hr.(1) The kinetics of this oxidation, which were observed to be markedly dependent upon the chloride ion concentration of the medium, have been studied, since apart from the interest concerning the mechanism of the reaction, data were required for some current work on the radiolytic oxidation of plutonium(III) in which chlorine is a possible intermediate.

Stoicheiometry of the oxidation

Excess chlorine was found to oxidize plutonium(III) at first to plutonium(IV) in hydrochloric acid. When the acid concentration was less than 3·5 M, the plutonium(IV), thus formed in a few hours, was then oxidized slowly to plutonium(VI); but no plutonium(VI) was formed in higher acidities (e.g. at 5·4 M) even when the reaction was allowed to proceed overnight. In the higher acid solutions the decrease in plutonium(III) concentration was found to be practically quantitative according to the reaction, $\mathrm{Pu(III)} + \tfrac{1}{2}\mathrm{Cl_2} \rightarrow \mathrm{Pu(IV)} + \mathrm{Cl^-}$ when the chlorine added varied between 0·012 to 0·12 mole/mole of plutonium.

Order of the reaction

The rate of reaction was measured at several hydrochloric acid concentrations. The linearity of the graphs of log plutonium(III) concentration against time (Fig. 1) indicates that at a given hydrochloric acid concentration, oxidation followed an apparently first order rate law with respect to both reactants. This was confirmed by calculating rate constant values to orders of 1·5 and 2. Although these graphs were linear the slopes of the lines were markedly dependent upon the hydrochloric acid concentration.

Effect of hydrogen ion concentration

Separate series of experiments were carried out in which the chloride concentration was maintained constant by addition of lithium or potassium chlorides to varying hydrochloric acid concentrations. The apparent specific reaction rate (k') was found

---

(1) R. E. Connick and W. H. McVey, *The Transuranium Elements*, paper 3.10, NNES, McGraw-Hill, New York (1949)

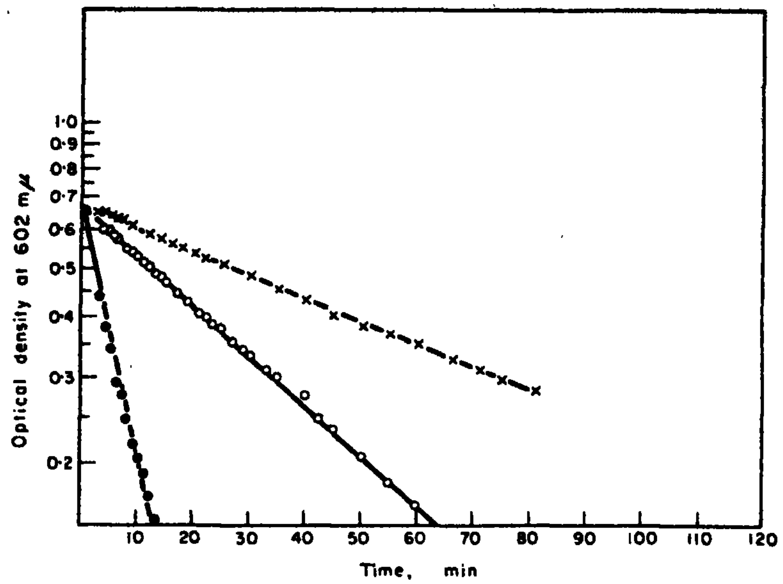

Fig. 1.—Rate of oxidation of Pu(III) by chlorine. Concentration of Pu(III): $1·67 \times 10^{-2}$ M; concentration of chlorine: $2·8 \times 10^{-2}$ N; concentration of HCl: × 3·0 M, O 4·5 M, ● 6·0 M.

not to depend significantly upon acidity when total chloride ion concentration was constant. Some typical data are shown below:

Total chloride ion (LiCl + HCl) conc. (M)	Range of varying HCl conc. (M)	Initial conc. of Pu(III) ($M \times 10^2$)	Initial conc. of chlorine ($M \times 10^2$)	$k'(\times 10^2$ min$^{-1})$
6·0	3·02 and 6·00	1·38	3·43	5·1
4·5	2·95 and 4·50	1·28	3·55	1·1

Effect of initial chlorine and of total plutonium concentration

Despite the first order rate dependence, k' increased gradually with the initial chlorine concentration and finally tended towards a constant value for a given plutonium concentration. This constant value was found to increase with increase in plutonium concentration in the range 0·002–0·02 M. k' values obtained in 3·04 M hydrochloric acid are shown in Fig. 2. At other hydrochloric acid concentrations also similar effect of initial chlorine concentration was observed.

Effect of chloride ion concentration

The rate of reaction was found to increase with increased concentrations of chloride ion. The variation of k' with chloride ion concentration at 0·01 M plutonium and about 0·02 M chlorine concentrations is shown in Fig. 3. k' increased from 0·5 to 0·9 10^{-2} min^{-1} and then rapidly to 27×10^{-2} min^{-1}, as the chloride ion concentration was increased from 1 to 4 M and then to 8 M respectively.

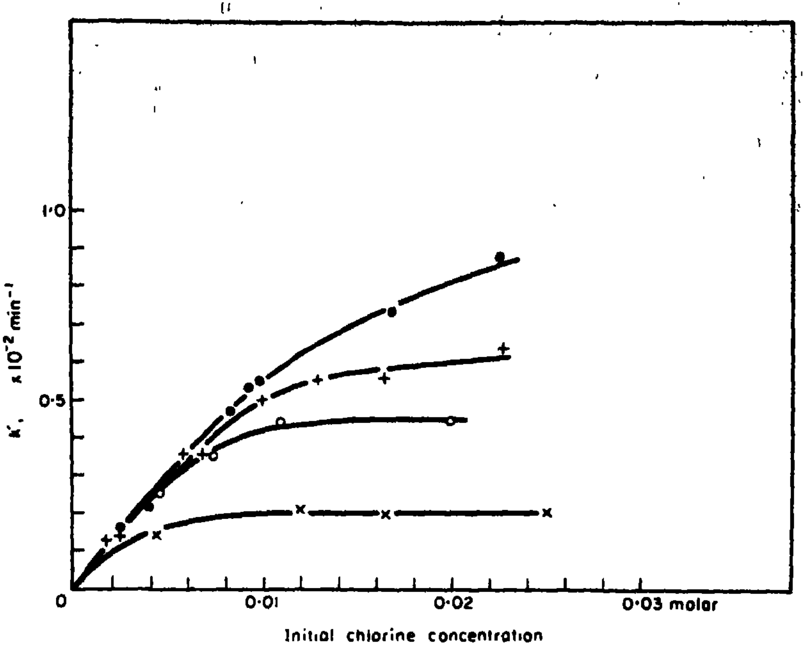

FIG. 2.—Variation of k' with initial concentration of chlorine at different initial concentrations of Pu(III); HCl concentration = 3·04 M; ● initial Pu(III) concentration 0·02 M; + initial Pu(III) concentration 0·01 M; ○ initial Pu(III) concentration 0·005 M; × initial Pu(III) concentration 0·002 M.

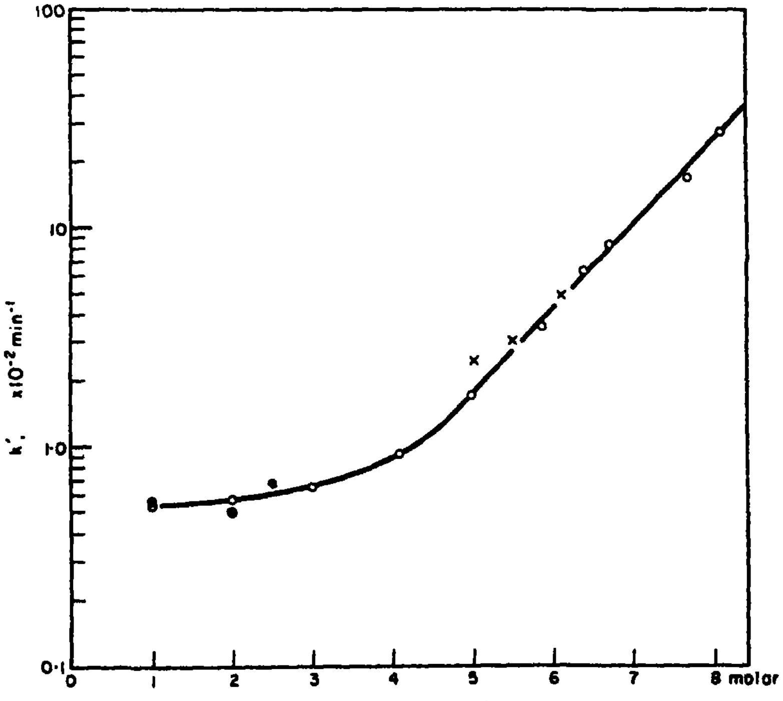

FIG. 3.—Variation of k' values with chloride ion concentration. ○ in hydrochloric acid; ● in hydrochloric-perchloric acid mixture, total anion concentration 3·0 M; × in hydrochloric-perchloric acid mixture, total anion concentration 6·5 M.

Rate in perchloric acid and in perchloric–hydrochloric acid mixtures

In perchloric acid alone, varying from 3·0 to 7·5 M, k' remained almost constant at 0·1 × 10^{-2} min.$^{-1}$. In acid mixtures, when the chloride ion concentration was varied at constant total anion concentration, variation of k' was of the same order of magnitude as in perchlorate-free medium (Fig. 3). Lastly, the variation in k' with total anion concentration and at a fixed chloride ion concentration was very slight as shown below:–

Range of total anion conc. (M)	Chloride ion conc. (M)	Observed variation in k' (× 10^2 min^{-1})
3·05 and 7·35	0·2	Almost constant at 0·2
4·0 and 6·1	4·0	0·8–1·1
5·1 and 6·1	5·1	1·3–1·5

Therefore, the observed rapid rise in k' with chloride ion concentration is mainly due to a specific effect of chloride ions rather than to any ionic strength influence or a general anion effect, contributed by these ions, on reaction rates.(2)

Halide ions facilitate kinetically many oxidation reduction reactions, electrochemical(3) as well as thermal.(4) Complexing could establish a new reaction path to accelerate the overall process of electron transfer since both plutonium(III) and (IV) ions are known to form chloride complexes.(5,6) The plutonium is probably oxidized by Cl_2^- ions which are known to form rapidly from chlorine and chloride ions,(7) thus qualitatively explaining the independence of the rate on acidity. Further work is proceeding.

EXPERIMENTAL

For the purification of plutonium, two procedures were followed. In one, anion exchange resin Dowex 1 × 4 was used. In the other, which excludes the possibility of any trace contamination with organic matter, fluoride precipitation method was adopted, following an oxidation reduction cycle.(8) The plutonium fluoride thus obtained was repeatedly heated with nitric acid to convert it to the nitrate form. In both cases, from the solution obtained, plutonium was precipitated twice as hydroxide and finally dissolved in hydrochloric acid. Trivalent plutonium was obtained by cathodic reduction, and was estimated by microtitration with ceric sulphate(9). Acidity was measured by micro-alkalimetry. For iodometric assay of dissolved chlorine in solutions, the gas was swept out with nitrogen into a series of potassium iodide solutions.

Laboratory reagent grade lithium chloride was purified by recrystallization. All other reagents used were of G.R. or AnalaR quality.

(2) V. K. La Mer, *Chem. Rev.* **10**, 179 (1932); R. Livingston, *J. Chem. Educ.* (Canada) 7, 2287 (1930); A. R. Olson and T. R. Simonson, *J. Chem. Phys.* **17**, 1167 (1949); R. L. Moore, *J. Am. Chem. Soc.* **77**, 1504 (1955).

(3) For bibliography see for example E. H. Lyons, *J. Electrochem. Soc.* **101**, 363 (1954); and A. S. Ghosh Mazumdar and M. Haissinsky, *J. Chim. Phys.* **53**, 979 (1956).

(4) For bibliography see for example B. J. Zwolinski, R. J. Marcus, and H. Eyring, *Chem. Rev.* **55**, 157 (1955); and H. Taube, *Advances in Inorg. Chem. and Radiochem.*, **1**, 1 (1959).

(5) M. Ward and G. A. Welch, *J. Inorg. Nucl. Chem.* **2**, 395 (1956).

(6) J. C. Hindman, "The Transuranium Elements", NNES, paper 4.7, McGraw-Hill (1949).

(7) F. A. Long and A. R. Olson, *J. Amer. Chem. Soc.* **58**, 2214 (1936); N. V. Sidgwick, *The Chemical Elements and Their Compounds*, Vol 2, p. 1167. Oxford (1932).

(8) G. T. Seaborg, A. C. Wahl, *The Transuranium Elements* NNES paper 1.6, McGraw-Hill, (1949); B. B. Cunningham and L. B. Werner, *ibid.* paper 1.8.

(9) C. W. Koch, *The Transuranium Elements*, NNES paper 17.4, McGraw-Hill (1949); P. V. Balakrishnan, A. S. Ghosh Mazumdar and R. N. Singh, AEET Report No. AEET/Radiochem/30. (1962).

Reaction rates were measured in the stoppered absorption cells of a Beckman DU Spectrophotometer. In a typical experiment, a measured volume of a solution of chlorine in hydrochloric acid was added by means of a pipette below the surface of a solution containing a known amount of plutonium (III) in an absorption cell, which was then stoppered and shaken to mix the reactants. No evolution of gas bubbles was noticed in these experiments which were performed at the laboratory temperature, conditioned to 25° ± 2°C. The time of start of the reaction was reckoned from the middle of the operation of adding chlorine and the progress of oxidation was followed by measuring the absorption due to plutonium(III) at 602 mμ.

Acknowledgement—The authors wish to express their gratitude to Dr. G. A. WELCH, Head of the Radiochemistry and Isotope Division for his interest in the work and valuable suggestions.

J. Inorg. Nucl. Chem., 1962, Vol. 24, pp. 1623 to 1633. Pergamon Press Ltd. Printed in Northern Ireland

THE CHEMISTRY OF PROTACTINIUM—VI

THE POLAROGRAPHY OF PROTACTINIUM†

C. FERRIERA DE MIRANDA* and A. G. MADDOCK
The University Chemical Laboratories, Cambridge

(*Received* 21 *August* 1961; *in revised form* 4 *June* 1962)

Abstract—Irreversible polarographic waves are observed in oxalate, citrate, sulphate and fluoride solutions of protactinium. Fluoride solutions show two waves, at −1·29 and −1·56 V vs. S.C.E., for a fluoride concentration of 3·8 M. The first wave can be attributed to the reduction of the fluoro complex of Pa(V) to the corresponding complex of Pa(IV). The second wave may be due to the reduction of Pa(IV) → Pa(III). Polarograms in oxalate and sulphate solutions give less meaningful results.

Most of the data that have so far been accumulated on the electrochemistry of protactinium have been obtained by HAISSINSKY, BOUISSIÈRES and FERRADINI, and their collaborators, working in the Institut du Radium, Paris. A concise summary of this information, together with full references, have been published by one of the above investigators(1) and no further work has been reported since this review. A large part of the work concerned deposition reactions, spontaneous, cathodic and anodic, at different metal electrodes.

The difficulty attending most of these studies was the certain identification of the electrode reactions involved. It is well known that protactinium compounds are generally very susceptible to hydrolysis. In fluoride solutions, where hydrolysis of the pentavalent state can be avoided, the tetravalent state forms an insoluble salt. Since the chemical identity of the deposits have not been thoroughly established, nor is there, in general, information on the reversibility of the electrode processes, the above chemical properties of the element indicate some of the uncertainties in deducing the electrode reactions involved. In the most recent and detailed of these studies FERRADINI(2) explored a cathodic deposition process with a standard electrode potential of −1·03 V. Her value for the coefficient in the Nernst equation led her to associate this potential with deposition of the metal, i.e. to refer it to the Pa/PaF_7^{2-} couple. As far as the Pa(V)/Pa(IV) potential is concerned no direct measurements have been reported.

Polarographic techniques have not been applied extensively in the study of this problem. GUÉRON and LEVÊQUE(3) were unable to find waves in fluoride or sulphate solutions. ELSON(4) was more successful in oxalate solutions. Working with solutions $0{\cdot}5 \times 10^{-3}$ to $2{\cdot}5 \times 10^{-3}$M in protactinium and 0·1–1·5M in oxalate, he obtained two waves, both irreversible. Rather arbitrarily he attributed the first to the reduction Pa(V) → Pa(IV) and the more negative to Pa(IV) → Pa(III). Surprisingly, on this interpretation, the first wave was independent of the hydrogen ion concentration, whereas the secondwave was not. The second wave, moreover, was almost superimposed on the oxalate ion reduction wave. No detailed account of this investigation has yet appeared.

---

* Present address: Laboratorio de Radioquimica, Faculdade de Ciencias, R. Escola Politechnica, Lisbon, Portugal.

† Presented, in part, at the XVIIth International Congress of Pure and Applied Chemistry, Munich, 1959.

(1) M. HAISSINSKY and G. BOUISSIÈRES, Protactinium section in *Nouveau traite de chimie minerale* (Edited by P. Pascal). Masson, Paris (1958).

(2) C. FERRADINI, *J. Chim. Phys.* **53**, 714 (1956).

(3) See M. HAISSINSKY and G. BOUISSIÈRES, *Bull. Soc. Chim. France* **18**, 146 (1951).

(4) R. E. ELSON, *Protactinium section, The Actinide Elements* (Edited by J. J. KATZ and G. T. SEABORG.) Chap. 5. N. N. E. S., Div. IV. Vol. 14A. McGraw-Hill, New York (1954).

EXPERIMENTAL

1. *Materials*

The protactinium-231, used throughout this work, was obtained from the pilot extraction and purification plant set up in this Laboratory.(5) Additional purification on the bench scale was accomplished by nine cycles of solvent extraction with di-isobutyl ketone (DIBK). The use of anhydrous aluminium chloride for complexing the fluoride ion prior to the extraction of the protactinium from 8M HCl + 0·5 M HF solution was avoided in the last two cycles, since some aluminium is bound to follow the protactinium in the extraction. Thus, ammonia was added to the aqueous phase, and the resulting precipitate was repeatedly treated with 8 M HCl until all the protactinium passed into solution. The protactinium was then extracted with DIBK, back-extracted with 8 M HCl + 0·5 M HF, and the process repeated. The organic phase was washed with 8 M HCl before each back-extraction from the third cycle onwards, in order to enhance the separation from zirconium and uranium. The *product of the solvent extraction treatment was further purified by ion exchange. The protactinium* was adsorbed from 8 M HCl solution onto a column of Amberlite IRA-400. The column was washed with 7 M HCl (elimination of zirconium,(6,7)) and the protactinium eluted with 10 column volumes of 9 M HCl + 0·1 M HF (separation from uranium, niobium, tantalum and iron).(8,9) Finally, the protactinium was precipitated as the peroxide and then as potassium fluoroprotactinate.(10)

Analytical grade reagents were employed throughout the work, but for the first few cycles of solvent extraction. DIBK, available as a technical grade reagent only, was washed with 8 M HCl before use. Ordinary distilled water proved suitable for the preparation of solutions. Platinum and polythene ware were used for some manipulations, and the fluoride solutions did not come into contact with glass except in the polarographic cell.

2. *Preparation of the solutions*

Fluoride solutions. Ammonium fluoride was chosen as a support electrolyte, since protactinium shows limited solubility in potassium fluoride and sodium fluoride solutions, which would be otherwise more convenient. Ammonium fluoride solutions of satisfactory purity were prepared by neutralizing hydrofluoric acid with ammonia to pH 7·2; fluoride was subsequently determined as lead chlorofluoride. Tetramethylammonium fluoride, prepared from a satisfactorily purified bromide, was also tried as a support electrolyte. However, it proved unsuitable owing to the difficulty experienced in obtaining solutions with lower residual currents than those given by ammonium fluoride.

For obtaining each polarogram, a convenient aliquot of a hydrofluoric acid stock solution of protactinium was taken and freeze dried. The residue was easily dissolved in 2 ml of the ammonium fluoride support electrolyte. The resulting solution was transferred to the polarographic cell, where 0·01 ml of a 2 per cent, freshly prepared gelatin solution was added. A polarogram was finally recorded, after complete de-aeration of the contents of the cell.

Sulphate solutions. Ammonium sulphate plus sulphuric acid solutions were used as support electrolyte. Protactinium was brought into solution in these media by three different techniques: (i), solid protactinium fluoride, obtained as described above, was directly dissolved in the base electrolyte: (ii), protactinium was extracted from 8 M HCl into DIBK, and back extracted into the sulphate solution; (iii), protactinium "carbonate" was precipitated from a hydrofluoric acid solution with ammonium carbonate, and the precipitate dissolved in the sulphate solution. In every case, gelatine was added as a maximum suppressor, and the samples de-aerated before registering the polarograms.

(5) A. G. Goble, J. Golden, A. G. Maddock and D. J. Toms, *Progress in Nuclear Energy, Series* III, *Process Chemistry*, Vol. 2, p. 86. Pergamon, London (1958).

(6) A. G. Maddock and W. Pugh, *J. Inorg. Nucl. Chem.* **2**, 114 (1956).

(7) S. Kahn and D. E. Hawkinson, *J. Inorg. Nucl. Chem.* **3**, 155 (1956).

(8) K. A. Kraus and G. E. Moore, *J. Amer. Chem. Soc.* **73**, 2900 (1951).

(9) K. A. Kraus, G. E. Moore and F. Nelson, *J. Amer. Chem. Soc.* **78**, 2692 (1956).

(10) J. S. Nairn, D. A. Collins, H. A. C. McKay and A. G. Maddock, *The Proceedings of the Second International Conference on Peaceful Uses of Atomic Energy, Geneva*, 1958, A/Conf. 15/1458 United Nations (1958).

Citrate solutions. These were obtained by dissolving protactinium "carbonate" in citric acid plus sodium citrate solutions.

Oxalate solutions. A stock solution of protactinium hydrated oxide in oxalic acid was prepared; convenient aliquots were taken and added to aqueous potassium oxalate.

The protactinium content of the solutions was determined after each polarogram had been recorded. In the case of fluoride solutions, two 0·01 ml aliquots were taken on platinum trays, evaporated to dryness, and gently ignited. Each sample was counted to within a standard deviation of 1 per cent in an α-scintillation counter whose geometry was established by means of a ^{241}Am standard. The deviation between the samples never exceeded 2 per cent. Thus, relative protactinium concentrations could be estimated with an accuracy of ~1 per cent. A half-life of $3 \cdot 43 \times 10^4$ years[11] was taken for the calculations. No self-absorption correction was needed, as the samples were virtually weightless. Solutions, other than the fluorides, which would not give weightless samples, were gamma assayed in a well type gamma scintillation counter. The activity at the half-width of the 0·3 MeV peak was compared with that of a protactinium source which was standardized by α-counting. The accuracy of this procedure was comparable to that achieved with the fluoride solution.

3. *Polarometer*

A home-made polarometer was employed. The applied e.m.f. could be read to 0·1 mV, and the current measured to within 0·5 per cent at mid-scale deflexion of the galvanometer. An auxiliary circuit provided for absolute calibration of the galvanometer sensitivity.

The dropping electrode was fashioned after SKOBETS and KAVETSKII,[12] having a glass "hoe" attached to its tip in order to improve regularity of dropping. The behaviour of this modified dropping electrode was tested with a cadmium solution. The half-wave potential and the diffusion current constant were found in good agreement with those reported in the literature. A saturated calomel electrode was used as anode. The connection between the cell and the S.C.E. was made via a bridge filled with the support electrolyte in the cell, stoppered with potassium chloride saturated agar–agar at the S.C.E. end. The resistance of the cell was such as to render negligible any correction due to an ohmic voltage drop across the cell.

The temperature of the sample under investigation was kept at 25 ± 0·2°C. De-aeration was effected by means of oxygen-free nitrogen, pre-saturated with the vapour of a blank matching the solution in the cell.

RESULTS

1. *Fluoride solutions*

(a) *Polarograms at constant ammonium fluoride concentration.* Polarograms were recorded under the following conditions: concentration of fluoride, 3·84 M; pH, 7·2; protactinium concentration, $2 \cdot 3$–$9 \cdot 5 \times 10^{-4}$ M.

Two waves are seen on the polarograms (Fig. 1). The height of the first wave is proportional to the concentration of protactinium within the range investigated. On the contrary, the height of the second step does not follow a similar law (Fig. 2).

It is seen in Fig. 3 that the plot of $\log i/(i_d - i)$ against $-E$ for the first wave approaches a straight line at each concentration of protactinium. All the plots give $E_{\frac{1}{2}} = -1 \cdot 29$ V. The slope increases with decreasing protactinium concentration, and tends to the theoretical value for a one-electron reduction. Though at the lowest concentration of $2 \cdot 3 \times 10^{-4}$ M the data are less accurate and the points more scattered than at higher concentration, the above trend is maintained. The diffusion coefficient of the fluoro-protactinate ion was calculated from the limiting diffusion current data by means of the Ilkovic equation and found equal to $(0 \cdot 71 \pm 0 \cdot 03) \times 10^{-5}$ cm^2 sec^{-1}, assuming a one-electron reduction.

The plot $\log i/(i_d - i) = f(-E)$ for the second wave also approaches a straight line whose slope is smaller than that corresponding to a one-electron reduction. Because this wave is smaller than the first one, the data are necessarily less accurate, and it is difficult to follow the trend of the slope down to the lowest protactinium

[11] Q. V. WINKLE, R. G. LARSON and L. I. KATZIN, *J. Amer. Chem. Soc.*, **71**, 2585 (1949).

[12] E. M. SKOBETS and N. S. KAVETSKII, *Savodskaya Lab.* **15**, 1299 (1949).

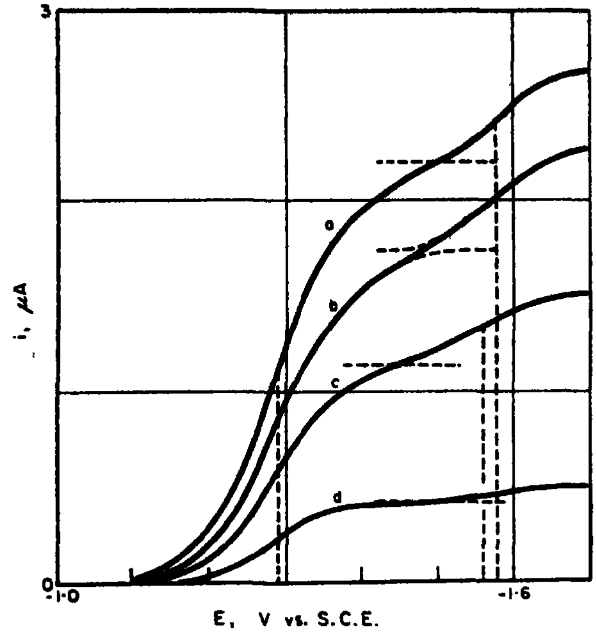

Fig. 1.—Polarograms of protactinium at constant ammonium fluoride concentration (3·84 M). Protactinium concentrations: *a*, $9{\cdot}4 \times 10^{-4}$ M; *b*, $7{\cdot}8 \times 10^{-4}$ M; *c*, $4{\cdot}9 \times 10^{-4}$ M; *d*, $2{\cdot}3 \times 10^{-4}$ M.

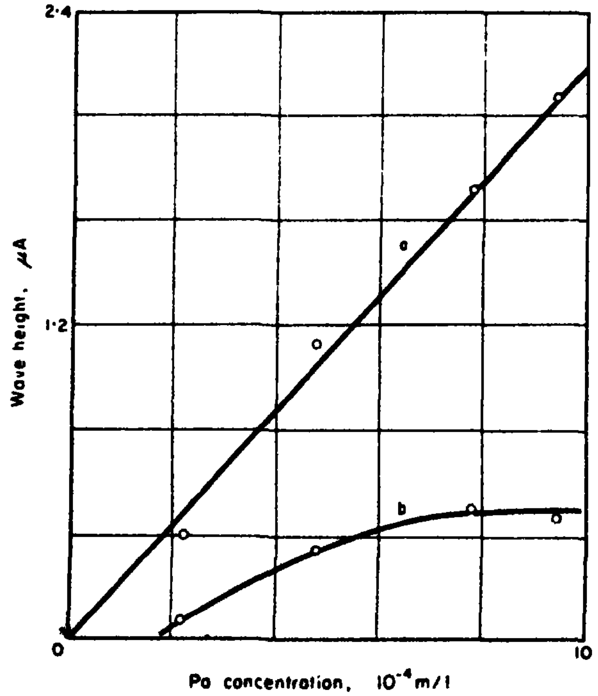

Fig. 2.—Dependence of the wave heights on protactinium concentration, in 3·84 M ammonium fluoride. *a*, first wave, $E_{\frac{1}{2}} = -1{\cdot}29$ V; *b*, second wave, $E_{\frac{1}{2}} = -1{\cdot}57$ V.

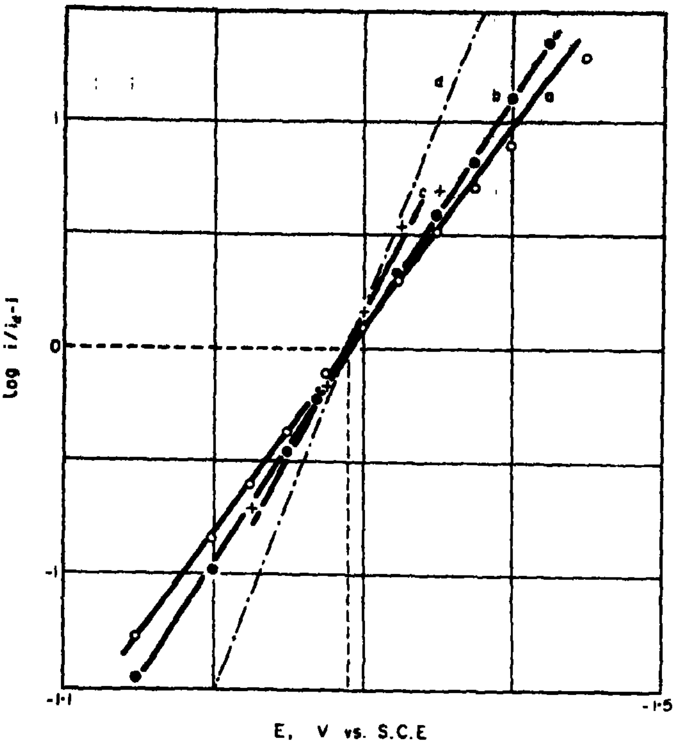

Fig. 3.—Reversibility test for the protactinium first wave in 3·84 M ammonium fluoride. *a*, $C_{Pa} = 9·4 \times 10^{-4}$ M; *b*, $C_{Pa} = 4·9 \times 10^{-4}$ M; *c*, $C_{Pa} = 2·3 \times 10^{-4}$ M; *d*, theoretical line for a one electron reduction with $E_{\frac{1}{2}} = -1·29$ V.

concentration. The half-wave potential determined from these plots varies between −1·58 and −1·56 V.

(b) *Polarograms at different concentrations of ammonium fluoride.* The effect of fluoride concentration on protactinium half-wave potentials was investigated in ammonium fluoride solutions of pH 7·2 and fluoride concentrations ranging from 1·02 to 7·94 M. The concentration of protactinium was kept between 5·9 and 7·8 × 10^{-4} M.

One or two waves are observed, depending on the fluoride concentration (Fig. 4). With fluoride concentration below 2 M, the second wave is either absent or, more likely, it is shifted to very negative potentials where satisfactory measurements cannot be carried out owing to the interfering reduction of NH_4^+. In 7·94 M ammonium fluoride the second wave can be observed; however, because the residual current of the support electrolyte decreased with time, it was difficult to register the wave accurately beyond −1·6 V. The half-wave potentials become more negative for both steps with decreasing fluoride concentration, this being the reverse of the expected behaviour (Table 1).

Table 1

Fluoride concentration (M)	$E_{\frac{1}{2}}$, first wave (V)	$E_{\frac{1}{2}}$, second wave (V)
1·02	−1·43	< −1·7
1·97	−1·36	< −1·7
3·84	−1·29	−1·57
7·94	−1·25	−1·54

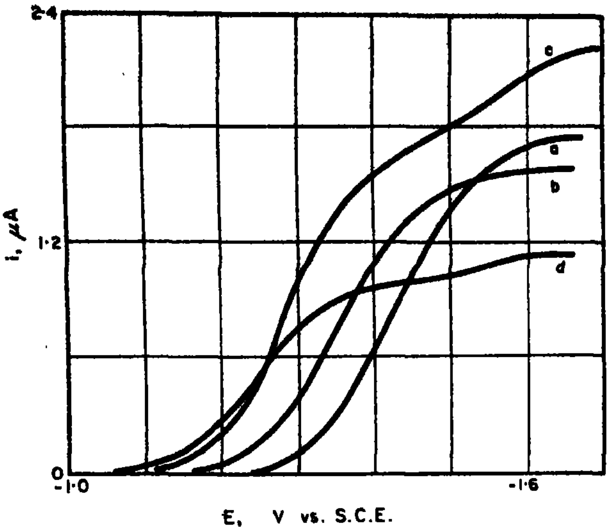

Fig. 4.—Polarograms of protactinium at different ammonium fluoride concentrations. *a*, 1·02 M ammonium fluoride, 7·1 × 10^{-4} M protactinium; *b*, 1·97 M ammonium fluoride, 7·0 × 10^{-4} M protactinium; *c*, 3·84 M ammonium fluoride, 7·8 × 10^{-4} M protactinium; *d*, 7·94 M ammonium fluoride, 5·9 × 10^{-4} M Pa.

(c) *Polarograms of protactinium in other fluoride media.* Attempts were made to record polarograms of protactinium in neutral fluoride. It was found, however, that sodium fluoro-protactinate has a rather limited solubility in neutral 1 M sodium fluoride ($\sim 10^{-4}$ M) and that the protactinium steps, though present, are accordingly too small.

Weakly acid ammonium fluoride solutions of protactinium were also investigated. No waves could be detected owing to the erratic behaviour of the dropping electrode under such conditions.

2. *Sulphate solutions*

(a) *Solutions prepared from the fluoride.* Polarograms were recorded for solutions of protactinium fluoride in the following support electrolytes: 3 M $(NH_4)_2SO_4$ + 10^{-2} M H_2SO_4; 1·5 M $(NH_4)_2SO_4$ + 10^{-2} M H_2SO_4; 3 M $(NH_4)_2SO_4$ + 1 M H_2SO_4. The polarograms (Fig. 5) show a well-defined wave whose half-wave potential is −0·97 V in the first support electrolyte, −0·94 V in the second, and −0·45 V in the third. All the polarograms suggest the presence of a second wave which cannot be plotted, however, due to the superposition of the hydrogen wave. The waves are irreversible. As can be anticipated, the half-wave potential is shifted to more negative values with higher sulphate concentrations, and with decreasing acidity.

(b) *Solutions prepared by solvent extraction.* Although partial precipitation occurred when protactinium was extracted from DIBK into 1·5 M $(NH_4)_2SO_4$ + 10^{-2} M H_2SO_4, a considerable amount of protactinium passed into the aqueous phase, yielding a 2·5 × 10^{-3} M solution. As the acidity of this solution was not easily controlled, the residual current of a support electrolyte blank treated in the same manner was not reproducible. It was impossible therefore to plot accurately the protactinium step(s).

(c) *Solutions prepared from the carbonate.* Solutions prepared by dissolving protactinium "carbonate" in the support electrolyte have the advantage of being free

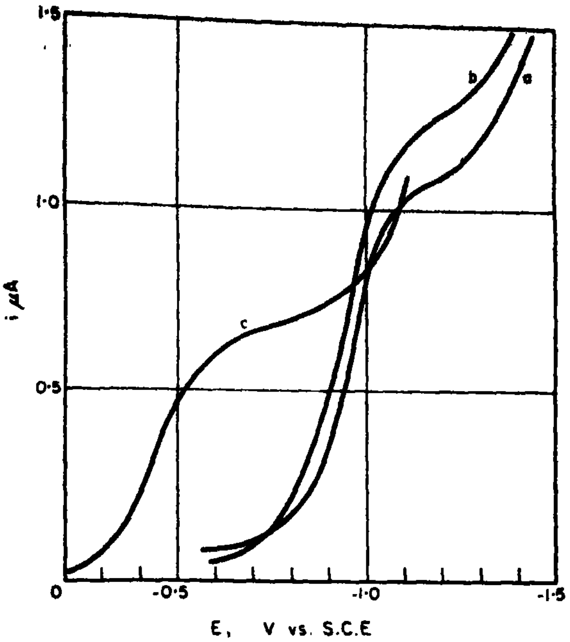

FIG. 5.—Polarograms of protactinium in sulphate solution. Solutions prepared from the fluoride. *a*, 3 M ammonium sulphate, 10^{-3} M sulphuric acid; $C_{Pa} = 5{\cdot}6 \times 10^{-4}$ M. *b*, 1·5 M ammonium sulphate, 10^{-3} M sulphuric acid; $C_{Pa} = 6{\cdot}0 \times 10^{-4}$ M. *c*, 3 M ammonium sulphate, 1 M sulphuric acid; $C_{Pa} = 5{\cdot}0 \times 10^{-4}$ M.

from fluoride or any anions other than the sulphate. Ammonium sulphate 1·5 M plus 0·3 M sulphuric acid was used as base electrolyte; solutions of lower H_2SO_4 concentrations were not employed as the acidity might be significantly changed when the carbonate was dissolved.

Two waves were observed, at −0·6 and −1·19 V (Fig. 6). The first small wave may be attributed to the same species as obtained upon dissolving protactinium fluoride in 1·5 M $(NH_4)_2SO_4$ + 0·3 M H_2SO_4 (*cf.* (a) above). The second wave is likely to correspond to the reduction of another species, more extensively hydrolysed, and present in greater proportion. The presence of a third wave is suggested by the polarograms, but it cannot be plotted owing to the interfering reduction of the hydrogen ion.

3. *Citrate solutions*

The above results indicate that polarograms of protactinium in slightly acid or neutral media are the more favourable ones for observing the reduction of Pa(IV) to Pa(III). Thus, citrate solutions seemed worth investigating as the protactinium citrate complex is rather stable(13) and likely to remain so even at low acidity. However, it was found that the reduction of protactinium in 0·5 M sodium citrate plus 0·5 M citric acid occurs at potentials very near to those corresponding to the interfering reduction of citrate ion. A maximum is present which is not suppressed by 0·02% gelatin (Fig. 7).

The unfavourable features of the polarograms discouraged further study of citrate solutions. Thus, alkaline solutions of the protactinium citrate complex were not

(13) A. G. MADDOCK and G. L. MILES, *J. Chem. Soc.* S 248 (1949).

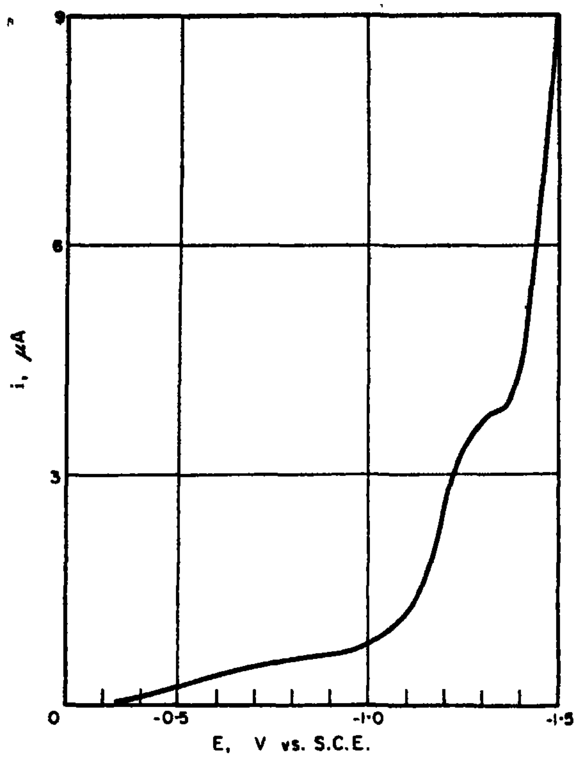

Fig. 6.—Polarogram of protactinium in 1·5 M ammonium sulphate, 0·3 M sulphuric acid. Solution prepared from the carbonate. $C_{Pa} = 1·3 \times 10^{-3}$ M.

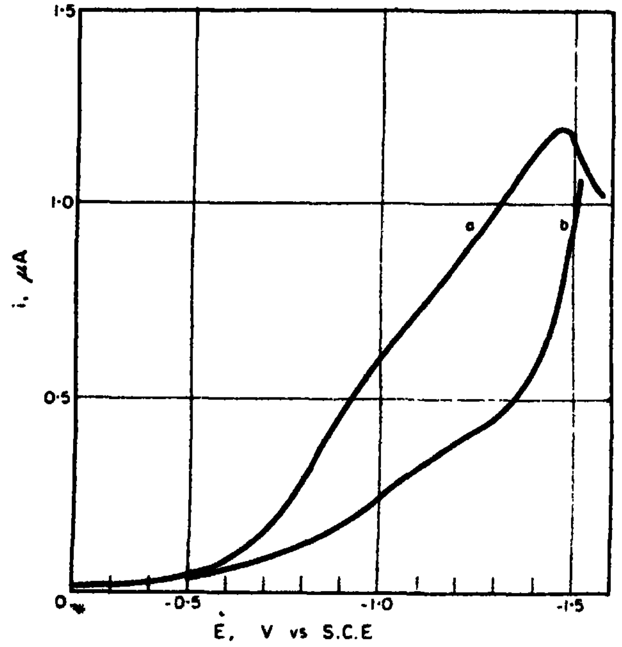

Fig. 7.—*a*, Polarogram of protactinium in 0·5 M sodium citrate, 0·5 M citric acid. $C_{Pa} = 4 \times 10^{-5}$ M. *b*, Polarogram of the support electrolyte.

investigated (although they were recognised as being surprisingly stable), because their only advantage over the acid solutions would have been the absence of the hydrogen wave which is not the chief source of interference.

4. *Oxalate solutions*

In agreement with Elson's observations,[4] a wave with $E_{\frac{1}{2}} = -1{\cdot}75$ V was obtained in 0·5 M potassium oxalate at a protactinium concentration of $1{\cdot}7 \times 10^{-4}$ M. This wave tended to present a maximum and was preceded by a small step at $-1{\cdot}2$ V. No attempt was made to record the second wave which has been observed by Elson at more negative potentials.

DISCUSSION

Fluoride solutions, which gave the best results both from the point of view of reproducibility and of significance will be discussed in some detail.

As far as the first wave is concerned, it is clearly suitable for the polarographic determination of protactinium, at least over the range of concentrations used in this investigation. Fig. 3 shows that wave is not polarographically reversible, but appears to be approaching such reversibility at low protactinium concentrations. The linearity of curve (a) in Fig. 2 and the normal dependence of wave height on the height of mercury show that the wave is in fact diffusion controlled. The slope of the log $i/(i_d - i)$ versus voltage plot at low concentrations suggests that the electrode process responsible for this wave is the one electron reduction of the Pa(V) fluoro-complex to the Pa(IV) state. This conclusion is supported by the reasonable value for the polarographic diffusion coefficient calculated for the Pa(V) ion on this basis using the Ilkovic equation. The value, $7{\cdot}1 \times 10^{-6}$ cm^2 sec^{-1}, may be compared with $7{\cdot}4 \times 10^{-6}$ for ferrocyanide and $8{\cdot}9 \times 10^{-6}$ for ferricyanide ions.

On the present data it is not possible to be confident as to the reason for the irreversibility of the wave, nor the reason for the influence of fluoride concentration. There is relatively little data in the literature regarding the polarography of fluoride solutions.[14,15] Much of it relates to the ferrifluoride system for which very conflicting results are reported.[16a,b] However, it does appear that irreversibility of the electrode reaction is not uncommon for the fluoro-complexes of metals. If the irreversibility arises from this cause it is not clear why the log $i/i_d - i$ versus voltage plots should approach the one electron slope at low protactinium concentrations.

The co-ordination number of the Pa(V) in the fluoro complex is high. It is known that the solid phase separating from the fluoride solution upon addition of potassium fluoride contains the PaF_7^{2-} ion.[17] We shall shortly publish evidence that the dominant ion present in the solution is very likely the PaF_8^{3-} anion. In either case it is quite improbable that the primary reduction product has more F^- ligands than the Pa(V) complex. Thus the effect of fluoride concentration on the half-wave potential cannot be ascribed to this cause. This effect might be due to the changing ionic strength of the solution but if one takes into account that the charge on the reduced ion is certainly greater than on the Pa(V) fluoro complex the change in the half-wave potential is again not of the expected sign.

[14] P. W. West, J. Dean and E. J. Breda, *Coll. Czech. Chem. Commun.* **13**, 1 (1948).

[15] J. T. Moelwyn-Hughes Thesis, Natal University, South Africa (1959).

[16a] C. E. Shoemaker, *Analyt. Chem.* **27**, 552 (1955).

[16b] C. L. Rolfs and G. A. Stoner, *J. Amer. Chem. Soc.* **77**, 2653 (1955).

[17] A. V. Grosse, *J. Amer. Chem. Soc.* **56**, 2501 (1934).

Other explanations of the polarographic irreversibility deserve attention. It must be remembered that even if the primary reduction product is the PaF_8^{4-} ion, this anion will be unstable with respect to PaF_4 deposition at quite low concentrations. A slow deposition reaction might lead to irreversibility with an approach to reversibility at a low enough protactinium concentration. It may be noted that the departure from linearity of the log $i/(i_d - i)$ versus voltage plot at the higher voltages (see Fig. 3, curve (a)) could arise in this way. The solubility of protactinium tetrafluoride in the supporting electrolyte was determined for the 3·84 M ammonium fluoride solution and found equal to $5{\cdot}8 \pm 0{\cdot}7 \times 10^{-4}$ M. Thus if the diffusion layer has a thickness of 0·05 mm, as suggested by Antweiler(18), deposition of PaF_4 could begin at a current of 2 μA. This explanation does not lead to an unequivocal prediction of the effect of fluoride concentration on the half-wave potential. Increasing fluoride concentration should drive the wave to more negative potentials in so far as it suppresses the dissociation of the PaF_8^{4-} ion, but it might lead to the opposite effect by accelerating the deposition of PaF_4 by lowering its solubility. The half-wave potential should also change with protactinium concentration but the range of concentrations investigated might be too small to show such an effect. However, with this explanation the slope of the log $i/i_d - i$ vs. voltages plots should assume the one electron value if the current is less than 2 μA. This does not appear to be the case.

The second wave is clearly irreversible and the diffusion current soon reaches a limiting value not dependent on the protactinium concentration. It was carefully confirmed that the wave is essentially connected with the protactinium by showing that the ratio of height of the second to that of the first wave was the same, under otherwise similar conditions, using protactinium from different purification treatments. A second possibility is that this wave is due to the reduction of another complex of Pa(V) not in rapid equilibrium with that responsible for the first wave. There are no quantitative data on the equilibria of the protactinium species in such fluoride solutions but the qualitative evidence(19) suggests that equilibrium, if indeed more than one complex ion is present in appreciable amounts at such F/Pa ratios, is very rapidly established, so that a single wave should result from the Pa(V) → Pa(IV) reduction.

A third possibility is that this is a catalytic reduction wave. Although the present data do not exclude this possibility and, indeed, the wave characteristics resemble those of catalytic waves, it is thought improbable because (a) the wave is not sensitive to modest changes in pH, (b) the height of the wave is always less than that of the Pa(V) → Pa(IV) stage, (c) existing information(19) suggests that fluoride ligand completely replaces OH ligand in the protactinium complexes.

It seems most likely that the second wave does represent another stage of the reduction of protactinium. It is not possible to say whether this wave is due to Pa(IV) → Pa(III) or some other process. However, PaF_3 will be even less soluble than PaF_4 and the formation of the two insoluble products round the drop would account for the diffusion current–protactinium concentration curves obtained.

The first half-wave potential is very close to the standard potential measured by Ferradini(2) and it seems quite possible that this potential refers to rather a Pa(V)/Pa(IV) couple, both valencies being present as their fluoro-complexes.

All the polarograms obtained with solutions other than the fluorides showed only

(18) H. J. Antweiler, *Z. Electrochem.* **44**, 719, 831–888 (1938).

(19) A. T. Casey, and A. G. Maddock, *J. Inorg. Nucl. Chem.* **10**, 289 (1959).

one irreversible wave corresponding to the reduction of Pa(V) to Pa(IV). Nevertheless, a rise in current following the Pa(V) reduction wave was systematically observed in the case of the sulphate solutions. This could be attributed to a catalytic reduction of the hydrogen ion promoted either by Pa(IV) or Pa(III). In the light of the behaviour of protactinium in fluoride solution, it seems likely than Pa(III) is formed in sulphate solutions as well, and that the corresponding wave would be detected were it not for the interfering reduction of hydrogen ion. Similar remarks apply to the case of oxalate solutions. Polarograms of citrate solutions are difficult to interpret owing to the presence of a persistent maximum, and do not contribute much to the general picture of the polarographic behaviour of protactinium.

On the whole, the present investigation shows that protactinium can be polarographically reduced to the tetravalent state, and that trivalent protactinium may possibly be obtained, at least at low acidities.

Acknowledgement—One of us (C. F. M.) is indebted to the "Instituto de Alta Cultura", Portugal for a fellowship. The investigation was partially supported by a contract from the A.E.R.E., Harwell.

J. Inorg. Nucl. Chem., 1962, Vol. 24, pp. 1635 to 1643. Pergamon Press Ltd. Printed in Northern Ireland

OBSERVATIONS ON THE RARE EARTHS—LXXVI(1)

THE STABILITIES OF THE *TRANS*-1,2-DIAMINOCYCLOHEXANE-N,N'-TETRAACETIC ACID CHELATES OF THE TRI-POSITIVE IONS*

T. Moeller and T. M. Hseu†
Noyes Chemical Laboratory, University of Illinois, Urbana, Illinois

(*Received* 3 *April* 1962; *in revised form* 17 *May* 1962)

Abstract—Interaction between *trans*-1,2-diaminocyclohexane-N,N' tetra-acetic acid (H_4DCTA or H_4Z) and tripositive rare-earth metal ions has been investigated. The formation constants of the hydrogen chelates (LnHZ) and of the normal chelates (LnZ^-) have been evaluated at 20°C, 30°C and 40°C and an ionic strength of 0·10(KNO_3), the former by a titration technique and the latter by a mercury indicator-electrode technique. Enthalpy and entropy changes characterizing the formation of the normal chelates have been calculated at 25°C. These and functions of the partial molal entropy of the normal chelates have been compared with corresponding values for related chelating agents. The significance of a configurational entropy contribution is particularly apparent for the complexes of this somewhat sterically limited ligand.

In previous communications in this series, variations in the entropy and enthalpy of formation, as judged by variations in formation constants as a function of both atomic number and temperature, of chelates of *N*-hydroxyethylethylenediaminetriacetic acid,(2) nitrilotriacetic acid(3) and diethylenetriaminepenta-acetic acid(4) have been examined in the light of possible steric changes as the size of the central cation changes. Contrary to the conclusions drawn earlier for the ethylenediaminetetra-acetic acid chelates,(5,6) these variations have been better correlated with a gradual weakening of the bond between the metal ion and a donor carboxyl group as cationic radius decreases than with complete rupture of such a bond at a specific cation in the series. These correlations, together with the somewhat nomadic behaviour of yttrium, have been related to configurational entropy.

The validity of this approach can be tested only through comparable studies involving related chelating agents of controlled structure. Inasmuch as ethylenediaminetetra-acetic acid (H_4EDTA) apparently behaves differently from the other agents described, it is, therefore, particularly important that the investigations also include donors that are structurally as nearly like this reagent as possible. Such a substance is

---

* After this work had been completed, it was learned that a similar study is described in the doctoral dissertation of R. H. Karraker, Iowa State University (1961).

† Present address: Department of Chemistry, National Taiwan University, Taipei, Taiwan, Republic of China.

(1) For the preceding paper in this series, see T. Moeller and L. C. Thompson, *J. Inorg. Nucl. Chem.* 24, 499 (1962).

(2) T. Moeller and R. Ferrús, *J. Inorg. Nucl. Chem.* 20, 261 (1961).

(3) T. Moeller and R. Ferrús, *Inorg. Chem.* 1, 49 (1962).

(4) T. Moeller and L. C. Thompson, *J. Inorg. Nucl. Chem.* In press.

(5) E. J. Wheelwright, F. H. Spedding and G. Schwarzenbach, *J. Amer. Chem. Soc.* 75, 4196 (1953).

(6) R. H. Betts and O. F. Dahlinger, *Canad. J. Chem.* 37, 91 (1959).

trans-1,2-diaminocyclohexane-N,N′-tetra-acetic acid (H_4DCTA), which differs essentially only in the ring-imposed rigidity between the two nitrogen atoms but which, in terms of the diagrammatic representation

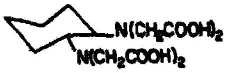

has these atoms ideally arranged for coordination. Although the two reagents may be expected to resemble each other closely,(7,8) both preorientation(9) and enhanced basicity of the nitrogen atoms should render the H_4DCTA chelates the more stable. The polarographically determined formation constants at 20°C for the $[Ln(DCTA)]^-$ species(10) are uniformly larger than those for the corresponding $[Ln(EDTA)]^-$ species.(5) It is significant that a plot of these values against atomic number closely parallels that for the H_4EDTA chelates, i.e., stability increases throughout the series with decreasing cationic radius but shows a marked discontinuity at gadolinium.(5,10,11) It is perhaps of even greater significance, however, that the entropy and enthalpy changes accompanying the formation of these chelates, as outlined later, are entirely different from those associated with the formation of the $[Ln(EDTA)]^-$ species.

In measuring the formation constants at several temperatures, certain of the complexities(12) inherent in the previously studied polarographic-exchange procedure(10) have been minimized through use of the mercury indicator-electrode method.(4,13) As an essential to application of this procedure, dissociation constants for the last two acidic protons of the chelating acid were measured as a function of temperature. These data were then used to evaluate the thermodynamic functions.

EXPERIMENTAL

Materials. Yttrium and rare-earth metal oxides of 99+–99·9 per cent purity were the same as those used in previous investigations.(2–4) *Trans*-1,2-diaminocyclohexane-N,N′-tetra-acetic acid, obtained as Chel-600 from Geigy Industrial Chemicals, was twice recrystallized from water to a product analysing to 99·8 per cent purity by potentiometric titration with potassium hydroxide in the presence of a slight excess of copper(II) chloride. Mercury was purified by the nitric acid-mercury(I) nitrate air-oxidation procedure.(14) All other chemicals were of analytical reagent quality.

Solutions. An approximately 2×10^{-3} M solution of the chelating acid was prepared by direct weighing and standardized by potentiometric titration with carbonate-free potassium hydroxide first in the presence of copper(II) chloride and then in the presence of neodymium chloride. Solutions of the rare-earth metal chelates were obtained by dissolving weighed quantities of the oxides and the chelating acid in known excess quantities of nitric acid. Each such solution was 2×10^{-3} M in the complex species and $1{\cdot}5 \times 10^{-2}$ M in total hydrogen ion. Previously described procedures(4) were used for the preparation of ca. 1×10^{-3} M mercury(II) nitrate, 5×10^{-3} M rare-earth metal nitrate, and 5×10^{-3} M mercury(II) chelate solutions.

Apparatus and procedure. These were the same as previously described.(4)

(7) G. Schwarzenbach, H. Ackermann and P. Ruckstuhl, *Helv. Chim. Acta* **32**, 1175 (1949).

(8) G. Schwarzenbach, A. Willi and R. O. Bach, *Helv. Chim. Acta* **30**, 1303 (1947).

(9) J. H. Holloway and C. N. Reilley, Project AF 49(638)-333, UNC-Chem. No. 2-CNR, TN-59-548, September 11 (1959).

(10) G. Schwarzenbach, R. Gut and G. Anderegg, *Helv. Chim. Acta* **37**, 937 (1954).

(11) G. Schwarzenbach and R. Gut, *Helv. Chim. Acta* **39**, 1589 (1956).

(12) R. W. Schmid and C. N. Reilley, *J. Amer. Chem. Soc.* **78**, 5513 (1956).

(13) G. Schwarzenbach and G. Anderegg, *Helv. Chim. Acta* **40**, 1773 (1957).

[illegible] Daniels, J. H. Mathews, J. W. Williams, P. Bender and R. A. Alberty, *Experimental Physical Chemistry*, p. 467. McGraw-Hill, New York (1956).

CALCULATIONS AND RESULTS*

Titration curves. Titration curves for solutions containing rare-earth metal ions and *trans*-1,2-diaminocyclohexane-N,N′-tetra-acetic acid show clearly the formation of comparatively stable 1:1 chelates and of protonated species of the type LnHZ ($Z = DCTA^{4-}$) but give no indication of the presence of species containing more than a single metal ion per chelating anion. The same observations have been reported for the thorium-H_4DCTA system.(15)

Stabilities of protonated chelates. Formation constants for the protonated chelates (LnHZ and $HgHZ^-$) were calculated from titration data for 1:1 mixtures of the metal ion with the chelating acid in the range of $a = 3$–4. In this region, the significant equilibria are

$$MHZ^{0 \text{ or } -} \rightleftharpoons MZ^{1- \text{ or } 2-} + H^+ \qquad \text{(I)}$$

(M = Hg or Ln). Previously developed equations(16) were used to convert the titration data to the formation constants listed in Table 1. Although the strongly acidic behaviour of all of these chelates renders the values only approximate, it is apparent that among the rare-earth metal species changing the cation is almost without effect. Inasmuch as the values for any particular cation are no more than very slightly temperature dependent, only the values at 20°C are included.

TABLE 1.—ACID FORMATION CONSTANTS FOR Hg(II)- AND Ln(III)-DCTA CHELATES AT 20°C

$\mu = 0{\cdot}10(KNO_3)$

M^{n+}	$\log K_H$ MHZ	M^{n+}	$\log K_H$ MHZ
Hg^{2+}	3·51	Tb^{3+}	2·11
		Dy^{3+}	2·16
La^{3+}	2·24	Ho^{3+}	2·41
Pr^{3+}	2·35	Er^{3+}	2·43
Nd^{3+}	2·22	Tm^{3+}	2·20
Sm^{3+}	2·18	Yb^{3+}	2·36
Eu^{3+}	2·17	Lu^{3+}	2·31
Gd^{3+}	2·23	Y^{3+}	2·18

Dissociation constants of H_4DCTA. Values for the dissociation constants of the free acid, as calculated by the method of DURHAM and RYSKIEWICH,(17) are summarized for several temperatures in Table 2. For this calculation, necessary hydroxyl ion concentrations were obtained from measured p_cH values as previously described.(4) The dissociation constants calculated agree closely with those reported by SCHWARZENBACH and ACKERMANN.(18)

Standard enthalpy values, ΔH_i° (where i refers to a particular dissociation step), were calculated from the third and fourth dissociation constants as before (Equation 2, Reference 4). Combination of these and the standard free energy changes, ΔF_i,

---

* The notation employed here is the same as that used for comparable situations in the DTPA study.(4) Continuing consultation of this reference will be helpful in following the treatment given.

(15) R. F. BOGUCKI and A. E. MARTELL, *J. Amer. Chem. Soc.* **80**, 4170 (1958).

(16) G. ANDEREGG, P. NAGELI, F. MÜLLER and G. SCHWARZENBACH, *Helv. Chim. Acta* **42**, 827 (1959).

(17) B. J. DURHAM and D. P. RYSKIEWICH, *J. Amer. Chem. Soc.* **80**, 4812 (1958).

(18) G. SCHWARZENBACH and H. ACKERMANN, *Helv. Chim. Acta* **32**, 1682 (1949).

TABLE 2.—DISSOCIATION CONSTANTS OF *Trans*-1,2,DIAMINOCYCLOHEXANE-N,N'-TETRA-ACETIC ACID

$\mu = 0{\cdot}1(KNO_3)$

Dissociation step	15°C	20°C	25°C	30°C	35°C	40°C
pK_1	—	2·40	—	—	—	—
pK_2	—	3·55	—	—	—	—
pK_3	6·15	6·14	6·12	6·10	6·08	6·07
pK_4	11·83	11·70	11·58	11·52	11·43	11·34

obtained from pK_i values, gave the entropy changes, ΔS_i°, involved. These thermodynamic values are given in Table 3 (± values indicate 95 per cent confidence intervals). Data for ethylenediaminetetra-acetic acid,(19) diethylenetriaminepenta-acetic acid,(4) and diethylenetriamine (den)(20) are included for comparison. The parallels among the three closely related amine polycarboxylic acids are apparent.

TABLE 3.—THERMODYNAMIC FUNCTIONS FOR THE DISSOCIATION OF 1,2-DIAMINOCYCLOHEXANE-N,N'-TETRA-ACETIC ACID, ETHYLENEDIAMINETETRA-ACETIC ACID, DIETHYLENETRIAMINEPENTA-ACETIC ACID AND DIETHYLENETRIAMINE(DEN)

Dissociation step	ΔF° (kcal/mole)	ΔH° (kcal/mole)	ΔS° (e.u./mole)	μ	t (°C)
H_4DCTA					
3rd	8·35 ± 0·02	1·34 ± 0·30	−23·51 ± 1·1	0·1	25
4th	15·80 ± 0·03	7·35 ± 0·50	−28·44 ± 1·7	(KNO_3)	
H_4EDTA					
3rd	8·26	4·39	−13·2	0·1	20
4th	13·76	5·69	−27·5	(KCl)	
H_5DTPA					
3rd	5·88 ± 0·03	1·49 ± 0·70	−14·7 ± 2·2	0·1	25
4th	11·64 ± 0·03	4·86 ± 0·70	−22·7 ± 2·4	(KNO_3)	
5th	14·23 ± 0·02	5·44 ± 0·42	−29·5 ± 1·4		
den					
1st	5	7·6	8	0·1	25
2nd	11	12·2	1	(KCl)	
3rd	13	11·1	−8		

Stability constants of chelates. The experimental cells and procedure involving the mercury electrode were the same as previously described.(4) The E_{Hg}° values, including the junction potentials E_j' and E_j, were −0·8387 V at 20°C, −0·8394 V at 30°C and −0·8400 V at 40°C.

The equilibrium

$$HgZ^{2-} + Ln^{3+} \rightleftharpoons Hg^{2+} + LnZ^- \qquad \text{(III)}$$

was established in solutions obtained by mixing the species HgZ^{2-}, LnZ^- and Ln^{3+}. For any specific determination, this equilibrium was studied by duplicate measurements involving each of four separate samples of the same compositional ranges as those used for the DTPA study.(4) As before, the tendency to form mixed chelates

---

(19) M. J. L. TILLOTSON and L. A. K. STAVELEY, *J. Chem. Soc.* 3613 (1958).

(20) G. H. MCINTYRE, Jr., B. P. BLOCK and W. C. FERNELIUS, *J. Amer. Chem. Soc.* 81, 529 (1959).

TABLE 4.—VALUES OF LOG $K_{\substack{\mathrm{Hg}\\ \mathrm{HgZ}}}$— AND —LOG K_{III}

$\mu = 0{\cdot}1(\mathrm{KNO_3})$

M^{n+}	log K		
	20·00°C	30·00°C	39·90°C
Hg^{2+}	23·59	23·25	22·92
La^{3+}	7·310	6·905	6·443
Pr^{3+}	6·436	6·013	5·526
Nd^{3+}	5·972	5·527	5·048
Sm^{3+}	5·039	4·608	4·127
Eu^{3+}	4·896	4·436	3·959
Gd^{3+}	4·865	4·409	3·930
Tb^{3+}	4·363	3·917	3·449
Dy^{3+}	3·949	3·552	3·126
Ho^{3+}	3·715	3·336	2·986
Er^{3+}	3·391	3·033	2·709
Tm^{3+}	3·127	2·849	2·530
Yb^{3+}	2·742	2·501	2·280
Lu^{3+}	2·651	2·479	2·219
Y^{3+}	4·246	3·826	3·370

under these conditions is sufficiently small to be neglected.[19] The equilibrium constant for this reaction

$$K_{III} = \frac{[\mathrm{Hg}^{2+}][\mathrm{LnZ}^-]}{[\mathrm{Ln}^{3+}][\mathrm{HgZ}^{2-}]} = K_{\substack{\mathrm{Ln}\\ \mathrm{LnZ}}}/K_{\substack{\mathrm{Hg}\\ \mathrm{HgZ}}} \tag{6}$$

was calculated in each instance from p_cH; the experimentally measured concentration of the Hg^{2+} ion; the initial concentrations of the ions Ln^{3+}, HgZ^{2-} and LnZ^-; and stoicheiometric Equations (7)-(9) of the previous paper.[4] Values of $K_{\substack{\mathrm{Ln}\\ \mathrm{LnZ}}}$ were then calculated as outlined there.[4] The results are summarized in Tables 4 and 5. The data in Table 5 are values interpolated[21] to 25°C. Variation of $K_{\substack{\mathrm{Ln}\\ \mathrm{LnZ}}}$ with atomic number is shown graphically in Fig. 1.

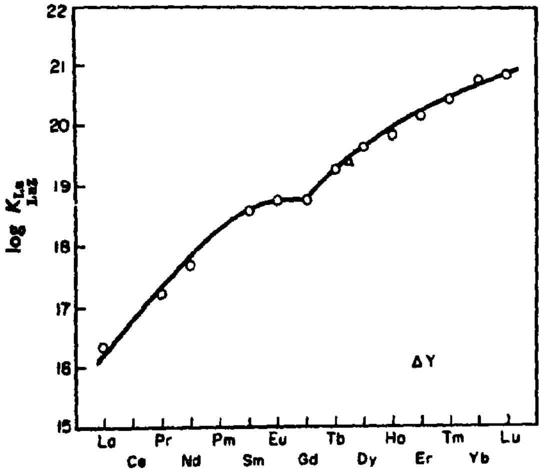

FIG 1.—Variation of log $K_{\substack{\mathrm{Ln}\\ \mathrm{LnZ}}}$ for tripositive cations.

---

[21] F. B. HILDEBRAND, *Introduction to Numerical Analysis*, pp. 35-48. McGraw-Hill, New York (1956).

Table 5.—Formation constants and values of the thermodynamic functions for Ln-DCTA and Hg(II)-DCTA chelates at 25°C $\mu = 0{\cdot}1(\mathrm{KNO_3})$

M^{n+}	$-\log K_{III}$	ΔH_{III}	$\log K^{\mathrm{M}}_{\mathrm{MZ}}$	$-\Delta F^{\circ}_{\mathrm{MZ}}$ (kcal/mole)	$\Delta H^{\circ}_{\mathrm{MZ}}$ (kcal/mole)	$\Delta S^{\circ}_{\mathrm{MZ}}$ (e.u./mole)	$(\Delta S^{\circ}_{\mathrm{LnZ}} + \bar{S}^{\circ}_{\mathrm{Ln}})$
Hg^{2+}	—	—	23·43 ± 0·03	31·97 ± 0·04	−14·07 ± 0·30	60·04 ± 1·0	—
La^{3+}	7·08 ± 0·04	17·62 ± 1·0	16·35 ± 0·05	22·3 ± 0·07	3·55 ± 1·04	86·7 ± 3·5	52·0
Pr^{3+}	6·20 ± 0·03	19·07 ± 0·8	17·23 ± 0·04	23·51 ± 0·06	5·00 ± 0·85	95·6 ± 2·9	58·2
Nd^{3+}	5·74 ± 0·05	19·07 ± 0·7	17·69 ± 0·06	24·13 ± 0·08	5·00 ± 0·76	97·6 ± 2·6	59·2
Sm^{3+}	4·80 ± 0·02	19·07 ± 0·8	18·63 ± 0·04	25·42 ± 0·06	5·00 ± 0·85	102·0 ± 2·9	61·8
Eu^{3+}	4·66 ± 0·02	19·61 ± 0·7	18·77 ± 0·04	25·61 ± 0·06	5·54 ± 0·76	104·5 ± 2·6	63·4
Gd^{3+}	4·63 ± 0·02	19·82 ± 0·6	18·80 ± 0·04	25·65 ± 0·06	5·75 ± 0·67	105·3 ± 2·3	63·5
Tb^{3+}	4·13 ± 0·03	19·07 ± 0·8	19·30 ± 0·04	26·33 ± 0·06	5·00 ± 0·85	105·1 ± 2·9	62·4
Dy^{3+}	3·74 ± 0·03	17·16 ± 0·7	19·69 ± 0·04	26·87 ± 0·06	3·09 ± 0·76	100·5 ± 2·6	56·9
Ho^{3+}	3·54 ± 0·02	15·25 ± 0·6	19·89 ± 0·04	27·14 ± 0·06	1·18 ± 0·67	95·0 ± 2·3	50·5
Er^{3+}	3·23 ± 0·02	14·19 ± 0·7	20·20 ± 0·04	27·56 ± 0·06	0·12 ± 0·76	92·8 ± 2·6	47·5
Tm^{3+}	2·97 ± 0·02	12·48 ± 0·7	20·46 ± 0·04	27·92 ± 0·06	−1·59 ± 0·76	88·3 ± 2·6	42·2
Yb^{3+}	2·63 ± 0·02	9·58 ± 0·7	20·80 ± 0·04	28·39 ± 0·06	−4·49 ± 0·76	80·2 ± 2·6	33·4
Lu^{3+}	2·52 ± 0·05	9·15 ± 1·0	20·91 ± 0·06	28·53 ± 0·08	−4·92 ± 1·04	79·2 ± 3·5	31·7
Y^{3+}	4·02 ± 0·02	18·30 ± 0·8	19·41 ± 0·04	26·48 ± 0·06	4·23 ± 0·85	103·0 ± 2·9	55·8

Thermodynamic functions. These were evaluated as previously outlined.(4) The ± variations indicated in Table 5 represent 95 per cent confidence intervals. The function $\Delta S^\circ_{\mathrm{LnZ}} + \bar{S}^\circ_{\mathrm{Ln}}$, introduced by BETTS and DAHLINGER(6) as a measure of the partial molal entropy of the chelate ($\bar{S}^\circ_{\mathrm{LnZ}}$), was evaluated as previously indicated,(2–4) using $\bar{S}^\circ_{\mathrm{Ln}}$ values calculated according to POWELL and LATIMER.(22) Variations of $\Delta H^\circ_{\mathrm{LnZ}}$ and $\Delta S^\circ_{\mathrm{LnZ}} + \bar{S}^\circ_{\mathrm{Ln}}$ with atomic number are indicated in Fig. 2 and 3, respectively.

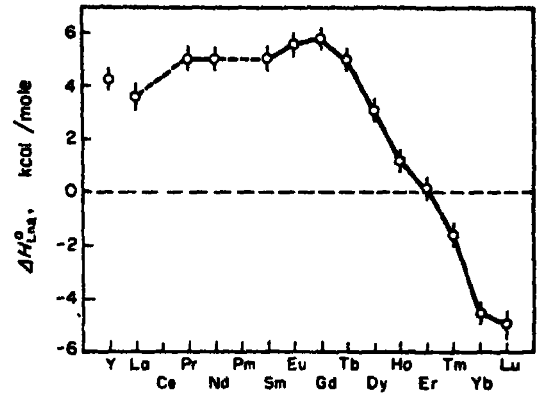

FIG. 2.—Enthalpy values for formation of chelates.

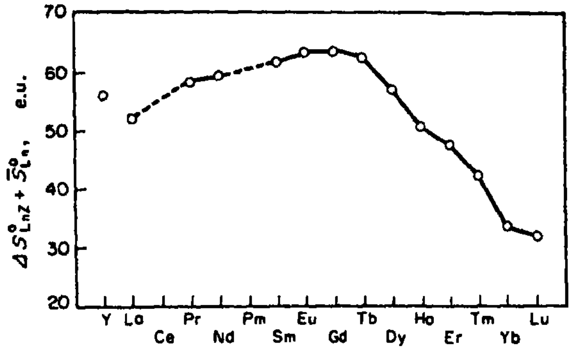

FIG. 3.—Variation in the function $\Delta S^\circ_{\mathrm{Ln}} + \bar{S}^\circ_{\mathrm{Ln}}$

DISCUSSION

Although it might be expected that the thermodynamic functions associated with the loss of the third and fourth protons of H_4DCTA would be comparable with the corresponding values for H_4EDTA, the data in Table 4 indicate substantial differences for the fourth proton. These differences may well arise from the structural rigidity imposed in the case of H_4DCTA by the cyclohexyl ring, which renders the hydrogen-bonded structure proposed by SCHWARZENBACH and ACKERMANN(18)

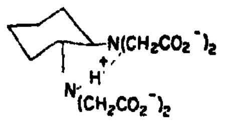

---

(22) R. E. POWELL and W. M. LATIMER, *J. Chem. Phys.* 19, 1139 (1951).

rather than the more usual zwitter-ion arrangement

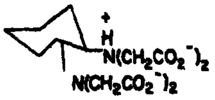

a logical way of accounting for differences in the properties of the fourth proton.

The general agreement between the $K_{\substack{\mathrm{Ln}\\\mathrm{LnZ}}}$ values obtained here and those previously reported(10) supports the validity of this experimental approach. The differences observed are compatible with those reported in other studies where the mercury indicator electrode technique has been compared with other techniques.(4,23) The variation in stability and the position of the yttrium chelate are comparable with what is reported for the EDTA system (Fig. 1). This may perhaps be expected because of similarities between the two reagents. However, when the log $K_{\substack{\mathrm{Ln}\\\mathrm{LnZ}}}$ values for the lighter cations are plotted against the summation of pK_2, pK_3, and pK_4 for the acid, they lie ca. 1 unit below the nearly linear curves obtained for the HEDTA-, EDTA-, and DTPA-systems.(4) This suggests that the number of chelate rings is not the same with the DCTA-chelates as with the others. Although such a suggestion is incapable of proof in terms of stability data alone, it is not incompatible with the structural limitations of the ligand and the differences found in the thermodynamic functions associated with chelate formation.

Although the limitations of such functions calculated from equilibrium data are well known, it is apparent from the values summarized in Table 5 that the entropy of chelation is more favorable in this system than it is in the other comparable systems previously studied.(2–4,6) It is apparent also that the entropy change is primarily responsible for the sizeable free energy change on chelation, particularly since the enthalpy change is positive in most instances and thus opposed to complex-ion formation. Although solution stability increases with atomic number among the rare-earth metal ions, with a small arrest at gadolinium, both $\Delta H^{\circ}_{\mathrm{LnZ}}$ and $\Delta S^{\circ}_{\mathrm{LnZ}}$ pass through maxima at the gadolinium chelate. The same is true of the partial molal entropy of the chelates, as measured by $\Delta S_{\mathrm{LnZ}} + S^{\circ}_{\mathrm{Ln}}$. This behaviour differs from that characterizing any previously described related system.(2–4,6)

Graphic representation of these data (Fig. 2, 3) indicates clearly that the "gadolinium break" is of some significance. In the range La-Gd, increase in entropy change favours stability, but increase in enthalpy change (positive) opposes it. Since solution stability does indeed increase, the entropy change must be a governing factor. In the sense that it undoubtedly reflects primarily the displacement of water molecules by the chelating ligand, this is reasonable. For the region Gd-Lu, it is reasonable to associate decrease in entropy with increasing solvation.(24) This could result from decrease in the multidentate character of the ligand, followed by entry of water molecules into the co-ordination sphere. Inasmuch as the values of $\Delta S^{\circ}_{\mathrm{LnZ}} + S^{\circ}_{\mathrm{Ln}}$ show no constancy in either region, but rather pass through a maximum at gadolinium, each of these

---

(23) J. E. Powell and J. L. Mackey, *Inorg. Chem.* 1, 418 (1962).

(24) A. E. Martell, *Ann. N.Y. Acad. Sci.* 88, 284 (1960).

processes must be a progressive one. Again it is apparent that configurational entropy(8) is of importance for chelates of the heavier cations, but neither the overall increase in solution stability with atomic number nor the position of yttrium can be completely rationalized in these terms. It is still impossible to do other than regard the latter as again the result of a fortuitous combination of contributing effects.

Acknowledgement—Fellowship support given to T. M. Hsu by the National Council on Science Development, Republic of China, is gratefully acknowledged.

J. Inorg. Nucl. Chem., 1962, Vol. 24, pp. 1645 to 1650. Pergamon Press Ltd. Printed in Northern Ireland

THE ASSOCIATION OF WATER MOLECULES WITH THE EXTRACTED BENZOHYDROXAMIC ACID CHELATES OF URANIUM(VI) AND IRON(III)

C. E. MELOAN*† and W. W. BRANDT
Department of Chemistry, Purdue University, Lafayette, Indiana

(*Received* 6 *September* 1960; *in revised form* 5 *April* 1962)

Abstract—The number of molecules of water associated with the benzohydroxamic acid chelates of uranium(VI) and iron(III) when extracted into alcohols was determined to be 6 ± 1 and 9 ± 3 respectively. A general relationship was established between the amount of chelate extracted by an alcohol and the amount of water soluble in it.

THE benzohydroxamic acid chelates of iron(III), vanadium(V) and uranium(VI) extract readily into aliphatic alcohols(1,2,3) and other polar organic compounds. The number of ligands per metal atom had been determined for iron(2), vanadium(3) and uranium(1) in aqueous and organic solutions. The possibility of determining the presence of water molecules associated with the metal chelates extracted into an organic layer was investigated. The results indicate that the benzohydroxamic acid chelates of uranium(VI) and iron(III) have 6 ± 1 and 9 ± 3 molecules of water associated with them respectively when extracted into n-decanol.

The results also indicate a general relationship between the solubility of water in the alcohol and the extractibility of the hydroxamic acid chelates. However, it is clear that this relationship is a secondary factor in the extraction.

Apparatus

The Karl Fischer technic used was described by MEYERS *et al.*(4) for a similar study. The dead stop method for endpoint detection(5) was substituted. The titration vessel of ZERBON and SATTLER(6) was modified by inverting the ball and socket joints. This allows any liquid that should happen to touch the joint to drain back into the flask. An automatic zeroing 10 ml microburette with graduations to 0·02 ml was used. (Ace Glass Co.).

Reagents

Dry methanol. The methanol was dried by the use of a fractionating column as suggested by Jones.(7) Distillation of reagent grade methanol in a 6 ft bead-packed column produced a product that contained 0·018 ± 0·002 per cent water.

Standard water solution. A standard solution of water in methanol was used to standardize the Karl Fischer reagent and to back titrate any excess Karl Fischer reagent during the water determination.

---

* Abstracted from a thesis submitted by C. MELOAN to the graduate school of Purdue University, January, 1959, in partial fulfillment of the requirements for the degree of Doctor of Philosophy.

† Present address: Kansas State University, Manhattan, Kansas.

(1) C. E. MELOAN, P. E. HOLKEBOER and W. W. BRANDT, *Analyt. Chem.* 32, 791 (1960).

(2) W. B. HOWSMON. Ph.D. Thesis, Purdue Universtiy (1955).

(3) W. M. WISE and W. W. BRANDT, *Analyt. Chem.* 27, 1392 (1955).

(4) R. J. MYERS, D. E. METZLER and E. N. SWIFT, *J. Amer. Chem. Soc.* 72, 3767 (1950).

(5) G. WERNIMONT and F. J. HOPKINSON, *Analyt. Chem.* 15, 272 (1943).

(6) F. ZERBON and L. SATTLER, *Industr. Engng. Chem. Analyt. Ed.* 18, 138–9 (1946).

(7) G. K. JONES, *Paint Manuf.* 15, 360–3 (1945).

Karl Fischer reagent. This reagent was prepared according to the procedure described by MITCHELL and SMITH.(8) The pyridinium iodide for this purpose was recovered from the aqueous preparation by evaporation to near dryness and recrystallization.*

System variables affecting the Karl Fischer reagent

Stabilizer for the Karl Fischer reagent. Some of the series of titrations of water lasted for 6 hr. The change in water equivalent of an unstabilized reagent was enough to make the results invalid. The BLOOMGREN and JENNER(9) method for stabilizing the Karl Fischer reagent was used. When using pyridinium iodide as the stabilizer, no detectable change in the strength of the Karl Fischer reagent was found over a six hour period.

Extractant. n-Decanol was chosen as the solvent for the extraction of the chelates because of all the substances tested (Table 1) this alcohol had the maximum absorbance for the extracted uranium benzohydroxamic acid chelate in relation to the amount of water soluble in it.

TABLE 1.—RESULTS OF KARL FISCHER TITRATION AND EXTRACTION STUDIES ON VARIOUS ALCOHOLS

Alcohol	*A* at 380 mμ†	Mg·H$_2$O per 5 ml of alcohol
n-amyl	2·03	396
n-hexyl	2·00	288
n-octyl	1·97	201
n-nonyl	1·85	178
n-decyl	1·85	161
n-hendecyl	1·6	144
n-dodecyl	0·06	128
isoamyl	2·00	458
t-amyl	2·34*	950
2-octyl	1·57	191
2-ethyl-n-hexyl	0·72	133
cyclohexyl	2·1	586
2-methyl cyclohexanol	2·00	337
4-heptyl	0·48	152
benzyl	1·94	638
2-ethyl butyl	1·52	221

* 10 ml of alcolol was used rather than 5 ml and Beer's law applied.
† *A* = Absorbance of extracted uranium benzohydroamic acid chelate.

Uranium chelate. The concentration of the uranium chelate solutions was limited to 2 × 10^{-5}–8 × 10^{-5} M in n-decanol by the sensitivity of the titration apparatus and the insolubility of the chelate respectively. The reagent solutions were prepared from aqueous stock solutions of 0·01 M uranyl acetate and 0·02 M benzohydroxamic acid. The proper quantities were diluted to 400 ml with distilled water. The pH was adjusted to 6 ± 0·1 using sodium hydroxide and a standardized Leeds and Northrup pH meter. The aqueous chelate was shaken 100 times with 40 ml of n-decanol and placed into a constant temperature bath at 25 ± 0·1°C for 30 minutes to separate and come to equilibrium. The water used for chelate preparation was brought to within

---

* On one occasion while purifying the hydriodic acid with a few drops of hypophosphorous acid a rather violent explosion occurred after prolonged standing of the reagents in the reaction flask. No such explosion ever occurred when the reaction was carried out immediately.

(8) J. MITCHELL and D. M. SMITH, *Aquametry*, p. 42. Interscience, New York (1948).

(9) BLOOMGREN and JENNER, *Brit.* 722, 983, Feb. 2 (1955).

2°C of the bath temperature to provide for a faster attainment of equilibrium. After equilibrium, the organic layer was separated and placed in a centrifuge for 1 min to remove suspended water droplets.

Iron chelate. For the same reasons as with uranium, the concentration of the iron chelate in n-decanol was limited to the range from 2×10^{-3} M to 5×10^{-3} M at pH 3 or to 2×10^{-3} M at pH 8. The chelate solutions were prepared in the same manner as uranium with two exceptions. At pH 3·5, 800 ml of aqueous chelate were prepared and at pH 8, 1600 ml. Because of the rapidity with which the more concentrated iron chelate solutions would form a precipitate after they had been extracted, it was necessary to titrate the most concentrated of a series first and the least concentrated last.

Experimentation and results

Solubility of water in the alcohols: The alcohols were saturated with water for three days at 25·0 ± 0·1°C with intermittent shaking. Five millilitre aliquots of the alcohol were then titrated with Karl Fischer reagent.

Interferences with the Karl Fischer titration

It was necessary to determine if any reaction would occur between the Karl Fischer reagent and the various constituents of the chelate systems.

Benzohydroxamic acid. Samples of 0·0516 M benzohydroxamic acid in dry methanol required the same amount of Karl Fischer reagent as a corresponding solution of dry methanol only.

Uranyl ion. Hydrogen iodide will not reduce uranium(VI) to uranium(IV) in aqueous solutions. However, no oxidation-reduction potentials were available for the uranium or iodide systems in the pyridine-methanol-SO_2 solvent to predict whether reaction might occur. Uranyl nitrate hexahydrate was dissolved in dry methanol and titrated with Karl Fischer reagent. The results are shown in Table 2.

TABLE 2.—EFFECT OF THE $UO_2(NO_3)_2 \cdot 6H_2O$ ON KARL FISCHER REAGENT

Predicted values	
If only the six hydrate molecules are titrated	22·0 mg
If UO_2^{2+} reacts as one equivalent of water	25·6 mg
If UO_2^{2+} reacts as two equivalents of water	29·3 mg
Experimental value	
Mg of water actually found in titration of $UO_2(NO_3)_2 \cdot 6H_2O$	22·2 mg

pH. The pH has to be controlled to ±0·1 pH unit for the chelate extractions(1,3) between pH 2 and 8. This range does not change the solubility of water in n-decanol significantly (Table 3).

Ionic strength. The effect of ionic strength was determined by using solutions of sodium perchlorate (Table 4). There is a noticeable effect only above a relative ionic strength of 0·1, however, the chelate systems used are less than 0·05.

TABLE 3.—EFFECT OF pH ON WATER SOLUBILITY IN DECANOL

pH	Mg·H_2O per 5 ml decanol
1	150·3
2	152·8
3	153·5
4	154·0
5	154·2
6	154·2
7	152·2
8	153·7
9	154·4

TABLE 4.—EFFECT OF IONIC STRENGTH ON THE AMOUNT OF WATER SOLUBLE IN DECANOL

Ionic strength	Mg H_2O per 5 ml decanol
0·001	158·8
0·005	158·0
0·01	157·7
0·05	158·5
0·1	157·8
0·5	151·6
1·0	143·8
2·0	133·2

TABLE 5.—WATER ASSOCIATED WITH THE URANIUM(VI)-BENZOHYDROXAMIC ACID CHELATE

Concentration of chelate	Mg H_2O per 5 ml decanol
1×10^{-5} M	146·1 146·1 146·3
2×10^{-5} M	147·2 147·3 147·2
3×10^{-5} M	148·2 148·2 148·4
4×10^{-5} M	149·2 149·1 149·0

Equilibria. Difficulty could arise if the half life of any co-ordinated water molecules were shorter than that of the organic–aqueous equilibrium as a whole. No water of co-ordination would be found. The decanol–water equilibrium is obtained in a matter of minutes if a very thorough shaking is performed. Tests conducted after a few minutes and after several hours showed no significant difference. It was assumed that no interference was present.

Associated water results

Water associated with the uranium(VI)-benzohydroxamic acid chelate. The solutions of different concentrations of the uranium benzohydroxamic acid chelate were extracted and the total water carried over into the organic phase determined (Table 5). The differences in water concentration were related to the differences in chelate concentration to obtain the stoicheioimetry. It was shown that there is no significant effect on the determination of water from the chelation agent, the metal ion, pH, ionic strength or temperature.

The average of the results indicate 1·04 mg of water for each 1 × 10^{-5} moles increase in amount of chelate present in the organic layer. The predicted value for six molecules of water is 1·08 mg. Other experiments of this type verified these results to within ±1 molecule of water.

The data in Table 5 would be significant to a 99 per cent confidence level with an *F* value of 7·59 or above. The *F* determined was 485.

TABLE 6.—WATER ASSOCIATED WITH THE IRON(III)-BENZOHYDROXAMIC ACID CHELATE AT pH 3·5

Concentration of chelate (Total moles present)	Mg H_2O per 5 ml decanol
0·5 × 10^{-5} M	156·1
	156·8
	156·5
1·25 × 10^{-5} M	157·5
	157·8
	157·7
2·0 × 10^{-5} M	159·5
	159·4
	159·4
2·75 × 10^{-5} M	160·4
	160·2
	160·4
Water co-ordinated around the iron(III)–benzohydroxamic acid chelate at pH 8·0	
0·5 × 10^{-5} M	159·6
	159·5
	158·7
1·0 × 10^{-5} M	159·4
	159·2
	159·9
1·5 × 10^{-5} M	160·2
	160·0
	159·8
2·0 × 10^{-5} M	162·3
	151·5

Water associated with the iron(III)–benzohydroxamic acid chelate. Iron(III) forms two species in aqueous solution, which extract into alcohols. HOWSMON(2) has shown that in aqueous solution a 2:1 chelate may exist in the organic phase in both cases.(2) Extraction studies were therefore carried out at pH 3·5 and 8.

The average of the results at pH 3·5 indicate 9 molecules of water for each molecule of chelate (Table 6). These results can be considered to be no more certain than ±3 molecules of water due to the spread of the values obtained. SWIFT(4) found that the hydrogen iodide in Karl Fischer reagent reduced ferric ion. The chelate was not reduced during the titration so this correction was not necessary.

The results at pH 8 also indicate 9 molecules of water (Table 6) although precipitation problems reduced the accuracy.

The fact that both pH systems gave essentially the same results supports the spectrophotometric data that the same chelate is present in the organic phase in both cases.

The top data of Table 6 require an F or 8·45 or above for a 99 per cent confidence level and give a value of 28·9. The bottom data require an F of 8·45 and give $F = 19{\cdot}8$. This would indicate that statistically the results are valid.

DISCUSSION

The preceding results indicate that a definite quantity of water is associated with the uranium(VI) and iron(III) benzohydroxamic acid chelates. It was known that many of the solvents used contained several percent of water.(11,12) A comparison of the solubility of water in an alcohol and its extractability for the complex showed that the best extracting agents dissolved the most water (Table 1).

However, many irregularities occur which cannot be explained simply on the basis of water solubility. In general the even-numbered straight chain alcohols extract somewhat better than the odd-numbered alcohols with the exception of C_8 and C_{12}. The C_{12} alcohol was checked several times. In view of the fact that there is only a 16 mg difference in water content between C_{11} ($A = 1{\cdot}61$) and C_{12} ($A = 0{\cdot}06$) it is hard to justify the large difference in extraction as being due only to water content unless a certain minimum amount of water must be present before extraction takes place.

With the alcohols other than the straight chain there appears to be a rough relationship between water content and extractability. There are discrepancies, however, in that while 2-ethyl butanol compares with n-heptanol, 2-ethyl-n-hexanol should give a lower absorbance than 4-heptanol but it does not.

No consideration has been made of the possibility that the absorptivity is changed by the properties of the solvent and therefore a direct correlation would not be expected. Dielectric properties and steric factors of the organic phase must also be considered and while there appears to be some relationship between the water content and extractability it is certain that water is not the only explanation.

Acknowledgement—The authors wish to express their appreciation for the financial support of this work by the Purdue Research Foundation.

(11) R. E. KIRK and D. F. OTHMER, *Encyclopedia of Chemical Technology*, Vol. 12, p. 675. Interscience Encyclopedia, New York (1953).

(12) R. E. KIRK and D. F. OTHMER, *Encyclopedia of Chemical Technology*, Vol. 10 p. 780. Interscience Encyclopedia, New York (1953).

J. Inorg. Nucl. Chem., 1962, Vol. 24, pp. 1651 to 1666. Pergamon Press Ltd. Printed in Northern Ireland

THE INFLUENCE OF DILUENT ON THE EXTRACTION OF IRON(III) FROM HYDROCHLORIC ACID SOLUTIONS BY TERTIARY AMINES

W. SMUŁEK AND S. SIEKIERSKI
Department of Radiochemistry, Institute of Nuclear Research, Warsaw 9, Poland

(*Received* 23 *March* 1962; *in revised form* 17 *May* 1962)

Abstract—A study has been made of the extraction of iron(III)—from hydrochloric acid solutions with tertiary amines in a series of diluents. From the experimentally determined extraction coefficients of iron, k, and the thermodynamic activities of the amines in the organic phase, a_0, the activity coefficients of the complex, y_c, have been calculated. The effect of diluent on a_0, y_c and k has been discussed from the point of view of intermolecular interactions.

HIGH molecular weight amines in organic diluents have been found to be efficient extractants for a wide variety of substances from aqueous solutions. The use of these amines for the extraction of many metals has been described in the literature. However there are only a few papers concerning the role of diluent in the extraction by amines. COLEMAN *et al.*(1) have investigated the extraction of several metals from sulphate solutions using a series of amines in kerosene, benzene and chloroform. He found that the extent of extraction can be influenced by the type of diluent. COLEMAN suggested that this influence can qualitatively be explained "if it is assumed that the diluent molecules associate with the amine, benzene more than kerosene, and chloroform more than benzene, in a way that is effectively similar to increased branching".

MADDOCK(2) while investigating the extraction of protactinium chloride from hydrochloric solutions using tri-n-butylamine in a number of diluents has found a linear dependency between the extraction coefficient and the dielectric constant of the diluent in a log–log plot.

TAUBE(3) has studied the effect of diluent on the extraction of plutonium, neptunium and uranium from sulphate and nitrate solutions using amines and other extractants. This author points out that the main factor influencing the extent of extraction is a dipole–dipole interaction between the complex extracted and the molecules of diluent.

One of the authors(4) has studied the mechanism of extraction of thorium and europium from nitrate solutions using tri-n-butylphosphate in various diluents. He has shown that in the extraction process the following two important factors must be taken into account.

(1) The interaction of the molecules of diluent with the extractant in the organic phase and (2) the interaction of the molecules of diluent with the complex extracted. To understand the influence of diluent both these factors must be known. This approach may have a more general character and may be applied to the extraction by amines.

---

(1) C. F. COLEMAN, K. B. BROWN, J. G. MOORE and K. A. ALLEN, *Proceedings of the Second International Conference on the Peaceful Uses of Atomic Energy, Geneva*, 1958 A/Conf. 15/510. United Nations (1958).

(2) A. G. GOBLE and A. G. MADDOCK, *J. Inorg. Nucl. Chem.* 7, 94 (1958).

(3) M. TAUBE, *J. Inorg. Nucl. Chem.* 12, 174 (1959).

(4) S. SIEKIERSKI, *J. Inorg. Nucl. Chem.* 24, 205 (1962).

If it is assumed that in the extraction of Fe(III) from HCl solutions by tertiary amines the only extracted species is $FeCl_4^-$ which associates with one amine cation to form an ion-pair, the following extraction reaction may be written:

$$R_3NHCl_{(o)} + Fe^{3+}_{(a)} + 4Cl^-_{(a)} \rightleftharpoons R_3NH^+FeCl^-_{4(o)} + Cl^-_{(a)} \tag{1}$$

The subscripts "o" and "a" refer to the organic and aqueous phase, respectively. Then the equilibrium constant for this reaction is

$$K = \frac{a_c}{a_{FeCl_3} \cdot a_{R_3NHCl}} = \frac{c_c \cdot y_c}{c_{Fe} \cdot c^3_{Cl^-} \cdot y^4_{\pm} \cdot a_{R_3NHCl}} \tag{2}$$

where: c_c is the concentration of the complex extracted, c_{Fe} is the total concentration of iron in the aqueous phase, y_c is the molar activity coefficient of the complex, $y_{\pm}$ is the mean molar stoicheiometric activity coefficient of $FeCl_3$. Although iron in the aqueous phase exists in many forms we can write $c_c/c_{Fe} = k$, where k is the experimentally determined ratio of the radioactivity from ^{59}Fe in the organic phase to that in the aqueous phase. This ratio will be called the extraction coefficient. It is possible to write the above because $y_{\pm}$ is defined as the mean molar stoicheiometric activity coefficient and it includes, therefore, any complexing of the iron in the aqueous phase. Since the composition of the latter was maintained constant in all experiments we can write

$$K = A \,.\, k \frac{y_c}{a_{R_3NHCl}} \tag{3}$$

or

$$k = K' . \frac{a_{R_3NHCl}}{y_c} \tag{4}$$

From the latter equation it follows that the extraction coefficient of iron is a function of the thermodynamic activity of the amine hydrochloride in the organic phase and the activity coefficient of the complex in the organic phase.

The present study was undertaken with the object of investigating the effect of the diluent on both these factors separately and its final effect on the extraction coefficient.

Measurements of the concentration of the amine hydrochlorides in the aqueous phase offer the possiblity of determining the term a_{R_3NHCl}. Having determined the thermodynamic activity it is possible, using Equation (4), to calculate the activity coefficient of the complex, provided k is known. To determine the thermodynamic activity of the amines their partition between 8 M hydrochloric acid and various diluents was measured. At equilibrium the amine salt distributes between the two phases so that we can write:

$$R_3NHCl_{(o)} \rightleftharpoons R_3NHCl_{(a)} \tag{5}$$

The equilibrium constant for this process is

$$K = \frac{a_o}{a_a} \tag{6}$$

where a_o and a_a stand for the thermodynamic activity of the amine hydrochloride in the organic and aqueous phase, respectively. Now, since the concentration of the amine salt in the aqueous phase was rather small in all experiments (the initial concentrations of the amines being within 10^{-5}–10^{-3} M) we may assume that the activity coefficient of the amine salt in the aqueous phase does not depend on the concentration of the amine. Consequently we can write

$$K' = \frac{a_0}{c_a} \tag{7}$$

Further if we choose for each amine a standard state in which the thermodynamic activity of the amine hydrochloride is assumed to be unity, then the amine salt activity in a given diluent is

$$a_0 = \frac{c_a}{c_a^s} \tag{8}$$

where c_a^s denotes the concentration of the amine hydrochloride in the aqueous phase corresponding to the standard state, and c_a the concentration of the amine hydrochloride in the aqueous phase, in equilibrium with the organic solutions of the amine salt. From the latter equation it is possible to calculate the values for a_0 provided c_a and c_a^s are known.

In the determination of c_a we encountered an inherent difficulty as the concentrations of the amine hydrochlorides in the aqueous phase were usually so small that no direct method could succesfully be used for this estimation. An indirect method was therefore developed. First the extraction coefficient, k, was plotted as a function of the initial concentration of the extractant diluted with chlorobenzene. The curve obtained was used as a calibration curve. Such calibration curves were constructed for all the amines used. From these curves it is possible to determine the extractant concentrations in the aqueous phase provided the secondary extraction coefficient, k', is known. The latter was measured as follows. An organic sample containing the amine at a given concentration was first contacted with 8 M HCl containing no iron. Part of the amine passes during equilibration to the aqueous phase. The latter is then separated and an aliquot of labelled iron added to make the metal concentration $5{\cdot}3 \times 10^{-5}$ M. This aqueous phase was then contacted with barren chlorobenzene, used as standard diluent in all experiments involving determination of the secondary extraction coefficients. After equilibration the radioactivity due to ^{59}Fe was assayed in both phases and the secondary extraction coefficient, k', determined. The values of the secondary extraction coefficient, k', were plotted as ordinates and the point of intersection with the calibration curve indicated on the abscissa the corresponding concentration of the amine in the aqueous phase, previously equilibrated with the organic phase. Using this technique it was possible to determine the concentrations of the amines in the aqueous phase after equilibration with a number of amine solutions in various diluents.

Standard states for the amines

As standard states for tribenzylamine, tri-n-hexylamine and tri-n-octylamine the amine hydrochlorides in equilibrium with 8 M HCl were chosen. The concentrations of the salts in the equilibrium aqueous phase were: $9{\cdot}0 \times 10^{-4}$ M, $6{\cdot}6 \times 10^{-4}$ M and $1{\cdot}0 \times 10^{-4}$ M, respectively.

Since the tri-n-butylamine hydrochloride is completely miscible with 8 M HCl, therefore, not the thermodymanic activity but only the value a_0/K, which is proportional to a_0, was determined in all experiments involving this amine.

EXPERIMENTAL

Materials. All the diluents presented in Table 1 were purified by fractional distillation. A.R. hydrochloric acid and $FeCl_3$ were used.

The radio-iron used was supplied by the Radiochemical Centre, Amersham, England, as ferric chloride solution and had a specific activity of 100 mC/g of iron. The activity was mainly due to ^{59}Fe.

The tertiary amines used: tribenzylamine, tri-n-butylamine, tri-n-hexylamine and tri-n-octylamine, hereafter denoted as TBA, TBuA, THA, TOA, were commercial products of BDH and Schuhardt. Only the TOA was additionally purified by distillation under vacuum. Using methyl violet saturated benzene solution as indicator, 0·1 M (by weight) solutions of these amines in benzene were titrated to a clear blue with 0·1 M perchloric acid dissolved in acetic acid. The titrant was standardized by titration against diphenylguanidine or potassium acid phthalate.

TABLE 1.—DILUENTS USED IN EXPERIMENTS

Diluent	Dielectric constant ε	Dipole moment μ	Solubility parameter σ
n-Hexane	1·89	0	7·3
n-Octane	1·95	0	7·55
n-Heptane	1·92	0	7·45
Carbon-tetrachloride	2·23	0	8·6
Benzene	2·28	0	9·15
Toluene	2·43	0·39	8·9
Cyclohexane	2·02	0	8·2
o-Xylene	2·56	0·52	9·0
Bromoform	4·38	0·99	10·5
Chloroform	4·81	1·21	9·3
Chlorobenzene	5·71	1·73	9·5
Ethyl iodide	7·82	1·93	9·4
Ethyl bromide	9·41	2·02	8·9
o-Dichlorobenzene	9·93	2·25	10·0
Nitrobenzene	34·82	4·23	10·0

From the neutralization equivalents of the amines it appears that their tertiary amine contents were: for TBA – 100% for TBuA – 98·4, for THA – 99·4 and for TOA – 98·7 per cent with the accuracy of ± 1 per cent in all cases.

Solutions. All experiments were conducted with aqueous phases 8 M in hydrochloric acid. In all cases the initial concentration of iron, containing ^{59}Fe, was $5{\cdot}3 \times 10^{-5}$ M. The iron concentration in the initial aqueous phase was determined spectrophotometrically. Standard 0·1 M solutions of the amines in various diluents were prepared on a weight basis and diluted as needed. Most of the experiments were conducted with amine solutions of concentration within 10^{-5}–10^{-2} M. The concentration of HCl bonded with the amines in the organic phase was determined by titrating 0·1 M solutions with 0·1 M NaOH using bromothymol blue as indicator. Before titration water and ethyl alcohol were added to the organic phase. From the results obtained it follows that the amines exist in the organic phase exclusively as amine hydrochlorides.

Procedure. All operations were carried out in glass separatory funnels. In most of the experiments 6 ml of each phase were equilibrated by shaking for 10 min. As test experiments have shown equilibration was complete in all cases in 4–5 min. Since change of temperature has only a small effect on the extraction coefficient no precautions were taken to thermostat the system. The laboratory temperature varied between 18 and 22°C. Separation of the phases after equilibration was generally good, only occasionally it was completed by centrifugation. No pre-equilibration with acid was found necessary when the usual amine concentrations (10^{-5}–10^{-2} M) were employed. If the concentration of amine exceeded 10^{-2} M the organic phase was initially pre-equilibrated with hydrochloric acid.

Measurements. Four ml samples from each phase were used for measurements. The aliquots were placed in polythene or glass cups and the γ activity measured using an "Ekco" type scintillation counter (thalium activated NaI crystal). The extraction coefficient of the iron was defined as the ratio of the concentrations of iron measured as activity per unit volumes, in the organic and the aqueous phases.

Accuracy and precision. In the extraction experiments the greatest source of error was in the analytical procedures. The estimated error in extraction coefficients does not exceed ±3·5 per cent, in thermodynamic activities does not exceed ~10 per cent, in amine distribution coefficient and in activity coefficient of the complex does not exceed ~20 per cent.

RESULTS AND DISCUSSION

1. *The effect of metal concentration*

The effect of metal concentration in the aqueous phase on the extraction coefficient by tribenzylamine in benzene is shown in Fig. 1. It follows from this figure that the extraction coefficient of iron is independent of the metal concentration when the latter is below 10^{-4} M. Therefore in all experiments an iron concentration of $5{\cdot}3 \times 10^{-5}$ M was used.

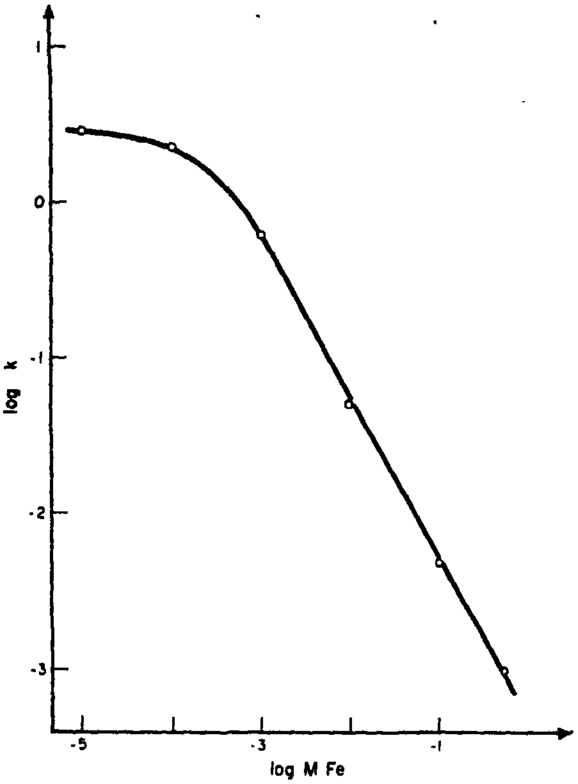

FIG. 1.—Extraction coefficient, *k*, for ^{59}Fe by 5×10^{-4} M tribenzylamine in benzene, for an aqueous phase 8·3 M in hydrochloric acid.

2. *The extraction coefficients*

In Tables 2, 3, 4 and 5 the extraction coefficient, *k*, is presented as a function of the initial concentration of the amines in a number of diluents. It follows from these Tables that in all the diluents the extraction coefficient increases with the length of the carbon chain of the amine. Very low extraction was observed when the amines were diluted with chloroform or bromoform. This observation resembles the results from this Laboratory[4] on the extraction of thorium and europium by tri-n-butylphosphate

TABLE 2.—EXTRACTION COEFFICIENTS OF Fe (III)—5·3 × 10^{-5} M FROM 8 M HCl BY TRIBENZYLAMINE IN VARIOUS DILUENTS

Initial concentration of TBA (M)	Diluents													
	Benzene	Toluene	*o*-Xylene	Chlorobenzene	*o*-Dichlorobenzene	Nitrobenzene†	Chloroform	Bromoform	Carbon tetrachloride	Ethyl bromide	Ethyl iodide	n-Hexane	Cyclohexane	n-Heptane
1·0 × 10^{-5}	0·03	0·025	0·01	0·06	0·11	0·18	0·003	0·007	0·003	0·14	0·02			
2·5 × 10^{-5}	0·07	0·06	0·03	0·16	0·22	0·47	0·007	0·01	0·005	0·62	0·19			
5·0 × 10^{-5}	0·14	0·12	0·06	0·34	1·0	1·0	0·01	0·015	0·006	1·5	0·41			
1·0 × 10^{-4}	0·33	0·25	0·13	0·80	2·4	1·9	0·03	0·02	0·009	2·6	1·0			
2·5 × 10^{-4}	0·94	0·62	0·34	3·1	14	3·6	0·05	0·04	0·02	5·0	4·4			
5·0 × 10^{-4}	2·2	1·5	0·80	10	85	5·6	0·11	0·09	0·04	11	18			
1·0 × 10^{-3}	6·9	4·1	1·4	40	206	7·3‡	0·24	0·18	*	88	55	<0·001	<0·001	<·001
2·5 × 10^{-3}	17	3·4*	1·4*	156			0·60	0·47		159	136			
5·0 × 10^{-3}							1·7	1·3						
1·0 × 10^{-2}							5·9							

* Precipitate occurred † 2·66 M HCl ‡ Emulsion

TABLE 3.—EXTRACTION COEFFICIENTS OF Fe (III)—5·3 × 10^{-5} M from 8 M HCl BY TRI-N-BUTYLAMINE IN VARIOUS DILUENTS

Initial concentration of TBuA (M)	Diluents										
	Benzene	Toluene	o-Xylene	Chlorobenzene	o-Dichlorobenzene	*n*-Heptane	Cyclohexane	Carbon tetrachloride	Chloroform	Ethyl iodide	Nitrobenzene*
5·0 × 10^{-5}	0·015	0·008	0·003	0·11					0·02		0·92
1·0 × 10^{-4}	0·03	0·02	0·007	0·23					0·03		2·1
2·5 × 10^{-4}	0·082	0·04	0·02	0·56	1·2				0·09	0·94	4·6
5·0 × 10^{-4}	0·16	0·08	0·03	1·2	2·7				0·18	2·3	8·1
1·0 × 10^{-3}	0·35	0·17	0·06	2·7	7·7				0·39	3·6	15
2·5 × 10^{-3}	0·87	0·45	0·16	7·1	27			0·01	1·15		21
5·0 × 10^{-3}	2·0	0·94	0·33	16				0·03	3·1		34
1·0 × 10^{-2}	4·7	2·2	0·79	45		0·005	0·007	0·07	8·8		

* 2·66 M HCl

TABLE 4.—EXTRACTION COEFFICIENTS OF Fe (III)—5·3 × 10^{-5} M FROM 8 M HCl BY TRI-N-HEXYLAMINE IN VARIOUS DILUENTS

Initial concentration of THA (M)	Diluents											
	Benzene	Toluene	*o*-Xylene	Chloro-benzene	n-Heptane	Cyclo-hexane	n-Octane	Carbon tetra-chloride	Chloro-form	Ethyl iodide	*o*-Di-chloro-benzene	Nitro-benzene
1·0 × 10^{-5}			0·13	0·13						0·7	0·28	0·26
2·5 × 10^{-5}	0·30	0·33	0·34	0·42	0·02	0·06		0·07		0·28	0·61	0·70
5·0 × 10^{-5}	0·54	0·59	0·72	1·0	0·027	0·13		0·27		0·68	1·27	1·4
1·0 × 10^{-5}	2·1	2·5	2·3	3·1	0·08	0·38	0·06	0·57	0·09	2·0	3·7	3·0
2·5 × 10^{-4}	10	12	12	12	0·40	2·1	0·36	3·0	0·13	5·2	16	9·8
5·0 × 10^{-4}	24	28	28	26	1·5	7·9	1·4	13	0·28	6·9	33	11
1·0 × 10^{-3}	44	85	53	44	7·0	23	5·0	28	0·68			
2·5 × 10^{-3}									2·0			
5·0 × 10^{-3}									5·0			

TABLE 5.—EXTRACTION COEFFICENTS OF Fe (III)—5·3. × 10^{-5} M FROM 8 M HCl BY TRI-N-OCTYLAMINE IN VARIOUS DILUENTS

Initial concentration of TOA (M)	Diluents										
	Benzene	Toluene	*o*-Xylene	Chloro-benzene	*o*-Dichlo-robenzene	n-Heptane	n-Hexane	n-Octane	Carbon tetra-chloride	Chloro-form	Nitro-benzene*
1·0 × 10^{-5}	0·13	0·14	0·13	0·13	0·21	0·07	0·28	0·08	0·06	0·007	0·18
2·5 × 10^{-5}	0·43	0·39	0·41	0·41	0·47	0·23	0·60	0·23	0·13	0·01	0·44
5·0 × 10^{-5}	0·87	1·0	1·0	1·1	1·1	0·63	2·0	0·56	0·34	0·02	1·12
1·0 × 10^{-4}	2·7	2·9	2·9	3·3	2·5	2·6	6·3	2·3	0·96	0·05	3·11
2·5 × 10^{-4}	17	15	12	13	25	86	28	33	6·9	0·12	8·74
5·0 × 10^{-4}	51	60	78	36	87	298	58	73	42	0·29	12·5
1·0 × 10^{-3}	103	137	152	90	207				251	0·61	23·3
2·5 × 10^{-3}	152	201								1·7	
5·0 × 10^{-3}										4·4	
1·0 × 10^{-2}										12	

* 2·66 M HCl

in $CHCl_3$ or $CHBr_3$, and those of Good and Bryan(5) on the extraction of Co(II) with amines. Another peculiarity was the fact that neither TBA nor TBuA extracts iron ($k < 0{\cdot}001$) when diluted with such aliphatic hydrocarbons as n-heptane or cyclohexane. Under the same conditions, however, THA or, in particular, TOA extracts iron fairly well. The lack of the extraction of iron(III) by TBA in cyclohexane was observed earlier by Maddock and Smułek(6) while concerned with the extraction of iron(III) and gold(III) from hydrochloric acid solutions with tribenzylamine in a number of diluents. There must be a qualitative change in the properties of the complex extracted connected with the length of the carbon chain. The behaviour of TBA or TBuA in carbon tetrachloride is worthy of notice. The properties of this diluent resemble those of the aliphatic hydrocarbons but the extraction by these amines in CCl_4 is considerably better than into the aliphatic hydrocarbons. It seems that the polarizability of CCl_4 may very likely account for this phenomenon.

3. *Distribution and thermodynamic activities of the amine hydrochlorides*

Distribution of the amine hydrochlorides between the two phases was determined by means of the secondary extraction coefficient technique. The amine concentration found in the aqueous phase was subtracted from the initial concentration and the extraction coefficient c_0/c_a was calculated. The results for the highest amine concentration employed are presented in Table 6. It follows from these data that the extraction coefficient of the amine increases with the length of the carbon chain of the amine. One of the most important factors for such a behaviour is the increase in the work needed to create a hole in the aqueous phase. This work should increase with the length of the carbon chain of the amine. It may be added that the data for the lower amine concentrations do not differ much from those given in Table 6. The highest extraction coefficients for all the amines are shown by chloroform and bromoform, the lowest by the aliphatic hydrocarbons. After equilibration with TBuA nearly all the amine was found to be present in the aqueous phase, except with chloroform. From the measured concentration of the amine hydrochloride in the aqueous phase its activity in the organic phase was calculated, using Equation (8). The results are presented for TBA and THA in Figs. 2 and 3, for TBuA and TOA in Table 7. As the solubility of TOA in the aqueous phase is very small only the amine concentration of 10^{-2} M was employed to determine its activity. On the basis of the above data the following conclusions can be drawn.

(1) The activity of tri-n-butylamine hydrochloride does not depend on the diluent. It seems that a higher solubility of this amine in the aqueous phase may very likely account for this behaviour.

(2) The activities of TBA-, THA- and TOA-hydrochlorides depend on the diluent. This dependency is more pronounced in the case of THA, than for tribenzylamine and TOA (Tables 2-5). Especially noteworthy are the differences in the activities for THA and TOA in the aromatic and aliphatic hydrocarbons. Generally, it can be said that the activities for all the amines decrease with increase in such physical parameters as the dielectric constant, dipole moment and solubility parameter of the diluent.

---

(5) M. L. Good and S. E. Bryan, *J. Inorg. Nucl. Chem* **20**, 140 (1961).

(6) A. G. Maddock and W. Smułek. Unpublished results.

TABLE 6.—DISTRIBUTION COEFFICIENTS FOR THE AMINES BETWEEN THE ORGANIC PHASE AND 8 M HCl

Amine	Amine concentration (M)	Diluents										
		Benzene	Toluene	*o*-Xylene	Chloro-benzene	*o*-Dichloro-benzene	Nitro-benzene	n-Heptane	Cyclo-hexane	Carbon tetra-chloride	Chloro-form	Ethyl iodide
TBA	$2·5 \times 10^{-4}$	0·6	0·2	0·2	1·6	4·8	16	<0·1	<0·1	<0·1		0·8
TBA	$5·0 \times 10^{-4}$	1·0	0·2	0·6	2·3	5·7	14	<0·1	<0·1	<0·1		1·4
TBA	$1·0 \times 10^{-3}$	1·0	0·2	0·6	2·3	4·5	19	0·8	0·2	<0·1	130	1·9
TBuA	$1·0 \times 10^{-2}$	0·2	<0·1	<0·1	0·2		0·2	<0·1	<0·1	<0·1	7·3	<0·1
THA	$2·5 \times 10^{-4}$	14	7·0	3·6	46			0·3	0·1	4·9		
THA	$5·0 \times 10^{-4}$	15	6·9	4·7	55			0·1	0·3	4·5		
THA	$1·0 \times 10^{-3}$	16	6·7	3·8	65	60	220	0·1	0·2	4·6	370	19
TOA	$1·0 \times 10^{-3}$	~1800	~1150	~1140	~1000			170		770	>13000	

TABLE 7.—ACTIVITIES OF TBuA ($\times 10^{+3}$) AND TOA IN VARIOUS DILUENTS

Amine	Amine concentration (M)	Diluents											
		Benzene	Toluene	*o*-Xylene	Chloro-benzene	*o*-Dichlo-benzene	Nitro-benzene	n-Hex-ane	n-Hep-tane	n-Octane	Cyclo hexane	Carbo-tetra-chloride	Chloro-form
TBuA	$1·0 \times 10^{-3}$	0·81	0·88	0·93	0·90	0·69	0·66		0·96		0·10	0·96	0·10
TBuA	$2·5 \times 10^{-3}$	2·2	2·7	2·4	1·8	1·8	1·8		2·4		2·4	2·2	0·25
TBuA	$5·0 \times 10^{-3}$	4·2	4·8	4·2	4·0		3·5		4·9		4·5	4·8	0·60
TBuA	$1·0 \times 10^{-2}$	8·9	10	10	8·7		8·1		10		10	10	1·3
TOA	$1·0 \times 10^{-3}$	0·017	0·027	0·029	0·026	0·027	0·027	0·17	0·18	0·19		0·04	0·002

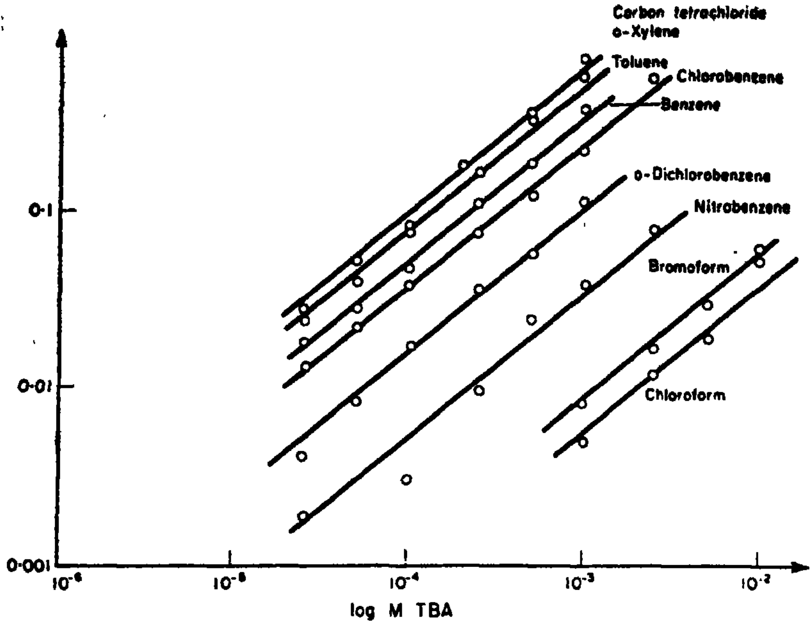

Fig. 2.—Relation between the tribenzylamine activity, *a*, and the concentration of the amine in the organic phase. Aqueous phase in all experiments, except where otherwise indicated, was maintained constant, Fe-5·3 × 10^{-5} M, 8·0 M HCl.

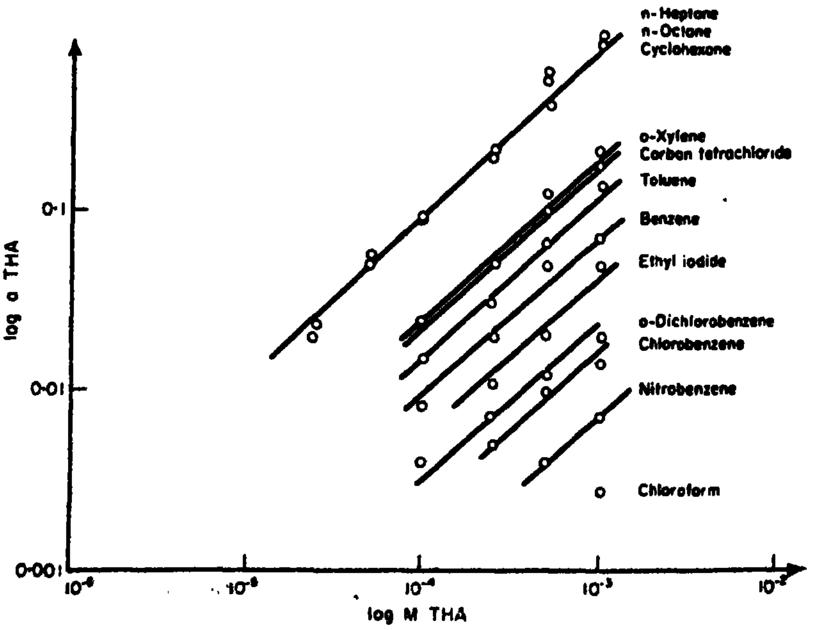

Fig. 3.—Relation between the tri-n-hexylamine activity, *a*, and the concentration of the amine in the organic phase.

(3) The activities of TBA-, THA- and TOA-hydrochlorides diluted with chloroform or bromoform were found to be remarkably lower in comparison with the other diluents. Since none of the physical parameters seems to account for this phenomenon the only reasonable assumption would be hydrogen bonding between the amine nitrogen and the acidic hydrogen in chloroform or bromoform. Similar assumptions were earlier advanced⁽⁴⁾ with respect to the low TBP activity in these solvents, and recently by GOOD and BRYAN in a study on the extraction of Co(II) from hydrochloric solutions by long chain alkyl amines, The hydrogen bonding in the latter study has, to some extent, been confirmed by an infra-red examination. The existence of hydrogen bonding between chloroform⁽⁷⁾ and the amine nitrogen seems to be understandable. However, as experiments have shown, the amine in the organic phase, at equilibrium with 8 M HCl, exists there as the salt: R_3NHCl. Thus it is obvious that the amine nitrogen is occupied by the molecule of HCl and no direct bond between the chloroform hydrogen and the amine nitrogen could be possible. If hydrogen bonding, in the case of haloforms, is still postulated it would be necessary to assume that this hydrogen bond is formed through the chlorine⁽⁷⁾ atom. The species formed might be represented by $R_3NHCl \ldots HCCl_3$. This hypothesis deserves further study.

In Figs. 2, 3 the activities of tri-n-hexylamine hydrochlorides and tribenzylamine hydrochlorides are plotted as a function of the initial amine concentration in the organic phase. The data for TBuA are not given because the activity of the amine hydrochloride depends only insignificantly on the diluent, except for chloroform. A number of superimposed curves of slope equal to 1·0 would be obtained in that case. From the slopes of the curves in Figs. 2, 3, a conclusion may be drawn as to the relation between the activity of the amine salts and their concentration. The slopes in the case of TBA, TBuA, THA and very probable, of TOA are close to 1·0. The latter value may mean that the activity is proportional to the concentration and that there is no dissociation or association of the amine hydrochloride in the organic phase. In the literature concerned with extraction by amines it is commonly supposed that the activity of amines in the organic phase is constant. This opinion seems to be true only for higher concentrations of amines (~ 0·1 M), but not for those employed in the present study. An experiment made by the authors with THA in benzene at concentrations ranging between 10^{-3} M and 10^{-1} M lends support to this suggestion.

4. *The effect of diluent on the activity coefficient, y_c*

The value of y_c can be calculated from Equation (4) on the assumption that $y_c = 1$ in the undiluted amine hydrochloride at equilibrium with 8 M hydrochloride acid. So defined y_c comprises the interaction with the diluent and the difference in the interaction of the complex with the undiluted and diluted amine hydrochloride. The activity coefficient was calculated assuming that one $FeCl_4^-$ anion associates with only one amine cation (Equation 1). If this is true y_c should be independent of the amine concentrations, at least at low concentrations. To examine this point the activity coefficient, y_c, was plotted as a function of the initial organic amine concentration (Figs. 4, 5, 6). It follows from these figures that in the range of small amine concentrations y_c is approximately constant, but it decreases with increasing amine

---

⁽⁷⁾ G. C. PIMENTAL and A. L. MC CLELLAN, *The Hydrogen Bond.* Freeman, San Francisco and London (1960).

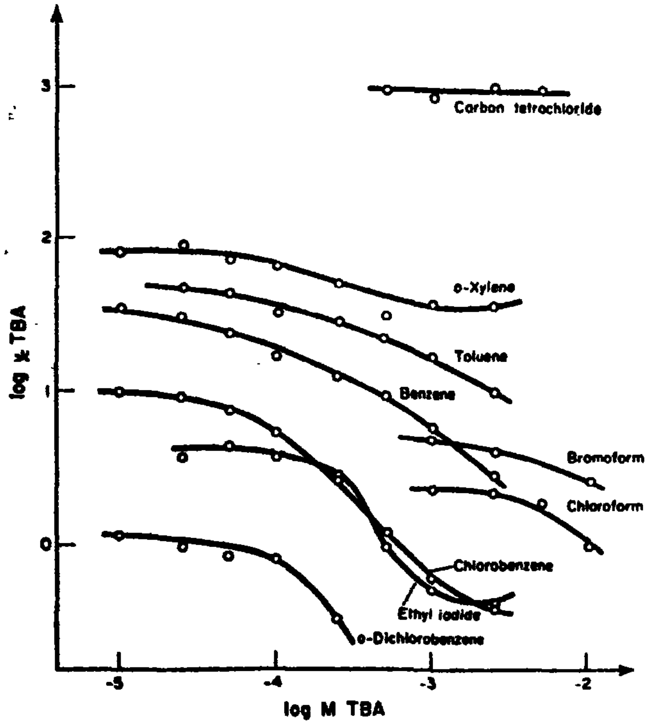

FIG. 4.—Relation between the activity coefficient of the complex, y_c, for tribenzylamine and the amine concentration in the organic phase.

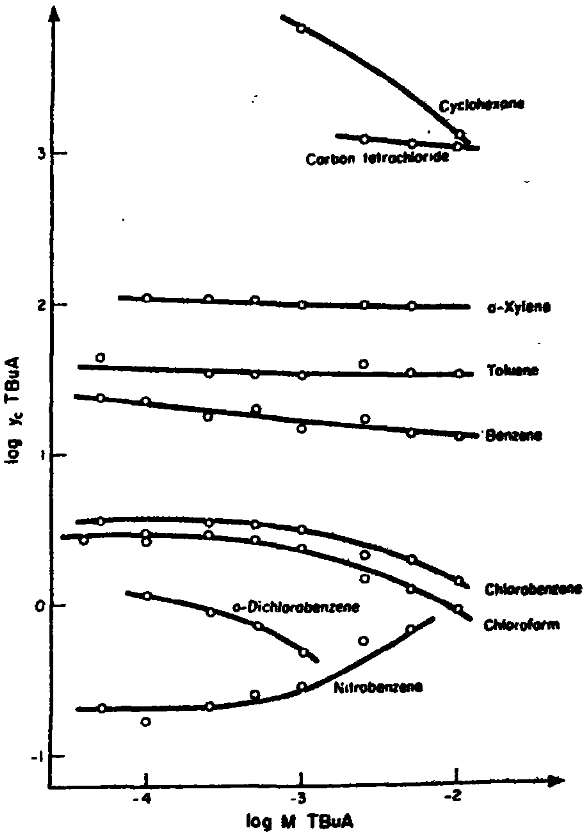

FIG. 5.—Relation between the activity coefficient of the complex, y_c, for tri-n-butylamine, and the amine concentration in the organic phase.

concentrations. This decrease may by explained by the complex–aminehydrochloride interaction. However, from these data it is difficult to decide whether this interaction leads to the formation of a well defined and stable compound containing more than one amine cation for one $FeCl_4^-$ to result in e.g. $R_3NHFeCl_4.R_3NHCl$, or whether this deviation arises only from the interaction between the complex and the amine hydrochloride which does not lead to the formation of any particular compound. Nevertheless it follows from Figs. 4, 5, 6, that owing to the constancy of y_c at small amine concentration, the 1 : 1 complex may be postulated in this range.

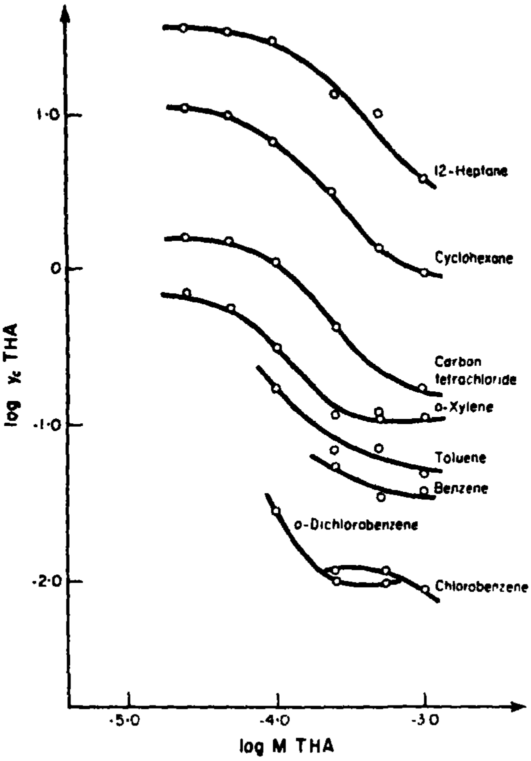

FIG. 6.—Relation between the activity coefficient, y_c, for tri-n-hexylamine, and the amine concentration in the organic phase.

The results obtained show that with all the amines used the diluent has a strong effect on the activity coefficient of the complex. To illustrate this point plots have been drawn of log y_c against the dipole moment (TBA and TBuA, Figs. 7 and 8) or the solubility parameter of the diluent (THA, Fig. 9). It is believed that similar behaviour at Fig. 9 also occurs in the case of TOA. The y_c for TOA were not calculated because the extraction coefficients of this amine were too high, at the appropriate amine concentration (10^{-3} M), to ensure reliable results.

The extraction coefficient, k, with TOA is less dependent on the diluent than that with THA. Especially noteworthy are the differences in k with THA and TOA in the aromatic and aliphatic diluents. With THA k in the aromatic diluents is much higher than in the aliphatic ones. However with TOA k in both series of the diluents is practically the same or even higher in the aliphatic diluents. On the other hand the thermodynamic activity of TOA-hydrochloride is less dependent on the diluent than in the case of THA-hydrochloride. Thus the activity coefficient, y_c, similarly as with THA, is dependent on the diluent, but to a lesser degree than with THA. This is very probably connected with the length of the carbon chain of the amine.

From the Figs. 7 and 8 it could be concluded that in the case of TBA and TBuA a dipole–dipole interaction, between the complex and diluent, may play a dominant role whereas in the long chain alkyl amine, THA, and probably in the case of TOA, dispersion forces seem to be the factor of primary importance.

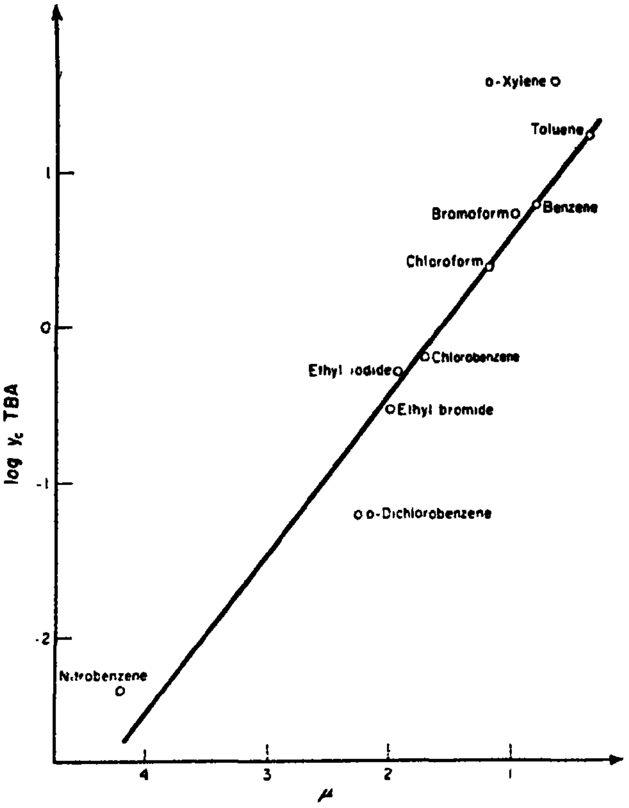

FIG. 7.—Activity coefficient, y_c, for the tribenzylamine-complex, for a constant amine concentration in the organic phase, 10^{-3} M, as a function of the dipole moment of the pure bulk diluent. The point referring to benzene was obtained by extrapolation.

5. *k as a function of the diluent*

From the two variable factors on which the extraction coefficient depends (Equation 4) the amine hydrochloride activity, a_0, was determined from its solubility in the aqueous phase and the activity coefficient, y_c, was determined from the known a_0, and the value k. If it is assumed that the reasoning which led to the derivation of Equation (4) is correct, it may still be assumed that y_c, determined directly from other experiments would be equal to that calculated in the present study. Now, bearing the above in mind, the effect of both these factors, a and y_c, on the extraction coefficient can be discussed.

In the case of THA and TOA both factors depend in a similar manner on the physical properties of the diluent (both decrease with increasing solubility parameter). Since k is directly proportional to the amine activity and inversely to y_c, therefore k is much less dependent on the diluent, particularly when the aromatic and aliphatic diluents are considered.

In the case of TBuA and TBA the activity coefficient of the polar complex depends very strongly on the diluent. On the other hand the amine salt activity of TBA depends only slightly on the diluent, whereas that of TBuA is roughly independent of the diluent.

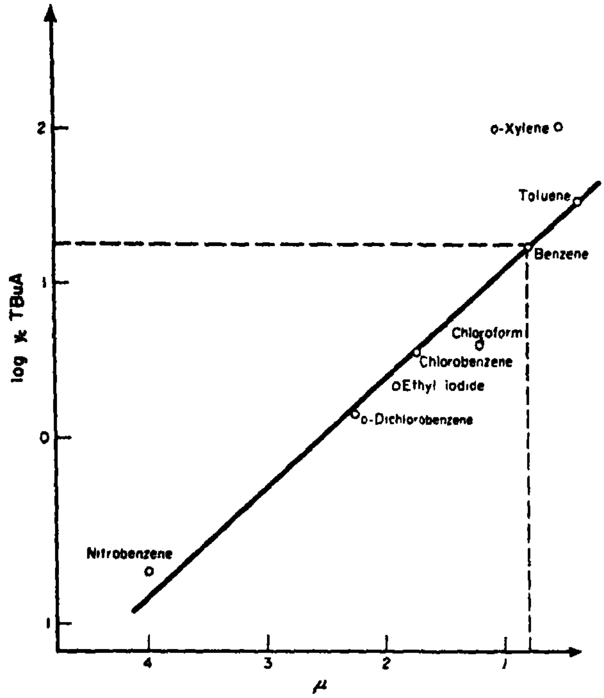

FIG. 8.—Activity coefficient, y_c, for the tri-n-butylamine complex, for a constant amine concentration in the organic phase, $2{\cdot}5 \times 10^{-4}$ M, as a function of the dipole moment of the pure bulk diluent. The point referring to benzene was obtained by extrapolation.

Thus, no compensation could be expected, like in the previous case, and as a result, the extraction coefficient is very dependent on the diluent. In the extraction by TBA and TBuA the more important factor is the interaction of the complex with the diluent, whereas for THA and TOA both the interaction of the amine and the complex with the diluent contribute roughly equally to the final effect. This explains the fairly good extraction into aliphatic hydrocarbons in the case of THA and TOA and the lack of extraction of the TBA or TBuA complexes into these diluents. If we take into account that there exists a specific and strong interaction between chloroform and the amines, i.e., hydrogen bonding, the remarkably low extraction into chloroform solutions of TBA, THA and TOA may easily be explained. The strong interaction between the amine and chloroform cannot be compensated for by a similar strong interaction between the complex and $CHCl_3$, since the latter behaves, with respect to the complex,

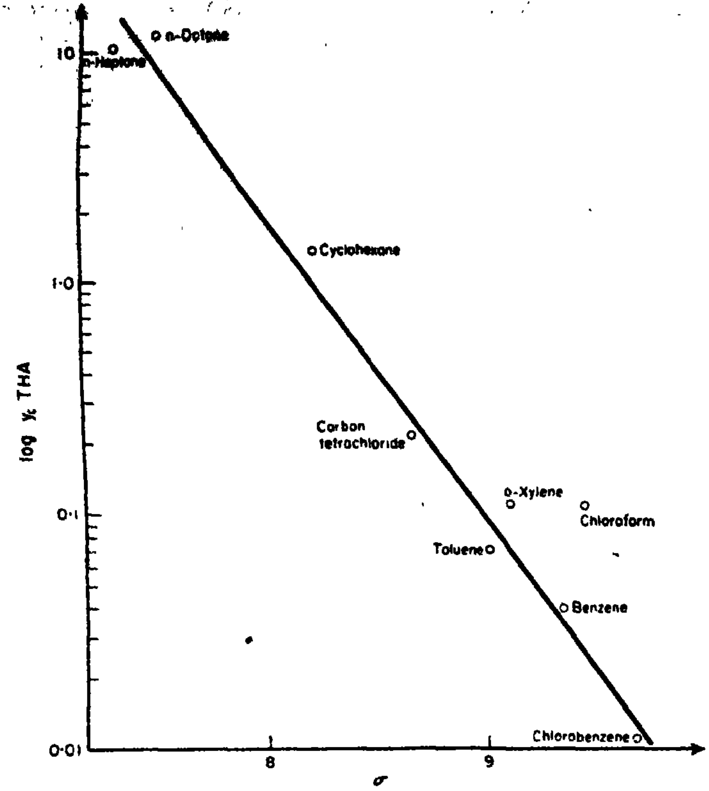

FIG. 9.—Activity coefficient, y_c, for the tri-n-hexylamine complex, for a constant amine concentration in the organic phase, 10^{-3} M, as a function of the solubility parameter of the pure bulk diluent.

"normally", as indicated by its physical parameters (e.g. the dipole moment, dielectric constant and solubility parameter).

This study shows the value of investigating the role of diluents in extraction processes by considering the activity of the extraction and the activity coefficient of the complex. Further studies in this field are in progress.

J. Inorg. Nucl. Chem., 1962, Vol. 24, pp. 1667 to 1674. Pergamon Press Ltd. Printed in Northern Ireland

POTENTIOMETRIC DETERMINATION OF BASICITY CONSTANTS IN ANHYDROUS FORMIC ACID*

A. I. POPOV† and J. C. MARSHALL
Chemistry Department, University of Iowa, Iowa City, Iowa

(*Received* 5 *March* 1962; *in revised form* 29 *May* 1962)

Abstract—A quinhydrone-sodium formate concentration cell in anhydrous formic acid was used for the determination of the relative basicity constants of several very weak bases. With one half-cell serving as the reference electrode, the e.m.f. of the cell was found to be a linear function of the log of the formate ion concentration. The pK_b values were obtained for caffeine, theobromine, urea, sodium sulphate, metrazole and nine substituted metrazoles. These values ranged from 0·55 to 2·24.

ANHYDROUS formic acid has been used by several investigators as a non-aqueous solvent for the study of acid-base equilibria.(1–5) While in all of these reports the authors have demonstrated, to varying degrees that the formic acid media does indeed enhance the strength of very weak bases, to our knowledge there are only two-reports in the literature(3,4) dealing with the measurements of basicity constants in this solvent. Yet, because of the strong protogenic character of formic acid it is to be expected that it will considerably enhance the strength of weak bases.

HAMMETT and DEYRUP(3), using the indicator method were able to determine the $pK_{b(HCOOH)}$ values for propionitrile, acetamide and water, as well as the $pK_{a(HCOOH)}$ value for the bisulphate ion. More recently SHKODIN *et al.*(4) reported the potentiometric determination of the $pK_{b(HCOOH)}$ values for a number of basic compounds. However, careful study of their procedure would seem to indicate that the significance of the results they obtained may be quite debatable. The values reported by these authors are given in Table 1.

TABLE 1.—$pK_{b(HCOOH)}$ VALUES FOR SEVERAL WEAK BASES ACCORDING TO SHKODIN *et al.*(4)

Base	$pK_{b(HCOOH)}$	Base	$pK_{b(HCOOH)}$
Diethyl Amine	0·74	Benzidine	0·75
Codeine	0·81	Aniline	0·44
Morphine	0·84	β-Naphthylamine	0·58
Urea	1·25	α-Naphthylamine	0·88
Sodium Formate	0·63	Glycocoll	0·58
Pyridine	0·45	Caffeine	0·78
		Theobromine	0·69

---

* Abstracted in part from the Ph.D. thesis of J. C. MARSHALL, State University of Iowa (1960).

† Present address: Department of Chemistry, Michigan State University, East Lansing, Michigan.

(1) L. P. HAMMETT and N. DIETZ, *J. Amer. Chem. Soc.* **52**, 4795 (1930).

(2) O. TOMICEK and P. VIDNER, Chem. Listy, **47**, 516 (1953).

(3) L. P. HAMMETT and A. J. DEYRUP, *J. Amer. Chem. Soc.* **54**, 2721, 4239 (1932).

(4) A. M. SHKODIN, N. A. IZMAILOV and N. P. DZYUBA, *Zhur. Obshchei Khimii* **20**, 1999 (1950); *Zhur. Anal. Khimii* **6**, 273 (1951).

(5) A. I. POPOV and J. C. MARSHALL, *J. Inorg. Nucl. Chem.* **19**, 340 (1961).

An examination of the results given in Table 1 reveals the surprising fact that two compounds (pyridine and aniline) are significantly stronger bases than sodium formate. This result is rather surprising since it would be expected that formic acid being a "levelling" solvent would reduce all strong proton acceptors to the basic strength of the formate ion. The only other explanation would be that sodium formate is incompletely dissociated in formic acid, but this is contrary to the conductivity data on sodium formate in formic acid published by Schlesinger and Martin[6] and to the indicator studies of Hammett and Deyrup.[3] Schlesinger and Martin report that sodium formate undergoes essentially complete dissociation in formic acid solution as concentrated as 0·1*M* (the concentration used by Shkodin *et al.*). The data of Hammett and Deyrup show that both aniline and sodium formate behave as strong bases in formic acid solutions and, in fact, find that solutions of aniline and sodium formate of the same concentration are of exactly the same basic strength.

Careful analysis of the method used to arrive at the values given in Table 1 seems to indicate the reason for the above discrepancies. All of the results obtained in that study are based on an equation originally proposed by Roller[7] which deals with the estimation of titration errors calculated from a known degree of uncertainty inherent in the measuring system. This equation is given below.

$$E = \pm 200\sqrt{\left(\frac{K_1}{K_b C_b}\right)} \,.\, \sinh \Delta \qquad (1)$$

Here E is the per cent error in titration, K_i is the dissociation constant of the solvent K_b the basicity constant of the base whose concentration in moles per litres is C_b and Δ is the *predetermined* error, expressed in millivolts, of the potentiometric measuring apparatus. However, the above authors[4] have applied Equation (1) in a somewhat different way. They first assume that an error of 1 per cent exists in their titrations, regardless of the strength of the base titrated, and substitute this value into Equation (1). Then they determine Δ by assuming that it is equal to the potential change on the titration curve corresponding to an error of 1 per cent. Using the known values for K_i and C_b they then calculate K_b. This would seem to violate both the intent and the meaning of Equation (1), since E in this equation represents a determinate error fixed by the predetermined uncertainty of the measuring system and whose magnitude depends on, among other things, the relative strengths of the acid and base involved in the titration. To make the assumption that this value is constant and then to use Equation (1) to calculate basicity constants would seem to be in error.

Another point worthy of mention is that the form of Equation (1) presumes the titration of a weak base with a strong acid. However, Shkodin *et al.* in a later paper[8] report the $pK_{a(HCOOH)}$ for *p*-toluene sulphonic acid (which was used by these authors as the titrant) to be either 0·34 or 0·73.* In either case most of the titrations involved reagents of approximately equivalent strength.

In view of the apparent lack of accurate potentiometric data on the strength of bases in anhydrous formic acid we thought it of interest to establish some empirical basis for such measurements. Also, in connection with some other studies in this laboratory on the physiochemical properties of a series of substituted metrazoles and tetrazoles, the investigation of their $\mathrm{p}K_{b(\mathrm{HCOOH})}$ values appeared to be of great interest.

---

* Respective results with quinhydrone and glass indicator electrodes.

[6] H. I. Schlesinger and A. W. Martin, *J. Amer. Chem. Soc.* **36**, 1589 (1914).

[7] P. S. Roller, *J. Amer. Chem. Soc.* **54**, 3485 (1932).

[8] A. M. Shkodin, N. A. Izmailov and N. P. Dzyuba, *Zhur. Obshchei Khim.* **23**, 27 (1953).

EXPERIMENTAL

Formic acid, 98 per cent, obtained from Eastman Kodak, was carefully purified and handled in a closed system under an inert atmosphere. The apparatus used in this investigation as well as the purification and the operating procedures have been previously described.(5) Because of the limited stability of the solvent it was always freshly distilled just prior to use. The details concerning the purification of other compounds used in this investigation are given in Table 2.

The $\mathrm{p}K_b$ values reported here are based on the measurement and the interpretation of the e.m.f. generated by the following electrochemical cell.

$$\mathrm{Pt}\Big/\begin{array}{c}\text{Sodium formate (0·25 M)}\\ \text{Quinhydrone (0·05 M)}\\ \text{(Formic acid)}\end{array}\Big/\Big/\begin{array}{c}\text{Base B (A M)}\\ \text{Quinhydrone (0·05 M)}\\ \text{(Formic acid)}\end{array}\Big/\mathrm{Pt} \qquad (2)$$

TABLE 2

Compound	Supplier	Grade	Purification	m.p. (uncorr) obs/reported (°C)
Sodium formate	J. T. Baker	Anal. Reagt.	Recryst. 3 times from conductivity water	
Caffeine	Eastman Kodak	White label	Recryst. 2 times from abs. ethanol	232–35/235–37
Theobromine	Eastman Kodak	White label	Recryst. 2 times from conductivity water	333–34/337
Strychnine	Merck		Recryst. as hydrochloride–Neut. with NH_3	267–68/268
Sodium sulphate	Mallinckrodt	Anal. Reagt.	Not purified	
Urea	J. T. Baker		Not purified	
Metrazole (Pentamethylene tetrazole)	Knoll. Pharm. Co.		Recryst. 2 times from ether	60–61/61
Substituted metrazoles and tetrazoles	Knoll Pharm. Co.		Not purified*	
Quinhydrone	Eastman Kodak	White label	Not purified†	

* These compounds were in such short supply that they could not be purified.

† Previous experiences(5) indicated that the product was of good quality and that purification seemed to have a negligible effect on the behavior of this compound in formic acid solutions.

The stability of the sodium formate reference electrode (SFRE) in formic acid has been previously investigated(8,9) and its performance was found to be entirely satisfactory.

The above cell was established in a closed system under inert atmosphere and the liquid junction between the two half cells was realized through an asbestos fibre sealed into the side arm of the reference electrode. Contamination of the sample solution by the flow of the junction was found to be negligible.(8) In all measurements bright platinum foil served as the electrode proper. The basicity constants of various bases were determined by preparing a solution of known concentration of the

(9) T. A. PINFOLD and F. SEBBA, *J. Amer. Chem. Soc.* 78, 2095, 5193 (1956).

base in the sample cell and determining the e.m.f. All the bases studied, with the exception of water, were solids. Solid samples along with an appropriate amount of quinhydrone were weighed into the sample cell and dissolved in a weighed amount of formic acid. Water was measured volumetrically and added to a formic acid solution of sodium formate of known concentration. The change in e.m.f. of the cell due to the addition of a known amount of water was interpreted in terms of the base strength of water. More complete details about the above operations have been given elsewhere.(5)

All measurements of cell potentials were made with a Leeds and Northrup type K-2 potentiometer accurate to ± 0·1 mV. A recently standardized Weston cell of the low resistance type served as a primary standard. Measurements were made at ambient room temperature of 25 ± 2°.

RESULTS AND DISCUSSION

The quantitative evaluation of base strengths using the electrolytic cell described above requires an assurance that in formic acid solution the quinhydrone electrode actually functions as a hydrogen ion indicator electrode. The potential of the concentration cell is given by Equation (3) where the subscripts S and R refer to the sample and reference cell respectively and E_j is the junction potential,

$$E_{\text{cell}} = E_R - E_S = -0{\cdot}0591 \log \frac{(H^+)_R}{(H^+)_S} + E_j \tag{3}$$

A series of sample solutions were prepared containing varying amounts of sodium formate. This gave liquid junction of the "first kind", which may be estimated from the following expression.(10)

$$E_j = [1 - \gamma N]0{\cdot}0591 \log \frac{C_R}{C_S} \tag{4}$$

Here γ is the number of ions per molecule of electrolyte, N is the transference number of the ion of the electrolyte involved in the electrode reaction and C_R and C_S are the respective concentrations of the electrolyte in the reference and sample cells. The value of N for the formate ion may be taken as 0·774.(11) Equation (4) may be substituted into Equation (3) giving the following simplified expression for the dependence of cell e.m.f. on the relative concentrations of sodium formate in the sample and reference cells.

$$E_{\text{cell}} = 0{\cdot}0271 \log \frac{(H^+)_S}{(H^+)_R} = 0{\cdot}0271 \log \frac{(\text{HCOO}^-)_R}{(\text{HCOO}^-)_S} \tag{5}$$

Therefore, when $(\text{HCOO}^-)_S$ is varied and $(\text{HCOO}^-)_R$ is held constant:

$$\left(\frac{\partial(E_{\text{cell}})}{\partial(\text{pHCOO}^-)}\right)_{(\text{HCOO}^-)_R, E_j} = +0{\cdot}027 \tag{6}$$

Implicit in the result of Equation (6) are the assumptions that quinhydrone does act as a hydrogen indicator electrode in formic acid, that sodium formate is a strong and completely dissociated base and finally that activity coefficients may be neglected. Equation (6) predicts that the plot of the e.m.f. values resulting between the SFRE and a series of sample solutions containing various amounts of sodium formate vs. p(HCOO⁻) in the sample solution, would yield a straight line of slope 0·027.

Experimental results are shown in Fig. 1. The experimental slope of 0·029 is in satisfactory agreement with the predicted slope. The concentration of the sample solution was kept low to avoid, as much as possible, the influence of activity coefficients.

---

(10) J. J. Lingane, *Electroanalytical Chemistry*, p. 43. Interscience, New York (1953).

(11) H. I. Schlesinger and E. N. Bunting, *J. Amer. Chem. Soc.* 41, 1934 (1919).

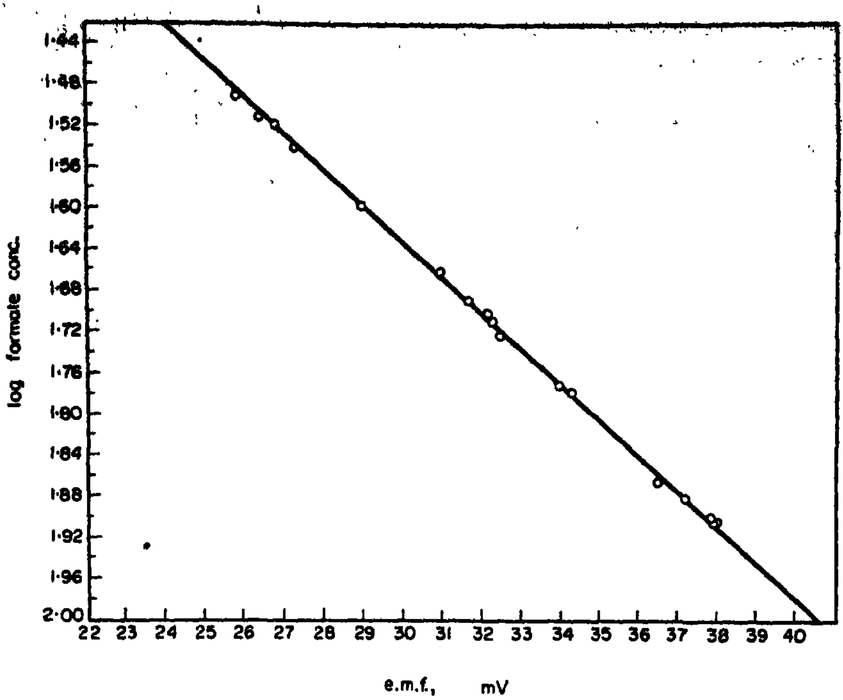

FIG. 1.—Calibration curve for the formate ion concentration in the concentration cell.

Base strengths may then be evaluated directly from potentiometric data in the following way. In general, if a base B is dissolved in formic acid the highly acidic nature of the media tends to favor the following reaction:

$$B + HCOOH \rightarrow BH^+ + HCOO^- \qquad (7)$$

The basicity constant, K_b, is given in terms of the following equilibrium concentrations:

$$K_b = \frac{(BH^+)(HCOO^-)}{(B)} \qquad (8)$$

The relationship between the cell potential and equilibrium formate ion concentration, consistent with the electrode system used, is shown in Fig. 1. If a known amount of a base is added to the sample cell so that the cell potential resulting from the combination of this cell with the SFRE is within the range of Fig. 1, the equilibrium formate ion concentration may be determined directly. This quantity along with the ion product if the solvent, K_t, and the analytical concentration of the base, B_t, may be used to calculate K_b:

$$K_b - \frac{(HCOO^-)^2 - K_t}{B_t = (HCOO^-) + K_t/(HCOO^-)} \qquad (9)$$

In view of the fact that most bases are relatively strong in formic acid, Equation (9) can, in general, be simplified to yield:

$$K_b = \frac{(HCOO^-)^2}{B_t - (HCOO^-)} \qquad (10)$$

The experimental data found for several bases and K_b values calculated from Equation (10) are given in Table 3.

Table 3.—The pK_b values of some weak bases in anhydrous formic acid

Compound	pK_b (This work)	pK_b av.	pK_b (ref. 4)	pK_b (ref 3).
Caffeine	0·56, 0·58, 0·53	0·55	0·78	
Theobromine	1·22, 1·20, 1·23	1·22	0·69	
Urea	1·72, 1·78, 1·76	1·75	1·25	
Sodium sulphate	1·90, 1·95	1·92		1·72*
Strychnine	———			
Metrazole	2·02, 2·04	2·03		
8-Tertiarybutyl Metrazole	2·08			
8-Isobutyl Metrazole	2·07			
7-Methyl-8-isopropyl Metrazole	2·27			
7-Methyl Metrazole	2·07			
8-Isopentyl Metrazole	2·18			
1-Cyclohexyl-5-ethyl Tetrazole	1·98			
1-Isobutyl-5-methyl Tetrazole	2·18			
1-Cyclohexyl-5-methyl Tetrazole	1·89			
1-Methyl-5-cyclohexyl Tetrazole	2·24			
Water	(3·9)†			4·77

* Assuming that sulphuric acid behaves as a strong monoprotic acid in formic acid solutions and taking sulphate ion as conjugate base of acid HSO_4^- for which these authors give pK_a = 4·70.
† Very approximate value.

The validity of the K_b value presented in Table 2 rests on the assumption that the junction potential remains constant when the protonated base BH^+ is substituted for the sodium ion, which is the cation present in the measurements used to establish the callibration curve shown in Fig. 1. This amounts to assuming that the ionic mobility of all positive ions is the same in this solvent. In general, it appears that the literature tends to support this assumption. Schlesinger *et al.*(6,12) report the limiting conductivities of sodium, potassium and phenylammonium ions to be 14·6, 17·5 and 13·9 mho cm^2 respectively. Lange(13) reports the limiting conductivity of tetramethylammonium ion as 17·4 mho cm^2. Taking the phenylammonium ion to most closely approximate the size of the cationic species encountered in this work, sodium rather than potassium formate was used to determine the callibration curve given in Fig. 1. The contention that the junction potential should remain fairly constant regardless of the base examined would then appear to be reasonable.

Table 3 gives a summary of the pK_b values found and such data as are found in the literature for comparison. There is very poor agreement between the values presented in this paper and those reported by Shkodin and his co-workers.(4) Fair agreement exists between the value obtained for the basicity of sulphate ion and the value calculated

(12) H. I. Schlesinger and R. D. Mullinix, *J. Amer. Chem. Soc.* 41, 72 (1919).
(13) J. Lange, *Z. Physik. Chem.* A 187, 27 (1940).

from the data of Hammett and Deyrup.[8] This is particularly significant because the above authors used an indicator method and this allows some comparison of the two independent methods.

The pK_b value obtained for water is only in very approximate agreement with the value found by Hammett and Deyrup. Because of the very slight base strength of water in formic acid, solutions had to be made as high as 1·5M in water to appreciably increase the formate ion concentration. The effect of such high water concentration on both the properties of the solvent and the junction potential is most difficult to assess. In the case of a base as weak as water the methods of Hammett and Deyrup would seem to be more reliable,

Strychnine is apparently completely dissociated as a base in the formic acid media. Solutions of strychnine in formic acid indicated equilibrium formate ion concentrations exactly coinciding with the analytical concentration of the base.

To make comparisons of relative base strengths in a non-aqueous solvent to those found in water would seem to have little meaning if the structures of the molecules differ greatly. However, in the case of caffeine and theobromine, where the two compounds have very similar structures, such a comparison should be at least of some interest. While both caffeine and theobromine are very weakly basic in water, caffeine ($K_{b(H_2O)} = 4{\cdot}1 \times 10^{-14}$) is a somewhat stronger base than theobromine ($K_{b(H_2O)} = 1{\cdot}3 \times 10^{-14}$). This same order is found in formic acid.

Strychnine, which is by far the strongest base in aqueous solution ($K_{b(H_2O)} = 10^{-7}$) of all bases examined, was the strongest base examined in formic acid. The fact that both sodium sulfate and urea are relatively, so weakly basic is somewhat difficult to interpret. The base strengths of the metrazoles and tetrazoles studied have not been determined in water although metrazole itself is known to be weakly basic in glacial acetic acid.(14)

It is difficult to estimate the absolute uncertainty in the pK_b values reported. The multiple values shown on Table 3 for caffeine, theobromine, metrazole, urea and sodium sulphate give an indication of the range of experimental error. The absolute uncertainty is, of course, dependent on the validity of the entire treatment.

The pK_b values for the substituted metrazoles and tetrazoles are based on a single measurement. This was necessary because of the limited amounts of these compounds which were available to us. While extreme care was used in making these measurements it must certainly be noted that the potential uncertainty is greater in these values than in cases where multiple determinations were possible.

Metrazole and several substituted metrazoles and tetrazoles were examined within the framework of a long standing investigation seeking to relate chemical properties and physiological activities. These compounds are of interest clinically as convulsants. While it is perhaps naive to assume that the base strength of these compounds in formic acid would be directly related to physiological activity, the formic acid media does allow a differentiation of the proton accepting tendencies of these compounds. The possibility then exists that base strength in formic acid could be in some way related to physiological activity. While it is perhaps of significance to note that the most physiologically active compound tested(15) 1-cyclohexyl-5-methyltetrazole, is the most basic and the most inactive of these compounds, 1-methyl-5-cyclohexyltetrazole is the least basic, some inversion of the order does exist with compounds of intermediate activity. The overall correlation, while it is certainly not clear-cut, may be significant. The authors feel that a great deal more work on a much larger number of compounds would be required before a more quantitative interpretation of these results can be offered.

---

(14) A. I. Popov and R. D. Holm, *J. Amer. Chem. Soc.* **81**, 3250 (1959).

(15) E. G. Gross and R. M. Featherstone, *J. Pharmac. Expert. Therap.* **87**, 291 (1946).

Acknowledgements—This work was supported by the Research Grant B-1095 from the National Institute of Neurological Diseases and Blindness, Public Health Service. The authors are also indebted to Dr. R. O. HAUCK of the Knoll Pharmaceutical Company for the substituted metrazole derivatives.

J. Inorg. Nucl. Chem., 1962, Vol. 24, pp. 1675 to 1681. Pergamon Press Ltd. Printed in Northern Ireland.

ELECTRODEPOSITION OF PLUTONIUM AND URANIUM FROM MOLTEN SALT SOLUTIONS OF DI-CHLORIDES*

M. B. BRODSKY and B. G. F. CARLESON†
Argonne National Laboratory, Argonne, Illinois

Abstract—The usefulness of molten salt solutions of Cs_2PuCl_6 and Cs_2UCl_6 for plutonium and uranium electrolyses has been investigated. Plutonium and uranium metal have been recovered from solutions without the use of soluble anodes. Up to 66 per cent of the Pu dissolved in salt solutions has been recovered with Ta cathodes. No net Pu was recovered from solution when Pu cathodes were used because of the reoxidation of the deposit by dissolved chlorine. Uranium metal was deposited on molten lead and solid molybdenum cathodes with high yields. The decomposition potentials for Pu(III)–Pu(O) and U(III)–U(O) were found to be in agreement with previous results for solutions of $PuCl_3$ and UCl_3.

STUDIES of the electrolysis of plutonium in molten salt solutions have been concerned, thus far, with the electrorefining of impure metal.(1–4) In those experiments, impure Pu anodes were electrolytically dissolved in the salt and purified metal was deposited on the cathodes. Solutions of PuF_4(1,2) and $PuCl_3$(3,4) in LiCl–KCl eutectic have been used as electrolytes. PuF_4 was used at this Laboratory because it is not hygroscopic and was available from Los Alamos. The presence of fluorine in solution with Pu, however, leads to a potential radiation hazard from the $^{19}F(\alpha,n)^{22}Na$ reaction. A flux of 20 fast neutrons/cm^2 sec, which is the maximum permissible limit for a 40 hr week, has been measured one foot from a cell which contained 100 g PuF_4.(1) Although the neutron hazard associated with $PuCl_3$–LiCl–KCl solutions is much smaller, the hygroscopic nature of $PuCl_3$(5) makes it difficult to handle and store the salt without it picking up moisture. Any moisture in the salt would have a detrimental effect on the cell operations.(2)

It has been shown(6) that the double chloride, Cs_2PuCl_6, is non-hygroscopic and can be crystallized in high yields from aqueous solution. Solutions of Cs_2PuCl_6 in LiCl–KCl contain Pu(IV) ions and will decompose to Pu(III) ions above 650°C.(7) It was suggested(6) that Cs_2PuCl_6 might be superior to either PuF_4 or $PuCl_3$ in plutonium electrolyses because it combines the best features of each. The double salt is non-hygroscopic easily prepared and causes fewer neutron problems.

---

* Work performed under the auspices of the United States Atomic Energy Commission.

† On leave from AB. Atomenergi Lovholmsv. 7, Stockholm, Sweden.

(1) B. BLUMENTHAL, Private communication (1958).

(2) B. BLUMENTHAL and M. B. BRODSKY, *Plutonium* 1960. (Edited by E. GRISON, W. B. H. LORD and R. D. FOWLER) pp. 171–186. Proceeding of the 2nd International Conference on Plutonium Metallurgy, Grenoble, France. Cleaver-Hume Press, London (1961).

(3) J. A. LEARY, R. BENZ, D. F. BOWERSOX, C. W. BJORKLUND, K. W. R. JOHNSON, W. J. MARAMAN, L. J. MULLINS and J. G. REAVIS. *Proc. of the Second International Conference on Peaceful Uses of Atomic Energy, Geneva*, 1958 Vol. 17, pp. 376–382 United Nations (1958).

(4) L. J. MULLINS, J. A. LEARY and C. W. BJORKLUND, LAMS-2441 (1960).

(5) B. M. ABRAHAM, B. B. BRODY, N. R. DAVIDSON, F. HAGEMAN, I. KARLE, J. J. KATZ and M. J. WOLF, *The Transuranium Elements.* (Edited by G. T. SEABORG, J. J. KATZ and W. M. MANNING) NNES, Plutonium Project Record, Vol. 14B., pp. 740–758. McGraw-Hill, New York (1949).

(6) J. KOOI, E. WEISSKOPF and D. M. GRUEN, *J. Inorg. Nucl. Chem.* 13, 310 (1960).

(7) D. M. GRUEN, R. L. MCBETH, J. KOOI and W. T. CARNALL, *Ann. N. Y. Acad. Sci.* 79, 941 (1960).

This study was undertaken to determine the behaviour of Cs_2PuCl_6 in electrolytic cells. The work reported here was based on electrodeposition experiments which attempted to recover the Pu which was present as Cs_2PuCl_6 in solution. This type of electrolysis differs from those described above(1–4) in that no soluble Pu anodes were used in the cells. A series of preliminary experiments were carried out with solutions of Cs_2UCl_6. This salt is also precipitated from aqueous solution without water of hydration(6) and was useful as a stand-in for the Pu salt.

EXPERIMENTAL

Electrolytic cells. Fig. 1 shows the cells used in this work. The arrangement in Fig. 1a was used for electrolyses with molten metal cathodes above the melting point of Pu, 640°C. The electrodes shown in Fig. 1b were used to deposit solid plutonium or uranium. The Vycor cells had standard-tapered, ground-glass tops which fitted a water-cooled brass cap. Holes were drilled in a tight fitting rubber stopper for electrode and gas leads.

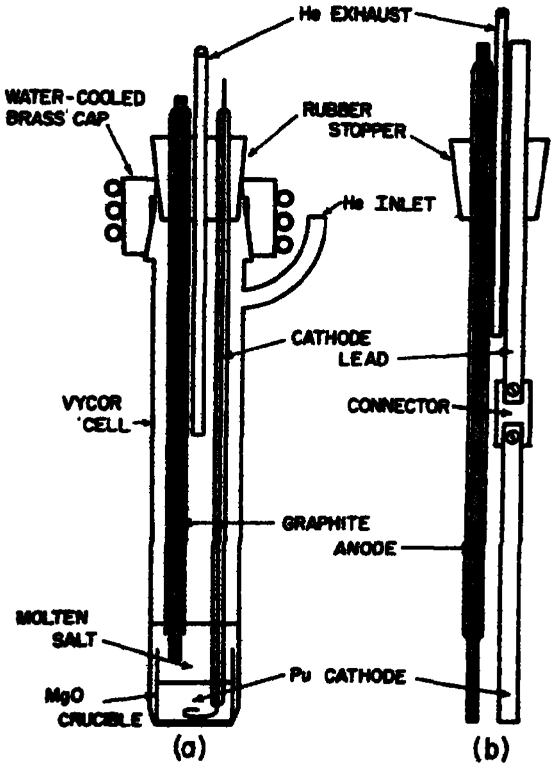

FIG. 1.

Cells were heated in a water cooled, resistance furnace inside a Pu glovebox.(8) The glovebox atmosphere was He containing a total of 0·1 w/o water, oxygen and nitrogen. Tank He (20 p.p.m. O_2) was passed directly through the cell. Uranium electrolyses were carried out in the open laboratory and a He atmosphere was maintained in the cell.

Electrodes. Spectroscopically pure graphite rods, 1/8 in. in diameter, were used as anodes in all runs. Close fitting silica tubes insulated the anodes and helped prevent them from being broken.

Solid metal cathodes were made of 1/8 in. Ta rod and 1/4 in. Pu rod. Molten metal cathodes of Pu and Pb were used. A silica insulated Ta wire was used to supply current to the molten metal. The molten Pb cathode was used in the uranium electrolyses and permitted the deposition of uranium onto a molten cathode at the same temperature of the molten Pu electrolyses, viz. 700°C. Several uranium electrolyses were made onto a cathode of Mo wire.

---

(8) L. R. KELMAN, *Gloveboxes and Shielded Cells* (Edited by G. N. WALTON). Academic Press, New York (1958).

Materials. Chemically pure CsCl, obtained from the American Potash and Chemical Corp., was filtered through a quartz frit at 700°C to remove the insoluble impurities. LiCl–KCl eutectic was prepared from J. T. Baker and Co. C.P. salts. The eutectic mixture was dried by bubbling HCl through the molten salt. The dried eutectic mixture was then filtered through a Pyrex frit.

Cs_2PuCl_6 was prepared by adding a solution of CsCl in HCl to a Pu(IV) solution.(8,9) The Pu(IV) solution was obtained by the dissolution of Pu metal in HCl and oxidation to Pu(IV) with HNO_3 followed by gentle evaporation to dryness. Batches of 11, 18, 25 and 36 g of Cs_2PuCl_6 were made with yields of 69, 80, 91 and 81 per cent, respectively. The highest yield was obtained by using minimum amounts of solvents. Analyses of the second batch showed 32·9% Pu and 29·3% Cl. These results compare favourably with theoretical values of 33·3% Pu and 29·6% Cl, and represent a Cl:Pu ratio of 6·01.

Ferraro(10) has described the Cs_2UCl_6 preparation. Yields of 85 and 92 per cent were obtained on 100 g batches. The salts analysed at 37·3 and 37·0% Cs; 33·5 and 33·6% U; and 29·3 and 29·1% Cl. The theoretical values are 37·10% Cs, 33·20% U and 29·69% Cl.

Experimental procedures. Cells were preheated at the electrolysis temperature overnight with the tank He being passed through the cell. Enough alkali halide was put into the cell to give the desired level. After the solvent had melted, approximately 5 m/o Cs_2PuCl_6 or Cs_2UCl_6 was added to the bath. The electrodes were pushed below the surface of the solution after the electrolyte had dissolved.

A six volt storage battery, in series with a suitable group of resistors, was used to furnish the cell potential. E.m.f.'s were measured with a Leeds and Northup millivolt potentiometer through an L. and N. voltbox. The number of coulombs passed through the cell was estimated from the cell current and time of electrolysis. The number of coulombs were exactly measured with a copper coulometer for the uranium runs. Potential–current curves were obtained for cells having Pu cathodes.

After the electrolysis, the deposit was melted under 50–50 m/o NaCl–KCl in Vycor and Pu beads were recovered by physical separation from the salt. This method of recovery has been used before to recover deposits(1,2) and is probably accurate to 0·01 g. The uranium content of the Pb cathode was determined after electrolysis by analysing the Pb–U alloy for total U.

RESULTS AND DISCUSSION

Results of U *cell runs.* The uranium cell data are summarized in Table 1. These runs were made at constant current at temperatures between 685° and 715°C. Cathodic current densities were usually 0·08 or 0·16 A/cm^2. Time–potential curves were obtained and are shown in Fig. 2.

The yields from runs 5 and 8 were recalculated using the amount of current which had passed through the cell when the potential curves showed the end of uranium deposition (above 2·5 V). This method of calculation gave current efficiencies of 90 and 95 per cent.

A considerable amount of the uranium was recovered as UO_2 and not U-Pb alloy. The amount of UO_2 formed was determined by analysing the salt for magnesium and measuring the weight change of the MgO crucible. Inclusion of the UO_2 in the yield calculations leads to very high recoveries. It is believed that most of the oxide was formed by reaction between the U-Pb alloy and the MgO. It is possible, however, that it might have been formed from UO_2^{2+} present in the salts. Run 7, which followed the pre-electrolysis run 6, still showed considerable UO_2 formation. Run 8, however, yielded only one-half as much UO_2, which implies that the amount of UO_2 formed does decrease with electrolysis in the same bath, but up to one-half of it is formed by reaction between the alloy and the crucible.

Fig. 2 leads to a measured decomposition potential for U(III)–U(O) of −2·34 to −2·43 V, compared to an expected value near −2·35 V.(7) If the potential at the end

---

(9) H. H. Anderson, *The Transuranium Elements* (Edited by G. T. Seaborg, J. J. Katz and W. M. Manning) NNES, Plutonium Project Record Vol. 14B., pp. 793–5. McGraw-Hill, New York (1949).

(10) J. Ferraro, *J. Inorg. Nucl. Chem.* 4, 283 (1957).

Table 1.—Summary of uranium cell results

Run No.	Cathode	U put into cell[a] (g)	U recovered at cathode (g)	U recovered as UO_2 (g)	Current efficiency (%)	
					[b]	[c]
1	Pb	3·0	1·41	1·6	56	121
2	Pb	4·39	1·55	2·5	42	109
3	Pb	4·44	1·01	2·5	26	88
4	Pb	8·04	0·10	2·8	3	67
5	Pb	4·50	3·40	1·1	72	96
6[d]	Mo	7·93	0·03	—	1	1
7	Pb	[e]	1·94	3·4	35	97
8	Pb	[e]	1·45	1·5	59	122
9	Mo	1·82	0·70	—	44	44
10	Mo	2·42	0·37	—	32	32

[a] Charged to cell as Cs_2UCl_6.

[b] Calculated from the total number of coulombs passed through the cell and the amount of uranium recovered at the cathode.

[c] Amount of UO_2 formed included in the yield.

[d] Pre-electrolysis run at 1·0 V.

[e] Electrolysis continued on solution from previous run.

of run 6 and beginning of run 7 is due to U(IV)-U(III), its value would be −1·22 to −1·29, compared to an expected −1·07 V. The potential governing reaction at the end of the electrolysis should be Cs(I)-Cs(O) with a potential of −3·48 V at 700°C.[11] The observed potential of −2·91 may be due to promotion of Cs deposition at a Pb cathode or to a reaction involving complex species.

Results of Pu cell runs. Table 2 summarizes the results of the Pu electrolyses. CsCl was used as the solvent in runs 1, 2, 3a and 3b, while LiCl-KCl eutectic was used in all other runs. It is evident that little or no Pu was recovered from the salt when Pu

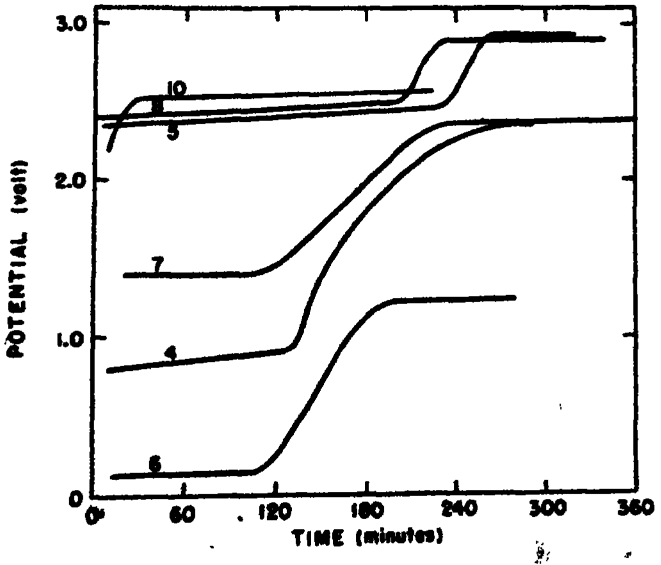

Fig. 2

---

[11] W. Hamer, M. S. Malmberg and B. Rubin, *J. Electrochem. Soc.* 103, 8 (1956).

cathodes were used but up to 66 per cent of the dissolved Pu was electrodeposited onto Ta cathodes. At the end of runs with Pu cathodes, a blue reaction product was always found on the upper part of the cathode. This material, undoubtedly $PuCl_3$, was not found on Ta cathodes.

The dark brown colour of the Cs_2PuCl_6 solutions changed to light tan after the electrolyses. The colour change generally occurred when enough current had passed through the cell to reduce twice as much Cs_2PuCl_6 as had been put into the cell. If the tan solution was kept at temperature overnight, the colour disappeared or changed to a very faint blue. During further electrolysis of the clear bath, Cl_2 gas evolved at the anode darkened the salt solution. When the current was then interrupted, the colour would fade after 10–15 min. When current to a cell was interrupted immediately after the solution had turned from dark brown to tan, a dark blue product was seen to come off the submerged Pu cathode.

TABLE 2.—SUMMARY OF Pu CELL RUNS

Run No.	Temp (°C)	Cathode(a)	Pu put(b) into cell (g)	Pu recovered (g)	Current efficiency (%)
1	700	Pu	5·04	−0·10	0
2	700	Pu	6·38	−0·30	0
3a	700	Ta	3·50	0·42	4·7
3b	740	Ta	(c)	0·00	0
4	500	Pu	0·53	−0·09	0
5	500	Pu	0·55	−0·01	0
6	450	Pu	0·53	0·01	0·1
7	504	Pu	0·53	−0·04	0
8	706	Pu	1·07	−0·17	0
9	445	Ta	0·53	0·23	20·6
10a	600	Ta	0·53	0·10	18·0
10b	591	Ta	(c)	0·14	25·1
10c	443	Ta	(c)	0·06	10·8
10d	442	Ta	(c)	0·05	9·0
10e	441	Ta	(c)	0·00	0

(a) Graphite anodes used in all runs.
(b) Charged to cell as Cs_2PuCl_6.
(c) Electrolysis continued on solution from previous run.

It is apparent that the solubility of chlorine in the salt was high enough to reoxidize Pu metal to Pu(III) or to Pu(IV). It seems likely that the liberated chlorine reacted with the Pu deposit or cathode to reverse the direction of the electrolytic reaction and to reduce the Pu yield. Naturally, it is to be expected that the reverse reaction would be more important with Pu cathodes because of the larger surface available for reaction. The redissolution of the deposit did not occur as much in the uranium electrolyses because the uranium formed UPb and UPb_3 particles which had a protective layer of Pb.(12)

Representative current–potential curves obtained in Pu cells are shown in Fig. 3. Breaks were observed consistently at −2·70 ± 0·08 and −2·98 ± 0·03 V. If one assumes that the activity coefficient for $PuCl_3$ in LiCl–KCl solutions is the same as in

---

(12) R. J. TEITEL, *Trans. Amer. Inst. Min. Met.* **194**, 397 (1952).

KCl[13] and NaCl[14] solutions and that the solutions obey Henry's Law below 50 m/o $PuCl_3$, the expected potential for Pu(III)–Pu(O) would be approximately −2·63 V in these experiments. This agreement with the observed value of −2·70 is excellent when one considers the assumptions made. The break at −2·98 V is probably due to a similar reaction as the −2·91 V break in the uranium cells, i.e., alkali metal deposition or complex species decomposition. There was no evidence of breaks for Pu(IV)–Pu(III) or Pu(IV)–Pu(O) which would be expected near 0·0 and −2·0 V, respectively.

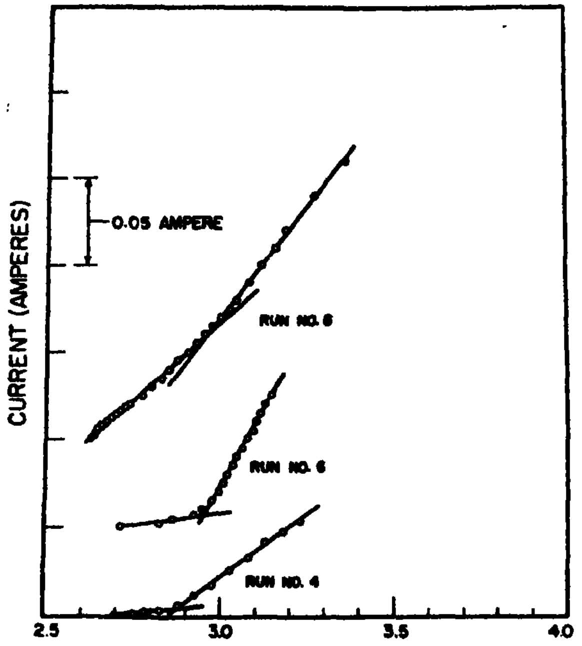

Fig. 3.

Purity of deposited metal. The small amount of Pu metal recovered in these studies made it difficult to obtain good samples for chemical analysis. Results from the analysis of run 3a are given, however, in Table 3. The surface cleanliness of the sample is seen from the low K and Na concentrations. Comparison of the data with the impurity content of the Pu used to make the Cs_2PuCl_6 shows improvement only for Ca, Mo and Ni. The high Zn content may be due to contamination of the salt bath by reaction between Cl_2 and the brass cell cap. The Cs impurity may have been due to codeposition of some Cs metal in run 3a.

Since the starting material for the salt used in run 3a was fairly pure, it is unknown if greater purification could have been obtained if less pure Pu had been used to make the Cs_2PuCl_6. Less pure Pu was used for the electrolyte of runs 4–10, but the very small recoveries did not permit adequate cleaning of the samples. Therefore, analytical results such as 200–1000 p.p.m. K and 150–500 p.p.m. Na were obtained. The other impurities were also high, e.g. Al—350 p.p.m., Cr—500 p.p.m., Fe—1000 p.p.m., Ni—150 p.p.m., etc., but were probably due to surface contamination. The only

---

(13) R. Benz, *J. Phys. Chem.* **65**, 81 (1961).

(14) R. Benz and J. A. Leary, *J. Phys. Chem.* **65**, 1056 (1961).

TABLE 3.—IMPURITY CONTENT OF DEPOSITED PU

Element(a)	Concentration in parts per million by weight	
	Pu used to make Cs_2PuCl_6	Deposited Pu
Al	29	40
Ca	13	L5
Cr	L0·01(b)	4
Fe	40	30
K	N.D.(c)	30
Li	0·02	0·02
Cs	N.D.	G500(d)
Mg	8	2
Mn	1	3
Mo	46	1
Na	13	15
Ni	10	L2
Rb	N.D.	20
Pb	L2	10
Zn	0	2000

(a) Elements not detected: Ag, B, Ba, Be, Bi, Co, Cu, Cd, Ga, La, Sb, Sn, Sr, Ti, V, W and Zr.

(b) Less than

(c) Not determined for this sample.

(d) Greater than.

impurity analyses made of U–Pb alloys showed 88 p.p.m. Mg, 20 p.p.m. Cs and <1500 p.p.m. Si.

CONCLUSIONS

This work has shown that U and Pu metal can be electrodeposited from solutions of Cs_2UCl_6 and Cs_2PuCl_6. Since the efficiency of the process is severely limited by reactions between the generated chlorine and deposited metal, it would be necessary to reduce the amount of the reverse reaction before the process could have wide use. It might be possible to prevent the chlorination of the metal by the use of anolyte or catholyte compartments; by removing the Cl_2 quickly with fast flushing or evacuation; by a process which removes the deposit frequently; etc. Greater recoveries of Pu would be obtained if a non-reactive molten metal cathode were used. Such an approach would be most useful if alloys of Pu with suitable cathode metals were desired.

It was seen that metal of fairly high purity could be obtained by the electrolysis of Cs_2PuCl_6 solutions. The removal of impurities from Pu by the crystallization of Cs_2PuCl_6 has been observed.(15) It would seem, therefore, that purification of starting materials, e.g. irradiated fuels, could be obtained by their conversion to Cs_2UCl_6 and Cs_2PuCl_6 followed by fused salt electrodeposition.

Since molten salt solutions of Cs_2PuCl_6 are suitable for Pu electrolysis, it would be desirable to demonstrate the electrorefining of impure Pu anodes in cells having the dihalide electrolyte. Such studies are in progress.

Acknowledgements—The authors wish to thank D. M. GRUEN and L. T. LLOYD for their useful discussions and interest in this work. The assistance of J. D. BADER in carrying out the experiments and E. A. HUFF and R. W. BANE for the analyses is gratefully acknowledged.

(15) J. A. LONG, Private communication (1961).

J. Inorg. Nucl. Chem., 1962, Vol. 24, pp. 1683 to 1690. Pergamon Press Ltd. Printed in Northern Ireland

NOTES

Anomolous solvent effects in the extraction of Co (II) from aqueous chloride solutions by long chain alkyl amines

(*Received* 12 *March* 1962)

A previous paper on the extraction of Co (II) from aqueous chloride solutions by long chain alkyl amines reported several effects of the organic solvent on the extraction efficiency of the system.[1] Non-polar aliphatic solvents formed three phase systems and the haloforms appeared to interact with the amines to form hydrogen bonds. Data on amines dissolved in 1-bromo-2-chloroethane showed exceptionally good extraction efficiency. A further study on the extraction efficiency obtained with amine systems dissolved in bromochloroalkane solvents has been done and is reported here.

EXPERIMENTAL

Materials

1. Long chain alkyl amines or quaternary salts used:
   - (a) Alamine 336 (tricapryl amine), General Mills Co.
   - (b) Aliquot 336 (tricapryl monomethyl ammonium chloride), General Mills Co.
   - (c) Tri-n-hexylamine, Eastman Organic Chemicals.
   - (d) Tri-iso-octylamine, Gulf Oil Corporation.
   - (e) Tri-iso-octyl monomethyl ammonium bromide was prepared by bubbling methyl bromide through an ether solution of tri-iso-octyl amine.
2. All solvents used were reagent grade and used without any further purification.

Procedure

Equal volumes of the cobalt (II) chloride in 0·25 M hydrochloric acid at various chloride ion concentrations (chloride ion was added as lithium chloride) were equilibrated with the alkyl amine dissolved in the organic solvent (usually 0·20 M). The percent extraction was determined by tracer techniques using Co^{58} isotope. This procedure is the same as described in a previous paper.[1]

RESULTS AND DISCUSSION

The percent extraction of Co (II) from aqueous solutions was observed to increase with the age of the amine solution for the bromochloroalkane solvents used. This is shown in Fig. 1. A possible explanation is that this increased extraction is caused by the formation of the hydrobromide salt of the amine, the hydrobromide being the result of a dehydrogenation of the bromochloroalkane solvent. However, treatment of the amine solution with hydrobromic acid before extraction produced no increase in the extraction efficiency. Although this evidence does not disprove the formation of the hydrobromide salt of the amine, it does show that this is not the cause of the increased extraction efficiency.

Another reaction which can occur in these solutions is nucleophilic displacement of the bromine in the solvent molecule. In this reaction a quaternary salt of the tertiary amine would be formed. Extraction experiments using the monomethyl quaternary salts of the amines in question did indeed show extraction efficiencies greater than those for the amines themselves. The results of these experiments are shown in Table 1. Also shown in Table 1 is the effect of age on a solution of tri-iso-octyl amine in 1-bromo-2-chloropropane. After 4 days the extraction efficiency of this amine solution approaches that of the corresponding quaternary salt.

Extraction values for an amine and a quaternary salt in toluene are also shown in Table 1. It can be seen that the extraction efficiency of the amine does not increase with age in this solvent but the efficiency of the quaternary salt is quite superior to that of the amine.

---

[1] M. L. Good and S. E. Bryan, *J. Inorg. Nucl. Chem.* **20**, 140 (1961).

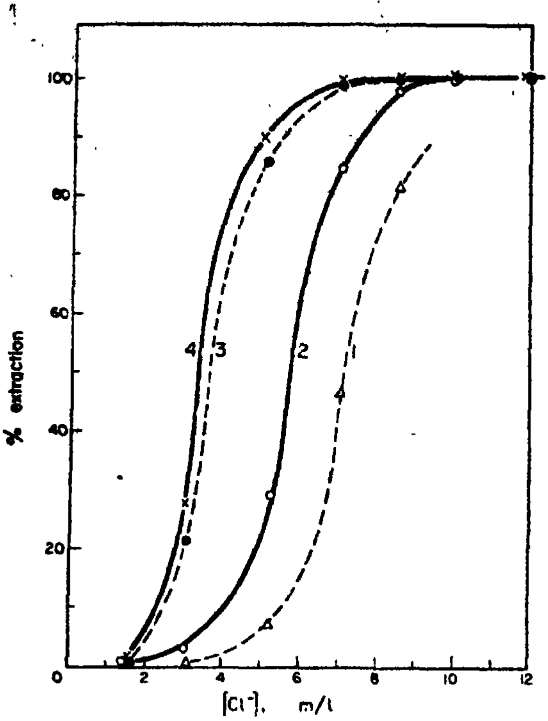

FIG. 1.—Extraction of Co (II) as a function of aqueous chloride concentration: 1 tricaprylamine in bromochloromethane, fresh solution; 2 tri-n-hexylamine in 1-bromo-2-chloroethane, fresh solution; 3 tricaprylamine in bromochloromethane, solution over 10 days old; 4 tri-n-hexylamine in 1-bromo-2-chloroethane, solution over 10 days old.

TABLE 1.—EXTRACTION OF Co (II) FROM AQUEOUS CHLORIDE MEDIA

Aqueous Cl^-*	Amine or Quaternary salt	Age of solution	Solvent	% Extraction
5 M LiCl	tricaprylamine	1 hr	bromochloro-	6·81
7 M LiCl			methane	67·7
5 M LiCl	tricaprylmonomethyl	1 hr	bromochloro-	82·6
7 M LiCl	ammonium chloride		methane	99·8
5 M LiCl	tri-iso-octylamine	1 hr	1-bromo-3-chloro	15·3
7 M LiCl			propane	94·1
5 M LiCl	tri-iso-octylamine	1 day	1-bromo-3-chloro	60·3
7 M LiCl			propane	98·7
5 M LiCl	tri-iso-octylamine	4 days	1-bromo-3-chloro	88·1
7 M LiCl			propane	99·7
5 M LiCl	tri-iso-octylmonomethyl	1 hr	1-bromo-3-chloro	90·2
7 M LiCl	ammonium bromide		propane	99·9
5 M LiCl	tri-n-octylamine	1 hr	toluene	33·9
7 M LiCl				97·9
5 M LiCl	tri-n-octylamine	41 days	toluene	34·8
7 M LiCl				98·2
5 M LiCl	tri-n-octylmonomethyl	1 hr	toluene	79·4
7 M LiCl	ammonium chloride			99·6
5 M LiCl	tri-n-octylmonomethyl	41 days	toluene	82·1
7 M LiCl	ammonium chloride			99·9

---

* Aqueous phase was 0·025 M $CoCl_2$ in 0·25 M HCl and enough LiCl was added to bring Cl^- concentration to 5 or 7 M.

Although positive identification of the quaternary salt in the aged amine solutions has not been made, these results certainly indicate that the salt is formed. The experiments reported here also point out the possibility of improving the extraction efficiency for selected metal ions in chloride media by substituting a quaternary salt for the corresponding long chain alkyl amine or simple amine salt. Similar results may also be obtainable for some metal ions in other anion systems, such as sulfate. We plan to investigate this possibility in our laboratory in the near future.

Acknowledgement—A major part of this work has been supported by the United States Atomic Energy Commission on Contract No. AT-(40-1)-2576.

Department of Chemistry
Louisiana State University
in New Orleans
New Orleans 22, Louisiana

M. L. Good
F. F. Holland, Jr.

The kinetics and heats of olation of some hydroxoaquotetramminecobalt (III) complexes

(*Received* 13 *November* 1961: *in revised form* 21 *May* 1962)

Werner[1,2] has shown that when hydroxoaquotetramminecobalt (III) complexes are heated to about 100°C, the following olation reaction takes place:

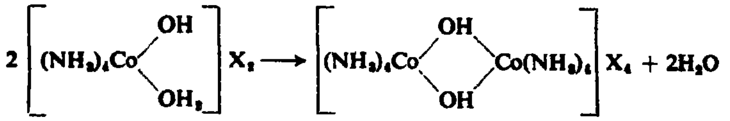

(1)

The products are water vapour and the binuclear cobalt (III complex containing two —OH bridging groups. Similar reactions have been observed for the hydroxoaquobis(ethylenediamine)cobalt (III)[3] and chromium (III)[4] complexes. More recently, the olation process has been used to explain the partial heterogeneous dehydration of various salt hydrates[5]. Since most olation processes have been observed in solution[6], it was of interest to examine the solid-state olation reaction in the cobalt (III) complexes and to determine the kinetics and heat of olation by the technique of differential thermal analysis (DTA).

EXPERIMENTAL

The complexes, $[Co(NH_3)_4OH(H_2O)]X_2$, where X is Cl^-, Br^-, and NO_3^-, and $[Co(NH_3)_4OH(H_2O)]SO_4$, were prepared by the method of Werner.[1,2]

Water contents of the complexes were determined by weight-loss on an automatic recording thermobalance.[7] The water contents found were: $[Co(NH_3)_4OH(H_2O)]Cl_2$, 7·64% found, 7·73% calc.; $[Co(NH_3)_4OH(H_2O)]Br_2$, 5·66% found, 5·60% calc.; $[Co(NH_3)_4OH(H_2O)]SO_4$, 6·74% found, 6·98% calc.; $[Co(NH_3)_4OH(H_2O)](NO_3)_2$, 6·26% found, 6·30% calc.

The DTA apparatus consisted of a nickel tube furnace, aluminium sample block, a Leeds and Northrup Model 9835-B low-level d.c. amplifier, and a Moseley Model 135R X-Y recorder.[8] Sample sizes ranged in weight from 50–70 mg and were pyrolysed in both helium and air atmospheres. A furnace heating rate of about 10°C/min was employed. The heats of olation were determined as previously described.[9] A "sandwich" type sample packing was employed. Sample sizes ranged in weight from 0·0300 to 0·500 g and were pyrolysed in a helium atmosphere under the same conditions as above. The areas of the curves were determined by tracing out the areas involved on good quality

[1] A. Werner, *Ber.* **40**, 4434 (1907).

[2] A. Werner, *Ann.* **375**, 1 (1910).

[3] A. Werner, *Ber.* **40**, 4426 (1907).

[4] P. Pfeiffer, *Z. anorg. allgem. Chem.* **29**, 107 (1901); **56**, 261 (1907).

[5] W. S. Castor and F. Basolo, *J. Amer. Chem. Soc.*, **75**, 4804, 4807 (1953).

[6] C. L. Rollinson, *Chemistry of the Coordination Compounds* (Edited by J. C. Bailar) Chap. 13, Reinhold, New York (1956).

[7] W. W. Wendlandt, T. D. George, G. R. Horton, *J. Inorg. Nucl. Chem.* **17**, 273 (1961).

[8] W. W. Wendlandt, *Anal. Chim. Acta*, in press.

[9] W. W. Wendlandt and T. D. George, *J. Inorg. Nucl. Chem.*, **19**, 245 (1961).

tracing paper, cutting them out, and weighing them on a Mettler semi-micro balance. Each such integration was performed three times per curve and the average value used in the calculations. The instrument was calibrated with $BaCl_2 \cdot 2H_2O$ crystals,(10) the ΔH of which is 26·83 kcal. mole^{-1}. An average value of 36·84 ± 0·20 cal g^{-1} of paper was obtained for the calibration constant.

The kinetic studies were performed on 0·0500 g samples, under a helium atmosphere, with the conditions the same as given above. The curves were integrated, up to temperature T or time t, in an identical manner as that used for the heats of olation studies.

RESULTS AND DISCUSSION

Since all of the compounds gave similar DTA thermograms, in an air atmosphere, only the bromide complex is shown in Fig. 1. The first endothermic peak, with a peak maximum temperature of 120°C, was due to the olation reaction as given in equation (1). The other endothermic peaks were not assigned to definite decomposition reactions but must be related to the total disruption of the binuclear complex. In the case of the nitrate compound, a pronounced exothermic peak was observed at 210°C.

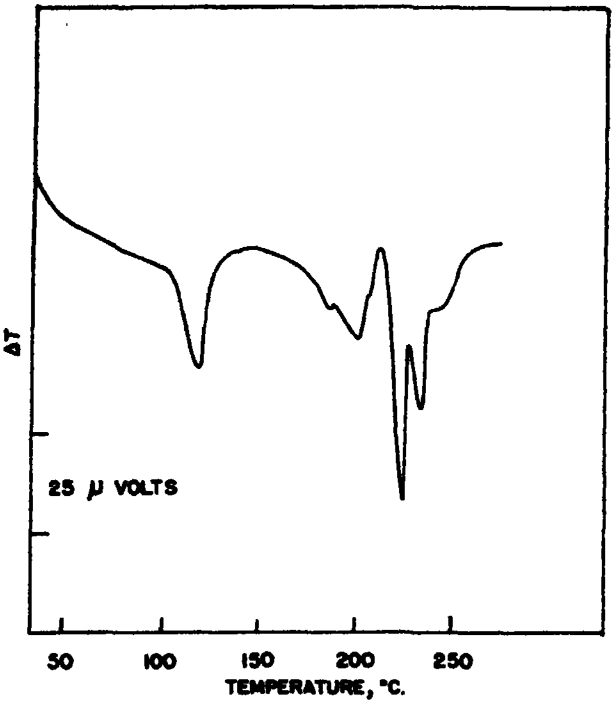

FIG. 1.—DTA curve of $[Co(NH_3)_4(OH_2)OH]Br_2$ (in air).

It is possible, by use of the technique of quantitative DTA, to determine the heat of reaction for the thermal transition involved, in this case, the heat of olation. From the various theories of DTA(11–13), the heat of reaction, ΔH, is related to the peak area by

$$\text{Peak area} = \int_{t_1}^{t_2} \Delta T\,dt = (\Delta HM)/(g\lambda_s)$$

where t_1 and t_2 are the time at the beginning and end of the peak (deviation from the base line), ΔT is the differential temperature, M is the mass of reactive sample, g is a constant dependent on the furnace and sample holder geometry, and λ_s is the thermal conductivity of the sample. Using a suitable reference material which has a known thermal transition in the temperature range being investigated, g and λ_s can be related to a constant so that

---

(10) *International Critical Tables*, 7, 263 (1926); *Selected Values of Chemical Thermodynamic Properties*, U.S. Bureau of Standards, Series 1, 1, Tables 87–5, 89–2, 3, 4 (1949).

(11) S. SPEIL, L. H. BERKELHAMER, J. A. PASK and B. DAVIS, *U.S. Bureau of Mines* Tech. Paper 664 (1945).

(12) M. J. VOLD, *Anal. Chem.* 21, 683 (1949).

(13) S. L. BOERSMA, *J. Amer. Ceram. Soc.* 38, 281 (1955).

$$\text{peak area} \times k = \Delta HM$$

Using the dehydration of $BaCl_2 \cdot 2H_2O$ as the reference material, the heats of olation in Table 1 were determined. No great accuracy is claimed for these results because of the number of variables involved in their determination. However, they are similar to those values obtained for the heat of deaquation of $[Co(NH_3)_5H_2O]X_3$[14] and $[Cr(NH_3)_5H_2O]X_3$.[15] The heats of deaquation for the above compounds ranged from 6·1 to 7·8 kcal mole^{-1}. The heats of olation found in this investigation were somewhat smaller than this, except in the case of the bromide. The comparison is not very rigorous however, since the olation reaction involves not only the breaking of Co^{3+}—OH_2 bonds but also the formation of Co^{3+}—OH—Co^{3+} bonds. In the aquopentamminecobalt (III) complexes, the first step is similar but the second step is the formation of Co^{3+}—X bonds to give $[M(NH_3)_5X]X_2$ type compounds instead of binuclear compounds.

TABLE 1.—HEATS OF OLATION FOR THE HYDROXOAQUOTETRAMMINECOBALT (III) COMPLEXES

Complex	ΔH (kcal. mole^{-1})
Chloride	3·3
	2·3
Bromide	6·1
	5·1
Nitrate	4·2
	4·8
Sulphate	2·4
	2·9

The kinetics of the olation reaction were determined by a modification of a method first described by BORCHARDT and DANIELS.[16] In this method, the rate constant, k, is equal to

$$k = [C_p(d\Delta T/dt) + K\Delta T]/[K(A - a) + C_p\Delta T]$$

where K is a constant characteristic of the experimental apparatus, A is the total curve area, C_p is the total heat capacity of the reactant or reference material, ΔT is the differential temperature, t is the time, and a is the area under the curve up to time t.

Several approximation of this method have been described.[17–19] Assuming that first order reaction kinetics are obeyed and that C_p is small, the original equation is reduced to

$$k = (\Delta T)/(A - a)$$

Using this method, the kinetics of the decomposition of the rare-earth oxalates[17,18] and calcium oxalate 1-hydrate[20] have been determined.

The results obtained here for the olation reaction are given in Fig. 2. From the slopes of the curves in Fig. 2, the activation energies, E_a, were calculated. The E_a values were as follows: chloride, 14; bromide, 15; nitrate, 33; and sulphate, 15 kcal mole^{-1}. Except for the nitrate, these values are quite close to those obtained by an isoteniscope method for the deaquation of the aquopentammine-cobalt and chromium complexes[14,15]. In the case of $[Co(NH_3)_5H_2O](NO_3)_3$, an E_a of 31 kcal was found, very close to that for the nitrate obtained in this investigation. Although the data is perhaps only approximate, it does seem to indicate that there is an anion effect in the solid-state olation reaction of the nitrate complex. The other anions involved do not appear to influence the activation energies.

In all cases, a first order reaction was assumed. This appears to be justified as tested by KISSINGER'S

---

[14] W. W. WENDLANDT and J. L. BEAR, *J. Phys. Chem.* **65**, 1516 (1961).

[15] W. W. WENDLANDT and J. L. BEAR, *J. Inorg. Nucl. Chem.* **22**, 77 (1961).

[16] H. J. BORCHARDT and F. DANIELS, *J. Amer. Chem. Soc.* **79**, 41 (1957).

[17] H. J. BORCHARDT, *J. Inorg. Nucl. Chem.* **12**, 252 (1960).

[18] V. M. PADMANABHAN, S. C. SARAIYA and A. K. SUNDARAM, *J. Inorg. Nucl. Chem.* **12**, 356 (1960).

[19] R. P. AGARWALA and M. C. NAIK, *Anal. Chim. Acta* **24**, 128 (1961).

[20] W. W. WENDLANDT, *J. Chem. Educ.* **38**, 571 (1961).

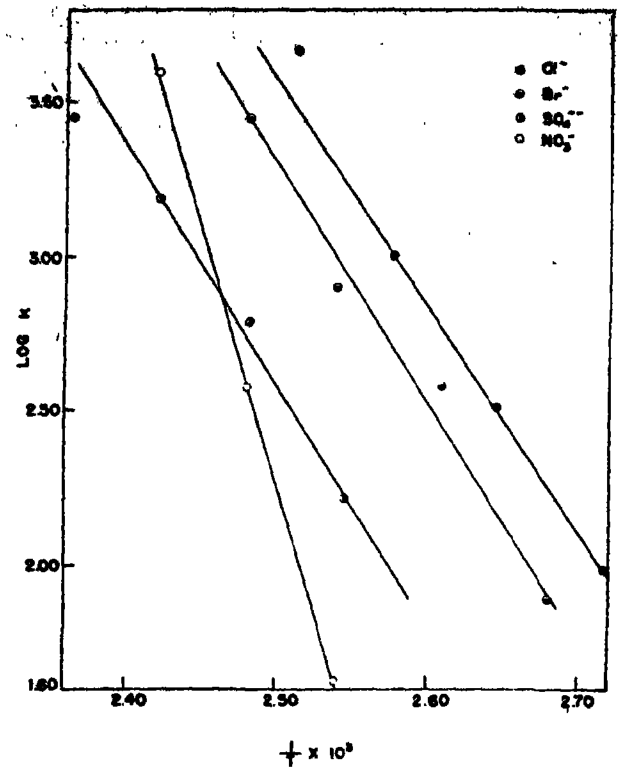

FIG. 2.—Arrhenius plots for the kinetics of olation of $[Co(NH_3)_4(OH_2)OH]^{2+}$ complexes.

method.(21) The asymmetry of the curve is described by the shape index, *S*, from which the reaction order, *n*, is related by the expression

$$n = 1{\cdot}26\, S^{1/2}$$

The values found here ranged from 0·95 to 1·09 from which it can be concluded that the reaction kinetics are probably first order with $n = 1$.

Acknowledgement—This work was supported by the U.S. Air Force, AFOSR, through Contract No. AF-49(638)-787.

W. W. WENDLANDT
J. K. FISHER

Department of Chemistry
Texas Technological College
Lubbock, Texas

(21) H. E. KISSINGER, *Anal. Chem.* 29, 1703 (1957).

Derivatives of nickelocene with thiols*

(*Received* 1 *March* 1962)

THE RECENT preparation of $(C_5H_5NiCO)_2$(1) and $(C_5H_5Ni)_2C_2R_2$ (R = alkyl, aryl)(2,3) suggested that similar dinuclear complexes might be prepared if one C_5H_5 ring in nickelocene is replaced by suitable bifunctional ligands capable of dπ—dπ bond formation. Thus, upon reaction of thiophenol, methyl- and ethyl-mercaptan with nickelocene in benzene at room temperature (method A), black complexes of composition $(C_5H_5NiSR)_2$ (R = CH_3, C_2H_5, C_6H_5) are obtained according to

---

* This research was sponsored by the International Nickel Company Inc., 67 Wall Street, New York 5, New York.

(1) E. O. FISCHER and C. PALM, *Chem. Ber.* 91, 1725 (1958).

(2) J. F. TILNEY-BASSET, *J. Chem. Soc.* 577, (1961).

(3) M. DUBECK, *J. Amer. Chem. Soc.* 82, 502 (1960).

$$(C_5H_5)_2Ni + 2RSH \rightarrow (C_5H_5NiSR)_2 + 2C_5H_6 \qquad (1)$$

Analytical results are given in Table 1.

TABLE 1.

	Compound		
Elemental Analyses	$(C_5H_5NiSC_6H_5)_2$	$(C_5H_5NiSC_2H_5)_2$	$(C_5H_5NiSCH_3)_2$
% Ni found (calc.)	24·3 (25·2)	30·8 (31·7)	33·6 (34·4)
% C found (calc.)	57·1 (56·7)	45·3 (45·5)	42·8 (42·2)
% H found (calc.)	4·7 (4·3)	5·5 (5·5)	5·0 (4·7)
% S found (calc.)	13·7 (13·7)	15·5 (17·3)	17·8 (18·8)
Melting Point, (°C)	125	78	118
Yield, (%)			
Method A	95	96	67
Method B	85	59	76
Mol. Wt. found (cal.) ebul. (benzene)	410 (465)	—	—

Magnetic measurements(4) at 330°K indicated that χ mole = -164×10^{-6} for $(C_5H_5NiSC_6H_5)_2$.

The non-polar nature of these complexes is indicated by their excellent solubility in common organic solvents. They are stable to air, even in solution, and exhibit moderate thermal stability. Above their melting points a slow disproportionation into the corresponding nickel(II)-thiolates and nickelocene takes place, as indicated by an observed sublimation of nickelocene. The molecular weight and diamagnetism confirm a dinuclear structure $(C_5H_5NiSC_6H_5)_2$. The dimerization is believed to occur via "sulphur-bridges" thus leading to a dsp^2-hybridization in the complexes. Evidence for the presence of a π-bonded cyclopentadienyl was obtained from the infra-red spectrum. The absorptions in the regions 780(*vs*), 835(*m*), 1400(*m*), and 3080(*w*) cm^{-1} are similar to those of nickelocene(5).

The splitting, not found in nickelocene, of the bands in the 1000–1100 cm^{-1} region, indicates a lower symmetry in these complexes. Although the information obtained is not sufficient to determine the structure, it seems reasonable to assume an arrangement whereby the nickel and sulphur atoms are in a plane perpendicular to the plane of the C_5H_5 ligand.

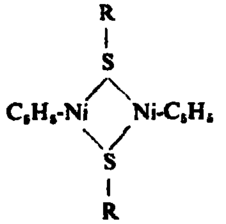

Another possibility would involve an out-of-plane position of the bridging sulphur atoms.

The same compounds can be prepared alternatively (method B) by reacting the cyclopentadienylcarbonyliodide, C_5H_5NiCOI(1), with the corresponding thiols in the presence of a base such as diethylamine. Their formation is illustrated in equation (2).

$$2C_5H_5NiCOI + 2RSH + 2B \rightarrow (C_5H_5NiSR)_2 + 2CO + 2B{\cdot}HI \qquad (2)$$

$$R = CH_3,\ C_2H_5,\ C_6H_5;\ B = (C_2H_5)_2NH$$

EXPERIMENTAL

Method A. Preparation of $(C_5H_5NiSR)_2$ (R = CH_3, C_2H_5, C_6H_5)

Equimolar amounts of nickelocene and methyl-, ethyl-, or phenyl-mercaptan were dissolved in the necessary amount of benzene and the solution stirred for 15 hr at 25°C. Immediate reaction is indicated by a colour change from green to dark brown. After removal of the solvent the residue was recrystallized from ether or hexane and dried in vacuo to give black crystals.

---

(4) The author is indebted to Dr. L. VASKA for the magnetic measurement.

(5) E. R. LIPPINCOTT and R. D. NELSON, *Spectrochim. Acta* **10**, 307 (1958).

Method B. (1) Preparation of C_5H_5NiCOI

A solution of 1·3 g of iodine (0·005 mole) in 50 ml of absolute ether was slowly dropped into a solution of 1·51 g of recrystallized $(C_5H_5NiCO)_2$[4] (0·005 mole) in 100 ml of ether, maintaining a temperature of −15°C. The resulting greenish-dark solution, containing some solid crystalline C_5H_5NiCOI, was used for the subsequent reactions.

(2) Reactions with Thiols

Equivalent amounts of thiol (0·01 mole) and 1 ml of anhydrous diethylamine were added to the stirred ethereal solution of C_5H_5NiCOI (0·01 mole) at −15°C. The colour of the solution immediately turned to a dark brown, while $(C_2H_5)_2NH{\cdot}HI$ precipitated. Excess water was added after 1 hr; the ethereal phase, containing the product, separated, was washed with dilute hydrochloric acid and water, and dried over calcium chloride. After evaporation of the solvent, the same black complexes are obtained. They can be recrystallized from ether or n-hexane.

W. K. Schropp

Mellon Institute
4400 Fifth Avenue
Pittsburgh 13, *Pennsylvania*

[4] For the preparation of $(C_5H_5NiCO)_2$ see references (1) and (2).

Cyclopentadienyl iodo nickel phosphines*

(*Received* 1 *March* 1962)

Whereas both carbon monoxide and iodine are displaced from C_5H_5NiCOI by thiols,[1] only carbon monoxide is displaced by reaction with triphenyl- and triethylphosphine. The products are monomeric, soluble in organic solvents, and exhibit remarkable thermal stability in contrast to the rather labile C_5H_5NiCOI.

Table 1

	Compound	
	$C_5H_5NiP(C_2H_5)_3I$	$C_5H_5NiP(C_6H_5)_3I$
Elemental Analyses		
% Ni found (calc.)	15·5 (15·9)	11·0 (11·4)
% C found (calc.)	36·2 (35·8)	54·0 (53·9)
% H found (calc.)	5·4 (5·5)	4·2 (3·9)
% I found (calc.)	34·2 (34·4)	24·6 (24·7)
Melting Point, °C	59	130 (decompn.)
Yield, %	88	84
Mol. Wt. found (calc.) ebul., benzene	—	522 (512)

EXPERIMENTAL

Reactions with phosphines

Triethyl phosphine (1·08 g, 0·01 mole) or triphenyl phosphine (2·26 g, 0·01 mole) dissolved in 100 ml of benzene were added with stirring to a solution of C_5H_5NiCOI (0·01 mole) in ether at −15°C. A red solution formed with liberation of carbon monoxide. After 1 hr the solvent was evaporated under reduced pressure. The maroon triethyl phosphine complex was recrystallized from n-hexane (−80°C), while the dark maroon triphenyl phosphine derivative, being insoluble in n-hexane, was recrystallized from benzene/n-hexane. The infra-red spectra of both complexes indicates the presence of π-bonded cyclopentadienyl groups.[2]

W. K. Schropp

Mellon Institute
4400 Fifth Avenue
Pittsburgh 13, *Pennsylvania*

* This research was sponsored by the International Nickel Company Inc., 67 Wall Street, New York, 5, New York.

[1] *J. Inorg. Nucl. Chem.* **24**, 1689 (1962).

[2] F. A. Cotton, *Modern Coordination Chemistry* 1960, Interscience Publ. Inc., New York, p. 355.